NUCLEAR SCIENCE ABSTRACTS

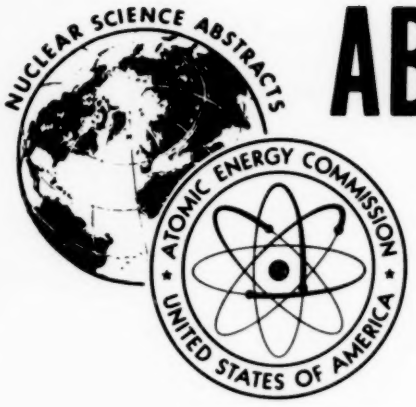

Volume 25 Number 6

Abstracts 10421-12920

March 31, 1971

UNITED STATES ATOMIC ENERGY COMMISSION
Division of Technical Information

REPORT COLLECTIONS IN THE UNITED STATES

The libraries listed below purchase and maintain microfiche collections of USAEC and foreign reports that are abstracted in *NSA*. Their collections also include *NSA* and its indexes, AEC's Technical Progress Reviews, AEC-sponsored translations, conference proceedings published by AEC, and various bibliographic tools. Most of these libraries have microfiche reader-printers or other photocopy facilities with which to reproduce enlarged copies from microfiche. Charges for reproduction services vary.

ALABAMA
Auburn, Auburn University
Tuskegee Institute, Tuskegee Institute

ALASKA
College, University of Alaska

ARIZONA
Tucson, University of Arizona

ARKANSAS
Fayetteville, University of Arkansas

CALIFORNIA
Davis, University of California
Los Angeles, University of California

COLORADO
Boulder, University of Colorado

DISTRICT OF COLUMBIA
Washington, Library of Congress (by deposit)

FLORIDA
Gainesville, University of Florida

GEORGIA
Atlanta, Georgia Institute of Technology

HAWAII
Honolulu, University of Hawaii

IDAHO
Pocatello, Idaho State University

ILLINOIS
Evanston, Northwestern University
Urbana, University of Illinois

INDIANA
Lafayette, Purdue University

IOWA
Ames, Iowa State University

KANSAS
Manhattan, Kansas State University

KENTUCKY
Lexington, University of Kentucky
Louisville, University of Louisville

LOUISIANA
Baton Rouge, Louisiana State University
New Orleans, Tulane University

MARYLAND
Baltimore, Johns Hopkins University
College Park, University of Maryland

MASSACHUSETTS
Cambridge, Massachusetts Institute of Technology

MICHIGAN
Ann Arbor, University of Michigan

MISSISSIPPI
State College, Mississippi State University

MISSOURI
Kansas City, Linda Hall Library

NEVADA
Las Vegas, University of Nevada

NEW JERSEY
Princeton, Princeton University

NEW MEXICO
Albuquerque, University of New Mexico

NEW YORK
Albany, New York State Library
Buffalo, State University of New York at Buffalo
Ithaca, Cornell University
New York, Columbia University
Rochester, University of Rochester
Syracuse, Syracuse University
Troy, Rensselaer Polytechnic Institute

NORTH CAROLINA
Raleigh, North Carolina State University

OHIO
Cincinnati, University of Cincinnati
Columbus, Ohio State University
Toledo, University of Toledo

OKLAHOMA
Norman, University of Oklahoma

PENNSYLVANIA
Philadelphia, University of Pennsylvania
Pittsburgh, Carnegie Library
University Park, Pennsylvania State University

PUERTO RICO
San Juan, University of Puerto Rico

SOUTH CAROLINA
Columbia, University of South Carolina

TENNESSEE
Knoxville, University of Tennessee
Nashville, Joint University Libraries
Oak Ridge, Oak Ridge Associated Universities

TEXAS
Austin, University of Texas
College Station, Texas A & M University
Houston, Rice University

UTAH
Salt Lake City, University of Utah

VIRGINIA
Blacksburg, Virginia Polytechnic Institute
Charlottesville, University of Virginia

WASHINGTON
Pullman, Washington State University
Seattle, University of Washington

WEST VIRGINIA
Morgantown, West Virginia University

WISCONSIN
Madison, University of Wisconsin

WYOMING
Laramie, University of Wyoming

The following governmental and international organizations offer for sale USAEC reports abstracted in *Nuclear Science Abstracts*:

National Technical Information Service, U. S. Department of Commerce
Springfield, Virginia 22151
International Atomic Energy Agency, Vienna, Austria
National Lending Library, Boston Spa, England

XUM

NOTICE

A title page for Volume 25, Numbers 1–6, is included at the back of this issue for use in binding those issues.

CORRECTIONS

NSA Vol. 20, No. 2, Abst. 37085, descriptive cataloging should read: DO-IT-YOURSELF EXTERNAL STANDARDIZATION FOR A LIQUID SCINTILLATION COUNTER. Paix, D. (Prince Henry Hospital, Little Bay, New South Wales, Australia). Int. J. Appl. Radiat. Isotop., 17: 486-8(Aug 1966).

NSA Vol. 24, No. 19, Abst. No. 39520, lines 2 and 3 should read: RADIOSENSITIVITY OF NORMAL AND TUMOR CELLS. Yarmonenko, S. P.; Pelevina, I. I. (Inst. of Experimental and Clini-

NSA Vol. 24, No. 24, Abst. 50360, line 6 should read: and F, in high-purity materials, such as Si, Ge, Fe, Ta, and Nb,

XUM

Volume 25, Number 6, March 31, 1971

NUCLEAR SCIENCE ABSTRACTS

A semimonthly publication of the USAEC Division of Technical Information, Edward J. Brunenkant, Director,
Published by the USAEC Division of Technical Information Extension, Robert L. Shannon, Extension Manager.

Nuclear Science Abstracts provides the only comprehensive abstracting and indexing coverage of international nuclear science literature. *Nuclear Science Abstracts* covers scientific and technical reports of the U. S. Atomic Energy Commission and its contractors, other U. S. Government agencies, other governments, universities, and industrial and research organizations. In addition, books, conference proceedings, individual conference papers, patents, and journal literature on a worldwide basis are abstracted and indexed. Each issue of *Nuclear Science Abstracts* includes four indexes: subject, personal author, corporate author, and report number.

The following organizations scan and abstract the nuclear science literature in their respective countries:

Atomic Energy of Canada Limited
Australian Atomic Energy Commission
Danish Atomic Energy Commission
Finnish Atomic Energy Commission
French Atomic Energy Commission
Japan Atomic Energy Bureau–Atomic Energy Research Institute
Institutt for Atomenergi (Norway)
Aktiebolaget Atomenergi (Sweden)
United Kingdom Atomic Energy Authority

Numerous organizations, societies, and publishers throughout the world provide *Nuclear Science Abstracts* with advance page-proof copy of their publications, e.g., in the United States the American Institute of Physics provides page-proof copy of its publications.

A list of the journals scanned regularly and the abbreviations used appears in Issue 1 (January 15) of each volume of *Nuclear Science Abstracts* and is supplemented in Issues 7, 13, and 19. Issue 1 of each volume also describes the scope and arrangement of the subject matter covered in *Nuclear Science Abstracts*. The subject matter covered is also described in TID-4552, *Subject Scope of Nuclear Science Abstracts*, available free from the USAEC Division of Technical Information Extension, P.O. Box 62, Oak Ridge, Tennessee 37830. An outline of the subject categories appears in the Contents of each issue.

AVAILABILITY OF PUBLICATIONS ABSTRACTED

Public availability of all U. S. Atomic Energy Commission reports is indicated in the report number indexes. The availability of other reports, when known, is also indicated. The availability of some unnumbered reports is given in the abstract.

Dissertations abstracted in *Dissertation Abstracts* and included in *Nuclear Science Abstracts* are available from University Microfilms, Inc., 315 N. First Street, Ann Arbor, Michigan 48103.

Information on the availability of the published literature and unpublished conference papers abstracted in *Nuclear Science Abstracts* can be obtained from the USAEC Division of Technical Information Extension, P.O. Box 62, Oak Ridge, Tennessee 37830.

HOW TO OBTAIN NUCLEAR SCIENCE ABSTRACTS

Nuclear Science Abstracts is available to the public on a subscription basis from the Superintendent of Documents, U. S. Government Printing Office, Washington, D. C. 20402.

For the 24 regular issues, the yearly rate is $42.00 for domestic subscribers and $52.50 for foreign subscribers. A single issue costs $1.75, domestic rates, or $2.19, foreign rates. Domestic rates apply to the United States, Canada, Mexico, and Central and South American countries except Argentina, Brazil, Guyana, French Guiana, Surinam, and British Honduras.

For a yearly subscription to the cumulative indexes, the rates are $38.00 for domestic subscribers and $47.50 for foreign subscribers.

The following cumulative indexes are available:

From Johnson Reprint Corporation, 111 Fifth Avenue, New York, N. Y. 10003:
Vols. 1–4, Subjects and Authors (1948–1950), $30.00.

From Superintendent of Documents, U. S. Government Printing Office, Washington, D. C. 20402:

Vols. 5–10, Subjects and Authors (1951–1956), $5.25.

Vols. 11–15, Subjects (1957–1961), $19.00.
Vols. 11–15, Personal Authors (1957–1961), $14.25.
Vols. 11–15, Corporate Authors (1957–1961), $2.50.

Vols. 16–20, Subjects (1962–1966), $36.00.
Vols. 16–20, Personal Authors (1962–1966), $22.50.
Vols. 16–20, Corporate Authors (1962–1966), $3.75.

Vol. 21, Subjects and Authors (1967), $16.00.
Vol. 22, Subjects and Authors (1968), $26.00.
Vol. 23, Subjects and Authors (1969), $25.75.
Vol. 24, Subjects and Authors (1970), $22.50.

Cumulative Report Number Index, Vols. 1-15 Revised, $4.00.
Cumulative Report Number Index, Vols. 16-20 Revised, $5.50.
Cumulative Report Number Index, Vols. 21-24, $4.25.

Nuclear Science Abstracts is available on an exchange basis to universities, research institutions, industrial firms, and publishers of scientific information. Government agencies may obtain *NSA* free of charge. Inquiries should be directed to the USAEC Division of Technical Information Extension, P. O. Box 62, Oak Ridge, Tennessee 37830.

INDEXES TO NSA

Comprehensive indexes appear in each issue and are cumulated quarterly and annually. Multivolume cumulations have been issued as indicated above.

All documents abstracted are indexed by subjects and personal authors. Report literature is indexed also by corporate author and report number. Each of these indexes in every issue is preceded by an introduction explaining in detail the organization of the index and the principles by which it is compiled. The reader is referred to these explanations for information not found in the brief summary below.

Personal Authors

Each author's name is indexed in the form appearing on the document abstracted:

ISHIHARA, T., Accumulation of fallout ^{137}Cs in newborn infants, 23:50538
ISHIHARA, Toyokuki, Shielding effect of paraffin, water, soil, concrete, Fe, and Pb for high-energy neutrons, 23:51748

Subjects

The subject index consisting of specific materials, objects, and processes is arranged alphabetically. Modifying phrases specific to these subjects in turn are arranged alphabetically under the subjects.

MELPHALAN
  effects on proliferation of cultured antigen-stimulated spleen cells from mice, dose-response curve for, 23:50820
MEMBRANE FILTERS
  design for removal of cell-free Streptococcus faecalus from bacteria cultures in fermentation tank, 23:49996 (UCRL-18667, pp 322-9)
MENDELEVIUM
  separation from einsteinium and fermium by electrolysis, 23:49772 (UCRL-18667, pp 277-312)
  separation from sodium acetate solutions by solvent extraction using sodium amalgam, 23:49772 (UCRL-18667, pp 277-312)
  stability of divalent state of, 23:49772 (UCRL-18667, pp 277-312)

Corporate Authors

Technical report literature is indexed from the name of the organization or institution responsible for the issuance of the report.

51093 (LA-4164) FABRICATION OF BORON CARBIDE RINGS AND DISKS. Sheinberg, H.; Herrera, T.; Kostacopoulos, J. (**Los Alamos Scientific Lab., N. Mex.**). Apr. 25, 1969. Contract W-7405-eng-36. 11p. Dep. CFSTI.

is indexed as:

LOS ALAMOS SCIENTIFIC LAB., N. MEX.
  Fabrication of boron carbide rings and disks, 23:51093 (LA-4164)

Report Numbers

Technical report literature is also indexed by report numbers. This index includes information on where individual reports may be obtained. While not reports, patents and conference papers are indexed here as a matter of convenience.

JPRS-	**(Non-AEC)**	
46949	23-51587	CFSTI
48330	23-52305	CFSTI
48331	23-52451	CFSTI
48481	23-50889	CFSTI
48743	23-51034	CFSTI
49025	23-51706	CFSTI (U. S. Sales Only)
JUL-	**(German)**	
571-RG	23-52269	Dep
578-PP	23-51624	Dep. CFSTI (U. S. Sales Only)
581-FN	23-51079	Dep. CFSTI (U. S. Sales Only)
584-RG	23-52313	Dep
586-FN	23-51035	Dep. CFSTI (U. S. Sales Only)
K-		
1777	23-50987	Dep. CFSTI
1778	23-50988	Dep. CFSTI
KFK-	**(German)**	
743	23-52461	Dep
743	23-52447	For translation see EURFNR-613
781/I	23-52462	Dep
824	23-52397	Dep. CFSTI (U. S. Sales Only)

XUM

TABLE OF CONTENTS

Volume 25, Number 6, March 31, 1971

Category	Page
CHEMISTRY	995
Analytical Chemistry	995
Chemical and Spectral Procedures	995
Isotope Dilution Procedures	999
Radiometric and Radiochemical Procedures	1000
Activation Procedures	1001
Inorganic, Organic, and Physical Chemistry	1004
Chemical Properties	1004
Isotope Effects and Exchange	1005
Physical Chemistry	1010
Radiation and Nuclear Chemistry	1011
Radiation Effects	1012
Radiation Processes	1013
Radiolysis	1017
Radioisotope Production	1020
Separation Processes	1020
EARTH SCIENCES	1024
Geology and Hydrology	1024
Meteorology	1025
Mineralogy and Exploration	1027
Oceanography	1027
Seismology	1027
ENGINEERING	1029
Nuclear Explosions	1029
Facilities and Equipment	1030
Heat Transfer and Fluid Flow	1032
Isotope Technology	1033
Materials Testing	1034
Protective Structures	1035
Radioactive Material Handling	1035
Vacuum Engineering	1036
INSTRUMENTATION	1037
Radiation Detection Instruments	1037
General Detectors and Monitors	1037
Nuclear Spectroscopic Instrumentation	1040
High Energy Physics Instrumentation	1042
Radiation Dosimeters	1043
Radiometric Instruments	1044
Miscellaneous Instruments and Components	1044
Radiation Effects on Instruments and Instrument Components	1045
LIFE SCIENCES	1047
Biochemistry, Physiology, and Molecular Biology	1047
Basic Processes	1047
Metabolism, Physiology, and Toxicology	1049
Radiation Effects	1053
Immunology	1055
Ecology	1056
Genetics and Cytogenetics	1057
Health Physics and Safety	1061
Radioactive Contamination and Decontamination	1061
Dosimetry and Monitoring	1062
Radiation Protection	1065
Safety Procedures	1065

Category	Page
LIFE SCIENCES (Cont'd.)	
Legal Aspects	1067
Medicine	1067
Protective Substances	1067
Radiation Sickness and Injuries	1069
Radiodiagnosis	1070
Radiotherapy	1081
Blast and Thermal Effects	1083
Radiation Effects on Animals	1084
Invertebrates	1084
Vertebrates	1085
Man	1090
Radiation Effects on Plants	1091
Radiation Effects on Microorganisms	1093
Radiosterilization and Radiopreservation	1093
METALS, CERAMICS, AND OTHER MATERIALS	1097
Metals and Alloys	1097
Corrosion and Erosion	1097
Preparation and Fabrication	1098
Properties Evaluations	1099
Structure and Phase Studies	1106
Radiation Effects	1110
Ceramics and Cermets	1112
Corrosion and Erosion	1112
Preparation and Fabrication	1112
Properties Evaluations	1114
Structure and Phase Studies	1118
Radiation Effects	1119
Plastics and Other Materials	1120
PHYSICS (GENERAL)	1121
Astrophysics and Cosmology	1121
Cosmic Ray Exposure Ages	1121
Stars	1121
Quasi-Stellar, Radio, and X-Ray Sources	1124
Solar Phenomena	1127
Galaxies	1130
Cosmology	1132
Planetary Phenomena	1134
Atomic and Molecular Physics	1135
Atomic, Electron, Ion, and Molecular Beams and Their Reactions	1135
Atomic and Molecular Properties	1136
Positronium, Muonium, and Mesic Atoms and Molecules	1138
Collision Phenomena	1138
Atomic Theory	1141
Cosmic Radiation	1142
Direct Energy Conversion	1143
Fluid Physics	1143
Geophysics (Upper Atmosphere)	1146
Low-Temperature Physics and Cryogenic Equipment	1151
Superfluidity	1151
Superconductivity	1151
Equipment and Devices	1154
Plasma and Thermonuclear Physics	1154
Confinement and Heating	1154
Diagnostics	1155

XUM

TABLE OF CONTENTS (continued)

Category	Page
PHYSICS (GENERAL) (Cont'd.)	
Kinetics (General)	1156
Kinetics (Experimental)	1156
Kinetics (Theoretical)	1157
Production	1159
Stability	1159
Thermonuclear Processes	1160
Wave Phenomena	1161
Shielding	1163
Solid-State Physics	1163
Radiation Effects	1163
Physical Properties	1166
Moessbauer Effects and NMR	1172
Theory	1173
Theoretical Physics	1173
PHYSICS (HIGH-ENERGY)	1176
Particle Interactions and Properties (Experimental)	1176
Electromagnetic	1176
Weak	1177
Strong (Baryon-Induced)	1178
Strong (Meson-Induced)	1179
Particle Interactions and Properties (Theoretical)	1182
General	1182
Electromagnetic	1183
Weak	1185
Strong (General)	1186
Strong (Baryon No. = 0)	1188
Strong (Baryon No. = 1)	1189
Strong (Baryon No. ≥ 2)	1191
Particle Invariance Principles and Symmetries	1192
General	1192
Applications (Electromagnetic and Weak)	1192
Applications (Strong)	1192
Field Theories	1192
General	1192
Quantum Field Theory	1193
Gravitation and General Relativity	1195
Scattering Theory	1197
Particle Accelerators	1198

Category	Page
PHYSICS (NUCLEAR)	1202
Neutron Interactions with Matter	1202
Nuclear Properties and Reactions, $A \leq 5$	1203
Nuclear Properties and Reactions, $6 \leq A \leq 19$	1205
Nuclear Properties and Reactions, $20 \leq A \leq 89$	1210
Nuclear Properties and Reactions, $A \geq 90$	1219
Nuclear Theory	1231
REACTOR TECHNOLOGY	1239
Commercial Power Reactors	1239
Operation and Economics	1240
Safety and Siting	1240
Steam and Power Conversion Systems	1242
Power Reactor Development	1242
Kinetics and Dynamics	1243
Control Systems	1244
Shielding	1244
Cooling Systems	1244
Fuels	1245
Auxiliary and Emergency Systems	1246
Safety and Siting	1246
Power Conversion Systems	1247
Research and Test Reactors	1247
Rocket and Space Reactors	1249
Marine and Portable Power Reactors	1250
Reactor Theory	1250
Kinetics	1250
Experimental Applications	1252
Reactor Components, Fuels, and Accessories	1252
GENERAL	1253
CORPORATE AUTHOR INDEX	INDEX-1
PERSONAL AUTHOR INDEX	INDEX-11
SUBJECT INDEX	INDEX-64
REPORT NUMBER INDEX	INDEX-168

XUM

STAFF OF NUCLEAR SCIENCE ABSTRACTS

John W. Norris
Managing Editor

Donald D. Davis
Assistant Managing Editor

David E. Bost
Production Manager

Sidney F. Lanier
Subject Heading Specialist

J. Paul Meredith
Descriptive Cataloging Specialist

Frederick E. Marsh, Jr.
Computer Index Coordinator

Clara L. Fox
Corporate Author Specialist

Helen W. White
Report Number Specialist

Section Editors

Everett J. Hoffman
Chemistry

Robert C. Kelly
Engineering; Earth Sciences; Metals, Ceramics, and Other Materials

Lee M. Thompson
General Physics

Charles E. Stuber
High Energy Physics; Instrumentation

Helen G. Donald
Life Sciences

Lawrence T. Whitehead
Nuclear Physics

James M. Jacobs
Reactor Technology

Evaluators

Thomas S. Chapman
Rose V. Jermain
John H. Mitchell
Mary H. Newman
Polly C. Summers

Abstractors

F. S. Armstrong*
Ellis R. Bedford
Mary M. Brown
Jane G. Buchanan
D. Lamar Cason
Gloria M. Caton
David C. Cunningham
James R. Dulaney
Helga B. Gerstner
Mary C. Grissom
Phyllis C. Hansen
Carolyn D. Houston
Elaine E. Huber
Rose V. Jermain
W. Hugh Kinser, Jr.
Lisbeth C. Lieberman
Betty L. McDowell
Patricia B. McEwen
Fay M. Martin
William D. Matheny
Dora H. Moneyhun
Jean F. Peckham
Henry D. Raleigh
Mona H. Raridon
Julia S. Redford
Jessie W. Rushing
Robert W. Rutkowski
Francis L. Sachs
Lila B. Smith
Anne G. Ward
Helen L. Ward
Milton O. Whitson
Juanita Wilson

*Atomic Energy of Canada, Ltd.

Charles R. Bruce
Publishing Coordinator

Communication concerning the editorial policy and content of *Nuclear Science Abstracts* should be addressed to the Managing Editor, *Nuclear Science Abstracts*, USAEC Division of Technical Information Extension, P. O. Box 62, Oak Ridge, Tennessee 37830.

Use of funds for printing this publication approved by the Director of the Bureau of the Budget, June 26, 1969.

Volume 25, Number 6 March 31, 1971

NUCLEAR SCIENCE ABSTRACTS

CHEMISTRY

Analytical Chemistry

Refer also to abstract 11539.

10421 (BRH/DMRE-70-5) USE OF RADIOACTIVE MATERIALS IN GAS CHROMATOGRAPHY. Pettigrew, George L.; Halperin, Jerome A. (Bureau of Radiological Health, Rockville, Md.). Oct 1970. 11p. NTIS.

Operating principles of gas chromatography, hazards from radioactive materials used in chromatographs, and safety precautions that could minimize the hazards are discussed. (M.C.G.)

10422 (NBS-TN-545) MICROCHEMICAL ANALYSIS SECTION. Summary of Activities, July 1969–June 1970. Taylor, John K. (ed.) (National Bureau of Standards, Washington, D. C.). Dec 1970. 126p. GPO $1.25.

The research activities and scientific programs of the Microchemical Analysis Section of the Analytical Chemistry Division of the National Bureau of Standards, Institute for Materials Research during the period July 1969 to June 1970 are described. General activities are reviewed in areas of gas analysis polarography, chemical microscopy, and classical microchemical analysis. Research activities described in some detail include: preparation and analysis of carbon monoxide mixture for standard reference materials; evaluation of sulfur dioxide permeation tubes as analytical standards; polarographic methods for determination of trace elements in a number of materials; certification of urea as a microchemical standard. A chapter reviewing the state-of-the art of analysis for air pollutants is also included. (auth)

10423 (ORNL-4636) ANALYTICAL CHEMISTRY DIVISION ANNUAL PROGRESS REPORT FOR PERIOD ENDING SEPTEMBER 30, 1970. Lyon, W. S. (comp. and ed.) (Oak Ridge National Lab., Tenn.). Jan 1971. Contract W-7405-eng-26. 82p. Dep. NTIS.

A separate abstract was prepared for each of the 10 sections. (M.C.G.)

For abstracts of individual sections see: 10424–10426, 10433–10438, and 10491.

10424 (ORNL-4636, pp 34-40) ANALYTICAL INSTRUMENTATION. (Oak Ridge National Lab., Tenn.).

From Analytical Chemistry Division annual progress report for period ending September 30, 1970.

Instrumentation research and development and computer analytical systems are discussed. (M.C.G.)

10425 (ORNL-4636, pp 40-2) METHODS DEVELOPMENT AND EVALUATION LABORATORY. (Oak Ridge National Lab., Tenn.).

From Analytical Chemistry Division annual progress report for period ending September 30, 1970.

Activities were carried out in three areas: LMFBR reactor fuel analysis, the transuranium program, and MSRE fuel analyses. (M.C.G.)

10426 (ORNL-4636, pp 54-7) PROCESS ANALYSES. (Oak Ridge National Lab., Tenn.).

From Analytical Chemistry Division annual progress report for period ending September 30, 1970.

Work is reported in the High-Level α Radiation Laboratory, the General Analyses Laboratory, the General Hot-Analyses Laboratory, the Radioisotopes–Radiochemistry Laboratories, and on radiation control and safety, quality control, and inorganic preparations. (M.C.G.)

10427 REVIEW OF PROBLEMS OF CONTAMINATION IN THE DETERMINATION OF TRACES. Pinta, M. (Office de la Recherche Scientifique et Technique Outre-Mer, Bondy, France). pp 25-40 of Dosage des Elements a l'Etat de Traces dans les Roches et les Autres Substances Minerales Naturelles. Paris; Centre National de la Recherche Scientifique (1970). (In French).

From National Conference on Measurement of Elements Occurring in Traces in Rocks, Nancy, France. See CONF-681205.

Every sample analyzed has to be related to the composition of the medium in its original state; the risks of contamination, particularly in the determination of traces, are present from the time of sampling up to measurement of the physical or chemical value defining the amount of the element determined. The contamination sources are numerous, often obvious, sometimes systematic or accidental, but often ignored. The resulting consequences in the determination of trace elements were analyzed one after another while trying to bring out the errors that can result and proposing, as far as possible, the best solution to the problem. The following factors were studied: sampling, bagging, transport; physical treatment, such as quartering, grinding, sifting (screening); chemical treatment, such as acid or alkaline attack, dissolution influence of glassware, chemical reagents; atmosphere; and staff personnel. Practical examples are given to illustrate these sources of error. The principal methods of determining trace elements are reviewed in an attempt to demonstrate the danger of contamination. (auth)

10428 TRACE ELEMENT CALIBRATIONS AND PROFILES AT THE GEOSECS TEST STATION IN THE NORTHEAST PACIFIC OCEAN. Spencer, Derek W. (Woods Hole Oceanographic Inst., Mass.); Robertson, D. E.; Turekian, K. K.; Folsom, T. R. J. Geophys. Res.; 36: 7688-96(20 Dec 1970).

Four laboratories collaborated on the trace element analysis of seawater samples obtained on the 1969 Geosecs test cruise in the northeast Pacific Ocean. The elements determined were Sr, Cs, Co, Ni, Sc, Cu, Sb, Zn, Fe, and U. Two or more laboratories reported on Sr, Cs, Zn, Fe, and U. The general agreement was good. Depth variations were noted for some elements. Acidified samples were higher in Fe, Zn, and Co than the unacidified samples. Except for surface iron values, filtering had no effect on concentration. (auth)

Chemical and Spectral Procedures

Refer also to abstracts 10671, 10686, and 10888.

10429 (BARC-468) SPECTROGRAPHIC ANALYSIS OF TUNGSTEN IN ORES AND THEIR CONCENTRATES: AN INTERMITTENT ac ARC METHOD. Chandola, L. C. (Bhabha Atomic Research Centre, Bombay (India)). 1970. 10p. Dep. NTIS (U. S. Sales Only).

A spectrographic method for the estimation of tungsten present in the concentration range 6 to 65% in ores and their concentrates is described. The sample is diluted tenfold with silica. It is mixed with buffer silver chloride and an internal standard nickel oxide is added. The mixture is glued to the flat ends of a pair of copper

electrodes and excited in an intermittent ac arc. The resulting spectrum is photographed on a large quartz spectrograph. The line pair W(3300.8Å)/Ni(3315.7Å) is used. The method gave an average coefficient of variation of ±6%. Iron, manganese, and calcium present in the sample are also estimated by the same procedure. It has been observed that oxides of manganese and calcium introduced systematic errors whereas iron oxide did not have any effect on the estimation of tungsten. (auth)

10430 (EUR-4541) SPECTROCHEMICAL ANALYSIS OF Zr AND ITS ALLOYS. I. DETERMINATION OF ORDINARY IMPURITIES AND OF Ta IN Zr AND IN ZIRCALOY-2. Ceccarelli, G.; Rossi, G. (European Atomic Energy Community, Ispra (Italy). Joint Nuclear Research Center). 1970. 36p. (In French). Dep. NTIS (U. S. Sales Only). EUR FF 5,60.

Spectrochemical methods for the determination of metal impurities in zirconium and Zircaloy-2 are presented. The carrier distillation technique of Scribner and Mullin has been successfully applied with proper modifications to the determination of Al, B, Be, Cd, Co, Cr, Cu, Fe, Mn, Mo, Ni, Pb, Si, Sn, and V in zirconium and of Al, B, Be, Cd, Co, Cu, Mn, Mo, Ti, and V in Zircaloy-2, In_2O_3 being used as carrier. Moreover, the use of a variable internal standard (Fe) in the case of Zircaloy-2 allowed a higher precision to be obtained. The methods for the determination of low Ta contents in the above-cited materials are also described. These methods are based on a fluorination procedure with teflon powder and dc arc excitation. The lowest Ta concentration (25 ppM) that can be measured does not represent the detection limit of the procedure described but compares favorably with the best sensitivity values in the literature. (auth)

10431 (IEA-208) SPECTROGRAPHIC DETERMINATION OF HAFNIUM IN ZIRCONIUM OXIDE. Deppe, Alzira Lourenco; Lordello, Antonio Roberto (Instituto de Energia Atomica, Sao Paulo (Brazil)). Apr 1970. 16p. (In Portuguese). Dep. NTIS (U. S. Sales Only).

A method is presented for the quantitative determination of hafnium in zirconium oxide by emission spectrography. The interval of concentration from 2000 to 100 ppM is covered, and a precision of roughly 10% is attained. An oxide sample of 15 mg is topped with graphite powder and is lightly pressed to prevent projection of particles into the plasma column to permit a slow volatilization and to be excited through the 15-A dc arc. The main advantage of the method derives from its relative simplicity when compared to others already published, such as Kingsbury-Temple and the "Porous Cup" procedures. (auth)

10432 (KFK-1261) EMISSION SPECTROSCOPIC DETERMINATION OF TRACES IN NUCLEAR FUEL MATERIALS. Mainka, E.; Mueller, H. G. (Kernforschungszentrum, Karlsruhe (West Germany). Institut fuer Radiochemie). Aug 1970. 34p. (In German). Dep. NTIS (U. S. Sales Only).

Two quantitative analytical methods using emission spectroscopy are described. These methods are applied on a routine basis for acceptance controls of plutonium-bearing nuclear fuels. Up to 17 trace impurities can be determined in a single analytical run. To minimize spectral interferences separation between matrix and impurities is needed. Separation is achieved by ion exchange on the one hand and by pre-evaporation on the other. As a result, the detection efficiencies were significantly increased for most trace elements as compared to the direct methods. Attention was given to the preparation of standard samples. It can be demonstrated that it was possible to use commercially available U_3O_8 standard samples Nr. 95 (1-7) of the NBL Laboratory for the determination of impurities. (auth)

10433 (ORNL-4636, pp 1-7) ANALYTICAL METHODOLOGY. (Oak Ridge National Lab., Tenn.).

From Analytical Chemistry Division annual progress report for period ending September 30, 1970.

Topics covered include: environmental activities, cigarette tobacco smoke analysis program, analytical research and support activities in the Transuranium Research Laboratory, electrochemical research, and gas chromatography. (M.C.G.)

10434 (ORNL-4636, pp 7-13) REACTOR PROJECTS. (Oak Ridge National Lab., Tenn.).

From Analytical Chemistry Division annual progress report for period ending September 30, 1970.

Topics covered include: determination of U in MSRE fuel samples and tritium in MSRE gas streams, reference electrodes for molten fluorides, measurement of U^{3+} in molten fluorides, spectrophotometric studies on actinide ions in molten fluorides, oxidation states of ions in molten fluorides, $NaBF_4$ coolant systems, and analysis of natural gas samples. (M.C.G.)

10435 (ORNL-4636, pp 14-20) ANALYTICAL BIOCHEMISTRY. (Oak Ridge National Lab., Tenn.).

From Analytical Chemistry Division annual progress report for period ending September 30, 1970.

Progress in analytical biochemistry is reported under the following headings: macromolecular separations, molecular anatomy (MAN) program, characterization and purity of biochemicals, and the GeMSAEC analyzer in the clinical development program. (M.C.G.)

10436 (ORNL-4636, pp 43-5) MASS SPECTROMETRY. (Oak Ridge National Lab., Tenn.).

From Analytical Chemistry Division annual progress report for period ending September 30, 1970.

Topics covered include: mechanisms of surface ionization, computer programs for mass spectrometry, a combined gas chromatograph-mass spectrometer, and various mass-spectral analyses. (M.C.G.)

10437 (ORNL-4636, pp 45-50) ELECTRON MICROSCOPY. (Oak Ridge National Lab., Tenn.).

From Analytical Chemistry Division annual progress report for period ending September 30, 1970.

Transmission and scanning electron microscopy, electron spectroscopy, x-ray diffraction studies, and electron microprobe analysis are discussed. (M.C.G.)

10438 (ORNL-4636, pp 51-3) SPECTROMETRY SERVICES. (Oak Ridge National Lab., Tenn.).

From Analytical Chemistry Division annual progress report for period ending September 30, 1970.

In order to obtain more quantitative results from the spark-source mass spectrometer used for impurity analyses, relative sensitivity factors were established for rare earths and certain actinides. Isotopic determinations are also discussed. (M.C.G.)

10439 DETERMINATION OF MOLYBDENUM IN IRON AND STEEL BY FLAME PHOTOMETRY. **Goto, Hidehiro; Kakita, Yachiyo; Namiki, Michiko (Tohoku Univ., Sendai). Jap. Anal.; 19: 1467-70(Nov 1970). (In Japanese).**

By using a Tokoshi-type oxygen-acetylene premixing burner, the flame photometric determination of Mo in iron and steel was investigated. Studies were also made on the effects of coexistent elements and the method of separation of molybdenum from matrix elements. The 379.82 mμ line was used for the determination, and the line intensity had good linearity with Mo concentration. Molybdenum was separated from matrix iron by methyl isobutyl ketone extraction of the precipitate of Mo-α-benzoin oxime complex from 2.5 N sulfuric acid. By this means, almost all elements did not interfere except for Cr, Bi, Co, Ce, and Nb, which gave low results. Influence by the latter elements was avoided by the standard addition method. The variation coefficient of the analytical results was 4.4%. (auth)

10440 DETERMINATION OF BERYLLIUM OXIDE INCLUSION IN Cu-Be ALLOY. IV. **Tsukahara, Iwao (Furukawa Electric Co., Ltd., Tokyo). Jap. Anal.; 19: 1502-7(Nov 1970). (In Japanese).**

A methanolic bromine method for the determination of beryllium oxide inclusion in Cu-Be alloy is described. In order to decide the optimum condition for extracting the inclusion, the effects of decomposition temperature, water in methanol, etc. on the solubility (recovery) of beryllium oxide have been studied by the use of synthesized pure beryllium oxides and internally oxidized Cu-Be alloys. The solubilities of metallic copper, metallic beryllium, and beryllium oxide with ester-bromine or with acid have also been studied and the applicability of the ester-bromine method or of the acid decomposition method to the determination of beryllium oxide inclusion in Cu-Be alloy is discussed. The recommended procedure is as follows: 2 ~ 5 g of Cu-Be alloy is decomposed with methanolic bromine (methanol 100 ml + bromine 10 ml) in a decomposition flask at 45 ~ 50°C for 5 hr or at 30 ~ 35°C for 20 hr. The solution is filtered by suction through Cella filter (CF, dense). The residue (beryllium oxide inclusion isolated) is washed with methanol, ignited in a platinum crucible, and fused with 5 ~ 8 g of potassium pyrosulfate. The melt is leached with 40 ml of 0.3 N HCl and made up to 100 ml with water. An aliquot of this solution containing 5 ~ 50 μg of beryllium is taken into a 100 ml beaker, and 5 ml of 4% KCN solution and 10 ml of 0.1% Arsenazo I solution are added. The pH of solution is adjusted to 12.5 ± 0.1 by adding dropwise 20% NaOH solution. It is transferred into a 100 ml volumetric flask and the volume is made up with diluted NaOH solution (pH = 12.5). The absorbance at 580 mμ is measured against the reagent blank and the amount of beryllium is determined from its calibration curve. (auth)

XUM

10441 FLUORESCENT X-RAY ANALYSIS OF TIN AND ZIRCONIUM IN ALUMINUM ALLOYS. Suzuki, Shuju; Matsumoto, Saburo; Itoh, Junichi (Central Research Lab., Tokyo). Jap. Anal.; 19: 1523-8(Nov 1970). (In Japanese).

Fluorescent x-ray analysis of Sn and Zr (below 0.3%) in aluminum alloys was investigated. Measurements were made for total x-ray intensities (I_{E+B}) at the wavelengths of SnK_α (n = 2) and ZrK_α (n = 1), and background intensities (I_B) in the vicinities of the characteristic lines. I_B's of individual samples were subtracted from corresponding I_{E+B}'s to obtain fluorescent x-ray intensities (I_E) of the elements of interest. Correlations of I_E to C_E, content of the elements, however, were poor due to the presence of heavy metals in some of the alloys. Correction for the absorbing constituents, Zn, Cu, and Ni, was made to establish satisfactorily linear relationship of corrected I_{Sn} to C_{Sn}. Further, application of an internal standard method was studied because the correction for absorption is not convenient in industrial analyses. I_B's of some metals and binary alloys of aluminum were investigated, and it was found that I_B was an adequate internal standard to eliminate the effect of absorption. Linear calibration lines were obtained by plotting I_E/I_B against C_E for both Sn and Zr. Precision data are given. (auth)

10442 SPECTROPHOTOMETRIC DETERMINATION OF TRACES OF NITROGEN IN ZIRCONIUM AND ZIRCALOY USING THYMOL. Hashitani, Hiroshi; Yoshida, Hideyo (Japan Atomic Energy Research Inst., Tokai). Jap. Anal.; 19: 1564-6(Nov 1970). (In Japanese).

The spectrophotometric method for the determination of ammonia nitrogen with thymol which had been established for uranium metal and its compounds was successfully applied to as low as 3 ppM of nitrogen in zirconium and zircaloy. Satisfactory results were obtained in the analysis of the NBS zircaloy-2 standard and other samples. Twenty milligrams of tin, 3 mg of iron, 4 mg of nickel, 2 mg of chromium, and 0.2 mg each of aluminum, copper, silicon, and titanium did not interfere. The molar absorptivity was the same as that previously reported (1.15×10^4 at 670 mμ). In the recommended procedure, up to 0.8 g of a sample was dissolved with 2 ml of sulfuric acid (18 N), 3 ml of hydrochloric acid, and 5 ml of fluoboric acid (10%) by heating in a water bath. After dissolution, 1 ml of hydrogen peroxide solution (30%) was added to oxidize iron and the solution was then evaporated to almost dryness to remove the excess peroxide and acids. The residue was dissolved with 50 ml of water, and 20 ml of sodium citrate solution (25 w/v%) was added. After adjusting the pH of the solution to 9.8 ~ 10.3, 0.5 ml of sodium hypochlorite solution containing 0.3% of active chlorine was added with stirring. After 20 seconds, 2.5 ml of a freshly prepared mixture of equal volumes of thymol solution (10% in acetone) and sodium hydroxide solution (1 N) was added. Sodium hydroxide solution (6 N) was then added to dissolve the deposited thymol, and the pH of the solution was adjusted to 11.6 ~ 11.9 with sodium phosphate solution (0.05 N) and sulfuric acid (6 N). Four milliliters of acetone was added and the resultant solution was diluted to 100 ml with water. After standing for 1.5 hours in darkness, the absorbance of the colored solution was measured against the blank at 670 mμ. (auth)

10443 USE OF RADIOISOTOPES FOR QUALITY AND PROCESS CONTROL ANALYSIS IN INDUSTRY. Kuusi, Juhani (Helsinki Univ. of Tech., Otaniemi, Finland). Arkhimedes, No. 1, 16-27(1970). (In Finnish).

Radioisotope methods of analysis and their potential use for quality and process control in industry are reviewed. Especially radioisotope x-ray spectrometry and radioisotope source neutron activation analysis are discussed. These methods of analysis and the research and development work done in this field at the Reactor Laboratory of the Technical University of Helsinki, Otaniemi, are further illustrated by more detailed description of some radioisotope instruments installed for routine use. (auth) (Finland)

10444 SPECTROCHEMICAL DETERMINATION OF TRACERS OF IMPURITY ELEMENTS IN PLUTONIUM BY THE COPPER SPARK METHOD. PRECISION AND LIMITATIONS. Andersson, L.; Johansson, I.; Soederlund, R. (Research Inst. of National Defence, Stockholm). FOA (Forsvarets Forsk.) Rep.; 4: No. 8, 1-7(Oct 1970).

The copper spark method was used for the spectrochemical determination of impurity elements in samples containing plutonium. The instrumentation, equipment, and procedure used in these determinations are described. Blank values for the whole procedure were determined as a matter of routine, and steps taken to reduce their size are described. The precision and limits of detection of the method in quantitative determination of several trace elements were evaluated. Large amounts of impurities and ion exchange decomposition products in the sample solution result in decreased precision and high limits of detection. (auth) (Sweden)

10445 STUDY OF THE PRECISE DETERMINATION OF MACRO-AMOUNTS OF PLUTONIUM IN SOLUTION BY THREE ELECTROMETRIC OXIDATION–REDUCTION TITRATION METHODS. Andersson, L.; Bauren, E.; Helleday, E. (Research Inst. of National Defence, Stockholm). FOA (Forsvarets Forsk.) Rep.; 4: No. 7, 1-6(Oct 1970).

The precise determination of macroamounts of plutonium in solution was studied by two potentiometric and one amperometric titration method. The potentiometric methods were, within the limits of experimental error, without bias, but the results obtained with the amperometric method were too high. When the amperometric method and one of the potentiometric methods were applied to the titration of dichromate solutions, a systematic difference was again found, the amperometric method giving low values. The discrepancies mentioned may be explained by assuming that small amounts of hydrogen peroxide are formed at the anode during the amperometric titration. For samples containing 20 to 30 mg of plutonium the precision of the two potentiometric methods in routine duplicate determinations was of the order of 0.1 percent or slightly better. The influence of americium was studied, but no definite conclusions can be drawn from the results obtained. (auth) (Sweden)

10446 DOSAGE DES ELEMENTS A L'ETAT DE TRACES DANS LES ROCHES ET LES AUTRES SUBSTANCES MINERALES NATURELLES. (Measurement of Elements Occurring in Traces in Rocks and Other Mineral Substances). National Conference on Measurements of Elements Occurring in Traces in Rocks, Nancy, France, 4–6 December 1968. Paris; Centre National de la Recherche Scientifique (1970). 466p. (CONF-681205).

Thirty-five papers are included; separate abstracts were prepared for 19. Four of the papers were previously abstracted in NSA as 23: 13617, 13619, 13670 and 13671. The remaining 12 papers contain information on: photoelectric emission spectrography; emission spectrography; atomic absorption spectrometry; polarography, chromatography, and titrimetry; and analysis of microscopic objects and point analysis. (P.C.H.)

For abstracts of individual papers see: 10427, 10447–10458, 10476, 10477, 10492–10494, and 10671.

10447 CORRECTION OF MATRIX EFFECTS IN X-RAY FLUORESCENCE. COMPARISON OF VARIOUS METHODS TRIED AT THE PAU RESEARCH CENTER. Sahores, J. (Societe Nationale des Petroles d'Aquitaine, Pau, France). pp 49-61 of Dosage des Elements a l'Etat de Traces dans les Roches et les Autres Substances Minerales Naturelles. Paris; Centre National de la Recherche Scientifique (1970). (In French).

From National Conference on Measurement of Elements Occurring in Traces in Rocks, Nancy, France. See CONF-681205.

A comparative study was made on the advantages and disadvantages of various methods of correction based on: multiple dilution (Tertian method); measurement of the transmittance; use of thin layers; and utilization of the background as internal standard. A few applications are then proposed. (auth)

10448 QUANTITATIVE DETERMINATION BY X-RAY FLUORESCENCE OF ELEMENTS IN LOW CONCENTRATIONS IN ROCKS. METHODS OF CORRECTION FOR THE MATRIX EFFECT. Tertian, R. (Produits Chimiques Pechiney-Saint-Gobain, Aubervilliers, France). pp 63-74 of Dosage des Elements a l'Etat de Traces dans les Roches et les Autres Substances Minerales Naturelles. Paris; Centre National de la Recherche Scientifique (1970). (In French).

From National Conference on Measurement of Elements Occurring in Traces in Rocks, Nancy, France. See CONF-681205.

The most appropriate working conditions are discussed, on a general basis, regarding the application of x-ray fluorescence analysis to quantitative determination of elements at lower concentrations in rocks and minerals. The use of homogeneous specimens, as obtained with relatively high concentrations of the sample fused in low absorbing fluxes such as $Li_2B_4O_7$ or $Na_2B_4O_7$, is recommended. Correction for matrix effect was obtained by using either the addition method, or the emission-transmission and simple transmission methods, or the so-called double dilution method. This last procedure, first developed for the determination of major elements, was altogether simple, rigorous, and of general value. It can be simplified for the determination of minor elements by the way of introducing a reference element, Co for instance, acting as a generalized internal standard. (auth)

10449 USE OF X-RAY FLUORESCENCE FOR THE NON-DESTRUCTIVE QUANTITATIVE DETERMINATION OF TRACE AMOUNTS OF ELEMENTS OF ATOMIC NUMBER GREATER

THAN 27 IN SILICATE, BAUXITE, AND CARBONATE ROCKS. Quintin, M. (Faculte des Sciences, Paris). pp 75-87 of Dosage des Elements a l'Etat de Traces dans les Roches et les Autres Substances Minerales Naturelles. Paris; Centre National de la Recherche Scientifique (1970). (In French).

From National Conference on Measurement of Elements Occurring in Traces in Rocks, Nancy, France. See CONF-681205.

In the determination of major elements of rocks, x-ray fluorescence is employed with success. This technique can also give good results in the determination of trace amounts of elements in geological materials. Special consideration was given to nondestructive analysis in an attempt to gain maximum information with a minimum of preparation. Hoover's method was theoretically justified then experimentally verified. The field of application and its validity are defined. A linear relation between intensity of the Compton WL β_1 ray diffused by the sample and the reverse of the relative absorption was confirmed. These principles are illustrated by the study of five international standards W_1, syenite, GR, DRN, and UBN, for several elements situated in the zone 1 of Hoover. (auth)

10450 METHOD FOR DETERMINATION OF 18 MAJOR ELEMENTS AND TRACES IN SEDIMETARY ROCKS AND DECAY PRODUCTS BY DIRECT-READING SPECTROMETRY. Besnus, Y.; Lucas, J. (CNRS, Strasbourg). pp 93-106 of Dosage des Elements a l'Etat de Traces dans les Roches et les Autres Substances Minerales Naturelles. Paris; Centre National de la Recherche Scientifique (1970). (In French).

From National Conference on Measurement of Elements Occurring in Traces in Rocks, Nancy, France. See CONF-681205.

In this method, the determination of trace elements requires previous knowledge of the major elements. The determination of major elements is briefly discussed: fusion with lithium tetraborate and arcing of a pellet in which the sample has been greatly diluted. The determination of trace elements is carried out on pellets of constant chemical composition, obtained by the addition of a buffer, formed by major oxides (SiO_2, Al_2O_3...) the addition of which is determined by the composition of the rock analyzed. The improvements brought to the method since its first development, such as preparation of the standards and better uniformisation of the samples are stressed. Finally, attention is drawn to a way in which research must be pursued for a better precision of the measures, such as control of grain-size distribution and preparation submitted to the arc. (auth)

10451 QUANTOMETER FOR DETERMINATION OF TRACE ELEMENTS IN NATURAL MATERIALS. Moal, J. Y.; Beguinot, J.; Ruel, G.; Vannier, M. (Bureau de Recherches Geologiques et Minieres, Orleans, France). pp 107-32 of Dosage des Elements a l'Etat de Traces dans les Roches et les Autres Substances Minerales Naturelles. Paris; Centre National de la Recherche Scientifique (1970). (In French).

From National Conference on Measurement of Elements Occurring in Traces in Rocks, Nancy, France. See CONF-681205.

After a brief survey of the equipment and of the experimental procedure, several ways of diminishing the matrix effect are discussed. The internal standardization has been abandoned because of the difficulty of finding one or even several elements capable of satisfying all the cases considered. Use of spectrographic buffer, essentially based on alkali and alkaline earth salts, in order to stabilize the discharge and reduce the effect of selective volatilization was considered, along with corrections of continuous background and of intensities of the signals obtained on the five programmed major elements and utilization of reference matrix of composition near those of the analyzed samples. Results obtained on the geochemical standards (U.S.G.S., C.R.P.G., and C.A.A.S.) are presented. (auth)

10452 USE OF FLUXES AND ION EXCHANGE RESINS FOR THE ELIMINATION OF THE MATRIX EFFECT AND QUANTOMETRIC DETERMINATION OF TRACE ELEMENTS IN SILICATES. Govindaraju, K. (CNRS, Vandoeuvre-les-Nancy, France). pp 133-47 of Dosage des Elements a l'Etat de Traces dans les Roches et les Autres Substances Minerales Naturelles. Paris; Centre National de la Recherche Scientifique (1970). (In French).

From National Conference on Measurement of Elements Occurring in Traces in Rocks, Nancy, France. See CONF-681205.

A new method is described which permits the elimination of the matrix effect by first destroying the crystalline structure of the sample by lithium borate fusion and then fixing the cations in a homogeneous manner on a cation exchanger. A cellulose tape impregnated with this organic resin passes between the electrodes at such a speed that each spark falls on new material. The use of this tape machine and of Li as internal standard and spectrochemical buffer considerably reduces selective vaporization. The analysis of samples as different as granites, basalts, micas, shales, carbonate rocks, and iron ores showed that the matrix effect is undiscernible. (auth)

10453 CORRECTION OF THE MATRIX EFFECT IN ULTRAVIOLET SPECTROGRAPHIC ANALYSIS. Jamond, C.; Roques, M. (Faculte des Sciences, Clermont-Ferrand, France). pp 151-7 of Dosage des Elements a l'Etat de Traces dans les Roches et les Autres Substances Minerales Naturelles. Paris; Centre National de la Recherche Scientifique (1970). (In French).

From National Conference on Measurement of Elements Occurring in Traces in Rocks, Nancy, France. See CONF-681205.

The simultaneous use of internal standardization and external standardization permit the reduction of the influence that variations in chemical composition and physical properties of material in consideration exercise on the result of quantitative analysis for trace elements in routine procedures. An account is given of the method carried out for twelve years in the "Département de Géologie et Minéralogie de la Faculté des Sciences de Clermont-Ferrand." (auth)

10454 USE OF SODIUM CHLORIDE AS A SPECTRAL BUFFER IN EMISSION SPECTROGRAPHY. APPLICATION TO THE DETERMINATION OF TRACE ELEMENTS IN SILICATE ROCKS. Martin, A.; Quintin, M. (Faculte des Sciences, Paris). pp 187-95 of Dosage des Elements a l'Etat de Traces dans les Roches et les Autres Substances Minerales Naturelles. Paris; Centre National de la Recherche Scientifique (1970). (In French).

From National Conference on Measurement of Elements Occurring in Traces in Rocks, Nancy, France. See CONF-681205.

A simplified emission spectrography method for the quantitative determination of 10 trace elements in silicate rocks is described. The use of NaCl as spectral buffer and of a three-step filter has allowed the number of analyses as well as reproducibility to increase. Powder sample was mixed with two parts of NaCl, four parts of graphite, and arcing mixture was burned into a graphite electrode as anode in a dc arc. The reproducibility and accuracy of the method have been tested with Rock Standard W_1 (U.S.G.S.). Results obtained with Syenite Rock (CAAS) and Rock Standards GR, DRN, UBN, prepared by the CRPG of Nancy France are reported. (auth)

10455 APPLICATION OF SPARK SOURCE MASS SPECTROGRAPHY TO CERTAIN GEOLOGIC PROBLEMS. Cornu, A.; Brun, J. C. (CEN, Grenoble, France). pp 215-23 of Dosage des Elements a l'Etat de Traces dans les Roches et les Autres Substances Minerales Naturelles. Paris; Centre National de la Recherche Scientifique (1970). (In French).

From National Conference on Measurement of Elements Occurring in Traces in Rocks, Nancy, France. See CONF-681205.

Spark source mass spectrography is a valuable analytical method whose exhaustivity and sensitivity (detection limit close to 10^{-9}) are appreciated. The possibility of obtaining an absolute semiquantitative analysis, without disposal of any standard sample extends the field of interest. For geological materials, different sparking devices are explained according to the sample. Examples are given with crystals (like diamond, sapphire, ruby), with natural glass (Ivory Coast Tektite), and with powdered rock samples for which homogeneous sample quantitative analysis can be performed if a correct photometric process is applied, involving pertinent corrections. (auth)

10456 DETERMINATION OF TRACES IN MINERALS, ESPECIALLY IN PHOSPHATES, BY MEANS OF SPARK SOURCE MASS SPECTROGRAPHY. Nalbantoglu, M. (Centre de Recherches Pechiney-Saint-Gobain, Antony, France). pp 225-33 of Dosage des Elements a l'Etat de Traces dans les Roches et les Autres Substances Minerales Naturelles. Paris; Centre National de la Recherche Scientifique (1970). (In French).

From National Conference on Measurement of Elements Occurring in Traces in Rocks, Nancy, France. See CONF-681205.

The technique of analysis of powders with spark source mass spectrometry is discussed. The application of this technique to the study of minerals with example of analysis of a few phosphates of various origins is presented. Using this method, almost all the trace elements can be determined in a phosphate with, in general, a precision of about 20%. (auth)

10457 MATRIX EFFECTS ON THE DETERMINATION OF TRACES BY ATOMIC ABSORPTION. Pinta, M. (Office de la Recherche Scientifique et Technique Outre-Mer, Bondy, France); Riandey, C. pp 237-49 of Dosage des Elements a l'Etat de Traces dans les Roches et les Autres Substances Minerales Naturelles. Paris; Centre National de la Recherche Scientifique (1970). (In French).

From National Conference on Measurement of Elements Occurring in Traces in Rocks, Nancy, France. See CONF-681205.

XUN

A definition is given of the matrix effect in physicochemical analysis, particularly in the case of atomic absorption. The different matrix effects are classified as functions of their consequences on the analysis: spectral interaction, molecular absorption, chemical reactions in the flame, and ionization phenomena. The matrix effects observed in the analysis of geological materials, especially of rocks and soils, are discussed. The methods of correction include electronic spectral or chemical buffer, standardization from complex synthetic medium, graphic correction, separation of interfering elements, and extraction of element. Examples of application in typical cases are given. (auth)

10458 ATOMIC ABSORPTION DETERMINATION OF POTASSIUM, RUBIDIUM, AND STRONTIUM FOR GEOCHRONOLOGICAL MEASUREMENTS. Gamot, E.; Philibert, J.; Vialette, Y. (Faculte des Sciences, Clermont-Ferrand, France). pp 287-99 of Dosage des Elements a l'Etat de Traces dans les Roches et les Autres Substances Minerales Naturelles. Paris; Centre National de la Recherche Scientifique (1970). (In French).

From National Conference on Measurement of Elements Occurring in Traces in Rocks, Nancy, France. See CONF-681205.

Quantitative determination in rocks and minerals for K, Rb, and Sr at concentrations lower than 1,000 ppM have been made with an atomic absorption spectrophotometer with accuracy better than 3% at 95% confidence. Measurement is carried out comparatively to external standards made from a rock low in the element to be determined. For Rb and Sr, the standard solutions and samples are buffered with Cs and La to eliminate interferences due to alkalines and Al. There is a very good agreement between results obtained by atomic absorption and isotopic dilution. Potassium quantitative determination in ultrabasic rocks gives results with a good precision if blank corrections are made and manipulations carried out under purified atmosphere. (auth)

10459 DETERMINATION OF TRACES OF FOREIGN MATTER IN MOLYBDENUM AND ITS COMPOUNDS. Horkay-Borsos, Klara; Hegedus, J. Andras (United Incandescent Lamp and Electric Co., Budapest). Kem. Kozlem.; 34: 107-21(14 Aug 1970). (In Hungarian).

The literature dealing with the determination of traces of foreign matter in molybdenum and its compounds is reviewed. The following subjects are covered: emission spectroscopy, absorption spectroscopy, x-ray spectroscopy, radiochemistry, and mass spectrometry as means for the determination of trace quantities of Ag, Al, As, B, Ba, Be, Bi, C, Ca, Cd, Cl, Co, Cr, Cs, Cu, Fe, Ga, Ge, H, Hf, Hg, In, K, Mg, Mn, N, Na, Nb, Ni, O, P, Pb, Rb, Re, S, Sb, Se, Si, Sn, SO_4^{2-}, Sr, Ta, Th, Tl, Tl, U, V, W, and Zn. (233 references.) (JPRS)

10460 ANALYTICAL CHEMISTRY OF MIXED LIGAND COMPLEXES. Alimarin, I. P.; Shlenskaya, V. I. (Moscow State Univ.). Pure Appl. Chem.; 21: 461-78(1970).

Mixed ligand complexes are characterized by their extreme stability. The chemical individuality of the central atom displays itself clearly, and peculiarities in extractions with organic solvents may be observed. Such properties open new routes to the solution of various theoretical and practical problems in analytical chemistry; true mechanisms and kinetics of analytical reactions can be elucidated and the selectivity and sensitivity of analytical methods can be improved. The process of complex formation and the properties of mixed complex compounds containing inorganic ligands are considered with reference to the platinum group elements. The formation of mixed complexes containing organic and inorganic ligands sometimes determines the mechanism of the analytical reaction and the composition of the end product; examples of such interaction are given. The sensitivity and selectivity of analytical methods can be improved by means of the formation of complex compounds of the ion-associate type, and unusual methods of separation and group concentration can be achieved. The study of mixed chelates has developed in two directions: (a) studies of improved extractability (synergy), and coextraction of elements as mixed chelates; and (b) studies of changes in the physicochemical properties of systems, e.g., absorbance and fluorescence. Various new analytical procedures are discussed. (auth) (UK)

10461 DETERMINATION OF BURN-UP OF NUCLEAR FUEL ON THE BASIS OF MASS SPECTROMETRIC MEASURING OF THE STABLE ISOTOPES OF NEODYMIUM. I. THE CALCULATION OF BURN-UP ON THE BASIS OF ISOTOPES OF NEODYMIUM. Bulovic, V. (Boris Kidric Inst. of Nuclear Sciences, Beigrade); Krtil, J.; Djordjevic, M.; Moravec, A. Radiochem. Radioanal. Lett.; 5: 223-8(15 Dec 1970).

Two methods for the calculation of the number of fissions in a sample of irradiated U from mass spectrometric data on neodymium-148 are given for the determination of burnup of nuclear fuels. (auth)

10462 SPECTROTITRATION OF ETHANE-1-HYDROXY-1,1-DIPHOSPHONIC ACID (EHDP) WITH THORIUM DIAMINOCYCLOHEXANETETRA-ACETATE. Liggett, S. L.; Libby, R. A. (Procter and Gamble Co., Cincinnati). Talanta; 17: 1135-40 (Nov 1970).

An automatic spectrotitration procedure for EHDP was developed. It is applicable to samples containing 50 μg or more of EHDP, with a relative standard deviation of 3% if no interfering materials are present. The sensitivity can be extended down to about 5 μg, but titration blanks become significant and the standard deviation increases markedly. Thorium diaminocyclohexanetetraacetate (Th–DCTA), indexed as the thorium complex of (1,2-cyclohexylenedinitrilo)tetraacetic acid, is used as the titrant, to give a ternary species (Th–DCTA)$_2$–EHDP. The end-point in the spectrotitration is due to deprotonation of xylenol orange indicator when it is incorporated into a weaker ternary species after all the EHDP has reacted. Salts such as NaCl, $NaClO_4$, Na_2SO_4, and $NaNO_3$ interfere if present at concentrations of 0.1 to 0.5 M. The method is much more sensitive to orthophosphate, but this interference can be averted by isolating the EHDP before titration by selectively adsorbing the phosphonate on calcium hydroxyapatite. (auth) (UK)

10463 AUTOMATIC MASS SPECTROMETER FOR THE ISOTOPIC ANALYSIS OF HYDROGEN IN NATURAL WATER SAMPLES. Lohez, P.; Hagemann, R.; Botter, R. (CEA, Saclay, France). Method. Phys. Anal.; 6: 291-4(Sep 1970). (In French).

An automatic mass spectrometer was developed at the CEA by which 32 samples of water can be analyzed in 24 hours. The D/H ratio of samples with a normal D concentration (150 D atoms per million H atoms) was measured with an accuracy of 0.5 ‰. Samples are introduced by a microsyringe in the mass spectrometer; this allows samples of some tens of mm^3 to be analyzed. The instrument is highly flexible because of the possibilities of programming the number of samples to be analyzed and the number of measurements to be made. (France)

10464 DETERMINATION OF TRACE ELEMENTS IN SERUM AND URINE WITH FLAMELESS ATOMIZATION. Welz, B.; Wiedeking, E. (Bodenseewerk Perkin-Elmer and Co. GmbH, Ueberlingen, Ger.). Z. Anal. Chem.; 252: 111-17(1970). (In German).

A graphite tube furnace for flameless atomic absorption spectroscopy and its application in the analysis of biological materials is described. The values obtained for copper in 12 sera are in good agreement with colorimetric results and flame atomic absorption spectroscopy. The sample volume needed for one determination is only 2 μl of serum. Several further application possibilities for the determination of trace elements and for smallest sample volumes are discussed. (auth)

10465 ARSENATE METHOD FOR IODOMETRIC DETERMINATION OF SCANDIUM IN THE PRESENCE OF IRON. Shakhtakhtinskii, G. B.; Valiev, B. S.; Aslanov, G. A.; Nadzhafkuliev, N. A. (Inst. of Inorganic and Physical Chemistry, Baku). Azerb. Khim. Zh.; Nos. 1-2, 150-4(1970). (In Russian).

The arsenate method is described for the iodometric determination of Sc without preliminary separation of iron by masking it with tartaric or sulfosalicylic acid. The method offers accurate results in a wide range of Sc and Fe concentrations. (R.V.J.)

10466 ISOTOPIC ANALYSIS OF MICROGRAM QUANTITIES OF LEAD IODIDE USING AN ELECTRON-BOMBARDMENT SOURCE MASS SPECTROMETER. Oversby, V. M.; Compston, W.; Penikis, E. (Australian National Univ., Canberra). Earth Planet. Sci. Lett.; 10: 121-8(Dec 1970).

A method for routine isotopic analysis of small amounts of lead using PbI_3^- ions in a modified commercial gas-source mass spectrometer was developed. Samples as small as 2 μg of lead were analyzed successfully. Mass fractionation averages +0.06% per mass unit with maximum observed fractionation of +0.13% per mass unit. Chemical separation of lead by a standard anion exchange column produces samples of sufficient purity for mass spectrometry by PbI_2. (auth)

Isotope Dilution Procedures

10467 DETERMINATION OF OXYGEN IN FERRO-BORON BY THE VACUUM FUSION ANALYSIS. Furuya, Keiichi; Kikuchi, Tadashi (Tokyo Univ.). Jap. Anal.; 19: 1533-7(Nov 1970). (In Japanese).

A graphite capsule method was applied to the determination of oxygen in ferro-boron powder by the vacuum fusion method in order to eliminate incomplete fusion and/or extraction of oxygen from samples. Neither tin foil nor iron capsule gave

good results from flashing-out of sample when the sample was dropped into the crucible. Good results were obtained when a high purity grade graphite capsule (20 mm × 10 mmϕ) loaded with 18 mg of sample powder and 1 g of platinum as bath metal was dropped at 1850°C. An isotope dilution method using aluminum oxide containing 70.9 at. % ^{18}O was applied to the same procedure and gave good agreement with the results obtained by the vacuum fusion analysis. (auth)

10468 BARIUM ANALYSES FROM THE FIRST GEOSECS TEST CRUISE. Wolgemuth, K. (Columbia Univ., Palisades, N. Y.). Contract AT(30-1)-2663. J. Geophys. Res.; 75: 7686-7 (20 Dec 1970).

A profile of barium concentration in the Pacific Ocean was determined from the first Geosecs test station southwest of San Dieg by the isotope dilution method. The shape of the profile agrees quite well with previous samples from the northeast Pacific. The absolute concentration is consistently lower than previous results. This is attributed to a combination of a blank problem and possible uptake of barium by polyethylene storage bottles. (auth)

10469 DETERMINATION OF BURN-UP OF NUCLEAR FUEL ON THE BASIS OF MASS SPECTROMETRIC MEASURING OF THE STABLE ISOTOPES OF NEODYMIUM. II. THE EXPERIMENTAL PROCEDURES FOR THE ISOLATION AND MEASURING OF STABLE ISOTOPES OF NEODYMIUM. Bulovic, V. (Boris Kidric Inst. of Nuclear Sciences, Belgrade); Krtil, J.; Djordjevic, M.; Moravec, A. Radiochem. Radioanal. Lett.; 5: 229-33(15 Dec 1970).

The use of the separation and mass spectrometric method of isotopic dilution for the isolation and determination of stable isotopes of neodymium for burnup analysis is described. (auth)

10470 DETERMINATION OF ^{32}P-LABELLED ADENINE NUCLEOTIDES BY CHROMATOGRAPHY WITH ISOTOPE DILUTION USING THE ^{14}C-LABELLED COMPOUNDS. Loeppert, H. G. (Univ., Vienna). Radiochem. Radioanal. Lett.; 5: 209-16(15 Dec 1970).

A very sensitive radiochemical method for the determination of free adenine nucleotides is described. After labeling with ^{32}P and extraction, the nucleotides are separated by ion exchange chromatography and measured with a liquid scintillation counter. Yields are determined through isotope dilution with ^{14}C-labeled nucleotides. The method is rapid and suitable for routine work. (auth)

10471 OPTIMUM EXACTNESS OF THE METHODS OF SIMPLE ISOTOPE DILUTION. Klas, J. (Slovak Technical Univ., Bratislava). Radiochem. Radioanal. Lett.; 5: 179-84 (15 Dec 1970).

The problems of optimum distribution of the total time of measuring the radioactivity of the samples and of the background are discussed. The aim is to reduce analytical error to the minimum possible. (auth)

Radiometric and Radiochemical Procedures

Refer also to abstracts 10819, 10833, 10843, 10849, and 10937.

10472 (BMBW-FBK-70-19) ANNUAL REPORT, 1969. (Mainz Univ. (West Germany). Institut fuer Anorganische Chemie und Kernchemie). Oct 1970. 141p. (In German). Dep. NTIS (U. S. Sales Only).

The report is composed of the following parts: performance of the TRIGA reactor (Mainz); rapid chemical separations and identification of short-lived nuclides; nuclear spectroscopy; mass- and charge-distribution in fission and cross sections; search for superheavy elements; activation analysis; and fallout studies. (auth)

10473 (CEA-R-4032) CONTINUOUS CONTROL OF LOW-URANIUM CONTENTS OF SOLUTIONS BY MEASUREMENT OF RADIOACTIVITY. Bouzigues, Henri; Toussaint, Claude (Commissariat a l'Energie Atomique, Pierrelatte (France)). Sep 1970. 23p. (In French). Dep. NTIS (U. S. Sales Only).

The continuous measurement of the alpha activity of solutions containing uranium with gas flow proportional counters has various industrial uses. The main components of the apparatus described are a flow cell with a working area of 6 dm^2, a measuring probe consisting of a methane flow semi-proportional counter with a 0.9 mg/cm^2 Mylar window with a 6 dm^2 working area, a preamplifier, a high-voltage power pack, and a recording integrator. For a 27 per cent ^{235}U enriched solution, the minimum sensitivity is less than 1 ppM. This method is superior to techniques such as x-ray fluorescence or absorption spectrophotometry. (auth) (France)

10474 DETERMINATION OF URANIUM CONTENTS IN SOME ROCKS BASED ON FISSION TRACK METHOD. Hashimoto, Tetsuo (Kyoto Univ.); Hayashi, Seiju; Iwata, Shiro. Jap. Anal.; 19: 1538-43(Nov 1970). (In Japanese).

Uranium contents in some rocks were determined by means of a conventional fission track method. For making the standard samples, an aliquot of standard uranium solution was mixed with the known amounts of fine silica gel powder. Both the standard and pulverized rock samples were pressed on muscovite into thin tablets using a hand press. These tablet samples were irradiated in a reactor, KUR, and then subjected to the chemical etching procedure of mica surface in HF solution. The number of fission tracks on mica was counted up a microscopic photograph. The relationship between uranium content and track number was linear as expected from the calculation. Thus the uranium content of rocks could be easily determined by the use of a standard calibration curve. The effects of powder grain and of thorium, which is the only fissile element in nature except uranium, were also investigated. Uranium contents of four U. S. Geological standard rocks together with JG-1 and JB-1 have been conveniently determined by this fission track technique and the results were compared with those by others. (auth)

10475 FIZICHESKIE METODY EKSPRESS-ANALIZA SOSTAVA VESHCHESTV. (Physical Methods for Rapid Analysis of Substances). Skripko, A. L. Frunze, USSR; Izdatel'stvo Ilim (1970). 111p.

Nine articles are included on determination of composition and properties of materials by radiospectroscopic, dielectrometric, and radioisotopic methods. Sensitivity and efficiency of volume analog and digital moisture meters are described. Moisture measurements by means of protonresonance are also described. Source selection for determining mercury and lead contents by recording K radiation excited by β particles, quality control of noncompact materials by γ-absorption methods, and an approach to the equation describing the nonlinear relation of inverse β scattering as a function of multicomponent mixtures are discussed. (R.V.J.)

10476 URANIUM DETERMINATION IN THIN LAYERS OF ROCKS BY DIELECTRIC DETECTORS. Neige, R. (Centre de Recherches Radiogeologiques, Nancy). pp 389-94 of Dosage des Elements a l'Etat de Traces dans les Roches et les Autres Substances Minerales Naturelles. Paris; Centre National de la Recherche Scientifique (1970). (In French).

From National Conference on Measurement of Elements Occurring in Traces in Rocks, Nancy, France. See CONF-681205.

Uranium was determined qualitatively or quantitatively in thin sections of micas (biotites and muscovites). Dielectric detectors were used for recording the fission product tracks. These tracks were then observed with an optical microscope. (auth) (France)

10477 USE OF LOW-LEVEL α SPECTROMETRY IN THE DETERMINATION OF ELEMENTS OCCURRING IN TRACES IN NATURAL MINERAL SUBSTANCES. Lalou, C.; Lambert, G.; Le Roulley, J. C.; Nguyen Huu Van; Sanak, J. (CNRS, Gif-sur-Yvette, France). pp 395-409 of Dosage des Elements a l'Etat de Traces dans les Roches et les Autres Substances Minerales Naturelles. Paris; Centre National de la Recherche Scientifique (1970) (In French).

From National Conference on Measurement of Elements Occurring in Traces in Rocks, Nancy, France. See CONF-681205.

The principles of low-level α spectrometry are discussed, and some examples of geophysical analysis are given. These include: measurement of the accumulation rate of snow in Antarctica using $^{210}Pb/^{210}Po$; and determination of Th and U isotopes in seawater, fluvial water, and stalagmites. (auth) (France)

10478 METHODS FOR FRACTIONATION AND SCINTILLATION COUNTING OF RADIOISOTOPE-LABELED POLYACRYLAMIDE GELS. Ward, Samuel; Wilson, David L.; Gilliam, James J. (California Inst. of Tech., Pasadena). Anal. Biochem.; 38: 90-7(Nov 1970).

Two polyacrylamide gel fractionators are described. A rapid method of preparing gel fractions for liquid-scintillation counting is presented. This procedure allows high-efficiency counting of both ^{3}H and ^{14}C, but does not require degradation of the gel prior to counting. (M.C.G.)

10479 SENSITIVITY OF RADIOISOTOPE X-RAY FLUORESCENCE ANALYSIS USING ROSS FILTERS FOR ENERGY SELECTION. Svitel, J.; Jombik, J. (Comenius Univ., Bratislava). Radiochem. Radioanal. Lett.; 5: 185-92(15 Dec 1970).

The concept of generalized sensitivity has been established when Ross filters are used for energy selection of characteristic radiation in radioisotope x-ray fluorescence analysis. The eval-

uation of the analysis is demonstrated by an example of iodine determination in models of pharmaceutical preparations. (auth)

10480 DETERMINATION OF LOW-LEVEL ^{90}Sr AND ^{137}Cs ACTIVATION IN MILK BY MEANS OF THIN PLASTIC SCINTILLATORS. Marinov, V.; Dimchev, T.; Vrigazov, A. Kernenergie; 13: 296-8(Sep 1970). (In Russian).

^{90}Sr and ^{137}Cs contents in cow's milk were studied in 50 Bulgarian settlements. A 2π β scintillation detector with thin plastic scintillators in unidirectional anticoincidence circuit was used for measuring the activity of ^{90}Y and ^{137}Cs isolated radiochemically. For the whole country, average ^{90}Sr content is (9.1 ± 4.0) pCi/l in the winter season, (9.5 ± 5.2) pCi/l in summer season, the data for ^{137}Cs being (9.2 ± 4.0) pCi/l and (11.4 ± 3.6) pCi/l, respectively. (auth)

10481 DETERMINATION OF TRACE AMOUNTS OF IODINE. II. DETERMINATION OF 12-2000 ng OF IODIDE BY EXTRACTIVE RADIOCHEMICAL TITRATION. Juette, B. A. H. G.; Agterdenbos, J.; Elberse, P. A. (Rijksuniversiteit, Utrecht). Talanta; 17: 1130-5(Nov 1970). (In German).

Theory and practice are described for a simple radiochemical determination of 12 to 2000 ng of iodide, based on the extraction of HgI_2. The iodide is titrated with Hg(II), labeled with ^{203}Hg. A determination takes about 45 min. The relative standard deviation is 1.5 to 5%, depending on the ^{203}Hg solution. (auth) (UK)

10482 ROUTINE METHOD FOR THE DETERMINATION OF LOW ^{137}Cs ACTIVITIES IN BIOLOGICAL SAMPLES. Mirna, A. (Federal Inst. for Meat Research, Kulmbach, Ger.). Analyst; 95: 1000-2(Dec 1970).

A routine method for the determination of low fallout activities of ^{137}Cs in biological materials is described. Radiocaesium is extracted by adsorption on ammonium molybdophosphate. The usual radiochemical purification of the alkaline ammonium molybdophosphate solution by anion exchange is omitted and caesium precipitated directly with bismuth tri-iodide in the presence of citric acid as complexing agent. A caesium chloroplatinate source is prepared for β counting. (auth) (UK)

10483 DETERMINATION OF BORON IN BORIC GLASSES BY A NEUTRON ABSORPTION METHOD. Dillinger, P.; Toelgyessy, J. (Technical Univ., Bratislava). Silikaty; 13: 339-46(Dec 1969). (In Slovak).

A neutron absorption method was used to determine B concentrations (ranging between 0 and 0.4%) in boric glasses. Samples were irradiated with a Pu-Be neutron source yielding 5.6×10^6 n/sec. Activation detectors (circular Ag foils) served to detect thermal neutrons. This technique is characterized by lower precision and greater simplicity than that using scintillation detectors. For samples with higher (lower) B concentrations the optimum sample thickness was 10 (25) mm. The complete analysis, including the plotting of the standard curve, does not take more than 2 hours. Individual determinations can be completed in 15 to 20 min. The mean quadratic error did not exceed ±1.5%. For B determinations in Sial and Simax glasses the calibration curve need not be plotted; two standards, one with minimum and one with maximum permissible B concentrations, are sufficient. (NSA of Czech)

10484 URANIUM ORE CONTRASTS. Omaljev, Veljko. Nukl. Energ.; 4: No. 6, 20-7(1967). (In Serbo-Croatian).

Methods for the measurement of the radioactivity of uranium ores at the pit are discussed. Fast radiometric analysis on the conveyor belt is described. Economic aspects of the radiometric analyses are analyzed. Optimum parameters for the distribution of the ore in barren rock were determined. (R.V.J.)

10485 GALACTOSEMIA: METABOLISM OF GALACTOSE ^{14}C IN BLOOD CELLS. APPLICATION TO THE DISTINGUISHING OF HETEROZYGOTES. Tron, P.; Milhaud, G. (CHU de Saint-Antoine, Paris. Hopital Parrot, Bicetre, France). Rev. Fr. Etud. Clin. Biol.; 14: 12-18(Jan 1969). (In French).

Blood cells incubated with galactose U ^{14}C were extracted in 80 and 20 percent ethanol and analyzed by chromatography on Whatman No. 4 paper, in two solvent systems: water-saturated phenol and n-butanol-propionic acid-water (2-1-1.4 V/V). Radioactive spots are localized by autoradiography, cut, eluted, and radioactivity is then measured in a liquid scintillation counter. In patients with galactosemia, UDP Gal spot radioactivity was almost absent. In normal subjects, there is a regression between UDP Gal and galactose-1-phosphate radioactivities. In the gene carriers the regression coefficient is different which enables them to be distinguished. Under test conditions, there is a more marked accumulation of galactose-1-phosphate in patients with galactosemia than in gene carriers and in the later, it is still more evident than in normal subjects. The comparison of results with the results of the uridyl-diphosphoglucose method shows a similar accuracy. (auth)

10486 MOISTURE DETERMINATION IN CERTAIN COMPOUNDS USED FOR PHARMACEUTICAL PURPOSES BASED UPON NEUTRON SCATTERING AND MODERATION. Dillinger, P.; Toelgyessy, J.; Sarsunova, M. (Technical Univ., Bratislava). Cesk. Farm.; 18: 517-21(Dec 1969). (In Slovak).

A Ra-Be neutron source was used containing 5 mg Ra and yielding ~6.5×0^4 n.sec^{-1}. Neutrons were detected with ZnS(Ag) scintillation detectors. The neutron source was placed in the center of the sample and the detector was situated under the sample. The sample volume amounted to 1 dm^3 and 5.5 cm was found to be the optimum source-to-detector distance. Moisture content was determined by means of a calibration curve. In samples of citric acid, lactose, sulphosalicylic acid, bentonite, and sodium citrate, the following values were found for the moisture content: 8.63, 8.78; 2.75, 2.71, 10.20, 9.90; 8.15, 8.43; and 12.18, 12.42%, respectively. Of each pair of values the former is the result of a gravimetric determination and the latter was obtained by the method presented. The absolute error or measurement ranges from 0.04 to 0.3% H_2O by weight. (NSA of Czech)

10487 NEUTRON ABSORPTION ANALYSIS OF PHARMACEUTIC PREPARATIONS CONTAINING BORON. Dillinger, P.; Toelgyessy, J.; Sarsunova, M. (Technical Univ., Bratislava). Ces. Farm.; 18: 433-7(Nov 1969). (In Slovak).

A Pu-Be neutron source yielding 5.6×10^6 n/sec was used. Neutrons were detected with a scintillation detector. Forty ml of the liquid was sampled into an open measuring cell. The sample thickness amounted to 2 cm. The cell was placed in irradiation apparatus between the source and the slow-neutron detector. A 5-cm plastic moderator layer between the sample and the neutron source was used. A neutron beam diameter of 3 cm was provided by a cadmium plate. Counting rates of I_0 and I were measured for water and for the sample, respectively. A calibration curve [I_0/I against boron concentration (from 1 to 5 mg/ml) of standard boric acid solutions] was plotted and used for analysis of liquid preparations containing boric acid and sodium tetraborate. (NSA of Czech)

Activation Procedures

Refer also to abstracts 10909 and 11472.

10488 (CEA-R-4072) STUDY OF ACTIVATION ANALYSIS USING CHARGED PARTICLES AND γ PHOTONS. Engelmann, Charles (Commissariat a l'Energie Atomique, Saclay (France). Centre d'Etudes Nucleaires). Oct 1970. 222p. (In French). Dep. NTIS (U. S. Sales Only).

Thesis. Submitted to Paris Univ., Orsay (France). Faculte des Sciences.

In order to study γ photon activation, a study was first made of the influence of conversion targets on the activities induced by irradiating C and Ag monitors behind Al, Cu, and Pt targets of various thicknesses. Using C and Ag monitors, a determination was made of the spatial distribution of the bremsstrahlung for Al and Pt targets irradiated with 25- to 45-MeV electron. The (γ,n) activation curves and the interference curves arising in the determination of C, N, and F by (γ,t) and $(\gamma,\alpha n)$ reactions on neighboring elements were determined. The integrated activation curves for the light elements Be, B, C, N, O, and F at a unit concentration of 10^{-6} μg/g were determined in a homogeneous medium with a moderating power equivalent to that of aluminum. Thick monitors were irradiated with p(5 to 15 MeV), d and ^{3}He (5 to 20 MeV), and α (25 to 42 MeV) particles. The detection of traces of C, N, O, and F using γ photons was compared to that using the charged particles p, d, ^{3}He, and α. It is possible to determine the oxygen in sodium by proton activation. Examples are given of the determination of light elements in very pure materials, in particular boron determination in silicon at a concentration of 10^{-4} μg/g and nitrogen determination at a concentration of 10^{-2} μg/g in iron and and niobium. (91 references). (France)

10489 (KFKI-70-25-NAC) PULSED REACTOR POTENTIALITIES FOR NEUTRON ACTIVATION ANALYSIS. Cheke, A.; Nad, A.; Sabo, E. (Magyar Tudomanyos Akademia Kozponti Fizikai Kutato Intezete, Budapest). [1970]. 30p. (In Russian). Dep. NTIS (U. S. Sales Only).

A brief review is given of characteristics of analytical methods using neutrons at various energies. Data are given of different areas in which pulsed reactors may prove to be more efficient than any other type. Studies were made of the feasibility of speci-

men irradiation in pulsed reactors and various suggestions are presented on the development of high-speed specimen conveyers. Descriptions are given of the design, specifications, and construction of specimen conveyers operating with 8 or 10 μsec speed. A general description is given of possible measuring devices. (R.V.J.)

10490 (LIB/Trans-334) RAPID ISOTOPIC SEPARATION METHOD FOR THE SELECTIVE DETERMINATION OF SHORT LIVED RADIOISOTOPES. Loepfe, E.; Monnier, D.; Haerdi, W. Translated by U. Engelbert for Australian Atomic Energy Commission Research Establishment, Lucas Heights, from Z. Anal. Chem.; 221: 109-19(1966). 12p. Dep. NTIS (U. S. Sales Only).

An abstract of this article prepared from the original appeared as NSA 21: 1276. (Australia)

10491 (ORNL-4636, pp 20-33) NUCLEAR AND RADIOCHEMISTRY. (Oak Ridge National Lab., Tenn.).

From Analytical Chemistry Division annual progress report for period ending September 30, 1970.

Topics covered include: trace element determinations in biological and environmental samples, cooperative isotopes program, radioisotopes characteristics and measurements, proton reaction analysis for $^{13}C/^{12}C$ and $^{15}N/^{12}C$ ratios in biological samples, gamma spectrometry and new facilities, nuclear safety support program, effects of radiation on analytical methods, and Cherenkov and phosphor studies. (M.C.G.)

10492 ACTIVATION ANALYSIS OF ROCKS AND DEGRADATION PRODUCTS, APPLICATION TO TWO TYPES OF SANDS WITH VARIOUS MINERALOGIC GRADES. Ricq, J. M. (l'Atome Industriel, Grenoble, France). pp 355-66 of Dosage des Elements a l'Etat de Traces dans les Roches et les Autres Substances Minerales Naturelles. Paris; Centre National de la Recherche Scientifique (1970). (In French).

From National Conference on Measurement of Elements Occurring in Traces in Rocks, Nancy, France. See CONF-681205.

After being activated by thermal neutrons, some trace amounts of elements were separated by a succession of ion exchange columns and determined by γ spectrometry. The elements included Cs, Na, Rb, K, Ni, Co, Zn, Cu, Al, Ga, Hf, Ta, W, Sb, Zr, U, Th, Mo, Ce, and others. A comparative study based on these analyses was made. (auth) (France)

10493 HIGHLY SENSITIVE RAPID METHODS FOR BORON AND LITHIUM DETERMINATION IN STONE METEORITES AND ROCKS. Quijano-Rico, M. (Max-Planck-Institut fuer Chemie, Mainz). pp 367-80 of Dosage des Elements a l'Etat de Traces dans les Roches et les Autres Substances Minerales Naturelles. Paris; Centre National de la Recherche Scientifique (1970). (In French).

From National Conference on Measurement of Elements Occurring in Traces in Rocks, Nancy, France. See CONF-681205.

A method was developed for the determination of boron in rocks and in the nonmetallic fraction of stone meteorites. In an especially designed apparatus the same sulfuric acid concentration was used for the attack of silicates, the separation of boron, and as detection medium. Very low blank values, equivalent to 5 nanograms boron and a determination limit at the nanogram level were obtained in routine analysis; a boron fluorimetric determination took about two hours per sample. Lithium was determined by thermal neutron activation, using the reactions $^{6}Li(n,\alpha)^{3}H$ and $^{16}O(T,n)^{18}F$. The separation of Cl after activation and F by pyrohydrolysis was complete in 15 minutes. Fluorine was determined by titration using thorium nitrate. The results obtained for the B, Li, Cl, and F contents of standard rocks G-1 and W-1 were in good agreement with those published by others and are summarized. Possible applications of the described methods to different problems are discussed. (auth) (France)

10494 URANIUM ISOTOPIC DETERMINATION IN ROCKS BY NEUTRON ACTIVATION. Deschamps, N. (CNRS, Vitry-sur-Seine, France); Rouchaud, J. C.; Ceard, P.; Neige, R. pp 381-7 of Dosage des Elements a l'Etat de Traces dans les Roches et les Autres Substances Minerales Naturelles. Paris; Centre National de la Recherches Scientifique (1970). (In French).

From National Conference on Measurement of Elements Occurring in Traces in Rocks, Nancy, France. See CONF-681205.

The ^{235}U and ^{238}U content of rocks was determined by measuring the radioactivity of ^{239}Np and ^{133}I after chemical separation of these isotopes. After irradiation of samples for 48 hours at a flux of 1.5 $10^{12}n/cm^2/sec$, 10^{-4} μg/g of ^{235}U and ^{238}U were determined. (auth) (France)

10495 NEUTRON ACTIVATION DETERMINATION OF SELENIUM IN BIOLOGICAL MEDIA. Maziere, B.; Comar, D.; Kellershohn, C. (CEA, Orsay, France). Bull. Soc. Chim. Fr.; 10: 3767-71(Oct 1970). (In French).

The determination of plasmatic selenium was made by activation analysis. The separation of selenium is achieved by substoichiometric extraction of the selenium–diethyldithiocarbamate complex. After 6 days of irradiation, in a $2 \times 10^{13}n \times cm^{-2} \times s^{-1}$ flux of thermal neutrons, the sample of lyophilized plasma is mineralized, in the presence of a known weight of carrier selenium, by a nitric acid-sulfuric acid mixture. The residue is filtered on a 2 × 8 Dowex column to eliminate zinc, gold, and mercury; selenium is then stoichiometrically complexed. The complex is extracted by carbon tetrachloride and its radioactivity measured by γ spectrophotometry. A series of 10 measurements made on the same sample of blood plasma gave the following results: 0.083 ± 0.005 μg/ml, (i.e., accuracy of ±6.05%) for a counting time of 20 min; the limit of sensitivity is about 10^{-1} μg. For direct spectrophotometry, a decrease of 2 to 3 weeks is necessary to eliminate the parasitic radioactivity of the shortlived radioelements. In the case of the determination of selenium in the blood plasma, for a weight of 0.1 μg the accuracy is 5.3% and the counting time is one hour. The comparison of date obtained by both methods is discussed. (auth) (France)

10496 THIN-LAYER CHROMATOGRAPHY AS AGENT IN RADIOCHEMISTRY. PART 5. SEPARATION OF Hg FROM A MIXTURE OF CATIONS. Seiler, H. (Univ., Basel). Helv. Chim. Acta; 53: 1893-5(1970). (In German).

The separation of Hg from a mixture of many cations by thin-layer chromatography, and its subsequent determination by activation analysis is described. (auth)

10497 ACTIVATION ANALYSIS. RECENT ADVANCES IN USING CHARGED PARTICLES, GAMMA PHOTONS, AND ^{252}Cf SOURCES. Ricci, Enzo (Oak Ridge National Lab., Tenn.). Energ. Nucl. (Madrid); 14: 303-10(Jul-Aug 1970). (In Spanish).

Following an introduction on the fundamentals of activation analysis there are comments on the origin and basic concepts of procedures that utilize neutrons from ^{252}Cf, gamma photons, and charged particles. In all cases there is a schematic description of the necessary instruments. A detailed account is given of the sensitivity and the limits of detection for various elements corresponding to the utilization of charged particles, gamma photons, and ^{252}Cf sources. (tr-auth)

10498 DETERMINATION OF FLUORINE BY NEUTRON ACTIVATION ANALYSIS IN FLUORINATED ORES AND CONCENTRATES. PART II. Simon, L.; Sok, V.; Filgas, R. (Mining Inst., Prague). Rudy (Prague); 17: 339-42(Nov 1969). (In Czech).

Activation analysis was applied to fluorine determinations in fluorite ores. A 2.75-Ci Po–Be source was used yielding 5.2 × 10^6 n/sec. The samples (100 to 200 g) were irradiated for 30 sec. The induced ^{16}N activity was measured with a scintillation γ spectrometer with a NaI(Tl) crystal for 30 sec. In 27 samples the CaF_2 concentration ranged between 2.5 and 97%. A linear course was found when plotting the measured activity against the sample weight for the range 0 to 200 g. (NSA of Czech)

10499 ACTIVATION ANALYSIS OF RARE-EARTH METALS. Bereznai, Tamas (United Incandescent Lamp and Electric Co., Budapest). Kem. Kozlem.; 34: 87-106(14 Aug 1970). (In Hungarian).

The literature dealing with the activation analysis of rare earth metals is reviewed. The following subjects are discussed: analysis with the aid of reactor neutrons, analysis with the aid of neutron generators, activation in accelerators, special techniques, and a comparative evaluation of the various techniques. (90 references) (JPRS)

10500 FEASIBILITY OF THE DETERMINATION OF COBALT AND SELENIUM BY ON-STREAM ACTIVATION ANALYSIS. Kliment, V. (Inst. of Physics, Bratislava); Toelgyessy, J. Radiochem. Radioanal. Lett.; 5: 259-63(15 Dec 1970).

Equipment has been designed and constructed for the continuous determination of cobalt and selenium by means of on-stream activation analysis. Measurements made with the equipment have confirmed the possibility of cobalt and selenium determination with sensitivities of 2.2 mg Co/ml and 2.7 mg Se/ml, respectively. (auth)

10501 PHOTO-NUCLEAR ACTIVATION ANALYSIS OF OXYGEN IN PURE MATERIALS WITH SENSITIVITIES OF 0.1 TO 0.01 PPM. Kapitza, S. P. (Inst. for Physical Problems, Moscow); Samosyuk, V. N.; Tsipenyuk, Yu. M.; (and others). Radiochem. Radioanal. Lett.; 5: 217-22(15 Dec 1970).

The determination of oxygen in various pure materials (copper, steel, tin) is described. "Mictrotron," a new electron accelerator, was used as a source of γ rays. For the rapid extraction of ^{18}O a carbon reduction method, using pulsed heating of the sample in an inert atmosphere, was employed. (auth)

10502 DETERMINATION OF MERCURY IN BIOLOGICAL MATERIAL BY NEUTRON ACTIVATION ANALYSIS. Haesaenen, Erkki (Helsinki Univ. of Tech., Otaniemi, Finland). Suomen Kem.; 43B: 251-4(1970).

A method was developed for determination of mercury in fresh biological material. After irradiation and addition of mercury as carrier, the sample is decomposed by wet oxidation with a mixture of nitric and sulfuric acids. Evaporation of the mercury is prevented by using a vertical condenser to which a capillary tube is connected. The resulting clear solution is diluted with water and the mercury allowed to precipitate on the surface of copper powder, which is isolated by filtration, washed, and enclosed in a plastic capsule. The gamma activity is measured using a NaI(Tl)-crystal and a multichannel analyzer. The mercury content of the sample is determined from the area of the 78-keV photopeak of ^{197}Hg. Simultaneously with the sample, a standard mercury solution is irradiated. The activity of this solution and that of the unknown sample is compared. The recovery of mercury after wet ashing and precipitation on copper powder was found to be 98.5%. The method is rapid, reliable, and suitable for routine analyses. It was used to analyze 12 samples, the mercury contents of which were also determined colorimetrically. (auth) (Finland)

10503 SURVIVAL OF ^{50}Cr-LABELED ERYTHROCYTES AS STUDIED BY INSTRUMENTAL ACTIVATION ANALYSIS. Glomski, Chester A. (State Univ. of New York, Buffalo); Pillay, Sivasankar K. K.; Hagie, Robert E. J. Nucl. Med.; 12: 31-4(Jan 1971).

The applicability of ^{50}Cr tagging of red blood cells and accurate quantitation of millimicrogram amounts of tracer ^{50}Cr bound to erythrocytes without having to resort to a chemical separation were investigated. Labeled blood samples were withdrawn, irradiated for 24 hr with a thermal flux of 3×10^{13} n/cm^2/sec, and counted using a Li-drifted Ge detector and a multichannel analyzer. (M. C.G.)

10504 ACTIVATION ANALYSIS BY CHARGED PARTICLES. Toelgyessy, Juraj; Salamon, Andras; Szabo, Elek. Chem. Listy; 64: 1121-46(1970). (In Czech).

A brief review is given on neutron irradiation and activation analysis. Nuclear techniques in analytical chemistry, radiochemical methods, and modern trends and instrumentation in charged-particle activation analysis are discussed. (189 references) (R.V.J.)

10505 STUDY ON IODINE AND BROMINE IN SOIL-PLANT SYSTEM IN RELATION TO THE RECLAMATION-AKAGARE DISEASE OF LOWLAND RICE BY MEANS OF RADIOISOTOPE-TECHNIQUES. Tensho, Kiyoshi; Yeh, Ko-ling (Japan Atomic Energy Research Inst., Tokyo). Radioisotopes (Tokyo); 19: 574-9(Dec 1970).

A study on iodine and bromine in soil-plant systems was performed by means of activation analysis and tracer techniques. The soils in volcanic ash origin from the Kanto District contained 14 to 23 ppM I and 55 to 139 ppM Br, and the ratios of I/Br were from 0.12 to 0.41. According to an incubation test using an Akagare-soil of Nishinasu, the oxidative retention and reductive liberation of soil iodine was well recognized, and the maximum of 60 to 70% of soil iodine was released under submerged condition, resulting in about 4 ppM I in soil solution. A plant culture test of rice revealed that the availabilities of iodine and bromine in soil as well as the applied ^{131}I were highly variable due to soil conditions, such as moisture status, accompanied chloride and calcium addition. Among these treatments, soil submergence was most predominant for increasing their uptake by root, especially in iodine. In the case of Nishinasu soil, the contents in dried plant ranged from 1.3 to 341 ppM I and from 46 to 2170 ppM Br. (auth)

10506 SIMULTANEOUS DETERMINATION OF ARSENIC AND ANTIMONY IN SOIL BY NEUTRON ACTIVATION ANALYSIS. Ohno, Shigeru (National Inst. of Radiological Sciences, Chiba, Japan); Yatazawa, Michihiko. Radioisotopes (Tokyo); 19: 565-9(Dec 1970).

Arsenic and antimony were determined in several soil samples by neutron activation analysis. A simple and rapid procedure is presented. After alkali fusion, the irradiated sample was dissolved in slightly acid solution and then arsenic was precipitated with quinoline molybdate solution, and antimony was separated as antimony sulfide. The precision of this method was calculated from analysis of a standard specimen to be about ±8% and the sensitivity of this method was estimated as 0.005 ppM for arsenic and 0.01 ppM for antimony. This method is also applicable to both geological and biological samples. (auth)

10507 NEUTRON-ACTIVATION ANALYSIS OF SEAWATER. Ryabinin, A. I.; Romanov, A. S. (Marine Hydrophysics Inst., Sevastopol). Geokhimiya; No. 7, 875-9(Jul 1970). (In Russian).

Unfiltered seawater samples 12 ml from the Black Sea were sealed in quartz tubes, and irradiated 1 hr at a thermal neutron flux of 1.8×10^{13} neutrons/sec/cm^2 in order to determine the antimony content (calculated amount of antimony is 10^{-9} g). The ampoules were set aside 4 days in order to allow the sodium and arsenic activities to decay. The ampoules were opened, transferred to 100 ml flasks, and distilled as stibine from a hydrochloric acid solution under reducing conditions. The antimony content was determined from the area under the 0.56-MeV photopeak. The sensitivity of the antimony determination was 1×10^{-10} g/ml. seawater. The results show an average antimony content of 5.3×10^{-6} g/l in the surface waters of the Black Sea along the 34th meridian. The antimony is probably absorbed on a ferric hydroxide sol. At greater depths animony is more likely to be present as the sulfide. (TTT)

10508 CONCENTRATION OF Cs IN HIGH GRADE METAMORPHIC ROCKS. Heier, K. S.; Brunfelt, A. O. (Mineralogisk-Geologisk Museum, Oslo). Earth Planet. Sci. Lett.; 9: 416-20 (11 Nov 1970).

Cesium concentrations have been determined by neutron activation analyses in 6 amphibolite facies gneisses and 16 rocks in medium to high pressure granulite facies. The Cs concentrations are discussed relative to K and Rb contents (determined previously by x-ray spectrography). Cs was significantly depleted relative to K in the granulite facies rocks. This depletion was greater, by about two orders of magnitude, than the previous values for K/Cs ratios in the crust. Cs was also low in the amphibolite facies gneisses. Fractionation between Cs and Rb was observed. (auth)

10509 SIMULTANEOUS DETERMINATION OF COPPER AND MANGANESE IN PLANTS BY NEUTRON-ACTIVATION ANALYSIS. Ohno, S. (National Inst. of Radiological Sciences, Anagawa, Japan); Suzuki, M.; Yatazawa, M. Analyst; 95: 995-9(Dec 1970).

By using the radioactivation technique, copper and manganese were determined simultaneously in plant leaves. A simplified and rapid procedure for the determination of both elements in plant leaves is presented. The copper and manganese in irradiated samples are separated by solvent extraction, the former being extracted with α-benzoinoxime–pyridine–chloroform and the latter with 8-hydroxyquinoline–chloroform. The time required for radiochemical separation from the end of irradiation to counting is less than 1 hour for ten samples. The precision of the method in the range of 0.1 to 0.2 ppM is about ±5 percent. The limits of detection calculated from the analysis of standard specimens are about 0.01 μg for copper and 0.001 μg for manganese. (auth) (UK)

10510 DETERMINATION OF ARSENIC IN BIOLOGICAL MATERIAL BY NEUTRON ACTIVATION ANALYSIS. Rakovic, M. (Charles Univ., Prague). Cas. Lek. Cesk.; 108: 1102-4(5 Sep 1969). (In Czech).

The sample of biological material is activated with thermal neutrons in a nuclear reactor for 20 hours. By the ^{75}As (n,γ) ^{76}As reaction, a beta–gamma emitter is formed with a half-life of 26.4 hours. After the activation a carrier (100 mg As) is added, the sample is decomposed, and the radioarsenic, ^{76}As, is separated by a precipitation procedure as arsenic pentasulfide. An integral measurement is carried out with both the precipitate obtained from the sample and the activated standard containing 1 μg As, using a scintillation detector with a NaI(Tl) crystal. The radiochemical purity of the preparation obtained by this one-step separation was checked by means of the decay curve. Radiophosphorus, ^{32}P, is the only radioactive impurity that can be observed. However, its effect on the result of measurement lies well below the total accuracy of the method. (NSA of Czech)

10511 NEUTRON ACTIVATION ANALYSIS OF MANGANESE AND SODIUM IN BACTERIAL CELLS. Krueger, Woodrow B.; Carey, Walter E.; Kolodziej, Bruno J. (Ohio State Univ., Columbus). Appl. Microbiol.; 20: 946-50(Dec 1970).

The application of neutron activation analysis for the determination of manganese and sodium in bacteria was investigated. Elements considered here were manganese and sodium. The sporeformer Bacillus megaterium ATCC 19213 was utilized. With this method, the manganese and sodium levels of whole and ashed vegetative cells, sporulating cells, and free spores

were determined. The culture medium was also analyzed for these two elements. The results indicate that neutron activation analysis is readily applicable to the study of mineral content of bacterial cells, spores, and culture media. The method has been shown to be ideal for the study of incorporation and egression of mineral elements during vegetative growth and secondary metabolism of sporulation. (auth)

10512 END-GROUP ANALYSIS BY NEUTRON ACTIVATION. DETERMINATION OF MOLECULAR WEIGHT OF α-LIN-POLY-p-XYLYLENE. Kobayashi, Mitsue (Kyoto Univ.). J. Polym. Sci., Part B; 8: 823-8(Nov 1970).

The determination of the molecular weight of α-lin-poly-p-xylylene synthesized by the Wurtz reaction of p-xylylene dichloride and sodium naphthalene by neutron activation analysis of chlorine in the two end-groups of this polymer is reported. After irradiation in a thermal neutron flux of 5×10^{12} n/cm²/sec, the samples were transferred into 5-ml capsules. Aliquots (2 to 100 ml) of the standard solutions were pipetted on filter papers. The γ spectrum of an irradiated polymer, together with that of ^{38}Cl in irradiated HCl, indicated that NaCl, a by-product of the polymerization reaction, has been removed completely from the polymer. An equation is given for calculating the weight of chlorine. Data are tabulated. (P.C.H.)

Inorganic, Organic, and Physical Chemistry

Refer also to abstract 10583.

Chemical Properties

Refer also to abstracts 10462, 10651, and 12034.

10513 (AERE-R-4887) THEORETICAL EXAMINATION OF IODINE–WATER PARTITION COEFFICIENTS. Eggleton, A. E. J. (Atomic Energy Research Establishment, Harwell (England)). Feb 1967. 16p. Dep. NTIS (U. S. Sales Only).

Examination of the various reactions of iodine in water leads to the selection of four fast reactions that control the equilibrium between elemental iodine and its hydrolysis products. On the assumption that elemental iodine is the only volatile species, water–gas phase partition coefficients were calculated from the equilibrium constants. At 25 the value increased from a minimum of 83 at high iodine concentrations and low pH to values in excess of 10,000 at high pH and low iodine concentrations. The values for 100°C are smaller than the 25°C values at high iodine concentration but increase more rapidly as the pH is raised and the iodine concentration lowered. The slow reaction leading to iodate formation is found to be of importance only at pH values greater than 7, both on equilibrium and rate grounds. The effects of traces of oxidizing and reducing agents were assessed on the basis of the redox potential of the final solution. (auth) (UK)

10514 (AERE-R-5320) THE POTENTIAL OF THE Pu(III)–Pu(IV) COUPLE IN NITRIC ACID SOLUTION AND EQUILIBRIUM CONSTANTS FOR THE NITRATO COMPLEXES OF Pu(IV). Wain, A. G. (Atomic Energy Research Establishment, Harwell (England)). Dec 1966. 9p. Dep. NTIS (U. S. Sales Only).

The formal potential of the Pu(III)–Pu(IV) couple in nitric acid solution versus the saturated calomel electrode (SCE) was measured at 25 ± 0.1 °C by titration of Pu(III) with standard potassium dichromate. The association between Pu^{4+} and the nitrate ion was investigated by measuring the shift in potential from nitric acid to perchloric acid medium. (auth) (UK)

10515 (COO-1780-14) ONE AND TWO ELECTRON TRANSFER REACTIONS. Progress Report, March 1, 1970–February 28, 1971. Gordon, Gilbert (Iowa Univ., Iowa City. Dept. of Chemistry). 19 Nov 1970. Contract AT(11-1)-1780. 20p. Dep. NTIS.

A systematic study is being made of electron transfer reactions that utilize oxygen-containing oxidizing agents and V(II), V(III), U(IV), and trisphenanthroline iron(II) as reducing agent. Mechanisms of the reactions of chlorine(III) with uranium(IV) were determined. The effect of sample reduction on diffusion coefficients of single crystals of TiO_2 was investigated. (M.C.G.)

10516 (IEA-185) DRY-WAY PREPARATION OF THORIUM TETRAFLUORIDE. Correa, Heleno S.; Costa, Eduardo C. (Instituto de Energia Atomica, Sao Paulo (Brazil)). Aug 1969. 26p. Dep. NTIS (U. S. Sales Only).

The dry preparation of ThF_4 via the action of anhydrous HF on ThO_2 was studied. Batch hydrofluorinations were conducted in graphite boats at constant HF flow rates and constant feed gas temperature. Time, temperature, and type of oxide were the variables studied. Oxides prepared by calcining the oxalate at 400, 600, and 800°C, and by calcining the hydroxide at 600 and 800°C, as well as a sulfate-activated hydroxide, and the original oxalate and hydroxide, were hydrofluorinated at temperatures of 400, 500, and 600°C for 1 and 3 hours. Conversions were determined by the weight change of samples. The highest conversions were obtained with the oxide derived by calcination of the oxalate at 800°C. Cross-plotting the experimental data in the form of time-temperature correlations at constant conversion allowed the determination of suitable combinations of time and temperature for a desired conversion level. Sintering of the tetrafluoride was observed at hydrofluorination temperatures higher than 525°C. (auth)

10517 (JUL-674-RC) PLANNING AN ATOMIC BEAM APPARATUS FOR INVESTIGATION OF ELEMENTARY CHEMICAL PROCESSES OF NEUTRAL PARTICLES AT TRANSLATION ENERGIES FROM 0.1 TO ABOUT 20 eV ("CHEMICAL ACCELERATOR"). Schmidt-Bleek, F.; Stoecklin, G.; Vogelbruch, K. (Kernforschungsanlage, Juelich (West Germany). Institut fuer Radiochemie). Jul 1970. 51p. (In German). Dep. NTIS (U. S. Sales Only).

The construction of a very flexible atomic beam device for the study of chemical reactions in the eV range was studied by applying the technology developed in molecular beam technology to higher energies and supplementing this technology by radiochemical methods. The principal possibilities for the production of a monoenergetic beam of neutral particles in the eV range were investigated, and the solid-body sputtering method was selected because of its wider usable energy range and the greater number of elements possible for application. The design of an atomic beam device using solid-body sputtering as the radiation source is given. The studies planned with this device are briefly outlined. (J.S.R.)

10518 (RD/B/N-1816) THE THERMODYNAMICS OF SOME METAL/COOLANT REACTIONS IN MK.III REACTORS. Hales, R.; Pearce, R. J. (Central Electricity Generating Board, Berkeley (England). Berkeley Nuclear Labs.). Oct 1970. 17p. Dep. NTIS (U. S. Sales Only).

A thermodynamic assessment of the compatibility of metals and gaseous impurities in a helium atmosphere is presented. It is shown that, assuming thermodynamic equilibrium can be attained, the constituent elements of an alloy may exhibit different reactions with the gaseous impurities present in reactor coolant atmospheres. Reactions may be reversed by fluctuations in either gas composition or temperature. The pressure dependency for the possible carburizing reactions is indicated. (auth) (UK)

10519 URANYL PYROPHOSPHATE COMPLEXES. II. INVESTIGATION OF THE FORMATION OF ANIONIC COMPLEXES. Dragulescu, C.; Vilceanu, N.; Julean, I. (Wissenschaftliche Forschungsstelle, Timisoara, Rumania). Z. Anorg. Allg. Chem.; 376: 196-204(Aug 1970). (In German).

The formation of complex anionic uranyl pyrophosphates was studied in solution at pH 1 to 10. The existence of uranyl mono pyrophosphate and bis pyrophosphate complexes, which may be represented by the general formula $[UO_2H_q(P_2O_7)_x]^{(4x-q-2)-}$ (x = 1; 2), was proved. (auth)

10520 AVIDITY OF FOLIC ACID FOR CARCINOGENIC METAL IONS, ALUMINIUM(III), CHROMIUM(III), BERYLLIUM(II), LEAD(II), AND URANIUM(VI). Nayan, Ram; Dey, Arun K. (Univ. of Allahabad, India). Z. Naturforsch.; 25b: 1453-7(Dec 1970).

Stepwise formation constants of folic acid, N-[p-[[(2-amino-4-hydroxy-6-pteridyl)methyl]amino]benzyl]glutamic acid, with the carcinogenic metal ions, aluminum(III), chromium(III), beryllium(II), lead(II), and uranium(VI) were determined at 30°C, and at various ionic strengths, viz. 0.01, 0.05, 0.10 M, maintained by potassium nitrate solution. The formation of the chelate is evident from the shift between the (i) ligand and (ii) ligand and metal titration curves. From the values for the stepwise protonation constants and metal-ligand stability constants at various ionic strengths, thermodynamic formation constants were evaluated by extrapolation to zero ionic concentration. Logarithms of the overall thermodynamic stability constants ($\log K^{\mu=0}$) are: 20.40 for H; 15.15 for Al; 10.10 for Cr; 9.35 for Be; 6.50 for Pb; 9.00 for U chelates. Corresponding free energy changes (ΔF^0) are −28.47, −21.14, −14.09, −13.05, −9.07, −12.56 kcal · mol^{-1}, respectively. (auth)

10521 STUDIES ON SOME N-ACYL N-PHENYLHYDROXYLAMINES AS METAL-COMPLEXING LIGANDS. IV. DETERMINATION OF FORMATION CONSTANTS OF U(VI) CHELATES. Ghosh, N. N.; Siddhanta, G. (University Coll. of Science, Calcutta). Z. Anorg. Allg. Chem.; 375: 197-201(Jul 1970).

The formation of uranyl complexes of N-acetyl, N-chloroacetyl, N-benzoyl, and N-o, -m, and -p nitrobenzoyl N-phenylhydroxylamines were studied potentiometrically in 1:1 aqueous acetone at constant ionic strength (μ = 0.5). Only the first step could be followed and the final results were evaluated by the projection strip method. The stabilities follow a general order. (auth)

Isotope Effects and Exchange

Refer also to abstracts 10622, 10637, 11696, 11825, 12042, and 12043.

10522 (COO-1008-13) THE DEPENDENCE OF SOLVOLYTIC α-DEUTERIUM RATE EFFECTS ON THE NATURE OF THE LEAVING GROUP. Shiner, V. J. Jr.; Dowd, W. (Indiana Univ., Bloomington. Dept. of Chemistry). [1970]. Contract AT(11-1)-1008. 7p. Dep. NTIS.

Experimental observations that confirm and extend earlier theoretical predictions of how the characteristic maximum α-deuterium isotope effect on solvolysis rate varies as a function of leaving group are reported. Studies were made on 3-pentyn-2-toluenesulfonate bromide and iodide in aqueous ethanol and trifluoroethanol solutions. Since the large isotope effects found indicated little or no covalent attachment in the rate determining step, the simplest interpretation of these findings was that the rate determining step is the interconversion of two ion pairs and that the product forming step is nucleophilic attack on the second formed ion pair. (P.C.H.)

10523 (COO-1008-15) α-DEUTERIUM EFFECTS ON THE RATE OF SOLVOLYSIS OF A 2-ADAMANTYL SULFONATE ESTER. Shiner, V. J. Jr.; Fisher, R. D. (Indiana Univ., Bloomington. Dept. of Chemistry). [1970]. Contract AT(11-1)-1008. 9p. Dep. NTIS.

Studies were made on the α-deuterium isotope effects on the rate of solvolysis of 2,2,2-trifluoroethylsulfonate (tresylate). The rate constants measured by the precise conductance method and isotope effects are tabulated. It was found that the isotope effects were exactly as predicted for the mechanism involving interconversion of ion pairs. It was therefore agreed that this reaction does not involve solvent nucleophilic participation in the rate-determining step. It was also found that in accord with this mechanism the isotope is not dependent on solvent polarity or nucleophilicity in the range studied. There is no reason to suspect that, within this mechanism, the effect should be much different in any other solvent. (P.C.H.)

10524 (COO-1008-16) DEUTERIUM AND TRITIUM EFFECTS ON THE RATES OF ORGANIC REACTIONS. Annual Technical Progress Report. (Indiana Univ., Bloomington). Dec 1970. Contract AT(11-1)-1008. 5p. Dep. NTIS

The solvolytic reaction mechanisms for a series of primary and secondary propargyl derivatives were investigated in a series of ethanol-water, trifluoroethanol-water, and hexafluoroisopropyl alcohol-water solvents. The α- and in some cases β and δ secondary deuterium isotope effects for these reactions were determined as were the yields of products. The steric result of substitution of chiral 3-butyn-2-yl p-bromobenzenesulfonate was determined through a range of solvents. The steric result of substitution in trifluoroacetolysis of chiral 2-octyl-p-bromobenzenesulfonate was also investigated. α-Deuterium isotope rate effects were also determined for two 1-adamantyl carbinyl derivatives. (P.C.H.)

10525 (COO-1008-17) DEUTERIUM EFFECTS ON BINDING OF NADH TO ALCOHOL DEHYDROGENASE ISOENZYME EE. Bush, Karen, Mahler, H. R.; Shiner, V. J. Jr. (Indiana Univ., Bloomington. Dept. of Chemistry). [1970]. Contract AT(11-1)-1008. 15p. Dep. NTIS.

The isotope effect for equilibrium dissociation constants with A-NADD (deuterium-labeled reduced NAD) was determined by both the Sephadex and the fluorimetric methods, and the two results were identical within experimental error: 0.65 ± 14 (Sephadex method) and 0.52 ± 0.07 (fluorimetric method). This kind of (inverse) isotope effect indicated that A-NADD is bound less tightly to the enzyme than is NADH: LADH + NADH $\underset{k_2}{\overset{k_1}{\rightleftharpoons}}$ LADH-NADH (LADH = horse liver alcohol dehydrogenase) and that the zero point energies for the isotopically sensitive vibrations are lower in the complex than in the free NADD. The results suggest that if the isotope effect on the dissociation reaction (rate constant k_2) is normal ($k_2 > 1$), then the isotope effect for the binding step (rate constant k_1) must also be normal and even larger, thus indicating an ability of the enzyme to discriminate kinetically against the coenzyme deuterated at the transferable hydrogen. (P.C.H.)

10526 ORGANIC OXALATES. IV. PYROLYSIS OF DIALLYL, DISUBSTITUTED-ALLYL, AND RELATED OXALATES. Trahanovsky, Walter S.; Ong, Ching Ching (Iowa State Univ., Ames). J. Amer. Chem. Soc.; 92: 7174-7(2 Dec 1970).

Products from the low-pressure gas-phase pyrolysis of diallyl, dicrotyl, dicinnamyl, and related oxalates are reported. The results indicated that these oxalates are a convenient source of substituted allyl radicals. The main products from allyl and crotyl radicals were coupling products, but no coupling products were observed from cinnamyl radicals. The main product from the pyrolysis of di-trans-cinnamyl oxalate was indene, which must result from an intramolecular cyclization of the cinnamyl radical. An isotope effect, K_H/k_D, of 2.92 is reported for the cyclization of o-deuteriocinnamyl radical to indene which suggests that formation of the intermediate cyclic radical from the cinnamyl radical is a reversible step. Several radicals generated from the appropriate oxalates that are similar to cinnamyl radicals also underwent cyclizations giving rise to cyclic products. (auth)

10527 ALKALINE HYDROLYSIS OF p-NITROACETANILIDE AND p-FORMYLACETANILIDE. Pollack, Ralph M.; Bender, M. L. (Northwestern Univ., Evanston, Ill.). J. Amer. Chem. Soc.; 92: 7190-4(2 Dec 1970).

The hydroxide ion catalyzed hydrolysis of p-nitroacetanilide (I) and p-formylacetanilide (II) has been investigated at 25.0° at [OH^-] ranging from about 10^{-3} to 1 M. The rates for both compounds showed a very marked dependence on the concentration of hydroxide ion. The kinetic order for I in hydroxide ion varied from 1.8 at low [OH^-] to 0.4 at high [OH^-]. The order for II was 1.9 throughout the range investigated. At [OH^-] below 0.1 M, I reacted 25 times faster than II. Both compounds reacted substantially faster than predicted from a previous study of ring-substituted acetanilides with more electron-donating substituents. These results were interpreted in terms of a mechanism involving nucleophilic attack of hydroxide ion to form a tetrahedral intermediate, followed by ionization to a dianion, and unimolecular breakdown to acetate ion and anilide ion. An inverse solvent isotope effect for p-nitroacetanilide (k_{H_2O}/k_{D_2O} = 0.61) at [OD^-] = 4.60 × 10^{-3} M supported this mechanism. The varying kinetic order in [OH^-] for I is explained by a change in the rate-determining step of the reaction at higher concentration of base, in conjuction with ionization of the substrate to give an unreactive anion. The pK_a's of p-nitroacetanilide and p-formylacetanilide were measured and found to be 13.8 and 14.3, respectively. (auth)

10528 ISOTOPE EFFECTS ON THE ELECTRON IMPACT INDUCED FRAGMENTATION OF ETHANOL. Corval, Madeline (Paris Univ.). Bull. Soc. Chim. Fr.; No. 8-9, 2871-82 (1970). (In French).

The mass spectra of CH_3CH_2OH, CH_3CHDOH, CH_3CD_2OH, CD_3CH_2OH, CD_3CD_2OH, and CD_3CD_2OD were recorded at 70 eV. The isotope effects on the breaking probability for the methylene C-X bond and for the C-C bond were determined. A calculation of the isotope effects in the case of CH_3CD_2OH and CH_3CHDOH indicates that, considering the two principal decomposition modes and adopting a simple function for the energy distribution, the calculated values are in satisfactory agreement with the experimental results. The use of a more specific distribution function for the molecules gives better agreement with experiment for the effect related to CH_3CHDOH. (auth)

10529 LOW-FREQUENCY VIBRATIONS OF MOLECULAR SOLIDS. X. CH_3CCl_3, CD_3CCl_3, CH_3CCl_2H, AND CH_3CF_3. Durig, J. R.; Craven, S. M.; Lau, K. K.; Bragin, J. (Univ. of South Carolina, Columbia). J. Chem. Phys.; 54: 479-87(15 Jan 1971).

The far-infrared spectra of solid CH_3CCl_3 and CD_3CCl_3 have been investigated from 33 to 400 cm^{-1}. Raman spectra of these solids have also been recorded. The internal torsional mode was observed at 290 and 206 cm^{-1} in the infrared spectra of solid methylchloroform and methylchloroform-d_3, respectively. The threefold periodic barrier to rotation was calculated to be 5.5 kcal/mole. This barrier was compared to those previously reported by other techniques for this molecule and the reported value was much larger than that currently accepted. Four lattice vibrations, 46.9, 53.4, 57.7, and 67.5 cm^{-1} were observed in the far-infrared spectrum of methylchloroform recorded at -190°C. Both the effects of temperature variation and deuterium substitution were investigated for these bands. These lattice modes shifted to lower frequency and became quite diffuse as the temperature approached the phase transition at -68°C. The low-frequency Raman spectrum of methylchloroform at -165°C showed one line at 38.6 cm^{-1}, which shifted to 37.0 cm^{-1} with deuteration. The infrared spectra of solid CH_3CHCl_2 and CH_3CF_3 have been recorded between 140 and 400 cm^{-1}. The internal torsional mode for 1,1-dichloroethane was observed at 232 and 231 cm^{-1} for the solid and vapor, respectively. The threefold barrier to rotation was calculated to be 3.50 kcal/mole. The internal torsion for methyl-

fluoroform was observed at 220 cm^{-1} for the solid, and the barrier was calculated to be 3.29 kcal/mole. Substituent effects on the barrier heights are discussed. (auth)

10530 CATALYTIC SITES FOR DEUTERIUM EXCHANGE WITH BENZENE OVER ALUMINA. Saunders, P. C.; Hightower, Joe W. (Rice Univ., Houston, Tex.). J. Phys. Chem.; 74: 4323-9(10 Dec 1970).

Some of the finer details of the interaction of benzene with the surface of an alumina catalyst have been investigated with the use of deuterium tracers. Exchange of benzene H atoms with D_2 occurred readily at room temperature, but intermolecular redistribution of H and D atoms between C_6H_6 and C_6D_6 occurred at least 10 to 20 times as rapidly under the same conditions. Both reactions apparently took place on the same sites whose concentration was 6 to 15 × 10^{12} sites/cm^2 as determined by CO_2 poisoning. Radioactive $C^{14}O_2$ was used to confirm complete adsorption. Several other compounds (NO, CO, O_2, H_2O, and NH_3) had little poisoning effect on the exchange reaction. The exchange reaction with D_2 exhibited a primary kinetic isotope effect by being faster than $C_6D_6-H_2$ exchange; the k_{CH}/k_{CD} = 2 was attributed to a dissociative exchange mechanism in which CH (or CD) cleavage was rate limiting. Benzene also poisoned the H_2-D_2 equilibration. Speculation about the active sites led to the conclusion that all these exchange reactions perhaps occur on exposed Al^{3+} surface ions. (auth)

10531 STUDIES ON HYDROGEN–OXYGEN SYSTEMS IN THE ELECTRICAL DISCHARGE. IV. SPECTROSCOPIC IDENTIFICATION OF THE MATRIX-STABILIZED INTERMEDIATES, H_2O_3 AND H_2O_4. Giguere, P. A.; Herman, K. (Univ., Laval, Quebec). Can. J. Chem.; 48: 3473-82(15 Nov 1970).

The infrared absorption of the products from electrically dissociated H_2O or D_2O vapor and other hydrogen–oxygen systems trapped at liquid nitrogen temperature was measured between 4000 and 300 cm^{-1}. Four new absorption bands were found in the deuterated systems at 857, 820, 760, and about 440 cm^{-1}. By isotopic substitution of ^{18}O the frequencies are shifted to 806, 775, 717, and ~420 cm^{-1} as expected for O–O vibrations. In the hydrogen systems this region is obscured by the strong libration bands of H_2O and H_2O_2 molecules. Temperature and composition effects show that more than one new species is involved. Accordingly the new spectra are assigned to the often postulated polyoxides, H_2O_3 and H_2O_4, stabilized in the water–peroxide matrix. The more abundant, and also more stable, H_2O_3 has a half-life of some 5 h at −65°C. The observed frequencies are consistent with zigzag chain structures linked by single covalent bonds as in hydrogen polysulfides. Relative concentrations of the polyoxides are estimated at 5 to 10 mole % depending on the composition of the starting material. Possible mechanisms of formation and decomposition are discussed. (auth) (Canada)

10532 MICROWAVE SPECTRUM, STRUCTURE, QUADRUPOLE COUPLING CONSTANT, AND FORCE CONSTANTS OF NSCl. Beppu, Tatsuro; Hirota, Eizi; Morino, Yonezo (Tokyo Univ.). J. Mol. Spectrosc.; 36: 386-97(Dec 1970).

Microwave spectra of the NSCl molecule were observed by pumping the products of thermally decomposing $N_3S_3Cl_3$ continuously through the cell. The rotational constants were obtained for $^{14}N^{32}S^{35}Cl$, $^{14}N^{32}S^{37}Cl$, $^{14}N^{34}S^{35}Cl$, and $^{15}N^{32}S^{35}Cl$, all in the ground vibrational states. The r_s structure calculated from these rotational constants is the configuration N ≡ S–Cl with r(NS) = 1.450 Å, r(SCl) = 2.161 Å and ∠NSCl = 117°42′. The nuclear quadrupole coupling constant of ^{35}Cl in the $^{15}N^{32}S^{35}Cl$ species is determined to be χ_{aa} = −38.51, χ_{bb} = 23.51, and χ_{cc} = 15.00 MHz, which corresponds to χ_{bond} of −43.36 MHz. In addition to the ground-state spectra, several sets of vibrational satellites were observed and assigned to the ν_2, ν_3, $2\nu_2$, and $2\nu_3$ states. The vibrational increments of the inertia defects, Δ_2 and Δ_3, are combined with two known vibrational frequencies, ω_1 and ω_2, to calculate the force constants. The value of ω_3, 261 cm^{-1}, calculated using the inertia defect increments is in agreement with 273 cm^{-1}, estimated by Müller and others from the infrared spectra. Redundancy among the three inertia-defect increments is noted for triatomic molecules with the C_s symmetry, and its consequence is discussed briefly. (auth)

10533 ν_4 BANDS OF $^{10}BF_3$ AND $^{11}BF_3$ AT HIGH RESOLUTION. Ginn, S. G. W.; Johansen, Dorothy; Overend, John (Univ. of Minnesota, Minneapolis). J. Mol. Spectrosc.; 36: 448-63(Dec 1970).

The perpendicular bands $\nu_4 \leftarrow 0$ at 480 cm^{-1} in the infrared spectra of $^{10}BF_3$ and $^{11}BF_3$ were measured with a resolution of ca. 0.03 cm^{-1}. The bands are similar in appearance and, in each case, the fine structure is almost fully resolved at low J values. The rotational constants of the $V_4 = 1$ state in both isotopic molecules were determined, in particular, $\zeta_{44}^{(z)}(^{10}BF_3) = -0.809$ and $\zeta_{44}^{(z)}(^{11}BF_3) = -0.789$ and the vibrational frequencies $\nu_4(^{10}BF_3)$ = 481.13 cm^{-1} and $\nu_4(^{11}BF_3)$ = 479.36 cm^{-1}. These results serve to fix the E species quadratic force constants of the BF_3 molecule. (auth)

10534 ETHYNYLBENZENE: THE VIBRATIONAL SPECTRA OF SOME DEUTERATED ISOMERS. King, G. W.; So, S. P. (McMaster Univ., Hamilton, Ont.). J. Mol. Spectrosc.; 36: 468-87 (Dec 1970).

The infrared and laser Raman spectra of four isomers of ethynylbenzene, C_6H_5CCH, C_6H_5CCD, C_6D_5CCH, and C_6D_5CCD were measured. From a comparative analysis of the spectra, together with those of other related molecules, assignments were made for the 36 normal frequencies of vibration of the molecule. (auth)

10535 SPECTRUM OF NEUTRAL ARGON HYDRIDE. Johns, J. W. C. (National Research Council of Canada, Ottawa). J. Mol. Spectrosc.; 36: 488-510(Dec 1970).

An emission spectrum near 7670 Å, arising from a transition between two excited states of neutral argon hydride was analyzed and the identity of the emitter confirmed by isotopic studies. The analysis shows that the transition is of the type $^2\Pi(b) - {}^2\Sigma^+$. The lower state, $A^2\Sigma^+$, is predissociated to the extent that the lines of ArH are diffuse whereas the lines of ArD are sharp. This predissociation is probably caused by interaction with the unstable ground state, $X^2\Sigma^+$. (auth)

10536 SOLVOLYSIS OF SULPHONYL HALIDES. VI. HYDROLYSIS AND DEUTEROLYSIS OF METHANESULPHONYL CHLORIDE AT PRESSURES TO 2000 ATM. Tonnet, Marie L.; Hambly, A. N. (Australian National Univ., Canberra). Aust. J. Chem.; 23: 2435-41(1970).

The solvent isotope effect for the solvolysis of methanesulphonyl chloride in H_2O and D_2O is not changed significantly when the pressure is raised from 1 to 2000 atm, though the rates of solvolysis at 25°C increase by a factor of about 2 to 3. This indicates that the isotope effect is not due mainly to the differences in the initial hydrogen-bonded structures of the two solvents. The maximum in the rate of solvolysis produced by the addition of small amounts of dioxane at 1 atm disappears at higher pressures. (auth) (Australia)

10537 SOLVOLYSIS OF SULPHONYL HALIDES. V. HYDROLYSIS AND DEUTEROLYSIS OF METHANESULPHONYL CHLORIDE. Tonnet, Marie L. (Australian National Univ., Canberra); Hambly, A. N. Aust. J. Chem.; 23: 2427-34(Dec 1970).

The values of the thermodynamic parameters of activation were determined for the solvolysis of methanesulphonyl chloride in H_2O and D_2O and their mixture with moderate amounts of dioxane. Some of the data are not in agreement with the postulate that the kinetic solvent isotope effect and the maximum in the rate of solvolysis produced by the addition of dioxane are due to changes in the state of the reacting system rather than to changes in the transition state. The reaction of dioxane does not produce a large reduction in the solvent isotope effect as reported for the hydrolysis of tert-butyl chloride and predicted to be general. The relative rates of solvolysis in mixtures of H_2O and D_2O are not in agreement with the analysis of such mixtures by Swann and Thornton. (auth) (Australia)

10538 ISOTOPE EFFECTS IN THE HYDROGEN-ATOM ADDITION TO OLEFINS AT LOW TEMPERATURES. Kelley, Richard D.; Klein, Ralph; Scheer, Milton D. (National Bureau of Standards, Washington, D. C.). J. Phys. Chem.; 74: 4301-9(10 Dec 1970).

The ratio of rates of addition of atomic hydrogen to the two possible sites of the double bond for several olefins has been measured over the temperature range 63 to 143°K. A pronounced isotope effect was found. In the comparison of addition ratios at a given temperature, the data show that the isotope effect was related to the value of the addition ratio, large ratios showing relatively large effects. The ratio of terminal to nonterminal addition of H to propylene at 90°K was 126, while for D it was 398. The ratio of H addition to carbon 2 relative to carbon 3 in cis-2-pentene at 90°K was 1.5 and that of D was the same. The results of these findings are discussed in terms of a one and two barrier model for the reaction of H with the olefinic bond. Both zero point energy effects and quantum tunneling of H through the reaction barriers were considered. It was concluded that a two barrier model with tunneling is most appropriate. The data generated from the H atom–olefin addition reactions in the low temperature region support the existence of chemical quantum tunneling. This is apart from the more equivocal arguments based on curvature of Arrhenius plots although indeed such curvature was found in the low-temperature H-atom additions. (auth)

10539 HYDROGEN–DEUTERIUM EXCHANGE OF MEDIUM RING CYCLOALKENES DURING DEUTEROGENATION WITH TRIS(TRIPHENYLPHOSPHINE)CHLORORHODIUM(I). Atkinson,

XUM

J. G.; Luke, M. O. (Merck Sharp and Dohme Canada Ltd., Pointe Claire, Quebec). Can. J. Chem.; 48: 3580-2(15 Nov 1970).

Cyclooctene, and, to a lesser extent, cycloheptene and cyclododecene undergo H–D scrambling during deuterogenation with tris(triphenylphosphine)chlororhodium(I), whereas this catalyst affords clean addition of two deuterium atoms to cyclohexene and 1-octene. Cyclooctene containing up to 0.4 deuterium atoms per molecule was isolated after 50% reduction and the isotope shown to be randomly distributed about the ring. This unexpected exchange reaction was accounted for in terms of the medium size ring effect (I-strain) and provides impressive further evidence for the reversible formation of a normally unobserved rhodium–alkyl species as an intermediate in the hydrogenation reaction. (auth) (Canada)

10540 EFFECT OF SOLVENT OF THE FREQUENCIES OF THE CD AND CH STRETCHING BAND IN SOME HALOFORMS. Rossi, I.; Nguyen-Van-Thanh; Brodbeck, C.; Haeusler, C. (Paris Univ., Orsay, France). Can. J. Chem.; 48: 3362-73(1 Nov 1970). (In French).

The frequencies of the fundamental C–D and C–H stretching band and the overtones were measured for $CDCl_3$, $CHCl_3$, and $CHBr_3$ in some nonpolar and some slightly polar solvents. The mechanical anharmonicity of these vibrations is strong and solvent-dependent. Therefore, the approximation $\Delta\omega/\omega \simeq \Delta v/v$ is not valid for the vibrators considered in this work. The solute–solvent interaction energy is the sum of induction, dispersion, and orientation energies (for polar solvents). Calculations based on the cell model for the liquid state showed that induction energy is of slight influence with respect to dispersion energy, which is greatly responsible for the observed frequency shift. (auth) (Canada)

10541 CONTRIBUTION TO THE ^{14}C EXCHANGE STUDIES IN THE SYSTEM: $^{14}CO_2$–CO–QUARTZ WALLS. Zielinski, Mieczyslaw; Wawer, Andrzej; Tabaka, Andrzej. Nukleonika; 15: 165-76(1970). (In Polish).

Kinetic data characterizing ^{14}C isotopic exchange between carbon monoxide and labeled carbon dioxide in a quartz vessel at 550 to 970°C are reported. The activation energy equals 112 kcal/mol. The average energy of activation decreased with decreasing exchange temperature. For example, in the temperature range 650 to 740°C, an average energy of activation of exchange equals 55.6 kcal/mol, and in the temperature range 900 to 823°C, this energy as determined from the temperature dependence of the rate constant k, equals 74.9 kcal/mol. This change of the average experimental energy of activation is interpreted by the dependence of the surface exchange reaction on the structure of the active centres on the surface of the vessel catalyzing the exchange reaction. By changing the total pressure of the gas in the vessel, keeping at the same time the $[CO_2]/[CO]$ ratio constant, the total order of the reaction was found to be 1.53 at 970°C. From a separate series of experiments it was established that, around 970°C, the reaction is first order with respect to CO_2 concentration and half order with respect to carbon monoxide. At 740°C, however, the order of the reaction with respect to CO_2 decreased to 0.8. A slight decrease in total order of the reaction with decreasing temperature was also observed. Further studies on the mechanism of the reaction were undertaken. (auth)

10542 LOW-FREQUENCY VIBRATION SPECTRA OF VARIOUS ISOTOPIC VARIETIES OF PRIMARY ALIPHATIC ETHERS. I. DIMETHYL ETHER. Perchard, J. P. (CNRS, Thiais, France. Faculte des Sciences, Paris). J. Mol. Struct.; 6: 359-74(Nov 1970). (In French).

The infrared spectra of four isotopic dimethyl ether species in various physical states were interpreted between 500 and 50 cm^{-1}. Crystals of three species at 80°K exhibit in their Raman spectra a few lines related to the torsion vibrations of methyl groups, in agreement with the absorption results. A calculation of the potential barrier from the frequency values was made and earlier work in this field is discussed. (auth)

10543 HYDROGEN BOND STUDIES. XXXXVI. THE CRYSTAL STRUCTURES OF NORMAL AND DEUTERATED SODIUM HYDROGEN OXALATE MONOHYDRATE $NaHC_2O_4.H_2O$ AND $NaDC_2O_4.D_2O$. Tellgren, Roland; Olovsson, Ivar (Univ. of Uppsala). J. Chem. Phys.; 54: 127-34(1 Jan 1971).

The crystal structures of $NaHC_2O_4 \cdot H_2O$ and $NaDC_2O_4 \cdot D_2O$ were determined from three-dimensional single crystal x-ray diffractometer data obtained at room temperature. Two formula units crystallize in a triclinic unit cell with the dimensions: a = 6.503, b = 6.673, c = 5.698 Å, α = 85.04, β = 110.00, γ = 105.02° for the hydrogen compound and a = 6.501, b = 6.671, c = 5.716 Å, α = 84.91, β = 109.93, γ = 105.00° for the deuterated compound. The space group is P$\bar{1}$. The hydrogen oxalate ions are linked end to end in infinite chains by hydrogen bonds (2.571 Å). The chains are cross linked to form layers by both O–H...O bonds from the water molecules (2.808, 2.826 Å) and by ionic bonds Na^+...O. These layers are in turn held together by Na^+...O bonds. The oxalate group is nonplanar with an angle of twist about the C–C bond of 12.9°. The only significant difference between the bond distances in the normal and deuterated compound occurs in the shortest hydrogen bond, which is 0.022 Å longer in the deuterated case. (auth)

10544 FAR-INFRARED SPECTRA OF ETHANE, ETHYLENE, AND ACETYLENE. Schwartz, Y. A.; Ron, A.; Kimel, S. (Technion–Israel Inst. of Tech., Haifa). J. Chem. Phys.; 54: 99-105 (1 Jan 1971).

The far-infrared spectra of crystalline C_2H_6, C_2D_6, C_2H_4, C_2D_4, C_2H_2, and C_2D_2 were recorded at various temperatures between 25 and 140°K. Each compound showed two absorption bands that were shown to be due to translational lattice modes. On heating, these bands broadened and decreased in intensity; they were also displaced toward lower frequencies by about 0.1 cm^{-1}/°K. For ethylene an analysis was carried out based on the "diatomic potential." Here each molecule was assumed to consist of a pair of centers separated by an effective distance d, each center interacting, through a Lennard-Jones-type potential, with the centers in all neighboring molecules. Frequencies and thermal frequency shifts were calculated as a function of d, and good agreement was attained with the observed values for ethylene, with d = 1.04 Å. (auth)

10545 REACTIONS OF SALTS OF DEUTERATED BENZENECARBOXYLIC ACIDS. Ratusky, J. (Inst. of Organic Chemistry and Biochemistry, Prague). J. Label. Compounds; 6: 124-34 (Apr-Jun 1970).

The course of transcarboxylation reactions of potassium salts of deuterated benzenecarboxylic acids was investigated. During the reaction rapid random exchange of hydrogen atoms of the benzene ring for deuterium takes place. The probable mechanism of this exchange, which involves the liberation of protons from the benzene ring and the formation of carbanions, is proposed. The mechanism of the deuterium for hydrogen exchange is in agreement with the intermolecular ionic mechanism of the transcarboxylation reaction itself since the formation of carbanions via liberation of protons is a part of this reaction. (auth)

10546 T. C. IN ACIDIC MEDIA. Hamada, Masayuki; Kiritani, Reiko (Radiation Center of Osaka Prefecture, Sakai, Japan). J. Label. Compounds; 6: 187-96(Apr-Jun 1970).

Tritium labeling of aromatic compounds in a few acidic media and the intramolecular distributions of radioactivities in the tritiated compounds were investigated. Various kinds of aromatic compounds were treated with powerful acid complex, $TH_2PO_4 \cdot BF_3$, or some other tritiated acids at room temperature. Aromatic compounds having electron-donating substituents were easily labelled with tritium and the radioactivity in each compound was predominantly found at the ortho- and para-positions of aromatic ring. Meanwhile, substituents which withdraw electrons from the aromatic ring inhibit the incorporation of tritium. Benzene and naphthalene were also labeled with tritium only when they were treated with $TH_2PO_4 \cdot BF_3$. This method was, however, not available for the nitrogen containing compounds. The reaction mechanism was also discussed. (auth)

10547 PHOSPHINE–BORANE DERIVATIVES. PART III. A PROTON MAGNETIC RESONANCE SPECTROSCOPIC STUDY OF METHYL- AND SILYL-PHOSPHINE WITH [$^1H_6$]- AND [$^2H_6$]-DIBORANE. Davis, J.; Drake, J. E.; Goddard, N. (Univ. of Windsor, Ont.). J. Chem. Soc., A; No. 18, 2962-4(1970).

The ^1H NMR spectra indicate that hydrogen–deuterium exchange occurs between silicon and boron sites in silylphosphine–borane but not between carbon and boron sites in methylphosphine–borane. Condensation of monosilylphosphine to trisilylphosphine can be catalysed by diborane. (auth) (UK)

10548 SECONDARY KINETIC DEUTERIUM ISOTOPE EFFECTS IN VINYL CATIONS. Hargrove, Robert J.; Dueber, Thomas E.; Stang, Peter J. (Univ. of Utah, Salt Lake City). J. Chem. Soc., D; No. 23, 1614-15(9 Dec 1970).

The β-deuterium isotope effect in the solvolysis of β-styryl trifluoromethanesulphonate, k_H/k_D = 1.42, is much larger than in normal carbonium ions. (auth) (UK)

10549 TEMPERATURE DEPENDENCES OF KINETIC ISOTOPE EFFECTS. Vogel, P. Christian; Stern, Marvin J. (Yeshiva Univ., New York). J. Chem. Phys.; 54: 779-96(15 Jan 1971).

Model-reaction calculations are used to investigate the ex-

pected incidence of temperature-dependence anomalies produced by the harmonic-vibrational contributions to kinetic isotope effects. These "anomalies" are defined as deviations from a smooth-monotonic log–log plot of isotopic rate-constant ratio vs temperature. Such deviations include inflections, extrema, and crossovers (inversions in direction with respect to the infinite-temperature, classical limit). The model systems studied represent a variety of mechanisms ranging from simple bond break to simultaneous rupture or formation of four bonds. The effects on the temperature-dependence-curve shapes of off-diagonal force-constant changes, variations in potential-barrier curvature, and tunneling corrections are examined. The major emphasis is on carbon and hydrogen isotope effects although some nitrogen and oxygen effects are also considered. Out of the 476 isotopic reaction pairs investigated, approximately 25% were found to be anomalous. Several examples of corresponding deuterium and tritium isotope effects exhibiting different types of temperature-dependence anomalies were found. Situations most likely to lead to anomalous temperature behavior are discussed. It was concluded that kinetic-isotope-effect temperature-dependence anomalies should occur fairly commonly although, at least for monosubstitution with carbon and hydrogen isotopes, probably less frequently than in equilibrium isotope effects. However, the anomalous region of a temperature-dependence curve might not fall within the range of experimental accessibility. No method of detecting an anomaly from observation of a portion of the temperature-dependence curve removed from the anomalous region has been found. It was found that the quality of data fitting with the gamma-bar approximation cannot be used as a reliable criterion of nonanomalous temperature behavior. The significance of kinetic-isotope-effect temperature-dependence anomalies to investigations of reaction mechanisms is discussed with respect to both approximation methods and model-calculation force-field-fitting procedures. (auth)

10550 TEMPERATURE EFFECTS ON THE PHOSPHORESCENCE OF BENZENE AND TOLUENE. Kilmer, Nelson G.; Spangler, John D. (Kansas State Univ., Manhattan). J. Chem. Phys.; 54: 604-12(15 Jan 1971).

Phosphorescence lifetimes have been measured as a function of temperature in the region 2 to 160°K for the following polycrystalline mixtures: C_6H_6 and C_6D_6 in cyclohexane and in cyclopentane; toluene-h_8, toluene-α-d_3, and toluene-d_8, in methylcyclohexane; and toluene-h_8 in perdeuteromethylcyclohexane. In each case the results can be reasonably fit by a formula of the form $1/\tau_P = K_0 + K_1 \exp(-\Delta E/kT)$, with the values of K_0, ΔE, and K_1 depending on both the solute and the solvent. An unexpected increase in lifetime at very low temperatures has been observed for benzene. For C_6H_6 and C_6D_6 in cyclohexane the ratio $\Phi_P/\Phi_F = k_p k_{ISC} \tau_P / k_F$ has been determined by numerical integration of the corrected emission spectra. Plots of Φ_P/Φ_F vs τ_P yield straight lines. (auth)

10551 MICROWAVE SPECTRA OF THE FIRST-EXCITED TORSIONAL STATES AND BARRIER TO INTERNAL ROTATION OF DIMETHYLAMINE. Wollrab, James E. (McDonnell Douglas Corp., St. Louis); Laurie, Victor W. J. Chem. Phys.; 54: 532-9(15 Jan 1971).

Rotational spectra in the first-excited torsional states of a number of isotopic species of dimethylamine have been assigned. Internal rotation splittings were observed and have been used to calculate a barrier of 3.22 ± 0.02 kcal mole^{-1}. Inversion splittings differ significantly from those observed in the ground state spectra while ^{14}N quadrupole effects are unchanged within experimental error. (auth)

10552 RELATIVE PROTON AFFINITY OF ARGON AND DEUTERIUM. Bowers, Michael T.; Elleman, Daniel D. (Univ. of California, Santa Barbara. California Inst. of Tech., Pasadena). J. Amer. Chem. Soc.; 92: 7258-62(16 Dec 1970).

In mixtures of Ar and D_2 at high pressures, the following ion-molecule reaction scheme is observed: $D_2^+ + D_2 \rightarrow (D_3^+)^* + D$ (1a); $(D_3^+)^* + (D_2)^2 \rightarrow (D_3^+) + D_2$(1b); $(D_3^+)^* + Ar \rightarrow ArD^+ + D_2$(5); $(D_3^+) + Ar \rightarrow ArD^+ + D_2$ (6); $ArD^+ + D_2 \rightarrow D_3^+ + Ar$ (4b). $(D_3^+)^*$ has of the order of 2 eV of energy according to the experiments of Leventhal and Friedman. (D_3^+) is the lowest vibrational state obtainable by collision of $(D_3^+)^*$ with D_2. The present results suggest that (D_3^+) is not the ground state but has at least 1 and possibly 2 quanta of vibrational energy (i.e., 10 to 20 kcal/mole). From pressure dependence studies it is shown that a maximum of three collisions is needed to moderate all $(D_3^+)^*$ to (D_3^+). From reaction 4b, PA (D_2) > PA(Ar). From threshold-double-resonance experiments on reaction 6, $PA(D_2)^+ \cong PA(Ar) + 7$ kcal/mole, with an uncertainty of ±5 kcal/mole $PA(D_2)$ is the energy required to remove D^+ from (D_3^+). The intrinsic proton (or deuteron) affinity of D_2, $PA(D_2)$, is felt to be 10 to 20 kcal/mole larger than $PA(D_2)$. (auth)

10553 MECHANISM OF ENZYMIC FORMATION OF HOMOGENTISATE FROM p-HYDROXYPHENYLPYRUVATE. Lindblad, Bengt; Lindstedt, Goeran; Lindstedt, Sven (Univ. of Goteborg). J. Amer. Chem. Soc.; 92: 7446-9(16 Dec 1970).

The mechanism for the enzymic formation of homogentisate from p-hydroxyphenylpyruvate was studied by carrying out the reaction in $^{18}O_2$ and in $H_2{}^{18}O$. Gas chromatography-mass spectrometry of the bistrimethylsilyl ether of the methyl ester of the formed homogentisate established that oxygen from $^{18}O_2$ is incorporated both in the new hydroxyl and in the carboxyl. The isolated homogentisate contained ^{18}O in only 30% of the new hydroxyl groups as a result of an exchange with water during the enzymic reaction, presumably in a hydrated quinonoid structure. It is proposed that incorporation of both atoms from an O_2 molecule into the homogentisate occurs through the formation of an intermediate cyclic peroxide and that the oxygen reduction occurs through the oxidative decarboxylation of the α-keto side chain in p-hydroxyphenylpyruvate. The mechanism is thus analogous to that proposed for 2-ketoglutarate dependent hydroxylations. (aut.)

10554 PHOTOCHEMISTRY OF SOME α-KETOPROPIOPHENONES. EVIDENCE FOR AN UNUSUAL CYCLIC TRANSITION STATE FOR HYDROGEN ABSTRACTION. Turro, Nicholas J.; Lee, Ta-jyh (Columbia Univ., New York). J. Amer. Chem. Soc.; 92: 7467-70(16 Dec 1970).

Results are summarized of a study of the photoreactions of some normal and deuterated α-ketopropiophenones in benzene. Of the various possibilities to explain the data, two are considered: intramolecular hydrogen abstraction from carbon 3 by the 1-keto or 2-keto groups via novel cyclic five- and four-membered transition states and intermolecular photoenolization or hydrogen abstraction. (M.C.G.)

10555 ELECTRON PARAMAGNETIC RESONANCE OF CD_2 AND CHD. ISOTOPE EFFECTS, MOTION, AND GEOMETRY OF METHYLENE. Wasserman, E.; Kuck, V. J.; Hutton, R. S.; Yager, W. A. (Bell Telephone Labs., Murray Hill, N. J. Rutgers–The State Univ., New Brunswick, N. J.). J. Amer. Chem. Soc.; 92: 7491-3(16 Dec 1970).

It was observed that the EPR spectra of CD_2 and CHD in a solid matrix differ significantly from the spectrum of CH_2. It was concluded that CH_2 has a significantly larger wobble of the long axis than CD_2. The x and z axes for CHD are tilted by 7° from those of the other species. (M.C.G.)

10556 PHOTOCHEMICAL EXCHANGE REACTION OF MICHLER'S KETONE. Koch, T. H.; Jones, A. H. (Univ. of Colorado, Boulder). J. Amer. Chem. Soc.; 92: 7503-5(16 Dec 1970).

Photon irradiation of Michler's ketone, 4, 4'-bis(N, N-dimethylamino) benzophenone, in the presence of ethanethiol-S-d exchanges up to 12 hydrogens of Michler's ketone for deuterium. The NMR spectra indicate that the methyl hydrogens are exchanged. In the absence of light, no exchange was observed. The quantum yield for hydrogen–deuterium exchange was dependent on Michler's ketone concentration. Data indicated that the primary photochemical process initiating the observed hydrogen–deuterium exchange is a reaction of excited triplet-state Michler's ketone with ground-state Michler's ketone. (M.C.G.)

10557 DEUTERIUM ISOTOPE EFFECT ON COMPETING HYDROGEN AND CARBOMETHOXY MIGRATION IN BENZOTROPILIDENE PHOTOCHEMISTRY. Madigan, Denise M.; Swenton, John S. (Ohio State Univ., Columbus). J. Amer. Chem. Soc.; 92: 7513-15(16 Dec 1970).

The change in product ratio on photolysis of normal and deuterated benzonorcaradiene and benzotropilidene indicated a primary isotope effect of 3.7. (M.C.G.)

10558 INTERMEDIATES IN ALLENE–ACETYLENE ISOMERIZATION OVER ZINC OXIDE. Chang, C. C.; Kokes, R. J. (Johns Hopkins Univ., Baltimore). J. Amer. Chem. Soc.; 92: 7517-18(16 Dec 1970).

Adsorption of normal and deuterated acetylene and methylacetylene on zinc oxide was studied. Perdeuterioacetylene gave rise to an OD band at a position close to that expected for a normal isotope shift. Adsorption of $CH_3-C \equiv C \cdot D$ gave rise to an OH band and no corresponding OD band was observed. (M.C.G.)

10559 LOW PRESSURE STUDY OF NON-STEADY STATE HYDROGEN–DEUTERIUM EXCHANGE ON A MOLYBDENUM SURFACE. Bergsnov-Hansen, B.; Pasternak, R. A. (Stanford Research Inst., Menlo Park, Calif.). Contract AT(04-3)-425. Surface Sci.; 17: 402-17(Oct 1969).

The heterogeneous hydrogen–deuterium exchange on a molybdenum surface was investigated under nonsteady-state conditions

at a constant gas pressure of 10^{-8} torr and sample temperature between −40 and 200°C. In one experimental series, an H_2-D_2 mixture was adsorbed on the originally clean surface, and in another series deuterium initially adsorbed on the surface was subsequently replaced by hydrogen from the gas phase. In both series, the rate of HD formation was measured with a mass spectrometer and related to surface coverage and temperature. The results of the quantitative analysis of the data can be summarized as follows: (1) The adsorption rate of hydrogen or deuterium, which is proportional to pressure, decreases linearly with surface coverage but is independent of temperature. Thus, the isosteric heat of adsorption is equal to the activation energy of desorption. (2) Desorption is second order in coverage, but the rate constant is a function of both temperature and coverage. (3) In the range of the experimental conditions employed, exchange proceeds by the atomic mechanism postulated by Bonhoeffer−Farkas. (auth)

10560 SYNTHESIS AND BIOLOGICAL ACTIVITY OF DEUTERIOBENZYL-d_7-PENICILLIN. Laskar, Paul A.; Mrtek, Robert G. (Univ. of Illinois, Chicago). J. Pharm. Sci.; 59: 1727-32(Dec 1970).

To investigate the deuterium isotope effect on the biological activity of penicillin G, this compound was chemically synthesized by first obtaining phenylacetyl-d_7-chloride from phenylacetic-d_7-acid and thionyl chloride, followed by condensation of the acid chloride with 6-aminopenicillanic acid. The penicillin was isolated as the 1-ethylpiperidine salt. Yield of the deuteriopenicillin was approximately 60% when a 2 : 1 (6-aminopenicillanic acid−acid chloride) molar ratio was used. The identity of the deuteriated penicillin was confirmed using several physical constants. From NMR data, the presence of deuterium in the benzyl moiety was found to be greater than 95 at. %. The biological activity of the deuteriopenicillin was compared to that of the protioanalog by a turbidimetric assay procedure using Staphylococcus aureus. The results of the biological assay indicate that a significant deuterium isotope effect operates in the antistaphylococcal action of benzylpenicillin. With the test organism chosen, the ratio of the antibiotic potencies was 125% H/D. (auth)

10561 EQUILIBRIUM GEOMETRIES OF THE METHYL HALIDES. Duncan, J. L. (Univ. of Aberdeen, Scotland). J. Mol. Struct.; 6: 447-56(Dec 1970).

Values of A_e and B_e for the H_3 and D_3 methyl chlorides, bromides, and iodides were calculated from the best present estimates of values of A_0, the microwave values of B_0, and the α_r^A and α_r^B data. The theoretical $A_e(CH_3X)/A_e(CD_3X)$ ratio is well obeyed in methyl iodide and bromide, but a discrepancy of 1% is observed in methyl chloride. It is concluded that $A_e(CD_3Cl)$ is slightly high, possibly as a result of the lack of precise data available from the strongly overlapped and Coriolis interacting fundamentals ν_2 and ν_5. The equilibrium rotational constants predict the molecular parameters: methyl chloride—$r_e(CH) = 1.086 \pm 0.004$ Å, $R_e(CCl) = 1.778 \pm 0.002$ Å, $\alpha_e(HCH) = 110° 40' \pm 40'$; methyl bromide—$r_e(CH) = 1.086 \pm 0.003$ Å, $R_e(CBr) = 1.933 \pm 0.002$ Å, $\alpha_e(HCH) = 111° 10' \pm 25'$; methyl iodide—$r_e(CH) = 1.085 \pm 0.003$ Å, $R_e(CI) = 2.133 \pm 0.002$ Å, $\alpha_e(HCH) = 111° 17' \pm 25'$. For methyl fluoride, for which the α_r^A and α_r^B data are not so complete, the A_0 and B_0 values were corrected to A_e and B_e by considering the trends in $(A_e - A_0)$ and $(B_e - B_0)$ in the other halides. Almost precise agreement with the theoretical ratio is obtained with the A_e values. The equilibrium rotational constants predict the molecular parameters: methyl fluoride $r_e(CH) = 1.095$ Å, $R_e(CF) = 1.382$ Å, $\alpha_e(HCH) = 110° 27'$. No estimates of uncertainty were made, as the results depend entirely on the validity of the extrapolation process used to obtain A_e and B_e values. The considerably larger CH bond length in comparison with the other halides is supported by the observations that the unperturbed CH_3 and CD_3 stretching vibration frequencies are much lower, and that the CH stretch force constant is significantly smaller than in the other halides. (auth)

10562 LOW-FREQUENCY VIBRATION SPECTRA OF VARIOUS ISOTOPIC TYPES OF PRIMARY ALIPHATIC ETHERS. II. METHYL ETHYL AND DIETHYL ETHERS. Perchard, J. P. (CNRS, Thiais, France. Faculte des Sciences, Paris). J. Mol. Struct.; 6: 457-70(Dec 1970). (In French).

The infrared spectra of seven deuterated and normal methyl ethyl ethers and of three diethyl ethers were recorded between 500 and 50 cm^{-1} and completely assigned. The internal rotation barrier of the methyl groups was calculated by two methods: harmonic approximation and the solving of Mathieu's equation. The values obtained are in good agreement with the experimental values and show the sensitivity of torsion vibrations to intermolecular effects. (auth)

10563 SOME FREQUENCY SHIFTS BY ^{13}C SUBSTITUTION IN THE IR SPECTRA OF C_2H_4, C_2D_4, AND C_2H_6; THEIR USE FOR FORCE CONSTANT CALCULATIONS. Becher, H. J.; Adrian, A. (Univ., Muenster, Ger.). J. Mol. Struct.; 6: 479-93(Dec 1970). (In German).

The infrared spectra of C_2H_4, C_2D_4, and C_2H_6, enriched with 56% ^{13}C, were examined in the region of B_{2u} and A_{2u} stretching and bending frequencies. The ^{13}C-shift was determined with a reliability of 0.15 cm^{-1}. After correction these results were used as additional data for the determination of symmetry-force constants. (auth)

10564 STUDIES ON THE SECONDARY STRUCTURE OF PHENYLALANYL TRANSFER RIBONUCLEIC ACID. Rosenfeld, Alita (Univ. of Pittsburgh); Stevens, Charles L.; Printz, Morton P. Biochemistry; 9: 4971-80(8 Dec 1970).

To investigate the secondary structure of Escherichia coli Phe tRNA the techniques of spectral analysis and tritium−hydrogen exchange were used on the reaction of 1% HCHO with Phe-tRNA at 35°C. The tritium-exchange measurements were made to determine the amount of base pairing before, during, and after reaction. As expected, there is a decreasing number of slowly exchanging hydrogens on increasing time of exposure to HCHO. Before reaction there were 84 H-bonded hydrogens in a 10^{-3} M Mg^{2+} solution and only 48 after reaction. The tritium exchange-out curve for Phe-tRNA in Mg^{2+}, treated with HCHO, coincided with unreacted Phe-tRNA in 0.03 M PO_4^{3-}. This suggested a stable "core" region of H bonding. The size of this core is that expected on the basis of a cloverleaf-like structure for tRNA. The thermal denaturation curve of Phe-tRNA in 0.03 M phosphate shows a coincidence with the theoretical curve obtained using a statistical mechanical theory of thermal transitions on the cloverleaf model of Phe-tRNA. Other thermal denaturation and tritium-exchange experiments suggest that the Phe-tRNA molecule may have tertiary folding of the cloverleaf in 0.2 M Na^+ solution. (auth)

10565 SOME THERMAL PROPERTIES OF DEUTERATED COPPER(II) SULFATE PENTAHYDRATE. Oki, Hisaya; Kyuno, Eishin; Tsuchiya, Ryokichi (Kanazawa Univ., Japan). Bull. Chem. Soc. Jap.; 43: 3263-4(Oct 1970).

Thermochemical functions were determined in the dehydration of copper(II) sulfate pentahydrate deuterated to different extents, in order to find differences in thermal properties of hydrates. The x-ray powder pattern and infrared spectra of several deuterated copper sulfate pentahydrates were compared with each other. (D.P.O.)

10566 HYDROLYSIS OF THE COPPER(II) ION IN HEAVY WATER. Kakihana, Hidetake; Amaya, Toshihiko; Maeda, Masunobu (Tokyo Inst. of Tech.). Bull. Chem. Soc. Jap.; 43: 3155-8(Oct 1970).

The hydrolysis equilibria of the copper(II) ion in heavy water were studied at 25°C by measuring the deuterium ion concentration by means of a commercial glass electrode. The total copper(II) concentration was varied between 50 and 90 mM, while the concentration of the perchlorate ion was held constant at 3M by the addition of $NaClO_4$. A hydrolyzed copper(II) perchlorate solution was gradually acidified up to the point where hydrolysis was negligible by the use of constant-current coulometry. The experimental data, which indicate a slight hydrolysis in the log d range from −4.0 to −5.26, can be explained by assuming these equilibria: $Cu^{2+} + D_2O = CuOD^+ + D^+$, $\log \beta_{1,1} = -7.71 \pm 0.07$; $2Cu^{2+} + 2D_2O = Cu_2(OD)_2^{3+} + 2D^+$, $\log \beta_{2,2} = -11.46 \pm 0.04$. (auth)

10567 EFFECT OF CONFORMATION ON ISOTOPIC EXCHANGE IN SYNTHETIC POLYPEPTIDES. Miller, Wilmer G. (Univ. of Minnesota, Minneapolis). Biochemistry; 9: 4921-30 (8 Dec 1970).

Calculated exchange rates are presented for amide isotopic exchange in synthetic polypeptide homopolymers and copolymers. The effects of pH, temperature, and ionic strength are considered. It is assumed that exchange does not occur from intramolecularly hydrogen-bonded (helical) amides and that the kinetics of the helix to random-coil conformation change is rapid compared with the isotopic exchange. The exchange rate law is considered to be a sum of independent parallel first-order terms with the apparent rate constants dependent on conformation as well as other factors. In homopolymers deviation from first-order behavior results from the high probability of residues near the end of a chain being in nonhelical conformation under all environmental conditions. The calculated rates are shown to be consistent with known experimental data with respect to apparent reaction order, ionic strength effects, and conformational contribution to the exchange activation energy. The effects of composition and sequence on the exchange kinetics are investigated in copolymers where one of the monomers has an ionizable side chain. Decreasing the amount of ionizable monomer increases the deviation from simple first-order be-

havior. Comparison with experimental data indicates that only the conformational thermodynamics, and not the conformational kinetics, need to be considered to understand the exchange kinetics in copolymers. (auth)

Physical Chemistry

Refer also to abstract 11384.

10568 (CEA-R-4051) STUDY OF NEPTUNIUM HEXAFLUORIDE FORMATION AND ITS ADSORPTION ON METALLIC FLUORIDES. Matcheret, Georges (Commissariat a l'Energie Atomique, Fontenay-aux-Roses (France). Centre d'Etudes Nucleaires). Nov 1970. 80p. (In French). Dep. NTIS (U. S. Sales Only).

Thesis. Submitted to Paris Univ. (France). Faculte des Sciences.

The action of elementary fluorine on neptunium compounds was studied by a thermogravimetric method. With neptunium tetrafluoride, the reaction proceeds in a single step. The kinetics corresponds to a uniform attack of the entire surface of the sample. The reaction with neptunium dioxide involves two steps, neptunium tetrafluoride being the intermediate compound. The kinetics of the first step corresponds to a diffusion process. The kinetics of the second step corresponds to a uniform attack of the entire surface of the sample. A study was made of the adsorption of uranium hexafluoride and neptunium hexafluoride on sodium, magnesium, and barium fluorides by a volumetric method. The adsorption of UF_6 on MgF_2 was investigated at 20°C. The isothermal curve obtained is characteristic of a physical monomolecular layer adsorption. In a way similar to the behavior of UF_6, the adsorption of NpF_6 involves in addition a chemical reduction with the formation of NpF_5 and release of fluorine. The reaction of NpF_6 with BaF_2 confirmed the influence of the polarizing power of the Ba^{2+} ion on the formation and stability of the product of addition. (63 references). (auth) (France)

10569 (CEA-R-4074) EFFECT OF α UO_3 IN THE PRODUCTION OF UO_2 AND UF_4 FROM β $UO_3 - 0.05$ H_2O. Nicolas-Jarleton, Jacques (Commissariat a l'Energie Atomique, Saclay (France). Centre d'Etudes Nucleaires). Dec 1970. 89p. (In French). Dep. NTIS (U. S. Sales Only).

Thesis. Submitted to Paris Univ. (France). Faculte des Sciences.

Various experiments showed that the structure of UO_3 influences both the chemical reduction and the reactivity of UO_2. Different crystalline UO_3 phases were studied and the presence of hexagonal α UO_3 in β $UO_3 - 0.5$ H_2O confirmed. An x ray diffraction method for determining the quantity of hexagonal UO_3 in the β $UO_3 - 0.5$ H_2O was developed. A comparative study was made of the kinetics of the NH_3 reduction of the α and β phases in UO_3 and of the reactivity of UO_2 with oxygen and hydrofluoric acid. The curves of reactivity of α and β UO_3 were established; the results were verified by three series of industrial tests using more than one metric ton of trioxide. The influence of the grinding process on the crystal structure (until it breaks), the absolute density, the specific surface, and the chemical reactivity of α UO_3 and β $UO_3 - 0.5$ H_2O are discussed. (auth) (France)

10570 (COO-294-10) STUDIES OF (1) ACTINIDE AND LANTHANIDE IONS AND (2) ORGANIC MOLECULES IN TRIPLET STATES BY MAGNETIC RESONANCE METHODS. Technical Progress Report. Hutchison, Clyde A. Jr. (Chicago Univ., Ill. Dept. of Chemistry). 16 Dec 1970. Contract AT(11-1)-294. 14p. Dep. NTIS.

Developments are reported for studies on: f electron systems in single crystals, including the electron nuclear double resonance (ENDOR) lines for La and Cl in single crystals of $LaCl_3$ and study of photoexcited states of Nd^{3+} and U^{3+} ions in $LaCl_3$ single crystals; and organic molecules in triplet states, including EPR spectra of benzene single crystals. (P.C.H.)

10571 (EUR-4550) NUCLEAR FUEL WITH BURNABLE POISON. PART 1. Gd_2O_3 MICROSPHERES PREPARATION FROM THE SOL-GEL METHOD. Topical Report, January 1, 1968-December 31, 1969. Abate-Daga, G.; Amato, I.; Grappiolo, G. (FIAT, Turin (Italy). Sezione Energia Nucleare. ANSALDO S.p.A., Genoa (Italy)). Nov 1970. 44p. Dep. NTIS (U. S. Sales Only). EUR FF 6.65.

Gd_2O_3 microspheres (95 to 98% of the theoretical value of the density) have been prepared through the sol-gel method. The process involves the following steps which have been optimized for the requested applications: sol preparation, gelation and spheroidization, and thermal treatment (presintering and sintering). The sol has been prepared by peptization at 80°C for 30 minutes of freshly precipitated gadolinium hydroxide with nitrate ions as stabilizing electrolyte. The concentration of sol was about 2 M and the NO_3^-/Gd molar ratio in the range 0.12 to 0.27. The gelation and spheroidization were carried out in a tapered column through dehydration and gelation by an aliphatic long chain alcohol. The gelled microspheres have been presintered under vacuum up to 950°C for a total time of about 10 hours in order to decompose the gadolinium hydroxide, nitrate, carbonate, and the adsorbed organic substances. The presintered microspheres have been hydrogen sintered for 2 to 3 hours at 1600 to 1700°C: microspheres with sintered density very near to the theoretical value have been obtained. 42 references. (auth)

10572 (IEA-184) CATALYTIC REDUCTION OF AQUEOUS SOLUTIONS OF URANYL NITRATE. Brown, Anthony E. P.; Costa, Eduardo C. (Instituto de Energia Atomica, Sao Paulo (Brazil)). Aug 1969. 41p. (In Portuguese). Dep. NTIS (U. S. Sales Only).

The catalytic reduction of aqueous solutions of uranyl nitrate has been studied employing hydrogen at low pressures as the reducing agent in the presence of 1% Pt-99% Al_2O_3 as a catalyst. The reductions were carried out in a 500-ml batch slurry reactor at constant over-all uranium concentration, constant agitation, and constant hydrogen flowrate. The variables studied were reaction time, temperature, Pt/U ratio, urea/U ratio, and the HNO_3/U ratio. Urea was used as a stabilizing agent for uranium(IV). The optimization procedure was based on the Steepest Ascent Method developed by Box and Wilson, utilizing data obtained from a quarter-replicate of a 2^3 factorial design. The analysis of the data indicated that the response optimum for a 0.25 M U(VI) solution was located around the point 235 ± 10 minutes, 39 ± 2°C, 3 ± 0.05 g/mole Pt/U, 0.06 ± 0.002 g/g urea/U and 2 ± 0.1 mole/mole HNO_3/U. Conversions higher than 99.9% were obtained around this point. (auth)

10573 (IEA-207) REDUCTION OF AMMONIUM DIURANATE WITH ANHYDROUS AMMONIA. Correa, Heleno S.; Costa, Eduardo C. (Instituto de Energia Atomica, Sao Paulo (Brazil)). Apr 1970. 16p. (In Portuguese). Dep. NTIS (U. S. Sales Only).

The preparation of uranium oxides by reduction of an ammonium diuranate with anhydrous NH_3 was investigated. The study was primarily aimed at establishing time-temperature correlations for the preparation of fluoride- and ceramic-grade oxides. Batch reduction was conducted in graphite boats placed inside a tubular reactor under a constant feed rate of the reducing gas in a thermostatically controlled system. Time and temperature variables were studied, keeping constant the external geometry of diffusion, and approximately constant the density and depth of the bed. The same uranate was employed in all experiments. In view of the high oxidation ability of the resulting oxides at room temperature, most of the reduction conditions were over-estimated. The reduction with anhydrous NH_3 presented inherent advantages over the usual reduction with hydrogen, among which include marked decrease of operational hazards, lower operating costs, and more favorable free energy of reaction. (auth)

10574 THERMAL CONDUCTIVITY OF CARBON DIOXIDE IN THE TEMPERATURE RANGE 100 TO 1075°C. Gupta, G. P. (Univ. of Rajasthan, India); Saxena, S. C. Mol. Phys.; 19: 871-80 (Dec 1970).

The thermal conductivity, k, of carbon dioxide was measured by adopting the conductivity column method in the temperature range 100 to 1075°C. The measurements were taken at various pressures between 12.5 and 50.5 cm of mercury where the k values were found to be independent of gas pressure. The estimated accuracy of k values is ±2% and these are correlated within an average absolute deviation of 0.5%. The present measurements agree well with the existing data. However, the latter have a large scatter and consequently the present work helps in resolving some of the controversies faced by correlators of k data. The theoretically calculated k values are appreciably smaller than the experimental results and this disagreement is attributed to a different value for the diffusion coefficient characterizing the transport of internal energy in comparison to the more familiar one associated with the diffusion coefficient measured in a tracer experiment. (auth) (UK)

10575 PRESSURE STUDIES IN SOLID D_2 AND SOLID H_2. Ramm, Dietolf. Durham, N. C.; Duke Univ. (1969). 205p. University Microfilms Order No. 70-20,283.

Thesis.

A sensitive strain gauge was used for the observation of pressure changes at constant volume ($(\partial P/\partial T)_V$) in solid deuterium and solid hydrogen at varying concentrations of paradeuterium and orthohydrogen which have a rotational angular momentum of J = 1. It is assumed that $(\partial P/\partial T)_V$ is the sum of the lattice contribution $(\partial P/\partial T)_{V,L}$ and a term due to other interactions. These interactions, which tend to order the angular momenta of the molecules, are thought to be electric quadrupole-quadrupole

interactions (EQQ). Thus, upon subtracting the lattice contribution from the experimental data, one obtains a quantity proportional to the specific heat due to the EQQ interaction, $(\partial P/\partial T)_{V,EQQ}$. The EQQ interaction is characterized by a parameter $\Gamma = 6e^2Q^2/25R^5$ where eQ is the quadrupole moment of the J = 1 molecule and R is the distance between two nearest neighbors. The calculated parameter for a rigid lattice is $\Gamma/k_B = 1.18$ K for deuterium and $\Gamma/k_B = 1.00$ K for hydrogen. The research includes a detailed study of the hcp-cubic transition as a function of paradeuterium concentration. The critical concentration below which there is no transition is c = 0.54. Samples were cycled through the transition many times without annealing. The results for hydrogen and deuterium were compared. The x-ray measurements of Schuch, Mills and Depatie in a similar cycling experiment are discussed. A study of the temperature and pressure hysteresis between the warming and cooling transition was made and the results for hydrogen and deuterium are compared. An examination of $(\partial P/\partial T)_V$ in the hcp phase shows a possible order-disorder transition in the paradeuterium concentrations between 0.4 and 0.52. Analysis of $(\partial P/\partial T)_V$ in the rotationally ordered cubic phase with rotational excitation theories gives $\Gamma/k_B = 1.05$ K. A study of solid hydrogen in a concentration range between 0.45 and 0.55 complements a previous study on hydrogen. This study does not indicate the order-disorder transition indicated in deuterium for the corresponding range of concentration of J = 1 molecules. The critical concentration for the hcp-cubic transition in hydrogen is c = 0.55. Evidence of molecular motion of orthohydrogen molecules at low ortho concentrations is confirmed by the measurement of $(\partial P/\partial t)_{V,T}$, where t = time. Pressure changes with the passage of time indicate that the ortho molecules, at a given temperature, are migrating from random distribution positions to configurations of lower free energy. The rate is $(\partial P/\partial t)_{V,T} = A\exp(-t/\tau)$ where τ is a characteristic time for rearrangement. A study was made of this time constant, τ, as a function of temperature for various concentrations of orthohydrogen. The pressure changes are discussed in terms of a simple theory utilizing the energy of isolated ortho molecules, that of isolated pairs and of triangular configurations. The results of the study of the time constant are consistent with those obtained from NMR data by Amstutz, Thompson and Meyer. In a similar investigation of deuterium, the molecular motion was found to be too small to be measured. (Diss. Abstr.)

10576 HALIDE COMPLEXES OF PENTAVALENT URANIUM. Ryan, Jack L. (Battelle-Northwest, Richland, Wash.). J. Inorg. Nucl. Chem.; 33: 153-77(Jan 1971).

New and simpler methods of preparing solutions and salts of the UF_6^- and UCl_6^- complexes are given. The preparation of the previously unknown hexahalide complexes UBr_6^- and UI_6^- and oxohalide complexes UOF_5^{3-}, $UOCl_5^{3-}$, and $UOBr_5^{3-}$ is described. The chemical properties and stabilities of all of these complexes are discussed. The stability of uranium(V) toward disproportionation in several nonaqueous halide solutions is demonstrated. Absorption spectra of these uranium(V) hexahalide and oxohalide complexes in the regions of electron transfer transitions, internal 5f electron transitions, metal–oxygen vibrational frequencies, and metal–halogen vibrational frequencies are presented. These spectra are interpreted and related to the observed chemical properties of uranium(V) in these halide complexes. (auth) (UK)

10577 CRYSTAL STRUCTURE OF ANHYDROUS UO_2F_2. Atoji, M.; McDermott, M. J. (Argonne National Lab., Ill.). Acta Crystallogr., Sect. B; 26: 1540(1970).

A neutron powder-diffraction study of UO_2F_2 has been carried out. The structure is trigonal with a unit-layer unit cell with a = b = 4.192 ± 0.001 and c/3 = 5.220 = 0.003 Å and bonding distances of U – O = 1.74 ± 0.02 and U – F = 2.429 ± 0.002 Å, confirming essentially a previous X-ray study but with considerably higher accuracy. The powder sample consisted of approximately equal cumulative volumes of four different types of ordered coherent domains, containing individually the layer sequences, $A^+B^+C^+$, $A^-B^-C^-$, $A^+B^+A^+B^+C^+B^+C^+A^+C^+$ and $A^-B^-A^-B^-C^-B^-C^-A^-C^-$, where (+) and (–) refer respectively to the right-side-up and upside-down unit-layer configurations. In each layer sequence, a backward stacking with the opposite-sign unit layer is equally possible in powder diffractometry. All structures belong to the centric trigonal space group $R\bar{3}m$ (D_{3d}^5). The polymorphic, multidomain structure is not necessarily unique, although an exhaustive search for other probable models was fruitless. (auth)

10578 DIFFUSION OF ^{24}Na IN A VISCOSITY STANDARD SILICATE GLASS. Winchell, P. (Gulf General Atomic Inc., San Diego, Calif.). Phys. Chem. Glasses; 11: 115-16(Aug 1970).

Diffusion coefficients for the transport of ^{24}Na in NBS 710 viscosity standard silicate glass were obtained in the temperature range 1041 to 1742°K. The results are summarized by: $D = 1.70 \times 10^{-2} \exp[-(2.35 \times 10^4/RT)]$. (auth) (UK)

10579 SOLUBILITY OF CARBON IN SODIUM. Longson, B.; Thorley, A. W. (United Kingdom Atomic Energy Authority, Culcheth, Eng.). J. Appl. Chem. (London); 20: 372-9(Dec 1970).

The solubility of carbon in sodium over the range 600 to 950°C may be expressed by the equation: log sol. = 7.20–5465/T where solubility is in ppM and T in °K. From plots of carbon activity versus concentration, and from observations that oxygen does not affect carbon solubility, it is proposed that carbon dissolves in sodium as single atoms. (auth) (UK)

10580 KHIMIYA REDKIKH I RASSEYANNYKH ELEMENTOV. (Chemistry of Rare Earths and Various Other Elements). Chalova, E. P. (ed.). Frunze, USSR; Izdatel'stvo Ilim (1969). 150p.

Sixteen articles are included on the chemistry and technology of rare earth elements, Sc, Y, Th, Se, and Te. Information is included on the separation of Au and Ag from Sb and Pb, reactions of Pt with O at high temperatures, and phase equilibria of ternary rare earth alloys. (P.C.H.)

10581 THERMOCHEMICAL STUDIES OF SOME URANIUM AND THORIUM COMPOUNDS. Athavale, V. T.; Kalyanaraman, R.; Sundaresan, M. (Bhabha Atomic Research Centre, Tronbay, India). Indian J. Chem.; 7: 386-91(Apr 1969).

The heats of formation of a series of uranium(VI), uranium(IV), and thorium compounds were determined by bomb calorimetry and some of the values so obtained were checked by another method involving the acid decomposition of the compounds in an isoperibol solution calorimeter. The vapor pressures of these compounds and the thermodynamic properties associated with their sublimation processes were determined. The mean bond energies of the bonds UO_2–O, U–O, Th–O, UO_2–N, U–N and Th–N were calculated by forming suitable empirical Born-Haber cycles. The transferability of the bond energies from one compound to another and certain structural considerations are discussed. (auth)

10582 TRANSMISSION OF ^{133}Xe THROUGH ACTIVATED CHARCOAL ADSORBER BEDS. Lee, K. B.; Madey, Richard (Clarkson Coll. of Tech., Potsdam, N. Y.). Nucl. Sci. Eng.; 43: 27-31(Jan 1971).

Experimental data of Cantelow on the time-dependent transmission of ^{133}Xe in air flowing steadily through fixed beds packed with activated charcoal adsorbent are reinterpreted on the basis of a dispersion model in terms of a dimensionless dispersion number and an effective adsorption capacity for the gas-adsorbent system. The transmission is the ratio of the concentration at the outlet of the adsorber bed to the concentration at the inlet to the bed. The dispersion model provides an alternative interpretation to the theoretical plate model for the transport of a gas through a packed bed. For the range of dimensionless dispersion numbers represented by the data, the two models lead to the same values for the effective adsorption capacity. The reciprocal of the dimensionless dispersion number is equal to twice the theoretical plate number. (auth)

Radiation and Nuclear Chemistry

Refer also to abstract 10517.

10583 (AECL–3776) CHEMISTRY AND MATERIALS DIVISION PROGRESS REPORT, JULY 1–SEPTEMBER 30, 1970. (Atomic Energy of Canada Ltd., Chalk River (Ontario). Chalk River Nuclear Labs.). 108p. (PR-CMa-14). Dep. NTIS (U. S. Sales Only). AECL $2.00.

ALUMINUM—crystal structure of quenched, vacancy formation in
ALUMINUM ALLOYS—Al–Mu, crystal structure of quenched, vacancy formation in
AMINES—radiolysis of, ESR studies on
CADMIUM ISOTOPES—yields from thermal fission of uranium-235
CALCIUM FLUORIDES—diffusion of calcium-45 in monocrystals of
CALCIUM-45—diffusion in calcium fluoride monocrystals
CHROMIUM-52—oxygen-16 reactions with
COBALT-58—neutron capture cross sections for, thermal
DEUTERIUM—separation from hydrogen, electrochemical
—exchange between hydrogen and water-d, effects of catalysts on
ELECTRON MICROSCOPY—research progress on
FILMS—ion scattering by thin
HELIUM-4—energy distributions from fission of uranium-236
HYDROGEN—separation from deuterium, electrochemical

IONS—scattering by thin films
LEAD—superconducting transition temperature and recovery of deformed
MANGANESE ALLOYS—Al–Mu, crystal structure of quenched, vacancy formation in
MOLYBDENUM—determination as fuel burnup monitor
NICKEL OXIDES—sorptive properties of aqueous suspensions of, for tellurium
NITRIDES—analysis of layers of, on silicon for oxygen by deuteron (d,p) reactions
OXYGEN—determination in nitride layers on silicon surfaces by deuteron (d,p) reactions
OXYGEN-16—reactions with chromium-52
REACTOR FUELS—burnup monitoring by molybdenum analysis
ROCKS—radioactivity of, measurements on
SEMICONDUCTORS—radiation effects on monocrystal
SILICON—analysis of nitride layers on, for oxygen by deuteron (d,p) reactions
TELLURIUM—sorption on nickel oxide suspensions in water
THORIUM OXIDES ThO_2—radiation effects on pure and doped
TRITIUM—energy distributions from fission of uranium-236
URANIUM-234—half-life of
URANIUM-235—neutron fission of, yields of cadmium isotopes from thermal
URANIUM-236—fission of, energy distribution of helium-4 and tritium from
WATER—D_2O-H_2O, radiolysis of
WATER-d_2—D_2O-H_2O, radiolysis of
WATER VAPOR—radiolysis of
ZIRCALOY—cracking of
ZIRCONIUM—oxidation by plasma anodization
—oxidation of, x-ray analysis of films formed in
ZIRCONIUM ALLOYS—oxidation by plasma anodization
—oxidation by molten salts
—radiation effects on hardness of (M.C.G.)

10584 (JAERI–5026) ANNUAL REPORT NO. 3 OF OSAKA LABORATORY FOR RADIATION CHEMISTRY, APRIL 1, 1969–MARCH 31, 1970. (Japan Atomic Energy Research Inst., Tokyo). 171p. (In Japanese). Dep. NTIS (U. S. Sales Only).

Twenty-seven papers and abstracts of 17 additional papers are included. Separate abstracts were prepared for 25 papers. The remaining papers covered emission spectra of excited species in a mass spectrometer and radical stability on silica gel. (M.C.G.)

For abstracts of individual papers see: 10585–10587, 10593–10610, and 10622–10625.

Radiation Effects

10585 (JAERI–5026, pp 153-5) OPTICAL RADIATION FROM GASES EXCITED BY HIGH-ENERGY ELECTRONS. II. IMPROVEMENT OF APPARATUS AND DETECTION OF OPTICAL EMISSION FROM CARBON MONOXIDE. Nakai, Yohta; Matsuda, Koji; Takagaki, Torao; Kimura, Ki-ichi (Japan Atomic Energy Research Inst., Tokyo). (In Japanese).

From Annual Report No. 3 of Osaka Laboratory for Radiation Chemistry, April 1, 1969–March 31, 1970.

Apparatus to measure the spectrum of light emitted from gases was constructed and tested. The overall sensitivity of the apparatus is greater than that of previous ones by a factor of three orders of magnitude. Spectra by 1.5-MeV electron impact on 430 torr CO were observed in the region from 2000 to 6000Å. The principal features were the singlets ($C^1\Sigma^+ \rightarrow A^1\Pi$, $B^1\Sigma^+ \rightarrow A^1\Pi$, and $A^1\Pi \rightarrow X^1\Sigma^+$) and the triplet ($b^3\Sigma^+ \rightarrow a^3\Pi$) bands of CO, as well as $B^2\Sigma^+ \rightarrow A^2\Pi_i$ and $A^2\Pi_i \rightarrow X^2\Sigma^+$) bands of CO^+, which were predominant for the low energy (~200 eV) electron impact at low pressure (~10^{-2} torr). (auth)

10586 (JAERI–5026, pp 155-7) OPTICAL RADIATION FROM GASES EXCITED BY HIGH-ENERGY ELECTRONS. III. COLLISIONAL EXCITATION TRANSFER IN N_2–NO, N_2–O_2, Ar–N_2 MIXTURES. Nakai, Yohta; Matsuda, Koji; Takagaki, Torao; Kimura, Ki-ichi (Japan Atomic Energy Research Inst., Tokyo). (In Japanese).

From Annual Report No. 3 of Osaka Laboratory for Radiation Chemistry, April 1, 1969–March 31, 1970.

The spectra induced by 1.5-MeV electron impact on N_2–NO, N_2–O_2, and Ar–N_2 mixtures were studied. Collisional energy transfer from the $A^3\Sigma^+$ state of N_2 to the $A^2\Sigma^+$ state of NO was observed in N_2–NO mixture at the total pressure between 20 and 300 torr. The second positive band system ($C^3\Pi_u \rightarrow B^3\Pi_g$) of N_2 has been quenched by the oxygen gas in N_2–O_2 mixtures. The results of Ar–N_2 mixture experiments support the notion that the energy of the electron-excited an atom is transferred to the $C^3\Pi_u$ state of N_2. (auth)

10587 (JAERI–5026, pp 167-8) RADIATION EFFECTS ON GRAMICIDIN. II. DILUTE AQUEOUS SOLUTION OF GRAMICIDIN. Sugimoto, Shun-ichi; Ohnishi, Shun-ichi; Nitta, Isamu (Japan Atomic Energy Research Inst., Tokyo). (In Japanese).

From Annual Report No. 3 of Osaka Laboratory for Radiation Chemistry, April 1, 1969–March 31, 1970.

Gramicidin becomes insoluble when irradiated in dilute aqueous solution. Formation of the insoluble fraction was studied as functions of dose, dose rate, and concentration. The minimum dose for the formation of the insoluble fraction was 4.3×10^7 R in 0.5 wt % aqueous solution. (auth)

10588 ESR STUDY OF RADICALS IN SOME IRRADIATED SINGLE CRYSTALS. Watson, James Clyde. East Lansing, Mich.; Michigan State Univ. (1970). 254p. University Microfilms Order No. 70-20,541.

Thesis.

ESR spectra of radicals produced by electron and γ irradiation in six single crystals were investigated as a function of temperature. The radicals produced in the crystals and the temperature range over which they are stable, are: Cl_2^- (77 to 123°K) and $CH_2-\overset{+NH_2}{\overset{\|}{C}}-NH_2$ (123 to 193°K) from acetamidine hydrochloride γ-irradiated at 77°K; $CH_3-\overset{CH_2O}{\overset{|}{\underset{CH_3}{\underset{|}{C}}}}-\overset{O}{\overset{\|}{C}}-NH_2$ (77 to 193°K) and t-butyl radical (77 to 300°K) from trimethylacetamide γ-irradiated at 77°K; $\overset{CH_2}{\underset{CH^3}{\diagup\diagdown}}CH-\overset{O}{\overset{\|}{C}}-NH_2$ (77 to 193°K) and $\overset{CH_3}{\underset{CH_3}{\diagup\diagdown}}\dot{C}-\overset{O}{\overset{\|}{C}}-NH_2$ (77 to 300°K) from isobutyramide γ-irradiated at 77°K; Cl_2^- (77 to 193°K) in γ-irradiated hydrazinium dichloride at 77°K; Br_2^- (77 to 113°K) in γ-irradiated hydrazinium dibromide at 77°K; and hydrogen atoms (77 to 193°K), an unidentified radical pair (77 to 193°K) and a radical, possibly $N_2H_6^+$, (193 to 300°K) in hydrazinium difluoride γ-irradiated at 77°K. In the case of the Cl_2^- radical anion in acetamidine hydrochloride it was found that the hyperfine splitting tensor and g tensor exhibited the anisotropy expected for a V center in a monoclinic crystal. The radical $\overset{CH_2-\overset{\|}{\underset{+NH_2}{C}}-NH_2}{\cdot}$, stable at intermediate temperatures, exhibited principal hyperfine splitting values of –35.9 gauss, –23.1 gauss, and –7.5 gauss for one proton and –36.2 gauss, –19.0 gauss, and –5.8 gauss for the second proton. These values are in reasonable agreement with predicted splittings for α-protons of π-electron radicals. A further interaction with the $-NH_2$ protons was detected giving principal proton hyperfine splittings of –6.4 gauss, –4.1 gauss and –1.7 gauss. In γ-irradiated trimethylacetamide single crystal both t-butyl radical and $CH_3-\overset{CH_2O}{\overset{|}{\underset{CH_3}{\underset{|}{C}}}}-\overset{O}{\overset{\|}{C}}-NH_2$ radical were present after irradiation at 77°K. Both radicals appear to be reorienting faster than 10^7 sec^{-1} since only the isotropic hyperfine splittings were observed in each case. The $CH_3-\overset{CH_2O}{\overset{|}{\underset{CH_3}{\underset{|}{C}}}}-\overset{O}{\overset{\|}{C}}-NH_2$ radical was stable only from 77 to 193°K. It was possible to obtain the maximum ^{13}C hyperfine splitting (92 gauss) for t-butyl radical at 77°K. This value was used to show that the t-butyl radical is probably slightly nonplanar with the C–C bonds tipped about 3 to 4° from the average radical plane. Isobutyramide single crystal gave two radicals upon irradiation at 77°K. In $\overset{CH_2}{\underset{CH_3}{\diagup\diagdown}}CH-\overset{O}{\overset{\|}{C}}-NH_2$ radical the equivalent α-proton principal hyperfine splittings of –24.2 gauss, –20.3 gauss, and –17.8 gauss show that the $-\dot{C}H_2$ group is reorienting slowly at 77°K. The β-proton principal hyperfine splittings of 22.8 gauss, 18.9 gauss and 12.2 gauss are characteristic of β-hyperfine splittings in $-\dot{C}-CH-XY$ type radicals. The isotropic β-hyperfine splitting of 18.0 gauss shows that the β-proton is oriented 93° from the plane containing the two carbon atoms and the p_π orbital of the α carbon. The $\overset{CH_3}{\underset{CH_3}{\diagup\diagdown}}\dot{C}-\overset{O}{\overset{\|}{C}}-NH_2$ radical exhibited essentially isotropic β-proton hyperfine splittings, the principal values being 23.0 gauss, 21.7 gauss, and 21.7 gauss. This is consistent with nearly free rotation of the CH_3- groups at 77°K. Hydrazinium dichloride and hydrazinium dibromide crystals contained V centers when γ-irradiated at

77°K. In the case of hydrazinium dichloride Cl_2^- radical anions were found to be oriented along (110) directions in the crystal. In hydrazinium dibromide Br_2^- exhibited principal values of the hyperfine splitting and g tensors which were consistent with the monoclinic symmetry of the crystal. In γ-irradiated hydrazinium difluoride hydrogen atoms were detected at 77°K, along with a radical pair. The presence of the pair was verified by the observation of lines at $g \cong 4$. Because of insufficiently resolved spectra over a range of orientations in the magnetic field it was not possible to identify the radical pair. Upon warming to −70° a spectrum was observed which indicated a radical in which the odd electron interacts with six equivalent protons and two equivalent nitrogen nuclei. Three possibilities which could explain the spectra observed were postulated; (a) formation of $N_2H_6^{3+}$ radical cation, (b) addition of an electron to $N_2H_5^{4+}$ cation to form the radical $N_2H_5^+$ with a three electron bond between the nitrogen atoms, or (c) formation of an F center by trapping an electron in a fluoride ion vacancy. (Diss. Abstr.)

10589 NEW INTERPRETATION OF THE BROAD-LINE NUCLEAR RESONANCE SPECTRA OF LINEAR POLYETHYLENE. PART II. Bergmann, Klaus (Badische Anilin- and Soda-Fabrik AG, Ludwigshafen, Rhine, Ger.). Ber. Bunsenges. Phys. Chem.; 74: 912-19(Sep 1970). (In German).

The decomposition of the wideline spectra of linear polyethylene into three components of different molecular mobility is theoretically further founded. It is shown that the three NMR-fractions can be obtained from the relaxation time spectra of the α-, β-, and γ-relaxation process. The protons with relaxation times $\lesssim 10^{-5}$ s are counted as mobile, all others as immobile. It is assumed that the α-process takes part in the crystalline and the β- and γ-process in the noncrystalline regions. For the dielectric active α- and γ-process good agreement between NMR- and dielectric measurements is obtained. The effects of different pretreatments (annealing, stretching, irradiation with fast electrons, crystallization from solution) on the relaxation behavior of the polyethylene are discussed. (auth)

10590 LUMINESCENCE OF Bi^{3+}-ACTIVATED LaOCl UNDER X-RAY EXCITATION. Simons, P. Y. (E. I. du Pont de Nemours and Co., Inc., Parlin, N. J.). J. Electrochem. Soc.; 118: 148-9 (Jan 1971).

The luminescence properties of Bi^{3+}-activated LaOCl over a wide composition range under x-ray excitation were studied. Broad-band emission occurred at 365 and 450 nm (measured at peak half-height). At all bismuth compositions below 25% the 365 nm is the more intense. The 365 nm emission intensity reaches a maximum at a bismuth concentration of 10 mole%, and with increasing bismuth this emission is severely quenched. On the other hand, the 450 nm emission intensity appears to reach a maximum at 25% bismuth. The assignment of emissions to electronic transitions between s^2 and sp states or activator−matrix states is discussed. (J.G.B.)

10591 THERMO-OXIDATION DEGRADATION OF POLY(VINYL ALCOHOL) IRRADIATED BY γ RAYS. Korodenko, G. D.; Narzullaev, B. N.; Karimov, S. N.; Zakharchuk, A. V. (Tadzhik State Univ., Stalinabad, USSR). Dokl. Akad. Nauk Tadzh. SSR; 13: No. 9, 23-7(1970). (In Russian).

Studies on the effects of γ radiation on poly(vinyl alcohol) (PVA) showed that the thermal stability of PVA increased due to increased crystallinity and reduction of the amount of the 1,2-glycol group. (R.V.J.)

Radiation Processes

10592 (BMBW-FBK-70-25) CONTRIBUTIONS TO THE RADIATION-INDUCED SULFOXIDATION OF PARAFFINS. Asinger, F.; Saus, A. (Technische Hochschule, Aachen (West Germany). Institut fuer Technische Chemie und Petrolchemie). Nov 1970. 59p. (In German). Dep. NTIS (U. S. Sales Only).

The sulfoxidation of paraffins for the manufacture of biologically soft detergents is of technical interest. The usual process with uv light as an initiator gives small yields per volume and time especially with paraffins within the washing active range. Experiments, performed with definite homologous n-alkanes as well as with technical paraffins of chain length $\bar{C}_{13}$ to C_{17} show that, in the presence of suitable additives, e.g., trichloromethane, dichloromethane, or tetrachloromethane, especially with acetic anhydride, the radioinduced reaction gives a considerable increase in yield of sulfoxidation product. Best results were obtained with γ rays and the addition of 1 to 5 vol % of acetic anhydride to the paraffin and the reaction temperature of 45 to 55°C. Comparative experiments with uv light, ozone, and γ rays showed that best results for increase in yield were obtained with γ rays. (auth)

10593 (JAERI-5026, pp 15-25) ON THE STABILITY OF POLYVINYL ACETATE EMULSIONS PRODUCED BY RADIATION-INDUCED POLYMERIZATION. I. EMULSIONS STABILIZED WITH THE CATIONIC SUFACTANT. Ohdan, Koji; Kamiyama, Hideo; Okamura, Seizo (Japan Atomic Energy Research Inst., Tokyo). (In Japanese).

From Annual Report No. 3 of Osaka Laboratory for Radiation Chemistry, April 1, 1969–March 31, 1970.

The process of particle formation and the stability of poly(vinyl acetate) (PVAc) emulsions prepared in the presence of cetyltrimethylammonium chloride (CTMAC) as cationic surfactant by γ-induced polymerization were studied mainly by turbidity measurement. The PVAc emulsions produced from dilue (1g/100 ml) a aqueous vinyl acetate solution were compared with those prepared in the presence of sodium dodecyl sulfate as an anionic surfactant and with emulsions obtained by polymerization induced by chemical initiators such as potassium persulfate (KPS). (auth)

10594 (JAERI-5026, pp 26-34) ON THE STABILITY OF POLYVINYL ACETATE EMULSIONS PRODUCED BY RADIATION-INDUCED POLYMERIZATION. II. RADIATION-INDUCED POLYMERIZATION OF VINYL ACETATE IN AQUEOUS SOLUTION. Kitajima, Masahiko; Kamiyama, Hideo; Okamura, Seizo (Japan Atomic Energy Research Inst., Tokyo). (In Japanese).

From Annual Report No. 3 of Osaka Laboratory for Radiation Chemistry, April 1, 1969–March 31, 1970.

Stability on aging and particle growth mechanisms of a polymer emulsion system obtained by radioinduced polymerization of vinyl acetate in aqueous solution were studied. Polymerization without surfactant proceeds with growth the size of negatively charged particles and with the degree of polymerization. The radioinduced initiation mechanism does not seem to have special contribution to the stability of the emulsion produced. The upper limit of stable concentration of polymer is very low (0.85 g/l) and can be increased by the exclusion of remaining monomer or by the addition of PVA. (auth)

10595 (JAERI-5026, pp 35-41) GRAFTING OF ACRYLONITRILE ONTO POLYVINYL CHLORIDE POWDER AND SPINNING OF FIBER FROM THE GRAFTS. Okada, Toshio; Kaji, Kanako; Sakurada, Ichiro (Japan Atomic Energy Research Inst., Tokyo). (In Japanese).

From Annual Report No. 3 of Osaka Laboratory for Radiation Chemistry, April 1, 1969–March 31, 1970.

Instead of grafting acrylonitrile on poly(vinyl chloride) fiber, grafting of acrylonitrile on poly(vinyl chloride) powder was carried out to obtain graft fiber using a simultaneous irradiation technique. The original poly(vinyl chloride) powder was a commercial product (DP = 980, diameter of particle-120 μ). The powder was suspended in water and the grafting was carried out with a mixture of acrylonitrile and ligroin by irradiation with γ rays from a ^{60}Co source. The total solid reaction product, which consisted of homo-poly (vinyl chloride), poly(vinyl chloride)-g-polyacrylonitrile, and homo-polyacrylonitrile was dissolved in dimethyl formamide and converted to fiber under application of the wet spinning process. The properties of the fiber were similar to those of fibers prepared by the fibrous grafting. The heat resistance of the fibers was much higher compared with that of conventional random copolymer fiber from vinyl chloride and acrylonitrile and the heat shrinkage was less than 10% even at 300°C. (auth)

10596 (JAERI-5026, pp 42-5) INFLUENCE OF THE DOSE RATE ON THE RATE OF RADIATION-INDUCED GRAFT POLYMERIZATION OF ACRYLONTRILE ONTO POLY(VINYL CHLORIDE) POWDER. Kaji, Kanako; Okada, Toshio (Japan Atomic Energy Research Inst., Tokyo). (In Japanese).

From Annual Report No. 3 of Osaka Laboratory for Radiation Chemistry, April 1, 1969–March 31, 1970.

Studies on the polymerization of acrylonitrile in a mixture of poly(vinyl chloride) powder, acrylonitrile, ligroin, and water were carried out over a range of dose rate of 7.4×10^3 to 8.0×10^7 rad/hr with the use of ^{60}Co γ rays and electron beams from a Van de Graaff machine. Rates of polymerization of acrylonitrile in the mixture were proportional to the 0.48 power of dose rates in the dose rate range studied. The molecular weight of polyacrylonitrile formed in the reaction was estimated from the intrinsic viscosity measurements of the graft product in the solution of dimethylformamide. The molecular weight depended only very slightly on the dose rate up to 2.1×10^6 rad/hr. (auth)

10597 (JAERI-5026, pp 46-51) RADIATION-INDUCED GRAFT COPOLYMERIZATION TO POLYESTER. IV. GRAFTING OF ACRYLIC ACID TO POLYETHYLENE TEREPHTHALATE FIBER WITH IMPREGNATION METHOD AT ROOM TEMPERATURE. Okada, Toshio; Sakurada, Ichiro (Japan Atomic Energy Research Inst., Tokyo). (In Japanese).

From Annual Report No. 3 of Osaka Laboratory for Radiation Chemistry, April 1, 1969–March 31, 1970.

Radiation grafting of acrylic acid at room temperature was studied by an impregnation method to improve the hygroscopic properties of polyester fibers. Polyester fabric was impregnated with acrylic acid or acrylic acid solution by immersion at 25 or 70°C, the impregnated fabric was irradiated under N_2 with γ rays from ^{60}Co or electron beams from a Van de Graaff accelerator at room temperature. Dimethylformamide, dimethyl sulfoxide, formic acid, and water were employed as solvents of acrylic acid for the impregnation. The highest value of the degree of grafting was only 8% at a dose of 6 to 7 Mrad in the case of impregnation with pure acrylic acid. Not only the use of a swelling agent such as dimethylformamide, dimethyl sulfoxide, or formic acid but also the use of water are effective to conduct the grafting up to 20% graft. In the case of the impregnation of a mixture of acrylic acid and water almost all polymer formed on the fabric by the irradiation could not be extracted with water at 100°C. Using aqueous solution of acrylic acid polyester fabric up to 30% apparent graft can be prepared with a graft yield greater than 90%. (auth)

10598 (JAERI–5026, pp 52-5) RADIATION-INDUCED GRAFT COPOLYMERIZATION TO POLYESTER. V. GRAFTING OF ACRYLIC ACID ONTO POLYESTER FILM WITH IMPREGNATION METHOD AT ROOM TEMPERATURE. Okada, Toshio (Japan Atomic Energy Research Inst., Tokyo). (In Japanese).

From Annual Report No. 3 of Osaka Laboratory for Radiation Chemistry, April 1, 1969–March 31, 1970.

Studies on impregnation grafting of acrylic acid on polyester film (degree of crystallinity 53%) were carried out by the irradiation of electron beams from a Van de Graaff accelerator at room temperature. Polyester films were immersed in pure acrylic acid at 20 to 70°C for 24 hr and the degree of swelling of polyester film was determined to be less than 2% at 20 to 35°C and 8 to 9% at 50 to 70°C. Polyester film was impregnated with acrylic acid at 50°C, the impregnated fabric was irradiated with electrons from a Van de Graaff accelerator at 50°C, and almost all polymer formed by the irradiation could not be extracted with water at 100°C. This indicates that the polyacrylic acid formed in the crystalline polyester matrix can hardly be extracted with water due to entanglement of their long-chain molecules between the crystalline parts of matrix polymer and is observed as apparently grafted on the polyester. (auth)

10599 (JAERI–5026, pp 56-62) RADIATION-INDUCED GRAFT COPOLYMERIZATION TO POLYESTER. VI. PROPERTIES OF ACRYLIC ACID GRAFT DRAWN POLYESTER FIBERS PREPARED BY IRRADIATION AT ELEVATED TEMPERATURE. Okada, Toshio; Sakurada, Ichiro (Japan Atomic Energy Research Inst., Tokyo). (In Japanese).

From Annual Report No. 3 of Osaka Laboratory for Radiation Chemistry, April 1, 1969–March 31, 1970.

Acrylic acid was grafted on drawn polyester fibers in acrylic acid solution in ligroin by irradiation with γ rays at 120°C and properties of the graft fibers were studied. From microscopic observation of cross-sections of dyed graft fiber, the grafting reaction seems to occur over the length and breadth of a polyester fiber when the degree of grafting is higher than 16.3% and polyacrylic acid to be distributed homogeneously throughout a fiber. Moisture regain of the grafts may be represented as a sum of moisture regains of component polyester and polyacrylic acid. The graft polyester fibers are converted to the corresponding Na or Ca salts by treatment with aqueous solutions of sodium bicarbonate or calcium acetate. The salts, especially the Na salt have enhanced hygroscopic properties. Graft fibers gave excellent acceptability toward basic, disperse, and metal complex dyes but still with poor lightfastness. The dry and wet tensile tenacity of the graft are similar to that of the original polyester fiber. The fiber melting temperature is raised from 256°C to a temperature higher than 500°C especially when the grafts are converted to Na or Ca salt. (auth)

10600 (JAERI–5026, pp 63-7) RADIATION INDUCED GRAFT COPOLYMERIZATION TO POLYESTER. VII. GRAFTING OF 2-HYDROXYETHYL METHACRYLATE ONTO POLYESTER FABRIC AS A STAIN RELEASE TREATMENT. Urakami, Motoaki; Okada, Toshio (Japan Atomic Energy Research Inst., Tokyo). (In Japanese).

From Annual Report No. 3 of Osaka Laboratory for Radiation Chemistry, April 1, 1969–March 31, 1970.

Grafting of 2-hydroxyethyl methacrylate on polyester fabrics was carried out with γ rays from ^{60}Co or electron beams from a Van de Graaff accelerator. Graft percent on irradiation at room temperature was 2%, but above 80°C the values were greater than 10% when an aqueous solution was employed for the reaction. The changes of hydrophilic properties on grafting of 2-hydroxyethyl methacrylate were studied by moisture regain, static electricity, and water contact angle measurements. Grafts with 2-hydroxyethyl metacrylate showed greater hydrophilicity than the original polyester but they were less hydrophilic than grafts of acrylic acid, as measured by moisture regain. Static electricity and water contact angle measurements showed that effective hydrophilization could be obtained with the grafts of 2 to 4%. Also grafts of 2 to 4% were found to show high release rate for oily stain. (auth)

10601 (JAERI–5026, pp 68-72) RADIATION-INDUCED GRAFT COPOLYMERIZATION TO POLYESTER. VIII. GRAFTING OF ACRYLIC ACID ONTO POLYESTER FABRIC BY ELECTRON BEAM IRRADIATION AND THE PROPERTIES OF THE GRAFT FABRIC. Urakami, Motoaki; Okada, Toshio (Japan Atomic Energy Research Inst., Tokyo). (In Japanese).

From Annual Report No. 3 of Osaka Laboratory for Radiation Chemistry, April 1, 1969–March 31, 1970.

The grafting of acrylic acid on polyester fabrics was carried out using an impregnation method. The fabrics impregnated with acrylic acid were irradiated in N_2 atmosphere at 60 to 100°C with 1.5-MeV, 50-μA electron beams from a Van de Graaff accelerator. The grafting on polyester fabric took place very smoothly in a very short irradiation time. At 100°C only 2 sec was required to obtain 25% graft. Hygroscopic properties of graft fabric were studied by moisture regain, contact angle of water, and frictional electricity measurements. Stain release property was also measured. The sodium salts of grafts are highly hydrophilic as measured by moisture regain. Fabrics with a small amount of graft such as 4% showed enhanced static dissipation in air and excellent oily stain release. Fabrics with graft greater than 4% had a good acceptability for basic dyes. (auth)

10602 (JAERI–5026, pp 73-9) UNCATALYZED GRAFTING OF ACRYLIC ACID ONTO POLYESTER FIBER. Urakami, Motoaki; Okada, Toshio; Sakurada, Ichiro (Japan Atomic Energy Research Inst., Tokyo). (In Japanese).

From Annual Report No. 3 of Osaka Laboratory for Radiation Chemistry, April 1, 1969–March 31, 1970.

It was found that not only homopolymerization but also grafting of acrylic acid took place, when drawn crystalline polyester fibers were heated without an addition of catalyst in a mixture of acrylic acid and ligroin at a temperature between 90 and 140°C. Examination of the fibers indicated that only a very small fraction of the apparent graft is truely chemically combined with the backbone polymer. The main fraction is not a graft copolymer but a homopolymer formed in the matrix of the backbone polymer and is insoluble in a solvent of the homopolymer due to molecular entanglement. Effect of temperature and monomer concentration [M] on the rates of overall polymerization and apparent graft copolymerization were studied. Activation energies in a temperature range between 100 and 130°C were for the overall polymerization at the monomer concentration [M] = 3.0 and 7.4 mole/l and for the apparent graft polymerization at the monomer concentration [M] = 7.4 mole/l, 15.7, 12.3, and 17.9 kcal/mole, respectively. The values are close to those found in conventional catalytic polymerization of acrylic acid. On the other hand the activation energy for the apparent graft polymerization at the monomer concentration of 3.0 mole/l was 28.1 kcal/mole, a value nearly the same as that for the diffusion process of disperse dyes into polyester fiber at 60 to 100°C. Up to [M] = 11.8 mole/l the rate of apparent graft polymerization was proportional to the square of the monomer concentration. The rate of the overall polymerization, which can be regarded roughly the same as that of the polymerization outside the fibers, was much more strongly dependent on monomer concentration. It suggests that the mechanism of polymerization outside and inside of the fibers are different. When γ irradiation was additionally used for the reaction, the promoting effect for the polymerization was remarkable especially when the reaction temperature was below 100°C or the monomer concentration was low. (auth)

10603 (JAERI–5026, pp 80-5) PREPARATION OF WOOD–POLYMER COMPOSITE BY IONIZING RADIATION. IV. RADIATION INDUCED POLYMERIZATION OF VINYLIDENE CHLORIDE IMPREGNATED IN LAUAN. Gotoda, Masao; Takeshita, Noboru (Japan Atomic Energy Research Inst.. Tokyo). (In Japanese).

From Annual Report No. 3 of Osaka Laboratory for Radiation Chemistry, April 1, 1969–March 31, 1970.

An investigation was undertaken to examine the radioinduced polymerization of vinylidene chloride (VDC) impregnated in lauan. Experiments were carried out in order to elucidate the effect of (1) the amount of moisture presoaked in wood (ca. 5 and 20%), and (2) type of radiations, i.e., γ rays from ^{60}Co (9.95×10^4 rad/hr) and electron beams (EB) from an accelerator (0.48 and 0.024 Mrad/sec) on polymerization in the wood and also the hygroscopic

XUM

properties of the composite thus obtained. It was found that the degree of impregnation of VDC in lauan was about the same in beech, and presoaked moisture promoted the impregnation. The conversion of VDC in lauan was nearly 100% by γ irradiation, while it was very low by EB irradiation especially at high dose rate, and the presoaked moisture did not affect the conversion in most cases except by EB with low dose rate, when strong bulking effect was observed for the composite formed. Hygroscopic properties of WPC thus prepared were shown to be generally improved. The studies on polymer loading, also proved that the required polymer loading was much reduced by presoaked moisture, especially in the case of EB with low dose rate. (auth)

10604 (JAERI–5026, pp 86-93) PREPARATION OF WOOD–POLYMER-COMPOSITE BY IONIZING RADIATION. PART V. EFFECT OF SOLVENT EXTRACTION OF WOOD AS A PRETREATMENT ON THE γ-RAY INDUCED POLYMERIZATION OF VINYLIDENE CHLORIDE IN WOOD. Gotoda, Masao; Tsuji, Tadashi; Toyonishi, Shigekazu (Japan Atomic Energy Research Inst., Tokyo). (In Japanese).

From Annual Report No. 3 of Osaka Laboratory for Radiation Chemistry, April 1, 1969–March 31, 1970.

The solvent extraction of woods as a pretreatment for the γ-induced polymerization of vinylidene chloride in wood was carried out. The extraction was effected by hot water, methanol, and benzene as solvents at 80°C. Increases in the extent of impregnation of vinylidene chloride and the reproducibility of the impregnation of the monomer were observed in the case of Yezo spruce and cedar after solvent extraction, but in the case of lauan the effect was less remarkable. The effect of extraction on polymerization in woods was remarkable when the wood specimens were long in the axial direction. Although in the case of lauan, hygroscopic properties of the wood itself were improved by benzene extraction, generally the effect of solvent extraction of wood on hygroscopic properties of wood–polymer composites was not remarkable. (auth)

10605 (JAERI–5026, pp 94-100) PREPARATION OF WOOD–POLYMER COMPOSITE BY IONIZING RADIATION. VI. IMPROVEMENT OF THERMAL STABILITY OF POLYVINYLIDENE CHLORIDE AND FLAME-RETARDANCY OF WOOD POLYVINYLIDENE CHLORIDE COMPOSITE. Gotoda, Masao; Takeshita, Noboru (Japan Atomic Energy Research Inst., Tokyo). (In Japanese).

From Annual Report No. 3 of Osaka Laboratory for Radiation Chemistry, April 1, 1969–March 31, 1970.

To improve the thermal stability of poly(vinylidene chloride) in wood, experiments were carried out to find suitable stabilizers, which did not hinder the γ-induced polymerization and retained its stabilizing ability in the final product. Among the stabilizers tested, phenylglycidyl ether was the most favorable, and the minimum required amount of addition was found to be 3% of the amount of the monomer. Wood–poly(vinylidene chloride) composites were prepared from Japanese red pine and beech to test the flame retardancy of the composites; char length, afterglow (time to cease burning), and weight loss by burning were measured. These properties were much improved with polymer loading of about 70 to 100%; a self-extinguishing property was observed even at smaller polymer loading. Finally, the tendency of smoke evolution from the lauan–PVDC composite was studied by a photometric method, with the results that more smoke was evolved from the composite than from the original wood in the lower temperature region of combustion, while the reverse was true in the higher temperature region of the combustion. (auth)

10606 (JAERI–5026, pp 101-7) RADIATION CURING OF MIXTURE OF DIALLYLPHTHALATE PREPOLYMER AND VINYL MONOMER. III. STUDIES ON ELECTRON BEAM CURING OF MIXTURE OF DIALLPHTHALATE PREPOLYMER AND MULTI COMPONENT MONOMERS, AND ITS APPLICATION TO DECORATIVE LAMINATE FOR WOOD VENEER (PART 2). Yokoyama, Kenji; Gotoda, Masao; Kodama, Takashi; Kono, Yoshimi (Japan Atomic Energy Research Inst., Tokyo). (In Japanese).

From Annual Report No. 3 of Osaka Laboratory for Radiation Chemistry, April 1, 1969–March 31, 1970.

A process was investigated for preparation of a decorative laminate on plywood by irradiation of a mixture of diallyl phthalate prepolymer and vinyl monomer on the wood in open air or in N_2 without pasting up the surface of the coating composition with plastic film. This was done to nearly simulate the conditions of a practical, high-speed continuous process of electron beam curing. However, without the presence of the plastic covering, foam formation took place. This, together with retardation of curing due to oxygen inhibition, posed serious problems. Surface-active agents, particularly MODAHURO (Nihon Monsanto Co.) were found to be most effective in producing bubble-free surfaces but caused an uneven, hammertone appearance. Oxygen concentrations in the air must be <5 mole % if curing with a dose of 6 Mrads is to be achieved. The product proved to be as good as that of a high-quality commercial laminate of polyester resin with the exception of the performance in a heat cycle test. (auth)

10607 (JAERI–5026, pp 108-20) RADIATION CURING OF MIXTURE OF DIALLYLPHTHALATE PREPOLYMER AND VINYL MONOMER. IV. STUDIES ON RADIATION (ESPECIALLY ELECTRON BEAM) CURING OF THE MIXTURE, IMPREGNATED IN WOOD, FOR PREPARING WOOD–POLYMER COMPOSITES. Gotoda, Masao; Yokoyama, Kenji; Toyonishi, Sigekazu (Japan Atomic Energy Research Inst., Tokyo). (In Japanese).

From Annual Report No. 3 of Osaka Laboratory for Radiation Chemistry, April 1, 1969–March 31, 1970.

Radiation curing of diallyl phthalate prepolymer–monomer mixture impregnated in woods (birch and beech) was developed for the purpose of preparing wood–polymer composites by electron irradiation, and studies as to the homogeneity and hygroscopic properties of the wood–polymer composites in relation to the preparation conditions were carried out. Diallyl phthalate prepolymer–acrylonitrile (1/1) mixture is easily cured by γ rays but rather difficultly by electron beams of high dose rate. In the latter case, however, it is nearly completely cured by adding benzoyl peroxide. The ratio of 1 : 1 for this mixture was found to be favorable for the curing of the mixture impregnated in wood. Homogeneity of wood–polymer composite is attained by pressure impregnation of the resin mixture. Experiments on hygroscopic properties of beech-polymer composites, prepared by using various mixtures of acrylonitrile and methyl acrylate as monomers in the impregnant mixture, show that acrylonitrile is very effective for the improvement of these properties; the dimensional stability of beech is much improved in proportion to the polymer loading. (auth)

10608 (JAERI–5026, pp 121-9) RADIATION CURING OF MIXTURE OF DIALLYLPHTHALATE PREPOLYMER AND VINYL MONOMER. V. STUDIES ON THE APPLICATION OF ELECTRON BEAM CURING OF MONOMER/DIALLYLPHTHALATE MIXTURE TO COATING ON METAL, ESPECIALLY TO SHOP PRIMER ON STEEL PANEL. Gotoda, Masao; Yokoyama, Kenji; Hiwano, Kunio; Shimoyama, Koitsu (Japan Atomic Energy Research Inst., Tokyo). (In Japanese).

From Annual Report No. 3 of Osaka Laboratory for Radiation Chemistry, April 1, 1969–March 31, 1970.

Diallyl phthalate prepolymer–vinyl monomer electron-beam-curable metal coatings were evaluated. As a constituent of vinyl monomers for this purpose, a mixture of acrylonitrile and alkyl acrylate was chosen and various organic vinyl phosphates were also employed as a comonomer to improve the adherability and corrosion inhibition of steel. A composition of diallyl phthalate prepolymer–acrylonitrile–butyl acrylate–bis(2-hydroxyethyl methacrylate) acid phosphate (50/10/40/2) with benzoyl peroxide, was found to give a suitable result in the physical properties of the cured coating. By examining several pigments, iron oxide was found to be suitable for the combination with this mixture. Electron-beam-cured coatings on steel panel, prepared from this resin mixture and iron oxide showed an excellent performance, when cured under an atmosphere with reduced O_2 concentration. Moreover, an overcoating of the so-called vinyl shipbottom paint could be applied over this cured coating. However, this cured coating is occasionally easily stripped after saltwater immersion; it seems that further improvement of the adherability of the coating is necessary. (auth)

10609 (JAERI–5026, pp 130-6) RADIATION CURING OF MONOMER–POLYBUTADIENE MIXTURE. I. FUNDAMENTAL STUDIES ON THE ELECTRON BEAM CURING OF THE MONOMER/POLYBUTADIENE MIXTURE. Gotoda, Masao; Azato, Ikuo; Takeuchi, Tamotsu (Japan Atomic Energy Research Inst., Tokyo). (In Japanese).

From Annual Report No. 3 of Osaka Laboratory for Radiation Chemistry, April 1, 1969–March 31, 1970.

To find a radiation-curable resin, monomer–oligo–1,2-polybutadiene (molecular weight 1000 to 4000) mixtures (ca. 1/1) were chosen and the effects of molecular weight of polybutadiene, kind and amount of monomer, and addition of comonomer, peroxide catalyst, and crosslinking agent were studied. Methyl acrylate was the most favorable monomer tested, and acrylic acid (and maleic acid anhydride) and trimethylolpropane trimethacrylate are effective as additives to improve the curing rate. Addition of small amounts of dicumyl peroxide also promotes the curing and increases the gel fraction. The gel formation is also influenced by the molecular weight of polybutadiene and increases linearly with it. A dose rate effect was also observed. In the case of γ irradiation, required dosage for the curing is low and gel fraction is very high. Thermal curing under suitable condition after electron-beam irradiation was found to be very effective to increase the gel fraction of electron-beam-irradiated specimen to nearly 100%. (auth)

10610 (JAERI-5026, pp 169-71) STUDIES ON RADIATION-INDUCED FREE-IONIC POLYMERIZATION BY ELECTRICAL CONDUCTIVITY MEASUREMENTS. II. STYRENE (PRELIMINARY REPORT). Hayashi, Kanae; Hayashi, Koichiro; Okamura, Seizo (Japan Atomic Energy Research Inst., Tokyo). (In Japanese).

From Annual Report No. 3 of Osaka Laboratory for Radiation Chemistry, April 1, 1969–March 31, 1970.

Free-ionic polymerization of bulk styrene was carried out at 0.25 and 40°C. Although the superdry condition was not achieved, the apparent activation energy of polymerization was tentatively estimated. A crude evaluation of activation energy for cationic propagation reaction was also made and it indicates that the propagation reaction of styrene in free cationic process may be characterized with lower activation energy as compared with that in other mechanisms while the frequency factor does not change so much in its magnitude from these in radical and free anionic mechanisms. (auth)

10611 RADIATION-INDUCED POSTPOLYMERIZATION OF TRIOXANE IN THE SOLID STATE. II. KINETIC STUDY OF RADIATION-INDUCED POSTPOLYMERIZATION OF TRIOXANE IN DRY AND HIGH-VACUUM SYSTEM. Ishigaki, Isao; Ito, Akihiko; Iwai, Tadashi; Hayashi, Koichiro (Japan Atomic Energy Research Inst., Takasaki). J. Polym. Sci., Part A-1; 8: 3061-77 (Nov 1970).

A kinetic study of the γ radioinduced postpolymerization of trioxane in the solid state has been made. Trioxane was purified by sublimation through Ag_2O and Na–K alloy in vacuo and was both irradiated and polymerized in a super-dry system under high vacuum. It was found that the initial rate of polymerization is larger than that reported previously. It is reasonably suggested that the postpolymerization of trioxane consists of two stages, i.e., a very large rate at the first stage and a relatively small one at the second stage. By using the kinetic sc' eme proposed previously, kinetic parameters at the second stage were determined. It was found that trioxane can be postpolymerized even at a temperature below 30°C with good reproducibility and that the overall activation energy of the polymerization was less than 15 kcal/mole. No chain-transfer reaction seems to occur except at low temperatures. These results are discussed in comparison with data reported previously. (auth)

10612 PARTICIPATION OF AN EXCITED MONOMER IN THE PROPAGATION REACTION OF THE γ-RAY INDUCED POLYMERIZATION OF ETHYLENE. Hagiwara, Miyuki; Okamoto, Hidemasa; Kagiya, Tsutomu (Atomic Energy Research Inst., Takasaki). J. Polym. Sci., Part A-1; 8: 3303-10(Nov 1970).

In the polymerization of ethylene, the reactivity of the growing radical produced by γ radiation was compared with that of the radical from 2,2′-azobisisobutyronitrile. The radicals produced in the polymerization at around room temperature were long-lived irrespective of the method of initiation. However, it was found that the radical produced by γ radiation became unreactive to ethylene when the reaction system was not exposed to γ rays. Irradiation with γ rays or ultraviolet light in a region below about 3900 Å was required for its chain growth. On the other hand, the radical from AIBN was always reactive, and the reactivity was little changed by γ radiation or by the presence of a trace amount of radiolysis products of ethylene. In explaining the characteristic differences between the nature of these radicals produced by two different methods of initiation, some other information on their reactivity was reviewed, and the participation of an excited ethylene in a dimer form is proposed for the propagation reaction of the γ-radioinduced polymerization. (auth)

10613 EFFECT OF SWELLING ON RADIATION-INDUCED GRAFTING OF STYRENE TO POLYETHYLENE. Machi, Sueo; Kamel, Ihab; Silverman, Joseph (Univ. of Maryland, College Park). J. Polym. Sci., Part A-1; 8: 3329-37(Nov 1970).

The radioinduced grafting of low-density polyethylene in contact with styrene solution was studied. The effects of the degree of swelling of the polymer on the rate of grafting were investigated by diluting the styrene with methanol and with n-octane. For styrene–methanol solution, the rate of grafting was found to increase with degree of swelling, passing through a maximum when the sorbed solvent reached 6.2 wt. % (70 vol % methanol in the outside solution) and decreasing thereafter. The methanol fraction of the sorbed liquid was far too small to cause precipitation of the grafted chains and inhibition of their termination rate. The dilution of styrene by octane had no effect on the swelling of polyethylene, but it decreased the grafting rate over the entire concentration range. The results are explained in terms of the concentration of sorbed monomer and the viscosity of the amorphous region of the polyethylene swollen by nonpolar liquids. Supporting evidence for the mechanism is presented in the form of grafting kinetic data as a function of dose rate ($2.8 \times 10^2 - 9.5 \times 10^4$ rad/hr), and post-irradiation grafting measurements for polyethylene in methanol–styrene (70/30 vol/vol). The data indicate that at the maximum grafting rate an optimum is achieved between a high concentration of sorbed monomer and a low viscosity for the poorly swelled polymer matrix. (auth)

10614 SULFOXIDATION OF LONG-CHAIN HYDROCARBONS WITH THE AID OF γ RADIATION. Roesinger, S. (Farbwerke Hoechst AG, Frankfurt am Main). Chem.-Ing.-Tech.; 42: 1236-9 (Oct 1970). (In German).

Mixtures of paraffins were treated with sulfur dioxide and oxygen to give the corresponding alkyl sulfonates (sulfoxidation) in an experimental system, the reaction mixtures being subjected to γ radiation from a ^{60}Co source. The space/time yield at 20°C is independent of the residence time in the reactor; however, it increases proportionally to the root of the dose rate and decreases with increasing temperature. As the gas throughput increases, the yield approaches a limiting value. (auth)

10615 ANALYTICAL METHOD APPLICABLE TO THE DETERMINATION OF INDIVIDUAL CONCENTRATIONS OF COMPONENTS, RESULTING FROM GAMMA INDUCED IODINATION OF METHANE. Vilenchich, R.; Venter, R. (McMaster Univ., Hamilton, Ont.). Can. J. Chem. Eng.; 48: 584-7(Oct 1970).

A method combining the least squares approach with the Monte Carlo technique applicable to a set of m simultaneous linear equations in n unknowns was developed to determine the n unknowns when the coefficients of the m equations are subject to a known distribution. The method was applied to the determination of the individual concentrations of components resulting from the gamma-induced iodination of methane. The concentrations calculated by this method are compared to the actual measured concentrations used during experimentation. (auth) (Canada)

10616 FORMATION OF TWO-DIMENSIONAL ORGANIC POLYMERS ON A MINERAL SURFACE. Thenk, B. K. G. (CSIRO, Melbourne). Nature (London); 228: 853-4(28 Nov 1970).

It is stated that planar organic macromolecules have attracted interest because of the unusual properties they are expected to possess, but they have proved difficult to synthesise. The polymerization of methyl methacrylate adsorbed in the interlayers of montmorillonite by means of γ-radiation was studied by Blumstein (J. Polymer Sci. A3: 2665(1965)), but the resulting interlayer polymer was resistant to the usual solvent extraction procedures and could be isolated only by dissolving out the silicate lattice with HF, a treatment liable to damage most polymers. Attempts to prepare organic sheet polymers on the surface of a synthetic calcium aluminate hydrate of composition 4CaO. Al_2O_3. × H_2O. are described. This mineral was selected because it can be made in a pure state, because it has a layer structure, and because it is capable of intercalating a wide range of organic materials, and is soluble in dilute HCl. It was found that only monomers containing polar groups were intercalated. Attempts to polymerize the interlayer monomers using conventional chemical initiators were only partially successful, but the use of γ-radiation at 2 MR/hr at a total dose of 20 MR was successful, employing benzene as extractor. Electron micrographs of polybutylene glycol dimethacrylate obtained from polymerization of the monomer in the mineral interlayers and in solution are shown, and the sheet-like structure of the former material is clearly visible, but there was a tendency to curl and fold around the edges. Other properties of the material are also described. (UK)

10617 RADIATION CHEMICAL PROCESSING, 1969. Whiting, R. Chemical Process Reviews, No. 41. Park Ridge, N. J.; Noyes Development Corporation (1969). 395p. $35.00.

Important details of processes related to the production of chemicals by radiation and based on U.S. patents issued since 1960 are presented. Information on the 252 patents is included under the following headings: polyolefins, other polymers, elastomers, hydrocarbons, organic chemicals, inorganic and organometallic compounds, and other processes. Company, inventor, and U.S. patent number indexes are also included. (J.G.B.)

10618 FUSION OF IRRADIATED LINEAR POLYETHYLENE CRYSTALLIZED BY HIGH SPEED STIRRING. Rijke, A. M.; Mandelkern, L. (Florida State Univ., Tallahassee). J. Polym. Sci., Part B; 8: 717-21(Oct 1970).

The fusion of irradiated linear polyethylene crystallized by high-speed stirring was investigated. The shapes of the fusion curves as a function of crystallization temperature and radiation dose are discussed. (D.P.O.)

10619 SPONTANEOUS GRAFTING IN THE PRESENCE OF SWELLING AGENTS. Williams, J. L.; Stannett, V. (Research

Triangle Inst., Triangle Park, N. C.). J. Polym. Sci., Part B: 8: 711-15(Oct 1970).

Under high swelling conditions and long contact times, a high degree of elasticity can be achieved with the wool–ethyl acrylate system without the use of any of the normal means of initiating grafting reactions. The grafting is essentially "spontaneous" after a long period of induction, as compared to a short induction period if the sample is preirradiated. The grafting reaction is initiated by free radical formation as a result of the strong anisotropic swelling brought about initially by water. Similar grafting behavior is obtained with cotton and rayon. (D.P.O.)

10620 GAMMA-INITIATED IODINATION OF METHANE IN THE GAS PHASE. Vilenchich, R.; Hodgins, J. W. (McMaster Univ., Hamilton, Ont.). Can. J. Chem. Eng.; 48: 588-90(Oct 1970).

Gamma radiation was used to initiate the gas-phase reaction between iodine and methane. Under appropriate conditions, the products are hydrogen iodide and the iodomethanes. The experiments were conducted over a range of temperature, concentration, and at two levels of total absorbed dose. The existence of a chain reaction is presumed, on the basis of G-values, which were as high as 7×10^3. In view of the propensity of iodine as a radical scavenger, this high efficiency might seem surprising, but may be attributable to the known autocatalytic effect of iodine in substitution reactions. (auth) (Canada)

10621 RADIATION-INDUCED GRAFT TERPOLYMERIZATION OF POLY(ETHYLENE TEREPHTHALATE). PART II. THE PRODUCTS OF GRAFT TERPOLYMERIZATION. Stolarczyk, L.; Achmatowicz-Szmajke, T. (Inst. of Nuclear Research, Warsaw). Nukleonika; 15: 267-77(1970).

The products appearing as a result of polyester grafting in aqueous solution of acryl- or methacrylamide and unsaturated dicarboxylic acids were studied. In a separated fraction of hydrolyzed polyester the functional groups, mainly amide and carboxyl groups, were determined. On the basis of data obtained from thin-layer chromatography and infrared spectrophotometry, it was stated that amides and CH_2 groups, originating probably from unsaturated dicarboxylic acids, take part in the grafting process. (auth)

Radiolysis

10622 (JAERI–5026, pp 6-10) ESR STUDY OF γ-IRRADIATED PYRIDINE–SILICA GEL SYSTEM. Nagai, Siro; Ohnishi, Shun-ichi; Nitta, Isamu (Japan Atomic Energy Research Inst., Tokyo). (In Japanese).

From Annual Report No. 3 of Osaka Laboratory for Radiation Chemistry, April 1, 1969–March 31, 1970.

The γ-irradiated pyridine–silica gel system was investigated by ESR. It was shown by use of pyridine-d_5 and deuterated silica gel that at least three kinds of radicals were produced; protonated pyridine anion 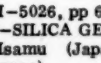 , α-pyridyl , and new species not previously reported. The ESR spectra of these species were observed in a γ-irradiated pyridine-d_5–D_2O system and have a characteristic feature that the hyperfine coupling constants of nitrogen nucleus are very large. These spectra were tentatively assigned to pyridine cation 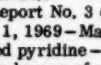 having different environments. (auth)

10623 (JAERI–5026, pp 157-60) ESR SPECTRA OF THE IRRADIATED BERYLLIUM ACETYLACETONATE SINGLE CRYSTAL. Hatada, Moyoyoshi; Nagai, Siro; Ohnishi, Shun-ichi; Nitta, Isamu (Japan Atomic Energy Research Inst., Tokyo). (In Japanese).

From Annual Report No. 3 of Osaka Laboratory for Radiation Chemistry, April 1, 1969–March 31, 1970.

Investigations were carried out on irradiated single crystals of beryllium acetylacetonate $Be(acac)_2$ to identify the species produced. The crystal irradiated at 77°K gave a double-septet ESR spectrum, which was similar to that observed for $Be(acac)_2$ powder, showing small anisotropy. The crystal irradiated at room temperature gave a well-resolved spectrum showing strong anisotropy. This spectrum is tentatively assigned to the $CH_3-CH_2-\dot{C}-C(CH_3)(=O)-Be$ radical occupying two sites of the crystal. (auth)

10624 (JAERI–5026, pp 160-4) RADIOLYSIS OF CHOLESTANOL. Takezaki, Jun'ichi; Hirota, Kozo (Japan Atomic Energy Research Inst., Tokyo). (In Japanese).

From Annual Report No. 3 of Osaka Laboratory for Radiation Chemistry, April 1, 1969–March 31, 1970.

The radiolysis of cholestanol was studied in air and in vacuum at room temperature. The total dose and dose rate dependences of products were investigated. The identified products were water, hydrogen, methane, propane, 2-methylheptane, cholestane, and 3-cholestanone. The mechanism of product formations is discussed. (auth)

10625 (JAERI–5026, pp 164-7) IRRADIATION EFFECTS OF OXYTOCIN. Sugimoto, Shun-ichi; Ohnishi, Shun-ichi; Nitta, Isamu (Japan Atomic Energy Research Inst., Tokyo). (In Japanese).

From Annual Report No. 3 of Osaka Laboratory for Radiation Chemistry, April 1, 1969–March 31, 1970.

Effects of γ-radiation on oxytocin were studied by ESR. The main ESR spectrum at both −196°C and room temperature consists of the same doublet (splitting 20.3 G measured at −196°C). The radical for this doublet can be assigned to the glycine radical, $(-NH-\dot{C}H-COONH_2)$. Radical accumulation curves were measured in various environments. Initial G_R values of the radical formation were 2.1 and 3.4 at −196°C and room temperature, respectively. Decay curves of the radical and the doublet splitting in the intact oxytocin and in the performic acid-treated oxytocin were different, reflecting difference in the molecular motion in the solid. (auth)

10626 (KFK–1285) RESONATOR FOR X-BAND ELECTRON SPIN RESONANCE SPECTROSCOPY FOR SIMULTANEOUS MEASUREMENT AND ELECTRON RADIATION OF THE SAMPLE. Mueller, O. (Kernforschungszentrum, Karlsruhe (West Germany). Labor fuer Elektronik und Messtechnik). Sep 1970, 42p, (In German). Dep. NTIS (U. S. Sales Only).

The design of a special resonator for electron spin resonance spectroscopy is described. It permits electron irradiation of the sample and measurement of the ESR signal simultaneously. In commercial ESR measurement resonators, sample measurements can be made only under irradiation with visible or ultraviolet light and with gamma quanta. However, in electron irradiation the magnetic field must be turned off, i.e., measurement and irradiation are possible only alternately. The measuring resonator described was designed for ESR measurement and electron irradiation of the sample at the same time. It permits the simultaneous production and measurement of free radicals during the process of irradiation. In two resonators of the H_{102} mode of oscillation the frequencies were 9.428 Gc/s and 9.401 Gc/s, reaching a maximum Q of 4500. This development was carried out for ESR measurement of transient free radicals. (auth)

10627 (NYO–2499-37) EFFECTS OF MERCAPTANS AND DISULFIDES ON PHOTOCHEMICAL AND HIGH ENERGY RADIATION INDUCED REACTIONS. Progress Report. Cohen, Saul G. (Brandeis Univ., Waltham, Mass. Dept. of Chemistry). 1 Nov 1970. Contract AT(30-1)-2499. 21p. Dep. NTIS.

Studies were made on the ^{60}Co γ irradiation of 0.1 and 0.01 M sec-bulytamine in water and the solutions were analyzed for 2-butanol and 2-butanone. The results indicated that the radiolysis converts the amine to the ketone and ammonia, the ketone is reduced to the alcohol. Some experiments were also carried out on irradiation of aqueous diisopropylamine in presence and absence of 2-mercaptoethanol. In the absence of mercaptan, acetone and 2-propanol were found in approximately equal quantities initially, with 2-propanol exceeding acetone after irradiation for 1 hr. In the presence of mercaptan, acetone was depressed to about 0.1 the concentration in the absence of mercaptan, and 2-propanol appeared little affected. Studies were also made on photoreduction in aqueous systems. Data are given on the photoreduction and quenching of 0.003 M fluorenone by para-substituted dimethylanilines in benzene. (P.C.H.)

10628 γ RADIOLYSIS OF LIQUIDS AT HIGH PRESSURES. IX. CYCLOPENTANE AND ITS SOLUTIONS WITH N_2O, ND_3, AND C_2H_5OD. Hentz, Robert R.; Brazier, David W. (Univ. of Notre Dame, Ind.). J. Chem. Phys.; 54: 554-8(15 Jan 1971).

The γ radiolysis of cyclopentane and its solutions with N_2O, ND_3, and C_2H_5OD was studied at room temperature at pressures in the range 0 to 6.2 kbar. For pure cyclopentane at 1 atm (0 kbar), $G(H_2)$ = 5.2, G(bicyclopentyl) = 1.3, G(cyclopentene) = 3.0, and G(pentene-1) = 0.70. The yields of hydrogen and bicyclopentyl were independent of pressure. The yields of cyclopentene and pentene-1 decreased with increase in pressure, and at 6.2 kbar both yields were ~10% smaller than the values at 1 atm. Yields of several unidentified minor products ($G < 0.1$ at 1 atm) showed the largest pressure dependence. Such results are discussed in terms of possible effects of pressure on competitive decay modes of cyclopentane excited states, and $\Delta V^{\ddagger}$(disproportionation) – $\Delta V^{\ddagger}$(com-

bination) for cyclopentyl radicals was estimated to lie in the range 0 to 1 ml mole^{-1}. For 0.06M N_2O solutions, the observed pressure independence of $G(N_2) = 3.0$ and $G(H_2) = 3.7$ indicated no effect of pressure on the yield of scavenged electrons. For both 0.006M ND_3 and 0.32M C_2H_5OD solutions, $G(H_2 + HD + D_2) = 5.2$ at all pressures. However, for both solutions, G(HD) increased with increase in pressure and at 6.2 kbar was ~35% larger than the value at 1 atm. The increase in G(HD) with pressure was attributed to an increase in the yield of cations scavenged from geminate cation–electron pairs. Such an effect of increased pressure can be understood in terms of a viscosity-independent decrease in the electron diffusion coefficient (via an effect on the depth and concentration of electron traps) or an increase in the positive-charge diffusion coefficient (via an enhancement of positive-hole conduction). (auth)

10629 RADIOLYSIS OF CHLOROFORM VAPOR. EFFECTS OF PHASE ON THE ARRHENIUS PARAMETERS OF THE HYDROGEN-ATOM ABSTRACTION REACTION OF DICHLOROMETHYL RADICALS WITH CHLOROFORM. **Dickey, Leland C.; Firestone, Richard F. (Ohio State Univ., Columbus). Contract AT(11-1)-1116. J. Phys. Chem.; 74: 4310-13(10 Dec 1970).**

The products of the radiolytic decomposition of air-free $CHCl_3$ vapor were the same as those formed in the radiolysis of liquid $CHCl_3$, except that CCl_4 was not formed in the irradiated vapor under conditions of the experiments. The effects of irradiation temperature on the rates of formation of major organic products were also the same as in the liquid phase. An interpretation of data based upon assumption of the homogeneous liquid phase radiolysis mechanism provided values of $A/A_c^{\frac{1}{2}}$ and $E - E_c/2$ for the reaction, $CHCl_2\cdot + CHCl_3 \rightarrow CH_2Cl_2 + CCl_3\cdot$, equal to 8.1 (±0.4) × 10^{-10} (cc molecule^{-1} sec^{-1})$^{\frac{1}{2}}$ and 6.4 ± 0.5 kcal mol^{-1}, respectively. The cross-combination ratio for $CHCl_2$ and CCl_3 radicals was equal to 2.1 ± 0.1 at 79 to 100°. Estimates of absolute values of the Arrhenius parameters indicated that the activation energy of the abstraction reaction is the same in both phases, but that the frequency factor is an order of magnitude smaller in the liquid phase. (auth)

10630 REACTIONS OF ELECTRONS AND FREE RADICALS IN GLASSY ETHANOL. **Fujii, S.; Willard, J. E. (Univ. of Wisconsin, Madison). J. Phys. Chem.; 74: 4313-19(10 Dec 1970).**

Experiments designed to increase understanding of the mechanisms of trapping and reaction of electrons and free radicals in γ-irradiated glassy ethanol at 77°K are reported. They show that the concentration of electrons grows with increasing γ dose to a maximum at 6×10^{20} eV g^{-1} and then decreases, accompanied by a decrease in G(free radicals). Free radicals are produced during thermal decay of trapped electrons, as well as by photobleaching. There is a blue shift in the optical absorption spectrum (λ_{max} 535 nm) of trapped electrons during thermal decay and also during photobleaching with 650-nm radiation, but not with 540 nm. Prolonged annealing of C_2H_5OH glass at 90°K prior to γ irradiation alters the available trapping sites in such a manner that the trapped electron spectrum is shifted to the red, the yield is reduced, and the decay rate is increased. CH_3CHOH radicals produced in the radiolysis decay by second-order kinetics. Parallel growth and decay of the ESR free-radical signal and absorption at 200 nm are consistent with the conclusion that the latter is in part attributable to free radicals. (auth)

10631 PHENYL AND HYDROXYPHENYL RADICALS. PULSE RADIOLYSIS STUDY OF THEIR SPECTRA AND REACTIVITY. **Cercek, B.; Kongshaug, M. (Christie Hospital and Holt Radium Inst., Manchester, Eng.). J. Phys. Chem.; 74: 4319-22(10 Dec 1970).**

The optical absorption spectra of the phenyl, $C_6H_5\cdot$, and hydroxyphenyl radicals, $HOC_6H_4\cdot$, in aqueous solutions have been obtained. Their spectra resemble those of benzene and phenol in water, but the absorptions are more intense, e.g., the molar extinction coefficients are $\epsilon(C_6H_5\cdot) = 630$ M^{-1} cm^{-1} at 260 nm and $\epsilon(HOC_6H_4\cdot) = 1950$ M^{-1} cm^{-1} at 275 nm. The following rate constants have been measured: $k(C_6H_5\cdot + C_6H_5I) = 7 \times 10^1$ M^{-1} sec^{-1} and $k(HOC_6H_4\cdot + HOC_6H_4Br) = 7 \times 10^7$ M^{-1} sec^{-1}. (auth)

10632 RADIOLYSIS OF ETHANE. II. LIQUID PHASE AT 195°K; EFFECT OF ELECTRON AND POSITIVE ION SCAVENGERS. **Holland, P. T.; Stone, J. A. (Queen's Univ., Kingston, Ont.). Can. J. Chem.; 48: 3277-81(1 Nov 1970).**

H atoms and $\cdot C_2H_5$ radicals in the radiolysis of liquid ethane have both ionic and nonionic precursors. The use of SF_6 as an electron scavenger leads to very low C_2H_4 yields which is consistent with the addition of $\cdot SF_5$ radicals to this product. H and D atoms produced by neutralization of ND_3H^+ can either add to C_2H_4 or abstract from C_2H_6 at 195°K. (auth) (Canada)

10633 IONIC REACTIONS OCCURRING IN THE IRRADIATION OF CARBON DIOXIDE–OXYGEN MIXTURES AT VERY HIGH DOSE RATES. **Willis, Clive; Bindner, P. E. (Atomic Energy of Canada Ltd., Chalk River, Ont.). Can. J. Chem.; 48: 3463-72(15 Nov 1970).**

Ozone yields were measured in CO_2–O_2 mixtures irradiated with single pulses from a Febetron 705 at a dose rate of 10^{20} eV g^{-1} s^{-1}. Low concentrations of carbon dioxide in oxygen rapidly reduced the yield from $G(O_3) = 12.8$ to $G(O_3) \approx 9$. At 300 torr total pressure, as the oxygen concentration was reduced, the ozone yield decreased from this yield of $G(O_3) \approx 9$ to an extrapolated yield, at zero oxygen, of close to $G(O_3) = 7.8$. Changes of yields with composition are explained in terms of ionic reactions, the main neutralization process being $O_2^+ + CO_4^- \rightarrow O + 2O_2 + CO$. At 700 to 1500 torr total pressure, the ozone yields were lower than that at 300 torr. It is proposed that clustering of the ionic species affects the products of the neutralization reaction. Sulfur hexafluoride suppresses the dissociative neutralization reaction and ozone yields from mixtures containing 1.5–2% SF_6 are those predicted from direct neutral dissociation processes in the pure gases. Computer calculations are used to compare the experimental results to the proposed mechanism and, in general, a good fit is obtained. (auth) (Canada)

10634 STABILITY OF PHENOPLAST MOLDING MATERIALS TOWARDS HIGH-ENERGY RADIATION. **Gilfrich, H.-P. (Chemische Werke Albert, Wiesbaden, Ger.); Wilski, H. Chem.-Ing.-Tech.; 42: 1231-3(Oct 1970). (In German).**

Phenoplast molding materials of Types 11, 15, 31, and 74 were irradiated in the absence of air with doses of up to 1,000 Mrad and in the presence of air at low dose rates (ca 1500 rad/h) with a dose of up to 32 Mrad. The molding compounds containing inorganic fillers (Types 11 and 15) proved very resistant to radiation, measured on the basis of tensile strength changes in samples, while Types 31 and 74 (with organic fillers) suffered considerable radiation damage, particularly in presence of atmospheric oxygen. (auth)

10635 RADIOLYTIC BEHAVIOR OF FERROUS AND FERRIC IONS IN VERY DILUTE SOLUTIONS. **Muller, J. C.; Ferradini, C. (Laboratoire Curie, Paris). Radiochem. Radioanal. Lett.; 5: 171-4(15 Dec 1970). (In French).**

Dilute acid solutions of iron (2×10^{-3} M, pH = 2.3) have been exposed to ^{60}Co γ rays. Reduction of ferric ions has been followed to the establishment of a stationary state. A qualitative interpretation of the results assumes competition between ferrous and ferric ions for the capture of H radicals. (auth)

10636 YIELD OF HYDROGEN PEROXIDE IN AERATED ACIDIFIED WATER EXPOSED TO TRITIUM β RAYS. **Lemaire, G.; Ferradini, C. (Laboratoire Curie, Paris). Radiochem. Radioanal. Lett.; 5: 175-8(15 Dec 1970). (In French).**

The yield of hydrogen peroxide obtained in aqueous 0.4 M H_2SO_4 exposed to tritium β rays was found to be $G_i(H_2O_2) = 1.5 \pm 0.01$. This value was one-half the yield of Ce(III) formed under the same conditions in a solution of 2×10^{-3} M Ce(IV). $\{G_i\,[Ce(III)] = 2.96 \pm 0.1\}$. (auth)

10637 FREE RADICALS PRODUCED BY GAMMA IRRADIATION IN THE BICYCLO[2,2,1]HEPTANE SERIES. **Gloux, J.; Guglielmi, M.; Lemaire, H. (CEN, Grenoble, France). Mol. Phys.; 19: 833-52(Dec 1970). (In French).**

Above the solid–plastic transition point, well-resolved ESR spectra are recorded when globular compounds are irradiated by γ-rays. The free radicals observed after γ-irradiation of 15 derivatives of bicyclo[2,2,1]heptane and eight deuterated homologues were studied. The ESR spectra are analysed; they are consistent with the appearance of a free valence localized on one carbon of the cyclohexane ring (C2 for the hydrocarbons, alcohols and chlorides, C3 for the ketones). A strong inequivalence for the β-proton couplings was noted and this is explained by a non-planarity of the three bonds surrounding the free radical centre; the deviation from planarity is estimated to be 20 to 30°. Strong hyperfine interactions were observed with γ-protons. Such long range interactions are inconsistent with the saturated model where spin density is transmitted by spin polarization of localized bonds; they are specific to the unsaturated character of bicyclic compounds which have an enhanced delocalization of the unpaired electron. (auth) (UK)

10638 EPR SPECTRA AND ELECTRONIC STRUCTURE OF SOME BICYCLIC RADICALS. **Marx, R.; Bonazzola, L. (Faculte des Sciences, Orsay, France). Mol. Phys.; 19: 899-909(Dec 1970). (In French).**

The ESR spectra of two new bicyclic hydrocarbon radicals produced by ^{60}Co γ irradiation of bicyclo[2.2.2]oct-2-ene and bicyclo-[2.2.1]heptane were studied. The main features were: long-range a_γ couplings still greater than in bicyclo[2,2,2]octane (6.3 and 15.1 gauss); inequivalence of the two β methyl proton coupling constants

$a_\beta^{CH_3}$; a_α^H coupling constants close to the usual hydrocarbon radicals. These results may be accounted for by a π-type radical (unpaired electron in a pure p_z orbital of the unsaturated carbon atom) slightly twisted around the C_1C_4 axis of the molecule. The rather low spin density on the trigonal carbon atom and the high value of the long-range coupling constants may be due to a partly unsaturated structure of these molecules, allowing some delocalization of the unpaired electron. (auth) (UK)

10639 AROMATIC ANIONS AND FREE RADICALS IN THE PULSE RADIOLYSIS OF AQUEOUS SOLUTIONS OF BENZONITRILE. Chutny, B. (Nuclear Research Inst., Rez, Czech.); Swallow, A. J. Trans. Faraday Soc.; 66: 2847-54(Nov 1970).

Studies were made on short-lived molecular species produced in aqueous benzonitrile solutions by electron-pulse radiolysis. It was found that hydrated electrons, hydrogen atoms, and hydroxyl radicals react with benzonitrile with rate constants of 1.7×10^{10}, 3.1×10^8, and 8.5×10^9 M^{-1} s^{-1} respectively. In alkaline solutions the hydrated electrons form an anion with a sharp absorption maximum at 315 nm and a broad one at 400 nm. This anion protonates with pK_a 7.2 and at pH 4 the reduced species present has an absorption maximum near 300 nm. A different form of the reduced species is seen at pH 3. In strongly acid solutions, H atoms add to benzonitrile yielding a mixture of isomers exhibiting an absorption maximum at 348 nm. Hydroxyl radicals (in neutral solution) add to benzonitrile yielding adducts showing an absorption maximum at 343 nm. The various adducts disappear in second-order reactions, with $2k = 1.1 \times 10^9$ M^{-1} s^{-1} for mutual reactions of H adducts and for reactions of H adducts with OH adducts. (auth) (UK)

10640 RADIOLYSIS OF GASEOUS ISOBUTENE BY ^{60}Co γ RAYS. III. LOW BOILING POINT CONDENSATION PRODUCTS. Herman, Jan A. (Univ., Laval, Quebec). Can. J. Chem.; 48: 3446-9(1 Nov 1970).

During the γ-ray irradiation of gaseous isobutene the following low-boiling-point condensation products are formed: 2-methyl-1-butene, 2-methyl-2-butene, 1,1-dimethylcyclopropane, 3-methyl-1-butene, neopentane, isopentane, and n-pentane. All these proudcts are formed in radical processes, as shown by the scavenging action of nitric oxide. The formation of the pentanes results from the reaction of the methylene radical with isobutene, whereas the reaction of the methyl radical with the monomer accounts for the production of pentanes. (auth) (Canada)

10641 STUDY OF THE STABILITY AND RADIOCHEMICAL PURITY OF SOME RADIOPHARMACEUTICALS. 2. LABELLED CHLORMERODRIN. Burianek, J.; Cifka, J. (State Inst. for Control of Drugs, Prague). J. Label. Compounds; 6: 224-39 (Jul-Sep 1970).

The chromatographic behavior of chlormerodrin and its radiochemical impurities was studied in various solvents. The main product of thermal decomposition of chlormerodrin was identified as 3-chloromercuri-2-hydroxypropylurea. The thermal decomposition of chlormerodrin is accelerated by the presence of theophylline and suppressed by sodium chloride. The main product of radiation decomposition of chlormerodrin is inorganic mercury. The yield of radiation decomposition was studied as a function of the concentration of chlormerodrin. The radiation decomposition of chlormerodrin is not essentially influenced by the presence of some other substances, however these substances can under certain circumstances support the formation of 3-chloromercuri-2-hydroxypropylurea as the product of the radiolysis. (auth)

10642 STUDY OF THE STABILITY AND RADIOCHEMICAL PURITY OF SOME RADIOPHARMACEUTICALS. 3. LABELLED DIIODOFLUORESCEIN. Rybakow, Z.; Cifka, J. (Nuclear Research Inst., Rez, Czech.). J. Label. Compounds; 6: 240-9(Jul-Sep 1970).

The thermal and radiation stability of diiodofluorescein was studied. The decomposition products were separated by paper chromatography. Inorganic iodine, mono-, tri- and tetrafluorescein were found as thermal decomposition products of diiodofluorescein. In addition, fluorescein and two unidentified compounds were separated from gamma-irradiated solutions of diiodofluorescein. The yields of radiation decomposition of diiodofluorescein and formation of monoiodofluorescein and inorganic iodine were estimated as a function of the concentration of diiodofluorescein. (auth)

10643 ABSORPTION SPECTRA AND KINETICS OF THE INTERMEDIATE PRODUCED FROM THE DECAY OF AZIDE RADICALS. Hayon, E.; Simic, M. (Army Natick Labs., Natick, Mass.). J. Amer. Chem. Soc.; 92: 7486-7(16 Dec 1970).

Azide ions in aqueous solution undergo a one-electron oxidation mechanism on reaction with hydroxyl radicals. This reaction was studied by generating OH radicals in the pulse radiolysis of aqueous solutions in the presence of 1 atm of nitrous oxide to convert >98% of e_{aq}^- to OH radicals. The spectra and structure of products are discussed. (M.C.G.)

10644 LOW-ENERGY ELECTRON RADIOLYSIS OF GASEOUS METHANE, ETHANE, AND ETHYLENE. Finney, Clifton Donald. Manhattan, Kans.; Kansas State Univ. (1970). 98p. University Microfilms Order No. 70-16,628.

Thesis.

Methods were developed to study and interpret the low-energy electron radiolysis of some simple gas phase organic systems. Two, high-flux, low-cathode-area photoelectron sources were developed. Product yields and ion currents were measured as a function of electron energy under single impact combinations for methane, ethane, and ethylene reactants. Results were obtained for product yields, total ionization cross sections, and reaction thresholds. For each reactant gas, products were observed above and below the ionization potential. With some reactants more than one product energy threshold was observed. Lowest product thresholds were 6.7, 6.4, and 3.3 eV for CH_4, C_2H_6, and C_2H_4 reactants, respectively. Acetylene was the product analyzed with ethylene reactant, and its very low appearance threshold of 3.3 eV suggests a primary triplet transition. The acetylene product yield with methane reactant declines to zero with the ion current and is interpreted as arising collectively from ionic, very-high-energy neutral, and superexcited primary processes. Results of this study are compared with those of a study on the low-energy solid-phase radiolysis of ethylene previously performed. Three salient features with respect to the energetics were found in the solid-phase system. The product distribution did not change within experimental error over the initial impacting energy range of 8.7 to 48.7 eV. The total cross sections for product formation were smaller than those observed in this gas study by about two orders of magnitude. The total G-values (product molecules per 100 eV absorbed) found in the solid phase study were about five times lower than those observed in the high-energy liquid-phase radiolysis and lower by a factor of ten for similar gas-phase studies. A qualitative model assuming approximate gas-phase excitation and ionization probabilities and complete energy deposition in the solid phase suitably accounts for the solid-phase observations. The constancy of the product distribution with energy is interpreted to mean the neutral excitation processes dominate. The model shows that ionization, even at the highest initial electron energies, is never a very probable process. The low G-values are the result of efficient solid phase quenching of the excited ethylene and a density effect causes the low cross section. (Diss. Abstr. Int., B)

10645 SATURATION PHENOMENA OF ELECTRON SPIN RESONANCE OF FREE RADICALS IN IRRADIATED CARBOHYDRATES. Neubacher, H. (Justus Liebig Univ., Giessen, Ger.). Biophysik; 7: 47-54(1970). (In German).

Saturation measurements of the electron spin resonance spectra of radioinduced free radicals in several carbohydrates are described. A saturation parameter is defined, which is applicable both in the cases of homogeneous and inhomogeneous line broadening. This saturation parameter is used for assessing relative changes of relaxation times. The saturation parameter was measured as a function of temperature and radical concentration. It may be concluded from the results obtained that a pronounced intermolecular energy transfer exists in carbohydrate crystals. (auth)

10646 EFFECT OF GAMMA RADIATION ON ION EXCHANGE RESINS. II. INVESTIGATION OF THE EFFECT OF GAMMA RADIATION ON ZEROLIT FF-IP BY THE IR-METHOD. Narebska, Anna; Basinski, Antoni; Litowska, Maria (Nicholas Copernicus Univ., Torun, Poland). Nukleonika; 15: 177-87(1970).

The radiation decomposition of the matrix of the anion exchange resin Zerolit FF-IP was investigated by the infrared spectrophotometric method. It was found that, in the irradiated resin, degradation of the chains following irradiation oxidation occurs and new groups, unsaturated bonds and further substituted benzene rings, appear. The data point to the significant participation of water radiolysis products in the irradiation decomposition of the resin. (auth)

10647 PROTECTIVE EFFECT OF ETHANOL AND POTASSIUM IODIDE ON THE RADIOLYSIS OF INDOLE-3-ACETIC ACID IN AQUEOUS SOLUTION. Yamaguchi, Hikoyuki; Miura, Kyoko (Tokyo Univ.). Radioisotopes (Tokyo); 19: 570-3(Dec 1970).

Aqueous solutions of IAA (indole-3-acetic acid) in the presence or the absence of oxygen were irradiated with ^{137}Cs gamma radiation. The apparent oxygen effect on the loss of biological activity of IAA was not observed. As the concentration of IAA was increased, a smaller proportion was affected. Both ethanol and potassium iodide protected almost completely the radiolysis of

IAA irradiated in aqueous solution. It was concluded that OH· radicals produced in the aqueous solution must produce damage to IAA. (auth)

10648 TRAPPED ELECTRONS AND FREE RADICALS IN γ-IRRADIATED ETHANOL GLASSES. Bernas, A. (Faculte des Sciences de Paris, Orsay, France); Grand, D.; Chachaty, C. J. Chem. Soc., D; No. 24, 1667-8(23 Dec 1970).

The absorption spectrum and extinction coefficients of trapped electrons and $CH_3\dot{C}HOH$ in γ-irradiated glassy ethanol were determined down to 210 nm and, by optical bleaching, the photodetachment threshold of the electrons was found to be about 2.3 eV. (auth (UK)

10649 γ-RADIOLYSIS OF AQUEOUS SOLUTIONS OF SODIUM SULFIDE. Natroshvili, G. R. (Inst. of Inorganic Chemistry and Electrochemistry, Tbilisi, USSR). Soobshch. Akad. Nauk Gruz. SSR; 59: 337-9(Aug 1970). (In Russian).

The products from the γ radiolysis of sodium sulfide in dilute aqueous solutions have been investigated. The formation of thiosulfates, sulfites, and molecular hydrogen has been established. The role of radiolytic products of water in the transformation of sulfide ion has been determined. (auth)

10650 MECHANISM OF BENZENE FORMATION IN THE RADIATION-INDUCED AND PHOTOCHEMICAL REACTIONS OF ACETYLENE. Shida, Shoji; Tsukada, Masao; Fujisaki, Noboru; Oka, Takefumi (Tokyo Inst. of Tech.). Bull. Chem. Soc. Jap.; 43: 3314(Oct 1970).

The distribution of isotopic benzenes formed in equimolar $C_2H_2-C_2D_2$ mixtures in radiation-induced and photochemical reactions of acetylene are given. The results suggest that benzene is formed by the same mechanism irrespective of the active rays. (D.P.O.)

10651 DISSOCIATION OF WATER VAPOUR BY PHOTOLYTIC, RADIOLYTIC, AND ELECTRON IMPACT METHODS. Dixon, R. S. (Whiteshell Nuclear Research Establishment, Pinawa, Manitoba). Radiat. Res. Rev.; 2: 237-96(Nov 1970).

This review encompasses studies of water vapor by the following methods: photochemistry, electron impact and mass spectrometry, and radiation chemistry. Despite limitations, both photochemistry and mass spectrometry have provided a source of background information that has made the elucidation of many gas-phase radiation-chemical problems somewhat simpler. This is adequately demonstrated for water vapor in the present review. (382 ref.) (D.P.O.)

10652 SCAVENGEABLE ELECTRON YIELD IN THE RADIOLYSIS OF LIQUID AND SOLID HYDROCARBONS. Kimura, Toyoaki; Fueki, Kenji; Kuri, Zen-ichiro (Nagoya Univ., Japan). Bull. Chem. Soc. Jap.; 43: 3090-5(Oct 1970).

Yields of scavenged electrons were measured in MCH (methylcyclohexane), 3MP (3-methylpentene), cumene, and tert-butylbenzene at 20 and −196°C. The yield of scavenged electrons is considerably lower at −196°C in the glassy state than at 20°C in the liquid state. The temperature effect on electron scavenging indicates that the difference in the yields of scavenged electrons between the liquid and glassy states is attributed to the variation not of temperature but of the physical conditions of the matrix. The effect of composition was also investigated in MCH−MTHF (methyltetrahydrofuran) mixtures along with the effect of the viscosity of the matrix on the yield of scavenged electrons at −196°C which led to the assumption that the extent of interactions between thermalized electrons and the matrix would affect the yield of scavenged electrons at −196°C. Since such interactions may be related to the mean free path of electrons, the contribution of the electron jump distance to the electron scavenging efficiency was calculated. The calculated results appear to explain qualitatively the experimental results. (auth)

Radioisotope Production

Refer also to abstracts 10674 and 10676.

10653 (BLG-442) DEVELOPMENT OF TECHNIQUES FOR PRODUCTION OF ^{131}I. Constant, R. (Centre d'Etude de l'Energie Nucleaire, Brussels (Belgium)). May 1970. 25p. (In French). Dep. NTIS (U. S. Sales Only).

A review is presented on methods developed since 1938 for the production of ^{131}I. The most important existing patents (20) are listed. (60 references) (P.C.H.)

10654 (ORNL-4588) TRANSURANIUM PROCESSING PLANT SEMIANNUAL REPORT OF PRODUCTION, STATUS, AND PLANS FOR PERIOD ENDING JUNE 30, 1970. Burch, W. D.; Bigelow, J. E.; King, L. J. (Oak Ridge National Lab., Tenn.). Jan 1971. Contract W-7405-eng-26. 35p. Dep. NTIS.

The total amounts of transuranium elements recovered during the period January 1, 1970, through June 30, 1970, are: 4.6 g of ^{242}Pu, 1.9 g of ^{243}Am, 34.5 g of ^{244}Cm, 3.8 mg of ^{249}Bk, 40.7 mg of ^{252}Cf, 298 μg of ^{253}Es, and 4×10^8 atoms of ^{257}Fm. Sixty-three shipments were made, which contained the following total amounts of nuclides: 2.3 mg of ^{244}Pu that had been isotopically enriched in a calutron and then irradiated in the HFIR prior to shipment; 26.48 g of ^{243}Am and 14.45 g of ^{244}Cm that had been separated and purified; a mixture of 5.1 g of ^{243}Am and 5.58 g of ^{244}Cm; 376.3 μg of ^{248}Cm; 3.6 mg of ^{249}Bk; 220 μg of isotopically pure ^{249}Cf; 161 μg of high-purity ^{250}Cf that was produced by irradiating ^{249}Bk in the HFIR hydraulic rabbit facility; 12.3 mg of ^{252}Cf in a mixture of californium isotopes; 259 μg of ^{253}Es in a mixture of einsteinium isotopes; 36 μg of isotopically pure ^{253}Es; and 3.7×10^8 atoms of ^{257}Fm. An unused cell in the TURF facility was equipped for purification and encapsulation of californium. The primary purpose of this cell is to provide a ^{244}Cm-free environment so that extremely pure ^{248}Cm may be recovered from aged ^{252}Cf neutron sources. A hydraulic rabbit tube was installed to permit the rapid transfer of small amounts of irradiated materials from the HFIR pool to a shielded cave in an alpha laboratory in TRU. Seven neutron sources were fabricated. About 155 μg of ^{250}Cf (isotopic purity, 87%) was produced for use as a target for transactinide element production in the Berkeley HILAC and about 6 μg of ^{250}Cf (isotopic purity, ~94%), part of which was sent to the Los Alamos Scientific Laboratory for use in fission cross-section studies. The values currently being used for transuranium-element decay data and for cross-section data in planning irradiation-processing cycles, calculating production forecasts, and assaying products are tabulated in the Appendix. (auth)

Separation Processes

Refer also to abstracts 10446, 10580, 11046, 11066, and 12520.

10655 (ANL-7751) ANION-EXCHANGE SEPARATION OF NEPTUNIUM FROM URANIUM AND THORIUM IN BASIC SOLUTION. Masino, A. P.; Orlandini, K. A.; Fried, S.; Cohen, D. (Argonne National Lab., Ill.). Oct 1970. Contract W-31-109-eng-38. 12p. Dep. NTIS.

The anion-exchange behavior of neptunium, uranium, plutonium, thorium, and several accompanying elements has been studied in an aqueous tetramethylammonium hydroxide (TMAH) medium and in this same basic medium containing various complexing agents. It has been found that the neptunium in the +5 oxidation state is not retained by Dowex-1 × 8 resin from slightly basic TMAH−citrate solution and is readily separated from uranium and thorium, which are retained by a column of this resin. (auth)

10656 (BM-IC-8502) METALLURGICAL APPLICATION OF SOLVENT EXTRACTION (IN TWO PARTS). 2. PRACTICE AND TRENDS. Rosenbaum, Joe B.; George, D. R.; May, Joan T. (Bureau of Mines, Salt Lake City, Utah. Salt Lake City Metallurgy Research Center). Jan 1971. 19p.

New applications and concepts of solvent extraction as a unit operation in extractive metallurgy have been developed in the last decade. Wider use is being made of established solvent extraction techniques in processing spent nuclear fuel elements and in winning columbium−tantalum, hafnium−zirconium, thorium, tungsten, uranium, and vanadium. Commercial application has been extended to recovery of beryllium, boron, bromine, copper, molybdenum, phosphorus, rare earth metals, and rhenium. Systems in use and proposed typically extract metals or salts as anion, cation, or neutral species from aqueous media by reaction with a recycleable organic reagent. (34 references). (auth)

10657 (BM-RI-7471) RECOVERY OF URANIUM FROM NATURAL MINE WATERS BY COUNTERCURRENT ION EXCHANGE. Ross, J. R.; George, D. R. (Bureau of Mines, Salt Lake City, Utah. Salt Lake City Metallurgy Research Center). [1971]. 17p.

Recovery of uranium from slightly alkaline mine water, available in the Ambrosia Lake district of New Mexico, was studied using countercurrent ion exchange columns developed by the Bureau of Mines. Approximately 5 million gallons of mine water containing 9 to 12 ppM U_3O_8 was treated by ion exchange using a 14-inch-diameter absorption column composed of five or six compartments each 4 feet deep. Uranium recoveries averaged in excess of 98% at solution flows ranging from 15 to 25 gallons per square foot per minute and resin loadings up to 3.6 pounds of U_3O_8 per cubic foot. In subsequent tests, loaded resin was continuously eluted in a countercurrent elution column with a diameter of 4 inches and con-

taining a bed of resin 9 feet deep. The resin was eluted to a residual loading of less than 0.06 pound of U_3O_8 per cubic foot, at a resin-retention time of 224 minutes, using only 1.9 volumes of 1.1 M NaCl–0.05 M $NaHCO_3$ solution per volume of resin. Compared with existing ion exchange practices for recovering uranium from mine waters in the Ambrosia Lake district of New Mexico, use of these improved ion exchange contactors would reduce ion exchange resin requirements at least 70% and allow further substantial reductions in capital and operating costs. (auth)

10658 (BNWL–1533) RESEARCH AND DEVELOPMENT ACTIVITIES FIXATION OF RADIOACTIVE RESIDUES. Quarterly Progress Report, August–October 1970. Blasewitz, A. G. (ed.) (Battelle-Northwest, Richland, Wash. Pacific Northwest Lab.). Nov 1970. Contract AT(45-1)-1830. 32p. Dep. NTIS.

The full level radioactive demonstrations were successfully completed in WSEP with the ninth pot solidification demonstration. A total of 33 runs was made in which 52 million curies of radionuclides were converted to solids. During the report period, the seventh, eighth, and ninth pot solidification demonstration runs in WSEP were completed. During Runs PC-7 and PC-8, simulated Purex Wastes containing 2.6 megacuries of radioactivity were reduced to a calcine product. During the ninth and final pot solidification run the rising level glass concept was demonstrated in which a simulated Purex Waste was fed to the pot where it was continuously concentrated, calcined, and fused to a borosilicate glass product. (auth)

10659 (CEA-N–1267) APPARATUS FOR AUTOMATIC LIQUID PHASE CHROMATOGRAPHY. Roliand, Marie Louise; Van Kote, Francis (Commissariat a l'Energie Atomique, Bruyeres-le-Chatel (France). Centre d'Etudes). Oct 1970. 18p. (In French). Dep. NTIS (U. S. Sales Only).

An apparatus for the automatic separation of fission products (Te, Cd, Pd, Mo, and Ru) by ion exchange is described. Four samples can be analyzed simultaneously. An electronic control, using a time-switch, injects very accurately equal volumes of the eluents into the four columns. Up to nine eluents can be used. A heating device allows the continuous evaporation of the eluents at the end of the column. After describing the apparatus, a typical experiment is presented to illustrate the working of the apparatus. (auth) (France)

10660 (DOCKET-50201–58) WEST VALLEY REPROCESSING PLANT. Low Level Liquid Waste Treatment Plant. Final Safety Analysis Report. (Nuclear Fuels Services, Inc., Rockville, Md.). Dec 1970. 45p. Dep. NTIS.

The construction and operation of a low-level waste treatment plant at West Valley is described. The process combines stages of carrier precipitation, flocculation and sludge removal, and ion exchange. Two streams leave the plant: clarified and treated waste and sludge bearing the removed radioactivity. The sludge is drummed and buried on the site. The treated waste is discharged at a controlled rate to the surface waters. (M.C.G.)

10661 (DOCKET-50201–59) WEST VALLEY REPROCESSING PLANT. Progress Report on Low Level Waste Treatment. (Nuclear Fuels Services, Inc., Rockville, Md.). 5 Jan 1971. 1p. Dep. NTIS.

Construction of the plant is on schedule, and the effects of the revised chemical treatment instituted as a temporary expedient are evaluated. (M.C.G.)

10662 (DOCKET-50201–71) WEST VALLEY REPROCESSING PLANT. GPC Crane Room Extension and Sump Collection Tank. Final Safety Analysis Report. (Nuclear Fuel Services, Inc., Rockville, Md.). Dec 1970. 10p. Dep. NTIS.

A safety analysis of an extension to the general purpose cell and crane room and a sump collection tank to be installed adjacent to it is presented. (M.C.G.)

10663 (DOCKET-50268–6) MIDWEST FUEL RECOVERY PLANT. Application for Conversion of Construction Permit to Operating License (Includes Final Safety Analysis Report). (General Electric Co., San Jose, Calif. Nuclear Energy Div.). 30 Dec 1970. 519p. Dep. NTIS.

In support of the application for an operating license, a final safety analysis report and a General Electric financial statement are given. Topics covered include: design criteria, site and environs, facility description, process systems description, radiological protection and confinement systems, auxiliary systems, safety analysis, management systems, preoperational testing, and technical specifications. (M.C.G.)

10664 (DP-MS–70-38) ON-LINE COMPUTER MONITORING OF PRESSURIZED ION EXCHANGE PROCESS. Peterson, S. F.; Wakat, M. A. (Du Pont de Nemours (E. I.) and Co., Aiken, S. C. Savannah River Lab.). 18 Aug 1970. 20p. (CONF-700911–1). Dep. NTIS.

From 160th National Meeting of the American Chemical Society, Chicago, Ill.

An on-line radiometric monitoring system has been developed to provide information for control of a pressurized ion exchange chromatographic process for the large-scale purification of ^{252}Cf, ^{244}Cm, and ^{243}Am. The effluent stream from the ion exchange chromatography columns is monitored by: a BF_3 neutron detector for detecting ^{252}Cf and ^{244}Cm; a NaI scintillation detector used with a single-channel analyzer; and a low-energy Ge(Li) photon detector (700 eV resolution at 42.9 keV). Information from these detectors is interfaced to a PDP-9 computer with an 8k memory capacity. The system calculates and prints out (as frequently as every 30 sec) concentrations of the radionuclides from the complex gamma and x-ray spectrum of the Ge(Li) detector and the BF_3 and NaI detector responses. Selected regions of the Ge(Li) pulse-height spectrum may be examined on an oscilloscope display. Data obtained from the computer system are compared with those from manual calculations. (auth)

10665 (INR-P–1209) EFFECT OF RESIN CROSS-LINKING ON ANION EXCHANGE SEPARATION OF RARE-EARTH–EDTA COMPLEXES. Dybczynski, R. (Institute of Nuclear Research, Warsaw (Poland)). 1970. 37p. Dep. NTIS (U. S. Sales Only).

Anion exchange separation of the rare earth complexes with EDTA on Dowex 1 resins with 2, 4, 8, 10, and 16 nominal crosslinks, respectively was investigated at tracer loadings. Selectivity coefficients, separation factors, plate heights, and resolutions for adjacent peaks were calculated from the elution curves. Although separation factors increased rather uniformly with the increase in resin crosslinking, best separations were obtained with Dowex 1 × 4 due to the most promising value of the plate height. Plate height, which was the lowest for X4 resin, was found to increase both with increase and decrease of resin crosslinking. The change from X4 to X16 resin resulted in drastic increase of plate height by nearly two orders of magnitude. It was found that the results obtained cannot be interpreted on the grounds of the classical Glueckauf equation. The introduction of a new term, accounting for longitudinal diffusion in the resin phase, into Glueckauf's equation was suggested and the qualitative agreement between theoretical prediction and experimental data was demonstrated. The existence of a sieve effect in the case of anion exchange of rare earth-EDTA complexes on highly crosslinked resins was also pointed out. (auth)

10666 (JINR–P6-5410) GASOCHROMATOGRAPHIC SEPARATION OF NONVOLATILE METAL CHLORIDES USING ALUMINUM CHLORIDE AS ELUENT. Zvarova, T. S.; Zvara, I. (Joint Inst. for Nuclear Research, Dubna (USSR). Lab. of Nuclear Reactions). 1970. 12p. (In Russian). Dep. NTIS (U. S. Sales Only).

It was found that a chromatographic method using a mixture of inert gas with aluminum chloride can be used for the separation of transition elements, which form only nonvolatile chlorides. The separation of elements (In–Zn, In–Tb, Zn–Co–Cu, Ga–Tl, and a mixture of elements containing In–Pd–Nb–Cd–Rh–Mo after irradiation of Nb foil by ^{23}N ions) by gas-adsorption chromatography in a glass column at <300°C using Al_2Cl_6 as a carrier gas is described. (R.V.J.)

10667 (LIB/Trans–310) THE TREATMENT OF THE IRRADIATED FUELS IN SPAIN. Translated by E. Monteleone for Australian Atomic Energy Commission Research Establishment, Lucas Heights, from Com. Naz. Energ. Nucl., Notiz.; 14: No. 4, 57-9(Apr 1968). 11p. Dep. NTIS (U. S. Sales Only).

An abstract of this article, prepared from the original, appeared as NSA 22: 33546. (Australia)

10668 (LYCEN–7034, pp 1-8) RAPID CHEMICAL SEPARATIONS: GENERAL ASPECTS. Moussa, A. (Grenoble Univ. (France). Institut des Sciences Nucleaires). (In French).

From Conference on low-energy spectrometry and nuclear spectrometry, Lyon, 18–20 February 1970.

Two separation methods are presented: ion exchange methods (reaction kinetics, effect of complexation) and solvent extraction methods (reaction kinetics, effect of pH, salt effects). Separations performed on columns were studied. They are very rapid when separation factors are high. When separation factors are low, a small column should be used and the amount to be treated should be limited. The use of separate isotopes for targets and high irradiation fluxes is recommended. (France)

10669 (LYCEN–7034, pp 9-22) DESCRIPTION OF VARIOUS TECHNIQUES, RECENT APPLICATIONS, AND TECHNOLOGICAL ASPECTS. Blachot, J. (Commissariat a l'Energie Atomique, Grenoble (France). Centre d'Etudes Nucleaires). (In French).

XUM

From Conference on low-energy spectrometry and nuclear spectrometry, Lyon, 18–20 February 1970.

Separation methods in the gaseous phase (rare gas emanation method, recoil in the solid or gaseous phase with formation of volatile species) and in the liquid phase (solvent extraction, ion exchange, chromatography, electrochemical methods, precipitation, isotopic exchange) are described. The physical methods used in the study of transuranium elements are based either on the electrostatic properties of the recoil atoms or on hydrodynamic properties (gas jet technique). (France)

10670 (LYCEN–7034, pp 23-33) ON-LINE NUCLEAR SPECTROSCOPY. Foucher, R. (Paris Univ., Orsay (France). Institut de Physique Nucleaire). (In French).

From Conference on low-energy spectrometry and nuclear spectrometry, Lyon, 18–20 February 1970.

Several of the motivations behind the world developments in on-line spectroscopy are discussed. The current wave of development in this domain in France is briefly described. (France)

10671 USE OF COMPLEXING AGENTS FOR DISSOLVING SILICATES AND ION EXCHANGE RESIN SEPARATIONS. Govindaraju, K. (CNRS, Vandoeuvre-les-Nancy, France). pp 269-85 of Dosage des Elements a l'Etat de Traces dans les Roches et les Autres Substances Minerales Naturelles. Paris; Centre National de la Recherche Scientifique (1970). (In French).

From National Conference on Measurement of Elements Occurring in Traces in Rocks. Nancy, France. See CONF-681205.

After decomposition of the sample by borate fusion, the fusion product is dissolved in complexing agents such as citric acid or ethylenediaminetetraacetic acid (EDTA). Ion exchange separations are favored in such complex solutions, particularly in EDTA medium. Without separation, Na and K are determined by flame photometry and Ca and Mg by atomic absorption. A certain number of separations realizable by column or batch method is discussed. In particular, the separation of Rb and Sr is described in detail for their atomic absorption determination. (auth)

10672 BASES OF A PROGRAM OF INVESTIGATION FOR THE DEVELOPMENT OF THE REPROCESSING OF FUELS IRRADIATED IN FAST REACTORS. Nogueira, Eduardo Diaz; Abellan, Jose Ortega. Energ. Nucl. (Madrid); 14: 311-28 (Jul-Aug 1970). (In Spanish).

The reprocessing of irradiated fuels from fast reactors presupposes 45 to 50% of the total fuel cycle cost. In a program for development of fast reactors fuel reprocessing is necessary since these reactors produce more fissionable material than they use and the only possible way to recover the new fissionable material is by reprocessing the irradiated fuels. The tendency in reprocessing irradiated fuels from fast reactors is adaptation of existing plants for reprocessing of fuels from thermal reactors to the specific characteristics of this type of irradiated fuel. From this point of view the most important differences result from a greater plutonium content (10 to 25%) and a greater burnup (10^5 MWd/metric ton) and a shorter cooling period (~30 days). A list of problems in connection with the development of the technology is: deactivation of sodium; methods of decladding; previous volatilization of fission products; studies on dissolution; removal of solid residues; influences of high concentrations of plutonium on the chemical process; degradation of the solvent; centrifugal equipment for solvent extraction; retention of iodine in the gaseous effluents; treatment of liquid residues of high activity; and recovery of by-products such as neptunium, americium, palladium, and rhodium. (tr-auth)

10673 FUTURE FOR THE REPROCESSING OF IRRADIATED FUELS IN EUROPE. Energ. Nucl. (Madrid); 14: 329-32(Jul-Aug 1970). (In Spanish).

A résumé is presented of the document entitled "The Future of Reprocessing in Europe," prepared in 1969 by the European Atomic Forum (FORATOM) and published in February 1970. It contains an examination of the market situation from the present to the near future; it next proceeds to a study of the cost structure (investment, operating, and total); and finally it includes a series of auxiliary factors, such as transport, control, and security. There is a series of recommendations referring to the adaptation of the reprocessing capacity to the demand, fields of technical development, safeguards, and security, among others. (tr-auth)

10674 PURIFICATION OF CYCLOTRON-PRODUCED ^{123}I BY LIQUID–LIQUID EXTRACTION. Neirinckx, R. D. (South African Council for Scientific and Industrial Research, Pretoria). Radiochem. Radioanal. Lett.; 5: 205-8(15 Dec 1970).

A procedure is described that allows higher chemical yields for ^{123}I separation from its antimony matrix than previously published procedures. The ^{123}I is produced by α bombardment of natural antimony metal in the variable energy cyclotron of the Council for Scientific and Industrial Research. The procedure is based on dissolution of the antimony target in hydrochloric acid to which hydrogen peroxide is added, reduction of the iodate by means of ferrous sulfate and extraction of the iodine by means of carbon tetrachloride. (auth)

10675 CO-PRECIPITATION OF CARRIER-FREE ^{31}Si WITH VARIOUS METAL HYDROXIDES. Sato, T.; Ichikawa, F. (Japan Atomic Energy Research Inst., Tokai). Radiochem. Radioanal. Lett.; 5: 165-70(15 Dec 1970).

The coprecipitation of anionic species of carrier-free ^{31}Si with various metal hydroxides was studied. The coprecipitation ratio varied according to the affinity of the silicate anion and metal cations. The mechanism of coprecipitation of lanthanum hydroxide is discussed in detail. (auth)

10676 SEPARATION OF ZIRCONIUM FROM HAFNIUM BY FRACTIONAL CRYSTALLIZATION OF POTASSIUM HEXAFLUOROZIRCONATE. Arsenie, Ioana (Institut de Physique Atomique, Bucarest); Leuca, I. Rev. Roum. Chim.; 15: 1263-73(Aug 1970). (In French).

A method is described for the separation of Zr from Hf by fractional crystallization of K_2ZrF_6/HfF_6. The method was developed for attaining a purity of 0.01% Hf/Zr (η = 80%). The effects of various parameters, such as pH, temperature, concentration, and rate of crystallization were also studied and conditions were established. (P.C.H.)

10677 SEPARATION OF PLUTONIUM FROM $^{95}Zr/+^{95}Nb/$ AND ^{106}Ru ON ZIRCONIUM PHOSPHATE SILICATE COLUMNS. Vaidyanathan, S.; Baetsle, L. H. (SCK/CEN, Mol, Belgium). Radiochem. Radioanal, 5: 247-57(15 Dec 1970).

The separation of ^{95}Zr and ^{106}Ru from Pu by inorganic ion exchange has been studied in order to develop an easy method for tail-end purification of the fissile nuclide after separation of the majority of fission products by liquid extraction. Zirconium phosphate silicate adsorbs ^{95}Zr and Pu(IV) quantitatively, while Ru passes the column unadsorbed; Pu(IV) is reduced to Pu(III) with ascorbic acid and eluted quantitatively with dilute HNO_3. The decontamination factors of Zr and Ru are 2.110 and 1.160, respectively. The breakthrough capacity of zirconium phosphate silicate for Pu amounts to 1.1 meq g^{-1}. (auth)

10678 PURIFICATION OF CYCLOTRON-PRODUCED ^{203}Pb FROM A THALLIUM METAL MATRIX. Neirinckx, R. D. (South African Council for Scientific and Industrial Research, Pretoria). Radiochem. Radioanal. Lett.; 5: 201-4(15 Dec 1970).

A method is described for the production of high-specific activity ^{203}Pb. The carrier-free product is separated from the thallium metal matrix by scavenging with iron hydroxide and subsequent solvent extraction of the iron. The ^{203}Pb is delivered in the acetate form for research work concerning lead metabolism in living organisms. (auth)

10679 EXTRACTION OF U(VI) AND SELECTED M(III) CATIONS BY BIS NEO-OCTYL PHOSPHORIC ACID IN TWO DIFFERENT HYDROCARBON DILUENTS. Mason, G. W.; Schofer, N. L.; Peppard, D. F. (Argonne National Lab., Ill.). J. Inorg. Nucl. Chem.; 32: 3911-22(Dec 1970).

The extraction of Ce^{3+}, Pm^{3+}, Eu^{3+}, Tm^{3+}, Y^{3+}, Am^{3+}, Cm^{3+}, and UO_2^{2+} from an aqueous chloride phase into a solution of $[C_4H_9C \times (CH_3)_2CH_2O)_2PO(OH)$, HDNOP, in benzene or in n-heptane was studied as a function of the concentration of extractant in the organic phase and of hydrogen ion in the aqueous phase, and the stoichiometries of extraction deduced. Corresponding to the stoichiometries, values of K, F and $[H^+]$ obtained from the hydrogen ion dependency plots were inserted in the equation: $K = K_x F^a / [H^+]^b$ to obtain values of K_x. (K is the observed distribution ratio, F the concentration of HDNOP in the organic phase and $[H^+]$ the concentration of hydrogen ion in the aqueous phase following equilibration, and a and b the respective extractant and hydrogen ion dependencies. The equation is applied specifically to a system embodying 1.0 F (NaCl + HCl) at 22 ± 2°C.) The K_x (n-heptane) value is higher than the K (benzene) value for each of the cations studied. However, although the ratio of the K_x values is large for each of the seven M(III) cations (in the 50 to 250 range), it is only 6 for U(VI). Comparison with extraction systems employing two other di octyl phosphoric acids, $(n\text{-}C_8H_{17}O)_2PO(OH)$ and $[C_4H_9CH \times (C_2H_5)CH_2O]_2PO(OH)$, as extractants are made in terms of: (1) acidity of the extractant, (2) steric effects within the extractant molecule, and (3) effect of diluent (aromatic or saturated hydrocarbon). (auth) (UK)

10680 THERMODYNAMICS OF URANYL ION EXCHANGE ON ZIRCONIUM PHOSPHATES OF VARIOUS CRYSTALLINITIES. Ruvarac, A. (Boris Kidric Inst. of Nuclear Sciences, Vinca,

XUM

Yugoslavia); Vesely, V. J. Inorg. Nucl. Chem.; 32: 3939-48 (Dec 1970).

The equilibrium exchange of UO_2^{2+} ions with the hydrogen forms of amorphous, semicrystalline, and crystalline zirconium phosphate at ionic strength 0.30 and 0.15 M was studied at 25, 50, 80, 100, 175, and 250°C. Thermodynamic equilibrium constants and changes of free energy, enthalpy, and entropy were calculated from the ion-exchange isotherms. The differences in thermodynamic quantities for zirconium phosphate samples of various crystallinities are discussed. (auth) (UK)

10681 SYNERGISTIC EFFECTS IN ION-EXCHANGE. PART I. ACETONE-METHANOL MIXTURES. Rao, A. P.; Dubey, S. P. (Indian Inst. of Tech., New Delhi). Indian J. Chem.; 7: 396-8 (Apr 1969).

Distribution coefficients of Cu(II), Ni(II), Co(II), UO_2(II), Fe(III), Zn(II), and Cd(II) in mixtures of acetone, methanol, and HCl were determined. The results obtained are discussed with respect to the various equilibria that exist in such mixtures. (auth)

10682 METHOD OF CONCENTRATING RADIOACTIVE WASTE. Doelgast, W. Canadian Patent 853,249. 6 Oct 1970. Priority date 29 Jun 1968, Germany.

A method of concentrating aqueous solutions and suspensions of radioactive waste by thickening and drying processes is described. The concentrate is dried on heated rollers, whereby a polyelectrolyte is added in a known manner, to adjust the viscosity. Bone glue is also added to prevent formation of dust and as an embedding mass. The rolled product is subsequently compressed into solid bodies. (F.S.A.) (Canada)

10683 RECOVERY OF URANIUM, THORIUM, AND CERIUM FROM EGYPTIAN MONAZITE SANDS. I. Saleh, F. A.; Farag, A. K. (Egyptian Atomic Energy Establishment, Cairo). Z. Anorg. Allg. Chem.; 375: 308-14(Aug 1970).

A process is described for the recovery of uranium, thorium, and cerium from Egyptian monazite sands. The process consisted of: (1) treatment of fine ground monazite sands with hot 50% caustic soda solution with a caustic soda to monazite sand ratio of 1 : 1; (2) dilution of the reaction slurry with 6 times the weight of the sand with water to dissolve the sodium phosphate formed; (3) filtration of the reaction slurry to remove the solid hydrous metal oxides from the sodium phosphate and excess sodium hydroxide; (4) drying of the mixed hydrous oxides at 150°C for 10 hours to oxidize cerium; (5) dissolution of the trivalent rare earths by addition of dilute nitric acid dropwise to an aqueous suspension of the dried hydrous oxides to pH 1.3; and (6) separation of uranium, thorium, and cerium by filtration of the dissolved tervalent rare earths from undissolved residue of the mixed hydrous oxides. (auth)

10684 VARIATIONS OF THE CARBON AND OXYGEN ISOTOPIC COMPOSITION IN STALAGMITES AND STALACTITES: EVIDENCE OF NON-EQUILIBRIUM ISOTOPIC FRACTIONATION. Fantidis, J.; Ehhalt, D. H. (Univ., Heidelberg). Earth Planet. Sci. Lett.; 10: 136-44(Dec 1970).

The variations of the ^{18}O and ^{13}C content along homogeneous layers of stalagmites and stalactites were studied. Both isotopes vary parallel, usually showing an increase, in one case a decrease, in the direction of water flow. Deposition of $CaCO_3$ under stalagmite growth conditions in the laboratory exhibits the same features. The laboratory experiments indicate that kinetic isotope fractionations during escape of CO_2 from the solution and in the reaction $H^+ + HCO_3^- \rightleftharpoons CO_2 + H_2O$ and $HCO_3^- \rightleftharpoons CO_2 + OH^-$ are partly responsible for the observed isotope variation. (auth)

10685 SEPARATION OF YTTRIUM, HOLMIUM, AND ERBIUM WITH DI-(2-ETHYLHEXYL) PHOSPHORIC ACID IN CHLORIDE AND NITRATE SYSTEMS. Michelsen, Odd B.; Smutz, Morton (Iowa State Univ., Ames). J. Inorg. Nucl. Chem.; 33: 265-78 (Jan 1971).

Distribution coefficients as a function of acidity were determined for Y, Ho, and Er in the system YCl_3-$HoCl_3$-$ErCl_3$-HCl-H_2O-D2EHPA-Amsco and $Y(NO_3)_3$-$Ho(NO_3)_3$-$Er(NO_3)_3$-HNO_3-H_2O-D2EHPA-Amsco. In both systems the distribution coefficients were found to go through minimum values at certain acidities. Separation factors tend to decrease at the higher acidities with the exception of the Er/Y separation factor in the chloride system, which shows a significant increase. The result was used to demonstrate a separation of Y from Ho and Er employing extraction chromatography and elution at different acidities. (auth) (UK)

10686 LIQUID-LIQUID EXTRACTION OF GOLD(III) WITH DILUTED TRIBUTYL PHOSPHATE. Yadav, A. A.; Khopkar, S. M. (Indian Inst. of Tech., Bombay). Separ. Sci.; 5: 637-43 (Oct 1970).

A method was developed for the solvent extraction of gold with dilute tributyl phosphate. In this method, 50% tributyl phosphate in toluene extracts gold quantitatively from 3 M hydrochloric acid containing 2 M lithium chloride as the salting-out agent. Gold from the organic phase is stripped with 1 M ammonium hydroxide and determined photometrically as its complex with stannous chloride. It is possible to extract gold in the presence of a large number of ions. (auth)

10687 SEPARATION OF THE OXIDATION STATES OF SOME ELEMENTS WITH THE USE OF TRI-n-BUTYL ORTHOPHOSPHATE. Thakur, Madhukar L. (Hammersmith Hospital, London). Separ. Sci.; 5: 645-51(Oct 1970).

The tributyl orthophosphate-acetic acid-acetone solvent system was studied for the paper chromatographic separation of the oxidation states of 16 elements. The separation of As^{3+}, As^{5+}; Cr^{3+}, Cr^{6+}; Fe^{2+}, Fe^{3+}; Hg^+, Hg^{2+}; Mn^{2+}, Mn^{3+}, and Mn^{7+}; Sb^{3+}, Sb^{5+}; Tl^+, Tl^{3+}; Cl^-, ClO_3^-; Br^-, BrO_3^-; I^-, IO_3^-; $P_2O_7^{4-}$ PO_4^{3-}, and PO_3^- was achieved. Multiple zones obtained with Fe^{3+} and Tl^{3+} species are discussed. (auth)

10688 FRACTIONATION OF TRITIUM IN THE CRYSTALLIZATION OF INORGANIC HYDRATES FROM A TRITIATED SOLUTION. Tanaka, Haruhiko; Negita, Hisao (Hiroshima Univ.). Bull. Chem. Soc. Jap.; 43: 3079-82(Oct 1970).

Bennema's theory of crystal growth from a solution was modified and used in explaining fractionation of tritiated water in the crystal-growth processes of several inorganic hydrated salts from concentrated aqueous solutions. It was suggested that some water molecules in the aqueous solutions were free to become growth units that are not necessarily activated for entering the crystal surface. The dilution of tritiated water in the crystal was observed; this was explained in a satisfactory way in terms of the surface-diffusion model originally proposed by Burton, Cabrera, and Frank. On the contrary, the volume diffusion model was inadequate for interpreting the fractionation of tritium. (auth)

10689 SEPARATION OF ZIRCONIUM FROM HAFNIUM BY THE TBP EXTRACTION METHOD. Deleon, Ana. Nukl. Energ.; 4: No. 6, 13-19(1967). (In Serbo-Croatian).

The separation of zirconium from hafnium using the TBP procedure is described. Imported zircon concentrate with an average hafnium content was used for the experiments. The extraction was performed from a nitric acid and sodium nitrate solution of zirconium nitrate with white-spirit diluted TBP. Following the adopted technological procedure for both elements the distribution and separation coefficients were determined, and a calculation made of the necessary number of stages for the extraction of zirconium and the scrubbing of hafnium from the organic phase. From published data and acquired experience a mixer-settler battery was prepared. From the experimental data of zirconium extraction, the efficiency of each battery stage was determined. On the basis of these experimental data and the calculated number of stages for zirconium extraction and hafnium separation from the organic phase, a mixer-settler battery for continuous separation of zirconium from hafnium was prepared. The experiments gave satisfactory results since a 94.5% zirconium yield with only 60 to 80 ppM of hafnium was obtained. (auth)

10690 ISOTOPE SEPARATION WITH THE cw HYDROGEN FLUORIDE LASER. Mayer, S. W.; Kwok, M. A.; Gross, R. W. F.; Spencer, D. J. (Aerospace Corp., El Segundo, Calif.). Appl. Phys. Lett.; 17: 516-19(15 Dec 1970).

A c-w hydrogen fluoride laser has been used successfully to separate deuterium from hydrogen by specific photocatalysis of the reaction of methanol with bromine. The strong absorption of H_3COH was demonstrated for the HF laser lines $P_1(5)$, $P_1(6)$, and $P_1(7)$ while no absorption by deutero-methanol of the HF beam was observed. Excitation of H_3COH by the absorbed beam increased the rate of H_3COH removal by reaction with bromine. Irradiation, at 90 W for 60 sec, with the c-w hydrogen fluoride laser of a 1 : 1 H_3COH : D_3COD gas mixture in the presence of bromine produced isotope enrichment to greater than 95% D_3COD. (auth)

EARTH SCIENCES

Geology and Hydrology

Refer also to abstracts 10446, 10477, 10508, 10741, 10825, 10849, and 10889.

10691 (BNWL-1345) EFFECT OF HANFORD PLANT OPERATIONS ON THE TEMPERATURE OF THE COLUMBIA RIVER 1964 TO PRESENT. Jaske, R. T.; Synoground, M. O. (Battelle-Northwest, Richland, Wash. Pacific Northwest Lab.). Nov 1970. Contract AT(45-1)-1830. 288p. Dep. NTIS.

Significant temperature information and effluent mixing data that have been performed under the study "Effect of Reactor Effluent on the Quality of Columbia River Water," begun in 1962, are compiled and reviewed. The basic information needed for a sound view of the temperature modification induced by reactor operation at Hanford and a technical basis for relating these modifications to the ecology are presented. The primary concern here is with physical changes; routine radiological aspects are not included except as they apply to the development of simulation models for effluent transport and dispersion and studies of the mechanics of related food chain transport. The development of the physical description of the plant effluents includes, among other factors, detailed knowledge of the concentration profiles and travel times of the effluents in the river below the reactors in order to: determine the extent of interaction between and among operating plants and the city of Richland water plant; permit prediction of potential exposures from partially diluted effluent to persons downstream, especially in the event of off-standard releases; and provide a basis for the accurate evaluation and mapping of the extent of zones in which aquatic life might be affected. (auth)

10692 ENVIRONMENTAL MOBILITY OF ^{106}Ru DURING IRRIGATION PROCESSES. Amy, Jean-Paul (CEA, Cadarache, France); Grauby, Andre; Jacquin, Fernand. Compt. Rend., Ser. D; 271: 644-7(17 Aug 1970). (In French).

Environmental mobility of ^{106}Ru in ruthenium nitrosyl complexes is very high. The results obtained show that the nuclide is only partly sorbed by the sediments of the irrigation canals and that it migrates rather deeply into the irrigated soils. (auth) (France)

10693 FAST DETERMINATION OF Zn + Cu MINERALIZATION BY GAMMA-GAMMA LOGGING. Simon, L. (Mining Inst., Prague). Rudy; 17: 188(Jun 1969). (In Czech).

The geophysical gamma-gamma method was shown to be applicable for direct measurement of Zn + Cu mineralization in small-diameter boreholes. The measurements were performed at the Jezírko Zn + Cu ore-bearing deposit near Staré Rancko. Two gamma-gamma logging instruments, the HOU 22 S and HOU P 22 S, were used. ^{75}Se was used as the radiation source. The measurements were compared with results of chemical analyses. It was shown that the gamma-gamma method is suitable for determining the Zn + Cu content in the Jezírko ore-bearing deposit. (NSA of Czech.)

10694 EFFECT OF CONCENTRATION SUPPLIED ON THE IODIDE SORPTION BY VARIOUS SOILS. Knaelmann, M. (Technische Hochschule, Hanover). Atomkernenergie; 16: 247-52(1970). (In German).

Among all fission products, ^{131}I is relatively easily transported in the soil. Therefore, its uncontrolled spreading in the soil constitutes a hazard. The sorption of I by 59 different soils was investigated. Iodine was supplied in form of aqueous iodide solutions of different concentrations. Differences in the relative sorption were noted among the various soils, however, the plot of concentration supplied versus relative sorption gave similar shaped curves for all soils. (auth)

10695 GEOMETRY FACTOR IN FISSION TRACK COUNTING. Reimer, G. M. (Univ. of Pennsylvania, Philadelphia); Storzer, D.; Wagner, G. A. Earth Planet. Sci. Lett.; 9: 401-4(11 Nov 1970).

Fission track density determinations of external and internal counting surfaces (2π and 4π geometry) were made for different glasses, apatite, zircon, sphene, and muscovite. The ratios between the two geometries range from 0.57 and 0.89 depending on the material and the etching time. Fission track ages using a factor of 0.5 between the two geometries must be corrected. (auth)

10696 ANNEALING OF FISSION TRACKS IN TEKTITES: CORRECTED AGES OF BEDIASITES. Durrani, S. A.; Khan, H. A. (Univ. of Birmingham, Eng.). Earth Planet. Sci. Lett.; 9: 431-45(11 Nov 1970).

Systematic annealing experiments have been carried out in an endeavor to obtain quantitatively reliable correction factors for the ages of tektites which may have been subjected to heat. The standardization of etching conditions, which is a prerequisite for making such corrections, is described. The application of the correction factors so obtained to a differentially-annealed bediasite gives self-consistent results. Inferences as to the possible thermal history of the bediasite are drawn from a careful analysis of the etch-pit diameter vs. track density histograms of natural as well as freshly irradiated samples. The mechanism of track shrinkage and fading is examined in some detail. (auth)

10697 URANIUM, THORIUM, AND RARE-EARTH ELEMENTS IN THERMAL WATERS OF THE KAMCHATKA PENINSULA. Udaltsova, N. I.; Leonova, L. L. (Inst. of Volcanology, Novosibirsk, USSR). Geokhimiya; No. 12, 1504-10(Dec 1970). (In Russian).

The rare earth elements, Th, and U contents were determined in chloride-sodic, sulfate-chloride-sodic sulfate and carbonate thermal waters of the Kamchatka peninsula. On the basis of these data Th/U and RE/Th ratios were calculated. The lowest concentrations of rare earth elements, Th, and U were found in chloride-sodic abyssal thermae; in sulfate waters the concentration of U increases by two orders, Th 10 times, and of rare earth elements 5 times. It is assumed that in all types of waters rare earth elements, Th, and U are present in a dissolved state and that rocks are the source of these elements. (auth)

10698 RADIOACTIVE ELEMENTS AND DEUTERIUM IN UNDERGROUND WATERS OF THE BUKHARA-KARSHIN ARTESIAN BASIN. Alekseev, F. A.; Gottikh, R. P.; Soifer, V. N.; Brezgunov, V. S. (All-Union Scientific Research Inst. of Nuclear Geophysics and Geochemistry, Moscow. Inst. of Water Problems, Moscow). Geokhimiya; No. 12, 1483-94 (Dec 1970). (In Russian).

The distribution of radioactive elements over the area of water-bearing complexes reflects well the change of geochemical conditions in the waters. A definite correlation between the radium and deuterium contents in waters was revealed. It was shown that the present character of the underground waters of the basin is a result of two infiltration periods (the Mesozoic and the recent one). The zones of intrusion of infiltration waters and the degree of sedimentation water dilution by them were determined. (auth)

10699 DATA. SECTION II. WATER. Radiol. Health Data Rep.; 11: 544(Oct 1970).

A list of Radiological Health Data and Reports issues is presented. These reports contain information on the gross β and gross α activities and specific radioisotope content of ground, surface, and treated waters measured at various US locations from 1967 to 1970. (L.C.L.)

10700 DETERMINATION OF THE AVERAGE VELOCITY OF GROUNDWATER FLOW AND PRELIMINARY ESTIMATION OF THE QUANTITY OF GROUNDWATER IN SHIGAYA AQUIFER IN KUWAIT USING RADIOISOTOPES. Hazzaa, I. B.; Sharhan, A. M.; Shuhaiber, Y. K. (Middle Eastern Regional Radioisotope Centre for the Arab Countries, Cairo). Isotop. Radiat. Res.; 3: 1-7 (Jun 1970).

The velocity of groundwater flow in the Shigaya aquifer in Kuwait was determined in ten localities. This velocity was calculated using the displacement r during a certain period γ. The velocity is then given by $\nu = r/\gamma$. The displacement r was measured by injecting a few millicuries of radioisotope ^{131}I into each well, letting the radioactivity be carried away by the groundwater stream during the period γ and then pumping from the well at a known rate. The radioactivity in the water pumped out was continuously monitored. From the (time, activity) record, the velocity was determined using the velocity equation. The measured velocity ranges between 0.7 m/d and 0.3 m/d; and the average velocity was found to be 0.4 m/d. Preliminary estimation of the quantity of groundwater flowing in the Shigaya aquifer under the existing conditions, was obtained. (auth)

10701 U-Th-Pb AND Rb-Sr SYSTEMATICS IN 2700 x 10^6-YEAR OLD PLUTONS FROM THE SOUTHERN WIND RIVER RANGE, WYOMING. Naylor, R. S. (California Inst. of Tech.,

XUM

Pasadena); Steiger, R. H.; Wasserburg, G. J. Geochim. Cosmochim. Acta; 34: 1133-59(Nov 1970).

To distinguish between episodic and continuous-diffusion loss mechanisms, and to compare the response of different parent–daughter systems to metamorphism, a series of well-exposed plutons were studied all about 2700×10^6 yr old and showing different degrees of metamorphism. The Louis Lake granodiorite pluton in the southern Wind River Range, Wyoming was selected to represent granitic rocks only slightly affected by later disturbances (intrusion of Precambrian diabase dikes and gentle Laramide uparching). Rb–Sr data on total-rock samples form a linear array on the Sr-evolution diagram, indicating that the pluton was emplaced $2630 \pm 20 \times 10^6$ yr ago ($\lambda^{87}Rb = 1.39 \times 10^{-11}$ yr^{-1}) with an initial $^{87}Sr/^{86}Sr$ ratio of 0.702 ± 0.001. Data on cogenetic zircon fractions form a linear array on a coupled Pb–U evolution diagram with a primary intercept of $2687 \pm 15 \times 10^6$ yr. The secondary intercept of $130 \pm 100 \times 10^6$ yr is distinctly lower than the 480 to 660×10^6 yr intercepts predicted by single-phase continuous-diffusion models. If the zircons reflect Laramide disturbance, this is not detected by the Rb–Sr data on mineral separates. Disturbance of these data is readily apparent only in rocks with high Rb/Sr ratios and has yielded no apparent secondary ages younger than 2000×10^6 yr. (auth) (UK)

Meteorology

Refer also to abstracts 10472, 10754, 10792, and 10999.

10702 (AD–708558) INTERACTION OF FALLOUT WITH FIRES. Final Report. Strom, Peter O.; Miller, Carl F. (URS Research Co., San Mateo, Calif.). Sep 1969. Contract DAHC20-70-C-0214. 71p. (URS–708–4). NTIS.

Parametric relationships describing the possible interactions of fallout particles with air and gas currents arising from fires of circular area and from line fires are discussed. The effects that result from fallout-fire interactions due to varying fire dimensions and intensities, ambient wind velocities, fallout particle sizes, height of particle-fire plume interaction and other variables are given. Fallout field dislocations caused by fires are estimated for a number of fallout, fire, and ambient wind conditions relative to fields postulated to exist in the absence of fires. Under a number of fire input, meteorological, and fallout parameter values, the model output suggests that considerable alterations in fallout patterns could be produced. (auth) (USGRDR)

10703 (EIR–185) INVESTIGATIONS OF AIR CURRENTS IN THE LOWER AARE RIVER VALLEY WITH REFERENCE TO MONITORING OF ATOMIC INSTALLATIONS. Nagel, E. (Eidgenoessisches Institut fuer Reaktorforschung, Wuerenlingen (Switzerland)). Jul 1970. 60p. (In German). Dep. NTIS (U. S. Sales Only).

The propagation of pollutants in the air is dependent on the prevailing currents to be expected at the site and in the vicinity of an apparent pollution source. The frequency and character of various current layers in the lower Aare River valley in northern Switzerland were studied on the basis of numerous measurements made with highly sensitive anenometers (starting velocity of 0.15 m/sec). The reactors of the Federal Institute for Reactor Research and the Northeast Swiss power plant are in this valley. The results emphasized the significance of the lower wind velocities; on the other hand they also emphasize the rareness of such current conditions, specifically those situations which are connected with an incoherent current picture. The dependence of the air motions on the terrain (hilly area with height variations up to 300 m wide, and differently oriented valleys) was shown in certain cases, such as at high wind velocities and with geotrophic parallel current, occur only slightly or even not at all. The persistence of a given current layer is essential for the propagation of possible pollutants; in practice, long persistence occurs only at those sites which show the most favorable dilution conditions, whereas less favored situations, such as low wind and irregular current behavior, are on much shorter duration for the most part. The results of the study also showed that the propagation within a given sector was determined by the wind direction and its oscillations and the relative terrain-dependence of the current; in the case of purely local currents, the propagation proceeds in a less simple fashion, i.e., along the valley bottom and corresponding weather conditions in the neighborhood. (tr-auth)

10704 (NP–18609) DIFFUSION OF THE MINOR CONSTITUENTS INTO THE TROPOSPHERE. Chanourdie, Jean-Claude; Crestia, Jean-Claude (Toulouse Univ. (France)). 1970. 152p. (In French). Dep. NTIS (U. S. Sales Only).

Thesis.

In order to study the behavior of various tracers in the troposphere, diffusion models were established. The natural radioactivity (radon, thoron and their daughters) and marine aerosols were studied. After analyzing the various parameters influencing the behavior of these minor constituents, a numerical solution of the diffusion equation was presented for various source geometries in time dependent and independent conditions. These models enable the influence of various parameters on the distribution of these tracer concentrations in the troposphere to be studied. In particular, a method of determining the diffusion coefficients was developed from these models. (auth) (France)

10705 (NYO–4061–3) PROGRESS REPORT. (Fraunhofer-Gesellschaft, Garmisch-Partenkirchen (West Germany). Physikalisch-Bioklimatische Forschungsstelle)). 1 Dec 1970. Contract AT(30-1)-4061. 18p. Dep. NTIS.

The results obtained from 1 Apr. to 15 Nov. 1970 by daily monitoring of the atmosphere at Zugspitze, Germany for ^7Be, fallout, and ^{32}P are presented. The ozone concentration was also measured, but not reported. The sampling and separation equipment and methods used are described. The analyzer used for determining the gamma spectrum of the chemically separated fallout radioactivity is discussed. Meteorological data were obtained from 2400 radiosonde ascents and used for deriving theoretical expresions for exchange processes in the atmosphere, particularly stratospheric–tropospheric exchange. Work on a computer program to evaluate the theoretical studies of the exchange processes and to correlate the results of the evaluations with ^7Be, fallout, and ^{32}P data is progressing. (L.C.L.)

10706 (ORO–2529–28) ATMOSPHERIC RADIOCHEMISTRY. Annual Progress Report. Kuroda, P. K. (Arkansas Univ., Fayetteville. Dept. of Chemistry). 31 Dec 1970. Contract AT(40-1)-2529. 169p. Dep. NTIS.

Experimental results from research conducted at the University of Arkansas on atmospheric radiochemistry, specifically the deposition and transport of radioactive fallout from nuclear explosions, are presented in nine appendixes. A separate abstract was prepared for each. (L.C.L.)

For abstracts of individual papers see: 10707–10715.

10707 (ORO–2529–28, App. 1) TEMPORAL DISTRIBUTIONS OF RADIOACTIVITY AND $^{89}Sr/^{90}Sr$ RATIOS DURING RAINSTORMS. Noyce, J. R.; Chen, T. S.; Moore, D. T.; Beck, J. N.; Kuroda, P. K. (Arkansas Univ., Fayetteville. Dept. of Chemistry). 23p.

From Atmospheric radiochemistry.

Radionuclide concentrations for ^{89}Sr, ^{90}Sr, ^{144}Ce, and ^{137}Cs were sequentially sampled from two different rainstorms to study the fallout behavior as a function of rainfall rate and type of storm during the summer of 1969, approximately seven months after the eighth Chinese nuclear explosion of Dec. 27, 1968. Great time variability in the ^{89}Sr, ^{90}Sr ratio was found in conjunction with a well-developed storm on July 21, but a nearly steady ratio was observed in a stratified, stable-type storm on Aug. 14. Trapping of stratospheric air appeared to be the cause of the ratio changes. For both storms, a strong trend was found to exist for concentrations of radioisotopes to decrease with increase in rainfall rate. Detailed discussions on meteorological factors, including a dilution effect, are given to interpret the experimental data. (auth)

10708 (ORO–2529–28, App. 2) JET STREAM AND RADIOACTIVE FALLOUT. Chen, T. S.; Kuroda, P. K. (Arkansas Univ., Fayetteville. Dept. of Chemistry). 8p.

From Atmospheric radiochemistry.

Data on the $^{89}Sr/^{90}Sr$ ratios in atmospheric precipitation at Fayetteville, Arkansas from 1964 to 1969 were correlated with information on meteorological conditions in the central region of Asia at the time of the first (Oct. 1964) through fifth (Dec. 1966) Chinese nuclear explosions to find reasons why a zig-zag time pattern (usually of 2 to 3 weeks duration) of variation in $^{89}Sr/^{90}Sr$ ratios in rain occurred after certain Chinese tests and not after others. It is concluded that the favorable position of the jet stream is one of the controlling factors which is closely related to the observed variations in the $^{89}Sr/^{90}Sr$ ratio in rain. (L.C.L.)

10709 (ORO–2529–28, App. 3) VARIATION OF THE RADIOCERIUM ISOTOPE RATIO IN RAIN CAUSED BY THE 27 DECEMBER 1968 CHINESE THERMONUCLEAR EXPLOSION. Moore, D. T.; Beck, J. N.; Kuroda, P. K. (Arkansas Univ., Fayetteville. Dept. of Chemistry). 20p.

From Atmospheric radiochemistry.

The $^{141}Ce/^{144}Ce$ ratio in the atmospheric precipitation after the 27 December 1968 Chinese thermonuclear explosion showed a very slow increase, which reached a maximum value of about 1

in April and May 1969, almost four months after the test. This suggested that the debris entered the upper stratosphere. The fallout pattern from this nuclear explosion was investigated using a three-compartment model of the atmosphere. (auth)

10710 (ORO–2529–28, App. 4) ^{89}Sr AND ^{90}Sr IN RAIN AT FAYETTEVILLE (36°N, 94°W), ARKANSAS. Moore, D. T. (Arkansas Univ., Fayetteville. Dept. of Chemistry). 4p.

From Atmospheric radiochemistry.

The concentrations of ^{89}Sr and ^{90}Sr in rain at Fayetteville, Arkansas, were measured during the period from Sept. 1969 to Aug. 1970. The results are presented. (auth)

10711 (ORO–2529–28, App. 5) ^{89}Sr AND ^{90}Sr IN AIR AT FAYETTEVILLE, ARKANSAS. Noyce, J. R. (Arkansas Univ., Fayetteville. Dept. of Chemistry). 6p.

From Atmospheric radiochemistry.

Measurements of certain fission products in ground-level were made in conjunction with the measurement of fission products in rain. A Gelman "Hurricane" air sampler was run continuously on the roof of the Chemistry Building of the University of Arkansas. All particles of 1 micron (μ) or larger were trapped on special filter paper. Filters were changed every two days. Approximately half of the samples collected during the period of August 1969 to July 1970 were radiochemically analyzed for strontium, cerium, and cesium. The results for Sr are shown in Table 1. $^{89}Sr/^{90}Sr$ ratios are plotted. Interpretation of this data is in progress. (auth)

10712 (ORO–2529–28, App. 6) ^{7}Be IN FAYETTEVILLE (36°N, 94°W), ARKANSAS. Swindle, D. L. (Arkansas Univ., Fayetteville. Dept. of Chemistry). 5p.

From Atmospheric radiochemistry.

Measurements of ^{7}Be in rain at Fayetteville, Arkansas, are reported for the time period from January 1969 to March 1970. The annual deposition during 1969 was 6.1×10^{5} atoms per cm^2. (auth)

10713 (ORO–2529–28, App. 7) RADIOCHEMICAL STUDIES ON ^{137}Cs IN RAIN. Sumerlin, Neal (Arkansas Univ., Fayetteville. Dept. of Chemistry). 37p.

From Atmospheric radiochemistry.

Radiocesium data in rain obtained during the past five years were brought up to date, compiled, and compared with ^{90}Sr data from the same period. The difference in fallout rates after individual nuclear detonations and in the stratospheric mean residence times is explained on the basis of relative volatility of the mass chains producing the two nuclides. The influence of the series of Chinese nuclear tests on the long-term observed concentrations of ^{137}Cs and ^{90}Sr is discussed. (auth)

10714 (ORO–2529–28, App. 8) FISSION PRODUCTS IN THE ATMOSPHERE. CHAPTER 1. EARLY FALLOUT STUDIES. Kuroda, P. K. (Arkansas Univ., Fayetteville. Dept. of Chemistry). 18p.

From Atmospheric radiochemistry.

The historical development of fallout studies is reviewed. Early papers, particularly from the 1950's on radioactivity monitoring in the atmosphere, the identification of fission products in atmospheric precipitation, and the effects of meteorological conditions on fallout transport and deposition, are discussed. (L.C.L.)

10715 (ORO–2529–28, App. 9) FISSION PRODUCTS IN THE ATMOSPHERE. CHAPTER 2. THE MEAN STRATOSPHERIC RESIDENCE TIME. Kuroda, P. K. (Arkansas Univ., Fayetteville. Dept. of Chemistry). 21p.

From Atmospheric radiochemistry.

Data on the ^{90}Sr content of atmospheric precipitation, acquired by many investigators at worldwide locations from 1956 to 1970 are compiled. Methods for using such data to establish the stratospheric residence time of ^{90}Sr are discussed. Finally, the residence time results reported by various investigators are tabulated and show a range of stratospheric residence time of ^{90}Sr from 10 yrs to 3 months, but with most investigations since 1961 resulting in residence times from 8 to 13 months. (L.C.L.)

10716 (UCRL–72534) DISTRIBUTION AND REDISTRIBUTION OF AIRBORNE PARTICULATES FROM THE SCHOONER CRATERING EVENT. Anspaugh, L. R.; Phelps, P. L.; Holladay, G.; Hamby, K. O. (California Univ., Livermore. Lawrence Radiation Lab.). 13 Nov 1970. 21p. (CONF-701106–5). Dep. NTIS.

From 5th Annual Midyear Topical Symposium on Health Physics Aspects of Nuclear Facility Siting, Idaho Falls, Idaho.

Project Schooner, a 31-kt nuclear cratering detonation, was conducted on December 8, 1968, at the Nevada Test Site. Twelve sampling stations consisting of 6 each, radiation activated, high-volume air samplers were established on arcs 6 and 50 miles downwind from the detonation site. Two stations were located upwind. The air samplers were electronically programmed to operate in a sequential fashion. Intensive sampling extended up to 6 weeks following the event. More than 20 gamma-emitting radionuclides were identified in the airborne particulates by the use of a Ge(Li) detector. Several days after the event, ^{181}W was the predominant radionuclide detected, and served as a unique tracer. Half-life of suspended radioactive particulates was observed to be 38 days. Resuspension factors were calculated and found to vary between 6×10^{-5} and 10^{-7} m^{-1}. Data showed that the passage of radioactive particulates does not occur as an abrupt event but that the air activity remains high for long periods of time after the detonation. Secondary peaks of air activity were seen as late as 2 to 4 days postshot and amounted to as much as 30 percent of the initial activity. Contributions of redistribution effects to the long-term radiological hazards associated with nuclear events are qualitatively discussed. (auth)

10717 PLUME RISE: A RECENT CRITICAL REVIEW. Briggs, Gary A. (National Oceanic and Atmospheric Administration, Oak Ridge, Tenn.). Nucl. Safety; 12: 15–24(Jan–Feb 1971).

Comparison of a large number of plume-rise observations and formulas indicated that a relatively simple model provided the best predictions of plume rise in a variety of meteorological conditions. The model predicts that near the stack the rise of a hot, buoyant plume is proportional to the reciprocal of the wind speed, to the one-third power of the heat emission, and to the two-thirds power of the distance downwind. This "$^{2}/_{3}$ law" of rise fits the bulk of published observations. Dependence on distance downwind gradually diminishes in neutral atmospheric conditions beyond the distance related to the heat emission and the stack height. In stable conditions, rather abrupt leveling of plumes occurs at a distance dependent on the wind speed and the atmospheric vertical temperature gradient. The model was also applied to the prediction of whether a hot plume will penetrate an elevated inversion and was found to agree with observations. (auth)

10718 DEPOSITION AND TRANSLOCATION OF THE RADIOACTIVE FALLOUT. Yamagata, Noboru (Inst. of Public Health, Tokyo); Chiba, Morito; Matsuda, Shunii. Koshu Eiseiin Kenkyu Hokoku; 18: 165–86(Dec 1969).

In order to estimate the contribution of the wind-blown surface soil to the monthly deposition of radioactive fallout, determination was made of iron content of the monthly collection of fallout at 25 localities throughout Japan during the period from April 1968 to March 1969. The iron content suggested that 10 to 15% of the measured ^{90}Sr deposition was contributed by the translocation of ground deposits through wind-blown dust. Discussion was also made on the $^{137}Cs/^{90}Sr$ ratios observed at various institutions in the world, and it was concluded that a representative value should be 1.6, ranging from 1.3 to 1.8 irrespective of the type of sample (deposition or air) and time of collection: higher values such as 2.7 were supposed improbable as an average for a set of determinations. (auth) (Japan)

10719 CALCULATION OF ^{90}Sr CONTENT CHANGES IN ATMOSPHERIC FALL OUT AND ON THE GROUND IN WEST SLOVAKIA UP TO THE YEAR 2000. Ussacev, Sergej; Dobiasova, Zlatica (Univ. Komenskeho, Bratislava). Jad. Energ.; 16: 420–1(Dec 1970). (In Czech).

Theoretical studies of measured data on ^{90}Sr distribution resulted in calculated values for ^{90}Sr hold-up time, T_m, in the atmosphere and of the ^{90}Sr content on the ground in West Slovakia to the year 2000, assuming no further nuclear tests. The values measured in Jaslovské Bohunice from 1962 to 1966 were used in the calculations. (auth)

10720 TRITIUM FALLOUT IN THE PACIFIC UNITED STATES. Leventhal, J. S.; Libby, W. F. (Univ. of California, Los Angeles). J. Geophys. Res.; 75: 7628–33(20 Dec 1970).

Tritium has been measured since the 1961 to 1962 nuclear tests to determine fallout patterns. Crater Lake tritium data are used for a model of mixing and fallout. Ocean-atmosphere-continent effects of stratosphere fallout and dilution by ocean water show continental and latitudinal variation. (auth)

10721 DATA, SECTION III, AIR AND DEPOSITION. Radiol. Health Data Rep.; 11: 545–62(Oct 1970).

Data are reported on the gross β activity in surface air samples collected throughout Central, North, and South America during June 1970. Data on the content of ^{238}Pu and ^{239}Pu in airborne particulates, sampled during April to December 1969, are included. (C.H.)

XUM

Mineralogy and Exploration

Refer also to abstracts 10484 and 10697.

10722 FAST DETERMINATION OF POLYMETALLIC Pb + Zn MINERALIZATION BY GAMMA–GAMMA LOGGING. Simon, L. (Mining Inst., Prague). Rudy (Prague); 17: 316-18(Oct 1969). (In Czech).

The geophysical gamma-gamma method was proved to be applicable for direct measurement of Pb + Zn mineralization in small-diameter boreholes. The measurements were performed at the Horní Benešov ore-bearing deposit. The HOÚ 22 Š gamma-gamma logging set was used for this purpose. As radiation source, ^{75}Se was used. The measurements were compared with results of chemical analyses. It was shown that the gamma-gamma method is suitable for determining the Pb + Zn content in the Horní Benešov ore-bearing deposit. (NSA of Czech.)

10723 LEACHING PATTERNS OF MONAZITE AND ZIRCON. Prasad, E. A. V.; Naidu, M. G. C. (Sri Venkateswara Univ., Tirupati, India). Curr. Sci. (India); 40: 14-15(5 Jan 1971).

Leaching patterns of monazite and zircon were studied. Beta activities of the mineral samples were measured after leaching with acetic, hydrochloric, nitric, and sulfuric acids at various concentrations. Acid concentration has no appreciable effects on losses of uranium. Beta activities are tabulated. (J.G.B.)

10724 URANIUM SUPPLIES. Bell, P. C. Nature (London); 228: 1007(5 Dec 1970).

Reference is made to the ENEA report on uranium resources as reported in Nature 228: 306(1970) and examples are given of the age of this report. (UK) (auth)

Oceanography

Refer also to abstract 10817.

10725 (CU–3139-4) INVESTIGATIONS OF U AND Th SERIES ISOTOPE DISEQUILIBRIA IN THE OCEAN AND IN PLEISTOCENE SEDIMENTS. Annual Progress Report. Broecker, Wallace S.; Feely, Herbert W. (Columbia Univ., Palisades, N. Y. Lamont-Doherty Geological Observatory). Oct 1970. Contract AT(30-1)-3139. 8p. Dep. NTIS.

The Th and U series isotope disequilibria in ocean water and Pleistocene sediments were investigated. The ^{226}Ra, ^{228}Ra, and ^{228}Th content of seawater samples from worldwide locations were measured. The results indicated that systematic trends in the areal and vertical distributions of ^{228}Ra in the oceans exist and that these trends reflect transport processes at work in the oceans. Results of experiments performed to evaluate the reliability of geologic ages obtained by measuring U-series radioisotopes in fossil mollusks, indicated that this dating method cannot be used safely on fossil mollusks. Preliminary experiments indicated that He/U dating is reliable for absolute age estimations for fossil corals. The composition of amino acids in fossil coral and in deep-sea sediments of known age was investigated. The Mn concentrations in deep-sea sediments were measured and proposals are made to explain the much higher Mn concentration in the sediments than in the continental rocks from which these sediments are derived. Ratios of $^{16}O/^{18}O$ in deep-sea sediments were measured to provide data on the history of ice volume fluctuations during the Pleistocene. A study of O isotopic fractionation between rutile and water was begun. (L.C.L.)

10726 ^{226}Ra MEASUREMENTS FROM THE 1969 NORTH PACIFIC GEOSECS STATION. Broecker, Wallace (Columbia Univ., Palisades, N. Y.); Kaufman, Aaron; Ku, Teh-lung; Chung, Yu-chia; Craig, Harmon. J. Geophys. Res.; 75: 7682-5(20 Dec 1970).

The profile of ^{226}Ra with depth at the 1969 Geosecs calibration station in the Pacific Ocean was determined by four different groups of investigators. The Lamont-Doherty group led by Broecker (LDGO-B) used the shipboard in situ method, the University of Southern California group (USC) and the Scripps Institution of Oceanography group (SIO) used the laboratory regenerated radon method, and the Lamont-Doherty group led by Kaufman (LDGO-K) used an isotope dilution method. Most measurements agreed to within 15%. (auth)

10727 NEAR-SURFACE AND NEAR-BOTTOM RADON RESULTS FOR THE 1969 NORTH PACIFIC GEOSECS STATION. Broecker, Wallace S.; Kaufman, Aaron (Columbia Univ., Palisades, N. Y.). J. Geophys. Res.; 75: 7679-81(20 Dec 1970).

Comparison of radon and radium results from the upper 100 meters of the water column at the Geosecs intercalibration station revealed deficiencies of radon consistent with those found at other places in the surface ocean. They suggest a gas exchange rate piston velocity of approximately 6 m/day. In the bottom 100 meters of the water column radon excesses were found. As a maximum in the excess radon was observed 50 meters above the bottom in two separate casts, a simple vertical diffusion model cannot account for the observations. Lateral influx must be taking place. (auth)

Seismology

Refer also to abstracts 10735–10737.

10728 (CEA-R-4059) MECHANICAL ACTIVITY IN A GRANITIC MASSIF SUBJECTED TO A NUCLEAR EXPLOSION. Perrier, Michel (Commissariat a l'Energie Atomique, Bruyeres-le-Chatel (France). Centre d'Etudes). Sep 1970. 30p. (In French). Dep. NTIS (U. S. Sales Only).

The indirect and direct, instantaneous and delayed seismic effects in the vicinity of the underground explosion in Sahara are presented. Interpretation and description are given of the different stages of the mechanical activity observed in the granitic batholith where the explosion took place. (auth) (France)

10729 (CEA-R-4105) SEISMIC COMPRESSION WAVES ASSOCIATED WITH UNDERGROUND NUCLEAR EXPLOSIONS IN THE SAHARA. Ferrieux, Henri (Commissariat a l'Energie Atomique, Grenoble (France). Centre d'Etudes Nucleaires). Nov 1970. 41p. (In French). Dep. NTIS (U. S. Sales Only).

A theoretical analysis was made on the generation of compression seismic waves. The influence of the various parameters (medium and explosion conditions) on the amplitude of the waves is demonstrated. Experimental results on the Sahara underground nuclear explosions are compared with the theoretical considerations. The amplitude relation has the classical form: $A = K W^{n} d^{-m}$ (W: explosive energy, d: distance between the measuring points). The amplitude laws vary with the location of the explosion in the mountain. (auth) (France)

10730 (NVO–1163-TM–22) SEISMIC RESPONSE CHARACTERISTICS AT NRDS FROM UNDERGROUND NUCLEAR DETONATIONS. Weetman, B. G.; Davis, L. L.; Hays, W. W.; Mueller, R. A. (Environmental Research Corp., Las Vegas, Nev.). Dec 1970. Contract AT(29-2)-1163. 99p. Dep. NTIS.

Ground motion generated by certain underground nuclear explosions at the Nevada Test Site (NTS) and recorded at the Engine Test Stand (Station ETS-1) located on the Nuclear Rocket Development Station (NRDS) exhibits a level of response higher than the level which would normally be expected on the basis of average NTS experience. Although the specific cause of this anomalous response is presently not clear, refined techniques have been developed for making ground motion predictions at NRDS. Characteristics of the anomaly include a spectrum unusually enriched in high frequency (3-5 Hz) components and velocity and acceleration seismograms having pulse-like first arrivals with a peak vector amplitude considerably greater than typically observed at that distance for stations with similar geologic settings. The anomalous response is greatest at ETS-1 and decreases in all directions away from it. Analysis of observed data suggests that the anomaly is related to physical parameters of the travel path rather than solely to parameters of the source or receiving station environments. The particular travel path between Pahute Mesa and ETS-1 appears to have a general bearing of N 18°W from ETS-1. (auth)

10731 THREE STUDIES OF MICROEARTHQUAKES: I. THE MICROEARTHQUAKE SEISMICITY OF THE DENALI FAULT. II. MICROEARTHQUAKE INVESTIGATIONS IN NEVADA. III. EARTHQUAKES ASSOCIATED WITH UNDERGROUND NUCLEAR EXPLOSIONS. Boucher, Gary Wynn. New York; Columbia Univ. (1969). 125p. University Microfilms Order No. 70-18,786. Thesis.

Three studies dealing with different aspects of microearthquake phenomena are discussed. The first study deals with the microearthquake activity along a 900 km long stretch of the great Denali fault in Alaska and western Canada. The rates of very local microearthquake activity (S-P times less than 2 sec) varied from 0 to about 40 events per day. The average microseismicity was found to be about the same as that recently found for the San Andreas fault. This result is surprising, because sizable earthquakes have not been reported in the last 70 years on the Denali fault east of Mt. McKinley National Park. A new fault is proposed in the Dezadeash Lake region of the Denali fault zone, based upon a concentration of microearthquake activity as well as topographic evidence. The new fault provides a mechanically more acceptable trend for large transcurrent displacements on the

southeast branch of the Denali fault. The second study reports on a microearthquake survey carried out in parts of Nevada, Utah, Idaho, Montana, and Wyoming. A procedure was developed for normalizing to a common basis microearthquake results obtained under different recording conditions. It was found that the details of microseismicity cannot necessarily be predicted from knowledge of previous major earthquake seismicity. Microearthquakes have a broader distribution than major earthquakes, and they tend to fill in the gaps between the larger events. The highest rate of aftershock occurrence ever recorded, nearly 20,000 events per day, was observed 8.5 days after the southeast Nevada earthquake of 1966. The aftershock zone was located and defined, providing additional constraint on the location of the epicenter of the main shock. The frequency of occurrence of aftershocks for this earthquake was found to decay with time according to an equation of the form $N(t) = N_0 t^{-0.85}$. Using this result, aftershock observations at the sites of 3 other major earthquakes in the western United States indicate that at least a few microaftershocks per day may be observed for centuries after a large earthquake. This suggests that microearthquake studies may provide information about the occurrence of prehistoric earthquakes. As an incidental result it was found that sonic booms from supersonic aircraft are accompanied by a low level 3–5 Hz seismic signal that precedes the arrival of the audible sonic boom by 1 minute or more. A low-flying supersonic aircraft can be detected in advance of its arrival at a distance of 20 km or more by means of this phenomena. In the third study, records of the University of Nevada seismographic station network provided evidence that underground nuclear explosions with magnitudes greater than 5.0 at the Nevada Test Site were followed by increased seismicity for at least 1 day following the explosions. For the most part this activity was confined to the test site and was probably located within 20 km of the shotpoint, although one or two of the larger tests may have influenced seismicity at somewhat greater distances. Most of the events recorded had very small magnitudes, and all earthquakes related to underground tests had magnitudes lower, by at least one magnitude unit, than those of the associated blasts. The study also showed that, if such explosions have any effect on seismicity in active areas distant from the shotpoint, the effects are probably minor compared with normal variations in seismicity. (Diss. Abstr. Int., B)

10732 SOIL STRAIN NEAR A NUCLEAR DETONATION. Olsen, C. W. (Univ. of California, Livermore). Bull. Seismol. Soc. Amer.; 60: 1999-2014(Dec 1970).

Radial and transverse strain seismometers using 6.1-m Invar rods were installed 457, 914, 1524 m from ground zero on a nuclear detonation at the Nevada Test Site. The detonation, Hutch, took place in alluvium at a depth of 548 m and gave a body-wave magnitude of 5.4 ± 0.2. Dynamic and quasi-static strain data were recorded along with triaxial accelerations at the 914-m location. The dynamic data show large strains (2×10^{-3}) and considerable shear-wave activity related to the subsurface structure. Decay with range, corrected for the inelastic region, shows dependence of peak amplitudes of about R^{-3}, but influence of the alluvium is present. The quasi-static data show large strain steps ($>10^{-6}$) at the two nearer stations and considerable dependence on alluvium depth. The strain decay with time is not consistent with that observed on Benham, and, at 914 m, appears to be a permanent step, similar to that observed on the Jorum event. (auth)

ENGINEERING

Nuclear Explosions

Refer also to abstracts 10702, 10716, 10728–10730, 10732, 10792, and 10893.

10733 (AD–708566) SOME PROPERTIES OF RADIOACTIVE FALLOUT: BALLOON-MOUNTED SHOT PRISCILLA. Final Report. Miller, Carl F. (URS Research Co., San Mateo, Calif.). Sep 1969. Contract DAHC20-69-C-0142. 20p. (URS–757-4). NTIS.

Radiochemical assay results from measurements on samples of fallout from the balloon-mounted (air) Shot Priscilla revealed the presence and relatively high abundance of induced activities from soil materials near ground zero. The decay rates at early times were, therefore, significantly slower and the relative exposure rates higher than for normal mixed fission products. On the other hand, the decay rate of the fallout at distances greater than 10 miles from ground zero was essentially parallel to that of unfractionated ^{235}U fission products. The bulk weight of the close-in fallout samples apparently consisted almost entirely of blast-raised dust that settled along with a few larger particles into the collecting trays. The measured specific activity of one single large particle with a diameter of about 750 microns was 40 terafissions/gm. (auth) (USGRDR)

10734 (AD–708567) SOME PROPERTIES OF RADIOACTIVE FALLOUT: SURFACE DETONATION COULOMB C. Final Report. Miller, Carl F. (URS Research Co., San Mateo, Calif.). Sep 1969. Contract DAHC20-69-C-0142. 21p. (URS–757-5). NTIS

Data on the ionization-rate decay, activity-particle size distributions, and exposure rate-conversion coefficient for soil and filter-collected samples of fallout from Shot Coulomb C have been presented. Radiochemical analyses of selected samples permitted the correlation of the results in terms of equivalent fission levels relative to the ^{99}Mo content of the samples. The gross fractionation ratio relative to normal ^{235}U fission products was generally lower than observed for the fallout from larger yield explosions at all times from 240 to 6,000 hours after detonation. Individual radionuclide–radiochemical "R" values were determined for ^{89}Sr, ^{95}Zr, ^{132}Te, and ^{140}Ba. No soil induced activities were detected to be present in significant amount at the time the analyses were carried out at around H + 270. (auth) (USGRDR)

10735 (PNE-R–39) MINE AND WELL EFFECTS EVALUATION FOR PROJECT RULISON. (Bureau of Mines, Denver, Colo. Denver Mining Research Center). Mar 1970. Contract AT(29-2)-914. 58p. Dep. NTIS.

Two reports on postshot evaluations of the effects of Project Rulison ground motions on nearby mines and gas wells are presented. A separate abstract was prepared for each. (L.C.L.)

For abstracts of individual sections see: 10736 and 10737.

10736 (PNE-R–39, Pt.1) MINE EFFECTS EVALUATION FOR PROJECT RULISON. Bolmer, R. L. (Bureau of Mines, Denver, Colo. Denver Mining Research Center). 39p.

The mine effects evaluation program for Project Rulison was designed to identify, evaluate, and eliminate or control all potential hazards to mining operations in the general project area and to document the effects of the nuclear explosion on such operations. An initial survey of the general area out to 50 miles from the emplacement well disclosed some 24 coal, oil shale, limestone, and vanadium mines which would be in active or standby status during event time and thus of concern in the effects evaluation program. Such mines were subsequently visited, and the operators were briefed on the general features of the project and its predicted effects on their operations. Recommendations for the evacuation of the mines during event time later were formulated, and preshot and postshot inspections eventually were made of several of the closer mines where structural damage was a possibility. Postshot inspections indicated structural damage during event time at only two mines—the Cameo and Red Canon coal mines at 27 and 32 miles respectively from the shot point. The rather extensive damage at Cameo reasonably could be attributed to the Rulison event, while the relatively minor damage at Red Canon may or may not be. Except for small landslides and isolated rock falls along certain access roads, no significant damage attributable to Rulison was observed at any of the other nearby mines inspected; nor was any reported by the operators of the fringe-area mines subsequently contacted. Effects of the Rulison event on the closer mines were somewhat less, and on the farther mines somewhat more, than had been expected from predicted ground motions. Azimuthal variations in the ground motion may account for most of these effects, but the lack of adequate damage criteria also could be a significant factor. Better criteria obviously were needed for relating ground motion to mine damage, and more restrictive safety measures were suggested for future shots until such criteria became available. Mine damages on the order of those experienced from the Rulison event would be expected from any future shot of the same yield. Nevertheless, the cumulative effects from a multitude of shots in this range could increase the overall damage potential. Both the severity and extent of such damages, of course, would tend to increase with the yield. Thus any escalation of the yield not only would cause greater damages to the affected mines but also could initiate damages at some of the closer but unaffected operations. (auth)

10737 (PNE-R–39, Pt.2) EFFECTS EVALUATION OF GAS WELLS AND ASSOCIATED FACILITIES FOR PROJECT RULISON. Ward, Don C. (Bureau of Mines, Denver, Colo. Denver Mining Research Center). 16p.

At the request of the Effects Evaluation Division of the Atomic Energy Commission's Nevada Operations Office, the Bureau of Mines inventoried gas wells and associated facilities within a 10-mile radius of Rulison surface ground zero (GZ). All wells and facilities within 5 miles of GZ were examined and photographed in detail, both preshot and postshot. No surface damage from the Rulison detonation was sustained by any of the field gas wells, the test well, or the emplacement well. No subsurface damage was evident or suspected at field wells. It is reasonable to assume that no damage should occur to similar wells and facilities that may be subjected to comparable ground motion. (auth)

10738 SCIENTIFIC AND INDUSTRIAL APPLICATION OF NUCLEAR EXPLOSIVES. Conference Held at Grenoble, France, 20–22 May 1970. Bull. Inform. Sci. Tech. (Paris); No. 149, 3-75 (Jun 1970). (In French). (CONF-700547).

Five papers on industrial and scientific uses of nuclear explosives were presented at the conference and are included in this issue. A separate abstract was prepared for each. (L.C.L.)

For abstracts of individual papers see: 10739–10743.

10739 SOME PHYSICAL ASPECTS OF NUCLEAR EXPLOSIVES. Boue, P. (CEA, Paris). Bull. Inform. Sci. Tech. (Paris); No. 149, 3-7(Jun 1970). (In French).

From 3rd Meeting on the Scientific and Industrial Applications of Nuclear Explosives, Grenoble, France. See CONF-700547.

Following a survey of the materials used, some details concerning fission and fusion reactions are given. The working phases of the explosive and the physical models used are described. The design of explosive charges for industrial or scientific use must respond to certain criteria of bulk or cleanliness, and the economic aspects will be of great importance. Experience gained in the Sahara has proved promising for the applications of these techniques. (auth) (France)

10740 CONTRIBUTION OF EARTH SCIENCES TO THE PEACEFUL APPLICATIONS OF NUCLEAR EXPLOSIONS. Dardel, J.; Sarcia, A. (CEA, Fontenay-aux-Roses, France). Bull. Inform. Sci. Tech. (Paris); No. 149, 9-15(Jun 1970). (In French).

From 3rd Meeting on the Scientific and Industrial Applications of Nuclear Explosives, Grenoble, France. See CONF-700547.

Because of its energy and the radioactivity it produces, a nuclear explosive can only be used under well-defined conditions For maximum yield and safety a thorough knowledge of the medium to be treated is necessary including its structure, lithology, hydrogeology, and chemical, physical, and mechanical properties. (auth) (France)

10741 MECHANICAL EFFECTS OF CONTAINED UNDERGROUND NUCLEAR EXPLOSIONS. Supiot, F. (CEA, Paris). Bull. Inform. Sci. Tech. (Paris); No. 149, 17-28(Jun 1970). (In French).

From 3rd Meeting on the Scientific and Industrial Applications of Nuclear Explosives, Grenoble, France. See CONF-700547.

The mechanical effects connected with the shock wave produced by a contained underground nuclear explosion of 100 kilotons are described and include creation of vaporized, fused, crushed and broken zones, formation of the cavity, and formation of the chimney. (auth) (France)

10742 DISTRIBUTION AND DEVELOPMENT OF RADIOELEMENTS AFTER A NUCLEAR EXPLOSION. Dupuis, M. (CEA, Montrouge, France). Bull. Inform. Sci. Tech. (Paris); No. 149, 41-52(Jun 1970). (In French).

From 3rd Meeting on the Scientific and Industrial Applications of Nuclear Explosives, Grenoble, France. See CONF-700547.

Methods for theoretically predicting the radioactivity due to an underground nuclear explosion are discussed, and are based on studies of: the reaction products of the explosive and of the neutron reaction products; the thermochemical changes in the cavity; and the behavior of the radioelements and their development, particularly the development of tritium. (auth) (France)

10743 SCIENTIFIC AND INDUSTRIAL APPLICATIONS OF NUCLEAR EXPLOSIVES: SAFETY PROBLEMS. Barthoux, A.; Cluchet, J.; Gerard, R.; Hubert, M. (CEA, Paris). Bull. Inform. Sci. Tech. (Paris); No. 149, 53-68(Jun 1970). (In French).

From 3rd Meeting on the Scientific and Industrial Applications of Nuclear Explosives, Grenoble, France. See CONF-700547.

The dangers due to the use of nuclear explosives are of several kinds: seismic effects, toxic and explosive gases, radiations. A thorough study of the meteorological, geological and hydrological parameters is necessary in order to evaluate the diffusion in air and water of the products formed. The special problems connected with excavation explosions and with contained explosions are reviewed. (auth) (France)

10744 SCIENTIFIC AND INDUSTRIAL APPLICATION OF NUCLEAR EXPLOSIVES. Conference Held at Grenoble, France, 20–22 May 1970. Bull. Inform. Sci. Tech. (Paris); No. 150, 3-71 (Jul-Aug 1970). (In French). (CONF-700547).

Eight papers on industrial and scientific uses of nuclear explosives were presented at the conference and are included in this issue. A separate abstract was prepared for each of six. Two abstracts appeared previously in NSA as 24: 22782 and 24: 50486. (L.C.L.)

For abstracts of individual papers see: 10745–10750.

10745 SCIENTIFIC AND INDUSTRIAL APPLICATIONS OF NUCLEAR EXPLOSIONS. Cally, J. C. (CEA, Fontenay-aux-Roses, France). Bull. Inform. Sci. Tech. (Paris); No. 150, 3-13 (Jul-Aug 1970). (In French).

From 3rd Meeting on the Scientific and Industrial Applications of Nuclear Explosives, Grenoble, France. See CONF-700547.

The performance expected from nuclear explosives and the calculation methods by which the effects of an explosion can be predicted are described. The research carried out in different countries on these new techniques is reported, with special reference to the United States. For industrial applications two different techniques are possible: contained explosions (stimulation of gas or oil deposits, storage, lixiviation of ore); and nuclear excavation (large-scale civil engineering operations or ore working). Scientific applications are generally carried out on the occasion of blasting for other purposes. (auth) (France)

10746 SOME ASPECTS OF THE USE OF NUCLEAR EXPLOSIVES IN THE PETROLEUM INDUSTRY. Soviche, G. (Societe ELF, Paris). Bull. Inform. Sci. Tech. (Paris); No. 150, 15-20(Jul-Aug 1970). (In French).

From 3rd Meeting on the Scientific and Industrial Applications of Nuclear Explosives, Grenoble, France. See CONF-700547.

Nuclear explosives can be applied to two branches of the petroleum industry: the stimulation of deposits and the storage of hydrocarbons. The most important technical and economic aspects of this technique already employed industrially in the United States and the Soviet Union are presented here. (auth) (France)

10747 APPLICATION OF NUCLEAR EXPLOSIVES IN THE MINING INDUSTRY. Cally, J. C.; Dardel, J.; Pello, H.; Sarcia, J. A. (CEA, Fontenay-aux-Roses, France). Bull. Inform. Sci. Tech. (Paris); No. 150, 21-8(Jul-Aug 1970). (In French).

From 3rd Meeting on the Scientific and Industrial Applications of Nuclear Explosives, Grenoble, France. See CONF-700547.

Nuclear explosives could be used to level deposits suitable for quarrying, to carry out underground blasting in large masses, or to break up mineral deposits before lixiviation in situ. Several American and Soviet industrial projects are planned for the very near future. (auth) (France)

10748 APPLICATION OF NUCLEAR EXPLOSIONS TO GEOPHYSICS (SEISMOLOGY, ACOUSTICS). Mechler, P. (Ecole Normale Superieure, Paris). Bull. Inform. Sci. Tech. (Paris); No. 150, 51-4(Jul-Aug 1970). (In French).

From 3rd Meeting on the Scientific and Industrial Applications of Nuclear Explosives, Grenoble, France. See CONF-700547.

From a study of geophysical phenomena following underground nuclear explosions it was possible to improve the tables giving the times of propagation of seismic waves between two given points and to develop a method of measuring the thickness of the earth's crust and of detecting the variations in this thickness on a small scale. A study of the propagation of the noise of explosions in the atmosphere showed up gravity waves and waves of a new type and allowed the theory of these phenomena to be established. (auth) (France)

10749 HIGH PRESSURE PHYSICS. Nelson, P. (CEA, Sevran, France). Bull. Inform. Sci. Tech. (Paris); No. 150, 55-8 (Jul-Aug 1970). (In French).

From 3rd Meeting on the Scientific and Industrial Applications of Nuclear Explosives, Grenoble, France. See CONF-700547.

The velocity of the shock wave in the target and at the free surface was measured. Materials under pressure up to 10 megabars were studied. These experiments allow the melting, fracturing, and the plasticity of compacting solid and porous bodies to be studied. (auth) (France)

10750 ECONOMICS OF INDUSTRIAL NUCLEAR EXPLOSIONS. Roynette, A. (CEA, Paris). Bull. Inform. Sci. Tech. (Paris); No. 150, 56-69(Jul-Aug 1970). (In French).

From 3rd Meeting on the Scientific and Industrial Applications of Nuclear Explosives, Grenoble, France. See CONF-700547.

Different methods can be used to carry out a nuclear explosion. The choice of the method depends upon several factors: economics, reliability, flexibility, information potentiality. The algorithms for the selection of a method are presented. (auth) (France)

10751 INTERNATIONAL ARRANGEMENTS AND CONTROL FOR THE PEACEFUL APPLICATIONS OF NUCLEAR EXPLOSIVES. Kalkstein, Marvin. Stockholm Papers. Stockholm; Almqvist and Wiksell (1970). 40p. Sw. Crs. 10.00.

The implications of peaceful nuclear explosives for arms control and disarmament are discussed. Considered in particular are the international arrangements and control measures that might be appropriate. The state of the art of nuclear explosives technology is described, proposed uses of nuclear explosives and their potential economic and social merits are reviewed, and the technical problems which remain to be solved before actual applications will be feasible are outlined. The arms control problems posed by peaceful nuclear explosives are dealt with in detail, as well as the difficulty of making arrangements for testing and use of nuclear explosives which will be compatible with the terms and purposes of the existing nuclear test ban or with a future comprehensive test ban treaty. Finally, the weapons control problems and some of the financial and political alternatives which would be involved in establishing international arrangements for conducting peaceful applications of nuclear explosives are examined. (Sweden)

Facilities and Equipment

Refer also to abstracts 10797, 10803, 11361, 11366, 11464, 11479, 11488, 11831, 11932, and 12708.

10752 (CEA-N-1360) TESTS ON AN AUTOMATIC AIR PURIFYING RESPIRATOR. Chretien, Louis; Le Bourdonnec, Yvon (Commissariat a l'Energie Atomique, Fontenay-aux-Roses (France). Centre d'Etudes Nucleaires). Oct 1970. 19p. (In French). Dep. NTIS (U. S. Sales Only).

Respiration rate can be measured, either from static characteristics (pressure-flow rate) or directly with a pump simulating human respiration. Both methods give an estimation of the relative gain due to the electric centrifugal blower included. The conditions ensuring a positive pressure in the half-mask, and the protection of the wearer against leakages are specified. A calculation was made of the work rate and relative gain in different air flow conditions. (auth) (France)

10753 (GAMD-7567) DYNA: A COMPUTER PROGRAM FOR DETERMINING THE MOTIONS OF THE HEAD OF A PCRV WITH A COMPLETE CIRCUMFERENTIAL CRACK. Read, J.; Katz, R. (Gulf General Atomic, Inc., San Diego, Calif.). 6 May 1969. Contract AT(04-3)-633. 61p. Dep. NTIS.

DYNA is a computer code written to investigate a postulated hypothetical accident in which a complete circumferential crack is assumed to develop in the PCRV liner and concrete. The code computes the transient pressure force and tendon restraining force on the PCRV head, the depressurization of the cavity, and the crack gap size as a function of time. (auth)

XUM

10754 (NP-18633) VARIOUS VERTICAL SAMPLING DEVICES FOR AEROSOLS. Julian, Alain (Toulouse Univ. (France)). 1970. 86p. (In French). Dep. NTIS (U. S. Sales Only).

Thesis.

The vertical distribution in the atmosphere of the long lived radioactive elements (^{7}Be, ^{32}P, ^{90}Sr, ^{210}Pb, and ^{210}Po) and the stable elements (Na, Br, Fe, P, Mn and Cl) was studied. The connection with certain atmospheric physics problems was envisaged. The sampling devices and their setting up were studied. The interest in these particular elements and the various procedures already used, were discussed. The experimental work carried out on the filters is described. Mathematical equations for calculating the rates of flow are solved. The experimental developments, performances obtained, and calibration procedures are presented. (auth) (France)

10755 (ORNL-TM-2803) PERFORMANCE CHARACTERISTICS OF CYLINDRICAL HEAT PIPES FOR NUCLEAR ELECTRIC SPACE AND UNDERSEA POWER PLANTS. LaVerne, M. E. (Oak Ridge National Lab., Tenn.). Jan 1971. Contract W-7405-eng-26. 75p. Dep. NTIS.

A preliminary investigation was made of the performance characteristics of cylindrical heat pipes with a view toward their incorporation as heat transport devices in nuclear electric space and undersea power plants, where reliable unattended operation is of prime importance. The basic operating principles of the heat pipe are summarized, together with an enumeration of the pertinent thermodynamic and transport fluid properties and a brief discussion of each. A number of capillary structures, of both the simple and composite type, is described and some of the advantages and disadvantages are delineated. The readily available heat pipe operating lifetime data are reviewed and are summarized in tabular form. The data show that the heat pipe is capable of the long-term reliability required for unattended operation. The theoretical bases for predicting several of the inherent heat pipe performance limits are reviewed and the resulting predictions compared with experimental data. In general, theory and experiment compare well. The optimization of heat pipe geometry with respect to performance is shown for the situation where heat pipe output is not limited by compressibility or entrainment effects. The effects of several geometric and fluid parameters are examined, primarily by means of the theoretical relations previously obtained. (auth)

10756 (ORNL-tr-2416) KARLSRUHE REPROCESSING PLANT: OBJECTIVES AND CONCEPTION OF THE WAK INSTALLATION. Eitz, A. W.; Ramdohr, H.; Schueller, W. Translated by R. Gregg Mansfield (Oak Ridge National Lab., Tenn.), from Atomwirt., Atomtech.; 15: 74-6(1970). 8p. Dep. NTIS.

An abstract of this paper, prepared from the original language, appeared as NSA 24: 22855.

10757 (RFP-1527) EQUIPMENT FORECASTING SIMULATION MODELS. FACILITIES: FACILITIES PLANNING. Hawes, Ralph W. (Dow Chemical Co., Golden, Colo. Rocky Flats Div.). 4 Dec 1970. Contract AT(29-1)-1106. 17p. Dep. NTIS.

A general description is given of a computerized modeling technique used to determine future equipment requirements. The technique has application also in manpower forecasting and in determining purchase requirements. Included is a simulation of a hypothetical product with related flow charts and illustrations of a computer modeling program. (auth)

10758 IMPACT OF NUCLEAR ENGINEERING ON DEVELOPMENTS IN STRUCTURAL MECHANICS. van Campen, D. H.; Latzko, D. G. (Technische Hogeschool, Delft, Netherlands). Ingenieur (Utrecht); 82: 111-20(16 Oct 1970). (In Dutch).

The need for detailed stress and deformation analysis in the design of nuclear power reactor components is discussed. Some important domains in nuclear engineering requiring further development in structural mechanics are briefly outlined. As an example, the main problems arising in the stress and deformation analysis of large high-pressure flanges are discussed in detail. These include a semi-empirical bolt tightening procedure for obtaining uniform bolt loading, as well as scale effects in flange model investigations and the influence of the gasket reaction location on the deformation behavior of flange joints. (auth) (Netherlands)

10759 IRRADIATION EQUIPMENT FOR STUDYING THE INFLUENCE OF RADIATION ON MARINE ORGANISMS. Vilquin, A.; Fraizier, A. (CEA, Cherbourg, France). Bull. Inform. Sci. Tech. (Paris); No. 151, 33-5(Sep 1970). (In French).

The Marine Radioecology Laboratory at The Hague possesses a panoramic irradiation system equipped with a 2000 Ci ^{137}Cs source designed for the experimental study of irradiation effects on marine organisms. A brief description of the apparatus and its accessory equipment, of the dosimetry methods used, and of the early experiments carried out, is given. (auth) (France)

10760 EXOTHERMAL REACTION TRIGGERING DEVICE. Meneret, Jean (to Desmarquest L. et Cie SA. Commissariat a l'Energie Atomique). French Patent 1,589,063. 23 Mar 1970. Filed 9 May 1968. (In French)

A device to trigger an exothermal reaction in a reaction mass is described, its purpose being to start up the calciothermy reactions involved in the manufacture of uranium or plutonium metal. It consists of a wire suspending a refractory bead above the reaction mass, a washer of given melting point holding the bead onto the wire, and a furnace to heat the bead and washer to a temperature high enough for the washer to melt or soften and release the bead, causing it to fall into the reaction mass. The bead slides on the wire and contains an inner cavity to house the washer and prevent it from heating more quickly than the bead. The furnace is heated electrically by Joule effect. (auth) (France)

10761 ANNULAR PACKED-BED FILTER. Ramaswami, Devabaktuni; Jonke, Albert A.; Levitz, Norman M. (to United States Atomic Energy Commission). U. S. Patent 3,541,762. 24 Nov 1970. Filed 18 Mar 1969.

Concentric cylindrical screens form an annulus which contains filter material. Gas is passed transversely through the filter material from the outer screen and exits axially upward through the inner screen. (Offic. Gaz.)

10762 IMPROVEMENTS IN OR RELATING TO STANDBY POWER SUPPLY SYSTEMS ARRANGEMENTS. Weinberg, Alan Henry (to Plessey Co. Ltd.). British Patent 1,214,880. 9 Dec 1970. Filed 11 Oct 1968.

Reference is made to emergency or standby electrical power supply systems. In conventional systems the supply is provided from an inverter powered by batteries constantly charged from the mains at a high current. In the event of a mains failure the battery continues to supply the load, via the inverter. A disadvantage of this system is that expensive battery charging rectifiers and charge control equipment must be provided to handle the heavy charging currents, that must be at least as large as the load current supplied by the inverter. The system described comprises an inverter, means for phase locking the inverter to the mains supply, and means including phase delay for maintaining the output current from the inverter substantially in phase quadrature with the voltage supply, so that little or no power is supplied to or drawn from the inverter while the supply is operating normally, but in the event of a supply failure the load is immediately provided by the inverter. If a 90° phase relationship is maintained precisely between inverter and supply no power will be transmitted there between, and the inverter "floats" on the supply voltage; in the event of a power failure full power will instantly be provided by the inverter. If the phase relationship is changed from 90° by a small amount it can be arranged for power to be provided via the inverter to charge the batteries while the supply voltage is supplying the load. The improvement over the circuit described in B.P. 1,214,646 for maintaining the desired phase relationship between supply and inverter consists in providing an alternative circuit therefor. A block schematic diagram is shown. The phase delay means may comprise a transducer and resistor arrangement. The systems may be employed as an emergency power supply for nuclear reactors, hospitals, etc. (UK)

10763 ENVIRONMENTAL RADIATION SURVEILLANCE LABORATORY. A Guide to Design, Layout, Staff, and Equipment Requirements. Kamath, P. R. Geneva, World Health Organization (1970). 44p. $2.00.

The rapid expansion of uses of nuclear energy and the tendency to site new nuclear installations close to population centers increases the importance of environmental surveillance near nuclear installations. The reasons for this are outlined. Basic considerations that influence the design of a surveillance laboratory are discussed and include: type of nuclear operations conducted, the density of population and proximity of population centers to the nuclear site; and nature of industrial and agricultural activities in the vicinity. Both regional and central type environmental surveillance laboratories are described in detail. Siting requirements, space requirements, use of individual rooms, staffing, and cost are discussed. Layout plans for laboratories in different climates are presented. The major laboratory equipment, chemicals, and equipment for sampling and emergency monitoring required in an environmental surveillance laboratory are listed in an annex. (L.C.L.)

10764 FURTHER DEVELOPMENT OF SULZER HEAVY WATER COLUMNS. Wartenweiler, M. Sulzer Tech. Rev.; 53: 84-6(1970).

The development of heavy water columns to be used with heavy water moderated nuclear power reactors is described. (D.C.C.)

Heat Transfer and Fluid Flow

Refer also to abstracts 10755, 10797, 11487, 12787, 12793, 12799, 12801, 12808, and 12833.

10765 (AD-709142) MACYL6 HYDRODYNAMIC CODE: A NUMERICAL METHOD FOR CALCULATING INCOMPRESSIBLE AXISYMMETRIC TIME-DEPENDENT FREE-SURFACE FLUID FLOWS AT HIGH REYNOLDS NUMBER. Pritchett, John W. (Information Research Associates, Inc., Berkeley, Calif.). 15 May 1970. Contract N00014-70-C-0260. 64p. (IRA-TR-1-70). NTIS.

A computer code was developed for solving incompressible two-dimensional axisymmetric time-dependent viscous fluid flow problems involving up to two free surfaces. Heuristic models for turbulence are employed to extend the method to indefinitely high Reynolds numbers. Scalar quantities (heat and solute concentrations) are also followed, and the fluid may be slightly nonhomogeneous in the Boussinesq approximation. The method is a second-order space, forward time explicit finite-difference scheme. Free surfaces are treated using the MAC ("Marker-and-Cell") technique. (auth) (USGRDR)

10766 (AERE-R-3984) SOME CALCULATIONS ON HOLDUP, HEAT TRANSFER, AND NUCLEATION FOR STEAM–WATER FLOW IN A 0.5 cm BORE TUBE. Hewitt, G. F. (Atomic Energy Research Establishment, Harwell (England)). Apr 1962. 38p. Dep. NTIS (U. S. Sales Only).

Using the theory of annular flow reported previously by Hewitt (1961) and assuming the Lockhart–Martinelli (1949) correlation for frictional pressure drop it was possible to calculate the holdup and heat transfer coefficient for simple hypothetical cases of steam-water flow in a tube. At zero entrainment the holdup correlation of Lockhart and Martinelli was predicted by the annular flow calculations and the reasons for this prediction are discussed. As entrainment increases the holdup falls and a mass flow rate effect occurs in the correlation. Heat transfer coefficient, on the other hand, is less affected by entrainment, since a large portion of the temperature drop occurs in the boundary layer. The heat transfer calculations reveal a correlation with the Martinelli parameter, X, of the ratio of two-phase to single phase coefficient; this correlation is some 30% higher than the empirical correlation of Collier et al. (1961). Some consideration has been given to the nucleation of steam bubbles in the annular liquid films. Using the theory of Hau (1961) it was possible to predict the heat flux for the onset of nucleation. Comparison of the nucleation heat flux with heat flux for burnout suggests a possible mechanism for burnout at the lower quality region which successfully explains both the reversal of the mass velocity effect, and the maxima, encountered in plots of burnout flux, versus exit quality. (auth) (UK)

10767 (BMBW-FBK-70-24) HEAT TRANSFER TO REFRIGERANTS AT NUCLEATE BOILING, FILM BOILING, AND SUPERCRITICAL CONDITION OF THE FLUID. Haffner, H. (Technische Universitaet, Munich (West Germany). Institut A fuer Thermodynamik). Nov 1970. 142p. (In German). Dep. NTIS (U. S. Sales Only).

In a natural circulation loop heat transfer from the inside of a vertical tube to the refrigerants R 12 and R 22 was studied. At reduced pressures p/p_c from about 0.2 to 2.0 experiments with nucleate boiling, film boiling and supercritical condition of the fluid were carried out. The results are presented in diagrams and tables. The pressure dependence of heat transfer with nucleate boiling is generalized by a relative function; the influence of surface roughness is discussed by microphotographs. The pressure dependence and the deterioration by buoyancy forces of heat transfer with film boiling and supercritical condition of the fluid are discussed. Whereas, heat transfer with nucleate and film boiling is strongly improved with increasing pressure, heat transfer in the studied supercritical region is nearly pressure independent. (auth)

10768 (JUL-657-MA) MATHEMATICAL TREATMENT OF THE STATIONARY THERMAL CONDUCTIVITY IN PIECEMEAL HOMOGENEOUS MEDIA. Walther, Georg Karl Heinrich (Kernforschungsanlage, Juelich (West Germany). Zentralinstitut fuer Angewandte Mathematik). Apr 1970. 64p. (In German). Dep. NTIS (U. S. Sales Only).

Problems of stationary thermal conductivity in piecemeal homogeneous media arising in the optimum thermal design of the pebble-bed reactor developed at Juelich are considered. The theory of the solution of the Laplace differential equation with transition conditions is discussed. The theory is generalized and the principles of numerical methods are developed. The numerical methods are then described. The heat conductivity processes in the pebble-bed reactor are discussed and treated with the help of the special numerical methods. (J.S.R.)

10769 (ORO-3911-3) ACOUSTIC EMISSIONS FROM BOILING BUBBLES. Progress Report, February–November 1970. Saxe, R. F. (North Carolina State Univ., Raleigh). Dec 1970. Contract AT(40-1)-3911. 32p. Dep. NTIS.

Activities are reported on programs to obtain information on parameters associated with generation of acoustic energy by boiling bubbles and to a further understanding of boiling bubble dynamics. Results of investigations on bubble sound emission, and bubble acoustic characteristics are included. (J.R.D.)

10770 COMPARATIVE HEAT EXCHANGE CHARACTERISTICS OF GLASSES WITH A RADIO-PROTECTIVE COATING AND WITHOUT ONE. Makhnavetskii, A. S.; Troshin, N. N. Steklo Keram.; No. 2, 11-14(Feb 1970). (In Russian).

Measurements of temperatures across the thickness of plane large dimension glass with and without coating showed that during continuous glass production with coating but without the secondary heating step, the existing installations for annealing the glass should be re-adjusted in order to complete the heat reflection during coating and to reduce the heat absorption of the coated glass. (tr-auth)

10771 THEORETICAL INVESTIGATION OF THE THERMAL ENTRANCE REGION IN STEADY, AXIALLY SYMMETRICAL SLUG FLOW WITH MIXED BOUNDARY CONDITIONS. Golos, S (Inst. of Nuclear Research, Swierk, Poland). Int. J. Heat Mass Transfer; 13: 1715-25(Nov 1970).

A theoretical analysis is made of the growth of the thermal boundary layer and the heat-transfer problem in a steady, axially symmetrical slug flow of an incompressible, isotropic medium with constant physical properties, without internal heat sources, and with mixed boundary conditions. The exact solution is obtained by use of the Laplace transformation. For comparative purposes, the same problem is solved in an approximate way, by applying the principle of restricted variation. The computations of the temperature field are carried out for liquid sodium flow in the case of Biot's number Bi = 0.5 and Pécelét's number Pe = 22600 using the exact and the approximate solution. The numerical results show that the principle of restricted variation can be applied in a case, in which an exact solution is not possible to find. (auth) (UK)

10772 GAZODINAMIKA DVUKHFAZNYKH SRED. (Gas Dynamics of Two-Phase Media). Deich, M. E.; Filippov, G. A. Moscow; Energiya (1968). 424p.

Problems concerning the flow of two-phase fluids at greater velocities are discussed, since they are important in stationary and transportable power engineering, atomic power plants, and in other fields of physics and heat engineering. The following are discussed in the first part of the book: theoretical bases of the mechanics of two-phase media; calculational methods giving the equations for problems concerning condensation at the greater flow rates; velocity of sound in two-phase media; and subsonic and supersonic flows of wet steam in quasi-one-dimensional formulation of the problem. The second part is concerned with the following applied problems: flow of two-phase media in nozzles, pipes, injectors, turbine networks, and turbine stages that operate on wet steam; problems concerning movement of films; and methods and results of experimental investigations of flow of two-phase media. 251 references. (tr-auth)

10773 TRANSIENT HEAT-TRANSFER PERFORMANCE OF A REACTOR COOLANT CHANNEL DURING ACCIDENTAL POWER EXCURSIONS. Gopalakrishnan, Adinarayantampi. Berkeley, Calif.; Univ. of California (1969). 313p. University Microfilms Order No. 70-17,569.

Thesis.

A detailed understanding of the transient heat transfer in the non-boiling domain within reactor channels is essential in the assessment of reactor safety during accidental power excursions. An approximate analytical solution and a comprehensive numerical solution for the heat transfer from a fuel plate, of appreciable thermal capacity and internal thermal resistance, to a fully developed turbulent channel flow have been obtained for the case of exponentially time-dependent heat generation rates within the plate. The analytical solution for the turbulent conduction re-

XUM

gime is based on a sectionalized flow region and the Karman-Martinelli relations for eddy diffusivity. Laplace transforms of the time-dependent wall heat flux and wall temperature rise are presented and comparison of the large-time analytical results with the numerical solution of the problem shows excellent agreement. A comprehensive computer program has been developed for the numerical solution of the general problem of transient heat transfer to steady fully developed turbulent flow through parallel wall channels. The program essentially solves for the two-dimensional transient temperature fields within the fuel region and the coolant, using either the Deissler or the Karman–Martinelli eddy diffusivity for heat in the fluid. The program has the built-in capability to handle arbitrary temperature dependence of the plate thermal properties, arbitrary space and time dependence of the wall heat source as well as time-dependent inlet coolant temperature distributions. Axial conduction effects are included both in the fuel plate and the coolant. Numerical results have been obtained primarily for exponentially increasing heat generation rates within the plate, with e-folding times in the range $1.0 \text{ msec} \leq t_0 \leq 50.0$, Reynolds numbers in the range $4.0 \times 10^4 \leq Re \leq 3.0 \times 10^5$ have been used and results are presented both for Pr = 0.82 (water) and Pr = 0.004 (liquid sodium). In this range of parameters, the effects of transverse conduction within the fuel plate and transverse turbulent conduction into the fluid are found to overshadow the convective and axial conduction effects during the transient. During exponentially increasing heat generation rates, there is an enhancement in the values of the local Nusselt numbers, this increase being greater for lower values of the exponential period. In all cases, the Nusselt numbers reach asymptotic steady values after a few periods from the beginning of the transient. For a heat generation rate which is exponentially decreased with time from an appreciable steady power level, there is a small decrease in the local Nusselt numbers from their steady state values, this decrease being higher for larger period transients. It is also observed that similar exponential transients, with positive periods, initiated from a steady power operation and from an isothermal low power state give identical results after a few initial periods. The asymptotic Nusselt numbers in the thermally developed region depend on Re, Pr and the non-dimensional channel thickness $(y_c/\sqrt{\alpha_f t_0})$. The effect of an axial distribution in heat generation on the local Nusselt numbers is found to be insignificant in the range $160 \leq Pe \leq 2.46 \times 10^5$. In the thermal entrance region, the nondimensional transverse fluid temperature distributions and the axial wall temperature profile are found to reach asymptotic stationary shapes. The effects due to a heat generation rate which follows the Fuchs' model can be explained in terms of the behavior of transients with positive and negative periods. Limited comparisons have been made between the transient non-boiling data of Schrock et al with the present numerical solutions and previous analytical approaches. The numerical results from the present program, using the Deissler formation of eddy diffusivity, are found to agree closely with the experimental data for average wall temperature rise and net heat flux. (Diss. Abstr. Int. B)

10774 DEVICE FOR LIMITING HEAT TRANSFERENCE BETWEEN TWO PARALLEL SURFACES. (to Compagnie des Ateliers et Forges de la Loire). British Patent 1,215,081. 9 Dec 1970. Priority date 1 Feb 1967, France.

A high efficiency barrier is described which is useful in limiting convective, conductive, and radiative heat transfer. A plurality of metal gauze elements are placed in parallel to form the barrier. Metal sheets without perforations are also used to effect thinner gas-filled compartments thereby reducing convection in the barrier. The barrier is useful in reactors, reheaters, and apparatus operating under pressure. (J.R.D.)

Isotope Technology

Refer also to abstracts 10443, 10755, 10759, 10842, 11227, and 11477.

10775 (KFKI–70–26–HP) QUANTITATIVE AUTORADIOGRAPHY OF Zr–T PARTICLES. Biro, J.; Feher, I. (Magyar Tudomanyos Akademia Kozponti Fizikai Kutato Intezete, Budapest). [1970]. 6p. Dep. NTIS (U. S. Sales Only).

The danger of tritium gas incorporation during the use and preparation of Zr–T targets for neutron production was investigated by the quantitative autoradiography of Zr–T particles. The active particles from the Zr–T targets were collected on membrane filters; the membrane filters were placed on a polyethylene foil and covered with a radiographic emulsion. The activity change of the Zr–T particles with the diameter as the dark spots in the radiogram was measured, and the particle diameter was determined in dependence on the dark spot diameter. The activity size distribution and the activity median diameter were determined from these measurements. (J.S.R.)

10776 (MLM–1779) APOLLO APPLICATIONS PROGRAM (ATM) UV MIRROR/GRATING RADIOISOTOPE HEATERS FABRICATION. Wyder, W. C. (Mound Lab., Miamisburg, Ohio). 8 Jan 1971. Contract AT–33–1–GEN–53. 10p. Dep. NTIS.

A summary is presented of the work performed on the fabrication of the Ta–10 wt % W inner liners for the 0.02-W source, and the Ta–10 wt % W inner liners and outer strength members for the 0.50-W source. Die dimensions, part dimensions, and recommendations for improvements are given. (auth)

10777 (NUMEC–4189–3) RADIOISOTOPE POWERED CARDIAC PACEMAKER PROGRAM. Quarterly Progress Report for Phase II, August 1–October 31, 1970. (Nuclear Materials and Equipment Corp., Apollo, Pa. Energy Conversion Div.). Contract AT(30–1)–4189. 73p. Dep. NTIS.

The results of developmental work on an implantable Radioisotope-Powered Cardiac Pacemaker (RPCP) are reported. During the period reported, 70% of the capsule components required for fuel, safety test, and weld verification capsules were completed. Ultrasonic inspection of all inner capsules materials was completed. Special equipment required for pilot plant production fabrication and testing was defined. Systems testing of units implanted in dogs continued. The safety testing program was further refined. Simulated cremation tests were performed on two RPCP units, from which it was concluded that the use of a Ta hot strap and Ti hot shoes, thereby eliminating most of the Cu in close proximity to the capsule, would result in a RPCP capsule capable of sustaining postulated cremation conditions. (L.C.L.)

10778 (ORNL–TM–3214) ISOTOPE KILOWATT PROGRAM QUARTERLY PROGRESS REPORT FOR PERIOD ENDING SEPTEMBER 30, 1970. (Oak Ridge National Lab., Tenn.). Dec 1970. Contract W–7405–eng–26. 24p. Dep. NTIS.

The design and fabrication of the shield block for a series of organic fluid capsule tests to evaluate the combined effects of temperature and radiation was completed. The radiation source has been prepared except for the closure weld for which a hot cell is scheduled. The materials for preparation of the fluid (a pure form of Dowtherm A) have been procured and several sample glass capsules have been fabricated. The detail design of the components for the organic fluid test loop has been initiated. A stainless steel Chempump of the proper capacity has been made available from another program that has been discontinued. The first tests of the aluminum screen thermal insulation—thermal fuse concept have been completed. Examination of the results indicates that the screen has sufficiently good insulating properties and yet will melt if the shield surface temperature rises to 1370°F, and thus it will provide the necessary safety provisions in the event of an accident that interrupts heat removal via the power conversion system. A new aluminum screen insulation test unit has been designed and is being built for further tests. This will be ready for test when new heater rods (which are on order) arrive, and the heater and wire screen test specimen are assembled in a vacuum-tight vessel. The latter will permit operating the thermal insulation under reduced pressure to determine the effect on the heat loss rate of eliminating thermal convection. The last series of tests on the reentry tube steam boiler has been completed and a report is being prepared. Three short lengths of wick for the heat pipe of the thermoelectric module have been fabricated and the first full-scale length has been drawn and sintered. Fabrication of the balance of the parts for the heat pipe test rig is largely completed and assembly has been initiated. The design and fabrication of a complete full-scale thermoelectric module making use of lead telluride junctions has been initiated. Analyses of the relative performance characteristics of iron and nickel heat block-shield assemblies have been completed. The study results show that nickel will be required if advanced thermoelectric materials become available and are to be operated with a hot junction temperature of 1350°F. Nickel is generally superior to steel, but steel is adequate for the other applications. The cost and delivery time are, of course, much greater for nickel, and the differences are being evaluated. The 4.10 in. diameter fuel capsule for the $SrTiO_3$ source has been evaluated and a detailed report of the capsule design and safety analysis is in preparation. (auth)

10779 HALF-LIFE OF ^{239}Pu BY CALORIMETRY. Oetting, Franklin L. (Dow Chemical Co., Golden, Colo.). Contract AT(29–1)–1106. Nucl. Met., Met. Soc. AIME; 17: 154–63(1970).

From 4th International Conference on Plutonium and Other Actinides, Santa Fe, N. Mex. See CONF-701001–(Pt.1).

The power output from two 1-kilogram samples of pure plutonium metal was determined by isothermal calorimetry. The

major isotopic constituent in both samples was plutonium-239, accounting for 93% in the first sample and 97% in the second sample. After making power corrections for the remaining isotopes, the specific power output of plutonium-239 was found to be $1.931 \pm 0.004 \times 10^{-3}$ watts/gram. The power emitted by the two samples remained essentially constant (±0.1%) for a period of four months. Using the alpha zero energy for plutonium-239 of 5.1556 MeV and the recoil energy of 0.0863 MeV, the alpha half-life of plutonium-239 was calculated to be 24,065 ± 50 years. This is compared to the currently accepted value of 24,400 ± 30 years as determined by absolute alpha (specific activity) low geometry counting techniques. (auth)

10780 ZASTOSOWANIE IZOTOPOW PROMIENIOTWORCZYCH W ODLEWNICTWIE. (Use of Isotopes in Casting Practice). Briks, Wojciech; Marcinkowski, Jan. Nowe Technika, Zeszyt 83. Warszawa; Wydawnictwa Naukowo-Techniczne (1969). 166p.

Radioisotopic tracer techniques used in the metallurgical industry are reviewed considering the methods, technical devices, and problems of personnel protection. The handling of radioactive materials, nondestructive activation analyses, autoradiographic techniques, aspects of nuclear fission of interest to metallurgists, radiotracer methods for metal cleaning, and control of charge cupola by means of γ rays are discussed as well as tracer studies of metal structure and phase transformation. The use of radioisotopes for evaluating the technology of continuous casting, and the protection of workers against ionizing radiation under industrial conditions are described. 204 references. (R.V.J.)

10781 COLLIMATION SYSTEM FOR IRRADIATION APPARATUS. Eymery, Rene (to Commissariat a l'Energie Atomique). French Patent 1,589,876. 6 Apr 1970. Priority date 23 Oct 1968, France. (In French).

A collimation device for irradiation apparatus was designed; it contains a radioactive source made up of a source holder frame in which radioactive elements in the form of cylindrical rods or point sources are arranged. This frame possesses the following features to be considered together or separately: it is equipped with a perforated mask placed parallel to and in front of one face of the source; the mask has screens extending in front of each of the parallel faces of the source holder frame; in the event that the source includes a number of radioactive elements in the form of parallel cylindrical rods the screens consist of metallic triangular-base prisms parallel to the rods; when the source contains radioactive point elements distributed over a regular network the screens form a grid, the perforations of which are placed in front of each point element and are prolonged by pyramidal or truncated cone shaped cells; the screens in the mask and the radioactive elements in the source can be oriented in such a way that they are inclined at a given angle to the traveling direction of the objects to be irradiated. (France)

10782 CASCADE RATE FUNCTIONS FOR SEPARATING MULTICOMPONENT ISOTOPIC MIXTURES. Kolokol'tsov, N. A.; Nikolaev, B. I.; Sulaberidze, G. A.; Tret'yak, S. A. At. Energ. (USSR); 29: 128-9(Aug 1970). (In Russian).

Individual elements of a countercurrent separation cascade were analyzed, determining the enrichment factor. The separating capacity is a characteristic of the element and thus it does not depend on the mass composition and the concentration of the components in the mixture. The separation potential Φ was derived from the differential equations of the partial derivatives. This potential indicates the contribution of the individual components to the overall degree of separation of the system. The expressions derived for the separation potential and the total rate function of the cascade allow an estimate to be made of the operating characteristics of optimized multicomponent cascades. (TTT)

10783 THERMAL DIFFUSION COLUMN. THEORY AND PRACTICE WITH PARTICULAR EMPHASIS ON ISOTOPE SEPARATION. Vasaru, Gheorghe; Mueller, Guenter; Reinhold, Guenther; Fodor, Traian. Physikalisch-Chemische Trenn- und Messmethoden, Band 13. Berlin, VEB Deutscher Verlag der Wissenschaften (1969). 210p.

Information is presented on the theory and practical aspects of thermal diffusion. Column theory is discussed along with multicomponent separation and operation of glass and metal columns. Process efficiency is examined. Emphasis is placed on isotope separation. (J.R.D.)

10784 PARTICLE SIZE OF SOLID AGGREGATES BY BETA-BACKSCATTERING. Banerji, S. K.; Chatterjee, A.; Das, S. K. (Fertilizer Corp. of India Ltd, Sindri). Technology (Sindri); 7: 55-6(Jan-Jun 1970).

A method of determining particle size in metal oxide and dolomitic limestone aggregates using beta backscattering from $^{90}Sr-^{90}Y$ sources is described. (J.R.D.)

10785 METHOD AND APPARATUS FOR MEASURING THE WEIGHT OF A LOAD ON A CONVEYOR BELT. Brunton, Donald C. (to Brun Sensor Systems, Inc.). U. S. Patent 3,541,332. 17 Nov 1970. Filed 1 Mar 1967.

Methods and apparatus for measuring and controlling the weight of irregular loads moving on conveyers are described. One or more radiation sources are used in a system in which the exponential radiation signal response to variations in load thickness on the conveyer in its movement is linearized by subjecting the output signal to a non-linear circuit. The output signal is then proportional to the weight of the incremental transverse vertical section of the load. (J.R.D.)

10786 EVALUATION OF THE INFLUENCE OF THE MODE OF GAS FLOW ON THE SEPARATION FACTOR OF A THERMAL DIFFUSION COLUMN. Shimizu, Masami (Showa Denko KK, Tokyo; Takashima, Yoichi. J. Nucl. Sci. Technol. (Tokyo); 7: 574-9(Nov 1970). (In French).

The transport equation relevant to the heavier of two elements forming a gaseous mixture was derived. The equation became that of Jones and Furry when the smaller terms were neglected. The influence on the separation factor brought by the axial gas velocity v_i along the hot wire surface was then analyzed. It was found that the maximum separation factor displaces toward lower operating pressures when the gas velocity v_i is increased to a certain degree. It appears that to obtain maximum separation, lower operating pressures should be combined with higher gas velocity v_i, while with increasing operating pressure, v_i should have to be gradually reduced, finally to reach zero at a certain pressure. (auth)

10787 CRITERIA FOR THE DESIGN OF A NH_3–H_2 TWO-TEMPERATURE PLANT FOR HEAVY WATER PRODUCTION. Folli, E. (Centro Informazione Studi Esperienze, Milan); Polastri, F.; Vaccaro, G. Energ. Nucl. (Milan); 17: 721-32(Dec 1970). (In Italian).

Criteria for the design of a dual temperature plant for heavy water production based on the $[NH_3]_l - [H_2]_g$ isotopic exchange reaction are presented. The reaction kinetics are examined and the temperatures of the hot and cold columns are optimized in relation to the overall exchange volume, which is a function of the recycle parameter, and in relation to the overall exchanger surface. Plant economic optimization parameters are correlated. (auth)

10788 SUBMERGED ENERGY CONVERTER. Majkrzak, Charles P. (to International Telephone and Telegraph Corp.). U. S. Patent 3,541,342. 17 Nov 1970. Filed 1 Dec 1967.

An arrangement is provided for converting the energy of radiation from a radioisotopic energy source into useful electrical energy using a mercury-vapor turbogenerator system, and means are provided in this system to enhance the heat transfer between the heat source and the boiler and superheater sections. (Office Gaz.)

10789 ISOTOPE SEPARATION APPARATUS. Combelles, Roland (to Entreprise Miniere et Chimique). French Patent 1,589,053. 22 Mar 1970. Filed 9 Apr 1968. (In French).

An isotope separation apparatus operating by exchange between a liquid phase and a gas or vapor phase is described. It consists essentially of one or more columns of general inverted conical form arranged in series, the section of the cylindrical stages decreasing from top to bottom and the height of the stages increasing with the isotope concentration. Each stage is provided with a partial reflux caused by chemical reaction or distillation, each flow-rate of which is adjusted independently either on the reflux volume or on the retrogression rate. (France)

Materials Testing

Refer also to abstracts 10784, 11364, 11369, 11488, and 12790.

10790 (RD/B/N–1795) DYNAMIC STRESS CONCENTRATION AT A CHAMFERED CHANGE OF SECTION. Stearn, S. M. (Central Electricity Board, Berkeley (England). Berkeley Nuclear Labs.). Oct 1970. 16p. Dep. NTIS (U. S. Sales Only).

The note re-examines the assumptions made previously in deriving the concentration of dynamic stress at a sharp change of section. It is concluded that the same analysis may be used to predict the dynamic stress concentration at a chamfered change of section, such as to be found on the gas baffle of Dungeness "B." The result is verified by experiment. (auth)

10791 ELECTRON-BEAM INDUCED STRESS WAVES IN SOLIDS. Perry, F. C. (Sandia Labs., Albuquerque, N. Mex.). Appl. Phys. Lett.; 17: 478-81(1 Dec 1970).

XUM

Large-amplitude stress waves have been generated in solids by means of a very high-current pulsed electron beam. The electron beam has an average energy of 3 MeV, current of 40,000 A, and pulse duration of approximately 70 nsec. The back surface velocity profiles were measured using a laser-Doppler interferometer. Data obtained for 6061-T6 aluminum indicated a slow rise of the plastic wave, thus suggesting the importance of strain rate effects. The utility of the technique for materials research at high pressures and temperatures is discussed. (auth)

Protective Structures

10792 (SC-RR-70-441) WIND AND AIRBLAST LOADS ON WINDOW PANES. Reed, Jack W. (Sandia Labs., Albuquerque, N. Mex.). Oct 1970. 21p. Dep. NTIS.

Proper perspective about the nuisance damage effects of explosion airblasts or sonic booms requires some understanding of background levels for this kind of deterioration. Many common instances of window breakage are caused by winds. Available data on winds and gustiness have been used to estimate wind load expectations for comparison with airblast experiences. In spite of many necessary uncertainties and assumptions, it is concluded that a recorded peak-to-peak airblast wave pressure of 4 mb, with wavelength typical of large explosions or sonic booms, gives damaging loads comparable to that from winds within the memory span of many people. (auth)

Radioactive Material Handling

Refer also to abstracts 10658, 10691, 10703, 10756, 10763, and 11062.

10793 (BARC-506) SYNTHESES OF PHYLLITIC MINERALS: THEIR UTILISATION IN RADIOACTIVE WASTE TREATMENT. PART I. FROM SILICA GEL AND MIXED GELS OF SILICA AND ALUMINA IN PRESENCE OF MAGNESIUM ACETATE. Brat, Satya; Balu, K. (Bhabha Atomic Research Centre, Bombay (India)). 1970. 22p. Dep. NTIS (U. S. Sales Only).

Syntheses of phyllitic silicate minerals have been carried out using silica gel and mixed gels of silica and alumina, in presence of different concentrations of magnesium acetate at atmospheric pressure and at a temperature of approximately 100°C. The products obtained were subjected to x-ray evaluations and have been found to be crystalline and belong to saponite–montmorillonite family. The suitability of the synthetic products for the decontamination of radioactive wastes with CsCl + ^{134}Cs, has been studied and the products are found to be promising for the removal of radioactive cesium from liquid wastes. (auth)

10794 (CEA-R-4120) ISODORE FACILITY. Brebant, Charles; Plumejeau, Jean; Ramus, Pierre; Roussel, Emile (Commissariat a l'Energie Atomique, Saclay (France). Centre d'Etudes Nucleaires). Dec 1970. 186p. (In French). Dep. NTIS (U. S. Sales Only).

The Isidore facility was constructed at the Irradiated Fuel Laboratories (L.E.C.I.) at Saclay, parallel with the K facility, which has been in use since 1959. A description is given of the general equipment, the ventilation circuits, the electrical circuits, the cell connections, the circuits for the disposing of contaminated liquids and the safety and radiological procedures. The Isidore and the K facility, which are composed of cells having very different characteristics, are complementary. (auth) (France)

10795 (CNEA-272) EZEIZA SEMI-INDUSTRIAL IRRADIATION PLANT. Papadopulos, Celso C. (Comision Nacional de Energia Atomica, Buenos Aires (Argentina)). 1970. 25p. (In Spanish). Dep. NTIS (U. S. Sales Only).

The Ezeiza semi-industrial irradiation plant is described in detail. The plant has some specific characteristics which distinguish it. The radiation source can produce up to 1 MCi. The irradiation enclosure and the access hall have large dimensions; the free passage section is more than 4 m^2, which permits the input and manipulation of large samples. The sample transport system consists of automatic carriers which integrate into a unit easily modified to adapt it to the variable conditions of the samples to be irradiated and to the dimensions of the source. (J.S.R.)

10796 (KFK-866) INCORPORATION OF MACHINE DATA HANDLING IN THE MONITORING OF FISSIONABLE MATERIAL IN LARGE RESEARCH CENTERS. Hagen, A.; Wickenhaeuser, A.; Winter, H. (Kernforschungszentrum, Karlsruhe (West Germany). Institut fuer Angewandte Reaktorphysik). Apr 1970. 19p. (In German). Dep. NTIS (U. S. Sales Only).

An Instrumented Nuclear Safeguards Project was developed at the Karlsruhe Nuclear Research Center. The modern control system evolved in the course of this work will be investigated not only in plants such as reactors, reprocessing and fabrication plants, but also in research installations, such as the Karlsruhe Nuclear Research Center which is used as an example. The multitude of users of fissile material within such establishment, the diversity of types and forms of fissile material, and the different origins and quantities give rise primarily to problems of data handling for control purposes. For processing the reports covering movements of fissile material within the Center and supplies from and to external agencies, a FORTRAN program was developed in its basic outlines which is capable of supplying information at any time about the fissile material within one research installation. The data processing program is flexible enough to allow the incorporation at any time of additional aspects, such as uncertainties in balancing because of errors in measurement, indications of criticality hazards, etc. (auth)

10797 (NYO-841-23) HARVARD AIR CLEANING LABORATORY SEMIANNUAL PROGRESS REPORT, MARCH 1–AUGUST 31, 1970. First, M. W.; Underhill, D. W.; Goldin, A. S.; Yusa, H.; Reist, P. C.; Baldwin, T.; Trindade, H. A.; Lee, S. H.; Moeller, D. W. (Harvard Univ., Boston, Mass. Harvard Air Cleaning Lab.). Oct 1970. Contract AT(30-1)-841. 83p. Dep. NTIS.

The experimental methods used and results obtained at the Harvard Air Cleaning Laboratory are described for the following studies: measurement of thermal conductivity of layers of elemental Na deposited on heat exchanger surfaces; behavior of I in Na systems; optical properties of Na aerosols; and evaluation of fission gas adsorption beds. In addition consultation services were provided to projects related to the Fast Flux Test Facility, and the 11th AEC Air Cleaning Conference was arranged. (L.C.L.)

10798 (ORNL-NSIC-84) INDEXED BIBLIOGRAPHY ON TRANSPORTATION AND HANDLING OF RADIOACTIVE MATERIALS–2. Seagren, R. D.; Shappert, L. B. (Oak Ridge National Lab., Tenn.). Jan 1971. Contract W-7405-eng-26. 123p. Dep. NTIS.

Abstracts of articles associated with shipping containers, transport regulations, criticality in handling, and transportation accidents are presented. Indexes of keywords, authors, and report numbers are included. (J.R.D.)

10799 SOLIDIFICATION OF RADIOACTIVE SLUDGES. Nomi, Mitsuhiko; Sano, Katsunori (Ebara Mfg. Co. Ltd., Tokyo). FAPIG (Tokyo); No. 54, 124-30(Sep 1969). (In Japanese).

With the advance of atomic industries, the problem of radioactive wastes is presenting increasing problems. For liquid wastes, the solidification in concrete was usually employed. Now, however, the solidification with asphalt is attracting general interest. Compared to the former technique, the solidification with asphalt has the advantages of a superior reduction in the volume and a higher water-repellant property. The state of worldwide developments on the method are reviewed, and then tests and studies are explained in detail, including the cold and the hot test. The process is as follows: a sludge is first prepared in a condensation-precipitation tank, followed by dehydration; asphalt is melted in a preheating tank; both the sludge and asphalt are admixed together in another tank, where moisture is also removed by heating; finally, the whole is allowed to solidify by cooling. Vapor and gas emitted during the process are suitably removed. (Japan)

10800 METHOD AND APPARATUS FOR TRANSFERRING SOLID RADIOACTIVE WASTE. Andriot, Roger; Besnier, Joseph (to Commissariat a l'Energie Atomique). British Patent 1,215,265. 9 Dec 1970. Priority date 5 Jun 1968, France.

Methods and apparatus for transferring radioactive waste incorporated in bitumens which soften at 40 to 65°C to non-recoverable containers are described. The material is transferred by gravity. When the container is full the waste is allowed to solidify and is cut at the coupling region to effect separation of the container and the filler chamber. (J.R.D.)

10801 CASK FOR NUCLEAR REACTOR FUEL ELEMENTS. Capet, Henri (to Commissariat a l'Energie Atomique). French Patent 1,586,456. 12 Jan 1970. Filed 30 Aug 1968. (In French).

A spent fuel element cask is described. It encloses a cylindrical container of radiation-shielding material fitted with cells to house the elements for transport, these being equidistant from a shaft fixed in the axis of the container. It also possesses a cover through which a tunnel is bored at the same distance from the shaft as the cells. Each cell in turn is brought in line with this tunnel for loading or unloading. (auth) (France)

10802 AMERICAN NATIONAL STANDARD FOR NUCLEAR CRITICALITY SAFETY IN OPERATIONS WITH FISSIONABLE

MATERIALS OUTSIDE REACTORS. ANSI N16.1-1969, Revision of N6.1-1964. Hinsdale, Ill.; American Nuclear Society (1970). 11p.

A standard to provide guidance for prevention of criticality accidents in handling, storing, processing, and transporting fissionable materials is presented. The scope of the standard is described and terms used are defined. Other sections contain information on nuclear criticality safety practices, single-parameter limits for fissile nuclides, and multiparameter control. (J.R.D.)

10803 IMPROVEMENTS TO RINGARD TRANSFER SYSTEMS. (to Commissariat a l'Energie Atomique. Societe Robatel SLPI, SA). French Patent 1,586,696. 19 Jan 1970. Filed 22 Aug 1968. (In French).

A flexible device was designed for the transfer of a radioactive element from a transport container to a cell where it is to be used. The elements or blocks, rigid and attachable by bolts, are fixed to a metallic ribbon of high tensile strength. The storage and conveyor mechanisms specially designed to cooperate with this device are described. (auth) (France)

Vacuum Engineering

10804 GETTER FOR VACUUM PUMPS AND ITS USE. Prevot, Francois; Sledziewski, Zbiniev (to Commissariat a l'Energie Atomique). French Patent 1,587,747. 16 Feb 1970. Filed 25 Sep 1968. (In French).

A titanium monoxide (TiO) vacuum pump getter is described. A procedure for obtaining an ultrahigh vacuum using this getter and the vacuum pumps used are described. (France)

10805 APPARATUS FOR EVAPORATION BY LEVITATION IN AN ULTRA-VACUUM. Van Audenhove, Jean; Joyeux, Jean; Parengh, Maurits (to EURATOM). British Patent 1,217,443. 31 Dec 1970. Priority date 5 Apr 1968, Belgium.

The design of equipment for use in deposition of thin coatings on substrates by levitation evaporation in ultrahigh vacuums is described. An inductor is provided to effect levitation and provision is made to transfer the coated piece and position a series of other pieces to be coated without the necessity of opening the vacuum chamber. (J.R.D.)

10806 DOUBLE-WALL ULTRA-HIGH VACUUM SYSTEM WITH ELECTRON GUN AND EVAPORATION RATE MONITOR. Hinoul, M.; Witters, J. (Univ., Louvain, Belg.). Thin Solid Films; 6: 213-16(Sep 1970).

An ultrahigh vacuum apparatus is described which is specially suited for film deposition in a clean and contamination-free atmosphere. It has an extremely rapid cycling time and provision for simultaneous evaporation from two sources by a new type of electron gun. (auth)

XUM

INSTRUMENTATION

Radiation Detection Instruments

Refer also to abstract 11056.

General Detectors and Monitors

Refer also to abstracts 10473, 10884, 10903, 11628, 12321, and 12826.

10807 (AD-708922) GEIGER COUNTERS: THEORY, OPERATION, AND MANUFACTURE. Final Report. Korff, Serge A. (New York Univ., N. Y. School of Engineering and Science). 30 Apr 1970. Contract DAHC20-68-C-0137. 160p. NTIS.

The theory, operation and the constructional details of Geiger counters are reviewed. Various types are discussed, and various manufacturing procedures are recommended. The fundamental characteristics of gas-discharge devices, and the details of quenching, the effects of gas fill and sizes and voltages are discussed. (auth) (USGRDR)

10808 (AERE-R-5561) TIME JITTER DUE TO NOISE IN TIMING SYSTEMS. Orman, P. R. (Atomic Energy Research Establishment, Harwell (England)). Aug 1967. 4p. Dep. NTIS (U. S. Sales Only).

Circuit noise gives rise to "time jitter" in the electrical signals used in timing systems. This may be significant especially when the transducer signals are amplified before being used to give time information. It is shown that because of the relation between amplifier noise and rise-time, minimum time jitter is obtained when the amplifier rise-time is equal to the rise-time of the transducer signal. (auth) (UK)

10809 (BNWL-SA-3565) INTERCOMPARISON OF PORTABLE RADIATION MONITORING INSTRUMENT EVALUATIONS. Thompson, I. M. G.; Larson, H. V.; Kathren, R. L. (Battelle-Northwest, Richland, Wash. Pacific Northwest Lab.). [1970]. 50p. (CONF-701112-2). Dep. NTIS.

From Symposium on New Developments in Physical and Biological Radiation Detectors, Vienna, Austria.

The evaluation procedures and results of the intercomparison of radiation protection instruments from Berkeley Nuclear Laboratories in the United Kingdom and the Pacific Northwest Laboratory of Battelle Memorial Institute are discussed. A low-level exposure ratemeter consisting of an energy-compensated G-M detector; a Cutie Pie β-photon survey meter (ionization chamber); a neutron dose-equivalent ratemeter consisting of a spherical helium-3 proportional detector in a polyethylene sphere; and a neutron dose-equivalent ratemeter consisting of a cylindrical boron trifluoride proportional detector in a polyethylene moderator were studied. (W.H.K.)

10810 (CEA-CONF-1688) STATIONARY GAS DETECTORS FOR MAPPING AND DYNAMIC STUDIES OF ORGANS USING X RAY OR LOW-ENERGY γ-RAY EMITTERS. Allemand, R.; Brey, C.; Gagelin, J. J.; Laval, M. (Commissariat a l'Energie Atomique, Grenoble (France). Centre d'Etudes Nucleaires). 8 June 1970. 13p. (In French). (CONF-700536-2). Dep. NTIS (U. S. Sales Only).

From 12th Meeting on Exploration Techniques Using Radioactive Isotopes, Strasbourg, France.

Work on the visualization process for thermal neutrons was adapted to the visualization of x or γ ray emitters using proportional gas detectors. Using induced charge effects, two signals on two different electrodes were associated for each event detected in the gas. These electrodes are interconnected and arranged to form a matrix; each point of this matrix is a detector cell. Each event thus corresponds to the coordinates (X Y). Each row and each column is associated with an electronic measurement channel and a coincidence logic (X Y), which allows the information to be located in the storage and visualization device. Results obtained with an experimental chamber led to the development of a detector for studying the thyroid using I-125. Tests are currently being made with this detector. The spatial resolution is 3 mm and the detection efficiency 35%. (France)

10811 (CEA-CONF-1685) NEUTRON DOSIMETRY AND SPECTROMETRY BY THE MULTISPHERE METHOD: PRESENT STATE OF THE STUDIES AT THE SERVICE D'ETUDES DE SURETE RADIOLOGIQUE. Benezech, Georges; Bricka, Michel; Dolias, Mylene (Commissariat a l'Energie Atomique, Saclay (France). Centre d'Etudes Nucleaires). 1970. 21p. (In French). (CONF-700939-1). Dep. NTIS (U. S. Sales Only).

From International Summer School on Radiation Protection, Dubrovnik, Yugoslavia.

Moderator spheres for neutron flux measurements in two principal directions are discussed. Attempts were made to measure directly the kerma fluence and the equivalent doses (rem) by using one or two or three spheres. Neutron spectra compatible with data from a more complete assembly of spheres were studied. The kerma fluences were obtained from those spectra. The multisphere technique led to an accuracy of 10% for the flux and 20% for the doses, measured in rem, and is particularly suitable for measurements in fields rich in intermediate energy neutrons. Multisphere spectrometry is of insufficient resolution for precise spectral analysis, but has been used successfully for the determination of fluences and doses in the 100 to 200 keV energy range. A rough estimation of dose can be made with a portable monitor which comprises a 4.2-inch sphere and which was developed for the routine detection of neutron leaks. Lithium iodide scintillation detectors, boron trifluoride proportional detectors, and activation detectors were used. (17 references) (auth) (France)

10812 (CEA-N-1401) X-RAY SPECTROMETRY USING Si (Li) DIODES. RESULTS RECENTLY OBTAINED AT THE GENERAL ELECTRONICS DEPARTMENT/REACTOR ELECTRONICS SERVICE. Friant, A.; Gras, R.; Lorin, A.; Saliou, C. (Commissariat a l'Energie Atomique, Saclay (France). Centre d'Etudes Nucleaires). 30 Oct 1970. 18p. (In French). Dep. NTIS (U. S. Sales Only).

The development of a very low noise preamplifier with optoelectronic negative feedback is described. Its field effect transistors are mounted on special ceramic bases and have led to a significant improvement in the resolution obtainable in nondispersive x ray spectrometry using the very low capacity Si(Li) detectors developed in the laboratory. The principal parameters of the assembly are indicated and the results obtained given: with 6 keV photons the electronic and nuclear resolutions were respectively 110 and 165 eV. (auth) (France)

10813 (JINR-P13-5378) TIME-COORDINATE COMPENSATOR FOR THE TIME SPECTROMETERS WITH LONG SCINTILLATORS. Ondrish, L.; Mukhin, S. V.; Rikhvitskii, S. V.; Semenyushkin, I. N.; Turala, M.; Khorvat, P.; Khrenov, A. N. (Joint Inst. for Nuclear Research, Dubna (USSR). Lab. of High Energy). 1970. 10p. (In Russian). Dep. NTIS (U. S. Sales Only).

A scheme of the time-coordinate compensator for the time spectrometer with the long plastic scintillators is described. The compensator is triggered by the pulses of standard amplitude and duration. The input pulses have the amplitude 0.3 V, the output one -1 V at 50 ohm, the duration being 15 ns and the polarity-negative. The time fluctuations of the output pulse are less than ±50 ns, the place of exposure of the 50 cm long scintillator being changed. (auth)

10814 (JINR-P13-5391) NEUTRON DETECTOR IN SEARCH FOR SUPERHEAVY ELEMENTS IN NATURE. Ter-Akop'yan, G. M.; Ivanov, M. P.; Popeko, A. G.; Subbotin, V. G.; Fefilov, B. V.; Vorob'ev, E. D. (Joint Inst. for Nuclear Research, Dubna (USSR). Lab. of Nuclear Reactions). 1970. 18p. (In Russian). Dep. NTIS (U. S. Sales Only).

The neutron fission detector constructed on the basis of proportional counters filled with ^{3}He is described. The detector has a sufficiently high sensitivity, small proper background and is meant for measurements of $\bar{\nu}$ (an average number of neutrons per act of fission). The measurements were performed in the shielded places at the depth of 10, 40 and 320 m of the water equivalent. The value $\bar{\nu} \leq 3$ is obtained for two samples in which an unknown natural spontaneously fissioning emitter was observed previously. (auth)

10815 (JUL-660-ZE) PULSE DISCRIMINATOR IN NUCLEAR ELECTRONICS. Abend, Klaus (Kernforschungsanlage, Juelich (West Germany). Zentrallabor fuer Elektronik). May 1970. 23p. (In German). Dep. NTIS (U. S. Sales Only).

The application of pulse discriminators to pulse form discrimination, particle identification, and measurement with position-resolving detectors is reviewed. Analog and digital discriminators are compared, and new circuit techniques are given. The comparison shows that with presently known discrimination methods, the discriminator with pure analog components is faster but more inaccurate than digital discriminators. (J.S.R.)

10816 HIGH SPEED 12 BIT REGISTER. Pozar, F.; Graichen, J. (Frieseke and Hoepfner GmbH, Erlangen, Ger.). Atompraxis; 16: 329(Sep-Oct 1970).

The circuitry of the 12 bit register with repetition rate higher than 100 MHz and adjustable threshold from 50 mV to 350 mV

is described. The instrument is made for a hodoscope array and for particle trajectories information. (auth)

10817 MEASURING INSTRUMENTS FOR THE CONTINUOUS CONTROL OF RADIOACTIVITY IN THE SUBSURFACE WATER OF THE OCEANS. Kautsky, H. (Deutsche Hydrographische Institut, Hamburg). Atompraxis; 16: 316-20(Sep-Oct 1970). (In German).

Radiation monitoring instruments for measuring radioactive pollution in seawater are described. Experience gained with these instruments over the past eight years is discussed. (W.H.K.)

10818 NUCLEAR ACCIDENT DOSIMETRY RESEARCH AND EXPERIENCE. Mehl, J. (Gesellschaft fuer Kernforschung, mbH, Karlsruhe, Ger.). pp 165-73 of Nuclear Accident Dosimetry Systems. Vienna; International Atomic Energy Agency (1970).

From Panel on Nuclear Accident Dosimetry Systems, Vienna, Austria. See STI/PUB-241; CONF-690223.

Specifications of criticality alarm systems, examples of portable instruments for neutron monitoring, personnel dosimetry and area monitoring, and assessment of neutron doses from induced body activity are discussed. (W.H.K.)

10819 POSSIBILITIES OF DETECTING LOW-LEVEL β-ACTIVITIES BY SCINTILLATION DETECTORS. Marinov, V.; Dimchev, T.; Vrigazov, A. (Inst. of Physics, Sofia). Kernenergie; 13: 330-4(Oct 1970). (In Russian).

The results of using some criteria for estimation of the reliability of ^{137}Cs determination are considered with a view to explanation of the applicability of scintillation technique in low-level activity measurement. Scintillation detectors with thin plastic scintillators in unidirectional anticoincidence circuits were used. Accuracy, reproducibility, and certainty of the results of radiochemical separation and physical measurement were studied for various activity levels. Average certainty is 69.0%. It resulted from analysis and measurement of matrix samples of recommended activity according to the LOWRA project. (auth)

10820 1/v DIELECTRIC TRACK DETECTORS FOR SLOW NEUTRONS. Schultz, W. W. (General Electric Co., Schenectady, N. Y.). J. Appl. Phys.; 41: 5260-9(Dec 1970).

The fabrication of track detectors with boron atoms uniformly dispersed throughout the volume of the track detector material has been successfully accomplished. Because of their small size they have little effect on the neutron flux one is trying to measure. It is possible to make measurements of neutron flux densities over a range of six to seven decades. Track density is found to be a function of the thickness of detector surface etched away and the ranges of the alpha particle and lithium recoil particle resulting from the capture of a neutron by a ^{10}B atom. At etching proceeds, track density may increase or decrease depending on the etching rate of the bulk material relative to the maximum etching rate perpendicular to the particle path. A new method of studying diffusion through thin layers at the surface of a solid is suggested. (auth)

10821 CALCULATION OF CHARGE AND CURRENT PULSES IN PLANAR AND COAXIAL Ge-(Li) DETECTORS. Kumar, Satinder; Garg, R. K. (Univ. of Delhi). Proc. Indian Nat. Sci. Acad., Part A; 36: 101-11(Mar 1970).

The charge and current pulses in a planar and a coaxial Ge-(Li) detector, due to a gamma quantum entering the detector, are calculated from a common theoretical approach. The pulse shapes and rise times of these pulses are also calculated and discussed for a special case in which the (e^-,h)-pairs are produced throughout the sensitive volume of the detector. (auth)

10822 MEASUREMENT OF THE ABSOLUTE RADIOLUMINESCENCE EFFICIENCY OF LIQUID BENZENE AND ALKYLBENZENE SCINTILLATORS. Fuchs, C.; Laustriat, G. (CNRS, Strasbourg). Rev. Phys. Appl.; 5: 617-23(Aug 1970). (In French).

An experimental method for the determination of the absolute scintillation yield η is presented. The values of η obtained on deoxygenated solutions of α-NPO in aromatic solvents ($\eta = 0.020 \pm 0.002$ in the case of oxygen-free benzene) are lower than those previously published. The radiolytic yields G_{s_1} for the formation of solvent lowest excited states ($G_{s_1} = 0.98$ for benzene) are deduced. (France)

10823 SOLID TRACK DETECTORS AND THEIR APPLICATIONS TO BIOLOGY. Monnin, Michel; Isabelle, Didier B. (Clermont-Ferrand Univ., France). Ann. Phys. Biol. Med.; 4: No. 2, 95-113(Apr-May-Jun 1970). (In French).

The mechanisms of track formation by ionizing particles in insulating materials are briefly described. Suitable materials and the corresponding etching reagents are listed. The use of this technique in the field of biology for dosimetry, autoradiography, and microanalysis is discussed, and special equipment is described. (France)

10824 A SEQUENTIAL NEUTRON AND GAMMA RAY MONITOR. Thonnard, N.; Hurst, G. S. (Univ. of Kentucky, Lexington). Health Phys.; 19: 671-3(Nov 1970).

A neutron dosimeter (Bragg-Gray proportional detector) and a gamma ray dosimeter were designed for mounting on the control panel of a Van de Graaff accelerator to monitor various work areas. By designing a special sequencing cycle and associated logic circuits, the instrument is fully automatic and will perform the operations of counting, timing, displaying and erasing alternate neutron dose rates or gamma dose rates from less than 0.1 mrad/hr to 10 rads/hr without operator assistance. (auth) (UK)

10825 SOLID TRACK DETECTORS: PRACTICAL APPLICATIONS. Blanc, D. (Toulouse Univ., France). Radioprotection; 5: 201-28(1970). (In French).

Because of their high sensitivity to fission fragments, solid track detectors can measure time interval measurements such as the spontaneous fission half-lives of ^{238}U and the isotope 260 of element 104. Their very high resolution power means that very short time intervals are measurable. These detectors can be used to study nuclear reactions of fission and spallation: neutron induced fission; fission and spallation induced by protons (3 and 18 GeV); fission induced by heavier nuclei; and photofission. Solid track detectors are used for measurements in balloon flights, recoverable-load rocket shots or space flights. In microanalysis, Rn and Tn and also U and Th were determined in natural crystals and the ^{235}U enrichment of metallic U measured. These detectors are employed in health physics for long-term space flights. Several types of dosimeters were designed for neutron detection and personnel protection (in mica, in plastic, threshold detectors and dosimeter glasses). A method of dating inorganic compounds based on the study of fossil tracks of spontaneous fission is being studied, together with a method to investigate minerals of extraterrestrial origin. The few existing applications in crystallography and aerosol physics are described. (France)

10826 REGISTRATION AND COUNTING OF ALPHA PARTICLE TRACKS IN CELLULOSE NITRATE. Anno, J. (Toulouse Univ., France); Commanay, L.; Teyssier, J. L. Radioprotection; 5: 147-65(1970). (In French).

The problem of alpha particle detection by track registration in cellulose nitrate was studied. From the analysis of the statistical errors due to track counting with an optical microscope, the number of fields to be observed is deduced in order to know the density of tracks with a given accuracy. This method was applied to the detection of alpha particles in air. (auth) (France)

10827 SOLID TRACK DETECTORS: ANALYSIS OF DATA AFTER DEVELOPMENT. Blanc, Daniel (Toulouse Univ., France). Radioprotection; 5: 115-46(1970). (In French).

The different methods used for the counting of developed tracks and the studies in spectrometry by solid track detectors are presented. A mechanism of track formation and development is established. (France)

10828 RADIOACTIVITY SENSING APPARATUS FOR MEASURING THE BLOOD FLOW. Vigoulet, Jacques Espagno; Espagno, Lucien; Chanh Trung, Huynh (to Societe Nationale des Petroles d'Aquitaine). U. S. Patent 3,528,407. 15 Sep 1970. Priority date 22 Feb 1965, France.

A device for measuring blood flow using radioactive isotopes is described. The radioactive tracer is injected into the organ through which blood flow is to be measured. A detector measures the level of radioactivity by passing pulses at selected intervals to a counter. Successive counts for successively equal time periods are accumulated into the counter wherein the counter is cleared between the accumulation of each count during the successively equal length time period. Any changes in the counts appear at an output meter to indicate a differentiated version of the count which is proportional to blood flow. Circuitry is provided for adjusting the rate of application of pulses to the counter to maintain the count near the capacity of the counter for more accurate measurement. Further means are provided for developing a count of the number of pulses generated during each time interval to provide an operator with the rate of change of decay occurring during succeeding time intervals. (auth)

10829 METHOD FOR IDENTIFICATION OF PARTICLES FROM A = 4 TO 20 BY TREATMENT OF DATA COLLECTED

XUM

FROM A ΔE–E SOLID-STATE DETECTOR. Galin, J.; Tarrago, X. (Institut Physique Nucleaire, Orsay, France). Nucl. Instrum. Methods; 89: 173-6(1970). (In French).

A two solid-state detector telescope is used to detect particles in the range A = 4 to 20, and to measure both the energy loss and the energy on a very wide range. The process used for mass identification is based on range energy curves. Data registered on magnetic tapes are treated on a computer. Every event which was formerly located in a ΔE–E space was transferred into a new space G(M)–E, in which all the nuclei having the same mass M were distributed along a single horizontal line parallel to the energy abscissa. With such a figuration, the computer can very quickly discriminate the mass corresponding to any particular event. (auth)

10830 ZERO CROSS TRIGGER WITH RISE TIME CORRECTION FOR TIMING OF Ge(Li)-DETECTOR PULSES. Dittner, A.; Hartmann, G.; Klein, J. W. (Frieseke and Hoepfner GmbH, Erlangen, Ger.). Nucl. Instrum. Methods; 89: 73-5(1970).

A method is proposed by which the timing signal from a Ge(Li)-detector may be improved by a factor of 8 compared with leading edge triggering. The detector pulse in the timing channel is limited and double delay-line clipped, so that the charge of the pulse between start and zero cross depends only on the slope of the pulse. This charge is integrated on a capacitor. At zero cross time, a constant current discharge of the capacitor is started, and a time correction is thus added to the zero cross signal, depending on the charge of the first part of the pulse corresponding to a rise time correction. The method is exact for pulses with linear slope and the maximal error is estimated for real Ge(Li) pulse form. (auth)

10831 OBSERVATION OF PROTON TRACKS BY A PLASTIC DETECTOR. Varnagy, M.; Csikai, J.; Szegedi, S.; Nagy, S. (Kossuth Univ., Debrecen, Hungary). Nucl. Instrum. Methods; 89: 27-8(1970).

Cellulose acetate (Cellit) has been found to be suitable for detecting protons with a threshold of about 300 keV and an efficiency of ≈100% within the error limits of the measurements. (auth)

10832 MEASUREMENTS OF THE ENERGY RESPONSE FUNCTIONS OF SCINTILLATORS FOR MONOENERGETIC ELECTRONS. Titus, F. (Union Coll., Schenectady, N. Y.). Nucl. Instrum. Methods; 89: 93-100(1970).

The energy response functions of plastic, anthracene, NaI(Tl), and CsI(Tl) scintillators for electrons of 0.25, 0.50, 0.75, 1.0 and 1.25 MeV at normal incidence and of plastic and NaI(Tl) scintillators for 0.50 and 1.0 MeV electrons at angles of incidence up to 70° from the normal are reported. The response functions are interpreted in terms of number and energy reflection coefficients and the latter are compared with the results of backscattering measurements by other methods and of Monte Carlo calculations. (auth)

10833 ON-LINE COMPUTER SYSTEM IN A LOW-LEVEL COUNTING LABORATORY. Ashkenazi, Y.; Carmi, I. (Weizmann Inst. of Science, Rehovot, Israel). Nucl. Instrum. Methods; 89: 125-30(1970).

A system has been developed at the Weizmann Institute of Science to provide on-line data acquisition and analysis from four independent tritium and ^{14}C experiments. It is based on a small general purpose digital computer (PDP-8/S) and a special interface. The design of the hardware and software was intended to optimize the acquisition and processing functions, and includes an objective data quality evaluation test. Several design and performance problems are discussed. The system resolution is analysed by using the renewal theory. Proportional counters surrounded by anticoincidence meson counters and enveloped by boron-loaded paraffin and lead and steel shields to attenuate neutrons and environmental radiation, respectively, were used. (auth)

10834 DESIGN PRINCIPLES OF FLUORESCENCE RADIATION CONVERTERS. Keil, G. (Technische Univ., Munich). Nucl. Instrum. Methods; 89: 111-23(1970).

Light collection e.g., from scintillators by systems using light conversion in fluorescent materials is discussed in detail. Especially the influence of optical contact media, reflectors and light attenuation is considered. Fluorescent acrylic glasses were found to be very well suited for such light collection systems–numerous experimental data are presented. A comparison of the light collection yield of a converter with common scintillator systems is presented. Interesting properties of a converter system e.g., for scintillation counting are the great possible reduction in the cross section of a light bundle and the high compactness of the design. (20 references) (auth)

10835 RESOLVING TIME MEASUREMENTS OF GEIGER COUNTERS USING A TIME ANALYZER. Tojo, T.; Nakajima, T.; Kondo, M. (Japan Atomic Energy Research Inst., Tokai). Nucl. Instrum. Methods; 89: 39-44(1970).

A new method of measuring the dead time, resolving time and recovering time of a Geiger counter using a time analyzer is reported. The dependence of the resolving time on the counting rate, applied voltage and discriminator level are described. (auth)

10836 EFFECTIVE NEUTRON TEMPERATURES IN REACTOR CORE MEASURED BY FISSION TRACK DETECTORS. Su, C. S.; Liu, T. C. (National Tsing Hua Univ., Hsinchu, China). Nucl. Instrum. Methods; 89: 233-6(1970).

The effective neutron temperature of a thermal reactor can be measured by directly counting the fission tracks of two fissile materials, ^{239}Pu and ^{235}U, irradiated in the reactor simultaneously. Glass slides were used as the fission track detectors. The effective neutron temperatures were measured at the reactor core of the open pool reactor. Results show that the effective neutron temperatures were 104°C at the positions near the control rods and 71°C at the center of the core, when reactor was operated at one kilowatt. (auth)

10837 ANGLE INFORMATION WITH A GRIDDED IONIZATION CHAMBER AND ITS APPLICATIONS. Mizuho, M.; Noguchi, M. (Japan Atomic Energy Research Inst., Tokyo). Nucl. Instrum. Methods; 89: 101-7(1970).

The characteristics of a gridded ionization chamber were studied, particularly, angle information by rise time analysis. An improvement was made to the alpha spectrum, demonstrating the effectiveness of the technique. The following was revealed by the study: a) The technique can give angle information for nuclear reactions and also serve as a neutron spectrometer with a thin radiator. b) Improvement of the alpha spectrum is fairly high in energy resolution, alpha background continuum, beta background, and background from the surrounding materials. c) The information obtained can be varied by a change in the setting of a rise time to pulse height converter (RHC). (auth)

10838 STATISTICS OF ELECTRON AVALANCHES AND ULTIMATE RESOLUTION OF PROPORTIONAL COUNTERS. Alkhazov, G. D. (Ioffe Inst. of Physics and Tech., Leningrad). Nucl. Instrum. Methods; 89: 155-65(1970).

The fundamental limitations set on the ultimate energy resolving power of a proportional counter are studied. An analysis of a few statistical models of electron avalanches in gases subjected to uniform electric fields is performed. A formula for gas amplification variance in non-uniform fields is derived. The relative variance of gas amplification in argon and methane filled cylindrical proportional counters for the case of $\overline{K} = 10^3 - 10^5$ and $pr_a = 1 - 4$ torr · cm is calculated to be 0.6 to 0.8. The present work shows that avalanche size distributions in uniform fields are close to those computed by Legler, but that the distributions in the non-uniform fields of cylindrical counters are close to those of Polya-type. (auth)

10839 SEMIAUTOMATIC SCANNING SYSTEM FOR NUCLEAR EMULSIONS. Yamaguchi, C.; Shintomi, T.; Masuda, M. (Tokyo Inst. of tech.). Nucl. Instrum. Methods; 89: 289-90(1970).

An electric apparatus for semiautomatic scanning of nuclear emulsions has been developed. It provides a high stability, a low drift and a good reproducibility. (auth)

10840 PROCESSING OF PULSE TRAINS USING RATE MULTIPLIERS IN NUCLEAR INSTRUMENTATION. Bhatt, S. J.; Taylor, D. (Univ. of Strathclyde, Glasgow). Nucl. Instrum. Methods; 89: 301-2(1970).

Some of the properties of binary rate multipliers in the generation of digital functions are studied. The binary rate multiplier, which comprises an assembly of flip-flops and gates is now much used in regular rate processing. Here attention is called to the fact that under certain conditions, it may also be employed for random rate processing, such as arise in nuclear instrumentation. As an example, a circuit is given for the automatic correction of deadtime losses. (auth)

10841 NOTE ON THE RESPONSE OF DETECTORS WITH CYLINDRICAL COLLIMATION TO NON-AXIAL POINT GAMMA RAY SOURCES. Bell, T. K. (Royal Victoria Hospital, Belfast); Johnston, A. R.; Spiers, E. W. Nucl. Instrum. Methods; 89: 315-16(1970).

A comparison is made of calculated and experimentally measured response curves of a NaI(Tl) crystal with cylindrical collimation for non-axial point sources close to the surface of the collimator. Good agreement is obtained for gamma energies 0.279, 0.662 and 1.11 MeV. (auth)

10842 ^{75}Se AS A CALIBRATION STANDARD FOR Ge(Li) DETECTORS. Nagpal, T. S.; Gaucher, R. E. (Bishop's Univ., Lennoxville, Quebec). Nucl. Instrum. Methods; 89: 311-13 (1970).

The use of ^{75}Se for calibrating Ge(Li) detectors is discussed. An example is given using its accurately measured energies and intensities. (auth)

10843 SYSTEM FOR $^{14}CO_2$ RADIOASSAY IN THE PRESENCE OF A HIGH BACKGROUND RADIATION. Clark, B. C. (Avco Corp., Tulsa, Okla.). Nucl. Instrum. Methods; 89: 225-31 (1970).

The detection system consists of a 30 cm^3 spherical proportional counter to measure the beta rays from ^{14}C labelled gas. This counter is built inside a plastic scintillator. Pulses from the photomultiplier tube which views this scintillator and from the wire anode of the proportional counter are amplified and fed to an anti-coincidence circuit which passes the proportional counter pulses only when no pulse occurs in the scintillator. The purpose of the scintillator and anti-coincidence circuitry is to reduce sensitivity to background radiation. Rejection factors of as high as 80 have been achieved for gamma radiation. Under optimum operating conditions, the detection system achieves a figure of merit of 6.2 in the presence of a SNAP-19 unit and 27 in the laboratory environment. This allows lower limits of detectability of 7 pCi and 1.4 pCi of $^{14}CO_2$, respectively, at a confidence level of 0.999999. The system has been designed for possible use on a Mars mission. (auth)

10844 CHARGE COLLECTION PROCESS IN pin JUNCTION RADIATION DETECTORS. Vass, D. G. (Univ. of Edinburgh). Nucl. Instrum. Methods; 89: 241-6(1970).

The electric intensity distribution and the width of the depletion layer in a pin junction radiation detector are calculated from the shape of the current pulses from the detector using the energy balance approach to the charge collection process. The results obtained are compared with those calculated using the Ramo theory of charge collection and also with the available experimental data. The charge density distribution in the detector is deduced from the static electric intensity distribution. A reasonable overall description of the charge collection process is obtained. (auth)

10845 NEW DETECTOR FOR keV NEUTRONS. van Hemert, R. L.; Bowman, C. D.; Baglan, R. J.; Berman, B. L. (Univ. of California, Livermore). Nucl. Instrum. Methods; 89: 263-75 (1970).

A neutron detector has been built and tested for use between 1 keV and 1 MeV which possesses the following properties: (1) useful neutron efficiency over the full energy range, (2) fast time response, (3) low sensitivity to gamma rays and gamma flash, and (4) good background rejection capability. It consists of a 1.25 cm thick by 25 cm diameter disk of ^{235}U positioned inside a cylindrical shell of plastic scintillator which has been divided into quarters. The axes of the disk and the cylinder are colinear. Neutron induced fission events in the ^{235}U are detected in the plastic scintillator by requiring a triple coincidence between prompt γ-rays and/or neutrons. (auth)

10846 ELECTROMAGNETIC DELAY LINE READOUT FOR PROPORTIONAL WIRE CHAMBERS. Grove, R.; Lee, K.; Perez-Mendez, V.; Speinde, J. (Univ. of California, Berkeley). Nucl. Instrum. Methods; 89: 257-62(1970).

The use of electromagnetic delay lines to read out the position of ionizing events in multi-wire proportional chambers is described. The delay line used is a ceramic core (non-magnetic) type with a delay of 80 nsec/cm. The readout accuracy achieved depends on the wire plane which is read out: for the positive plane which forms the electron avalanche, the accuracy is ±1 mm (half the wire spacing). For the negative plane, which records the induced signal produced on a number of adjacent wires by the positive ions, the interpolation property of the delay line permits an accuracy of ±0.15 mm. (auth)

10847 STUDIES CONCERNING THE BEHAVIOUR OF PHOTOMULTIPLIER WITH LARGE PHOTOCATHODE. Paul, J. M. (Louisiana State Univ., Baton Rouge). Nucl. Instrum. Methods; 89: 285-7(1970).

The results from a series of measurements show that the relative sensitivity of a large cathode photomultiplier varies as much as 50%; although, according to the manufacturer, this should not be more than 10–15%. This latter figure might include only that part of the variation which arises out of non-uniformity of the photosensitive material of the cathode. But, in reality, the variation arises also due to the variation in the photoelectron collection efficiency onto the first dynode even under the optimum conditions of focusing and accelerating voltages. Moreover, the optimum focusing and accelerating voltages set for a particular zone, does not fulfill the requirements for an adjacent zone and, as such, there is no ideal setting for the whole cathode surface. (auth)

Nuclear Spectroscopic Instrumentation

Refer also to abstract 10670.

10848 (ANL–7704) HARDWARE AND SOFTWARE FOR NUCLEAR SPECTROSCOPY ON THE VARIAN DATA MACHINES 622/i COMPUTER. Cohn, C. E.; Bennett, E. F.; Yule, T. J. (Argonne National Lab., Ill.). Aug 1970. Contract W-31-109-eng-38. 37p. Dep. NTIS.

A Varian Data Machines 622/i computer has been interfaced with a dual analog-digital converter (ADC) and a display oscilloscope for use as a pulse-height-analysis system. Two binary counters have also been provided as general-purpose input channels. The interfaces and a representative machine-language pulse-height-analysis program are described. (auth)

10849 (CEA-CONF–1694) GAMMA-RAY SPECTROMETRY IN DRILLINGS USING Ge–Li SEMICONDUCTOR PROBES. Andrieux, Claude; Dumesnil, Patrice (Commissariat a l'Energie Atomique, Saclay (France). Centre d'Etudes Nucleaires). 1 Jul 1970. 26p. (In French). (CONF-701030–1). Dep. NTIS (U. S. Sales Only).

From Meeting on the Use of Radioelements and Nuclear Methods in Geophysics for the Prospection and Exploitation of the Minerals, Nancy, France.

A Ge-Li semiconductor well logging probe possessing excellent energy resolution characteristics is described. The method used to determine the uranium content of rocks is discussed. In order to demonstrate the superiority of this method of analysis, comparisons were made between the spectra obtained from a sample containing 0.5% uranium using a scintillographic probe, and the Ge-Li semiconductor probe. (France)

10850 (JUL–684–FF) PSEUDORANDOM AND MARKOV SEQUENCES OPTIMIZING CORRELATION TIME-OF-FLIGHT SPECTROMETRY. Hossfeld, F.; Amadori, R. (Kernforschungsanlage, Juelich (West Germany). Institut fuer Festkoerperforschung). Jul 1970. 149p. Dep. NTIS (U. S. Sales Only).

The principles of the correlation method are summarized on the basis of a generalized theory yielding a gain factor from the comparison of the conventional time-of-flight technique with the correlation method. This gain factor depends on the structure of the time-of-flight spectrum, on the level of the unmodulated background, and on the duty cycle of the chopper sequence and thus can be used as a criterion for the optimization of the correlation experiments leading to optimum duty cycles. The generalization of the correlation method to a double correlation time-of-flight technique using uncorrelated pseudorandom sequences is outlined. A comprehensive survey on the properties and the duty cycles of all classes of binary pseudorandom sequences so far known is given including the tables of all explicitly generated integer difference sets which are associated with the sequences interesting for time-of-flight applications. It is proved that binary pseudorandom sequences with coprime periods satisfy the conditions for the applications in the double correlation time-of-flight technique. Finally, the correlation properties of sequences generated by finite stationary Markov chains are discussed. (193 references) (auth)

10851 (NP–18570) ADVANCES IN THE STUDY OF GERMANIUM DETECTORS AND THEIR USE FOR CHARGED PARTICLES, EXPERIMENTAL STUDY OF (d,d'), (d,p), (d,t) REACTIONS ON ^{12}C AT 80 MeV. Marcus, Luc (Paris Univ., Orsay (France)). 1970. 87p. (In French). Dep. NTIS (U. S. Sales Only).

Thesis. Submitted to Paris Univ., Orsay (France). Faculte des Sciences.

Ge(Li) detectors for gamma-ray spectrometry were studied. The methods used in their manufacture (ion implantation) and the difficulties encountered in selecting types which could be used for deuteron detection were discussed. An 80-MeV deuteron beam revealed the existence of randomly distributed nondetecting "dead zones" in certain detector crystals; the resolution of the active zones was 130 keV. The positions of the peaks depended upon whether the particles impinged upon the face or the sides of the crystal. It was shown that these variations were due to preferential trapping of the holes and the electrons. A calculation on the charge collection confirmed the predominant trapping of the electrons and led to values for the trapping factors which were admissible with the resolution sought. When these detectors were used in deuteron scattering experiments, a peak-to-valley ratio of about 1000 and an efficiency of 86% were achieved. Over a large excitation energy range, the spectra of protons (E_p > 28 MeV), deuterons (E_D > 28

XUM

MeV), and tritons ($E_T > 40$ MeV) associated with reactions induced by 80-MeV deuterons with ^{12}C between 11° and 42° lab. were studied. The differential cross sections of inelastic scattering for the first excited ^{12}C levels were calculated from the results. An oscillatory structure was revealed from the angular distributions. The excitation of the nonnatural parity level at 12.7 MeV and the three groups of high excitation energy levels (T = 0) at 18.2 MeV, 20.3 MeV and 21.6 MeV were observed. In the angular region explored, the stripping reactions $^{12}C(d,p)^{13}C$ were characterized by decreasing differential cross sections and very little structure. An exception occurred with the 3.09-MeV ($\frac{1}{2}^+$, 1 = 0) level, which had much structure. These results were interpreted in terms of the loose deuteron structure in a weakly bound projectile (WBP) model. The angular distributions of the pick-up reaction $^{12}C(d,t)^{11}C$ were similar to those related to ^{12}C at 50 MeV, but had less structure. The distribution of the first excited levels of ^{11}C, compared with those obtained for ^{11}B by the $^{12}C(d,He)^{11}B$ reaction at the same energy, indicated the analogue states corresponding to quasi-identical cross sections, which are in agreement with results reported for ^{12}C at 50 MeV. (France)

10852 (NP-18617) SEMICONDUCTOR DETECTOR TELESCOPE ELECTRON SPECTROMETER. Kantele, J.; Passoja, A. (Jyvaskyla Univ. (Finland). Dept. of Physics). Oct 1970. 16p. Dep. NTIS (U. S. Sales Only).

A simple dE/dx + E type semiconductor detector telescope electron spectrometer featuring high detection efficiency and effective discrimination against γ-rays and heavy particles is described. The line shape of the spectrometer is better than that of a single detector of corresponding size; at 1 MeV, the peak-to-total ratio is approximately 0.8. The device is suited to the study of beta-ray spectra and conversion electron lines at energies above about 0.4 MeV. (auth) (Finland)

10853 (RT/PROT-(70)21) METHODS OF QUANTITATIVE ANALYSIS OF A GAMMA SPECTRUM. Frittelli, L. (Comitato Nazionale per l'Energia Nucleare, Rome (Italy)). 14 Jul 1970. 47p. (In Italian). Dep. NTIS (U. S. Sales Only).

Numerical methods of quantitative analysis of digital gamma spectra are described and compared. (auth)

10854 SPECTROMETER FOR THERMAL NEUTRONS. Gailliard, Jean-Pierre (to Commissariat a l'Energie Atomique). French Patent 1,586,182. 5 Jan 1970. Filed 30 Aug 1968. (In French).

This spectrometer functions satisfactorily even with a low flux of thermal neutrons. A rotating disc with an aperture is placed in the neutron flux. A second disc is placed at a given distance from the first. A fixed collimator situated between the two discs guides the neutron beam from the first to the second. The distribution of the points of impact on the second disc gives the neutron distribution in terms of velocity and hence energy. (France)

10855 ELECTRON-TRANSPORT SOLENOID-Si(Li) DETECTOR SPECTROMETER AND ON-LINE CONVERSION ELECTRON AND γ-RAY SPECTROSCOPY. Klank, Benno Ernst. Boulder, Colo.; Univ. of Colorado (1969). 175p. University Microfilms Order No. 70-16,497.

Thesis.

An internal conversion electron spectrometer incorporating a solenoidal magnetic field along the target-detector axis for transporting electrons from a target placed in a cyclotron beam to a liquid nitrogen cooled Si(Li) detector has been constructed and successfully operated in experimental nuclear structure research. A time-varying magnetic field is employed to avoid fluctuations of the electron transmission for different energies, and the time-averaged value of the magnetic induction is approximately 5500 gauss. For a 0.9 cm diameter detector 54 cm away from the target the measured solid angle of electrons collected on the detector face is 45 percent, 22 percent, and 9 percent of 2π for 100 keV, 500 keV and 1500 keV electrons respectively. During work with radioactive sources and during on-line experiments an energy resolution of approximately 3 keV FWHM has been obtained for electron lines over a wide range of energies. For on-line measurements a baffle is located on the solenoid axis between the target and the detector to discriminate against delta-rays, and the compiling of a prompt internal conversion electron spectrum (approximately 10^5 counts above background in the strongest peaks) typically requires one to two hours. The computation of the time-averaged values for the solid angle of electrons collected on the detector face is reduced to a static, two-dimensional problem. Approximate formulas for these values as a function of energy and explanations for the differences between these values and the measured efficiency of the instrument are presented and applied to the discussion of possible improvements of the transmission of the spectrometer. For γ-e and X-e coincidence measurements a liquid nitrogen cooled Si(Li) or Ge(Li) photon spectrometer can be located as close as 1.5 cm from the target on that side of the target opposite to the electron detector. A description of details of the construction and performance of the electron transport solenoid-Si(Li) spectrometer and of the photon spectrometer is given. The application of the spectrometer to experimental nuclear structure research is discussed. To demonstrate some of the capabilities of the instrument, the investigations of the isomeric photon transitions in ^{73}Se and ^{179}W, and the study of prompt transitions between levels excited by the $^{181}Ta(p,2n)^{180}W$ transition are described. (Diss. Abstr. Int., B)

10856 HIGH EFFICIENCY TIME-OF-FLIGHT NEUTRON SPECTOMETRY FOR RANDOM SOURCES. Picot, A. (Univ., Nancy). Rev. Phys. Appl.; 5: 693-703(Aug 1970). (In French).

A time-of-flight spectrometer for random source analysis is described. The efficiency between 0.2 and 20 MeV is about 10^{-5} to 10^{-6} and the energy resolution is about 15%. A conventional apparatus with only two diffusors is used, but the shapes, dimensions, and distances between the two scintillators and the source were carefully chosen and verified using a Monte-Carlo method to obtain the highest energy resolution for a given efficiency. (France)

10857 GAMMA-RAY DISCRIMINATION IN A PROTON-RECOIL SPECTROMETER FOR A FAST REACTOR SPECTRUM MEASUREMENT. Oebu, M.; Ichimori, T.; Shirakata, K. (Japan Atomic Energy Research Inst., Tokai). Nucl. Instrum. Methods; 89: 131-9(1970).

Studies have been made on gamma-ray discrimination for a proton-recoil neutron spectrometer with pulse-shape discrimination electronics for in-core measurements. A small proportional counter filled with hydrogen, in conjunction with a pulse-shape discrimination system, was used in experiments to examine the characteristics of gamma-ray discrimination in the energy region below 100 keV. Characteristics of the discrimination by two types of systems, using the "dividing" and the "rise time" methods respectively, were compared with each other under the same conditions. Distributions of relative specific ionization or rate of rise in various energy bands and gamma elimination ratios in the energy region from 5 to 30 keV are obtained. The results of the experiments indicate that the two methods are able to distinguish completely between neutron and gamma events above 40 keV and the gamma elimination ratios decrease rapidly at energies below 10 keV. The dividing method is observed to be slightly better than the rise time method with respect to the pulse-shape discrimination. (auth)

10858 NON-PARAMETRIC METHOD FOR THE EXTRACTION OF INFORMATION FROM DIGITIZED SPECTRA. Goss, D. (Nebraska Wesleyan Univ., Lincoln). Nucl. Instrum. Methods; 89: 221-4(1970).

A method for determining the location and calibration of peaks in digitized spectra is discussed. It is based on the use of interpolating polynomials to represent experimental data. As an application of method, the treatment of Ge(Li) spectrometer data taken from a multichannel analyzer is briefly discussed. (auth)

10859 SPECTROMETER PERMITTING THE ANALYSIS OF LOW-ENERGY GAMMAS IN THE PRESENCE OF A STRONG HIGH-ENERGY GAMMA BACKGROUND. Grenier, G.; Poussier, C. (CEA, Villeneuve-Saint-Georges, France). Nucl. Instrum. Methods; 89: 199-203(1970). (In French).

A gamma ray spectrometer for a wide range energy is described. This device permits in particular to analyze the low energy gammas in the presence of a strong high energy photon background. It can operate simultaneously in the following modes: low energy gamma ray spectrometer from 30 to 500 keV; Compton spectrometer or "duode" from 0.3 to 4 MeV; and pair spectrometer for $E_\gamma > 2$ MeV. With simultaneously two sources, ^{57}Co and ^{60}Co, the limit of detection for the ^{57}Co 136 keV gammas is obtained for an intensity 7000 times weaker than that of the ^{60}Co 1.17 and 1.33 MeV gammas. The duode operation gives approximately a peak-to-Compton continuum ratio of 100:1 for the ^{137}Cs line, which is a good compromise between the Compton suppression and the efficiency. The possible improvements for this spectrometer are given. (auth)

10860 IDENTIFICATION OF NUCLEAR FRAGMENTS BY A COMBINED TIME-OF-FLIGHT, ΔE-E TECHNIQUE. Butler, G. W.; Poskanzer, A. M.; Landis, D. A. (Univ. of California. Berkeley). Nucl. Instrum. Methods; 89: 189-98(1970).

Nuclear fragments of Z = 5 to 10 that resulted from the interaction of 5.5-GeV protons with uranium have been identified by a combined time-of-flight, ΔE-E technique. A thin ΔE detector

was used so that the ΔE–E information provided only element resolution, not isotopic resolution. However, the measurement of the time-of-flight between the ΔE and E detectors together with the energy deposited in the E detector allowed the fragment mass to be determined. This technique enabled one to observe not only the major isotopes of these elements but also such neutron-rich nuclei as ^{18}C and ^{20}N. An improved algorithm for power-law particle identification is also described. (auth)

10861 ENERGY MEASUREMENTS OF THE 20 TO 60 MeV NEUTRON BEAM OF THE DAVIS 76-INCH ISOCHRONOUS CYCLOTRON. Brady, F. P.; Knox, W. J.; Johnsen, S. W. (Univ. of California, Davis). Nucl. Instrum. Methods; 89: 309-10 (1970).

The time-of-flight reference time is derived from an electromagnetic beam pick-off which monitors the protons incident on the lithium-7 target. The neutrons from the $^7Li(p,n)^7Be$ reaction are detected with a NE102 scintillation detector. Energy measurements are achieved to an absolute precision of 0.1%. (W.H.K.)

10862 COINCIDENCE SPECTROMETER FOR FAST NEUTRONS. Richter, B.; Schneider, H. (Univ., Giessen, Ger.). Nucl. Instrum. Methods; 89: 69-72(1970). (In German).

A spectrometer for fast neutrons is described. The energy is measured by proton-recoil in a stilbene-crystal. A coincidence circuit with a ^6Li-glass-scintillator detects those neutrons which are scattered in the stilbene-crystal. Neutron energies are measured in the range from 0.8 to 14 MeV. (auth)

10863 MOESSBAUER EFFECT STUDIES FOLLOWING COULOMB EXCITATION USING A CLOSED CYCLE HELIUM REFRIGERATOR. Wender, S. A.; Oberley, L. W.; Hershkowitz, N. (Univ. of Iowa, Iowa City). Nucl. Instrum. Methods; 89: 61-4 (1970).

An improved apparatus based on a closed cycle helium refrigerator has been developed to cool targets and absorbers for Moessbauer effect studies following Coulomb excitation. The system is capable of maintaining the target at a temperature of 15 K with no heat input. There is a temperature increase of 1.5 K/W. The major problem of vibrations has been reduced to an acceptable level. (auth)

10864 SEMICONDUCTOR DETECTOR SPECTROMETER WITH MAGNETIC ELECTRON LENS. Waldschmidt, M.; Osterman, P. (Univ., Frankfurt am Main). Nucl. Instrum. Methods; 89: 65-7(1970). (In German).

An electron spectrometer with a strong suppression of γ-background is described. The electrons are guided by the magnetic field of a superconducting coil and are detected with great efficiency. (auth)

10865 SOME DETAILS ABOUT ANGULAR DISTRIBUTION MEASUREMENTS IN INVERSE PHOTONUCLEAR REACTIONS. Kernel, G.; Mason, W. M.; Tanner, N. W. (Nuclear Physics Lab., Oxford). Nucl. Instrum. Methods; 89: 1-8(1970).

The determination of the absolute value of the cross section for inverse photonuclear reactions, and the rejection of the cosmic-ray background are discussed. Examples of experimentally determined finite solid angle correction coefficients for NaI(Tl) crystals are given and their application to the analysis of angular distributions of gamma rays is studied. (auth)

10866 COMPUTERIZED MOESSBAUER SPECTROMETER EMPLOYING A DOUBLE ENDED TRANSDUCER. Biran, A.; Shoshani, A.; Montano, P. A. (ELSCINT Labs., Haifa, Israel). Nucl. Instrum. Methods; 89: 21-6(1970).

A new computerized double ended Moessbauer effect spectrometer is described. The system utilizes a small computer and interface, which act as a double multiscaler analyzer recording two Moessbauer spectra simultaneously. The transducer is double-ended carrying two sources, one at either end, enabling accurate simultaneous calibration with a standard absorber while performing Moessbauer experiments. Thus, small differences in center shifts may be measured. The system was used to measure the center shift between $^{57}Co:Cu$ and $^{57}Co:Pd$, and a value of 0.043 ± 0.001 mm/sec was found. Small differences in the center shift of potassium ferrocyanide trihydrate single crystal for different crystal orientation, due to the presence of an unresolved O. S. were also measured with this Moessbauer spectrometer. (auth)

High Energy Physics Instrumentation

10867 (CEA-R-4081) GEOMETRIC CORRECTION FACTORS RELATING TO THE RECOIL OF PROTONS IN NUCLEAR EMULSIONS. Vialettes, Henry; Le Thanh, Phung (Commissariat a l'Energie Atomique, Saclay (France). Centre d'Etudes Nucleaires). Oct 1970. 29p. (In French). Dep. NTIS (U. S. Sales Only).

The geometric correction factors relative to measurements carried out on the spectra of recoil protons, obtained using nuclear emulsions, are discussed; these factors take into account the probability of a proton track being wholly contained within the emulsion. Two aspects relative to radioprotection are considered: the case of a quasi-point source for which a single rectangular shaped emulsion surface is used (the length of this surface is along the same axis as that of the incident neutrons); the case of an incident flux of neutrons of indeterminate direction. The first case is only briefly reviewed. The second case is extensively treated. The numerical values obtained for the correction factor relative to the length of proton tracks in emulsions of 200, 400 and 600 μm are indicated. The validity of these corrections is demonstrated in the determination of the neutron emission spectra of an americium fluorine source, and by the $D(d,n)^3He$ reaction. (auth)

10868 (IFVE-SEF/OP-70-13) INVESTIGATION OF A PARTICLE BEAM WITH ENERGY UP TO 70 GeV WITH A SPARK SPECTROMETER. Aleksandrov, I. A.; Bolotov, V. N.; Devisheva, M. N.; Devishev, M. I.; Isakov, V. V.; Samoilov, A. V. (Gosudarstvennyi Komitet po Ispol'zovaniyu Atomnoi Energii SSSR, Serpukhov. Institut Fiziki Vysokikh Energii). 1970. 22p. (In Russian). Dep. NTIS (U. S. Sales Only).

The paper describes a magnetic spark spectrometer installed in the beam for the search for quarks, the measurement results of the beam parameters and the comparison with the calculated ones are reported. Differential cross-sections of the negative production by protons on Al nuclei are derived. (auth)

10869 (JINR-E13-5459) MEASUREMENT OF THE SCATTERING ANGLE OF PARTICLES BY VAVILOV-CHERENKOV RADIATION AT HIGH ENERGIES. Ivanov, V. I.; Moroz, N. S.; Radomanov, V. B.; Stavinskii, V. S.; Zubarev, V. N. (Joint Inst. for Nuclear Research, Dubna (USSR). Lab. of High Energy). 1970. 10p. Dep. NTIS (U. S. Sales Only).

Angular resolution characteristics and efficiencies of the 6-channel Cherenkov hodoscope in the interval of angles from 0 to 30 mrad were obtained. (auth)

10870 (JINR-P13-5420) FAST VALVE OF HIGH PRESSURE FOR BUBBLE CHAMBER. Balandin, M. P.; Ganichev, V. I.; Moiseenko, V. A.; Solov'ev, M. I.; Trifonov, V. L.; Shmidtke, B. (Joint Inst. for Nuclear Research, Dubna (USSR). Lab. of Nuclear Problems). 1970. 12p. (In Russian). Dep. NTIS (U. S. Sales Only).

The fast valve, operating at a pressure of 100 atm with a 20-cm^2 passage cross section, is described. The plunger is stopped in the valve with the aid of an air damper. To adjust the impactless stopping of the plunger the valve is equipped with a piezoelectric pressure detector. The opening time of the pressing window, at the operating pressure being 5 atm, is 5.10^{-3}s. The valve was tested for resource. After 5.10^5 cycles the air-tightness of all the joints remained within the required limits. (auth)

10871 CONSTRUCTION OF A SCINTILLATION COUNTER TELESCOPE FOR THE REGISTRATION OF THE MESON COMPONENT OF COSMIC RAYS. Kokkoniemi, J.; Kananen, H. (Oulu Univ., Finland). Geophysica; 11: 107-17(1970)

A scintillation counter telescope has been constructed at the Department of Physics, University of Oulu, to register the hard component of cosmic rays. It is a standard equipment for cosmic ray measurements consisting of a so called wide angle telescope, four cubical telescopes and east–west, west–east, north–south and south–north directional telescopes. Integrated circuit electronics has been applied. The average counting rates are about $1.07 \cdot 10^6$ particles per hour (p.p.h.) for the wide angle telescope, $1.61 \cdot 10^5$ p.p.h., for cubical telescopes and $9.54 \cdot 10^4$ p.p.h. for directional telescopes. The soft component of the radiation has been absorbed by a 10 cm layer of lead. (auth) (Finland)

10872 OPERATION OF CYLINDRICAL WIRE SPARK-CHAMBERS IN LOW-PRESSURE HELIUM. Dahlgren, S.; Kullander, S.; Lorenzi, R. (CERN, Geneva). Nucl. Instrum. Methods; 89: 29-38(1970).

A pair of cylindrical wire spark-chambers is used for detecting alpha particles emitted in high-energy π ^4He interactions. A particular feature of the system is the low gas pressure employed, corresponding to a thickness of 0.7 mg/cm^2. The angular error for 5.48-MeV alpha particles is 1.2° fwhm. The chambers are insensitive to minimum-ionizing particles. (auth)

10873 SPARK CHAMBER SPECTROMETER FOR HEAVY COSMIC IONS. Lecleach, X. (CEN, Saclay, Gif-sur-Yvette, France). Nucl. Instrum. Methods; 89: 13-19(1970). (In French).

XUM

A new heavy cosmic ray spectrometer with a large geometry factor is proposed. This spectrometer includes more particularly two magnetostrictive wire spark chambers. The encoding system is designed for low power drain and for reducing the bulk of the information to be transmitted by telemetry. A spark chamber has been experimented on particles of various specific ionization, and from these results its behavior with heavy cosmic rays has been evaluated. (auth)

10874 STUDIES CONCERNING THE BEHAVIOUR OF GAS CHERENKOV COUNTERS FOR ELECTRONS. Paul, J. M. (Louisiana State Univ., Baton Rouge). Nucl. Instrum. Methods; 89: 277-83(1970).

A pair of gas Cherenkov counters, C_1 and C_2 of radiating length 35 cm and 40 cm respectively, were constructed by dividing optically the total radiating length (≈105 cm) of a gas holder for detection of electrons. The efficiency of the counters attains the maximum values at a pressure of 5 atm for Freon 13 at 20°C. The efficiency neither increases with higher gas pressure nor does the ratio of the photomultiplier output voltage to the density of the gas remain constant. The latter effect was found to be due to the characteristic behaviour of large cathode photomultipliers, whereby the optimum focusing and accelerating voltages for a particular zone of a photocathode do not satisfy the requirements of an adjacent zone. The lowest values of the rejection ratio, i.e., the number of particles not detected by a counter to the number of particles registered by the scintillation counter telescope in coincidence, were 5×10^{-3} for C_1 3×10^{-3} for C_2 and 2.5×10^{-4} for C_1 & C_2 (combined). These values could be attributed to the secondary processes in the material of the gas holder as well as in the radiating medium. It was also found that the rejection ratio of a counter could be arbitrarily increased by placing an absorber in the beam and is affected by the presence of matter in the vicinity of the counter. (auth)

10875 ACHIEVING UNIFORM SPATIAL RESPONSE FROM LARGE AREA LIQUID SCINTILLATION DETECTORS. LaPointe, M. H.; Rennex, B. G.; Siohan, F.; Wayland, J. R. (Univ. of Maryland, College Park). Nucl. Instrum. Methods; 89: 291-3(1970).

A method of obtaining uniform spatial response from large, thin (1 m × 2 m × 8 cm), liquid scintillator detectors is described. Lucite steps are used to vary the depth of the scintillator and compensate for geometrical non-uniformities. (auth)

10876 THERMODYNAMIC PROPERTIES OF PROPANE AS BUBBLE CHAMBER LIQUID IN ANALYTICAL REPRESENTATION. Christenn, G.; Scheer, M. M. (Univ. of Wuerzburg, Ger.). Nucl. Instrum. Methods; 89: 295-6(1970).

Thermodynamic properties of propane important for creation and growth of bubbles are represented by analytical expressions. (auth)

10877 HIGH ENERGY PARTICLE IDENTIFICATION BY MEANS OF X-RAY TRANSITION RADIATION (XTR) DETECTORS. Alikhanian, A. I.; Ispirian, K. A.; Oganessian, A. G.; Tamanian, A. G. (Yerevan Physical Inst., Armenia, USSR). Nucl. Instrum. Methods; 89: 147-53(1970).

The results of an experiment on the investigation of a XTR-detector are given. On the basis of these results and theoretical calculations the possibilities of using XTR-detectors for identifying particles with various masses in the momentum region $P \geq 100$ GeV/c are analyzed. (auth)

10878 VIDICON DEVICE FOR IONIZATION MEASUREMENTS. Diamond, R. N.; Erwin, A. R.; Thompson, M. A. (Univ. of Wisconsin, Madison). Nucl. Instrum. Methods; 89: 45-52(1970).

A vidicon device which measures the relative ionization of tracks on bubble chamber film has been constructed and used at the University of Wisconsin. It is mounted on a manual film-plane measuring machine on-line with a CDC 924 computer. The section of film being scanned is displayed on a TV monitor along with a digital representation of the track being measured. Ionization reproductibility gives a standard deviation less than 3%. In actual experimental measurements the agreement with the ionization calculated from the kinematics is limited by the number of gaps measured being typically within 10%. (auth)

Radiation Dosimeters

Refer also to abstracts 10811, 10825, 11056, 11958, and 12773.

10879 THERMOLUMINESCENT DOSIMETRY WITH POLYCRYSTALLINE LiF. Stolz, W.; Lohse, U.; Demko, M.; Walter, R. (Technische Univ., Dresden. VEB Fluorwerke, Dohna, Ger.). Atompraxis; 16: 309-12(Sep-Oct 1970). (In German).

The preparation and properties of polycrystalline LiF for thermoluminescent dosimetry are described. Phosphor preparation and analytical results are reported. Polycrystalline LiF may be used for dosimetry either embedded in polytetrafluorethylene (PTFE) or as powder. It allows measurements of the absorbed dose over the range from 1 mrad to 10^5 rad. The following properties of the phosphor are discussed: glow curve, fading, sensitivity, dose response, measuring of low absorbed doses and energy dependence. The possibility of reutilization and the order for regeneration are discussed. (auth)

10880 NEUTRON PERSONNEL DOSIMETRY ON TISSUE-EQUIVALENT PHANTOMS BY SOLID-STATE TRACK DETECTORS. Doerschel, B.; Stolz, W. (Technische Univ., Dresden). Kernenergie; 13: 290-5(Sep 1970). (In German).

Phantom studies by means of solid-state track detectors in the neutron field of a Pu–Be source and of a nuclear reactor are described. Detector material was mica, and fissile materials were ^{235}U and natural uranium. Indication of a neutron personnel dosemeter worn on the front side of the body was studied for routine and emergency dosimetry. Body burden is shown to be estimated for any depth within the body from depth distributions of dose equivalent measured. The body orientation effect in the neutron field may be corrected by determining direction factors. If conclusions for doses absorbed in the human body should be drawn from health physics measurements made in air, backscattering has to be taken into account for thermal and intermediate neutrons, and build-up factors must be considered for fast neutrons. A comparison of measured and calculated build-up factors is made. (auth)

10881 EMERGENCY PERSONAL n-γ RADIATION DOSIMETERS. Keirim-Markus, I. B. (Inst. of Biophysics, Moscow); Knyazev, V. A.; Kozlov, B. F.; Obaturov, G. M.; Turkin, A. D. pp 103-15 of Nuclear Accident Dosimetry Systems. Vienna; International Atomic Energy Agency (1970). (In Russian).

From Panel on Nuclear Accident Dosimetry Systems, Vienna, Austria. See STI/PUB-241; CONF-690223.

Work on emergency personal n-γ radiation dosimeters, including activation (Cu, P) track dielectrics of glass or mica, placed in contact with layers of fissionable materials (^{235}U, ^{238}U, natural U and ^{237}Np), photographic dosimeters (M3-32-1 film type), and IKS-A thermoluminescent dosimeters, which have been investigated in the USSR and put to practical use, are reviewed. The track dosimeter containing ^{237}Np with a boron filter can be used to advantage in the measurement of neutron kerma as can the IKS-A thermoluminescent dosimeter in the measurement of γ-radiation dose. (auth)

10882 DEVELOPMENTS IN THRESHOLD DETECTORS FOR PERSONAL DOSIMETERS. Cross, W. G. (Chalk River Nuclear Labs., Ont.). pp 117-29 of Nuclear Accident Dosimetry Systems. Vienna; International Atomic Energy Agency (1970).

From Panel on Nuclear Accident Dosimetry Systems, Vienna, Austria. See STI/PUB-241; CONF-690223.

A technique is described which makes visible and automatically counts the damage-track holes made by fission fragments through a thin, plastic sheet. This method considerably reduces the time required to read damage-track neutron detectors and overcomes some of the restrictions of using ^{237}Np in a dosimeter to be worn regularly by people. The reaction $^{103}Rh(n,n')^{103m}Rh$ has a threshold close to that of ^{237}Np and gives roughly equivalent performance in combination with U and S threshold detectors. Addition of either Np or Rh to an In-S dosimeter significantly improves the accuracy of dose measurements on moderated fission spectra. For a criticality accident the remaining error in such measurements is expected to arise mainly from neutrons with energies between 0.1 and 0.6 MeV. (auth)

10883 CHEMICAL DOSIMETERS FOR ACCIDENT DOSIMETRY. Dvornik, I. (Institut Ruder Boskovic, Zagreb). pp 131-3 of Nuclear Accident Dosimetry Systems. Vienna; International Atomic Energy Agency (1970).

From Panel on Nuclear Accident Dosimetry Systems, Vienna, Austria. See STI/PUB-241; CONF-690223.

A chemical dosimeter which can measure the first-collision gamma plus neutron absorbed dose is described. The dosimeter is composed of an ethanol–chlorobenzene–saturated hydrocarbon–thymolsulphon–phthalein indicator solution. (W.H.K.)

10884 NUCLEAR ACCIDENT DOSIMETRY BY FOIL GROUP. Shibata, T. (Kyoto Univ.). pp 135-45 of Nuclear Accident Dosimetry Systems. Vienna; International Atomic Energy Agency (1970).

From Panel on Nuclear Accident Dosimetry Systems, Vienna, Austria. See STI/PUB-241; CONF-690223.

Some foil activation methods are proposed for the measurement of the neutron fluence and its energy spectrum, which is important not only for dose estimation but also for accident analysis. After a nuclear accident, induced activities of foils, which are mounted around reactors, are measured, and the information for the neutron fluence and the whole neutron energy spectrum are obtained by the combination of different activation foils each of which has a different response to the neutron spectrum. The techniques are examined by using the Kyoto University Reactor at normal operation. Further possibilities for nuclear accident dosimetry are also discussed. (auth)

10885 PERSONNEL MONITORING FOR RADIATION ACCIDENTS. Krishnamoorthy, P. N. (Bhabha Atomic Research Centre, Trombay, India). pp 147-52 of Nuclear Accident Dosimetry Systems. Vienna; International Atomic Energy Agency (1970).

From Panel on Nuclear Accident Dosimetry Systems, Vienna, Austria. See STI/PUB-241; CONF-690223.

A personnel monitoring system for radiation accidents used at the Bhabha Atomic Research Centre is described. It consists of (i) a conventional film badge mounted in a multi-filter cassette; and (ii) a number of other detector elements for measuring high exposures of gamma-rays and neutrons. (auth)

10886 MULTI-LABORATORY INTERCOMPARISONS AND STANDARDIZATION: NUCLEAR ACCIDENT DOSIMETRY SYSTEMS. Auxier, J. A. (Oak Ridge National Lab., Tenn.). pp 153-64 of Nuclear Accident Dosimetry Systems. Vienna; International Atomic Energy Agency (1970).

From Panel on Nuclear Accident Dosimetry Systems, Vienna, Austria. See STI/PUB-241; CONF-690223.

The most significant advances in the physical dosimetry of neutrons during the past 20 years have been (1) the development of proportional counter techniques; (2) the improvement of threshold and activation detector techniques; (3) the development of spectrometers; and (4) the development and improvement of solid-state detectors. However, some of the most widely used detectors of the 1940s are still used (viz., nuclear emulsions and ionization chambers). Just as important as the instrumentation has been the search for greater understanding of the principles of radiation interaction with matter, and the rate of progress has improved rapidly during the last five years. Several national and international intercomparisons of dosimetry systems, particularly those for nuclear accident dosimetry, have been made at ORNL. The results show that approximately three-fourths of all major nuclear facilities are prepared to evaluate dose due to neutron exposures from nuclear accidents with a standard deviation of about ±15%. The remaining one-fourth obtains results in test excursions which may be high or low, depending on the neutron spectrum, by 25% to a factor of three or more. Gamma radiation exposures are measured to within ±25% by all of those who have participated in intercomparisons (15 to 20 major installations). Intercomparison studies for small nuclear installations are now being arranged at the DOSAR Facility. (auth)

Radiometric Instruments

Refer also to abstracts 10785 and 11421.

10887 (INP-709) ACCURACY OF THE NEUTRON METHOD OF MOISTURE MEASUREMENT. Sciesinska, E. (Institute of Nuclear Physics, Krakow (Poland)). 1970. 43p. Dep. NTIS (U. S. Sales Only).

A discussion is given of the influence of density and chemical composition of the medium, as well as of the measurement geometry, on the accuracy of the neutron method of moisture measurement. Experimental and theoretical calibration curves obtained for foundry mass in finite 4π-geometry were compared for this purpose. The influence of density was investigated for all variants of the 4π-geometry employed whereas the influence of absorbents of thermal neutrons was studied only for the simplest geometry. The incompatibility of the obtained results with the Fermi age theory is interpreted. Accuracies of the epithermal and thermal variant of the neutron method are compared. (auth)

10888 UTILIZATION OF GEIGER COUNTERS FOR THE DETECTION OF NON-RADIOACTIVE EFFLUENTS FROM A GAS CHROMATOGRAPH. Lubkowitz, J. A.; Parker, W. C.; Findeis, A. F. (Instituto Venezolano de Investigaciones Cientificas, Caracas). Radiochem. Radioanal. Lett.; 5: 235-41 (15 Dec 1970).

A Geiger counter has been used to detect non-radioactive impurities that eluted at the exit of a column of a gas chromatograph. The detector is simple and of comparable sensitivity to the thermal conductivity detector. The detector response is linear indicating that it can be used as detector for gas chromatography. (auth)

10889 METHOD AND APPARATUS FOR SIMULTANEOUS POROSITY AND CHLORINITY LOGGING. Moran, James H. (to Schlumberger Tech. Corp.). U. S. Patent 3,529,160. 15 Sep 1970. Filed 10 May 1967.

One embodiment of the invention shows a well logging tool that contains a source for emitting neutron pulses of equal duration and spacing. An epithermal or thermal and epithermal neutron detector signal registered during each pulse is added to a detector signal registered between each pulse in order to produce an indication of formation porosity. The difference between these detector signals is divided by the detector signal sum to provide a normalized log of thermal neutron decay time that characterizes the chlorine concentration in the formation. The technique also can be applied to measure epithermal or thermal and epithermal neutron slowing down time. The neutron population, moreover, can be measured through the gamma radiation that results from neutron interaction with the nuclear structure of the earth formation. (auth)

10890 RADIATION GAUGE SYSTEM FOR TUBULAR PLASTIC FILM. Hannula, Fred W.; Stanko, Alfred F.; Kelleher, Daniel F. (to Lee Corp.). U. S. Patent 3,529,163. 15 Sep 1970. Filed 14 Sep 1967.

A beta backscatter gage for the measurement of the thickness of plastic film which is extruded in tubular form by the blown film process is described. (W.H.K.)

Miscellaneous Instruments and Components

Refer also to abstracts 10626, 11850, 12299, and 12792.

10891 (AERE-R-5422) MEASUREMENT OF TIME-OF-FLIGHT USING 300 Mc/s SCALERS. Richards, J. M.; Hinton, J. H.; Bowker, A. J. (Atomic Energy Research Establishment, Harwell (England)). Dec 1967. 13p. Dep. NTIS (U. S. Sales Only).

A time-of-flight encoder that digitizes the time interval using a 300 mc/s pulse train and a 300 mc/s scaler is described. The basic encoder was extended to time several events after each start pulse. A method of automatic spectrum correction is discussed. This eliminates the distortion of the time-of-flight spectrum which is introduced whenever more events occur in the time range than can be accepted by the time-of-flight encoder. (auth) (UK)

10892 (CEA-N-1363) VISUALIZATION OF SPECTRA IN NUCLEAR PHYSICS. A PROGRAM SYSTEM ADAPTED TO GIVE A GRAPHICAL OUT PUT WITH A CII-90-10 COMPUTER. Morvan, Pierre (Commissariat a l'Energie Atomique, Saclay (France), Centre d'Etudes Nucleaires). Oct 1970. 57p. (In French). Dep. NTIS (U. S. Sales Only).

A general description of the visualization unit is given including the general design with the oscilloscope and analog and logic units, the generators of visual functions, the methods of associated dialog. Also a system of programs for the unit is described. (J.F.P.)

10893 (EGG-1183-484) THREE-BAND SOURCE SPECTRA FROM COLOR FILM. Buckner, J.; Maciel, R. (EG and G, Inc., Bedford, Mass.). 31 Mar 1969. Contract AT(29-1)-1183. 29p. Dep. NTIS.

This report demonstrates how the LASL-EG&G effective exposure method may be utilized to obtain the source radiance in three broad spectral bands from color photographic images. The demonstration consists of developing a matrix solution of the effective exposure equation which does not depend on a priori knowledge of the spectral radiance but which does yield the absolute radiance amplitudes of the three bands. For EDER film, these bands are 3800–5000 Å, 5000–5900 Å, and 5900–6800 Å. When applied to color photographs of a standard radiance source, this three-band approach yields spectral radiance values to within 10% of the known values over the range 3800–6800 Å. The usefulness of this approach is demonstrated by applying it to an important feature recorded during Operation Dominic. This application results in the gross spectral resolution of a source in time and space, making it possible to quote power-time histories in three bands spanning the interval 3800–6800 Å. (auth)

10894 (NP-18614) SIMULTANEOUS RECORDING OF TRUE AND RANDOM COINCIDENCES USING A TWO-PARAM-

XUM

ETER ANALYZER SYSTEM. Hattula, J.; Helppi, H. (Jyvaskyla Univ. (Finland). Dept. of Physics). Jun 1970, 9p. Dep. NTIS (U. S. Sales Only).

A description is given of a simple fast coincidence method which allows the simultaneous recording of coincidence and random coincidence spectra. The method is based on the properties of a standard two-parameter pulse-height analyzer system, and no special electronics is required. The method is tested in connection with angular correlation measurements. (auth) (FINLAND)

10895 (ORNL-TM-3101) CONTROLS DEPARTMENT HYBRID COMPUTER: HARDWARE AND APPLICATIONS. Stone, R. S. (Oak Ridge National Lab., Tenn.). 24 Aug 1970. 23p. Dep. NTIS.

An analog-digital hybrid computer was added to the computation facility of the ORNL Controls Department. By combining the speed, parallel operations, and on-line interaction of the analog computer with the accuracy, memory, and preprogramming of the digital computer, the hybrid becomes more effective than the sum of its components for certain classes of problems. In general, the problems best suited to the hybrid computer are those involving (1) the dynamics of large multidimensional distributions, (2) problems wherein one aspect calls for high accuracy and another aspect requires high speed, or (3) large families of differential equations whose coupling coefficients are to be determined. The system includes a digital computer with 32K words of 36-bit fast memory, plus an analog computer with 153 operational amplifiers, 16 quarter-square multipliers, and 148 coefficient devices. (auth)

10896 (RD/B/N-1720) INDUCTIVE LIQUID METAL LEVEL DETECTOR. Walker, R. C. (Central Electricity Generating Board, Berkeley (England). Berkeley Nuclear Labs.). Jun 1970. 27p. Dep. NTIS (U. S. Sales Only).

Instruments were designed and developed to detect and measure levels of liquid metal coolants. These instruments measure the level to accuracies of $\pm\frac{1}{8}$ in. without the necessity of inserting contacts or couplings into the sealed containment vessels, so reducing the risk of leakage through seals or weak points in its surrounding walls. (auth)

10897 MILLIMETER AND SUBMILLIMETER RADIOSPECTROSCOPY. Krupnov, A. F. (Gorky State Univ., USSR). Izv. Vyssh. Ucheb. Zaved., Radiofiz.; 13: 961-1000(1970). (In Russian).

Aspects of development of millimeter and submillimeter radiospectroscopy are briefly reviewed. The methods of gas, radio, and laser spectroscopy are discussed and various spectroscopic devices and their performance are described. (247 references) (R.V.J.)

10898 DELAY CIRCUITS FOR NUCLEAR APPLICATIONS. Grose, K. D. (Univ. of Birmingham, Eng.). J. Phys., E (London); 4: 57-8(Jan 1971).

The use of an integrated circuit TTL monostable module for producing signal delays for pulsed nuclear experiments is described. (auth) (UK)

10899 GENERATOR FOR STUDYING SUPERCONDUCTIVITY BY A PULSE METHOD. Frantsevich, V. M.; Klyushnikov, O. I.; Romanov, E. P. (Inst. of Metal Physics, Sverdlovsk, USSR). Cryogenics; 10: 506-7(Dec 1970).

A generator was developed, which gave a saw tooth current of maximum amplitude 70A with a large off period, to study the resistive state and to determine the critical current in hard superconductors. A circuit diagram is given and discussed. (UK)

10900 OPTIMIZATION OF TIME ANALYZER PARAMETERS IN MULTI-CYCLE EXPERIMENTS WITH EXPONENTIAL DECAY. Bull, S. R.; Lu, K. K. (Univ. of Missouri, Columbia). Nucl. Instrum. Methods; 89: 253-6(1970).

A method has been devised to determine the optimum channel dwell time and number of analysis channels of the time analyzer in multi-cycle experiments with exponential decay. The optimization was accomplished by minimizing the total experiment time with the constraint that the error in the decay constant was a constant. Calculations were restricted to the parameters commonly available on multichannel analyzers in the multiscale mode. The results indicate that experiments would often be more efficient and valuable experiment time would be conserved if larger channel dwell times were employed. (auth)

10901 DESIGNING METHOD OF SWITCHING CIRCUITS CASCADE FOR ANALOG PARAMETER DISCRIMINATION. Abbattista, N. (Istituto di Fisica, Bari, Italy); Marino, D.; Plantamura, V. L.; Coli, M. Nucl. Instrum. Methods; 89: 215-19(1970).

A method of analyzing the cascade switching circuit configurations specializing in the discrimination of an analog input parameter is described. The method is based on the transfer of the resolution curve from the input to the output. This allows an iterative process for describing n cascading stages. The behavior of a resolution figure is given for a better design of these systems. (auth)

10902 ANALYSIS OF ACCIDENTAL COINCIDENCES BY MEASUREMENTS WITH TIME-TO-PULSE HEIGHT CONVERTERS. II. Braunsfurth, J. (Univ., Hamburg). Nucl. Instrum. Methods; 89: 305-7(1970). (In German).

The influence of noise pulse length on background in time spectra obtained with time to pulseheight converters and performance differences between Start/Stop- and Square-Overlap-Converters are discussed. (auth)

10903 ION-MOBILITY SPECTROMETER FOR RADIOCHEMICAL APPLICATIONS. Stevenson, P. C. (Univ. of California, Livermore); Thomas, R. A.; Lane, S. Nucl. Instrum. Methods; 89: 177-87(1970).

The design of a novel instrument for measuring mobilities of ionic species in gases at pressures of about 1 atm is reported. The device is designed especially, although not exclusively, for the measurement of the mobility of the ions of radioactive species recoiling from a source into a gas subsequent to a nuclear reaction. Measurements have been obtained on a variety of fission fragment species in helium and also on the major charge-carrying nonradioactive species present. (auth)

Radiation Effects on Instruments and Instrument Components

Refer also to abstract 11951.

10904 (HMI-B-97) INVESTIGATIONS OF RADIATION RESISTANCE OF OPTOELECTRONIC DEVICES FOR AN ELECTRONICALLY SCANNING STAR SENSOR IN SATELLITES. [DIODES: 663(ENL), 602-5D, PIN 6LC(UDT) MULTIPLIER: XP 1117 (VALVO)]. Braeunig, D.; Spencker, A.; Wagemann, H. G. (Hahn-Meitner-Institut fuer Kernforschung, Berlin (West Germany)). Jul 1970. 170p. (In German). Dep. NTIS (U. S. Sales Only).

Several optoelectronic devices (photomultipliers and photocells) were submitted to electrical (especially noise and dark-current) and to optical (relative spectral sensitivity and photoelectric current generated by means of Johnson light) measurements before and after they had absorbed irradiations of X-rays (100 keV), electrons (600 keV), and electrons (1.5 MeV). The results of the irradiations are discussed and evaluated concerning the different technology of the devices. (auth)

10905 EFFECT OF RADIATION IN REACTIVELY SPUTTERED Al_2O_3–Si STRUCTURES. Hattori, Takeshi; Iwauchi, Shigeki; Tanaka, Toshio (Sophia Univ., Tokyo). Jap. J. Appl. Phys.; 9: 1538(Dec 1970).

MOS structures consisting of reactively sputtered Al_2O_3–Si were irradiated with 1-MeV electrons and the resulting induced changes and surface state densities measured at various bombardment biases. The induced change is low compared with best steam-grown SiO_2 and plasma-anodized Al_2O_3, and the density of interface states does not exceed twice the initial value at a fluence of 10^{14} e/cm^2. (D.L.C.)

10906 MECHANISMS OF RADIATION-INITIATED SEMICONDUCTOR DEVICE FAILURES. Tarka, John Edward. Philadelphia; Univ. of Pennsylvania (1969). 252p. University Microfilms Order No. 70-16,219.

Thesis.

An experimental study of the radiation initiated failure modes of approximately 120 actively biased and instrumented integrated circuits, which included both linear and logic types, junction isolation and dielectric isolation, encompassing several manufacturers, resulted in the hypothesis that radiation initiated second breakdown is the mechanism which many of these failures had in common. In several cases of these failures, direct evidence of the effects of a mesoplasma formed during the second breakdown mode was observed through crater like formations that originated in the active region of the junction. It is inferred through experiment that the phenomenon referred to as latchup in dielectrically isolated integrated circuits is due to the action of a self sustaining mesoplasma, and may or may not lead to a catastrophic failure mode, depending on the circuit configuration in which it is tested. A series of experiments performed on discrete devices, which included pulsed radiation and pulsed elec-

XUM

trical verification tests, exclusive of one another, served as the basis for proof that radiation initiated second breakdown is the primary failure mechanism for several of the commonly observed semiconductor failure modes. A unique experimental method for using a super flash x-ray machine operating in the electron mode was developed in the course of this work. Essentially the electromagnetic coupling effects of a 16,000 ampere electron plasma were reduced so that a relatively noise free radiation field was realized. Specifically the electromagnetic coupling of this electron beam into the monitoring electronics, at a pulsed radiation level of 50,000 rads (Al), was less than 20 millivolts peak to peak. (Diss. Abstr. Int., B)

XUM

LIFE SCIENCES

Biochemistry, Physiology, and Molecular Biology

Refer also to abstract 10435.

Basic Processes

Refer also to abstracts 10505, 10511, 11046, 11066, 11118, 11121, 11132, 11133, 11138, 11142, 11157, 11159, 11192–11194, and 11208.

10907 (N-70-31814) STUDY TO DEVELOP NEUTRON ACTIVATION FOR MEASURING BONE CALCIUM CONTENT. Lukens, H. R. Jr.; Fleishman, D. M.; MacKenzie, J. K. (Gulf General Atomic, Inc., San Diego, Calif.). Jun 1970. Contract NAS2-5178. 84p. (NASA-CR-1606). NTIS.

A study of the feasibility of utilizing neutron activation analysis for the in vivo determination of bone calcium in the macaque monkey was carried out. Theoretical calculations showed that the absolute determination of bone calcium by in vivo neutron activation analysis is highly dependent on the use of comparator standards that accurately represent the size, shape, and composition of the specimen. Accurate models of a vertebra and a femur were constructed of calcium-loaded plastic, and analyses of two vertebrae and a femur were carried out under simulated in vivo conditions using the models as comparator standards. The absolute calcium values were confirmed by both high-flux neutron activation analysis and atomic absorption analyses. With sufficiently accurate comparator standards, it is estimated that in vivo neutron activation analysis is capable of determining absolute calcium levels in the whole body to within 2% to 3% of the actual value. (auth)

10908 METHOD FOR STUDYING PHAGOCYTOSIS WITH ^{51}Cr-LABELLED YEAST CELLS. Nordenfelt, Erik (Univ. of Lund, Sweden). Acta Pathol. Microbiol. Scand.; 78B: 247-52 (1970).

A new method is described for measuring phagocytosis in vitro. Leukocytes obtained by peritoneal irrigation of the rabbit were allowed to phagocytize ^{51}Cr-labeled yeast cells. The subsequent ^{51}Cr-activity of the leukocytes was taken as a measure of phagocytic activity. The method was tried in the presence of some factors known to be capable of affecting phagocytic activity. The results obtained agreed well with those reported in previous investigations. The method is suitable for studies of the course of events during phagocytosis. (auth)

10909 RAPID DETERMINATION OF ALUMINIUM, MANGANESE, AND SODIUM IN SOILS BY NEUTRON ACTIVATION ANALYSIS. Khera, A. K. (Agricultural Coll. of Norway, Vollebekk); Steinnes, E. Agrochimica; 13: 524-9(Oct 1969).

A simple and rapid method for the determination of aluminium, manganese and sodium in soils by reactor neutron activation and γ-spectrometry was presented. The method gave a precision on the order of 1 to 2% and few sources of systematic error were inherent in the method. (auth)

10910 WHOLE-BODY COUNTER FOR SERIAL STUDIES OF TOTAL BODY POTASSIUM. Johny, K. V.; Worthley, B. W.; Lawrence, J. R.; O'Halloran, M. W. (Queen Elizabeth Hosptial, Woodville, Australia). Clin. Sci.; 39: 319-26(Aug 1970).

The use of a whole-body counter in total body potassium estimations was described. The accuracy and value of the counter in measuring serial changes in total body potassium were assessed. Serial study of twelve normal subjects at varying intervals revealed a normal variability in total body potassium of up to 1.23% (4-weekly measurements over 3 mos.). The error involved in counting statistics alone was 4%. The whole-body counter appeared to be an accurate and useful method of assessing total body potassium in clinical studies. (auth) (UK)

10911 DETERMINATION OF CORONARY BLOOD FLOW WITH RADIOACTIVE INDICATORS AS MEASURED BY EXTERNAL COUNTING. Hundeshagen, H. (Medizinische Hochschule, Hanover). Nucl.-Med.; 32: Suppl. 7, 9-16(1968). (In German).

From 5th Conference of the Society of Nuclear Medicine, Vienna, Austria. See CONF-670996.

To determine the coronary blood flow, two scintillation crystals with collimators are used. One is located over the left ventricle, while the other one is centered on the right heart at the level of the coronary sinus. Through the cubital vein, a catheter is passed into the pulmonary artery. Either 150 μCi ^{131}I albumen or 500 to 100 μCi ^{99m}Tc albumen is injected rapidly. The left detector records cardiac minute volume while the right detector indicates coronary blood flow. In normal persons, the coronary flow ranges from 5 to 9% of the minute volume. Patients suffering from either arteriosclerosis or angina pectoris display values between 3.5 and 5.5%. (H.B.G.)

10912 STUDIES ON PERIPHERAL CIRCULATION WITH RADIOISOTOPES. Pabst, H. W. (Univ., Munich). Nucl.-Med.; 32: Suppl. 7, 141-64(1968). (In German).

From 5th Conference of the Society of Nuclear Medicine, Vienna, Austria. See CONF-670996.

Studies of peripheral blood circulation with radioisotopes are presented and reviewed. The survey includes determination of circulation time, measurement of blood flow in the extremities, scintigraphy of extremities following administration of ^{131}I albumen macroaggregate, quantitative determination of blood volume in the extremities, and clearance methods for the study of peripheral blood flow. A special clearance method, based on the simultaneous injection of ^{133}Xe and ^{131}I, is described. The double isotope method allows quantitative assessment of circulatory defects and predictions about feasibility of correction by surgical intervention. 52 references are given. (H.B.G.)

10913 SIMULTANEOUS BLOOD FLOW MEASUREMENTS WITH ^{133}Xe IN FLEXORS AND EXTENSORS OF THE LOWER LEG UNDER POSITIVE AND NEGATIVE LOAD. Hengst, W.; Kaltenbach, M. (Medizinische Klinik des Krankenhauses Nordwest, Frankfurt an Main. Medizinische Univ., Frankfurt am Main). Nucl.-Med.; 32: Suppl. 7, 187-94(1968). (In German).

From 5th Conference of the Society of Nuclear Medicine, Vienna, Austria. See CONF-670996.

A method was developed by which ^{133}Xe clearance was measured simultaneously in flexors and extensors during work. In addition, blood flow through the lower extremities was measured under positive and negative load; that means during active and passive work. Under the same load, active work produced twice the increase of blood flow found during negative work. Blood flow was affected significantly by the rate of work. The length of rest periods between working phases was especially influential. (tr-auth).

10914 STUDIES ON VASOACTIVE DRUGS WITH THE ^{133}Xe MUSCLE CLEARANCE METHOD. Zerkowitz, A.; Hoppe, G.; Bublitz, G. (Staedt. Auguste-Viktoria-Krankenhauses, Berlin). Nucl.-Med.; 32: Suppl. 7, 195-200(1968). (In German).

From 5th Conference of the Society of Nuclear Medicine, Vienna, Austria. See CONF-670996.

Xenon-133 clearance from the anterior tibial muscle was measured at rest and under work. Three types of vasilator drugs were administered intraarterially and it was shown that they caused different reactions in rest and work phases. Vasodilation was not striking in normal persons and diminished with severity of pathological processes. Muscle activity caused more vasodilation than any of the drugs. The Xe clearance method proved to be suitable for evaluating vasoactive drugs. (H.B.G.)

10915 RESULTS AND IMPORTANCE OF QUANTITATIVE BLOOD FLOW MEASUREMENTS THROUGH PARABIOTIC TISSUE CONNECTIONS. Kuni, H.; Graul, E. H.; Linke, R. (Philipps-Univ., Marburg, Ger.). Nucl.-Med.; 32: Suppl. 7, 201-7(1968). (In German).

From 5th Conference of the Society of Nuclear Medicine, Vienna, Austria. See CONF-670996.

Parabiotic pairs of mice were injected with ^{51}Cr-labeled erythrocytes. Total blood volume as well as exchange through the tissue bridge were measured by external counting and by determination of activity in blood samples. Up to 50 hours post parabiotic connection, no blood exchange occurred. Then, quite rapidly, the exchange was established and reached a maximum between 70 and 80 hours post surgery. It was concluded that the capillary systems of the two animals interconnected rather suddenly. If one of the partners was sacrificed, the other one went into shock because of blood loss through the parabiotic connection. (H.B.G.)

10916 RADIOISOTOPE STUDIES ON HYPEREMIA PRODUCING TREATMENT. Grebe, S. F.; Kern, W.; Schellman, R. (Justus Liebig-Univ., Giessen, Ger.). Nucl.-Med.; 32: Suppl. 7, 209-14(1968). (In German).

From 5th Conference of the Society of Nuclear Medicine, Vienna, Austria. See CONF-670996.

XUM

Following injection of 20 μCi ^{131}I RISA, radioactivity was measured over the hepatic and cardiac regions. A series of patients received 10 min. microwave radiation to the liver area, another series was treated for 30 min. with hot compresses to the same area. Results showed that the minute volume of hepatic blood flow increased significantly while total blood content of the liver decreased. Reduction of hepatic blood volume lasted throughout 90 min. post microwave radiation, and throughout 50 min. post application of hot compresses. (H.B.G.)

10917 PRINCIPALS OF BLOOD FLOW MEASUREMENTS THROUGH ORGANS BY CLEARANCE METHODS. Wolf, R. (Univ., Mainz). Nucl.-Med.; 32: Suppl. 7, 215-23(1968). (In German).

From 5th Conference of the Society of Nuclear Medicine, Vienna, Austria. See CONF-670996.

Single and double compartment models are analyzed with respect to errors that might occur during the determination of blood flow through organs with radioactive isotope clearance methods. Mathematical formulas are developed for the effect of uneven extraction, simultaneous accumulation in several organs, inhomogeneity of the tracer material, disassociation of the isotope label in vitro and in vivo, and incomplete or delayed dilution of the isotope. (tr-auth).

10918 COLLOID CLEARANCE: EFFECT OF PARTICLE SIZE AND EXTRAHEPATIC DEPOSITION. Hoefer, R.; Ogris, E.; Pfeiffer, G.; Probst, P. (Medizinische Univ., Vienna). Nucl.-Med.; 32: Suppl. 7, 225-9(1968). (In German).

From 5th Conference of the Society of Nuclear Medicine, Vienna, Austria. See CONF-670996.

Hepatic clearance of radioactive colloidal gold was determined for particle sizes of 50 Å and 300 Å. The study comprised eight patients without liver diseases and four with hepatic or hematic disorders. For 300 Å particles, half time of hepatic clearance was 1.7 min.; accumulation in bone marrow was about 2%. For 50 Å particles, half time of hepatic clearance was 2.2 min. and accumulation in bone marrow was 5.3%. In almost all cases studied, hepatic clearance was delayed for smaller particles and bone marrow accumulation was increased. In liver clearance studies, errors caused by extrahepatic deposition increased with decreasing particle size. Attempts should be made to produce colloidal gold smaller than 50 Å for improved scintigraphy of bone marrow. (H.B.G.)

10919 STUDIES ON LIVER FUNCTION WITH COMPUTER-SCINTIGRAPHY. Rommel, K.; Adam, W. E.; Lorenz, W. J.; Bitter, F. (Univ., Ulm, Ger. Deutsche Krebsforschungszentrums, Heidelberg). Nucl.-Med.; 32: Suppl. 7, 231-6(1968). (In German).

From 5th Conference of the Society of Nuclear Medicine, Vienna, Austria. See CONF-670996.

In dogs, 200 μCi ^{131}I-Rose Bengal was injected intravenously. The liver area was counted with an Anger camera. A special computer program allowed differentiation of activity in various areas. The method was valuable for determining localized pathological liver changes and for the differential diagnosis between intrahepatic and extrahepatic occlusions. (H.B.G.)

10920 SIMULTANEOUS DETERMINATION OF TOTAL POTASSIUM AND EXCHANGEABLE SODIUM IN MAN. Kunkel, R.; Oberhausen, E. (Univ. des Saarlandes, Homburg, Ger.). Nucl.-Med.; 32: Suppl. 7, 411-15(1968). (In German).

From 5th Conference of the Society of Nuclear Medicine, Vienna, Austria. See CONF-670996.

Throughout ten minutes, total K content of patients is measured by determining the ^{40}K activity in a whole-body counter. Subsequently, 0.1 μCi of ^{22}Na is injected. Twenty-four hours later, whole-body counting is performed for one hour. Total K values ranged from 43 to 60 m/equiv./kg. Exchangeable Na ranged from 41 to 46 m/equiv./kg. (H.B.G.)

10921 TUMOR-SPECIFIC LOCALIZING AGENT FOR RADIOISOTOPE IMAGE. IV. WHOLE BODY AUTORADIOGRAPHY BY 5-^{131}IU AND 6-^{131}IP. Maeda, Tatsuo; Kono, Akira; Nagao, Koichiro; Kojima, Masaharu (Kyushu Univ., Fukuoka). Radioisotopes (Tokyo); 19: 507-10(Nov 1970). (In Japanese).

The distribution of ^{131}I-labeled uridine or uridine phosphates in the bodies of mice in which Ehrlich ascites tumor was implanted was studied by mean of the whole-body autoradiography. After intraperitoneal injection of ^{131}I-uridine and ^{131}I-phosphates considerable radioactivity was detected in the tumor tissues, although higher radioactivities were found in the stomach, thyroid, and salivary gland. Whole-body autoradiography is as useful as the scinticamera technique for investigations of tumor localizing radioactive agents. (auth)

10922 DETERMINATION OF MONOAMINE OXIDASE ACTIVITY IN HUMAN BLOOD SERUM WITH ^{14}C-BUTYLAMINE AS SUBSTRATE. Tufvesson, G. (Central Hospital, Kristiansand, Norway). Scand. J. Clin. Lab. Invest.; 25: 231-5(May 1970).

A method for determining monoamine oxidaze in human serum with ^{14}C-butylamine as substrate is described. The optimal experimental conditions for the determination are given. (auth)

10923 DETERMINATION OF TESTOSTERONE IN PERIPHERAL BLOOD OF SWINE AND BOVINES WITH A DOUBLE ISOTOPE DERIVATIVE DILUTION METHOD. Hoffmann, B.; Claus, R.; Karg, H. (Technische Hochschule, Munich). Acta Endocrinol.; 64: 377-84(1970). (In German).

Using a double-isotope-dilution derivative method combined with a crystallization technique testosterone was measured in pig and bovine peripheral blood. In the male pig the values varied from 0.94 to 1.61 μg per 100 ml plasma and were 7- resp. 11-times higher than in castrated and female animals. Values increased with age. The concentration measured in a bull was 0.59 μg per 100 ml plasma. (auth)

10924 USE OF RADIOACTIVE TRACERS IN IMMUNOLOGY AND ALLERGY. Cirstea, M. (Inst. of Normal and Pathological Physiology, Bucharest). Stud. Cercet. Fiziol.; 14: 439-53(1969). (In Rumanian).

Tracer techniques have been used with good success to solve research problems in the fields of immunology and allergy. The applications of the technique include radioimmunological studies involving analyses similar to the classical methods but offering higher sensitivity and increased speed, and completely new uses which make it possible to investigate previously inaccessible areas. The fields described include the determination of the behavior of antigens in the organism by using ^{131}I-labeled proteins; formation and metabolism of antibodies involving the incorporation of exogenous nitrogen, studied by feeding animals with ^{15}N-labeled glycine; the use of ^{35}S-labeled methionine and of several ^{131}I-labeled antigens. Valuable information was obtained on the nature of cells which trigger the immunological response by in-vivo labeling, followed by histoautoradiography, using tritium-labeled thymidine. The in-vitro synthesis of antibodies was investigated by using ^{14}C-labeled lysine and L-isoleucine. The other applications reviewed include fixation of antibodies in tissues and cells, their detection and determination, the primary antigen–antibody interactions, and radioimmunological determination. (Review article, 53 references) (TTT)

10925 RADIOCHEMICAL PROBLEMS OF THE WATER SOLUTIONS OF RADIONUCLIDES USED FOR BIOLOGICAL EXPERIMENTS. Severa, J. (Military-Medical Research Inst., Hradec Kralove, Czech.). Sb. Ved. Pr. VLVDU Hradci Kralove; 47: 175-93(1970). (In Czech).

Tracer amounts of radionuclides can exist in water solutions in the form of ions or complexes, neutral molecules, and colloids. Under definite conditions these forms can coexist and create polydispersed solutions. The investigation of tracer amounts in water solutions is complicated and must be conducted by using various methods such as adsorption, desorption, dialysis, ultrafiltration, centrifugation, diffusion, and electrophoresis. The significance of these studies rests in the differences in properties and behavior of the individual forms. These facts must be respected when applying the radionuclides in biological experiments. If, for example, the concentration of ^{85}Sr in a water solution is 10^{-8} M at pH 6, then the radioisotope is found in the ionic form. On the other hand, 10^{-10} M ^{144}Ce at pH 6 exists in the partly hydrolyzed or neutral forms of the $[CE(OH)_x Cl_{3-x}]o$ type. (tr-auth)

10926 DOUBLE ISOTOPE DILUTION TECHNIQUE IN THE STUDY OF A PERIPHERAL VASCULAR SYSTEM IN VIVO. Brakkee, A. J. M.; Vendrik, A. J. H. (Univ., Nijmegen, Netherlands). Bibl. Anat.; No. 10, 528-31(1969).

From 5th European Conference on Microcirculation, Goteborg, Sweden. See CONF-680670.

Experimental data are presented on arterio-venus shunt systems performed on feet of hindlegs of dogs. Procedures for a double isotope method are described and evaluated. ^{24}NaCl and ^{131}I-albumin are used as indicators. The measurements are analyzed in terms of the blood flow through as well as the volume of the shunt vessels and the capillary system. (H.B.G.)

10927 THE APPLICATION OF RADIATION TECHNIQUES TO WATER USE EFFICIENCY STUDIES. THE EVAPOTRANSPIRATION STUDIES ON MAIZE CROP IN GIZA, U. A. R. Zein el Abedine, A.; Abdalla, M. M.; Abd-el-al, Sh. I. (Middle Eastern Regional Radioisotope Centre for the Arab Countries, Cairo). Isotope Radiat. Res.; 1: 25-32(Oct 1968).

The evapotranspiration for maize crop is determined using, the

XUM

direct method or the actual E.T., the calculated E.T. by tracing the moisture contents in the soil profile, or the E.T. potential using the Penman's equation. From the obtained data the following trends are presented: the actual E.T. is very close to the E.T.P. (as total amounts), yet they vary in different age periods of plant growth. The actual E.T. exceeds the E.T.P. in the period when the ears of maize start to appear. The actual E.T. becomes less than the E.T.P. if the wind velocity is decreased and transpiration is not great. The calculated E.T. determined by the use of neutron moisture meter is less than the E.T.P. as the water-table rise increases the amount of water in the soil. Both actual E.T. and calculated E.T. are less than the E.T.P. in the second treatment where the soil was subjected to high water stress. (auth)

10928 SEQUENTIAL USE OF THE ANGER CAMERA IN DOUBLE-TRACER STUDIES. Schenck, P.; Lange, D.; Schnabel, K. (Univ., Heidelberg). Nucl.-Med.; 9: 120-8(30 Jun 1970). (In German).

The simultaneous registration by a modified Anger camera of two simultaneously administered radioisotopes permits diagnostic conclusions with respect to function as well as morphology. This fact is illustrated by the combined injection of ^{99m}Tc-pertechnetate and ^{113m}In for the diagnosis of tumor metastases. Efficiency of the double isotope method also is demonstrated by simultaneous injection of ^{131}I-hippuric acid and ^{68}Ga-EDTA that allows assessment of glomerular damage. (H.B.G.)

10929 QUANTIFICATION OF FUNGUS: SMALL ARTHROPOD FOOD CHAINS IN THE SOIL. Coleman, David C.; McGinnis, John T. (Univ. of Georgia, Athens). Oikos; 21: 134-7(1970).

Fungal mycelium was labeled in a culture medium, and placed in the soil of a broomsedge field. After several time intervals, cores of litter and soil were extracted and microarthropods counted for radioactivity in species groups. Six of 13 species or groups were consistently labeled, taking up, in some cases, as much as 16 to 22% of the initial fungal activity density. Another 12 to 14 species were never labeled in the course of the experiment. The labeled groups included Acaridae, Oribatei, and Mesostigmata. A very low percentage of the total food placed in the soil was consumed by the mites, indicating they probably have a minor direct role in grazing the soil mycoflora. (auth)

Metabolism, Physiology, and Toxicology

Refer also to abstracts 10983, 11037, 11038, 11047–11049, 11169, 11263, 11308, and 11309.

10930 (CEA-CONF-1517) THE FIXATION AND MIGRATION OF ^{42}K APPLIED TO THE LEAVES OF CORN. Chamel, Andre R. (Commissariat a l'Energie Atomique, Saclay (France). Centre d'Etudes Nucleaires). [1970]. 12p. (In French). (CONF-700327-1). Dep. CFSTI (U. S. Sales Only).

From 6th International Colloquium on Plant Analysis and Fertilizer Problems, Tel Aviv, Israel.

The fixation and migration of ^{42}K in the form of KNO_3 solutions applied to the leaves of corn was studied in corn of different ages. The results show that the age of the leaf has no effect on the fixation of ^{42}K, but the migration of ^{42}K from the leaves is differentiated progressively with the development of the plant. The greatest part of the radioactivity is found in the stem of the leaf treated. A potassium deficiency in the nutritive milieu does not affect the fixation, but the migration decreases very sharply when the plants are cultivated in a K-deficient milieu. The temperature of the milieu surrounding the roots affects the fixation but less sharply than it affects the migration; both are less at low temperatures. (J.S.R.)

10931 (CEA-CONF-1557) STUDY OF TWO CASES OF CONTAMINATION BY ^{241}Am. Jeanmaire, L.; Ballada, J. (Commissariat a l'Energie Atomique, Fontenay-aux-Roses (France). Centre d'Etudes Nucleaires). [nd]. 13p. (In French). (CONF-700505-13). Dep. CFSTI (U. S. Sales Only).

From 2nd Congress of the International Radiation Protection Association, Brighton, England.

Two technicians were accidentally exposed to an aerosol of a soluble salt of ^{241}Am. The technicians were hospitalized nine days later for medical surveillance. The radioactivity of the excreta was measured, and whole-body spectrometry was made in a shielded chamber using a sodium iodide crystal detector. The detection device was first calibrated with two phantoms. The whole-body measurement showed that the Am seemed to be localized essentially in the lungs and perhaps at the level of the head. A study of the fecal excretion, the lack of effect by DTPA on the fecal excretion, the lack of evidence of Am in the bony tissue, and the negative results from the hepatic localization tests indicated that the contamination was deposited exclusively in the lungs. The initial quantity inhaled was estimated to be of the order of 180,000 pCi. (J.S.R.)

10932 (CEA-CONF-1558) EVALUATION OF THE IRRADIATION OF BONE MARROW RESULTING FROM MILK CONTAMINATION BY ^{90}Sr AFTER CONTINUOUS OR UNEVEN DEPOSITION ON PASTURES. Odievre, M.; Planet, J.; Uzzan, G. (Commissariat a l'Energie Atomique, Fontenay-aux-Roses (France). Centre d'Etudes Nucleaires). [1970]. 15p. (In French). (CONF-700505-14). Dep. CFSTI (U. S. Sales Only).

From 2nd Congress of the International Radiation Protection Association, Brighton, England.

The permanent contamination of milk in the case of continuous ^{90}Sr deposition and the short-duration contamination in the case of accidental deposition of the isotope were estimated. Dose calculations were made by considering the bone marrow as representative of the risks caused by the contamination of the human organism by ^{90}Sr. The results obtained are shown graphically for the newly born and for a subject 20 years of age at the commencement of contamination. The evolution of the dose to the bone marrow of the newly born increases more rapidly in the newly born than in the adult. The dose received by long-term contamination is about 5 times weaker than short-term contamination in the newly born. In the adult the dose received by long-term contamination is about 1.5 times higher than that received by short-term contamination. (J.S.R.)

10933 (COO-1339-45) INTESTINAL ABSORPTION OF ^{47}Ca AND ^{85}Sr IN ESTRADIOL TREATED RATS. (Illinois Univ., Urbana. Coll. of Veterinary Medicine). 3 Sep 1970. Contract AT(11-1)-1339. 5p. Dep. NTIS.

Pre-treatment of male and female rats with 17B-estradiol for 4 days caused increased intestinal absorption and femur uptake of ^{47}Ca and ^{85}Sr in females only. Low levels of estradiol facilitated absorption in females to levels comparable with those of untreated males, but absorption of either radionuclide was not increased further by higher doses. (auth)

10934 (NP-18380) DIETARY INTAKE OF ^{90}Sr BY THE POPULATION OF THE USSR OVER THE PERIOD 1959–1967 AS A RESULT OF STRATOSPHERIC FALLOUT. Knizhnikov, V. A.; Petukhova, E. V.; Stepanov, Yu. S.; Barkhudarov, R. M. (Gosudarstvennyi Komitet po Ispol'zovaniyu Atomnoi Energii SSSR, Moscow). 1969. 11p. (In Russian). Dep. CFSTI (U. S. Sales Only).

The maximum contamination of food products was observed in 1963 to 1964. The contamination of grain products and milk decreased in 1967, 3 to 4 times and that of potatoes and fish in 1965 to 1967 remained practically without change. The maximum intake of ^{90}Sr with food was in 1964. In 1967 it had decreased 2.5 to 3 times. The ^{90}Sr content of grain, milk, and potatoes from some regions of the country (for example, in the Far East, in mountain regions of northern Asia, and Transcaucasia) was 1.5 to 3 times higher than the average. The contamination of food products, obtained from mountain regions, as a rule, was sometimes higher than the contamination of products from adjacent plains. The rural population of the country received during all periods of observation 10 to 20% more ^{90}Sr than the city population. The same quantity of ^{90}Sr was found in the city populations in different regions of the country. The contamination with ^{90}Sr of rural populations of isolated republics exceeds by 1.5 to 2 times that of the national average of the food. The principal amount of ^{90}Sr in 1963 to 1967 of the population of the Soviet Union was received with grain products and not with milk. In 1966 to 1967, the role of potatoes and fish as source of ^{90}Sr was significantly increased. Together with grain products and milk they constituted the principal source of ^{90}Sr. The characteristics of the contamination of different contingents of the population with ^{90}Sr with expressions in comparative magnitudes (Sr units) and in absolute magnitudes (curies) in a series of cases gives a substantial difference which is connected with the dissimilar content in K allowance, the intake of which was determined in the basic consumption of milk. (tr-auth)

10935 (NP-18388) VALIDATION OF METHODS FOR MASS MEASUREMENT OF ^{90}Sr CONTENT IN THE ORGANISM OF ADULT PERSONS. Marei, A. N.; Borisov, B. K. (Gosudarstvennyi Komitet po Ispol'zovaniyu Atomnoi Energii SSSR, Moscow). 1969. 19p. (In Russian). Dep. CFSTI (U. S. Sales Only).

Under conditions of general protracted contamination of surface media with ^{90}Sr, the use of teeth for the mass control of the level of concentration of this isotope in bony tissue of the population has a number of advantages over the use of bony tissue samples and can be recommended as a basic method. The relation between the concentration of ^{90}Sr in teeth, individual bones, and

skeleton of adults does not depend on the geographic range of their residence. The sizes of the bone/skeleton and teeth/skeleton normalization coefficients with the passage of time changed somewhat and depends on periodic adjustments. The method proposed for the calculation of the normalization coefficients, taking into consideration the weight relation of the bone to the skeleton of adults, combines in itself simplicity of utilization and the necessary reliability of the results. (tr-auth)

10936 (UCB-34-P-23-15) [BEHAVIOR AND EFFECTS OF RADIONUCLIDES IN SOILS AND PLANTS.] Technical Summary, 1969-70. (California Univ., Berkeley). Contract AT(04-3)-34. 45p. Dep. CFSTI.

Seedlings of beans and tomatoes were placed for four days in media containing ^{137}Cs, ^{106}Ru, or ^{85}Sr. The plants were then transferred to normal culture solution and four weeks later the distribution of the isotopes was determined. Results were compared with those of earlier experiments on the forage plants, Adenostoma and Ceanothus. Retention of ^{85}Sr and ^{137}Cs by the root was much less pronounced in beans and tomatoes than in forage plants; however, retention of ^{106}Ru by the root was very pronounced in all plants. Within the shoot both ^{85}Sr and ^{137}Cs were more mobile in the forage plants than in beans or tomatoes. Experiments on the distribution and effects of ^{89}Sr on growth of dwarf peas showed that there were no effects on yield even at the highest concentrations. Both the root and shoot meristems remained uncontaminated and no deleterious effects on growth were observed. Roots of dwarf pea seedlings exposed to solutions of ^{32}P were observed, one week after treatment, to be thicker and shorter than normal and to have produced very few laterals. Standardization and readout procedures were developed for β radiation dosimeters; this involved the construction of a 4-π exposure chamber to provide known doses of radiation from ^{90}Y in solution. A preliminary dose-depth curve was obtained using polyethylene absorbers. Field experiments on ^{90}Y β damage to corn, wheat, and lettuce crops showed that there was a severe reduction in the yield of lettuce and wheat, but no reduction in yield of corn was observed. (H.L.W.)

10937 (UCRL-50957) FORTRAN CODE FOR THE ANALYSIS OF COUNTING DATA FROM ANIMAL TISSUES. Martin, W. H.; Fleshman, D. G.; Silva, A. J. (California Univ., Livermore. Lawrence Radiation Lab.). 16 Oct 1970. 28p. Dep. NTIS.

A Fortran code designed to run under the monitor system of the CDC 6600 computer was developed for processing counting data from studies involving the metabolism of radionuclides in animals. This report includes the mathematics and input parameters necessary to reduce these data. The program applies calculations required to derive uptake, retention, distribution, and excretion data from animals which were administered radionuclides. (auth)

10938 A CONTRIBUTION TO THE MECHANISM OF RADIOSTRONTIUM RESORPTION IN RATS. Popelka, M. (Military Medical Research and Postgraduate Inst., Hradec Kralove, Czech). Sb. Ved. Pr. VLVDU Hradci Kralove; 41: 23-42(1969). (In Czech).

The mechanism of ^{85}Sr transport through the rat intestinal epithelial membrane was studied. Experiments were carried out in vitro on 6 cm segments of duodenum. The accumulation process reached its equilibrium after an incubation in medium for 40 to 60 min. Sr was mostly bound by weak physical sorption forces to the surface. Sr linkage to the low-molecular fraction represented by amino acids and phosphates was proved. The excretion of amino acids was found to be a biochemically controlled process. The hypothesis of an active role of amino acids was supported by experiments involving inhibitions of their chelating groups, however, a lesser importance of phosphates was observed. Thus, ^{85}Sr is bound with amino acids into complexes which are subsequently transported. No evidence was found about a direct role of the lipoid barrier in the membrane. When damaging the surface structure either by a prolonged incubation period of 130 min or by adding CH_3Cl, the adsorption increased. A role of the controlled permeability of cell membranes was obvious from an inhibition of ^{85}Sr accumulation with uranyl acetate. An inhibition of ^{85}Sr accumulation occurs when that stage of metabolic pathway is inhibited that directly results in amino acid formation. The energetic system of cells did not take part in the accumulation. One can conclude that there exists an active ^{85}Sr transport through the membrane studied. (NSA of Czech.)

10939 STUDIES ON INHIBITION OF INTESTINAL ABSORPTION OF RADIOACTIVE STRONTIUM. IX. RELATIONSHIP BETWEEN BIOLOGICAL ACTIVITY AND ELECTRON MICROSCOPIC APPEARANCE OF ALGINIC ACID COMPONENTS. Tanaka, Y.; Inoue, S.; Skoryna, S. C. (McGill Univ., Montreal. Univ., Montreal). Can. Med. Ass. J.; 103: 484-6(12 Sep 1970).

The inhibitory action of alginate on intestinal absorption of radioactive strontium was investigated in order to correlate the biological activity with the chemical composition. Alginate from Laminaria hyperborea was partially hydrolyzed with oxalic acid and the degradation products were fractionated into polymannuronic and polyguluronic acid. The activity of these products was assessed biologically in rats and morphologically by electron microscopy. Sodium polymannuronate was found to be less effective than sodium polyguluronate in preventing absorption of radiostrontium. The inhibition of absorption of radiocalcium was low and not affected by hydrolysis or fractionation. When dried from dilute aqueous solutions, the polymannuronate retained the original helical structure of alginate, while the polyguluronate showed a strong tendency to coagulate, forming granules. The variation in the biological activity was attributed to the morphological differences between these alginic acid components and it is suggested that the degree of uncoiling of the polyguluronate chain in water is greater than that of the polymannuronate chain, thus making the carboxylate ions more accessible to strontium. (auth) (Canada)

10940 DECREASE IN RADIOSTRONTIUM ACCUMULATION DUE TO ACTIVATED BARIUM SULPHATE DURING REPEATED AND CONTINUOUS PERORAL CONTAMINATION OF RATS. Knajfl, J.; Smid, A. (Military Medical Research and Postgraduate Inst., Hradec Kralove, Czech.). Sb. Ved. Pr. VLVDU Hradci Kralove; 41: 67-82(1969). (In Czech).

Experiments on rats dealt with the influence of repeated applications of activated $BaSO_4$ on the accumulation of ^{85}Sr applied either repeatedly into the stomach or continuously with the diet. In a group where rats received ^{85}Sr for 28 days and were killed one week after the last application, the retention was decreased by 65 to 70% by the action of activated $BaSO_4$. Portions of 1.5 and 0.45% of ^{85}Sr were found in the femur of controls and of $BaSO_4$-treated animals, respectively. In the second experiment the animals received ^{85}Sr and ^{45}Ca with drinking water; the experimental animals were fed with a diet containing either 2 or 12% of activated barium sulphate. Experimental animals exhibited a significant decrease of the ^{85}Sr level in bones as compared with controls. No differences were found in the case of ^{45}Ca. (NSA of Czech)

10941 MECHANISMS OF THE ACCUMULATION OF ^{239}Pu AND ^{210}Po BY THE BROWN ALGA ASCOPHYLLUM NODOSUM AND MARINE PHYTOPLANKTON. Zlobin, V. S.; Mokanu, O. V. (Polar Scientific Research Inst. of Marine Fish Farming and Oceanography, Murmansk, USSR). Radiobiologiya; 10: 584-9 (Jul-Aug 1970). (In Russian).

The accumulation of plutonium-239 by Ascophyllum nodosum and marine phytoplankton and of polonium-210 by macrophytes under the influence of inhibitors of cellular respiration was investigated. It was established that plutonium and polonium exist in sea water in the form of colloidal particles. Sodium cyanide induced uniform suppression of the accumulation of ^{239}Pu and ^{210}Po in plant cells, while ammonium chloride briefly stimulated accumulation. It was demonstrated that the accumulation of plutonium-239 by marine algae is an active process, and it involves an energy expenditure by the cell. (tr-auth)

10942 MICRODISTRIBUTION AND MORPHOLOGICAL CHANGES IN RATS IN THE CASE OF INTRAVENOUS INJECTION OF ^{241}Am. Rudnitskaya, E. I.; Moskalev, Yu. I. (Inst. of Biophysics, Moscow). Radiobiologiya; 10: 570-4(Jul-Aug 1970). (In Russian).

Americium chloride ($^{241}AmCl_3$) existed primarily in the finely divided state and was diffusely distributed in the organs and tissues of animals after intravenous injection. Over long-term periods, a tendency for aggregation of particles of the substance in the medullar layer of the kidneys and liver as well as in the basic substance of the cartilage was detected. (tr-auth)

10943 FUNCTIONAL STUDIES WITH SHORT-LIVED REACTOR ISOTOPES. Krauss, O.; Maier-Borst, W.; Lorenz, W. J.; Prpic, B.; Harbst, H. (Deutsche Krebsforschungszentrums, Heidelberg). Nucl.-Med.; 32: Suppl. 7, 449-53(1968). (In German).

From 5th Conference of the Society of Nuclear Medicine, Vienna, Austria. See CONF-670996.

By (n,γ) reaction in the reactor, short-lived radioisotopes for diagnostic use were produced. Especially studied and discussed were biological behavior of ^{18}F. Its accumulation in bone tissue was demonstrated by several clinical examples. These studies were performed by scanning and Anger camera display within 0.5 to 2 hours following injection of 1 to 2 μCi of ^{18}F. (H.B.G.)

XUM

10944 STUDIES ON l-TRIIODO-THYRONINE SUPPRESSION IN ITS DEPENDENCY ON THYROIDAL FUNCTION, IODINE STORAGE, THYROID SIZE, AND AGE OF PATIENTS. Heinze, H. G.; Pabst, H. W.; Klemm, J. (Univ., Munich). Nucl.-Med.; 32: Suppl. 7, 491-8(1968). (In German).

From 5th Conference of the Society of Nuclear Medicine, Vienna, Austria. See CONF-670996.

In 395 patients, ^{131}I thyroid uptake was measured at 6, 24, and 48 hours following isotope administration. Four weeks later, thyroid function was suppressed by daily doses of 60 μg l-triiodothyronine throughout a period of ten days. On the 8th day of suppression, ^{131}I uptake was again measured. Euthyroid patients without increased ^{131}I metabolism showed no effect of suppression; euthyroid patients with increased ^{131}I metabolism showed a suppression of more than 20%. Degree of suppression was independent of thyroidal shape and size as well as age of the patient. (H.B.G.)

10945 METHOD FOR MEASUREMENT OF IODINE, IODOTYROSINE, AND IODOTHYRONINS IN HUMAN SERUM. Gloebel, B. (Univ. des Saarlandes, Homburg, Ger.). Nucl.-Med.; 32: Suppl. 7, 499-502(1968). (In German).

From 5th Conference of the Society of Nuclear Medicine, Vienna, Austria. See CONF-670996.

Following oral administration of 25 μCi of ^{131}I, the time course of various ^{131}I components was measured in the serum by using ion exchange columns and thin layer chromotography. Distribution of ^{131}I was determined by β radiation measurements. In addition, distribution of compounds containing ^{127}I was assessed semiquantitatively by measuring the area of color spots. A discrepancy existed between the distribution of ^{131}I and ^{127}I that remained unexplained. (tr-auth).

10946 MECHANISM OF CONJUGATION AND RECOMBINATION IN BACTERIA. IX. THE ROLE OF DNA SYNTHESIS IN POST-CONJUGAL GENETIC RECOMBINATION. Wlodarczyk, Miroslawa; Kunicki-Goldfinger, Wladyslaw (Univ., Warsaw). Mol. Gen. Genet.; 106: 263-73(1970).

Development of resistance to ^{32}P-decay of donor genetic determinants after their transfer into the female cell is dependent on unabated DNA synthesis. A similar dependence upon DNA synthesis was found in recombinational events. Both processes show a similar time-course. The DNA synthesis, involved, seems distinct from physiological replication of the chromosome. The formation of the structure resistant to ^{32}P-decay is going on concomitantly with recombinational process and is completed within 45 to 55 minutes after transfer, before beginning of the replication of recombinant structure. The bearing of these facts on the molecular mechanism of genetic recombination is discussed. (auth)

10947 CONTRIBUTION TO THE ABSORPTION OF RADIOSTRONTIUM IN IRRADIATED ORGANISM. Vondracek, V.; Neruda, O. (Military-Medical Research Inst., Hradec Kralove, Czech.). Sb. Ved. Pr. VLVDU Hradci Kralove; 47: 65-78(1970). (In Czech).

The absorption of radiostrontium from the gastrointestinal tract of dogs was investigated. A double isotope method for the measurement of intestinal absorption was used. Dogs, who had been situated in large metabolic cages, received intravenously $^{85}SrCl_2$ and simultaneously $^{89}SrCl_2$ orally, both radioisotopes in tracer amounts. The animals were starved for 24 hr before the beginning of the experiment and the first food came 4 hr after radiostrontium administration. Determinations of ^{85}Sr and ^{89}Sr were made on samples of plasma; ^{85}Sr in urine and stool. Plasma samples were drawn at 10, 30 min, 1, 2, 3, 4, 5, 12, 24, 48, and 72 hr, and urine and stool samples were obtained for 24-hr periods during the 6 day period after administration of radiostrontium. Each dog was the subject of two investigations of absorption. The first examination was done before irradiation and the second one after 350 R whole-body irradiation. For dogs H 4 to H 9 renal and gastrointestinal clearance of ^{85}Sr were calculated. After irradiation the absorption of radiostrontium is time dependent. In the first hours after irradiation with 350 R the amount of absorbed radiostrontium did not change in comparison with values before irradiation. Three days after irradiation the values of radiostrontium absorption increased in five of six cases. The decreased values of gastrointestinal clearances of ^{85}Sr correspond to changes of radiostrontium absorption in the irradiated dogs. (tr-auth)

10948 CONTRIBUTION TO THE ASSESSMENT OF RADIOTELLURIUM AS A FISSION PRODUCT. Slouka, V.; Knajfl, J. (Military-Medical Research Inst., Hradec Kralove, Czech.). Sb. Ved. Pr. VLVDU Hradci Kralove; 47: 45-64(1970). (In Czech).

The four fission products critical for internal contamination are ^{131}I, ^{89}Sr, ^{90}Sr, and ^{137}Cs. Mixed fission products contain also a considerable amount of tellurium radioisotopes, which in the time interval from 24 hr to 7 days, represent 10 to 20% of the total activity. Out of 11 tellurium radioisotopes, 9 are precursors of radioiodine. The condensation of tellurium in the radioactive cloud occurs in relatively late intervals and it appears therefore on the surface of primary particles. The main chemical form of tellurium in fission products is tellurium oxide (TeO_2), which is soluble water and readily enters into food chains. Tellurium compounds contained in radioactive fallout are well absorbed from the respiratory route and from the gastrointestinal tract as well. The organ distribution of tellurium is nearly uniform with a somewhat higher concentration in the kidney, liver, spleen, and in the blood. The retention in the skeleton has a low-rate component and lasts for a long time. Tellurium is excreted at a relatively fast rate and biological half-lives do not exceed 15 to 30 days, except in the skeleton. According to the metabolic and radiation characteristics, tellurium radioisotopes can be rated among less toxic radionuclides. Their importance consists mainly in generating iodine radioisotopes in food chains. Iodine-129 has a long half-life 1.7×10^7 yr; its fission yield is low and, from the standpoint of the thyroid dose, is insignificant. The half-lives of ^{134}Te and ^{134}I are less than 1 hr and they can be significant only immediately after a fission. The pair $^{132}Te-^{132}I$ can be assessed similarly. ^{131}I, ^{132}I, ^{133}I, and their tellurium precursors are more important. The doses to the thyroid gland from radionuclides of iodine contained in unfractionated mixed fission products as fractions of the total dose from all radionuclides of iodine after an inhalation are given. The radiobiological affect of ^{132}I is limited by its short half-life 2.4 hr. If, however, its precursor (^{132}Te) enters the body (T = 78 hr), the new ^{132}I is generated for several days and the risk of damaging the thyroid is much greater. Radioiodine can enter the body directly from the atmosphere, as radioiodine generated in the food chain (e.g., in cow's milk), and can be formed also in the human body after an internal contamination by its precursors. The importance of radiotellurium for man lies above all in the fact that it generates radioiodine in food chains. From the point of view of the comparative radiotoxicology, radiotellurium can be rated just behind radioisotopes of Sr, I, and Cs. (tr-auth)

10949 KINETICS OF ORALLY ADMINISTERED RADIOTELLURIUM IN THE RAT. Slouka, V.; Hradil, J. (Military-Medical Research Inst., Hradec Kralove, Czech.). (In Czech). Pr. VLVDU Hradci Kralove; 47: 21-43(1970). (In Czech).

The kinetics of orally administered $Na_2{}^{132m}TeO_3$ was studied in the rat and it was compared with the kinetics of radiotellurium after intravenous injection. The models of organ distribution after oral and intravenous administration are similar. The uptake from the gastrointestinal tract is relatively rapid and takes place mainly in the duodenum and jejunum. The fraction absorbed from the gastrointestinal tract was determined by comparing the whole-body retention, the amount retained in main organs of retention, and excretion after intravenous and oral administration. The results are in a good agreement, about 25% of orally administered Te is absorbed from the gastrointestinal tract. The retention can be described by a three-term exponential with half-lives $T_1 = 0.28$ day (68%), $T_2 = 0.9$ day (19%) and $T_3 = 14.7$ days (13%). Orally administered radiotellurium is excreted mainly via the feces, about 65% during the first week, via the urine about 9% of the dose. The unabsorbed fraction is excreted in the first 2 days and largely in the first 24 hr, where the fecal excretion amounts to 58% of the dose. Finally, a simple compartmental model for the kinetics of orally administered pair radiotellurium–radioiodine and the possibilities of its solution are discussed. (tr-auth)

10950 DISTRIBUTION AND EXCRETION OF INTRAVENOUS RADIOTELLURIUM IN THE RAT. Slouka, V. (Military-Medical Research Inst., Hradec Kralove, Czech.). Sb. Ved. Pr. VLVDU Hradci Kralove; 47: 3-19(1970). (In Czech).

The organ distribution of intravenously injected radiotellurium in the rat was studied in 11 intervals from 5 min to 7 days. The retention was studied by whole-body counting and excreta were assayed daily for a period of 7 days. The main results may be briefly summarized as follows: The whole body retention can be expressed as the sum of two exponentials with half-lives 0.75 day (45%) and 15.4 days (58% of the administered amount), respectively. Intravenously administered radiotellurium is excreted during the first week largely via the urine (about 33%), but also via the feces (about 14%). The greatest activity is excreted in the first 24 hr (more than 14%), in subsequent days always 2 to 3% of the administered amount. The organ distribution of intravenously administered radiotellurium is nearly uniform, the greatest concentration is in the kidney, liver, bone, and thyroid gland. The study of biliary excretion showed that biliary excretion is the main mechanism by which Te enters the intestine. The binding to eryth-

rocytes in vivo is rapid; in the second hour it reaches 90%. The binding with hemoglobin was proved using biochemical methods. Experiments in vitro demonstrated that the binding is conditioned by an active metabolic process. The radiotoxicological significance of radiotellurium lies in the fact that nine of its radionuclides formed in nuclear fission generate radioiodine and the daughter radionuclide can be formed in food chains. (tr-auth)

10951 CALCULATION OF ABSORPTION RATE OF STRONTIUM FROM GASTROINTESTINAL TRACT. Neruda, O.; Hradil, J. (Military-Medical Research Inst., Hradec Kralove, Czech.). Sb. Ved. Pr. VLVDU Hradci Kralove; 47: 219-41(1970). (In Czech).

The fractional absorption of radiostrontium was examined from various points of view in numerous studies. Solving some problems, the determination of the kinetics of passage from gastrointestinal lumen into the circulating blood, revealing the absorption rate has proved to be very useful and valuable information. For example, some pathological states of calcium absorption have not only different fractional absorptions of calcium with respect to strontium, but they are characterized by an earlier or later absorption as well. These conclusions were based on a simple scope of the curve of plasma specific activity after oral administration. The time, when these curves had reached a maximum, was the most employed semiquantitative criterion of an earlier or later absorption. The determination of the absorption course is very important for the assessment of the inhibitory effect of various substances on the absorption, when the substances are given orally after the ingestion of radiostrontium. The method which enables the determination of the time course v(t) of the passage through the intestinal wall was used. The curves of plasma specific activity I(t) and P(t) were determined after intravenous and oral administration of ^{87m}Sr and v(t) were calculated using the deconvolution method. (tr-auth)

10952 EARLY DETECTION OF INJURY AFTER NITROGEN MUSTARD (HN2) THERAPY: THE RADIOIRON DISAPPEARANCE RATE AS A DOSIMETER. Woods, A. H.; O'Bar, P. R. (Veterans Administration Hospital, Tucson, Ariz. Univ. of Arizona, Tucson). Int. J. Appl. Radiat. Isotop.; 21: 213-17(Apr 1970).

The radioiron plasma disappearance rate was studied as a potential dosimetry system in 14 patients with terminal cancer given doses of HN2 up to 1.5 mg/kg. Results indicate this rate rises to a sharp maximum 72 hr after therapy, that it provides a linear dose-response relationship at high dose and reflects changes in individual sensitivity at low doses. (auth) (UK)

10953 AUTORADIOGRAPHY AS A HELP FOR ANALYSING THE DISTRIBUTION OF α-ACTIVE MATERIAL IN THE HUMAN BODY AFTER AN AIR CONTAMINATION. Vaane, J. P.; De Ras, E. M. M.; Von Brandenstein, Chr. (Europaeische Institut fuer Transurane, Karlsruhe, Ger.). Atompraxis; 16: 249-57(Jul-Aug 1970). (In German).

According to the lungmodel of the ICRP the size distribution of the particles of an aerosol is an important parameter for calculating the distribution of radioactive dust in the respiratory tract. A review and a short description of autoradiographic methods used to determine the distribution of α particles collected by dust filters, and an example of such a calculation after the release of α activity into the respiratory air are given. (auth)

10954 INCORPORATION OF TRITIUM IN HAIR. Jaworowski, Z.; Bilkiewicz, J.; Zylicz, E. (Inst. of Nuclear Research, Warsaw). Int. J. Radiat. Biol.; 18: 487-90(1970).

The anagen hair from each of 11 rabbits was collected twice from a previously plucked area: the first fleece on the 28th day and the second fleece from the same area on the 68th day after administration of tritium. A sample of resting (telogen) hair was also plucked from each animal on the 28th day. The influence of washing procedures on the elution of tritium from internally and externally contaminated hair was investigated and a table is given. In internally contaminated anagen hair, tritium was not strongly bound to the hair structure as 13 to 69% of the activity was eluted by one of the methods tested. The elution of externally contaminated hair ranged from 80.2 to 86.6%. A table showing the uptake of tritiated water by growing and resting hair is given. In the first anagen fleece the increase of tritium varied from 0.0017 to 0.0058% of the injected dose per gramme of hair, increasing with increasing dose. However, in the anagen fleece the incorporation of tritium was highest in animals injected with the lowest dose. In metabolically inactive telogen hair the incorporation of tritium, between the 1st and 28th day after administration was found to be 3.5 to 39 times lower than the hair of the first anagen fleece. It was deduced that the lowest detectable amount of tritium entering a human body 1 month before collecting a 1 g hair sample is 5μ Ci which is 400 times lower than the maximum permissible body burden, and that hair may be used for the detection and evaluation of the internal contamination of the body with tritium. (auth) (UK)

10955 TRANSLOCATION OF CARRIER-FREE ^{85}Sr, ^{137}Cs, AND ^{106}Ru IN WOODY PLANTS. Handley, R.; Babcock, K. L. (Univ. of California, Berkeley). Radiat. Bot.; 10: 577-83(Nov 1970).

Carrier-free solutions of ^{137}Cs and ^{106}Ru were applied to the foliage of three genera of woody shrubs (Ceanothus, Adenostoma, and Quercus) and subsequent translocation into untreated portions of the plants was measured. In all cases the bulk of the retained dose remained with the directly treated material. The results indicate that in these genera foliarly applied ^{137}Cs is no more mobile than Sr while ^{106}Ru is considerably less mobile than either. In another series of experiments the distribution of ^{85}Sr, ^{137}Cs, and ^{106}Ru between the root, the old growth and the new growth was determined after incorporation of the isotopes into Ceanothus and Adenostoma via their root systems. ^{137}Cs and especially ^{106}Ru were largely retained in the root. A relatively large fraction of the retained dose of ^{85}Sr was found in the shoot. In both series of experiments a preferential movement of ^{137}Cs into new growth was observed. (auth) (UK)

10956 EXPERIMENTAL SUBSTANTIATION OF PREVENTIVE DIET IN CASE OF INTERNAL IRRADIATION WITH ^{137}Cs AND ^{90}Sr. Danetskaya, E. V.; Kolesnikov, V. V.; Shakalova, V. V.; Kupriyanov, I. N. (Leningrad Research Inst. of Radiation Protection). Gig. Sanit.; No. 7, 42-6(Jul 1970). (In Russian).

It was found that the accumulation of ^{137}Cs and ^{90}Sr in the body of an animal is indirectly proportional to the quantity of protein contained in the diet. The addition of a vegetable protein, as soya bean, to the diet of experimental animals brought about a considerable fall in the accumulation of these radionuclides in their body. A daily introduction into the diet of experimental animals of methionine in a dose of 0.224 gm per rat decreased the accumulation of ^{90}Sr by 50 per cent and that of ^{137}Cs by 28 per cent. When calcium triphosphate in a dose of 0.240 gm per rat per day was added to the food ration the accumulation of ^{90}Sr was decreased by 70 per cent and that of ^{137}Cs by 15 per cent. (auth)

10957 BIOLOGICAL TESTS OF PHARMACEUTICAL RADIO COLLOIDS. Chivot, J. J.; Cohen, Y. (Commissariat a l'Energie Atomique, Paris). Int. J. Appl. Radiat. Isotop.; 21: 459-69(Aug 1970). (In French).

A kinetic method employing unilateral carotid–carotid circulation outside the body is described. This method estimates the elimination of colloid from the blood after intravenous injection. A phagocytosis coefficient K_S is defined by calculation and is used, under specified experimental conditions, as a constant of the preparations tested. A second determination K_H is made simultaneously by external hepatic counting. On injecting 20 μg of colloid per 100 g body weight in rats, the following results were obtained: for preparations of gold with particle diameters 20–40 nm, $K_S = 0.254$; for particle diameters 3–5 nm, $K_S = 0.112$; for the polydispersed gold preparation of particle diameters 5–50 nm, $K_S = 0.107$. By hepatic counting K_H values of 0.268, 0.119 and 0.102 were respectively obtained. With a 2 mg/100 g dose of albumin degraded by heat and labelled with iodine 131 (C.A. ^{131}I) the values $K_S = 0.132$ and $K_H = 0.137$ were found in rats and $K_S = 0.200$ in guinea pigs. A significant variation in the K_S values according to the heating methods used during preparation of the C.A. ^{131}I was observed. Cumulative injections made in the same animal showed build-up of the colloid in the ion of the C.A. ^{131}I. Cumulative injections made in the same animal also showed build-up of the colloid in the organism as a function of its nature. The biological tests proposed give a precise idea of the properties of the preparation in vivo and can serve either to define the possible applications of a new colloid or to check the manufacture of a known colloidal radiopharmaceutical product when the physiochemical criteria are difficult to determine. (auth) (UK)

10958 FATE OF ^{60}Co 1-NITROSO 2-NAPHTHOL CHELATE IN ALBINO RATS AFTER INTRAVENOUS ADMINISTRATION. Jagadeesan, V.; Sivaramakrishnan, V. M. (Cancer Inst., Madras). Indian J. Exp. Biol.; 7: 217-20(Oct 1969).

The metabolism ^{60}Co 1-nitroso 2-naphthol chelate in albino rats after intravenous administration was studied. The radioactivity accumulates initially in liver, then moves over to bones, muscles and skin and is subsequently excreted slowly through urine and feces. Employing dialysis, chloroform extraction and other methods to distinguish between the ionic cobalt and the chelate, the exact state in which the radioisotope occurs in the various tissues was studied. Cobalt-60 administered in the ionic form has a generalized distribution and occurs in the various tissues mostly in

XUM

the bound state. The chelate, on administration, is instantaneously bound as a whole to the blood proteins almost completely. It is released in liver where it occurs predominantly in the free state initially, but with progress of time, most of the radioactivity is present in the bound state. In other tissues like skin, bone and muscle, the isotope occurs partly as the free chelate, but mostly as the bound form. In kidneys, the free chelate predominates initially, but the bound and the free ionic forms are more significant later. The chelate is completely split up in the body before excretion. The cobalt ions arising from the splitting occur in various tissues only to a very limited extent in the free form, but are mostly protein-bound. There is complete absence of the free chelate in both urine and feces. (auth)

Radiation Effects

Refer also to abstracts 10560, 10587, 10625, 10647, 11096, 11285, 11307, 11324, and 11341.

10959 (BNL-50203, pp 27-40) ENZYMATIC MECHANISMS FOR THE REPAIR OF UV-IRRADIATED DNA. Grossman, Lawrence; Kaplan, Joan; Kushner, Sidney; Mahler, Inga (Brandeis Univ., Waltham, Mass. Graduate Dept. of Biochemistry).

From Conference on time and dose relationships in radiation biology as applied to radiotherapy held at Carmel, California, September 15-18, 1969.

Studies were conducted on the isolation of enzymes that can recognize localized regions of distortion in damaged DNA. Micrococcus luteus was chosen as the bacterial source because of its low endogenous nuclease levels, that permit the detection of small amounts of distortion-specific endo- and exonucleases. The properties of two enzymes that together excise photoproducts from uv-irradiated double-stranded DNA are described. Methods for purification of the endonuclease and exonuclease are discussed. These enzymes were studied with regard to the combined action of the two enzymes, site of uv endonuclease action, mechanism of exonuclease action, and involvement of nucleases in repair in vivo. (H.L.W.)

10960 (BNL-50203, pp 82-90) ON THE ROLE OF DNA IN CELL KILLING BY RADIATION. Terasima, Toyozo (National Inst. of Radiological Sciences, Chiba (Japan)).

From Conference on time and dose relationships in radiation biology as applied to radiotherapy held at Carmel, California, September 15-18, 1969.

A review is presented on the role of DNA in radioinduced lethality. Studies on Salmonella and L cells showed that the administration of highly polymerized DNA significantly increased the survival of cells irradiated with x rays. Experiments on mammalian and yeast cells showed that the RBE-LET relationship for killing of these cells was very similar to that for transforming DNA. Other studies reviewed include the following: radiosensitizing effects of halogenated pyrimidines; x ray survival responses of Bacillus subtilis cells and of their transforming DNA grown in the presence or absence of BUdR; ultraviolet-induced damage in DNA and repair by photoreactivation and dark reactivation; and effects of x-ray dose on sedimentation rate of DNA. (H.L.W.)

10961 (ORO-3329-6) EFFECT OF RADIATION ON MUCOSAL PHOSPHOLIPASE ACTIVITY. Progress Report. (Duke Univ., Durham, N. C. Dept. of Physiology and Pharmacology). Oct 1970. Contract AT(40-1)-3329. 17p. Dep. NTIS.

In order to obtain evidence of the relation between hematopoietic tissue and intestinal levels of phospholipase, that were indicated by previous studies on x-irradiated animals, experiments were begun employing bone marrow depressant drugs and agents capable of affecting peripheral levels of eosinophils. Following administration of single and fractionated doses of cyclophosphamide to rats, the phospholipase B content of the bone marrow, spleen, and intestine was determined. A single dose of 150 mg/kg body weight induced a reduction in spleen and marrow cellularity accompanied by a fall in phospholipase B content. Effects on the intestine were relatively minor. Fractionation of the same dose in two or three successive administrations at 3-day intervals brought about a pronounced loss of body weight, hematuria, anorexia, and decrease in eosinophils and phospholipase B. Effects of dexamethazone and a combination of the two drugs were also studied. Studies on correlations between phospholipase B content and eosinophilic cell population in the rat intestine are also being conducted. (H.L.W.)

10962 EFFECT OF CHLORIDE IONS ON THE γ RADIATION-INDUCED DESTRUCTION OF DNA, NUCLEOSIDES, AND NUCLEOTIDES IN AQUEOUS SOLUTION. Ward, J. F.; Kuo, I. (Univ. of California, Los Angeles). Contract AT(04-1)-GEN-12. Int. J. Radiat. Biol.; 18: 381-90(1970).

Deoxyribonucleic acid in oxygenated aqueous solution is protected from the effects of ionizing radiation by chloride ions, as measured by chromophore destruction. The mechanism of this protection is probably a change in the mode of decay of the DNA-OH radicals and not a change in the primary attacking species. Chloride ions have no effect on the radioinduced destruction of nucleosides and nucleotides in neutral solution. The chloride effects observed for these compounds in acid solution can be attributed to conversion of OH radicals to Cl_2^- ion radicals, and differences in the reaction of the latter species with solutes. There is no observable chloride effect on thymine or adenine compounds. The reaction of Cl_2^- with pyrimidine nucleosides and nucleotides results in destruction of the glycosidic bond and the release of undamaged base. This effect is not observed with the purine compounds or with the deoxyribose compounds. The radical which results from the reaction of Cl_2^- with guanine compounds reacts efficiently to reform the parent compound. (auth) (UK)

10963 EFFECT OF A UREMIC ENVIRONMENT ON PHOSPHATE EXCRETION BY A SMALL POPULATION OF INTACT AND SEVERELY DISEASED NEPHRONS. Morrin, P. A. F.; Joynt, Margaret S. K.; Frame, J. (Queen's Univ., Kingston, Ont.). Nephron; 7: 248-57(1970).

The effect of a uremic environment on phosphate excretion by a decreased nephron population was studied in dogs with either subtotal renal infarction or extensive radiation nephritis. No significant difference was observed between the two groups. In the uremic environment, phosphate reabsorption decreased despite an increase in the filtered load of phosphate. It was concluded that both damaged and intact nephrons respond comparably to changes in phosphate load and that parathyroid activity plays an important regulatory role in decreasing phosphate reabsorption in the uremic state. (auth)

10964 INACTIVATION OF β-FRUCTOFURANOSIDASE AND GLUCOSIDASE BY MEANS OF γ RADIATION IN THE TISSUES OF BETA VULGARIS. Giovanozzi-Sermanni, G.; Tomati, U.; Catoni, M. (Univ., Rome). Agrochimica; 13: 485-90(Oct 1969). (In Italian).

The possibilities of radiation processing of sugar beets to avoid loss of sucrose during storage were investigated. Results of radioinduced inactivation, in vitro and in vivo, showed an inactivation of 80% in β-fructofuranosidase and a 60% inactivation of glucosidase following 300 kR of ^{60}Co γ radiation. This method would be economically feasible for sugar refineries. (E.E.H.)

10965 GROWTH, SURVIVAL, AND CONTENT OF ASCORBIC ACID IN NORMAL AND TUMOR TISSUE CULTURES OF TOBACCO AFTER GAMMA IRRADIATION. Rennert, A.; Antoshevskaya, L. (Univ. of Lodz, Poland). Radiobiologiya; 10: 580-3(Jul-Aug 1970). (In Russian).

The effects of γ irradiation with ^{60}Co on callus and tumor (bacterial) tissues of Nicotiana tabacum var White Burley cultured in vitro on standard medium and enriched with an extract from bee pollen (EBP) were compared. After influences at doses of 500, 1000, and 2000 rad, all the tissues resumed their normal growth after several passages, while after a dose of 5000 rad, only the tumor cells cultured on enriched medium survived. The callus tissue was more sensitive than the tumor tissue, this was evident from its lower ability for survival and the small stimulation of growth at doses of 1000 and 2000 rad. In bacterial tumor tissues, the ascorbic acid (AA) content increased depending on the dose of irradiation. In tissues of the normal type, the amount of AA decreased. It was assumed that there was a direct relationship between the concentration of AA and the postradiation resistance of the investigated plant material. (tr-auth)

10966 ANALYSIS OF THE RADIOSENSITIVITY OF DNA IN THE CASE OF ITS IRRADIATION IN VIVO AND IN VITRO. Ryabchenko, N. I.; Ivannik, B. P. (Inst. of Medical Radiology, Obninsk, USSR). Radiobiologiya; 10: 483-9(Jul-Aug 1970). (In Russian).

A comparative analysis was made of the radiosensitivity of DNA during irradiation in vivo and in vitro. The contribution of the direct action to the degradation of DNA in vivo was calculated on the basis of the data obtained. It was shown that 43 ± 6% residual breaks in DNA in the case of its irradiation in vivo arise on account of the direct interaction of radiation with the DNA. (tr-auth)

10967 MECHANISM OF THE CHANGE IN THE HISTAMINE LEVEL IN THE BLOOD AND TISSUES OF ANIMALS UNDER THE ACTION OF RADIOACTIVE ISOTOPES. Fedorova, A. V.; Zapol'skaya, N. A. (Scientific Research Inst. of Radiation Hygiene, Leningrad). Radiobiologiya; 10: 600-2(Jul-Aug 1970). (In Russian).

XUM

The mechanism of the increase in the free histamine level in the blood and tissues of the liver, kidneys, and intestines of rats after the introduction of a mixture of radionuclides in an amount of 5 μCi was studied. The mechanism of the increase in the free histamine content differed for different tissues. In some organs it was due primarily to the liberation of histamine, in others to the activation of its formation. (tr-auth)

10968 INFLUENCE OF A MIXTURE OF RADIONUCLIDES ON CERTAIN ENZYMES OF RAT BLOOD AND TISSUES. Fedorova, A. V.; Mikhailov, V. G. (Scientific Research Inst. of Radiation Hygiene, Leningrad). Radiobiologiya; 10: 592-5(Jul-Aug 1970). (In Russian).

Experimental data were presented on the study of the influence of a mixture of radionuclides on the cholinesterase and alkaline phosphatase activity in the blood and tissues. It was shown that more pronounced changes in the activity of the enzymes were noted in animals that received 1.5 μCi of the mixture of radionuclides. Significant decreases in the cholinesterase activity occurred earlier than those in the alkaline phosphatase activity. (tr-auth)

10969 NATURE OF POSTRADIATION HYPERGLYCEMIA. Kendysh, I. N. (Inst. of Biophysics, Moscow). Radiobiologiya; 10: 552-5(Jul-Aug 1970). (In Russian).

Postradiation hyperglycemia in rabbits is due to an intensification of gluconeogenesis resulting from the reutilization of metabolites. These metabolites are liberated as a result of the destruction of radiosensitive tissues. (tr-auth)

10970 EFFECTS OF AN IRRADIATED NUTRIENT MEDIUM ON THE FREQUENCY OF CHROMOSOME ABERRATIONS IN MAMMALIAN CELLS IN VITRO. Yasnova, L. N.; Kozlova, A. A.; Trofimova, O. S. (Inst. of Cytology and Genetics, Novosibirsk, USSR). Radiobiologiya; 10: 504-11(Jul-Aug 1970). (In Russian).

The work was devoted to a study of the possibility of mediated mutagenic effects in the irradiation of mammalian cells. The effects of an irradiated nutrient medium on cells in tissue culture were studied. An increase in the frequency of chromosome rearrangements and a change in the spectrum of chromosome aberrations in the cells of the primary culture were observed. This was similar to the changes arising after direct irradiation at a dose of 50 R. The amino acid composition of the nutrient mixture was studied after its irradation at a dose of 500 R. (tr-auth)

10971 EFFECTS OF GAMMA RADIATION ON THE PHYSICOCHEMICAL PROPERTIES OF HISTONES FROM RAT THYMUS NUCLEI. Korol, B. A.; Tarshis, M. A.; Kuzin, A. M.; (and others) (Inst. of Biological Physics, Pushchino, USSR). Radiobiologiya; 10: 490-4(Jul-Aug 1970). (In Russian).

The effects of irradiation on the physicochemical properties of the histones of rat thymus nuclei were investigated. It was shown that the irradiation of animals at doses of 400 and 1000 R leads to a decrease in the amount of histones that can be isolated and a redistribution of the individual histone fractions in the case of chromatography of the summary histones. A pronounced decrease in the yield of the arginine fraction f_3 is observed. Radiation produced a change in the composition of the histones during electrophoresis in polyacrylamide gel, changed the electrophoretic mobility and increased the content of sulfhydryl groups. The amino acid concentration of the fraction f_3 was investigated. (tr-auth)

10972 INFLUENCE OF THE REGULATION OF CORTICISM AND GLYCEMIA BY INSULIN AND DIANABOL ON CERTAIN HEMATOLOGICAL INDICES DURING ACUTE RADIATION SICKNESS. Barkalaya, A. I. (Inst. of Biophysics, Moscow). Radiobiologiya; 10: 603-5(Jul-Aug 1970). (In Russian).

Certain hormonal-metabolic and hematological indices of rats were investigated following administration of insulin during acute radiation sickness, administration of dianabol 10 days before irradiation, and their combined use. It was found that the restoration of hematopoiesis depended to a definite degree on the level of corticosterone and glucose in the blood of the irradiated rats. Normalization of corticism and glycemia by insulin and dianabol increased the rate of restoration of bone marrow hematopoiesis. (tr-auth)

10973 PARTICIPATION OF NATURAL INHIBITORS OF PEROXIDASE AND ITS ACTIVATION IN ROOTLETS OF GAMMA-IRRADIATED BROAD BEAN SEEDLINGS. Fomenko, B. S. (Inst. of Biological Physics, Pushchino, USSR). Radiobiologiya; 10: 495-9(Jul-Aug 1970). (In Russian).

It was shown that in the γ irradiation of four-day old broad bean seedlings (10 kR), peroxidase was activated in the primary rootlets as a result of a decrease in the inhibitors of this enzyme in the irradiated seedlings, not as a result of synthesis of the enzyme. (tr-auth)

10974 INFLUENCE OF γ-RADIATION ON THE ACTIVITIES OF SEVERAL GLYCOLYTIC ENZYMES IN RESTING AND SPROUTING RYE SEEDS. Bancher, E.; Washuetti, J.; Stachelberger, H. (Technische Hochschule, Vienna). Mikrochim. Acta; No. 3, 582-7(1970). (In German).

The influence of γ radiation on the activity of hexokinase, phosphofructokinase, phosphoglucomutase, and phosphoglucose isomerase in rye seeds during storage and sprouting was studied. There was a decrease in the activity of hexokinase and phosphofructokinase following γ irradiation of rye seeds, both in the dormant and sprouting stages. Phosphoglucomutase and phosphoglucose isomerase undergo activation immediately after irradiation. During sprouting, phosphoglucomutase activity varies with differing doses of radiation. On the eleventh day following sprouting, the enzyme activity values were approximately the same as those of the nonirradiated specimens. During the first and third day of storage, phosphoglucomutase activity showed a strong increase, but decreased rapidly thereafter. In the storage experiment, phosphoglucose isomerase activity was highest immediately after radiation and above that of the controls. Its values were lowest on the third day of storage and lower than its initial values. (E.E.H.)

10975 ULTRA-VIOLET-LIGHT-INDUCED DNA-TO-PROTEIN CROSS-LINKING IN HeLa CELLS. Habazin, Vlasta; Han, Antun (Institute Ruder Boskovic, Zagreb). Int. J. Radiat. Biol.; 18: 569-75(1970).

The extractability of DNA from uv-irradiated HeLa cells following lysis is an inverse function of the uv-dose. The effect was examined immediately after exposures ranging from 500 ergs/mm^2 to 3000 ergs/mm^2, and the cells were irradiated either at room temperature (22°C) or in cold (4°C). The unextracted DNA was recovered from the protein fraction with 0.5 percent trypsin solution. Dose-response curves show that the magnitude of the effect increased linearly with dose, and the amount of DNA recovered from irradiated cells decreased for about 1 percent for every 100 ergs/mm^2 of uv light for cells exposed at room temperature. The effect is twice as large, when the cells are irradiated in cold. The amount of DNA cross-linked to proteins remained unchanged from 0 up to 10 hours after exposure, i.e., for as long as the experiments were carried out. (auth) (UK)

10976 ANNUAL REVIEW OF PLANT PHYSIOLOGY. VOLUME 19. Machlis, Leonard (ed.). Palo Alto, Calif.; Annual Reviews, Inc. (1968). 563p.

A separate abstract was prepared for one paper on the use of ionizing radiation in research. An additional 21 papers are included on various aspects of plant physiology. (H.L.W.)

For an abstract of one paper see: 10977.

10977 IONIZING RADIATIONS AS RESEARCH TOOLS. Haber, Alan H. (Oak Ridge National Lab., Tenn.). Annu. Rev. Plant Physiol.; 19: 463-89(1968).

A number of examples of uses of ionizing radiations for biological investigations at molecular, organelle, cellular, and organismal levels are discussed. Topics discussed are: calculation of apparent sensitive volumes using x or γ radiation and hit or target theories; determining cross sections, thickness, shape, and internal structure using charged particles; molecular weight dependence of genetic transcription from radioinduced chain breaks in DNA; determining time of chromosome strand splitting and investigations of chromatid fine structure; somatic mutations in studying cell lineages in plant development; determining times of organogenesis; studies of nuclear-cytoplasmic interrelations; and use of mitotic inhibition for developmental studies. (H.L.W.)

10978 PRESENCE OF SUBSTANCES THAT REACT WITH THIOBARBITURIC ACID IN IRRADIATED FLOUR. Deschreider, A. R.; Meaux, R. (Ministere des Affaires Economiques, Brussels). Ind. Aliment. Agr. (Paris); 86: 519-23(Apr 1969). (In French).

Irradiation of flour with γ rays produce substances volatile with water vapor. Some of these react with thiobarbituric acid (ATB) giving two complexes; one yellowish with maximum absorption at 454 nm, the other reddish with maximum absorption at 534 nm. The chromogene 454 nm is the most abundant; it probably derives from a degradation product of starch, such as glyoxal. The chromogene 534 nm results from the reaction of ATB with malonic aldehyde, which itself is a by-product of the oxidation of lipids and glucides. The fate of these two colored complexes was followed

XUM

over a storage period of 1 yr. The relation between radiation dose and complex formation was also studied. (auth)

10979 EFFECTS OF γ RADIATION ON PENICILLIUM EXPANSUM L. II. SOME ENZYMATIC CHANGES IN THE FUNGUS. Chou, T. W.; Singh, B.; Salunkhe, D. K.; Campbell, W. F. (Utah State Univ., Logan). Radiat. Bot., 10: 517-20(Nov 1970).

The spore suspensions of Penicillium expansum were irradiated with 50 and 100 krad of γ radiation. Rates of growth (mycelial dry weight), pectinesterase, polygalacturonase, and tissue macerating enzymes were measured 1 to 7 days after inoculation in Czapek–Dox broth. Mycelial dry weight in irradiated cultures was lower than those in the controls. The activities of polygalacturonase and tissue macerating enzymes were higher than those in the controls after 3 days of post-irradiation incubation. Evidence indicates that the enzyme synthesis rather than the enzyme release causes an increase in the activities of pectolytic enzymes. (auth) (UK)

10980 METABOLIC STUDIES ON THE CONTINUOUSLY IRRADIATED RAT. Ziller, Henry Hubert. College Station, Tex.; Texas A and M Univ. (1969). 99p. University Microfilms Order No. 70-11,594.

Thesis.

Male albino rats were continuously irradiated on a 60 R per 20-hr day schedule for 27 days and tested on days 21, 23, 25 and 27. Active transport of ^{14}C glucose was measured using the inverted gut technique. Oxygen utilization of diaphragm muscle strips was measured using the Gilson Respirometer. Carbon-14 labeled CO_2 production was measured following an intraperitoneal injection of ^{14}C glucose. Blood levels of ^{14}C were compared. Mitochondria were isolated and their activity was measured. These studies were correlated to a depression in the rate of weight gain or of weight loss seen in rats irradiated at these continuous levels. There was no difference between the controls and irradiated animals in their ability to absorb glucose. The irradiated rats exhibited a depression in the amount of $^{14}CO_2$ produced, the amount of O_2 used, and in mitochondrial function, when compared to the controls. It was suggested that irradiation was impairing some metabolic pathway involved in the electron transport chain. (Diss. Abstr.)

10981 EFFECT OF SMALL X-RAY DOSES UPON STORED BLOOD. Szotor, Maria; Albinowska, Miroslawa; Skatulska-Surmacka, Teresa; Leyko, Wanda (Univ., Lodz, Poland). Pol. Przegl. Radiol. Med. Nukl.; 34: 427-34(May-Jun 1970). (In Polish).

The effect of small doses of x rays upon changes occurring during the storage of human blood in ACD conservant was studied. The irradiation was performed using an XD_{12} apparatus (Polish production); the parameters were: 80 KV, 120 mA, aluminium filter 0.5 mm, and tube focus distance 0.5 m. Time of exposure was 2 sec, which corresponded to a dose of about 40 R. The examinations of the blood samples were carried out after 1, 7, 14, and 21 days after collection and irradiation of the blood. In the examined samples, the concentration of phosphate compounds of the acid-soluble fractions of erythrocytes was estimated together with the evaluation of the degree of hemolysis, and the potassium level in whole blood and in plasma. The only change that was observed, in comparison with the control samples, was an increase in the degree of hemolysis in the irradiated blood. (auth)

10982 DIFFERENTIATION BETWEEN MATERNAL, PLACENTAL, AND EMBRYONAL HORMONE PRODUCTION. Kaiser, R.; Geiger, W. (Univ., Munich). Geburtsh. Frauenheilk.; 30: 307-16(Apr 1970). (In German).

Hormonal analysis of the urine in human chorionic gonadotropin-pseudopregnancies, normal early pregnancies and irradiated pregnancies showed qualitative and quantitative differences in the hormone production of mother, placenta, and embryo or fetus. In early pregnancy the human chorionic gonadotropin doubles every third day. The corpus luteum of pregnancy produces about twice as much estrogen and one third more progesterone than the corpus luteum of the menstrual cycle. The tropho-blast produces steroid hormones as early as 4 weeks after ovulation. The embryo starts to secrete precursors of estrogens 8 weeks after ovulation. DHE in the urine of pregnant women is of maternal origin. HCG, pregnandiol, pregnanolone, and estradiol-estron are of placental origin and estriol is mostly of fetal origin. (auth)

Immunology

10983 IN VITRO RADIOPROTECTION OF MOUSE TAIL BONES BY DIMETHYL SULPHOXIDE, GLYCERAL, AND ANOXIA. Noel, Janet F.; Wright, E. A. (St. Mary's Hospital Medical School, London). Int. J. Radiat. Biol.; 18: 301-9(1970).

Tail bones from 7 day old mice were irradiated in vitro by x rays under oxygenated and anoxic conditions and in various concentrations of glycerol and dimethyl sulphoxide. After irradiation the bones were transplanted under the renal capsules of syngeneic animals and allowed to grow for 3 wks. The relative growth in length of the irradiated and control bones was used to draw dose response curves, from which radioprotective factors were assessed. The following radioprotective factors were found: oxygen 1.0; 2 molar glycerol 1.32; 2 molar DMSO 2.25; anoxia 2.65; anoxia plus 2 molar DMSO 3.23. (auth)

10984 IMMUNOSUPPRESSIVE EFFECT OF CHRONIC ^{90}Sr ADMINISTRATION TO MINIATURE SWINE. Howard, E. B.; Jannke, C. C. (Battelle-Northwest, Richland, Wash.). Experientia; 26: 785(15 Jul 1970).

A study was conducted to determine the immunocompetence of miniature swine that had received chronic ^{90}Sr exposure. Six animals were fed a daily dose of 625 μCi of ^{90}Sr for ten months then were given a single i.m. inoculation of 0.4 cm^3 strain 19 Brucella abortus vaccine. This experiment demonstrated that prolonged ^{90}Sr exposure results in a significant immunodepression. Since the marrow is the hematopoietic tissue receiving the greatest radiation dose, it was suspected that the defect in antibody response was a result of irradiating sensitive immunocompetent cells in this site. Both myeloid and lymphoid neoplasms were produced in miniature swine receiving chronic ^{90}Sr exposure, possibly indicating that this radiation damage affects the pluripotent stem cell population in the marrow. (E.E.H.)

10985 REACTION OF CONSUMPTION OF THE COMPLEMENT IN LOCALLY IRRADIATED ANIMALS. Ivanov, A. A. (Inst. of Biophysics, Moscow). Radiobiologiya; 10: 556-60(Jul-Aug 1970). (In Russian).

The dynamics of the change in the concentration of tissue autoantibodies and autoantibodies to DNA in rabbits was studied following local irradiation of the liver with x rays at a dose of 2000 R. Phase changes in the concentration of autoantibodies were established: a decrease in the initial normal concentration in the first days (3 to 7 days) after irradiation and a significant increase in the autoantibody concentration at 15 to 19 days. (tr-auth)

10986 SUPPRESSION OF THE ENDOCOLONIZATION OF THE SPLEEN IN SUBLETHALLY IRRADIATED MICE IN THE CASE OF TRANSPLANTATION OF ALLOGENIC LYMPHOID CELLS. Petrov, R. V.; Khaitov, R. M.; Seslavina, L. S. (Inst. of Biophysics, Moscow). Radiobiologiya; 10: 532-5(Jul-Aug 1970). (In Russian).

Mice of the CBA and C57BL lines and their F_1 hybrids (CBAx C57BL) were irradiated with the γ rays of ^{60}Co at doses of 400, 500, 600, and 700 R. An increase in the number of endogenous colonies with decreasing dose of radiation and increase in length of time elapsed after irradiation was shown on all the investigated lines of mice. Transplantation of the allogenic lymphoid cells during the first four days after irradiation suppressed endogenous colony formation in the spleens of F_1 recipients. Substantial differences in the inhibition of the endocolonization of the spleens of lymphoid cells of various genotypes were demonstrated. (tr-auth)

10987 RADIORESISTANCE OF COOPERATIVE FUNCTION OF CARRIER-SPECIFIC LYMPHOCYTES IN ANTIHAPTEN ANTIBODY RESPONSES. Katz, David H.; Paul, William E.; Goidl, Edmond A.; Benacerraf, Baruj (National Institutes of Health, Bethesda, Md.). Science; 170: 462-4(23 Oct 1970).

Transfer of lymphoid cells from strain-2 guinea pigs immunized to bovine gamma globulin into syngeneic recipients immunized with dinitrophenyl ovalbumin markedly enhances the secondary antidinitrophenyl response of the recipient to challenge with dinitrophenyl–bovine gamma globulin. This function of the carrier bovine gamma globulin-specific cells is resistant to irradiation with up to 5000 rads, although the capacity of the irradiated cell population to transfer immunologic memory for bovine gamma globulins or to be stimulated by antigen to synthesize DNA in vitro is abolished by this treatment. (auth)

10988 STERILIZATION OF QUAILS BY X-RAYS AND INTERRACIAL GRAFTS. Brard, Emile; Benoit, Jacques. Bull. Biol. Fr. Belg.; 103: 313-21(1969). (In French).

Immature quails tolerated 1200 R x irradiation 600/R twice within 5 days. This dose caused very pronounced emaciation and a delay in laying eggs. Experiments on ovarian fertile grafts in the quail are reported. Fertile testicular grafting in young male chickens was reported previously. The possibility of obtaining in two species of birds, in both sexes, a lineage derived from different races in the graft-carrier animal is discussed. Testicular grafts of young chickens inserted in gonads of adult cocks and

quails after previous exposure to x rays, or ovarian grafts after the removal of the normal ovary in the quail have a proper physiological and zoological interest. (tr-auth)

10989 NONSPECIFIC ALLERGIC REACTIONS IN SHEEP IN CHRONIC RADIATION SICKNESS. Kruglov, V. T.; Kartashov, P. A.; Kos'yanov, A. N.; Kudryashov, Yu. I. Veterinariya; 1: 44-7(Jan 1970). (In Russian).

Exposure of the organism to ionizing radiation results in the destruction of the tissues and the increased penetrability of blood and lymph vessels, allowing toxic, sensitizing and immunizing cell products to enter the blood stream. Reaction to allergenic agents may be distorted by the radiation; this is important because the irradiated animals may be affected by infectious diseases that are diagnosed by allergy skin tests. Experiments were carried out to confirm the appearance of nonspecific allergic reactions in the case of domestic animals suffering from radiation sickness. Some of the sheep used for the experiments were fed with ^{90}Sr while others were exposed to 300 R of external γ radiation. The lambs were fed milk containing radiotoxin obtained from irradiated ewes. It was found that all animals free from brucellosis and tuberculosis but suffering from radiation sickness exhibited the nonspecific allergic reaction; no such reaction to brucellin and tuberculin were observed in healthy animals. Thus, radiation causes deep and long-lasting pathological changes in the organism. (TTT)

10990 TARGET LYMPHOID CELL POPULATION OF CARCINOGEN INDUCED IMMUNODEPRESSION IN MICE. Rowland, G. F.; Hurd, C. M. (St. Bartholomew's Hospital, London). Nature (London); 227: 167-8(11 Jul 1970).

In a study designed to show whether carcinogen-induced immunodepression is a process linked to cells involved in the immune response and, if so, which of the interacting classes of cell is the target for this effect, spleen cells were extracted from mice treated with DMBA (dimethylbenzanthracene) and the viable cells were injected into heavily irradiated (800 R, total body) syngeneic mice together with sheep red cells (SRBC). After 7 days the mice were killed and their spleens assayed for PFC (plaque forming cells) content. The PFC response in irradiated mice receiving spleen cells plus SRBC is shown in tabular form, together with data on the attempted reversal of depressed PFC response in irradiated mice by injection of normal thymus or bone marrow cells. A degree of immune depression was observed identical with that found in mice receiving DMBA, and it is concluded that the depression was a cell-mediated process which can be transferred to the irradiated recipients. According to the two-cell theory of immunocompetence lymphocytes extracted from the spleen consist of both thymus and marrow-derived populations. It was therefore possible to test if DMBA induced immunodepression is the result of deficiency in one or both of these cell lines by attempting to reverse the depression with normal thymus or marrow cells. (UK)

10991 ISOTOPE BIOASSAY FOR THROMBOPOIETIN. Pennington, D. G. (St. Vincent's Hospital, Melbourne). Brit. Med. J.; 1: 606-8(7 Mar 1970).

An assay system has been developed in mice for the humoral agent thrombopoietin. This is based on utilization in newly-formed platelets of the radio-amino-acid ^{75}Se selenomethionine 24 hours after intravenous injection. The possibility that the results could be due to the effects of species antibody, to foreign protein, or to an effect primarily on selenomethionine metabolism, has been explored, but the findings are consistent with the presence of a physiological humoral factor. Thrombopoietin has been shown to be present in the plasma of patients suffering from severe thrombocytopenia of varied aetiology. (auth) (UK)

10992 ISOENZYMATIC SPECTRUM OF LACTIC DEHYDROGENASE IN XENOGENIC RADIATION CHIMERAS. Mayanskii, D. N. (Kazan Medical Inst., USSR). Byull. Eksp. Biol. Med.; 70: No. 7, 47-50(Jul 1970). (In Russian).

In C3H mice irradiated with a lethal dose of 850 R and protected in 24 hours with Wistar rat myeloid cells at a dose of 2.8×10^7, in the bone marrow, spleen, liver and erythrocytes new chimeric spectra of isoenzymes of lactic dehydrogenase were seen. They gradually stabilized in 30 to 60 days of the post-transplantation period. With the aid of an isoenzymatic marker one could reveal all types of donor hematopoietic cells, sufficiently accurately evaluate the distribution of donor cells and the quantitative ratio of hematopoietic series of the donor and recipient at different periods of chimerism. The employment of an isoenzymatic tag is based on differences in electrophoretic motility and on percentage ratios of isoenzymes of lactic dehydrogenase in the organs of rats and mice in fractionation in agar gel. (auth)

10993 SEROLOGICAL STUDY OF SPECIFIC SURFACE ANTIGENS IN CELLS OF METHYLCHOLANTHRENE-INDUCED TUMORS. Lezhneva, O. M. (Inst. of Epidemiology and Microbiology, Moscow). Tsitologiya; 12: 666-74(May 1970). (In Russian).

A study was made of specific surface antigens in methylcholanthrene-induced tumors with indirect fluorescent antibody technique being applied. Antisera were produced in mice by inoculating these with syngeneic tumor of recent origin (1st to 9th transfer generation), irradiated with γ rays. Specific surface antigens were shown to be, as a rule, individually specific and weakly cross-reactive. These data are in agreement with those obtained with transplantation test. The application of the fluorescent antibody technique is believed to reveal the antigens identical to transplantation ones responsible for immunity. (auth)

10994 ANTIBODY PRODUCTION BY HOST CELLS IN X-IRRADIATED RECIPIENTS OF ALLOGENEIC SPLEEN CELLS. Storb, U.; Weiser, R. S. (Univ. of Washington, Seattle). J. Immunol.; 105: 957-63(Oct 1970).

Experiments were performed to test the hypothesis that two different cells, a radiosensitive antigen reactive cell and a radioresistant precursor of the antibody producing cell collaborate in antibody synthesis. Twenty-four hours following 500 R x-irradiation, experimental recipient group C mice were injected with normal allogeneic spleen cells and sheep red blood cells (SRBC). Control recipients of group A were irradiated similarly and injected with SRBC alone while control recipients of group B were irradiated similarly and injected simultaneously with SRBC and allogeneic spleen cells from heavily irradiated (1000 R) mice. Five to 10 days after antigen injection, the numbers of plaque-forming cells (PFC) of donor and host origin were determined in the spleens of the three groups. The contribution of donor and host PFC was distinguished by the use of anti-histocompatibility sera. On day 5, the spleens of mice in group C contained 26 times as many PFC as did the spleens of mice in group A. Of these, 80% were donor cells and 20% were of host type. Thus more than five times as many host PFC developed in group C than in group A. At least some of the stimulatory effect on host PFC was independent of the normal donor spleen cells because the spleens of control group B contained twice as many PFC as did those of control group A. On days 6 and 7, the PFC in group C decreased, while those in control group A increased, possibly due to alloimmune reactions between donor graft and recipient. The injection of antidonor H-2 serum into group C on day 3 suppressed the development of PFC of both donor and recipient type. Evidently survival of donor cells beyond day 3 was necessary for the enhanced recipient PFC response. It is concluded that existing data establish the importance of cell interactions in the immune response but do not prove the existence of an antigen-sensitive cell capable of transmitting antigen-specific information to the precursor of the antibody-producing cell. (auth)

Ecology

Refer also to abstracts 11038–11042, 11045, 11074, and 12763.

10995 (BMI-171-45) ESTIMATION OF POTENTIAL RADIONUCLIDE INGESTION BY NATIVE POPULATIONS OF EASTERN PANAMA AND NORTHWESTERN COLOMBIA. Bioenvironmental and Radiological-Safety Feasibility Studies, Atlantic-Pacific Interoceanic Canal. Levin, A. A.; Bloom, S. G.; Martin, W. E.; Raines, G. E. (Battelle Memorial Inst., Columbus, Ohio). 15 Sep 1970. Contract AT(26-1)-171. 73p. Dep. NTIS.

A summary of studies is presented on the development of mathematical models that simulate the redistribution of radionuclides deposited in tropical ecosystems and their transport to people via food and water. The objective of the program was to assess the radiological safety feasibility of using nuclear explosives to excavate a sea-level canal in Panama and Colombia. Potential external and internal radiation doses were estimated to people living in the areas most likely to be contaminated by radionuclides resulting from nuclear excavations. Dose estimates were compared with existing radiological criteria. (H.L.W.)

10996 (BNWL-1537) GROWTH OF THE COLUMBIA RIVER LIMPET, FISHEROLA NUTTALLI (HALDEMAN), IN NORMAL AND REACTOR-WARMED WATER. Coutant, C. C.; Becker, C. D. (Battelle-Northwest, Richland, Wash. Pacific Northwest Lab.). 15 Aug 1970. Contract AT(45-1)-1830. 11p. Dep. NTIS.

Limpet snails (Fisherola nuttalli) were collected through 1969 to 70 at locations above and below thermal additions from reactor discharges in the central Columbia River above Richland, Wash-

XUM

ington. Temperatures of the mixed river water below the reactor operations were increased about 0.5 to 2.5 C. Limpet sizes and growth rates at any collecting period did not differ significantly between the two areas. Growth of young limpets was most rapid from July to October when Columbia River temperatures were high. Growth rates stabilized during the fall and winter when temperatures dropped and became minimum, then increased with warming temperatures of early spring. Adult limpets collected from downstream areas and held in the warmed water in the laboratory reproduced successfully. Deposition of egg cases by mature limpets occurred on rising temperatures in April, May, and June during the period of maximum river flows. High mortality occurred among mature limpets during and following the reproductive period. The Columbia River limpet, like many other gastropod molluscs, has a predominantly one year life cycle. (auth)

10997 (RLO-2225-T-14-1) STUDIES OF THE NATURAL ALPHA-EMITTING RADIOISOTOPES IN MARINE ORGANISMS. Annual Progress Report, 1970-1971. Beasley, Thomas M. (Washington Univ., Seattle. Lab. of Radiation Ecology). 10 Dec 1970. Contract AT(45-1)-2225. 46p. Dep. NTIS.

Sample collections were made of zooplankton (copepods, euphausiids, mysids, and zoea), pelagic fishes (smelt, rock fish, herring, cod, whiting, and sablefish), and benthic organisms (sole, flounder, hake, sea urchins, sea cucumbers, and crabs). Tissues from these specimens were analyzed for ^{210}Po, ^{210}Pb, and stable lead. An increase in ^{210}Po concentrations from copepods to euphausiids and from mysids to pelagic fishes occurred. In contrast, ^{210}Pb levels decreased through the same chain. A higher concentration of radionuclides was found in the internal organs than in the muscles. Reduced concentrations of ^{210}Po were found in the late spring and summer months. Radiometric and trace element measurements were made on protein concentrates prepared from pelagic fishes collected both offshore and from estuaries and lakes. Studies on analysis of blood specimens from residents of Rongelap Atoll revealed unusually high body burdens of ^{55}Fe. (H.L.W.)

10998 DYNAMIC CONCENTRATION PROCESS OF RADIOACTIVE SUBSTANCES IN AQUATIC ORGANISMS. TENTATIVE APPROACH FROM STOCHASTIC THEORY. Aoyama, Isao; Yoshikawa, Susumu; Inoue, Yoriteru; Iwai, Shigehisa (Kyoto Univ.). Hoken Butsuri; 5: 135-40(Sep 1970). (In Japanese).

A concentration factor of radioactive nuclides in aquatic organisms is affected by various factors. The distribution and daily change of the concentration factors are discussed. The distribution of the concentration factor of individual organisms showed the logarithmic normal distribution or the Poisson distribution. An attempt is made to explain the dynamics of concentration of radioactive substances in the organisms using a Markov process. The phenomenon is well depicted with the stationary Markov process defined by the initial distribution of the concentration factor $Q_i(0)$ and the conditional probability P_{ij}. (auth) (Japan)

10999 ^{95}Zr IN UTAH VEGETATION PRODUCED DURING THE 1966 GROWING SEASON. Pendleton, R. C.; Lloyd, R. D. (Univ. of Utah, Salt Lake City). Radiol. Health Data Rep.; 11: 277-81(Jun 1970).

Levels of ^{95}Zr in crops and dust from farm implements indicated widespread contamination of Utah with fresh fission products during May or June 1966. Although the exact origin and date of arrival of the ^{95}Zr in these vegetation samples cannot be determined from available evidence, at least part was probably from the May 9, 1966 atmospheric nuclear detonation on the Chinese mainland. No important increase of iodine-131, cesium-137, or strontium-90 has been reported for these months, but there is evidence that farm workers could have been exposed to secondary aerosols containing relatively high levels of radioactivity. This indicates that a potential radiological hazard may have occurred in the past and that highly contaminating incidents may recur, if a highly contaminating incident takes place in the future. (auth)

11000 DOSIMETRIC CONTROL IN BRACHYCURIETHERAPY BY ESCARGOT ISODOSES. Schlienger, M.; Rosenwald, J. C.; Miclutia, M.; Quint, R.; Pierquin, B. (Institut Gustave Roussy, Villejuif, France). Acta Radiol., Ther., Phys., Biol.; 9: 282-8 (Jun 1970). (In French).

The dosimetric control in brachycurietherapy with iridium-192 can be simplified by the use of isodose curves. Dosimetry can be carried out with great precision by means of computer calculation and tracing of the curves. The costs and space requirements are negligible and the method can be used in all radiotherapeutic centres where iridium-192 is employed. (auth) (Sweden)

11001 DATA. SECTION IV. OTHER DATA. Radiol. Health Data Rep.; 11: 563-70(Oct 1970).

The content of ^{137}Cs, ^{89}Sr, and ^{90}Sr in samples of caribou and reindeer meat collected in Alaska between May and December 1969 is reported. Whole-body counting of natives of Alaska was continued. Results of monitoring of radioactivity in the environs of Goodyear Atomic Corporation, Piketon, Ohio during July through December 1969 and Knolls Atomic Power Laboratory, Schenectady, N. Y. during 1968 are reported. (C.H.)

11002 DATA. SECTION I. MILK AND FOOD. Radiol. Health Data Rep.; 11: 533-43(Oct 1970).

Tabulated data are included on the content of ^{137}Cs, ^{131}I, and ^{90}Sr in milk samples collected at various sites throughout Central, North, and South America during July 1969 to July 1970. (C.H.)

11003 ELEVATED LEVELS OF CESIUM-137 IN COMMON MUSHROOMS (AGARICACEAE) WITH POSSIBLE RELATIONSHIP TO HIGH LEVELS OF CESIUM-137 IN WHITETAIL DEER, 1968-1969. Johnson, Wallace; Nayfield. Chester L. Radiol. Health Data Rep.; 11: 527-31(Oct 1970).

High levels of cesium-137 exist in game animals of the southeastern United States. The highest levels, ranging from 250 to 152,940 picocuries per kilogram, have been found in muscle tissue of the Whitetail deer. Levels in Florida range from 10 to 100 times those encountered in Alabama. An important factor in the diet of these animals in Florida is the common gill mushroom, Agaricaceae. Examination of these fungi revealed cesium-137 levels higher by an order of magnitude than levels in vegetation. Similar concentrations of potassium-40 do not occur, indicating a selective effect. (auth)

11004 SOME MEASUREMENTS ON RADIOACTIVITY IN SWEDEN CAUSED BY NUCLEAR TEST EXPLOSIONS. Magi, Attilio (Soedersjukhuset, Stockholm); Snihs, Jan Olof; Swedjemark, Gun Astri. Radiol. Health Data Rep.; 11: 487-509(Oct 1970).

Data on environmental radioactivity levels in Sweden during the period 1959 to 1968 are summarized. Emphasis is placed on γ radiation from the ground and concentrations of cesium-137 and strontium-90 in some foodstuffs of special interest, such as dairy milk and reindeer meat. Various empirical correlations between the concentrations of radioactivity in milk and meat and those found in precipitation are discussed; such correlations may be used in planning environmental sampling programs. The radiation dose contribution to the population caused by fallout is assessed and discussed. (auth)

11005 BIOLOGY OF POPULATIONS. The Biological Basis of Public Health. Sladen, Brenda K.; Bang, Frederik B. (eds.). New York; American Elsevier Publishing Company, Inc. (1969). 466p. $17.50.

Separate abstracts were prepared for two abstracts of the book. An additional 28 chapters are included on various aspects of population growth, population genetics, social behavior and organization, and diseases of populations. Author and subject indexes are appended. (H.L.W.)

For abstracts of individual chapters see: 11006 and 11025.

11006 ECOLOGY OF ANIMAL COMMUNITIES. Sladen, Brenda K. (Johns Hopkins Univ., Baltimore). pp 87-100 of Biology of Populations. /Sladen, Brenda K. (ed.). New York; American Elsevier Publishing Co., Inc. (1969).

Accumulation of radioactive substances in an aquatic animal community is described as an example of the practical significance of community interrelationships. A Canadian lake contained radionuclides from seepage from a liquid disposal area of an atomic reactor. There was a constant input of radionuclides and lake water was regularly depleted in nuclide levels during the warmer months because of biological activity. The content of ^{90}Sr in bones of perch reached a constant after five years. In shorter-lived animals an equilibrium was reached in two years or less. A diagram is presented to show the cycling of ^{90}Sr from species to species in the community. The concentration of ^{90}Sr in bones of perch and muskrats was 3,000 to 3,500 times that of the water. General discussions are given of ecological succession, cycling and energy flow in ecosystems, food webs, and other ecological concepts. (H.L.W.)

Genetics and Cytogenetics

Refer also to abstracts 10946, 10970, 11005 and 11074.

11007 (BNL-50203, pp 1-13) REPAIR AND RECONSTRUCTION OF CHROMOSOMAL DNA AFTER REPLICATION. Rupp, W. Dean; Zipser, Edith; von Essen, Carl; Reno, Donna; Prosnitz, Leonard; Howard-Flanders, Paul (Yale Univ., New Haven, Conn.).

From Conference on time and dose relationships in radiation biology as applied to radiotherapy held at Carmel, California, September 15–18, 1969.

For studies on effects of heat treatment on the yield of single-strand breaks, Escherichia coli cells were exposed to 52°C for 10 min before x irradiation. The heat treatment did not reduce the viability nor the molecular weight of the DNA, but it increased five-fold the yield of single-strand breaks as deduced from the alkaline sedimentation data. Studies on radioinduced single and two-strand breaks in DNA, radiosensitive mutants of Escherichia coli, excision repair, recombinational repair, radiosensitization by organic nitroxides, and DNA repair in mouse leukemia cells are reviewed. It was concluded that the excision mechanism repairs the DNA before replication and that a second mechanism acts following replication past defective bases to reconstruct a functional chromosome by a recombinational process involving sister exchanges. (H.L.W.)

11008 (BNL–50203, pp 14–26) DNA REPAIR IN MAMMALIAN CELLS. Painter, Robert B. (California Univ., San Francisco. Radiological Lab. California Univ., San Francisco. Medical Center).

From Conference on time and dose relationships in radiation biology as applied to radiotherapy held at Carmel, California, September 15–18, 1969.

Four kinds of DNA repair are discussed. The first is photoreactivation which occurs in marsupials and corrects only for ultraviolet damage. The second is the repair of single-strand breaks; this kind of repair seems to occur in all cells thus far tested and seems to be very efficient. The third kind of DNA repair is known as repair replication. This is described for DNA damage in uv-irradiated Escherichia coli, and occurs in all mammalian cells thus far tested with the exception of xeroderma pigmentosum cells. Repair of DNA by this method was studied using uv-irradiated cultured cells incubated with tritium-labeled BUdR. The fourth kind of DNA repair, known as recombination repair, appears to be of great importance in mammalian cells. Interrelations of the various repair systems are considered and their possible roles in the recovery of mammalian cells from ionizing radiation damage are discussed. (H.L.W.)

11009 (COO–1512–22) APPLICATION OF BIOMETRICAL GENETICS TECHNIQUES TO IRRADIATED AND NON-IRRADIATED POPULATIONS OF CORN TO PROVIDE INFORMATION ON NATURE OF GENE ACTION INVOLVED IN THE INHERITANCE OF QUANTITATIVE TRAITS AND IN HETEROSIS. Final Report, 1970. Gardner, C. O. (Nebraska Univ., Lincoln. Dept. of Agronomy). Contract AT(11–1)–1512. 61p. Dep. NTIS.

Results are reported for research on the following projects: effects of thermal neutron irradiation and recurrent mass selection on random mating populations of corn; effects of mass selection for prolificacy on a random mating population of corn; effects of recurrent x-ray seed treatment and mass selection on a random mating population of corn; effects of thermal neutron irradiation and mass selection on genetic variation and genetic correlation in the Hays Golden variety and selected populations; modification of the Gardner–Eberhart model to evaluate changes in genetic parameters resulting from selection; effects of plant population density on quantitative traits in irradiated and selected populations compared to Hays Golden and a hybrid check; development of homozygous lines from Hays Golden and selected populations for genetic studies; effect of thermal neutron irradiation, recombination, and selection on means and genetic variation in populations developed from a cross of two inbred lines; effects of thermal neutron irradiation of seeds and of ultraviolet irradiation of pollen on homozygous lines of corn; genetic study of necrotic leaf spot mutation induced by thermal neutron irradiation; genetic studies of plant height mutants induced by thermal neutron irradiation and ultraviolet light treatments; effect of the chemical mutagen EMS on genetic variation in quantitative traits of corn, sorghum, and Arabidopsis; mutation breeding in allogamous species; and quantitative genetic procedures in studying populations treated with a mutagenic agent. (H.L.W.)

11010 (ORO–2583–8) CYTOLOGICAL STUDY OF RADIATION INDUCED ALTERATIONS IN CYTOPLASMIC FACTORS CONTROLLING MALE STERILITY IN CORN. Progress Report. Edwardson, J. R. (Florida Univ., Gainesville. Dept. of Agronomy). 1 Dec 1970. Contract AT(40–1)–2583. 15p. Dep. NTIS.

Cytoplasmic male sterility in corn was studied. Sterility factors may be linked to cytoplasmic factors controlling susceptibility, or sterility factors may be located at different cytoplasmic sites. In either case, factors controlling susceptibility should be subject to alternation by irradiation. Fertile lines derived from irradiated corn containing T-type cytoplasm should provide information on whether the sterility factors are involved in the susceptibility reactions. Corn seedlings carrying T, normal, and S-type cytoplasms were inoculated with asexual spores of Phyllosticta and Helminthosporium maydis and susceptibility reactions were studied. (P.B.M.)

11011 SOMATIC MUTATIONS IN PETUNIA AFTER SEED TREATMENT. Cornu, A. (INRA, Dijon, France). Ann. Amelior. Plant.; 20: 189–214(1970). (In French).

Petunia seeds treated by two different mutagenic agents, ethyl methane sulfonate and gamma rays, produce plants showing somatic mutations (chlorophyllian or anthocyanic). It is observed that: the frequency of appearance of these mutations is effectively proportional to the dose applied; presoaking of the seeds increases the mutagenic effects of gamma rays; the optimum gamma dose is 6 KR; large differences are found between the effects of gamma rays and ethyl methane sulfonate according to whether homozygous descendants or heterozygous material is involved; the somatic mutations obtained take the form of periclinic or mericlinic chimera. Isolated chlorophyllian mutations are usually carried by the subepidermal layer and can be transmitted to the next generation. Floral mutations affect only the epidermal layer and cannot be sexually transmitted. In vitro cultivation techniques to obtain buds from the changed epidermal layer alone are under investigation. (France)

11012 PUTATIVE DELETIONS OF THE PROXIMAL HETEROCHROMATIN OF CHROMOSOME THREE IN DROSOPHILA MELANOGASTER. Baldwin, Madeline Carol. Vancouver, B. C.; Univ. of British Columbia (1969). Thesis.

A scheme involving the use of attached-autosomes to select for those third chromosomes that have sustained breaks in the proximal heterochromatin was devised. Virgin females were irradiated and attached-third chromosomes were selected for by mating these females to attached-third males. Female progeny carrying these newly synthesized attached-autosomes were irradiated and newly reconstituted chromosomes were selected for by mating the females to males carrying normal third chromosomes. Thus, each newly reconstituted chromosome has sustained a number of breaks at different positions in the proximal heterochromatin. Using this procedure, 66 homozygous lethal chromosomes were recovered. Fifty-three of these 66 lethals may be placed in one of the six complementation groups, two of which appear to be multisite deletions. In addition, these 53 lethals appear to be located, by the results of genetic mapping, in the region spanning the centromere. These two pieces of evidence suggested that the method used here does, indeed, select for deletions in the proximal heterochromatin. (Diss. Abstr.)

11013 EFFECTS OF INCORPORATED RADIONUCLIDES ^{90}Sr–^{90}Y ON THE CHROMOSOMES OF CREPIS CAPILLARIS. Shevchenko, V. V. (Inst. of Developmental Biology, Moscow). Radiobiologiya; 10: 575–9(Jul-Aug 1970). (In Russian).

The cytogenetic effect of incorporated strontium-90–yttrium-90 was investigated. The chromosome rearrangements were analyzed in the first and second mitoses after placement of the seedlings in the solution of radionuclides with activity 1.5×10^{-4} Ci/ml. The localization of breaks induced by incorporated radionuclides in the second cellular cycle was analyzed. The effect of irradiation by incorporated radionuclides proved to be qualitatively similar to the effect of irradiation by external radiation sources. (tr-auth)

11014 DOSE VERSUS EFFECTS CURVES FOR EHRLICH'S ASCITES CARCINOMA CELLS IRRADIATED WITH GAMMA RAYS AT VARIOUS TEMPERATURES. Alekseeva, S. I.; Tsarapkin, L. S. (Inst. of Medical Radiology, Obninsk, USSR). Radiobiologiya; 10: 518–21(Jul-Aug 1970). (In Russian).

Based on dose-effect curves obtained at 10° and 37°C, it was concluded that lowering the temperature of the cell suspension during irradiation enhanced the effect of radiation damage to the chromosomes in cells of Ehrlich's ascites carcinoma. The results were independent of the individual peculiarities of the mice in which the irradiated cells were incubated. (tr-auth) (TSS)

11015 MODIFICATION OF RADIATION DAMAGE TO THE CHROMOSOMES IN ROOTLETS OF CREPIS CAPILLARIS BY CAFFEINE. Eliseenko, N. N. (Inst. of General Genetics, Moscow). Radiobiologiya; 10: 499–503(Jul-Aug 1970). (In Russian).

When seedlings of C. capillaris were treated with a solution of caffeine during irradiation and 4 and 6 hrs. after irradiation, the number of cells with aberrations increased (in the anaphases, the number of bridges approximately doubled; no increase in the number of fusions was detected by the metaphase method). When the cells were treated with caffeine 2 hrs after irradiation, the effect of modification was not detected. Prolonged treatment with caffeine led to a doubling of the number of cells with gaps. (tr-auth)

XUM

11016 MUTAGENESIS OF THE T4B PHAGE IN GAMMA IRRADIATED CELLS OF ESCHERICHIA COLI B. Kuzin, A. M.; Yurov, S. S.; Veksler, A. M. (Inst. of Biological Physics, Pushchino, USSR). Radiobiologiya; 10: 624-7(Jul-Aug 1970). (In Russian).

It was shown that in the case of infection of γ-irradiated cells of E. coli B with nonirradiated T4Br$^+$ phage, mutations of the phage arise, and the yield of r-mutants was higher in bacteria irradiated on solid medium than on liquid medium. The distribution of r-mutants according to groups and their testing for fII → rII$^+$ reversion (obtained in γ-irradiated cells, spontaneously and under the direct action of radiation) indicated different mechanisms of mutagenesis. The radiotoxins formed in the irradiated bacteria induced transition mutations in the phage DNA. (tr-auth)

11017 INVESTIGATION OF THE RADIOSENSITIVITY OF THE GRAPE IN THE CASE OF CHRONIC GAMMA IRRADIATION. Arkhangel'skaya, V. V. (All-Union Scientific Research Inst. of Viniculture and Viticulture, Moscow). Radiobiolcgiya; 10: 622-4 (Jul-Aug 1970). (In Russian).

The radioresistance of certain varieties of the grape was investigated in the case of chronic γ irradiation. Morphological forms arising at irradiation doses of 1900 to 3500 R during vegetation at rates of 1.2 to 1.6 R/hr were described. The response to irradiation of from one to three year old plantings of four grape varieties was characterized. The lethal and inhibiting doses of chronic irradiation for one year old plants were refined. The dependence of the level of lethal doses on the irradiation rate was detected. The results of the experiments were used to refine the method of obtaining somatic radiomutants in the grape. (tr-auth)

11018 COMPARISON OF THE EFFECTIVENESS OF THE ACTION OF FAST NEUTRONS AND X-RAYS ACCORDING TO THE FORMATION OF CHROMOSOME ABERRATIONS IN THE CORNEAL EPITHELIUM OF MICE. Domareva, O. P.; Dmitrieva, T. I. (Inst. of Biological Physics, Pushchino, USSR). Radiobiologiya; 10: 614-16(Jul-Aug 1970). (In Russian).

The work presents data on the influence of X-rays and neutrons on the formation of chromosome aberrations in the corneal epithelium of mice. A linear dose dependence of the formation of chromosome aberrations under the influence of X rays and an exponential dependence under the influence of neutrons were established. The calculated relative biological effectiveness proved equal to 3.3. (tr-auth)

11019 MICROBIOLOGICAL EVOLUTION UNDER RADIATION: A PHENOTYPE OF A RADIORESISTANT MUTANT OF ESCHERICHIA COLI K_{12} INDUCED AND SELECTED BY SUCCESSIVE EXPOSURES TO GAMMA RADIATION FROM ^{60}Co. Mouton, R. F.; Tremeau, O. (CEN de Saclay, Gif-sur-Yvette, France). Int. J. Radiat. Biol.; 17: 237-48(1970). (In French).

The mutant Escherichia coli K12/30 R, selected after 30 successive exposures to γ rays from a ^{60}Co source, shows a doubling of its radiation resistance to both γ (^{60}Co) and uv (2537 Å) radiation. Nevertheless, its repair capacity for phage λ_{vir}, previously exposed extracellularly to uv is not increased. This rules out the hypothesis of a stimulation of the HCR function of the parent strain E. coli K12 Hfr H. The mutant presents a modified cellular division leading to an important percentage of elongated forms; a loss of autotrophy is also noticeable for histidine, tryptophan, and methionine. Preliminary tests did not reveal the presence of suppressor mutations of amber or ochre mutants capable of explaining the observed increase of resistance by a functional repair at the translation level. (auth) (UK)

11020 RADIOSENSITIVITY OF THREE PAIRS OF DIPLOID AND TETRAPLOID PLANT SPECIES: CORRELATION BETWEEN NUCLEAR AND CHROMOSOMAL VOLUME, ROENTGEN EXPOSURE, AND ENERGY ABSORPTION PER CHROMOSOME. Miller, M. W. (Univ. of Rochester, N. Y.). Radiat. Bot.; 10: 273-9 (Jun 1970). (UR-49-1125).

Diploid and tetraploid seedlings of marigold (Tagetes erecta, 2n; T. patula, 4n), zinnia (Zinnia elegans, 2n and 4n), and petunia (Petunia spp., 2n and 4n) were irradiated with increasing exposures of x rays and then scored several weeks later for survival (LD_{50} and LD_{100}). The LD_{50} for each diploid and tetraploid form was: 2n marigold−7.3 kR, 4n marigold−6.4 kR; 2n zinnia−2.2 kR, 4n zinnia−7.2 kR, 2n petunia−3.5 kR, 4n petunia−4.0 kR; the corresponding LD_{100} was 2n marigold−12 kR, 4n marigold−14 kR; 2n zinnia−3 kR, 4n zinnia−15 kR; and 2n petunia−9 kR, 4n petunia−10 kR. Nuclear and interphase chromosome volumes of shoot apices were determined from seedlings at the stage in which they were irradiated. In all three genera, the nuclear volume increased with increased ploidy (69.9 ± 16.8 μ^3 for 2n marigold to 140.3 ± 10.8 μ^3 for 4n marigold; 121.8 ± 28.1 μ^3 for 2n zinnia to 153.9 ± 29.5 μ^3 for 4n zinnia; and 121.6 ± 29.6 μ^3 for 2n petunia to 234.4 ± 49.4 μ^3 for 4n petunia) but interphase chromosome volume either stayed about the same (2.9 ± 0.9 μ^3 for 2n marigold to 2.9 ± 0.2 μ^3 for 4n marigold; and 8.7 ± 2.1 μ^3 for 2n petunia to 8.4 ± 1.8 μ^3 for 4n petunia) or decreased (5.1 ± 1.2 μ^3 for 2n zinnia to 3.2 ± 0.6 μ^3 for 4n zinnia). Two of the three pairs of diploids and tetraploids (marigolds and petunia) absorbed similar amounts of energy per chromosome at LD_{50} and LD_{100} within each genus; the diploid zinnia absorbed significantly less energy per chromosome at LD_{50} (0.7×10^6 eV) than its tetraploid (1.4×10^6 eV) and at LD_{100}, (0.9×10^6 eV) for the diploid and (2.9×10^6 eV) for the tetraploid. (auth) (UK)

11021 FREQUENCY AND SPECTRUM OF CHLOROPHYLL MUTATIONS INDUCED BY MUTAGENS IN SUMMER BARLEY. Danko, V. (Komensky Univ., Bratislava). Genet. Slechteni; 6: 95-101(May 1970). (In Czech).

The effects of x-ray radiation, of ethyl methane sulphonate and nitrosomethyl urea on the frequency and spectrum of chlorophyll mutations in summer barley of the "Slovenský Dunajský trh" variety were investigated. The results obtained showed that the frequency of chlorophyll mutations induced by chemomutagens was higher than after x-ray irradiation. The number of mutations of the albina type was higher after x-ray irradiation. We found that in one spike strain there may occur several mutation types. Nitrosomethyl urea was proved to be most effective. The number of chlorophyll mutations in the third generation was lower than in the second one. However, the frequency of the albina type increased. A more pronounced change in favor of the albina type takes place in the case of lower doses, but the total number of chlorophyll mutations in the case of lower doses decreases visibly compared with higher doses. (auth)

11022 GAMMA RAY-INDUCED MUTATIONS IN DROSOPHILA MELANOGASTER OOCYTES: THE PHENOMENON OF DOSE RATE. Markowitz, Eleanor Himoe (Univ. of Wisconsin, Madison). Genetics; 64: 313-22(Feb 1970).

Drosophila melanogaster females were irradiated with cesium-137 gamma rays at dose rates ranging from 4.8R per minute to over 300R per minute. The frequencies of sex-linked lethal mutations recovered from treated stage 7 oocytes were measured, and indicated no difference due to the dose rate of the irradiation. (auth)

11023 EFFECTS OF X RAYS ON THE BRONZE AND SHRUNKEN LOCI IN MAIZE. Mottinger, J. P. (Univ. of Rhode Island, Kingston). Genetics; 64: 259-71(Feb 1970).

A study was made of the effects of x-irradiation on the Bz locus in chromosome 9 of maize. Pollen of Sh Bz Wx homozygotes was x-irradiated and applied to silks of sh bz wx tester plants. Of 132957 F_1 plants, 837 exhibited the bronze phenotype. Two plants of Sh bz*Wx/sh bz wx constitution (the bz-x1 and bz-x2 mutants) were selected for more intensive study as well as two plants with nearly normal pollen in which both Sh and Bz markers were mutated (sh−bz-x1 and sh−bz-x2). All of the remaining plants proved to be double mutants of sh*bz*/sh bz or bz* wx*/bz wx constitution with high pollen abortion. They were assumed to be heterozygous for deletions in chromosome 9 and were not analyzed further. The bz-x1, bz-x2 and sh−bz-x1 mutants were classified as small deletions on the basis of results from pollen analysis, gametophytic transmission and cross-over studies. The nature of sh−bz-x2 cannot be categorically defined because of contradictory evidence from genetic tests. A deficiency hypothesis and an interpretation of sh−bz-x2 as a suppressed state of Sh and Bz are considered. (auth)

11024 LONG-TERM STORING OF PEA SEED AFTER CHRONIC γ IRRADIATION. Vlk, J.; Kupec, V. (Agricultural Coll., Prague). Genet. Slechteni; 6: 111-13(May 1970). (In Czech).

In the M_2 generation of garden peas the effect of storing of seeds after chronic irradiation with gamma rays on the frequency of the chlorophyll mutations was investigated. After irradiation on gamma-field at Strnady the seeds of two varieties were stored for four years in a constant temperature and moisture. According to the isodoses the frequency of chlorophyll mutations amounted to 0.74 to 11.6 percent. This value does not differ from the current results obtained immediately after application of the mutagen (2 to 14 percent). (auth)

11025 GENETIC EFFECTS OF RADIATIONS IN HUMAN POPULATIONS. Hillis, William D. (Johns Hopkins Univ., Baltimore). pp 221-31 of Biology of Populations. /Sladen, Brenda K. (ed.). New York; American Elsevier Publishing Co., Inc. (1969).

Introductory explanations are given of basic principles such as

kinds of ionizing radiation, measurement of radiation, sources of natural and artificial radiation, mutation production by radiation, and relationship of radiation to spontaneous mutations. The role of natural selection in removing deleterious radioinduced mutants from populations is discussed. Equations are presented to show relationships between mutation rates and selection rates following exposure of biological populations to radiation. A discussion is presented of the establishment of genetic equilibrium in human populations based on data from research on radioinduced mutations in Drosophila. Evidence for genetic effects in human populations is presented from data on survivors of the atomic explosions at Hiroshima and Nagasaki and data from studies on offspring of American radiologists. (H.L.W.)

11026 EFFECT OF A POTENT CARCINOGEN, 4-NITROQUINOLINE 1-OXIDE, AND ITS REDUCED FORM, 4-HYDROXYLAMINOQUINOLINE 1-OXIDE, ON BACTERIAL AND BACTERIOPHAGE GENOMES. Yamamoto, Nobuto; Fukuda, Shizuo; Takebe, Hiraku (Temple Univ., Philadelphia. Southwest Center for Advanced Sciences, Dallas). Cancer Res.; 30: 2532-7(Oct 1970).

4-Nitroquinoline 1-oxide (4NQO)-sensitive mutants of Salmonella typhimurium were found to be sensitive to ultraviolet light (uv) and β-propiolactone. These mutants were subdivided into two groups: host cell reactivation minus (hcr⁻) mutants lacking repair activity for the uv-damaged superinfecting phage and recombination-deficient (rec⁻) mutants. The hcr⁻ mutant is known to lack an enzyme to excise pyrimidine dimers formed in uv-irradiated DNA. 4NQO, β-propiolactone, and uv induced prophages from hcr⁻ and wild-type strains but not from rec⁻ strains. Prophage induction from hcr⁻ strains was far more efficient than that from wild-type strain. A metabolic intermediate of 4NQO, 4-hydroxylaminoquinoline 1-oxide (4HAQO), which is highly carcinogenic, inactivated Salmonella phage P22 in vitro whereas 4NQO did not. When 4HAQO-treated P22 was assayed simultaneously on hcr⁻, rec⁻, and wild-type strains lysogenic for P221b, no difference in inactivation rates on these indicator hosts was found. This indicates that the 4HAQO-damaged phage genome is not repairable by the hosts. Moreover, although a greatly increased frequency of recombination was found between the 4HAQO-treated P22 and the prophage P221b in wild-type and hcr⁻ hosts, no significant increase of recombination was found in rec⁻ strains. Thus, it was concluded that the bacterial recombination mechanism plays an important role in recombination between the damaged P22 and the prophage P221b. (auth)

11027 MUTAGENIC ACTION OF LASER RADIATION ON THE SEEDS OF ARABIDOPSIS THALIANA (L) HEYNH. Usmanov, P. D.; Startsev, G. A.; Shabalov, V. V.; Nasyrov, Yu. S. (Inst. of Plant Physiology and Biophysics, Dushanbe, USSR). Dokl. Akad. Nauk SSSR; 193: 455-7(11 Jul 1970). (In Russian).

Although the visible light does not affect the genetic apparatus of the cells, the heat and electric field generated by laser radiation was considered as an important factor: therefore, the mutagenic action of lasers on Arabidopsis thaliana (L.) seeds was investigated. The airdried seeds were irradiated by a ruby laser (λ = 6943 Å), at $t = 6 \times 10^{-9}$ and 5×10^{-4} sec., corresponding to an energy density of 0.55 and 2.2 J/cm^2. The seeds were planted on filter paper with a 0.1% KNO_3 solution, agar-medium and soil. Analysis of the results indicates that the pigmented mutations obtained are due not only to the heating effect but also to nonlinear optical processes. Mutants with germinating ability had light green, yellow, and white leaves. Thus the laser radiation may be considered a new physical agent, able to induce variations in the above seeds. (TTT)

11028 OCCURRENCE OF SINGLE-STRAND BREAKS IN THE TEMPLATE LABELLED DNA OF P388F CELLS AFTER LOW DOSES OF ELECTRONS. Fox, B. W.; Fox, M. (Christie Hospital and Holt Radium Inst., Manchester, Eng.). Int. J. Radiat. Biol.; 18: 479-82(1970).

The effect of doses of 10 MeV electrons on the DNA of P388F cells was examined. The use of high dose rate radiation (one 1μ sec pulse) enabled rapid changes to be detected and eliminated the occurrence of repair during exposure and hence the obscuring of any damage produced. To investigate strand rejoining in the template DNA, cells in log-phase growth were incubated with ^{14}C thymidine, washed free of precursor and incubated further to allow cell doubling to occur before irradiation. Doses of 100R, 200R, and 300R showed increasing evidence of single-strand breakage which was clearly visible at about 200R. Evidence for the repair of this damage after 30 min was found. (UK)

11029 MUTANTS OF ESCHERICHIA COLI WITH ALTERED SURFACE PROPERTIES WHICH ARE REFRACTORY TO COLICIN E2, SENSITIVE TO ULTRAVIOLET LIGHT, AND WHICH CAN ALSO SHOW RECOMBINATION DEFICIENCY, ABORTIVE GROWTH OF BACTERIOPHAGE λ, AND FILAMENT FORMATION. Holland, I. B.; Threlfall, E. J.; Holland, Eva M.; Darby, Valerie; Samson, A. C. R. (Univ. of Leicester, Eng.). J. Gen. Microbiol.; 62: 371-82(Aug 1970).

Mutants refractory to colicin E2, previous phenotypic symbol RefII, were divided into two major phenotypic groups. CetC mutants in distinction to CetB mutants showed increased sensitivity to uv and to a detergent (DOC). CetC mutants sometimes showed other properties, including abortive growth of bacteriophage λ and defective division. CetB mutants were refractory to E2 at 30° but largely sensitive at 37°. CetC mutants were also refractory at 30° but either sensitive or completely refractory at 37°. In contrast to Rec⁻ mutants, CetC strains were not sensitive to γ rays but two mutants show enhanced DNA breakdown after uv irradiation. CetC mutants seemed defective in a specific membrane component which rendered them insensitive to E2 and alteration of which could affect several aspects of DNA metabolism. (auth) (UK)

11030 INDUCED MUTATIONS IN SUGAR CANE. Jagatbesan, D.; Sreenivasan, T. B. (Sugarcane Breeding Inst., Coimbatore, India). Indian J. Agr. Sci.; 40: 165-72(Feb 1970).

Results of a breeding programme for sugar cane initiated to improve some of the varieties under cultivation by induced mutations are reported. Single budded seeds of the varieties "Co 312", "Co 418", "Co 527" and "Co 997" were treated with 1 to 5 Kr gamma rays and X rays. Data on germination, plant height, and seedling abnormalities were recorded 15, 30, 45 days after irradiation. The changes in cane, leaf, and bud characters were recorded in the first generation when the crop was about 10 months old. Representative buds from each cane of every plant in this generation were planted and the changes in the next generation studied. The experiment was repeated for the third generation also. It was observed that low doses of x rays stimulated the growth of the main shoot in some varieties. Mutants affecting cane and leaf sheath characters were isolated. Yielding ability of "Co 418" glabrous leaf-sheath mutant was similar to that of the parent. A glabrous leaf-sheath mutant was isolated in "Co 527". The genetic nature of these mutants and possibility of inducing desirable mutants in sugarcane is discussed. (INIS)

11031 VARIATION IN SOMATIC CHROMOSOME NUMBER FOUND IN RADIATION-INDUCED MUTANTS OF CHRYSANTHEMUM MORIFOLIUM HEMSL. CV. YELLOW DELAWARE AND DELAWARE. Ichikawa, S. (Kyoto Univ.); Yamakawa, K.; Sekiguchi, F.; Tatsuno, T. Radiat. Bot.; 10: 557-62(Nov 1970).

Young plants of Chrysanthemum morifolium CV. Yellow Delaware and Delaware were irradiated chronically with ^{60}Co gamma rays in the gamma field. The total exposures were 5, 10, and 20 kR. Many whole-type sports were produced after irradiation, thus the method of internal disbudding by radiation treatments was confirmed to be efficient in enlarging mutation sectors. Cytological examination of 19 mutant and 12 apparently produced normal shoots after irradiation revealed that the somatic chromosome numbers ranged from 49 to 55 with an exceptional doubled number of 110. Some of the shoots were chimeric cytologically. None of the shoots examined had higher chromosome numbers than the control plants (2n = 55) except for the 110 chromosome shoot. More reduction of chromosome number was caused with higher exposures. Reduction of chromosome number was also correlated with the type of mutation and with the size of inflorescence. (auth) (UK)

11032 MUTAGENIC EFFECTS OF NEAR ULTRAVIOLET AND VISIBLE RADIANT ENERGY ON CONTINUOUS CULTURES OF ESCHERICHIA COLI. Webb, Robert B.; Malina, Mylan M. (Argonne National Lab., Ill.). Photochem. Photobiol.; 12: 457-68(Dec 1970).

The induction of mutation to phage T5 resistance by near uv and visible light was studied in chemostat cultures of Escherichia coli strains B/r and B/r/1, trp. The visible light mutation rate to phage T5 resistance was independent of growth rate over the range studied. This result is consistent with a photochemical mechanism of mutagenesis. Change overs, in which a faster growing subpopulation takes over the culture, usually causing the mutant frequency to decline sharply, occur more frequently in chemostat cultures irradiated with visible light than in cultures treated with far uv or caffeine. A preliminary action spectrum was obtained with aerated chemostats that revealed effective wavelengths to be between 330 nm and 500 nm. Wavelengths longer than 500 nm were not effective. Wavelengths longer than 340 nm were not mutagenic in anaerobic chemostats. This oxygen requirement for mutagenesis between 340 nm and 500 nm is consistent with a photodynamic mechanism of action. In aerated cultures, wavelengths between 400 nm and 500 nm were as effec-

XUM

tive as wavelengths between 330 nm and 400 nm. A number of naturally occurring compounds, including riboflavin and vitamin K, are consistent with the data as candidates for the chromophore responsible for near uv and visible light mutagenesis. (auth) (UK)

11033 RADIO INDUCED MUTATION OF HARD WHEAT. Mugnozza, G. T. S. (to CNEN). French Patent 2,000,473. 5 Sep 1969. Priority date 20 Jan 1968, Italy. (In French).

A new variety of hard wheat of the Triticum durum Desf. class was obtained by radioinduced mutation of the latent caryopsis of the cv. Cappelli variety with thermal neutrons at a dose of $1.05 \times 10^{13}/cm^2$ and with a flux of $5.82 \times 10^8/cm^2/sec$. The hard wheat is characterized by mean height-small 105 to 115 cm, yellow-brown awn at maturation with semi-compact, oblong barb, upright with small tightened awns, good fertility, dark green leaves, amber caryopsis, translucent, and slightly curved in growth with protuberant dorsal profile. (P.C.H.)

11034 RADIO-INDUCED MUTATION OF HARD WHEAT. Mugnozza, G. T. S. (to CNEN). French Patent 2,000,475 5 Sep 1969. Priority date 20 Jan 1968, Italy. (In French).

A new variety of hard wheat of the Triticum durum Desf. class was obtained by radioinduced mutation of the latent caryopsis of the cv. Cappelli variety with thermal neutrons at a dose of $8.38 \times 10^{12}/cm^2$ and a flux of $5.82 \times 10^8/cm^2/sec$. The new variety is characterized by mean height-small 85 to 95 cm, yellow-brown awn at maturation, with semi-compact, oblong barb, upright with tightened small awns, fertility, dark green leaves, amber caryopsis, translucent, long, elliptical, with protuberant dorsal profile. (P.C.H.)

11035 EFFECT OF ENVIRONMENT ON DIPLONTIC SELECTION IN IRRADIATED GLADIOLUS CORMS. Buiatti, M.; Baroncelli, S.; Tesi, R.; Boscariol, P. (Univ., Pisa, Italy). Radiat. Bot.; 10: 531-8(Nov 1970).

The effect of two different growing conditions (greenhouse and open field) on mutation frequency and mutated sector size was studied on spikes of Gladiolus plants, var. Oscar, raised from gamma-irradiated corms. Faster growth in the first part of the life cycle (from planting to spike emergence) generally led to an increase in mutation frequencies and a decrease in mutated sector areas. This general situation, however, led to different results when the first 6 flowers in order of emergence or the later formed ones were taken into consideration. In the first case slower growth resulted in larger sectors in terms of per cent of total petal area per flower, in the second in a higher number of mutated flowers within the same spike. The aforementioned data are discussed in view of the possibility of different ontogenetic situations in the two flower classes at the time of irradiation. (auth) (UK)

Health Physics and Safety

Refer also to abstract 10421.

Radioactive Contamination and Decontamination

Refer also to abstracts 10721, 10797, 10953, 10954, 10995, 10997–10999, 11001–11004, 11006, and 11073.

11036 (CEA-Bib-185) MAIN MECHANICAL AND ELECTRICAL PROPERTIES OF AEROSOLS. APPLICATION TO HEALTH PHYSICS. Lasseur, Claude (Commissariat a l'Energie Atomique, Saclay (France). Centre d'Etudes Nucleaires). Oct 1970. 63p. (In French). Dep. NTIS (U. S. Sales Only).

Stokes law and the limits to its application, diffusion and coagulation are reviewed. The main theories concerning the mobility of the ions and the charge of the particles are briefly reviewed. Polarization phenomena are studied. The corrections associated with these properties are given. Examples are then given of the applications to health physics of the various aerosol properties and of the results obtained in the study of natural radioactive aerosols, and in the methods used for collecting the aerosols (filters, impactors, precipitators). (France)

11037 (NP-18381) ^{137}Cs IN THE LICHEN-REINDEER MAN IN THE EXTREME NORTH OF THE USSR (1962–1968). Nizhnikov, A. I.; Nevstrueva, M. A.; Ramzaev, P. V.; Moiseev, A. A.; Troitskaya, M. N.; Litver, B. Ya.; Ibatullin, M. S.; Kharchenko, L. A.; Dmitriev, I. M. (Gosudarstvennyi Komitet po Ispol'zovaniyu Atomnoi Energii SSSR, Moscow). 1969. 16p. (In Russian). Dep. CFSTI (U. S. Sales Only).

The dynamics of the ^{137}Cs contamination levels in all links of the chain specific for pre-arctic regions in a series of summers confirmed the previously assumed hypotheses that the minimal period of semi-decontamination of the chain in a given period of time is 2.5 yrs. For a series of eastern regions of the north the decontamination rate of the food chain can be significantly less ($T_{\frac{1}{2}}$ of more than 2.5 yrs.). The amount of absorbed dose in reindeer herdsmen from ^{137}Cs in extreme northern regions continues to remain high and amounts to 67 to 350 Mrad/yr, approximately 30 to 170 times higher than in inhabitants of temperate latitudes of the northern hemisphere. (tr-auth)

11038 (UCRL-72716(Rev.1)) RADIONUCLIDE BODY BURDENS AND HAZARDS FROM INGESTION OF FOODSTUFFS CONTAMINATED BY FALLOUT. Ng, Yook C.; Tewes, Howard A. (California Univ., Livermore. Lawrence Radiation Lab.). 2 Oct 1970. 79p. (CONF-700908-3). Dep. NTIS.

From Symposium on Survival of Food Crops and Livestock in the Event of Nuclear War, Upton, N. Y.

A method was developed for predicting the internal dose that could result when radionuclides are released to the atmosphere and deposited on agricultural land. This approach was used to extend earlier studies on the problems associated with food contamination following a nuclear attack. The study considers activation products as well as fission products. It attempts to take into account recent data on the retention and rate of loss by weathering of both small and large particles on plants, on the uptake of nuclides into dietary constituents, and on the biological availability of nuclides in nuclear debris. Potential levels of food contamination and internal dose commitment are estimated both for the immediate postattack period and during the year closely following the attack when the initial deposition rates of stratospheric debris would be highest. The results are discussed in the light of the modifying factors that would influence them. (auth)

11039 DATA. SECTION III. AIR AND DEPOSITION. Radiol. Health Data Rep.; 11: 305-12(Jun 1970).

Data are presented on the gross β activity in atmosphere and precipitation sampled throughout North and South America during February 1970. Data are also included on the content of tritium in precipitation during January to July 1969 and the content of ^{238}Pu and ^{239}Pu in airborne particulates during July through December 1968 in the United States. (C.H.)

11040 DATA. SECTION I. MILK AND FOOD. Radiol. Health Data Rep.; 11: 283-99(Jun 1970).

Data are presented on the content of ^{140}Ba, ^{137}Cs, ^{131}I, ^{89}Sr, and ^{90}Sr in milk samples collected throughout the United States during February 1970. The content of ^{137}Cs, ^{89}Sr, and ^{90}Sr in institution total diets at eight sampling sites throughout the United States during July to September 1969 and of ^{90}Sr in various food classes and individual diets in New York City and San Francisco during November and December 1969 is reported. (C.H.)

11041 DATA. SECTION II. WATER. Radiol. Health Data Rep.; 11: 301-4(Jun 1970).

Data are presented on the content of ^{137}Cs, ^{90}Sr, and tritium in samples of surface water collected from various locations throughout New York State during January to July 1969. (C.H.)

11042 DATA. SECTION IV. OTHER DATA. Radiol. Health Data Rep.; 11: 313-24(Jun 1970).

Data are summarized on the content of ^{131}I in thyroid glands from cattle slaughtered at various locations throughout the United States from 1962 to 1969 and on the content of ^{90}Sr in samples of human bones collected throughout the United States from July through September 1969. Environmental levels of radioactivity at Mound Laboratory, Miamisburg, Ohio from January through June 1969 and at the National Reactor Testing Station, Idaho Falls, Idaho from July through December 1968 are reported. During May 1970, nine underground nuclear explosions at the Nevada Test Site were announced by the U. S. AEC. A small amount of radioactivity escaped to the atmosphere following the May 26 explosion. (C.H.)

11043 RADIATION IN URANIUM MINES. Thompkins, R. W. (Queen's Univ., Kingston, Ont.). Can. Mining J.; 91: 103-5(Oct 1970).

A review is given of some pertinent facts about environmental radiation with an assessment of the knowledge required and how it can be used for economically designing controls of concentration levels. Radiation in mines was measured in terms of radon daughters present in the atmosphere breathed. A theoretical level of their allowable concentration, called a working level (W.L.), was accurately defined. Measurement errors and sources of radon gas in various mining situations are discussed with supporting examples. Adequate ventilation and design criteria for new mines are outlined. It was concluded that with proper basic

measurements of radon emanation rates the required acceptable figure of 0.3 W. L. could be attained. (Canada)

11044 ESTIMATION OF RADIOACTIVITY OF BIOLOGICAL SAMPLES CONTAINING A MIXTURE OF ^{144}Ce, ^{144}Pr, AND ^{59}Fe. Kollar, J.; Chorvat, D.; Klemova, L. (Research Inst. for Industrial Hygiene and Occupational Medicine, Bratislava. Inst. for Tech. Cybernetics, Bratislava). Atompraxis; 16: 247-9 (Jul-Aug 1970).

In many radiobiological experiments it was possible to determine the amount of radionuclides in a mixture sample using a radiometric γ scintillation spectrometry method based on the assumption of equilibrium of radionuclides ^{144}Ce and ^{144}Pr. Due to the very short half-life of ^{144}Pr there were no practical difficulties. The described method was used for routine analysis of large series of biological samples. (auth)

11045 ENVIRONMENTAL SURVEY OF URANIUM MILL TAILINGS PILE, MONUMENT VALLEY, ARIZ. Snelling, Robert N. (Bureau of Radiological Health, Las Vegas, Nev.). Radiol. Health Data Rep.; 11: 511-17(Oct 1970).

At the request of the Navajo Tribal Council through the Public Health Service Division of Indian Health at Window Rock, Ariz., an environmental radiological survey was conducted on the Foote Mineral Company's uranium tailings pile, Monument Valley, Ariz., in May 1968. The purpose of the survey was to identify any radiation hazards which might exist and recommend methods for their control. The survey included evaluation of external γ radiation, airborne radioactivity, and waterborne radioactivity. The results of the survey indicate that existing radiation levels do not exceed recommended exposure limits. However, to minimize the possibility of increased activity from weather conditions different from those existing during the survey, it was recommended that the mill tailings be stabilized against wind erosion. Otherwise, periodic monitoring will be necessary in the future. (auth)

11046 DETECTION AND REMOVAL OF RADIOACTIVE CONTAMINANTS IN REACTOR-IRRADIATED NaCl, KCl/K_2CO_3, AND NH_4Br. Assheuer, J.; Leistner, G. H. (Medizinische Univ., Bonn). Nucl.-Med.; 32: Suppl. 7, 417-20(1968). (In German).

From 5th Conference of the Society of Nuclear Medicine, Vienna, Austria. See CONF-670996.

A neutron activation method is described for determination of impurities in ^{82}Br, ^{42}K, and ^{24}Na. Following neutron activation in the reactor, solutions of ^{24}Na and ^{42}K were purified satisfactorily from radioactive anions by an Amberlite IRA column. The eluate was then transferred to columns of Bio-Rad 2T 1 and ^{24}Na and ^{42}K were eluted with 0.1 mol and 0.3 mol ammonium chloride solution, respectively. For ^{82}Br, removal of radioactive cations was achieved with a column of Amberlite IRA 120. The degree of purity was judged by the half-life of the final product. (H.B.G.)

11047 USE OF ACTIVATED BARIUM SULFATE IN ORAL CONTAMINATION WITH RADIOSTRONTIUM. III. DECREASE IN ABSORPTION IN MAN. Neruda, O.; Knajfl, J. (Military-Medical Research Inst., Hradec Kralove, Czech.). Sb. Ved. Pr. VLVDU Hradci Kralove; 47: 113-27(1970). (In Czech).

The effect of activated barium sulphate was investigated in man. In the control, studies a single tracer dose of ^{87m}Sr was given orally in 50 ml of water. The plasma levels of ^{87m}Sr were determined at 4 and 8 hr after the ingestion and the activity of 12 hr urine was measured. In the experimental studies, the same persons were given another tracer dose. An amount of activated barium sulphate suspended in 150 ml of water was administered at different times before and after the tracer as well. The measurement of ^{87m}Sr in plasma and urine was performed like that in the control studies. All subjects fasted overnight and breakfast was always given 1 hr after ^{87m}Sr or after activated barium sulphate, if this substance was given later than ^{87m}Sr. Altogether 36 of the administration of ^{87m}Sr were carried out in eight subjects. The reduction factor of absorption was calculated as the ratio of the control and experimental values of plasma specific activity and activity in urine. Percents of decrease were obtained by equation. Comparing the results with those obtained by aluminum phosphate gel and sodium alginate, different conditions of the examinations must be taken into account, because even a meal is known to decrease absorption of radiostrontium. In spite of this activated barium sulphate may be a more effective substance in decrease of strontium absorption than the others. (tr-auth)

11048 USE OF ACTIVATED BARIUM SULFATE IN ORAL CONTAMINATION WITH RADIOSTRONTIUM. II. TIME INTERVALS AND DOSAGE. Smid, A.; Knajfl, J. (Military-Medical Research Inst., Hradec Kralove, Czech.). Sb. Ved. Pr. VLVDU Hradci Kralove; 47: 103-11(1970). (In Czech).

The dose effect of the orally administered activated barium sulphate (ABS) upon the decrease of radiostrontium deposition in the bones of rats was studied. The experimental animals were given 25, 50, 100, 200, 500, and 800 mg of ABS/1 rat. The ABS suspension was given 10 min following oral contamination with ^{85}Sr. The rats were killed at 48 hr after the contamination. The results indicate that the optimum dose of ABS for one rat (180 to 200 g) is 200 mg. The rats were divided into groups containing 10 animals each of which were given 200 mg of ABS per os in intervals varying from 10 min to 12 hr before the oral contamination. The animals were killed at 24 hr. The results demonstrated that the deposition of ^{85}Sr was decreased significantly even after application 6 hr before contamination. The application of ABS (200 mg) up to 2 hr following the ingestion of ^{85}Sr decreased the deposition of radiostrontium in the bones. In cases of oral contamination with radiostrontium, a significant decrease in deposition can be obtained if ABS is applied in the intervals from 6 hr before to 2 hr after contamination. A sufficient dose is represented by 200 mg of ABS. (tr-auth)

11049 USE OF ACTIVATED BARIUM SULFATE IN ORAL CONTAMINATION WITH RADIOSTRONTIUM. I. PREPARATION OF ACTIVATED BARIUM SULFATE AND ITS PROPERTIES. Knafjl, J. (Military-Medical Research Inst., Hradec Kralove, Czech.). Sb. Ved. Pr. VLVDU Hradci Kralove; 47: 79-102 (1970). (In Czech).

A number of substances was tested for decreasing the absorption of radiostrontium from the gastrointestinal tract. Most favorable effects were observed when using alginates and aluminium phosphate. Activated barium sulphate (ABS) was proved previously to be a very effective substance in preventing the absorption of radiostrontium. Some properties of ABS, which was prepared by precipitation of barium chloride and calcium chloride, appear to be very effective in vivo; the most effective results were observed following precipitation of 1 M $BaCl_2$ and $CaCl_2$ in the ratio 6:4. An application of non-dried ABS suspension prepared immediately before use was also tested. Its effect was the same as that of a crushed dried preparation in particles not greater than 0.1 mm. A conclusion can be made that ABS is a very effective substance, the properties of which are not affected essentially by the changes of $BaCl_2/CaCl_2$ ratio at precipitation. There is no difference in effectiveness when stored ABS is used or when it is prepared immediately before the application. (tr-auth)

11050 ^{90}Sr UPTAKE BY AGRICULTURAL PLANTS AND ANIMALS. Kruglov, V. T.; Vikhrenko, N. M. Veterinariya; 46: 93-5(1969). (In Russian).

Tabulated data are given for concentrations of ^{90}Sr in 10,000 specimens of plants and forage tested during 1965 to 1967. The highest content of ^{90}Sr was found in rough forage; the content was five to seven times lower in concentrated fodder. It was also found that the uptake of ^{90}Sr by cattle and the contamination of agricultural products were reduced about two to three fold during the last four years. A higher level of radioactivity was observed in mountainous regions than in lowland regions. (R.V.J.)

11051 SUBSTANTIATION OF THE MAXIMUM PERMISSIBLE CONCENTRATION OF ^{232}Th AND OF NATURAL THORIUM IN THE DRINKING WATER. Lyarskii, P. P.; Pavlovskaya, N. A.; Petushkov, A. A.; Zel'tser, M. R.; Provotorov, A. V.; Makeeva, L. G. (Inst. of Labor Protection and Occupational Diseases, Moscow). Gig. Sanit.; No. 7, 46-51(Jul 1970). (In Russian).

On the basis of analysis of published data and of results of observations, the parameters necessary for calculating the maximum permissible concentration (MPC) of ^{232}Th and of natural thorium in drinking water were defined. The defined constants made it possible to calculate the MPC ^{232}Th and of natural thorium in water. By means of these calculations the MPC of ^{232}Th in drinking water was found to amount to $1.0 \cdot 10^{-11}$ curie/l or 0.1 mg/l, that of natural thorium to amount to $0.35 \cdot 10^{-11}$ curie/l or 0.082 mg/l, if the maximum permissible dose (MPD) is equal to Lber/yr. If the MPD amounts to 3 ber/yr the calculation results should be increased three times. (auth)

Dosimetry and Monitoring

Refer also to abstracts 10699, 10763, 10818, 10881, 10883–10886, 10934, 10936, 11001, 11037, 12320, and 12757.

11052 (AERE-R-5069) RADIATION DOSE RATES FROM PLUTONIUM OXIDE–BERYLLIUM OXIDE MIXTURES. Douglas, J. A.; McLaren, J. R.; Robotham, F. P. J. (Atomic Energy Research Establishment, Harwell (England)). Oct 1966. 18p. Dep. NTIS (U. S. Sales Only).

The fast neutron, gamma, and x ray dose rates from various

mixtures of plutonium oxide and beryllium oxide were measured and compared with theoretical estimates of fast neutron emission. The results obtained were used to estimate the radiological hazard that may be encountered in the small scale manufacture of plutonium oxide–beryllium oxide fuel pellets. (auth) (UK)

11053 (BNWL-B-12) BUILD-UP OF AMERICIUM-241 IN LUNG CONTAINING PLUTONIUM-241. Nelson, I. C. (Battelle-Northwest, Richland, Wash. Pacific Northwest Lab.). 23 Sep 1970. Contract AT(45-1)-1830. 11p. Dep. NTIS.

Estimations of the lung burden of ^{241}Am following accidental inhalation of a mixed ^{241}Pu–^{241}Am aerosol are discussed. Equations are developed for calculating the lung burden of ^{241}Pu based on measurements of ^{241}Am in the lung at various times after inhalation of the mixed aerosol. For purposes of lung counting, the amounts of radionuclides in the model pulmonary and lymph compartments constitute the material of measurement interest. (H.L.W.)

11054 (JINR-P16-5383) DOSE CHARACTERISTICS OF PROTONS WITH ENERGY 200 MeV. Zel'chinskii, M.; Pshona, S.; Komochkov, M. M.; Sychev, B. S.; Cherevatenko, A. P. (Joint Inst. for Nuclear Research, Dubna (USSR). Lab. of Nuclear Problems). 1970. 16p. (In Russian). Dep. NTIS (U. S. Sales Only).

The dose characteristics of protons with energy 200 MeV are found experimentally by recombination methods for which there are detailed theoretical calculations. The absorbed dose rate, related to unit density proton flux (P) and quality factor (QF) at the depth 5 cm in an infinite tissue-equivalent slab 30 cm thick for the case of normal irradiation with a broad parallel monoenergetical proton beam are taken as compared parameters. The values $P = 81 \pm 8$ nrad · prot^{-1} cm^2 and $QF = 1.40 \pm 0.25$ rem/rad, obtained experimentally, testify that theoretical calculations have been based on the right assumptions with respect to cross section values and model of interaction process. (auth)

11055 (ORNL-4579) DOSE-ESTIMATION STUDIES RELATED TO PROPOSED CONSTRUCTION OF AN ATLANTIC–PACIFIC INTEROCEANIC CANAL WITH NUCLEAR EXPLOSIVES: PHASE III. Kaye, Stephen V.; Rohwer, Paul S. (Oak Ridge National Lab., Tenn.). Dec 1970. Contract W-7405-eng-26. 145p. Dep. NTIS.

Potential doses to indigenous populations along Route 17 in eastern Panama and Route 25 in northwestern Colombia were estimated for a combination of hypothetical exposures to radiation. The studies attempted to determine when it might be appropriate for the evacuated populations to reenter areas adjacent to the two routes. The only modes of exposure considered were external exposure to a contaminated land surface and internal exposure from the ingestion of four types of contaminated foods and beverages. Parameters in the internal dose models were adjusted to differentiate five age groups within each of four indigenous populations and nine reference organs. These populations were further differentiated on the basis of diet and estimates of time- and age-dependent concentrations of radioactivity in dietary items. Intake functions (μCi ingested per day) for internal dose estimates were average values for watersheds with the highest initial areal concentration of fallout along each route, whereas external doses were computed for 13 locations (towns and villages) in watersheds of the exclusion zone of Route 17 only. Estimates of potential external doses were based on 170 radionuclides; only 31 radionuclides were considered in detail for the estimation of potential internal doses, with an approximate estimate of total dose from the radionuclides not included in the list of 31. Estimates of potential total doses (internal dose from ingestion + external dose from land surface) were assessed in terms of radiation safety criteria recommended for members of the public by recognized authorities. The basic criteria were: annual dose limit for the total body of 0.17 rem/year and a genetic dose limit of 5 rems/30 years. Assessments based on somatic doses suggest reentry may be appropriate 8 to 10 years after the last detonation. Children less than 5 years of age at the time of reentry may be the critical age group among the age groups for which doses were estimated. Within this age group, no single ethnic group emerged as the most critical. Assessments based on genetic dose appear to be less limiting, suggesting that reentry may be possible within months following the last detonation. These assessments are based on comparisons with the total doses allowed under the radiation safety criteria. In actual practice, however, some apportionment of these criteria might be likely. Such an apportionment should be undertaken by the countries involved (Panama and Colombia). (auth)

11056 (STI/PUB-241) NUCLEAR ACCIDENT DOSIMETRY SYSTEMS. Panel Proceedings Series. Proceedings of a Panel Held in Vienna, 17–21 February 1969. (International Atomic Energy Agency, Vienna (Austria)). May 1970. 199p. (In several languages). (CONF-690223). IAEA $5.00.

Separate abstracts were prepared for 15 papers presented at this conference. (C.H.)

For abstracts of individual papers see: 10818, 10881–10886, 11057, 11079–11084, and 12343.

11057 EXPERIENCE GAINED DURING A CRITICALITY ACCIDENT WHICH AFFECTED A CRITICAL ASSEMBLY IN MOL. Boulenger, R. (Centre d'Etude l'Energie Nucleaire, Mol, Belg.). pp 1-23 of Nuclear Accident Dosimetry Systems. Vienna; International Atomic Energy Agency (1970). (In French).

From Panel on Nuclear Accident Dosimetry Systems, Vienna, Austria. See STI/PUB-241; CONF-690223.

The measurements of external exposure of a person made after a criticality accident at Mol on 30 December, 1965, are described together with the results. The circumstances of the accident are summarized. High γ radiation doses (550 R) were recorded on the film dosimeter worn on the breast by the person. Several irradiations of Rando and Remcal phantoms, fitted out with internal and external dosimeters, were done; the aim was to seek guidance for appropriate medical treatment and to allow a comparison of biological effects. The γ and neutron dosimetry methods used are described with some examples of the results. The irradiations presented several peculiarities: inhomogeneity owing to the proximity of the source, which entailed a knowledge of the doses at the different areas of the body; instantaneous exposure, which made possible a fairly precise reconstitution with a phantom; and an absorbed γ dose much higher than the neutron dose. (auth)

11058 COMPUTATION OF DOSE DISTRIBUTION AND ITS EVALUATION BY DIGITAL COMPUTER FOR THE INTRACAVITARY IRRADIATION OF UTERINE CERVIX CANCER. Machida, Takako (National Cancer Center, Tokyo). Nippon Igaku Hoshasen Gakkai Zasshi; 30: 33-45(Apr 1970). (In Japanese).

The application of computer techniques to the dose computation has improved the accuracy of γ intracavitary irradiation for cervix cancer. The three dimensional doses computation system for the intracavitary irradiation of uterine cervix cancer which is now in operation at National Cancer Hospital is described in detail. The conception of index of merit is defined for the purpose of evaluating the quality of dose distribution. This index can be calculated by the computer. The calculated index showed good correlation with clinical experiences. The quantitative estimation of radiation injury on the rectum and bladder was tried using an index of radiation injury. This index can be calculated from the dose matrix confined within the target volume. Further study is required to ascertain the usefulness of this index. (auth) (Japan)

11059 INVESTIGATION OF IONIZING RADIATION EXPOSURE FROM CATHETERIZATION OF THE HEART. Kukacka, R. (Regional Hygienic Station, Ostrava, Czech.). Cas. Lek. Cesk.; 108: 1251-5(10 Oct 1969). (In Czech).

Ionizing radiation exposures to personnel engaged in radiography during the catheterization of heart were measured. The local doses measured by means of film dosimeters in various regions of the body of members of the working team are summarized in a table. The maximum doses (in hands) were 330 to 550 mR. An image amplifier with an amplification factor of 8000 coupled to closed-loop television should be used to provide a safe operation. (NSA of Czech)

11060 DOSIMETRIC STUDIES OF MANTLE FIELDS IN ^{60}Co THERAPY OF MALIGNANT LYMPHOMAS. Svahn-Tapper, Gudrun (Univ. of Lund, Sweden). Acta Radiol., Ther., Phys., Biol.; 9: 190-204(Jun 1970).

The dosimetry for mantle fields in the supradiaphragmatic treatment of malignant lymphomas with cobalt 60 γ was analysed. Isodose charts for the mantle field were constructed in sagittal and in different transverse planes. Studies of the agreement between planned and measured doses in a thorax phantom were performed both with and without beam flattening filters. (auth) (Sweden)

11061 TISSUE-AIR RATIO FORMULAE IN ^{60}Co TELETHERAPY DOSIMETRY. Melski, J. (John Hopkins Hospital, Baltimore). Brit. J. Radiol.; 43: 825-6(1970).

An input requirement for computer calculations of teletherapy dosimetry is the provision of tissue-air ratios and off axis ratios in the form of tables. It has to be decided whether to leave a table as it is, making linear interpolation between values, or to use an empirical formula. A simple expression is presented for

tissue-air ratios as a function of depth. The mean and standard deviations of the percentage differences between the published and formula-calculated tissue-air ratios for any given field size were less than 0.3 and 0.4 respectively. (UK)

11062 ESTIMATE OF THE DOSE OF IONOGENIC RADIATION ABSORBED BY AIRPORT PERSONNEL CARRYING OUT THE GROUND OPERATIONS CONNECTED WITH THE TRANSPORT OF PACKAGES CONTAINING RADIOACTIVE MATERIALS. Perini, A. (Ispettorato Medico Centrale del Lavoro, Rome); Susanna, A. Securitas; 54: 821-40(1969). (In Italian).

A study was made at the Forlanini Airport at Milan-Linate of the conditions under which various operations connected with the air transport of packages containing radioactive materials were carried out. The operations studied included embarkation and disembarkation, handling and storage, as well as acceptance and delivery of the packages, and particular attention was paid to the problems of protecting the personnel against radiation. The study indicated that the critical group of workers was the one concerned with handling the arriving packages in the store. At the actual level of traffic involving packages with radioactive contents, it was found that the dose absorbed was of the order of 350 mrem/annum. The study also arrived at an estimate of the radiation dose absorbed by the whole of the airport staff affected by the traffic between April 1967 and April 1968 and determined the frequency of such transports from both a quantitative and a qualitative point of view. (auth)

11063 RESULTS OF A STUDY OF COLOR TELEVISION SET ASSEMBLY AND REPAIR WORKERS X-RAY SAFETY. Savic, Stanley D. (Zenith Radio Corp., Chicago). Radiol. Health Data Rep.; 11: 519-25(Oct 1970).

A study was conducted to determine the degree of exposure of television set assemblers and repairmen to low levels of low energy x radiation. Two independent companies supplied the x-ray film badges on a biweekly basis. In addition, some television repairmen were also asked to wear thermoluminescent (TLD) ring badges so that the degree of hand exposure to x rays could be determined. In two large service shops, detailed records were also kept of the number and models of television receivers which were serviced. The largest total exposure recorded by film badges worn by any repairman during the one and a half year duration of the survey, was 34 mR. During that same time, no other badge showed any radiation, and therefore, we assume that this one was inadvertently exposed to heat or some other element. In a later survey, there were a few scattered hand exposure readings ranging from 10 to 70 mR for TLD rings which were continuously worn over a 3-month period. These readings are also suspected to be false, because they were not repeatable with the same individuals and because hundreds of other TLD rings registered no dosage. During the eight months duration of the factory assemblers' survey, over half a million color television receivers were produced by the 1,000 monitored employees. Not a single film badge worn in the factory assemblers' survey showed any radiation. We conclude that occupational x-radiation exposure of television repairmen and assemblers is virtually nonexistent. (auth)

11064 RECENT TENDENCY OF RADIATION UNIT. Moriuchi, Yasuyuki (Electrotechnical Lab., Tokyo). Oyo Butsuri; 39: 141-9(Feb 1970). (In Japanese).

Revisions were made in 1967 for the international radiation unit by ICRU. The ICRU congress was held in October, 1969, in Japan, and the revisions were reconfirmed. Based on the most recent information, the ICRU recommendation was discussed in this article. First, ionizing radiation was classified according to the particle involved. Then, various radiation units were classified into four groups. The first group was concerned with the ionizing radiation itself. The second group included those regarding the interaction of radiation with matters, for example, mass absorption coefficient, mass stopping power, etc. The third group was concerned with the effect of radiation on matter, and was divided into three categories. The fourth group was concerned with radioactivity, etc. Each group was described and discussed. The Japanese translation for each unit and term was shown. Several examples of the abuse of the units were described. (auth) (Japan)

11065 ESTIMATION OF EXPOSURE FROM ^{147}Pm-ACTIVATED SELF-LUMINOUS PAINTS. Iida, Hiroyoshi (National Inst. of Radiological Sciences, Chiba, Japan); Shiraishi, Yoshiyuki; Koshijima, Tokusaburo; (and others). J. Nucl. Sci. Technol. (Tokyo); 7: 588-91(Nov 1970).

The majority of radioactive self-luminous paints produced in Japan uses ^{147}Pm. The characteristics of the radiation from a ^{147}Pm-activated self-luminous paint layer sandwiched between polyvinyl chloride layers with Al backing with a luminous area of 12 × 8 cm^2 and having radioactivity of 12.5 mCi were examined. Bremsstrahlung was produced from the luminous area absorbing the 220 keV β-particles of ^{147}Pm. The energy of the bremsstrahlung was analyzed with use of both NaI scintillation and Ge solid state detectors: the spectrum obtained showed a peak at around 50 keV and also a small peak due to γ rays emitted from the ^{147}Pm at 121 keV. Measurements of the bremsstrahlung made with Lauritsen electroscope, film badges, fluoroglass dosimeters, and thermoluminescent dosimeters gave estimated exposure rates of at most only 0.5 and 0.3 mR/hr respectively at distances from the plate of 3 and 7 cm. (NSA of Japan)

11066 METHOD FOR SIMULTANEOUS ACTIVITY MEASUREMENTS OF ^{24}Na, ^{42}K, AND ^{82}Br IN LIQUID SAMPLES. Leistner, G. H.; Assheuer, J. (Medizinische Univ., Bonn). Nucl.-Med.; 32: Suppl. 7, 473-6(1968). (In German).

From 5th Conference of the Society of Nuclear Medicine, Vienna, Austria. See CONF-670996.

The liquid to be analyzed for ^{82}Br, ^{42}K, and ^{24}Na, 20 ml of urine, or at least 5 ml of plasma or saliva, was pipetted into a series of ion exchange columns consisting of an upper part filled with Amberlite IR 120 and a lower part filled with Amberlite IRA 400. After the columns were emptied, 20 ml of distilled water were applied twice to eliminate all radioactivity from the container vessel and connecting tubes and to wash out all anions from the upper parts of the column. In the Ir 120 column, the entire radioactivity of Na and K was retained and measured in a well counter; in the IRA 400 column, only ^{82}Br was retained. When doses of 120 μCi of ^{42}K, 100 μCi of ^{24}Na, or 10 μCi of ^{82}Br were administered, standard deviations were as follows: ^{24}Na 1.8%, ^{42}K 2.7%, and ^{82}Br 1.7%. The method eliminated time consuming purification procedures and permitted the handling of large numbers of samples. (H.B.G.)

11067 USE OF A TISSUE EQUIVALENT PHANTOM TO ESTIMATE RADIOACTIVE CONTAMINATION AND THE DOSE ABSORBED AT THE SITE OF CERTAIN ORGANS. Radioprotection; 5: 167-74(1970). (In French).

A study based chiefly on the use of an original tissue equivalent phantom of human body geometry, with an incorporated skeleton and removable organs, was undertaken. The detection possibilities of a system from the known content of a given radionuclide in a phantom organ were investigated. The influence of localization of the element on the count rate was studied and the geometry most suitable for diagnosis defined. The absorbed dose distribution in an organ contaminated uniformly or otherwise was determined. The mean dose delivered to the organ was estimated from physical measurements by calculation. The result was compared with that obtained by theoretical methods. (auth) (France)

11068 DETERMINATION OF ENVIRONMENTAL RADIOACTIVITY. Gil, Francisco Parra. Rev. Ecuator. Hig. Med. Trop.; 25: 31-60(Jan-Apr 1968). (In Spanish).

In Ecuador there are no nuclear reactors and no industrial use of radioisotopes, while their application in research and medicine is insignificant. In spite of this the environmental radioactivity of the country has increased steadily since the release of radioactive particles into the atmosphere by atomic explosions. Of special interest was the radioactivity in air and milk. Because of the damaging effects of radioactivity to human health the Ecuadorian Government has established a special Department of Radiobiology within the National Hygienic Institute Leopoldo Izquieto Pérez, a part of its National Health Service. The Department monitors environmental radioactivity in Ecuador and as such is part of the Panamerican Radiation Supervising Institute and works in cooperation with the OPS/PHS in Washington that issues regular reports on radiological health in the Americas. Also these studies have been made in collaboration with OPH/PHS. Of greatest importance are the β-activities of the atmosphere that were measured on air samples from various places in Ecuador by Geiger–Müller counters through comparison with a standard activity of 1.04 mCi ^{79}Se (the atomic weight, missing in the original text, was supplied by F.J.W.). A waiting time of 60 hours between sampling and measurement was observed to allow the disappearance of the natural radioactivity of Ra B that in this period passes through 10 half-lives. The β-activity of milk was measured by separating the more important radioactivity sources, namely ^{90}Sr and ^{140}Ba through a Dowex ion exchange resin. Comparative results of radioisotopes found in milk are given for Chile, Columbia, and Ecuador in tabular form showing the monthly mean values for these countries in 1967 for the radioisotopes ^{89}Sr, ^{90}Sr, ^{131}I, ^{137}Cs, and ^{140}Ba. The values are given in pCi/l milk. The greatest contamination of air and milk was found in October, November, and part of December with the peak in

XUM

October. The values for Ecuador are in good agreement with those for other countries in the Western part of South America. (F.J.W.)

11069 DOSIMETRIC REQUIREMENTS TO THE ACCURACY OF ROENTGENOMETRIC INVESTIGATIONS IN RADIUM THERAPY. Kuznetsov, E. A.; Sinitsyn, R. V.; Malevich, M. A.; Konnov, B. A. Med. Radiol.; 15: No. 4, 67-70(Apr 1970). (In Russian).

The accuracy of roentgenometric measurements was discussed and the values for error during dose determination due to displacement of the target were given. The calculations were made for electromagnetic radiation and heavy charged particles in the instance of shift of the target in the direction of the beam axis and in a perpendicular direction. (auth)

11070 RADIOLOGICAL PROTECTION CONDITIONS IN THE MANAGEMENT OF ^{60}Co TELETHERAPY EQUIPMENT "GRAVICERT." Peszynski, Jerzy; Patyra, Ryszard. Pol. Przegl. Radiol. Med. Nukl.; 34: 421-5(May-Jun 1970). (In Polish).

The dose recording was performed in the building accommodated for the teletherapeutic ^{60}Co equipment "Gravicert." The radiation measurement was performed in the working and protected positions of the source. Based on the results, the irradiation hazard (leakage and dispersed) to the staff was evaluated. (auth)

11071 DOSE FRACTIONATION IN RADIOTHERAPY: BIOLOGICAL BASES AND EQUIVALENCE NOMOGRAMS. Bagni, B.; De Bellis, N.; Biolcati, A. (Arcispedale Sant'Anna, Ferrara, Italy). Minerva Radiol.; 15: 68-76(Mar 1970). (In Italian).

After recalling recent findings in experimental radiobiology, the equivalence nomograms regarding fractionated doses are illustrated. Their current utility and limitations in radiotherapy are then discussed and stress laid on the mathematics that underlie them. It is held that the lack of correspondence between the theoretical model, based on simple survival of cell cultures, and experimental results, based on isoeffect curves, depends on the continuous variation in radioexistence induced during the cycle of fractionated treatment. (auth)

11072 DETERMINATION OF ABSORBED DOSES OF LONG-WAVE ROENTGEN RADIATION WITH THE AID OF TISSUE-EQUIVALENT PLASTIC SCINTILLATORS. Frolova, A. V.; Kolotilova, V. G.; Krongauz, A. N. (Moscow Research Inst. of Roentgen-Radiology). Med. Radiol.; 15: No. 4, 57-61(Apr 1970). (In Russian).

The problems of using tissue-equivalent scintillators for determining the absorbed energy and the distribution of absorbed doses of long-wave roentgen radiation are outlined. It is shown that the ratio between the value of absorbed energy and the technical efficiency of the scintillator is determined by a number of parameters. The values of these parameters for some radiation regimes used in radium therapy are given. (auth)

11073 POPULATION DOSE OF IRRADIATION OF THE POPULATION IN THE USSR DUE TO GLOBAL CESIUM. Ushakova, A. P.; Likhtarev, I. A.; Moiseev, A. A. Gig. Sanit.; No. 7, 54-9(Jul 1970). (In Russian).

The population doses of irradiation of all the population in the USSR from incorporated global ^{37}Cs was assessed. (auth)

Radiation Protection

11074 (AECL-3777) BIOLOGY AND HEALTH PHYSICS DIVISION PROGRESS REPORT, JULY 1-SEPTEMBER 30, 1970. (Atomic Energy of Canada Ltd., Chalk River (Ontario). Chalk River Nuclear Labs.). 56p. (PR-B-87). Dep. NTIS (U. S. Sales Only). AECL $1.50.

Studies on thermoluminescent dosimetry included development of personal dosimetry using lithium fluoride and advances in portable instruments for estimating radiation hazards. Studies on biochemistry and molecular biology included comparison of RNA molecules in animal cells by oligonucleotide analysis; preparation of lysis-sensitive yeast cells; use of a laser light scattering method for the study of ribosomal ribonucleic acid solutions; and radiation biochemistry of Escherichia coli. Genetics, development, and population studies were carried out on yeast (Schizosaccharomyces pombe) and insects (blackflies, mosquitoes, and Dahlbominus). Population research included studies on hereditary changes in irradiated rat populations and low dose genetic effects in fish embryos from irradiated sperm. Research on methods for the study of somatic and genetic harm in human populations included development of linked files of British Columbia vital and health records; studies of threshold diseases; collaboration with outside agencies; and methods for detecting long-term harm from working environments. The environmental research branch conducted studies on off-site monitroing for ^{137}Cs and ^{90}Sr; liquid effluent monitoring; uptake of ^{60}Co by edible plants; fate of radionuclides in aquatic communities; radioecological studies on Perch Lake; distribution of radium in surface water and aquatic organisms; and experimental studies on the effect of ^{226}Ra on fresh water organisms. The health physics branch conducted research on damage track measurements of doses from fission neutrons; intercomparison experiments on nuclear accident dosimetry systems; derivation of fast neutron kerma from Rh, In, and S activities; semiconductors detectors; irradiation jig for gamma meters; tritium monitoring; routine film exposure; and hand monitoring with thermoluminescence dosimeters. (H.L.W.)

11075 (NCRP-36) RADIATION PROTECTION IN VETERINARY MEDICINE. (National Council on Radiation Protection and Measurements, Washington, D. C.). 15 Aug 1970. 52p. NCRP $1.50.

A report is presented on the protection of personnel exposed to γ or x-ray equipment and sealed radioactive sources in the practice of veterinary medicine. The recommendations for maximum permissible dose equivalents (MPD) were developed by the National Council on Radiation Protection and Measurements and by the International Commission on Radiological Protection. Recommendations for radiation protection surveys of x-ray equipment and sealed sources of radiation are outlined. Recommendations are also outlined for shielding procedures, radiography with fixed diagnostic equipment, radiography with portable and mobile diagnostic equipment, fluoroscopic installations, x-ray therapy equipment, and use of sealed sources of radiation. Appendices are included for definitions, tables, and shipping regulations. (H.L.W.)

11076 RADIATION STANDARDS AND PUBLIC HEALTH. Eisenbud, Merril (New York Univ., N. Y.). Nucl. Safety; 12: 1-8(Jan-Feb 1971).

The radiation-safety record of the AEC has been good, but changes in the present regulatory system are needed to reconcile differences between public attitudes and the AEC. AEC regulations are based on the recommendations of the ICRP and the NCRP, and the standards contain extensive built-in conservatism. However, the emphasis on the maximum permissible concentrations of radionuclides in air and drinking water should be changed to specify the maximum permissible daily intake from all sources to take into consideration multiple sources and ecological factors. Further, the dual responsibility of the AEC for the development of nuclear power and the protection of the public has contributed to lack of public confidence in the AEC. Accordingly, it is recommended that responsibilities for setting radiation limits be shifted to another agency of the federal government. The same agency, in cooperation with the states, should assume responsibility for environmental monitoring in the vicinity of AEC-licensed facilities. (auth)

11077 CYTOKINETIC ANALYSIS OF SLOWLY PROLIFERATING BONE MARROW CELLS DURING RECOVERY FROM RADIATION INJURY. Haas, R. J.; Bohne, F.; Fliedner, T. M. (Univ., Ulm, Ger.). Cell Tissue Kinet.; 4: 31-45(Jan 1971).

A continuous administration of tritium-labeled thymidine (^{3}H-TdR) into pregnant rats results in a complete labeling of the offspring. Further injections with ^{3}H-TdR for 26 days maintained the 100% labeling. Four weeks after discontinuation of ^{3}H-TdR application, distinct classes of cytokinetically resting labeled bone marrow cells were detected. These animals received x irradiation of the body with 750 R with one leg shielded, or x irradiation of one leg with 750 R, or x irradiation of one leg with 1500 R. In none of the experiments did the reticular and endothelial cells show indications of destruction or stimulation. In all x-irradiated parts, the small bone marrow lymphocytes decreased their labeling intensity. The same behavior was seen in the marrow of the shielded leg. After 1500 R to one leg, a subsequent rise of mean grain count was detected after 3 days. No change of the labeling pattern of lymphocytes of other organs could be observed. The behavior of labeled bone marrow lymphocytes during recovery from radiation injury suggests that these cells play a role in the regenerative process of bone marrow. There may be a migration from shielded areas into x-irradiated parts if the dose is high enough to prevent efficient endogenous regeneration. (auth)

Safety Procedures

Refer also to abstract 11109.

11078 (Y-1754) X-RAY AND NUCLEAR RADIATION FACILITIES, PERSONNEL SAFETY FEATURES. Mason, W. J.; Pipes, E. W.; Rucker, T. R.; Smith, D. N.; West, C. W. (Union

Carbide Corp., Oak Ridge, Tenn. Y-12 Plant). 18 Dec 1970. Contract W-7405-eng-26. 71p. Dep. NTIS.

The development and implementation of these standards are described and the general philosophy and approach to these standards are outlined. The use of a matrix (type of installation versus radiation safety feature) to facilitate equipment classification and personnel safety feature requirements is presented. Included is a set of the standards showing formats, matrices, etc., and the detailed standards for each safety feature. (auth)

11079 DOSIMETRY IN NUCLEAR ACCIDENTS. Candes, P. (CEA, Saclay, France); Lamberieux, J. pp 25-56 of Nuclear Accident Dosimetry Systems. Vienna; International Atomic Energy Agency (1970). (In French).

From Panel on Nuclear Accident Dosimetry Systems, Vienna, Austria. See STI/PUB-241; CONF-690223.

Since, it appears in spite of all precautions and regulations, a criticality accident can still occur, French radiological safety experts have been concentrating their efforts on two main areas: limitation of the dose received when the accident occurs (criticality detection and alarm system), and evaluation of the dose received after the accident (dosimetric system). Since the use of inexpensive dosimetric units for a grid survey of the suspected areas results in a spectrometric system with only restricted possibilities, one must attempt to compensate this deficiency by endeavoring to ascertain whether the spectra obtained during accidents can be classed in a relatively narrow range of models. It should then be possible to accord greater accuracy to the formulae based on these detectors for calculating the doses. These are the basic ideas which have made necessary the studies which are now being carried out. Dosimetry experts from the main CEA centers have drafted a document having the form of recommendations covering all the problems connected with dosimetry and criticality after an accident. The document is annexed to the present paper. To enable them to carry out their various tasks, the experts are provided with suitable equipment to simulate full-scale accidents, in the liquid phase; the associated electronic equipment is also capable of providing all the relevant data (power rise, excursion dynamics, etc.). The over-all program of experiments is entitled CRAC (Radiological Consequences of a Criticality Accident). The research on zone dosimetry within the framework of this program aims at establishing laws for describing the field at a point in space, when the field is known at other points in the same space. The instruments and methods applied are presented together with comments on the first experimental results. To attain the objectives in view and to ensure that the results are in universally communicable form, i.e. amenable to exchange, comparison and assessment, the authors advocate employing investigators for the improvement of detection techniques, the study of irradiation fields in criticality installations, and studies on radiation metrology. Particularly in this latter connection, they advocate periodic intercomparison programs for suitable installations; in this connection, the Cadarache Centre has an irradiation station (STIRCA) with powerful sources capable of operation in free air. (auth)

11080 RADIATION ACCIDENT DOSIMETRY IN POLAND. Siwicki, R. (Inst. of Nuclear Research, Swierk, Poland). pp 57-60 of Nuclear Accident Dosimetry Systems. Vienna; International Atomic Energy Agency (1970).

From Panel on Nuclear Accident Dosimetry Systems, Vienna, Austria. See STI/PUB-241; CONF-690223.

In the only plant where a radiation accident can be regarded as possible, the criticality dosimetry is based on film-badge and individual activation detectors and simultaneous area measurements. In addition the organization and administrative units are prepared for an emergency. (auth)

11081 REVIEW OF EXPERIENCE AND RESEARCH ON NUCLEAR ACCIDENT DOSIMETRY IN JAPAN. Shibata, T. (Kyoto Univ.). pp 61-6 of Nuclear Accident Dosimetry Systems. Vienna; International Atomic Energy Agency (1970).

From Panel on Nuclear Accident Dosimetry Systems, Vienna, Austria. See STI/PUB-241; CONF-690223.

Some recent studies related to nuclear accident dosimetry systems in Japan are reviewed. In the Japan Atomic Energy Research Institute, research on film badges, glass dosimeters, and thermoluninescence dosimeters has been developed. At the Tokyo Atomic Industry Corporation, dose estimates for neutron irradiation of the human body have been studied by using activation techniques. In Kyoto University, at the Research Reactor Institute, foil activation methods for measuring neutron flux and spectrum in fast, epithermal, and thermal neutron energy regions have been established. At the Toshiba Electric Company, the glass dosimeter has been developed for wide-range γ radiation dosimetry. (auth)

11082 NUCLEAR ACCIDENT DOSIMETRY SYSTEM AT EUROCHEMIC. Hunzinger, W. (Eurochemic, Mol, Belg.). pp 67-73 of Nuclear Accident Dosimetry Systems. Vienna; International Atomic Energy Agency (1970).

From Panel on Nuclear Accident Dosimetry Systems, Vienna, Austria. See STI/PUB-241; CONF-690223.

The nuclear accident dosimetry system in use at the Eurochemic nuclear fuel reprocessing plant has been designed to enable the assessment of individual radiation doses from accidents delivering high γ doses and/or neutron doses from critical excursions. The neutron energies cover the entire range from thermal energies to a few MeV with various energy destructions depending on the moderation properties of the system that become critical and the shield properties interposed. The most important specifications imposed on the accident dosimetry system included: simplicity, light weight if to be worn by persons, and economy; rapidity in assessments (commonly used reading, measuring, or counting equipment should serve the accident dosimetry system); precision and accuracy. No special research work is carried out at Eurochemic in the field of accident dosimetry. As no satisfactory accident dosimeters that met the specifications sufficiently well were available on the market, it was decided to develop a system, which is described in detail. (auth)

11083 ACCIDENT DOSIMETRY IN YUGOSLAVIA. REVIEW OF WORK. Miric, I.; Miric, P. (Boris Kidric Inst. of Nuclear Sciences, Vinca, Yugoslavia). pp 75-7 of Nuclear Accident Dosimetry Systems. Vienna; International Atomic Energy Agency (1970).

From Panel on Nuclear Accident Dosimetry Systems, Vienna, Austria. See STI/PUB-241; CONF-690223.

Current planning with respect to dose estimation following a criticality accident is summarized. Rapid selection of exposed persons and a rough estimate of dose levels will be done by measuring activation of indium foils or by direct survey of body activity. The total neutron doses will be evaluated by using an activation foil system, while the evaluation of γ doses will be done with film dosimeters. (auth)

11084 REVIEW OF UNITED KINGDOM RESEARCH AND EXPERIENCE IN CRITICALITY DOSIMETRY. Adams, N. (United Kingdom Atomic Energy Authority, Harwell, Eng.). pp 79-101 of Nuclear Accident Dosimetry Systems. Vienna; International Atomic Energy Agency (1970).

From Panel on Nuclear Accident Dosimetry Systems, Vienna, Austria. See STI/PUB-241; CONF-690223.

The requirements to be met by a criticality dosimetry system are established; the research that has been done to develop and verify the system adopted in the United Kingdom is described in relation to a connected account of the physical measurements and interpretation which that system employs. Two recent examples of the application of the United Kingdom dosimetry system to simulated criticality accidents are described in some detail. (auth)

11085 CONTROLLING EMPLOYEE EXPOSURE TO ALPHA RADIATION IN UNDERGROUND URANIUM MINES. VOLUME I. Rock, R. L.; Walker, D. K. Washington, D. C.; Department of the Interior, Bureau of Mines (1970). 76p. GPO $0.40.

The Bureau of Mines presented a general discussion of the radon-daughter hazard associated with underground uranium mining and the control measures that were effective in eliminating this danger. The problem of employee exposure to radiation in underground uranium mines was reviewed, methods of determining atmospheric α radiation levels were discussed, and practical methods of reducing radon and radon-daughter influx into active mine openings were presented. Other pertinent subjects in radiation control were discussed, such as mine ventilation, mine planning, miner education, and individual exposure protection. (auth)

11086 PROVISION OF SOLAR FLARE RADIATION INFORMATION IN SUPPORT OF SUPERSONIC TRANSPORT OPERATIONS: A REVIEW OF DEVELOPMENTS. Buley, L. E. (International Civil Aviation Organisation, Montreal). pp 375-81 of Proceedings of XVII International Congress on Aviation and Space Medicine, Oslo, 1968. /Hannisdahl, Birger (ed.). Oslo; Universitetsforlaget (1968).

The fundamental difference between the radiobiological problems for SST operations posed by heavy-nuclei components of galactic cosmic radiation and by proton-/neutron flux associated with solar flares (SF) is stated. In the absence of information needed to evaluate the former problem, only the latter is dealt with. Expert evaluations of the SF radiation hazard to SST crew and passengers, potentialities of present technology on-board and

ground-based SF radiation prediction-monitoring-measuring-warning systems, and the state of the art in both areas are reviewed. The trend of competent international opinion towards a consensus favoring on-board equipment as the prime means of ensuring biological safety in SST operations is traced; at the same time the potential value of predictive information for flight planning by SST operators is recognized. The much-discussed problem of interference with SST R/T communications during SF activity is mentioned only to dismiss it. Although no ICAO operational requirement for SF radiation measuring-warning has been formulated at the time of writing, it is suggested, without seeking to prejudge the issue, that this may occur in the future. (auth) (Norway)

Legal Aspects

11087 (CONF-700408-3) STATES AND RADIATION CONTROL. Coleman, James R. (NUS Corp., Washington, D. C. Environmental Safeguards Div.). [1969]. 19p.

From 2nd Conference on Radiation and Man's Environment, Buck Hill Falls, Pa.

Northern States Power Company of Minnesota has initiated a court action to contest the jurisdiction of the State of Minnesota over nuclear power plants and the radioactive wastes discharged from them. This will be a landmark decision in the nuclear industry. The purpose of this paper was to consider the problems involved in the construction, use, and environmental hazards of nuclear plants and what steps other states have taken to control them. Only three states are presently without enabling legislation for radiation protection regulations. The main points raised by the Minnesota controversy are the right of the individual states to set standards for nuclear reactor discharges, the technical feasibility of reducing discharges, and the adequacy of AEC standards as applied to power reactors. A survey was taken to determine the reactions of other states to this controversy. On the basis of this survey, it was concluded that the issue is the right of states to set standards and not an issue of health, safety, or the adequacy of AEC standards and, if Minnesota is upheld, a profusion of standards, developed on slightly different bases, is a possibility. (E.E.H.)

11088 REVIEW OF INTERNATIONAL MICROWAVE EXPOSURE GUIDES. Swanson, Jon R.; Rose, Vernon E.; Powell, Charles H. (International Labour Office, Geneva. Public Health Service, Cincinnati). Amer. Ind. Hyg. Ass. J.; 31: 623-9(Sep-Oct 1970).

A review of microwave exposure criteria used in the United States and other western countries in the past ten yrs. indicates a general acceptance of a power density exposure level of 10mW/cm^2. The U.S.S.R. and Poland specify permissible levels lower by a factor of 1000 at 10 μW/cm^2, while Czechslovakia has proposed a sliding scale allowing 25 μW/cm^2 for an average working day exposure. The first U. S. standards considered only the power density level of microwave energy and did not consider other factors affecting biological response such as multifrequency exposures, time of exposure, frequency used, and environmental factors such as the heat load or cooling capacity of the workplace. The effects of severe heat stress or intense cold on the body's cooling capacity were noted in the latest U. S. standards, although the definitive recommendations for applying the concepts were not provided. Future standards should reflect environmental stress as well as other factors found to affect the biological response to microwave energy. (E.E.H.)

11089 RADIATION PROTECTION WHEN HANDLING CAPSULED RADIOISOTOPES IN NONDESTRUCTIVE TESTING. Kolb, K. Materialpruefung; 12: No. 5, 163-9(1970). (In German).

After a brief description of legal internal and general regulations that must be observed when working with encapsulated radioisotopes, the fundamental principles of all available types of gammagraphic devices are treated. Possible defects are specified with regard to the construction of the devices, and the way of their recognition and the conclusions to be drawn are pointed out. Finally regulations on behavior in the case of accidents and a possible classification of the accidents, with respect to the scale of danger, are discussed. (auth) (INIS)

11090 RADIOSENSITIVITY AND SPATIAL DISTRIBUTION OF DOSE. ICRP Publication 14. Oxford; Pergamon Press (1969). 118p.

The subject is discussed under the following main headings: basic considerations; current recommendations on non-uniform exposure; scheme for non-uniform exposure based on risk considerations; range of linearity of dose response; non-uniformity of dose within organs and tissues; additivity; expression of radiation damage; radiosensitivities of different organs and tissues in man; relative sensitivity to different kinds of biological damage by radiation and the overall assessment of radiation damage; revision of currently recommended dose limits; and summary and general conclusions. Appendices cover: radiation cataract in man; radiation and human fertility; relative sensitivity of different tissues to tumor induction by radiation—the human evidence; derivation of numerical values for dose limits—example for discussion; and further helpful information. (UK)

Medicine

11091 RADIATSIONNAYA MEDITSINA (POSOBNE DLYA VRACHEI I STUDENTOV). IZDANIE CHETVERTOE, PERERABOTANNOE I DOPOLNENNOE. (Radiation in Medicine. (Reference Book for Doctors and Students). The Fourth Improved and Expanded Edition). Burnazyan, A. I. (ed.). Moscow; Atomizdat (1968). 388p.

The book is intended for use as a textbook in medical schools and a reference work for physicians specializing in radiobiology. It covers the physical principles of ionizing radiations, their biological action, the pathophysiology of radiation injury and the bases of radiation protection and therapy. Sections of the book are devoted to immunological problems of radiation sickness and the toxicology of radioactive isotopes. The present fourth edition has been revised; the chapter on dosimetry covers also radiation from atomic explosions and the methods used for the detection of neutron radiation on the basis of induced activity. Recent data on the metabolism of radioactive materials and their excretion are also included. The chapter on the immunity of irradiated animals includes a section on chemical radioprotection techniques and therapy of exposed humans, including bone marrow transplants. (TTT)

Protective Substances

Refer also to abstracts 10960, 10962, 11239, 11240, 11243, 11252, 11258, 11288, 11304, and 11323.

11092 (BNL-50203, pp 41-53) RECOVERY FROM RADIATION DAMAGE IN MAMMALIAN CELLS. Whitmore, G. F.; Gulyas, S.; Kotalik, J. (Ontario Cancer Inst., Toronto).

From Conference on time and dose relationships in radiation biology as applied to radiotherapy held at Carmel, California, September 15–18, 1969.

A review is presented of studies on potentially lethal lesions, whose potential for killing the cell could be altered by the physiological condition of the cell before and after irradiation. Experiments are described on the effects of temperature changes on survival of irradiated L cells. The role of RNA synthesis in determining lethality in the cell was studied using the inhibitor, methotrexate. By combining low temperature experiments with methotrexate effects, it was found that potentially lethal lesions are responsible for the rapid increase in radiosensitivity, once RNA synthesis has recommenced. It was confirmed that there is a class of lesions having a variable probability of becoming lethal, the lethality being in some way connected to the metabolic activity of the cell and especially to the rate of RNA synthesis. Properties of potentially lethal lesions are compared with those of sublethal lesions. (H.L.W.)

11093 (BNL-50203, pp 97-116) DEPENDENCE OF RADIOSENSITIVITY UPON CELL AGE. Sinclair, Warren K. (Argonne National Lab., Ill.).

From Conference on time and dose relationships in radiation biology as applied to radiotherapy held at Carmel, California, September 15–18, 1969.

A review is presented of studies on responses to ionizing radiation of mammalian cells depending upon their age or position within the generation cycle. Chinese hamster cells were most sensitive to x radiation in mitosis, while the survival rate increased after DNA synthesis (S period) rose to a peak near the end of S. Graphs are presented to show single-cell survival for various stages of the cell cycle. The relationship between variations in cell sensitivity to age and other factors known to modify radiation response is examined with regard to linear energy transfer, dose fractionation, oxygen, radioprotective agents, radiosensitizers, and inhibitors of macromolecular synthesis. The significance for radiotherapy of the dependence of radiosensitivity upon cell age is discussed and the potential usefulness of the combined effects of hydroxyurea and x rays is examined. (H.L.W.)

11094 (BNL-50203, pp 215-33) EFFECT OF pO_2 ON CELL PROLIFERATION KINETICS. Tannock, Ian F. (Anderson (M.D.) Hospital and Tumor Inst., Houston, Tex.).

From Conference on time and dose relationships in radiation biology as applied to radiotherapy held at Carmel, California, September 15-18, 1969.

Thymidine-labeling results are presented for two mouse mammary tumors. Each was grossly necrotic and had cords of viable tissue separating blood vessels and connective tissue from the necrosis. Radii of the tumor cords approximated oxygen diffusion distances. Special staining techniques were used to recognize endothelial cells in a tumor grown in C3H mice, and their turnover time was estimated in a repeated labeling experiment to be 53 hr. Proliferation of carcinoma cells in the same tumor was investigated by the labeled-mitoses and repeated-labeling techniques; the median cell cycle time was 13 hr, and the growth fraction was 50%. The same techniques were used to study cell proliferation in different regions of the cords of a tumor grown in Strong A mice. Labeling and mitotic indices decreased with distance from a blood vessel, and cells migrated centrifugally toward the necrosis. The median cell cycle time was relatively constant in all regions of the cords. The labeling index and cord radius were reduced in animals breathing 10% oxygen, and tumors grew more slowly; the median cell cycle time did not increase. These results suggest that the tissue oxygen tension might influence cell proliferation through the growth fraction and that anoxia might be a cause of cell death at the cord periphery. The C3H tumor was studied at intervals after being irradiated with 600 rads. The labeling index and cord radius were reduced between 6 and 24 hr but returned to control values by 48 hr. Most of the radiation-killed cells were in well-oxygenated regions near blood vessels, while cells near the necrosis remained intact. The reduction in cord radius suggests that the oxygenation of these surviving cells might improve shortly after irradiation. (auth)

11095 (BNL-50203, pp 308-17) CELL KILLING AT VERY LOW DOSE RATES. Hall, Eric J. (Columbia Univ., New York. Coll. of Physicians and Surgeons).

From Conference on time and dose relationships in radiation biology as applied to radiotherapy held at Carmel, California, September 15-18, 1969.

A review is presented of cell killing or reproductive death and various factors influencing the cell survival curve. Figures are presented to show dose response curves for mouse leukemia and other types of cells. It was predicted that the cell survival curve for low dose rates would be less steep than that for acute exposures. Examination of the survival curve for 30 rad/hr showed that the data were more closely fitted by a two-phase line or a continuously bending curve than by the simple exponential function. Experiments with synchronously dividing cells show the important influence of cell age on cell sensitivity. Experiments using lymphoma cells and Vicia faba cells showed that the accumulated dose per cell cycle was a more appropriate parameter for determining cell lethality than the dose per unit time. The oxygen enhancement ratio was measured for acute and protracted exposures of Vicia faba seedlings to neutrons and γ rays, and results are shown by means of graphs. Implications of radiobiological factors in the success of radium implant techniques are discussed, and the replacement of radium by ^{252}Cf for low dose interstitial and intracavitary techniques is considered. (H.L.W.)

11096 (EUR-4491) STUDY OF THE EFFECT OF RADIATIONS ON THE EMBRYO AND ITS ORGANS IN VIVO AND IN VITRO. Final Activity Report Concerning Researches Effectuated From 1 October 1964-31 December 1968. (College de France, Nogent-sur-Marne. Laboratoire d'Embroyologie Experimentale). 11 Feb 1969. 10p. (In French). Dep. CFSTI (U. S. Sales Only). EUR FF 2.80.

The respiration of x-irradiated organs was studied by two methods: the consumption of oxygen and the enzymatic activity of lactic dehydrogenase. Both methods show that at doses below 8000 to 10,000 R, the respiration of the organ decreases immediately followed by a more or less complete or partial recovery. The radioprotective power of cysteamine on the lactic dehydrogenase activity is considerable whether the enzyme is exposed to the radiation in place of the cells or in solution. A radioprotective action was also observed at the level of the ultrastructure of the cells. Nicotinamide adenine dinucleotide acts as a coenzyme, especially in the respiration cycle. Cysteamine also has a radioprotective power on the metabolism of the nucleic acids. In morphogenesis and organogenesis studies under x irradiation, differences observed in the sensitivity of the mesoderm and the ectoderm member rudiments give an explanation of the genesis of the malformations obtained after action of nitrited yperite. In cancerous tissues the incorporation of thymidine is not modified by doses up to 15,000 R. Other observation confirmed the very great sensitivity of the mitosis to x rays in cancerous tissues in culture although the metabolic differences remain almost insensitive to radiation in the first two days after irradiation. (J.S.R.)

11097 ACTINOMYCIN D AND RADIATION FRACTIONATION STUDIES IN ASYNCHRONOUS AND SYNCHRONIZED CHINESE HAMSTER CELLS. Elkind, M. M.; Kano, E. (Brookhaven National Lab., Upton, N. Y.). Radiat. Res.; 44: 484-97(Nov 1970).

Using Chinese hamster cells grown, treated, and assayed in culture, we have examined the fractionation response relative to cell killing of two 30 min exposures of actinomycin D, or a single exposure to this drug followed by a dose of x rays. Asynchronous cells and cells synchronized by hydroxyurea treatment were used. We found that while an increase in 2-dose survival in 2 hrs is observed with two actinomycin D exposures, this was very likely not due to repair of sublethal damage. It appeared, rather, that cell progression in the growth cycle to more resistant ages was probably responsible for the fractionation survival increase. Fractionation experiments in which a first dose of actinomycin D was followed at varying intervals by an x ray dose supported this interpretation since we found that the drug damage able to interact with radiation damage persisted in time. In contrast to the situation when radiation is administered first, the DNA binding ability of actinomycin D probably accounts for the persistence of drug damage and the lack of significant sublethal damage repair during periods long enough for appreciable x ray damage repair. (auth)

11098 EFFECT OF GLUTATHIONE ON THE PROTECTION AGAINST RADIATION. Kawasaki, Shoji; Sakurai, Ko; Nakada, Taishi; Nishimura, Sanae; Okita, Isao (Yamaguchi Univ., Ube, Japan). Shinyaku To Rinsho; 19: No. 1, 119-22(Jan 1970). (In Japanese).

The radioprotective effects of reduced glutathione were studied. Mice of the dd strain were given intraperitoneal injections of glutathione before x irradiation with 500 R. The glutathione-treated mice survived for 16.7 days in comparison with 9.1 days for the controls. Injection of 30 mg. of reduced glutathione 30 min to 3 hr before irradiation was effective. The protective result was assumed to result from the reaction of the SH group to form an -SS- group. Glutathione increased the mitotic index of Ehrlich's ascites carcinoma, repressed the lowering of the index induced by radiation, and then accelerated the recovery of the index. (Japan) (TSS)

11099 PECULIARITIES OF THE FORMATION OF ENDOGENOUS COLONIES OF HEMATOGENIC TISSUE IN THE SPLEENS OF IRRADIATED INBRED ($CC_{57}W$) AND NONINBRED MICE UNDER CONDITIONS OF THE USE OF RADIOPROTECTORS AND THE SIGNIFICANCE OF THE DOSE OF THE LATTER. Zherebchenko, P. G.; Zaitseva, K. K.; Zaitseva, T. G. (Military Medical Academy, Leningrad). Radiobiologiya; 10: 522-6(Jul-Aug 1970). (In Russian).

It was established that 5-methoxytryptamine (mexamine) was three times as effective with respect to the number of endogenous colonies of hematogenic tissue formed in the spleen when it was administered to noninbred mice in comparison with inbred mice ($CC_{57}W$), whereas the effectiveness of cystaphos was the same in both cases. The differences in the effectiveness of mexamine were explained by its more pronounced vaso-constrictive action in noninbred mice than in inbred mice. Increasing the dose of mexamine above 0.1 mmole/kg, and that of cystaphos above 2 mmoles/kg was not accompanied by any further increase in the protective effect; however, it was achieved by the combined administration of these substances. (tr-auth)

11100 OXIDATIVE PHOSPHORYLATION IN THE SPLEEN MITOCHONDRIA IN THE TREATMENT OF ACUTE RADIATION SICKNESS WITH BONE MARROW TRANSPLANTS. Malovichko, I. I.; Shampai, A. E. (Kiev Medical Inst.). Radiobiologiya; 10: 590-2(Jul-Aug 1970). (In Russian).

The influence of homotransplantation of bone marrow on the processes of oxidative phosphorylation of mitochondria isolated from the spleen of rats irradiated at doses of 800 to 850 R was studied. The experiments were conducted on the 8, 13, 20, and 30th days after irradiation. At all the investigated periods, the injection of a suspension of bone marrow cells into irradiated animals prevented the disturbance of respiration and oxidative phosphorylation in the spleen mitochondria. The possible biological role of metabolites of transplanted bone marrow was discussed. (tr-auth)

11101 IDENTIFICATION OF NONPROTEIN THIOL COMPOUNDS IN TISSUES AFTER THE ADMINISTRATION OF CYSTAMINE. Titov, A. V.; Golubentsev, D. A.; Mordukhovich, V. V.

(Military Medical Academy, Leningrad). Radiobiologiya; 10: 606-8(Jul-Aug 1970). (In Russian).

The nature of the nonprotein thiol compounds in the tissues of the spleen, small intestine, kidneys, and bone marrow of mice was studied after intraperitoneal injection of cystamine in the optimum radioprotective dose. Three methods were used to determine the protector: chromatographic, according to the increase in thiols, and according to the values of the radioactivity of labeled sulfur. Using the chromatographic method, it was established that in the period of manifestation of the radioprotective effect, the increase in nonprotein thiols in the tissues was due chiefly to the reduction product of cystamine-β-mercaptoethylamine (MEA). During this period, from 72 to 90% of the labeled sulfur in the tissues was contained in MEA. (tr-auth)

11102 PROTECTIVE EFFECTS OF BIOGENIC AMINES IN THE RADIATION INTESTINAL SYNDROME. Ovakimov, V. G.; Airapetyan, G. M.; Ivanov, V. N.; (and others) (Inst. of Labor Hygiene and Occupational Diseases, Moscow). Radiobiologiya; 10: 561-5(Jul-Aug 1970). (In Russian).

In experiments on mice and rats subjected to a single total γ irradiation at a dose rate of 710 R/min, a pronounced protective effect of 5-methoxytryptamine, serotonin, adrenalin, histamine, and acetylcholine was detected at doses of irradiation inducing predominant death of the animals from the intestinal syndrome. The mechanisms of the pharmacological radioprotection were discussed from the standpoint of the temporary and differently directed peculiarities of the vascular responses of individual organs to the introduction of the same chemical agent. (tr-auth)

11103 CALCIUM ALGINATE AS THE PROTECTIVE AGENT IN THE CASE OF CHRONIC INTAKE OF RADIOISOTOPES OF STRONTIUM WITH THE DIET. Malkin, P. M.; Dolmatova, M. Yu.; Dubrovina, Z. V.; Frolova, E. I. (Inst. of Biophysics, Moscow). Radiobiologiya; 10: 565-9(Jul-Aug 1970). (In Russian).

Preparations that selectively bind radioactive strontium in the gastrointestinal tract and do not affect the assimilation of calcium were essential for the protection of the organism in the case of long-term intake of radioisotopes of strontium with the diet. The acid calcium salt of alginic acid (calcium alginate) was investigated as such a preparation. It was shown that in the case of prolonged intake of the preparation, for a period of 98 days, its protective effect remained constant. Prolonged administration of the preparation did not disturb the calcium balance in the organism and had no effect on the vital activity of the animals. (tr-auth)

11104 INHIBITION OF ESTROGEN-INDUCED RADIOPROTECTION OF PLACENTAL NUCLEIC ACIDS AND PROTEINS BY THE ANTIESTROGEN CLOMIPHENE. Mitznegg, Peter; Saebel, Manfred; Heim, Fritz (Univ., Erlangen, Ger.). Life Sci., Part II; 9: 815-20(22 Jul 1970).

The 500 rad whole-body ^{60}Co γ irradiation of pregnant rats on the 20th day of gestation as well as the treatment of the animals with 0.5 mg Clomiphene per kg per day between the 18th and 21st day, measured on the 22nd day of pregnancy, was ineffective on placental weight and its contents of DNA, RNA, and proteins. The combination of both treatments led to a significant decrease in placental weight and its contents of DNA, RNA, and proteins. Clomiphene, a 1(p-β-diethylaminoethoxy-phenyl)-2.2-diphenyl-2-chloro-ethylen-citrate, in the presence of estrogen showed antiestrogenic effects by blocking estrogen-specific receptors. These experiments provided evidence that endogenous estrogens were radioprotective during pregnancy, when the content of endogenous estrogen was increased 300 to 500 times. Because of functional relations to the nucleo-proteins, estrogens may decrease the effect of radioinduced radicals on the DNA. (auth)

11105 HEMORRHAGIC SYNDROME IN RADIATION SICKNESS. II. EXPERIMENTAL STUDY OF THE RADIOPROTECTIVE EFFECT OF CYSTAMINE AND TREATMENT WITH NUCLEIC ACIDS OF HOMOLOGOUS BONE MARROW ON COAGULATION AND FIBRINOLYSIS IN RATS EXPOSED TO LETHAL X-RAY DOSES. Cuteudache, Caliopi; Boldescu, Gabriela; Popa, Rodica; (and others). Fiziol. Norm. Patol. (Bucharest); 16: 169-77(Mar-Apr 1970). (In Hungarian).

The protective effects of cystamine and nucleic acids from homologous bone marrow on coagulation and fibrinolysis was determined in rats exposed to lethal doses of x radiation (700 R). Results obtained 2, 5, 10, and 15 days after irradiation showed that oral administration of cystamine had a favorable effect on blood coagulation. Differential coagulation tests showed that cystamine protected proaccelerin and stimulated thrombocytic recovery in the irradiated animal and did not inhibit prothrobin. The decrease of antithrobin III and the possible mechanism of cystamine action on blood coagulation in vivo are discussed. Homologous marrow nucleic acids, at the molecular weight and dose administered, did not confer satisfactory protection against lethal doses of x radiation. (E.E.H.)

11106 CHANGES IN LETHAL EFFECT OF IRRADIATION OF CELLS CULTIVATED OUTSIDE OF ORGANISM DUE TO CHEMICAL COMPOUNDS. Gotlib, V. Ya.; Pelevina, I. I.; Afanas'ev, G. G.; Lipchina, L. P. (Inst. of Chemical Physics, Moscow). Dokl. Akad. Nauk SSSR; 192: 1367-70(21 Jun 1970). (In Russian).

Treatment by certain chemical compounds may enhance or decrease the reaction of cells to ionizing radiation. This problem was examined by investigating changes in the radiosensitivity of cells in cell cultures treated with a radical-reaction inhibitor. Cells of the LL line, obtained in the MKLy lympholeukosis of mice, were used in the experiments, carried out with monodispersed cells exposed to γ radiation doses ranging from 100 to 700 R within 18 hr after inoculation. The effect of the irradiation was modified by adding propylester of gallic acid to the cells before exposure at the ratio of 2.0×10^{-4} M. The colonies formed after 10 days of incubation were dyed with toluidine blue. Study of the survival rate and of the non-lethal effects indicated that the time of contact of the compound affects the lethal action: D_0, the dose required to reduce survival rate by a factor of e, $-1/2.72 = 0.37$, ranged from 120 rad in a single exposure to 74 and 223 rad. Injuries are accumulated before the lethal effect becomes observable. (TTT)

11107 INFLUENCE OF SIN-ESTROL DOSE ON THE DEVELOPMENT OF CHANGES IN IRRADIATED OVARIES. Gubareva, A. V. Vop. Onkol.; 16: No. 2, 85-6(1970). (In Russian).

The influence of various doses of sin-estrol (diethylstilbestrol) on the development of ovaries was studied using 1609 mature mice irradiated with 200 R of ^{60}Co γ rays and injected with 0.62, 0.25, or 0.062 mg of the hormone. The weekly injections of 0.062 mg doses into irradiated mice inhibited the development of hyperplastic processes in the sterilized ovaries. The latent period of tumor formation was extended. (R.V.J.)

11108 STUDIES OF RADIOPROTECTIVE ACTION OF POLYMER SALT OF CYSTAMINE AND SULPHOPROPYL ESTER OF DEXTRANE. Trushina, M. N.; Khomyakov, K. P.; Virnik, A. D.; Rogovin, Z. A.; Rogozkin, V. D. (Moscow Inst. of Biophysics). Vop. Med. Khim.; 16: 195-8(Mar-Apr 1970). (In Russian).

The radioprotective effects of a salt-like adduct of cystamine to a sulfopropyl ester of dextran were studied. Addition of cystamine to the polymer leads to an increase in the radioprotective effect of cystamine at small doses injected 10 to 15 min before irradiation. The cystamine and dextran complex is characterized by a prolonged period of action as compared to cystamine dihydrochloride. This allows for administration of the polymer 1 hr before irradiation instead of 15 min as for cystamine dihydrochloride. (auth)

Radiation Sickness and Injuries

Refer also to abstract 11077.

11109 FIRST AID MEASURES IN RADIATION ACCIDENTS, ESPECIALLY ON RADIOACTIVELY CONTAMINATED WOUNDS. Ohlenschlaeger, L. (Kernforschungszentrum, Karlsruhe, Ger.). Atompraxis; 16: 236-41(Jul-Aug 1970). (In German).

First aid measures to be taken in radiation accidents that may occur in nuclear facilities and in the fabrication and reprocessing of nuclear fuel elements were discussed. For quick and effective first aid, the medical measures were subdivided into three steps: first aid by trained laymen on the spot of the accident, first medical care at the casualty ward, further treatment of severely and very severely injured persons with the help of an expert team in suitable central surgeries. The establishment of regional and supra-regional central consulting and therapeutic agencies was discussed. (auth)

11110 EFFECTS OF KALLIKREINE ON THE IRRADIATED SKIN OF SWINE (LARGE WHITE). Goffin, J. C.; Ledoux-Corbusier, M. (Univ., Brussels). J. Belge Radiol.; 53: 300-10(Jul-Aug 1970). (In French).

The effects of callicrein were studied in normal skin and radioinduced, cicatrized, chronic dermatitis in pigs. It was believed that the pharmacodynamic action of callicrein consisted of a vasodialating action and stimulation of the synthesis of mucopolysaccharides in the collageneous tissue. Observations showed that callicrein has a vasodialating action only on normal skin. Cicatrized radiolesions treated with callicrein, as com-

pared with untreated radiolesions, showed better irrigation and thicker scar tissue consisting of capillaries, newly formed collageneous fibers, and an increased number of fibrocytes producing polysaccharides. (E.E.H.)

Radiodiagnosis

Refer also to abstracts 10810, 10828, 10910–10912, 10918, 10926, 10928, 11275, and 11300.

11111 CLINICAL VALUE OF LIVER FUNCTION APPRAISAL BY MEANS OF ^{131}I-ROSE BENGAL. II. COMPARISON OF THE RESULTS OF ^{131}I-ROSE BENGAL TEST WITH OTHER BIOCHEMICAL TESTS. Dobrzanski, Z.; Toth, Z. (Postgraduate Medical Training Inst., Warsaw). Pol. Med. J.; 9: 595-8(1970).

Experiments were conducted to determine the value of the ^{131}I-rose bengal test for the assessment of the degree of liver parenchymal damage in comparison with other hepatic function tests. The ^{131}I-rose bengal test was found to be the most sensitive and universal test of the liver parenchymal function. In order of decreasing sensitivity, the results of the compared tests were: ^{131}I-rose bengal- half-time excretion by the liver, ^{131}I-rose bengal— half-time of blood clearance, bilirubin level, γ-globulin level, albumin level, thymol test, cadmium test, and alanine aminotransferase activity. (E.E.H.)

11112 LONG-TERM EFFECTS OF LOCAL IRRADIATION OF THE MARROW ON ERYTHRON AND RED CELL FUNCTION. Nelp, Wil B.; Gohil, Mahendra N.; Larson, Steven M.; Bower, Rae Ellen (Univ. of Washington, Seattle). Blood; 36: 617-22 (Nov 1970).

Changes in erythron and reticulo-endothelial (RE) cell function were examined in the marrow of the rabbit after 250 to 5000 R of localized irradiation by comparing the amount of ^{59}Fe and ^{99m}Tc sulfur colloid concentrated in the irradiated tibiofibula to that in the unirradiated control. At all levels of irradiation, there was immediate and severe loss of erythron function while RE cell activity remained nearly intact. Erythron function showed prompt partial recovery to a maximum level at approximately 8 days but with doses greater than 1000 R there was a secondary decline to 20% of normal during the next 8 wks. After 15 days, RE cell function had decreased to the same level as the erythron and subsequently fell in parallel with it. After 15 mo, the marrow showed a secondary recovery of both RE cell and erythron function to 50 and 66% of normal. The results of these experiments suggest that radiocolloid photoscans of the marrow showing decreased or absent RE cell activity will reflect a similar degree of erythropoietic damage if the studies are obtained wks or mos following radiation therapy. (auth)

11113 CHROMOSOME ABNORMALITIES OBSERVED IN CHILDREN RECEIVING ROENTGENOSCOPE. Komiya, Hisako (Tokyo Univ.). Nippon Shonika Gakkai Zasshi; 73: 2027-31 (Dec 1969). (In Japanese).

Irradiation for diagnostic purposes is in a low dose, but there have been many cases of abnormality in peripheral lymphocytes. Chromosome analysis was carried out on seven cytogenetically normal children 4 to 15 yrs of age, following cardiac catheter examination. For this test, 5 ml of venous blood was collected before, directly after, and 24 hr after x irradiation and leucocyte cultures were made for 50 hr. The number of cells examined was 437 before irradiation, 597 immediately after, and 254 after 24 hr. The cells were classified into three groups. Group A cells were those without structural abnormality. They could be divided into modal and non-modal cells. Group B cells were those cells that showed chromatid gap, chromatid break, or isochromatid gap. Group C cells were those that showed other structural abnormalities, divided into unstable C_u and stable C_s abnormalities. Frequency of the appearance of non-modal A cells to the total number of cells examined was 7.3% before irradiation, 4.8% immediately after, and 4.3% 24 hr after irradiation. Frequency of B cells was 1.8% before, 0.8% immediately after, and 1.1% 24 hr after irradiation. Frequency of C_u cells was 9.4% before, 1.3% immediately after, and 0% 24 hr after irradiation. There was no statistically significant difference in B and C group cells. Only one C_s cell was observed before irradiation and none appeared after irradiation. (Japan)

11114 DETERMINING BODY COMPOSITIONS BY RADIATION ABSORPTION SPECTROMETRY. Mazess, R. B.; Cameron, J. R.; Sorenson, J. A. (Univ. of Wisconsin, Madison). Nature (London); 228: 771-2(21 Nov 1970).

The fractional composition of a multi-component absorber can be determined from the attenuation of γ-radiation at various energies, and it was shown that absorption measurements at two energies can accurately indicate the relative lean-fat composition of soft tissue. A scanning method was developed for determining fat, lean, cellular and bone mineral mass in vivo. Sources used were ^{241}Am (59.6 keV) and tin-filtered ^{125}I (27.4 keV), together with a conventional detector and single channel analyser. Instead of solving simultaneous equations for each set of observations the ratio (R) of ^{125}I absorbance to ^{241}Am absorbance was used as a direct index by establishing a calibration curve relating R to composition. Since absorption coefficients of fat and lean are nearly equal with ^{241}Am γ-rays, the relationship between the ratio and relative composition of a mixture is linear. The accuracy of this new method was high; in soft tissue phantoms the standard error was <0.02; and for seven meat samples was 0.03, whilst the measured values of R in the mixtures tested corresponded closely to values derived from published absorption coefficients. In measurements of tissue composition in vivo at single points on human limbs reproducibility was high, but composition changed with small position changes. In order to eliminate this problem a scanning method was developed, which permitted measurements of the mass of the components as well as their proportions, including bone mineral. The dose from such scans was about 10mR and confined to a narrow area across the limb. The measurements were highly correlated with some indirect measure of composition. (UK)

11115 RADIONUCLIDE SCANNING IN RENAL SPACE-OCCUPYING LESIONS. Dugdale, L. M. (Alfred Hospital, Melbourne). Australas. Radiol.; 14: 281-5(Aug 1970).

The development of radioisotope methods for detecting kidney lesions is reviewed. Scanning is considered to be complementary to other radiological investigations. (Australia)

11116 GAMMA DENSITOMETRY IN THE STUDY OF VENTILATION AND THE PULMONARY CIRCULATION. Cattrell, V. G.; Franklin, D. H.; Kirkpatrick, A. E. (Royal Infirmary, Edinburgh). Clin. Radiol.; 21: 396-402(Oct 1970).

A new method for fluorodensitometry of the lungs is briefly described. The method differs from conventional techniques by employing a small source of γ radiation (^{137}Cs) in place of x rays. Ventilatory and circulatory studies in normal subjects, and circulatory studies in a case of pulmonary embolism, are presented. (auth)

11117 IDENTIFICATION OF CASES OF ACQUIRED FUNCTIONAL ASPLENIA. Spencer, Richard P.; Pearson, Howard A.; Binder, Henry J. (Yale Univ., New Haven). J. Nucl. Med.; 11: 763-6(Dec 1970).

Functional asplenia, defined as the presence of the spleen (by palpation or by radiographic evidence) that fails to accumulate standardized ^{99m}Tc-sulfur colloid was identified in three individuals with diseases other than sickle cell anemia. A case of acquired functional asplenia was found in a woman 24 years after the injection of Thorotrast. A second case was noted in a child who had surgical transposition of the spleen. A third case was found in a woman with rapidly progressing reticulum cell sarcoma receiving antineoplastic agents and radiation therapy. Criteria in attempting to identify such individuals on the basis of hematologic findings or past history were discussed. Recording of counts over the liver and spleen, from anterior and posterior views, should be a routine part of liver and spleen scans to identify these patients. Although it has been reported that hematologic evidence of hyposplenia can occur in celiac-sprue disease, six cases of this disorder (in remission) all had normal splenic uptake of the radiocolloid. It may also be of value for patients with celiac-sprue to have spleen scans made during remission and exacerbation of the disease to determine whether accumulation of the radiocolloid changes as the disease waxes and wanes. (auth)

11118 RADIONUCLIDES IN CIRCULATION RESEARCH AND CIRCULATION DIAGNOSIS. Fifth Conference of the Society of Nuclear Medicine, Vienna, Austria, September 21–23, 1967. Hoffmann, G.; Hoefer, R. Nucl.-Med.; 32: Suppl. 7, 1-560(1968). (In several languages). (CONF-670996).

Separate abstracts were prepared for 79 of the 86 papers appearing in this conference. The other papers discuss radiocardiography, ^{131}I therapy of the endolymphatics, and malignant complications in Cushing's Syndrome. (E.R.B.)

For abstracts of individual papers see: 10911–10920, 10943–10945, 11046, 11066, 11119–11180, 11230, and 11275.

11119 QUANTITATIVE RADIOCARDIOGRAPHIC STUDIES WITH A SCINTILLATION CAMERA. Adam, W. E.; Lorenz, W. J.; Scheer, K. E. (Univ., Ulm, Ger. Deutsche Krebsforschungszentrums, Heidelberg). Nucl.-Med.; 32: Suppl. 7, 17-22(1968). (In German).

From 5th Conference of the Society of Nuclear Medicine, Vienna, Austria. See CONF-670996.

Three mCi of ^{99m}Tc were injected into models of the heart and into patients. The activity was measured with an Anger camera. The information was stored in analog form on magnetic tape. Through an analog-digital converter, data were fed into a computer. Computer programming allowed separation of activity values for all four chambers of the heart. Improvement of the method should allow scintigraphic representation of the various phases of cardiac action. (H.B.G.)

11120 VISUALIZATION BY IMAGE INTENSIFIER OF RADIOACTIVE INDICATOR FLOW THROUGH THE CARDIAC CHAMBERS AND THE LARGE VESSELS. Kellershohn, C. (Service Hospitalier Frederic Joliot, Orsay, France); de Vernejoul, P.; Lansiart, A.; Roux, G.; Lequais, J. Nucl.-Med.; 32: Suppl. 7, 23-9(1968). (In French).

From 5th Conference of the Society of Nuclear Medicine, Vienna. Austria. See CONF-670996.

The main advantage in using stationary detectors in nuclear medicine is the possibility of making an image of the distribution of a radioisotope within the organism in very short exposure times, these can be on the order of 1 sec when short lived radioisotopes with high activity are used. In this way, images of a radioactive embolus transversing the heart cavity have been obtained using a Bender autofluoroscope and an Anger camera. (tr-auth)

11121 ANGIOCARDIOGRAPHY WITH A SCINTILLATION CAMERA. Schenck, P.; Zum Winkel, K.; Maier-Borst, W.; Szegvari, M. (Univ., Heidelberg. Deutsche Krebsforschungszentrums, Heidelberg). Nucl.-Med.; 32: Suppl. 7, 31-4(1968). (In German).

From 5th Conference of the Society of Nuclear Medicine, Vienna, Austria. See CONF-670996.

To differentiate simultaneously activities in the right heart, the left heart, and the aorta, the patient was positioned at a 45° angle with the left side of the thorax nearer to the Anger camera. Ten mCi of ^{99m}Tc pertechnetate were injected into the cubital vein and pictures were taken at 0.5 sec. intervals. In normal persons the following values were found with respect to arrival at the subclavical vein: right ventricle 1.4 sec., lungs 5.2 sec., left ventricle 6.2 sec., and aorta 6.8 sec. These values agreed with angiographic measurements. Significant differences indicated cardiac insufficiency. Several pathological examples were presented. (H.B.G.)

11122 COMPUTER EVALUATION OF SCINTIGRAPHIC STUDIES OBTAINED WITH A SCINTILLATION CAMERA. Ammann, W.; Lorenz, W. J.; Adam, W. E.; Schmidlin, P.; Scheer, K. E. (Deutsche Krebsforschungszentrums, Heidelberg. Medizinisch-Naturwissenschaftlichen Hochschule, Ulm, Ger.). Nucl.-Med.; 32: Suppl. 7, 35-8(1968). (In German).

From 5th Conference of the Society of Nuclear Medicine, Vienna, Austria. See CONF-670996.

Two methods for digital evaluation of high-speed scintigrams are described. In each of the methods, the signals, obtained with an Anger camera, are registered in an analog form on magnetic tape. Subsequently, they are fed to an analog-digital converter into the computer. The first method allows the analysis of entire scintigrams at 3 sec. intervals. For the second method, only small sections of the scintigrams, possessing particular interest, are selected and analyzed at 0.1 sec. intervals. Several examples are given. (H.B.G.)

11123 DETERMINATION OF CENTRAL CIRCULATION PARAMETERS AND PERIPHERAL BLOOD FLOW BY SIMULTANEOUS APPLICATION OF ^{133}Xe AND ^{131}I-LABELED RISA. Alexander, K.; Fabel, H.; Feuerhake, I.; Hundeshagen, H.; Pixberg, H. U. (Medizinische Hochschule, Hanover). Nucl.-Med.; 32: Suppl. 7, 39-43(1968). (In German).

From 5th Conference of the Society of Nuclear Medicine, Vienna, Austria. See CONF-670996.

Simultaneous studies were performed on central and peripheral circulation as well as on metabolic factors with patients suffering from occlusion of peripheral arteries. Measurements were performed under normal conditions and under the influence of various drugs. Recorded were: cardiac minute volume after injection of ^{131}I RISA; the blood flow through the quadriceps muscle and the gastrocnemius by ^{133}Xe clearance; skin blood flow with a thermal probe; oxygen, carbon dioxide, and pH in both femoral artery and vein with special electrodes. In addition, glucose, lactate, and pyruvate concentrations were measured in the same blood vessels. Results were compiled in one diagram and two tables. It was concluded that only the combination of metabolic studies with blood flow measurements permits complete assessment of the circulatory system. (H.B.G.)

11124 DIAGNOSIS OF MITRAL INSUFFICIENCY WITH ^{85}Kr. Weichert, G. (Max-Planck-Gesellschaft und der Kerckhoff-Klinik, Bad Nauheim, Ger.). Nucl.-Med.; 32: Suppl. 7, 65-71 (1968). (In German).

From 5th Conference of the Society of Nuclear Medicine, Vienna, Austria. See CONF-670996.

To assess the degree of insufficiency in a combined defect of the mitral valve, measurement of regurgitation by the ^{85}Kr method proved valuable. Left ventricle as well as left atrium were catheterized. Through the left ventricle catheter ^{85}Kr in normal saline was infused at 5 ml/minute and 10 to 25 μCi/ml. Total activity never exceeded 800 μCi. During infusion, blood samples were withdrawn at 1 min. intervals from the left atrium and the brachial artery for counting. In combination with pressure measurements, the ^{85}Kr method contributed significantly to the evaluation of valve efficiency. (H.B.G.)

11125 LUNG CIRCULATION STUDIES USING RADIOACTIVE GASES. West, J. B. (Royal Postgraduate Medical School, London). Nucl.-Med.; 32: Suppl. 7, 73-9(1968).

From 5th Conference of the Society of Nuclear Medicine, Vienna, Austria. See CONF-670996.

Both pulmonary circulation and ventilation were studied with ^{15}O-labeled carbon dioxide and with ^{133}Xe. In the upright position, three regions of the lung could be distinguished, with ventilation and blood circulation increasing from the apex to the base of the lung. Reasons for this behavior were discussed. In a prone position and in various diseases, the three-region pattern was significantly altered as demonstrated by several case histories. ^{15}O-labeled carbon dioxide, because of its rapid uptake by blood, proved especially useful for detection of septal defects with left to right shunts. The technique was particularly useful in congenital heart disease because only one or two inhalations of radioactive gas were required. In addition, it was used frequently to determine effectiveness of surgical repair of shunts. (H.B.G.)

11126 LUNG SCINTIGRAPHY FOR STUDIES OF NORMAL AND PATHOLOGICAL BLOOD DISTRIBUTION IN THE PULMONARY CIRCULATORY SYSTEM. Ernst, H. (Freie Univ., Berlin). Nucl.-Med.; 32: Suppl. 7, 81-6(1968). (In German).

From 5th Conference of the Society of Nuclear Medicine, Vienna, Austria. See CONF-670996.

To study pulmonary circulation, radioactive particles were injected and scintigrams obtained. The method proved diagnostically very sensitive but not specific. Even small centrifugal forces led to detectable distortions in pulmonary blood distribution. Clinically significant emboli could be localized in 80 to 90% of the patients. In 250 patients with bronchial carcinoma, abnormal scintigrams were obtained even though angiography did not show compression of major pulmonary vessels. (H.B.G.)

11127 SCINTIGRAPHIC STUDIES OF BLOOD DISTRIBUTION IN THE PULMONARY SYSTEM. Winkler, C.; Felix, R.; Duex, A. (Univ., Bonn). Nucl.-Med.; 32: Suppl. 7, 87-93(1968). (In German).

From 5th Conference of the Society of Nuclear Medicine, Vienna, Austria. See CONF-670996.

After intravenous injection of ^{131}I albumen macroaggregate, pulmonary scans were obtained, stored on magnetic tape, and evaluated by a computer. In addition, ventilation of one side of the lung was performed with a gas mixture of 5% O_2, 7% CO_2, and 88% N_2. This functional blockage of one pulmonary section together with the scintigraphy permitted quantitative evaluation of lung circulation. As demonstrated by several cases of bronchial carcinoma, the technique possessed great clinical significance, especially in the preoperative diagnosis of pulmonary tumors. (H.B.G.)

11128 APPLICATION OF ^{99m}Tc FOR SCINTIGRAPHIC STUDIES OF PULMONARY CIRCULATION. de Vernejoul, P.; Ruff, F.; Kellershohn, C. (Service Hospitalier Frederic Joliot, Orsay, France). Nucl.-Med.; 32: Suppl. 7, 95-101(1968). (In French).

From 5th Conference of the Society of Nuclear Medicine, Vienna, Austria. See CONF-670996.

The fact that particles of a diameter greater than 20 μ may stop at the level of the pulmonary capillaries has already been exploited for the study of pulmonary circulation by scintigraphy. Iodine-131-labeled macroaggregates of human serum albumin were usually used. The use of ^{99m}Tc for labeling has, as was previously pointed out, genuine advantages over the use of ^{131}I. Its very short half-life (6 hr) permits the injection of relatively high doses, several mCi, without any danger to the patient and makes very rapid scanning possible. The energy of the γ rays (140 keV) is much

weaker than that of ^{131}I allowing pulmonary scintigrams to be made from different aspects (front, profile, back) without the interference of one pulmonary region on another. This proves to be of basic concern in the clinical interpretation of scintigrams. (tr-auth)

11129 STUDIES ON TECHNIQUES FOR LUNG SCINTIGRAPHY. Leb, G.; Eber, O.; Wascher, H.; Tillich, G. (Medizinische Univ., Graz). Nucl.-Med.; 32: Suppl. 7, 103-7(1968). (In German).

From 5th Conference of the Society of Nuclear Medicine, Vienna, Austria. See CONF-670996.

In 12 patients, the pressure of the pulmonary artery was measured during and following injection of ^{131}I albumen macroaggregate. With the exception of one patient, who showed a moderate transitory rise, arterial pressure was not affected by injection of the labeled particles. In certain pulmonary diseases, the scintigram frequently showed a defect larger than the actual pathological process. Injection of ^{131}I RISA demonstrated contraction of pulmonary vessels in the affected area. This contraction was either caused by external compression as in tumors, or by reflex action in lung areas with reduced ventilation. (H.B.G.)

11130 COMPARATIVE STUDIES BETWEEN HEART AND LUNG SCINTIGRAPHY. Zita, Gerlinde (Krankenhauses der Stadt, Vienna). Nucl.-Med.; 32: Suppl. 7, 109-12(1968). (In German).

From 5th Conference of the Society of Nuclear Medicine, Vienna, Austria. See CONF-670996.

The heart chambers and large blood vessels were scintigraphically depicted following injection of ^{131}I RISA. Lung scintigraphy was performed following administration of ^{131}I albumen macroaggregate. The combination of the two methods allowed not only differential diagnosis between mediastinal processes and pericardial effusion but also contributed to evaluation of pulmonary circulation and decreased radioactivity in neoplastic diseases. In addition, activity distribution in the blood pool was evaluated. (tr-auth)

11131 DETERMINATION OF LUNG CIRCULATION WITH THE DYNAPIX RAPID SCANNER IN PULMONARY RESTRICTIONS. Hundeshagen, H.; Stender, H. St.; Cruetzig, H. (Medizinische Hochschule, Hanover). Nucl.-Med.; 32: Suppl. 7, 113-17(1968). (In German).

From 5th Conference of the Society of Nuclear Medicine, Vienna, Austria. See CONF-670996.

Following administration of ^{131}I albumen macroaggregate, lung scintigrams were obtained with a ten-crystal scanner. Evaluation of the scintigrams was performed either with a 4096 channel analyzer or with a computer. With each patient the measurements included the following positions: anterior-posterior, posterior-anterior, right-left, and left-right. The entire procedure was completed within 16 minutes. Efficiency of the method was demonstrated in patients with tumors. (tr-auth)

11132 SCINTIGRAPHIC STUDIES IN PULMONARY TUBERCULOSIS. Kutzim, H. (Univ., Cologne). Nucl.-Med.; 32: Suppl. 7, 119-24(1968). (In German).

From 5th Conference of the Society of Nuclear Medicine, Vienna, Austria. See CONF-670996.

Lung scintigraphy was performed 30 min. following intravenous injection of 100 μCi of ^{131}I albumen particles with a size ranging from 5 to 50 microns. As a method for differential diagnosis in pulmonary tuberculosis, radioisotope scanning was inferior to conventional procedures. However, the isotope technique proved to be significant for evaluation of pulmonary function. Especially, reduction in pulmonary blood flow could be easily demonstrated. Therefore, lung scintigraphy is an important contributing factor to establish indication for surgery. (H.B.G.)

11133 PERFUSION SCINTIGRAM OF LUNGS DURING VARIOUS STAGES OF PULMONARY SARCOIDOSIS (MORBUS BOECK). Novak, D.; Schneider, C.; Brandenburg, H. (Radiologische Univ. und des Strahleninstitus, Hamburg. Krankenhaus der LVA, Hamburg). Nucl.-Med.; 32: Suppl. 7, 125-30(1968). (In German).

From 5th Conference of the Society of Nuclear Medicine, Vienna, Austria. See CONF-670996.

Suitability of lung scintigraphy following administration of ^{131}I albumen macroaggregate was studied in 25 patients suffering from pulmonary sarcoidosis. In stage I, distribution of radioactivity deviated not significantly from normal. In stage II, an inhomogenous distribution of activity was seen that ranged from small to large size spots. In stage III, irregular but sharply outlined areas of reduced activity were found ranging in size from moderate to large. The lung scintigraphy supplied valuable information about severity of the disease and functional condition of the lungs. (tr-auth)

11134 RESULTS OF LUNG SCINTIGRAPHY IN SILICOSIS. Hennig, K.; Fritz, H.; Woller, P.; Franke, W.-G.; Kemnitz, H.-P. (Medizinische Akademie Carl Gustav Carus, Dresden). Nucl.-Med.; 32: Suppl. 7, 131-5(1968). (In German).

From 5th Conference of the Society of Nuclear Medicine, Vienna, Austria. See CONF-670996.

In 95 patients, suffering from silicosis, lung scintigraphy was performed following administration of ^{131}I albumen macroaggregate. Scintigraphic findings paralleled to a certain degree those obtained with x-radiography and measurements of ventilation. However, in individual cases, close agreement frequently did not exist. In approximately one fourth of the patients, scintigraphically determined reduction of pulmonary function was more pronounced than that obtained through ventilation measurements. To reduce the risk of misinterpretation of the patients pulmonary condition, scintigraphy should be an integral part in the routine examination of persons professionally exposed to silicon producing materials. (tr-auth)

11135 LUNG SCINTIGRAPHY WITH ^{131}I-LABELED MAA IN LATE SEQUELAE FOLLOWING BLUNT CHEST CONCUSSIONS. Kappey, F.; Schenck, P. (Univ., Heidelberg). Nucl.-Med.; 32: Suppl. 7, 137-9(1968). (In German).

From 5th Conference of the Society of Nuclear Medicine, Vienna, Austria. See CONF-670996.

In twelve patients, lung scintigraphy was performed after administration of 300 μCi of ^{131}I albumen macroaggregate. At least one year prior to examination, the patients received blunt injuries to the chest cage with multiple fractures and pleural effusions. Routine radiography showed reduced mobility of the lungs as well as thickening of the pleura. In nine of the patients, scintigraphy revealed reduction of radioactivity in the injured area indicating diminished blood flow. Lung scintigraphy, together with radiography and ventilation measurements, proved to be an important procedure for evaluating late sequelae following blunt chest concussions. (H.B.G.)

11136 BLOOD FLOW DETERMINED BY LOCAL INJECTION OF ^{133}Xe IN SKELETAL MUSCLE. COMPARISON TO DIRECTLY METERED FLOW. Sejrsen, P.; Toennesen, K. H. (Bispebjerg Hospital, Copenhagen. Univ. of Copenhagen). Nucl.-Med.; 32: Suppl. 7, 165-7(1968).

From 5th Conference of the Society of Nuclear Medicine, Vienna, Austria. See CONF-670996.

Xenon-133 was applied by means of a small chamber to the gastrocnemius surface of a cat. The venous outflow was recorded continuously by a photoelectric drop recorder and the relative ^{133}Xe concentration in the tissue was monitored by external counting. It was concluded that blood flow in 0.3% of the muscle corresponds to that in the whole muscle, and that xenon clearance values agreed closely with the directly measured venous blood flow. Direct injection of ^{133}Xe into the muscle led to disturbances of circulation in the area of deposition and to significant disagreements between xenon clearance and directly measured blood flow. (H.B.G.)

11137 BLOOD FLOW DETERMINED BY INTRA-ARTERIAL-INJECTION AND EXTERNAL RECORDING OF ^{133}X: COMPARISON TO DIRECTLY METERED FLOW. Toennesen, K. H.; Sejrsen, P. (Univ. of Copenhagen. Bispebjerg Hospital, Copenhagen). Nucl.-Med.; 32: Suppl. 7, 169-71(1968).

From 5th Conference of the Society of Nuclear Medicine, Vienna, Austria. See CONF-670996.

The blood flow was calculated from the Height over Area equation of Zieler following a rapid intraarterial injection of ^{133}Xe with a well defined volume of distribution such as inert gases. Following complete saturation of muscle tissue, blood flow calculated from the initial slope of the clearance curves was identical to the directly measured blood flow. The hypothesis of gas shunting was used to explain the shape of the clearance curves. (auth)

11138 IS ^{133}Xe CLEARANCE A ROUTINE TECHNIQUE FOR STUDYING MUSCULAR BLOOD FLOW? Klemm, J. (Medizenische Univ., Munich). Nucl.-Med.; 32: Suppl. 7, 173-6(1968). (In German).

From 5th Conference of the Society of Nuclear Medicine, Vienna, Austria. See CONF-670996.

On a series of patients, blood flow in the lower extremities was determined following injection of ^{133}Xe into the anterior tibial muscle. Results showed that the procedure is reproducible, not time consuming, relatively inexpensive, free of complications, and insignificant from the standpoint of radiation burden. Routine clinical use of the muscle clearance method with ^{133}Xe was strongly recommended. (H.B.G.)

11139 EVALUATION OF ARTERIAL INSUFFICIENCY OF THE LEGS. A COMPARISON OF ARTERIOGRAPHY AND THE

XUM

^{133}Xe WALKING TEST. Larsen, O. A.; Alpert, J. S.; Lassen, N. A. (Bispebjerg Hospital, Copenhagen). Nucl.-Med.; 32: Suppl. 7, 177-85(1968).

From 5th Conference of the Society of Nuclear Medicine, Vienna, Austria. See CONF-670996.

The ^{133}Xe standardized walking test was used to study the muscle blood flow in the lateral head of the gastrocnemius muscle in 28 patients with symptomatic occlusive arterial disease. Five parameters calculated from the ^{133}Xe clearance curves for each individual leg were compared with aortographic studies. On the basis of this comparison, three classes of ^{133}Xe clearance curves were distinguished, corresponding to three groups of arteriographically observed arterial abnormalities: mild to moderate arterial changes without clinical significance, distal arterial occlusions or significant main artery stenoses, combined proximodistal arterial occlusions and significant stenoses. It was suggested that a test of arterial function such as the ^{133}Xe standardized walking test is more effective in the clinical evaluation of arterial insufficiency than is a knowledge of the presence of vessel stenoses or occlusions. Consequently, radiologic techniques for the visualization of these arterial abnormalities should only be employed pre-operatively where the surgeon has need of a road map. Even in these cases, however, a functional test such as the ^{133}Xe standardized walking test is of value as it points to lesions of functional significance. (auth)

11140 COMPARATIVE DETERMINATION OF HEPATIC BLOOD FLOW WITH COLLOIDAL ^{198}Au AND COLLOIDAL ^{99m}Tc-S. Haas, J. P.; Brod, K. H.; Wolf, R.; Schmidt, K. J. (Johannes Gutenberg-Univ., Mainz). Nucl.-Med.; 32: Suppl. 7, 237-41(1968). (In German).

From 5th Conference of the Society of Nuclear Medicine, Vienna, Austria. See CONF-670996.

In 63 patients, accumulation of colloidal gold-198 was compared with that of a ^{99m}Tc-sulfur colloid. The acid colloidal solution was neutralized by sodium hydroxide. This method produced a solution that was isotonic and possessed high specific activity. The patients received 400 μCi ^{99m}Tc colloid followed, 30 to 45 min. later, by liver scintigraphy. After 25 hours, 50 μCi of ^{198}Au was given and scintigraphy was again performed. Clearance from blood and specific accumulation in the liver was significantly higher for technetium than for gold. It was concluded that ^{99m}Tc colloid is the superior isotope for diagnosis of liver diseases. (H.B.G.)

11141 DETERMINATION OF HEPATIC BLOOD FLOW IN HYPERTHYROIDISM WITH THE ^{198}Au BLOOD EXTRACTION METHOD. Kostamis, P.; Kralios, A.; Darsinos, J.; Konstantinides, K.; Binopoulos, D.; Sfondouris, J.; Malamos, B. (Univ. of Athens). Nucl.-Med.; 32: Suppl. 7, 243-6(1968). (In German).

From 5th Conference of the Society of Nuclear Medicine, Vienna, Austria. See CONF-670996.

In 28 patients, heart minute volume was determined following administration of ^{131}I RISA and, two days later, liver blood flow was measured by injection of ^{198}Au and by the determination of its disappearance rate from the blood. Eighteen of the patients were hyperthyroid, while ten were euthyroid. Results showed a significant increase in the heart minute volume for the hyperthyroid group while the hepatic blood flow revealed no significant difference. (H.B.G.)

11142 DETERMINATION OF SPLENIC BLOOD FLOW WITH ^{51}Cr LABELED AND HEAT TREATED ERYTHROCYTES. Fischer, J.; Wolf, R.; Leon, A. (Johannes Gutenberg-Univ., Mainz). Nucl.-Med.; 32: Suppl. 7, 247-51(1968). (In German).

From 5th Conference of the Society of Nuclear Medicine, Vienna, Austria. See CONF-670996.

Splenic blood flow was determined by external counting following injection of heat treated and ^{51}Cr-labeled erythrocytes. In healthy and resting persons, minute volume of the spleen was 500 to 700 ml; thus, the specific blood flow was about 3 ml/g/min. In splenomegalie, the minute volume increased, while the specific blood flow decreased significantly. (H.B.G.)

11143 REGIONAL CEREBRAL BLOOD FLOW. A COMPARISON OF 8-DETECTOR AND 16-DETECTOR EQUIPMENTS. Paulson, O. B.; Cronqvist, S.; Risberg, J.; Jeppesen, F. (Bispebjerg Hospital, Copenhagen. University Hospital, Lund, Sweden). Nucl.-Med.; 32: Suppl. 7, 253-8(1968).

From 5th Conference of the Society of Nuclear Medicine, Vienna, Austria. See CONF-670996.

An 8-detector equipment and a 16-detector equipment for measuring regional cerebral blood flow, using an intraarterial injection of Xenon-133, were compared in a group of patients with focal cerebral disease. The analysis of the results showed that it is possible to obtain a better resolution and to obtain more information using the equipment with 16 smaller detectors. Perhaps even better resolution and results may be obtained by using more than 16 detectors. (auth)

11144 BRAIN BLOOD FLOW MEASUREMENTS (CEREBRAL CLEARANCE) WITH ^{133}Xe. Klemm, J. (Medizinische Univ., Munich). Nucl.-Med.; 32: Suppl. 7, 259-63(1968). (In German).

From 5th Conference of the Society of Nuclear Medicine, Vienna, Austria. See CONF-670996.

After injection of 250 to 300 μCi of ^{133}Xe into the internal carotid artery, radioactivity of the brain was recorded by a frontal and a lateral detector connected with rate meters. Normal persons showed a cerebral blood flow of 75 to 80 ml/100g/minute for grey matter and of 20 to 25 ml/100g/minute for white matter. Degenerative brain processes, such as sclerosis, atrophy, endangiitis obliterans, and periarteritis nodosa, showed a symmetrical and homogenous reduction in blood flow. Tumors caused a pronounced diminution of blood flow at lateral recording but not at the frontal recording. Grey and white matter were approximately evenly affected. Occlusion of larger intracerebral vessels led to sharp reduction of blood flow mainly in white matter. It was assumed that grey matter is better compensated by collateral vessels. (H.B.G.)

11145 DIAGNOSIS OF BRAIN TUMORS WITH ^{131}I-LABELED ALBUMEN PARTICLES AND WITH ^{75}Se. Doering, P.; Lorenz, B. (Barmherzigen Brueder, Regensburg, Ger.). Nucl.-Med.; 32: Suppl. 7, 265-71(1968). (In German).

From 5th Conference of the Society of Nuclear Medicine, Vienna, Austria. See CONF-670996.

After injection of ^{131}I albumen macroaggregate particles into the internal carotid artery, brain scans were performed. In eleven tumor patients, metastatic carcinomas appeared as areas of reduced radioactivity, while glioblastomas appeared as spots of increased activity. In six patients with hemiparesis following cerebral infarction, the brain scans closely resembled those of patients with larger tumors; therefore, difficulties in differential diagnosis could arise. In a second series of patients, 3 μCi/kg of ^{75}Se was injected intravenously. Brain scintigraphy was performed at 25 hours following injection. In eight patients, confirmed tumors were detected scintigraphically. In six cases with cerebral infarction, brain scans were negative. It was concluded that ^{75}Se is a promising radioisotope for detection of cerebral tumors. (H.B.G.)

11146 OBJECTIVE DETECTION OF CEREBRAL BLOOD FLOW DISTURBANCES WITH ^{99m}Tc. Montz, R.; Prevot, H.; Schneider, C. (Radiologische Univ. und des Strahleninstitutes, Hamburg). Nucl.-Med.; 32: Suppl. 7, 273-6(1968). (In German).

From 5th Conference of the Society of Nuclear Medicine, Vienna, Austria. See CONF-670996.

In five normal persons and in forty patients with cerebral lesions, brain scintigraphy was performed following administration of 0.5 mCi ^{99m}Tc. With 4 detectors, located over the heart, the nape of the neck, and various regions of the head, radioactivity was recorded by rate meters. In normal persons, blood transit time through the brain ranged from 6 to 8 seconds. In patients suffering from cerebral lesions, transit times were either normal or deviated from normal too inconsistently to be of diagnostic value. Differential diagnosis between vascular processes and tumors was impossible. (H.B.G.)

11147 DETERMINATION OF REGIONAL BLOOD FLOW WITH ^{133}Xe IN THE BRAIN OF PARKINSON AND TUMOR PATIENTS. Mundinger, F.; Schmidt, K.; Walter, E.; Dietz, K.; Kaiser, G. (Neurochirurgische Univ., Freiburg i. B. Univ., Freiburg i. B.). Nucl.-Med.; 32: Suppl. 7, 277-81(1968). (In German).

From 5th Conference of the Society of Nuclear Medicine, Vienna, Austria. See CONF-670996.

In twelve patients with Parkinson's disease and in six patients, from whom brain tumors were surgically removed, cerebral blood flow was measured by the ^{133}Xe method. In patients with Parkinson's cerebral blood flow was reduced to 62% of the normal value. Administration of an amphetamine derivative did not improve blood flow; L-dopa, combined with the amphetamine, caused significant increase in cerebral blood flow. After brain surgery, cerebral blood flow was reduced to 53% of normal. It was concluded that the ^{133}Xe method represented a reliable tool for measuring cerebral blood and for evaluating effectiveness of drugs. (H.B.G.)

11148 INTERRELATIONSHIP BETWEEN CEREBRAL CIRCULATION TIME, PULMONARY CIRCULATION, AND BLOOD PRESSURE. Baggio, G. F.; Morgando, E. (Univ., Turin). Nucl.-Med.; 32: Suppl. 7, 283-7(1968). (In German).

From 5th Conference of the Society of Nuclear Medicine, Vienna, Austria. See CONF-670996.

Several groups of patients with various brain diseases received injections of 50 μCi ^{131}I RISA into the antecubital vein. Three detectors, one over the heart region, the other two at each side of the head, recorded the time course of radioactivity. The delay between the peak in the left ventricle and the peak in the head detectors was defined as cerebral circulation time. The delay between the peak in the right ventricle and the peak in the left ventricle was defined as pulmonary circulation time. Thrombosis of one of the major cerebral arteries caused striking prolongation of cerebral circulation time that paralleled severity of the disease; on the unaffected side, circulation time was shortened especially between ten to thirty days following occlusion. Patients with nonocclusive vascular pathology showed no difference between the two hemispheres. In mild forms of the disease, circulation times were within normal range; in severe forms, significant prolongation occurred. No relationship between mean blood and cerebral circulation time existed. In thrombosis and other vascular diseases, cerebral and pulmonary circulation times were equally prolonged. (H.B.G.)

11149 DIFFERENTIAL DIAGNOSIS OF BRAIN ALTERATIONS CAUSED BY TUMOR AND VASCULAR PROCESSES WITH RADIOACTIVE ISOTOPE BLOOD FLOW MEASUREMENTS. Koch, R. D.; Abraham, K.; Otto, H. J. (Medizinische Akademie, Magdeburg, Ger.). Nucl.-Med.; 32: Suppl. 7, 289-93(1968). (In German).

From 5th Conference of the Society of Nuclear Medicine, Vienna, Austria. See CONF-670996.

In more than 200 patients, the cerebral blood transit time was measured with ^{131}I hippuran or ^{131}I RISA. In normal persons, transit times ranged from 8 to 12 sec. In 94 patients with vascular diseases, mean transit time was prolonged to 30.5 sec. In 47 patients with cerebral tumors, transit time was strikingly prolonged and ranged from 14 to 27 sec. It was concluded that moderately prolonged transit time and reduction of radioactivity indicate pathological vascular processes; while strikingly prolonged transit time with increased brain radioactivity indicated neoplasms. (H.B.G.)

11150 COMPARISON OF CEREBRAL BLOOD FLOW MEASUREMENTS WITH INTRAVENOUSLY ADMINISTERED ^{131}I-LABELED HIPPURAN BETWEEN ARTERIOSCLEROTIC AND NORMAL PATIENTS. Dubansky, B.; Kuba, J.; Svozil, O.; Setlik, L.; Vyhnankova, M. (Palacky Univ., Olomouc, Czech. Univ. of Olomouc, Czech. Militaerkrankenhauses, Olomouc, Czech.). Nucl.-Med.; 32: Suppl. 7, 295-9(1968). (In German).

From 5th Conference of the Society of Nuclear Medicine, Vienna, Austria. See CONF-670996.

Iodine-131 hippuran was injected either into the internal carotid or intravenously and cerebral circulation time determined with two detectors and rate meters. It was concluded that the method yielded only semiquantitative information about cerebral blood flow. Between normal persons and patients suffering from moderate pathological processes in brain vessels, no significant difference in radioactivity recordings was found. Only in the case of advanced vascular impairment reliable differences were observed. (H.B.G.)

11151 VARIATIONS IN REGIONAL CEREBRAL BLOOD VOLUME DURING MENTAL ACTIVITY. Risberg, J.; Ingvar, D. H. (University Hospital, Lund, Sweden). Nucl.-Med.; 32: Suppl. 7, 301-4(1968).

From 5th Conference of the Society of Nuclear Medicine, Vienna, Austria. See CONF-670996.

Eighteen healthy male students received 100 μCi of ^{131}I RISA for measurements of regional cerebral blood flow. Gamma radiation was recorded from eight regions of the brain by means of eight scintillation detectors, mounted in parallel cylindrical holes within a block of lead at a right angle to the lateral surface of the subject's head. The measuring fields had a diameter of about 4 cm and they covered frontal, precentral, central, postcentral, parietal, and occipital parts of the hemisphere. Specific patterns of regional cerebral blood were demonstrated that were characteristic for specific forms of mental activity. (H.B.G.)

11152 DIAGNOSTIC SIGNIFICANCE OF VENTRICULAR RESORPTION OF ^{131}I-LABELED HIPPURAN AS COMPARED TO OTHER PATHOLOGICAL CHANGES IN CHILDHOOD HYDROCEPHALUS. Anlauf, M.; Mundinger, F.; Jesdinsky, H. J. (Neurochirurgische Univ., Freiburg i. B. Univ., Freiburg i. B.). Nucl.-Med.; 32: Suppl. 7, 305-10(1968). (In German).

From 5th Conference of the Society of Nuclear Medicine, Vienna, Austria. See CONF-670996.

In hydrocephalic children, 5 to 10 μCi ^{131}I hippuran was injected through the large fontanelle into one of the lateral ventricles. Resorption of ^{131}I hippuran was then recorded by external counting. The examination was performed prior to and at various times following surgical establishment of a ventriculo-atrial shunt. Resorption depended strongly on ventricle volume and protein content of the cerebro-spinal fluid. The method permitted reliable assessment of surgical shunts. Radiation burden to the ventricular walls was approximately 0.1 rad. (H.B.G.)

11153 ASSESSMENT OF RENAL BLOOD FLOW WITH RADIOACTIVE LABELED COMPOUNDS EXCRETED BY GLOMERULAR FILTRATION. Haas, J. P.; Schmidt, K. J.; Wolf, R.; Pierach, C. A. (Johannes Gutenberg-Univ., Mainz). Nucl.-Med.; 32: Suppl. 7, 311-16(1968). (In German).

From 5th Conference of the Society of Nuclear Medicine, Vienna, Austria. See CONF-670996.

In approximately 100 hypertensive patients, renal blood flow was assessed after injection of various radioisotope-labeled compounds that were excreted by glomerular filtration. Compounds used were ^{57}Co-labeled vitamin B_{12}, ^{131}I hippuran, ^{125}I-labeled iothalamate, ^{51}Cr-labeled EDTA, and ^{51}Cr-labeled inulin. It was concluded that some of the compounds were superior to inulin in diagnosing obstruction of the renal artery. (H.B.G.)

11154 DETERMINATION OF GLOMERULAR CLEARANCE WITH RADIOISOTOPE LABELED SUBSTANCES ACCORDING TO THE SLOPE METHOD. Kampmann, H.; Grebe, S. F. (Justus-Liebig-Univ., Giessen, Ger.). Nucl.-Med.; 32: Suppl. 7, 317-21(1968). (In German).

From 5th Conference of the Society of Nuclear Medicine, Vienna, Austria. See CONF-670996.

With the slope method, glomerular clearance was determined for ^{57}Co-labeled vitamin B_{12} and ^{51}Cr-labeled EDTA. The results were compared with those obtained with a steady state method of inulin clearance. Results obtained on 32 patients showed no significant difference between the two techniques. The ^{51}Cr-labeled EDTA slope method proved to be superior because of brief mixture time, small protein binding, and lower radiation burden. (H.B.G.)

11155 DETERMINATION OF RENAL CLEARANCE BY EXTERNAL γ-RAY MEASUREMENTS. Oberhausen, E.; Romahn, A. (Univ. des Saarlandes, Homburg, Ger.). Nucl.-Med.; 32: Suppl. 7, 323-6(1968). (In German).

From 5th Conference of the Society of Nuclear Medicine, Vienna, Austria. See CONF-670996.

To determine renal clearance, a new method based on ^{51}Cr-labeled EDTA is described and mathematically formulated. The principle consists in whole-body counting by two large sodium iodide crystals. During the counting, a lead shield covers the patients kidneys and bladder because the activity in this area is considered already eliminated from the body. Total time required for clearance determination is about twenty minutes. (H.B.G.)

11156 CLEARANCE STUDIES WITH ^{131}I-LABELED HIPPURAN, ^{203}Hg-SALYRGAN, ^{51}Cr- EDTA, AND ^{51}Cr-INULIN. Hoer, G.; Pabst, H. W.; Steinhoff, H.; Haubold, U.; Heinze, H. G. (Univ., Munich). Nucl.-Med.; 32: Suppl. 7, 327-34(1968). (In German).

From 5th Conference of the Society of Nuclear Medicine, Vienna, Austria. See CONF-670996.

In a comparative study, renal clearance was determined with ^{131}I-labeled hippuran, ^{203}Hg-labeled Salyrgan, ^{51}Cr-labeled EDTA, and ^{51}Cr-labeled inulin. ^{131}I-labeled hippuran and radiosalyrgan showed values that were too different from those obtained by standard procedures and varied too much to be of diagnostic value. ^{51}Cr-labeled EDTA and ^{51}Cr-labeled inulin yielded reliable identical results. It was concluded that clearance methods with radioisotopes require further refinement before they can compete with commonly used diagnostic procedures. (H.B.G.)

11157 SIMULTANEOUS DETERMINATION OF GLOMERULAR FILTRATION RATE AND RENAL BLOOD FLOW WITH ^{60}Co-CYANOCOBALAMINE AND ^{131}I-ORTHOHIPPURIC ACID: COMPARATIVE CLEARANCE STUDIES IN THE "STEADY STATE" WITH INULIN AND PAH. Huenig, R.; Weidmann, P. (Kantonsspitals, Zurich). Nucl.-Med.; 32: Suppl. 7, 335-40(1968). (In German).

From 5th Conference of the Society of Nuclear Medicine, Vienna, Austria. See CONF-670996.

To determine glomerular filtration rate, ^{57}Co-labeled vitamin B_{12} was injected; simultaneously, ^{131}I-labeled orthohippuric acid was administered for determination of tubular excretion. The time course of radioactivity in blood plasma was determined by four samples taken in succession. Studies on sixteen patients showed excellent correlation of tubular excretion values obtained with paraaminohippuric acid and ^{131}I-labeled hippuric acid. This part of the technique was recommended for routine clinical ap-

plication. In contrast, clearance of ^{57}Co-labeled vitamin B_{12} showed such a poor correlation to inulin clearance that its clinical use was not justified. (H.B.G.)

11158 RENAL CLEARANCE OF ^{133}Xe. Steinhoff, H.; Pabst, H. W. (Univ., Munich). Nucl.-Med.; 32: Suppl. 7, 341-8(1968). (In German).

From 5th Conference of the Society of Nuclear Medicine, Vienna, Austria. See CONF-670996.

To determine renal blood flow, ^{133}Xe dissolved in saline is injected through a catheter into the renal artery. Radioactivity is determined by external counting and recorded by a rate meter. The initial rise of radioactivity indicates blood flow through the renal cortex. In normal persons, mean values are 4 ml/g/min. In 23 hypertensive patients with angiographically confirmed stenosis of the renal artery, renal blood flow is decreased to about 2.4 ml/g/min. for moderate to severe forms of the disease. It is concluded that Xenon clearance contributes significantly to the diagnostic evaluation of renal angiograms. (H.B.G.)

11159 QUANTITATIVE ANALYSIS OF THE RADIORENOGRAM BASED ON ^{131}I-ORTHOHIPPURIC ACID CLEARANCE. Fischer, W.; Roesler, H.; Mueller-Duysing, W. (Univ., Zurich). Nucl.-Med.; 32: Suppl. 7, 349-53(1968). (In German).

From 5th Conference of the Society of Nuclear Medicine, Vienna, Austria. See CONF-670996.

Renograms were recorded following administration of ^{131}I-labeled orthohippuric acid and, simultaneously, total clearance with the slope method was performed on two blood samples taken 7 to 17 minutes, respectively, after injection of the radioisotope. From the rate of activity increase between 30 seconds and 90 seconds after injection, renal clearance was determined. (H.B.G.)

11160 QUANTITATIVE EVALUATION OF ^{131}I-HIPPURAN RENAL CLEARANCE BASED ON A MODEL. Praeg, R.; Wolf, F.; Kroenert, E. (Univ., Erlangen, Ger.). Nucl.-Med.; 32: Suppl. 7, 355-9(1968). (In German).

From 5th Conference of the Society of Nuclear Medicine, Vienna, Austria. See CONF-670996.

Instead of compartment models, mathematical treatment of renal clearance of ^{131}I-labeled hippuran was based on concepts with the following principles: radioactivity, eliminated either by glomerular filtration or tubular secretion, enters the renal pelvis without mixing with previously or subsequently eliminated activity. The renal pelvis empties, corresponding to its peristalsis, periodically, but not necessarily completely. The model allows a very satisfactory approximation of all renograms even those showing extremely pathological behavior. (tr-auth)

11161 RESULTS OF RENOGRAMS EVALUATED BY COMPUTER ANALYSIS BASED ON A NON-COMPARTMENTAL MODEL. Wolf, F.; Kroenert, E.; Praeg, R. (Univ., Erlangen, Ger.). Nucl.-Med.; 32: Suppl. 7, 361-5(1968). (In German).

From 5th Conference of the Society of Nuclear Medicine, Vienna, Austria. See CONF-670996.

Renograms of 103 patients were subjected to computer analysis based on a non-compartmental model. For normal renograms, agreement with the model is excellent. Conditions after nephrectomy also were well displayed. The occlusion type of renogram generally showed satisfactory agreement. It was concluded that the computer program and the basic model were well suited for interpretation of pathologic processes. (H.B.G.)

11162 QUANTITATIVE RADIORENOGRAMS AS FUNCTION TESTS FOLLOWING KIDNEY TRANSPLANTATION. Roesler, H. (Univ., Zurich). Nucl.-Med.; 32: Suppl. 7, 367-73(1968). (In German).

From 5th Conference of the Society of Nuclear Medicine, Vienna, Austria. See CONF-670996.

In 17 kidney transplant patients, renograms were obtained after administration of ^{131}I hippuran. Renograms proved suitable for assessment of transplant function. Degree of tubular damage and its therapeutic control was recognized by means of total clearance. One day after transplantation, total clearance gave important prognostic indications. Seven patients with normal clearance developed neither hypertension nor serious complications during the first three months following transplantation. Five patients with reduced initial clearance became hypertensive and two died within three months post transplantation. Pending transplant rejection as well as its therapeutic control was detected early from the elimination index of the renogram. Complete stenosis of the transplanted kidney as well as obstruction of the ureter produced characteristic abnormalities of the renograms. (H.B.G.)

11163 COMPARISON OF RENAL ISOTOPE DIAGNOSIS WITH VASOCONSTRICTOR CONTENT IN THE RENAL VEIN OF HYPERTENSIVE PATIENTS. Pierach, C. A.; Schmidt, K. J.; van de Weyer, K. H.; Haas, J. P. (Univ., Mainz). Nucl.-Med.; 32: Suppl. 7, 375-8(1968). (In German).

From 5th Conference of the Society of Nuclear Medicine, Vienna, Austria. See CONF-670996.

Renograms obtained with ^{57}Co-labeled vitamin B_{12}, ^{131}I hippuran, ^{131}I-iothalamate, and ^{51}Cr EDTA, or ^{51}Cr inulin were compared with kidney scintigrams after administration of ^{99m}Tc and with vasoconstrictor substances obtained from the renal vein. In 18 patients, a good correlation was found between the three techniques. However, it was pointed out that occasionally atypical renogram and scintigram findings were obtained through vascular changes that represented no causative factor for development of hypertension. (H.B.G.)

11164 ASSESSMENT OF FUNCTIONAL SIGNIFICANCE FOR RENAL ARTERY STENOSIS CONFIRMED BY ANGIOGRAPHY. COMPARISON OF THE RADIORENOGRAM WITH THE ANGIOTENSININFUSION TEST AND WITH THE PLASMA RENIN CONTENT IN BOTH PERIPHERAL AND RENAL VENUS BLOOD. Weidmann, P.; Roesler, H.; Siegenthaler, W.; Endres, P. (Kantonsspitals, Zurich). Nucl.-Med.; 32: Suppl. 7, 379-83(1968). (In German).

From 5th Conference of the Society of Nuclear Medicine, Vienna, Austria. See CONF-670996.

Eighteen hypertensive patients with stenosis of the renal artery were subjected to the following tests: renin activity in the plasma of peripheral blood as well as in blood of the renal vein, angiotensin infusion, and renograms. Renograms as well as total clearance studies with the slope method were performed after injection of ^{131}I orthoiodohippuric acid. Measurement of plasma renin, especially in the venous blood, proved to be the most reliable, but also the most complicated method. Angiotensin infusion was only of secondary importance for screening tests. Because of certain ambiguities, radiorenograms possessed high reliability. If possible, renograms should be complemented with renin studies prior to surgery. (H.B.G.)

11165 SCINTIGRAPHY OF RENAL FUNCTION EVALUATED BY DIGITAL AND ANALOG COMPUTERS. Lorenz, W. J.; Adam, W. E.; Ammann, W.; zum Winkel, K.; Scheer, K. E. (Deutche Krebsforschungszentrums, Heidelberg. Medizinisch-Naturwissenschaftliche Hochschule, Ulm, Ger.). Nucl.-Med.; 32: Suppl. 7, 391-6(1968). (In German).

From 5th Conference of the Society of Nuclear Medicine, Vienna, Austria. See CONF-670996.

Following injection of ^{131}I hippuran, renal function was studied with an Anger scintillation camera. The camera impulses were stored in analog fashion on magnetic tape. Two methods for evaluating the data were developed. In the first one, the tape was displayed on an oscilloscope connected with an image intensifier, photomultiplier, and printout. In the second one, the tape was evaluated by a computer. Diagnostic value of the digital and analog processing of camera data was discussed and demonstrated on two patients. (H.B.G.)

11166 CONTRIBUTION OF SCINTIGRAPHY FOR EVALUATION OF VASCULAR RENAL DISEASES. Schmidt, K. J.; Haenze, S.; Pierach, C. A.; Wolf, R.; Haas, J. P.; Brod, K. H. (Johannes-Gutenberg-Univ., Mainz). Nucl.-Med.; 32: Suppl. 7, 397-401 (1968). (In German).

From 5th Conference of the Society of Nuclear Medicine, Vienna, Austria. See CONF-670996.

In seventeen patients with unilateral stenosis of the renal artery, scintigraphy was performed after administration of a ^{99m}Tc-iron complex. In 14 patients, the diseased kidney appeared smaller and its radioactivity generally was diminished. It was concluded that scintigrams represent an important diagnostic tool for evaluation of the cause of hypertension, especially in young people. Atypical scintigrams should be confirmed by renal angiography. (tr-auth)

11167 EXAMINATION OF VARIOUS PROCEDURES FOR LOCALIZATION OF THE COUNTER IN ISOTOPE RENOGRAMS. Tan, A. H.; Becker, G. (Medizinische Univ., Wuerzlung, Ger.). Nucl.-Med.; 32: Suppl. 7, 403-10(1968). (In German).

From 5th Conference of the Society of Nuclear Medicine, Vienna, Austria. See CONF-670996.

Quantitative evaluation of renograms following administration of ^{131}I hippuran is possible when two requirements are fulfilled. The patient must be sufficiently hydrated to produce a urinary excretion of not less than 3 ml/min. The detector must be localized as accurately as possible. Deviations of less than 2 cm from the ideal position do not affect the renogram significantly. Deviations in excess of 3 cm make evaluation of the renogram impossible both qualitatively and quantitatively. The rising phase of the

renogram is more affected than the falling one. The best method for localization of the kidney is injection of a test dose of 5 μCi ^{131}I hippuran followed by determination of maximal activity with a laboratory monitoring device. (H.B.G.)

11168 CLINICAL AND EXPERIMENTAL INVESTIGATION OF $^{14}CO_2$ EXHALATION. Glaubitt, D.; Freudenberg, V. (Medizinische Univ., Hamburg). Nucl.-Med.; 32: Suppl. 7, 421-5 (1968). (In German).

From 5th Conference of the Society of Nuclear Medicine, Vienna, Austria. See CONF-670996.

Both healthy controls and patients received orally either 10 μCi ^{14}C-labeled oleic acid or 11 μCi of ^{14}C-labeled glyceryltrioleate. In the exhaled air, total carbon dioxide was determined by infrared absorption and ^{14}C was determined by a methane flow counter. The measurements were recorded throughout a period of 6 to 10 hours. It was concluded that this method permits recognition of disturbances in intermediary metabolism as well as in digestion and resorption of fats. (H.B.G.)

11169 ANIMAL EXPERIMENTS ON THE SUITABILITY OF ^{68}Ga COMPOUNDS FOR DIAGNOSIS IN NUCLEAR MEDICINE. Prpic, B.; Maier-Borst, W.; Scheer, K. E. (Deutsche Krebsforschungszentrums, Heidelberg). Nucl.-Med.; 32: Suppl. 7, 455-8(1968). (In German).

From 5th Conference of the Society of Nuclear Medicine, Vienna, Austria. See CONF-670996.

Renograms were performed in rats. Various ^{68}Ga compounds were analyzed as to suitability for scintigraphy. The excretion mechanism for ^{68}Ga EDTA as compared to ^{131}I hippuran was examined by means of renograms and autoradiography. Results showed that ^{68}Ga EDTA was eliminated exclusively by glomerular filtration. (tr-auth)

11170 DEPENDENCY OF PROTEIN RESORPTION ON ACIDITY AND RETENTION TIME OF THE STOMACH: STUDIES WITH ^{131}I-LABELED HUMAN ALBUMIN AND INTRAGASTRIC Ph MEASUREMENTS. Hemmati, A. (Univ., Cologne). Nucl.-Med.; 32: Suppl. 7, 459-66(1968). (In German).

From 5th Conference of the Society of Nuclear Medicine, Vienna, Austria. See CONF-670996.

In 44 persons, resorption of human albumin and retention time in the stomach were determined by oral administration of ^{131}I RISA, pH measurements, and x-ray pictures with contrast medium. The total amount of resorbed albumin was independent of hydrochloric acid production. Equality of time for maximal resorption was explained by the shortened stomach retention in sub- or anacid cases and by the enhanced proteolytic activity in superacidic and normal acidic stomach secretion. (tr-auth)

11171 ^{59}Fe DEXTRANE TEST AS INDICATOR OF ENTERAL PROTEIN LOSS. Glaubitt, D. (Medizenische Univ., Hamburg). Nucl.-Med.; 32: Suppl. 7, 467-72(1968). (In German).

From 5th Conference of the Society of Nuclear Medicine, Vienna, Austria. See CONF-670996.

Various groups of patients received intravenously 5 μCi of ^{59}Fe-labeled dextran. Throughout six days following injection, radioactivity in the feces was determined as well as activity in liver, spleen, and kidney regions. It was concluded that the ^{59}Fe-dextran test represents a reliable indicator for protein loss into the gastrointestinal tract. In contrast to other radioisotope methods, only insignificant amounts were removed by renal excretion; therefore, the test was especially suited for patients with urinary incontinence. (H.B.G.)

11172 THYROID DIAGNOSIS WITH A WHOLE-BODY COUNTER IN CHILDREN. Romahn, A.; Kunkel, R.; Oberhausen, E. (Univ. des Saarlandes, Homburg, Ger.). Nucl.-Med.; 32: Suppl. 7, 481-4(1968). (In German).

From 5th Conference of the Society of Nuclear Medicine, Vienna, Austria. See CONF-670996.

Children received 0.5 to 1 μCi of ^{131}I. Three to four hours after administration, whole-body counting was started and repeated throughout several days. Fourteen infants and children with clinical suspicion of thyroidal disfunction were examined. Of these, five showed euthyroid condition. In the other ones, various pathological findings were established. At 0.5 μCi total radiation burden to the thyroid was 12 rads. It was concluded that whole-body counting is a relatively safe and reliable screening procedure for thyroidal function in early childhood. (H.B.G.)

11173 DETERMINATION OF THYROIDAL CLEARANCE DURING AN AUTOMATICALLY CONTROLLED AND CONSTANT ^{131}I BLOOD LEVEL. Oeff, K.; Scholz, A. (Freie Univ., Berlin). Nucl.-Med.; 32: Suppl. 7, 485-90(1968). (In German).

From 5th Conference of the Society of Nuclear Medicine, Vienna, Austria. See CONF-670996.

To determine ^{131}I clearance at steady state plasma levels, ^{131}I radioactivity of the blood was kept constant by means of an infusion pump regulated by feed back control. Simultaneously, ^{131}I activity of the thyroid gland was recorded continuously and from the rate of activity increase, clearance was calculated. Suitability of the method was analyzed for evaluation of thyroid depressing drugs as well as for the study of iodine metabolism in the thyroid gland. (H.B.G.)

11174 DIFFERENTIAL DIAGNOSIS OF ^{85}Sr ACCUMULATING PROCESSES WITH THE WHOLE-BODY SCINTIGRAM. Walther, E. (Univ., Zurich). Nucl.-Med.; 32: Suppl. 7, 511-15(1968). (In German).

From 5th Conference of the Society of Nuclear Medicine, Vienna, Austria. See CONF-670996.

Whole-body scintigraphy was performed after administration of ^{85}Sr. In 60 patients, scintigraphy confirmed bone metastases diagnosed by x-radiography; however, the scintigraphic changes frequently exceeded in extent the roentgenologically determined defects. In 6 patients with roentgenologically established bone metastases, the scintigram was negative. In 9 patients with negative radiographic findings, scintigraphy revealed multiple bone metastases. After blunt injuries to muscles, calcification was recognized easily by scintigraphy. Degenerative changes in bones and joints appeared clearly in the scintigram and presented frequently difficult differential diagnostic problems against metastases. (H.B.G.)

11175 STUDIES WITH ^{85}Sr OF DISEASES BELONGING TO THE RHEUMATIC COMPLEX. Eickenbusch, W.; Mueller, W.; Lahrtz, Hg. (Univ., Kiel). Nucl.-Med.; 32: Suppl. 7, 517-22 (1968). (In German).

From 5th Conference of the Society of Nuclear Medicine, Vienna, Austria. See CONF-670996.

Patients received intravenously 50 to 100 μCi ^{85}Sr chloride. Several days later, after emptying of bladder and colon, scintigraphy was performed. In Bechterews disease, high amounts of radioactivity appeared in the sacroiliac area during the inflammatory phase of the disease. In ankylosing spondylitis, chronic polyarthritis, and arthrosis deformans findings were less consistent. It was concluded that ^{85}Sr scintigraphy plays a significant role in differential diagnosis of rheumatic processes involving bones, joints, and soft tissues. (H.B.G.)

11176 DIFFERENTIAL SCINTIGRAPHIC REPRESENTATION OF THE PANCREAS BY MEANS OF A COMPUTER. Roth, G.; Eber, O.; Wascher, H.; Leb, G. (Medizinische Univ., Graz). Nucl.-Med.; 32: Suppl. 7, 523-7(1968). (In German).

From 5th Conference of the Society of Nuclear Medicine, Vienna, Austria. See CONF-670996.

Selenium-75-methionine is accumulated by both pancreas and liver. Because of overlapping of the two organs, scintigraphy of the pancreas frequently is difficult or impossible. A relatively simple computer method prints the difference between the simultaneous labeling with ^{198}Au and ^{75}Se. Since ^{198}Au is preferentially accumulated in the liver, the differential scintigram clearly outlines the pancreas alone, as demonstrated by clinical application. (tr-auth)

11177 SOME ASPECTS OF ABDOMINAL LYMPHO-SCINTIGRAPHY. Firusian, N.; Schmidt, C. G. (Univ., Muenster, Ger.). Nucl.-Med.; 32: Suppl. 7, 529-33(1968). (In German).

From 5th Conference of the Society of Nuclear Medicine, Vienna, Austria. See CONF-670996.

Possible errors in performance and interpretation of scintigrams involving the abdominal lymphatic system are analyzed. Evaluation of filling defects can only be made in combination with that of clinical findings and other diagnostic procedures. Cold spots can be produced not only by tumor metastases and granulomatosis, but also by varicosis with lymphedema of the lower extremities, obesity, ascites, size of colloidal particles of ^{198}Au in excess of 50 Å, condition after x-ray therapy, and congenital aplasia. (H.B.G.)

11178 LYMPH DRAINAGE FOLLOWING NECK SURGERY. Wascher, H.; Eber, O.; Leb, G.; Siegl, H. (Medizinische Univ., Graz. Univ., Graz). Nucl.-Med.; 32: Suppl. 7, 535-39(1968). (In German).

From 5th Conference of the Society of Nuclear Medicine, Vienna, Austria. See CONF-670996.

To study lymphatic drainage following radical neck dissection, 21 patients received 100 to 150 μCi of ^{198}Au colloid injected subcutaneously into the mastoid region. To facilitate resorption, 100 units of hyaluronidase were added. 24 hours following injection, the neck area was scanned. Results showed that satisfactory lymph drainage was reestablished, at the earliest five months, at

XUM

the latest 13 months, following radical neck dissection. Salvage of the jugular vein seemed to facilitate reestablishment of lymph drainage. In several patients, collateral lymph drainage could be detected. (H.B.G.)

11179 STUDIES ON THE UPTAKE OF ^{203}Hg-CHLORMERODRIN BY BRAIN TUMORS. Riccabona, G.; Scharfetter, F. (Chirurgische Univ., Innsbruck). Nucl.-Med.; 32: Suppl. 7, 541-5 (1968). (In German).

From 5th Conference of the Society of Nuclear Medicine, Vienna, Austria. See CONF-670996.

In eleven patients with brain tumors, ^{203}Hg chlormerodrin was injected and brain scans obtained. Surgical removal of the tumor was performed in 4 patients at 2 hours following isotope injection, in 3 patients at 4 hours, and in 4 patients at 24 hours. The tumor material was homogenized and its radioactivity analyzed. Results showed that ^{203}Hg was rapidly bound to an α-globulin. This labeled mercury-globulin complex disappeared from the tumor at a half time of 12 hours. Since removal of ^{203}Hg chlormerodrin from the plasma occurred with a half time of approximately 30 min., differential diagnosis between brain tumors and other brain lesions was possible. (H.B.G.)

11180 SCINTIGRAPHIC FINDINGS IN LIVER DISEASES IDENTIFIED BY LAPAROSCOPY AND HISTOLOGY. Kempe, H.; Dischler, W.; Gehring, D. (Medizinische Univ., Freiburg i. B.). Nucl.-Med.; 32: Suppl. 7, 547-52(1968). (In German).

From 5th Conference of the Society of Nuclear Medicine, Vienna, Austria. See CONF-670996.

Scintigraphy of the liver was performed at 10 to 15 min. following administration of ^{131}I Rose Bengal in doses from 100 to 200 μCi. In comparison with findings through laparoscopy and biopsy it was concluded that in the majority of patients abnormal scintigraphic findings could be confirmed by both laparoscopy and histology. Occasionally, inconspicuous scintigrams were obtained in spite of severe liver damage. In a few patients with normal clinical laparoscopic and histologic findings, abnormal scintigrams were obtained that could not be explained. Significance of scintigraphy increased when pathological processes exceeded a diameter of 2 to 3 cm. (H.B.G.)

11181 NORMAL-PRESSURE HYDROCEPHALUS. ROLE OF CISTERNOGRAPHY IN DIAGNOSIS. James, A. Everette Jr.; DeLand, Frank H.; Hodges III, Fred J.; Wagner, Henry N. Jr. (Johns Hopkins Medical Institutions, Baltimore). J. Amer. Med. Ass.; 213: 1615-22(7 Sep 1970).

Normal-pressure hydrocephalus is characterized by neurological symptoms of dementia and awkwardness of movement, cerebrospinal fluid pressure in the normal range, and ventricular enlargement without cortical atrophy. Pneumoencephalograms reveal enlarged ventricles with failure of air to pass over the cerebral convexities. The cisternographic abnormalities are the presence of radioactivity in the enlarged ventricles, abnormality of movement of the injected radioactivity over the cerebral hemispheres, and failure of the radioactivity to concentrate in the sagittal area on delayed scans (24 or 48 hrs.). Since normal-pressure hydrocephalus is a treatable form of dementia, accurate diagnosis based on clinical manifestations, findings from lumbar puncture, pneumoencephalography, and cisternography is mandatory. (auth)

11182 USE OF THE SCINTILLATION CAMERA FOR FUNCTIONAL INVESTIGATION IN MEDICINE. Delaloye, B. (Univ., Lausanne, Switzerland). Helv. Med. Acta; 35: No. 1, 43-54 (1969).

The value of the scintillation camera in medical diagnosis is reviewed. Stationary detectors permit dynamic and functional investigations which are impossible with scintigraphy. The use of the scintillation camera is discussed in the diagnosis of the placental insertion, of cerebral tumors, in the examination of the bile ducts, pancreas, lymphatic tracts and in the evaluation of renal and cardiopulmonary function. Numerous examples are presented. (Excerpta Med.)

11183 DIAGNOSTIC VALUE OF HEPATIC SCINTIGRAPHY IN THE LIGHT OF PERSONAL EXPERIENCES. Austoni, M. (Univ., Padua). Minerva Med. Giuliana; 8: 364-74(Sep-Oct 1968). (In Italian).

Notwithstanding the great advances in systematology the differential diagnosis of liver affections offers great difficulties. Recent progress in hepatic scintigraphy offers prospects for improving diagnosis and therapy of liver diseases. Availability of a wide range of radioisotopes and tagged molecules in combination with improved methods of isotopic analysis, autoradiography, scanning methods, gammagraphy and the use of computers in image interpretation, above all the possibility to suppress radiation effects at any desired level of activity and thus obtaining sharper and clearer images have greatly expanded the diagnostic value of hepatic scintigraphy. The time has come to give the clinician a better idea of what scintigraphy can accomplish in the diagnosis of abdominal diseases. For the purpose of scintigraphy the pathogenic liver conditions are classified in two groups: those of a diffuse nature such as cirrhosis, where one can determine with Rose-Bengal-^{131}I alterations in volume, form and structure of the liver; those of circumscribed nature such as tumors, cancer, adenomas, where the use of ^{198}Au produces images localizing exactly the respective malignancies. In general one can say that scintigraphy has become an important help in the diagnosis of hepatic diseases, but does not replace other methods; its particular value lies in the possibility to observe evolvement of pathogenic changes within certain time periods; pre-operative scanning of suspected areas will help the surgeon immensely in his task; in combination with splenoportography it greatly facilitates differential diagnoses; it offers also corollary data concerning bile functions; it allows tridimensional projections of otherwise unobtainable visceral conditions, particularly in cases of obesity or dropsy; and it allows evaluation of therapeutic results and post-operative regeneration. It makes the differential diagnosis between liver cirrhosis and jaundice possible. (F.J.W.)

11184 HEMODYNAMIC FUNCTION STUDIES. Mundschenk, H.; Fischer, J.; Wolf, R. (Univ., Mainz). Int. J. Appl. Radiat. Isotop.; 21: 471-85(Aug 1970). (In German).

The multichannel function test device described allows the simultaneous measurement of radioactivity at several sites of the body and the observation of very fast hemodynamic processes. The data, stored in the memory of a multiscaler, are smoothed as regards the statistical fluctuations by means of 2 procedures. The activity curves are read out logarithmically by an XY-plotter and evaluated graphically with respect to the rate constants, and complementary exponential functions are differentiated, read out logarithmically and evaluated in the same manner. In some selected cases it is demonstrated how the measured activity curves can be decomposed, interpreted and correlated to the corresponding biological processes. Furthermore it is pointed out how using two different and labeled particles, further information can be obtained in hemodynamic function studies. The set-up used also allows the registration of processes with rate constants in the msec-range. By careful positioning of the detectors above the heart and spleen the activity fluctuations, caused by periodical contractions of the organs, can be observed clearly. Such observations indicate that in certain circumstances the spleen is able to contract periodically. (auth) (UK)

11185 VALIDITY OF THE ISOTOPE DILUTION METHOD OF MEASURING EXTRACELLULAR FLUID VOLUME AFTER ACUTE HAEMORRHAGE. Furneaux, R. W.; Tracy, G. D. (New South Wales Univ., Kensington, Australia). Aust. J. Exp. Biol. Med. Sci.; 48: 407-15(Aug 1970).

Estimations of extracellular fluid volumes were made before and after three levels of acute hemorrhage in anesthetized, splenectomized dogs. Three different radioactive isotopes, $^{35}SO_4$, ^{125}I, and ^{24}Na were used. The reduction in sulfate space after 10% and 27% blood loss was replenished in less than two hours. However, after 46% blood loss, the sulfate space was markedly reduced and showed no evidence of recovery. The rate loss of the isotope after equilibration declined from 12.7% to 9% per hour. When ^{125}I or ^{24}Na were used the results were different. These isotope dilution spaces were reduced two hours after hemorrhage only by an amount equal to the volume of plasma water removed by the hemorrhage. Delay in equilibration of all three isotopes occurred after hemorrhage, and possible explanations for the anomalous behavior of sulfate after 46% hemorrhage are discussed. From this it is concluded that immediately after severe hemorrhage an accurate assessment of extracellular fluid partitioning may not be possible without a marker which is instantly distributed into the total extracellular fluid space. (auth) (Australia)

11186 PROGNOSTIC VALUE OF RADIOISOTOPIC RENAL FUNCTION STUDIES FOR SELECTING PATIENTS WITH RENAL ARTERIAL STENOSIS FOR SURGERY. Farmelant, Melvin H.; Sachs, Charles; Burrows, Belton A. (Boston Univ. Boston Veterans Administration Hospital). Contract AT(20-1)-3099. J. Nucl. Med.; 11: 743-8(Dec 1970).

The achievement of normotension in hypertensive patients with renal arterial stenosis by surgical restoration of renal blood flow or nephrectomy is quite variable. The relationship of preoperative renal function to the blood pressure response to surgery was considered in a group of patients undergoing operations for renal arterial stenosis. In addition to usual clinical estimates, ^{131}I-Hippuran studies were used to evaluate renal function. Nineteen of the 20 patients who were cured of renovascular hypertension by

XUM

surgery had preoperative ^{131}I-Hippuran studies with an initial half-time of 4.3 min. or less. All 25 patients with persistent hypertension after similar surgery had half-time values 4.4 min. or more. The ^{131}I-Hippuran studies provided a sensitive measure of renal function; this measure predicts the blood pressure response to surgery for renovascular hypertension with acceptable accuracy. The response to surgery is dependent on the functional state of the kidneys. (E.E.H.)

11187 RADIOISOTOPIC ANGIOCARDIOGRAPHY: FINDINGS IN MITRAL STENOSIS AND MITRAL INSUFFICIENCY. Matin, Philip; Kriss, Joseph P. (Stanford Univ., Calif.). J. Nucl. Med.; 11: 723-30(Dec 1970).

Using the scintillation camera and the variable time-lapse videoscintiscope and a special positioning technique, intravenous radioisotope (^{99m}Tc) angiocardiography was performed in a group of 22 patients with documented disease of the mitral valve. The purpose of this paper was to describe this technique and show its application in the study of three categories of patients with mitral valvular disease: pure mitral stenosis, pure mitral unsufficiency and combined mitral stenosis and insufficiency. The technique offers promise as a simple, safe screening procedure for patients with known or suspected disease of the mitral valve. (E.E.H.)

11188 RADIOIODINATED TOLUIDINE BLUE: AN UNSATISFACTORY SCANNING AGENT. Larose, James H.; Whitaker, Robert H.; Reba, Richard C. (Johns Hopkins Medical Institutions, Baltimore). J. Nucl. Med.; 11: 731-2(Dec 1970).

To be considered as an effective scanning agent, a radiopharmaceutical should concentrate significantly in the organ or area of interest in relation to the background radioactivity for the duration of the expected observation. These experiments were designed to evaluate the use of ^{125}I-labeled toluidine blue as a possible scanning agent for the parathyroid or pancreas. The concentration ratios of toluidine blue in pancreas to liver and parathyroid to thyroid were less than 2:1 and there was frequent overlap in the relative concentrations at 1 s.d. These results were considered unsatisfactory. (E.E.H.)

11189 EVALUATION OF /sup 99m/Tc-DTPA ACID AS A BRAIN SCANNING AGENT. Brookeman, Valerie A.; Williams, Clyde M. (Univ. of Florida, Gainesville. Veterans Administration Hospital, Gainesville, Fla.). J. Nucl. Med.; 11: 733-8(Dec 1970).

The chelating agent, diethylenetriaminepentaacetic acid (DTPA), when complexed with ^{99m}Tc was advocated as a brain scanning agent superior in clinical use to ^{99m}Tc-pertechnetate. Paired brain images were obtained with $^{99m}TcO_4^-$ and ^{99m}Tc-DTPA, two days apart, in 14 patients with a variety of intracranial lesions. Lesion-to-brain and lesion-to-blood ratios were calculated from digitized computer-processed data matrices after suitable correction for inequalities in detector-system response. All lesions were visualized equally well with both scanning agents. Lesion-to-brain and lesion-to-blood ratios obtained at postinjection times from 10 min. to 3½ hr. did not differ significantly between $^{99m}TcO_4^-$ and ^{99m}Tc-DTPA. When lesions were divided into two groups, tumors and infarcts, it was observed that $^{99m}TcO_4^-$ tumor-to-brain and tumor-to-blood ratios increased significantly from 30 min. to 1 hr., after which time no further significant increase occurred. Infarct-to-brain and infarct-to-blood ratios did not increase significantly with time over the period from 30 min. to 3 hr. The data suggested that the optimal time to begin scanning is about 1 hr. after injection of $^{99m}TcO_4^-$ since no significant improvement was obtained in lesion-to-brain and lesion-to-blood ratios after that time. (E.E.H.)

11190 RADIATION BURDEN IN NUCLEAR MEDICINE INVESTIGATIONS IN CHILDHOOD. Wolf, R. (Univ., Mainz). Monatsschr. Kinderheilk.; 118: 221-4(Jun 1970). (In German).

Even during childhood, thyroid examination represents the most frequent application of radioisotopes. Detection of thyroid deficiency is most decisive for both mental and physical development of the child. Administration of even 1 μCi ^{131}I leads to doses between 10 and 24 rad to the thyroid. Use of ^{125}I reduces the burden to one third. Most favorable appears application of ^{99m}Tc that reduces the radiation burden to the thyroid to 1% of that of ^{131}I. Similar considerations are applied to diagnostic renal procedures in children. ^{203}Hg-labeled compounds as well as ^{75}Se-methionine should be avoided. In comparison to radiological procedures, certain radioisotope methods pose less of a radiation burden and may be applied when diagnostic significance is carefully balanced against the risk. (H.B.G.)

11191 DETECTION OF THROMBOSIS WITH ^{125}I FIBRINOGEN. O'Brien, J. R. Lancet; 2: 396-8(22 Aug 1970).

The injection of ^{125}I-fibrinogen with subsequent scanning of the legs is a valuable method of detecting thrombosis. A new method of analysing the data is put forward and related to clinical events in selected patients. The method assumes that the counts registered over a thrombus are contaminated by an almost normal amount of circulating blood in the thrombosed and other veins. Thus the normal count for the area scanned, estimated from counts above or below or contralateral counts, is subtracted from the observed count. This excess count, expressed as a percentage of the excess counts on the 1st day of thrombosis, most accurately reflects any change in the amount of deposited fibrin. (auth) (UK)

11192 5th EUROPEAN CONFERENCE ON MICROCIRCULATION. International Conference, Goteborg, Sweden, June 24-29, 1968. Harders, H. (ed.). Bibliotheca Anatomica, No. 10. Basel; S. Karger AG (1969). 617p. $45.60. (CONF-680670).

One hundred and two papers were presented in the conference. Four separate abstracts were prepared. The papers not included for NSA deal with rheology, viscometry, clinical rheology, ultrastructure, vascular anatomy, properties of blood vessels, nervous system, experimental and clinical microscopy, coagulation, fibrinolysis, and platelets. (H.B.G.)

For abstracts of individual papers see: 10926 and 11193–11195.

11193 ALLERGIC INFLAMMATION. I. SIMULTANEOUS MEASUREMENT OF VASCULAR PERMEABILITY TO ISOTOPE-LABELLED CELLS AND PROTEIN IN IMMEDIATE AND DELAYED HYPERSENSITIVITY. Morley, J.; Dumonde, D. C. (Kennedy Inst., London. St. Mary's Hospital Medical School, London). Bibl. Anat.; No. 10, 244-51(1969).

From 5th European Conference on Microcirculation, Goteborg, Sweden. See CONF-680670.

The application of quantitative physiological techniques to study the development of inflammation in response to immunological reactions is discussed. Isotope-labeling of erythrocytes can readily be accomplished with $Na_2Cr^{51}O_4$. Intravascular injection of these labeled cells provides a simple technique for measuring the local accumulation of cells during the development of an inflammatory lesion. Intravascular injection of ^{125}I-labeled protein permits simultaneous measurement of increased vascular permeability to protein in the same lesion. These techniques were applied to the study of vascular permeability to cells and protein in skin reactions of immediate and delayed hypersensitivity. (auth)

11194 MEASUREMENT OF HYPOTHALAMIC BLOOD FLOW IN THE CONSCIOUS RABBIT BY A RADIOACTIVE INERT GAS CLEARANCE TECHNIQUE. Rosendorff, C.; Cranston, W. I. (St. Thomas' Hospital Medical School, London). Bibl. Anat.; No. 10, 292-7(1969).

From 5th European Conference on Microcirculation, Goteborg, Sweden. See CONF-680670.

Diffusible indicators were used to provide estimates of total cerebral blood flow, compartmental flow, regional flow, and legal flow in the cortex and subcortical white matter. The present method is an adaptation of the ^{133}Xe clearance technique, and was used to assess local blood flow in the anterior hypothalamus of the conscious rabbit, without craniotomy. Microlitre volumes of a saline solution of ^{133}Xe were injected into the hypothalamus through a stereotaxically placed cannula, and the γ emission counted using an external probe. The clearance of radioactivity from the injection site was mono-exponential, and the derived values for hypothalamic blood flow varied from 0.21 to 0.43, with a mean of 0.31 ml/g tissue/min. The accuracy of absolute values for blood flow depends upon a knowledge of λ for the hypothalamus, which is not yet available. However, the technique allows for measurement of changes in flow in a variety of experimental situations, some of which were described. (auth)

11195 SIGNIFICANCE OF RED CELL AGGREGATION IN THE VASCULAR COMPLICATIONS OF ANGIOGRAPHY. Langsjoen, P. H.; Best, E. B. (Scott and White Hospital, Temple, Tex.). Bibl. Anat.; No. 10, 449-57(1969).

From 5th European Conference on Microcirculation, Goteborg, Sweden. See CONF-680670.

Two hundred ninety-eight patients subjected to angiography were randomized by the sealed envelope system into three groups. Group A received no preliminary hydration. Group B received 500 cc 5% glucose in distilled water immediately prior to angiography. Group C received 500 cc 10% low molecular weight dextran in 5% glucose immediately prior to angiography. Serial measurements of venous blood hematocrit and viscosity showed changes which were compatible with, though not clearly diagnostic of, immediate red cell aggregation in Groups A and B only. No statistically significant difference in the incidence of complications was noted between Groups A and B, indicating that hydration alone has no prophylactic value. Statistically significant

XUM

reduction in the incidence of complications was noted in Group C when compared with either Group A, Group B or Group A and B combined. Low molecular weight dextran given intravenously as a 10% solution in 5% glucose immediately prior to angiography significantly reduced the incidence of complications from these procedures. (auth)

11196 SCINTIGRAPHY WITH ^{198}Au FOR CHRONIC HEPATITIS. Torsoli, A.; Cassano, C. C.; Arzano, S. (Univ., Rome). Minerva Med. Giuliana; 8: 409-10(Sep-Oct 1968). (In Italian).

There exist numerous pathological conditions with similar scintigraphic manifestations such as non-cirrhotic chronic hepatitis with obstruction of the portal vein and systemic diseases of the liver (reticuloses) which involve both liver and spleen. Scintigrams produced by the same dose of ^{198}Au per kg body weight are a function of two parameters: local blood circulation and number of active granulated elements. For liver diagnoses the first parameter is of greater importance. In suspected cases of cirrhosis where the scintigram shows no abnormality, one may either increase the dose thus increasing the contrast; or reduce it to get a clearer image of existing heterogeneities. The scintigraphic effect of ^{198}Au on the spleen depends in contrast to that of the liver on the number of granulated elements. For a systematic scintigraphic appraisal of the liver one must distinguish between cirrhosis and non-cirrhotic chronic liver affections; establish the existence of a congestive cirrhosis; exclude all forms of neoplastic processes; and closely observe the evolution of the pathologic condition. (F.J.W.)

11197 SCINTIGRAPHY FOR DIAGNOSIS OF HEPATIC AND PANCREATIC CONDITIONS OF SURGICAL INTEREST. Fegiz, G. F. (Univ., Rome). Minerva Med. Giuliana; 8: 439-40(Sep-Oct 1968). (In Italian).

Pre-operation scanning of the liver using colloidal ^{198}Au or rose bengal-^{131}I is of great importance for surgery. It reveals not only the exact dimension of the liver but also under-fixation areas which may correspond to echinococcus cysts, abscesses, angiomas, primary and secondary tumors. Cysts can be recognised by their sharply demarcated spherical form. Of special interest are those in the hepatic cupola which tend to penetrate the diaphragm of the lung and invade the bronchial tubes. Though the symptoms are pulmonary, a diagnosis cannot be reached by bronchiography, but only by hepatigraphy. Post-operative scintigraphic control of the patient is necessary since cysts have the tendency to reappear. A neoplasm can be distinguished from a cyst by its ragged form and by the fact that the surrounding healthy tissue is not displaced. Evidence of hepatic abscesses is detected in the scintigram by a round area of underfixation without sharp boundaries and infiltration into the surrounding inflammation. Interpretation of pancreatic scintigraphy with methionine-^{75}Se is very difficult since liver and other organs have a stronger competitive affinity to this tracer than the pancreas. In acute cases of pancreatitis fixation is reduced and the image ill-defined. In chronic or neoplastic cases under-fixation may be observed of the entire organ or only parts of it together with various lacunae. Finally the scintigraphic appearance of the seldom observed pancreas calcification is described. (F.J.W.) (TSS)

11198 CONTRIBUTION OF SCINTIGRAPHY FOR THE DIAGNOSIS OF LIVER DISEASES. Benassi, E.; Sannazzari, G. L. (Univ., Turin). Minerva Med. Giuliana; 8: 375-77(Sep-Oct 1968). (In Italian).

Hepatic tracers can be divided into two groups: epitelliotropic compounds that are rapidly excreted such as rose bengal-^{131}I, phenolphthaleine-tetraiodide-^{131}I or ^{64}Cu, and ^{99}Mo as precursor of ^{99m}Tc; histocytotropic compounds that are picked up by the cytoplasm and remain there, depending on their half-life. The most important are colloidal ^{198}Au, serum al bumin-^{131}I or -^{125}I, and a colloidal suspension of ^{99m}Tc in form of insoluble Tc_2S_7. Labeled rose bengal is now very little used since it is too rapidly eliminated. Since many pathological conditions in the liver reveal themselves through the absence of activity, it is essential to know how the response would be to normal tissue. The symptomatological conditions revealed by scintigraphy can be classified as follows: modification of liver position, revealed by roentgenscintigraphy, showing the entire hepatic region on a single film; modification of form and size of the liver as for instance in cirrhosis using colloidal ^{198}Au; and structural changes in the liver such as diffuse alterations appearing as irregular crosshatchings with diminished blackening of the film or localized structural alterations due to liver abscesses or malignancies. If the difference in shading is so slight that it does not allow any judgement, magnetic registration with subsequent close-circuit TV provides greater contrasts. However good the scintographic images may be, their value can be obliterated by erroneous interpretation. (F.J.W.) (TSS)

11199 CONSIDERATION OF THE CLINICAL INTERPRETATION OF SCINTIGRAMS OF THE PANCREAS UNDER NORMAL AND PATHOLOGICAL CONDITIONS. Centi Colella, A.; Pigorini, F.; Tomisdili, A. (Univ., Rome). Minerva Med. Giuliana; 8: 411-15(Sep-Oct 1968). (In Italian).

Pancreas scintigraphy began in 1963, but only in the last three years it became clinically important. This is due: to a better preparation of the patient before examination by high protein diet to increase the avidity of absorption of methionine-^{75}Se for enzyme synthesis and increased retention of the formed enzyme by administration of anticolinergic agents; to improved instrumentation by using larger crystals, focalizing collimators, and photographic registration; greater purity of tagged selenomethionine of which 3.5 μCi per 1 kg body weight are administered. Pancreas morphology can be of three basic types: classic or pistol form; club form; horse-shoe form. Interference with the pancreatic image may result from an enlarged liver or parasitic activities in the gastrointestinal mucosa. Under pathological conditions such as sclerosis or neoplasia, the pancreatic image is greatly enlarged compared to that of the stomach or small intestines. In case of swelling of extra-pancreatic organs pressure is exerted on the pancreas and the images show deformation or displacement. For instance an enlarged spleen makes the tail of the pancreas appear smaller which may lead to misinterpretation in various ways, if no account were taken of the existing splenomegaly. (F.J.W.) (TSS)

11200 SCINTIGRAPHY OF LIVER, SPLEEN, AND PANCREAS. Melli, G. (Univ., Milan). Minerva Med. Giuliana; 8: 381-5(Sep-Oct 1968). (In Italian).

Two types of instruments are used in liver, spleen, and pancreas scintigraphy: the movable scanner which rapidly explores the field of interest; and the fixed scintigraph with large crystal (γ-chamber). The former have superior resolution, while the latter have the advantage of recording distinctively the accumulation and disappearance of radioactive tracers. In clinical use are also photoscanners which have great versatility and high resolution. For liver scintigraphy one uses as tracers colloidal solution of ^{198}Au or ^{111}Ag, serum albumin-^{125}I, and others. Pathological conditions are indicated by anomalies of position, form, and structure. Positional changes may consist in prolapse, inversion, or displacement, the latter an indication of abscesses or tumors. For spleen scintigraphy one uses as tracers erythrocytes tagged with ^{51}Cr and also bromo-mercury-hydroxypropane-^{197}Hg which attaches itself to the erythrocytes. Since the clearance of the spleen from radioactive matter is completed in 6 hours, it is necessary to carry out the spectrographic examination within this time. In this way one can determine pathological processes that change form, volume, and position of this organ, but also localised processes such as malignancies, necroses, cysts, abscesses, etc. Total invisibility indicates complete functional exclusion. The most common tracer for pancreas scintigraphy is methionine-^{75}Se. In order to make the pancreas more conspicuous with this weak radioactive tracer, the patient is usually given before its administration an intravenous injection of 30g glucose. A serious difficulty in pancreas scintigraphy is the fact that the liver has a greater affinity to ^{75}Se than the pancreas and in cases of liver enlargement the pancreas image may become completely obscured. In such cases one extinguishes the liver image obtained with ^{198}Au electronically and superimposes it upon the ^{75}Se picture of the pancreas. The scintigraphic picture of the pancreas shows greatest variability. In general the following conditions may appear in the images: total underfixation or irregular fixation could indicate edema, acute pancreatitis or diabetes of long duration. The presence of voids within the pancreas may be an indication of tumors, cysts, or septic ulcers. Complete absence of fixation may be caused by obstructing tumors or destructive atrophia. However, the images of all these pancreas diseases are extremely difficult to differentiate on the basis of scintigraphic findings only. These constitute only hints indicating to the clinician strong possibilities, but deserving close scrutiny by other diagnostic methods. (F.J.W.)

11201 ON THE SCINTIGRAPHY OF PARENCHYMATOUS ORGANS AND IN PARTICULAR OF THE SPLEEN. Ratti, A. (Univ., Milan). Minerva Med. Giuliana; 8: 386-8(Sep-Oct 1968). (In Italian).

General problems of radiography of parenchymatous organs (thyroid and adrenal glands, liver, pancreas, and spleen) are discussed. During the last few years new methods have been developed that make it possible to recognize pathological changes in these organs. In the first place it is necessary to find a suitable gamma-radioisotope for the fixation of the outlines of the organ in question. Secondly, one has to apply a suitable radioactively tagged compound which would reveal the internal structure of the organ. Limiting factors for scintigraphic scanning

are the resolving capacity of the instruments, i.e., the possibility of a point by point determination of small differences of radioactivity and the system of reconstruction of the thus obtained information in form of a map or a profile. Considering the contours of an organ on a scintigraphic map, it cannot be ascertained whether areas of major or minor activity give the true contour of this organ or perhaps cold spots are formed by infection as, for instance, in cysts. There is also the possibility that areas in the map appearing abnormal are due to the enormous variability of parenchymatous tissue in healthy individuals. Erythrocytes were tagged with ^{51}Cr or with bromo-mercury-hydroxypropane-^{197}Hg. Fifteen patients suffered from lymphogranuloma, 10 from lymphosarcoma, 2 had lymphatic leukemia and the rest other splenic diseases. Of the 25 lymphatic cases 8 showed a normal scintigraphic picture and 17 clearly visible pathological conditions. In four cases cold areas of irregular size were found. An examination of the liver of these patients, using ^{198}Au as tracer, revealed severe damage. In general it can be stated that scintigraphic examination of the spleen is a useful diagnostic method. (F.J.W.) (TSS)

11202 SCINTIGRAPHIC METHOD FOR DETERMINATION OF THE REGENERATIVE ABILITY OF THE LIVER. Cirenei, A.; Bernardini, P. (Pio Istituto di S. Spirito ed OO.RR., Rome). Minerva Med. Giuliana; 8: 430-8(Sep-Oct 1968). (In Italian).

Among the methods to determine the actual regeneration as well as the regenerative capacity of the liver after hepatectomies the most efficient and precise is angiography, particularly splenoportography and arteriography. But this method is extremely complicated and also hazardous so that other means have to be found for the control of the recovery process. A simple, rapid, and repeatable method consists in a systematic evaluation of portion of the scintigraphic image of the liver in comparison to the macroscopic findings during the operation and the histological appearance of the hypertrophic parenchyma. The correlation between scintigraphic, bioptic, and histological findings before and after hepatectomies is shown in numerous graphs and photographs. But it is pointed out that in the case of water-filled cysts apparent hypertrophies cannot be considered as signs of regeneration. Scintigraphic methods hold great promise, in combination with other clinical findings, for the evaluation of recovery prospects after liver operations. (F.J.W.) (TSS)

11203 SOME PARTICULAR ASPECTS OF SCINTIGRAPHY IN CIRRHOSIS OF THE LIVER. Girolami, M.; de Dominicis, A. (Univ., Rome). Minerva Med. Giuliana; 8: 378-80(Sep-Oct 1968). (In Italian).

The patients were given 3 uCi ^{198}Au per kg body weight in colloidal solution. A common feature of the scintigraphs was the uneven distribution of the tracer on the liver surface. Another characteristic was the abnormal position of the liver, due to prolapse. Its morphology was completely changed by a missing lobe or part. In some cases the intraparenchymatous area was more or less voluminous, but the radiocolloid completely absent or reduced. In many cases irregularities or morphological alterations were actually due to the pick-up of relatively large amount of radioactive matter by an enlarged spleen. Spleen hyperactivity in cirrhosis has the most profound effect on structural appearance of the liver in the scintigraph, due to the fixation of a distinct amount of ^{198}Au at the margin of the hemopoietic zones. In many cases a remarkable increase of erythroblast was actually observed that also explains the diffuse radioisotope pick-up. Many patients with liver cirrhosis were treated with testosterone propionate or vitamin B_1. In many so treated subjects an increase in liver volume and greater homogeneity of tracer distribution was observed. In general the scintigraphic picture improves corresponding to the clinical symptoms of improvement of the patient. (F.J.W.) (TSS)

11204 ^{69m}Zn-CHLORIDE. A NEW SCANNING AGENT: A STUDY OF ITS DOSIMETRY AND BIOLOGICAL FATE. Lorber, Steven A.; Gold, Fred M.; Maglione, Anthony A.; Rubenfeld, Sidney (New York Univ., N. Y.). J. Nucl. Med.; 11: 699-703 (Dec 1970).

Zinc chloride in the form of radioactive ^{69m}Zn-chloride when injected into mature male dogs and female rabbits was found to concentrate most in the liver and less in the prostate, pancreas and kidney. The ^{69m}Zn β-γ absorbed doses of the target organs studied were found to be within the acceptable ranges of other commonly used radioisotopes. Satisfactory γ-camera scans of the prostate were obtained. The possibility of morphological evaluation of the prostate by scanning is especially promising. (auth)

11205 ^{68}Ga-LABELED MACROAGGREGATES FOR LUNG STUDIES. Colombetti, Lelio G.; Goodwin, David A.; Togami, Edwin (Veterans Administration Hospital, Palo Alto, Calif. Stanford Univ., Palo Alto, Calif.). J. Nucl. Med.; 11: 704-7(Dec 1970).

A simple and rapid technique for the preparation of sterile, pyrogen-free ^{68}Ga-labeled particles suitable for lung studies in humans was presented. This technique for preparation of positron-labeled particles permits a tomographic display of pulmonary perfusion by means of the Anger positron camera. Preliminary studies suggest that perfusion tomograms will have great value in accurately determining the size and location of perfusion abnormalities in the lung. (auth)

11206 USE OF THE GAMMA CAMERA FOR ^{131}I RENOGRAPHY: A CASE STUDY ON A NEPHRECTOMIZED PATIENT. Short, M. D.; Glass, H. I.; Vernon, P. (Hammersmith Hospital, London). J. Nucl. Med.; 11: 758-60(Dec 1970).

A case study was presented which allowed examination of the validity of existing techniques in ^{131}I renography and to test the feasibility of using the gamma camera as an alternative method. A comparison of small (7-cm-dia) and large (14-cm-dia) collimator fields of view showed a reduction in the kidney-to-tissue background counting-rate ratio by a factor of five for normal function when the larger field size was used. Errors in tissue background estimates were evident using the γ camera even when a double tracer method using labeled albumin and Hippuran is adopted. The use of a double tracer method was considered essential when renal function is poor. It was suggested that to obtain maximum accuracy in the quantitation of poor renal function, a suitably located additional probe used in association with the γ camera may prove to be a more useful type of system. Quantitative studies of renal function or plasma flow with ^{131}I-Hippuran using a γ camera system alone are unlikely to be of value unless a factor can be found which relates the albumin counting rate at the subclavicular site to that at the selected tissue background site within the camera field of view. The feasibility of establishing such a factor is being investigated at the present time using ^{131}I- and ^{123}I-labeled Hippuran and Albumin. (auth)

11207 FALSE-POSITIVE PULMONARY PHOTOSCANS OBTAINED WITH A DUAL-PROBE DETECTOR SYSTEM. Krishnamurthy, G. T.; Winston, Martin A.; Weiss, Edward R.; Blahd, William H. (Veterans Administration Center, Los Angeles. Univ. of California, Los Angeles. Univ. of Southern California, Los Angeles). J. Nucl. Med.; 11: 719-22(Dec 1970).

Investigations were made on the effects of posture and patient positioning on the results obtained with a dual-probe scanning system. Iodinated ^{131}I-serum albumin aggregate was injected intravenously into eight patients with suspected pulmonary embolisms. A Picker Dual-Probe-500 Magnascanner was used for pulmonary photoscans. Artifactual defects were present in at least one-half of the photoscans obtained with the bottom probe, whereas no artifacts were noted when the same lung was scanned with the top probe. In some instances, abnormalities were exaggerated in the photoscan obtained with the bottom probe when only minimal abnormalities were noted with the top probe. Abnormal pulmonary photoscans obtained by the bottom probe of a dual-probe scanning system should be interpreted with caution and confirmed by a repeat study with the top probe. The findings indicate that patient posture or position may significantly alter pulmonary photoscan morphology when the dual-probe scanning system is used. (E.E.H.)

11208 FIRST ATTEMPTS OF CLINICAL APPLICATION OF A METHOD FOR THE QUANTITATIVE INTERPRETATION OF RENOGRAM WITH RADIOHIPPURAN. Meldolesi, U.; Roncari, G.; Fidanza, M. A.; Conte, L. (Univ., Milan). J. Nucl. Biol. Med.; 13: 94-102(Jul-Sep 1969).

Results are reported of a first attempt of clinical application of a method for the digital computing elaboration of renograms. This method allows an estimate, for each kidney, of the radiohippuran clearance and of some physiological parameters of the urinary excretion. Besides a group of normal subjects, patients with glomerulonephritis, pyelonephritis, tuberculosis, polycystic disease and calculosis were examined. The method used for the renogram analysis has allowed in these cases a quantitative estimate of the functional conditions of the kidneys and of the urinary excretion. Nevertheless the results obtained showed a wide dispersion within the groups, that limits, at the present time, the usefulness of this method in clinical diagnostic work. (auth)

11209 YEAR BOOK OF NUCLEAR MEDICINE. VOLUME 4. 1969. Quinn III, James L. (ed.). Chicago; Year Book Medical Publishers, Inc. (1969). 387p. $12.00.

A literature review of nuclear medicine is presented. A separate chapter is devoted to each of the following systems: en-

XUM

docrine, hematopoietic, genitourinary, nervous, gastrointestinal, circulatory, pulmonary, and skeletal. A chapter on health physics is concerned with accidental radiation, cellular effects of ionizing radiation, effects of radiation on the fetus, incidence of leukemia following treatment of hyperthyroidism, photon dosimetry, short-lived radioisotopes, radiopharmaceutical dosimetry, and radiation exposure of the patient in clinical scintigraphic investigation. Other chapters are included on the role of the chemist in nuclear medicine, radiation physics and instrumentation, and radiochemistry and radiopharmacology. (H.L.W.)

11210 REVIEW ON EVALUATION OF ^{131}I LABELLED HIPPURAN IN THE DIAGNOSIS OF RENAL DISEASE. Hamid, Mohamed Khairi (Radioisotopes Centre, Baghdad). Isotope Radiat. Res.; 1: 73-80(Oct 1968).

Radioisotope renography and isotope clearance procedures for the diagnosis of renal diseases are reviewed. The instrumentation, position and state of hydration of the patient are discussed for the use of iodine-131-labeled Hippuran and a calculated dose of 0.3 μc/Kgm. body wt is given as adequate for reproducible renograms. For the isotope-clearance procedure, formulae for calculating clearance are given as well as interpretations of renograms. The diagnostic value of renography is discussed. (F.M.M.)

11211 LATERAL LIVER SCANNING: AN INDEX TO HEPATIC AND RETROHEPATIC DISEASE. Blum, Manfred; George, Ajax (New York Univ., N. Y.). J. Nucl. Med.; 11: 753-7(Dec 1970).

An analysis of 1,088 liver scans performed during the past 2½ yrs. revealed that 15% of 597 positive examinations had no discernible abnormality in the frontal projection while the lateral projection was abnormal. Forty-three of these patients in whom only the lateral scan was abnormal were followed and have demonstrated metastatic disease, renal pathology, intrahepatic mass lesions, gallbladder pathology, and retroperitoneal space-occupying lesions. An accurate estimate of false-positive scans has not been possible. The importance of biplane scanning of the liver was stressed. (auth)

11212 TECHNICAL ADVANCES OF PANCREATIC SCINTIGRAPHY WITH A FAST SCANNER (DYNAPIX). Schnabel, K.; Schenck, P.; Lange, D. (Univ., Heidelberg). Nucl.-Med.; 9: 129-35(30 Jun 1970). (In German).

In 101 patients the pancreas was scanned using a Dynapix-scanner. Of these, 64 patients were positioned on their right side with the lower end of the table elevated by 15°. No pretreatment with drugs or diet was used. In some cases the pancreas scan after intravenous injection of 200 to 250 μCi of ^{75}Se-selenomethionine was followed by a visualization of the gastrointestinal tract after oral administration of colloidal ^{198}Au, the position of the patients remaining unchanged. The resulting scintigrams of the pancreas and the gastrointestinal tract were exactly superimposed. The results obtained indicated that two of the four scintigraphically demonstrable shapes of the pancreas as described by King, i.e., the sigmoidal and the horse-shoe form, are most likely artefacts caused by the superposition of the gastrointestinal tract. The additional scintigraphy of the GI-tract enables in many cases a clear separation of the pancreas from the GI-tract which also concentrates ^{75}Se-selenomethionine. By using this method the contours of the pancreas could be evaluated in 78% of the patients. (auth)

11213 SCINTIGRAPHIC AND ANGIOGRAPHIC STUDIES OF THE LIVER OF DOGS WITH EXPERIMENTALLY PRODUCED OBSTRUCTIVE JAUNDICE. Kampmann, H.; Beduhn, D. (Institut fuer Nuklearmedizin, Heidelberg. Univ., Heidelberg). Nucl.-Med.; 9: 156-66(30 Jun 1970). (In German).

In dogs, the bile duct was ligated shortly before its entrance into the duodenum. For four weeks, liver function was studied with the scintillation camera following injection of ^{131}I-labeled Rose Bengal and the blood circulation time from the portal vein to the right ventricle was determined with ^{113m}In-labeled EDTA. Scintigraphically, early as well as delayed disturbances of liver function could be detected. Radioactivity was increased in the extrahepatic bile channels while it was decreased in the liver parenchyma. Scintigraphic studies appear to be useful for the differentiation of obstructive jaundice in its early stages, while angiographic studies of the hepatic arteries and the vein of the porto-caval system can contribute little to the early diagnosis. (H.B.G.)

11214 EXPERIMENTAL SCINTIGRAPHY OF THROMBI IN ANIMALS. Nuri, M.; Kampmann, H.; Sinn, H. (Deutsche Krebsforschungszentrum, Heidelberg). Nucl.-Med.; 9: 167-76(30 Jun 1970). (In German).

Thrombi were experimentally produced in hindlegs of rabbits using the method of Gottlob and May. ^{131}I- and ^{113m}In-fibrinogen were used to label the thrombi. The distribution of activity was determined in vivo with a scintillation camera connected to a computer. It was found possible to visualize scintigraphically thrombi labeled with fibrinogen in the rabbit normally up to 48 hours after their production. Iodine-labeled and indium-labeled fibrinogen are equally useful. In order to evaluate the clinical usefulness of thromboscintigraphy as a screening method for the early diagnosis of thrombi, the method should also be used in man. (auth)

11215 DISCREPANCY BETWEEN RADIOLOGICAL AND SCINTIGRAPHIC FINDINGS IN A CASE OF HONEY-COMB LUNG. Chone, B. (Univ., Heidelberg). Nucl.-Med.; 9: 177-85(30 Jun 1970). (In German).

The case history of one patient is reported. Radiology showed pulmonary fibrosis with multiple cystic cells. The tentative diagnosis was between congenital honey-comb lung and progressive pulmonary dystrophy. Scintigraphy after injection of ^{131}I-MAA showed a decreased pulmonary blood flow through the left lung, in sharp contrast to the fact that radiological findings indicated greater damage to the right lung. The final diagnosis was pulmonary emphysema and localized honey-comb lung. (H.B.G.)

11216 EXPERIMENTAL BONE SCINTIGRAPHY IN ANIMALS. Georgi, P.; Sinn, H.; Matzku, S.; Maier-Borst, W.; Bahk, Y. W. (Deutsche Krebsforchungszentrum, Heidelberg). Nucl.-Med.; 9: 194-201(30 Jun 1970). (In German).

The uptake of ^{18}F, ^{47}Ca, ^{85}Sr, and ^{177}Lu was determined 11 days after artificial fracture of the tibia and fibula in rats. The highest uptake rates were found with ^{18}F, ^{47}Ca and ^{85}Sr. The largest difference between the uptake by the callus and that by the healthy diaphysis was found with ^{18}F. The uptake curves of ^{47}Ca and ^{85}Sr had a maximum between 2 and 24 hours. At this time the uptake difference between healthy diaphasis and callus was largest. (auth)

11217 BODY SCANNER USING A MATRIX SYSTEM. Cronquist, A. G. (University Coll. Hospital, London). Bio-Med. Eng.; 5: 552-5(Nov 1970).

A semi-automated body scanner is described, in which counting only takes place when the counting head is stationary. The head moves across a rectangular matrix of counting positions, and results are printed out in matrix form suitable for superimposition on to an outline of the scanned anatomical structures. The method is of particular value when, for instance, small residues of thyroid cancer tissue are being sought close to normal sites of radio-iodine concentration. (auth) (UK)

Radiotherapy

Refer also to abstracts 11058, 11060, 11070–11072, 11296, 11302, and 11303.

11218 (BNL–50203) CONFERENCE ON TIME AND DOSE RELATIONSHIPS IN RADIATION BIOLOGY AS APPLIED TO RADIOTHERAPY HELD AT CARMEL, CALIFORNIA, SEPTEMBER 15–18, 1969. (Brookhaven National Lab., Upton, N. Y.). 372p. (CONF-690915). Dep. CFSTI.

Separate abstracts were prepared for the 26 papers presented at the conference. (H.L.W.)

For abstracts of individual papers see: 10959, 10960, 11007, 11008, 11092–11095, 11219–11224, 11239, 11240, 11252–11260, and 11304.

11219 (BNL–50203, pp 130-53) KINETICS OF CELL PROLIFERATION IN TUMORS. Steel, G. Gordon (Institute of Cancer Research, Sutton (England). Surrey Branch).

From Conference on time and dose relationships in radiation biology as applied to radiotherapy held at Carmel, California, September 15–18, 1969.

A review is presented of the structure of tumor cell populations, the place of models in cell population kinetics, and the cell cycle in tumors. A table is presented to show results of computer analysis of labeled mitoses curves by the SAB model for Ehrlich ascites tumors, transplanted tumors in mice and rats, primary tumors in laboratory animals, spontaneous dog tumors, and tumors in man. The relevance of these studies to radiotherapy of tumors is discussed. (H.L.W.)

11220 (BNL–50203, pp 234-41) REOXYGENATION DURING FRACTIONATED IRRADIATION. Howes, A. E. (Anderson (M.D.) Hospital and Tumor Inst., Houston, Tex.).

From Conference on time and dose relationships in radiation biology as applied to radiotherapy held at Carmel, California, September 15–18, 1969.

Theoretical implications of effects of reoxygenation in fractionated radiotherapy are discussed. In a cell population containing 99% well-oxygenated cells and 1% hypoxic cells, the effects of assuming either that none of the hypoxic cells becomes reoxygenated during the treatment or that the proportion of hypoxic cells returns to its original value of 1% by the beginning of each successive treatment are considered. Effects of reoxygenation on the shape of the curve relating total dose and numbers of fractions are discussed. Results from various experimental systems are described. A discussion is presented of the effects of hypoxia, air, and high-pressure oxygen on the TCD_{50}, or dose required to produce local tumor control in 50% of the treated population for 120 days. It is suggested that the rate and extent of reoxygenation varies between tumors of different biological types, but for most, significant improvements in oxygenation probably take place in one day. It is thought that human tumors treated by radiotherapy may, with use of conventional techniques, reoxygenate sufficiently during treatment to make unnecessary other attempts at overcoming hypoxic cells, such as hyperbaric oxygen breathing. (H.L.W.)

11221 (BNL–50203, pp 268-79) INTERIM PROGRESS REPORT (1969) ON THE BRITISH INSTITUTE OF RADIOLOGY FRACTIONATION STUDY ON 3-FRACTIONS/WEEK OR 5-FRACTIONS/WEEK TREATMENT OF LARYNX AND PHARYNX. Ellis, F.; Brindle, J.; Churchill-Davidson, I. F. J. (British Inst. of Radiology, London (England)).

From Conference on time and dose relationships in radiation biology as applied to radiotherapy held at Carmel, California, September 15–18, 1969.

An examination was made of available data on cell cycle times and cell turnover times in human tumors and normal tissues. In order to obtain retrospective information, radiotherapists were asked to make their records available or to provide data on past cases. A prospective trial was considered desirable to decide whether some fractionation regimes could produce better results than others, and whether the same results might be produced by different numbers of fractions in the same overall time. A program was established which aimed at comparison of five with three fractions per week. Clinical forms to provide data on identification, diagnosis, and planned treatment are shown. The forms indicate effects on the tumor and normal tissues and record the patients' symptoms during and soon after the course of treatment. Tables are presented to show preliminary results. The interim conclusion was reached that there were no significant differences between the effects of 3F/wk and 5F/wk. (H.L.W.)

11222 (BNL–50203, pp 280-5) STUDIES ON THE RELATIONSHIPS BETWEEN DOSE-TIME, FRACTIONATION, AND REST PERIOD IN RADIATION THERAPY. Marcial, Victor A. (Puerto Rico Nuclear Center, San Juan).

From Conference on time and dose relationships in radiation biology as applied to radiotherapy held at Carmel, California, September 15–18, 1969.

Clinical observations on effects of dose fractionation, rest-period, and dose-time on patients with carcinoma of the esophagus, head and neck, breast, cervix, and bladder are tabulated. Fractionation studies were based on three versus five fractions per week, and one versus five fractions per week. Rest-period studies were conducted using split-course techniques with exposures of 3000 R in 2 weeks followed by a 2 to 3 week rest period and a repetition of the previous treatment of 3000 R in 2 weeks. Studies on rest periods between external and intracavitary irradiation in cervical carcinoma showed that the optimal interval was from one to two weeks. Dose-time studies were conducted by comparing two total-dose levels for periods of 4 to 6 weeks. Studies on fractionation in external irradiation of carcinoma of the uterine cervix are described, and three-year results are presented of three versus five fractions per week. (H.L.W.)

11223 (BNL–50203, pp 292-307) SPLIT-COURSE TECHNIQUES. Holsti, Lars R. (University Central Hospital, Helsinki (Finland). Radiotherapy Clinic).

From Conference on time and dose relationships in radiation biology as applied to radiotherapy held at Carmel, California, September 15–18, 1969.

Split-course therapy involves dividing the treatment into two or more phases separated by one or more rest periods of two weeks or longer. The biological basis of split-course therapy is discussed with regard to the following aspects: mitotic and metabolic suppression and recovery with restoration of radiosensitive elements of the tumor; avoidance of complete suppression of the tumor-bed effect; utilization of differential recovery rates between normal and malignant tissues; and improvement in tumor cell oxygenation. Clinical trials were made to compare the split-course therapy given by daily fractionation with that in which the first part is given in two fractions a week and the second part as daily fractionation. Results are tabulated for carcinomas of the esophagus, larynx, and lung. Cell survival observations were made on autopsy material from 67 lung cancer cases and an equation was developed for estimating the proportion of surviving cells in relation to the total therapeutic dose. (H.L.W.)

11224 (BNL–50203, pp 318-38) REOXYGENATION AND ITS POTENTIAL ROLE IN RADIOTHERAPY. Elkind, M. M. (Brookhaven National Lab., Upton, N. Y.).

From Conference on time and dose relationships in radiation biology as applied to radiotherapy held at Carmel, California, September 15–18, 1969.

Radiobiological factors observed with single-cell systems are reviewed and implications for radiotherapy are discussed. The reduced oxygen enhancement ratio associated with high LET radiation is utilized in radiotherapy for improvement of the therapeutic ratio by enhancing the degree of damage in tumors. Procedures for estimating the proportion of hypoxic cells in a tumor and for detecting and estimating the extent of reoxygenation are described. Relationships between survival curves for oxygenated cells to those for hypoxic cells are discussed. Graphs are presented to show results of studies using hamster cells for age-density distribution of hypoxic cells, survival variation curves for oxygenated cells, and survival variation curves for irradiation under nitrogen. Requirements for accurate hypoxic fraction assessments are listed and discussed. Reoxygenation is discussed with regard to human tumor treatment. Data needed to assess tumor fractionation are the aerobic survival curve, the oxygen enhancement ratio, and whether these depend upon the region of the tumor sampled. It is proposed that tumors can be treated more effectively if contribututions to cell killing from reoxygenation can be increased by allowing more time between fractions for cell lysis and tumor shrinkage to set in. (H.L.W.)

11225 RADIOTHERAPY OF MALIGNANT DISEASE OF THE KIDNEY AND URETER. Sandeman, T. F. (Univ. of Melbourne). Australas. Radiol.; 14: 285-93(Aug 1970).

Post operative x-ray therapy of the upper urinary tract over a 35 year period (but predominantly 1951-65), was analyzed. Cases were categorized as carcinoma of the renal pelvis and ureter, sarcomas of the kidney, carcinoma of the renal parenchyma and Wilms tumour. Increase in survival rates is attributed predominantly to use of Actinomycin D. (Australia)

11226 RADIOSENSITIVITY OF MEDIASTINAL LYMPHOMAS IN HODGKIN'S DISEASE TREATED WITH SPLIT-COURSE RADIOTHERAPY. A RETROSPECTIVE STUDY. Landberg, Torsten; Forslo, Hans. (Univ. of Lund, Sweden). Acta Radiol., Ther., Phys., Biol.; 9: 177-89(Jun 1970).

Doses delivered to the centres of the target volumes were calculated retrospectively in nineteen patients followed up for at least three years after split-course irradiation for mediastinal Hodgkin's disease. Eleven patients without recurrences were compared with eight patients in whom recurrences had been diagnosed clinically. The development or absence of a recurrence seems to depend mainly on the size of the dose to the centre of the target volume. (auth) (Sweden)

11227 APPLICATORS FOR REMOTE AFTERLOADING TECHNIQUE FOR OPTIMUM PELVIC DOSE DISTRIBUTION IN CARCINOMA OF THE UTERINE CERVIX. Joelsson, Ingemar; Baeckstroem, Anders (Radiumhemmet, Stockholm). Acta Radiol., Ther., Phys., Biol.; 9: 233-46(Jun 1970).

Selective shielding with gold screens considerably increased the pelvic dose in relation to the rectal dose in the treatment of carcinoma of the cervix uteri with two different intracavitary afterloading applicator systems. The vaginal part of the applicator device represents one phase in continued efforts towards optimum dose distribution. Different types and sizes must become available so as to facilitate individualized treatment by the remote afterloading technique. (auth) (Sweden)

11228 VISUALISATION OF THE PLACENTA WITH A GAMMA SCINTILLATION CAMERA AND INDIUM (^{113m}In). Sundsfjord, Johan A.; Nilsen, Per Agnar (Aker Hospital, Oslo). J. Norw. Med. Ass.; 7: 1687-9(15 Sep 1970). (In Norwegian).

A method of placental scintigraphy using a gamma scintillation camera and ^{113m}In is presented. Placental localisation has been carried out in 36 women with suspected placenta praevia. An accuracy of 94.9% was found when the results of this method were correlated with observations made post partum or during caeserean section. (auth) (Norway)

11229 POLICY AND RESULTS OF TREATMENT BY RADIOTHERAPY OF CARCINOMA OF THE BLADDER IN LEEDS.

XUM

Frank, H. G. (Cookridge Hospital, Leeds, Eng.). Clin. Radiol.; 21: 425-30(Oct 1970).

One-hundred-and-eighty-one patients suffering from carcinoma of the bladder were treated by radiotherapy, the majority by high-energy x ray therapy. The number treated by transvesical implantation was small. Radiotherapy was the primary treatment method in 138 patients. The remaining cases represent the failure of surgery to control the growth, except those where radiotherapy was given as a prophylactic measure after a partial cystectomy. Of those patients treated radically, the 5-year survival rates were: stage T.2 57%; T.3 31%; and T.4 10%. These figures compare favorably with other series, especially those for the stage T.3 patients. The incidence of complications was 19%, none being severe or disabling. The advent of high-energy x ray therapy has improved the cure rate and reduced the morbidity. Radiotherapy is the treatment of choice in all stages except those tumors in stages T.1 and T.2, which can be controlled endoscopically and for multiple, well differentiated, papillary tumors which require total cystectomy. The closest cooperation between the urologist and radiotherapist is essential in the management of these patients. (auth)

11230 SUCCESSES AND FAILURES OF FRACTIONATED RADIOIODINE THERAPY AMONG 700 HYPERTHYROID PATIENTS. Horster, F. A.; Reinwein, D.; Klein, E.; Miss, H. D.; Oberdisse, K. (Univ., Duesseldorf, Ger.). Nucl.-Med.; 32: Suppl. 7, 477-80(1968). (In German).

From 5th Conference of the Society of Nuclear Medicine, Vienna, Austria. See CONF-670996.

Seven hundred hyperthyroid patients were treated with ^{131}I. Those without goiter received 2 to 4 μCi; those with goiter received 3 to 7 μCi. Ten days following radioiodine therapy, treatment with methylmercaptoimidazol and desiccated thyroid was started. Three months later, a clinical examination was performed. The results were as follows: as to function, euthyroid 91%, hyperthyroid 6%, hypothyroid 3%; as to goiter, disappearance 78%, exacerbation 6%, unchanged 16%; as to exophthalmus, disappearance 51%, exacerbation 20%, unchanged 29%. Experience over a ten year period showed a surprisingly low incidence of hypothyroidism. Reasons for these results were explained by selection of patients, administration of the smallest effective dose of ^{131}I, and interval therapy with antithyroidal drugs supported by thyroid hormones. (H.B.G.)

11231 ACCUMULATION AND EXCRETION OF ^{224}Ra (THORIUM X) DURING TREATMENT OF ANKYLOSING SPONDYLITIS. Klemm, C.(Rheumaklinik Landesbad, Aachen); Michel, K.; Rose, E.; Meringdal, J. Z. Rheumaforsch.; 29: 234-40(Jul-Aug 1970). (In German).

Whole-body counting and excretion measurements were performed during radium 224 treatment of two patients, who were sent because of an advanced ankylosing spondylitis so far resistant to therapy. Former information that the main part of the excreted activity is excreted with the feces and only an unimportant portion in the urine could be confirmed. Whole-body measurements made with an intensification of 3.8 and 2.4 gave similar results. The results of the total body measurements are presented and discussed. It appeared that 7 days after the 9th injection only 5% of the incorporated radium 224 doses were detectable in the whole-body spectrum. The spectra measured on the 9th and 10th day before and after the injection were nearly the same. (auth)

11232 THE CURRENT STATE AND PROSPECTS OF NEUTRON AND NEUTRON-CAPTURE THERAPY. Ryabukhin, Yu. S. (Inst. of Medical Radiology, Moscow). Med. Radiol.; 15: No. 5, 74-6(May 1970). (In Russian).

Prospect of neutron and neutron-capture therapy are evaluated. On the basis of pertinent literature data some modern approaches to the solution of these problems, mainly elaborated in the laboratory, are discussed. (auth)

11233 EVALUATION OF RESULTS OF TREATMENT OF THYROID CARCINOMA. Hoffmann, G.; Gehring, D.; Pfannenstiel, P. (Univ., Freiburg i. B.). Nucl.-Med.; 9: 186-93 (30 Jun 1970). (In German).

Out of a group of 244 patients with malignant goitre 87 patients were evaluated who were treated exclusively with ^{131}I and thyroid medication. It appeared that a prognosis as to the success of radioiodine therapy is possible only if the tumor was properly classified histologically. An evaluation of the survival rate of the patient is possible only if the age of the patient is taken into consideration. Under these conditions it was found that 90% of the patients with organoid thyroid carcinoma without metastases and aged below 50 years may at the beginning of the treatment be expected to live for more than 10 years. (auth)

11234 TREATMENT OF THYROID CANCER. DEATH RATES AFTER SURGERY AND AFTER SURGERY FOLLOWED BY SODIUM IODIDE ^{131}I. Varma, Vijay M.; Beierwaltes, William H.; Nofal, Mohammed M.; Nishiyama, Ronald H.; Copp, Jeanne E. (Univ. of Michigan, Ann Arbor). J. Amer. Med. Ass.; 214: 1437-42(23 Nov 1970).

A total of 263 patients with histopathologically proved, well-differentiated papillary and follicular thyroid carcinoma were treated with sodium iodide ^{131}I after surgery. A 100% follow-up was achieved with a mean of 6.3 years, and an observation period of 0 to 20 yrs. The death rate in these patients was compared with the death rate in 50 patients with papillary and follicular carcinoma of the thyroid treated surgically before introduction of sodium iodide ^{131}I (control group), and followed for a mean of 6.7 years (0 to 20 years). These groups were matched in sex, but not in age distribution. In patients 40 years of age and older, the group treated with sodium iodide ^{131}I had a significantly lower death rate than the surgery-only group ($P < 0.005$). There was no significant difference in death rate between patients treated with sodium iodide ^{131}I and control patients 39 years of age and under. (auth)

11235 ROLE OF RADIATION THERAPY IN THE MANAGEMENT OF HEMANGIOMAS OF THE LIVER. Park, Won C.; Phillips, Ralph (Memorial Hospital for Cancer and Allied Diseases, New York. James Ewing Hospital, New York). J. Amer. Med. Ass.; 212: 1496-8(1 Jun 1970).

Hemangiomas are the most common benign tumors of the liver, and they are usually of the cavernous type. At autopsy, they are often encountered as an incidental finding and only occasionally do they cause symptoms such as pain in the right upper quadrant of the abdomen, abdominal mass, hepatomegaly, low grade fever, and chills. The large ones may rupture and thus produce a surgical emergency. Of 89 cases available for review, only 12 (13.5%) had symptoms referable to the hemangioma. In 77 (86.5%) cases the hemangioma was an incidental finding either at laparotomy for some other condition or at autopsy. Both sexes are equally affected in our series. Certain hemangiomas of the liver are not resectable, depending upon their size, location, and the surgical risks involved. Radiation therapy of five patients with nonresectable hemangiomas of the liver is reported. All patients but one had satisfactory results. (P.B.M.)

11236 RADIOTHERAPY OF CANCER OF THE OESOPHAGUS. Vitale, V.; Ricci, G. (Ospedali Galliera, Genoa). Minerva Radiol.; 15: 86-97(Mar 1970). (In Italian).

Comparison is drawn between the radiotherapy of oesophageal cancer employed in the Galliera Hospital and the methods described in the literature. A brief reference is made to the different radiological and surgical indications for such treatment and is followed by the presentation of a personal series. Emphasis is placed on the need for planned treatment as soon as the diagnosis has been made. Therapy cycles should be interspersed with brief rest periods to enable an assessment of the evolution of the site to be made. (auth)

Blast and Thermal Effects

11237 (ABCC-68-69) ANNUAL REPORT, JULY 1, 1968-JUNE 30, 1969. (Atomic Bomb Casualty Commission, Hiroshima, Nagasaki (Japan)). 440p. (In Japanese and English). Dep. NTIS.

The status of research program of the Atomic Bomb Casualty Commission between July 1968 and July 1969 is reviewed. The objective of the program is to collect, accumulate, and analyze data on the health status of survivors of the atomic bombings at Hiroshima and Nagasaki, including those exposed in utero and the offspring of survivors. Brief summaries are presented for 70 active and eight completed studies. A list is included of some 36 publications during the period that report the findings from some of these studies, including data on the radiation dose received by the survivors as a function of distance from the bomb hypocenter and shielding; the growth and development of those exposed in utero; radiation doses to survivors from medical uses of radiation; various disease conditions in the exposed population, with emphasis on the incidence of leukemia and cancers; mortality data; the frequency of chromosome aberrations in peripheral blood cells; indications of aging; and other genetic and hematological studies. (C.H.)

11238 MEDICAL EXPERIENCE OF THE ATOMIC BOMBINGS. Ilbery, P. L. T. (Univ. of Sydney). Australas. Radiol.; 14: 233-40(Aug 1970).

Radiation effects on the human population following the bombing

XUM

of Hiroshima are analyzed. Aspects of the radiation syndrome following whole-body radiation exposure to various dosages are considered. (Australia)

Radiation Effects on Animals

Refer also to abstracts 10960, 10975, 11092, 11093, 11095, 11097, 11106, and 11330.

11239 (BNL-50203, pp 117-29) RADIOBIOLOGY OF MAMMALIAN CELLS IN THE PLATEAU PHASE OF GROWTH. Hahn, George M. (Stanford Univ., Calif. Dept. of Radiology).

From Conference on time and dose relationships in radiation biology as applied to radiotherapy held at Carmel, California, September 15-18, 1969.

Cultures of Chinese hamster cells were used for studies on growth limitation in vitro. Reasons for the drop in growth rate as the cell density increases were examined; it appeared that crowding was the chief reason for the plateau in the growth curve. Experiments on the uptake of labeling precursors of RNA, DNA, and proteins by cells under conditions of progressive crowding showed that as long as exponential growth was maintained, the uptake of all precursors was independent of cell density. However, after one or two days in plateau, no uptake of leucine or uridine could be detected. Studies on cell viability and cell kinetics showed that cell viability dropped almost linearly with time after the cell number reached its plateau. Experiments on response of Chinese hamster cells and HeLa cells to single doses of x radiation emphasized the importance of nutritional state. Studies on ability to sustain and repair sublethal damage and repair of potentially lethal damage are reviewed. The relevance of in vitro studies on mammalian cells to radiotherapy is discussed. It is pointed out that these data offer at least a partial explanation for the tremendous variation in responses of tumors to fractionated courses of radiotherapy. (H.L.W.)

11240 (BNL-50203, pp 339-52) RADIOBIOLOGICAL BASES IN THE DESIGN OF NEW CLINICAL TRIALS. Barendsen, G. W. (Gezondheidsorganisatie TNO, Rijswijk (Netherlands). Radiobiologisch Instituut).

From Conference on time and dose relationships in radiation biology as applied to radiotherapy held at Carmel, California, September 15-18, 1969.

Results of radiobiological research on mammalian cells in vitro are discussed with regard to clinical applications. A table is presented to show factors that may cause differences in responses of tumors and normal tissues to fractionated treatments with ionizing radiation. Proliferation characteristics and radiation responses of R-1 rhabdomyosarcomas growing in rats are described with emphasis on the following: the experimental tumor system and proliferation parameters of cells; effects produced by single exposures of R-1 rhabdomyosarcomas to 300 kV x rays or 15 MeV neutrons; effects produced by exposures of tumors to fractionated treatments with equal doses applied five days per week for three weeks; tumor volume changes after irradiation with daily doses of 300 kV x rays, five times per week for different treatment periods; and relative effectiveness of different treatment regimes for reduction of the numbers of clonogenic cells. (H.L.W.)

11241 MICROSPECTROPHOTOMETRIC STUDY OF OXIDATIVE ENZYMES IN IRRADIATED EPIDERMIS. Klein-Szanto, A. J. P.; Cabrini, R. L. (Comision Nacional de Energia Atomica, Buenos Aires). Int. J. Radiat. Biol.; 18: 235-41(1970).

Enzyme variations produced by local x irradiation on epidermis were studied by a microspectrophotometric technique. Analysis of enzyme response as a function of the post-irradiation time showed clear changes after 2 days using 16,000 rads. A consistent total enzyme content (TEC) increase was found in all irradiation conditions, for the four oxidative enzymes under study succinate dehydrogenase, lactate dehydrogenase, glucose-6-phosphate dehydrogenase, and NADP diaphorase (SDH, LDH, G-6-phDH, and NADP diaph). The mean enzyme concentration (MEC = TEC/epithelial thickness) increased for NADP diaph and G-6-phDH, while decreasing for LDH and SDH activities. These findings suggest a metabolic adjustment to other oxidative pathways. (auth) (UK)

11242 ARGON LASER MICRO-IRRADIATION OF MITOCHONDRIA IN RAT MYOCARDIAL CELLS IN TISSUE CULTURE. Berns, Michael W.; Gamaleja, Nicolai; Olson, Robert; Duffy, Cecilia; Rounds, Donald E. (Pasadena Foundation for Medical Research, Calif.). J. Cell. Physiol.; 76: 207-10(Oct 1970).

Three types of lesions produced by argon laser micro-irradiation of single mitochondria are described. A correlation between lesion severity and optical phase density and/or laser output power was observed. Cell survival was generally not affected by mitochondrial irradiation. As many as ten mitochondria were irradiated without cell death resulting. Absorption of the laser radiation was attributed to the natural chromophores, cytochromes c and c_1. (auth)

11243 NEW EVIDENCE CONCERNING THE MOLECULAR BASIS OF THE RESTORATIVE EFFECT OF DNA IN CULTURED MAMMALIAN CELLS. Petrovic, Danilo; Ferle-Vidovic, Ana; Habazin, Vlasta; Vukovic, Biserka (Inst. Rudjer Boskovic, Zagreb). Int. J. Radiat. Biol.; 18: 243-58(1970).

The effect of post-irradiation treatments with exogenous DNA, deoxyribonucleotides, and deoxyribonucleosides on the rate of DNA synthesis and on the survival of x-irradiated L-V166 cells was studied. The addition of either DNA or deoxyribonucleosides to the cells immediately after irradiation increased the rate of DNA synthesis. The magnitude of this effect is not dose-dependent and can be related to the increase in the cell survival. The experiments with synchronized cultures showed that the increase in survival is a function of cell position in the intermitotic cycle: the highest increase in survival was observed in S-phase cells. Further experiments were concerned with the fate of DNA, when added to the serum-containing growth medium. The results show that most of DNA was broken down to the level of deoxyribonucleosides. When DNA breakdown was prevented, the addition of DNA had no effect on either survival or on the rate of DNA synthesis. All these results indicate that small molecules, probably deoxyribonucleosides, are utilized by irradiated cells and are involved in the repair of the induced damage. (auth) (UK)

Invertebrates

Refer also to abstracts 11012 and 11338.

11244 (NP-18607) STUDIES ON THE KILLING EFFECT OF GAMMA RADIATION ON ORYZAEPHILUS SURINAMENSIS (L.) COLEOPTERA, SILVANIDAE IN STORED DATES. Ahmed, Mohamed S. H. (Atomic Energy Commission, Baghdad (Iraq). Nuclear Research Inst.). Sep 1970. 5p. (B-2). Dep. NTIS (U. S. Sales Only).

Adults of the grain beetle, Oryzaephilus surinamensis, were collected from infested dates and exposed to ^{60}Co γ radiation in doses of 16 to 320 krad. A table is presented to show accumulated mortality percentages of males and females following exposure to six different doses. It was estimated that the doses of 16 to 320 krad would cause 100% mortality in 17 to 4 days respectively. (H.L.W.)

11245 EFFECTS OF X AND γ RADIATIONS ON THE RESISTANCE AND LONGEVITY OF ORPHAN WORKERS OF THE ANT DOLICHODERUS QUADRIPUNCTATUS. Torossian, Claude (Univ., Toulouse). Compt. Rend., Ser. D; 271: 987-90(21 Sep 1970). (In French).

A study is given of the resistance of workers to ionizing radiations administered at doses varying between 1,000 and 150,000 Rads. The results obtained are presented in table form. (France)

11246 EFFECTS OF X IRRADIATION ON DNA SYNTHESIS IN SALIVARY GLAND CELLS OF DROSOPHILA HYDEI. Wong, Patrick Tin-choi. Corvallis, Oreg.; Oregon State Univ. (1970). 87p. University Microfilms Order No. 70-14,144.

Thesis.

The effect of x-irradiation on DNA synthesis in larval salivary glands of Drosophila hydei was studied using the technique of liquid scintillation spectrometry and autoradiography. DNA synthesis in salivary glands of synchronized larvae was measured at successive stages of third instar development by in vitro uptake of ^{3}H-thymidine for a period of 30 minutes in ten pooled glands. A major period of DNA synthesis, which lasted for about 5% of larval life, was found in glands just before the mid-point of third instar development. DNA synthesis before and after this period was relatively low. (Diss. Abstr. Int., B)

11247 EFFECTS OF GAMMA RADIATION ON THE LARVAL STAGE OF THE LESSER COTTON LEAF WORM, SPODOPTERA EXIGUA Hb. Zaki, M. M. (Ain Shams Univ., Cairo); El-Badry, E. A.; Wakid, A. M.; Ahmed, M. Y. Y. Z. Angew. Entomol.; 66: 54-9(Jul 1970).

Newly hatched larvae of Spodoptera exigua treated with different doses of gamma radiation (2 to 8 Krad) suffered from reduction in the percentage pupation and adult emergence. Sublethal doses retarded the development of the immature stages, reflected itself on larval weight, body length and head capsule width of the third and fifth instar larvae. There was a gradual decrease in egg production with the increase of dose. The average number of eggs laid per female reached 0.8 at 8 krad. The viability of the eggs laid

decreased with increasing the dose up to 4 krad that prevented egg hatching. Adult longevity was also reduced by irradiation of newly hatched larvae. Irradiation of mature larvae with 1 to 3 krad decreased the percentage pupation and adult emergence. Thirty krad prevented pupation, while 15 krad prevented adult emergence. Pupal duration was slightly affected with doses 2 and 3 krad, while adult longevity was shortened at all doses tested. All doses reduced the number of eggs laid per female and percentage hatchability. The reduction increased progressively with the increase of dose. (auth)

11248 EFFECTS OF LOW- AND HIGH-LET CYCLOTRON-ACCELERATED α PARTICLES ON LONGEVITY OF DROSOPHILA MELANOGASTER. Atlan, H. (Ames Research Center, Moffett Field, Calif.); Miquel, J.; Welch, G. Int. J. Radiat. Biol.; 18: 423-31 (1970).

An investigation of the effects of exposing Drosophila melanogaster to γ rays and α particle radiation of low and high LET resulted in dose-mean longevity curves of the exponential type. The effect of low LET particles was similar to that of ^{60}Co, whereas the high LET α particles were more effective than the two other types of radiation with an RBE of 1·3. No protective effect of low doses (3 and 5 krads) was observed. No dose-rate effect was observed in the range 4 to 256 krads/min. (auth) (UK)

11249 FORMATION OF SUPERNUMERARY SURFACE LAYERS IN IRRADIATED AMOEBAE. Mookerjee, Sivatosh; Chatterjee, Samar (Presidency Coll., Calcutta). Curr. Sci. (India); 39: 468-9(20 Oct 1970).

Soil amoebae, Acanthamoeba sp, were x-irradiated at various doses. A peeling-off of the surface layer was observed and supernumerary new surface membranes were formed within the cell body to replace the shredded-off limiting membrane. The peeling-off of the surface layer suggests overproduction of surface-forming material induced as an after-effect of radiation. (F.M.M.)

11250 APPEARANCE OF SENSITIVITY TO THE TUMOR-INDUCING ACTION OF X RAYS IN THE ZYGOTE OF DROSOPHILA. Gbelelovitch, S. (Institut du Radium, Paris). Int. J. Radiat. Biol.; 18: 331-45(1970). (In French).

X irradiation of the parental gametes does not produce in Drosophila any tumorigenic effect in the progeny. The tumorigenesis is, on the contrary, stimulated in individuals that develop from irradiated zygotes. Three different explanations of these findings are discussed: elimination of gametes with lesions, otherwise able to favour the tumorigenesis; repair of such lesions in gametes; impossibility to induce such lesions in gametes. The first hypothesis can be excluded. The two others believe that the penetration of the sperm into the egg of Drosophila establishes the intracellular conditions necessary for the production of the tumorigenic effect. (auth) (UK)

Vertebrates

Refer also to abstracts 10933, 10947, 10963, 10967–10972, 10980, 10983–10986, 10988, 10989, 10992, 10994, 11014, 11018, 11077, 11094, 11096, 11098–11105, 11107, 11110, 11112, 11188, 11204, 11220, and 11321.

11251 (AD-705976) WHOLE-BODY IRRADIATION EFFECT RELATED TO CANINE TREADMILL PERFORMANCE DECREMENT: AN ANNOTATED BIBLIOGRAPHY. Final Report, September 1969–February 1970. Watters, J. W.; Bennett, C. H.; Hudson, R. F. (School of Aerospace Medicine, Brooks AFB, Tex.). Apr 1970. 14p. (SAM-TR-70-22). NTIS.

A literature survey was made for the years 1958 through 1968 as part of a study to determine the effects of radiation on canine locomotion. A compilation of 15 titles and abstracts on canine performance decrement following high doses of radiation is included. The following reference sources were used: Biological Abstracts, Excerpta Medica, Index Medicus, and Nuclear Science Abstracts. (auth) (STAR)

11252 (BNL-50203, pp 54-69) CAPACITY FOR REPAIR IN CELLS OF NORMAL AND MALIGNANT TISSUES. Withers, H. R. (Anderson (M.D.) Hospital and Tumor Inst., Houston, Tex.).

From Conference on time and dose relationships in radiation biology as applied to radiotherapy held at Carmel, California, September 15–18, 1969.

A review of studies on repair of sublethal damage in animal tissues indicated that all normal and malignant tissues, with the probable exception of bone marrow, contain cells capable of extensive repair of sublethal damage. This capacity for repair by a proportion of cells may be the same for cells of most tissues, both normal and malignant, but the density distributions of these cells with the large repair capacity probably vary from tissue to tissue. The size of the preceding dose will determine the amount of recovery occurring during a fractionation interval. Recovery occurring in a steady-state tissue during the 24 hr interval between first and second doses is probably attributable to repair of sublethal radiation injury. Isoeffect curves reflect repair of sublethal damage as a function of dose per fraction. (H.L.W.)

11253 (BNL-50203, pp 154-73) BIOLOGY OF DOSE-LIMITING TISSUES. Mendelsohn, Mortimer L. (Pennsylvania Univ., Philadelphia. Dept. of Radiology).

From Conference on time and dose relationships in radiation biology as applied to radiotherapy held at Carmel, California, September 15–18, 1969.

The possibility that dose limitation is determined by an underlying common denominator of all tissues is discussed. Chief candidates for this role are blood vessels, lymphatics, and connective tissue. A second possibility is that alteration of cellular reproductive integrity is the common basis for deleterious effects. This mechanism is thought to be chiefly responsible for radiation effects on tumors. The importance of clonogenicity and reproductive integrity in the acute response of bone marrow, skin, and intestine is emphasized. A third factor is based on clinical data collected by radiotherapists over a period of 70 yrs. Time–dose studies for various organs and tissues are reviewed, and graphs are presented to show time–dose relationships for radiotherapy of various pathological conditions. (H.L.W.)

11254 (BNL-50203, pp 174-80) EFFECT OF 14-MeV ELECTRONS ON THE BLOOD VESSELS OF THE MOUSE EARLOBE. Lindop, Patricia J.; Jones, Arthur; Bakowska, Anna (Saint Bartholomew's Hospital Medical Coll., London (England)).

From Conference on time and dose relationships in radiation biology as applied to radiotherapy held at Carmel, California, September 15–18, 1969.

In order to determine the effects of radiation on the microcirculatory units, arterioles, venules, and capillaries, experiments were performed on irradiation of the mouse earlobe. Single and fractionated doses of 14 MeV electrons were administered to one earlobe of each mouse and changes in blood vessels were observed at intervals up to 55 wks. The outstanding change was the dilated venule; other changes were narrowing and tortuosity of the arterioles and dilation of capillaries. Graphs are presented to show effects of various radiation doses on lumen diameter of arterioles, venules, and capillaries. Results suggested that part of the mechanism of necrosis is a result of a circulatory imbalance. It was concluded that local irradiation of the mouse earlobe can be used as a convenient model to study the morphological and physiological interaction of vessel and tissue damage in the acute, intermediate, and late periods post irradiation. (H.L.W.)

11255 (BNL-50203, pp 181-5) EFFECTS OF RADIATION ON VASCULATURE OF INTESTINE. Casarett, George W.; Eddy, Hubert A. (Rochester Univ., N. Y. Dept. of Radiation Biology and Biophysics).

From Conference on time and dose relationships in radiation biology as applied to radiotherapy held at Carmel, California, September 15–18, 1969.

Exteriorized loops of small intestine of rats were exposed to single doses of 600, 1000, and 1400 R x radiation and the rats were killed at intervals up to one year. The following effects were observed: acute destruction and hypoplasia of mucosal epithelium; acute damage and obstruction of fine vasculature; progressive arteriolar degeneration, fibrosis, and vascular obstruction; delayed infarction with necrosis of intestinal wall and subsequent stenosis. Arterial vessels were filled with a radio-opaque medium and changes following irradiation were noted. Degeneration and swelling of endothelial cells, edematous thickening of the wall, and occasional thrombi were observed. Although recovery of the mucosal epithelium was essentially complete within the first week after 600 R and largely complete by the third week after 1000 R, the degree of recovery was variable after 1400 R and seemed to depend upon the degree of vascular damage. (H.L.W.)

11256 (BNL-50203, pp 186-203) LATE EFFECTS ON VASCULAR TISSUE. Brecher, George (California Univ., San Francisco, Medical Center); Tessmer, Carl F. (Anderson (M.D.) Hospital and Tumor Inst., Houston, Tex.).

From Conference on time and dose relationships in radiation biology as applied to radiotherapy held at Carmel, California, September 15–18, 1969.

In summary, radiation damage may involve vessels of all sizes from capillaries to the aorta and affect all coats from the endo-

XUM

thelium to the adventitia. There does not seem to be a predictable sequence in the involvement of the various coats or in the temporal progression of the lesions. Although radiation injury to a large vessel may contribute to a fatal outcome, as in the rupture of the carotid artery, concomitant lesions such as infection or a breakdown of the surrounding tissue also contribute. Conversely, the vascular lesion may be aggravated by injury to adjacent tissues. The degree of vascular damage may be a function of the reactivity of the particular region irradiated and may vary from one region to another. Thus, no common denominator has yet emerged from a study of radiation damage to blood vessels which would support a uniform or general role of vascular injury in the production of late radiation lesions. Certainly an adequate blood supply is essential to the recovery of any tissue or to the survival of grafts. The ability of the tissues to produce normal granulation tissue which encompasses the formation of both connective tissues and blood vessels is essential to the healing after surgical intervention or after destruction of a tumor. In association with fibrosis, vascular damage may also interfere with function. In this restricted sense the extent of vascular lesions may indeed determine the ability of the tissue to withstand further irradiation. A much more detailed analysis of the effects of radiation and of general modifiers such as diets and drugs is needed before this general concept can become helpful in the management of radiation therapy. (H.L.W.)

11257 (BNL–50203, pp 210-14) RESPONSE OF TUMOR BLOOD SUPPLY TO FRACTIONATED IRRADIATION. Reinhold, Huibert S. (Gezondheidsorganisatie TNO, Rijswijk (Netherlands). Radiobiologisch Instituut).

From Conference on time and dose relationships in radiation biology as applied to radiotherapy held at Carmel, California, September 15–18, 1969.

Improvement of tumor microcirculation during a course of fractionated radiotherapy was demonstrated in the C3HBA mouse mammary carcinoma, grown in a sheetlike fashion in a modified Algire chamber system. The microcirculation in these sandwich tumors was quantified from fluorescent microangiography recordings. Once it has been shown possible to grow tumors in a sheetlike fashion, more techniques become feasible for the study of tumor oxygenation and reoxygenation. (auth)

11258 (BNL–50203, pp 242-54) REOXYGENATION AS A FUNCTION OF TUMOR SIZE AND HISTOPATHOLOGICAL TYPE. Thomlinson, R. H. (Medical Research Council, London (England). Experimental Radiopathology Research Unit).

From Conference on time and dose relationships in radiation biology as applied to radiotherapy held at Carmel, California, September 15–18, 1969.

Patterns of change in proportions of hypoxic cells following x irradiation are considered for three types of tumors: mammary carcinoma in mice, van Putten's osteogenic sarcoma, and rat fibrosarcoma RIB_5. In all three types the proportion of hypoxic cells rises after a single dose of x rays and in all three there is evidence of reoxygenation, but the pattern of events is different in each case. Results are shown by means of a graph. Factors influencing oxygen consumption in normal tissues and various types of tumors are considered. A discussion is presented of oxygen supply to tissues with regard to different histological types of tumors and arrangement of cells in relation to capillaries. Factors such as nutritional failure and rate of cell death affecting the falling demand for oxygen in necrotic tissues are discussed. Following therapy of tumors reoxygenation occurs because the tumor shrinks and the pathway for red cells is shortened. It is pointed out that processes leading to necrosis are reversed during treatment of tumors resulting in reoxygenation and improved blood supply. (H.L.W.)

11259 (BNL–50203, pp 260-7) BACKGROUND OF PRESENT DOSE-TIME FRACTIONATION PRACTICE. Fletcher, Gilbert H. (Anderson (M.D.) Hospital and Tumor Inst., Houston, Tex.).

From Conference on time and dose relationships in radiation biology as applied to radiotherapy held at Carmel, California, September 15–18, 1969.

A brief historical background for determining response curves for tumor control in radiotherapy is presented. A review of isoeffect studies includes studies on fractionation curves for calculation of equivalent doses in squamous cell carcinomas and skin reactions. The slopes of fractionation curves were estimated for various types of tumors. The basic principle of radiotherapy, which is to obtain maximum control of tumors with a minimum of complications, is discussed. A review of studies on tolerance of normal tissues is presented with emphasis on mucous membrane reactions to ^{60}Co γ radiation. Criticality of tumor control versus normal tissue tolerance is reviewed with emphasis on studies on radiotherapy of lesions of the larynx, uterine cervix, and cancer of mammary glands. (H.L.W.)

11260 (BNL–50203, pp 286-91) EARLY RECOVERY OF SKIN REACTIONS IN MICE AFTER 15 SESSIONS OF SPLIT-DOSE IRRADIATION. Dutreix, J.; Eschwege, F.; Wambersie, A.; Salamon, E. (Institut Gustave Roussy, Villejuif, (France)).

From Conference on time and dose relationships in radiation biology as applied to radiotherapy held at Carmel, California, September 15–18, 1969.

The experiments deal with recovery of skin reaction of mice (Swiss strain) irradiated in 15 sessions in an overall time of 35 days. The magnitude and kinetics of recovery were investigated by comparing the single dose and split dose per session resulting in the same skin reaction. It is concluded that the recovery is the same for each of the 15 sessions; recovery starts immediately after irradiation, without any delay; the recovered dose increases to a maximum at about 3 hr, equal to 140 rads for a split dose of 2 × 240 rads; the recovery half-time is $\frac{3}{4}$ hr. (auth)

11261 CHANGES IN THE SLEEP PATTERN FOLLOWING γ IRRADIATION IN CATS. Riotte, M.; Arnaud, S.; Sassard, J.; Cier, A. (Centre de Recherches du Service de Sante des Armees, Lyon). J. Physiol. (Paris), Suppl.; 62: 310(1970). (In French).

Adult cats were given whole body γ irradiations at a lethal dose of 750 R after being subjected to a continuously recorded encephalogram. The recording was then resumed until death by irradiation. Quantitative observations showed: increased wakefulness during the last days of life; few changes in the percentages of slow sleep; a slow decrease in paradoxical sleep during the first 4 days followed by a sharp drop on the 5th day; this is succeeded by a variable rebound, itself followed by a decrease in the amount of paradoxical sleep. The qualitative aspect showed: an alteration in the electroencephalogram tracks, on which can be seen a dissociation between the tonic and phasis activities of sleep and a disturbance in the succession of the different hypnic states. (France)

11262 IRRADIATION IN VITRO OF NERVOUS TISSUE. Berger, J. P. (Univ., Lausanne, Switzerland). J. Physiol. (Paris); 62: 189-218(May-Jun 1970). (In French).

The superior cervical sympathetic ganglia of rats were exposed in vitro in Krebs oxygenated solution, to the β radiation of ^{90}Sr. Dose-rate was maintained in all cases at 2.7 Krads/min.; only time of exposure varied, from 7.30 to 300 min. The height of the action potential from the postganglionic nerve was recorded during the hours following irradiation. Glucose uptake and lactate production were measured during the same period. Five hrs of continuous irradiation (720 Krads) result in loss of the electro-physiological response. On the other hand, 15 min of irradiation is sufficient to modify that response, bringing about an increase of the action potential recorded from the postganglionic nerve. Compared with the metabolic controls, the glucose utilization decreases and lactate production increases with an increasing dose of β-radiation, incubation being in an oxygenated Krebs-solution. If the tissue irradiated in the oxygenated solution is then incubated in the presence of N_2 (in which glucose uptake is maximal), one observes an impairment of the glucose uptake and lactate production after only 20 Krads. With that dose there is no apparent ultra-structural lesion. There is no evidence of a decrease in the activity of either LDH or SDH. There appears to be, simultaneously, a radioresistance of the tissue (when one considers the amount of radiation necessary to abolish the electrophysiological function itself), and a very early sensitivity shown by the glucose uptake. A correlation between the impairment of glucose uptake and a loss of electrophysiological activity only appears at higher doses of radiation, when the tissue is incubated in the presence of oxygen. Then the amount of glucose needed is lower than the highest possible uptake. (France) (auth)

11263 A CONTRIBUTION TO THE KINETICS OF RADIOSTRONTIUM IN RATS AFTER EXTERNAL IRRADIATION. Vondracek, V. (Military Medical Research and Postgraduate Inst., Hradec Kralove, Czech.). Sb. Ved. Pr. VLVDU Hradci Kralove; 41: 3-21(1969). (In Czech).

Male rats were exposed to 400 R of ^{60}Co γ rays. ^{85}Sr was applied either intravenously or perorally in indicator amounts of 1 to 5 μCi per rat. The animals were killed and the activity in bones and the whole-body activity were determined. The accumulation of ^{85}Sr in bones of irradiated rats was increased (by 38.2 to 68.3% in one to 14 days after irradiation) only in the case of peroral application. Pylorospasm and decreased intestinal motility and passage are probably responsible. The results agree with those obtained by measuring retained ^{85}Sr and calculating the amount resorbed. In the first week after peroral application, no differences were observed between the urinary excretion of ^{85}Sr in irradiated animals and that in controls. After internal contamination with ^{85}Sr, an increased bone marrow dose should be expected in the irradiated organism as compared with the non-irradiated one. (NSA of Czech)

XUM

11264 ACATALASEMIA IN THE MOUSE AND OTHER SPECIES. Feinstein, Robert N. (Argonne National Lab., Ill.). Biochem. Genet.; 4: 135-55(Feb 1970).

Genetic control of the level of blood catalase activity was first demonstrated in 1927. At present, such control has been demonstrated or suggested for nine different species, including man, the most studied. The development of an acatalasemic strain of mice has permitted a wide variety of experimental approaches, including most of those used in humans. Among those approaches which cannot readily be applied to man but have been used in acatalasemic mice are investigations of sensitivity to radiation lethality, mechanism of awareness to radiation, possible use as a model for replacement therapy for inborn errors of metabolism, and catalase in tissues other than erythrocytes. These are described, together with genetic, immunological, and other studies comparable to similar work on acatalasemic humans. (auth)

11265 COURSE OF PULMONARY ASCARIASIS IN AN IRRADIATED ORGANISM. I. INFLUENCE ON VIABILITY, BODY WEIGHT, AND VARIATION IN THE NUMBER OF BLOOD ELEMENTS. Radvan, Rostislav. Sb. Ved. Pr. Lek. Fak. Karlovy Univ. Hradci Kralove, Suppl.; 12: 519-32(1969). (In Czech).

The effect of x radiation and simultaneous invasion of larvae of Ascaris suum was studied in experiments on white mice. The death rate, weight loss, number of migrating larvae in the lungs, and changes in the number of blood elements were followed up in the experimental mice. (auth)

11266 COURSE OF HEALING OF MANDIBULAR FRACTURES IN RADIATION SICKNESS. Bobrowski, Antoni. Czas. Stomatol.; 23: 547-54(May 1970). (In Polish).

Experiments were carried out on 49 rabbits, 11 of which served as controls. In the remaining 38 rabbits, a 600 rads x ray dose to the whole body was given and the mandible was fractured at its angle. Clinical observations, radiological examinations, and histological investigations showed that in control animals the union of the mandibular fragments occurred by connective tissue union much earlier than in the experimental animals. In the experimental rabbits, heating of mandibular fractures occurred by development of cartilage first and it was much slower than in controls and complications (abscesses and osteitis) developed more frequently. (auth)

11267 RADIATION DAMAGE TO THE SURFACTANT SYSTEM OF THE RABBIT LUNG. Forsberg, Sven-Ake; Johansson, John M.; Lindskoug, Bengt (Univ., Goteborg). Life Sci., Part II: 9: 795-803(22 Jul 1970).

Therapeutic irradiation of the human lung often leads to such clinical manifestations as coughing and dyspnoea. It is also attended by roentgenologically visible opacities in the irradiated fields. These reactions have been ascribed to exudation into irradiated alveoli and bronchioles. In a preliminary study on radiation injuries to rabbit lungs, it was found that atelectasis was probably part of the acute reaction. The hypothesis that alteration of the pulmonary surfactant system contributes to the radiation injury was tested. Experiments were conducted on 60 albino rabbits in which the right lobe of the lung was irradiated with a 5 MeV linear accelerator at doses of 2500, 5000, and 10,000 rads. Results showed that radiation injury does include damage to the pulmonary surfactant system. (E.E.H.)

11268 STUDIES ON NUTRITIONAL MANAGEMENT IN OPERATION. PART 1. STUDY ON THE INFLUENCE OF 19-NOR-ANDROSTENOLONE PHENYLPROPIONATE ADMINISTRATION ON THE SUPRARENAL GLAND. SECTION 1. HISTOLOGICAL CHANGES OF THE ADRENAL CORTEX INDUCED BY A CONTINUOUS LARGE DOSE ADMINISTRATION. Mizugaki, Hiroshi (Sapporo Medical Coll.). Sapporo Igaku Zasshi, 32: No. 1, 1-20(Jul 1967). (In Japanese).

Animal experiments using rats were conducted in an attempt to study the influence of 19-nor-androstenolone (19 NAPP), an anabolic steroid, on the suprarenal gland. At the same time, an investigation was made to study the relation, if any, between predonisolone sodium hemisuccinate (predonine, an adrenal cortex hormone) and stress. While 19 NAPP produced a slight shrinking of the adrenal cortex in normal rats, this change returned to normal levels after 10 days. Predonine produced an atrophy of the adrenal cortex especially in the zona glomerulosa and zona fasciculata; however, when 19 NAPP was used jointly a remarkable diminishing of the symptoms was seen. When whole-body x irradiation was administered as a stressor, an atrophy in the zona glomerulosa and zona fasciculata and localized lesions were found in the adrenal cortex. However, a pre-treatment by predonine prevented the above. On the other hand, an atrophy that may be attributed to the influence of predonine itself was found. This also can be prevented by joint treatment with 19 NAPP. (NSA of Japan)

11269 VULNERABILITY OF THE ENDOTHELIUM OF THE LARGE VESSELS IN RADIOSENSITIVE AND RADIORESISTANT ANIMALS. Shcherbova, E. N.; Gruzdev, G. P.; Ivanov, Yu. V. (Inst. of Biophysics, Moscow). Radiobiologiya; 10: 548-51(Jul-Aug 1970). (In Russian).

A decrease in the number of endothelial cells of the thoracic aorta was noted in guinea pigs and rabbits injured by radiation. Elimination of endothelial cells in the guinea pigs was noted at lower doses of irradiation than in rabbits. A cytometric analysis of the endothelial lining of the aorta of healthy animals indicated that in rabbits the volume of cytoplasm of the cell is greater than in guinea pigs. It was suggested that as the volume of the cytoplasm of the cell increases, its radioresistance increases. (tr-auth)

11270 DAMAGE TO NERVE GANGLIA OF THE INTESTINES AND ITS SIGNIFICANCE IN THE DEVELOPMENT OF THE INTESTINAL SYNDROME IN MICE AFTER NEUTRON IRRADIATION. Ulitovskaya, I. I.; Simonenkova, V. A. (Military Medical Academy, Leningrad. Ioffe Inst. of Physics and Tech., Leningrad). Radiobiologiya; 10: 536-40(Jul-Aug 1970). (In Russian).

A morphological investigation was made of the intestines of mice irradiated with a lethal dose of neutrons. The number of mitoses was counted and the thickness of the muscle layer was measured. It was established that there was no full correspondence between the nature of the injury and the periods of restoration of the epithelium of the mucous membrane and intramural nerve cells. The thinning of the muscle layer and delay of secretion in the crypts correspond in degree of expression and periods to damage to the nerve apparatus. Plethora of the vessels of the intestines was observed in all phases of the process. (tr-auth)

11271 RADIATION DAMAGES AND REPAIR OF INTESTINAL TISSUES IN THE EARLY AND LONG-TERM PERIODS AFTER THE CHRONIC INFLUENCE OF RADIOACTIVE SUBSTANCES. Lavrent'ev, L. N. (Scientific Research Inst. of Radiation Hygiene, Leningrad). Radiobiologiya; 10: 612-14(Jul-Aug 1970). (In Russian).

The results of morphological investigations of the intestines of rats in the case of the prolonged influence of a mixture of various radioactive isotopes are presented. Attention is paid to certain mechanisms of the observed damages and recovery processes. A number of changes preceding the appearance of malignant neoplasms are followed. (tr-auth)

11272 DELAYS OF MITOSIS IN A CULTURE OF MAMMALIAN CELLS UNDER THE ACTION OF ALPHA AND GAMMA RAYS. Popov, A. S.; Mikhailova, A. A.; Soboleva, G. B. (Inst. of Biophysics, Moscow). Radiobiologiya; 10: 512-17(Jul-Aug 1970). (In Russian).

In the case of α irradiation of SOTs (SCH-E) cells, the duration of the drop in the mitotic index coincides with the duration of mitosis; in the case of γ irradiation it is four times as great. The delay of mitosis increases linearly with increasing dose for γ radiation, and increases with the square root of dose for α radiation. It was suggested that the delay of divisions under γ and α irradiation arises as a result of a disturbance of various mechanisms. For γ irradiation, the damage was associated with disturbances in nucleus components; for α irradiation some other starter mechanism of mitosis was affected. The literature data on the processes leading to the disturbance of the first mechanism were discussed. (tr-auth) (TSS)

11273 INFLUENCE OF X IRRADIATION IN FRACTIONAL DOSES ON THE DEVELOPMENT AND CONSERVATION OF A MAZE HABIT IN RATS. Skobeev, E. M. (Inst. of Biological Physics, Pushchino, USSR). Radiobiologiya; 10: 619-21(Jul-Aug 1970). (In Russian).

Rats were subjected to three whole-body irradiations at single doses of 50 R. The interval between the first and second irradiations was 14 days. The interval between the second and third irradiations was seven days. After the first exposure, the number of errors in the maze was significantly reduced. The latent period of running and the time of passage through the maze were insignificantly reduced. After the second and third irradiations, the average indices of conservation of the maze habit slightly and insignificantly deteriorated. It was suggested that the behavior of irradiated rats in a maze was greatly influenced by compensation processes. (tr-auth)

11274 INFLUENCE OF NORMAL CELLS ON THE PROLIFERATION OF TUMOUR CELLS IN CULTURE. Weiss, R. A. (University Coll., London). Exp. Cell Res.; 63: 1-18(Nov 1970).

The effect of population density of normal fibroblastic cells on the proliferation of x-irradiated Rous, polyoma, and sarcoma 180 cells was studied. The growth of Rous-transformed chick,

XUM

rat, and hamster cells was not inhibited by dense sheets of normal mouse or chick cells. Polyoma and S180 cell growth was inhibited by crowded mouse or rat cells, but not by crowded chick, quail, or goose cells. Contact or close apposition of cells was essential for the transmission of growth-inhibitory influences. The transformation of chick cells freshly infected with Rous sarcoma virus was inhibited by dense mouse cells but not chick cells. Both mouse and chick cells exerted a feeder effect on tumor cell growth in monolayer and suspension. The proliferation of mouse and chick cells seeded at different densities was analysed. (P.B.M.)

11275 ASSESSMENT OF THE COURSE OF EXPERIMENTALLY INDUCED RADIONEPHRITIS WITH ISOTOPE RENOGRAPHY. Bargon, G.; Emrich, D. (Medizinische Univ., Goettingen, Ger.). Nucl.-Med.; 32: Suppl. 7, 385-9(1968). (In German).

From 5th Conference of the Society of Nuclear Medicine, Vienna, Austria. See CONF-670996.

In 30 rabbits, local ^{60}Co γ radiation of 4000 r was administered to the left kidney. Subsequently, renograms were obtained with ^{131}I hippuran. Within the observation time of 36 days postradiation, the vascular phase as well as the secretory phase became increasingly impaired in the irradiated kidney, while the non-irradiated right organ showed a corresponding compensatory enhancement of function. Histological findings in the glomeruli and tubular system were described. It was concluded that the radiorenogram is a suitable method for early detection of renal damage after therapeutic radiation for abdominal and retroperitoneal tumors. (H.B.G.)

11276 EFFECT OF X-RAYS OF 1000 R ON MALE GERM CELLS IN THE MOUSE, WITH PARTICULAR ATTENTION TO THE DIFFERENCE IN X-RAY SENSITIVITY OF SPERMATOGONIA. Itagaki, Gentaro (Hirosaki Univ., Japan). Jap. J. Genet.; 45: 239-54(Aug 1970).

The quantative changes in spermatogenetic cell populations in mice following a 1000 R dose of x radiation and the mechanism of depletion and recovery of spermatogonia were studied with particular emphasis on the radiosensitivity of spermatogonia. A decrease in spermatogenetic cell populations occurred according to their developmental stages. Spermatogonia began to decrease 12 hrs after irradiation and showed a large loss at the third day On the twelfth day, spermatocytes disappeared completely. Depletion of spermatids and spermatozoa occurred in the third and fourth wk., respectively. In comparing the sensitivity of spermatogonia, intermediate and type B cells were more sensitive to radiation than type A cells. This supported the hypothesis that a few spermatogonia of type A, showing heterogeneous sensitivity, survive after radiation and repopulate new spermatogenetic cell elements. Some spermatocytes become abnormal spermatids, suggesting the formation of abnormal spermatozoa. Sertoli cells and interstitial cells were seen in considerable numbers in severely damaged testes. Their apparent increase seems to be a relative increase due to the shrinkage of seminiferous tubules accompanied by depletion of the tubule constituents. The rate of decrease of the tubule diameter after radiation depends on the dose. Therefore, the tubule diameter may serve as a useful parameter in comparison of radiation effects. (E.E.H.)

11277 SPECIES DIFFERENCES OF THE EFFECTS OF X-IRRADIATION UPON THE RAT AND MOUSE EMBRYO. Hoshino, Kiyoshi; Kameyama, Yoshiro; Murakami, Ujihiro. (Nagoya Univ., Japan). Annu. Rep. Res. Inst. Environ. Med., Nagoya Univ.; 17: 25-34(1969).

The present experiment was designed to examine species differences of radiosensitivity between the rat and mouse embryo by comparing the mortality and malformations manifested. Pregnant rats and mice were irradiated with a single exposure of 200 or 300 R x rays during the period of organogenesis. Fetuses were removed on day 20 in rats and on day 18 in mice. The mortality of the rat embryo was higher than that of the mouse in the groups exposed in the early stages of organogenesis, but there was no apparent difference between the two species in those treated in the later periods. The incidence of malformations in the rat fetus treated with 200 R was higher than that in the mouse treated with the same dose. These differences in mortality, incidence of malformations, critical period of malformations, and type of malformations cannot be explained only by species differences of development rate and radiosensitivity. Genetic factors producing specific malformations may also play a role in the species differences in teratogenesis. (E.E.H.)

11278 CHANGE IN THE RED BLOOD IN THE CASE OF PROLONGED AND BRIEF IRRADIATION OF GUINEA PIGS. Rogozkin, V. D.; Ostroumova, L. M. (Inst. of Biophysics, Moscow). Radiobiologiya; 10: 608-12(Jul-Aug 1970). (In Russian).

The changes in the number of erythrocytes and reticulocytes in the peripheral blood, as well as the changes in the acid stability of the erythrocytes in guinea pigs subjected to prolonged irradiation with the γ rays of ^{137}Cs at a dose of 576 R with a constant dose rate of 0.27 R/min, were studied in comparison with animals irradiated briefly with the γ rays of ^{60}Co at a dose of 385 R with a dose rate of 606 R/min. Under these conditions of irradiation of guinea pigs at equally effective average lethal doses, no significant difference was detected in the postradiation changes in the erythrocytes and reticulocytes in the peripheral blood. (tr-auth)

11279 CHANGE IN THE CELLULAR POPULATIONS OF THE BONE MARROW OF MICE AFTER SINGLE AND REPEATED IRRADIATION. Barakina, N. F.; Khao, Yu. (Inst. of Developmental Biology, Moscow. Univ., Liege). Dokl. Akad. Nauk SSSR; 192: 213-5(1 May 1970). (In Russian).

One group of mice were given a single x-ray dose of 500 R, and a second group of mice were given two doses of 500 R each separated by a time of 14 days. The mice were killed on 2, 4, 6, 8, 10, 12, 14, 16, 18, 20, 24 and 28 days after irradiation. Bone marrow was taken from the femur to determine mature cell forms (metamyelocytes and mature leukocytes) and the proliferative forms that included all the other cellular elements of the bone marrow. The mitotic index was determined on 2000 cells. No change in the behavior of the mitotic index with time could be observed in mice irradiated a single time as compared to the mice who were given two irradiations. It was found that the mature cellular elements do not play a role in determining the radioresistance of the animal organism. On the other hand, the increase in radioresistance of the animal to repeated irradiation can be explained by the state of the hematopoietic system, that is, by the proliferative pool. (TTT)

11280 NECESSITY OF USING DIRECT CORRELATIONS BETWEEN THE RESULTING DAMAGE AND THE TRAJECTORIES IN THE STUDY OF THE BIOLOGICAL EFFECTS OF THE HEAVY IONS IN COSMIC RADIATION. Deltour, G.; Kaiser, R.; Pfister, A.; Miro, L. (Laboratoires, Marcoussis, France). pp 382-5 of Proceedings of XVII International Congress on Aviation and Space Medicine, Oslo, 1968. /Hannisdahl, Birger (ed.). Oslo; Universitetsforlaget (1968). (In French).

Experiments carried out in France using balloons have indicated some radiobiological hazard in space and high altitude flights. This hazard is mainly due to the heavy ion components of primary cosmic radiation and from giant chromospheric eruptions. Until now only purely qualitative results have been obtained, either from small laboratory animals or from bacteriological preparations. It is necessary to work out quantitative techniques in order to be able to evaluate the hazard with instrumentation used in classical radioprotection. Because of their high energy, and weak and non-homogeneous flux, the heavy particles cause intense, but very local, injuries. The extent of biological damage can only be measured by a study of the effects produced in ionization cylinders by each particle in living matter. The best correlation should be obtained using homogeneous mixtures of nuclear emulsion and bacteria. (auth)

11281 NATURE OF THE EARLY GLYCEMIC RESPONSE OF THE IRRADIATED ORGANISM. Barkalaya, A. I. (Inst. of Biophysics, Moscow). Radiobiologiya; 10: 386-9(May-Jun 1970). (In Russian).

The dynamics of the glycemic response and the response of the adrenal cortex immediately after γ irradiation and electroshock were compared in noninbred white rats. These same responses were also determined in adrenalectomized irradiated rats. The data suggest that the early glycemic response of the irradiated organism is associated with the phase of alarm of the nonspecific response of adaptation. (tr-auth)

11282 MATERIALS OF THE INTERRELATIONSHIP OF THE INTEROCEPTIVE UNCONDITIONED REFLEXES AT VARIOUS PERIODS AFTER IRRADIATION. Lapshin, N. A. (Military Medical Academy, Leningrad). Radiobiologiya; 10: 390-4(May-Jun 1970). (In Russian).

In the presence of interacting interoceptive reflexes that arise from two receptor fields, the final reflect effect, as a rule, is represented in the form of a new summary response, the magnitude of which is not equal to the simple sum of the initial reflexes. The degree of change in the final effects of interacting reflexes depended on the periods of irradiation. This conclusion is based on experiments in which the mechanoreceptors of the duodenum, rectum, a segment of the small intestine, and the urinary bladder were stimulated at various times after the cats were x-irradiated. Stimulation was produced by stretching the walls of the organ with air. (tr-auth)

11283 SOME PECULIARITIES OF THE ACTIVITY OF THE ELEMENTS OF THE OPTICAL CORTEX IN ANIMALS IRRADI-

XUM

ATED IN THE MIDDLE OF EMBRYOGENESIS. Kolomeitseva, I. A. (Inst. of Higher Nervous Activity and Neurophysiology, Moscow). Radiobiologiya; 10: 400-3(May-Jun 1970). (In Russian).

Neuronal activity of the optical cortex of rabbits irradiated on the 15th day of embryogenesis was characterized by: a slowing of the background pulsed activity and a predominance of group discharges; the presence of a distinct overcharging in response to a light stimulus in 55.4% of the cells; a decrease in the number of elements responding to a light stimulus; a lower probability of charging to light; and the predominance of elements that respond with primary inhibition. (tr-auth)

11284 TREATMENT OF REACTIONS AND INJURIES TO THE EYE AFTER ACTION OF IONIZING RADIATIONS. Wollensak, J. (Univ., Erlangen, Ger.). Arbeitsmed. - Sozialmed. - Arbeitshyg.; 4: 90-1(Mar 1969). (In German).

The relative radiosensitivities of the mammalian hematopoietic system, gonads, gastrointestinal tract, hair, and eyes were compared and the possibilities for radiotherapy were reviewed briefly. The major injury of the eye following x irradiation with acute doses from 1000 to 2000 R was seen as keratoconjunctivitis. At higher doses, injuries included corneal ulcers, symblepharon, necrosis of connective tissue, increased vascularity of the iris and ciliary body, and tissue atrophy. Lens cataracts were produced after irradiation with 500 to 600 R of γ irradiation, or after only 15 to 45 R of neutron irradiation. Irradiation injuries of the lens were irreversible, and maximum doses of lens irradiation exposure were established as 200 R for children, and in adults as 200 R for a single dose, 300 R for doses fractionated over 3 months, 500 R for doses fractionated over more than 3 months, and 800 R for doses received over a period of one year. The most radiosensitive lens region was the germinative zone of the equator, where changes could be noted within a few hr of exposure. Very high doses caused severe lenticular degeneration. The possibility of medical personnel receiving cataractogenic doses over long periods of low level irradiation exposure was discussed. In rats, retinal injuries that ranged from inflammation to destruction of sensory cells were reported after irradiation with doses from 1200 to 6000 R. The tolerance dose for short-term irradiation of the choroid was from 2500 to 3000 R. The optic nerve was less radiosensitive. (BBB)

11285 EFFECT OF ROUTE OF ADMINISTRATION AND RADIATION OF ^{3}H-ACTINOMYCIN D BINDING BY MOUSE HEPATOCYTE DNA. Yatvin, Milton B. (Univ. of Wisconsin, Madison. CEN, Mol, Belgium). Proc. Soc. Exp. Biol. Med.; 135: 42-5(Oct 1970).

The ability of hepatocyte nuclei from irradiated mice to bind ^{3}H-actinomycin D was investigated at various times after exposure. Shortly after irradiation (1 to 3 hr), there was a marked drop in the amount of actinomycin bound by liver nuclei of ip-injected mice. The decreased binding after ip injection was probably an indirect action of radiation since it had no effect on binding iv-administered material. The decrease in actinomycin movement from the peritoneal cavity of similarly treated animals supports the hypothesis of an indirect action of radiation on binding by liver nuclei of ip-injected ^{3}H-actinomycin D. Further evidence for the hypothesis derives from the in vitro experiments using nuclei irradiated either in vivo or in vitro, in which there was no influence of exposure on binding. When iv administration is used, the amount of actinomycin bound to nuclei is three times that when the drug is given ip. These data call attention to the importance of the route used to administer compounds when interpreting either the action of the compound or those of radiation in animals. (auth)

11286 RADIATION NEPHRITIS. II. CHRONIC CHANGES AFTER HIGH DOSES OF RADIATION. Madrazo, A.; Suzuki, Y.; Churg, J. (St. Vincent's Hospital, New York. Barnert Memorial Hospital, Paterson, N. J. City Univ., New York). Amer. J. Pathol.; 61: 37-44(Oct 1970).

Large doses of radiation (4800 or 9600 rads) to an exposed kidney induce progressive changes, terminating in almost complete destruction of the organ in 5 to 6 months. Glomerular lesions become apparent a few days after the procedure and consist of detachment of cells, especially the endothelial cells, from the basement membranes; progressive formation of secondary basement membranes; and wrinkling and eventual collapse of the capillaries. This is accompanied by mesangial lysis and later, sclerosis. Tubular damage is also an early manifestation, with detachment of cells and formation of secondary basement membranes, necrosis and collapse. Lesions of arteries and arterioles appear late, 3 to 4 months after radiation. They consist of endothelial detachment, fibrinoid necrosis of the wall and luminal thrombosis. It is suggested that damage to both the cells and the intercellular substances, with loss of contact between the two and eventual overproduction of the intercellular material, constitutes one of the forms of tissue response to radiation. (auth)

11287 IMPLICATIONS OF RADIATION-INDUCED MODIFICATIONS IN THE COMPARATIVE TERATOLOGY OF THE NERVOUS SYSTEM. Ostertag, B. (Univ., Tuebingen, Ger.). Deut. Z. Nervenheilk; 197: 239-54(1970). (In German).

Changes of the nervous system in mouse embryos and in infant mice, brought about by single doses of x-radiation, were discussed. The strictly hemilateral exposure to radiation of the pregnant animal allowed for accurate comparisons between irradiated and untreated animals of the same litter. As to the teratogenic variation the age of individual embryos appeared to be more crucial than the duration of the pregnancy. However, it was this variation that made it possible to study sequentially the dysontogenetic effects when a large number of litters was used. Both a phase specificity in the maturation of organs and, in particular, cortical disorders may be recognized in the already present pallium. Here deviations, defects and transient overshooting developments of structures become manifest. The radiation-induced spinal cord lesions corresponded to dysraphias found in man at young age. The surviving infant animals, irradiated on the 11th day after conception, were generally retarded compared to their litter mates, displaying multiple malformations and functional lesions of the nervous system in addition to conjugated deformities. (auth)

11288 CHANGES IN THE NUMBER OF BONE MARROW CELLS AFTER A SINGLE INJECTION OF METHIONINE SULPHOXIMINE AS COMPARED WITH THE EFFECT OF WHOLE BODY IRRADIATION WITH X-RAYS IN MICE. Zak, M.; Kolousek, J. (Charles Univ., Prague). Neoplasma; 17: 339-43(1970).

The changes in the number of bone marrow cells were studied in mice after a single i.p. application of DL-methionine sulphoximine in a dose of 400 mg per kg of body weight and after a single whole body irradiation with x-rays in a dose of 600 R as compared with the controls. The changes were followed on the 1st, 5th, 14th and 28th day after the treatment and in the control group. Cyclical decrease in the number of bone marrow cells in mice was observed both after the x-irradiation and also after the single administration of methionine sulphoximine. (auth)

11289 COMPARISON OF THE HEART RATE, MEAN ARTERIAL PRESSURE, AND RESPIRATORY FREQUENCY AFTER ZIRCONIUM CITRATE ADMINISTRATION IN IRRADIATED AND NON-IRRADIATED RABBITS. Kuna, P.; Vokrouhlicky, L. (Military-Medical Research Inst., Hradec Kralove, Czech.). Sb. Ved. Pr. VLVDU Hradci Kralove; 47: 159-73(1970). (In Czech).

Zirconium citrate (50 mg Zr per 1 kg body weight) produced, after intravenous administration in rabbits 24 hr following 1000 R whole-body γ irradiation, analogous changes in heart rate (retardation and later acceleration), disorders of mean arterial pressure (hypo- and hypertension), and respiratory arrest for 5 sec. to 3 min., in the first 5 min. after injection as in non-irradiated animals. Synchronous zirconium citrate and calcium gluconate (1 ml of 10% solution per 1 kg b.w.) administration had very favorable effect on the observed physiological changes also in irradiated rabbits. (auth)

11290 KINETIC MODEL OF STEM-CELLS POPULATION IN THE POSTIRRADIATION BONE MARROW INJURY. II. Smid, A.; Hradil, J. (Military-Medical Resarch Inst., Hradec Kralove, Czech.). Sb. Ved. Pr. VLVDU Hradci Kralove; 47: 129-58(1970). (In Several languages).

A universal program was constructed to examine the tolerance of a model stem cell population to biological effects of single and continuous irradiations acting simultaneously. Attempts were made to solve some problems of erythropoiesis kinetics with a view to the relations between the stem cell and proerythroblast compartments under steady state conditions and after a simulated irradiation. Then an attempt was made to test some results obtained in experimental therapy of irradiated rats given homologous bone marrow cells. In building up the model, the classic conception of hemopoietic cell division and differentiation was used. It was determined that inside the system of stem-cell and proerythroblast populations, a persistent structural renewal is going on under steady state conditions caused by a continuous physiological decrease of the final cells. If a disturbance is acting from without, then the feed-back control operates to compensate for the unfavorable effect and to bring the system back into equilibrium. (tr-auth)

11291 REVIEW ON RADIOBIOLOGY OF THE THYROID GLAND. Al-Hindawi, Ali Y. (Republic Hospital, Baghdad). Isotope Radiat. Res.; 1: 81-5(Oct 1968).

The thyroid gland is difficult to investigate in radiobiology because of its tough capsule, the adherent cells, and the low mitotic index. The effects of internal irradiation by ^{131}I on the thyroid of animals and man are reviewed. DNA synthesis is impaired and the lifespan of irradiated thyroid cells is shortened. The effects of external irradiation by x rays on the thyroid of animals are also reviewed. (F.M.M.)

11292 EFFECTS OF CYSTEAMINE GIVEN BEFORE AND AFTER X IRRADIATION UNDER DIFFERENT TEMPERATURE CONDITIONS ON MORTALITY OF THE FISH, ORYZIAS LATIPES. Egami, N. (Tokyo Univ.). Int. J. Radiat. Biol.; 18: 391-4 (1970).

All fish irradiated with 2.8 kR of x rays at 23°C, and kept at the same temperature died within 30 days. One third survived for 30 days if cysteamine (20 mg/10 ml Ringer's solution) were injected intraperitoneally 10 min before irradiation. No radioprotective action was seen if cysteamine were given 3 min after irradiation. In the group of fish irradiated and kept alive at 4°C for 3 weeks after irradiation before being transferred to 23°C, the majority died within 15 days after transfer. In fish injected with cysteamine 15 min before irradiation at 4°C, radioprotection was marked. There was no significant effect on survival when fish were injected 21 days after irradiation, and just before transfer from 4°C to 23°C. Other series of experiments were carried out with radiation doses of 3.0 kR and 2.5 kR and similar results were obtained. The protective action of cysteamine was marked provided the fish were treated before irradiation. Two doses of cysteamine after irradiation appeared to have toxic effects on the fish and did not show radioprotective effects. Numbers of fish in each group varied from 41 to 120. (UK)

11293 MULTI-COMPONENT RADIATION SURVIVAL CURVE USING AN IN VITRO TUMOUR MODEL. Sutherland, R. M.; Inch, W. R.; McCredie, J. A.; Kruuv, J. (Univ. of Western Ontario, London, Can.). Int. J. Radiat. Biol.; 18: 491-95(1970).

Chinese hamster V79 cells were grown for periods up to 30 days to produce multicell spheroids. Spheroids of similar size were selected after various periods of growth and given graded doses of ^{60}Co irradiation. They were then broken up into single cells by trypsinization and mechanical shaking. Unirradiated control spheroids were similarly treated. After an incubation period of 8 days colonies were stained and counted. Survival was expressed as a fraction of the control population. Single cells and multicell spheroids after growing for 3, 5 and 9 days were irradiated. Survival curves for spheroids of various sizes compared with single cell curves irradiated in air with ^{60}Co at a dose rate of 135 rads/min are given. The change in slope in the high dose region of the curve indicated that a resistant cell population was present when the spheroids reached a diameter of about 200μ. They then contained cells in different nutritional states, indicated by the start of central necrosis. The curves are multi-component and similar to those obtained from solid tumours. It is concluded that this in vitro system is a good model to study the complex interaction among the factors modifying radiosensitivity and repair, during radiotherapy of solid tumours. (UK)

Man

Refer also to abstracts 10953, 10982, 11025, 11057, 11063, 11086, 11109, 11111, 11113, 11181, 11187, 11189, 11190, 11205–11207, 11209, 11222, 11228, 11237, and 11926.

11294 (EUR-4542) PATHOGENESIS OF GENETIC AND SOMATIC RADIATION DAMAGE. Annual Report, 1969. (Gesellschaft fuer Strahlenforschung m,b,H., Neuherberg bei Munich (West Germany). Institut fuer Biologie). 1970. 28p. (In German). Dep. NTIS (U. S. Sales Only). EUR DM 3,70.

As part of the research program, experimental studies are being conducted on the frequency and genesis of somatic and genetic radiation damage by exposure to external radiation sources and after the incorporation of radioactive nuclides. The studies deal with selected questions covering the following fields: radiation genetics of vertebrates; functional disturbances of the nervous system after radiation exposure; radiotoxicity; and radiation damage in man resulting from the supply of ^{224}Ra. (auth)

11295 ^{90}Sr AND INFANT MORTALITY IN CANADA. Shaw, R. F.; Smith, A. P. (Univ. of Dalhousie, Halifax, Nova Scotia). Nature (London); 228: 667-9(14 Nov 1970).

Evidence is presented against the findings of Sternglass and others regarding ^{90}Sr in fall-out and infant mortality. Examination of Canadian data showed that although the ^{90}Sr levels were higher than in the USA, this appeared to have had no effect on the mortality and there appeared to be no real association between the two variables. A large rise in ^{90}Sr did not appear to be associated with a large rise in excess mortality, and if anything the reverse appears to hold. There was a slight negative association between the amount of change in the two variables over the period 1946-55, which is regarded by Sternglass as the most appropriate period for such studies. The possibility is discussed as to whether the association asserted by Sternglass does, in fact, hold for the USA. Analysis of the somewhat limited available data indicated a similar result, in that the mortality and ^{90}Sr variables did not rise together and, if anything, showed a small negative association (regression coefficient = –0.81). (UK)

11296 WHOLE BODY SKIN ERUPTION COMBINED WITH RADIOTHERAPY. WITH A SPECIAL REFERENCE TO 6 CASES OF OUR OWN INVESTIGATION. Kiyono, Kunihiro; Watanabe, T. (Shinshu Univ., Nagano, Japan). Rinsho Hoshasen; 14: 944-50 (Dec 1969). (In Japanese).

Of 527 cases of malignant tumors subjected to radiotherapy in the Radiological Department of Shinshu University Hospital during the last 2 yr, whole-body skin eruption due to irradiation occurred in six cases. There were three cases of esophageal cancer, and one case each of breast, cervical, and epipharyngeal cancer. The dose at the time of occurrence of skin reaction ranged from 1,200 to 12,000 R, and there was no correlation between the site irradiated and the occurrence of skin reaction. Fever was observed in all six cases, and in two cases, the exacerbation of skin reaction was found following the fever. Most of the skin reactions observed were papula with erythema and, occasionally, vesicula. Three cases complained of itching. Seven to 15 days were required for healing of the skin eruptions. The pathogenesis of this reaction is not well understood. Allergic response to radiation, autoantibody or toxin production by irradiation, non pathogenic microbes (virus, bacterium, fungus) obtaining pathogenic properties following irradiation, or lowering of the resistance of tissues and whole body to drugs or bacteria by irradiation are being considered. (Japan)

11297 INTENSE RADIATIONS AND OCULAR EXPOSURE HAZARDS. Armstrong, C. E. Nat. Saf. News; 100: No. 4, 90-5(Oct 1969).

A survey of the traumatic effects of eye exposure to various types of electromagnetic radiation, describing the role of the optometrist, the structure of the eye, injuries which can be caused and the mechanism of their formation, types of radiation and doses causing damage to various parts of the eye. Preventive measures are briefly discussed for a few types of radiation sources. (Occup. Safety and Health Abstr.)

11298 ACTION OF SOME FACTORS IN SPACE FLIGHT ON THE CENTRAL NERVOUS SYSTEM. Livshits, N. N.; Apanasenko, Z. I.; Klimovitskii, V. Ya.; Korolevskii, A. P.; Kuznetsova, M. A.; Luk'yanova, L. D.; Meizerov, E. S. Usp. Sovrem. Biol.; 67: 256-72(Mar-Apr 1969). (In Russian).

Ionizing radiation effects on the central nervous system during cosmic flights depend on various factors (the type of radiation, the duration of dose distribution, and preliminary effects of dynamic factors, acceleration, and vibration). Accelerated peripheral pulsation plays an important role in the vibration effects on the reaction of the central nervous system. Repetition of vibration effects reduced their effectiveness and simultaneously reduced the excitation of the higher centers of the brain by peripheral excitations. (R.V.J.)

11299 CHANGE IN THE TYPE OF RADIATION CELL-KILLING ON HUMAN LYMPHOCYTES AFTER BLAST FORMATION BY PHYTOHAEMAGGLUTININ. Sato, C. (Aichi Cancer Research Inst., Nagoya, Japan). Int. J. Radiat. Biol.; 18: 483-5(1970).

Leukocytes in the upper layer of heparinized human venous blood were purified to make the lymphocyte content 90 to 99% of nucleated cells. Irradiation was performed soon after the addition of phytohaemagluttinin (PHA). Following incubation the cumulative fraction of mitotic cells was expressed as a fraction of the original lymphocytes which entered the mitotic phase in a certain culture time with PHA. The time-course of cell death is shown graphically. Small lymphocytes without PHA began to die 10h after 500R irradiation and 95% of cells died during 40h of exposure. However, lymphocytes stimulated by PHA survived longer and began to decrease 40h after the addition of PHA and irradiation. (UK)

11300 MATERNAL DIAGNOSTIC X IRRADIATION BEFORE CONCEPTION AND THE FREQUENCY OF MONGOLISM IN

XUM

CHILDREN SUBSEQUENTLY BORN. Stevenson, Alan C.; Mason, Rita; Edwards, Kathleen D. (Medical Research Council, Oxford). Lancet; 2: 1335-7(26 Dec 1970).

Follow-up of 1052 children born to mothers who had x ray investigations involving doses to ovaries before conception showed that 3 children had Down's syndrome. It is estimated that this number is not significantly different from that which would be expected when the high proportion of older mothers in the study is taken into account. (auth) (UK)

11301 SPECULATED RISK TO BONE AND LIVER FROM ^{239}Pu. Mays, Charles W.; Taylor, Glenn N.; Jee, Webster S. S.; Dougherty, Thomas F. (Univ. of Utah, Salt Lake City.). Contract AT(11-1)-119. Health Phys.; 19: 601-10(Nov 1970).

The permissible body burden of ^{239}Pu in radiation workers is 0.04 μCi. A literature survey indicates that the Pu reaching the circulatory system from occupational exposure may redeposit roughly half in bone and half in liver. For a constant 0.02 μCi ^{239}Pu in bone and 0.02 μCi ^{239}Pu in liver, the 50-yr doses to man are 14 and 57 rads, averaged over these respective organs. Estimated probabilities of radioinduced tumors from these doses are given. The threshold model is based on radium-containing humans, whereas the dose-rate and lifespan dose models are extrapolated from plutonium-containing dogs. These risks refer to adult, not childhood, exposures. The hazards to the lung from inhaled plutonium, and the hazards to wound puncture sites are not estimated. Improved estimates of the actual risks are urgently needed. (auth) (UK)

11302 CASE OF MYELOCYTIC LEUKEMIA SIMULATING THE MOUSE MODEL DISEASES. Bennett, Michael (Buffalo General Hospital. Roswell Park Memorial Inst., Buffalo). J. Surg. Oncol.; 2: 239-43(1970).

A case of myeloid leukemia is reported that occurred in a woman whose previous experiences are known to increase the incidence of myeloid leukemia in the mouse. Ovariectomy and sterile turpentine abscess formation increase the incidence of myeloid leukemia in mice exposed to ionizing radiation. In addition, antigenic similarities exist between certain variants of murine leukemia virus and mammary tumor virus. This patient experienced ovariectomy, thigh abscess formation, and partial body irradiation for carcinoma of the breast a few years before she developed leukemia. An association between human breast cancer and myelocytic leukemia has been described. While this case certainly does not prove that similar pathogenetic mechanisms of myeloid leukemia occur in mice and man, the events preceding the development of leukemia in this patient certainly mimicked the mouse models well. (auth)

11303 LATE EFFECTS OF RADIOPHOSPHORUS THERAPY OF POLYCYTHEMIA VERA. Hoefer, R.; Kuehboeck, J. (Univ., Vienna). Blut; 20: 237-41(Apr 1970). (In German).

It is concluded that radiophosphorus therapy is still the treatment of choice for polycythemia. No other type of therapy has yet resulted in a similar prolongation of life together with a low incidence of leukemia in such patients. (auth)

Radiation Effects on Plants

Refer also to abstracts 10965, 10973, 10974, 10976, 10977, 10979, 11009–11011, 11013, 11015, 11017, 11020, 11027, 11030, 11031, 11033–11035, and 11095.

11304 (BNL-50203, pp 70-81) ROLE OF OXYGEN IN THE REPAIR PROCESS. Howard, Alma (Christie Hospital and Holt Radium Inst., Manchester (Eng.) Paterson Labs.).

From Conference on time and dose relationships in radiation biology as applied to radiotherapy held at Carmel, California, September 15–18, 1969.

Split-dose experiments on recovery from sublethal damage were performed using the alga, Oedogonium cardiacum. Data were obtained for effects of oxygen during the first irradiation and during the interval between the two doses. Results indicated that the damage done hypoxically was less recoverable than damage done aerobically. A review of the literature is presented on the effects of hypoxia on recovery of mammalian cells, Vicia, Chlamydomonas, and yeast. It is concluded that cells that are severely hypoxic during irradiation suffer less recoverable damage than cells that are better aerated. Well-aerated cells are maximally sensitive to radiation, but are also able to repair a maximum proportion of their sublethal damage. Cells that are severely hypoxic during the interval between doses have a reduced capacity for repair. Experiments indicate that sublethal damage may remain open during hypoxic intervals and subsequently be repaired when oxygen is restored. (H.L.W.)

11305 (NP-18394) STUDY OF ELECTRON EPR PARAMAGNETIC RESONANCE OF IRRADIATED SEEDS OF DAHLIA COCCINEA. Orlando de la Teja Angeles, Carlos (Universidad Nacional Autonoma de Mexico, Mexico City. Facultad de Ciencias). 1970. 111p. (In Spanish). Dep. CFSTI (U. S. Sales Only).

Thesis.

The principles on which the electron paramagnetic resonance (EPR) method is based are briefly analyzed and some examples of its application in biology are presented. The results of experiments with seeds of Dahlia coccinea both whole and in sections (stamen, cotyledon, and embryo) irradiated with electrons at 1 MeV and without irradiation are presented. The behavior of the free radicals produced in the unirradiated forms and induced by irradiation is analyzed. It was observed that the dahlia seeds produce a simple EPR single without hyperfine structure and is of greatest intensity in the stamen. The intensity of the signal of the whole seeds is inversely proportional to the humidity content of the sample, and the same effect is observed in the samples treated with the complex of serotonine-sulfate of creatinine but to a lesser degree than in samples treated with distilled water. The number of free radicals in the samples increase proportionally with the radiation dose, increasing consequently the intensity of the resonance signals. The average life of the free radicals induced by the radiation is sufficiently large when the samples are maintained in dessicators with calcium chloride. As it is thought the free radicals produced by the radiation contribute directly or indirectly to the radiation damage in living organisms, the behavior of various protective substances was examined by the EPR method to determine the radioprotection mechanism. The results obtained and the conclusions drawn are compared with those of previous studies. (tr-auth)

11306 HOST-BACTERIA RELATIONSHIP IN THE TISSUES OF X-IRRADIATED JERUSALEM ARTICHOKES. Jonard, Robert; Parrot-Miche, Francoise (Univ., Montpellier, France). Physiol. Veg.; 8: 231-4(Apr-Jun 1970). (In French).

Jerusalem artichoke tissues treated by x ray doses that inhibit their proliferation can, under certain conditions, recover the ability to proliferate. However this restoration does not allow them to produce tumors by inoculation of Agrobacterium tumefaciens cells (strain B_6). This is a new example of the selectivity of x rays with regard to tumoral processes. (France)

11307 GAMMA RADIATION EFFECTS ON THE CONTENT OF PYRIMIDINE OLIGONUCLEOTIDES IN LOW-POLYMER FRACTION OF LABILE DNA IN COTTON SPROUTS. Ibragimov, A. P.; Divavin, I. A.; Aripdzhanov, Sh. A. (Inst. of Biochemistry, Tashkent). Dokl. Akad. Nauk Uzb. SSR; No. 1, 48-9(1970). (In Russian).

The effects of γ radiation on the oligonucleotide composition and various fractions of DNA in cotton were studied using seven day sprouts of Gossypium hirsutum from seed irradiated at 6 kR before planting. Tabulated data are given on the content of pyrimidine nucleotide isofractions and the composition and quantitative content of various oligonucleotides. Possible reaction mechanisms involved are discussed. (R.V.J.)

11308 BIOELECTRIC POTENTIAL OF ZEA MAYS ROOTS: CHARACTERIZATION AND RADIATION EFFECTS. Carlton, William Herbert. New Brunswick, N. J.; Rutgers-The State Univ. (1969). 46p. University Microfilms Order No. 70-10,050.

Thesis.

The bioelectric potential associated with untreated and x-irradiated Zea mays roots was characterized, correlated with cell growth, and evaluated in terms of the uptake of an inorganic ion. The bioelectric potential pattern surrounding the root of Zea mays was specified as either transient, steady state, or oscillating, depending upon the method and time of measurement. A transient potential existed during the first few minutes after a root was placed in a monitoring solution; then a steady state potential existed following equilibration. An oscillating potential, with a 17 min period, could only be observed when both probes are placed in a stationary position near the root. X irradiation caused the peak in the bioelectric potential pattern, that occurred at the point of maximum rate of elongation, to move nearer the root tip. This movement was explained by an analysis of cell growth in the root. The bioelectric potential pattern was not directly related to mitosis since a cessation of mitotic activity following irradiation did not affect the potential pattern for several hours. Because of the lack of cell division, the process of elongation moved nearer the tip, corresponding to the movement of the potential peak. In order to test the correlation between inorganic ion transport and bioelectric potential, uptake experiments with ^{42}K were performed. There was very little correlation between the bioelectric potential pattern and ^{42}K uptake, however, uptake experiments demonstrated a partial correlation between ^{42}K concentration in the root and the positive peak of the bioelectric potential pattern. RNA and protein

content and oxygen uptake were at a maximum in the portion of the root where the negative peak of the bioelectric potential occurred. (Diss. Abstr.)

11309 IONIZING RADIATION AND NITROGEN METABOLISM DURING THE INITIAL PERIODS OF GROWTH IN CORN. Babenko, V. I.; Sivolap, Yu. M. Vestn. Sel'skokhoz. Nauki (Moscow); No. 11, 44-6(1969). (In Russian).

Data are presented on the metabolism of different nitrogen compounds in the endosperm and seedlings of corn (Zea mays) grown from seeds exposed to ionizing radiation. It was concluded that there is decomposition of proteins in the endosperm that results in the significant accumulation of free amino acids in seedlings and in the endosperm after irradiation. (auth)

11310 PHOTODESTRUCTION OF CHLOROPLAST ULTRASTRUCTURE BY RED LIGHT: LOCATION OF CHLOROPHYLL. Walne, Patricia L.; Haber, Alan H.; Triplett, Larry L. (Oak Ridge National Lab., Tenn. Univ. of Tennessee, Knoxville). Proc. Nat. Acad. Sci. U. S. A.; 67: 1501-4(Nov 1970).

A lethal dose (1 Mrad) of gamma rays was given to wheat leaf tissue to restrict migration of the energy of red light photoexcitation to the photosynthetic pigment system. This dose of gamma radiation had no apparent effect on chloroplast ultrastructure in tissue that received no illumination. Subsequent illumination with red light, used to induce chlorophyll-sensitized photodestruction of ultrastructure, permitted inferences about the location of chlorophyll within the chloroplast. The red light produced extensive disruption in chloroplasts but not in any other cellular organelles. The sequence of events in this photodestruction was different from that which occurs when chloroplasts are destroyed by methods that do not involve illumination. The red light caused peculiar abnormalities only in the internal lamellar system of the chloroplast and not in the envelope or any other regions. These findings support other studies which suggest that chlorophyll is located exclusively in grana and stroma lamellae. (auth)

11311 EFFECTS OF ACUTE GAMMA RADIATION ON CHRYSANTHEMUM INFLORESCENCE MORPHOGENESIS. Naskali, Richard John. Columbus, Ohio; Ohio State Univ. (1969). 232p. University Microfilms Order No. 70-14,080.
Thesis.

Chrysanthemum morifolium plants were irradiated with an acute 2500 R γ dose at 0, 7, 14, 21, 28, 35, 42, or 49 days after daily photoinduction commenced in order to relate microscopic ontogenetic events with induced variations in intact flowering plants. Histological materials were studied from eight weekly collections of controls and all previously irradiated plants. In non-irradiated plants, there was little anatomical change in apices from zero through seven short days. With onset of photoinduction, mean plastochron decreased from the 2.1 days of foliage leaves to a 0.4 day mean involucral bract plastochron. Between the 15th and 20th short days, after approximately 38 involucral bracts formed, rapid acropetal initiation of floret primordia commenced. Florets formed in cycles of 22 to 40 florets each, at the rate of about 23 hours per cycle, until approximately 367 florets were present. Florets, the last of which formed between the 28th and 35th short days, differentiated into either perfect (disc) or pistillate (ray) florets by the 35th short day concomitant with decreasing growth of involucral bracts. In irradiated plants, first floret initiation was not delayed by treatment at zero or seven short days; there was no evidence that phytochrome-mediated photoperiodism was directly affected. Initiation of last florets was delayed in plants irradiated after zero, seven, 14, and 21 short days, presumably due to mitotic inhibition. Radiosensitivity varied greatly among treatment times and among criteria considered. Irradiation-induced genotype changes were attributable to several possible genetic phenomena other than the breaking of a periclinal chimera. Typical and supernumerary involucral bracts appear to play a role in the usual differentiation of florets into discs or rays, as well as in the induction of sex reversals. During inflorescence ontogeny, there are phasic changes in levels of at least four endogenous hormones. Auxin, some of which may form in rapidly growing involucral bracts, appears to enhance ray floret differentiation at high concentrations; disc florets appear to differentiate during periods of low or declining levels of auxin. Ray floret growth initially is apical; subsequently, there is intercalary growth over the entire ray floret corolla. Maturation of leaves was a linear process. (Diss. Abstr. Int., B)

11312 DIFFERENTIAL AND COMBINED EFFECTS OF BETA, GAMMA, AND FAST NEUTRON IRRADIATION OF SOYBEAN SEEDLINGS. Witherspoon, J. P.; Corney, A. Kathleen (Oak Ridge National Lab., Tenn. Emory Univ., Atlanta). Radiat. Bot.; 10: 429-35(Sep 1970).

Young soybean (Glycine max, L., Dare variety) seedlings were acutely irradiated with various doses of $^{90}Sr-^{90}Y$ β rays, ^{60}Co γ rays, and fission neutrons. The radiation types were given in combination as well as singly. Biological effects were evaluated on the basis of apical meristem mortality, dry weight, and height. The dose necessary to produce a 50% effect was calculated, and RBE values were derived. Gamma and beta radiation were essentially equally effective in producing these end points, but fission neutrons were 6.0, 15.7 and 7.7 times more effective in producing a 50% effect on apical meristem mortality, height, and shoot weight, respectively. The effects of combined radiation types were not directly additive. With β doses of 1500 rads, a 10% increment of γ or fast neutron doses gave greater effects than were expected. (auth) (UK)

11313 RELATIVE BIOLOGICAL EFFECTIVENESS OF X-RAYS AND 0.43-MeV MONOENERGETIC NEUTRONS ON SOMATIC MUTATIONS AND LOSS OF REPRODUCTIVE INTEGRITY IN TRADESCANTIA STAMEN HAIRS. Underbrink, A. G.; Sparrow, Rhoda C.; Sparrow, A. H.; Rossi, H. H. (Brookhaven National Lab., Upton, N. Y. Columbia Univ., New York). Radiat. Res.; 44: 187-203(Oct 1970).

Young inflorescences of Tradescantia clone 02 were irradiated with 0.43 MeV neutrons at doses of 0.163, 0.54, 1.07, 2.16, 4.34, 7.97, 12.7, 17.2, and 24.4 rads. Data from this experiment were compared with data from 250 kVp x rays with doses of 11.5, 24.0, 48.0, 96.0, 144.0, 192.0, 240.0, 288.0, and 432.0 rads. In both experiments, the stamen hairs were scored daily from day 7 through day 23 postirradiation. Relative biological effectiveness (RBE) values were determined for four cellular aberrations: the color change from blue to pink and to colorless, and the morphological change from normal-sized blue cells to either blue dwarf or blue giant cells. Maximum RBE values found were 23.5 for blue dwarf, 30.7 for pink, 39.1 for colorless, and 120.5 for blue giant cells. In all cases, the RBE decreased with increasing dose but only slightly so for blue dwarf cells. Survival curves were constructed with hairs of three different lengths (cell numbers) being considered as the surviving fraction. RBE values of about 10 were found for 50% loss of reproductive integrity. The reasons for the large variation in RBE obtained with the different criteria used as end points are not understood. (auth)

11314 SIMPLIFIED METHOD FOR PREDICTING THE RADIATION EFFECT IN THE IRRADIATION OF SEEDS OF CEREAL GRASSES WITH IONIZING RADIATIONS. Kavats, G. E. (Inst. of Biology, Riga). Radiobiologiya; 10: 426-8(May-Jun 1970). (In Russian).

A comparison was made of certain methods for predicting the survival of plants on the basis of indices of the initial growth. It was shown that the most accurate results are given by the method of Osborn and Lunden. The possibility of a substantial simplication of this method was demonstrated. (tr-auth)

11315 INFLUENCE OF IONIZING RADIATION AND CHEMICAL MUTAGENES ON BARLEY SEEDS. Pitirimova, M. A.; Batygin, N. F. Vestn. Sel'skokhoz. Nauki (Moscow); No. 4, 97-9 (1969). (In Russian).

The influence of γ radiation and of chemical mutagenes on the growth of barley seeds in various soils was studied using dry seeds. Irradiation was carried out at 1, 5, 10, 15, and 20 kR at 950 R/min. After either exposing the seeds to γ radiation or soaking the seeds in solutions of ethylenimine, ethylmethane sulfonate, or diethylsulfate at concentrations of 0.01, 0.03, 0.1, 0.3, and 0.6%, they were planted in highly- and normally fertilized soils. Data obtained confirmed that the physiological reactions of plants to γ radiation and to chemical mutagenes depended on the dose factor. Soil conditions also produced a modifying influence on the chemical and radiobiological effects of the seed treatment. High concentrations of fertilizer enhanced the damaging effects of both radiation and the chemical mutagenes. (R.V.J.)

11316 SIMULTANEOUS RECOVERY OF YEAST CELLS FROM SUBLETHAL AND LETHAL DAMAGES AFTER IRRADIATION. Barsukov, V. S.; Malinovskii, O. V.; Mityushova, N. M. (Physical-Technical Inst., Moscow. Inst. of Physiology, Leningrad). Tsitologiya- 12: 658-65(May 1970). (In Russian).

The increased survival of resting yeasts following irradiation with fractionated doses and the plating of cells on nutrient medium immediately after the second dose may be explained by the simultaneous recovery of lethal and sublethal damages. The process of recovery from lethals slows down the recovery from sublethals. This fact may be explained by a gradual elimination of lethals by conversion into sublethals. Suggesting that lethals appear as the result of interreaction between sublethals, the above facts may be easily accounted for. (auth)

11317 SYNERGISTIC INHIBITION OF GROWTH OF MUNG BEAN SEEDLINGS AFTER A COMBINATION OF LOW-LEVEL X IRRADIATION AND LOW-LEVEL SHOCK TREATMENT. Mur-

ray, Sylvia A.; Newcombe, C. L. (San Francisco State Coll., Calif.). Radiat. Bot.; 10: 563-7(Nov 1970).

Seedlings of Phaseolus aureus were studied for the effect of low level irradiation, shock, and combined treatments. Low levels of x irradiation (100 R and 1000 R) decreased seedling height, hypocotyl length, and root dry weight linearly, with significant curvilinear responses for the internode and leaf length. Low shock pressure levels (20 psi and 40 psi) inhibited growth of all plant characters. The radiation × shock interactions were significant for all plant characters except root dry weights. The combined treatments acted additively or synergistically to inhibit seedling height, hypocotyl, epicotyl, internode and leaf lengths, and shoot and root dry weights in at least one treatment level for each plant character. (auth) (UK)

11318 EFFECT OF ACUTE γ IRRADIATION ON SELF-INCOMPATIBILITY AND RELATED CHARACTERS IN BROWN SARSON. Rao, T. Swamy (Indian Agricultural Research Inst. New Delhi). Radiat. Bot.; 10: 569-75(Nov 1970).

The patterns of response to radiation in 3 varieties of Brassica campestris var. brown sarson representing different degrees of self-incompatibility were distinctly diverse in M_1, M_2, and M_3 generations for chlorophyll recessives and other quantitative characters including the measures of self-incompatibility. The results confirmed that changes in the genetic architecture of the irradiated populations are as important as the initial differences for the degrees of self-incompatibility among the parental populations. The studies showed that it is possible to get a greater response in a direction opposite to the previous history of selection, in both self-compatible and self-incompatible types. (auth) (UK)

11319 EFFECTS OF IONIZING RADIATION ON DRIED SPORES OF OSMUNDA REGALIS. I. ELECTRON SPIN RESONANCE STUDY OF SPORES. Dodd, N. J. F.; Ebert, M. (Christie Hospital and Holt Radium Inst., Manchester, Eng.). Int. J. Radiat. Biol.; 18: 451-61(1970).

Spores were irradiated and their ESR signals studied. The radio-produced radicals fall into 6 distinct groups, only one of which reacts with O_2. The groups were characterized by their behaviour in N_2, O_2, and NO. These gases were chosen for their ability to modify biological radiation damage. In control experiments with unirradiated spores the endogenous radical populations were examined. Surface radicals were observed which react reversibly with O_2, NO, and NO_2. (auth) (UK)

Radiation Effects on Microorganisms

Refer also to abstracts 10959, 10960, 11007, 11008, 11016, 11019, 11026, 11029, 11032, 11280, 11306, and 11328.

11320 NATURE OF REPARABLE AND NON-REPARABLE LETHAL DAMAGE IN E. COLI AND BACTERIOPHAGE INDUCED BY THE PHOTODYNAMIC ACTION OF ACRIDINE ORANGE. Janovska, Eva; Zhestjanikov, Vladimir; Vizdalova, Milena (Inst. of Biophysics, Brno). Int. J. Radiat. Biol.; 18: 317-29(1970).

Experiments were carried out to determine the lethal photodynamic effect of acridine orange on 10 strains of Escherichia coli of the groups B and K12, differing in their ability to repair lesions caused by uv and ionizing radiation. The strains vary in their sensitivity to the photodynamic action of acridine orange. These differences are at variance with the ability of the bacteria to repair their radiation damage. The experiments on extracellular phages of E. coli revealed no multiplicity, uv, v and x gene reactivations after the photodynamic action of acridine orange. In phage T3, repair by the host cell was observed in bacterial strains capable of repairing uv-irradiated phage (hcr^+); this did not occur in phage T7. In bacteria and DNA of phages T2, T4, and T7, acridine orange-induced lesions differ in their nature from damage caused by uv light. On the other hand, in DNA of phage T3, higher doses of visible light induced damage which could be partly repaired by bacterial enzymes of the excision repair system. (auth)

11321 INTERFERENCE OF COCAL VIRUS WITH FRIEND LEUKEMIA VIRUS-INDUCED SPLENOMEGALY IN DBA/2J MICE. Stim, Thomas B. (Yale Univ., New Haven). Proc. Soc. Exp. Biol. Med.; 134: 413-20(Jun 1970).

In studying the inhibitory effect of a single infectious or uv-inactivated arbovirus (Cocal) dose on Friend leukemia virus-induced leukemia in DBA/2J mice, the greatest degree of interference (reduction of splenomegaly) occurred when Cocal virus was administered 24–48 hr prior to Friend leukemia virus. The percentage and duration of splenomegaly inhibition was dependent on the dose and state (infectious or inactivated) of the Cocal virus. (auth)

11322 SELECTIVE EXTIRPATION OF ORAL CILIATURE OF BLEPHARISMA BY LASER MICROBEAM. Jenkins, R. A.; Sawyer, H. R. (Univ. of Wyoming, Laramie). Exp. Cell Res.; 63: 192-5(Nov 1970).

The superiority of laser microbeams over uv microbeams for selected area cell irradiation has been cited. Laser microbeams have also been used in investigations of particular cellular phenomena. The purpose of the present study was to ascertain the feasibility of using the laser microbeam as a means of educing a specific cellular process, kinetosome and cilium formation. It is reported here that the use of the laser microbeam for the selective extirpation of kinetosomes and associated cilia of the oral apparatus of Blepharisma japonicum was demonstrated and the added precision of the device as a microsurgical tool in a study of the replacement of these organelles was studied. (P.B.M.)

11323 RADIOSENSITIZATION OF SHIGELLA FLEXNERI AND ESCHERICHIA COLI BY METHYL HYDRAZINE, INDANE TRIONE, AND ACRIFLAVINE. Cramp, W. A. (Hammersmith Hospital, London). Int. J. Radiat. Biol.; 17: 559-67(1970).

Three compounds which differ widely in their chemical reactions with cellular constituents were found to sensitize Shigella flexneri Y6R, Escherichia coli B/r and E. coli B_{s-1} to the effects of ionizing radiation. The radiosensitivity of survivors from bacteria treated with toxic concentrations of these compounds and then washed was the same as untreated bacteria. However, bacteria treated with non-toxic concentrations of indane trione and acriflavine and then thoroughly washed were more resistant to the effects of uv-light. Since the bacteria were sensitized to ionizing radiation only in the presence of the free compounds, it was concluded that sensitization to ionizing radiation could be by means of an energy-transfer mechanism between the sensitizing compound and neighboring but not bonded vital macromolecules. Alternatively sensitization may involve interaction between short-lived, radiation-induced radicals and the sensitizing compound. (auth) (UK)

11324 THERMOGENESIS OF IRRADIATED YEAST CELLS IN THE PROCESS OF RECOVERING THEIR REPRODUCTIVE CAPACITY. Platonov, A. L.; Seliverstova, L. A.; Protasevich, I. I.; Meisel, M. N.; Tumerman, L. A. (Inst. of Molecular Biology, Moscow. Inst. of Microbiology, Moscow). Dokl. Akad. Nauk SSSR; 192: 209-12(1 May 1970). (In Russian).

Radioresistant cells of Saccharomyces vini, and the more radiosensitive cells of Torulopsis sphaerica were given x-ray doses of 70 or 150 KR. The cells were suspended in sterile water, and placed in a calorimeter to determine the heat output of the cells with time. On four series of experiments the results show that in cells of S. vini the heat evolution per unit dry weight of biomass was a factor of 2.5 greater than in unirradiated control cells under the same conditions. The radiosensitive culture of T. sphaerica showed a 30 to 40% heat decrease as compared with control cells. The S. vini cells showed an ability to recover their reproductive ability after irradiation, while the T. sphaerica did not reproduce after irradiation. From the literature data it is possible to conclude that the heat evolution under these experimental conditions can be correlated with endogenous respiratory processes in the cell. (TTT)

11325 NOTE ON A RADIO-RESISTANT AUXOTROPHIC STRAIN OF RHIZOBIUM LEGUMINOSARUM. Bose, Paromita; Venkataraman, G. S. (IARI, New Delhi). Curr. Sci. (India); 39: 542-3(5 Dec 1970).

During the studies on the induction of radio-resistance in Rhizobium leguminosarum, using the cyclic irradiation technique, a number of radioresistant mutants were obtained, of which about 8% from the 14th cycle of irradiation were found to be auxotrophs. The present communication describes the level of radioresistance and the essential requirement of a radioresistant auxotrophic strain, R 14/1, of R. leguminosarum. (P.B.M.)

Radiosterilization and Radiopreservation

Refer also to abstracts 10964, 10978, 11244, and 11247.

11326 (NP-18393) PRESERVATION OF FOOD BY IRRADIATION: PRELIMINARY STUDIES ON COMMERCIAL SHRIMP. Woodhouse, Denise Micheline Rostan (Universidad Nacional Autonoma de Mexico, Mexico City. Facultad de Ciencias). 1970. 111p. (In Spanish). Dep. CFSTI (U. S. Sales Only).

Thesis.

Studies were made to determine the radiation dose needed for

the preservation of commercial shrimp, using ^{60}Co source with γ energy of 1.25 MeV. The interaction of γ radiation with matter and the chemical and biological effects of radiations are first reviewed. A detailed description is then given of the techniques used. The sterilization dose for shrimp was established as 3 Mrads. Irradiated samples were then stored for seven mon at room temperature and 0°C and compared with non-irradiated samples stored under the same conditions. There was a significant discoloration and a decrease of the odor in the non-irradiated samples. A normal consistency was however maintained in the irradiated samples, whereas the non-irradiated controls were almost completely disintegrated. The type of modifications caused by the irradiation in the volatile nitrogen constituents was also determined. There was a decrease of from 5 to 40% in the total volatile nitrogen; from 5 to 25% in trimethylamine nitrogen; and from 9 to 49% in the aminic nitrogen. (J.S.R.)

11327 (STI/PUB-247) STERILIZATION AND PRESERVATION OF BIOLOGICAL TISSUES BY IONIZING RADIATION. Panel Proceedings Series. Report of a Panel on Radiation Sterilization of Biological Tissues for Transplantation Held in Budapest, 16–20 June 1969. (International Atomic Energy Agency, Vienna (Austria)). Jul 1970. 129p. (CONF-690646). IAEA $4.00.

Separate abstracts were prepared for 10 of 11 papers dealing with radiosterilization and radiopreservation of biological and medical supplies. (P.B.M.)

For abstracts of individual papers see: 11328–11337.

11328 RADIATION RESISTANCE OF BACTERIA AND THE MICROBIOLOGICAL CONTROL OF IRRADIATED MEDICAL PRODUCTS. Christensen, E. A. (Statens Seruminstitut, Copenhagen. Accelerator Dept., Risoe, Denmark). pp 1-13 of Sterilization and Preservation of Biological Tissues by Ionizing Radiation. Vienna; International Atomic Energy Agency (1970).

From Panel on Radiation Sterilization of Biological Tissues for Transplantation, Budapest. See STI/PUB-247; CONF-690646.

The value of sterility tests on random samples of sterilized products is very limited. Much higher safety can be obtained by placing the emphasis on the bacteriological control of the contamination possibilities prior to sterilization, and control of the type and number of microorganisms on and within the product before sterilization. The radiation resistance of different types of cells under various environmental conditions is compared and related to the doses, which can be applied for sterilization or preservation of medical products. The most radiation-resistant bacteria isolated from dust contaminations are described. Stress is laid on the special problems related to the microbiological control of products derived from human tissue. (auth)

11329 FREE RADICALS EVOKED BY RADIOSTERILIZATION IN PRESERVED BONE GRAFTS. Stachowicz, W. (Inst. of Nuclear Research, Warsaw); Ostrowski, K.; Dziedzic-Goclawska, A.; Komender, A. pp 15-27 of Sterilization and Preservation of Biological Tissues by Ionizing Radiation. Vienna; International Atomic Energy Agency (1970).

From Panel on Radiation Sterilization of Biological Tissues for Transplantation, Budapest. See STI/PUB-247; CONF-690646.

One of the modern techniques used for preservation of human tissues for grafting is lyophilization and radiosterilization. A dose of about 3 Mrad is used for sterilization. One of the physicochemical changes caused by irradiation is the induction of free radicals in irradiated tissues. The peculiar feature of some of these radicals is their unusual stability. Apart from the theoretical aspects of these changes, free radicals are looked upon as potential mutagenic agents; therefore they are potentially oncogenic. Their nature and fate are of great clinical interest. The authors analysed the electron-spin resonance (ESR) signals in irradiated bone samples and tried to identify their origin. Two long-lasting signals were found. One lasting several minutes is connected with molecular changes in collagen, the second, stable for months, is connected with apatite. The results are compared with those known from the literature. It is suggested that the stable signals evoked in bone grafts by irradiation could be used for quantitative estimation of resorption and substitution of the graft in experimental research on bone transplantation. (auth)

11330 SPECIFIC EFFECT OF RADIATION-STERILIZED TISSUES ON CELLULAR MULTIPLICATION. Revesz, L. (Karolinska Inst., Stockholm). pp 29-36 of Sterilization and Preservation of Biological Tissues by Ionizing Radiation. Vienna; International Atomic Energy Agency (1970).

From Panel on Radiation Sterilization of Biological Tissues for Transplantation, Budapest. See STI/PUB-247; CONF-690646.

Mammalian cells injured lethally by radiation retain the capacity to synthetize cellular constituents and also to perform several divisions during the period before they disintegrate. Owing to these properties, radiation-sterilized tissues exert a specific influence on cellular proliferation and are capable of both enhancing and inhibiting the growth of a graft in the host organism. This paper surveys a series of model experiments performed with the purpose of investigating the mechanism underlying these effects. Observations are described which suggest that enhancement of cell multiplication can be attributed to a cell-to-cell interaction, the actively metabolizing, radiation-sterilized cells acting as feeders and/or conditioners of the micro-environment of adjacent viable cells. Enhancement is also attributable to an indirect action, transplanted sterilized cells being capable of provoking a local inflammatory tissue reaction and/or a systemic immunological reaction in the host organism, which favor the growth of a concomitant graft. Inhibition of growth is due to a homograft reaction which can be readily elicited by radiation-sterilized tissues under appropriate immunogenetic conditions. The bearing of these observations upon the experimental and clinical approaches towards cancer therapy and tissue transplantation is discussed. (auth)

11331 SOME EFFECTS OF STERILIZING DOSES OF RADIATION ON BIOLOGICAL TISSUES. Little, K. (United Kingdom Atomic Energy Authority, Wantage, Eng.). pp 37-41 of Sterilization and Preservation of Biological Tissues by Ionizing Radiation. Vienna; International Atomic Energy Agency (1970).

From Panel on Radiation Sterilization of Biological Tissues for Transplantation, Budapest. See STI/PUB-247; CONF-690646.

The doses being considered are in the 1.5–5 Mrad range. All cells are killed so that organ grafts are not under consideration, but only tissues that when implanted will remain inert, or be gradually replaced by cells from the host (e.g. nerves, bone, heart valves). Various cellular activities in the body are stimulated by specific chemicals or combinations of chemicals. These are different for different cell types. The osteogenic factor, which is destroyed by the radiation, is needed for bone formation; certain tissue breakdown products are needed for the production of granulation tissue or vascular proliferation, but not for nerve regeneration; and so on. Radiation affects the production and type of these chemicals. The effects of radiation are two-fold. Under some conditions intercellular materials are rendered more inert, while they may also be degraded. There is a need to find a balance between the two. The radiation initiates chain reactions which continue for some time afterwards. (auth)

11332 RADIATION STERILIZATION OF IMPLANTS FOR RECONSTRUCTIVE SURGERY OF KINESTHETIC ORGANS. Balint, J. B. (National Inst. of Traumatology, Budapest). pp 43-5 of Sterilization and Preservation of Biological Tissues by Ionizing Radiation. Vienna; International Atomic Energy Agency (1970).

From Panel on Radiation Sterilization of Biological Tissues for Transplantation, Budapest. See STI/PUB-247; CONF-690646.

The properties of mesenchymal tissues are important to the regeneration of bones, tendons, and ligaments following surgery on them. When surgery is anticipated, concern should be given to the function of tissues that are to be used for substitution and the function of the tissue into which the implant is to take place. In tissues where changes in mechanical loading are expected, the quantitative and qualitative effects of radiation sterilization of the implant must be evaluated. Bone fragments may become more fragile and the mechanical properties of the intercellular material may be altered; therefore, the implant must be larger than usual. (auth)

11333 RADIOSTERILIZATION OF FIBRINOGEN AND ITS PRACTICAL USE. Frischauf, H. (First Univ., Vienna). pp 47-58 of Sterilization and Preservation of Biological Tissues by Ionizing Radiation. Vienna; International Atomic Energy Agency (1970).

From Panel on Radiation Sterilization of Biological Tissues for Transplantation, Budapest. See STI/PUB-247; CONF-690646.

Serum hepatitis is rather frequent after transfusions of plasma proteins. Chemical sterilization of plasma proved to be either unsatisfactory or to damage extensively the biological activity of coagulation factors. This fact initiated an examination of the effect of gamma-rays (^{60}Co) on the clottability of fibrinogen, factor VIII activity, and virus infectivity, using canine hepatitis virus as a model. The biological activity of fibrinogen irradiated in solution was decreased to a high degree by low radiation doses, which lowered the infectivity titre of virus less than one order of magnitude. Clottability of dried fibrinogen irradiated at low temperature was reduced to about 60% of the initial value with a dose of 3 Mrad, which decreased the virus activity by about three orders of magnitude. In the second part of the paper clinical aspects of

XUM

the substitution therapy with coagulation factors are discussed. (auth)

11334 FROZEN IRRADIATED PERIPHERAL NERVE AND CALVARIAL HOMOGRAFTS IN CLINICAL SURGERY. Campbell, J. B. (New York Univ., N. Y.); Bassett, C. A. L.; Luzio, J. pp 59-69 of Sterilization and Preservation of Biological Tissues by Ionizing Radiation. Vienna; International Atomic Energy Agency (1970).

From Panel on Radiation Sterilization of Biological Tissues for Transplantation, Budapest. See STI/PUB-247; CONF-690646.

Laboratory studies show that freezing, -76°C, and irradiation, 2 Mrad delivered by a 3-MeV Van de Graaff accelerator, diminish the antigenicity of peripheral nerve and skull bone homografts to a level which is tolerated by the recipient. In addition, irradiation sterilizes the homografts. Maintenance in the frozen state permits storage until required for use. In the case of nerve, the non-viable tissue is replaced by host connective tissue, capillaries and Schwann cells. The latter digest the graft gradually and later form myelin which encases the axons migrating centrifugally through it to enter the distal stump of the nerve. In the case of irradiated skull bone, inflammatory reaction to the implants in animals is minimal. Following capillary penetration, perivascular new bone formation utilizes the microscopic scaffold of the implant. At the end of the osteogenetic process, the implant is replaced and remodelled to conform with the host skull including a deposition of marrow in the new middle table. Clinical methods using frozen irradiated nerve and skull implants are demonstrated and the results are described. (auth)

11335 IONIZING RADIATION FOR STERILIZATION OF BONE. Buring, K. (General Hospital, Malmoe, Sweden). pp 71-8 of Sterilization and Preservation of Biological Tissues by Ionizing Radiation. Vienna; International Atomic Energy Agency (1970).

From Panel on Radiation Sterilization of Biological Tissues for Transplantation, Budapest. See STI/PUB-247: CONF-690646.

With recent evidence that osteogenic inductors are present and active in the organic matrix of allogenic bone implants it is clearly vital to know what effect treatment and storage may have upon this inductive capacity. Lyophilization and deep-freezing are useful methods for preservation of bone grafts but do not secure sterility. Ionizing radiation from linear accelerators or ^{60}Co sources assures sterility in a dose of 2-4 Mrad but possible effects on the organic matrix deserves less attention. The present experimental investigation shows changes from three different points of view. Biological: The inductive capacity of decalcified, lyophilized allogenic rat and rabbit implants was totally destroyed at a dose of 2 Mrad. The implants either evoked a heavy foreign body reaction or were totally resorbed. Chemical: The solubility of collagen and glycosaminoglycans was investigated by neutral and weak acid extractions. It was found to increase continuously with a marked rise at 2 Mrad. The sub-units of collagen were determined by electrophoresis and chromatography, the findings suggesting scission of covalent bonds in the alpha chain as well as dearrangement of intra and intermolecular helical structure. Ultrastructural: The regular fibrillar network of bone matrix was destroyed by doses exceeding 2 Mrad. (auth)

11336 HOMOGRAFT HEART-VALVE REPLACEMENT. REPORT ON 110 CONSECUTIVE REPLACEMENTS USING GAMMA-IRRADIATED GRAFTS. Gibbons, J. R. P. (Brompton Hospital, London); Alladine, F. A. pp 95-105 of Sterilization and Preservation of Biological Tissues by Ionizing Radiation. Vienna; International Atomic Energy Agency (1970).

From Panel on Radiation Sterilization of Biological Tissues for Transplantation, Budapest. See STI/PUB-247; CONF-690646.

Homograft valves have been used to replace diseased or congenitally abnormal heart valves for over seven years. Sterilization of homografts and their subsequent preservation in a state suitable for grafting, has presented problems and most surgeons are still undecided on the best method to treat these grafts. After six months' experimental work, gamma-irradiated grafts were first used four years ago to replace diseased aortic valves. Since that time a technique was developed, using inverted irradiated aortic or pulmonary homografts, to replace the atrio-ventricular valves. Over one hundred patients now have these valves in situ and were observed for periods of three months to four years following operation. The clinical results were good. Those patients having failure of the graft after operation are discussed and compared with a similar group who have had homografts, prepared by other methods, inserted at operation. (auth)

11337 CO-OPERATIVE STUDIES IN THE USE OF IONIZING RADIATION FOR STERILIZATION AND PRESERVATION OF BIOLOGICAL TISSUES. TWENTY YEARS' EXPERIENCE. Wright, K. A.; Trump, J. G. (Massachusetts Inst. of Tech., Cambridge). pp 107-18 of Sterilization and Preservation of Biological Tissues by Ionizing Radiation. Vienna; International Atomic Energy Agency (1970).

From Panel on Radiation Sterilization of Biological Tissues for Transplantation, Budapest. See STI/PUB-247; CONF-690646.

Physical studies were carried out since the early 1940s in order to enable delivery of controlled doses of ionizing radiation to produce sterilization of biological materials. Co-operative studies, begun initially with members of the Massachusetts Institute of Technology, Department of Food Technology, have continued with many different groups. This work indicated that a dose of two million roentgens would destroy high concentrations of microorganisms even at dry-ice temperatures. Irradiation of viruses and blood derivatives was carried out to establish a range of dose which would be considered adequate to inactivate the hepatitis virus in blood derivatives and to determine which derivatives could tolerate such a dose. No controlled clinical tests of known infected material were carried out. In co-operation with Drs. Gross and Meeker of the Children's Medical Center, Boston, studies were carried out to determine dosage levels and conditions of irradiation to produce sterility and provide suitable arterial segments for surgical procedures. Aortic segments irradiated while frozen to a minimum dosage level of 1.3 million rad were clinically satisfactory, but at maximum dosage levels above three million rad vessel-wall destruction was encountered. Other surgeons have successfully used blood vessels, bone segments, skull flaps, nerve sections and aortic valves irradiated at dosage levels of two million rad and stored for extended periods of time. (auth)

11338 STUDIES ON THE ECOLOGY OF INSECT WHICH WAS STERILIZED ARTIFICIALLY (GAMMA RADIATION). 4. SEXUAL BEHAVIOR OF SPODOPTERA LITTORALIS (BOISD.) STERILIZED AS PUPAE BY THE GAMMA RADIATION. Kiyoku, Masao (Okayama Univ., Japan); Tsukuda, Ritsuko; Wada, Tohru. Okayama Daigaku Nogakubu Gakujutsu Hokoku; No. 34, 15-21 (Oct 1969). (In Japanese).

The mating ability of males sterilized by gamma radiation — ^{137}Cs was examined. A male moth sterilized by a dose of 20Kγ applied to pupae could mate with 3 ~ 5 virgin females in succession. The female mated with the sterilized male laid no viable eggs. Significant differences occurred in the egg production curves of females mated with sterilized or unsterilized males. Both the beginning and maximum time for egg production were delayed by two and four days, respectively, as compared with the control. Virgin females were mated first with unirradiated males and two days later with irradiated ones. In most cases they produced many viable eggs even after the second mating with irradiated males. When females were mated first with irradiated males and two days later with unirradiated ones, females of not less than 50 percentages produced non-viable eggs in spite of the mating with unirradiated males, but the others produced viable eggs after the second mating. The structure of reproductive organs, development of germ cells and behavior of sperms in the reproductive organ of females were observed. It was found that the eggs of females mated with irradiated males did not hatch for two different reasons. One was due to sterility of sperm and another to lack of sperm in a receptaculum seminis according to abnormality of ejaculatory duct or spermatophore by the gamma radiation. It seemed to be necessary for the successful sterile male technique that the ejaculatory duct or spermatophore was not injured but only sperm were sterilized by the gamma radiation. (auth) (Japan)

11339 EFFECT OF GAMMA IRRADIATION ON CHANGES IN THE AMINO ACID COMPOSITION OF COOKED MEAT. Gel'fand, S. Yu.; Frumkin, M. L. Vop. Pitan.; 27: 81-2(Jul-Aug 1968). (In Russian).

Studies carried out with cooled meat, broiled in an infrared oven, γ-irradiated at 800 R/sec with the total dose of .08 rad showed a reduction of the content of glutamic acid (17%) and of valine (13%), while the amount of the histidine and asparagine increased (12 to 13%). The rest of the amino acids remained unchanged. (R.V.J.)

11340 QUANTITATIVE EVALUATION OF IRRADIATED BONE GRAFTS RESORPTION RATE BY THE ELECTRON SPIN RESONANCE TECHNIQUE. Ostrowski, K.; Dziedzic-Goclawska, A.; Michalik, J.; Stachowicz, W. (School of Medicine, Warsaw. Inst. of Nuclear Research, Warsaw). Experientia; 26: 822(15 Aug 1970).

Fragments of cancellous bone were γ-irradiated and used for allogeneic grafts in rabbits At intervals of 3, 6, 9, 12, and 15 weeks after grafting, samples were taken for ESR measurements

of resorption rate. A linear decrement of spin concentration per mg of bone was obtained. It is suggested that the method based on the use of radioinduced stable ESR signals in bone tissue as a new biological label might be useful in experimental as well as in clinical research. (H.L.W.)

11341 BIOCHEMICAL CHANGES IN HETEROLOGOUS AORTIC VALVE TRANSPLANTS FOLLOWING APPLICATION OF VARIOUS STERILIZATION METHODS. Hehrlein, F. W.; Haas, H. Langenbecks Arch. Chir.; 325: 1183-5(1969). (In German).

Hydroxyproline determinations were carried out on heterologous calf aorta transplants in order to assess the collagen damage produced by sterilization and storage. Particularly after the action of gamma rays and beta-propiolactone considerable irritation was observed. Preservation with cialit appears to produce only minimal changes on the heart valve tissue. (auth)

XUM

METALS, CERAMICS, AND OTHER MATERIALS

Metals and Alloys

Refer also to abstract 11474.

11342 FIZIKO-KHIMICHESKIE OSNOVY PRIMENENIYA ZHIDKOMETALLICHESKIKH TEPLONOSITELEI. (Physicochemical Analysis of Handling Liquid Metal Coolants). Subbotin, V. I.; Ivanovskii, M. N.; Arnol'dov, M. N. Moscow; Atomizdat (1970). 296p.

Physicochemical processes taking place in liquid metal coolants circulating through nuclear power installations is described. Properties of liquid metal coolants, impurities in coolants, preliminary purification, and chemical and cold purification are discussed as well as the influence of the physicochemical condition of the coolant on heat transfer during convection, boiling, and condensation. (375 references) (R.V.J.)

Corrosion and Erosion

Refer also to abstracts 10583 and 10658.

11343 (AECL–3778) MATERIALS RESEARCH IN ATOMIC ENERGY OF CANADA LIMITED. (Atomic Energy of Canada Ltd., Chalk River (Ontario)). Fall 1970. 24p. Dep. NTIS (U. S. Sales Only). AECL $0.50.

Reviews are presented on technologies concerned with corrosion of water reactor in-core and out-of-core materials, corrosion of Zr alloys by organic coolants, liquid metals, H diffusion in corrosion processes, and plasma anodization. (J.R.D.)

11344 (AWRE-O-46/66) EFFECT OF HUMIDITY ON THE DUCTILITY OF URANIUM. Whitlow, G. A.; Willows, R. (Atomic Weapons Research Establishment, Aldermaston (England)). 1966. 11p. Dep. NTIS (U. S. Sales Only).

The mechanical properties of uranium have been shown to be markedly affected by the presence of moisture in the testing environment. The elongation in high humidity air is reduced to half the value in air at ambient temperature and humidity. It is suggested that atomic hydrogen acting at the preferential sites for corrosion formed by localized stress concentrations may be responsible for what may well be stress corrosion or hydrogen embrittlement in uranium. (auth) (UK)

11345 (AWRE-O-49/66) STRESS CORROSION OF URANIUM ALLOYS. Whitlow, G. A. (Atomic Weapons Research Establishment, Aldermaston (England)). 1966. 18p. Dep. NTIS (U. S. Sales Only).

The phenomenon of stress corrosion in binary uranium–molybdenum alloys was examined, revealing acicular precipitation associated with fracture. This may be due to reaction between uranium and moisture, not oxygen, producing atomic hydrogen. A uranium–7½ wt % niobium–2½ wt % zirconium alloy is also shown to be susceptible to stress corrosion in high humidity environments. (auth) (UK)

11346 (AWRE-O-100/66) ATMOSPHERIC OXIDATION OF UNALLOYED PLUTONIUM AT LOW HUMIDITIES. Raynor, J. B.; Sackman, J. F. (Atomic Weapons Research Establishment, Aldermaston (England)). 1966. 15p. Dep. NTIS (U. S. Sales Only).

The rate of oxidation at 90°C of unalloyed plutonium over a number of desiccants was measured. The results confirm the sigmoidal shape of the oxidation rate versus relative humidity curve and place the position of the knee, which indicates the level below which the humidity must be reduced to obtain a significant decrease in oxidation rate, at about 2%. The vapor pressure (of water) above the desiccants used was determined over a range of temperatures up to 90°C. (auth) (UK)

11347 (CISE-R-222) EXPERIMENTS ON BEHAVIOR OF METALLIC URANIUM–ZIRCALOY-2 FUEL ELEMENT DEFECTS AND EXPOSURE TO AQUEOUS CORROSION AT HIGH TEMPERATURE. Technical Report No. 30. Cerrai, E.; Ghersini, G.; Scaroni, A. (Centro Informazioni Studi Esperienze, Milan (Italy)) Jan 1967. Contract 008.65.1-NTRI. 157p. (In Italian). Dep. NTIS (U. S. Sales Only).

The compatibility of tubular fuel elements of metallic uranium clad with Zircaloy-2 (of the Cirene type) and water–steam mixtures was investigated. Three specimens of the fuel elements were selectively flawed and placed in a water–steam circuit (the vapor content in correspondence to the defects was about 15% in weight at 285°C and 71 atm). The thermal gradient characteristics for power generation from a fuel element were simulated. The results, particularly a metallographic study of the defects due to corrosion, are reported. A brief description of the circuit, of the test sections, and of the techniques used for the flawing of the samples is given. The thermodynamic and kinetic data obtained on the reactions involved in corrosion phenomenon are used in an attempt to interpret the corrosion process. A bibliographic review is given of the data available in the literature on the corrosion of uranium and its alloys by water and steam. (tr-auth)

11348 (GEAP-13539-13) SODIUM TECHNOLOGY DEVELOPMENT PROGRAM MASS TRANSFER INVESTIGATIONS IN LIQUID METAL SYSTEMS. Quarterly Progress Report No. 13, March–May 1970. (General Electric Co., Sunnyvale, Calif. Breeder Reactor Development Operation). Jun 1970. Contract AT(04-3)-189. 45p. Dep. NTIS.

Activities in programs devoted to improvements of empirical and rational models for use in predicting corrosion and mass transfer in Na systems are summarized. Work is also reported on improved sampling and monitoring systems for Na systems. Results of investigations on the integrity of LMFBR materials such as Types 304 and 316 stainless steel are reported. (J.R.D.)

11349 (WAPD-TM-906) INFLUENCE OF PRIOR CORROSION HISTORY UPON THE HYDROGEN PICKUP BY ZIRCALOY DURING SUBSEQUENT EXPOSURE IN HOT WATER. Kass, Stanley (Bettis Atomic Power Lab., Pittsburgh, Pa.). Dec 1970. Contract AT(11-1)-Gen-14. 34p. Dep. NTIS.

Experiments were conducted to investigate the influence of prior corrosion history upon the aqueous corrosion and hydrogen absorption characteristics of Zircaloy. These experiments confirmed prior studies describing the aqueous corrosion behavior of Zircaloy containing oxide films formed at temperatures different from that of the final exposure. A 1-day, 750°F, 1500-psi steam corrosion test before exposure to hot pressurized water produced measurably lower hydrogen pickup values during the pre- and post-transition corrosion regions. Any prior water-formed film prevented the beneficial effect of the subsequent 750°F treatment upon hydrogen absorption. The post-transition hydriding rates also were found not to be measurably altered by prior corrosion treatments involving water-plus-steam exposure. Test data suggest that the 750°F steam tests were conducted in an oxidizing media which decreased the hydrogen permeability characteristics of the oxide film, in contrast with other data which showed that oxides very permeable to hydrogen can be formed. (auth)

11350 CORROSION OF PLUTONIUM IN ARGON WITH SMALL AMOUNTS OF MOISTURE. Vesterberg, Viveka; Ekbom, Lars (Research Inst. of the Swedish National Defence, Stockholm). Nucl. Met., Met. Soc. AIME; 17: 164-73(1970).

From 4th International Conference on Plutonium and Other Actiides, Santa Fe, N. Mex. See CONF-701001-(Pt.1).

The corrosion of the alpha, beta, and gamma phases of plutonium in argon was studied with various low moisture contents of the atmosphere at 760 mm Hg. The reaction rates varied within wide ranges for specimens from different castings. In the alpha phase and lower part of the beta phase two linear rate laws were obeyed, while in the upper part of the beta phase and in the gamma phase a parabolic rate law followed by a linear rate law was established. A minimum in the second linear oxidation rate was observed at about 160°C. (auth)

11351 ELLIPSOMETRIC STUDIES OF ANODIC OXIDE FILMS FORMED ON TANTALUM IN DILUTE PHOSPHORIC ACID. Dell'Oca, C. J.; Young, L. (Univ. of British Columbia, Vancouver). J. Electrochem. Soc.; 117: 1545-8(Dec 1970).

Further ellipsometric data which confirm the two-layer nature of the anodic oxide films grown on tantalum in dilute phosphoric acid are reported. The two layers are believed to arise, respectively, from growth at the oxide/solution interface due to metal ion transport and from growth at the metal/oxide interface due to oxygen ion transport. The outer layer has a lower refractive index and dielectric constant due to phosphate incorporation. The effects have been observed in dilute phosphoric acid but not in the previous work in dilute sulfuric acid and citric acid of comparable concentration since phosphate is incorporated relatively strongly during the growth process. A model with a linear gradient of index is shown not to give an adequate representation of the optical results. (auth)

11352 EFFECTS OF URANIUM ON THE CORROSION OF RESULFURIZED STAINLESS STEELS. Biefer, G. J.; Crawford, W. M. (Dept. of Energy, Mines, and Resources, Ottawa). Mem. Sci. Rev. Met.; 67: 253-9(Apr 1970). (In French).

As an alloying element in resulfurized stainless steels, uranium was almost entirely incorporated in sulfides with melting point high enough so that they retained their form. The improvement in corrosion resistance which was large for AISI-430 F steels, was smaller in the case of uranium steels of Types 416 (martensitic) and 316 F (austenitic) and absent for Type 303 steel (austenitic). For nonuraniferous steels of Types 316 F and 303, the anticorrosive effects of molybdenum in nitric acid were much greater than those of uranium in the same medium. Molybdenum also improved corrosion resistance to a significant extent during tests on a limited scale in normal sulfuric acid, hydrochloric acid, and ferric chloride, whereas additions of uranium proved ineffective in these media. (auth) (France)

11353 MEZHKRISTALLITNAYA KORROZIYA I KORROZIONNOE RASTRESKIVANIE NERZHAVEYUSHCHIKH STALEI V VODNYKH SREDAKH. (Intercrystalline Corrosion and Corrosion Cracking of Stainless Steel in Aqueous Solutions). Pogodin, V. P.; Bogoyavlenskii, V. L.; Sentyurev, V. P. Moscow; Atomizdat (1970). 424p.

Aspects of intercrystalline corrosion and corrosion cracking of stainless steel by water and aqueous salts, acids, and alkalis at 20 to 700°C, are examined. These conditions are considered typical for water reactors and industrial steam power plants. The effects of composition, corrosive media parameters, microstructure, heat treatments, stresses, deformation, and radiation on stainless steel stability are analyzed. Protective measures for use under these conditions are surveyed. (tr-auth)

11354 KINETICS OF CORROSION OF NIOBIUM IN AQUEOUS SOLUTIONS AT TEMPERATURES UP TO 250°C. Heusler, Konrad E. (Max-Planck-Institut fuer Metallforschung, Stuttgart). Z. Metallk.; 61: 828-32(Nov 1970). (In German).

The stationary corrosion rate of oxide-covered niobium and the transients following a perturbation of the stationary state were measured electrochemically at temperatures up to 250°C in dilute neutral and weakly alkaline buffer-solutions. The transient currents caused by small changes of the electrode potential were calculated in a general form. The analysis of the experiments showed that the passivating oxide had the same ionic conductivity as the usual anodic oxide film. The electronic conductivity of the oxide layer was high at elevated temperatures. The exchange current density of oxygen ions between the oxide and the aqueous solution was much greater than the steady state corrosion current density. (auth)

11355 INTERPRETATION OF ELLIPSOMETRIC OBSERVATIONS OF ABSORBED OXYGEN IN NIOBIUM. Lederich, R. J.; Bellina, J. J. Jr. (McDonnell Douglas Corp., St. Louis). J. Opt. Soc. Amer.; 60: 1697m-8(Dec 1970).

The oxidation of niobium and molybdenum at 200 to 600°C and pressures of 10^{-6} to 10^{-4} torr oxygen was studied by using ellipsometry. The results for niobium, in which oxygen was soluble, indicated that the changes of the ellipsometric parameters were not entirely related to film growth. In contrast, the results for molybdenum, in which the oxygen solubility was small, could be interpreted by simple film growth. (G.M.C.)

Preparation and Fabrication

Refer also to abstracts 10760, 10776, 10780, and 11479.

11356 (CONF-700546-1) AN INVESTIGATION OF METHODS OF PREPARING HIGH PURITY VANADIUM. Beale, H. A.; Arsenault, R. J. (Maryland Univ., College Park, Engineering Materials Group). [1969]. Contract AT(40-1)-3612. 33p. Dep. NTIS.

From 4th International Conference on Electron and Ion Beam Science and Technology, Los Angeles, Calif.

High purity vanadium single crystals (resistance ratios in excess of 600) were grown in an electron beam float zone refiner. Numerous parameters were varied and their effects on the purification process studied. Also hydrogen and ammonia gases were introduced during the first molten zone pass and pumped back out on subsequent molten zone passes. Most experiments were performed twice, once with, and then without, pedestal rod rotation. (auth)

11357 FIRST INTERNATIONAL CONFERENCE ON PRESSURE VESSEL TECHNOLOGY. PART III. DISCUSSION. First International Conference, Delft, Netherlands, September 29-October 2, 1969. New York; American Society of Mechanical Engineers (1970). 263p. $20.00. (CONF-690906-(Pt.3)).

Lectures on pressure vessels are presented concerning welding, uses of high-strengtlf steels, design, and stress analysis. Summaries of discussions are included on plasticity, pressure vessel auxiliaries, computer analysis, piping, material failure, and testing. (J.R.D.)

11358 PREPARATION AND SOME PROPERTIES OF BERKELIUM METAL. Peterson, J. R.; Fahey, J. A.; Baybarz, R. D. (Univ. of Tenn., Knoxville, Oak Ridge National Lab., Tenn.). Nucl. Met., Met. Soc. AIME; 17: 20-34(1970).

From 4th International Conference on Plutonium and Other Actinides, Santa Fe, N. Mex. See CONF-701001-(Pt.1).

The first bulk (5 μg) samples of berkelium metal were prepared by the reduction at ~1025°C of BkF_3 with lithium metal in a tantalum crucible system. The BkF_3 starting material was obtained by air ignition of individual resin beads to BkO_2 followed by treatment with a H_2(g)-HF(g) mixture at 600°C. All samples prepared to date exhibited a face-centered cubic phase with a lattice parameter of 4.999 ± 0.005 Å. In addition, several samples exhibited a double hexagonal close packed phase with lattice parameters of a_0 = 3.416 ± 0.005 Å and c_0 = 11.068 ± 0.009 Å. Present data indicated that the fcc phase was the high-temperature phase with respect to the dhcp phase. Magnetic susceptibility studies showed that the dhcp phase had more +4 character than the fcc phase, in agreement with calculated metallic radii of 1.704 Å (dhcp) and 1.764 Å (fcc). During the course of this work and in some similar with Am, Cm and Es, it was found that, under the above described conditions for the preparation of microgram quantities of these metals, the relative volatilities were given by Cm ≪ Bk < Am ≪ Cf < Es. The melting point of Bk metal was determined to be 986 ± 22°C. (auth)

11359 FABRICATION AND MECHANICAL PROPERTIES OF DISPERSION HARDENED Pu-1 WT. PERCENT Ga ALLOY. Faiers, M. E.; Davies, N.; Moore, A. D. L. (Atomic Weapons Research Establishment, Aldermaston, Eng.). Nucl. Met., Met. Soc. AIME; 17: 468-77(1970).

From 4th International Conference on Plutonium and Other Actinides, Santa Fe, N. Mex. See CONF-701001-(Pt.1).

The low creep strength and tensile strength of δ-Pu at high temperatures are well known. Powder metallurgy techniques are described which were used to produce dispersion hardened 1 wt % Ga stabilized δ-phase plutonium. Initially powder was produced by ball milling fine Pu swarf. The use of lubricants, both wet and dry, and surface de-activators was examined, and sieve sizing data obtained. An alternative method of powder production employing a hydride-dehydride route was also examined and found to be very satisfactory. Consolidation of the powder by cold compaction, sintering, and hot pressing was performed and the fabrication variables examined. Rolling and hot extrusion of the compacted material was also accomplished. PuO_2, Al_2O_3, and ThO_2 were used as the dispersed phase for hardening. Compressive yield strength data indicated pronounced hardening at room temperature compared with the starting material, strengthening factors of 5X being obtained. At higher temperature, i.e., at 400°C, strengthening factors of ~5X were obtained using additions of fine Al_2O_3. Methods of producing higher strength material are discussed. (auth)

11360 SPUTTERED PLUTONIUM-GALLIUM ALLOYS. Busch, R. A. (Battelle-Northwest, Richland, Wash.). Contract AT(45-1)-1830. Nucl. Met., Met. Soc. AIME; 17: 1037-44(1970).

From 4th International Conference on Plutonium and Other Actinides, Santa Fe, N. Mex. See CONF-701001-(Pt.2).

Plutonium-gallium alloy deposits were formed by triode sputtering under a range of deposition conditions. The phase composition and grain structure were examined in the as-sputtered and heat treated conditions. Substrate temperatures greater than 100°C combined with deposition rates below 1.0 mil/hr produced the equilibrium delta-phase structure. The inverse conditions resulted in the formation of highly strained, fine grain beta-phase structures. The distortion of these structures increased with the gallium content from 1.0 to 2.5 wt %. These structures were metastable, transforming to the delta phase upon heat treating at temperatures as low as 200°C. (auth)

11361 SINTERING OF DIE-PRESSED Co_5Sm MAGNETS. Cech, R. E. (General Electric Co., Schenectady, N. Y.). J. Appl. Phys.; 41: 5247-9(Dec 1970).

An experimental program was carried out to establish the conditions necessary to achieve successful sintering of Co_5Sm powder. The objective was to sinter the as-pressed powder to the highest possible density without having the powder suffer a loss of coercive force. It was found that to maintain coercive force it was neces-

sary to have an oxygen scavenging agent intimately dispersed throughout the powder. This was accomplished by adding either samarium metal or samarium hydride powder to nominally stoichiometric Co_5Sm to give an average composition in the range of 36 to 37.5 wt % Sm. In addition, it was found that highest sintered densities were achieved with a total samarium content slightly greater than that needed to maintain a high coercive force in the densified compacts. (auth)

11362 METHOD OF MAKING METAL ALLOY POWDERS. Whitfield, Cyrus E. (to United States Atomic Energy Commission). U. S. Patent 3,535,103. 20 Oct 1970. Filed 10 Apr 1968.

A method of making a metal alloy in powder form is described. It consists of heating a powder mixture comprising a substrate metal, a mobile metal, and a halide capable of reacting with the mobile metal to a temperature at which a halide is formed. The resulting mixture is cooled to a temperature at which a reaction occurs producing a mobile metal in fluid form from the mobile metal halide, thereby depositing a metal film on the particles of the substrate metal. The heating and cooling cycles are repeated until an alloy powder of the desired composition is obtained. (Official Gazette)

11363 VANADIUM BASE ALLOY. (to Westinghouse Electric Corp.). British Patent 1,218,605. 6 Jan 1971. Priority date 16 Mar 1967, United States.

Preparation of solution and precipitation hardened V-base alloys having good resistance to creep at elevated temperatures is described. The alloy contains 1 to 4% Zr; 3 to 20% C, N, and O; and one element from the group Nb, Cr, W, Mo, Fe, Ni, Ti or Ta. (J.R.D.)

11364 REACTOR-USE STRUCTURAL MATERIALS VIEWED FROM THEIR FABRICATION. Usuda, Hiroshi (Mitsubishi Heavy Industries, Ltd., Kobe, Japan). Karyoku Hatsuden; 20: 1257-66(Dec 1969). (In Japanese).

The fabrication of a reactor pressure vessel has to take the following into consideration concerning the structural materials: the characteristics, workability, and operational performance. Two topics concerning the technology of such structural materials are explained. Program testing technique for steel plates in quenching is described. Compared to the conventional one, it had the advantage of high accuracy in testing and only required a small number of test specimens. The program testing technique was studied for charges of pressure vessel steels: with a special heat-and-cool device, a simulation of the small specimens was made with regard to the quenching-cooling curves, and application of wedge opening loading (WOL) for surveillance tests is discussed. The WOL as compared to the ductile-fragile transition temperature approach is attracting interest as a means of obtaining the fracture toughness. (Japan)

11365 ELECTROLYTIC AND CHEMICAL POLISHING OF METALS. Shchigolev, P. V. Holon, Israel; Freund Publishing House (1970). 274p. $18.00.

Theoretical and practical aspects of electropolishing and chemical polishing of metals are discussed. Actual chemical polishing methods used in the laboratory and in industry are given for: aluminum, copper and its alloys, iron, steels, rare and non-ferrous metals, nickel, silver, lead, zirconium, beryllium, germanium, tantalum, magnesium, zinc, and cadmium. Specific information is given on the composition of electrolytes and process conditions for the electropolishing of various metals and alloys. (G.M.C.)

11366 ROLLED CHANNEL JOINTS. (to Atomic Energy of Canada Ltd.). British Patent 1,218,514. 6 Jan 1971. Priority date 29 Apr 1968, United States.

An improved end fitting for fuel channels in reactors is described. A method of effecting strong leaktight joints between thin tubular elements and end fittings is provided. The end fitting or hub member is hollow, having a cylindrical inner surface, provided with grooves for joining with tubular elements rolled into the grooves and a hard cylindrical insert having a surface concentric with the cylindrical inner surface. (J.R.D.)

11367 NEW ETCHANTS FOR IRRADIATED URANIUM ALLOYS. Cheney, Donald M. (Argonne National Lab., Idaho Falls, Idaho). Metallography; 3: 371-4(Sep 1970).

Two new etchants were found effective in revealing the microstructure of irradiated uranium-5% fissium alloys. A solution of nitric acid and hydrogen peroxide in water with some added EDTA to slow down the reaction could be applied either by immersion or by swabbing. A solution of lactic acid, orthophosphoric acid, water, and dioxane at 5 to 25 V dc was very effective in resolving the fine structure in the grain boundaries. (G.M.C.)

Properties Evaluations

Refer also to abstracts 10778, 11983, 12001–12006, 12008, 12020, 12021, 12030, 12032, and 12783.

11368 (AECL-3688) THEORY FOR A "LEAST SQUARES" DESCRIPTION OF RADIAL DISTORTIONS IN IRRADIATED FUEL SHEATHS. Jarvis, R. G. (Atomic Energy of Canada Ltd., Chalk River (Ontario). Chalk River Nuclear Labs.). Oct 1970. 19p. Dep. NTIS (U. S. Sales Only). AECL $0.50.

The theory for a standard method to describe distortions in irradiated fuel sheaths is developed. The departures from roundness are measured by deviations from least-squares-circles and the radial displacements of the circle centers from the original element axis describe the bowing and twisting. (auth)

11369 (BMI-1892) INVESTIGATION OF THE INITIATION AND EXTENT OF DUCTILE PIPE RUPTURE. PHASE II. Progress Report, July-September 1970. Eiber, Robert J.; Maxey, Willard A.; Duffy, Arthur R. (Battelle Memorial Inst., Columbus, Ohio). Oct 1970. Contract W-7405-eng-92. 8p. Dep. NTIS.

An experiment was designed to permit measurement of the rate of rupture area development. The published data on the fracture behavior of flawed tees and elbows were reviewed. (G.M.C.)

11370 (CEA-CONF-1689) DETERMINATION OF LIMITING SOLUBILITIES USING HETERODIFFUSION COEFFICIENT MEASUREMENTS. Zanghi, Jean-Pierre; Van Craeynest, Annick; Calais, Daniel (Commissariat a l'Energie Atomique, Fontenay-aux-Roses (France). Centre d'Etudes Nucleaires). 1970. 15p. (In French). (CONF-700941-5). Dep. NTIS (U. S. Sales Only).

From Meeting on Metallurgy, Paris, France.

Using the coefficients of heterodiffusion and the Jost method the solubility of U in Ni was measured. Heterodiffusion coefficients for U in Ni at infinite dilution were obtained using the technique of making a thin deposit of U, between two semi-infinite Ni media, by evaporation under vacuum. The concentration-penetration curves were determined. The heterodiffusion coefficients varied between 1.2 and 7.5 10^{-10} $cm^2 \cdot s^{-1}$ in the temperature range 975 to 1075°C. The diffusion range ϵ in the diffusion couples which consisted of a pure nickel side and a two-phase Ni–U alloy side (the Ni matrix being saturated with U and UNi_5 precipitates) was measured from 975 to 1075°C; the solubility of U in Ni was found to be between 0.7 and 1.4 wt % or between 0.18 and 0.33 at. %. An accuracy of 15% was achieved, which is superior to that obtained by x-ray microanalysis or metallography. The dissolution enthalpy was found to be 20 kcal/mole and the vibrational entropy 3.60 $cal^{\circ} k^{-1}$ $mole^{-1}$. (France)

11371 (CEA-CONF-1690) SELF DIFFUSION, UNDER HYDROSTATIC PRESSURE, OF BODY CENTERED CUBIC Pu. Cornet, Jean-Andre; Calais, Daniel (Commissariat a l'Energie Atomique, Fontenay-aux-Roses (France). Centre d'Etudes Nucleaires). 1970. 14p. (In French). (CONF-700941-2). Dep. NTIS (U. S. Sales Only).

From Meeting on Metallurgy, Paris, France.

The activation volume for the self-diffusion of Pu ϵ phase (bcc) was determined using the hydrostatic pressure parameter. Samples containing different quantities of ^{240}Pu were studied. The activities of the faces of the sample, in the 17 keV range (L conversion line of uranium) were compared using a 400 channel scintillation detector. In the first approximation the $D = f(P)_T$ curves reveal an exponential increase in the diffusion coefficient D with respect to pressure. This unusual result and the low value of the activation enthalpy characterize this phase as being abnormal from the point of view of diffusion. The activation volume $\Delta V = -4.9$ cm^3 is 34 per cent of the molar volume. In order to explain this result it is necessary to introduce the following hypothesis: that the atoms in the ϵ phase are subjected to a modification in their electronic structure, which gives to them the same valence as in the liquid phase (the slope of the liquidus line of the pressure-temperature diagram is negative). Thus their displacement into interstitial positions in octahedral sites of bcc phase can take place with a negative activation volume and a small activation enthalpy. (auth) (France)

11372 (CONF-701001-(Pt.1)) PLUTONIUM 1970 AND OTHER ACTINIDES. NUCLEAR METALLURGY, VOLUME 17. Proceedings of the 4th International Conference, Sante Fe, New Mexico, October 5–9, 1970. Miner, William N. (ed.) (Los Alamos Scientific Lab., N. Mex.). 532p. (In English and French).

A total of 48 papers are included in Part I. A separate abstract was prepared for each of 42 papers. Six papers were previously abstracted in NSA. For abstracts of these see CONF-701001 in the Report Number Index. (G.M.C.)

For abstracts of individual papers see: 10779, 11350, 11358, 11359, 11381–11391, 11435, 11436, 11451–11498, 11520, 11991–12005, and 12036.

11373 (COO-2048-1) PLASTIC-STRAIN CONTROLLED FAILURE CRITERIA AND DESIGN PARAMETERS. Technical Progress Report. Meyerer, W. P.; Kobayashi, S.; Vanecko, J.; Chakrabarti, A.; Firrao, D.; Spretnak, J. W. (Ohio State Univ. Research Foundation, Columbus). 2 Jul 1970. Contract AT-(11-1)-2048. 88p. Dep. NTIS.

The role of plastic instability in pure shear in limiting allowable plastic strain, particularly at a discontinuity (notch effect) is being studied. Previous research has revealed that this instability is basic in the strength transition in notch toughness in heat-treatable high-strength steel. The subjects reported on include the theory of plastic instability, effects of elevated temperatures and strain rate, effects of degree of saturation of terminal solid solutions, the role of instability in the temperature transition in toughness, and evaluation of the Gerard–Papirno characterization of notch ductility by their "ductility ratio." (auth)

11374 (DP-Report-530) STUDY OF CATALYTIC DECOMPOSITION OF CARBON MONOXIDE ON PURE IRON, MILD STEELS, AND ALLOYED STEELS. Project DRAGON. Warzee, M.; Sonnen, C.; Hennaut, J.; Ruston, W. R. (Atomic Energy Establishment, Winfrith (England)). Mar 1967. 36p. (CONF-670341-2). Dep. NTIS.

From Conference on Gas-Metal Reactions in Environments Containing CO_2, London, England.

Carbon monoxide decomposed at 550°C in contact with iron and steels. The steel was carburized and carbon deposited on the surface. Oxidizing impurities, i.e., O_2, H_2O and CO_2, produced, in certain cases, partially or fully protecting oxide films by reaction with oxidizable alloying elements, i.e., chromium, manganese, silicon and aluminum. The factors governing the formation of protective oxide films were temperature, surface structure of the steel (cold-worked or annealed), content of alloying elements or impurities in the steel, and composition of the reactant gas mixtures. (auth)

11375 (IN-1437, pp 24-59) METALLURGICAL DEVELOPMENT. (Idaho Nuclear Corp., Idaho Falls).

From Metallurgy and Materials Science Branch annual report, fiscal year 1970.

Results of development work are summarized on use of electron beam welding in reclamation of rejected fuel plates, fission product release from UAl fuels, thermal expansion of ATR fuel plates, surface defects in fuel plates, fabrication of fuel plates, use of UAl_x fines in fuel plates, production of ZrH, and nondestructive testing. (J.R.D.)

11376 (JUL-661-RW) SOLUBILITY AND CORROSION BEHAVIOR OF IRON, STEEL, MOLYBDENUM, NIOBIUM, TANTALUM, VANADIUM, TUNGSTEN, AND CHROMIUM IN MOLTEN LEAD AT HIGH TEMPERATURES. Khan, I. Ali (Kernforschungsanlage, Juelich (West Germany). Institut fuer Reaktorwerkstoffe). May 1970. 62p. (In German). Dep. NTIS (U. S. Sales Only).

In the temperature range between 350 and 1100°C, the solubility of Armco iron, steel X 7 Cr 14, and steel X 20 Cr 13 in lead was determined. The solvent properties of lead for iron in the X 8 CrTi 17 and X 8 CrNb 17 steels was also determined at 650°C. A lower iron solubility was established in the carbon-free steel X 20 Cr 13 than in the steel X 7 Cr 14 and in Armco iron. In Armco iron the temperature dependence in lead over and below 910°C shows a different pattern. Therefore a different solubility of the α- and γ-phases of the iron in lead was deduced. The samples were investigated metallographically with respect to their corrosion behavior. In general, they show higher corrosion attack at the places at which they were placed under tension. In an Armco iron sample which was in contact with lead for 520 hrs at a temperature of 950°C, intercrystalline corrosion was established. The X 8 CrTi 18 and X 8 CrNb 17 steels were corroded by the lead melt at 650°C during a period of 1000 hrs in the same manner. In both steels the penetration depth was about 38 μm. The high-melting metals, such as Mo, Nb, Ta, V, and W, show no solubility in liquid lead up to about 1000°C. The metallographic study showed that V was corroded by lead at 950°C. At 1110°C it was deeply corroded even after only 20 hrs. In Ta fissures occur at 925°C after 324 hrs in the bent part of the sample. At a temperature of 985°C Cr was strongly corroded by lead during a research period of 233 hrs. (tr-auth)

11377 (MLM-1778) ELECTRON BEAM WELDING STUDY ON U–Nb–Zr ALLOY. Final Report. McDougal, J. R.; Greene, L. A. (Mound Lab., Miamisburg, Ohio). 23 Dec 1970. Contract AT(33-1)-Gen-53. 17p. Dep. NTIS.

An electron beam welding study was conducted on Mulberry alloy (U–7.5% Nb–2.5% Zr). The study was conducted on 0.080 and 0.250-in. thick sheet stock. The purpose of the study was to determine what effect the variation of welding parameters would have on weld characteristics in partial penetration welds. The use of a straight beam of electrons or ac deflection resulted in weld spiking and cold shut area in the 0.250-in. thick material. Circle generation drastically reduced the number of weld defects. The 0.080-in. thick Mulberry welded easily except when ac deflection was used where the amount of weld porosity in the fusion area was high. (auth)

11378 (ORNL-TM-2989) URANIUM AND THORIUM DIFFUSION IN COLUMNAR PYROCARBONS AS INFLUENCED BY ACTINIDE CONCENTRATION. Evans III, R. B.; Stiegler, J. O. (comps.) (Oak Ridge National Lab., Tenn.). Jan 1971. Contract W-7405-eng-26. 45p. Dep. NTIS.

Studies of the diffusion behavior of uranium and thorium in two columnar pyrocarbons are described. Thin-layer depletion experiments were conducted that yield coefficients at low actinide concentrations applicable in the stabilized regime, where the coefficients are true constants, and also at intermediate concentrations (or regions), where coefficients are concentration dependent. Constant-potential experiments were also conducted that yield diffusion coefficients applicable at very high concentrations and also an apparent solubility C_0. The C_0 corresponds to the maximum uranium concentration the pyrocarbon can attain without undergoing detectable structural changes. The densities of the pyrocarbons were greater than 2.0 g/cm³. Results from uranium thin-layer experiments in the stabilized diffusion region for pyrocarbon A show good agreement with results for this system reported elsewhere. The uranium diffusion coefficient D_U, in cm²/sec, is given as a function of temperature T, in °K, by the equations $(D_U)_{\langle a\rangle} = 1.84 \times 10^4 \exp(-119{,}000/RT)$, and $(D_U)_{\langle c\rangle} = 1.29 \times 10^0 \exp(-103{,}000/RT)$. The anisotropic pyrocarbons were well oriented, and the subscripts $\langle a\rangle$ and $\langle c\rangle$ refer to diffusion along directions parallel and perpendicular, respectively, to the average position of the basal surfaces. Similar experiments with thorium and pyrocarbon A along with other published results demonstrate that values of the coefficients increase as the average actinide concentration is increased. Careful examination of all results indicates that the upper limit for stabilized diffusion is around 0.14 mg of actinide per cubic centimeter of pyrocarbon. Results from constant-potential experiments show that $\langle a\rangle$ direction diffusion is so rapid that the pyrocarbons do not attain a true saturation value with respect to C_0; the only reliable C_0 results emanate from $\langle c\rangle$ direction experiments. Data from the latter produce three different Arrhenius plots of the coefficients for various actinide–pyrocarbon systems. Regardless of this, the average apparent solubility was nearly the same for all systems, and it was definitely independent of the experimental temperature. The value was ~1.3 mg/cm³, which is about nine to ten times the maximum value for stabilized diffusion. Several complementary studies with emphasis on autoradiography and detection of structural changes of the pyrocarbons contacted by materials with very high actinide concentrations were carried out. Results of autoradiographs indicated nonuniform diffusion patterns for $\langle c\rangle$ direction diffusion and gave justification for elimination of $\langle a\rangle$ direction diffusion at high concentrations. Results of studies using the electron microscope demonstrated that dramatic changes occurred when the material was contacted directly by actinide carbide. Similar, but less dramatic, effects were observed on the source-exposed surfaces of constant-potential experiments. From the latter it was concluded that the pyrocarbon matrix undergoes an actinide-catalyzed reformation when C_0 is drastically exceeded. In some cases the reformation might be reversible. It is nevertheless possible to discount supersaturation effects in diffusion specimens by extrapolation, so that all constant-potential diffusion parameters will refer to pyrocarbon matrices with unaltered structures (but degenerative with respect to diffusion behavior). Accordingly, one may view C_0 as the concentration which delineates a diffusion region and a chaotic ill-defined migration zone containing some perfected graphitic regions. A qualitative description of the process in all diffusion regimes is presented to rationalize findings in an orderly and logical fashion. This required a careful study of the "as-deposited" pyrocarbons, which exhibited complicated structural characteristics. The structural changes in supersaturated regions are presented and discussed in detail. Although a defini-

tive description of migration in such zones is not given, comparison with the as-deposited structures and thermally treated specimens gave considerable insight as to the degree of reformation that occurs. A major finding is that results of trace-level diffusion do not give an adequate description of impurity atom diffusion under applied conditions where impurity atom (particularly actinide) concentrations can be very high. (auth)

11379 (UCRL-72477) SHEAR STRENGTH OF BERYLLIUM, URANIUM, AND TUNGSTEN AS A FUNCTION OF STRAIN, STRAIN RATE, AND PRESSURE. Abey, A. E.; Stromberg, H. D. (California Univ., Berkeley. Lawrence Radiation Lab.). 22 May 1970. 23p. (CONF-701110-1). Dep. NTIS.

From ASME Winter Annual Meeting, New York, N. Y.

The shear strengths of beryllium, uranium, and tungsten were measured at strain rates of 3.5×10^{-5}, 3.6×10^{-3}, and 3.7×10^{-1} sec^{-1}. The measurements were taken under nearly hydrostatic pressures of 21, 44, and 63×10^8 N/m^2. The shear strength vs shear strain curves are presented along with the pressure and ln strain rate derivatives of the experimental parameters. (auth)

11380 (WCAP-7578) HEAVY SECTION STEEL TECHNOLOGY PROGRAM. TECHNICAL REPORT NO. 10. FRACTURE TOUGHNESS CHARACTERIZATION STUDY OF A533, GRADE B, CLASS 1 STEEL. Mager, T. R. (Westinghouse Electric Corp., Pittsburgh, Pa. PWR Systems Div.). Oct 1970. Contract W-7405-eng-26; Subcontract 3196. 39p. Dep. NTIS.

The fracture toughness of various plates of material from the HSST program was characterized. The plate materials evaluated were HSST Plates 01, 02, and 03. Fracture toughness (K_{Ic}) properties were obtained at −150°F utilizing 1T Compact Tension specimens and at +10°F utilizing 4T Compact Tension specimens. Fracture mechanics was utilized to characterize the various HSST plate materials as a function of location throughout the thickness and throughout the length and breadth of the material. The effects of orientation of the specimen's notch with the primary working direction of the material on the fracture toughness were evaluated. The results indicate that the fracture toughness, K_{Ic}, was essentially the same for HSST Plates 01, 02, and 03. Specimen orientation did not have an effect on the measured K_{Ic} values at −150°F. (auth)

11381 EARLY ACTINIDES: THE PERIODIC SYSTEM'S *f* ELECTRON TRANSITION METAL SERIES. Hill, H. Hunter (Los Alamos Scientific Lab., N. Mex.). Nucl. Met., Met. Soc. AIME; 17: 2-19(1970).

From 4th International Conference on Plutonium and Other Actinides, Santa Fe, N. Mex. See CONF-701001-(Pt.1).

The physical properties of the metals in the first half of the transactinium (actinide) series are discussed in relation to the properties of the 5f electrons in these metals. Emphasis is placed on the unique nature of the 5f electrons in this part of the series, with particular attention paid to their influence on the crystal structures, melting points, and superconductivity and magnetism exhibited by this group of metals. The results of recent band structure calculations by Kmetko are utilized to expand on the idea that the 5f electrons in the transactinium metals are often better compared to the 3d electrons of the first transition series than to the 4f electrons of the rare-earth series. This proposal, that the early transactinium metals in many ways constitute an f electron transition metal series, is used to cast a new light, perhaps, on several of their known properties, to provide a basis for predicting some new properties, and to speculate on the nature of the metals in the last half of the transactinium series. (auth)

11382 THERMAL CONDUCTIVITY IN THE ACTINIDE ELEMENTS. Hall, R. O. A.; Lee, J. A. (Atomic Energy Research Establishment, Harwell, Eng.). Nucl. Met., Met. Soc. AIME; 17: 35-47(1970).

From 4th International Conference on Plutonium and Other Actinides, Santa Fe, N. Mex. See CONF-701001-(Pt.1).

Existing information on the thermal conductivity of the actinide elements at low temperatures is reviewed and compared with new results reported here for high-purity uranium and plutonium. The data showed for high-purity uranium an anomaly associated with the α/α_0 transition at 43°K, and a maximum conductivity of 65 W/m°K at the low temperature purity peak. For the highest purity plutonium, a small peak (3.4 W/m°K) in the thermal conductivity-temperature curve was seen at ~10°K, followed by a shallow minimum at ~40°K. (auth)

11383 THERMAL CONDUCTIVITY OF PLUTONIUM AT HIGH TEMPERATURE. Wittenberg, Layton J.; Engel, Thomas K.; Vaughn, Glen A. (Mound Lab., Miamisburg, Ohio). Contract AT(33-1)-Gen-53. Nucl. Met., Met. Soc. AIME; 17: 48-57(1970).

From 4th International Conference on Plutonium and Other Actinides, Santa Fe, N. Mex. See CONF-701001-(Pt.1).

The thermal diffusivity of Pu was determined between 400 and 800°C from the temperature difference measured radially across a cylindrical specimen during transient heating conditions. Thermal conductivity was calculated from the thermal diffusivity values and accepted values for the density and heat capacity. The thermal conductivity values obtained for δPu, εPu, and the liquid phase at 700°C were 0.014 ± 0.002, 0.012 ± 0.002, and 0.016 ± 0.001 cal/cm-sec-°C, respectively. The thermal conductivity of liquid Pu was the lowest value reported for any liquid metal but was 16 times greater than for a fused salt; consequently, electronic conduction is assumed to be the principal mode of thermal transport. The ratio of the thermal conductivity of solid to liquid was only 0.8 while it was usually greater than 1.0 for normal metals. The lower conductivity of the solid phase is compatible with a correlation based upon the Debye temperatures for the solid and liquid phases. The thermal conductivity results indicate nearly constant values for αPu at 25°C, δPu, εPu, and liquid Pu. This trend is normal for most metals. Conversely, the electrical resistivity reported for Pu is abnormal since it decreases from αPu to εPu; consequently, the Lorenz number which is nearly normal for αPu at 25°C decreases to 40% of its normal value for δPu and εPu. The significance of the low Lorenz numbers is difficult to interpret until the band structures of δPu and εPu are better defined. (auth)

11384 REVIEW OF LOW TEMPERATURE SPECIFIC HEATS OF THE ACTINIDES. Lee, J. A. (Atomic Energy Research Establishment, Harwell, Eng.); Sutcliffe, P. W.; Martin, D. J.; Mendelssohn, K. Nucl. Met., Met. Soc. AIME; 17: 58-67(1970).

From 4th International Conference on Plutonium and Other Actinides, Santa Fe, N. Mex. See CONF-701001-(Pt.1).

A review is made of the specific heat measurements below room temperature for the actinide elements, Th, U, Np, and Pu. The temperature dependence of C_P for these elements is presented together with the derived characteristic Debye temperature, θ_D, and the electronic coefficients, γ. The anomalous behavior of C_P of α-uranium at ~43°K and of α-plutonium at ~60°K showed marked similarities and is probably due to the same mechanism. (auth)

11385 HEAT CAPACITY BEHAVIOR OF ^{242}Pu BETWEEN 10^0 AND 373°K. Sandenaw, Thomas A.; Gibney, Robert B. (Los Alamos Scientific Lab., N. Mex.). Nucl. Met., Met. Soc. AIME; 17: 68-77(1970).

From 4th International Conference on Plutonium and Other Actinides, Santa Fe, N. Mex. See CONF-701001-(Pt.1).

Although the self irradiation rate of ^{242}Pu was approximately $1/18$ that of normal ^{239}Pu, the ^{242}Pu metal did not give a completely straight-forward heat capacity versus temperature curve. Storage of self-induced radiation damage was considerably greater in ^{242}Pu than was expected and could be clearly seen in runs made above room temperature. In addition there was a discernible difference between C_P vs T runs starting after liquid nitrogen quenches and those started after cooling to ~4°K with liquid helium. There was a divergence in these curves at ~170°K. It appears that if some treatment is not given to α-Pu metal to achieve a standard state, results of measurements are applicable only to that specimen at that time. (auth)

11386 ENTHALPIES OF SOLUTION OF CARBON, THULIUM, TITANIUM, MANGANESE, ZIRCONIUM, AND RHENIUM IN LIQUID PLUTONIUM. Bowersox, D. F.; Leary, J. A. (Los Alamos Scientific Lab., N. Mex.). Nucl. Met., Met. Soc. AIME; 17: 120-34(1970).

From 4th International Conference on Plutonium and Other Actinides, Santa Fe, N. Mex. See CONF-701001-(Pt.1).

The partial molar enthalpies of solution of several elements which form compounds with plutonium were calculated by regular solution theory from solubility data. The calculated enthalpies are (in kcal/mole): carbon, 10.5; thulium, 9.2; manganese, 4.8; and rhenium, 10.5. The partial molar enthalpies of solution of titanium and zirconium, which form solid solutions with plutonium, were also calculated in liquid plutonium from solubility data. An extra entropy term was added to regular solution theory to account for the configurational entropy due to the solubility of the solute in the solid solution. The calculated enthalpies are (in kcal/mole): zirconium, 4.2; titanium, 4.1 from 700 to 750°C, and 5.3 from 800 to 1000°C. (auth)

11387 CHEMICAL DIFFUSION IN THE ε PHASE OF THE PLUTONIUM-COPPER SYSTEM. Lataillade, F.; Despres, J.; Hocheid, B. (Commissariat a l'Energie Atomique, Bruyeres-le-Chatel, France). Nucl. Met., Met. Soc. AIME; 17: 144-53(1970). (In French).

From 4th International Conference on Plutonium and Other Actinides, Santa Fe, N. Mex. See CONF-701001-(Pt.1).

The diffusion was studied in ϵ phase on welded couples composed of unalloyed plutonium and of a biphased plutonium-copper alloy. The diffusion coefficients were determined according to Wagner and Matano. The values determined were high, about 10^{-7} cm^2 s^{-1}, with low activation energies ranging from 13,900 to 18,000 cal/at. g according to copper concentration. Copper solubility in ϵ phase is derived from the penetration curves as established by punctual microanalysis. (auth)

11388 EXPANSION PROPERTIES OF SEGREGATED Pu-Ga ALLOYS. Taylor, J. M. (Battelle-Northwest, Richland, Wash.). Contract AT(45-1)-1830. Nucl. Met., Met. Soc. AIME; 17: 183-93(1970).

From 4th International Conference on Plutonium and Other Actinides, Santa Fe, N. Mex. See CONF-701001-(Pt.1).

Expansion properties were determined from 25 to 475°C for segregated and rolled Pu-1 wt % Ga and Pu-1.9 wt % Ga alloys. The expansion curves for the segregated and rolled alloys were compared to expansion curves for fully homogenized alloys of the same composition. No difference was observed between the segregated alloy expansion curves and that of the fully homogenized curves when no alpha phase was present. When alpha phase was present the total length change was greater than the length change observed in the homogenized alloys and depended on the amount of alpha phase present in any one direction. The expansion curves of rolled, segregated Pu-1 wt % Ga and Pu-1.9 wt % Ga alloys exhibited anisotropic expansion properties. The anisotropic expansion was the result of alpha phase being present in greater amounts in the transverse direction. Dilatometry coupled with x-ray diffraction proved to be a sensitive and quantitative method for determining the amounts of metastable phase present in segregated Pu-Ga alloys. In this study the expansion data indicated that only alpha and delta phases existed in as-cast and segregated, rolled Pu-Ga alloys. (auth)

11389 DEFORMATION OF PLUTONIUM ALLOTROPES. Merz, M. D.; Nelson, R. D. (Battelle-Northwest, Richland, Wash.). Contract AT(45-1)-1830. Nucl. Met., Met. Soc. AIME; 17: 387-405(1970).

From 4th International Conference on Plutonium and Other Actinides, Santa Fe, N. Mex. See CONF-701001-(Pt.1).

The deformation behavior of alpha, beta, and gamma plutonium is discussed. The hardness of alpha plutonium was measured over the temperature range -196 to 100°C for different grain sizes. The hardness of fine grained metal was lower than that of coarse grained metal above -133°C. Alpha plutonium recrystallized when deformed around room temperature and above, resulting in a much smaller grain size than can be obtained by casting. Alpha plutonium was extruded and the resultant fine grained metal exhibited elongations over 200% at 108°C. The hardness of the extruded material increased with time after extrusion from 200 to 235 dph. The creep rate of alpha plutonium was measured over the temperature range 50 to 108°C, for both fine grained (2 to 5 micron) extruded metal and chill-cast metal (5 to 20 micron grain size). The fine grained metal was found to creep about 100 times faster than the coarser grained metal and the creep rate decreased markedly below 60°C. The superplasticity of β_α plutonium (beta formed from alpha) was explained on the basis of grain size: β_α had a finer grain size than non-superplastic β_γ. The creep behavior of gamma plutonium was studied. The activation energy for creep was about twice the reported value for self diffusion in gamma. The stress exponent, n, was 8.9, much higher than is usually observed. (auth)

11390 EFFECT OF HOT WORKING ON ROOM-TEMPERATURE STRENGTH AND DUCTILITY OF A PLUTONIUM-1 WT. PERCENT GALLIUM DELTA-STABILIZED ALLOY. Wheeler, A. D.; Thayer, W. L.; Robbins, J. L. (Univ. of Calif., Livermore). Nucl. Met., Met. Soc. AIME; 17: 437-48(1970).

From 4th International Conference on Plutonium and Other Actinides, Santa Fe, N. Mex. See CONF-701001-(Pt.1).

High-purity Pu-1 wt % Ga specimens (annealed for 24 hours at 460°C) were hot-worked to a torsional strain of 63 (at a torsional strain rate of 0.04 sec^{-1}) at temperatures of 300, 400, and 500°C and quenched to room temperature within 20 seconds. The effects of this hot working were evaluated by measuring the room-temperature strength and ductility of the quenched specimens by torsion, tension, and compression testing; all three methods showed excellent agreement. Hot working at 300°C appreciably increased the room-temperature yield and ultimate strength without loss of ductility. Hot working at 400 and 500°C significantly increased room-temperature ductility with some concurrent increase in strength. The high capacity for deformation during hot working is associated with a dynamic restoration process which results in a very fine-grained equiaxed room-temperature structure. The mechanism of this restoration process is believed to be concomitant recrystallization. The final grain size increased with increasing hot-working temperature. This grain size increase is due to the fact that grain size is a function of the steady state hot-working stress, and increases with decreasing stress. The effect of grain size on room-temperature yield strength can be described by the Hall-Petch relation. (auth)

11391 HOT SHORTNESS IN PLUTONIUM-1 WEIGHT PERCENT GALLIUM. Beitscher, S. (Dow Chemical Co., Golden, Colo.). Contract AT(29-1)-1106. Nucl. Met., Met. Soc. AIME; 17: 449-56(1970).

From 4th International Conference on Plutonium and Other Actinides, Santa Fe, N. Mex. See CONF-701001-(Pt.1).

Uniaxial tensile tests were performed at temperatures up to 550°C to determine the ductility and strength of rolled Pu-1 w/o Ga containing 135 to 800 ppM of Fe plus Ni. Hot shortness was observed at temperatures from 400 to 500°C in specimens that contained 235 ppM or greater total concentration of these elements. Fracture elongations in some of the hot-short alloys decreased by a factor of about 50 between 390 and 410°C. Relatively minor effects of Fe-plus-Ni content on ultimate strengths were observed. Optical metallography and electron microprobe analyses showed that the hot-short alloys contained grain-boundary constituents of the Pu-Pu_6Fe eutectic composition (410°C melting point). It is believed that the constituents are non-equilibrium phases in these alloys that result from Fe and Ni coring after casting. Hot shortness results from the ease of grain boundary crack propagation from these liquid-filled crack initiators. (auth)

11392 THERMODYNAMICS AND ALLOY BEHAVIOR OF THE bcc AND fcc PHASES OF PLUTONIUM AND THORIUM. Brewer, Leo (Univ. of California, Berkeley). Nucl. Met., Met. Soc. AIME; 17: 650-8(1970).

From 4th International Conference on Plutonium and Other Actinides, Santa Fe, N. Mex. See CONF-701001-(Pt.2).

Sufficient spectroscopic data have now accumulated to allow application of the Engel theory of metals to the predictions of portions of the phase diagrams of the lanthanide and actinide metals. Pu and Th will be used as examples. For bcc thorium the electronic configuration is predominately $6d^37s$ with a promotion energy of 16 kcal. Bcc Pu with a configuration f^5d^2s with only 3 bonding electrons and a promotion energy of 43 kcal is much less strongly bound. No spectroscopic data are available to verify the electronic configurations of the fcc phases, but the Engel correlation indicates that the fcc phases will have more s and p electrons and fewer d electrons than the bcc phases. On the basis of the above electronic configurations, one can predict that all twenty-four transition metals from the Ti-Hf group to the Cu-Au group would make fuller use of their bonding d electrons in bcc Th or Pu than in the corresponding fcc phases with fewer d electrons and these transition metals will stabilize the bcc phases relative to the fcc phases. On the other hand, non-transition metals or interstitial electron-donating elements, which cannot provide d electron bonding, will stabilize the fcc phases of Pu and Th relative to the bcc phases. The effect of internal pressure differences upon solubilities will be discussed and the effect of pressure upon the bcc-fcc transition of Th and Pu will be predicted. (auth)

11393 EFFECT OF β PHASE-RETAINING OR δ PHASE STABILIZING ELEMENTS ON PLUTONIUM DURING ALPHA-BETA THERMAL CYCLING. Prunier, C.; Hay, S.; Hocheid, B. (Commissariat a l'Energie Atomique, Bruyeres-le-Chatel, France). Nucl. Met., Met. Soc. AIME; 17: 1013-26(1970). (In French).

From 4th International Conference on Plutonium and Other Actinides, Santa Fe, N. Mex. See CONF-701001-(Pt.2).

Advantage is taken of the slow $\alpha \rightleftharpoons \beta$ heat cycles imposed by enthalpic analysis to follow retained phases and physical damages suffered by non-alloyed or slightly-alloyed plutonium samples. The elements chosen promote β phase retention (titanium, uranium) or may stabilize the δ phase at a sufficiently high concentration (gallium). Kinetic interpretation of the differential enthalpic analysis thermograms leads to an estimation of stabilized and retained phases. From density measurements, accompanied by micrographic examination it is possible to evaluate the volume of cracks caused by alpha-beta thermal cycling. Concerning the behavior of non-alloyed plutonium, β phase retention and cracking were observed to the greatest extent in the presence of titanium. While gallium had a little effect, it seemed that uranium reduced the formation of cracks in plutonium. (auth)

XUM

11394 EFFECT OF PRESSURE AND STRAIN RATE ON THE SHEAR STRENGTH OF BERYLLIUM. Abey, A. E. (Univ. of California, Livermore). J. Appl. Phys.; 41: 5254-9(Dec 1970).

The shear strength of beryllium was measured at strain rates of 3.5×10^{-5}, 3.6×10^{-3}, and 3.7×10^{-1} sec^{-1}. Measurements were taken under nearly hydrostatic pressures of 21, 44, and 63×10^8 neutrons/m^2. The shear strength was found to increase with both pressure and strain rate. A sample dislocation model was used to find an activation energy of 0.19 eV for dislocation motion. The model also gives an activation volume of 2.4×10^{-30} m^3 per unit length of moving dislocation. Data taken at a strain rate of 3.7×10^{-1} sec^{-1} to strains of approximately 40 indicate no ductile strain below a pressure of 6×10^8 neutrons/m^2 and an increase in ductile strain of 1.2 for each increase in pressure of 10^9 neutrons/m^2 above this value. (auth)

11395 SPECTRAL EMISSIVITY OF Ta IN THE RED AND IN GREEN AND CHANGE IN EMISSIVITY RESULTING FROM CHANGE IN SURFACE STRUCTURE INDUCED BY HEAT TREATMENT. Martinez, J. M.; Madjid, A. H. (Pennsylvania State Univ., University Park). J. Appl. Phys.; 41: 5322-6(Dec 1970).

The spectral emissivity ϵ_λ of tantalum for $\lambda = 0.645\ \mu$ and $\lambda = 0.546\ \mu$ has been measured by using a De Vos blackbody in ultra-high vacuum. Changes of the emissivity with heat treatment are related to changes in surface structure, and the reproducibility of results is demonstrated by making measurements on two different blackbodies of identical construction that have been subjected to similar heat treatment. The data presented are compared to previously published results. It is found that $\epsilon_{0.645\mu}$ between 1100 and 1700°K for tantalum that is not heated above 1700°K ranges from 0.420 to 0.411; that $\epsilon_{0.645\mu}$ between 1100 and 2400°K for tantalum that is heat treated one hour at 2450°K ranges between 0.394 and 0.370; and that $\epsilon_{0.546\mu}$ in the latter temperature interval, also for heat-treated tantalum, ranges from 0.456 to 0.423. (auth)

11396 THERMODYNAMIC PROPERTIES OF SOLID PALLADIUM-RICH Pd–Cd, Pd–In, Pd–Sn, AND Pd–Sb ALLOYS. Darby, J. B. Jr. (Argonne National Lab., Ill.); Myles, K. M.; Pratt, J. N. Acta Met.; 19: 7-14(Jan 1971).

Vapor pressure measurements were employed to determine the activities and the free energies of formation, at 1350°K, of palladium-rich Pd–Cd alloys. Entropy of formation values was computed by combining the free-energy data with heats of formation determined calorimetrically at 298°K. Heats of formation at 298°K were determined also for the α-phase palladium-rich alloys of the polyvalent solutes indium, tin, or antimony and for the intermediate phases PdSb and $PdSb_2$. A comparison of the thermodynamic and electronic properties of the four alloy systems suggests that a correlation exists between them. The major contribution to the heats of formation appears to be derived from a redistribution of electrons upon alloying of palladium. (auth)

11397 MINIMUM-CREEP-RATE BEHAVIOR OF POLYCRYSTALLINE VANADIUM FROM 0.35 TO 0.87 T_m. Wheeler, K. R. (Battelle-Northwest, Richland, Wash.); Gilbert, E. R.; Yaggee, F. L.; Duran, S. A. Contract AT(45-1)-1830. Acta Met.; 19: 21-6(Jan 1971).

The minimum creep-rate behavior of polycrystalline vanadium was investigated over the temperature range of 477 to 1600°C (0.35–0.87 T_m). The uncorrected or apparent activation energy for creep was found to increase linearly with temperature from 56 to 121 kcal/mole over this temperature range as the stress was decreased from 14.7 to 0.25×10^8 dyne/cm^2. A fifth power dependence of minimum creep-rate on applied tensile stress was observed when the ratio of strain rate to diffusivity was less than 10^9 cm^{-2}; however, above this ratio a stronger dependence was found. The creep-rate data are in agreement with contemporary correlations between creep and diffusion activation energies if the nonlinearity of the Arrhenius type plot for the diffusivity is taken into account. Mechanistically, the creep behavior was ascribed to dislocation climb by divacancy diffusion at high temperatures. As temperature decreased, the climb became controlled by single vacancy diffusion and eventually at low temperatures the climb was controlled by short-circuited diffusion. At any given temperature, the activation energy for creep was larger than that for self-diffusion. This effect was attributed to the larger vacancy concentration during creep, shifting the high-temperature divacancy diffusion mechanism to lower temperatures during creep. (auth)

11398 ELECTRICAL CONDUCTIVITY OF LIQUID INDIUM–BISMUTH ALLOYS. Romanova, A. V.; Kuchak, G. M. (Inst. of Physics of Metals, Kiev). Ukr. Fiz. Zh.; 15: 1526-9(Sep 1970). (In Russian).

The electrical conductivity of 13 indium–bismuth alloys corresponding to all characteristic points of the phase diagram was measured by an induction method with rotating magnetic field at temperatures from liquidus to 700 to 850°C. The electrical conductivity vs concentration isotherms plotted at 200, 400, 600, and 700°C indicate no singular points. It was shown that alloys with a quasi-eutectic structure after fusion have the same type of temperature dependence of electrical conductivity, which is characterized by two different temperature coefficients of resistivity. The conductivity of the alloys, rich in indium and bismuth which apparently have no quasi-eutectic atomic distribution after fusion is characterized either by a linear decrease in conductivity with a temperature rise, or a certain change in the 450 to 500°C temperature range. (auth)

11399 DIFFUSION OF NICKEL IN BERYLLIUM. Anan'in, V. M.; Gladkov, V. P.; Zotov, V. S.; Skorov, D. M. At. Energ. (USSR); 29: 220-1(Aug 1970). (In Russian).

The diffusion of nickel in beryllium was studied in pure beryllium and 2 Be–Ni alloys containing 10 and 36 wt % of nickel, respectively. The specimens were subjected to a high-temperature homogenizing, annealing and after placing ^{63}Ni on the surface, to diffusion annealing. The concentration curves were determined by removing layers of the metal and measuring the integral activity of the remaining specimen. The diffusion coefficients were calculated for all 3 cases in both α and β phases. The data indicated that the mobility of nickel in the Be + 10 wt % nickel alloy and in pure beryllium was quite close; this was found true also for the energies of activation of the diffusion process. In the Be + 36 wt % Ni the mobility of nickel was higher; it was also higher in the β phase of all 3 materials. Concentration measurements and autoradiographic tests revealed that nickel atoms diffusing through the grains play the most important role in the process; migration at the grain boundaries was less important. (TTT)

11400 CONTINUOUSLY-ACTIVE INDICATOR FOR THE DIFFUSION OF HYDROGEN IN SODIUM. Subbotin, V. I.; Kozlov, F. A.; Kuznetsov, E. K.; Ivanovskii, N. N.; Matyukhin, V. V. At. Energ. (USSR); 29: 210-12(Aug 1970). (In Russian).

A continuously acting indicator of hydrogen in sodium was developed on the basis of the diffusion of that gas from the liquid metal through a nickel wall into an argon stream, which in turn carried the hydrogen to a secondary detecting instrument. The overpressure of argon prevented the entry of air into the system. The other nonmetallic impurities in the sodium, such as oxygen, nitrogen and carbon passed much more slowly through the nickel film. The material balance under steady-state conditions allowed the determination of the partial pressure of hydrogen in the argon atmosphere above the sodium. The hydrogen was identified by means of a heat-conductivity detector which was sensitive toward this gas. The instrument was tested in a circulating sodium loop which included a centrifugal pump, heater, hold trap, and other secondary components; the total weight of the sodium in the loop amounted to 150 kg. The instrument reacted correctly to the introduction of 2 g of water with response time of 3 minutes. The sensitivity threshold of the instrument was 7×10^{-5} wt % of hydrogen in the sodium. (TTT)

11401 EFFECT OF A THORIA DISPERSION ON THE YIELDING AND FLOW OF IRON. Place, Thomas Alan. Vancouver, B. C.; Univ. of British Columbia (1969).

Thesis.

A technique for the preparation of iron containing a fine dispersion of thoria particles was developed. The method involved coprecipitation, hydrogen reduction, and hot rolling in a reducing atmosphere at 1373°K. The mechanical properties of iron and iron-thoria strip were investigated over the temperature range 77 to 373°K. The dispersion increased the strength and work hardening rate of iron, and reduced the ductility. The yield strength of the alloy was explained in terms of dislocation multiplication rates and the stress dependence of dislocation velocity. The work hardening rate was regarded as a balance between the yield stress behavior at low temperatures and recovery processes at the higher temperatures. The mechanics of neck and Luders band formation were examined, and the observed fracture angles explained in terms of this analysis. The ductile-to-brittle transition temperature was found to be improved in the iron-thoria, as a consequence of both a finer grain size and the direct influence of the particles. (Diss. Abstr. Int. B)

11402 SUBSTRUCTURE STRENGTHENING IN NICKEL ALLOYS. Clegg, Maurice Alexander. Vancouver, B. C.; Univ. of British Columbia (1969).

Thesis.

Pure nickel, Ni-20% Cr, Ni-2% ThO_2, and Ni-20% Cr-2% ThO_2 were studied to compare the mechanisms of dispersion strength-

ening in the latter two materials. All four materials were subjected to a wide range of thermomechanical treatments including cold rolling reductions up to 90% and annealing treatments which in the case of the materials containing ThO_2 were at temperatures up to 0.97 Tm (1400°C). In each condition the materials were examined by an x-ray line profile technique to determine the distribution of nonuniform lattice strain, the coherent crystallite domain size, and the twin and stacking fault probabilities. The x-ray data were also interpreted in terms of dislocation configurations. Supporting transmission electron microscopy was carried out on each material. Tensile tests were done at room temperature and at an elevated temperature on all materials to determine the strength properties and initial work hardening rate. It was concluded that the room temperature strength and the high temperature strength of all materials were determined by the presence of a fine domain or cell size and that the high temperature strength was also determined by the degree of polygonization of the fine substructure boundaries. In the case of the dispersion strengthened alloys the substructure boundaries were stabilized by the presence of ThO_2. It was observed that the Ni–Cr–ThO_2 material developed a different lattice strain distribution during cold rolling than did the Ni–ThO_2. This was characterized by a very small domain size and a high level of lattice strain averaged over short distances. It is proposed that this strain distribution favors recrystallization and grain growth and leads to the inferior structural stability in cold rolled Ni–Cr–ThO_2 at elevated temperatures compared to Ni–ThO_2. (Diss. Abstr. Int., B)

11403 REHEATING PROCESS OF Fe–Cr AND Fe–Cr–V ALLOYS AGED AROUND 500°C. Yamaguchi, Masaharu; Mima, Genjiro (Osaka Univ.). J. Jap. Inst. Metals; 34: 988-92(Oct 1970). (In Japanese).

The 475°C embrittlement of Fe–Cr and Fe–Cr–V alloys can be removed completely by reheating the alloys around 600°C. The process occurring in reheating of Fe–Cr and Fe–Cr–V alloys aged at 480°C is discussed. The electrical resistivity and hardness changes produced during reheating were measured. The process of the recovery of electrical resistivity during reheating was found to obey a first order chemical rate equation and was characterized by a considerably higher activation energy than that for the diffusion of chromium and vanadium in iron. From such an analysis the reheating process of Fe–Cr and Fe–Cr–V alloys aged around 500°C was confirmed to be associated with the resolution of Cr-rich precipitates into Fe-rich matrix. (auth)

11404 ELECTROTRANSPORT IN LIQUID Na–K. Olson, D. L.; Blough, J. L.; Rigney, D. A. (Ohio State Univ., Columbus). Scr. Met.;4: 1023-32(Dec 1970).

The liquid Na–K electrotransport problem was considered theoretically. The calculations of Epstein and Dickey were extended by the computation of the back-scattering differential cross-section, S, for Na and K as functions of composition, temperature, and pressure. The calculated composition dependence of S for the liquid Na–K system predicted the correct direction of migration for each species in dilute alloys, and it predicted the existence of a migration reversal at some intermediate composition. At 100°C the predicted cross-over was 68 at % K. (G.M.C.)

11405 CHEMISORPTION OF IODINE ON TUNGSTEN(100). Lander, J. J.; Morrison, J. (Bell Telephone Labs., Murray Hill, N. J.). Surface Sci.; 17: 469-73(Oct 1969).

The analysis of a series of LEED patterns observed in the chemisorption of iodine on a clean tungsten (100) crystal surface at room temperature in the pressure range between 1×10^{-5} and 1×10^{-8} torr is given. The results were preproducible and were reversible at 800 to 1100°C. (G.M.C.)

11406 DISTRIBUTION OF IRON AND ALUMINUM DURING ZONE MELTING OF URANIUM. Duzi, P.; Kuchar, L. (Inst. of Mining and Metallurgy, Ostrava, Czech.). Hutn. Listy; 24: 437-41(Jun 1969). (In Czech).

The distribution of Al and Fe in the course of zone melting of U was investigated. Fe was distributed very uniformly, Al was not distributed. For a zone travel rate of 2.22 cm/hr, the effective distribution coefficient of Fe in U amounts to 0.36 ± 0.06. For comparison of zone-melting efficiency an equilibrium distribution coefficient of Fe in U was established. (NSA of Czech)

11407 EFFECT OF MATRIX STRENGTHENING AND FIBER COATING ON MECHANICAL BEHAVIOR OF BORON–MAGNESIUM COMPOSITES. Dhingra, Ashok Kumar. Seattle; Washington Univ. (1970). 227p. University Microfilms Order No. 70-18,944. Thesis.

Unidirectionally aligned continuous composites of boron fibers magnesium metal matrix were developed by liquid infiltration techniques. Reproducible quality composites with uniform periodic distribution of boron fibers were fabricated in the form of rods, tensile bars, and plates. The mechanical properties of the composites were optimized by optimizing the volume fraction of fibers and by strengthening the matrix. It was found that composites containing 70% boron fibers showed flexural strengths in excess of 350,000 psi and Young's modulus of over 45×10^6 psi. The specific mechanical properties of the magnesium-boron composites were found to be higher than any other existing composite or bulk material. Fracture studies of the composites by scanning electron micrography showed that boron was fully wetted without any degradation by the molten magnesium and developed strong metallurgical bonds with the matrix at the interface. It was found that nickel coated boron composites showed loss in strength as compared to the uncoated boron composites. The loss in strength increased with increase in coating thickness on the boron fibers and occurred due to the formation of the brittle intermetallic phases at the interface and not due to fiber degradation. The failure mechanism of the various composites was studied by examining the fracture surface under a scanning electron microscope. The transverse and shear strengths of the composites were found to be much higher than the corresponding strength of the case bulk matrix. The matrices used were pure magnesium, magnesium alloy AZ31B, magnesium alloy ZK, and precipitation hardened alloy ZK. This substantial increase in the strength of the matrix was attributed to its ultra fine grain size in the composite. The transverse and shear strength for each composite system were found to be equal to the corresponding strength of the wrought matrix. The experimental data for the shear modulus and the transverse modulus of the composites were found to be in agreement with the hexagonal array micromechanics analysis of Hashin and Rosen. Under transverse loading, three types of composite failures have been observed: matrix failure, matrix and fiber failure, and fiber failure. Each of these failure mechanisms operated progressively as the strength of the magnesium matrix was increased. Therefore, by developing boron fibers with higher strengths in the transverse direction, the anisotropic strengths of the boron-magnesium system can be further improved. (Diss. Abstr. Int. B)

11408 STUDY OF HIGH-TEMPERATURE CREEP OF NICKEL–TUNGSTEN SOLID SOLUTIONS. Johnson, William Robert. Stanford, Calif.; Stanford Univ. (1970). 235p. University Microfilms Order No. 70-18,422.

Thesis.

Constant stress tensile creep tests were conducted for several dilute nickel-tungsten (0 to 6 wt % W) solid solutions in vacuum and argon at temperatures exceeding one-half the absolute melting temperature. In vacuum the steady state creep rate, $\dot{\epsilon}_s$, decreased slightly with increasing grain size and became essentially constant for specimens with grain sizes larger than a critical value. This decrease of $\dot{\epsilon}_s$, with increasing grain size, was attributed to a decreasing contribution of grain boundary sliding to the total strain or to the occurrence of recrystallization during testing. In addition, the initial strain on loading increased and the extent of primary creep and strain to rupture decreased with increasing grain size. In argon the minimum creep rate, $\dot{\epsilon}_m$, exhibited a U-shaped dependence with grain size. The increase of $\dot{\epsilon}_m$ with decreasing grain size was attributed to an increased grain boundary sliding contribution to the total strain while the increase of $\dot{\epsilon}_m$ for grain sizes larger than an optimum value was associated with an increased degree of cavitation due to the influence of the gas and an early initiation of tertiary creep before the steady state stage was reached. The initial strain on loading increased and the extent of primary creep decreased with increasing grain size. The strain to rupture also decreased with increasing grain size and was less in argon than in vacuum. In vacuum, the steady state creep rate, $\dot{\epsilon}_s$, obeyed a power law dependence on stress with a stress exponent, n, which decreased with increasing tungsten content. This decrease of n was attributed to a corresponding decrease of the stacking fault energy with tungsten addition. The effect of testing in an argon atmosphere was to increase the apparent value of n. The increase was attributed to an enhancement of grain boundary cavitation which led to a decrease in rupture strain and higher minimum creep rates. The apparent activation energy for creep, Q_c, corrected for the temperature dependence of the elastic modulus, increased with increasing tungsten content and was excellent agreement with the activation energy for diffusion in the alloy. Recrystallization during testing increased the minimum creep rate and caused an anomalous increase in Q_c and n. The effect of carbon is to increase the steady state creep rate and extent of primary creep. For tests conducted in vacuum at constant diffusivity and constant stress/modulus the steady state creep rate and extent of primary creep decreased with decreasing stacking fault energy. This influence was attrib-

XUM

uted to a decrease in the recovery rate and/or decrease in the dislocation generation rate with decreasing stacking fault energy. The effect of stacking fault energy on steady state creep rate, taken as the ratio of creep rates for pure nickel and the Ni-6 wt % W alloy, was approximately a factor of 70 and the creep rate appeared to obey a power law dependence on stacking fault energy with an exponent of about 4. (Diss. Abstr. Int. B)

11409 MEASUREMENT OF THE KINETICS OF OXIDATION OF MOLYBDENUM BY MEANS OF THE REACTING, ROTATING DISK TECHNIQUE. Schofill, John Luther Jr. Berkeley, Calif.; Univ. of California (1969). 142p. University Microfilms Order No. 70-17,649.

Thesis.

A rotating disk system was developed to study heterogeneous chemical reactions subject to the gas phase diffusion limitations. The system operated at temperatures up to 2000°K and disk speeds up to 15,000 rpm to investigate the reaction of oxygen and molybdenum. The independence of reaction or diffusion on radial position in the rotating disk system permitted kinetic data to be obtained from simple weight loss measurements as a function of disk temperature, oxygen partial pressure, and disk speed. Because of the availability of an exact solution of the diffusion-convection equation for the rotating disk, the diffusional contribution to the overall rate can be accurately assessed when both diffusion and surface reaction offer resistances of comparable magnitude. The surface process was shown to be consistent with the overall reaction $Mo(s) + O_2(g) \rightarrow MoO_3(g)$. The order of this reaction with respect to oxygen partial pressures from 0.002 to 0.05 atm at one atmosphere total pressure was found to be 1.00 ± 0.03 and the activation energy of the reaction was determined as 40 ± .3 kcal/mole for the temperature range 1100 to 1500°K. At temperatures above ~1650°K, the overall rate of corrosion was temperature independent, and predicted by rotating disk theory to within 15%. The results of this study demonstrated the importance of studying heterogeneous reactions at atmospheric pressure and high temperature in a flow system for which accurate prediction of diffusional limitations is possible. The rotating disk is an eminently satisfactory tool for such theoretical and experimental studies. (Diss. Abstr. Int. B)

11410 YAVLENIYA PERENOSA V ZHIDKIKH METALLAKH I POLUPROVODNIKAKH. (Transport Phenomena in Liquid Metals and Semiconductors). Belashchenko, D. K. Moscow; Atomizdat (1970). 400p.

Transport phenomena in metallic and semiconductor melts and the properties (electric, viscosity, and thermal) of these melts are discussed. Diffusion and interdiffusion of the melts, viscosity energy parameters of pure metals and liquid compounds, electric conductivity, and emf of the metallic compounds are analyzed considering various structural materials and their applications. The influence of corrosion in liquid metals on the mechanical properties of structural materials including liquid metal coolants in nuclear reactors is discussed. 1156 references. (R.V.J.)

11411 DIFFUSION IN SOLID METALS AND ALLOYS. Woehlbier, F. H. (ed.). Diffus. Data; 4: 296-405(1970).

Information is summarized on chemical diffusion, electrotransport, gas diffusion in metals, impurity diffusion, internal friction, radiation effects, diffusion in metals and alloys, and diffusion in oxides. (J.R.D.)

11412 TRANSIENT CREEP OF Cd SINGLE CRYSTALS AT ROOM TEMPERATURE. Hamersky, M. (Univ., Brno). Czech. J. Phys.; B20: 1327-9(1970).

The transient creep was studied at 24°C using the gradual loading method, and the activation volume and velocity-stress exponent were determined as functions of resolved shear stress. The maximum value of the exponent m (m = 0.6 for $\dot{\epsilon} \sim t^{-m}$) is obtained when the resolved shear stress is ~100 p/mm². From the activation volume, the rate-controlling process is either dislocation intersection or nonconservative jog motion. (D.L.C.)

11413 SLIDING FRICTION AND WEAR OF PURE METALS UNDER VACUUM OF 5 x 10^{-6} TORR. Duebler, Horst; Feller, Heinz Gerhard; Hack, Klaus; Matschat, Elke (Technische Univ., Berlin). Z. Metallk.; 61: 861-5(Nov 1970). (In German).

The wear of different metal pairs was investigated by gravimetric and electron optical techniques. The friction coefficient was determined. The results showed the strong influence of the structure on friction and wear. Metal transfer was found in almost all cases by means of microprobe analysis. (auth)

11414 STEADY-STATE CREEP OF ALPHA ZIRCONIUM. Gilbert, Edgar Robert. Pullman, Wash.; Washington State Univ. (1970). 77p. University Microfilms Order No. 70-16,783. Thesis.

The uniaxial tensile creep behavior of zirconium was investigated through the range of temperatures corresponding to the beta-to-alpha transformation to 50°C. Three materials were employed in the investigation: commercially pure zirconium annealed in the stable beta-phase region, commercially pure zirconium annealed in the stable alpha-phase region, and iodide zirconium annealed in the stable alpha-phase region. A discontinuity in the temperature dependence of the creep rate was observed as the temperature was lowered through the beta-to-alpha phase transformation. Upon completion of the beta-to-alpha phase change, the creep behavior was consistent with a dislocation climb mechanism controlled by divacancy diffusion. As the temperature was decreased, the creep behavior became consistent with climb by single vacancy diffusion. The change from divacancy to single-vacancy diffusion was rationalized in terms of the greater effectiveness of an undissociated dislocation as a vacancy sink. At high temperatures partial dislocations were more common and diffusion paths became long due to the reduced density of undissociated dislocations which served as local vacancy sinks. As a consequence, the faster-diffusing divacancy provided a greater contribution to creep. Brief periods of recovery were observed after several percent strain. Recovery resulted in an increased creep rate and may give the appearance of a low apparent activation energy; however, when recovery was not occurring, creep was characteristic of a discrete mechanism. Recovery was more pronounced at low strain rates and in the higher purity iodide zirconium. Below a stress of 70 kg/cm² at 840°C the creep behavior was characterized by a linear stress dependence and the creep rate appeared to be strongly dependent upon grain size. Below 500°C, creep is possibly controlled by a cross slip mechanism with a superimposed strain-ageing phenomenon at 450 and 300°C. The activation energy decreased from 105 kcal/mole at 450°C to approximately 30 kcal/mole at 50°C with a peak of 70 kcal/mole appearing at 300°C. These peaks of 105 and 70 kcal/mole are associated with the activation energy for cross slip being increased by a solute-dislocation interaction. Analysis of activation areas indicated that the stress dependence of the creep rate reflects the stress dependence of the dislocation density as well as dislocation velocity. At low stress levels between 300 and 400°C, creep behavior for a zirconium alloy Zr-2.5 Nb is consistent with a dislocation-climb mechanism controlled by diffusion along dislocation cores. This behavior is observed only when the ratio of strain rate to effective diffusivity is less than 10^9 cm^{-2}. (Diss. Abstr. Int., B)

11415 GAS-METAL REACTIONS IN SYSTEMS OF HIGH-MELTING METALS WITH NITROGEN OR OXYGEN. Hoerz, Gerhard; Fromm, Eckehard (Max-Planck-Institut fuer Metallforschung, Stuttgart). Z. Metallk.; 61: 819-27(Nov 1970). (In German).

A review is given of the mechanisms and kinetics of some engassing and degassing reactions and of the thermodynamic equilibria and steady states in the nitrogen and oxygen systems of the high-melting metals V, Nb, and Ta (VA group) and Mo and W (VIA group). The marked differences existing between the nitrogen and the oxygen systems as well as between the group VA metals and group VIA metals are discussed. Simultaneous engassing and degassing reactions caused thermodynamic equilibria in the nitrogen systems, but steady states in the oxygen systems. In the nitrogen systems of VA metals the dissolution reaction of nitrogen was exothermic, whereas in the nitrogen systems of the VIA metals it was endothermic. Furthermore, the rate of nitrogen degassing of VA metals in thin specimens was determined by the recombination of nitrogen with subsequent desorption whereas with VIA metals the diffusion of nitrogen in the metal determined the rate. In the ternary system Nb–Mo–N a continuous transition in characteristics from the Nb–N to the Mo–N binary system was observed. The relationships for the thermodynamic equilibria and steady states and also for the kinetics of engassing and degassing in the gas-metal systems compiled in this review permit estimations of the minimum gas contents attainable by high vacuum annealing and estimations of the annealing times required to reach a given degree of degassing. (auth)

11416 SUPERCONDUCTIVITY AND METALLURGICAL PROBLEMS WITH TITANIUM–NIOBIUM ALLOYS WHICH MAY SERVE AS MATERIALS FOR THE PRODUCTION OF SUPERCONDUCTING MAGNETS. Zwicker, Ulrich; Loehberg, Reinhold; Heller, Wolfram (Univ., Erlangen, Ger.). Z. Metallk.; 61: 836-47(Nov 1970). (In German).

The influence of crystal segregation, impurities, temperature of swaging, swaging rate, annealing between different swaging steps, and final annealing on the critical current density in magnetic fields of about 100 kG of 1 mm diameter wires of titanium-

niobium alloys was investigated. The sample annealed between swaging steps showed maximum critical current at 100 kG besides the smallest increase of voltage and, therefore, almost no tendency for flux jumping of large flux bundles. By additions, hardness and elastic modulus of titanium–niobium alloys may be increased. The additions of copper and germanium were investigated in greater detail. By these additions the intermetallic compounds Ti_2Cu or Ti_3Ge_3 were precipitated. By a small particle size of these intermetallic compounds the critical current of titanium–niobium alloys at 100 kG can be increased. (auth)

11417 ADSORPTION OF OXYGEN AND NITROGEN ON TANTALUM FILMS. PART III. INVESTIGATIONS WITH NITROGEN. Fromm, Eckehard; Fischer, Konrad; Treschau, Elmar (Max-Planck-Institut fuer Metallforschung, Stuttgart). Z. Metallk.; 61: 811-14(Nov 1970). (In Germann).

The adsorption of nitrogen on tantalum films was an irreversible chemisorption process between 273 and 370°K. When the amount of adsorbed nitrogen was less than 10^{13} molecules/cm^2, the sticking probability was between 0.2 and 0.5 and did not depend on pressure and temperature. At higher degrees of coverage the sticking probability decreased exponentially with increasing nitrogen adsorption and increased with temperature, but it remains independent of pressure. (auth)

11418 ADSORPTION OF OXYGEN AND NITROGEN ON TANTALUM FILMS. PART II. INVESTIGATIONS WITH OXYGEN. Fischer, Konrad; Fromm, Eckehard (Max-Planck-Institut fuer Metallforschung, Stuttgart). Z. Metallk.; 61: 805-10(Nov 1970). (In German).

The sticking probability of oxygen on clean thin tantalum films was about 1 between 77 and 295°K. At room temperature a chemisorption layer of oxygen was formed even at pressures below 10^{-4} torr, which contained more than one monolayer of tantalum atoms. The oxygen atoms of this layer were fixed to their sites and did not move over macroscopic distances. (auth)

11419 ADSORPTION OF OXYGEN AND NITROGEN ON TANTALUM FILMS. PART IV. TEMPERATURE DEPENDENCE OF THE RATE OF CHEMISORPTION AND PHYSICAL ADSORPTION OF NITROGEN. Fromm, Eckehard; Bauder, Ulrich; Fischer, Konrad (Max-Planck-Institut fuer Metallforschung, Stuttgart). Z. Metallk.; 61: 815-18(Nov 1970). (In German).

The rate of chemisorption of nitrogen on tantalum films was measured as a function of temperature between 150 and 500°K. When the amount of adsorbed nitrogen was low (<10^{14} molecules/cm^2), a non-activated chemisorption process was observed and at higher degrees of coverage activated chemisorption processes with activation energies up to 20 kcal/mole N_2 occurred. At temperatures below 300°K in addition to the chemisorption processes the reversible reaction of physical adsorption was determined. The dependence of N_2 coverage on pressure (in torr) is: $\Theta = 0.5 \cdot p \cdot \exp(2500/RT)$. The heat of physical adsorption is $\Delta H = 2.5 \pm 1$ kcal/mole N_2. (auth)

11420 STAGE I RECOVERY OF DEFORMED METALS. I. Swanson, M. L. (Atomic Energy of Canada, Ltd., Chalk River, Ont.). Phys. Status Solidi (a); 3: 287-98(16 Oct 1970).

A review is presented of defects and dislocations induced in deformed metals and the stage I recovery below 60°K. Experimental methods which can distinguish between effects produced by dislocations and these produced by point defects, are surveyed, and their use in studying stage I recovery and defect symmetry is discussed. 65 refs. (D.L.C.)

11421 USE OF ELECTRON MICROPROBE ANALYSIS TO DETERMINE LAYER THICKNESSES DOWN TO THE MONOLAYER RANGE. Butz, R.; Wagner, H. (Kernforschungsanlage, Juelich, Ger.). Phys. Status Solidi (a); 3: 325-31(16 Oct 1970).

Electron microprobe analysis was performed on Mo layers of 2 to 157 Å thickness deposited on tungsten. The x-ray intensity of the Mo–$L_{\alpha 1}$ and W–$M_{\alpha 1}$ line were investigated as a function of the Mo layer thickness and the electron-beam voltage of 2.9 to 40 kV. Mo layers could be detected down to the monolayer range. A linear relation between the layer thickness and the x-ray intensity is found. The greatest sensitivity in the determination of the layer thickness is attained for beam voltages 3 to 4 times the excitation energy of the characteristic Mo radiation. (auth)

11422 CORRELATION BETWEEN DISLOCATION STRUCTURE AND WORK-HARDENING BEHAVIOR OF MOLYBDENUM SINGLE CRYSTALS DEFORMED AT 293°K. Luft, A. (Zentralinstitut fuer Festkoerperphysik, Berlin. Werkstofforschung der Deutsche Akademie der Wissenschaften, Berlin. Institutsteil fuer Metallphysik und Reinstmetalle, Dresden). Phys. Status Solidi; 42: 429-40(1 Nov 1970).

The dislocation structure of high-purity molybdenum single crystals after tensile deformation at 293°K was studied by transmission electron microscopy. Dislocation and debris densities were determined as function of strain. The stress–strain curve is characterized by a high initial work-hardening rate and a subsequent stress plateau. At low strains long jogged screw dislocations and dislocation debris predominate while at higher strains additionaly large dislocation tangles are formed. The resolved flow stress τ and screw dislocation density ρ_1 obey $\tau = \tau_0 + \alpha_1 G b\sqrt{\rho_1}$ with $\alpha_1 = 1.1$. It is suggested that the interaction between primary and secondary screws involving the formation of jogs, debris, and attractive dislocation junctions is the relevant dislocation strengthening mechanism. (auth)

11423 EQUILIBRIUM VACANCIES IN LANTHANUM. Akimov, A. I.; Kraftmakher, Ya. A. (Inst. of Inorganic Chemistry, Novosibirsk, USSR). Phys. Status Solidi; 42: K41-2 (1 Nov 1970).

The thermal capacity of β–La was measured at high temperatures and found to increase strongly with temperature. The data were fitted to the equation $C_p = A + BT + (c/T)^2 \exp(-E/kT)$, where E is the defect formation energy. The parameters were found to be: $A = 0.1777$, $B = 4.7 \times 10^{-5}$, $c = 2.66 \times 10^3$, and $E = 1$ eV. The equilibrium concentration of the point defects can be found from the equation $c = 320 \exp(-1eV/kT)$; it is 1.2% at 1137°K. (D.L.C.)

11424 INVESTIGATION OF INTERDIFFUSION IN Nb–Zr SYSTEM BY THE LOCAL X-RAY SPECTRAL ANALYSIS METHOD. Ronami, G. N.; Gryzunov, V. I.; Sokolovskaya, E. M.; Tatarkina, A. L.; Raevskaya, M. V. Vestn. Mosk. Univ., Ser. III. Fiz. Astron.; 11: 251-5(May-Jun 1970). (In Russian).

A Kameka MS-46 microanalyzer was used in studies of mutual diffusion of Nb and Zr at 1600°C (45 hr), 1000°C (123, 390, and 483 hr), 900°C (360 hr), and 800°C (500 hr). The mutual diffusion as a function of Nb concentration was determined. (R.V.J.)

11425 THERMAL PROPERTIES OF TANTALUM AT HIGH TEMPERATURES. Arutyunov, A. V.; Makarenko, I. N.; Trukhanova, L. N.; Filippov, L. P. Vestn. Mosk. Univ., Ser. III. Fiz. Astron.; 11: 340-3(May-Jun 1970). (In Russian).

The thermal conductivity, anharmonic lattice oscillations, electronic specific heat, and the influence of vacancies in liquid- and solid-state metals were analyzed. Results of systematic studies of the thermal properties of tantalum, measured at high temperatures (from 1100 to 2945°C), are tabulated. (R.V.J.)

11426 IZLUCHATEL'NAYA SPOSOBNOST' VYSOKOTEMPERATURNYKH MATERIALOV. (Emissivity of High-Temperature Materials). Petrov, V. A. Moscow; Izdatel'stvo Nauka (1969). 80p.

Methods for measuring the emissivity of high-temperature reactor materials are described. Results of measurements using these methods are presented for investigations at 3500°K. Results of theoretical work on the emissivity of solid metals and nonmetals are reviewed along with methods for determining the emissivity. References are included for calculations associated with fabrication of high-temperature experimental equipment. (tr-auth)

11427 EFFECT OF IRON ON THE HOT CRACKING OF URANIUM WELD METAL. PART I. Turner, P. W. (Union Carbide Corp., Oak Ridge, Tenn.); Lundin, C. D. Weld. J. (N.Y.); 49: 579s-87s(Dec 1970).

The influence of iron on the hot-cracking tendency of uranium weld metal was investigated. Iron was added in calculated amounts to electron-beam welds to produce weld-metal compositions ranging from 50 to 7,700 ppM iron. Hot cracking susceptibility was determined with a spot-Varestraint test device. Intermediate iron concentrations in the weld metal caused severe cracking at low levels of strain. Welds having high and low concentrations of iron were not prone to hot cracking. The cracking tendencies of actual welds on partial penetration butt joints compared favorably with the results of the Varestraint test. (auth)

Structure and Phase Studies

Refer also to abstracts 11979, 11995, 11998, 12006, and 12025.

11428 (AWRE-O-29/67) ELECTRON METALLOGRAPHY OF PRECIPITATES IN IRRADIATED AND IN UNIRRADIATED 20 WT. PERCENT Cr–25 WT. PERCENT Ni–0.7 WT. PERCENT Nb STAINLESS STEEL. Ranzetta, G. V. T.; Scott, V. D. (Atomic Weapons Research Establishment, Aldermaston (England)). 1967. 17p. Dep. NTIS (U. S. Sales Only).

The parallel application of electron microscopy, diffraction and

electron-probe microanalysis to the study of precipitates extracted by a replica technique from a stainless steel containing 20 wt % Cr, 25 wt % Ni, and 0.7 wt % Nb is described. Two types of precipitate were present in both irradiated and unirradiated material, one in the form of a fine dispersion, the other as coarser grain-boundary particles. The fine precipitates were identified as niobium carbide. The coarse particles were shown to contain mainly nickel and niobium, which together with the corresponding electron diffraction data, indicated that they were based on the carbide phase $[Ni + (Fe + Cr)]_6Nb_2C$, but containing very little iron and chromium. (auth) (UK)

11429 (CEA-CONF-1687) CHEMICAL DIFFUSION AND HETERODIFFUSION AT INFINITE DILUTION OF Pu IN BODY CENTERED CUBIC β Ti. Languille, Alain (Commissariat a l'Energie Atomique, Fontenay-aux-Roses (France). Centre d'Etudes Nucleaires). 1970. 14p. (In French). (CONF-700941-3). Dep. NTIS (U.S. Sales Only).

From Meeting on Metallurgy, Paris, France.

The Pu-Ti phase diagram presents a body centered cubic TiPuβ solid solution ranging from 0 per cent to 50 per cent Pu by weight at 900°C. Heterodiffusion at infinite dilution of Pu in this phase was carried out on alloys containing 0.3 per cent and 3 per cent by weight of Pu. The examinations are made by x ray microanalysis and autoradiography. The results obtained between 900 and 1200°C give a very low activation energy of the order of 20 kcal, which confirms the abnormal body-centered cubic structure of β titanium where diffusion is concerned. In the case of chemical diffusion, the diffusion coefficient depends little on the concentration although the slope of the liquidus curve is steep. (auth) (France)

11430 (CEA-CONF-1688) CRYSTALLOGRAPHIC ANALYSIS OF THE SEGREGATIONS OBSERVED IN DILUTE ZrPu ALLOYS DURING MARTENSITIC TRANSFORMATION. Cornet, Jean-Francois; Calais, Daniel (Commissariat a l'Energie Atomique, Fontenay-aux-Roses (France). Centre d'Etudes Nucleaires). 1970. 21p. (In French). (CONF-700941-1). Dep. NTIS (U. S. Sales Only).

From Meeting on Metallurgy, Paris, France.

Zirconium alloys with small Pu contents (from 0.3 to 3 wt. %) in the β phase (bcc) were studied. After heat treatment segregations appeared. The form of the segregations (needles) demonstrated that the diffusion anisotropy was due to the martensitic nature of the Zr $\beta \rightarrow \alpha$ phase change. In order to confirm this the following two approaches were adopted: A 3 per cent ZrPu alloy which had been quench hardened when in the β phase was analyzed using x-ray crystallography; this sample did not exhibit segregation because the rate of cooling had been too rapid; a 0.3 per cent ZrPu alloy which had been slowly cooled was similarly analyzed; the macroscopic segregation observed in the solute was attributed to an anisotropic diffusion phenomena. The microscopic and x-ray crystallographic data obtained were compared and discussed. (France)

11431 (CEA-CONF-1691) EFFECT OF A $\beta \rightarrow \alpha$ TRANSFORMATION AND OF OXYGEN ON PLUTONIUM DISTRIBUTION IN DILUTE Zr-Pu AND Ti-Pu ALLOYS. Languille, Alain; Remy, Clotilde; Calais, Daniel (Commissariat a l'Energie Atomique, Fontenay-aux-Roses (France). Centre d'Etudes Nucleaires). 1970. 16p. (In French). (CONF-700941-4). Dep. NTIS (U.S. Sales Only).

From Meeting on Metallurgy, Paris, France.

Allotropic $\alpha \rightarrow \beta$ transformations in Ti and Zr are of the martensitic type. After a sufficiently rapid $\beta \rightarrow \alpha$ transformation, micrographic observation revealed a needle structure whose direction varied in relation to the relative positions of the β grains in the previous phase. Some segregation in solute appeared with dilute PuTi, PuZr, and UTi alloys after heating at a temperature superior to that of the transformation for the pure metal. Each β grain led, after cooling, to a series of α needles, whose orientation was well defined. X ray microanalysis and α autoradiography revealed the needles to be alternatively deficient and enriched with β active solute. The zones may vary between 1 and 10. The macroscopic and anisotropic displacement of the solute atoms observed cannot be explained by only thermal diffusion accounting for the diffusion coefficients and the cooling rate during the phase change. Two hypotheses were proposed to explain the phenomena: an accelerated diffusion resulting from the supersaturation in point defects caused by the phase change; contamination by α active oxygen. (France)

11432 (CEA-N-1310) STRUCTURE TRANSFORMATIONS OF Zr-Cu BINARY ALLOYS WITH LOW Cu CONTENTS AND TERNARY ALLOYS DURING CONTINUOUS COOLING. Decours, Jacques; Brun, Gilbert; Gratias, Denis (Commissariat a l'Energie Atomique, Saclay (France). Centre d'Etudes Nucleaires). Sep 1970. 23p. (In French). Dep. NTIS (U. S. Sales Only).

The phase transformations occurring in the β phase of Zr-Cu binary alloys (Cu = 0.5 to 2.33%) and ternary alloys (Zr-0.5% Cu-0.5% Mo; Zr-2% Cu-0.5% Mo; Zr-2% Cu-0.5% Ni; Zr-2% Cu-0.5% Cr) during continuous cooling were investigated using different physical methods such as thermal analysis, dilatometry, and optical and electron microscopy. (auth) (France)

11433 (CONF-701001-(Pt.2)) PLUTONIUM 1970 AND OTHER ACTINIDES. NUCLEAR METALLURGY, VOLUME 17. Proceedings of the 4th International Conference, Sante Fe, New Mexico, October 5-9, 1970. Miner, William N. (ed.) (Los Alamos Scientific Lab., N. Mex.). 548p. (In English and French).

A total of 42 papers are included in Part II. A separate abstract was prepared for each of 35 papers. Seven papers were previously abstracted in NSA. For abstracts of these see CONF-701001 in the Report Number Index. (G.M.C.)

For abstracts of individual papers see: 11360, 11392, 11393, 11437-11447, 11467, 11468, 11499-11507, 11521-11525, 11535-11537, 11960, and 12006.

11434 (SU-326-P-17-X-1) STRUCTURE DEPENDENCE OF HIGH TEMPERATURE DEFORMATION OF METALS. Progress Report, March 1, 1969-March 1, 1970. Nix, William D.; Barrett, Craig R. (Stanford Univ., Calif. Dept. of Materials Science). 1 Mar 1970. Contract AT(04-3)-326. 44p. Dep. NTIS.

Progress in a research program concerned with the structure dependence of high-temperature deformation of metals and alloys is summarized. Work toward development of a deeper understanding of the relation between structure and high-temperature creep and creep rupture of metals is described along with work on new ways of improving the creep resistance of metals through structural control. An extensive portion of the study has been concerned with determining the rate controlling creep mechanism operating in metals and alloys at very high temperatures and low stresses. Completed work on Al, Al-0.5% Fe, Cu and Cu-Si alloys has shown conclusively that Newtonian viscous deformation can occur in metals as the result of dislocation motion and does not necessarily involve the stress directed diffusion of vacancies between interfaces. Extensive work is currently underway extending these observations to the Fe-3% Si system. Results of the work carried out thus far on Fe-3% Si (creep tests, etch pit observations of dislocation substructure, and comparison of the creep behavior of single and polycrystals) indicate that high-temperature-low stress creep in this system is also controlled by dislocation motion with grain boundary shearing also contributing extensively to the observed strain rate, especially during primary creep. A theoretical interpretation of high-temperature deformation due to the directed diffusion of vacancies between dislocations and based on Nabarro's earlier but incorrect treatment has also been completed. Research on the structure dependence of creep at intermediate temperatures has been carried out in three areas including effects of shock loading, high temperature solid solution hardening, and high-temperature recovery. (J.R.D.)

11435 LOW-TEMPERATURE DEFORMATION MECHANISMS IN DELTA STABILIZED Pu-Ga ALLOYS. Seery, William N.; Rafalski, Anthony L. (Dow Chemical Co., Golden, Colo.). Contract AT(29-1)-1106. Nucl. Met., Met. Soc. AIME; 17: 426-36 (1970).

From 4th International Conference on Plutonium and Other Actinides, Santa Fe, N. Mex. See CONF-701001-(Pt.1).

Deformation mechanisms in delta-stabilized fcc Pu-Ga alloys were studied over the temperature range, -196 to 25°C. Both optical and electron microscopy were used to observe the deformation features. Slip, twinning, and a martensitic transformation of the fcc delta phase to the monoclinic alpha phase were observed on compressive loading. The operating deformation mechanism was found to be dependent on temperature, gallium content, and strain rate. The effects of stress, strain, strain rate, and grain size on the martensitic delta to alpha transformation were studied to define the M_D temperature of this reaction. The effect of temperature and deformation on the reverse reaction, alpha to delta, was also investigated. (auth)

11436 ANNEALING AND DEFORMATION TWINNING IN DELTA-STABILIZED PLUTONIUM-GALLIUM ALLOYS. Moment, Roger L. (Dow Chemical Co., Golden, Colo.). Contract AT(29-1)-1106. Nucl. Met., Met. Soc. AIME; 17: 457-67(1970).

From 4th International Conference on Plutonium and Other Actinides, Santa Fe, N. Mex. See CONF-701001-(Pt.1).

Conditions under which annealing and deformation twins were

observed in Pu-1, 2, and 3 wt % Ga alloys are discussed. Twins were found in all three alloys after casting and homogenization, but large variations in the grain size prevented using these structures to estimate the stacking fault energy (SFE). Annealing twins were also seen in the primary recrystallization grains of the Pu-2 and 3 wt % Ga alloys, in higher density than in the original cast structure. However, the secondary recrystallization grains contained very few twins. Deformation twinning was observed in the Pu-2 wt % Ga alloy rolled at −196°C, and is thought to occur in the Pu-3 wt % Ga alloy rolled at −196°C as well. In the Pu-1 wt % Ga alloy rolled at this temperature, formation of the alpha phase prevented identifying any deformation twins. All three alloys showed a change in rolling texture with reduced temperature of rolling, paralleling the behavior of Cu under similar conditions. This, plus the similar occurrence of deformation twinning at low temperatures in Cu, suggests a similarity of deformation mechanisms between the two metal systems. (auth)

11437 PHASE RELATIONSHIPS IN URANIUM, NEPTUNIUM, AND PLUTONIUM. Wittenberg, Layton J.; Vaughn, Glen A.; DeWitt, Robert (Mound Lab., Miamisburg, Ohio). Contract AT(33-1)-Gen-53. Nucl. Met., Met. Soc. AIME; 17: 659-68(1970).

From 4th International Conference on Plutonium and Other Actinides, Santa Fe, N. Mex. See CONF-701001-(Pt.2).

A quantitative differential thermal analysis technique was used to determine the temperatures and heats of transformation of Np. The heats of transformation for the $\alpha \rightarrow \beta$(280°C), the $\beta \rightarrow \gamma$ (575°C) and the $\gamma \rightarrow$ liquid(640°C) transformations were 1.34 ± 0.13, 1.26 ± 0.04, and 1.24 ± 0.03 kcal/g-at., respectively. When the information on Np is combined with that of U and Pu, several anomalous properties are noted for these transuranium elements when compared with the other groups of elements in the Periodic Table. Several semi-empirical relationships are used to compare various properties of these elements in order to acquire a better understanding of their behavior. The observation that the $\alpha \rightarrow \beta$ transformations in Np and Pu have larger heats and entropies of transformation than the fusion reactions is explained as due to a semi-metallic → metallic electronic transformation in the solid state. The low melting point of Pu is shown to be a consequence of the low vibrational frequencies of the atoms in the high temperature bcc solid phase. The bcc phases of U and Np are expected to show similar correlations. Additionally, the volume decrease at the melting point of Pu was assigned to a contraction in the atomic radius. The size of the metallic atom in the liquid was calculated from transport measurements and does explain the effect of pressure upon the melting temperature. (auth)

11438 CONSTITUTION OF PLUTONIUM-RICH PLUTONIUM–OSMIUM ALLOYS. Ellinger, F. H.; Land, C. C. (Los Alamos Scientific Lab., N. Mex.). Nucl. Met., Met. Soc. AIME; 17: 679-85(1970).

From 4th International Conference on Plutonium and Other Actinides, Santa Fe, N. Mex. See CONF-701001-(Pt.2).

The Pu–Os phase diagram from 0 to 15 at. % Os was constructed from thermal, dilatometric, micrographic, and x-ray diffraction data. The principal features of the diagram are: a eutectic at ~10 at. % and 515°C; a maximum solubility of ~7 at. % Os in ϵPu; the eutectoidal decomposition of ϵ solid solution at 427°C; an elevated-temperature intermediate phase that corresponded to ~$Pu_{19}Os$ and was stable between 195 and 434°C; and an intermediate phase that also corresponded to ~$Pu_{19}Os$ and was stable up to 300°C. (auth)

11439 PLUTONIUM–ZIRCONIUM PHASE DIAGRAM. Ellinger, F. H.; Land, C. C. (Los Alamos Scientific Lab., N. Mex.). Nucl. Met., Met. Soc. AIME; 17: 686-98(1970).

From 4th International Conference on Plutonium and Other Actinides, Santa Fe, N. Mex. See CONF-701001-(Pt.2).

Arc cast and heat treated Pu–Zr alloys were studied by the methods of dilatometry, microscopy, and x-ray diffraction. The lattice parameter vs composition relationships of the fcc δPu solid solution and the limits of the δ phase field were determined. The formation of the ζ phase by the peritectoid reaction γPu + δPu → ζ was confirmed. A new intermediate low-temperature phase somewhat richer in zirconium than the θ phase was discovered. The ϵPu(βZr) solid solution was found to transform congruently into δ phase at 55 at. % Zr and 643°C, and to transform eutectoidally into $\delta + \alpha$Zr at 70 at. % Zr and 621°C. (auth)

11440 Pu–Sc SYSTEM: DIAGRAM AND PROPERTIES. Ballagny, Alain; Boucher, Rene; Carrard, Claude (Centre d'Etudes Nucleaires, Fontenay-aux-Roses, France). Nucl. Met., Met. Soc. AIME; 17: 699-706(1970).

From 4th International Conference on Plutonium and Other Actinides, Santa Fe, N. Mex. See CONF-701001-(Pt.2).

Phase studies of the Pu–Sc system were based on x-ray diffraction, metallography, dilatometry and density techniques. The limits of the delta stabilized phase were fixed, at room temperature, between 4 and 19.4 at. % scandium. The domain of zeta phase was determined to be between 43.4 and 47.4 at. % Sc. An equilibrium diagram is presented. The following properties were studied: lattice constants, densities, coefficients of thermal expansion, electrical resistivity, atmospheric corrosion between 20 and 550°C, hardness, and workability by rolling. (auth)

11441 INVESTIGATION OF THE PLUTONIUM–SILVER SYSTEM. Wood, David H.; Cramer, Eugene M.; Wallace, Peter L. (Univ. of California, Livermore). Nucl. Met., Met. Soc. AIME; 17: 707-19(1970).

From 4th International Conference on Plutonium and Other Actinides, Santa Fe, N. Mex. See CONF-701001-(Pt.2).

Metallographic, x-ray diffraction, and differential thermal analyses were used in a limited investigation of the plutonium–silver phase diagram. Two compounds were observed: $PuAg_{3.6}$, which melted congruently at 977°C, and $PuAg_2$, which melted peritectically at 817°C. A region of liquid immiscibility extended from about 2 to 59 at. % silver, at which composition there was a monotectic reaction at 795°C. A eutectic between $PuAg_{3.6}$ and silver was found at 801°C and 90.8 at. % silver. These results are at variance with the literature in several respects. The occurrence of liquid immiscibility is explained in accordance with the thermodynamic reasoning of Hume–Rothery and Anderson. (auth)

11442 URANIUM–PLUTONIUM–ZIRCONIUM TERNARY ALLOY SYSTEM. O'Boyle, D. R.; Dwight, A. E. (Argonne National Lab., Ill.). Nucl. Met., Met. Soc. AIME; 17: 720-32(1970).

From 4th International Conference on Plutonium and Other Actinides, Santa Fe, N. Mex. See CONF-701001-(Pt.2).

Electron-microprobe analysis, x-ray diffraction, and optical metallography techniques were used to study high-purity U–Pu–Zr alloys in order to establish the equilibrium phases and transformations in the ternary alloy system. Below the solidus temperature, the three elements show complete miscibility of the bcc high-temperature allotropes (γ–U, ϵ–Pu, β–Zr). The bcc gamma phase was stabilized by additions of zirconium and plutonium. With decreasing temperatures from 700 to 600°C, the gamma single-phase boundary swept rapidly from the U–Zr and U–Pu binary sides of the system toward the Zr–Pu side of the system. Isothermally annealed alloys were examined by means of quantitative electron-microprobe analysis to determine the extent of the U–Zr $\gamma_1 + \gamma_2$ miscibility gap in the ternary system and to establish the composition of phases in equilibrium with the zirconium-rich gamma phase. Four-phase reactions that occurred in the uranium corner of the system below 700°C are outlined in a solid-state reaction scheme that is in agreement with the phases found in the ternary system and with the published transformations in the three limiting binary systems. The αU + ζ(U–Pu) + δ(U–Zr) three-phase region was stable from 595°C (the lowest four-phase reaction temperature) to room temperature. Isothermal sections are presented to show the phases in equilibrium over the range of temperatures from 700 to 500°C. (auth)

11443 LOW TEMPERATURE TRANSFORMATIONS IN PLUTONIUM. Rechtien, J. J.; Friddle, R. J.; Harkreader, W. F. (Argonne National Lab., Ill.). Nucl. Met., Met. Soc. AIME; 17: 983-90(1970).

From 4th International Conference on Plutonium and Other Actinides, Santa Fe, N. Mex. See CONF-701001-(Pt.2).

The crystallography of the $\alpha \rightleftharpoons \beta$ transformation in plutonium was investigated by x-ray and metallographic observations on a single crystal. X-ray patterns in the β phase were not interpretable, but observations in the product α phase have allowed some conclusions concerning reversibility and previously reported orientation relationships to be made. The alpha to beta plutonium transformation can be studied correctly by Laue techniques. The beta grains resulting from a single alpha grain are very coarse, but a very subgrained single grain cannot be entirely ruled out. An orientation relationship probably exists between alpha and beta plutonium. Neither of the two product orientations analyzed can be formed reversibly with the orientation relationship previously suggested by Nelson and Bowman. (auth)

11444 BETA GRAIN SIZE AND THE $\beta \rightarrow \alpha$ TRANSFORMATION IN UNALLOYED PLUTONIUM. Allen, R. P.; Nelson, R. D. (Battelle-Northwest, Richland, Wash.). Contract AT(45-1)-1830. Nucl. Met., Met. Soc. AIME; 17: 991-1000(1970).

From 4th International Conference on Plutonium and Other Actinides, Santa Fe, N. Mex. See CONF-701001-(Pt.2).

An elevated temperature x-ray metallographic technique was

XUM

used to compare the grain size of beta plutonium (β_γ) formed from the higher temperature gamma phase with the grain size of beta plutonium (β_α) formed from the lower temperature alpha phase. In all cases the grain size of the β_γ was found to be larger than that of the β_α. The effect of gamma-phase heat treatments on the kinetics of subsequent $\beta \rightarrow \alpha$ transformations was also investigated using alpha-phase extruded plutonium as a reference material. The incubation time for the initial $\beta \rightarrow \alpha$ transformations of the extruded metal was about 2 minutes at an isothermal transformation temperature of 71°C. After a gamma-phase heat treatment, the incubation time for the corresponding $\beta_\gamma \rightarrow \alpha$ transformation was less than 2 seconds. Specimens quenched from β_γ to ambient or subzero temperatures had incubation times of 2 minutes or longer for the subsequent $\beta \rightarrow \alpha$ transformations. However, specimens slowly cooled $\gamma \rightarrow \beta_\gamma \rightarrow \alpha$ or quenched from β_γ to high alpha temperatures had an incubation time of less than 10 seconds for the first $\alpha \rightarrow \beta \rightarrow \alpha$ transformation cycle. The incubation time then progressively increased with further $\alpha \rightleftharpoons \beta$ cycling to the 2 minute value characteristic of the initial as-extruded plutonium. The results of both the x-ray investigation and the kinetic study are consistent with a beta grain size explanation for the difference in $\beta_\gamma \rightarrow \alpha$ and $\beta_\alpha \rightarrow \alpha$ transformation kinetics. (auth)

11445 COMPARED STUDY OF THE PLUTONIUM TRANSFORMATION HEATS AS DETERMINED BY ENTHALPIC ANALYSIS AND BY THE USE OF HIGH PRESSURES. Prunier, C.; Roux, C.; Rapin, M. (Commissariat a l'Energie Atomique, Bruyeres-le-Chatel, France). Nucl. Met., Met. Soc. AIME; 17: 1001-12(1970). (In French).

From 4th International Conference on Plutonium and Other Actinides, Santa Fe, N. Mex. See CONF-701001-(Pt.2).

By differential enthalpic analysis, temperatures and heats of plutonium transformations may be determined not only while heating but also during cooling. With this method, it is possible to separate all the transformations and to show up: the influence of the γ phase origin (γ_β or γ_δ) on $\gamma \rightarrow \beta$ transformation temperature and heat; and the low energies involved in part of the $\beta \rightarrow \alpha$, $\delta \rightarrow \gamma$, and $\delta' \rightarrow \delta$ transformations, which in spite of the high sensitivity of the calorimetric method hinders complete measurement of the corresponding transformation heat. After the slope evaluation at the origin of the pressure-temperature diagram, transformation heats may be obtained by Clapeyron's formula application. On heating $\delta \rightarrow \delta'$ transformation escapes detection and during cooling only $\epsilon \rightarrow \delta'$ and $\beta \rightarrow \alpha$ limits can be defined. The transformation heats obtained by these two methods on plutonium samples from the same source differ widely for the $\alpha \rightarrow \beta$ transformation. Tentative explanations (complete transformation of the retained phases during high pressure experiments, difficulty of applying Clapeyron's formula to transformations which are not perfectly reversible) are inadequate to account for such a difference. (auth)

11446 PHASE TRANSFORMATIONS IN METASTABLE PLUTONIUM-GALLIUM ALLOYS. Ekbom, Lars; Bogegard, Sven (Research Inst. of the Swedish National Defence, Stockholm). Nucl. Met., Met. Soc. AIME; 17: 1027-36(1970).

From 4th International Conference on Plutonium and Other Actinides, Santa Fe, N. Mex. See CONF-701001-(Pt.2).

The relation between the metastable and the equilibrium phases in the Pu-1 at. % Ga alloy is discussed. Hot hardness measurements indicated that gallium additions had no effects on the typical properties of β_α and β_γ. An equilibrium diagram for the plutonium-rich end of the Pu-Ga system is proposed. (G.M.C.)

11447 SPUTTERED PLUTONIUM-TANTALUM ALLOYS. Busch, R. A. (Battelle-Northwest, Richland, Wash.). Contract AT(45-1)-1830. Nucl. Met., Met. Soc. AIME; 17: 1045-55(1970).

From 4th International Conference on Plutonium and Other Actinides, Santa Fe, N. Mex. See CONF-701001-(Pt.2).

Plutonium was alloyed with tantalum, which is insoluble in the solid state, by cosputtering the elements. The alloy deposits exhibited unusual phase transformation properties. When the substrate temperature was in the normal alpha region, the deposit was beta phase at room temperature. On subsequent heating, the first transformation observed was at about 250°C; subsequently the sample exhibited normal allotropic behavior. The phase stabilization effect depended on the tantalum content and substrate temperature. The results are discussed in terms of lattice strain and particle-grain boundary interactions. (auth)

11448 CRYSTAL STRUCTURE AND MARTENSITIC TRANSFORMATION IN NEAR-EQUIATOMIC AuCd. Ledbetter, Hassell Marion Jr. Urbana, Ill.; Univ. of Illinois (1970). 170p. University Microfilms Order No. 70-21,006.

Thesis.

The crystallography of the interrelationships among the β, β' and β'' phases in near-stoichiometric AuCd alloys has been studied experimentally and theoretically. Particular emphasis was placed on the crystal structure of the β''-AuCd phase and the geometrical aspects of the $\beta \rightarrow \beta''$ martensitic transformation. Guinier-DeWolff (powder) and oscillation-rotation (single crystal) x-ray diffraction techniques were used for the crystal structure determinations. Quantitative metallographic procedures were used for the martensite crystallography. Theoretical calculations were made according to the theory of Bowles and Mackenzie programmed for electronic machine computation. The crystal structures of β and β' were verified, β having an ordered body-centered cubic (CsCl) crystal structure with 2 atoms per unit cell, and β' having a base-centered orthorhombic crystal structure with 4 atoms per unit cell. The β'' phase was found to have trigonal or hexagonal point-symmetry with 18 atoms in the unit cell. The lattice parameters for the equiatomic alloy are in a hexagonal basis: $C_H = 5.7984$ Å, $a_H = 8.1083$ Å, and $C_H/a_H = 0.7151$. This phase can be considered to be a slightly distorted form of the β phase which has a c/a ratio of $\sqrt{2}/2 = 0.7071$ when referred to a hexagonal basis. The present study is believed to be the first observation of the lattice correspondence

$$\overset{C}{\beta}-\beta'' = \begin{bmatrix} 1 & 1 & 1 \\ -2 & 1 & 1 \\ 1 & -2 & 1 \end{bmatrix}$$

for a martensitic transformation of a beta-phase alloy. The mode of the lattice invariant deformation was verified to be $\{110\}_\beta$ twinning. Coupled with the observed lattice correspondence this requires that the direction of the twinning shear be $\langle 00\bar{1}\rangle_\beta$, contrary to previously reported results. The predicted crystallographic features of the $\beta \rightarrow \beta''$ transformation were found to be extremely sensitive to the input data (the lattice parameters of the two phases, once the lattice correspondence and system of lattice invariant deformation are specified). For example, the habit plane sweeps through about 21° if the errors in the lattice parameters are ±0.0005 Å. This strain sensitivity reflects the small principal strains accompanying the transformation, $\epsilon_1 = \epsilon_2 = -0.0015$ and $\epsilon_3 = +0.0098$. Because of the small strains the only crystallographic features of the transformation subject to accurate measurement are the habit plane and the twin ratio. Predictions of the present study are in accord with existing measurements of these parameters. (Diss. Abstr. Int., B)

11449 LOW-TEMPERATURE PHASE TRANSITIONS IN ALPHA URANIUM. Steinitz, M. O.; Burleson, C. E.; Marcus, J. A. (Northwestern Univ., Evanston, Ill.). J. Appl. Phys.; 41: 5057-9(Dec 1970).

From Conference on Thermal Expansion of Solids, Santa Fe, N. Mex. See CONF-700633.

Strain-gage thermal expansion and anisotropy of susceptibility measurements indicate the existence of three phase transitions below 50°K in alpha uranium. Two of the transitions are of first order and one is of second order. (auth)

11450 TEXTURE OF Zn-Cd ALLOY INGOT SOLIDIFIED FROM THE FLOWING LIQUID. Abe, Hideo; Togano, Kazumasa (Tokyo Univ.). J. Jap. Inst. Metals; 34: 993-6(Oct 1970). (In Japanese).

The texture of the columnar crystal zone in a Zn-1.5% Cd alloy ingot solidified from the flowing melt was studied by the x-ray pole figure method. The texture, represented by a plane parallel to the chilled surface and an axis parallel to the flow direction of the melt, can be described as the $(10\bar{1}0)[0001]$ orientation tilted approximately 27° to the upstream of the melt, while the columnar crystals are tilted by 24 to 28° to the same direction. The development of this texture can be interpreted by the selective growth of the columnar crystals with cellular dendritic interface which have the ledges vertical to the flow direction of the melt. (auth)

11451 BEHAVIOR OF α URANIUM UNDER LIGHT STRESSES DURING THE RECRYSTALLIZATION PROCESS OR DURING THE ALLOTROPIC α/β TRANSFORMATION. Collot, J.; Cizeron, G.; Lacombe, P. (Ecole Nationale Superieure des Mines, Paris). Mem. Sci. Rev. Met.; 67: 519-39(Jul-Aug 1970). (In French).

This study was carried out with a vacuum extrusion micromachine serving as a dilatometer under stress. The two main parameters liable to affect the dilatometric curves recorded under stress were studied systematically: rate of temperature rise and value of the load applied. It was possible to analyze the phenomena associated with the recrystallization of electrolytically pure uranium having previously undergone various degrees of compression by unidirectional rolling; in these experi-

ments, the heating rate was set at 20°C/hr and the load applied was uniformly 14.8 N/mm^2. The various curves obtained showed up clear variations of slope corresponding to the transitory development of a super-ductility of very fine grains dispersed inside a recovered matrix. The effect of tensile stresses applied during the allotropic $\alpha \rightleftharpoons \beta$ transformation was considered particularly. The amplitude of the dilatometric anomalies associated with the phase change was measured during successive cycles; an increase in applied stress led to a gradual increase in the expansion anomaly connected with the $\alpha \rightarrow \beta$ change whereas the contraction associated with the reverse transformation $\beta \rightarrow \alpha$, still observable for low applied stress values, canceled out when the latter reached about 7 to 9 N/mm^2 and became an expansion for higher values. Micrographic examinations showed mainly that after an $\alpha \rightarrow \beta \rightarrow \alpha$ cycle the specimens were polycrystalline if the applied load was great enough; on the other hand for low stresses (~1 N/mm^2) large polygonized crystals developed. (auth) France)

11452 INITIAL STAGES OF ORDERING IN THE ALLOY Ni_4Mo. Okamoto, Paul Rokuro. Berkeley, Calif.; Univ. of California (1969). 132p. University Microfilms Order No. 70-17,629.

Thesis.

Transmission electron and field ion microscopy techniques were used to study the nature of short range order (SRO) in as-quenched Ni_4Mo and the changes which occurred during the very initial stages of the transition to the long range ordered state. Field ion images of both as-quenched and alloys aged for very short times below 750°C showed a strong tendency for clustering of well defined groups of atoms about the ⟨420⟩ fcc poles. The effect was most pronounced in aged alloys where ordered regions were directly resolved in dark field electron micrographs. However, the effect was also observed in the alloys in which ordered regions were not directly resolved in transmission electron micrographs. The unique orientation dependence of the distribution of the well defined groups of atoms was evidence that the disordered alloy consisted of tiny regions possessing a layered type of atomic arrangement in which the Mo concentration was varying on the (420) matrix planes. The electron diffraction patterns of the as-quenched alloy exhibited both sharp $1\frac{1}{2}0$ SRO spots and very weak satellites near superlattice positions. However, the latter were detectable only in microphotometer traces and then only in diffraction patterns of certain favorable orientations. These satellites were not observed on 002 diffraction patterns as they were obscured by neighboring $1\frac{1}{2}0$ SRO spots. As ordering proceeded, the satellites eventually sharpened into superlattice reflections at the expense of the $1\frac{1}{2}0$ SRO spots. During the very early stages the satellites were streaked in the 210 directions of the fcc lattice, however, satellites which eventually developed into superlattice reflections corresponding to domains of a particular orientational variant were not initially streaked in the same 210 direction. An explanation for this is given in terms of a composition modulation normal to the 420 planes of the fcc lattice. A diffraction model based on this idea explains not only the $1\frac{1}{2}0$ SRO intensity maxima but also the presence of the weak satellites near superlattice positions. The model is also compatible with the FIM results and suggests that the bright well defined groups of atoms correspond to planes possessing a high Mo concentration. A physical basis for the diffraction model is given in terms of a recent spinodal approach to order-disorder transformations. The physical connection between the present results and the theoretical prediction of the Clapp–Moss theory of SRO is also discussed. (Diss. Abstr. Int. B)

11453 STRAIN-INDUCED PHASE TRANSFORMATIONS IN Ti-6Al-4V. Roberts, E. C.; Kellerer, H.; Walsh, F. D. (Boeing Co., Seattle). Metallography; 3: 291-305(Sep 1970).

Metallographic studies of sections of tensile specimens tested in the temperature range of 1000 to 1400°F showed that the transition from the metastable to the stable condition in quenched Ti–6Al–4V was strain- and temperature-sensitive. The time of preheating prior to testing at 1200°F was influential in determining the strain required to effect the changes that occurred. (auth)

Radiation Effects

Refer also to abstracts 11957, 11960, 12823, and 12862.

11454 (AECL–3734) THE EFFECT OF IRRADIATION ON THE TENSILE AND IMPACT PROPERTIES OF $3\frac{1}{2}$ PERCENT AND 9 PERCENT NICKEL STEEL WELDMENTS. Watson, M. B.; Wotton, B. L. (Atomic Energy of Canada Ltd., Chalk River (Ontario). Chalk River Nuclear Labs.). Oct 1970. 33p. Dep. NTIS (U. S. Sales Only). AECL $1.00.

A study was made on the effects of fast neutron irradiation at temperatures below 140°C on the tensile and impact properties of $3\frac{1}{2}$% nickel steel (A-203) and 9% nickel steel (A-353) weldments. Data were determined for three neutron fluences, 4.7×10^{19}, 9.3×10^{19}, and 1.2×10^{20} n/cm^2 > 1 MeV. Results indicated that saturation of fast neutron damage may occur in the $3\frac{1}{2}$% nickel steel by a neutron fluence of 9.3×10^{19} n/cm^2 > 1 MeV. At this level the change in the 0.2% yield strength was about 120%, and the increase in transition temperature about 280°C. Only the tensile properties of the 9% nickel steel may be near saturation at this fluence. The change in the 0.2% yield strength was about 60% and the increase in transition temperature about 170°C. The latter value could be increased by a prolonged post-weld heat treatment. Significant variations in impact properties were observed for different forms of steel (weld metal, heat affected zone, and base metal) of the same nominal compositions. (auth)

11455 (AERE-R–4982) EFFECTS OF STRAIN RATE, NEUTRON DOSE, AND IRRADIATION TEMPERATURE ON THE TENSILE PROPERTIES OF NIMONIC PE16. Broomfield, G. H. (Atomic Energy Research Establishment, Harwell (England)). Jul 1965. 20p. Dep. NTIS (U. S. Sales Only).

Work on a low boron double vacuum melted cast is described that covers tensile tests at varying strain rate in the range 1×10^{-7} sec^{-1} to 2×10^{-4} sec^{-1} before and after irradiation to a dose of 1.5×10^{20} thermal n/cm^{-2} and 5×10^{19} fission n/cm^{-2} at 45°C; the effects of increasing neutron dose in the range 4×10^{17} to 6×10^{20} thermal n/cm^{-2} at 45°C and a comparison of the effects of irradiation at 650°C with those at 45°C for a dose of 6×10^{20} thermal n/cm^{-2} and 2×10^{20} fission n/cm^{-2}, on the alloy with two different heat treatments. (auth) (UK)

11456 (AERE-R–5622) INTERGRANULAR EMBRITTLEMENT OF AN AUSTENITIC STEEL DUE TO IMPREGNATION WITH HELIUM. Probyn, J. E. B.; Roberts, A. C. (Atomic Energy Research Establishment, Harwell (England)). Jan 1968. 9p. Dep. NTIS (U. S. Sales Only).

Strip tensile specimens of 20% Cr, 25% Ni, Nb stabilized austenitic steel were neutron irradiated with one of their faces in contact with boron. Helium, which is responsible for the elevated temperature embrittlement of neutron irradiated steels, is formed by the $^{10}B(n\alpha)^7Li$ reaction and injected as α-particles into the surface layer. The helium impregnated surfaces were compared after straining at 750°C, both directly and using tapered sections, with surfaces which have only been irradiated with an equivalent number of neutrons. The technique using tapered sections from the gage length provides a method of determining the amount of strain, for a given helium concentration, to cause intergranular failure due to helium bubbles at the grain boundaries. As a result of surface contamination of the specimens, which occurred during straining and which could not be removed without also removing some of the underlying metal, no intergranular cracks were found by surface examination. (auth) (UK)

11457 (CISE-R–278) EXPERIMENTAL IRRADIATION OF METALLIC URANIUM FUEL ELEMENTS IN THE HALDEN HBWR REACTOR. Technical Report No. 73. Morandi, G.; Scaroni, A. (Centro Informazioni Studi Esperienze, Milan (Italy)). Aug 1969. Contract 008.65.1-NTRI. 88p. (In Italian). Dep. NTIS (U. S. Sales Only).

The first phase of the irradiation experiments of two metallic uranium fuel elements, made within the framework of the CIRENE program, is described. The experiments were conducted in the HBWR reactor at Halden in Norway. A brief description of the experimental equipment is given and data on the preirradiation characteristics of the fuel elements and the data developed from the experiments are reported. At the end of the first phase, the mean burnup was 1130 and 1568 MWd/ton U (maximum equal burn-up at 1503 and 1991 MWd/ton U). (tr-auth)

11458 (IN–1437) METALLURGY AND MATERIALS SCIENCE BRANCH ANNUAL REPORT, FISCAL YEAR 1970. Francis, W. C. (ed.) (Idaho Nuclear Corp., Idaho Falls). Nov 1970. Contract AT(10-1)-1230. 75p. Dep. NTIS.

Research and development is reported in six sections. A separate abstract was prepared for each section. (J.R.D.)

For abstracts of individual sections see: 11375 and 11459–11463.

11459 (IN–1437, pp 1-4) AXIAL FATIGUE OF IRRADIATED STAINLESS STEELS TESTED AT ELEVATED TEMPERATURES. Beeston, J. M.; Brinkman, C. R. (Idaho Nuclear Corp., Idaho Falls).

From Metallurgy and Materials Science Branch annual report, fiscal year 1970.

Efforts devoted to determining the effects of irradiation on the

XUM

high-temperature fatigue properties of stainless steels for use in LMFBR are summarized. Specimens of Types 304, 304L, and 316 were irradiated and tested. Typical microstructures associated with these steels are illustrated in microphotographs and data on fatigue life are included. (J.R.D.)

11460 (IN-1437, pp 5-12) SURVEILLANCE OF TEST REACTOR BERYLLIUM AND HAFNIUM. Korth, G. E.; Beeston, J. M. (Idaho Nuclear Corp., Idaho Falls).

From Metallurgy and Materials Science Branch annual report, fiscal year 1970.

Results of examination of beryllium specimens being irradiated showed clean and bright surfaces, continued linear growth rate, and adequate temperature thresholds (>700°C) for fluences up to 1.3×10^{22} n/cm^2 (E > 1 MeV). Swelling behavior appears to be strongly dependent on grain size, the large grains exhibiting a more detrimental effect. Results of examination of a fixed hafnium shim rod showed no significant length change after irradiation to 3.6×10^{21} n/cm^2 (E > 1 MeV) while tensile tests on other hafnium specimens with fluences of 1.4×10^{21} n/cm^2 (E > 1 MeV) gave ultimate strength increases of 30%, yield strength increases of 240% while maintaining total elongation constant at 35%. (auth)

11461 (IN-1437, pp 13-23) PROTOTYPE ELEMENTS. (Idaho Nuclear Corp., Idaho Falls).

From Metallurgy and Materials Science Branch annual report, fiscal year 1970.

Results of tests on B_4C-impregnated Al foils as controllable neutron absorbers for fuel elements, are presented. Investigations of core breakup during fabrication of ETR fuel plates are summarized along with work devoted to development of 2219 Al alloy as fuel cladding. (J.R.D.)

11462 (IN-1437, pp 59-70) IRRADIATION TESTING. (Idaho Nuclear Corp., Idaho Falls).

From Metallurgy and Materials Science Branch annual report, fiscal year 1970.

Results of radiation testing are reported on fuel plates, uranium-silicon-aluminum powders, boron compounds in foils, uranium-aluminum alloys, and hydrated aluminum oxide, as fuel plate cladding. (J.R.D.)

11463 (IN-1437, pp 70-5) FAILURE ANALYSIS. (Idaho Nuclear Corp., Idaho Falls).

From Metallurgy and Materials Science Branch annual report, fiscal year 1970.

Results of failed ETR fuel element investigations are discussed along with properties of four operational fuel elements irradiated during ATR startup, and effects of steam at 980 to 1340°C on Zircaloy. (J.R.D.)

11464 (KFK-1281) IN-PILE ARRANGEMENT FOR STRAIN MEASUREMENTS IN NUCLEAR FUEL AND STRUCTURAL MATERIALS. Will, H. (Kernforschungszentrum, Karlsruhe (West Germany). Institut fuer Reaktorentwicklung). Oct 1970. 33p. (In German). Dep. NTIS (U. S. Sales Only).

The design criteria of a creep capsule are presented. The possible methods of measurement for in-pile expansion measurements are discussed in detail with respect to suitability and applicability in an irradiation rig. A description of finished models of irradiation rigs is included. (auth)

11465 (ORNL-TM-3109) VOIDS IN NEUTRON IRRADIATED ALUMINUM. Packan, Nicolas Hayes (Oak Ridge National Lab., Tenn.). Jan 1971. Contract W-7405-eng-26. 155p. Dep. NTIS.

Thesis. Submitted to Univ. of Missouri, Rolla.

Void formation in high-purity aluminum resulting from irradiation to fluences between 1.5×10^{19} and 1.6×10^{22} neutrons/cm^2 (E > 0.1 MeV) at a temperature of 55 ± 5°C was studied, primarily by means of transmission electron microscopy. In particular the effects of neutron fluence and flux were examined, as well as the possible influences of both preexisting and transmutation-produced impurities. A very low concentration of voids (about 10^{12}/cm^3) resulted from irradiation to 1.5×10^{19} neutrons/cm^2; they averaged about 150 Å in diameter. Void concentrations and sizes increased with fluence, reaching values of 6×10^{14} voids/cm^3 averaging 500 Å in diameter at 1.6×10^{22} neutrons/cm^2. Void formation initially was nonuniform in distribution, but tended to be homogeneous at higher fluences. The void shapes were always consistent with those of octahedra bounded by {111} planes, sometimes with the vertices truncated by {100} planes. Void size distribution curves were obtained for all fluences, and from these the mean void size was found to increase in proportion to the fluence raised to the one-sixth power. The void concentration displayed a fluence dependence best described by a power law, $N \sim (\phi t)^a$, in which the exponent decreased from 2 at 1.5×10^{19} neutrons/cm^2 (E > 0.1 MeV) down to only 0.1 at 1.6×10^{22} neutrons/cm^2. Treating the swelling with a similar power law, $\Delta V/V \sim (\phi t)^b$, a similar saturation effect was observed, with the fluence exponent b decreasing roughly from 2.5 to 0.5 over the range of fluence studied. At 1.6×10^{22} neutrons/cm^2 the total void volume or swelling amounted to 7.4%. Microhardness increases in the irradiated specimens can be explained on the basis of void contributions to the impeding of dislocation motions. Irradiation at a factor-of-ten lower flux produced effects upon the void morphology (e.g., half as many but larger and more elongated voids) much like those resulting from irradiation at a higher temperature. In each case, the lowering of the vacancy supersaturation during irradiation is a consequence. Irradiation, annealing to remove damage, and reirradiation of a specimen, each exposure to a fluence of 5×10^{20} neutrons/cm^2 (E > 0.1 MeV), yielded twice as many voids of smaller maximum size, having the same total void volume as those produced by the first irradiation alone. The effect is attributed to submicroscopic remnants of the original voids surviving the anneal and serving as preexisting nuclei in the second irradiation. In postirradiation void annealing experiments performed inside a high vacuum electron microscope, the rate at which void radius changed, dr/dt, varied considerably from void to void. A transient effect in dr/dt was observed upon abrupt changes in the annealing temperature. Both effects are ascribed to the actions of local vacancy sinks near the voids, such as a suggested population of submicroscopic gas bubbles. The experimental observations are compared with the current models for void formation. The two models most consistent with the experimental evidence both involve transmutation-produced helium playing a crucial role in void nucleation—one involving helium-stabilized spikes and the other small helium bubbles as the nuclei of voids. Effects were found which demonstrate a strong influence of impurities upon void formation in high-purity aluminum. (auth)

11466 (SRARI-P-78) EFFECT OF IRRADIATION ON THE MECHANICAL PROPERTIES OF fcc ALLOYS OF THE Fe-Cr-Ni SYSTEM. PART I. Balashov, V. D.; Votinov, S. N.; Prokhorov, V. I. (Scientific Research Atomic Reactor Inst., Melekess (USSR)). 1970. 40p. (In Russian). Dep. NTIS (U. S. Sales Only).

The results of mechanical tests of Fe-Cr-Ni system alloys (X2OH15, X2OH40, X2OH60, X2OH80, and nickel) unirradiated and irradiated in water at 70°C with the dose of 7×10^{21} n/cm^2 are presented. It is shown that the effect of high temperature irradiation embrittlement was typical for all the investigated materials and decreased from low nickel alloys to unalloyed nickel. The deformation mechanisms of the irradiated and unirradiated alloys were related. (auth)

11467 INFLUENCE OF THERMAL NEUTRON IRRADIATION ON THE EQUILIBRIUM TEMPERATURE OF THE $\alpha \rightarrow \beta$ TRANSFORMATION IN PLUTONIUM. Robinson, A. C.; Stacey, R.; Taylor, J. C. (Atomic Weapons Research Establishment, Aldermaston, Eng.). Nucl. Met., Met. Soc. AIME; 17: 606-15(1970).

From 4th International Conference on Plutonium and Other Actinides, Santa Fe, N. Mex. See CONF-701001-(Pt.2).

Some effects of thermal neutron irradiation on the $\alpha \rightarrow \beta$ transformation in unalloyed plutonium containing 450 ppM of impurity are reported and compared with transformation data obtained using conventional oil bath heating. The transformations were monitored by electrical resistance measurements on 0.004-in. thick foil samples at temperatures from 40 to 145°C. The irradiation was provided by a thermal neutron flux of 10^{10} n per cm^2 per second. Transformations were studied during irradiation and also in samples 14 days after an integrated irradiation of 18×10^{12} n per cm^2 at 40°C. At temperatures below the $\alpha \rightleftharpoons \beta$ equilibrium temperature of 112°C no indication of the $\alpha \rightarrow \beta$ transition was observed suggesting that the high temperatures in the thermal spikes produced by the fission fragments were not sufficiently long-lived to form metastable regions of the β-phase even though more than sufficient fission energy was deposited to complete the transformation. Above the $\alpha \rightleftharpoons \beta$ equilibrium temperature, plutonium transformations during irradiation were characterized by shorter incubation periods and faster transformation rates than observed in unirradiated material using conventional oil bath heating techniques. Similar though less marked effects were exhibited by foils transformed using oil bath heating 14 days after irradiation. As an explanation of these effects it is suggested that regions of disturbed atoms formed by energetic fission fragments serve as nuclei for formation of the β phase above the $\alpha \rightleftharpoons \beta$ equilibrium temperature. Some permanent increases were observed in the electrical resistivity of samples irradiated in the α phase but these effects were not studied in detail. (auth)

11468 LENGTH CHANGES IN THE ACTINIDE METALS DUE TO SELF-IRRADIATION DAMAGE AT 4°K. Marples, J. A. C.;

Hough, A.; Mortimer, M. J.; Smith, A.; Lee, J. A. (Atomic Energy Research Establishment, Harwell, Eng.). Nucl. Met., Met. Soc. AIME; 17: 623-34(1970).

From 4th International Conference on Plutonium and Other Actinides, Santa Fe, N. Mex. See CONF-701001-(Pt.2).

Measurements were made of the length changes due to self-irradiation damage in α- and δ-plutonium (stabilized by aluminum) and in α-uranium and α-thorium containing ^{238}Pu in solution. The results for δ-plutonium are remarkable in that they show a contraction due to self-damage. (auth)

11469 CHARACTERIZATION AND ANNEALING BEHAVIOR OF VOIDS IN NEUTRON-IRRADIATED NICKEL. Kulcinski, G. L.; Mastel, B.; Kissinger, H. E. (Battelle-Northwest, Richland, Wash.). Contract AT(45-1)-1830. Acta Met.; 19: 27-36(Jan 1971).

Transmission electron microscopy (TEM) and small angle scattering (SAS) techniques were used to determine the size and density of voids in high purity nickel that was irradiated to 3×10^{21} n/cm^2 (>0.1 MeV) at 450°C and subsequently annealed for 2 hr at 650 to 1150°C. The as-irradiated material contained 1.8×10^{14} truncated octahedral voids cm^3 whose average size was 400 Å. TEM revealed that the dissolution of the voids during high temperature anneals was rather inhomogeneous with those voids nearest the grain boundaries disappearing first. This resulted in a grain boundary denuded zone whose width depended on temperature, varying from 1 μ at 650°C to 15 μ at 975°C and complete denuding at 1050°C. Both TEM and SAS revealed that the voids in the center of the grains did not coarsen during annealing, and the average size remained at ~400 Å up to the temperature of complete annealing (1050°C). Such behavior was predicted for voids that are partially gas-filled, and annealing studies at 1050 and 1150°C did indeed reveal gas bubbles at the recrystallized grain boundaries. Microhardness measurements were also made on the samples after various anneals, and a good correlation was found between the hardness increase, ΔH, and the quantity $(Nd)^{\frac{1}{2}}$, where N is the number of voids/cm^3 and d is their diameter. More specifically, $\Delta H = 6\ \mu b\ (Nd)^{\frac{1}{2}}$, where μ is the shear modulus and b is the burgers vector. (auth)

11470 EVALUATION BY LINEAR ELASTIC FRACTURE MECHANICS OF RADIATION DAMAGE TO PRESSURE VESSEL STEELS. Mager, T. R.; Hazelton, W. S. (Westinghouse Electric Corp., Pittsburgh). Contract AT(30-1)-3677. Atompraxis; 16: 257-63(Jul-Aug 1970).

The hardening and embrittlement of mild steels are important in connection with the safety of reactor pressure vessels. A much more sophisticated and quantitative approach to the brittle fracture problem, developed by Westinghouse research personnel, is described. (auth)

11471 TRANSMUTATION-PRODUCED SILICON PRECIPITATES IN IRRADIATED ALUMINUM. Farrell, K.; Stiegler, J. O.; Gehlbach, R. E. (Oak Ridge National Lab., Tenn.). Metallography; 3: 275-84(Sep 1970).

Commercially pure aluminum and an aluminum-1% nickel alloy exposed to high-fluence neutron irradiation contained a finely divided precipitate phase. This precipitate coarsened markedly during postirradiation annealing. Chemical analyses, electron diffraction, and electron probe microanalyses were used to identify the precipitate as silicon, produced by the transmutation reaction with thermal neutrons $^{27}Al(n,\gamma)^{28}Al\ ^{28}Al \rightarrow {}^{28}Si + \beta$. (auth)

Ceramics and Cermets

11472 (AD-708705) CENTER OF EXCELLENCE IN CERAMIC AND COMPOSITE MATERIALS. Progress Report No. 8 and Summary Report, September 1, 1968-August 31, 1969. Report on Project THEMIS. McGee, Thomas D. (Iowa State Univ. of Science and Technology, Ames. Engineering Research Inst.). 31 Aug 1969. Contract F33615-68-C-1034. 129p. (ERI-551). NTIS.

Reports are presented on initial creep and recovery experiments on rutile and MgO, chromium diffused into the surface of Al_2O_3, water adsorption on Fiberglas E, and neutron activation analysis of NaCl, MgO, CaF_2, and Al_2O_3. An arc transfer method has successfully produced single crystals of NiO and CoO. The electronic conductivity of Gd-doped $BaTiO_3$ has been successfully compensated with additions of Cu. Coulombic titrations have been successfully made using an electrical potential to control the oxygen pressure in a solid electrolyte. A solid galvanic cell oxygen pressure gage has been designed and tested. A review of the conductivity domains of various solid electrolytes is presented along with a general theoretical treatment of the conditions necessary to produce a pure Rayleigh wave. High strength surface waves have been produced in an $LiNbO_3$ crystal. (USGRDR)

11473 (AD-708712) PROPERTIES OF CERAMIC MATERIALS. Progress Report No. 11, March 1-May 31, 1970. Report on Project THEMIS. McGee, Thomas D. (Iowa State Univ. of Science and Technology, Ames. Engineering Research Inst.). May 1970. Contract F33615-68-C-1034. 67p. (ERI-76500). NTIS.

Research is summarized on: reversible emf measurements made over a range of temperatures for solid-state displacement reactions (going from left to right) $M + M'F \pm MF + M'$ where $M \pm$ Ni, Mn, Co, Fe, and Y measurements of weight loss at 10 to -40 atmospheres O_2 at 1300°C which show agreement with the estimates of others by wet chemical techniques. It was found that when MgO is used to control the sintering of dense high purity aluminum oxide it produces poor thermal shock resistance. The initial phase of analysis of the sorption of H_2O on Fiberglas E was completed, and a new plot of energy vs thickness is proposed to fit water sorption on Fiberglas E. For water on Fiberglas E, the computed isosteric entropies of adsorption indicate the adsorbed phase is intermediate between the solid and liquid state and reaches the liquid state at higher coverage. Recovery of creep of stoichiometric rutile at zero stress was found and is primarily due to migration and coalescence of dislocation walls during the recovery period. An exact analysis of surface waves in piezoelectric crystals has been completed and compared with a quasi-static analysis. (auth) (USGRDR)

11474 (BNWL-842) REACTOR FUELS AND MATERIALS DEVELOPMENT PROGRAMS FOR FUELS AND MATERIALS BRANCH OF USAEC DIVISION OF REACTOR DEVELOPMENT AND TECHNOLOGY. Quarterly Progress Report, April-June 1968. Cadwell, J. J.; de Halas, D. R.; Nightingale, R. E.; Worlton, D. C. (Battelle-Northwest, Richland, Wash. Pacific Northwest Lab.). Aug 1968. Contract AT(45-1)-1830. 150p. Dep. NTIS.

Research and development progress is reported on nuclear graphite, fuels for gas-cooled reactors, nuclear ceramics, nitride fuels for fast reactors, nondestructive testing, metallic fuels, radioinduced fuel swelling, ATR gas loop operation, dosimetry and materials damage in fast reactors, radiation effects on metals and alloys, and fast reactor program support. (J.R.D.)

Corrosion and Erosion

11475 (AERE-R-5173) COMPATIBILITY STUDIES BETWEEN ARC CAST $(U_{0.85}Pu_{0.15})$-C AND TYPE 316L STAINLESS STEEL. Hodkin, D. J.; Evans, J. P.; Mardon, P. G. (Atomic Energy Research Establishment, Harwell (England)). Oct 1966. 26p. Dep. NTIS (U. S. Sales Only).

Arc cast $(U_{0.85}Pu_{0.15})C$ with carbon contents of 4.72 to 5.06 wt % is compatible with Type 316L stainless steel at temperatures up to 900°C. However some carburization of the steel was observed and this is believed to be due to a gas phase originating from hydrolysis of the carbide by its own absorbed moisture. When a sodium bond is introduced gross carburization of the steel is observed for hyperstoichiometric carbides, the rate of carburization depending primarily on the MC_2 content of the carbide. For cermets of mixed carbide dispersed in a steel matrix some reaction was observed at temperature as low as 700°C. (auth) (UK)

11476 REDISTRIBUTION OF BORON IN THE DIFFUSED LAYER DURING THERMAL OXIDATION. Huang, J. S. T.; Welliver, L. C. (Solid State Electronics Center, Plymouth, Minn.). J. Electrochem. Soc.; 117: 1577-80(Dec 1970).

The impurity redistribution process in a two step p-type diffusion was investigated. A theoretical model is formulated from which a closed form expression for the impurity profile is obtained. The experimental results verify the theoretical prediction of the profile. From these results, the segregation coefficient of boron at the oxide-silicon interface is determined, and the total number of impurity atoms that have escaped into the oxide can also be estimated. (auth)

Preparation and Fabrication

Refer also to abstracts 10571, 11962, and 12795.

11477 (ALO-(2510)-T-2) SILICON GERMANIUM THERMOELECTRIC MATERIALS AND MODULE DEVELOPMENT PROGRAM. (Radio Corp. of America, Harrison, N. J.). 1 Jun 1970. Contract AT(29-2)-2510. 60p. Dep. NTIS.

A SiGe air-vac thermoelectric converter was designed, fabricated and performance mapped at design and off-design temperature conditions. The converter employed 63.5 at. % zone-leveled Si-SiGe air-vac thermocouples, multi-layer foil heat shunt in-

sulation, and a simulated heat source and heat source support system. The converter was performance mapped for electrical and thermal characteristics over a range of hot-shoe temperatures from 500 to 1100°C and then placed on stability life test at a hot-shoe temperature of 1100°C. During the stability test at 1100°C, significant leakage-to-ground developed causing the converter performance to substantially degrade in only 300 hours of life testing. The converter was analyzed for the causes of this leakage which was traced to increasing electrical conductivity of the thermocouple wrap insulation, corrective procedures were developed and the converter was reassembled and put back on test. The performance mapping at various hot shoe temperatures showed results similar to the first performance run. The converter has subsequently completed over 2100 hours of stability life testing at 1100°C hot shoe temperature with no evidence of performance degradation attributable to leakage or shorts. After rebuilding, the converter performance at the design objective operating conditions of 1000 and 250°C hot- and cold-junction temperatures was 33.6 watts power output, 5.82% converter efficiency and a converter specific power of 2.65 watts/pound. The converter will be subjected to shock and vibration loadings to simulate actual launch conditions and then placed on long term stability life test. (auth)

11478 (BNWL-843) FORMATION OF UO_2–CARBON MIXTURES AND CARBIDE OR NITRIDE FUEL MATERIAL IN A SPRAY REACTOR. Coppinger, E. A. (Battelle-Northwest, Richland, Wash. Pacific Northwest Lab.). Dec 1968. Contract AT(45-1)-1830. 35p. Dep. NTIS.

The production of an intimate mixture of UO_2 and carbon directly from a nitrate solution containing sugar was investigated in 15 exploratory runs in a spray calciner. This mixture of UO_2 and carbon is a key intermediate in the one-step production of carbides or nitrides in a modified spray reactor. The mixture is also a necessary intermediate in other equipment arrangements for production of nitrides and carbides by the carbothermic reaction. Results indicate that an intimate UO_2-carbon mixture can be produced. The carbon content can be readily varied over a wide range bracketing the amount required for subsequent carbide or nitride production. Two small samples of the UO_2-carbon mixture with slightly different carbon content were tested for conversion to uranium nitride in a high-temperature furnace. The samples were held at 1600°C in flowing nitrogen until CO evolution ceased. The product was primarily uranium nitride. Analytical results from one sample indicate a final composition of 5.34 wt % nitrogen, 7800 ppM oxygen, and 350 ppM carbon. The carbon and oxygen contents were reasonably low for this initial attempt to convert powder from the spray calciner to nitride. Further improvement can be expected by adjustment of the initial carbon content. A thermodynamic investigation was made to determine the feasibility of producing nitrides directly from nitrates in a spray calciner. A standard calciner design consisting of a heated tower with an atomizing nozzle at the top and a filter section at the bottom was assumed. While calculation results indicate the process to be thermodynamically possible, minimum temperatures of 1800 to 2000°C are required even when methane is substituted for much of the sugar in order to reduce the partial pressure of CO in the equilibrium gas mixture. Indications are that the partial pressure of CO has a significant effect on the minimum temperature required for relatively complete conversion. As a result of the thermodynamic investigation, a novel modification of a spray calciner has been conceived for operation at more reasonable temperatures. The favorable results of the experimental program have demonstrated the feasibility of the upper portion of the modified spray reactor. Further development work is required to determine the feasibility of the lower high-temperature section and a one-step process. Such work will require study of reaction kinetics and nitride or carbide production in the high-temperature section. A criticality and design study is also needed to determine the feasibility of producing uranium–plutonium nitrides or carbides in a spray reactor in a glove box. (auth)

11479 (JUL-669-RW) MODEL INVESTIGATIONS ON CONICAL FLUIDIZED BEDS. A REPORT ON COATING OF FUEL PARTICLES. Wallroth, Carl-Friedrich (Kernforschungsanlage, Juelich (West Germany). Institut fuer Reaktorwerkstoffe). Jul 1970. 173p. (In German). Dep. NTIS (U. S. Sales Only).

The motion processes in high-temperature coating beds at room temperature were studied by simulation. Efforts directed toward optimization of the fluidizing conditions for improvement of the separation conditions with respect to the polyhedritate of the coated particles are discussed. The theoretical bases for the determination of the conditions in the coating bed and for the production of physical similarity in the model bed are reported. The similarity characteristics for description of the state in the coating and model beds are derived, numerical methods for the determination of the material value—especially at high temperatures—are described, and formulas for the calculation of the gas and particle velocities in the fluidized beds are given. Variation calculations showed that with petunia hybrida (Petunin) and a nitrogen-hydrogen mixture in the model, the same constants can be introduced as in the fluidized bed. In the model study the same motion forms (spouting, bubbling, slugging) as in the fluidized bed were observed. For knowledge of the processes, which occur in the coating in conical fluidized beds, the effect of the gas current and gas distribution, the particle load, and the bed and nozzle geometry on the particle motion in the model experiment, was studied. It was found that three motion forms can be introduced by the gas distribution between the central and ring nozzles. With increasing gas velocity the effect of the particle load on the motion form was decreased. Research on modified nozzle geometry showed that the nozzle output velocities determine the motion form. With large central nozzle surface the spouting motion disappears. Study on various cone slit angles gave for $\alpha = 30$ (grd) the best proportions (stable bubble motion, good circulation of the particles). Studies on various bed dimensions showed that in the 1-inch bed relatively good fluidized beds are produced, in the larger bed geometries however, very inhomogeneous proportions and, therefore, unfavorable coating conditions appeared as a result of the poor particle concentration in the central coating zone. A cyclone bed was developed for improvement of the fluidizing conditions. By the production of drift currents by auxiliary nozzles and a spiral ring gas input, the sliding coats can be fluidized and the conditions homogenized. In coating studies with various motion forms, bubbling was found to be the best and slugging gave the poorest results with respect to the polyhedritate of the coated particles. Coatings in cyclone beds also gave low polyhedritate values for large coat thicknesses. (tr-auth)

11480 (ORNL-4608) SYNTHESIS, CHARACTERIZATION, AND FABRICATION OF UN. Tennery, V. J.; Godfrey, T. G.; Potter, R. A. (Oak Ridge National Lab., Tenn.). Dec 1970. Contract C-51092-B. 67p. (NASA-CR-72764). Dep. NTIS.

Procedures were developed for synthesizing fine uranium nitride powders that contain less than 200 ppM O from uranium metal by the hydride-dehydride-nitride process. A method based on the principle of gas sedimentation was established as suitable for measuring the distribution of particle sizes. It was found that 80% of the particles were between 1 and 7 μm in diameter. Scanning electron microscopy showed that the particles were very irregularly shaped and that each particle had several protrusions from the surface, which explains the difficulty in fabricating these powders. Uranium mononitride (UN) cylinders were fabricated by both uniaxial and isostatic pressing. Uniaxial pressing required additives such as camphor to act as a binder and die lubricant, but the addition of camphor resulted in about 1000 ppM O in the sintered product. Isostatic pressing required no additives and typically resulted in a sintered product with less than 300 ppM O. It was found that the precision and accuracy possible in the analyses for uranium and nitrogen were the limiting factors for adequate quantitative chemical analysis of UN. The microstructure of UN bodies of about 85% theoretical density was very stable when subjected to 1400°C for 100 hr in vacuum; very small shrinkages of about ½ to 1% were accompanied by very small increases in grain size. Conventional grinding of UN produced minute cracks in the machined surface, but electrodischarge machining produced very smooth surfaces with a thin coating of an unidentified phase. (auth)

11481 IMPROVEMENTS IN OR RELATING TO PROCESSES FOR THE PREPARATION OF CERAMICS OF MATERIALS, IN PARTICULAR OF FISSIONABLE MATERIALS. (to Commissariat a l'Energie Atomique). British Patent 1,215,343. 9 Dec 1970. Priority date 9 Mar 1967, France.

A process for preparing of sintered products such as UO_2 is described. The starting material is powder which is compressed to produce a conglomerate of compacted particles. The conglomerate is crushed and recompressed at a lower pressure to obtain a compact of desired porosity. The compact is then sintered. (J.R.D.)

11482 CHANGES IN RESIDUAL CARBON CONTENT IN UO_2 PELLETS DURING DECARBONIZATION AND INITIAL PHASES OF SINTERING. Landspersky, Hanus; Bezucha, Jaromir (Inst. of Nuclear Research, Rez, Czech.). Jad. Energ.; 16: 408-13(1970).

Decarbonization of UO_2 pellets compacted with 2% of binders at temperatures between 500 and 800°C was studied at different heating rates, followed by sintering at temperatures up to 1600°C in hydrogen. During the decarbonization, the content of carbon decreased, but at 800°C the residual carbon content still exceeded several times the limit of 100 ppM. At temperatures above 1000°C, the decarbonization continued and at 1200 to 1400°C the residual carbon content reached ~50 ppM. (auth)

11483 HIGH-TEMPERATURE SOLUTION GROWTH OF SINGLE-CRYSTAL NEPTUNIUM DIOXIDE. Finch, C. B.; Clark, G. W. (Oak Ridge National Lab., Tenn.). J. Cryst. Growth; 6: 245-8(Mar-Apr 1970).

Single crystals of $^{237}NpO_2$ up to 2 × 2 × 3 mm in size with well-developed faces were grown from $PbF_2-B_2O_3-NpO_2$ and $Li_2O-MoO_3-NpO_2$ solutions at 1250 to 1350°C. Magnetic susceptibility, x-ray diffraction, and chemical analysis data indicated that crystals from either system were very near stoichiometric ($NpO_{2.00\pm0.04}$). Crystals grown from the first solution contained as solvent impurities 200 ppM B, 1000 ppM Pb, and an undetermined amount of F; those from the second solution contained only 10 ppM Mo and 2 ppM Li. The growth parameters for NpO_2 approximately paralleled those previously reported for the isostructural CeO_2 and ThO_2 from the same solvents. (auth)

11484 USE OF HOLLOW CATHODE DC PLASMA DISCHARGE FLOAT ZONING FOR THE GROWTH OF MATERIALS WITH HIGH MELTING POINTS: THE GROWTH OF SINGLE CRYSTALS OF Ta_2C. Storey, R. N.; Laudise, R. A. (Bell Telephone Labs., Inc., Murray Hill, N. J.). J. Cryst. Growth; 6: 261-5(Mar-Apr 1970).

A hollow cathode heat source was used to zone melt TiC, HfC, TaC, MoC, WC, and MoB_2 rods. The technique was shown to be easily capable of melting materials with melting points in the vicinity of 3800°C, and preliminary results on TiC, HfC, and TaC gave indications that crystals could be grown from melts of their own composition. TaC growth was studied more extensively, and it was shown that after about six passes the composition of the melt had shifted to a range where Ta_2C was the stable phase due to incongruent volatilization. However, after about nine passes in rods of this composition, single crystals of Ta_2C whose dimensions were about 3 mm × 1 mm × 1 cm were produced. (auth)

Properties Evaluations

Refer also to abstracts 10578, 11372, 11410, 11411, 11433, 11991, 11993, 11994, 11996, 12010, 12014, 12015, 12031, 12033, and 12316.

11485 (CEA-CONF-1670) MECHANICAL PROPERTIES OF PLUTONIUM-BASED CERAMICS AT HIGH TEMPERATURE. APPLICATION TO FUEL ELEMENTS. de Novion, Charles; Lallement, Robert (Commissariat a l'Energie Atomique, Fontenay-aux-Roses (France). Centre d'Etudes Nucleaires). 1970. 17p. (In French). (CONF-701028-1). Dep. NTIS (U. S. Sales Only).

From Meeting of the French Society of High Temperatures, Clermont-Ferrand, France.

Results of creep rate measurements carried out under compression and at high temperature on mixed uranium and plutonium oxides and carbides are presented. The creep rate depends to a large extent on the composition and porosity of the compounds studied. It is shown how neutron irradiation modifies the results of experiments outside the pile. From these results it should be possible to estimate the swelling caused by fission products and to foresee the deformation of fuel element cladding as a function of burnup. (auth) (France)

11486 (CEA-R-4095) APPLICATION OF THE $^{18}O(p,\alpha)^{15}N$ REACTION TO THE STUDY OF THE SELF-DIFFUSION OF OXYGEN IN URANIUM DIOXIDE. Ligeon, Emile; Fontenille, Jean; Bontemps, Andre; Contamin, Pierre (Commissariat a l'Energie Atomique, Grenoble (France). Centre d'Etudes Nucleaires). Nov. 1970. 26p. (In French). Dep. NTIS (U. S. Sales Only).

The $^{18}O(p,\alpha)^{15}N$ reaction was applied to the study of the O self-diffusion in UO_2 samples. A comparison between calculated and experimental spectra of α particles allowed low diffusion coefficients to be determined ($D \leq 10^{-13}$ cm²/sec). The following values of D were obtained: $D = 10^{-15}$ cm²/sec for $UO_{2.000}$ at 650°C ± 15; $D = 9.3\ 10^{-12}$ cm²/sec for $UO_{2.000}$ at 400°C ± 1; $D = 9.6\ 10^{-10}$ cm²/sec for $UO_{2.12}$ at 600°C ± 1. These results are in good agreement with those obtained with the ion mass analyzer developed by Slodzian. (auth) (France)

11487 (GA-9168) LASER-PULSE METHOD OF DETERMINING THERMAL DIFFUSIVITY AND THERMAL CONDUCTIVITY OF GRAPHITE BETWEEN 300° AND 3300°K. Koyama, Karl; Tuckfield, R. G. (Gulf General Atomic, Inc., San Diego, Calif.). 1 Feb 1969. 9p. (CONF-690447-1). Dep. NTIS.

From 6th Conference of the Temperature Measurements Society, Hawthorne, Calif.

The laser-pulse method was used to determine thermal diffusivity and thermal conductivity of graphite over a continuous temperature range of 300 to 3300°K. A thin-disk specimen was pulsed with a neodymium laser, and the transient temperature rise is detected with a photovoltaic indium antimonide device. The InSb detector, normally used in the low temperature region, was extended to also include measurements at high temperatures. The method was tested with OFHC copper and Armco iron of various thicknesses at low temperatures; the results of the measured thermal diffusivities agreed within an experimental error of approximately 5% with reported values. At high temperatures, the technique was tested with H-327 graphite. The thermal conductivity of the graphite computed from the measured thermal diffusivity was in good agreement with results from other methods. (auth)

11488 (KFK-1211) OBSERVATION WINDOWS OF SYNTHETIC SAPPHIRE (LEUCOSAPPHIRE) IN HIGH-PRESSURE VESSELS. Schmidt, H. (Kernforschungszentrum, Karlsruhe (West Germany). Institut fuer Reaktorbauelemente). Sep 1970. 86p. (In German). Dep. NTIS (U. S. Sales Only).

High-speed photographs are required for a study of the phenomena of direct material and heat exchange during the dispersion of a gas in a liquid so that the geometric events can be followed. Investigations of this type are performed in the water-steam system at operating pressures up to some 200 atm. The sight glasses in this case are panes of synthetic sapphire (leucosapphire). Experiments have shown that some panes do not stand up to the stress despite good resistance to pressure, temperature, and the attacking medium, the rupture behavior observed varying over a rather wide range of pressures. The characteristics of colorless corundum are described. For a given geometric setup the rupture behavior of the sapphire is discussed. A new disk geometry is suggested and its testing is reported. The forces occurring during bursting are calculated for a given design. The choice of a suitable safety device and its experimental testing are reported. (auth)

11489 (WHAN-FR-20) EVALUATION OF PuO_2 HOMOGENEITY IN PuO_2-UO_2 FAST REACTOR FUEL BY SCANNING ELECTRON MICROPROBE. Stranik, D. A.; Powers, H. G.; Last, G. A. (WADCO Corp., Richland, Wash.). Oct 1970. Contract AT(45-1)-2170. 43p. Dep. NTIS.

Quantitative characterization of a $(Pu_{0.25}U_{0.75})O_2$ fuel pellet matrix was accomplished by scanning pellets with an electron microprobe for PuO_2 concentration sizes of PuO_2 enriched or depleted zones and separation distance of such zones. Statistical analyses of the data indicated less than 1 percent probability of occurrence of zones with peak PuO_2 concentration greater than 50 wt % and less than 1 percent probability of occurrence of PuO_2 enriched or depleted zones having diameters greater than 50 microns. This technique enabled a mathematical model to be developed relating fuel pellet characteristics to a figure of merit which describes the homogeneity of mixed oxide fuel in terms of the degree of uniformity of energy deposition (or temperature rise) under reactor transient conditions in the UO_2 content of the fuel. A test was designed to verify the model and to determine the homogeneity of pellets with a wide range of homogeneities based upon previous alpha-autoradiographs. The powder preparation varied for the four pellets. Results of the test indicated that the approach was feasible. In order for industry to use this model to establish homogeneity in the fuel for the FFTF, it was determined that the correlation between figure of merit and alpha-autoradiography would be developed. This would permit the utilization of a relatively inexpensive and simple test method. Standards were made having a range of figures of merit which were then alpha-autoradiographed. These standards of known homogeneity are compared to pellets with unknown homogeneity by using alpha-autoradiographs taken at the same time. From this visual comparison with the standards, a figure of merit for the unknown pellets can be determined. This method of relating the figure of merit to alpha-autoradiography makes the homogeneity specification feasible for industrial measurement and use. (auth)

11490 DYNAMIC YIELD STRENGTHS OF B_4C, BeO, AND Al_2O_3 CERAMICS. Gust, W. H.; Royce, E. B. (Univ. of California, Livermore). J. Appl. Phys.; 42: 276-95(Jan 1971).

The dynamic yield strengths for several ceramics were measured under shock-wave compression. The Hugoniot elastic limit (HEL), taken as the amplitude of the observed elastic precursor traveling ahead of the compressional wave, was 154 and 82 kbar for B_4C and BeO ceramics, respectively, and ranged from 61 to 134 kbar for several Al_2O_3 ceramics. These values apply to 6-mm-thick samples; in some cases there were variations with sample thickness. The offset of the Hugoniot from the isotropic compression curve in the stress-volume plane indicates a nonzero yield strength above the HEL for Al_2O_3. This yield strength is somewhat less than the yield strength at the HEL. The compaction of porous ceramics is found to follow a quadratic variation with stress, full compaction being reached at about four times the HEL. (auth)

XUM

11491 HIGH-TEMPERATURE HEAT CONTENT OF PLUTONIUM DIOXIDE. Ogard, Allen E. (Los Alamos Scientific Lab., N. Mex.). Nucl. Met., Met. Soc. AIME; 17: 78-83(1970).

From 4th International Conference on Plutonium and Other Actinides, Santa Fe, N. Mex. See CONF-701001-(Pt.1).

The high-temperature heat content of PuO_2 was measured from 1500 to 2715°K in an isoperibol drop calorimeter. The equation $H_T - H_{298} = -6.36 + 0.0180T + 1.95 \times 10^{-6}T^2 + 2.46 \times 10^{3}T^{-1}$ kcal $mole^{-1}$ expresses the results. (auth)

11492 THERMOPHYSICAL PROPERTIES OF (UPu)N. Alexander, C. A.; Ogden, J. S.; Pardue, W. M. (Battelle Memorial Inst., Columbus, Ohio). Contract W-7405-eng-92. Nucl. Met., Met. Soc. AIME; 17: 95-103(1970).

From 4th International Conference on Plutonium and Other Actinides, Santa Fe, N. Mex. See CONF-701001-(Pt.1).

Thermochemical and thermophysical determinations were performed on UN, PuN, and $U_{0.8}Pu_{0.2}N$. For the most part it was established that the properties of $U_{0.8}Pu_{0.2}N$ are intermediate between that of UN and PuN. Heat capacity seemed to be a near-linear function of composition and the thermochemical determinations indicated that UN and PuN formed a near ideal solution. The ideal solution concept does not apply to the individual elements plutonium and uranium, however. The metal/nitrogen ratio seems governed by the plutonium while mass transport is governed predominantly by diffusion of plutonium through a surface layer of uranium nitride. (auth)

11493 LOW-TEMPERATURE HEAT CAPACITY OF $PuC_{0.81}$. Sandenaw, Thomas A.; Gibney, Robert B. (Los Alamos Scientific Lab., N. Mex.). Nucl. Met., Met. Soc. AIME; 17: 104-12(1970).

From 4th International Conference on Plutonium and Other Actinides, Santa Fe, N. Mex. See CONF-701001-(Pt.1).

The composition $PuC_{0.81}$ is close to the lower C/Pu atom ratio phase boundary and most runs appear to be representative of an irreproducibly varying phase mixture of PuC and Pu_2C_3 and/or traces of Pu metal. Ease in crossing the phase boundary on cooling below room temperature may be attributed in part to radioactive decay energy and also in part to the properties of nonstoichiometric compounds. The heat capacity data indicated that $PuC_{0.81}$ was single phase at room temperature under some conditions and became single phase above 320°K under most processing conditions. A published correlation between lattice parameter and magnetic susceptibility behavior explains the absence of heat capacity peaks in rapidly quenched $PuC_{0.81}$. Cooling in a 300 Oe field only effected heat capacity values below 75°K. Thermodynamic property values at 298°K were very close to previously made estimates. A comparison of the low temperature heat capacity curves of UC (Westrum et al.), $NpC_{0.89}$ and $PuC_{0.81}$ is shown. (auth)

11494 ELECTRICAL AND THERMAL PROPERTIES OF THE NaCl STRUCTURED METALLIC ACTINIDE COMPOUNDS. Fulkerson, W.; Kollie, T. G.; Weaver, S. C.; Moore, J. P.; Williams, R. K. (Oak Ridge National Lab., Tenn.). Nucl. Met., Met. Soc. AIME; 17: 374-85(1970).

From 4th International Conference on Plutonium and Other Actinides, Santa Fe, N. Mex. See CONF-701001-(Pt.1).

Literature data for the NaCl structured metallic compounds UC, PuC_{1-x}, (U,Pu)C, and UN are reviewed and, where data permit, preferred thermal conductivity, λ, and electrical resistivity, ρ, values are assigned. These values are then analyzed in order to estimate the relative proportions of electronic and phonon conductivity in these materials. Gaps in the state of knowledge are pointed out. In addition, some preliminary results on the ρ and λ of ThN and (Th,U)N alloys are reported. (auth)

11495 COMPRESSIVE CREEP PROPERTIES OF UO_2-PuO_2 COMPOUNDS. Bohaboy, P. E.; Evans, S. K. (General Electric Co., Sunnyvale, Calif.). Nucl. Met., Met. Soc. AIME; 17: 478-87 (1970).

From 4th International Conference on Plutonium and Other Actinides, Santa Fe, N. Mex. See CONF-701001-(Pt.1).

The steady state creep of mixed plutonium-uranium oxide samples was measured in a compression test as a function of temperature, stress, density, stoichiometry, and plutonium content. Experimental results indicated that these variables have definite and predictable effects on the measured creep rate. From this data an empirical expression was generated which describes the behavior of the material for certain combinations of the test parameters. This description is in general agreement with existing theoretical creep models. (auth)

11496 THERMAL CREEP OF POLYCRYSTALLINE UO_2-PuO_2. Houston, M. D.; Kruger, O. L.; Pardue, W. M. (Battelle Memorial Inst., Columbus, Ohio). Contract W-7405-eng-92 Nucl. Met., Met. Soc. AIME; 17: 488-96(1970).

From 4th International Conference on Plutonium and Other Actinides, Santa Fe, N. Mex. See CONF-701001-(Pt.1).

The compressive creep properties of UO_2-22 wt % PuO_2 were studied in the temperature range from 1100 to 1330°C and with stresses from 1100 to 3200 psi. Test specimens were fabricated from mechanically blended powder by normal ceramic cold pressing and sintering techniques. Two types of mixed oxide material were prepared by selected sintering parameters: high density (94 ± 1 percent of theoretical) and small grain size (3 to 5 microns); and lower density (90 ± 1 percent of theoretical) and larger grain size (10 to 15 microns). Creep rates for the fine-grain material (O/M = 1.99) indicated a stress dependence of 1.4. The activation energy for creep with this material was determined to be 77 kcal/mole. The observed creep rates for the two types of material indicated a relationship proportional to the reciprocal of the square of the grain size ($1/D^2$). (auth)

11497 CREEP OF UO_2 AND $(U,Pu)O_2$. Marples, J. A. C.; Hough, A. (Atomic Energy Research Establishment, Harwell, Eng.). Nucl. Met., Met. Soc. AIME; 17: 497-508(1970).

From 4th International Conference on Plutonium and Other Actinides, Santa Fe, N. Mex. See CONF-701001-(Pt.1).

The compressive creep of UO_2 and $(U,Pu)O_2$ was studied as a function of temperature, stress, composition, oxygen to metal ratio, density, and grain size. Substitution of PuO_2 for UO_2 was found to have a marked softening effect. (auth)

11498 FACTORS AFFECTING THE HARDNESS OF URANIUM MONONITRIDE AT ELEVATED TEMPERATURES. Harrison, J. D. L.; Pape, R. P. (Atomic Energy Research Establishment, Harwell, Eng.). Nucl. Met., Met. Soc. AIME; 17: 518-29(1970).

From 4th International Conference on Plutonium and Other Actinides, Santa Fe, N. Mex. See CONF-701001-(Pt.1).

The Vickers Pyramid hardness numbers (VHN) of UN prepared from four different purity grades of uranium metal were measured at temperatures between 20 and 1400°C, using hot-hardness machines. The grades of metal were: commercial, electrodeposited, and two batches depleted in ^{235}U. Specimens were fabricated from UN produced by reaction of nitrogen with fine metal powder, the resulting UN powder being cold pressed and sintered to ~95% density. The variation of VNH with temperature did not follow the behavior indicated by other workers, namely $\log(VHN) \alpha (-T°)$. For all grades, there was a similar decrease in hardness as the temperature rose to 600°C, with $\log(VHN) \alpha 1/T°K$. Above 700°C, there was a considerable difference between the pure and impure materials. For the former, between 600 and 700°C there was an increase (by an order of magnitude) in the proportionality constant for log $VHN \alpha 1/T°K$, which led to rapid softening as the temperature rose to 1400°C. For the impure material, the relationship between hardness and temperature was complex above 700°C, and the rate of softening with increase in temperature was slower than for pure UN. It is suggested that the factor controlling hardness changes at ~700°C, with impurities imparting more resistance to deformation above this temperature. (auth)

11499 HELIUM RELEASE FROM $^{238}PuO_2$ MICROSPHERES. Stark, W. A. Jr. (Sandia Labs., Albuquerque, N. Mex.). Nucl. Met., Met. Soc. AIME; 17: 554-62(1970).

From 4th International Conference on Plutonium and Other Actinides, Santa Fe, N. Mex. See CONF-701001-(Pt.2).

In a first attempt to characterize the release of helium gas from production grade plasma-torch fused $^{238}PuO_2$ microspheres, the results of a series of annealing experiments were analyzed using a simple diffusion model. The analytical approach is outlined, and the experimental technique and results are briefly reviewed. A temperature dependent diffusion coefficient, D', is obtained as $D' = D'_0 \exp[-\Delta E/RT]$ sec^{-1} for $T \geq 800°C$, where $D'_0 \approx 824$ $sec^{-1} \pm 600\%$ and $\Delta E \approx 55$ kcal/mole ± 10%. Possible causes of the scatter in the data are reviewed. (auth)

11500 CALCULATIONS OF HELIUM RELEASE FROM $^{238}PuO_2$ MICROSPHERES. Williams, David C. (Sandia Labs., Albuquerque, N. Mex.). Nucl. Met., Met. Soc. AIME; 17: 563-74(1970).

From 4th International Conference on Plutonium and Other Actinides, Santa Fe, N. Mex. See CONF-701001-(Pt.2).

The helium release data were obtained employing plasma-torched $^{238}PuO_2$ microspheres which were subjected to complex thermal histories prior to the experiment, and which were far from uniform in physical nature. It is shown that these facts can lead to sizable errors in the value of the diffusion parameters extracted from the data, and they can also result in behavior which might otherwise be regarded as anomalous. However, it is not possible to account for all the erratic behavior which

was observed by means of the effects considered here. Some recommendations are made for minimizing these problems in future experiments. (auth)

11501 HELIUM DIFFUSION IN $^{238}PuO_2$. Northrup, C. J. M., Jr. (Sandia Labs., Albuquerque, N. Mex.); Amos, D. E.; Zielinski, R. E. Contract AT(33-1)-Gen-53. Nucl. Met., Met. Soc. AIME; 17: 575-84(1970).

From 4th International Conference on Plutonium and Other Actinides, Santa Fe, N. Mex. See CONF-701001-(Pt.2).

The behavior of helium that was self-introduced by alpha decay in $^{238}PuO_2$ was investigated in the temperature range from 25 to 2000°C. Computer simulation of diffusion in a sphere containing bubbles was accomplished by a generalization of Hurst's trapping model applicable to alpha emitting solids. These results were then compared with experiment. It was found that the porosity produced in fabrication of sol-gel microspheres could not alone account for the anomalous diffusion behavior of helium in $^{238}PuO_2$ during temperature transients. The anomalous changes in the diffusion properties of the microsphere were observed during transients in the temperature range from 25 to 800°C. This suggests that at these temperatures, the alpha radiation damage and bubble formation can play significant roles on the release of helium from $^{238}PuO_2$. (auth)

11502 HELIUM RELEASE FROM ALPHA-BOMBARDED ThO_2. Clinard, F. W. Jr.; Douglass, Dana L.; Woods, R. (Los Alamos Scientific Lab., N. Mex.). Nucl. Met., Met. Soc. AIME; 17: 585-95(1970).

From 4th International Conference on Plutonium and Other Actinides, Santa Fe, N. Mex. See CONF-701001-(Pt.2).

Two samples of bulk polycrystalline ThO_2 were injected with 5-MeV alpha particles to a dose of 9.4×10^{16} ions/cm^2. One sample was then heated to ~1650°C and the helium escape monitored. Gas was released both continuously and in bursts, with the bursts for the most part preceding the maximum in the continuous release curve at 1400°C. The other sample was heated similarly, except that it was rapidly cooled after attaining 1390°C in order to freeze in the conditions which existed near the time of maximum continuous gas release. The second sample was examined by transmission electron microscopy, and it was found that helium escaped by two modes: bubble migration within the grains, and grain boundary separation resulting from bubble coalescence. It is concluded that the gas bursts resulted from boundary separation. Modes of intragranular bubble migration to the surface are considered, and the most feasible found to be motion by surface diffusion down a stress gradient. (auth)

11503 MASS SPECTROMETRIC INVESTIGATION OF THE VOLATILIZATION BEHAVIOR OF $(U_{0.8}Pu_{0.2})O/sub\ 2-x/$. Battles, J. E.; Shinn, W. A.; Blackburn, P. E.; Edwards, R. K. (Argonne National Lab., Ill.). Nucl. Met., Met. Soc. AIME; 17: 733-42 (1970).

From 4th International Conference on Plutonium and Other Actinides, Santa Fe, N. Mex. See CONF-701001-(Pt.2).

The volatilization behavior of the mixed oxide $(U_{0.8}Pu_{0.2})O_{2-x}$ was investigated in the temperature range from 1905 to 2411°K and for $1.92 \leq O/M \leq 2.00$ by combined mass-loss and mass-spectrometric Knudsen effusion studies. The partial enthalpies of vaporization for the primary vapor species PuO, PuO_2, UO_2, and UO_3 were determined as a function of the O/M atom ratio. Partial vapor pressures were measured as a function of the O/M ratio at constant temperature. These data are combined with the partial enthalpies to yield equations for the partial pressures as a function of temperature. The vapor phase was predominantly $UO_3(g)$ and $UO_2(g)$ for O/M ratios greater than about 1.97; whereas, at lower O/M ratios, (<1.94) the ratios of U/Pu in the solid and vapor phase were about equal. (auth)

11504 EVAPORATION BEHAVIOR OF SUBSTOICHIOMETRIC $(U,Pu)O_2$. Ohse, Roland W. (EURATOM, Karlsruhe, Ger.); Olson, William M. Nucl. Met., Met. Soc. AIME; 17: 743-52(1970).

From 4th International Conference on Plutonium and Other Actinides, Santa Fe, N. Mex. See CONF-701001-(Pt.2).

The evaporation behavior of the ternary oxide system $(U_{0.88}Pu_{0.12})O_{2-y}$, where y = 0 to 0.06, was studied between 1800 and 2350°K by an effusion collection technique combined with mass spectrometric analysis of the vapor phase. The general behavior of the system was analyzed by following pressure and composition changes as a function of time. A quasi-congruently vaporizing composition was found at $(O/M)_s = 1.97$ when following the change of composition in the solid at constant temperature starting at $(O/M)_s = 1.94$ and 2.08. The ion intensities of UO_3^+, UO_2^+, PuO_2^+, and PuO^+ were measured as a function of both temperature and composition. The partial molar enthalpies of evaporation, $\Delta H(UO_3) = 115.8$ kcal/mole, $\Delta H(UO_2) = 148.4$ kcal/mole, $\Delta H(PuO_2) = 141.9$ kcal/mole, and $\Delta H(PuO) = 124.5$ kcal/mole, were obtained from the least-squares equations of the log (I · T) vs 1/T data at $(O/M)_s = 1.969$. The absolute pressures of uranium- and plutonium-bearing species were measured by the effusion collection method, and were combined with the ion intensity determinations to yield the partial pressures at $(O/M)_s = 1.969$. The consistency of the thermodynamic data of the binary Pu–O and ternary U–Pu–O system is discussed. The standard free energy of formation of $PuO_2(g)$ was recalculated to be $\Delta G_{f,PuO_2(g)} = -102,700 - 3.16\ T$ kcal/mole. (auth)

11505 THERMODYNAMIC BEHAVIOR OF PLUTONIUM OXIDE SYSTEMS IN A TEMPERATURE GRADIENT. Aitken, E. A.; Evans, S. K. (General Electric Co., Pleasanton, Calif.). Nucl. Met., Met. Soc. AIME; 17: 772-80(1970).

From 4th International Conference on Plutonium and Other Actinides, Santa Fe, N. Mex. See CONF-701001-(Pt.2).

Preferential migration of oxygen and plutonium were observed in U–Pu–O systems when exposed to a temperature gradient. Thermomigration mechanisms are described for each of two cases and are related to experimental observations as tests for their validity where experimental data are sufficient. For the case of oxygen thermomigration, both solid and gas phase diffusion paths were important for hypostoichiometric compositions in establishing the heat of transport. The heat of transport can be derived from reversible thermodynamic quantities in the U–Pu–O system. For the case of Pu/U thermomigration it is not clear whether gas phase or solid phase diffusion is dominant. Both processes are capable of explaining observed preferential migration of Pu to the hot end. The solid phase diffusion mechanism requires inclusion of irreversible terms which are not readily predicted from activation energies. The gas phase diffusion mechanism utilizes thermodynamic vaporization data to arrive at a composition gradient. (auth)

11506 THERMODYNAMIC PROPERTIES OF THE PLUTONIUM–CARBON SYSTEM. Campbell, G. M.; Kent, R. A.; Leary, J. A. (Los Alamos Scientific Lab., N. Mex.). Nucl. Met., Met. Soc. AIME; 17: 781-90(1970).

From 4th International Conference on Plutonium and Other Actinides, Santa Fe, N. Mex. See CONF-701001-(Pt.2).

Mass spectrometric-Knudsen effusion and emf techniques were used to measure Pu activities in the Pu–C system over the temperature range 900 to 2200°K and composition range Pu to PuC_2 + C. Thermodynamic properties at 298°K were estimated. (auth)

11507 MELTING BEHAVIOR OF (U,Pu) MONOCARBIDES. Reavis, J. G.; Johnson, K. A.; Leary, J. A. (Los Alamos Scientific Lab., N. Mex.). Nucl. Met., Met. Soc. AIME; 17: 791-8 (1970).

From 4th International Conference on Plutonium and Other Actinides, Santa Fe, N. Mex. See CONF-701001-(Pt.2).

Solidus and liquidus temperatures were determined for (U,Pu)C solid solutions containing 0 to 50 mole % PuC. Differential thermal analysis and metallographic techniques were used. Solidus and liquidus temperatures of UC were 2520 and 2540°C, respectively. Solidus and liquidus temperatures of UC–20% PuC were 2275 and 2485°, respectively. (auth)

11508 SYMPOSIUM ON THERMAL EXPANSION OF SOLIDS. 1970 Symposium Held in Santa Fe, New Mexico, 10–12 June 1970. J. Appl. Phys.; 41: 5043-5154(Dec 1970). (CONF-700633).

In this proceedings, covering theoretical and experimental studies of thermal expansion and its relation to other properties of solids, 31 full papers, 4 abstracts, and 8 titles–only are presented. The papers are arranged in the following sections: low temperature; defects and diffraction; molecular solids and graphite; standards, copper, methods; composites and carbides; magnetism; and theory. Separate abstracts were prepared for 7 of the papers. (D.L.C.)

For abstracts of individual papers see: 11449, 11509–11513, and 12015.

11509 ANISOTROPIC THERMAL EXPANSION OF REFRACTORY CARBIDES BY HIGH-TEMPERATURE NEUTRON DIFFRACTION. Bowman, A. L.; Arnold, G. P.; Krikorian, N. H. (Los Alamos Scientific Lab., N. Mex.). J. Appl. Phys.; 41: 5080-1(Dec 1970).

From Conference on Thermal Expansion of Solids, Santa Fe, N. Mex. See CONF-700633.

The anisotropic thermal expansion of U_2PtC_2 (tetragonal), and $UMoC_2$ (orthorhombic) has been measured using a high-temperature neutron diffractometer. Coefficients of thermal expansion (units of 10^{-6}/°C) are U_2PtC_2, $\alpha_{11} = 9.3 \pm 0.1$, $\alpha_{33} = 10.1 \pm 0.8$; $UMoC_2$, $\alpha_{11} = 8.6 \pm 0.2$, $\alpha_{22} = 15.5 \pm 0.5$, $\alpha_{33} = 10 \pm 3$. (auth)

XUM

11510 ANISOTROPIC THERMAL EXPANSION OF PYROLYTIC GRAPHITE AT LOW TEMPERATURES. Bailey, A. C.; Yates, B. (Univ. of Salford, Eng.). J. Appl. Phys.; 41: 5088-91(Dec 1970).

From Conference on Thermal Expansion of Solids, Santa Fe, N. Mex. See CONF-700633.

Interferometric measurements of the linear thermal-expansion coefficients $\alpha_{||}$ and $\alpha_{\perp}$ in the "c" and "a" axial directions of well-oriented pyrolytic graphite between approximately 20 and 270°K are reported. Grüneisen parameters $\gamma_{||}$ and $\gamma_{\perp}$, defined for strain coordinates parallel and perpendicular to the "c" axis, respectively, have been calculated from the present thermal expansion coefficients and related data. Between 30 and 270°K, $\gamma_{||}$ is positive, indicating the preponderance of longitudinal modes of vibration, while $\gamma_{\perp}$ is negative, indicating the predominance of transverse modes. The quasiharmonic approximation has been applied to calculate the characteristic temperatures $\theta(n)$ corresponding to the maximum frequencies $\omega_D(n)$ of the Debye distributions having the same nth moments $\langle\omega^n\rangle$ as the specimens, which vary between approximately 420 and 2270°K as n increases from −3 to +6. The dimensional dependence of the moments, defined by $\gamma(n) = \Sigma\gamma_j\omega_j^n / \Sigma\omega_j^n$ corresponding to $\gamma_{||}(n)$ and $\gamma_{\perp}(n)$, and their variations with n, are consistent with the existence of low-frequency modes of vibration between planes of atoms perpendicular to the "c" axis, and high-frequency modes within the planes, a result supported by calculations of the rms displacements of the atoms. (auth)

11511 THERMAL EXPANSION OF POLYCRYSTALLINE GRAPHITE. Naum, Robert G.; Jun, Choll K. (Carborundum Co., Niagara Falls, N. Y.). J. Appl. Phys.; 41: 5092-5(Dec 1970).

From Conference on Thermal Expansion of Solids, Santa Fe, N. Mex. See CONF-700633.

Thermal expansion characteristics of a group of polycrystalline graphites have been measured to 2400°C by a method which permits acquisition of meaningful expansion data without resorting to reference standards. Direct measurements on specimens while in the furnace were accomplished by using two 8-in. focal length Gaertner optical micrometers. Thermal expansion behavior is discussed in relation to orientation, impurity, degree of crystallinity, and grain size. Specimens were heated from room temperature to 2400°C, then cooled to room temperature, taking measurements of thermal expansion throughout both heating and cooling cycles. The existence of hysteresis is observed and discussed. (auth)

11512 THERMAL EXPANSION OF EXTRUDED GRAPHITE–ZrC CARBIDE COMPOSITES. Cowder, L. R.; Zocher, R. W.; Kerrisk, J. F.; Lyon, L. L. (Los Alamos Scientific Lab., N. Mex.). J. Appl. Phys.; 41: 5118-21(Dec 1970).

From Conference on Thermal Expansion of Solids, Santa Fe, N. Mex. See CONF-700633.

The thermal expansion of extruded graphite–ZrC composites was measured over the temperature range 20 to 2500°C and over a composition range 0–0.4 volume fraction of carbide, for directions parallel and transverse to the extrusion axis. The thermal-expansion furnace was 4-in.-I. D. by 60-in.-long horizontal graphite resistance heater in which a 30-in.-long sample was passively heated. Measured thermal expansion of the composite are compared with those calculated. Calculations using elastic-constant data of the composite material are in good agreement with the measurements. (auth)

11513 THERMAL EXPANSION AND PHASE EQUILIBRIA OF THE CARBON-SATURATED PLUTONIUM CARBIDES. Green, J. L.; Leary, J. A. (Los Alamos Scientific Lab., N. Mex.). J. Appl. Phys.; 41: 5121-4(Dec 1970).

From Conference on Thermal Expansion of Solids, Santa Fe, N. Mex. See CONF-700633.

An x-ray diffractometer furnace was developed for use in the study of the high-temperature properties of refractory compounds of plutonium. The furnace design is based on a resistance heated strip which serves as the sample support. The mechanics of the support system are such that the location of the scattering center of the sample is maintained throughout the temperature range of the instrument, i.e., room temperature to 2500°C. The thermal expansion characteristics of carbon-saturated Pu_2C_3 and PuC_2 were determined. A least-squares fit of the lattice dimension data for Pu_2C_3 in the temperature interval from room temperature to 1600°C yielded $\Delta a/a_0 = (1.29 \pm 0.02 \times 10^{-5})(T - 25) + (2.07 \pm 0.14 \times 10^{-9})(T - 25)^2$, where a is the lattice dimension in Å, and T is the temperature in °C. A least-squares fit of the lattice dimension data for fcc PuC_2 in the temperature interval from 1660°C to 2000°C yielded $\Delta a/a_0 = (17.9 \pm 1.6 \times 10^{-6})(T - 1660)$. (auth)

11514 MICROFRACTOGRAPHIC ASPECT OF REFRACTORY CARBIDES: CASE OF THE TiC AND WC–Co ALLOYS. Chermant, Jean-Louis; Coster, Michel; Deschanvres, Alfred (Caen Univ., France). Compt. Rend., Ser. C; 271: 885-8(12 Oct 1970). (In French).

Microfractographic examinations of TiC and WC–Co samples broken under different conditions were carried out by electron microscopy. The aspect and manner of breaking of these different materials were studied as a function of the size of the carbide crystals. (auth) (France)

11515 FURTHER LOOK AT WC–Co FROM THE CONTINUUM VIEWPOINT. Butler, Thomas Wesley. Providence; Brown Univ. (1969). 81p. University Microfilms Order No. 70-8698. Thesis.

The flow and fracture of sintered tungsten carbide–cobalt are discussed and analyzed by applying continuum mechanics on the microscale. A plane model of rigid, hexagonal inclusions in an elastic-perfectly plastic matrix is taken to represent WC particles in a Co matrix. The continuum model employed here is used to extend earlier work by Drucker to include effects due to non-uniform particle spacings on the behavior of WC–Co in tension and bending. Effects on the bending strength due to change of the yield strength of the matrix are discussed. Also, the fracture strength of WC–Co in compression is predicted by using the continuum model and found to be in reasonable agreement with published compressive strength data. (Diss. Abstr. Int., B)

11516 NEW TECHNIQUE FOR MEASURING OXYGEN DIFFUSION COEFFICIENTS. Derry, Dennis J. (Univ. of Manchester, Eng.). Emen; No. 5, 40-9(Oct 1970).

Oxygen diffusion coefficients were measured by a proton resonance method that used nuclear bombardment to determine the tracer profile in the oxide. This method was useful because it was nondestructive and enabled quite low diffusion coefficients to be determined after relatively short anneals and gave the concentration profile of the solute directly. The diffusion coefficient of oxygen in monocrystalline TiO_2 was determined. (G.M.C.)

11517 PROPERTIES AND STRUCTURES OF La_2O_3–CdO–B_2O_3 GLASSES. Deneka, Charles William. New Brunswick, N. J.; Rutgers–The State Univ. (1970). 252p. University Microfilms Order No. 70-16,927.

Thesis.

Experimental compositions were prepared from analyzed frit with additions of La_2O_3, CdO, and H_3BO_3 in some cases. A special technique was used to obtain homogeneous glasses which were then given equivalent heat treatments. Several physical properties were measured from which structural inferences were drawn. Density, index of refraction, and indentation hardness were determined at room temperature while coefficients of linear thermal expansion were determined from room temperature to 300°C. Glass transition temperatures were determined from thermal expansion curves. Dielectric constant and dielectric dissipation factor were determined over a frequency range of 50 KHz to 50 MHz. The fluorescent lifetime of Tb^{3+} was determined for selected compositions and electron microscopy was used to determine the existence and nature of subsolidus phase separation at selected compositions near the region of stable immiscibility. The results of the physical measurements strongly suggested that the structure of these ternary glasses was a mixture of $La_2O_3 \cdot xB_2O_3$ and $CdO \cdot yB_2O_3$ matrices. Changes in nature of various property measurements as La replaced Cd suggested that lanthanum began to take some part in the network at the lowest boron concentrations studied. (auth)

11518 INFRA-RED REFLECTANCE SPECTRA (IRRS) OF ANODIC OXIDE FILMS FORMED ON PURE TANTALUM. Kihara-Morishita, H. (Tokyo Shibaura Electric Co., Ltd., Kawasaki, Japan); Takamura, T.; Takeda, T. Thin Solid Films; 6: R29-31(Sep 1970).

A study was made of the effects of anodization conditions on the infrared reflectance spectra of anodic Ta oxide films. Significant changes in the spectra occur when the anodization voltage ~100 V: below 100 V, there are two absorptions centered at 1050 and 810 cm^{-1}, while above 100 V, the 1100 cm^{-1} absorption is very weak, and the other absorptions shift to 950 cm^{-1} and lower frequencies. The bands are assigned to ν Ta–O stretching. The broad 1100–1020 cm^{-1} band of oxides formed below 70 V is also found in natural Ta oxide films. The effects of thickness on the optical density of each band were also studied. It is concluded that the anodic films formed at the lower voltage are mostly a lower oxide. (D.L.C.)

11519 INTERACTIONS OF REFRACTORY METAL SILICIDE COATINGS WITH SUBSTRATES. Schwartz, Leon Joseph. New York; City Univ. of New York (1970). 227p. University Microfilms Order No. 70-15,465.

Thesis.

The growth rate of Ta_5Si_3 in the $Ta/TaSi_2$ system was accurately measured. This was accomplished by contacting dense $TaSi_2$ wafers and wafers of Ta, holding the couple at a controlled temperature for the desired time and later measuring the thickness of the resultant intermediate zone. In the Arrhenius form the parabolic growth constant is: $k = 5e^{-77,000/RT}$ where the activation energy is known with 95% confidence to be between 74,000 and 80,000 cal/mole and the pre-exponential constant is known with the same confidence to be between 2 and 11 cm^2/sec. The rate of degradation of $TaSi_2$ in the $Ta/TaSi_2$ system was measured separately and may be expressed as $k_1 = 2e^{-81,000/RT}$. The 95% confidence intervals are 74,000 to 88,000 cal/mole for the activation energy and 0.2 to 16 cm^2/sec for the pre-exponential constant. Marker experiments indicated that only silicon diffuses. Six metals were tested as barriers to the degradation of $TaSi_2$. They were: tungsten, rhenium, molybdenum, niobium, zirconium, and titanium. None of the metals tested was effective in lowering the rate of loss of $TaSi_2$. In all but the $Ti/TaSi_2$ system, Si alone was shown to diffuse. Incompatibility in the $W/TaSi_2$ and $Re/TaSi_2$ systems interrupted solid state diffusion and resulted in the vapor transport of Si, particularly during the early stages of the diffusion anneal. Fundamental activation energies for diffusion of silicon in four silicides were determined. The four compounds are: Ta_5Si_3, $Q_{Si} = 77,000$ cal/mole; Mo_3Si, $Q_{Si} = 58,000$ cal/mole; Nb_5Si_3, $Q_{Si} = 49,000$ cal/mole; and Ti_5Si_3, $Q_{Si} = 44,000$ cal/mole. (Diss. Abstr. Int., B)

Structure and Phase Studies

Refer also to abstracts 11999 and 12039.

11520 LATTICE DEFECTS IN THE FLUORITE STRUCTURE OF UO_2 AND UO/sub 2+x/. Ronchi, C.; Blank, H. (EURATOM, Karlsruhe, Ger.). Nucl. Met., Met. Soc. AIME; 17: 174-82(1970).

From 4th International Conference on Plutonium and Other Actinides, Santa Fe, N. Mex. See CONF-701001-(Pt.1).

Dislocations in {111} glide planes of UO_{2+x} can move at least as easy as dislocations on {100} planes of $UO_{2.00}$. Deformation of UO_2 by several glide systems {110}, ⟨110⟩ produces a high density of point defects. Extended defects in UO_2 and UO_{2+x} show a mixture of stacking fault and antiphase boundary contrast in the electron microscope. The model of a non glissile stacking fault in UO_2 is proposed. (auth)

11521 STUDIES OF MIXED ACTINIDE OXIDES: Am/sub y/Cm/sub 1-y/O/sub x/ AND Pu/sub y/Cm/sub 1-y/O/sub x/. Mosley, W. C. (E. I. du Pont de Nemours and Co., Aiken, S. C.). Contract AT(07-2)-1. Nucl. Met., Met. Soc. AIME; 17: 762-71 (1970).

From 4th International Conference on Plutonium and Other Actinides, Santa Fe, N. Mex. See CONF-701001-(Pt.2).

The systems $Am_yCm_{1-y}O_x$ and $Pu_yCm_{1-y}O_x$ were investigated by thermogravimetric analysis and high-temperature x-ray diffraction. The solid solution dioxides had the fluorite structure typical of actinide dioxides. Another apparently fcc phase with composition $1.93 \geq O/M \geq 1.80$ was produced on thermal decomposition of the Am-Cm and Pu-Cm dioxides in oxygen and helium. A rhombohedral phase was produced on further reduction to compositions with $1.80 \geq O/M \geq 1.685$. A disordered phase related to the bcc C-type sesquioxide formed near 900°C for $O/M \sim 1.7$ and at lower temperatures for more-reduced oxide. Variations in the lattice parameters with oxygen content for intermediate phases between dioxide and sesquioxide exhibited positive deviations from predictions based on Vegard's Law. Mixed americium-curium sesquioxides existed in all three polymorphic forms observed for rare-earth sesquioxides. Americium addition to curium sesquioxide had no apparent effect on the temperature for the irreversible transformation of the bcc C-type form to the monoclinic B-type form between 800 and 1000°C, but the transformation temperature at which the hexagonal A-type form appeared was lowered with increasing americium content from 1600°C for Cm_2O_3 to 800 to 1000°C for Am_2O_3. All three crystallographic forms of $(Am, Cm)O_{1.5}$ exhibited decreasing molecular volumes with decreasing americium content. The presence of Pu^{4+} stabilized the bcc structure for reduced oxide and hindered formation of stoichiometric plutonium-curium sesquioxide. Monoclinic B-type $(Pu, Cm)O_{1.5}$ and a modification of hexagonal A-type $(Pu, Cm)O_{1.5}$ were observed. (auth)

11522 DIFFERENTIAL THERMAL ANALYSIS OBSERVATIONS OF U-Pu DICARBIDES. Reavis, J. G.; Leary, J. A. (Los Alamos Scientific Lab., N. Mex.). Nucl. Met., Met. Soc. AIME; 17: 809-17(1970).

From 4th International Conference on Plutonium and Other Actinides, Santa Fe, N. Mex. See CONF-701001-(Pt.2).

The UC_2-PuC_2 pseudobinary was studied by differential thermal analysis techniques throughout the composition range UC_2 to PuC_2. X-ray powder diffraction and metallographic studies were used to obtain information about structures of species present in the system. Transformations were observed at 1660 ± 10° and 2230 ± 20°C in PuC_2(+C) and at 1785 ± 20° and 2480 ± 20°C in UC_2(+C). (auth)

11523 URANIUM-PLUTONIUM-CARBON PHASE DIAGRAM, PART I, MELTING BEHAVIOUR AND THE ISOPLETH FOR THE DICARBIDE REGION. Dalton, J. T.; Harper, E. A.; Hedger, H. J.; Stannard, R. W. (Atomic Energy Research Establishment, Harwell, Eng.). Nucl. Met., Met. Soc. AIME; 17: 829-41(1970).

From 4th International Conference on Plutonium and Other Actinides, Santa Fe, N. Mex. See CONF-701001-(Pt.2).

The melting temperatures of alloys having nominal compositions on the tie UC_2-PuC_2 are reported and discussed. A minimum was observed in the liquidus temperatures at high Pu concentrations because of the peritectic melting behavior of PuC_2. The isopleth for the region, UC_2-PuC_2, was determined using dilatometry and high temperature x-ray diffractometry. The temperatures for the reactions $(UPu)C_2 \rightarrow (UPu)C_{1.5} + 0.5C$ as a function of Pu content were determined using a dilatometer. At low Pu concentrations, examinations of rapidly quenched alloys were made using x-ray powder photography and ceramography. This region, with low Pu concentrations, was the only region where the tetragonal $(UPu)C_2$ phase appeared to be thermodynamically stable. Studies using a high temperature x-ray diffractometer showed that except for Pu concentrations less than ~10 at. % the only stable dicarbide phases had face-centered cubic structures, but at low Pu concentrations, dicarbides with a stable tetragonal structure were found. At 1800°C, the lattice parameters of cubic UC_2 and PuC_2 were close, 0.548 and 0.570nm, but did not form a complete range of solid solution. High temperature diffractometry showed conclusively that the tetragonal dicarbides observed at room temperature were metastable phases. All the cubic dicarbide alloys cooled to room temperature showed the presence of the tetragonal dicarbide and sesquicarbide. At high Pu concentrations it was increasingly difficult to prevent the decomposition of the tetragonal dicarbide to the sesquicarbide and carbon. (auth)

11524 URANIUM-PLUTONIUM-CARBON PHASE DIAGRAM, PART II. THE FREEZING OF THE ALLOYS AND CALCULATION OF SOME EQUILIBRIA. Mardon, P. G.; Potter, P. E. (Atomic Energy Research Establishment, Harwell, Eng.). Nucl. Met., Met. Soc. AIME; 17: 842-58(1970).

From 4th International Conference on Plutonium and Other Actinides, Santa Fe, N. Mex. See CONF-701001-(Pt.2).

The experimentally determined liquidus values for the ternary, together with the published data for the U-C and Pu-C binaries, were employed to postulate several possible isotherms indicating the most likely freezing behavior for the ternary alloys with carbon contents greater than 40 at. %. The equilibria in the UC_2-PuC_2 region are discussed, and the temperature of the decomposition of the dicarbide to sesquicarbide and carbon as a function of Pu concentration was calculated. A regular solution model with a small interaction parameter must be employed to describe either the dicarbide or sesquicarbide solid solutions in order to obtain a fit to the experimental data. The transformation from the tetragonal to cubic dicarbides is also considered. The equilibria in the two phase regions, metal + monocarbide and monocarbide + sesquicarbide, were calculated. The calculations predict that the Pu concentration is always greater in the metal than in the monocarbide, and greater in the sesquicarbide than in the monocarbide. These predictions were confirmed by experiment. The significance of these equilibria to the Pu and U pressures above the systems together with the variations of carbon potential in these regions is discussed and illustrated by calculation. (auth)

11525 ON THE U-Pu-C-O SYSTEMS. Potter, P. E. (Atomic Energy Research Establishment, Harwell, Eng.). Nucl. Met., Met. Soc. AIME; 17: 859-73(1970).

From 4th International Conference on Plutonium and Other Actinides, Santa Fe, N. Mex. See CONF-701001-(Pt.2).

A knowledge of the phase relationships in the U-Pu-C-O system is of significance to the preparation of carbide nuclear fuels by the carbothermic reduction of the oxides, and in the interpretation of the behavior of alloys of the system at high temperatures. Some of the equilibria in the U-Pu-C-O system are considered together with the relevant ternary systems. An analysis was made of the equilibria in the U-C-O system, and these equilibria were consistent with the thermodynamic

XUM

data for the binary U–C and U–O systems providing a regular solution model was employed to describe the UC–UO solid solution. The interaction parameter was estimated to be –20 kcals. At the temperatures where UC_2 was a phase of the system the activity must be less than unity in order to fit the experimental data. The calculations also predicted that C could not be in equilibrium with the UC–UO solid solution even at temperatures lower than 1000°C. A similar analysis of the Pu–C–O system indicated that an interaction parameter of –2.5 kcals was required to describe the PuC–PuO solid solution in order that the binary thermodynamic data were consistent with the experimentally determined phase diagram. The data for the free energies of formation of the hypothetical monoxides of U and Pu, together with the published data on the U–Pu–C and U–Pu–O systems were utilized to predict some of the equilibria in the quaternary U–Pu–C–O system. In a phase field containing 3 condensed phases the amounts of the phases must be known in order to determine the gas pressure above the system at a given temperature. The U and Pu concentrations in each of the coexisting condensed phases will in general be different; these differences were calculated. These calculations will serve as a basis for the interpretation of experimental studies on the system. (auth)

11526 SYSTEMS B_2O_3–MO–MS BORACITES M–S (M = Mg, Mn, Fe, Cd) AND SODALITES M–S (M = Co, Zn). Fouassier, C.; Levasseur, A.; Joubert, J. C.; Muller, J.; Hagenmuller, P. Z. Anorg. Allg. Chem.; 375: 202-8(Jul 1970). (In French).

In the B_2O_3–MO–MS (M = Mg, Mn, Fe, Co, Zn, Cd) systems six ternary phases were isolated, four of them having the structure of the cubic variety of the boracite, $Mg_3B_7O_{13}Cl$, and two the structure of the sodalite, $Na_4(SiAlO_4)_3Cl$. Some properties of the new phases were investigated. (auth)

11527 SYSTEM V_2O_5–K_2SO_4. Haehle, S.; Meisel, A. Z. Anorg. Allg. Chem.; 375: 24-31(Jul 1970). (In German).

The phase diagram of the system V_2O_5–K_2SO_4 was established by x-ray diffraction and DTA. An endothermal reaction led to the compound $5\ V_2O_5 \cdot 3\ K_2SO_4$ which melted at 510°C, crystallized needle-shaped and formed hydrates. Eutecties occurred at 31 (505°) and 55 mole-% K_2SO_4 (455°C). (auth)

11528 STRESS INDUCED α–U_3O_8–β–U_3O_8 TRANSFORMATION. Herak, R. (Boris Kidric Inst. of Nuclear Sciences, Belgrade). J. Inorg. Nucl. Chem.; 32: 3793-7(Dec 1970).

It was found that the action of pressure and shear on the α–U_3O_8 phase induces a transition to β–U_3O_8, a modification usually obtained by heating uranium oxides of different stoichiometric compositions. In the identification of phases the x-ray diffraction, neutron diffraction, and infrared spectrometry data were used. The possible mechanism of α–U_3O_8–β–U_3O_8 transformation was discussed. (auth) (UK)

11529 CARBONACEOUS MESOPHASE FORMED IN THE PYROLYSIS OF GRAPHITIZABLE ORGANIC MATERIALS. Dubois, J.; Agache, C.; White, J. L. (Joint Nuclear Research Center, Petten, Netherlands). Metallography; 3: 337-69(Sep 1970).

Observations by polarized light of the microstructures formed during the pyrolysis of materials used to fabricate graphitic artifacts have directed attention to the narrow range of temperature during which the carbonizing liquid exists as a liquid crystal called the carbonaceous mesophase. The poor polishing characteristics of the unhardened mesophase required modifications to the preparation methods used for carbons and graphites. A temperature-gradient heat-treatment technique was employed to obtain specimens representative of the various mesophase morphologies developed in the short plastic range. Three mechanisms (the mesophase transformation itself, the coalescence of the initial spherules to bulk mesophase, and the plastic flow before hardening) act to establish the principal features of the lamelliform morphology of a graphitizable coke. Fine insoluble particles are segregated by the mesophase transformation, and the effect of graphite substrate particles is to align the mesophase layers parallel to the layer planes of the substrate. On heat-treatment of the hardened mesophase to graphitizing temperatures, shrinkage-cracking and fine-scale mechanisms of fold-sharpening and polygonization take place to yield the final microstructure of the graphitic product. (auth)

Radiation Effects

Refer also to abstracts 10583, 11458, 11462, 11464, and 12795.

11530 (AECL–3732) MULTI-CYCLE IRRADIATION OF HOLLOW UO_2 PELLETS IN COLLAPSIBLE ZIRCALOY-2 SHEATHING. Bain, A. S.; Mizzan, E. (Atomic Energy of Canada Ltd., Chalk River (Ontario). Chalk River Nuclear Labs.). Nov 1970. 49p. Dep. NTIS (U. S. Sales Only). AECL $1.50.

Zircaloy sheathed elements containing UO_2 pellets with an axial void (4 vol %) were irradiated in a series of tests in the X-2 loop of NRX. Because of defects several elements were removed before their scheduled dates. The irradiation confirmed that the hollow pellet fuel elements had lower diametral expansions than solid pellet fuel irradiated at the same power. Circumferential ridges and fission gas release were similar to previous data of other highly rated fuel. The tests also confirmed that instability of the sheathing occurred if the fuel was operated above the melting point. Four defect mechanisms were considered: internal contamination, faulty tubing, stress rupture, and internal attack by fission products. One element almost certainly defected because of a tubing fault, and others probably contained a small amount of an internal hydrogenous contaminant. The most probable cause of the majority of the defects was the inability of the specific batch of tubing to yield during a slight power increase. The influence of any internal attack could not be assessed. (auth)

11531 (AERE-R-4913) EFFECT OF SOME STRUCTURE VARIATIONS ON THE TENSILE PROPERTIES OF IRRADIATED NIMONIC PE16. Broomfield, G. H. (Atomic Energy Research Establishment, Harwell (England)). Jun 1965. 36p. Dep. NTIS (U. S. Sales Only).

Nimonic PE16 is a precipitation hardening nickel–iron–chromium–molybdenum high-temperature alloy, and is a potential nuclear fuel canning material. Its high temperature ductility is decreased by neutron irradiation, and the degree of embrittlement at neutron doses of 5×10^{19} thermal n/cm^{-2} and 1.5×10^{20} thermal n/cm^{-2} is a function of the grain size in the fine grain region (down to 3.5 μ grain diameter). The degree of embrittlement is not reduced by over-ageing, nor by the presence of wide grain boundary zones denuded of precipitation in the as-heat treated structure. The strength of 14 μ grain diameter material is not affected by irradiation, but the 3.5 μ grain diameter material has a 22% lower strength before irradiation and a 36% lower strength after irradiation, in tests at 650°C and 4×10^{-6} sec^{-1} initial strain rate. Stress-directed diffusion strain (Herring–Nabarro creep) is considered to have occurred in the 3.5 μ grain size material, in both the unirradiated and irradiated conditions, and to account for a few percent of the strain observed in tests at 650°C and 4×10^{-6} sec^{-1} initial strain rate. Helium arising from the $^{10}B(n,\alpha)^7Li$ reaction is assumed to be the cause of the high temperature embrittlement. It is considered that this embrittlement can be explained on the basis of the helium bubble model proposed by Barnes (1963 and 1964). (auth) (UK)

11532 (AERE-R-5677) TECHNIQUE FOR THE PREPARATION OF THIN FILMS FOR TRANSMISSION ELECTRON MICROSCOPY FROM HIGHLY IRRADIATED URANIUM DIOXIDE FUEL ELEMENTS. Bainbridge, J. E. (Atomic Energy Research Establishment, Harwell (England)). Sep 1970. 13p. Dep. NTIS (U. S. Sales Only).

Techniques have been developed for the preparation of thin films suitable for transmission electron microscopy from highly irradiated, cracked uranium dioxide fuel elements. The essential feature of the various stages of the technique—impregnation, slicing, trepanning and thinning—is that the number and complexity of the handling operations are reduced to a minimum. In the thinning operation this is achieved by electropolishing with a reversible polarity double jet electrolyte process which eliminates the need for mechanical contact. (auth) (UK)

11533 (ORNL-TM-2635(Suppl.)) EXPERIMENT DESCRIPTION AND HAZARDS EVALUATION FOR THE SERIES I ORNL OXIDE FUELS IRRADIATION IN EBR-II. Olsen, A. R.; Homan, F. J. (Oak Ridge National Lab., Tenn.). Jun 1970. Contract W-7405-eng-26. 16p. Dep. NTIS.

The operating conditions and safety of the Series I capsules were reevaluated to justify inclusion in a new subassembly to extend the target burnup level from 5% FIMA to an average of 10.5% FIMA. The analysis shows that such an extension is safe for these capsules in the peak flux position in an EBR-II A-19 subassembly located in row 5, with the reactor operating at a power level of 62.5 MW. (auth)

11534 (WAPD-TM-979) ANALYSIS OF THE TRANSIENT CAPABILITY OF ROD-TYPE FUEL ELEMENTS (LWBR DEVELOPMENT PROGRAM). Campbell, W. R.; Goldberg, I. (Bettis Atomic Power Lab., Pittsburgh, Pa.). Dec 1970. Contract AT(11-1)-Gen-14. 11p. Dep. NTIS.

The capability of a bulk-oxide, rod-type fuel element to sustain a series of up-power transients that induces high strain rate in

the cladding has been evaluated by comparing peak clad stresses and strains calculated by the CYGRO computer program with a set of stress-strain limits used for this evaluation. The generalized data of depletion capability developed herein are useful in determining fuel rod performance capability for a wide range of geometries and operating conditions, without having to run specific CYGRO calculations for each fuel element. (auth)

11535 IRRADIATION STUDIES OF (U,Pu)N. Bauer, A. A.; Storhok, V. W. (Battelle Memorial Inst., Columbus, Ohio). Contract W-7405-eng-92. Nucl. Met., Met. Soc. AIME; 17: 532-44 (1970).

From 4th International Conference on Plutonium and Other Actinides, Santa Fe, N. Mex. See CONF-701001-(Pt.2).

The irradiation behavior of solid-solution uranium-20 wt % plutonium nitride was investigated in a series of four capsule irradiations performed in the MTR and ETR. The nitride fuel, prepared by a hydride–nitride cycle from uranium–plutonium alloy castings, was irradiated in the form of pellets contained within stainless steel cladding. Pellet densities were in the ranges of 80 to 84 and 93 to 97 percent of theoretical. Fuel specimens were prepared and irradiated in which either helium or sodium served as the fuel-to-cladding bond medium. Fuel burnups ranged from 11.0 to 34.5 $\times 10^{20}$ fissions/cm^3, average linear heat ratings from 13.5 to 32.2 kW/ft, and average fission heat densities from 1.7 to 4.4 kW/cm^3. Fuel surface temperatures were between 395 and 825°C while fuel centerline temperatures were at least as high as 1260°C. No evidence of reaction between fuel and stainless steel cladding or between the fuel and bonding media was observed. Fuel microstructural changes were minimal. Fuel swelling rates were uniformly low at a maximum of 0.48 percent $\Delta V/V$ per 10^{20} fissions/cm^3. This swelling rate is apparently characteristic of fuel growth associated with the locating of individual fission-product atoms at interstitial and substitutional sites of the nitride lattice. No evidence of fuel swelling associated with the formation of fission gas bubbles was obtained. Fission-gas-release values ranged from 0.09 to 13.5 percent, the release percentage varying with fuel density. Gas release was 0.09 to 0.8 percent for the high-density fuel and 1.55 to 13.5 percent for low-density fuel. (auth)

11536 FISSION GAS BUBBLE PRECIPITATION AND GROWTH IN PuO_2–UO_2 UNDER IRRADIATION. Bullington, D. C.; Leggett, R. D. (WADCO, Richland, Wash.). Nucl. Met., Met. Soc. AIME; 17: 545-53(1970).

From 4th International Conference on Plutonium and Other Actinides, Santa Fe, N. Mex. See CONF-701001-(Pt.2).

The intergranular pore density was determined at two axial positions in a mixed oxide fuel pin irradiated in EBR-II to a peak burnup of 1 percent of the heavy atoms. The pore size was approximately that calculated; however, no dependence of pore size distribution with local temperature or temperature gradient was found. The volumetric average intergranular pore volume was found to be greater in the fuel operating at the lower burnup rate. The study indicated that unetched fuel is more suitable for measurement of spatial pore distributions than etched samples. (auth)

11537 ELECTRON MICROSCOPY OF ALPHA PARTICLE DAMAGE IN ACTINIDE OXIDES. Douglass, Dana L.; Bronisz, S. E. (Los Alamos Scientific Lab., N. Mex.). Nucl. Met., Met. Soc. AIME; 17: 596-605(1970).

From 4th International Conference on Plutonium and Other Actinides, Santa Fe, N. Mex. See CONF-701001-(Pt.2).

Three actinide oxides, ThO_2, NpO_2, and PuO_2, irradiated with 5.5 MeV alpha particles to a dose of ~10^{15} α's/cm^2, were examined by means of transmission electron microscopy. Both the primary defects produced by radiation and the secondary defects, dislocation loops, produced by post-irradiation annealing at ~$T_m/2$ were similar in the three oxides. Voids were observed only in NpO_2 after short post-irradiation exposure to ~400°C. The loops were larger in ThO_2 (up to 300 Å dia) than in either NpO_2 or PuO_2. The loops were generally situated on {113}, {110}, and {012} planes in ThO_2; {012} and {110} in NpO_2; and {110}, {012}, and {111} in PuO_2. (auth)

Plastics and Other Materials

Refer also to abstracts 10609, 11952, 11961, and 12804.

XUM

PHYSICS (GENERAL)

Astrophysics and Cosmology

11538 ASTRONOMIYA I GEODEZIYA V ESTONSKOI SSR (1940–1966). (Astronomy and Geodesy in Estonian SSR (1940–1966)). Kuzmin, G. G. (ed.). Tartu, USSR; Institut Fiziki i Astronomii, Akademiya Nauk Estonskoi SSR (1969). 180p.

Eight articles are included on the development of astronomy in the Estonian SSR. The physics of stars and nebulae, the structure and dynamics of star systems, cosmology and relativistic astrophysics, and small bodies of the solar system are discussed in the first five articles. Geodesy, astronomy, instrumentation manufacturing, and the history of astronomy and geodesy are covered in the last three articles. Extensive references are included. (R.V.J.)

Cosmic Ray Exposure Ages

11539 RADIONUCLIDES IN METEORITES AND IN THE LUNAR SURFACE. Lindstrom, Richard Mark. San Diego, La Jolla, Calif.; Univ. of California (1970). 213p. University Microfilms Order No. 70-15,445.

Thesis.

This thesis consists of three specific parts: production of ^{129}I in meteorites and the neutron capture cross section of ^{128}I; gas proportional counting of transition-metal x-ray emitters; and ^{36}Cl, ^{55}Fe, and ^{210}Pb in Mare Tranquillitatis. (TSS)

11540 GAMMA SPECTROMETRY MEASUREMENT OF THE RADIOACTIVITY OF A RECENTLY FALLEN CARBONATED CHONDRITE: ALLENDE. Tobailem, Jacques; Nordemann, Daniel (CEA, Saclay, France). Compt. Rend., Ser. D; 271: 1249-51(12 Oct 1970). (In French).

The γ emitters ^{22}Na, ^{26}Al, ^{40}K, ^{54}Mn, and ^{60}Co were determined in the meteorite Allende (February 8, 1969) by low-background γ spectrometry. The results are discussed. The minimum pre-atmospheric mass of the meteorite was estimated at 5,000 kg. (auth) (France)

Stars

Refer also to abstracts 11637 and 12188.

11541 (CSIRO-Trans-10286) DENSITIES AND MASSES OF COMET-SHAPED NEBULAE. Dibai, E. A. Translated by G. Losonci from Astron. Tsirk.; No. 502, 1-3(11 Apr 1969). 3p. Dep. NTIS (U. S. Sales Only).

A tabulation is presented of the estimated masses, intensities, ionized-gas densities, and neutral-gas densities of some comet-shaped nebulae. Notes on some of the measurements are included. (Australia)

11542 (NP-18591) ON THE NUCLEOSYNTHESIS OF LITHIUM, BERYLLIUM, AND BORON. Bernas, R.; Gradsztajn, E. (Paris Univ., Orsay (France). Laboratoire Joliot-Curie de Physique Nucleaire); Reeves, H. (Centre National de la Recherche Scientifique, Orsay (France). Centre de Spectrometrie Nucleaire et de Spectrometrie de Masse. Centre National de la Recherche Scientifique, Paris (France). Institut d'Astrophysique); Schatzman, E. (Centre National de la Recherche Scientifique, Paris (France). Institut d'Astrophysique). [nd]. 73p. Dep. NTIS (U. S. Sales Only).

The nuclear physics of the spallation reactions, which lead to the formation of Li, Be, and B by the proton bombardment of light nuclei, is reviewed. A large amount of experimental data was gathered. A simple rule was devised for classifying the cross sections in terms of their isotopic spin parameters. This rule can be used to predict the results of reactions. The physical meaning of this rule is discussed, using calculations based on statistical models. The ratios of the Li, Be, and B isotopes produced by protons of fixed energies or by cosmic-ray protons with an extended energy spectrum were determined. The exact shape of the spectrum, which gives rise to these isotopes, was not known; it was assumed to be power energy spectrum with exponents ranging from (–1) to about (–4). The probable nuclear reactions responsible for the change in the ratios after formation are discussed. The abundance of these elements in nature is discussed and results compared and summarized in terms of creation and decay rates. The meteoritic ^{11}B to ^{10}B ratio is shown to be equal to its formation ratio, and the ^{7}Li to ^{6}Li formation ratio is shown to be smaller than the meteoritic ratio. A tentative picture of the history of the solar system is given from these results. An alternative picture is also sketched, based on the assumption of a much steeper type of spectrum. (France)

11543 STELLAR SPECTROSCOPY: NORMAL STARS. Hack, Margherita; Struve, Otto. Trieste, Italy; Osservatorio Astronomico di Trieste (1969). 203p.

The purpose of the book is to give to graduate students a review of the main results obtained in stellar physics through the study of stellar spectra. It is complementary to books on theory of stellar atmospheres in that it describes spectra and observational facts and their interpretation, as well as their use in constructing theories of stellar atmospheres. Topics considered in this volume include stellar atmospheres and methods for the study of stellar spectra, spectral classification, stellar rotation, and quantitative analysis of stellar spectra. (W.D.M.)

11544 SOME NUCLEOSYNTHETIC EFFECTS OF ENERGETIC PROTON FLUXES ON STELLAR SURFACES AND ON THE SOLAR SYSTEM. Audouze, Jean (Institut d'Astrophysique, Paris. Service d'Electronique Physique, Saclay, France). Astron. Astrophys.; 8: 436-57(Oct 1970).

Taking advantage of recent developments (both experimental and theoretical) in the determination of spallation cross sections of atomic nuclei, the rate of isotope formation generated when a flux of fast protons irradiates material of various compositions was computed. These calculations were applied to various types of physical conditions, simulating models of astrophysical processes. The abundances of Li, Be, and B) were taken as monitors for the total (time-integrated) flux intensity. The abundance of elements produced by such a flux on a standard "cosmic" gas (simulating the effect of the galactic cosmic rays on the interstellar gas) was extremely small, way below the observed abundance of even the rarest isotopes except ^{50}V. Models of the early solar system and of particular stars were also considered; under specific assumptions the isotopes D, ^{49}K, ^{50}V and heavy p-elements in the solar system and the Tc in cold S stars could be of spallogenic origin. The effect of proton-induced nuclear reactions in solar flares and the consequent γ-ray flux were considered, in reference to the proton flux observed at the Earth. The predicted γ fluxes are often appreciably higher than the present upper limits quoted from observations. Recent measurements of stellar Li and Be in F and G stars are discussed; the abundance differences could be explained by assuming a variation of the mean spectral index with spectral class. The spallogenetic role of secondary neutrons is usually found to be negligible; after thermalization these particles are photocaptured into deuterons. (auth)

11545 SUPERFLUID STATE IN NEUTRON STAR MATTER. I. GENERALIZED BOGOLYUBOV TRANSFORMATION AND EXISTENCE OF $^3P_2$ GAP AT HIGH DENSITY. Tamagaki, Ryozo (Kyoto Univ.). Progr. Theor. Phys. (Kyoto); 44: 905-28(Oct 1970).

A superfluid state originating from the $^3P_2$ pairing was investigated for the high-density core of neutron stars ($\rho \gtrsim \frac{1}{2}\ \rho$(nuclear matter) $= 1.6 \times 10^{14}$ gcm^{-3}), where the pairing interaction is most attractive in the $^3P_2$ state due to spin-orbit forces. In order to treat such a nonzero angular momentum pairing, generalization of the Bogolyubov transformation was developed. Applications of this formalism to several cases are given. For the $^3P_2$ pairing in neutron star matter, calculations were made for a special but characteristic coupling leading to an anisotropic energy gap. The results show that the $^3P_2$ gap exists with $1 \sim 3$ MeV for the density $\rho \gtrsim 2\ 10^{14}$ gcm^{-3} ($E_F \gtrsim 50$ MeV). (auth)

11546 ATMOSPHERES OF METAL-DEFICIENT STARS: GIANT STARS. Krishna Swamy, K. S. (Rice Univ., Houston, Tex.). Astron. Astrophys.; 8: 375-80(Oct 1970).

Model atmospheres were constructed for effective temperatures 4000, 4500, and 5000°K and for hydrogen-to-metal ratios of 1, 5, 10, 40, and 100 times the solar value, and for surface gravities of 2×10^3 and 2×10^2. The effect of metal deficiency on the atmospheric structure of these stars was studied. (auth)

11547 STUDY OF NOVA HER 1963 IN THE EARLY DECLINE AND IN THE TRANSITION STAGE. Tremko, J. (Hamburger Sternwarte, Hamburg). Astron. Astrophys.; 8: 381-8(Oct 1970).

The radial velocities in the shell of Nova Her 1963 were studied on the basis of the principal, the diffuse enhanced, and the Orion spectrum during the early decline and transition phase, and the radial-velocity systems were determined. The influence of emission on the radial velocities derived from the hydrogen absorption lines was studied. This effect was only –9.6 km for the lines H_δ,

H_γ, H_δ, and H_β. There was some correlation between the radial velocities of the principal spectrum and the excitation potential. Possible correlations between photometric and spectroscopic data were investigated. Changes of brightness and radial velocity were not closely correlated and there was a discrepancy in the phase. An acceleration of 21 cm/sec^2 in the principal and diffuse enhanced spectrum during the first part of the early decline stage was present. A considerable acceleration in the Orion spectrum during the transition phase was observed. (auth)

11548 ENERGETICS OF L-NUCLEI FORMATION IN STELLAR ATMOSPHERES AND ITS RELEVANCE TO X-RAY ASTRONOMY. Ryter, C.; Reeves, H.; Gradsztajn, E.; Audouze, J. (CEN, Saclay, France. Institut d'Astrophysique, Paris. Centre de Spectrometrie Nucleaire, et de Spectrometric de Masse, Orsay, France). Astron. Astrophys.; 8: 389-97(Oct 1970).

The energy required to generate the light nuclei Li, Be, and B by fast-particle-induced nuclear reactions on atoms of the stellar atmospheres was evaluated in various physical conditions (energy spectra, gas temperature). In the most optimistic case, where hard spectra in very hot flares are present, the energy of formation of one lithium atom requires at least 0.1 erg; in more realistic cases, values of ten to hundreds of ergs are found necessary. This result has an important bearing on the nucleosynthesis of the light elements in young stars (T Tauri). If these stars have generated these elements by particle acceleration in their own atmosphere (the so-called autogenetic model for the origin of the light elements) they must have used in this accelerating process an amount of energy comparable to, if not larger than, the total amount of gravitational energy released since their birth. The presence of hot flares in T-Tauri stars involving the amount of energy and the temperature required by the autogenetic model would lead to x-ray emission. The flux for a typical T-Tauri star was evaluated and falls just below present observational threshold. If real, it should be observable in a near future. (auth)

11549 THERMODYNAMICS OF WHITE DWARF MATTER. Kovetz, A.; Shaviv, G. (Tel Aviv Univ., Israel). Astron. Astrophys.; 8: 398-403(Oct 1970).

An equation of state for white-dwarf matter of high density and finite temperature, in which the ions form a cubic body centered lattice, was derived. Some thermodynamic quantities are discussed with numerical examples. The passage from gas to solid is treated as a quasi-static phase transition and the effect of latent heat release on stellar evolution is briefly discussed. (auth)

11550 VARIABLE STARS IN A FIELD CENTERED AT $l^{II} = 0°$, $b^{II} = -10°$ (FIELD 3 OF THE PALOMAR-GRONINGEN VARIABLE-STAR SURVEY $\alpha = 18^h24^m04^s$, $\delta = -33°58'.6$). Plaut, L. (Kapteyn Astronomical Lab., Groningen, Netherlands). Astron. Astrophys.; 8: 341-57(OCt 1970).

This paper is the fourth one in a series giving results of the Palomar–Groningen variable-star survey. It deals especially with the results obtained from the observations of variables in field 3 centered at $l^{II} = 0°$, $b^{II} = -10°$. Results on the RR Lyrae variables are given, especially a discussion on their spatial distribution in the direction of field 3. The long-period variables are considered in the same way. Results are compared with those from fields 1 and 2, which are on other galactic latitudes but the same longitude, and with results from other investigators. The agreement is fairly good, although the accuracy of the densities is not yet satisfying. Suggestions to obtain more accurate results are given. Other types of variables found are mentioned. Details on all variables will be given in a subsequent paper in the Supplement Series. (auth)

11551 METAL-TO-HYDROGEN RATIO FOR STARS IN THE HYADES AND COMA OPEN CLUSTERS. Nissen, P. E. (Kitt Peak National Observatory, Tucson, Ariz.). Astron. Astrophys.; 8: 476-9(Oct 1970).

Photoelectric observations of the strength of a group of weak metal lines were carried out with the 60-inch McMath Solar Telescope for 9 Hyades stars and 10 Coma stars. No evidence was found for any composition variations among individual members for any of the clusters. An average difference of the logarithm of the metal-to-hydrogen ratio (Hyades – Coma = 0.19 ± 0.04) was derived with the aid of a model-atmosphere analysis of the observations. (auth)

11552 STABILITY OF ROTATING STARS. III. NONAXISYMMETRIC MODES AND DIFFUSIVITY IN MAGNETIC STARS. Fricke, K. (Univ., Goettingen, Ger.); Schubert, G. Astron. Astrophys.; 8: 480-5(Oct 1970).

A local analysis was used to investigate the stability to nonaxisymmetric perturbations of differentially rotating stellar interiors in the presence of toroidal and poloidal magnetic fields. In the case of toroidal magnetic fields it was found that the nonaxisymmetric modes can be unstable under conditions which guarantee stability to axisymmetric perturbations. The effect of nonzero magnetic diffusivity was also investigated. The stability criteria exhibit the proper behavior in the limit of zero magnetic field. It is shown that stabilization of rotation laws satisfying the Ferraro isorotation condition is likely only if the rotation is slow and the poloidal magnetic field is large. (auth)

11553 EXTENSIVE AIR SHOWER ARRAYS AS DETECTORS OF PROMPT GAMMA RAYS FROM SUPERNOVAE EXPLOSIONS. Oegelman, H. (Middle East Tech. Univ., Ankara). Nature (London); 228: 1181(19 Dec 1970).

From the considerations discussed it is concluded that high-altitude extensive air shower arrays are capable of use for investigating the very early phases of cosmic-ray acceleration in supernova explosions. The initial pulses could be extremely short and contain energies $>10^{46}$ ergs as high-energy photons. It would seem worthwhile to examine past and future data of extensive air shower arrays for this type of event. The operational time of the BASJE array at Mt. Chacaltaya, Bolivia, has been sufficient to see several such events. It is conceivable that such events have been overlooked or rejected during automated analysis procedures. (UK)

11554 SPHERICAL VORTEX MOTIONS OF A CONDUCTING FLUID. Ranger, K. B. (Univ. of Toronto). J. Fluid Mech.; 44: 481-92(26 Nov 1970).

Some exact solutions of the steady MHD equations for an inviscid infinitely conducting fluid are discussed, and a generalization of the Prendergast model for an idealized magnetic star is obtained, in which there is a finite azimuthal swirl velocity of the fluid. The flow in all examples is bounded by a sphere and expressions are found for the distribution of energy between the fluid motion and magnetic field. (auth) (UK)

11555 PHOTOMETRIC HISTORY OF BL LACERTAE. Shen, B. S. P. (Univ. of Pennsylvania, Philadelphia); Usher, P. D. Nature (London); 228: 1071-2(12 Dec 1970).

Previous studies of BL Lac are briefly summarised. The non-thermal nature of the radiation and the optical variability resemble the characteristics of compact galaxies and quasars, and the variability is found to be extremely irregular over periods of a few hundred days of continuous observation. In view of interest being shown in the past variability of BL Lac, photometric data are presented derived from the archive plate collection of Harvard College Observatory. Conclusions reached are as follows: (1) the brightness is fainter than 14 magnitude for most of the time, reaching or exceeding magnitude 13 during two periods in its history; (2) during the second outburst, the brightness increased secularly throughout practically the entire known range of variability and subsequently decreased again, the whole episode lasting about 10 years; and (3) there is a similarity in the optical behaviour of BL Lac and the N-galaxy 3C371. (UK)

11556 ATMOSPHERES OF WHITE DWARFS. II. THE EFFECTS OF CONVECTION. Wickramasinghe, D. T.; Strittmatter, P. A. (Inst. of Theoretical Astronomy, Cambridge, Eng.). Mon. Notic. Roy. Astron. Soc.; 150: 435-41(1970).

The effect of convection on the structure and observable features of DA (hydrogen line) and DB (He I line) white dwarf atmospheres is examined on the basis of mixing length theory and of constant flux model atmospheres. It is concluded that (in comparison to models in pure radiative equilibrium) convection has important effects on the atmospheric structure in the temperature ranges $8000° \lesssim T_{eff} \lesssim 13{,}000°K$ and $15{,}000° \lesssim T_{eff} \lesssim 25{,}000°K$ for DA's and DB's respectively. In all cases convection causes the visual spectrum to mimic that of a hotter star. Equivalent widths of Hγ and He I λ 4472 respectively are increased by ~10%. The predicted U–B, B–V colors are hardly affected however, since convection is important only when the colors are insensitive to temperature changes. (auth) (UK)

11557 METHOD FOR DETERMINING THE SIZES OF THE GASEOUS ENVELOPES SURROUNDING Be STARS. Kitchin, C. R. (Univ. of Leicester, Eng.). Mon. Notic. Roy. Astron. Soc.; 150: 455-80(1970).

A simple, direct method of obtaining the sizes of the emitting or absorbing regions of the rarefied gaseous envelopes around Be stars is outlined. The method allows the size of the emitting or absorbing region to be found directly in terms of the ratio of the intensities in the outer parts of a line, arising in the envelope, to the intensity of the inner part. The method has possible applications to other fast-rotating stellar systems with gaseous envelopes. In particular, it is suggested that the method outlined might be applicable to the envelopes of Of, P Cygni, T Tauri, and

XUM

possibly Ap stars, and to close binary systems. The method was applied to the O I 8446 line of ξ Tauri, and a radius of II stellar radii was found for the region of the envelope emitting this line. (auth) (UK)

11558 MASSES OF PULSATING STARS. Rodgers, A. W. Mon. Notic. Roy. Astron. Soc.; 151: 133–40(1970).

Observations of period, color, and luminosity of classical Cepheids and RR Lyrae stars are compared with the predictions of linear and nonlinear pulsation theory computed by Christy. There is a discrepancy between the pulsational mass and that inferred from evolutionary tracks computed by Iben; the pulsation masses range between 60 and 70% of the evolutionary masses. Pulsation theory, using radiative envelopes, fails to predict the correct stellar parameters for the amplitude-modulated-beat Cepheids, which are in the transition between fundamental and overtone pulsation. Pulsation theory predicts a variation of mass of RR Lyrae stars as a function of color. It is concluded that quantitative deductions of the masses of pulsating stars cannot yet be made from a comparison of observations and pulsation theory based on radiative envelopes and diffusive radiation transfer. (auth) (UK)

11559 INTERNAL STRUCTURE OF UPPER MAIN-SEQUENCE STARS. Stothers, R. (Goddard Space Flight Center, New York). Mon. Notic. Roy. Astron. Soc.; 151: 65-80(1970).

In main-sequence stars heavier than 9 $M_\odot$, convective instability develops just outside the zero-age convective core as hydrogen depletion proceeds. At least ten schemes are available in the literature to treat the unstable intermediate zone that results; a detailed investigation, utilizing physical, laboratory, stellar-model, and observational considerations, is presented here. Only two schemes survive, both of which are semiconvective: the modified Schwarzschild–Härm (SH) prescription and the modified Ledoux–Sakashita–Hayashi (LSH) prescription. The former scheme is tentatively favored by the weight of laboratory evidence. In either case, the earliest stages of hydrogen depletion are characterized by a semiconvective zone that joins continuously the convective core and the outer radiative envelope. The later stages are characterized by a radiative detachment of the semiconvective zone from the core, except for masses above 15 $M_\odot$ in the SH scheme. At any given mass, the final hydrogen profiles resulting from each of the two schemes are very similar. (auth) (UK)

11560 GRAVITATIONAL INSTABILITY OF POLYTROPIC GAS SPHERES UNDER EXTERNAL PRESSURE. Horedt, Gp. (Observatorul Astronomic, Lomami, Congo). Mon. Notic. Roy. Astron. Soc.; 151: 81-6(1970).

The behavior of polytropic gas spheres under an external pressure is studied. For a polytropic index n greater than three, gravitational instability occurs and a criterion exists similar to the Jeans criterion for the isothermal medium. The critical masses and densities for n = 4, 5 are obtained. Infinitely long nonrotating polytropic cylinders under external pressure have no gravitational instability along their radius. (auth) (UK)

11561 B-TYPE STARS WITHIN TEN DEGREES OF THE GALACTIC CENTRE. I. Dixon, M. E. (Australian National Univ., Canberra). Mon. Notic. Roy. Astron. Soc.; 151: 87-92 (1970).

Ages, distances, and space motions are presented for a sample of B-type stars with 10° of the galactic center. (auth) (UK)

11562 ORIGIN OF THE IRON BANDS IN SUPERNOVAE SPECTRA. Manning, P. G. (Dept. of Energy Mines and Resources, Ottawa). Nature (London); 228: 844-5(28 Nov 1970).

Three absorption bands (at 6200, 4430, and 3800 Å) in the optical spectra of Type 1 supernovae have recently been assigned to transitions within octahedral Fe^{3+} ions in andradite garnet, whilst two other bands (at 5100 and 5700 Å) were attributed to Fe^{2+} ions in almandine garnet. It has also been suggested that the bands may mark transitions in Fe^{2+} ions in pyroxene minerals. Spectra are presented for two supernovae and two terrestrial Fe^{2+}-bearing minerals, together with their resolved band components, and peak heights for bands in four supernova spectra and absorbance ratios for pairs of bands in the four spectra are tabulated. From a discussion of the data it is concluded that band intensity relationships confirm an earlier suggestion that at least two Fe-bearing minerals condense from ejected supernova shells. The 6200-, 4430-, and 3800-Å bands would seem to characterize octahedral Fe^{3+} ions and possibly an andradite garnet. Garnets on Earth form under restricted conditions of temperature and high pressure, conditions that might exist in the atmospheres of cool stars. It is conceivable that the silicates that give rise to supernova spectra may have pre-existed the supernova explosion, the circumstellar grains being rendered transparent by evaporation of condensed volatiles on grain surfaces. (UK)

11563 TWO INFRARED SOURCES IN NEBULAE. Cohen, M.; Dewhirst, D. W. (Cambridge Univ., Eng.). Nature (London); 228: 1077(12 Dec 1970).

In a systematic survey of the Caltech infrared catalog, using the prints of the National Geographic Society–Palomar Observatory sky survey, some errors of identification were indicated, and these are briefly reviewed. Two particularly interesting sources were found to coincide with small nebulae on the sky survey prints, details of which are given. The first was IRC + 40091, which was identified with NGC 1579, a small, irregular, diffuse nebulosity, about 10 arc-min across. The second source, closely associated with NGC 6857, was IRC + 30407, of extent about 40 arc-sec, and the recognition of an infrared source in this nebulosity strengthens the evidence from radio observations that NGC 6857 is a region of active star formulation. (UK)

11564 COMPOSITION OF δ PAVONIS. Harmer, D. L.; Pagel, B. E. J.; Powell, A. L. T. (Royal Greenwich Observatory, Sussex, Eng.). Mon. Notic. Roy. Astron. Soc.; 150: 409-18(1970).

The old subgiant δ Pavonis, which has an ultraviolet deficiency on the UBV system, was found by Rodgers (1969) to have the same composition as the Sun, but enhanced microturbulent velocity. A new analysis, however, suggests that the star is metal rich, compared to the Sun, by a factor of about 2, and this result is confirmed by a reanalysis of Rodgers' measurements. (auth) (UK)

11565 ENERGY OF THE SECOND EXCITED STATE OF ^{12}C AND THE RATE OF THE TRIPLE-ALPHA REACTION. Austin, Sam M. (Univ. of Copenhagen. Michigan State Univ., East Lansing); Trentelman, G. F.; Kashy, E. Astrophys. J.; 163: L79-82(15 Jan 1971).

The excitation energy of the second excited state of ^{12}C was measured to be $E_x = 7.6562 \pm 0.0021$ MeV. This value of E_x leads to a factor of $\exp(-0.138/T_8)$ change in the 3α reaction rate quoted by Fowler, Caughlan, and Zimmerman and a substantial change in the products of helium-burning nucleosynthesis. (auth)

11566 HAGEDORN EQUATION OF STATE IN NEUTRON STARS. Rhoades, Clifford E. Jr. (Princeton Univ., N. J.); Ruffini, Remo. Astrophys. J.; 163: L83-7(15 Jan 1971).

At a density of $\sim 5 \times 10^{12}$ g cm^{-3} neutron-star matter can be described (Harrison and Wheeler) by a system of three noninteracting degenerate gases—namely, electrons, protons, and neutrons. At a density of $\sim 10^{14}$ g cm^{-3}, strong interactions between particles can give a significant contribution (Cameron, Cohen, Langer, and Rosen). At densities of $\gtrsim 10^{15}$ g cm^{-3}, production of new particles has to be taken into account. Hagedorn has recently given an analytic equation of state for this regime. The effect of this new equation of state for supranuclear densities on the equilibrium configurations of neutron stars was explored. (auth)

11567 FURTHER RADIO OBSERVATIONS OF PLANETARY NEBULAE. Thomasson, P.; Davies, J. G. (Manchester Univ., Jordell Bank, Eng.). Mon. Notic. Roy. Astron. Soc.; 150: 359-71(1970).

The Jodrell Bank Mark I and Mark II telescopes were used both as an interferometer and as total power instruments to measure the spectra of planetary nebulae over the frequency range 408 MHz to 7800 MHz. Any previous indication of nonthermal spectra was shown to be the effect of confusing sources. A spherical shell model, the thickness of which is variable from zero up to the radius of the nebula, was adopted and values for the parameters of the model were derived. From the relationship between the linear dimensions of a nebula and the "turn-over" frequency of its spectrum, it is concluded that three nebulae—IC 418, NGC 6210, and NGC 40—have ionized masses significantly different from those of other nebulae. (auth) (UK)

11568 OBSERVATION OF CO EMISSION AT 2.6 MILLIMETERS FROM IRC +10216. Solomon, Philip (Columbia Univ., New York); Jefferts, Keith B.; Penzias, Arno A.; Wilson, Robert W. Astrophys. J.; 163: L53-6(15 Jan 1971).

The CO J = 1 to J = 0 rotational transition at 2.6 mm was observed in IRC + 10216. The spectral line was broad and fairly flat, which indicated thermal emission from a shell expanding at 15 km sec^{-1}, with an age of approximately 500 years. The mass in the CO emitting region was estimated to be in the range expected for planetary nebulae. (auth)

11569 INFRARED STUDIES OF GALACTIC NEBULAE. II. THE COMPACT NEBULAE IC 4997, VV 8, AND FG SAGITTAE. Gillett, F. C. (Univ. of California, San Diego, La Jolla); Knacke, R. F.; Stein, W. A. Astrophys. J.; 163: L57-9(15 Jan 1971).

Three compact nebulae, IC 4997, VV 8 (M1 – 2), and FG Sge, were observed at 3.5 and 11.0 μ. IC 4997 and VV 8 emit more energy at infrared wavelengths than at visual wavelengths. The energy detected from FG Sge at λ = 3.5 μ appears to be consistent with the radiation expected from a 5500°K blackbody normalized at the observed visual magnitude of the object. The upper limit set at λ = 11 μ from FG Sge is also consistent with no large infrared excess. In addition, Sharpless 71 has also been found to emit more energy in the infrared than at visual wavelengths. (auth)

11570 NOTE ON THE CENTRAL STAR OF NGC 3132. Brown, S.; Higginbotham, N.; Lee, P. (Louisiana State Univ. Observatory, Baton Rouge). Publ. Astron. Soc. Pac.; 82: 1372-4(Dec 1970).

Observations are reported which suggest that the central star of NGC 3132 may be a member of a binary. (auth)

11571 OBSERVATIONAL CONFIRMATION OF A MECHANISM FOR THE PRODUCTION OF EXTENDED STELLAR ATMOSPHERES. Hillendahl, R. W. (Lockheed Palo Alto Research Labs., Palo Alto, Calif.). Publ. Astron. Soc. Pac.; 82: 1231-52 (Dec 1970).

A recently reported mechanism for the production of extended stellar atmospheres is discussed in some detail and compared with presently available observations. The mechanism involves the outward acceleration of material in a rarefaction wave which follows the arrival of a shock wave at the edge of the atmosphere. It is shown that the rarefaction wave will generate a secondary shock wave of atmospheric origin as it moves back into the star. Observational evidence is cited for the existence of the secondary shock waves. The rarefaction waves also provide a mechanism for mass loss to the interstellar medium. An observational criterion is discussed for identifying the existence of this mechanism and for distinguishing it from other mechanisms for mass loss. (auth)

11572 PHOTOELECTRIC OBSERVATIONS OF STARS WITH VARIABLE H AND K EMISSION COMPONENTS. Blanco, C.; Catalano, S. (Univ., Catania, Italy). Publ. Astron. Soc. Pac.; 82: 1293-1304(Dec 1970).

On the hypothesis that spectral and photometric variations might be connected, as in the Sun, to a stellar cycle of activity, photoelectric observations of stars showing variable H and K emission components were carried out. Results on the observations of HD 119850, α Boo, and α Tau are reported. (auth)

11573 PHOTOMETRIC CLASSIFICATION OF THE FEIGE BLUE STARS. Graham, J. A. (Cerro Tololo Inter-American Observatory, La Serena, Chile). Publ. Astron. Soc. Pac.; 82: 1305-23(Dec 1970).

A photometric classification scheme for high-latitude blue stars is described with reference to the properties of the Strömgren uvby system, uvby photometry is presented for 94 stars from the Feige list of blue stars. When the classification procedure is applied to these stars, a large number of interesting objects are detected. Nineteen of the Feige stars are probable sdO or sdB stars. Eight are low-gravity horizontal branch stars. The Feige stars numbered 7, 87, 90, and 109 have peculiar color indices and spectra are needed for further study of their nature. (auth)

11574 NATURE OF THE NEBULOSITY ABOUT FG SAGITTAE. Faulkner, D. J.; Bessell, M. S. (Australian National Univ., Canberra). Publ. Astron. Soc. Pac.; 82: 1333-40(Dec 1970).

Two independent methods were used to verify the conclusion of Herbig and Boyarchuk (1968) that the nebulosity surrounding FG Sge is an old planetary shell, indicating that shell formation is a repetitive phenomenon. It is suggested that nebula ejection takes place at the thermal relaxation oscillation stage of a helium shell-burning star, through the action of radiation pressure. (auth)

11575 EXISTENCE OF AN UPPER LIMIT IN THE ACTIVITY OF SOLAR NEIGHBORHOOD FLARE STARS. Kunkel, William E. (Cerro Tololo Inter-American Observatory, La Serena, Chile). Publ. Astron. Soc. Pac.; 82: 1341-5(Dec 1970).

Flare incidence was examined for 21 dMe stars in the solar neighborhood. Flare activity was found to have an upper bound in that the time-averaged energy radiated by flares is 1% or less of the energy radiated by the quiescent photosphere. (auth)

11576 INFERRED PRESENCE OF BALMER EMISSION FEATURES IN THE SPECTRA OF EARLY-TYPE STARS. I. THE HAMBURG-CASE SURVEY. Wackerling, Lloyd R. (Northwestern Univ., Evanston, Ill.). Publ. Astron. Soc. Pac.; 82: 1352-6(Dec 1970).

A comparison was made between the sample of spectra noted as peculiar in the Hamburg–Case survey and a collation of early-type stars whose spectra have shown emission lines. The results of the comparison are presented and briefly discussed. (auth)

11577 INFERRED PRESENCE OF BALMER EMISSION FEATURES IN THE SPECTRA OF EARLY-TYPE STARS. II. MK SPECTRAL CLASSIFICATION AND BALMER-LINE PHOTOMETRY. Wackerling, Lloyd R. (Northwestern Univ., Evanston, Ill.). Publ. Astron. Soc. Pac.; 82: 1357-9(Dec 1970).

Spectroscopic observations were made of 15 stars noted by Andrews (1968) as probably showing Hα emission. The results of these observations tend to bear out Andrews' interpretation of his line-photometry data. (auth)

11578 NEW Ap STARS IN NGC 3114. Frye, Roland L. (Univ. of Michigan, Ann Arbor); Mac Connell, Darrell J.; Humphreys, Roberta M. Publ. Astron. Soc. Pac.; 82: 1360-3(Dec 1970).

Two previously unsuspected peculiar A stars were discovered in NGC 3114 as a result of a southern hemisphere objective prism survey carried out with the Michigan Curtis telescope. On the basis of their location and of their position in the H–R diagram, both stars are probable members of the cluster and should be included in the lists of known Ap stars in clusters. (W.D.M.)

11579 MAGNITUDE SEQUENCES FOR THE VARIABLE STARS UZ BOOTIS AND W PISCIUM. Landolt, Arlo U. (Louisiana State Univ. Observatory, Baton Rouge). Publ. Astron. Soc. Pac.; 82: 1364-7(Dec 1970).

UBV photoelectric sequences were established for the variable stars UZ Bootis and W Piscium. (auth)

Quasi-Stellar, Radio, and X-Ray Sources

Refer also to abstract 11812.

11580 (CSIRO-Trans-10204) FREQUENCY CORRELATION OF INTERPLANETARY SCINTILLATIONS IN METRE WAVELENGTH RANGE. Antonova, T. D. Translated by M. Hintze from Astron. Tsirk.; No. 486, 1-4(15 Oct 1968). 4p. Dep. NTIS (U. S. Sales Only).

An estimate of the value of the mean square of phase incursion fluctuation was made by simultaneous observations of scintillations at two wavelengths. Correlation coefficients for recorded pairs at 3.5 and 5 m are listed for source 3C 48, together with corrected values (assuming normal random processes). The ratio of the mean squares of intensity fluctuation at each wavelength had an average value = $1 \neq \lambda_2/\lambda_1 = 1.42$. This is attributed to the dimensions of 3C 48 being comparable with the angular dimension of inhomogeneities ($\Theta_{source} \sim 0.5''$); so 3C 48 cannot be used as a standard calibration source. (Australia)

11581 (CSIRO-Trans-10247) CONNECTION BETWEEN ABSOLUTE RADIOLUMINOSITY OF EXTRAGALACTIC SOURCES AND REDSHIFT. Braude, S. Ya.; Vaisberg, V. V.; Zhuk, I. N.; Men, A. V. Translated by M. Hintze from Astron. Tsirk.; No. 492, 5-7(25 Dec 1968). 3p. Dep. NTIS (U. S. Sales Only).

The dependence of absolute radioluminosity L, on redshift Z, is plotted for 96 quasars and over 100 galaxies at 16.5, 400, and 1410 Mc indicating that L increases with distance for Z < 2.2. (Australia)

11582 TURBULENCE IN H II REGIONS. Louise, R.; Monnet, G. (CNRS, Marseille). Astron. Astrophys.; 8: 486-8(Oct 1970). (In French).

Using the values of radial velocity given by Courtès (1960) in M8 it was found that the Kolmogoroff law $u(\Lambda) = k\Lambda^{\frac{1}{3}}$ is satisfied in this nebula. On the other hand, the internal motions integrated along the line of sight was measured recently by means of $H_\alpha(\lambda = 6563)$ and [NII](λ = 6584) line widths (Courtès et al., 1968; Louise and Monnet, 1969; Louise, 1970). These measures showed that the turbulence integrated along the line of sight is several times larger than the values predicted by the Kolmogoroff law. This is certainly due to the fact that the conditions of incompressibility and homogeneity in HII regions are not satisfied. The line widths measure the velocity dispersion along the line of sight and certainly indicate the existence of expanding condensations, which of course is consistent with the evidence of inhomogeneous density (Osterbrock and Flather, 1959). (auth)

11583 THERMAL EMISSION FROM GRAINS IN H-II REGIONS. Krishna Swamy, K. S. (Rice Univ., Houston, Tex.). Astron. Astrophys.; 8: 358-63(Oct 1970).

The thermal emission from the grain models of dirty ice, graphite, and graphite core-dirty ice mantle was calculated for different radiation fields of the central star. (auth)

11584 QUASI-STELLAR OBJECTS AND GRAVITATIONAL LENSES. de Silva, L. N. K. (Univ. of Sussex, Brighton, Eng.). Nature (London); 228: 1180-1(19 Dec 1970).

It has been suggested that QSOs are images of the nuclei of Seyfert galaxies, resulting from a gravitational lens mechanism, and expressions have been found for the intensification and angular size of the image when the path of the photons from the object to the observer passes outside the intervening object that acts as the gravitational lens. It was considered worthwhile to investigate whether there are enough Seyfert galaxies to produce the QSOs by this mechanism, where the deflectors are galaxies of every sort. The upper limit for the ratio of the number of QSOs to the number of Seyfert galaxies would appear to lie between 10^{-7} and 10^{-3}, and even if it is assumed that the density of matter in the universe is 10^{-29} g/cm^3, which is the upper bound usually quoted, and even if all this matter is in the form of deflectors, the ratio is down by at least a factor of ten from the required estimate. Apart from the small chance of finding a deflector between a Seyfert galaxy and the observer, other problems arise when it is attempted to explain QSOs by the gravitational lens mechanism. Although a point source would give rise to such a phenomenon, an extended source of size comparable with that of the deflector would not, and even if the source can be regarded as a point source for the optical radiation, this cannot be done for the radio emission from an extended source. It is not considered possible, therefore, to explain the radio emission by the gravitational lens mechanism. (UK)

11585 EQUILIBRIUM OF AN IONIZED ATMOSPHERE SUBMITTED TO AN INTENSE RADIATION FIELD. **Peyraud, Nelly (Laboratoire de Physique des Plasmas, Orsay, France). Astron. Astrophys.; 8: 428-35(Oct 1970). (In French).**

The problem of the stability of ionized matter in an intense radiation field opposed to the gravitational field has applications in astrophysics because it can explain some properties of quasars. It is considered that the quasar is a stellar object composed of a nucleus of antimatter surrounded by matter; the annihilation between particles and antiparticles in the intermediary region produces hard photons constituting the radiation field. This representation of matter–antimatter is sufficient for the energy balance, but it does not explain the electromagnetic radiation of the quasar, which needs the existence of magnetic fields of about one gauss in the external region. The external region of the quasar is a slab of ionized matter in a gravitational field and is subjected to the action of photons issued from the center and producing Compton effects on electrons. This situation is very similar to that of the Rayleigh–Taylor density instability, the light media being the radiation. The principle of the instabilities is thus similar to the Rayleigh–Taylor one, despite the fact that the dispersion relation is quite different. The main consequences of this instability are: control of the flow of matter through antimatter (analogous to a dense fluid flowing through a light one); production of turbulent magnetic fields by the dynamo effect (the dense fluid-plasma can be considered as a perfect conductor); in a first evaluation, the magnetic fields are of about one gauss. The brightness of the quasar fluctuates and is associated with variations of the shape of the external slab. The scale time of these variations, which is in good agreement with those observed experimentally (about one day to one month), was determined. This theory incorporates, in the same description, the most important properties of quasars. (auth)

11586 PECULIAR PULSE BURST IN PSR 1237 + 25. **Backer, D. C. (Arecibo Observatory, Puerto Rico). Nature (London); 228: 1297-8(26 Dec 1970).**

A peculiar change of mode in the pulsar PSR 1237 + 25, occurring infrequently in its pulse sequence, is described. The mode changes were observed on several occasions; in one case they lasted for about 250 pulses, and in another case for about 1,300 pulses. Mode changes lasting for five to ten pulses were also detected. The general features of short-term variations in pulsars are briefly summarized, and a detailed analysis is given of PSR 1237 + 25 pulse systems. (UK)

11587 OBSERVATIONS OF HIGH VELOCITIES IN H II REGIONS. **Meaburn, J. (Univ. of Manchester, Eng.). Nature (London); 228: 1069-70(12 Dec 1970).**

Investigations using a variety of optical instruments have indicated that small components of the ionized matter in H II regions are in a highly turbulent condition. Shcheglov, using a photographic single-etalon Fabry–Perot instrument at Hα, in combination with a telescope, found such components with turbulence up to 100 km/sec in NGC 6618, 6523, 1976, and 6611. An exact measurement of the line shapes from the dense cores of bright H II regions was considered to be desirable to examine this turbulence further and, if confirmed, to indicate its nature. For this purpose modified instrumentation was necessary, consisting essentially of a two-etalon propane scanned photoelectric Fabry–Perot, combined with a 1-m reflecting telescope. The [O III] (5007-Å) line was chosen for the studies, in preference to Hα, for reasons given, including the fact that this line could be detected at three times the quantum efficiency of Hα. Twenty-eight positions in the bright cores of three nebulae (NGC 6523, 6611, and 6618) in the Sagittarius arm were observed and a scan of the 5007-Å line from four positions in the centre of NGC 6618 is shown. For one position the line is clearly split into two components, the fainter being emitted by ionized matter approaching at 35 km/sec with respect to the bulk of the nebular material. It was apparent that the nebular lines were, in some cases, strongly split; in other cases, they showed turbulently broadened wings. The bulk of the matter appeared to emit an asymmetric 5007-Å line approximately 0.35-Å wide. Further observations are necessary to resolve the nature of these interesting features. It is considered that unambiguous confirmation of highly turbulent components and of Gershberg and Shcheglov's observations of NGC 6611 and 6618 was obtained, together with their preliminary explanations. (UK)

11588 PULSAR EJECTION IN SUPERNOVA EVENTS. **Michel, F. C. (Cambridge Univ., Eng. Rice Univ., Houston, Tex.). Nature (London); 228: 1072-3(12 Dec 1970).**

It is stated that although pulsar formation is generally attributed to supernova events, only two pulsars are convincingly associated with known supernova remnants (the Crab Nebula and Vela). Other pulsars are close enough to remnants to suggest association, but only if they are moving away at velocities of the order of 10^3 km/sec. Another problem is that a supernova core may be too massive to form a gravitationally stable object, such as a neutron star, and gravitationally collapsing objects (black holes) do not seem promising candidates as pulsars. It was suggested (Fowler and Hoyle, Nature 197: 533(1963)) that the symmetric ejection of radio-luminous material from galaxies could be caused by asymmetrical processes occurring in the collapse of very massive objects. Such an imploding system is Rayleigh–Taylor unstable, and the more massive core could fission into several less massive objects. The same idea can be applied to a supernova event, the core fragmenting into a distribution of neutron stars, black holes, and general debris. The number of fragments should be few, since the disparity between core mass and neutron star masses is not large. Such a multiple system would be readily detectable either directly as superimposed pulsars or indirectly from the orbital perturbations of the observed pulsar period. It is shown that the resultant system can be expected to become unbound, the component objects being ejected with velocities of the order of 10^3 km/sec. In this connection the binary fission of a supernova core into equal mass neutron stars is considered. The absence of observed pulsars associated with supernova remnants could be attributed to the formation of non-pulsar objects or of pulsars not beamed towards the Earth. (UK)

11589 ABSENCE OF AVERAGE POLARISATION AT 111.5 MHz IN PULSAR NP 0532. **Heiles, C. (Arecibo Observatory, Puerto Rico); Rankin, J. M.; Campbell, D. B. Nature (London); 228: 1074(12 Dec 1970).**

A brief review is given of previous studies of the polarization properties of NP 0532, followed by a report on the measurement of the four Stokes parameters of the average pulse at 111.5 MHz. A feed giving two orthogonal linear polarizations was employed. Observations were made over a period of 3 hours on Jan. 7 and 11, 1970. Allowance was made for Faraday rotation. No appreciable linear or circular polarization was found. Several explanations for the lack of observed polarization are plausible; the precursor polarization previously observed at about 400 MHz may have become weak relative to the other pulse components at 111.5 MHz, or it may not be strongly polarized on emission at the pulsar, or a strongly polarized precursor may have become dipolarized in transit to Earth. None of these possibilities is subject to direct confirmation, but measurements of the integrated flux density of the precursor relative to the main pulse showed that this ratio is more or less independent of frequency in the interval 430 to 196.5 MHz, and from this it was argued that although the main pulse and precursor cannot be resolved at 111.5 MHz it is unlikely that the relative flux changes greatly between 196.5 and 111.5 MHz. A strongly polarized precursor is severely broadened by scattering in the interstellar medium, and although the scattering itself will not change the fraction of linear polarization, or its sense, it introduces the possibility that differential Faraday rotation may occur on propagation paths. The scattering angle would be expected to be about 6×10^{-7} radians and it seems unlikely that depolarization due to differential Faraday rotation occurs over such a small angular extent. It seems probable that either the 111.5-MHz radiation is depolarized in the Crab Nebula, or in the immediate vicinity of the pulsar, or that the pulsar radiation at low frequency is not strongly polarized on emission. A need for further polarization measurements at intermediate frequencies is indicated. (UK)

XUM

11590 DISTRIBUTION OF BRIGHTNESS AND POLARIZATION IN CASSIOPEIA A AT 5.0 GHz. Rosenberg, Ivan (Cavendish Lab., Cambridge, Eng.). Mon. Notic. Roy. Astron. Soc.; 151: 109-22 (1970).

Cas A (3C 461) was observed at a frequency of 5.0 GHz with a resolving power of 6.5 × 7.6″ arc. Further resolution of the fine structure is revealed in the distribution of total intensity, and a study of the variations of structure with frequency is presented. Linear polarization of about 5% was found around the rim of the source, consistent with a radial component of magnetic field. The distribution of total emission from the source is shown to be consistent with this configuration of magnetic field. (auth) (UK)

11591 BATTERY EFFECT IN NEUTRON STARS. Sedrakian, D. M. (Cambridge Univ., Eng.). Nature (London); 228: 1074-6 (12 Dec 1970).

Reference is made to an interesting problem of intense magnetic fields in gravitationally collapsed bodies; radio emission from pulsars suggests magnetic fields of the order of 10^{12} G. The battery effect for nonuniformly rotating early main-sequence stars has been considered (Roseburgh, Mon. Not. Roy. Astron. Soc. 132: 201 and 133 (1966)). In the present communication a possible battery effect in neutron stars, having a different physical cause, is considered. A model is considered for a rotating star composed only of neutrons, protons, and electrons, assumed completely degenerate, leading to a possibility that a nonstationary magnetic field of the order of 10^{12} G can be generated. The effect of gravity is considered, using the post-Newtonian approximation, and the space–time metric is derived. Maxwell's equations are applied, together with the equation of motion for plasma in the space considered. A toroidal magnetic field is generated in the star, and the speed at which the magnetic field increases depends on the central density of the matter of the neutron star, and is found to be of the order of 10^{-4} G/sec. The Hall effect is also considered. For this model, the time over which the Ohm effect balances the battery effect is 10^{15} years and the time in which the Hall effect becomes equal to the battery effect is of the order of 10^{9} years. In order to find the magnitude of the maximum magnetic field it can be assumed that, on the time scale of 10^{9} years, the growth of the magnetic field depends linearly on time, and this gives a field of ~10^{12} G. The Crab Nebula pulsar has an age of the order of 10^{3} years, and if it is supposed that its angular velocity decreases linearly from 6×10^{3}/sec to 30/sec, then in 10^{3} years the magnetic field can grow to ~10^{12} G. (UK)

11592 STRONG NEW X-RAY OBJECT IN THE CETUS REGION. Shukla, P. G.; Wilson, B. G. (Univ. of Calgary, Alberta). Nature (London); 228: 1077-9(12 Dec 1970).

In a flight of a Black Brant rocket (AKF-IIIB-51) a new intense x-ray source with a photon flux of 16.9/cm²/sec in the 1.5- to 5.0-keV range was observed. The count rate in the region of highest intensity was about six times normal value, and the data for this region were analyzed separately after substraction of the contribution of both the diffuse x radiation and the instrumental background. Attempts were made to fit the data to the predictions of theoretical models of synchrotron emission, blackbody radiation, and thermal bremsstrahlung from a hot thin plasma. The fit was poor with the first two models, but consistent with the third model, with a plasma temperature of $(8.3 \pm 0.7) \times 10^{7}$K. The fitted energy spectrum is shown. The estimated position of the object was $l^{II} = 159°$ and $b^{II} = -52°$. The object is designated Cet-XR2, and showed an intensity comparable with that of Sco-XR1. The data are compared with these reported for Cet-1 (Cet-XR1) (Proc. Astron. Soc. Austral. 1: 236 (1969)), and within the experimental errors the two sets of measurements could refer to the same object. Neither of the two experiments yielded sufficiently precise information to clarify the situation, but it is tentatively considered that two different sources were involved. Further experiments with more precise position determination are indicated. (UK)

11593 MICROWAVE DETECTION OF INTERSTELLAR FORMIC ACID. Zuckerman, B. (Univ. of Maryland, College Park); Ball, John A.; Gottlieb, Carl A. Astrophys. J.; 163: L41-5 (15 Jan 1971).

An emission line was observed in the direction of the continuum source Sgr B2, and identified with the $1_{11} - 1_{10}$ transition of interstellar formic acid at 1638.805 MHz. This is the first organic acid detected in interstellar space. (auth)

11594 OBSERVATIONS OF RADIO EMISSION FROM INTERSTELLAR HYDROGEN CYANIDE. Snyder, Lewis E. (Univ. of Virginia, Charlottesville); Buhl, David. Astrophys. J.; 163: L47-52(15 Jan 1971).

Radio emission spectra from the J = 1 – 0 transitions of $H^{12}C^{14}N$ and $H^{13}C^{14}N$, two molecular isotopes of hydrogen cyanide, were detected at 88.6 and 86.3 GHz, respectively. The preliminary survey resulted in the detection of six interstellar $H^{12}C^{14}N$ sources; to date, two of these have been found to contain detectable amounts of $H^{13}C^{14}N$. (auth)

11595 GENERATION OF RADIO WAVES IN PULSARS. Smith, F. G. (Univ. of Manchester, Eng.). Nature (London); 228: 913-16(5 Dec 1970).

Pulsars generate radio waves by an unknown process which gives the highest volume emissivity known in astrophysics. The radiation forms a beam the width and polarization of which are independent of frequency. This article assembles the observational facts which any theory of emission must explain. (auth) (UK)

11596 FREE DYNAMICS OF PULSARS. Burns, J. A. (Cornell Univ., Ithaca, N. Y.). Nature (London); 228: 986-8(5 Dec 1970).

The rotational dynamics of freely spinning pulsars are discussed, including the effects of pulsar nonrigidity and some possible consequences of viscosity. In this connection, expressions for the period of the Eulerian free oscillation or precession of pulsars are of particular interest; this oscillation is a permitted solution of the free rotational dynamics since, as a result of centrifugal effects, pulsars are somewhat oblate, and any nonspherically symmetric body that is not a perfect fluid and is spinning freely in a space will wobble about the constant direction of its angular momentum vector. This may account for some of the amplitude and time variations observed in pulsar signals and, if observable, could give the first fairly accurate measurement of pulsar size. Other authors have discussed the rotational dynamics of pulsars under the action of torques caused by the electromagnetic forces present and have considered the alignment of the magnetic dipole in the oblique rotator model and decay of the spin itself, which indicates the pulsar age. The discussion presented in this communication supplements such calculations by presenting the solutions to the homogeneous equations of motion and, because the actual torques are so weak, represents more clearly a pulsar's rotational motion over a short time. Before considering the effects of fluidity and viscosity, the motion of a rotationally symmetric rigid body spinning freely is discussed. The effect of nonrigidity is to lengthen the Eulerian free-precession period, while leaving the qualitative picture of the dynamics unchanged. An estimate of the crystal rigidity is obtained, and it is indicated that a pulsar surface, although very strong by terrestrial standards, behaves like a fluid in the presence of the pulsar's very large gravitational field. The free-precession period would be substantially increased by the fluid-like character of the crust. The question as to whether viscous effects can prevent the body from acting like a fluid causing the body to maintain a rigid configuration is discussed; this can happen only if frictional forces dominate the inertial forces. Little information is, however, available on neutron-star viscosities, beyond an estimate of the viscosity of the inner core. Whatever the initial amplitude of the Eulerian oscillation, it will decay in time because of viscous dissipation and electromagnetic torques and, if this oscillation is to be significant, there must be an impulsive energy input from time to time. The influence of starquakes is discussed in connection with the abrupt jumps in frequency observed in several pulsars. The picture obtained for a rotating neutron star is a body whose angular momentum vector is constant from an external point of view; the magnetic moment axis appears to wobble in space because of the combined motions of spin and precession, and this wobble can produce time variations in the signal period. The wobbling will also permit the emissions from a narrow angular source on the pulsar to sweep out a larger angular area of the sky during one precession period, and this will increase the probability of seeing any pulsar which has a narrow emission core, and the pulsar number density may be less than is currently thought on the assumption that the emission is beamed. Even if the amplitude of the precession is small it may be of considerable interest, if its period is measurable, in connection with measurement of pulsar radius for the first time. The results could be useful as a constraint on future neutron star models. (UK)

11597 EXTRAGALACTIC RADIO SOURCES. II. THE INTERACTION OF RADIO SOURCES WITH THE COSMICAL BLACK-BODY RADIATION. Rowan-Robinson, M. (Queen Mary Coll., London). Mon. Notic. Roy. Astron. Soc.; 150: 389-408(1970).

The effect of the interaction of relativistic electrons in radio sources with the cosmic blackbody radiation on the lifetime of sources, radio source-counts, and the integrated radio and x-ray backgrounds, is discussed for a variety of source models, including the effects of expansion losses and continuous injection of electrons. It is suggested that the x-ray background is due

XUM

primarily to the weaker radio galaxies: a model in which the radio luminosity of sources is an increasing function of magnetic field is consistent with all the present data. A sharp break in the x-ray background spectrum leads to difficulties for all models of this type. (auth) (UK)

11598 OBSERVATIONS OF THE CRAB PULSAR AT 410 AND 1664 MHz. Manchester, R. N. (National Radio Astronomy Observatory, Green Bank, W. Va.). Astrophys. J.; 163: L61-3(15 Jan 1971).

The Crab pulsar was detected at 1664 MHz. Comparison of mean pulse profiles at 410 and 1664 MHz shows that the components of the pulse have quite different spectral indices. (auth)

11599 FURTHER RADIO OBSERVATIONS OF NOVAE. Wade, C. M.; Hjellming, R. M. (National Radio Astronomy Observatory, Green Bank, W. Va.). Astrophys. J.; 163: L65-7(15 Jan 1971).

Radiation from Nova Serpentis 1970 was detected at wavelengths of 3.5 and 9.5 mm, and from Nova Delphini 1967 at 9.5 mm. Further observations of Nova Serpentis 1970 at centimeter wavelengths showed that the flux from this object has increased markedly since its original detection in June 1970. No significant change in the flux from Nova Delphini 1967 was seen. (auth)

11600 SPECTROSCOPIC OBSERVATIONS OF SCORPIUS X-1. Mook, D. (Dartmouth Coll., Hanover, N. H.); Hiltner, W. A.; Lynds, R. Astrophys. J.; 163: L69-71(15 Jan 1971).

Preliminary results of a program of simultaneous optical spectroscopic and photometric observations of Sco X-1 are presented. Equivalent widths of the Hα and He II λ4686 emission lines change in a pattern related to the brightness of the continuum. Line profiles also change, and an instance of hydrogen-line doubling is presented. No correlation was found between the radial velocity of the emission lines and the brightness of the object. (auth)

11601 OCCURRENCE OF HIGH-LATITUDE IONOSPHERIC IRREGULARITIES GIVING RISE TO SATELLITE SCINTILLATION. Frihagen, Jon (Norwegian Defence Research Establishment, Kjeller). J. Atmos. Terrest. Phys.; 33: 21-30(Jan 1971).

The variation of mean scintillation depth at 40 MHz with geomagnetic latitude, geomagnetic local time, and K_p was found. Scintillation peaks were found in two regions, a polar region above 80° geomagnetic latitude and one resembling the auroral oval. Between these there is a nighttime scintillation trough. This trough may separate regions where different production mechanisms for ionospheric irregularities predominate. The regions expand especially on the dayside with increasing K_p. (auth) (UK)

Solar Phenomena

Refer also to abstract 11817.

11602 SEPARATION OF RELATIVITY EFFECTS AND EFFECTS DUE TO A QUADRUPOLE MOMENT OF THE SUN IN TIME-DELAY MEASUREMENTS. Richard, J.-P. (Univ. of Maryland, College Park). Contract NGR-21-002-214. Phys. Rev., D; 2: 2743-5(15 Dec 1970).

The general-relativistic corrections and the effects due to a quadrupole moment of the Sun in measurements of the travel time of electromagnetic signals sent from Earth to artificial planets on circular and coplanar orbits are considered. It is found that a relativistic correction due to a term in the metric of second order in the mass of the Sun could not be separated from the effect due to a quadrupole moment unless additional information were available. The use of previous optical determinations of the motion of the node and perihelion of Mercury is considered and seen as adequate for a separation of the two effects to an accuracy of a few percent of the relativistic "nonlinear" effect. (auth)

11603 COMPARISON OF THE MEAN PHOTOSPHERIC MAGNETIC FIELD AND THE INTERPLANETARY MAGNETIC FIELD. Severny, A. (Crimean Astrophysical Observatory, Nauchny, USSR); Wilcox, J. M.; Scherrer, P. H.; Colburn, D. S. Solar Phys.; 15: 3-14(Nov 1970).

The mean photospheric magnetic field of the Sun seen as a star was compared with the interplanetary magnetic field observed with spacecraft near the Earth. Each change in polarity of the mean solar field was followed about 4½ days later by a change in polarity of the interplanetary field (sector boundary). The scaling of the field magnitude from Sun to near Earth was within a factor of two of the theoretical value, indicating that large areas on the Sun have the same predominant polarity as that of the interplanetary sector pattern. An independent determination of the zero level of the solar magnetograph yielded a value of 0.1 ± 0.05 G. An effect attributed to a delay of approximately one solar rotation between the appearance of a new photospheric magnetic feature and the resulting change in the interplanetary field was observed. (auth)

11604 MAGNETIC FIELDS AND THE STRUCTURE OF THE SOLAR CORONA. II. OBSERVATIONS OF THE 12 NOVEMBER 1966 SOLAR CORONA. Newkirk, Gordon Jr. (High Altitude Observatory, Boulder, Colo); Dupree, Robert G.; Schmahl, Edward J. Solar Phys.; 15: 15-39(Nov 1970).

During the eclipse of November 12, 1966, the solar corona was photographed at an effective wavelength of 6500 Å with an f/16, 11.1-cm-aperture camera. Reduction of the observations yielded coronal radiances and polarizations from 1.4 to 3.5 solar radii. Standard techniques were used for the separation of F and K coronas, determination of coronal electron densities and temperatures, and estimation of the orientation of the major streamers in space. (auth)

11605 CORONAL MAGNETIC FIELD PATTERNS INFERRED FROM RADIO OBSERVATIONS. Lantos-Jarry, M. F. (Meudon-Nancay Observatory, France). Solar Phys.; 15: 40-7(Nov 1970).

A noise storm center clearly associated with an active center was followed from January 2 to January 8, 1969. The study of the mean distribution of continuum and of type-1 bursts showed a global and systematic displacement interpreted in terms of the coronal magnetic structure. This structure was formed by field lines connecting the active center to a stable region of inverse polarity, characterized by the existence of a coronal condensation. These results show the possibility of using this method for the systematic study of coronal magnetic structures, the knowledge of which is vital as far as the problems of particle propagation in the corona and in the interplanetary medium are concerned. (auth)

11606 ORIGIN OF INTERPLANETARY SECTORS FROM RADIO OBSERVATIONS. Martres, M. (Meudon Observatory, France); Pick, M.; Parks, G. K. Solar Phys.; 15: 48-60(Nov 1970).

The interplanetary sectors were correlated to observations of solar coronal active centers and condensations in the metric wavelengths. It was found that (1) a sector boundary is always located to the west of a coronal condensation, and (2) the effect of active centers is to displace systematically the boundary toward the east, thus enlarging the sector. A physical interpretation is discussed. (auth)

11607 MAGNETIC AND THERMAL PRESSURES IN THE SOLAR WIND. Burlaga, L. F.; Ogilvie, K. W. (Goddard Space Flight Center, Greenbelt, Md.). Solar Phys.; 15: 61-71(Nov 1970).

Explorer 34 solar-wind data for the period June to December, 1967 show that (a) the magnetic pressure, $P_B \equiv B^2/8\pi$, and thermal pressure, $P_k \equiv n_p kT_p + n_\alpha kT_\alpha + n_e kT_e$, are variable and positively correlated on a scale of $\gtrsim$2 days, but (b) changes in P_B and P_k are anticorrelated on a scale ~1 hr (~0.01 AU). Thus, dynamical hydromagnetic processes ($dv/dt \neq 0$) must occur on the mesoscale, but the solar wind tends to be in equilibrium ($P_B + P_k \sim$ constant) on a smaller scale, the microscale. The 3-hr averages show that the most probable value of $\beta \equiv P_k/P_B$ is $\beta' = 1.0 \pm 0.1$, which implies that the most probable state of the solar wind at 1 AU is not one of equipartition between the thermal energy and magnetic energy. The average total pressure for a given bulk speed ($\overline{P}$ (V) = $P_k + P_B$) is essentially independent of V, implying that P is not determined by the heating or acceleration mechanisms of the solar wind; the average pressure is $\overline{P} = (2.9 \pm 1.5) \times 10^{-10}$ dyne/cm^2. (auth)

11608 UNIFIED THEORY OF THE INTERPLANETARY MAGNETIC FIELD. Rosenberg, Ronald L. (Univ. of California, Los Angeles). Solar Phys.; 15: 72-8(Nov 1970).

A simple model is used to present a unified picture of the polarity pattern of the interplanetary magnetic field observed during the solar cycle. Emphasis is on the field near solar maximum. The heliographic latitude dependence of the dominant polarity of the interplanetary magnetic field is explained in terms of weak poloidal (dipolar) field sources in the photosphere. Unlike the Babcock theory, the author hypothesizes that the dipolar field exists at equatorial latitudes (0 to 20°), too, (as well as in polar regions) and that the major source of the interplanetary magnetic field observed near the ecliptic plane is the dipolar field from equatorial latitudes. The polarity of the interplanetary field data taken in 1968 and in the first half of 1969 near solar maximum may possibly be explained in terms of a depression of the dipolar field boundary in space. The effect on the solar wind of the greater activity in the northern hemisphere of the Sun that existed in 1968 and in the first half of 1969 is believed responsible for this hypothesized depression,

especially near solar maximum, of the plane separating the + and – dipolar polarity below the solar equatorial plane in space. Predictions are made concerning the interplanetary field to be observed near the ecliptic plane in each portion of the next solar cycle. (auth)

11609 TRANSFORMATION OF THE ABSOLUTE SOLAR RADIATION DATA INTO THE INTERNATIONAL PRACTICAL TEMPERATURE SCALE OF 1968. Labs, Dietrich (Landessternwarte, Heidelberg); Neckel, Heinz. Solar Phys.; 15: 79-87(Nov 1970).

Corrections are given for transforming the tables of the solar radiation data (Labs and Neckel, 1968) into the "International Practical Temperature Scale of 1968". Additionally, for the adjustment of the data of the "true continuum" and the corresponding line blanketing as well, the veiled line effect mentioned first by Carbon et al. (1968), but studied in more detail by Holweger (1970a), was considered also. The corresponding corrections of the solar irradiance result in an improved value of the spectrophotometric solar constant: $S = 1.947$ cal cm^{-2} min^{-1} or 0.1358 W cm^{-2}. Two tables presenting the "highest (window-) intensities" and the corrected irradiance data were added. (auth)

11610 SOME CONSIDERATIONS FROM THE DIRECT COMPARISON BETWEEN THE OBSERVATIONS AND THE THEORY OF SOLAR DISK POLARIZATION. Pecker, Jean-Claude (College de France, Paris. Univ. of Colorado, Boulder). Solar Phys.; 15: 88-96(Nov 1970).

Simple considerations of observed variation with wavelength of polarization on the solar disc, computed continuum polarization, and estimated line polarization have led to the following simple conclusions (more qualitative than quantitative); (a) The metal abundances in the photosphere are five times larger than the "classical" values adopted in the BCA model of the solar photosphere. (b) The depolarization factor k in lines is an increasing function of wavelength. (c) Assuming that k varies as λ^2, an additional polarization (which can be either solar or instrumental) has to be taken into account. (auth)

11611 IMPROVED SOLAR WAVELENGTHS BETWEEN 7780 AND 7925 A. Young, A. T.; Schorn, R. A. (California Inst. of Tech., Pasadena). Solar Phys.; 15: 97-101(Nov 1970).

By utilizing the known rotational constants for the 7820- and 7883-Å CO_2 bands, substantially improved wavelengths for solar lines in the 7780 to 7925 Å region were derived. (auth)

11612 LINE FORMATION IN A MAGNETIC FIELD AND THE INTERPRETATION OF MAGNETOGRAPHIC MEASUREMENTS. III. CALCULATIONS FOR DIFFERENT SPOT MODELS AND ARBITRARY DEPTH DEPENDENCE OF THE MAGNETIC FIELD VECTOR. Staude, J. (Zentralinstitut fuer Solar-Terrestrische Physik, Potsdam, Ger.). Solar Phys.; 15: 102-12(Nov 1970).

The strong temperature dependence of the line Fe I λ 5250.2 Å was studied by calculating line contours and magnetographic calibration curves for different spot models and the BCA. Line contours calculated for arbitrary depth dependence of the magnetic field vector show depolarization effects within the Zeeman components for transverse fields with variable direction and changes of the observed plane of polarization if anomalous dispersion is taken into account. The observed anomalous splitting of the π-component may be interpreted best by suggesting discrete inhomogeneities of the magnetic field within sunspots. (auth)

11613 EUROPIUM AND LANTHANUM IN SUNSPOT AND IN THE UNDISTRUBED PHOTOSPHERE. Bachmann, G.; Pflug, K.; Staude, J. (Zentralinstitut fuer Solar-Terrestrische Physik, Potsdam, Ger.). Solar Phys.; 15: 113-19(Nov 1970).

Line profiles of Eu II λ4129.7 Å and La II λ4086.7 Å were observed photoelectrically and photographically in the photosphere and within sunspots and after corrections were compared with calculated profiles. The observed large hyperfine structure broadening and isotope shift of λ4129.7 Å confirm the Eu origin of this line and suggest a larger Eu abundance than that recently published by Grevesse and Blanquet (1969). The line profiles within the spot may be well represented by means of the spot model of Hénoux (1969), while older spot models are not able to do it. An abundance difference between spot and photosphere has not been observed. (auth)

11614 SOLAR LYMAN CONTINUUM AND THE STRUCTURE OF THE SOLAR CHROMOSPHERE. Noyes, Robert W.; Kalkofen, Wolfgang (Smithsonian Astrophysical Observatory, Cambridge, Mass. Harvard Coll. Observatory, Cambridge, Mass.). Solar Phys.; 15: 120-38(Nov 1970).

Data on the spectrum and center-to-limb variation of the solar Lyman continuum were analyzed. They show: (a) the brightness temperature of the Lyman continuum is about 6500 K, but the kinetic temperature, as deduced from the slope of the continuum, lies between 8000 and 9000 K; the difference between the kinetic temperature and the brightness temperature requires that the source function be smaller than the Planck function by a factor of several hundred; (b) the Lyman continuum exhibits slight limb darkening longward of 825 Å, and slight limb brightening shortward of 750 Å; the crossover point varies from equator to pole and with solar activity; and (c) the slope $d \ln I(\lambda)/d\lambda$ of the Lyman continuum decreases toward the limb, implying that the kinetic temperature increases outward in the region of Lyman continuum formation. Using radiative-transfer calculations for a plane-parallel atmosphere in hydrostatic equilibrium, a homogeneous model of the upper chromosphere was derived that reproduces the main features of the observations. It is characterized by a temperature of 8300 K and a pressure of about 0.15 dyne/cm^2 at $\tau_{Lyc} = 1$, and it has an abrupt temperature rise at a height of 1500 km above the limb. More precise agreement with the observations will require a detailed treatment of the inhomogeneous nature of the upper chromosphere. (auth)

11615 THREE-COMPONENT MODEL FOR THE FORMATION OF THE CHROMOSPHERIC Ca II K LINE. Wilson, P. R. (Univ. of Sydney). Solar Phys.; 15: 139-47(Nov 1970).

A recent two-component model for the formation of the Ca II K line in the solar chromosphere put forward by Beebe and Johnson is discussed. Although this model is a great advance on existing one-component models, it is pointed out that observations require a minimum of three components in order to understand the formation of the K_2 peaks. In order to make some progress in the study of multicomponent models an adaptation of the empirical (or analytic) approach is suggested. This relates the line source function directly to observations and places a secondary importance (at this stage) on the synthetic approach to the problem. A model is obtained which is in adequate agreement with observed mean profiles and its features are briefly discussed. (auth)

11616 POLARIMETRY IN SOLAR ACTIVE REGIONS. III. CIRCULAR POLARIZATION IN DIFFERENT LINES; DEVELOPMENT OF MAGNETIC FIELDS. Wiehr, E. (Univ., Goettingen, Ger.). Solar Phys.; 15: 148-57(Nov 1970).

Measurements of the circular polarization V in different lines show that the deduced magnetic field strength and flux are systematically influenced by variations of the line absorption coefficient from photosphere to spot and faculae. Disbalances between preceding and following flux seem to be due mainly to such variations rather than to real physical conditions in active regions. The spatial distribution of the normal component of the magnetic field in an active region near the disc center was observed during two days using the temperature insensitive line Fe λ6302.5. The initial field structure seems to become more and more bipolar. The increase of the flux exceeds that of the area thus suggesting the appearance of new magnetic fields. Backward extrapolation in time leads to a date of first appearance of the magnetic field which agrees with the appearance of first Hα anomalies. (auth)

11617 ORIENTATION OF MAGNETIC FIELDS IN QUIESCENT PROMINENCES. Tandberg-Hanssen, E.; Anzer, Ulrich (National Center for Atmospheric Research, Boulder, Colo.). Solar Phys.; 15: 158-66(Nov 1970).

The longitudinal component, $B_{||}$, of the magnetic field in quiescent prominences was measured and a relationship between $B_{||}$ and θ was obtained, where θ is the angle between the long axis of the prominence and the north–south direction on the Sun. From this relationship a distribution function for the magnetic field vector in quiescent prominences was deduced in terms of the angle α between the field and the long axis of the prominence. The mean angle $\bar{\alpha}$, for the data was small, ≈15°, indicating that the magnetic field traverses quiescent prominences under a small, but finite angle. (auth)

11618 STRUCTURE OF THE MONOCHROMATIC CORONA IN THE SURROUNDINGS OF PROMINENCES. Waldmeier, M. (Swiss Federal Observatory, Zurich). Solar Phys.; 15: 167-75 (Nov 1970).

It is well known that in the immediate surroundings of stationary filaments the white light of the corona is strongly reduced. The same effect is observed in the monochromatic emissions of the lines 5303 and 6374 Å, for which some examples are given. This diminuation of light can only be explained by a corresponding diminuation of the density. As the density in the vicinity of the prominence may be as small as one tenth of that of the undisturbed corona, or even smaller in some cases, these features are called cavities. The intensity distribution of

the line 5303 Å in the region of a stable prominence observed on October 6, 1969 was analysed. The cavity turns out to be of the shape of a half-ellipsoid. Its length (in heliographic longitude) was found to be 0.68, its width (in heliographic latitude) 0.20 and its height 0.16 $R_\odot$. The corresponding dimensions of the enclosed filament were 0.56 (length), 0.10 (width), and 0.08 (height) $R_\odot$. (auth)

11619 WHITE-LIGHT EVENTS AS PHOTOSPHERIC FLARES. Najita, Kazutoshi; Orrall, Frank Q. (Univ. of Hawaii, Honolulu). Solar Phys.; 15: 176-94(Nov 1970).

The possibility is considered that white light flares are due to heating of the photosphere by a flux of energetic ions and electrons impinging on it from above. Particles with energy in the range 10 MeV to 1 BeV release most of their energy to the ambient gas at about optical depth unity in the photosphere. This increase in energy produces a temperature perturbation of several hundred degrees in the layer and results in a re-radiation of the energy with a radiative relaxation time of several seconds. The consequences of this model are applied to a study of the great flare of May 23, 1967 and to the very fast event of August 11, 1954. Large numbers of very energetic electrons or protons must be produced in the first few minutes of the primary flare event if the interpretation (or one based on synchrotron emission) is correct. (auth)

11620 CHANGES IN CORONAL CONDENSATIONS EMISSION AFTER SOLAR BURSTS AT MICROWAVES. Kaufmann, Pierre; Scalise, E. Jr.; Dos Santos, P. Marques (Mackenzie Univ., Sao Paulo, Brazil). Solar Phys.; 15: 195-201(Nov 1970).

The amount of circular polarization of the total solar radio emission at 7 GHz presents permanent changes after the occurrence of certain radio bursts associated with larger flares. For isolated S components associated with such flares the changes of the polarization degree $\Delta\Pi_c$ ranges between 0.004 to 0.1, and appears to be a function of the flare importance. A semi-qualitative interpretation associates $\Delta\Pi_c$ with magnetic field reductions at the S component, agreeing fairly well with a flare mechanism based on collisionless dissipation of magnetic energy, corresponding to energies in the range of 10^{30} to 10^{32} ergs, assuming an average model for the coronal condensations. (auth)

11621 TOWARDS A THEORY FOR TYPE III SOLAR RADIO BURSTS. I. NATURE OF THE EXCITING AGENCY. Smith, D. F. (Shternberg Astronomical Inst., Moscow). Solar Phys.; 15: 202-21(Nov 1970).

The possibilities for Type-III-burst excitors are reviewed, and it is concluded that particle streams are the most likely excitor. Possible methods of resolving the apparent discrepancy between the number of particle events observed in interplanetary space in the vicinity of the Earth and the number of Type-III bursts are indicated. Observations relevant to the excitor are reviewed and translated into requirements for a theory of the exciting stream. Possibilities for an electron stream excitor are considered and it is concluded that, while such an excitor cannot be eliminated at the present time, there are definitely theoretical difficulties with it that can be overcome only by seemingly ad hoc and improbable assumptions. Possibilities for a proton-stream excitor are examined, and it is found that all theoretical difficulties can be overcome in a natural manner. The number of ≈50-MeV protons required to explain a strong Type-III burst is estimated conservatively as 3×10^{25} which, after diffusion in interplanetary space, would be undetectable by the instruments flown thus far. This number is consistent with some theoretical ideas about the flare mechanism and also with present observational data. (auth)

11622 TYPE III SOLAR RADIO BURST STORMS OBSERVED AT LOW FREQUENCIES. I. STORM MORPHOLOGY. Fainberg, Joseph; Stone, R. G. (Goddard Space Flight Center, Greenbelt, Md.). Solar Phys.; 15: 222-33(Nov 1970).

Storms of Type-III solar radio bursts observed from 5.4 to 0.2 MHz, indicate the quasi-continuous production of Type-III events observable for a half solar rotation but persisting in some cases for well over a complete rotation. The characteristics of these storms, including the dependence of occurrence and apparent drift rates on the disc position of the associated active region are discussed. The drift-rate dependence is shown to be a consequence of the propagation time of emission from the source to the observer. The occurrence rate of a burst every 10 sec observed near CMP implies that, if this level of activity persists, then about a quarter of a million exciter packets are released into the interplanetary plasma during a complete rotation. Storm bursts are less intense than most isolated Type III's and occur over a more limited frequency range. There appears to be a very close relation between these storms and decametric continuum. (auth)

11623 POLARIZATION AND ANISOTROPY OF SOLAR X RADIATION DURING FLARES. Elwert, Gerhard; Haug, Eberhard (Univ., Tuebingen, Ger.). Solar Phys.; 15: 234-48(Nov 1970).

Starting from the idea that the electrons accelerated during a solar flare have originally a preferred direction, the angular distribution and the polarization of bremsstrahlung below 10 Å are calculated, taking into account the influence of the magnetic field. The energy distribution of the nonthermal electrons is based on x-ray spectra measured by the Leicester group during flares in 1962 and 1967. In addition to the case of a fixed angle α between the electron velocity and the magnetic field, an angular distribution of the form $\sin^n\alpha$ is considered. The results may be used to test flare models. Recent measurements of the polarization of solar x radiation yield the expected order of magnitude. (auth)

11624 ACCELERATION OF PROTONS BY INTERPLANETARY SHOCKS. Ogilvie, K. W.; Arens, J. F. (Goddard Space Flight Center, Greenbelt, Md.). J. Geophys. Res.; 76: 13-20(1 Jan 1971).

Short-duration increases in particle flux at 1-MeV energy, detected by Explorer 34 just before the time of passage of interplanetary shocks are discussed. The effect is interpreted as particle acceleration associated with the shocks; most of the increase is found to be consistent in many ways with the idea of energy gain by successive reflection between the Earth's bow shock and the interplanetary shock. Other mechanisms are not excluded, however. From the small sample observed, it appears that shocks occurring when the interplanetary magnetic field at the observer's position does not intersect the Earth's bow shock did not show particle flux increases, and that the particles accelerated to 1 MeV by the observed shocks did not come from solar wind energies, but rather from solar particles in the hundred-keV energy region which were available in the medium. (auth)

11625 SOLAR COSMIC-RAY PHENOMENA. McCracken, K. G.; Rao, U. R. (Physical Research Lab., Ahmedabad, India). Space Sci. Rev.; 11: 155-233(Oct 1970).

This review attempts to present an integrated view of the several types of solar cosmic-ray phenomena. The relevant large- and small-scale properties of the interplanetary medium are first surveyed, and their use in the development of a quantitative understanding of the cosmic-ray propagation processes is summarized. Solar cosmic-ray events, in general, are classified into two phenomenological categories: (a) prompt events, and (b) delayed events. The properties of both classes of events are summarized. The properties considered are the frequency of occurrence, dependence on parent-flare position, the time profile, energy spectra, anisotropies, particle species, velocity dispersions, etc. A single model is presented to explain the various species of delayed event. Thus the halo and core events, energetic storm particle events, EDP events, and proton recurrent regions are suggested to be essentially of common origin. The association of flare particle events with electromagnetic phenomena, including optical, x-ray, and microwave emissions is summarized. The conditions in a sunspot group, and solar flare that are considered to be conducive to cosmic-ray acceleration processes are discussed. Considerable discussion is devoted to physical processes occurring near the Sun. Near-Sun particle storage, diffusion, and secondary injection processes that are triggered by a far distant solar flare are reviewed. In order to explain the considerable differences between aspects of the prompt and delayed events, selective diffusion processes are proposed that only occur at early times in a solar flare. The Type IV radio emissions at metric wavelengths are suggested to yield direct evidence for the storage processes that are necessary to explain the properties of the delayed events, and also as yielding direct evidence of secondary injection processes. The ionospheric effects of the solar cosmic radiation are summarized. (auth)

11626 MICROSCOPIC STRUCTURE OF THE SOLAR WIND. Scarf, Frederick L. (TRW Systems Group, Redondo Beach, Calif.). Space Sci. Rev.; 11: 234-70(Oct 1970).

As the solar wind flows out from the coronal base, the Coulomb collision frequencies rapidly become small and particle–particle collisions can no longer maintain local statistical equilibrium. At 1 AU the particle distribution functions have important non-Maxwellian characteristics and the firehose instability, a cyclotron resonance whistler-mode instability, and several heat flux current instabilities should be operative. Superthermal particle populations also provide large wave levels, and other forms of enhanced plasma turbulence develop at shock fronts and discontinuities. This report contains a review of the theoretical concepts and a progress report on the experimental study of interplanetary wave–particle interactions. (auth)

XUM

11627 STUDY OF THE STRUCTURE OF INTERPLANETARY SPACE BY MEANS OF COSMIC RADIATION. Somogyi, Antal (Central Research Inst. for Physics, Budapest). Fiz. Szemle; 20: 247-9(Aug 1970). (In Hungarian).

Changes in the intensity of cosmic radiation with an energy of >1 GeV reflect variations of the electromagnetic states of the solar system. The changes are caused by scattering on mobile magnetic inhomogeneities, consisting of magnetic fields sealed within the plasma emitted by the Sun (solar wind), and moving with a velocity of 300 to 500 km/sec. The space and time intensity variations follow the 11-year cycle of solar activity, the 27-day rotation of the Sun, and the Forbush effect. The study, started in 1958 and still in progress, covers the 10^{11}-eV range, and is carried out with two telescopes placed 20 m underground and containing 120 G–M tubes each. The soil and the lead shield used represent an absorber of about 4000 g/cm^2. The results point toward the existence of scattering centers of the order of 2 AU in interplanetary space. They are attributed to events on the surface of the Sun because they were found to reappear after several rotations of the Sun. No permanent inhomogeneity was observed near the Sun. The results were evaluated by means of a newly developed statistical technique. (TTT)

11628 CONCERNING ONE EXPERIMENTAL POSSIBILITY IN NEUTRINO ASTRONOMY. Zatsepin, G.; Pontecorvo, B. (Joint Inst. for Nuclear Physics, Moscow). JETP Lett. (USSR) (Engl. Transl.); 12: 236-8(5 Oct 1970).

Translated from Zh. Eksp. Teor. Fiz., Pis'ma Red.; 12: 347-9 (5 Oct 1970).

The desirable properties of a solar-neutrino detector based on electronic methods are listed. A liquid ionization instrument, preferably with internal multiplication, is proposed to satisfy the requirements. The problem of background discrimination is discussed. (W.D.M.)

11629 SUN AS A MAGNETIC ROTATOR. Tuominen, J. (Univ. of Helsinki). Nature (London); 228: 1179-80(19 Dec 1970).

Comments are offered on the paper by Severnyi (Nature 224: 53 (1969)), particularly concerning the observation that, at most times, the integrated field of sunspots appears to be opposite to the field of the Sun as a whole, and also concerning the lifetime of the large-scale magnetic regions. (UK)

11630 CORRELATIONS BETWEEN THE INDEX OF THE SPOT AREAS AND THE NUMBER OF PROTON FLARES, THE VARIATION OF THE RADIO DIAMETER OF THE SOLAR CORONA, AND THE INTENSITY OF THE COSMIC RAYS. Xanthakis, Jean (Research Center for Astronomy and Applied Mathematics, Athens). Compt. Rend., Ser. B; 271: 1009-12(9 Nov 1970). (In French).

Sunspot area indices, when used in the same way as solar activity indices, were shown to be of interest, particularly in the study of chromospheric phenomena and the corona. (auth) (France)

11631 LONG-TERM FORECASTING OF THE CYCLES OF SUNSPOTS. PARAMETERS OF THE 21st CYCLE. Halley, Pierre; Risson, Frederic (Centre National d'Etudes des Telecommunications, Issy-les-Moulineaux, France). Ann. Telecommun.; 25: No. 7-8, 265-8(Jul-Aug 1970). (In French).

The principal results of a study carried out in 1963 that predicted the 20th solar cycle were resumed. Predictions about the 21st solar cycle were made by the same method. This method depends upon the existence of a secondary cycle of about 16 elementary cycles and predicts the minimum and the maximum of the next cycle. If, in addition, an empirical relation between the duration of the rising phase and the amplitude of the maximum is considered, then the maximum value of the sliding mean of the Wolf number over a period of 12 months may be estimated. The estimated dates for the minimum and the maximum are respectively 1976.6 (±0.06) and 1982.0 (±1.4). The estimated maximum value of the Zurich number $\bar{R}_{12}$ is 80 (62 to 98). (France)

11632 SIMPLIFIED THERMAL CONTINUUM FUNCTION FOR THE X-RAY EMISSION FROM CORONAL PLASMAS. Culhane, J. L.; Acton, L. W. (Lockheed Palo Alto Research Lab., Calif.). Mon. Notic. Roy. Astron. Soc.; 151: 141-7(1970).

At temperatures below 30.0×10^6°K, the free–bound process makes an increasingly significant contribution to the total continuum flux. While the free–free spectrum may be represented by a relatively simple expression, a detailed calculation of the free–bound spectrum requires a lengthy summation process over all the ionization stages and levels of the abundant coronal ions. A simple empirical expression is presented that gives the magnitude and spectral slope of the free–bound contribution over the energy interval 1.5 to 15 keV for the temperature range 4.0 to 20.0×10^6°K. This expression gives results that agree to better than 15% with more detailed calculations of the thermal continuous spectrum. (auth) (UK)

11633 SYROVATSKII PROCESS. Schatzmann, E. (CNRS, Paris). pp 73-81 of La Magnetohydrodynamique Classique et Relativiste. Paris; Centre National de la Recherche Scientifique (1970). (In French).

From Symposium on Classical and Relativistic Magnetohydrodynamics, Lille, France. See CONF-690648.

The Syrovatskii mechanism involved in the production of high-energy particles along a neutral line of the magnetic field is presented. It is shown that the discharge mechanism results from a modification of the limiting-time conditions, which are related to an energy conversion mechanism rather than an instability. Two conditions must be fulfilled if dynamic dissipation of the magnetic field is to take place: these concern the speed at which the modification takes place and the physical conditions about the neutral line. Solar explosions are examined. The process considered takes place when the magnetic flux varies in a disturbed region of the surface of the sun. The variations in the magnetic flux produce a displacement in space of the neutral line and the compression of the magnetic field. The explosion takes place when the two critical conditions are fulfilled. (auth) (France)

Galaxies

11634 (CSIRO-Trans-10206) MASSES OF GALAXIES ACCORDING TO RADIO AND OPTICAL OBSERVATIONS. Vorontsov-Vel'yaminov, B. Translated by A. K. Rothfield from Astron. Tsirk.; No. 466, 3-5(5 Apr 1968). 3p. Dep. NTIS (U. S. Sales Only).

Values of mass, mass–brightness correlation, and association with type of galaxy were determined, using the 21-cm-line profile and including the mean statistical value $\bar{r}_p = \bar{a} x r_H$ with the proportionality factor (optical) $\bar{a}_{op} = 0.2$. However $\bar{a}_{rad} = 0.73$, gives a 2.5 to 3.5 times increase in mass. The change is not smaller than the possible distance error, estimated at moderate redshift. It is considered improbable that the value of $\bar{a}$ for galaxies should vary from 0.5 (NGC 4826-optical) to 4.26 (NGC 4449-radio) and that it should be the same for M31 and M33. It is suggested that dynamic models of plane galaxies may need revision. (Australia)

11635 MEAN ROTATIONAL VELOCITIES OF 56 GALAXIES. Mayall, N. U. (Kitt Peak National Observatory, Tucson, Ariz.); Lindblad, P. O. Astron. Astrophys.; 8: 364-74(Oct 1970).

Mean rotational velocities for 56 galaxies as given by line inclinations in their spectra are presented mainly as guidance for future work in the field of the rotation of galaxies. The low angular velocities of SBc systems are emphasized. (auth)

11636 DISCRETE SOURCE INTERPRETATION OF THE ISOTROPIC COMPONENT OF THE DIFFUSE γ-RADIATION. Cavallo, G. (Univ. of California, San Diego, La Jolla). Astron. Astrophys.; 8: 489-90(Oct 1970).

Gamma-ray observations in the 100-MeV range suggest that a strong and possibly extended source exists in the center of the Galaxy. The total γ-luminosity of the Galaxy is then such that a superposition of discrete sources like the Galaxy is a plausible explanation of the isotropic background. (auth)

11637 FREQUENCY OF SUPERNOVAE AS A FUNCTION OF THE INTEGRAL PROPERTIES OF INTERMEDIATE AND LATE TYPE SPIRAL GALAXIES. Tammann, G. A. (Univ., Basel. Carnegie Institution of Washington, D. C. California Inst. of Tech., Pasadena). Astron. Astrophys.; 8: 458-75(Oct 1970).

The frequency of supernovae was investigated in all 65 Sb and 108 Sc galaxies that have known luminosity classes and that lie within the distance range of the Virgo Cluster. By September, 1969, a total of 45 supernovae was known in them. It was found that the frequency is a strong function of the luminosity class and about linearly dependent on the luminosity and the mass of the parent galaxy. Although, strictly speaking, this dependence could only be established for Sc galaxies, it is believed to hold equally for Sb galaxies. The frequency in Sb galaxies is about three times lower than in comparable Sc galaxies which is probably caused by the lower number of massive stars in Sb galaxies. Apparently, supernovae of type II as well as of type I contribute to the higher frequency in Sc galaxies since the ratio of 2:1 between the two types does not seem to vary with the type of the galaxy. Even without corrections for incompleteness, the present results indicate very high supernova frequencies in supergiant Sc systems, i.e., one supernova per 16 years or, in some cases, even higher, whereas only one supernova per several hundred years is expected in small Sb galaxies. The true supernova frequencies per 100 years per unit luminosity ($10^{\frac{1}{2}}_{pg,\odot}$) and per unit mass ($10^{10}M_\odot$) of the parent galaxy are found to be in Sc spirals 0.022 and 0.35, respectively, and in Sb spirals 0.007 and 0.09, respectively (if H = 75 km s^{-1} Mpc^{-1} and after correcting for incompleteness and, in the case of the frequencies per unit luminosity, to face-on luminosi-

ties). Supernova frequencies in E and Ir galaxies were not determined. Therefore, nothing can be said about the average overall frequency of supernovae. It is shown, however, that this quantity is strongly dependent on the mean intrinsic luminosity of the galaxies considered. An application of the present results to the Galaxy yields one supernova per 26 (±10 estimated error) years in very good agreement with the evidence from historical supernovae. The corresponding frequency of type II supernovae is one event per 38 to 60 years and is compatible with the assumption that all stars in the mass range $4\ M_\odot < M < 9M_\odot$ become supernovae and eventually pulsars. Type I supernovae are tentatively identified with exploding white dwarfs whose parent stars had masses $\geq 9M_\odot$. The total mass involved in all galactic supernovae is estimated. The influence of supernovae on the chemical history of the Galaxy is briefly discussed. A few remarks on possible supernova search programs are given. (auth)

11638 21-cm NEUTRAL HYDROGEN LINE OBSERVATIONS OF COMPACT GALAXIES. Chamaraux, P.; Heidmann, J.; Lauque, R. (Observatoire de Paris, Meudon, France). Astron. Astrophys.; 8: 424-7(Oct 1970).

Five compact galaxies or galaxies with compact parts were observed with the 21-cm line of neutral hydrogen. For the first time one, and possibly three, were detected. Their hydrogen mass and hydrogen mass to light ratio are comparable to those of late type galaxies. The apparent velocity dispersion of the neutral hydrogen is an order of magnitude smaller than the velocity dispersion measured for the stars in other compact galaxies. From an upper limit set on the neutral hydrogen extent of one of them (II Zw 40), an upper estimate of its total mass is 10^{10} solar masses. (auth)

11639 STRUCTURE OF HYDROMAGNETIC SHOCKS IN REGIONS OF VERY LOW IONIZATION. Mullan, Dermott Joseph. College Park, Md.; Univ. of Maryland (1969). 173p. University Microfilms Order No. 70-16,026.
Thesis.

Gas flows in the interstellar medium in all likelihood contain shocks. These shocks compress not only the gas they encounter, but also the magnetic field which is convected with the gas. The pressure available to compress the field resides mainly in the momentum of the neutral gas. The magnetic field has, however, no direct link with the neutral atoms, but only with the ions. The transfer of neutral momentum to magnetic pressure must occur through the ions. In an H I region, where photoionization is the dominant ionizing mechanism, the atoms outnumber the ions by about 2000 to 1. Each ion is therefore required to transfer the momentum of about 2000 atoms to the magnetic field. The transient momentum flux in the ions appears as both thermal and kinetic pressure. Detailed models of several shocks are computed to determine the heating and drifting of ions relative to the atoms resulting from the momentum transfer. The hydromagnetic approximation is used to derive the equations describing the spatial variations of temperature and velocity of ions and atoms in the rest frame of the shock. The shock is assumed to move transverse to the field lines. Linearization of the equations shows the kinds of shocks that are possible. The full equations are integrated numerically for cases of interest in the interstellar medium. Gas velocities range from 5 to 10 km/sec, magnetic fields from 2×10^{-6} to 40×10^{-6} gauss, atom densities from 10 to 1000 cm^{-3}, and degrees of ionization from 5×10^{-4} to 5×10^{-3}. It is found that the ions temporarily become several hundred degrees hotter than the atoms in a shock that heats the gas from 100 to 1000°K. Ions much heavier than the atoms are heated by a greater amount than ions of the same mass as the atoms. Relative velocities of ions and atoms up to 3 km/sec occur in these shocks. It is concluded that the magnetic field is compressed more efficiently by ion–atom drift than by high ion temperatures. The ion temperatures do not remain high for a sufficiently long time to give observable effects. The results are of interest in star formation. A magnetic field in an interstellar cloud must be removed before contraction of normal stars is permitted. The ion–atom drift produced by shocks provides a mechanism for removing the field. The results are also of interest in the reconnection of field lines in interstellar space and in the solar chromosphere. The regions of field-line reconnection are estimated to be on the order of 0.01 pc and 1 km in size, respectively. Finally a possible interpretation of a laboratory experiment is given. (Diss. Abstr. Int., B)

11640 GALACTIC LYMAN ALPHA AND THE INTERSTELLAR SHOCK WAVE. Bowers, B. (Weapons Research Establishment, Salisbury, Australia). Nature (London); 228: 1182-3(19 Dec 1970).

It has been suggested that the collision of interstellar hydrogen with the solar system produced an anisotropic distribution of fast neutral-H atoms, and this suggestion has been used to interpret Vela 7 Lyman-alpha results. It is shown that a peak in the Lyman-alpha brightness occurs in a direction very close to the velocity vector of the solar system, implying that the radiation originates in the shock front that surrounds the solar system. Reasons are given, however, why such an interpretation may be erroneous. (UK)

11641 INTERSTELLAR MEDIUM. Kaplan, S. A.; Pikelner, S. B. Cambridge, Mass.; Harvard University Press (1970). 475p. $20.00.

An attempt is made to give a comprehensive review of the interstellar medium in all its aspects and to bring unity to a broad field of research in which investigation has tended to be highly specialized and fragmented. Using data derived from optical and radio-astronomical techniques, a wide range of topics are discussed, including: the presence and origin of molecules in space; the distribution of interstellar gas and dust; the diffusion of cosmic rays in the Galaxy and their interaction with interstellar gas; and the application of the theory of gravitational instability to the formation of stars and galaxies. (W.D.M.)

11642 CAN THE COSMOLOGICAL CONSTANT STABILISE GALAXY CLUSTERS? Noerdlinger, P. D. (Ames Research Center, Moffett Field, Calif.). Nature (London); 228: 845(28 Nov 1970).

A discussion is presented on the recent proposal by Jackson that the cosmological constant is negative and so large as to stabilise clusters of galaxies without "hidden mass" (Mon. Not. Roy. Astron. Soc., 148: 249(1970)). The discussion is based primarily on factors arising from the Hubble constant, Hubble expansion, and Hubble motions. Jackson proposed a reduction of the Hubble constant, but it is argued that such a reduction cannot result in stabilisation of galaxy clusters. (UK)

11643 ORIGIN OF THE DIFFUSE INTERSTELLAR BAND AT 4430A. Runciman, W. A. (Atomic Energy Research Establishment, Harwell, Eng.). Nature (London); 228: 843(28 Nov 1970).

It was recently suggested that the 4430-Å interstellar absorption line might be due to transitions in Fe^{3+} ions in a silicate matrix (Nature, 226: 829(1970)). The present author considers this from a slightly different point of view, and the two lines of argument are compared. It is concluded that the identification is still inconclusive, and that very careful measurements of the absorption spectra of iron-containing silicates, and in particular orthopyroxene inosilicates, are needed before a convincing case can be made. (UK)

11644 RADIO OBSERVATIONS OF THE CLUSTER OF GALAXIES IN COMA BERENICES: THE 5C4 SURVEY. Willson, M. A. G. (Cavendish Laboratory, Cambridge, Eng.). Mon. Notic. Roy. Astron. Soc.; 151: 1-44(1970).

High-resolution observations of the Coma cluster enabled the detection of 189 radio sources with $S_{408} > 16 \times 10^{-29}$ W m^{-2} Hz^{-1}. Twenty-four were also detected at 1407 MHz. Most of them are believed to be field objects unconnected with the cluster. Optical identifications are suggested for many and the counts and spectra are compared with the results of earlier $_5$C surveys. Two components of the complex of radio sources Coma C coincide with the bright galaxies NGC 4874 and NGC 4869, and about nine other cluster galaxies have radio luminosities $P_{408} \gtrsim 10^{21}$ W Hz^{-1} sr^{-1}. It is shown that the other component of Coma C, a large diameter source observed at low frequencies, must be intergalactic emission rather than the integrated radiation from normal galaxies. Such extensive sources appear to be a common feature of rich clusters. The extended source, and the emission associated with NGC 4869, may be due to the ejection of relativistic particles from NGC 4874 at a mean rate of 10^{51} erg yr^{-1} for the past 3.5×10^9 yr. (auth) (UK)

11645 SPIRALS MADE SIMPLE. Harrison, E. R. (Univ. of Massachusetts, Amherst). Mon. Notic. Roy. Astron. Soc.; 150: 443-53(1970).

The origin of spiral waves in galaxies is studied with the aid of a simple model. It is argued that the problem of generating inclined waves in a system of uniform flow, and the problem of generating spiral waves in a rotating fluid system are fundamentally equivalent. Thus, the complex environment of a differentially rotating disk of stars and gas is not essential in order to understand the origin of spiral waves. Hence "spirals made simple" are inclined waves generated in fluids of uniform motion. A simplified model has the virtue of immediately disclosing a mechanism of "crossed-stream" interactions capable of exciting and maintaining inclined waves. On the basis of this model, it is proposed that spiral waves are generated within the inner galaxy by the interaction of the radial flow from the galactic center with the

galactic rotation flow. The spiral waves trail and are propagated outward. Gravitational stability in multistream collisionless fluids is discussed. (auth) (UK)

11646 STUDIES OF THE NEUTRAL HYDROGEN CONTENT OF THE GALAXIES M31 AND M33. I. GENERAL OBSERVATIONAL METHODS AND DATA REDUCTION PROCEDURES. Gottesman, S. T.; de Jager, G. (Univ. of Manchester, Jodrell Bank, Eng.). Mem. Roy. Astron. Soc.; 74: 67-72(1970).

Results are presented of a series of neutral hydrogen observations of the galaxies M31 and M33. Observations were carried out during June 1965 and May–June 1966 with the Jodrell Bank Mark I telescope. A bandwidth of 40 kHz (8.4 km s^{-1}) and a 14′ × 18′ arc telescope beamwidth made possible an investigation of the detailed structure of these galaxies. The observational data were reduced to a series of spectra and of contour maps at constant velocity. These can be compared with optical features and used to obtain rotation laws from which mass distributions can be derived. The general observational techniques, the equipment used, and the method of data analysis are described. (auth) (UK)

11647 STUDIES OF THE NEUTRAL HYDROGEN CONTENT OF THE GALAXIES M31 AND M33. II. OBSERVATIONS OF THE GALAXY M31. Gottesman, S. T. (Univ. of Manchester, Jodrell Bank, Eng.). Mem. Roy. Astron. Soc.; 74: 73-122(1970).

In Part I (Gottesman and de Jager 1970) of this series of papers the general instrumental, observational and analytical techniques employed in these investigations were discussed. The particular methods used for the observations of the galaxy M31 are described here, and results of the data reduction procedures are given. These are in the form of contour maps at each observing frequency, spectra along selected lines, and a table of median velocity and integral of the spectrum at closely spaced points in the galaxy. (auth) (UK)

11648 STUDIES OF THE NEUTRAL HYDROGEN CONTENT OF THE GALAXIES M31 AND M33. III. OBSERVATIONS OF THE GALAXY M33. de Jager, G. (Univ. of Manchester, Jodrell Bank, Eng.). Mem. Roy. Astron. Soc.; 74: 123-38(1970).

The study of neutral hydrogen in M33 forms part of a series of neutral hydrogen studies of nearby galaxies made at Jodrell Bank with the 250-ft telescope. The instrumentation and the methods of observation and data reductions are described in Part I (Gottesman & de Jager 1970). Part II (Gottesman 1970) gives the observations of M31. The present paper presents the basic observational results for M33. (auth) (UK)

11649 GALAXIES IN THE DIRECTION OF QSO'S WITH SMALL REDSHIFTS. Bahcall, Neta A.; Bahcall, John N. (Inst. for Advanced Study, Princeton, N. J. California Inst. of Tech., Pasadena). Publ. Astron. Soc. Pac.; 82: 1276-92(Dec 1970).

Accurate positions are given for the brightest galaxies that are likely to be associated with all known QSO's with redshifts less than or equal to 0.2. Special attention is drawn to the galaxies in the direction of 3C 273. It is shown that the probability is small that purely by chance coincidence a galaxy redshift will be measured to be approximately equal to that of a quasar in its direction. (auth)

11650 CLOUD–INTERCLOUD PHASE CHANGE IN THE INTERSTELLAR MEDIUM. Penston, M. V.; Brown, F. Elizabeth (Royal Greenwich Observatory, Sussex, Eng.). Mon. Notic. Roy. Astron. Soc.; 150: 373-88(1970).

Pressure equilibrium is not the only condition necessary for the equilibrium of an interstellar cloud—the interface between cloud and intercloud medium as a whole must be in thermal balance as heat diffuses from regions of the interface that are heated excessively to those that would otherwise cool. On the other hand this equilibrium is only attained on a very long time-scale so that earlier treatments of clouds as discrete particles are quite justified. Use of an improved equation of state shows that interstellar clouds are always gravitationally unstable if their mass exceeds ~2000 $M_{\odot}$. Such a figure would indicate star formation to be a more efficient process than hitherto thought but inclusion of effects such as magnetism and rotation would increase this mass and modify this conclusion. (auth) (UK)

11651 SCANNER OBSERVATIONS OF THE λ 4430 DIFFUSE INTERSTELLAR FEATURE. Kellman, Sanford A. (Univ. of California, Berkeley). Publ. Astron. Soc. Pac.; 82: 1368-71 (Dec 1970).

The variation of the λ 4430 diffuse interstellar feature with color excess was investigated with a photoelectric spectrum scanner. In addition, the variation of the ratio of λ 4430 feature strength to color excess with galactic longitude was investigated in twelve selected longitude regions between l^{II} = 20° and 220°. Significant variations in this ratio were found to occur among the different regions. (auth)

11652 OPTICAL QBSERVATIONS OF THE PAIR OF GALAXIES ASSOCIATED WITH THE RADIO SOURCE 4C 31.04. van den Bergh, Sidney (Univ. of Toronto). Publ. Astron. Soc. Pac.; 82: 1374-5(Dec 1970).

An image-tube spectrogram obtained with the 200-inch telescope yielded redshifts of Z = 0.0548 and Z = 0.0586 for the pair of galaxies associated with the radio source 4C 31.04. (auth)

11653 EXCESS BACKGROUND RADIATION OF SOFT X RAYS AT THE GALACTIC POLE AND PLANE. Henry, Richard C. (E. O. Hulburt Center for Space Research, Washington, D. C. Johns Hopkins Univ., Baltimore); Fritz, Gilbert; Meekins, John F.; Chubb, Talbot; Friedman, H. Astrophys. J.; 163: L73-7(15 Jan 1971).

A Teflon-windowed proportional counter was used to measure a flux of 18 Å (0.68 keV) x rays from regions near the North Galactic Pole. This flux is significantly in excess of what is predicted by extrapolation of the x-ray background spectrum between 2 and 10 keV, which was observed simultaneously by both a Teflon- and a Mylar-windowed counter. A possible source of this soft x-ray background is thermal emission from a dense intergalactic medium. The spectrum between 2 and 10 keV suggests that the break toward higher energies occurs closer to 10 keV than 40 keV. A flux of soft x rays is also observed in the galactic plane near l^{II} = 190°. Unexplained line features at 6 and 7 keV are present in the data. (auth)

Cosmology

Refer also to abstracts 11597, 11642, and 12239.

11654 ABSORPTION AND SCATTERING OF ULTRAVIOLET AND X-RAY PHOTONS BY INTERGALACTIC GAS. Rees, M. J. (Cambridge, Univ., Eng.); Setti, G. Astron. Astrophys.; 8: 410-19(Oct 1970).

The state of ionization and the temperature of the intergalactic gas as a result of photoionization processes are discussed. It is shown that, under reasonable assumptions, there should be a nonthermal ultraviolet background with an intensity at the Lyman limit of 1 to 4 × 10^{-23} ergs/cm^2 s ster Hz, sufficient to ionize a uniform intergalactic medium (with concentration $n \cong 3 \times 10^{-5}$ at a redshift $z \cong 2$) at the level required by the absence of Lyman absorption in QSO spectra. The origin of this background is either Compton scattering by relativistic electrons produced in radio sources at early epochs of the microwave photons of the universal radiation field, and/or the integrated contribution from QSO's at $z \gtrsim 2$. In the former case the estimate is based on an extrapolation towards lower energies of the observed x-ray background, while in the latter case the estimate is made by extrapolating toward higher energies the optical continua of QSO's and making use of the available data on their optical luminosity function. In both cases strong evolutionary cosmological effects are assumed to be present. If the intergalactic gas had a density $n \cong 3 \times 10^{-4}$ H atoms/cm^3 (necessary to close the Universe at z = 2), the high level of ionization could be maintained assuming an ultraviolet flux ~100 times as great, which might be associated with intrinsically weak objects at large redshift, such as O stars in young galaxies. This flux would be greater than the indirect limit set by Sunyaev (1969), but it is shown that there are several ways to evade Sunyaev result. If the photoionization process represents also the main source of heat input (adiabatic expansion being the main source of cooling), it is shown that the temperature of the intergalactic gas at $z \cong 2$ would be raised to approximately (1 to 4) × 10^4°K (depending on the density and on the primeval helium content), while at present it could be as low as ~2 × 10^3°K, and the gas might have largely recombined at present. In this case it would be opaque to ultraviolet radiation, and no conflict with the Sunyaev limit would arise. If the distribution of the gas is not uniform, but it is mainly concentrated in clusters of galaxies, the previous conclusions are not essentially changed, except for the fact it would have almost certainly recombined at the present epoch. This may have important consequences for the opacity of the gas up to high energies. Further the implications for the opacity of the gas of the possible presence of heavy elements are discussed. (auth)

11655 COLLIDING GRAVITATIONAL WAVES. Szekeres, P. (Kings Coll., London). Nature (London); 228: 1183-4(19 Dec 1970).

A coordinate system is described in which the problem of colliding plane waves may be discussed in general relativity, and a particular solution, expressible in elementary functions and representing at least a part of such a collisional situation, is given. It is pointed out that nowhere should the nonlinear features of general

relativity be seen more clearly than in the collisional interaction of two gravitational waves. The nonlinearity of the interaction is best shown by calculating the physical components of the curvature tensor in a null tetrad carried by a timelike observer. Singularities must of necessity develop in this type of coordinate system, and they can frequently be transformed away by using more than one coordinate patch, but this cannot be done in the present case since the physical components of the curvature tensor, relative to a geodesic observer, become singular at the boundaries. The problem is not, however, serious since the metric could be curtailed and joined smoothly to flat space to give a completely regular space–time representing two sandwich waves in collision. A problem of interest is whether it is possible for real singularities to develop in the interaction zone even when the incoming sandwich waves are completely regular. (UK)

11656 CAN THE LUMPY DISTRIBUTION OF GALAXIES BE RECONCILED WITH THE SMOOTH X-RAY BACKGROUND? Wolfe, A. M.; Burbidge, G. R. (Univ. of California, San Diego, La Jolla. Cambridge Univ., Eng.). Nature (London); 228: 1170-4 (19 Dec 1970).

The fluctuations in x-ray background intensity that would be generated by clusters or superclusters of galaxies exceed those observed. It may be that the x-ray background arises from low-luminosity objects that are distributed much more smoothly and are more numerous than bright optical galaxies. Hierarchical universe models in which the distribution of x-ray sources follows the cosmological mass distribution are ruled out. (auth) (UK)

11657 ORIGIN OF THE X RADIATION OF THE METAGALAXY. Gnedin, Yu. N.; Dolginov, A. Z. (Ioffe Inst. of Physics and Tech., Leningrad). JETP Lett. (USSR) (Engl. Transl.); 12: 264-6(5 Oct 1970).

Translated from Zh. Eksp. Teor. Fiz., Pis'ma Red.; 12: 838-6(5 Oct 1970).

The hypothesis that the background x radiation is produced by leakage electrons from the radio galaxies is considered. It is sufficient to assume, for this purpose, that the electrons are accelerated and scattered by inhomogeneities of the magnetic field of a moving plasma; this process was considered earlier by the authors (1970). It is assumed that the dimensions of the electron-acceleration region is much smaller than the dimensions of the galaxy, and the magnetic field in the remainder of the galaxy is more homogeneous, so as to make the leakage time $\sim 10^6$ years. (W.D.M.)

11658 MOMENTUM CONSERVATION AND SOME PROBLEMS OF METAGALACTIC ASTRONOMY. Shklovskii, J. (Sternberg Astronomical Inst., Moscow). Nature (London); 228: 1174-5(19 Dec 1970).

It is explained that bodies of plasma in active galactic nuclei and quasi-stellar objects, "magnetoids," will attain large momenta because of anisotropy in the generation of relativistic particles and in synchrotron emission. "Magnetoids" may therefore be expected to be ejected from the nuclei with high velocities, thus accounting for several puzzling observations in astronomy. (auth) (UK)

11659 VACUUM-LIKE STATE OF A MEDIUM AND FRIEDMAN COSMOLOGY. Gliner, E. B. (Ioffe Inst. of Tech. Physics, Leningrad). Dokl. Akad. Nauk SSSR; 192: 771-4(1970). (In Russian).

The purpose of this note is to show that the vacuum-like state of a physical medium can be the initial state of any of the three models of Friedman. In distinction from a "singular state" (in cosmology on describing gravitational collapse, etc.), a vacuum-like state is described within the framework of general relativity theory. If the pressure changes sign at high density of the medium, it is very probable that a vacuum-like state will occur. It is incorrect to believe that a negative pressure should lead to unlimited compression of the medium. The mechanical properties of the vacuum-like and previous states are different. It is assumed that the vacuum-like state of the medium is a particular phase which in principle can exchange energy, momentum, baryon charge, etc. with other phases of the medium. The local rise in density of one phase is accompanied by a corresponding change in density of another phase. A feature of the vacuum-like state is the negative value of the effective gravitating density, as a result of which any system of free particles is brought to a state of expansion. The local density of a medium falls by initiating a phase transition to the ordinary phase. Explosions in galactic nuclei may be typical features of an initial, unstationary transition of a vacuum-like phase to an ordinary phase. (TTT)

11660 FORMATION OF GEONS AND BLACK HOLES. Gerlach, Ulrich H. (Battelle Memorial Inst., Columbus, Ohio). Phys. Rev. Lett.; 25: 1771-4(28 Dec 1970).

The dynamics of a spherically symmetric, thin-shelled ensemble of collisionless particles are determined. All the stable and unstable equilibrium configurations (which are found to be stable against single-particle decay) are classified with the help of a variational principle. Applying this principle to zero-rest-mass particles (e.g., gravitational geon), it is found that quantum geometrodynamics must be applied when the geon has low angular momentum and is in its ground state. (auth)

11661 SEPARATION OF MATTER AND ANTIMATTER. Defouw, R. J. (Harvard Coll. Observatory, Cambridge, Mass.). Nature (London); 228: 1068-9(12 Dec 1970).

The question is discussed as to whether or not the Universe contains equal amounts of matter and antimatter. Unless an asymmetric initial condition is assumed, charge symmetry follows from the conservation of baryons, but an asymmetric initial condition cannot be ruled out and, in fact, is postulated in big-band cosmology. Observations yield essentially no information on the relative amounts of matter and antimatter beyond the solar system, but do indicate that they are rarely, if ever, found together; stringent upper limits on the amount of mixed matter and antimatter can be derived from dynamical arguments and from γ-ray observations. Furthermore, condensed objects such as stars must be composed exclusively of either matter or antimatter, and this high degree of separation cannot be explained by statistical fluctuations. It is therefore important from the standpoint of charge-symmetric cosmologies to explore possible physical mechanisms by which matter and antimatter can be separated. Several such mechanisms have been suggested, and one of these is discussed. The case is considered of a gas composed of protons, antiprotons, electrons, and positrons sufficiently dilute that annihilation can be neglected. In general such a gas will be located in a magnetic field $\underline{B}$, a gravitational field $\underline{g}$, and an electromagnetic radiation field of flux $\underline{F}$, and the effects of these fields are discussed for both protons and antiprotons and for electrons and positrons, and drift velocities are derived. There is a natural tendency for $\underline{g}$ and $\underline{F}$ to be antiparallel, and it follows that protons and electrons will drift in one direction whilst antiprotons and positrons drift in the opposite direction, resulting in a separation of matter and antimatter. $\underline{B}$ must be very small if this separation mechanism is to have any cosmological significance and, in this respect, the mechanism contrasts sharply with Alfven's electrolytic mechanism. Reasons why $\underline{g}$ and $\underline{F}$ may, in general, be expected to be antiparallel are discussed. The findings are considered for supergiant stars, main-sequence stars of types O and B, and objects deriving their luminosity from annihilation, such as quasars. A possibility provided by the cosmology of Alfven and Klein is also discussed (Arkiv. Fysik, 23: 187(1963)); in this case the scale of matter–antimatter separation is determined by the magnetic field and is likely to be much more local. The effect of the black-body radiation of the Universe is also discussed. (UK)

11662 POSSIBLE IMPLICATIONS OF THE 3K BACKGROUND RADIATION. Stephenson, L. M. (University Coll., London). J. Phys., A (London); 3: L49-50(Nov 1970).

An explanation for the anomalies that have been observed in the approximately 3°K microwave background radiation is proposed. A possible observational test, for the theoretical model on which the explanation is based, is indicated. (auth) (UK)

11663 GRAVITATIONAL COLLAPSE AGAINST A COSMOLOGICAL BACKGROUND. Barnes, A. (Imperial Coll. of Science and Tech., London). J. Phys., A (London); 3: 653-61 (Nov 1970).

The propagation of light in a spherically symmetric dust distribution is investigated. A sufficient condition for light to escape from a collapsing region to an expanding region of the system is obtained. This corrects the result of Raychaudhuri (1966). It is also shown that, contrary to the conclusion drawn by Som (1968), no event horizon other than that associated with the Schwarzschild radius occurs. These results are illustrated by some numerical calculations for particular models. (auth) (UK)

11664 LUMINOSITY–VOLUME TEST FOR QUASI-STELLAR OBJECTS. Longair, M. S.; Scheuer, P. A. G. (Cavendish Lab., Cambridge, Eng.). Mon. Notic. Roy. Astron. Soc.; 151: 45-63 (1970).

The luminosity–volume test for a complete sample of quasi-stellar objects, which consists of all those brighter-than-prescribed limiting radio and optical flux densities, is investigated. The best available sample of QSOs that fulfil the completeness criteria, that was discussed by Schmidt, is used in the analysis. It is shown that: the luminosity–volume test does not depend upon the association of a particular redshift with a particular QSO—all that is important is the range of redshifts of the QSOs; the luminosity–volume test and the counts of radio sources and of QSOs are very

closely related; the two tests are not independent methods of investigating the evolution of QSOs over cosmological time scales; "luminosity" and "density" evolution hypotheses are indistinguishable from the present QSO data and, in principle, it is very doubtful if they can be distinguished; the counts of radio sources are inconsistent with the predictions of realistic Lemaitre models in which the distribution of sources is assumed uniform; and the luminosity–volume test for QSOs in Lemaitre world models is not consistent with a uniform distribution of sources, in agreement with the above. (auth) (UK)

11665 POSSIBLE METHOD FOR DETERMINING THE PLANCK CONSTANT OF COSMIC PHOTONS. Harwit, M. (Astronomical Inst., Prague). Nature (London); 228: 845-7(28 Nov 1970).

The theme of this discussion is that astronomical evidence may indicate variations of the Planck constant ($\hbar$). Bahcall and Salpeter (Astrophys. J., 142: 1677(1965)) suggested that photons arriving from distant quasars might not have the same $\hbar$ that is normally measured in the laboratory, and suggested a test that might be used to determine a dependence of $\hbar$ on the redshift parameter z of photons arriving from these objects. It is interesting that $\hbar$ serves as a measure of the spin angular momentum ($\hbar/2\pi$) along a photon's direction of propagation. Questions discussed include how photons under certain spin conditions would interact with matter; how would they be absorbed by an astronomical radiation detector, and how would the quantum mechanical angular momentum conservation relationships be obeyed in such an interaction. The first question discussed is whether or not the photons can, in fact, interact with normal matter. It is suggested that photons are not absorbed by some interstellar constituents. Absorption by interstellar gases is chosen as a test, since only under such tenuous conditions can it be assessed that atoms must interact with radiation individually. Data discussed include those for 3C 273B, the Crab Nebular pulsar, and a supernova that erupted in NGC 1058. (UK)

11666 SPECTRUM OF THE EXTRAGALACTIC BACKGROUND RADIATION AT LOW RADIO FREQUENCIES. Clark, T. A.; Brown, L. W.; Alexander, J. K. (Goddard Space Flight Center, Greenbelt, Md.). Nature (London); 228: 847-9(28 Nov 1970).

An analysis of the cosmic noise background radiation from 0.5 to 100 MHz, using a model for the effects of free–free absorption in the galactic disk, led to an estimate of the spectrum of the extragalactic radiation over this range in good agreement with independent determinations from meter-wave measurements. The isotropic brightness was found to vary with the -0.8 ± 0.1 power of frequency above 10 MHz and was $5.5 \pm 2.0 \times 10^{-22}$ W/m^2 Hz sr at 100 MHz. Below 10 MHz the isotropic spectrum turned over in a manner similar to that expected from free–free absorption between the sources and the Galaxy, with an optical depth of order 5 at 1 MHz. This result provides independent confirmation of similar conclusions derived from observations at 2 MHz and suggests that the isotropic radiation may be absorbed by electrons in the sources and/or the intergalactic medium. From the shape of the spectrum of the radiation component coming from outside the galactic disk, it is deduced that any galactic halo radiation must constitute less than 15% of the minimum total brightness observed at 100 MHz. If the radius of the galactic halo is >10 kpc and the semi-thickness of the galactic disk is <0.5 kpc, the volume emissivity of the halo radiation must be not greater than 1% of the synchrotron emissivity in the disk. (UK)

11667 USE OF WORLD MODELS WITH ANTIPOLES IN DERIVING AN UPPER BOUND FOR THE COSMOLOGICAL DENSITY PARAMETER. Baylis, D. J. (Univ. of Sussex, Eng.). Mon. Notic. Roy. Astron. Soc.; 151: 93-107(1970).

If the Universe can be adequately described by one of the isotropic zero-pressure models arising from the field equations of general relativity (with the cosmological constant), then it corresponds to a point of a plane whose coordinates can be taken as the familiar acceleration and density parameters, q_0 and σ_0. A large area corresponding to some of the singular "big-bang" models can be ruled out by considering lower bounds for the age of the Universe, and most of the nonsingular models are ruled out since observed redshifts are in excess of the theoretical maximum redshifts of these models. This still leaves an infinite area of the q_0, σ_0 diagram in which the Universe may lie, and an upper bound for the mean density of matter would reduce this to a finite region. However, the bounds obtained by most of the recent direct observational work are unsatisfactory, and this leaves an important gap in the available tests of cosmological models. The main conclusion of this paper is that the gap could be filled with the aid of a new test involving only those models with observable antipoles (models in which photons have had time to travel at least halfway around the Universe). The proposed test is completely independent of density estimates. (auth) (UK)

11668 SEARCH OF ELECTRODYNAMIC RADIATIVE CORRECTIONS FOR TIME VARIATIONS. Aurela, A. M. (Univ. of Turku, Finland). Nature (London); 228: 985-6(5 Dec 1970).

Reference is made to a simple model of electrodynamic radiative corrections formulated recently by combining several hypotheses of neutrinos of nonzero mass and electromagnetic properties with the hypothesis of a neutrino sea. The central notion of this model is that the magnitudes of the corrections will depend on the temperature and density of the neutrino sea at the point in question, and these properties of the neutrino sea will vary in space and time. The model predicts, amongst other things, that the different radiative corrections and, in particular, the Lamb shifts and the anomalous magnetic moments of the electron and muon should show simultaneous correlated time variations. Ways of forming working hypotheses concerning the origin of the proposed time variation of the neutrino sea are discussed, and the hypothesis that solar activity would be associated with activity in the neutrino sea is accepted; thus, the transient large-scale activity of the Sun might conceivably correlate with changes in radiative correction on the Earth. In this context, the model of solar energy production due to Sheldon (Nature 221: 650(1969)) is considered, which proposes that the solar nuclear reactions and the neutrino production are "switched on" only for a comparatively short period during each 11-year cycle. The predictions of the model are compared with observations. It is concluded that, in spite of the suggestive agreement between predictions and observations, only new experimental data can settle the problems. Other kinds of time variation could exist. (UK)

Planetary Phenomena

Refer also to abstract 12057.

11669 FLUX OF LOW-ENERGY PROTONS NEAR THE MOON ON DECEMBER 13, 1966. Grigorov, N. L.; Kurt, V. G.; Lutsenko, V. N.; Maduev, V. L.; Pisarenko, N. F.; (and others). Cosmic Res. (USSR) (Engl. Transl.); 7: 123-7(Jan-Feb 1969).

Translated from Kosm. Issled.; 7: 137-42(Jan-Feb 1969).

The results of measurements of low-energy protons on the artificial lunar satellite Luna 12 are analyzed. The composition, temporal change, and angular distribution of radiation fluxes indicate that the observed proton burst was associated with the transit of the satellite through a region of magnetized plasma populated by low-energy protons (0.5 to 10 MeV). The character of the angular distribution of the proton flux precludes the possibility of radiation trapped by a magnetic trap moving with a stream of solar plasma. It is noted that this event has a number of characteristics in common with earlier-studied bursts of low-energy protons coinciding with the onset of a Forbush decrease. (tr-auth)

11670 WAVEFORM AND SOURCE-SIZE STUDIES OF JUPITER'S DECAMETRIC RADIATION. Paul, Madhabendra Prasad. Gainesville, Fla.; Univ. of Florida (1969). 145p. University Microfilms Order No. 70-14,908.

Thesis.

The waveform characteristics of the Jovian decametric radiation were studied, and the source sizes using long-baseline radio interferometer were determined. It was found that Jovian S bursts can be further subdivided into two types: recurrent and nonrecurrent. In the recurrent type the bursts are spaced very close to each other and occur fairly regularly, whereas in the nonrecurrent type the bursts are randomly spaced and occur less frequently. Statistical analyses regarding the duration and separation of these bursts and also their relationship with System III (1957.0) longitude were also made. The nature of radio noise composing these two types of bursts and also of L bursts was investigated and from comparison with noise obtained from a band-limited noise generator it was found that there is no significant difference between the different types of radio noise within Jovian bursts. Further evidence was found that S bursts do not acquire their burstiness due to interplanetary scintillations, but rather to an intrinsic emission mechanism of the source itself. (TSS) (Diss. Abstr. Int., B)

11671 HABIT AND TEXTURE STUDIES OF LUNAR AND METEORITIC MATERIALS WITH A 1 MeV ELECTRON MICROSCOPE. Dran, J. C. (CNRS, Orsay, France); Durrieu, L.; Jouret, C.; Maurette, M. Earth Planet. Sci. Lett.; 9: 391-400 (11 Nov 1970).

Some habit and texture features of the finest and uncrushed grains in the lunar dust samples 10084 and 12070 were studied with a 1-MeV electron microscope. These features were then

compared with those observed in broken fragments extracted either from lunar rocks 10047 and 12063 or from different types of meteorites (Orgueil; Pesyanoe, Shergotty). The finest fraction of the Apollo 11 lunar soil samples is constituted of about 80% of well-ordered but rounded crystals which are frequently overlaid by a thin skin of amorphous material. In the Apollo 12 soil the grains are coarser, the fraction of crystalline material is higher (~90%) and the proportion of crystals showing an amorphous skin is smaller, but both lunar soil samples are very different from meteoritic or lunar rock matter. Some implications of the present results concerning the fabric fraction of the lunar regolith, the ancient solar wind and meteoritic research are briefly outlined. (auth)

Atomic and Molecular Physics

Atomic, Electron, Ion, and Molecular Beams and Their Reactions

Refer also to abstracts 10517 and 12017.

11672 INELASTIC ELECTRON SCATTERING AND SECONDARY ELECTRON EMISSION OF Mg AND MgO. Bronshtein, I. M.; Brozdnichenko, A. N. Radiotekh. Elektron.; 15: 1721-6(Aug 1970). (In Russian).

Certain relationships were found for the secondary electron emissions of Mg and MgO for incident electron energies of 0.25 to 4 keV. The effective yields of $\lambda_{Mg} = 50$ Å and $\lambda_{MgO} = 320$ Å of truly secondary electrons were determined. The role of the inelastic reflection of electrons in the secondary electron emission of Mg and MgO was analyzed. Effects of surface structure and temperature on the secondary electron emission of MgO are discussed. (tr-auth)

11673 PENETRATION OF ELECTRONS INTO ANTHRACENE CRYSTALS. Kawabe, Mitsuo; Masuda, Kohzoh; Namba, Susumu (Osaka Univ.). J. Appl. Phys.; 42: 501-2(Jan 1971).

Penetration depths and energy-loss profiles were determined for electrons of 25, 30, 35, and 40 keV energies in anthracene crystals, using cathodoluminescence photographed through a microscope. Tetracene was introduced as an impurity to suppress the exciton diffusion length. The range–energy relation is in excellent agreement with the theoretical curve. (D.L.C.)

11674 BASE OF MULTIPLE COMPONENT SYSTEM ANALYSIS BY ELECTRON AND BETA RAY INTERACTION. I. CALCULATION OF THE EFFECTIVE ATOMIC NUMBER FOR THE BACKSCATTERING PROCESS. Thuemmel, H.-W. (Institut fuer Angewandte Radioaktivitaet, Leipzig). Isotopenpraxis; 6: 214-19 (Jul 1970). (In German).

Formulas for calculating the effective atomic number of complex substances assuming single-scattering and diffusion models, respectively, are derived and evaluated, considering the dependence of scattering and differential energy-loss cross section on primary energy E_0, scattering angle Θ, and atomic number Z. It is shown that single scattering and diffusion processes lead to different atomic numbers ($\overline{Z}_E$ and Z_D, resp.), which are functions of E_0 and Θ. The effective atomic number $\overline{Z}_\Sigma$ valid for the whole backscattering process may be expressed as $\overline{Z}_\Sigma = p_E\overline{Z}_E + p_D Z_D$, where p_E and p_D are the relative intensity contributions to the backscattering process of single scattering and diffusion processes, respectively. Calculation methods of other authors for the effective atomic number are discussed; they may be explained as approximations of $\overline{Z}_\Sigma$. Filtering of backscattered radiation before being detected changes p_E and p_D because of the different mean energy of single-scattered and backdiffused parts; thus, the methods of analyzing three-component systems by measuring unfiltered backscattered beta particles can be understood. (auth)

11675 INTERACTION OF ATOMIC PARTICLES WITH SOLID SURFACES AT INTERMEDIATE ENERGIES. III. ANGULAR AND ENERGY DISTRIBUTIONS OF PARTICLES SCATTERED WITH ELECTRIC CHARGE FROM POLYCRYSTALLINE AND CRYSTALLINE PLATINUM. Cawthron, E. R.; Cotterell, D. L.; Oliphant, Sir Mark (Australian National Univ., Canberra). Proc. Roy. Soc. (London), Ser. A; 319: 435-59(10 Nov 1970).

The distributions in angle and energy for charged particles emitted from polycrystalline and crystalline platinum (100 face) bombarded with ions of hydrogen, nitrogen, and argon were measured, in continuation of previous work. Hydrogen ions incident on polycrystalline platinum, with energy of the order of 10 keV, gave distributions with angle of incidence, α, and angle of scattering, Θ, in general accord with what might be expected, but the heavier ions showed marked differences, probably due to some sputtered atoms escaping with electric charge. With the crystalline target, effects of channelling observed in the angular distribution of emitted charged particles were accompanied by marked changes in the energy distribution of these scattered particles. (auth) (UK)

11676 EJECTION OF ATOMIC PARTICLES FROM ION-BOMBARDED SOLIDS. MacDonald, R. J. (Australian National Univ., Canberra). Advan. Phys.; 19: 457-524(Jul 1970).

An account of the work being done on the particles ejected from a single crystal, following ion bombardment is presented. These particles include sputtered atoms and ions, scattered atoms and ions, and secondary electrons. An attempt is made to indicate the similarities and differences, particularly between the energy and angular distributions of these ejected particles. The major link involving the dependence of these distributions of all particles on crystallography is stressed. (auth) (UK)

11677 ELECTRON ENERGY LOSS DUE TO SURFACE MODES IN A THIN IONIC CRYSTAL FILM. Chase, J. B.; Kliewer, K. L. (Ames Lab., Iowa). Phys. Rev., B; 2: 4389-4400(1 Dec 1970).

A local theory for the energy loss of a relativistic electron beam, incident normally on a thin ionic crystal film, is developed and applied to the energy region of the surface modes of vibration. It is found that the loss function, including retardation, is essentially the same as that without retardation. Important effects associated with experimental resolution in energy and momentum are included in the analysis. With the inclusion of the characteristics of the apparatus, the theoretical line shapes and positions are in good agreement with the experimental results on LiF obtained by Boersch, Geiger, and Stickel. A study of the effects of substrate thickness and conductivity is reported. A good conductor, like aluminum, has a strong effect on the loss function, whereas a poor conductor, like carbon, has little effect. (auth)

11678 SURFACE AND VACUUM PHYSICS INDEX. VOLUME 5, NO. 10, 1970. Bibliography, Author Index, Subject Index in Alphabetical Order, Cumulative Subject Index in Logical Order. Frankfurt am Main; Zentralstelle fuer Atomkernenergie-Dokumentation (1970). 64p.

This listing includes 266 articles on various aspects of the title subjects. (M.O.W.)

11679 PHOTON RADIATION BY ELECTRONS UPON REFLECTION FROM A MAGNETIC FIELD. Loskutov, Yu. M.; Zakhartsov, V. M. Vestn. Mosk. Univ., Ser. III, Fiz. Astron.; 11: 53-6(Jan-Feb 1970). (In Russian).

The effect of electron reflection from a magnetic field that fills half-space is examined. The differential cross sections were found for bremsstrahlung production and total loss for a single reflection. Photon emission during reflection leads to preferred polarization of electrons in a direction opposite to the field. For nonrelativistic electrons, the degree of such a polarization is close to unity. (tr-auth)

11680 MODEL FOR ELECTRONIC STOPPING POWER OF HEAVY IONS. Reese, Glen Patrick. Manhattan, Kans.; Kansas State Univ. (1970). 109p. University Microfilms Order No. 70-16,643.

Thesis.

A theoretical model for the electronic stopping power, S_e, for heavy ions in the velocity range $v \lesssim v_0$ is proposed. The Hartree–Fock–Slater description of the atom is used. Two sets of calculations are presented, where the only difference is the inclusion of contributions of all orbital electrons compared with a scheme selectively using only outer-shell contributions. A criterion is proposed for the selection of participating subshells. The requirement of a lower limit on the impact parameter of the projectile in the stopping medium is pointed out, and scattering theory is used to obtain this limit. Unlike the theories of Lindhard and Scharff, and Firsov, the present calculations exhibit an oscillatory structure in S_e as a function of projectile atomic number. These results are compared with experiment for amorphous carbon and nitrogen gas targets, for projectile atomic number $36 \gtrsim Z_1 \gtrsim 6$, and velocities $v/v_0 = 0.41$, 0.63, and 0.91. The positions of the maxima and minima are well predicted. Agreement with experimental values is improved with respect to existing theories. In addition to the stopping power results, the calculated energy loss of the projectile is presented as a function of the distance of closest approach in a two-atom collision. A critical comparison is made with theories using nodeless one-parameter wave functions. It is concluded that the one-parameter wave functions underestimate the average electron velocity when the radial wave function has nonzero nodes. (Diss. Abstr. Int. B)

11681 EXACT SCREENED CALCULATIONS OF ATOMIC-FIELD BREMSSTRAHLUNG. Tseng, H. K.; Pratt, R. H. (Univ. of Pittsburgh). Phys. Rev., A; 3: 100-15(Jan 1971).

A discussion of relativistic bremsstrahlung cross sections is given for incident-electron kinetic energies in the range 5 keV to 1 MeV, based on an exact numerical calculation using screened potentials. Comparisons are made with previous authors' results, extending the discussion of a preliminary note. Exact point-Coulomb and Born-approximation results are contrasted. The present results show that the Born approximation significantly underestimates the bremsstrahlung cross sections in the energy region considered. Screening effects are somewhat larger than expected, and when large are not well described by a form factor. (auth)

11682 SPATIAL DISTRIBUTION OF ENERGY DEPOSITED BY ATOMIC PARTICLES IN ELASTIC COLLISIONS. Winterbon, K. B.; Sigmund, Peter; Sanders, J. B. Kgl. Dan. Vidensk. Selsk., Mat.-Fys. Medd.; 37: 14-(1970).

Energetic atomic particles slowing down in a solid or a gas create cascades of atomic collisions. This paper deals with the spatial distribution of the energy dissipated within the cascades at the end of the slowing-down process. This distribution is of central interest in the theory of radiation damage and sputtering. An integrodifferential equation determining the distribution function is derived under the assumption of random slowing down in an infinite medium. A set of equations is derived determining spatial moments over the distribution functions, and the moment equations are solved explicitly under the assumption of elastic scattering with power-law cross sections. The theory applies to heavy ions or recoil atoms in the keV range (for lighter ions only in the lower keV range) slowing down in a (monatomic or polyatomic) target under conditions where crystal lattice effects may be neglected. Moments over the distribution are tabulated for a wide range of mass ratios and several exponents in the Lindhard power cross section and are compared to corresponding moments over the distribution of ion ranges. Several methods of constructing distributions from spatial moments are discussed, and some typical energy and range distributions are presented, both in one dimension (depth distribution) and three dimensions. A brief discussion of the experimental situation concludes the paper. (auth)

11683 SCATTERING OF THE RARE GASES (He, Ne, Ar, Kr, AND Xe) FROM PLATINUM (111) SURFACES. Stoll, A. George; Smith, Donald L.; Merrill, Robert P. (Univ. of California, Berkeley). J. Chem. Phys.; 54: 163-9(1 Jan 1971).

The scattering of He, Ne, Ar, Kr, and Xe from Pt (111) surfaces characterized by LEED was measured for surface temperatures between 100°C and 500°C using effusive thermal-energy beams of 23°C and 700°C. The LEED and helium scattering indicate that the surfaces are geometrically smooth, regular, and free from low-molecular-weight contaminants. Results are in qualitative agreement with some of the predictions of the "cube" scattering theories but at variance with the effect of incident angle and surface mass. Data agree qualitatively in these respects with the finite range interaction (FRI) models. Approximate mass balances between the total scattered flux and the incident flux permit estimates of the initial trapping probabilities. No diffraction of He was observed. (auth)

Atomic and Molecular Properties

Refer also to abstract 12398.

11684 P-STATE WAVE FUNCTION OF THE TWO-ELECTRON ATOM AND THE ABSORPTION COEFFICIENT OF H^- NEGATIVE HYDROGEN ION. Postma, Richard William. Lexington, Ky.; Univ. of Kentucky (1969). 61p. University Microfilms Order No. 70-16,982.

Thesis.

A continuum-state wave function is developed using the same general method as that employed by James E. Miller to develop the bound S-state wave function. The procedure is to take the partially separated two-electron wave function given by G. Breit and expand the function as a series in the Legendre polynomials of the cosine of the angle between the radius vectors of the two electrons. This results in explicit representation of the dependence of the wave function on all four angle variables and leaves only the two radius variables to be determined. When the function is substituted into the Schroedinger equation and the equation is integrated over the angles, the result is a system of coupled partial differential equations of second order in the two independent variables, the radius distances to the two electrons. The singlet (symmetric) solutions are then sought by substituting difference operators for the differential operators and applying the result to a grid of function values. This results in a set of linear equations in the functions to be determined, the coefficients depending on the value of the functions at the surrounding points. At each point the functions may be calculated, and the results used as new values at that particular point. Then the procedure is iterated using the new values. The iteration procedure is repeated, using a high-speed computer, until the solution becomes stationary. The wave function is thus calculated at approximately 180,000 points. The local energy is calculated at a large number of these points and is found to vary only slightly over a major part of the region. The variation became large only near the origin. This is in contrast to variational or perturbation calculations where the local energy may vary from $-\infty$ to ∞. The virial theorem is used to test the solution. The absorption coefficients are calculated for the transition from the bound S-state to the continuum P-state. Miller's S-state bound function is used together with the P-state continuum function calculated herein. The value for K_M was found to come satisfactorily close to the values for K_A and K_L. As a large amount of computer time was required only two continuum functions were calculated, those corresponding to absorption of light of 8000-Å and of 12,000-Å wavelengths. (TSS) (Diss. Abstr. Int., B)

11685 RELATIVISTIC CALCULATIONS OF ATOMIC X-RAY AND AUGER TRANSITION RATES. Rosner, Herbert Reginald. Manhattan, Kans.; Kansas State Univ. (1970). 228p. University Microfilms Order No. 70-16,645.

Thesis.

The transition rates for the characteristic x-ray spectra of the elements are computed relativistically by using the Dirac formulation of the orbital electrons and the radial wave functions and energies of the relativistic Hartree–Fock–Slater atomic model. The calculations are carried out to all orders of contributing multipoles, for transitions between final states ranging from the K shell to the N_6 subshell and initial states ranging from the L_1 subshell to the N_7 subshell. Results are obtained for the elements with atomic number Z = 21, 30, 35, 41, 48, 55, 63, 70, 80, and 93. In a similar manner and for the same elements, the transition rates for the Auger groups K–LM, K–MM, and L_1–MM are calculated relativistically, with the use of two-electron retarded interaction theory. The calculations again make use of the wave functions and energies of the relativistic Hartree–Fock–Slater model. The K-shell and L_1-subshell fluorescence yields are calculated for the same range of elements with the results obtained for the total respective x-ray and Auger transition rates, as described above. Detailed comparisons are made between these calculations and some of the earlier theoretical results of other workers. In the x-ray case, there is good agreement with the limited relativistic results of Massey and Burhop for the heavier elements, Z > 50. In the Auger case, the agreement with the nonrelativistic results of Rubenstein is better than with the results of Asaad and Burhop. It is inferred that the latter calculations may be in error. Comparisons are also made between the present results and the available experimental data. In the x-ray case, the calculated relative transition rates are in very good agreement with the experimental values. In the Auger case, the agreement is also reasonably good for Z > 40. In the cases of the lighter elements, there is less agreement, which is ascribable to the fact that the jj-coupling scheme contained in the present relativistic calculations is not appropriate. The calculated fluorescence yields, in which the results of the x-ray and Auger calculations are combined, are in very good agreement with experiment, indicating that the presently calculated total x-ray and Auger transition rates are correct. (Diss. Abstr. Int., B)

11686 AB INITIO CALCULATIONS OF HARMONIC FORCE CONSTANTS. IV. COMPARISON OF DIFFERENT METHODS. Bishop, David M.; Macias, A. (Univ. of Ottawa). J. Chem. Phys.; 53: 3515-21(1 Nov 1970).

Five different ab initio methods of calculating force constants are considered. The advantages and disadvantages of these methods are brought out by their application to a calculation of the force constant of the hydrogen molecule using a basis set of Gaussian functions. Particular attention is drawn to both the accuracy and time involved in the different methods. (auth)

11687 FINE STRUCTURE MEASUREMENT OF SINGLY IONIZED HELIUM, n = 4. Jacobs, Ralph Raymond. New Haven; Yale Univ. (1969). 118p. University Microfilms Order No. 70-16,283.

Thesis.

Precision measurements of the energy differences $\mathscr{I}_4 = 4^2S_{\frac{1}{2}} - 4^2P_{\frac{1}{2}}$ and $\Delta E_4 - \mathscr{I}_4 = 4^2P_{\frac{1}{2}} - 4^2S_{\frac{1}{2}}$ in $(He^4)^+$ are reported. The experimental results, $\mathscr{I}_4 = (1768 \pm 5)$ MHz and $\Delta E_4 - \mathscr{I}_4 = (20179.7 \pm 1.2)$ MHz, are compared with the values determined by quantum electrodynamic theory, $\mathscr{I}_4 = 1768.34 \pm 0.51$ MHz and $\Delta E_4 - \mathscr{I}_4 = 20180.78 \pm 0.56$ MHz. An electron gun is operated in a section of waveguide containing helium gas. For appropriate electron energies, a process of simultaneous ionization and excitation of some

atoms to He^+, n = 4 results. An external magnetic field applied perpendicular to the waveguide axis helps to focus the electron beam, but more importantly, for a fixed frequency of oscillating electric field in the waveguide, allows one to scan a microwave resonance between suitable Zeeman levels. The electric dipole transitions $4^2S_{\frac{1}{2}} \rightarrow 4^2P_{\frac{1}{2}}$ or $4^2S_{\frac{1}{2}} \rightarrow 4^2P_{\frac{3}{2}}$ cause a reduction in the intensity of 1215-Å radiation emitted in the natural decay of 4S to 2P. This radiation passes through holes in the waveguide and is focused by an ellipsoidal light pipe onto a suitable ultraviolet detector. Following the phototube is a lock-in detection system for which the synchronous signal is provided by square-wave amplitude modulation of the microwave field. The resonances so obtained are fitted by various theoretical line shapes in a computerized least squares program. The resulting "best fit" parameters include either $\mathscr{S}_4$ or $\Delta E_4 - \mathscr{S}_4$ depending on the transition studied. (Diss. Abstr. Int. B)

11688 FINE STRUCTURE MEASUREMENT IN IONIZED HELIUM. Mader, David Lyle. New Haven; Yale Univ. (1969). 50p. University Microfilms Order No. 70-16,305.

Thesis.

The fine structure splitting $\Delta E - \mathscr{S}(^2S_{\frac{1}{2}} - ^2P_{\frac{1}{2}})$ in the n = 3 level of ionized helium, He^+, was measured to 17 ppM with a microwave-optical technique. Here ΔE is the fine structure interval $(^2P_{\frac{3}{2}} - ^2P_{\frac{1}{2}})$ and $\mathscr{S}$ is the Lamb shift. Electron bombardment of helium gas produces excited ions. The light from the n = 3 to n = 2 decay shows a decrease when a microwave field induces transitions among the fine structure levels. Enough data were taken to permit an extrapolation to zero gas pressure, bombarding current, and microwave power for each of the transitions αc and βd, resulting in $\Delta E - \mathscr{S} = 47843.76 \pm 0.81$ (68% confidence) MHz. This value is 1.37 ± 0.93 MHz lower than the theoretical value of 47845.13 ± 0.46 MHz calculated with the Taylor, Parker, and Langenberg value of $\alpha^{-1} = 137.03602$. If a value of $\mathscr{S}$ is extracted from the $\Delta E - \mathscr{S}$ measurement, it is 0.033 ± 0.022% higher than the current theoretical value. (Diss. Abstr. Int. B)

11689 PROFILES OF THE He I 4471.5- AND 4922-A LINES IN A dc ARC. Birkeland, J. W.; Bacon, M. E.; Braun, W. G. (Aerospace Research Labs., Wright-Patterson AFB, Ohio). Phys. Rev., A; 3: 354-8(Jan 1971).

Measurements were made of the profiles of the He I 4471.5- and 4922-Å lines in a dc arc for electron densities in the range of 0.4 to 2×10^{16} cm^{-3}. Concurrent determinations of the electron densities and temperatures by various methods could not be fully reconciled and are critically discussed. The normalized experimental and theoretical profiles, when compared on the basis of equal peak separation, show increased broadening of the forbidden component and filling in of the dip in the observed profile. (auth)

11690 ELECTRONIC RECOMBINATION OF He_2^+. Gerardo, J. B.; Gusinow, M. A. (Sandia Labs., Albuquerque, N. Mex.). Phys. Rev., A; 3: 255-67(Jan 1971).

The electronic recombination coefficient of He_2^+ under thermalized conditions at 80°K is $(3.4 \pm 1.5) \times 10^{-6}$ cm^3 sec^{-1}. The electron-temperature dependence of this coefficient is $T_e^{-\chi}$, $\langle\chi\rangle = 1.22$, $0.98 < \chi < 1.60$. This is applicable when both the gas and ion temperatures are near 80°K. The fragments of the recombination process have not been identified but the results indicate dissociation into He_2^* + He. (auth)

11691 MEASUREMENT OF THE $2^2S_{\frac{1}{2}} - 2^2P_{\frac{1}{2}}$ ENERGY SEPARATION ($\Delta E - S$) IN HYDROGEN (n = 2). Shyn, T. W.; Rebane, T.; Robiscoe, R. T.; Williams, W. L. (Univ. of Michigan, Ann Arbor). Phys. Rev., A; 3: 116-22(Jan 1971).

The $2S_{\frac{1}{2}} - 2P_{\frac{1}{2}}$ energy separation ($\Delta E - S$) in the n = 2 state of atomic hydrogen was measured by an atomic-beam radio-frequency method. A beam of metastable atoms in the single hyperfine state $\beta_A(F, m_F = 0, 0)$ was used. The electric dipole transitions $\beta_A - b(F, m_F = 1, +1)$ and $\beta_A - d(F, m_F = 1, -1)$ were observed at fixed frequencies by sweeping the Zeeman magnetic field parallel to the beam axis. Measurements of the frequencies of the rf field used to drive the transition and the magnetic fields at the line centers of the resonance curves, along with the theory of Zeeman splitting, were used to determine the zero-field splitting ($\Delta E - S$). The final value of ($\Delta E - S$) is 9911.250 ± 0.063 MHz, where the quoted uncertainty is one average deviation from the mean. Using the revised experimental value of the Lamb shift, $S_H = 1057.90 \pm 0.10$ MHz, the value $\Delta E = 10{,}969.15 + 0.12$ MHz was obtained. The corresponding value for α^{-1} is 137.0356 ± 0.0007. (auth)

11692 THEORETICAL CONSIDERATIONS FOR AUTOIONIZING STATES WITH MICROSECOND LIFETIMES. Manson, Steven Trent (Columbia Univ., New York. Georgia State Univ., Atlanta). Phys. Rev., A; 3: 147-53(Jan 1971).

Analytic Hartree–Fock wave functions were used to perform model calculations on the structure and lifetimes of the slowly auto-ionizing states arising from (1s, 2s, 2p) ^4P in He^- and Li. The effect of mixing with the associated ^2P's is considered, and the phenomenon of differential metastability is discussed. A framework is provided to interpret experimental observations. (auth)

11693 HYPERFINE AND ZEEMAN STUDIES OF LOW-LYING ATOMIC LEVELS OF ^{139}La AND THE NUCLEAR ELECTRIC-QUADRUPOLE MOMENT. Childs, W. J.; Goodman, L. S. (Argonne National Lab., Ill.). Phys. Rev., A; 3: 25-45(Jan 1971).

The atomic-beam magnetic-resonance technique was used to determine the hyperfine-interaction constants A, B, and C and electron g values g_j for all previously unstudied atomic levels of ^{139}La below 9000 cm^{-1}. The results are analyzed in detail in terms of a set of eigenvectors spanning the three configurations $5d6s^2$, $5d^26s$, and $5d^3$. Corrections for hyperfine and Zeeman interactions between all low-lying states are carried out in intermediate coupling. The value deduced from the observed hyperfine structure for Q, the ^{139}La nuclear ground-state electric-quadrupole moment, is influenced strongly by taking account of (a) the large recently found configuration mixing between $5d6s^2$, $5d^26s$, and $5d^3$ and (b) the rather substantial Sternheimer shielding effects. The effects (a) and (b), though both about 30%, are in opposite directions and partially cancel. The value obtained is Q = (+0.22 ± 0.03)b. Although the order of consistency between the experimental results and theory is encouraging, a number of problems remain. (auth)

11694 LS-TERM DEPENDENCE OF HYPERFINE-INTERACTION PARAMETERS IN d^2s CONFIGURATIONS. Wilson, M. (Argonne National Lab., Ill.). Phys. Rev., A; 3: 45-50(Jan 1971).

Hartree–Fock calculations have been made for the configurations $3d^24s$ of Sc I and $5d^26s$, $5d6s^2$, and $5d^3$ of La I. Attention is drawn to the variation of atomic quantities that influence hyperfine structures owing to the LS-term dependence of the radial wave functions. Theoretical calculations of the level structure of $(5d + 6s)^3$ of La I are also presented. (auth)

11695 LIFETIME OF THE 2^1P_1 AND 3^1P_1 STATES OF ATOMIC HELIUM. Burger, James M.; Lurio, Allen (Columbia Univ., New York). Phys. Rev., A; 3: 64-75(Jan 1971).

The radiative lifetime of the 2^1P_1 and 3^1P_1 state of atomic helium was measured by the level-crossing technique. In the experiment, a beam of 2^1S_0 metastable atoms was first produced and then excited to the 2^1P_1 or 3^1P_1 state with resonance radiation. The lifetimes were measured by observing the zero-field level-crossing signals in the detected 584- or 537-Å fluorescent radiation when these $^1P_1$ states decayed to the 1^1S_0 ground state. The results are $\tau(2^1P_1) = (5.57 \pm 0.15) \times 10^{-10}$ sec and $\tau(3^1P_1) = (1.73 \pm 0.11) \times 10^{-9}$ sec. These values are in excellent agreement with theory. (auth)

11696 ISOTOPE SHIFT IN THE $(2^1S_0 - 2^1P_1)$ LINE OF ATOMIC HELIUM. Burger, James M.; Lurio, Allen (Columbia Univ., New York). Phys. Rev., A; 3: 76-81(Jan 1971).

A measurement of the isotope shift in the $(2^1S_0 - 2^1P_1)$ line of atomic helium was made and is in excellent agreement with theory. Both ^4He and ^3He 2^1S_0 metastable beams were irradiated in a magnetic field with 20582-Å $(2^1S_0 - 2^1P_1)$ radiation from ^3He and ^4He resonance lamps, respectively. In each case, a magnetic sublevel of the 2^1P_1 state was Zeeman-shifted so as to scan the resonance-lamp profile. The 584-Å $(2^1P_1 - 1^1S_0)$ decay photons served to monitor the excitation. A shift $\nu(^3He) - \nu(^4He) = 0.1408 \pm 0.0019$ cm^{-1} was obtained. (auth)

11697 HIGHER-ORDER FINITE-DIFFERENCE SOLUTIONS OF THE SCHROEDINGER EQUATION FOR THE HELIUM ATOM. Barraclough, C. G.; Mooney, J. R. (Univ. of Melbourne). J. Chem. Phys.; 54: 35-44(1 Jan 1971).

Higher-order finite-difference solutions of the Schrödinger equation for the helium atom were obtained. For the S-limit equation the ground- and first-excited-state energy values were found. There was a substantial reduction in the difference error in comparison with the treatment of Winter, Diestler, and McKoy (1968). For the complete (nonrelativistic) Schrödinger equation for He finite-difference expressions of error $O(h^6)$ gave the ground-state energy to five significant figures (−2.9038 hartree). This problem seems to be near the limit of practical solution by the finite-difference method. (auth)

11698 OPTICAL ABSORPTION OF CERIUM, CERIUM OXIDE, PRASEODYMIUM, PRASEODYMIUM OXIDE, NEODYMIUM, NEODYMIUM OXIDE, AND SAMARIUM IN THE EXTREME ULTRAVIOLET. Haensel, R.; Rabe, P.; Sonntag, B. (Deutsches

Elektronen-Synchrotron, Hamburg. Univ., Hamburg). Solid State Commun.; 8: 1845-8(15 Nov 1970).

The optical absorption of the rare earths Ce, Pr, Nd, and Sm was measured in the energy region 100 to 180 eV. The absorption spectra of the oxides of Ce, Pr, and Nd were determined in the same energy region. Synchrotron radiation of the 7.5-GeV electron synchrotron DESY was used as a light source. Transitions from the 4d level of the rare earths contribute the main part of the absorption in this energy region. At the onset of these transitions a number of sharp absorption maxima were found. This fine structure is followed by a broad absorption maximum about 15 eV above the onset of 4d transitions, which is due to d → f continuum transitions. The absorption spectra of Ce and Ce oxide show a marked difference, whereas the absorption spectra of Pr and Nd are very similar to those of their oxides. (auth) (UK)

Positronium, Muonium, and Mesic Atoms and Molecules

Refer also to abstract 12041.

11699 EFFECT OF PHONONS ON THE e^+-e^- ANNIHILATION RATE IN METALS. Hede, B. B. J.; Carbotte, J. P. (McMaster Univ., Hamilton, Ont.). Can. J. Phys.; 48: 2661-72(15 Nov 1970).

An estimate of the effect of positron–phonon and electron–phonon interactions on the positron partial annihilation rate in metals is presented in an effort to explain the smearing of the two-photon counting rate at the Fermi cutoff which remains at low temperatures. The lowest-order phonon diagrams in the expansion of the electron–positron correlation function are studied. It is found that such phonon effects do not account for a significant part of the smearing. In fact, it seems sensible to assume that even a more complete treatment of phonon diagrams would not appreciably change this result. (auth) (Canada)

11700 DETECTION OF POSITRONIUM HYDRIDE. Schrader, David M.; Petersen, Teri (Marquette Univ., Milwaukee). Phys. Rev., A; 3: 61-3(Jan 1971).

Annihilation converts positronium hydride into photons and a hydrogen atom. The probability that the residual hydrogen atom will relax to each of number of bound states is calculated. The results suggest an experiment for detecting positronium hydride in a system in which excited hydrogen atoms do not exist except as the residue after annihilation. The experiment consists of measuring the intensity increase of the Lyman-α line upon quenching the 2s atoms to 2p atoms. It is predicted that the intensity will increase by a factor of 35. (auth)

Collision Phenomena

11701 IMPORTANCE OF THE KINETIC-ENERGY EXPRESSION FOR A BOUND ELECTRON IN CLASSICAL THEORY. Tripathi, D. N.; Rai, D. K. (Banaras Hindu Univ., Varanasi, India). J. Quant. Spectrosc. Radiative Transfer.; 10: 1329-34 (Dec 1970).

Electron-impact ionization cross sections of alkali-metal atoms and noble-gas atoms were calculated using Gryzinski's, Vriens', and Burgess' formulas. The kinetic energy of the bound electron was estimated by using Slater's rule. Comparisons were made with experimental results. (auth) (UK)

11702 EXCITATION PROCESSES IN HELIUM AND HYDROGEN. Weaver, Lawrence D. Jr. Fayetteville, Ark.; Univ. of Arkansas (1970). 122p. University Microfilms Order No. 70-17,206.

Thesis.

The absolute cross sections for the production of the He I $4^3S \rightarrow 2^3P$ (λ4713Å) and the He II $n = 4 \rightarrow n = 3$(λ4686Å) emissions were determined for the energy range from threshold to several hundred electron volts. The experimental results for the 4^3S excitation are compared with those of other investigators. The $4^3S \rightarrow 2^3P$ relative excitation function at the higher energies was found to decrease faster than those determined by other investigators. The excitation cross section, in the energy range from 50 to 200 eV, has an $E^{-2.50 \pm .15}$ energy dependence, whereas the Ochkur theory predicts an E^{-3} dependence. The cross sections obtained for the production of the He II line (λ4686Å) are compared to the Born calculations of Lee and Lin. The experimental cross sections are about 2 to 3 times larger than those obtained from theory. The absolute cross sections for the production of the H_α (λ6563Å) and H_β (λ4861Å) emissions by electron impact on molecular hydrogen were measured in the range from 20 to 400 eV. Using the techniques of time-resolved spectroscopy the 3s → 2p and 4s → 2p contributions to the H_α and H_β emissions, respectively, were determined. The possible effect of ion–atom collisions on the 3s and 4s radiative lifetimes was determined. It appears that such collisions have no effect on the radiative lifetimes under suitable conditions for excitation. Under other than suitable conditions, the 3s and 4s lifetimes are found to be shortened. (Diss. Abstr. Int., B)

11703 ANALYTIC CROSS SECTIONS FOR INELASTIC COLLISIONS OF PROTONS AND HYDROGEN ATOMS WITH ATOMIC AND MOLECULAR GASES. Green, A. E. S. (Univ. of Florida, Gainesville). J. Geophys. Res.; 76: 133-44(1 Jan 1971).

Analytic formulas are given for inelastic cross sections for collisions of protons and hydrogen atoms with atomic and molecular gases in the energy range 0.5 keV to 5 MeV. They are convenient interpolation formulas that span the broad energy region important in atmospheric physics, astrophysics, radiation physics, and plasma physics. The asymptotic form of the analytic expressions is shown to be equivalent in appropriate cases to theoretical results obtained with the well-known Born approximation. The parameters of the formulas are evaluated for noble gases and for diatomic atmospheric gases with the aid of electron impact data and recent results of proton and hydrogen atom impact experiments. The systematics of the parameters are discussed. (auth)

11704 COINCIDENCE STUDY OF NITROGEN ION–ARGON ATOM COLLISIONS AT KILOVOLT ENERGIES. Knystautas, Emile John. Storrs, Conn.; Univ. of Connecticut (1970). 55p. University Microfilms Order No. 70-15,542.

Thesis.

Single collisions are studied between nitrogen ions scattering from argon atoms at laboratory energies $10 \text{ keV} \leq T_\theta \leq 150 \text{ keV}$ and laboratory scattering angles $9° \leq \theta \leq 40°$. A collision is specified by fixing T_θ and θ. In an (m,n) reaction, the nitrogen ion scatters into angle θ with charge +m, and the argon target recoils into angle $\phi = \beta - \theta$ with charge +n. After collision, both ions are detected in coincidence and are charge-state analyzed. A "coincidence profile" plots relative coincidence counts versus β and is generally Gaussian-shaped. Two types of data result. The area under a coincidence profile for an (m,n) reaction is proportional to the relative probability of that reaction. A classically derived expression gives that portion Q of the incident kinetic energy lost to inelastic processes in terms of β (for a given collision). Thus from the center-value $\bar{\beta}_{mn}$ of the Gaussian coincidence profile is obtained the average inelastic energy $\bar{Q}_{mn}$ for that reaction. For classically calculated distances of closest approach $R_\theta \sim 0.15$ Å, the coincidence profiles indicate unresolved structure. Plots of average inelastic energy $\bar{Q}$ and estimated natural profile linewidths δQ^N versus R_θ show sudden changes of slope in that region. The fraction of inelastic energy received by each ion is estimated on the basis of several models, and the results are compared. (Diss. Abstr. Int. B)

11705 SMALL-ANGLE DIFFERENTIAL CHARGE EXCHANGE MEASUREMENTS FOR He^+ ON He, Ne, AND Kr IN THE LOW-keV REGION. Nagy, Stephen William. Storrs, Conn.; Univ. of Connecticut (1970). 109p. University Microfilms Order No. 70-15,547.

Thesis.

Differential charge-exchange measurements were made in the angular range of −1.00° to +3.00° at various energies ranging from 1 to 3 keV for He^+ on He, Ne, and Kr. The He^+ signal was recorded at angles greater than 0.50°, and the He signal was measured over the entire angular range. The angular range was limited by the low scattered-particle count rate at angles greater than 3.00°. Measurements were not taken below 1 keV because of the instability and low intensity of the beam; the upper limit was set by the maximum range of the accelerator. The probability of charge exchange is reported for the He^+ on He and Ne collisions and in both cases is shown to oscillate as a function of angle and to be independent of energy for the range of angles and energies described above. The most notable feature of the He^+ + Kr collision was the obvious lack of oscillatory structure in the count rate of the neutral signal. In addition, the three collisions are classified as symmetric or asymmetric and the charge-exchange process as resonant, quasi-resonant, and nonresonant. The results of the experiment are related to the existing theories. (Diss. Abstr. Int. B)

11706 MEASUREMENT OF THE TOTAL CROSS SECTION FOR LOW-ENERGY ELECTRONS ON METASTABLE ARGON. Celotta, Robert James. New York; New York Univ. (1969). 120p. University Microfilms Order No. 70-16,044.

Thesis.

Measurements are presented of the total cross section for scattering of low-energy electrons by $^3P_{0,2}$ metastable argon. The

XUM

atomic-beam recoil method was used to make an absolute measurement. The cross section was measured from 0.35 to 6.75 eV with an angular resolution of 16.1° in the electron polar scattering angle at an electron energy of 1 eV. A ground-state argon beam was metastabilized by electron bombardment, and the metastable atoms were detected by the Auger ejection of an electron from the cathode of an electron multiplier. A second electron gun, located approximately half way between the source and detector, produced the scattering electrons. Electron beams had typical energy distributions of 0.3 eV, full width at half maximum. The energy distributions of the electron beam, as well as the absolute energy of the electrons, were determined by a retarding potential technique. The absolute energy determination is believed accurate to ±0.150 eV. The metastable atom beam intensity was measured with the scattering electrons alternately turned off and on. The difference between the off and on beam signals is a measure of the number of atoms scattered out of the beam. The data were accumulated digitally by switching the electrons on and off and monitoring the detector current with a multichannel analyzer. The multichannel analyzer served as a signal averager; it integrated the signal over many on–off cycles. In some cases the energy of the scattering electrons was varied over each cycle to obtain an accurate measurement of the shape of the cross-section curve. The velocity distribution of the atom beam was measured by time-of-flight spectrometry. The multichannel analyzer was used to store signal pulses as a function of the corresponding atom's transit time. The velocity distribution was integrated numerically in order to calculate the atom beam density in the interaction region. The statistical error in the data, the errors in the velocity and the electron current measurements, and the miscellaneous errors combine to give an estimated overall error in the cross section of ±13%. (Diss. Abstr. Int. B)

11707 ELECTRON–POTASSIUM INELASTIC DIFFERENTIAL CROSS SECTION MEASUREMENTS WITH SPIN ANALYSIS. Goldstein, Marvin. New York; New York Univ. (1969). 125p. University Microfilms Order No. 70-16,065.

Thesis.

Measurements were made of the fractional depolarization of a polarized atom beam by electron impact for the $^2S_{1/2} - {}^2P_{1/2}$ transition in potassium. These measurements were related to the various direct and exchange scattering amplitudes necessary to describe differential inelastic electron–potassium collisions. The measurements yielded the ratio $R(\theta)$ where $R(\theta) = (4/9 + 1/9) \times [(6|g^1|^2 + |go|^2 - 4|t^1 - g^1|^2 - 4|f^1|^2)/(|f^0 - g^0|^2 + |f^0|^2 + 2(|f^1 - g^1|^2 + |g^1|^2 + |f^1|^2))]$ where f^μ and g^μ are the direct and exchange scattering amplitudes, respectively, for an event where the atom is left in a state with z component of orbital angular momentum μ. Measurements were made in the energy range 1.6 to 20 eV for a nominal electron scattering angle of 0° and in the energy range 3 to 10 eV for nominal electron scattering angles in the range 0 to 20°. The measurements for a nominal electron scattering angle of 0° showed $R(\theta)$ to be between the theoretical limits (neglecting exchange) of 4/9 and 2/9 except near to threshold where it exceeded 4/9. This effect can be explained by including exchange effects. The measurements for finite angles showed $R(\theta)$ to decrease with increasing θ. Corrections for the detection of elastically scattered atoms were made for 3, 4, and 5 eV. These corrections yielded a relative increase in $R(\theta)$ for $\theta \geq 10°$. This structure is again believed to be due to exchange effects. Corrections to the data for energies above 5 eV are not presently available. The crossed-beam atomic recoil technique was used. A polarized and velocity-selected atom beam was cross-fired at 90° by an unpolarized electron beam. The scattered atoms were spin analyzed with an E–H gradient magnet. (Diss. Abstr. Int. B)

11708 ELECTRON CAPTURE CROSS SECTIONS INTO THE n = 3 LEVEL OF HYDROGEN FOR 30- TO 120-keV PROTON IMPACT ON GAS TARGETS. Stigers, Charles Arthur. Fayetteville, Ark.; Univ. of Arkansas (1970). 111p. University Microfilms Order No. 70-17,190. Thesis.

Electron-capture cross sections into the 3p and 3d states of H, by 30- to 100-keV proton impact on He, Ne, Ar, N_2, O_2, and H_2, were measured. Except for He, these cross sections appear to vary as $\exp[-(E/k)^{1/2}]$ in this energy range, within experimental error. For each individual cross section X is a constant between 2.9 and 7.8 keV. The polarization of the H_α radiation due to the 3p → 2s and 3d → 2p transitions of fast atoms formed by electron capture was measured in the same energy range. The cross sections for electron capture into the 3s state of H and of D, by 30- to 120-keV proton and deuteron impact on these gases, were also measured. The cross sections for these two events were found to be equal, for equal projectile velocities. When compared with earlier measurements of 4s cross sections, the 3s cross sections support the Born prediction that the s-state cross sections should be proportional to n^{-3} where n is the principal quantum number. (Diss. Abstr. Int. B)

11709 FAST ELECTRON–SCATTERED ION COINCIDENCE STUDIES OF THE ARGON ION–ATOM COLLISION. Thomson, George Michael. Storrs, Conn.; Univ. of Connecticut (1970). 83p. University Microfilms Order No. 70-15,557.

Thesis.

Coincidence techniques were used to obtain the fast-electron energy spectrum emitted by the ions colliding with a known scattering angle θ, incident-ion energy T_0, and final scattered charge state m. The reactions studied were of the type: $Ar^+ + Ar \rightarrow Ar^{+m} + Ar^{+n} + (m + n - 1)e^-$. Fixing θ at 21°, T_0 was chosen between 10 and 30 keV. Final scattered charge states from m = 1 to m = 4 were available. Fast-electron spectra in the energy range 100 to 250 eV were obtained from those collisions. The inelastic energy-loss excitation probability and the fast-electron production probability are compared as a function of the distance of closest approach. This demonstrates conclusively the relation between the inelastic energy-loss structure and fast-electron emission. Furthermore, fixing θ and T_0, it was found that the peak of the distribution of electron energies depends upon the charge state of the ion from which the electron is emitted. The molecular approximation of Fano and Lichten is used to interpret this result. Finally, the number of fast electrons emitted exhibited a dependence upon final ion charge state (θ, T_0 held constant). An empirical explanation for this effect is proposed on the basis of an examination of the various possible processes that may produce a given ion charge state combined with data from the Kessel–Everhart ion–ion coincidence experiment. (TSS) (Diss. Abstr. Int., B)

11710 CROSS SECTIONS FOR ELECTRON CAPTURE AND LOSS BY FAST BROMINE AND IODINE IONS TRAVERSING LIGHT GASES. Betz, Hans D. (Massachusetts Inst. of Tech., Cambridge); Ryding, G.; Wittkower, A. B. Phys. Rev., A; 3: 197-206(Jan 1971).

Bromine and iodine ions, accelerated to energies between 6 and 15 MeV, were passed through thin gas targets of H_2 and He. Nonequilibrium charge distributions were measured, from which cross sections for capture and loss of one or more electrons by the heavy ions were determined by means of a least-squares fitting technique. The cross sections are discussed with regard to their functional dependence on the charge and velocity of the ions. Owing to the unprecedented precision of the results, characteristic irregularities were revealed in the charge dependence of the cross sections for both capture and loss of one and two electrons. These effects are attributed to the influence of shell structure and residual excitation of the ions. (auth)

11711 ANALYSIS OF THE N^+–Ar AND O^+–Kr COLLISIONS. Hayden, H. C.; Knystautas, E. J. (Univ. of Connecticut, Storrs). Phys. Rev., A; 3: 206-16(Jan 1971).

A statistical model, similar to that of Everhart and Kessel (EK), is described for N^+–Ar and O^+–Kr collisions of the type $X^+ + Y \rightarrow X^{+m} + Y^{+n} + (m + n - 1)e$. The EK model utilizes coincidence data on inelastic energy distributions (usually Gaussian) and average probabilities $\bar{P}_n(\bar{E})$ for n-fold ionization to construct (by an unfolding procedure) intrinsic ionization probabilities $P_n(E)$ for collisions wherein X and Y are of the same species. In the present case of asymmetric collisions, it is necessary to devise a scheme to determine the manner in which the average inelastic energy $(\bar{Q})$ is divided (into $\bar{E}'$ and $\bar{E}''$) between the two colliding partners. Three such schemes (shown to be mutually consistent) are presented, one of which assumes that the average inelastic energy associated with an m, n event varies linearly with the spectroscopic energy deficits for the ions in charge states m and n ($\bar{Q}_{mn} = A + BU'_m + CU''_n$) and calculates the required coefficients by a least-squares procedure. Values of $\bar{E}'_m$ and $\bar{E}''_n$ are then calculated from the assumption that the outer shell electrons in the two atoms contribute equally to A. The EK model is then applied to each atomic species investigated. Statistical assumptions tested are that $\bar{E}'_m$ is independent of n (and $\bar{E}''_n$ is independent of m), and that the intrinsic ionization probabilities depend only upon the inelastic energy E received by the atoms even when the atom collides with one of another species. The probabilities obtained for argon ions in N^+–Ar collisions agree reasonably well with those obtained for Ar^+–Ar collisions. The data available on the O^+–Kr and Kr^+–Kr reactions are somewhat sparse and preclude a thorough analysis, although the results are encouraging enough to warrant further experimental investigation. (auth)

11712 DISTRIBUTIONS IN ENERGY AND ANGLE OF ELECTRONS EJECTED FROM MOLECULAR NITROGEN BY 0.3- TO 1.7-MeV PROTONS. Toburen, L. H. (Battelle-Northwest, Richland, Wash.). Phys. Rev., A; 3: 216-28(Jan 1971).

Cross sections, differential in ejection energy and angle, for electron emission from nitrogen following proton impact were measured for protons with energies from 0.3 to 1.7 MeV. Electrons were detected at emission angles from 20° to 130° with en-

ergies from a few eV to approximately 4000 eV. Cross sections differential in energy were obtained from the doubly differential cross sections by integration with respect to the emission angle. These results were compared with cross sections calculated from binary-encounter theory. Agreement between the calculated and measured cross sections was within experimental uncertainties (25%) throughout most of the energy range of the ejected electrons. K-shell ionization cross sections for nitrogen were also estimated from the intensity of the K Auger electrons emitted following proton impact. (auth)

11713 ABSOLUTE EXCITATION CROSS SECTIONS OF He^+ IN 20- TO 100-keV He^+–He COLLISIONS USING ENERGY-LOSS SPECTROMETRY. Schoonover, D. R.; Park, John T. (Univ. of Missouri, Rolla). Phys. Rev., A; 3: 228-32(Jan 1971).

Application of positive-ion energy-loss spectrometry was extended to include experimental determination of absolute excitation cross sections of ground-state helium ions. Helium ion–atom collisions were studied for impact energies ranging between 20 and 100 keV, in 10-keV intervals. The data were taken with an apparatus resolution between 0.6 and 0.8 eV full width at half maximum. Cross sections for transitions from the ground state to the second and third principal quantum levels of the ion plotted as a function of impact energy were still rapidly increasing at 100 keV. The cross sections at this energy were $(1.64 \pm 0.28) \times 10^{-18}$ cm^2 for $He^+(1^2s_{1/2}) \rightarrow He^+$ (n = 2) and $(3.46 \pm 0.45) \times 10^{-19}$ cm^2 for He^+ $(1^2s_{1/2}) \rightarrow He^+$ (n = 3). (auth)

11714 EXCITATION OF THE 2s STATE OF ATOMIC HYDROGEN BY ELECTRON IMPACT IN THE DISTORTED-WAVE APPROXIMATION: ANGULAR DISTRIBUTIONS. Shelton, W. N.; Leherissey, E. S.; Madison, D. H. (Florida State Univ., Tallahassee). Phys. Rev., A; 3: 242-50(Jan 1971).

The excitation of ground-state hydrogen atoms to the 2s state by the impact of electrons with energies of 1 to 50 Ry (13.6 to 680.3 eV) was calculated in the distorted-wave approximation with exchange included. The angular distributions of the scattered electrons at 1 and 4 Ry are compared with those derived from the close-coupling calculations by Burke, Schey, and Smith and are compared with four different plane-wave theories at all energies calculated. Taking the close-coupling results as a standard, it is found that the distorted-wave angular distributions represent an improvement over those of the plane-wave theories. (auth)

11715 INELASTIC SCATTERING OF ELECTRONS AND PROTONS BY THE ELEMENTS He TO Na. McGuire, Eugene J. (Sandia Labs., Albuquerque, N. Mex.). Phys. Rev., A; 3: 267-79(Jan 1971).

Discrete and continuum generalized oscillator strengths were calculated for all the occupied shells of the elements He to Na and the 3s and 3p continuum generalized oscillator strengths for Ar. The calculations are done with a one-electron common-central-potential unrelaxed-core approximation. The generalized oscillator strengths were used to compute proton-excitation and -ionization cross sections and stopping power, electron-ionization cross sections, and neutral–neutral ionization and stripping cross sections. For proton ionization above 200 keV and electron ionization above 200 eV, the calculated cross sections are in better than 20% agreement with experiment. The calculated proton stopping power is lower than experiment by 25% at 100 keV and within 10% at 1 MeV. The computed He–He ionization cross section agrees with the measurement by Wittkower, Levy, and Gilbody, while the computed He–Ar ionization cross section is a factor of 5 higher than the measurement by Puckett, Taylor, and Martin. (auth)

11716 SMALL-ANGLE CHARGE-EXCHANGE SCATTERING OF He^+ BY He, Ne, AND Kr AT ENERGIES BETWEEN 1.00 AND 3.00 keV. Nagy, Stephen W.; Fernandez, Salvador M.; Pollack, Edward (Univ. of Connecticut, Storrs). Phys. Rev., A; 3: 280-8(Jan 1971).

The scattering of He^+ by He, Ne, and Kr is studied in the energy range 1.00 to 3.00 keV and in an angular region from 0° to about 3°. These studies yield information on the probability of charge exchange P_θ as a function of beam energy and scattering angle. For the He^+ + He case, the positions of the maxima and minima of P_θ generally agree with those of previous experiments. A wider range of P_θ values is obtained, however, and the current results lend more credence to a two-state resonant-charge-exchange theory for the He^+ + He collision. In the He^+ + Ne collision, the charge-exchange differential cross section is found to increase with increasing energy, while the non-charge-exchange differential cross section decreases. An unexpected result of the current studies on Ne is that the positions of the maxima and minima of the scattered neutral He (and of P_θ) are independent of energy. These results are not consistent with a curve-crossing model for the charge-exchange process, which predicts an angular structure dependent on energy. Studies of the He^+ + Kr collision show a broad forward He peak with no pronounced structure in the energy and angular region investigated. (auth)

11717 LOW-ENERGY PHOTO-IONIZATION OF THE 1^1S AND 2^1S STATES OF He. Jacobs, Verne (Weizmann Inst. of Science, Rehovoth, Israel). Phys. Rev., A; 3: 289-98(Jan 1971).

The photo-ionization cross sections of the 1^1S and 2^1S states of He were evaluated in the energy regions 0.20 to 2.40 Ry and 3.15 to 3.30 Ry. The 56-term ^1S bound-state wave functions obtained by Pekeris were used for the initial states. An expansion into a complete discrete basis set (a modification of the close-coupling method used in electron–atom scattering) was carried out for the ^1P final-state continuum wave functions. Particular attention was given to the processes where the ejected photoelectron leaves the He^+ ion in an n = 2 excited state. The results obtained from the length and velocity expressions for the photo-ionization cross sections show an agreement to within 1% in the lower-energy region. Good accuracy is achieved for the negative-power moments of the oscillator-strength distributions. (auth)

11718 INFINITE-CHANNEL CLOSE-COUPLING THEORY IN THE SECOND BORN APPROXIMATION. I. CHARGE POLARIZATION IN THE ELASTIC ELECTRON SCATTERING FROM H AND He. Bonham, R. A. (Tokyo Univ. Indiana Univ., Bloomington). Phys. Rev., A; 3: 298-309(Jan 1971).

One of the oldest methods suggested for treating the effect of charge polarization on elastic scattering is revived by the use of certain physically reasonable assumptions and is shown to lead to results, in the limit of small scattering angles and high incident energies, which are in quantitative agreement with experimental and theoretical expectations. The theory is worked out in detail for one- and two-electron atoms, and the extension to more complex systems is also discussed. The effect of charge polarization on the elastic differential cross section for 500-eV incident electrons on He is calculated and compared with the experimental results of Bromberg and the theoretical results of LaBahn and Callaway. The agreement is good over the angular range $0° \leq \theta < 6°$ if exchange scattering contributions are included. (auth)

11719 GENERALIZED VARIATIONAL BOUNDS ON THE POSITRON–HYDROGEN REACTION MATRIX. II. EFFECTIVE DISTORTIONS. Dirks, Johan F.; Hahn, Yukap (Univ. of Connecticut, Storrs). Phys. Rev., A; 3: 310-19(Jan 1971).

The problem of the two-channel positron–hydrogen rearrangement collision is studied with the formalism of the generalized variational bounds. For the zero total partial wave, a reasonably complete treatment of this scattering system is presented, including a detailed discussion of the energy spectrum of the closed-channel Hamiltonian M. The coupling of the open channels to the closed channels gives rise to the effective interaction potentials, and these distortion terms are estimated variationally using the bound property of M. The orthogonality of M to the open-channel space is maintained by the presence of the energy-shift operator S, and the role of S is demonstrated in detail numerically, which produces essential cancellation of various terms. Partly owing to the crudity of the trial functions used, it has not been possible to find resonance states below the first excitation threshold. Bounds on the diagonal K matrix elements and eigenphase shifts are presented. (auth)

11720 NUCLEAR-SPIN EFFECTS ARE IMPORTANT IN ANALYZING SPIN-EXCHANGE EXPERIMENTS. Gibbs, Hyatt M. (Bell Telephone Labs., Inc., Murray Hill, N. J.). Phys. Rev., A; 3: 500-2(Jan 1971).

Lambert's proof that the inclusion of nuclear spin does not alter the equation of motion for the electronic polarization is shown to be valid only when the hyperfine interaction is negligible. Usually the hyperfine frequency is much greater than the frequency of spin-exchange collisions; then the effect of the hyperfine interaction between collisions invalidates Lambert's proof. In general, spin exchange with a second depolarized species relaxes the electronic polarization as the sum of two exponentials, as shown by Gibbs and Grossetête. (auth)

11721 SPIN-EXCHANGE EFFECTS ON DENSITY-MATRIX ELEMENTS. Valberg, Peter A. (Harvard Univ., Cambridge, Mass. Amherst Coll., Mass.). Phys. Rev., A; 3: 505-8(Jan 1971).

The work of Balling, Hanson, and Pipkin on the density-matrix equations for spin-exchange collisions is extended and is simplified in the case of $^2S_{1/2}$ atoms. The results allow straightforward calculation of the detailed effects of spin exchange on the density-matrix elements. The equations are useful when dealing with an ensemble of atoms such as in the hydrogen maser, in the rubidium maser, and in optical pumping cells. (auth)

XUM

11722 ADDENDUM TO POTENTIAL-SCATTERING MODEL FOR ELECTRONS ON HELIUM AND OTHER ATOMS. Berg, R. A.; Purcell, J. E.; Green, A. E. S. (Univ. of Florida, Gainesville). Phys. Rev., A; 3: 508-10(Jan 1971).

It is shown, as an extension to a previous paper by the authors (Phys. Rev., A2: 107(1970)), that a relatively simple analytic potential obtained from studies of bound electron states in atoms gives differential cross sections in good agreement with experimental values for the rare gases Ar, Kr, and Xe. (auth)

11723 COLLISIONAL-QUENCHING PROCESSES IN H(2s). Baragiola, R. A.; Salvatelli, E. R. (Univ. Nacional de Cuyo, San Carlos de Bariloche, Argentina). Phys. Rev., A; 3: 514-15 (Jan 1971).

Quantitatively different collisional-quenching processes of H(2s) were resolved by means of a calculation using measured charge equilibrium fractions and cross sections. The results show that at 5 keV and for neon as a target quenching to the ground state H(1s) is the dominant process. (auth)

11724 EVOLUTION OF ELECTRON ANGULAR MOMENTUM DUE TO SPIN-EXCHANGE COLLISIONS INVOLVING NUCLEAR SPIN. Crampton, S. B. (Williams Coll., Williamstown, Mass.). Phys. Rev., A; 3: 515-18(Jan 1971).

The evolution of electronic angular momentum due to spin-exchange collisions between two species of ground-state alkali atoms is shown to depend substantially on nuclear spin when the effects of spin precession between collisions are included with the effects of the collisions themselves. General results are illustrated for nuclear spin $\frac{1}{2}$ and 1. (auth)

11725 ADIABATIC THEORY OF ROTATIONAL EXCITATION OF NON-Σ STATES. Temkin, A.; Faisal, F. H. M. (Goddard Space Flight Center, Greenbelt, Md.). Phys. Rev., A; 3: 520-1(Jan 1971).

The formulas for the rotational excitation of diatomic molecules in the adiabatic theory are generalized to include rotational excitation within molecular states of arbitrary Λ symmetry. For Λ not equal to zero (non-Σ states), the rotational quantum number can change by any integer, and not only an even integer as is the case for Σ states. (auth)

11726 PRECISION ENERGY LOSS MEASUREMENTS FOR NATURAL ALPHA PARTICLES IN ARGON. Hanke, C. C.; Bichsel, H. Kgl. Dan. Vidensk. Selsk., Mat.-Fys. Medd.; 38: 3-(1970).

Energy losses of natural alpha particles from ^{212}Bi and ^{212}Po were determined in argon gas with an accuracy of about 0.2%. The Lewis correction and the multiple-scattering correction are briefly discussed. The data are compared with the Bethe theory, formulated with two different shell-correction functions. I values of 182 eV and 167 eV are obtained, respectively. Northcliffe's measurements at higher energies favor I = 182 eV. Comparison with hydrogen-ion stopping power data confirms the recently discovered dependence on the particle charge. (auth)

11727 MEAN ENERGY OF ELECTRONS EJECTED FROM ATOMS AT IONIZATION BY ELECTRON IMPACT. Grechikhin, L. I.; Kudryashov, V. V. (Minsk School of Rocket Construction). Izv. Vyssh. Ucheb. Zaved., Fiz.; No. 9, 158-60(1970). (In Russian).

In order to understand plasma formation processes related to ionization of atoms and molecules by electron impact, it is important to know the number of ionization events and the mean energy of ejected electrons. It is known that the number of ionization events is described mainly by the total ionization cross section and the electron energy distribution by differential cross sections. Various theoretical descriptions of differential cross sections of ionization by electron impact are compared and used for calculating the mean energy of ejected electrons. (R.V.J.)

11728 ADVANCES IN ATOMIC AND MOLECULAR PHYSICS. VOLUME 6. Bates, D. R.; Esterman, Immanuel (eds.). New York; Academic Press Inc. (1970). 349p. $18.00.

A separate abstract was prepared for each of the six papers included. (A.G.W.)

For abstracts of individual papers see: 11729–11733 and 11875.

11729 DISSOCIATIVE RECOMBINATION. Bardsley, J. N.; Biondi, M. A. (Univ. of Pittsburgh). Advan. At. Mol. Phys.; 6: 1-57(1970).

Both experimental and theoretical studies of the reaction $AB^+ + e \rightleftharpoons AB'' \rightarrow A + B$ are reviewed. Experimental methods surveyed are classified broadly into plasma-afterglow and electron–ion beam techniques. Experimental results on noble gases and atmospheric gases are summarized in sections on establishing the recombination mechanism, recombination measurements near thermal energies, recombination measurements as a function of electron temperature, recombination measurements at elevated ion temperatures. Theoretical work reviewed is concerned with general theory, magnitude of the recombination rate, temperature dependence of the recombination rate, calculation of potential energy curves, and the role of Rydberg states in recombination. Recombination in the ionosphere and the various factors that affect it are discussed briefly. 132 references. (A.G.W.)

11730 ROTATIONAL EXCITATION OF MOLECULES BY SLOW ELECTRONS. Takayanagi, Kazuo; Itikawa, Yukikazu (Tokyo Univ.). Advan. At. Mol. Phys.; 6: 105-53(1970).

Theoretical work, published by early 1969, on rotational excitation of molecules by electrons having a velocity comparable to or below that of the molecular electrons is reviewed. An outline of the general mathematical formulation of the problem and the derivation of the basic equations is followed by consideration of more specific calculational methods such as the Born approximation, the adiabatic approximation, the distorted-wave method, and close-coupling calculations. Conclusions from theoretical calculations are summarized and compared with experimental data. Resonance effects and effects of molecular vibration and unpaired electron spin are discussed briefly. 89 references. (A.G.W.)

11731 DIFFUSION OF ATOMS AND MOLECULES. Mason, E. A.; Marrero, T. R. (Brown Univ., Providence). Advan. At. Mol. Phys.; 6: 155-232(1970).

A brief historical sketch of the physics of gaseous diffusion of atoms and molecules is followed by a survey of recent experimental and theoretical work. The phenomenological aspect is considered first; emphasis is on the simplest physical explanations that are essentially correct without resort to the full kinetic theory of gases. Two sections deal with the molecular aspect of diffusion, whose task is to relate the phenomenological coefficients to atomic and molecular properties. Methods for determination of diffusion coefficients are reviewed. Some of the most reliable experimental results on binary gaseous diffusion coefficients are summarized. 271 references. (A.G.W.)

11732 THEORY AND APPLICATION OF STURMIAN FUNCTIONS. Rotenberg, Manuel (Univ. of California, San Diego, La Jolla). Advan. At. Mol. Phys.; 6: 233-68(1970).

A general review of the mathematics of Sturmian functions is followed by discussion of several applications to scattering problems. The close-coupling method for scattering of electrons and positrons by hydrogen atoms, application of Sturmians to the Faddeev equations, and charge transfer in $(H-H^+)$ collisions are considered. Sturmian functions with more than one potential are discussed briefly. 63 references. (A.G.W.)

11733 USE OF CLASSICAL MECHANICS IN THE TREATMENT OF COLLISIONS BETWEEN MASSIVE SYSTEMS. Bates, D. R.; Kingston, A. E. (Queen's Univ., Belfast). Advan. At. Mol. Phys.; 6: 269-321(1970).

An extensive set of comparisons between calculated and measured cross sections is presented in an attempt to determine the value of classical mechanics for atom–ion and atom–atom collisions. Four types of fast collisions are considered: removal of an electron from an atomic or molecular system, excitation, electron loss, and electron capture. The only slow collision process treated is symmetrical resonance charge transfer. No generally applicable conclusions are reached. 105 references. (A.G.W.)

11734 THREE-PHOTON IONIZATION OF A HELIUM ATOM IN THE EXCITED 2S STATE. Bakos, J.; Kantor, J.; Kiss, A. (Lebedev Inst. of Physics, Moscow). JETP Lett. (USSR) (Engl. Transl.); 12: 255-7(5 Oct 1970).

Translated from Zh. Eksp. Teor. Fiz., Pis'ma Red.; 12: 371-3(5 Oct 1970).

The He atoms of a discharge-afterglow plasma, in the 2^1S and 2^3S states, were exposed to focused radiation of a Q-switched ruby laser. The ions produced in the plasma by the laser radiation were registered by a probe as a function of pulsed radiation energy. From these data the cross section for three-photon ionization was calculated to be $4.7 \times 10^{-71\pm1}$ cm^6 sec^2 photon^{-3}. This value is larger than that previously calculated by others. (A.G.W.)

Atomic Theory

Refer also to abstracts 12052 and 12056.

11735 TRANSFORM FOR TREATING A WIDE CLASS OF PERTURBATION PROBLEMS, WITH APPLICATION TO THE EXCHANGE EQUATIONS FOR H_2^+ AND H_2. Rosenthal, Carey M. (Univ. of Wisconsin, Madison). J. Chem. Phys.; 53: 3709-16 (1 Nov 1970).

A transform is introduced to solve the H_2^+ and H_2 exchange functions of Certain and Hirschfelder. The solution obtained for H_2^+ is inverted numerically. The properties of this transform are derived and its applicability to other perturbation problems is discussed. (auth)

11736 SINGLE-PARAMETER FREE-ELECTRON EXCHANGE APPROXIMATION IN FREE ATOMS. Kmetko, E. A. (Los Alamos Scientific Lab., N. Mex.). Phys. Rev. A; 1: 37-8(Jan 1970).

The optimum scale factor for the Slater free-electron exchange approximation for atoms has been obtained by minimizing the total electronic energy. In general, the scale factor lies between the Slater and the Gaspar–Kohn–Sham limit of 1 and $\frac{2}{3}$, respectively. The variation that occurs as the different shells are populated is qualitatively understandable in terms of the inhomogeneity of the overall charge distribution. (auth)

11737 THEORY OF ATOMIC STRUCTURE INCLUDING ELECTRON CORRELATION. Oeksuez, Iskender. New Haven; Yale Univ. (1969). 145p. University Microfilms Order No. 70-2781.

Thesis.

There are anomalous correlation effects in nonclosed shells, especially in excited configurations and states of atoms, not found in closed shells. This thesis presents an N-body theory of correlation effects for excited states of atoms, applicable also to ground states. The method is applied to 113 species arising from configurations of the type $1s^2 2s^n 2p^m$ (n = 0, 1, 2; m = 0, 1,...,6). The types of correlations indicated by the theory are evaluated and analyzed. They are then used for predictions of energies and related quantities such as electron affinities, intermultiplet separations, energies of excited states of negative ions, excitation energies, and term splitting ratios of excited configurations. Transformation properties of pair correlation functions and energies among various orbital pair descriptions are investigated. (Diss. Abstr. Int. B)

11738 RELATIVISTIC INDEPENDENT-PARTICLE MODEL FOR ATOMS BASED ON ANALYTICAL POTENTIALS. Darewych, J. W. (York Univ., Toronto); Green, A. E. S.; Sellin, D. L. Phys. Rev., A; 3: 502-5(Jan 1971).

A two-parameter analytic potential for electrons in atoms, introduced by Green, Sellin, and Zachor, is used in conjunction with Dirac's equation to determine independent-particle-model electronic energy levels for neutral atoms in their ground states. The parameters are determined for each atom so that the predicted energy levels approximate observed electronic separation energies in accordance with a weighted least-squares sum. The agreement with experimental data is as good as for relativistic Hartree–Fock results. Electronic energies are given for a random selection of elements with Z = 10, 20, ..., 90. (auth)

11739 SEMI-EMPIRICAL ATOMIC-ENERGY FORMULA. Green, A. E. S.; Sellin, D. L.; Darewych, G. (Univ. of Florida, Gainesville). Phys. Rev., A; 3: 159-65(Jan 1971).

The Thomas–Fermi–Dirac statistical model of the atom is studied in the energy-functional formulation. Minima of the total energy are obtained for five combinations of analytic screening function and density. Total energies, average radii, and rms radii vary from model to model quite markedly and depart quite substantially from "data" based upon Hartree–Fock or Hartree–Fock–Slater calculations. For the model based upon the analytic screening function due to Green, Sellin, and Zachor and for a closely related "regularized" model, the dependence of the component energies upon the electron number N, the model parameters, and certain integral constants is represented analytically. Minimization of the total energy with respect to the potential parameters leads to simple algebraic equations. The results again are poor. However, by making reasonable semiempirical modifications in the component terms, stability can be achieved with binding energies and potential parameters close to the data obtained from Hartree–Fock or Hartree–Fock–Slater studies. (auth)

11740 NUMERICAL COEFFICIENT OF THE FIRST EXCHANGE INHOMOGENEITY TERM. Smith, John R. (Lewis Research Center, Cleveland). Phys. Rev., A; 3: 513(Jan 1971).

A simple approximate derivation of the numerical coefficient of the first inhomogeneity term in the exchange energy and the Kohn–Sham–Gaspar exchange potential is provided. It is much closer to the numbers estimated by Herman et al. than to that suggested by Darewych. (auth)

11741 RELATIVISTIC CALCULATION OF ATOMIC STRUCTURES. Grant, I. P. (Oxford Univ.). Advan. Phys., No. 82, 747-811(Nov 1970).

The current state of the art in relativistic calculation of atomic structures is surveyed. The theory is modeled on the practice in nonrelativistic calculations, using many-particle wave functions built from Dirac central field spinors. The Hamiltonian includes quantum electrodynamic effects in the form of the Breit approximation for the interaction energy of two electrons. Within the limits for which this is valid, it is possible to construct matrices for one- and two-particle operators and hence to perform atomic structure calculations that automatically include the major relativistic effects. The theory can be greatly simplified by using Racah's tensor operators. Major applications have utilized the Hartree or Hartree–Fock methods, and the relevant equations are formulated in detail. Numerical Hartree–Fock solutions for the average of the ground configuration have now been obtained for most elements with atomic number less than 103, and some solutions have also been obtained for ions. The same methods were used to investigate the likely configurations of superheavy elements with atomic numbers as high as 168. A few calculations were also done using a relativistic analogue of Roothaan's method. Methods of solution and numerical results are described for both types of calculation. A brief description is also given of some problems in which it has been necessary to take relativistic effects into account including, in particular, elastic scattering of low- and medium-energy electrons from heavy elements, the calculation of x-ray-scattering factors, and the probability of electron shake-off following sudden perturbations. (auth) (UK)

Cosmic Radiation

Refer also to abstracts 11553, 11627, 11636, 12071, 12082, and 12093.

11742 (KFKI-70-21-HEP) HIGH-STABILITY APPARATUSES TO INVESTIGATE THE ANGULAR DI:TRIBUTION OF CHARGED PARTICLES OF ENERGIES 10^{13}–10^{14} eV IN THE GALAXY. Koch, J.; Kota, J.; Somogyi, A.; (and others) (Magyar Tudomanyos Akademia Kozponti Fizikai Kutato Intezete, Budapest). [1970]. 8p. (CONF-700708-4). Dep. NTIS (U. S. Sales Only).

From 6th Interamerican Seminar on Cosmic Rays, La Paz, Bolivia.

Two sets of apparatus designed to study the angular distribution of primaries of energies 10^{13} to 10^{14} eV in the Galaxy are described in detail. One of them is an extensive air shower detector of conventional design with Geiger–Müller counters covering extremely large areas; the other is an EAS detector consisting of a combination of G–M counters and scintillators allowing the directions of EAS axes, i.e., directions of high-energy primaries, to be determined individually with a high repetition rate. Both sets of apparatus have been set up and are running in the northern hemisphere. The paper ends with an invitation for other research groups to join the project and to build similar instruments near the equator and in the southern hemisphere so as to extend measurements to all directions of the celestial sphere. (auth)

11743 EXAMINATION OF THE LEAKAGE-LIFETIME APPROXIMATION IN COSMIC-RAY DIFFUSION. Jones, Frank C. (Goddard Space Flight Center, Greenbelt, Md.). Phys. Rev., D; 2: 2787-2802(15 Dec 1970).

The diffusion of cosmic-ray particles in a finite volume of space with a simultaneous diffusion and/or transport in energy is considered. The solution of the appropriate differential equation may be expressed as an expansion in eigenfunctions of the differential operator. If one approximates the solution by keeping only the lowest or fundamental eigenfunction, one obtains the common "leakage-lifetime" approximation. In some situations this approximation can be justified, but in others (e.g., synchrotron or inverse-Compton losses) it cannot. The reason for the failure in this case can be seen from the point of view of the expansion. The solution of the general case of Fermi acceleration, synchrotron losses, and energy fluctuation acting together is also obtained by this method. (auth)

11744 IDENTIFICATION AND RELATIVE ABUNDANCES OF C, N, AND O NUCLEI TRAPPED IN THE GEOMAGNETIC FIELD. Mogro-Campero, Antonio; Simpson, J. A. (Univ. of Chicago). Phys. Rev. Lett.; 25: 1631-5(7 Dec 1970).

The nuclei C, N, and O were detected in the energy range 13 to 33 MeV/nucleon trapped in the radiation belt near the geometric equator in the region $2.5 \leq L \leq 5.5$ with an intensity ≥ 160 times the CNO flux level of interplanetary nuclei. The data were obtained over a 10-month period in 1968 by the University of

XUM

Chicago nuclear composition telescope on the satellite OGO-5. The measured abundance ratio for these nuclei was O/C ≃ 0.5; this ratio was consistent only with an extraterrestrial origin for these nuclei. (auth)

11745 SPHERICAL HARMONIC ANALYSIS OF WORLDWIDE COSMIC-RAY VARIATIONS DURING GEOMAGNETIC STORMS. Yoshida, S. (Univ. of Alaska, College); Akasofu, S.-I.; Ogita, N.; Outi, A. J. Geophys. Res.; 76: 1-12(1 Jan 1971).

The spherical harmonic analysis is performed on a number of cosmic-ray storms on the basis of the records collected from 26 stations whose asymptotic directions are reasonably uniformly distributed in the geographic coordinates. Detailed results are reported for 2 events, September 21 to 25, 1966, and March 20 to 26, 1966; the results for 8 other events are given in tabular form. It is shown that the worldwide component (C_0) varies closely with the simultaneous cosmic-ray variation observed by the Pioneer 7 space probe and for the September 23, 1966, event. The analysis also provides the maximum anisotropic component flux (P) and its asymptotic direction; both vary considerably even during single events. On September 23, 1966, P temporarily reached a value as large as 4.3%. (auth)

11746 SOLAR MODULATION OF GALACTIC COSMIC RAYS, 2. Fisk, L. A. (Goddard Space Flight Center, Greenbelt, Md.). J. Geophys. Res.; 76: 221-6(1 Jan 1971).

A numerical technique for solving the Fokker–Planck equation, which governs the solar modulation of galactic cosmic rays, is outlined. As examples of the use of this technique, some numerical solutions are presented that provide reasonable fits to observed spectra of protons and helium ions. (auth)

11747 SYNCHROTRON EMISSION FROM HIGH ENERGY COSMIC-RAY ELECTRONS AS AN EXPLANATION OF THE COSMIC X-RAY EXCESS. De Freitas Pacheco, J. A. (Observatoire de Nice). Astron. Astrophys.; 8: 420-3(Oct 1970).

Possible emission mechanisms to explain the excess x radiation observed by Cooke et al. (1969) in the galactic plane are discussed. It is suggested that the most probable mechanism is the synchrotron emission of high-energy electrons traveling in the galactic disk and it provides evidence for a break in the cosmic-ray electron spectrum for energies greater than 10^7 MeV. (auth)

11748 STATIONARY RELATIVISTIC GAS IN COSMIC OBJECTS AND γ BACKGROUND IN THE 1- TO 20-MeV REGION. Syunyaev, R. A. (Applied Mathematics Inst., Moscow). JETP Lett. (USSR) (Engl. Transl.); 12: 262-4(5 Oct 1970).

Translated from Zh. Eksp. Teor. Fiz., Pis'ma Red.; 12: 381-3 (5 Oct 1970).

As is known, the x- and γ-ray background spectra at 40 keV to 1 MeV and the points at 30 and 100 MeV are in good agreement with the power law $I_\nu \sim \nu^{-1.2}$. Recent measurements have revealed an increase of the background radiation in the region 1 to 6 MeV. In this paper this fact is interpreted as a superposition of the summary radiation from discrete sources of bremsstrahlung γ rays on the general power-law spectrum of the background. (W.D.M.)

11749 MEAN TRANSVERSE MOMENTUM OF SECONDARIES FROM COSMIC-RAY INTERACTIONS IN THE REGION OF 2×10^5 GeV. Adcock, C. (Univ. of Durham, Eng.); Coats, R. B.; Wolfendale, A. W.; Wdowczyk, J. J. Phys., A (London); 3: 697-707(Nov 1970).

The variation with separation of the rate of pairs of cosmic-ray muons of energies above 1000 GeV was measured at a mean angle to the vertical of 45° by Coats et al. (1970). The variation was most sensitive to the mean transverse momentum of the parent pions in the initial nucleon–air nucleus interactions and the value determined from comparison with a theoretical analysis was $\langle p_t \rangle = 0.60 \pm 0.05$ GeV/c, the median primary energy in question being approximately 2×10^5 GeV. The form of the distribution in transverse momentum giving a best fit to the experimental data is that proposed by Elbert et al. (1968). The value found for $\langle p_t \rangle$ confirms the slow increase in this quantity with increasing interaction energy suggested by previous work. (auth) (UK)

11750 HIGH TRANSVERSE MOMENTA OBSERVED IN AIR SHOWER CORES. Bakich, A. M.; McCusker, C. B. A.; Winn, M. M. (Cornell-Sydney Univ. Astronomy Centre, Sydney). J. Phys., A (London); 3: 662-88(Nov 1970).

Evidence is presented for the occurrence of very high transverse momenta at energies above 10^{14} eV, which indicate the operation of a super-strong force. Detailed results are given of the last three years of operation of the Sydney 64-scintillator array and of the Monte Carlo simulations of air showers. These are compared with earlier results. It is shown that: Two main types of core exist which can conveniently be called single cores and multi cores. All groups observe both types. The two types can be distinguished objectively if the highest (Δ_1) and second highest (Δ_2) particle densities, observed over areas of 0.25 m^2, are compared. At a given shower size single-cored showers have a more marked radial symmetry, a much higher mean Δ_1, a steeper electron structure function within 3 meters of the core, a much higher mean hadron energy and many more high-energy hadrons in the core. For simulated showers (of total primary energy 10^{15} eV) these characteristics are shared by the showers with proton primaries. Simulated showers with heavy primaries behave like real multi-cored showers. The experimental distribution of Δ_1/Δ_2, at shower sizes around 10^5 particles, cannot be reproduced by a pure simulated beam of protons or a pure beam of heavy primaries. It can be reproduced by a beam of chemical composition similar to that of lower-energy cosmic radiation. At shower sizes above 10^6 particles the Russian, Sydney, and Kiel groups find an increase in the fraction of multi-cored showers. The hypothesis that the high transverse momenta observed in scintillator experiments are due to fluctuations in the scintillators was investigated and shown to be untenable. The effect of local hadronic interactions on core type is shown to be negligible. (auth) (UK)

Direct Energy Conversion

Refer also to abstracts 11755 and 11766.

11751 ELECTRICAL PARAMETERS IN AN MHD GENERATOR WITH GAS NONUNIFORMITY IN y OR z DIRECTION. Celinski, Z. N. (Inst. of Nuclear Research, Swierk, Poland). Nukleonika; 15: 237-51(1970).

When the gas parameters are nonuniformly distributed in the channel cross section of the MHD generator, its electrical performance may be considerably deteriorated. The expressions that enable the calculation of the electrical parameters of the generator are constructed. The dimensionless parameters λ, ϵ, and D (or ζ) that measure the performance, depend only on the distribution of the gas velocity, the gas conductivity, and the Hall parameter. The numerical calculation of their values was performed for boundary layers of various thicknesses and for various wall temperatures. The calculated parameters make it possible to find all electrical parameters of the generator on the ground of one-dimensional generator theory. Constant channel cross section, subsonic gas flow, and uniform distribution of gas parameters along the channel were assumed in the calculations. The distribution of the gas parameters was assumed to be independent of the generator loading. The channel end effects were neglected. (auth)

11752 MODERN PLASMA PHYSICS AS A BRANCH OF NUCLEAR ENGINEERING. Rothhardt, L. (Zentralinstitut fuer Elektronenphysik, Berlin). Kernenergie; 13: 269-74(Sep 1970). (In German).

Modern plasma physics is reviewed in detail with special respect to a later use and utilization of its fundamental principles for nuclear energy production. Recent state in the evolution of MHD generators working in conjunction with gas-cooled high-temperature nuclear fission reactors and in fusion research is discussed. (auth)

Fluid Physics

Refer also to abstracts 11901–11903.

11753 (EUR-CEA-FC-571) PARTICULAR MHD SOLUTIONS. Pantuso Sudano, J. (Commissariat a l'Energie Atomique, Fontenay-aux-Roses (France). Centre d'Etudes Nucleaires). Nov 1970. 10p. (In French). Dep. NTIS (U. S. Sales Only).

A particular solution of the linearized MHD system inside a neutral sheet is given. The perturbation of the vector potential is described by a partial differential equation with variable coefficients. This equation is transformed into a wave equation by a transformation of the space variable. (auth) (France)

11754 THERMOMAGNETIC GAS TORQUE FOR COLLINEAR STATIC AND ALTERNATING MAGNETIC FIELDS. Hess, S.; Waldmann, L. (Univ., Erlangen-Nuernberg, Ger.). Z. Naturforsch.; 25a: 1367-9(Oct 1970).

Results obtained within the framework of kinetic theory are presented for the part of the thermomagnetic gas torque that stems from the thermal pressure and is associated with the influence of the magnetic fields on the viscosity (Senftleben–Beenakker effect). Good qualitative agreement and quantitative

agreement within a factor of roughly 1.5 are found between the theory and the experimental data of Smith and Scott [1969]. (auth)

11755 IONIZATIONAL AND ELECTRON THERMAL NONEQUILIBRIUM EFFECTS IN COMPRESSIBLE MAGNETOHYDRODYNAMIC BOUNDARY LAYERS. Cott, Donald Wing. Knoxville, Tenn.; Univ. of Tennessee (1969). 141p. University Microfilms Order No. 70-20,300.

Thesis.

The effects of thermal nonequilibrium (elevated electron temperature), and ionizational nonequilibrium (finite-rate recombination) are studied in the insulator boundary layer of the potassium-seeded nitrogen MHD accelerator. The nonsimilar, compressible boundary layer is assumed steady, laminar, and two-dimensional. The conservation equations are derived from Boltzmann's equation in a two-fluid formulation. A collisionless sheath is assumed and matched with the boundary-layer equations, which are solved numerically for a core flow Hall-neutralized Faraday accelerator. The relative importance of the various terms in the electron energy equation are assessed, and the overall effect of the nonequilibrium phenomena on the boundary layer parameters is described. It is concluded that thermal nonequilibrium can lead to significant B-wall shorting in long channels, and that Hall effects should not be neglected, but that operation is not noticeably affected by ionizational nonequilibrium or the physics of the electrostatic sheath. (Diss. Abstr. Int., B)

11756 NORMAL VORTICITY JUMP CONDITION ACROSS A MAGNETOGASDYNAMIC DISCONTINUITY. Ram, Rishi; Sharma, V. D. (Banaras Hindu Univ., India). Experientia; 26: 1049 (15 Oct 1970).

Hayes (J. Fluid Mech., 2: 595(1957)) showed that the normal jump in the vorticity across a gasdynamic discontinuity is zero. In this note it is shown that the same conclusion is not true across a magnetogasdynamic discontinuity. (auth)

11757 EQUATIONS GOVERNING THE SECOND-ORDER CORRELATION FUNCTIONS FOR THE VELOCITY AND THE MAGNETIC FIELD OF ISOTROPIC HYDROMAGNETIC TURBULENCE IN AN INCOMPRESSIBLE FLUID. Codreanu, S. (Univ. of Cluj). J. Phys., A (London); 3: L50-2(Nov 1970).

By applying the Smirnov method (1970) the equations describing the correlation functions of the velocity and the magnetic field for an isotropic nonhomogeneous hydromagnetic turbulence in an incompressible conducting fluid are derived. (auth) (UK)

11758 MAGNETIC-FIELD RECONNEXION IN A HIGHLY CONDUCTING INCOMPRESSIBLE FLUID. Sonnerup, Bengt U. Oe. (Dartmouth Coll., Hanover, N. H.). J. Plasma Phys.; 4: 161-74(Feb 1970).

A theoretical model is proposed for the process of re-connection of frozen-in magnetic-field lines at an X-type null point in the field. The model involves a diffusion region, immediately adjacent to the null point and an outer wave-dominated region. For the latter an exact solution to the magnetohydrodynamic equations is obtained; for the former an approximate relationship is derived between the field-re-connection rate, measured by the Alfvén number of the incident flow, and the magnetic Reynolds number, based on the width of the diffusion region. The maximum field-re-connection rate is determined entirely by conditions near the null point and may under suitable conditions become large. A condition for maximum conversion of magnetic energy is derived. (auth) (UK)

11759 LA MAGNETOHYDRODYNAMIQUE CLASSIQUE ET RELATIVISTE. (Classical and Relativistic Magnetohydrodynamics). International Symposium on Classical and Relativistic Magnetohydrodynamics, Lille, France, 16–20 June 1969. Paris; Centre National de la Recherche Scientifique (1970). 312p. (In French and English). (CONF-690648).

Twenty-five papers are included, and twenty of them are abstracted. The topics covered are (1) in classical magnetohydrodynamics: flow, linearization, multiple scales, airfoils in magnetogasdynamics, and magnetostatics; (2) in relativistic magnetohydrodynamics: variational principles, waves and discontinuities, magnetohydrodynamic shocks, and the Hugoniot function; (3) mathematical problems such as hyperbolic systems, the KWB method for the nonlinear equations of fluid mechanics, and the existence theorems, and (4) energy-stress tensor, kinetic theory of charged gases, and Boltzmann equations. (France)

For abstracts of individual papers see: 11633, 11760–11774, 11901–11903, and 12058.

11760 FLUID FLOWS AROUND A SPHERE IN FLUID MAGNETOHYDRODYNAMICS. Cabannes, H. (Univ., Paris). pp 19-30 of La Magnetohydrodynamique Classique et Relativiste. Paris; Centre National de la Recherche Scientifique (1970). (In French).

From Symposium on Classical and Relativistic Magnetohydrodynamics, Lille, France. See CONF-690648.

Stationary flow with axial symmetry of an incompressible fluid around a sphere was studied. Two cases were considered: first, a perfect fluid, with the sphere solid and velocity and magnetic field uniform to infinity and reducible to a dipole at the center of the sphere; second, a viscous fluid, with the sphere hollow and velocity uniform to infinity and the magnetic field zero at infinity. In both cases the calculation explaining the drag demonstrated the influence of the magnetic field and the magnetic permeability of the sphere on the problem. (auth) (France)

11761 RESISTANCE BETWEEN TWO CIRCULAR ELECTRODES IN PRESENCE OF A STRONG MAGNETIC FIELD. Stewartson, K. (University Coll., London). pp 31-43 of La Magnetohydrodynamique Classique et Relativiste. Paris; Centre National de la Recherche Scientifique (1970).

From Symposium on Classical and Relativistic Magnetohydrodynamics, Lille, France. See CONF-690648.

The space between two circular electrodes was filled with mercury and a current was passed through the mercury from one electrode to the other. The structure of the current and velocity fields in the mercury was examined when, in addition, a strong magnetic field was applied across the electrodes. Using boundary-layer techniques, the resistance was determined and found to be in good agreement with experiment. (auth) (France)

11762 WAVES AND DISCONTINUITIES IN RELATIVISTIC MAGNETOHYDRODYNAMICS. Pham Mau Quan (Univ., Lille, France). pp 45-59 of La Magnetohydrodynamique Classique et Relativiste. Paris; Centre National de la Recherche Scientifique (1970). (In French).

From Symposium on Classical and Relativistic Magnetohydrodynamics, Lille, France. See CONF-690648.

Waves and shocks are described with respect to their distributions by weak and continuous solutions, both differentiable by parts, respectively. An existence theorem was established for the continuous solutions in a differential system of a Riemann variety. The results obtained were used to study relativistic magnetohydrodynamic waves and discontinuities. (auth) (France)

11763 SHOCK WAVES IN RELATIVISTIC MAGNETOHYDRODYNAMICS. Lichnerowicz, A. (College de France, Paris). pp 61-71 of La Magnetohydrodynamique Classique et Relativiste. Paris; Centre National de la Recherche Scientifique (1970). (In French).

From Symposium on Classical and Relativistic Magnetohydrodynamics, Lille, France. See CONF-690648.

Magnetohydrodynamic shock waves were rigorously studied; certain aspects became apparent more easily than in the corresponding classical study. The relativistic form of the fluid compressibility played a major role. These conditions and a simple relativistic form of the Hugoniot equation led to a complete study of the thermodynamics of the shocks and the velocity properties of the different waves. (auth) (France)

11764 RELATIVISTIC EFFECTS FOR MAGNETOHYDRODYNAMIC WAVES. Shikin, I. S. (Moscow State Univ.). pp 93-122 of La Magnetohydrodynamique Classique et Relativiste. Paris; Centre National de la Recherche Scientifique (1970).

From Symposium on Classical and Relativistic Magnetohydrodynamics, Lille, France. See CONF-690648.

The relativistic magnetohydrodynamics of an ideal fluid (nonviscous, nonthermally conducting, and infinitely electrically conducting) are considered in a general covariant form. The general equations, the simple waves (Riemann waves) within the limits of special relativity, and the relations at the surface of strong discontinuities are examined. Purely relativistic effects in the MHD waves are discussed; these effects disappear in the Newtonian version. In particular, these effects are polarization and specific relativistic waves (super rapids). Relativistic effects may occur for MHD waves even under laboratory conditions. (auth) (France)

11765 BOLTZMANN EQUATION IN GENERAL RELATIVITY. Vignon, B. (Univ., Dijon, France). pp 141-4 of La Magnetohydrodynamique Classique et Relativiste. Paris; Centre National de la Recherche Scientifique (1970). (In French).

From Symposium on Classical and Relativistic Magnetohydrodynamics, Lille, France. See CONF-690648.

The thermodynamic eigenvalues of a relativistic gas are defined, and an approximate solution to the relativistic Boltzmann equation is given. (France)

XUM

11766 ABOUT ONE-DIMENSIONAL APPROXIMATION FOR MAGNETOHYDRODYNAMIC CHANNEL FLOW. Lyubimov, G. A. (Moscow State Univ.). pp 157-60 of La Magnetohydrodynamique Classique et Relativiste. Paris; Centre National de la Recherche Scientifique (1970).

From Symposium on Classical and Relativistic Magnetohydrodynamics, Lille, France. See CONF-690648.

The principal results from a mathematical model, giving the equations of motion of an inhomogeneous one-dimensional flow in the pipe of an MHD generator, whose walls are imperfect, are presented. (auth) (France)

11767 MAGNETODYNAMICS OF FLUIDS WITHOUT INERTIA. Ludford, G. S. S. (Univ., Paris). pp 161-76 of La Magnetohydrodynamique Classique et Relativiste. Paris; Centre National de la Recherche Scientifique (1970). (In French).

From Symposium on Classical and Relativistic Magnetohydrodynamics, Lille, France. See CONF-690648.

The flow of an electrically conducting liquid of small kinematic viscosity, in a channel, was considered. An important difference appeared between the cases of planar and three-dimensional flow in the presence of an intense transverse magnetic field. If inertia is neglected, this difference manifests itself in the asymptotic behavior of the double Orseen equation, which is a fourth-order linear partial differential equation. This fact was ascertained from the general solution of the equations of motion without inertia. With a knowledge of certain asymptotic properties, the essential mathematical difference between planar and three-dimensional flow was demonstrated for a model, whose boundary conditions were much simpler than those encountered in the physical problem considered. (auth) (France)

11768 LIMITING PROCESS LEADING TO THE EQUATIONS OF RELATIVISTIC AND NONRELATIVISTIC FLUID DYNAMICS. Friedrichs, K. O. (New York Univ., N. Y.). pp 177-88 of La Magnetohydrodynamique Classique et Relativiste. Paris; Centre National de la Recherche Scientifique (1970).

From Symposium on Classical and Relativistic Magnetohydrodynamics, Lille, France. See CONF-690648.

The magnetohydrodynamic equations were derived by a limit process from the equations describing the interaction of an electromagnetic field and a charged fluid. The specific charge was allowed to extend to infinity, while the charge density, the current, the mass, and the moment were restricted. The interaction equations, which are symmetric hyperbolics, degenerate in passing through the limits. However, they may be transformed into symmetric hyperbolics by eliminating the electrical charge and the current. This process is equally valuable for the classical or relativistic case, under the hypothesis of the absence of electrical resistivity. (auth) (France)

11769 VARIATIONAL PRINCIPLES AND RELATIVISTIC MAGNETOHYDRODYNAMICS. Taub, A. H. (Univ. of California, Berkeley). pp 189-200 of La Magnetohydrodynamique Classique et Relativiste. Paris; Centre National de la Recherche Scientifique (1970).

From Symposium on Classical and Relativistic Magnetohydrodynamics, Lille, France. See CONF-690648.

A general variational principle is given from which the Einstein field equations, the Maxwell equations, and the equations of motion for self-gravitating charged fluids with electric permittivity and magnetic permeability may be derived. It is shown that the ponderomotive forces are not obtained from the divergence of the nonsymmetric Minkowski stress–energy tensor, but rather from a symmetric one. The variational principle makes use of those discussed previously for a general relativistic fluid. The computations are simplified by the use of moving coordinates. (auth) (France)

11770 BOUNDARY-VALUE PROBLEMS IN MAGNETOHYDRODYNAMICS. Kanwall, R. P. (Univ. of Pennsylvania, Philadelphia). pp 201-12 of La Magnetohydrodynamique Classique et Relativiste. Paris; Centre National de la Recherche Scientifique (1970).

From Symposium on Classical and Relativistic Magnetohydrodynamics, Lille, France. See CONF-690648.

Two kinds of boundary-value problems are considered. The first pertains to the internal interfaces that separate the fluid in two regions. These wave fronts exist in space physics, e.g., the shock fronts on the surface of the sun and the magnetospheric boundaries. The second kind of boundaries considered are the physical boundaries such as a sphere or a disk. The flow and magnetic fields set up in the fluid is interesting because of the motion of these boundaries. For viscous fluids it is shown that many modern and classical methods of applied mathematics can be used to solve the canonical problems of longitudinal and rotational motion of bodies of various shapes. Drag and torque formulas are collected and presented. It is shown that the motion of physical boundaries in a nonviscous fluid can be developed on the same lines as done for viscous fluids. An interesting feature of the boundary-value problems in nonviscous fluids is the appearance of the deflection forces on the solids. These forces tend to orient the solids along the lines of force. (auth) (France)

11771 MULTIPLE-SCALE METHOD APPLIED TO MAGNETOHYDRODYNAMIC FLOW INSIDE DUCTS. Peyret, R. (CNRS, Paris). pp 235-49 of La Magnetohydrodynamique Classique et Relativiste. Paris; Centre National de la Recherche Scientifique (1970). (In French).

From Symposium on Classical and Relativistic Magnetohydrodynamics, Lille, France. See CONF-690648.

The flow of an electrically conducting but perfect, compressible fluid, in a semi-infinite channel under the action of an electromagnetic field is studied. The induced fields are assumed negligible. Two situations are considered: progressing fields, inducing a nonstationary one-dimensional flow, and oblique crossed fields, inducing a steady two-dimensional flow. The solution is obtained in the form of an asymptotic expansion in terms of the interaction parameter, which is assumed small. The multiple-scale method employed permits an expansion valid near the entry of the duct as well as at large distances. (auth) (France)

11772 THIN AIRFOIL THEORY IN MAGNETOAERODYNAMICS. Imai, Isao (Tokyo Univ.). pp 263-79 of La Magnetohydrodynamique Classique et Relativiste. Paris; Centre National de la Recherche Scientifique (1970).

From Symposium on Classical and Relativistic Magnetohydrodynamics, Lille, France. See CONF-690648.

Thin airfoil theory in magnetoaerodynamics is presented in a systematic way comparable to that of ordinary fluid dynamics. The steady two-dimensional flow of a compressible, perfectly conducting, inviscid fluid past a thin airfoil in the presence of a uniform magnetic field in an arbitrary direction is considered. Explicit expressions for the velocity and magnetic fields, as well as for the lift, drag, and moment of the airfoil are obtained for the general case of oblique fields. As examples of the applications of the theory, special consideration is given to the flow past an inclined flat plate and a circular arc airfoil at zero incidence. The remarkable feature of the transition from "hyperliptic" to "hyperbolic" flow conditions is explained for the case of the inclined flat plate. (auth) (France)

11773 LINEARIZED MAGNETOGASDYNAMIC CHANNEL AND JET FLOW. Ehlers, F. E. (Univ. of Texas, Austin). pp 281-95 of La Magnetohydrodynamique Classique et Relativiste. Paris; Centre National de la Recherche Scientifique (1970).

From Symposium on Classical and Relativistic Magnetohydrodynamics, Lille, France. See CONF-690648.

The equations of motion for a conducting gas in the presence of magnetic and electric fields are linearized, when the magnetic Reynolds number is small and the flow nearly parallel, by expanding the perturbation flow quantities in power series in the magnetic interaction parameter. In the first approximation the magnetic and electric fields act as internal forces in the gas. The solution is obtained for subsonic flow in a coaxial channel. A turbulent flow results if an electric potential is established between the two cylinders. By reducing the electric field and allowing the inner radius to approach zero, the solution for the subsonic flow in the tube is found. Graphs are given for the perturbation velocity components and pressure in the tube induced by the magnetic field from a single current loop or a toroidal coil. The general solutions are given for the subsonic axially symmetric free jets and for both the subsonic and supersonic two-dimensional free jets. The perturbation velocity components and jet shape are described for the magnetic field due to a current in a wire. (auth) (France)

11774 FLOW OF FLUIDS WITH CONDUCTIVITY TENSORS IN PRESENCE OF A THIN AIRFOIL. Dragos, L. (Univ. of Bucharest). pp 297-309 of La Magnetohydrodynamique Classique et Relativiste. Paris; Centre National de la Recherche Scientifique (1970). (In French).

From Symposium on Classical and Relativistic Magnetohydrodynamics, Lille, France. See CONF-690648.

A general study was made of the flow of compressible fluids with conductivity tensors in the presence of an aerofoil, using the hypothesis of orthogonal fields. The solution is given in terms of Fourier integrals that were determined by using an integral equation corresponding to the boundary conditions. The kernel of this equation is a distribution. Using results obtained from distribution theory, the integral equation reduces to a Fredholm equation (for supersonic and subsonic flow), whose kernels are expressed in

terms of convergent integrals. The results obtained without the intervention of the Hall effect (electrically resistive fluid and negligible electrically resistive fluid) and the results of classical aerodynamics appear as special cases. (auth) (France)

11775 MAGNETIC CONTROL OF A CONDUCTING JET. Kamil, J.; Erlicki, M. S.; Schieber, D. (Technion–Israel Inst. of Tech., Haifa). J. Phys., D (London); 1981-4(Dec 1970).

The speed of a conducting jet in a special disk-shaped tube is determined. The results show that the mobility of the ionized jet depends, among other things, on the form of its movement in the tube. For specific electromagnetic parameters, and also for given dimensions of the tube, it is possible to obtain a movement where the conducting jet behaves as a body moving in a fluid medium (mode I). In this case, the speed of the jet is very high. On the other hand, for different specific electromagnetic and geometric parameters of the experimental system, it is possible to obtain a low speed of the ionized jet, and the fluid in the tube appears to move as a single whole (mode II). It must be noted that in each of the two types of the jet movement, both laminar and turbulent motion can occur, with the transition between them determined by the critical Reynolds number, which differs markedly for the two modes. An expression for the opposing force (due to viscosity) was derived from the experiments in both modes. (auth) (UK)

Geophysics (Upper Atmosphere)

Refer also to abstract 11744.

11776 (AD–708495) MODEL RELATING THE RADIAL CHANGES OF THE PLASMAPAUSE AT DUSK TO GEOMAGNETIC ACTIVITY. Mendillo, Michael; Papagiannis, Michael D. (Boston Univ., Mass. Dept. of Physics and Astronomy). Apr 1970. Contract F19628-68-C-0097. 18p. (AFCRL–70-257). NTIS.

The theory of magnetospheric convection is reviewed with special attention paid to the dusk sector. A model is presented that relates the dawn–dusk electric field, which drives the convection, to the square of the solar-wind speed. Assuming that the plasmapause is located at the equatorial distance where the dawn–dusk electric field conceals the electric field due to the rotation of the Earth, the changes of the plasmapause for various values of solar-wind speed are computed. Furthermore, using a previously obtained empirical relation between the solar-wind speed and the geomagnetic index Kp, the equatorial radius of the plasmapause in the dusk sector vs the Kp index is plotted. Extrapolating along L shells to ionospheric heights, the predictions of this model are found to be in good agreement with a statistical relation between Kp and the invariant latitude of the ionospheric trough. (USGRDR)

11777 (AD–708496) INFLUENCE OF THE NEUTRAL WINDS IN THE FORMATION AND DISTRIBUTION OF THE IONOSPHERIC EVENING ANOMALY. Mullaney, Henry; Papagiannis, Michael D. (Boston Univ., Mass. Dept. of Physics and Astronomy). Jun 1970. Contract F19628-68-C-0097. 19p. (AFCRL–70-2063). NTIS.

By plotting world-contour maps of the index that describes the magnitude of the evening anomaly (the higher than expected evening values of the critical ionospheric frequency in the summer hemisphere), patterns were obtained that show that the anomaly is more pronounced in regions of westward declination in the northern hemisphere and eastward declination in the southern hemisphere, as well as in regions where there is a poleward divergence of the magnetic meridians. By studying neutral-wind patterns computed by other authors, the conclusion is reached that the neutral winds, by dragging the ionospheric plasma that is essentially constrained to move along the lines of force of the Earth's magnetic field, play a very important role in determining the geographic variations in the intensity of the evening anomaly. (auth) (USGRDR)

11778 (AD–709105) COORDINATED EXPERIMENT ON RADAR CLUTTER AND AURORAL PARTICLE FLUXES. Final Report. Shook, G. B. (Lockheed Missiles and Space Co., Palo Alto, Calif. Lockheed Palo Alto Research Lab.). 30 Apr 1970. Contract N00014-69-C-0207. 15p. (LMSC-N-6-P-70-1). NTIS.

A series of coordinated experiments were performed, consisting of simultaneous radar-echo and auroral-particle flux measurements over Alaska. The radar data were obtained by Stanford Research Institute, based at Homer, Alaska; the particle-flux data were obtained from the Lockheed group of instruments aboard the polar-orbiting satellite OV1-18, during the spring and fall of 1969. Both radar and satellite data are of good to excellent quality, and general agreement is observed between location and intensity of radar echoes and the precipitating particles producing the aurora. Detailed analysis (not a part of this work) appears worthwhile to determine a characteristic signature for radar returns from aurora, as distinguished from solid-body returns. (USGRDR)

11779 RING CURRENT IN THE MAGNETOSPHERE AND LOW-LATITUDE MAGNETIC RAYS. Troshichev, O. A.; Fel'dshtein, Ya. I. Cosmic Res. (USSR) (Engl. Transl.); 7: 277-80 (Mar-Apr 1969).

Translated from Kosm. Issled.; 7: 309-12(Mar-Apr 1969).

Variations in the particle density are given for the orbit of the ATS-1 and the corresponding variations in the magnetic field on the satellite orbit and at the Honolulu and College observatories on Dec. 24, 1966. Comparison at various other observatories showed a correspondence between the particle-flux peaks and magnetic disturbances on the Earth's surface and on the satellite. These results were interpreted as an indication of the motion of an extensive current of plasma into the magnetosphere from the direction of the geomagnetic belt. It was assumed that this motion should give rise to an increase in the particle energy, and hence to an increase in the centrifugal and gradient drift of the particles, resulting in the appearance of a ring current. A model is proposed for a ring current that will explain the magnetic field disturbances observed on the Earth's surface and on the satellite. It may be concluded that low-latitude bays, which appear during the period of auroral disturbances, can be explained by ring current flowing outside the limits of the stable particle-capture region. The diamagnetic effect due to the particles forming the ring current is the reason for the depression of the magnetic field on the satellite. The fact that the magnetic disturbances on the Earth's surface and on the satellite are synchronous is a consequence of the varying particle density in the arriving plasma current. (J.C.W.)

11780 VLF MEASUREMENTS OF THE POYNTING FLUX ALONG THE GEOMAGNETIC FIELD WITH THE INJUN 5 SATELLITE. Mosier, Stephen Russell. Iowa City, Ia.; Univ. of Iowa (1970). 134p. University Microfilms Order No. 70-15,627.

Thesis.

The direction of the Poynting flux, up or down the geomagnetic field, was determined for several types of vlf (30 H_z to 10 kHz) radio-noise phenomena observed with the Injun 5 satellite, thereby providing information about the source region of these waves and their propagation in the magnetosphere. Determinations of the Poynting-flux direction of short-fractional-hop whistlers and proton whistlers show that they propagate up the geomagnetic field in accordance with the accepted theories of these phenomena, thereby providing a good check on the experimental technique. Measurements are presented on the Poynting-flux direction of subprotonospheric whistlers, periodic emissions, elf hiss, chorus, vlf hiss, and a new type of emission called a saucer. A new propagation phenomenon was found in which elf hiss may propagate across the plasmapause boundary to lower latitudes and become subsequently reflected and trapped within the plasmasphere. A new type of subauroral-zone vlf hiss was found, and it is shown that the observations of vlf hiss are consistent with emission mechanisms proposed by other investigators in which hiss is generated by Cherenkov radiation. The saucer-shaped emissions are found to be propagating upward from a source below the satellite. A qualitative explanation of the frequency–time shape of this new type of emission is presented. (Diss. Abstr. Int., B)

11781 ELECTRON DENSITY MEASUREMENTS IN THE IONOSPHERE WITH AN IMPROVED RF IMPEDANCE PROBE. Melzner, F.; Rabben, H. H. (Max-Planck-Institut fuer Physik und Astrophysik, Garching, Ger.). Z. Geophys.; 36: 135-50 (Apr 1970). (In German).

Eleven successful experiments for measuring the electron density along the rocket's trajectory were performed within the auroral zone (northern Sweden and northern Canada) as well as near the equator (southern India) by a swept frequency rf impedance probe improved by introducing a guard ring between the electrodes. The principle of the measurement procedure and a description of the probe are given. The impedance probe must be large enough to avoid transit-time effects, e.g., the characteristic linear dimensions of the probe system must not be less than the relative velocity of the electrons divided by angular frequency. The experiments show the applied electrode configuration to be similar to a (hemi)-spherical probe. The calculations, carried out for a spherical condenser, may be applied to the rf probe described, even if it is within a magneto-active plasma. This is demonstrated by comparing the calculated spectra for a spherical condenser, with the spectra recorded during rocket flights with the improved impedance probe. In addition to the main resonances, the frequency of which depends on the electron density, several more resonances were frequently observed. They arise at the harmonics of the electron gyrofrequency and mostly at those harmonics that are adjacent to the main resonances. Another type of resonance has been observed at a

XUM

frequency between the electron gyrofrequency and the Larmor frequency, which is one-half the electron gyrofrequency. (TSS) (tr-auth)

11782 BOUNDARY OF CAPTURED 280-keV ELECTRONS AND POSITION OF CURRENT ELECTROJETS IN THE IONOSPHERE. Afonina, R. G.; Fel'dshtein, Ya. I. Cosmic Res. (USSR) (Engl. Transl.); 7: 281-2(Mar-Apr 1969).

Translated from Kosm. Issled.; 7: 312-14(Mar-Apr 1969).

Experimental results on captured energetic electrons ($E \geq 280$ keV) in the outer radiation zone at a height of 1100 km are discussed. The mutual disposition is considered of the high-latitude boundary of the capture region for these electrons and the current electrojet in the ionosphere, which is important for the understanding of the nature of physical processes responsible for the appearance and development of DP and for the variations in the ionosphere and magnetosphere during magnetic disturbances. Observations obtained with the satellite 1963 38C, which was launched on September 23, 1963, into a circular polar orbit are used. The corrected geomagnetic latitude Φ' of the capture boundary was determined for the period between March 15 and April 28, 1964, when the satellite orbit lay on the night side of the earth at midnight during the appearance of negative bay disturbances on the surface. It was assumed that the counting rate on the boundary of the capture region was $1/100$ of the maximum counting rate in the outer radiation zone. This corresponds to the definition of the capture region in accordance with a reduction in the electron counting rate for electrons with $E \geq 280$ keV by two orders of magnitude relative to the maximum of the latitude distribution of the counting rate. The latitude Φ' of the capture boundary was determined by interpolation between the latitudes at which the counting rate was equal to 1 and 10, respectively. The position of the electrojet, regarded as an equivalent linear current, was determined from magnetograms obtained at Barrow and College Observatories and at the Tiksi Observatory which lay no further than 15° in longitude from the meridian of the intersection of the capture boundary by the satellite. (J.C.W.)

11783 ACCESS OF SOLAR ELECTRONS TO CLOSED FIELD LINES. Vampola, A. L. (Aerospace Corp., El Segundo, Calif.). J. Geophys. Res.; 76: 36-43(1 Jan 1971).

Observations of solar electron fluxes, spectra, pitch-angle distributions, and temporal and spatial behavior are used in investigating the quasi-trapping region of the geomagnetosphere. Several features of this region are demonstrated using data from magnetic electron spectrometers on the polar-elliptical orbiting satellite OV1-19 (1969-25C) during the period April 12 to April 17, 1969. The results indicate that, although solar electrons have ready access to closed field lines, they do not become stably trapped in significant quantities. Sharp persistent gradients between the quasi-trapped zone and the polar plateau (a region of uniform isotropic fluxes) are regarded as indicating an abrupt transition between a region of the geomagnetic field that consists entirely of closed field lines (i.e., permit conjugate-point mirroring) and a second region in which the field lines either connect directly to the interplanetary field or extend into a tail that is very turbulent on the scale of the gyroradius of 0.1- to 2-MeV electrons. (auth)

11784 MAGNETOPAUSE CROSSING OF THE GEOSTATIONARY SATELLITE ATS 5 AT 6.6 R_E. Skillman, T. L.; Sugiura, M. (Goddard Space Flight Center, Greenbelt, Md.). J. Geophys. Res.; 76: 44-50(1 Jan 1971).

During the moderate magnetic storm of September 29–30, 1969, an unusually large magnetic field decrease preceded by an impulsive increase of about 100 γ was observed by the geostationary satellite ATS 5 at about 1733 UT on September 29. The field remained low for about 1 min and returned to the pre-event level as abruptly as it decreased. From the ATS 1 and ATS 5 observations and magnetograms from ground observatories, it is inferred that the magnetosphere was greatly compressed before the event; the magnetopause distance was probably near 7 R_E at the subsolar point. By comparing the changes observed by ATS 5 with the field measured by ATS 1, which was 3 hours behind ATS 5 in local time, the event is interpreted as a magnetopause crossing of ATS 5 caused by a localized rapid inward motion of the magnetopause and its subsequent recession, temporarily creating an identation on the magnetopause surface and briefly exposing ATS 5 to the magnetosheath field. It is suggested that the apparent "holes" in the magnetic field observed by Ogo 3 and Ogo 5 in the magnetosphere near the magnetopause may have been caused, at least in some instances, by similar localized magnetopause motions. (auth)

11785 STORMTIME DISTURBANCE FIELDS AT ATS 1. Coleman, Paul J. Jr. (Univ. of California, Los Angeles); Cummings, W. D. J. Geophys. Res.; 76: 51-62(1 Jan 1971).

Magnetic field measurements made at the synchronous equatorial satellite ATS 1 during nine geomagnetic storms are compared with simultaneous field measurements made at low-latitude observatories. The nine storms occurred during the first six months of 1967. The results indicate that the sudden-commencement (sc) compression of the cavity persists through the initial phase and well into the main phase decrease, perhaps until the time of the main phase minimum. The sc is often accompanied by an increase in the tail current, which then also persists through the initial phase. The tail current increases further during the main phase decrease. However, both the compression and particularly the tail current are sometimes intermittently variable during this part of the storm. There is some evidence that the neutral-sheet current in the tail and the ring current are contiguous while the ring current is developing. As the recovery phase begins, or shortly thereafter, the compression and the tail current return to their respective quiet-day states. As the tail current decreases the ring current and neutral-sheet current apparently separate. During the rest of the recovery phase, the compression and the tail current remain at typical quiettime levels, and the decreasing ring current moves inward. (auth)

11786 ENERGY SPECTRUMS FOR PROTON (200 eV $\leq E \leq 1$ MeV) INTENSITIES IN THE OUTER RADIATION ZONE. Pizzella, G.; Frank, L. A. (Univ. of Iowa, Iowa City). J. Geophys. Res.; 88-91(1 Jan 1971).

The directional differential spectrums of proton intensities mirroring near the magnetic equator in the outer radiation zone are obtained for the energy range 200 eV $\lesssim E \lesssim 1$ MeV with measurements from the spacecrafts Ogo 3, Explorer 12 and 14, and Mariner 4. The average proton spectrum is characterized by a single maximum of differential intensities at 5 to 10 keV and monotone decreasing intensities with lower and higher proton energy. It is suggested that the appropriate boundary region for models of radial diffusion of protons into the outer radiation zone is located in the vicinity of the earthward edge of the quiettime extraterrestrial ring current at $L \approx 6.5$ R_E. (auth)

11787 IRREGULARITIES IN PROTON DENSITY DEDUCED FROM CYCLOTRON DAMPING OF PROTON WHISTLERS. Lucas, Christopher; Brice, Neil (Cornell Univ., Ithaca, N. Y.). J. Geophys. Res.; 76: 92-9(1 Jan 1971).

The damping of proton whistlers is found to be much more gradual than predicted by the cyclotron damping theory of Gurnett and Brice (1966) for an assumed homogeneous plasma with an isotropic Maxwellian proton velocity distribution. Several possible causes of the discrepancy are: nonlinear effects, anisotropy, a non-Maxwellian velocity distribution, and irregularities in proton density. It is concluded that plasma density irregularities are responsible for the observed gradual damping. When these effects are included, the deduced proton temperature increases significantly (about a factor of 2) and the magnitudes of the variations in proton plasma frequency estimated are about 15 to 20%. (auth)

11788 RELATION OF THE Pc1 MICROPULSATION SOURCE REGION TO THE PLASMASPHERE. Heacock, R. R. (Univ. of Alaska, College). J. Geophys. Res.; 76: 100-9(1 Jan 1971).

Amplitude and polarization measurements of structured Pc1 micropulsations obtained in Alaska and in Finland imply that the Pc1 source lines are near or inside the plasmapause. The measurements give the source lines significantly closer to the Earth than are given by Pc1 dispersion calculations. Specific Pc1 events are compared with plasmapause positions determined by the Ogo 3 and Ogo 5 satellites. Some evidence is presented that implies that structured Pc1 source lines corotate with the Earth. (auth)

11789 OBSERVATION OF THE HELIUM I 584-A DAYGLOW RADIATION BETWEEN 400 AND 1000 km. Donahue, T. M.; Kumer, J. B. (Univ. of Pittsburgh). J. Geophys. Res.; 76: 145-62(1 Jan 1971).

Retarding potential analysis of photoelectrons created by the Earth's euv airglow permitted the measurement of the height profile of the He I 584-A and H I 1216-A dayglow lines from 400 to 1016 km. Maximum 584-A emission occurred at 500 km during rocket ascent and amounted to 0.7 ± 0.3 kR. The large uncertainty reflects several experimental difficulties, one of which was the presence of a large and variable background signal. This background is believed to have been caused by photoelectrons produced at the instrument baffles by direct sunlight. It is concluded that there is no important contribution to the signal from ionospheric electrons. The height profile of the 584-A line was consistent with that expected for resonance scattering of solar 584-A radiation by telluric helium in diffusive equilibrium at 927°K. The helium density required was $6.5 \pm 0.7 \times 10^6$ cm^{-3} at 176 km. However, the very large emission rates observed demand that the solar 584-A (full) line width be 0.023 ± 0.007 A if the flux was 10^9 photons cm^{-2} sec^{-1}. Lyman-α air-

XUM

glow (14 kR at 1000 km) varied in a way consistent with expectations for resonance scattering in an atmosphere containing 3×10^7 H atoms cm^{-3} at 100 km. There is some evidence in the Lyman-α data for a rather strong dependence of exospheric hydrogen abundance on the solar zenith angle. (auth)

11790 ATMOSPHERIC X-RAY FLUORESCENCE. Tomblin, F. F. (Bellcomm, Inc., Washington, D. C.). J. Geophys. Res.; 76: 163-9(1 Jan 1971).

Solar-stimulated fluorescence by photoelectric ionization in the Earth's upper atmosphere generates fluxes of up to 9×10^4 photons cm^{-2} sec^{-1} $ster^{-1}$ at 110 km for nitrogen K-α emission. The corresponding maximum flux for oxygen is 1×10^4 photons cm^{-2} sec^{-1} $ster^{-1}$ at approximately the same altitude. Recent observations have confirmed the fluorescence at a somewhat lower level than that computed here. This flux may place some limitations on low-energy (0.1 to 1 keV) x-ray astronomy experiments performed during the daytime at altitudes below 300 km. (auth)

11791 SCINTILLATION BOUNDARY DURING QUIET AND DISTURBED MAGNETIC CONDITIONS. Aarons, Jules; Allen, Richard S. (Air Force Cambridge Research Labs., Bedford, Mass.). J. Geophys. Res.; 76: 170-7(1 Jan 1971).

Earlier studies of ionospheric scintillations outlined the lower boundary of the high-latitude region where intense scintillations at 40 MHz were observed. The quiet-day scintillation boundary reached a lower position of 57° invariant latitude at 2200 LT. Dyson's (1969) recent observations with a Langmuir probe have verified the existence of a lower-latitude boundary of small-scale irregularities. The boundary concept has been extended to include the effects of magnetic storms. Observation of satellite beacon signals at 40 and 54 MHz during 1961 to 1966 indicate that the mean change in the lower-boundary latitude of the irregularity region is a decrease of approximately 1.6° per unit change in local K index. This is quite similar to the change of 1.8° per unit change in Kp noted for the trough position by Rycroft and Thomas (1970). In examining the data available from high-inclination and synchronous satellites, it was noted that the change in latitude with K index is a function of time. The maximum change of latitude as a function of K index, approximately 2° to 3° per unit K, occurred between 0300 and 0600 LT; the minimum change, about 1° per unit K, occurred over a broad interval from 1600 to 0200 LT. If the irregularity structure is produced by an interaction of the plasmapause with the ionosphere, the morphologic behavior of this region of the magnetosphere can be studied by reviewing the large inventory of scintillation and spread-F data that has been amassed in the course of ionospheric research. (auth)

11792 INCLINATION OF THE GEOMAGNETIC FIELD MEASURED BY AN INCOHERENT SCATTER TECHNIQUE. Woodman, Ronald F. (Instituto Geofisico del Peru, Lima). J. Geophys. Res.; 76: 178-84(1 Jan 1971).

A technique to measure the direction of the geomagnetic field by using incoherent scatter techniques is described. The technique has been used to measure the inclination of the magnetic field at the Jicamarca Radar Observatory with an accuracy of the order of 1 minute of arc in the height range from 200 to 800 km. The corresponding inclinations obtained from the Goddard Space Flight Center (12/66) and the International Geomagnetic Reference Field (10/68) models are found to be about 1° in error. (auth)

11793 DIURNAL VARIATION OF THE NEUTRAL TEMPERATURE PROFILE AT ARECIBO FROM INCOHERENT SCATTER MEASUREMENTS AND ITS RELEVANCE TO THE 1400-HOUR DENSITY MAXIMUM. Swartz, Wesley E.; Nisbet, John S. (Pennsylvania State Univ., University Park). J. Geophys. Res.; 76: 185-96(1 Jan 1971).

High-resolution electron and ion temperature and electron density measurements at Arecibo are used to derive profiles of the neutral temperature from 116 to 400 km throughout the day. In this technique, least-squares fitting is used to calculate a smooth temperature profile and a neutral atmospheric model. The availability of a complete profile allows calculation of the thermal-energy storage and downward heat conduction throughout the day. Two methods are employed to calculate the density profile. The first assumes that the density at 120 km is known and solves for the diffusion-equilibrium model that best fits the data. The second method requires only the assumption of the relative densities of the neutral constituents at the lower boundary but has a somewhat higher experimental variance. It is shown that density and temperature do not generally peak at the same time, though current atmospheric models such as Cira 1965 suggest that they do. These models are based mainly on satellite orbital-decay measurements and indicate a density maximum around 1400 hours. Neutral temperatures derived from incoherent sounding have indicated a temperature maximum near 1600 hours. It is now suggested that these two phenomena may be self-consistent when the entire temperature profile affecting the neutral density is considered. (auth)

11794 ATMOSPHERIC DENSITY AND ROTATION BELOW 195 km FROM A HIGH-RESOLUTION DRAG ANALYSIS OF THE SATELLITE OVI-15 (1968-059A). Ching, Barbara K. (Aerospace Corp., El Segundo, Calif.). J. Geophys. Res.; 76: 197-201(1 Jan 1971).

A drag analysis using high-accuracy C-band radar-transponder data yielded densities at heights between 135 and 195 km at approximately 1-day intervals over a 4-month period in 1968. On the average, the results were in reasonable agreement with currently used model atmospheres, but the variability of the density was found to be much larger than was predicted by the models. Density variations of the order of 10% to 20% at 170 km were observed to correlate with moderate geomagnetic activity and the semiannual effect. A large increase of about 35% at 140 km was observed during a major geomagnetic storm. Increases in the density at times of geomagnetic activity were significantly larger in the northern auroral region than elsewhere. The effects of solar activity, the diurnal bulge, and latitude were not apparent in the data. The atmospheric rotation rate at 175 km was found to be higher than that of the Earth by a factor of about 1.3. (auth)

11795 ROCKET MEASUREMENTS OF UPPER ATMOSPHERIC NITRIC OXIDE AND THEIR CONSEQUENCES TO THE LOWER IONOSPHERE. Meira, Luiz Gylvan Jr. (Univ. of Colorado, Boulder). J. Geophys. Res.; 76: 202-12(1 Jan 1971).

The nitric oxide density profile in the upper atmosphere between 70 and 110 km was measured with scanning ultraviolet spectrometers aboard two Nike–Apache rockets on February 6 and January 31, 1969. The observed nitric oxide density profile has a maximum of about 10^8 cm^{-3} at 105 km, and a minimum of about 10^7 cm^{-3} at 85 km. Photochemical equilibrium is prevalent at about 85 km while mixing dominates below that altitude. A model in which nitric oxide is formed from $N(^2D)$ atoms can explain the observed features of the height profile. The contribution of nitric oxide ionization by solar Lyman-α to the total ion production is dominant in the middle D region (below 90 km) for the solar activity level at the time of the experiments. Dissociative recombination of nitric oxide ions is the main loss process in the region above 85 km. Below that height, a faster mechanism is required. (auth)

11796 GROUP RAYS OF INTERNAL GRAVITY WAVES IN A WIND-STRATIFIED ATMOSPHERE. Cowling, D. H.; Webb, H. D.; Yeh, K. C. (Univ. of Illinois, Urbana). J. Geophys. Res.; 76: 213-20(1 Jan 1971).

The propagation of internal gravity waves in a model atmosphere with stratified neutral winds is studied. The waves are subjected to a ray-tracing analysis and, as a result, are grouped into three types: (1) those that penetrate the F region of the ionosphere, (2) those that are reflected, and (3) those that nearly reach the critical-layer condition and are absorbed. Examples of the three types of ray paths are shown. The traveling waves observed in the ionosphere are excited by the propagating acoustic–gravity waves launched at lower levels in the atmosphere. The characteristics of the waves, such as period and velocity, are dependent on atmospheric conditions, as well as on the nature of the source. Extensive computations show that neutral winds provide a directional-filter effect as depicted in several contour plots. From Faraday-rotation data taken during the summer of 1968, the characteristics of 13 traveling waves that were observed fit into the calculated contours reasonably well. (auth)

11797 STRUCTURE OBSERVED IN SOLAR-PARTICLE LATITUDE PROFILES AND ITS DEPENDENCE ON RIGIDITY. McDiarmid, I. B.; Burrows, J. R.; Wilson, Margaret D. (National Research Council of Canada, Ottawa). J. Geophys. Res.; 76: 227-31(1 Jan 1971).

Latitude profiles of solar protons with energies greater than 1, 33, and 114 MeV and solar electrons with energies greater than 35 keV are discussed and compared with the cutoff-rigidity calculations of D. F. Smart et al. (1969). The measurements indicate that a field model could be chosen to give agreement between trajectory calculations and measured knee latitudes for 114-MeV protons and 35-keV electrons but that 1- and 33-MeV protons penetrate more deeply into the magnetic field than could be accounted for on the basis of such calculations. Sometimes intensity changes, not associated with the knee latitude, occur in the 1- and 33-MeV distributions at latitudes that coincide approximately with calculated cutoffs. (auth)

XUM

11798 IONIZATION DISTURBANCES CAUSED BY GRAVITY WAVES IN THE PRESENCE OF AN ELECTROSTATIC FIELD AND BACKGROUND WIND. Whitehead, J. D. (Univ. of Queensland, St. Lucia, Australia). J. Geophys. Res.; 76: 238-41(1 Jan 1971).

Internal gravity waves in the neutral air propagating through the ionosphere cause a corresponding disturbance in the ionization. This note discusses additional effects that arise owing to the presence of an electrostatic field and background wind and in particular the possibility of a "spatial resonance" when the natural drift of ionization irregularities equals the phase velocity of the gravity wave. The electrostatic field may be the one associated with the tidal motions that drive the S_q current system. It is shown that short-period ($\tau < 30$ min) disturbances in the F region may be appreciably affected by spatial resonance, if the component of $E \times B/B^2$ drift in the wave normal direction is equal to the phase velocity of the wave. In the E region a similar coincidence between the ion-drift velocity and the wave-phase velocity may cause intense patches of sporadic E to drift almost with the background wind at the sporadic-E height. (auth)

11799 OBSERVATIONS OF CONJUGATE EXCITATION OF THE O I 1304-A AIRGLOW. Meier, R. R. (Naval Research Lab., Washington, D. C.). J. Geophys. Res.; 76: 242-7(1 Jan 1971).

Observations of the O I $^3P-^3S$ 1304-A airglow were made from the Ogo 4 spacecraft that was launched into a near twilight polar orbit on July 28, 1967. Orbital apogee and perigee were about 920 and 420 km, respectively. The Ogo 4 ultraviolet detectors were oriented toward the center of the Earth and observed the airglow backscattered from the atmosphere. By August 20, 1967, the orbit had precessed sufficiently for spacecraft ellipse to occur. Observations are reported of a 1304-A emission at night when the Earth is normally black in the uv. The emission was observed only when the conjugate ionosphere was still sunlit, thus suggesting excitation by photoelectrons traveling along magnetic field lines to the night hemisphere. (auth)

11800 QUASI-STAGNATION LEVELS IN THE ION MOTION INDUCED BY INTERNAL ATMOSPHERIC GRAVITY WAVES AT IONOSPHERIC HEIGHTS. Hooke, William H. (National Oceanic and Atmospheric Administration, Boulder, Colo.). J. Geophys. Res.; 76: 248-50(1 Jan 1971).

A theoretical demonstration is given of the existence, under appropriate ionospheric conditions, of a height or heights at which the vertical ion motion induced by a single internal atmospheric gravity wave vanishes identically, at all phases of the wave cycle. The heights are called quasi-stagnation levels because the horizontal ion motions there are, in general, nonzero. Such quasi-stagnation levels can exist because of two properties of internal atmospheric gravity waves: (1) Hines, 1960, reports that those waves have small vertical wavelength ($4k_z^2 \gg 1/H^2$, where k_z is the vertical angular wave number, and H is the neutral-gas scale height) are very nearly transverse; and (2) the waves all have nonzero horizontal components of phase propagation, and hence from Hines, have nonzero vertical components for their associated winds. The analysis outlined was developed for waves traveling in any azimuthal direction and, for the present example, a specialization to the case of zonal (magnetic east–west) wave propagation is used. (J.C.W.)

11801 PROTON DRIFT ECHOES IN THE MAGNETOSPHERE. Lanzerotti, L. J.; Maclennan, C. G.; Robbins, M. F. (Bell Telephone Labs., Murray Hill, N. J.). J. Geophys. Res.; 76: 259-63 (1 Jan 1971).

The first observational evidence of drift periodic echoes in the energetic proton fluxes in the magnetosphere is reported. The data were obtained at synchronous altitude by ATS 1 launched Dec. 6, 1966. The proton data included measurement of significant fluxes of solar protons with the onset of the large solar proton event on Nov. 18, 1968. The data confirm previous conjectures that these solar particles are apparently trapped for several drift periods. Since the drift echoes presented resulted from a compression of the magnetosphere produced by a sudden commencement, the event indicates that these protons, when present in the outer zone, respond to sc and sudden impulses in a manner similar to the outer-belt electrons. This implies that some of the energetic solar protons can be transported, by sc- and si-produced third invariant-violating radial diffusion, across L shells, and deep into the magnetosphere from a source at $L \sim 6$. By using the longitudinal drift times determined for the magnetosphere (boundary at 9 R_E and a 40-γ tail field), a model of the proton drift echoes was constructed. The model predicted the response of the actual experimental proton energy channels as a spectrum of protons drifted past the detector telescope. The calculations show that the observed peak enhancements after the sc were proton drift echoes. (J.C.W.)

11802 TRANSPORT AND LOSS PROCESSES FOR MAGNETOSPHERIC HELIUM. Cornwall, John M. (Aerospace Corp., El Segundo, Calif.). J. Geophys. Res.; 76: 264-7(1 Jan 1971).

The anomalously low α/p flux ratio measured at $L \simeq 3$ by Krimigis and Van Allen (Krimigis, 1970) and by Blake and Paulikas (1970) can be understood qualitatively in terms of radial diffusion driven primarily by fluctuating electrostatic convection fields when proper account is taken of charge exchange and pitch-angle loss processes. It is shown that electrostatic radial diffusion seems to explain proton-flux profiles better than magnetic diffusion for energies less than a few MeV. Studies of the distribution and charge composition of ionized helium and other heavy ions on closed field lines and in the auroral zone shed light not only on the origin, transport, and loss processes of the ions, but also on corresponding processes for protons. The three sources of helium at the outer boundary of the trapping zone, where radial diffusion is considered to begin, are discussed. Even though the large cross section for conversion of He^{++} to He^+ does not result in a direct loss of ionized helium, it can profoundly affect the magnetospheric-helium concentration since other loss processes and the radial diffusion coefficient depend on Z, the charge number. (J.C.W.)

11803 PITCH-ANGLE DISTRIBUTIONS OF PROTONS AND HELIUM IONS IN THE MAGNETOSPHERE. Gregory, C. T. (Univ. of California, San Diego, La Jolla). J. Geophys. Res.; 76: 268-71(1 Jan 1971).

The loss of energetic protons and helium ions from the magnetosphere resulting from charge exchange and pitch-angle diffusion is discussed. The pitch-angle distribution is determined by the Fokker–Planck equation and a numerical solution is obtained for protons and He^{++} and He^+ ions that are assumed to be injected into the magnetosphere during the early phase of a geomagnetic storm. It is assumed that the pitch-angle distribution is initially isotropic, that the particles remain on the L shell on which they are injected, and that their energy is constant. Numerical solutions to the Fokker–Planck equation are shown for protons, He^{++}, and He^+. To estimate the contribution of pitch-angle diffusion to the loss process, the equation is solved both with and without the diffusion factor. In solutions using both charge exchange and diffusion, the decay time decreased; pitch-angle scattering decreased the particle pitch angles. (J.C.W.)

11804 AURORAL PHENOMENA DRIVEN BY THE MAGNETOSPHERIC PLASMA. Taylor, Harold E.; Perkins, Francis W. (Princeton Univ., N. J.). J. Geophys. Res.; 76: 272-7(1 Jan 1971).

Auroral phenomena involve an interaction between the magnetosphere and the ionosphere. These two regions are linked by the magnetic field along which currents flow to close the open part of the transverse currents in the magnetosphere. Dimensional analysis is used to examine the solution of the magnetohydrodynamic equations for fields and plasmas in the magnetosphere. Ionospheric conductivity is low and allows a polarization electric field of the order of one volt per meter to develop. To limit the electric field to the observed values (~30 millivolts per meter), one is forced to the important conclusion that surfaces of constant $\int dl/B = V$ must approximately coincide with surfaces of constant plasma pressure. The $\int dl/B$ is taken along a field line and is proportional to the volume of a flux tube. It is a scalar function to be denoted by V and has a single value for each field line so it is convenient to specify it as a function of position in the magnetic equatorial plane. Currents flowing along magnetic field lines imply the existence of particle fluxes of 10^8 particles/(cm^2 sec) or greater. These parallel currents are identified with an auroral arc in a model where the electric field in the background plasma will be larger than the field in the arc by the ratio of conductivity in the arc to that in the background—a number of the order of 60. (J.C.W.)

11805 ELECTROMAGNETIC DRIFT OF THE MIDLATITUDE F2 LAYER DURING A STORM. VanZandt, T. E.; Peterson, V. L.; Laird, A. R. (National Oceanic and Atmospheric Administration, Boulder, Colo.). J. Geophys. Res.; 76: 278-81(1 Jan 1971).

Two reasons given for the uncertainty of what causes the variations in the F2 layer during a magnetic storm include (1) the electric fields in the F2 layer have not yet been measured simultaneously with storm-related F2-layer variations, and (2) the observed variations might be caused by several other processes. A middle-latitude nighttime F2-layer event during a moderate magnetic storm (Oct. 23, 1965) is reported here that almost certainly was caused by electromagnetic drift of the ionospheric plasma. The most direct and easily observed effects of electromagnetic drift are changes in the height of the F2 layer. These are seen in h'F, which is defined to be the virtual height at 1.6 MHz of the ordinary-mode F2-layer trace on ionograms. Ionization by

XUM

particle bombardment can hardly cause a rise of the F2 layer. It might have caused the low h'F's immediately preceding the rise. Two arguments against this are (1) ionization by particle bombardment would also have caused an appreciable enhancement of the nightglow emissions; and (2) a height increase by the eating away of the bottom of the F2 layer by recombination is far too slow. This brief study shows a rough estimate of the magnitude and direction of the ionospheric electric field during a storm. (J.C.W.)

11806 ROLE OF PLASMA INSTABILITIES IN IONOSPHERIC HEATING BY RADIO WAVES. Perkins, F. W.; Kaw, P. K. (Princeton Univ., N. J.). J. Geophys. Res.; 76: 282-4(1 Jan 1971).

The relevance of recent theoretical results on the anomalous absorption of electromagnetic waves in plasmas to ionospheric heating is demonstrated. When sufficiently intense long-wavelength transverse electromagnetic waves with frequencies almost equal to the plasma frequency are incident on a plasma, instabilities involving both ion and electron density fluctuations can occur and are known as parametric instabilities. The presence of parametric instabilities can lead to an enhanced heating of the plasma. The incident power in the Boulder heating experiment is sufficient to cause a plasma instability whose result is ionospheric heating and the attenuation of radio waves. Because both the heating and the thermal conductivity depend, through the effective collision frequency, on the incident power, the heating should be equally effective during daytime or nighttime. (J.C.W.)

11807 EFFECT OF IONOSPHERIC HEATING BY RADIO WAVES ON ABSORPTION OF PROBING WAVES OF DIFFERENT POLARIZATION. Fejer, J. A. (Univ. of California, San Diego, La Jolla). J. Geophys. Res.; 76: 285-6(1 Jan 1971).

A theoretical prediction related to the presence of the Earth's magnetic field observed during the Boulder ionospheric heating experiment is presented. An important observation is the strong absorption of the probing wave of ordinary polarization, about 10 sec after switching on the heating transmitter, and the total absence of absorption of the probing wave of extraordinary polarization. The presence of the Earth's magnetic field requires a modification of the existing theories. The absorption and reflection phenomena of the probing waves are given briefly and explain the absence of absorption for waves of extraordinary polarization; they also present strong evidence in favor of the suggestion that the energy of the probing wave is scattered into plasma oscillations and is eventually dissipated. (J.C.W.)

11808 CORRELATION STUDY OF AURORAL LUMINOSITY AND X RAYS. Rosenberg, T. J. (Univ. of Bergen, Norway); Bjordal, J.; Trefall, H.; (and others). J. Geophys. Res.; 76: 122-32(1 Jan 1971).

Simultaneous observations of λ5577 O I and X-ray bremsstrahlung reveal that postbreakup quasi-periodic 5- to 15-sec pulsations in these two phenomena are positively correlated. Cross-correlation analysis of the fluctuations shows that λ5577 O I pulses lag corresponding x-ray pulses by ~0.5 to 1 sec, a value consistent (within experimental uncertainties) with the effective lifetime of oxygen atoms in the 2^1S state. The percentage modulation of x rays >25 keV was usually 2 to 5 times larger than the percentage modulation of auroral light. Estimates of the energy distribution in the primary electron-precipitation pulsations indicate that at times as much as 50% of the energy needed to account for the luminosity variations may be carried by electrons with energies greater than 25 keV. It is concluded that pulsating auroras and x rays result from a single process modulating both the low-energy (<25 keV) and the high-energy (>25 keV) primary electron flux. From these observations, gross intensity changes of a slowly varying nature appear to be largely unrelated, in agreement with the majority of previous findings. (auth)

11809 ENERGY SPECTRA AND ANGULAR DISTRIBUTIONS OF PARTICLES IN THE PLASMA SHEET AND THEIR COMPARISON WITH ROCKET MEASUREMENTS OVER THE AURORAL ZONE. Hones, E. W. Jr.; Asbridge, J. R.; Bame, S. J.; Singer, Sidney (Los Alamos Scientific Lab., N. Mex.). J. Geophys. Res.; 76: 63-87(1 Jan 1971).

Examples are presented of electron and proton differential energy spectra between ~100 eV and 18 keV measured with hemispherical plate electrostatic analyzers on the Vela satellites at a geocentric distance of ~18 R_E in the magnetotail plasma. The spectra were obtained under several conditions of geomagnetic activity during very quiet conditions, during the expansive phase of substorms, and following a sudden impulse at the Earth. Most of the published auroral-particle differential energy spectra measured by rockets are sketched for easy comparison with the plasma sheet spectra. The plasma sheet particle fluxes generally, but not always, appear nearly isotopic to a wide-angle detector such as the analyzer used here. Comments cite features of these sample spectra, referring to averages of measurements made in the antisolar direction and perpendicular to these directionally averaged results. Plasma sheet electron spectra are usually smooth single-peaked distributions often resembling Maxwellian distributions from several hundred eV to a few keV and frequently becoming power-law spectra above several keV. In quiet times peak electron intensities were ~10^8 el/cm^2 sec ster keV and occurred from 100 to several hundred eV. Proton peak fluxes during quiet times were ~10^6 p/cm^2 sec ster keV and appeared near or below 1 keV. After a sudden impulse the electron and proton energy densities rose to unusually high values. The electron and proton fluxes measured at rocket altitudes typically exceed fluxes in the plasma sheet by factors of 10 to 100 over most of the energy range of the Vela measurements. A careful analysis of the data shows that the angular distribution of the plasma sheet electrons can be sharply peaked along the presumed direction of the magnetic field lines. (auth)

11810 ELEMENTARY PROCESSES INVOLVING ELECTRONS IN THE IONOSPHERE. Takayanagi, Kazuo; Itikawa, Yukikazu (Tokyo Univ.). Space Sci. Rev.; 11: 380-450(Oct 1970).

The production, slowing-down, and disappearance processes of ionospheric electrons are discussed. Emphasis is placed on the individual elementary processes, especially on electron collisions with other atmospheric constituents, rather than on other topics involving the gross structure of the real ionosphere. (auth)

11811 NIGHT AIRGLOW PHENOMENOLOGY. Silverman, S. M. (Air Force Cambridge Research Labs., Bedford, Mass.). Space Sci. Rev.; 11: 341-79(Oct 1970).

The phenomenology of the night airglow is reviewed with particular emphasis on the work of recent years. The major topics discussed are the spectrum; latitudinal dependency; diurnal variation; correlations in time and space; the effects of magnetic activity and of the sunspot cycle and solar activity; and conjugacy and the airglow. A number of other topics are also discussed briefly. (auth)

11812 NIGHT-TIME ANOMALIES IN VERY LOW FREQUENCY PROPAGATION PRODUCED BY A GALACTIC X-RAY SOURCE AT CENTAURUS. Kaufmann, P.; Paes de Barros, M. H.; Vianna, E. N. (Mackenzie Univ., Sao Paulo, Brazil). Nature (London); 228: 1080-1(12 Dec 1970).

It was observed that night-time propagation of vlf waves in the ionosphere shows considerable variability, both in phase and amplitude, in comparison with the relatively stable day-time conditions. The night-time anomalies are not well understood; some are associated with the presence of energetic particles originating from solar proton events, but explanations of others remain obscure. It has been demonstrated, however, that the night-time ionisation at heights around the upper boundary of the Earth–ionosphere waveguide may contain appreciable contributions from the stronger celestial x-ray sources and these may have an effect on both phase and amplitude. In this connection, the effect of a very strong x-ray source that appeared in the southern sky between July 6 and 9, 1969 is discussed. This source was associated with Centaurus and produced a night-time disturbance on vlf transmissions received at Sao Paulo. Only the night-time phase showed a significant departure from normal, and the effect on amplitude was much less marked. The data obtained are discussed in detail, and it was concluded that short-period anomalies produced by hard and intense galactic x rays are more pronounced and definite than long-term effects. The studies reported should encourage a detailed search of other night-time anomalies that could be associated with the appearance of celestial x-ray sources. vlf data on long propagation paths, controlled by atomic frequency standards, appear very suitable for the purpose. (UK)

11813 SATELLITE EQUIPMENT FOR THE MEASUREMENT OF HIGH ENERGY ELECTRONS AND PROTONS. Dalziel, R.; Harden, B. N.; Page, D. E.; Thomas, G. R.; Thorpe, D. G. (SRC Radio and Space Research Station, Slough, Eng.). J. Atmos. Terrest. Phys.; 33: 71-87(Jan 1971).

Two experiments are described that were flown on the satellites ESRO-IA (Aurorae) and ESRO-IB (Boreas). The experiments measured the intensity and energy spectrum of electrons in the range 40 to 400 keV with pitch angles of about 10 and 90°, and of protons in the energy range 1 to 30 MeV with pitch angles <30°. Details are given of the electron and proton detectors, and of the design parameters and methods of measurement. The electronics system and the calibrations of the experiments are described, and the paper includes some results that illustrate the functioning of the experiments in orbit. (auth) (UK)

XUM

11814 ACCESSIBILITY TO THE ELECTRON PLASMA RESONANCE IN THE F REGION OF A WAVE EMITTED FROM THE EARTH. Bouchet, P. (Thomson-CSF, Orsay, France). J. Atmos. Terrest. Phys.; 33: 89-100(Jan 1971). (In French).

The influence of a flux of pseudo-acoustic energy on the accessibility to the plasma resonance in the F region of a wave emitted from the Earth is analyzed in the adiabatic approximation with pressure taken as a scalar. The rays involved in the plasma resonance as well as their attenuation by collisions are treated using a parabolic density profile for the ionosphere. The analysis leads to new experimental possibilities allowing one to control the existence of particular rays. (auth) (UK)

11815 ASPECT SENSITIVITY OF SPREAD-F IRREGULARITIES. Bates, Howard F. (Stanford Research Inst., Menlo Park, Calif.). J. Atmos. Terrest. Phys.; 33: 111-15(Jan 1971).

A high-latitude oblique incidence echo, previously shown to be produced by irregularities strongly aligned along the magnetic field, is found to occur whenever vertical incidence spread-F is recorded from the same volume of the F layer. Frequently, the southern boundary of the irregular region is sharp, and occasionally large-scale structure can be detected within the irregular region. King (1970) recently concluded that the irregularities producing spread-F are large-scale surfaces that are not field aligned. These various results suggest that the agent responsible for spread-F produces large-scale F-layer irregularities that are at times sharply bounded and contain small-scale, weak-scattering, field-aligned irregularities. (auth) (UK)

11816 OBSERVATIONS OF IONOSPHERIC ELECTRON CONTENT ACROSS THE EQUATORIAL ANOMALY AT SUNSPOT MINIMUM. Golton, E.; Walker, G. O. (SRC Radio and Space Research Station, Slough, Eng.). J. Atmos. Terrest. Phys.; 33: 1-11(Jan 1971).

Observations of the Faraday rotation of signals from the satellite Transit 4A recorded at three stations within the South East Asian equatorial zone were analyzed to show the latitudinal variation of electron content at sunspot minimum. By day an anomaly is apparent, analogous to that found in f_0F2, consisting of two maxima and an intermediate minimum. The structure is centered on the magnetic equator and has on average a nearly symmetrical form during northern summer and the equinoxes; this differs from results found by other workers in the East African zone, where asymmetry was found in northern summer. A regular diurnal variation is observed between 1000 and 1800 LMT, the anomaly reaching a maximum latitudinal extent just after noon. By night data appear quite irregular, changes of 15% in total content per degree of latitude being common. (auth) (UK)

11817 VARIATIONS OF HARD SOLAR X RAYS DEDUCED FROM RADIO-WAVE ABSORPTION. Nestorov, G. (Geophysical Inst., Sofia). J. Atmos. Terrest. Phys.; 33: 119-22(Jan 1971).

The strength of radio waves of frequency 164 kHz received at a distance of 1720 km over a period 1966-69 was analysed to show that the D-region electrons produced by hard solar x rays varied quasi-periodically with periods 10 and 5 months. (auth) (UK)

Low-Temperature Physics and Cryogenic Equipment

Superfluidity

Refer also to abstract 11545.

11818 SUM RULE ANALYSIS OF TWO-BRANCH EXCITATION SPECTRUM OF LIQUID ^{4}He. Soda, Toshio; Sawada, Katsuro; Nagata, Tsuneo (Tokyo Univ. of Education). Progr. Theor. Phys. (Kyoto); 44: 860-4(Oct 1970).

The experimental intensity curves for the two-branch peaks of excitation spectrum for liquid ^{4}He obtained by Cowley and Woods (Phys. Rev. Lett., 24: 646(1970)) are explained from the two-branch spectrum and the experimental form factor in a manner consistent with sum rules, by assuming that the sum rules are exhausted by "real" one- and two-phonon excitations. (auth)

Superconductivity

Refer also to abstracts 10899, 11381, 11416, and 12032.

11819 (CALT-822-22) SUPERCONDUCTING METASTABLE SIMPLE CUBIC ALLOYS. AEC Research and Development Report No. 17. Tsuei, C. C.; Yen, Huan-Chun; Duwez, Pol (California Inst. of Tech., Pasadena. W. M. Keck Lab. of Engineering Materials). Feb 1971. Contract AT(04-3)-822. 4p. Dep. NTIS.

Four new simple cubic superconducting alloys were obtained by rapid quenching (10^7 °C/sec) from the liquid state: $AuSb_2$, $Pd_{16.5}Sb_{83.5}$, $InSb_3$, and $Au_{1-x}Pd_xTe_2$. Critical temperatures and lattice parameters are listed for these alloys and for previous experimental cubic alloys. (D.L.C.)

11820 (LNF-70/18) PRELIMINARY RESULTS REGARDING DEVELOPMENT OF SUPERCONDUCTING RIBBONS OF Nb_3Sn. Note No. 474. Pasotti, G.; Ricci, M. V.; Sacchetti, N.; Sacerdoti, G.; Spadoni, M. (Comitato Nazionale per l'Energia Nucleare, Frascati (Italy). Laboratori Nazionali di Frascati). 5 May 1970. 12p. (In Italian). Dep. NTIS (U. S. Sales Only).

Preliminary results on the development of superconducting ribbons of Nb_3Sn were obtained, using the method of diffusion of tin into the niobium. The production apparatus and techniques and the measuring apparatus and techniques are described. Characteristics of the superconducting ribbons produced were determined with respect to temperature. (J.S.R.)

11821 SUPERCONDUCTIVITY IN SILVER. Wolf, Stuart Alan. New Brunswick, N. J.; Rutgers-The State Univ. (1970). 124p. University Microfilms Order No. 70-16,962.

Thesis.

Thermal conductivity and critical field measurements were made on triple-layer films consisting of two outer layers of a PbBi alloy and an inner layer of silver. Superconductivity is induced in the silver and disappears at a magnetic field sufficiently low that the conductivity of the PbBi layers is the same as in zero field. K_S/K_N for the silver layer can therefore be measured directly and from its temperature dependence information on the excitation spectrum in the silver can be obtained. The results indicate a complex spectrum that was approximated by assuming the existence of two gaps. From the dependence on silver layer thickness of these gaps, one gap was associated with excitations traveling perpendicular to the normal/superconductor interface. This is the gap that is determined by tunneling experiments, and its thickness dependence qualitatively fits the tunneling theory of McMillan. The other gap is associated with excitations traveling parallel to the interface and reflects the intrinsic properties of the silver. Both gaps were determined in this experiment, and from the gap associated with the parallel excitations, the value of NV for silver was calculated to be $.107 \pm .015$. The measurements of critical field as a function of temperature show that supercooling appears below a temperature T^* and that the supercooling field is proportional to temperature down to a temperature T_1, below which it stays constant. These results indicate that between T_c and T^* the field transition is of first order and is very well described by a temperature-dependent κ. A simple theoretical model is proposed to explain the saturation observed below T_c as well as the observed amount of supercooling. According to this model, the value of T_1 depends on the value of $(NV)_{Ag}$. The experimental results therefore lead to a second, independent estimate of NV for silver, equal to +.10, thus confirming the result from the gap analysis. The model further suggests that a $1/x$ spatial dependence of the order parameter should be observed in the ^{3}He temperature range and below. (Diss. Abstr. Int., B)

11822 RESPONSE OF HIGHLY DAMPED JOSEPHSON JUNCTIONS TO EXTERNAL, LOW-FREQUENCY NOISE CURRENTS. Kanter, H.; Vernon, F. J. Jr. (Aerospace Corp., El Segundo, Calif.). Phys. Rev., B; 2: 4694-6(1 Dec 1970).

The dc characteristics of superconducting point-contact junctions subjected to external noise currents are measured under the condition that the noise-frequency spectrum is below the Josephson frequency. It is shown that the curves are in agreement with a model based on modulation of the noise-free dc characteristic. Although in the low-bias-voltage region the shape of the curves is qualitatively similar to previous theoretical predictions for the case of high-frequency noise, for higher voltages the shapes are different. Quantitative differences exist over the whole range of bias voltage. (auth)

11823 SUPPRESSION OF AC HYSTERESIS ENERGY LOSS IN NONIDEAL TYPE-II SUPERCONDUCTOR WITH THE APPLICATION OF LONGITUDINAL MAGNETIC FIELD. Sugahara, Masanori (Yokohama National Univ., Japan); Yamada, Naohei. Jap. J. Appl. Phys.; 9: 1531(Dec 1970).

It is shown that the ac hysteresis losses in a 0.025-cm dia Nb-25% Zr wire, which limits the use of the alloy, are virtually eliminated at ~8°K if a longitudinal magnetic field of ~4 kG is applied to the wire. The critical current curve shows a maximum of ~140 A at 4 kG. (D.L.C.)

11824 INFRARED OPTICS OF HIGH-T_c SUPERCONDUCTORS. Hopfield, J. J. (Princeton Univ., N. J.). Comments Solid State Phys.; 111: 48-52(Jun-Jul 1970).

The major gap between theory and experiment for high-T materials is defined, and an attempt is made to show why the infrared optical properties of metals (from 2 to 20 μ) are of importance for bridging this gap. (M.H.R.)

11825 ISOTOPE EFFECT IN SUPERCONDUCTING CADMIUM. Fassnacht, R. E.; Dillinger, J. R. (Univ. of Wisconsin, Madison). Phys. Rev., B; 2: 4442-4(1 Dec 1970).

The superconducting transitions of ^{110}Cd, naturally occurring Cd, ^{114}Cd, and ^{116}Cd were measured. The transition temperatures T_c were found to be 0.5218, 0.5173, 0.5148, and 0.5115°K, respectively, giving $z = 0.385 \pm 0.015$ and $\zeta = 0.23$ as parameters in $T_c \propto M^{-z} = M^{-0.5(1-\zeta)}$. These results are compared with various theoretical predictions. (auth)

11826 SUPERCONDUCTING Pb–Pb TUNNELING NEAR T_c. Wyatt, P. W.; Yelon, A. (Yale Univ., New Haven). Phys. Rev., B; 2: 4461-7(1 Dec 1970).

Electron tunneling from Pb films into (111)-oriented Pb films was measured at temperatures from 1.2 to 7.2°K. Above 6°K, structure in dV/dI at voltages greater than 2Δ is observed which is not the same as that found at low temperature. One new feature, a resistance maximum just outside 2Δ, is shown by a numerical calculation to arise from the occupation of excited states above the gap. The other, a resistance peak at 3.5 mV, is shown by further calculation to be associated primarily with the phonon-emission structure described by strong-coupling theory. It is found that the effect of the previously predicted recombination process, also located at 3 to 4 mV, is too broad to be clearly identified. (auth)

11827 rf-INDUCED EFFECTS IN SUPERCONDUCTING TUNNEL JUNCTIONS. Hamilton, C. A.; Shapiro, Sidney (Univ. of Rochester, N. Y.). Phys. Rev., B; 2: 4494-503(1 Dec 1970).

Arguments are presented to resolve experimental discrepancies with the theory of photon-assisted tunneling. A standing-wave model is suggested as a more realistic picture of the rf fields in a thin-film tunnel junction. By including the effects of this model in the theories of Tien and Gordon and of Werthamer, qualitative agreement is obtained with data on both the Josephson effects and the photon-assisted tunneling effects in the same junction. In an experiment with a junction sufficiently small to maintain a uniform rf field, excellent agreement with the unmodified theory was found. The low-frequency equivalence of the photon-assisted tunneling phenomenon and classical rf detection is also pointed out and used to demonstrate that the magnitude of the rf voltage appears correctly in the theory. It is concluded that the Werthamer theory of rf-induced effects in superconducting tunnel junctions is on very firm experimental ground. (auth)

11828 SURFACE IMPEDANCE OF A CLEAN TWO-BAND SUPERCONDUCTOR NEAR H_{c_2}. Tang, I-ming (Reed Coll.; Portland, Oreg.). Phys. Rev., B; 2: 4505-7(1 Dec 1970).

The surface impedance is calculated for two-band superconductors in the mixed state near H_{c_2}. The electromagnetic response function for the two-band system is seen to be the sum of the electromagnetic response in the individual bands. The individual response functions are then evaluated using a technique developed by Caroli and Maki. The resulting two-band expression for the surface impedance in the mixed state near H_{c_2} is used to analyze surface-impedance measurements on niobium. Both the purity dependence and the anisotropy in the surface impedances observed by Hibler and Maxwell can be accounted for qualitatively by the two-band expression. (auth)

11829 FLUX MOTION THROUGH THE SUPERCONDUCTING SURFACE SHEATH. Gosselin, J.; Silcox, J.; Trefny, J. U. (Cornell Univ., Ithaca, N. Y.). Phys. Rev., B; 2: 4508-10(1 Dec 1970).

The response $\bar{b}$ of Pb–2% In alloy specimens in the superconducting surface-sheath state to a small ac field $\bar{h}$ with a triangular waveform was studied. Features noted with this approach include a precursor, a plateau, and an exponential approach of $\bar{b}$ to $\bar{h}$. These observations and others point to the necessity of a more complete model for flux passage through the sheath. An analytical expression, based on a model of creep of flux spots in the sheath, is found to give an excellent quantitative description for Pb–2% In alloy specimens. The activation energy for the process is 10^{-3} eV < U_0 < 10^{-2} eV and the activation distance is greater than 10 Å. This latter value is regarded as low but may result from geometrical effects within the sheath. (auth)

11830 CASE FOR A SECOND ENERGY GAP IN SUPERCONDUCTING NIOBIUM. Hafstrom, J. W.; MacVicar, M. L. A. (Massachusetts Inst. of Tech., Cambridge). Phys. Rev., B; 2: 4511-16(1 Dec 1970).

Low-temperature tunneling studies of high-purity single crystals of niobium indicate the existence of two energy gaps Δ_s and Δ_d, one for each of the two bands lying at the Fermi level. The value of Δ_s is approximately $\Delta_d/10$. The crystallographic dependence of Δ_s indicates that Δ_s does not appear in directions where there is no s–d overlap at E_F. The behavior of Δ_s with temperature and magnetic field indicates that interband coupling is significant in niobium. The results are related to current theories of multiband superconductivity. (auth)

11831 MULTICORE SUPERCONDUCTORS FOR LABORATORY-SCALE MAGNETS AND FOR BIG MAGNETS. Hillmann, H. (Vacuumschmelze GmbH, Hanau, Ger.). Z. Angew. Phys.; 30: 233-8(16 Nov 1970). (In German).

Multicore superconductors will be used for large magnets and laboratory coils. In magnet coils with high stored energies, fully stabilized superconductors will be used. The stability criterion from Stekly will be applied for designing fully stabilized composites. The physical properties, especially the critical current densities and the recovery density of some fully stabilized composites, are discussed. Intrinsically filament composites based on new theoretical considerations were developed. They show no flux jumps when flux penetrates, and heat losses are low. Properties and designing of these intrinsically stable composites are discussed. (auth)

11832 MICROSTRUCTURAL EFFECTS IN CRITICAL FIELDS OF NIOBIUM FILMS. Connella, M. J.; Deck, R. J.; Morriss, R. H. (Tulane Univ., New Orleans). J. Appl. Phys.; 41: 5346-8(Dec 1970).

It was found that critical fields are higher in the perpendicular direction ($H_{c\perp}$) than in the parallel direction ($H_{c\parallel}$) at 4.2°K in oriented Nb films grown on MgO substrates. The epitaxial-growth pattern was (001) bcc Nb parallel to (001) MgO. The difference between $H_{c\perp}$ and $H_{c\parallel}$ tends to increase with decreasing grain size. (D.L.C.)

11833 EXAMINATION OF FLUXON BEHAVIOUR BY ANALOGY WITH A FLOATING MAGNETIC MODEL. Melville, P. H. (Central Electricity Research Labs., Leatherhead, Eng.); Taylor, M. T. Cryogenics; 10: 491-7(Dec 1970).

Work on a floating magnet model of a lattice of fluxons in type II superconductors by Rose–Innes and Stangham was extended, and the effects of flux pinning and flux motion were examined. Fluxon–fluxon forces appear very important in determining the way the lattice is pinned, and a theory is developed to show how this effect works in a simple case. Motion of fluxons through the model is restricted to movement in narrow channels. This provides a better understanding of the forces on fluxons during flux flow. (auth) (UK)

11834 SOME EXPERIMENTAL INVESTIGATIONS OF THE KAPITZA RESISTANCE OF LEAD. Cheeke, J. D. N. (CNRS, Grenoble, France). Cryogenics; 10: 463-72(Dec 1970).

Results are presented of the Kapitza resistance of lead specimens between 1 and 2°K. The specimens underwent surface treatments that included annealing, electropolishing, argon ion bombardment, and finally surface preparation by guillotining under liquid helium. The difference in Kapitza resistance between normal and superconducting states is seen to be compatible with the presence of a bulk thermal resistance due to mechanical strain which is operative in the superconducting state only. A preliminary result on a Pb–20 at. % In alloy is also given. (auth) (UK)

11835 VOLTAGES INDUCED IN SUPERCONDUCTORS BY SUPERIMPOSED ac AND dc MAGNETIC FIELDS. Joiner, W. C. H.; Ohmer, Melvin C. (Univ. of Cincinnati). Solid State Commun.; 8: 1811-14(15 Nov 1970).

The superposition of ac and dc magnetic fields on superconducting foils produces dc and harmonic voltages in those foils. The dc voltage reverses sign with a reversal of polarity of the dc magnetic field. These voltages are identified with the decay of shielding currents. The harmonic voltages are thus a result of the nonlinear relationship between the magnetization and the fields. (auth) (UK)

11836 DEPENDENCE OF s–f EXCHANGE ON ATOMIC NUMBER IN RARE EARTH DIALUMINIDES. Maple, M. B. (Univ. of California, San Diego, La Jolla). Solid State Commun.; 8: 1915-17(15 Nov 1970).

The relative variation of the magnitude of the s–f exchange coupling parameter $|J_{sf}|$ with rare earth (RE) atomic number was determined within the deGennes model from the depression of the superconducting transition temperature of the cubic Laves-phase compound $LaAl_2$ by RE impurities. The results compare favorably with measurements of $|J_{sf}|$ made on the isostructural series of compounds $(RE)Al_2$. (auth) (UK)

11837 EFFECT OF NOISE ON THE CURRENT–VOLTAGE CHARACTERISTICS OF A JOSEPHSON JUNCTION. Lee, Patrick A. (Univ. of Arizona, Tucson). J. Appl. Phys.; 42: 325-34(Jan 1971).

The effect of noise on the current–voltage characteristic of a Josephson junction is investigated (1) when the temperature is near the transition temperature of the superconductors and (2) when the junction is driven by an external signal. In case (1) the noise source is the quasi-particle tunneling current but in case (2) there is in addition the noise arising from the finite linewidth of the external signal. This latter noise source is shown to dominate when the junction is operating at high harmonics. The problem is treated in the limits of small and large capacitance, and a criterion is obtained to determine under what circumstances each limit applies. A solution that includes a first-order correction due to a finite capacitance is given. In the limit of large capacitance the existence and lifetime of hysteresis curves are discussed. (auth)

11838 MAXIMAL OUTPUT POWER OF POINT-CONTACT JOSEPHSON JUNCTIONS. Fack, H.; Kose, V. (Physikalisch-Technische Bundesanstalt, Brunswick). J. Appl. Phys.; 42: 322-3(Jan 1971).

A simple model is considered in order to describe point-contact Josephson junctions as oscillators. The maximal output power of these generators into a matched load is determined as a function of frequency. (auth)

11839 PULL-IN PHENOMENA OF JOSEPHSON OSCILLATORS. Fack, H.; Kose, V. (Physikalisch-Technische Bundesanstalt, Brunswick). J. Appl. Phys.; 42: 320-2(Jan 1971).

Constant voltage steps in dc current–voltage characteristics occur by assuming pull-in phenomena. Based on this concept, steps above the gap voltage and frequency dependence of the step amplitudes are found. (auth)

11840 TRANSITION-FIELD ENHANCEMENT AND SHAPE EFFECTS DUE TO MAGNETIC INCLUSIONS IN A SUPERCONDUCTOR. Lebeau, C.; Pinel, J.; Rosenblatt, J. (Institut National des Sciences Appliquees, Rennes, France). J. Appl. Phys.; 42: 323-4(Jan 1971).

Magnetization curves of spherical and cylindrical superconductors made of a fine suspension of Fe grains in Hg were measured. The experiments show that the transition field depends strongly on both the magnetization of the ferromagnetic system and on shape of the sample. (auth)

11841 BOUND STATES IN A SUPERCONDUCTOR CONTAINING A MAGNETIC IMPURITY. Sato, Hirokazu; Maki, Kazumi (Tohoku Univ., Sendai). Progr. Theor. Phys. (Kyoto); 44: 865-78 (Oct 1970).

The bound states associated with a magnetic impurity in a superconductor are studied, by making use of the Bethe–Salpeter equation for a quasi particle (in the BCS state) and a quasi fermion describing the impurity spin. The bound-state energy is determined as a function of the s–d exchange potential J. In particular it is found that the triplet bound state appears for all positive J(i.e., in the case of ferromagnetic coupling) and for J negative and $T_K > T_{c0}$ where T_K is the Kondo temperature and T_{c0} is the superconducting transition temperature of the host metal, and that the singlet bound state appears for a negative J and $T_K < T_{c0}$. These results are in complete agreement with recent calculations in the framework of the S-matrix theory. Furthermore, the wave function of the bound state is calculated; this will be of importance in calculation of the transition probability associated with the local interaction. (auth)

11842 ELECTRON TUNNELING INVESTIGATION OF QUENCH-CONDENSED SUPERCONDUCTORS. Leslie, J. D.; Chen, J. T.; Chen, T. T. (Univ. of Waterloo, Ont.). Can. J. Phys.; 48: 2783-2803(1 Dec 1970).

An electron-tunneling investigation was carried out on quench-condensed Bi, Ga, Pb, $Pb_{.75}Bi_{.25}$, $Pb_{.50}Bi_{.50}$, and $Pb_{.25}Bi_{.75}$. The energy gap and transition temperature were measured for each sample. The tunneling derivative data were analyzed in terms of the strong-coupling theory of superconductivity by means of a computer program of W. L. McMillan. The effective phonon spectrum, the Coulomb pseudopotential, the complex energy gap function, the pairing self-energy function, and the electron renormalization function were determined for each sample. Certain parameters based on integrals over the phonon spectrum were also calculated for each sample. (auth) (Canada)

11843 ELECTRODYNAMICS OF STRONG-COUPLING SUPERCONDUCTING ALLOYS IN HIGH MAGNETIC FIELDS. Usadel, Klaus D. (Univ. of Montreal). Can. J. Phys.; 48: 2809-11 (1 Dec 1970).

The electromagnetic response of superconducting alloys in the electron–phonon model is investigated for situations where the electric field is parallel to the static magnetic field. It is shown that for ordinary microwave frequencies strong-coupling only renormalizes physical quantities, but does not change the form of the weak-coupling response function. (auth) (Canada)

11844 CRITICAL CARRIER CONCENTRATION FOR SUPERCONDUCTIVITY IN MIXED METAL–SEMICONDUCTOR SYSTEMS. van Maaren, M. H.; Harland, H. B.; Havinga, E. E. (Philips Research Labs., Eindhoven, Netherlands). Solid State Commun.; 8: 1933-5(15 Nov 1970).

The appearance of superconductivity in the systems $CuRh_{2-x}Sn_xSe_4$ and $Rh_{1-x}Ru_xSe_2$ coincides with anomalies in the normal Hall coefficient. The strong increase of the electronic heat-capacity coefficient in the superconducting part of the system appears to be entirely caused by phonon enhancement. The results imply that superconductivity occurs only if both electrons and holes are present at the Fermi surface. (auth) (UK)

11845 TRANSITION TEMPERATURE AND TEMPERATURE DEPENDENCE OF THE ENERGY GAP IN THIN FILM SUPERCONDUCTORS. Rajput, J. S. (Banaras Hindu Univ., India); Gupta, A. K. Phys. Status Solidi (a); 3: 485-91(16 Oct 1970).

The Gorkov equations are solved for a superconducting film. The important role of the energy-level quantization of single-particle states in thin films is explicitly taken into account from the beginning. The single-particle Green function is expanded in terms of the complete set of orthonormal wave functions. The Gorkov equations are then iterated to an arbitrary order. The energy gap in the quasi-particle spectrum is determined. The transition temperature for thin films is determined from the iteration to the lowest order, while the temperature dependence of the energy gap near the transition temperature is determined from iteration up to the third order. The temperature dependence of the energy gap can be determined up to lowest temperatures; thanks to the orthonormality of the eigenfunctions, it is possible to write down all the terms of the series in quite a simple form. Numerical results are presented for thin films by taking the iterated solution up to the third order only. (auth)

11846 SUPERCONDUCTIVITY FOR TERNARY fcc Bi–Pb–Tl ALLOYS. Claeson, T.; Munkby, L.; Wingbro, T. (Chalmers Univ. of Tech., Goteborg). Phys. Status Solidi; 42: 321-7(1 Nov 1970).

The superconducting transition temperatures were measured for several fcc ternary Bi–Pb–Tl alloys. The transition temperature is essentially determined by the number of valence electrons per atom. A phase transition to a hcp phase extends from $BiTl_3$ into the ternary system giving rise to broad transitions to the superconducting state. The T_c of a hypothetical fcc Tl phase was extrapolated to 1.75°K. The electron–phonon coupling strength could be estimated from T_c and the Debye temperature using a theory by McMillan. The variation of the coupling strength with concentration of Tl in Pb shows a greater similarity with expectations regarding the density of electron states at the Fermi level than with an empirical curve by McMillan based upon the phonon distribution. (auth)

11847 HEAVY HOLES AND SUPERCONDUCTIVITY IN GeTe AND SnTe. Lewis, J. E. (State University Coll., Plattsburgh, N. Y.). Phys. Status Solidi; 42: K97-9(1 Nov 1970).

The observed superconducting transition temperature T_c dependence on Hall carrier concentration p^* can be fitted for SnTe but not GeTe using the theory of Koonce et al. for low-carrier-density, many-valley systems. An explanation is offered which is based on the minority heavy hole carriers. The second valence band which occurs in both SnTe and GeTe has a heavier effective mass and lower mobility in GeTe than the upper band, and thus it becomes densely occupied only above a threshold carrier concentration. It is argued that the superconductivity in GeTe and SnTe is due to the heavy-mass holes only, the light holes behaving normally. Hence, superconductivity in SnTe is observed at all carrier concentrations, while in GeTe, T_c should increase with $\exp(p^{\frac{1}{3}})$, where p is the heavy hole carrier density. A plot of $\ln T_c$ vs p confirms this hypothesis. (D.L.C.)

11848 EFFECT OF NEUTRON IRRADIATION AT 4.6 K ON THE CRITICAL TEMPERATURE OF SUPERCONDUCTING NIOBIUM. Berndt, H.; Sernetz, F. (Zentralinstitut fuer Teiftemperaturforschung, Garching, Ger.). Phys. Lett.; 33A: 427-8(14 Dec 1970).

The critical temperature T_c of superconducting Nb decreases with increasing residual resistance ρ_0 produced by neutron irradiation. In agreement with theory the parameter for the energy-

gap anisotropy $\langle a^2 \rangle = 0.006$ was found. Subsequent annealing shows a hysteresis of T_c versus ρ_n. (auth)

11849 PRESSURE DEPENDENCE OF THE SUPERCONDUCTING TRANSITION TEMPERATURE FOR NIOBIUM. Smith, T. F. (Univ. of California, San Diego, La Jolla). Phys. Lett.; 33A: 465-6(14 Dec 1970).

Since disagreement exists regarding the pressure dependence of the superconducting transition temperature for niobium, data taken under what is believed to be the closest to hydrostatic pressure conditions as yet employed are presented. From measurements on five samples of niobium, it is found that $\partial T_c/\partial P = -0.20 \pm 0.03 \times 10^{-5}$ °K/bar. (M.H.R.)

Equipment and Devices

Refer also to abstract 12034.

11850 SUPERCONDUCTING WIRED-WALL CAVITY FOR V-BAND ENDOR EXPERIMENT. Yagi, Hisao; Inoue, Masasi; Tatsukawa, Toshiaki; Yaeguchi, Osami; Kato, Susumu (Fukui Univ., Japan). Jap. J. Appl. Phys.; 9: 1534(Dec 1970).

The Q of the wired-wall cavity for V-band (50 GHz) ESR and ENDOR is ~3500. In an attempt to improve this Q, superconducting Nb–Ti wire was used; its surface impedance was estimated to be small enough at 4.2°K. From the synchroscope traces, Q below T_c was found to increase remarkably. No difference in the ESR shape was observed, and the ENDOR signals were much stronger. (D.L.C.)

11851 SUPERCONDUCTING MAGNET RESEARCH. Coles, W. D.; Laurence, J. C.; Brown, G. V. (Lewis Research Center, Cleveland). Cryog. Ind. Gases; 5: 15-20(Nov-Dec 1970).

Research at NASA's Lewis Research Center is described under the following headings: cryogenically cooled coils, superconducting magnets, magnet design and construction, magnet system, and liquid helium consumption. (M.H.R.)

11852 TEMPERATURE SCALE FOR NEODYMIUM ZINC NITRATE BELOW 1K. Sapp, R. C. (Univ. of Kansas, Lawrence); Tschanz, J. F. Cryogenics; 10: 498-500(Dec 1970).

The thermodynamic temperature scale, as a function of initial conditions for adiabatic demagnetization, was constructed for single crystals of $Nd_2Zn_3(NO_3)_{12} \cdot 24H_2O$ between 0.01 and 1°K using, as a thermometer, the anisotropy of gamma rays following the decay of ^{60}Co. This material should be useful for orientation of nuclides of rare earth and iron transition series elements by thermal equilibrium methods. (auth) (UK)

11853 PHASE FLUCTUATIONS OF THE SIGNAL OF A TRAVELLING WAVE TUBE GENERATOR WITH SUPERCONDUCTING RESONATOR. Kukushkin, A. V.; Nasonov, V. S. (Physical Tech. Inst., Leningrad). Cryogenics; 10: 503-4(Dec 1970).

The oscillator system comprises superconducting resonators connected in negative feedback with a travelling tube. A graph is given to show the dependence of the voltage standing wave ratio at two inputs of the superconducting resonator on tuning. Graphs are also given showing the dependence of oscillator frequency on the change in phase advance in the negative feed back circuit and on the voltage on the travelling-wave tube control electrode. The spectral distributions of phase fluctuations of the oscillator signals were also measured and a graph is given. The system was found to have a signal comparable in spectral characteristics to the signal of a quartz oscillator. (UK)

Plasma and Thermonuclear Physics

11854 (EUR-CEA-FC-542(Pt.1)) EURATOM–CEA ASSOCIATION PLASMA PHYSICS AND CONTROLLED FUSION DEPARTMENT (FONTENAY-AUX-ROSES). Progress Report of the Research Group for 1st of April 1969–28th of February 1970. (European Atomic Energy Community. Commissariat a l'Energie Atomique, Fontenay-aux-Roses (France). Centre d'Etudes Nucleaires). 1970. 121p. (In French). Dep. NTIS (U. S. Sales Only).

The scientific results obtained by the Services and Sections in 1969 are presented. The Ionized Gas Theory Section presents a brief account of published and current work. The Plasma Physics Section gives an account of the work undertaken: interaction mechanisms between radiation and matter, nonlinearities associated with the propagation of waves in plasmas, and microinstabilities and spectroscopy. The activities of the Plasma Confinement Group are presented in three chapters: confinement in an open configuration, confinement in a closed configuration, and formation and heating of the plasma. (auth) (France)

11855 (EUR-CEA-FC-542(Pt.2)) EURATOM–CEA ASSOCIATION PLASMA PHYSICS AND CONTROLLED FUSION DEPARTMENT (GRENOBLE). Progress Report of the Research Group for 1st of April 1969–28th of February 1970. (European Atomic Energy Community. Commissariat a l'Energie Atomique, Fontenay-aux-Roses (France). Centre d'Etudes Nucleaires). 1970. 118p. (In French). Dep. NTIS (U. S. Sales Only).

The scientific results obtained during 1969 and up until March 1970 by the Plasma Physics and Controlled Fusion Department of Grenoble are presented. The Department consists of the General Ion Technology Service and the Wave–Plasma Interaction Section. The following subjects were studied: turbulent diffusion, microinstabilities and stabilization using curvature and shear effects in the confining magnetic fields; the acceleration, confinement, and heating of a plasma using the pairing action of the high-frequency fields associated with the static magnetic fields in the region of a characteristic resonance (electron cyclotron or a lower hybrid); the stabilization of drift instabilities by the action of an oscillating electric field, parallel to the confining magnetic field; the properties of the plasmas; advanced technology, production of strong magnetic fields, cryogenic pumping, high power oscillators and the applications of optical methods to the microwaves. (France)

11856 TECHNOLOGY INDEX FOR PLASMAPHYSICS RESEARCH AND FUSION REACTORS. VOLUME 4, NO. 11, 1970. Bibliography, Author Index, Subject Index, Appendix. Frankfurt am Main; Zentralstelle fuer Atomkernenergie-Dokumentation (1970). 55p.

This listing includes 204 articles on various aspects of plasma physics and fusion reactors. (M.O.W.)

11857 PLASMA PHYSICS INDEX. VOLUME 5, NO. 10, 1970. Bibliography, Author Index, Subject Index. Frankfurt am Main; Zentralstelle fuer Atomkernenergie-Dokumentation (1970). 112p.

This listing includes 525 articles on various aspects of plasma physics. (M.O.W.)

11858 TECHNOLOGY INDEX FOR PLASMAPHYSICS RESEARCH AND FUSION REACTORS. VOLUME 4, NO. 10, 1970. Bibliography, Author Index, Subject Index, Appendix. Frankfurt am Main; Zentralstelle fuer Atomkernenergie-Dokumentation (1970). 45p.

This listing includes 233 articles on various aspects of plasma physics and fusion reactors. (M.O.W.)

Confinement and Heating

Refer also to abstract 12045.

11859 (EUR-CEA-FC-563) FILLING OF A MAGNETIC WELL BY INJECTION OF NEUTRAL ATOMS AT VARIOUS ANGLES AND ENERGIES. Dei-Cas, R.; Hennion, F. (European Atomic Energy Community. Commissariat a l'Energie Atomique, Fontenay-aux-Roses (France). Centre d'Etudes Nucleaires). Nov 1970. 54p. (In French). Dep. NTIS (U. S. Sales Only).

Numerical calculations concerned with filling a magnetic well (minimum B configuration) using multi-injection by ten sources at different energies injected at different angles, are presented. The model enables spatial–temporal changes in density, anisotropy, and energy distribution to be studied. The real geometry of the magnetic field, ion pumping effects, and the bombardment of the walls by the particles are taken into consideration. Stable plasmas with densities up to the order of 10^{12} cm^{-3} ($\omega_{pi}/\omega_{ci} \simeq 10$) could be achieved with total currents of the order of 700 mA, when the initial residual pressure was 3×10^{-8} mm of Hg. With these injection conditions, the final characteristics of the plasma were: ion density at the center 10^{13} cm^{-3}; plasma decay time 0.1 to 1 second; and mean ion temperature 10 keV. (auth) (France)

11860 (FTI-282) HIGH FREQUENCY PLASMA HEATING NEAR THE LOW-HYBRID FREQUENCY. Galaktionov, B. V.; D'yachenko, V. V.; Shcherbinin, O. N. (Akademiya Nauk SSSR, Leningrad. Fiziko-Tekhnicheskii Institut). 1970. 14p. (In Russian). Dep. NTIS (U. S. Sales Only).

Some experiments on the hf heating of a hydrogen plasma are described. The boundary of efficient heating was found at the magnetic fields corresponding to the low hybrid frequency. The energy input decreased considerably below the critical field. The plasma density was determined when the efficiency of the coupling circuit was at a maximum. From an analysis of the diamagnetic pressure distribution along the discharge tube, it became possible to separate the diamagnetic effects due to ions and elec-

trons. The energy of ions and electrons was nearly the same. (auth)

11861 (NP–18635) CONDITIONS OF PLASMA HEATING AT ELECTRON CYCLOTRON RESONANCE. Vinogradov, N. I.; Podushnikova, K. A.; Poloskin, B. P. (Akademiya Nauk SSSR, Leningrad. Fiziko-Tekhnicheskii Institut). 1970. 15p. (In Russia). Dep. NTIS (U. S. Sales Only).

Conditions of formation of a group of fast particles (up to 100 keV) and heating dynamics of this group and of the main electron plasma component (up to 100 eV) were studied during electron cyclotron heating. It was found that the efficiency of heating of the main component and of the group of fast electrons depends on the position of the resonance region in the chamber. The rate of heating of the main group is ~10^8 eV/sec and the rate of heating of the fast particles is ~7×10^9 eV/sec. Analysis of the data revealed that heating of the main component may occur in a nonresonance region and, for the fast particles, in a resonance region. (R.V.J.)

11862 STUDIES OF TURBULENT HEATING OF HYDROGEN PLASMA BY NUMERICAL SIMULATION. Morse, R. L.; Nielson, C. W. (Los Alamos Scientific Lab., N. Mex.). Phys. Rev. Lett.; 26: 3-6(4 Jan 1971).

One-dimensional numerical simulation of the development of the ion–acoustic instability in a plasma with mass ratio 1836 shows considerable electron heating but only small high-temperature tails or large-amplitude, undamped ion–acoustic waves in the ion distribution. (auth)

11863 PLASMA CONTAINMENT IN A SPHERICAL MULTIPOLE MAGNETIC TRAP. Sadowski, M. (Inst. of Nuclear Research, Warsaw). J. Plasma Phys.; 4: 1-12(Feb 1970).

A method of plasma containment by means of spherical multipole (SM) magnetic fields was developed. The analysis of the confining field geometry proved that the high-order SM-configurations constitute minimum-B traps with a given number of point cusps instead of linear loss gaps which occur in a standard minimum-B geometry. Injection and trapping of a gun-produced plasma in the SM magnetic trap were investigated and compared with those in a spindle-cusp trap. (auth) (UK)

11864 RADIO-FREQUENCY HEATING OF A PLASMA. Cross, R. C. (Univ. of British Columbia, Vancouver). Can. J. Phys.; 48: 2888-93(1 Dec 1970).

It is shown that if a uniform plasma is surrounded by a heating coil in the presence of a steady axial magnetic field, a considerable increase in power absorption may be expected if the operating frequency is chosen to be close to a magneto-acoustic resonance of the plasma column. This effect is due to a very large increase in the oscillating field at the center of the plasma column. For an initially cool plasma, heating is due to a combination of ohmic and collisional heating, while at higher temperatures, collisional heating by magnetic pumping is the dominant heating mechanism. (auth) (Canada)

Diagnostics

Refer also to abstract 11690.

11865 (CEA-R–4058) THOMSON SCATTERING IN LASER CREATED PLASMA. Decroisette, Michel (Commissariat a l'Energie Atomique, Limeil-Brevannes (France). Centre d'Etudes). Sep 1970. 22p. (In French). Dep. NTIS (U. S. Sales Only).

The scattered spectrum of monochromatic radiation incident from a laser-created plasma is computed, using the Salpeter theory and taking into account the inhomogeneity of the plasma. The FORTRAN program can be used to calculate the average parameters of the plasma from a given profile. The shape of the complex spectrum is shown to be generally associated with the most dense zone, which is also the hottest. (tr-auth) (France)

11866 (EUR-CEA-FC–570) REVIEW ON CORRELATION MEASUREMENTS IN PLASMA. Bernard, M.; Briffod, G.; Bussac, J. P.; Frank, R.; Gregoire, M.; Touzeau; Weisse, J. (Commissariat a l'Energie Atomique, Fontenay-aux-Roses (France). Centre d'Etudes Nucleaires). Oct 1970. 25p. (CONF-700548–1). Dep. NTIS (U. S. Sales Only).

From Symposium on Plasma Diagnostics, Sukhumi, USSR.

Two ways in which correlation techniques are particularly useful are presented: turbulent diffusion studies (measurement of particle losses and diffusion coefficients); and investigation of fluctuations and instabilities. In the first case it is necessary to measure the correlation time and correlation lengths of the fluctuating electric field as well as the correlation coefficient $\langle \tilde{N}\,\tilde{V}\rangle = \langle \tilde{N}\,\tilde{E}\theta/B_0\rangle$. In the second case, the measured autocorrelation and cross-correlation functions of the plasma parameters are time and space Fourier transformed. Hence, either the energy spectrum of the fluctuations and their dispersion relation for a linear model or the structure of the wave packets for nonlinear cases, can be deduced. Correlation measurement systems and the experimental work are reviewed. The results which were obtained in the laboratory on a hydrogen diffusion plasma with static magnetic field are then more precisely described. (auth) (France)

11867 (MATT–818) MEASURING CURRENT DISTRIBUTION IN A TOKAMAK PLASMA. Perkins, F. W. (Princeton Univ., N. J. Plasma Physics Lab.). Dec 1970. Contract AT(30-1)-1238. 17p. Dep. NTIS.

It is proposed to measure the current distribution in a tokamak plasma by measuring the (pitch) angle which the magnetic field makes with respect to the direction of a purely toroidal magnetic field, and then using Ampere's law. This measurement is carried out by observing the spectrum of CO_2 laser light scattered by the plasma. As the difference between the incident and scattered wave vectors of the laser light approaches perpendicularity with the magnetic field, the spectrum changes qualitatively from the usual Gaussian spectrum to a series of sharp lines separated by the electron gyrofrequency. An angular resolution of ~0.5° may be obtained. A feasibility study produces a signal-to-noise ratio of 80. (auth)

11868 (SC-T–70-4054) A METHOD FOR INFRARED DIAGNOSTICS OF A PLASMA AND ITS APPLICATION FOR INVESTIGATION OF IONIZATION AND RECOMBINATION OF XENON BEHIND THE FRONT OF A SHOCK WAVE. Generalov, N. A.; Zimakov, V. P.; Kozlov, G. I. Translated by Marcel I. Weinreich (Sandia Labs., Albuquerque, N. Mex.), from Zh. Eksp. Teor. Fiz.; 58: 1928-37(1970). 26p. Dep. NTIS.

An abstract of this paper, prepared from the original language, appeared as NSA 24: 40045. (M.O.W.)

11869 CO_2 LASER HETERODYNE PLASMA DIAGNOSTICS IN AN ADVERSE ENVIRONMENT. Zucker, O. S. (Univ. of California, Livermore). J. Appl. Phys.; 42: 306-7(Jan 1971).

A CO_2 laser heterodyne system was successfully used to measure plasma density-length product (DLP) in the 10^{13} to 10^{14}-cm^{-2} range, with μsec response. This was done in the extremely adverse environment of the Astron-controlled fusion experimental area at the Lawrence Radiation Laboratory, Livermore. The results indicate that the system is capable of covering a plasma DLP range of 10^{12} to 10^{16} cm^{-2} with 20-nsec response. (auth)

11870 MULTILAYER TARGETS AS A DIAGNOSTIC TOOL FOR LASER-PRODUCED PLASMAS. Seka, W.; Schwob, J.-L.; Breton, C. (EURATOM–CEA, Fontenay-aux-Roses, France). J. Appl. Phys.; 42: 315-19(Jan 1971).

A novel experimental method employing multilayer targets was developed permitting a more detailed study of laser-produced plasmas through analysis of the spectrum emitted by a given layer as a function of its location. This method allows one to study the progression of the interaction phenomena into the interior of the target and to examine the plasma expansion phase. It could thus be demonstrated that the plasma produced at different depths within the target has essentially the same characteristic parameters and that the hot plasma region is delimited by very sharp gradients towards the interior of the target. In the expansion phase the importance of recombination phenomena has been well established up to certain limits beyond which these observations are compatible with the notion of freezing of the degree of ionization at closed-shell electron configurations in carbon and aluminum plasmas. A comparison of the experimental results with simple theoretical models is included. (auth)

11871 INTERFEROMETRIC INVESTIGATIONS OF PLASMA IN A COAXIAL HIGH-CURRENT ACCELERATOR USING A HELIUM–NEON LASER. Zavenyagin, Yu. A.; Dontsov, Yu. P. Zh. Prikl. Spektrosk.; 12: 622-6(Apr 1970). (In Russian).

The methodology of measurement of plasma density by means of a gas laser and a multiray interferometer, placed in a vacuum chamber, was established. The radial distribution of electron density at specific periods of time was obtained. (tr-auth)

11872 CHARGED-PARTICLE DISTRIBUTION FUNCTION MEASUREMENT IN A TOROIDAL OCTUPOLE AND IN A STREAMING PLASMA. Kuswa, Glenn Wesley. Madison, Wis.; Univ. of Wisconsin (1970). 195p. University Microfilms Order No. 70-19,159.

Thesis.

Electrostatic energy analyzers were used to measure the distribution functions of ions and electrons in an inductively excited

toroidal octupole. Plasmas injected by external guns, heated by microwaves, created by microwave breakdown of gas, and injected by miniature guns placed within the octupole were examined. Most measurements were made in the low magnetic field region near the center of the octupole. The results of the distribution function measurements were compared, when possible, with results obtained using Langmuir probes, scintillator probes, and microwave diagnostics. Several types of mass spectroscopy were used to estimate impurity content in the hydrogen plasma. Parameters of interest were density, electron and ion temperatures or average energies, anisotropy of the distributions, and floating and plasma potentials. The effects of obstacles, background gas density, induced electric fields, and the magnetic field strength of the octupole were examined and compared with theoretical estimates. Proton loss rates proportional to velocity were found to hold above ~10 eV and below ~500 eV, the containment limit for the usual magnetic strength. A similar loss dependence was noted for electrons from ~50 eV up to at least 40 keV, the upper limit of the measuring equipment. The effects of aperture contamination and space-charge expansion on distribution function measurements were established. The effect of probe material upon floating-potential measurements was examined, and corrected values of floating potential were related to plasma potential measurements made using particle cutoff techniques. The flow of plasma through a 0.64-cm-i.d. by 45-cm-long high-magnetic-permeability tube, used to guide particles from the magnetic well to the outside of the octupole, was examined. On the basis of this work, a new simplified version of a gridded probe is suggested. A conical θ-pinch plasma source producing a single burst (typically 3×10^5 m/sec) of hydrogen plasma was developed and examined with an electron energy analyzer at various distances from the source. A novel detector, employing a flexible fiber optic light guide to couple a scintillator, held at high potential, to a photomultiplier, gave the necessary sensitivity, time response, and freedom from ground loops to make possible measurements at positions arbitrarily close to the gun. Useful measurements were obtained at densities beyond the range of Langmuir probes. (Diss. Abstr. Int., B)

11873 BEHAVIOR OF LOW-DENSITY PLASMAS IN THE PRESENCE OF CYLINDRICAL LANGMUIR PROBES. Szuszczewicz, Edward Paul. St. Louis, Mo.; St. Louis Univ. (1969). 160p. University Microfilms Order No. 70-20,427.

Thesis.

An electron-bombardment conical-anode plasma generator was systematically studied as a source of low-density Maxwellian argon plasmas. The electron densities and temperatures measured by the standard techniques of Langmuir probes were in the range $10^5 \lesssim N_e[cm^{-3}] \lesssim 10^9$ and $500 \lesssim T_e[°K] \lesssim 10^5$. Homogeneous radial profiles of approximately 12 cm cross section were observed for N_e and T_e when $P > 10^{-4}$ torr. When the pressure was in the range $P \leq 10^{-4}$ torr, density gradients were observed which increased with decreasing pressure. The plasma generator was subsequently used to investigate the validity of the theoretical prediction of orbital-motion-limited (OML) currents by Laframboise for an ion-collecting cylindrical Langmuir probe imbedded in a collisionless, Maxwellian plasma. The experimental investigation was conducted under conditions for which $(R_p/\lambda_{ee})_{max} = 1/330$, $(R/\lambda_{ii})_{max} = 1/32$, and $(R_p/\lambda_{ia})_{max} = 1/29.4$, and yielded results which substantiate the existence of OML currents. This agreement with the theoretical prediction of Laframboise is believed to be primarily a result of careful adherence to the conditions imposed upon a laboratory plasma in the collisionless limit. Previous investigations of Sonin and Bell showed no evidence of OML current behavior. It is demonstrated that the charged particle collision frequencies in their plasmas were too large to permit a collision-free description in the presence of Langmuir probes. Specifically it is shown that values of R_p/λ_{ia} as small as 0.2 can lead to plasma behavior totally different from that expected in the collision-free case. (Diss. Abstr. Int., B)

11874 USE OF OPTICAL SPECTRA TO MEASURE LARGE ELECTRIC FIELDS IN A HOT-ION PLASMA. Scott, F. R. (Oak Ridge National Lab., Tenn.); Neidigh, R. V.; McNally, J. R. Jr.; Cooper III, William S. J. Appl. Phys.; 41: 5327-9(Dec 1970).

Intense electric fields found in the beam–plasma interface of Burnout V give rise to satellite spectra of the helium 2^3P-4^3D, ^3F triplet (4471 Å), and the 2^1P-4^1D, ^1F singlet (4922 Å) emission lines. Electric-field strengths increasing from near zero on the magnetic axis to about 7 kV cm^{-1} at 1 cm, and then decreasing to less than 2 kV cm^{-1} at 2-cm radial distance, are found. An Abel inversion giving intensity of the satellite lines as a function of plasma radius, together with displacement and intensity of π and σ components in the Zeeman structure of the satellites, gives the electric-field strength and implies that the direction of the electric field is perpendicular to the magnetic axis. (auth)

11875 ANALYSIS OF THE VELOCITY FIELD IN PLASMAS FROM THE DOPPLER BROADENING OF SPECTRAL EMISSION LINES. Kaufman, A. S. (Bar-Ilan Univ., Ramat-Gan, Israel. Hebrew Univ., Jerusalem). Advan. At. Mol. Phys.; 6: 59-104 (1970).

The meaning of kinetic temperature and mass motion in a plasma is discussed, and a criterion is established for distinguishing between thermal motion and mass motion in a measurement of line broadening. Experimental methods of separating thermal motion from random mass motion are classified into two main classes according to whether the motion is examined by its average properties or statistically. The only method in the first class, the method of different ionic species, is then described in some detail. 130 references. (A.G.W.)

11876 MEASUREMENT OF LTE PLASMA TEMPERATURES BELOW 10,000 K. Johnston, P. D. (Electricity Council Research Centre, Capenhurst, Eng.). J. Phys., D (London); 3: 1999-2004(Dec 1970).

The technique described for measuring the temperature of a discharge in local thermodynamic equilibrium uses the total continuum emitted by the discharge when seeded with hydrogen. The combined intensity of the continuum caused by the negative hydrogen ion and the positive ion from the discharge gas, when divided by the intensity of a spectral line from either of the constituents, produces a function with a well-defined maximum at a certain temperature, from which other temperatures corresponding to other ratios can be determined. (auth) (UK)

11877 FEASIBILITY OF USING THE SUPER-HIGH-FREQUENCY RADIATION OF A PLASMA FOR AN ACCURATE MEASUREMENT OF ITS TEMPERATURE. Iosel'son, G. L. Meas. Tech. (USSR) (Engl. Transl.); No. 5, 703-7(May 1970).

Translated from Izmer. Tekh.; No. 5, 48-50(May 1970).

Certain problems in measuring the electron temperature of a plasma, based on its thermal shf radiation, are discussed. The efficiency of the method is described, taking into account the plasma emissivity. (M.O.W.)

Kinetics (General)

Refer also to abstract 11910.

11878 INTERACTION BETWEEN A FULLY IONIZED PLASMA AND A NEUTRAL GAS BLANKET. Lehnert, B.; Bergstroem, J.; Holmberg, S.; Wilner, B. (Royal Inst. of Tech., Stockholm). Phys. Scr.; 1: 39-45(1970).

Experimental studies were performed on a fully ionized magnetized plasma generated in a poloidal magnetic field by a transverse electric field applied between two electrodes and surrounded by a neutral gas blanket. The rotating plasma generated in the crossed fields is released from its energy source and its rotation stopped. The plasma decay is then studied in the absence of macroscopic motions, with the exception of those from a slow diffusion process. The state of ionization is determined by suddenly giving the plasma a small pulse of angular momentum which, after a short time, is recovered as a current pulse being extracted by means of a short circuit between the electrodes. The pulse becomes a measure of the state of ionization and shows that the rate of penetration of neutral gas into the plasma is strongly delayed at high plasma densities, in agreement with theory. The velocity field of a quasi-stationary, rotating plasma was investigated spectroscopically by observing the Doppler shifts of various spectral lines. The results agree with theoretical predictions of the velocity and temperature distributions within the plasma region. The results also support the prediction that the interior of the plasma should be screened from the surrounding neutral gas. (auth) (Sweden)

Kinetics (Experimental)

Refer also to abstract 11755.

11879 SCATTERING OF FAST ELECTRONS BY A GAS PLASMA. Boersch, H.; Geiger, J.; Topschowsky, M. (Technische Univ., Berlin). Z. Naturforsch.; 25a: 1411-17(Oct 1970). (In German).

The elastic and inelastic scattering of 25-keV electrons by argon and by an argon discharge was measured in the small angular region $\theta \leq 2 \times 10^{-2}$ rad. The angular resolution was 5×10^{-5} rad. The experimental result for scattering by neutral argon atoms is in agreement with theory. In the case of the argon plasma, where free charge carriers (ions and electrons) are present, the number of electrons scattered into the angular range $\theta \leq 10^{-3}$ rad increases enormously. It is shown that, because of

XUM

the large differential Rutherford cross section at small scattering angles, multiple scattering occurs by the free charge carriers. The densities of ions and of electrons in the plasma can be obtained from the width of the multiple scattering distribution. (auth)

11880 ION SCATTERING BY ELECTRIC FIELDS IN AN INERTIALLY CONFINED PLASMA. Stallings, Charles Henry. Madison, Wis.; Univ. of Wisconsin (1970). 177p. University Microfilms Order No. 70-19,174.

Thesis.

The plasma used in these experiments was produced with a conical theta-pinch gun. Two meters from the gun, a small amount of plasma passed through a slit of variable width. This slit was typically 0.2 mm in width. The analyzing system, after the slit, consisted of a 3-meter-long Faraday cage with an ion detector or electrostatic energy analyzer at the end. It was found that the ion energy distribution was a function of the width of the slit separating the main body of the plasma from the measuring apparatus. When the plasma passed through a slit, the perpendicular motion of the electrons caused them to move away from the ions. This charge separation produced an electric field perpendicular to the motion of the ions. The electric field changed the paths of the ions and therefore, changed the measured ion energy distribution. With a very small-acceptance-angle analyzer, the peak of the measured ion energy spectrum could be shifted from 300 to 400 eV by changing the size of a slit. The shape of the spectrum was also changed When the slit was five Debye lengths wide, 30% of the ions were scattered more than 15°, even though the ions had several hundred electron volts of energy and the electron temperature was only 2.3 electron volts. The correct ion energy distribution could be determined by taking curves of the ion flux at each energy as a function of slit width. A model was developed to calculate the ion scattering. This model ignored the detailed motion of the electrons. Good agreement was obtained between this model and experiment. A simple formula was obtained which approximated the variation of ion flux on centerline as a function of slit width. When measurements were taken at two different slit widths, this formula could be used to determine Debye length and electron temperature at the slit. These electric fields were observed by using a low-energy electron-beam probe. The potentials were found to oscillate in an irregular fashion. However, the deflection of the electron beam was used to determine the potential and charge density as a function of radius for a number of cases. (Diss. Abstr. Int., B)

11881 MEASUREMENT OF THE LINE SHAPES OF THE NITROGEN II AND CARBON II RESONANCE MULTIPLETS FROM A PLASMA. Fortna, John David Edward. College Park, Md.; Univ. of Maryland (1969). 84p. University Microfilms Order No. 70-15,484.

Thesis.

The spectral line shapes of the nitrogen II and carbon II resonance multiplets, which occur in the vacuum-ultraviolet region of the spectrum, were measured. The Stark widths were deduced from the optically thin Lorentz wings. The source of radiation was the hot plasma produced by reflecting the shock wave generated by an electromagnetic T-type shock tube operating at a moderate pressure of helium gas to which the test elements (and hydrogen) were added. The electron temperature was determined from the ratio of the total intensities of the He I 4713-Å and the hydrogen Hβ 4861-Å lines. The electron density was obtained from the halfwidth of the He I 3889-Å line. The electron temperature and density of the test plasma was such as to provide a critical test of a recent semi-empirical theory of Stark broadening of isolated ion lines under conditions in which the broadening electron collisions are predominantly elastic and without classical analogue. Agreement was found within the expected precision of the theory. (Diss. Abstr. Int., B)

11882 PLASMA ACCELERATION BY MEANS OF EXTERNAL MAGNETIC FIELD. Maloch, J.; Sestak, B.; Sobra, K.; Stanek, Z. (Czech Tech. Univ., Prague). Czech. J. Phys.; B20: 1342-4 (1970).

An experimental study was made of the possibility of the plasma cluster acceleration in rail accelerators by the use of the external transverse magnetic field is reported. The assumption was made that maximum luminosity of the plasma cluster is in the place of the maximum mass density. (M.O.W.)

11883 EXPERIMENTAL STUDIES OF PLASMA GENERATED BY THE RPI SYSTEM. Sadowski, Marek; Skladnik-Sadowska, Elzbieta (Inst. of Nuclear Research, Swierk, Poland). Nukleonika; 15: 145-60(1970).

Magnetic probes and photomultipliers were used to study a plasma generated by the Multi-Rod Plasma Injector (RPI). The average and local magnetic fields as well as the space and time-distributions of currents in plasma jets are determined. Also determined are the propagation velocities of uncompensated charges in the absence of an external magnetic field and the velocities of plasmoids in the presence of the external field. Time correlations of plasma visible radiation, discharge currents, and diamagnetic signals are considered. It is found that the azimuthal currents play an essential role in the plasma generated by the RPI system. (auth)

Kinetics (Theoretical)

Refer also to abstract 11765, 11930, and 12058.

11884 (CEA-N-1399) LASER-MATTER INTERACTION: STIMULATED AND NONLINEAR EFFECTS. Guillaneux, Pierre (Commissariat a l'Energie Atomique, Limeil-Brevannes (France). Centre d'Etudes). [1970]. 17p. (In French). Dep. NTIS (U. S. Sales Only).

High flux laser-plasma interaction is studied. The various effects produced are listed: nonlinear or stimulated Compton scattering, nonlinear bremsstrahlung, and electron-positron pair creation. Possible effects of these phenomena on energy changes in the plasma particles are considered. (auth) (France)

11885 (NYO-4077-1, Paper 3) NONLINEAR BEAM-PLASMA INTERACTIONS AND STOCHASTIC ACCELERATION. Dum, Christian T.; Sudan, R. N. (Cornell Univ., Ithaca, N. Y. Lab. of Plasma Studies). 35p.

From Theoretical studies on Astron stability.

The development of an electron beam-plasma instability beyond the stage described by quasi-linear theory was investigated by means of kinetic equations for waves and particles which include the effects of spontaneous emission and scattering of waves. Characteristic times were calculated for the formation of a high-energy tail, which at late times may extend significantly beyond the original beam velocity. Reasonable agreement is obtained with experiments. (auth)

11886 (NYO-4077-1, Paper 4) RETURN CURRENT INDUCED BY A RELATIVISTIC BEAM PROPAGATING IN A MAGNETIZED PLASMA. Lee, Roswell; Sudan, R. N. (Cornell Univ., Ithaca, N. Y. Lab. of Plasma Studies). 59p.

From Theoretical studies on Astron stability.

The propagation of a high-current relativistic beam in a cold magnetized plasma is investigated, using a model developed by Hammer and Rostoker for the unmagnetized case. In this model, the beam electrons are assumed to be undeflected from their zero-order orbits and the fields associated with the beam are switched on at time $t = 0$. The return current induced in the plasma is calculated as a function of beam and plasma parameters. It is demonstrated that the return current does not extend indefinitely but dies away inversely as the distance from the head of the beam with a characteristic length $L_n = v_0 \tau a^2/\lambda_E^2$, where v_0 and a are the beam velocity and radius, τ is a phenomenological momentum relaxation time for the plasma electrons, $\lambda_E = c/\omega_p$, and ω_p is the plasma frequency of the plasma electrons. When the beam is injected either parallel or perpendicular to a static magnetic field B_0, it is found to be magnetically neutralized by a return current over a length of order L_n if $a^2/[\lambda_E^2 (1 + \Omega^2/\omega_p^2)] \gg 1$, where $\Omega = eB_0/m_0c$. (auth)

11887 (NYO-4077-1, Paper 5) FINITE BETA EQUILIBRIA OF RELATIVISTIC ELECTRON BEAMS IN TOROIDAL GEOMETRY. Ott, Edward; Sudan, R. N. (Cornell Univ., Ithaca, N. Y. Lab. of Plasma Studies). 41p.

From Theoretical studies on Astron stability.

Vlasov equilibria of axisymmetric toroidal plasma pinches are obtained by a perturbation expansion with the inverse aspect ratio, r_p/R, as the small parameter (r_p and R are the minor and major toroid radii). The particle distribution function is a delta function in the two constants of motion, the canonical azimuthal angular momentum and the total energy. The equilibria studied include a plasma pinch contained within a conducting toroidal vessel and a plasma ring such as might be formed by transverse injection into a mirror field (e.g., Astron). (auth)

11888 INVERSE COMPTON SCATTERING AND GYRO-SYNCHROTRON EMISSION BY FAST ELECTRONS IN A COLD PLASMA. Goldstein, Melvyn Lee. College Park, Md.; Univ. of Maryland (1970). 97p. University Microfilms Order No. 70-21,328.

Thesis.

The theories and astrophysical importance of inverse Compton scattering in a vacuum and of synchrotron radiation in a cold plasma are reviewed. A theory is then derived for inverse Comp-

XUM

ton scattering in a cold collisionless plasma. The general shape of the scattered photon spectrum is qualitatively similar to the vacuum spectrum. The average electron energy loss rate is $\frac{3}{4}$ of the vacuum value if the ambient photon frequency is equal to the plasma frequency. The theory is given of gyrosynchrotron emission by monoenergetic electrons in a cold magnetoactive plasma, emphasizing the spectrum below the plasma frequency. Using this emission process as a source of ambient photons, the spectrum of inverse Compton scattered photons is calculated. If the ambient photons are propagating in the extraordinary mode, the resulting spectrum is very similar to the one obtained in a cold plasma with no magnetic field. When the ambient photons are propagating in the ordinary mode below the plasma frequency, the spectrum of inverse Compton scattered photons can be suppressed at low frequencies. For some values of electron energy and ambient photon frequency, there will be no inverse Compton scattering. (Diss. Abstr. Int., B)

11889 DOUBLE LAPLACE TRANSFORMATION IN MIXED-BOUNDARY INITIAL-VALUE PROBLEMS AND ITS APPLICATION TO MULTI-COMPONENT PLASMAS. Evans, Kenneth Edward Jr. Urbana, Ill.; Univ. of Illinois (1970). 89p. University Microfilms Order No. 70-20,962.

Thesis.

The application of the double Laplace transform (Laplace transformation in both space and time) to the solution of systems of linear, homogenous, hyperbolic, partial differential equations with real, constant coefficients is treated. The purpose of this treatment is to discuss comprehensively a method whereby the mixed-boundary initial-value problem for these equations can be solved. The treatment is limited to one-dimensional systems. Certain features of the double Laplace transform method, which regularly appear in the solution of equations of the type described, are examined in detail. Two of these features are the important role played by the characteristics of the partial differential equations and the restrictions among the boundary and initial conditions that are necessary for a well-defined solution. The method is applied to the moment equations for a multicomponent plasma, and the relation between the general solution and the usual "normal mode" solution is discussed. The case of a monoenergetic beam injected into a cold, semi-infinite plasma is treated in detail. The effect of the collisions of the plasma particles with the background is included. A solution for the growth of an initial thermal disturbance in the plasma is obtained in the asymptotic limit $t \to \infty$. The dominant feature of this solution is a growth proportional to $\exp(\gamma x^{\frac{1}{3}} t^{\frac{1}{3}} - \frac{1}{2}\nu t)$, where γ is a constant and ν is the collision frequency. The relationship between this solution and the spatially inhomogenous stationary state resulting from recurring thermal disturbances is discussed. This treatment yields the first picture of the relationship between the temporal and spatial growth in a finite, unstable plasma. (Diss. Abstr. Int., B)

11890 ELECTROMAGNETIC RADIATION FROM HETEROGENEOUS PLASMA. Ishii, T. Koryu; Birr, Michael P. (Marquette Univ., Milwaukee). Proc. IEEE (Inst. Elec. Electron. Eng.); 58: 1848-9(Nov 1970).

It was found that the electromagnetic radiation frequency, strength, and waveforms from a heterogeneous plasma were independent of the circuit but were influenced by the material of the electrodes. Using the same circuit for various electrodes, radiation ranging from 10 to 50 MHz, power from 0.5 to 200 mW, and sinusoidal to spiked waves were observed. (auth)

11891 WAVE-MECHANICAL FORMULATION OF PLASMA DYNAMICS IN LONGITUDINAL ELECTRIC FIELDS. Wilhelm, H. E. (Colorado State Univ., Fort Collins). Z. Phys.; 241: 1-8(1971).

The macroscopic dynamics of classical many-component plasmas, in which the particles interact by the self-consistent electric field, is formulated in terms of scalar, complex wave equations. The wave equation of each component is shown to be mathematically equivalent to its nonlinear conservation equations for mass, vector momentum, and energy. Thus, the description through wave equations leads to a considerable mathematical simplification compared to the conventional many-fluid hydrodynamics. As an elementary illustration of the wave-mechanical formalism, the dispersion of electrostatic waves in an electron plasma is treated. (auth)

11892 STARK-BROADENING FUNCTIONS FOR NONHYDROGENIC IONS. Klarsfeld, S. (Institut de Physique Nucleaire, Orsay, France). Phys. Lett.; 33A: 437-8(14 Dec 1970).

Rapidly convergent integral representations are given for several functions used in calculating profiles of isolated ion lines. (auth)

11893 RELAXATION OF A TEMPERATURE ANISOTROPY IN A COLLISIONLESS PLASMA. Montes, C.; Coste, J.; Diener, G. (Faculte des Sciences, Orsay, France). J. Plasma Phys.; 4: 21-41(Feb 1970).

The quasi-linear relaxation of an aperiodic instability, namely the instability caused by the temperature anisotropy of a collisionless electron plasma, is studied in the absence of an external magnetic field. A detailed description of the relaxation process is given and the validity of the quasi-linear theory (existence of separate time scales, quasi linearity of the particles' orbits) is examined. (auth) (UK)

11894 CURRENT INDUCED IN A PLASMA BY A PENETRATING ELECTRON BEAM. Cox, James L. Jr.; Thomas, L. H. (Old Dominion Univ., Norfolk, Va. North Carolina State Univ., Raleigh). Proc. Nat. Acad. Sci. U. S. A.; 67: 1651-5(15 Dec 1970).

The passage of a single pulse of relativistic electrons through a plasma is considered, and the total current in the axial direction it induces in the plasma is calculated. This calculation is valid for an injected beam current density that has arbitrary functional dependence on the radial and azimuthal coordinates. For the special case of a beam current density that is uniform in the radial direction out to the beam radius a, these results agree with results of others published previously. This calculation is simple because the equation for the variation with time of the plasma charge density at any point, independent of what happens at other points, is only slightly more complicated than the familiar equation for an ohmic conduction. (auth)

11895 KINETIC THEORY OF SPATIALLY INHOMOGENEOUS PLASMA WITH TIME-INDEPENDENT AVERAGE PROPERTIES. Cairns, R. A. (Univ. of Glasgow). J. Plasma Phys.; 4: 51-65(Feb 1970).

Kinetic equations are obtained that describe the variation in one spatial direction of a plasma whose average properties are independent of time and do not vary in the perpendicular direction. These equations consist of a coupled set giving the variation of the electric field fluctuation spectrum and the particle distribution functions. They take into account particle discreteness effects and describe the plasma both when it is stable and weakly unstable. It is suggested that they may be used to describe an infinite plane shock wave in a plasma. (auth) (UK)

11896 APPLICATION OF THE COLLECTIVE APPROACH TO THE THERMODYNAMICS OF AN ELECTRON GAS. Carroff, Lawrence J. (Ames Research Center, Moffett Field, Calif.). Liboff, Richard L. J. Plasma Phys.; 4: 83-107(Feb 1970).

The collective approach of Pines and Bohm was applied to the problem of the thermodynamics of the N-particle electron gas including transverse radiation. Partitioning of the internal energy and certain of the other thermodynamic quantities is discussed generally. Analytical expressions for the energy, pressure, and constant-volume specific heat of the transverse oscillators are given, together with approximate expressions applicable to the high-density–low-temperature and low-density–high-temperature limits. Detailed numerical calculations of the internal energy and pressure of the longitudinal modes are presented. In addition, the contributions to the energy and pressure from the particle portion are evaluated in the low-density–high-temperature limit as functions of the cutoff wave vector k_c; k_c is the maximum k-vector of the longitudinal oscillators. (auth) (UK)

11897 NOTE ON THE SEMI-LAGRANGIAN FORMULATION OF THE VLASOV EQUATION. Lewak, G. J. (Univ. of California, San Diego, La Jolla). J. Plasma Phys.; 4: 143-4(Feb 1970).

It can be shown that the Vlasov equation in the semi-Lagrangian formulation may be written in a form resembling the fluid equations and the form of these equations assume, for simplicity, a uniform fixed ion background. A modification of the equations is derived, which can account for the presence and motion of the ions. (UK)

11898 SOLUTION OF THE BOLTZMANN EQUATION FOR ELECTRONS IN EXTERNAL ELECTRIC FIELDS. Stenflo, L. (Inst. of Physics, Uppsala). J. Plasma Phys.; 4: 145-59 (Feb 1970).

A plasma in a time-dependent external electric field is considered. Collisions are described by means of Fokker–Planck and BGK models. Longitudinal and transverse wave propagation is treated by means of exact analytical solutions of the linearized Boltzmann equation. The results generalize previous calculations on dispersion relations and density fluctuation spectra. (auth) (UK)

11899 WAVE-MECHANICAL FORMULATION OF MANY-FLUID PLASMA THEORY IN ELECTROMAGNETIC FIELDS.

XUM

Wilhelm, H. E. (Colorado State Univ., Fort Collins). Phys. Rev., A; 3: 399-404(Jan 1971).

The macroscopic dynamics of classical many-component plasmas in electric and magnetic fields is formulated in terms of scalar complex wave equations that contain pressure and electromagnetic potentials. The complex wave equation of each particle component is shown to be mathematically equivalent to the nonlinear conservation equations of mass, vector momentum, and energy. Thus, the description of a plasma by wave equations leads to a considerable mathematical simplification compared to the conventional many-fluid electromagnetohydrodynamics. As an elementary illustration of the wave-mechanical formalism, the dispersion of longitudinal and transverse electromagnetic waves in an electron plasma is treated. (auth)

11900 DERIVATION OF THE VLASOV EQUATION. Wilson, Robert N. (Lockheed Research Labs., Palo Alto, Calif.); Futterman, Walter I.; Yue, John T. Phys. Rev., A; 3: 453-70(Jan 1971).

The solution of the Liouville equation is expressed in the interaction representation. It is shown that the early-time behavior of the single-particle distribution function F_1 for a classical gas consisting of particles interacting through weak two-body central forces is governed by the Vlasov equation. The two-body potentials are assumed to be "good" functions. The derivation fails if initial correlations are present. The argument is carried out in configuration space. The analysis is extended to the derivation of differential equations governing the time evolution of the multiparticle distribution functions F_k. In this "Vlasov approximation" to the solution of the Liouville equation, one finds that the Vlasov equation for F_1, together with the differential equations for the $F_k (k < 1)$, amounts to the statement that the multiparticle distribution functions are factorable into products of single-particle distribution functions. (auth)

11901 GRAD METHOD EXTENSION TO SOLVING THE RELATIVISTIC BOLTZMANN EQUATION. Marle, C. pp 129-34 of La Magnetohydrodynamique Classique et Relativiste. Paris; Centre National de la Recherche Scientifique (1970). (In French).

From Symposium on Classical and Relativistic Magnetohydrodynamics, Lille, France. See CONF-690648.

The method of solving the Boltzmann equation due to Grad was extended to the case of a relativistic gas: this extension led to a system of equations, which at each order of approximation, comprised as many equations as there were unknowns. The second-order approximation describes the state of a gas by fourteen parameters and not thirteen, such as in a nonrelativistic gas. In consequence, the two coefficients of viscosity are not linked by the Stokes relation ($3\lambda + 3\mu = 0$) as in the case of a nonrelativistic gas. (auth) (France)

11902 CAUCHY PROBLEM FOR THE LINEARIZED RELATIVISTIC BOLTZMANN EQUATION. Pichon, G. (Univ., Orleans, France). pp 135-40 of La Magnetohydrodynamique Classique et Relativiste. Paris; Centre National de la Recherche Scientifique (1970). (In French).

From Symposium on Classical and Relativistic Magnetohydrodynamics, Lille, France. See CONF-690648.

A method of studying the Boltzmann equation about a distribution equilibrium is indicated. The linearized equation is studied by means of functional analysis. (auth) (France)

11903 RELATIVISTIC PLASMA IN A STRONG MAGNETIC FIELD. Bertotti, B. (European Space Research Inst., Rome). pp 251-62 of La Magnetohydrodynamique Classique et Relativiste. Paris; Centre National de la Recherche Scientifique (1970).

From Symposium on Classical and Relativistic Magnetohydrodynamics, Lille, France. See CONF-690648.

The guiding center theory of a plasma immersed in a strong magnetic field is generalized in the framework of special relativity. The method is based upon the canonical decomposition of the electromagnetic tensor in two simple vectors and leads to simplified Lorentz-invariant equations. When the heat flow is neglected, a closed set of MHD equations is obtained; the pressure tensor for each species depends upon four scalars and the transport equations have only one constant of motion. The connection between this general theory and the dynamics of emission processes in pulsars is discussed. (auth) (France)

11904 INVERSE PROBLEM FOR A CYLINDRICAL PLASMA. Degasperis, Antonio (Indiana Univ., Bloomington). J. Math. Phys. (N. Y.); 11: 3392-3400(Dec 1970).

The Maxwell equation for the electric potential inside a neutral nonuniform cylindrical plasma in an external oscillating electric field was studied from the point of view of the inverse problem. The logarithmic derivatives of the radial Fourier components of the electric potential at the edge of the cylinder are considered as experimental data. An explicit and exact representation of the electron density was obtained in terms of the high-frequency behavior of the experimental data. The general analyticity properties in the complex-frequency plane are also discussed. (auth)

Production

11905 EFFECT OF ARC DISCHARGE PARAMETERS ON THE FORM OF THE PLASMA CLUSTER IN DC ARCS WITH APPLIED INHOMOGENEOUS MAGNETIC FIELDS. Kharizanov, Yu.; Zadgorska, Z. (Inst. of General and Inorganic Chemistry, Sofia). Zh. Prikl. Spektrosk.; 12: 610-14(Apr 1970). (In Russian).

The shape of a plasma cluster of a constant-current arc in an inhomogeneous magnetic field as related to magnetic field strength, diameter of front surface of the anode, and the distances between electrodes is discussed. A premise is made concerning the probable mechanism of formation of the plasma cluster. The form of the plasma cluster that shows maximum enhancement of intensity of the spectral lines was determined, and the visual criterion for finding optimum parameters of the arc discharge was established. (tr-auth)

11906 NEODYMIUM GLASS LASER WITH HIGH RADIATION INTENSITY FOR PRODUCING A HIGH-TEMPERATURE PLASMA. Vanyukov, M. P.; Venchikov, V. A.; Isaenko, V. I.; Serebryakov, V. A.; Starikov, A. D. Opt. Spectrosc. (USSR) (Engl. Transl.); 28: 544-7(May 1970).

Translated from Opt. Spektrosk.; 28: 1008-12(May 1970).

The apparatus developed consists of a low-power neodymium glass laser with a divergence close to the diffraction limit and four stages of amplification with gradually increasing rod diameter. A Galilean telescope tube is used to increase the cross section of the light beam. The output radiation of the laser included in the diffraction core of the beam has a brightness $B = 1.3 \times 10^{17}$ W/cm^2 sr, and an axial brightness of the order of 10^{18} W/cm^2 sr. The system generates 100 J of energy with a power of 10 GW. The diameter of the output beam is 27 mm. Using a specially designed objective, a light flux of density 10^{15} to 10^{16} W/cm^2 can be produced. (auth)

11907 LASER-PRODUCED PLASMAS AT NRC'S PHYSICS DIVISION. Alcock, A. J. (National Research Council, Ottawa). Can. Res. Develop.; 3: 19-22(Nov-Dec 1970).

Commercial lasers now available can produce nanosecond pulses with an energy of several hundred joules which, by means of a short focal length lens, can be concentrated in a volume of approximately 10^{-6} cm^3. Thus, the interaction of high-power laser radiation with matter offers a completely new approach to the production of high-temperature plasmas. Laser-induced gas breakdown and the mechanisms involved in the development of the plasma produced in this manner were investigated. Free electrons, naturally present in the gas due to cosmic rays, gain energy from the high-frequency electric field and produce additional electrons by means of ionizing collisions with neutral atoms. This leads to a chain reaction, known as cascade ionization, which can result in a very rapid growth in the degree of ionization of the gas. This is capable of producing at least one electron well before the end of the laser pulse. The requirement is satisfied by a process known as multiphoton ionization, which permits a single atom to absorb simultaneously a number of photons having a total energy equal to the ionization potential of the atom. Velocities of ~10^7 cm/sec were recorded on a high-speed image-converter streak camera. (Canada)

11908 PLASMA PRODUCTION USING A STANDING HELICON WAVE. Boswell, R. W. (Flinders Univ., South Australia). Phys. Lett.; 33A: 457-8(14 Dec 1970).

A standing helicon wave was excited by applying a transverse rf field to a cylindrical plasma immersed in a steady axial magnetic field. The predictions of the hydrodynamic theory are found to be inadequate in describing the damping. (auth)

Stability

11909 (COO-1695-31) PLASMA INSTABILITIES AND WAVES EXCITED BY AN ANISOTROPIC ENERGY DISTRIBUTION PRODUCED BY ELECTRON CYCLOTRON RESONANCE. Quarterly Progress Report No. 14. Shohet, J. L.; Sprott, J. C. (Wisconsin Univ., Madison. Dept. of Electrical Engineering). 15 Sep 1970. Contract AT(11-1)-1695. 53p. Dep. NTIS.

During the report period, the off-resonance heating phenomena

has been studied in detail, both experimentally and theoretically. Bremsstrahlung measurements were made and compared with theoretical predictions. A new experimental facility has become operational, and studies of computer simulation of plasmas have continued. (M.O.W.)

11910 (COO-1695-32) PLASMA INSTABILITIES AND WAVES EXCITED BY AN ANISOTROPIC ENERGY DISTRIBUTION PRODUCED BY ELECTRON CYCLOTRON RESONANCE. Annual Progress Report. Shohet, J. L.; Sprott, J. C.; Seshadri, S. R. (Wisconsin Univ., Madison. Dept. of Electrical Engineering). 15 Dec 1970. Contract AT(11-1)-1965. 133p. Dep. NTIS.

The research performed under this contract involves the study of plasmas produced by electron cyclotron resonance heating in a magnetic mirror device. Specifically, the work has centered on four major problems: (1) measurement of the intensity and polarization of free-free bremsstrahlung from the plasma and the theoretical problem of relating the results to the electron energy distribution; (2) behavior of the plasma produced by cyclotron resonant heating when subjected to microwave radiation at a frequency displaced from the cyclotron frequency; both experimental and theoretical results have been obtained; (3) investigation and identification of an electromagnetic instability; and (4) numerical simulation and experimental diagnostic techniques used in conjunction with the above work. (M.O.W.)

11911 (EUR-CEA-FC-569) MHD EQUILIBRIUM AND STABILITY OF TOROIDAL PLASMAS WITH A QUASI-TRIANGULAR CROSS SECTION IN TOKAMAK TYPE MAGNETIC CONFIGURATIONS. Luc, H. (European Atomic Energy Community. Commissariat a l'Energie Atomique, Fontenay-aux-Roses (France). Centre d'Etudes Nucleaires). Oct 1970. 34p. (In French). Dep. NTIS (U. S. Sales Only).

The MHD equilibrium of an axisymmetric toroidal plasma is studied. Its stability against local perturbations is strongly dependent upon the existence of triangular deformations (even slight) in its cross section. The displacement of the magnetic axis in relation to the central axis is not necessarily small and the plasma pressure may be near the equilibrium pressure limit. (auth) (France)

11912 (MPI/PA-7/62) INFLUENCE OF ELECTRICAL CONDUCTIVITY ON THE EQUILIBRIUM OF LOW-PRESSURE PLASMA IN STELLARATORS. Pfirsch, D.; Schlueter, A. (Max-Planck-Institut fuer Physik und Astrophysik, Munich (West Germany)). [nd]. 14p. (In German). Dep. NTIS (U. S. Sales Only).

In finite-electric-conductivity plasma there is no static, but only stationary, equilibrium in stellarators. The currents arising in such configurations, the related diffusion, and the electric fields were calculated by means of a simple model. The duration of the acceleration process up to the attainment of the current velocities was estimated. The general results are that the diffusion is larger by the factor Br^2/l^2 than the normal diffusion (l is the rotation transformation of the magnetic field) and that, in plasmas of high density and low temperature, the duration of the acceleration process can be so great that the plasma drifts to the wall before attainment of the equilibrium state. Certain experiments of Remy, Lotz, and Wolf could be explained by these results. (tr-auth)

11913 (UUIP-722) STUDY OF NONLINEAR INSTABILITIES. Oestberg, Kjell (Uppsala Univ. (Sweden). Inst. of Physics). Aug 1970. 33p. Dep. NTIS (U. S. Sales Only).

Equations describing resonant interaction between three waves in a plasma in the fixed-phase approximation were investigated. It is assumed that the coupling is explosively unstable and that dissipative effects can be neglected. The development in time of the wave amplitudes and phases is studied by means of numerical methods. An analytic expression is derived for the time of explosion and it is shown how this time depends on the initial values. (auth) (Sweden)

11914 SOLUTION OF EQUATIONS DESCRIBING EXPLOSIVE INSTABILITIES. Stenflo, L.; Weiland, J.; Wilhelmsson, H. (Uppsala Univ.). Phys. Scr.; 1: 46(1970).

The basic equations that describe three-wave interactions in a plasma, where collisional effects have to be taken into account, are studied. An analytical solution is found and compared with computer results. (auth) (Sweden)

11915 QUASI-LINEAR DYNAMICS OF ION CYCLOTRON INSTABILITY IN AN ANISOTROPIC PLASMA. Preinhaelter, J.; Vaclavik, J. (Inst. of Plasma Physics, Prague). J. Plasma Phys.; 4: 175-86(Feb 1970).

It is shown that in a dense magnetoactive plasma $c/c_A \gg 1$ with cold electrons and ions with an anisotropic temperature $1 \ll T_{||}/T_{\perp} \ll (n_0 T_{\perp}/H_0^2)^{1/3}$ the ion cyclotron waves propagating along the magnetostatic field are excited with a maximum increment. The dynamics of the quasi-linear stage of this instability is investigated. It turns out that, at any moment, the ion distribution function is of the form of a step with the steep front. The speed of the front in the velocity space and the characteristic time of the relaxation process are found. It is ascertained that the distribution function arising in the course of the relaxation is stable with respect to the ion cyclotron waves propagating obliquely to the magnetostatic field. (auth)(UK)

11916 TEMPERATURE-ANISOTROPY INSTABILITY FOR ELECTROMAGNETIC WAVES PROPAGATING ACROSS A STATIC MAGNETIC FIELD. Landau, R. W.; Cuperman, S. (Inst. of Planetary and Space Science, Tel-Aviv Univ., Israel). J. Plasma Phys.; 4: 13-20(Feb 1970).

The instability of electromagnetic waves propagating across a static magnetic field in the presence of a thermal anisotropy ($T_{||} > T_{\perp}$) is investigated. The marginal stability criterion as well as the rate of growth of the instability are derived. When compared with the firehose instability (of electromagnetic waves propagating along the static magnetic field) it is found that higher electron pressures are required for this new instability to be set up; however, the maximal rate of growth is much larger than in the firehose case. The interplanetary plasma is stable to this thermal anisotropy instability; high-β plasma devices may be unstable. (auth) (UK)

Thermonuclear Processes

Refer also to abstract 11752.

11917 (CEA-R-4024) CONTRIBUTION TO THE UNDERSTANDING OF THE HIGH-MAGNETIC FIELD COMPRESSION PRODUCED BY THE IMPLOSION OF A THIN METAL TUBE. Besancon, Jacques (Commissariat a l'Energie Atomique, Limeil-Brevannes (France). Centre d'Etudes). Dec 1970. 208p. (In French). Dep. NTIS (U. S. Sales Only).

Thesis. Submitted to Paris Univ., Orsay (France). Faculte des Sciences.

The following essential phenomena occurring during a magnetic flux compression obtained by the implosion of a thin conducting liner are presented: acceleration time, dynamic changes, heating and instability behavior of the liner, field diffusion through the conducting walls and the resulting flux losses which control the increasing field in the cavity. Various implosion models are proposed; the most elaborate model leads to the numerical computation of the flux compression. Repeated experiments have led to improvements in the flux injection techniques, the optical and electrical diagnostics, and consequently the final compressed field. Techniques are now available for obtaining and recording reproducible fields of 12 MOe in 0.8-cm-diameter cavities. All the implosions are compared with theoretical predictions. The final phase of the liner turnaround is of particular interest. It is concluded that the electrical conductivity of the liner determines the final flux value. (auth) (France)

11918 (EUR-CEA-FC-543) STRAIGHT STELLARATORS WITH STRONG HELICAL CURRENTS. Maschke, E. K. (European Atomic Energy Community. Commissariat a l'Energie Atomique, Fontenay-aux-Roses (France). Centre d'Etudes Nucleaires). Oct 1970. 38p. Dep. NTIS (U. S. Sales Only).

A type of toroidal stellarator configurations, called Torsatron, is produced by helical windings with all currents circulating in the same direction around the torus. Straight stellarator and Torsatron configurations are studied for large ratios of helical current to B_z-coil current, and the limiting case of the Torsatron without B_z coils is investigated. (auth) (France)

11919 (EUR-CEA-FC-566) VACUUM PROBLEMS ENCOUNTERED IN NUCLEAR FUSION RESEARCH. Prevot, F. (European Atomic Energy Community. Commissariat a l'Energie Atomique, Fontenay-aux-Roses (France). Centre d'Etudes Nucleaires). Oct 1970. 29p. (In French). (CONF-700928-6). Dep. NTIS (U. S. Sales Only).

From 6th Symposium on Fusion Technology, Aachen, Germany.

Research in plasma physics and future developments in fusion power plants pose important vacuum technique problems, which are briefly reviewed. The characteristics of these problems are contrasted with conventional vacuum technology. (auth) (France)

11920 (EUR-CEA-FC-567) PRODUCTION OF INTENSE BEAMS OF FAST NEUTRAL PARTICLES USING PLASMA ACCELERATORS OF THE PLEIADE TYPE. Geller, R.; Jacquot, B.; Jacquot, C. (European Atomic Energy Community. Commis-

XUM

sariat a l'Energie Atomique, Fontenay-aux-Roses (France). Centre d'Etudes Nucleaires). Oct 1970. 33p. (In French). Dep. NTIS (U. S. Sales Only).

The performance of Pleiade-type cyclotron resonance devices in producing intense beams of energetic neutral particles is studied. It is shown that a two-fold increase in the present performance can be achieved for neutral-particle beams with energies less than 20 keV. The optimum region for coherent acceleration is determined. The influence of wavelength and uhf power on the performance is studied. (auth) (France)

11921 (IPPJ-T-2) FEEDBACK CONTROL OF THE PIG DISCHARGE OF THE QP MACHINE. Matsuura, Kiyokata; Horikoshi, Genichi; Kuroda, Tsutomu; Sato, Teruyuki (Nagoya Univ. (Japan). Inst. of Plasma Physics). Nov 1970. 34p. Dep. NTIS (U. S. Sales Only).

Operational principles, technical problems, and electronic circuitry of the feedback control system for a high-current PIG discharge are discussed. In the PIG discharge with an electron-bombarded hot cathode, the discharge current is kept constant by controlling the cathode temperature by means of the bombardment control. Important parameters for regulation of the cathode temperature are the back heating on the cathode due to ion current in the plasma and on the filament by radiation from the high-temperature cathode. The circuit with an available open loop gain, 10^2, is designed to control the discharge current. The characteristics of the control system are examined and experimental results for the response time and the time constant of every part in the system are summarized for the discharge parameters. A simple analysis for the stability of the system was made by considering the time constant of elementary circuits and the open-loop gain of the system. The observed stability of the system is quite satisfactory with a small drift less than 6×10^{-3}/hour. In this system, the adjustment of discharge voltage or current can easily be made by a selector switch. Some physical problems of the hot cathode discharge are also discussed. (auth) (Japan)

11922 (KHFTI-70-25) EFFECT OF TOROIDAL STATE ON VACUUM MAGNETIC CONFIGURATION OF A VINTOTRON (HELICOTRON). Aleksin, V. F.; Nemov, V. V.; Shishkin, A. A. (Akademiya Nauk Ukrainskoi SSR, Kharkov. Fiziko-Tekhnicheskii Institut). 1970. 19p. (In Russian). Dep. NTIS (U. S. Sales Only).

The magnetic configuration of a toroidal helicotron was studied. In the Mercier system of coordinates, linked with the helical line on the torus, expressions were developed for the components of a magnetic field. Equations were solved for the force lines with an accuracy to the terms $\delta l n \delta^{-1}$ and δ, where $\delta = a/R \ll 1$ (a and R = the small and large radii of the torus). It is shown that the force lines near the magnetic axis form closed magnetic surfaces and that the separation of the toroidal helicotron's magnetic axis from the position of the straight (uniflow) helicotron comprises a value of the order of $r_0 \delta l n \delta^{-1}$ for the elliptical surfaces and $r_0[\delta l n \delta^{-1}]^{1/4}$ for those parameters of the helicotron when in the direct (straight) helicotron the surfaces are circular (r_0 = distance from axial flow to magnetic axis of direct helicotron). (tr-auth) (JPRS)

11923 (NYO-4077-1) THEORETICAL STUDIES ON ASTRON STABILITY. Progress Report, January 1, 1970–December 31, 1970. (Cornell Univ., Ithaca, N. Y. Lab. of Plasma Studies). Contract AT(30-1)-4077. 180p. Dep. NTIS.

Separate abstracts were prepared for the five individual papers. (M.O.W.)

For abstracts of individual papers see: 11885–11887, 11924, and 11925.

11924 (NYO-4077-1, Paper 1) PRECESSION OF A STRONG E-LAYER. Lovelace, R. V.; Sudan, R. N. (Cornell Univ., Ithaca, N. Y. Lab. of Plasma Studies). 20p.

From Theoretical studies on Astron stability.

Observed precession of weak E layers in the Astron is compatible with the "super-particle" model of Furth in which the electrons constituting the layer precess as a rigid body with a frequency appropriate for the precession of a single electron in the external fields. By perturbation of the Vlasov equation for an E layer of arbitrary strength, the assumptions involved in the super-particle model are investigated. A dispersion relation is obtained, and this has a single real low-frequency solution which equals the single-electron precession frequency in the weak E-layer limit, but for stronger E layers approaching field reversal, the frequency may be significantly reduced from that for a single electron. In addition there may be an imaginary damping part to the precession frequency which corresponds to nonrigid motion of the layer. This damping may occur in the absence of external forces on the layer. (auth)

11925 (NYO-4077-1, Paper 2) E-LAYER PRECESSION IN A PLASMA. Berk, H. L.; Sudan, R. N. (Cornell Univ., Ithaca, N. Y. Lab. of Plasma Studies). 22p.

From Theoretical studies on Astron stability.

A weak E layer in a nonuniform magnetic field will tend to precess as a rigid body in response to the radial focusing of external magnetic fields and fields due to wall currents. The interaction of this precessional mode with a background plasma is studied, and dissipation mechanisms in the plasma, walls, and external resistors are included. When the plasma background is treated in the MHD approximation one finds that the mode changes character from a precessional mode at low density to a compressional Alfvén wave at high density. For a very weak E layer, instability is found, even without dissipation, when a sufficiently high background plasma density is present. However, for moderate E layer strengths the modes are found to be stable, even with dissipation. (auth)

11926 RADIATION FROM BALL LIGHTNING. Hill, C. R.; Sowby, F. D. Nature (London); 228: 1007(5 Dec 1970).

Reference is made to Altschuler (Nature 228: 545(1970)) who suggested that ball lightning may be due to formation of ^{15}O and ^{17}F within a localized plasma capable of yielding radioactive decay energy of the order of 10^7 J. The authors of this letter state that the mean γ radiation absorbed dose rate in the human body at 2m distance from such a source would be about 175 R/sec for ^{15}O or 325 R/sec for ^{17}F, in which case signs of radiation sickness would have been expected, even becoming lethal. Therefore, it is suggested that medical evidence of radiation effects should be sought in persons exposed at close quarters to ball lightning. It might also be interesting to look for thermoluminescence effects in suitable materials in the vicinity of a suspected ball lightning strike. (UK)

Wave Phenomena

Refer also to abstracts 11909, 11916, 12055, 12332, and 12782.

11927 (FTI-295) DETERMINATION OF THE BOUNDARY OF HIGH FREQUENCY WAVE ABSORPTION BETWEEN THE ELECTRON CYCLOTRON AND THE LOW-HYBRID FREQUENCY. Galaktionov, B. V.; Golant, V. E.; D'yachenko, V. V.; Shcherbinin, O. N. (Akademiya Nauk SSSR, Leningrad. Fiziko-Tekhnicheskii Institut). 1970. 11p. (In Russian). Dep. NTIS (U. S. Sales Only).

The boundary of the absorption of high-frequency waves by plasma was determined from the study of conditions under which plasma was maintained by hf power. From the variation of plasma parameters, some critical values were found when the plasma density decreased abruptly. The results can be related to the theory of absorption by linear wave transformation. (auth)

11928 (IAE-1949) PROPAGATION AND ABSORPTION OF IONIC-HYBRID WAVES IN A SLIGHTLY-HETEROGENEOUS PLASMA LAYER. Glagolev, V. M. ([Gosudarstvennyi Komitet po Ispol'zovaniyu Atomnoi Energii SSSR] Moscow. Institut Atomnoi Energii). 1970. 44p. (In Russian). Dep. NTIS (U. S. Sales Only).

The problem of propagation and absorption of ionic-hybrid waves in a slightly heterogeneous plasma layer is considered. The plasma's density increases in a direction perpendicular to the magnetic field. Excitation of the electromagnetic waves is accomplished in a region having a low plasma density. It is demonstrated that for the wave penetration into a plasma, the retardation of a wave along the magnetic field is necessary. Conditions are stipulated for transforming the electromagnetic wave to a plasma wave; calculations are made of the collisionless ionic and electron absorption of a wave both in the presence and in the absence of transformation. (tr-auth) (JPRS)

11929 ELECTRIC AND MAGNETIC RESONANCES OF A PARTICULATE MAGNETOPLASMA: IDENTIFICATION BY MICROWAVE PROPAGATION IN THE VOIGT CONFIGURATION. Galeener, F. L.; Saraikar, A. A.; Furdyna, J. K. (Purdue Univ., Lafayette, Ind.). Appl. Phys. Lett.; 17: 486-8(1 Dec 1970).

A theoretical model is presented for the propagation of plane electromagnetic waves through a discontinuously inhomogeneous magnetoplasma. The model predicts selective excitation of magnetic resonances in the ordinary Voigt configuration and electric resonances in the extraordinary. Measurements of microwave transmission through powdered n-type InSb in an applied magnetic field verify this prediction and establish the character of related resonances previously observed in the Faraday configuration. It is concluded that the particle-size-independent resonances of the system are electric dipole in character and thus appear in its effective permittivity, while the size-dependent resonances are

XUM

magnetic and contribute to the effective permeability. Formulas for effective wave propagation constants are given. (auth)

11930 LAMINAR SHOCKS AND OTHER NONLINEAR WAVES IN WARM PLASMAS. Crevier, William Francis. College Park, Md.; Univ. of Maryland (1970). 138p. University Microfilms Order No. 70-21,325.

Thesis.

A two-fluid model for collisionless shock waves in warm plasmas is presented. Dissipation is included by assuming an effective collision frequency. The model is capable of describing waves over a wide range of Mach numbers and angles of propagation. The wave behavior is compared to the motion of a particle moving in a somewhat complicated force field. A part of this force can be written as the gradient of a potential. The response of the plasma to a small perturbation is analyzed by linearizing the equations of motion about their equilibrium values. Comparing the shape of the potential well near the origin with the results of the linearized equations of motion provides considerable physical insight into the initial-wave behavior. The Rankine–Hugoniot relations for a shock transition in a warm plasma are derived and used to study the possible down-stream equilibrium states. Again, the potential-well analogy proves useful by providing information on the stability of the final equilibrium states. The usual two-fluid model is expanded to include high-Mach-number shock waves. By including a thin region of intense electrostatic turbulence in an otherwise laminar shock (21), one is able to produce shock waves with Alfvén Mach numbers up to 40 or more. A digital computer is used to provide examples of the various kinds of wave behavior predicted analytically. Examples of waves with and without dissipation are given. (TSS) (Diss. Abstr. Int., B)

11931 ANOMALOUS TRANSMISSION AND REFLECTION OF CYCLOTRON WAVES. Marsh, Jeffrey Brian. Princeton, N. J.; Princeton Univ. (1970). 89p. University Microfilms Order No. 70-19,791.

Thesis.

A formalism is developed to describe the propagation along a slowly varying field of purely transverse cyclotron waves. Starting from the coupled set of linearized Vlasov–Maxwell equations, expansions are made in terms of the two small parameters $(\Omega_{max} - \omega)/\omega$ and $(k_\infty L)^{-1}$, where Ω_{max} is the maximum value of the gyro frequency, ω is the wave frequency, k_∞ is the wave number at infinity, and L is the scale length of variation of the magnetic field. This results in the derivation of a one-dimensional wave equation, which is applied to the case where the field configuration is a magnetic mirror with small field variation that includes points of cyclotron resonance where the local gyro frequency is equal to the wave frequency, and the collisionless low-β plasma that supports the wave in the regions outside these points is made up of both trapped and untrapped particles. Processes by which the trapped particles can cause anomalous transmission and reflection of the wave by a nonlocal mechanism are investigated. The trapped particles participate in the damping of the incident wave in the propagation region before cyclotron resonance and, after free-streaming across the central region of the mirror where the wave is evanescent, excite transmitted and reflected waves by coherently releasing the electromagnetic energy they have previously acquired from the incident wave in the damping process. (TSS) (Diss. Abstr. Int., B)

11932 COUPLING OF A HIGH-CURRENT RELATIVISTIC ELECTRON BEAM TO A SLOW WAVE STRUCTURE. Nation, John A. (Cornell Univ., Ithaca, N. Y.). Appl. Phys. Lett.; 17: 491-4(1 Dec 1970).

Annular relativistic electron beams carrying currents of 30 to 40 kA at energies of 200 to 500 keV were propagated through a cylindrically symmetric, annular, ridged waveguide. An interaction between the electron beam and a backward wave in the guide was observed. This leads to oscillations in the range 7.8- to 9.7-GHz at power levels of about 10 MW in a 30-nsec pulse. (auth)

11933 PERTURBATION APPROACH TO NONLINEAR VLASOV EQUATION. II. NONLINEAR PLASMA OSCILLATION OF FINITE AMPLITUDE. Kawakami, Ichiro; Yagishita, Takashi (Nihon Univ., Tokyo). J. Phys. Soc. Jap.; 30: 244-53(Jan 1971).

A perturbation method based on a canonical transformation, which has been developed in a previous paper for the infinitesimal expansion parameter ϵ, proportional to the amplitude of wave, is extended to the case where ϵ is small but finite. Under the transformation, the original system is transformed into a new system where off-resonant particles are almost in free motion, while resonant particles are under the influence of an almost monochromatic wave. The solution for the off-resonant particles is essentially the same as that found in the previous paper, while the solution for the resonant particles is essentially the same as that found by O'Neil. (auth)

11934 PARAMETRIC EXCITATION OF BERNSTEIN WAVES IN PLASMAS. Sugaya, Reiji; Mizuno, Katsuhiro; Tanaka, Shigetoshi (Kyoto Univ.). J. Phys. Soc. Jap.; 30: 253-8(Jan 1971).

The parametric excitation of Bernstein waves with the frequency f_d are observed experimentally when the intense pump signal with the frequency $f_{pump} = (2/m)f_d (m = 1, 3 \text{ and } 5)$ is applied to a non-uniform plasma in a magnetic field. The threshold values are very small as compared with those expected from theory, though they increase with m. As the pump field increases, the amplitude of the excited signal becomes saturated and the signal disappears. The frequency conservation among the pump and excited signals is certified. The experimental results are interpreted on the basis of the Mathieu equation derived from the electrostatic hydrodynamic approximation, assuming the spatial gradient of the electron density. (auth)

11935 MEASUREMENT OF THE PHASE CONSTANT ALONG A CONDUCTING WIRE IN A MAGNETOPLASMA. Ishizone, T.; Adachi, S.; Mushiake, Y. (Tohoku Univ., Sendai). Proc. IEEE (Inst. Elec. Electron. Eng.); 58: 1852-4(Nov 1970).

The phase constant of the electromagnetic wave along a conducting wire in a plasma magnetized parallel or perpendicularly to the wire was measured. Fairly good agreement is found between the measured results and theoretical predictions when the effect of the surrounding ion sheath is taken into account. (auth)

11936 HELICON WAVE PROPAGATION: EFFECT OF ELECTRON INERTIA. Davies, B. (Flinders Univ. of South Australia, Bedford Park). J. Plasma Phys.; 4: 43-50(Feb 1970).

The dispersion relation for traveling helicon waves in a uniform non-resistive plasma is investigated, and it is shown that the effect of electron inertia for a cylindrical plasma bounded by conducting walls is qualitatively different from the plane wave case, leading to significant differences in the dispersion relation at all frequencies in the range $0 < \omega < \Omega_e$. (auth) (UK)

11937 ONE-DIMENSIONAL ION-ACOUSTIC MODES OF BOUNDED PLASMAS. Rosa, Rui; Allen, J. E. (Oxford Univ.). J. Plasma Phys.; 4: 195-203(Feb 1970).

One-dimensional ion–acoustic normal modes of bounded plasmas are theoretically investigated in plane, cylindrical and spherical geometries. The characteristic frequencies, damping constants, and spatial structure of the oscillatory modes are obtained. (auth) (UK)

11938 NOTE ON ION RAREFACTION WAVES. Allen, J. E. (Oxford Univ.); Andrews, J. G. J. Plasma Phys.; 4: 187-94 (Feb 1970).

A theory is given of an ion rarefaction wave in a low-pressure plasma under conditions where ionization processes are unimportant. (auth) (UK)

11939 REFLEXION OF A PLANE WAVE AT A PLASMA HALF-SPACE. Clemmow, P. C.; Karunarathne, V. B. (Cambridge Univ.. Eng.). J. Plasma Phys.; 4: 67-81(Feb 1970).

The problem of a monochromatic plane electromagnetic wave incident from a vacuum on the plane boundary of a plasma half-space is considered. The method of solution is based on the representation of the disturbance in the plasma half-space as that generated by some current source in the complementary half-space into which, for the purpose of the representation, the plasma is conceived to extend. The specular reflection boundary conditions and the diffuse scattering boundary conditions are treated in turn, first for normal incidence and then for oblique incidence. (auth) (UK)

11940 NONLINEAR DISPERSION OF COLD PLASMA WAVES. Tam, Christopher K. W. (Massachusetts Inst. of Tech., Cambridge). J. Plasma Phys.; 4: 109-25(Feb 1970).

The propagation of a packet of weakly nonlinear dispersive cold plasma waves is studied by means of a two-time scale expansion. The effects of amplitude dispersion and the coupling to the mean plasma motion are taken into account. The governing equations are put into a conservation form. It is found that this system of equations is elliptic or hyperbolic depending on the wave number of the dispersive waves. It is shown that except for waves which have their wave vectors nearly at right angle to the unperturbed magnetic field only fast waves with wave-number less than 0.585 $(\Omega_i \Omega_e)^{1/2}/V_a$ are stable; where V_a is the Alfvén velocity and Ω_i, Ω_e are the ion and electron cyclotron frequencies respectively. A process of steepening of these waves into shocks with dissipation due to wave turbulence at the head of the wave packet is suggested. (auth) (UK)

11941 LANDAU DAMPING OF RESONANCE OSCILLATIONS IN INHOMOGENEOUS PLASMAS. Dorman, G. (Brooklyn Polytechnic Inst.). J. Plasma Phys.; 4: 127-42(Feb 1970).

XUM

A self-consistent solution of the Vlasov–Poisson equations is obtained for a low-temperature, bounded, Maxwellian plasma of arbitrary nonuniform density. An eigenvalue equation for the central frequencies and electric fields of the resonance oscillations is obtained, which agrees with the equation obtained by a low-temperature expansion of the orbital-integral solution. The Landau damping rate is given in a general, explicit form in terms of the central frequencies and fields of the resonances. (auth) (UK)

11942 NONLINEAR DAMPING OF TONKS–DATTNER RESONANCES. Decker, J. F.; Mendel, C. W. Jr. (Bell Telephone Labs., Whippany, N. J.). Phys. Rev., A; 3: 471-7(Jan 1971).

A nonlinear damping of Tonks–Dattner resonances was observed in active and afterglow plasmas. The damping is found to decrease with increasing strength of the exciting microwave electric field with no change in resonant frequency. A decrease in the Landau damping due to a flattening of the steady-state electron velocity distribution appears to be responsible. It is believed that a balance between the wave–particle interaction and electron–particle collisions is important in determining the steady-state slope of the velocity distribution, and therefore the Landau damping. Order-of-magnitude comparisons are made with a simplified quasilinear analysis based upon this idea. (auth)

11943 KINEMATICS AND DYNAMICS OF NONLINEAR MODE COUPLING. Van Hoven, Gerard (Univ. of California, Irvine). Phys. Rev., A; 3: 153-8(Jan 1971).

A general treatment is given for the interaction of two propagating modes when they are nonlinearly coupled by a large-amplitude driving wave. The equations describing the space–time development of the mode amplitudes have a certain symmetry due to the constraints of small-signal energy conservation. The wave solutions, given the vector coupling relations ($\omega_d = \omega_a \pm \omega_b$, $k_d = k_a \pm k_b$), are of four possible types, depending on the signs of the energy densities and group velocities of the individual modes. The periodicity imposed by the driving wave is used to construct a spatial–temporal harmonic dispersion diagram in which these interactions are displayed. The results are then shown to be generalizations of the wave–wave couplings of linear theory. (auth)

11944 MEASUREMENT OF GROWTH RATE, NONLINEAR SATURATION COEFFICIENTS, AND MODE–MODE COUPLING COEFFICIENTS OF A VAN DER POL PLASMA INSTABILITY. Keen, B. E.; Fletcher, W. H. W. (United Kingdom Atomic Energy Authority, Abingdon, Eng.). J. Phys., D (London); 3: 1868-85(Dec 1970).

Results presented show that a self-excited ion–sound instability in a plasma behaves in a similar manner to a classical Van der Pol oscillator, both (a) in a single-mode régime, and (b) in a multi-mode régime. In the single-mode régime, various methods that enable the linear growth rate α_0 to be measured are described. These were checked by direct measurement and a consistent value is obtained. In the multi-mode régime, values are obtained for mode–mode coupling coefficients and nonlinear saturation coefficients for each mode present in the system, as well as for the parameters associated with the growth rates of these modes. Comparison with a theory developed to describe these two systems shows good agreement. (auth) (UK)

11945 EIGENVALUES OF BOUNDED PLASMAS WITH RANDOM PROPERTIES. Poularikas, A. D. (Univ. of Rhode Island, Kingston). Int. J. Electron.; 29: 581-5(Dec 1970).

The relation for the eigenvalues of slow waves in longitudinally magnetized plasmas with random plasma properties was developed. It was found that the phase characteristics of the wave are influenced by the type of the assumed correlation function. (auth) (UK)

11946 COUPLED WAVE EQUATIONS FOR MAGNETOPLASMA WITH ANISOTROPIC PRESSURE. Talekar, V. L.; Rawat, S. S. (Malaviya Regional Engineering Coll., Jaipur, India). Int. J. Electron.; 29: 533-9(Dec 1970).

The unified approach applied to magnetoplasma with isotropic pressure given in the earlier work of the authors (NSA 23: 42315) is extended to include the case of anisotropic pressure. General coupled-wave equations were deduced for such a type of magnetoplasma. Cases of propagation parallel and transverse to the static magnetic field are examined in some detail giving expressions for velocity of various modes. It is shown that the electromagnetic modes, ordinary as well as extraordinary, and the plasma mode are modified due to coupling when propagated in a general direction with respect to the static magnetic field. For the propagation along the static magnetic field the coupling vanishes and the modes are unmodified. Also the waves propagated in this direction do not experience the anisotropic effects of pressure. (auth) (UK)

Shielding

11947 GAMMA-RAY ATTENUATION AT ENERGIES OF APPROXIMATELY 6 AND 8 MeV. Johnson, W. Reed; Risher, Daniel H.; Rogers, James E.; Thompson, William L. (Univ. of Virginia, Charlottesville). Nucl. Sci. Eng.; 43: 32-41(Jan 1971).

Well-collimated beams of thermal-neutron-capture gamma rays from titanium and nickel, having average energies of about 6 to 8 MeV, respectively, were used to measure narrow-beam and total gamma-ray dose attenuation. Slab shields of lead, iron, and concrete were investigated for normal and oblique beam incidence. Total dose measurements were made by traversing an exposure-responsive detector through a plane behind and parallel to the shield. Monte Carlo and moments-method calculations were used to compare analytical and experimental total dose results. Good agreement was found for iron and concrete shields, but experimental results for the lead shield were higher than those predicted by the moments method by a factor of ~1.2 for 6 MeV and ~1.5 for 8 MeV. The reason for this disagreement is believed to be primarily bremsstrahlung produced by energetic secondary electrons slowing down in lead. (auth)

11948 LAYOUT OF RADIATION SHIELDS AGAINST GAMMA-RADIATION FROM SPENT NUCLEAR FUEL. Krueger, F. W. (VEB Kombinat Kraftwerksanlagenbau, Berlin). Kernenergie; 13: 287-90(Sep 1970). (In German).

The gamma-ray spectra from fission products formed after an arbitrary reactor working period and the dose rates behind a shield due to this radiation are shown to be simply calculable from the spectra or dose rates from fission products formed after an infinite reactor working period. Using this relationship, the number of initial data necessary for the layout of shields against gamma radiation from fission products, may essentially be reduced. As an example, the initial data for shielding point sources of gamma rays from fission products by ordinary concrete are given. (auth)

Solid-State Physics

Refer also to abstract 12427.

Radiation Effects

Refer also to abstracts 10905, 11673, 11676, and 11682.

11949 (AI-Trans-267) SOME STUDIES ON COBALT ELECTRON IRRADIATED AT 20°K. Sulpice, G.; Minier, C.; Moser, P.; Bilger, H. (Commissariat a l'Energie Atomique, Grenoble (France). Centre d'Etudes Nucleaires). Translated for Atomics International, Canoga Park, Calif., from a French report. 9p. Dep. NTIS.

An abstract of this paper, prepared from the original language, appeared as NSA 22: 26466.

11950 (CEA-R-3937) ELECTRON SPIN RESONANCE STUDY OF DEFECTS PRODUCED BY IRRADIATION IN AN IONIC SOLID: BERYLLIUM OXIDE. Herve, Alain (Commissariat a l'Energie Atomique, Grenoble (France). Centre d'Etudes Nucleaires). Dec 1970. 160p. (In French). Dep. NTIS (U. S. Sales Only).

Thesis. Submitted to Grenoble Univ. (France). Faculte des Sciences.

Using electron spin resonance, models were established for different types of defects (donor or acceptor centers, anion and cation vacancies) created by gamma or neutron irradiation in single crystals of beryllium oxide. It is shown that ionizing radiations liberate electrons and holes that are trapped by imperfections in the lattice (impurities, vacancies) and that neutron bombardments produce displacements of atoms in the crystal lattices. (auth) (France)

11951 THERMOLUMINESCENCE OF PURIFIED LiF POWDER EXPOSED TO THERMAL NEUTRONS AND GAMMA RAYS. Harasawa, Susumu (Rikkyo Univ., Tokyo); Kitahara, Akiharu; Saitoh, Masashi. Jap. J. Appl. Phys.; 9: 1552-3(Dec 1970).

The difference between the glow curves of pure LiF powders exposed to thermal neutrons and gamma rays was studied. It was found that the 140°C peak is sensitive to gamma rays, while the 335°C peak is sensitive only to thermal neutrons. The relation between the area of the 335°C peak and the total neutron flux is linear up to 10^{15} nvt. (D.L.C.)

11952 EFFECTS OF NUCLEAR RADIATION ON THE THERMOELECTRIC PROPERTIES OF MOLTEN SALTS AND P-TYPE

CUPROUS SULFIDE. Plummer, Mitty Charles. College Station, Tex.; Texas A and M Univ. (1970). 103p. University Microfilms Order No. 70-22,948.

Thesis.

Cobalt-60 γ irradiation of the molten salts, CuI, AgBr, and AgCl, at a dose rate of 1.4×10^3 R/sec produced changes in the electrical conductivity of 0.1 to 0.3%. The change in conductivity could not be accounted for by simple models. No change in the Seebeck effect was observed during irradiation. Hall mobilities for AgBr, CuCl, and AgCl were measured to be +.027, +.023, and +.031 (cm^2/volt-sec), respectively, at 50°C above the melting temperature of each. Zinc-doped Cu_2S exposed to cobalt-60 γ radiation was annealed at temperatures between 23 and 73°C to determine activation energies for annealing of radiation-induced resistivity increases. The activation energies 0.79 and 0.415 eV were used in predicting a damage cross section of 0.212 ± 0.02 barns for cobalt-60 γ radiation. Cu_2S was then exposed to reactor radiation. Comparison to reactor irradiations of other thermoelectric materials showed the resistance of Cu_2S to be less effected by neutrons. (Diss. Abstr. Int., B)

11953 WAVELENGTHS OF TRANSVERSE OSCILLATIONS OF FAST PROTONS IN PLANAR CHANNELING. Sone, Kazuho (Kyoto Univ.). Jap. J. Appl. Phys.; 9: 1533(Dec 1970).

Wavelength distributions were calculated for transverse oscillations of 200-keV and 1-MeV protons in a Si(110) planar channel at various incident angles Ψ_{in} up to the critical angle (0.68 and 0.30°, respectively). The results show that the distribution peaks shift to lower λ with increasing Ψ_{in}. (D.L.C.)

11954 ACTIVATION ENERGY AND THE FREQUENCY FACTOR OF THE 100°K ANNEALING STAGE OF SIMPLE DEFECTS IN n-TYPE GERMANIUM. Jaworowski, Andrzej (Univ., Warsaw); Wojcik, Krystyn; Rzewuski, Henryk. Nukleonika; 15: 253-8 (1970).

The Hall-mobility annealing stage at 100°K in Sb-doped germanium irradiated with 1-MeV electrons was investigated. The activation energy for the process $E = (0.11 \pm 0.02)$ eV and the frequency factor $A = (10 - 10^3)$ sec^{-1} were found. (auth)

11955 LUMINESCENCE OF CaF_2–TRF_3 IN THE GAMMA-RAY FIELD OF ^{60}Co. Vakhidov, Sh. A.; Kaipov, B.; Tavshunskii, G. A. Opt. Spectrosc. (USSR) (Engl. Transl.); 28: 515-17(May 1970).

Translated from Opt. Spektrosk.; 28: 949-54(May 1970).

The luminescence of CaF_2–ErF_3 and CaF_2–HoF_3 crystals was studied in a gamma-ray field in the temperature range 77 to 500°K. The gamma luminescence (GL) spectra are compared with photoluminescence (PL) data on the same samples. The temperature and concentration dependences of the quantum yield of GL in the visible portion of the spectrum were studied. The electron–hole and ionic processes leading to GL are discussed. It is concluded that the processes of luminescence in a γ-ray field are mainly due to the Er^{3+} and Ho^{3+} centers of cubic symmetry. (auth)

11956 INVESTIGATION OF M AND F' CENTERS IN ALKALI HALIDES BY LASER EXCITATION. Borms, Francois Leon. Ghent; State Univ. of Ghent (1970).

Thesis.

Measurements were performed on the repopulation rate of the M-center ground state after excitation in the M_1 band with a ruby laser. The M centers were created by irradiation with a ^{60}Co γ source. A description of the recovery of the M absorption requires the assumption of different processes with different decay times. About 40% of the excited M centers decay exponentially with a time constant 5×10^{-8} sec, presumably the decay of the $^1\Sigma\mu^+ \rightarrow {}^1\Sigma g^+$ transition. This decay time was independent of the concentration and temperature between 4 and 200°K as expected for an allowed dipole transition. The slow recovery of the M band is associated with the formation of new temporary bands at 1.02 and 4 μ. The 1.02-μ band is attributed to a transition of the F_2^+ center. The maximum of this band shifts to higher energies with increasing temperature. The 4 μ band is attributed to a transition of the center formed by an electron in a shallow trap. Decay times were measured simultaneously in M, F_2^+, and 4-μ bands. They indicate a bimolecular decay with the same time constant for the three bands. The decay time, which is strongly temperature-dependent, is 1.7 sec at 87°K and 7×10^{-3} sec at 110°K. By a supplementary excitation in the F or in the 4-μ band, the decay time decreases strongly. The formation of the 4-μ band in NaCl was detected by excitation in each of the bands associated with the electron-excess centers. Simultaneous absorption measurements were made with polarized light in the F, 4-μ, and M bands after laser excitation in the M band and in the F, the 4-μ, and the F' band after laser excitation in the F' band. From these measurements, it was concluded that the shallow trap is the F center. This implies the existence of a metastable form of the F' center. A triplet state is postulated. Absorption bands analogous to the 4-μ band in NaCl were seen in KCl at 6 μ (decay time at LNT = 8 sec), in NaF at 2,4 μ (decay time = 1 min), in KI at 4.8 μ (decay time $\approx$ 1 sec), and in KBr (decay time = 4.5 sec). (Diss. Abstr. Int., B)

11957 DETAILED INVESTIGATION OF STAGE I_D–I_E RECOVERY IN ELECTRON-IRRADIATED COPPER. Parkin, Don Merrill. Salt Lake City; Univ. of Utah (1970). 91p. University Microfilms Order No. 70-20,580.

Thesis

The work was conducted to study the annealing behavior of Frenkel distant pairs in copper as a function of initial defect concentration and incident electron energy. After an irradiation near 4.2°K, isothermal resistivity recovery curves were obtained in the range between 30°K and 60°K. The I_D–I_E recovery region (30 to 60°K) was found to be governed by a single activation energy, E = 0.117 eV, for interstitial migration. Based upon this observation, the I_D–I_E region is accounted for by the three-dimensional free diffusion of interstitials. The I_D recovery is described as being due to interstitials that are able to freely migrate, but which are spatially correlated to their vacancies and, upon activation, recombine with their vacancies. I_E is described as being due to interstitials that freely migrate and recombine with foreign vacancies. The experimental result that, although interstitials are able to freely migrate to vacancies, complete recovery was not achieved, is accounted for by including i–i interactions and impurity trapping in addition to i–v recombination. A theoretical expression including all of the above processes is presented. This expression includes a parameter that describes the initial correlation of interstitials and vacancies, as well as capture radii for i–v recombination, i–i interactions, and impurity trapping. It was found that this expression was able to fit the recovery data for initial defect concentrations of 2.2, 7, and 25 ppm after a 0.6-MeV electron bombardment. It was observed that the character of the I_D–I_E recovery was only slightly changed for incident electron energies of 0.6, 1.0, and 1.4 MeV. This result is interpreted as indicating that distant pairs in copper are mainly produced by knock-ons in or near the ⟨110⟩ direction. (TSS) (Diss. Abstr. Int., B)

11958 COLOR CENTERS AND THERMOLUMINESCENCE IN LiF. Mayhugh, Michael Ray. Hanover, N. H.; Dartmouth College (1970). 74p. University Microfilms Order No. 70-20,684.

Thesis.

A study was made of the radiation-induced optical absorption from 2 to 12 eV and the thermoluminescence from room temperature to about 300°C in pure and dosimetry-grade LiF. Irradiating the pure LiF induces the F-absorption band at 5.0 eV, a second band at 11.0 eV which is identified as the V_3 band in LiF, and a broad absorption from 6 to 10 eV, which also appears to be intrinsic. By observing the optical absorption in the pure and dosimetry LiF after various thermal and optical treatments, and by also ascertaining the attendant changes in the thermoluminescence, several conclusions can be made about the thermoluminescence process in the dosimetry-grade LiF. The two thermoluminescence peaks near 200°C, which are usually used for dosimetry, correlate with 4.0-eV impurity absorption bands that are induced by irradiation in the dosimetry material. In the case of the most prominent glow peak, the correlation is supported by an equality of thermal activation energies between the band and peak. Further, the centers causing these bands and peaks contain trapped electrons. Destruction of the V_3 band is shown to accompany release of these trapped electrons, and it is concluded that V_3 centers are involved in the luminescence process. Trap structures, the detailed luminescence mechanism, and a mechanism for supralinearity and sensitization are suggested. (Diss. Abstr. Int., B)

11959 SPUTTERING AND STRAIN OF SILICON BY ION IMPLANTATION. EerNisse, E. P. (Sandia Labs., Albuquerque, N. Mex.). J. Appl. Phys.; 42: 480-2(Jan 1971).

Sputtering yields of amorphous Si films by Ar^+, Kr^+, and Xe^+ ions were investigated in the 50- to 300-keV energy range. The yields were determined from the mass change measured by a quartz resonator microbalance which was used as the substrate for the Si films. The large frequency shifts at the lower ion fluences are evidence of strain introduced by the ion implantations. The results can be used as upper limits to estimate the sputtering yield of other ions in the periodic table. (D.L.C.)

11960 SELF-IRRADIATION DAMAGE INDUCED RESISTIVITY CHANGES IN ACTINIDE METALS AT LOW TEMPERATURES. Griffin, C. S. (Oxford Univ.); Mendelssohn, K.; Lee, J. A.; Mortimer, M. J. Nucl. Met., Met. Soc. AIME; 17: 635-48(1970).

From 4th International Conference on Plutonium and Other Actinides, Santa Fe, N. Mex. See CONF-701001-(Pt.2).

The results of recent low-temperature measurements on the actinide elements uranium, protactinium, neptunium, and plutonium are given. The changes in resistivity with time show saturation effects which may be correlated with changes seen in other properties. (auth)

11961 CORRECTION OF OPTICAL ABERRATIONS BY NEUTRON IRRADIATION. Sinai, P. Appl. Opt.; 10: 99-104(Jan 1971).

The refractive index of optical materials can be modified by means of neutron irradiation. By varying the radiation dose over selected areas of a lens according to some given law, the local change in the refractive index can be adjusted to correct for different types of optical aberrations. The particular case of spherical aberration is treated in detail. It is shown that irradiation leads to index modifications of the required order of magnitude and that irradiation times are acceptable. Moreover, the stability of the index modifications, the possibility of bleaching —without curing the index —and the absence of residual radioactivity make an irradiated lens suitable for optical applications. (auth)

11962 GROWTH OF EPITAXIAL LAYERS BY ION BEAM SPUTTERING. Unvala, B. A.; Pearman, K. (Imperial Coll. of Science and Tech., London). J. Mater. Sci.; 5: 1016-18(Nov 1970).

High-quality epitaxial silicon layers were grown by a novel technique of sputtering by an argon ion beam of high current density in a vacuum in the range of 10^{-4} torr at controlled rates of up to 400 Å per min, and at substrate temperatures between 700 and 900°C. The bombardment of the substrate surface by positive ions during deposition, which has been shown to have an adverse effect on the quality of the layers, was eliminated. A transition from polycrystalline to single-crystal structure was found in the temperature range of 700 to 730°C. The single-crystal layers were free from twinning, including grains and stacking faults. The layers, however, contained a number of small crystallographic defects, the nature of which is not clearly understood. Both p-type layers on n-type substrates and n-type layers on p-type substrates were deposited. The mesa section (~1-mm diameter) exhibited sharp diode characteristics, giving reverse breakdown voltages of between 30 and 150 V. The reverse current at voltages just below the breakdown voltages was about 10 μA. (UK)

11963 CHANGES OF SURFACE CONDUCTIVITY IN Ge DURING X-IRRADIATION. Kreutz, E. W.; Pagnia, H.; Waidelich, W. (Technische Hochschule, Darmstadt, Ger.). Z. Angew. Phys.; 30: 145-50(16 Nov 1970). (In German).

Changes of electrical conductivity in p-type Ge single crystals were measured during x-irradiation at liquid nitrogen temperature. Magnitude and sign of the changes in electrical conductivity depend on the radiation intensity, bulk carrier concentration, crystal thickness, and surface treatments. Thermally stimulated recovery measurements are presented. Field-effect measurements and thermal annealing indicate that surface phenomena are responsible for the σ changes. Charge transfers are excited between slow surface states and the underlying bulk. (auth)

11964 PRODUCTION OF LITHIUM OXIDE BY ELECTRON IRRADIATION OF LITHIUM FLUORIDE. Russell, G. J.; Martin, K. J.; Bowen, D. H. (Portsmouth Polytechnic, Eng.). J. Mater. Sci.; 5: 972-7(Nov 1970).

Observations of electron damage occurring in LiF single crystals within an electron microscope are recorded. A number of irradiation-induced defects were observed, but a new feature is the identification, by electron diffraction, of Li_2O distributed in precipitates and as a dispersed phase. (auth) (UK)

11965 TEMPERATURE DEPENDENCE OF THE KINETICS OF THE F-CENTER ACCUMULATIONS UNDER PROTON IRRADIATION. Alekseev, P. D. (Tomsk Polytechnic Inst., USSR). Izv. Vyssh. Ucheb. Zaved., Fiz.; No. 2, 144-6(1970). (In Russian).

Coloration processes induced by ionizing radiation were studied, using KI crystals irradiated by 3.5-MeV protons with a constant intensity of 1.12×10^{15} eV/cm^3 · sec at 90 to 300°K. The optimum temperature for maximum effective production of F centers was 130 ± 3°K, identical to the optimum temperature of x-ray and uv colorations. The only difference observed was that, in the case of proton irradiation, the efficiency curve was more symmetric and revealed greater difference in efficiency between the room and optimum temperatures. (R.V.J.)

11966 ISOCHRONAL ANNEALING OF THE ELECTRICAL PROPERTIES OF ELECTRON-IRRADIATED SEMICONDUCTING DIAMOND. Horszowski, S. M. (Diamond Research Lab., Johannesburg); Lourens, J. A. J. Phil. Mag.; 22: 1243-59(Dec 1970).

Two semiconducting diamonds were irradiated with 1-MeV electrons. The specimen temperature during the irradiation was 77°K and the cumulative dose was of the order of 8 μAhr/cm^2. The resistivity ρ and the Hall coefficient R were measured at ambient temperature before the irradiation, at half the cumulative dose and at the end of the irradiation. The specimens were subsequently subjected to a series of isochronal heatings at successively increasing temperatures in the range 200 to 1200°C. Each heating lasted for 30 min. Rho and R were measured at ambient temperature after each heating. From these measurements the concentration N_R of radiation-induced donor levels and the mobility μ_H of the charge carriers (positive holes) were calculated. N_R was found to increase approximately linearly with the dose D. This is consistent with the radiation-induced donor centers being vacancies or carbon interstitials. μ_H decreased with D, presumably larger due to an increase in ionized center scattering. Both N_R and μ_H exhibited reverse annealing, i.e., annealing producing changes in the same direction as the radiation damage. Reverse annealing in both specimens was first observed after heating at 400°C. The behavior of N_R on annealing was not found to correlate with that of μ_H in either specimen. However, the qualitative behavior of N_R was identical in both specimens. The same applies to the behavior of μ_H. The values of N_R after heating at 1200°C were equal to those before irradiation in both specimens. The value of μ_H after heating at 1200°C was higher than that before irradiation for one specimen and approximately equal to that before irradiation for the other specimen. (auth) (UK)

11967 DYNAMIC STUDIES OF THE OPTICAL ABSORPTION ASSOCIATED WITH TRAPPED ELECTRONS. Bieringer, R. J. (Owens-Illinois Tech. Center, Toledo); Montgomery, C. G. Phys. Rev., B; 2: 4988-94(15 Dec 1970).

Studies of electron traps in fused silica, populated via x irradiation, are reported. The silica was doped with several concentrations of the rare earths Tb, Tm, and Dy in order to measure thermoluminescence, which was correlated with the radiation-induced optical absorption. The traps were found to be host-associated, rather than dopant associated. The absorption spectrum was obtained both under static conditions (at room temperature) and under dynamic conditions (at elevated temperatures) for which, in addition to thermal broadening, the densities of the populated traps change with time. The dynamic measurements were made using a rapid-scan monochromator, designed to obtain the spectrum in ~1 msec. The results of these measurements demonstrated unambiguously the existence of a redistribution of electrons among the traps at elevated temperatures, implying the existence of nonlocalized intermediate states. (auth)

11968 RECOMBINATION PARAMETERS IN LOW-RESISTIVITY GAMMA-IRRADIATED n-TYPE GERMANIUM. Srour, J. R.; Curtis, O. L. Jr. (Northrop Corporate Labs., Hawthorne, Calif.). Phys. Rev., B; 2: 4977-87(15 Dec 1970).

Detailed studies of recombination in ~0.2-Ω cm As- and Sb-doped ^{60}Co γ-irradiated Ge are reported. The principal experimental techniques used were measurement of the variation of minority-carrier lifetime with temperature (at low excess density) and with excess density (using temperature as a parameter). The temperature dependence of the electron capture probability c_n was obtained for both dopant cases. The hole capture probability c_p was found, in both cases, to be approximately independent of temperature over the range examined. For Sb-doped material at 323°K, the recombination-center energy-level position (neglecting statistical weight) was found to be 0.361 ± 0.005 eV above the valence band, with a possible slight temperature dependence corresponding roughly to one-half the variation of the band gap with temperature. The capture-probability ratio c_p/c_n at this same temperature was 740. For the As-doped case, two different levels appear to dominate the recombination process in annealed and unannealed low-resistivity material. The energy-level positions relative to the valence band (neglecting statistical weight) are 0.327 ± 0.005 and 0.37 ± 0.01 eV at room temperature for the annealed and unannealed samples, respectively. The corresponding capture-probability ratios are 650 and 810. As in the case of Sb doping, the energy level appears to shift with temperature at about one-half the rate of the shift in band-gap energy. (auth)

11969 TEMPERATURE DEPENDENCE OF DECHANNELING COEFFICIENT IN CHANNELING PHENOMENA OF PROTONS IN SILICON CRYSTALS. Fujimoto, F. (Tokyo Univ.); Komaki, K.; Nakayama, H.; Ishii, M. Phys. Lett.; 33A: 432-3(14 Dec 1970).

The variations of dechanneling coefficient with temperature are studied for the ⟨111⟩ axial channeling of protons for silicon crystals. The result shows that the dechanneling coefficient is represented by $A\rho^2 + B$, where ρ is the mean amplitude of thermal vibrations. (auth)

11970 DENSITY INCREASE IN THE Si(111) SURFACE REGION CREATED BY Ar ION BOMBARDMENT. Andersson, S. (Chalmers Univ. of Technology, Goteborg). Phys. Lett.; 33A: 455-6(14 Dec 1970).

When the Si(111) surface is bombarded with doses $>10^{15}$ Ar ions/cm^2 (150 eV), the electron energy loss spectra exhibit an increase in the plasmon loss energy revealing an increased density of Si atoms in the surface region. (auth)

11971 ANOMALOUS TRANSMISSION OF PARTICLES THROUGH PERFECT CRYSTALS. Pathak, A. P.; Yussouff, M. (Indian Inst. of Tech., Kanpur). Phys. Rev., B; 2: 4723-30(15 Dec 1970).

A formalism for the transmission of particles through perfect crystals at low temperatures is presented, assuming a Debye model for the lattice vibrations. The results are compared with a similar calculation by DeWames et al. in which the Einstein model is used to depict lattice vibrations. It is shown that the requirements of high particle energy and localization of the interaction potential for producing anomalous transmission are justified in the present model. The temperature dependence of the process and its dependence on the energy of the incident particles are established. A comparison is made between the relative effects of the atomic mean-square displacement and the range of the interaction potential. (auth)

11972 LUMINESCENT RESPONSE OF ANTHRACENE TO CHANNELED α PARTICLES. Wille, Klaus (Univ., Goettingen, Ger.). Z. Phys.; 241: 55-64(1971).

Luminescent response of anthracene to channeled α particles transmitted parallel to the [001] axis is investigated. A simple theoretical model is presented and comparisons made with experiment. For a given specific energy loss dE/dx, the luminescent response to channeled α particles is the same as to randomly incident particles. This result is concluded from the good agreement of theoretical calculations and experimental measurements within the accuracy of about ±3%. The relationship between specific luminescence dS/dx of anthracene and specific energy loss dE/dx is used for the calculations. It is obtained by fitting experimental values to the theoretical expression. (auth)

11973 LOW-TEMPERATURE LITHIUM DRIFT IN SILICON. Klimkova, O. A.; Niyazova, O. R. (Inst. of Nuclear Physics, Tashkent). Phys. Status Solidi (a); 3: K93-6(16 Oct 1970).

Lithium drift stimulated by soft x rays in p-type (B-doped) Si single-crystal plates at 200 and 300°K was studied. The lithium penetration into the crystals was detected by means of capacitance vs voltage characteristics. It was found that the x radiation does increase the lithium mobility; the activation energy is estimated to be 0.1 eV. (D.L.C.)

11974 CATHODOLUMINESCENCE OF ION IMPLANTED SiC. Brander, R. W.; Callaghan, M. P. (General Electric Co. Ltd., Wembley, Eng.). Phys. Status Solidi (a); 3: K143-6(16 Oct 1970).

Crystals of SiC were implanted with Kr and He ions and their cathodoluminescence spectrum examined. The implanted regions were found to be black and opaque in the originally transparent crystals. Annealing was carried out at 400 to 1400°C. The cathodoluminescence before annealing was weaker than the residual luminescence, but during annealing it increased greatly, and its color was green. The spectrum showed a broad band and several sharp peaks and is independent of the type of implanted ion. Crystals that exhibited strong yellow cathodoluminescence before implantation did not exhibit green luminescence; the yellow luminescence reappeared on annealing above 800°C. No change in polytype occurred over the annealing. The spectrum could be due to a vacancy complex and exciton transitions. (D.L.C.)

11975 SOME FEATURES OF RADIATION HARDENING OF NaCl SINGLE CRYSTALS. Boyarskaya, Yu. S.; Zhitaru, R. P. (Inst. of Applied Physics, Kishinev, USSR). Phys. Status Solidi; 42: K29-32(1 Nov 1970).

NaCl crystals were irradiated by 30-kV x rays at an intensity of 10^{14} eV/cm-sec. Microhardness was measured on the irradiated surfaces, and the accumulation of F and M centers was studied in a 20-μm surface layer. A graph of microhardness vs irradiation time shows two plateaus, while the F- and M-center growth curves show no such plateaus. The hardening is not affected by bleaching with light. A plausible mechanism for these observations is given. The concentration of hardening defects is calculated, using Fleisher's theory, and found to be of the same order of magnitude as in the case of interstitials or interstitial clusters. (D.L.C.)

11976 ENERGY LOSS AND ENERGY STRAGGLING OF WELL-CHANNELED HYDROGEN, HELIUM, AND LITHIUM IONS IN GOLD. Hoegberg, G.; Norden, H.; Skoog, R. (Chalmers Univ. of Tech., Goteborg). Phys. Status Solidi; 42: 441-51(1 Nov 1970).

The stopping cross sections of well-channeled H^+, D^+, He^+, and Li^+ ions were determined in thin gold single crystals along the ⟨110⟩, ⟨112⟩, and ⟨111⟩ directions. The energy range studied was 2 to 54 keV. The energy straggling was investigated as a function of energy loss for different mean energies, kinds of ions, and crystallographic directions. In some cases, the energy loss spectrum showed a structure. (auth)

11977 ENERGY RELEASE AND ELECTRICAL RESISTIVITY RECOVERY IN NICKEL AND NICKEL WITH SILICON IMPURITY CONTENTS FOLLOWING ELECTRON IRRADIATION AT 20°K. Cotignola, J. M.; Minier, C.; Paillery, A.; Bonjour, E. (CEN, Grenoble, France). Phys. Status Solidi; 42: 167-71(1 Nov 1970).

The stored energy release in Ni and Ni−(0.014, 0.073, and 0.29) at. % Si was measured in the temperature range 40 to 400°K after irradiation with 2-MeV electrons. The resistivity of the samples was measured simultaneously between 40 and 70°K. The ratios of stored energy and resistivity obtained in stage I are 3.9 cal/g per $\mu\Omega$cm for pure Ni, 2.2 cal/g per $\mu\Omega$cm for Ni−0.014 at. % Si, 2.0 cal/g per $\mu\Omega$cm for Ni−0.073 at. % Si, and 1.1 cal/g per $\mu\Omega$cm for Ni−0.29 at. % Si. (auth)

11978 BARKHAUSEN EFFECT IN FERROELECTRICS DURING CONTINUOUS X IRRADIATION. Komlyakova, N. S.; Kharitonov, Yu. N. (Abakan Teachers Inst., USSR). Izv. Vyssh. Ucheb. Zaved., Fiz.; No. 2, 458-60(1970). (In Russian).

The Barkhausen effect in Seignette salts and triglycinesulfate (TGS) crystals under continuous x irradiation was studied. Curves of the number of amplitude jumps as a function of the x-ray dose are presented for the Seignette and TGS crystals. Multiple measurements revealed a general rule for all specimens: at doses up to 1.5 to 2 Ci, the total number of jumps increased, reaching the maximum after which it monotonically diminished. A similar picture was observed for the TGS crystal. However, in contrast to the Seignette salts, the increased number of jumps in TGS was due to small jumps. The extreme dependence of the number of oscillation jumps on the dose of the x radiation was observed only in well-annealed specimens. In the nonannealed and deformed specimens, the number of jumps during irradiation usually began to drop immediately with the irradiation. It was concluded that the maximum of Barkhausen jumps depend strongly on the irradiation dose. (R.V.J.)

Physical Properties

Refer also to abstracts 11372, 11381, 11403, 11423, 11440, 11472, 11477, 11494, 11510, 11677, and 11847.

11979 (CEA-CONF-1704) COLINEAR AND NONCOLINEAR MAGNETIC STRUCTURES IN THE RARE EARTH COMPOUNDS RNi_3 AND R_2Ni_7. Paccard, D. (Centre National de la Recherche Scientifique, Grenoble (France)); Schweizer, J.; Yakinthos, J. (Commissariat a l'Energie Atomique, Grenoble (France). Centre d'Etudes Nucleaires). 1970. 6p. (In French). (CONF-700940-3). Dep. NTIS (U. S. Sales Only).

From International Conference on Magnetism, Grenoble, France.

The crystalline structures of the compounds RNi_3 and R_2Ni_7 (R = rare earth element) can be represented by a superposition of hexagonal RNi_5 cells with ordered substitutions of atoms. These substitutions lead to a hexagonal site and a pseudocubic site for the rare earth atoms. Two spin arrangements (colinear and canted) are possible due to the strong anisotropy of the rare earth in both crystallographic sites. A colinear structure was found to exist for $HoNi_3$ and canted structures for Er_2Ni_3 and $ErNi_7$. In these compounds, the nickel moment is almost zero and exchange interactions between rare earth atoms are small. In erbium compounds, local anisotropy favors different moment directions in both sites. In isomorphous compounds with cobalt, exchange interactions are enhanced by the magnetic moment of the cobalt and stabilize the colinear structure. A strong magnetic field can induce the change from a colinear to a canted structure with $ErCo_3$. (auth) (France)

11980 (CEA-R-4113) ELECTRONIC PROPERTIES OF ACTINIDE CARBIDES AND NITRIDES. de Novion, Charles-Henri (Commissariat a l'Energie Atomique, Fontenay-aux-Roses (France). Centre d'Etudes Nucleaires). Dec 1970. 153p. (In French). Dep. NTIS (U. S. Sales Only).

Thesis. Submitted to Paris Univ., Orsay (France). Faculte des Sciences.

Measurements were made on the following properties: magnetic susceptibilities of ThN, UN, U_2C_3, $NpC_{0.95}$, NpN, $U(C_{1-x}N_x)$, $(U_xTh_{1-x})N$; electrical resistivities of NpN, U_2C_3, $U(C_{1-x}N_x)$; specific heat (between 1.3 and 10°K) of ThN, UN, $U(C_{1-x}N_x)$, YN,

$(Y_{0.94}U_{0.06})N$. The results are discussed from two points of view: random and localized 5 f electrons. The calculated crystal field effect with a localized 5 f^2 configuration gave the right order of magnitude for the specific heat anomaly of UN at 52°K. The electronic specific heat, magnetic susceptibility (at 4°K), and residual resistivity for $U(C_{1-x}N_x)$ carbonitrides are maxima for x = 0.88 (concentration for which the long range antiferromagnetic order at 0°K disappears): it is probably a paramagnon effect. (France)

11981 (ORO-3674-4) MAGNETIC PHENOMENA AT METAL SURFACES. Technical Progress Report, February 1–December 31, 1970. Spooner, Stephen (Georgia Inst. of Tech., Atlanta. Engineering Experiment Station). Contract AT(40-1)-3674. 94p. Dep. NTIS.

COBALT — magnetic torque measurements on films of, on copper single-crystal substrate
COMPUTER PROGRAMS — FOCAL, for control of neutron diffraction experiments
IRON CARBONATES — neutron inelastic scattering study of magnons and phonons in siderite
MANGANESE CHLORIDES — magnetic spin structure of $MnCl_2 \cdot 4H_2O$, neutron diffraction study of
NEUTRON DIFFRACTION ANALYSIS — control of experiments, FOCAL interpreter for (D.L.C.)

11982 PHOTOEMISSION AND OPTICAL INVESTIGATION OF THE ELECTRONIC STRUCTURE OF MOLYBDENUM AND RUTHENIUM. Kress, Kenneth Albert. Bozeman, Mont.; Montana State Univ. (1970). 152p. University Microfilms Order No. 70-14,698.

Thesis.

The photoemission and optical properties of vapor-deposited films of Mo and Ru were measured at room temperature. The photoemission properties measured are in the spectral range of the threshold (4.3 and 5.4 eV for Mo and Ru, respectively) to 11.8 eV. The optical properties are measured from 0.5 to 11.8 eV. The data from both Mo and Ru are found to be consistent with, and analyzed by, the nondirect transition model. Corrections for the escaping scattered electrons are included in the optical density of states (ODS) analysis. Peaks in the ODS are found at $E - E_F$ = −0.5 eV, −1.6 eV, and −3.9 eV for Mo; and −0.4 eV, −1.3 eV, and a third tentatively placed at −3.6 eV for Ru. The ODS for $E > E_F$ is determined by direct numerical inversion of the nondirect model expression for the dielectric constant. Several peaks appear in the ODS of Mo for $E > E_F$ while only one is observed in the ODS of Ru. The ODS of Mo and Ru is compared with the band calculations of Matthesis for tungsten (Matthesis, 1965) and rhenium (Matthesis, 1966) respectively. The relation of the measured ODS's to the explanations based on the electronic density of states for the anomalous isotopic mass dependence of the superconducting transition temperature is discussed. For Mo the volume loss function has a peak at 10.8 eV while the absorption coefficient has a minimum at 11.3 eV, which correlates with a minimum in the quantum yield at approximately 11.0 eV. The energy distribution of the photoemitted electrons shows slight structural changes in the spectral range 10 to 11 eV. In the same spectral region a similar but weaker correlation between structure in the loss function, absorption coefficient, yield, and the energy distributions of Ru is noted. (Diss. Abstr. Int., B)

11983 COMPOSITION RANGES WITH SIMILAR CONSTRICTED HYSTERESIS LOOPS IN Mn–Al–B ALLOYS. Narita, Kenji; Sasaki, Tadashi; Setoguchi, Yoshinori (Kyushu Univ., Fukuoka). Jap. J. Appl. Phys.; 9: 1536(Dec 1970).

The change of hysteresis loop form with B additions to 55 at. % Mn–Al alloys was studied. The transition from the hysteresis loop of Mn–Al to the constricted loop at high B contents (21 at. %) proceeds through two loops with knees in the second and third quadrants. A phase diagram of the composition ranges with the four hysteresis loop types is presented. The Mn content for maximum saturation magnetization changes from 55 at. % Mn at no B to 53 at. % Mn at 21 at. % B. (D.L.C.)

11984 TEMPERATURE DEPENDENCE OF THE ROTATIONAL HYSTERESIS OF THE ALLOYS OF $SmCo_5$–$SmCu_5$ SYSTEM. Uehara, Mitsuru; Morimoto, Ichiro (National Research Inst. for Metals, Tokyo). Jap. J. Appl. Phys.; 9: 1539(Dec 1970).

The magnetic torque and rotational hysteresis losses of $SmCo_4Cu_1$ and $SmCo_{3.5}Cu_{1.5}$ were studied over a wide temperature range, from 500 to 0°K. The losses and the critical fields at which the hysteresis occurs were found to increase at the lower temperatures. The temperature dependence of the critical field is very pronounced, decreasing as T^{10}. (D.L.C.)

11985 STUDY OF IN-BAND RESONANT MODES IN CHROMIUM–TUNGSTEN ALLOYS BY INELASTIC NEUTRON SCATTERING. Cunningham, Robert Martin. Columbia, Mo.; Univ. of Missouri (1970). 139p. University Microfilms Order No. 70-20,774.

Thesis.

The modifications, additions, and supplementary programs necessary for preparing the Mitsubishi Dual-Arm Neutron Diffractometer for use at the University of Missouri's 5-MW Reactor (MURR) were completed. The first investigation to be undertaken on the MURR diffractometer was a study of the in-band resonant modes in chromium–tungsten alloys by inelastic neutron scattering. The mean positions and full widths at half maximum for fourteen phonon groups in the transverse branch in the (001) direction in Cr, Cr–0.3 at. % W, Cr–0.8 at. % W, and Cr–1.6 at. % W were determined, and the frequency shifts and natural widths were plotted as functions of the frequency of pure Cr for these concentrations. The results seem to substantiate the contention of Behera and Deo that the discrepancy between the theory and the experiment is not a concentration effect. The magnitude of the negative frequency shifts appears to be in fair agreement, but these negative shifts occur at a higher frequency than indicated by theory and there is very little positive shift observed. The measured natural widths also peak at a higher frequency than predicted. The qualitative features of the frequency shifts and natural widths seem to be in much better agreement with the theory of first-neighbor force constant changes considered by Behera and Deo. (TSS) (Diss. Abstr. Int., B)

11986 PHONON SPECTRA IN TaC AND HfC. Smith, H. G.; Glaeser, W. (Oak Ridge National Lab., Tenn.). Phys. Rev. Lett.; 25: 1611-13(7 Dec 1970).

Phonon dispersion curves were measured by one-phonon coherent inelastic neutron scattering in the high-symmetry directions of TaC at room temperature and at 4.2°K (superconducting transition temperature $T_c \approx 10$°K). Pronounced structure is observed in the [001] and [110] directions for the longitudinal acoustic modes and, to some extent, for the longitudinal optic modes. By contrast, HfC ($T_c < 1$°K) exhibits little or no structure in these modes. (auth)

11987 OPTICAL PROPERTIES OF ANTIFERROMAGNETIC CHROMIUM AND DILUTE Cr–Mn AND Cr–Re ALLOYS. Bos, Laurence W.; Lynch, David W. (Ames Lab., Iowa). Phys. Rev., B; 2: 4567-77(1 Dec 1970).

The antiferromagnetic energy gap and optical properties of single crystals of Cr and of Cr alloyed with 0.45, 0.94, 2.5, and 4.5% Mn and with 1.05 and 2.0% Re have been investigated by measuring the optical absorption over a photon energy range of 0.08 to 5 eV. The data were taken at 4.2°K by a calorimetric technique. It is found that at 4.2°K, approximately 1% Mn or Re will cause commensurate antiferromagnetic ordering, and the energy gap shifts abruptly from 0.13 to 0.36 eV near this concentration of diluent. Evidence is given for indirect transitions occurring across a double energy gap in the noncommensurate samples, and the results are explained in terms of a band model. The widths of the absorption peak and the peak in ϵ_2 in the commensurate samples are discussed in terms of a gap anisotropy and impurity broadening. Optical absorption peaks near 1, 2, and 3.4 eV are associated with direct interband transitions originating from the N_1', Γ_{25}', and P_4 symmetry points, with a contribution to the 1-eV absorption from transitions from the Fermi surface to the flat unoccupied band extending through N_4, Γ_{12}, P_3, and H_{25}'. (auth)

11988 MAGNETIC ORDERING IN PrB_6. Lee, K. N. (Stanford Univ., Calif.); Bachmann, R.; Geballe, T. H.; Maita, J. P. Phys. Rev., B; 2: 4580-5(1 Dec 1970).

Measurements of the specific heat and resistivity ρ of PrB_6 at low temperatures are presented. The extreme sharpness of the specific-heat anomaly at the antiferromagnetic ordering temperature indicates that PrB_6 may undergo a first-order transition of the type predicted by Wang and Cooper. A comparison of $d\rho/dT$ with the heat capacity in the critical region gives qualitative agreement with the theory of Fisher and Langer. (auth)

11989 VIRTUAL-BOUND-STATE FORMATION IN Pd–U ALLOYS. Nellis, W. J. (Argonne National Lab., Ill.); Brodsky, M. B.; Montgomery, H.; Pells, G. P. Phys. Rev., B; 2: 4590-6 (1 Dec 1970).

Measurements were made from below 2°K to 300°K of the electrical resistivity and magnetic susceptibility of Pd–U alloys. Low-temperature specific heats were also measured for Pd–U and Pd–Th alloys. At low-actinide compositions, the electronic specific-heat coefficient and the magnetic susceptibility decrease with concentration and are the same as those of Pd–Ag versus electron/atom ratio, provided valences of 1, 4, and 6 are

used for silver, thorium, and uranium, respectively. However, at compositions above 7.5 at. % uranium, the electronic specific-heat coefficient and susceptibility rose quickly with composition, and minima are found in the resistivity–temperature curves. The susceptibility indicates no localized-moment behavior. The results are interpreted by the formation at the Fermi level of uranium-5f virtual bound-state levels, whose width decreases with uranium concentration. The specific-heat data give evidence for a term due to interactions between conduction electrons and spin fluctuations. The negative resistivity–temperature derivatives are attributed to localized spin fluctuations. (auth)

11990 KONDO EFFECT IN $La_{1-x}Ce_x$ ALLOYS UNDER PRESSURE. Kim, K. S.; Maple, M. B. (Univ. of California, San Diego, La Jolla). Phys. Rev., B; 2: 4696-9(1 Dec 1970).

The low-temperature electrical resistance of $La_{1-x}Ce_x$ alloys in both the fcc and the dhcp phase was measured under pressure. Between normal pressure and 19 kbar the resistance always exhibited a minimum at T_{min}, which initially increased slightly under pressure, but remained constant above 7 kbar. The resistance R(T) for $T < T_{min}$ varied as lnT down to the superconducting transition temperature T_c or the limiting measuring temperature (1.3°K). The slope, $-dR(T)/d\ lnT$, varied appreciably and nonmonotonically with pressure; the relationship between the depression of T_c and $-dR(T)/d\ lnT$ as a function of pressure is discussed. (auth)

11991 SOME ELECTRICAL PROPERTIES OF THE URANIUM–PLUTONIUM MIXED OXIDES. Kurihara, Masayoshi; Abe, Jiro; Fukushima, Susumu; Sasayama, Tatuo; Shimokawa, Junichi (Japan Atomic Energy Research Inst., Tokai). Nucl. Met., Met. Soc. AIME; 17: 84-94(1970).

From 4th International Conference on Plutonium and Other Actinides, Santa Fe, N. Mex. See CONF-701001–(Pt.1).

Both the electrical resistivity and thermoelectrical power of hypostoichiometric uranium–plutonium mixed oxides containing from 19 to 40 wt. % plutonium were measured at temperatures from room temperature to about 800°C. The data were not reproducible in the low temperature during the temperature cycle, and a cause for this was attributed to the effect of self-irradiation damage due to plutonium. Temperature of about 350°C for a sharp break in resistivity vs 1/T was very similar to that for the p–to–n conductivity transition, and this temperature agreed approximately with temperature for the phase reaction, $MO_{2-y} \rightleftharpoons MO_2 + MO_{2-y}$ (fcc) in the U–Pu–O system. Two conductivity mechanisms are possible in this temperature range. Below about 350°C the conductivity is extrinsic and may be explained in terms of hopping mechanism. At temperatures above 350°C the conductivity becomes intrinsic with an energy gap of 1.1 eV. (auth)

11992 ELECTRONIC BAND STRUCTURE OF THE ACTINIDE METALS. Koelling, D. D. (Northwestern Univ., Evanston, Ill.); Freeman, A. J.; Arbman, G. O. Nucl. Met., Met. Soc. AIME; 17: 194-208(1970).

From 4th International Conference on Plutonium and Other Actinides, Santa Fe, N. Mex. See CONF-701001–(Pt.1).

The electronic band structures of fcc americium and thorium and bcc uranium were calculated. A basic method using the relativistic augmented plane wave basis set in a variational formalism was employed. Calculations on fcc plutonium and curium are in progress. (G.M.C.)

11993 ELECTRONIC BAND STRUCTURE CALCULATIONS FOR PARAMAGNETIC URANIUM COMPOUNDS WITH THE NaCl-TYPE SYMMETRY. Davis, Harold L. (Oak Ridge National Lab., Tenn.). Nucl. Met., Met. Soc. AIME; 17: 209-18(1970).

From 4th International Conference on Plutonium and Other Actinides, Santa Fe, N. Mex. See CONF-701001–(Pt.1).

Motivated by a desire to investigate possible correlations between calculated band structures and the diverse physical properties of actinide compounds, first-attempt band structure calculations were performed for the uranium compounds UX, with X = C, N, P, As, S, and Se. The calculations correspond to the paramagnetic states, and were done using the nonrelativistic form of the Korringa–Kohn–Rostoker method. Some features of the calculations having qualitative correlations with physical properties are given. All the investigated compounds have sufficient band overlap, in the vicinity of their calculated Fermi energies, to account for their observed metallic behaviors. The calculations for all the compounds have completely occupied U 5f—X np bands, whose electron density distributions resemble covalent chemical bonds. This feature correlates with the hardness and brittleness of the compounds. The calculated Fermi energies intersect strongly hybridized f-d bands, which give high density of states at the Fermi energies and correlate with the observed high low-temperature specific heat coefficients. In addition, comments are made comparing the present calculations with previous band structural models for these and similar actinide compounds. (auth)

11994 CRYSTAL-FIELD EFFECT AND THE MAGNETIC PROPERTIES OF NaCl-TYPE ACTINIDE COMPOUNDS. Chan, S.-K.; Lam, D. J. (Argonne National Lab., Ill.). Nucl. Met., Met. Soc. AIME; 17: 219-32(1970).

From 4th International Conference on Plutonium and Other Actinides, Santa Fe, N. Mex. See CONF-701001–(Pt.1).

The effects of strong spin–orbit coupling and strong crystal-field perturbation on the low-lying states of 5f ions in a cubic crystal environment were investigated theoretically. The energy-level scheme was applied to the magnetic properties of actinide ions in NaCl-type compounds. (auth)

11995 METALLIC VALENCIES OF THE EARLY TRANS-ACTINIUM METALS: THEORETICAL VS. EMPIRICAL CORRELATIONS. Kmetko, E. A.; Hill, H. H. (Los Alamos Scientific Lab., N. Mex.). Nucl. Met., Met. Soc. AIME; 17: 233-43(1970).

From 4th International Conference on Plutonium and Other Actinides, Santa Fe, N. Mex. See CONF-701001–(Pt.1).

Nonrelativistic band structure calculations were performed for the metals Ra through Cm by the augmented plane wave method incorporating an optimized Slater exchange potential. The band charge hybridizations found were compared with those implied by empirical assignments of metallic valency based on measured atomic radii, such as the well-known correlation due to Zachariasen. Serious disagreement between these two approaches was revealed in the results for the metals Pa through Cm. This apparently indicates that empirical correlations of the Zachariasen type fail to fully take into account the apparently vast differences between the 4f electrons of the rare-earth metals and the 5f electrons in the transactinium series. (auth)

11996 INFRARED PROPERTIES AND SPECIFIC HEAT OF PLUTONIUM DIOXIDE. Manes, Livio (EURATOM, Karlsruhe, Ger.). Nucl. Met., Met. Soc. AIME; 17: 254-63(1970).

From 4th International Conference on Plutonium and Other Actinides, Santa Fe, N. Mex. See CONF-701001–(Pt.1).

Measurements of normal reflection and absorption on stoichiometric PuO_2 were performed. The values of the vibrational frequencies of the oxide at K = 0, and of ϵ_∞ and $(\epsilon_0 - \epsilon_\infty)$ are reported. This set of values was used to calculate the vibrational specific heat of PuO_2. An analysis of the experimental c_p vs T curves of Sandenaw and of Kruger permits the presence of an additional contribution, having an Arrhenius dependence at low temperature, in the range 300 to 1000°K. An interpretation of this effect is advanced as a Schottky electronic excitation in levels resulting from the crystal-field splitting of the 5I4 state of the free Pu(IV) ion. (auth)

11997 POSITRON ANNIHILATION IN PLUTONIUM. Barnes, G. T.; Gustafson, D. R. (Wayne State Univ., Detroit). Nucl. Met., Met. Soc. AIME; 17: 271-8(1970).

From 4th International Conference on Plutonium and Other Actinides, Santa Fe, N. Mex. See CONF-701001–(Pt.1).

The angular correlation of positron annihilation radiation in plutonium was measured at several temperatures ranging from 4.2 to 623°K in order to examine the part played by the conduction electrons in the anomalous properties of plutonium. No apparent difference was observed between the α-phase angular correlation curves measured at 4.2, 53, 77, and 232°K indicating that little or no repopulation of electrons between conduction and 5f states occurred. These temperatures are both above and below the critical temperature of ~65°K associated with the various low-temperature anomalies in plutonium. Zachariasen's promotional model for the negative coefficient of thermal expansion in δ- and δ′-plutonium predicts a change of valence of 8% in addition to a 7% change in conduction electron density due to lattice expansion when going from γ- to δ-plutonium. The observed difference of 7.0 ± 1.6% in the conduction electron density calculated from a comparison of angular correlation curves of γ-plutonium (520°K) and δ-plutonium (623°K) can be explained by the lattice expansion associated with the γ- to δ-phase transition alone without assuming any significant change in valence. (auth)

11998 POSITRON ANNIHILATION IN PLUTONIUM–ALUMINUM DELTA PHASE ALLOYS. Loree, T. R. (Los Alamos Scientific Lab., N. Mex.). Nucl. Met., Met. Soc. AIME; 17: 279-85(1970).

From 4th International Conference on Plutonium and Other Actinides, Santa Fe, N. Mex. See CONF-701001–(Pt.1).

The delta-phase Pu–Al alloys (1 to 10 at. % Al) were investigated at room temperature by the technique of positron annihilation. Two distinct groups of valence electrons were found, which

XUM

were interpreted to be a group of plane-wave-like electrons and a larger group of hybridized valence electrons. The data suggest that all the valence electrons from the aluminum go into the plane-wave-like group in the alloys, and that in pure delta plutonium this group contains one electron. (auth)

11999 LOW ENERGY SECONDARY ELECTRON DISTRIBUTION STUDIES OF SOME LIGHT ACTINIDES. Ellis, W. P.; Jackson, D. D. (Los Alamos Scientific Lab., N. Mex.). Nucl. Met., Met. Soc. AIME; 17: 286-95(1970).

From 4th International Conference on Plutonium and Other Actinides, Santa Fe, N. Mex. See CONF-701001-(Pt.1).

At incident beam energies below 1000 eV, only 5 to 15% of electrons are scattered elastically from solid surfaces. These are the coherently reflected electrons normally displayed in low-energy electron diffraction, LEED, in studies of surface crystallography. The remaining 95 to 85% of the secondary current contains extractable information about atomic core energy levels and the chemical nature of the surface. Two main types of peaks are observed in the energy distribution curves: Auger and inner-shell ionization characteristic losses. For ThO_2(~111) at $E_p < 1000$ eV, there are some twenty readily detectable transitions among which nine are Auger peaks and eleven are characteristic losses. The following text describes the transitions present in the inelastic secondary-electron spectra from ThO_2 (~111), briefly compares them with previous UO_2 data, and discusses the results in terms of reported x-ray levels. (auth)

12000 DETERMINATION OF ELECTRONIC PROPERTIES OF THE ACTINIDES WITH THE MOESSBAUER EFFECT. Kalvius, G. Michael (Argonne National Lab., Ill.). Nucl. Met., Met. Soc. AIME; 17: 296-330(1970).

From 4th International Conference on Plutonium and Other Actinides, Santa Fe, N. Mex. See CONF-701001-(Pt.1).

The application of Moessbauer spectroscopy for the determination of electronic properties of the actinides is outlined. It is shown how Moessbauer spectroscopy enables the deduction of the electron charge density, the electric field gradient, and the magnetic hyperfine field at the actinide nucleus. To achieve this goal a brief outline of the basic physical principles governing the Moessbauer effect is given. Then the most important aspect of the usual experimental arrangement is discussed. Hyperfine spectra are explained and the origin of the hyperfine parameters in the actinides in general is discussed. Some typical examples of recent experimental results in this field are shown. Finally a brief summary is given of the most promising isotopes that can be used in Moessbauer spectroscopy of the first half of the actinide series. (auth)

12001 MAGNETIC BEHAVIOR OF Np METAL AND DILUTE Np ALLOYS FROM MOESSBAUER EFFECT STUDIES. Dunlap, B. D.; Brodsky, M. B.; Kalvius, G. M.; Shenoy, G. K. (Argonne National Lab., Ill.). Nucl. Met., Met. Soc. AIME; 17: 331-7(1970).

From 4th International Conference on Plutonium and Other Actinides, Santa Fe, N. Mex. See CONF-701001-(Pt.1).

The Moessbauer effect of the 59.6 keV γ-ray in ^{237}Np was used to study the magnetic behavior of α-Np metal as well as alloys of Np in Pd and Np in Am. Measurements of the magnetic hyperfine field as a function of an externally applied field showed no localized moment in α-Np. A localized moment was present for Np in Pd, and the effects of the formation of a Kondo state were seen in the field and temperature dependence of the hyperfine field. Comparison of the Moessbauer data with the bulk susceptibility showed the formation of a spatially extended spin density below the Kondo temperature. Isomer-shift measurements indicated that approximately two f electrons were localized on Np in Pd. A small local moment was found on Np in Am, and a Kondo state was also indicated in this system. (auth)

12002 INTERPRETATION OF MEASUREMENTS OF MAGNETIC SCATTERING FROM ACTINIDE IONS. Lander, G. H. (Argonne National Lab., Ill.); Brun, T. O. Nucl. Met., Met. Soc. AIME; 17: 338-45(1970).

From 4th International Conference on Plutonium and Other Actinides, Santa Fe, N. Mex. See CONF-701001-(Pt.1).

The use of neutron diffraction to study the magnetic properties of actinide compounds is limited by experimental and theoretical problems. Experimentally, plutonium is particularly difficult to use because of the high neutron absorption cross section of the most abundant isotope ^{239}Pu, and the isotopes ^{240}Pu or ^{242}Pu have to be used. Theoretically, the large perturbations that arise from the spin-orbit coupling and crystal field are impossible to handle with the conventional methods of calculating magnetic scattering amplitudes. However, the scattering from the ground-state configurations may be evaluated by using a new tensor method. Plutonium is of special interest since, in certain configurations, the magnetic scattering amplitude increases as the scattering angle increases. Neutron diffraction may thus provide information about the ground-state configuration of the ion as well as about the spatial extent of the 5f wave functions. (auth)

12003 MAGNETISM IN PALLADIUM-ACTINIDE ALLOYS. Nellis, W. J.; Brodsky, M. B. (Argonne National Lab., Ill.). Nucl. Met., Met. Soc. AIME; 17: 346-54(1970).

From 4th International Conference on Plutonium and Other Actinides, Santa Fe, N. Mex. See CONF-701001-(Pt.1).

The electrical resistivities, magnetic susceptibilities, and magnetoresistances of Pd(U), Pd(Np), and Pd(Pu) solid solutions containing 2 to 13 at. % actinide solute are reported. The resistivity and susceptibility measurements were made in the range 2 to 300°K. The magnetoresistances were measured at 5°K in applied fields up to 77 kOe. In addition to the minimum found in the resistivity-temperature curves for dilute Pd(Np) alloys, the alloys near 5% neptunium had a resistivity maximum as well. The minimum was suppressed as neptunium was added and it disappeared near 10% neptunium. The low-temperature resistivities of Pd(Pu) decreased with decreasing temperature for concentrations up to 9% plutonium, the highest composition investigated. Resistivity minima were found in Pd(U) for concentrations greater than 8% uranium. The magnetoresistances of the 5 and 10% neptunium alloys were negative ($\Delta\rho/\rho(o) \simeq -0.01$ at 77 kOe). The magnetoresistance of a Pd(6.8% Pu) alloy was two orders of magnitude smaller and positive. Pd(9%U) and Pd(11%U) alloys also had small and positive magnetoresistances. All the alloys are proposed to have actinide-5f virtual bound states at the Fermi level, with only neptunium atoms forming localized magnetic moments in palladium. The similarity in the properties of Pd(U) alloys and pure plutonium suggests strongly that the resistivity of plutonium can be explained by conduction electron-paramagnon interactions. (auth)

12004 STUDY OF THE OCCURRENCE OF THE KONDO EFFECT IN Ti, Zr, AND Hf ALLOYS CONTAINING Pu. Elliott, R. O.; Hill, H. H. (Los Alamos Scientific Lab., N. Mex.). Nucl. Met., Met. Soc. AIME; 17: 355-63(1970).

From 4th International Conference on Plutonium and Other Actinides, Santa Fe, N. Mex. See CONF-701001-(Pt.1).

The electrical resistivities of Ti, Zr, and Hf alloys containing Pu were measured in a study of the occurrence of the Kondo effect (resistance minimum phenomenon) in alloys containing transactinium metals as solutes. Minima were observed only in the Zr-Pu alloys and then only within a limited concentration range (5 to 10 at. % Pu). The latter behavior was in contrast to that observed in two other Pu alloy systems previously found to exhibit the Kondo effect. Ternary (Zr, Ti) Pu alloys were prepared to determine the effect on the minimum phenomenon produced by substitution of Ti for Zr in a Zr-7.5 at. % Pu alloy. The results of the investigation are discussed in relation to those of a similar study conducted on transition metal solutes by Cape and Hake. (auth)

12005 ELECTRONIC AND MAGNETIC PROPERTIES OF SINGLE-CRYSTAL ALPHA PLUTONIUM. Arko, A. J.; Brodsky, M. B. (Argonne National Lab., Ill.). Nucl. Met., Met. Soc. AIME; 17: 364-73(1970).

From 4th International Conference on Plutonium and Other Actinides, Santa Fe, N. Mex. See CONF-701001-(Pt.1).

The electrical resistivity, ρ, and magnetic susceptibility, χ, of single crystal α-Pu were investigated as a function of crystallographic orientation in specimens having resistance ratios ranging from 20 to 50. Anisotropy was observed in both properties. For J nearly along the b-axis $d\rho/dT$ was positive at all temperatures, while the familiar resistivity maximum was observed for all other orientations. A large (~6%) temperature-dependent anisotropy was observed in χ at all temperatures, with the a-axis being the high susceptibility axis. Susceptibilities along the other two axes were nearly equal. No abrupt changes in the slope of $\Delta\chi$ vs T were observed. Some single-crystal Hall effect and magnetoresistivity data are also presented. Insufficient evidence is found to lend support to antiferromagnetism as the cause of resistivity anomalies in Pu, nor does the interband scattering model seem to be the answer. A spin fluctuation model is suggested as a reasonable alternative. (auth)

12006 STUDY OF THE OCCURRENCE OF DIFFERENT α-PHASES OF URANIUM AT LOW TEMPERATURES BY THERMOPOWER AND RESISTIVITY EXPERIMENTS. Sze, N. H.; Meaden, G. T. (Dalhousie Univ., Halifax, Nova Scotia). Nucl. Met., Met. Soc. AIME; 17: 974-82(1970).

From 4th International Conference on Plutonium and Other Actinides, Santa Fe, N. Mex. See CONF-701001-(Pt.2).

Experiments were conducted on high-purity polycrystalline U at various rates of cooling and warming with the measurements

made under both static and dynamic conditions. They provided evidence for the contention that quenched α-U transforms to an intermediate form (α'_0) at ~7 to 10°K, which later reverts back to α at around 60°K, a temperature considerably higher than the normal $\alpha \rightleftharpoons \alpha_0$ phase transition (43 to 50°K). The $\alpha'_0 \rightarrow \alpha$ reversion was exothermic and caused a huge thermopower anomaly due to the occurrence of the anomalous ΔT effect which is associated with first-order transitions. The various thermopower and resistivity anomalies corresponded to one previously reported for the thermal expansion and elastic moduli. These results are explained by a model based on the multiplicity of the orthorhombic phases combined with the conception of the development of 5f virtual-bound states associated with the $\alpha \rightarrow \alpha_0$ transition. Support for the latter might be strengthened by the observation, reported here, of a susceptibility increase between 50 and 4°K, which could correspond to the formation of 0.04 Bohr magnetons in the α_0 phase. (auth)

12007 POSSIBILITY OF POLARIZING NUCLEI WITH ULTRASOUND. Buishvili, L. L.; Giorgadze, N. P. JETP Lett. (USSR) (Engl. Transl.); 12: 215-17(20 Sep 1970).

Translated from Zh. Eksp. Teor. Fiz., Pis'ma Red.; 12: 318-20(20 Sep 1970).

In normal diamagnetic materials two-phonon processes of electron-spin relaxation, and also the relaxation of nuclei via the electron dipole–dipole reservoir, prevent polarization of the nuclei. It is shown here, however, that under certain conditions and with a sufficiently high-intensity ultrasound signal, a noticeable polarization can be attained. (L.M.T.)

12008 EFFECTS OF TANTALUM ADDITIONS ON THE PROPERTIES OF NEW MAGNETIC PERMEABILITY ALLOYS NIMALLOY IN NICKEL AND MANGANESE SYSTEM. Masumoto, Hakaru; Murakami, Yuetsu; Hinai, Masakatsu (Research Inst. of Electric and Magnetic Alloys, Sendai). J. Jap. Inst. Metals; 34: 1029-33(Oct 1970). (In Japanese).

The results showed that with increasing Ta content, the permeability of Ni–Mn alloys increased gradually at the beginning and later rapidly attained a maximum, and then decreased gradually. The highest initial permeability of 20470 was obtained on the alloy composed of 75.88% Ni, 19.47% Mn, and 4.65% Ta when cooled at a rate of 240°C/hr from 900°C and baked at 440°C for 64 hr, and the highest maximum permeability of 84800 on the alloy of 75.37% Ni, 19.08% Mn, and 5.55% Ta when cooled at a rate of 240°C/hr from 900°C and baked at 440°C for 65 hr. The latter alloy showed a coercive force of 0.0253 Oe and a magnetic hysteresis loss of 50.85 erg/cm^3/cycle for the maximum magnetic induction of 5000 G, and its electrical resistivity was 52.7 $\mu\Omega$-cm at 20°C. (auth)

12009 CALCULATION OF THE INFLUENCE OF THE CRYSTALLINE ELECTRIC FIELD ON THE SPIN-DISORDER RESISTIVITY OF RARE-EARTH ALLOYS AND COMPARISON WITH RESULTS ON $CeAl_2$. Rao, V. U. S.; Wallace, W. E. (Univ. of Pittsburgh). Phys. Rev., B; 2: 4613-16(1 Dec 1970).

An expression is developed for the spin-disorder resistivity for metallic rare-earth systems; it takes into account the effect of the crystalline electric field. The expression, which is general, is made use of to treat the case of Ce^{+3} in $CeAl_2$; its resistivity–temperature behavior is adequately accounted for on the basis of a Γ_7 doublet ground state. (auth)

12010 MAGNETIC SUSCEPTIBILITY OF BORON NITRIDE. Zupan, J.; Komac, M.; Kolar, D. (Inst. Josef Stefan, Ljubljana, Yugoslavia). J. Appl. Phys.; 41: 5337-8(Dec 1970).

The magnetic susceptibility of BN was measured by the Gony method at room temperature in five different field strengths. Heat treatments up to 1100°C were used to remove ferromagnetic impurities, by oxidizing Fe to Fe_2O_3. The susceptibility of pure BN was determined to be $-0.48 \pm 0.02 \times 10^{-6}$ emu/g. (D.L.C.)

12011 DISCLINATION STRUCTURES IN BLOCH WALL LATTICES IN $BaFe_{12}O_{19}$ AND $SmCo_5$. Hirth, J. P. (Ohio State Univ., Columbus); Wells, R. G. J. Appl. Phys.; 41: 5250-4 (Dec 1970).

Domain walls in barium hexaferrite ($BaFe_{12}O_{19}$) and $SmCo_5$ are shown to form a lattice. Defects observed in the Bloch wall patterns are interpreted geometrically as dislocations and disclinations. The elastic properties of these defects are briefly discussed The faceted appearance of some Bloch wall patterns is analyzed on the basis of a surface energy torque term arising from an anisotropy in the Bloch wall energy. The anisotropy is deduced to arise from high-order coefficients in the anisotropy energy and the magnetostriction. (auth)

12012 X-RAY SPECTRA AND BAND STRUCTURE OF REFRACTORY VANADIUM COMPOUNDS. Zhurakovskii, E. A.; Dzeganovskii, V. P.; Bondarenko, T. N. (Inst. of Problems in Studies of Solids, Kiev). Ukr. Fiz. Zh.; 15: 1477-87(Sep 1970). (In Russian).

K_{β_5}- and $L_{\alpha 1,2}$-emission bands and K-absorption edges of vanadium were investigated in carbides VC_x and V_2C_x in their regions of homogeneity, in nitrides V_2N and VN, boride VB_2 and oxide VO_x. K_α-emission bands of carbon and nitrogen are also presented in the investigated carbides and nitrides. Some conclusions on the nature of chemical bonds in these compounds were drawn on the basis of analysis and comparison of the experimental data with the theoretical calculations. The band schemes of VC, TiC, TiN, TiB_2 were constructed, using x-ray spectroscopic and ESCA data. K-absorption edges of vanadium in the region of homogeneity of V_2C and V_2N were taken first. So were CK_α-bands of both carbides. (auth)

12013 MAGNETIZATION IN Yb–Eu ALLOYS. Unterreiner, K. H.; Elschner, B. (Technische Hochschule, Darmstadt, Ger.). Z. Angew. Phys.; 30: 239-41(16 Nov 1970). (In German).

The field dependence of the Eu_x-Yb_{1-x} magnetization was measured at different Eu concentrations (x = 0.01 to 0.2) in the temperature range from 2.5° K to 50° K. All alloys investigated showed magnetic transition points which depend on the Eu concentration. In samples with less than 10 at.% Eu, these transition points separate a ferromagnetic low-temperature phase from a paramagnetic high-temperature phase. In comparison with pure europium, the europium in ytterbium—especially in samples with small Eu concentration—shows an increase of the magnetic moment. μ_{eff}, calculated from the increase of the reciprocal susceptibility with temperature in the paramagnetic range, is raised by a factor of 1.4 in the sample with 1 at.% Eu. (auth)

12014 HIGH RESOLUTION PRINT-OUT OF THE ELECTRONIC CONDUCTIVITY DISTRIBUTION OF ANODIC TANTALUM OXIDE. Klein, Gerhart P. (P. R. Mallory and Co. Inc., Burlington, Mass.). J. Electrochem. Soc.; 117: 1581-3(Dec 1970).

An improvement of the redox printout technique, using KI/starch gel electrolyte, is reported. A microscope was used in the printing experiments to obtain high resolution. Microprints were obtained for anodized Ta foils, and pretreatments were used to introduce heterogeneities or impurities. The maximum resolution is estimated to be 10^7 to 10^8 conducting sites/cm^2. (D.L.C.)

12015 ELECTRONIC STRUCTURE AND ANOMALOUS THERMAL EXPANSION IN FeF_2 AND VO_2. Hazony, Y.; Perkins, H. K. (Princeton Univ., N. J.). J. Appl. Phys.; 41: 5130-1 (Dec 1970).

From Conference on Thermal Expansion of Solids, Santa Fe, N. Mex. See CONF-700633.

The negative thermal expansion coefficient (TEC) in FeF_2 and the large positive one in VO_2, along the c axis, are explained by a model which emphasizes the changes in force constants, resulting from the spatial rearrangement of the electronic charge surrounding the cation, when low-lying electronic states are thermally populated. The TEC data are compared for 14 rutile-type crystals. It is significant that all the compounds studied, which involve unequally occupied t_{2g} electronic orbitals, display TEC anomalies. (auth)

12016 CONDENSATION INTO A HIGH-TEMPERATURE SPIN-COMPENSATED STATE: α-Ce. Edelstein, Alan S. (Univ. of Illinois, Chicago. Argonne National Lab., Ill.). Solid State Commun.; 8: 1849-52(15 Nov 1970).

The molar susceptibility of Ce_xTh_{1-x} (x = 0.261, 0.398, and 0.664) exhibits a Curie law behavior above 300°K, decreases with decreasing temperature between 300 and 60°K, and fits $A + BT^{-\frac{1}{2}}$ at low temperatures. It is suggested that these alloys at low temperatures are similar to αCe and all these systems, including αCe, are in high-temperature spin-compensated states. (auth) (UK)

12017 MEAN SQUARE THERMAL DISPLACEMENT FOR SURFACE ATOMS IN THE NICKEL (001) SURFACE. Andersson, S.; Kasemo, B. (Chalmers Univ. of Tech., Goteborg). Solid State Commun.; 8: 1885-8(15 Nov 1970).

The temperature dependence of the specular electron reflectivity of low-energy electrons from a Ni (001) surface was investigated for two regions of different electron penetration. A Debye temperature $\theta_D = (415 \pm 20)$°K for Ni was determined. In the direction [001], the mean square thermal displacement of the surface atoms was found to be 2.20 ± 0.25 times the value for bulk atoms. These results agree with theoretical predictions. (auth) (UK)

12018 MAGNETIC SUSCEPTIBILITY OF CERIUM METAL UNDER PRESSURE. MacPherson, M. R. (Univ. of California, Riverside); Everett, G. E.; Wohlleben, D.; Maple, M. B. Phys. Rev. Lett.; 26: 20-3(4 Jan 1971).

The demagnetization of the 4f state of metallic Ce as function of pressure was studied by magnetic susceptibility measurements. In contrast to the β and γ phases, the collapsed α phase does not show a local moment but exhibits instead a strong local exchange enhancement of the susceptibility. The susceptibility decreases linearly with increasing pressure in the measured range and is estimated to decrease by 80% between the boundaries of the magnetic and the superconducting phases. The results are consistent with the Anderson model of local moment formation over the entire range of interest of the parameter $E_{4f}-E_F$. (auth)

12019 INVESTIGATION OF IN-BAND RESONANT MODES IN Cr–W ALLOYS BY INELASTIC NEUTRON SCATTERING. Cunningham, R. M.; Muhlestein, L. D.; Shaw, W. M.; Tompson, C. W. (Univ. of Missouri, Columbia). Phys. Rev., B; 2: 4864-70(15 Dec 1970).

Transverse phonon groups in the [001] and [011] symmetry directions were measured for Cr and three Cr–W alloys by inelastic neutron scattering using the triple-axis neutron diffractometer at the Missouri University Research Reactor. The tungsten concentration for the alloys is 0.3-, 0.8-, and 1.6- at. % W. The shifts in the phonon frequencies for each alloy showed the expected in-band resonant mode behavior. However, on extending the measurements of the shifts to the zone boundary in the [011] direction, additional structure was observed as well as a substantial increase in the magnitude of the negative shifts as one approaches the zone boundary. These frequency shifts are compared to the theory of Elliott and Maradudin using the frequency distribution function of chromium. The agreement between theory and experiment is no better for the lower tungsten concentrations than for previous results for Cr–3-at.% W. Thus, for the Cr–W system, the mass-defect theory appears to be inadequate to predict the measured frequency shifts. (auth)

12020 ELECTRICAL PROPERTIES OF HYDRIDES AND DEUTERIDES OF ZIRCONIUM. Bickel, P. W. (Atomics International, Canoga Park, Calif.); Berlincourt, T. G. Phys. Rev., B; 2: 4807-13(15 Dec 1970).

Electrical properties of hydrides and deuterides of zirconium have been investigated between 1.1 and 410°K. The metallic nature of these materials is evident in the fact that for compositions approaching ZrH_2, the hydride is a better conductor than is high-purity zirconium. Above ~150°K, the electrical resistivity exhibits an interesting upturn, which arises from scattering from the optical-mode lattice vibrations. Excellent fits to the ideal-resistivity data are obtained with a simple additive combination of Grueneisen and Howarth–Sondheimer functions for the respective acoustical- and optical-mode scattering contributions. The corresponding acoustical- and optical-mode characteristic temperatures are in good accord with expectations based on earlier inelastic neutron scattering data. Moreover, the optical-mode characteristic temperature exhibits the expected hydride-deuteride isotope shift of $\sqrt{2}$. The observed Hall coefficients are large in magnitude (much greater than for pure Zr), and indicate majority hole conduction for the fcc δ phase and majority electron conduction for the face-centered tetragonal ϵ phase. The thermoelectric power also changes from positive to negative with increasing hydrogen concentration in the range $ZrH_{1.5}-ZrH_2$. (auth)

12021 ELECTRICAL PROPERTIES OF Ta_2H. Berlincourt, T. G. (North American Rockwell Corp., Thousand Oaks, Calif.); Bickel, P. W. Phys. Rev., B; 2: 4838-43(15 Dec 1970).

Data were obtained on the electrical resistivity, Hall effect, and thermoelectric power in Ta_2H from low temperatures to above the hydrogen sublattice order–disorder transformation temperatures. Prominent manifestations of the $\beta_1-\beta_2$ and $\beta_2-\alpha$ transformations are evident in the data, but no clear evidence was found for a splitting of the upper transition such as that reported in the calorimetric studies of Saba et al. Several features of the electrical properties are consistent with the existence of similar conduction-electron dispersions in Ta_2H and Ta metal, but other factors appear to be inconsistent with this possibility. Hysteresis was observed in the electrical resistivity in the vicinity of the order–disorder transformations, and possible origins of this hysteresis are discussed. The Hall-effect data show that the majority charge carriers in Ta_2H are holes. (auth)

12022 DOPPLER-SHIFTED ACOUSTIC CYCLOTRON RESONANCE IN TUNGSTEN. Hui, S. W.; Rayne, J. A. (Carnegie-Mellon Univ., Pittsburgh). Phys. Lett.; 33A: 459-60(14 Dec 1970).

Doppler-shifted cyclotron resonances were observed acoustically in high-purity tungsten single crystals. The resulting Fermi surface area derivatives agree generally with those obtained from magnetomorphic size-effect experiments and with calculations based on an empirical model fitted to de Haas–van Alphen data. Detailed discrepancies with the latter suggest corrections to the shapes of the noncentral orbit zones on the Fermi surface model. (auth)

12023 EPITAXY BY PERIODIC ANNEALING. Cho, A. Y. (Bell Telephone Labs., Inc., Murray Hill, N. J.). Surface Sci.; 17: 494-503(Oct 1969).

A HEED study was made of the stages of amorphous-crystalline transition during the annealing of GaAs films deposited on a GaAs substrate at room temperature. The film thickness was varied from 2 to 100 monolayers (6 to 300 Å). The amorphous films were found to recrystallize to single crystal on heating to 580°C, with single- and multiple-twinning on the way. Similar results were obtained for GaP films on GaAs substrate. (D.L.C.)

12024 CONDUCTION BAND OF IVa AND Va SUBGROUP TRANSITION METAL MONOCARBIDES. I. Geld, P. V.; Tskhai, V. A.; Borukhovich, A. S.; Dubrovskaya, L. B.; Matveenko, I. I. (Inst. of Chemistry, Sverdlovsk, USSR). Phys. Status Solidi; 42: 85-93(1 Nov 1970).

Based on the general conceptions of the band structure of stoichiometric IVa subgroup transition metal monocarbides, and assuming two types of atomic interactions, a conduction-band model for nonstoichiometric carbides is elaborated that takes into account the vacancies in the carbon sublattice. It is assumed that the formation of vacancies is accompanied by the appearance of local electronic levels in the vicinity of the Fermi level of stoichiometric carbide which, in the case of high concentrations of C vacancies, form a subband of unscreened Me–Me bonds. This results in a filling of the Me–C band, a shift of the Fermi level into the Me–Me band, followed by an increase of the electron density of states and an increase of the Fermi level. The increasing density of states leads to an increase in the magnetic susceptibility. On the basis of the above band model, the results of measurements of the Hall effect (in the range 20 to 300°K), thermopower (77 to 300°K), and electric resistivity (77 to 1200°K) of zirconium monocarbide of different composition are discussed. The observed temperature dependence of the Hall coefficient of ZrC_x samples indicates that two types of carriers take part in the conduction process, their mutual contribution to this phenomenon changing with the composition of the sample. (auth)

12025 CRYSTAL STRUCTURE AND MAGNETIC PROPERTIES OF CERIUM–IRON COMPOUNDS. Buschow, K. H. J.; van Wieringen, J. S. (Philips Research Labs., Eindhoven, Netherlands). Phys. Status Solidi; 42: 231-9(1 Nov 1970).

The crystal structure, magnetic properties, and phase relations of cerium–iron compounds were investigated. A phase diagram is presented. Lattice constants are given for $CeFe_2$, α-Ce_2Fe_{17}, and β-Ce_2Fe_{17}. The compound $CeFe_2$ is ferromagnetic with T_c = 230°K. Investigations by means of the Moessbauer effect and bulk magnetization indicate an antiferromagnetic–ferromagnetic transition near 70°K and an antiferromagnetic–paramagnetic transition close to 270°K for the compound β-Ce_2Fe_{17}. The ordering temperatures and saturation moments for the Ce–Fe compounds are compared with magnetic data presented for the isostructural Y–Fe compounds. (auth)

12026 LATTICE DYNAMICS OF ZIRCONIUM. Bezdek, H. F. (Univ. of Colorado, Boulder); Schmunk, R. E.; Finegold, L. Phys. Status Solidi; 42: 275-80(1 Nov 1970).

Using coherent inelastic neutron scattering, phonon dispersion curves for zirconium, at room temperature, were measured for two high-symmetry directions, [0001] and [01$\bar{1}$0]. The data were analyzed on the basis of a six-neighbor modified axially symmetric model. A frequency distribution calculated from the parameters obtained from the model is also presented. (auth)

12027 STRUCTURE, ENERGY, AND PERIODIC POTENTIAL OF KINKS IN SCREW DISLOCATIONS FOR BCC LATTICES. Hartmann, O. (Technische Univ., Dresden. Zentralinstitut fuer Feskoerphysik und Werkstofforschung, Dresden). Pegel, B. Phys. Status Solidi; 42: 315-20(1 Nov 1970).

The widths, energies, and periodic potentials of kinks in undissociated screw dislocations are numerically computed within a modified Dietze and Leibfried model. The kinks considered are assumed to lie in a {110} plane. Results are presented for Nb, Mo, and Fe. The kink widths range between 0.8 and 2.6 lattice constants while the amplitudes of the periodic potential felt by the kink when moving along the dislocation are found to be 6, 15, and 2 MeV for Nb, Mo, and Fe, respectively. The kinks are short and the kink widths differ, depending on the kink position, by about 100%. The kink energies range between 0.5 and 4 eV. (auth)

12028 NOTE ON THE MAGNETIC STRUCTURE OF U_3P_4. Dobrzynski, L.; Przystawa, J. (Joint Inst. for Nuclear Re-

search, Dubna, USSR). Phys. Status Solidi; 42: K15-18(1 Nov 1970).

The neutron diffraction data of Ciszewski et al. (Phys. Status Solidi, 10: K85 (1965)) on U_3P_4 are analyzed. It is shown that the poor agreement with the collinear model can be improved by assuming the multiaxial models admissible by the R3c' symmetry. The magnetic moments of the U atom in these models, 1.64 and 1.74 μ_B, are high compared with that of the collinear model (1.50 μ_B), but the moment along (111) is in agreement with Buhrer (J. Phys. Chem. Solids 30: 1273 (1969)). (D.L.C.)

12029 OPTICAL ANISOTROPY OF β-RHOMBOHEDRAL BORON. Werheit, H.; Hausen, A.; Binnenbruck, H. (Univ. Cologne). Phys. Status Solidi; 42: K57-60(1 Nov 1970).

A study was made of the optical properties of B single crystals oriented with the crystallographic c-axis parallel to the surface. No optical rotation could be detected in the 0.55- to 13-μm range, in contrast with Bachan et al. (Phys. Status Solidi 35: K37 (1969)), who found optical activity. Linear birefringence was found, and the difference between the refractive indices of the principal axes was determined as a function of wavelength. The results agree with the D_{3d}^5–R$\bar{3}$m structure proposed by Hoard and Hughes (Boron, Vol. 2, G. K. Gaulé, ed., P. 81, Plenum Press, 1965). (D.L.C.)

12030 RESISTIVITY DECREASE DUE TO GRAIN GROWTH IN TUNGSTEN. Uray, L.; Gaal, I. (Research Inst. for Technical Physics, Budapest). Phys. Status Solidi (a); 3: K123-7(16 Oct 1970).

A study was made of the stage VI annealing between 1800 and 2600°K in drawn W wires doped with K, Si, and Al. The resistivity decrease is independent of the impurities. The resistivity of the grain boundaries is calculated to be 140 nΩcm, which is nearly equal to the stage VI value (170 nΩcm). It is concluded that the stage VI is due to grain growth. (D.L.C.)

12031 DIELECTRIC PROPERTIES OF ELECTRON-BEAM-EVAPORATED YTTRIUM OXIDE THIN FILMS. Campbell, C. K. (Univ. of British Columbia, Vancouver). Thin Solid Films; 6: 197-202(Sep 1970).

Thin films of yttrium oxide were fabricated by the direct electron-beam evaporation, in an oxygen atmosphere, of 99.9% yttrium oxide powder. Such films, ranging in thickness from about 2000 to 15,000 Å, were observed to be quite stable and free of pinholes over areas as large as 0.5 in. × 0.5 in. At 1000 Hz and 25°C the lowest value of dielectric dissipation factor (tan δ) obtained was 0.00255, decreasing to a value of 0.0024 at 100 kHz. Bridge measurements on such films forming capacitors of the type $Al/Y_2O_3/Au$ further yielded an average dielectric permittivity value $\epsilon' = 13.5 \pm 1.5$ and a temperature coefficient of capacitance of +320 ppm/°C. Typical breakdown field strengths were in the order of 2.8×10^6 volt/cm for such capacitors as large as 0.065 μF, while the measured resistivity of the dielectric was estimated to be $>2 \times 10^{14}$ Ω cm. (auth)

12032 FERMI SURFACE TOPOLOGY CHANGES IN In ALLOYS DEDUCED FROM THE BEHAVIOR OF In ALLOY WHISKERS UNDER STRAIN. Overcash, Danny Ray. Clemson, S. C.; Clemson Univ. (1969). 53p. University Microfilms Order No. 70-17,450.

Thesis.

The effect of elastic stress (σ) to 0.3 kbar on the resistivity (ρ) at room and helium temperatures and on the superconducting transition temperature (T_c) of In and dilute In alloy whiskers was measured. These whiskers had diameters of about 1 μm and axes parallel to a closest-packed or ⟨101⟩ direction. Alloy contents ranged up to 0.1 at. % Ag, 1.5 at. % Sn, and 3 at. % Cd. At room temperature $\Delta\rho/\rho\sigma = a + b\sigma$, where $a = (-0.4 \pm .2) \times 10^{-5}$ bars^{-1} and $b = (14 \pm 2) \times 10^{-9}$ bars^{-2}. The $\partial T_c/\partial\sigma$ was 51 ± 7 mK/kbar, in disagreement with results obtained by measuring the change in length of In crystals as they passed through the superconducting transition. The addition of Ag and Sn did not change $(\partial T_c/\partial\epsilon)$ from the pure In result, but the addition of Cd had a large effect. The initial slope of the T_c vs strain (ε) curve, $(\partial T_c/\partial\epsilon)_{\epsilon=0}$, decreased with increasing Cd content until at 0.9 at. % it was one fourth of its value for pure In. As the amount of Cd was increased from 0.9 to 2.0 at. % $(\partial T_c/\partial\epsilon)_{\epsilon=0}$ increased to nearly the value for pure In. The transition temperature was linear in ε for ε as high as ¾% for alloys with less than 0.1 at. % Cd. From 0.1 to 0.9 at. % Cd $(\partial T_c/\partial\epsilon)$ decreased with increasing ε, and for alloys with between 0.9 and 2.0 at. % Cd $(\partial T_c/\partial\epsilon)$ increased with increasing ε. For alloys with greater than about 2.0 at. % Cd T_c was linear in ε. This behavior is attributed to a change in the topology of the Fermi surface occurring at about 0.9 at. % Cd in In. (Diss. Abstr. Int. B)

12033 STUDIES OF THE DEFECT STRUCTURE OF NONSTOICHIOMETRIC CERIUM DIOXIDE. Blumenthal, R. N.; Lee, P. W.; Panlener, R. J. (Marquette Univ., Milwaukee). J. Electrochem. Soc.; 118: 123-9(Jan 1971). (COO-1441-6).

The electric conductivity of sintered specimens of $Ce_{1+y}O_2$ was measured over the temperature range 800 to 1500°C and from 1 to 10^{-21} atm of oxygen. Based on the agreement between these experimental data and theoretically derived relations obtained using the law of mass action, the nonstoichiometric defect structure of $Ce_{1+y}O_2$ was interpreted in terms of a defect structure consisting of triply and quadruply ionized cerium interstitials and localized electrons. The standard enthalpies of formation for the following defect reactions in $Ce_{1+y}O_2$ were determined: (a) $V_i + 5Ce_{Ce} + 2O_0 = Ce_i \ldots + 4Ce'_{Ce} + O_2(g)$; $\Delta H_a^0 = 10.4$ eV ± 0.3, (b) $V_i + 4Ce_{Ce} + 2O_0 = Ce_i \ldots + 3Ce'_{Ce} + O_2(g)$; $\Delta H_b^0 = 8.5$ eV[3], and (c) $Ce_{Ce} + Ce_i \ldots = Ce_i \ldots + Ce'_{Ce}$; $\Delta H_c^0 = 1.9$ eV[3]. (auth)

Moessbauer Effects and NMR

Refer also to abstracts 10863 and 10866.

12034 (CEA-R-3855) NUCLEAR MAGNETIC RESONANCE AT 310 MHz IN A SUPERCONDUCTING SOLENOID. Dunand, Jean-Jacques (Commissariat a l'Energie Atomique, Grenoble (France). Centre d'Etudes Nucleaires). Nov 1970. 104p. (In French). Dep. NTIS (U. S. Sales Only).

Thesis. Submitted to Grenoble Univ. (France). Faculte des Sciences.

The development of a NMR spectrometer with a superconducting magnet is discussed in the first section. The methods used to obtain the most homogeneous magnetic field and to minimize the sources of error due to the spectrometer are described. The second section is devoted to the study of elastomers and free nitroxide radicals. The elastomers exhibited a variation in transition temperature with respect to the magnetic field. The large paramagnetic shifts enabled a complete study by NMR of piperidinic and pyrrolidinic nitroxide free radicals to be made. (auth) (France)

12035 MOESSBAUER-EFFECT STUDIES OF THE HYPERFINE INTERACTIONS AND RELAXATION PHENOMENA IN DYSPROSIUM METAL AND $DyCo_2$, AND NUCLEAR MOMENTS MEASUREMENT OF THE 75-keV STATE OF ^{161}Dy. Loh, Eddie Lei, Baltimore; Johns Hopkins Univ. (1970). 138p. University Microfilms Order No. 70-20,165.

Thesis.

Temperature dependences of the nuclear hyperfine splitting of ^{161}Dy have been studied in dysprosium metal and in the intermetallic Laves phase compound $DyCo_2$. Magnetic relaxation phenomena were observed in both compounds starting at temperatures around 30°K below the ordering temperature. The experimental temperature dependence of the hyperfine fields was compared to the modified Brillouin function with spin $^5/_2$. The experimental data points were found to lie higher than the Brillouin curve. In the cubic Laves compound, $DyCo_2$, crystal field effects were taken into account and a good fit between the data points and the modified Brillouin curve was obtained. From the fit, the exchange splitting was found to correspond to a temperature of about 400°K. The internal magnetic field in Dy metal and $DyCo_2$ extrapolated to T = 0°K were found to be (6.2 ± 0.15) MOe and (6.51 ± 0.15) MOe, respectively. Present values are in agreement with previous results. The quadrupole interaction constants in Dy metal and $DyCo_2$ were found to be (679 ± 40) MHz and (725 ± 40) MHz, respectively. In this case, the present results are higher than previous Moessbauer data. Using the observed internal magnetic field in Dy metal, a value of $\langle r^{-3}\rangle_{eff} = (9.29 \pm 0.20)$ a.u. was obtained. Hyperfine structures of the 74.57-keV state of ^{161}Dy in $DyFe_2$ and $DyCo_2$ were obtained by using an unsplit source of $^{161}Dy_2O_3$. The hyperfine structures were analyzed by assuming electric field gradients having axial symmetry about the direction of the internal magnetic field. Using a value of $g_0 = -0.189 \pm 0.005$ and $Q_g = 1.9 \pm 0.1$ barns, the nuclear magnetic dipole and electric quadrupole moments were found to be: $\mu = -0.391 \pm 0.009$ n.m. and $Q = 1.32 \pm 0.12$ barns, respectively. The rotational and intrinsic gyromagnetic ratios were deduced on the basis of the unified model to be: $g_R = 0.160 \pm 0.040$ and $g_K = 0.542 \pm 0.050$, respectively. This work indicates that the mean radius of the ground state is greater than that of the 75-keV state, but less than that of the 26-keV state. (TSS) (Diss. Abstr. Int., B)

12036 NUCLEAR MAGNETIC RESONANCE OF ACTINIDE COMPOUNDS. Fradin, F. Y. (Argonne National Lab., Ill.). Nucl. Met., Met. Soc. AIME; 17: 264-70(1970).

From 4th International Conference on Plutonium and Other Actinides, Santa Fe, N. Mex. See CONF-701001-(Pt.1).

The results of nuclear magnetic resonance measurements on actinide compounds with the NaCl-type structure are reviewed.

The Knight shift and spin–lattice relaxation time of carbon, nitrogen, or phosphorous combined with either plutonium or uranium are related to the magnetic susceptibility and spin fluctuations, respectively. The results indicate that the interactions between the conduction electrons and the 5f electron moments play an important role in the coupling between the magnetic moments. (auth)

12037 COMMENTS ON MAGNETIC PROPERTIES OF Nb_3X COMPOUNDS. Ehrenfreund, E.; Gossard, A. C.; Wernick, J. H. (Bell Telephone Labs., Inc., Murray Hill, N. J.). Solid State Commun.; 8: 1925-7(15 Nov 1970).

^{93}Nb NMR in Nb_3X (X = Al, Sn, Au, Ir) compounds was observed using the spin-echo technique. The pattern observed is typical of a quadrupole pattern at high magnetic fields. The ^{93}Nb resonances in Nb_3X compounds (X = Os, Ir, Pt, Pt–Au, Au) reported recently by Bernasson, Descouts, Fluckiger and Treyvand (1970) are shown not to arise from Nb nuclei on the A sites of the A_3B β–W structure. (auth) (UK)

12038 NUCLEAR MAGNETIC RESONANCE INVESTIGATION OF THE METAL-TO-SEMICONDUCTOR TRANSITION IN CRYSTALLINE CdO. Benedict, R. P. (Air Force Inst. of Tech., Wright-Patterson AFB, Ohio); Look, D. C. Phys. Rev., B; 2: 4949-59(15 Dec 1970).

Measurements of the ^{113}Cd nuclear-spin–lattice relaxation time (T_1) and resonance frequency shift (K) were carried out in several samples of polycrystalline n-type CdO over the temperature (T) range 1.4 to 300°K, frequency (ν) range 2 to 10 MHz, and carrier concentration (N_c) range 3.3 to 44 × 10^{18} cm^{-3}. For $N_c > 10^{19}$ cm^{-3}, it was found that $T_1 \propto N^{-\frac{1}{3}} T^{-1}$ and $K \propto N_c^{\frac{2}{3}}$, showing that the nuclei are interacting with degenerate conduction electrons. Furthermore, the Korringa relationship holds and the calculated electron density at a nucleus is almost the same as that in a free atom, indicating that the electrons are in the host-lattice conduction band. The Hall constant is independent of temperature, also suggesting that there is no separate impurity band. Conversely, for $N_c < 10^{19}$ cm^{-3}, none of the above-mentioned relationships holds and a model must be invoked in which the electrons are concentrated near impurity centers, forming an impurity band, with nuclei near the centers experiencing strong contact interactions while nuclei far from the centers experience only indirect interactions through nuclear-spin diffusion. These two groups of nuclei do not maintain a common spin temperature and, thus, the recovery of the magnetization is nonexponential. Finally, the concentration (N) at which the impurity wave functions no longer form a band is estimated from the Mott criterion to be about 2 × 10^{18} cm^{-3}, slightly below the lowest-concentration sample. Thus, assuming that $N_c \simeq N$, it was found that for $N < 2 \times 10^{18}$ cm^{-3} the impurity wave functions are localized, for $2 \times 10^{18} < N < 10^{19}$ cm^{-3} the electrons are free to move in an impurity band, and for $N > 10^{19}$ cm^{-3} the Fermi level crosses into the host-lattice conduction band. (auth)

12039 INVESTIGATION OF THE METAL–INSULATOR TRANSITION IN V_2O_3 BY NUCLEAR MAGNETIC RESONANCE. Rubinstein, Mark (Naval Research Lab., Washington, D. C.). Phys. Rev., B; 2: 4731-41(15 Dec 1970).

The metal-to-insulator phase transitions have been investigated in Cr- and Al-doped V_2O_3 by nuclear magnetic resonance. Two distinct transitions exist in this system: a low-temperature antiferromagnetic insulator–metal transition, and a high-temperature metal–insulator transition. An abrupt change in the Knight shift is noted at the high-temperature transition, while the resonance signal completely vanishes in the low-temperature antiferromagnetic phase. A theoretical model is developed that explains the existence of both transitions, and the anomalous properties of the metallic state. The magnitude of the magnetic moment in the antiferromagnetically ordered state is discussed. (auth)

Theory

Refer also to abstract 11699.

12040 CALCULATION OF PHOTOELECTRIC EMISSION FROM TUNGSTEN, TANTALUM, AND MOLYBDENUM. Petroff, Irene Karmilof. Los Angeles; Univ. of California (1970). 145p. University Microfilms Order No. 70-19,881.

Thesis.

Photoelectric emission due to direct transitions between volume states of the crystal is calculated for tungsten, tantalum, and molybdenum. The data required for such a calculation include the energy band structure and the corresponding electron eigenfunctions for the materials considered. In this study, therefore, the crystal potentials are first constructed from tabulated free-atom data. The band structures are then calculated by the APW method and the Fermi energies and density of states curves are obtained. The transition probabilities for direct interband transitions are then found, and the photoelectric emission arising from these transitions is calculated by applying a standard simplified analysis to the transport properties and escape probability of the excited electrons. The results obtained show that the magnitude of the direct transition probability varies widely as a function of the k vector, and indicate that considerable inaccuracies are introduced when the matrix element for the transition probability is taken as a constant. The photoelectric emission curves also indicate that much of the structure observed experimentally is due to the direct transition contribution to the photoemission. (Diss. Abstr. Int., B)

12041 ELECTRON DISTRIBUTION AROUND POSITRONS IN METALS. Sjoelander, A.; Stott, M. J. (Inst. of Theoretical Physics, Goteborg). Solid State Commun; 8: 1881-4(15 Nov 1970).

A new approach is presented to calculate the induced charge density around a charged point particle in the electron gas beyond linear response. The method can be used to treat finite mass impurities as well as those with infinite mass. Calculations were performed for a positron in an electron gas. The positron annihilation rates thereby obtained are compared with results of other authors and with experiment. (auth) (UK)

12042 CALCULATED ISOTOPE EFFECT FOR DIFFUSION IN SOLID ARGON. Burton, J. J. (Columbia Univ., New York). Phys. Rev., B; 2: 5010-11(15 Dec 1970).

The isotope effect was calculated for diffusion in solid argon using a formalism developed by Glyde. The computed values of ΔK are 0.99 for self-diffusion via a single-vacancy mechanism, 0.88 for self-diffusion via a divacancy mechanism, 0.999 for neon impurity diffusion via single vacancies, and 0.94 for krypton impurity diffusion via single vacancies. These calculated values are compared with experimental data and suggest that diffusion in solid argon may be via either a single-vacancy or divacancy mechanism; neither the calculations nor the experiments are sufficiently precise to establish the mechanism with certainty. (auth)

12043 ISOTOPE EFFECTS IN DEFECT-INDUCED INFRARED ABSORPTION. Benedek, Giorgio (Univ., Milan). Phys. Status Solidi; 42: 389-99(1 Nov 1970).

Splitting of the defect-induced infrared absorption peaks produced by the isotope mixture of defect ions (defect isotope effect) or nearest-neighbor ions (nn isotope effect) is investigated. The defect isotope effects in the systems KI : Cl^-, KI : Br^-, KBr : Li^+, and KCl : Li^+ are calculated within the harmonic approximation by means of a defect model in which the elastic relaxation is taken into account. Concerning the nn isotope effect, the F-center is found to be a suitable system for the detection of relatively large nn isotope effects. (auth)

12044 ENERGY BANDS OF VANADIUM OXIDE. Norwood III, Thomas Ellis. Baton Rouge, La.; Louisiana State Univ. (1970). 152p. University Microfilms Order No. 70-18,551.

Thesis.

Energy bands of vanadium oxide are calculated by the tight binding method. For this purpose, the method of Lafon and Lin is extended to include 3p, 3d, and 4s functions so that three-center integrals could be included in the calculations. All matrix elements are summed to convergence, and the core functions of both vanadium and oxygen are explicitly included. The crystal potential is constructed from a superposition of spherically averaged atomic potentials. The exchange potential used consists of the $\rho^{\frac{1}{3}}$ approximation of Slater, together with an adjustable factor λ. Band structures are calculated, using three different crystal potentials. The density of states is computed from a sample of 505 points in $\frac{1}{48}$ of the Brillouin zone. The effect of including core states is examined in detail, as are the effects of varying the factor λ in the exchange potential. Using the three different computed band structures, an estimate of the self-consistent potential is made. (Diss. Abstr. Int., B)

Theoretical Physics

Refer also to abstracts 12162, 12263, and 12624.

12045 (IPPJ-T-4) USE OF COMFORMAL MAPPING TO IMPROVE UNIFORMITY OF ELECTRIC FIELD. Kawasaki, Sunao (Nagoya Univ. (Japan), Inst. of Plasma Physics). Nov 1970. 13p. Dep. NTIS (U. S. Sales Only).

The form of simple auxiliary electrodes attached to two parallel plates for deflecting charged particles is determined by a conformal-mapping technique so that the end effect of the electric

field can be cancelled. It is shown that the uniformity of the field is much improved only by a small modification of the shape of the parallel plates at their ends. (auth) (Japan)

12046 (NP-18619) NOTES ON QUANTUM MECHANICAL SUM RULES. Lilja, I. A.; Haemaelaeinen, R. M. K. (Jyvaskyla Univ. (Finland). Dept. of Physics). Sep 1970. 15p. Dep. NTIS (U. S. Sales Only).

Sum rules for expressions of the form $\Sigma_j (E_j - E_n)^s \times \langle n|B|j\rangle \langle j|A|n\rangle$ are investigated. New derivations by using a simple and useful technique are given. Applications of the sum rules are given for an electric dipole operator and for the operator function e^A, where A is an antihermitian operator. Applicability of the sum rules in general is discussed. (auth) (Finland)

12047 (NYO-3829-65) RELATIVISTIC QUANTUM MECHANICS OF DYONS: EXACT SOLUTIONS. Bialynicki-Birula, I. (Pittsburgh Univ., Pa. Dept. of Physics. Warsaw Univ. (Poland). Inst. for Theoretical Physics). Nov 1970. Contract AT(30-1)-3829. 9p. Dep. NTIS.

Relativistic quantum mechanics of dyons (hypothetical particles endowed with both electric and magnetic charges) is formulated. The hydrodynamical formulation of quantum mechanics is used to overcome all problems created by the simultaneous presence of both electric and magnetic charges. In the case of one dyon moving in the electromagnetic field of another dyon, the exact solutions are found and the energy levels are determined. (auth)

12048 MATHEMATICAL AND THEORETICAL PHYSICS. VOLUME I. Hylleraas, Egil A. New York; John Wiley and Sons, Inc. (1970). 505p. $15.00.

This volume begins with a condensed exposition on the required mathematical preparations for theoretical physics—the nature of vectors and vector fields, tensor and tensor fields, linear transformation, and basic theories of functions. Supplemented by a historical overview, the section on classical mechanics opens with mechanical fundamentals and proceeds through a series of more complex forms of Lagrangian and Hamiltonian mechanics. Included in the discussion of thermodynamics is a significant set of applications of quantitative statistics to gas kinetics: the photon gas and the law of radiation, the virial theorem in quantum statistics, sums of states in quantum statistics, ideal gases with weak degeneracy and strong degeneracy of both a Bose–Einstein and a Fermi gas. (M.O.W.)

12049 MATHEMATICAL AND THEORETICAL PHYSICS. VOLUME II. Hylleraas, Egil A. New York; John Wiley and Sons, Inc. (1970). 491p. $15.00.

This volume begins with a section on electricity and magnetism. A concise explication of electrostatics and magnetostatics is followed by a treatment of electromagnetic radiation. A commentary on the origin of wave mechanics precedes an expertise on the absorption and emission of an atom in a radiation field, refraction and dispersion, as well as scattering principles. (M.O.W.)

12050 APPROACH TO THE QUANTUM-MECHANICAL FOUR-BODY BOUND-STATE PROBLEM. I. DISTINGUISHABLE PARTICLES. Magyari, E. (Univ., Craiova, Rumania). Acta Phys. Pol.; A38: 703-13(Nov 1970).

An earlier approach to the three-body bound-state problem, developed by Eyges and Jasperse and Friedman, is generalized to the N-body case. This approach is then developed in detail for a system of four distinguishable particles. (auth)

12051 INTEGRAL EQUATIONS FOR WAVE VECTORS OF A QUANTUM SYSTEM WITH A DISCRETE SET OF STATES. Garczynski, W. (Wroclaw Univ.). Acta Phys. Pol.; A38: 795-7 (Nov 1970).

The Feller-type equations for wave vectors of a quantum system with a discrete set of states are written. They are of the Volterra integral of the second kind that may be solved by means of an iteration procedure or by the Laplace transformation. (auth)

12052 KVANTOVAYA MEKHANIKA I ATOMNAYA FIZIKA. (Quantum Mechanics and Atomic Physics). Sokolov, A. A.; Ternov, I. M. Moscow; Izdatel'stvo Prosveshchenie (1970). 424p.

The first chapter covers nonrelativistic quantum mechanics and considers quantum optical theory, wave properties of particles, the Schroedinger equation, particle passage through potential barriers, particle motion, transition processes, elastic scattering, perturbation theory, and atoms in a magnetic field. Relativistic quantum mechanics including the Klein–Gordon equation, Dirac equation, Dirac electron motion in the central force field, fine structure of hydrogen-like atoms, Lamb shift, and complete solutions for the Dirac equation are covered in the second chapter. The third chapter is devoted to the theory of many particles, the theory of helium atoms with and without spin, and the structure of complex atomic and molecular spectra. (R.V.J.)

12053 FLUCTUATIONS OF BEAMS OF QUANTUM PARTICLES. Benard, Christine (Faculte des Sciences, Orsay, France). Phys. Rev., A; 2: 2140-53(Nov 1970).

A beam of noninteracting particles, bosons or fermions, is described by the superposition of stochastic wave packets. This description allows in each case (bosons or fermions), the determination of the detection process of the particles. This process is defined by the set of the p-order coincidence probability densities, a general formulation of which is given. In the case of a stationary and weak incoherent beam, these coincidence probability densities are studied thoroughly and several results are obtained. The well-known bunching effect for bosons and the "antibunching effect" for fermions are shown to come from the detection of indistinguishable particles. In the boson case, all the well-known results for thermal light are found. In the fermion case, the detection process is, under certain conditions, identical to a renewal process. (auth)

12054 TIME-DEPENDENT PERTURBATION THEORY. Sen Gupta, N. D. (Tata Inst. of Fundamental Research, Bombay). J. Phys., A (London); 3: 618-24(Nov 1970).

It is shown that if the time-dependent perturbation Hamiltonian admits of Fourier resolution, then the solution of the wave equation possesses perturbation expansions, without any secular term. Further, each term can be expressed in terms of its Fourier resolution. (auth) (UK)

12055 PARTICULAR SOLUTIONS OF THE MONOENERGETIC TRANSPORT EQUATION WITH ANISOTROPIC SCATTERING. Leuthaeuser, Klaus-Dieter (Univ., Kiel). Atomkernenergie; 16: 253(1970).

In a source-free medium the neutron transport is governed by the homogeneous Boltzmann equation whose general solution is given by Case's normal-mode expansion. In the presence of an inhomogeneous source term, a particular solution has to be added in order to obtain the complete solution to which the boundary conditions have to be applied. Particular solutions have been obtained for various source terms of practical interest in the case of isotropic and linearly anisotropic scattering. These results are generalized here for scattering kernels that can be approximated by finite sums of Legendre polynomials. (M.H.R.)

12056 SIMPLE APPROXIMATE EIGENFUNCTIONS FOR AN ELECTRON IN A FINITE DIPOLE FIELD. Fox, Kenneth (California Inst. of Tech., Pasadena. Oak Ridge National Lab., Tenn.). Phys. Rev., A; 3: 13-15(Jan 1971).

Ground-state energy eigenvalues for an electron in a stationary finite electric-dipole field are calculated by a novel variational approach. The physical model is taken to be a perturbed hydrogen atom. Accurate energy eigenvalues are obtained for a large range of dipole moments. The simple variational functions used compare favorably with more nearly exact eigenfunctions obtained in complex calculations. (auth)

12057 EQUILIBRIUM SOLUTIONS OF THE SECULAR VARIATIONS IN THE RESTRICTED THREE-BODY PROBLEM AND THEIR STABILITY. Antonacopoulos, Gr. A. (Univ. of Athens, Greece). Mon. Notic. Roy. Astron. Soc.; 151: 123-32(1970).

The equilibrium solutions of the secular variations in the restricted three-body problem and their stability are discussed in relation to the Delaunay variable H and the ratio of the semi-major axes α. For each value of α there is a limiting value of the eccentricity and the inclination, for which there exists an equilibrium solution besides that of the origin of the rectangular type variables used here. For a given α there exists a value i^* such that circular orbits are stable or unstable according as $i < \text{or} > i^*$. Results on i are valid only for those values less than the limiting values imposed by convergence requirement. (auth) (UK)

12058 RELATIVISTIC KINETIC THEORY OF CHARGED GASES. Ehlers, Jurgen (Univ. of Texas, Austin). pp 221-9 of La Magnetohydrodynamique Classique et Relativiste. Paris; Centre National de la Recherche Scientifique (1970).

From Symposium on Classical and Relativistic Magnetohydrodynamics, Lille, France. See CONF-690648.

The basic concepts and theorems of general relativistic kinetic theory of gases are reviewed. The underlying kinematics in phase space, the statistics, Liouville's equation, the Boltzmann equation, conservation laws, an H-theorem, and equilibrium distributions are treated from a geometrical, space–time point of view. (auth) (France)

12059 RADIATION OF A PARTICLE IN A STRONG MAGNETIC FIELD AT LOW ENERGY LEVELS. Mkrtchyan, M. M. Vestn. Mosk. Univ., Ser. III. Fiz. Astron.; 11: 281-4(May-Jun 1970). (In Russian).

Formulas were obtained for the total energy and polarization of radiation from electrons and spin-free particles, in second excitation state, moving in a superhigh magnetic field. (tr-auth)

12060 RADIATIVE POLARIZATION OF FREE RELATIVISTIC ELECTRONS IN A MAGNETIC FIELD. Gal'tsov, D. V.; Nikitina, N. S. Vestn. Mosk. Univ., Ser. III. Fiz. Astron.; 11: 329-35 (May-Jun 1970). (In Russian).

The influence of external electromagnetic radiation on the spin state of weakly relativistic electrons in a homogeneous magnetic field is studied. It is shown that, under certain conditions, the electron beam must become strongly polarized. Expressions are developed for the probability of radiative transitions with spin reorientation for arbitrary particle energies. (tr-auth)

12061 APPLICATION OF SPECTRAL DENSITY METHOD TO SYSTEMS WITH PAIR INTERACTION. Kalashnikov, O. K.; Fradkin, E. S. (Lebedev Inst. of Physics, Moscow). Teor. Mat. Fiz.; 5: 417-38(Dec 1970). (In Russian).

The method of spectral densities is formulated and the simplest approximations are pointed out for systems of Fermi (Bose) particles with pair interaction. The method is illustrated by the solution of the Hubbard model and the "pair Hamiltonian" model. The spectrum of the system of interacting bosons is investigated in the simplest approximation. (auth)

12062 CLASSICAL APPROACH TO THE EQUATIONS OF QUANTUM MECHANICS IN AN ELECTROMAGNETIC FIELD. Kaliski, S. (Inst. of Basic Tech. Problems, Warsaw). Bull. Acad. Pol. Sci., Ser. Sci. Tech.; 18: 561-6(1970).

A generalization was made of equations from an earlier paper (S. Kaliski, Proc. Vibr. Probl., 11(1970) No. 1), which correspond to the Schroedinger equation, and from the paper (S. Kaliski, Proc. Vibr. Probl., 11(1970) No. 2), which corresponds to the Klein-Gordon equation. (M.O.W.)

12063 WKB METHOD IN THE CLASSICAL APPROACH TO QUANTUM MECHANICS. Kaliski, S. (Inst. of Basic Tech. Problems, Warsaw). Bull. Acad. Pol. Sci., Ser. Sci. Tech.; 18: 553-9(Nov 1970).

The WKB method is applied to equations of an earlier paper (S. Kaliski, Proc. Vibr. Probl. 11: 1(1970)). It is then shown that this method can be transferred, with some minor modifications, directly to the equations expressed in terms of the complex variable v. It is also shown that the WKB method can be modified in a manner that enables the discussion of a solution in the neighborhood of a turning point to be omitted. (M.O.W.)

PHYSICS (HIGH ENERGY)

Particle Interactions and Properties (Experimental)

Refer also to abstracts 12123 and 12124.

12064 SEARCH FOR QUARKS IN FERROMAGNETICS USING AN ELECTROMETER WITH THE BEAMS SUSPENSION METHOD. Braginsky, V. B.; Kornienko, L. S.; Poloskov, S. S. (Moscow Stat Univ.). Phys. Lett.; 33B: 613-14(21 Dec 1970).

Using a ferromagnetic electrometer an upper limit of concentration of quarks was measured. The negative results was at the level 10^{-20}. (auth)

Electromagnetic

Refer also to abstracts 11749 and 11750.

12065 (CNRS-CPT-70-P-339) SIXTH-ORDER RADIATIVE CORRECTIONS TO THE ANOMALOUS MAGNETIC MOMENT OF THE ELECTRON. Calmet, J.; Perrottet, M. (Centre National de la Recherche Scientifique, Marseilles (France). Centre de Physique Theorique). 1970. 8p. Dep. NTIS (U. S. Sales Only).

The sixth-order contributions to the anomalous magnetic moment of the electron from the Feynman diagrams with vacuum polarization insertions were computed. This computation was done by means of a program devoted to the calculation of the Feynman diagrams finite contributions. (France)

12066 (DESY-HERA-70-1) COMPILATION OF PHOTOPRODUCTION DATA ABOVE 1.2 GeV. Joos, Peter (Deutsches Elektronen-Synchrotron, Hamburg (West Germany)). 23 Sep 1970. 142p. Dep. NTIS (U. S. Sales Only).

A compilation is presented of 3477 existing data from 243 references on experimental photoproduction above 1.2 GeV. (auth)

12067 (LAL-1239) π^+ MESON PHOTOPRODUCTION AT 180° ON H FROM 450 MeV TO 3 GeV. D'Almagne, B. (Paris Univ., Orsay (France). Laboratoire de l'Accelerateur Lineaire). Oct 1970. 113p. (In French). Dep. NTIS (U. S. Sales Only).

Thesis. Submitted to Paris Univ., Orsay (France). Faculte des Sciences.

The photoproduction of π^+ at 180° with protons is described. The aim of the experiment was to complete over a large energy range (450 MeV to 3 GeV) previously obtained data on the first resonance zone and to determine the structure of the cross sections observed in the region of the second resonance. The three distributions obtained by the integration of the 810 to 880 MeV, the 1625 to 1850 MeV, and the 1970 to 2230 MeV angular distributions were without structure. The experiment demonstrated that the second resonance is dominated by the D13 wave in the $^3/_2$ helical state and the S11 wave but did not allow the effect of the P11 resonance to be determined. The structure in the 700 MeV region is explained by a cusp effect at the threshold energy for η_0 meson photoproduction. The third resonance is essentially photoproduced in the $^3/_2$ states of helicity, but at energies in excess of 1 GeV the effect due to resonances at higher energies becomes significant. At energies in excess of 900 MeV a strong structure was observed. The cross section decreased by a factor approaching 100 between 950 and 1650 MeV, increased to a factor of 3 to 2 GeV and decreased again at energies between 2.3 and 3 GeV. The experiment demonstrated the importance of exchanges occurring in the direct channel at energies less than 2.5 GeV. The Regge pole model explained the experimental data for energies in excess of 4 GeV. A description is given which unites the two models. (France)

12068 (SLAC-PUB-842) RECENT DEVELOPMENTS IN INELASTIC ELECTRON-NUCLEON SCATTERING. Gilman, Frederick J. (Stanford Linear Accelerator Center, Calif.). Nov 1970. 30p. (CONF-700937-1). Dep. NTIS.

From Symposium on Hadron Spectroscopy, Balatonfured, Hungary.

A review is given of the experimental and theoretical aspects of inelastic electron-nucleon scattering. In this discussion particular attention is devoted to some theoretical consequences of recent experimental data and to duality and resonance behavior. (J.F.P.)

12069 BACKWARD PHOTOPRODUCTION OF π^0 MESONS AT 6 TO 18 GeV. Tompkins, Donald Harvey. Philadelphia; Univ. of Pennsylvania (1969). 128p. University Microfilms Order No. 70-16,227.

Thesis.

Differential cross sections for π^0 photoproduction at backward angles were measured in the momentum transfer range $u = 0$ to -1 $(GeV/c)^2$, for incident photon energies of 6, 8, 12 and 18 GeV. A collimated bremsstrahlung beam from the Stanford linear accelerator was passed through a 40-in.-long liquid-hydrogen target, and the momentum spectrum of the forward moving protons was measured in the SLAC 20-GeV/c magnetic spectrometer. Single pion production is separated from other processes on the basis of kinematics and the spectrum shape. (Diss. Abstr. Int., B)

12070 FORM-FACTOR RATIO $G_E(n)/G_E(p)$ AT LOW MOMENTUM TRANSFERS. Bumiller, F. A. (Naval Postgraduate School, Monterey, Calif.); Buskirk, F. R.; Stewart, J. W.; Dally, E. B. Phys. Rev. Lett.; 25: 1774-8(28 Dec 1970).

Measurements of the ratio of the deuteron to proton electric form factors, $G_E(d)/G_E(p)$, were made from elastic electron-deuteron scattering to a precision of approximately 1% for the range of momentum transfers $0.10 \leq q^2 \leq 0.8$ F^{-2}. Within experimental errors the slope as obtained from the ratio $G_E(n)/G_E(p)$ agrees with the extrapolated thermal neutron–electron interaction slope when relativistic corrections and Feshbach–Lomon deuteron wave functions are applied. The deuteron radius was found to be 1.95 ± 0.02 F, the same as predicted by the Feshbach–Lomon calculation. (auth)

12071 HORIZONTAL AIR SHOWERS OF ENERGIES ABOVE 10^{13} eV. Nagano, Motohiko (Tokyo Univ.); Hara, Tadao; Kawaguchi, Setsuo; (and others). J. Phys. Soc. Jap.; 30: 33-55(Jan 1971).

An observation of horizontal air showers was continued during four years with the air shower array at the Institute for Nuclear Study, University of Tokyo. The integral size spectrum is expressed by $(4.9 \pm 0.7) \times 10^{-13}(N/10^4)^{-2.8\pm0.3}$ cm^{-2} sec^{-1} $ster^{-1}$ for the showers of sizes 10^3 to 10^5 and zenith angles above 70°. The zenith angle distributions for three size regions $(0.5 \sim 1) \times 10^4$, $(1 \sim 2) \times 10^4$ and $(2 \sim 4) \times 10^4$ indicate that the intensities are proportional to sec θ from 60 to 75° and decrease at above $75 \pm 5°$ with attenuation mean free path of 5,000 to 10,000 g/cm^2. The proportion of nuclear cascade showers to the total showers is estimated to be $(20 \sim 70)\%$ in the range of size 3×10^3 to 6×10^4. The implications of an effect of possible anomalous muon interactions and of, as an alternative, a possibility of heavy mass particles being the parent particles of the horizontal air showers are discussed. (auth)

12072 π^0 PHOTOPRODUCTION FROM HYDROGEN WITH LINEARLY POLARIZED PHOTONS. Anderson, R. L. (Stanford Univ. of Calif.); Gustavson, D.; Johnson, J.; (and others). Phys. Rev. Lett.; 26: 30-3(4 Jan 1971).

The asymmetry in the process $\gamma + p \rightarrow \pi^0 + p$ with polarized photons was measured at 6 GeV for momentum transfers from $t = -0.4$ $(GeV/c)^2$ to $t = -1.1$ $(GeV/c)^2$, using coherent bremsstrahlung from a diamond crystal. A coincidence was made between the recoil proton in a 1.6-GeV/c spectrometer and one of the π^0 decay photons in a Lucite shower counter. The measured asymmetry $(\sigma_\perp - \sigma_{||})/(\sigma_\perp + \sigma_{||})$ is consistent with strongly dominant natural parity exchange in the t channel. (auth)

12073 ELECTRON–POSITRON ELASTIC SCATTERING AT HIGH ENERGIES. Bartoli, B. (CNEN, Frascati, Italy); Coluzzi, B.; Felicetti, F.; (and others). Nuovo Cim.; 70A: 603-14 (21 Dec 1970).

In an experiment performed at Adone, the Frascati 2×1.5 GeV electron–positron storage ring, the e^+e^- wide-angle elastic-scattering process was investigated. The analysis of approximately 1700 e^+e^- Bhabha scattering events collected at several energies of the incident electron and positron beams between 0.8 and 1.0 GeV is presented; this corresponds in our experimental apparatus to an averaged momentum transfer to the virtual spacelike photon ranging within $\sim(1.0 + 1.7)$ $(GeV/c)^2$. In the energy range explored the experimental data show a slope and an absolute value in agreement with the predictions of quantum electrodynamics to within the experimental errors of ~10%. (auth)

12074 UPPER LIMIT ON ϕ IN TWO-π BRANCHING RATIO. Bizot, J. C.; Delcourt, B.; Jeanjean, J.; (and others) (Laboratoire de l'Accelerateur Lineaire, Orsay, France). Lett. Nuovo Cim.; 4: 1273-4(26 Dec 1970).

From a fit of Orsay measurements on the $e^+ + e^- \rightarrow \pi^+ + \pi^-$ interaction the $\pi^+ + \pi^-$ cross section at the ϕ energy is computed to be (0.38 ± 0.03) (10^{-31}). It is pointed out that a possible destructive interference between the ρ and ϕ 2π decays may lead to the same result as a vanishing $\phi \rightarrow 2\pi$ amplitude. (J.F.P.)

12075 PRECISION MEASUREMENT OF THE g-FACTOR OF THE FREE POSITRON. Gilleland, John Rogers. Ann Arbor, Michigan; Univ. of Michigan (1969). 103p. University Microfilms Order No. 70-21,665.

Thesis.

A precision measurement of the g-factor of the free positron was recently completed. The basic experimental technique is that developed in an earlier positron measurement: A group of positrons from a ^{58}Co source is confined in a magnetic mirror trap. On emission from the source, the positron "beam" is polarized parallel to its "average" velocity $\langle\vec{v}\rangle$, with polarization $\vec{P} = \langle\vec{v}\rangle/c$. While in the field the beam undergoes cyclotron orbital motion at an angular frequency ω_c. Simultaneously $\vec{P}$ precesses at an angular frequency ω_s. Since these two frequencies are slightly different the polarization $\vec{P}$ rotates about the velocity $\vec{v}$ at the beat or difference frequency $\omega_D = \omega_s - \omega_c$. After a controlled length of time, the particles are ejected from the trap and sent into a plastic stopping scintillator. This scintillator is situated in a 10-kG magnetic field $\vec{B}_p$, which served to define a fixed direction in the laboratory. Since the beam always enters the field $\vec{B}_p$ in the same direction, the rotation of $\vec{P}$ about $\vec{v}$ implies an identical rotation of $\vec{P}$ about $\vec{B}_p$. Roughly half of the incident positrons form positronium. A fast coincidence counter measures that fraction of positronium atoms which survives in the scintillator longer than some fixed time t. This fraction depends linearly upon $\vec{P} \cdot \vec{B}_p$. Thus a plot of the coincidence counter output versus trapping time is a cosine curve of angular frequency ω_D. This measurement of ω_D, when combined with a measurement of the time average field B experienced by the positrons in the trap, is the basis of the experiment. More explicitly, if the g-factor is written as g = 2(1 + a), where "a" is the g-factor anomaly, then $a = (m_0c/eB)\,\omega_D$. The principal difference between the present experiment and previous work is the use of a pulsed coil instead of a dc magnet to generate the 10-kG magnetic field of the polarization analyzer. In the previous experiment fringe fields from the dc magnet caused severe drifting of the trapped beam so that only 8 cycles of the ω_D curve could be recorded before loss of all usable beam intensity. Under the new arrangement, such fringe fields are not present and trapping times corresponding to 80 cycles of the curve are feasible. This increase in the observable number of cycles accounts for a factor of five improvement in measurement accuracy. After evaluation of small relativistic corrections, the results of the experiment may be written as $a = (11{,}603 \pm 12) \times 10^{-7}$. Invariance under TCP requires equality of the electron and positron g-factors. The results, when compared to previous electron measurements, serve to confirm this prediction at the 1 ppm level in the g-factor. Furthermore, since the M^+ and M^- g-factors are equal to 0.7 ppm, any violation of TCP which manifests itself in a lepton-antilepton g-factor asymmetry is ruled out at the 1 ppm level. (Diss. Abstr. Int., B)

Weak

12076 VECTOR–AXIAL VECTOR CURRENT RATIO IN THE DECAY $\Sigma^- \to ne^-\nu$. Knop, Robert Edward. College Park, Md.; Univ. of Maryland (1969). 105p. University Microfilms Order No. 70-14,942. Thesis.

An experiment to measure the magnitude of the ratio of vector to axial vector coupling in the weak decay $\Sigma^- \to ne^-\nu$ is described. The analysis is based on an exposure of ~550,000 frames of K^- stopping in the 30″ Brookhaven National Laboratory hydrogen bubble chamber. The determination of the vector to axial vector ratio required the identification of np scatters associated with the $\Sigma^- \to ne^-\nu$ decay. The results of this experiment are favorable for the SU3 based model of Cabibbo. (Diss. Abstr. Int., B)

12077 MEASUREMENT OF THE RELATIVE RATE $K^+_{e2}/K^+_{\mu 2}$ AND AN UPPER LIMIT FOR THE STRUCTURE DEPENDENT RADIATION IN $K \to e\nu\gamma$. Roberts, Jabus Bridges Jr. Philadelphia; Univ. of Pennsylvania (1969). 165p. University Microfilms Order No. 70-16,203. Thesis.

The K^+_{22} branching ratio was measured in a counter and spark chamber experiment at the Princeton-Pennsylvania accelerator. A 500-MeV/c unseparated K^+ beam produced by the collision of the external proton beam with a platinum target was brought to rest in a beryllium stopper by means of a copper degrader. The K^+ mesons were identified by range and time of flight from the external target. Decay particles from the stopper at right angles to the beam passed through a momentum analyzing spectrometer consisting of wire spark chambers located on opposite sides of a magnet. Positrons were identified by three low pressure threshold gas Cherenkov counters, one adjacent to the stopping region to suppress background from muon decays in flight. A γ-ray detector on the opposite side of the stopper from the spectrometer identified decays accompanied by gamma rays. Wire spark chambers with magnetostrictive digital readout made possible computer monitoring of the experiment and rapid analysis of the many K_{e3} events that were necessarily detected. The solid angle subtended by the decay detecting apparatus was 2.7 percent of 4π. The K_{e2} rate was normalized against the well known high energy part of the K_{e3} positron spectrum. K_{e2} and K_{e3} events were identified by momentum and having the K^+ lifetime. A value of $1.7^{+.7}_{-.4} \times 10^{-5}$ was obtained for the $K_{e2}/K_{\mu 2}$ relative rate, to be compared with V– A prediction of 2.1×10^{-5}, including radiative corrections. An upper limit was also placed on the structure dependent radiation in $K \to e\nu\gamma$ of $(K \to e\nu\gamma/\text{All } K^+ \text{ Decays}) < 7.1 \times 10^{-5}$. (Diss. Abstr. Int., B)

12078 STUDY OF $K^0 \to \pi^+\pi^-$ TIME DEPENDENCE. Lowenstein, Derek Irving. Philadelphia; Univ. of Pennsylvania (1969). 108p. University Microfilms Order No. 70-16,181.

Thesis.

A sample of 9731 $K^0 \to \pi^+\pi^-$ decays in the 0–10 K^0_S lifetime region was collected using magnetostrictive wire spark chambers. Of these, that were produced in reactions $\pi^- + p \to \Lambda^0 + K^0$ and $\pi^- + p \to \Sigma^0 + K^0$ by 1.45 BeV/c π^- mesons on copper, 3725 were used in the calculation of the K^0_S lifetime, τ_s, and the CP violating parameter phase, Φ_+. By a least squares fitting procedure to the $K^0 \to \pi^+\pi^-$ time distribution $\tau_s = (.870 \pm .019) \times 10^{-10}$ sec. and $\Phi_+ = 65^0 \pm 75^0$ were obtained. (Diss. Abstr. Int., B)

12079 STUDY OF INTERFERENCE BETWEEN AMPLITUDES FOR $K_L \to 2\pi^0$ AND $K_S \to 2\pi^0$. Green, Daniel Raymond. Rochester, N. Y.; Univ. of Rochester (1970). 136p. University Microfilms Order No. 70-17,882.

Thesis.

The proper time dependence of the decays $K \to \pi^+\pi^-$ and $K \to \pi^0\pi^0$ over a proper time interval of 2 to 8 K_S lifetimes was investigated. Kaons, K^0 or $\bar{K}^0$, were produced by charge exchange of a K^+ or K^- beam with a momentum of 2 GeV/c. Charged and neutral decays were simultaneously detected in a system of spark chambers. No statistically significant difference in the proper time dependence of the charged and neutral decay modes was observed. This result has implications for the structure of the CP violating interaction. In terms of the usual complex phenomenological parameters for CP violation, $\eta = |\eta|e^{i\Phi} \equiv A(K_L \to \pi\pi)/A(K_S \to \pi\pi)$, this result resolves a previous two-fold ambiguity for ϕ_{00}; the phase ϕ_{00} is equal to the phase ϕ_{+-} within errors, $\phi_{00} - \phi_{+-} = -70^{+10}_{-11}{}^{\circ}$. Alternatively, it is concluded that the amplitude for the CP violating decay $K_L \to 2\pi$, with the final state pions having total isotopic spin = 2, is, at most, 35% of the analogous decay amplitude with isotopic spin = 0. (Diss. Abstr.)

12080 THE $|\Delta\vec{I}| = \frac{1}{2}$ RULE AND Λ^0 DECAY. Olsen, Stephen Lars. Madison, Wis.; Univ. of Wisconsin (1970). 92p. University Microfilms Order No. 70-13,931. Thesis.

A test of the $|\Delta\vec{I}| = \frac{1}{2}$ rule was performed by measuring α_0/α_-, the ratio of the parity violating Λ^0 decay parameters. The rule predicts this ratio to be 1. Polarized Λ^0's were produced by 1.0 GeV/c π^+'s in deuterium, using the reaction $\pi^+ + n + (p) \to K^+ + \Lambda^0 + (p)$. Either neutrons from $\Lambda^0 \to n\pi^0$ or protons from $\Lambda^0 \to p\pi^-$ were detected in a spark chamber with 33 polyethylene plates, each 1 gm/cm^2 thick. The ratio α_0/α_- was then determined by comparing the up-down asymmetry, relative to the production plane, of the decay neutrons and the decay protons. The result was $\alpha_0/\alpha_- = .977 \pm .071$, in good agreement with the $|\Delta\vec{I}| = \frac{1}{2}$ rule. (Diss. Abstr.)

12081 DETERMINATION OF THE AXIAL VECTOR TO VECTOR RATIO IN THE BETA DECAY OF THE LAMBDA HYPERON. Stevens, Alan Jerald. Columbus, Ohio; Ohio State Univ. (1970). 142p. University Microfilms Order No. 70-19,367. Thesis.

A counter-optical spark chamber experiment to study the β decay of the Λ hyperon was performed at the Zero Gradient Synchrotron at the Argonne National Laboratory. $\Lambda\beta$ events are identified by a combination of fiducial volume, time-of-flight, and kinematic requirements. The axial vector to vector ratio (C_A/C_V) is determined from the up-down asymmetries of the decay products with respect to the polarized lambdas. Analysis of 44 identified $\Lambda\beta$ events gives $C_A/C_V = -.41^{+.23}_{\infty}$ which is consistent with, but does not confirm, the theoretical prediction of Cabibbo. (auth)

12082 LATERAL DISTRIBUTION OF MUON PAIRS IN UNDERGROUND COSMIC-RAY SHOWERS. Coats, R. B.; Ozaki, S.; Stenerson, R. O.; (and others) (Univ. of Utah, Salt Lake City). J. Phys., A (London); 3: 689-96(Nov 1970).

The lateral distribution of cosmic-ray muon showers underground was studied by measuring the separations between about 5000 pairs of muons. Results are presented in terms of a counting rate for an equivalent pair of one meter-square detectors beneath 2500 hg cm^{-2} rock and orientated at 45° zenith. For separations from 0 to 50 m an approximately exponential dependence of the counting rate on detector separation is observed which decreases by a factor e in the order of 10 m. (auth) (UK)

XUM

12083 OBSERVATION OF MUON TRIDENT PRODUCTION IN LEAD AND THE STATISTICS OF THE MUON. Russell, J. J. (Harvard Univ., Cambridge, Mass.); Sah, R. C.; Tannenbaum, M. J.; (and others). Contracts AT(30-1)-2752; AT(30-1)-3651. Phys. Rev. Lett.; 26: 46-50(4 Jan 1971).

The production of muon tridents in lead with an effective cross section of 51 ± 7 nb per nucleus was observed in agreement with the predictions of quantum electrodynamics. This measurement is sufficiently accurate that the interference term due to the presence of two identical muons in the final state is seen. The size of the measured interference term is 1.15 ± 0.25 times the value predicted for Fermi statistics. (auth)

12084 PROTON POLARIZATION IN $\Sigma^+ \rightarrow p\pi^0$. Harris, Frederick Allan. Ann Arbor, Mich.; Univ. of Michigan (1970). 86p. University Microfilms Order No. 70-21,677.

Thesis.

The decay parameters of $\Sigma^+ \rightarrow p\pi^0$ were measured by observing the polarization of the decay protons by scattering in a carbon plate spark chamber. A sample of 1335 useful scatters gave $\alpha_0 = -0.98^{+0.01}_{-0.02}$, $\beta_0 = 0.08^{+0.16}_{-0.12}$, and $\gamma_0 = 0.19^{+0.33}_{-0.33}$. The value of β_0 is consistent with time reversal invariance, which predicts $\beta_0 \simeq -0.03 \pm 0.03$. Using data on $\Sigma^+ \rightarrow n\pi^+$ and $\Sigma^- \rightarrow n\pi^-$ and fitting to the $|\Delta\vec{I}| = 1/2$ rule gave $\chi^2 = 0.8$ for two degrees of freedom, which is in good agreement with the $|\Delta\vec{I}| = 1/2$ rule. Further, the present experimental data require the upper limits on possible $|\Delta\vec{I}| = 3/2$ amplitudes to be less than about 10% of the $|\Delta\vec{I}| = 1/2$ amplitudes. (Diss. Abstr. Int., B)

12085 SEARCH FOR DIRECT PROCESSES IN TWO-PION RADIATIVE DECAYS OF POSITIVE AND NEGATIVE KAONS. Edwards, Ralph Thomas. Urbana, Ill.; Univ. of Illinois (1970). 79p. University Microfilms Order No. 70-20,958.

Thesis.

Decays of the type $K^\pm \rightarrow \pi^\pm\pi^0\gamma$ were observed in an experiment performed at Argonne National Laboratory using a scintillation counter-optical spark chamber arrangement, and a 3.5 GeV/c $K^\pm$ beam. These decays are interesting because the interference of two competing mechanisms for this decay may produce asymmetries in the partial decay rates for K^+ and K^- into this mode. The mechanisms are internal bremsstrahlung and a hypothetical direct process in which the gamma is produced within the decay vertex. The experiment was performed to compare the partial rates of $K^+ \rightarrow \pi^+\pi^0\pi^0$ and $K^- \rightarrow \pi^-\pi^0\pi^0$ as a method of observing CP asymmetries. Among the 3π decays we have found 33 events of the type $K^+ \rightarrow \pi^+\pi^0\gamma$ and 31 of the type $K^- \rightarrow \pi^-\pi^0\gamma$. These events were separated from the 3π decays by observing an angle of the charged pion relative to the $K^\pm$ direction larger than that kinematically allowed for the 3π decays. The angles of the decay product in $K^\pm \rightarrow \pi^\pm\pi^0\gamma$ were used to calculate the K rest system energies and angles of the decay products. The distribution of the cosine of the angle between the charged pion and the gamma in the center of mass was used to fit parameters corresponding to the fraction of direct decays in the sample. The fraction of direct decays is consistent with zero, and the partial decay rate for direct decay, excluding interference between direct and internal bremsstrahlung amplitudes, is less than 10% (to 1 standard deviation) of the partial rate for internal bremsstrahlung for the kinetic energy of the charged pion between 58 and 90 MeV. The resulting upper limit for the asymmetries in the partial decay rates for $K^+ \rightarrow \pi^+\pi^0\gamma$ and $K^- \rightarrow \pi^-\pi^0\gamma$ is $[\Gamma(K^- \rightarrow \pi^-\pi^0\gamma)]/[\Gamma(K^+ \rightarrow \pi^+\pi^0\gamma)] - 1 = 0 \pm .24$ to one standard deviation for the same energy region. So, although the size of the direct process is small relative to internal bremsstrahlung, CP asymmetries were not shown to be unobservable. (Diss. Abstr. Int., B)

12086 TEST OF THE $|\Delta\vec{I}| = 1/2$ RULE IN LAMBDA DECAY. Smith, James Alan. Ann Arbor, Mich.; Univ. of Michigan (1970). 91p. University Microfilms Order No. 70-21,792.

The asymmetry parameter α_0 for $\Lambda^0 \rightarrow n\pi^0$ measured relative to α_- by comparing the neutron distribution to the proton distribution from the decay $\Lambda^0 \rightarrow p\pi^-$ for polarized Λ^0 hyperons. The polarized lambda particles were produced in liquid deuterium by the reaction $\pi^+ + n + (p) \rightarrow K^+ + \Lambda^0 + (p)$, where (p) represents the spectator proton. A sample of 4760 neutron events and 8500 proton events gave $\alpha_0/\alpha_- = 0.977 \pm 0.071$, in good agreement with the $|\Delta\vec{I}| = 1/2$ rule. The spark chamber-scintillation counter experiment was performed at the Princeton-Pennsylvania Accelerator. (Diss. Abstr. Int., B)

12087 STUDY OF THE DECAY MODE $K_L^0 \rightarrow \pi^+\pi^-\pi^0$. Buchanan, C. D. (Univ. of California, Los Angeles); Drickey, D. J.; Rudnick, F. D.; (and others). Phys. Lett.; 33B: 623-6(21 Dec 1970).

The decay process $K_L^0 \rightarrow \pi^+\pi^-\pi^0$ was studied in the 3° K_L^0 beam at the Stanford Linear Accelerator Center using a wire chamber magnetic spectrometer. The three pion decay was separated from leptonic decays using kinematics and muon identification. The average detection efficiency is 58.5% with a variation of less than 10% over the Dalitz plot. For a matrix expressed expanded in terms of a power series in the kinetic energy of the π^0, the parameter of the expansion a_0 was found to be -0.257 ± 0.005. (auth)

12088 MEASUREMENT OF THE FORM FACTORS FOR THE DECAY $K_L^0 \rightarrow \pi\mu\nu$. Chien, C.-Y. (Johns Hopkins Univ., Baltimore); Cox, B.; Ettlinger, L.; (and others). Phys. Lett.; 33B: 627-30(21 Dec 1970).

The decay process $K_L^0 \rightarrow \pi\mu\nu$ was studied in a wire chamber experiment using the three-degree K_L^0 beam at SLAC. A sample of 26,500 $K_{\mu 3}$ events have been identified to obtain information on the form factors $f_\pm$ associated with the V−A hypothesis for this decay. Expressing the energy dependence of the form factors as $f_\pm + f_\pm(0)(1 + \lambda_\pm q^2/m^2)$, where $q^2 = (p_K - p_\pi)^2$, the experiment yields the value $\lambda_+ = 0.08 \pm 0.01$ and reveals a strong coupling between λ_- and $\xi(0) = f_-(0)/f_+(0)$. (auth)

12089 SMALL-ANGLE SCATTERING OF RELATIVISTIC PARTICLES. Hickey, Francis Roger. Potsdam, N. Y.; Clarkson Coll. of Tech. (1970). 307p. University Microfilms Order No. 70-22,585.

Thesis.

The scattering of high-energy muons through extremely small angles in solids was investigated. The projected angular deviations of muons with momenta 2.5, 5, 10, and 14.8 GeV/c through thicknesses of 500, 1000, 2000, 4000, 8000, and 16,000 microns were measured using nuclear emulsions both as a track recording device and scattering material. The measured angular distributions (0.1 − 4.0 mrad) include contributions from single scatters by individual nuclei as well as plural and multiple scattering. The data in all three regions were found to be in excellent agreement with the early and mathematically simple scattering theory developed by E. J. Williams (1939, 1940) when suitable modification for the finite dimensions of the emulsion nuclei is made. These results were used to study multiple scattering techniques in nuclear emulsions including problems connected with the scattering constant and spurious scattering. Finally, this investigation suggests a new method of determining a particle's energy from standard multiple scattering measurements. (Diss. Abstr. Int. B)

Strong (Baryon-Induced)

Refer also to abstract 10868.

12090 (INR-P-1223) HYPERNUCLEI AND HYPERNUCLEAR SPECTROSCOPY. Pniewski, J. (Institute of Nuclear Research, Warsaw (Poland)). 1970. 25p. Dep. NTIS (U. S. Sales Only).

The review of experimental studies of hypernuclei covers identification, binding energies, and production of hypernuclei, spins, lifetimes, nonmesic and π^+ decays, and the AN interaction. Also discussed are excited and resonant states, hypernuclear isomers, and the gamma spectroscopy of hypernuclei. (J.F.P.)

12091 STUDY OF EVENTS WITH TWO OR FOUR CHARGED PRONGS FROM 28.5-GeV/c pp INTERACTIONS. Ellis, William Edwin Nashville; Vanderbilt Univ. (1970). 123p. University Microfilms Order No. 70-16,422.

Thesis.

The Brookhaven 80-inch hydrogen bubble chamber at the BNL-AGS was exposed to a proton beam with a momentum of 28.5 GeV/c. Approximately 83,000 pictures were taken and scanned for pp interactions with two or four charged outgoing particles. The presence of outgoing particles with high laboratory momentum made positive kinematic fitting of the events difficult. In particular, the high momentum positive tracks could be interpreted as either protons or positive pions. Only the four-constraint fits to the final state $pp\pi^+\pi^-$ were taken to be reliable. These difficulties were overcome by analyzing the events with neutral particles by a missing mass technique. This consists of selecting a low-momentum recoil proton which could be well measured and calculating the remaining missing mass as indicated in the reaction $p + p \rightarrow p_R + MM$. Results of this analysis were compared with the missing mass data from the higher statistic counter experiments. The use of bubble chamber data allows one to determine that the 1.4-GeV enhancement seen in the missing mass spectrum is predominantly composed of $N\pi$ rather than $N\pi\pi$ systems. Selection of events with the mass of the $(p\pi^+)$ combination in the region of the Δ^{++} (1236) isobar allowed the analysis of these events in the form $p + p \rightarrow \Delta^{++} + M$. The virtual scattering of a π^- to produce the system M was compared with the real π^-p scattering that gives the system M. Good agreement was seen between this off-shell and on-shell scattering. The momentum distributions for the individual particles from several final states are presented. These include distributions of the longitudinal and transverse components of the center-of-mass momentum. The method suggested by van Hove for analysis based on the use of the

longitudinal components of center-of-mass momentum was applied to the intermediate state $\Delta^{++}\pi^-p$. Systems of particles such as $(n\pi^+)$, $(\Delta^{++}\pi^-)$, and $(n\pi^+\pi^+\pi^-)$ can be produced by the diffraction dissociation of a proton. This diffraction dissociation is investigated by making comparisons with the results of a Monte Carlo program using an empirically formulated expression for the differential cross section. (Diss. Abstr. Int., B)

12092 DEUTERON–DEUTERON ELASTIC SCATTERING AT 2.20 GeV/c. Oddone, Piermaria Jorge. Princeton, N. J.; Princeton Univ. (1970). 143p. University Microfilms Order No. 70-19,797.

Thesis.

The deuteron-deuteron differential cross section was obtained at an incident laboratory momentum of 2.20 GeV/c. The data cover a momentum transfer range from 0.07 $(GeV/c)^2$ to the kinematic limit at 90° CM scattering angle. The data were obtained in the 15-inch Princeton-Pennsylvania rapid cycling bubble chamber in an exposure corresponding approximately to 2.5 events/microbarn. This exposure contains thirty times more data than previously available above an incident laboratory momentum of 2.0 GeV/c. The uncertainties in the experimental cross section are much smaller than the uncertainties and ambiguities which exist in the theoretical models that have been applied up to the present time. The features of the observed differential cross section were interpreted using the Glauber multiple scattering theory. In applying this theory it was extended to include the quadrupole deformation of the deuteron which up to now has been neglected in theoretical studies of deuteron-deuteron collisions. Theoretically it was found that the quadrupole deformation of the deuteron plays a significant role in the region where interference occurs in the multiple scattering amplitudes. This theoretical conclusion is borne out by the experimental data. The theoretical predictions agree qualitatively with the experimental data. Quantitative agreement is obtained only for momentum transfers below 0.2 $(GeV/c)^2$. The question whether quantitative agreement may be obtained for larger momentum transfers remains open since the computations are subject to refinement by including a spin dependent parametrization of the nucleon-nucleon amplitudes. (Diss. Abstr.)

12093 SYSTEMATIC INVESTIGATION OF ULTRA HIGH ENERGY INTERACTIONS. II. Nozaki, Tadao; Koshiba, Masatoshi (Tokyo Univ.). J. Phys. Soc. Jap.; 30: 1-33(Jan 1971).

The composition of secondary particles produced in the backward cone of nuclear interactions of 10^{12} eV to 10^{13} eV was investigated by means of a large emulsion stack. The angular distributions in the center of mass system of protons, $K^\pm$ mesons and $\pi^\pm$ mesons were observed to have their respective peaks in the narrow, $\lesssim$0.2 radian, angular region around the backward direction. The $K^\pm/\pi^\pm$ ratio in the peak was found to be 0.71 ± 0.20. The $K^\pm$ mesons in the peak are likely to be the decay products of ϕ mesons produced with small emission angles. Finally the "Aleph" isobar proposed previously is examined with additional experimental data. (auth)

12094 ESTABLISHMENT OF UPPER LIMITS FOR TWO PARITY-VIOLATING PARAMETERS IN THE NUCLEON–NUCLEON SCATTERING MATRIX AT 210 MeV. Gucker, Edward Joseph. Rochester, N. Y.; Univ. of Rochester (1970). 164p. University Microfilms Order No. 70-17,883.

Thesis.

This experiment constituted a test of parity conservation in the strong nucleon-nucleon interaction in that it placed upper limits on the magnitudes of two parameters which are directly related to the mixing of scattering states of opposite parity. A longitudinally polarized beam of 210 MeV protons was prepared by passing the vertically polarized beam from the Rochester synchrocyclotron through a sequence of vertical and solenoidal magnetic fields. The preparation of the beam was such that the polarization could be reversed by reversing the direction of the current in the coils of the solenoid magnet. This beam was then allowed to strike targets of polyethylene and of carbon, with the scattered protons being detected by two triple coincidence counter telescopes located on either side of the beam line. The asymmetry a_k was measured between the counting rates generated by the forward polarized beam and the backward polarized beam. (TSS) (Diss. Abstr.)

12095 LOW-MOMENTUM ANTIPROTON–PROTON SCATTERING. English, Jane Butterfield. Madison, Wis.; Univ. of Wisconsin (1970). 61p. University Microfilms Order No. 70-13,912.

Thesis.

Results are presented from a study of $\bar{p}p$ interactions between 100 and 750 MeV/c. A total of 125,000 pictures were taken in the hydrogen-filled 30" bubble chamber at Brookhaven. Two classes of events were studied, backward hemisphere elastic scattering and very low momentum annihilation events coming from antiprotons that had already scattered elastically. For the annihilation events 0, 2, 4 and 6 prong cross sections were measured from 100 MeV/c to 550 MeV/c. All these cross sections fall steeply from 100 MeV/c to 300 MeV/c, then with a rather abrupt break fall less sharply from 300 MeV/c to 550 MeV/c. The differential elastic cross section was measured from 250 MeV/c to 750 MeV/c. Comparison of the data with previous experiments lends some support for the existence of two resonances with masses 1927 and 1950 MeV and widths 10 and 50 MeV respectively. It is noted that the mass and spin are right for the first Regge recurrence of the A_2 meson. (TSS) (Diss. Abstr.)

12096 EXPERIMENTAL DETERMINATION OF THE INELASTIC NEUTRON FORM FACTOR BY THE SCATTERING OF 12-GeV MUONS ON HYDROGEN, CARBON, AND COPPER. Lakin, W. L. (Stanford Univ., Calif.); Braunstein, T. J.; Cox, J.; (and others). Phys. Rev. Lett.; 26: 34-8(4 Jan 1971).

Results for the ratios of the muon inelastic-scattering cross sections on carbon and copper to the cross sections on hydrogen, measured in the same experiment, are presented. The data are consistent with ratios of cross sections for real photoabsorption. In the kinematical region where coherent diffractive effects should be small or absent it is found that the inelastic cross section varies as $A^{0.99\pm0.01}$ and that $\sigma_n/\sigma_p = 0.91 \pm 0.6$. (auth)

12097 ANNIHILATION OF 1.6- TO 2.2-GeV/c ANTIPROTONS INTO K_1 MESONS. Ring, Harvey Michael. Ann Arbor, Mich.; Univ. of Michigan (1970). 333p. University Microfilms Order No. 70-21,775.

Thesis.

In an exposure of the ANL 30-inch hydrogen bubble chamber to a beam of antiprotons at six beam momenta (invariant masses) 1.63 (2300), 1.77 (2350), 1.83 (2370), 1.88 (2390), 1.95 (2410), 2.20 (2510) GeV/c (MeV), all reactions resulting in one or more $K_1 \to \pi^+\pi^-$ accompanied by at least two charged tracks at the main interaction origin were analyzed. Cross sections as a function of energy are presented for all of the following reactions and their charge conjugates (c.c): $\bar{p}p \to \bar{K}^0K^+\pi^-$ + c.c, $\bar{p}p \to \bar{K}^0K^+\pi^-\pi^0$ + c.c, $\bar{p}p \to K_1K_2\pi^+\pi^-$, $\bar{p}p \to K_1K_1\pi^+\pi^-$, $\bar{p}p \to \bar{K}^0K^+\pi^-\pi^+\pi^-$, $\bar{p}p \to K_1K_1\pi^+\pi^-\pi^0$, $\bar{p}p \to K_1K_1\omega$, $\bar{p}p \to \bar{K}^0K^+\pi^-\pi^+\pi^-\pi^0$ + c.c, $\bar{p}p \to K_1(K^0)\pi^+\pi^-\pi^+\pi^-$, $\bar{p}p \to K_1K_1\pi^+\pi^+\pi^-\pi^-$, $\bar{p}p \to \bar{K}^0K^+\pi^-(n\pi^0)n \geq 2$ + c.c, $\bar{p}p \to K_1\pi^+\pi^-(K_2 + n\pi^0)$ $n \geq 1$, and $\bar{p}p \to K_1(K^0)K^+K^-$. The energy dependence of the cross sections is used to investigate the formation of direct-channel boson resonances. Evidence is found for an odd-C resonance of mass (2370 ± 10) MeV and width, $\Gamma < 40$ MeV, decaying into $K_1K_1\pi^+\pi^-\pi^0$. Mass distributions for each channel are presented to investigate resonance formation in the various channels. Only the $K^*(892)$, ω, and ρ mesons are strongly produced in the data. All other resonances are either weakly produced or otherwise not evident in the data. Angular distributions and their interpretation with respect to the annihilation process are also presented. (Diss. Abstr. Int., B)

Strong (Meson-Induced)

12098 (CEA-R-4068) RESONANCE IN THE REACTIONS $K^-p \to \Sigma^\pm\pi^\pm$ BETWEEN 440 AND 1230 MeV/c. Granet, Pierre (Commissariat a l'Energie Atomique, Saclay (France). Centre d'Etudes Nucleaires). Oct 1970. 133p. (In French). Dep. NTIS (U. S. Sales Only).

Thesis. Submitted to Paris Univ., Orsay (France). Faculte des Sciences.

The analysis of the reactions presented is part of a systematic study of $\bar{K}N$ interactions in hydrogen bubble chambers undertaken by the CERN–HEIDELBERG–SACLAY collaboration. Analysis of energy-dependent partial waves revealed six baryonic resonances of strangeness −1 and isospins 0 and 1 (two had never been detected before). These resonances can be classified in four octets of the baryonic states of the unitary symmetry SU(3); the two new A resonances found were assigned to the two 0-hypercharge baryons missing in the octets $\frac{3}{2}^-$ and $\frac{5}{2}^-$. Finally, the branching ratio of the nonleptonic decay of the Σ^+ and the $\Sigma^\pm$ lifetimes were accurately determined. (auth)

12099 (JINR-P1-5398) OBSERVATION OF $\pi^-p \to e^+e^-n$ REACTION AT 275 MeV. Akimov, Yu. K.; Vertogradov, L. S.; Dem'yanov, A. V.; (and others) (Joint Inst. for Nuclear Research, Dubna (USSR). Lab. of Nuclear Problems). 1970. 24p. (In Russian). Dep. NTIS (U. S. Sales Only).

A system consisting of scintillation and Čerenkov counters, Čerenkov total absorption spectrometers and spark chambers was used for the $\pi^- + p \to e^+e^-n$ reaction detection. Electrons and positrons were registered at an angle close to 90° relative to the π^--meson beam. The energy and the angle of emission of electrons and positrons were measured. The analysis of the data obtained allows one to identify 55 events of the reaction with the

(e^+e^-) pair effective mass about 300 MeV and to determine the differential cross section of the reaction at an electron energy more than 40 MeV. (auth)

12100 (NP-18629) THE PRODUCTION OF STRANGE PARTICLES IN π^+d INTERACTIONS AT 5.1 GeV/c: 2-BODY AND QUASI-2-BODY REACTIONS. Mettel, Denyse (Paris Univ. (France)). 1970. 172p. (In French). Dep. NTIS (U. S. Sales Only).

Thesis.

Strange particles produced by π^+d interactions at 5.1 GeV/c were studied. The principal interest of experiments with a deuterium target is the possibility of obtaining interactions in which either the deuteron remains intact or the incident beam interacts with the neutron. If the impulse approximation model is used a quasi-free neutron target may be used in conjunction with the last hypothesis. Cross sections for all the π^+n interactions in the final state with 2, 3, 4, and 5 bodies, were evaluated. The analysis of reactions associated with K $\bar{K}$ and Y K is described in detail. A systematic study was made of resonances which could lead to the observation of quasi-2-body reactions; the various results of the 5.1 GeV/c experiment were deduced. In particular, the angular distributions of the disintegration products of a resonance and the evaluation of the spin density matrix allowed comparisons to be made with the previous OME model. All the experimental results of the two-body and quasi-two-body reactions were used in a more general π-nucleon interaction model and the values deduced were compared with the more simple Regge pole model. A more complicated Regge pole model using a double pole was studied in order to explain results concerning the polarization of the Λ^0 of the two body $\pi^+n \rightarrow \Lambda^0K^+$ interaction. In this way very important additional information about the nature of the exchanges involved in the process was obtained. Nevertheless, for various experimental and theoretical reasons the models are limited. (France)

12101 STUDY OF THE REACTION $\pi^-p \rightarrow \pi^+\pi^-\pi^-\pi^0p$ AT 6 GeV/c. Lee, Kyu Yul. Bloomington, Ind.; Indiana Univ. (1970). 126p. University Microfilms Order No. 70-14,967.

Thesis.

The reaction $\pi^-p \rightarrow \pi^+\pi^-\pi^-\pi^0p$ at the beam momentum 6 GeV/c is studied in detail. Approximately 95,000 usable frames of pictures were taken with the MURA hydrogen bubble chamber exposed to 6 GeV/c negative pions, at Argonne National Laboratory. About 20,000 4-prong events were scanned and measured, and 2454 events for the above reaction were selected. The cross section for the reaction is found to be 1.52 ± 0.13 mb. The final state is characterized by an abundance of resonance production; Δ^{++} (1236), ω (783), ρ^- (765), ρ^0, and ρ^+ production channels are 21, 15, 23, 20, and 6 percent of the reaction. The clean appearance of the ρ^+ enhancement is worthy of note, since it is not frequently observed in this type of reaction. Enhancement of an η-meson is also observed, and there is evidence for A_2, Δ^0, and Δ^+. The enhancement of g′ (1700) in the 4-pion effective mass spectrum is not clear, due to the large background. Evidence for its existence is presented by analyzing its decay modes. The cross section for $g' \rightarrow \rho^-\rho^0$ decay mode is found to be 23 ± 8 μb; $g' \rightarrow \rho\pi\pi$ and $g' \rightarrow A_2\pi$ are also possible. A negative result is obtained for the $g' \rightarrow \omega\pi$ mode. A very clean enhancement is observed at the mass 1.26 GeV in the ($\omega\pi^-$) effective mass spectrum. This is identified as the B-meson. Approximately 65% of the Δ^{++} isobar appear to be produced in association with a ρ^-. The corresponding reaction $\pi^-p \rightarrow \rho^-\pi^-\Delta^{++}$ is tested on the much-publicized double Regge pole exchange model. Events were grouped into different Regge diagrams according to the ordering of the longitudinal momenta of the final state particles. Since this method can be applied only to the very high energy regions, a sizeable background was inevitable. The experimental data are compared with the predictions given by E. L. Berger's model, as well as by H. M. Chan's. Chan's model gives the better fit to the data. (Diss. Abstr. Int., B)

12102 STUDY OF DIFFRACTIVELY PRODUCED THREE-BODY FINAL STATES IN K^+p INTERACTIONS AT 13 GeV/c. Farber, Morton S. Rochester, N. Y.; Univ. of Rochester (1970). 232p. University Microfilms Order No. 70-17,876.

Thesis.

Results are presented of a study of the four-pronged topology produced in K^+-proton interactions at an incident beam momentum of 12.7 GeV/c, using Brookhaven National Laboratory's 80-inch hydrogen filled bubble chamber. The reactions discussed in detail are: (1) $K^+p \rightarrow K^+p\pi^+\pi^-$, (2) $K^+p \rightarrow K^+p\pi^+\pi^-\pi^0$, and (3) $K^+p \rightarrow K^+p\,K^+K^-$. Reaction (1) is found to proceed largely via quasi-three body production leading to the final states $K^+\rho^0p$, $\pi^+K^*(890)p$, $K^+\pi^-\Delta^{++}(1236)$ and is characterized by large low-mass enhancements in the $K^+\pi^+\pi^-$ and $p\pi^+\pi^-$ systems. For both the K$\pi\pi$ (Q meson) and p$\pi\pi$(N*(1400)) enhancements, the data suggest a diffraction type of production mechanism, similar to the mechanism used to explain elastic scattering. The data are compared for Q and N*(1400) production to the predictions of a double-Regge model and to a nonresonant diffraction model suggested by Ross and Yam. It is found that these models fail to give a completely satisfactory description of the data. A spin-parity analysis was done for the K$\pi\pi$ low-mass region in which the entire enhancement was interpreted as consisting of a Q meson resonant state plus an incoherent mixture of K*(1420) and phase space background. From an analysis of the Dalitz plots in the Q region it is found that the data are consistent with a spin-parity assignment for the Q of 1^+. It is also found that if the Q is a member of an SU(3) octet then it belongs in the octet in which the neutral nonstrange member has C = +1. The mass and width obtained for the Q are M_0 = 1270 ± 20, and Γ_0 = 180 ± 20 MeV, respectively. Using reactions (2) and (3) the three-body states $K^+\omega^0p$, $K^+\eta^0p$ (reaction (2) and $K^+\phi^0p$ (reaction (3)) are studied. It is found that a prominent feature in these reactions is low-mass enhancements in the $K^+\omega^0$, $K^+\eta^0$ and $K^+\phi^0$ systems. Low-mass enhancements in the $p\omega^0$ and $p\eta^0$ systems are also observed. All these low mass enhancements are indicative of diffraction phenomena. (Diss. Abstr. Int., B)

12103 STRANGE-PARTICLE PRODUCTION IN 7.3-GeV/c K^- INTERACTIONS IN DEUTERIUM. Eide, Age Jostein. Boulder, Colo.; Univ. of Colorado (1969). 243p. University Microfilms Order No. 70-16,479.

Thesis.

Three prong events with one or more neutral decays associated, were studied in 50,000 pictures taken at the Brookhaven National Laboratory 80-inch bubble chamber, filled with deuterium and exposed to an incoming negative kaon beam of 7.3 GeV/c momentum. Partial cross sections are measured and resonance production is studied. The cross section for production of one neutral hyperon of strangeness −1 or of one neutral kaon is (1.59 ± 0.03) mb. Total cross section is (37.4 ± 1.5) mb. (Diss. Abstr. Int.,B)

12104 STRANGE-PARTICLE FINAL STATES FROM π^+p INTERACTIONS AT 1.7 GeV/c. Forman, Fred Leslie. Philadelphia; Univ. of Pennsylvania (1969). 172p. University Microfilms Order No. 70-16,146.

Thesis.

The strange particle final states from π^+p interactions at an incident π^+ momentum of 1.7 GeV/c were studied. Cross sections for all observed channels are presented. In the Σ^+K^+ channel the model of Louie gave good quantitative agreement with the experimentally observed differential cross section and polarization. The $\pi^+K^+\Lambda^0$ channel is dominated by $Y_1^*(1385)$ production. The $Y_1^*(1385)$ production and decay angular distributions are presented and compared with the models of Stodolsky and Sakurai, and Reininger and Sarma. A new particle state was observed in the $\Lambda^0\pi^+$ mass distribution in the $\pi^+K^+\Lambda^0$ channel at 1475 ± 15 MeV, with a width of 30 ± 15 MeV. This new state, the $Y_1^*(1475)$, as well as the $Y_1^*(1385)$, was also observed in the $(\Sigma\pi)^+$ system from the $\pi^+\Sigma^0K^+$ and $\pi^+\Sigma^0K^+$ channels. Indications of the $Y_1^*(1475)$ were also seen in the $p\bar{K}^0$ system from the $pK^+\bar{K}^0$ channel. Branching ratios were determined. No statistically significant evidence for resonance production was found in the $(K\pi)^+$ [below the K* (890)], $(K\pi)^{++}$, $(\Sigma K)^+$, $(\Sigma K)^{++}$ or $(\Sigma\pi)^{++}$ systems from the various channels studied. (Diss. Abstr. Int., B)

12105 PION INTERACTIONS IN DEUTERIUM AT 330 MeV. Brunhart, Gunter. Lexington, Ky.; Univ. of Kentucky (1962).

Thesis.

Pion interactions in deuterium were investigated and compared with the free nucleon assumption and the impulse approximation. It could be shown that the interactions do not proceed as free particle reactions; i.e., the incident pion does not interact with either the proton or the neutron in the deuterium but it interacts with both. Total cross sections and differential cross sections were determined and are compared with the predictions of the impulse approximation. The elastic differential cross section appears to be in good agreement with a theory advanced by Bransden and Moorhouse, however, it is in definite disagreement with the predictions of the theory by Rockmore based on the impulse approximation. The total cross section was found to be 51.2 mb compared to a cross section of 77 mb for the free particle assumption. Momentum and angular distributions are given for the elastic as well as the inelastic events. The momentum cutoff is compared with the statistical model and good agreement is found if the reactions are assumed to involve the deuteron as a whole. Pion production was found to be possible. A separation of the pion production events was attempted and differential cross sections are given for definitely identified events. (auth)

12106 K^- ABSORPTION ON NEON. Tucker, Lee Mewbourne Jr. Knoxville, Tenn.; Univ. of Tennessee (1969). 93p. University Microfilms Order No. 70-17,854.

Thesis.

XUM

Results of a bubble chamber study of K^- meson interactions with neon nuclei are presented. The exposure was obtained in the Brookhaven National Laboratory 30-inch bubble chamber filled with a 24 mole per cent mixture of neon in hydrogen. The general systematics of K^- neon interactions are discussed and compared with results obtained in experiments with other nuclei. In particular, results on Λ^0 trapping (hyperfragment formation), single and multinucleon absorption rates, and the $\Sigma - \Lambda$ conversion process are discussed. (Diss. Abstr.)

12107 RESONANCE PRODUCTION IN THE REACTION $\pi^+ d \rightarrow pp\pi\pi$ FROM 1.1 TO 2.3 GeV/c. I. AND II. Manning, Robert Jerome. Berkeley, Calif.; Univ. of California (1969). 139p. University Microfilms Order No. 70-17,616.

Thesis.

In an analysis of 229,000 pictures of π^+ at incident momenta of 1.1 to 2.3 GeV/c in the deuterium-filled 72-in. bubble chamber, 41,045 examples of the reaction $\pi^+ d \rightarrow pp\pi^+\pi^-$ were identified. A phase shift analysis was attempted on the angular distribution moments of off-mass-shell π-π scattering for low momentum transfer events (production angle cosine from beam to outgoing mesons >0.8). This resulted in 4 distinct solutions for the I = 0, J = 0 π-π scattering phase shift. The solution which rises slowly to nearly 90° at a π-π mass of 700 MeV and remains near 90° for π-π masses between 700 and 1000 MeV is preferred over the other solutions by comparison with the subtracted $\pi^0\pi^0$ mass spectrum reported. At values of center-of-mass energy >2.1 Gev forward peaking is found in the single meson exchange forbidden reaction $\pi^+ N \rightarrow \Delta^{++}(1238)\pi^-$. In the same reaction backward peaking was also observed inconsistent with simple J = ½ baryon exchange in the u-channel. In an analysis of 229,000 pictures of π^+ at incident momenta of 1.1 to 2.3 GeV/c in the deuterium-filled 72-inch bubble chamber, 8433 examples of the reaction $\pi^+ d \rightarrow pp$ (neutrals) were identified. An application of the impulse approximation and the selection 1.831 < ECM < 2.285 Gev gives 4956 events of the type $\pi^+ N \rightarrow P$ (neutrals). At small momentum transfers (≤0.2 and 0.08 Gev^2/c^2) to the neutrals system, no direct evidence is found for an enhancement near the reported position of the ϵ^0, ≈ 730 MeV. A detailed subtraction of $3\pi^0$ and $\Delta^+(1238)$ background based on cross sections from other experiments results in a $2\pi^0$ mass spectrum which is in disagreement with two other experiments at nearly the same center-of-mass energy, and which is consistent with a δ§ π-π phase shift which rises slowly to near 90° at a π-π mass of 700 MeV and remains near 90° for π-π masses between 700 and 1000 Mev. (Diss. Abstr.)

12108 K^--NEUTRON ELASTIC SCATTERING FROM $K^- d \rightarrow K^- d$ AND $K^- d \rightarrow K^- pn$ AT 1 GeV/c. Jew, Nathan Nay Shew. Berkeley, Calif.; Univ. of California (1969). 109p. University Microfilms Order No. 70-17,586.

Thesis.

Experimental angular distributions are presented for $K^- d \rightarrow K^- d$ and $K^- d \rightarrow K^- pn$ at incident K^- momenta of 810, 910, 1010, and 1110 MeV/c. These distributions are analyzed simultaneously in terms of free nucleon scattering parameters, using Glauber's impact parameter formalism as starting point. This formalism was modified to make it applicable to the data, which contained a proton momentum cut made during scanning. In addition, two other modifications to this formalism were incorporated into the analysis. One of these arose from the difference in flux factors between $K^- d$ and K^- nucleon scattering, the other from the smearing of the nucleon cross sections due to Fermi momentum. Finally, this formalism was extended to include spin dependence. The method of analysis required both the $K^- p$ and $K^- n$ elastic scattering amplitudes. The $K^- p$ amplitudes were input from two models based on experiment. These were held fixed during the fitting. Then the $K^- n$ amplitudes were parametrized and the data fitted by varying the $K^- n$ parameters to get a minimum for the fitting χ^2. The analysis included both the single and double scattering effects. (Diss. Abstr.)

12109 STUDY OF $\pi^- + p \rightarrow \Lambda + K^0$ FROM 944 TO 1170 MeV/c. Doyle, Joseph Cecil. Berkeley, Calif.; Univ. of California (1969). 66p. University Microfilms Order No. 70-17,547.

Thesis.

The process $\pi^- + p \rightarrow \Lambda + K^0$ was studied at incident beam momenta of 944, 966, 986, 991, 1006, and 1170 MeV/c in the Lawrence Radiation Laboratory 72-inch hydrogen bubble chamber. Differential and total cross sections and polarizations are presented. An attempted partial-wave analysis incorporating previously reported data at 1030 MeV/c is described and two solutions found are compsared with other results. (Diss. Abstr.)

12110 STRANGE-PARTICLE FINAL STATES PRODUCED BY 7-GeV/c π^- ON PROTONS. Peekna, Andres. Madison, Wis.; Univ. of Wisconsin (1970). 167p. University Microfilms Order No. 70-12,746.

Thesis.

Production of resonances involving strange particles is surveyed. Only well established resonances were clearly seen. Data from the University of Toronto and the University of Colorado were included, for some reactions. There is an indication that the $\eta_{0+}(1070)$ may be produced most strongly in association with a nucleon and a pion. Data on quasi-two-body reactions were found to be generally consistent with the Regge pole model but there are some indications that the highest-lying trajectory (K^*) does not always exclusively dominate at this energy. (Diss. Abstr.)

12111 BACKWARD PION PRODUCTION FROM $\pi^- p$ INTERACTIONS. Anthony, R. W. (Univ. of Michigan, Ann Arbor); Coffin, C. T.; Meanley, E. S.; (and others). Phys. Rev. Lett.; 26: 38-41 (4 Jan 1971).

The cross section for backward inelastic production of π^+ by π^- on protons was measured at eleven beam momenta between 2.15 and 6.0 GeV/c. It is found that the laboratory cross sections $d^2\sigma/dp_{||}dp_\perp^2$ at fixed transverse momentum $p_\perp$ and longitudinal momentum $p_{||}$ have little or no dependence on beam momentum between 3.5 and 6.0 GeV/c, and are sharply peaked toward zero $p_\perp^2$. The backward π^+ distributions in the laboratory from the experiment are nearly identical in shape to those obtained in the beam frame from pp experiments. (auth)

12112 MESON AND BARYON PRODUCTION IN THE $\pi^+ d \rightarrow pp\pi^+\pi^-\pi^0$ REACTION AT 4.19 GeV/c. Gordon, Howard Allan Urbana, Ill.; Univ. of Illinois (1970). 129p. University Microfilms Order No. 70-20,968.

Thesis.

A study of 1809 events of the reaction $\pi^+ d \rightarrow pp\pi^+\pi^-\pi^0$ at 4.19 GeV/c incident pion moment is reported. The experiment was done in the Lawrence Radiation Laboratory 72 in. deuterium bubble chamber. A significant amount of beam contamination is found but shown not to be present in the events selected for analysis. A considerable amount of ρ production is found. The clearest feature of the data is the ω^0 production with a cross section of $\sigma(\pi^+ n \rightarrow \omega^0 p) = 0.36 \pm 0.05$ mb. There is a 2-standard deviation dip in ρ_{00} for the ω^0 between $-0.2 < |t| < -0.3(GeV/c)^2$ and a small negative value of $Re\rho_{10}$ for $|t| < -1.0(GeV/c)^2$. The dip in ρ_{00} is consistent with the vanishing, in that region of t, of an exchanged trajectory with unnatural parity. A simple Regge model calculation with ρ + B exchange does not reproduce the data. Evidence is given for simultaneous $\rho\Delta(1236)$ production produced by one-pion exchange. Enhancements are seen in the three pion spectrum corresponding to the A_1, A_2 and $\varphi(1650)$. The data alone cannot prove that the I = O assignment for the φ is correct. (Diss. Abstr. Int., B)

12113 PRODUCTION OF NEUTRAL MESONS IN BACKWARD $\pi^- p$ SCATTERING. Romer, Henry Fiske. Minneapolis; Univ. of Minnesota (1970). 102p. University Microfilms Order No. 70-20,231.

Thesis.

Inelastic scattering of π^- mesons on protons is studied at incident pion momenta of 2, 3, 4, 5, and 6 GeV/c, for events with scattering angles greater than 120° in the center-of-mass system. An optical spark chamber array surrounding a liquid hydrogen target is used to record all the final state particles from the reactions $\pi^- p \rightarrow n\gamma\gamma$, and $\pi^- p \rightarrow n\pi^+\pi^-$. Production of η^0 mesons in the two gamma ray final state is observed and comparison of this rate with that for π^0 production yields a ratio of the two cross sections, for the region studied of 0.18 ± 0.05. Production of ρ^0 and f^0 mesons is observed in the two pion system. Differential cross sections for these processes show a backward peak characteristic of baryon exchange. Analysis of the energy dependence of these cross sections indicates that this exchange is consistent with the Regge trajectory N_γ. Decay angular distributions of the two pions in the dipion rest frame are used to compute spin density matrix elements for these productions. (Diss. Abstr. Int., B)

12114 K^0 PROTON π^+ CHANNEL IN K^+ PROTON INTERACTIONS AT 3.2 GeV/c. Shufeldt, Warren Eugene. Urbana, Ill.; Univ. of Illinois (1970). 76p. University Microfilms Order No. 70-21,062.

Thesis.

The reaction $K^+ p \rightarrow K^0 p\pi^+$ was studied with a 3 GeV/μb exposure in the ANL 30-inch hydrogen bubble chamber. The 5700 two-prong V^0 events in this film sample were measured on SMP's and processed with the Illinois programs SPACE-ILLFIT-GNUS. The reaction is found to be dominated by production of the quasi-two body final states K^*p and K^0N^*. The absorptive peripheral model was compared to the K^* production data and although the spin density matrix elements show general agreement with its predictions, the differential cross section does not. The N^* production data are well described by the ρ and A_2 Regge pole model of Krammer and Maor. The dependence of momentum transfer distributions upon invariant masses is also discussed. (Diss. Abstr. Int., B)

12115 K^+–PROTON ELASTIC SCATTERING AT 2.53, 2.76, AND 3.20 GeV/c. Whitmore, James Jonathan. Urbana, Ill.; Univ. of Illinois (1970). 142p. University Microfilms Order No. 70-21,085.

Thesis.

Presented in this report are the results of a study of K^+p elastic scattering at incident kaon momenta of 2.53, 2.76, and 3.20 GeV/c. The data were obtained from exposures of the MURA 30" hydrogen bubble chamber at the Argonne National Laboratory, Illinois. Differential and total elastic cross sections are given. Characterizing the kaon center-of-mass angular distributions are peaks in both forward and backward directions. The momentum dependence of both the diffraction and backward peaks in K^+p elastic scattering is compared with the calculations of Regge pole exchange models. Also presented are some preliminary results of a phase shift analysis at 2.50 GeV/c. (Diss. Abstr. Int., B)

12116 A_2 MASS SPECTRUM IN 7-GeV/c π^+p INTERACTIONS. Alston-Garnjost, M.; Barbaro-Galtieri, A.; Buhl, W. F.; (and others). (Univ. of California, Berkeley). Phys. Lett.; 33B: 607-12(21 Dec 1970).

The A_2 mass spectrum is studied in the reaction $\pi^+p \rightarrow A_2^+p$ at 7 GeV/c in a hydrogen bubble chamber in order to investigate previously reported structure. A report is given on 1400 A_2 events with mass resolutions of 3.8, 6.7, and 9.2 MeV in the $K^+\bar{K}^0$, 3π and $\eta\pi^+$ channels. (auth)

12117 REACTIONS $\pi^-p \rightarrow n\pi^0$ and $\pi^-p \rightarrow n\eta^0$ IN THE BACKWARD HEMISPHERE. Boright, J. P.; Bowen, D. R.; Groom, D. E.; (and others) (Cornell Univ., Ithaca, N. Y.). Phys. Lett.; 33B: 615-19(21 Dec 1970).

Cross sections for $\pi^-p \rightarrow n\pi^0$ at 5.9, 10.1 and 13.8 GeV/c incident momentum are presented in the angular region from 180° to u, the crossed four-momentum transfer squared, of -2 $(GeV)^2$ and the energy dependence is discussed. The cross section for $\pi^-p \rightarrow n\eta^0$ integrated over the same angular region at 5.9 GeV/c is also presented. (auth)

12118 EVIDENCE FOR B(1220) PRODUCTION IN AN ANALYSIS OF THE REACTION $K^-d \rightarrow p_S\Lambda\pi^+\pi^-\pi^-\pi^0$ AT 3 GeV/c. Hoogland, W. (Zeeman Lab., Amsterdam); Kluyver, J. C.; De Vries, T.; (and others). Phys. Lett.; 33B: 631–4(21 Dec 1970).

In an analysis of the reaction $K^-n \rightarrow \Lambda 4\pi$ at 3 GeV/c evidence is found for the production of the B(1220) resonance, mainly decaying in $\omega\pi$. For the mass and width $(1236 \pm 15)MeV/c^2$ and $(132 \pm 20)MeV/c^2$, respectively, are found. The cross section for the reaction $K^-n \rightarrow \Lambda + B(1220)$ is found to be (102 ± 26) μb. (auth)

12119 SPIN-PARITY ANALYSIS OF THE B-MESON PRODUCED IN π^+p REACTIONS. Werbrouck, A. (Univ., Turin. Instituto Nazionale di Fisica Nucleare, Turin); Rinaudo, G.; van de Walle, R. T.; (and others). Lett. Nuovo Cim.; 4: 1267-72 (26 Dec 1970).

It is shown that the analysis of some specific angular functions which are little affected by the strong $\Delta^{++} + \omega$ background permits in the studied $\pi^+ + p$ interactions a spin-parity determination for the B meson in agreement with $\pi^- + p$ results and at a comparable confidence level. The reaction $\pi^+ + p \rightarrow 2\pi^+ + \pi^- + \pi^0 + p$ from incident π^+ momenta between 3 and 5 GeV/c is studied. The $\pi^+\omega$ mass spectrum is shown, and a clear B signal is visible. The spin-parity assignment found for the B meson is 1^+. (J.F.P.)

12120 KAON NUCLEON TOTAL CROSS SECTIONS AT LOW MOMENTUM. Peterson, Douglas Vernon Tucson, Ariz.; Univ. of Arizona (1970). 50p. University Microfilms Order No. 70-22,849.

Thesis.

The K^+ and K^- total cross sections were measured on both hydrogen and deuterium at a series of momenta between 360 MeV/c and 720 MeV/c by the transmission method. The data were corrected for Coulomb and decay effects, and the pure isospin states extracted. The K^+N I = 1 cross section was found to be free from resonances though the existence of a small dip at about 700 MeV/c was confirmed. No convincing evidence was found for structure in the K^+N I = 0 cross section, which was seen to be steeply rising with increasing momentum throughout this range. However, a small enhancement near 600 MeV/c cannot be ruled out. The prominence of the $\Lambda'(1520$ at 390 MeV/c) was verified in the K^-N I = 0 system in which no additional structure was seen. In the K^-N I = 1 system no new structure was clearly established, though a small enhancement at 580 MeV/c, which corresponds to a mass of about 1600 MeV, is strongly suggested. (Diss. Abstr. Int., B)

12121 PION–NUCLEON INTERACTIONS IN DEUTERIUM AT 3.65 GeV/c. Chaudhary, Banvir Singh. Minneapolis; Univ. of Minnesota (1970). 99p. University Microfilms Order No. 70-20,183.

Thesis.

The interaction $\pi^+d \rightarrow \pi^+\pi^-\pi^0$ pp (1) at 3.65 GeV/c was studied. In particular there was interest in the existence of a boson resonance H(990) decaying into $\pi^+\pi^-\pi^0$. A total of 1211 events were found to satisfy (1) with the three pion mass less than 1.2 GeV. A study of the contribution of η' to the 1 GeV region in 3π effective mass was made by fitting the events to the reaction $\pi^+ d \rightarrow \pi^+\pi^-\gamma$ pp (2). Also Monte-Carlo calculations were made to observe the distortion of phase space due to the cuts made in the data to reduce background. The analysis shows a peak of less significance at 1 GeV in three pion effective mass than previously reported in the reaction (1). The enhancement at 1 GeV in the data can be explained almost entirely by the phase space and the η' contamination. (Diss. Abstr. Int., B)

Particle Interactions and Properties (Theoretical)

General

Refer also to abstract 12294.

12122 (NYO–2262-TA-228) EXISTENCE OF COMPLEX POLES AND OSCILLATORY AVERAGE MULTIPLICITY IN MULTIPERIPHERAL MODELS. Goldberger, Marvin L. (Princeton Univ., N. J. Joseph Henry Labs.); Silverman, Dennis (California Univ., La Jolla, San Diego. Dept. of Physics); Tan, Chung-I (Brown Univ., Providence, R. I. Dept. of Physics). [1970]. Contract AF49(648)-1545. 11p. Dep. NTIS.

Using only the general factorization and nondegenerate thresholds properties of multiperipheral models, the existence of damped oscillatory components is demonstrated for both the total cross section and the rate of growth of average multiplicity, with identical frequencies and relative amplitudes. For weak oscillation, however, they are shown to be 180° out of phase. Relevant experimental information on these fine structures is also discussed. (auth)

12123 HIGH ENERGY PHYSICS INDEX. VOLUME 8, NO. 25, 1970. Frankfurt am Main; Zentralstelle fuer Atomkernenergie-Dokumentation (1970). 87p.

12124 HIGH ENERGY PHYSICS INDEX. VOLUME 8, NO. 24, 1970. Frankfurt am Main; Zentralstelle fuer Atomkernenergie-Dokumentation (1970). 91p.

12125 REPRESENTATIONS OF LOCAL NONRELATIVISTIC CURRENT ALGEBRAS. Grodnik, Jesse. Philadelphia; Univ. of Pennsylvania (1969). 133p. University Microfilms Order No. 70-16,155.

Thesis.

It is shown how to specify the particle content of a nonrelativistic quantum theory of N identical particles, both spinless and with spin $\frac{1}{2}$, in terms of observables such as the particle number density, spin density, and the flux density of particles. The approach to this problem is through a study of the irreducible representations of the local, equal-time, current algebra. It is shown how these representations define a functional representation of the current algebra, and that the Hamiltonian can be written in terms of the currents in a nonsingular fashion in any irreducible representation. It is argued that bosons and fermions belong to inequivalent representations of the current algebra. Constraint equations abstracted from a second-quantized many body formulation of nonrelativistic quantum mechanics are used to distinguish boson from fermion representations of the current algebra. (Diss. Abstr. Int., B)

12126 OVERLAPPING RESONANCES. Snoke, J. Arthur. New Haven; Yale Univ. (1969). 94p. University Microfilms Order No. 70-16,256.

Thesis.

An example of overlapping resonances is considered: namely a system of three particles in which one of the particles can form a two-particle resonance with either of the other two. There have been claims that overlapping two-particle resonances can cause an enhancement in the three-particle mass spectrum, and part of the motivation for this work was to investigate such a possibility. It is shown that when the calculations are done correctly and the results given the proper interpretation, the enhancements of previous models do not appear. It is concluded, therefore, that enhancements in the three-particle mass can not be caused by overlapping two-particle resonances. (TSS) (Diss. Abstr. Int., B)

12127 REPRESENTATIONS OF LOCAL CURRENTS AND RELATED ALGEBRAS. Mendes, Rui Vilela de L. Austin, Tex.;

Univ. of Texas (1970). 120p. University Microfilms Order No. 70-18,270.

Thesis.

An approach to the problem of representation of the algebra of currents (and other local operators) that puts essential emphasis on the study of infinite-parameter Lie algebras is proposed. As a first example a class of irreducible Hermitean representations of the algebra of I-spin charge densities $[V^i(\phi_1), V^j(\phi_2)] = i\,\epsilon^{ijk}V^k(\phi_1\phi_2)$ is studied. After the isospin dependence of the reduced matrix elements is separated the dependence on the algebra $\{\phi\}$ is completely characterized by two functional equations that are explicitly solved for $\{\phi\}$ an algebra of polynomials. States of well defined momentum and angular momentum properties are then constructed using translational and rotational invariance and forming direct integral spaces. The representations are seen to belong to two distinct subclasses, distinguished by the vanishing or nonvanishing of a length-parameter. The subclass with $|\eta| = 0$ is unbounded in isospin and has a trivial momentum transfer dependence. On the other hand, the spaces with $|\eta| \neq 0$ are bounded in isospin and have nontrivial form factors. Invariant form factors are derived by choosing a particular frame to ensure covariances of the results. The same results are then applied to two other algebras of local operators: the canonical commutation relations of an uncharged scalar field and the Lee, Weinberg and Zumino algebra of fields (restricted to the isospin part). For the canonical commutation relations one is led to a classification of the representations in an infinite number of classes that are completely characterized by systems of functional equations. For the algebra of fields, a negative result is proved forbidding a nontrivial representation of Schwinger terms in spaces that are direct sums of representations of the integrated subalgebra. A continuous measure is then used to form a direct integral space and a representation of the algebra is derived. The implications of the results on the physical applications of the algebra of fields, in particular the Sugawara model, are discussed. (Diss. Abstr.)

12128 RELATIVISTIC LIMIT OF SPIN TENSOR OPERATORS ASSOCIATED WITH A VECTOR PARTICLE. Beckers, J.; Pirotte, Ch. (Univ., Liege). Bull. Soc. Roy. Sci. Liege; 39: 279-87(1970). (In French).

The relativistic limit of spin tensor operators associated with vector particles is studied following recent developments for arbitrary spin particles. The difficulties related to redundant components, projection operators, singular matrices, are solved through a (6 × 6) reformulation of the corresponding Cini-Touschek representation. (auth)

12129 CURRENT STRUCTURE OF PHENOMENOLOGICAL LAGRANGIANS. Volkov, D. V.; Gershun, V. D.; Tkach, V. I. (Inst. of Physics and Tech., Kiev). Teor. Mat. Fiz.; 5: 321-8 (Dec 1970). (In Russian).

It is shown that the phenomenological Lagrangians invariant with respect to the group G, when realized on homogeneous (with respect to transformations from G) irreducible symmetrical spaces G/H, can be represented as the products of currents. In general case of homogeneous spaces, the requirement of representability of a phenomenological Lagrangian in the form of the product of currents is satisfied only if the phenomenological constants are chosen in a special way. In certain cases this leads to enlargement of the symmetry group of the initial Lagrangian. (auth)

12130 OPERATORIAL EXPANSION OF THE PRODUCT OF TWO CURRENTS. Bonora, L.; Vendramin, I. (Univ., Padua). Nuovo Cim.; 70A: 441-52(21 Dec 1970).

On the grounds of general principles and a certain set of hypotheses the most general expansion of the product of two $U_3 \otimes U_3$ currents in neighboring space-time points is constructed, following the Wilson method. By means of this expansion a certain number of current–current and current–derivative-of-current equal-time commutators is determined. These are in agreement with the results obtained by other methods. As an application, it is shown that the structure of stress-energy tensor suggested by Sugawara can be embodied as a limiting case in Wilson's theory. (auth)

12131 DUAL AMPLITUDES FOR 6 PIONS WITH EPSILON-TENSOR COUPLINGS. Dorren, J. D. (Weizmann Inst. of Science, Rehovot, Israel); Rittenberg, V.; Rubinstein, H. R.; Chaichian, M.; Squires, E. J. Nuovo Cim.; 1A: 149-54(1 Jan 1971).

A dual amplitude is constructed for 6 pions which contains the normal-parity trajectories ω-A_3 in the three-body channels and ρ-f^0 in the two-body ones. The leading trajectory is ghost free and has no parity doubling. Taking into account previous work, a complete solution of the construction of a 6-pion amplitude with all required physical properties in the tree approximation is now available. (auth)

12132 THEORY OF HIGHLY CHARGED SUBNUCLEAR PARTICLES. Yock, P. C. M. (Univ. of Auckland, New Zealand). Ann. Phys. (N. Y.); 61: 315-28(Dec 1970).

A new quantum field theory of matter was recently proposed which predicts the existence of an as yet experimentally unconfirmed set of highly charged subnuclear particles. Previously only the mathematical foundation of the theory has been discussed. The more directly physical aspects of the theory are presented. In particular, the identification of nuclear particles as bound states of subnuclear particles is made. Conservation laws are also treated. The structure of the weak interactions implied by the new theory is derived. Possible experimental evidence of highly charged subnuclear particles is pointed out. Characteristic sizes of bound subnucleonic structures are discussed. Finally, comparison is made with conventional theory, and various distinguishing features are pointed out. (auth)

12133 SINGULARITY STRUCTURE OF CAUSAL DISTRIBUTIONS AND RESTRICTED EQUAL-TIME LIMITS. Otterson, P. J. (New York Univ., New York); Sucher, J. J. Math. Phys. (N. Y.); 11: 3307-16(Dec 1970).

Aspects of the space–time singularity structure of several classes of causal distributions are studied including the cases usually encountered in perturbation theory. Various definitions of restricted equal-time limit are considered which allow for the presence of highly singular Schwinger terms. It is shown that, with one definition, every causal distribution has a restricted equal-time limit. A form of sum rule valid even in the presence of singular Schwinger terms is given. (auth)

12134 MONTE CARLO METHOD FOR EVALUATING SCATTERING CROSS SECTIONS FOR MULTI-PARTICLE PRODUCTION PROCESSES. Long, W. F.; Kovacs, J. S. (Michigan State Univ., East Lansing). Progr. Theor. Phys. (Kyoto); 44: 952-8(Oct 1970).

A Monte Carlo algorithm is constructed for evaluating the integrals which arise in calculations of total and differential scattering cross sections. The method is especially valuable for use with theories which give the matrix element for production of three or more particles. (auth)

12135 RELATIVISTIC CALCULATIONS OF ANGULAR DISTRIBUTIONS AND CORRELATIONS IN A THREE-BODY PHASE SPACE WITH CONSTRAINT FUNCTIONS. Proriol, J. (Institut Univ. de Tech., Montlucon, France); Laverriere, R. Amer. J. Phys.; 39: 89-93(Jan 1971).

A method is derived for computation of angular distributions and angular correlations in a three-body phase space. Earlier work did not take account of a constraint function connected with the dynamics of the problem. With the relations given one can easily compute the integrals giving the angular distribution and correlation. Some applications are presented. (auth)

Electromagnetic

Refer also to abstracts 12068, 12249, 12272, and 12322.

12136 (CNRS-CPT-70-P-336) COMPUTATIONAL ANALYSIS OF FEYNMAN DIAGRAMS. APPLICATION TO THE CALCULATION OF THE ANOMALOUS MAGNETIC MOMENT OF THE ELECTRON AND OF THE MUON. Calmet, Jacques (Centre National de la Recherche Scientifique, Marseilles (France). Centre de Physique Theorique). 1970. 131p. (In French). Dep. NTIS (U. S. Sales Only).

Thesis. Submitted to Aix-Marseilles Univ., Faculte des Sciences, France.

If the anomalous part of the magnetic moment of the electron and muon is to be measured, theoretical knowledge of the contributions proportional to $\alpha 3$ (α is the fine structure constant) is required. Programs for constructing Feynman diagrams of a given order in the series of the perturbations are presented. The theory of the renormalization formulas in the framework of the functional formalism leads to a recurrence relation defining the fine contributions of preceding orders and the correction terms. The diagrams can be generated from this equation, which is written directly in LISP language. The problem of radiative corrections for the case of three interacting fields is treated. The contributions of the Feynman diagrams to the anomalous magnetic moment of the electron are calculated. The internal uv divergences are eliminated by using a numerical method to evaluate the multiple integrals. The results obtained for the contributions of the diagrams containing vacuum polarization are given. (France)

12137 (DESY-70/56) DUAL MODEL FOR DIFFRACTIVE TWO-PION ELECTROPRODUCTION. Bartl, A.; Iso, C. (Deutsches Elektronen-Synchrotron, Hamburg (West Germany)). Nov 1970. 10p. Dep. NTIS (U. S. Sales Only).

A recent dual model for diffractive two-pion photoproduction, treating the pomeron as having O^+ structure, is generalized to two-pion electroproduction. Taking into account gauge invariance and kinematical singularity free condition in a strict way, a cross section for ρ' production is obtained which is an order of magnitude higher than the experimental value. (auth)

12138 (NYO-2262-TA-222) SCATTERING OF ELECTROMAGNETIC AND GRAVITATIONAL WAVES BY A STATIC GRAVITATIONAL FIELD: COMPARISON BETWEEN THE CLASSICAL (GENERAL-RELATIVISTIC) AND QUANTUM FIELD-THEORETIC RESULTS. Westervelt, Peter J. (Brown Univ., Providence, R. I. Dept. of Physics). [1970]. 18p. Dep. NTIS.

The classical general-relativistic cross sections for the scattering of either an electromagnetic wave or a gravitational wave by a scalar particle are calculated and found to agree with the results of the quantized-linearized field theory. (auth)

12139 EFFECTIVE FIELD EQUATIONS FOR ONE-ELECTRON MULTIPHOTON STATIONARY STATES WITH APPLICATION TO COMPTON SCATTERING. Brett, Alistair Morley. Philadelphia; Drexel Inst. of Tech. (1970). University Microfilms Order No. 70-19,675.

Thesis.

The nonperturbative Rayleigh-Ritz procedure for functionalities is applied to the quantum theory of the interaction of an electron with the electromagnetic field in certain approximations. The procedure yields effective field equations, the solutions to which enable one to evaluate quantities of physical significance. For an unquantized description of the electron, taking a single wave function for the electron throughout the interaction process, effective stationary state field equations for the electron interacting with one or two real photons are found. An effective vector potential which may take the form of a plane wave is found in the Dirac equation yielded by the Rayleigh-Ritz procedure. Taking the full second quantized Hamiltonian of quantum electrodynamics again produces, via the above procedure, a set of effective stationary state field equations. Possible solutions to these equations in the one photon approximation are discussed. If the state functional for the complete system is modified to explicitly take account of the different momentum states of the electron and photon in the particular scattering process considered, then it is found that a solution for the scattered photon wave function to order e^2 can be obtained. The differential cross section for the scattered photon in this approximation is then found from the solution. This cross section is in agreement with the standard S-matrix perturbation theory calculation for such a system. (Diss. Abstr.)

12140 VERIFICATION OF VECTOR DOMINANCE. Ryndin, R. M. (Ioffe Inst. of Physics and Tech., Moscow). JETP Lett. (USSR) (Engl. Transl.); 12: 223-5(20 Sep 1970).

Translated from Zh. Eksp. Teor. Fiz., Pis'ma Red.; 12: 329-32(20 Sep 1970).

Reactions are discussed in which, at a constant internal parity the vector particle has only transverse polarization. The reactions $\gamma + He \rightarrow He + \pi^0$, $\pi^+ + He \rightarrow \rho^+ + He$, $\pi^- + He \rightarrow \rho^- + He$, and $e + He \rightarrow e + He + \pi^0$ are considered. In such reactions it is possible to formulate the consequences of the vector dominance in explicitly covariant fashion as well as to attempt to resolve the question of whether the hadron amplitude depends on the square of the vector-particle mass. (J.F.P.)

12141 KAON AND NUCLEON FORM FACTORS USING VECTOR DOMINANCE. Buchl, R. A.; Nigam, B. P. (Arizona State Univ., Tempe). Nuovo Cim.; 70A: 542-8(21 Dec 1970).

The nucleon form factors $G_E(t)$ and $G_M(t)$ are related to the K-meson isoscalar and isovector electromagnetic form factors in the vector-dominance model assuming the existence of universality among form factors. The mean charge radius of the nucleon is calculated along with that of the K-meson. Relationships among the total cross sections for the processes $e^+e^- \rightarrow KK$, $\pi\pi$ are stated. (auth)

12142 CONFORMAL INVARIANT FORM FACTORS IN TWO DIMENSIONS. Castell, L. (Max-Planck-Institut fuer Physik und Astrophysik, Munich). Nuovo Cim.; 70A: 564-8(21 Dec 1970).

The integral representations for the "conformal" invariant form factors in two dimensions are derived. The high-energy limit of these expansions is uniquely determined. For particles with "spin" $\frac{1}{2}$ and mass $m \neq 0$ the asymptotic q^2-dependence $(m^2/(-q^2), (m^2/(-q^2))^2$, etc., is obtained. (auth)

12143 MULTIPLE PARTICLE PRODUCTION FROM e^+e^- INTERACTIONS AT C.M. ENERGIES BETWEEN 1.6 AND 2 GeV. Bartoli, B. (CNEN, Frascati, Italy); Coluzzi, B.; Felicetti, F.; (and others). Nuovo Cim.; 70A: 615-31(21 Dec 1970).

Multiple particle production in electron-positron interactions was observed in an experiment performed at Adone, the Frascati 2×1.5 GeV e^+e^- storage ring. A total number of 239 events collected at several energies of the incident electron and positron beams between 0.8 and 1.0 GeV were analyzed. The distribution of the multiplicity of charged particles produced in the final state is discussed and some upper limits on these multiplicities are reported. The observed lower limit to the total cross section for multiple particle production in e^+e^- interactions, averaged over the energy range explored, is $3 \cdot 10^{-32}$ cm^2 with a statistical error of ±10% and a systematic uncertainty of ±25%. (auth)

12144 NUCLEON FORM FACTORS IN THE VENEZIANO MODEL. Konetschny, W. (Technische Hochschule, Vienna); Majerotto, W. Nuovo Cim.; 1A: 188-201(1 Jan 1971).

Pole dominance and a Veneziano model for the scattering amplitudes $\pi N \rightarrow \pi N$, $\pi N \rightarrow NA_1$ and $\pi N \rightarrow N\rho$ are used to derive the electromagnetic nucleon form factors. The technique is based on a method proposed by Rosner and Suura. Correction terms to the pole-dominance assumption are necessary and therefore included. Their specific form strongly influences the final result. With the simplest assumptions for them the electric form factor contains a dipole term instead of an infinite sequence of poles as encountered in the meson case, and drops off at infinity like t^{-1}. However, to get a reasonable magnetic form factor some correction terms have to be modified. As a by-product an expression for the axial form factor is obtained. (auth)

12145 SIXTH-ORDER CORRECTIONS TO THE ANOMALOUS MAGNETIC MOMENT OF THE ELECTRON. De Rujula, A.; Lautrup, B.; Peterman, A. (CERN, Geneva). Phys. Lett.; 33B: 605-6(21 Dec 1970).

The gauge-invariant contribution to the anomalous magnetic moment of the electron (or muon) from four diagrams was calculated. The result is infrared convergent and numerically equal to: $(\alpha/\pi)^3\{0.477 \pm 0.023\}$. (auth)

12146 FIXED-t DISPERSION RELATIONS FOR PION PHOTOPRODUCTION IN THE SECOND RESONANCE REGION. Devenish, R. C. E. (Univ. of Lancaster, Eng.); Leigh, W. J.; Lyth, D. H.; Rankin, A. Nuovo Cim.; 1A: 155-70(1 Jan 1971).

Fixed-t dispersion relations are evaluated for π^+ and π^0 photoproduction in the second resonance region. Only resonances in the first, second and third resonance regions are included. The predictions are in approximate agreement with experiment. It is argued that a major part of the discrepancy will come from resonances in the fourth resonance region, rather than from Regge tails or nonresonant effects. (auth)

12147 MODEL OF NUCLEON ELECTROMAGNETIC FORM FACTORS. Zovko, N. (Inst. Rudjer Boskovic, Zagreb). Lett. Nuovo Cim.; 4: 1278-80(26 Dec 1970).

It is shown how simple pole terms add in order to obtain a faster decreasing sum with increasing momentum transfer by superconvergent dispersion sum rules. The simplest two-pole model coincides with the one-parameter dipole formula. It is assumed that there is vector meson dominance in a dispersion approach and that the form factors decrease asymptotically at least as t^{-3}. (J.F.P.)

12148 DEEP INELASTIC e-p SCATTERING AND A REGGEIZATION SCHEME FOR PHOTON PROCESSES. Akiba, T.; Sakuraoka, M.; Ebata, T. (Tohoku Univ., Sendai). Lett. Nuovo Cim.; 4: 1281-4(26 Dec 1970).

The kinematical constraints imposed by gauge invariance on the virtual Compton scattering, to which the inelastic e + p scattering is related, is discussed along the general Reggeization scheme for photon processes. Also some immediate consequences from the analysis of inelastic scattering, which includes the ordinary Regge exchanges in addition to the Pomeranchuk exchange, are described. (J.F.P.)

12149 STUDY OF SCALE INVARIANCE IN A $\lambda\phi^4$ THEORY. Choudhury, S. Rai (Univ. of Delhi). Lett. Nuovo Cim.; 4: 1285-8(26 Dec 1970).

Results of calculations in the ladder approximation for scalar Compton scattering in the $\lambda\phi^4\phi x^2$ theory, where ϕ and x are charged and neutral scalar bosons respectively, are given. (J.F.P.)

12150 SIMPLE PICTURE FOR DIRAC'S CHARGE-POLE QUANTIZATION LAW. Lubkin, Elihu (Univ. of Wisconsin, Milwaukee). Amer. J. Phys.; 39: 94-6(Jan 1971).

If something appears to bear a magnetic monopole of strength g not equal to a multiple of $(2e)^{-1}$, as a result of measurement of the magnetic field about it over most of the 4π solid angle, then at least one visible bar magnet will be found by the electron-optical interferometric experiment of Aharonov and Bohm, in the remaining solid angle. (auth)

XUM

12151 HIGH-ENERGY PHOTONUCLEAR REACTIONS AND VECTOR-MESON DOMINANCE. Henley, E. M. Comments Nucl. Particle Phys.; 4: 107-15(May-Jun 1970).

Two main considerations for studying high energy interactions of photons with nuclei and nucleons are discussed: the quantum-mechanical interference phenomena which occur in this energy region; and testing basic theoretical postulates of photon-hadron interactions. Two methods for testing VMD are also briefly discussed: measurements of the total photon absorption cross sections and photoproduction of vector mesons. (L.B.S.)

12152 DIFFRACTIVE TWO-PION PHOTOPRODUCTION AND FIVE-BODY DUALITY. Kagiyama, Shigenori (Kyushu Univ., Fukuoka). Progr. Theor. Phys. (Kyoto); 44: 1103-5(Oct 1970).

A model given by Pokorski, Satz, and Schilling in which the four-body Veneziano amplitude was introduced into diffraction dissociation processes is modified to include the sub-energy dependence in the diffraction part of the amplitude. It is shown that the modification gives a better mass dependence of the diffraction slope in the process $\gamma p \rightarrow \pi^+\pi^- p$. (L.B.S.)

12153 PHENOMENOLOGICAL ANALYSIS OF THE INFINITE RESONANCE MODEL FOR THE NUCLEON ELECTROMAGNETIC FORM FACTOR. Miyake, Shogo; Takagi, Fujio (Tohoku Univ., Sendai). Progr. Theor. Phys. (Kyoto); 44: 1096-8(Oct 1970).

A phenomenological analysis is made of the electromagnetic form factor for the proton in the infinite resonance model. The form factor in this model is expressed in terms of gamma functions, and calculated values are presented for the Suura type and the DiVecchia–Drago–Oyanagi type. (L.B.S.)

12154 COMMENTS ON THE ELECTROMAGNETIC FORM FACTORS AND MASS DIFFERENCES. Hori, Setsuko; Hosoda, Masataka (Osaka Univ.). Progr. Theor. Phys. (Kyoto); 44: 1098-9(Oct 1970).

An estimate is made of the contribution of the Born term to the π, K, and N mass differences, using new expressions for the form factor. (L.B.S.)

12155 ELECTROMAGNETIC MASS DIFFERENCE OF HADRONS AND THE PARTON MODEL. Muta, Taizo (Kyoto Univ.). Progr. Theor. Phys. (Kyoto); 44: 1022-33(Oct 1970).

The parton model is used to calculate the forward virtual Compton scattering amplitude of hadrons in the deep inelastic region. Inserting it into the Cottingham formula for the electromagnetic mass difference of hadrons, the vanishing deep-inelastic contribution to the $\Delta I = 2$ mass difference and the logarithmically divergent contribution to the $\Delta I = 1$ mass difference are obtained, the sign of which depends on the choice of specific models for the parton: the quark, quartet, two-triplet and three-triplet models. The quartet-type model proposed by Namiki and Tanaka seems to be preferable. (auth)

12156 ELECTRODYNAMIC ANALOG OF WAVE DIFFRACTION PHENOMENA. Robinson, L. C. (Sydney Univ.). Ann. Phys. (N. Y.); 61: 265-76(Dec 1970).

The interaction of a charged particle orbiting in cyclotron motion with a transverse rotating field is analyzed from an elemental impulse approach and by solving the linear equations of motion. A close analogy is shown between the motion of a particle undergoing a sequence of N such interactions and effects produced by an N-slit diffraction grating. The analogy suggests a new method of velocity and mass spectrometry to which such optical concepts and phenomena as the Rayleigh criterion of resolving power, overlapping orders and Babinet's principle may be applied. (auth)

12157 ANOMALOUS MAGNETIC MOMENT AND NONPOLYNOMIAL INTERACTIONS. Calucci, G.; Furlan, P. (Univ., Trieste, Italy). Nuovo Cim.; 1A: 171-6(1 Jan 1971).

An evaluation of the anomalous magnetic moment of a lepton in a version of Q.E.D. in which a cut-off is introduced through a field with nonpolynomial interaction is presented. The numerical results are compared with the actual experimental situation in order to set an upper limit for the new coupling constant. (auth)

12158 SCATTERING OF γ-QUANTUM IN THE FIELD OF NUCLEUS WITH CREATION OF e^-e^+ PAIR AND SEVERAL PHOTONS. Nadzhafov, I. M. Moscow State Univ. Izv. Vyssh. Ucheb. Zaved., Fiz.; No. 8, 148-50(1970). (In Russian).

The process of e^-e^+-pair photoproduction in the nuclear field with one, two, and three photons was studied considering longitudinal polarization of electron and positron and circular polarization of γ quanta. The studies are the continuation of previous works on the $\gamma + (Ze) \rightarrow (Ze)' + e^+ + e^- + \gamma$, for all four kinematic cases considering polarization of all particles and in which it was shown that the density of the process has a maximum value for the zero angle and with the increase of the angle of scattering from 0 to 8° it drops by several orders of magnitude. This work was limited to small angles θ_i between particle pulses [$\sin\theta_i| \ll |\cos\theta_i|$. It was found that during γ-quantum scattering on the nuclear Coulomb field forming e^+e^- pair and several photons at small angles resulted in the emission of the odd number of hard photons. (R.V.J.)

12159 POLARIZATION OF PHOTONS DURING SCATTERING IN GRAVITATIONAL FIELD OF SPHERICAL SYMMETRY. Vladimirov, Yu. S.; Iskhakov, I. F. (Moscow State Univ.). Izv. Vyssh. Ucheb. Zaved., Fiz.; No. 8, 45-9(1970). (In Russian).

Studies were made of quantum electromagnetic field interactions with classical Einstein's gravitational field, or more specific, of the photon scattering on spherical, symmetric Schwarzschild field. In contrast to the previous works, which were limited to the effects of the first order or magnitude $\sqrt{\mathcal{K}}$, the present calculations were expanded to the magnitudes of the second order, considering the larger gravitational radius of the source $R \gg 2\gamma m/c^2$ and, also, polarization effects which were not considered in previous works. (R.V.J.)

12160 FORCED RADIATION OF NEUTRAL FERMI-PARTICLES MOVING IN PLANAR WAVE. Bagrov, V. G.; Klimenko, Yu. I.; Pavlova, O. S.; (Moscow State Univ.). Izv. Vyssh. Ucheb. Zaved., Fiz.; No. 8, 50-3(1970). (In Russian).

An induced radiation of a neutral Fermi particle possessing an abnormal moment (neutron) in motion in a strong electromagnetic wave and acted upon by a second electromagnetic wave of lesser intensity was studied. It is shown that such a process results in preferred orientation of particle spin. (R.V.J.)

12161 EFFECT OF INDUCED RADIATION OF ELECTRONS MOVING IN PLANAR ELECTROMAGNETIC WAVE ON ORIENTATION OF THEIR SPINS. Ternov, I. M.; Bagrov, V. G.; Pavlova, O. S.; Khalilov, V. R. (Moscow State Univ.). Izv. Vyssh. Ucheb. Zaved., Fiz.; No. 8, 54-8(1970). (In Russian).

It was shown that induced emission of electrons moving in a plane monochromatic wave of circular polarization resulted in a preferred electron spin orientation and under certain conditions the electron beams became completely polarized. Thus, it was confirmed that induced emission and absorption of electrons moving in a plane electromagnetic wave can be used for producing electrons with oriented spin. (R.V.J.)

Weak

Refer also to abstracts 12252, 12280, and 12281.

12162 (AD-710572) WEAK INTERACTION HAMILTONIAN IN L-MATRIX THEORY. Ramakrishnan, Alladi (RAND Corp., Santa Monica, Calif.). Jul 1970. 6p. (P-4407). NTIS.

A systematic study was made of matrices A and B which satisfy the Clifford conditions $A^2 = B^2 = I$ $AB = -BA$. It was demonstrated that there is a "shell structure" in the anticommuting matrices and a consequent telescoping of eigenvalues of an L matrix which is a linear combination of anticommuting matrices. It is now observed that the form of the weak interaction Hamiltonian in elementary particle physics is an interesting manifestation of the shell structure. (auth) (USGRDR)

12163 (COO-264-563) HYPERON BETA DECAY. Frampton, Paul (Chicago Univ., Ill. Enrico Fermi Inst. European Organization for Nuclear Research, Geneva (Switzerland)); Tung, Wu-ki (Chicago Univ., Ill.). Nov 1970. Contract AT(11-1)-264. 34p. (EFI-70-65). Dep. NTIS.

Polarized hyperon beta-decay is considered in the center of mass frame of the outgoing leptons. Simple and exact expressions are obtained for the differential intensity distribution function under the assumption of local current-current interaction and two component neutrinos. It is shown that by exploiting only the fully integrated data, it is possible to make a large number of tests on the structure of the $\Delta s = 1$ current even with somewhat limited statistics. These include direct tests on the locality and V–A nature of the interaction without additional assumptions as well as detailed and rather stringent tests on the Cabbibo theory. (auth)

12164 (COO-264-563(Add.)) HYPERON BETA-DECAY. Tung, Wu-ki (Chicago Univ., Ill. Enrico Fermi Inst. Chicago Univ., Ill. Dept. of Physics). Dec 1970. Contract AT(11-1)-264. 7p. Dep. NTIS.

To make a previous analysis of hyperon beta-decay complete, the q^2-spectrum of the decay rate and asymmetry functions are discussed. It is shown that these spectra provide a valuable source of information on the hard to measure form factors f_2 and g_2. (auth)

12165 HADRONIC HELICITY CONSERVATION AND INELASTIC LEPTON-NUCLEON REACTIONS. Pais, A. (Rockefeller

XUM

Univ., New York). Contract AT(30-1)-4204. Phys. Rev. Lett.: 26: 51-3(4 Jan 1971).

It has been suggested that hadronic s-channel helicity is conserved in the diffractive region. If applicable to inelastic lepton-nucleon processes, such conservation has many implications which are illustrated for π and 2π production. Polarization information is not needed for a first verification. (auth)

12166 SCALING LAWS IN HIGH-ENERGY NEUTRINO REACTIONS. Landshoff, P. V. (CERN, Geneva). Nuovo Cim.; 70A: 525-41(21 Dec 1970).

Bjorken has proposed that the structure functions F_1, F_2, F_3 of deep inelastic neutrino scattering are functions of $\omega = -2Mv/q^2$ only. These scaling laws are studied in Veneziano-like models and are found to emerge naturally for the scattering of neutrinos on a neutron or of antineutrinos on a proton, together with the Callan-Gross sum rule for $\int_1^\infty d\omega F_2/\omega^2$, the Gross-Llewellyn Smith sum rule for $\int_1^\infty d\omega F_3/\omega^2$ and the relation $F_1 = \frac{1}{2}\omega F_2$. (It is assumed that certain equal-time commutators of currents contain no operator Schwinger terms.) The models suggest the possibility that the structure functions for the scattering of neutrinos on a proton, or of antineutrinos on a neutron, are small in the deep inelastic limit. (auth)

12167 GENERAL TESTS OF THE $\Delta I = \frac{1}{2}$ AND $\Delta S = \Delta Q$ RULES IN K_{l3} DECAYS. Field, J. H. (Rutherford High Energy Lab., Chilton, Eng.). Nuovo Cim.; 1A: 89-96(1 Jan 1971).

A complete phenomenological description of K_{l3} decays (relative decay rates, angular distributions, momentum spectra and polarizations) can be given in terms of 5 (reduced) form factor ratios ξ^0, y_i^0, x_i^0 with respective isospin transformation properties I, I_3 = $\frac{1}{2}$, $\frac{1}{2}$; $\frac{3}{2}$, $\frac{1}{2}$; $\frac{3}{2}$, $\frac{3}{2}$. Shortcomings of the well-known tests of the $\Delta I = \frac{1}{2}$ rule for K_{l3} decays are discussed, and a general test of the form $y_i^0 = x_i^0 = 0$ is proposed. A method is described of extracting the reduced form factor ratios from experimental data. A relation between y_i^0 and x_i^0 is given for the case in which the $I = \frac{3}{2}$ currents have definite SU_3 transformation properties. (auth)

12168 DISCUSSION OF SOME RECENT RESULTS ON COSMIC-RAY MUONS. Castagnoli, C. (CNR, Turin); Etim, E.; Picchi, P. Nuovo Cim.; 1A: 133-48(1 Jan 1971).

The unexpected results of recent experiments on cosmic-ray muons of very high energy and the consistency of some of their interpretations are studied. It is found that although these interpretations cannot be dismissed outright as untenable, their physical bases will have to await more refined data, hopefully from many experimental groups, before they can be finally established. (auth)

12169 TWO-BODY WEAK-ELECTROMAGNETIC HYPERON DECAYS. Ozaki, Kazuhiko; Kunimasa, Tosaku (Osaka Univ.). Progr. Theor. Phys. (Kyoto); 44: 1102-3(Oct 1970).

A phenomenological estimation is made of the asymmetry parameters and branching ratios in the two-body weak-electromagnetic hyperon decays by using the experimental data on the nonleptonic hyperon decays. (L.B.S.)

12170 THEORY OF NEUTRAL WEAK CURRENT. Iwao, Syurei (Kanazawa Univ., Japan). Progr. Theor. Phys. (Kyoto); 44: 1092-4(Oct 1970).

The $K^+ \to \pi^0 e^+ \nu_e$, $K^+ \to \pi^+ \nu\bar{\nu}$, and $K^+ \to \pi^+ e^- e^+$ processes are discussed, assuming the existence of the neutral lepton current. (L.B.S.)

12171 ANALYSIS OF HYPERON NONLEPTONIC DECAY AMPLITUDES. Takahashi, Junji (Osaka Univ.). Progr. Theor. Phys. (Kyoto); 44: 1034-46(Oct 1970).

Hyperon nonleptonic decay amplitudes are analyzed including relative phases and signs under the assumption of CP-invariance. Magnitudes of S- and P-wave amplitudes and their relative phases are evaluated, by taking account of the final state interactions. In Λ- and Ξ-decays, the $\Delta I = \frac{1}{2}$ rule holds in good accuracy. The relative sign of the amplitude $\Lambda \to n\pi^0$ to $\Lambda \to p\pi^-$ is likely to be minus than plus, and the P-wave amplitudes of $\Sigma^+ \to n\pi^+$ and $\Sigma^+ \to p\pi^0$ seem to be of equal sign. Both are consistent with the signs predicted by the $\Delta I = \frac{1}{2}$ rule. In Σ^+-decay, the large phase shift difference between the $I = \frac{1}{2}$ and $\frac{3}{2}$ S-wave states leads to $|S(\Sigma\ddagger)/S(\Sigma_0^\ddagger)| \geq 0.16$, and it is found that $S(\Sigma\ddagger)$ is mainly imaginary. No evidence of large violation of CP is found in any processes. (auth)

12172 UNITARITY AT THRESHOLD AND VENEZIANO-TYPE FORM FACTORS FOR MESONS. Hama, Mitsuru (Dalhousie Univ., Halifax, Nova Scotia). Progr. Theor. Phys. (Kyoto); 44: 1047-52(Oct 1970).

A simple form of Veneziano type form factors is investigated and applied to K_{l3}-decay form factors. The p-wave part is determined by using the unitarity condition at threshold and the Veneziano model for scattering amplitudes. The PCAC condition and the broken chiral symmetry with current commutation relations are used for determining the s-wave part. The results are $f_K/f_\pi f_+(0) = 1.24$ and $\xi = -0.15$. Suura's method is also applied and shown to give $f_K/f_\pi f_+(0) = 1.41$. (auth)

12173 PERTURBATION THEORY ABOUT THE SYMMETRY LIMIT AND K_{l3} FORM FACTORS. Sirlin, A. (New York Univ., N. Y.). Ann. Phys. (N. Y.); 61: 294-314(Dec 1970).

General properties of form factors associated with a vector current are discussed in the framework of off-mass shell perturbative methods. A number of theorems, valid in the symmetry limit, are first derived. As an illustration, it is shown that these results, when applied to K_{l3} decays in conjunction with a previous relation, lead in a simple manner to the Dashen–Weinstein theorem for the parameter ξ, in the context of a perturbative expansion about the $SU_3 \otimes SU_3$ limit. The effect of $SU_3 \otimes SU_3$ breaking on the mass extrapolation of the K_{l3} form factors is also studied and a formula involving ξ and other observable quantities with a theoretical error $O(\epsilon_1\epsilon_2, \epsilon_1^2, \epsilon^2 \sin^2\theta, \epsilon^3)$ is discussed. The first-order corrections are then studied in the general framework of relativistic perturbation theory and a field theoretic derivation of the nonrenormalization theorem is obtained. Under the assumption of octet behavior of the symmetry-breaking interaction, some general symmetry properties of the off- and on-mass shell form factors are discussed. These results lead to some relations between the physical electromagnetic and $\Delta S = 1$ weak form factors which are valid for arbitrary momentum transfers, with an error of the second order in the symmetry-breaking interactions. In order to illustrate some assumptions underlying the derivation of the nonrenormalization theorem, a particular model of symmetry breaking is discussed in which the charge algebra is broken and the theorem does not obtain. A necessary and sufficient condition for the validity of this theorem in the case of SU_3 is then pointed out. (auth)

12174 ISOBAR NEUTRINO PRODUCTION PROCESSES. Ershov, D. K. (Smolensk State Teacher's Inst., USSR). Izv. Vyssh. Ucheb. Zaved., Fiz.; No. 8, 82-6(1970). (In Russian).

Processes of isobar production during neutrino and antineutrino collisions with nucleons were studied. Differential and total cross sections of the processes were calculated. The form factors were selected as ordinary Hoffstadter ones and by diminishing exponential. Graphs were constructed of the cross section as a function of the neutrino (antineutrino) energy for isobar production processes $N_{\frac{1}{2}}^*$ and Y_1^*. (R.V.J.)

Strong (General)

12175 (COO–1764–81) CONSISTENCY BETWEEN LOW-ENERGY AND HIGH-ENERGY HADRON SCATTERING. Rosner, Jonathan L. (Minnesota Univ., Minneapolis. School of Physics and Astronomy. Tel Aviv Univ. (Israel). Dept. of Physics). [1969]. Contract AT(11-1)-1764. 78p. (CONF-691033-2). Dep. NTIS.

From 8th Eastern Theoretical Physics Conference, Syracuse, N. Y.

A brief review is given of some results of duality regarding internal symmetries for low- and high-energy hadron scattering. The quark model, superconvergence, finite-energy sum rules, and duality, exchange degeneracy and the quark model, and applications of quark graphs and duality are treated. (J.F.P.)

12176 RELATIVISTIC CALCULATIONS OF ANGULAR CORRELATIONS OF PARTICLES ISSUED FROM AN INTERACTION-FREE RESONANCE DECAY. Proriol, J. (Institut Universitaire de Technologie, Montlucon, France. Laboratoire de Physique Nucleaire Fondamentale et Developpement, Clermont-Ferrand, France); Laverriere, R. J. Comput. Phys.; 6: 329-32(Oct 1970).

The Jacobian method is used to find results on the angular correlations between the particles of an interaction-free particle decay. Decays into two particles with equal and different masses are considered. (J.F.P.)

12177 VECTOR CURRENTS AND CURRENT ALGEBRA IN A ZERO-WIDTH MODEL. Brower, Richard Comfort. Berkeley, Calif.; Univ. of California (1969). 158p. University Microfilms Order No. 70-13,021.

Thesis.

The S matrix for photon and vector current processes is considered directly in terms of Lorentz covariance, analyticity, crossing, Regge asymptotics, and consistency with a dual, zero-width model for the hadron bootstrap. The direct use of local field and current operators is avoided, although occasionally consistency with the results of current algebra is imposed. Since only limited use of unitarity is made, no determination of the ultimate redundancy or inconsistency of the results of current

algebra with the unitary S matrix can be made. The covariant photon amplitude is proved to be the smooth limit of the helicity amplitude for a massive vector boson. The kinematical consequences of this zero mass limit and crossing are shown to include conservation of charge (or the equivalence principle in the case of the graviton), and the low energy theorems for photoproduction and Compton scattering. Consequently, the zero mass limit is a practical alternative to the use of on-mass-shell gauge invariance. Moreover, the zero-mass limit provides a technique for the construction of Regge expansion and Veneziano parameterization for photon amplitudes from the corresponding amplitudes for a massive vector boson. Also a parameterization of the amplitude for Compton scattering of off-mass-shell charged currents off pions is presented which satisfies the current algebra sum rule of Fubini, Dashen, and Gell-Mann. Amplitudes for one or two vector currents and an arbitrary number of spinless hadrons are considered. The investigation of the properties of vector currents consistent with the hadron bootstrap assuming duality and zero resonance widths is begun. First, on general grounds (unitarity and the conserved vector current hypothesis), it is proven that two current amplitudes must have fixed singularities in the angular momentum plane. This result is consistent with the space-time and time-time commutation relations of vector currents, but it is far less restrictive. Then some general consequences for current amplitudes of duality and the zero-width approximation are discussed. In particular, the relation between the internal symmetries and the external line insertion terms (poles at vanishing four-momenta of the current, $q_\mu \to 0$) is investigated. A simple N-point beta function model (generalized Veneziano model) of the hadron bootstrap is assumed and the properties of vector currents consistent with it are investigated. It is found that this hadron bootstrap admits conserved vector currents satisfying the Gell-Mann current algebra in an approximation which assumes single vector meson poles in the form factors and requires factorization only at resonances on leading Regge trajectories. It is believed that the results of this simplified model give some important indication of the expected behavior of currents in general dual zero-width models. In addition, a model for the Pomeranchuk contribution which does not fall off at large q^2 is proposed. This suggests a unique role for the Pomeranchuk in deep inelastic electroproduction, with no counterpart in purely hadronic processes. (Diss. Abstr. Int., B)

12178 THREE-DIMENSIONAL FIELD EMISSION IN THE PERTURBED SCATTERING MODEL. Politzer, Jay Lester. University Park, Pa.; Pennsylvania State Univ. (1969). 118p. University Microfilms Order No. 70-19,450.

Thesis.

A three-dimensional Green's function solution is obtained for field emission from a spherical tip with arbitrary perturbative potentials. The unperturbed problem is a spherical well, representing the tip, with a coulomb barrier outside the tip, and is solved exactly. The formulation is in terms of scattering theory, and a differential scattering probability is used to replace the usual transmission coefficient. Statistical averaging is accomplished without recourse to kinetic arguments which are shown to be generally invalid. A simple expression for the perturbed energy distribution is obtained. The perturbed distribution is the unperturbed distribution multiplied by energy- and angle-dependent pre-factors. The pre-factors are related to radial integrals of the perturbation and may be deduced from experiments which measure the angular distribution of field emitted electrons. An important three-dimensional perturbation arises from patch-fields. The patch-fields for a multi-faceted tip are derived in a completely general manner. These fields are expressed in terms of a constant facet independent bulk work-function, and a facet dependent dipole moment density. It is demonstrated that, even in the one-dimensional Fowler-Nordheim theory, patch-fields may greatly alter present values for measured work-functions. (Diss. Abstr.)

12179 CHARGE DISTRIBUTIONS AND MULTIPERIPHERALISM. Caneschi, L.; Schwimmer, A. (Stanford Univ., Calif.). Phys. Lett.; 33B: 577-81(21 Dec 1971).

A new distribution of charged and neutral pions is proposed on the basis of a resonance dominated Amati-Fubini-Stanghellini multiperipheral model. The model is in good agreement with the present experimental data. (auth)

12180 CHARACTERIZATION OF THE PHYSICAL STATES IN DUAL-RESONANCE MODELS. Del Giudice, E.; De Vecchia, P. (Massachusetts Inst. of Tech., Cambridge). Nuovo Cim.; 70A: 579-91(21 Dec 1970).

In the framework of dual-resonance models the necessary conditions that the physical states on the mass shell have to satisfy are derived. The orthogonality with the spurious states is required. By using these conditions it is shown that the first "daughter" is empty, while the second daughter contains at least three particles for each level ($N > 4$). The first three excited levels are analyzed in some detail. (auth)

12181 REPRESENTATIONS OF LOCAL I-SPIN CHARGE DENSITIES. I. SPACES WHERE EACH I OCCURS ONLY ONCE. Mendes, Rui V. (Univ. of Texas, Austin); Ne'eman, Yuval. J. Math. Phys. (N. Y.); 11: 3371-82(Dec 1970).

An approach to the problem of representation of the algebra of currents that puts essential emphasis on the study of infinite-parameter Lie algebras is proposed. As an example, a class of irreducible Hermitian representations of the commutation relations $[V^i(\phi_1), V^j(\phi_2)] = ic^{ijk}V^k(\phi_1\phi_2)$, where the ϕ's are elements of a commutative algebra with identity, is derived. The dependence of the representations on the algebra $\{\phi\}$ is completely characterized by two functional equations that are explicitly solved, for $\{\phi\}$ an algebra of polynomials. States of well-defined momentum and rotational properties are constructed using translational and rotational invariance and forming direct integral spaces. The representations so constructed are seen to belong to two distinct subclasses, distinguished by the vanishing or nonvanishing of a length parameter $|\eta|$. The subclass with $|\eta| = 0$ is unbounded in isospin and has the trivial momentum-transfer structure characteristic of field-theoretical point particles. On the other hand, the spaces characterized by $|\eta| \neq 0$ are bounded in isospin and suited to describe particles with structure. A brief discussion on how to derive invariant form factors from the results is included. (auth)

12182 LEVEL STRUCTURE OF HADRONS. Nagasaki, Masayuki; Taketani, Mituo (Rikkyo Univ., Tokyo). Progr. Theor. Phys. (Kyoto); 44: 1112-14(Oct 1970).

An attempt is made to investigate the phenomena of elementary particles from the standpoint of the dynamics of the composite system, and thereby to study the mode of dynamics of the ur-baryon. It is supposed that the hadronic matter extends over the region with the radius $a = 1/M_N$ (M_N = the nucleon mass); and the excitation of the hadronic matter is treated as due to its density oscillation. Experimental and theoretical results for meson mass levels are compared, assuming that the intrinsic spin and parity of the meson are given by the Sakata model. (L.B.S.)

12183 EXOTIC RESONANCES: URBARYON REARRANGEMENT AND HADRON STRUCTURE. Imachi, Masahiro; Oroguchi, Takashige; Otsuki, Shoichiro; Toyoda, Fumihiko (Kyushu Univ., Fukuoka). Progr. Theor. Phys. (Kyoto); 44: 1107-9(Oct 1970).

A new type of urbaryon rearrangement diagram induced by $t\bar{t}$ pair excitation is considered, where t denotes triplet urbaryon. This mechanism is characterized by a rather large excitation energy and rather small impact parameters. The urbaryon rearrangement diagram is applied to K^+p scattering. The mass of baryon resonances is plotted against the number of excited $t\bar{t}$ pairs. It is shown that the breaking of the Iizuka-Okubo rule is closely related to the existence of exotic resonances. (L.B.S.)

12184 TWISTING INVARIANT FACTORIZATION IN DUAL RESONANCE MODEL. I. THE GAUGE PROPERTY AND THE LOOP AMPLITUDES. Sakai, Sunao (Tokyo Univ. of Education). Progr. Theor. Phys. (Kyoto); 44: 1053-67(Oct 1970).

The factorization of multi-point dual resonance model in new basis vectors which are eigenstates of twisting transformation is proposed. In this factorization the twisting operator has a simple form, and it is easily seen that the generator of infinitesimal gauge transformation changes sign under the twisting transformation. It is easy to calculate the non-planar loop amplitudes without contribution of the spurious states in this factorization. It is found that by inserting the projection operator the divergence is decreased only by one power for the non-planar loop amplitudes with even numbers of twisting operators, and the divergence is not decreased at all for the non-planar loop amplitude with odd numbers of twisting operators. (auth)

12185 PROPER-TIME FORMULATION IN DUAL RESONANCE MODEL AND THE SUBSIDIARY CONDITIONS. Biyajima, Minoru; Kenmoku, Masakatsu (Tokyo Univ. of Education). Progr. Theor. Phys. (Kyoto); 44: 1100-1(Oct 1970).

The invariance properties of the proper-time equation under the transformations of the generators of the conformal group of infinite dimensions are discussed. Using these new properties, the general conserved currents and the Ward-like identities in the proper-time formulation are derived. (L.B.S.)

12186 MULTIPLE PRODUCTION PROCESSES AND REARRANGEMENT OF SAKATONS. Kobayashi, Akizo; Matsuoka, Takeo; Ninomiya, Kansuke; Sawada, Shoji (Nagoya Univ., Japan). Progr. Theor. Phys. (Kyoto); 44: 1094-5(Oct 1970).

An analysis of multiproduction processes πp, Kp, pp, and $\bar{p}p$ in terms of rearrangement of sakatons is presented. The energy dependence of the cross sections is discussed. (L.B.S.)

12187 HADRON SCATTERING AT EXTREMELY HIGH ENERGIES IN THE PARTON MODEL. Okumura, Yoshitaka (Kyoto Univ.). Progr. Theor. Phys. (Kyoto); 44: 995-1005(Oct 1970).

The total cross section for hadron scattering at extremely high energies is calculated in the parton model. It is concluded that the total cross section at extremely high energies is constant or logarithmically divergent and the ratio of the total cross section for hadron scattering is determined only from the normalization constant of P_N which is the distribution function of partons in a hadron. The ratio of the total cross section for baryon-baryon scattering to that of meson-baryon scattering is in fairly good agreement with the experimental data. (auth)

12188 QUARK STARS. Ivanenko, D. D.; Kurdgelaidze, D. F. (Moscow State Univ.). Izv. Vysah. Ucheb. Zaved., Fiz.; No. 8, 39-44(1970). (In Russian).

An attempt was made of developing a hypothesis on quark regions inside of massive stars indicating the possibility of the presence of superconductance. The properties of quark atoms are also discussed. (R.V.J.)

12189 FEYNMAN-LIKE DIAGRAMS IN DUAL-RESONANCE MODELS. Mandelstam, Stanley (Univ. of California, Berkeley). Comments Nucl. Particle Phys.; 4: 95-101(May-Jun 1970).

The construction of Feynman-like diagrams for a Born term, a single-loop planar amplitude, and a single-loop nonplanar amplitude in dual-resonance models is briefly discussed. (L.B.S.)

12190 MULTIPERIPHERAL MODEL. Fubini, Sergio (Massachusetts Inst. of Tech., Cambridge). Comments Nucl. Particle Phys.; 4: 102-6(May-Jun 1970).

A brief survey is given of some of the properties and main results of the multiperipheral model. (L.B.S.)

Strong (Baryon No. = 0)

Refer also to abstract 12269.

12191 (INR-P-1207) FURTHER ANALYSIS OF D^0 MESON IN REACTION $\pi^+p \to p\pi^+\pi^+\pi^+\pi^-\pi^-\pi^0$ AT 8 GeV/c. Otwinowski, S. (Institute of Nuclear Research, Warsaw (Poland)). 1970. 6p. Dep. NTIS (U.S. Sales Only).

The existence of the intermediate $\delta\pi$ state in the decay $D^0 \to \eta\pi\pi$ is discussed. It is shown that the reflection of the ω production cannot produce a spurious maximum in the $(\eta\pi)$ mass distribution at the position of the δ. (auth)

12192 (NYO-2262-TA-232) SINGULAR OFF-MASS-SHELL EQUATION WITH VECTOR-MESON EXCHANGE. Chen, T. C. (Brown Univ., Providence, R. I. Dept. of Physics); Raman, K. (Wesleyan Univ., Middletown, Conn.). Oct 1970. 46p. Dep. NTIS.

A method is suggested for handling the singular Blankenbecler-Sugar-Logunov-Tavkhelidze (BSLT) equation for the scattering of two spin-zero particles through the exchange of a vector meson. First the Born term describing vector-meson exchange is defined in such a way as to minimize the degree of singularity of the equation. A distorted-wave method is then used for the modified equation, which is still marginally singular. This reduces the problem to that of solving a Fredholm equation. Numerical solutions are obtained for the low-energy S-wave and P-wave amplitudes and resonances. (auth)

12193 (SU-1206-234) INEQUALITIES FOR THE s- AND p-WAVE $\pi\pi$ PARTIAL-WAVE AMPLITUDES. Balachandran, A. P. (Syracuse Univ., N. Y. Dept. of Physics, Tata Inst. of Fundamental Research, Bombay (India)); Blackmon, Maurice L. (Syracuse Univ., N. Y. Dept. of Physics). Aug 1970. 25p. (NYO-3399-234). Dep. NTIS.

An infinite number of inequalities for integrals over the s- and p-wave $\pi\pi$ amplitudes in the interval $0 \le s \le 4m_\pi^2$ in terms of the $\pi\pi$ total cross sections and other experimentally accessible data are derived. The main ingredients in the derivations are crossing symmetry, the positivity of the even $l \ge 2$ partial waves of the reactions $\pi^0\pi^0 \to \pi^0\pi^0$ and $\pi^0\pi^0 \to \pi^+\pi^-$ in the interval $0 \le s \le 4m_\pi^2$ and some known bounds on the crossed channel absorptive parts of these reactions. It is shown that if the partial-wave sum over any subset of $\pi^0\pi^0 \to \pi^0\pi^0$ partial waves is itself invariant under permutations of s, t, and u and this subset contains the s-wave, then the entire $\pi^0\pi^0 \to \pi^0\pi^0$ amplitude has to vanish identically. (Actually, a somewhat stronger result is proved for the amplitudes of both the processes $\pi^0\pi^0 \to \pi^0\pi^0$ and $\pi^0\pi^0 \to \pi^+\pi^-$ or for any linear combination of these amplitudes with positive coefficients.) (auth)

12194 CHIRAL DYNAMICS, SU(3) SYMMETRY BREAKING AND THE Kl_4 FORM FACTORS; ALSO, A COMPARISON OF CLASSICAL AND QUANTAL PREDICTIONS FOR RESCATTERING PROBABILITIES IN 3-BODY PROCESSES. Wood, Louvan Elbert Jr. College Park, Md.; Univ. of Maryland (1969). 181p. University Microfilms Order No. 70-14,952.

Thesis.

The strong decay rates of spin-one resonances are correlated with the Kl_3 and Kl_4 decay amplitudes using the chiral Lagrangian approach. The basic assumptions of the model are SU(3) ⊗ SU(3) field algebra, PCAC and PCVC, that chiral symmetry is broken by a term transforming as (3,3*) ⊕ (3*,3), and the single particle saturation consequences of Weinberg's second sum rule. A further approximation is the use of a nonlinear realization of SU(3) ⊗ SU(3) appropriate to the symmetry breaking assumptions. The chiral Lagrangian approach provides a method of obtaining current algebra results in the physical region of the decay, i.e., all particles are on their mass shell. By using experimental information on the strong spin-one decays, one can predict values of the Kl_3 parameters in agreement with experiment. Results for Kl_4 are more uncertain. For the form factor F_1, one finds for the s-wave part $F_1^{(s)}(s) = -3.8 + 3.8(s - \bar{s})$ for a K_A mass of 1320 MeV and $F_1^{(s)} = -3.6 + 3.5(s - \bar{s})$ for a K_A mass of 1230 MeV (to within about 10%), where s is the dipion effective mass in $(GeV)^2$ and $\bar{s} = 0.10(GeV)^2$. The form factor F_2 contains unknown parameters, and if they are not unreasonably large, one finds $F_2 \simeq -4.8 + x(s - \bar{s})$. The constant term is not particularly sensitive to the unknown parameters; the coefficient x of $(s - \bar{s})$ is. There is a significant numerical difference between the soft and hard pion results. The model used to obtain the above predictions has been constrained to give the values of the $\pi-\pi$ scattering lengths found by Weinberg. This assumption could be relaxed, but only at the cost of adding several undetermined parameters to the model. The Kl_4 vector form factor "d" is estimated by the vector dominance model of Sakurai. In contrast to previous such calculations all lowest-order Feynman graphs which contribute to the process, for the first time are included. It is found that d is between .94 and 1.4, depending on methods and experimental numbers used. Comparisons with previous estimates and present experimental data are made. The 2-stage process $b + t \to R + 2$, $R \to 1 + 3$ is considered. Classically, it may be possible for particle 3 to catch up with particle 2, and rescatter. If R has lifetime τ_0, and width $\Gamma = 1/\tau_0$, then classically the rescattering probability $P_{cl} = K/\tau_0^2$, where K is determined by the kinematics. The nonrelativistic quantal matrix element is known, and P_{QM} was evaluated from this. For small Γ, one finds $P_{QM} = a\Gamma + b\Gamma^2 \ln \Gamma + c\Gamma^2 + \ldots$. Attempts to reconcile these two predictions do not lead to useful results. Numerically, in regions of interest, P_{cl} is smaller than P_{QM} by a factor of up to 10^3. The conclusion is that, in general, there is no useful relation between the quantal and classical predictions. (Diss. Abstr. Int., B)

12195 BRANCHING RATIOS OF TRACKS OF π MESONS EMITTED FROM PROTON-ANTIPROTON ANNIHILATION. Vandermeulen, J. (Univ., Liege). Bull. Soc. Roy. Sci. Liege; 39: 274-8(1970). (In French).

The necessity is shown of taking into account the production of resonances in order to study the relations among the various charge configurations and diverse multiplicities in the annihilations into π mesons. A table of branching ratios relative to the production of 4 to 10 π mesons is presented. (tr-auth)

12196 CROSSING-SYMMETRIC UNITARIZATION OF THE VENEZIANO AMPLITUDE. Carpenter, K. M.; Negrine, S. M. (Cambridge Univ., Eng.). Nuovo Cim.; 1A: 13-37(1 Jan 1971).

By using the Veneziano formula for $\pi\pi$ scattering as an approximation to the crossing-symmetric K-matrix, it is possible to obtain a model that satisfies two-body unitarity and is approximately crossing symmetric. The model contains very little freedom, but nevertheless gives good predictions for resonance masses and widths. (auth)

12197 TWO-VARIABLE CROSSING-SYMMETRIC EXPANSION OF THE $\pi\pi$ SCATTERING AMPLITUDE AND LOW-ENERGY PARAMETER SUM RULES. Maiella, G. (Univ. of Texas, Austin). Nuovo Cim.; 70A: 507-24(21 Dec 1970).

A two-variable crossing-symmetric expansion of the $\pi-\pi$ scattering amplitude in the interior of the Mandelstam triangle is obtained. From this expansion, sum rules are derived for the low-energy parameters, assuming the "weakness" of the threshold unitarity cut. Finally, these sum rules are compared with experimental data and theoretical predictions. (auth)

12198 K_{l3} FORM FACTORS, F_K/F_π AND THE SYMMETRY-BREAKING PARAMETER OF THE VACUUM STATES. Lai, C. S.; Lin, H. E.; Lin, W. C. (Univ. of Prince Edward Island, Charlottetown). Nuovo Cim.; 70A: 549-63(21 Dec 1970).

Solving four sets of relations involving the K_{13} form factors $F_i(q^2)$ and the ratio F_K/F_π obtained in a previous paper, the values of $F_+(0)$ and F_K/F_π are found to be functions of the symmetry-breaking parameter $b = \langle 0|S_8(0)|0\rangle/\langle 0|S_0(0)|0\rangle$. Near a value of

b = −0.22, which is close to the one estimated by Mathur et al., it is found that the form factor $F_+(0)$ is almost nonrenormalizable and $F_K/F_\pi \simeq 1.28$. (auth)

12199 EXTENSION OF KEMMER-SYMMETRIC COUPLING TO MESON DECAYS. MacGregor, M. H. (Univ. of California, Livermore). Lett. Nuovo Cim.; 4: 1309-15(26 Dec 1970).

By extending the Kemmer symmetry and studying the η, η', K_1^0, K_2^0, K^+, K^-, and δ^- decays, all of which fall into $^2/_3$ and $^1/_3$ groupings, internal charge configurations can be deduced for these particles. Using a basic mass quantum μ = 71 MeV the masses can be accurately reproduced, and the striking ratios that occur for the lifetimes can be explained phenomenologically. (J.F.P.)

12200 MESON AND KAON STRUCTURE. MacGregor, M. H. (Univ. of California, Livermore). Lett. Nuovo Cim.; 4: 1249-58(26 Dec 1970).

The mass matrix elements are used to systematically construct the meson and kaon resonances. These are tabulated and illustrated. In addition to well-known levels, several low-lying levels recently reported or not yet extracted from the data are accounted for. All identified meson resonances up to 1600 MeV and several examples above this energy, and all kaon resonances up to 1800 MeV are included. Meson and kaon resonances are also grouped according to their observed widths; and the systematics are illustrated and discussed. (J.F.P.)

12201 DISCOVERY OF THE S^0 MESON. Gemesy, Tibor (Central Research Inst. for Physics, Budapest). Fiz. Szemle; 20: 249-51(Aug 1970). (In Hungarian).

Classification of the more than 200 elementary particles represents the most interesting field of theoretical physics; in this connection, discovery of the S^0 meson is reviewed. Comparison of the angular distributions of the 2 types of ρ meson revealed significant differences. They were attributed to the existence of another type of neutral resonance, possessing the same mass as the neutral ρ meson and designated variously as ϵ, S^0 or η meson. The decay of the S^0 meson into 2 neutral π mesons was studied in a cooperative study at Dubna, Warsaw and Budapest; the study involved irradiation of the 25-liter liquid-xenon-filled bubble chamber at Dubna with 2.34 GeV/c pulses of positive pions. Decay of the neutral pions yielded 2 photons which may be detected by means of the xenon chamber with a 94% probability. About 500,000 stereo pictures taken between 1964 and 1969 were subjected to a computerized analysis at the 3 cooperating institutes. Measurement of the cascade energy and of the angle of 2 cascades allowed the determination of the mass of the particles yielding 2 photons. The effective mean $M(\pi^0\pi^0)$ distribution histogram revealed a significant S^0 peak at 730 MeV. The data agree with results reported by about 20 western laboratories. (TTT)

12202 UNITARITY AND A TIGHTLY BOUND PION. Han, Sook Jong. Amherst, Mass.; Univ. of Massachusetts (1970). 50p. University Microfilms Order No. 70-23,034.

Thesis.

The dynamical mechanism of a tightly bound-state of a pion was studied based on the multichannel N/D equations. The emphasis is given to the production process $\pi\rho \rightleftharpoons N\bar{N}$ rather than the elastic channels. Since the two channels are strongly coupled to each other, the forces from the production channel $\pi\rho \rightleftharpoons N\bar{N}$ play a crucial role in forming a pion bound-state. The forces from the elastic channel $\pi\rho \to \pi\rho$ are taken to be zero because of the instability of ρ-meson decay into two pions, which introduces enormous difficulties such as overlapping cuts and anomalous thresholds. In order to examine the effect of the forces from the $N\bar{N}$-elastic channel on the pion, bound-state mass, the forces from the work of Ball, Scotti, and Wong were used as a check. As for the input forces from the production process $\pi\rho \rightleftharpoons N\bar{N}$, which are generated by the exchanges of nucleon in the t- and u-channels, the well established experimental mass of π, ρ, and N, and coupling constant $g_{\pi NN}$ were taken as fixed values, while a less certain coupling constant, $f_{\rho NN}$ is viewed as a parameter. With these input forces, the standard N/D equations were solved numerically since no analytic approximation method can be a real substitute for the exact solutions. The bound-state mass of the pion is found close to the physical pion mass within a reasonable range of coupling constant $f_{\rho NN}$ ($f^2_{\rho NN}/4\pi$ = 2.05, Λ^2 = 2500 μ^2). The bound-state mass of the pion shows a lower and an upper bound. In particular, the lower bound corresponds to a soft pion for both cut-off parameters. As one expects from the importance of nearby singularities, the effect of the forces from the $N\bar{N}$-elastic channel on the pion, bound-state mass is insignificant. (Diss. Abstr. Int., B)

12203 RELATION AMONG CROSS SECTIONS OF PRODUCTION OF THE 2^+, 1^+, 0^+, AND 1^-, 0^- NONETS MESONS IN MESON–BARYON INTERACTIONS IN NONRELATIVISTIC MODEL OF QUARKS. Levin, E. S. (Leningrad State Teacher's Inst.). Izv. Vyssh. Ucheb. Zaved., Fiz.; No. 8, 100-4(1970). (In Russian).

A nonrelativistic model was used for meson classifications according to the L-S bond type. A ratio between the meson formations with L = 0 and L = 1 (which was described by the ratio of meson form factors with L = 0 and L = 1) was obtained within the limits of the classification. The ratio of form factors was calculated on the basis of the nonrelativistic quark model and the hypothesis on ρ dominance in electromagnetic hadron interactions. The meson formation reactions during πN-collisions, with the cross sections related to the established ratios are described. (R.V.J.)

Strong (Baryon No. = 1)

12204 (JINR-P1-5431) ANALYSIS OF $\pi^-p \to n\pi^+\pi^-m\pi^0$ (m = 1, 2, 3) AND $\pi^-p \to n2\pi^+2\pi^-m\pi^0$ (m = 1,2) REACTIONS AT pc = 4 GeV ACCORDING TO THE STATISTICAL AND ANISOTROPIC MODELS. Grishin, V. G.; Inogamov, Sh. V.; Kopylova, D. K.; Lyubimov, V. B.; Yuldashev, B. S. (Joint Inst. for Nuclear Research, Dubna (USSR). Lab. of High Energy). 1970. 19p. (In Russian). Dep. NTIS (U. S. Sales Only).

The $\pi^-p \to n\pi^+\pi^-m\pi^0$ (m = 1,2,3) and $\pi^-p \to n2\pi^+2\pi^-m\pi^0$ (m = 1,2) reactions at pc = 4 GeV are analyzed in the framework of the statistical and anisotropic models. It is shown that the basic characteristics of these processes can be described by using the anisotropic model. (auth)

12205 PARTICLE MULTIPLE AND DIFFRACTION SCATTERING AND DIPS. Dorfman, Ronald Sherman. New York; Yeshiva Univ. (1970). 127p. University Microfilms Order No. 70-17,105.

Thesis.

A model for high-energy pion nucleon charge exchange scattering is introduced. The model employs the asymptotic generalized optical eikonal model of Chou and Yang (for elastic scattering). Energy dependence was introduced by combining this model with Regge theory. The model can be looked upon as a Reggeized generalized eikonal picture or optical model. The Regge term could correspond to a single scattering term, and the whole amplitude to generalized multiple scattering. (TSS) (Diss. Abstr. Int., B)

12206 DECISIVE TESTS OF HIGH-ENERGY MODELS. Berger, Edmond L.; Fox, Geoffrey (Argonne National Lab., Ill.). Phys. Rev. Lett.; 25: 1783-7(28 Dec 1970).

Regge-pole and strong-absorption (diffractive) models are based upon fundamentally different physical postulates. Although both reproduce available $d\sigma/dt$ and polarization data, profound differences are evident in basic amplitude structure. It is shown that measurements of the spin-rotation parameters R and A, for any high-energy exchange process, will determine structure of amplitudes and thus provide unambiguous tests of essential assumptions in the models. The experimentally feasible reactions $\pi N \to K(\Lambda,\Sigma)$, $\bar{K}N \to \pi(\Lambda,\Sigma)$, and $\gamma p \to K(\Lambda,\Sigma)$ are examined explicitly as well as multiparticle processes. (auth)

12207 CONTINUOUS MOMENT SUM RULES. Liu, Yu-chien. Rochester, N. Y.; Univ. of Rochester (1970). 182p. University Microfilms Order No. 70-17,893.

Thesis.

A new type of dispersion sum rule—the continuous moment sum rule (CMSR)—is developed. The main ingredient consists of putting the real part of the scattering amplitude on an equal footing with the imaginary part, with both of them appearing in the physical region; introducing a continuous parameter, and therefore an infinite number of sum rules which contain both ordinary and inverse dispersion relations as special cases. Use was found in determining the low-energy parameters (coupling constants, scattering lengths) and the high energy ones (Regge trajectories, residues, . . .). The main formalism is developed for forward pion–nucleon scattering, for which confrontation with experiment is clean. Extensions to nonforward directions as well as to other interesting processes (single pion-photoproduction, nucleon–nucleon scattering, proton Compton scattering and pion–pion scattering) are discussed. A detailed presentation is made for the kinematics of each process, from which the derivation of CMSR and the use of experimental data should be very simple. (Diss. Abstr.)

12208 INFLUENCE OF ρ^0–ω MIXING ON THE SPIN DENSITY MATRIX ON THE ω MESON IN THE REACTIONS $\pi N \to \omega N$ AND $\pi N \to \omega\Delta$. Achasov, N. L.; Shestakov, G. N. (Mathematics Inst., Novosibirsk, USSR). JETP Lett. (USSR) (Engl. Transl.); 12: 218-21(20 Sep 1970).

Translated from Zh. Eksp. Teor. Fiz., Pis'ma Red.; 12: 323-7(20 Sept 1970).

It is pointed out that previous experimental evidence allows one to expect a strong effect of electromagnetic $\rho^0-\omega$ mixing on the spin density matrix of the meson (ω) in the reactions $\pi + N \rightarrow \omega + N(\Delta)$. The consequences of the two kinds of effects from the electromagnetic $\rho^0 - \omega$ mixing are discussed; namely, the change of the mass spectrum of the decay pions and the change of the amplitudes of vector meson production. (J.F.P.)

12209 DISCREPANCIES BETWEEN πN CHARGE EXCHANGE FORWARD SCATTERING DATA AND THE DISPERSION RELATION PREDICTION. Hoehler, G.; Strauss, R. (Univ., Karlsruhe, Ger.). Z. Phys.; 240: 377-91(1970).

The πN charge-exchange forward scattering amplitude was recalculated, using the most recent total cross section data, charge independence and the forward dispersion relation. In general the prediction agrees rather well with the data, but there are several discrepancies which are considerably larger than the errors. Some of these discrepancies follow from the fact that a structure at small $|t|$ was ignored in the extrapolation. —The new fit gives an accurate value for the subtraction constant of the integral. It agrees with the evaluation of the unsubtracted integral at threshold, if, at high energies, the Regge behavior for $\sigma(\pi^-p)-\sigma(\pi^+p)$ is inserted. This result favors the validity of Pomeranchuk's theorem. —An improved value for f^2 cannot be obtained at present because of the uncertainty following from charge-dependent effects at low energies. (auth)

12210 CONSTANCY OF TOTAL CROSS SECTIONS AT HIGH ENERGIES AND K-MESON CHARGE EXCHANGE. Babaev, Z. R. JETP Lett. (USSR) (Engl. Transl.); 12: 257-9(5 Oct 1970).

Translated from Zh. Eksp. Teor. Fiz., Pis'ma Red.; 12: 374-7(5 Oct 1970).

A detailed analysis is made for the reaction $K^- + p \rightarrow \overline{K}^0 + n$. The charge-exchange amplitude is related with the $K^- + n$ and $K^- + p$ elastic scattering amplitudes. Curves showing the different parametrization of the difference $\Delta\sigma$ between the $K^- + p$ and $K^- + n$ total cross sections are shown. Also the differential cross section of the forward $K^- + p \rightarrow \overline{K}^0 + n$ interactions are shown for different parametrizations and in accordance with the Regge pole model. It is found that the assumed constancy of $\Delta\sigma$ leads to a strong deviation of the differential charge-exchange cross section from the predictions of the Regge pole model. The effect of the constancy of $\Delta\sigma$ on the behavior of the forward elastic KN scattering is much weaker than in the case of charge exchange. (J.F.P.)

12211 REGGE PARAMETRIZATION FOR LOW-ENERGY πN SCATTERING. Minkowski, P. (SIN, Zurich); Halzen, F. Nuovo Cim.; 1A: 59-77(1 Jan 1971).

It is shown that the complementary aspect of high-energy Regge behavior and low-energy resonance saturation known as "duality" from finite-energy sum rules can be advanced in a unifying direction. The Regge parametrization of low-energy partial waves is deduced reversing the path leading to asymptotic Regge behavior in the crossed channel by means of the Khuri-Jones representation. The P_{11} and S_{11} waves in πN scattering are analyzed. They show evidence for a pattern of trajectories characteristic for a model of oscillatory excitations. (auth)

12212 NONEVASIVE CONTRIBUTIONS TO FORWARD RHO-PRODUCTION AND VECTOR DOMINANCE. Froggatt, C. D. (University Coll., London); Morgan, D. Phys. Lett.; 33B: 582-6(21 Dec 1970).

It is shown that the small t background to rho production as determined from fits to experiment agrees rather well with the predictions from simple theoretical models, leading to a quantitative agreement with the vector dominance model and an overall picture of the background to OPE for use in $\pi\pi$ phenomenology. (auth)

12213 SIMPLE MODEL OF LOW-ENERGY K^-N SCATTERING ON BOUND NUCLEONS. Revai, J. (CEN de Saclay, Gif-sur-Yvette, France). Phys. Lett.; 33B: 587-90(21 Dec 1970).

The presence of the Y* (1405) resonance in the K^-N system not far below the threshold suggests the existence of important binding effects on low-energy K^-N scattering on bound nucleons. This question was studied in a framework of an exactly soluble three-body model. It has been shown that for the experimental value of $K^-N - \Sigma\pi$ coupling the effect of the resonance on the K^-N scattering length is small while for smaller couplings the effect can be considerable. (auth)

12214 SCALE AND CHIRAL SYMMETRY BREAKING. Ellis, J. (CERN, Geneva). Phys. Lett.; 33B: 591-5(21 Dec 1970).

The absence of a q-number δ term in the hadronic energy momentum density $\theta_{00} = \theta_{00} + \delta + u$ is compatible with the meson-baryon scattering analysis of von Hippel and Kim. (auth)

12215 IMPLICATIONS OF DUALITY FOR $\overline{K}$N RESONANCES. Capps, R. H. (Weizmann Inst. of Science, Rehovot, Israel); Dixit, V. V. (Phys. Lett.; 33B: 596-8(21 Dec 1970).

A local duality condition, and a semilocal duality condition, are applied to the resonance contributions to backward $\overline{K}$N scattering amplitudes. Predictions concerning the relative partial widths of different Σ^* resonances, and of different Λ^* resonances, are made. (auth)

12216 EMPIRICAL TEST OF TENSOR MESON DOMINANCE. Renner, B. (Univ., Hamburg). Phys. Lett.; 33B: 599-600 (21 Dec 1970).

The assumption of meson pole dominance for matrix elements of the energy momentum tensor is tested using empirical results on tensor meson decay widths and nucleon coupling constants. Its most significant consequence is the decoupling of the f-exchange contribution from the A-amplitude in pion-nucleon scattering. (auth)

12217 REGGE-PHENOMENOLOGICAL STUDIES OF SU(3), EXCHANGE DEGENERACY, AND CONSPIRACY. Jackson, Jane Chapman. Tempe, Ariz.; Arizona State Univ. (1970). 47p. University Microfilms Order No. 70-21,957.

Thesis.

Three independent but related Regge-phenomenological studies of SU(3), exchange degeneracy and conspiracy are presented. In the first study, from the formalism combining SU(3) symmetry, exchange degeneracy, and Regge poles, it is found that a single parameter can fit all the existing data in meson-nucleon reactions in the forward direction. In the second study, Regge-pole fits to π^-p charge-exchange differential cross section and polarization data were given at moderately high energies and over a wide range of momentum transfers. Besides the ρ trajectory, whose slope and intercept are determined by exchange degeneracy, a conspiring ρ' trajectory of the same slope but intercept near zero was taken into account. In the spirit of the Veneziano formula, the residues are assumed to be of the form const/$\Gamma(\alpha)$. A four-parameter fit gives good agreement with the experimental data. In the third study, a phenomenological study of SU(3) and exchange degeneracy is made in a Regge pole-cut model. The high energy data of pion-nucleon, kaon-nucleon, nucleon-nucleon, and nucleon-antinucleon total cross sections, including the new Serpukhov data, are analyzed by means of least-squares fits with parameters corresponding to the P, P^1, ρ, A_2, and ω Regge poles and a subtractive vacuum cut. The data are fitted adequately with the assumptions of SU(3) and exchange degeneracy. For completeness, the data are analyzed with the assumptions of SU(3) alone, exchange degeneracy alone, and also without either of these assumptions. (Diss. Abstr. Int., B)

12218 HADRON SPECTROSCOPY AND HIGH-ENERGY SCATTERING IN THE QUARK MODEL. Chylek, Petr. Riverside, Calif.; Univ. of California (1970). 92p. University Microfilms Order No. 70-22,857.

Thesis.

The Roper resonance is interpreted as a radially excited three-quark state. For its octet counterparts the resonances $\Sigma(1700)$, $\Lambda(1745)$, and $\Xi(1930)$ are suggested. Thus the unusually large widths of these resonances are explained and the spin-parity is predicted to be $\frac{1}{2}^+$. The double-peaked A_2 meson is explained by the $(q\bar{q})^3$ meson structure. Consequences of this assignment are discussed. The quark model numerical selection rule for the three-hadron vertex is derived and a new graphical approach to high energy scattering in the framework of the quark model is suggested. The method is applied to elastic forward meson-nucleon scattering and several reasonably well satisfied relations between total cross sections are derived. The same model is applied to backward meson-nucleon scattering and backward $N\bar{N}$ production. Whenever comparison with experimental data is possible, good agreement is found. The model also gives a connection between the possible violation of the Pomeranchuk theorem and isospin dependence of total cross sections at high energy. (Diss. Abstr. Int., B)

12219 DIP–BUMP STRUCTURE OF CROSS SECTION AND URBARYON REARRANGEMENT. II. Imachi, Masahiro; Oroguchi, Takashige; Otsuki, Shoichiro; Toyoda, Fumihiko (Kyushu Univ., Fukuoka). Progr. Theor. Phys. (Kyoto); 44: 1110-12 (Oct 1970).

The dynamic structure of urbaryon-rearrangement-diagram amplitude is examined for elastic πN scattering. The results are compared with experiment on $d\sigma/dt$ and P(t) of elastic $\pi^\pm p$ interactions at $P_L = 5.0$ GeV/c. The importance of the generalized Ogawa rule, which gives the dip-bump structure of $d\sigma/dt$ and P(t), is stressed. (L.B.S.)

12220 REGULARITY OF THE COUPLING CONSTANTS OF THE $N^* \rightarrow N + \pi$ DECAYS. Kaiba, Masayuki (Shizuoka Women's Coll., Japan). Progr. Theor. Phys. (Kyoto); 44: 1006-11(Oct 1970).

It is pointed out that the coupling constant of an effective Hamiltonian suitable for the decay interactions $N^* \rightarrow N + \pi$ exhibits a

certain kind of regularity, when the nucleon resonances are assigned by the quantum numbers of a harmonic oscillator quark model. (auth)

12221 THREE-CHANNEL MODEL FOR P_{33} πN SCATTERING. Hori, Setsuko; Kanki, Takeshi (Osaka Univ.). Progr. Theor. Phys. (Kyoto); 44: 1012-21(Oct 1970).

A static three-channel model is presented for the πN $I = J = \frac{3}{2}$ p-wave scattering at low and intermediate energies. The (ρN) and (πN^*) states are taken into account as inelastic channels. Only the nucleon-exchange poles in each channel are retained as the most effective nearby singularities, but static ND^{-1} is solved exactly. Some of these poles exist on the righthand cut and give very important contributions. A very small value is found for the ($\pi N^* N^*$) coupling constant compared with the SU(6) prediction. It is also discussed that this value is quite consistent with small experimental inelasticity of P_{33} πN collision in the intermediate energy region. (auth)

12222 INELASTIC π-N and N-N COLLISIONS IN THE PARTON MODEL. Niegawa, Akira (Kyoto Univ.). Progr. Theor. Phys. (Kyoto); 44: 977-94(Oct 1970).

The deep inelastic N-N scattering cross section at high energies is calculated by using the parton model. The one-boson exchange interaction is expediently assumed between partons. The result is shown to be consistent with the experimental data. The cross section is also calculated in the usual 3-quark model to show that the parton model is better than the usual 3-quark model. The constant asymptotic behavior of the π-N total cross section at high energies is obtained by taking into account the contribution of the non-"wee" partons. This constant asymptotic behavior comes essentially from the "background" part in agreement with the Freund-Harari conjecture. (auth)

12223 $\pi^+ p \rightarrow \pi^0 N^{*++}$ REACTION AT HIGH ENERGY AND CORRECTION TO ρ-EXCHANGE CONTRIBUTION. Hama, Mitsuru; Iwaki, Atsuko (Rikkyo Univ., Tokyo). Progr. Theor. Phys. (Kyoto); 44: 959-76(Oct 1970).

The reaction $\pi^+ p \rightarrow \pi^0 N^{*++}$ at high energies is investigated by using a model in which some of the assumptions used in the absorption model are removed and the transition amplitudes take a form connected with the transition amplitudes for $\pi^- p$ charge exchange scattering. It is shown that the model can reproduce the experimental energy dependence of the differential cross section and gives good agreement with almost all of the data including those on the spin density matrix of N^* decay. (auth)

12224 INVESTIGATION OF POSSIBLE ANAPOLE AND ELECTRIC DIPOLE MOMENT OF PROTON WITH THE HELP OF THE ANNIHILATION REACTION $p\bar{p} \rightleftharpoons e^+e^-$. Kerimov, B. K.; Kasumov, Yu. M.; Sadykhov, F. S. (Moscow State Univ.). Izv. Vyssh. Ucheb. Zaved., Fiz.; No. 8, 59-65(1970). (In Russian).

A single-photon approximation was used for obtaining differential and total cross sections for the electron-positron pair formation during annihilation of the arbitrary polarized proton and antiproton ($\bar{p}p \rightarrow e^+e^-$), and the inverse process of $e^+e^- \rightarrow \bar{p}p$), taking into account disturbing C-, P-, and T-parities of the anapole and electric dipole proton moments. The means for determination of the quadratic modulus for form factors of anapole (G,q^2) and electric dipole $|G_2(q^2)|$ moments and the relative phase between form factors $F_e(q^2)$, and $G_2(q^2)$, $F_m(q^2)$ and $G_1(q^2)$, are analyzed. Estimations of $G_1(q^2)$ and $|G_2(q^2)|^2$ at $q^2 = 6.8$ $(GeV/2)^2$ are included. (R.V.J.)

Strong (Baryon No. ≥ 2)

Refer also to abstracts 12393 and 12668.

12225 ANALYSIS OF PION–HELIUM SCATTERING FOR THE PION CHARGE FORM FACTOR. Mottershead, Charles Thomas. Berkeley, Calif.; Univ. of California (1969). 80p. University Microfilms Order No. 70-17,624.

Thesis.

Elastic scattering of π^+ and π^- on ^{4}He is analyzed for information on the charge radius of the pion using a new method based on boundary conditions near the nuclear surface. The pion radius enters the calculation via the electrostatic potential of the pion and helium charge distributions, which is assumed to be the only charge-dependent interaction. Since ^{4}He is isoscalar the strong nuclear interaction is assumed charge independent. Differential cross section data for both signs of the charge are fit simultaneously by a program that uses the logarithmic derivatives of the pion radial wave function for each charge as free parameters. If the nuclear interaction operator is symmetric (i.e., $\langle \underline{r}' | U_N | \underline{r} \rangle = \langle \underline{r} | U_N | \underline{r}' \rangle$), the difference in the logarithmic derivative for a given partial wave due to changing the sign of the charge may be expressed as an integral of the internal Coulomb potential weighted by the wave function. Nuclear model dependence is greatly reduced by the constraints imposed by the empirical boundary conditions on the internal wave function. The Crowe Group's data at beam momenta of 130 to 163 MeV/c are analyzed by this method using both local potential and Kisslinger models for the strong interaction, and Gaussian and Yukawa pion charge distributions. The results indicate $2.2 < r_\pi < 3.2$ F, depending on theoretical model, with an experimental precision of ~±0.5 F. In the course of the analysis, the singular point difficulty with the Kisslinger model was examined and found to be serious. A simple treatment of the relativistic reduced mass (two body problem) is given. (Diss. Abstr.)

12226 ESTIMATE OF A INTERACTION IN THE p STATE. Khrylin, B. A. JETP Lett. (USSR) (Engl. Transl.); 12: 221-3 (20 Sep 1970).

Translated from Zh. Eksp. Teor. Fiz., Pis'ma Red.; 12: 327-8(20 Sep 1970).

For the study of Λ + N interactions in the p state of hypernuclei, the Λ binding energy of the Λ-0^{17} hyperfragment is calculated using the main approximation of the method of K harmonics. It is found that for all the sets of the ΛN potentials the Λ binding energy of Λ-0^{17} hyperfragments is approximately 15.5. (J.F.P.)

12227 CALCULATIONS ON NEUTRON–DEUTERON SCATTERING. Laroze, Luciano B. Troy, N. Y.; Rensselaer Polytechnic Inst. (1970). 186p. University Microfilms Order No. 70-19,942.

Thesis.

Using separable tensor two-nucleon potentials, the neutron-deuteron system was studied in states of total angular momentum and parity $\frac{1}{2}^+$. Scattering equations of the Lovelace type appropriate to this case were obtained and solved to determine the elastic scattering amplitudes for a wide energy range up to 100 MeV. Different form factor shapes were used to investigate the sensitivity of the results of the two-nucleon potential. The percent D-state of the deuteron was also varied. In analogy to the previous parametrization of the two-nucleon phase shifts, a convenient parametrization scheme for the elastic scattering amplitude matrix was developed in terms of two complex eigenphase shifts and a complex mixing parameter. Results are compared to a previous phase shift analysis and with previous computations using central spin dependent interactions. The calculations with tensor forces show much better agreement with the experimental values than do those using only central potentials. The n-d doublet scattering length and its relation with the triton binding energy were studied using a variety of potential shapes. The results agree with previous findings in that whenever the correct triton energy is obtained the old value of 0.7 ± 0.3F is obtained for the doublet scattering length. The triton energy and the newer experimental value of 0.15 ± 0.05F were unable to be fitted simultaneously. In order to test whether this result arises from the use of separable potentials, calculations were performed using the unitary pole expansion for the Reid singlet potential. It is found that the inclusion of additional separable terms produces little change in the result suggesting that a separable approximation is valid. Motivated by this inability to simultaneously fit the triton binding energy and the newer doublet scattering length, the effects of including a three-nucleon potential in a phenomenological separable form were investigated. Appropriately adjusting the parameters in this interaction both experimental quantities could be fitted. (Diss. Abstr.)

12228 LIGHT-CONE ANALYSIS OF MASSIVE μ-PAIR PRODUCTION. Altarelli, Guido; Brandt, Richard A.; Preparata, Giuliano (Rockefeller Univ., New York). Phys. Rev. Lett.; 26: 42-6(4 Jan 1971).

An operator representation for the behavior of the product of two electromagnetic currents near the light cone is used to discuss massive μ-pair production in hadron-hadron interactions. Restrictions from the Stanford Linear Accelerator Center electroproduction experiments and from Regge theory are incorporated. The predictions are in agreement with the recent Columbia–Brookhaven Laboratory experiment. (auth)

12229 PRODUCTION OF MUON PAIRS IN INTERACTIONS OF HADRONS OF HIGH ENERGY. Budnev, V. M.; Ginzburg, I. F.; Meledin, G. V.; Serbo, V. G. (Novosibirsk State Univ., USSR). JETP Lett. (USSR) (Engl. Transl.); 12: 238-40(5 Oct 1970).

Translated from Zh. Eksp. Teor. Fiz., Pis'ma Red.; 12: 349-51(5 Oct 1970).

The cross sections for two different types of interaction processes in proton–proton interactions with the production of muon pairs are written and compared. (J.F.P.)

12230 MECHANISM OF PARTICLE PRODUCTION IN NUCLEON–NUCLEON INTERACTIONS AT VERY HIGH ENERGIES. Jain, P. L.; Shivpuri, R. K. (State Univ. of New York, Buffalo). Nuovo Cim.; 70A: 632-50(21 Dec 1970).

A mechanism of particle production in nucleon–nucleon interactions for 18 very-high-energy (~10^{12} eV) cosmic-ray jets is discussed. The analysis is given in terms of production of two centers (fireballs). The separation of the two centers is clearly shown through the analytical discussion of the theoretical curves fitted to the angular distribution of the secondary particles produced in these jets. This method gives a clear distinction of the two centers which is quite different from the standard techniques used in the past for separating the two centers from the population density of the particles in their angular distribution. The experimental parameters (angle, momentum, mass) of these two fireballs are estimated in all the interactions. The cross section of production of a pair of fireballs as a function of available energy in the center of mass and fireball mass is estimated. The four-momentum transfer between the fireballs and its variation with multiplicity have been studied. The center-of-mass longitudinal and transverse momenta of the secondary particles is discussed. The results seem to indicate the exchange of a Pomeranchuk pole between the two fireballs. (auth)

12231 THEORETICAL CALCULATION OF THE CROSS SECTION FOR PAIR PRODUCTION IN A PROTON–PROTON COLLISION. Parker, B. R. (Idaho State Univ., Pocatello); Chatelaine, J. Nuovo Cim.; 70A: 502-3(21 Dec 1970).

The differential cross section for electron-pair production in a proton–proton collision is calculated. Standard perturbation methods with retarded interactions are used throughout the calculation. A typical result is of the order of a tenth of a microbarn. (auth)

12232 LIGHT Λ^0 HYPERNUCLEI AND THE LAMBDA-NUCLEON POTENTIAL. Porter, L. E. (Los Alamos Scientific Lab., N. Mex.). Amer. J. Phys.; 39: 97-102(Jan 1971).

Characteristics of light hypernuclei are described. Exploitations of hypernuclei in studies of the lambda–nucleon force are reviewed, with emphasis on phenomenological potential well parameters. Results of studies of lambda–nucleon scattering and final state interactions are summarized. Properties of the lambda–nucleon force are discussed briefly. (auth)

Particle Invariance Principles and Symmetries

General

Refer also to abstract 12253.

12233 WIGNER'S ROTATIONS AND THE LIMITING PROCESS m → O. Beckers, J. (Univ., Liege). Physica; 92-7(12 Oct 1970).

The limiting process m → O is applied to Wigner's rotations written in exponential form in the timelike case. The results are then interpreted in the lightlike case and their physical meaning is given in connection with previous works on [m,s]- and [O,s]-irreducible unitary representations of the Poincaré group. (auth)

12234 DIAGRAMMATIC TECHNIQUE FOR CONSTRUCTING MATRIX ELEMENTS. Gilmore, Robert (Massachusetts Inst. of Tech., Cambridge. Alabama Agricultural and Mechanical Univ., Normal). J. Math. Phys. (N. Y.); 11: 3420-7(Dec 1970).

A diagrammatic technique is presented for computing the matrix elements of the generators of the unitary, orthogonal, symplectic, and symmetric groups (A_n, D_n, B_n, C_n, and S_n) within any of their unitary irreducible representations. Examples are worked out. (auth)

12235 NOTE ON MATRIX ELEMENTS OF FINITE U(n) TRANSFORMATIONS. Flores, J. (Instituto de Fisica, Mexico City); Niederle, J. Czech. J. Phys.; B20: 1241-50(1970).

Matrix elements of finite transformations of the group U(n) in an arbitrary unitary irreducible representation of U(n) are discussed and a technique for their determination is presented. As a byproduct a recursion relation for a special Racah coefficient of U(n) is obtained. (auth)

12236 PHOTONS AND TACHYONS WITH CONTINUOUS SPIN. Mukunda, N. (Tata Inst. of Fundamental Research, Bombay). Ann. Phys. (N. Y.); 61: 329-50(Dec 1970).

Lightlike and spacelike representations of the Poincaré group, describing photons and tachyons with continuous spin, are considered. The conditions are examined under which these representations can assume a form analogous to the Shirokov–Foldy form for the timelike representations, namely a form in which the generators of the appropriate little group show no mixing of the momentum and internal degrees of freedom. While every continuous spin lightlike representation can be put into this form, only those spacelike ones can, which correspond to using a continuous series representation of the little group appropriate to this case. (auth)

Applications (Electromagnetic and Weak)

Refer also to abstracts 12075 and 12171.

12237 SPIN-ZERO MESONS AND BROKEN CHIRAL $SU_3 \times SU_3$. Rodenberg, R.; Zerwas, P. (Technische Hochschule, Aachen). Nuovo Cim.; 70A: 569-78(21 Dec 1970).

Using the Fubini-Furlan method of the dispersive sum rules for N-point functions, some properties of the spin-zero mesons are discussed in the framework of broken chiral $SU_3 \times SU_3$ by means of field-current divergence identities. The masses of the $\varkappa$ and η' mesons and the ($K\pi$) S-wave scattering lengths are estimated. These results are applied to the K_{l3} decay parameters. (auth)

Applications (Strong)

12238 $n + p \rightarrow d + \gamma$: A TEST OF TIME REVERSAL INVARIANCE. Friedberg, Carl E. Princeton, N. J.; Princeton Univ. (1969). 166p. University Microfilms Order No. 70-14,207.

Thesis.

The process $n + p \rightarrow d + \gamma$ was investigated at the Princeton Pennsylvania Accelerator as a test of time reversal invariance. The differential and total cross sections obtained were compared with those for the process $\gamma + d \rightarrow n + p$, as a test of reciprocity, for neutron energies between 160 and 640 MeV. The total cross sections measured are in agreement with existing data. The differential cross sections measured are in agreement except in the energy range $520 < T_n < 640$ MeV. (Diss. Abstr.)

12239 CP NONINVARIANCE AND BARYON ASYMMETRY OF THE UNIVERSE. Kuz'min, V. A. (Lebedev Inst. of Physics, Moscow). JETP Lett. (USSR) (Engl. Transl.); 12: 228-30(20 Sep 1970).

Translated from Zh. Eksp. Teor. Fiz., Pis'ma Red.; 12: 335-7(20 Sep 1970).

A model is described which explains in a natural way the occurrence of the baryon asymmetry and its magnitude. It is assumed that at the present time the universe as a whole has a nonzero baryon number. In the model the universe is initially symmetrical with respect to the baryon number, and later becomes asymmetrical. This is attained by introducing an interaction that does not conserve the baryon number and contains a CP-noninvariant admixture. (J.F.P.)

Field Theories

General

12240 PHASE OF THE CHARGE IN ELECTRODYNAMICS. Mavrychev, Yu. S. (Ivanov Power Engineering Inst., USSR). Izv. Vyssh. Ucheb. Zaved., Fiz.; No. 9, 129-30(1970). (In Russian).

The phase of the charge in electrodynamics was examined considering the equations of free electromagnetic field covariance in relation to the intensity conversions $E \rightarrow E \cos\theta - H \sin\theta$ and $H \rightarrow E \sin\theta + H \cos\theta$ and developing the law of conservation based on the conversion $e \rightarrow e \cos\theta - e_+ \sin\theta$; and $e_+ \rightarrow e \sin\theta + e_+ \cos\theta$ (where e is the electric charge and e_+ is the magnetic charge), which connected the phases of the charges in interacting particles. (R.V.J.)

12241 EQUIVALENCE BETWEEN TWO FIELD-THEORETICAL MODELS INVOLVING PURE FERMION FIELDS. Manoukian, E. B. (Univ. of Toronto). Lett. Nuovo Cim.; 4: 1289-92 (26 Dec 1970).

A simple field-theoretical model with an interaction Lagrangian density of the form $\lambda(\bar{\psi}_1\psi_2 + \bar{\psi}_2\psi_1)$ is considered, and it is shown that this theory may be reduced to a free-field theory of a massless spinor particle after mass and wave function renormalization if the bare masses of the spinor fields ψ_1, ψ_2 are infinite. The model is exactly solvable by Schwinger's external-source technique. (J.F.P.)

12242 SOLUTION TO THE INITIAL-VALUE PROBLEM FOR NONLINEAR CLASSICAL FIELD EQUATIONS. Rosen, G. (Drexel Univ., Philadelphia). Lett. Nuovo Cim.; 4: 1301-4(26 Dec 1970).

XUM

It is stated that the functional differential calculus enables one to give a formal general solution to the initial-value problem for a generic system of nonlinear field equations. The derivation of this formal general solution is given. (J.F.P.)

12243 SUPERPROPAGATORS. Karowski, M. (Univ., Hamburg). Commun. Math. Phys.; 19: 289-300(1970). (In German).

Some mathematical properties of superpropagators for any mass in field theories with exponential coupling are investigated. The principle of minimal singularity is discussed. (auth)

12244 CLASSICAL SCHWINGER TERMS. Boulware, David G. (Univ. of Washington, Seattle); Deser, S. Contract AT(45-1)-1388B. Commun. Math. Phys.; 19: 327-31(1970).

Schwinger terms must be present in equal time ground state Poisson brackets among currents unless the latter are stationary in that state. (auth)

Quantum Field Theory

Refer also to abstracts 12132, 12133, 12149, 12157, 12180, and 12236.

12245 (CNRS-CPT-70-P-318) COMPUTATION OF RENORMALIZED RADIATIVE CORRECTIONS: APPLICATION TO THE SCALAR THEORY $\lambda\phi^3$. Perrottet, Michel (Centre National de la Recherche Scientifique, Marseilles (France). Centre de Physique Theorique). 1970. 87p. (In French). Dep. NTIS (U.S. Sales Only).

Thesis. Submitted to Aix-Marseilles Univ., Faculte des Sciences, France.

Programs for calculating the Feynman diagrams of a scalar field interacting with itself for any order in the perturbation series are presented. The interaction term used is $\lambda\phi^3\psi$ where λ is coupling constant, and ϕ and ψ are the two interacting fields. The FRENEY program was written in FORTRAN and uses combinatorial analysis to obtain all the nonrenormalized diagrams associated with a given order in the perturbation series of a predetermined physical process. The ACOFIS program used for calculating the diagrams (the Feynman parametrization) was written in LISP language. The program is not concerned with algebraic calculations. The LISP programs were used with IBM 360-67 and the FORTRAN program with UNIVAC 1108. The ACOFIS program used in conjunction with the $\lambda\phi^3$ enabled a treatment in 80 seconds of all the vertexes up to the 7th order, all the eigen energies up to the 6th order, a numerical study of the asymptotic behavior of higher order diagrams, and calculations on the Delbruck effect up to the 4th order. This program was incorporated with a program for calculating anomalous magnetic moments and yielded satisfactory results. (France)

12246 FORMULATION OF LOCAL FIELDS DESCRIBING AN INFINITE TOWER OF PARTICLES. Wu, Ning. College Park, Md.; Univ. of Maryland (1969). 59p. University Microfilms Order No. 70-15,515.

Thesis.

A local infinite component field theory is formulated. The fields are the explicit realizations (as quantum fields) of the wave functions with mass-spin relation discussed by Bacry and Nuyts. Although the theory is trivial in that the fields are composed of an infinite stack of free fields, it serves as a simple example of an infinite component field theory with a nondegenerate mass spectrum, in which strong locality, the PCT theorem, and the spin-statistics theorem all hold. An application is made to Van Hove's model of Regge poles. It is shown that the locality requirement invalidates the reggeization via the Watson-Sommerfeld transform in Van Hove's model. (Diss. Abstr. Int., B)

12247 FINITE QUANTUM ELECTRODYNAMICS. Samuel, Mark Aaron. Rochester, N. Y.; Univ. of Rochester (1970). 101p. University Microfilms Order No. 70-17,907.

Thesis.

The question of the finiteness of quantum electrodynamics is examined from several points of view. To sixth order, one finds that there is no possibility of satisfying the eigenvalue condition $\phi(\alpha_0) = 0$ ($\alpha_0 > 0$), which is necessary for finite charge renormalization. The high k^2 behavior of the renormalized photon propagator is considered in the context of the renormalization group. One can thereby show that the coefficients in the perturbation expansion of this quantity are not all independent. In particular, in $2n^{th}$ order ($n > 1$), where n coefficients appear, there are $n - 2$ independent relations connecting these coefficients to lower-lying ones. Thus, in each order there are only 2 independent coefficients, namely the finite and the single-log terms. The leading coefficient in each order is given. The question of finite charge renormalization is further studied in the case that the domain of pure electrodynamics is enlarged to include other particles. Several models are considered. It is shown that if one includes two spin-one-half particles with unequal charge and unequal mass, the possibility of finite charge renormalization in sixth order exists. A detailed calculation is performed which indicates how strong interaction effects can enter this question. It suggests the reasonableness of the possibility that the charge renormalization may be finite only after strong interactions (and perhaps even weak interactions) are included in the theory. (Diss. Abstr.)

12248 QUANTUM FIELD THEORY WITHOUT CUTOFFS FOR SELF-INTERACTING BOSONS. Rosen, Lon Michael. New York; New York Univ. (1970). 113p. University Microfilms Order No. 70-19,026.

Thesis.

A $P(\phi)$ model in two-dimensional space-time is considered, that is, a scalar boson field with self-interaction given by an arbitrary Wick polynomial $P(\phi)$ of even degree in the field. First the hamiltonian is defined on Fock space by imposing three cutoffs: a box cutoff; an ultraviolet cutoff; and a space cutoff given by a cutoff function g(x). These are subsequently removed, yielding a quantum field theory with cutoffs. As the first two are removed the resolvents of the cutoff Hamiltonians converge uniformly and this leads to the essential self-adjointness of the spatially cutoff hamiltonian H(g). The spatially cutoff theory in Fock space is studied. For ϕ^4 and $\lambda\phi^6$ (for small λ) it is shown that H(g) is essentially self-adjoint on the set of C^∞ vectors of the free Hamiltonian and that powers of the number operator and the free Hamiltonian can be dominated by powers of H(g). The Heisenberg picture field $\phi(x,t)$ exists as a bilinear form continuous in x and t, and gives rise to a self-adjoint operator when smeared with a real function. The field equations are satisfied, and expectation values of products of the fields exist as tempered distributions. In this spatially cutoff theory, functions of the local fields are independent of g(x) provided that $g(x) = 1$ on a sufficiently large set. As the space cutoff g is removed, the Hamiltonians H(g) do not converge to an operator in Fock space. However, the vacuum expectation values converge and enable one to obtain a representation of the $P(\phi)$ theory without cutoffs on a new Hilbert space. On this physical Hilbert space the hamiltonian is a positive self-adjoint operator with a physical vacuum. (Diss. Abstr.)

12249 ASYMPTOTIC STATES IN QUANTUM ELECTRODYNAMICS. Eriksson, K.-E. (Inst. of Theoretical Physics, Goteborg). Phys. Scr.; 1: 3-12(1970).

The time evolution of a system of charged particles due to the long-range part of the Coulomb interaction and the interaction with the soft part of the transverse radiation field is studied within the frame-work of first-quantized theory of the charged particles and second-quantized theory of the electromagnetic field. States are defined which may serve as asymptotic states in a scattering theory. They differ from the free states by a phase factor (generalization of the Coulomb phase) and by the presence of a coherent soft radiation field. The time development of the phase factor and of the wave function that describes the coherent field is studied in detail and expressed in terms of elementary functions. An outline is made of an S-matrix theory based on the asymptotic states thus defined. (auth) (Sweden)

12250 RENORMALIZATION PROBLEM OF THE YANG-MILLS THEORY WITH NON-ZERO MASS: THE SPECTRAL APPROACH. Perveen, Suraiya (International Centre for Theoretical Physics, Trieste, Italy). J. Phys., A (London); 3: 625-9(Nov 1970).

By using the spectral representation the vertex operator is investigated in lowest-order perturbation theory of a massive Yang-Mills field. On examining the behavior for large momenta the nonrenormalizability of off-shell S-matrix for the massive Yang-Mills field is established. (auth) (UK)

12251 INTERPRETATION OF THE ENERGY-MOMENTUM TENSOR OF THE DIRAC FIELD WITH ANOMALOUS MAGNETIC MOMENT. Rashid, Khalid (Univ., Marburg, Ger.). Z. Phys.; 240: 342-7(1970).

An interpretation of the energy-momentum tensor is sought by splitting the tensor into its orbital and spin parts and relating the various components to the particle density. (auth)

12252 DISCRETE TRANSFORMATIONS IN SIX-DIMENSIONAL MODEL OF MINKOWSKI SPACE. Konopel'chenko, B. G. (Novosibirsk State Univ., USSR). Teor. Mat. Fiz.; 5: 366-71 (Dec 1970). (In Russian).

It is shown that the analysis of invariance properties of the massless particle equation in six-dimensional Dirac model leads to the introduction of two types of the neutrino, which may be called the plus and minus neutrino. The inversion $R\{Rx^\mu = [x^\mu/(x \cdot x)]\}$ with respect to the unit hypersphere in Minkowski space is connected closely with the reflections in six-dimensional

space. The operation K, which transforms the plus-neutrino into the minus-neutrino and vice versa, is introduced. One can suppose that the existence of the plus- and minus-neutrino is connected with the existence of the electron and muon neutrino in nature. (auth)

12253 PHYSICAL SYMMETRIES IN FIELD THEORY FRAMEWORK. Lopushinski, Ya. (Wroclaw Univ.). Teor. Mat. Fiz.; 5: 343-55(Dec 1970). (In Russian).

Earlier results are generalized to the case of many fields with arbitrary covariance properties relative to the Poincaré group. Bound states are taken into account. A number of local conserving tensor currents corresponding to physical symmetries are considered. The main result obtained consists in the proof of the assertion that free fields, which are obtained from asymptotical ones by means of symmetry transformation, are connected linearly with asymptotical fields. This assertion can be interpreted as the proof of the fact that nonlinear n-dimensional realizations of symmetry group, for which linear n-dimensional representations of this group do not exist, cannot be realized if the interaction theory possesses a mass gap. The result obtained shows the close connection between nonlinear realizations and the presence of zero-mass particles, under the condition that fields and points leave local and charges leave translational-invariant. (auth)

12254 SYSTEMES A UN NOMBRE INFINI DE DEGRES DE LIBERTE. (Systems With an Infinite Number of Degrees of Freedom). International Conference, Gif-sur-Yvette, France, 7–10 May 1969. Paris; Centre National de la Recherche Scientifique (1970). 200p. (CONF-690558).

Sixteen papers were presented at the conference. A separate abstract was prepared for four of them: model estimates and results, renormalized Hamiltonian dynamics and representations of the canonical (anti-) commutation relations, analyticity in the coupling constant, elementary examples of renormalizations and dressing transformations. (France)

For abstracts of individual papers see: 12255–12258.

12255 MODEL ESTIMATES AND RESULTS. Jaffe, A. (Harvard Univ., Cambridge, Mass.). pp 37-47 of Systemes a un Nombre Infini de Degres de Liberte. Paris; Centre National de la Recherche Scientifique (1970). (In French).

From Conference on Systems With an Infinite Number of Degrees of Freedom, Gif-sur-Yvette, France. See CONF-690558.

Some recent advances in constructing quantum field theories with interaction are described. The $(\varphi^4)2$ theory is particularly studied. (France)

12256 RENORMALIZED HAMILTONIAN DYNAMICS AND REPRESENTATIONS OF THE CANONICAL (ANTI-) COMMUTATION RELATIONS. Hepp, K. (Institut des Hautes Etudes Scientifiques, Bures-sur-Yvette, France. Eidgenoessische Technische Hochschule, Zurich). pp 49-62 of Systemes a un Nombre Infini de Degres de Liberte. Paris; Centre National de la Recherche Scientifique (1970). (In French).

From Conference on Systems With an Infinite Number of Degrees of Freedom, Gif-sur-Yvette, France. See CONF-690558.

The representations of the canonical (anti-) commutation relations which arise on the proper domain of the renormalized space cut-off Hamiltonian in quantum field theory are investigated. For theories with infinite wave function renormalizations, these representations are shown to be locally Fock in momentum space, but globally unitarily inequivalent to a direct sum of Fock representations. Quadratic Hamiltonians provide simple and completely analyzable examples for this phenomenon. (France)

12257 ANALYTICITY IN THE COUPLING CONSTANT. Wightman, A. S. (Institut des Hautes Etudes Scientifiques, Bures-sur-Yvette, France). pp 63-73 of Systemes a un Nombre Infini de Degres de Liberte. Paris; Centre National de la Recherche Scientifique (1970). (In French).

From Conference on Systems With an Infinite Number of Degrees of Freedom, Gif-sur-Yvette, France. See CONF-690558.

The analyticity and singularities in the coupling constants of the functions, characterizing a finite system, are studied. The case of the anharmonic oscillator is seen in detail. (auth)

12258 ELEMENTARY EXAMPLES OF RENORMALIZATIONS AND DRESSING TRANSFORMATIONS. Guenin, M. (Univ., Geneva). pp 105-11 of Systemes a un Nombre Infini de Degres de Liberte. Paris; Centre National de la Recherche Scientifique (1970). (In French).

From Conference on Systems With an Infinite Number of Degrees of Freedom, Gif-sur-Yvette, France. See CONF-690558.

The perturbation of a quadratic Hamiltonian by quadratic counterterms is studied. It is shown that the Hamiltonian formalism breaks down in the $\square : \Phi^2$ interaction. (auth)

12259 POINCARE COVARIANCE AND QUANTIZATION OF ZERO-MASS FIELDS. I. THE ELECTROMAGNETIC FIELD. Bertrand, J. (Institut H. Poincare, Paris). Nuovo Cim.; 1A: 1-12(1 Jan 1971).

The covariant quantization of the electromagnetic field is studied by means of a 4-vector potential, starting from the general results of Wigner on Poincaré invariance. From this sole hypothesis, it is deduced that such a quantization may only be performed using indefinite metrics and requiring the Lorentz condition (in the form given by Gupta and Bleuler) together with gauge invariance. Moreover, all the possible indefinite metrics are exhibited: they form a two-parameter family which of course includes Gupta-Bleuler's metric and they all lead to the same physically significant results. (auth)

12260 CELLULAR SPACE–TIME AND QUANTUM FIELD THEORY. Cole, E. A. B. (Univ. of Leeds, Eng.). Nuovo Cim.; 1A: 120-32(1 Jan 1971).

The cellular aspect of space-time is introduced by replacing partial differentials with respect to position and time by partial central finite differences. A modified solution of the field equations for spinless mesons is then found in terms of the annihilation and creation operators of these particles. A form of the continuous-theory divergence theorem is found for the cellular case and this is used to obtain the cellular equivalent of the continuity equation for the charge-current density. In order that this equation be satisfied it is found that the definition of the charge-current density has to be modified by adding an extra term which turns out to be of the order of the square of the cell lengths. This term is calculated exactly for the charged-meson case. (auth)

12261 SPINOR POTENTIALS WITH LOGARITHMIC REGULARIZATION. Saller, H. (Max-Planck-Institut fuer Physik und Astrophysik, Munich). Nuovo Cim.; 1A: 97-119(1 Jan 1971).

A spinor theory is formulated with spinor potentials as fundamental constituents. To avoid logarithmic inconsistencies in the self-consistency considerations of the fermion propagator the theory is modified with additional logarithmic terms for big momenta. The two sorts of boson poles are interpreted as hadronic bosons and as a photon. (auth)

12262 GAUGE-INVARIANT SPINOR THEORIES. Duerr, H. P.; Winter, N. J. (Max-Planck-Institut fuer Physik und Astrophysik, Munich). Nuovo Cim.; 70A: 467-501(21 Dec 1970).

It is demonstrated that in spinor theories with nonlinear quadratic self-interaction, gauge symmetries connected with x-dependent internal symmetry transformations can be established without the introduction of additional vector fields if the spinor field operator has the noncanonical length dimension $-\frac{1}{2}$. In this case the theory is scale invariant at small distances and hence formally renormalizable. Operator products can be defined according to prescriptions given by Zimmermann and Wilson. The usual role of the gauge fields in these spinor theories is taken over by the formally constructed vector and axial-vector "currents" of the noncanonical spinor fields which have the correct length dimension of boson operators. Physical fermion fields are related to derivatives of these spinor fields or to 3-products of these fields. The noncanonical spinor field hence may be regarded as a "spinor potential" in the sense that its relation to a physical spinor field is similar to the relation of the vector potential to the physical electromagnetic field. The unobservable "spinor potential" acts in a state space with indefinite metric. Examples for $SU_n \otimes SU_n$ gauge-invariant theories are given. The Heisenberg nonlinear spinor theory is shown to be SU_2 gauge-invariant, and hence the parity symmetry version of Dürr to be $SU_2 \otimes SU_2$ gauge-invariant. This formal invariance, however, does not necessarily imply that the symmetry holds in Hilbert space. (auth)

12263 GENERALIZED OPERATORS. Svetlichny, George (Univ. of Maryland, College Park). J. Math. Phys. (N. Y.); 11: 3433-86(Dec 1970).

A formal expression T in creation and annihilation operators (e.g., the Hamiltonian for a field theory model) is generally not a densely defined bona fide Hilbert space operator but is usually a densely defined sesquilinear form; as such it is convenient to consider it as a linear map from a dense domain Φ_- of a Hilbert space Φ_0 to a still larger space Φ_+ of antilinear functionals on Φ_-; that is, $T: \Phi_- \to \Phi_+ \supset \Phi_0$. The basis of a mathematical structure theory of such generalized operators is given. The idea which is explored is that, associated with T, there is a (not necessarily unique) analytic family R_λ of generalized operators called the resolvent of T. Formally, $R_\lambda = (\lambda - T)^{-1}$, an equation to which is given more precise interpretations. The ambiguities in determining R_λ are associated with the arbitrary adjustments that are characteristic of renormalization programs. When appropriate

XUM

conditions are met, one can construct from R_λ a new Hilbert space Ψ_0 and a bona fide operator T_R (the renormalized T) which is related to T by a formal intertwining equation $T_R\Delta = \Delta T$, where Δ maps Φ_- into a space containing Ψ_0. Given several generalized operators, a procedure is outlined by which a subset of these can be renormalized to bona fide operators while the rest are reinterpreted as new generalized operators in the new Hilbert space. These are the rudiments of a multiplicity theory. Numerous examples illustrate the methods; in particular, the $N\theta$ sector of the Lee model with arbitrary cutoff (including none) is treated in detail. (auth)

12264 PROPERTIES OF CONSERVED LOCAL CURRENTS AND SYMMETRY TRANSFORMATIONS. Maison, D.; Reeh, H. (Max-Planck-Institut fuer Physik und Astrophysik, Munich). Nuovo Cim.; 1A: 78-88(1 Jan 1971).

The connection between integrals over conserved local currents and generators of symmetry transformations is discussed. It is shown that this connection is simpler in the case of the Hamiltonian than in other cases. It is also shown that conserved symmetric-tensor currents of second rank never lead to spontaneously broken symmetries. (auth)

12265 EMPIRICAL FOUNDATIONS OF SPECIAL RELATIVITY. Breitenberger, E. (Ohio Univ., Athens. Univ., Bonn). Nuovo Cim.; 1B: 1-22(11 Jan 1971).

It is known that the Lorentz transformation can be derived from purely topological and kinematical axioms, without reference to the velocity of light or to electrodynamics. The major consequences of this approach are discussed, and some deeply ingrained ideas are found wanting. The value of the kinematical limiting velocity c_0 must be determined empirically; the usual assumption, here called the "signal postulate," identifies it with the light velocity c, but the evidence is fragmentary. The weakest link is the "second postulate" stating the independence of c from the state of motion of the source; further work is desirable under circumstances where nonelectrodynamical forces, radiative reactions and changes of source acceleration play prominent roles. The signal postulate holds if and only if c does not depend on frequency. Recent observations on the Crab Nebula pulsar, an effectively stationary flash source, have established a constancy of c in the visible region which can plausibly be interpreted as implying a photon rest mass of less than 2 MHz. However, a smaller limit may be surmised from the consistency of quantum electrodynamics as known at present; thus the pulsar work should be extended. It is also possible to determine c_0 directly; the best way seems to be a calculation from combined nuclear transmutation energies and accurate m/e values. The kinematical approach also calls for sharper verifications of the direct consequences of the Lorentz transformation, such as Doppler effect, time dilatation and Einstein addition law; any observed violation would mean a failure of the underlying assumptions about the topological nature of space and time. (auth)

12266 THIRD-ORDER CALCULATION IN A NONPOLYNOMIAL LAGRANGIAN THEORY. Sakai, Norisuke (Tokyo Univ.). Progr. Theor. Phys. (Kyoto); 44: 1068-76(Oct 1970).

The third-order Feynman amplitude is considered in a simple model of a massless scalar field. Triple contour integrations are obtained. It is shown that the amplitude decreases in certain inverse power in $(-p^2)$ in the space-like direction $p^2 \to -\infty$, but the dependence of the power on the number of external lines differs from the case of the second-order amplitude. The behavior in time-like direction $p^2 \to +\infty$ is expected to be marginally singular. Automatic quenching of the possible infrared catastrophe in nonpolynomial Lagrangian theories is also noted. (auth)

12267 ELECTROMAGNETIC INTERACTION OF A SPIN-3/2 FIELD. Dormuth, Kenneth; Takahashi, Yasushi (Univ. of Alberta, Edmonton). Progr. Theor. Phys. (Kyoto); 44: 1077-89(Oct 1970).

The formalism of hyperquantization is applied to the quantum electrodynamics of a spin $\frac{3}{2}$ field. The result is a quantized theory in which the difficulty of negative field anticommutation relations does not appear. It is explicitly demonstrated to lowest order in the perturbation expansion that the S-matrix of this theory satisfies probability conservation. (auth)

12268 POSSIBLE MODEL OF A DIVERGENCELESS NONLOCAL QUANTUM FIELD THEORY. Gallaher, D. F. (Univ. of Western Ontario, London). Progr. Theor. Phys. (Kyoto); 44: 1090-1(Oct 1970).

A connection between the construction of propagators of the type $\exp\{-[L^{*2}(K^2 - m^2)]^{2n}\}/(K^2 - m^2)$ with commutation relations generalized to violate the commutativity condition is suggested. A possible mathematical model is proposed for resolving the ultraviolet divergence difficulty. (L.B.S.)

12269 ENERGY–MOMENTUM SPECTRUM AND VACUUM EXPECTATION VALUES IN QUANTUM FIELD THEORY. Glimm, James (New York Univ., New York); Jaffe, Arthur. J. Math. Phys. (N. Y.); 11: 3335-8(Dec 1970).

Nonlinear boson self-interactions with a periodic spatial cutoff are considered. It is proven that the energy–momentum spectrum lies in the forward light cone. A momentum cutoff does not influence this result. For theories with finite-field strength renormalization, bounds are obtained on the vacuum expectation values of products of the ϕ_t's and $\nabla\phi$'s. These bounds are uniform in the volume (and possible momentum) cutoff. (auth)

Gravitation and General Relativity

Refer also to abstracts 11602, 11655. 11660, 12138, and 12159.

12270 MACH'S PRINCIPLE IN THE SCALAR TENSOR THEORY OF GRAVITY. Toton, Edward Thomas. College Park, Md.; Univ. of Maryland (1969). 108p. University Microfilms Order No. 70-15,492.

Thesis.

It is pointed out that there are two dominant themes in most formulations of Mach's principle. On the one hand the emphasis is laid on the influence of matter in determining inertial frames; on the other hand it is believed that inertia arises through the interaction of matter and, as such, should be a theoretically determinable quantity. Since both general relativity and the scalar-tensor theory entail the use of metric spaces influenced by the presence of matter, the significant differences between the theories, from the viewpoint of Mach's principle, must lie in the inertial implications. Inquiry is therefore made into whether the inertia of a body is due to the interaction with other bodies in the universe. More precisely, is its inertia zero in the absence of all other bodies? The canonical formalism as developed by Arnowitt, Deser and Misner is used because, with the assumption of flat space at "spatial infinity" it is possible to obtain a well-defined concept of inertia. From the canonical form one obtains the generators of space and time translations; when evaluated for the actual fields these give the energy and momentum of a localized system. These four quantities constitute a four-vector with respect to a Lorentz frame at infinity. The magnitude of the four-vector is of course the inertia of the system and can be evaluated in the rest frame by calculating the energy there. The scalar-tensor theory is first cast into the representation in which masses can in fact vary. From there the canonical form is obtained as well as the constraint relations from which the energy of a system can be computed. The models of a neutral point particle and a charged point particle are discussed with the result that the inertia of each of these bodies is unchanged in passing from general relativity to the scalar-tensor theory. Because of this it is concluded that, from the viewpoint of Mach's principle, the scalar-tensor theory affords no substantial improvement over general relativity. Finally, exact solutions of the Brans-Dicke equations are given for a static, spherically symmetric, charged-mass distribution, external to the source which correspond to the generalization of the Reissner– Nordstrom solution. (Diss. Abstr. Int., B)

12271 INTERACTION PICTURE FOR GRAVITY INTERACTING WITH FERMIONS. Bergere, Michel Charles Vincent. Lafayette, Ind.; Purdue Univ. (1970). 286p. University Microfilms Order No. 70-18,595.

Thesis.

The interaction between gravitons and fermions is described by a Lagrangian function of the tetrad field and of the fermion field. It is more convenient to use the tetrad field instead of the metric field to describe the interaction because of the use of tetrads in the formulation of the fermion Lagrangian density in curved space. A canonical formalism is developed defining field momenta and Hamiltonian operators on a spatial three-hypersurface. The dynamics of the system is given by the commutators of the fields and momenta with the Hamiltonian. (TS5) (Diss. Abstr. Int., B)

12272 CONVERSION OF PHOTONS INTO GRAVITONS AND VICE VERSA IN A STATIC ELECTROMAGNETIC FIELD. Boccaletti, D. (Istituto Nazionale di Fisica Nucleare, Bologna. Univ., Bologna); De Sabbata, V.; Fortini, P.; Gualdi, G. Nuovo Cim., 60B: 129-46(11 Dec 1970).

Production of gravitational waves by photons incident on a static electromagnetic field as well as the production of photons by gravitational waves incident on a static electromagnetic field are studied. The possibility of using these results for the detection of gravitational waves is also examined. (auth)

12273 SOLUTION OF PROBLEMS WITH THE DICKE THEORY. Magnon, Anne (Clermont-Ferrand Univ., France). Compt. Rend., Ser. A; 271: 1033-5(16 Nov 1970). (In French).

The problem of determinism, problems concerning regions of space with particular uniform internal space-times and singular fields, was studied in the framework of relativistic gravitational theory proposed by Dicke. (auth)

12274 CENTRIFUGAL FORCE AND GENERAL RELATIVITY. Cohen, J. M. (Inst. for Advanced Study, Princeton, N. J.); Sarill, W. J. Nature (London); 228: 849(28 Nov 1970).

Reference is made to Thirring's solution for a rotating mass shell, which is frequently used to illustrate the appearance of centrifugal and Coriolis force in general relativity. In the equations of motion of test particles within the shell terms appear that are of second order in shell angular velocity (ω). These terms are conventionally identified with "centrifugal force", but bear the relation to "Coriolis force" expected from Mach's principle. Resolution of this paradox has an important bearing on the foundations of general relativity; the extreme position was previously taken that either general relativity or Mach's principle must be abandoned. In this communication the paradox is resolved without abandoning either. Because the geometry of the shell remains spherical it was previously argued that the ω^2 terms cannot represent quadrupole terms, but it is argued that the ω^2 terms are solely quadrupole terms. The quadrupole moment arises as a consequence of the special relativistic mass increase with velocity of the shell. The mass on the equator moves faster than that on the poles. Because the ω^2 terms vanish when the quadrupole moment (in the rest frame of a distant observer) vanishes and are present when the quadrupole moment is present, it is reasonable to conclude that the ω^2 terms are quadrupole. A further indirect way in which this conclusion can be reached is discussed, showing that the ω^2 terms cannot be correctly interpreted as "centrifugal force" terms. Thus the ω^2 terms do not represent "centrifugal forces" in any sense, and Thirring's ω^2 terms are due solely to the quadrupole moment associated with the special relativistic mass increase of the shell, and there is no conflict with Mach's principle. (UK)

12275 INVESTIGATIONS INTO GRAVITATIONAL WAVES AND THE SOLUTIONS OF EINSTEIN'S EQUATIONS. Dangvu, Huyen; Dangvu-Delcarte, Claudine. Compt. Rend., Ser. A; 271: 906-8(2 Nov 1970). (In French).

It is shown that Einstein gravitational equations admit a plane wave solution. This solution is constructed. The Riemann tensor is considered as a gravitational field tensor. (France)

12276 GROUND STATE FUNCTIONAL OF THE LINEARIZED GRAVITATIONAL FIELD. Kuchar, Karel (Princeton Univ., N. J.). J. Math. Phys. (N. Y.); 11: 3322-34(Dec 1970).

The ground state functional of the linearized Einstein theory of gravitation is given as a functional of the gauge invariant Ricci tensor, and compared with the corresponding electromagnetic expression. The connection of the canonically quantized nonlinear theory of gravitation with the linearized theory is exhibited. Time is treated as a momentum variable rather than as a superspace coordinate, which leads to an "extrinsic time representation" h_{ik}^{TT}, h_i, $t = -\frac{1}{2}\Delta^{-1}\pi^T$. The state functional of the linearized theory is shown to be the initial value of the state functional of the canonical theory on a constant extrinsic time hypersurface in the lowest order of a perturbation expansion. By means of the Einstein-Schrödinger equation, this functional can be integrated off this initial hypersurface. (auth)

12277 EINSTEIN TENSOR AND 3-PARAMETER GROUPS OF ISOMETRIES WITH 2-DIMENSIONAL ORBITS. Goenner, Hubert (Temple Univ., Philadelphia); Stachel, John. J. Math. Phys. (N. Y.); 11: 3358-70(Dec 1970).

The algebraic classification of the Weyl and Ricci tensors and the relation between them in a Riemann space with an isometry group possessing a nontrivial isotropy group are reviewed. All metrics with Minkowski signature, invariant under a 3-parameter isometry group with 2-dimensional orbits having nondegenerate metrics, are constructed from the group properties and are shown to have Ricci tensors with a double eigenvalue, and the orbits are shown to be surfaces of constant curvature. The null orbits are shown to have a triply degenerate eigenvalue of the Ricci tensor. The various additionally degenerate metrics are classified in further detail, extending the work of Plebański and Stachel. (auth)

12278 SPINOR TREATMENT OF STATIONARY SPACE-TIME. Perjes, Z. (Central Research Inst. for Physics, Budapest). J. Math. Phys. (N. Y.); 11: 3383-91(Dec 1970).

A generalized SU(2) spinor calculus is established on the "background space" V_3 of the stationary space-time. The method of spin coefficients is developed in three dimensions. The stationary field equations can be put to a form which in V_3 is analogous to the Newman-Penrose equations. A V_3 filling family of curves is determined by the gravitational field and is called the eigenray congruence. Stationary space-times may be characterized by the geometric properties of eigenrays. The relation of this classification to the algebraic ones is discussed. The method of solving the equations obtainable for various classes is illustrated on the case of nonshearing geodetic eigenrays. Assuming asymptotic flatness, one obtains the Kerr metric. (auth)

12279 NEWMAN-PENROSE CONSTANTS AND THEIR INVARIANT TRANSFORMATIONS. Glass, Edward N.; Goldberg, Joshua N. (Syracuse Univ., N. Y.). J. Math. Phys. (N. Y.); 11: 3400-13(Dec 1970).

The origin and significance of the Newman-Penrose (N-P) constants of the motion are examined from the point of view that constants of the motion generate invariant transformations. The calculation makes use of a generalization of Green's theorem to a situation applicable to the coupled Einstein-Maxwell fields in general relativity. One finds strictly electromagnetic constants generated by an incoming electromagnetic shock wave, with dipole symmetry, at future null infinity. The gravitational constants contain an admixture from the electromagnetic field. They are generated by an incident quadrupole gravitational shock wave at future null infinity (J^+). Both the electromagnetic dipole field and the gravitational quadrupole field behave like linearized fields at J^+. All higher-multipole fields do not uncouple from the nonlinear corrections induced by the self-coupling of the gravitational field and its coupling with the electromagnetic field. It is shown that the gravitational constants are related to the rate of shear of the null rays near J^+ a result which suggests a connection with sources. Finally, the supertranslation invariance of the result is discussed. (auth)

12280 ARE THE NEUTRINOS AN ASPECT OF RIEMANNIAN GEOMETRY? Oektem, F. (Middle East Technical Univ., Ankara, Turkey). Nuovo Cim.; 1A: 38-48(1 Jan 1971).

Space-time with a 1-parameter holonomy group and vanishing scalar curvature is interpreted as describing the neutrinos. An algebraic condition in the curvature tensor is obtained which, for perfect holonomy groups, characterizes the 1-parameter group. Physical interest in recurrent and symmetric spaces is emphasized. (auth)

12281 NEUTRINO RADIATION IN GRAVITATIONAL FIELDS. Audretsch, J.; Graf, W. (Univ., Freiburg i. B.). Commun. Math. Phys.; 19: 315-26(1970).

A differential equation representing radiation solutions of the general relativistic Weyl equation is derived. Their optical properties and the group of motion of the corresponding energy-momentum tensor are studied. If there exists neutrino radiation the Riemann space must be algebraically special and the propagation of the neutrinos occurs only along one of the principal null directions. Gravitational- and neutrino pp-waves taken together represent an exact solution of the Weyl-Einstein system of field equations. (auth)

12282 EVENT HORIZONS IN STATIC SCALAR-VACUUM SPACE-TIMES. Chase, J. E. (Univ. of Alberta, Edmonton). Commun. Math. Phys.; 19: 276-88(1970).

The following theorem is established. Every zero-mass scalar field which is gravitationally coupled, static and asymptotically flat, becomes singular at a simply connected event horizon. In the special case where the gravitational coupling of the scalar energy density is neglected, the solutions are computed explicitly. Some properties of the singular event horizons are discussed, and a brief mention of related work with nonstatic scalar fields is given. (auth)

12283 GRAVITATIONAL FIELD OF A MASSLESS PARTICLE. Aichelburg, P. C.; Sexl, R. U. (Univ., Vienna). Lett. Nuovo Cim.; 4: 1316-18(26 Dec 1970).

The gravitational field produced by a single photon (more precisely the field of a point particle moving with the velocity of light) is given. To obtain this metric the Schwarzschild solution is used, and to it is applied a Lorentz transformation. As the velocity tends to 1, the rest mass is allowed to approach zero in such a way that the energy of the particle remains finite. The result is that the gravitational field of the particle is nonvanishing only on a plane containing the particle and orthogonal to the direction of motion. On this hypersurface the Riemann tensor has a δ-like singularity. It is also pointed out that for this particular problem the linearized and the full Einstein equations give the same result. (J.F.P.)

12284 MATHEMATICAL PROBLEMS OF THE RELATIVISTIC BOLTZMAN EQUATION. Pichon, G. (Faculte des Sciences, Orleans, France). Commun. Math. Phys.; 19: 189-203(1970). (In French).

XUM

The relativistic Boltzmann equation and more particularly the integral operator of the complete equation and the integral operator of linearized equation are considered. These operators depend on the differential cross section $h(\langle p,q\rangle, \cos\theta)$ which is a function of energy $\langle p,q\rangle$ and of the deviation angle θ. The only hypothesis is that h is a symmetric function of $\cos\theta$. The linearized equation in special relativity is considered. For the distribution function: $F(x,p) = ae^{-\lambda p/2}[e^{-\lambda p/2} + \epsilon f(x,p)]$ is taken where a is a constant, λ a constant vector and ϵ a small constant so that ϵ^2 can be neglected. The equation $[(p^\alpha/p^0)(\partial f/\partial x^\alpha)] = -K(p) \cdot f + G(f)$ is obtained where K(p) is a positive function and G a Hilbert–Schmidt operator. Then Cauchy's problem is resolved by taking the Fourier's transformation of f, and by investigating properties of the resolvent of $-K + G$. It is established that as $x^0 \to +\infty$ the solution of this problem has for limit the equilibrium distribution $ae^{-\lambda p}$. (auth)

12285 CLASSIFICATION OF THE CURVATURE TENSOR BY MEANS OF PRINCIPAL CONGRUENCES. Polishchuk, R. F. Dokl. Akad. Nauk SSSR; 194: 62-5(Sep-Oct 1970). (In Russian).

The Petrov type curvature tensor of a V_4 Riemann space is classified algebraically on the basis of canonic ortho-references. Such a classification of the canonical or principal tensor vectors may be derived not only for a given point but for the finite V_4 range. Division by a suitable counting system of the tensor to be classified is used for this purpose. The counting system is defined according to A. L. Zel'manov as the congruence of the time-like lines; it is determined by the field of the intersecting vector which divides the curvature tensor into three chronometrically invariant incomplete χ tensors. The principal congruence simplifies the geometric description of the V_4 range with the physical interpretation requires the derivation of an unequivocally determinable canonical counting system. The existence of a separate counting system is required by the general theory of relativity on the basis of the inhomogeneity of the curvature of space. It was confirmed that the tensor of dually asymmetric spaces becomes zero if and only if the dividing vector is specific for the Ricci tensor. (TTT)

Scattering Theory

Refer also to abstracts 12178, 12189, 12249, and 12673.

12286 FEYNMAN PATH INTEGRALS AND SCATTERING THEORY. Gelman, Donald. New York; New York Univ. (1969). 109p. University Microfilms Order No. 70-16,063.

Thesis.

The Feynman path integral formulation of nonrelativistic quantum mechanics is applied to scattering theory. A particularly appealing result of Feynman's is a variational upper bound (VUB) on the ground state energy, with the bound expressed in terms of path integrals containing a trial functional $\tilde{S}$. When $\tilde{S}$ is of the standard form $\int \{(KE) + \tilde{V}\}\, dt/\hbar$, with KE the kinetic energy and $\tilde{V}$ a trial potential, the bound reduces to the Rayleigh-Ritz result. Since $\tilde{S}$ need not be of that form, Feynman's result has interesting new possibilities. For central potentials, Feynman's analysis is extended to the subspace $\mathfrak{H}^{(L)}$ of states of a given angular momentum L, obtaining a VUB on the energy of the lowest energy bound state within $\mathfrak{H}^{(L)}$. By exploiting the analogy between the lowest energy bound state and the zero energy scattering state in the no bound state case, a VUB on A_L is obtained, the parameter which characterizes low energy scattering in $\mathfrak{H}^{(L)}$. The bound on A_L is expressed in terms of modified path integrals containing a trial functional $\tilde{S}_L$, and it reduces to the usual result if and only if $\tilde{S}_L$ is of the standard form $\int \{(KE)_L + \tilde{V}\}\, dt/\hbar$, where $(KE)_L$ is the kinetic energy corresponding to motion with fixed angular momentum $\{L(L+1)\hbar^2\}^{1/2}$. The bound therefore contains new features. Finally, a similar but much simpler bound on A_L is derived by using the regularization $\mathrm{Tr}\{\exp(-\beta H_L) - \exp(-\beta H_L^0)\}$ of the divergent function $\mathrm{Tr}\exp(-\beta H_L)$, with Tr the trace, H_L^0 the (reduced) free particle Hamiltonian in $\mathfrak{H}^{(L)}$, and $H_L = H_L^0 + \tilde{V}$. (Diss. Abstr. Int., B)

12287 RELATION BETWEEN THE THIRD VIRIAL COEFFICIENT AND THE SCATTERING MATRICES. Buslaev, V. S.; Merkur'ev, S. P. (Leningrad State Univ.). Teor. Mat. Fiz.; 5: 372-87(Dec 1970). (In Russian).

The connection between the third virial coefficient and the scattering matrices of two- and three-particle systems is established. (auth)

12288 ON THE α-REPRESENTATION OF FEYNMAN INTEGRALS. Stepanov, B. M. (Inst. of Mathematics, Moscow). Teor. Mat. Fiz.; 5: 356-65(Dec 1970). (In Russian).

Graph theory is used for the rigorous proof of an explicit formula for the integral over internal momenta in the α-representation of Feynman integral. The formula is perfectly symmetric with respect to the choice of a tree in the graph. (auth)

12289 TWO-PARTICLE UNITARITY IN THE ITERATED REGGE-CUT MODEL. Mason, A. L. (Cambridge Univ., Eng.). Nuovo Cim.; 70A: 453-66(21 Dec 1970).

The iterated cut model of Landshoff and Polkinghorne is generalized to allow external particles with spin, and it is verified that certain consequences of unitarity are satisfied. (auth)

12290 S MATRIX IN THE HEISENBERG REPRESENTATION. Borie, Edith (Univ. of North Carolina, Chapel Hill). J. Math. Phys. (N. Y.); 11: 3487-96(Dec 1970).

The elements of the S matrix are calculated directly from an operator formalism, using the method of Yang and Feldman. This method has the advantage of providing a simple and direct justification of the Feynman rules for gauge fields, which express the contribution to the S matrix from a diagram containing closed loops in terms of sums over lowest-order physical amplitudes (tree amplitudes) in which all external lines are on the mass shell and have physical polarizations. This guarantees unitarity. A condensed notation due to DeWitt is used. First, the one- and two-loop contributions to the amplitude for production of a single quantum, and the amplitudes for pair production and scattering of a single particle by a classical background field are calculated in the absence of an invariance group. Noncausal chains (loops of cylically connected advanced or retarded Green's functions) never appear at any stage of the calculation, thus giving the decomposition into sums over tree amplitudes directly. This result is then generalized in an obvious way to the case in which an invariance group is present. The amplitudes are expressed in terms of a noncovariant propagator which propagates only physical (transverse) quanta. Rewriting these expressions in terms of covariant propagators leads to the formal appearance of "fictitious quanta," which compensate the nonphysical modes carried by these propagators. All results are in agreement with those obtained by other methods. (auth)

12291 COMMENTS ON THE PROBLEM OF RISING TRAJECTORIES AND SINGULAR POTENTIALS. Watt, C. S.; Brown, D. J. (Carleton Univ., Ottawa). Lett. Nuovo Cim.; 4: 1298-1300(26 Dec 1970).

In previous work an attempt was made to investigate the nature of the Regge trajectories arising from potentials singular at the origin. The results indicated that potentials of the form g^2r^{-n} $(n > 3)$ yielded indefinitely rising trajectories. It is found that these results are apparently not justified within the framework of the model used. (J.F.P.)

12292 GENERAL THEOREMS ON FACTORIZATION. Benayoun, M.; Leruste, Ph. (College de France, Paris). Lett. Nuovo Cim.; 4: 1305-8(26 Dec 1970).

It is proven that several previous results in scattering theory can be obtained through a general fratorization theorem which deals with the whole principal part of the S- (or T-) matrix Laurent expansion in the neighborhood of a pole of any order. (J.F.P.)

12293 SOME PHYSICAL REGION MASS SHELL PROPERTIES OF RENORMALIZED FEYNMAN INTEGRALS. Chandler, Colston (Eidgenoessische Technische Hochschule, Zurich). Commun. Math. Phys.; 19: 169-88(1970).

Certain properties proved in S-matrix theory on the basis of macroscopic causality are verified for renormalized Feynman integrals. The technique uses the analytic renormalization of Speer and a specific distortion of the contour of integration. It is proved for an arbitrary Feynman graph G that the corresponding renormalized Feynman integral is holomorphic in the (mass shell) physical region except on the positive-α Landau surface $\mathfrak{L}^+\{G\}$. Under a certain assumption about the geometry of $\mathfrak{L}^+\{G\}$ an "$i\epsilon$-prescription" is constructed for continuing (in the mass shell) around $\mathfrak{L}^+\{G\}$. The difficulties involved in removing this assumption are discussed. (auth)

12294 SOME DISTRIBUTION THEORETIC ASPECTS OF CURRENT ALGEBRA. Otterson, Paul James. College Park, Md.; Univ. of Maryland (1970). 133p. University Microfilms Order No. 70-23,309.

Thesis.

The role of Schwinger terms in the derivation of sum rules and asymptotic limits of scattering amplitudes is studied. New methods for obtaining equal-time limits of current commutators from spectral representations are derived and examples given. These methods are used to derive Schwinger terms in perturbation theory. Particular care is taken in making precise definitions—e.g., LSZ equal-time terms and Schwinger terms are carefully distinguished. It is shown that: the usual current algebra calculations may be generalized to apply when Schwinger terms are present, ambigui-

ties inherent in such calculations may be resolved by demanding consistency with the Feynman rules. Finally, it is shown that, as an alternative to the use of spectral representations, commutator identities such as [AB,C] = A[B,C] + [A,C]B may be used to obtain Schwinger terms. (Diss. Abstr. Int., B)

Particle Accelerators

Refer also to abstracts 10824, 10861, 10863, and 12156.

12295 (BNL–15438) PARTICLE SEPARATION IN A SYSTEM OF CONVENTIONAL IRIS-LOADED DEFLECTORS INTERSPERSED WITH ALTERNATE GRADIENT MAGNETS. Lazarus, D. (Brookhaven National Lab., Upton, N. Y.). 12 Nov 1970. 26p. Dep. NTIS.

A long-pulse, room-temperature rf separator based on a series of conventional S-band iris-loaded deflectors with magnets of a strong focusing channel between them is considered. A calculation of particle motion in such a system has been carried out which is exact except for aberrations whose effect on the results is shown to be negligible. Performance parameters and particle fluxes are given for separators designed for the 1 to 5 GeV/c and 5 to 15 GeV/c ranges. Implications for purified beams for counter and spark chamber experiments are discussed. (auth)

12296 (BNL–15464) ECONOMICAL BEAM TRANSPORT FOR UTILIZATION OF THE POST CONVERSION AGS. Allinger, J. E.; Danby, G. T.; Jackson, J. W.; Smith, L. W. (Brookhaven National Lab., Upton, N. Y.). 8 Dec 1970. 70p. Dep. NTIS.

Conclusions and recommendations from a study on the design and installation of a new external beam transport system to effectively utilize the forthcoming beam intensity gain (a factor of 10 gain) of the Brookhaven AGS are presented. Topics discussed include a review of some simple scaling laws on magnet sizes and strengths; some implications for optical properties due to variations of magnet strengths, lengths, and aperture sizes; cryogenic technology and beam transport; cost and performance criteria; power supply and facility costs; quadrupole magnet costs and parameters; dipole magnet costs and parameters; and parameter and cost curves. (W.H.K.)

12297 (CEA-N–1389) DIGITAL MEASUREMENT OF THE PEAK CURRENT IN A LINEAR ELECTRON ACCELERATOR. Gourcy, Georges (Commissariat a l'Energie Atomique, Saclay (France). Centre d'Etudes Nucleaires). Dec 1970. 40p. (In French). Dep. NTIS (U. S. Sales Only).

In a linear electron accelerator, peak current values can be obtained from the peak voltage generated by an appropriate electron beam monitoring system. A target type monitor intercepts the electron beam whereas a ferrite type monitor does not affect the beam. A toroidal ferrite monitoring system and its associated digital equipment is described. It is shown that such a system is more accurate and reliable than the usual standard oscilloscope methods. Moreover, this system allows simultaneously the direct reading in current units, the recording in analog form and the sequential recording in digital form. (France)

12298 (CERN-Trans–70-7) COLLECTIVE EFFECTS IN ACCELERATORS. Kolomenskii, A. A.; Lebedev, A. N. Translated by O. Barbalat (CERN, Geneva, Switzerland), from pp 261–73 of the National Particle Accelerator Conference, Moscow, 9–16 October 1968, Vol. 2. 26p. (In French). (CONF-681029–4). Dep. NTIS (U. S. Sales Only).

A systematic description is given of collective effects in accelerator beams. The material reviewed is divided into effects relative to longitudinal and transverse motion. Included in the discussion are static equilibrium, Coulomb, and resonator effects, resistive instabilities, synchrotron radiation, and space-charge effects. (J.F.P.)

12299 (IPP–7/2) CALCULATION OF THE ION-TRAJECTORIES IN FRONT OF A FIELD EMISSION TIP. Vernickel, H.; Welter, H. (Institut fuer Plasmaphysik, G.m.b.H., Garching (West Germany)). Jun 1970. 26p. (In German). (CONF-690968–1; IPP–6/88). Dep. NTIS (U. S. Sales Only).

From 16th Field-Emission Symposium, Pittsburgh, Pa.

The equations of motion of the ions produced by ionization of the gas between tip and screen of a field-emission microscope have been numerically integrated for two tip geometries (drop-like and rounded-off cone). Based on these results, the ion-current density and the energy distribution of the ions impinging on the tip were calculated. Results: all ions hitting the imaged part of the tip originate within a small "pencil" around the emitter axis; the maximum of the energy distribution is, depending on tip geometry, between 0.03 and 0.2 of the energy corresponding to the voltage between anode and tip. (auth)

12300 (JINR–P8-5212) PRECISION APPARATUS WITH LIQUID HYDROGEN TARGET. Borzunov, Yu. T.; Golovanov, L. B.; Mazarskii, V. L.; Tsvinev, A. P. (Joint Inst. for Nuclear Research, Dubna (USSR). Lab. of High Energy). 1970. 17p. (In Russian). Dep. NTIS (U.S. Sales Only).

Liquid hydrogen targets are used to determine the total cross section of interaction on the basis of the absorption of particles emitted by an accelerator. The precision of the measurements depends on the exact determination of the amount of hydrogen in the path of the particles. An installation was built to confine the liquid hydrogen with a precision of 0.05%. It consisted of 2 targets, one of which was filled with liquid hydrogen while the empty one was used for measuring the background. The operating target was refilled by gravity flow by means of a 50-liter storage tank. A mobile support made it possible to place the system in the path of the beam. The 50-liter tank ensured continuous operation of the system for about 50 hours. The valves, measurement and control devices and auxiliary equipment were located at the panel, using siphons for interconnection. The actual target consisted of an internal cylindrical container, covered with multilayered insulation and a vacuum housing, and kept at a pressure of 1×10^5 mm of Hg. Steps were taken to prevent interference by bubbles from the boiling hydrogen and to keep the pressure constant. Special windows were provided to reduce the amount of foreign matter in the path of the beam. (TTT)

12301 (JINR–P9-5394) MOTION OF THE CHARGED ELECTION RING IN THE RIPPLE MAGNETIC FIELD. Reshetnikova, K. A. (Joint Inst. for Nuclear Research, Dubna (USSR)). 1970. 17p. (In Russian). Dep. NTIS (U. S. Sales Only).

The effect of the fields, appearing when the charged electron ring passes through the ripple magnetic field, on the motion of electrons inside the ring is considered. (auth)

12302 (JINR–P9-5405) CALCULATION OF THE PHASE VOLUME OF THE ELECTRON–ION BUNCHES IN THE COLLECTIVE ACCELERATOR AND THE PROBLEMS OF SEPARATION. Iovnovich, M. L.; Rubin, N. B.; Sarantsev, V. P. (Joint Inst. for Nuclear Research, Dubna (USSR)). 1970. 8p. (In Russian). Dep. NTIS (U. S. Sales Only).

Motion of protons in the plane of the charged ring, accelerated up to high energies, is investigated. The proton phase volume is calculated. Separation of high energy secondary particles is considered. (auth)

12303 (JINR–P9-5442) ACCELERATION AND EXTRACTION OF THE DEUTERONS FROM THE JINR PROTON SYNCHROTRON. Baldin, A. M.; Beznogikh, Yu. D.; Zinov'ev, L. P.; Issinskii, I. B.; Kazanskii, G. S.; Mikhailov, A. I.; Moroz, V. I.; Pavlov, N. I.; Puchkov, G. P. (Joint Inst. for Nuclear Research, Dubna (USSR)). 1970. 8p. (In Russian). Dep. NTIS (U. S. Sales Only).

In August 1970 the works were completed on improvement of the linear accelerator and high-frequency systems of the JINR PS which allowed the previously suggested regime of deuteron acceleration at momentum of 11 GeV/c to be realized. The accelerated deuteron beam has been extracted from PS and physical experiments were started. (auth)

12304 (JINR–P9-5446) METHOD FOR PULSED POLARIZED ION BEAM PRODUCTION FOR HIGH-ENERGY ACCELERATORS. Donets, E. D.; Plis, Yu. A. (Joint Inst. for Nuclear Research, Dubna (USSR)). 1970. 9p. (In Russian). Dep. NTIS (U. S. Sales Only).

A method for the atomic beam ionization with the storage of polarized ions in the electron beam and their pulsed extraction during the capture time of the accelerator is proposed. It is shown that a confined charge is equal approximately to 2×10^{11} ions for the ionizer 20 cm long. Estimates for the phasotron with spatial variation of the magnetic field, designed in the Laboratory of Nuclear Problems, show that the external polarized proton beam will be equal approximately to 0.5 μ A, which is 400 times the value for the polarized proton beam produced by the scattering at the target. (auth)

12305 (JINR–P9-5558) EXPERIMENTS ON α-PARTICLE ACCELERATION BY THE COLLECTIVE METHOD. Sarantsev, V. P.; Rashevskii, V. P.; Kaminskii, A. K.; Mironov, V. I.; Fartushnyi, V. P.; Sergeev, A. P.; Novikov, V. G.; Tyutyunnikov, S. I.; Kaminskaya, A. M. (Joint Inst. for Nuclear Research, Dubna (USSR)). 1971. 13p. (In Russian). Dep. NTIS (U.S. Sales Only).

The results of experiments on α-particle acceleration by the collective method in the adgesator model and the technique of α-particle detection are presented. (auth)

XUM

12306 (KFK-tr-334) INFLUENCE OF THE RADIAL SLOTS IN THE IRIS DISK OF A WAVEGUIDE ON THE DISPERSION PROPERTIES AND THE QUALITY FACTOR OF A SYSTEM OF AXIALLY-SYMMETRIC AND NONAXIALLY-SYMMETRIC WAVES. Kramskoi, G. D.; Zykov, A. I.; Kolot, Z. M. (Akademiya Nauk Ukrainskoi SSR, Kharkov. Fiziko-Tekhnicheskii Institut). Translated by Rosemarie Corssen (Kernforschungszentrum, Karlsruhe, Ger.), from report KHFTI-69-24. 10p. (In German). Dep. CFSTI (U. S. Sales Only).

On the basis of the data determined for the quality factor and the group velocity of the highest modes EH_{11} and EH_{12}, the dependence of their damping coefficients on the length and type of the radial slits can be established. The geometry of the radial slits in the iris disk of the accelerator wave guide can also be selected on the basis of these data. (tr-auth)

12307 (KHFTI-69-27) RESEARCH ON THE 100-MeV ELECTRON STORAGE RING OF THE TECHNICAL PHYSICS INSTITUTE OF THE UKRAINIAN ACADEMY OF SCIENCES. Grigor'ev, Yu. N.; Grishaev, I. A.; Koba, I. I.; Kononenko, S. G.; Mocheshnikov, N. I.; Reprintsev, L. V.; Tarasenko, A. S.; Terekhov, B. A.; Shenderovich, A. M. (Akademiya Nauk Ukrainskoi SSR, Kharkov. Fiziko-Tekhnicheskii Institut). 1969. 9p. (In Russian). Dep. CFSTI (U. S. Sales Only).

Studies of low-intensity beam parameters were carried out; the longitudinal motion of particles under various conditions was investigated; and experiments were begun on a beam of synchrotron radiation. The basic parameters of the storage ring are as follows: (1) particle energy of 100 MeV, (2) radius of curvature of the equilibrium orbit R = 50 cm, (3) lengths of rectangular intervals L_1 = 50 cm and L_2 = 80 cm, (4) index of the fall in field η = 0.17 to 0.37, (5) frequency of the radial betatron oscillations ν_z = 1.143 to 1.213, (6) frequency of vertical betatron oscillations ν_z = 0.62 to 0.72, (7) amplitude of high-frequency field V = 50 to 1000 volts, (8) frequency of high-frequency field equal to 52.25 megacycles per second, (9) parameters characterizing the non-linearity of the magnetic field of about ±0.01 I/cm, and (10) a Q-factor of the accelerating system of about 20. The radial dimensions of the beam are given as a function of the electron energy. Data are given to characterize the effect of resonances on the life time of the beam. The most dangerous resonances were those with $\nu_z = 3/4$ and $\nu_z = 5/4$. It is shown that phase dampening takes place much faster, and energy dampening takes place slower than at small oscillations. Interferometer experiments show the presence of interference in synchrotron radiation. (TTT)

12308 (LAL-RT-5-70) BEAM-BEAM EFFECT. THE POTENTIAL IN A BI-GAUSSIAN BEAM. Buffet, X.; Potaux, D. (Paris Univ., Orsay (France). Laboratoire de l'Accelerateur Lineaire). 13 Feb 1970. 12p. (In French). Dep. NTIS (U. S. Sales Only).

An infinitely long beam of uniform density in the direction of the azimuth and of bi-gaussian charge distribution in the transverse plane is considered. The potential produced is calculated from the Poisson equation. (France)

12309 (LYCEN-6909) STUDY AND DEVELOPMENT OF A SOURCE OF POLARIZED DEUTERONS FOR A SYNCHROCYCLOTRON, ITS APPLICATION IN ELASTIC SCATTERING. Kouloumdjian, Jacques (Lyon Univ. (France). Institut de Physique Nucleaire). Mar 1969. 91p. (In French). Dep. NTIS (U. S. Sales Only).

Thesis.

A source of polarized deuterons adapted for a synchrocyclotron was constructed. The theoretical aspects of polarization, polarization method for a deuteron beam, the construction of a polarized deuteron source, and the adaptation of the source for synchrocyclotron measurements, were discussed. Experimental results were also obtained using the deuteron source for the asymmetries appearing in deuteron elastic scattering on carbon-12, silicon-28, and calcium-40 at 28 MeV. The results were analyzed using the optical model. (J.F.P.)

12310 (NP-18612) PARTICLE DYNAMICS IN THE ORSAY HEAVY-ION LINEAR ACCELERATOR, ALICE: FOCUSING AND ACCELERATION. Goldstein, Charles (Paris Univ., Orsay (France)). 1970. 107p. (In French). Dep. NTIS (U. S. Sales Only).

Thesis.

The work done at Saclay using the heavy ion linear accelerator in conjunction with the ALICE project is presented. The geometrical characteristics of the accelerator and its grid focusing system were determined using the method of calculation of Smith and Gluckstern already applied to the Berkeley grid. The limiting factors in the calculation are indicated. The technological parameters of the Orsay grid are defined: temperature and transparence. The tests carried out on the mock-up are described. The program concerning the dynamics of the particles, which explains the characteristics of the extracted beam, is described. Using measurements of potential made in the electrolytic tank, the assembly of electric fields of the accelerator was simulated and the motion of the particles studied by integrating their equations of motion using the Runge Kutta method. The electric field was measured in two planes of symmetry and the calculations made in only one plane. The MORAD program developed for this study is presented. Measurements made on the characteristics of the beam confirm calculations and the possibility of making significant improvements to the injector characteristics: output and overall yield. (France)

12311 LONGITUDINAL INSTABILITIES IN ANNULAR CHARGED BEAMS. II. RADIATION INSTABILITY. Bonch-Osmolovskii, A. G.; Perel'shtein, E. A. Izv. Vyssh. Ucheb. Zaved., Radiofiz.; 13: 1089-95(1970). (In Russian).

The azimuthal instability associated with coherent synchrotron radiation is studied for the beam of relativistic particles rotating in the magnetic field inside a metal tube. Expressions are derived for the increments at different energy distribution functions of the beam for variable distances from the camera wall. It is shown that the thermal spread in the beam decreases the increments of instability and far from the camera wall (transition to the free space) leads to stopping the instability due to Landau damping. (auth)

12312 LONGITUDINAL INSTABILITIES IN ANNULAR CHARGED BEAMS. I. THE NEGATIVE MASS EFFECT. Bonch-Osmolovskii, A. G.; Perel'shtein, E. A. Izv. Vyssh. Ucheb. Zaved., Radiofiz.; 13: 1080-8(1970). (In Russian).

A longitudinal instability of a thin ring of electrons rotating in the magnetic field inside a perfectly conducting metal tube is analyzed. In the frames of a self-consistent problem a general dispersion equation is derived for oscillations of the beam density, which is analysed for the case when the conditions of radiation of transverse wave are not satisfied. The instability of the negative mass occurs near the wall for a thin ring of monoenergetic electrons both in nonrelativistic and relativistic cases. In the ultra-relativistic case, the instability stopping in the E-region, however, the instability increments for the ring are considerably less. Far from the wall there takes place the sequence of bands of the negative mass instability in the vicinity of the camera resonance lines. (auth)

12313 PROTON CURRENTS THAT MAY BE OBTAINED WITH HIGH EQUILIBRIUM PHASES IN A LINEAR ACCELERATOR WITHOUT PARTICLE LOSSES. Vlasov, A. D. At. Energ. (USSR); 29: 141-3(Aug 1970). (In Russian).

Action of the specific charge of the accelerating clusters which limits the proton current in a linear accelerator has been estimated in an earlier study. The author has attempted to estimate the maximum attainable current without particle losses. In the present work, earlier results which were derived for only small phases were generalized for any equilibrium phase between 0 and 90° using a nonrelativistic approximation method. The results indicated that increase of the equilibrium phase allows to increase considerably the currents which may be obtained in the case of neutral equilibrium of the clusters at the beginning of the acceleration. Specific numerical examples are presented for the Serpukhov I-100 accelerator and the I-2 accelerator of the Institute for Theoretical and Experimental Physics. Increase of the equilibrium phase is probably related to the corresponding elongation of the initial portion of the accelerator or with the increase of the amplitude of the accelerating field. (TTT)

12314 SHIELDING AGAINST HIGH ENERGY RADIATIONS PRODUCED BY A 30 MeV LINEAR ACCELERATOR AT HIROSHIMA UNIVERSITY. Takeshita, Kenji; Antoku, Shigetoshi; Sunayashiki, Tadashi (Hiroshima Univ.). Proc. Res. Inst. Nucl. Med. Biol.; No. 11, 27-34(1970). (In Japanese).

A 30 MeV NEC-Varian linear accelerator is being used in biological studies of extremely high intensity radiations and for radiation therapy. To shield high energy x-rays and neutrons from photodisintegration reactions, the room housing the linear accelerator is located below ground. By theoretical calculation, stray radiations outside the building are well within the maximum permissible dose according to Japanese regulations and the International Commission on Radiological Protection. This was confirmed by measurements of stray radiation using survey meters. However, considerable induced radioactivity in the exposure room was detected immediately after irradiation. This emphasizes the necessity of monitor systems and restrictions of working time of personnel after exposure. The accelerator is briefly described. (auth)

12315 LINEINYE USKORITELI ELEKTRONOV S INTENSIVNYMI PUCHKAMI (FIZICHESKIE OSNOVY TEORII). (Linear Electron Accelerators with Intense Beams (Physical Principles of the Theory)). Burshtein, E. L.; Voskresenskii, G. V. Moscow; Atomizdat (1970). 192p.

The characteristics of high-current electron linear accelerators are studied. These characteristics are affected by the self-field of the electron beam and are dependent upon increases in current and acceleration energy. Field calculations in complex waveguide structures are considered. Beam loading in high-current accelerators is discussed. Beam instability and methods of suppression of the instability are also considered. (tr-auth)

12316 PRESSED BORIDE CATHODES. Wolski, W. (Royal Inst. of Tech., Stockholm). Elektronika; No. 4, 149-55(1970). (In Polish).

The results of the examinations of boride emission cathodes from LaB_6, YB_6 and GdB_6 for electron accelerators are presented. The technology was based on the hot pressing in vacuum. The stability of the obtained cathodes is characterized. (auth)

12317 STUDY OF RADIATION PRODUCED BY HIGH-ENERGY ELECTRONS IN A DISK-LOADED WAVEGUIDE. Mahaffey, William Raymond. University, Ala.; Univ. of Alabama (1970). 46p. University Microfilms Order No. 70-17,941.

Thesis.

Results are presented for the radiation emitted when a fast beam is in close synchronism with the fundamental azimuthally symmetric space harmonic. The effects of beam velocity and diameter are illustrated. (auth)

12318 METHOD OF LOCALIZED IRRADIATION OF MATERIAL BY LOW ENERGY OR SHORT RANGE CHARGED PARTICLES. Chuang, L. S. (Chinese Univ., Hong Kong). Health Phys.; 19: 439-42(Sep 1970).

A 4.23 MeV Van de Graaff positive-ion accelerator was used to separately accelerate triton beams and singly charged ^3He beams to energies ranging from 1 to 3.5 MeV. The inside dimensions of the scattering chamber used are given. The scattering gas in this experiment was a mixture of ^4He and air, with the air forming a small fraction of the total gas pressure of 10 mm of Hg. Recoil nuclei could be eliminated to obtain irradiating particles with a monoenergetic component. Typical examples of the energy spectra for $T-^4He$ and $^3He-^4He$ scattering are shown graphically. The attainable dosages were computed from the component peaks of the energy spectra and the detector counts. The dosages were about 10^{-3} to 10 rad. for T^+ and 1 to 10^4 rad. for $^3He^+$ with a mean beam current of about 10^{-3} to μA. Typical energy spectra for $^3He-^{14}N$ (air) scattering are shown. In the irradiation of living biological specimens, air is the scattering medium and as Rutherford scattering is predominant the number of detector counts can be calculated without actual measurement. Difficulties in accurate dosage calculation are considered. (UK)

12319 ENERGY DISTRIBUTION OF FAST ELECTRONS PRESENT IN BEAMS FROM HOLLOW-ANODE GAS DISCHARGE ELECTRON GUNS. Allen, W. D.; Hale, D. P. (Univ. of Reading, Eng.). J. Phys., D (London); 3: 1912-18(Dec 1970).

Energy distributions of electrons in beams from hollow-anode gas discharge electron guns were determined for electron flight paths of 0.1, 0.3 and 0.6 m. Guns were operated at potentials between 5 kV and 20 kV in hydrogen, helium, oxygen, air, nitrogen and argon at pressures in the approximate range 10 to 100 $\underline{N}\ m^{-2}$. A typical spectrum obtained has a sharp peak at an energy equivalent to that achieved by electrons accelerated to the full cathode potential. A second peak of amplitude 0.05 to 0.5 times the primary peak amplitude occurs at an energy lower by approximately one ionization potential. This secondary peak is broader, the amplitude falling to approximately zero within an energy range of about 100 eV. (auth) (UK)

12320 NEUTRON RADIATION PRODUCED BY THE 32 MeV ROENTGEN BEAM OF A MEDICAL BETATRON. Loefgren, Kaj-Erik; Spring, Erik (University Central Hospital, Helsinki). Acta Radiol., Ther., Phys., Biol.; 9: 247-56(Jun 1970).

Solid state track detectors, consisting of 1 per cent uranium soda-lime-silica glass, have been used for investigation of the neutron fluence and the corresponding neutron doses and dose equivalents inside, outside and in the neighborhood of the roentgen beam of the medical betatron. (auth) (Sweden)

12321 DETECTOR SENSITIVITY FOR MEASURING ELECTRON CURRENT IN A BETATRON. Sokolov, O. V.; Chastokolenko, B. L. (Tomsk Polytechnic Inst., USSR). Izv. Vyssh. Ucheb. Zaved., Fiz.; No. 9, 106-10(1970). (In Russian).

Results are given of the calibration of detector (magnetic belt, acceleration chamber loops, and electrostatic electrode signals) designed for measuring the current circulating in the acceleration chamber of the 15-MeV betatron at various phases of acceleration. The calibration was taken during accelerator operation considering the current of electrons during a single rotation cycle. Measurements of electron current captured by the loops in the chamber by means of electrostatic electron dumping are described. Aspects of the detector use during betatron adjustment are discussed. (tr-auth)

12322 TRAJECTORIES OF CHARGED PARTICLES IN MAGNETIC FRINGE FIELDS. Bosi, G. (Univ. of Moncton, New Brunswick, Can.). J. Phys., D (London); 3: 1925-30(Dec 1970).

A generalized treatment of the influence of magnetic fringe fields on particle trajectories is proposed. The behavior of the real field is compared with the ideal field, whose boundary is assumed to be curved. The position and shape of the virtual boundary are thus determined to simplify the resulting formulas. Third-order effects are disregarded. (auth) (UK)

12323 FIELD HARMONIC ANALYSIS OF SHORT, CURRENT-DOMINATED, BEAM TRANSPORT MAGNETS. Goodman, B. B. (BOC Ltd., London). Nucl. Instrum. Methods; 89: 9-12(1970).

The theory of long, current-dominated, beam transport magnets is generalized to include the case of short magnets for which end effects are important. It is shown that the effect of a current-dominated beam transport magnet on a high momentum charged particle beam is conveniently characterized by a complex "parallel trajectory field integral" whose real and imaginary parts are the integrals of the transverse components of the magnetic field along a trajectory parallel to the axis of the magnet. This function is an analytic function of the position of the intersection of the parallel trajectory with the complex plane normal to the magnet axis. Furthermore, its relationship to the Fourier components of the longitudinal integral of the longitudinal current density in the magnet is identical to the relationship between the complex field and the Fourier components of the longitudinal current density in an infinitely long magnet. (auth)

12324 CALCULATION OF TARGET EFFICIENCY AND MULTIPLE TRAVERSALS IN THE CERN 600 MeV SYNCHRO-CYCLOTRON. Michaelis, E. G.; Skarek, P. (CERN, Geneva). Nucl. Instrum. Methods; 89: 81-6(1970).

Target efficiencies and the number of target traversals in the CERN synchro-cyclotron are calculated by following particles directly with step by step integration and Monte-Carlo scattering at various targets. The computed results agree fairly well with the values found by experiments made in that energy region. (auth)

12325 PHYSICS WITH AND PHYSICS OF COLLIDING ELECTRON BEAMS. Pellegrini, Claudio; Sessler, Andrew M. (Univ. of California, Berkeley). Comments Nucl. Particle Phys.; 4: 55-68(Mar-Apr 1970).

The physics experiments which can be performed using colliding electron beams are discussed including previous and future experiments. The physics of colliding beams is considered covering synchrotron radiation, radio-frequency fields, and particle motion, the injected current limit, the beam lifetime, coherent instabilities, and the incoherent two-beam limit. (J.F.P.)

12326 INFLUENCE OF STATISTICAL FIELD ERRORS ON THE STABILITY OF LONGITUDINAL PHASE OSCILLATIONS OF A LINEAR ACCELERATOR (FLATNESS-PROBLEM. Sauter, E. (Kernforschungszentrum, Karlsruhe, Ger.). Nucl. Instrum. Methods; 89: 247-52(1970).

The influence of random errors caused by construction and adjustment tolerances on the size of the stability region of longitudinal phase oscillations is investigated analytically and numerically. A linear approximation leads to the stability problem of an harmonic oscillator, whose frequency changes at random. No influence is found on that region of the phase-plane, which is used for acceleration, even for relatively large initial errors. (auth)

12327 GENERATION OF FIRST AND SECOND ORDER TRANSFORMATION ELEMENTS FROM A GIVEN MAGNETIC FIELD. Close, E. R. (Univ. of California, Berkeley). Nucl. Instrum. Methods; 89: 205-14(1970).

Equations of motion and a simple elimination scheme suitable for obtaining first and second order transformation elements by numerically integrating through a magnetic field are developed. The results are applied to ideal magnets with a constant field, a quadrupole field, and a sextupole field. The results obtained by numerical integration are compared with analytically obtained values. (auth)

XUM

12328 PENNING TYPE STRONG IONIZING FIELD FOR POLARIZED ATOMIC BEAMS. **Bruandet, J. F. (Institut des Sciences Nucleaires, Grenoble, France); Bouchez, R.; Danielou, R. Nucl. Instrum. Methods; 89: 297-9(1970). (In French).**

Oscillating electrons confined by strong magnetic fields in a Penning source with no filament are used to ionize a coaxial atomic beam. High efficiency ($\gtrsim 10^{-3} \approx 8\ \mu A\ D^+$), low background ($\lesssim 5\%$) and excellent stability is obtained. (auth)

12329 METHOD OF MEASURING THE PHASE ANGLE OF A CHARGED PARTICLE BEAM IN A CYCLOTRON. **Stuessi, H. P.; Schutte, F. (Eindhoven Univ. of Tech., Netherlands). Nucl. Instrum. Methods; 89: 87-91(1970).**

Computer control of a cyclotron necessitates a number of probes to measure those parameters of the accelerator which provide the input signals for the computer. One of these parameters is the phase angle between the accelerating dee-voltage and the particle bunches. A method is described of measuring rapidly this phase angle without destroying the beam. The phase of the signal produced by an inductive pick-up coil inside the vacuum chamber is compared with the phase of the dee-voltage by applying a mixing technique and transforming the phase angle into an amplitude of a low frequency signal. Some requirements of the electronic circuits, the limitations of the method and a basic measurement carried out with the device are discussed. This preliminary measurement shows that at 3 μA internal beam current, the phase angle of the particle bunches can be determined with a sensitivity of approx. 0.5 degree. With further improvement of this device we hope to get the current limit to below 0.5 μA internal beam current. With the present device, field fluctuations of less than 10^{-5} Wb m^{-2} can be observed. (auth)

12330 CENTRAL REGION OF THE DELFT 12 MeV ISOCHRONOUS CYCLOTRON. **Lubach, B. (Technische Hogeschool, Delft, Netherlands). Nucl. Instrum. Methods; 89: 141-6(1970).**

In the Delft isochronous cyclotron two regions may be distinguished with respect to trajectory calculations: first, a main region characterized by an intricate magnetic field, a simple electric field and negligible space charge; second, a central region where things are just reversed. For the central region of this cyclotron two computer programmes have been written without taking space charge into account. In the first programme the trajectories in the median plane are calculated for various source-puller situations and for various initial positions and start phases. In the second programme the vertical motion is calculated for any trajectory computed in the first programme. In both programmes the equations of motion are solved by means of a fourth order Runge–Kutta procedure. The field data in the equations of motion are obtained from electrolytic tank measurements. Absence of a central magnetic field cone is the only particular supposition made, so application of the results to some other machines will probably be possible. Two typical results are: 1. A beam quality of 54 mm · mrad at 12 MeV for a source hole diameter of 2 mm and a symmetrical electric field; and 2. A better steadiness of the centre of curvature for a more symmetrical electric field. (auth)

12331 MEDIUM-ENERGY NEUTRON FACILITY. **Jungerman, J. A.; Brady, F. P. (Univ. of California, Davis). Contract AT(11-1)-GEN-10. Nucl. Instrum. Methods; 89: 167-72 (1970).**

A facility for producing variable energy neutron beams in the energy range 20 to 60 MeV using protons from the 76″ Isochronous Cyclotron at the University of California, Davis is described. The $^7Li(p,n)^7Be$ reaction is used to produce nearly monoenergetic beams with approximately 60% of the neutrons in a well defined peak. (auth)

12332 LATERAL SPREAD OF HIGH-ENERGY (≤400 MeV) NEUTRON BEAMS AND EARTHSHINE. **Alsmiller, R. G. Jr. (Oak Ridge National Lab., Tenn.); Mynatt, F. R.; Gritzner, M. L.; Pace, J. V.; Barish, J. Nucl. Instrum. Methods; 89: 53-9(1970).**

Calculated results obtained using the method of discrete ordinates are presented for the cases of zero-width beams of 100- and 400-MeV neutrons normally incident along the axis of a cylindrical shield of silicon dioxide with 5% water by weight. The results include the omnidirectional neutron flux per unit energy as a function of depth and radius in the shield and the neutron and photon dose equivalents as a function of depth and radius in the shield. In the vicinity of well shielded target areas of high-energy accelerators, the neutrons and photons which diffuse through the ground under the shield, "earthshine," often pose a radiation hazard. Calculated results of the earthshine from a 400-MeV neutron source in a specific geometry are presented and discussed. (auth)

12333 PARAMETRIC EFFICIENCY LIMIT OF RESONANCE CHARGING OF PULSE-FORMING NETWORK IN PULSE GENERATORS. **Borisov, D. G.; Grislov, A. I. (Efremov Scientific Research Inst. of Electrophysical Apparature, Leningrad). Nucl. Instrum. Methods; 89: 77-9(1970).**

The equivalent circuit of pulse generators with pulse forming network (PFN) is described. It is shown that resonance charging application of the pulse forming network is effective only for a determined range of the pulse rates. This range of pulse rates is determined by parameters of the device. (auth)

12334 LEADING OF ACCELERATED ELECTRONS OUT OF SMALL -GABARITE BETATRONS BY MEANS OF MAGNETIC METHOD. **Solomatin, V. I. (Tomsk Polytechnic Inst., USSR). Izv. Vyssh. Ucheb. Zaved., Fiz.; No. 8, 77-81(1970). (In Russian).**

An equation was obtained for electron motion in a betatron which could be used for calculating the orbits for small electron deflection from the equilibrate orbit $x \ll r_0$ and for large deflections $x \geq r$. Theoretical and experimental data are given for the possible extraction of the electron beam from the acceleration chamber and betatron of a special construction and PMB-6 parameters. It was found that for extraction of accelerated electrons from a PMB-6 betatron by asymmetric shifting of the equilibrate orbit it was necessary to increase the angle of emergence and the beam trajectory spacing by reducing the time of the pulse rise in the perturbation field. It was concluded that an additional extracting device of a pulse bypass or electrostatic capacitor should be installed for effective electron extraction from PMB-6 type betatron. (R.V.J.)

XUM

PHYSICS (NUCLEAR)

Neutron Interactions with Matter

Refer also to abstracts 10861, 11056, 11986, 12019, 12026, and 12331.

12335 (AECL–3671) FORGOD: A FORTRAN IV PROGRAM FOR SOLVING THE FOUR GROUP NEUTRON DIFFUSION EQUATIONS IN ONE DIMENSION. Smith, N. (Atomic Energy of Canada Ltd., Chalk River (Ontario). Chalk River Nuclear Labs.). Nov 1970. 56p. Dep. NTIS (U. S. Sales Only). AECL $1.50.

FORGOD, written in Fortran IV for the CDC 6600 computer, solves the neutron diffusion equation in one-dimensional geometry. Up to four energy groups can be used, with single downscatter removal between groups. The solution is based on standard finite-difference techniques. Since the program is described in full detail, users can incorporate the methods and adapt them to their own needs. The program is intended to be simple and general. Input and output are minimized, and a straight eigenvalue solution is the only option available. (auth)

12336 (ANL–7645) RABID: AN INTEGRAL TRANSPORT-THEORY CODE FOR NEUTRON SLOWING DOWN IN SLAB CELLS. Olson, Arne P. (Argonne National Lab., Ill.). Apr 1970. Contract W-31-109-eng-38. 116p. Dep. NTIS.

This report consists of the theory behind the methods used in the RABID code to solve the integral transport equation in slab geometry for cells with repeating boundary conditions, together with a user's guide, sample problems, and code listings. Space- and lethargy-dependent slowing-down sources are used with cross sections obtained by the single-level Breit–Wigner formalism for s- and p-wave resonances to calculate resonance absorption, broad-group average fluxes and cross sections, and foil reaction rates. RABID is coded in FORTRAN-IV for the IBM/360-75. A core requirement of 420K bytes permits up to 300 resonances, 20 materials having resonances, 10 materials without resonances, 30 regions in the cell, and 25 broad groups. (auth)

12337 (ANL–7654) SERVICE ROUTINES FOR THE MULTIGROUP CROSS-SECTION CODE MC^2. Pennington, E. M.; Gajniak, J. C.; Cohen, A. B.; Bohl, W. (Argonne National Lab., Ill.). Apr 1970. Contract W-31-109-eng-38. 74p. Dep. NTIS.

The FORTRAN codes MERMC2 and MAGIC are service routines for binary cross-section library tapes used by the MC^2 multigroup cross-section code. MERMC2 requires as input two MC^2 library tapes and produces another library tape containing data from the input tapes with deletion of some materials if desired. Alternately, MERMC2 may be used to produce a library tape by deleting materials from a single input tape. The MAGIC code yields listings and Calcomp plots of selected data from an input MC^2 library tape. (auth)

12338 (CNEA–266) OPERATIONAL FORMULATION OF RESONANCE ABSORPTION OF NEUTRONS. Corcuera, R. Paviotti; Solanilla, R. (Comision Nacional de Energia Atomica, Buenos Aires (Argentina)). 1970. 24p. (In Spanish). Dep. CFSTI (U. S. Sales Only).

The use of operation calculations makes it possible to obtain exact expressions for the resonance integral and the intermediary resonance parameters. These expressions can be applied to the most general case of a heterogeneous system formed by a resonant absorbent mixed with N diluents and M moderators. The test functions for the fluxes are obtained by means of a linear approximation by the moderation operators. In this approximation the resonance parameters with physical significance are introduced. Three approximations are also given for the calculation of the resonance integrals which are directly applied to various resonances in homogeneous and heterogeneous systems. The three approximations are compared with Monte Carlo results. One of the approximations agrees very well with the Monte Carlo values. The general formulation given includes many of the I–R methods developed up to the present. (tr-auth)

12339 (EUR–4521) CODAC: A FORTRAN IV PROGRAMME TO PROCESS A TIMOC LIBRARY FROM THE ENDF/B FILE. Krainer, H. (European Atomic Energy Community, Ispra (Italy). Joint Nuclear Research Center). 15 Jun 1970. 52p. Dep. NTIS (U. S. Sales Only). EUR FF 7.75.

The processing of nuclear data from standard cross section libraries is of particular importance for Monte Carlo programs which can handle a large number of nuclear input parameters. The CODAC code is designed to produce these parameters from the ENDF/B data file in the form of group averaged cross sections and scattering models. The output formats of CODAC agree with the input specifications of the Monte Carlo code TIMOC. CODAC generates the group averaged values of σ_c, σ_{el}, σ_{in}, α and ν, the angular distribution function for elastic scattering and different inelastic scattering models. With this code one has the possibility to obtain group averaged data for special, problem orientated group limits. CODAC is written in FORTRAN IV for an IBM 360/65 using no programming tricks and nearly no machine features, so that it will run, except for minor modifications, on any other machine which is large enough. For the sake of saving computer space, it is built up in an overlay structure. CODAC uses the retrieval subroutines developed by H. C. Honeck and parts of the ETOM-ETOG code of Westinghouse which produces inputs for MUFT and GAM. (auth)

12340 (KFK–1223) MODAL DEVELOPMENT OF THE NEUTRON TRANSPORT EQUATION FOR PLANE GEOMETRY. Schwetje, W. (Kernforschungszentrum, Karlsruhe (West Germany). Institut fuer Neutronenphysik und Reaktortechnik). Jul 1970. 118p. (In German). Dep. NTIS (U. S. Sales Only).

Thesis. Submitted to Karlsruhe Univ., Ger.

The problem of solving the neutron transport equation is reduced to the problem of solving systems of linear first-order differential equations or systems of Fredholm integral equations of the second type with degenerate kernel by four different half-range expansions of low order. The expansion functions or modes may be specifically adapted to each problem in both half-spaces. Numerical methods are given for solving the reduced systems of equations. It is demonstrated for several representative examples that these expansions — with suitably chosen modes — yield the same accuracy as numerical discrete ordinate methods, but with much less computing time. (auth)

12341 (LFEN-NI–46-a) BEHAVIOR OF NEUTRONS IN A MULTIPLYING MEDIUM: DEFINITION OF KINETIC PARAMETERS. Oliveira, Jaime M. Costa (Junta de Energia Nuclear, Sacavem (Portugal). Laboratorio de Fisica e Engenharia Nucleares). 1969. 22p. (In Portuguese). Dep. NTIS (U. S. Sales Only).

The behavior of neutrons in a multiplying medium is theoretically considered and the definitions of kinetic parameters are derived. The Boltzmann equation is applied to the evolution, production, and loss of neutrons in a multiplying medium. The effect of the introduction of neutrons to a multiplying medium is derived. The kinetic equations are given, and approximations are made of the kinetic equations. The prompt kinetic equations are derived. (J.S.R.)

12342 (RPI–328-210) TEMPERATURE DEPENDENCE OF NEUTRON INELASTIC SCATTERING FROM WATER. Esch, L. J.; Yeater, M. L. (Rensselaer Polytechnic Inst., Troy, N. Y.); Moore, W. E.; Seemann, K. W. (Knolls Atomic Power Lab., Schenectady, N. Y.). [1969]. Contracts AT(30-1)-328; W-31-109-eng-52. 34p. Dep. NTIS.

The double differential neutron scattering cross section for water has been measured at temperatures of 27°C, 170°C and 270°C. The RPI Linear electron accelerator provided the pulsed neutron source for a time-of-flight analysis of neutron energy. By phasing the LINAC with a high speed chopper, incident neutron energies ranging from 0.04 eV to 0.632 eV were selected. Energy distributions of scattered neutrons were obtained at scattering angles of 10, 14, 25, 40, 60, 90, 120 and 150 degrees. The relatively wide range of incident energies with good resolution made it possible to observe clearly the molecular energy levels. The structure was seen to be broadened considerably in going from 27°C to 170°C, but was little changed by the further temperature increase. In order to fit these data, a model has been developed in which the water scattering system is considered as consisting of aggregates of molecules. These clusters have temperature dependent sizes, and diffuse according to a temperature dependent diffusion constant. The energy levels of the molecules bound in the clusters are represented by a multi-Gaussian frequency distribution which varies with temperature. The internal vibrations of the individual water molecules are represented by delta functions. A new approach has been taken in comparing this and other models with the data, involving the application of recent improvements in methods of treating resolution and multiple scattering: A Monte Carlo technique has been used to impose these conditions on the models. These comparisons, and comparisons with integral data, indicate that the new model should have advantages for reactor calculations. (auth)

XUM

12343 IAEA PROGRAMS IN THE COMPILATION AND REVIEW OF NUCLEAR DATA. Lorenz, A. (International Atomic Energy Agency, Vienna). pp 175-8 of Nuclear Accident Dosimetry Systems. Vienna; International Atomic Energy Agency (1970).

From Panel on Nuclear Accident Dosimetry Systems, Vienna, Austria. See STI/PUB-241; CONF-690223.

A brief description of the world-wide effort in the collection, compilation and dissemination of neutron data information, as performed by the IAEA Nuclear Data Section in cooperation with three other regional data centers, is presented in the light of the implications of future developments. The concept of a complete nuclear data information system is suggested, highlighting the potential benefits to nuclear data users in the field of physical dosimetry. (auth)

12344 TOTAL NEUTRON CROSS SECTIONS AND THE NUCLEAR RAMSAUER EFFECT. Angeli, I.; Csikai, J. (Kossuth Univ., Debrecen, Hungary). Nucl. Phys.; A158: 389-92(1970).

A simple empirical formula is given to describe the mass-number dependence of total neutron cross sections at 14 MeV. It is shown that this expression can be well interpreted in terms of the nuclear Ramsauer effect with a reasonable value of the real optical-potential depth and a finite surface thickness. A value of $r_0 = 1.26$ fm was found, in agreement with the electromagnetic radii. The calculated energy dependence of the total neutron cross section for Bi agrees with the experimental values within a few percent. (auth)

12345 MULTIGROUP NEUTRON TRANSPORT EQUATION IN THE DIFFUSION AND P_1 APPROXIMATION. Obradovic, D. (Boris Kidric Inst., Belgrade). Fizika (Zagreb); 2: 119-220 (Oct 1970).

Investigations of the properties of the multigroup-transport operator, with and without delayed neutrons in the diffusion and P_1 approximations, are performed using Keldiš's theory of operator families as well as a technique recently used for investigations into the properties of the general linearized Boltzmann operator. It is shown that, in the case without delayed neutrons the multigroup transport operator in the diffusion and P_1 approximations possesses a complete set of generalized eigenvectors. A formal solution to the initial value problem is also given. (auth)

12346 SOME EXACT AND APPROXIMATE SOLUTIONS OF THE NEUTRON SLOWING DOWN EQUATION IN RESONANT ABSORBING MEDIA. Finkelstein, L.; Shatz, M. (Soreq Nuclear Research Center, Yavne, Israel). Nucl. Sci. Eng.; 42: 260-6 (Dec 1970).

A class of resonant absorption cross sections was found for which there are simple exact solutions of the neutron moderation equation. Some of these solutions are compared with corresponding numerical solutions obtained by the methods of Rowlands, Nordheim, and Finkelstein. The first two methods are accurate for narrow and intermediate absorption resonances but develop instability when relatively strong (with respect to scattering) absorption extends for a few or more collision intervals. Then only the third method may be used with confidence. (auth)

12347 MULTIPLE SCATTERING AND COLLISION PROBABILITY METHOD FOR NEUTRON TRANSPORT PROBLEMS. Lefvert, T. (Research Inst. of National Defence, Stockholm). Nucl. Sci. Eng.; 42: 267-71 (Dec 1970).

A multigroup, collision-probability, order-of-scattering approach is made to the slowing-down solution of the neutron transport equation in a heterogeneous, nonmultiplying medium with sources. After the introduction of first-collision probabilities into the Liouville–Neumann series solution of the neutron flux, the series may be summed, and a transport matrix defined. If a flat source distribution in the region is assumed, this matrix is typical of the medium and of the geometrical configuration only and links, in an explicit way, sources and resultant fluxes. In a multiplying system without external sources it is also possible to use the above transport model when determining the effective neutron multiplication factor by the fission-probability-matrix method. (auth)

12348 CALCULATION OF NEUTRON AGES AND SLOWING DOWN SPECTRA IN LIGHT WATER FOR A FISSION SOURCE AND A D–T SOURCE. Yamamura, Yasunori; Sekiya, Tamotsu (Osaka Univ.). J. Nucl. Sci. Technol. (Tokyo); 7: 564-73 (Nov 1970).

Numerical calculations on neutron age and neutron spectra for a fission source and a D–T source in light water are performed by means of a stochastic method of calculation for the slowing-down process. The formulas for calculation are derived through direct operational treatment. In dealing with neutron degradation, account is taken of both inelastic scattering and anisotropy of elastic scattering in the center-of-mass system. To elucidate the effects brought by these factors, and to compare the present exact results with those by G.G. approximation for isotropic scattering, numerical calculations are performed and discussions on the results are given. The results obtained on neutron age are in good agreement with values from experiment by other authors. The neutron ages from a fission source and a D–T source to I_0 resonance are found to be 26.34 and 156.4 cm^2, respectively. (auth)

12349 ATTENUATION OF 14.7-MeV NEUTRONS IN WATER. Gomaa, M. A. (Middlesex Hospital, London). Isotop. Radiat. Res.; 3: 63-4(Jun 1970).

The measured attenuation of 14.7-MeV neutrons was compared with the results of Goldstein (1959) in which he solved the neutron transport equation using the moments method. The agreement was reasonably good. From the experimental results, the microscopic apparent (or removal) cross section was found to be 0.71 ± 0.01 b. (L.T.W.)

12350 EFFECT OF NUCLEAR MOTION ON THE DAMPING OF A NEUTRON PULSE. Kostritsa, A. A.; Neimotin, E. I. This paper was summarized in At. Energ. (USSR); 27: 50-1(Jul 1969) as paper No. 317/4669. (In Russian).

The effect of the uniform flow of isotropically scattering nuclei on the change in the scalar density and the mean square velocity of a neutron beam is examined. A pulse of monoenergetic neutrons is considered, as well as a source with a Maxwellian velocity distribution. The development of the neutron behavior with time is discussed under various conditions. (R.W.R.)

12351 SLOWING DOWN OF NEUTRONS TO VERY LOW TEMPERATURE BY COLD SOLID HYDROGENOUS MODERATORS. Inoue, Kazuhiko (Hokkaido Univ., Sapporo). J. Nucl. Sci. Technol. (Tokyo); 7: 580-7(Nov 1970).

The slowing-down of neutrons to very low energy is examined with particular reference to cold-neutron production. The neutron spectrum formed in very cold light water ice was measured with time-of-flight techniques. It is observed that at extremely low temperature the neutron temperature is much higher than the moderator temperature, whereas in the intermediate range of temperature the neutron temperature does not differ much from the moderator temperature. It is suggested that there is a limiting neutron temperature below which it does not fall, even when the moderator temperature drops further. This observation can lead to information on the nature of the mechanism for removing small amounts of energy from slow neutrons in cold, solid, hydrogenous moderators. By using a simplified model for the cold, solid hydrogenous moderators, it is shown that low-frequency lattice vibrations play an important role in producing cold neutrons. Also, quantitative analysis indicates that, while the cold-neutron temperature depends only slightly on the neutron absorption, the gain in cold-neutron flux is strongly affected by the neutron absorption. (auth)

12352 PYROLYTIC GRAPHITE AS A HIGH EFFICIENCY FILTER FOR 13 TO 15 MeV NEUTRONS. Shirane, G.; Minkiewicz, V. J. (Brookhaven National Lab., Upton, N. Y.). Nucl. Instrum. Methods; 89: 109-10(1970).

Highly oriented pyrolytic graphite is shown to be an extremely efficient $\lambda/2$ filter in the energy range between 13 and 15 MeV. The transmission ratios for neutrons with energies of 13.7 and 14.8 MeV are shown to be typically 3:4 for a filter 2″ thick and with a mosaic spread (fwhm) of 3.5°. The $\lambda/2$ component on the other hand suffers a transmission ratio of approximately 1:1500. The efficiency of the filter for a given thickness increases as the mosaic spread is decreased. The filtering process is a result of the high Bragg reflectivity of pyrolytic graphite for those neutrons that are directed along the c axis and that have certain specified wavelengths. Riste and Otnes have recently shown that pyrolytic graphite is an exceptionally good neutron monochromator. The present results demonstrate that highly oriented graphite can also be used as a selective single crystal filter to obtain a "clean" low energy neutron beam. (auth)

Nuclear Properties and Reactions, $A \leq 5$

Refer also to abstracts 10892, 12519, 12549, and 12686.

12353 (NP-18616) TABLE OF CROSS SECTIONS OF SOME REACTIONS INDUCED BY 14-15 MeV NEUTRONS. Leppaemaeki, H.; Kantele, J. (Jyvaskyla Univ. (Finland). Dept. of Physics). Jul 1970. 50p. Dep. NTIS (U. S. Sales Only).

Values of cross sections of reactions measured for neutrons having a mean energy in the range of 14 to 15 MeV are listed in two tables: cross sections of some reactions, and cross sections (in millibarns) of the reaction (n,n') and of some "rare" reactions induced by 14- to 15-MeV neutrons. References are listed. (Finland)

12354 POLARIZATION MEASUREMENTS OF 16.5- AND 22.1-MeV NEUTRONS ELASTICALLY SCATTERED FROM LIQUID TRITIUM AND LIQUID DEUTERIUM. Walter, Roger Kenneth. Provo, Utah; Brigham Young Univ. (1970). 192p. University Microfilms Order No. 70-16,898.

Thesis.

Cryogenic scattering samples of approximately one mole of liquid tritium and liquid deuterium were used in the measurement of $T(\vec{n},\vec{n})T$ and $D(\vec{n},\vec{n})D$ scattering. The source of 16.5-MeV, −54% polarized neutrons and of 22.1-MeV, +40% polarized neutrons was the $T(d,\vec{n})^4He$ reaction with an incident deuteron energy of 6.0 MeV. The left-right scattering asymmetries for laboratory angles from 40° to 118.5° were measured with a two-detector, time-of-flight spectrometer; and after neutron-gamma-ray discrimination was applied, the pulse height spectra were routed to an on-line computer for preliminary data analysis. The measured asymmetry for $T(\vec{n},\vec{n})T$ at E_n = 22.1 MeV is negative at angles forward of 95° (lab) and positive at larger angles. The extrema of the n-T polarizations are −60% at 85° (lab) and +98% at 110° (lab). $T(\vec{n},\vec{n})T$ polarizations for E_n = 16.5 MeV are negative at forward angles. $D(\vec{n},\vec{n})D$ polarizations at E_n = 22.1 MeV are measured to be small and negative at forward angles and small and positive at back angles. (Diss. Abstr. Int., B)

12355 DISTORTED-WAVE ANALYSIS OF CHARGE ASYMMETRY EFFECTS IN THE REACTION $d(\alpha,t)^3He$. Richter, A.; Vincent, C. M. (Argonne National Lab., Ill.). Phys. Rev. Lett.; 25: 1460-3(16 Nov 1970).

The fore–aft asymmetry of the angular distribution for the reaction $d(\alpha,t)^3He$ at 82 MeV is compared with the result of a simple distorted-wave Born-approximation calculation. If Coulomb effects are included, the general features of the asymmetry can be reproduced. (auth)

12356 ABSOLUTE TENSOR-POLARIZATION CALIBRATION OF A POLARIZED DEUTERON BEAM. Darden, S. E.; Prior, R. M.; Corrigan, K. W. (Univ. of Notre Dame, Ind.). Phys. Rev. Lett.; 25: 1673-4(14 Dec 1970).

The tensor analyzing power A_{yy} of $^4He(d,d)^4He$ was calibrated absolutely at θ_{lab} = 55°, E = 7.07 MeV using the reaction $^{16}O(d,\alpha_1)^{14}N^*(2.31)$. A value of A_{yy} = −1.066 ± 0.034 was obtained. (auth)

12357 $^3He(d,p)^4He$ REACTION PROTON ASYMMETRY USING A POLARIZED ^3He GAS TARGET. Watt, B. E.; Leland, W. T. (Los Alamos Scientific Lab., N. Mex.). Phys. Rev., C; 2: 1680-1(Nov 1970).

Angular asymmetries were measured for the reaction protons, using a polarized ^3He gas target and an unpolarized deuteron beam. Deuteron (lab) energies were 6, 8, and 10 MeV. Observations were made in the angular range $57° \leq \theta_{c.m.} \leq 137°$. Present and earlier data are compared with Plattner and Keller's data using vector-polarized deuterons. (auth)

12358 DEUTERON SCATTERING FROM A POLARIZED ^3He GAS TARGET. Watt, B. E.; Leland, W. T. (Los Alamos Scientific Lab., N. Mex.). Phys. Rev., C; 2: 1677-9(Nov 1970).

Scattering asymmetries in the angular range $78° \leq \theta_{c.m.} \leq 127°$ were measured for 9.9- and 11.9-MeV (lab energy) unpolarized deuterons incident on a polarized ^3He gas target. (auth)

12359 SEPARABLE POTENTIAL CALCULATIONS ON THE $\frac{1}{2}^+$ NEUTRON–DEUTERON SYSTEM. Laroze, L.; Harms, E.; Levinger, J. S. (Rensselaer Polytechnic Inst., Troy, N. Y.). Nucl. Phys.; A158: 615-24(1970).

Various rank-three separable potentials containing tensor forces and repulsion are used to calculate phase shifts and mixing parameters over a range of energies above and below breakup in the $J^\pi = \frac{1}{2}^+$ neutron–deuteron system. The calculated phase shifts agree well with the phase-shift analysis of van Oers and Seagrave although the calculated phase shifts display a somewhat different energy dependence. Calculated quantities are sensitive to the deuteron percent D-state but are relatively insensitive to the shape of the form factors used once repulsion has been included. (auth)

12360 NEUTRON–HELIUM INTERACTION. II. ANGULAR DISTRIBUTIONS AND PHASE SHIFTS FROM 0.2 TO 7.0 MeV. Morgan, G. L. (North Carolina State Univ., Raleigh. Triangle Universities Nuclear Lab., Durham, N. C.); Walter, R. L. Phys. Rev., C; 2: 2034-5(Nov 1970).

Previously reported helium recoil energy distributions produced by neutron elastic scattering from ^4He in a gaseous scintillator have been modified to provide cross-section data suitable for use in current phenomenological investigations of the nucleon–helium interaction. (auth)

12361 POLARIZATION OF PROTONS FROM THE REACTION $^2H(d,p)^3H$ AT DEUTERON ENERGIES BETWEEN 1.35 TO 2.00 MeV. Dietze, G.; Lorenzen, K. (Univ., Hamburg). Nucl. Phys.; A158: 577-83(1970). (In German).

The polarization of protons from the reaction $^2H(d,p)^3H$ was measured at six deuteron energies between 1.35 and 2.00 MeV. Elastic scattering from ^{12}C was used as a polarization analyzer. The polarization shows a maximum of about −17% at an angle of $\theta_{c.m.}$ = 50° and changes sign near $\theta_{c.m.}$ = 70°. (auth)

12362 PHOTODISINTEGRATION OF DEUTERIUM: ABSOLUTE CROSS SECTION AND ANGULAR DISTRIBUTION. Weissman, Barry. New Haven; Yale Univ. (1969). 186p. University Microfilms Order No. 70-17,224.

Thesis.

Absolute differential cross sections were measured for the $D(\gamma,p)$ reaction in the photon energy range from 25 to 55 MeV at seven laboratory angles between 30 and 150°. Bremsstrahlung was produced by a 60-MeV electron beam from the Yale University linac. The Schiff thin target bremsstrahlung spectrum, integrated over all angles of photons and incident electrons was assumed. Photoprotons from the gas target were detected in thick lithium drifted silicon counters. Measured angular distributions were fitted with sums of Legendre polynomials and the results are compared with the calculations of Partovi. At 35 MeV the measured total cross section is in excellent agreement with Partovi. At lower energy the total cross section is somewhat below calculated values, while above 35 MeV it is higher. The measured angular distribution is more asymmetric (forward peaked) than calculations predict. (Diss. Abstr. Int., B)

12363 STUDY OF N + α SYSTEM WITH THE RESONATING-GROUP METHOD. Reichstein, I.; Tang, Y. C. (Univ. of Minnesota, Minneapolis). Nucl. Phys.; A158: 529-45(1970).

The n + α and p + α systems are considered with the resonating-group method in the one-channel approximation. The nucleon-nucleon potential used has both a central part and a spin-orbit component. From the results it is found that very good agreement with experiment can be obtained in the energy region below the reaction thresholds. In fact, even above the reaction thresholds, where the validity of the one-channel approximation may be questioned, the results are quite satisfactory. An effective potential between the clusters is also constructed. From this potential it is determined that the requirement of antisymmetry for the total wave function is very important. In particular, it creates an odd-even feature, wherein the effective central and the effective one-body spin-orbit potentials in the odd-l states are appreciably different from those in the even-l states. (auth)

12364 TRITON WAVE FUNCTION IN THE FESHBACH–RUBINOW APPROXIMATION. McMillan, Malcolm; Maroun, David (Univ. of British Columbia, Vancouver). Nucl. Phys.; A159: 661-72(1970).

Previous work on the triton wave function using the Feshbach–Rubinow equivalent two-body method was extended to include all of the symmetric and mixed symmetric S- and D-state components. The modified Feshbach–Rubinow method and the potential deepening procedure used previously are found to yield reasonably accurate results for the triton energy and wave function corresponding to the Feshbach–Pease potentials. A method for handling soft-core potentials is used to find an approximate symmetric S-state component of the triton wave function corresponding to the Bressel–Kerman–Rouben potential. The body form factor calculated with this function has a zero for q^2 = 13.8 fm^{-2}. (auth)

12365 EXPERIMENTAL STUDIES OF THE REACTIONS $^3H(p,p)^3H$, $^3He(p,p)^3He$, AND $^3H(p,n)^3He$ AT 156 MeV. Langevin-Joliot, H.; Narboni, Ph.; Didelez, J. P.; (and others) (Institut de Physique Nucleaire, Orsay, France). Nucl. Phys.; A158: 309-20 (1970). (In French).

A comparative experimental study of the reactions $^3H(p,p)^3He$, $^3He(p,p)^3He$, and $^3H(p,n)^3He$ was performed at 156 MeV with gaseous ^3He and ^3H targets at low temperature. The experimental set-up is described. Elastic differential cross sections are given from 15.8° c.m. to 178° c.m.; and charge-exchange ones, from 83.4° c.m. to 178° c.m. First order calculations are done, with direct scattering and the pick-up terms and S states for the three-body wave functions taken into account. Theoretical curves reproduce the angular distributions well enough in the forward range, absolute values being nearly a factor two higher.

XUM

In the backward range, the $^3H(p,n)^3He$ differential cross sections are about three to four times smaller than elastic ones. This result is not expected by first-order theory. (auth)

12366 REACTION LIST FOR CHARGED-PARTICLE-INDUCED NUCLEAR REACTIONS Z = 1 TO Z = 98 (H TO Cf), MAY 1969–JUNE 1970. McGowan, F. K.; Milner, W. T. (Oak Ridge National Lab., Tenn.). Nucl. Data, Sect. A; 8: 199-322(Nov 1970).

This reaction list for charged-particle-induced nuclear reactions has been prepared from the journal literature for the period from May 1969 through June 1970. Each published experimental paper is listed under the target nucleus in the nuclear reaction with a brief statement of the type of data in the paper. The nuclear reaction is denoted by A(a,b)B, where $M_a \geq$ (one-nucleon mass). There is no restriction on energy. Nuclear reactions involving mesons in the outgoing channel are not included. (auth)

12367 KINEMATICALLY COMPLETE EXPERIMENT ON THE REACTION n + d → n + n + p. Lunke, C.; Egger, J. P.; Rossel, J. (Univ. Neuchatel, Switzerland). Nucl. Phys.; A158: 278-88(1970).

The energy of the three nucleons produced in the break-up reaction $^2H(n, nnp)$ at 14.1 MeV is measured in coincidence for an experimental configuration which enhances the final-state interaction of one n–p pair and gives a two-fold redundancy, essential for the rejection of false events. The analysis of the shape of the distribution in the Watson approximation, with due consideration of the influence of the other pairs in triplet or singlet states, gives the value –23.0 ± 1.7 Fm for the singlet n–p scattering length. The absolute value of $d^3\sigma/dE_1 d\Omega_1 d\Omega_2$ at the peak of the n–p pole is 5.1 ± 0.7 mb · sr^{-2} · MeV^{-1}. (auth)

12368 $^2H(d,p)^3H$ ANISOTROPY AT LOW ENERGIES. Pixley, R. E.; Mann, F.; Glavish, H. F. (Stanford Univ., Calif.). Nucl. Phys.; A160: 222-4(1971).

The angular distribution of protons from the $^2H(d, p)^3H$ reaction was measured for deuteron lab energies in the range 90 to 120 keV in steps of 2 keV and with a resolution of less than 3 keV. A resonance as reported in other measurements was not reproduced. (auth)

12369 MEASUREMENT AND POLE DIAGRAM ANALYSIS OF THE $^2H(n,p)2n$ REACTION CROSS SECTION AT 14.5 MeV. Arai, E. (Tokyo Inst. of Tech.). Nucl. Phys.; A160: 161-70 (1971). (In German).

The deuteron break-up reaction was investigated by means of the two-dimensional measurement of proton and neutron energy distributions at neutron emission angles of 10, 20, 30 and 40°. The pole diagram approximation was applied to analyze the measured cross sections for a bombarding neutron energy of 14.5 MeV. Reasonable agreement between the observed and calculated cross sections was obtained. (auth)

12370 DEUTERON ELASTIC SCATTERING AND THE (d,p) REACTION WITH A POLARIZED ^3He TARGET. Hardy, D. M.; Baker, S. D.; McSherry, D. H.; Spiger, R. J. (Rice Univ., Houston, Tex.). Nucl. Phys.; A160: 154-60(1971).

Measurements of deuteron elastic scattering from polarized ^3He are reported for the energy range 4.78 to 11.88 MeV. The left-right asymmetries observed bear a striking similarity to the values of the deuteron vector analyzing power (iT_{11}) measured by Plattner and Keller. Also reported are measurements of asymmetries in the (d,p) reaction, which augment earlier measurements. (auth)

12371 EVEN-PARITY STATES OF THE FIVE-NUCLEON SYSTEM; AN APPLICATION TO DEUTERON–TRITON PHOTOCAPTURE. Wagner, Robert F. Washington, D. C.; Catholic Univ. of America (1970). 61p. University Microfilms Order No. 70-14,155.

Thesis.

A two particle-one hole shell model calculation was carried out for the five nucleon system. Spurious shell model states were constructed and projected out by the Schmidt orthogonalization method. The separable, smooth, two-body interaction of Tabakin was taken as the residual force. The resulting theoretical spectrum reproduces the first excited state in ^5He with $J^\pi = 3/2^+$. It also predicts structure in the neighborhood of 20–22 MeV which carries the preponderance of the dipole strength. One experiment for locating the dipole state in this system is the photo-capture of deuterons by tritons. Until now this experiment was performed with deuterons of insufficient energy for checking this prediction. In anticipation of such work a detailed calculation of the dependence of the cross section for this reaction upon energy and angle was carried out using a many-level generalization of the R-matrix formalism. This required a knowledge of the coupling of the shell model states to the physical single particle and deuteron channels; a semi-quantitative calculation of this coupling involving transformations from j-j to L-S coupling and from occupation to coordinate space yielded results compatible with the experimentally known make-up of the first excited state. It is suggested that deuterons of at least 12 MeV laboratory energy be used to look for the features of the dipole state which is predicted. (Diss. Abstr. Int., B)

12372 DIRECT RADIATIVE CAPTURE OF ^3He BY TRITONS AND t + ^3He CLUSTER STATES IN ^6Li. Young, A. M.; Blatt, S. L.; Seyler, R. G. (Ohio State Univ., Columbus). Phys. Rev. Lett.; 25: 1764-7(28 Dec 1970).

A direct-capture model is used to calculate the cross section for the capture of ^3He by tritons. Comparisons with data to 20 MeV show that the energy dependence of the ground-state capture cross section is well accounted for and that there exists substantial t + ^3He clustering in the first three ^6Li states. (auth)

12373 THIRD-ORDER CORRECTIONS TO THE HARTREE–FOCK APPROXIMATION FOR THE BINDING ENERGY OF ^4He. Kreuzer, H. J. (Univ. of Alberta, Edmonton). Can. J. Phys.; 48: 2123-9(15 Sep 1970).

Third-order calculations of the binding energy of ^4He with an effective (finite) nucleon–nucleon interaction of the Hamada–Johnston type are presented. The intermediate (unoccupied) states are approximated by plane waves in a first calculation and in a second by oscillator functions. In both approximations third-order graphs contribute only a few percent of the second-order terms to the binding energy. (auth) (Canada)

12374 PHOTONEUTRON ANGULAR DISTRIBUTIONS FROM THE $^2H(\gamma,n)H$ REACTION. Shin, Y. M.; Rawlins, J. A.; Buss, W.; Evwaraye, A. O. (Saskatchewan Accelerator Lab., Saskatoon, Can.). Nucl. Phys.; A154: 482-96(1970).

The angular distributions of neutrons from the $^2H(\gamma,n)^1H$ reaction were measured from E_γ = 10 to 95 MeV, using neutron time-of-flight spectrometers at five angles. The results were compared with current theory. Although the theory predicts general features of the reaction significant discrepancies between theoretical predictions and experimental results were found. (auth)

12375 QUASIELASTIC DEUTERON BREAKUP BY PROTONS AT 100 MeV. Pan, P. J.; Crawford, J. E. (McGill Univ., Montreal). Nucl. Phys.; A150: 216-24(1970).

Two-parameter energy spectra of the outgoing protons in the d(p,2p)n reaction have been collected at 11 angle pairs for an incident proton beam energy of 100 MeV. For angle separations close to 88.5°—the free proton–proton scattering angle—a spectator model calculation predicts two-parameter cross sections $d^3\sigma/d\Omega_1 d\Omega_2 dE_1$ which agree in shape with those measured, but which are high by a factor of about 1.5. A Chew–Low extrapolation of the data has been performed. The cross sections are compared with results at other incident energies. (auth)

Nuclear Properties and Reactions, 6 ≤ A ≤ 19

Refer also to abstracts 10851, 10892, 11565, 12309, 12353, 12366, 12372, 12441, 12497, 12498, 12519, 12549, 12663, 12686, 12689, 12692, and 12694.

12376 (AD-710383) ELASTIC ELECTRON SCATTERING FROM ^{13}C. Heisenberg, J.; McCarthy, J. S.; Sick, I. (Stanford Univ., Calif. High-Energy Physics Lab.). Jul 1970. Contract Nonr-225(67). 32p. (HEPL-628). NTIS.

Cross sections for elastic scattering of electrons from the charge and magnetic distribution of ^{13}C were measured. The data, covering a range of q of 0.4–3.4 F^{-1} are fitted by a phenomenological charge distribution. The difference between ^{12}C and ^{13}C is analyzed in terms of the change in parameters of the Woods–Saxon potential used in a shell model description of the nuclei. (auth) (USGRDR)

12377 (INP–711) POLARIZATION OF PROTONS FROM $^{12}C(d,p)^{13}C$ REACTION AT E_d = 12.4 MeV. Budzanowski, A.; Freindl, L.; Karcz, W.; Lazarska, B.; Zipper, W. (Institute of Nuclear Physics, Krakow (Poland)). 1970. 27p. Dep. NTIS (U. S. Sales Only).

The polarization of protons from the $^{12}C(d,p)^{13}C$ reaction at 12.4 MeV was measured for the ground state (in the angular range 20° to 136° lab) and the first excited state (in the angular range 20° to 90° lab) transitions. The results obtained are compared to the vector analyzing power data for the same reaction and at the same energy of the incident deuterons. An attempt to fit the polarization data with the DWBA theory is also presented. (auth)

12378 (JINR-P1-4872) INVESTIGATION OF THE ^{8}Li RECOIL NUCLEI IN THE ^{9}Be(p,2p)^{8}Li REACTION AT THE PROTON ENERGIES OF 180 AND 660 MeV. Grigoriev, E. L.; Lozhkin, O. V.; Maric, Z.; Suslenko, V. C.; Kochkin, V. I. (Joint Inst. for Nuclear Research, Dubna (USSR)). 1969. 25p. (In Russian). Dep. NTIS (U. S. Sales Only).

The results of the experimental analysis of the ^{9}Be(p,2p)^{8}Li reaction are presented. The ^{8}Li recoil nuclei were detected by means of photoemulsions; and the data on their energy distributions at the angles $\theta_{\frac{1}{2}}$ = 50°, 90°, and 120° (for incident protons of the kinetic energy T = 660 MeV), $\theta_{\frac{1}{2}}$ = 50° and 90° (T = 180 MeV), and their angular distributions are reported. Theoretical analysis based on the pole Feynman diagram is carried out. Qualitative agreement of the theoretical analysis with the given experimental data has been obtained. (R.W.R.)

12379 (KAPL-P-3901) NOTES ON THE CARBON TOTAL CROSS SECTION FROM 0-2 MeV. Francis, Norman C. (Knolls Atomic Power Lab., Schenectady, N. Y.). [1970]. Contract W-31-109-eng-52. 17p. (CONF-701002-2). Dep. NTIS.

From EANDC Symposium on Neutron Standards and Flux Normalization, Argonne, Ill.

Because of its smooth energy dependence, the total cross section of carbon is a good candidate for a primary standard for the measurement of neutron cross sections from 0 to 2 MeV. The ^{13}C content of natural C can be ignored for errors greater than 1%. The results of several measurements of the thermal cross section are given, and polynomial fits are made to the data. The binding energy and n + C elastic scattering are also considered. It is concluded that, if the energies of the ^{13}C resonances are avoided, the carbon total cross section is known to about 1%, and the angular distribution to about 10%. (29 references) (R.W.R.)

12380 (KFK-1222) INVESTIGATION OF THE β SPECTRUM OF ^{14}C WITH A PROPORTIONAL COUNTER WITH INNER ANTICOINCIDENCE SCREENS. Gramm, W. R.; Thio, S. K.; Rebel, H.; Loehken, R. (Kernforschungszentrum, Karlsruhe (West Germany). Zyklotron-Laboratorium. Heidelberg Univ. (West Germany). Physikalisches Institute (II)). Sep 1970. 33p. (In German). Dep. NTIS (U. S. Sales Only).

The β spectrum of ^{14}C was measured using a multiwire proportional counter and gaseous ^{14}C sources. The spectrum measurements at different pressures result in clear deviations from the statistical shape. The shape factor has been analyzed in terms of higher-order nuclear matrix elements contributing to allowed Gamow-Teller transitions. (auth)

12381 (NP-18541) INVESTIGATIONS OF SOME ONE-NEUTRON-TRANSFER REACTIONS WITH ^{18}O AND ^{19}F BEAMS. Knoth, Helmut (Eidgenoessische Technische Hochschule, Zurich (Switzerland)). 1970. 43p. (In German). Dep. NTIS (U. S. Sales Only).

Thesis.

Single-neutron-transfer reactions at and just below the Coulomb barrier are examined. Angular distributions are presented for the following reactions at 12 to 24 MeV: ^{13}C(^{18}O,^{19}O)^{12}C, ^{9}Be(^{18}O,^{19}O) × ^{8}Be, ^{9}Be(^{18}O,^{17}O)^{10}Be, ^{10}B(^{18}O,^{17}O)^{11}B, and ^{10}B(^{19}F,^{18}F)^{11}B. Elastic scattering of ^{18}O and ^{19}F was also measured between 12 and 31 MeV; angular distributions are given for the scattering of ^{18}O by ^{9}Be, ^{10}B, and ^{13}C and the scattering of ^{19}F by ^{10}B. The reactions are analyzed by the DWBA method, and spectroscopic factors are obtained. (R.W.R.)

12382 (NP-18546) TRANSFER OF A NEUTRON BETWEEN ^{9}Be, ^{13}C, AND ^{17}O. Matter, Ulrich (Eidgenoessische Technische Hochschule, Zurich (Switzerland)). 1970. 42p. (In German). Dep. NTIS (U. S. Sales Only).

Thesis.

The elastic scattering of ^{12}C by ^{9}Be, and of ^{16}O by ^{9}Be and ^{13}C, was measured in the neighborhood of the Coulomb barrier. These data were analyzed by the optical model and the smooth-cutoff model. The one-neutron-transfer reactions ^{9}Be(^{12}C,^{13}C)^{8}Be, ^{9}Be(^{16}O,^{17}O)^{8}Be, and ^{13}C(^{16}O,^{17}O)^{12}C to ground and excited states were also measured, and the angular distributions were analyzed by the DWBA method. Spectroscopic factors for ^{9}Be, ^{13}C, and ^{17}O are found. (R.W.R.)

12383 PHENOMENOLOGICAL WAVE FUNCTION OF ^{6}Li. Cheon, Il-tong (Kyung Hee Univ., Seoul). Progr. Theor. Phys. (Kyoto); 44: 549-51(Aug 1970).

In an attempt to reproduce both the quadrupole moment and the charge form factor of ^{6}Li, the usual cluster model is modified by introducing a deformation in the relative motion between the spherical alpha particle and the deformed deuteron having the positive value of the quadrupole moment. The parameters in the trial wave function are adjusted so as to give the theoretical value of the quadrupole moment of the bound deuteron as +0.278 F^{-2}. The charge form factor shows a diffraction minimum at 8.3 F^{-2}. (R.W.R.)

12384 NUMERICAL ANALYSIS OF THE INELASTIC SCATTERING OF NUCLEONS FROM ^{7}Li. Kinkaid, Donald Eugene. Clemson, S. C.; Clemson Univ. (1969). 57p. University Microfilms Order No. 70-17,448.

Thesis.

One of the primary goals of low-energy nuclear physics is to obtain a representation of internucleon forces by defining a single particle potential and a set of two-body potentials. It has been assumed that a single set of potentials can be used to predict both the stationary properties of low-lying energy levels and scattering results. A numerical analysis of the structure of 1P shell nuclides has been performed which defined a set of potentials that can be used to perform scattering calculations. The set of potentials consist of a single particle potential which follows the shape of the nuclear density and a set of exchange parameters. In this study, a numerical analysis of the inelastic scattering of nucleons from ^{7}Li was performed using the set of potentials defined by the structure calculations. The distorted-wave Born approximation was used to calculate the differential inelastic scattering cross sections. The scattering states were combinations of coulomb distorted waves and the bound shell model states which were defined by the structure calculations cited above. The j-j coupling scheme was used throughout the calculations. The strength and range parameters of the potentials were varied to determine whether or not the potentials could be used to obtain descriptions of both structure and scattering. The results of the calculations indicate that the two-body forces between the positive energy nucleon and the bound nucleons are considerably stronger than the two-body forces between the bound nucleons. Apparently, realistic nucleon-nucleon interactions should be used for scattering calculations. (Diss. Abstr. Int., B)

12385 PROTON PICK-UP FROM ^{19}F, ^{20}Ne, AND ^{22}Ne. Kaschl, G. Th. (Max-Planck-Institut fuer Kernphysik, Heidelberg); Wagner, G. J.; Mairle, G.; Schmidt-Rohr, U.; Turek, P. Nucl. Phys.; A155: 417-42(1970).

Energy spectra and angular distributions of the ^{3}He particles from the (d,^{3}He) reactions on ^{19}F, ^{20}Ne and ^{22}Ne were measured at an incident energy of 52 MeV. Excitation energies up to 15 MeV (^{18}O), 7 MeV (^{19}F) and 9 MeV (^{21}F) and pick-up from seven different shell-model orbits were observed. Several previously unknown negative parity states were found in ^{18}O. A $(^{3}/_{2},^{1}/_{2})^{-}$ level at 4.56 MeV was found in ^{19}F, while the known J = $^{3}/_{2}$ level at 3.91 MeV was not observed which suggests a positive parity assignment. The hole state spectrum of ^{21}F resembles closely that of ^{19}F. The spectroscopic factors are compared to the predictions from a simple rotational model and from various effective shell-model calculations. All models describe the positive parity transitions leading to ^{19,21}F reasonably well, but those leading to ^{18}O are only understood by the inclusion of excited core contributions of 4p-2h character in ^{18}O. The low-lying negative parity states, containing essentially the $1p_{\frac{1}{2}}$ hole strengths, are also nicely described by the weak coupling calculations. Higher excited negative parity states show deviations which are discussed in terms of 2p particle-1p hole admixtures. (auth)

12386 GAMMA-NEUTRINO CORRELATION IN MUON CAPTURE IN ^{14}N. Dmitrieva, T. A.; Oziewicz, Z.; Pikulski, A. (Joint Inst. for Nuclear Research, Dubna, USSR). Nucl. Phys.; A155: 205-8(1970).

The capture rate and the gamma-neutrino angular correlation for the process $^{14}N(1^{+}) \xrightarrow{\mu^{-}} {}^{14}C^{*}(2^{+}) \xrightarrow{\gamma} {}^{14}C(0^{+})$ are calculated by taking into account the second-forbidden terms, and it is shown that the inclusion of these terms is necessary. (auth)

12387 ENERGY AND ANGULAR DISTRIBUTIONS OF PHOTONEUTRONS FROM ^{6}Li AND ^{7}Li. Mecca, Stephen J. Troy, N. Y.; Rensselaer Polytechnic Inst. (1969). 171p. University Microfilms Order No. 70-11,327.

Thesis.

Photoneutron spectra from ^{6}Li and ^{7}Li were measured at several angles from 30 to 152° and at several bremsstrahlung endpoint energies from 20 to 75 MeV. A method of obtaining the differential cross section to various states in the residual nuclei was developed. The maximum possible use is made of the yield spectra, even in energy regions where neutrons can go to more than one final state. The ^{6}Li and ^{7}Li yield data were used with this method to obtain the differential cross section to various residual energy states or residual energy regions. The results indicate small cross sections, ranging from microbarns to tens of

XUM

microbarns, having "gentle tail-off" features much like the ^{4}He and ^{3}He photoneutron cross sections. Integrated cross sections obtained are as follows: for a ^{6}Li two-final-state separation, σ_{int} = 2.618 ± .066 MeV-mb from 28.7 to 72.0 MeV; for a ^{6}Li three-final-state separation, σ_{int} = .770 ± .094 MeV-mb from 43.3 to 74.4 MeV; for a ^{7}Li three-final-state separation, σ_{int} = .508 ± .068 MeV-mb from 41.9 to 56.6 MeV; for a ^{7}Li two-final-state separation, σ_{int} = .280 ± .046 MeV-mb from 44.4 to 57.5 MeV. Comparison of the present analyses with previous total photoneutron data suggests that reactions such as (γ,np), where the neutron takes off substantially less than its maximum allowable energy, are of major importance. (auth) (Diss. Abstr. Int., B)

12388 HIGHLY EXCITED STATES OF ^{12}C AND ^{16}O FROM ^{3}He CAPTURE STUDIES. Moon, Kuk Jin. Columbus, Ohio; Ohio State Univ. (1969). 98p. University Microfilms Order No. 70-14,077.

Thesis.

The differential cross sections from the ^{9}Be(^{3}He,γ)^{12}C reaction were measured from 3 to 6 MeV of ^{3}He bombarding energy. Two resonances were observed: one from which decays via gamma rays to the ground and second excited states of ^{12}C at 3.5 MeV of ^{3}He bombarding energy and the other which decays to the first excited state of ^{12}C at 5.5 MeV of ^{3}He bombarding energy. These 3.5 and 5.5 MeV ^{3}He bombarding energies correspond to 28.9 and 30.4 MeV of excitation energy of ^{12}C. Angular distribution measurements were also made at these resonances and analysis of the angular distribution measurements led to the assignments of 1^- or 2^+ to the 28.9 MeV state of ^{12}C and 3^- to the 30.4 MeV state of ^{12}C as the spins and parities of the resonances respectively. Differential cross section measurements from the ^{13}C-(^{3}He,$\alpha\gamma_{15.11,\ 12.71}$)^{12}C reaction were also made and two prominent broad peaks were observed in the 15.11-MeV gamma ray excitation curve at about 5.5 and 9.5 MeV of ^{3}He bombarding energy. The result of the 12.71-MeV gamma ray yield curve reveals a peak around 6.0 MeV ^{3}He bombarding energy. The radiative capture reaction ^{13}C(^{3}He,γ)^{16}O was also studied at several points. (Diss. Abstr. Int., B)

12389 STUDY OF THE EXCITED STATES BETWEEN 18 AND 22 MeV IN ^{10}B. Ling, Samuel Chen-ying. Columbus, Ohio; Ohio State Univ. (1969). 93p. University Microfilms Order No. 70-14,065.

Thesis.

The cross-section measurements of radiative capture of ^{3}He by ^{7}Li were extended from 3 to 6 MeV in bombarding energy and angular distributions were taken at strong resonances seen in this reaction between 1 and 6 MeV with a NaI(Tl) detector system specially designed for such high Q-value and low capture cross-section experiments. The detector system is capable of providing 7% energy resolution for 20.5 MeV gamma radiation, cosmic rejection ratio of 1 to 1000, and a resolving time for pileup suppression of 5 or 20 nanoseconds depending on the type of pileup pulses. To remove ambiguities arising from unresolved gamma radiations by the NaI(Tl) detector system, a Ge(Li) detector equipped with a segmented NaI(Tl) annulus was also used to obtain 90° spectra at the peaks of the resonances under study. A broad resonance which decays to the third and fourth excited states in ^{10}B was found at the bombarding energy (lab.) of 3.4 MeV with an experimental width (cm) of 0.91 MeV. Analysis of the angular distribution measurements together with results from the ^{7}Li(^{3}He,α)^{8}B reaction led to the assignment of 1^- as the spin and parity of the resonance. Similar analysis applied to data of strong resonances previously reported at 1.1 and 2.2 MeV yielded the following results: 2.1 MeV in resonance energy with width 0.23 MeV and spin and parity assignment 1^-; 1.0 in resonance energy with width 0.26 MeV and probable spin and parity assignment 1^- or 2^-, the first value somewhat favored. In addition, lower limits of the radiative widths of these resonances were also established. (Diss. Abstr. Int., B)

12390 INVESTIGATION OF STATES IN ^{17}O BETWEEN 8.6 AND 10.1 MeV VIA NEUTRON POLARIZATION MEASUREMENTS FOR THE ^{13}C(α,n)^{16}O REACTION. Baker, William Lewis. Columbus, Ohio; Ohio State Univ. (1969). 102p. University Microfilms Order No. 70-13,975.

Thesis.

Excited states in the compound nucleus ^{17}O were investigated by measuring the polarization of the neutrons from the ^{13}C(α,n)^{16}O reaction. Polarization excitation functions were measured for bombarding energies between 2.9 and 4.9 MeV, and six polarization angular distributions were measured in this energy interval. An S-matrix search program was used to analyze the polarization data simultaneously with previous cross section data. This method of analysis allowed the determination of a consistent set of J^π assignments to levels in ^{17}O at excitation energies between 8.6 and 10.1 MeV. J^π assignments of $\frac{3}{2}^-$, $\frac{3}{2}^+$, and $\frac{7}{2}^-$ for the resonances at 3.1, 3.38, and 3.42 MeV were consistent with the assignments of Walton et al., but evidence was seen for an additional $J^\pi = \frac{1}{2}^-$ resonance in this region. Evidence was also seen for a new $J^\pi = \frac{3}{2}^-$ resonance near 4.3 MeV. The assignments of $\frac{1}{2}^+$, $\frac{3}{2}^+$, and $\frac{5}{2}^+$, made to the resonances at 4.38, 4.42, and 4.58 MeV, respectively, were consistent with those of Kerr et al. The simultaneous analysis of the polarization and cross-section data at 4.7 MeV indicates that the preferred J^π assignment to this resonance should be $\frac{5}{2}^+$. The usefulness of polarization measurements in checking J^π assignments and resolving possible ambiguities is demonstrated. (auth) (Diss. Abstr. Int., B)

12391 STUDY OF THE ^{14}N(p,2p)^{13}C REACTION AT 46 MeV. Welch, L. C. (Univ. of Southern California, Los Angeles); Chang, C. C.; Forster, H. H.; (and others). Nucl. Phys.; A158: 644-56(1970).

The ^{14}N(p,2p)^{13}C quasi-elastic reaction at 46 MeV was investigated using symmetric coplanar geometry. For those events where $|E_1 - E_2| \leq 5$ MeV, the cross section was measured for laboratory angles from 20° to 75° by 5° steps. A calculation of the angular distribution is performed using approximate optical-model waves and a non-local p−p effective interaction. The formalism used is the distorted-wave t-matrix approximation (DWTA) in the static limit, where the distorted waves are approximated by relatively simple analytic forms. The parameters in these waves describe the distortion present in the reaction. The effects of these parameters on the (p,2p) cross section are studied, and it is noticed that the various aspects of distortion are discernible. Since a reasonable fit to the data is obtained, the approximate optical-model waves are capable of describing distortion at the energies involved. The effects of absorption and focusing are complimentary, and the left-to-right peak ratio in the (p,2p) distribution is greatly controlled by the final state focus phase φ. (auth)

12392 ^{10}B(α,^{6}Li)^{8}Be REACTION AT 46 MeV AND THE CONFIGURATION OF THE ^{10}B GROUND STATE. Zeidman, B.; Fortune, H. T.; Richter, A. (Argonne National Lab., Ill.). Phys. Rev., C; 2: 1612-16(Nov 1970).

Differential cross sections for the reactions ^{10}B(α,^{6}Li)^{8}Be$_g$ and ^{10}B(α,^{6}Li)^{8}Be$_{2,9}$ were measured in the angular range from 9 to 25° (lab system) in 1° steps at E_α = 46 MeV. The shapes of the angular distributions are typical of a direct reaction, and the pickup processes are analyzed in distorted-wave approximations on the basis of an extreme cluster model, i.e., on the assumption that a deuteron is picked up from the target nucleus ^{10}B. Calculations using proper two-particle form factors are also performed, and the results agree with the former method. From the ratio of the experimental to the theoretical cross section, a relative spectroscopic factor (^{9}Be-core-plus-deuteron-cluster parentage) is obtained and compared with two-particle fractional-parentage coefficients calculated in intermediate coupling. (auth)

12393 BINDING ENERGIES OF THE p-SHELL ΛΛ HYPERNUCLEI. Hsieh, S. T.; Lee, T. Y.; Chen-tsai, C. T. (Tsing Hua Univ., Hsinchu, Taiwan). Phys. Rev., C; 2: 1597-1600(Nov 1970).

Using the results of a shell-model analysis of the p-shell hypernuclei, the binding energies of the two Λ particles in the p-shell ΛΛ hypernuclei are calculated. A consistent account of the binding energies of the two known ΛΛ hypernuclei, $^{\ 6}_{\Lambda\Lambda}$He and $^{10}_{\Lambda\Lambda}$Be (or $^{11}_{\Lambda\Lambda}$Be) is obtained. Close agreement with the results of other investigators who used different methods is also pointed out. The effects of the noncentral potentials in the effective two-body Λ−N interaction are discussed. (auth)

12394 HALF-LIVES OF ^{11}Be, ^{15}C, ^{16}N, ^{19}O, AND ^{28}Al. Alburger, D. E.; Engelbertink, G. A. P. (Brookhaven National Lab., Upton, N. Y.). Phys. Rev., C; 2: 1594-6(Nov 1970).

The half-lives of several radioactivities induced by Van de Graaff bombardment were measured using plastic and NaI(Tl) scintillation detectors, together with a time-channel analyzer controlled by a quartz-crystal clock. The half-lives obtained are as follows: ^{11}Be, 13.81 ± 0.08 sec; ^{15}C, 2.46 ± 0.01 sec; ^{16}N, 7.13 ± 0.04 sec; ^{19}O, 27.1 ± 0.1 sec; and ^{28}Al, 2.252 ± 0.006 min. (auth)

12395 EXPERIMENTAL TEST OF THE ANALOGY BETWEEN RADIATIVE PION ABSORPTION AND MUON CAPTURE IN ^{12}C. Hilscher, H.; Krebs, W.-D.; Sepp, G.; Soergel, V. (Univ., Heidelberg). Nucl. Phys.; A158: 584-92(1970).

The yields of the analogous reactions $\mu^-_{at\ rest} + {}^{12}C \rightarrow \nu + {}^{12}B_{stable}$ and $\pi^-_{at\ rest} + {}^{12}C \rightarrow \gamma + {}^{12}B_{stable}$ were determined by detecting the ^{12}B activity produced in a plastic scintillator by stopping π^- and μ^-. Under certain assumptions about the strength of the π^- absorption from the mesic 2P level and about the contribution of the particle-stable excited ^{12}B states, the ratio of the 1S capture rates

obtained is $R = (\Lambda_\gamma^\pi/\Lambda^\mu)(^{12}C \rightarrow {}^{12}B_{g.s.}) = (1.99 \pm 0.53) \times 10^{12}$. The theoretically expected value is $R = (1.27 \pm 0.17) \times 10^{12}$. (auth)

12396 PROJECTED HARTREE–FOCK CALCULATION FOR LIGHT NUCLEI. V. NON-NORMAL PARITY STATES AND INTERLOPERS IN ^{10}Be. Bouten, M.; Bouten, M.-C.; Depuydt, H.; Schotsmans, L. (SCK/CEN, Mol, Belgium). Nucl. Phys.; A158: 561-7(1970).

A projected Hartree–Fock calculation is made for the ground state band of ^{10}Be as well as for the non-normal parity band and the interloper states. A satisfactory energy spectrum is obtained. There exists, however, a discrepancy with experiment about the order of the L = 2 states from the lowest configuration. (auth)

12397 SEARCH FOR THE EXCITATION OF THE ISOSPIN TRIPLET ^{12}B, ^{12}C*(15.11 MeV), ^{12}N BY PION CHARGE EXCHANGE AND INELASTIC SCATTERING ON ^{12}C AT 70 MeV. Hilscher, H.; Krebs, W.-D.; Sepp, G.; Soergel, V. (Univ., Heidelberg). Nucl. Phys.; A158: 593-601(1970).

In a search for ^{12}N beta activity induced by a 70-MeV π^+ beam through the reaction $^{12}C(\pi^+,\pi^0)^{12}N$, an upper limit of 120 μb was obtained for the integrated cross section, to be compared with 38 μb expected from an impulse approximation estimate. For the mirror reaction $^{12}C(\pi^-,\pi^0)^{12}B$, $\sigma = 0.80 \pm 1.85$ mb was obtained. Upper limits of 705 μb and 810 μb, respectively, for π^+ and π^- inelastic scattering by ^{12}C by excitation of the 15.11-MeV level resulted from a search for 15-MeV γ rays. In addition, the inelastic scattering by ^{12}C leading to the 4.44-MeV state was measured for π^+ and π^- of 70 MeV, again by detecting the γ rays. If a $|X_2^0|^2$ angular distribution is used for the γ rays, the cross sections found are 14.5 ± 3.0 mb for π^+ and 17.9 ± 3.1 mb for π^-. (auth)

12398 DETERMINATION OF THE RELATIVE ELECTRON DENSITY AT THE Be NUCLEUS IN DIFFERENT CHEMICAL COMBINATIONS, MEASURED AS CHANGES IN THE ELECTRON-CAPTURE HALF-LIFE OF ^{7}Be. Johlige, H. W.; Aumann, D. C.; Born, H.-J. (Technische Hochschule, Munich). Phys. Rev., C; 2: 1616-22(Nov 1970).

Differences in the decay constant of ^{7}Be in various states of chemical combination were measured using the differential-ionization-chamber technique. The results are: $\lambda(BeO) - \lambda(BeF_2)_{amorph} = (1.130 \pm 0.058) \times 10^{-3}\lambda(Be)$, $\lambda(BeO) - \lambda[Be_4O(CH_3COO)_6] = (-0.724 \pm 0.057) \times 10^{-3}\lambda(Be)$, $\lambda(BeO) - \lambda(BeBr_2) = (1.472 \pm 0.063) \times 10^{-3}\lambda(Be)$, $\lambda[Be_4O(CH_3COO)_6] = \lambda(BeF_2)_{amorph} = (1.852 \pm 0.082) \times 10^{-3}\lambda(Be)$, $\lambda(BeO) - \lambda(Be(C_5H_5)_2) = (0.795 \pm 0.074) \times 10^{-3}\lambda(Be)$, $\lambda(BeO) - \lambda[Be^{2+}(OH_2)_4] = (-0.374 \pm 0.077) \times 10^{-3}\lambda(Be)$, $\lambda[Be(C_5H_5)_2] - \lambda[Be^{2+}(OH)_4] = (-1.169 \pm 0.106) \times 10^{-3}\lambda(Be)$. The decay constant of ^{7}Be is proportional to the electron density at the nucleus. These results can therefore be used to establish a scale for the relative electron density at the Be nucleus in different chemical combinations. (auth)

12399 PHOTODISINTEGRATION OF ^{9}Be. Salyers, A. (St. Mary's Coll., St. Mary's City, Md.). Phys. Rev., C; 2: 1653-6(Nov 1970).

The photoneutron cross section of ^{9}Be is calculated using the Dirac model. It is found to have a form that differs somewhat from the standard Breit–Wigner form near threshold. A good fit to the data is obtained. (auth)

12400 CROSS SECTIONS FOR THE $^7Be(p,\gamma)^8B$ REACTION. Vaughn, F. J.; Chalmers, R. A.; Kohler, D.; Chase, L. F. Jr. (Lockheed Palo Alto Research Lab., Calif.). Phys. Rev., C; 2: 1657-65(Nov 1970).

Cross sections for the $^7Be(p,\gamma)^8B$ reaction were measured at 20 proton energies ranging from 0.953 to 3.281 MeV. Measurements were made relative to the cross section for the $^7Li(d,p)^8Li$ reaction at the 0.770-MeV resonance peak. The results were analyzed in two ways to obtain values for S(0), the zero-energy cross-section factor. The first type of analysis, based on the assumption that the observed cross section was composed of a nonresonant part and resonant contributions from the first two excited states of ^{8}B, gave an S(0) of 0.0263 ± 0.0027 keV b. The second type of analysis assumed an additional resonance contribution from a higher-lying state and led to an S(0) of 0.0226 ± 0.0043 keV b. The result obtained from the second analysis represents the best estimate for the value of S(0) obtainable from the present measurements. (auth)

12401 DIFFERENTIAL CROSS SECTIONS OF 3.0- TO 6.9-MeV NEUTRONS SCATTERED FROM ^{12}C, AND EXCITED STATES OF ^{13}C. Galati, William. Lexington, Ky.; Univ. of Kentucky (1969). 117p. University Microfilms Order No. 70-12,351. Thesis.

Thirty-two elastic and nine inelastic angular distributions of the scattering of neutrons from carbon were measured in the neutron energy range 3.03 to 6.95 MeV and at angles from 15 to 155°. The incident neutrons had an energy spread of 60 keV, except in the region of the 4.93- and 5.37-MeV resonances where it was approximately 35 keV. A biased liquid-scintillator detector and time-of-flight techniques were used. The corrected cross sections have a 3 to 6% relative error and 5 to 8% absolute error. A phase-shift analysis of the whole set of elastic angular distributions was carried out. Complex phase shifts were used above a neutron bombarding energy of 4.8 MeV, the threshold for inelastic scattering. Level parameters derived from the analysis yield the following spins and parities for excited ^{13}C levels: $E_x = 8.2$ MeV, $3/2^+$; $E_x = 8.89$ MeV, $1/2^-$; $E_x = 9.51$ MeV, $(1/2^-, 3/2^-)$; $E_x = 9.90$ MeV, $3/2^-$; $E_x = 10.75$ MeV, $1/2^-$; $E_x = 11.00$ MeV, $(1/2^+)$. Identifications of analogs of levels in the mirror nucleus ^{13}N are presented. Polarizations are calculated using phase-shift values read from smooth curves drawn through the measured phase shifts. Comparisons with available polarization measurements are presented. (auth) (Diss. Abstr. Int., B)

12402 PRECISION DETERMINATIONS OF NUCLEAR REACTION CALIBRATION ENERGIES BY VELOCITY MEASUREMENTS. Roush, M. L.; West, L. A.; Marion, J. B. (Univ. of Maryland, College Park). Nucl. Phys.; A147: 235-48(1970).

Precision measurements of the $^{27}Al(p,\gamma)^{28}Si$ resonance energy and the $^7Li(p,n)^7Be$ threshold energy have been made using an absolute velocity technique. The results for these two energies are 991.907 ± 0.049 keV and 1880.612 ± 0.090 keV, respectively. A precision of 1 part in 10^4 in such measurements has been exceeded for the first time. The $^{12}C(^3He, n)^{14}O$ threshold was observed at 1437.9 ± 0.6 keV. (auth)

12403 GAMMA RAYS FROM THERMAL-NEUTRON CAPTURE IN NATURAL AND ^{28}Si ENRICHED SILICON. Spits, A. M. J.; Op Den Kamp, A. M. F.; Gruppelaar, H. (Rijksuniversiteit, Utrecht). Nucl. Phys.; A145: 449-60(1970).

The γ-radiation following thermal-neutron capture in natural and in ^{28}Si enriched silicon was investigated with a Ge(Li) detector. Altogether 49 γ-transitions were found, most of which could be fitted into the level schemes of ^{29}Si, ^{30}Si or ^{31}Si. The excitation energies of ^{29}Si levels were determined precisely. The Q-values of the $^{28}Si(n,\gamma)^{29}Si$, $^{29}Si(n,\gamma)^{30}Si$ and $^{30}Si(n,\gamma)^{31}Si$ reactions have been determined as: Q = 8473.5 ± 0.5, 10609.5 ± 0.7 and 6587.5 ± 0.8 keV, respectively. (auth)

12404 DIFFERENTIAL SCATTERING OF NEUTRONS AT NARROW LEVELS IN ^{17}O. Fowler, J. L.; Johnson, C. H. (Oak Ridge National Lab., Tenn.). Phys. Rev., C; 2: 124-31(Jul 1970).

The differential cross sections for scattering of neutrons from ^{16}O at or near four narrow resonances were measured. The energy spread of the incident neutrons ranges from 5 to 13 keV full width at half maximum. Scattered neutrons were detected as a function of angle with a stilbene crystal. Using phase shifts from previous work, were detected the differential data were analyzed and resonant parameter assignments made as follows (in order: excitation energy of ^{17}O in keV, J value, parity, and c.m. resonant width in keV: 5867 ($5/2$+, 6.6), 7164 ($5/2$−, 1.4), 7377 ($5/2$+, 0.5), and 7380 ($5/2$−, 1.1)). In table form are given level assignments of ^{17}O up to 7380-keV excitation energy and estimates of reduced widths in single-particle units. (auth)

12405 DWBA ANALYSIS OF THE CROSS SECTION AND POLARIZATION DATA FOR THE $^{14}N(d,n)^{15}O$ REACTION AT 3.5 MeV. Meier, M. M. (Duke Univ., Durham, N. C.); Walter, R. L.; Donoghue, T. R.; Seyler, R. G.; Drisko, R. M. Nucl. Phys.; A159: 273-304(1970).

The differential cross section for elastic scattering of 3.5 MeV deuterons from ^{14}N was analyzed using the optical-model formalism and taking account of the compound elastic contribution in a consistent way. The analysis was conducted over a broad range of parameter space, and several distinct families were discovered. Representative sets from each of these families were used to provide initial state wave functions for DWBA calculations of the $^{14}N(d, n_0)^{15}O$ (g.s.) reaction. The results of the calculations are correlated with the families from which the particular sets were drawn. The calculations are compared to experimental cross section and polarization data and spectroscopic factors are extracted. The best agreement with the experimental results occurs for sets in a family which has a representative member with a real well depth of 100 MeV and a real well radius of 1.6 A$^{\frac{1}{3}}$ fm. Calculational sensitivities of the DWBA to parameter variation are investigated to provide a critique of the assumptions used in the $^{14}N(d, n)$ work, as well as to provide insight into some features of (d, n) reactions for neighboring nuclei. (auth)

XUM

12406 GAMMA-RAY PRODUCTION CROSS SECTIONS FOR THE $^{16}O(n,x\gamma)$ REACTION FROM 6.35- TO 16.52-MeV NEUTRON ENERGY. Orphan, V. J.; Hoot, C. G.; John, Joseph (Gulf Energy and Environmental Systems, Inc., San Diego, Calif.). Nucl. Sci. Eng.; 42: 352-66(Dec 1970).

Gamma-ray production cross sections were measured for the $^{16}O(n,x\gamma)$ reaction from 6.35- to 16.52-MeV neutron energy. The Gulf General Atomic LINAC was used to produce a pulsed source of neutrons having a continuous distribution of neutron energies. A 30-cm^3 Ge(Li) detector, placed at 125 deg to the incident neutron beam, was used to measure the γ-ray spectra. The corresponding neutron energy was determined by the time-of-flight technique. The two-parameter data (γ-ray energy, neutron energy) were processed with an on-line computer and sorted into 10 γ-ray spectra spanning the range 6.35 MeV $\leq E_n \leq$ 16.52 MeV. From these data average differential gamma-ray production cross sections were obtained for 9 gamma rays from the $^{16}O(n,x\gamma)$ reaction. The cross sections are in good agreement with other recent measurements, but show rather large disagreement with some earlier measurements. The total nonelastic cross section obtained by summing the partial cross sections is consistent with the nonelastic cross section obtained from the difference between the total cross section and the total elastic cross section for $E_n <$ 11 MeV. However, in the range 11 MeV $\leq E_n \leq$ 16.5 MeV, there is a serious discrepancy for which a possible explanation is discussed. (auth)

12407 PHOTOPRODUCTION OF CHARGED PIONS FROM ^{12}C. Rao, K. Srinivasa (Inst. of Mathematical Sciences, Madras); Devanathan, V.; Prasad, G. N. S. Nucl. Phys.; A159: 97-103(1970).

The photoproduction of π^+ from $^{12}C(0^+, g.s.)$ leading to the five bound states $J^\pi = 1^+, 2^+, 2^-, 1^-, 3^-$ of ^{12}B and the photoproduction of π^- from $^{12}C(0^+, g.s.)$ leading to the ground state of $^{12}N(J^\pi = 1^+)$ are studied by means of a transition amplitude obtained in the impulse approximation. It is suggested that these reactions are favorable for experimental study from which definite conclusions regarding the photopion production process can be drawn. (auth)

12408 OPTICAL-MODEL ANALYSIS FOR ^6Li ELASTIC SCATTERING BY ^{16}O AT 20 MeV. Schmidt, W.; Strohbusch, U. (Univ., Freiburg i. B.). Nucl. Phys.; A159: 104-12(1970).

$^6Li-^{16}O$ elastic scattering data were analyzed using the optical model without the spin-orbit term. Good fits were obtained for both surface and volume absorption. Continuous and discrete ambiguities similar to those known for d, ^3He and α scattering were found. The influence of uncertainties in the normalization of the cross sections on the parameters was investigated. (auth)

12409 EFFECT OF PAIRING CORRELATIONS ON THE LEVEL DENSITY OF THE SYSTEM OF INTERACTING NUCLEONS IN A p-SHELL. Zivanovic, D. (Boris Kidric Inst., Belgrade). Fizika (Zagreb); 2: 177-98(Oct 1970).

The level density of the model consisting of interacting nucleons in a p-shell is calculated, with pairing correlations taken into account through the Hartree–Bogoliubov canonical transformation. The grand partition function is first calculated by the suitably generalized Bloch–Dominicis perturbation formalism, and the level density is then obtained by the saddle-point method. The level-density curves corresponding to the 1st and 2nd order perturbation calculation are discussed. (auth)

12410 HARTREE–FOCK MODEL OF THE ^6Li NUCLEUS. Suzuki, Yasuyuki; Kubodera, Kuniharu (Tokyo Univ.). Progr. Theor. Phys. (Kyoto); 44: 617-45(Sep 1970).

The ^6Li nucleus is investigated in the projected Hartree–Fock model. In view of the partial successes of the deformed Hartree–Fock and the cluster models, an extension of the deformed orbits and construction of the molecule-like orbits is attempted. Energy variation and the calculation of the elastic and inelastic charge form factors are carried out in both the extended deformed orbits and the newly introduced molecule-like orbits. Conventional effective two-body forces are assumed in energy calculations. The results are compared with experiment and detailed discussions are made on the comparative merits of the above two orbits. Expansion of the Hartree–Fock states in terms of shell-model configurations is presented. The use of the density-dependent forces is discussed in connection with the underbinding of ^6Li. (auth)

12411 REACTION MATRIX THEORY FOR CLUSTER STATES IN LIGHT NUCLEI. I. ^8Be. Bando, Hiroharu; Nagata, Sinobu; Yamamoto, Yasuo (Kyoto Univ.). Progr. Theor. Phys. (Kyoto); 44: 646-62(Sep 1970).

Reaction-matrix theory is applied to the cluster model of ^8Be with the aim of founding it on a realistic nuclear force. The model wave function consists of the s orbits around two centers corresponding to two α clusters separated by distance 2d. For each value of d, self-consistent calculations are made for the reaction matrix and the single-particle energies; and then the generator-coordinate method is applied for the relative motion between two α clusters. The nuclear forces adopted are OPEG and H-J potential. The dependence of the effective interaction on clusterization is shown and discussed. (auth)

12412 LOW-LYING 0^+ STATES IN ^{12}C AND ^{16}O. Bouten, M.; Bouten, M.-C.; Depuydt, H.; Schotsmans, L. (SCK/CEN, Mol, Belgium). Nucl. Phys.; A158: 217-24(1970).

A projected Hartree–Fock calculation is carried out for the 0^+ states of the 0p–0h, 2p–2h, and 4p–4h configurations in ^{12}C and ^{16}O. The interaction B1 of Brink and Boeker is used. The 4p–4h states are lowered to energies which agree well with the first excited 0^+ states in ^{12}C and ^{16}O. The 2p–2h states, on the other hand, stay at about 20 MeV excitation. (auth)

12413 INVESTIGATION OF THE $^{12}C(\gamma,n)^{11}C$ REACTION FOR E_γ UP TO 1 GeV. Hylten, Gunnar (Lund Inst. of Tech., Sweden). Nucl. Phys.; A158: 225-9(1970).

The yield per equivalent quantum of the reaction $^{12}C(\gamma, n)^{11}C$ was determined between 100 and 1050 MeV. The cross section integrated throughout this energy region is calculated; and the cross section as a function of energy, derived. (auth)

12414 EFFECT OF THE DEUTERON D-STATE ON DWBA CALCULATIONS FOR $^{16}O(p,d)^{15}O$ AND $^{40}Ca(d,p)^{41}Ca$. Delic, G. (Australian National Univ., Canberra). Nucl. Phys.; A158: 117-28(1970).

The effect of the deuteron D-state on exact finite-range DWBA calculations is studied for l = 1 transitions in the following two reactions: $^{40}Ca(d, p)^{41}Ca$ leading to the 2.47($3/2^-$)- and 3.95-MeV($1/2^-$) levels for incident deuteron energies of 7 and 9 MeV and $^{16}O(p, d)^{15}O$ leading to the ground ($1/2^-$) and 6.18-MeV($3/2^-$) states for incident proton energies of 25.52, 30, and 31.82 MeV. Spectroscopic factors are extracted for calculations with and without a lower radial cut-off and compared to the corresponding zero-range predictions. The effect of the deutron D-state on the j-dependence shown by the differential cross sections, analyzing powers, and polarizations is investigated. (auth)

12415 EFFECT OF RESCATTERING AND THE ABSORPTION MECHANISM OF STOPPED π^- MESONS BY Li NUCLEI. Kopaleishvili, T. I.; Machabeli, I. Z. (Tbilisi State Univ., USSR). Nucl Phys.; A160: 204-10(1971).

The relative significance of the rescattering effect and of the interaction of nucleons emitted in the process (π^-, 2N) was studied on ^6Li and ^7Li nuclei. It was shown that when the rescattering effect is taken into account, interactions between outgoing nucleons may be neglected. The pair and α-particle mechanisms of π^- meson absorption by the ^6Li nucleus are discussed. These mechanisms lead to different excited states of residual nuclei. Some advantages of the two-particle mechanism of absorption are pointed out, while explaining the experimental features. (auth)

12416 GAMMA DECAY OF THE FIRST TWO $T = 3/2$ STATES OF ^{15}N. Kuan, H. M.; Umbarger, C. J.; Shirk, D. G. (Univ. of Kansas, Lawrence). Nucl. Phys.; A160: 211-21(1971).

Gamma transitions from the first two $T = 3/2$ states of ^{15}N were studied via the reaction $^{14}C(p,\gamma)^{15}N$. The angular distributions of the three transitions from the lowest $T = 3/2$ state at $E_x = 11.61$ MeV are isotropic, in agreement with the $J^\pi = 1/2^+$ assignment for the state. For the second $T = 3/2$ state at $E_x = 12.52$ MeV the angular distributions are in agreement with $J^\pi = 1/2^+$. The transitions 12.52 → 5.27 and 12.52 → 6.33 MeV are essentially pure M1 and pure E1, respectively. A comparison of the strength of the allowed β^- decay of the ^{15}C ground state (the supposed parent analog state of the 11.61 MeV state of ^{15}N) to the 5.30 MeV state of ^{15}N with the strength of the 11.61 → 5.30 MeV γ-transition in ^{15}N suggests a considerable contribution from the orbital part in the M1 matrix element. The Zuker–Buck–McGrory shell-model wave functions for ^{15}N give a qualitative description of the observed γ-decay. But the disagreement in decay strengths between theory and experiment and the omission of the known $1p_{\frac{1}{2}}$ hole state (6.33 MeV) suggest the need of ^{12}C core excitation in the ZBM calculation. (auth)

12417 DIRECT PHOTODISINTEGRATION OF ^6Li IN THE LOW AND SUB-GIANT DIPOLE RESONANCE REGION. Aurdal, A. (NORDITA, Copenhagen). Nucl. Phys.; A160: 99-108(1971).

Using a single-particle model for ^6Li, electric dipole cross sections for the reactions $^6Li(\gamma,p)^5He$ and $^6Li(\gamma,n)^5Li$ were evaluated in the photon energy range from the respective thresholds to 20 MeV. The interaction between the outgoing nucleon and the rest of the nucleus was in each case represented by a Saxon–Woods potential, a Coulomb term being added in the (γ,p) case. With potential parameters adapted from optical-model analyses, good agreement was obtained between the theoretical estimates and experimental

data by assuming a rather high percentage of α–d clustering in ^{6}Li. (auth)

12418 STUDY OF REACTIONS ^{6}Li + ^{12}C AT BOMBARDING ENERGIES FROM 9.0 TO 14.0 MeV. Johnson, David John. Iowa City, Ia.; Univ. of Iowa (1970). 212p. University Microfilms Order No. 70-15,608.

Thesis.

A comprehensive investigation of the ^{6}Li + ^{12}C reaction was carried out at bombarding energies above the Coulomb barrier for particle groups corresponding to the following states of the residual nuclei involved: 0.0, 0.871, 3.058, and 3.846 MeV for ^{17}O; 0.0, 6.05 + 6.13 (unresolved), 6.92 + 7.12, and 8.88 MeV for ^{16}O; 0.0 MeV for ^{15}O; and 0.0, 3.945, and 4.91 + 5.10 MeV for ^{14}N. Yield curves were measured for protons, deuterons, and α particles at laboratory angles of 0 and 40°, at ^{6}Li bombarding energies from 5.6 to 14.0 MeV. Angular distributions were measured at 9.0, 10.0, 11.2, 12.0, 13.0, and 14.0 MeV. An attempt was made to interpret the accumulated α particle data in terms of two-mode plane wave and single-mode distorted wave direct reaction theories. The proton, deuteron, and α particle data corresponding to individual states of the residual nuclei were also compared to Hauser–Feshbach-averaged angular distributions. It was concluded that the data could not be represented by a direct reaction mechanism alone. A similar conclusion was reached for the Hauser–Feshbach formalism. An Ericson fluctuation analysis of the yield curve gives a coherence width Γ_0 = 400 keV ± 100 keV for ^{18}F at 15.9 to 22.5 MeV excitation. An angular cross correlation analysis of the angular distributions gives a coherence angle of 15 to 20° for protons and 14 to 16° for α particle groups. (Diss. Abstr. Int., B)

12419 ELASTIC SCATTERING OF ALPHA PARTICLES BY ^{16}O. Takeda, Minoru; Kato, Syohei; Yamazaki, Takashi (Osaka Univ.). J. Phys. Soc. Jap.; 30: 56-61(Jan 1971).

Differential cross sections for the elastic scattering of alpha particles by ^{16}O have been measured at laboratory angle of 176° as a function of incident energy in the range 20 to 24.5 MeV. Six resonances have been observed. Angular distributions have been measured at eight energies. Tentative spin and parity assignments of the compound ^{20}Ne nucleus have been made. (auth)

12420 PION SCATTERING BY NUCLEI IN THE REGION OF THE (3,3) RESONANCE. Ericson, T. E. O. (CERN, Geneva); Huefner, J. Phys. Lett.; 33B: 601-4(21 Dec 1970).

The salient features of pion scattering by nuclei around $E_\pi \approx 180$ MeV are discussed within the frame of a simple model. It is found that the experimentally observed phenomena are essentially due to strong absorption and are rather insensitive to details of the scattering mechanism. (auth)

12421 BETA DECAY AND NUCLEAR STRUCTURE IN THE MASS-14 SYSTEM. Huffaker, J. N. (Oklahoma Univ., Norman); Laird, C. E. Nucl. Phys.; A150: 61-7(1970).

The β-decay correction factor for a very-much-hindered Gamow–Teller allowed transiton was calculated, including higher-order effects usually ignored. The results were used to analyze the decay of ^{14}O to the ^{14}N ground state, using various models of the nuclear structure. Also, the class of such models agreeing with both the ft-value and spectral shape was determined. A discussion is given of the ambiguities involved in determining the Gamow–Teller allowed matrix element. (auth)

12422 Al(α,α')Al* COMPOUND-NUCLEUS REACTIONS. Benveniste, J. (Physics International Co., San Leandro, Calif.); Merkel, G.; Mitchell, A. Phys. Rev., C; 2: 500-11(Aug 1970).

The energy and angular distribution of α particles inelastically scattered from Al were measured from 30 to 170° for 20.0- and 27.5-MeV bombarding energies. Angular distributions of the inelastic α particles corresponding to residual nuclei excited to the continuum are found to be symmetric around 90°. For a number of angular distributions, the magnitude of the anisotropy is large; i.e., the ratio of differential cross sections at 170 to 90° is greater than 2.5. In the interpretation of the experimental results, the nuclear-level-density parameter and the spin cutoff parameter are derived by application of the semiclassical compound-nucleus theory of Ericson and Strutinski. This cutoff parameter is consistent with the rigid-rotor model of the nucleus. In order to obtain agreement between the magnitudes of the calculated and the experimentally measured cross sections, it was necessary to incorporate nuclear shell effects into the statistical-theory calculations. (auth)

12423 R-MATRIX SHELL-MODEL CALCULATIONS OF SCATTERING AND REACTION CROSS SECTIONS. Takeuchi, K.; Moldauer, P. A. (Argonne National Lab., Ill.). Phys. Rev., C; 2: 925-41(Sep 1970).

The Wigner–Eisenbud R-matrix theory was applied to the calculation of neutron total and inelastic scattering cross sections for a system consisting of two neutrons interacting with an inert ^{16}O core through a spherically symmetric Woods–Saxon potential and interacting with each other through a δ-function force. The calculational method employed has the advantages that it includes the effects of shell-model configurations in which both neutrons are unbound, that it presents no obstacles to inelastic or reaction calculations, that it permits antisymmetrization of the compound space wave functions, and that it requires only one shell-model diagonalization for the computation of cross sections up to 5-MeV neutron energy. Use of antisymmetrized wave functions is shown to reduce substantially the number of compound-nucleus resonances and to reduce the magnitude of the inelastic cross section. By the correct calculation of the distant resonance contribution to the R matrix, it is shown that the calculated cross sections are independent of the choice of channel radii. Application of the method to more complex systems with larger numbers of neutrons as well as protons and holes and also with direct coupling between channels is discussed. A selection rule encountered in the calculations suggests a possible J^π dependence of the absorptive part of the optical-model potential. (auth)

12424 STUDY OF THE REACTION ^{15}N(τ,α)^{14}N. Bohne, W.; Homeyer, H.; Lettau, H.; Morgenstern, H.; Scheer, J.; Sichelschmidt, F. (Hahn-Meitner-Institut fuer Kernforschung, Berlin). Nucl. Phys.; A154: 105-12(1970).

The reaction ^{15}N(τ,α)^{14}N was studied at an incident energy of 11 MeV. For 13 final states spectroscopic factors were determined. The results were compared to other pick up reactions. It was found that the reaction is described quantitatively by DWBA, contrary to (τ,α) reactions on neighboring nuclei. (auth)

12425 LEVEL STRUCTURE OF ^{17}O AND THE ^{13}C(^{6}Li,d) AND ^{13}C(^{7}Li,t) REACTIONS. Bethge, K.; Pullen, D. J.; Middleton, R. (Univ. of Pennsylvania, Philadelphia). Phys. Rev., C; 2: 395-401(Aug 1970).

The reactions ^{13}C(^{7}Li,t)^{17}O and ^{13}C(^{6}Li,d)^{17}O were studied at 17 and 18 MeV, respectively. Both reactions are selective in the states they populate, although this is more evident in the (^{7}Li,t) case. Angular distributions were extracted for 15 levels below 8.5-MeV excitation. These exhibit pronounced structures and are generally indicative of direct-reaction mechanisms. Transitions to the negative-parity states at 3.06, 3.85, and 4.55 MeV are the strongest observed below 7-MeV excitation. These levels are discussed within the framework of the weak-coupling model and the transitions compared with those from the ^{12}C(^{7}Li,t) and ^{12}C(^{6}Li,d) reactions leading to the first K = 0 rotational band in ^{16}O. Strong transitions are also observed to levels at 7.38, (8.46, 8.49), (8.87, 8.95), and (9.14, 9.20) MeV. (auth)

12426 MONOPOLE EXCITATIONS IN ^{16}O. Gerace, W. J. (Univ. of Massachusetts, Amherst); Sparrow, D. A. Contract AT(30-1)-2098. Nucl. Phys.; A154: 576-86 (1970).

The monopole matrix elements and electron scattering form factors of the excited 0^+ states in ^{16}O were calculated using the Brown and Green valence wave functions in a triaxial potential. Although the use of triaxial intrinsic states increases the monopole matrix elements and form factors over the axially symmetric case, the overall agreement with experiment is still not good. The shape of the electron scattering form factors is found to be insensitive to the degree or type of deformation and to the details of the mixing of the intrinsic states. (auth)

Nuclear Properties and Reactions, 20 ≤ A ≤ 89

Refer also to abstracts 10892, 11693, 12309, 12353, 12366, 12394, 12402, 12403, 12414, 12419, 12519, 12520, 12529, 12549, 12554, 12607, 12624, 12627, 12635, 12664, 12686, 12689, and 12691.

12427 (AECL-3666) PHYSICS DIVISION PROGRESS REPORT, OCTOBER 1–DECEMBER 31, 1969. (Atomic Energy of Canada Ltd., Chalk River (Ontario). Chalk River Nuclear Labs.). 100p. (PR-P-84). Dep. CFSTI (U. S. Sales Only). AECL $2.00.

Studies made by the nuclear physics branch, the general physics branch, the neutron physics branch, the theoretical physics branch, and the mathematics and computation branch of the physics division at Atomic Energy of Canada Limited in the period Oct. 1 to Dec. 31, 1969 are briefly described. (J.W.R.)

12428 (CNEA-278) CROSS SECTION AND YIELD RELATIONS FOR THE ISOMERIC PAIR ^{90m}Y/^{90}Y OBTAINED BY THE

(d,p) REACTION. Corazza, C.; Nassiff, S. J. (Comision Nacional de Energia Atomica, Buenos Aires (Argentina)). 1970. 12p. (In Spanish). Dep. NTIS (U. S. Sales Only).

The excitation functions and the cross section ratios for the isomeric pair $^{90m}Y/^{90}Y$ produced by the (d,p) reaction were measured up to deuteron energies of 27.0 MeV. The stacked foil method was used and no chemical separation was made of the reaction products. (tr-auth)

12429 (COO-7-565) MAGNETIC MOMENTS OF THE 7/2$^-$ MIRROR STATES IN ^{37}Ar AND ^{37}K. Randolph, W. L. Jr.; Borchers, R. R. (Wisconsin Univ., Madison). [1970]. 7p. (CONF-700933-2). Dep. NTIS.

From Conference on Hyperfine Interactions Detected by Nuclear Radiation, Rehovot and Jerusalem, Israel.

The magnetic moments of the $^1/_2^-$ states in ^{37}K and ^{37}Ar are reported. The latter was determined to be -1.35 ± 0.06 nm from the reaction ^{37}Cl(p,n)^{37}Ar at E_p of 4.850 MeV; the lifetime of ^{37}Ar was measured as 4.66 ± 0.16 ns. The magnetic moment of ^{37}K, from the ^{40}Ca(p,α)^{37}K reaction at 13.0 MeV, was found to be 5.29 ± 0.26 nm. The lifetime determined for the 1.380-MeV state in ^{37}K was 10.82 ± 0.43 ns. (R.W.R.)

12430 (INR-P-1091) EXCITATION OF ISOMERIC ACTIVITIES IN ^{71}Ge, ^{78}Br, AND ^{79}Br USING 14.8-MeV NEUTRONS. Rurarz, E.; Haratym, Z.; Kozlowski, T.; Wojtkowska, J. (Institute of Nuclear Research, Warsaw (Poland)). 1969. 26p. Dep. NTIS (U. S. Sales Only).

The cross sections for the production of the isomeric states in ^{71}Ge, ^{78}Br and ^{79}Br were measured using 14.8-MeV neutrons. The half-lives and energies of these isomeric activities were remeasured for checking the assignments. Data were obtained for the following: ^{72}Ge(n,2n)^{71m}Ge, ^{79}Br(n,2n)^{78m}Br, and ^{79}Br(n,n') × ^{79m}Br. (auth)

12431 (INSJ-124) NUMERICAL DIFFERENTIAL CROSS SECTIONS OF THE REACTION ^{58}Ni(p,t)^{56}Ni WITH 51.9 MeV PROTONS. Suehiro, T.; Ishizaki, Y.; Ogata, H.; Kokame, J.; Stricker, A.; Saji, Y.; Sugiyama, Y.; Nonaka, I.; Saeki, B.; Nakamura, H. (Tokyo Univ. (Japan). Inst. for Nuclear Study). 31 Oct 1970. 17p. Dep. NTIS (U. S. Sales Only).

Numerical values of the differential cross sections for the reaction ^{58}Ni(p,t)^{56}Ni with 51.9-MeV protons are analyzed using the proton beam extracted from the INS synchrocyclotron. Momentum analysis of the emitted tritons was made with a broad-range magnetic spectrometer. The typical energy resolution was about 100 keV. (L.T.W.)

12432 (LYCEN-7034, pp 117-46) REVIEW OF EXPERIMENTAL WORKS ON CLOSED-SHELL NUCLEI AND THE ALMOST CLOSED SHELL NUCLEI FROM ^{40}Ca TO ^{210}Pb. Petit, G. Y. (Bordeaux Univ., Gradignan (France). Centre d'Etudes Nucleaires). (In French).

From Conference on low-energy spectrometry and nuclear spectrometry, Lyon, 18-20 February 1970.

Several experiments are reviewed which revealed the structure of nuclei of neutron numbers or proton numbers corresponding to almost closed shells. Five mass domains were revealed: nuclei in the ^{40}Ca region, the ^{89}Y region, the ^{118}Sn region, the ^{140}Ce region, and the ^{208}Pb region. There were certain parallels between the elements for which N = 50 and Z = 50, and also between the elements for which N = 82 and Z = 82 (which are doubly magic). (France)

12433 (NP-18552) POLARIZATION OF PROTONS INELASTICALLY SCATTERED ON ^{24}Mg, ^{52}Cr, AND ^{58}Ni. Ruh, Arthur Walter (Eidgenoessische Technische Hochschule, Zurich (Switzerland)). 1970. 56p. (In German). Dep. NTIS (U. S. Sales Only).

The polarization of protons inelastically scattered by ^{24}Mg, ^{52}Cr, and ^{58}Ni (with the residual nucleus left in its first excited state) was measured with a carbon polarimeter. The polarization of the elastically scattered protons was also measured. The energy of the incident protons was varied between 5.38 and 5.95 MeV; and the laboratory scattering angle, between 45° and 120°. In addition, the excitation functions were measured for ^{24}Mg(p,p$_1$)^{24}Mg* between 5 and 6 MeV and for ^{52}Cr(p,p$_0$)^{52}Cr and ^{52}Cr(p,p$_1$)^{52}Cr* between 5 and 6.5 MeV. Large values of the polarization were determined for the protons scattered by ^{24}Mg; and, in agreement with the predictions of the statistical CN model, no polarization was observed for the protons inelastically scattered by ^{58}Ni. Relatively large polarizations were found in the inelastic scattering by ^{52}Cr: this result seems to indicate a violation of the statistical assumptions. The latter had been believed to be fulfilled, since (p,p'γ)-angular-correlation measurements on ^{52}Cr had given excellent agreement with the statistical CN theory. On the other hand, the angular cross-correlation function of the cross-section fluctuations also does not agree with the statistical theory. The correlated intermediate structure of the excitation functions can probably be interpreted as an excitation of doorway states; this assumption, in turn, would also explain the measured polarizations. (auth)

12434 STUDY OF THE TRANSFER REACTIONS (α,t), (α,^{3}He) IN THE fp SHELL: MECHANISM AND SPECTROSCOPIC USE. Roussel, P.; Bruge, G.; Bussiere, A.; Faraggi, H.; Testoni, J. E. (CEN, Saclay, France). Nucl. Phys.; A155: 306-36(1970). (In French).

A study of (α,t) and (α,^{3}He) reactions at 44 MeV on the target nuclei ^{54}Fe and ^{58,60,62,64}Ni, with the use of solid-state identifier, is described. A critical study of optical-model and distorted-wave analysis is performed. The complementarity of different transfer reactions, the ambiguity of the spectroscopic factors, and the importance of the problem of the reaction mechanism are demonstrated. (auth)

12435 STRUCTURE OF ^{51}Cr VIA ^{49}Ti(^{4}He,nγ) AND ^{51}V(p,nγ) PROMPT γ-RAY SPECTROMETRY. Sarantites, D. G.; Winn, W. G. (Washington Univ., St. Louis). Contracts AT(11-1)-1530; AT(11-1)-1760. Nucl. Phys.; A155: 257-96(1970).

The level structure of ^{51}Cr was studied in some detail via prompt γ-ray energy and intensity measurements by utilizing a NaI(Tl)-Ge(Li) anti-Compton spectrometer and a 511-γ-511 escape peak spectrometer via the ^{51}V(p,nγ) reaction with proton energies in the range 2.6 to 6.0 MeV and via the ^{49}Ti(^{4}He,nγ) reaction with ^{4}He^{++} energies in the range 12.0 to 15.0 MeV. Many of the γ rays associated with levels in ^{51}Cr were identified with the (^{4}He,nγ) or the (p,nγ) reaction by means of nγ coincidence measurements employing an organic phosphor as the fast-neutron detector and a Ge(Li) γ-ray detector. Characterization of many levels populated in the (p,nγ) reaction was achieved by means of thresholds for individual γ rays obtained from measurement of excitation functions of individual γ rays, and from the $\gamma\gamma$ coincidence relationships established in on-beam $\gamma\gamma$ coincidence measurements in the ^{51}V(p,nγ) reaction at E_p = 5.0 MeV employing a NaI(Tl) and a Ge(Li) detector. It was thus established that 39 levels in ^{51}Cr are populated in these reactions. The levels at 2255.7, 2385.6, 2767.1, and 3001.6 or 3004.1 keV, which were observed in these experiments, have not been reported previously. The rest of the levels studied in this work have been studied previously by means of (d,p), (p,d), and (n_{th},γ) reactions. With the exception of the first six levels, the levels reported here have not been reported previously in the (p,nγ) or the (^{4}He,nγ) reactions. For the levels below 2704 keV in ^{51}Cr branching ratios for deexcitation of these levels by γ decay were obtained by averaging the measured angular correlation of each γ ray about the beam direction. The new γ-ray information from the present study was used in conjunction with the results of previously reported (d,p) reaction studies to make definite J$^\pi$ assignments to many stripping levels in ^{51}Cr, and to place limits to the J$^\pi$ values for many levels that were reported earlier to exhibit proton-angular-distribution patterns from the (d,p) reaction non-characteristic of a stripping reaction. In this work a number of γ rays were assigned to deexcite levels in ^{51}V that are populated via the ^{51}V(p,p'γ) and ^{49}Ti(^{4}He,pγ) reactions and which were found to compete to a small extent with the (p,nγ) and (^{4}He,nγ) reactions. A tentative decay scheme for the deexcitation of levels in ^{51}V is offered. The level structure of ^{51}Cr and of ^{51}V is compared with previously reported results of the Coriolis coupling model for the $f_{\frac{7}{2}}$ shell, and good qualitative agreement in the level ordering is found. (auth)

12436 STRUCTURE OF THE CALCIUM ISOTOPES. Federman, P. (Weizmann Inst. of Science, Rehovot, Israel); Pittel, S. Nucl. Phys.; A155: 161-81(1970).

The calcium isotopes for A = 41 to 50 are studied in the framework of the shell model by using the method of effective interactions. Particular attention is focused on some of the puzzles provided by recent (t,p) data. The model is extremely successful in reproducing the observed features of the Ca isotopes. The reproduction of energy levels is very good, as is the reproduction of single-particle spectroscopic factors and (t,p) strengths calculated by using the resulting wave functions. Finally, the two-particle matrix elements obtained exhibit all the features that are desired of them. (auth)

12437 INVESTIGATION OF PROTON INDUCED RESONANCE REACTIONS ON ^{39}K. De Meijer, R. J.; Sieders, A. A.; Landman, H. A. A.; De Roos, G. (Rijksuniversiteit, Utrecht). Nucl. Phys.; A155: 109-28(1970).

The ^{39}K(p,α_0)^{36}Ar reaction was investigated in the energy region E_p = 1.75 to 3.23 MeV; 52 resonances were observed. Resonance and excitation energies, yields, J$^\pi$ values, and formation parameters were determined, the latter two from angular distribution

measurements. A $\Delta E-E$ counter telescope system was used to reduce the background arising from proton pile-up. The yield of the $^{39}K(p,p_0)^{39}K$ reaction was measured simultaneously with the (p,α_0) yield; 25 (p,p_0) resonances could be analyzed in the region E_p = 1.75 to 3.23 MeV. Resonance and excitation energies, yields, widths, J^π values, and orbital angular momenta were determined. In the energy region E_p = 1.03 to 1.75 MeV the (p,p_0) reaction was measured simultaneously with the yield of the $^{39}K(p,\gamma)^{40}Ca$ reaction. The resonances at E_p = 1103, 1130, 1153, 1238, 1306, and 1307 keV appear in both reactions. Some of the possible J^π values, obtained from the (p,p_0) analysis, could be excluded with the help of the known γ decay. A comparison is made with data obtained from a study of delayed proton emission following the positron decay of ^{40}Sc and with data from the $^{39}K(d,n)^{40}Ca$ reaction. A number of resonances can be explained as the analogs of known ^{40}K levels. (auth)

12438 EXCITATION FUNCTIONS FOR RADIOACTIVE NUCLIDES PRODUCED BY DEUTERON-INDUCED REACTIONS IN COPPER. Fulmer, C. B.; Williams, I. R. (Oak Ridge National Lab., Tenn.). Nucl. Phys.; A155: 40-8(1970).

Cross sections were measured for the production of radioactive nuclides by deuteron-induced reactions in natural copper at bombarding energies up to 40 MeV. Stacked foil targets were bombarded with deuterons from the Oak Ridge Isochronous Cyclotron. Gamma spectra of individual foils were measured with a Ge(Li) spectrometer. Excitation functions were obtained for ^{61}Cu, ^{62}Cu, ^{64}Cu, ^{66}Cu, ^{62}Zn, ^{63}Zn, and ^{65}Zn. Yields for $^{63}Cu(d,xn)$ reactions show a strong dependence on level density of the residual nucleus. (auth)

12439 CROSS SECTIONS FOR THE PRODUCTION OF NUCLIDES FROM MEDIUM-WEIGHT ELEMENTS BY HIGH-ENERGY PROTON BOMBARDMENT. Gupta, B. K. (Univ. of Calcutta); Das, S.; Biswas, M. M. Nucl. Phys.; A155: 49-69 (1970).

By starting from a simplified and idealized model an expression for the formation cross section of nuclides by the bombardment of high-energy protons on a medium-weight nucleus is derived from a statistical approach, which, with the help of a few reliable experimental data, could give the cross sections of the whole series of the nuclides that might be formed from such target. It is applied to the targets V, Mn, Fe, Co, Ga, As, Y, and Nb. In view of the level of accuracy of the experimental cross sections, the calculated values agree fairly well with the experimental ones. (auth)

12440 SPINS, PARITIES, AND ELECTROMAGNETIC TRANSITION PROBABILITIES IN ^{35}Cl. Wiesehahn, Willem Jacobus. Toronto; Univ. of Toronto (1968).

Thesis.

The spins and parities of levels in ^{35}Cl and the multipolarities, mixing ratios, and branching ratios of the gamma rays emitted in the deexcitation of these levels were studied. The levels were populated at four resonances in the $^{34}S(p,\gamma)^{35}Cl$ reaction at proton energies E_p = 1019 keV, 1214 keV, 1267 keV and 1510 keV. The levels up to and including the 3163-keV level were also populated by the $^{34}S(d,n)^{35}Cl$ reaction. The yield of this reaction was measured in the deuteron energy range from 3.8 MeV to 5.2 MeV and found to be nonresonant. The angular distributions of the neutrons leading to the various excited levels up to 3.163 MeV were studied at a deuteron energy of 4.95 MeV. For three of the resonances the angular distributions of one or more gamma rays were determined. The negative parities of the 7545-keV level (E_p = 1214 keV resonance) and the 3163-keV level were determined by measuring the linear polarization of the cascade gamma rays via these levels. The parities and spins of the levels below 4 MeV were also determined by a study of the angular distribution of the neutrons in the $^{34}S(d,n)^{35}Cl$ reaction. The doppler shift attenuation was used to measure the mean lifetime of several levels or to determine limits. A summary of all the experimental results is presented. The shell model with core excitation is applied to the decay scheme of ^{35}Cl nucleus. It appears that the description of the properties of the ^{35}Cl nucleus using this model is the best of all models available; however, the 3006-keV level is not accounted for. (TSS) (Diss. Abstr. Int., B)

12441 STUDY OF HIGH ISOSPIN STATES BY ISOSPIN-FORBIDDEN RADIATIVE CAPTURE REACTIONS. Snover, Kurt Albert. Stanford, Calif.; Stanford Univ. (1969). 109p. University Microfilms Order No. 70-10,528.

Thesis.

The low-lying T = 2 levels in several light, self-conjugate nuclei were investigated by means of isospin-forbidden radiative-capture reactions. Proton particle-capture reactions were investigated in the vicinity of the lowest T = 2 states of ^{12}C, ^{20}Ne, ^{24}Mg, and ^{32}S; and both proton and alpha-particle capture reactions into ^{28}Si were studied in the vicinity of the lowest two T = 2 levels. In addition, alpha-induced charged-particle reactions were studied in the immediate vicinity of the lowest T = 2 level in ^{28}Si. In ^{20}Ne and ^{28}Si the lowest T = 2 levels were located and studied, and in ^{24}Mg additional measurements of the properties of the lowest T = 2 level were made. Evidence for a tentative assignment for the lowest T = 2 level in ^{32}S is presented, along with negative results for ^{12}C and the second T = 2 level in ^{28}Si. These measurements provide accurate excitation energies of the observed T = 2 levels, small upper limits (typically about 2 keV) on the total widths of the states, radiative-capture strengths, and both qualitative and quantitative information on the sizes of the isospin-forbidden particle decay modes of these states. Also reported are the first measurements which test the basic selection rule for electromagnetic decay, $\Delta T = 0, \pm 1$. The excitation-energy measurements are discussed in terms of Coulomb-energy calculations and the quadratic mass formula, and are used in computations of masses of missing members of the isobaric multiplets. The measured radiative-decay strengths and branching ratios are discussed and compared to theoretical calculations. The isospin-forbidden radiative and particle decays are discussed, along with a qualitative model for the latter. (auth) (Diss. Abstr., Int., B)

12442 LEVELS IN ^{34}Cl AND ^{35}Cl FROM THE REACTIONS $^{34}S(p,n)$ AND $^{31}P(\alpha,n)$. Umbarger, Cecil John Jr. Tallahassee; Florida State Univ. (1969). 120p. University Microfilms Order No. 70-11,170.

Thesis.

Ground- and excited-state threshold energies for the reactions $^{34}S(p,n)^{34}Cl$ and $^{31}P(\alpha,n)^{34}Cl$ were investigated by detection of the positron decay of ^{34}Cl. The 1.57-second super-allowed positron activity was observed with a plastic scintillator as a function of beam energy. The (p,n) ground-state threshold was found to be 6,438 ± 10 keV; and the (α,n) ground-state threshold, 6,360 ± 10 keV. The values for the mass of ^{34}Cl, calculated from the two measurements, agree with each other and previous results. Excited-state thresholds in the two excitation functions correspond to known levels at 460, 670, and 1,230 keV. The positron end-point energy for the superallowed decay of ^{34}Cl was measured in a plastic scintillator. The resulting value of 4.44 MeV agrees with the end-point energy calculated from the (p,n) and (α,n) threshold measurements. The gamma energy of the first excited state in ^{34}Cl was measured to be 146 ± 2 keV with a Ge(Li) detector. Absolute total cross sections were measured for the production of the ground state of ^{34}Cl (1.57-second half-life) and its first excited state (32-minute half-life) for both the (p,n) and (α,n) reactions. Resonance structures were found in both the (p,n) and (α,n) excitation functions, indicating that the reaction mechanism contains a compound-nucleus component. The prominent resonances correspond to levels near 12.9, 13.3, 13.5, and 13.9 MeV in the compound nucleus ^{35}Cl. The elastic scattering of alpha particles on phosphorus was studied to help determine the nature of the states near 12.9 MeV in ^{35}Cl responsible for the observed resonances. The lack of any prominent structure in the $^{31}P(\alpha,\alpha_0)^{31}P$ excitation functions, plus the results of the (p,n) and (α,n) cross-section measurements, suggests tentative isospin and angular-momentum assignments of $[T,J] = [3/2, 7/2]$ or $[3/2, 5/2]$ for the levels. (auth) (Diss. Abstr. Int., B)

12443 STUDY OF DOPPLER-BROADENED GAMMA RAYS RESULTING FROM THE $^{23}Na(p,\alpha\gamma)^{20}Ne$ REACTION. Stark, Werner Joseph. Lawrence, Kan.; Univ. of Kansas (1969). 101p. University Microfilms Order No. 70-11,090.

Thesis.

A Ge(Li) detector was used to find the spin and parity for several states in the ^{24}Mg compound nucleus formed by means of the $^{23}Na(p,\alpha\gamma)^{20}Ne$ reaction. Arguments are made showing that the pulse-height distribution resulting from Doppler-broadened gamma rays depends on the $\alpha-\gamma$ angular correlation. This correlation was determined at several resonances from an analysis of the pulse-height distribution. Supplementary information on the possible spin and parity and the mixing parameters was obtained from conventional angular distribution measurements at each resonance. The results show that this method was successful in finding the spin and parity of several states in ^{24}Mg in the energy range $12.7 < E_x < 13$ MeV. Three previous spin and parity assignments were confirmed and new assignments were made at three resonances. These are $J^\pi = 2^+$, 1^+, and 3^- at Ep = 1.163, 1.254, and 1.458 MeV, and $J^\pi = 2^+$, (2^-), and 2^- at Ep = 1.091, 1.210, and 1.328 MeV. In addition, new information on the orbital angular momentum of the protons in the formation process and the α particles in the decay was obtained for all the states investigated. (TSS) (Diss. Abstr. Int., B)

12444 DISINTEGRATION OF THE TWO ISOMERS OF ^{84}Br (31.8 MIN AND 6.0 MIN). Hattula, T.; Andre, S.; Schussler, F.;

XUM

Moussa, A. (CEN, Grenoble, France). Nucl. Phys.; A158: 625-43(1970). (In French).

The study of β and γ activity, associated with the disintegration of the two isomers of ^{84}Br produced by fission of ^{235}U and by the reaction natural Rb(n,α), allowed determination of 16 states of ^{84}Kr. The use of magnetic spectrometers enabled assignment of spin 2$^-$ to the isomer of 31.8-min half-life and a precise measurement of its Q value (4650 ± 30 keV). (auth)

12445 DECAY OF 6.5 MIN ^{78}Br. Pan, P. J.; Taylor, H. W. (Univ. of Toronto). Nucl. Phys.; A158: 664-72(1970).

The decay of 6.5-min ^{78}Br was studied with a Ge(Li) spectrometer and a Ge(Li)-NaI(Tl) coincidence spectrometer. Levels in ^{78}Se are proposed at 613.9, 1308.3, 1498.7, 2329, 2454, 2510, 2537.9, 3090.4, 3220, 3345, and 3528 keV. Positron branchings to the first three states of ^{78}Se were established experimentally. (auth)

12446 CHARGE EXCHANGE OF 70 MeV π^- ON C, Al, Cu, AND Pb. Hilscher, H.; Krebs, W.-D.; Sepp, G.; Soergel, V. (Univ., Heidelberg). Nucl. Phys.; A158: 602-6(1970).

The integrated cross sections for the total charge exchange of 70-MeV π^- on natural carbon, aluminum, copper, and lead were measured by detecting the π^0-decay γ rays. For lead, the cross section per proton was found to be about 12 times smaller than for a free proton. The dependence of the cross section per proton on the mass number A is compared with theoretical predictions, and a value for the cross section of the elementary pion-nucleon interaction inside the nucleus is derived. (auth)

12447 RADIATION WIDTHS OF BOUND NUCLEAR LEVELS IN THE VICINITY OF THE NEUTRON THRESHOLD. Schlesinger, Y. (Soreq Nuclear Research Centre, Yavne, Israel); Szichman, H.; Ben-David, G.; Hass, M. Phys. Rev., C; 2: 2001-9(Nov 1970).

The radiation widths of bound nuclear levels excited by (γ,γ') reactions in nuclei ^{139}La, ^{130}Te, ^{120}Sn, ^{86}Sr, ^{80}Se, and ^{66}Zn were measured. The present results together with results published by other authors using (γ,γ') reactions are summarized and compared with similar results obtained in capture reactions of thermal and resonance neutrons. The expected properties of the nuclear levels obtained by extrapolation of the giant-dipole resonance to lower energies are compared with the present experimental data. The fluctuation in partial radiative widths from these bound levels is shown to be compatible with the Porter-Thomas distribution. (auth)

12448 SEARCH FOR THE DOUBLE BETA DECAY OF ^{48}Ca AND LEPTON CONSERVATION. Bardin, R. K.; Gollon, P. J.; Ullman, J. D.; Wu, C. S. (Columbia Univ., New York). Nucl. Phys.; A158: 337-63(1970).

Although recent mass-spectrometer experiments have shown convincingly that double beta decay does take place, observation of the decay-electron spectrum is necessary to be certain whether two neutrinos are emitted (as expected if one assumes lepton conservation) or none (if leptons are not conserved). An attempt to measure the electron spectrum from the double beta decay of ^{48}Ca was made in a deep salt mine by means of a streamer chamber in a magnetic field. In 1150 hours of observation with a 10.6-g source, only one event was seen which might be neutrinoless double beta decay; this implies a half-life of $>2 \times 10^{21}$ y at the 80% confidence level. This in turn implies that any violation of lepton conservation must be of the order of 10^{-3} or less. A half-life limit of $>3.6 \times 10^{19}$ y for the two-neutrino mode of ^{48}Ca double beta decay was also obtained. (auth)

12449 ROTATIONAL STRUCTURE IN ^{28}Si. Main, I. G.; Dawson, N.; Davis, C. K.; (and others) (Univ. of Liverpool). Nucl. Phys.; A158: 364-84(1970).

Properties of excited states below 5.3 MeV in ^{28}Si were deduced from proton-γ angular correlations in inelastic proton scattering, and from γ-ray angular distributions in the ^{26}Mg(α,nγ) reaction. Spins $^1/_2$, $^3/_2$, $^3/_2$, $^5/_2$, and $^1/_2$ are assigned to the levels at 4.08 MeV, 4.74 MeV, 4.84 MeV, 4.89 MeV, and 5.28 MeV, respectively; and previous spin assignments are confirmed for all other levels below 5.3 MeV. Branching ratios were measured for all these levels. A number of multipole mixing ratios are deduced, and are supplemented by angular-correlation data from inelastic α-particle scattering. The results are shown to be consistent with some predictions of the strong-coupling rotational model. (auth)

12450 STUDY OF THE T = $^3/_2$ STATES OF ^{25}Mg AND ^{29}Si. Detraz, C.; Richter, R. (Max-Planck-Institut fuer Kernphysik, Heidelberg). Nucl. Phys.; A158: 393-402(1970).

Magnetic-spectrograph analysis of the (^{3}He,α) reaction at 15.4 MeV was used to investigate T = $^3/_2$ states in ^{25}Mg and ^{29}Si. Eight T = $^3/_2$ levels in ^{25}Mg and five in ^{29}Si are characterized. For almost all of them, l-transfer assignments and spectroscopic factors could be extracted. The level scheme and spectroscopic properties of the T = $^3/_2$ ^{25}Mg and ^{29}Si levels closely correspond to those of the parent ^{25}Na and ^{29}Al nuclei, respectively. Some observed Coulomb displacements between the parent and analog states are discussed in relation with the configuration of these states. (auth)

12451 NUCLEAR-STRUCTURE CALCULATIONS FOR ^{58}Cu AND ODD NICKEL ISOTOPES. Singh, R. P.; Raj, R.; Rustgi, M. L.; Kung, H. W. (State Univ. of New York, Buffalo). Phys. Rev., C; 2: 1715-24(Nov 1970).

A detailed shell-model calculation is carried out to discuss the properties of the low-lying states of ^{58}Cu and ^{59}Ni nuclei. An inert ^{56}Ni core is assumed and the three extracore particles are considered to occupy the $1p_{3/2}$, $0f_{5/2}$, and $1p_{1/2}$ orbitals. The effect of including the $0g_{9/2}$ orbital is studied. The renormalized reaction matrix elements as derived by Kuo and Brown for this mass region are used. A comparison between the observed and calculated energy levels is made and the wave functions obtained are used to calculate the spectroscopic factors for the ^{58}Ni(^{3}He,d)^{58}Cu and ^{58}Ni(d,p)^{59}Ni reactions. The odd-mass Ni isotopes (^{59}Ni,^{61}Ni,^{63}Ni, ^{65}Ni) are then described by the modified Tamm-Dancoff approximation (MTDA) method. The MTDA results for odd Ni isotopes are found to be in quite satisfactory agreement with experiment. These results together with the previous results for even Ni isotopes by Roy, Raj, and Rustgi lead one to believe that the Kuo-Brown matrix elements in conjunction with the MTDA method give a good description of all the Ni isotopes. (auth)

12452 NUCLEAR STRUCTURE OF ^{48}Sc FROM THE ^{49}Ti(d,^{3}He)^{48}Sc REACTION. Ohnuma, H. (Univ. of Minnesota, Minneapolis); Yntema, J. L. Phys. Rev., C; 2: 1725-8(Nov 1970).

The ^{49}Ti(d,^{3}He)^{48}Sc reaction was studied at 19.45 and 22.4 MeV, and spectroscopic factors were obtained. There are serious discrepancies between the present result and previous work. The present experiment supports a simple picture of the ^{48}Sc nucleus. (auth)

12453 BETA DECAY OF ^{20}O. Mak, H. B. (California Inst. of Tech., Pasadena); Spinka, H.; Winkler, H. Phys. Rev., C; 2: 1729-33(Nov 1970).

^{20}O was produced in the reaction ^{18}O(^{18}O,^{16}O)^{20}O and its half-life measured by observing the decay of the 1.06-MeV γ transition in ^{20}F in a Ge-Li counter. The result is $t_{1/2}$ = 13.57 ± 0.1 sec, log ft = 3.73. Upper limits were obtained for weak β-decay branches of ^{20}O to other states in ^{20}F between E_x = 0.984 and 2.195 MeV. (auth)

12454 SPIN DEPENDENCE IN INELASTIC SCATTERING. Legg, J. C. (Kansas State Univ., Manhattan); Abraham, D. R.; Yntema, J. L.; Bearse, R. C.; Fortune, H. T. Phys. Rev., C; 2: 1733-7(Nov 1970).

The inelastic scattering of deuterons, ^{3}He, and α particles from ^{63}Cu, ^{65}Cu, and ^{67}Zn was investigated to determine whether spin-dependent effects similar to those observed for protons were observable for these projectiles. The inelastic deuteron scattering shows an effect that is similar to, but stronger than, that seen for proton scattering. The angular distributions for $^1/_2^-$ states are quite different from those for $^5/_2^-$ and $^1/_2^-$ states in ^{63}Cu and ^{65}Cu. The inelastic ^{3}He scattering exhibits no real structure in its angular distributions for any of the states, so no conclusions may be reached concerning spin-dependent effects for ^{3}He scattering. The inelastic α scattering shows no spin-dependent effect. No definite theoretical explanation for these observations is apparent. (auth)

12455 OPTICAL-MODEL ANALYSIS OF ALPHA-PARTICLE SCATTERING BY ^{36}Ar FROM 12.83 TO 17.83 MeV. Wallace, W. J.; Knuth, K. R.; Davis, R. H. (Florida State Univ., Tallahassee). Phys. Rev., C; 2: 1738-46(Nov 1970).

Forty-six-point angular distributions for the elastic scattering of α particles by ^{36}Ar were measured with a gas target from 12.83 to 17.83 MeV in 20-keV intervals throughout the angular range from 29.0 to 167.8° (c.m.). Optical-model fits to the data smoothed in energy with a Lorentzian weighting function were obtained. The computed cross sections were obtained from an incoherent sum of a direct contribution calculated from the optical model and a compound-elastic term based on Hauser-Feshbach theory. Parameters found for the compound-elastic-scattering term are consistent with the systematics for such parameters determined from fluctuation theory. The importance of compound-nuclear processes in the inelastic scattering is confirmed by a coupled-channel calculation. Although there is some indication of discrete ambiguous potentials in the analysis, no set exists for which the fits are com-

parably good. Fits to the data were not improved by the inclusion of l-dependence in the imaginary potential. Parameter values determined by the analysis were U = 182.2 MeV and W_S = 36.4 MeV (surface imaginary), with a fixed real well-radius value of 4.9 F chosen to be consistent with previous analyses of electron scattering data. (auth)

12456 PHOTONEUTRON CROSS SECTION OF STRONTIUM. Hicks, R. S.; Spicer, B. M. (Univ. of Melbourne, Parkville, Australia). Nucl. Phys.; A159: 265-72(1970).

The photoneutron cross section of natural Sr was measured from threshold to 27 MeV using bremsstrahling and direct neutron detection. The measurement is compared with theoretical dipole spectra of ^{88}Sr calculated using the particle-hole formalism and the dynamic collective model. Although all structure observed can be accounted for by either one or both models, neither offers a complete explanation of the observed cross section. The relevance of the conservation of isospin is discussed. (auth)

12457 GENERALIZED DWBA MODEL APPLIED TO THE ^{24}Mg(d,p)^{25}Mg REACTION AT E_d = 13.5 MeV. Schulz, H. (Joint Inst. for Nuclear Research, Dubna, USSR); Wiebicke, H. J.; Fuelle, R.; Netzband, D.; Schlott, K. Nucl. Phys.; A159: 324-36(1970).

Angular distributions of the reaction ^{24}Mg(d,p)^{25}Mg were calculated by the code POLLUX and compared with the experimental data covering the $5/2^+$[202], $1/2^+$[211], $1/2^+$[200] and $1/2^-$[330] rotational bands. The code considers indirect transitions arising via intermediate rotational excitations of the target and final nuclei. The optical and deformation parameters for both the entrance and exit channel were taken from the elastic and inelastic scattering data. The wave function of the transferred neutron was obtained in a deformed Saxon-Woods potential. The experimental data are sufficiently well described as is shown by the comparison between calculation and measurement. This concerns the shape as well as the absolute cross section. In particular a remarkable agreement was obtained for the stripping forbidden transition to the $1/2$ $5/2^+$[202] state. (auth)

12458 ANGULAR MOMENTUM PROJECTION FROM NON-AXIAL INTRINSIC STATES: A CALCULATION FOR ^{20}Ne. Watt, A. (Univ. of Glasgow). Nucl. Phys.; A159: 202-8(1970).

Projected Hartree-Fock calculations are reported for ^{20}Ne. States of definite angular momentum are projected from non-axial intrinsic wave functions and their energies are then minimized. The results are compared with exact shell-model calculations and good agreement is obtained. (auth)

12459 SHELL-MODEL STUDY OF ^{65}Cu AND ^{63}Cu. Wong, S. S. M. (Univ. of Toronto. Univ. of Rochester, N. Y.). Nucl. Phys.; A159: 235-48(1970).

The low-lying states of ^{65}Cu and ^{63}Cu are studied in the framework of the ($1f_{\frac{1}{2}}2p_{\frac{3}{2}}2p_{\frac{1}{2}}$) shell model with realistic effective interaction. Good agreement is obtained with the observed level structure, E2 and M1 decay rates and spectroscopic strengths. The weak-coupling scheme of coupling a proton to the quadrupole vibrations of nickel is found to be valid provided admixtures of $2p_{\frac{1}{2}}$ and $1f_{\frac{5}{2}}$ proton states are allowed in addition to the usual $2p_{\frac{3}{2}}$ state. This implies that it is possible to treat more complicated vibrational nuclei by first calculating the individual proton and neutron vibrational modes microscopically and then coupling them with a residual proton-neutron force. (auth)

12460 AVERAGE CROSS SECTIONS OF THE ^{28}Si(n,p)^{28}Al AND THE ^{29}Si(n,p)^{29}Al REACTIONS IN A FISSION NEUTRON SPECTRUM. Bruggeman, A.; De Soete, D.; Hoste, J. (Ghent Univ.). Radiochim. Acta; 14: 147-51(Nov 1970).

The average cross sections in an undisturbed fission neutron spectrum were experimentally determined for the reactions ^{28}Si(n,p)^{28}Al and ^{29}Si(n,p)^{29}Al, with the ^{32}S(n,p)^{32}P reaction as a reference. The thermal to fast flux ratio was evaluated in the irradiation facility, by means of the (n,γ) reaction on ^{23}Na and the (n,p) reaction on ^{32}S respectively, and was found to be approximately 5. As short irradiations were required, only the thermal flux monitor was applied for the sample irradiations, and the equivalent fission flux was determined by means of the thermal to fast flux ratio. This was possible as the shape of the neutron energy spectrum in the reactor remained unchanged for small fluctuations in the neutron flux density. The ^{28}Al and ^{29}Al disintegration rates were measured by means of a calibrated gamma spectrometer, without chemical separation of the matrix. Average cross sections of 6.68 mb and 3.41 mb were found for the respective reactions, with a standard deviation of about 1.2% (on the basis of $\bar{\sigma}$ = 65 mb for the reaction ^{32}S(n,p)^{32}P). (auth)

12461 STUDY OF PROTONS AND ALPHA PARTICLES EMITTED FROM ^{75}Br COMPOUND NUCLEI WITH DIFFERING ANGULAR-MOMENTUM DISTRIBUTIONS. Reedy, R. C.; Fluss, M. J.; Herzog, G. F.; Kowalski, L.; Miller, J. M. (Columbia Univ., New York). Phys. Rev.; 188: 1771-83(20 Dec 1969).

The energy spectra and angular distributions of protons and α particles emitted from the compound nucleus ^{75}Br formed at the excitation energies of 49 and 88 MeV have been studied. The ^{75}Br compound nuclei were formed in three different ways: ^{11}B + ^{64}Zn, ^{12}C + ^{63}Cu, and ^{16}O + ^{59}Co. The differences in the angular-momentum distributions of the compound nuclei formed in each of the entrance channels permitted the study of the particles emitted from specific ranges of angular momentum of the compound nuclei. The yield of α particles from the high-angular-momentum states was found to be significantly enhanced relative to that from the low-angular-momentum states and the average energy of the α particles emitted increased with the angular momentum of the compound nucleus. The yield of protons and their average energy was not significantly affected by angular momentum. These results are consistent with results calculated using an angular-momentum-dependent statistical theory of nuclear reactions. (auth)

12462 ON-LINE SEPARATION AND IDENTIFICATION OF SEVERAL SHORT-LIVED FISSION PRODUCTS: DECAY OF ^{84}Se, ^{91}Kr, ^{97}Y, ^{99}Nb, ^{99}Zr, ^{100} ^{101}Nb, and ^{101}Zr. Eidens, J.; Roeckl, E.; Armbruster, P. (Kernforschungsanlage, Juelich, Ger.). Nucl. Phys.; A141: 289-324(1970).

A device for nuclear spectroscopy of short-lived fission products was run at the focus of the gas-filled on-line mass separator at the FRJ-2 reactor. By the known γ-lines of long-lived fission products, a mass calibration of the separator was carried out. Several unknown short-lived fission products could be identified by investigating some very intense γ-lines. For these lines, the decay curves were measured, and β−γ coincidence spectra as well as γ−γ coincidence spectra were recorded. The data were assigned to eight nuclides for which the following half-lives, β-decay Q-values and γ-lines were determined:

^{84}Se $T_{\frac{1}{2}}$ = 3.5 min, Q_β = 1.8 MeV, E_γ = 406 keV,
^{91}Kr $T_{\frac{1}{2}}$ = 7.9 sec, Q_β = 5.7 MeV, E_γ = 111 and ≈630 keV,
^{97}Y $T_{\frac{1}{2}}$ = 1.11 sec, Q_β = 5.7 MeV, E_γ = 125 and 810 keV,
^{99}Nb $T_{\frac{1}{2}}$ = 14.3 sec, Q_β = 3.7 MeV, E_γ = 137 keV,
^{99}Zr $T_{\frac{1}{2}}$ = 2.4 sec, Q_β = 4.5 MeV, E_γ = 468, 548, 595 and ≈430 keV,
^{100}Nb $T_{\frac{1}{2}}$ = 6.6 sec, Q_β = 6.5 MeV, E_γ = 159 and 533 keV,
^{101}Nb $T_{\frac{1}{2}}$ = 7.0 sec, Q_β = 4.6 MeV, E_γ = 273 and 399 keV,
^{101}Zr $T_{\frac{1}{2}}$ = 3.3 sec, Q_β = 6.5 MeV, E_γ = 293 and ≈400 keV.

In three of the eight cases, the decay curves permitted the following estimates for the half-lives of the precursors: ^{97}Sr, $T_{\frac{1}{2}} \approx 0.4$ sec; ^{99}Y, $T_{\frac{1}{2}} \approx 0.8$ sec and ^{100}Zr, $T_{\frac{1}{2}} \approx 1.0$ sec. For all these values, the corresponding errors are given. The results obtained in this investigation are compared, if possible, with published data from earlier β-decay or nuclear-reaction measurements; discrepancies are discussed. Using the new results and the published data, decay schemes are proposed for the eight nuclides. (auth)

12463 STUDY OF THE GIANT RESONANCE BY PHOTON SCATTERING IN MEDIUM SPHERICAL NUCLEI. Arenhoevel, H. (Max-Planck Institut fuer Chemie, Mainz. Univ., Frankfurt am Main); Maison, J. M. Nucl. Phys.; A147: 305-25(1970).

Differential scattering cross sections for natural Ti, ^{51}V, Cr, ^{75}As, Se, ^{89}Y, Cd, In, and Sn have been measured at $\theta \approx 150°$ using a bremsstrahlung photon beam of 32-MeV maximum energy. From angular distribution measurements the inelastic scattering cross sections are extracted, which prove the existence of a tensor polarizability for vibrational spherical nuclei. General agreement is found with the predictions of the dynamic collective model calculations. The influence of the mean square quadrupole amplitude β on the shape of the giant resonance and on the strength of the inelastic scattering is shown. Some parameters are discussed, and a better estimate of the giant dipole state width is given. Discrepancies around 21 MeV for the lighter nuclei and for ^{89}Y are interpreted as evidence for isobaric spin splitting of the giant dipole resonance. (auth)

12464 DECAY SCHEME OF ^{59}Fe AND ^{192}Ir. Legrand, Jean; Morel, Jean; Clement, Christophe (CEN, Saclay, France). Nucl. Phys.; A142: 63-71(1970). (In French).

Gamma-ray transitions following the decay of ^{59}Fe to ^{59}Co, ^{192}Ir to ^{192}Pt, and ^{182}Os were investigated with calibrated Ge(Li) detectors. The new transitions of ^{59}Co at 381 and 1481 keV were confirmed. The absolute intensities for γ-rays and transitions were deduced. Particularly, the electron capture intensity in ^{192}Ir: (4.7 ± 0.4)%. The K-capture probability is calculated: P_K = 0.811 ± 0.05. (auth)

12465 ANGULAR CORRELATION MEASUREMENTS ON THE EXCITED STATES OF ^{42}Ca. Lawley, N.; Dawson, N.; Jones, G.

XUM

D.; (and others) (Univ. of Liverpool). Nucl. Phys.; A159: 385-98(1970).

The excited states of ^{42}Ca up to an excitation of 4.2 MeV were studied with a particle–γ-ray angular correlation technique in order to measure their spin values and electromagnetic decay properties. Unique spin assignments were obtained for states at 3.25 MeV (J = 4), 3.88 MeV (J = 1) and 4.23 MeV (J = 1). Possible spin values were restricted for the states at 4.00 MeV (J = 2 or 3) and 4.11 MeV (J = 1, 2 or 3). Gamma-ray branching and mixing ratios were measured. The mixing ratios for the transitions $2_2^+ \rightarrow 2_1^+$, $2_3^+ \rightarrow 2_1^+$, $2_4^+ \rightarrow 2_1^+$, were found to be $+0.09 \pm 0.08$, $-1.7^{+0.3}_{-0.5}$ and 0.00 ± 0.10, respectively. The results are discussed with reference to two sets of theoretical calculations, firstly those assuming an inert ^{40}Ca core and then those considering core excitation. The core excitation model gives reasonably good agreement with the experimental results. (auth)

12466 E.C./e^+ RATIOS IN THE NON-UNIQUE FIRST-FORBIDDEN DECAY OF ^{84}Rb. Goedbloed, W.; Goverse, S. C.; Brinkman, A.; Blok, J. (Vrije Univ., Amsterdam). Nucl. Phys.; A159: 409-16(1970).

The K/e^+ ratio of the non-unique first-forbidden ($2^- - 2^+$) transition to the first excited state of ^{84}Kr was measured by means of an internal source scintillation spectrometer in coincidence with a Ge(Li) crystal. A mass separator was used to purify the source material. The result K/$e^+ = 3.96 \pm 0.16$ is about 20% lower than earlier results of Welker and Perlman and of Konijn, it agrees with a theoretical prediction of Perlman et al. (auth)

12467 MEASUREMENTS ON THE ELECTRON CAPTURE RATIOS OF ^{83}Rb AND ^{84}Rb. Goedbloed, W.; Goverse, S. C.; Gerner, C. P.; Brinkman, A.; Blok, J. (Vrije Univ., Amsterdam). Nucl. Phys.; A159: 417-21(1970).

The electron capture decays of ^{83}Rb and ^{84}Rb were investigated by means of an internal source scintillation spectrometer. The capture ratios were measured in a 4π geometry by way of a construction of three CsI(Na) disks, enveloping a small crystal of either CsI(Na) or NaI(Tl) containing the radioactive material. These so-called source crystals were grown from the melt. (auth)

12468 BETA DECAY AND M1 DECAY RATES FOR A = 20 NUCLEI. Ananthanarayanan, K. (McGill Univ., Montreal). Nucl. Phys.; A159: 45-8(1970).

The Tabakin potential and a Serber–Yukawa potential are used to calculate the shell-model wave functions of A = 20 nuclear states with quantum numbers $J^\pi = 0^+$, T = 0, $J^\pi = 0^+$, T = 1, $J^\pi = 0^+$, T = 2 and $J^\pi = 1^+$ and T = 1. The former is found to give good fits for the energies. The log ft values for β-decays from ^{20}O to low-lying levels of ^{20}F and M1 decay rates in ^{20}Ne are calculated in reasonable agreement with observed values. (auth)

12469 PHOTONEUTRON CROSS SECTIONS OF ^{28}Si AND ^{24}Mg. Webb, D. V.; Muirhead, E. G.; Spicer, B. M. (Univ. of Melbourne). Nucl. Phys.; A159: 81-96(1970).

The photoneutron cross sections of ^{28}Si and ^{24}Mg were obtained with good resolution from threshold to 25 MeV and with coarser resolution to 31 MeV. Activation techniques were used to detect the annihilation γ-quanta both singly and in coincidence. The yield curves for each reaction were analyzed using the Leiss–Penfold method with bin widths of 200 keV and 100 keV for the good resolution and data, and 500 keV for the coarser data. Absolute cross sections, assigned by comparison with ^{12}C(γ,n)^{11}C data, give integrated cross sections which are in good agreement with previous estimates. The cross sections for both ^{28}Si and ^{24}Mg show considerably fine structure which is remarkably similar. A broader "intermediate" structure is observed up to 31 MeV. The silicon and magnesium data are compared with predictions of the collective correlations model and the random phase approximation model respectively, suggesting that the degree of agreement in each case depends to a large extent on the inclusion of core excitations generally, either phenomenologically or by consideration of np-nh transitions. It is concluded that the extent and nature of the dipole excitations do not differ markedly between the two nuclides in spite of apparent differences in the interpretation of the low-energy collective core spectra. (auth)

12470 INTERMEDIATE STRUCTURE AND THE REACTION ^{28}Si(p,p')^{28}Si. Shotter, A. C.; Fisher, P. S.; Scott, D. K. (Oxford Univ.). Nucl. Phys.; A159: 577-97(1970).

Angular distributions are reported for the reaction ^{28}Si(p,p')^{28}Si* measured over the incident energy range 12.0 to 15.0 MeV, at 100 keV intervals with a beam resolution of 100 keV. Total cross sections are determined for all residual states from 0.0 to 8.25 MeV. Cross-correlation analysis between the cross sections reveals structure similarities between the different excitation functions; this structure has a width of several hundred keV. An attempt is made to interpret the structure within the framework of the conventional statistical model. When the spacing of the compound levels is described by a Poisson distribution the model gives a fairly good representation of the data. (auth)

12471 BETA–GAMMA CIRCULAR POLARIZATION CORRELATION IN THE DECAY OF ^{48}V. Koopmann, E. W.; van Krugten, H.; van Nooijen, B. (Technische Hogeschool, Delft, Netherlands). Nucl. Phys.; A159: 609-14(1970).

The $\beta\gamma$ circular polarization correlation (695 keV, $4^+ \rightarrow 4^+$, β^+)–(1312 + 983 keV, γ) in the decay of ^{48}V was measured with a sector-focusing magnetic β-ray spectrometer. The use of this spectrometer, replacing the anthracene crystal usually employed for this kind of measurements, strongly reduces the systematic errors which are inevitable when an anthracene crystal is used. The resulting value of the asymmetry parameter is $A = -0.080 \pm 0.023$ which supports the validity of the conserved vector current theory. (auth)

12472 GAMMA-RAY SPECTRA FROM THE RADIATIVE CAPTURE OF 14 MeV NEUTRONS IN ^{28}Si AND ^{40}Ca. Cvelbar, F.; Hudoklin, A. (Jozef Stefan Nuclear Inst., Ljubljana, Yugoslavia. Univ., Ljubljana, Yugoslavia). Nucl. Phys.; A159: 555-60(1970).

Gamma-ray spectra from the radiative capture of 14-MeV neutrons in ^{28}Si and ^{40}Ca were calculated according to the direct-semi-direct and statistical model and compared with the experimental values. In the case of ^{28}Si the agreement between the experimental spectrum and the one calculated according to the direct-semi-direct model agree within about 10% in the region of the excitation energies of the final nucleus from 0 to about 4 MeV. In the case of ^{40}Ca the experimental value is about two times lower than the calculated one. This discrepancy is discussed. The intensity calculated according to the statistical model is dominant in the region of higher excitation energies. (auth)

12473 LIFETIME OF A NEW 194.9 keV LEVEL IN ^{77}As. Drost, H.; Weyer, G. (Hahn-Meitner-Institut fuer Kernforschung, Berlin). Nucl. Phys.; A159: 540-4(1970).

On the basis of $\gamma\gamma$ delayed coincidence measurements with NaI(Tl) and Ge(Li) detectors a 194.9 keV transition in ^{77}As is determined to be a transition to the ground state. The half-life of this state is $T_{\frac{1}{2}} = 7.4 \pm 0.3$ ns. Spin and parity are proposed to be $J^\pi = (\frac{1}{2}^-)$ in analogy with the first excited state of ^{75}As. The half-lives of known states at 215.51 keV and 264.45 keV are found to be shorter than 0.3 ns. (auth)

12474 COMPARISON BETWEEN THE ACTIVATION CROSS SECTIONS AND INTEGRATED CROSS SECTIONS FOR THE RADIATIVE CAPTURE OF 14 MeV NEUTRONS. Cvelbar, F.; Hudoklin, A.; Potokar, M. (Institut Josef Stefan, Ljubljana, Yugoslavia. Univ., Ljubljana, Yugoslavia). Nucl. Phys.; A158: 251-6(1970).

Cross sections obtained by the integration of prompt γ-ray spectra from the radiative capture of 14-MeV neutrons in a series of elements are presented and compared with the activation cross sections reported by different authors. In contrast to the activation cross-section values, which are scattered between 1 mb and 10 mb as a function of mass number, the integrated cross-section values show a smooth mass dependence. For targets with $A \gtrsim 50$ the two cross sections agree within some 10% only for nuclei near closed neutron shells. In other cases the activation cross sections are several times higher than the integrated ones. (auth)

12475 DECAY OF ^{104}Cd. Muennich, F.; Kjelberg, A.; Hnatowich, D. J. (CERN, Geneva). Nucl. Phys.; A158: 183-92 (1970).

The decay scheme of 57.7-min ^{104}Cd was investigated using isotopically separated samples. The seven γ rays observed in this decay are placed in a level scheme involving five excited states in ^{104}Ag. The Q value of ^{104}Cd was determined to be 1.56 ± 0.05 MeV. (auth)

12476 INVESTIGATION OF LEVELS IN ^{51}Cr, ^{55}Fe, AND ^{59}Ni BY MEANS OF (p,n) AND (p,nγ) REACTIONS. Tepel, J. W.; Malan, J. G.; de Villiers, J. A. M. (Atomic Energy Board, Pelindaba, S. Afr.). Nucl. Phys.; A158: 129-45(1970).

The level structures of ^{51}Cr, ^{55}Fe, and ^{59}Ni were investigated by yield and angular-distribution measurements of neutrons and decay γ rays from (p,n) reactions on ^{51}V, ^{55}Mn, and ^{59}Co at $E_p \leq 3.3$ MeV. Excitation energies as well as γ-decay schemes and branching ratios are presented. Several new spin assignments are made. In particular, the low-lying $\frac{9}{2}^-$ and $\frac{11}{2}^-$ states predicted for odd-

mass nuclei in the $f_{\frac{7}{2}}$ shell are identified in ^{51}Cr at 1165.0 ± 0.5 keV and 1479.1 ± 0.5 keV, respectively. (auth)

12477 RE-EXAMINATION OF THE ^{66}Ge DECAY. de Boer, F. W. N.; Lingeman, E. W. A.; van Lieshout, R.; Ricci, R. A. (Instituut voor Kernphysisch Onderzoek, Amsterdam). Nucl. Phys.; A158: 166-82(1970).

The energies and relative intensities of 89 γ rays following the decay of ^{66}Ge to ^{66}Ga were measured using Ge(Li) and Si(Li) spectrometers. The positron spectrum could be separated into four branches. Coincidence measurements were performed. By measuring the conversion electron spectrum with a Si(Li) detector the conversion coefficients and multipolarities of some intense transitions could be determined. The total disintegration energy was calculated to be 2102 ± 13 keV. The existence of levels with the following energies was deduced: 43.89 ± 0.04(1^+), 66.32 ± 0.04(2^+), 108.95 ± 0.04(1^+), 162.60 ± 0.06, 234.15 ± 0.05(2^+), 290.96 ± 0.05 (2^+), 381.91 ± 0.03(1^+), 536.74 ± 0.06(1^+), 664.0 ± 0.5, 706.09 ± 0.04(1^+), 866.04 ± 0.10(1^+), 974.65 ± 0.16(1), 1001.4 ± 0.3(0,1), 1062.2 ± 0.2(0,1), 1076.7 ± 0.1(0,1), 1164.4 ± 0.1(0,1), 1210.3 ± 0.1(0,1), 1456.54 ± 0.12(1^+), 1556.71 ± 0.04(0^+,1^+), 1573.9 ± 0.1 (0^+,1^+), and 1769.39 ± 0.16 keV(1^+). The half-life of ^{66}Ge was measured to be 2.27 ± 0.05 h; the lifetime of the 43.89-keV level, as <12 ns. (auth)

12478 RADIATIVE WIDTHS OF LEVELS IN ^{58}Ni AND ^{60}Ni. Metzger, F. R. (Franklin Inst., Swarthmore, Pa.). Nucl. Phys.; A158: 88-96(1970).

The radiative widths of six levels in ^{58}Ni and four in ^{60}Ni at excitation energies below 4.2 MeV were measured using the resonance scattering of bremsstrahlung. From the angular distribution of the resonance radiation, the 4.020-MeV level in ^{60}Ni was shown to have spin 1. The experimental B(M1) values for the ground state transitions from four 1^+ states exhibit considerably less variation from level to level than expected on the basis of a modified Tamm–Dancoff approximation calculation using the two-body matrix elements of a Kuo and Brown. (auth)

12479 j-DEPENDENCE IN l = 2 (^{3}He,d) REACTIONS ON ^{24}Mg, ^{28}Si, AND ^{30}Si. Mertens, B. (Univ., Cologne); Mayer-Boericke, C.; Kattenborn, H. Nucl. Phys.; A158: 97-109(1970).

Angular distributions of (^{3}He,d) reactions on the target nuclei ^{16}O, ^{24}Mg, ^{28}Si, ^{30}Si, and ^{32}S were measured at incident energies of 18 and 20 MeV. The stability of structures in the angular distributions against variations of the incident energy suggests that a direct reaction mechanism dominates. j-dependent differences in the shape of l = 2 angular distributions with $\Delta j = l \pm \frac{1}{2}$ appear distinctly in a plot of quotients of cross sections. They are the same for all investigated cases. Quite satisfactory DWBA fits are obtained in some cases; but the j effect, in particular, is not reproduced so well. (auth)

12480 ANGULAR CORRELATION STUDY OF THE LOW-LYING LEVELS OF ^{29}P. Lamaze, G. P. (Duke Univ., Durham, N. C. Triangle Universities Nuclear Lab., Durham, N. C.); Gould, C. R.; Moss, C. E.; Roberson, N. R.; Tilley, D. R. Nucl. Phys.; A158: 43-50(1970).

The low-lying levels of ^{29}P were investigated by ^{32}S(p,$\alpha\gamma$)^{29}P angular-correlation measurements using a collinear geometry. The spin assignments for the 1.38- and 1.96-MeV levels are in agreement with the known values of $\frac{3}{2}$ and $\frac{5}{2}$, respectively. A $J^\pi = \frac{3}{2}^+$ assignment is made to the third excited state at 2.40 MeV. Branching ratios for these levels are presented as well as γ-ray multipole mixing ratios for some of the transitions. Predictions of the vibration–particle coupling model are compared with these results. (auth)

12481 DECAY OF 3.2 sec ^{58}Cu AND AN UNUSUALLY HINDERED E2 TRANSITION IN ^{58}Ni. Raman, Subramanian (Oak Ridge National Lab., Tenn.). Nucl. Phys.; A158: 65-76(1970).

Ten γ rays from the decay of 3.2-sec ^{58}Cu were observed with high-resolution Ge(Li) detectors. These γ rays are incorporated into the known level scheme of ^{58}Ni. The 0_2^+, 2942.5-keV level in ^{58}Ni decays strongly (84%) to the 1_1^+, 2901.9-keV level and only weakly (8% each) to the 2_2^+, 2775.4- and 2_1^+, 1454.1-keV levels. The mean lifetime of the 2942.5-keV level was measured as 2.1 ± 0.2 nsec. The measured lifetime and branching ratios imply that the 1488.3-keV, $0_2^+ \rightarrow 2_1^+$, E2 transition is hindered by a factor of 3.3×10^3 compared to the Weisskopf estimate. The experimental level energies and transiton rates are compared with the results of shell-model calculations based on a ^{56}Ni core and two valence neutrons in the $p_{\frac{3}{2}}$, $f_{\frac{5}{2}}$, and $p_{\frac{1}{2}}$ orbits. Whereas the correspondence between the experimental and calculated energy level spectrum is reasonably good, that between the transition rates is not. (auth)

12482 APPLICATION OF THE UNIFIED MODEL WITH CORIOLIS COUPLING TO ^{22}Na, ^{26}Al, AND ^{30}P. Wasielewski, P. (Yale Univ., New Haven); Malik, F. B. Nucl. Phys.; A160: 113-36(1971).

The collective rotational model of Bohr, Mottelson and Nilsson is applied to the doubly odd sd shell nuclei ^{22}Na, ^{26}Al, and ^{30}P. The odd neutron and odd proton are placed in Nilsson orbitals generated by the axially symmetric deformed core. The Hamiltonian is composed of the collective rotational energy, including the Coriolis terms; the single-particle Nilsson energies; and a residual interaction between the last odd neutron and proton. The effective matrix elements calculated by Kuo and Brown from the Hamada–Johnston nucleon–nucleon potential are used for the residual interaction between the last two nucleons. Nuclear energy levels and wave functions are calculated by diagonalizing this Hamiltonian on a basis consisting of the rotational bands built on single-particle states obtained by placing the odd neutron and odd proton in all available sd shell Nilsson single-particle and single-hole orbitals. The deformation parameter β is determined for each nucleus by fitting the experimental energy spectrum. The other model parameters are assigned the same value for all the nuclei treated, except for the coefficient D of the $\mathbf{l} \cdot \mathbf{l}$ term in the Nilsson Hamiltonian, which must be varied to produce a satisfactory spectrum for ^{30}P. Magnetic moments, electric quadrupole moments, and M1 and E2 transition rates and mixing ratios are calculated. The calculated results are compared with experimental data. Agreement between the theoretical and experimental energy spectra is satisfactory for all three nuclei for states below 2 MeV, but there are discrepancies for states above 2 MeV in ^{22}Na. For the electromagnetic properties, agreement is satisfactory for transitions from states below 2 MeV in ^{22}Na and ^{30}P, but there are discrepancies for states above 2 MeV in ^{30}P and for low-lying states in ^{26}Al. (auth)

12483 ELECTROMAGNETIC PROPERTIES OF ^{55}Fe. Robertson, B. C.; Carola, T. P. G.; Sheppard, D. M.; Olsen, W. C. (Univ. of Alberta, Edmonton). Nucl. Phys.; A160: 137-53(1971).

Measurements of level positions, lifetimes, decay modes and the deduction of spins in ^{55}Fe were carried out using the ^{55}Mn(p,nγ)^{55}Fe reaction. Lifetimes of 12 levels between 1.3 and 3.1 MeV excitation are reported. Spin and mixing ratio assignments are made for levels above 2.2 MeV excitation using a statistical compound nuclear calculation. The measured lifetimes are compared with recent shell-model and intermediate-coupling predictions. (auth)

12484 SECOND-ORDER CALCULATION OF THE ISOTOPE EFFECT IN THE Ca ISOTOPES. Dieperink, A. E. L. (Duke Univ., Durham, N. C.). Nucl. Phys.; A160: 171-80(1971).

The difference of the charge distributions of ^{40}Ca and ^{42}Ca is calculated up to second order in perturbation theory. The Tabakin interaction is used to evaluate the two-body matrix elements. One- and two-body effects are taken into account. One-body renormalization diagrams tend to decrease the rms radius while the calculated two-body effects are found to increase the rms radius, but are much smaller in magnitude than experimental data indicate. (auth)

12485 LEVELS IN ^{87}Rb POPULATED IN THE DECAY OF ^{87}Kr. Shihab-Eldin, Adnan (Univ. of California, Berkeley); Prussin, S. G.; Bernthal, F. M.; Rasmussen, J. O. Nucl. Phys.; A160: 33-52(1971).

The γ-ray transitions following β-decay of 78 min ^{87}Kr were studied with Ge(Li) spectrometers. Thirty-three transitions between levels in ^{87}Rb were observed and $\gamma\gamma$ coincidence relations were obtained for the prominent lines. A level scheme is presented that incorporates 28 of these transitions between thirteen levels in ^{87}Rb. The level scheme is qualitatively interpreted according to the predictions of a simple weak-coupling model for excited states in ^{87}Rb. Also, the results from an exact diagonalization of the seniority-one pairing force Hamiltonian matrix are compared with the proposed experimental single-particle energy levels in ^{87}Rb and ^{89}Y. (auth)

12486 LIFETIMES OF THE FIRST FOUR EXCITED STATES OF ^{32}S. Garvey, G. T.; Jones, K. W.; Carlson, L. E.; (and others) (Oxford Univ.). Nucl. Phys.; A160: 25-32(1971).

The mean lifetimes of the first four excited states of ^{32}S were obtained using the attenuated Doppler shift method and the reaction ^{32}S(α,α')^{32}S. The results are τ_m = 0.23 ± 0.06, 1.05 ± 0.30, 0.048 ± 0.013 and 0.18 ± 0.04 ps for the levels at excitation energies 2230, 3777, 4278 and 4458 keV, respectively. Deduced E2 transition rates are compared with the predictions of collective and shell-model descriptions of these levels. (auth)

XUM

12487 NUCLEAR SPINS, $^3P_1$ AND $^3P_2$ HYPERFINE STRUCTURES, AND NUCLEAR MOMENTS OF ^{69}Ge AND ^{75}Ge, AND $^3P_2$ HYPERFINE STRUCTURE OF ^{71}Ge. Oluwole, Abiodun Francis. Berkeley, Calif.; Univ. of California (1969). 98p. University Microfilms Order No. 70-17,633.

Thesis.

The atomic-beam magnetic-resonance (ABMR) technique was used to measure the nuclear spin, I, and the $^3P_2$ hyperfine structure (hfs) constants, a and b, for 37-hr ^{69}Ge, the $^3P_2$ hfs constant a for 11-day ^{71}Ge, and the nuclear spin and hfs constant a for ^{75}Ge in the $^3P_1$ and $^3P_2$ electronic states. The nuclear moments were inferred by the use of the Fermi-Segrè formula from the corresponding hfs interaction constants. Relativistic effects account for about 25% of the a values while the remainder is attributed to effects of configuration interaction. The nuclear spins are predicted correctly by the shell model, while the quasi-particle nuclear theory of Migdal is found to predict the nuclear moments more accurately than the shell model. (Diss. Abstr. Int., B)

12488 X-RAY EMISSION INDUCED BY 30- TO 80-MeV ALPHA PARTICLES. Watson, R. L.; Lewis, C. W.; Natowitz, J. B. (Texas A and M Univ., College Station). Nucl. Phys.; A154: 561-75(1970).

Cross sections for the production of K- and L-shell vacancies by α particles were determined from measurements of K x-ray yields from thin targets of Fe, Ni, Cu, Zr, Nb, Rh, Pd, Ag, and Sn and L x-ray yields from thin targets of Sn, Tm, Ta, and Au. The measurements were carried out at α energies of 30, 40, 50, 60, 70, and 80 MeV using a Si(Li) semiconductor x-ray spectrometer. In general, the α-particle ionization cross sections were found to be consistent with available proton ionization cross-section data although systematic differences have been observed. The experimental excitation functions were compared with the theoretical excitation functions based on the Born approximation and found to rise more steeply than predicted, thus giving cross sections that are larger than the theoretical values. (auth)

12489 MEAN LIVES AND ANGULAR CORRELATIONS IN ^{35}S WITH THE ^{34}S(d,pγ)^{35}S REACTION. Burton, K. S.; McIntyre, L. C. Jr. (Univ. of Arizona, Tucson). Nucl. Phys.; A154: 551-60(1970).

The ^{34}S(d,pγ)^{35}S reaction at incident energies between 2 and 3.25 MeV was used to investigate the properties of the first three excited states in ^{35}S. The Doppler-shift attenuation method of measuring mean lives gives the following results for the levels at 1.57, 1.99 and 2.35 MeV: $\tau \geq 1.8$ ps, $\tau \geq 4.5$ ps and $\tau = 0.8 \pm 0.2$ ps, respectively. Angular correlation measurements were also performed using a collinear geometry. The 2.35 MeV level was found to have $J^\pi = \frac{3}{2}^-$. (auth)

12490 STUDY OF HIGHLY EXCITED NUCLEAR STATES USING γ RAYS FROM NEUTRON CAPTURE. Begzhanov, R. B.; Akhrarov, S. M. (Inst. of Nuclear Physics, Tashkent). Yadern. Fiz.; 12: 449-54(Sep 1970). (In Russian).

The widths of levels near the neutron binding energy in a number of intermediate and heavy nuclei are first determined using the method γ-ray resonance scattering from the neutron radiative capture. Experimental values of radiative widths of highly excited levels are compared with various theoretical estimates. (auth)

12491 LEVELS IN ^{47}Ca AND ^{41}Ca POPULATED IN THERMAL NEUTRON CAPTURE. Cranston, F. P.; Birkett, R. E.; White, D. H.; Hughes, J. A. (Univ. of California, Livermore). Nucl. Phys.; A153: 413-23(1970).

Gamma radiation from the ^{46}Ca(n,γ)^{47}Ca and ^{40}Ca(n,γ)^{41}Ca reactions was measured with Ge(Li) detectors. The ^{47}Ca γ rays observed can be placed in a decay scheme with levels at 2013.62 ± 0.20, 2875.27 ± 0.25, 4057.9 ± 0.3, 4809.2 ± 0.3 and 5503.4 ± 0.3 keV. The neutron binding energy of ^{47}Ca is 7276.0 ± 0.5 keV. The primary γ intensities populating intermediate $\frac{1}{2}^-$ and $\frac{3}{2}^-$ states are strongly correlated with $l_n = 1$ transitions in ^{46}Ca(d,p)^{47}Ca studies, which is consistent with the common unique parent assumption and suggests a direct process (channel capture) in the (n,γ) reaction. The decay of the low-lying negative parity states is consistent with their shell-model interpretation as $2p_{\frac{3}{2}}$ and $2p_{\frac{1}{2}}$ one-particle two-hole excitations in the ^{48}Ca inert core. Energies of the previous established levels in ^{41}Ca are 1942.69 ± 0.14, 2009.88 ± 0.24, 2462.15 ± 0.17, 2669.82 ± 0.18, 3400.08 ± 0.26, 3613.42 ± 0.17, 3944.20 ± 0.25, 4603.7 ± 0.7, and 4752.6 ± 0.2 keV. The neutron binding energy of ^{41}Ca is 8363.1 ± 0.5 keV. (auth)

12492 MEASUREMENT AND INTERPRETATION OF ELECTROMAGNETIC TRANSITIONS IN ^{51}V. Horoshko, R. N.; Cline, D.; Lesser, P. M. S. (Univ. of Rochester, N. Y.). Nucl. Phys.; A149: 562-84(1970).

Angular correlation measurements in the 180° geometry for the ^{48}Ti(α,pγ)^{51}V reaction were used to determine the γ decay properties of states in ^{51}V at 0.32, 0.93, 1.61, 1.81, 2.41, 2.55, 2.68, and 2.70 MeV. Coulomb excitation measurements with ^{32}S ions, using a thick ^{51}V target and a Ge(Li) detector, were used to deduce the B(M1) and B(E2) reduced transition probabilities for the decays of the 0.32, 0.93, 1.61, and 1.81 MeV states. For these states the M1 transitions are retarded by factors ranging from about 400 to over 10,000, while the E2 transitions are enhanced by about an order of magnitude relative to the Weisskopf estimate. Shell-model calculations were performed for ^{51}V considering all basic three proton states in the f−p shell and assuming a ^{48}Ca core. Kuo and Brown two-body matrix elements were used. Remarkably good agreement was obtained between the calculated and measured transition rates, supporting the shell-model predictions of a high-configuration purity for the six levels of the basic $f_{\frac{7}{2}}^3$ multiplet. By contrast, the B(M1) values predicted by the strong Coriolis coupling model of Scholz and Malik strongly disagreed with the measured values, generally being two or three orders of magnitude too large. It was concluded that the spherical shell model provides an excellent description of the low-lying states in ^{51}V and, contrary to Scholz and Malik, no evidence was found for deformation in this nucleus. (auth)

12493 GAMMA-RAY TRANSITION STRENGTHS IN ^{34}Cl. Brandolini, F.; Engmann, R. G. R.; Signorini, C. (Rijksuniversiteit, Utrecht). Nucl. Phys.; A149: 411-17(1970).

Gamma-ray transitions in ^{34}Cl have been studied with p−γ coincidence measurements in the ^{32}S(τ,pγ)^{34}Cl reaction. A new level, at $E_x = 2179.4 \pm 1.4$ keV has been found. From DSA measurements mean lives of $\tau_m = 940 \pm 400$, 46 ± 15, 400 ± 100, and 260 ± 75 fs were found for the ^{34}Cl levels at $E_x = 1.89$, 2.16, 2.18, and 2.38 MeV, respectively. Branchings are given for the three upper states. From the presently known information it is possible to identify the 2.16 MeV level with the 2^+, T = 1 state expected in this region. Even parity can be deduced for the 0.46, 1.89, and 2.38 MeV levels. The M1 and E2 strengths for a number of transitions in ^{34}Cl have been compared with calculations performed with many-particle shell-model wave functions. (auth)

12494 CORE-PLUS-PARTICLE MODEL AND THE LOW-LYING LEVELS OF ^{53}Cr. Philpott, R. J. (Florida State Univ., Tallahassee); True, William W. Phys. Rev., C; 2: 512-21 (Aug 1970).

Experimental energies, spectroscopic factors, and electromagnetic data associated with the low-lying levels of ^{53}Cr were fitted by means of a model in which the basis states are taken to be single-particle orbits vector-coupled to states of the ^{52}Cr core. Unknown properties of the core states are treated as parameters. A least-squares minimization procedure is used to determine optimum fits to the data. Although most of the low-energy data can be fitted quite successfully, the spectroscopic factors and quadrupole moment are not well reproduced. The observed levels appear to be more highly mixed than is suggested by the model. It is also found to be necessary to introduce an effective charge in order to reproduce the B(E2) data. (auth)

12495 SEARCH FOR DOUBLE GAMMA EMISSION FROM THE FIRST EXCITED STATES OF ^{40}Ca AND ^{90}Zr. Harihar, P.; Ullman, J. D.; Wu, C. S. (Columbia Univ., New York). Phys. Rev., C; 2: 462-7(Aug 1970).

A search for double γ emission from the first excited 0^+ states in ^{40}Ca and ^{90}Zr was carried out using a NaI(Tl) scintillation spectrometer and a sum-coincidence technique. No definite evidence for double γ emission was found in either case. In the 3.35-MeV, 0^+-to-ground-state transition in ^{40}Ca, an upper limit of 4×10^{-4} was established for the branching ratio of double γ emission with respect to internal pair emission. For the 1.75-MeV 0^+-to-ground-state transition in ^{90}Zr, an upper limit of 1.8×10^{-4} was obtained for the branching ratio of double γ emission with respect to the sum of internal-conversion electrons and internal pairs. The significance of these results in the light of existing theories is discussed. (auth)

12496 BREMSSTRAHLUNG AND PHOTONEUTRONS FROM THICK TUNGSTEN AND TANTALUM TARGETS. Berger, Martin J.; Seltzer, Stephen M. (National Bureau of Standards, Washington, D. C.). Phys. Rev., C; 2: 621-31(Aug 1970).

Monte Carlo calculations were made of electron−photon cascades in thick tungsten targets bombarded by electrons with energies up to 60 MeV. The following information was obtained: the bremsstrahlung efficiency, the angular distribution of the emitted bremsstrahlung intensity, the spectra of the bremsstrahlung emitted in various directions, the transmission of primary and secondary electrons through the target, energy deposition as function of the depth in the target, the differential photon track length distri-

XUM

bution inside the target, and the yield of photoneutrons. Comparisons with experimental data are also included. (auth)

12497 PROTON TOTAL REACTION CROSS SECTIONS IN THE 10 TO 20 MeV RANGE: ^{40}Ca AND ^{12}C. Dicello, J. F.; Igo, G. (Los Alamos Scientific Lab., N. Mex.). Phys. Rev., C; 2: 488-99(Aug 1970).

Total reaction cross sections for protons on ^{40}Ca were measured at 15 energies between 10.3 and 21.6 MeV by the beam-attenuation method. The total reaction cross section for ^{40}Ca rises sharply at low energies, reaches a maximum value around 13 MeV, and reaches a minimum value around 16 MeV. The rise at the lower energies is a result of the Coulomb barrier. The dip at 16 MeV is probably associated with the (p,n) threshold for ^{40}Ca. A comparison is made between the present experimental values and preliminary optical-model predictions based on available elastic-scattering data and polarization data. The variation in the reaction cross section is also compared with the integrated partial cross sections for elastic scattering. Total reaction cross sections for protons on carbon were measured at ten energies between 9.88 and 19.48 MeV. Resonances in the total reaction cross section were observed in the neighborhood of 10.4 and 13.8 MeV. Variations of 200 mb are seen in the cross sections with changes in energy of the incident protons of about 200 keV. A comparison is made of the present total reaction cross sections and the integrated partial cross sections for elastic scattering and inelastic scattering to the first excited state of ^{12}C. (auth)

12498 (^{3}He,t) REACTIONS ON THE T = 1 NUCLEI ^{18}O, ^{22}Ne, ^{26}Mg, AND ^{30}Si. Duhm, H. H.; Peterseim, K.; Seehars, R.; Finlay, R.; Detraz, C. (Max-Planck-Institut fuer Kernphysik, Heidelberg). Nucl. Phys.; A151: 579-608(1970).

The (^{3}He,t) reactions were investigated on ^{18}O, ^{22}Ne, ^{26}Mg, and ^{30}Si at 16 and 30 MeV. Angular distributions were obtained for levels up to about 4 MeV. The diffraction patterns were consistent with most of the previous spin and parity assignments for the ^{18}F, ^{22}Na, ^{26}Al, and ^{30}P states with the exception of a few discrepancies, e.g., for the 0$^-$ state at 1.08 MeV in ^{18}F, which are not understood. Elastic and inelastic ^{3}He scattering was also measured for ^{26}Mg at both incident energies. Results are interpreted in terms of macroscopic and microscopic DWBA calculations. The systematic preference of the higher l-values for (^{3}He,t) transitions to the lowest states of non-normal parity was observed in the $d_{\frac{5}{2}}$ nuclei, whereas the ^{30}P ground state shows a predominant l = 0 pattern in the angular distribution. Both of these results seem to be understandable in terms of a tensor exchange term contributing to the reaction mechanism. (auth)

12499 ^{43}Ar AND ^{44}Ar. Hudis, J.; Hageboe, E.; Patzelt, O. (CERN, Geneva). Nucl. Phys.; A151: 634-40(1970).

The half-lives and γ spectra of ^{43}Ar and ^{44}Ar were measured. The first information on the half-life of ^{43}Ar was obtained using the reaction Ti(p,spallation)^{43}Ar and the isotope separator on-line facility (ISOLDE) at the CERN 600-MeV synchrocyclotron. Precise measurements of the half-lives and γ energies, and also of the relative γ intensities were made on samples produced by the reaction V(p,spallation)^{43,44}Ar with 600-MeV protons followed by mass separation in the CERN off-line isotope separator. The half-life of ^{43}Ar is 5.37 ± 0.06 min, and that of ^{44}Ar is 11.87 ± 0.05 min. The γ spectrum accompanying the decay of ^{43}Ar is complex; 18 γ rays were found. The γ spectrum accompanying ^{44}Ar decay has only five γ rays. Partial decay schemes for ^{43}Ar and ^{44}Ar are presented. (auth)

12500 ANGULAR DISTRIBUTION OF RECOIL PRODUCTS FROM SOME SIMPLE REACTIONS OF 400 MeV PROTONS WITH ^{58}Ni AND ^{197}Au. Yu, Y.-W. (Carnegie-Mellon Univ., Pittsburgh); Caretto, A. A. Jr.; Church, L. B. Nucl. Phys.; A152: 295-304 (1970).

The angular distribution of the recoil products from (p,pn) and (p,p2n) reactions of ^{58}Ni and (p,pn) and (p,p3n) reactions on ^{197}Au were measured at 400 MeV in order to study the mechanisms of these reactions. The ^{58}Ni(p,pn)^{57}Ni reaction appears to proceed completely via a clean knock-out mechanism while the (p,pn) reaction on ^{197}Au is only about 50% clean knock-out. The apparent change in the (p,pn) reaction mechanism with target mass is studied and correlated with the total (p,pn) reaction cross section. The isomeric ratio of the ^{196}Au is constant with respect to recoil angle. The mechanisms of the more complex (p,p2n) and (p,p3n) reactions are also discussed. (auth)

12501 ANGULAR AND ENERGY DISTRIBUTION OF PHOTOPROTONS FROM ^{27}Al. Costa, S.; Ferrero, L.; Garfagnini, G.; (and others). (Univ., Turin. Istituto Nazionale di Fisica Nucleare, Turin). Nuovo Cim.; 70A: 517-24(21 Dec 1970).

The angular and energy distribution of photoprotons from ^{27}Al irradiated with 85 MeV bremsstrahlung was measured using two different techniques, solid-state detectors telescope and diffusion cloud chamber in magnetic field. There is some experimental evidence of high-energy excited levels beyond the giant resonance. The proton angular distribution suggests a rather important interference between the main E1 and E2 or M1 photonuclear excitations. The results were also compared with the theoretical predictions of the quasi-deuteron and one-particle interactions models. This latter model is in good agreement with experimental data. (auth)

12502 MUON CAPTURE PROBABILITY IN ISOTOPES OF BROMINE. Povel, H. P.; Koch, H.; Hamilton, W. D.; Charalambus, S.; Backenstoss, G. (CERN, Geneva. Univ., Karlsruhe, Ger. Kernforschungszentrum, Karlsruhe, Ger.). Phys. Lett.; 33B: 620-2(21 Dec 1970).

The muon capture probabilities in ^{79}Br and ^{81}Br were measured by observing the time distribution of γ-rays with respect to the stopped muons. The γ-rays predominantly occur following (μ^-,n) reactions. A natural bromine target was used and a Ge(Li) detector recorded x-rays and γ-rays. The capture lifetimes $\tau(^{79}\text{Br})$ = 143.9 ± 7.4 nsec and $\tau(^{81}\text{Br})$ = 132.8 ± 8.9 nsec were obtained; they indicate that nuclear structure may be influencing the process. (auth)

12503 LOW-ENERGY SPECTRUM OF ^{29}Si AND THE EXISTENCE OF LARGE OBLATE DISTORTIONS ASSOCIATED WITH CERTAIN INTRINSIC ORBITALS. Ragnarsson, Ingemar; Nilsson, Sven Goesta (Lund Inst. of Tech., Sweden). Nucl. Phys.; A158: 155-60(1970).

Equilibrium calculations involving different odd-particle excitations for ^{29}Si and neighboring nuclei are reported. Minima corresponding to very large oblate distortions are confirmed to be associated with a recently found rotational band in ^{29}Si. (auth)

12504 TITANIUM (n,p) CROSS-SECTION MEASUREMENTS. Lukic, Yovan (Instituto Venezolano de Investigaciones Cientificas, Caracas); Carroll, Edward E. Nucl. Sci. Eng.; 43: 233-5(Feb 1971).

Cross sections for the reactions ^{46}Ti(n,p)^{46}Sc and ^{48}Ti(n,p)^{48}Sc were measured at six different energies ranging from 4.91 ± 0.20 to 7.04 ± 0.12 MeV with a 4.0-MeV Van de Graaff accelerator using the D(d,n)^{3}He reactions. Measurements were made relative to the ^{56}Fe(n,p)^{56}Mn, ^{27}Al(n,α)^{24}Na, and ^{58}Ni(n,p)^{58}Co reactions. (L.T.W.)

12505 FINITE-RANGE CALCULATION OF THE TWO-NEUTRON TRANSFER REACTION. Bayman, B. F. (Univ. of Minnesota, Minneapolis). Phys. Rev. Lett.; 25: 1768-71(28 Dec 1970).

Distorted-wave Born-approximation calculations are done for the reactions ^{40,48}Ca(t,p)^{42,50}Ca$_{g.s.}$. A finite-range interaction is used, which acted between the proton and each transferred neutron. The results support conclusions of zero-range (t,p) calculations, both with respect to the shapes of the angular distributions and the relative cross sections for stripping into different shells. The calculated absolute cross section, however, is about one-third of that observed. (auth)

12506 ISOSPIN-FORBIDDEN ANALOGUE RESONANCES IN ^{33}Cl. I. THE LOWER T = 3/2 ANALOGUE RESONANCE. Abbondanno, U. (Univ., Trieste, Italy. Instituto Nazionale di Fisica Nucleare, Trieste, Italy); Giacomich, R.; Granata, L.; (and others) Nuovo Cim.; 70A: 391-404(1 Dec 1970).

Details are reported on a search for an isospin-forbidden resonance in ^{33}Cl, reached by means of (p,p) elastic scattering on ^{32}S. The corresponding level, which is one of the T = 3/2, A = 33 quartet, has been already singled out via an isospin-allowed reaction and localized at an excitation energy of 5.55 MeV in ^{33}Cl. Examination of the excitation curve over the energy interval of the incoming proton, 3200 to 3385 keV, revealed the existence of an anomaly at a proton bombarding energy of E_p = (3370 ± 1) keV in the laboratory system. An R-matrix analysis of the anomaly allows one to state that it represents the required resonance. (auth)

12507 DECAY OF THE GROUND STATE OF ^{82}Rb. Hryniewicz, A. Z. (Jagellonian Univ., Krakow. Inst. of Nuclear Physics, Krakow); Styczen, J.; Walus, W.; Broda, R. Acta Phys. Pol.; A38: 501-13(Nov 1970).

An investigation of the decay scheme of ^{82}Rb by means of a Ge(Li) detector, NaI(Tl) counters, and coincidence techniques establishes, besides the levels at 776.9 and 1475.1 keV known from the decay of ^{82}Br, levels characterized by the following energies (in keV): 1487.4, 2172.4, 2481.0, 2945.0, and 3188.0. The spins and parities to these levels are proposed on the basis of

log ft values and disintegration modes. Furthermore, correlation experiments were performed which furnish the 0 spin value to the 2172.4 keV level. The 1487.4 keV level is tentatively assigned as 0^+ spin and parity. (auth)

12508 LIFETIME OF THE 2007-keV LEVEL FOR THE ^{46}Ti NUCLEUS. Berlovitch, E. E.; Lukashevitch, V. V.; Popov, A. V.; Romanov, V. M. (Ioffe Inst. of Phsics and Tech., Leningrad). Acta Phys. Pol.; A38: 651-4(Nov 1970).

The lifetime of the 2007 keV excited state for the ^{46}Ti nucleus was measured by the centroid method using a differential converter described earlier. The half-life was found to be: $(3.8 \pm 1.5) \times 10^{-12}$ sec $< T_{\frac{1}{2}} < (7.2 \pm 1.5) \times 10^{-12}$ sec. (auth)

Nuclear Properties and Reactions, A ≥ 90

Refer also to abstracts 10472, 10491, 10583, 10779, 10814, 10825, 10860, 10892, 12035, 12353, 12366, 12403, 12432, 12446, 12447, 12462–12464, 12474, 12488, 12490, 12495, 12500, 12626, 12630, 12664, 12672, 12674, 12685, 12689, and 12703.

12509 (ANL-Trans-855) SCATTERING OF NEUTRONS WITH AN ENERGY OF 4 MeV AT ANGLES CLOSE TO 180°. Morozov, V. M.; Gorlov, G. V.; Zubov, Yu. G.; Lebedeva, N. S. (Akademiya Nauk SSSR, Moscow. Institut Atomnoi Energii). Translated for Argonne National Lab., Ill., from report IAE-1962. 5p. Dep. NTIS.

The elastic scattering of a polarized beam of neutrons with an energy of 4 MeV by In, Sn, Pb, Bi, and U nuclei was measured at scattering angles of 146–177°. The differential cross sections were determined for a non-polarized beam, along with the (scattered neutron) polarization of the nuclei investigated. A maximum was found in the cross section for backward scattering on all nuclei except uranium. The experimentally determined cross section values differ from the calculated ones obtained by means of an optical potential selected to describe the elastic scattering by nuclei of neutrons with an energy of 4 MeV. The behavior of the differential cross section of uranium does not agree either qualitatively or quantitatively with the predictions of several variants of the spherical optical potential. (auth)

12510 (BNL-tr-366) OPTIMUM PARAMETERS OF THE NEUTRON OPTICAL POTENTIAL FOR ^{238}U. Anikin, G. V. Translated by Stephen J. Amoretty (Brookhaven National Lab., Upton, N. Y.), from At. Energ. (USSR); 420-1(1970). 3p. Dep. CFSTI.

An optical-model analysis is done for neutron elastic scattering by ^{238}U from 0.075 to 15 MeV. Energy-independent parameters are given which describe the total cross sections with accuracy of ~3% and the angular distributions with accuracy of 10 to 15%. (R.W.R.)

12511 (CEA-N-1368) MEASUREMENT AND ANALYSIS OF THE CAPTURE TO FISSION CROSS SECTION RATIO α FOR ^{239}Pu BETWEEN 20 keV AND 500 keV. Lottin, Andre (Commissariat a l'Energie Atomique, Saclay (France). Centre d'Etudes Nucleaires). Nov 1970. 12p. (In French). Dep. NTIS (U. S. Sales Only).

The ratio $\alpha = \sigma_c/\sigma_f$ of ^{239}Pu measured at Oak Ridge National Laboratory exhibited a negative slope with respect to the incident neutron energy between 20 and 500 keV. The energy of the 1^+ transition state explaining this slope was calculated, assuming a Hill and Wheeler fission barrier. It was 250 ± 50 keV above the neutron binding energy assuming $\hbar\omega$ = 500 keV. (France)

12512 (CERN-70-29) MAIN DECAY CHARACTERISTICS OF MERCURY ISOTOPES AND THEIR DAUGHTER PRODUCTS ($182 \leq A \leq 192$). Finger, M.; Foucher, R.; Husson, J. P.; (and others) (European Organization for Nuclear Research, Geneva (Switzerland)). 3 Nov 1970. 53p. Dep. NTIS (U. S. Sales Only).

Isotopically pure mercury isotopes and their radioactive daughter products in the mass range 182 to 192 were produced by use of the ISOLDE facility. As part of the nuclear spectroscopic investigations of these nuclides, a large amount of information was gathered on half-lives of ground states and some excited states, on gamma-ray energies and intensities, and on conversion-electron energies and intensities, by the use of high-resolution detectors. Simplified decay schemes obtained on this basis are also presented. (79 references.) (R.W.R.)

12513 (CNEA-269) CROSS SECTIONS FOR NUCLEAR REACTIONS PRODUCED BY DEUTERONS ON TANTALUM. de Bentancourt, I.; Nassiff, S. J. (Comision Nacional de Energia Atomica, Buenos Aires (Argentina)). 1970. 11p. (In Spanish). Dep. CFSTI (U. S. Sales Only).

The cross sections for the nuclear reactions ^{181}Ta(d,p)^{182}Ta and ^{181}Ta(d,2n)^{181}W were determined experimentally. The deuteron energy in the incident beam was 27.2 MeV. The stacked foil technique was used to reduce its energy to the value corresponding to the threshold. The results obtained are tabulated and agree well with the experimental values obtained by Lange and Munzel. (tr-auth)

12514 (COO-1672-21) RADIOCHEMICAL INVESTIGATIONS OF NUCLEAR PROPERTIES. Progress Report, October 1969–September 1970. Daly, Patrick J. (Purdue Univ., Lafayette, Ind. Dept. of Chemistry). Sep 1970. Contract AT(11-1)-1672. 20p. Dep. NTIS.

Research progress at the Purdue University Chemistry Dept. in the period Oct. 1969 to Sept. 1970 is reported. Some previously unreported data on ^{184,187}Os levels from ^{184,187}Ir decays, ^{200}Hg and ^{200}Au levels from ^{200m}Au decay, and ^{185}Re (p,nγ) reactions are given. (J.W.R.)

12515 (COO-1746-51) E2/M1 MULTIPOLE MIXING RATIOS IN THE "SPHERICAL" NUCLEI ^{124}Te, ^{126}Te, AND ^{126}Xe. Grabowski, Z. W.; Krane, K. S.; Steffen, R. M. (Purdue Univ., Lafayette, Ind. Dept. of Physics). [1970]. Contract AT(11-1)-1746. 25p. Dep. NTIS.

E2/M1 mixing ratios of the 709-keV, 714-keV, and 723-keV transitions in ^{124}Te, the 754-keV transition in ^{126}Te, and the 491-keV transition in ^{126}Xe were measured using the $\gamma-\gamma$ directional correlation technique. In addition, the measurements on the 646-keV–603-keV, 1691-keV–603-keV, and 2091-keV–603-keV $\gamma-\gamma$ cascades in ^{124}Te are in agreement with pure E2 character of 646-keV transition and with pure E1 character of the 1691-keV and 2091-keV transitions in ^{124}Te. Coaxial Ge(Li) and NaI(Tl) scintillation detectors were used in different combinations depending on the energy resolution required for a particular measurement. The results for the mixing ratios are $\delta_{709} = +0.04^{+0.03}_{-0.05}$, $\delta_{714} = +0.98 \pm 0.19$, and $\delta_{723} = -3.4 \pm 0.1$ for the transitions in ^{124}Te, $\delta_{754} = -5.5^{+0.4}_{-0.3}$ for the $2^{+\prime} \rightarrow 2^+$ transition in ^{126}Te, and $\delta_{491} = +27^{+30}_{-8}$ for the $2^{+\prime} \rightarrow 2^+$ transition in ^{126}Xe. There is an indication that the mixing ratios for the $2^{+\prime} \rightarrow 2^+$ transitions in even–even tellerium isotopes are negative and the mixing ratios of similar transitions in even–even Xe isotopes have positive values. (auth)

12516 (EUR-4525) ANNUAL PROGRESS REPORT, 1969. (European Atomic Energy Community, Geel (Belgium). Central Nuclear Measurements Bureau). 1970. 72p. Dep. NTIS (U. S. Sales Only). EUR FF 11.-.

The different activities of the Central Bureau for Nuclear Measurements during the year 1969 are described. The progress and trends of the research program are presented together with a description of the operational, service and administrative activities of the Laboratory. (auth)

12517 (INP-714) PARITY NONCONSERVING EFFECTS IN NUCLEI ^{175}Lu AND ^{181}Ta. Grabowski, J. (Institute of Nuclear Physics, Krakow (Poland)). 1970. 10p. Dep. NTIS (U. S. Sales Only).

The nuclear part R of the parity-nonconserving circular polarization in 343-keV and 396-keV gamma transitions in ^{175}Lu and 482-keV gamma transition in ^{181}Ta have been calculated. The Saxon–Woods type single-particle wave functions were used. (auth)

12518 (INS-J-123) QUASI-GAMMA BANDS IN ^{152}Gd AND POSSIBLE PRESENCE OF QUASI-K QUANTUM NUMBER. Sakai, Mitsuo; Ishii, Kameo; Aoki, Takayoshi (Tokyo Univ. (Japan). Inst. for Nuclear Study). 7 Sep 1970. 16p. Dep. NTIS (U. S. Sales Only).

Nuclear properties of low-lying excited levels of ^{152}Gd are discussed based on the beta transition probabilities of ^{152}Eu. The log ft values of the beta transitions to the so-called quasi-gamma band clearly show up to be smaller than those to the members of the quasi-ground-state rotational and quasi-beta bands. As ^{152}Eu is known to have K = 3, this fact can be explained if one assumes that the properties of the K quantum number are still alive in this transitional nucleus in the form of a quasi-K quantum number K_q, namely K_q = 2 for the quasi-gamma band and K_q = 0 for the quasi-ground-state rotational band and the quasi-beta band, of which the selection rules are similar to those of the K quantum number of deformed nuclei. (auth)

12519 (KFK-1247) A COMPUTER PROGRAM FOR DISCOVERY OF EXCITED NUCLEAR STATES ACCORDING TO THE

RITZ COMBINATION PRINCIPLE. Heck, Dieter (Kernforschungszentrum, Karlsruhe (West Germany). Institut fuer Angewandte Kernphysik). Jul 1970. 35p. (In German). Dep. NTIS (U. S. Sales Only).

With a set of measured γ-ray energies and a few known level energies as a starting point, the Ritz combination principle may be used to construct a more nearly complete level scheme. This problem is well suited for application of a computer, since certain operations—forming a sum or a difference of two γ-ray energies, forming a difference of two level energies, and comparing these two quantities—must be performed many thousands of times in most cases. The program developed, which is especially adapted to the data obtained from the (n,γ) reaction, is listed herein. (auth)

12520 (LYCEN-7034) CONFERENCE ON LOW-ENERGY SPECTROMETRY AND NUCLEAR SPECTROMETRY, LYON, 18–20 FEBRUARY 1970. (Lyon Univ. (France). Institut de Physique Nucleaire). 1970. 172p. (In French). (CONF-700219).

Ten articles are included; an abstract was prepared for each. (P.C.H.)

For abstracts of individual papers see: 10668–10670, 12432, 12521–12525, and 12634.

12521 (LYCEN-7034, pp 34-41) NUCLEAR MAGNETIC MOMENTS AND HYPERFINE INTERACTIONS. Berkes, I. (Lyon Univ. (France). Institut de Physique Nucleaire). (In French).

From Conference on low-energy spectrometry and nuclear spectrometry, Lyon, 18–20 February 1970.

Several rotational magnetic moments were studied and the hyperfine anomaly defined. The principles by which it was measured using NMR destruction of the nuclear orientation are described. (France)

12522 (LYCEN-7034, pp 42-57) NUCLEAR REORIENTATION. Vanhorenbeeck, Jean (Paris Univ. (France). Laboratoire Joliot-Curie de Physique Nucleaire). (In French).

From Conference on low-energy spectrometry and nuclear spectrometry, Lyon, 18–20 February 1970.

The theory of the reorientation effect was recalled. This technique appeared to be very useful in measuring quadrupolar moments of excited states, however its use was somewhat limited by the mathematical complexity, when a large number of states were considered. (France)

12523 (LYCEN-7034, pp 58-83) EXPERIMENTAL DETERMINATION OF COUPLINGS IN DEFORMED NUCLEI. Valentin, J. (Grenoble Univ. (France). Institut des Sciences Nucleaires). (In French).

From Conference on low-energy spectrometry and nuclear spectrometry, Lyon, 18–20 February 1970.

A bibliography of French publications in the field of the nuclear spectroscopy of rare earths is given. The different types of experiment used for studying the problems of nuclear structure were recalled: nuclear spectroscopy by the study of radioactive disintegrations, gamma ray spectroscopy of nuclear reactions, and reactions involving the transfer of a single nucleon. (France)

12524 (LYCEN-7034, pp 84-93) THE WORK CARRIED OUT IN FRANCE DURING RECENT YEARS ON ISOTOPES WITH $Z \geq 83$. Walen, R. J. (Centre National de la Recherche Scientifique, Orsay (France). Centre de Spectrometrie Nucleaire et de Spectrometrie de Masse). (In French).

From Conference on low-energy spectrometry and nuclear spectrometry, Lyon, 18–20 February 1970.

A brief summary is given on the work which has been carried out in France on isotopes with $Z \geq 83$. Difficulties were encountered, no matter what method of study was chosen: nuclear reactions, decay series, production of isotopes, and α emission. (France)

12525 (LYCEN-7034, pp 94-116) STUDY OF DIFFERENT COMPETING COUPLING MECHANISMS IN DEFORMED NUCLEI OF ODD MASS. Piepenbring, R. (Centre National de la Recherche Scientifique, Strasbourg (France). Centre de Recherches Nucleaires). (In French).

From Conference on low-energy spectrometry and nuclear spectrometry, Lyon, 18–20 February 1970.

The competition between the different coupling mechanisms taking place in deformed nuclei of odd mass was studied. The coupling, which can take place between the different shells (principally between states whose principal quantum numbers differ by two), the coupling between quasi-particle states and those of the vibrational mode, and Coriolis coupling, were individually analyzed. The manner in which the competition aids the understanding of certain levels of complex structure in the ^{155}Gd and ^{165}Er deformed nuclei was studied. (France)

12526 (MNC-3783-7) DIRECT INTERACTION EFFECTS IN THE FISSION OF ^{238}U WITH 63.5-MeV ^{4}He IONS. Viola, V. E. Jr.; Minor, M. M.; Salwin, A. E. (Maryland Univ., College Park. Dept. of Chemistry); Bondelid, R. O.; Theus, R. B. (Naval Research Lab., Washington, D. C.). Sep 1970. Contract AT(40-1)-3783. 29p. Dep. NTIS.

Position-sensitive semiconductor detectors were used to measure both in-plane and out-of-plane angular correlations for binary-fission events from 63.5-MeV ^{4}He-induced fission of ^{238}U. From these data a value of 7.5 ± 1.0 percent is derived for the contribution of direct-interaction mechanisms to the total fission cross section at 63.5 MeV. When this result is included with recent theoretical expressions, the interpretation of fission-fragment angular-distribution data is found to be consistent with both theory and low-energy results up to this energy. The most probable total kinetic-energy release was found to be 173.3 ± 5.4 MeV for the compound nucleus ^{242}Pu. The measured variations in the average fission-fragment kinetic energies and the widths of the fragment spectra as a function of correlation angle are interpreted in terms of effects arising from direct interaction, neutron evaporation, and the reaction kinematics. (auth)

12527 (NP-18613) DIRECTIONAL CORRELATIONS OF SOME γ-RAY CASCADES IN ^{200}Hg. Hattula, J.; Helppi, H.; Kantele, J. (Jyvaskyla Univ. (Finland). Dept. of Physics). Sep 1970. 13p. Dep. NTIS (U. S. Sales Only).

Directional correlation functions of 10 γ-ray cascades in ^{200}Hg have been measured using a ^{200}Tl source and a Ge(Li)–NaI(Tl) coincidence spectrometer arrangement. Values of the mixing parameter δ for several transitions are determined, and the spin assignments for the following levels in ^{200}Hg are established (level energies are given in keV): 1029.4(0^+), 1254.2(2^+), 1573.7(2^+), 1593.4(2^+), 1641.5(2^+), 1730.9(2^+) and 1775.6(3^+). (auth) (Finland)

12528 (NP-18647) REINVESTIGATION OF THE DECAY OF ^{200}Tl. Research Report No. 13/1970. Komppa, T.; Pakkanen, A.; Kantele, J. (Jyvaskyla Univ. (Finland). Dept. of Physics). Nov 1970. 18p. Dep. NTIS (U. S. Sales Only).

A detailed study of γ rays and γ-ray cascades from 26.1-h ^{200}Tl was carried out employing Ge(Li) detectors, an anti-Compton spectrometer, and a Ge(Li)–NaI(Tl) coincidence spectrometer. A decay scheme is proposed which incorporates six new excited states in ^{200}Hg. The energies and γ-ray decay branching ratios of some of the levels are compared with values calculated from the model of Covello and Sartoris who describe ^{200}Hg as two proton holes coupled to surface vibrations. (auth) (Finland)

12529 (ORNL-tr-3020) ESTIMATION OF UNKNOWN EXCITATION FUNCTIONS FOR (α,xn)-, (α,pxn)-, (d,xn)-, (d,pxn)-, AND (p,xn)-REACTIONS. Lange, Juergen; Muenzel, Helmut (Kernforschungszentrum, Karlsruhe (West Germany)). Translated by J. J. Pinajian and Lynda H. Kern (Oak Ridge National Lab., Tenn.), from report KFK-767. 43p. Dep. NTIS.

Excitation functions for the reactions (α,xn), (α,pxn), (d,xn), (d,pxn), and (p,xn) are presented. Experimental results obtained over a period of twelve years have been compiled, and from these theoretical curves are deduced for the various reaction types. Yields produced by the irradiation of thick targets by the above processes are also presented. (78 references) (R.W.R.)

12530 (RLO-1388-130) SPIN ISOMERS OF THE SHAPE ISOMER ^{237m}Pu. Russo, P. A.; Vandenbosch, R.; Mehta, M.; Tesmer, J. R.; Wolf, K. L. (Washington Univ., Seattle. Nuclear Physics Lab.). [1970]. 28p. Dep. NTIS.

Two components in the spontaneous fission decay of ^{237m}Pu are investigated. The half-lives of the two isomers are 82 ± 8 nsec and 1120 ± 80 nsec. The production ratio of the two components was determined for three different bombarding conditions: ^{235}U + 24-MeV α, ^{235}U + 27-MeV α, and ^{237}Np + 12.1-MeV d. The dependence of the production ratio on angular-momentum deposition for the various reactions shows that the two shape isomers differ in spin with the short-lived component corresponding to the lower spin state. The experimental isomer ratios are compared with statistical model calculations. It is shown that, if a future threshold measurement demonstrates that the high spin isomer cannot decay to the low spin isomer, the deformation associated with shape isomerism can be deduced from isomer-spin information extracted from the present experiment and reference to the Nilsson diagram at large deformation. (auth)

XUM

12531 (TID-25586) GAMMA-RAY SPECTROSCOPIC STUDY OF THE DECAYS OF ^{124}Sb AND ^{126}I. Auer, Ivan Paul (Michigan Univ., Ann Arbor). 1969. 122p. Dep. NTIS.

Thesis.

Gamma-ray intensity and coincidence measurements associated with the decay of ^{124}Sb and ^{126}I are reported, as well as the analysis and interpretation of the resulting data. The results are compared with various nuclear models. (R.W.R.)

12532 (TID-25592) DECAY SCHEMES OF ^{131}Ba AND ^{192}Ir NUCLEI. Lee, Sabrina Lin (Michigan Univ., Ann Arbor). 1969. 158p. Dep. NTIS.

Thesis.

In the study of the electron-capture decay of ^{131}Ba to levels in ^{131}Cs, energy and relative-intensity measurements were performed on 36 gamma rays with a 4-cc Ge(Li) detector. New transitions at 797 keV and 954 keV were observed. Precision energy determinations were made for the four strongest transitions using a 2-meter curved-crystal spectrometer. Gamma–gamma coincidence studies were performed utilizing a 17-cc and a 40-cc coaxial Ge(Li) detector, a 4-cc planar Ge(Li) detector, and NaI crystals. All observed gamma rays are placed into the decay scheme, including the new transitions. The 1047-keV peak is concluded to be a doublet. A new decay scheme is proposed, which is consistent with the presently established decay scheme, with the addition of a new level at 1170 keV. The previously uncertain transitions at 323 keV, 461 keV, and 969 keV are confirmed to belong to the decay. In the study of the beta decay and electron-capture decay of ^{192}Ir to levels in ^{192}Pt and ^{192}Os, respectively, 21 gamma transitions were observed, including new transitions at 110 keV, 177 keV, and 280 keV. Energy and relative-intensity measurements were made using a 17-cc and a 40-cc coaxial Ge(Li) detector. Precision curved-crystal gamma-ray energy determinations were made for 19 gamma transitions. In addition, a search was performed using a curved-crystal spectrometer for all gamma rays reported in Nuclear Data Sheets (1963) and by other authors, and for possible missing transitions between existing levels. Upper intensity limits are given. The singles and coincidence results confirm the presently established decay scheme. Furthermore, a level at 905 keV in ^{192}Os is confirmed by gamma–gamma coincidence results. While there is no experimental evidence for the existence of 1055-keV and 1360-keV levels in ^{192}Pt, there is some evidence for a level at 1090 keV. Lifetime measurements were performed on all gamma-rays except the fore-mentioned possible new transitions. Transition multipolarities and spins and parities of excited states were deduced for ^{131}Cs, ^{192}Pt, and ^{192}Os. The experimental results of this work are compared with theoretical assignments of levels of these nuclei obtained from a consideration of various nuclear models. (auth)

12533 (TKK-F-A-123) USE OF NUCLEAR POLARIZATION IN NEUTRON SCATTERING AND TRANSMISSION MEASUREMENTS. Tiainen, O. J. A.; Anttila, M.; Tunkelo, E. (Technical Univ. of Helsinki, Otaniemi (Finland). Dept. of Technical Physics). 1 Oct 1970. 13p. Dep. NTIS (U. S. Sales Only).

The use of nuclear polarized targets in connection with a polarization spectrometer, and measurements of scattering lengths, b_+ and b_-, for two different resultant spin states of the neutron and the target nucleus are discussed. The depolarization of the neutron beam has been calculated in some special cases. It can be concluded that the use of polarized targets with a polarization spectrometer may be useful in separation of a weak coherent-scattering component from an incoherent background. The measurements of the spin dependence of thermal absorption and the scattering lengths, b_+ and b_-, by using brute-force polarization of the target seem to be promising in experiments with nuclei having short enough spin–lattice relaxation times. (auth) (Finland)

12534 (TUNL-2) ANNUAL PROGRESS REPORT, OCTOBER 1, 1968–SEPTEMBER 1, 1969. (Triangle Universities Nuclear Lab., Durham, N. C.). 31 Dec 1969. Contract AT(40-1)-1067. 72p. Dep. NTIS.

Research at the Triangle Universities Nuclear Laboratory from Oct. 1, 1968 to Sept. 1, 1969 is described. The research included work in neutron physics, charged-particle reactions, radioactivity, general physics, and nuclear theory. The papers published and submitted for publication in the period are listed. (J.W.R.)

12535 COMPUTER METHOD FOR ANALYSIS OF HIGHLY RESOLVED γ SPECTRA AND ITS APPLICATION TO FISSION-FRAGMENT MIXTURES. Winiger, P.; Huber, O.; Halter, J. (Univ., Fribourg, Switzerland). Helv. Phys. Acta; 43: 693-712 (1 Oct 1970). (In German).

γ-spectroscopic methods offer considerable advantages compared to other procedures in the analysis of unknown mixtures of radionuclides. There exists, in particular, the possibility of computer programs to achieve a complete analysis of highly resolved spectra even with rather small installations. The principles of peak location, approximation of the peaks with Gaussian distributions, and energy calibration and determination, which allow an identification of the peaks with a suitable catalogue of γ-ray energies, are outlined. Besides the calculation of the activity of the identified nuclides and the necessary time corrections, a comparison with normal mixtures of fission fragments is made. To do this, a special fission mode is assumed, and for every measured nuclide the corresponding number of fissions is calculated; the expected value for normal mixtures is a constant Q if the chosen fission mode is correct. The accuracy of this procedure was tested experimentally with a normal mixture of fission fragments of ^{235}U irradiated with thermal neutrons. The mean deviation of the Q values is about $\pm 10\%$ if the most recent data are used. The analysis of three airfilter samples with fission fragments and neutron-induced nuclides (^{239}Np, ^{237}U) from nuclear explosions allowed their attribution to two different types of bombs. (auth)

12536 DETERMINATION OF THE LEVEL DENSITY PARAMETERS FOR GERMANIUM, HOLMIUM, AND TANTALUM. Sobottka, H.; Grimes, St.; Huber, P.; Mangold, E.; Schacher, J.; Wagner, R. (Univ., Basel). Helv. Phys. Acta; 43: 559-82 (1 Oct 1970). (In German).

Germanium, holmium, and tantalum samples were bombarded with 14-MeV neutrons; and the resulting neutron spectra measured with a time-of-flight spectrometer. Use of a Monte Carlo computer program permitted the calculation of multiple-scattering effects. Application of the assumptions of the Fermi-gas and superconductor model led to a level-density formula, which was used to calculate the (n,n′) and (n,2n) spectra. These calculations for various values of the level-density parameter a were fitted to the experimental data. As a second, independent method to determine the level-density parameter the relation of Lang and Le Couteur was used to obtain a value for the nuclear temperature, which can be related to the density parameter a'_p of the Fermi-gas model. The resulting values are compared with the magnitudes calculated from the shell model. The values for the density parameters are $a = 12.5 \pm 0.7$, 23.0 ± 1.7, and 27.0 ± 2.0 MeV^{-1} and $a'_p = 12.3 \pm 1.2$, 17.4 ± 1.7, and 22.9 ± 1.6 MeV^{-1} for Ge, Ho, and Ta, respectively. (auth)

12537 PARTICLE–HOLE INTERACTIONS IN ^{90}Zr. Rhodes, Wesley. University Park, Pa.; Pennsylvania State Univ. (1969). 96p. University Microfilms Order No. 70-19,455.

Thesis.

The energy levels of the $(d_{5/2}\nu)(g_{9/2}\nu)^{-1}$ multiplet in ^{90}Zr are calculated with the nonlocal Tabakin interaction representing the bare nucleon interaction. In the shell model calculation second-Born terms are taken into account in the plane wave approximation, and, in addition, a microscopic approach is employed for the treatment of core polarization effects. Microscopic calculations are also carried out for states of the $(d_{5/2}\nu)(g_{9/2}\pi)$ configuration in ^{92}Nb. The resulting spectrum for the particle-hole states in ^{90}Zr agrees well with the experimental data except for the 2^+ level which lies ~0.3 MeV too high. Excellent agreement is obtained for the six low-lying energy levels associated with the $(d_{5/2}\nu)(g_{9/2}\pi)$ multiplet of ^{92}Nb. Comparison of the isospin dependence of the two-body force for identical particles (T = 1) and nonidentical particles (T = 0, 1) is presented. (Diss. Abstr. Int., B)

12538 SPONTANEOUS FISSION OF ^{238}U AND ^{241}Am. Galliker, D. (Univ., Freiburg i. B.); Hugentobler, E.; Hahn, B. Helv. Phys. Acta; 43: 593-606(1 Oct 1970). (In German).

With the spinner method, which is based on the principle of cavitation of liquids induced by energy deposition by particles, the spontaneous-fission half-lives of ^{238}U and ^{241}Am were measured. The values found were $(8.19 \pm 0.06)\ 10^{15}$ years for ^{238}U and $(9.0 \pm 0.4)\ 10^{13}$ years for ^{241}Am. In order to search for possible systematic errors, the measurements were done under different experimental conditions. (auth)

12539 NONRESONANT NEUTRON CAPTURE IN ^{207}Pb? Allen, B. J. (Australian Atomic Energy Commission, Sutherland. Oak Ridge National Lab., Tenn.); Macklin, R. L. Phys. Rev. Lett.; 25: 1675-7(14 Dec 1970).

The neutron-capture cross section of the 41-keV resonance in ^{207}Pb was measured with improved resolution. Resonance asymmetry is not observed within the accuracy of the measurement and, consequently, there is no evidence for a significant nonresonant-capture cross section. (auth)

12540 STUDY OF THE 190-keV TRANSITION IN ^{141}La. Berg, V. (Univ. of Stockholm. Aktiebolaget Atomenergi, Studsvik, Sweden); Hoeglund, A.; Fogelberg, B. Nucl. Phys.; A155: 297-305(1970).

The γ-ray spectrum from the decay of 18 min ^{141}Ba was studied. Seventeen transitions were found below 900 keV, with energies and (intensities) as follows: 112.9 ± 0.2(3.0), 163.1 ± 0.3(1.0), 165.7 ± 0.4(0.7), 180.5 ± 0.2(0.9), 190.3 ± 0.1(100), 276.9 ± 0.1(52.2), 304.2 ± 0.1(55.8), 343.6 ± 0.1(30.8), 364.4 ± 0.6(1.6), 389.7 ± 0.2(2.8), 457.7 ± 0.2(10.4), 462.3 ± 0.2(10.5), 467.3 ± 0.1(11.4), 625.1 ± 0.2 (6.1), 647.9 ± 0.2(10.7), 739.1 ± 0.3(8.7), and 876.5 ± 0.3(6.7). The K- and L-shell conversion coefficients were measured for the 190.3-keV transition, which shows a multipolarity of M1 + <8% E2. Half-life measurements using a delayed-coincidence technique gave the following results: $T_{½}$ (190 keV level) = $1.27^{+0.06}_{-0.10}$ ns, $T_{½}$ (304 keV level) <200 ps, $T_{½}$ (467 keV level) <120 ps. A level scheme of ^{141}La is constructed, and the spin–parity assignments of the ground state and first excited state are discussed in terms of the shell model. (auth)

12541 LIFETIMES OF ROTATIONAL STATES IN ^{229}Th AND ^{235}U. Ton, H.; Roodbergen, S.; Brasz, J.; Blok, J. (Vrije Univ., Amsterdam). Nucl. Phys.; A155: 245-56(1970).

The lifetimes of the $\frac{7}{2}^+$ and $\frac{9}{2}^+$ rotational states in ^{229}Th and the $\frac{5}{2}^+$ rotational state in ^{235}U were measured by using the delayed-coincidence technique. The following half-lives were obtained: $T_{½}(\frac{7}{2}^+; ^{229}\text{Th})$ = 172 ± 6 ps, $T_{½}(\frac{9}{2}^+; ^{229}\text{Th})$ = 147 ± 12 ps, $T_{½}(\frac{5}{2}^+; ^{235}\text{U})$ = 191 ± 5 ps. From the transition probabilities electric and magnetic parameters could be determined. The magnetic parameters are compared with predictions from the Nilsson model. (auth)

12542 LIFETIMES OF 2^+ AND 4^+ ROTATIONAL STATES IN HEAVY DOUBLY EVEN NUCLEI. Ton, H.; Beens, W.; Roodbergen, S.; Blok, J. (Vrije Univ., Amsterdam). Nucl. Phys.; A155: 235–44(1970).

The lifetimes of the 2^+ rotational states in ^{228}Th, ^{234,236}U, ^{238,240}Pu, and ^{248}Cm and of the 4^+ rotational states in ^{228}Th and ^{236}U were measured by using the delayed-coincidence technique. From the 2^+ lifetimes the quantities B(E2; $2^+ \rightarrow 0^+$), Q_0, and β are derived and compared with theoretical predictions. The values of the ratio B(E2; $4^+ \rightarrow 2^+$)/B(E2; $2^+ \rightarrow 0^+$) in ^{228}Th and ^{236}U are found to be 1.42 ± 0.16 and 1.27 ± 0.16, respectively, in good agreement with the rotational-model prediction. (auth)

12543 HOLE-VIBRATION COUPLING IN ^{115}In. Dietrich, F. S. (Niels Bohr Inst., Copenhagen. Stanford Univ., Calif.); Herskind, B.; Naumann, R. A.; Stokstad, R. G.; Walker, G. E. Nucl. Phys.; A155: 209-34(1970).

The collective states of ^{115}In were studied by Coulomb excitation with ^{16}O and ^{12}C ions and by inelastic scattering of 12-MeV deuterons. In both experiments the excitation strength is strongly concentrated on a group of levels in the region of 900 to 1500 keV. A number of additional levels were observed in the (d,d′) reaction. Several strong M1 transitions between the excited levels were observed in the γ-decay spectra. The levels directly excited by Coulomb excitation (in keV), their B(E2↑) transition probabilities (in 10^{-2} $e^2 \cdot b^2$), and the inferred spin–parity assignments are as follows: 941.7(0.27)$\frac{5}{2}^+$, 1078.2(2.2)$\frac{5}{2}^+$, 1133.1(10.0)$\frac{11}{2}^+$, 1290.6(5.0)$\frac{13}{2}^+$, 1449.4(1.24)$\frac{9}{2}^+$, 1463.7(1.24)$\frac{7}{2}^+$, and 1486.6(0.60)$\frac{9}{2}^+$. Large Doppler broadenings were observed in the decays of the 1133- and 1464-keV levels, indicating predominantly M1 downward transitions. A calculation of the ^{115}In spectrum involving strong coupling of a $1g_{9/2}$ proton hole to the vibrational states of ^{116}Sn was performed. The results are in good agreement with the level positions, B(E2) values, and ground-state quadrupole moment, and with the relative spectroscopic factors observed in the ^{116}Sn(d,^{3}He)^{115}In reaction. The M1 transition strengths are also predicted reasonably well. No support is found for the existence of a proposed rotational band in ^{115}In. (auth)

12544 ROTATIONAL STATES OF ^{158}Dy, ^{164}Er, ^{168}Yb, AND ^{174}Hf EXCITED BY EVAPORATION REACTIONS. Jett, J. H.; Lind, D. A. (Univ. of Colorado, Boulder). Nucl. Phys.; A155: 182-204(1970).

A series of rotational bands in ^{158}Dy, ^{164}Er, ^{168}Yb, and ^{174}Hf was studied by excitation with neutron evaporation reactions initiated by protons, deuterons, ^{3}He, and α particles with energies between 16 and 28 MeV. The resulting prompt γ-ray spectra were analyzed with a curved crystal diffraction spectrometer and with lithium-drifted germanium detectors. Transitions from levels in the ground-state bands were seen up to 10^+ in ^{168}Yb, 12^+ in ^{158}Dy and ^{174}Hf, and 14^+ in ^{164}Er. The γ-vibrational bands in three of the nuclei were strongly excited and several β bands were weakly excited. The energy levels deduced from the measurements were successfully fit by the empirical formulas of Holmberg and Lipas and of Sood for the ground-state band as well as for the higher bands. The cross sections for transitions in the ground-state band agree with the statistical-model calculations made. Within the validity of the calculations, no large angular momentum deficit was observed. (auth)

12545 DECAY OF ^{95}Ru. Tucker, A. B.; Hein, W. W. (Ames Lab., Iowa). Nucl. Phys.; A155: 129–44(1970).

Ge(Li) detectors were used singly and in coincidence to study γ rays in the decay of ^{95}Ru to ^{95}Tc. A NaI(Tl) anticoincidence shield was used to suppress the Compton background in the singles spectrum—this procedure increased sensitivity to low-intensity gammas. Energies and intensities were determined for 36 transitions. A decay scheme is proposed which accommodates 33 of these transitions. Spins and parities for these levels are assigned from calculated log ft values and measured γ-ray branching ratios. (auth)

12546 DIRECTIONAL CORRELATION AND MULTIPOLE MIXING OF THE GAMMA TRANSITIONS IN ^{102}Ru. Singh, B.; Taylor, H. W. (Univ. of Toronto). Nucl. Phys.; A155: 70-88(1970).

Directional correlation measurements were made on sixteen gamma cascades in ^{102}Ru; these determined the spins of the levels at 944, 1581, 1837, 1873, 2037, 2219, and 2261 keV. The multipole mixtures were deduced for the gamma transitions with energies 418.8, 627.8, 680.6, 739.2, 766.7, 1046.5, 1106.1, 1112.9, 1158.0, and 1562.0 keV. The values of δ^2 for these transitions are compared with those obtained theoretically from the collective model in the hydrodynamical approximation. The predicted electron conversion coefficients are compared with the experimentally measured values, and the parities of the levels are discussed. (auth)

12547 THERMAL NEUTRON CAPTURE IN ^{151}Eu. Michaelis, W. (Kernforschungszentrum, Karlsruhe, Ger.). Nucl. Phys.; A155: 21-32(1970).

The γ-ray spectrum from the radiative capture of thermal neutrons in 96.83% enriched ^{151}Eu was investigated in the energy range 150 keV to 880 keV by using a Ge(Li) detector in Compton-suppression technique. The structure of the spectrum was found to be extremely complex. Two hundred seventy three full-energy peaks were resolved in the energy interval studied. The data are believed to provide a useful contribution to the still unsettled problem of constructing a reliable transition diagram for the odd nucleus ^{152}Eu. (auth)

12548 REORIENTATION EFFECT IN THE CADMIUM ISOTOPES. Steadman, S. G. (Rutgers–The State Univ., New Brunswick, N. J. Univ., Erlangen-Nuernberg, Ger.); Kleinfeld, A. M.; Seaman, G. G.; de Boer, J.; Ward, D. Nucl. Phys.; A155: 1-20(1970).

A thick target of natural cadmium metal was bombarded with 9- to 10-MeV ^{4}He, 38- to 40-MeV ^{16}O, 64-MeV ^{32}S and 101-MeV ^{40}Ar ions. Relative γ-ray intensities from the decay of the Coulomb-excited first 2^+ state in all six natural even-mass cadmium isotopes were measured. (The γ rays from isotopes 106 and 108 could not be resolved.) For each isotope the relative γ-ray intensities for the different projectiles are compared with those for ^{114}Cd, and the deviations are interpreted in terms of the reorientation effect. This determines the difference in the static quadrupole moments of the 2^+ state in ^{114}Cd and the other isotopes. If a value of $Q_{2+} = -0.38$ b is assumed for ^{114}Cd, the values for the other isotopes are given in barns following the mass number of each isotope—106 and 108: −0.84 ± 0.28; 110: −0.24 ± 0.09; 112: −0.15 ± 0.07; 116: −0.88 ± 0.25. (auth)

12549 166-MeV ELASTIC AND INELASTIC ALPHA-PARTICLE SCATTERING; MACROSCOPIC AND MICROSCOPIC ANALYSIS. Tatischeff, B.; Brissaud, I. (Institut de Physique Nucleaire, Orsay, France). Nucl. Phys.; A155: 89-108(1970).

Alpha-particle elastic scattering by ^{12}C, ^{28}Si, Sn, Pb, and ^{2}H was studied in order to obtain optical potential parameters. For each nucleus only one potential gives a good fit, the situation being rather different from that existing at smaller energies. The first 2^+ levels of C, Si, and Sn and the first 3^- level of C were observed, and the angular distribution of scattered α-particles was analyzed using the DWBA. Comparison is made between theoretical and experimental deformation parameters. Optical potentials are calculated with an effective αN interaction and a matter distribution of the Fermi, shell-model, or Hartree–Fock type. The agreement with elastic scattering results is very good. Differential cross sections for inelastic scattering obtained by using these optical potentials and the same effective αN interaction in the DWBA matrix elements are compared with the experimental ones. (auth)

12550 TOTAL NEUTRON CROSS SECTION AND RESONANCE PARAMETERS OF ^{147}Pm. Codding, J. W. Jr.; Tromp, R. L.;

XUM

Simpson, F. B. (Idaho Nuclear Corp., Idaho Falls). Nucl. Sci. Eng.: 43: 58-65(Jan 1971).

The total neutron cross section of ^{147}Pm has been measured from 0.01 to 1000 eV, using compacted oxide samples in the Materials Testing Reactor (MTR) fast chopper. After correcting the data for decay product ^{147}Sm content and water contaminant bias, the total cross section of ^{147}Pm at 0.0253 eV was found to be 200^{+8}_{-7} b. Resonance parameters were determined up to 250 eV by shape-fitting and area analysis, and a negative energy resonance has been postulated to fit the data at thermal. From these parameters a resonance absorption integral of 2192 ± 100 b and a neutron s-wave strength function ($\bar{\Gamma}^0_n/D$) of 2.37×10^{-4} have been obtained. (auth)

12551 INVESTIGATION ON THE GAMMA-RAY SPECTRUM OBTAINED FROM THE THERMAL NEUTRON CAPTURE IN NATURAL CERIUM. Chintalapudi, Surya N.; Sastry, D. L.; Jnanananda, Swami (Andhra Univ., Waltair, India). Indian J. Pure Appl. Phys.; 7: 542-64(Aug 1969).

The low-energy gamma-ray spectrum, obtained from thermal neutron capture in natural cerium, was investigated with a scintillation system and a multi-channel pulse-height analyser. The spectrum exhibits gamma components at energies 0.828, 0.668, 0.628, 0.510, 0.448, 0.352, 0.179, 0.145, and 0.091 MeV. Some of the gamma rays were found to fit into the level structure of the nucleus ^{141}Ce, reported from the (d,p) and (d,t) reaction studies. The relative intensities of these gamma rays are estimated. (auth)

12552 NUCLEAR STRUCTURE OF ^{140}Ce, ^{139}La, AND ^{138}Ba DETERMINED WITH (d,^{3}He) AND (^{3}He,d) TRANSFER REACTIONS. Borgman, Lawrence William. Ann Arbor, Mich.; Univ. of Michigan (1969). 107p. University Microfilms Order No. 70-14,479.

Thesis.

The nuclear structure of three nuclei, each having a closed shell of eighty-two neutrons, was studied using the proton transfer reactions ^{139}La(^{3}He,d)^{140}Ce, ^{140}Ce(d,^{3}He)^{139}La, and ^{139}La(d,^{3}He)^{138}Ba. Excitation spectra were measured up to 4.36 MeV in ^{140}Ce, to 1.95 MeV in ^{139}La, and to 3.05 MeV in ^{138}Ba. Angular momentum transfers were determined from analysis of the characteristic angular distributions with distorted-wave calculations for levels observed in each of these nuclei. Shell-model calculations for each of the nuclei studied were made in a generalized seniority basis space. In these calculations a combination of the surface delta interaction and the generalized pairing interactions were used as residual interactions. There was good agreement between the measured and calculated spectra for the nuclei studied. (auth) (Diss. Abstr. Int., B)

12553 TRANSITIONS FEEDING THE GROUND-STATE ROTATIONAL BAND FOLLOWING (α,xn) REACTIONS WHICH LEAD TO DISTORTED EVEN-EVEN NUCLEI. Ferguson, Stephen Mason. Seattle; Univ. of Washington (1969). 262p. University Microfilms Order No. 70-14,751.

Thesis.

The transition strength for transitions in and from some well-known vibrational-state bands and transition strengths from some high-K isomeric states were measured. Measurements of the transition strengths in the ground-state band were made and extended to transitions from states with spin as high as 16. The angular distributions of these radiations were studied, and the intensities of transitions in certain residual nuclei excited by both (α,3n) and (α,4n) reactions were compared. The studies included ^{154}Gd, ^{160}Dy, and ^{176}Hf, which were created by (α,4n) reactions, and ^{158}Dy, ^{164}Er, ^{168}Yb, ^{174}Hf, and ^{180}W, which were created in both (α,3n) and (α,4n) reactions. Beams of 5 to 20 μA of 42 MeV alpha particles were used. A simplified model was developed by taking into account nonstatistical photon decays in the last few MeV of the photon cascade. The basic assumption of the model is that certain transitions which remove angular momentum are collective and, therefore, enhanced. This assumption is handled in the calculation by the introduction of fairly strict K selection rules. This so-called K-band model can account with moderate success for the radiation intensities and angular distributions. The half-life of a new isomer in ^{174}Hf was measured, as well as the branching ratios of the transitions from the high-spin states in the β band of ^{154}Gd. The photon decay in the (α,pn) reaction in oxygen was also studied. (TSS) (Diss. Abstr. Int., B)

12554 RESONANCE FLUORESCENCE IN Cd AND Ni USING NEUTRON-CAPTURE GAMMA RAYS. Estes, Guy Phillips. Charlottesville, Va.; Univ. of Virginia (1969). 162p. University Microfilms Order No. 70-8060.

Thesis.

The nuclear resonance fluorescence technique was used to study three highly excited nuclear energy levels in cadmium and nickel isotopes by employing neutron capture gamma rays as the exciting radiation. For the 7.64-MeV level of ^{112}Cd, excited by iron capture gamma rays, 11 deexcitation transitions were observed. Angular momentum assignments were made for the resonant level and three lower-lying levels, and the multipole natures of the photon transitions leading to these states were determined. Furthermore, the branching ratios for the 11 observed decay transitions were determined. The 7.64-MeV level in ^{62}Ni was observed to decay by 3 transitions, and the respective branching ratios were determined. In addition, angular momenta were assigned for the resonant level and for the 2.06-MeV level to which inelastic scattering occurred. The photon transitions involved were found to be essentially pure dipole in both instances. A 6.98-MeV level in ^{113}Cd was attributed to the scattering of cobalt capture gamma rays from a natural cadmium target. The resonant isotope had been previously unassigned, and the resonant energy had been given as 6.95 MeV. A spin assignment of $\frac{5}{2}$ was made for the 6.98-MeV resonant level in contrast to a previous assignment of 1, which would necessarily have been associated with an even-A isotope. In addition, the spin of a 0.52-MeV level was found to be $\frac{3}{2}$ in agreement with a known level of that energy in ^{113}Cd. A previously unobserved level at 0.72 MeV with a probable spin of $\frac{3}{2}$ is tentatively suggested on the basis of inelastic scattering to a level at that energy. All photon transitions observed appeared to be mixtures of dipole and quadrupole radiation. (Diss. Abstr. Int., B)

12555 NUCLEAR STRUCTURE STUDIES THROUGH DIRECTIONAL CORRELATIONS. Gupta, Nand Kishore. Amherst, Mass.; Univ. of Massachusetts (1970). 151p. University Microfilms Order No. 70-10,034.

Thesis.

In the decay of ^{209}Tl, $\beta-\gamma$ correlations involving the 1.795-MeV, 1.520-MeV, and 1.286-MeV β groups with appropriate cascade γ rays were measured. These correlations are found to be small ($A_2 \lesssim 2\%$); this result is consistent with the ξ approximation. These results, in conjunction with the known structure of the ground state of ^{209}Tl, are discussed in terms of particle-hole structure of low-lying excited states of ^{209}Pb. The data are consistent with $[\nu g_{9/2}, \nu p^{-1}_{1/2}]$ or $[\pi h_{9/2}, \pi s^{-1}_{1/2}]$ configurations for the first 5^- and 4^- states at 3.198 MeV and 3.475 MeV in ^{209}Pb. The second 5^- state at 3.708 MeV seems to be more complex. In the decay of ^{126}Sb, $\beta-\gamma$ correlation involving the 1.9-MeV β group with the 415-keV γ ray ($A_2 = -0.042 \pm 0.013$) clearly rules out an 8^- assignment for the ground state of ^{126}Sb. A 7^- assignment for this state is indicated. In the decay of ^{214}Bi, $\beta-\gamma$ correlations involving the 1.8-MeV β group with the 769-keV stop-over γ ray and also with the 1378-keV cross-over γ ray were measured. Assignment of 1^- for the spin and parity of the ground state of ^{214}Bi is most consistent with our measurements and the shape of the ground state β-transition. An analysis of the shape of the ground state β transition suggests that the structure of the ground state of ^{214}Bi may be very similar to that of ^{210}Bi. $\gamma-\gamma$ correlations involving 769-keV-609-keV, 806-keV-609-keV, 1120-keV-609-keV, 1155-keV-609-keV, and 1238-keV-609-keV cascades in ^{214}Po were also measured. These correlations indicate that the 1120-keV, 1155-keV, and 1238-keV γ transitions are essentially of M1 nature. The value of δ(E2/M1) for the 769-keV transition was determined to be $-1.7^{+}_{-}{}^{+}_{-}{}^{0.4}_{0.3}$ and $-2.6^{+0.4}_{-0.3}$ from our $\beta-\gamma$ and $\gamma-\gamma$ correlation measurements. This value confirms the collective nature of the 1378-keV second 2^+ excited state of ^{214}Po. Preliminary results of the $\beta-\gamma$ correlation in the second-forbidden β decay of ^{94}Nb are presented. The relation between matrix elements of the Vector interaction ($\int iA_{ij} = -A\xi \int R_{ij}$) is discussed in the light of the Conserved Vector Current theory. The β-decay properties are insensitive to the choice of the value of A. The set of matrix elements ($C_V \int R_{ij}/C_A \int iT_{ij} \approx 0.19$, $\int S_{ij}/\int iT_{ij} \approx 1$ and $A \approx 2.3$) is consistent with the β-decay properties and the CVC theory. Unfortunately, the value of A cannot be determined uniquely in this case. The β-decay rate is calculated as a function of A. The experimental rate is hindered by a factor of 4 to 14 in the range A = 1 to 4 compared to the theoretical estimates. (TSS) (Diss. Abstr. Int., B)

12556 REORIENTATION EXPERIMENTS IN THE EVEN-MASS CADMIUM ISOTOPES: THICK TARGET YIELDS AND GAMMA-RAY ANGULAR DISTRIBUTIONS. Steadman, Stephen Geoffrey. New Brunswick, N. J.; Rutgers-The State Univ. (1969). 119p. University Microfilms Order No. 70-10,106.

Thesis.

The reorientation effect in Coulomb excitation was utilized to obtain the differences in the static electric quadrupole moments of the 2^+ states Q_{2+} for the even-mass cadmium isotopes. The total gamma-ray yields, relative to ^{114}Cd, from the deexcitation of the 2^+ states were measured for bombardment of a thick natural cadmium target with 9- to 10-MeV ^{4}He ions, 38- to 40-MeV ^{16}O

ions, 64-MeV ^{32}S ions, and 101-MeV ^{40}Ar ions. The gamma rays were detected with a Ge(Li) counter located at 0 and 55 degrees relative to the beam. With the aid of a computer program, the expected gamma-ray yield was calculated for each isotope for two values of the diagonal reduced matrix element $\langle 2^+ || M(E2) || 2^+ \rangle$, namely, 0 and −0.5 e−barns. A perturbation theory calculation indicates that the gamma-ray yield depends approximately linearly on the matrix element $\langle 2^+ || M(E2) || 2^+ \rangle$. By extrapolation, the value of Q_{2^+} for each isotope relative to ^{114}Cd was obtained. If a value of $\langle 2^+ || M(E2) || 2^+ \rangle = -0.5$ e−barns is assumed for ^{114}Cd, the values for the isotopes, in barns, are −0.76 ± 0.33 for $^{106,108}Cd$, −0.28 ± 0.10 for ^{110}Cd, −0.15 ± 0.06 for ^{112}Cd, −0.38 for ^{114}Cd (assumed), and −0.68 ± 0.23 for ^{116}Cd. An analysis in terms of perturbation theory gives similar results. The yields for $^{106,108}Cd$ could not be separated; the composite result has relative weights of about 57% for ^{106}Cd and 43% for ^{108}Cd. This is the first measurement of Q_{2^+} for ^{110}Cd; the other values agree with previous measurements. All observed values are negative and the magnitudes form a U-shaped curve with ^{112}Cd as the minimum value. The isotope ^{112}Cd, with 64 neutrons, completes the $1g_{\frac{9}{2}}$ shell. An attempt was made to observe the reorientation effect in the gamma-ray angular distribution of the $2^+ \rightarrow 0^+$ transition in ^{114}Cd in coincidence with 36-MeV ^{16}O ions scattered at 90 degrees in the laboratory system. Calculations were made using both a computer program and perturbation theory. From the perturbation-theory calculation, an anisotropy in the angular distribution is predicted which contains a term that is approximately linear in the reduced matrix element $\langle 2^+ || M(E2) || 2^+ \rangle$. Both calculations indicate a rotation of the angular distribution by 0.44 degrees for a change in $\langle 2^+ || M(E2) || 2^+ \rangle$ equal to −0.5 e−barns. In this case, the expected shift was too small to be observed. (auth) (Diss. Abstr. Int., B)

12557 PROPERTIES OF THE EXCITED STATES OF ^{147}Sm AND ^{149}Pm. Begzhanov, R. B.; Gaffarov, D. G.; Il'khamdzhanov, N.; Muminov, A. I. (Inst. of Nuclear Physics, Tashkent). Izv. Akad. Nauk Uzb. SSR, Ser. Fiz.-Mat. Nauk; No. 2, 65-8(1970). (In Russian).

The fast−slow coincidence method was used to measure the angular correlations of the γ cascade transitions and the magnetic moments of some excited states of the ^{147}Sm and ^{149}Pm nuclei. The ^{147}Eu source for the study of the excited states of ^{147}Sm was obtained by the cyclotron irradiation of natural samarium with 18-MeV protons. The results agree with some of the previously reported data. The quadrupole moments of the ground states of the two nuclei indicate that they are spherical. Predictions of the simplified one-particle model with respect to the M1 and E2 transition probabilities and the magnetic moments of the lower excited states do not agree satisfactorily with the experimental data. The properties of the excited states of such nuclei of the transition region may be explained on the basis of the phonon model of Kissinger and Sorensen by taking into account the superfluidity of spherical nuclei, polarization of the shell, and the relation of the quasiparticles with phonons. (TTT)

12558 NUCLEAR STRUCTURE OF ^{140}Ce, ^{141}Pr, AND ^{142}Nd DETERMINED BY (d,^{3}He) AND (^{3}He,d) REACTIONS. Jones, William Philip. Ann Arbor, Mich.; Univ. of Michigan (1969). 96p. University Microfilms Order No. 70-14,558.

Thesis.

The nuclear structure of the N = 82 isotones ^{140}Ce, ^{141}Pr, and ^{142}Nd were studied with the reactions ^{141}Pr,(d,^{3}He)^{140}Ce, ^{140}Ce(^{3}He,d)^{141}Pr, and ^{141}Pr(^{3}He,d)^{142}Nd. Excitation energies and absolute cross sections were measured for states with excitation energy below 4.0 MeV in ^{140}Ce, 2.0 MeV in ^{141}Pr, and 4.5 MeV in ^{142}Nd. Angular distributions were measured for these states and the techniques of distorted wave analysis used to extract spectroscopic information. Shell model calculations were performed in a generalized seniority basis using either a surface delta interaction or a generalized pairing Hamiltonian. The agreement between the experimentally derived information and results of the calculations for ^{140}Ce and ^{142}Nd was quite good. The calculation for ^{141}Pr was somewhat less satisfactory than hoped for. Suggestions for improving that calculation are presented. (Diss. Abstr. Int., B)

12559 STUDIES OF THE FIRST 2^+ STATES OF ^{154}Sm AND ^{238}U USING THE MOESSBAUER EFFECT FOLLOWING COULOMB EXCITATION. Wheeler, Richard Merrill. Baltimore; Johns Hopkins Univ. (1969). 152p. University Microfilms Order No. 70-11,806.

Thesis.

The hyperfine interactions of the first excited 2^+ states of ^{154}Sm and ^{238}U were studied using the Moessbauer effect following Coulomb excitation (ME-CE). The magnetic dipole and electric quadrupole hyperfine interactions of ^{154}Sm were measured in $SmCl_3 \cdot 6H_2O$ at 30° and 4.2°K and in SmIG at 4.2°K. With a value for the internal magnetic field acting on the Sm nucleus in $SmCl_3 \cdot 6H_2O$ reported by Ofer and Nowik and a free ion value for the electric field gradient in Sm calculated by Ofer et al., the results in $SmCl_3 \cdot 6H_2O$ were used to determine the magnetic dipole and electric quadrupole moment, $\mu^{154} = (.778 \pm .036)\mu_N$ and $^{154}Q(1-R) = (-1.33 \pm .46)$ barns, respectively. μ^{154} was used to determine $H_{eff}(SmIG) = (3.04 \pm .12)$ MG at 4.2°K. This value for H_{eff}(SmIG) agrees with the value used by Atzmony et al., to measure g_R^{152} in SmIG; thus, their value for g_R^{152} is confirmed. The isomer shift of the 82 keV transition in ^{154}Sm between Sm_2O_3 and SmB_6 was measured as $\delta = (-1 \pm 1)$ mm/sec. The uncertainty in this value arises from difficulty in analyzing the complex spectrum of Sm_2O_3 at 4.2°K. Since the Sm^{2+} ion is expected to have no hyperfine interaction the observation of a single line supports the hypothesis that SmB_6 is divalent at 0°K. ^{238}U was studied in the compounds α-uranium metal, U_3O_8, $(UO_2)(NO_3)_2 \times 6H_2O$ and UO_2 above 30° and UO_2 at 4.2°K. The Moessbauer absorption spectra of U_3O_8 and $(UO_2)(NO_3)_2 \cdot 6H_2O$ were interpreted in terms of pure quadrupole interactions with $e^2qQ/4$ equal to (2.64 ± .19) cm/sec and (−4.26 ± .29) cm/sec, respectively. Recent ME measurements by S. L. Ruby et al., of UO_2 at 77° and 4.2°K were interpreted in terms of a pure magnetic hyperfine interaction. This measurement is confirmed in the present work. A new ME-CE technique featuring independent target and absorber cryogenic supplies is reported. (Diss. Abstr. Int., B)

12560 NUCLEAR-RESONANCE FLUORESCENCE IN ^{130}Xe. Kenealy, P. F. (Wayne State Univ., Detroit); Beard, G. B.; Parsons, Karl. Phys. Rev., C; 2: 2009-15(Nov 1970).

The 536-keV (2^+) first excited state of ^{130}Xe was investigated by means of nuclear-resonance-fluorescence scattering experiments. The use of a Ge(Li) detector allowed a good determination of the Rayleigh scattering contribution which amounted to about 30% of the resonant peak. The level width was found to be $(5.2 \pm 0.9) \times 10^{-5}$ eV, corresponding to a mean life of $(1.3 \pm 0.3) \times 10^{-11}$ sec and a B(E2) ↑ of $(0.69 \pm 0.15)e^2 \times 10^{-48}$ cm^4. From this result and the relative transition probabilities determined previously in a Coulomb-excitation experiment by Pieper, Anderson, and Heydenburg, the absolute B(E2) values for the first excited states of ^{128}Xe and ^{132}Xe were obtained. (auth)

12561 RESONANCE NEUTRON CAPTURE IN ^{103}Rh. Rimawi, K. (State Univ. of New York, Albany); Garg, J. B.; Chrien, R. E.; Graves, R. G. Phys. Rev., C; 2: 1793-1808(Nov 1970).

The γ-ray spectra following slow-neutron capture in a target of ^{103}Rh were measured with the fast-chopper time-of-flight facility at the high flux beam reactor at Brookhaven National Laboratory. A total of 145 radiative intensities, involving transitions from seven resonances and 16 unresolved resonances, to levels in ^{104}Rh were recorded. A neutron binding energy of 6999.3 ± 1.5 keV is obtained. From these high-energy γ-ray data, several spin assignments for levels in ^{104}Rh are made. The distribution of transition probabilities in rhodium is not consistent with the Porter-Thomas distribution; values of $\nu = 2.70$ and $\nu = 2.45$ are obtained as best fits to the class of χ^2 distribution functions to spin-0 and spin-1 resonances, respectively. The gross shape of the γ-ray spectrum shows an enhancement of strength to states near 1 MeV in excitation energy, both for thermal and resonance capture. It is shown that this enhancement is not due to a direct-reaction process, and it is suggested that the presence of doorway states may be responsible for this enhancement. (auth)

12562 THRESHOLD PHOTODISINTEGRATION OF ^{208}Pb. Shakin, C. M. (Massachusetts Inst. of Tech., Cambridge); Weiss, M. S. Phys. Rev., C; 2: 1809-14(Nov 1970).

The threshold photodisintegration of ^{208}Pb and the thermal-neutron capture by ^{207}Pb is considered. It is shown that the magnitude of the thermal capture cross section and the asymmetry of the resonance observed in the (γ,n) reaction at 41 keV above threshold may be explained by extrapolating the giant resonance amplitude and the amplitude of a subthreshold resonance into the appropriate energy domains. It is found that the direct (optical) processes are small compared with the effects of the "resonance tails." (auth)

12563 COMPARISON OF ASYMMETRIC SHAPES FOR DEFORMED NEGATIVE-PARITY STATES IN HEAVY EVEN NUCLEI. Davidson, Melvin G. (Univ. of Kansas, Lawrence. Western Washington State Coll., Bellingham). Phys. Rev., C; 2: 1814-22(Nov 1970).

The predictions of asymmetric collective models with pure quadrupole, pure octupole, and mixed quadrupole-plus-octupole shapes are developed for negative-parity states in deformed even nuclei in an effort to determine the usefulness of the asymmetric model as a tool to distinguish surface shapes. The models are ap-

XUM

plied to the data for ^{228}Th, ^{232}U, and ^{234}U, and the comparison indicates that the energy and electric quadrupole branching-ratio predictions are independent of surface-shape multipolarity. (auth)

12564 PROTON DECAY OF ISOBARIC ANALOG RESONANCES IN ^{85}Nb. **Lieb, Klaus-Peter (Univ. of Texas, Austin. Univ. Nacional, Bogota); Kent, James J.; Hausmann, Till; Watson, Charles E. Phys. Rev., C; 2: 1822-41(Nov 1970).**

Differential cross sections for elastic and inelastic proton scattering on ^{94}Zr were measured between 6.0- and 8.5-MeV bombarding energy. The decay of analogs of states in ^{95}Zr to the ground state and the 0.92 MeV (2^+), 1.30 MeV (0^+), 1.66 MeV (2^+), and 2.06 MeV (3^-) states in ^{94}Zr was investigated. In the analysis of the inelastic proton groups, the enhancement of the Hauser–Feshbach background, as well as the interference of the resonance amplitude with direct nuclear excitation was taken into account. Spins, spectroscopic factors, and possible weak-coupling configurations in the parent system are derived and compared with results previously obtained for ^{91}Zr and ^{93}Zr. (auth)

12565 TOTAL NEUTRON CROSS SECTION OF ORIENTED ^{165}Ho FROM 2 TO 135 MeV. **Marshak, H. (National Bureau of Standards, Washington, D. C.); Langsford, A.; Tamura, T.; Wong, C. Y. Phys. Rev., C; 2: 1862-81(Nov 1970).**

The difference in the total neutron cross section due to nuclear orientation, $\Delta\sigma_{def}$, was measured for ^{165}Ho over the energy range of 2 to 135 MeV. The results show that $\Delta\sigma_{def}$ oscillates as well as changing sign, contrary to the classical concept of the interaction. The data, both σ_t and $\Delta\sigma_{def}$, are successfully fitted by adiabatic coupled-channel calculations using the optical model. The parameters for the optical model were determined by fitting σ_t and σ_R data (over approximately the same energy range as in the present work) for the two spherical nuclei Cd and Pb. The only additional quantity introduced was the quadrupole deformation parameter for ^{165}Ho which is known to be 0.33. The data for $\Delta\sigma_{def}$ can also be explained quite well by a simple semiempirical model which makes use of the black-nucleus model, the nuclear Ramsauer effect, and the experimental σ_t data. The temperature dependence of $\Delta\sigma_{def}$ agrees very well with our calculated values for the degree of nuclear orientation, which is consistent with ^{165}Ho being almost a pure quadrupole-shaped nucleus. (auth)

12566 DECAY OF ^{117}In ISOMERS AND SEARCH FOR A LOW-LYING $9/2^-$ LEVEL IN ^{117}Sn. **Baedecker, P. A.; Pakkanen, A.; Walters, W. B. (Massachusetts Inst. of Tech., Cambridge). Nucl. Phys.; A158: 607-14(1970).**

The decay of 40-min ^{117g}In and 117-min ^{117m}In to the excited states of ^{117}Sn was investigated in a search for a low-lying $9/2^-$ level. New β branches to several levels previously identified in ^{117}Sn were observed; but no evidence was obtained for the presence of any additional states, including any $9/2^-$ level. M2–E2 competition was observed in the decay of the $7/2^+$ level at 711.5 keV in ^{117}Sn, and its half-life was determined to be 1.0 ± 0.1 nsec. (auth)

12567 GAMMA–GAMMA DIRECTIONAL CORRELATIONS IN THE DECAY OF ^{147}Nd. **Blaskovich, Nick Jr.; Arya, Atam P. (West Virginia Univ., Morgantown). Phys. Rev., C; 2: 1881-6(Nov 1970).**

A 10-cc coaxial Ge(Li) detector and a 2-in. × 2-in. NaI(Tl) detector were used in conjunction with a multichannel coincidence configuration to investigate the following $\gamma-\gamma$ directional correlations in the decay of 11.1-day ^{147}Nd: 319-91, 398-91, 440-91, 121-319, and 276-319 keV. Using the well-established values of $7/2$ and $5/2$ for the ground and 91-keV levels, respectively, and an admixture of (1.6 ± 0.4)% E2 for the 91-keV transition, this experiment favored the following spin assignments to the various levels: 410 ($3/2$), 489 ($5/2$), 531 ($5/2$), and 686 keV ($5/2$). The M1 + E2 multipolarity mixtures obtained, which are in agreement with nuclear-orientation and internal-conversion measurements reported by previous investigators, for each of the respective γ transitions are: 121 (1.5 ± 0.5)% E2, 276 (~1)% E2, 319 (11 ± 2)% E2, 398 (3 ± 2)% E2, and 440 keV (27 ± 7)% E2. A 310-keV γ ray proposed by several investigators was directly observed in the Ge(Li) spectrum; measurements indicate that this peak decays with the half-life of ^{147}Nd. (auth)

12568 NUCLEAR-STRUCTURE AND HYPERFINE-FIELD STUDIES WITH ^{95}Mo. **Bond, Peter; Jha, S. (Case Western Reserve Univ., Cleveland). Phys. Rev., C; 2: 1887-97(Nov 1970).**

Excitation functions for (α, xn), (α, αn), and (α, 2p) reactions upon niobium targets were measured for incident α-particle energies from 15 to 41 MeV. Excited states in ^{95}Mo were studied by observing the decay of the 61-day isotope ^{95m}Tc, which was produced by the ^{93}Nb(α, 2n) reaction. The energies and the intensities of the γ rays resulting from this decay were measured. The angular-correlation coefficients of the two strongest cascades in ^{95}Mo were found to be $A_{22} = -0.292 \pm 0.005$ and $A_{44} = -0.001 \pm 0.006$ for the 582–204-keV cascade, and $A_{22} = -0.196 \pm 0.006$ and $A_{44} = -0.003 \pm 0.008$ for the 835–204-keV cascade. The mean life of the 204-keV state was measured by the delayed-coincidence technique and found to be 1.09 ± 0.02 nsec. The g factor of the 204-keV state was measured to be −0.26 ± 0.02. A summary of a number of calculations concerning the nuclear structure of ^{95}Mo is given, and some predictions of the Kisslinger–Kumar model of near-spherical nuclei for ^{95}Mo are presented. The technique of perturbed angular correlations was used to measure the hyperfine fields at the molybdenum nucleus in iron and nickel hosts. These fields were found to be B_{eff} (Mo in Fe) = −236 ± 19 kG and B_{eff} (Mo in Ni) = −29.9 ± 5.1 kG at 55°C. (auth)

12569 EXCITATION OF STATES IN ^{207}Pb BY ^{208}Pb(d,t), ^{206}Pb(d,p), AND ^{207}Pb(d,d') REACTIONS. **Moyer, R. A.; Cohen, B. L.; Diehl, R. C. (Univ. of Pittsburgh). Phys. Rev., C; 2: 1898-1916(Nov 1970).**

States up to 5.6 MeV in excitation energy in ^{207}Pb were studied by the ^{208}Pb(d,t), ^{206}Pb(d,p), and ^{207}Pb(d,d') reactions at a deuteron bombarding energy of 17 MeV. Over 100 states were observed and 70 angular distributions were measured and compared with distorted-wave Born approximation calculations for the (d,p) and (d,t) reactions. Special emphasis was placed on obtaining accurate excitation energies to compare those states excited in more than one reaction. In ^{208}Pb(d,p), some of the two-hole–one-particle (2h-1p) states are found to be fragmented. The $i_{13/2}$ and $j_{15/2}$ 2h-1p states are tentatively identified. Many of the weaker (less than 5 μb/sr) transitions in (d,t) have angular distributions which do not follow DWBA–possibly indicating other than one-step reaction mechanisms. Observation of the 2h-1p states in (d,t) indicates that the ^{208}Pb closed shell contains about 4.7% $(2g_{9/2})^2$, ≲4.7% $(3d_{5/2})^2$, and ≲1.2% $(4s_{1/2})^2$ particle-^{206}Pb core admixture. (auth)

12570 NUCLEAR STRUCTURE EFFECTS IN (p,2 NUCLEON) REACTIONS ON THE SEPARATED ISOTOPES OF CADMIUM AT 400 MeV. **Nieckarz, W. J. Jr.; Caretto, A. A. Jr. (Carnegie-Mellon Univ., Pittsburgh). Phys. Rev., C; 2: 1917-23(Nov 1970).**

The cross sections of (p,2p), (p,pn), and (p,2n) reactions at 400 MeV on the separated isotopes of cadmium were determined. The (p,pn) cross sections exhibit abrupt variations within a narrow target mass range. The data are examined in terms of the currently accepted mechanisms for high-energy (p,2 nucleon) reactions. An estimate is made of the relative contribution of direct knockout processes versus the two-step inelastic scattering and neutron evaporation mechanism. There does not appear to be any obvious explanation for the abrupt cross-section variations. The cross section of the cadmium (p,2p) reactions is inversely proportional to the neutron skin thickness. This is consistent with the conclusion that these reactions take place predominantly by direct knockout processes and in the peripheral region of the nucleus. (auth)

12571 SINGLE NUCLEON TRANSFER REACTIONS: THE EXTRACTION OF RELIABLE SPECTROSCOPIC FACTORS AND CHARGE EXCHANGE EFFECTS. **Hinrichs, Roger Albert. Seattle; Univ. of Washington (1969). 219p. University Microfilms Order No. 70-14,763.**

Thesis.

The single nucleon transfer reactions (d,p) and (p,d) on Zr and Mo isotopes were studied with an interest in spectroscopic and reaction mechanism information. The effects of charge exchange upon the excitation functions for such transfer reactions were observed not only in the outgoing proton channel but also in the incident proton channel. Tentative evidence for such isospin coupling was obtained for proton induced reactions on ^{98}Mo, ^{95}Mo, ^{100}Mo and ^{94}Zr. The shapes of the anomalies are similar in most all cases. For ^{98}Mo(p,d), anomalous behavior in the excitation function was observed not only at the threshold for the (p,n) reaction to the isobaric analog state but possibly also at the quasi-inelastic threshold to collective states. The absence of structure in the proton scattering from these nuclei reduces the possibility that the anomalies arise from interference with isobaric analog type resonances in the incident channel. However such resonance effects were observed in the ^{208}Pb(p,d) reaction and masked any evidence of charge exchange effects. Evidence of non-analogous coupling was observed in ^{90}Zr(d,p) angular distributions at the (d,n) threshold to the ground state analog. These dips in the angular distributions at forward angles in several channels imply a need for an analysis more complicated than the simple two channel approach. In the ^{90}Zr(d,p) reaction a procedure is developed for the extraction of reliable spectroscopic factors. By using the constraint that these values should be constant with bombarding

energy, several sets of optical model parameters obtained from elastic scattering analyses for use in the DWBA could be eliminated, and the spectroscopic factors determined to an accuracy of better than ±15%. The difficulty with the strong dependence of the cross-section upon the bound state parameters could be removed by using values of the mean square radius obtained from the reformulated optical model of Greenlees and constraining the bound state parameters. The allowed variation in the spectroscopic factors for the states in ^{91}Zr was then less than 15%. (Diss. Abstr. Int., B)

12572 ISOMERS OF ^{136}I AND ^{136}Xe. Carraz, L. C.; Blachot, J.; Monnand, E.; Moussa, A. (CEN, Grenoble, France). Nucl. Phys.; A158: 403-17(1970). (In French).

The β decay of ^{136}I isomers was studied with Ge(Li) detectors. Beta-gamma and γ-γ coincidences were carried out. Delayed coincidences between the β spectrum and some γ rays show a metastable state in ^{136}Xe, the period of which is 2.8 μsec. A level scheme is proposed for ^{136}Xe and compared with results of the ^{136}Xe (p,p') reaction. (auth)

12573 HIGH-ENERGY PHOTOFISSION CROSS SECTIONS OF URANIUM AND THORIUM. Methasiri, T. (Lund Inst. of Tech., Sweden). Nucl. Phys.; A158: 433-9(1970).

The photofission cross sections per equivalent quantum of uranium and thorium were measured in the bremsstrahlung energy range 200 to 900 MeV. A glass detector was used to detect the fission fragments. Fission cross sections are obtained from the integrated cross section using Penfold and Leiss's method. It is found that the photofission cross sections of both uranium and thorium show resonance peaks at a photon energy of 350 MeV, with peak values of 80 and 60 mb, respectively. It is suggested that, in a high-energy photofission, the fission mechanism can, at least in part, be due to photomeson production processes. (auth)

12574 TEST OF THE SHELL MODEL FOR ^{206}Pb BY THE ^{208}Pb(p,t) REACTION. Smith, S. M. (Univ. of Maryland, College Park); Roos, P. G.; Bernstein, A. M.; Moazed, Cyrus. Nucl. Phys.; A158: 497-515(1970).

The ^{208}Pb(p,t)^{206}Pb reaction induced by 40-MeV protons was studied with 40-keV triton energy resolution. The experimental energies and transition strengths for the natural parity levels below 3.4 MeV are compared with the predictions obtained from four sets of shell-model wave functions. The overall agreement for each set is good. The insensitivity of the energy-level positions and (p,t) transition strengths to the differences in the shell-model calculations considered made determination of the most satisfactory set of wave functions for ^{206}Pb difficult. However, through the use of an approximate sum rule, it is concluded that the wave-function sets derived from the calculations which employ a larger model space produce a better agreement with the experimental transition strengths. (auth)

12575 STUDY OF THE ^{208}Pb(d,^{3}He)^{207}Tl AND ^{204}Pb(d,^{3}He)^{203}Tl REACTIONS AT 80 MeV. Royer, D.; Arditi, M.; Bimbot, L.; (and others) (Institut de Physique Nucleaire, Orsay, France). Nucl. Phys.; A158: 516-28(1970). (In French).

The ^{208,204}Pb(d,^{3}He)^{207,203}Tl reactions were studied at E_d = 80 MeV. Five previously reported single-proton hole states in the former reaction and eight excited states up to 3 MeV in excitation energy in the latter reaction were observed. The l transfers were deduced from their angular distributions. The DWBA was applied, and absolute spectroscopic factors were obtained which are in good agreement with shell-model predictions for ^{207}Tl. A proton bound-state well radius of 1.286 F had to be used, which is larger then the usual neutron radius. For ^{203}Tl, spectroscopic factors were in good agreement with the predictions of the model of a single-proton hole coupled with quadrupole and octupole vibrations of the core. (auth)

12576 M1 ADMIXTURES IN TRANSITIONS FROM γ-VIBRATIONAL STATES IN ^{152}Sm, ^{154}Gd, AND ^{156}Gd. Rud, N.; Bonde Nielsen, K. (Univ. of Aarhus, Denmark). Nucl. Phys.; A158: 546-60(1970).

Measurements of M1 admixtures in a number of transitions depopulating 2, 3$^+$ and 2, 2$^+$ γ-vibrational states in ^{152}Sm, ^{154}Gd, and ^{156}Gd are presented. In the case of ^{152}Sm, it is verified that the intrinsic static quadrupole moments of the γ band and the ground-state band are equal to within 10%. It is concluded that the small M1 admixtures present in transitions between the two bands can be accounted for in first-order perturbation theory as a result of K = 1 impurities. The M1 admixture in the intraband transition 2, 3$^+$-2, 2$^+$ of ^{152}Sm and ^{154}Gd is estimated and attributed to $|g_K - g_R| \approx 0.15$ in both cases. (auth)

12577 LIFETIMES OF SOME EXCITED STATES IN ^{182}W. Abou-Leila, H.; Darwish, S. M.; El-Haliem, A. Abd; Awwad, Z. (Atomic Energy Establishment, Cairo). Nucl. Phys.; A158: 558-76(1970).

The lifetimes of five excited states in ^{182}W were measured using a magnetic double-lens spectrometer coupled to a pulse-height converter and a fast-slow coincidence system. The half-lives of the 100-keV, 1289-keV, 1374-keV, 1488-keV, and the 1553-keV levels were found to be 1.48 ± 0.03 ns, 1.06 ± 0.02 ns, 1.70 ± 0.05 ns, ≤1.70 ns, and 1.35 ± 0.04 ns, respectively. Some nuclear parameters are deduced and discussed. (auth)

12578 TWO-QUASIPARTICLE STATES IN ^{159}Tb. Jones, H. D.; Sheline, R. K. (Florida State Univ., Tallahassee). Phys. Rev., C; 2: 1747-58(Nov 1970).

Thirty-four levels in ^{159}Tb were observed up to an excitation energy of 1166 keV utilizing 12-MeV deuterons and the reaction ^{159}Tb(d,t)^{158}Tb. The ground-state Q value was determined to be −1870 ± 15 keV. The spectrum was interpreted in terms of the coupling of the [411↑] Nilsson proton orbital with the neutron orbitals prominent in the (d,t) spectrum of ^{157}Gd. This interpretation has resulted in the determination of relative energies due to the residual neutron-proton interaction for eight different configurations. The observed singlet-triplet splitting energies for the [521↑], [402↓], and [400↑] neutron orbitals coupled to the [411↑] proton orbital were measured to be +132, −111, and +136 keV, respectively. Theoretical calculations of these energies made for a zero-range spin-dependent central potential gave values of +174, −186, and +136 keV, respectively. (auth)

12579 FISSION OF ODD-A URANIUM AND PLUTONIUM ISOTOPES EXCITED BY (d,p), (t,d), AND (t,p) REACTIONS. Britt, H. C.; Cramer, J. D. (Los Alamos Scientific Lab., N. Mex.). Phys. Rev., C; 2: 1758-68(Nov 1970).

Fission-fragment angular correlations and fission probabilities were measured for a series of odd-A uranium and plutonium isotopes excited by (d,p), (t,d), and (t,p) reactions. The following fissioning nuclei were studied: (1) ^{235}U from (d,pf), (t,pf); (2) ^{237}U from (d,pf), (t,df), (t,pf); (3) ^{239}U from (d,pf); (4) ^{241}Pu from (d,pf), (t,df), (t,pf); and (5) ^{243}Pu from (d,pf), (t,df). Fission probabilities and angular-correlation coefficients for each case are compared with previously reported (n,f) results. The direct-reaction experiments show fission thresholds at excitation energies equal to or less than threshold energies observed in (n,f) experiments. Some qualitative characteristics of the transition-state spectrum for the nuclei studied are determined from comparisons of the direct-reaction and (n,f) results. (auth)

12580 PRODUCTION OF ^{149}Tb FROM GOLD BY 2.2-GeV PROTONS. Crespo, V. P. (Brookhaven National Lab., Upton, N. Y.); Cumming, J. B.; Alexander, J. M. Phys. Rev., C; 2: 1777-92(Nov 1970).

Angular distributions and differential range spectra at angles of 15, 60, 90, 120, and 165° to the beam direction were measured for ^{149}Tb recoiling from thin gold targets irradiated with 2.2-GeV protons. The observed mean velocities decrease monotonically from a value of 0.264 (MeV/amu)$^{\frac{1}{2}}$ at 15° to 0.149 (MeV/amu)$^{\frac{1}{2}}$ at 165°. The ratio of integrated intensity in the forward hemisphere to that backward is 3.10. The experimental results are consistent with the symmetry requirements of a two-step model for the reaction, provided that there is a positive correlation between $v_{||}$, the forward component of velocity due to the first step, and V, the velocity due to the second step. However, there are substantial quantitative discrepancies between the experimental results and calculations based on the cascade-evaporation model which is commonly used to describe the two steps of a high-energy nuclear reaction. The calculations predict a value of $\langle v_{||} \rangle$ twice as large as that observed and a much weaker correlation between V and $v_{||}$. These effects are discussed in terms of possible contributions from heavy-fragment emission in both steps of the reaction. Systematics of the average energies of various recoil products suggest an empirical correlation that may be useful in distinguishing fission from "deep spallation." (auth)

12581 NUCLEAR STRUCTURE EFFECTS IN (p,2 NUCLEON) REACTIONS ON THE SEPARATED ISOTOPES OF TELLURIUM AT 300 MeV. Schall, Roy F. Jr.; Caretto, Albert A. Jr. (Carnegie-Mellon Univ., Pittsburgh). Phys. Rev., C; 2: 1924-9 (Nov 1970).

The cross sections of (p,2p), (p,pn), and (p,2n) reactions at 300 MeV on the separated isotopes of tellurium were determined. The total (p,pn) cross sections, for those cases in which it was only possible to measure one of the isomeric states in the product, was calculated by assuming that the direct knockout mechanism was predominant. Both the total (p,pn) cross sections and the (p,2n) cross sections are directly proportional to the neutron skin thickness. This is consistent with the assumption that these reactions take place by direct knockout processes in the diffuse or peripheral

XUM

region of the nucleus. The tellurium (p,2p) reactions were observed to be inversely proportional to the neutron skin thickness. (auth)

12582 EXPERIMENTAL STUDIES OF THE NEUTRON-DEFICIENT GADOLINIUM ISOTOPES. II. ^{145m}Gd. Eppley, R. E.; McHarris, Wm. C.; Kelly, W. H. (Michigan State Univ., East Lansing). Phys. Rev., C; 2: 1929-34(Nov 1970).

The N = 81 isomer ^{145m}Gd is characterized as having a half-life of 85 ± 3 sec and an M4 isomeric transition of 721.4 ± 0.4 keV. It also has a direct β^+/ϵ branch to the $h_{\frac{11}{2}}$ state at 716.1 keV in ^{145}Eu. The intensity of this branch is 4.7% of the decay, implying a log ft of 6.2. The M4 transition probability is calculated and compared with the trends among other isomeric transitions in this region. (auth)

12583 LIFETIME MEASUREMENTS IN ^{131}Xe AND ^{129}Xe. Langhoff, H. (Franklin Inst., Swarthmore, Pa.). Nucl. Phys.; A158: 657-63(1970).

By means of the centrifuge technique nuclear resonance fluorescence was observed from the levels at 364 keV, 637 keV, and 723 keV in ^{131}Xe and from the 411-keV level in ^{129}Xe. The following lifetimes were determined: τ_{364} = 73 ± 6 psec, τ_{637} = 6.0 ± 0.6 psec, τ_{723} = 0.76 ± 0.13 psec, and τ_{411} = 72 ± 15 psec. The results are compared with predictions from a recent calculation by Paradellis and Hontzeas using the intermediate coupling model. (auth)

12584 HIGH-ORDER DEFORMATIONS AND ELECTRIC MONOPOLE TRANSITIONS IN DEFORMED NUCLEI. Aveledo, C. E.; Davidson, J. P. (Univ. of Kansas, Lawrence). Phys. Rev., C; 2: 1934-7(Nov 1970).

Calculation of electric monopole X ratios in deformed nuclei using the higher-order shape deformations Y_4 and Y_8 yields much better agreement with measured values than is obtained when only pure quadrupole surfaces are assumed. Use was made of recently measured values of β_4, and β_8. (auth)

12585 USE OF THE (γ,γ) REACTION FOR STUDYING THE ENERGY LEVELS OF ^{139}La. Moreh, R.; Nof, A. (Nuclear Research Centre, Beer Sheva, Israel). Phys. Rev., C; 2: 1938-47(Nov 1970).

Elastic and inelastic scattering of monochromatic photons were used for studying nuclear energy levels in ^{139}La; the photons were produced by thermal-neutron capture in titanium and iron. Two independent resonance lines at 6418 and 6760 keV were excited with the titanium γ source, and three independent resonances at 6018, 7279, and 7632 keV were excited with the iron γ source. Some 18 known low-lying levels were populated by deexcitation of these resonance levels. The angular distribution of some intense elastic and inelastic lines was measured and the following spin and parity determinations (keV, J^π) were made: 166, $\frac{5}{2}$; 1220, $\frac{5}{2}$, ($\frac{3}{2}$); 1384, $\frac{7}{2}$; 1419, $\frac{7}{2}$, ($\frac{11}{2}$); 1536, $\frac{7}{2}$; 1580, $\frac{9}{2}$; 2232, ($\frac{7}{2}$, $\frac{11}{2}$); 6018, $\frac{1}{2}^-$; 6418, $\frac{9}{2}^-$; and 6760, $\frac{7}{2}$, where parentheses denote uncertainties. The parities of the 6018- and 6418-keV levels were directly determined using a Compton polarimeter. The total radiative widths of the 6018- and 6418-keV levels were measured and found to be Γ_γ = 0.051 and 0.081 eV, respectively. The ^{139}La levels are compared with recent theoretical calculations. (auth)

12586 AVERAGE-RESONANCE METHOD OF NEUTRON-CAPTURE γ-RAY SPECTROSCOPY: STATES OF ^{106}Pd, ^{156}Gd, ^{158}Gd, ^{166}Ho, AND ^{168}Er. Bollinger, L. M.; Thomas, G. E. (Argonne National Lab., Ill.). Phys. Rev., C; 2: 1951-2000 (Nov 1970).

The average-resonance method of neutron-capture γ-ray spectroscopy is critically examined by means of measurements on stable isotopes of palladium, gadolinium, holmium, and erbium. A mathematical model of the capture process is developed. This model shows that the intensities of the lines in average-resonance-capture spectra can yield the parities and set narrow limits on the spins of states in almost all nuclides with A > 100 if the γ-ray strength function is a smooth function of γ-ray energy and if the random fluctuations in intensity result only from the Porter-Thomas distribution of partial radiation widths. The measurements give extensive data for ^{106}Pd, ^{156}Gd, ^{158}Gd, ^{166}Ho, and ^{168}Er, and some for ^{103}Pd, ^{105}Pd, ^{155}Gd, ^{157}Gd, ^{165}Er, ^{167}Er, and ^{169}Er. These data are examined for information relating to the mechanisms of radiative capture. All of the data are consistent with the hypothesis that the radiation widths are a smooth function of γ-ray energy and that the random fluctuations in intensity are well described by the Porter-Thomas distribution. The intensities of E1 transitions vary with γ-ray energy more rapidly than E_γ^3, as expected from a giant-resonance description of the radiative process. The intensity of M1 radiation was measured over a 2-MeV range for ^{106}Pd and ^{168}Er, and the reduced M1 widths for ^{106}Pd form a giant-resonance-like curve that peaks at ~7.8 MeV. Ratios of widths for E1 and M1 radiation and for E1 and E2 radiation are obtained for several nuclides. These properties of radiative capture are used to obtain spectroscopic information about final states. The most complete results are for ^{166}Ho, for which 16 rotational bands are identified and interpreted in terms of the collective model. Similar but less extensive data are obtained for ^{156}Gd, ^{158}Gd, and ^{168}Er. The measurements on ^{106}Pd show that the shapes of the observed γ-ray lines may be used to determine the parities of final states. (auth)

12587 STATIC QUADRUPOLE MOMENT OF THE FIRST 2+ STATES OF THE EVEN TIN NUCLEI. Stelson, P. H.; McGowan, F. K.; Robinson, R. L.; Milner, W. T. (Oak Ridge National Lab., Tenn.). Phys. Rev., C; 2: 2015-22(Nov 1970).

Measurements of the relative thick-target yields of γ rays deexciting the 2+ first excited states in ^{112,116,118,120,122,124}Sn, following Coulomb excitation by α particles and ^{16}O ions, were interpreted in terms of the relative static quadrupole moments of these states. The absolute static quadrupole moment of the 2+ state in ^{120}Sn was determined to be +(0.09 ± 0.10) b. With this value it was then possible to obtain the absolute static quadrupole moments for the 2+ state in the other even tin nuclei. The resulting values are closer to the vibrational-model prediction (static quadrupole moment of zero) than to values predicted by the rotational model. A set of absolute B(E2, 0 → 2) values was also obtained with assigned errors between 2 and 3%. (auth)

12588 CHARGE-EXCHANGE THRESHOLD EFFECT IN ^{93}Nb(d,p)^{94}Nb. Coker, W. R.; Kent, J. J. (Univ. of Texas, Austin). Phys. Rev., C; 2: 2023-4(Nov 1970).

A charge-exchange threshold cusp is observed in the summed 160° excitation curve for ^{93}Nb(d,p)^{94}Nb(6^+, g.s. -2^+, 0.31 MeV) at ~7.1 MeV, the threshold of the analogous ^{93}Nb(d,n)^{94}Mo^A(6^+, 13.2 MeV $-$ 2^+, 13.5 MeV) reaction. As predicted by theory, it is essentially identical in shape to the excitation curve previously measured for ^{90}Zr(d,p)^{91}Zr($d_{\frac{5}{2}}$, g.s.) in the same energy region. (auth)

12589 LOW-ENERGY GAMMA RAYS FROM RESONANT NEUTRON CAPTURE IN ^{169}Tm. Bhat, M. R.; Chrien, R. E.; Garber, D. I.; Wasson, O. A. (Brookhaven National Lab., Upton, N. Y.). Phys. Rev., C; 2: 2030-3(Nov 1970).

Low-energy γ rays following slow-neutron capture in thulium were used to check the angular-momentum assignments of the neutron resonances. A previous discrepancy in the spin of the 17.5-eV resonance was resolved. The correlation between reaction widths noted in previous work was recalculated and found to be substantially unchanged. An isomeric state at 183.2 keV was investigated by measuring the delay in the low-energy transitions involving this state, and a half-life of 3.2 ± 0.3 μsec is obtained, in fair agreement with previous work. (auth)

12590 LIFETIMES OF ^{193}Ir LEVELS. Metzger, F. R. (Franklin Inst., Swarthmore, Pa.). Phys. Rev., C; 2: 2024-5 (Nov 1970).

Using new information concerning the decay modes of the 460-, 557-, and 559-keV levels in ^{193}Ir, previous resonance-fluorescence data were reevaluated in terms of the mean lives of these levels. (auth)

12591 UPPER LIMIT FOR A K-ELECTRON-CAPTURE BRANCH IN ^{113m}In. der Mateosian, E.; Goldhaber, M. (Brookhaven National Lab., Upton, N. Y.). Phys. Rev., C; 2: 2026-7(Nov 1970).

An improved search for the K-capture branch in ^{113m}In has established a new upper limit for this decay mode of 0.0036%, from which one may conclude log ft >6.5 for this first-forbidden transition. (auth)

12592 PRODUCTION AND DECAY PROPERTIES OF PROTACTINIUM ISOTOPES OF MASS 222 TO 225 FORMED IN HEAVY-ION REACTIONS. Borggreen, Joern; Valli, Kalevi; Hyde, Earl K. (Univ. of California, Berkeley). Phys. Rev., C: 2: 1841-62(Nov 1970).

Four α-decay chains initiated by ^{225}Pa, ^{224}Pa, ^{223}Pa, and ^{222}Pa were produced by the bombardment of thallium, lead, and bismuth targets with beams of ^{22}Ne, ^{20}Ne, ^{19}F, ^{18}O, ^{16}O, ^{15}N, and ^{14}N at the Berkeley heavy-ion linear accelerator. The reaction products were transported from the reaction cell by the helium-jet technique and their decay was measured with a semiconductor detector. Energy values, excitation functions, half-lives, and genetic relationships of individual peaks were determined. Two new techniques based on the use of a time-to-amplitude converter were developed for the measurement of μsec half-lives of daughter products, and five half-lives in the μsec range were measured. These new α data help to determine the trends in α-decay energies for isotopes of odd-Z elements, particularly in the poorly defined region just

above the 126-neutron shell. This allows more accurate predictions of α-decay properties of many unknown nuclei. Some anomalous behavior of the apparent α-decay energies for nuclei with 133 and 135 neutrons is pointed out. (auth)

12593 NEW ISOTOPES ^{241}Cf AND ^{240}Cf. Silva, R. J.; Hahn, R. L.; Toth, K. S.; (and others) (Oak Ridge National Lab., Tenn.). Phys. Rev., C; 2: 1948-51(Nov 1970).

Two new isotopes of californium were identified through bombardments of ^{235}U, ^{234}U, and ^{233}U with ^{12}C ions from the Oak Ridge isochronous cyclotron. They decay with half-lives of 3.78 ± 0.70 and 1.06 ± 0.15 min and with the emission of α particles of 7.335 ± 0.005 and 7.590 ± 0.010 MeV, respectively. Analysis of the excitation functions for these α emitters favors the assignment of mass 241 to the former and mass 240 to the latter; also, the 7.335-MeV activity was shown to be chemically similar to californium. New values for the α-particle energies of ^{242}Cf were obtained: 7.385 ± 0.004 and 7.351 ± 0.006 MeV, assigned, respectively, to α-decay transitions to the ground and first excited states of ^{238}Cm. (auth)

12594 ODD PARITY STATES IN ^{238}Pu. Bengtson, B.; Jensen, J.; Moszynski, M.; Nielsen, H. L. (Univ. of Aarhus, Denmark). Nucl. Phys.; A159: 249-56(1970).

The decay of 2.1 d ^{238}Np was investigated by means of singles and coincidence spectrometry with Ge(Li) counters and a six-gap orange beta-spectrometer. Fast lifetime techniques with Ge(Li) detectors were used. New ^{238}Pu levels were established at 1082.6 keV (K, I^π = 4, 4$^-$; $t_{\frac{1}{2}}$ = 8.5 ± 0.5 ns) and 1202.4(3, 3$^-$), they are interpreted as the Σ = 0 and Σ = 1 doublet of the $[743]7/2^-$, $[631]1/2^+$ two-neutron configuration. Other odd parity levels were established at 661.4(0, 3$^-$), 962.7(1, 1$^-$), 985.5(1, 2$^-$) and 968(2, 2$^-$). (auth)

12595 EXCITATION FUNCTIONS FOR ^{159}Tb(d,p)^{160}Tb AND ^{159}Tb(d,4n)^{157}Dy REACTIONS. Siri, L. Nicola; Nassiff, S. J. (Comision Nacional de Energia Atomica, Buenos Aires. Univ. Nacional, Buenos Aires). Radiochim. Acta; 14: 159-60(Nov 1970).

The cross sections for the (d,p) and (d,4n) reactions on ^{159}Tb were experimentally determined by activation. The stacked foil technique was used, and the incident energy of deuterons was 27.2 MeV. Experimental excitation functions are reported. (auth)

12596 LEVEL STRUCTURE OF ^{101}Rh FROM THE DECAY OF 8.5 h ^{101}Pd. Phelps, Michael E.; Sarantites, Demetrios G. (Washington Univ., St. Louis). Contracts AT(11-1)-1530; AT(11-1)-1760. Nucl. Phys.; A159: 113-42(1970).

The level structure of ^{101}Rh was investigated from the decay of 8.5 h ^{101}Pd. Singles γ-ray energy and intensity measurements were taken with a 25 cm^3 high-resolution Ge(Li) detector in an anti-Compton arrangement which employed a large NaI(Tl) annular detector. Extensive $\gamma\gamma$ coincidence measurements were made with a Ge(Li)–Ge(Li) and a NaI-Ge(Li) arrangement with the Ge(Li) detector under Compton suppression. Triple $\gamma\gamma\gamma$ coincidence measurements were taken in a NaI-Ge(Li)-NaI arrangement with the Ge(Li) detector under Compton suppression. The low-energy γ-rays and x-rays were studied with a high-resolution Si(Li) x-ray spectrometer. Conversion electron measurements were made with Si(Li) detectors and α_K values were determined for the most intense transitions. From these data it was concluded that levels at 157.32, 181.78, 305.3, 355.14, 478.00, 747.67, 905.61, 974.7, 978.42, 1035.5, 1057.7, 1320.4, 1359.31, 1470.82, 1696.27, 1789.26, 1820.22 and 1911.23 keV are populated in the decay of 8.5 h ^{101}Pd. From log ft and α_K values determined in this work and from γ-ray intensity information definite J^π assignments were made to a number of levels and limits for the J^π values were placed for the rest of the levels in ^{101}Rh. The fraction of decay of the 4.5 d isomeric state by an isomeric transition was measured to be 0.072 ± 0.004. The level structure and the level trends in the ^{99,101,103,105}Rh isotopes are examined and discussed in relation to recently published results on calculated levels in these isotopes on the basis of an extended pairing-plus-quadrupole model for the nucleus. (auth)

12597 NUCLEAR MATRIX ELEMENTS IN THE FIRST FORBIDDEN BETA DECAY OF ^{198}Au. Smith, H. A.; Simms, P. C. (Purdue Univ., Lafayette, Ind.). Contract AT(11-1)-1746. Nucl. Phys.; A159: 143-52(1970).

Nuclear matrix elements for the 2$^-$(0.959 MeV β^-)2$^+$ beta transition in ^{198}Au were extracted and comparison was made with CVC theory predictions for the vector matrix element ratio $\Lambda_{CVC} = \int\alpha/\int ir/\rho$. It was found that the ratio Λ_{CVC} was consistent with the CVC prediction based on the assumption that the Coulomb Hamiltonian is diagonal. However, contributions from off-diagonal matrix elements of the Coulomb Hamiltonian could not be ruled out. Fairly good limits were placed on the nuclear matrix elements in spite of the fact that the Coulomb-enhanced combinations of matrix elements dominate the transition. (auth)

12598 INVESTIGATIONS OF THE EXCITED STATES OF THE ^{96}Mo NUCLEUS FROM THE REACTION ^{95}Mo(n,γ)^{96}Mo. Heck, D.; Ahmed, N.; Fanger, U.; (and others) (Kernforschungszentrum, Karlsruhe, Ger.). Nucl. Phys.; A159: 49-80(1970). (In German).

The gamma radiation following thermal neutron capture in ^{95}Mo was studied using an enriched sample of MoO_3 in external target geometry at the Karlsruhe reactor FR 2. Energies and intensities of the gamma rays in the energy ranges 0.15 to 2.70 MeV and 4.87 to 8.90 MeV were determined with Ge(Li) diodes in Compton-suppression and singles mode. Cascade relationships were studied with a Ge(Li)–Ge(Li) coincidence setup. A level scheme of ^{96}Mo is proposed which includes 37 levels and 138 gamma transitions. Gamma–gamma angular correlation measurements with an apparatus consisting of two NaI(Tl) detectors were used to determine the spin values of 7 levels and the mixing ratios of the involved transitions. The most striking result is the observation of a second 2$^+$ level in the region of the two-phonon states. This level is separated only by 2.3 keV from the well known 4$^+$ state at 1628 keV. A level at 1148 keV appears to have spin and parity 0$^+$. The results are compared with earlier shell-model calculations and are discussed in terms of collective nuclear motions. (auth)

12599 GAMMA-RAY STUDIES OF THE γ-VIBRATIONAL BAND OF ^{166}Er. Reich, C. W.; Cline, J. E. (Idaho Nuclear Corp., Idaho Falls). Nucl. Phys.; A159: 181-201(1970).

Improved energy and intensity values were obtained for the γ-radiation emitted in the decay of 1200 y ^{166}Ho, 27 h ^{166}Ho and 7.7 h ^{166}Tm. These data were used to investigate the mixing between the ground state band and the γ-vibrational band of ^{166}Er. The effect of this mixing on the interband E2 transition probabilities is discussed from the points of view of the conventional $\Delta K = 2$ band-mixing picture and of the generalized approach of Mikhailov. The former picture was extended to treat the situation in which the intrinsic quadrupole moments of the two bands are unequal, and the resultant expressions are presented. The analysis yields a value of 0.041 ± 0.002 for the band-mixing parameter z_γ and indicates that, contrary to the conclusions of some previous analyses, the intrinsic quadrupole moments of these two bands in ^{166}Er are equal. An odd–even shift in the energies of the members of the γ-vibrational band is observed and is found to be well described by a term of the form $(-)^I A_4(I-1)I(I+1)(I+2)$ with A_4 = +(0.079 ± 0.007) eV. This value is roughly an order of magnitude smaller than that expected based on the results of the band-mixing analysis of the interband γ-ray transition probabilities. Evidence for the existence of M1 transitions within the γ-vibrational band of ^{166}Er is presented. These data suggest that $|g_K - g_R|$ is constant within the band and has the value ≈0.11. A hindrance factor of ≈400 with respect to the single-particle estimate is inferred for these M1 transition probabilities. (auth)

12600 EFFECTS OF MAGNETIC DIPOLE CORE POLARIZATION IN ^{206}Pb AND ^{207}Pb. Harada, K.; Pittel, S. (Franklin Inst., Swarthmore, Pa.). Nucl. Phys.; A159: 209-21(1970).

The effects of magnetic dipole core polarization on dipole moments and M1 transition rates in ^{206}Pb and ^{207}Pb are studied in the framework of the weak-coupling model. The coupling potential between a particle and the M1 states of the core nucleus ^{208}Pb is calculated microscopically and used to estimate the admixtures of these magnetic dipole states in the relevant states of ^{206}Pb and ^{207}Pb. The qualitative agreement with experiment is good, except for the $p_{\frac{1}{2}}^{-1} \rightarrow p_{\frac{1}{2}}^{-1}$ transition strength and the $f_{\frac{5}{2}}^{-1}$ dipole moment. The calculations also yield some general features of magnetic moments, M1 decays and their interrelation based on purely geometrical considerations. Finally, exchange effects are studied and found to be rather small. (auth)

12601 MEASUREMENT OF THE AVERAGE CIRCULAR γ-POLARIZATION AND DETERMINATION OF SPINS FOR COMPOUND STATES FORMED IN THERMAL NEUTRON CAPTURE. Eichler, J.; Djadali, F. (Kernforschungszentrum, Karlsruhe, Ger. Univ., Karlsruhe, Ger.). Nucl. Phys.; A147: 150-60(1970).

The circular polarization averaged over the γ-spectrum after capture of polarized thermal neutrons was measured for some nuclei. It is shown that from the experimental results, conclusions about the spin of the compound state can be drawn. The method can be applied to the determination of the spin of neutron resonances. (auth)

12602 STUDY OF ELASTIC AND INELASTIC SCATTERING OF PROTONS FROM ^{128}Te AND ^{130}Te AT ISOBARIC ANALOGUE RESONANCES. Burde, J.; Engler, G.; Ginsburg, A.; Jaffe, A. A.;

XUM

Marinov, A.; Birstein, L. (Hebrew Univ., Jerusalem). Nucl. Phys.; A141: 375-99(1970).

Isobaric analog states in ^{129}I and ^{131}I were studied by (p,p') and (p,p) scattering from ^{128}Te and ^{130}Te in the incident energy ranges 7.66 to 11.87 MeV and 7.48 to 12.65 MeV, respectively. The energy differences between the resonances and the orbital momentum transferred in their formation agree very well with the corresponding analog states which have been previously observed by the (d,p) reaction on the same target nuclei. There is fairly good agreement between the corresponding spectroscopic factors. The Coulomb displacement energies were found to be 13.949 and 13.898 MeV for the pairs of isotopes ^{129}Te–^{129}I and ^{131}Te–^{131}I, respectively. The spins of the resonances at E_p^{cm} = 10.199 and E_p^{cm} = 10.545 MeV in ^{129}I and those at E_p^{cm} = 10.455 and E_p^{cm} = 10.520 MeV in ^{131}I were found to have spin and parity $3/2^-$. The angular distribution of the inelastic protons from the resonances at E_p^{cm} = 9.96 and E_p^{cm} = 10.07 MeV in ^{129}I and at E_p^{cm} = 10.20 MeV in ^{131}Te are consistent with an assignment of $7/2^-$ to these levels and with a $1/2^-$ assignment to the resonance at E_p^{cm} = 10.915 MeV in ^{131}I. The modes of the de-excitation of the two-phonon states and other higher states in ^{128}Te and in ^{130}Te were studied by observing the gamma-ray spectra and by coincidence measurements between the gamma rays and the inelastic protons at the various resonances. The states at 1498 and 1520 keV in ^{128}Te were found to have spins and parities of 4^+ and 2^+, respectively. The 1634 keV level in ^{130}Te was found to have spin and parity 2^+. Upper limits were placed on the ratios of the gamma-ray transitions $I_\gamma(2_2^+ \rightarrow 0^+)/I_\gamma(2_2^+ \rightarrow 2_1^+)$ in ^{128}Te and ^{130}Te of 3%. Seven odd-parity resonances in ^{129}I and ^{131}I are discussed in terms of the core excitation model. (auth)

12603 COULOMB EXCITATION OF ^{123}Te AND ^{125}Te. Sergolle, H.; Albouy, G.; Lagrange, J. M.; Pautrat, M.; Poffe, N.; Vanhorenbeeck, J. (Institut de Physique Nucleaire, Orsay, France). Nucl. Phys.; A145: 351-61(1970). (In French).

Coulomb excitation experiments have been performed on the two stable odd-mass tellurium isotopes using a N^{3+} beam from the Orsay cyclotron. The reduced excitation probabilities of the following levels: 439.2 keV ($3/2^+$) and 505.2 keV ($5/2$ or $3/2^+$) in ^{123}Te, 443.5 keV ($3/2^+$), 463.4 keV ($5/2^+$) and 671.3 keV ($5/2^+$) in ^{125}Te were measured by this method. Some B(E2) and B(M1) transition probabilities are deduced from experiments. The results are discussed in terms of de Shalit's model and Kisslinger and Sorensen's calculations. (auth)

12604 HIGHLY INELASTIC SCATTERING OF MEDIUM-ENERGY ^{3}He AND ^{4}He PARTICLES BY HEAVY NUCLEI. Chenevert, Gary Milo. Seattle; Univ. of Washington (1969). 221p. University Microfilms Order No. 70-14,742.

Thesis.

The energy spectra of ^{3}He and ^{4}He particles emitted by heavy nuclei (Sn, Ta, Pt, Au, and Pb) when bombarded by 50- and 75-MeV ^{3}He particles and 42-, 50-, 65-, and 90-MeV ^{4}He particles were measured. Emphasized in the experiment were the inelastic scattering reactions (^{3}He,^{3}He') and (α,α'); however, data were also obtained for the transfers (^{3}He,α) and (α,^{3}He). By means of a (dE/dX)–E semi-conductor detector telescope in conjunction with a Goulding particle identifier, the helium ions were detected and identified in the energy range from the energy of the Coulomb barrier for the emitted particles to that of the ground state. Study of the angular distributions, spectrum shapes, and absolute cross sections indicated that the spectra could be clearly separated into direct and evaporation components. Comparison of the features of the evaporation component with statistical theory predictions confirms that the statistical model is an accurate description of the evaporation process. At forward angles the direct component is dominant, and it displays several features that have not been observed previously. In the energy spectrum (at angles less than 50°) a broad prominent structure between 9 and 32 MeV excitation is seen, and the ^{4}He spectra have a greater proportion of low-energy particles than do the ^{3}He spectra. Attempts to attribute the direct component to specific processes are not definitive. (auth) (Diss. Abstr. Int., B)

12605 QUADRUPOLE AND HEXADECAPOLE DEFORMATIONS IN RARE EARTH NUCLEI. Aponick, A. A. Jr. (Yale Univ., New Haven); Chesterfield, C. M.; Bromley, D. A.; Glendenning, N. K. Contract AT(30-1)-3223. Nucl. Phys.; A159: 367-84(1970).

Precision studies of the inelastic scattering of alpha particles from selected rare earth nuclei were interpreted to yield quantitative determinations of the hexadecapole term in the mass distributions of these nuclei in addition to the now familiar, and dominant, quadrupole term. Cross sections for scattering to the 0^+, 2^+ and 4^+ states of the ground state rotational bands of ^{154}Sm, ^{166}Er and ^{176}Yb were measured at 27.5, 30.0 and 32.5 MeV incident α-particle energy, and over the angular range from 20 to 140°. These data were analyzed with a theory which models the nucleus as a rigid rotor, and the interaction as a deformed, complex optical potential. The parameters of the undeformed potential were determined from an optical-model analysis of elastic scattering from the essentially spherical ^{148}Sm, measured over the same α-particle angle and energy ranges. The analysis of the data has as its foundation the utilization of the interferences among Coulomb excitation, nuclear quadrupole and nuclear hexadecapole inelastic scattering amplitudes leading to the lower members of the ground state band. The characteristically different energy dependence of the interfering amplitudes has led to a determination of deformation parameters of these nuclei. The parameters so determined simultaneously fit the data obtained at all three incident energies. They are, moreover, in complete accord with parameters previously extracted from 50 MeV inelastic α-particle scattering data. Additional credence is therefore given to the interpretation of the parametrization as a physical representation of the nuclear shape. (auth)

12606 MECHANISM OF SINGLE-NUCLEON AND MULTI-NUCLEON TRANSFER REACTIONS IN GRAZING COLLISIONS OF HEAVY IONS ON SILVER. Galin, J. (Institut Physique Nucleaire, Orsay, France); Guerreau, D.; Lefort, M.; (and others). Nucl. Phys.; A159: 461-80(1970).

A large number of products of transfer reactions was identified when bombarding natural Ag and ^{109}Ag by 86 MeV ^{12}C and by 78 and 113 MeV ^{14}N ions. From the analysis of angular and energy distributions, it was shown that both multi-nucleon and single-nucleon transfer processes are ruled by two different mechanisms. When the products are formed at the ground state or at relatively low excited states, the angular distribution can be interpreted in terms of a DWBA analysis of a quasi-elastic scattering. This first mechanism is responsible for the preferential emission at a particular angle which depends on the bombarding energy. When the products are formed with a very large defect of kinetic energy (more than 10 MeV) they are observed at very small angles. A qualitative explanation of this "grazing" process is tentatively given. The relative importance of the second mechanism is higher for a large number of transferred nucleons than for single-nucleon transfers and increases with the bombarding energy. (auth)

12607 MASS DETERMINATIONS OF THE NEUTRON-DEFICIENT NUCLIDES ^{88}Zr AND ^{140}Nd BY (p,2n) THRESHOLD MEASUREMENTS. Russo, P. A.; Vandenbosch, R. (Univ. of Washington, Seattle). Nucl. Phys.; A159: 153-60(1970).

Masses of ^{140}Nd and ^{88}Zr were determined from measured thresholds of ^{141}Pr(p,2n) and ^{89}Y(p,2n) reactions. Thresholds extracted from fits of the data with the Jackson neutron evaporation model produce mass excess values of -83.57 ± 0.04 MeV for ^{88}Zr and -84.26 ± 0.06 MeV for ^{140}Nd. Measured masses are compared to existing data and to calculations based upon several semi-empirical mass formulas. (auth)

12608 EFFECT OF INTERFERENCE ON THE AVERAGE NEUTRON CROSS SECTIONS OF FISSILE NUCLEI. Garrison, John D. (Gulf General Atomic Inc., San Diego, Calif. San Diego State Coll., Calif.). Nucl. Phys.; A159: 305-23(1970).

The ratio of the average fission, capture and resonance scattering cross sections to the corresponding average cross sections obtained neglecting resonance–resonance interference were calculated by a Monte Carlo method for a variety of interference conditions typical of fissile nuclei. It is shown in general that the average total cross section is unaffected by interference. The importance of interference increases with the number of open fission channels. The effective number of resonances with which a given resonance interferes is obtained for different numbers of open channels. Results for the cross-section ratios for both S- and P-wave neutrons were obtained for the common fissile nuclei by fitting calculated cross sections to the average capture and fission cross sections over the neutron energy range from 0.3–100 keV. The ratios for S-wave neutrons at low energy (≈500 eV) are: $^{233}_{92}$U: $R_{fiss} = 0.95 \pm 0.01$, $R_{capt} = 1.23 \pm 0.03$, $R_{scatt} = 1.45 \pm 0.10$; $^{235}_{92}$U: $R_{fiss} = 0.94 \pm 0.01$, $R_{capt} = 1.11 \pm 0.01$, $R_{scatt} = 1.10 \pm 0.01$; $^{239}_{94}$Pu: $R_{fiss} = 0.99 \pm 0.005$, $R_{capt} = 1.00 \pm 0.002$, and $R_{scatt} = 1.02 \pm 0.005$. The process of cross-section fitting also yields values for the average resonance parameters for these nuclei. The effect of the (n,γf) process is presented. (auth)

12609 MAGNETIC MOMENTS OF THREE EXCITED STATES IN ^{149}Pm. Seo, T. (Kyoto Univ., Osaka); Hayashi, T.; Aoki, A. Nucl. Phys.; A159: 494-512(1970).

The magnetic moments of three excited states in ^{149}Pm were determined through the measurements of g-factors of the corresponding states by the perturbed $\gamma\gamma$ angular correlation method

using a Ge(Li) detector and an NaI(Tl) scintillation counter. The results obtained are μ = 2.0 ± 0.2, 2.2 ± 0.6 and 3.6 ± 0.2 nm for the 114, 189 and 270 keV states, respectively. The experimental values are discussed in comparison with contemporary models of the nucleus. (auth)

12610 PHOTONEUTRON CROSS SECTIONS OF ^{208}Pb AND ^{197}Au. Veyssiere, A.; Beil, H.; Bergere, R.; Carlos, P.; Lepretre, A. (CEN, Saclay, France). Nucl. Phys.; A159: 561-76(1970).

Partial photoneutron cross sections $\sigma_{\gamma,n}$, $\sigma_{\gamma,2n}$, $\sigma_{\gamma,3n}$ and $\sigma_{\gamma,4n}$ of ^{208}Pb and ^{197}Au were measured using a monochromatic photon beam and a neutron detecting system capable of analyzing directly and simultaneously interactions of the type (γ,xn) in the photon energy range 6 MeV ≤ E ≤ 35 MeV. Nuclear information extracted from these data includes threshold values, integrated cross sections and giant dipole resonance parameters obtained by means of Lorentz line fitting. A tentative analysis of the structure observed on the rising shoulder of the giant resonance of ^{208}Pb is presented. The level density parameters a as well as the non-statistical neutron contributions obtained from a study of the competition between the (γ,n) and (γ,2n) decay modes, are also given. (auth)

12611 ^{182}W(t,d)^{183}W REACTION AT 20 MeV TRITON ENERGY. Flynn, E. R. (Los Alamos Scientific Lab., N. Mex.); Igo, G.; Barnes, P. D.; Casten, R. F.; Erskine, J. R. Nucl. Phys.; A159: 598-608(1970).

Spectroscopic factors for the lowest six excited states of ^{183}W were obtained by means of the ^{182}W(t,d)^{183}W reaction. Elastic scattering measurements also were carried out and optical-model parameters thus obtained are used in the DW analysis. The results agree with previous (d,p) experiments and maintain the discrepancy which exists between the usual distorted-wave calculations on deformed nuclei and the expected spectroscopic values. When average value triton and deuteron optical-model parameters are used, this discrepancy becomes smaller. (auth)

12612 REACTIONS ^{152}Sm(p,t)^{150}Sm AND ^{154}Sm(p,t)^{152}Sm. McLatchie, William (Queen's Univ., Kingston, Ont. Oxford Univ.); Darcey, W.; Kitching, J. E. Nucl. Phys.; A159: 615-24 (1970).

The reactions ^{152,154}Sm(p,t) were carried out at a bombarding energy of 20.6 MeV. The angular distributions of the outgoing tritons appear characteristic of the angular momentum transfer but for L = 2 exhibit some variety. The L = 0 cross sections from the present work are compared with existing (t,p) cross sections and support the suggestion of shape coexistence in the transitional nuclei ^{150}Sm and ^{152}Sm. (auth)

12613 REACTION ^{90}Zr(^{3}He,d)^{91}Nb AT 18 MeV. Knoepfle, K. T. (Max-Planck-Inst. for Nuclear Physics, Heidelberg); Rogge, M.; Mayer-Boericke, C.; Pedersen, J.; Burch, D. Nucl. Phys.; A159: 642-52(1970).

The ^{90}Zr(^{3}He,d)^{91}Nb reaction was investigated using incident ^{3}He ions of 18 MeV. The ground-state Q-value was measured to be −0.227 ± 0.020 MeV. Deuteron spectra were obtained at 16 scattering angles between 5 and 80°. A distorted-wave analysis of the data was carried out to obtain l_p values and spectroscopic factors; j values were deduced. A comparison of these results with shell-model calculations of the low-lying states in ^{91}Nb gave additional information about the ground-state wave function of ^{90}Zr. The higher excited l_p = 0, 2, 4 transitions were found to be the T < components of the single-particle states of the next major shell ($2d_{5/2}$, $2d_{3/2}$, $1g_{9/2}$, $3s_{1/2}$). (auth)

12614 STROBOSCOPIC DETERMINATION OF THE MAGNETIC MOMENT OF THE 8$^+$ ISOMERIC STATE OF ^{208}Po. Nagamiya, S. (Inst. of Physical and Chemical Research, Saitama, Japan); Nomura, T.; Yamazaki, T. Nucl. Phys.; A159: 653-60(1970).

The g-factor of the $[h_{9/2}(p)^2\ p_{1/2}(n)^{-2}]8^+$ isomeric state of ^{208}Po was determined to be 0.902 ± 0.006 by the stroboscopic resonance method, in which the aligned isomeric state of 380 ns half-life was generated by the reaction ^{206}Pb(α,2n)^{208}Po in microscopic beam bursts of a cyclotron. The observed g-factor agrees with that of the $[h_{9/2}(p)^2]8^+$ state of ^{210}Po within an accuracy of 1%, indicating that the effect of the $[p_{1/2}(n)^{-1}\ p_{1/2}(n)]1^+$ type spin polarization on the magnetic moment is negligibly small, as expected from the theoretical predictions. (auth)

12615 BETA SPECTRUM OF ^{206}Tl. Flothmann, D. (Univ., Heidelberg); Loehken, R.; Wiesner, W.; Rebel, H. Phys. Rev. Lett.; 25: 1719-20(21 Dec 1970).

The spectrum shape of the β particles emitted in the 0$^-$ → 0$^+$ decay of ^{206}Tl was determined using a 4π solid-state β spectrometer. The sources used were isotopically separated and extremely thin. The shape factor shows only small deviations from a statistical form. The half-life was determined as $\tau_{1/2}$ = 4.27 ± 0.05 min. (auth)

12616 REALISTIC QTDA CALCULATIONS IN THE ODD-MASS N = 82 ISOTONES. Freed, N.; Miles, W. (Pennsylvania State Univ., University Park). Nucl. Phys.; A158: 230-50(1970).

The quasi-particle Tamm−Dancoff approximation (QTDA) is applied to a calculation of the low-lying states of the odd-mass N = 82 isotones ^{137}Cs, ^{139}La, ^{141}Pr, ^{143}Pm, and ^{145}Eu. The realistic Elliott interaction is diagonalized exactly in a space of one and three quasi-particles from which spurious components have been removed. Single-particle energies are determined through the use of Gambhir's modification of the inverse-gap-equation method. Results are presented for level schemes, selected eigenvectors, electromagnetic moments and transition rates, and spectroscopic factors for (^{3}He,d) stripping reactions. (auth)

12617 PROPERTIES OF ^{96,98}Rh FROM THE ^{96,98}Ru(p,n) REACTION. Ashkenazi, J.; Friedman, E.; Nir, D.; Zioni, J. (Hebrew Univ., Jerusalem). Nucl. Phys.; A158: 146-54(1970).

The threshold energies for the ^{96}Ru(p,n)^{96}Rh and ^{98}Ru(p,n)^{98}Rh reactions were measured as 7.30 ± 0.01 and 5.90 ± 0.01 MeV, respectively; the values for the mass excess of the Rh isotopes are thus −79.622 ± 0.011 MeV (^{96}Rh) and −83.16 ± 0.011 MeV (^{98}Rh). By observation of delayed γ rays following the β^+ decay of the produced Rh isotopes, two half-lives of 1.55 ± 0.15 min and 9.25 ± 0.10 min were found in the activity of ^{96}Rh and a half-life of 9.05 ± 0.30 min was found for the ^{98}Rh. The above results, together with Hauser−Feshbach analyses of the (p,n) excitation functions, suggest the value 3$^+$ for the spins and parities of ^{96,98}Rh. (auth)

12618 ISOMERIC CROSS-SECTION RATIOS FOR THE REACTIONS ^{192}Os(n,2n)^{191}Os AND ^{198}Pt(n,2n)^{197}Pt AT 14 MeV. Winiwarter, P. (Institut fuer Radiumforschung und Kernphysik, Vienna). Nucl. Phys.; A158: 77-80(1970).

The activation cross sections for (n,2n) reactions induced by 14.7-MeV neutrons were measured in ^{192}Os and ^{198}Pt. The isomeric cross-section ratios for both reactions were determined. (auth)

12619 REORIENTATION EFFECT MEASUREMENTS IN ^{106,114}Cd. Kleinfeld, A. M.; Rogers, J. D.; Gastebois, J.; Steadman, S. G.; de Boer, J. (Rutgers−The State Univ., New Brunswick, N. J.). Nucl. Phys.; A158: 81-7(1970).

The static electric quadrupole moments Q_{2^+} of the first 2$^+$ states of ^{106}Cd and ^{114}Cd were measured by the reorientation effect, using a particle−γ coincidence technique. The attenuation of the γ-ray angular distribution due to the hyperfine interaction was measured; and its effect, found to be important for the determination of the quadrupole moments. The values of Q_{2^+} obtained range from −0.69 b to −0.99 b for ^{106}Cd and from −0.21 b to −0.52 b for ^{114}Cd. The measured value for ^{114}Cd is 46% of the value obtained without accounting for the hyperfine attenuation. (auth)

12620 SYNTHESIS OF ELEMENT 105. Flerov, G. N.; Oganesian, Yu. Ts.; Lobanov, Yu. V.; (and others) (Joint Inst. for Nuclear Research, Dubna, USSR). Nucl. Phys.; A160: 181-92(1971).

In bombardments of a ^{243}Am target with ^{22}Ne ions a spontaneous fission activity with a half-life of 1.8 ± 0.6 s was observed. The yield corresponds to a formation cross section of (5.0 ± 1.5) × 10^{-34} cm^2, for the spontaneous fission decay. Integral angular distributions of products from the reaction ^{243}Am + ^{22}Ne and the formation cross section for the new isotope as a function of the bombarding ion energy were measured. From these data and the results of test experiments it is concluded that the atomic number of the new spontaneous fission activity with $T_{1/2} \approx 2$ s, is 105. The spontaneous fission decay of the isotopes ^{256,257}103 was also investigated. The spontaneous fission half-lives of these nuclei are shown to be larger than 10^5 s. (auth)

12621 PARITY VIOLATION IN THE TRANSITION OF ^{181}Ta AT 482 keV. de Saintignon, P.; Lucas, J. J.; Viano, J. B.; Chabre, M.; DePommier, P. (Institut des Sciences Nucleaires, Grenoble, France). Nucl. Phys.; A160: 53-64(1971). (In French).

The parity-violating component of the 482-keV gamma transition of ^{181}Ta was investigated by measuring its degree of circular polarization. Two Compton forward scattering analyzers were used and the scattered gamma rays were detected by eight lead-loaded plastic scintillators, each one connected to an independent energy selection and counting system. Because of the small asymmetry expected a careful investigation of the various sources of systematic errors were minimized or eliminated. False asymmetries of the polarimeters and detectors were measured using the 498-keV gamma transition from a ^{103}Ru source. A calculation of the asymmetry due to bremsstrahlung shows that it is negligible, due to the

XUM

energy selection. The efficiency of the polarization analyzers was calculated and experimentally measured by beta–gamma circular polarization correlation on ^{198}Au. The result for the polarization of the 482-keV transition of ^{181}Ta is: $P = -(0.21 \pm 0.11) \cdot 10^{-4}$. Comparisons with theoretical estimates and previous experiments are made. (auth)

12622 STUDY OF SOME EVEN ISOTOPES OF NEODYMIUM BY ELECTRON SCATTERING. Madsen, David William. New Haven; Yale Univ. (1969). 140p. University Microfilms Order No. 70-16,306.

Thesis.

The Yale University Electron Accelerator was used to study the ground-state charge distributions and properties of some low-lying states in ^{142,146,150}Nd. The incident electron energy was varied between 15 and 60 MeV and angular distribution measurements were made at angles between 70 and 150°. If the charge distribution is described in terms of a half-density radius c and a skin thickness t, the present results indicate anomalously small values of t in all three neodymium isotopes. A comparison with the effect of dispersion corrections on the interpretation of muonic x-ray results suggests that similar corrections are needed in the present case. Reduced gamma transition probabilities, B(EL ↑), and transition radii, R_{tr}^2, are presented for the following low-lying levels: ^{142}Nd, 1.57 MeV (2^+), 2.09 MeV [3^-, (2^+?)]; ^{146}Nd, 0.45 MeV (2^+); ^{150}Nd, 0.13 MeV (2^+). (Diss. Abstr. Int., B)

Nuclear Theory

Refer also to abstracts 12007, 12158, 12235, 12363, 12371, 12384, 12386, 12409–12411, 12423, 12432, 12434, 12439, 12520, 12532, 12543, 12549, 12552, 12555, and 12556.

12623 (AECL-3730) ELMOS: A CDC-6600 FORTRAN-IV CODE TO MANIPULATE SINGLE PARTICLE WAVEFUNCTIONS AND SOLVE THE ELLIPSOIDAL MODIFIED OSCILLATOR PROBLEM. Cusson, R. Y. (Atomic Energy of Canada Ltd., Chalk River (Ontario). Chalk River Nuclear Labs.). Oct 1970. 44p. Dep. NTIS (U. S. Sales Only). AECL $1.50.

A general set of subroutines was constructed to handle operations on a state vector which is stored as a set of quantum numbers characterising the basis states and the corresponding real amplitudes. A novel basis, called the spin-cartesian basis, is defined and used to deal with fermions in a 3-dimensional non-isotropic harmonic oscillator basis. This new basis has the desirable feature that the unitary transformation which connects it to the usual spherical basis is a real orthogonal transformation. These subroutines are used to solve the problem of the motion of a single spin-½ nucleon in an ellipsoidal harmonic oscillator potential with spin-orbit and $|\mathbf{l}|^2$ interaction terms, namely Nilsson's modified oscillator potential. The expansion coefficients of these eigenstates on the spherical oscillator basis with major shell q.n. ≤ 6 are computed. The total energy sums are performed so that the energy surfaces in the β-γ plane can be obtained readily. The routines necessary to compute all the multipole moments up to L = 6 are also described. An appendix to this report is a 2400 foot reel of ½, 7 track, BCD magnetic tape containing most of the results needed to deal with the nuclei with A ≤ 70, and a set of card images for the code. The structure of the tape is described. (auth)

12624 (ANU-P-497) SCATTERING AND POLARIZATION OF NUCLEONS AND DEUTERONS. A Series of Lectures. Robson, B. A. (Australian National Univ., Canberra. Research School of Physical Sciences). Oct 1970. 122p. Dep. NTIS (U. S. Sales Only).

A section on polarized light, including Stokes parameters and Jones and Mueller calculi, precedes sections on the quantum theory of light, elastic scattering of spin-½ particles by complex nuclei, elastic scattering of deuterons, targets with spin, and polarization phenomena in (d,p) and (p,d) reactions with particular reference to the DWBA description. (Australia)

12625 (COO-1764-85) TREATMENT OF TWO-PARTICLE CONTINUUM STATES IN THE SHELL MODEL APPROACH TO NUCLEAR REACTIONS. Fuller, R. C. (Minnesota Univ., Minneapolis. School of Physics). [1969]. Contract AT(1-11)-1764. 60p. Dep. NTIS.

To consider deuteron-induced reactions within the shell model it is necessary to include single-particle states with two particles in continuum single-particle states. Expressions are derived for operators whose matrix elements give the transition amplitudes for the processes encountered in deuteron-induced reactions. Each of these operators can be written in terms of a single operator which satisfies an integral equation whose kernel involves the Green's function for two non-interacting particles in the presence of a common potential. This operator is discussed at length. A method using single-particle Gamow states is formulated to approximate the connected part of this operator by an operator of finite rank. This approximation is then tested numerically and is found to be effective. Finally, there is a discussion of the implications of the approximation in the scattering amplitudes of interest. (auth)

12626 (FMRB-33/70) GAMMA RADIATION FOLLOWING THE CAPTURE OF NEUTRONS, ESPECIALLY OF POLARIZED REACTOR NEUTRONS BY ORIENTED NUCLEI. Weise, Klaus (Physikalisch-Technische Bundesanstalt, Brunswick (West Germany)). Jun 1970. 120p. (In German). Dep. NTIS (U. S. Sales Only).

Thesis. Submitted to Technische Universitaet, Hanover, Ger.

The ratio $\sigma_{\alpha,I+½}/\sigma_{\alpha,I-½}$ of the cross sections of the (n,γ) process at low neutron energies outside the resonances, and for the different total angular momenta $J = I \pm ½$ of the neutron–target-nucleus system for nuclei with ground state spin I > 0, can be simply derived from the integral $v = \int F(U)Z(U)dU$, which has to be determined by means of polarized neutrons and oriented nuclei in a thin target for two different degrees of neutron polarization. Z(U) is a linear combination of the gamma radiation pulse-height spectra measured at two definite angles to the direction of the nuclear orientation. F(U) is arbitrary if the function Z(U) varies only slightly (except for normalization) when neutron polarization is altered. That this can be expected follows from the cascade theory of neutron-capture gamma radiation, which can be deduced from the theory of stochastic processes. With several neutron-capture mechanisms (direct, compound, valence-nucleon, and doorway capture, and one- and more-particle deexcitation processes) included, the gamma spectrum is calculated from the solution of a system of integral equations given by the cascade theory. The characteristic properties of the spectrum and its dependence on the various parameters are discussed. The 5-MeV anomaly seems to arise from the valence-nucleon capture mechanism. (auth)

12627 (INP-720) REAL PART OF THE ALPHA-NUCLEUS POTENTIAL OBTAINED BY DOUBLE FOLDING PROCEDURE. Budzanowski, A.; Dudek, A.; Grotowski, K.; Strzalowski, A. (Institute of Nuclear Physics, Krakow (Poland)). 1970. 10p. Dep. NTIS (U. S. Sales Only).

A microscopic analysis of the elastic scattering of 27.5-MeV alpha particles by ^{59}Co nuclei is presented. The real part of the α-nucleus optical-model potential was obtained from the elementary nucleon–nucleon interaction using the so-called double-folding procedure. The matter-density distributions for the target nucleus and alpha particles were taken from recent experimental data. Calculations were made for several simple forms of the effective nucleon–nucleon interaction. The best agreement with the experimental angular distributions was obtained using the effective two-nucleon potential of Slanina and McManus. (auth)

12628 (INR-P-1201) GAMMA VIBRATION OF NUCLEI AT EQUILIBRIUM AND SADDLE POINT. Zielinska-Pfabe, M. (Institute of Nuclear Research, Warsaw (Poland)). 1970. 25p. Dep. NTIS (U. S. Sales Only).

The γ-vibrational parameters B_γ, C_γ and the energy E_γ of the γ-vibrational state of deformed nuclei have been calculated as functions of the β deformation in the whole region between equilibrium and the saddle point. Both the microscopic and macroscopic descriptions have been used. The following result is obtained: when β increases from its equilibrium value to the saddle point, the nucleus begins to be more stiff with respect to the gamma vibration. The quadrupole coupling constant should increase with the deformation of the nucleus. (auth)

12629 (JINR-E4-5135) ALPHA AND GAMMA DECAYS OF THE HIGH EXCITED STATES OF COMPLEX NUCLEI. Soloviev, V. G. (Joint Inst. for Nuclear Research, Dubna (USSR)). 1970. 28p. Dep. NTIS (U. S. Sales Only).

A possibility of obtaining information on the structure of the states of complex nuclei with excitation energies close to or higher than the nucleon binding energy from the experimental data on (n,α) and (n,γ) reactions on resonances is studied. The wave function of the high excited state is constructed, and the matrix elements for the alpha and gamma transitions from the high excited states to the ground one-phonon and two-quasiparticle ones are given. It is shown that the alpha and gamma transitions involve a small number of the components of the wave function of the high excited state. Therefore, the reduced probabilities data on alpha and gamma transitions may give information on the magnitude of definite type components of the wave functions of high excited states. (auth)

12630 (JINR–E4-5469) COMPLICATION OF THE NUCLEAR STATE STRUCTURE WITH INCREASING EXCITATION ENERGY. Soloviev, V. G. (Joint Inst. for Nuclear Research, Dubna (USSR). Lab. of Theoretical Physics). 1970. 30p. Dep. NTIS (U. S. Sales Only).

The tendency towards the complication of the structure of nuclear states and the growth of their density with increasing excitation energy is demonstrated by a simple model. It is shown that the description of the excited states by means of the wave functions containing few- and many-quasi-particle components is efficient for the study of their structure. The behavior of the s-neutron strength function depending upon the mass number A is explained without recourse to the optical model. It is shown that the experimental data on the reduced alpha widths give evidence on the structure of highly excited states. The correlations between various processes proceeding through the same state are studied. Some cases are indicated in which there must be correlations between the reduced neutron, alpha, and gamma widths. (auth)

12631 (JINR–P4-5008) CLASSIFICATION OF STATES AND INTERACTIONS IN THE NUCLEAR COLLECTIVE MODEL. Afanasjev, G. N. (Joint Inst. for Nuclear Research, Dubna (USSR)). 1970. 20p. (In Russian). Dep. NTIS (U. S. Sales Only).

The symmetry properties of the nuclear collective model are studied. It is assumed that the dynamics of this model is correctly described by means of the noncompact group Sp (5,5). The energy spectrum is vibrational or rotational depending on whether the invariance group is isomorphic to SU_5 or to $SO(2.1) \times R_5$. (auth)

12632 (JINR–P4-5084) AVERAGE FIELD OF THE EXCITED NUCLEI. Vagradov, G. M.; Kalinkin, B. N. (Joint Inst. for Nuclear Research, Dubna (USSR)). 1970. 30p. (In Russian). Dep. NTIS (U. S. Sales Only).

The dependence of the potential describing the average nuclear field on the excitation energy is discussed. It is shown that this dependence can be explained by the presence of "polarization" of the nucleus interacting with a particle or a "hole." One can thus connect the results of recent experiments on elastic nucleon scattering with the results on quasi-elastic knocking out of protons in (e,e'p) and (p, 2p) processes. Possible examples of this effect in nuclear properties at small energies and large deformations are also discussed. (auth)

12633 (JINR–P4-5346) MASS COEFFICIENT IN THE NUCLEUS COLLECTIVE HAMILTONIAN AND SUM RULES FOR THE PROBABILITIES OF E2-TRANSITIONS AND OF QUADRUPOLE MOMENTS. Dzholos, R. V. (Joint Inst. for Nuclear Research, Dubna (USSR). Lab. of Theoretical Physics). 1970. 18p. (In Russian). Dep. NTIS (U. S. Sales Only).

In the framework of the collective model for certain assumptions on the kinetic energy structure, different relations were obtained for the matrix elements of the quadrupole moment operator and the collective state energies. The dependence of the mass coefficient in the collective Hamiltonian on the deformation parameters is investigated. (auth)

12634 (LYCEN–7034, pp 147-72) THEORETICAL DEVELOPMENTS IN SPECTROSCOPY OF SPHERICAL NUCLEI. Arvieu, R. (Paris Univ., Orsay (France). Institut de Physique Nucleaire). (In French).

From Conference on low-energy spectrometry and nuclear spectrometry, Lyon, 18–20 February 1970.

A rapid survey was made of the calculations involved in shell models: exact calculations and approximate calculations bringing in the method of quasi-particle interaction or the calculation of the excited states in a deformed field model. The quantity and the quality of the experimental results made it necessary to use very precise theoretical calculations. (France)

12635 (NP–18545) ENERGIES OF NUCLEI WITH DIFFERENT NEUTRON AND PROTON NUMBER IN THOMAS FERMI APPROXIMATION. Nemeth, J.; Erba, E. Gadioli (Roland Eotvos Univ., Budapest (Hungary). Inst. for Theoretical Physics). Mar 1970. 10p. (ITP–274). Dep. NTIS (U. S. Sales Only).

The Thomas–Fermi method is applied to calculate the energies of nuclei with density-dependent effective forces. The terms of the semiempirical mass formula are determined. They are in good agreement with experiment. The neutron–proton density distributions are given for the mass range A = 50 to 240. In the same mass-number domain, nuclei far off the β-stability line are examined. (auth)

12636 (NP–18580) NUCLEAR FORCES AND SATURATION. Note No. 274. Calogero, F. (Rome Univ. (Italy). Istituto di Fisica. Istituto Nazionale di Fisica Nucleare, Rome (Italy)). 6 Jul 1970. 27p. Dep. NTIS (U. S. Sales Only).

Rigorous conditions that the nuclear interaction must satisfy to be consistent with saturation are reported. The implications of these results for current models of the nuclear force are assessed. (auth)

12637 (NYO–2171-328) PROGENITOR SUM-RULES IN NUCLEAR PHYSICS. Noble, J. V. (Pennsylvania Univ., Philadelphia. Dept. of Physics). [1970]. 28p. Dep. NTIS.

The classic method for generating relations like the Thomas–Reiche–Kuhn dipole sum rule or the f sum rule used in many-body theory is generalized. By considering the double commutators of various current-density operators $J_a(q)$ with the nuclear Hamiltonian $\{J_a(-q'), [H, J_b(q)]\}$ and concentrating on those which have simple forms, a more general class of sum-rules than any previously applied to nuclear physics is established. These so-called "progenitor" sum rules act as generating functions for all the previously known sum rules. With the hypothesis that certain "giant" states saturate the sum rules, approximate dynamical relations between various form factors are derived. Several examples are given by way of illustration, and some further applications are suggested. (auth)

12638 (NYO–2171-334) THEORETICAL FOUNDATION OF VARIABLE MOMENT OF INERTIA MODELS. Das, T. K.; Dreizler, R. M.; Klein, A. (Pennsylvania Univ., Philadelphia. Dept. of Physics). 18 Dec 1970. 10p. Dep. NTIS.

A derivation of the VMI model is presented which is general enough to account for its successful application to both deformed and spherical nuclei. A derivation of multiband generalizations is also outlined. (auth)

12639 (ORO–3765-28) PROGRESS REPORT FOR THEORETICAL STUDIES IN NUCLEAR REACTIONS AND STRUCTURE. (Maryland Univ., College Park. Dept. of Physics and Astronomy). Sep 1970. Contract AT(40-1)-3765. 35p. Dep. NTIS.

Studies on the Bethe–Goldstone equation in finite nuclei, major shell mixing with a density dependent effective G-matrix, the generator coordinate method for light nuclei, relativistic formulation of the many-body problem using excitation as variational parameters, relativistic Green's function approach to nuclear matter, three-body forces in nuclear matter, spin-orbit splitting in nuclei, reactions involving elementary particles and nuclei, extraction of the two-nucleon T-matrix from reaction data, shell model reaction theory, three-body effect, model three-body problem with break-up, reactions induced by multi-nucleon projectiles, and nuclear fission and statistical nuclear reactions are briefly described. (J.W.R.)

12640 (OU-LNS-70-2) SYSTEMATIC PROPERTIES OF NUCLEI. II. GROUND STATE BANDS IN EVEN–EVEN NUCLEI. Yoshizawa, Y. (Osaka Univ. (Japan). Lab. of Nuclear Studies). [1969]. 82p. Dep. NTIS (U. S. Sales Only).

Ground state bands of 0^+, 2^+, 4^+, ... in even-even nuclei are analyzed by the power series of spin I, $E = aI + bI^2 - cI^3 + dI^4$. Four-parameter and three-parameter analyses (d = 0) give very good fits for all even-even nuclei except magic number nuclei. In the deformed region, this result shows $a \simeq b$, and also three-parameter analysis ($a \equiv b$) gives a good fit. It is concluded that $a \gg b \gg c$ for the non-deformed nuclei and $a \simeq b \gg c$ for the deformed nuclei. The I term is essential for the difference between the deformed and the non-deformed nucleus, and the I^3 term (not $I^2 (I+1)^2$ term) gives the deviation from $aI + bI^2$ at higher energy levels. From these results the following expression is proposed for the ground state bands of even-even nuclei in all regions except magic number nuclei: $E = AI + BI(I+1) - CI^2(I+1)$. (auth)

12641 (RLO–1388–595) VALIDITY OF THE SOPKOVICH APPROXIMATION. Blair, J. S. (Washington Univ., Seattle. Dept. of Physics). Sep 1970. 30p. Dep. NTIS.

Distorted-wave Born-approximation calculations for high-energy peripheral collisions are frequently circumvented by a simple prescription, emerging from the high-energy WKB approximation, in which the plane-wave Born-approximation amplitudes are multiplied by the factor $\exp(i[\delta_l + \delta_{l'}])$, where δ_l and $\delta_{l'}$ are phase shifts characteristic of elastic scattering in the incident and final channels, respectively. The validity of this recipe for medium-energy nuclear reactions is tested through numerical calculations with a simple non-relativistic potential model. For sufficiently weak potentials, the recipe appears quantitatively reliable; but in realistic situations of moderate or strong absorption, although it frequently approximates the exact angular distribution well, this prescription can give quan-

XUM

titatively unreliable values for the important partial-wave amplitudes as well as miss important features of the cross section. The implications of the numerical results for several related approximations are also discussed. (auth)

12642 MODEL DEPENDENCE OF THE BINDING ENERGY OF NUCLEAR MATTER. Miller, Michael David. East Lansing, Mich.; Michigan State Univ. (1969). 84p. University Microfilms Order No. 70-15,086.

Thesis.

It is possible to produce hard-core, soft-core, finite-core, and momentum-dependent potentials which fit the two-nucleon elastic scattering data equally well and which are, therefore, indistinguishable from that standpoint. This thesis examines the feasibility of using nuclear matter calculations to distinguish between potentials which cannot be distinguished through two-nucleon elastic scattering experiments. Using the method described by Brueckner and Masterson for the static potentials and, with modifications, for the momentum-dependent potentials, the mean binding energy per nucleon in nuclear matter is calculated for each of the S, P, and D states using several phenomenological two-nucleon potentials which have identical on-energy-shell matrix elements. The binding energy is found to be very sensitive to the form of the short range repulsion in the potential. Replacing a hard core potential by a short range momentum-dependent one having identical on-energy-shell matrix elements is found to increase the contribution of the S and P states to the binding energy of nuclear matter. There was little change in the contribution of the D states. With the proper form for the momentum dependence, increases in the binding energy of over 12 MeV per particle were obtainable. The hard core Hamada–Johnston potential predicts a binding energy of 8.5 MeV per particle for a Fermi momentum of 1.4 F^{-1}. This is fairly typical of hard core potentials which fit the two-nucleon elastic scattering data fairly well, but is in poor agreement with the empirical value of 16 MeV per nucleon. Replacing the S state potential alone by an equivalent momentum-dependent one results in a calculated value for the binding energy which is in excellent agreement with the empirical value. (auth)

12643 UNITARITY CONSTRAINTS FOR MULTIPLE RESONANCES. Rosdolsky, Hans (Univ., Bern). Helv. Phys. Acta; 43: 631-51(1 Oct 1970).

The unitarity constraints for any number of overlapping resonances are derived. These are the necessary and sufficient conditions on the resonance masses, widths, and couplings for the S-matrix to satisfy unitarity. The unitarity constraints for an isolated resonance, two overlapping resonances, and the dipole are studied in greater detail. The eigenphase behavior for an isolated resonance and a degenerate dipole is also discussed. (auth)

12644 ANGULAR-MOMENTUM DECOMPOSITION OF THE THREE-BODY PROBLEM. Depp, Joseph George. Pittsburgh; Carnegie-Mellon Univ. (1970). 96p. University Microfilms Order No. 70-17,139.

Thesis.

A formalism is developed which enables the use of an antisymmetrized potential in the calculation of the three-body contribution to the binding energy per particle of nuclear matter. An angular momentum decomposition is done in the center of mass of the three particle system. And a three-body angle-averaged Pauli operator is also developed and utilized. Appropriate numerical approximations are introduced and the numerical methods used are discussed. The calculation has been performed using the Reid soft-core potential. At normal density a repulsive contribution of 2.913 MeV is obtained for the binding energy per particle. (Diss. Abstr. Int., B)

12645 ADIABATIC THEORY OF FISSION. Ohta, Kohichi (Tokyo Univ.). Progr. Theor. Phys. (Kyoto); 44: 389-412(Aug 1970).

The time-dependent Hartree–Fock–Bogolyubov theory is developed by assuming that the fission process from the saddle point to the scission point is adiabatic with respect to the degrees of freedom of elongation and rotation of the nucleus as a whole, and that the state wave function remains a quasi-particle vacuum throughout the process. A representation of the nucleon destruction operator in terms of the fragment single-particle wave functions is introduced; this representation is suitable for the description of the density localization of the nucleus. Furthermore, it is assumed that the nascent fragments interact through the exchange of the valence nucleons near the Fermi energy and that the remaining nucleons form inert closed cores of the fragments. A simple model of the equations of motion for the density matrices is solved, and it is shown that the valence nucleon system has an asymmetric oscillation mode that leads to asymmetric mass divisions of the nucleus. (auth)

12646 UNIFIED DERIVATION OF THE CRANKING MODEL AND THE PEIERLS–YOCCOZ METHOD. II. ENERGIES. Shono, Yoshiyuki (Hiroshima Univ.). Progr. Theor. Phys. (Kyoto); 44: 413-18(Aug 1970).

Expressions for the energy obtained by the cranking-model method and the Peierls–Yoccoz method are derived in a unified way, and at the same time a relation between them is established. (auth)

12647 LIPKIN'S CONDITION AND A MICROSCOPIC THEORY OF THE NUCLEAR ROTATIONAL MOTION. Shono, Yoshiyuki (Hiroshima Univ.). Progr. Theor. Phys. (Kyoto); 44: 553-5(Aug 1970).

A microscopic theory of nuclear rotational motion is described in which the emphasis is on the structure of the elementary excitations responsible for the rotational motion. A creation operator of the rotational motion is introduced which consists of operators for particle excitations within a degenerate single-particle level. As an example, the method is applied to the single j-shell pairing-plus-quadrupole-force model. (R.W.R.)

12648 SHAPES OF ANGULAR DISTRIBUTIONS OF (^{3}He,t) AND (p,n) TRANSITIONS TO 0^+ ANTIANALOG STATES. Noble, J. V. (Univ. of Pennsylvania, Philadelphia). Phys. Rev. Lett.; 25: 1458-9(16 Nov 1970).

The anomalous shapes of the angular distributions of tritons from the $0^+ \rightarrow 0^+$ ^{3}He-induced charge-exchange transitions to antianalog states of ^{64,66}Ga and ^{40}K can be understood on the basis of the structural relation between analog and antianalog states, together with the assumption of a pure charge-exchange (i.e., no knockout) mechanism. (auth)

12649 LIMITS OF VALIDITY OF SIEGERT'S THEOREM IN THE NUCLEAR PHOTOABSORPTION. Haemaelaeinen, R. M. K.; Lilja, I. A. (Univ. of Jyvaeskylae, Finland). Lett. Nuovo Cim.; 4: 947-9(21 Nov 1970).

The standard derivation of Siegert's theorem is discussed, and the erroneous neglect of a term is pointed out. It is concluded that calculations of absorption cross sections according to Siegert's theorem can contain errors which vary from the order of 10% at 50 MeV to about 60% at 200 MeV. (R.W.R.)

12650 NEW DERIVATION OF AN APPROXIMATE EXPRESSION IN CLOSED FORM FOR THE BINDING ENERGY OF AN IMPURITY PARTICLE IN NUCLEAR MATTER. Grypeos, M. E. (Democritus Nuclear Research Center, Athens. International Centre for Theoretical Physics, Trieste, Italy). Lett. Nuovo Cim.; 4: 973-6(21 Nov 1970).

The calculation of the binding energy B = –E of an impurity particle (for example, a Λ hyperon) in its ground state in an infinitely extended uniform host medium of identical particles (usually taken to be nuclear matter) is considered. A new, simpler derivation is given for the trial expression for the energy of the Λ particle in the form of a power series of the density of nuclear matter. The first two terms of the original expression for the energy are included exactly; other terms are included only approximately, but the result has the desired asymptotic behavior. (R.W.R.)

12651 MICROSCOPIC DESCRIPTION OF THE CHARGE FORM FACTOR OF ^{4}He. Boffi, S. (Univ., Pavia, Italy. Istituto Nazionale di Fisica Nucleare, Pavia, Italy); Rimini, A.; Weber, T. Lett. Nuovo Cim.; 4: 988-90(21 Nov 1970).

A microscopic description of the charge form factor of ^{4}He is possible if one takes into account 2p–2h configurations in the nuclear ground-state wave function. The calculation is done with the Tabakin interaction in a suitably large Hartree–Fock (H.F.) basis. No attempt is made to take c.m. corrections into account. No significant difference is seen between the zeroth-order and first-order calculations. It is impossible to determine the energy of the nucleus, its radius, and all the single-particle energies, together with its charge form factor, not only in zeroth-order H.F. approximation, but also up to first order. (R.W.R.)

12652 NUCLEAR REACTIONS WITH POLARIZED PARTICLES OF ARBITRARY SPIN. Lindner, Albrecht (Univ., Hamburg). Nucl. Phys.; A155: 145-60(1970).

Cross sections and polarization of reaction products are given for two-particle reactions in terms of S-matrix elements. The beam and target may be polarized. (auth)

12653 APPLICATION OF THE HARTREE–FOCK VARIATIONAL METHOD TO CENTER-OF-MASS MOTION. Dreizler, R. M. (Univ. of Pennsylvania, Philadelphia); Krejs, F. R.; Klein, A. Contract AF48(638)-1545. Nucl. Phys.; A155: 33-9(1970).

A one-particle wave equation for c.m.s. motion is derived from the Hartree–Fock variational principle by assuming that the Hartree–Fock solution defines an exact intrinsic state for c.m.s. motion. The result is applied to a calculation of the c.m.s. correction to the mean square charge radius predicted by the shell model. (auth)

12654 EXTENDED CRANKING MODEL AND THE MOMENT OF INERTIA OF THE HIGH SPIN ROTATIONAL STATES OF DEFORMED NUCLEI. Ma, Chin-wah. Berkeley, Calif.; Univ. of California (1969). 137p. University Microfilms Order No. 70-13,105.

Thesis.

A matrix diagonalization method based on the cranking model is used to calculate theoretically the effective moment of inertia up to high-spin rotational states for rare earth nuclei. Any use of expansion in the rotational velocity ω is avoided, since the usual perturbation methods become questionable for high spin. On the other hand some approximations are introduced including the truncation of the number of quasiparticles and the use of a simplified Nilsson scheme in which the single particle angular momentum is kept as a good quantum number in the basis. The results indicate the following: (1) The large high-order admixtures in cranking solutions make the usual lowest order cranking formula unreliable for spin $I \gtrsim 6$-8. (2) The Coriolis-Anti-Pairing effect makes the major contribution to the increase of moment of inertia with spin. However, the C-A-P effect is generally overestimated by the BCS method, and the fixed-particle-number correction considerably reduces the C-A-P effect. The collective gyromagnetic ratio g_r and the rotational-vibrational coefficient B associated with the $I^2(I+1)^2$ term were also calculated. (Diss. Abstr. Int., B)

12655 MACROSCOPIC SELF-CONSISTENCY OF THE COLLECTIVE MODEL OF DEFORMED NUCLEI. Bow, Y. F. (Univ. of Western Ontario, London). Phys. Rev., C; 2: 1600-8(Nov 1970).

It has been suggested, in effect, that in a deformed nucleus the number of protons (or the amount of charge) which are carried along by the rotational motion may, on the average, be approximated as the product of the atomic number Z and the deformation parameter δ. The theoretical justification of this suggestion is discussed, and a more accurate expression is obtained. Assuming that the interaction of the rotational motion with an external magnetic field is entirely due to the current associated with the amount of charge following the rotational motion, on the average, and also in accordance with the cranking approximation, a macroscopic expression for the rotational gyromagnetic ratio g_R is derived. This expression, supplemented by the usual macroscopic formula for the intrinsic quadrupole moment Q_0, may constitute a macroscopic self-consistency relation among the collective parameters in a rotational band, namely, Q_0, g_R, and the moment of inertia J. The values of g_R calculated from the experimental values of J and Q_0 are tabulated for the ground-state rotational bands of both even–even and odd-mass nuclei. The aforementioned macroscopic self-consistency is then tested by comparing these calculated values of g_R with both empirical values and previous microscopic calculations. According to the present approach, the well-known lowering of g_R from the usual fluid-model value is mainly due to the limitation on the number of protons which can follow the rotational motion, on the average. It is not clear, however, whether there is any direct connection between this limitation and the pairing interaction which seems to play a rather essential role in the current microscopic calculations. This puzzling situation is further illustrated by considering the moments of inertia of even–even nuclei. (auth)

12656 MAGNETIC DIPOLE TRANSITION PROBABILITIES OF DEFORMED ODD-MASS NUCLEI. Bow, Y. F. (Univ. of Western Ontario, London). Phys. Rev., C; 2: 1608-11(Nov 1970).

Based on the ground-state magnetic moments, the magnetic dipole transition probabilities in the ground-state rotational bands of deformed odd-mass nuclei are analyzed assuming that the rotational gyromagnetic ratios are given by a theoretical expression derived previously. (auth)

12657 COULOMB-DISTORTION EFFECTS IN MAGNETIC MULTIPOLE ELECTROEXCITATION. Chertok, B. T.; Johnson, W. T. K.; Sarkar, D. (American Univ., Washington, D. C.). Phys. Rev., C; 2: 2028-30(Nov 1970).

Computer calculations of Coulomb-distortion effects are presented for inelastic electron scattering inducing M2 transitions in light nuclei. The distortion effect is presented over $1 < Z < 20$, $40\ \text{MeV} < E_0 < 140\ \text{MeV}$, $10 < k < 19\ \text{MeV}$, and for two large angles of scatter. The dependence of the calculation on the assumed nuclear transition current is displayed. (auth)

12658 EQUIVALENT LOCAL POTENTIALS FROM NONLOCAL SEPARABLE ONES. Husain, D. (Univ. of Dacca, Pakistan); Ali, S. Phys. Rev., C; 2: 1587-90(Nov 1970).

Explicit expressions for the calculation of equivalent local potentials corresponding to given nonlocal separable potentials were derived. Using these expressions, equivalent local potentials were calculated for a test case and a self-consistency check of the formulation was made. An effective-range formalism for nonlocal separable potentials was also presented following the coordinate representation. (auth)

12659 HARD-CORE POTENTIAL REPRESENTATION BY δ' IN VARIATION AND HARTREE CALCULATIONS. Schenter, R. E. (Battelle-Northwest, Richland, Wash.); Ford, W. F. Phys. Rev., C; 2: 1590-3(Nov 1970).

The δ' interaction was used to represent the hard-core potential in variation and Hartree calculations. These calculations were compared with exact calculations for a two-body boundstate problem and a soluble three-body problem. The trial wave function in the variational problem with the δ' interaction is shown to approach rapidly its hard-core limit with increasing number of trial parameters. The δ' interaction is superior to current soft-core representations of the nucleon–nucleon potential in the Hartree calculations. (auth)

12660 FOUR-BODY CORRELATIONS IN LIGHT NUCLEI. THE GROUND-STATE CORRELATIONS AND THE EXCITED LEVEL STRUCTURE. Fukushima, Yoshihiro; Kamimura, Masayasu; Takada, Kenjiro (Kyushu Univ., Fukuoka). Mem. Fac. Sci., Kyushu Univ., Ser. B; 4: No. 2, 39-45(Dec 1969).

Using the theory of the four-body correlations in light nuclei proposed by Marumori and Suzuki, the effect of the ground-state correlations on the level structure in the nucleus of the closed core plus four particles is investigated. A very simplified two-level model is used for this aim. It is clarified that the ground-state correlations have little influence on the relative level structure. A brief discussion on the relation between the model and the surface-delta-interaction model is also presented. (auth) (Japan)

12661 MACROSCOPIC MODEL FOR THE ANELASTIC SCATTERING OF HEAVY IONS. Gadioli-Erba, E.; Sona, P. G. (CISE, Milan. Univ., Milan). Energ. Nucl. (Milan); 17: 601-5 (Oct 1970).

The anelastic scattering and transfer reactions between two nuclei are treated in a macroscopic model. The model assumes maximum anelasticity compatible with conservation of orbital angular momentum. Related possible experiments are discussed. (auth)

12662 PHYSICS OF NUCLEI AND PARTICLES. VOLUME II. Marmier, Pierre; Sheldon, Eric. New York; Academic Press Inc. (1970). 681p. $19.50.

Chapters are included in Volume II on nuclear particles and their interactions, nuclear forces and potentials as deduced from nuclear dynamics, scattering and reaction models in nuclear physics, and nuclear models. (J.W.R.)

12663 NOTE ON THE ALPHA-PARTICLE MODEL OF ^{12}C. Lim, T. K. (Florida State Univ., Tallahassee). Nucl. Phys.: A158: 385-8(1970).

The binding energy with respect to alpha-particle breakup of ^{12}C, calculated from a three-alpha model with the alpha particles interacting via pairwise soft-core potentials, does not agree with experiment. This tri-particle representation of the ground state of the A = 12 nuclear system also fails to give the elastic form factor and the experimental rms radius. Although the model is attractive in its conception, it is apparently too simple to have much physical validity. (auth)

12664 NUCLEAR SIZE EFFECTS IN THE POLARIZATION OF ELASTICALLY SCATTERED ELECTRONS. Ugincius, P. (Naval Weapons Lab., Dahlgren, Va); Ueberall, H.; Rawitscher, G. H. Nucl. Phys.; A158: 418-32(1970).

Exact numerical values of the polarization functions S (θ) and R (θ) for electron scattering from ^{208}Pb and ^{51}V are calculated with a computer phase-shift program for elastic scattering, with the extension of the nuclear charge taken into account. Considerable deviations from point-nuclear values appear above 10 MeV for ^{208}Pb and above 40 MeV for ^{51}V. These deviations, however, are important only for scattering angles close to 180° where the polarization functions are large. The results are compared with previous calculations which used the second Born approximation. In the case of ^{51}V, the influence of magnetic-moment scattering on the polarization effects is also considered. (auth)

XUM

12665 SOME COMMENTS ON THE SIGNS OF MIXING RATIOS AND ON PAIRING FACTORS FOR ELECTROMAGNETIC TRANSITIONS AND MOMENTS. Brussaard, P. J. (State Univ., Utrecht). Nucl. Phys.; A158: 440-8(1970).

A survey is given of various phase conventions that are in use for mixing ratios of electromagnetic radiation. The mixing ratios that are defined as parameters in the most common formulas for the analysis of angular correlations are compared to the expressions in terms of reduced matrix elements of customary transition operators. Explicit formulas for the multipole operators in quasiparticle representation are given. It is pointed out that the pairing factors for electric multipole moments are different from those for electric multipole transitions; the latter are the same as for magnetic multipole operators. (auth)

12666 NEW QUASIPARTICLE FACTORIZATION OF THE j-SHELL. Hecht, K. T.; Szpikowski, S. (Univ. of Michigan, Ann Arbor). Nucl. Phys.; A158: 449-75(1970).

The new Elliott–Evans classification scheme by means of a quasi-particle factorization of the j shell of both protons and neutrons is developed further. The needed reduced matrix elements follow from the equivalence between quasi-particle isospins and quasi-particle quasi-spins. The transformation to states of good particle number n is simplified by imbedding the quasi-particle quasispins in the five-dimensional quasi-spin group R(5). This leads to a factoring of the transformation coefficients. One factor is independent of J and other subgroup labels of Sp(2j + 1) and carries the dependence on the subgroup labels of R(5). Simple recursion formulas are derived from which this factor can be calculated in complete generality. The second factor carries the dependence on the subgroup labels of Sp(2j + 1) and must be calculated for each j. Since it is independent of n and T, it is sufficient to calculate this factor for particular (most convenient) values of n and T. A calculation of the coefficients is illustrated with $j = 5/2$, for which complete tables are given. An extension of the quasi-particle factorization technique to the nuclear LST scheme is discussed. (auth)

12667 EVALUATION OF FINITE NUCLEAR SIZE EFFECTS IN ALLOWED β-DECAY. Wilkinson, D. H. (Nuclear Physics Lab., Oxford). Nucl. Phys.; A158: 476-86(1970).

Analytical parameterizations are given that reproduce with good accuracy the exact value of $[f_1^2 + g_{-1}^2]_{r=R}$ for electron and positron wave functions generated in the field of a uniform spherical nuclear charge distribution. Formulas are presented for the corrections to the conventional f function for allowed β decay due to the finite extension of the nuclear charge distribution, to the finite de Broglie wave length, and to the variation of the β-particle and neutrino wave functions inside the nucleus. (auth)

12668 AN TENSOR FORCES FOR SCATTERING AND THE Λ-PARTICLE BINDING IN NUCLEAR MATTER. Bodmer, A. R. (Univ. of Illinois, Chicago. Argonne National Lab., Ill.); Rote, D. M.; Mazza, A. L. Phys. Rev., C; 2: 1623-48(Nov 1970).

The effect of ΛN tensor forces on the Λ-particle binding in nuclear matter is studied with the use of second-order perturbation theory and the Brueckner–Bethe reaction-matrix approach in the g-matrix approximation. The g matrix is calculated self-consistently by use of the Kallio-Day version of the reference-spectrum method. The free kinetic energies are assumed for the unoccupied states. One-boson-exchange (OBE) models indicate that the ΛN tensor force is expected to be of short range and moderate strength. For short-range tensor forces the dominant momentum components are very large, and the effects of such forces are only slightly modified by the nuclear medium. On the other hand, if the ΛN tensor forces were of rather long range, they would be quite strongly suppressed in nuclear matter. These features are very clearly exhibited by consideration of the effective nonlocal central potentials that represent the (s-state) effect of tensor forces for nuclear matter and for scattering. The ratio of the (nuclear-matter) expectation values of these two effective potentials is a good measure of the suppression. The expectation value of the effective potential for nuclear matter is just the second-order perturbation-theory energy. Reaction-matrix calculations show that higher-order effects may become quite important for shorter ranges. Such calculations have, in particular, been made for various mixtures of central and tensor forces chosen to give a constant s-wave scattering length. Yukawa shapes corresponding to the kaon and one- and two-pion masses were used, as well as "realistic" OBE potentials with a hard core and a tensor component due to kaon exchange (and also approximately due to η exchange). For a particular mixture, the suppression is measured by the reduction in the well depth relative to the depth for a purely central potential which has the same hard core and the same scattering length and effective range as the mixture. For the short-range tensor forces there is rather little suppression even for very strong tensor forces which account for all the triplet scattering. Different assumptions about the d-state interaction have an almost negligible effect on the s-state well depth if the same assumption is made for both scattering and nuclear matter. Similar considerations are made for the effect of tensor forces in the p wave, for which very little suppression ($\lesssim$1 MeV) is found. It is concluded that if central and short-range tensor forces are chosen to compensate each other for low-energy scattering, they will also compensate each other quite closely for nuclear matter. In particular, for the OBE potentials with strengths consistent with the phenomenological values of the $\Lambda N\overline{K}$ coupling constants, the reduction in the well depth is at most about 4 MeV. The conclusions about the ΛN interaction obtained from a comparison of the calculated and phenomenological well depths are, therefore, effectively unchanged by the presence of a ΛN tensor force. Consequently, in order to bring the two numbers into agreement, it is necessary to invoke a substantial short-range repulsion, a rather weak p-state interaction, and suppression of the $\Lambda N - \Sigma N$ coupling and/or repulsive ΛNN three-body forces. (auth)

12669 PROPERTIES OF THE K MATRIX IN NUCLEAR-REACTION THEORY. Payne, G. L.; Schlessinger, L. (Univ. of Iowa, Iowa City). Phys. Rev., C; 2: 1648-53(Nov 1970).

Expressions are derived for the K matrix for the general case where the Hamiltonian is separated as $H = H_0 + V$, and H_0 can have discrete as well as continuum states. It is shown that the correct handling of the bound states in the continuum eliminates one of the correction terms proposed by Tobocman and Nagarajan. In addition, some of the properties of the K matrix evaluated at complex energies are discussed. (auth)

12670 OFF-SHELL EFFECTS IN KNOCKOUT REACTIONS. Redish, Edward F.; Stephenson, G. J. Jr.; Lerner, Gerald M. (Univ. of Maryland, College Park). Phys. Rev., C; 2: 1665-77(Nov 1970).

The amplitude for a knockout reaction in the plane-wave impulse approximation is derived from the Faddeev equations. It factorizes into the product of an off-shell two-body t matrix times the bound-state wave function in momentum space. Results are derived for the (p, 2p) experiment from a realistic potential and compared with those arising from some current approximations. Distortion effects are ignored in order to isolate the off-shell effects. It is found that for incident protons with lab energy below 200 MeV using an off-shell amplitude can change the cross section significantly as compared with the on-shell approximations in current use. The effect increases with the binding energy of the struck proton and with the recoil momentum. This indicates that (p,2p) reactions below 200 MeV are sensitive to the off-shell behavior of the two-body amplitude and that they should not be used to obtain nuclear information using on-shell approximations. (auth)

12671 NUCLEAR ROTATION AND BOSON EXPANSIONS. I. Marshalek, Eugene R. (Univ. of Notre Dame, Ind.); Weneser, Joseph. Phys. Rev., C; 2: 1682-1714(Nov 1970).

The Beliaev–Zelevinsky method, which represents fermion-pair operators by infinite expansions in exact bosons, is applied to the problem of nuclear rotation. In the harmonic order, which is essentially the random-phase approximation (RPA), the rotation, viewed as infinitesimal, is decoupled from the collective vibrations. The higher orders, however, give rise to various band-mixing terms, which may be interpreted as rotation-vibration and higher-order Coriolis interactions, as well as to vibrational anharmonicities and renormalization of the moment of inertia. A systematic approach is given for extracting these higher-order corrections for the idealized case of a two-dimensional system of interacting particles. Both the Hamiltonian and transition operators are treated. The self-consistent-field approximation is then formulated in the boson picture and applied to the cranking model. The advantage of this formulation is that it allows one to establish the correctness of the higher-order cranking model, which is shown to provide the ground-state-band rotational energies with an error of the order of the small boson-expansion parameter (or the square of this paremeter, depending on its definition). The usefulness of the cranking model for obtaining the angular momentum dependence of transition operators is also demonstrated. The Appendix illustrates some of the ideas by way of application to a system of particles interacting through a two-dimensional analog of the quadrupole-quadrupole force. (auth)

12672 SELF-CONSISTENT CALCULATIONS OF SHELL EFFECTS INCLUDING THE PROPOSED ISLAND OF STABILITY. Bassichis, W. H. (Massachusetts Inst. of Tech., Cambridge.

Univ. of California, Livermore); Kerman, A. K. Phys. Rev., C; 2: 1768-76(Nov 1970).

A study is made of the characteristics of magic nuclei displayed in a Hartree–Fock calculation. It is seen that the known doubly-closed-shell nuclei are clearly distinguished by the behavior of the energy as a function of neutron and proton number. The existence of these characteristics for the superheavy nucleus with Z = 120 and N = 178 indicates that this may also be a magic nucleus. Single-particle-model calculations have indicated Z = 114 as the magic nucleus. Possible reasons for this difference are discussed. (auth)

12673 CONSTRUCTION OF THE T-MATRIX FROM ITS SYMMETRIC PART. Van Dijk, W.; Razavy, M. (Oxford Univ.). Nucl. Phys.; A159: 161-80(1970).

The symmetric and the anti-symmetric parts of the transition matrix, for an uncoupled state, can be related to each other by certain singular integral equations. Thus the scattering matrix can be described and parametrized in terms of the symmetric part of the T-matrix, instead of a potential function. The off-diagonal elements of the symmetric part are arbitrary except for a weak condition imposed on them by the range of the force, while the diagonal elements are directly related to the experimental phase shifts. These phase shifts also determine the bound state energy, but not its form factor. From a given set of phase shifts for the lth partial wave, one can construct a class of T-matrices having the same diagonal elements, but differing in the off-diagonal elements. The difference between any two T-matrices belonging to the same class is a transparent T-matrix, which has no observable effect in two-body scattering. Methods of constructing transparent interactions are discussed, and their effect in the nuclear many-body problem is briefly mentioned. (auth)

12674 HEXADECAPOLE DEFORMATION AND ROTATION-PARTICLE COUPLING IN THE RARE EARTH NUCLEI. Davis, A. D. (Univ. of California, Los Angeles). Nucl. Phys.; A159: 257-64(1970).

Calculations of the energy spectra for odd-A nuclei in the rare earth region were made using a rotational model for deformed nuclei. Both pairing and band mixing were included in detail. A hexadecapole (P_4) deformation was considered in addition to the usual quadrupole (P_2) deformation. In most cases, this additional hexadecapole deformation proved to be quite necessary to achieve a good fit to the experimental spectra. Thirty nuclei in this region were investigated. Good results were obtained for twenty-seven. With the parameters found in achieving a fit to the energy spectra, reduced transitions rates and spectroscopic factors were calculated. Band mixing made it possible to investigate K-forbidden transitions. In most cases there was good agreement with experimental values. (auth)

12675 TWO-BODY SPIN–ORBIT POTENTIALS AND SEMI-INFINITE NUCLEAR MATTER. Stocker, W. (Univ., Munich). Nucl. Phys.; A159: 222-34(1970).

The single-particle potential in semi-infinite nuclear matter resulting from realistic two-body spin-orbit potentials in first order perturbation theory is shown to be of the form $(\sigma \times k) \cdot e_z W(z)$ if only the contribution of the direct part is included. The strength of the single-particle potential is comparable to that of shell model and optical potentials. The development of W(z) into a series of derivatives of the nuclear density is given. A variational procedure to obtain the Weizsäcker surface energy coefficient is carried through starting with two-body potentials containing spin-orbit parts. The spin-orbit potential brings about a lowering of several MeV of the surface energy coefficient. The density is changed in such a way that it falls off more steeply at first than the density obtained without spin-orbit part; the tail of the density distribution, however, extends further. (auth)

12676 EXCHANGE EFFECTS WITH A REALISTIC INTERACTION FOR INELASTIC SCATTERING. Love, W. G.; Satchler, G. R. (Oak Ridge National Lab., Tenn.). Nucl. Phys.; A159: 1-44(1970).

The long-range part of the Hamada–Johnston potential was used as an effective interaction in a microscopic description of the inelastic and charge exchange scattering of protons. The present paper investigates the knock-on exchange amplitudes due to this force and compares the results with those for Gauss and Yukawa interactions. Exchange is very important. A Gaussian which fits low-energy nucleon–nucleon scattering gives results close to the HJ interaction provided its strength is renormalized. A Yukawa interaction is less satisfactory. The formalism for including exchange in the distorted-wave approximation is outlined. (auth)

12677 NOTE ON THE CALCULATION OF THE EFFECTIVE MASS IN NUCLEAR MATTER. Baeckman, S.-O.; Sjoeberg, O. (Aabo Akademi, Turku, Finland). Acta Acad. Abo., Ser. B; 30: No. 2, 1-5(1970).

A simplified model for the calculation of the effective mass of a nucleon in infinite nuclear matter is given. Brueckner's theory is used as a starting point, but a continuous quasi-particle spectrum at the Fermi surface is demanded. In a preliminary calculation an effective mass close to the free nucleon mass was found. (auth) (Finland)

12678 MICROSCOPIC FIRST-ORDER CORE POLARIZATION CORRECTIONS TO DWBA FOR (p,p') SCATTERING. Agassi, D.; Schaeffer, R. (Centre d'Etudes Nucleaires de Saclay, Gif-sur-Yvette, France). Nucl. Phys.; A145: 401-22 (1970).

The importance of full antisymmetrization (taking also into account the exchange nature of the nuclear forces), and first-order corrections to the DWBA matrix element are examined in the case of (p,p') and nuclei with two identical particles outside closed shells. These corrections correspond to core polarization and clustering of the projectile with the valence particles. ^{18}O, ^{54}Fe, ^{90}Zr, and ^{206}Pb are considered as examples. The results indicate an increase by a factor 2–10 in the cross-section normalization if all contributions are added, whereas, the angular distribution is practically insensitive to the various corrections. The agreement with experiment is fair for the angular distributions, but off about a factor 4 or more in the cross-section normalization. (auth)

12679 SPECTRAL THEORY FOR THE KLEIN–GORDON EQUATION WITH AN EXTERNAL ELECTROSTATIC POTENTIAL. Veselic, K. (Ruder Boskovic Inst., Zagreb. Univ., Zagreb). Nucl. Phys.; A147: 215-24(1970).

It has been shown that the energy operator for the Klein–Gordon particle in the presence of an external electrostatic potential satisfying some suitable conditions possesses a spectral decomposition. The spectrum is shown to cover $(-\infty, -mc^2] \cup [mc^2, \infty)$, whereas the gap $(-mc^2, mc^2)$ possibly contains isolated eigenvalues, each of them having a finite multiplicity. It has also been proved that in the non-relativistic limit the spectral projections of the Klein–Gordon Hamiltonian tend in a sense to those of the Schrödinger operator with the same potential. (auth)

12680 COULOMB EFFECT ON THE PROTON–PROTON LOW-ENERGY SCATTERING PARAMETERS. Vo-Dai, Thien; Nogami, Y. (McMaster Univ., Hamilton, Ont.). Nucl. Phys.; A141: 369-74(1970).

The effect of the Coulomb force on the proton–proton low-energy scattering parameters is examined when the nuclear interaction is represented by a separable potential. Naqvi's two-term potential as well as Yamaguchi's one-term potential are considered, following Harrington's method. After removing the Coulomb effect, the "nuclear" scattering length and effective range are both found to be somewhat larger (in absolute values) than those previously obtained by using hard-core local nuclear potentials. (auth)

12681 POTENTIAL LANDSCAPE FOR FISSIONING NUCLEI. I. GENERAL METHOD, SYMMETRIC SHAPES. Andersen, B. L. (Niels Bohr Inst., Copenhagen); Dickmann, Friedrich; Dietrich, Klaus. Nucl. Phys.; A159: 337-66(1970).

The potential energy of a nucleus is calculated as a function of its shape using the method of Strutinski. The nuclear shapes are composed of two spheroids (centres $z = \pm z_1$; z-axis = symmetry axis) smoothly joined by a central hyperboloid (neck) or a central spheroid (belly). The corresponding shell-model potential is constructed from two harmonic oscillators centered around $z = \pm z_1$ and smoothly joined by a third oscillator centered around z = 0. A generalized form of Nilsson's spin-orbit and l^2 term is used. (auth)

12682 PARTICLE-HOLE ADMIXTURES TO HARTREE–FOCK IN THE 2s-1d SHELL. Friedman, Marvin I. (Yale Univ., New Haven). Contract AT(30-1)-3223. Nucl. Phys.; A159: 422-48 (1970).

One- and two-particle/hole excitations are considered as a mechanism for scattering nucleons across the finite energy gap appearing between Hartree–Fock deformed orbitals of doubly even, N = Z nuclei in the 2s-1d shell. Admixtures of these configurations to the Hartree–Fock state are found to be minimal and inadequate to account for the discrepancies between theoretically predicted and experimentally observed states of the nucleus. They do, however, give qualitative explanation to the low-energy excited nuclear configurations found to lie within or above the quasi-rotational Hartree–Fock spectrum. (auth)

XUM

12683 TEST OF A DWBA-TYPE MODEL FOR ANALYSIS OF HEAVY-ION TRANSFER REACTIONS. Da Silveira, R. (Institut de Physique Nucleaire, Orsay, France); Galin, J.; Ngo, C. Nucl. Phys.; A159: 481-93(1970).

A DWBA-type model with distorted waves given in the Glauber approximation is tested. This has been proposed for analysis of heavy-ion transfer reactions well above the Coulomb barrier, in order to avoid the laborious conventional calculations. Consideration is given to the comparison of the Glauber result for elastic scattering with essentially exact calculations. Good agreement with experiment is obtained both in elastic scattering and transfer reactions. (auth)

12684 STRENGTH OF THE TENSOR INTERACTION IN THE DEUTERON OPTICAL POTENTIAL. Stamp, A. P. (Oxford Univ.). Nucl. Phys.; A159: 399-408(1970).

The strength of the quadratic (L · S) tensor interaction in the deuteron optical potential arising from the spin-orbit interaction in the nucleon–nucleus potential is estimated. It is found that the strength is considerably weaker and of opposite sign to the phenomenological tensor potential obtained from the optical-model analysis of elastically scattered deuterons. (auth)

12685 ELECTRON-NUCLEUS QUADRUPOLE INTERACTION AND ITS INFLUENCE ON β-DECAY. Martinsen, P. O.; Randrup, J. (Univ. of Aarhus, Denmark). Nucl. Phys.; A159: 449-60 (1970).

The problem of an outgoing electron in the field of a quadrupole deformed nucleus is solved by means of an exact numerical method. It is found that the results for one nucleus are rather representative. Typical results for ^{166}Er are tabulated. Further, general formulas for β-decay of deformed nuclei are developed, and the corrections to spectra and ft-values are estimated. The quadrupole coupling gives rise to discontinuities in the β-spectra, and as an illustration the decay ^{170}Tm → ^{170}Yb is considered. (auth)

12686 SHELL-MODEL DATA FROM A REALISTIC N–N INTERACTION. Irvine, J. M.; Pucknell, V. F. E. (Univ. of Manchester, Eng.). Nucl. Phys.; A159: 513-39(1970).

Using a local density-dependent reaction matrix calculated by Siemens and Negele from the Reid potential Hartree–Fock calculations are carried out on the closed-shell nuclei ^{4}He, ^{16}O and ^{40}Ca and on the closed-shell plus one-nucleon nuclei ^{5}He, ^{17}O and ^{41}Ca. These calculations yield a set of single-particle wave functions which may be used in shell-model calculations. Tables of interaction matrix elements for such calculations up to, and including, the 0f–1p shell are presented. (auth)

12687 THREE-NUCLEON EQUATIONS WITH SEPARABLE TWO-BODY POTENTIALS. Harms, Edward (Rensselaer Polytechnic Inst., Troy, N. Y.). Nucl. Phys.; A159: 545-54(1970).

Assuming separable two-body potentials, a general derivation is given of the three-nucleon equations. The derivation allows for the full complexity, in separable form, of the two-nucleon interaction including an arbitrary number of (possibly coupled) partial waves and an arbitrary number of separable terms in each partial wave. All three-body partial waves are considered. Using a convenient notation, the three-body equations and their angular momentum decomposition are easily derived. (auth)

12688 SHELL-MODEL NUCLEAR LEVEL DENSITY. Baba, H. (Japan Atomic Energy Research Inst., Tokai). Nucl. Phys.; A159: 625-41(1970).

A nuclear level-density formula was derived by introducing a stepwise single-particle level structure. It was found to be formally identical to the well-known Fermi gas level density, when the level-density parameter a was regarded as a function of the excitation energy E instead of a constant. The computed level-density parameter was compared with that deduced from neutron resonance data. (auth)

12689 EXCHANGE EFFECTS IN THE NUCLEON–NUCLEUS OPTICAL POTENTIAL. Owen, L. W.; Satchler, G. R. (Oak Ridge National Lab., Tenn.). Phys. Rev. Lett.; 25: 1720-4 (21 Dec 1970).

A simple model of the nucleon–nucleus optical potential is used to explore the effects of exchange. The resulting potential is close to those found from analysis of actual scattering. Exchange effects are important. (auth)

12690 GROSS THEORY OF β DECAY AND ITS APPLICATION TO THE FERMI MATRIX ELEMENT. Koyama, Shin-Ichiro; Takahashi, Kohji; Yamada, Masami (Waseda Univ., Tokyo). Progr. Theor. Phys. (Kyoto); 44: 663-88(Sep 1970).

The gross theory of nuclear β decay proposed by Takahashi and Yamada is reinvestigated. A revised model for treating the even–odd mass difference is set up and applied to the calculation of the squared Fermi matrix elements. The results for the superallowed transitions agree well with those expected from the isospin formalism except for the transitions from odd–odd to even–even nuclei. The isospin-forbidden Fermi transitions are also studied. The results are consistent with the existence of the gross structure in the Fermi transitions. (auth)

12691 EXCHANGE EFFECTS FOR COMPOSITE PARTICLES. Schaeffer, Richard (Univ. of California, Berkeley). Nucl. Phys.; A158: 321-36(1970).

Inelastic and charge-exchange scattering of light projectiles by a nucleus are considered. Among the contributions to the scattering amplitude which arise from the antisymmetrization of the projectile and target wave functions and from the exchange nature of the nuclear force, the process where the interacting projectile nucleon and target nucleon are exchanged is shown to be important. This contribution changes the angular distribution only slightly, but it may increase the cross-section strength up to a factor 4. Other processes similar to the transfer of two particles should be included in order to estimate the magnitude of all the exchange effects. (auth)

12692 FADDEEV EQUATIONS FOR SPIN-DEPENDENT FORCES: CALCULATION OF ^{9}Be BINDING ENERGY. Grubman, Ronald; Witten, Thomas Jr. (Univ. of California, San Diego, La Jolla). Nucl. Phys.; A158: 289-308(1970).

A new angular-momentum decomposition of the Faddeev equations for the general case of three particles with spin is described. The formalism is applied to calculate the binding energy of two α-particles and a neutron. In this calculation the n–α and α–α interactions are represented phenomenologically by local potentials, and the corresponding two-body T matrices are approximated by a Sturmian expansion. The potentials were determined from two-body scattering data at low energies. The calculation yields a binding energy of 1.22 ± 0.05 MeV. This is comparable to the experimental value of 1.571 MeV for the three-body breakup energy of ^{9}Be. It thus appears that ^{9}Be may be crudely described as a bound state of three simple particles. (auth)

12693 STUDIES TO A NEW APPROACH FOR THE THREE-BODY PROBLEM. Gloeckle, W. (Centre d'Etudes Nucleaires de Saclay, Gif-sur-Yvette, France). Nucl. Phys.; A158: 257-77 (1970).

Eigenvalue problems for Hilbert–Schmidt kernels in two variables related to the three-body problem are investigated numerically. With the aid of these eigenfunctions the solution of the three-body problem is constructed in a purely algebraic manner. (auth)

12694 INTERNAL BREMSSTRAHLUNG AND THE MECHANISM OF DIRECT NUCLEAR REACTIONS: THE TRIANGLE MECHANISM. Janouch, F.; Mach, R. (Nuclear Research Inst., Rez, Czech.). Nucl. Phys.; A158: 193-216(1970).

The IBS spectrum accompanying a direct nuclear reaction is studied in a model using the non-relativistic Feynman–Shapiro-diagram technique. Attention is centered on the triangle diagrams. The threshold singularities and the magnitudes of angular momenta of particles interacting in vertices are investigated with regard to their influence on the shape of the IBS spectrum. The pole- and the triangle-diagram contributions to the total radiative amplitude are compared. The possibility of the experimental identification of the nuclear reaction mechanism is discussed. (auth)

12695 REMARK ON THE VILLARS THEORY OF NUCLEAR COLLECTIVE ROTATION AND ITS RELATION TO THE VARIABLE MOMENT OF INERTIA MODEL OF MARISCOTTI ET AL. da Providencia, J.; Urbano, J. N. (Univ., Coimbra, Portugal). Nucl. Phys.; A158: 161-5(1970).

A critical analysis is made of the Villars elementary quantum theory of nuclear collective rotation, and a new method for determining the rotational-state excitation energies is proposed which may provide a theoretical foundation for the phenomenological variable moment of inertia (VMI) model of Mariscotti, Scharf–Goldhaber, and Buck. (auth)

12696 NUMERICAL EVALUATION OF RADIATIVE CORRECTIONS OF ORDER α TO ALLOWED NUCLEAR β-DECAY. Wilkinson, D. H.; Macefield, B. E. F. (Nuclear Physics Lab., Oxford). Nucl. Phys.; A158: 110-16(1970).

The "outer," model-independent, radiative corrections to allowed nuclear β decay are evaluated for all Z in the multiplicative approximation. Results are presented in graphical and tabular form. (auth)

12697 BOSON METHOD AND THE ANTISYMMETRIZATION PROBLEM. Banville, M.; Simard, P. A. (Univ., Sherbrooke, Quebec). Nucl. Phys.; A158: 51-64(1970).

The transcription of the quasi-particle in the ideal space is studied for systems containing up to five quasi-particles. A way is found to introduce properly the Pauli exclusion principle, and the states are completely antisymmetrized. The quasi-particle operators and their products appearing in the Hamiltonian are also transcribed in that space. The matrix elements of the products of quasi-particle operators evaluated in the ideal space are exactly the same as those evaulated in the quasi-particle space. This enables one to determine many anharmonic corrections. (auth)

12698 NUCLEAR SATURATION AND THE SMOOTHNESS OF NUCLEON–NUCLEON POTENTIALS. Haftel, Michael I. (Naval Research Lab., Washington, D. C.); Tabakin, Frank. Nucl. Phys.; A158: 1-42(1970).

The two-nucleon and nuclear-matter problems are solved by matrix inversion in momentum space. Direct matrix inversion of the Lippman–Schwinger and Brueckner equations is shown to be useful for general nuclear potentials including ones that are local, nonlocal, weak, strong, central, or noncentral. This flexibility is employed to study the relationship between nuclear saturation and the smoothness of the two-nucleon interaction. Five potentials are considered that give approximately equivalent phase shifts but differ in their smoothness. Two examples of smooth potentials with very weak nonlocal tensor terms are given. The potentials are classified according to their smoothness by calculating the wave function defect and the wound integral for each case. The binding energy of nuclear matter is calculated for each potential by using the effective mass and angle-averaged Pauli operator approximations. A self-consistent hole spectrum and a free-particle spectrum are used. A systematic dependence of saturation on the smoothness of the two-nucleon interaction is found. Only strong potentials with strong tensor terms yield correct saturation, whereas very smooth potentials produce overbinding and large equilibrium densities. (auth)

12699 POLARIZATION AND THE STATISTICAL MODEL. Goldfarb, L. J. B. (Univ. of Manchester, Eng.); Seyler, R. G. Nucl. Phys.; A160: 109-12(1971).

Using familiar statistical assumptions regarding averages of reaction matrix elements, attention is given to polarization phenomena involving particles with spins greater than one half. Description of a particular test, involving only channel-spin incoherence, obtained when deuterons are emitted in association with spin-one nuclei is given. The polarizations of the deuteron and the residual nucleus are completely identical. (auth)

12700 SYSTEMATIC BEHAVIOUR OF THE MOST PROBABLE CHARGE IN THE MEDIUM-ENERGY FISSION. Umezawa, H.; Baba, S.; Baba, H. (Japan Atomic Energy Research Inst., Tokai). Nucl. Phys.; A160: 65-98(1971).

The most probable charge Z_p observed in the medium energy fission of various nuclides was studied in comparison with the thermal-neutron-induced and the spontaneous fission. In the course of study, the systematics in the numbers of neutrons emitted before and after fission for the former was found to show no saw-tooth structure as found for the latter. It was found that the Z_p showed rather clear systematic behavior with respect to the fragment mass fraction. The number of neutrons evaporated during the competition against fission was calculated using Jackson–Vandenbosch model and was compared with that deduced from the neutron systematics. (auth)

12701 THEORY OF INELASTIC NUCLEON–NUCLEUS SCATTERING. Emrich, Kurt (Technische Univ., Hanover). Nucl. Phys.; A160: 1-24(1971).

The formalism of quantum Green functions is used to derive exact formulas for the S-matrix describing the scattering of nucleons on odd-mass and doubly even nuclei. From the exact equations approximate formulas are derived and the conditions under which these go over into the formulas of the distorted-wave Born approximation are discussed. (auth)

12702 COUPLING OF COLLECTIVE MODES IN DEFORMED NUCLEI. Nadjakov, E.; Mikhailov, I. N. (Inst. of Physics, Sofia. Joint Inst. of Nuclear Research, Dubna, USSR). Compt. Rend. Acad. Bulg. Sci.; 23: 767-70(1970).

A microscopic collective model for deformed nuclei is discussed. The model employs transition operators to describe the coupling of collective modes. The use of roton–phonon transition operators to describe the coupling of nuclear rotation to other modes is illustrated. (J.W.R.)

12703 SPIN-VIBRATIONAL I^+ STATES IN DEFORMED EVEN–EVEN NUCLEI. Gabrakov, S. (Inst. of Physics, Sofia). Compt. Rend. Acad. Bulg. Sci.; 23: 923-6(1970).

Energies and wave functions for I^+ states in deformed even–even nuclei were calculated. In addition, transition probabilities for M1 transitions to the ground state were calculated. Some results for ^{164}Er and ^{170}Yb are presented and compared with other calculations. (J.W.R.)

XUM

REACTOR TECHNOLOGY

Commercial Power Reactors

12704 (BMBW-FBK-70-11) RESEARCH AND DEVELOPMENT WORK FOR OBRIGHEIM NUCLEAR POWER STATION. Kafka, P. (Siemens A. G., Erlangen (West Germany)). Jul 1970. 138p. (In German). Dep. NTIS (U. S. Sales Only).

A description is given of the research and development work carried out by Siemens Aktiengesellschaft and its subcontractors for Obrigheim Nuclear Power Station which is equipped with a light-water-cooled PWR. 14 references. (auth)

12705 (JAERI-Memo-4197) DEVELOPMENT OF REACTOR ENCLOSURE HIGH VOLTAGE POWER CABLE PENETRATION. Futamura, Yoshiaki; Watanabe, Masaaki; Takano, Masami (Japan Atomic Energy Research Inst., Tokyo). Oct 1970. 44p. (In Japanese). Dep. NTIS (U. S. Sales Only).

In case of an incident the penetration shall be capable of maintaining electrical and mechanical integrity, enduring the stress imposed by the increase of pressure, temperature and humidity inside the enclosure. Newly developed porcelain type penetration is used for high voltage power cable at JPDR-II plant. The detail description of seal mechanism, stress analysis of porcelain, test result of porcelain under stress imposed and nonimposed for high voltage power cable is reported. (auth) (Japan)

12706 WIND-TUNNEL MEASUREMENTS OF REACTOR COMPONENTS TO DETERMINE FLOW LOADS AND FLOW DISTRIBUTION. Klein, H. (Siemens, AG, Erlangen, Ger.). Atomkernenergie; 16: 306-10(1970). (In German).

In order to determine the required strength of certain reactor components for the Stade Nuclear Power Station, it was necessary to obtain information on the flow loads to which these parts would be subjected during service. To do this, it was decided to make use of a low-velocity wind tunnel which was employed, for example, to measure the drag coefficients of the control-rod guide inserts. Knowing these values and also the nature of flow distribution in the upper header room, it is possible to calculate the forces which the control-rod guide inserts will be subject to. In addition the nature of the flow distribution at three different zones of a fuel assembly was determined. This information also contributes towards understanding the flow loads and cooling effects that will be encountered. (auth)

12707 WHAT FUTURE FOR ADVANCED REACTORS IN EUROPE? Vichney, N. New Sci.; 48: 434-5(10 Dec 1970).

American technology of light water reactors is being adopted in Western Europe and future reactors are being investigated. As it is thought unwise to rely completely on fast breeder reactors, the high temperature reactor is being developed. In Europe two reactors of this type are being tested: the Dragon reactor, built at Winfrith, which uses fuel in the form of a pile of small prisms, and the AVR built in Julich, which uses fuel in the form of pebbles. The reactor situation in Germany and France is discussed and future cooperation between Britain, Germany and France is considered. (UK)

12708 50 MW SODIUM COMPONENT TEST FACILITY. Nucl. Eng. Int.; 15: 1007-8(Dec 1970).

The facility, which is being built at Hengels by Neratom, is to test Na–Na heat exchangers and steam generators for the prototype 300MW(e) SNR fast reactor. Details are given of the facility and a flow diagram is included. Test results of the steam generator can be easily extrapolated from 50MW to 60MW, which is approximately the power transferred in one generator. By use of a special regenerative coupling it is possible to test the heat exchanger at about a third of its nominal power. An air cooler, or the evaporator, can be used as the heat sink. (UK)

12709 OT NAUCHNOGO POISKA K ATOMNOI PROMYSHLENNOSTI. RAZVITIE I SOVREMENNYE PROBLEMY ATOMNOI NAUKI I TEKHNIKI V SSSR. (From Scientific Research to Nuclear Industry. Development and Problems of Nuclear Science and Technology in USSR). Petros'yants, A. M. Moscow; Atomizdat (1970). 312p.

A general review is given on the nuclear research carried out in U. S. S. R. Descriptions are given of various types of reactors, high-energy physics and charged particle accelerators. Thermonuclear fusion as a new source of energy, nuclear power plants, and small dimension nuclear power installations are discussed as well as the nuclear submarines, isotopes in agriculture, waste disposal and various other aspects of nuclear science including the international cooperation in atomic studies and techniques. (R.V.J.)

12710 OSKARSHAMN REACTORS I AND II SALIENT FEATURES. Haga, I. (AB ASEA-ATOM, Vasteras, Sweden). Nucl. Eng. Int.; 15: 989-92(Dec 1970).

Principal technical data for the two units of the direct cycle light water BWR are tabulated. Special features which were developed for the first unit are retained in all later plants. These are described. They include fuel design of small fuel geometry, each assembly consisting of 64 rods, O.D. 12.25 mm; the electro-hydraulic control rod drive system; the primary water clean-up system; and the containment design which is based on the pressure suppression system. (UK)

12711 WORLD'S REACTORS. Nucl. Eng. Int.; 15: 994 (Dec 1970).

A chart is presented showing a large coloured cut-away drawing of the Oskarshamn Power Reactor and listing parameters for both units. (UK)

12712 RESEARCH AND DEVELOPMENT WORK LEADING UP TO THE ASEA-ATOM BWR. Leine, L.; Tenerz, E. (AB ASEA-ATOM, Vasteras, Sweden). Nucl. Eng. Int.; 15: 999-1002(Dec 1970).

Development work leading to the design of Oskarshamn Unit I included both out-of-pile loop tests and in-pile testing in Sweden's research reactors and in the Halden reactor. Computer programmes were also developed and correlated with this work. Examples are given of the work undertaken on core design, reactor physics and fuel element development. Out-of-pile loops are illustrated and details presented of a gamma ray void measuring system. Methods of determining power distribution are described. Full scale testing was undertaken on the electro-hydraulic control rod drive and on the steam-water separator. (UK)

12713 DEVELOPMENT OF THE U.K. NUCLEAR POWER INDUSTRY. McTighe, E. P. (United Kingdom Atomic Energy Authority, Risley, Eng.). Atom (London); No. 170, 242-53(Dec 1970).

The present structure of the nuclear power industry in the U.K. and the historical trends that have shaped it are discussed. The present U.K. nuclear program and its future development are described. The lessons of the U.K. experience are discussed with a view to the future needs of Finnish industry. (auth) (UK)

12714 UNDERWATER PLASMA-ARC CUTTING AS A POWERFUL DISMANTLING TOOL FOR WATER REACTORS. Adorni, N. (CISE, Milan); Germani, G.; Parmeggiani, A.; Possa, G.; Turricchia, A. Energ. Nucl. (Milan); 17: 695-706 (Dec 1970).

Plasma-arc cutting of thick stainless steel plates can be performed underwater, in a relatively simple way, retaining all the well-known advantages of cutting in air, such as high working speed, easy automation and small encumbrance. The experiments aimed to assess the feasibility of the underwater plasma-arc cutting, as well as the design, construction, and test of a machine based on this method for the underwater dismantling of a reactor thermal shield, are described. This work was performed in connection with the repair of the Trino (Italy) pressurized water reactor. (auth)

12715 ELIMINATION OF THE THERMAL SHIELD FROM THE TRINO VERCELLESE PRESSURIZED WATER REACTOR BY MECHANICAL CUTTING. Donega, G.; Giuriato, A.; Morandi, G. (Ente Nazionale per l'Energia Elettrica, Rome). Energ. Nucl. (Milan); 17: 707-20(Dec 1970).

On the first refueling shutdown of the Trino Vercellese nuclear power station, the joints of the thermal shield in the reactor pressure vessel were found broken. Since the repair appeared to be difficult and not reliable, the elimination of the thermal shield was decided. Any dangerous effect on the reactor pressure vessel has been prevented by replacing the eight outermost fuel assemblies with dummies, the plant power capability being not affected by this change. The three segments of the thermal shield were cut underwater into long slices, transferred outside the reactor plant container and stored on a special rack in the spent fuel pit. For the cutting operation a milling machine designed, built and set up at the plant was used. The work performed in connection with the thermal shield elimination is described. (auth)

12716 CONSTRUCTION AND INSTALLATION WORK AT OSKARSHAMN. Wassberg, R. (AB ASEA-ATOM, Vasteras, Sweden); Nilsson, L. B. Nucl. Eng. Int.; 15: 995-8(Dec 1970).

Some parameters are tabulated which illustrate the overall size difference between the two units of the station. A plan and elevation illustrate the station layout of Unit I. Details are given of con-

struction of the containment and of the installation of the reactor vessel, together with an outline of the pressure and leak testing methods employed. Brief descriptions are given of the radiographic and ultrasonic inspection of pipework and of the method of installation of the STAL-LAVAL contra-rotating turbine. (UK)

Operation and Economics

12717 (DOCKET-50231-66) SOUTHWEST EXPERIMENTAL FAST OXIDE REACTOR. Quarterly Plant Operations Report No. 2, August 1–October 31, 1969. (General Electric Co., Sunnyvale, Calif. Breeder Reactor Development Operation). 30 Dec 1969. 15p. Dep. NTIS.

12718 (DOCKET-50237-127) DRESDEN NUCLEAR POWER STATION, UNIT 2. Failure of "A" Standby Gas Treatment System Discharge Damper Motor. (Commonwealth Edison Co., Chicago, Ill.). 2 Jan 1971. 1p. Dep. NTIS.

12719 (DOCKET-50237-128) DRESDEN NUCLEAR POWER STATION, UNIT 2. Receipt of Operational Neutron Sources in Excess of Allowance under License DPR-19. (Commonwealth Edison Co., Chicago, Ill.). 12 Jan 1971. 2p. Dep. NTIS.

12720 (DOCKET-50237-129) DRESDEN NUCLEAR POWER STATION, UNIT 2. Shut Down by Instrument Air Leak. (Commonwealth Edison Co., Chicago, Ill.). 8 Jan 1971. 2p. Dep. NTIS.

12721 (DOCKET-50245-51) MILLSTONE NUCLEAR POWER STATION, UNIT 1. Abnormal Occurrence Report No. 9. (Millstone Point Co., Hartford, Conn.). 6 Jan 1971. 1p. Dep. NTIS.

The failure of the main steam bypass valves to operate properly during a startup test at 75 percent rated output is discussed. Maintenance required on the pivot point for the bypass valve mechanical operating linkage is described. (D.C.C.)

12722 (TID-25636) SENA NUCLEAR POWER PLANT MONTHLY REPORT, OCTOBER 1970. (Societe d'Energie Nucleaire Franco-Belge des Ardennes, Chooz-liz-Givet (France)). 18p. Dep. NTIS.

The plant operated almost continuously throughout the month at a net power of 245 MW(e). One scheduled shutdown for maintenance and one accidental manual trip interrupted operation for only a few hours. The operating data are tabulated. (H.D.R.)

12723 (TID-25637) GUNDREMMINGEN NUCLEAR POWER PLANT MONTHLY REPORT, OCTOBER 1970. (Kernkraftwerk RWE-Bayernwerk G.m.b.H., Gundremmingen (West Germany)). 24 Nov 1970. 41p. (In German). Dep. NTIS.

The plant was operated at full load. The power was briefly reduced to 70 MW(e) for the purpose of changing control rods and carrying out the quarterly repeat tests, such as scram time measurements, closing time measurements on the main steam valves and the tripping test on the turbine. The activity of the reactor water and waste gas remained constantly low. Preparations were made for the transport of the spent fuel elements and the solid and liquid wastes. (auth)

12724 (TRG-Report-2090) ASSESSING THE ECONOMICS OF NUCLEAR POWER STATIONS IN AN ELECTRICITY GENERATING SYSTEM. Iliffe, C. E. (United Kingdom Atomic Energy Authority, Risley (England). Reactor Group). 1970. 29p. (CONF-701031-1). Dep. NTIS (U. S. Sales Only).

From Symposium on Economic Integration of Nuclear Power Stations in Electric Power Systems, Vienna, Austria.

Use of discounted cash flow techniques is shown to lead to a mean generating or "system" cost, for any installation within an electricity generating system extending over a given period of time such as to yield a prescribed rate of return on investment. The system cost can be expressed in terms of the mean generating costs of the individual types of station within the system and their mean load factors. The contribution of any type of station to the overall results can thus be readily assessed. For a single station the system cost is shown to reduce to the generating cost as normally employed. The extent to which a value of Pu affects the system cost is examined and a digression is made on the interpretation of indifference curves. A description is given of the calculation of trading prices for any quantities of Pu entering or leaving the system. These principles have been applied by means of the program DISCOUNT. The latest version of this is described together with an example of input and output. Within a defined system, the program enables the build-up of the nuclear and fossil fuelled sectors to be calculated subject to certain preferences for commissioning a particular type of station and considering Pu supply and demand. The program quotes the overall system cost, the contribution to it from the different station types, and also, for every instant of time and for each type of station, number of stations installed, load factor, cash flows to which they give rise, highest and lowest, or "marginal" durations and marginal costs. The Pu stocks are also quoted for each instant of time. By use of a subsidiary program CASHFLO the rate of return provided by any improved station on the development expenditure needed to achieve it can be calculated. (10 references) (auth) (UK)

Safety and Siting

Refer also to abstract 11087.

12725 (DOCKET-50155-58) BIG ROCK POINT NUCLEAR PLANT. Sensitized Stainless Steel Components Within Primary Coolant Pressure Boundary. (Consumers Power Co., Jackson, Mich.). 12 Jan 1971. 19p. Dep. NTIS.

12726 (DOCKET-50155-59) BIG ROCK POINT NUCLEAR PLANT. License No. DPR-6; Technical Specifications Change Nos. 21, 22, and 24, Additional Information. (Consumers Power Co., Jackson, Mich.). 19 Jan 1971. 4p. Dep. NTIS.

Revised physics calculations for the $Gd_2O_3-UO_2$ fuel elements are presented. Permission for use of the new fuel storage racks is requested. (D.C.C.)

12727 (DOCKET-50213-89) CONNECTICUT YANKEE ATOMIC POWER PLANT. Thermal Stress Evaluation of the Reactor Vessel During a Cooldown Transient. (Connecticut Yankee Atomic Power Co., Hartford). 5 Jan 1971. 30p. Dep. NTIS.

12728 (DOCKET-50213-92) CONNECTICUT YANKEE ATOMIC POWER PLANT. License No. DPR-14. Technical Specifications Proposed Change No. 17. (Connecticut Yankee Atomic Power Co., Hartford). 6 Jan 1971. 10p. Dep. NTIS.

Revised technical specifications concerning the inspection and testing of cooling system components are presented. (D.C.C.)

12729 (DOCKET-50213-93) CONNECTICUT YANKEE ATOMIC POWER PLANT. Preliminary Safety Analysis Report, Suppl. No. 1. (Connecticut Yankee Atomic Power Co., Hartford). 14 Jan 1971. 34p. Dep. NTIS.

Revised and additional data on the Connecticut Yankee Power Reactor are presented. Financial statements for the owners are included. (D.C.C.)

12730 (DOCKET-50214-2) MALIBU NUCLEAR PLANT, UNIT NO. 1. Preliminary Safety Summary Report. (Department of Water and Power, Los Angeles, Calif.). 31 May 1965. Contract AT(30-1)-3266. 454p. Dep. NTIS.

Information on Malibu Power Reactor is presented under the following broad topics: introduction and summary; site; containment; reactor design; nuclear steam supply systems; shielding; instrumentation and controls; secondary systems; tests and operation; administration and training; and accidents and potential hazards. Included also are additional data on the reactor requested by the Division of Reactor Licensing. (D.C.C.)

12731 (DOCKET-50231-65) SOUTHWEST EXPERIMENTAL FAST OXIDE REACTOR. Quarterly Plant Operations Report No. 1, May 1–July 31, 1969. (General Electric Co., Sunnyvale, Calif. Breeder Reactor Development Operation). 7 Nov 1969. 11p. Dep. NTIS.

12732 (DOCKET-50237-126) DRESDEN NUCLEAR POWER STATION, UNIT 2. Refueling. Proposed Modification No. 71-1 to Final Safety Analysis Report. (Commonwealth Edison Co., Chicago, Ill.). 15 Jan 1971. 25p. Dep. NTIS.

Safety analysis and predicted performance characteristics for operations with $Gd_2O_3-UO_2$ replacement fuel are presented. (D.C.C.)

12733 (DOCKET-50244-54) ROBERT EMMETT GINNA NUCLEAR POWER PLANT, UNIT NO. 1. Request for Approval of Respiratory Protection Procedure. (Rochester Gas and Electric Corp., N. Y.). 15 Jan 1971. 4p. Dep. NTIS.

12734 (DOCKET-50249-53) DRESDEN NUCLEAR POWER STATION, UNIT 3. Facility Operating License No. DPR-25. (Division of Reactor Licensing (AEC), Washington, D. C.). 12 Jan 1971. 186p. Dep. NTIS.

The facility operating license is presented. Technical specifications are included. (D.C.C.)

12735 (DOCKET-50259-21) BROWNS FERRY NUCLEAR PLANT, UNITS 1, 2, AND 3. Environmental Radioactivity Levels. Semiannual Report, January–June 1970. (Tennessee Valley Authority, Chattanooga. Office of Power). 18 Jan 1971. 32p. (DOCKET-50260-21; DOCKET-50296-20). Dep. NTIS.

12736 (DOCKET-50267-24) FORT ST. VRAIN NUCLEAR GENERATING STATION, UNIT 1. Preliminary Safety Analysis Report, Amendment 17. (Public Service Co. of Colorado, Denver). 21 Dec 1970. 356p. Dep. NTIS.

XUM

Revised design parameters of the Fort St. Vrain Power Reactor Unit 1 are presented. Included also are additional data on the reactor requested by the Division of Reactor Licensing. (D.C.C.)

12737 (DOCKET-50267-25) FORT ST. VRAIN NUCLEAR GENERATING STATION, UNIT 1. Applicant's Environmental Report: Operating License Stage. (Public Service Co. of Colorado, Denver). 22 Dec 1970. 124p. Dep. NTIS.

Information concerning radioactive discharges from the reactor is presented. The effects of reactor operations on the environment are analyzed. (D.C.C.)

12738 (DOCKET-50271-35) VERMONT YANKEE NUCLEAR POWER STATION. Preliminary Safety Analysis Report, Amendment 17 (Includes Additional Revisions to Final Safety Analysis Report). (Vermont Yankee Nuclear Power Corp., Rutland). 11 Jan 1971. 211p. Dep. NTIS.

Revised and additional information concerning instrumentation and piping systems and standby gas treatment system control and instrumentation is presented. (D.C.C.)

12739 (DOCKET-50280-32) SURRY POWER STATION, UNITS 1 AND 2. Applicant's Environmental Report, Operating License Stage. (Virginia Electric and Power Co., Richmond). 31 Dec 1970. 169p. (DOCKET-50281-32). Dep. NTIS.

Information concerning radioactive and thermal discharges from the reactor is presented. The effects of reactor operations on the environment are analyzed. (D.C.C.)

12740 (DOCKET-50280-33) SURRY POWER STATION, UNITS 1 AND 2. Preliminary Safety Analysis Report, Amendment 17. (Virginia Electric and Power Co., Richmond). 14 Jan 1971. 360p. (DOCKET-50281-33). Dep. NTIS.

Revised and additional design parameters of the Surry Power Reactor Units 1 and 2 are presented. (D.C.C.)

12741 (DOCKET-50293-33) PILGRIM NUCLEAR POWER STATION. Recommendations for Power Piping Code. (Boston Edison Co., Mass.). 12 Jan 1971. 4p. Dep. NTIS.

12742 (DOCKET-50295-22) ZION STATION, UNITS 1 AND 2. Resolution of Void at Concrete/Buttress Plate Joint. (Commonwealth Edison Co., Chicago, Ill.). 31 Dec 1970. 30p. (DOCKET-50304-22). Dep. NTIS.

12743 (DOCKET-50295-23) ZION STATION, UNITS 1 AND 2. Information Relative to a Liner Bulge in Containment Structure. (Commonwealth Edison Co., Chicago, Ill.). 15 Jan 1971. 25p. (DOCKET-50304-23). Dep. NTIS.

12744 (DOCKET-50301-26) POINT BEACH NUCLEAR PLANT, UNIT NO. 2. Preliminary Safety Analysis Report, Amendment 11. (Wisconsin Electric Power Co., Milwaukee. Wisconsin Michigan Power Co., Appleton, Wis.). 15 Jan 1971. 61p. Dep. NTIS.

Revised and additional information for Point Beach Power Reactor Unit 2 is presented. Additional design parameters for the high safety injection system piping are included. (D.C.C.)

12745 (DOCKET-50324-18) BRUNSWICK STEAM ELECTRIC PLANT, UNITS 1 AND 2. Containment Design Report. Design Report No. 7. (Carolina Power and Light Co., Raleigh, N. C.). 31 Dec 1970. 130p. (DOCKET-50325-18). Dep. NTIS.

12746 (DOCKET-50335-17) HUTCHINSON ISLAND PLANT, UNIT NO. 1. Replies to Questions on Unresolved Design and Construction Items. (Florida Power and Light Co.). 10 Dec 1970. 11p. Dep. NTIS.

12747 (DOCKET-50341-24) ENRICO FERMI ATOMIC POWER PLANT, UNIT 2. Preliminary Safety Analysis Report, Amendment 13. (Detroit Edison Co., Mich.). 4 Dec 1970. 54p. Dep. NTIS.

Information concerning radioactive discharges from the reactor is presented. The effects of reactor operations on the environment are analyzed. (D.C.C.)

12748 (DOCKET-50348-15) JOSEPH M. FARLEY NUCLEAR PLANT, UNITS 1 AND 2. Preliminary Safety Analysis Report, Amendment 9. (Alabama Power Co., Birmingham). 5 Jan 1971. 349p. (DOCKET-50364-9). Dep. NTIS.

Revised design parameters of the Joseph M. Farley Power Reactor Units 1 and 2 are presented. Included also are additional data on the reactor requested by the Division of Reactor Licensing. (D.C.C.)

12749 (DOCKET-50358-10) WM. H. ZIMMER NUCLEAR POWER STATION, UNIT 1. Preliminary Safety Analysis Report, Amendment 4. (Cincinnati Gas and Electric Co., Ohio. Columbus and Southern Ohio Electric Co., Columbus, Ohio. Dayton Power and Light Co., Ohio). 6 Jan 1971. 958p. Dep. NTIS.

Revised design parameters of the William H. Zimmer Power Reactor Unit 1 are presented. Included also are additional data on the reactor requested by the Division of Reactor Licensing. (D.C.C.)

12750 (DOCKET-50361-13) SAN ONOFRE NUCLEAR GENERATING STATION, UNITS 2 AND 3. Preliminary Safety Analysis Report, Amendment 5. (Southern California Edison Co., Los Angeles. San Diego Gas and Electric Co., Calif.). 29 Dec 1970. 139p. (DOCKET-50362-12). Dep. NTIS.

Additional information concerning the quality assurance program for the San Onofre Power Reactor Units 2 and 3 is presented. (D.C.C.)

12751 (DOCKET-50363-10) FORKED RIVER NUCLEAR GENERATING STATION, UNIT 1. Preliminary Safety Analysis Report, Amendment 4. (Jersey Central Power and Light Co., Morristown, N. J.). 28 Dec 1970. 69p. Dep. NTIS.

Additional data on the reactor requested by the Division of Reactor Licensing are presented. (D.C.C.)

12752 (DOCKET-50376-7) AGUIRRE NUCLEAR PLANT, UNIT NO. 1. Preliminary Facility Description and Safety Analysis Report, Amendment 1. (Puerto Rico Water Resources Authority, San Juan). 11 Jan 1971. 328p. Dep. NTIS.

Revised and additional information for the Aguirre Power Reactor Unit 1 is presented. (D.C.C.)

12753 (DOCKET-50382-2) WATERFORD STEAM ELECTRIC STATION, UNITS 3 AND 4. Preliminary Safety Analysis Report, Vol. 1. (Louisiana Power and Light Co., New Orleans). Jan 1971. 500p. (DOCKET-50383-2). Dep. NTIS.

Information on Waterford Power Reactor Units 3 and 4 is presented under the headings of introduction and summary, and site and environment. Seismic information concerning the site and surrounding area is included. (D.C.C.)

12754 (DOCKET-50382-3) WATERFORD STEAM ELECTRIC STATION, UNITS 3 AND 4. Preliminary Safety Analysis Report, Vol. 2. (Louisiana Power and Light Co., New Orleans). Jan 1971. 314p. (DOCKET-50383-3). Dep. NTIS.

Information on Waterford Power Reactor Units 3 and 4 is presented under the following broad topics: reactor; reactor coolant system; containment and plant structures; and engineered safety features. (D.C.C.)

12755 (DOCKET-50382-4) WATERFORD STEAM ELECTRIC STATION, UNITS 3 AND 4. Preliminary Safety Analysis Report, Vol. 3. (Louisiana Power and Light Co., New Orleans). Jan 1971. 228p. (DOCKET-50383-4). Dep. NTIS.

Information on Waterford Power Reactor Units 3 and 4 is presented under the following broad topics: instrumentation and control; electrical systems; auxiliary systems; steam and power conversion system; boron and waste management systems and radiation protection; conduct of operations; and initial tests and operations. (D.C.C.)

12756 (DOCKET-50382-5) WATERFORD STEAM ELECTRIC STATION, UNITS 3 AND 4. Preliminary Safety Analysis Report, Vol. 4. (Louisiana Power and Light Co., New Orleans). Jan 1971. 286p. (DOCKET-50383-5). Dep. NTIS.

Information on the Waterford Power Reactor Units 3 and 4 is presented under the broad topics of safety analysis and proposed technical specifications. (D.C.C.)

12757 (SSI-70-27) ON THE SWEDISH POLICY WITH REGARD TO THE LIMITATION OF RADIOACTIVE DISCHARGES FROM NUCLEAR POWER STATIONS: AN INTERPRETATION OF CURRENT INTERNATIONAL RECOMMENDATIONS. Hedgran, Arne; Lindell, Bo (National Inst. of Radiation Protection, Stockholm (Sweden)). Jun 1970. 25p. Dep. NTIS (U. S. Sales Only).

The protection measures applied to the normal operation of nuclear reactors guarantee that no individuals will suffer acute radiation injury. The remaining risks relate to the late occurrence of cancer or hereditary damage. Since they are very low and of random nature, they are controlled by limitation of the activity output rather than by limiting activity concentrations in the environment. The restrictions on the discharges of radioactive material are intended to satisfy the following criteria: no individual in the neighborhood shall receive a radiation dose such that the dose contribution from the operation of the reactor exceeds a certain fraction of the ICRP dose limits (0.5 rems per year in the case of whole body exposure); the total population exposure caused by the activity released from a reactor shall not exceed $\frac{1}{3}$ manrem per MW-year (thermal power); and all appropriate measures should be taken to reduce both the individual doses and the number of manrems as much as practicable, considering that a justifiable expense in the field of radiation protection is often about $200 per manrem. For accidental

situations some compulsory action levels for doses and activity concentrations in the environment have been recommended. Remedial action is often appropriate at lower levels; however, deliberate action levels cannot be specified until the actual situation is known. For widespread contamination non-action levels have been mentioned, one recommendation on a non-action level relates to iodine-131 in dairy milk. (auth) (Sweden)

12758 NEEDED: NUCLEAR ENGINEERING STANDARDS. Schmidt, R. A. (Oak Ridge National Lab., Tenn.). Power Eng.; 74: No. 12, 42-5(Dec 1970).

The requirement of nuclear engineering standards in the development of nuclear power plants is reviewed. The roles of international codes and standards, RDT standards, and AEC regulatory standards are analyzed. (D.C.C.)

12759 HOW TO OBTAIN NUCLEAR SAFETY DATA. Buchanan, J. R. (Oak Ridge National Lab., Tenn.). Power Eng.; 74: No. 12. 46-9(Dec 1970).

Operations of the Nuclear Safety Information Center are described. Products and services available are discussed. (D.C.C.)

12760 OSKARSHAMN NUCLEAR POWER STATION. Gimstedt Olle, G. Nucl. Eng. Int.; 15: 987-8(Dec 1970).

Sweden's first commercial nuclear power station consists of two direct cycle light water BWR's, a 440MW(e) unit now undergoing commissioning and a 560MW(e) unit under construction. The commercial background to the enterprise is discussed. Details of the site are given. (UK)

12761 POWER,POLLUTION, AND THE IMPERILED ENVIRONMENT. II. EAST, MIDWEST, AND WEST COAST: POLLUTION-CONTROL PLANS OF SOME MAJOR UTILITIES; ROLE OF GOVERNMENT IN ENVIRONMENTAL MATTERS; OTHER PROPOSED SYSTEMS FOR REDUCING STACK EMISSIONS. Friedlander, Gordon D. IEEE (Inst. Elec. Electron. Eng.), Spectrum; 7: No. 12, 65-75(Dec 1970).

Utilities in the U. S. are very aware of the public anxiety concerning the deteriorating environment. Some of the specific programs being evolved in coping with this grave problem are examined. (auth)

12762 ACTION ON REACTOR AND OTHER PROJECTS UNDERGOING REGULATORY REVIEW OR CONSIDERATION. Blakely, J. P. (Comp.). Nucl. Safety; 12: 59-71(Jan-Feb 1971).

12763 ECOLOGICAL CONSIDERATIONS IN SITING NUCLEAR POWER PLANTS: THE LONG-TERM BIOTIC EFFECTS PROBLEM. Auerbach, Stanley I. Nucl. Safety; 12: 25-34(Jan-Feb 1971).

One of the current concerns over the increasing installation of nuclear power stations is the potential impact of radioactive waste releases on local ecosystems. In particular, the question has been raised whether waste releases at maximum permissible concentration (MPC) levels would cause ecological problems due to the radioactivity. Hypothetical annual submersion dose rates from water assumed to be maintained at the occupational MPC × 1/30 were calculated for organisms living continuously in these waters. These hypothetical doses are used as a basis for comparison in a variety of ecological studies of low doses of ionizing radiation and are analyzed and evaluated in terms of detectability of biological effects at MPC levels. Present knowledge based on these and similar studies of the ecological effects of low-level chronic doses, such as could result from routine reactor releases under current standards, guidelines, and operational experience, indicates that any possible biological effects would be undetectable. Although the data in support of this contention are limited, they consistently point to this conclusion. 23 references. (auth)

12764 FUEL MELTDOWN AT ST. LAURENT I. Corbett, B. L. Nucl. Safety; 12: 35-9(Jan-Feb 1971).

The St. Laurent I plant, Électricité de France's 500-MW(e) gas-cooled nuclear generating facility, suffered a fuel meltdown on Oct. 17, 1969. During a routine refueling operation, graphite absorbers, including a graphite flow restrictor, were mistakenly loaded at the top of a fuel-element channel. The coolant-flow reduction damaged 6 of the 10 fuel elements in this channel, and there was some evidence that up to 10 kg of uranium (equivalent to a complete fuel element) completely melted. Subsequent cleanup and plant modifications were expected to require about 1 year of reactor downtime. 6 references. (auth)

12765 OFFSHORE SITING OF NUCLEAR ENERGY STATIONS. Anderson, T. D. Nucl. Safety; 12: 9-14(Jan-Feb 1971).

Questions involving environmental quality, priority of land uses, and public safety have created and will continue to create difficulties in finding acceptable sites for nuclear power plants. Interest is increasing in offshore stations as one solution to the siting problem. Investigations of offshore stations have included both artificial islands and floating platforms and have touched on environmental effects, economics, and safety. Indications are that many of the problems associated with siting nuclear power plants could be alleviated by offshore stations. The floating-station concept, in particular, seems to have significant potential for the future. Before this potential can be realized, however, considerable development of the concept will be needed. 13 references. (auth)

Steam and Power Conversion Systems

12766 NEW STEAM GENERATING SYSTEM FOR THE FRENCH NUCLEAR POWER STATION EL-4. Profos, O. Sulzer Tech. Rev.; 53: 69-83(1970).

Fabrication procedures for steam generators for the Britanny Power Reactor (EL-4) are described. Testing programs for the prototype steam generator are discussed. (D.C.C.)

Power Reactor Development

Refer also to abstracts 10434, 10758, and 11348.

12767 (BMBW-FBK-70-20) DEVELOPMENT PROGRAM: STEAM-COOLED FAST REACTOR. SUMMARY REPORT, PART 1. TECHNICAL DESCRIPTION. Affeldt, B.; Agemar, F.; Amon, F.; (and others) (Allgemeine Elektricitaets-Gesellschaft, AEG-Telefunken, Frankfurt am Main (West Germany). Gutehoffnungshuette Sterkrade A.G., [Oberhausen (West Germany)]. Maschinenfabrik Augsburg-Nuernberg A. G., Nuremberg (West Germany)). Oct 1970. 433p. (In German). Dep. NTIS (U. S. Sales Only)

In commission of the Bundesministerium the companies AEG, GHH and MAN designed a 300 MWe steam cooled fast breeder prototype reactor. The technical design of the plant as seen in early 1969 is described. Important features of the design are: safety containment with pressure suppression system, turbine in direct cycle, half integrated primary loop system, system pressure of 120 ata, steam outlet temperature of 470°C, cladding material Incoloy, max. cladding temperature 660°C, fuel rod outer diameter 7 mm, max. burnup of 85 MWd/kg. Most important results of design: plant efficiency of about 36%, Pu fiss-inventory 1.14 t, breeding ratio 1.2. (auth)

12768 (EURFNR-855) FAST REACTOR PROGRAMME. First Quarter 1970 Progress Report. Hoekstra, E. K. (comp.) (Reactor Centrum Nederland, Petten). Oct 1970. 73p. (RCN-130). Dep. NTIS (U. S. Sales Only).

Work performed under United States–Euratom Fast Reactor Exchange Program.

The RCN program on fast reactor physics, fuel performance, radiation damage in canning materials, corrosion behavior in canning materials, aerosol research, and heat transfer and hydraulics is summarized. (auth)

12769 IMPROVEMENTS IN AND RELATING TO NUCLEAR REACTOR FUEL ELEMENT DEBRIS RECEPTACLES. Appleby, George Graham; Brown, Arthur James (to Atomic Power Constructions Ltd.). British Patent 1,214,998. 9 Dec 1970. Filed 9 Mar 1967.

Some disadvantages of conventional arrangements for dealing with fuel element debris are mentioned, including the risk that the receptacles may lift and be forced up the fuel channel by coolant gas when replacing a fuel element stringer. If this happens the receptacle may tilt and become wedged in the fuel channel and block the coolant flow, or the receptacle may damage other reactor components or handling equipment. The receptacle described has perforated side walls, forming inlets for coolant, some of these perforations having surfaces above and/or below them so inclined that, in use, coolant flowing over these surfaces exerts a downward force on them. The side walls of the receptacle may be formed from expanded metal mesh or perforated metal sheet, with diamond-shaped perforations. Strips of metal may be provided above and below each perforation, strips beneath the opening being slightly concave on their upper surfaces. The side walls of the receptacle may be apertured to form coolant inlet ports, some of these ports being covered by a perforated sheet having surfaces inclined upwards or downwards towards the interior of the vessel. The side walls may be lined internally or externally with perforated sheet. Several alternative geometrical arrangements are described. (UK)

12770 NUCLEAR REACTORS. Willson, Charles Frederick (to Atomic Power Constructions Ltd.). British Patent 1,215,138. 9 Dec 1970. Filed 8 Mar 1967.

XUM

The disadvantages of conventional keying systems for the graphite blocks of gas-cooled reactors are pointed out, and an improved keying system is described. In this system the distances between centers of the graphite blocks in adjacent columns are held substantially constant by keying means in keyways in the sides of the blocks. Each keyway is shorter than the length of the block and each keying means is shorter than the keyway. The blocks in at least some of the columns may have holes which form continuous channels through the columns. The keying means may be integral with the side walls of the blocks, or may be separate from the blocks and disposed in oppositely facing keyways in two adjacent blocks; if desired a combination of these keying means may be employed. The keyways may be manufactured with parallel side walls to the upper surface of the blocks in which they are located, so as to provide slots in the upper surface; alternately the keying means may have side walls that diverge slightly outwards from the floor of the keyway. The opposite side walls of some keyways are preferably joined by a curved lower wall terminating the lower ends of the keyways, and the keying means in such arrangements are preferably shaped to prevent them being jammed in the curved portion. (UK)

12771 IMPROVEMENTS RELATING TO NUCLEAR REACTORS. **Webb, John; Stacey, John (to United Kingdom Atomic Energy Authority). British Patent 1,214,136. 2 Dec 1970. Filed 24 Feb 1967.**

Reference is made to closure plugs for reactor vessels. The inner face of such plugs may become exposed to high levels of temperature and radiation, and the plug must incorporate thermal and radiation shielding in order that the temperature and radiation may be reduced to acceptable levels at the outer face. The plug therefore has considerable depth and cannot be a perfect fit, but there must be a narrow clearance to preserve radiation shielding integrity. If deposits can collect in the clearance they may interfere with free rotation of the plug. The plug described has a main dip seal adjacent to its outer face, a secondary dip seal adjacent to its inner face, and a thermally insulated annular trough for containing the liquid of the secondary seal, for ensuring that the temperature of the liquid is lower than that of the inner face of the plug. For a liquid cooled reactor this liquid may be the same as that employed as reactor coolant. Where the reactor is Na-cooled the closure plug may be a rotatable shield closing the upper end of the Na tank, the secondary seal containing Na and the main seal containing Hg. A layer of an organic liquid of specific gravity lower than Hg may be floated on the Hg; this liquid may be liquid paraffin. A substance that has a lower specific gravity and higher freezing point than Hg and a freezing point higher than the ambient temperature during normal operation, and which if immiscible with Hg may be added to the Hg of the main seal, may be employed, with means for heating the main seal to keep this substance in the liquid state during normal operation. Removal of the heating causes this substance to freeze and thereby provide a seal against a reactor pressure surge. This substance may be paraffin wax. Means may also be provided for bleeding cool inert gas into the clearance annulus of the closure plug so as to build up a pressure sufficient to unbalance the secondary seal but not the main seal, the gas then bubbling through the secondary seal into the interior of the reactor vessel. (UK)

Kinetics and Dynamics

Refer also to abstract 12830.

12772 (BAW-3867-9(Vol.1)(Rev.1)) FAST BREEDER REACTOR STATIC PHYSICS METHODS DEVELOPMENT AND ANALYSIS PROJECT. VOLUME 1. FARED: ONE-DIMENSIONAL FAST REACTOR PHYSICS DESIGN AND ANALYSIS CODE. **Roy, D. H.; Tilford, J. M.; Livolsi, A. Z.; Colpo, P. N.; Carmichael, C. D.; Jacobsen, J. A. (Babcock and Wilcox Co., Lynchburg, Va. Nuclear Power Generation Dept.). Dec 1970. Contract AT-(30-1)-3867. 197p. Dep. NTIS.**

The computer program FARED is described. The program is a one-dimensional static physics design code with an internal cross section collapse program; criticality, depletion, and search routines; fuel management capability; and a variety of edits including an extensive perturbation edit. Execution of the various routines in FARED is controlled by user directives, and all input is free format. Limitations and applications for the program are described. 12 references. (D.C.C.)

12773 (BNWL-1403) EBR-II DOSIMETRY TEST REACTION RATE MEASUREMENTS (REACTOR RUNS 31E AND 31F). **Kellogg, L. S.; Zimmer, W. H. (Battelle-Northwest, Richland, Wash. Pacific Northwest Lab.). Jun 1970. Contract AT(45-1)-1830. 65p. Dep. NTIS.**

The data have been analyzed from ~800 foils irradiated during an EBR-II dosimetry test. A standard deviation of ±7% has been assigned to the majority of the reaction rate data. In most instances where a rigid statistical evaluation could be made, it indicated a calculated accuracy estimate with errors less than the assigned 7% standard deviation. However, comparisons using other techniques indicated that the 7% value could be reasonably expected to encompass most of the data. Discrepancies noted in the decay scheme data used by the various participants must be resolved, perhaps by continuation of "Round Robin" interlaboratory comparison programs. 25 references. (auth)

12774 (CEA-N-1344(1)) COREGRAF 2: A CODE FOR COMPUTING GRAPHITE LATTICES AND THEIR EVOLUTION FOR IBM 360 AND CDC 6600. **Cogne, Francois; Hoffmann, Alain; Reuss, Paul (Commissariat a l'Energie Atomique, Saclay (France). Centre d'Etudes Nucleaires). Dec 1970. 103p. (In French). Dep. NTIS (U. S. Sales Only).**

The Coregraf 2 code is used for lattices and lattice evolution calculations in the natural uranium graphite moderated gas cooled reactors. It was written in FORTRAN IV for either IBM 360 or CDC 6600 computers. Owing to the very short computing time (about 0.5 sec. on IBM 360-91), it is most convenient for calculations with power reactor lattices. The code uses the secondary model of thermalization (CADILHAC model) and rapidly calculates the diffusion coefficients using the BENOIST formalism. The resonant range is treated in a simple way by using the formulation of the resonance integral, obtained from the set of experiments performed on the critical assemblies of MARIUS and CESAR. This procedure leads to an accuracy of between 100.10^{-5} to 200.10^{-5} for the reactivity of the graphite gas-cooled reactors. 37 references. (auth) (France)

12775 (CEA-N-1395) EL 600: STUDY OF THE CORE NEUTRONIC PROPERTIES. **Chabrillac, Marcel; Goldstein, Stephen; Naudet, Roger; Tran Tuc Vi (Commissariat a l'Energie Atomique, Fontenay-aux-Roses (France). Centre d'Etudes Nucleaires). Dec 1970. 57p. (In French). Dep. NTIS (U. S. Sales Only).**

EL 600 is a heavy water moderated and cooled power reactor of the same type as the Canadian Pickering reactor. Results of fundamental neutronic calculations are given: lattice calculations and reactivity coefficients for the fresh fuel; burnup calculations; balance of absorption and reactivity coefficients for the irradiated core; and study of the power and flux distributions in the core at equilibrium. 14 references. (auth) (France)

12776 (JUL-678-RG) HANDLING OF FISSION PRODUCTS IN CALCULATION OF BURNUP WITH REGARD TO NEW NUCLEAR DATA APPLIED TO GRAPHITE REACTORS. **Liu, Yosen (Kernforschungsanlage, Juelich (West Germany). Institut fuer Reaktorentwicklung). Jul 1970. 248p. (In German). Dep. NTIS (U. S. Sales Only).**

Thesis. Submitted to Technische Hochschule, Aachen, Ger.

The nuclear data of all fission products were newly compiled and processed. The data thus obtained were used for an extensive study of reactor poisoning by fission products. An accurate evaluation of the reactor poisoning was made on the basis of the burnup calculations with consideration of the complete fission product decay schemes. Approximation versions for practical application were developed; these can be used for fuel cycle studies in thermal reactors. (25 references) (tr-auth)

12777 (TRG-Report-2060(Rev.)) COMPUTATION OF ASYMMETRIC POWER DIVERGENCES IN LARGE NUCLEAR REACTORS. **Thornton, D. E. J. (United Kingdom Atomic Energy Authority, Risley (England). Reactor Group). Mar 1968; Revised 1970. 25p. (CONF-701019-3). Dep. NTIS (U. S. Sales Only).**

From CREST Meeting on Reactivity Effects in Large Power Reactors, Ispra, Italy.

A method is described for calculating the course of rapid asymmetrical power divergences in large nuclear reactors without a specially written multi-dimensional kinetics computer code. The computer codes used are a steady-state two-dimensional azimuthal-plane flux and reactivity code and a one-dimensional axial kinetics code. An example is given of the application of the method to a control-rod withdrawal fault in the Advanced Gas-Cooled Reactor, and the validity of the method is discussed. (auth)

12778 CALCULATION OF THE STATIONARY STATE THERMAL NEUTRON SPECTRUM GENERATED BY A PLUTONIUM PHOENIX MIXTURE IN HIGH TEMPERATURE REACTORS. **Penndorf, K. (GKSS, Institut fuer Reaktorphysik, Geesthacht, Ger.). Atomkernenergie; 16: 291-302(1970). (In German).**

A procedure is developed, which is apt for production of satisfying thermal group constants of certain HTR fuel element geometries even at high Plutonium contents within a reasonable time of calculation. Technologically interesting applications are given. 14 references. (auth)

12779 USE OF ACOUSTIC WAVES IN NUCLEAR POWER REACTORS TO DETERMINE AVERAGE VOID FRACTIONS. Bonnet, J. A. Jr.; Osborn, R. K. (Univ. of Michigan, Ann Arbor). Nucl. Sci. Eng.; 43: 1-4(Jan 1971).

A method for estimating the average void fraction in water-moderated power reactors is presented. The method might be useful to determine departure from normal boiling conditions or nucleate boiling in boiling and pressurized water reactors, respectively. A standing acoustic wave is introduced in the core and the neutron density is measured, squared, time-averaged, and compared with the same quantity without an acoustic wave. The ratio is inversely proportional to the sixth power of the acoustic velocity; and the acoustic velocity depends on the average void fraction in the core. Consequently, this ratio is very sensitive to the average void fraction in the core. (auth)

12780 SUCCESSIVE SPACE-ENERGY SYNTHESIS FOR NEUTRON FLUXES IN FAST REACTORS. Cockayne, J. E.; Ott, K. O. (Purdue Univ., West Lafayette, Ind.). Nucl. Sci. Eng.; 43: 159-72(Feb 1971).

A new zero-dimensional procedure was developed for the calculation of neutron spectra in a fast reactor. The procedure yields a good approximation to the spectrum at a given "point" in a fast reactor rather than for a larger "region." Therefore, the procedure is especially suitable for the calculation of spectra in transition areas where other methods are very inaccurate. These close approximations to actually occurring spectra have been found to be good trial functions for the space-energy synthesis method of approximately solving the multigroup equations. The new procedure is based on an approximate flux from a 2-mode synthesis solution; high accuracy is not required for this initial flux. A single-group diffusion kernel is applied as weight function in the derivation of the zero-dimensional multigroup equations for the spectrum at a given point. Application of this procedure for two or more points yields an excellent set of trial functions for a subsequent space-energy synthesis calculation. Normally, M modes (with $M > 2$) are used in the second synthesis calculation. The complete synthesis procedure is therefore called "successive 2-M mode space-energy synthesis." Application of a successive 2−3 mode synthesis to a two-region fast reactor model yielded very high accuracy when compared with a numerical multigroup (diffusion) reference solution. Two substantially different 2-mode solutions used as basis for the calculation of the new set of trial spectra gave approximately the same final accuracy. The high accuracy and the small computation time give the successive synthesis method a good chance to compete with the multigroup method either by a reduction in computation time or by an increase in accuracy through a more detailed description of the energy dependence. (auth)

Control Systems

Refer also to abstract 10895.

12781 (ANL/EBR-25) INSTRUMENT PROBE FOR MEASURING TEMPERATURE AND PRESSURE IN THE UPPER PLENUM OF THE EBR-II REACTOR VESSEL. EBR-II Project. Wallin, W. R.; Haroldsen, R. O.; Moriarty, K. J. (Argonne National Lab., Ill. Argonne National Lab., Idaho Falls, Idaho). May 1970. Contract W-31-109-eng-38. 30p. Dep. NTIS.

Instrumentation has been installed to measure temperature and pressure of sodium in the upper plenum of the EBR-II reactor vessel. The instrumentation includes eight thermocouples, positioned at eight different elevations, and two pressure detectors. These instruments are mounted in a thimble-like probe, which replaces a plug in an auxiliary hole designed for the fuel-handling gripper. The probe extends from the operating floor of the reactor building through the primary-tank cover and the reactor vessel cover. Performance of the instrumentation is described. (auth)

Shielding

12782 (CEA-CONF-1683) REACTOR SHIELDING IN THE COMMISSARIAT A L'ENERGIE ATOMIQUE. Devillers, C. (Commissariat a l'Energie Atomique, Fontenay-aux-Roses (France). Centre d'Etudes Nucleaires). 1970. 23p. (CONF-700711-1). Dep. NTIS (U. S. Sales Only).

From Meeting of the European-American Committee on Reactor Physics, Richland, Wash.

The different codes used at the CEA for calculations concerning reactor protection are examined: NIOBE, ZEUS, TRIPOLI, ANISN, SABINE, MERCURE, as well as the PEPIN LE BREF code which is intended for the study of fission products. The results obtained from calculations of the neutron flux in the thermal column of the Harmonie reactor using the NIOBE, ANISN, and POKER codes are compared. The results obtained from a three-dimensional Monte Carlo calculation of neutron streaming towards Phenix heat exchangers are presented. (France)

Cooling Systems

Refer also to abstracts 10513, 10518, 10764, and 10896.

12783 (GEAP-10207-22) REACTOR PRIMARY COOLANT SYSTEM RUPTURE STUDY. Quarterly Report No. 22, July-September 1970. (General Electric Co., San Jose, Calif. Atomic Power Equipment Dept.). Oct 1970. Contract AT(04-3)-189. 46p. Dep. NTIS.

PIPES—failure in reactor cooling systems
—crack initiation and growth in reactor cooling systems, effects of low cycle fatigue on, (E)
REACTORS, BOILING—cooling systems for, effects of corrosion on low cycle fatigue life of piping in, (E)
REACTORS, WATER-COOLED—cooling systems for, failure mechanisms in piping of, (E/T)
STEEL—crack initiation and growth in A106B carbon and Type 304 stainless, effects of low cycle fatigue on (D.C.C.)

12784 (KFKI-70-20-RPT) COBRA: COMPUTER PROGRAM FOR COOLANT BOILING IN ROD ARRAYS. Vigassy, J. (Magyar Tudomanyos Akademia Kozponti Fizikai Kutato Intezete, Budapest). Jun 1970. 14p. Dep. NTIS (U. S. Sales Only).

Status report is given about the existing versions of the COBRA code for the computer ICL-1905 of the CRIP. A short code description, user's manual as well as some ideas for the code development are shown. 6 references. (auth)

12785 (ORNL-TM-3221) ENGINEERING PRACTICES FOR LARGE (4 INCHES AND OVER) GATE, GLOBE, AND CHECK VALVES IN WATER-COOLED NUCLEAR REACTOR SYSTEMS. (Oak Ridge National Lab., Tenn. NUS Corp., Rockville, Md.). Jan 1971. Contract W-7405-eng-26. 327p. Dep. NTIS.

Considerations relevant to the design, fabrication, and use of gate, globe, and check valves of 4-in. size and larger for water-cooled nuclear reactor systems are presented. Long-term reliability of these valves is a major design objective reflected in the discussions of their applications with respect to functional requirements, flow characteristics, design criteria and analyses, material requirements, fabrication, maintenance, and special design features. Techniques which can be used to determine how well these guidelines for achieving high reliability have been followed are also outlined. 37 references. (auth)

12786 (ORNL-TM-3273) GUIDE FOR SPECIFYING VALVES FOR WATER-COOLED NUCLEAR REACTOR SYSTEMS. (Oak Ridge National Lab., Tenn. NUS Corp., Rockville, Md.). Jan 1971. Contract W-7405-eng-26; Subcontract 2904. 129p. Dep. NTIS.

The requirements to be included in a specification for the procurement of valves for nuclear service are described, and technical considerations relative to the design, fabrication, testing, and inspection of gate, globe, and check valves of 4-in. size and larger are discussed. The technical considerations are directed primarily toward the requirements necessary for the use of these valves in water-cooled nuclear reactor systems. The material presented covers the requirements to be included in the six major sections of the procurement specification. (auth)

12787 CRITICAL HEAT FLUX AND PRESSURE DROP TESTS WITH PARALLEL UPFLOW OF HIGH PRESSURE WATER IN BUNDLES OF TWENTY ½-IN. RODS. LeTourneau, B. W.; Green, S. J. (Westinghouse Electric Corp., West Mifflin, Pa.). Nucl. Sci. Eng.; 43: 90-104(Jan 1971).

As a part of the Light Water Breeder Reactor (LWBR) development program, basic pressure drop, mixing, and critical heat flux (CHF) data were obtained with upflow of water in parallel-flow rod bundles. The test series reported simulated a "wet" region of relatively large diameter, low heat flux rods with a relatively large water-to-solid ratio. The test series included tests with a uniform heat flux to obtain basic CHF and pressure drop data for the geometry, and tests with a transversely nonuniform heat flux to obtain mixing and flow redistribution data. These data would permit evaluation of existing two- and three-dimensional hydrodynamic digital computer programs, such as COBRA and HAMBO, applicable to rod geometries. (auth)

12788 REACTOR PRESSURE VESSELS MADE OF CONCRETE. Margen, P. (Aktiebolaget Atomenergi, Studsvik, Sweden); Menon, S.; Tarandi, T. Tek. Tidskr.; 100: No. 13, 24-8(Sep 1970). (In Swedish).

Steel reactor pressure vessels and prestressed concrete pressure vessels are compared. Advantages with a concrete pressure

XUM

vessel and applications for water reactors are discussed. Construction problems such as high pressure, equipment for loading, heat insulation, and piping are considered. The Scandinavian shared model vessel in Studsvik is presented as well as planned tests and developments. Use for PWR and BWR is compared. Developments outside the Scandinavian countries are briefly reviewed. (Sweden)

12789 HELIUM FORCES STEAM FROM TOMORROW'S STATIONS. Engineer; 231: 35-7(10 Dec 1970).

In considering the pattern of power station development in the next twenty-five years it is suggested that while the fast breeder will probably be the one chosen in the longer term, during the interim period an advanced gas-cooled type, such as the Mark III AGR, will be required. High operating temperatures of HTR type reactors leads to the use of He as coolant. Possible disadvantages are problems of cost, impurity levels, and supply. The direct use of He coolant as a working gas in a He gas turbine is a future possibility. An initial design for an HTR gas turbine is illustrated. (UK)

12790 ULTRASONIC INSPECTION OF WELDS IN NUCLEAR REACTOR PRESSURE VESSELS. (NEWLY-DEVELOPED EQUIPMENT FOR AUTOMATIC SCANNING AND RECORDING OF BUTT WELDS). de Sterke, A. (Rontgen Technische Dienst N. V., Rotterdam). Brit. J. Non-Destruct. Test.; 12: 114-24(1970).

Possible scanning procedure for the detection of flaws in welds, including techniques with both a single and a double probe system was investigated. It was concluded that a combination of the two systems is necessary to detect planar defects of different orientation. The requirements of the system are considered and the following aspects discussed: registration of echoes; the keeping of the main and cross-sectional records; calibration and checking; use of the removable-test-condition-determination strip; automated scanning; the influence of parent metal and cladding on sensitivity. (UK)

12791 THERMAL ANALYSIS OF PRESSURIZED WATER REACTORS. Tong, L. S.; Weisman, Joel. AEC Monograph Series on Nuclear Science and Technology. Hinsdale, Ill.; American Nuclear Society (1970). 313p. $24.00. (TID-25635).

The basic principles underlying thermal and hydraulic design of pressurized water reactors are presented. Included are discussions of: (1) basic power distributions in these reactors; (2) fuel element behavior under steady-state and transient conditions; (3) basic coolant flow characteristics in the core; (4) heat transfer and transport in the core; and (5) maximum heat removal capability of a core design. (H.D.R.)

12792 SODIUM FLOW MONITORING. Dean, S. A.; Harrison, E.; Stead, A. (United Kingdom Atomic Energy Authority, Risley, Eng.). Nucl. Eng. Int.; 15: 1003-6(Nov 1970).

Although the PFR primary circuit flow may be determined by the transit time analysis technique, two additional types of fast response flowmeters are needed in the primary circuit. One is to be inserted in the pump ducts, which are located well down in the reactor, immersed in the sodium pool, to monitor the delivery rate of each of the impeller-type sodium pumps during normal running. The other type is needed to monitor the total core flow and to trip the reactor should this flow fall below a prescribed value or at a rate exceeding a given safe limit, and is to be installed in a suitably modified and gagged control rod guide tube in the core. Descriptions are given of two a-c operated flowmeters developed for these specific applications. The electronic system for the drive and amplifier units of each is presented. Performance data is summarised. (UK)

12793 STABLE NUMERICAL INTEGRATION OF CONSERVATION EQUATIONS FOR HYDRAULIC NETWORKS. Porsching, T. A.; Murphy, J. H.; Redfield, J. A. (Westinghouse Electric Corp., West Mifflin, Pa.). Nucl. Sci. Eng.; 43: 218-25(Feb 1971).

Hydraulic-network models have been used to study transient flow phenomena in pressurized water reactor plants. The nature of the differential equations associated with these networks imposes severe time-step restrictions on explicit numerical integration methods. A convergent, implicit method is described which, when used in conjunction with a block inversion technique, produces an efficient numerical integration procedure for the network equations. (auth)

Fuels

12794 (ANL-7736) LIFE-I: A FORTRAN-IV COMPUTER CODE FOR THE PREDICTION OF FAST-REACTOR FUEL-ELEMENT BEHAVIOR. Jankus, V. Z.; Weeks, R. W. (Argonne National Lab., Ill.). Nov 1970. Contract W-31-109-eng-38. 63p. Dep. NTIS.

LIFE-I is designed to predict the in-pile behavior of cylindrical fast-reactor fuel elements. Assuming axial symmetry, the generalized plane-strain analysis combines models for fuel restructuring, migration of fuel constituents, fuel swelling due to the accumulation of fission products, fission-gas release, hot pressing of the fuel, and cladding swelling due to void nucleation and growth. An iterative procedure allows the code to compute the detailed thermal and mechanical response of the fuel element during any specified history of normal reactor power cycling. Up to 10 axial sections are allowed to account for variations in power and coolant temperature, and an option is included for the treatment of encapsulated elements. Typical input for mixed-oxide stainless steel clad elements, some preliminary results, and a discussion of the input and output for LIFE-I are included. (25 references) (auth)

12795 (BMI-1893) PROGRESS ON DEVELOPMENT OF FUELS AND TECHNOLOGY FOR ADVANCED REACTORS DURING JULY-SEPTEMBER 1970. Progress Report. Keller, Donald L. (Battelle Memorial Inst., Columbus, Ohio). Oct 1970. Contract W-7405-eng-92. 112p. Dep. NTIS.

EXPERIMENTAL BREEDER REACTOR-II — fuel elements for, fabrication of Type 316 stainless steel clad plutonium nitride (PuN) - uranium nitride (UN) pin type
LIQUID METAL FAST BREEDER REACTOR — fuels for, development of plutonium nitride (PuN) - uranium nitride (UN) and plutonium oxide (PuO_2) - uranium oxide (UO_2)
PLUTONIUM NITRIDES — PuN - UN, fabrication of Type 316 stainless steel clad fuel pins of
— PuN - UN, irradiation testing in liquid sodium cooled fast reactor environment
PLUTONIUM OXIDES PuO_2 — PuO_2 - UO_2, irradiation testing in liquid radium cooled fast reactor environment
— PuO_2 - UO_2, creep testing of
REACTOR FUEL ELEMENTS — fabrication of Type 316 stainless steel clad plutonium nitride (PuN) - uranium nitride (UN) pin type
— creep testing of uranium oxide (UO_2) and plutonium oxide (PuO_2) - uranium oxide (UO_2)
REACTOR FUELS — irradiation testing of plutonium nitride (PuN) - uranium nitride (UN) and plutonium oxide (PuO_2) - uranium oxide (UO_2) and uranium carbide (UC)
STAINLESS STEEL — fabrication of cladding of type 316, for plutonium nitride (PuN) - uranium nitride (UN) fuel pins
URANIUM CARBIDES — irradiation testing at high temperatures of loose packed particles of
URANIUM NITRIDES — PuN - UN, fabrication of Type 316 stainless steel clad fuel pins of
URANIUM NITRIDES — PuN - UN, irradiation testing in liquid sodium cooled fast reactor environment
URANIUM OXIDES UO_2 — PuO_2 - UO_2, irradiation testing in liquid sodium cooled fast reactor environment
— creep testing of
— PuO_2 - UO_2, creep testing of
— fission gas diffusion and bubble growth in (D.C.C.)

12796 (EURAEC-2145) EXPERIMENTAL AND THEORETICAL PHYSICS WORK ON PLUTONIUM ENRICHED LWR'S, LATTICES. Final Report. Bindler, L.; Leenders, L.; Van Den Broeck, H. (Centre d'Etude de l'Energie Nucleaire, Brussels (Belgium)). Jun 1970. 220p. (EUR-4034; BN-7006-3; BLG-440). Dep. NTIS.

The activities up to 1968 of the Belgian program for studying technical and economic aspects of recycling plutonium in thermal light water reactors are summarized. The reactor physics theoretical methods and codes development studies are described. Included are: the preparation of the VENUS critical facility and associated installations; the initial code calibration on the basis of previous experimental data; and experimental and theoretical work on the VENUS-program study of 4% UO_2 fuel and mixed 3% UO_2 - 1% PuO_2 fuel. (H.D.R.)

12797 (IEA-186) FUEL DEVELOPMENT. PROGRAM FOR CALCULATION OF A LATTICE OF NATURAL URANIUM AND HEAVY WATER AND FOR THE CALCULATION OF THE PRODUCTION OF PLUTONIUM. Hehl, Wilma Sonia Caiaffa (Instituto de Energia Atomica, Sao Paulo (Brazil)). Sep 1969. 40p. (In Portuguese). Dep. NTIS (U. S. Sales Only).

A digital program is presented that calculates the variation, as a function of the irradiation, of the mean parameters relevant to burnup studies of an initially clean heavy water pressure tube reactor. The program gives the values of the four factors of k infinite, of the k effective, moderation and diffusion areas, geometrical and material bucklings, maximum and effective fluxes. The concentrations, in g/ton UO_2, of the fissile and fertile nuclides are also calculated as a function of the irradiation. The program is written in FORTRAN 2 for the IBM 1620. (auth)

12798 (IAE-1942) PROCEDURE FOR CALCULATING CERTAIN PARAMETERS OF HEAT-PRODUCING ELEMENTS OF VVER TYPE. Vinokhodov, E. V. ([Gosudarstvennyi Komitet po Ispol'zovaniyu Atomnoi Energii SSSR] Moscow. Institut Atomnoi Energii). 1969. 48p. (In Russian). Dep. NTIS (U. S. Sales Only).

A technique for calculating the temperature field, the power reserve prior to fusion of the fuel, the radial and diametral clearances, and the pressure of gaseous fission products in the VVER type of fuel elements is presented. The procedure is exemplified with a calculation of the VVER fuel elements at a power of 1375 MW(t). 9 references. (tr-auth) (JPRS)

12799 (TUBIK-17) STATIONARY HEAT TRANSFER IN INFINITELY LONG FUEL ELEMENTS WITH LOCALLY VARYING HEAT SOURCES AND BOUNDARY CONDITIONS. Wolf, L.; Johannsen, K. (Technische Universitaet, Berlin (West Germany). Institut fuer Kerntechnik). Mar 1970. 8p. (In German). Dep. NTIS (U. S. Sales Only).

A collection of papers previously published in the years 1968 to 1970 is presented. Some different models for the heat transport in fuel element rods with a circumferentially varying gap geometry are presented and possible methods of solution are proposed which can be used from case to case in view of the desirable accuracy. The influence of the hyperfine structure of the heat source distribution, the eccentric position of the fuel pellet within the canning and an elliptical deformation of the canning on the temperature fields in the fuel and the canning are analyzed. The limitations of the simplified gap model and "linearized" method of solution are presented by comparison with a sophisticated model and method of solution. (auth)

12800 NUCLEAR REACTOR FUEL ELEMENTS. Cobb, Edward Clifford; Quick, Martin Vinicombe (to Nuclear Power Group Ltd.). British Patent 1,213,557. 25 Nov 1970. Filed 11 Jul 1968.

The object is to provide a fuel element in which the fuel is encapsulated and in which the temperature difference between the fuel and the coolant flowing over the element is kept to a minimum and the pressure drop over the fuel element is also kept to a minimum by reducing the length of the fuel bearing section through which the coolant passes, other than axial passages of relatively large hydraulic mean diameter. The fuel element described comprises coated fuel particles located in a space between two walls that have openings to permit flow of coolant through the walls and over the surface of the particles; the space between the walls is tapered to maintain a substantially constant coolant velocity. The walls may be tubular and may define an annular space for the fuel particles. The inner and outer walls may be tapered so that the cross-sectional area of the space enclosed by the inner wall diminishes in the direction of coolant flow, while that of the annular space between the walls remains constant. The walls may take the form of flat plates. (UK)

12801 THERMOKINETICS OF THE FUEL ELEMENT CASETTE OF THE FAST REACTOR. Novotny, P.; Mantlik, F. (Inst. of Nuclear Research, Rez, Czech.). Jad. Energ.; 16: 397-408(Dec 1970). (In Czech).

The determination of hydrodynamic and temperature conditions in a fuel casette of a fast reactor is studied. The elements is of the form of a rod bundle arranged in a triangular lattice and mounted in a hexagonal casing. In the first part fundamental relations are formulated which are valid for a nominal calculation. The calculation method is based on following assumptions and simplifications; A stationary case is assumed and coolant flow through the fuel element is developed. The starting point is the given distribution of heat sources along the height and along the core diameter. Heat sources within the fuel casette and within individual fuel elements are assumed constant along the diameter. Temperature gradient in the axis direction is neglected, the temperature variations along the fuel element length, however, are accounted for. Temperature gradient along the fuel rod perimeter is also neglected. Fuel heat conductivity is assumed to be dependent on its temperature only. Coolant cross-mixing between cooling cells is not considered. The second part deals with the method of the determination of maximum cladding temperature with respect to possible deviations of the parameters from their nominal values. The numerical values of the total factor of uncertainty and of the maximum overheat possible are evaluated for the cladding of the fuel element type given. 9 references. (auth)

Auxiliary and Emergency Systems

12802 IMPROVEMENTS IN OR RELATING TO NUCLEAR REACTOR PLANT. Porter, William Hugh Lancelot (to United Kingdom Atomic Energy Authority). British Patent 1,214,459. 2 Dec 1970. Filed 16 May 1967.

Reference is made to means of containment in the event of a rupture in the pressurised coolant circuit of a reactor. It is common practice to provide a double containment system for this purpose, and in some cases a pond of water is provided in the interspace between the inner and outer containments, with a duct or lute communicating between the inner containment and the pond water. The disadvantages of such a system are described. In the system described a further condensing means is provided to condense steam or other vapour arising from the free surface of the pond. A water droplet disentrainment device may also be located above the pond surface. (UK)

Safety and Siting

12803 (BNWL-1457) NATURAL TRANSPORT EFFECTS ON FISSION PRODUCT BEHAVIOR IN THE CONTAINMENT SYSTEMS EXPERIMENT. Hilliard, R. K.; Coleman, L. F. (Battelle-Northwest, Richland, Wash. Pacific Northwest Lab.). Dec 1970. Contract AT(45-1)-1830. 184p. Dep. NTIS.

The results of six experiments in the 26,500 ft^3 Containment Systems Experiment (CSE) containment vessel are reported. In these tests, no active safety feature operated and all transport was by natural passive processes. The time dependence of iodine, methyl iodide, cesium, ruthenium, and uranium concentrations was measured at various locations in the vapor space and in the steam condensate. Parameters which were varied from test to test included the ratio of surface area to volume, temperature and pressure of the atmosphere, heat transfer rate to walls, paint age, and initial iodine concentration. Most of the tests were at steady temperature with steam feed to replace heat losses, but in one experiment the steam feed was zero and the temperature and pressure decreased with time. The results are compared with theoretical predictions with good agreement for iodine behavior and reasonable agreement for particulate materials when suitable particle sizes are used in predictive calculations. The initial rate controlling mechanism for elemental iodine is shown to be gas phase diffusion across boundary layers. For particles, gravitational settling dominated, with turbulent deposition and diffusiophoresis being of secondary importance. Whether the temperature and pressure were held constant or allowed to decrease with time had essentially no effect on the iodine behavior; but particle deposition was significantly slower in the temperature decay case. The best estimates of the 2-hr dose reduction factor (DRF) due to fission product removal by natural processes for large PWR containment systems are about 2.6 for inorganic iodine, 1.15 for particulate matter and 1.0 for methyl iodide. At longer times the estimates for DRF are considerably larger. 36 references. (auth)

12804 (ORNL-TM-3104) EVALUATION OF BURGESS FOBES PAINT COMPANY PROTECTIVE COATINGS FOR NUCLEAR PLANT APPLICATION. Row, T. H.; Griess, J. C. (Oak Ridge National Lab., Tenn.). Jan 1971. Contract W-7405-eng-26. 23p. Dep. NTIS.

Protective coatings on steel coupons supplied by the Burgess Fobes Paint Company were tested in a spray test loop facility. Coupons coated with the various protective coatings were exposed to a solution containing 2960 ppM boron with a pH of 9.5 under conditions that simulated the temperature and pressure transients of a design-basis accident. There were no observable failures of a number of the coatings, but those with a zinc-rich primer indicate the need for additional investigation because of their high failure rate. (auth)

12805 PROGRESS SUMMARY OF NUCLEAR SAFETY RESEARCH AND DEVELOPMENT PROJECTS. Savolainen, A. W.; Whetsel, H. B. (Comps. and Eds.). Nucl. Safety; 12: 42-55(Jan-Feb 1971).

12806 GENERAL ADMINISTRATIVE ACTIVITIES. Blakely, J. P. (Comp.). Nucl. Safety; 12: 56-8(Jan-Feb 1971).

12807 SAFETY-RELATED OCCURRENCES REPORTED IN AUGUST-SEPTEMBER 1970. Casto, W. R. (Comp.). Nucl. Safety; 12: 39-41(Jan-Feb 1971).

12808 PRESSURE DISTRIBUTION FOR AXISYMMETRIC TWO-DIMENSIONAL FLOW IN A PLENUM DURING COOLANT EXPULSION. Chawla, T. C.; Hoglund, B. M. (Argonne National Lab., Ill.); Nucl. Sci. Eng.; 43: 87-90(Jan 1971).

During coolant expulsion due to rapid fission gas release or due to the sudden vaporization of superheated coolant in the reactor fuel assembly, the transient times of the event are very short and the expulsion process is inertia dominated. Consequently, one must properly include the inertial contribution of the fluid in the

plenum to the expulsion process. With this in view, the above-mentioned inertial contribution of the fluid in the plenum is determined by assuming the flow in the plenum to be axisymmetric two dimensional. (auth)

Power Conversion Systems

12809 STUDIES FOR THE OPTIMUM DESIGN OF THERMODYNAMIC CYCLES OF HELIUM-COOLED HIGH-TEMPERATURE NUCLEAR POWER STATIONS. Wlezek, Camil (Technische Univ., Hanover). Atomkernenergie; 16: 311-22(1970). (In German).

In order to determine the best thermal efficiency of thermodynamic cycles for nuclear power stations with helium-cooled high-temperature reactors the one-cycle system, the two-cycle system, and the combined system were investigated depending on the properties and thermodynamic data of the reactor. Present and also future stages of development of high-temperature reactors with reactor outlet temperatures raised to 1000°C or 1100°C are included. 13 references. (auth)

12810 IMPROVEMENTS IN AND RELATING TO NUCLEAR REACTORS INCORPORATING STEAM RAISING UNITS. Bilsborough, Roy (to Nuclear Power Group Ltd.). British Patent 1,215,176. 9 Dec 1970. Filed 20 Nov 1968.

Reference is made to plants of the type in which the reactor and tubular steam raising units are housed in the same pressure vessel, which is usually of prestressed concrete construction. Where the steam is used to drive steam turbines using re-heat, banks of reheater tubes are included in the path of the coolant in order to reheat steam passing from one turbine to a lower pressure turbine. The tube banks and connecting pipes must be capable of withstanding the high velocity coolant flow and must be sufficiently flexible to permit differential thermal expansion. In the improved system described at least one steam reheater unit is in the form of a U-shaped bank of tubes, with the legs of the U vertical and connected to anchor points in the wall of the pressure vessel by vertical connecting tubes within the wall; the coolant is directed across the tubes in each leg in a generally horizontal direction. Where coolant flows vertically downward over the steam raising units the reheater banks may be arranged above the steam raising banks, or below where the coolant flows vertically upwards. In the former case anchorage is above the tube banks, and in the latter case below the tube banks. The steam raising units and the reheater are preferably arranged in vertical "pods" within the pressure vessel walls and the reheater bank is suspended vertically in the "pod" from anchor points in a removable concrete plug at the upper end of the "pod." The reheater unit may take the form of two or more banks of tubes disposed around the central axis of the "pod," and inlet and outlet connections for the steam raising units may pass between the units and through the plug. (UK)

12811 IMPROVEMENTS IN OR RELATING TO HEAT EXCHANGERS. Byran, J. A.; Evans, D. B. (to Babcock and Wilcox Ltd.). British Patent 1,214,993. 9 Dec 1970. Filed 9 Dec 1966.

In heat exchangers where the inlets and outlets of the tubes are at the same end, with the result that fluid flows generally in one direction in some tubes, in the reverse direction in other tubes, and from one tube to another through cross tubes, expansion problems may arise due to heating of the tubes to different temperatures. In the system described the ends of the tubes to which the cross tubes are connected can move relatively to each other during operation of the heat exchanger. The heat exchanger includes a helically wound tube length with means for maintaining predetermined spacings between the convolutions of the helix. A further tube length is connected in series with, and extends in the same general direction as, the helical tube length, and the ends of the tube lengths between the series connection are displaced laterally from each other. The series connection is effected by a cross tube which, at least for part of its length, is bowed and can flex to accommodate relative movement of the main tube ends. The helically wound tube lengths may be mounted so that the helices are disposed within one another on a common axis. The series connected tube lengths may be straight, or may lie within the helix, and the cross tube lengths may include a part lying on an arc of which the center is the axis of the helices. The cross tubes may include a further part lying radially with regard to the helix, and disposed between the arcuate portion and the further tube length. The arcs may be aligned with the outermost helix. The helically wound tube lengths, the further tube lengths and the cross tubes may lie between the inlet and outlet of a container, with baffles to form passages so that fluid by-passes the cross tubes. The heat exchanger described is intended especially for use in a gas-cooled reactor plant having a concrete pressure vessel, and the container may comprise a cavity in the wall of the pressure vessel. (UK)

Research and Test Reactors

Refer also to abstracts 10472, 10836, 11463, and 11533.

12812 (BNWL-1479) FAST FLUX TEST FACILITY CONTAINMENT SYSTEM ALARM AND TRIP CRITERIA (ATMOSPHERIC RADIOACTIVITY MEASUREMENT STUDY). Hendrickson, M. M.; Gustafson, V. W. (Battelle-Northwest, Richland, Wash. Pacific Northwest Lab.). Oct 1970. Contract AT(45-1)-2170. 31p. Dep. NTIS.

Potential radioactive releases within the various cells and containment vessel of the Fast Flux Test Facility have been reviewed and a basis has been selected for identifying radioactivity release rates which require containment action. Noble gases were selected as the control isotopes and alarm and ventilation containment trip levels determined on the basis of calculated estimates of the airborne activity at a control point approximately ¼ mile from the stack assuming all the activity has the characteristics of ^{41}Ar. Alarm and containment trip levels are 10^{-4} Ci/sec emission and 1.0 Ci/sec emission, respectively. An alarm level was chosen which would result in $\frac{1}{10}$ the yearly average permissible concentration at the control point, ¼ mile from the stack. If activity levels greater than the alarm level, up to the trip level, persisted for the period of up to 8 hours, a manual ventilation containment trip would be recommended. 9 references. (auth)

12813 (CEA-CONF-1673) IN-PILE LOOP BANJO. Lalere, J.; Rousseau, J. (Commissariat a l'Energie Atomique, Saclay (France). Centre d'Etudes Nucleaires). 30 Sep 1970. 22p. (In French). (CONF-701029-1). Dep. NTIS (U. S. Sales Only).

From Euratom Working Group on Irradiation Devices, Karlsruhe, Germany.

The Banjo loop is described; it consists of a liquid sodium loop and was designed for irradiation in OSIRIS of fuel pins intended to be used in fast neutron reactors. The loop will be placed in the pool around the reactor core in a zone where the thermal neutron flux is high (3.10^{14}) and where the heating is small (about 2W/gram). The loop allows several successive irradiations of pins which have or have not already been irradiated. Pins whose external diameters lie between 5 and 10 mm may be accepted without modifying the circuit. The fissile height may reach 600 mm. A total power of 70 Kw can be obtained. Three entirely independent controls allow the sodium input and output temperatures to be set at desired values. (France)

12814 (DOCKET-50184-24) NATIONAL BUREAU OF STANDARDS REACTOR. Inlet Filter Strainer Torn Loose. (National Bureau of Standards, Washington, D. C.). 14 Jan 1971. 2p. Dep. NTIS.

12815 (DUN-7149) OPERATING PROCEDURES: HANFORD TEST REACTOR. Brown, A. E. (Douglas United Nuclear, Inc., Richland, Wash.). 1 Jul 1970. 36p. Dep. NTIS.

A brief and up-to-date guide for the safe and efficient operation of the HTR is presented. Topics discussed include: fuel and material handling; emergency procedures; and special procedures and routine testing. (D.C.C.)

12816 (EACRP-L-74) PROPOSAL FOR A STANDARD SPECTRUM TO CHECK TECHNIQUES OF FAST NEUTRON SPECTRUM MEASUREMENTS. Kuechle, M.; Wattecamps, E. (Kernforschungszentrum, Karlsruhe (West Germany)). [nd]. 14p. (CONF-690225-1). Dep. NTIS (U. S. Sales Only).

From 11th EACRP Meeting, London, England.

In order to allow a cross check of neutron spectra measurements in fast critical assemblies, a standard assembly is proposed. The assembly composition which is concluded to be the optimum for a standard spectrum is U with a 10% average enrichment moderated with polyethylene so that the atomic ratio of H to U is 0.15. (H.D.R.)

12817 (EUR-4326) MEASURE OF THE FACTOR OF FAST FISSION "ϵ" IN A D_2O URANIUM LATTICE. Rustichelli, F.; Maracci, G. (European Atomic Energy Community, Ispra (Italy). Joint Nuclear Research Center). 1969. 52p. (In Italian). Dep. NTIS (U.S. Sales Only).

An analysis of the different definitions of the fast fission factor ϵ is first performed. Then the method of measurement used in the determination of the fast fission ratio δ^{28} in ORGEL heavy water natural U lattices is described. Such a method is based on the integral γ, counting of irradiated U detectors. A description is then given of the back-to-back fission chamber which has been built in

order to determine the calibration factor P(t). Finally the experimental values of δ^{28} obtained at different pitches are compared with the theoretical data of PINOCCHIO code; the agreement is satisfactory. The reported values for ϵ were calculated by using the OLDEKOP theory. 25 references. (auth)

12818 (FMRB–34/70) REACTIVITY MEASUREMENT IN REACTOR CORES ON MTR FUEL ELEMENTS WITH A ONE-SIDED HEAVY WATER REFLECTOR. Roethemeyer, H.; Hollnagel, R.; Wendt, W. (Physikalisch-Technische Bundesanstalt, Brunswick (West Germany)). Nov 1970. 54p. (In German). Dep. NTIS (U. S. Sales Only).

The FMRB is operated by two MTR-cores weakly coupled with a heavy water-tank. The reactivity parameters of the two uncoupled cores facing the tank are analyzed. They are determined by means of asymptotic period and pulsed source measurements. Results are given of extensive control rod calibrations and of the reactivity contribution of the heavy water tank. If the subcriticality is achieved by means of control rods the known effect of increasing reduced neutron generation time with increasing subcriticality is observed. But decreasing the heavy water level in the tank shows a decreasing neutron generation time with increasing subcriticality. Finally, the shutdown and excess reactivity of the coupled core configuration is discussed. The electronic apparatus used had been developed in view of the later use with coupled core experiments. This allows all measurements to be simultaneously performed with two detectors. The program PROVYM evaluates the pulsed source experiments accordingly. 24 references. (auth)

12819 (JAERI-Memo–4196) DETECTION OF FAILED FUEL AT JRR-4. Morozumi, Minoru (Japan Atomic Energy Research Inst., Tokyo). Nov 1970. 31p. (In Japanese). Dep. NTIS (U. S. Sales Only).

The Japan Research Reactor No. 4 (JRR-4) is a swimming pool type reactor using MTR type fuel elements. The reactor has a fuel failure detection (FFD) system consisting of delayed neutron detection. The system does not indicate the failed fuel element. The FFD's indication had gradually increased for the period between July 1968 and March 1969. The following tests were applied: flux-tilting method, sipping method for in-core fuels, and sipping method for a fuel held in the ruptured fuel test can. The failed fuel element was then identified. (auth) (Japan)

12820 (KFK–1255) CAN FAILURE–STEAM LOOP. Jacobi, S.; Rautenberg, I.; Beitner, H.; (and others) (Kernforschungszentrum, Karlsruhe (West Germany)). Aug 1970. 92p. (In German). Dep. NTIS (U. S. Sales Only).

The release of fission products and fuel particles from a failed reactor fuel element, their transport and detection in steam, their deposition and decontamination of circuit components, the corrosion resistance of reactor materials, and the behavior of failed fuel elements are important design parameters of steam cooled reactors. For experiments of this kind a superheated steam test loop has been installed at the FR 2 reactor at Karlsruhe. This loop consists of a steam generator unit, an in-pile test bed for accommodation of the fuel pins, and an expansion unit, condenser and low pressure section. The loop is controlled automatically and is run with indirect supervision. A two-out-of-three selection circuit actuates shutdown of the FR 2 reactor as soon as unsafe operating conditions are approached. 12 references. (auth)

12821 (LIB/Trans–335) TREATMENT OF WATER IN A NUCLEAR PLANT FOR THE TESTING OF FUEL ELEMENTS. di Pietro, R.; Gadda, F.; Ronchetti, C. (Centro Informazioni Studi Esperienze, Milan (Italy)). Translated by W. Buykx for Australian Atomic Energy Commission Research Establishment, Lucas Heights, from report CISE-N–137. 21p. Dep. NTIS (U. S. Sales Only).

The treatment of water in an experimental testing loop for nuclear fuel element components, such components being sensitive to the chemical-physical characteristics of the coolant, must be carried out according to such criteria as to guarantee conditions closely approaching reality. The nuclear reactor referred to is CIRENE; this is a prototype of 130 MW(t), direct cycle, which burns natural UO_2. This reactor is of the type moderated by cold heavy water and cooled by boiling light water under phase boundary conditions. The experimental loop CART for the testing of fuel elements for the CIRENE reactor, in which chemical tests on water were also carried out, is described. It was installed in the research reactor ESSOR at Ispra. (tr-auth)

12822 (NP–18499) SAFETY ENGINEERING CONSIDERATIONS ON THE ESTABLISHMENT OF A HEAVY WATER SYSTEM IN THE BRAUNSCHWEIG RESEARCH AND MEASUREMENT REACTOR AND ON THE OPERATION OF THE REACTOR WITH TWO CORES. May, J.; von Roenne, P.; Thein, W. (Technischer Ueberwachungs-Verein Hannover e. V. (West Germany)); Franzen, L. F.; Patzelt, A.; Ullrich, W. (Technischer Ueberwachungs-Verein e. V., Cologne (West Germany). Institut fuer Reaktorsicherheit). Jun 1969. 24p. (In German). Dep. NTIS (U. S. Sales Only).

The Braunschweig Research and Measurement Reactor has incorporated a heavy water system and a double core in the reactor. The safety of the reactor with these major changes was evaluated. The reactor physics data, mechanical and thermodynamic data, and radiation protection were considered. Specific proposals to improve the safety of the reactor operation were made. (J.S.R.)

12823 (RCN–125) POST-FAILURE EXAMINATION OF THE IN-PILE SECTION OF THE PRESSURIZED WATER LOOP IN THE H.F.R. AT PETTEN. van der Linde, A. (Reactor Centrum Nederland, Petten). Aug 1970. 67p. Dep. NTIS (U. S. Sales Only).

After 637 days in-core service the stainless steel in-pile section of a pressurized water loop failed. The loop was mounted in the H-5 and H-6 positions of the H.F.R. core at Petten. The U-shaped in-pile part was operated at a loop water temperature of 275 ± 5°C, a pressure of 140 kg/cm^2 and a water flow of 15 m^3/hr. The maximum fuel bundle power rating in each leg was 80 kW. Post failure examination of in-pile components in situ and after dismantling in the hot laboratory revealed that failure was most likely caused by H.F.R. water leakage, through a leak in an insulation pipe, into the space between the pressure tubes and their mantle pipes. This leaking insulating pipe, fabricated from AISI-347 material, was located 60 cm above the top of the H.F.R. core at a position where the inlet and outlet branches are connected with the vertical U-shaped section. Measurement of the room temperature tensile properties of specimens made out of the pressure tubes showed that alternate irradiation, up to 1.5.10^{21} nvt (>1 MeV) at 200–300°C and about 50°C results in a smaller increase in yield strength and decrease in total elongation than that encountered for comparable stainless steel which was irradiated continuously at 290°C up to the same fluence level. (auth)

12824 (STI/PUB–248) DIRECTORY OF NUCLEAR REACTORS. VOL. VIII. RESEARCH, TEST AND EXPERIMENTAL REACTORS. (International Atomic Energy Agency, Vienna (Austria)). 1970. 233p. IAEA $7.00.

Supplement to Vols, II, III, V, and VI.

The eighth volume of the IAEA's Directory of Nuclear Reactors is devoted to research, test and experimental reactors. It is a continuation of Volumes II, III, V and VI and, although primarily concerned with 57 new reactors, also contains revised data on power and flux levels of reactors already covered in the previous volumes. The individual data sheets are presented in a manner identical to that in Volumes II, III, V and VI. The first page gives general information, reactor physics data, and core and fuel element details. Subsequent pages provide: diagrams of the fuel element and sections of the reactor; information on core heat transfer, control, reactor vessel and overall dimensions, reflector and shielding, containment and cost estimate; a table of research and experimental facilities; a simplified diagram and data on fluid flow. The description of each reactor is concluded with a bibliography and remarks. For a reactor of a type already described in detail elsewhere in the Directory, a suitable cross-reference is made and only differences and modifications are given. For reactors with variable parameters only design values are stated and data subject to change are identified. (auth)

12825 ANALYSIS OF HETEROGENEITY AND SODIUM-VOID EFFECTS IN A 2700-LITER URANIUM CARBIDE FAST CORE, ZPR-6 ASSEMBLY 5. Karam, R. A.; Marshall, J. E.; Dance, K. D. (Argonne National Lab., Ill.). Nucl. Sci. Eng.; 43: 5-26(Jan 1971).

The heterogeneity and sodium void effects in ZPR-6 Assembly 5, a 2700-liter UC core, were analyzed using ENDF/B data. The cross-section sets used were generated for the homogeneous composition of this assembly, corrected for resonance spatial self-shielding in ^{238}U via equivalence theory, and weighted with the fine structure of the fluxes in the unit-cell. Bilinear weighting with the unit-cell fine structure of the real and adjoint fluxes was also performed. The calculated critical mass was 18% greater than the measured value. The calculated k_{eff} of the as-built system was 0.988. The calculated ratio of fission in ^{238}U to fission in ^{235}U was, depending on the loading pattern in the unit-cell, 13 to 26% less than the measured value. The calculated ratio of capture in ^{238}U to fission in ^{235}U was 7 to 10% greater than the measured value. The measured reactivity difference between a small homogeneous sample and another matched plate heterogeneous sample was a factor of 4 greater than the calculated value, indicating the analytical tools used for treating the heterogeneity effects were not adequate. The reactivity difference between homogeneous and rodded samples was nil. The calculated reactivity worths of ^{235}U samples are in a reasonable agreement with measurements. The predicted ^{238}U reactivity worth was 15 to 20%

XUM

greater than the measured value. The measured sodium-void coefficient was about 25% greater than the calculated value. The magnitude of this coefficient is quite sensitive to the particular loading pattern in the unit-cell and it is strongly dependent on the effective capture rates in ^{238}U. The dependence of the void coefficient on loading patterns is predictable in direction but not magnitude. The void coefficient in a rodded sample was the same as that in a plate heterogeneous sample. The void coefficient in a homogeneous sample was 56% greater than that in the rodded or the plate samples. (13 references) (auth)

12826 RELATIVE THERMAL NEUTRON FLUX DISTRIBUTION IN THE CORE OF THE RV-1 REACTOR. Mazur, Claude; David, Lubomir (Instituto Venezolano de Investigaciones Cientificas, Caracas). Acta Cient. Venez.; 21: 139-44(1970). (In Spanish).

The results of measurements of the relative thermal neutron flux distribution in the core of the RV-1 reactor are presented. Axial and radial flux mapping were carried out over the whole 5 × 7 fuel element array at 100 kW power level using the Co-Al wire activation techniques. The activity of the in-core irradiated wires was measured by counting gamma rays that result from radioactive decay of ^{60}Co. Included is also a description of the experimental conditions and the semi-automatic scanning equipment. The results are given in the form of curves. 14 references. (auth)

12827 CONSIDERATIONS ON PULSED REACTOR OPTIMIZATION. Asaoka, T.; Larrimore, J. A. (EURATOM-CCR, Ispra, Italy). J. Nucl. Energy, 24: 439-72(Dec 1970).

An overall figure-of-merit is proposed as a basis for optimization of pulsed reactors and accelerator pulsed reactors, as low energy pulsed neutron sources for beam experiments using time-of-flight methods. This figure-of-merit contains the fast neutron source and the moderator characteristics almost independently of each other which facilitates its application. A moderator optimization study in terms of the figure-of-merit is carried out using the j_N method, which is a simple but accurate analytic approach to neutron transport in a finite system. The calculations are performed in the j_1 approximation with seven energy groups (one thermal group) to obtain the thermal neutron yield leaking from a hydrogenous moderator slab, and the variance of the leakage time distribution. Parameters studied are moderator thickness and material, lateral leakage, input source characteristics and homogeneous poisoning. The figure-of-merit peaks at a moderator thickness between 3 and 4.5 cm for all cases considered. The effects of reactor core parameters on the figure-of-merit are also considered through comparison of the IBR and SORA reactors. (auth)

12828 BUCKLING AND FINE STRUCTURE MEASUREMENTS IN THE HELEN I FACILITY. Dodd, B. (Queen Mary Coll., London). Nucl. Energy; 11: 175-81(Nov-Dec 1970).

The short experimental program described was carried out on the HELEN I subcritical facility with the aim of illustrating some of the basic experimental techniques used in buckling and fine structure measurements. These types of measurement are performed with the aim of checking the performance of calculation methods used to predict the nuclear behavior of power reactors, and in the present case a preliminary comparison of the experimental results is made with some straightforward core calculations. (auth) (UK)

12829 OPTIMUM DIMENSIONS OF THE OPERATIONAL VOLUMES OF RADIATION CIRCUIT JOINTS. Sakharov, E. S.; Chuchalin, I. P. At. Energ. (USSR); 29: 125-7(Aug 1970). (In Russian).

The optimum size of irradiation positions in a reactor is studied in relation to attaining the highest specific activity of the target samples. Equations are developed for calculating the activation of the target in relation to the target size, the neutron flux spectra, and the properties of the surrounding medium. Measurements in the water reflector of an IRT type reactor using indium targets of various thicknesses and the calculated values were used to construct a nomogram for deriving optimum target thickness and maximum specific activity as a function of irradiation position volume in water, beryllium, and graphite. (H.D.R.)

12830 POSITIVE REACTIVITY FROM REPLACEMENT OF HEAVY WATER BY LIGHT WATER IN THE COOLANT CHANNELS OF A HEAVY-WATER-MODERATED REACTOR. Talboy, James H.; Donahue, Edward J.; Pierce, Albert W.; Vronich, John J. (Argonne National Lab., Ill.). Nucl. Sci. Eng.; 43: 227-9(Feb 1971).

A reactivity increase caused by introducing ordinary water into a fuel assembly coolant channel has been measured using the CP-5 reactor at Argonne National Laboratory. This reactor uses 17 cylindrical fuel assemblies arranged on a 6-in. triangular pitch in a tank of heavy water, which is used as both a moderator and a coolant. Fuel enrichment in ^{235}U is nominally 93%. A special fuel assembly was constructed for this investigation. Reactivity change effects are listed. (auth)

Rocket and Space Reactors

12831 IMPROVEMENTS IN AIRCRAFT NUCLEAR PROPULSION SYSTEM HAVING AN ALTERNATIVE POWER SOURCE. (to General Electric Co.). British Patent 1,215,499. 9 Dec 1970. Priority date 18 Sep 1967, United States.

REACTORS, AIRCRAFT—description of fuselage mounted, with wing mounted propulsion units and auxiliary gas turbine systems

12832 IMPROVEMENTS IN NUCLEAR POWER PLANT SUITABLE FOR USE IN AIRCRAFT PROPULSION SYSTEMS. (to General Electric Co.). British Patent 1,214,892. 9 Dec 1970. Priority date 18 Sep 1967, United States.

REACTORS, AIRCRAFT—description of fuselage mounted, with wing mounted propulsion units

12833 PREDICTED COOLANT HEAT TRANSFER AND FRICTION COMPARED WITH NUCLEAR ROCKET TEST RESULTS. Taylor, Maynard F. (Lewis Research Center, Cleveland). J. Spacecraft Rockets; 7: 1472-5(Dec 1970).

Correlation equations are brought together and used to revise the coolant side calculations in an existing digital computer program for design and evaluation of convectively cooled rocket nozzles. Gas-side wall temperature, coolant pressure drop, and coolant temperature rise predicted by this revised code are compared with measured values from several NERVA nuclear tests. Wall temperatures were not measured in Phoebus 2 and Pewee nuclear tests, so that only measured coolant temperature rise and pressure drop are compared with predictions. It should be noted that, although Pewee, NERVA, and Phoebus 2 vary a great deal in size and power, their nozzles have similar geometry; these calculation procedures should be compared with experiments for other geometries when available. 12 references. (auth)

12834 GAS-CORE NUCLEAR ROCKET ENGINE TECHNOLOGY STATUS. McLafferty, George H. (United Aircraft Research Labs., East Hartford, Conn.). J. Spacecraft Rockets; 7: 1391-6(Dec 1970).

A review is presented of the status of research on the nuclear light bulb and coaxial-flow gaseous-core nuclear rocket engines. Both proposed engines are based on the transfer of energy by thermal radiation from gaseous nuclear fuel to seeded hydrogen propellant. Reference configurations for both engines are calculated to provide a specific impulse of ~1800 sec and a thrust-to-weight ratio of ~1.4. Two recently investigated flow configurations show promise of improving the containment of the gaseous nuclear fuel in a coaxial-flow engine. These configurations involve the use of foam inlets at the gas entrance to reduce the turbulence in the flow, and the use of a spherical, rather than a cylindrical, cavity. Substantial progress has been made in simulating the thermal environment of a nuclear light bulb engine during tests employing rf induction-heated and arc-heated plasmas. During one rf test, 85% of the energy deposited in the plasma was emitted as thermal radiation with a radiant flux of 48 kw/in.^{2}. This flux is slightly greater than the radiant flux at the surface of the sun, and is 20 times that which has been obtained from any other rf tests. Initial low-power arc tests have resulted in heating of seeded simulated propellant by thermal radiation to a temperature of ~2200°R. 21 references. (auth)

12835 NUCLEAR ROCKET EXPERIMENTAL ENGINE TEST RESULTS. Durkee, W. E.; Damerval, F. B. (Aerojet Nuclear Systems Co., Sacramento, Calif.). J. Spacecraft Rockets; 7: 1397-1402(Dec 1970).

An extensive series of tests of a nuclear rocket experimental engine, XE-Prime, were completed in 1969. The main emphasis of the series was upon characteristics of starting from various conditions and upon operation of the test facility under nuclear firing conditions; however, engine performance at full power and throttled pressure were also investigated. Selected startup test results are compared with predictions made by computer simulation of the test system. Full-power and high-specific-impulse operations are described. Representative startup data are presented for automatic temperature startups performed with initial levels of 0.1 and 2.7 MW, initial core temperatures of approximately 250° and 1250°R, and drum exponential set points of +11° and −8.5° from critical. The test results showed that startup can be controlled over a wide range of initial conditions. (auth)

Marine and Portable Power Reactors

12836 NUCLEAR SHIP PROPULSION. Pocock, R. F. London; Ian Allan (1970). 176p. 50s.

The subject is considered under the following headings: atomic bombs and power reactors, the atomic submarine and Admiral Rickover, the British reactor program, the world's nuclear fleets, the NS "Savannah," nuclear merchant shipping in the UK, development of the marine reactor, submarine operations in the arctic ocean, the "Thresher" disaster, progress towards the nuclear merchant ship, present trends and future prospects. (UK)

Reactor Theory

12837 (RISO-M-1279) FORTRAN IV VERSION OF THE SUM-OF-EXPONENTIAL LEAST-SQUARES CODE EXPOSUM. Kirkegaard, Peter (Danish Atomic Energy Commission, Risoe, Research Establishment). Sep 1970. 57p. Dep. NTIS (U. S. Sales Only).

An improved version of the computer program AEK P-513 EXPOSUM is described. The program carries out a least-squares fitting of the parameters in a sum-of-exponentials to given table values. The new EXPOSUM code is written in FORTRAN IV and replaces the old GIER-ALGOL III version. 13 references. (auth) (Denmark)

12838 COARSE MESH ACCELERATION OF ITERATIVE SOLUTION OF NEUTRON DIFFUSION EQUATION. Nakamura, Shoichiro (Ohio State Univ., Columbus). Nucl. Sci. Eng.; 43: 116-20(Jan 1971).

Modified pyramid functions were previously used to formulate rebalancing functions to accelerate the iterations of neutron diffusion equations. Numerical studies show this method to be quite effective when it is applied to the outer iterations of multidimensional diffusion codes. The same method should be effective in reducing the number of inner iterations as well. However, the advantage of the reduced number of inner iterations may be lost because of the longer computer time for one coarse mesh procedure compared with that for one inner iteration. In fact, the use of the modified pyramid functions requires more computer time than does the disjunctive partitioning method, mainly due to the multiple overlapping of the pyramid functions. The previous method is reformulated by combining the simple aspect of the disjunctive partitioning method with the advantage of using the modified pyramid functions. (auth)

12839 DETERMINING COLLISION VARIANCES FROM ADJOINTS. Amster, Harvey (Univ. of California, Berkeley). Nucl. Sci. Eng.; 43: 114-16(Jan 1971).

A method is presented for estimating statistical errors in Monte Carlo calculations of neutron collision histories. The method is based on a derivation of the adjoint equation for the mean number of collisions per history and then generalizing the procedure for larger collision numbers. (H.D.R.)

12840 FAST METHOD OF COMPUTING THE CONTRIBUTION FROM INTERFERENCE SCATTERING OF NEUTRONS TO THE INTEGRAL $J(\theta, \alpha, \beta)$. Wasastjerna, Frej (Technical Univ. of Helsinki, Otaniemi, Finland). Nucl. Sci. Eng.; 43: 106-8(Jan 1971).

A method of computing the resonance integral $J(\theta, \alpha, \beta)$ in the form $J(\theta, \alpha, \beta) = J(\theta, 0, \beta) + R$ is proposed. The method is based on a series approximation of R that is both fast and accurate to within a few percent. (H.D.R.)

Kinetics

Refer also to abstracts 12772, 12774, and 12780.

12841 (IAE-1938) MULTIGROUP DESIGN OF UNIDIMENSIONAL NUCLEAR REACTORS WITHOUT USE OF GRID METHOD. Gluchkov, E. S. ([Gosudarstvennyi Komitet po Ispol'zovaniyu Atomnoi Energii SSSR] Moscow. Institut Atomnoi Energii). 1969. 40p. (In Russian). Dep. NTIS (U. S. Sales Only).

A technique is presented for solving the unidimensional multigroup reactor equations, based on an analytical solution to the diffusion type of equations with the right-hand part being known. On the basis of this procedure, an algorithm (subroutine) was developed, the formulas and relationships needed for the calculation were written, and a block-diagram for the computer program is given. Results are adduced for the calculations based on the given technique as compared with the results obtained from the calculations using the grid method; the results shown substantiate the effectiveness of the method proposed. (tr-auth) (JPRS)

12842 (INR-1193) BIGG CODE IN GIER-ALGOL 4 FOR THE GIER COMPUTER. Kulikowska, T. (Institute of Nuclear Research, Warsaw (Poland)). 1970. 65p. (In Polish and English). Dep. NTIS (U. S. Sales Only).

BIGG is a multigroup spectral code solving the Bi equations for a bare slab reactor with slowing down described by Grueling-Goertzel approach. The program works together with a 40 group library. The present version of the code is based on the BIGG II code written in FORTRAN for the CDC-3600 computer. A short scope of the algorithm applied and the users manual including the program listing are given. (5 references) (auth)

12843 (INR-1206) VOLTERRA FUNCTIONAL SERIES FOR REACTORS WITH LINEAR FEEDBACK. Kielkiewicz, M. (Institute of Nuclear Research, Warsaw (Poland)). 1970. 9p. Dep. NTIS (U. S. Sales Only).

The Volterra kernels for the general case of a reactor with delayed neutrons and a linear absolutely integrable reactivity feedback were determined. The convergence of the Volterra functional series was investigated. (auth)

12844 (TKK-F-A-121) SYNTH2: A TWO DIMENSIONAL MULTIGROUP FLUX SYNTHESIS CALCULATION CODE. Salo, Seppo (Technical Univ. of Helsinki, Otaniemi (Finalnd). Dept. of Technical Physics). 11 Aug 1970. 44p. Dep. NTIS (U. S. Sales Only).

SYNTH2, an IBM S/360 Fortran IVG program, is described. SYNTH2 is a two-dimensional multigroup flux synthesis calculation code. It synthesizes, by using diffusion theory, a two-dimensional (r,z) neutron flux distribution from given one-dimensional (r) flux distributions. The synthesis techniques used are based on the formulation of J. B. Yasinsky and S. Kaplan. (auth) (Finland)

12845 BOUNDED POSITIVE SOLUTIONS OF NUCLEAR REACTOR KINETICS EQUATIONS. Kielkiewicz, M. (Technical Univ., Warsaw). Bull. Acad. Pol. Sci., Ser. Sci. Tech.; 18: 655-8 (1970).

Existence of bounded positive solutions of nuclear reactor kinetics equations is investigated. A nuclear reactor with Newton's law of cooling model and one group of delayed neutrons is analyzed. (auth)

12846 PERIODIC POSITIVE SOLUTIONS OF NUCLEAR REACTOR KINETICS EQUATIONS. Kielkiewicz, M. (Technical Univ., Warsaw). Bull Acad. Pol. Sci., Ser. Sci. Tech.; 18: 659-65(1970).

Existence of positive periodic solutions of nuclear reactor kinetics equations is investigated. A nuclear reactor with xenon feedback and without delayed neutrons is considered. 5 references. (auth)

12847 SUPPLEMENTS TO THE THEORY OF SWELLING. Matthies, S. (Zentralinstitut fuer Kernforschung, Rossendorf, Ger.). Kernenergie; 13: 320-4(Oct 1970). (In German).

Within the scope of Barnes' swelling model description (bubble fusion by collision) generalized by August by taking fission gas bubble spectrum into account, the asymptotic time behavior of swelling and of other quantities of physical interest is exactly derived as an analytical function and discussed. An equation is given for determination of asymptotic bubble spectrum. 3 references. (auth)

12848 PROBLEMS OF PERSISTING MODE TIME CONSTANT IN MONTE CARLO CALCULATIONS. Barz, H. U. (Zentralinstitut fuer Kernforschung, Rossendorf, Ger.). Kernenergie; 13: 316-19(Oct 1970).

A reformulation of the concept of persisting solution time constant α proper for Monte Carlo calculation is given. Approximations of α according to statistical averages of stationary systems are given. A calculation procedure is proposed based on a static Monte Carlo calculation in which the estimation of average times and squares of times is included. 7 references. (auth)

12849 CALCULATION OF K_{eff} FOR A BARE Pu SPHERE BY COLLISION PROBABILITY METHOD. Navalkar, M. P.; Iyengar, S. B. D. (Bhabha Atomic Research Center, Trombay, India). Atomkernenergie; 16: 303-5(1970).

The method of calculation of k_{eff} for a Pu sphere based on the collision probability method is presented. The effect of density variation (studied experimentally by changing temperature) and of the concentration and nature of impurities can also be taken into account in the calculations. 4 references. (auth)

XUM

12850 EFFECT OF RANDOM AMPLITUDES AND PHASES OF VIBRATING FUEL ELEMENTS UPON MULTIGROUP NEUTRON LATTICE PARAMETERS. Barrett, P. R. (Univ. of New South Wales, Sydney). Atomkernenergie; 16: 285-90(1970).

The effect of the randomness of fuel element vibrations upon spatially averaged homogenized lattice multigroup cross sections is calculated. The theory is restricted to arrays of fuel rods or widely spaced plates for which it is a sufficient approximation to assume that the random components of the vibration of a fuel element are statistically uncorrelated with those of any other fuel element. It is assumed that the fuel elements are vibrating at a frequency close to that of their fundamental mode but with an amplitude of vibration that is Gaussian distributed, with a randomly distributed initial phase of oscillation and, in the case of fuel rods, with a randomly distributed direction of oscillation. It is shown that the effect of the random components of the vibrations is to increase the fuel-to-fuel first flight neutron collision probability owing to the increased fuel element interaction effect for neutrons of any energy. 6 references. (auth)

12851 TRANSPORT PROPERTIES OF CAVITIES. Breitenhuber, L. (Institut fuer Kernphysik, Graz). Atomkernenergie; 16: 270-2(1970).

It is shown that for homogeneous infinite systems a cavity of arbitrary shape has no influence on the differential flux and its adjoint inside and outside the cavity. Hence, this applies also to the scalar flux and its adjoint as well. No assumption about weak absorption is necessary. The approximate validity for small cavities in finite regions (and channels as regards the scalar flux) is discussed. Numerical examples illustrate the general theorem. 4 references. (auth)

12852 REDUCTION OF THE RAY EFFECT IN DISCRETE ORDINATES CALCULATIONS. Sullivan, Robert E. (Lewis Research Center, Cleveland); Albers, Lynn U.; Yu, Dahsoong. Nucl. Sci. Eng.; 43: 108-14(Jan 1971).

A method for reducing the ray effect based on separation of the characteristic directions used in the discrete ordinates angular quadratures is presented. For some types of problems, the procedure is capable of yielding more accurate results from a given number of directions without significantly increasing the computation time. (8 references) (H.D.R.)

12853 PHASE-SPACE REDUCTION IN NEUTRON DIFFUSION CALCULATIONS. Harms, A. A.; Babb, A. L. (Univ. of Washington, Seattle). Nucl. Sci. Eng.; 43: 66-73(Jan 1971).

A method of analysis associated with the specification of optimal energy-group and space-interval structures in neutron diffusion calculations is presented. Initially, an extremal algorithm is formulated to minimize the integrated error between two arbitrary piecewise-constant functions of two variables. The minimization is attained by steepest descent in piecewise-constant, non-convex, multidimensional phase-space. It is found that given an initial reference neutron diffusion calculation, the extremal algorithm may be effectively used to specify a reduced energy-group structure and/or a reduced space-interval structure such that the error in the effective multiplication constant is minimized. The extremal-nodal analysis discussed appears to be particularly useful for repetitious nuclear reactor calculations which seek to maximize numerical accuracy and minimize computer execution time. (13 references) (auth)

12854 MULTIPLE WEIGHTING FUNCTIONS IN FAST REACTOR SPACE-ENERGY SYNTHESIS. Neuhold, R. J. (Babcock and Wilcox Co., Lynchburg, Va.). Nucl. Sci. Eng.; 43: 74-86(Jan 1971).

The weighted residual procedure was used to expand the fast reactor space-energy synthesis approach to include multiple (discontinuous) weighting functions with continuous trial functions. In the past (except for discontinuous trial function applications) the number of weighting functions was chosen equal to the number of trial functions, and all region and current residuals were weighted with the same set of weights. In the present procedure the region residuals are weighted with region reaction rates, and the current boundary conditions are weighted with a boundary "reaction rate." Numerical results are presented for a typical two-region (core and blanket) fast reactor in which multiple reaction rate weighting and a special use of reaction rate weighting are compared with previously used fast reactor space-energy synthesis weighting forms. The results, based on using realistic trial functions, show that multiple reaction rate weighting is generally better than Galerkin or reaction rate weighting, and approaches or exceeds the accuracy of adjoint weighting for the cases examined. Although the group balance or weighted group balance weighting is improved with an application of reaction rate weighting, preliminary results based on an extension of the two techniques to multiple reaction rate weighted group balance were not encouraging. Applications of various weighting functions using poor trial functions show the necessity of realistic trial spectra if weighting functions are to be improved. Multiple reaction rate weighting maintains the "easy to use" feature of Galerkin weighting with considerable potential for multiregion error reduction. (39 references) (auth)

12855 SOLUTION OF THE ONE-DIMENSIONAL, MULTI-ZONE, MULTI-GROUP DIFFUSION EQUATION USING THE LIE SERIES METHOD. Lemanska, Miriam (Soreq Nuclear Research Centre, Yavne, Israel). J. Nucl. Energy; 24: 431-8 (Dec 1970).

The one-dimensional G-group diffusion equation for the multizone reactor is solved using the Lie series technique. The flux vector at any point of the arbitrary zone z of the reactor is given by the $G \times G$ transfer matrix multiplied by the flux vector at the origin. This matrix is a product of the transfer matrices of the first z zones. It is presented explicitly for each geometry separately; for slab and sphere with the help of the trigonometric functions, for cylinder with the help of the Bessel functions, whose arguments are matrices. The critical equations are derived and compared with the corresponding ones in the monoenergetic reactor theory. The critical sizes of several reactors in spherical geometry are calculated using the corresponding critical equation. (auth)

12856 RELATIONSHIPS BETWEEN VARIOUS DEFINITIONS OF PROMPT-NEUTRON LIFETIME. Nelson, Paul Jr. (Oak Ridge National Lab., Tenn.). Nucl. Sci. Eng.; 43: 154-8(Feb 1971).

The mean time to destruction of a neutron is shown to be equal to the reciprocal unity-weighted loss rate for a general neutron transport problem. The mean production time and reciprocal importance-weighted loss rate are shown to be similar, but slightly different. The results are illustrated for a simple model problem. (auth)

12857 ENERGY-DEPENDENT NEUTRON TRANSPORT THEORY IN ADJACENT HALF-SPACES. Jauho, Pekka; Rajamaeki, Markku (Technical Univ. of Helsinki, Otaniemi, Finland). Nucl. Sci. Eng.; 43: 145-53(Feb 1971).

The solutions to the one-dimensional energy-dependent Boltzmann equations for two different media are shown to possess such a full-range completeness property that an arbitrary function satisfying a Hölder condition can be expanded in terms containing solutions to both equations. These solutions are given by Leonard and Ferziger. This property makes it possible to solve energy-dependent neutron transport problems for two adjacent media. In comparison with half-space problems, one must solve two more inhomogeneous Fredholm integral equations. The scheme of the extension to multilayer system is also represented. In using the multigroup method, the series solutions of the Fredholm equations are rapidly convergent, if the energy dependences of the total cross sections in both adjacent media are roughly of the same form. (auth)

12858 VARIATIONAL DERIVATION OF DISCRETE ORDINATE-LIKE APPROXIMATIONS. Natelson, M. (Westinghouse Electric Corp., West Mifflin, Pa.). Nucl. Sci. Eng.; 43: 131-44(Feb 1971).

The derivation of discrete ordinate and discrete ordinate-like approximations from variational principles for the one-speed transport equation is explored. Standard discrete ordinate approximations are derived from a first-order stationary variational principle. The derivation yields a prescription for ordinates to be used given a selection of weights. Resultant quadrature schemes are compared numerically with those in common use. These new schemes derived using the weights of S_N quadratures do not show significant variations in performance from the parent S_N schemes. A new "modified" discrete ordinate approximation, MD_N, is found by applying the same techniques as in the derivation of the standard approximation, this time, however, using an extremum second-order variational principle. The new approximation is compared through several numerical examples with standard discrete ordinate, simplified P_N, and standard P_N approximations. The MD_N results do show a mitigation of the ray effects associated with standard discrete ordinate calculations (D_N), but for gross region-wise absorption rates its accuracy for low orders is more like that of simplified P_N rather than of P_N or D_N approximations. It is concluded that a low-order MD_N approximation should not be a candidate to replace diffusion theory. The approximation may, however, have some application as a calculational standard. (auth)

Experimental Applications

12859 MONTE CARLO CALCULATION OF THE THERMAL NEUTRON ACTIVATION IN LIGHT-WATER-MODERATED URANIUM CELLS USING ENDF/B CROSS-SECTION DATA. Volpe, John J.; Baer, William (Westinghouse Electric Corp., West Mifflin, Pa.). Nucl. Sci. Eng.; 43: 105-6(Jan 1971).

Experimental and Monte Carlo calculated thermal cell activations are compared for water moderated natural uranium fuel lattices. The thermal activation disadvantage factors of ^{164}Dy, ^{176}Lu, and ^{239}Pu and the thermal spectral indices in the fuel and moderator regions are tabulated. (H.D.R.)

12860 CONSISTENT CRITICALITY ESTIMATES IN PULSED NEUTRON EXPERIMENTS. Harms, A. A. (McMaster Univ., Hamilton, Ont.). Nucl. Sci. Eng.; 43: 122-4(Jan 1971).

An algebraic procedure is proposed for the selection of a time interval for fitting detector response in a pulsed neutron experiment to the fundamental-mode decay process. The procedure is amenable to computer operation and ensures objective consistency for comparative criticality analyses of pulsed systems. (H.D.R.)

12861 PULSED DETERMINATION OF CONSTANTS OF NEUTRON DIFFUSION INTO HETEROGENEOUS WATER LATTICES. Khristov, V. (Inst. of Physics, Sofia). Compt. Rend. Acad. Bulg. Sci.; 23: 667-9(1970). (In Russian).

Pulsed experiments were made with one of the horizontal beams of the IRT reactor in Sophia. Neutron pulses were obtained by means of a fast mechanical selector of the "Agnes" type. A steel selector rotor operating at 6000 rotations per minute produced rectangular shape pulses of 160 microseconds duration. Statistical data during 1500 kW reactor operations for 5 to 8 hours for the lattice with R = 0.5 cm show diffusion elongations $D||D_0$ = 1.489 and $D\perp D_0$ = 1.264, which are lower than the data calculated by the Behrens theory (1.587 and 1.384). The anisotropic factor $D||D_\perp$ = 1.178 was in good agreement with the magnitudes calculated by Stepanov formulas, 1.181. The lattices were also studied using the poison method. 8 references. (R.V.J.)

Reactor Components, Fuels, and Accessories

Refer also to abstracts 10571, 10753, 10768, 10773, 10794, 11366, 11368, 11457, 11470, 11474, 11475, 11478, 11485, 11532, and 11534.

12862 (JAERI-Memo-4192) IRRADIATION TESTS OF DOMESTIC ZIRCALOY-2 CLADDING MATERIALS IN JPDR. Nomura, Sueo; Ito, Noboru; Honma, Kenzo (Japan Atomic Energy Research Inst., Tokyo). Nov 1970. 20p. (In Japanese). Dep. NTIS (U. S. Sales Only).

In order to perform surveillance tests of Zircaloy-2 fuel cladding material, three types of Zircaloy-2 sample coupons for corrosion, tensile, and Charpy impact tests were inserted into the three positions of different neutron flux in the JPDR. The coupons were removed after one year, then mechanical tests and corrosion examination were conducted. Corrosion of irradiated samples was accelerated with increase of neutron dose. Results of tensile tests indicated increases of ultimate and yield strengths and a decrease of total elongation with increase of neutron exposure. No clear conclusion was obtained on the effects of neutron irradiation on impact properties. The results of induced activity measurement and γ-ray spectrometric analysis of coupons and crud are also presented. (auth) (Japan)

12863 HERMETICALLY-SEALED THROUGH-PASSAGE ASSEMBLY FOR TRANSMITTING MOTION THROUGH A NUCLEAR REACTOR VESSEL WALL. Cavy, Claude; Rouge, Pierre; Tissot, Roland (to Commissariat a l'Energie Atomique). British Patent 1,215,960. 16 Dec 1970. Priority date 11 Dec 1967, France.

PRESSURE VESSELS—penetrations in reactor, description of hermetically sealed drive shaft assembly for
REACTORS—pressure vessel penetrations for, description of hermetically sealed drive shaft assembly for
SEALS AND GLANDS—description of reactor pressure vessel penetration hermetic, for drive shaft assembly (D.C.C.)

XUM

GENERAL

12864 (ANL–7725) TRAINING MANUAL FOR FABRICATION OF PRINTED-CIRCUIT BOARDS. Nelson, C. A.; Yannitell, T. W.; Rudnick, S. J. (Argonne National Lab., Ill.). Jul 1970. Contract W-31-109-eng-38. 28p. Dep. NTIS.

12865 (ANL–Trans–873) COULOMETRIC TITRATIONS FOR THE DETERMINATION OF THE HOMOGENEITY REGION OF SOLID SILVER SULFIDE, SILVER SELENIDE, AND SILVER TELLURIDE. Valverde, Nilo. Translated for Argonne National Lab., Ill., from Z. Phys. Chem. (Frankfort); 70: 113-27(1970). 14p. Dep. NTIS.

12866 (BDX–613–198) SPLIT FIBERGLASS HOLDER. Darbyshire, H. F. (Bendix Corp., Kansas City, Mo.). Aug 1970. Contract AT(29-1)-613. 17p. Dep. NTIS.

12867 (BDX–613–213) DESIGN OF AN INSULATOR WHICH MUST SURVIVE HIGH g-FORCES. Guzzo, V. J.; Thorne, L. F. (Bendix Corp., Kansas City, Mo.). Jun 1970. 39p. Dep. NTIS.

12868 (BMI–171–101) SEA OTTER NATURAL MORTALITY AT AMCHITKA ISLAND, ALASKA. Annual Progress Report, February 20, 1968–June 20, 1968. Ailton, Wayne H. (Battelle Memorial Inst., Columbus, Ohio). Jul 1968. Contract AT(26-1)-171. 5p. Dep. NTIS.

12869 (BMI–171–102) STUDIES OF THE AVIFAUNA ON AMCHITKA ISLAND, ALASKA. Annual Progress Report, August 14, 1967–June 9, 1968. Williamson, Francis S. L. (Johns Hopkins Univ., Baltimore, Md. Dept. of Pathobiology). Jul 1968. Contract AT(26-1)-171. 53p. Dep. NTIS.
For Battelle Memorial Inst., Columbus, Ohio.

12870 (BMI–171–103) THE FRESHWATER ECOLOGY OF AMCHITKA ISLAND. Annual Progress Report. Koob, Derry D. (Ohio State Univ., Columbus). Jul 1968. Contract AT(26-1)-171. 70p. Dep. NTIS.
For Battelle Memorial Inst., Columbus, Ohio.

12871 (BMI–171–104) FRESHWATER VERTEBRATE AND INVERTEBRATE ECOLOGY OF AMCHITKA ISLAND. Annual Progress Report, August 30, 1967–June 30, 1968. Neuhold, John M.;Helm, William T. (Utah State Univ., Logan). Jul 1968. Contract AT(26-1)-171. 60p. Dep. NTIS.
For Battelle Memorial Inst., Columbus, Ohio.

12872 (BMI–171–105) REVEGETATION OF DISTURBED AREAS OF AMCHITKA ISLAND. Annual Progress Report. Kazmaier, H. E. (Battelle Memorial Inst., Columbus, Ohio). 22 Jul 1968. Contract AT(26-1)-171. 34p. Dep. NTIS.

12873 (BMI–171–106) GEOMORPHOLOGY AND PEDOLOGY OF AMCHITKA ISLAND. Annual Progress Report. Everett, K. R. (Ohio State Univ., Columbus). Jun 1968. Contract AT-(26-1)-171. 82p. Dep. NTIS.
For Battelle Memorial Inst., Columbus, Ohio.

12874 (BMI–171–107) PLANT ECOLOGY OF AMCHITKA ISLAND, ALASKA. Annual Progress Report, August 1, 1967–June 30, 1968. Clebsch, Edward E. C. (Tennessee Univ., Knoxville, Dept. of Botany). Jul 1968. Contract AT(26-1)-171. 21p. Dep. NTIS.
For Battelle Memorial Inst., Columbus, Ohio.

12875 (BMI–171–108) A FEASIBILITY TEST TO DETERMINE THE AMCHITKA SEA OTTER POPULATION THROUGH PHOTOGRAMMETRIC TECHNIQUES. Annual Progress Report. Stephan, Joachim G. (Battelle Memorial Inst., Columbus, Ohio). 26 Jul 1968. Contract AT(26-1)-171. 30p. Dep. NTIS.

12876 (BMI–171–111) EFFECTS OF UNDERWATER OVERPRESSURES ON THE SEA OTTER AND ITS PRINCIPAL FOOD SPECIES. Annual Progress Report. Wright, Ronald A. (Battelle Memorial Inst., Columbus, Ohio). 31 Jul 1968. Contract AT(26-1)-171. 30p. Dep. NTIS.

12877 (BMI–171–114) RESEARCH PROGRAM ON MARINE ECOLOGY AND OCEANOGRAPHY, AMCHITKA. Annual Progress Report, July 1, 1967–June 30, 1968. Burgner, Robert L.; (and others) (Washington Univ., Seattle. Coll. of Fisheries). 13 Sep 1968. Contract AT(26-1)-171. 79p. Dep. NTIS.
For Battelle Memorial Inst., Columbus, Ohio.

12878 (BNWL–1469) TRANSFORMATION (ANALYZER) DEVICE USING POST-DETECTOR SIGNAL PATTERN ROTATORS FOR MULTIPARAMETER EDDY CURRENT TESTER. Libby, H. L.; Wandling, C. R. (Battelle-Northwest, Richland, Wash. Pacific Northwest Lab.). Sep 1970. Contract AT(45-1)-1830. 19p. Dep. NTIS.

12879 (BNWL–1525) INTERACTIVE GRAPHICS DISPLAY SYSTEM FOR HYDROLOGIC ANALYSIS. Business, K. M. (Battelle-Northwest, Richland, Wash. Pacific Northwest Lab.). Dec 1970. Contract AT(45-1)-1830. 90p. Dep. NTIS.

12880 (BNWL–SA–3539) MATHEMATICAL MODEL FOR APPROXIMATING TRANSIENT, THREE-DIMENSIONAL GROUNDWATER SYSTEMS. Reisenauer, A. E.; Cearlock, D. B. (Battelle-Northwest, Richland, Wash. Pacific Northwest Lab.); Bryan, C. A. (Montana Univ., Missoula). 2 Dec 1970. Contract AT(45-1)-1830. 14p. (CONF-701201–1). Dep. NTIS.
From American Geophysical Union National Fall Meeting, San Francisco, Calif.

12881 (COO–1198–777) THE EFFECT OF PRESSURE ON THE ELECTRONIC STRUCTURE OF FERRIC HYDROXAMATES AND FERRICHROME A. Grenoble, D. C.; Drickamer, H. G. (Illinois Univ., Urbana). [1970]. Contract AT(11-1)-1198. 23p. Dep. NTIS.

12882 (COO–1339–44) ^{47}Ca TURNOVER OF A READILY EXCHANGEABLE CALCIUM POOL IN PREGNANT AND LACTATING COWS. Anderson, J. J. B.; Crackel, W. C. (Illinois Univ., Urbana. Dept. of Veterinary Physiology and Pharmacology). [1970]. Contract AT(11-1)-1339. 20p. Dep. NTIS.

12883 (COO–1440-21) INVESTIGATION OF MIXED CONDUCTION IN SOLID ELECTROLYTES. Progress Report, December 1, 1970–November 30, 1971. Rapp, Robert A. (Ohio State Univ., Columbus. Dept. of Metallurgical Engineering). 30 Sep 1970. Contract AT(11-1)-1440. 20p. Dep. NTIS.

12884 (COO–1599–31) UTILIZATION OF BENTHIC DETRITUS IN A MARL LAKE. Rich, Peter Hamilton (Michigan State Univ., East Lansing). 1970. 78p. Dep. NTIS.
Thesis.

12885 (COO–2032–6) THEORETICAL AND EXPERIMENTAL STUDY OF FILM CONDENSATION OF LIQUID METAL VAPORS. Annual Progress Report. Springer, George S. (Michigan Univ., Ann Arbor. Dept. of Mechanical Engineering). Dec 1970. 13p. Dep. NTIS.

12886 (COO–2092–1) DYNAMICS OF CHEMICAL REACTIONS. I. DYNAMICS OF FLUORINE ATOM REACTIONS. II. INTERMOLECULAR POTENTIALS FROM HIGH RESOLUTION DIFFERENTIAL CROSS SECTIONS. III. COLLISION INDUCED DISSOCIATIONS OF DIATOMIC MOLECULES. Technical Progress Report, April 1–December 31, 1970. Lee, Yuan Tseh (Chicago Univ., Ill. James Franck Inst.). Contract AT(11-1)-2092. 8p. Dep. NTIS.

12887 (COO–2094–2) ICR QUARTERLY REPORT NUMBER 26. Ashenhurst, Robert L. (Chicago Univ., Ill. Inst. for Computer Research). 1 Aug 1970. Contract AT(11-1)-2094. 169p. Dep. NTIS.

12888 (CU–1804–34) TRIENNIAL REPORT, 1968–1970. (Columbia Univ., Irvington-on-Hudson, N. Y. Nevis Biological Station). Contract AT(30-1)-1804. 9p. Dep. NTIS.

12889 (EGG–1183–542) OPTIMIZATION OF IMAGE LOCATION RELATIVE TO ROTOR SURFACE MODEL 739 FRAMING CAMERA. Pierson, Arthur (EG and G, Inc., Bedford, Mass.). Jun 1970. Contract AT(29-1)-1183. 11p. Dep. NTIS.
For Univ. of California Lawrence Radiation Lab., Livermore.

12890 (LA–4524) MUX: A SIMPLE APPROACH TO ON-LINE COMPUTING. Christman, Ronald D. (Los Alamos Scientific Lab., N. Mex.). Sep 1970. Contract W-7405-eng-36. 16p. Dep. NTIS.

12891 (NP–18608) INVESTIGATION OF HEAT TRANSFER AUGMENTATION THROUGH USE OF INTERNALLY FINNED AND ROUGHENED TUBES (Final Summary Report). Report No. DSR 70790-69. Bergles, A. E.; Brown, G. S, Jr.; Lee, R. A.; Simonds, R. R.; Snider, W. D. (Massachusetts Inst. of Tech., Cambridge. Heat Transfer Lab.). Aug 1970. 98p.
For French (F. W.) Tube Co., Newtown, Conn.

12892 (NYO–2150–65) DIRECT ELECTROMAGNETIC GENERATION OF ULTRASOUND IN CONDUCTING LIQUIDS. Report No. 1482. Gaerttner, M. R.; Maxfield, B. W. (Cornell Univ., Ithaca, N. Y.). Nov 1970. 8p. Dep. NTIS.

12893 (NYO–2471–47) ULTRASONIC MEASUREMENTS ON PARAELASTIC IMPURITIES IN ALKALI HALIDES. Report

No. 1469. Shuman, Henry E. (Cornell Univ., Ithaca, N. Y. Materials Science Center). Jan 1971. 86p. Dep. NTIS.
Thesis.

12894 (NYO-3087-16) EFFECT OF DISLOCATIONS ON THE COERCIVITY OF SINGLE CRYSTALS OF NICKEL. Geiss, Roy Howard (Cornell Univ., Ithaca, N. Y. Materials Science Center). Jan 1968. 174p. Dep. NTIS.
Thesis.

12895 (NYO-3087-17) SOME FERROMAGNETIC EFFECTS IN THE ELECTRICAL RESISTIVITY OF NICKEL. Schwerer III, Frederick Carl (Cornell Univ., Ithaca, N. Y. Materials Science Center). Jan 1968. 208p. Dep. NTIS.
Thesis.

12896 (NYO-3087-21) STRUCTURAL AND RELATED MAGNETIC PROPERTIES OF HIGH ANGLE EVAPORATED COBALT FILMS. Report No. 1110. Snyder, Keith Alan (Cornell Univ., Ithaca, N. Y. Materials Science Center). Jun 1969. 73p. Dep. NTIS.
Thesis.

12897 (NYO-3087-23) LOW FIELD MAGNETORESISTANCE OF NICKEL POLYCRYSTALS. Report No. 1295. Schwerer, F. C.; Silcox, J. (Cornell Univ., Ithaca, N. Y. Materials Science Center). 16 Dec 1969. 25p. Dep. NTIS.

12898 (NYO-3661-33) PRELIMINARY STUDY ON THE TEMPERATURE EFFECT ON POSITRON ANNIHILATION IN $KClO_4$. Tao, S. J.; Chuang, S. Y. (New England Inst., Inc., Ridgefield, Conn.). May 1970. 6p. Dep. NTIS.

12899 (NYO-4185-1) OBSERVATION OF VOID FORMATION INDUCED BY ELECTROMIGRATION IN METALLIC FILMS. Report No. 1447. Ho, P. S.; Glowinski, L. D. (Cornell Univ., Ithaca, N. Y. Materials Science Center). 1 Sep 1970. 14p. Dep. NTIS.

12900 (NYO-4185-2) APPLICATION OF PSEUDOPOTENTIALS TO CALCULATION OF VACANCY FORMATION ENERGY AND VOLUME FOR ALKALI METALS. Report No. 1486. Ho, Paul S. (Cornell Univ., Ithaca, N. Y. Materials Science Center). Nov 1970. 31p. Dep. NTIS.

12901 (ORNL-TM-3210) CHARACTERIZATION AND BEHAVIOR OF ALKALIZED ALUMINA DURING THE SULFUR DIOXIDE SORPTION-REGENERATION PROCESS: A SUMMARY REPORT. Godfrey, T. G.; Ernst, W. S.; Tennery, V. J.; Harris, L. A. (Oak Ridge National Lab., Tenn.). Jan 1971. Contract W-7405-eng-26. 45p. Dep. NTIS.

12902 (ORO-2036-20) ACTIVITY COEFFICIENT AND VACANCY FLOW EFFECTS ON TRACER DIFFUSION IN SILVER-GOLD ALLOYS. Greene, Marvin H. (North Carolina Univ., Chapel Hill). 1970. 76p. Dep. NTIS.
Thesis.

12903 (ORO-3935-4) INTERFACES ASSOCIATED WITH ORDERED ALLOYS. Marcinkowski, M. J. (Maryland Univ., College Park). 24 Dec 1970. Contract AT(40-1)-3935. 46p. (CONF-700809-5). Dep. NTIS.
From 7th International Congress on Electron Microscopy, Grenoble, France.

12904 (RFP-1568) VAPOR-ION METHODS OF FILM DEPOSITION. Summary and Annotated Bibliography. Kurtz, Robert G. (Dow Chemical Co., Golden, Colo. Rocky Flats Div.). 18 Dec 1970. Contract AT(29-1)-1106. 12p. Dep. NTIS.

12905 (SC-CR-70-6137) FINAL REPORT ON THE DEVELOPMENT OF PELLETIZED HEAT SOURCES FOR THERMAL BATTERIES. Rittenhouse, C. T. (Unidynamics, Phoenix, Ariz.). Nov 1970. Contract 25-8652. 95p. Dep. NTIS.
For Sandia Labs., Albuquerque, N. Mex.

12906 (SC-M-70-868) ANNOUNCEMENT OF THE AVAILABILITY OF RUNKUT: A COMPUTER ROUTINE FOR INTEGRATING SYSTEMS OF FIRST ORDER ORDINARY DIFFERENTIAL EQUATIONS. Jones, R. E. (Sandia Labs., Albuquerque, N. Mex.). Dec 1970. 4p. Dep. NTIS.

12907 (SC-M-70-886) ROTATING MIRROR FRAMING CAMERA. (Sandia Labs., Albuquerque, N. Mex.). Dec 1969. 8p. Dep. NTIS.

12908 (SC-RR-70-163) OUTDOOR AGING OF ADHESIVE SEALANTS. DeLollis, Nicholas J.; Montoya, Orelio (Sandia Labs., Albuquerque, N. Mex.). Apr 1970. 25p. Dep. NTIS.

12909 (SC-RR-70-471) STRAIN HARDENING AND STRAIN RATE IN ONE-DIMENSIONAL WAVE PROPAGATION CALCULATIONS. Herrmann, W.; Lawrence, R. J.; Mason, D. S. (Sandia Labs., Albuquerque, N. Mex.). Nov 1970. 119p. Dep. NTIS.

12910 (SC-T-71-3002) GROUP THEORY OF PARAMAGNETIC RESONANCE: A COMPARISON. Bieri, A.; Kneubuehl, F. K. Translated for Sandia Labs., Albuquerque, N. Mex., from Phys. Kondens. Mater.; 4: 230-46(1965). 22p. Dep. NTIS.

12911 (SC-T-71-3003) NATURAL VIBRATIONS OF THE R(t)CL-CIRCUIT. Haeusler, J. Translated by Marcel I. Weinreich (Sandia Labs., Albuquerque, N. Mex.), from Frequenz; 24: No. 3, 71-7(1970). 28p. Dep. NTIS.

12912 (SRIA-106-76) THALLIUM-IODINE PHASE DIAGRAM. Cubicciotti, Daniel (Stanford Research Inst., Menlo Park, Calif.). 15 Dec 1970. Contract AT(04-3)-106. 17p. Dep. NTIS.

12913 (SRO-475-9) POWDER METALLURGY COMPACTION. Quarterly Progress Report, September 1-November 30, 1970. Schwartz, E. G.; Wilson, Kenneth L.; Hornsby, James B.; Ni, Tiee-Bor (South Carolina Univ., Columbia. Coll. of Engineering). Contract AT(38-1)-475. 26p. Dep. NTIS.

12914 (TID-25633) DIFFERENTIAL QUADRATURE AND LONG-TERM INTEGRATION. Bellman, Richard (University of Southern California, Los Angeles); Casti, John (RAND Corp., Santa Monica, Calif.). Mar 1970. Contract AT(11-1)-113. 6p. Dep. NTIS.

12915 (UCLA-34-P-122-X-1) ELECTROABSORPTION AND ELECTRO-PHOTOLUMINESCENCE IN HgI_2. Coleman, Charles Clyde (University of Southern California, Los Angeles. Dept. of Physics). Oct 1968. Contract AT(11-1)-34. 150p. Dep. NTIS.
Thesis.

12916 (UCRL-19115) ROLE OF CALORIMETRY IN THE THERMODYNAMICS OF METALS AND ALLOYS. Hultgren, Ralph (California Univ., Berkeley. Lawrence Radiation Lab.). Oct 1969. Contract W-7405-eng-48. 16p. (CONF-691130-1). Dep. NTIS.
From 5th Japanese Calorimetry Conference, Osaka, Japan.

12917 (UCRL-72393) COMPUTER PROCESSING OF GAS CHROMATOGRAPHIC DATA: QUANTITATIVE ANALYSIS OF FATTY ACID METHYL ESTERS USING AN OFF-LINE MAGNETIC TAPE SYSTEM. Nelson, Gary J. (California Univ., Livermore. Lawrence Radiation Lab.). 22 Oct 1970. 43p. (CONF-700938-1). Dep. NTIS.
From Fall Meeting of the American Oil Chemists Society, Chicago, Ill.

12918 (WAPD-TM-987) UIS: THE BETTIS CDC-211 DISPLAY PACKAGE. DeVries, R. G. (Bettis Atomic Power Lab., Pittsburgh, Pa.). Nov 1970. Contract AT(11-1)-Gen-14. 34p. Dep. NTIS.

12919 (WHAN-IR-47) DPB: A DYNAMIC PROGRAMMING CODE FOR OPTIMIZING THE SHORT-TERM OPERATION OF A POWER UTILITY. Little, W. W. Jr.; Hardie, R. W. (WADCO Corp., Richland, Wash.). Nov 1970. 51p. Dep. NTIS.

12920 (Y-1752) OBSERVATION OF ABLATION BEHAVIOR OF FIBROUS CARBON-CARBON COMPOSITES. Cook, J. L.; Theis, J. D. (Union Carbide Corp., Oak Ridge, Tenn. Y-12 Plant). 4 Jan 1971. Contract W-7405-eng-26. 165p. Dep. NTIS.

CORPORATE AUTHOR INDEX

In the Corporate Author Index, technical report literature is indexed by the organization or institution responsible for issuing the report. Entries are given for all report literature and for published literature for which a corporate author approach is especially desirable, e.g., symposium and conference proceedings.

Each entry under a corporate author gives the publication title and the *NSA* volume and abstract numbers. Report numbers, where applicable, are given in parentheses at the end of the entry.

A

AIX-MARSEILLES UNIV. (FRANCE). FACULTE DES SCIENCES.
Computation of renormalized radiative corrections, 25:12245 (CNRS-CPT-70-P-318)
Computational analysis of Feynman diagrams, 25:12136 (CNRS-CPT-70-P-336)
AKADEMIYA NAUK SSSR, LENINGRAD. FIZIKO-TEKHNICHESKII INSTITUT.
Conditions of plasma heating at electron cyclotron resonance, 25:11861 (NP-18635)
Determination of the boundary of high frequency wave absorption between the electron cyclotron and the low-hybrid frequency, 25:11927 (FTI-295)
High frequency plasma heating near the low-hybrid frequency, 25:11860 (FTI-282)
AKADEMIYA NAUK SSSR, MOSCOW. INSTITUT ATOMNOI ENERGII.
Scattering of neutrons with an energy of 4 MeV at angles close to 180°, 25:12509 (ANL-Trans-856)
AKADEMIYA NAUK UKRAINSKOI SSR, KHARKOV. FIZIKO-TEKHNICHESKII INSTITUT.
Effect of toroidal state on vacuum magnetic configuration of vintotron, 25:11922 (KHFTI-70-25)
Influence of radial slots in iris disk of waveguide on dispersion properties and quality factor of system of axially-symmetric and nonaxially-symmetric waves, 25:12306 (KFK-tr-334)
Research on 100-MeV electron storage ring of Technical Physics Institute of Ukrainian Academy of Sciences, 25:12307 (KHFTI-69-27)
ALABAMA POWER CO., BIRMINGHAM.
Joseph M. Farley Nuclear Plant, Units 1 and 2. Preliminary safety analysis report, Amendment 9, 25:12748 (DOCKET-50348-15)
ALLGEMEINE ELEKTRICITAETS-GESELLSCHAFT, AEG-TELEFUNKEN, GROSSWELZHEIM (WEST GERMANY).
Development program: steam-cooled fast reactor. I, 25:12767 (BMBW-FBK-70-20)
AMERICAN NUCLEAR SOCIETY, HINSDALE, ILL.
American National Standard for nuclear criticality safety in operations with fissionable materials outside reactors, 25:10802
ANDERSON (M. D.) HOSPITAL AND TUMOR INST., HOUSTON, TEX.
Dose-time fractionation practice, 25:11259 (BNL-50203, pp 260-7)
Effects of pO_2 on cell proliferation kinetics, 25:11094 (BNL-50203, pp 215-33)
Late effects on vascular tissue, 25:11256 (BNL-50203, pp 186-203)
Reoxygenation during fractionated irradiation, 25:11220 (BNL-50203, pp 234-41)
Repair in cells of normal and malignant tissues, 25:11252 (BNL-50203, pp 54-69)
ANSALDO S.p.A., GENOA (ITALY).
Nuclear fuel with burnable poison. I, 25:10571 (EUR-4550)
ARGONNE NATIONAL LAB., IDAHO FALLS, IDAHO.
Instrument probe for measuring temperature and pressure in the upper plenum of the EBR-II reactor vessel. EBR-II Project, 25:12781 (ANL-EBR-25)
ARGONNE NATIONAL LAB., ILL.
Anion-exchange separation of neptunium from uranium and thorium in basic solution, 25:10655 (ANL-7751)
Dependence of radiosensitivity upon cell age, 25:11093 (BNL-50203, pp 97-116)
Hardware and software for nuclear spectroscopy on the Varian Data Machines 622/i Computer, 25:10848 (ANL-7704)
Instrument probe for measuring temperature and pressure in the upper plenum of the EBR-II reactor vessel. EBR-II Project, 25:12781 (ANL-EBR-25)
LIFE-I: a FORTRAN-IV computer code for the prediction of fast-reactor fuel-element behavior, 25:12794 (ANL-7736)
RABID: an integral transport-theory code for neutron slowing down in slab cells, 25:12336 (ANL-7645)
Service routines for multigroup cross-section code MC², 25:12337 (ANL-7654)
Training manual for fabrication of printed-circuit boards, 25:12864 (ANL-7725)
ARKANSAS UNIV., FAYETTEVILLE. DEPT. OF CHEMISTRY.
Beryllium-7 in Fayetteville, (36°N, 94°W), Arkansas, 25:10712 (ORO-2529-28, App. 6)
Fission products in atmosphere. I, 25:10714 (ORO-2529-28, App. 8)
Fission products in atmosphere. II, 25:10715 (ORO-2529-28, App. 9)
Jet stream and radioactive fallout, 25:10708 (ORO-2529-28, App. 2)
Prog. rpt. on atmospheric radiochemistry, annual, 12/70, 25:10706 (ORO-2529-28)
Radiochemical studies on ^{137}Cs in rain, 25:10713 (ORO-2529-28, App. 7)
Strontium-89 and ^{90}Sr in air at Fayetteville, Arkansas, 25:10711 (ORO-2529-28, App. 5)
Strontium-89 and ^{90}Sr in rain at Fayetteville (36°N, 94°W), Arkansas, 25:10710 (ORO-2529-28, App. 4)
Temporal distributions of radioactivity and $^{89}Sr/^{90}Sr$ ratios during rainstorms, 25:10707 (ORO-2529-28, App. 1)
Variation of radiocerium isotope ratio in rain, 25:10709 (ORO-2529-28, App. 3)
ATOMIC BOMB CASUALTY COMMISSION, HIROSHIMA (JAPAN).
Prog. rpt., annual, 7/68--6/69, 25:11237 (ABCC-68-69)
ATOMIC BOMB CASUALTY COMMISSION, NAGASAKI (JAPAN).
Prog. rpt., annual, 7/68--6/69, 25:11237 (ABCC-68-69)
ATOMIC ENERGY COMMISSION, BAGHDAD (IRAQ). NUCLEAR RESEARCH INST.
Killing effect of γ radiation on Oryzaephilus surinamensis, 25:11244 (NP-18607)
ATOMIC ENERGY ESTABLISHMENT, WINFRITH (ENGLAND).
Catalytic decomposition of carbon monoxide on pure iron, mild steels, and alloyed steels, 25:11374 (DP-Report-530)
ATOMIC ENERGY OF CANADA LTD., CHALK RIVER (ONTARIO).
Materials research in AECL, 25:11343 (AECL-3778)
ATOMIC ENERGY OF CANADA LTD., CHALK RIVER (ONTARIO). CHALK RIVER NUCLEAR LABS.
Effect of irradiation on tensile and impact properties of $3^1/_2$ percent and 9 nickel steel weldments, 25:11454 (AECL-3734)
ELMOS: code to manipulate single particle wavefunctions and solve the ellipsoidal modified oscillator problem, 25:12623 (AECL-3730)
FORGOD: FORTRAN IV program for solving the four group neutron diffusion equations in one dimension, 25:12335 (AECL-3671)
Multi-cycle irradiation of hollow UO_2 pellets in collapsible Zircaloy-2 sheathing, 25:11530 (AECL-3732)
Prog. rpt. on biology and health physics, 7--9/70, 25:11074 (AECL-3777)
Prog. rpt. on chemistry and materials, 7--9/70, 25:10583 (AECL-3776)
Prog. rpt. on physics, 10--12/69, 25:12427 (AECL-3666)
Theory for least squares description of radial distortions in irradiated fuel sheaths, 25:11368 (AECL-3688)
ATOMIC ENERGY RESEARCH ESTABLISHMENT, HARWELL (ENGLAND).
Compatibility studies between arc cast $(U_{0.85}Pu_{0.15})$--C and type 316L stainless steel, 25:11475 (AERE-R-5173)
Effect of some structure variations on tensile properties of irradiated Nimonic PE16, 25:11531 (AERE-R-4913)
Effects of strain rate, neutron dose, and irradiation temperature on tensile properties of Nimonic PE16, 25:11455 (AERE-R-4982)
Holdup, heat transfer, and nucleation for steam--water flow in a 0.5 cm bore tube, 25:10766 (AERE-R-3984)
Intergranular embrittlement of an austenitic steel due to impregnation with helium, 25:11456 (AERE-R-5622)
Measurement of time-of-flight using 300 Mc/s scalers,

25:10891 (AERE-R-5422)
Potential of Pu(III)--Pu(IV) couple in nitric acid solution and equilibrium constants for nitrato complexes of Pu(IV), 25:10514 (AERE-R-5320)
Radiation dose rates from plutonium oxide--beryllium oxide mixtures, 25:11052 (AERE-R-5069)
Technique for the preparation of thin films for transmission electron microscopy from highly irradiated uranium dioxide fuel elements, 25:11532 (AERE-R-5677)
Theoretical examination of iodine--water partition coefficients, 25:10513 (AERE-R-4887)
Time jitter due to noise in timing systems, 25:10808 (AERE-R-5561)

ATOMIC WEAPONS RESEARCH ESTABLISHMENT, ALDERMASTON (ENGLAND).
Atmospheric oxidation of unalloyed plutonium at low humidities, 25:11346 (AWRE-O-100/66)
Effect of humidity on the ductility of uranium, 25:11344 (AWRE-O-46/66)
Electron metallography of precipitates in irradiated and unirradiated 20 wt. percent Cr--25 wt. percent Ni--0.7 wt. percent Nb stainless steel, 25:11428 (AWRE-O-29/67)
Stress corrosion of uranium alloys, 25:11345 (AWRE-O-49/66)

AUSTRALIAN NATIONAL UNIV., CANBERRA. RESEARCH SCHOOL OF PHYSICAL SCIENCES.
Scattering and polarization of nucleons and deuterons, 25:12624 (ANU-P-497)

B

BABCOCK AND WILCOX CO., LYNCHBURG, VA. NUCLEAR POWER GENERATION DEPT.
Fast breeder reactor static physics methods development and analysis project. Volume 1. FARED: one-dimensional fast reactor physics design and analysis code, 25:12772 (BAW-3867-9(Vol.1)(Rev.1))

BATTELLE MEMORIAL INST., COLUMBUS, OHIO.
Estimation of potential radionuclide ingestion by native populations of Eastern Panama and Northwestern Colombia. Bioenvironmental and Radiological-Safety Feasibility Studies, Atlantic-Pacific Interoceanic Canal, 25:10995 (BMI-171-45)
Prog. rpt. on development of fuels and technology for advanced reactors,7--9/70, 25:12795 (BMI-1893)
Prog. rpt. on effects of underwater overpressures on the sea otter and its principal food species, annual, 7/68, 25:12876 (BMI-171-111)
Prog. rpt. on feasibility test to determine Amchitka Sea otter population through photogrammetric techniques, annual 7/68, 25:12875 (BMI-171-108)
Prog. rpt. on freshwater ecology of Amchitka Island, annual, 7/68, 25:12870 (BMI-171-103)
Prog. rpt. on freshwater vertebrate and invertebrate ecology of Amchitka Island, annual, 8/30/67--6/30/68, 25:12871 (BMI-171-104)
Prog. rpt. on geomorphology and pedology of Amchitka Island, annual, 6/68, 25:12873 (BMI-171-106)
Prog. rpt. on investigation of initiation and extent of ductile pipe rupture, Phase II, 7--9/70, 25:11369 (BMI-1892)
Prog. rpt. on plant ecology of Amchitka Island, Alaska, annual, 8/1/67--6/30/68, 25:12874 (BMI-171-107)
Prog. rpt. on research program on marine ecology and oceanography, Amchitka, annual, 7/1/67--6/30/68, 25:12877 (BMI-171-114)
Prog. rpt. on revegetation of disturbed areas of Amchitka Island, annual, 7/68, 25:12872 (BMI-171-105)
Prog. rpt. on sea otter natural mortality at Amchitka Island, Alaska, 2/20/68--6/20/68, 25:12868 (BMI-171-101)
Prog. rpt. on the avifauna on Amchitka Island, Alaska, 8/14/67--6/9/68, 25:12869 (BMI-171-102)

BATTELLE-NORTHWEST, RICHLAND, WASH. PACIFIC NORTHWEST LAB.
Build-up of americium-241 in lung containing plutonium-241, 25:11053 (BNWL-B-12)
EBR-II dosimetry test reaction rate measurements (reactor runs 31E and 31F), 25:12773 (BNWL-1403)
Effect of Hanford Plant operations on the temperature of the Columbia River 1964 to present, 25:10691 (BNWL-1345)
FFTF containment system alarm and trip criteria, 25:12812 (BNWL-1479)
Formation of UO_2--carbon mixtures and carbide or nitride fuel material in spray reactor, 25:11478 (BNWL-843)
Interactive graphics display system for hydrologic analysis, 25:12879 (BNWL-1525)
Intercomparison of portable radiation monitoring instrument evaluations, 25:10809 (BNWL-SA-3565)
Mathematical model for approximating transient, three-dimensional groundwater systems, 25:12880 (BNWL-SA-3539)
Natural transport effects on fission product behavior in the containment systems experiment, 25:12803 (BNWL-1457)
Prog. rpt. on fixation of radioactive residues, 8--10/70, 25:10658 (BNWL-1533)
Prog. rpt. on reactor fuels and materials development, 4--6/68, 25:11474 (BNWL-842)
Transformation device using post-detector signal pattern rotators for multiparameter eddy current tester, 25:12878 (BNWL-1469)

BENDIX CORP., KANSAS CITY, MO.
Design of an insulator which must survive high g-forces, 25:12867 (BDX-613-213)
Split fiberglass holder, 25:12866 (BDX-613-198)

BETTIS ATOMIC POWER LAB., PITTSBURGH, PA.
Analysis of the transient capability of rod-type fuel elements (LWBR Development Program), 25:11534 (WAPD-TM-979)
Influence of prior corrosion history upon the hydrogen pickup by Zircaloy during subsequent exposure in hot water, 25:11349 (WAPD-TM-906)
UIS: Bettis CDC-211 display package, 25:12918 (WAPD-TM-987)

BHABHA ATOMIC RESEARCH CENTRE, BOMBAY (INDIA).
Spectrographic analysis of tungsten in ores and their concentrates: an intermittent ac arc method, 25:10429 (BARC-468)
Syntheses of phyllitic minerals: their utilization in radioactive waste treatment. I, 25:10793 (BARC-506)

BORDEAUX UNIV., GRADIGNAN (FRANCE). CENTRE D'ETUDES NUCLEAIRES.
Review of experimental works on closed-shell nuclei and the almost closed shell nuclei from ^{40}Ca to ^{210}Pb, 25:12432 (LYCEN-7034, pp 117-46)

BOSTON EDISON CO., MASS.
Pilgrim Nuclear Power Station. Recommendations for power piping code, 25:12741 (DOCKET-50293-33)

BOSTON UNIV., MASS. DEPT. OF PHYSICS AND ASTRONOMY.
Influence of the neutral winds in the formation and distribution of the ionospheric evening anomaly, 25:11777 (AD-708496)
Model relating the radial changes of the plasmapause at dusk to geomagnetic activity, 25:11776 (AD-708495)

BRANDEIS UNIV., WALTHAM, MASS. DEPT. OF CHEMISTRY.
Prog. rpt. on effects of mercaptans and disulfides on photochemical and high energy radiation induced reaction, annual, 11/69--11/70, 25:10627 (NYO-2499-37)

BRANDEIS UNIV., WALTHAM, MASS. GRADUATE DEPT. OF BIOCHEMISTRY.
Repair of UV-irradiated DNA, 25:10959 (BNL-50203, pp 27-40)

BRITISH INST. OF RADIOLOGY, LONDON (ENGLAND).
Fractionation treatment of larynx and pharynx, 25:11221 (BNL-50203, pp 268-79)

BROOKHAVEN NATIONAL LAB., UPTON, N. Y.
Conference on time and dose relationships in radiation biology as applied to radiotherapy, Carmel, Calif., 9/69, 25:11218 (BNL-50203)
Economical beam transport for utilization of post conversion AGS, 25:12296 (BNL-15464)
Particle separation in a system of conventional iris-loaded deflectors interspersed with alternate gradient magnets, 25:12295 (BNL-15438)
Reoxygenation in radiotherapy, 25:11224 (BNL-50203, pp 318-38)

BROWN UNIV., PROVIDENCE, R. I. DEPT. OF PHYSICS.
Existence of complex poles and oscillatory average multiplicity in multiperipheral models, 25:12122 (NYO-2262-TA-228)
Scattering electromagnetic and gravitational waves by a static gravitational field, 25:12138 (NYO-2262-TA-222)
Singular off-mass-shell equation with vector-meson exchange, 25:12192 (NYO-2262-TA-232)

BUREAU OF MINES, DENVER, COLO. DENVER MINING RESEARCH CENTER.
Effects evaluation of gas wells and associated facilities for Project Rulison, 25:10737 (PNE-R-39, Pt.2)
Mine and well effects evaluation for Project Rulison, 25:10735 (PNE-R-39)
Mine effects evaluation for Project Rulison, 25:10736 (PNE-R-39, Pt.1)

BUREAU OF MINES, SALT LAKE CITY, UTAH. SALT LAKE CITY METALLURGY RESEARCH CENTER.
Metallurgical application of solvent extraction. II, 25:10656 (BM-IC-8502)
Recovery of uranium from natural mine waters by countercurrent ion exchange, 25:10657 (BM-RI-7471)

BUREAU OF MINES, WASHINGTON, D. C.
Controlling employee exposure to alpha radiation in underground uranium mines. Volume I, 25:11085

BUREAU OF RADIOLOGICAL HEALTH, ROCKVILLE, MD.
Use of radioactive materials in gas chromatography, 25:10421 (BRH/DMRE-70-5)

C

CALIFORNIA INST. OF TECH., PASADENA. W. M. KECK LAB. OF ENGINEERING MATERIALS.
Superconducting metastable simple cubic alloys, 25:11819 (CALT-822-22)

CALIFORNIA UNIV., BERKELEY.
Behavior and effects of radionuclides in soils and plants, summary, 1969--70, 25:10936 (UCB-34-P-23-15)

CALIFORNIA UNIV., BERKELEY. LAWRENCE RADIATION LAB.
Role of calorimetry in the thermodynamics of metals and alloys, 25:12916 (UCRL-19115)
Shear strength of beryllium, uranium, and tungsten as a function of strain, strain rate, and pressure,

25:11379 (UCRL-72477)
CALIFORNIA UNIV., LA JOLLA, SAN DIEGO. DEPT. OF PHYSICS.
Existence of complex poles and oscillatory average multiplicity in multiperipheral models, 25:12122 (NYO-2262-TA-228)
CALIFORNIA UNIV., LIVERMORE. LAWRENCE RADIATION LAB.
Computer processing of gas chromatographic data: quantitative analysis of fatty acid methyl esters using an off-line magnetic tape system, 25:12917 (UCRL-72393)
Distribution and redistribution of airborne particulates from the Schooner cratering event, 25:10716 (UCRL-72534)
FORTRAN code for analysis of counting data from animal tissues, 25:10937 (UCRL-50957)
Optimization of image location relative to rotor surface Model 739 framing camera, 25:12889 (EGG-1183-542)
Radionuclide body burdens and hazards from ingestion of foodstuffs contaminated by fallout, 25:11038 (UCRL-72716(Rev.1))
CALIFORNIA UNIV., SAN FRANCISCO. MEDICAL CENTER.
DNA repair in mammalian cells, 25:11008 (BNL-50203, pp 14-26)
Late effects on vascular tissue, 25:11256 (BNL-50203, pp 186-203)
CALIFORNIA UNIV., SAN FRANCISCO. RADIOLOGICAL LAB.
DNA repair in mammalian cells, 25:11008 (BNL-50203, pp 14-26)
CAROLINA POWER AND LIGHT CO., RALEIGH, N.C.
Brunswick Steam Electric Plant, Units 1 and 2. Containment design report. Design report No. 7, 25:12745 (DOCKET-50324-18)
CENTRAL ELECTRICITY GENERATING BOARD, BERKELEY (ENGLAND). BERKELEY NUCLEAR LABS.
Dynamic stress concentration at a chamfered change of section, 25:10790 (RD/B/N-1795)
Inductive liquid metal level detector, 25:10896 (RD/B/N-1720)
Thermodynamics of some metal/coolant reactions in Mk.III reactors, 25:10518 (RD/B/N-1816)
CENTRE D'ETUDE DE L'ENERGIE NUCLEAIRE, BRUSSELS (BELGIUM).
Development of techniques for production of ^{131}I, 25:10653 (BLG-442)
Experimental and theoretical physics work on Pu enriched LWR's lattices, 25:12796 (EURAEC-2145)
CENTRE NATIONAL DE LA RECHERCHE SCIENTIFIQUE, GRENOBLE (FRANCE).
Colinear and noncolinear magnetic structures in rare earth compounds RNi_3 and R_2Ni_7, 25:11979 (CEA-CONF-1704)
CENTRE NATIONAL DE LA RECHERCHE SCIENTIFIQUE, MARSEILLES (FRANCE). CENTRE DE PHYSIQUE THEORIQUE.
Computation of renormalized radiative corrections, 25:12245 (CNRS-CPT-70-P-318)
Computational analysis of Feynman diagrams, 25:12136 (CNRS-CPT-70-P-336)
Sixth-order radiative corrections to the anomalous magnetic moment of the electron, 25:12065 (CNRS-CPT-70-P-339)
CENTRE NATIONAL DE LA RECHERCHE SCIENTIFIQUE, ORSAY (FRANCE). CENTRE DE SPECTROMETRIE NUCLEAIRE ET DE SPECTROMETRIE DE MASSE.
Nucleosynthesis of Li, Be, and B, 25:11542 (NP-18591)
Work carried out in France during recent years on isotopes with Z greater than or equal to 83, 25:12524 (LYCEN-7034, pp 84-93)
CENTRE NATIONAL DE LA RECHERCHE SCIENTIFIQUE, PARIS (FRANCE).
Conference on classical and relativistic magnetohydrodynamics, Lille, France, 6/69, 25:11759
Conference on measurements of elements occurring in traces in rocks, Nancy, 12/68, 25:10446
Conference on systems with an infinite number of degrees of freedom, Gif-sur-Yvette, France, 5/69, 25:12254
CENTRE NATIONAL DE LA RECHERCHE SCIENTIFIQUE, PARIS (FRANCE). INSTITUT D'ASTROPHYSIQUE.
Nucleosynthesis of Li, Be, and B, 25:11542 (NP-18591)
CENTRE NATIONAL DE LA RECHERCHE SCIENTIFIQUE, STRASBOURG (FRANCE). CENTRE DE RECHERCHES NUCLEAIRES.
Study of different competing coupling mechanisms in deformed nuclei of odd mass, 25:12525 (LYCEN-7034, pp 94-116)
CENTRO INFORMAZIONI STUDI ESPERIENZE, MILAN (ITALY).
Behavior of metallic U--Zircaloy-2 fuel element defects and exposure to aqueous corrosion, 25:11347 (CISE-R-222)
Experimental irradiation of metallic U fuel elements in the Halden HBWR reactor, 25:11457 (CISE-R-278)
Treatment of water in a nuclear plant for the testing of fuel elements, 25:12821 (LIB/Trans-335)
CHICAGO UNIV., ILL.
Hyperon beta decay, 25:12163 (COO-264-563)
CHICAGO UNIV., ILL. DEPT. OF CHEMISTRY.
Prog. rpt. on actinide and lanthanide ions and organic molecules in triplet states by magnetic resonance methods, 12/70, 25:10570 (COO-294-10)
CHICAGO UNIV., ILL. DEPT. OF PHYSICS.
Hyperon beta-decay, 25:12164 (COO-264-563(Add.))
CHICAGO UNIV., ILL. ENRICO FERMI INST.
Hyperon beta decay, 25:12163 (COO-264-563)
Hyperon beta-decay, 25:12164 (COO-264-563(Add.))
CHICAGO UNIV., ILL. INST. FOR COMPUTER RESEARCH.
Prog. rpt. on computer research, 8/70, 25:12887 (COO-2094-2)
CHICAGO UNIV., ILL. JAMES FRANCK INST.
Prog. rpt. on dynamics of chemical reactions, annual, 4--12/70, 25:12886 (COO-2092-1)
CHRISTIE HOSPITAL AND HOLT RADIUM INST., MANCHESTER (ENGLAND). PATERSON LABS.
Role of oxygen in repair process, 25:11304 (BNL-50203, pp 70-81)
CINCINNATI GAS AND ELECTRIC CO., OHIO.
Wm. H. Zimmer Nuclear Power Station, Unit 1. Preliminary safety analysis report, Amendment 4, 25:12749 (DOCKET-50358-10)
COLLEGE DE FRANCE, NOGENT-SUR-MARNE. LABORATOIRE D'EMBROYOLOGIE EXPERIMENTALE.
Prog. rpt. on embryo and its organs, 10/64--12/68, 25:11096 (EUR-4491)
COLUMBIA UNIV., IRVINGTON-ON-HUDSON, N. Y. NEVIS BIOLOGICAL STATION.
Prog. rpt., triennial, 1968--1970, 25:12888 (CU-1804-34)
COLUMBIA UNIV., NEW YORK. COLL. OF PHYSICIANS AND SURGEONS.
Cell killing at very low dose rates, 25:11095 (BNL-50203, pp 308-17)
COLUMBIA UNIV., PALISADES, N. Y. LAMONT-DOHERTY GEOLOGICAL OBSERVATORY.
Investigations of U and Th series isotope disequilibria in the ocean and in pleistocene sediments. Annual Progress report, 25:10725 (CU-3139-4)
COLUMBUS AND SOUTHERN OHIO ELECTRIC CO., COLUMBUS, OHIO.
Wm. H. Zimmer Nuclear Power Station, Unit 1. Preliminary safety analysis report, Amendment 4, 25:12749 (DOCKET-50358-10)
COMISION NACIONAL DE ENERGIA ATOMICA, BUENOS AIRES (ARGENTINA).
Cross section and yield relations for the isomeric pair /sup 90m/Y/^{90}Y obtained by the (d,p) reaction, 25:12428 (CNEA-278)
Cross sections for nuclear reactions produced by deuterons on tantalum, 25:12513 (CNEA-269)
Ezeiza semi-industrial irradiation plant, 25:10795 (CNEA-272)
Operational formulation of resonance absorption of neutrons, 25:12338 (CNEA-266)
COMITATO NAZIONALE PER L'ENERGIA NUCLEARE, FRASCATI (ITALY). LABORATORI NAZIONALI DI FRASCATI.
Preliminary results regarding development of superconducting ribbons of Nb_3Sn, 25:11820 (LNF-70/18)
COMITATO NAZIONALE PER L'ENERGIA NUCLEARE, ROME (ITALY).
Methods of quantitative analysis of a gamma spectrum, 25:10853 (RT/PROT-(70)21)
COMMISSARIAT A L'ENERGIE ATOMIQUE, BRUYERES-LE-CHATEL (FRANCE). CENTRE D'ETUDES.
Apparatus for automatic liquid phase chromatography, 25:10659 (CEA-N-1267)
Mechanical activity in a granitic massif subjected to a nuclear explosion, 25:10728 (CEA-R-4059)
COMMISSARIAT A L'ENERGIE ATOMIQUE, FONTENAY-AUX-ROSES (FRANCE). CENTRE D'ETUDES NUCLEAIRES.
Chemical diffusion and heterodiffusion at infinite dilution of Pu in body centered cubic β Ti, 25:11429 (CEA-CONF-1687)
Crystallographic analysis of segregations observed in dilute ZrPu alloys during martensitic transformation, 25:11430 (CEA-CONF-1688)
Determination of limiting solubilities using heterodiffusion coefficient measurements, 25:11370 (CEA-CONF-1689)
Effect of a β → α transformation and of oxygen on plutonium distribution in dilute Zr--Pu and Ti--Pu alloys, 25:11431 (CEA-CONF-1691)
EL 600: study of core neutronic properties, 25:12775 (CEA-N-1395)
Electronic properties of actinide carbides and nitrides, 25:11980 (CEA-R-4113)
Evaluation of the irradiation of bone marrow resulting from milk contamination by ^{90}Sr after continuous or uneven deposition on pastures, 25:10932 (CEA-CONF-1558)
Filling of a magnetic well by injection of neutral atoms at various angles and energies, 25:11859 (EUR-CEA-FC-563)
Mechanical properties of plutonium-based ceramics at high temperature, 25:11485 (CEA-CONF-1670)
MHD equilibrium and stability of toroidal plasmas with a quasi-triangular cross section in Tokamak type magnetic configurations, 25:11911 (EUR-CEA-FC-569)
Particular MHD solutions, 25:11753 (EUR-CEA-FC-571)
Production of intense beams of fast neutral particles using plasma accelerators of the pleiade type, 25:11920 (EUR-CEA-FC-567)
Prog. rpt. on plasma physics and controlled fusion, 4/1/69--2/28/70, 25:11854 (EUR-CEA-FC-542(Pt.1))
Prog. rpt. on plasma physics and controlled fusion, 4/1/69--2/28/70, 25:11855 (EUR-CEA-FC-542(Pt.2))
Reactor shielding in the CEA, 25:12782 (CEA-CONF-1683)
Review on correlation measurements in plasma, 25:11866 (EUR-CEA-FC-570)
Self diffusion, under hydrostatic pressure, of body centered cubic Pu, 25:11371 (CEA-CONF-1690)
Straight stellarators with strong helical currents,

25:11918 (EUR-CEA-FC-543)
Study of neptunium hexafluoride formation and its adsorption on metallic fluorides, 25:10568 (CEA-R-4051)
Study of two cases of contamination by ^{241}Am, 25:10931 (CEA-CONF-1557)
Tests on an automatic air purifying respirator, 25:10752 (CEA-N-1360)
Vacuum problems encountered in nuclear fusion research, 25:11919 (EUR-CEA-FC-566)

COMMISSARIAT A L'ENERGIE ATOMIQUE, GRENOBLE (FRANCE). CENTRE D'ETUDES NUCLEAIRES.
Application of $^{18}O(p,\alpha)^{15}N$ reaction to study of self-diffusion of oxygen in uranium dioxide, 25:11486 (CEA-R-4095)
Cobalt electron irradiated at 20°K, 25:11949 (AI-Trans-267)
Colinear and noncolinear magnetic structures in rare earth compounds RNi_3 and R_2Ni_7, 25:11979 (CEA-CONF-1704)
Description of various techniques, recent applications, and technological aspects, 25:10669 (LYCEN-7034, pp 9-22)
Electron spin resonance study of defects produced by irradiation in an ionic solid: beryllium oxide, 25:11950 (CEA-R-3937)
Nuclear magnetic resonance at 310 MHz in a superconducting solenoid, 25:12034 (CEA-R-3855)
Seismic compression waves associated with underground nuclear explosions in the Sahara, 25:10729 (CEA-R-4105)
Stationary gas detectors for mapping and dynamic studies of organs using x ray or low-energy γ-ray emitters, 25:10810 (CEA-CONF-1668)

COMMISSARIAT A L'ENERGIE ATOMIQUE, LIMEIL-BREVANNES (FRANCE). CENTRE D'ETUDES.
High-magnetic field compression produced by implosion of a thin metal tube, 25:11917 (CEA-R-4024)
Laser--matter interaction: stimulated and nonlinear effects, 25:11884 (CEA-N-1399)
Thomson scattering in laser created plasma, 25:11865 (CEA-R-4058)

COMMISSARIAT A L'ENERGIE ATOMIQUE, PIERRELATTE (FRANCE).
Continuous control of low-uranium contents of solutions by measurement of radioactivity, 25:10473 (CEA-R-4032)

COMMISSARIAT A L'ENERGIE ATOMIQUE, SACLAY (FRANCE). CENTRE D'ETUDES NUCLEAIRES.
Activation analysis using charged particles and γ photons, 25:10488 (CEA-R-4072)
COREGRAF 2: code for computing graphite lattices and their evolution for IBM 360 and CDC 6600, 25:12774 (CEA-N-1344(1))
Digital measurement of the peak current in a linear electron accelerator, 25:12297 (CEA-N-1389)
Effect of α UO_3 in production of UO_2 and UF_4 from β UO_3--0.05 H_2O, 25:10569 (CEA-R-4074)
Fixation and migration of ^{42}K applied to leaves of corn, 25:10930 (CEA-CONF-1517)
Gamma-ray spectrometry in drillings using Ge--Li semiconductor probes, 25:10849 (CEA-CONF-1694)
Geometric correction factors relating to the recoil of protons in nuclear emulsions, 25:10867 (CEA-R-4081)
In-pile loop BANJO, 25:12813 (CEA-CONF-1673)
Isodore facility, 25:10794 (CEA-R-4120)
Measurement and analysis of capture to fission cross section ratio α for ^{239}Pu between 20 keV and 500 keV, 25:12511 (CEA-N-1368)
Mechanical and electrical properties of aerosols: application to health physics, 25:11036 (CEA-Bib-185)
Neutron dosimetry and spectrometry by multisphere method, 25:10811 (CEA-CONF-1685)
Resonance in reactions $K^-p \to \Sigma^+\pi^-$ between 440 and 1230 MeV/c, 25:12098 (CEA-R-4068)
Structure transformations of Zr--Cu binary alloys with low Cu contents and ternary alloys during continuous cooling, 25:11432 (CEA-N-1310)
Visualization of spectra in nuclear physics, 25:10892 (CEA-N-1363)
X-ray spectrometry using Si (Li) diodes, 25:10812 (CEA-N-1401)

COMMONWEALTH EDISON CO., CHICAGO, ILL.
Dresden Nuclear Power Station, Unit 2. Failure of "A" standby gas treatment system discharge damper motor, 25:12718 (DOCKET-50237-127)
Dresden Nuclear Power Station, Unit 2. Receipt of operational neutron sources in excess of allowance under License DPR-19, 25:12719 (DOCKET-50237-128)
Dresden Nuclear Power Station, Unit 2. Refueling. Proposed Modification No. 71-1 to final safety analysis report, 25:12732 (DOCKET-50237-126)
Dresden Nuclear Power Station, Unit 2. Shut down by instrument air leak, 25:12720 (DOCKET-50237-129)
Zion Station, Units 1 and 2. Information relative to a liner bulge in containment structure, 25:12743 (DOCKET-50295-23)
Zion Station, Units 1 and 2. Resolution of void at concrete/buttress plate joint, 25:12742 (DOCKET-50295-22)

CONNECTICUT YANKEE ATOMIC POWER CO., HARTFORD.
Connecticut Yankee Atomic Power Plant. License No. DPR-14. Technical specifications Proposed Change No. 17, 25:12728 (DOCKET-50213-92)
Connecticut Yankee Atomic Power Plant. Preliminary safety analysis report, Suppl. No. 1, 25:12729 (DOCKET-50213-93)
Connecticut Yankee Atomic Power Plant. Thermal stress evaluation of the reactor vessel during a cooldown transient, 25:12727 (DOCKET-50213-89)

CONSUMERS POWER CO., JACKSON, MICH.
Big Rock Point Nuclear Plant. License No. DPR-6; technical specifications Change Nos. 21, 22, and 24, additional information, 25:12726 (DOCKET-50155-59)
Big Rock Point Nuclear Plant. Sensitized stainless steel components within primary coolant pressure boundary, 25:12725 (DOCKET-50155-58)

CORNELL UNIV., ITHACA, N. Y.
Direct electromagnetic generation of ultrasound in conducting liquids, 25:12892 (NYC-2150-65)

CORNELL UNIV., ITHACA, N.Y. LAB. OF PLASMA STUDIES.
E-layer precession in a plasma, 25:11925 (NYO-4077-1, Paper 2)
Finite beta equilibria of relativistic electron beams in toroidal geometry, 25:11887 (NYO-4077-1, Paper 5)
Nonlinear beam--plasma interactions and stochastic acceleration, 25:11885 (NYO-4077-1, Paper 3)
Precession of a strong E-layer, 25:11924 (NYO-4077-1, Paper 1)
Prog. rpt. on theoretical studies on Astron stability, 1--12/70, 25:11923 (NYO-4077-1)
Relativistic beam propagation in magnetized plasma, 25:11886 (NYO-4077-1, Paper 4)

CORNELL UNIV., ITHACA, N. Y. MATERIALS SCIENCE CENTER.
Application of pseudopotentials to calculation of vacancy formation energy and volume for alkali metals. report no. 1486, 25:12900 (NYO-4185-2)
Effect of dislocations on the coercivity of single crystals of nickel, 25:12894 (NYO-3087-16)
Low field magnetoresistance of nickel polycrystals, 25:12897 (NYO-3087-23)
Observation of void formation induced by electromigration in metallic films. report no. 1447, 25:12899 (NYO-4185-1)
Some ferromagnetic effects in the electrical resistivity of nickel, 25:12895 (NYO-3087-17)
Structural and related magnetic properties of high angle evaporated cobalt films, 25:12896 (NYO-3087-21)
Ultrasonic measurements on paraelastic impurities in alkali halides, 25:12893 (NYO-2471-47)

D

DANISH ATOMIC ENERGY COMMISSION, RISOE. RESEARCH ESTABLISHMENT.
FORTRAN IV version of sum-of-exponential least-squares code EXPOSUM, 25:12837 (RISO-M-1279)

DAYTON POWER AND LIGHT CO., OHIO.
Wm. H. Zimmer Nuclear Power Station, Unit 1. Preliminary safety analysis report, Amendment 4, 25:12749 (DOCKET-50358-10)

DEPARTMENT OF WATER AND POWER, LOS ANGELES, CALIF.
Malibu Nuclear Plant, Unit No. 1. Preliminary safety summary report, 25:12730 (DOCKET-50214-2)

DETROIT EDISON CO., MICH.
Enrico Fermi Atomic Power Plant, Unit 2. Preliminary safety analysis report, Amendment 13, 25:12747 (DOCKET-50341-24)

DEUTSCHES ELEKTRONEN-SYNCHROTRON, HAMBURG (WEST GERMANY).
Compilation of photoproduction data above 1.2 GeV, 25:12066 (DESY-HERA-70-1)
Dual model for diffractive two-pion electroproduction, 25:12137 (DESY-70/56)

DIVISION OF REACTOR LICENSING (AEC), WASHINGTON, D. C.
Dresden Nuclear Power Station, Unit 3. Facility Operating License No. DPR-25, 25:12734 (DOCKET-50249-53)

DOUGLAS UNITED NUCLEAR, INC., RICHLAND, WASH.
Operating procedures: Hanford Test Reactor, 25:12815 (DUN-7149)

DOW CHEMICAL CO., GOLDEN, COLO. ROCKY FLATS DIV.
Equipment forecasting simulation models, 25:10757 (RFP-1527)
Vapor--ion methods of film deposition, 25:12904 (RFP-1566)

DU PONT DE NEMOURS (E.I.) AND CO., AIKEN, S. C. SAVANNAH RIVER LAB.
On-line computer monitoring of pressurized ion exchange process, 25:10664 (DP-MS-70-38)

DUKE UNIV., DURHAM, N. C. DEPT. OF PHYSIOLOGY AND PHARMACOLOGY.
Prog. rpt. on the effect of radiation on mucosal phospholipase activity, 10/70, 25:10961 (ORO-3329-6)

E

EG AND G, INC., BEDFORD, MASS.
Optimization of image location relative to rotor surface Model 739 framing camera, 25:12889 (EGG-1183-542)
Three-band source spectra from color film, 25:10893 (EGG-1183-484)

EIDGENOESSISCHE TECHNISCHE HOCHSCHULE, ZURICH (SWITZERLAND).
Investigations of some one-neutron-transfer reactions with ^{18}O and ^{19}F beams, 25:12381 (NP-18541)
Polarization of protons inelastically scattered on ^{24}Mg, ^{52}Cr, and ^{58}Ni, 25:12433 (NP-18552)
Transfer of a neutron between ^{9}Be, ^{13}C, and ^{17}O, 25:12382 (NP-18546)
EIDGENOESSISCHES INSTITUT FUER REAKTORFORSCHUNG, WUERENLINGEN (SWITZERLAND).
Investigations of air currents in the lower Aare river valley with reference to monitoring of atomic installations, 25:10703 (EIR-185)
ENVIRONMENTAL RESEARCH CORP., LAS VEGAS, NEV.
Seismic response characteristics at NRDS from underground nuclear detonations, 25:10730 (NVO-1163-TM-22)
EUROPEAN ATOMIC ENERGY COMMUNITY.
Filling of a magnetic well by injection of neutral atoms at various angles and energies, 25:11859 (EUR-CEA-FC-563)
MHD equilibrium and stability of toroidal plasmas with a quasi-triangular cross section in Tokamak type magnetic configurations, 25:11911 (EUR-CEA-FC-569)
Production of intense beams of fast neutral particles using plasma accelerators of the pleiade type, 25:11920 (EUR-CEA-FC-567)
Prog. rpt. on embryo and its organs, 10/64--12/68, 25:11096 (EUR-4491)
Prog. rpt. on pathogenesis of genetic and somatic radiation damage, annual, 1969, 25:11294 (EUR-4542)
Prog. rpt. on plasma physics and controlled fusion, 4/1/69--2/28/70, 25:11854 (EUR-CEA-FC-542(Pt.1))
Prog. rpt. on plasma physics and controlled fusion, 4/1/69--2/28/70, 25:11855 (EUR-CEA-FC-542(Pt.2))
Spectrochemical analysis of Zr and its alloys. I, 25:10430 (EUR-4541)
Straight stellarators with strong helical currents, 25:11918 (EUR-CEA-FC-543)
Vacuum problems encountered in nuclear fusion research, 25:11919 (EUR-CEA-FC-566)
EUROPEAN ATOMIC ENERGY COMMUNITY, GEEL (BELGIUM). CENTRAL NUCLEAR MEASUREMENTS BUREAU.
Prog. rpt. on Central Bureau of Nuclear Measurement, annual, 1969, 25:12516 (EUR-4525)
EUROPEAN ATOMIC ENERGY COMMUNITY, ISPRA (ITALY). JOINT NUCLEAR RESEARCH CENTER.
CODAC: program to process TIMOC library from ENDF/B file, 25:12339 (EUR-4521)
Measure of the factor of fast fission epsilon in a D_2O uranium lattice, 25:12817 (EUR-4326)
Spectrochemical analysis of Zr and its alloys. I, 25:10430 (EUR-4541)
EUROPEAN ORGANIZATION FOR NUCLEAR RESEARCH, GENEVA (SWITZERLAND).
Hyperon beta decay, 25:12163 (COO-264-563)
Main decay characteristics of mercury isotopes and their daughter products (182 less than or equal to A less than or equal to 192), 25:12512 (CERN-70-29)

F

FIAT, TURIN (ITALY). SEZIONE ENERGIA NUCLEARE.
Nuclear fuel with burnable poison. I, 25:10571 (EUR-4550)
FLORIDA POWER AND LIGHT CO.
Hutchinson Island Plant, Unit No. 1. Replies to questions on unresolved design and construction items, 25:12746 (DOCKET-50335-17)
FLORIDA UNIV., GAINESVILLE. DEPT. OF AGRONOMY.
Prog. rpt. on cytological study of radiation induced alterations in cytoplasmic factors controlling male sterility in corn, annual, 12/70, 25:11010 (ORO-2583-8)
FRAUNHOFER-GESELLSCHAFT, GARMISCH-PARTENKIRCHEN (WEST GERMANY). PHYSIKALISCH-BIOKLIMATISCHE FORSCHUNGSSTELLE.
Prog. rpt., 12/70, 25:10735 (NYO-4061-3)
FRENCH (F.W.) TUBE CO., NEWTON, CONN.
Investigation of heat transfer augmentation through use of internally finned and roughened tubes, 25:12891 (NP-18698)

G

GENERAL ELECTRIC CO., SAN JOSE, CALIF. ATOMIC POWER EQUIPMENT DEPT.
Prog. rpt. on reactor primary coolant system, 7--9/70, 25:12783 (GEAP-10207-22)
GENERAL ELECTRIC CO., SAN JOSE, CALIF. NUCLEAR ENERGY DIV.
Midwest Fuel Recovery Plant. Application for conversion of construction permit to operating license (includes final safety analysis report), 25:10663 (DOCKET-50268-6)
GENERAL ELECTRIC CO., SUNNYVALE, CALIF. BREEDER REACTOR DEVELOPMENT OPERATION.
Prog. rpt. on sodium technology development program, 3--5/70, 25:11348 (GEAP-13539-13)
Southwest Experimental Fast Oxide Reactor. Quarterly plant operations report No. 1, May 1--July 31, 1969, 25:12731 (DOCKET-50231-65)
Southwest Experimental Fast Oxide Reactor. Quarterly plant operations report No. 2, August 1--October 31, 1969, 25:12717 (DOCKET-50231-66)
GEORGIA INST. OF TECH., ATLANTA. ENGINEERING EXPERIMENT STATION.
Prog. rpt. on magnetic phenomena at metal surfaces, 2--12/70, 25:11981 (ORO-3674-4)
GESELLSCHAFT FUER STRAHLENFORSCHUNG M.B.H., NEUHERBERG BEI MUNICH (WEST GERMANY). INSTITUT FUER BIOLOGIE.
Prog. rpt. on pathogenesis of genetic and somatic radiation damage, annual, 1969, 25:11294 (EUR-4542)
GOSUDARSTVENNYI KOMITET PO ISPOL'ZOVANIYU ATOMNOI ENERGII SSSR, MOSCOW.
Cesium-137 in lichen-reindeer man in the extreme north of the USSR, 1962--68, 25:11037 (NP-18381)
Dietary intake of ^{90}Sr by population of the USSR, 1959--1967 as a result of stratospheric fallout, 25:10934 (NP-18380)
Measurement of ^{90}Sr content in organism of adult persons, 25:10935 (NP-18388)
GOSUDARSTVENNYI KOMITET PO ISPOL'ZOVANIYU ATOMNOI ENERGII SSSR, MOSCOW. INSTITUT ATOMNOI ENERGII.
Multigroup design of unidimensional nuclear reactors without use of grid method, 25:12841 (IAE-1938)
Procedure for calculating certain parameters of heat-producing elements of VVER type, 25:12798 (IAE-1942)
Propagation and absorption of ionic-hybrid waves in a slightly-heterogeneous plasma layer, 25:11928 (IAE-1949)
GOSUDARSTVENNYI KOMITET PO ISPOL'ZOVANIYU ATOMNOI ENERGII SSSR, SERPUKHOV. INSTITUT FIZIKI VYSOKIKH ENERGII.
Investigation of a particle beam with energy up to 70 GeV with a spark spectrometer, 25:10868 (IFVE-SEF/OP-70-13)
GRENOBLE UNIV. (FRANCE). FACULTE DES SCIENCES.
Electron spin resonance study of defects produced by irradiation in an ionic solid: beryllium oxide, 25:11950 (CEA-R-3937)
Nuclear magnetic resonance at 310 MHz in a superconducting solenoid, 25:12034 (CEA-R-3855)
GRENOBLE UNIV. (FRANCE). INSTITUT DES SCIENCES NUCLEAIRES.
Experimental determination of couplings in deformed nuclei, 25:12523 (LYCEN-7034, pp 58-83)
Rapid chemical separations: general aspects, 25:10668 (LYCEN-7034, pp 1-8)
GULF GENERAL ATOMIC, INC., SAN DIEGO, CALIF.
DYNA: computer program for determining motions of head of PCRV with complete circumferential crack, 25:10753 (GAMD-7867)
Laser-pulse method of determining thermal diffusivity and thermal conductivity of graphite between 300° and 3300°K, 25:11487 (GA-9168)
Neutron activation for measuring bone calcium content, 25:10907 (N-70-31814)
GUTEHOFFNUNGSHUETTE STERKRADE A.G., OBERHAUSEN (WEST GERMANY).
Development program: steam-cooled fast reactor. I, 25:12767 (BMBW-FBK-70-20)

H

HAHN-MEITNER-INSTITUT FUER KERNFORSCHUNG, BERLIN (WEST GERMANY).
Investigations of radiation resistance of optoelectronic devices for an electronically scanning star sensor in satellites, 25:10904 (HMI-B-97)
HARVARD UNIV., BOSTON, MASS. HARVARD AIR CLEANING LAB.
Prog. rpt. on air cleaning, semiannual, 3--8/70, 25:10797 (NYO-841-23)
HEIDELBERG UNIV. (WEST GERMANY). PHYSIKALISCHES INSTITUT (II).
Investigation of β spectrum of ^{14}C with a proportional counter with inner anticoincidence screens, 25:12380 (KFK-1222)

I

IDAHO NUCLEAR CORP., IDAHO FALLS.
Axial fatigue of irradiated stainless steels tested at elevated temperatures, 25:11459 (IN-1437, pp 1-4)
Failure analysis, 25:11463 (IN-1437, pp 70-5)
Irradiation testing, 25:11462 (IN-1437, pp 59-70)
Metallurgical development, 25:11375 (IN-1437, pp 24-59)
Prog. rpt. on metallurgy and materials science, annual, FY 1970, 25:11458 (IN-1437)
Prototype elements, 25:11461 (IN-1437, pp 13-23)
Surveillance of test reactor beryllium and hafnium, 25:11460 (IN-1437, pp 5-12)
ILLINOIS UNIV., URBANA.
Effect of pressure on electronic structure of ferric hydroxamates and ferrichrome A, 25:12881 (COO-1198-777)
ILLINOIS UNIV., URBANA. COLL. OF VETERINARY MEDICINE.
Intestinal absorption of ^{47}Ca and ^{85}Sr in estradiol treated rats, 25:10933 (COO-1339-45)
ILLINOIS UNIV., URBANA. DEPT. of VETERINARY PHYSIOLOGY AND PHARMACOLOGY.
Calcium-47 turnover of a readily exchangeable calcium pool in pregnant and lactating cows, 25:12882 (COO-1339-44)

INDIANA UNIV., BLOOMINGTON.
Prog. rpt. on deuterium and tritium effects on rates of organic reactions, annual, 12/70, 25:10524 (COO-1008-16)
INDIANA UNIV., BLOOMINGTON. DEPT. OF CHEMISTRY.
α-deuterium effects on rate of solvolysis of 2-adamantyl sulfonate ester, 25:10523 (COO-1008-15)
Dependence of solvolytic α-deuterium rate effects on nature of the leaving group, 25:10522 (COO-1008-13)
Deuterium effects on binding of NADH to alcohol dehydrogenase isoenzyme EE, 25:10525 (COO-1008-17)
INFORMATION RESEARCH ASSOCIATES, INC., BERKELEY, CALIF.
MACYL6 hydrodynamic code, 25:10765 (AD-709142)
INSTITUT FUER PLASMAPHYSIK, G.M.B.H. GARCHING (WEST GERMANY).
Calculation of the ion-trajectories in front of a field emission tip, 25:12299 (IPP-7/2)
INSTITUT GUSTAVE ROUSSY, VILLEJUIF (FRANCE).
Recovery of skin reactions in mice after split-dose irradiation, 25:11260 (BNL-50203, pp 286-91)
INSTITUTE OF CANCER RESEARCH, SUTTON (ENGLAND). SURREY BRANCH.
Kinetics of cell proliferation in tumors, 25:11219 (BNL-50203, pp 130-53)
INSTITUTE OF NUCLEAR PHYSICS, KRAKOW (POLAND).
Accuracy of the neutron method of moisture measurement, 25:10887 (INP-709)
Parity nonconserving effects in nuclei ^{175}Lu and ^{181}Ta, 25:12517 (INP-714)
Polarization of protons from ^{12}C(d,p)^{13}C reaction at E/sub d/ = 12.4 MeV, 25:12377 (INP-711)
Real part of the alpha-nucleus potential obtained by double folding procedure, 25:12627 (INP-720)
INSTITUTE OF NUCLEAR RESEARCH, WARSAW (POLAND).
Analysis of D^0 meson in reaction π^+p + $p\pi^+\pi^+\pi^+\pi^-\pi^-\pi^0$ at 8 GeV/c, 25:12191 (INR-P-1207)
BIGG code in GIER-ALGOL 4 for the Gier computer, 25:12842 (INR-1193)
Effect of resin cross-linking on anion exchange separation of rare-earth--EDTA complexes, 25:10665 (INR-P-1209)
Excitation of isomeric activities in ^{71}Ge, ^{78}Br, and ^{79}Br using 14.8-MeV neutrons, 25:12430 (INR-P-1091)
Gamma vibration of nuclei at equilibrium and saddle point, 25:12628 (INR-P-1201)
Hypernuclei and hypernuclear spectroscopy, 25:12090 (INR-P-1223)
Volterra functional series for reactors with linear feedback, 25:12843 (INR-1206)
INSTITUTO DE ENERGIA ATOMICA, SAO PAULO (BRAZIL).
Catalytic reduction of aqueous solutions of uranyl nitrate, 25:10572 (IEA-184)
Dry-way preparation of thorium tetrafluoride, 25:10516 (IEA-185)
Fuel development. Program for calculation of a lattice of natural uranium and heavy water and for the calculation of the production of plutonium, 25:12797 (IEA-186)
Reduction of ammonium diuranate with anhydrous ammonia, 25:10573 (IEA-207)
Spectrographic determination of hafnium in zirconium oxide, 25:10431 (IEA-208)
INTERNATIONAL ATOMIC ENERGY AGENCY, VIENNA (AUSTRIA).
Conference on nuclear accident dosimetry systems, Vienna, 2/69, 25:11056 (STI/PUB-241)
Conference on sterilization and preservation of biological tissues by ionizing radiation, Budapest, 6/69, 25:11327 (STI/PUB-247)
Directory of nuclear reactors. VIII, 25:12824 (STI/PUB-248)
IOWA STATE UNIV. OF SCIENCE AND TECHNOLOGY, AMES. ENGINEERING RESEARCH INST.
Prog. rpt. on center of excellence in ceramic and composite materials, 9/68--8/69, 25:11472 (AD-708705)
Prog. rpt. on properties of ceramic materials, 3--5/70, 25:11473 (AD-708712)
IOWA UNIV., IOWA CITY. DEPT. OF CHEMISTRY.
Prog. rpt. on one and two electron transfer reactions, annual, 3/70--2/71, 25:10515 (COO-1780-14)
ISTITUTO NAZIONALE DI FISICA NUCLEARE, ROME (ITALY).
Nuclear forces and saturation, 25:12636 (NP-18580)

J

JAPAN ATOMIC ENERGY RESEARCH INST., TOKYO.
Detection of failed fuel at JRR-4, 25:12819 (JAERI-Memo-4196)
Development of reactor enclosure high voltage power cable penetration, 25:12705 (JAERI-Memo-4197)
ESR spectra of irradiated beryllium acetylacetonate single crystal, 25:10623 (JAERI-5026, pp 157-60)
ESR study of γ-irradiated pyridine--silica gel system, 25:10622 (JAERI-5026, pp 6-10)
Grafting acrylonitrile onto polyvinyl chloride powder and spinning fiber, 25:10595 (JAERI-5026, pp 35-41)
Grafting of acrylic acid onto polyester fiber, 25:10602 (JAERI-5026, pp 73-9)
Irradiation effects of oxytocin, 25:10625 (JAERI-5026, pp 164-7)
Irradiation tests of domestic Zircaloy-2 cladding materials in JPDR, 25:12862 (JAERI-Memo-4192)
Optical radiation from gases excited by high-energy electrons. II, 25:10585 (JAERI-5026, pp 153-5)
Optical radiation from gases excited by high-energy electrons. III, 25:10586 (JAERI-5026, pp 155-7)
Preparation of Wood--Polymer composite by ionizing radiation. VI, 25:10605 (JAERI-5026, pp 94-100)
Preparation of Wood--Polymer Composite by ionizing radiation. IV, 25:10603 (JAERI-5026, pp 80-5)
Preparation of Wood--Polymer-Composite by ionizing radiation. V, 25:10604 (JAERI-5026, pp 86-93)
Prog. rpt. on radiation chemistry, annual, 4/69--3/70, 25:10584 (JAERI-5026)
Radiation curing of mixture of diallylphthalate prepolymer and vinyl monomer. IV, 25:10607 (JAERI-5026, pp 108-20)
Radiation curing of mixture of diallylphthalate prepolymer and vinyl monomer. III, 25:10606 (JAERI-5026, pp 101-7)
Radiation curing of mixture of diallylphthalate prepolymer and vinyl monomer. V, 25:10608 (JAERI-5026, pp 121-9)
Radiation curing of monomer--polybutadiene mixture. I, 25:10609 (JAERI-5026, pp 130-6)
Radiation effects on gramicidin. II, 25:10587 (JAERI-5026, pp 167-8)
Radiation induced graft copolymerization to polyester. VII, 25:10600 (JAERI-5026, pp 63-7)
Radiation-induced graft copolymerization to polyester. IV, 25:10597 (JAERI-5026, pp 46-51)
Radiation-induced graft copolymerization to polyester. V, 25:10598 (JAERI-5026, pp 52-5)
Radiation-induced graft copolymerization to polyester. VI, 25:10599 (JAERI-5026, pp 56-62)
Radiation-induced graft copolymerization to polyester. VIII, 25:10601 (JAERI-5026, pp 68-72)
Radiation-induced graft polymerization of acrylonitrile onto poly(vinyl chloride) powder, 25:10596 (JAERI-5026, pp 42-5)
Radiolysis of cholestanol, 25:10624 (JAERI-5026, pp 160-4)
Stability of polyvinyl acetate emulsions produced by radiation-induced polymerization. I, 25:10593 (JAERI-5026, pp 15-25)
Stability of polyvinyl acetate emulsions produced by radiation-induced polymerization. II, 25:10594 (JAERI-5026, pp 26-34)
Studies on radiation-induced free-ionic polymerization by electrical conductivity measurements. II, 25:10610 (JAERI-5026, pp 169-71)
JERSEY CENTRAL POWER AND LIGHT CO., MORRISTOWN, N. J.
Forked River Nuclear Generating Station, Unit 1. Preliminary safety analysis report, Amendment 4, 25:12751 (DOCKET-50363-10)
JOHNS HOPKINS UNIV., BALTIMORE, MD. DEPT. OF PATHOBIOLOGY.
Prog. rpt. on the avifauna on Amchitka Island, Alaska, 8/14/67--6/9/68, 25:12869 (BMI-171-102)
JOINT INST. FOR NUCLEAR RESEARCH, DUBNA (USSR).
Acceleration and extraction of deuterons from the JINR proton synchrotron, 25:12303 (JINR-P9-5442)
Alpha and gamma decays of the high excited states of complex nuclei, 25:12629 (JINR-E4-5135)
Average field of excited nuclei, 25:12632 (JINR-P4-5084)
Calculation of the phase volume of the electron--ion bunches in the collective accelerator and the problems of separation, 25:12302 (JINR-P9-5405)
Classification of states and interactions in the nuclear collective model, 25:12631 (JINR-P4-5008)
Experiments on α-particle acceleration by collective method, 25:12305 (JINR-P9-5558)
Investigation of ^{8}Li recoil nuclei in ^{9}Be(p,2p)^{8}Li reaction at proton energies of 180 and 660 MeV, 25:12378 (JINR-P1-4872)
Method for pulsed polarized ion beam production for high-energy accelerators, 25:12304 (JINR-P9-5446)
Motion of the charged election ring in the ripple magnetic field, 25:12301 (JINR-P9-5394)
JOINT INST. FOR NUCLEAR RESEARCH, DUBNA (USSR). LAB. OF HIGH ENERGY.
Analysis of π^-p + $n\pi^+\pi^-m\pi^0$ (m = 1,2,3) and π^-p + $n2\pi^+2\pi^-m\pi^0$ (m = 1,2) reactions, 25:12204 (JINR-P1-5431)
Measurement of scattering angle of particles by Vavilov--Cherenkov radiation, 25:10869 (JINR-E13-5459)
Precision apparatus with liquid hydrogen target, 25:12300 (JINR-P8-5212)
Time-coordinate compensator for the time spectrometers with long scintillators, 25:10813 (JINR-P13-5378)
JOINT INST. FOR NUCLEAR RESEARCH, DUBNA (USSR). LAB. OF NUCLEAR PROBLEMS.
Dose characteristics of protons with energy 200 MeV, 25:11054 (JINR-P16-5383)
Fast valve of high pressure for bubble chamber, 25:10870 (JINR-P13-5420)
Reaction π^-p + e^+e^-n at 275 MeV, 25:12099 (JINR-P1-5398)
JOINT INST. FOR NUCLEAR RESEARCH, DUBNA (USSR). LAB. OF NUCLEAR REACTIONS.
Gasochromatographic separation of nonvolatile metal chlorides using aluminum chloride as eluent, 25:10666 (JINR-P6-5410)
Neutron detector in search for superheavy elements in nature, 25:10814 (JINR-P13-5391)

XUM

JOINT INST. FOR NUCLEAR RESEARCH, DUBNA (USSR). LAB. OF THEORETICAL PHYSICS.
Complication of the nuclear state structure with increasing excitation energy, 25:12630 (JINR-E4-5469)
Mass coefficient in nucleus collective Hamiltonian and sum rules for probabilities of E2-transitions and of quadrupole moments, 25:12633 (JINR-P4-5346)
JUNTA DE ENERGIA NUCLEAR, SACAVEM (PORTUGAL). LABORATORIO DE FISICA E ENGENHARIA NUCLEARES.
Behavior of neutrons in multiplying medium, 25:12341 (LFEN-NI.-46-a)
JYVASKYLA UNIV. (FINLAND). DEPT. OF PHYSICS.
Directional correlations of some γ-ray cascades in ^{200}Hg, 25:12527 (NP-18613)
Notes on quantum mechanical sum rules, 25:12046 (NP-18619)
Reinvestigation of the decay of ^{200}Tl, 25:12528 (NP-18647)
Semiconductor detector telescope electron spectrometer, 25:10852 (NP-18617)
Simultaneous recording of true and random coincidences using a two-parameter analyzer system, 25:10894 (NP-18614)
Table of cross sections of some reactions induced by 14 to 15 MeV neutrons, 25:12353 (NP-18616)

K

KARLSRUHE UNIV. (WEST GERMANY).
Modal development of the neutron transport equation for plane geometry, 25:12340 (KFK-1223)
KERNFORSCHUNGSANLAGE, JUELICH (WEST GERMANY). INSTITUT FUER FESTKOERPERFORSCHUNG.
Pseudorandom and Markov sequences optimizing correlation time-of-flight spectrometry, 25:10850 (JUL-684-FF)
KERNFORSCHUNGSANLAGE, JUELICH (WEST GERMANY). INSTITUT FUER RADIOCHEMIE.
Planning an atomic beam apparatus for investigation of elementary chemical processes of neutral particles, 25:10517 (JUL-674-RC)
KERNFORSCHUNGSANLAGE, JUELICH (WEST GERMANY). INSTITUT FUER REAKTORENTWICKLUNG.
Handling of fission products in calculation of burnup with regard to new nuclear data applied to graphite reactors, 25:12776 (JUL-676-RG)
KERNFORSCHUNGSANLAGE, JUELICH (WEST GERMANY). INSTITUT FUER REAKTORWERKSTOFFE.
Model investigations on conical fluidized beds, 25:11479 (JUL-669-RW)
Solubility and corrosion behavior of iron, steel, molybdenum, niobium, tantalum, vanadium, tungsten, and chromium in molten lead at high temperatures, 25:11376 (JUL-661-RW)
KERNFORSCHUNGSANLAGE, JUELICH (WEST GERMANY). ZENTRALINSTITUT FUER ANGEWANDTE MATHEMATIK.
Mathematical treatment of the stationary thermal conductivity in piecemeal homogeneous media, 25:10768 (JUL-657-MA)
KERNFORSCHUNGSANLAGE, JUELICH (WEST GERMANY). ZENTRALLABOR FUER ELEKTRONIK.
Pulse discriminator in nuclear electronics, 25:10815 (JUL-660-ZE)
KERNFORSCHUNGSZENTRUM, KARLSRUHE (WEST GERMANY).
Can failure--steam loop, 25:12820 (KFK-1255)
Estimation of unknown excitation functions for (α,xn)-(α,pxn)-, (d,xn)-, (d,pxn)-, and (p,xn)-reactions, 25:12529 (ORNL-tr-3020)
Proposal for a standard spectrum to check techniques of fast neutron spectrum measurements, 25:12816 (EACRP-L-74)
KERNFORSCHUNGSZENTRUM, KARLSRUHE (WEST GERMANY). INSTITUT FUER ANGEWANDTE KERNPHYSIK.
Computer program for discovery of excited nuclear states according to Ritz combination principle, 25:12519 (KFK-1247)
KERNFORSCHUNGSZENTRUM, KARLSRUHE (WEST GERMANY). INSTITUT FUER ANGEWANDTE REAKTORPHYSIK.
Incorporation of machine data handling in the monitoring of fissionable material in large research centers, 25:10796 (KFK-866)
KERNFORSCHUNGSZENTRUM, KARLSRUHE (WEST GERMANY). INSTITUT FUER NEUTRONENPHYSIK UND REAKTORTECHNIK.
Modal development of the neutron transport equation for plane geometry, 25:12340 (KFK-1223)
KERNFORSCHUNGSZENTRUM, KARLSRUHE (WEST GERMANY). INSTITUT FUER RADIOCHEMIE.
Emission spectroscopic determination of traces in nuclear fuel materials, 25:10432 (KFK-1261)
KERNFORSCHUNGSZENTRUM, KARLSRUHE (WEST GERMANY). INSTITUT FUER REAKTORBAUELEMENTE.
Observation windows of synthetic sapphire (leucosapphire) in high-pressure vessels, 25:11488 (KFK-1211)
KERNFORSCHUNGSZENTRUM, KARLSRUHE (WEST GERMANY). INSTITUT FUER REAKTORENTWICKLUNG.
In-pile arrangement for strain measurements in nuclear fuel and structural materials, 25:11464 (KFK-1281)
KERNFORSCHUNGSZENTRUM, KARLSRUHE (WEST GERMANY). LABOR FUER ELEKTRONIK UND MESSTECHNIK.
Resonator for x-band electron spin resonance spectroscopy for simultaneous measurement and electron radiation of the sample, 25:10626 (KFK-1285)
KERNFORSCHUNGSZENTRUM, KARLSRUHE (WEST GERMANY). ZYKLOTRON-LABORATORIUM.
Investigation of β spectrum of ^{14}C with a proportional counter with inner anticoincidence screens, 25:12380 (KFK-1222)
KERNKRAFTWERK RWE-BAYERNWERK G.M.B.H., GUNDREMMINGEN (WEST GERMANY).
KRB technical operating report, 10/70, 25:12723 (TID-25637)
KNOLLS ATOMIC POWER LAB., SCHENECTADY, N. Y.
Notes on the carbon total cross section from 0-2 MeV, 25:12379 (KAPL-P-3901)
Temperature dependence of neutron inelastic scattering from water, 25:12342 (RPI-328-210)

L

LOCKHEED MISSILES AND SPACE CO., PALO ALTO, CALIF. LOCKHEED PALO ALTO RESEARCH LAB.
Coordinated experiment on radar clutter and auroral particle fluxes, 25:11778 (AD-709105)
LOS ALAMOS SCIENTIFIC LAB., N. MEX.
Conference on plutonium and other actinides, Santa Fe, N. Mex., 10/70, 25:11433 (CONF-701001-(Pt.2))
Conference on plutonium and other actinides, Santa Fe, N. Mex., 10/70, 25:11372 (CONF-701001-(Pt.1))
MUX: simple approach to on-line computing, 25:12890 (LA-4524)
LOUISIANA POWER AND LIGHT CO., NEW ORLEANS.
Waterford Steam Electric Station, Units 3 and 4. Preliminary safety analysis report, Vol. 3, 25:12755 (DOCKET-50382-4)
Waterford Steam Electric Station, Units 3 and 4. Preliminary safety analysis report, Vol. 2, 25:12754 (DOCKET-50382-3)
Waterford Steam Electric Station, Units 3 and 4. Preliminary safety analysis report, Vol. 4, 25:12756 (DOCKET-50382-5)
Waterford Steam Electric Station, Units 3 and 4. Preliminary safety analysis report, Vol. 1, 25:12753 (DOCKET-50382-2)
LYON UNIV. (FRANCE). INSTITUT DE PHYSIQUE NUCLEAIRE.
Conference on low-energy spectrometry and nuclear spectrometry, Lyon, 2/70, 25:12520 (LYCEN-7034)
Development of source of polarized deuterons for a synchrocyclotron, 25:12309 (LYCEN-6909)
Nuclear magnetic moments and hyperfine interactions, 25:12521 (LYCEN-7034, pp 34-41)

M

MAGYAR TUDOMANYOS AKADEMIA KOZPONTI FIZIKAI KUTATO INTEZETE, BUDAPEST.
COBRA: computer program for coolant boiling in rod arrays, 25:12784 (KFKI-70-20-RPT)
High-stability apparatuses to investigate the angular distribution of charged particles of energies 10^{13}--10^{15} eV in the Galaxy, 25:11742 (KFKI-70-21-HEP)
Pulsed reactor potentialities for neutron activation analysis, 25:10489 (KFKI-70-25-NAC)
Quantitative autoradiography of Zr--T particles, 25:10775 (KFKI-70-26-HP)
MAINZ UNIV. (WEST GERMANY). INSTITUT FUER ANORGANISCHE CHEMIE UND KERNCHEMIE.
Prog. rpt. on inorganic chemistry and nuclear chemistry, annual, 1969, 25:10472 (BMBW-FBK-70-19)
MARYLAND UNIV., COLLEGE PARK.
Interfaces associated with ordered alloys, 25:12903 (ORO-3935-4)
MARYLAND UNIV., COLLEGE PARK. DEPT. OF CHEMISTRY.
Direct interaction effects in the fission of ^{238}U with 63.5-MeV ^{4}He ions, 25:12526 (MNC-3783-7)
MARYLAND UNIV., COLLEGE PARK. DEPT. OF PHYSICS AND ASTRONOMY.
Prog. rpt. on theoretical studies in nuclear reactions and structure, 9/70, 25:12639 (ORO-3765-28)
MARYLAND UNIV., COLLEGE PARK. ENGINEERING MATERIALS GROUP.
An investigation of methods of preparing high purity vanadium, 25:11356 (CONF-700546-1)
MASCHINENFABRIK AUGSBURG-NUERNBERG A. G., NUREMBERG (WEST GERMANY).
Development program: steam-cooled fast reactor. I, 25:12767 (BMBW-FBK-70-20)
MASSACHUSETTS INST. OF TECH., CAMBRIDGE. HEAT TRANSFER LAB.
Investigation of heat transfer augmentation through use of internally finned and roughened tubes, 25:12891 (NP-18608)
MAX-PLANCK-INSTITUT FUER PHYSIK UND ASTROPHYSIK, MUNICH (WEST GERMANY).
Influence of electrical conductivity on the equilibrium of low-pressure plasma in stellarators, 25:11912 (MPI-PA-7/62)
MEDICAL RESEARCH COUNCIL, LONDON (ENGLAND). EXPERIMENTAL RADIOPATHOLOGY RESEARCH UNIT.
Reoxygenation as a function of tumor size and histopathological type, 25:11258 (BNL-50203, pp 242-

54)
MICHIGAN STATE UNIV., EAST LANSING.
Utilization of benthic detritus in a mari lake, 25:12884 (COO-1599-31)
MICHIGAN UNIV., ANN ARBOR.
Decay schemes of ^{131}Ba and ^{192}Ir nucleus, 25:12532 (TID-25592)
Gamma-ray spectroscopic study of decays of ^{126}Sb and ^{126}I, 25:12531 (TID-25586)
MICHIGAN UNIV., ANN ARBOR. DEPT. OF MECHANICAL ENGINEERING.
Prog. rpt. on theoretical and experimental study of film condensation of liquid metal vapors, annual, 12/70, 25:12885 (COO-2032-6)
MILLSTONE POINT CO., HARTFORD, CONN.
Millstone Nuclear Power Station, Unit 1. Abnormal occurrence report No. 9, 25:12721 (DOCKET-50245-51)
MINNESOTA UNIV., MINNEAPOLIS. SCHOOL OF PHYSICS.
Treatment of two-particle continuum states in the shell model approach to nuclear reactions, 25:12625 (COO-1764-85)
MINNESOTA UNIV., MINNEAPOLIS. SCHOOL OF PHYSICS AND ASTRONOMY.
Consistency between low-energy and high-energy hadron scattering, 25:12175 (COO-1764-81)
MISSOURI UNIV., ROLLA.
Voids in neutron irradiated aluminum, 25:11465 (ORNL-TM-3109)
MONTANA UNIV., MISSOULA.
Mathematical model for approximating transient, three-dimensional groundwater systems, 25:12880 (BNWL-SA-3539)
MOUND LAB., MIAMISBURG, OHIO.
Electron beam welding study on U--Nb--Zr alloy, 25:11377 (MLM-1778)
UV mirror/grating radioisotope heaters fabrication, 25:10776 (MLM-1779)

N

NAGOYA UNIV. (JAPAN). INST. OF PLASMA PHYSICS.
Feedback control of the PIG discharge of the QP machine, 25:11921 (IPPJ-T-2)
Use of comformal mapping to improve uniformity of electric field, 25:12045 (IPPJ-T-4)
NATIONAL BUREAU OF STANDARDS, WASHINGTON, D. C.
Microchemical Analysis Section. Summary of activities, July 1969--June 1970, 25:10422 (NBS-TN-545)
National Bureau of Standards Reactor. Inlet filter strainer torn loose, 25:12814 (DOCKET-50184-24)
NATIONAL COUNCIL ON RADIATION PROTECTION AND MEASUREMENTS, WASHINGTON, D.C.
Radiation protection in veterinary medicine, 25:11075 (NCRP-36)
NATIONAL INST. OF RADIATION PROTECTION, STOCKHOLM (SWEDEN).
Swedish policy with regard to the limitation of radioactive discharges from nuclear power stations, 25:12757 (SSI-70-27)
NATIONAL INST. OF RADIOLOGICAL SCIENCES, CHIBA (JAPAN).
Role of DNA in cell killing by radiation, 25:10960 (BNL-50203, pp 82-90)
NAVAL RESEARCH LAB., WASHINGTON, D. C.
Direct interaction effects in the fission of ^{238}U with 63.5-MeV ^{4}He ions, 25:12526 (MNC-3783-7)
NEBRASKA UNIV., LINCOLN. DEPT. OF AGRONOMY.
Prog. rpt. on genetic effect of irradiated corn, final, 1970, 25:11009 (COO-1512-22)
Netherlands. Gezondheidsorganisatie, TNO. Radiobiologisch Instituut, Rijswijk.
Radiobiological bases in design of clinical trials, 25:11240 (BNL-50203, pp 339-52)
Response of tumor blood supply to fractionated irradiation, 25:11257 (BNL-50203, pp 210-14)
NEW ENGLAND INST., INC., RIDGEFIELD, CONN.
Preliminary study on temperature effect on positron annihilation in $KClO_4$, 25:12898 (NYO-3661-33)
NEW YORK UNIV., N. Y. SCHOOL OF ENGINEERING AND SCIENCE.
Geiger counters: theory, operation, and manufacture, 25:10807 (AD-708922)
NORTH CAROLINA STATE UNIV., RALEIGH.
Prog. rpt. on acoustic emissions from boiling bubbles, 2--11/70, 25:10769 (ORO-3911-3)
NORTH CAROLINA UNIV., CHAPEL HILL.
Activity coefficient and vacancy flow effects on tracer diffusion in silver-gold alloys, 25:12902 (ORO-2036-20)
NUCLEAR FUEL SERVICES, INC., ROCKVILLE, MD.
West Valley Reprocessing Plant. GPC crane room extension and sump collection tank. Final safety analysis report, 25:10662 (DOCKET-50201-71)
West Valley Reprocessing Plant. Low level liquid waste treatment plant. Final safety analysis report, 25:10660 (DOCKET-50201-58)
West Valley Reprocessing Plant. Progress report on low level waste treatment, 25:10661 (DOCKET-50201-59)
NUCLEAR MATERIALS AND EQUIPMENT CORP., APOLLO, PA. ENERGY CONVERSION DIV.
Prog. rpt. for radioisotope powered cardiac pacemaker, 8--10/70, 25:10777 (NUMEC-4189-3)
NUS CORP., ROCKVILLE, MD.
Engineering practices for large (4 inches and over) gate, globe, and check valves in water-cooled nuclear reactor systems, 25:12785 (ORNL-TM-3221)
Guide for specifying valves for water-cooled nuclear reactor systems, 25:12786 (ORNL-TM-3273)
NUS CORP., WASHINGTON, D.C. ENVIRONMENTAL SAFEGUARDS DIV.
States and radiation control, 25:11087 (CONF-700408-3)

O

OAK RIDGE NATIONAL LAB., TENN.
Analytical biochemistry, 25:10435 (ORNL-4636, pp 14-20)
Analytical instrumentation, 25:10424 (ORNL-4636, pp 34-40)
Analytical methodology, 25:10433 (ORNL-4636, pp 1-7)
Characterization and behavior of alkalized alumina during sulfur dioxide sorption--regeneration process, 25:12901 (ORNL-TM-3210)
Controls Department hybrid computer: hardware and applications, 25:10895 (ORNL-TM-3101)
Dose-estimation studies related to proposed construction of Atlantic--Pacific Interoceanic Canal with nuclear explosives: Phase III, 25:11055 (ORNL-4579)
Electron microscopy, 25:10437 (ORNL-4636, pp 45-50)
Engineering practices for large (4 inches and over) gate, globe, and check valves in water-cooled nuclear reactor systems, 25:12785 (ORNL-TM-3221)
Evaluation of Burgess Fobes Paint Company protective coatings for nuclear plant application, 25:12804 (ORNL-TM-3104)
Experiment description and hazards evaluation for the Series I ORNL oxide fuels irradiation in EBR-II, 25:11533 (ORNL-TM-2635(Suppl.))
Growth of Columbia River Limpet, Fisherola nuttalli (Haldeman), in normal and reactor-warmed water, 25:10996 (BNWL-1537)
Guide for specifying valves for water-cooled nuclear reactor systems, 25:12786 (ORNL-TM-3273)
Heavy section steel technology program. Technical report No. 10. Fracture toughness characterization study of A533, grade B, class 1 steel, 25:11380 (WCAP-7578)
Indexed bibliography on transportation and handling of radioactive materials--2, 25:10798 (ORNL-NSIC-84)
Mass spectrometry, 25:10436 (ORNL-4636, pp 43-5)
Methods development and evaluation laboratory, 25:10425 (ORNL-4636, pp 40-2)
Nuclear and radiochemistry, 25:10491 (ORNL-4636, pp 20-33)
Performance characteristics of cylindrical heat pipes for nuclear electric space and undersea power plants, 25:10755 (ORNL-TM-2803)
Process analyses, 25:10426 (ORNL-4636, pp 54-7)
Prog. rpt. on analytical chemistry, annual, 9/30/70, 25:10423 (ORNL-4636)
Prog. rpt. on isotope kilowatt program, 9/70, 25:10778 (ORNL-TM-3214)
Reactor projects, 25:10434 (ORNL-4636, pp 7-13)
Spectrometry services, 25:10438 (ORNL-4636, pp 51-3)
Synthesis, characterization, and fabrication of UN, 25:11480 (ORNL-4608)
Transuranium processing plant semiannual report of production, status, and plans for period ending June 30, 1970, 25:10654 (ORNL-4588)
Uranium and thorium diffusion in columnar pyrocarbons as influenced by actinide concentration, 25:11378 (ORNL-TM-2989)
Voids in neutron irradiated aluminum, 25:11465 (ORNL-TM-3109)
OHIO STATE UNIV., COLUMBUS.
Prog. rpt. on freshwater ecology of Amchitka Island, annual, 7/68, 25:12870 (BMI-171-103)
Prog. rpt. on geomorphology and pedology of Amchitka Island, annual, 6/68, 25:12873 (BMI-171-106)
OHIO STATE UNIV., COLUMBUS. DEPT. OF METALLURGICAL ENGINEERING.
Prog. rpt. on mixed conduction in solid electrolytes, annual, 12/1/70, 25:12883 (COO-1440-21)
OHIO STATE UNIV. RESEARCH FOUNDATION, COLUMBUS.
Plastic-strain controlled failure criteria and design parameters. Technical progress report, 25:11373 (COO-2048-1)
ONTARIO CANCER INST., TORONTO.
Recovery from radiation damage in mammalian cells, 25:11092 (BNL-50203, pp 41-53)
OSAKA UNIV. (JAPAN). LAB. OF NUCLEAR STUDIES.
Systematic properties of nuclei. II, 25:12640 (OU-LNS-70-2)

P

PARIS UNIV. (FRANCE).
Production of strange particles in π^+d interactions at 5.1 GeV/c, 25:12100 (NP-18629)
PARIS UNIV. (FRANCE). FACULTE DES SCIENCES.
Effect of α UO_3 in production of UO_2 and UF_4 from β UO_3--0.05 H_2O, 25:10569 (CEA-R-4074)
Study of neptunium hexafluoride formation and its adsorption on metallic fluorides, 25:10568 (CEA-R-4051)

PARIS UNIV., ORSAY (FRANCE).
Focusing and acceleration in ALICE, 25:12310 (NP-18612)
Germanium detectors and their use for charged particles, experimental study of (d,d'), (d,p), and (d,t) reactions on ^{12}C, 25:10851 (NP-18570)
PARIS UNIV., ORSAY (FRANCE). FACULTE DES SCIENCES.
Activation analysis using charged particles and γ photons, 25:10488 (CEA-R-4072)
Electronic properties of actinide carbides and nitrides, 25:11980 (CEA-R-4113)
Germanium detectors and their use for charged particles, experimental study of (d,d'), (d,p), and (d,t) reactions on ^{12}C, 25:10851 (NP-18570)
High-magnetic field compression produced by implosion of a thin metal tube, 25:11917 (CEA-R-4024)
Meson π^+ photoproduction at 180° on H from 450 MeV to 3 GeV, 25:12067 (LAL-1239)
Resonance in reactions $K^-p \to \Sigma^+\pi^-$ between 440 and 1230 MeV/c, 25:12098 (CEA-R-4068)
PARIS UNIV., ORSAY (FRANCE). INSTITUT DE PHYSIQUE NUCLEAIRE.
On-line nuclear spectroscopy, 25:10670 (LYCEN-7034, pp 23-33)
Theoretical developments in spectroscopy of spherical nuclei, 25:12634 (LYCEN-7034, pp 147-72)
PARIS UNIV., ORSAY (FRANCE). LABORATOIRE DE L'ACCELERATEUR LINEAIRE.
Beam--beam effect, 25:12308 (LAL-RT-5-70)
Meson π^+ photoproduction at 180° on H from 450 MeV to 3 GeV, 25:12067 (LAL-1239)
PARIS UNIV., ORSAY (FRANCE). LABORATOIRE JOLIOT-CURIE DE PHYSIQUE NUCLEAIRE.
Nuclear reorientation, 25:12522 (LYCEN-7034, pp 42-57)
Nucleosynthesis of Li, Be, and B, 25:11542 (NP-18591)
PENNSYLVANIA UNIV., PHILADELPHIA. DEPT. OF PHYSICS.
Progenitor sum-rules in nuclear physics, 25:12637 (NYO-2171-328)
Theoretical foundation of variable moment of inertia models, 25:12638 (NYO-2171-334)
PENNSYLVANIA UNIV., PHILADELPHIA. DEPT. OF RADIOLOGY.
Biology of dose-limiting tissues, 25:11253 (BNL-50203, pp 154-73)
PHYSIKALISCH-TECHNISCHE BUNDESANSTALT, BRUNSWICK (WEST GERMANY).
Gamma radiation following capture of neutrons, especially of polarized reactor neutrons by oriented nuclei, 25:12626 (FMRB-33/70)
Reactivity measurement in reactor cores on MTR fuel elements with a one-sided heavy water reflector, 25:12818 (FMRB-34/70)
PITTSBURGH UNIV., PA. DEPT. OF PHYSICS.
Relativistic quantum mechanics of dyons: exact solutions, 25:12047 (NYO-3829-65)
PRINCETON UNIV., N.J. JOSEPH HENRY LABS.
Existence of complex poles and oscillatory average multiplicity in multiperipheral models, 25:12122 (NYO-2262-TA-228)
PRINCETON UNIV., N. J. PLASMA PHYSICS LAB.
Measuring current distribution in a Tokamak plasma, 25:11867 (MATT-818)
PUBLIC SERVICE CO. OF COLORADO, DENVER.
Fort St. Vrain Nuclear Generating Station, Unit 1. Applicant's environmental report: operating license stage, 25:12737 (DOCKET-50267-25)
Fort St. Vrain Nuclear Generating Station, Unit 1. Preliminary safety analysis report, Amendment 17, 25:12736 (DOCKET-50267-24)
PUERTO RICO NUCLEAR CENTER, SAN JUAN.
Relations between dose-time, fractionation, and rest period in radiation therapy, 25:11222 (BNL-50203, pp 280-5)
PUERTO RICO WATER RESOURCES AUTHORITY, SAN JUAN.
Aguirre Nuclear Plant, Unit No. 1. Preliminary facility description and safety analysis report, Amendment 1, 25:12752 (DOCKET-50376-7)
PURDUE UNIV., LAFAYETTE, IND. DEPT. OF CHEMISTRY.
Prog. rpt. on radiochemical investigation of nuclear properties, 10/69--9/70, 25:12514 (COO-1672-21)
PURDUE UNIV., LAFAYETTE, IND. DEPT. OF PHYSICS.
E2/M1 multipole mixing ratios in spherical nuclei ^{124}Te, ^{126}Te, and ^{126}Xe, 25:12515 (COO-1746-51)

R

RADIO CORP. OF AMERICA, HARRISON, N. J.
Silicon germanium thermoelectric materials and module development program, 25:11477 (ALO-2510-T-1)
RAND CORP., SANTA MONICA, CALIF.
Differential quadrature and long-term integration, 25:12914 (TID-25633)
Weak interaction Hamiltonian in L-matrix theory, 25:12162 (AD-710572)
REACTOR CENTRUM NEDERLAND, PETTEN.
Post-failure examination of the in-pile section of the pressurized water loop in the HFR at Petten, 25:12823 (RCN-125)
Prog. rpt. on fast reactor program, 1--3/70, 25:12768 (EURFNR-855)
RENSSELAER POLYTECHNIC INST., TROY, N. Y.
Temperature dependence of neutron inelastic scattering from water, 25:12342 (RPI-328-210)
ROCHESTER GAS AND ELECTRIC CORP., N. Y.
Robert Emmett Ginna Nuclear Power Plant, Unit No. 1. Request for approval of respiratory protection procedure, 25:12733 (DOCKET-50244-54)
ROCHESTER UNIV., N. Y. DEPT. OF RADIATION BIOLOGY AND BIOPHYSICS.
Effects of radiation on vasculature of intestine, 25:11255 (BNL-50203, pp 181-5)
ROLAND EOTVOS UNIV., BUDAPEST (HUNGARY). INST. FOR THEORETICAL PHYSICS.
Energies of nuclei with different neutron and proton number in Thomas Fermi approximation, 25:12635 (NP-18545)
ROME UNIV. (ITALY). ISTITUTO DI FISICA.
Nuclear forces and saturation, 25:12636 (NP-18580)

S

SAINT BARTHOLOMEW'S HOSPITAL MEDICAL COLL., LONDON (ENGLAND).
Effect of 14-MeV electrons on blood vessels of the mouse earlobe, 25:11254 (BNL-50203, pp 174-80)
SAN DIEGO GAS AND ELECTRIC CO., CALIF.
San Onofre Nuclear Generating Station, Units 2 and 3. Preliminary safety analysis report, Amendment 5, 25:12750 (DOCKET-50361-13)
SANDIA LABS., ALBUQUERQUE, N. MEX.
Development of pelletized heat sources for thermal batteries, 25:12905 (SC-CR-70-6137)
Outdoor aging of adhesive sealants, 25:12908 (SC-RR-70-163)
Rotating mirror framing camera, 25:12907 (SC-M-70-886)
RUNKUT: computer routine for integrating systems of first order ordinary differential equations, 25:12906 (SC-M-70-868)
Strain hardening and strain rate in one-dimensional wave propagation calculations, 25:12909 (SC-RR-70-471)
Wind and airblast loads on window panes, 25:10792 (SC-RR-70-441)
SCHOOL OF AEROSPACE MEDICINE, BROOKS AFB, TEX.
Bibliography on whole-body irradiation effect related to canine treadmill performance decrement, 25:11251 (AD-705976)
SCIENTIFIC RESEARCH ATOMIC REACTOR INST., MELEKESS (USSR).
Effect of irradiation on mechanical properties of fcc alloys of Fe--Cr--Ni system. I, 25:11466 (SRARI-P-78)
SIEMENS A.G., ERLANGEN (WEST GERMANY).
Research and development work for Obrigheim Nuclear Power Station, 25:12704 (BMBW-FBK-70-11)
SOCIETE D'ENERGIE NUCLEAIRE FRANCO-BELGE DES ARDENNES, CHOOZ-LEZ-GIVET (FRANCE).
SENA technical operating report, 10/70, 25:12722 (TID-25636)
SOUTH CAROLINA UNIV., COLUMBIA. COLL. OF ENGINEERING.
Prog. rpt. on powder metallurgy compaction, 9--11/70, 25:12913 (SRO-475-9)
SOUTHERN CALIFORNIA EDISON CO., CAMP PENDLETON, CALIF.
San Onofre Nuclear Generating Station, Units 2 and 3. Preliminary safety analysis report, Amendment 5, 25:12750 (DOCKET-50361-13)
STANFORD LINEAR ACCELERATOR CENTER, CALIF.
Recent developments in inelastic electron--nucleon scattering, 25:12068 (SLAC-PUB-842)
STANFORD RESEARCH INST., MENLO PARK, CALIF.
Thallium--iodine phase diagram, 25:12912 (SRIA-106-76)
STANFORD UNIV., CALIF. DEPT. OF MATERIALS SCIENCE.
Prog. rpt. on structure dependence of high temperature deformation of metals, 3/69--3/70, 25:11434 (SU-326-P-17-X-1)
STANFORD UNIV., CALIF. DEPT. OF RADIOLOGY.
Radiobiology of mammalian cells, 25:11239 (BNL-50203, pp 117-29)
STANFORD UNIV., CALIF. HIGH-ENERGY PHYSICS LAB.
Elastic electron scattering from ^{12}C, 25:12376 (AD-710383)
SYRACUSE UNIV., N. Y. DEPT. OF PHYSICS.
Inequalities for s- and p-wave π π partial-wave amplitudes, 25:12193 (SU-1206-234)

T

TATA INST. OF FUNDAMENTAL RESEARCH, BOMBAY (INDIA).
Inequalities for s- and p-wave π π partial-wave amplitudes, 25:12193 (SU-1206-234)
TECHNICAL UNIV. OF HELSINKI, OTANIEMI (FINLAND). DEPT. OF TECHNICAL PHYSICS.
SYNTH2: two dimensional multigroup flux synthesis calculation code, 25:12844 (TKK-F-A-121)
Use of nuclear polarization in neutron scattering and transmission measurements, 25:12533 (TKK-F-A-123)
TECHNISCHE HOCHSCHULE, AACHEN (WEST GERMANY).
Handling of fission products in calculation of burnup with regard to new nuclear data applied to graphite reactors, 25:12776 (JUL-678-RG)
TECHNISCHE HOCHSCHULE, AACHEN (WEST GERMANY). INSTITUT FUER TECHNISCHE CHEMIE UND PETROLCHEMIE.
Contributions to the radiation-induced sulfoxidation of

paraffins, 25:10592 (BMBW-FBK-70-25)
TECHNISCHE UNIVERSITAET, BERLIN (WEST GERMANY). INSTITUT FUER KERNTECHNIK.
Stationary heat transfer in infinitely long fuel elements with locally varying heat sources and boundary conditions, 25:12799 (TUBIK-17)
TECHNISCHE UNIVERSITAET, HANOVER (WEST GERMANY).
Gamma radiation following capture of neutrons, especially of polarized reactor neutrons by oriented nuclei, 25:12626 (FMRB-33/70)
TECHNISCHE UNIVERSITAET, MUNICH (WEST GERMANY). INSTITUT A FUER THERMODYNAMIK.
Heat transfer to refrigerants at nucleate boiling, film boiling, and supercritical condition of the fluid, 25:10767 (BMBW-FBK-70-24)
TECHNISCHER UEBERWACHUNGS-VEREIN E. V., COLOGNE (WEST GERMANY). INSTITUT FUER REAKTORSICHERHEIT.
Safety of heavy water system in Braunschweig research reactor, 25:12822 (NP-18499)
TECHNISCHER UEBERWACHUNGS-VEREIN HANNOVER E.V. (WEST GERMANY).
Safety of heavy water system in Braunschweig research reactor, 25:12822 (NP-18499)
TEL AVIV UNIV. (ISRAEL). DEPT. OF PHYSICS.
Consistency between low-energy and high-energy hadron scattering, 25:12175 (COO-1764-81)
TENNESSEE UNIV., KNOXVILLE. DEPT. OF BOTANY.
Prog. rpt. on plant ecology of Amchitka Island, Alaska, annual, 8/1/67--6/30/68, 25:12874 (BMI-171-107)
TENNESSEE VALLEY AUTHORITY, CHATTANOOGA. OFFICE OF POWER.
Browns Ferry Nuclear Plant, Units 1, 2, and 3. Environmental radioactivity levels. Semiannual report, January--June 1970, 25:12735 (DOCKET-50259-21)
TOKYO UNIV. (JAPAN). INST. FOR NUCLEAR STUDY.
Numerical differential cross sections of reaction $^{58}Ni(p,t)^{56}Ni$ with 51.9 MeV protons, 25:12431 (INSJ-124)
Quasi-gamma bands in ^{152}Gd and possible presence of quasi-K quantum number, 25:12518 (INSJ-123)
TOULOUSE UNIV. (FRANCE).
Diffusion of the minor constituents into the troposphere, 25:10704 (NP-18609)
Various vertical sampling devices for aerosols, 25:10754 (NP-18633)
TRIANGLE UNIVERSITIES NUCLEAR LAB., DURHAM, N.C.
Prog. rpt., annual, 10/68--9/69, 25:12534 (TUNL-2)

U

UNIDYNAMICS, PHOENIX, ARIZ.
Development of pelletized heat sources for thermal batteries, 25:12905 (SC-CR-70-6137)
UNION CARBIDE CORP., OAK RIDGE, TENN. Y-12 PLANT.
Observation of ablation behavior of fibrous carbon--carbon composites, 25:12920 (Y-1752)
X-ray and nuclear radiation facilities, personnel safety features, 25:11078 (Y-1754)
UNITED KINGDOM ATOMIC ENERGY AUTHORITY, RISLEY (ENGLAND). REACTOR GROUP.
Assessing the economics of nuclear power stations in an electricity generating system, 25:12724 (TRG-Report-2090)
Computation of asymmetric power divergences in large nuclear reactors, 25:12777 (TRG-Report-2060(Rev.))
UNITED STATES-EURATOM FAST REACTOR EXCHANGE PROGRAM.
Prog. rpt. on fast reactor program, 1--3/70, 25:12768 (EURFNR-855)
UNIVERSIDAD NACIONAL AUTONOMA DE MEXICO, MEXICO CITY. FACULTAD DE CIENCIAS.
EPR of irradiated seeds of Dahlia coccinea, 25:11305 (NP-18394)
Preservation of food by irradiation: preliminary studies on commercial shrimp, 25:11326 (NP-18393)
UNIVERSITY CENTRAL HOSPITAL, HELSINKI (FINLAND). RADIOTHERAPY CLINIC.
Split-course techniques, 25:11223 (BNL-50203, pp 292-307)
UNIVERSITY OF SOUTHERN CALIFORNIA, LOS ANGELES.
Differential quadrature and long-term integration, 25:12914 (TID-25633)
UNIVERSITY OF SOUTHERN CALIFORNIA, LOS ANGELES. DEPT. OF PHYSICS.
Electroabsorption and electro-photoluminescence in HgI_2, 25:12915 (UCLA-34-P-122-X-1)
UPPSALA UNIV. (SWEDEN). INST. OF PHYSICS.
Study of nonlinear instabilities, 25:11913 (UUIP-722)
URS RESEARCH CO., SAN MATEO, CALIF.
Interaction of fallout with fires, 25:10702 (AD-708558)
Properties of radioactive fallout: balloon-mounted Shot Priscilla, 25:10733 (AD-708566)
Properties of radioactive fallout: surface detonation Coulomb C, 25:10734 (AD-708567)
UTAH STATE UNIV., LOGAN.
Prog. rpt. on freshwater vertebrate and invertebrate ecology of Amchitka Island, annual, 8/30/67--6/30/68, 25:12871 (BMI-171-104)

V

VERMONT YANKEE NUCLEAR POWER CORP., RUTLAND.
Vermont Yankee Nuclear Power Station. Preliminary safety analysis report, Amendment 17 (includes additional revisions to final safety analysis report), 25:12738 (DOCKET-50271-35)
VIRGINIA ELECTRIC AND POWER CO., RICHMOND.
Surry Power Station, Units 1 and 2. Applicant's environmental report, operating license stage, 25:12739 (DOCKET-50280-32)
Surry Power Station, Units 1 and 2. Preliminary safety analysis report, Amendment 17, 25:12740 (DOCKET-50280-33)

W

WADCO CORP., RICHLAND, WASH.
DPB: dynamic programming code for optimizing short-term operation of a power utility, 25:12919 (WHAN-IR-47)
Evaluation of PuO_2 homogeneity in PuO_2--UO_2 fast reactor fuel by scanning electron microprobe, 25:11489 (WHAN-FR-20)
WARSAW UNIV. (POLAND). INST. FOR THEORETICAL PHYSICS.
Relativistic quantum mechanics of dyons: exact solutions, 25:12047 (NYO-3829-65)
WASHINGTON UNIV., SEATTLE. COLL. OF FISHERIES.
Prog. rpt. on research program on marine ecology and oceanography, Amchitka, annual, 7/1/67--6/30/68, 25:12877 (BMI-171-114)
WASHINGTON UNIV., SEATTLE. DEPT. OF PHYSICS.
Validity of Sopkovich approximation, 25:12641 (RLO-1388-595)
WASHINGTON UNIV., SEATTLE. LAB. OF RADIATION ECOLOGY.
Prog. rpt. on natural alpha-emitting radioisotopes in marine organisms, annual, 1970--71, 25:10997 (RLO-2225-T-14-1)
WASHINGTON UNIV., SEATTLE. NUCLEAR PHYSICS LAB.
Spin isomers of the shape isomer /sup 237m/Pu, 25:12530 (RLO-1388-130)
WESLEYAN UNIV., MIDDLETOWN, CONN.
Singular off-mass-shell equation with vector-meson exchange, 25:12192 (NYO-2262-TA-232)
WESTINGHOUSE ELECTRIC CORP., PITTSBURGH, PA. PWR SYSTEMS DIV.
Heavy section steel technology program. Technical report No. 10. Fracture toughness characterization study of A533, grade B, class 1 steel, 25:11380 (WCAP-7578)
WISCONSIN ELECTRIC POWER CO., MILWAUKEE.
Point Beach Nuclear Plant, Unit No. 2. Preliminary safety analysis report, Amendment 11, 25:12744 (DOCKET-50301-26)
WISCONSIN MICHIGAN POWER CO., APPLETON, WIS.
Point Beach Nuclear Plant, Unit No. 2. Preliminary safety analysis report, Amendment 11, 25:12744 (DOCKET-50301-26)
WISCONSIN UNIV., MADISON.
Magnetic moments of the 7/2- mirror states in ^{37}Ar and ^{37}K, 25:12429 (COO-7-565)
WISCONSIN UNIV., MADISON. DEPT. OF ELECTRICAL ENGINEERING.
Prog. rpt. on plasma instabilities, 9/15/70, 25:11909 (COO-1695-31)
Prog. rpt. on plasma instabilities, annual, 12/15/70, 25:11910 (COO-1695-32)
WORLD HEALTH ORGANIZATION, GENEVA (SWITZERLAND).
Environmental radiation surveillance laboratory, 25:10763

Y

YALE UNIV., NEW HAVEN, CONN.
Repair and reconstruction of chromosomal DNA, 25:11007 (BNL-50203, pp 1-13)

Z

ZENTRALSTELLE FUER ATOMKERNENERGIE-DOKUMENTATION, FRANKFURT AM MAIN (WEST GERMANY).
High energy physics index, Vol. 8, No. 24, 1970, 25:12124
High energy physics index, Vol. 8, No. 25, 1970, 25:12123
Plasma physics index, Vol. 5, No. 10, 1970, 25:11857
Surface and vacuum physics index, Vol. 5, No. 10, 1970, 25:11678
Technology index for plasmaphysics research and fusion reactors, Vol. 4, No. 10, 1970, 25:11858
Technology index for plasmaphysics research and fusion reactors, Vol. 4, No. 11, 1970, 25:11856

XUM

PERSONAL AUTHOR INDEX

Authors' names are indexed in the form appearing in the abstracted publication. Each entry under an author's name gives the publication title and the *NSA* volume and abstract numbers. Report numbers, where applicable, are given in parentheses at the end of the entry.

Because of problems involved in the mechanical preparation of this index, all accent marks are omitted. The following changes in spelling have been introduced to reduce some of the confusion which might result from omitting the accents:

Germanic	ä appears as	ae
Germanic	ö	oe
Germanic	ü	ue
Scandinavian	ϕ	oe

A

AARONS, Jules, Scintillation boundary during quiet and disturbed magnetic conditions, 25:11791

ABATE-DAGA, G., Nuclear fuel with burnable poison. I, 25:10571 (EUR-4550)

ABBATTISTA, N., Designing method of switching circuits cascade for analog parameter discrimination, 25:10901

ABBONDANNO, U., Isospin-forbidden analogue resonances in ^{33}Cl. I, 25:12506

ABDALLA, M. M., Application of radiation techniques to water use efficiency studies, 25:10927

ABD-EL-AL, Sh. I., Application of radiation techniques to water use efficiency studies, 25:10927

ABE, Hideo, Texture of Zn--Cd alloy ingot solidified from the flowing liquid, 25:11450

ABE, Jiro, Some electrical properties of the uranium--plutonium mixed oxides, 25:11991

ABELLAN, Jose Ortega, Bases of a program of investigation for the development of the reprocessing of fuels irradiated in fast reactors, 25:10672

ABEND, Klaus, Pulse discriminator in nuclear electronics, 25:10815 (JUL-660-ZE)

ABEY, A. E., Effect of pressure and strain rate on the shear strength of beryllium, 25:11394

Shear strength of beryllium, uranium, and tungsten as a function of strain, strain rate, and pressure, 25:11379 (UCRL-72477)

ABDU-LEILA, H., Lifetimes of some excited states in ^{182}W, 25:12577

ABRAHAM, D. R., Spin dependence in inelastic scattering, 25:12454

ABRAHAM, K., Differential diagnosis of brain alterations caused by tumor and vascular processes with radioactive isotope blood flow measurements, 25:11149

ACHASOV, N. I., Influence of rho^0--w mixing on spin density matrix of w meson, 25:12208

ACHMATOWICZ-SZMAJKE, T., Radiation-induced graft terpolymerization of poly(ethylene terephthalate). II, 25:10621

ACTON, L. W., Thermal continuum function for x-ray emission from coronal plasmas, 25:11632

ADACHI, S., Measurement of the phase constant along a conducting wire in a magnetoplasma, 25:11935

ADAM, W. E., Computer evaluation of scintigraphic studies obtained with a scintillation camera, 25:11122

Quantitative radiocardiographic studies with a scintillation camera, 25:11119

Scintigraphy of renal function evaluated by digital and analog computers, 25:11165

Studies on liver function with computer-scintigraphy, 25:10919

ADAMS, N., United Kingdom research and experience in criticality dosimetry, 25:11084

ADCOCK, C., Transverse momentum of secondaries from cosmic-ray interactions in region 2 x 10^5 GeV, 25:11749

ADORNI, N., Underwater plasma-arc cutting as a powerful dismantling tool for water reactors, 25:12714

ADRIAN, A., Some frequency shifts by ^{13}C substitution in the ir spectra of C_2H_4, C_2D_4, and C_2H_4, 25:10563

AFANAS'EV, G. G., Changes in lethal effect of irradiation of cells cultivated outside of organism due to chemical compounds, 25:11106

AFANASJEV, G. N., Classification of states and interactions in the nuclear collective model, 25:12631 (JINR-P4-5008)

AFFELDT, B., Development program: steam-cooled fast reactor. I, 25:12767 (BMBW-FBK-70-20)

AFONINA, R. G., Boundary of captured 280-keV electrons and position of current electrojets in the ionosphere, 25:11782

AGACHE, C., Carbonaceous mesophase formed in the pyrolysis of graphitizable organic materials, 25:11529

AGASSI, D., Core polarization corrections to DWBA for (p,p') scattering, 25:12678

AGEMAR, F., Development program: steam-cooled fast reactor. I, 25:12767 (BMBW-FBK-70-20)

AGTERDENBOS, J., Determination of trace amounts of I. II, 25:10481

AHMED, M. Y. Y., Effects of gamma radiation on cotton leaf worm, 25:11247

AHMED, Mohamed S. H., Killing effect of γ radiation on Oryzaephilus surinamensis, 25:11244 (NP-18607)

AHMED, N., Investigations of excited states of ^{98}Mo nucleus from reaction ^{98}Mo(n,γ)^{99}Mo, 25:12598

AICHELBURG, P. C., Gravitational field of a massless particle, 25:12283

AIRAPETYAN, G. M., Protective effects of biogenic amines in the radiation intestinal syndrome, 25:11102

AITKEN, E. A., Thermodynamic behavior of plutonium oxide systems in a temperature gradient, 25:11505

AKASOFU, S.-I., Cosmic-ray variations during geomagnetic storms, 25:11745

AKHRAROV, S. M., Study of highly excited nuclear states using γ rays from neutron capture, 25:12490

AKIBA, T., Deep inelastic e-p scattering and a reggeization scheme for photon processes, 25:12148

AKIMOV, A. I., Equilibrium vacancies in lanthanum, 25:11423

AKIMOV, Yu. K., Reaction π$^-$p → e$^+$e$^-$n at 275 MeV, 25:12099 (JINR-P1-5398)

ALBERS, Lynn U., Reduction of the ray effect in discrete ordinates calculations, 25:12852

ALBINOWSKA, Miroslawa, Effect of x-ray upon stored blood, 25:10981

ALBOUY, G., Coulomb excitation of ^{123}Te and ^{125}Te, 25:12603

ALBURGER, D. E., Half-lives of ^{11}Be, ^{15}C, ^{16}N, ^{19}O, and ^{28}Al, 25:12394

ALCOCK, A. J., Laser-produced plasmas at NRC'S Physics Division, 25:11907

ALEKSANDROV, I. A., Investigation of a particle beam with energy up to 70 GeV with a spark spectrometer, 25:10868 (IFVE-SEF/OP-70-13)

ALEKSEEV, F. A., Radioactive elements and deuterium in underground waters of the Bukhara--Karshin artesian basin, 25:10698

ALEKSEEV, P. D., Temperature dependence of kinetics of F-center accumulations under proton irradiation, 25:11965

ALEKSEEVA, S. I., Dose effects curves for Ehrlich's ascites cells irradiated with γ rays, 25:11014

ALEKSIN, V. F., Effect of toroidal state on vacuum magnetic configuration of vintotron, 25:11922 (KHFTI-70-25)

ALEXANDER, C. A., Thermophysical properties of (UPu)N, 25:11492

ALEXANDER, J. K., Spectrum of the extragalactic background radiation at low radio frequencies, 25:11666

ALEXANDER, J. M., Production of ^{149}Tb from Au by 2.2-GeV protons, 25:12580

ALEXANDER, K., Determination of central circulation parameters and peripheral blood flow by simultaneous application of ^{133}Xe and ^{131}I-labeled RISA, 25:11123

AL-HINDAWI, Ali Y., Radiobiology of thyroid gland, 25:11291

ALI, S., Equivalent local potentials from nonlocal separable ones, 25:12658

ALIKHANIAN, A. I., High energy particle identification by x-ray transition radiation (XTR) detectors, 25:10877

ALIMARIN, I. P., Analytical chemistry of mixed ligand complexes, 25:10460

ALKHAZOV, G. D., Statistics of electron avalanches and ultimate resolution of proportional counters, 25:10838

ALLADINE, F. A., Homograft heart--valve replacement, 25:11336
ALLEMAND, R., Stationary gas detectors for mapping and dynamic studies of organs using x ray or low-energy γ-ray emitters, 25:10810 (CEA-CONF-1668)
ALLEN, B. J., Nonresonant neutron capture in ^{207}Pb, 25:12539
ALLEN, J. E., Ion rarefaction waves, 25:11938
One-dimensional ion--acoustic modes of bounded plasmas, 25:11937
ALLEN, R. P., Beta grain size and β → α transformation in unalloyed Pu, 25:11444
ALLEN, Richard S., Scintillation boundary during quiet and disturbed magnetic conditions, 25:11791
ALLEN, W. D., Energy distribution of fast electrons present in beams from hollow-anode gas discharge electron guns, 25:12319
ALLINGER, J. E., Economical beam transport for utilization of post conversion AGS, 25:12296 (BNL-15464)
ALLTON, Wayne H., Prog. rpt. on sea otter natural mortality at Amchitka Island, Alaska, 2/20/68--6/20/68, 25:12868 (BMI-171-101)
ALPERT, J. S., Evaluation of arterial insufficiency of the legs, 25:11139
ALSMILLER, R. G. Jr., Lateral spread of high-energy (less than or equal to 400 MeV) neutron beams, 25:12332
ALSTON-GARNJOST, M., A_2 mass spectrum in 7-GeV/c π⁺p interactions, 25:12116
ALTARELLI, Guido, Light-cone analysis of massive μ-pair production, 25:12228
AMADORI, R., Pseudorandom and Markov sequences optimizing correlation time-of-flight spectrometry, 25:10850 (JUL-684-FF)
AMATO, I., Nuclear fuel with burnable poison. I, 25:10571 (EUR-4550)
AMAYA, Toshihiko, Hydrolysis of Cu(II) ion in heavy water, 25:10566
AMMANN, W., Computer evaluation of scintigraphic studies obtained with a scintillation camera, 25:11122
Scintigraphy of renal function evaluated by digital and analog computers, 25:11165
AMON, F., Development program: steam-cooled fast reactor. I, 25:12767 (BMBW-FBK-70-20)
AMOS, D. E., Helium diffusion in $^{238}PuO_2$, 25:11501
AMSTER, Harvey, Determining collision variances from adjoints, 25:12839
AMY, Jean-Paul, Environmental mobility of ^{106}Ru during irrigation processes, 25:10692
ANAN'IN, V. M., Diffusion of nickel in beryllium, 25:11399
ANANTHANARAYANAN, K., Beta decay of M1 decay rates for A = 20 nuclei, 25:12468
ANDERSEN, B. L., Potential landscape for fissioning nuclei. I, 25:12681
ANDERSON, J. J. B., Calcium-47 turnover of a readily exchangeable calcium pool in pregnant and lactating cows, 25:12882 (COO-1339-44)
ANDERSON, R. L., Pi^0 photoproduction from H with linearly polarized photons, 25:12072
ANDERSON, T. D., Offshore siting of nuclear energy stations, 25:12765
ANDERSSON, L., Spectrochemical determination of tracers of impurity elements in Pu by Cu spark method, 25:10444
Study of the precise determination of macroamounts of plutonium in solution by three electrometric oxidation--reduction titration methods, 25:10445
ANDERSSON, S., Density increase in Si(111) surface region created by Ar ion bombardment, 25:11970
Mean square thermal displacement for surface atoms in nickel (001) surface, 25:12017
ANDRE, S., Disintegration of the two isomers of ^{80}Br (31.8 min and 6.0 min), 25:12444
ANDREWS, J. G., Ion rarefaction waves, 25:11938
ANDRIEUX, Claude, Gamma-ray spectrometry in drillings using Ge--Li semiconductor probes, 25:10849 (CEA-CONF-1694)
ANDRIOT, Roger, Transferring solid radioactive waste, 25:10800
ANGELI, I., Total neutron cross sections and nuclear Ramsauer effect, 25:12344
ANIKIN, G. V., Optimum parameters of neutron optical potential for ^{238}U, 25:12510 (BNL-tr-366)
ANLAUF, M., Diagnostic significance of ventricular resorption of ^{131}I-labeled hippuran, 25:11152
ANNO, J., Registration and counting of alpha particle tracks in cellulose nitrate, 25:10826
ANSPAUGH, L. R., Distribution and redistribution of airborne particulates from the Schooner cratering event, 25:10716 (UCRL-72534)
ANTHONY, R. W., Backward pion production from π⁻p interactions, 25:12111
ANTOKU, Shigetoshi, Shielding against high energy radiations produced by 30 MeV linear accelerator at Hiroshima University, 25:12314
ANTONACOPOULOS, Gr. A., Secular variations in restricted three-body problem and stability, 25:12057
ANTONOVA, T. D., Frequency correlation of interplanetary scintillations in metre wavelength range, 25:11580 (CSIRO-Trans-10204)
ANTOSHEVSKAYA, L., Growth, survival, and content of ascorbic acid in cultures of tobacco after γ irradiation, 25:10965
AHTTILA, M., Use of nuclear polarization in neutron scattering and transmission measurements, 25:12533 (TKK-F-A-123)
ANZER, Ulrich, Orientation of magnetic fields in quiescent prominences, 25:11617
AOKI, A., Magnetic moments of three excited states in ^{149}Pm, 25:12609
AOKI, Takayoshi, Quasi-gamma bands in ^{152}Gd and possible presence of quasi-K quantum number, 25:12518 (INSJ-123)
ADYAMA, Isao, Dynamic concentration process of radioactive substances to aquatic organisms, 25:10998
APANASENKO, Z. I., Effects of space flight on the central nervous system, 25:11298
APONICK, A. A. Jr., Quadrupole and hexadecapole deformations in rare earth nuclei, 25:12605
APPLBY, George Graham, Improvements fuel element debris receptacles, 25:12769
ARAI, E., Measurement and pole diagram analysis of the ^{2}H(n,p)2n reaction cross section at 14.5 MeV, 25:12369
ARBMAN, G. O., Electronic band structure of the actinide metals, 25:11992
ARDITI, M., Study of the ^{208}Pb(d,^{3}He)^{207}Tl and ^{206}Pb(d,^{3}He)^{205}Tl reactions at 80 MeV, 25:12575
ARENHOEVEL, H., Giant resonance by photon scattering in medium spherical nuclei, 25:12463
ARENS, J. F., Acceleration of protons by interplanetary shocks, 25:11624
ARIPDZHANOV, Sh. A., Gamma radiation effects on pyrimidine oligonucleotides in low-polymer fraction of DNA, 25:11307
ARKHANGEL'SKAYA, V. V., Gamma-radiosensitivity of grape, 25:11017
ARKO, A. J., Electronic and magnetic properties of single-crystal alpha plutonium, 25:12005
ARMBRUSTER, P., Decay of ^{84}Se, ^{91}Kr, ^{97}Y, ^{99}Nb, ^{99}Zr, ^{100} ^{101}Nb, and ^{101}Zr, 25:12462
ARMSTRONG, C. E., Intense radiations and ocular exposure hazards, 25:11297
ARNAUD, S., Sleep pattern following γ irradiation in cats, 25:11261
ARNOLD, G. P., Anisotropic thermal expansion of refractory carbides by high-temperature neutron diffraction, 25:11509
ARNOL'DOV, M. N., Physico-chemical analysis of handling liquid metal coolants, 25:11342
ARSENAULT, R. J., An investigation of methods of preparing high purity vanadium, 25:11356 (CONF-700546-1)
ARSENIE, Ioana, Separation of Zr from Hf by fractional crystallization, 25:10676
ARUTYUNOV, A. V., Thermal properties of tantalum at high temperatures, 25:11425
ARVIEU, R., Theoretical developments in spectroscopy of spherical nuclei, 25:12634 (LYCEN-7034, pp 147-72)
ARYA, Atam P., Decay of ^{147}Nd, 25:12567
ARZANO, S., Scintigraphy with ^{198}Au for chronic hepatitis, 25:11196
ASAOKA, T., Considerations on pulsed reactor optimization, 25:12827
ASBRIDGE, J. R., Energy spectra and angular distributions of particles in the plasma sheet, 25:11809
ASHENHURST, Robert L., Prog. rpt. on computer research, 8/70, 25:12887 (COO-2094-2)
ASHKENAZI, J., Properties of ^{94} ^{98}Rh from ^{94} ^{98} Ru(p,n) reaction, 25:12617
ASHKENAZI, Y., On-line computer system in a low-level counting laboratory, 25:10833
ASINGER, F., Contributions to the radiation-induced sulfoxidation of paraffins, 25:10592 (BMBW-FBK-70-25)
ASLANOV, G. A., Arsenate method for iodometric determination of scandium in the presence of iron, 25:10465
ASSHEUER, J., Detection and removal of radioactive contaminants in reactor-irradiated NaCl, KCl/K_2CO_3, and NH_4Br, 25:11046
Method for simultaneous activity measurements of ^{24}Na, ^{42}K, and ^{82}Br in liquid samples, 25:11066
ATHAVALE, V. T., Thermochemical studies of some U and Th compounds, 25:10581
ATKINSON, J. G., Hydrogen--deuterium exchange of medium ring cycloalkenes during deuterogenation with tris(triphenylphosphine)chlororhodium(I), 25:10539
ATLAN, H., Effects of α particles on longevity of Drosophila melanogaster, 25:11248
ATOJI, M., Crystal structure of anhydrous UO_2F_2, 25:10577
AUDOUZE, J., Energetics of L-nuclei formation in stellar atmospheres and its relevance to x-ray astronomy, 25:11548
AUDOUZE, Jean, Some nucleosynthetic effects of energetic proton fluxes on stellar surfaces and on the solar system, 25:11544
AUDRETSCH, J., Neutrino radiation in gravitational fields, 25:12281
AUER, Ivan Paul, Gamma-ray spectroscopic study of decays of ^{124}Sb and ^{126}I, 25:12531 (TID-25586)
AUERBACH, Stanley I., Ecological considerations in siting nuclear power plants: the long-term biotic effects problem, 25:12763
AUMANN, D. C., Electron density at the Be nucleus, 25:12398
AURDAL, A., Direct photodisintegration of ^{6}Li, 25:12417
AURELA, A. M., Search of electrodynamic radiative corrections for time variations, 25:11668

AUSTIN, Sam M., Energy of the second excited state of ^{12}C and the rate of the triple-alpha reaction, 25:11565
AUSTONI, M., Diagnostic value of hepatic scintigraphy in the light of personal experiences, 25:11183
AUXIER, J. A., Multi-laboratory intercomparisons and standardization: nuclear accident dosimetry systems, 25:10886
AVELEDO, C. E., Electric monopole transitions in deformed nuclei, 25:12584
AWWAD, Z., Lifetimes of some excited states in ^{182}W, 25:12577
AZATO, Ikuo, Radiation curing of monomer--polybutadiene mixture. I, 25:10609 (JAERI-5026, pp 130-6)

B

BABA, H., Shell-model nuclear level density, 25:12688
Systematic behaviour of the most probable charge in the medium-energy fission, 25:12700
BABA, S., Systematic behaviour of the most probable charge in the medium-energy fission, 25:12700
BABAEV, Z. R., Constancy of total cross sections at high energies and K-meson charge exchange, 25:12210
BABB, A. L., Phase-space reduction in neutron diffusion calculations, 25:12853
BABCOCK, K. L., Translocation of carrier-free ^{85}Sr, ^{137}Cs, and ^{106}Ru in woody plants, 25:10955
BABENKO, V. I., Ionizing radiation and nitrogen metabolism in corn, 25:11309
BACHMANN, G., Europium and lanthanum in sunspot and in the undisturbed photosphere, 25:11613
BACHMANN, R., Magnetic ordering in PrB_6, 25:11988
BACKENSTOSS, G., Muon capture probability in isotopes of bromine, 25:12502
BACKER, D. C., Peculiar pulse burst in PSR 1237 + 25, 25:11586
BACON, M. E., Profiles of the He I 4471.5- and 4922-A lines in a dc arc, 25:11689
BAECKMAN, S.-O., Calculation of effective mass in nuclear matter, 25:12677
BAECKSTROEM, Anders, Applicators for optimum pelvic dose distribution in uterine cervix, 25:11227
BAEDECKER, P. A., Decay of ^{117}In isomers and search for a low-lying $9/2^-$ level in ^{117}Sn, 25:12566
BAER, William, Monte Carlo calculation of the thermal neutron activation in light-water-moderated uranium cells using ENDF/B cross-section data, 25:12859
BAETSLE, L. H., Separation of Pu from ^{95}Zr/+ ^{95}Nb/ and ^{106}Ru, 25:10677
BAGGIO, G. F., Interrelationship between cerebral circulation time, pulmonary circulation, and blood pressure, 25:11148
BAGLAN, R. J., New detector for keV neutrons, 25:10845
BAGNI, B., Dose fractionation in radiotherapy, 25:11071
BAGROV, V. G., Effect of induced radiation of electrons moving in planar electromagnetic wave on orientation of their spins, 25:12161
Forced radiation of neutral Fermi-particles moving in planar wave, 25:12160
BAHCALL, John N., Galaxies in the direction of QSO's with small redshifts, 25:11649
BAHCALL, Neta A., Galaxies in the direction of QSO's with small redshifts, 25:11649
BAHK, Y. W., Experimental bone scintigraphy in animals, 25:11216
BAILEY, A. C., Anisotropic thermal expansion of pyrolytic graphite at low temperatures, 25:11510
BAIN, A. S., Multi-cycle irradiation of hollow UO_2 pellets in collapsible Zircaloy-2 sheathing, 25:11530 (AECL-3732)
BAINBRIDGE, J. E., Technique for the preparation of thin films for transmission electron microscopy from highly irradiated uranium dioxide fuel elements, 25:11532 (AERE-R-5677)
BAKER, S. D., Deuteron elastic scattering and the (d,p) reaction with polarized ^3He target, 25:12370
BAKER, William Lewis, States in ^{17}O via the $^{13}C(\alpha,n)^{16}O$ reaction, 25:12390
BAKICH, A. M., High transverse momenta observed in air shower cores, 25:11750
BAKOS, J., Three-photon ionization of a He atom in excited 2S state, 25:11734
BAKOVSKA, Anna, Effect of 14-MeV electrons on blood vessels of the mouse earlobe, 25:11254 (BNL-50203, pp 174-80)
BALACHANDRAN, A. P., Inequalities for s- and p-wave π π partial-wave amplitudes, 25:12193 (SU-1206-234)
BALANDIN, M. P., Fast valve of high pressure for bubble chamber, 25:10870 (JINR-P13-5420)
BALASHOV, V. D., Effect of irradiation on mechanical properties of fcc alloys of Fe--Cr--Ni system. I, 25:11466 (SRARI-P-78)
BALDIN, A. M., Acceleration and extraction of deuterons from the JINR proton synchrotron, 25:12303 (JINR-P9-5442)
BALDWIN, Madeline Carol, Putative deletions of the proximal heterochromatin of chromosome three in Drosophila melanogaster, 25:11012
BALDWIN, T., Prog. rpt. on air cleaning, semiannual, 3--8/70, 25:10797 (NYO-841-23)
BALINT, J. B., Radiation sterilization of implants for reconstructive surgery of kinesthetic organs, 25:11332
BALL, John A., Microwave detection of interstellar formic acid, 25:11593
BALLADA, J., Study of two cases of contamination by ^{241}Am, 25:10931 (CEA-CONF-1557)
BALLAGNY, Alain, Pu--Sc system: diagram and properties, 25:11440
BALU, K., Syntheses of phyllitic minerals: their utilization in radioactive waste treatment. I, 25:10793 (BARC-586)
BAME, S. J., Energy spectra and angular distributions of particles in the plasma sheet, 25:11809
BANCHER, E., Influence of γ-radiation on activities of several glycolytic enzymes in rye seeds, 25:10974
BANDO, Hiroharu, Reaction matrix theory for cluster states in light nuclei. I, 25:12411
BANERJI, S. K., Particle size of solid aggregates by beta-backscattering, 25:10784
BANG, Frederik B., Biology of populations, 25:11085
BANVILLE, M., Boson method and the antisymmetrization problem, 25:12697
BARAGIOLA, R. A., Collisional-quenching processes in H(2s), 25:11723
BARAKINA, N. P., Change in the cellular populations of the bone marrow of mice after single and repeated irradiation, 25:11279
BARBARO-GALTIERI, A., A_2 mass spectrum in 7-GeV/c π^+p interactions, 25:12116
BARDIN, R. K., Double beta decay of ^{48}Ca, 25:12448
BARDSLEY, J. N., Dissociative recombination, 25:11729
BARENDSEN, G. W., Radiobiological bases in design of clinical trials, 25:11240 (BNL-50203, pp 339-52)
BARGON, G., Assessment of the course of experimentally induced radionephritis with isotope renography, 25:11275
BARISH, J., Lateral spread of high-energy (less than or equal to 400 MeV) neutron beams, 25:12332
BARKALAYA, A. I., Early glycemic response of the irradiated organisms, 25:11281
Regulation of corticism and glycemia by insulin and dianabol during acute radiation sickness, 25:10972
BARKHUDAROV, R. M., Dietary intake of ^{90}Sr by population of the USSR, 1959--1967 as a result of stratospheric fallout, 25:10934 (NP-18380)
BARNES, A., Gravitational collapse against a cosmological background, 25:11663
BARNES, G. T., Positron annihilation in Pu, 25:11997
BARNES, P. D., Reaction $^{182}W(t,d)^{183}W$ at 20 MeV triton energy, 25:12611
BARONCELLI, S., Diplontic selection in irradiated Gladiolus corms, 25:11035
BARRACLOUGH, C. G., Higher-order finite-difference solutions of Schroedinger equation for He atom, 25:11697
BARRETT, Craig R., Prog. rpt. on structure dependence of high temperature deformation of metals, 3/69--3/70, 25:11434 (SU-326-P-17-X-1)
BARRETT, P. R., Effect of random amplitudes and phases of vibrating fuel elements upon multigroup neutron lattice parameters, 25:12850
BARSUKOV, V. S., Recovery of yeast cells after irradiation, 25:11316
BARTHOUX, A., Scientific and industrial applications of nuclear explosives, 25:10743
BARTL, A., Dual model for diffractive two-pion electroproduction, 25:12137 (DESY-70/56)
BARTOLI, B., Electron--positron elastic scattering at high energies, 25:12073
Multiple particle production from e^+e^- interactions, 25:12143
BARZ, H. U., Problems of persisting mode time constant in Monte Carlo calculations, 25:12848
BASINSKI, Antoni, Effect of gamma radiation on ion exchange resins. II, 25:10646
BASSETT, C. A. L., Frozen irradiated peripheral nerve and calvarial homografts in clinical surgery, 25:11334
BASSICHIS, W. H., Self-consistent calculations of shell effects, 25:12672
BATES, D. R., Advances in atomic and molecular physics. VI, 25:11728
Use of classical mechanics in the treatment of collisions between massive systems, 25:11733
BATES, Howard F., Aspect sensitivity of spread-F irregularities, 25:11815
BATTLES, J. E., Mass spectrometric investigation of volatilization behavior of $(U_{0.8}Pu_{0.2})O/sub\ 2-x/$, 25:11503
BATYGIN, N. F., Radiation and chemical mutagenes in barley seeds, 25:11315
BAUDER, Ulrich, Adsorption of O and N on Ta films. IV, 25:11419
BAUER, A. A., Irradiation studies of (U,Pu)N, 25:11535
BAUREN, E., Study of the precise determination of macroamounts of plutonium in solution by three electrometric oxidation--reduction titration methods, 25:10445
BAYBARZ, R. D., Preparation and some properties of berkelium metal, 25:11358
BAYLIS, D. J., Deriving upper bound for cosmological density parameter, 25:11667
BAYMAN, B. F., Finite-range calculation of the two-neutron transfer reaction, 25:12505

BEALE, H. A., An investigation of methods of preparing high purity vanadium, 25:11356 (CONF-700546-1)
BEARD, G. B., Nuclear-resonance fluorescence in ^{130}Xe, 25:12560
BEARSE, R. C., Spin dependence in inelastic scattering, 25:12454
BEASLEY, Thomas M., Prog. rpt. on natural alpha-emitting radioisotopes in marine organisms, annual, 1970--71, 25:10997 (RLO-2225-T-14-1)
BECHER, H. J., Some frequency shifts by ^{13}C substitution in the ir spectra of C_2H_4, C_2D_4, and C_2H_4, 25:10563
BECK, J. N., Temporal distributions of radioactivity and $^{89}Sr/^{90}Sr$ ratios during rainstorms, 25:10707 (ORO-2529-28, App. 1)
Variation of radiocerium isotope ratio in rain, 25:10709 (ORO-2529-28, App. 3)
BECKER, C. D., Growth of Columbia River Limpet, Fisherola nuttalli (Haldeman), in normal and reactor-warmed water, 25:10996 (BNWL-1537)
BECKER, G., Examination of various procedures for localization of the counter in isotope renograms, 25:11167
BECKERS, J., Relativistic limit of spin tensor operators associated with a vector particle, 25:12128
Wigner's rotations and the limiting process m → 0, 25:12233
BEDUHN, D., Scintigraphic and angiographic studies of the liver of dogs with experimentally produced obstructive jaundice, 25:11213
BEENS, W., Lifetimes of 2^+ and 4^+ rotational states in heavy doubly even nuclei, 25:12542
BEESTON, J. M., Axial fatigue of irradiated stainless steels tested at elevated temperatures, 25:11459 (IN-1437, pp 1-4)
Surveillance of test reactor beryllium and hafnium, 25:11460 (IN-1437, pp 5-12)
BEGUINOT, J., Quantometer for determination of trace elements in natural materials, 25:10451
BEGZHANOV, R. B., Properties of the excited states of ^{147}Sm and ^{149}Pm, 25:12557
Study of highly excited nuclear states using γ rays from neutron capture, 25:12490
BEIERWALTES, William H., Treatment of thyroid cancer. Death rates after surgery and after surgery followed by sodium iodide ^{131}I, 25:11234
BEIL, H., Photoneutron cross sections of ^{208}Pb and ^{197}Au, 25:12610
BEITNER, H., Can failure--steam loop, 25:12820 (KFK-1255)
BEITSCHER, S., Hot shortness in Pu--1 wt percent Ga, 25:11391
BELASHCHENKO, D. K., Transport phenomena in liquid metals and semiconductors, 25:11410
BELL, P. C., Uranium supplies, 25:10724
BELL, T. K., Response of detectors with cylindrical collimation, 25:10841
BELLINA, J. J. Jr., Interpretation of ellipsometric observations of absorbed oxygen in niobium, 25:11355
BELLMAN, Richard, Differential quadrature and long-term integration, 25:12914 (TID-25633)
BENACERRAF, Baruj, Radioresistance of cooperative function of carrier-specific lymphocytes in antihapten antibody responses, 25:10987
BENARD, Christine, Fluctuations of beams of quantum particles, 25:12053
BENASSI, E., Contribution of scintigraphy for the diagnosis of liver diseases, 25:11198
BENAYOUN, M., General theorems on factorization, 25:12292
BEN-DAVID, G., Radiation widths of bound nuclear levels, 25:12447
BENDER, M. L., Alkaline hydrolysis of p-nitroacetanilide and p-formylacetanilide, 25:10527
BENEDEK, Giorgio, Isotope effects in defect-induced infrared absorption, 25:12043
BENEDICT, R. P., Nuclear magnetic resonance investigation of the metal-to-semiconductor transition in crystalline CdO, 25:12038
BENEZECH, Georges, Neutron dosimetry and spectrometry by multisphere method, 25:10811 (CEA-CONF-1685)
BENGTSON, B., Odd parity states in ^{239}Pu, 25:12594
BENNETT, C. H., Bibliography on whole-body irradiation effect related to canine treadmill performance decrement, 25:11251 (AD-705976)
BENNETT, E. F., Hardware and software for nuclear spectroscopy on the Varian Data Machines 622/i Computer, 25:10848 (ANL-7704)
BENNETT, Michael, Case of myelocytic leukemia simulating the mouse model diseases, 25:11302
BENOIT, Jacques, Sterilization of quails by x-rays and inter-racial grafts, 25:10988
BENVENISTE, J., $Al(\alpha,\alpha')Al^*$ compound-nucleus reactions, 25:12422
BEPPU, Tatsuro, Microwave spectrum, structure, quadrupole coupling constant, and force constants of NSCl, 25:10532
BEREZNAI, Tamas, Activation analysis of rare-earth metals, 25:10499
BERG, R. A., Addendum to potential-scattering model for electrons on helium and other atoms, 25:11722
BERG, V., 190-keV transition in ^{141}La, 25:12540
BERGER, Edmond L., Decisive tests of high-energy models, 25:12206
BERGER, J. P., Irradiation in vitro of nervous tissue, 25:11262
BERGER, Martin J., Bremsstrahlung and photoneutrons from thick tungsten and tantalum targets, 25:12496
BERGERE, Michel Charles Vincent, Interaction picture for gravity interacting with fermions, 25:12271
BERGERE, R., Photoneutron cross sections of ^{208}Pb and ^{197}Au, 25:12610
BERGLES, A. E., Investigation of heat transfer augmentation through use of internally finned and roughened tubes, 25:12891 (NP-18608)
BERGMANN, Klaus, Broad-line nuclear resonance spectra of linear polyethylene. II, 25:10589
BERGSNOV-HANSEN, B., Hydrogen--deuterium exchange on Mo, 25:10559
BERGSTROEM, J., Interaction between a fully ionized plasma and a neutral gas blanket, 25:11878
BERK, H. L., E-layer precession in a plasma, 25:11925 (NYO-4077-1, Paper 2)
BERKES, I., Nuclear magnetic moments and hyperfine interactions, 25:12521 (LYCEN-7034, pp 34-41)
BERLINCOURT, T. G., Electrical properties of hydrides and deuterides of zirconium, 25:12020
Electrical properties of Ta_2H, 25:12021
BERLOVITCH, E. E., Lifetime of 2007-keV level for ^{44}Ti nucleus, 25:12508
BERMAN, B. L., New detector for keV neutrons, 25:10845
BERNARD, M., Review on correlation measurements in plasma, 25:11866 (EUR-CEA-FC-570)
BERNARDINI, P., Scintigraphic method for determination of the regenerative ability of the liver, 25:11202
BERNAS, A., Trapped electrons and free radicals in γ-irradiated ethanol glasses, 25:10648
BERNAS, R., Nucleosynthesis of Li, Be, and B, 25:11542 (NP-18591)
BERNDT, H., Effect of neutron irradiation on critical temperature of superconducting Nb, 25:11848
BERNS, Michael W., Argon laser micro-irradiation of mitochondria in rat myocardial cells in tissue culture, 25:11242
BERNSTEIN, A. M., Test of the shell model for ^{208}Pb, 25:12574
BERNTHAL, F. M., Levels in ^{87}Rb populated in decay of ^{87}Kr, 25:12485
BERTOTTI, B., Relativistic plasma in a strong magnetic field, 25:11903
BERTRAND, J., Poincare covariance and quantization of zero-mass fields. I, 25:12259
BESANCON, Jacques, High-magnetic field compression produced by implosion of a thin metal tube, 25:11917 (CEA-R-4024)
BESNIER, Joseph, Transferring solid radioactive waste, 25:10800
BESNUS, Y., Determination of 18 major elements and traces in rocks, 25:10450
BESSELL, M. S., Nature of the nebulosity about FG Sagittae, 25:11574
BEST, E. B., Significance of red cell aggregation in the vascular complications of angiography, 25:11195
BETHGE, K., Level structure of ^{17}O and the $^{13}C(^6Li,d)$ and $^{13}C(^7Li,t)$ reactions, 25:12425
BETZ, Hans D., Electron capture and loss by fast Br and I ions traversing light gases, 25:11710
BEZDEK, H. F., Lattice dynamics of zirconium, 25:12026
BEZNOGIKH, Yu. D., Acceleration and extraction of deuterons from the JINR proton synchrotron, 25:12303 (JINR-P9-5442)
BEZUCHA, Jaromir, Changes in residual carbon content in UO_2 pellets during decarbonization and sintering, 25:11482
BHAT, M. R., Gamma rays from resonant neutron capture in ^{169}Tm, 25:12589
BHATT, S. J., Processing of pulse trains using rate multipliers, 25:10840
BIALYNICKI-BIRULA, I., Relativistic quantum mechanics of dyons: exact solutions, 25:12047 (NYO-3829-65)
BICHSEL, H., Precision energy loss measurements for natural alpha particles in argon, 25:11726
BICKEL, P. W., Electrical properties of hydrides and deuterides of zirconium, 25:12020
Electrical properties of Ta_2H, 25:12021
BIEFER, G. J., Effects of uranium on the corrosion of resulfurized stainless steels, 25:11352
BIERI, A., Group theory of paramagnetic resonance, 25:12910 (SC-T-71-3002)
BIERINGER, R. J., Dynamic studies of the optical absorption associated with trapped electrons, 25:11967
BIGELOW, J. E., Transuranium processing plant semiannual report of production, status, and plans for period ending June 30, 1970, 25:10654 (ORNL-4588)
BILGER, H., Cobalt electron irradiated at 20°K, 25:11949 (AI-Trans-267)
BILKIEWICZ, J., Incorporation of tritium in hair, 25:10954
BILSBOROUGH, Roy, Improvements in nuclear reactors, 25:12810
BIMBOT, L., Study of the $^{208}Pb(d,^3He)^{207}Tl$ and $^{206}Pb(d,^3He)^{203}Tl$ reactions at 80 MeV, 25:12575
BINDER, Henry J., Identification of cases of acquired functional asplenia, 25:11117
BINDLER, L., Experimental and theoretical physics work on Pu enriched LWR's lattices, 25:12796 (EURAEC-2145)
BINDNER, P. E., Ionic reactions occurring in the irradiation of carbon dioxide--oxygen mixtures at very

XUM

high dose rates, 25:10633
BINNENBRUCK, H., Optical anisotropy of β-rhombohedral B, 25:12029
BINOPOULOS, D., Determination of hepatic blood flow in hyperthyroidism with the ^{198}Au blood extraction method, 25:11141
BIOLCATI, A., Dose fractionation in radiotherapy, 25:11071
BIONDI, M. A., Dissociative recombination, 25:11729
BIRAN, A., Computerized Moessbauer spectrometer, 25:10866
BIRKELAND, J. W., Profiles of the He I 4471.5- and 4922-A lines in a dc arc, 25:11589
BIRKETT, R. E., Levels in ^{47}Ca and ^{41}Ca, 25:12491
BIRO, J., Quantitative autoradiography of Zr--T particles, 25:10775 (KFKI-70-26-HP)
BIRR, Michael P., Electromagnetic radiation from heterogeneous plasma, 25:11890
BIRSTEIN, L., Scattering of protons from ^{120}Te and ^{130}Te, 25:12602
BISHOP, David M., Ab initio calculations of harmonic force constants. IV, 25:11686
BISWAS, M. M., Production of nuclides by high-energy proton bombardment, 25:12439
BITTER, F., Studies on liver function with computer-scintigraphy, 25:10919
BIYAJIMA, Minoru, Proper-time formulation in dual resonance model and the subsidiary conditions, 25:12185
BIZOT, J. C., Upper limit on phi in two-ν branching ratio, 25:12074
BJORDAL, J., Correlation study of auroral luminosity and x rays, 25:11808
BLACHOT, J., Description of various techniques, recent applications, and technological aspects, 25:10669 (LYCEN-7034, pp 9-22)
Isomers of ^{126}I and ^{134}Xe, 25:12572
BLACKBURN, P. E., Mass spectrometric investigation of volatilization behavior of ($U_{0.8}Pu_{0.2}$)O/sub 2-x/, 25:11503
BLACKMON, Maurice L., Inequalities for s- and p-wave ν ν partial-wave amplitudes, 25:12193 (SU-1206-234)
BLAHD, William H., False-positive pulmonary photoscans obtained with a dual-probe detector system, 25:11207
BLAIR, J. S., Validity of Sopkovich approximation, 25:12641 (RLO-1388-595)
BLAKELY, J. P., Action on reactor and other projects undergoing regulatory review or consideration, 25:12762
General administrative activities, 25:12806
BLANC, D., Solid track detectors: practical applications, 25:10825
BLANC, Daniel, Solid track detectors: analysis of data after development, 25:10827
BLANCO, C., Photoelectric observations of stars with variable H and K emission components, 25:11572
BLANK, H., Lattice defects in fluorite structure of UO_2 and UO/sub 2+x/, 25:11520
BLASEWITZ, A. G., Prog. rpt. on fixation of radioactive residues, 8--10/70, 25:10658 (BNWL-1533)
BLASKOVICH, Nick Jr., Decay of ^{147}Nd, 25:12567
BLATT, S. L., Direct radiative capture of ^{3}He by tritons and t + ^{3}He cluster states in ^{6}Li, 25:12372
BLOK, J., E.C./β^+ ratios in non-unique first-forbidden decay of ^{84}Rb, 25:12466
Lifetimes of 2^+ and 4^+ rotational states in heavy doubly even nuclei, 25:12542
Lifetimes of rotational states in ^{229}Th and ^{235}U, 25:12541
Measurements on electron capture ratios of ^{83}Rb and ^{84}Rb, 25:12467
BLOOM, S. G., Estimation of potential radionuclide ingestion by native populations of Eastern Panama and Northwestern Colombia. Bioenvironmental and Radiological-Safety Feasibility Studies, Atlantic-Pacific Interoceanic Canal, 25:10995 (BMI-171-45)
BLOUGH, J. L., Electrotransport in liquid Na--K, 25:11404
BLUM, Manfred, Lateral liver scanning: an index to hepatic and retrohepatic disease, 25:11211
BLUMENTHAL, R. N., Studies of the defect structure of nonstoichiometric cerium dioxide, 25:12033
BOBROWSKI, Antoni, Course of healing of mandibular fractures in radiation sickness, 25:11266
BOCCALETTI, D., Conversion of photons into gravitons and vice versa in a static electromagnetic field, 25:12272
BODNER, A. R., Λ-particle binding in nuclear matter, 25:12668
BOERSCH, H., Scattering of fast electrons by a gas plasma, 25:11879
BOFFI, S., Microscopic description of charge form factor of ^{4}He, 25:12651
BOGEGARD, Sven, Phase transformations in metastable plutonium--gallium alloys, 25:11446
BOGOYAVLENSKII, V. L., Intercrystalline corrosion and corrosion cracking of stainless steel in aqueous solutions, 25:11353
BOHABOY, P. E., Compressive creep properties of UO_2--PuO_2 compounds, 25:11495
BOHL, W., Service routines for multigroup cross-section code MC², 25:12337 (ANL-7654)
BOHNE, F., Cytokinetic analysis of slowly proliferating bone marrow cells during recovery from radiation injury, 25:11077
BOHNE, W., Reaction ^{15}N(tau,α)^{14}N, 25:12424
BOLDESCU, Gabriela, Hemorrhagic syndrome in radiation sickness. II, 25:11105
BOLLINGER, L. M., States of ^{106}Pd, ^{154}Gd, ^{158}Gd, ^{160}Ho, and ^{168}Er, 25:12586
BOLMER, R. L., Mine effects evaluation for Project Rulison, 25:10736 (PNE-R-39, Pt.1)
BOLOTOV, V. N., Investigation of a particle beam with energy up to 70 GeV with a spark spectrometer, 25:10868 (IFVE-SEF/OP-70-13)
BONAZZOLA, L., EPR spectra of some bicyclic radicals, 25:10638
BONCH-OSMOLOVSKII, A. G., Longitudinal instabilities in annular charged beams. II, 25:12311
Longitudinal instabilities in annular charged beams. I, 25:12312
BOND, Peter, Hyperfine-field studies with ^{99}Mo, 25:12568
BONDARENKO, T. N., X-ray spectra and band structure of refractory vanadium compounds, 25:12012
BONDELID, R. O., Direct interaction effects in the fission of ^{238}U with 63.5-MeV ^{4}He ions, 25:12526 (MNC-3783-7)
BONDE NIELSEN, K., M1 admixtures in transitions from γ-vibrational states in ^{152}Sm, ^{154}Gd, and ^{156}Gd, 25:12576
BONHAM, R. A., Infinite-channel close-coupling theory in second Born approximation. I, 25:11718
BONJOUR, E., Energy release and electrical resistivity recovery in Ni following electron irradiation, 25:11977
BONNET, J. A. Jr., Use of acoustic waves in nuclear power reactors to determine average void fractions, 25:12779
BONORA, L., Operatorial expansion of the product of two currents, 25:12130
BONTEMPS, Andre, Application of ^{18}O(p,α)^{15}N reaction to study of self-diffusion of oxygen in uranium dioxide, 25:11486 (CEA-R-4095)
BORCHERS, R. R., Magnetic moments of the 7/2⁻ mirror states in ^{37}Ar and ^{37}K, 25:12429 (COO-7-565)
BORGGREEN, Joern, Production and decay of protactinium isotopes, 25:12592
BORGMAN, Lawrence William, Nuclear structure of ^{140}Ce, ^{139}La, and ^{138}Ba determined with (d,^{3}He) and (^{3}He,d) transfer reactions, 25:12552
BORIE, Edith, S matrix in Heisenberg representation, 25:12290
BORIGHT, J. P., Reactions ν⁻p → nν⁰ and ν⁻p → neta⁰ in the backward hemisphere, 25:12117
BORISOV, B. K., Measurement of ^{90}Sr content in organism of adult persons, 25:10935 (NP-18388)
BORISOV, D. G., Parametric efficiency limit of resonance charging of pulse-forming network in pulse generators, 25:12333
BORNS, Francois Leon, Investigation of M and F' centers in alkali halides by laser excitation, 25:11956
BORN, H.-J., Electron density at the Be nucleus, 25:12398
BORUKHOVICH, A. S., Conduction band of IVa and Va subgroup transition metal monocarbides. I, 25:12024
BORZUNOV, Yu. T., Precision apparatus with liquid hydrogen target, 25:12300 (JINR-P8-5212)
BOS, Laurence W., Optical properties of antiferromagnetic chromium and dilute Cr--Mn and Cr--Re alloys, 25:11987
BOSCARIOL, P., Diplontic selection in irradiated Gladiolus corms, 25:11035
BOSE, Paromita, Radio-resistant auxotrophic strain of R. leguminosarum, 25:11325
BOSI, G., Trajectories of charged particles in magnetic fringe fields, 25:12322
BOSWELL, R. W., Plasma production using a standing helicon wave, 25:11908
BOTTER, R., Automatic mass spectrometer for the isotopic analysis of hydrogen in natural water samples, 25:10463
BOUCHER, Gary Wynn, Three studies of microearthquakes: I, II, III, 25:10731
BOUCHER, Rene, Pu--Sc system: diagram and properties, 25:11440
BOUCHET, P., Accessibility to the electron plasma resonance in the F region of a wave emitted from the Earth, 25:11814
BOUCHEZ, R., Penning type strong ionizing field for polarized atomic beams, 25:12328
BOUE, P., Some physical aspects of nuclear explosives, 25:10739
BOULENGER, R., Experience gained during a criticality, 25:11057
BOULWARE, David G., Classical Schwinger terms, 25:12244
BOUTEN, M., Low-lying 0^+ states in ^{12}C and ^{16}O, 25:12412
Projected Hartree--Fock calculation for light nuclei. V, 25:12396
BOUTEN, M.-C., Low-lying 0^+ states in ^{12}C and ^{16}O, 25:12412
Projected Hartree--Fock calculation for light nuclei. V, 25:12396
BOUZIGUES, Henri, Continuous control of low-uranium contents of solutions by measurement of radioactivity, 25:10473 (CEA-R-4032)
BOW, Y. F., Collective model of deformed nuclei, 25:12655
Transition probabilities of deformed odd-mass nuclei, 25:12656
BOWEN, D. H., Production of lithium oxide by electron irradiation of lithium fluoride, 25:11964
BOWEN, D. R., Reactions ν⁻p → nν⁰ and ν⁻p → neta⁰ in the backward hemisphere, 25:12117

BOWER, Rae Ellen, Long-term effects of local irradiation of the marrow on erythron and red cell function, 25:11112
BOWERS, B., Galactic Lyman alpha and interstellar shock wave, 25:11640
BOWERS, Michael T., Relative proton affinity of argon and deuterium, 25:10552
BOWERSOX, D. F., Enthalpies of solution of C, Tm, Ti, Mn, Zr, and Re in liquid Pu, 25:11386
BOWKER, A. J., Measurement of time-of-flight using 300 Mc/s scalers, 25:10891 (AERE-R-5422)
BOWMAN, A. L., Anisotropic thermal expansion of refractory carbides by high-temperature neutron diffraction, 25:11509
BOWMAN, C. D., New detector for keV neutrons, 25:10845
BOYARSKAYA, Yu. S., Radiation hardening of NaCl single crystals, 25:11975
BRADY, F. P., Energy measurements of 20 to 60 MeV neutron beam of Davis 76-inch isochronous cyclotron, 25:10861
Medium-energy neutron facility, 25:12331
BRAEUNIG, D., Investigations of radiation resistance of optoelectronic devices for an electronically scanning star sensor in satellites, 25:10904 (HMI-B-97)
BRAGIN, J., Low-frequency vibrations of molecular solids. X, 25:10529
BRAGINSKY, V. B., Search for quarks in ferromagnetics using an electrometer with the beams suspension method, 25:12064
BRAKKEE, A. J. M., Double isotope dilution technique in the study of a peripheral vascular system in vivo, 25:10926
BRANDENBURG, H., Perfusion scintigram of lungs during various stages of pulmonary sarcoidosis (Morbus boeck), 25:11133
BRANDER, R. W., Cathodoluminescence of ion implanted SiC, 25:11974
BRANDOLINI, F., Gamma-ray transition strengths in ^{34}Cl, 25:12493
BRANDT, Richard A., Light-cone analysis of massive μ-pair production, 25:12228
BRARD, Emile, Sterilization of quails by x-rays and interracial grafts, 25:10988
BRASZ, J., Lifetimes of rotational states in ^{229}Th and ^{238}U, 25:12541
BRAT, Satya, Syntheses of phyllitic minerals: their utilization in radioactive waste treatment. I, 25:10793 (BARC-506)
BRAUDE, S. Ya., Connection between absolute radioluminosity of extragalactic sources and redshift, 25:11581 (CSIRO-Trans-10247)
BRAUN, W. G., Profiles of the He I 4471.5- and 4922-A lines in a dc arc, 25:11689
BRAUNSFURTH, J., Analysis of accidental coincidences by measurements with time-to-pulse height converters. II, 25:10902
BRAUNSTEIN, T. J., Determination of inelastic neutron form factor by scattering of 12-GeV muons on H, C, and Cu, 25:12096
BRAZIER, David W., γ radiolysis of liquids at high pressures. IX, 25:10628
BREBANT, Charles, Isodore facility, 25:10794 (CEA-R-4120)
BRECHER, George, Late effects on vascular tissue, 25:11256 (BNL-50203, pp 186-203)
BREITENBERGER, E., Empirical foundations of special relativity, 25:12265
BREITENHUBER, L., Transport properties of cavities, 25:12851
BRETON, C., Multilayer targets as a diagnostic tool for laser-produced plasmas, 25:11870
BRETT, Alistair Morley, Effective field equations for one-electron multiphoton stationary states with application to Compton scattering, 25:12139
BREWER, Leo, Thermodynamics and alloy behavior of the bcc and fcc phases of plutonium and thorium, 25:11392
BREY, C., Stationary gas detectors for mapping and dynamic studies of organs using x ray or low-energy γ-ray emitters, 25:10810 (CEA-CONF-1668)
BREZGUNOV, V. S., Radioactive elements and deuterium in underground waters of the Bukhara--Karshin artesian basin, 25:10698
BRICE, Neil, Irregularities in proton density deduced from cyclotron damping of proton whistlers, 25:11787
BRICKA, Michel, Neutron dosimetry and spectrometry by multisphere method, 25:10811 (CEA-CONF-1685)
BRIFFOD, G., Review on correlation measurements in plasma, 25:11866 (EUR-CEA-FC-570)
BRIGGS, Gary A., Plume rise: a recent critical review, 25:10717
BRIKS, Wojciech, Use of isotopes in casting practice, 25:10780
BRINDLE, J., Fractionation treatment of larynx and pharynx, 25:11221 (BNL-50203, pp 268-79)
BRINKMAN, A., E.C./e$^+$ ratios in non-unique first-forbidden decay of ^{86}Rb, 25:12466
Measurements on electron capture ratios of ^{83}Rb and ^{86}Rb, 25:12467
BRINKMAN, C. R., Axial fatigue of irradiated stainless steels tested at elevated temperatures, 25:11459 (IN-1437, pp 1-4)
BRISSAUD, I., 166-MeV elastic and inelastic alpha-particle scattering, 25:12549
BRITT, H. C., Fission of odd-A U and Pu isotopes, 25:12579
BROD, K. H., Comparative determination of hepatic blood flow with colloidal ^{198}Au and colloidal /sup 99m/Tc-S, 25:11140
Contribution of scintigraphy for evaluation of vascular renal diseases, 25:11166
BRODA, R., Decay of ground state of ^{82}Rb, 25:12507
BRODBECK, C., Effect of solvent on frequencies of CD and CH stretching band in some haloforms, 25:10540
BRODSKY, M. B., Electronic and magnetic properties of single-crystal alpha plutonium, 25:12005
Magnetic behavior of Np metal and dilute Np alloys from Moessbauer effect studies, 25:12001
Magnetism in Pd-actinide alloys, 25:12003
Virtual-bound-state formation in Pd--U alloys, 25:11989
BROECKER, Wallace, Radium-226 measurements from the 1969 North Pacific Geosecs Station, 25:10726
BROECKER, Wallace S., Investigations of U and Th series isotope disequilibria in the ocean and in pleistocene sediments. Annual Progress report, 25:10725 (CU-3139-4)
Near-surface and near-bottom radon results for the 1969 North Pacific Geosecs Station, 25:10727
BROMLEY, D. A., Quadrupole and hexadecapole deformations in rare earth nuclei, 25:12605
BRONISZ, S. E., Electron microscopy of alpha particle damage in actinide oxides, 25:11537
BRONSHTEIN, I. M., Inelastic electron scattering and secondary electron emission of Mg and MgO, 25:11672
BROOKEMAN, Valerie A., Evaluation of /sup 99m/Tc-DTPA acid as a brain scanning agent, 25:11189
BROOMFIELD, G. H., Effect of some structure variations on tensile properties of irradiated Nimonic PE16, 25:11531 (AERE-R-4913)
Effects of strain rate, neutron dose, and irradiation temperature on tensile properties of Nimonic PE16, 25:11455 (AERE-R-4982)
BROWER, Richard Comfort, Vector currents and current algebra in a zero-width model, 25:12177
BROWN, A. E., Operating procedures: Hanford Test Reactor, 25:12815 (DUN-7149)
BROWN, Anthony E. P., Catalytic reduction of aqueous solutions of uranyl nitrate, 25:10572 (IEA-184)
BROWN, Arthur James, Improvements fuel element debris receptacles, 25:12769
BROWN, D. J., Rising trajectories and singular potentials, 25:12291
BROWN, F. Elizabeth, Cloud--intercloud phase change in the interstellar medium, 25:11650
BROWN, G. S. Jr., Investigation of heat transfer augmentation through use of internally finned and roughened tubes, 25:12891 (NP-18608)
BROWN, G. V., Superconducting magnet research, 25:11851
BROWN, L. W., Spectrum of the extragalactic background radiation at low radio frequencies, 25:11666
BROWN, S., Note on the central star of NGC 3132, 25:11570
BROZDNICHENKO, A. N., Inelastic electron scattering and secondary electron emission of Mg and MgO, 25:11672
BRUANDET, J. F., Penning type strong ionizing field for polarized atomic beams, 25:12328
BRUGE, G., Transfer reactions (α,t), (α, ^{3}He) in the fp shell, 25:12434
BRUGGEMAN, A., Average cross sections of ^{28}Si(n,p)^{28}Al and ^{29}Si(n,p)^{29}Al reactions, 25:12460
BRUN, Gilbert, Structure transformations of Zr--Cu binary alloys with low Cu contents and ternary alloys during continuous cooling, 25:11432 (CEA-N-1310)
BRUN, J. C., Application of spark source mass spectrography to geologic problems, 25:10455
BRUN, T. O., Interpretation of measurements of magnetic scattering from actinide ions, 25:12002
BRUNFELT, A. O., Concentration of Cs in high grade metamorphic rocks, 25:10508
BRUNHART, Gunter, Pion interactions in deuterium at 330 MeV, 25:12105
BRUNTON, Donald C., Method and apparatus for measuring the weight of a load on a conveyor belt, 25:10785
BRUSSAARD, P. J., Some comments on the signs of mixing ratios and on pairing factors for electromagnetic transitions and moments, 25:12665
BRYAN, C. A., Mathematical model for approximating transient, three-dimensional groundwater systems, 25:12880 (BNWL-SA-3539)
BUBLITZ, G., Studies on vasoactive drugs with the ^{133}Xe muscle clearance method, 25:10914
BUCHANAN, C. D., Study of decay mode K/sub L/^{0} + $\pi^+\pi^-\pi^0$, 25:12087
BUCHANAN, J. R., How to obtain nuclear safety data, 25:12759
BUCHL, R. A., Kaon and nucleon form factors using vector dominance, 25:12141
BUCKNER, J., Three-band source spectra from color film, 25:10893 (EGG-1183-484)
BUDNEV, V. M., Production of muon pairs in interactions of hadrons of high energy, 25:12229
BUDZANOWSKI, A., Polarization of protons from ^{12}C(d,p)^{13}C reaction at E/sub d/ = 12.4 MeV, 25:12377 (INP-711)
Real part of the alpha-nucleus potential obtained by double folding procedure, 25:12627 (INP-720)
BUFFET, X., Beam--beam effect, 25:12308 (LAL-RT-5-70)
BUHL, David, Observations of radio emission from interstellar hydrogen cyanide, 25:11594
BUHL, W. F., A_2 mass spectrum in 7-GeV/c π^+p interactions,

XUM

25:12116
BUIATTI, M., Diplontic selection in irradiated Gladiolus corms, 25:11035
BUISHVILI, L. L., Possibility of polarizing nuclei with ultrasound, 25:12007
BULEY, L. E., Solar flare radiation information in support of supersonic transport operations, 25:11086
BULL, S. R., Optimization of time analyzer parameters in multi-cycle experiments with exponential decay, 25:10900
BULLINGTON, D. C., Fission gas bubble precipitation and growth in PuO_2--UO_2 under irradiation, 25:11536
BULOVIC, V., Determination of burn-up of nuclear fuel on basis of stable isotopes of Nd. I, 25:10461
Determination of burn-up of nuclear fuel on the basis of stable isotopes of Nd. II, 25:10469
BUMILLER, F. A., Form-factor ratio G/sub E/(n)/G/sub E/(p) at low momentum transfers, 25:12070
BURBIDGE, G. R., Can the lumpy distribution of galaxies be reconciled with the smooth x-ray background, 25:11656
BURCH, D., Reaction $^{90}Zr(^3He,d)^{91}Nb$ at 18 MeV, 25:12613
BURCH, W. D., Transuranium processing plant semiannual report of production, status, and plans for period ending June 30, 1970, 25:10654 (ORNL-4588)
BURDE, J., Scattering of protons from ^{128}Te and ^{130}Te, 25:12602
BURGER, James M., Isotope shift in the (2^1S_0--2^1P_1) line of atomic He, 25:11696
Lifetime of the 2^1P_1 and 3^1P_1 states of atomic He, 25:11695
BURGNER, Robert L., Prog. rpt. on research program on marine ecology and oceanography, Amchitka, annual, 7/1/67--6/30/68, 25:12877 (BMI-171-114)
BURIANEK, J., Stability and radiochemical purity of some radiopharmaceuticals. II, 25:10641
BURING, K., Ionizing radiation for sterilization of bone, 25:11335
BURLAGA, L. F., Magnetic and thermal pressures in the solar wind, 25:11607
BURLESON, C. E., Low-temperature phase transitions in alpha uranium, 25:11449
BURNAZYAN, A. I., Radiation in medicine, 25:11091
BURNS, J. A., Free dynamics of pulsars, 25:11596
BURROWS, Belton A., Prognostic value of radioisotopic renal function studies for selecting patients with renal arterial stenosis for surgery, 25:11186
BURROWS, J. R., Structure observed in solar-particle latitude profiles, 25:11797
BURSHTEIN, E. L., Linear electron accelerators with intense beams, 25:12315
BURTON, J. J., Calculated isotope effect for diffusion in solid argon, 25:12042
BURTON, K. S., Mean lives and angular correlations in ^{35}S, 25:12489
BUSCH, R. A., Sputtered plutonium--gallium alloys, 25:11360
Sputtered plutonium--tantalum alloys, 25:11447
BUSCHOW, K. H. J., Crystal structure and magnetic properties of Ce--Fe compounds, 25:12025
BUSH, Karen, Wahler, H. R., Deuterium effects on binding of NADH to alcohol dehydrogenase isoenzyme EE, 25:10525 (COO-1008-17)
BUSKIRK, F. R., Form-factor ratio G/sub E/(n)/G/sub E/(p) at low momentum transfers, 25:12070
BUSLAEV, V. S., Relation between the third virial coefficient and the scattering matrix, 25:12287
BUSNESS, K. M., Interactive graphics display system for hydrologic analysis, 25:12879 (BNWL-1525)
BUSS, W., Photoneutron angular distributions from $^2H(\gamma,n)H$ reactions, 25:12374
BUSSAC, J. P., Review on correlation measurements in plasma, 25:11866 (EUR-CEA-FC-570)
BUSSIERE, A., Transfer reactions (α,t), (α, ^3He) in the fp shell, 25:12434
BUTLER, G. W., Identification of nuclear fragments, 25:10860
BUTLER, Thomas Wesley, Further look at WC--Co from continuum viewpoint, 25:11515
BUTZ, R., Electron microprobe to determine layer thicknesses down to monolayer range, 25:11421
BYRAN, J. A., Improvement in heat exchangers, 25:12811

C

CABANNES, H., Fluid flows around a sphere in fluid magnetohydrodynamics, 25:11760
CABRINI, R. L., Microspectrophotometric study of oxidative enzymes in irradiated epidermis, 25:11241
CADWELL, J. J., Prog. rpt. on reactor fuels and materials development, 4--6/68, 25:11474 (BNWL-842)
CAIRNS, R. A., Kinetic theory of spatially inhomogeneous plasma with time-independent average properties, 25:11895
CALAIS, Daniel, Crystallographic analysis of segregations observed in dilute ZrPu alloys during martensitic transformation, 25:11430 (CEA-CONF-1688)
Determination of limiting solubilities using heterodiffusion coefficient measurements, 25:11370 (CEA-CONF-1689)
Effect of a β → α transformation and of oxygen on plutonium distribution in dilute Zr--Pu and Ti--Pu alloys, 25:11431 (CEA-CONF-1691)
Self diffusion, under hydrostatic pressure, of body centered cubic Pu, 25:11371 (CEA-CONF-1690)
CALLAGHAN, M. P., Cathodoluminescence of ion implanted SiC, 25:11974
CALLY, J. C., Application of nuclear explosives in the mining industry, 25:10747
Scientific and industrial applications of nuclear explosions, 25:10745
CALMET, J., Sixth-order radiative corrections to the anomalous magnetic moment of the electron, 25:12065 (CNRS-CPT-70-P-339)
CALMET, Jacques, Computational analysis of Feynman diagrams, 25:12136 (CNRS-CPT-70-P-336)
CALOGERO, F., Nuclear forces and saturation, 25:12636 (NP-18580)
CALUCCI, G., Anomalous magnetic moment and nonpolynomial interactions, 25:12157
CAMERON, J. R., Determining body compositions by radiation absorption spectrometry, 25:11114
CAMPBELL, C. K., Dielectric properties of electron-beam-evaporated yttrium oxide thin films, 25:12031
CAMPBELL, D. B., Absence of average polarization at 111.5 MHz in pulsar NP 0532, 25:11589
CAMPBELL, G. M., Thermodynamic properties of Pu--C system, 25:11506
CAMPBELL, J. B., Frozen irradiated peripheral nerve and calvarial homografts in clinical surgery, 25:11334
CAMPBELL, W. F., Effects of γ radiation on Penicillium expansum. II, 25:10979
CAMPBELL, W. R., Analysis of the transient capability of rod-type fuel elements (LWBR Development Program), 25:11534 (WAPD-TM-979)
CANDES, P., Dosimetry in nuclear accidents, 25:11079
CANESCHI, L., Charge distributions and multiperipheralism, 25:12179
CAPET, Henri, Cask for nuclear reactor fuel elements, 25:10801
CAPPS, R. H., Implications of duality for anti KN resonances, 25:12215
CARBOTTE, J. P., Effect of phonons on the e^+--e^- annihilation rate in metals, 25:11699
CARETTO, A. A. Jr., Nuclear structure effects in (p,2 nucleon) reactions on isotopes of Cd, 25:12570
Reactions of 400 MeV protons with ^{58}Ni and ^{197}Au, 25:12500
CARETTO, Albert A. Jr., Nuclear structure effects in (p,2 nucleon) reactions on isotopes of Te, 25:12581
CAREY, Walter E., Neutron activation analysis of manganese and sodium in bacterial cells, 25:10511
CARLOS, P., Photoneutron cross sections of ^{208}Pb and ^{197}Au, 25:12610
CARLSON, L. E., Lifetimes of first four excited states of ^{32}S, 25:12486
CARLTON, William Herbert, Bioelectric potential of Zea mays roots, 25:11308
CARMI, I., On-line computer system in a low-level counting laboratory, 25:10833
CARMICHAEL, C. D., Fast breeder reactor static physics methods development and analysis project. Volume 1. FARED: one-dimensional fast reactor physics design and analysis code, 25:12772 (BAW-3867-9(Vol.1)(Rev.1))
CAROFF, Lawrence J., Application of the collective approach to the thermodynamics of an electron gas, 25:11896
CAROLA, T. P. G., Electromagnetic properties of ^{55}Fe, 25:12483
CARPENTER, K. M., Crossing-symmetric unitarization of the Veneziano amplitude, 25:12196
CARRARD, Claude, Pu--Sc system: diagram and properties, 25:11440
CARRAZ, L. C., Isomers of ^{134}I and ^{136}Xe, 25:12572
CARROLL, Edward E., Titanium (n,p) cross-section measurements, 25:12504
CASARETT, George W., Effects of radiation on vasculature of intestine, 25:11255 (BNL-50203, pp 181-5)
CASSANO, C. C., Scintigraphy with ^{198}Au for chronic hepatitis, 25:11196
CASTAGNOLI, C., Discussion of some recent results on cosmic-ray muons, 25:12168
CASTELL, L., Conformal invariant form factors in two dimensions, 25:12142
CASTEN, R. F., Reaction $^{182}W(t,d)^{183}W$ at 20 MeV triton energy, 25:12611
CASTI, John, Differential quadrature and long-term integration, 25:12914 (TID-25633)
CASTO, W. R., Safety-related occurrences reported in August--September 1970, 25:12807
CATALANO, S., Photoelectric observations of stars with variable H and K emission components, 25:11572
CATONI, M., Inactivation of β-Fructofuranosidase and Glucosidase by γ radiation of Beta vulgaris, 25:10964
CATTRELL, V. G., Gamma densitometry in the study of ventilation and the pulmonary circulation, 25:11116
CAVALLO, G., Discrete source interpretation of the isotropic component of the diffuse γ-radiation, 25:11636
CAVY, Claude, Transmitting motion through reactor wall, 25:12863
CAWTHRON, E. R., Interaction of atomic particles with solid surfaces at intermediate energies. III, 25:11675
CEARD, P., Uranium isotopic determination in rocks by

neutron activation, 25:10494
CEARLOCK, D. B., Mathematical model for approximating transient, three-dimensional groundwater systems, 25:12880 (BNWL-SA-3539)
CECCARELLI, G., Spectrochemical analysis of Zr and its alloys. I, 25:10430 (EUR-4541)
CECH, R. E., Sintering of die-pressed Co_5Sm magnets, 25:11361
CELINSKI, Z. N., Electrical parameters in MHD generator, 25:11751
CELOTTA, Robert James, Total cross section for low-energy electrons on metastable Ar, 25:11706
CENTI COLELLA, A., Consideration of the clinical interpretation of scintigrams of the pancreas under normal and pathological conditions, 25:11199
CERCEK, B., Phenyl and hydroxyphenyl radicals. Pulse radiolysis study of their spectra and reactivity, 25:10631
CERRAI, E., Behavior of metallic U--Zircaloy-2 fuel element defects and exposure to aqueous corrosion, 25:11347 (CISE-R-222)
CHABRE, M., Parity violation in the transition of ^{181}Ta at 482 keV, 25:12621
CHABRILLAC, Marcel, EL 600: study of core neutronic properties, 25:12775 (CEA-N-1395)
CHACHATY, C., Trapped electrons and free radicals in γ-irradiated ethanol glasses, 25:10648
CHAICHIAN, M., Dual amplitudes for 6 pions with epsilon-tensor couplings, 25:12131
CHAKRABARTI, A., Plastic-strain controlled failure criteria and design parameters. Technical progress report, 25:11373 (COO-2048-1)
CHALMERS, R. A., Cross sections for ^{7}Be(p,γ)^{8}B, 25:12400
CHALOVA, E. P., Chemistry of rare earths and various other elements, 25:10580
CHAMARAUX, P., 21-cm neutral hydrogen line observations of compact galaxies, 25:11638
CHAMEL, Andre R., Fixation and migration of ^{42}K applied to leaves of corn, 25:10930 (CEA-CONF-1517)
CHAN, S.-K., Crystal-field effect and magnetic properties of NaCl-type actinide compounds, 25:11994
CHANDLER, Colston, Some physical region mass shell properties of renormalized Feynman integrals, 25:12293
CHANDOLA, L. C., Spectrographic analysis of tungsten in ores and their concentrates: an intermittent ac arc method, 25:10429 (BARC-468)
CHANG, C. C., Intermediates in allene--acetylene isomerization over zinc oxide, 25:10558
Study of the ^{14}N(p,2p)^{13}C reaction at 46 MeV, 25:12391
CHANH TRUNG, Huynh, Radioactivity sensing apparatus for measuring the blood flow, 25:10828
CHANOURDIE, Jean-Claude, Diffusion of the minor constituents into the troposphere, 25:10704 (NP-18609)
CHARALAMBUS, S., Muon capture probability in isotopes of bromine, 25:12502
CHASE, J. B., Electron energy loss due to surface modes in a thin ionic crystal film, 25:11677
CHASE, J. E., Event horizons in static scalar-vacuum space--times, 25:12282
CHASE, L. F. Jr., Cross sections for ^{7}Be(p,γ)^{8}B, 25:12400
CHASTOKOLENKO, B. L., Detector sensitivity for measuring electron current in a betatron, 25:12321
CHATELAINE, J., Cross section for pair production in proton--proton collision, 25:12231
CHATTERJEE, A., Particle size of solid aggregates by beta-backscattering, 25:10784
CHATTERJEE, Samar, Formation of supernumerary surface layers in radiated amoebae, 25:11249
CHAUDHARY, Banvir Singh, Pion--nucleon interactions in deuterium at 3.65 GeV/c, 25:12121
CHAWLA, T. C., Pressure distribution for axisymmetric two-dimensional flow in a plenum during coolant expulsion, 25:12808
CHEEKE, J. D. N., Kapitza resistance of Pb, 25:11834
CHEKE, A., Pulsed reactor potentialities for neutron activation analysis, 25:10489 (KFKI-70-25-NAC)
CHEN, J. T., Electron tunneling investigation of quench-condensed superconductors, 25:11842
CHEN, T. C., Singular off-mass-shell equation with vector-meson exchange, 25:12192 (NYO-2262-TA-232)
CHEN, T. S., Jet stream and radioactive fallout, 25:10708 (ORO-2529-28, App. 2)
Temporal distributions of radioactivity and ^{89}Sr/^{90}Sr ratios during rainstorms, 25:10707 (ORO-2529-28, App. 1)
CHEN, T. T., Electron tunneling investigation of quench-condensed superconductors, 25:11842
CHENEVERT, Gary Milo, Highly inelastic scattering of medium-energy ^{3}He and ^{4}He particles by heavy nuclei, 25:12604
CHENEY, Donald M., New etchants for irradiated uranium alloys, 25:11367
CHEN-TSAI, C. T., Binding energies of p-shell hypernuclei, 25:12393
CHEON, Il-tong, Phenomenological wave function of ^{6}Li, 25:12383
CHEREVATENKO, A. P., Dose characteristics of protons with energy 200 MeV, 25:11054 (JINR-P16-5383)
CHERMANT, Jean-Louis, Microfractographic aspect of refractory carbides, 25:11514
CHERTOK, B. T., Magnetic multipole electroexcitation, 25:12657
CHESTERFIELD, C. M., Quadrupole and hexadecapole deformations in rare earth nuclei, 25:12605
CHIBA, Morito, Deposition and translocation of the radioactive fallout, 25:10718
CHIEN, C.-Y., Form factors for the decay K/sub L/^{0} + νμν, 25:12088
CHILDS, W. J., Hyperfine and Zeeman studies of low-lying atomic levels of ^{139}La, 25:11693
CHING, Barbara K., Atmospheric density and rotation below 195 km, 25:11794
CHINTALAPUDI, Surya N., Gamma spectrum from the thermal neutron capture in cerium, 25:12551
CHIVOT, J. J., Biological tests of pharmaceutical radio colloids, 25:10957
CHO, A. Y., Epitaxy by periodic annealing, 25:12023
CHONE, B., Discrepancy between radiological and scintigraphic findings in a case of honey-comb lung, 25:11215
CHORVAT, D., Estimation of radioactivity of biological samples, 25:11044
CHOU, T. W., Effects of γ radiation on Penicillium expansum. II, 25:10979
CHOUDHURY, S. Rai, Study of scale invariance in lambdaphi^{4} theory, 25:12149
CHRETIEN, Louis, Tests on an automatic air purifying respirator, 25:10752 (CEA-N-1360)
CHRIEN, R. E., Gamma rays from resonant neutron capture in ^{169}Tm, 25:12589
Resonance neutron capture in ^{103}Rh, 25:12561
CHRISTENN, G., Thermodynamic properties of propane as bubble chamber liquid, 25:10876
CHRISTENSEN, E. A., Radiation resistance of bacteria and the microbiological control of irradiated medical products, 25:11328
CHRISTMAN, Ronald D., MUX: simple approach to on-line computing, 25:12890 (LA-4524)
CHUANG, L. S., Localized irradiation of material, 25:12318
CHUANG, S. Y., Preliminary study on temperature effect on positron annihilation in $KClO_4$, 25:12898 (NYO-3661-33)
CHUBB, Talbot, Excess background radiation of soft x rays at the galactic pole and plane, 25:11653
CHUCHALIN, I. P., Optimum dimensions of the operational volumes of radiation circuit joints, 25:12829
CHUNG, Yu-chia, Radium-226 measurements from the 1969 North Pacific Geosecs Station, 25:10726
CHURCH, L. B., Reactions of 400 MeV protons with ^{58}Ni and ^{197}Au, 25:12500
CHURCHILL-DAVIDSON, I. F. J., Fractionation treatment of larynx and pharynx, 25:11221 (BNL-50203, pp 268-79)
CHURG, J., Radiation nephritis. II. Chronic changes after high doses of radiation, 25:11286
CHUTNY, B., Pulse radiolysis of aqueous solutions of benzonitrile, 25:10639
CHYLEK, Petr, Hadron spectroscopy and high-energy scattering in the quark model, 25:12218
CIER, A., Sleep pattern following γ irradiation in cats, 25:11261
CIFKA, J., Stability and radiochemical purity of some radiopharmaceuticals. II, 25:10641
Stability and radiochemical purity of some radiopharmaceuticals. III, 25:10642
CIRENEI, A., Scintigraphic method for determination of the regenerative ability of the liver, 25:11202
CIRSTEA, M., Use of radioactive tracers in immunology and allergy, 25:10924
CIZERON, G., Behavior of α U under light stresses during recrystallization process or during the allotropic α/β transformation, 25:11451
CLAESON, T., Superconductivity for ternary fcc Bi--Pb--Tl alloys, 25:11846
CLARK, B. C., System for $^{14}CO_2$ radioassay, 25:10843
CLARK, G. W., High-temperature solution growth of single-crystal neptunium dioxide, 25:11483
CLARK, T. A., Spectrum of the extragalactic background radiation at low radio frequencies, 25:11666
CLAUS, R., Determination of testosterone in peripheral blood of swine and bovines with a double isotope derivative dilution method, 25:10923
CLEBSCH, Edward E. C., Prog. rpt. on plant ecology of Amchitka Island, Alaska, annual, 8/1/67--6/30/68, 25:12874 (BMI-171-107)
CLEGG, Maurice Alexander, Substructure strengthening in nickel alloys, 25:11402
CLEMENT, Christophe, Decay scheme of ^{59}Fe and ^{192}Ir, 25:12464
CLEMMOW, P. C., Reflexion of a plane wave at a plasma half-space, 25:11939
CLINARD, F. W. Jr., Helium release from alpha-bombarded ThO_2, 25:11502
CLINE, D., Electromagnetic transitions in ^{51}V, 25:12492
CLINE, J. E., Gamma-ray studies of the γ-vibrational band of ^{166}Er, 25:12599
CLOSE, E. R., Generation of first and second order transformation elements from a given magnetic field, 25:12327
CLUCHET, J., Scientific and industrial applications of nuclear explosives, 25:10743
COATS, R. B., Lateral distribution of muon pairs in underground cosmic-ray showers, 25:12082
Transverse momentum of secondaries from cosmic-ray interactions in region 2 x 10^{5} GeV, 25:11749

XUM

COBB, Edward Clifford, Nuclear reactor fuel elements, 25:12800
COCKAYNE, J. E., Successive space-energy synthesis for neutron fluxes in fast reactors, 25:12780
CODDING, J. W. Jr., Total neutron cross section and resonance parameters of ^{147}Pm, 25:12550
CODREANU, S., Velocity and magnetic field of isotropic hydromagnetic turbulence in an incompressible fluid, 25:11757
COFFIN, C. T., Backward pion production from π^-p interactions, 25:12111
COGNE, Francois, COREGRAF 2: code for computing graphite lattices and their evolution for IBM 360 and CDC 6600, 25:12774 (CEA-N-1344(1))
COHEN, A. B., Service routines for multigroup cross-section code MC², 25:12337 (ANL-7654)
COHEN, B. L., Excitation of states in ^{207}Pb, 25:12569
COHEN, D., Anion-exchange separation of neptunium from uranium and thorium in basic solution, 25:10655 (ANL-7751)
COHEN, J. M., Centrifugal force and general relativity, 25:12274
COHEN, M., Two infrared sources in nebulae, 25:11563
COHEN, Saul G., Prog. rpt. on effects of mercaptans and disulfides on photochemical and high energy radiation induced reaction, annual, 11/69--11/70, 25:10627 (NYO-2499-37)
COHEN, Y., Biological tests of pharmaceutical radio colloids, 25:10957
COHN, C. E., Hardware and software for nuclear spectroscopy on the Varian Data Machines 622/i Computer, 25:10848 (ANL-7704)
COKER, W. R., Threshold effect in $^{93}Nb(d,p)^{94}Nb$, 25:12588
COLBURN, D. S., Comparison of the mean photospheric magnetic field and the interplanetary magnetic field, 25:11603
COLE, E. A. B., Cellular space--time and quantum field theory, 25:12260
COLEMAN, Charles Clyde, Electroabsorption and electro-photoluminescence in HgI_2, 25:12915 (UCLA-34-P-122-X-1)
COLEMAN, David C., Quantification of fungus: small arthropod food chains in the soil, 25:10929
COLEMAN, James R., States and radiation control, 25:11087 (CONF-700408-3)
COLEMAN, L. F., Natural transport effects on fission product behavior in the containment systems experiment, 25:12803 (BNWL-1457)
COLEMAN, Paul J. Jr., Stormtime disturbance fields at ATS 1, 25:11785
COLES, W. D., Superconducting magnet research, 25:11851
COLI, M., Designing method of switching circuits cascade for analog parameter discrimination, 25:10901
COLLOT, J., Behavior of α U under light stresses during recrystallization process or during the allotropic α/β transformation, 25:11451
COLOMBETTI, Lelio G., ^{68}Ga-labeled macroaggregates for lung studies, 25:11205
COLPO, P. N., Fast breeder reactor static physics methods development and analysis project. Volume 1. FARED: one-dimensional fast reactor physics design and analysis code, 25:12772 (BAW-3867-9(Vol.1)(Rev.1))
COLUZZI, B., Electron--positron elastic scattering at high energies, 25:12073
Multiple particle production from e^+e^- interactions, 25:12143
COMAR, D., Neutron activation determination of selenium in biological media, 25:10495
COMBELLES, Roland, Isotope separation apparatus, 25:10789
COMMANAY, L., Registration and counting of alpha particle tracks in cellulose nitrate, 25:10826
COMPSTON, W., Isotopic analysis of microgram quantities of lead iodide using an electron-bombardment source mass spectrometer, 25:10466
CONNELLA, M. J., Microstructural effects in critical fields of niobium films, 25:11832
CONSTANT, R., Development of techniques for production of ^{131}I, 25:10653 (BLG-442)
CONTAMIN, Pierre, Application of $^{18}O(p,\alpha)^{15}N$ reaction to study of self-diffusion of oxygen in uranium dioxide, 25:11486 (CEA-R-4095)
CONTE, L., First attempts of clinical application of a method for the quantitative interpretation of renogram with radiohippuran, 25:11208
COOK, J. L., Observation of ablation behavior of fibrous carbon--carbon composites, 25:12920 (Y-1752)
COOPER III, William S., Use of optical spectra to measure large electric fields in a hot-ion plasma, 25:11874
COPP, Jeanne E., Treatment of thyroid cancer. Death rates after surgery and after surgery followed by sodium iodide ^{131}I, 25:11234
COPPINGER, E. A., Formation of UO_2--carbon mixtures and carbide or nitride fuel material in spray reactor, 25:11478 (BNWL-843)
CORAZZA, C., Cross section and yield relations for the isomeric pair /sup 90m/Y/^{90}Y obtained by the (d,p) reaction, 25:12428 (CNEA-278)
CORBETT, B. L., Fuel meltdown at St. Laurent I, 25:12764
CORCUERA, R. Paviotti, Operational formulation of resonance absorption of neutrons, 25:12338 (CNEA-266)
CORNET, Jean-Andre, Self diffusion, under hydrostatic pressure, of body centered cubic Pu, 25:11371 (CEA-CONF-1690)
CORNET, Jean-Francois, Crystallographic analysis of segregations observed in dilute ZrPu alloys during martensitic transformation, 25:11430 (CEA-CONF-1688)
CORNEY, A. Kathleen, Differential and combined effects of beta, gamma, and fast neutron irradiation of soybean seedlings, 25:11312
CORNU, A., Application of spark source mass spectrography to geologic problems, 25:10455
Somatic mutations in petunia, 25:11011
CORNWALL, John M., Transport and loss processes for magnetospheric helium, 25:11802
CORREA, Helano S., Dry-way preparation of thorium tetrafluoride, 25:10516 (IEA-185)
Reduction of ammonium diuranate with anhydrous ammonia, 25:10573 (IEA-207)
CORRIGAN, K. W., Absolute tensor-polarization calibration of a polarized deuteron beam, 25:12356
CORVAL, Madeline, Isotope effects on the electron impact induced fragmentation of ethanol, 25:10528
COSTA, Eduardo C., Catalytic reduction of aqueous solutions of uranyl nitrate, 25:10572 (IEA-184)
Dry-way preparation of thorium tetrafluoride, 25:10516 (IEA-185)
Reduction of ammonium diuranate with anhydrous ammonia, 25:10573 (IEA-207)
COSTA, S., Angular and energy distribution of photoprotons from ^{27}Al, 25:12501
COSTE, J., Relaxation of a temperature anisotropy in a collisionless plasma, 25:11893
COSTER, Michel, Microfractographic aspect of refractory carbides, 25:11514
COTIGNOLA, J. M., Energy release and electrical resistivity recovery in Ni following electron irradiation, 25:11977
COTT, Donald Wing, Nonequilibrium effects in compressible MHD boundary layers, 25:11755
COTTERELL, D. L., Interaction of atomic particles with solid surfaces at intermediate energies. III, 25:11675
COUTANT, C. C., Growth of Columbia River Limpet, Fisherola nuttalli (Haldeman), in normal and reactor-warmed water, 25:10996 (BNWL-1537)
COWDER, L. R., Thermal expansion of extruded graphite--ZrC carbide composites, 25:11512
COWLING, D. H., Group rays of internal gravity waves in a wind-stratified atmosphere, 25:11796
COX, B., Form factors for the decay K/sub L/^{0} + $\pi\mu\nu$, 25:12088
COX, J., Determination of inelastic neutron form factor by scattering of 12-GeV muons on H, C, and Cu, 25:12096
COX, James L. Jr., Current induced in a plasma by a penetrating electron beam, 25:11894
CRACKEL, W. C., Calcium-47 turnover of a readily exchangeable calcium pool in pregnant and lactating cows, 25:12882 (COO-1339-44)
CRAIG, Harmon, Radium-226 measurements from the 1969 North Pacific Geosecs Station, 25:10726
CRAMER, Eugene M., Investigation of the plutonium--silver system, 25:11441
CRAMER, J. D., Fission of odd-A U and Pu isotopes, 25:12579
CRAMP, W. A., Radiosensitization of Shigella Flexneri and Escherichia coli, 25:11323
CRAMPTON, S. B., Evolution of electron angular momentum due to spin-exchange collisions involving nuclear spin, 25:11724
CRANSTON, F. P., Levels in ^{47}Ca and ^{41}Ca, 25:12491
CRANSTON, W. I., Measurement of hypothalamic blood flow in the conscious rabbit by a radioactive inert gas clearance technique, 25:11194
CRAVEN, S. M., Low-frequency vibrations of molecular solids. X, 25:10529
CRAWFORD, J. E., Quasielastic deuteron breakup by protons, 25:12375
CRAWFORD, W. M., Effects of uranium on the corrosion of resulfurized stainless steels, 25:11352
CRESPO, V. P., Production of ^{149}Tb from Au by 2.2-GeV protons, 25:12580
CRESTIA, Jean-Claude, Diffusion of the minor constituents into the troposphere, 25:10704 (NP-18609)
CREVIER, William Francis, Laminar shocks and other nonlinear waves in warm plasmas, 25:11930
CRONQUIST, A. G., Body scanner using a matrix system, 25:11217
CRONQVIST, S., Regional cerebral blood flow, 25:11143
CROSS, R. C., Radio-frequency heating of a plasma, 25:11864
CROSS, W. G., Developments in threshold detectors for personal dosimeters, 25:10882
CRUETZIG, H., Determination of lung circulation with the dynapix rapid scanner in pulmonary restrictions, 25:11131
CSIKAI, J., Observation of proton tracks by a plastic detector, 25:10831
Total neutron cross sections and nuclear Rensauer effect, 25:12344
CUBICCIOTTI, Daniel, Thallium--iodine phase diagram, 25:12912 (SRIA-106-76)
CULHANE, J. L., Thermal continuum function for x-ray emission from coronal plasmas, 25:11632

CUMMING, J. B., Production of ^{149}Tb from Au by 2.2-GeV protons, 25:12580
CUMMINGS, W. D., Stormtime disturbance fields at ATS 1, 25:11785
CUNNINGHAM, R. M., Investigation of in-band resonant modes in Cr--W alloys by inelastic neutron scattering, 25:12019
CUNNINGHAM, Robert Martin, In-band resonant modes in Cr--W alloys, 25:11985
CUPERMAN, S., Temperature-anisotropy instability for em waves propagating across static magnetic field, 25:11916
CURTIS, O. L. Jr., Recombination parameters in low-resistivity gamma-irradiated n-type germanium, 25:11968
CUSSON, R. Y., ELMOS: code to manipulate single particle wavefunctions and solve the ellipsoidal modified oscillator problem, 25:12623 (AECL-3730)
CUTEUDACHE, Calliopi, Hemorrhagic syndrome in radiation sickness. II, 25:11105
CVELBAR, F., Activation cross sections and integrated cross sections for radiative capture of 14 MeV neutrons, 25:12474
Gamma-ray spectra from radiative capture of 14 MeV neutrons in ^{28}Si and ^{40}Ca, 25:12472

D

DAHLGREN, S., Operation of cylindrical wire spark-chambers in low-pressure helium, 25:10872
DALLY, E. B., Form-factor ratio G/sub E/(n)/G/sub E/(p) at low momentum transfers, 25:12070
D'ALMAGNE, B., Meson π^+ photoproduction at 180° on H from 450 MeV to 3 GeV, 25:12067 (LAL-1239)
DALTON, J. T., Uranium--plutonium--carbon phase diagram. I, 25:11523
DALY, Patrick J., Prog. rpt. on radiochemical investigation of nuclear properties, 10/69--9/70, 25:12514 (COO-1672-21)
DALZIEL, R., Satellite equipment for the measurement of high energy electrons and protons, 25:11813
DAMERVAL, F. B., Nuclear rocket experimental engine test results, 25:12835
DANBY, G. T., Economical beam transport for utilization of post conversion AGS, 25:12296 (BNL-15464)
DANCE, K. D., Analysis of heterogeneity and sodium-void effects in a 2700-liter uranium carbide fast core, ZPR-6 Assembly 5, 25:12825
DANETSKAYA, E. V., Preventive diet in internal irradiation with ^{137}Cs and ^{90}Sr, 25:10956
DANGVU, Huyen, Gravitational waves and the solutions of Einstein's equations, 25:12275
DANGVU-DELCARTE, Claudine, Gravitational waves and the solutions of Einstein's equations, 25:12275
DANIELOU, R., Penning type strong ionizing field for polarized atomic beams, 25:12328
DANKO, V., Chlorophyll mutations in summer barley, 25:11021
DA PROVIDENCIA, J., Villars theory of nuclear collective rotation and its relation to variable moment of inertia model of Mariscotti et al, 25:12695
DARBY, J. B. Jr., Thermodynamic properties of solid palladium-rich Pd--Cd, Pd--In, Pd--Sn, and Pd--Sb alloys, 25:11396
DARBY, Valerie, Mutants of E. coli with altered surface properties and sensitive to uv light, 25:11029
DARBYSHIRE, H. F., Split fiberglass holder, 25:12866 (BDX-613-198)
DARCEY, W., Reactions ^{152}Sm(p,t)^{150}Sm and ^{154}Sm(p,t)^{152}Sm, 25:12612
DARDEL, J., Application of nuclear explosives in the mining industry, 25:10747
Contribution of earth sciences to the peaceful applications of nuclear explosions, 25:10740
DARDEN, S. E., Absolute tensor-polarization calibration of a polarized deuteron beam, 25:12356
DAREWYCH, G., Semi-empirical atomic-energy formula, 25:11739
DAREWYCH, J. W., Relativistic independent-particle model for atoms based on analytical potentials, 25:11738
DARSINOS, J., Determination of hepatic blood flow in hyperthyroidism with the ^{198}Au blood extraction method, 25:11141
DARWISH, S. M., Lifetimes of some excited states in ^{182}W, 25:12577
DAS, S., Production of nuclides by high-energy proton bombardment, 25:12439
DAS, S. K., Particle size of solid aggregates by beta-backscattering, 25:10784
DAS, T. K., Theoretical foundation of variable moment of inertia models, 25:12638 (NYO-2171-334)
DA SILVEIRA, R., Test of DWBA-type model for analysis of heavy-ion transfer reactions, 25:12683
DAVID, Lubomir, Relative thermal neutron flux distribution in core of RV-1 reactor, 25:12826
DAVIDSON, J. P., Electric monopole transitions in deformed nuclei, 25:12584
DAVIDSON, Melvin G., Deformed negative-parity states in heavy even nuclei, 25:12563
DAVIES, B., Helicon wave propagation: effect of electron inertia, 25:11936
DAVIES, J. G., Further radio observations of planetary nebulae, 25:11567
DAVIES, N., Fabrication and mechanical properties of dispersion hardened Pu--1 wt. percent Ga alloy, 25:11359
DAVIS, A. D., Hexadecapole deformation and rotation-particle coupling in the rare earth nuclei, 25:12674
DAVIS, C. K., Rotational structure in ^{29}Si, 25:12449
DAVIS, Harold L., Electronic band structure calculations for paramagnetic U compounds with NaCl-type symmetry, 25:11993
DAVIS, J., Phosphine--borane derivatives. III, 25:10547
DAVIS, L. L., Seismic response characteristics at NRDS from underground nuclear detonations, 25:10730 (NVO-1163-TM-22)
DAVIS, R. H., Alpha-particle scattering by ^{38}Ar, 25:12455
DAWSON, N., Angular correlation measurements on excited states of ^{42}Ca, 25:12465
Rotational structure in ^{29}Si, 25:12449
DEAN, S. A., Sodium flow monitoring, 25:12792
DE BELLIS, N., Dose fractionation in radiotherapy, 25:11071
DE BENTANCOURT, I., Cross sections for nuclear reactions produced by deuterons on tantalum, 25:12513 (CNEA-269)
DE BOER, F. W. N., Re-examination of ^{66}Ge decay, 25:12477
DE BOER, J., Reorientation effect in the cadmium isotopes, 25:12548
Reorientation effect measurements in ^{106,110}Cd, 25:12619
DECK, R. J., Microstructural effects in critical fields of niobium films, 25:11832
DECKER, J. F., Nonlinear damping of Tonks--Dattner resonances, 25:11942
DECOURS, Jacques, Structure transformations of Zr--Cu binary alloys with low Cu contents and ternary alloys during continuous cooling, 25:11432 (CEA-N-1310)
DECROISETTE, Michel, Thomson scattering in laser created plasma, 25:11865 (CEA-R-4058)
DE DOMINICIS, A., Some particular aspects of scintigraphy in cirrhosis of the liver, 25:11203
DEFOUW, R. J., Separation of matter and antimatter, 25:11661
DE FREITAS PACHECO, J. A., Synchrotron emission from high energy cosmic-ray electrons as an explanation of the cosmic x-ray excess, 25:11747
DEGASPERIS, Antonio, Inverse problem for a cylindrical plasma, 25:11904
DE HALAS, D. R., Prog. rpt. on reactor fuels and materials development, 4--6/68, 25:11474 (BNWL-842)
DEI-CAS, R., Filling of a magnetic well by injection of neutral atoms at various angles and energies, 25:11859 (EUR-CEA-FC-563)
DEICH, M. E., Gas dynamics of two-phase media, 25:10772
DE JAGER, G., Neutral H content of galaxies M31 and M33. I, 25:11646
Neutral H content of galaxies M31 and M33. III, 25:11648
DELALOYE, B., Use of the scintillation camera for functional investigation in medicine, 25:11182
DELAND, Frank H., Normal-pressure hydrocephalus. Role of cisternography in diagnosis, 25:11181
DELCOURT, B., Upper limit on phi in two-π branching ratio, 25:12074
DELEON, Ana, Separation of Zr from Hf by the TBP extraction method, 25:10689
DEL GIUDICE, E., Characterization of the physical states in dual-resonance models, 25:12180
DELIC, G., Effect of deuteron D-state on DWBA calculations for ^{16}O(p,d)^{15}O and ^{40}Ca(d,p)^{41}Ca, 25:12414
DELL'OCA, C. J., Ellipsometric studies of anodic oxide films formed on tantalum in dilute phosphoric acid, 25:11351
DELOLLIS, Nicholas J., Outdoor aging of adhesive sealants, 25:12908 (SC-RR-70-163)
DELTOUR, G., Biological effects of the heavy ions in cosmic radiation, 25:11280
DE MEIJER, R. J., Proton induced resonance reactions on ^{39}K, 25:12437
DEMKO, M., Thermoluminescent dosimetry with polycrystalline LiF, 25:10879
DEM'YANOV, A. V., Reaction π^-p + e$^+$e$^-$n at 275 MeV, 25:12099 (JINR-P1-5398)
DENEKA, Charles William, Properties and structures of La_2O_3--CdO--B_2O_3 glasses, 25:11517
DE NOVION, Charles, Mechanical properties of plutonium-based ceramics at high temperature, 25:11485 (CEA-CONF-1670)
DE NOVION, Charles-Henri, Electronic properties of actinide carbides and nitrides, 25:11980 (CEA-R-4113)
DEPOMMIER, P., Parity violation in the transition of ^{181}Ta at 482 keV, 25:12621
DEPP, Joseph George, Angular-momentum decomposition of the three-body problem, 25:12644
DEPPE, Alzira Lourenco, Spectrographic determination of hafnium in zirconium oxide, 25:10431 (IEA-208)
DEPUYDT, H., Low-lying 0$^+$ states in ^{12}C and ^{16}O, 25:12412
Projected Hartree--Fock calculation for light nuclei. V, 25:12396
DE RAS, E. M. M., Autoradiography as help for analysing distribution of α-active material in human body after air contamination, 25:10953
DER MATEOSIAN, E., Upper limit for a K-electron-capture

branch in /sup 113m/In, 25:12591
DE ROOS, G., Proton induced resonance reactions on ^{39}K, 25:12437
DERRY, Dennis J., New technique for measuring oxygen diffusion coefficients, 25:11516
DE RUJULA, A., Sixth-order corrections to the anomalous magnetic moment of the electron, 25:12145
DE SABBATA, V., Conversion of photons into gravitons and vice versa in a static electromagnetic field, 25:12272
DE SAINTIGNON, P., Parity violation in the transition of ^{181}Ta at 482 keV, 25:12621
DESCHAMPS, N., Uranium isotopic determination in rocks by neutron activation, 25:10494
DESCHANVRES, Alfred, Microfractographic aspect of refractory carbides, 25:11514
DESCHREIDER, A. R., Substances that react with thiobarbituric acid in irradiated flour, 25:10978
DESER, S., Classical Schwinger terms, 25:12244
DE SILVA, L. W. K., Quasi-stellar objects and gravitational lenses, 25:11584
DE SOETE, D., Average cross sections of $^{28}Si(n,p)^{28}Al$ and $^{29}Si(n,p)^{29}Al$ reactions, 25:12460
DESPRES, J., Chemical diffusion in epsilon phase of Pu--Cu system, 25:11387
DE STERKE, A., Ultrasonic inspection of welds in nuclear reactor pressure vessels, 25:12790
DETRAZ, C., Reactions ($^{3}He,t$) on ^{16}O, ^{22}Ne, ^{26}Mg, and ^{30}Si, 25:12498
T = 3/2 states of ^{25}Mg and ^{29}Si, 25:12450
DEVANATHAN, V., Photoproduction of charged pions from ^{12}C, 25:12407
DE VECCHIA, P., Characterization of the physical states in dual-resonance models, 25:12180
DEVENISH, R. C. E., Fixed-t dispersion relations for pion photoproduction in the second resonance region, 25:12146
DE VERNEJOUL, P., Application of /sup 99m/Tc for scintigraphic studies of pulmonary circulation, 25:11128
Visualization by image intensifier of radioactive indicator flow through the cardiac chambers and the large vessels, 25:11120
DEVILLERS, C., Reactor shielding in the CEA, 25:12782 (CEA-CONF-1683)
DE VILLIERS, J. A. M., Investigation of levels in ^{51}Cr, ^{55}Fe, and ^{59}Ni, 25:12476
DEVISHEV, M. I., Investigation of a particle beam with energy up to 70 GeV with a spark spectrometer, 25:10868 (IFVE-SEF/OP-70-13)
DEVISHEVA, M. N., Investigation of a particle beam with energy up to 70 GeV with a spark spectrometer, 25:10868 (IFVE-SEF/OP-70-13)
DEVRIES, R. G., UIS: Bettis CDC-211 display package, 25:12918 (WAPD-TM-987)
DE VRIES, T., Evidence for B(1220) production in an analysis of reaction K-d + p/sub s/Ar+$\pi^-\pi^-\pi^0$ at 3 GeV/c, 25:12118
DEWHIRST, D. W., Two infrared sources in nebulae, 25:11563
DEWITT, Robert, Phase relationships in U, Np, and Pu, 25:11437
DEY, Arun K., Avidity of folic acid for carcinogenic metal ions, Al(III), Cr(III), Be(II), Pb(II), and U(VI), 25:10520
DHINGRA, Ashok Kumar, Effect of matrix strengthening and fiber coating on mechanical behavior of boron--magnesium composites, 25:11407
DIAMOND, R. M., Vidicon device for ionization measurements, 25:10878
DIBAI, E. A., Densities and masses of comet-shaped nebulae, 25:11541 (CSIRO-Trans-10286)
DICELLO, J. F., Proton total reaction cross sections of ^{40}Ca and ^{12}C, 25:12497
DICKEY, Leland C., Radiolysis of chloroform vapor. Effects of phase on the arrhenius parameters of the hydrogen-atom abstraction reaction of dichloromethyl radicals with chloroform, 25:10629
DICKMANN, Friedrich, Potential landscape for fissioning nuclei. I, 25:12681
DIDELEZ, J. P., Experimental studies of reactions $^{3}H(p,p)^{3}H$, $^{3}He(p,p)^{3}He$, and $^{3}H(p,n)^{3}He$ at 156 MeV, 25:12365
DIEHL, R. C., Excitation of states in ^{207}Pb, 25:12569
DIENER, G., Relaxation of a temperature anisotropy in a collisionless plasma, 25:11893
DIEPERINK, A. E. L., Second-order calculation of isotope effect in Ca isotopes, 25:12484
DIETRICH, F. S., Hole-vibration coupling in ^{115}In, 25:12543
DIETRICH, Klaus, Potential landscape for fissioning nuclei. I, 25:12681
DIETZ, K., Determination of regional blood flow with ^{133}Xe in the brain of Parkinson and tumor patients, 25:11147
DIETZE, G., Polarization of protons from the reaction $^{2}H(d,p)^{3}H$ at deuteron energies between 1.35 to 2.00 MeV, 25:12361
DILLINGER, J. R., Isotope effect in superconducting cadmium, 25:11825
DILLINGER, P., Determination of boron in boric glasses by a neutron absorption method, 25:10483
Moisture determination in certain compounds used for pharmaceutical purposes based upon neutron scattering and moderation, 25:10486
Neutron absorption analysis of pharmaceutic preparations containing boron, 25:10487
DIMCHEV, T., Determination of low-level ^{90}Sr and ^{137}Cs activation in milk, 25:10480
Possibilities of detecting low-level β-activities by scintillation detectors, 25:10819
DI PIETRO, R., Treatment of water in a nuclear plant for the testing of fuel elements, 25:12821 (LIB/Trans-335)
DIRKS, Johan F., Generalized variational bounds on positron--H reaction matrix. II, 25:11719
DISCHLER, W., Scintigraphic findings in liver diseases identified by laparoscopy and histology, 25:11180
DITTNER, A., Timing of Ge(Li)-detector pulses, 25:10830
DIVAVIN, I. A., Gamma radiation effects on pyrimidine oligonucleotides in low-polymer fraction of DNA, 25:11307
DIXIT, V. V., Implications of duality for anti KN resonances, 25:12215
DIXON, M. E., B-type stars within ten degrees of galactic centre. I, 25:11561
DIXON, R. S., Dissociation of water vapour by photolytic, radiolytic, and electron impact methods, 25:10651
DJADALI, F., Circular γ-polarization spins for compound states in thermal neutron capture, 25:12601
DJORDJEVIC, M., Determination of burn-up of nuclear fuel on the basis of stable isotopes of Nd. II, 25:10469
Determination of burn-up of nuclear fuel on basis of stable isotopes of Nd. I, 25:10461
DMITRIEV, I. M., Cesium-137 in lichen-reindeer man in the extreme north of the USSR, 1962--68, 25:11037 (NP-18381)
DMITRIEVA, T. A., Muon capture in ^{14}N, 25:12386
DMITRIEVA, T. I., Action of fast neutrons and x-rays in formation of chromosome aberrations in mice, 25:11018
DOBIASOVA, Zlatica, Calculation of ^{90}Sr content changes in atmospheric fallout and on ground in West Slovakia up to year 2000, 25:10719
DOBRZANSKI, Z., Clinical value of liver function appraisal by means of ^{131}I-rose bengal. II, 25:11111
DOBRZYNSKI, L., Magnetic structure of U_3P_4, 25:12028
DODD, B., Buckling and fine structure measurements in the Helen I facility, 25:12828
DODD, W. J. F., Effects of ionizing radiation on dried spores of Osmunda regalis. I, 25:11319
DOELLGAST, W., Method of concentrating radioactive waste, 25:10682
DOERING, P., Diagnosis of brain tumors with ^{131}I-labeled albumen particles and with ^{75}Se, 25:11145
DOERSCHEL, B., Neutron personnal dosimetry on tissue-equivalent phantoms by solid-state track detectors, 25:10880
DOLGINOV, A. Z., Origin of the x radiation of the metagalaxy, 25:11657
DOLIAS, Mylene, Neutron dosimetry and spectrometry by multisphere method, 25:10811 (CEA-CONF-1685)
DOLMATOVA, M. Yu., Protective effects of calcium alginate against chronic ^{90}Sr ingestion, 25:11103
DOMAREVA, O. P., Action of fast neutrons and x-rays in formation of chromosome aberrations in mice, 25:11018
DONAHUE, Edward J., Positive reactivity from replacement of heavy water by light water in the coolant channels of a heavy-water-moderated reactor, 25:12830
DONAHUE, T. M., Helium I 584-A dayglow radiation between 400 and 1000 km, 25:11789
DONEGA, G., Elimination of thermal shield from Trino Vercellese pressurized water reactor, 25:12715
DONETS, E. D., Method for pulsed polarized ion beam production for high-energy accelerators, 25:12304 (JINR-P9-5446)
DONOGHUE, T. R., DWBA analysis of the cross section and polarization data for the $^{14}N(d,n)^{15}O$ reaction at 3.5 MeV, 25:12405
DONTSOV, Yu. P., Interferometric investigations of plasma in a coaxial high-current accelerator using a helium--neon laser, 25:11871
DORFMAN, Ronald Sherman, Particle multiple and diffraction scattering and dips, 25:12205
DORMAN, G., Landau damping of resonance oscillations in inhomogeneous plasmas, 25:11941
DORNUTH, Kenneth, Electromagnetic interaction of a spin-$^3/_2$ field, 25:12267
DORREN, J. D., Dual amplitudes for 6 pions with epsilon-tensor couplings, 25:12131
DOS SANTOS, P. Marques, Changes in coronal condensations emission after solar bursts at microwaves, 25:11620
DOUGHERTY, Thomas F., Risk to bone and liver from ^{239}Pu, 25:11301
DOUGLAS, J. A., Radiation dose rates from plutonium oxide--beryllium oxide mixtures, 25:11052 (AERE-R-5069)
DOUGLASS, Dana L., Electron microscopy of alpha particle damage in actinide oxides, 25:11537
Helium release from alpha-bombarded ThO_2, 25:11502
DOVD, W., Dependence of solvolytic α-deuterium rate effects on nature of the leaving group, 25:10522 (COO-1008-13)
DOYLE, Joseph Cecil, Study of $\pi^- + p \rightarrow \Lambda + K^0$ from 944 to 1170 MeV/c, 25:12109
DRAGOS, L., Flow of fluids with conductivity tensors in presence of a thin airfoil, 25:11774
DRAGULESCU, C., Uranyl pyrophosphate complexes. II, 25:10519
DRAKE, J. E., Phosphine--borane derivatives. III,

25:10547
DRAN, J. C., Habit and texture of lunar and meteoritic materials, 25:11671
DREIZLER, R. M., Application of the Hartree--Fock variational method to center-of-mass motion, 25:12653
Theoretical foundation of variable moment of inertia models, 25:12638 (NYO-2171-334)
DRICKAMER, H. G., Effect of pressure on electronic structure of ferric hydroxamates and ferrichrome A, 25:12881 (COO-1198-777)
DRICKEY, D. J., Study of decay mode K/sub L/^{0} + $\pi^{+}\pi^{-}\pi^{0}$, 25:12087
DRISKO, R. M., DWBA analysis of the cross section and polarization data for the ^{14}N(d,n)^{15}O reaction at 3.5 MeV, 25:12405
DROST, H., Lifetime of new 194.9 keV level in ^{77}As, 25:12473
DUBANSKY, B., Comparison of cerebral blood flow measurements with intravenously administered ^{131}I-labeled hippuran between arteriosclerotic and normal patients, 25:11150
DUBEY, S. P., Synergistic effects in ion-exchange. I, 25:10681
DUBOIS, J., Carbonaceous mesophase formed in the pyrolysis of graphitizable organic materials, 25:11529
DUBROVINA, Z. V., Protective effects of calcium alginate against chronic ^{90}Sr ingestion, 25:11103
DUBROVSKAYA, L. B., Conduction band of IVa and Va subgroup transition metal monocarbides. I, 25:12024
DUDEK, A., Real part of the alpha-nucleus potential obtained by double folding procedure, 25:12627 (INP-720)
DUEBER, Thomas E., Secondary deuterium isotope effects in vinyl cations, 25:10548
DUEBLER, Horst, Sliding friction and wear of pure metals under vacuum of 5 x 10^{-8} torr, 25:11413
DUERR, H. P., Gauge-invariant spinor theories, 25:12262
DUEX, A., Scintigraphic studies of blood distribution in the pulmonary system, 25:11127
DUFFY, Arthur R., Prog. rpt. on investigation of initiation and extent of ductile pipe rupture, Phase II, 7--9/70, 25:11369 (BMI-1892)
DUFFY, Cecilia, Argon laser micro-irradiation of mitochondria in rat myocardial cells in tissue culture, 25:11242
DUGDALE, L. M., Radionuclide scanning in renal lesions, 25:11115
DUHM, H. H., Reactions (^{3}He,t) on ^{18}O, ^{22}Ne, ^{26}Mg, and ^{30}Si, 25:12498
DUM, Christian T., Nonlinear beam--plasma interactions and stochastic acceleration, 25:11885 (NYO-4077-1, Paper 3)
DUMESNIL, Patrice, Gamma-ray spectrometry in drillings using Ge--Li semiconductor probes, 25:10849 (CEA-CONF-1694)
DUMONDE, D. C., Allergic inflammation. I, 25:11193
DUNAND, Jean-Jacques, Nuclear magnetic resonance at 310 MHz in a superconducting solenoid, 25:12034 (CEA-R-3855)
DUNCAN, J. L., Equilibrium geometries of the methyl halides, 25:10561
DUNLAP, B. D., Magnetic behavior of Np metal and dilute Np alloys from Moessbauer effect studies, 25:12001
DUPREE, Robert G., Magnetic fields and the structure of the solar corona. II, 25:11604
DUPUIS, M., Distribution and development of radioelements after a nuclear explosion, 25:10742
DURAN, S. A., Minimum-creep-rate behavior of polycrystalline vanadium from 0.35 to 0.87 T/sub m/, 25:11397
DURIG, J. R., Low-frequency vibrations of molecular solids. X, 25:10529
DURKEE, W. E., Nuclear rocket experimental engine test results, 25:12835
DURRANI, S. A., Annealing of fission tracks in tektites: corrected ages of bediasites, 25:10696
DURRIEU, L., Habit and texture of lunar and meteoritic materials, 25:11671
DUTREIX, J., Recovery of skin reactions in mice after split-dose irradiation, 25:11260 (BNL-50203, pp 286-91)
DUWEZ, Pol, Superconducting metastable simple cubic alloys, 25:11819 (CALT-822-22)
DUZI, P., Distribution of iron and aluminum during zone melting of uranium, 25:11406
DVORNIK, I., Chemical dosimeters for accident dosimetry, 25:10883
DWIGHT, A. E., Uranium--plutonium--zirconium ternary alloy system, 25:11442
D'YACHENKO, V. V., Determination of the boundary of high frequency wave absorption between the electron cyclotron and the low-hybrid frequency, 25:11927 (FTI-295)
High frequency plasma heating near the low-hybrid frequency, 25:11860 (FTI-282)
DYBCZYNSKI, R., Effect of resin cross-linking on anion exchange separation of rare-earth--EDTA complexes, 25:10665 (INR-P-1209)
DZEGANOVSKII, V. P., X-ray spectra and band structure of refractory vanadium compounds, 25:12012
DZHOLOS, R. V., Mass coefficient in nucleus collective Hamiltonian and sum rules for probabilities of E2-transitions and of quadrupole moments, 25:12633 (JINR-P4-5346)
DZIEDZIC-GOCLAWSKA, A., Free radicals evoked by radiosterilization in preserved bone grafts, 25:11329
Quantitative evaluation of irradiated bone grafts resorption rate by the electron spin resonance technique, 25:11340

E

EBATA, T., Deep inelastic e-p scattering and a reggeization scheme for photon processes, 25:12148
EBER, O., Differential scintigraphic representation of the pancreas by means of a computer, 25:11176
Lymph drainage following neck surgery, 25:11178
Studies on techniques for lung scintigraphy, 25:11129
EBERT, M., Effects of ionizing radiation on dried spores of Osmunda regalis. I, 25:11319
EDDY, Hubert A., Effects of radiation on vasculature of intestine, 25:11255 (BNL-50203, pp 181-5)
EDELSTEIN, Alan S., Condensation into high-temperature spin-compensated state: α-Ce, 25:12016
EDWARDS, Kathleen D., Maternal x irradiation and the frequency of mongolism, 25:11300
EDWARDS, R. K., Mass spectrometric investigation of volatilization behavior of ($U_{0.8}Pu_{0.2}$)O/sub 2-x/, 25:11503
EDWARDS, Ralph Thomas, Direct processes in two-pion radiative decays of K^{+-}, 25:12085
EDWARDSON, J. R., Prog. rpt. on cytological study of radiation induced alterations in cytoplasmic factors controlling male sterility in corn, annual, 12/70, 25:11010 (ORO-2583-8)
EERNISSE, E. P., Sputtering and strain of silicon by ion implantation, 25:11959
EGAMI, N., Effects of cysteamine and x irradiation on mortality of fish, 25:11292
EGGER, J. P., Kinematically complete experiment on reaction n + d → n + n + p, 25:12367
EGGLETON, A. E. J., Theoretical examination of iodine--water partition coefficients, 25:10513 (AERE-R-4887)
EHHALT, D. H., Variations of the carbon and oxygen isotopic composition in stalagmites and stalactites: evidence of non-equilibrium isotopic fractionation, 25:10684
EHLERS, F. E., Linearized magnetogasdynamic channel and jet flow, 25:11773
EHLERS, Jurgen, Relativistic kinetic theory of charged gases, 25:12058
EHRENFREUND, E., Magnetic properties of Nb_3X compounds, 25:12037
EIBER, Robert J., Prog. rpt. on investigation of initiation and extent of ductile pipe rupture, Phase II, 7--9/70, 25:11369 (BMI-1892)
EICHLER, J., Circular γ-polarization spins for compound states in thermal neutron capture, 25:12601
EICKENBUSCH, W., Studies with ^{89}Sr of diseases belonging to the rheumatic complex, 25:11175
EIDE, Age Jostein, Strange-particle production in 7.3-GeV/c K^{-} interactions in deuterium, 25:12103
EIDENS, J., Decay of ^{84}Se, ^{91}Kr, ^{97}Y, ^{99}Nb, ^{99}Zr, ^{100} ^{101}Nb, and ^{101}Zr, 25:12462
EISENBUD, Merril, Radiation standards and public health, 25:11076
EITZ, A. W., Karlsruhe reprocessing plant: objectives and conception of WAK installation, 25:10756 (ORNL-tr-2416)
EKBOM, Lars, Corrosion of plutonium in argon with small amounts of moisture, 25:11350
Phase transformations in metastable plutonium--gallium alloys, 25:11446
EL-BADRY, E. A., Effects of gamma radiation on cotton leaf worm, 25:11247
ELBERSE, P. A., Determination of trace amounts of I. II, 25:10481
EL-HALIEM, A. Abd, Lifetimes of some excited states in ^{182}W, 25:12577
ELISEENKO, N. N., Radiation damage to chromosomes in Crepis capillaris, 25:11015
ELKIND, M. M., Actinomycin D and radiation fractionation studies in asynchronous and synchronized Chinese hamster cells, 25:11097
Reoxygenation in radiotherapy, 25:11224 (BNL-50203, pp 318-38)
ELLEMAN, Daniel D., Relative proton affinity of argon and deuterium, 25:10552
ELLINGER, F. H., Constitution of plutonium-rich plutonium--osmium alloys, 25:11438
Plutonium--zirconium phase diagram, 25:11439
ELLIOTT, R. O., Kondo effect in Ti, Zr, and Hf alloys containing Pu, 25:12004
ELLIS, F., Fractionation treatment of larynx and pharynx, 25:11221 (BNL-50203, pp 268-79)
ELLIS, J., Scale and chiral symmetry breaking, 25:12214
ELLIS, W. P., Low energy secondary electron distribution studies of some light actinides, 25:11999
ELLIS, William Edwin, Events with two or four charged prongs from 28.5-GeV/c pp interactions, 25:12091
ELSCHNER, B., Magnetization in Yb--Eu alloys, 25:12013
ELWERT, Gerhard, Polarization and anisotropy of solar x radiation during flares, 25:11623
EMRICH, D., Assessment of the course of experimentally

XUM

induced radionephritis with isotope renography, 25:11275
EMRICH, Kurt, Theory of inelastic nucleon--nucleus scattering, 25:12701
ENDRES, P., Assessment of functional significance for renal artery stenosis confirmed by angiography. comparison of the radiorenogram with the angiotensininfusion test and with the plasma renin content in both peripheral and renal venus blood, 25:11164
ENGEL, Thomas K., Thermal conductivity of plutonium at high temperature, 25:11383
ENGELBERTINK, G. A. P., Half-lives of ^{11}Be, ^{15}C, ^{16}N, ^{19}O, and ^{28}Al, 25:12394
ENGELMANN, Charles, Activation analysis using charged particles and γ photons, 25:10488 (CEA-R-4072)
ENGLER, G., Scattering of protons from ^{128}Te and ^{130}Te, 25:12602
ENGLISH, Jane Butterfield, Low-momentum antiproton--proton scattering, 25:12095
ENGMANN, R. G. R., Gamma-ray transition strengths in ^{34}Cl, 25:12493
EPPLEY, R. E., Neutron-deficient Gd isotopes. II, 25:12582
ERBA, E. Gadioli, Energies of nuclei with different neutron and proton number in Thomas Fermi approximation, 25:12635 (NP-18545)
ERICSON, T. E. O., Pion scattering by nuclei in region of (3,3) resonance, 25:12420
ERIKSSON, K.-E., Asymptotic states in quantum electrodynamics, 25:12249
ERLICKI, M. S., Magnetic control of a conducting jet, 25:11775
ERNST, H., Lung scintigraphy for studies of normal and pathological blood distribution in the pulmonary circulatory system, 25:11126
ERNST, W. S., Characterization and behavior of alkalized alumina during sulfur dioxide sorption--regeneration process, 25:12901 (ORNL-TM-3210)
ERSHOV, D. K., Isobar neutrino production processes, 25:12174
ERSKINE, J. R., Reaction ^{182}W(t,d)^{183}W at 20 MeV triton energy, 25:12611
ERWIN, A. R., Vidicon device for ionization measurements, 25:10878
ESCH, L. J., Temperature dependence of neutron inelastic scattering from water, 25:12342 (RPI-328-210)
ESCHWEGE, F., Recovery of skin reactions in mice after split-dose irradiation, 25:11260 (BNL-50203, pp 286-91)
ESPAGNO, Lucien, Radioactivity sensing apparatus for measuring the blood flow, 25:10828
ESTERMAN, Immanuel, Advances in atomic and molecular physics. VI, 25:11728
ESTES, Guy Phillips, Resonance fluorescence in Cd and Ni using neutron-capture gamma rays, 25:12554
ETIN, E., Discussion of some recent results on cosmic-ray muons, 25:12168
ETTLINGER, L., Form factors for the decay K/sub L/^{0} → $\pi\mu\nu$, 25:12088
EVANS, D. B., Improvement in heat exchangers, 25:12811
EVANS, J. P., Compatibility studies between arc cast ($U_{0.85}Pu_{0.15}$)--C and type 316L stainless steel, 25:11475 (AERE-R-5173)
EVANS, Kenneth Edward Jr., Double Laplace transformation and its application to multi-component plasmas, 25:11889
EVANS, S. K., Compressive creep properties of UO_2--PuO_2 compounds, 25:11495
Thermodynamic behavior of plutonium oxide systems in a temperature gradient, 25:11505
EVANS III, R. B., Uranium and thorium diffusion in columnar pyrocarbons as influenced by actinide concentration, 25:11378 (ORNL-TM-2989)
EVERETT, G. E., Magnetic susceptibility of cerium metal under pressure, 25:12018
EVERETT, K. R., Prog. rpt. on geomorphology and pedology of Anchitka Island, annual, 6/68, 25:12873 (BMI-171-106)
EVWARAYE, A. O., Photoneutron angular distributions from ^{2}H(γ,n)H reactions, 25:12374
EYMERY, Rene, Collimation system for irradiation apparatus, 25:10781

F

FABEL, H., Determination of central circulation parameters and peripheral blood flow by simultaneous application of ^{133}Xe and ^{131}I-labeled RISA, 25:11123
FACK, H., Maximal output power of point-contact Josephson junctions, 25:11838
Pull-in phenomena of Josephson oscillators, 25:11839
FAHEY, J. A., Preparation and some properties of berkelium metal, 25:11358
FAIERS, M. E., Fabrication and mechanical properties of dispersion hardened Pu--1 wt. percent Ga alloy, 25:11359
FAINBERG, Joseph, Type III solar radio burst storms observed at low frequencies. I, 25:11622
FAISAL, F. H. M., Adiabatic theory of rotational excitation of non-I states, 25:11725
FANGER, U., Investigations of excited states of ^{96}Mo nucleus from reaction ^{95}Mo(n,γ)^{96}Mo, 25:12598
FANTIDIS, J., Variations of the carbon and oxygen isotopic composition in stalagmites and stalactites: evidence of non-equilibrium isotopic fractionation, 25:10684
FARAG, A. K., Recovery of U, Th, and Ce from Egyptian monazite sands. I, 25:10683
FARAGGI, H., Transfer reactions (α,t), (α, ^{3}He) in the fp shell, 25:12434
FARBER, Morton S., Three-body final states in K^{+}p interactions at 13 GeV/c, 25:12102
FARMELANT, Melvin H., Prognostic value of radioisotopic renal function studies for selecting patients with renal arterial stenosis for surgery, 25:11186
FARRELL, K., Transmutation-produced silicon precipitates in irradiated aluminum, 25:11471
FARTUSHNYI, V. P., Experiments on α-particle acceleration by collective method, 25:12305 (JINR-P9-5558)
FASSNACHT, R. E., Isotope effect in superconducting cadmium, 25:11825
FAULKNER, D. J., Nature of the nebulosity about FG Sagittae, 25:11574
FEDERMAN, P., Structure of the calcium isotopes, 25:12436
FEDOROVA, A. V., Histamine level in blood and tissues of animals under action of radioisotopes, 25:10967
Influence of radionuclides on enzymes of rat blood and tissues, 25:10968
FEELY, Herbert W., Investigations of U and Th series isotope disequilibria in the ocean and in pleistocene sediments. Annual Progress report, 25:10725 (CU-3139-4)
FEFILOV, B. V., Neutron detector in search for superheavy elements in nature, 25:10814 (JINR-P13-5391)
FEGIZ, G. F., Scintigraphy for diagnosis of hepatic and pancreatic conditions of surgical interest, 25:11197
FEHER, I., Quantitative autoradiography of Zr--T particles, 25:10775 (KFKI-70-26-HP)
FEINSTEIN, Robert N., Acatalasemia in the mouse and other species, 25:11264
FEJER, J. A., Effect of ionospheric heating by radio waves on absorption of probing waves of different polarization, 25:11807
FEL'DSHTEIN, Ya. I., Boundary of captured 280-keV electrons and position of current electrojets in the ionosphere, 25:11782
Ring current in the magnetosphere and low-latitude magnetic rays, 25:11779
FELICETTI, F., Electron--positron elastic scattering at high energies, 25:12073
Multiple particle production from e^{+}e^{-} interactions, 25:12143
FELIX, R., Scintigraphic studies of blood distribution in the pulmonary system, 25:11127
FELLER, Heinz Gerhard, Sliding friction and wear of pure metals under vacuum of 5 x 10^{-9} torr, 25:11413
FERGUSON, Stephen Mason, Transitions feeding ground-state rotational band following (α,xn) reactions, 25:12553
FERLE-VIDOVIC, Ana, New evidence concerning the molecular basis of the restorative effect of DNA in cultured mammalian cells, 25:11243
FERNANDEZ, Salvador M., Charge-exchange scattering of He^{+} by He, Ne, and Kr, 25:11716
FERRADINI, C., Radiolytic behavior of ferrous and ferric ions in very dilute solutions, 25:10635
Yield of hydrogen peroxide in aerated acidified water exposed to tritium β rays, 25:10636
FERRERO, L., Angular and energy distribution of photoprotons from ^{27}Al, 25:12501
FERRIEUX, Henri, Seismic compression waves associated with underground nuclear explosions in the Sahara, 25:10729 (CEA-R-4105)
FEUERHAKE, I., Determination of central circulation parameters and peripheral blood flow by simultaneous application of ^{133}Xe and ^{131}I-labeled RISA, 25:11123
FIDANZA, M. A., First attempts of clinical application of a method for the quantitative interpretation of renogram with radiohippuran, 25:11208
FIELD, J. H., General tests of the ΔI = 1/2 and ΔS = ΔQ rules in K/sub t3/ decays, 25:12167
FILGAS, R., Determination of fluorine by neutron activation analysis in fluorinated ores and concentrates. II, 25:10498
FILIPPOV, G. A., Gas dynamics of two-phase media, 25:10772
FILIPPOV, L. P., Thermal properties of tantalum at high temperatures, 25:11425
FINCH, C. B., High-temperature solution growth of single-crystal neptunium dioxide, 25:11483
FINDEIS, A. F., Geiger counters for detection of non-radioactive effluents from gas chromatograph, 25:10888
FINEGOLD, L., Lattice dynamics of zirconium, 25:12026
FINGER, M., Main decay characteristics of mercury isotopes and their daughter products (182 less than or equal to A less than or equal to 192), 25:12512 (CERN-70-29)
FINKELSTEIN, L., Some exact and approximate solutions of the neutron slowing down equation in resonant absorbing media, 25:12346
FINLAY, R., Reactions (^{3}He,t) on ^{18}O, ^{22}Ne, ^{24}Mg, and ^{30}Si, 25:12498
FINNEY, Clifton Donald, Low-energy electron radiolysis of gaseous methane, ethane, and ethylene, 25:10644
FIRESTONE, Richard F., Radiolysis of chloroform vapor. Effects of phase on the arrhenius parameters of the hydrogen-atom abstraction reaction of dichloromethyl

radicals with chloroform, 25:10629
FIRRAO, D., Plastic-strain controlled failure criteria and design parameters. Technical progress report, 25:11373 (COO-2046-1)
FIRST, M. W., Prog. rpt. on air cleaning, semiannual, 3--8/70, 25:10797 (NYO-841-23)
FIRUSIAN, N., Some aspects of abdominal lympho-scintigraphy, 25:11177
FISCHER, J., Determination of splenic blood flow with ^{51}Cr labeled and heat treated erythrocytes, 25:11142
Hemodynamic function studies, 25:11184
FISCHER, Konrad, Adsorption of O and N on Ta films. IV, 25:11419
Adsorption of O and N on Ta films. III, 25:11417
Adsorption of O and N on Ta films. II, 25:11418
FISCHER, W., Quantitative analysis of the radiorenogram based on ^{131}I-orthohippuric acid clearance, 25:11159
FISHER, P. S., Intermediate structure and reaction $^{28}Si(p,p')^{28}Si$, 25:12470
FISHER, R. D., α-deuterium effects on rate of solvolysis of 2-adamantyl sulfonate ester, 25:10523 (COO-1008-15)
FISK, L. A., Solar modulation of galactic cosmic rays. II, 25:11746
FLEISHMAN, D. M., Neutron activation for measuring bone calcium content, 25:10907 (N-70-31814)
FLEROV, G. N., Synthesis of element 105, 25:12620
FLESHMAN, D. G., FORTRAN code for analysis of counting data from animal tissues, 25:10937 (UCRL-50957)
FLETCHER, Gilbert H., Dose-time fractionation practice, 25:11259 (BNL-50203, pp 260-7)
FLETCHER, W. H. W., Van der Pol plasma instability, 25:11944
FLIEDNER, T. M., Cytokinetic analysis of slowly proliferating bone marrow cells during recovery from radiation injury, 25:11077
FLORES, J., Matrix elements of finite U(n) transformations, 25:12235
FLOTHMANN, D., Beta spectrum of ^{204}Tl, 25:12615
FLUSS, M. J., Protons and alpha particles emitted from ^{75}Br compound nuclei with differing angular-momentum distributions, 25:12461
FLYNN, E. R., Reaction $^{182}W(t,d)^{183}W$ at 20 MeV triton energy, 25:12611
FODOR, Traian, Thermal diffusion column, 25:10783
FOGELBERG, B., 190-keV transition in ^{141}La, 25:12540
FOLLI, E., Design of NH_3--H_2 two-temperature plant for heavy water production, 25:10787
FOLSOM, T. R., Trace element calibrations and profiles at Geosecs Test Station in Northeast Pacific Ocean, 25:10428
FOMENKO, B. S., Peroxidase activation in γ-irradiated broad beans, 25:10973
FONTENILLE, Jean, Application of $^{18}O(p,\alpha)^{15}N$ reaction to study of self-diffusion of oxygen in uranium dioxide, 25:11486 (CEA-R-4095)
FORD, W. F., Hard-core potential representation, 25:12659
FORMAN, Fred Leslie, Strange-particle final states from π^+p interactions at 1.7 GeV/c, 25:12104
FORSBERG, Sven-Ake, Radiation damage to the surfactant system of the rabbit lung, 25:11267
FORSLO, Hans, Radiosensitivity of mediastinal lymphomas treated with split-course radiotherapy, 25:11226
FORSTER, H. H., Study of the $^{14}N(p,2p)^{13}C$ reaction at 46 MeV, 25:12391
FORTINI, P., Conversion of photons into gravitons and vice versa in a static electromagnetic field, 25:12272
FORTNA, John David Edward, Line shapes of N II and C II resonance multiplets from plasma, 25:11861
FORTUNE, H. T., Reaction $^{10}B(\alpha,^6Li)^8Be$, 25:12392
Spin dependence in inelastic scattering, 25:12454
FOUASSIER, C., Systems B_2O_3--MO--MS boracites M--S (M = Mg, Mn, Fe, Cd) and sodalites M--S (M = Co, Zn), 25:11526
FOUCHER, R., Main decay characteristics of mercury isotopes and their daughter products (182 less than or equal to A less than or equal to 192), 25:12512 (CERN-70-29)
On-line nuclear spectroscopy, 25:10670 (LYCEN-7034, pp 23-33)
FOWLER, J. L., Differential scattering of neutrons at narrow levels in ^{17}O, 25:12404
FOX, B. W., Single-strand breaks in DNA of P388F cells after low doses of electrons, 25:11028
FOX, Geoffrey, Decisive tests of high-energy models, 25:12206
FOX, Kenneth, Simple approximate eigenfunctions for an electron in a finite dipole field, 25:12056
FOX, M., Single-strand breaks in DNA of P388F cells after low doses of electrons, 25:11028
FRADIN, F. Y., Nuclear magnetic resonance of actinide compounds, 25:12036
FRADKIN, E. S., Application of spectral density method to systems with pair interaction, 25:12061
FRAIZIER, A., Irradiation equipment for studying the influence of radiation on marine organisms, 25:10759
FRAME, J., Effect of a uremic environment on phosphate excretion by a small population of intact and severely diseased nephrons, 25:10963
FRAMPTON, Paul, Hyperon beta decay, 25:12163 (COO-264-563)
FRANCIS, Norman C., Notes on the carbon total cross section from 0-2 MeV, 25:12379 (KAPL-P-3901)
FRANCIS, W. C., Prog. rpt. on metallurgy and materials science, annual, FY 1970, 25:11458 (IN-1437)
FRANK, H. G., Treatment by radiotherapy of carcinoma of the bladder, 25:11229
FRANK, L. A., Energy spectrums for proton intensities in outer radiation zone, 25:11786
FRANK, R., Review on correlation measurements in plasma, 25:11866 (EUR-CEA-FC-570)
FRANKE, W.-G., Results of lung scintigraphy in silicosis, 25:11134
FRANKLIN, D. H., Gamma densitometry in the study of ventilation and the pulmonary circulation, 25:11116
FRANTSEVICH, V. M., Generator for studying superconductivity by a pulse method, 25:10899
FRANZEN, L. F., Safety of heavy water system in Braunschweig research reactor, 25:12822 (NP-18499)
FREED, N., Realistic QTDA calculations in odd-mass N = 82 isotones, 25:12616
FREEMAN, A. J., Electronic band structure of the actinide metals, 25:11992
FREINDL, L., Polarization of protons from $^{12}C(d,p)^{13}C$ reaction at E/sub d/ = 12.4 MeV, 25:12377 (INP-711)
FREUDENBERG, V., Clinical and experimental investigation of $^{14}CO_2$ exhalation, 25:11168
FRIANT, A., X-ray spectrometry using Si (Li) diodes, 25:10812 (CEA-N-1401)
FRICKE, K., Stability of rotating stars. III, 25:11552
FRIDDLE, R. J., Low temperature transformations in plutonium, 25:11443
FRIED, S., Anion-exchange separation of neptunium from uranium and thorium in basic solution, 25:10655 (ANL-7751)
FRIEDBERG, Carl E., n + p + d + γ: a test of time reversal invariance, 25:12238
FRIEDLANDER, Gordon D., Power, pollution, and the imperiled environment. II. East, Midwest, and West Coast: pollution-control plans of some major utilities; role of government in environmental matter; other proposed systems for reducing stack emissions, 25:12761
FRIEDMAN, E., Properties of ^{94} ^{99}Rh from ^{94} ^{99} Ru(p,n) reaction, 25:12617
FRIEDMAN, H., Excess background radiation of soft x rays at the galactic pole and plane, 25:11653
FRIEDMAN, Marvin I., Particle-hole admixtures to Hartree--Fock in 2s-1d shell, 25:12682
FRIEDRICHS, K. O., Limiting process leading to equations of fluid dynamics, 25:11768
FRIHAGEN, Jon, Occurrence of high-latitude ionospheric irregularities giving rise to satellite scintillation, 25:11601
FRISCHAUF, H., Radiosterilization of fibrinogen and its practical use, 25:11333
FRITTELLI, L., Methods of quantitative analysis of a gamma spectrum, 25:10853 (RT/PROT-(70)21)
FRITZ, Gilbert, Excess background radiation of soft x rays at the galactic pole and plane, 25:11653
FRITZ, H., Results of lung scintigraphy in silicosis, 25:11134
FROGGATT, C. D., Nonevasive contributions to forward rho-production and vector dominance, 25:12212
FROLOVA, A. V., Use of plastic scintillators in x-ray dosimetry, 25:11072
FROLOVA, E. I., Protective effects of calcium alginate against chronic ^{90}Sr ingestion, 25:11103
FROMM, Eckehard, Adsorption of O and N on Ta films. II, 25:11418
Adsorption of O and N on Ta films. III, 25:11417
Adsorption of O and N on Ta films. IV, 25:11419
Gas-metal reactions in systems of high-melting metals with nitrogen or oxygen, 25:11415
FRUMKIN, M. L., Effect of γ irradiation on cooked meat, 25:11339
FRYE, Roland L., New Ap stars in NGC 3114, 25:11578
FUBINI, Sergio, Multiperipheral model, 25:12190
FUCHS, C., Absolute radioluminescence efficiency of liquid benzene and alkylbenzene scintillators, 25:10822
FUEKI, Kenji, Scavengeable electron yield in radiolysis of hydrocarbons, 25:10652
FUELLE, R., DWBA model applied to the $^{24}Mg(d,p)^{25}Mg$ reaction at E/sub d/ = 13.5 MeV, 25:12457
FUJII, S., Reactions of electrons and free radicals in glassy ethanol, 25:10630
FUJIMOTO, F., Temperature dependence of dechanneling coefficient in protons in silicon crystals, 25:11969
FUJISAKI, Noboru, Benzene formation in radiation-induced and photochemical reactions of acetylene, 25:10650
FUKUDA, Shizuo, Effect of a potent carcinogen, 4-nitroquinoline 1-oxide, and its reduced from, 4-hydroxylaminoquinoline 1-oxide, on bacterial and bacteriophage genomes, 25:11026
FUKUSHIMA, Susumu, Some electrical properties of the uranium--plutonium mixed oxides, 25:11991
FUKUSHIMA, Yoshihiro, Four-body correlations in light nuclei, 25:12660
FULKERSON, W., Electrical and thermal properties of NaCl structured metallic actinide compounds, 25:11494
FULLER, R. C., Treatment of two-particle continuum states in the shell model approach to nuclear reactions, 25:12625 (COO-1764-65)
FULMER, C. B., Deuteron-induced reactions in copper, 25:12438
FURDYNA, J. K., Electric and magnetic resonances of a particulate magnetoplasma, 25:11929
FURLAN, P., Anomalous magnetic moment and nonpolynomial

XUM

interactions, 25:12157
FURNEAUX, R. W., Validity of the isotope dilution method of measuring extracellular fluid volume, 25:11185
FURUYA, Keiichi, Determination of oxygen in ferro-boron by the vacuum fusion analysis, 25:10467
FUTAMURA, Yoshiaki, Development of reactor enclosure high voltage power cable penetration, 25:12705 (JAERI-Memo-4197)
FUTTERMAN, Walter I., Derivation of the Vlasov equation, 25:11900

G

GAAL, I., Resistivity decrease due to grain growth in tungsten, 25:12030
GABRAKOV, S., Spin-vibrational I+ states in deformed even--even nuclei, 25:12703
GADDA, F., Treatment of water in a nuclear plant for the testing of fuel elements, 25:12821 (LIB/Trans-335)
GADIOLI-ERBA, E., Macroscopic model for the anelastic scattering of heavy ions, 25:12661
GAERTTNER, M. R., Direct electromagnetic generation of ultrasound in conducting liquids, 25:12892 (NYO-2150-65)
GAFFAROV, D. G., Properties of the excited states of ^{147}Sm and ^{149}Pm, 25:12557
GAGELIN, J. J., Stationary gas detectors for mapping and dynamic studies of organs using x ray or low-energy γ-ray emitters, 25:10810 (CEA-CONF-1668)
GAILLIARD, Jean-Pierre, Spectrometer for thermal neutrons, 25:10854
GAJNIAK, J. C., Service routines for multigroup cross-section code MC^2, 25:12337 (ANL-7654)
GALAKTIONOV, B. V., Determination of the boundary of high frequency wave absorption between the electron cyclotron and the low-hybrid frequency, 25:11927 (FTI-295)
High frequency plasma heating near the low-hybrid frequency, 25:11860 (FTI-282)
GALATI, William, Cross sections of 3.0- to 6.9-MeV neutrons scattered from ^{12}C, 25:12401
GALEENER, F. L., Electric and magnetic resonances of a particulate magnetoplasma, 25:11929
GALIN, J., Mechanism of single-nucleon and multi-nucleon transfer reactions in grazing collisions of heavy ions on silver, 25:12606
Method for identification of particles from A = 4 to 20, 25:10829
Test of DWBA-type model for analysis of heavy-ion transfer reactions, 25:12683
GALLAHER, D. F., Possible model of a divergenceless nonlocal quantum field theory, 25:12268
GALLIKER, D., Spontaneous fission of ^{238}U and ^{241}Am, 25:12538
GAL'TSOV, D. V., Radiative polarization of free relativistic electrons in a magnetic field, 25:12060
GAMALEJA, Nicolai, Argon laser micro-irradiation of mitochondria in rat myocardial cells in tissue culture, 25:11242
GAMOT, E., Atomic absorption determination of K, Rb, and Sr, 25:10458
GANICHEV, V. I., Fast valve of high pressure for bubble chamber, 25:10870 (JINR-P13-5420)
GARBER, D. I., Gamma rays from resonant neutron capture in ^{169}Tm, 25:12589
GARCZYNSKI, W., Integral equations for wave vectors of a quantum system with a discrete set of states, 25:12051
GARDNER, C. D., Prog. rpt. on genetic effect of irradiated corn, final, 1970, 25:11009 (COO-1512-22)
GARFAGNINI, G., Angular and energy distribution of photoprotons from ^{27}Al, 25:12501
GARG, J. B., Resonance neutron capture in ^{103}Rh, 25:12561
GARG, R. K., Calculation of charge and current pulses in planar and coaxial Ge-(Li) detectors, 25:10821
GARRISON, John D., Effect of interference on the average neutron cross sections of fissile nuclei, 25:12608
GARVEY, G. T., Lifetimes of first four excited states of ^{32}S, 25:12486
GASTEBOIS, J., Reorientation effect measurements in $^{104-114}$Cd, 25:12619
GAUCHER, R. E., Selenium-75 as a calibration standard for Ge(Li) detectors, 25:10842
GEBALLE, T. H., Magnetic ordering in PrB_6, 25:11988
GEHLBACH, R. E., Transmutation-produced silicon precipitates in irradiated aluminum, 25:11471
GEHRING, D., Evaluation of results of treatment of thyroid carcinoma, 25:11233
Scintigraphic findings in liver diseases identified by laparoscopy and histology, 25:11180
GEIGER, J., Scattering of fast electrons by a gas plasma, 25:11879
GEIGER, W., Differentiation between maternal, placental, and embryonal hormone production, 25:10982
GEISS, Roy Howard, Effect of dislocations on the coercivity of single crystals of nickel, 25:12894 (NYO-3087-16)
GELD, P. V., Conduction band of IVa and Va subgroup transition metal monocarbides. I, 25:12024
GEL'FAND, S. Yu., Effect of γ irradiation on cooked meat, 25:11339
GELLER, R., Production of intense beams of fast neutral particles using plasma accelerators of the pleiade type, 25:11920 (EUR-CEA-FC-567)
GELMAN, Donald, Feynman path integrals and scattering theory, 25:12286
GEMESY, Tibor, Discovery of S^0 meson, 25:12201
GENERALOV, N. A., Method for infrared diagnostics of plasma, 25:11868 (SC-T-70-4054)
GEORGE, Ajax, Lateral liver scanning: an index to hepatic and retrohepatic disease, 25:11211
GEORGE, D. R., Metallurgical application of solvent extraction. II, 25:10656 (BM-IC-8502)
Recovery of uranium from natural mine waters by countercurrent ion exchange, 25:10657 (BM-RI-7471)
GEORGI, P., Experimental bone scintigraphy in animals, 25:11216
GERACE, W. J., Monopole excitations in ^{16}O, 25:12426
GERARD, R., Scientific and industrial applications of nuclear explosives, 25:10743
GERARDO, J. B., Electronic recombination of He_2, 25:11690
GERLACH, Ulrich H., Formation of geons and black holes, 25:11660
GERMANI, G., Underwater plasma-arc cutting as a powerful dismantling tool for water reactors, 25:12714
GERNER, C. P., Measurements on electron capture ratios of ^{83}Rb and ^{84}Rb, 25:12467
GERSHUN, V. D., Current structure of phenomenological Lagrangians, 25:12129
GHELELOVITCH, S., Sensitivity to x rays in the zygote of Drosophila, 25:11250
GHERSINI, G., Behavior of metallic U--Zircaloy-2 fuel element defects and exposure to aqueous corrosion, 25:11347 (CISE-R-222)
GHOSH, N. N., Studies on some N-acyl N-phenylhydroxylamines as metal-complexing ligands. IV, 25:10521
GIACOMICH, R., Isospin-forbidden analogue resonances in ^{33}Cl. I, 25:12506
GIBBONS, J. R. P., Homograft heart--valve replacement, 25:11336
GIBBS, Hyatt M., Nuclear-spin effects are important in analyzing spin-exchange experiments, 25:11720
GIBNEY, Robert B., Heat capacity behavior of ^{242}Pu between 10° and 373°K, 25:11385
Low-temperature heat capacity of $PuC_{0.81}$, 25:11493
GIGUERE, P. A., Hydrogen--oxygen systems in electrical discharge. IV, 25:10531
GIL, Francisco Parra, Determination of environmental radioactivity, 25:11068
GILBERT, E. R., Minimum-creep-rate behavior of polycrystalline vanadium from 0.35 to 0.87 T/sub m/, 25:11397
GILBERT, Edgar Robert, Steady-state creep of alpha zirconium, 25:11414
GILFRICH, H.-P., Stability of phenoplast molding materials towards high-energy radiation, 25:10634
GILLELAND, John Rogers, Precision measurement of the g-factor of the free positron, 25:12075
GILLETT, F. C., Infrared studies of galactic nebulae. II. The compact nebulae IC 4997, VV 8, and FG sagittae, 25:11569
GILLIAM, James J., Methods for fractionation and scintillation counting of radioisotope-labeled polyacrylamide gels, 25:10478
GILMAN, Frederick J., Recent developments in inelastic electron--nucleon scattering, 25:12068 (SLAC-PUB-842)
GILMORE, Robert, Diagrammatic technique for constructing matrix elements, 25:12234
GIMSTEDT OLLE, G., Oskarshamn nuclear power station, 25:12760
GINN, S. G. W., N_{u_1} bands of $^{10}BF_3$ and $^{11}BF_3$ at high resolution, 25:10533
GINSBURG, A., Scattering of protons from ^{128}Te and ^{130}Te, 25:12602
GINZBURG, I. F., Production of muon pairs in interactions of hadrons of high energy, 25:12229
GIORGADZE, N. P., Possibility of polarizing nuclei with ultrasound, 25:12007
GIOVANOZZI-SERMANNI, G., Inactivation of β-Fructofuranosidase and Glucosidase by γ radiation of Beta vulgaris, 25:10964
GIROLAMI, M., Some particular aspects of scintigraphy in cirrhosis of the liver, 25:11203
GIURIATO, A., Elimination of thermal shield from Trino Vercellese pressurized water reactor, 25:12715
GLADKOV, V. P., Diffusion of nickel in beryllium, 25:11399
GLAESER, W., Phonon spectra in TaC and HfC, 25:11986
GLAGOLEV, V. M., Propagation and absorption of ionic-hybrid waves in a slightly-heterogeneous plasma layer, 25:11928 (IAE-1949)
GLASS, Edward N., Newman--Penrose constants and their invariant transformations, 25:12279
GLASS, H. I., Use of the gamma camera for ^{131}I renography: a case study on a nephrectomized patient, 25:11206
GLAUBITT, D., Clinical and experimental investigation of $^{14}CO_2$ exhalation, 25:11168
Iron-59 dextrane test as indicator of enteral protein loss, 25:11171
GLAVISH, H. F., Anisotropy ^{2}H(d,p)^{3}H at low energies, 25:12368
GLENDENNING, N. K., Quadrupole and hexadecapole deformations in rare earth nuclei, 25:12605
GLIMM, James, Energy--momentum spectrum and vacuum expectation values in quantum field theory, 25:12269

GLINER, E. B., Vacuum-like state of medium and Friedman cosmology, 25:11659
GLOEBEL, B., Method for measurement of iodine, iodotyrosine, and iodothyronins in human serum, 25:10945
GLOECKLE, W., Studies to a new approach for the three-body problem, 25:12693
GLOMSKI, Chester A., Survival of ^{50}Cr-labeled erythrocytes as studied by instrumental activation analysis, 25:10503
GLOUX, J., Free radicals produced by gamma irradiation in bicyclo[2,2,1]heptane, 25:10637
GLOWINSKI, L. D., Observation of void formation induced by electromigration in metallic films. report no. 1447, 25:12899 (NYO-4185-1)
GLUCHKOV, E. S., Multigroup design of unidimensional nuclear reactors without use of grid method, 25:12841 (IAE-1938)
GNEDIN, Yu. N., Origin of the x radiation of the metagalaxy, 25:11657
GODDARD, N., Phosphine--borane derivatives. III, 25:10547
GODFREY, T. G., Characterization and behavior of alkalized alumina during sulfur dioxide sorption--regeneration process, 25:12901 (ORNL-TM-3210)
Synthesis, characterization, and fabrication of UN, 25:11480 (ORNL-4608)
GOEDBLOED, W., E.C./e$^+$ ratios in non-unique first-forbidden decay of ^{84}Rb, 25:12466
Measurements on electron capture ratios of ^{83}Rb and ^{84}Rb, 25:12467
GOENNER, Hubert, Einstein tensor and 3-parameter groups of isometries with 2-dimensional orbits, 25:12277
GOFFIN, J. C., Effects of Kallikreine on the irradiated skin of swine (large white), 25:11110
GOHIL, Mahendra N., Long-term effects of local irradiation of the marrow on erythron and red cell function, 25:11112
GOIDL, Edmond A., Radioresistance of cooperative function of carrier-specific lymphocytes in antihapten antibody responses, 25:10987
GOLANT, V. E., Determination of the boundary of high frequency wave absorption between the electron cyclotron and the low-hybrid frequency, 25:11927 (FTI-295)
GOLD, Fred M., /sup 69m/Zn-chloride. A new scanning agent: a study of its dosimetry and biological fate, 25:11204
GOLDBERG, I., Analysis of the transient capability of rod-type fuel elements (LWBR Development Program), 25:11534 (WAPD-TM-979)
GOLDBERG, Joshua N., Newman--Penrose constants and their invariant transformations, 25:12279
GOLDBERGER, Marvin L., Existence of complex poles and oscillatory average multiplicity in multiperipheral models, 25:12122 (NYO-2262-TA-228)
GOLDFARB, L. J. B., Polarization and the statistical model, 25:12699
GOLDHABER, M., Upper limit for a K-electron-capture branch in /sup 113m/In, 25:12591
GOLDIN, A. S., Prog. rpt. on air cleaning, semiannual, 3--8/70, 25:10797 (NYO-841-23)
GOLDSTEIN, Charles, Focusing and acceleration in ALICE, 25:12310 (NP-18612)
GOLDSTEIN, Marvin, Electron--potassium inelastic differential cross section measurements with spin analysis, 25:11707
GOLDSTEIN, Melvyn Lee, Inverse Compton scattering and synchrotron emission by fast electrons in plasma, 25:11888
GOLDSTEIN, Stephen, EL 600: study of core neutronic properties, 25:12775 (CEA-N-1395)
GOLLON, P. J., Double beta decay of ^{48}Ca, 25:12448
GOLOS, S., Thermal entrance region in steady, axially symmetrical slug flow, 25:10771
GOLOVANOV, L. B., Precision apparatus with liquid hydrogen target, 25:12300 (JINR-P8-5212)
GOLTON, E., Observations of ionospheric electron content across the equatorial anomaly at sunspot minimum, 25:11816
GOLUBENTSEV, D. A., Nonprotein thiols in tissues after administration of cystamine, 25:11101
GOMAA, M. A., Attenuation of 14.7-MeV neutrons in water, 25:12349
GOODMAN, B. B., Short, current-dominated, beam transport magnets, 25:12323
GOODMAN, L. S., Hyperfine and Zeeman studies of low-lying atomic levels of ^{139}La, 25:11693
GOODWIN, David A., ^{68}Ga-labeled macroaggregates for lung studies, 25:11205
GOPALAKRISHNAN, Adinarayantampi, Transient heat-transfer performance of a reactor coolant channel during accidental power excursions, 25:10773
GORDON, Gilbert, Prog. rpt. on one and two electron transfer reactions, annual, 3/70--2/71, 25:10515 (COO-1780-14)
GORDON, Howard Allan, Meson and baryon production in π^+d + pp$\pi^+\pi^-\pi^0$ reaction, 25:12112
GORLOV, G. V., Scattering of neutrons with an energy of 4 MeV at angles close to 180°, 25:12509 (ANL-Trans-855)
GOSS, D., Non-parametric method for the extraction of information from digitized spectra, 25:10858
GOSSARD, A. C., Magnetic properties of Nb_3X compounds, 25:12037
GOSSELIN, J., Flux motion through the superconducting surface sheath, 25:11829
GOTLIB, V. Ya., Changes in lethal effect of irradiation of cells cultivated outside of organism due to chemical compounds, 25:11106
GOTO, Hidehiro, Determination of Mo in Fe and steel by flame photometry, 25:10439
GOTODA, Masao, Preparation of Wood--Polymer composite by ionizing radiation. VI, 25:10605 (JAERI-5026, pp 94-100)
Preparation of Wood--Polymer Composite by ionizing radiation. IV, 25:10603 (JAERI-5026, pp 80-5)
Preparation of Wood--Polymer-Composite by ionizing radiation. V, 25:10604 (JAERI-5026, pp 86-93)
Radiation curing of mixture of diallylphthalate prepolymer and vinyl monomer. IV, 25:10607 (JAERI-5026, pp 108-20)
Radiation curing of mixture of diallylphthalate prepolymer and vinyl monomer. III, 25:10606 (JAERI-5026, pp 101-7)
Radiation curing of mixture of diallylphthalate prepolymer and vinyl monomer. V, 25:10608 (JAERI-5026, pp 121-9)
Radiation curing of monomer--polybutadiene mixture. I, 25:10609 (JAERI-5026, pp 130-6)
GOTTESMAN, S. T., Neutral H content of galaxies M31 and M33. I, 25:11646
Neutral H content of galaxies M31 and M33. II, 25:11647
GOTTIKH, R. P., Radioactive elements and deuterium in underground waters of the Bukhara--Karshin artesian basin, 25:10698
GOTTLIEB, Carl A., Microwave detection of interstellar formic acid, 25:11593
GOULD, C. R., Angular correlation study of low-lying levels of ^{29}P, 25:12480
GOURCY, Georges, Digital measurement of the peak current in a linear electron accelerator, 25:12297 (CEA-N-1389)
GOVERSE, S. C., E.C./e$^+$ ratios in non-unique first-forbidden decay of ^{84}Rb, 25:12466
Measurements on electron capture ratios of ^{83}Rb and ^{84}Rb, 25:12467
GOVINDARAJU, K., Complexing agents for dissolving silicates and ion exchange resin, 25:10671
Elimination of matrix effect and quantometric determination of trace elements in silicates, 25:10452
GRABOWSKI, J., Parity nonconserving effects in nuclei ^{175}Lu and ^{181}Ta, 25:12517 (INP-714)
GRABOWSKI, Z. W., E2/M1 multipole mixing ratios in spherical nuclei ^{124}Te, ^{126}Te, and ^{126}Xe, 25:12515 (COO-1746-51)
GRADSZTAJN, E., Energetics of L-nuclei formation in stellar atmospheres and its relevance to x-ray astronomy, 25:11548
Nucleosynthesis of Li, Be, and B, 25:11542 (NP-18591)
GRAF, W., Neutrino radiation in gravitational fields, 25:12281
GRAHAM, J. A., Photometric classification of the Feige blue stars, 25:11573
GRAICHEN, J., High speed 12 bit register, 25:10816
GRAMM, W. R., Investigation of β spectrum of ^{14}C with a proportional counter with inner anticoincidence screens, 25:12380 (KFK-1222)
GRANATA, L., Isospin-forbidden analogue resonances in ^{33}Cl. I, 25:12506
GRAND, D., Trapped electrons and free radicals in γ-irradiated ethanol glasses, 25:10648
GRANET, Pierre, Resonance in reactions K$^-$p → Σ$^+\pi^-\pi^+$ between 440 and 1230 MeV/c, 25:12098 (CEA-R-4068)
GRANT, I. P., Relativistic calculation of atomic structures, 25:11741
GRAPPIOLO, G., Nuclear fuel with burnable poison. I, 25:10571 (EUR-4550)
GRAS, R., X-ray spectrometry using Si (Li) diodes, 25:10812 (CEA-N-1401)
GRATIAS, Denis, Structure transformations of Zr--Cu binary alloys with low Cu contents and ternary alloys during continuous cooling, 25:11432 (CEA-N-1310)
GRAUBY, Andre, Environmental mobility of ^{106}Ru during irrigation processes, 25:10692
GRAUL, E. H., Results and importance of quantitative blood flow measurements through parabiotic tissue connections, 25:10915
GRAVES, R. G., Resonance neutron capture in ^{103}Rh, 25:12561
GREBE, S. F., Determination of glomerular clearance with radioisotope labeled substances according to the slope method, 25:11154
Radioisotope studies on hyperemia producing treatment, 25:10916
GRECHIKHIN, L. I., Mean energy of electrons ejected from atoms at ionization by electron impact, 25:11727
GREEN, A. E. S., Addendum to potential-scattering model for electrons on helium and other atoms, 25:11722
Cross sections for inelastic collisions of protons and H atoms with gases, 25:11703
Relativistic independent-particle model for atoms based on analytical potentials, 25:11738
Semi-empirical atomic-energy formula, 25:11739
GREEN, Daniel Raymond, Interference between amplitudes for

XUM

K/sub L/ + 2ν^0 and K/sub S/ + 2ν^0, 25:12079
GREEN, J. L., Thermal expansion and phase equilibria of the carbon-saturated plutonium carbides, 25:11513
GREEN, S. J., Critical heat flux and pressure drop tests with parallel upflow of high pressure water in bundles of twenty 1/2-in. rods, 25:12787
GREENE, L. A., Electron beam welding study on U--Nb--Zr alloy, 25:11377 (MLM-1778)
GREENE, Marvin H., Activity coefficient and vacancy flow effects on tracer diffusion in silver-gold alloys, 25:12902 (ORO-2036-20)
GREGOIRE, M., Review on correlation measurements in plasma, 25:11866 (EUR-CEA-FC-570)
GREGORY, C. T., Pitch-angle distributions of protons and helium ions in the magnetosphere, 25:11803
GRENIER, G., Spectrometer permitting the analysis of low-energy gammas in the presence of a strong high-energy gamma background, 25:10859
GRENOBLE, D. C., Effect of pressure on electronic structure of ferric hydroxamates and ferrichrome A, 25:12881 (COO-1198-777)
GRIESS, J. C., Evaluation of Burgess Fobes Paint Company protective coatings for nuclear plant application, 25:12804 (ORNL-TM-3104)
GRIFFIN, C. S., Self-irradiation damage induced resistivity changes in actinide metals at low temperatures, 25:11960
GRIGOR'EV, Yu. N., Research on 100-MeV electron storage ring of Technical Physics Institute of Ukrainian Academy of Sciences, 25:12307 (KHFTI-69-27)
GRIGORIEV, E. L., Investigation of ^{8}Li recoil nuclei in ^{9}Be(p,2p)^{8}Li reaction at proton energies of 180 and 660 MeV, 25:12378 (JINR-P1-4872)
GRIGOROV, N. L., Flux of low-energy protons near the Moon on December 13, 1966, 25:11669
GRIMES, St., Level density parameters for Ge, Ho, and Ta, 25:12536
GRISHAEV, I. A., Research on 100-MeV electron storage ring of Technical Physics Institute of Ukrainian Academy of Sciences, 25:12307 (KHFTI-69-27)
GRISHIN, V. G., Analysis of π^-p + $n\nu^+\pi^-m\nu^0$ (m = 1,2,3) and π^-p + $n2\nu^+2\pi^-m\nu^0$ (m = 1,2) reactions, 25:12204 (JINR-P1-5431)
GRISLOV, A. I., Parametric efficiency limit of resonance charging of pulse-forming network in pulse generators, 25:12333
GRITZNER, M. L., Lateral spread of high-energy (less than or equal to 400 MeV) neutron beams, 25:12332
GRODNIK, Jesse, Representations of local nonrelativistic current algebras, 25:12125
GROOM, D. E., Reactions π^-p + $n\nu^0$ and π^-p + neta^0 in the backward hemisphere, 25:12117
GROSE, K. D., Delay circuits for nuclear applications, 25:10898
GROSS, R. W. F., Isotope separation with the cw hydrogen fluoride laser, 25:10690
GROSSMAN, Lawrence, Repair of UV-irradiated DNA, 25:10959 (BNL-50203, pp 27-40)
GROTOWSKI, K., Real part of the alpha-nucleus potential obtained by double folding procedure, 25:12627 (INP-720)
GROVE, R., Electromagnetic delay line readout for proportional wire chambers, 25:10846
GRUBMAN, Ronald, Faddeev equations for spin-dependent forces: calculation of ^{3}Be binding energy, 25:12692
GRUPPELAAR, H., Gamma rays from thermal-neutron capture in natural and ^{28}Si enriched silicon, 25:12403
GRUZDEV, G. P., Vulnerability of endothelium of large vessels in radiosensitive and radioresistant animals, 25:11269
GRYPEOS, M. E., New derivation of an approximate expression in closed form for the binding energy of an impurity particle in nuclear matter, 25:12650
GRYZUNOV, V. I., Interdiffusion in Nb--Zr system, 25:11424
GUALDI, G., Conversion of photons into gravitons and vice versa in a static electromagnetic field, 25:12272
GUBAREVA, A. V., Development of changes in irradiated ovaries, 25:11107
GUCKER, Edward Joseph, Parity-violating parameters in nucleon--nucleon scattering matrix at 210 MeV, 25:12094
GUENIN, M., Elementary examples of renormalizations and dressing transformations, 25:12258
GUERREAU, D., Mechanism of single-nucleon and multi-nucleon transfer reactions in grazing collisions of heavy ions on silver, 25:12606
GUGLIELMI, M., Free radicals produced by gamma irradiation in bicyclo[2,2,1]heptane, 25:10637
GUILLANEUX, Pierre, Laser--matter interaction: stimulated and nonlinear effects, 25:11884 (CEA-N-1399)
GULYAS, S., Recovery from radiation damage in mammalian cells, 25:11092 (BNL-50203, pp 41-53)
GUPTA, A. K., Transition temperature and temperature dependence of the energy gap in thin film superconductors, 25:11845
GUPTA, B. K., Production of nuclides by high-energy proton bombardment, 25:12439
GUPTA, G. P., Thermal conductivity of carbon dioxide in temperature range 100 to 1075°C, 25:10574
GUPTA, Nand Kishore, Nuclear structure studies through directional correlations, 25:12555
GUSINOW, M. A., Electronic recombination of He_2, 25:11690
GUST, W. H., Dynamic yield strengths of B_4C, BeO, and Al_2O_3 ceramics, 25:11490
GUSTAFSON, D. R., Positron annihilation in Pu, 25:11997
GUSTAFSON, V. W., FFTF containment system alarm and trip criteria, 25:12812 (BNWL-1479)
GUSTAVSON, D., Pi^0 photoproduction from H with linearly polarized photons, 25:12072
GUZZO, V. J., Design of an insulator which must survive high g-forces, 25:12867 (BDX-613-213)

H

HAAS, H., Biochemical changes in aortic valve transplants following sterilization, 25:11341
HAAS, J. P., Assessment of renal blood flow with radioactive labeled compounds excreted by glomerular filtration, 25:11163
Comparative determination of hepatic blood flow with colloidal ^{198}Au and colloidal /sup 99m/Tc-S, 25:11140
Comparison of renal isotope diagnosis with vasoconstrictor content in the renal vein of hypertensive patients, 25:11163
Contribution of scintigraphy for evaluation of vascular renal diseases, 25:11166
HAAS, R. J., Cytokinetic analysis of slowly proliferating bone marrow cells during recovery from radiation injury, 25:11077
HABAZIN, Vlasta, New evidence concerning the molecular basis of the restorative effect of DNA in cultured mammalian cells, 25:11243
UV-induced DNA-to-protein cross-linking in HeLa cells, 25:10975
HABER, Alan H., Ionizing radiations as research tools, 25:10977
Photodestruction of chloroplast ultrastructure by red light: location of chlorophyll, 25:11310
HACK, Klaus, Sliding friction and wear of pure metals under vacuum of 5 x 10^{-8} torr, 25:11413
HACK, Margherita, Stellar spectroscopy: normal stars, 25:11543
HAEHLE, S., System V_2O_5--K_2SO_4, 25:11527
HAEMAELAEINEN, R. M. K., Limits of validity of Siegert's theorem in nuclear photoabsorption, 25:12649
Notes on quantum mechanical sum rules, 25:12046 (NP-18619)
HAENSEL, R., Optical absorption of Ce, Ce oxide, Pr, Pr oxide, Nd, Nd oxide, and Sm in extreme ultraviolet, 25:11698
HAENZE, S., Contribution of scintigraphy for evaluation of vascular renal diseases, 25:11166
HAERDI, W., Rapid isotopic separation method for the selective determination of short lived radioisotopes, 25:10490 (LIB/Trans-334)
HAESAENEN, Erkki, Determination of mercury in biological material by neutron activation analysis, 25:10502
HAEUSLER, C., Effect of solvent on frequencies of CD and CH stretching band in some haloforms, 25:10540
HAEUSLER, J., Natural vibrations of the R(t)CL-circuit, 25:12911 (SC-T-71-3003)
HAFFNER, H., Heat transfer to refrigerants at nucleate boiling, film boiling, and supercritical condition of the fluid, 25:10767 (BMBW-FBK-70-24)
HAFSTROM, J. W., Case for a second energy gap in superconducting niobium, 25:11830
HAFTEL, Michael I., Nuclear saturation and the smoothness of nucleon--nucleon potentials, 25:12698
HAGA, I., Oskarshamn reactors I and II salient features, 25:12710
HAGEBOE, E., Argon-43 and ^{44}Ar, 25:12499
HAGEMANN, R., Automatic mass spectrometer for the isotopic analysis of hydrogen in natural water samples, 25:10463
HAGEN, A., Incorporation of machine data handling in the monitoring of fissionable material in large research centers, 25:10796 (KFK-866)
HAGENMULLER, P., Systems B_2O_3--MO--MS boracites M--S (M = Mg, Mn, Fe, Cd) and sodalites M--S (M = Co, Zn), 25:11526
HAGIWARA, Miyuki, Participation of an excited monomer in propagation reaction of the γ-ray induced polymerization of ethylene, 25:10612
HAGLE, Robert E., Survival of ^{51}Cr-labeled erythrocytes as studied by instrumental activation analysis, 25:10503
HAHN, B., Spontaneous fission of ^{238}U and ^{241}Am, 25:12538
HAHN, George M., Radiobiology of mammalian cells, 25:11239 (BNL-50203, pp 117-29)
HAHN, R. L., New isotopes ^{241}Cf and ^{249}Cf, 25:12593
HAHN, Yukap, Generalized variational bounds on positron--H reaction matrix. II, 25:11719
HALE, D. P., Energy distribution of fast electrons present in beams from hollow-anode gas discharge electron guns, 25:12319
HALES, R., Thermodynamics of some metal/coolant reactions in Mk.III reactors, 25:10518 (RD/B/N-1816)
HALL, Eric J., Cell killing at very low dose rates, 25:11095 (BNL-50203, pp 308-17)
HALL, R. O. A., Thermal conductivity in the actinide elements, 25:11382
HALLEY, Pierre, Long-term forecasting of cycles of sunspots, 25:11631

HALPERIN, Jerome A., Use of radioactive materials in gas chromatography, 25:10421 (BRH/DMRE-70-5)
HALTER, J., Computer method for analysis of γ spectra application to fission-fragment mixtures, 25:12535
HALZEN, F., Regge parametrization for low-energy νN scattering, 25:12211
HAMA, Mitsuru, Reaction $\pi^+p \to \pi^0N^{2+}$ at high energy and correction to rho-exchange contribution, 25:12223
Unitarity at threshold and Veneziano-type form factors for mesons, 25:12172
HAMADA, Masayuki, TC in acidic media, 25:10546
HAMBLY, A. N., Solvolysis of sulphonyl halides. VI, 25:10536
HAMBY, K. O., Distribution and redistribution of airborne particulates from the Schooner cratering event, 25:10716 (UCRL-72534)
HAMERSKY, M., Transient creep of Cd single crystals at room temperature, 25:11412
HAMID, Mohamed Khairi, Evaluation of ^{131}I labelled Hippuran in diagnosis of renal disease, 25:11210
HAMILTON, C. A., rf-induced effects in superconducting tunnel junctions, 25:11827
HAMILTON, W. D., Muon capture probability in isotopes of bromine, 25:12502
HAN, Antun, UV-induced DNA-to-protein cross-linking in HeLa cells, 25:10975
HAN, Sook Jong, Unitarity and a tightly bound pion, 25:12202
HANDLEY, R., Translocation of carrier-free ^{85}Sr, ^{137}Cs, and ^{106}Ru in woody plants, 25:10955
HANKE, C. C., Precision energy loss measurements for natural alpha particles in argon, 25:11726
HANNULA, Fred W., Radiation gauge system for tubular plastic film, 25:10890
HARA, Tadao, Horizontal air showers of energies above 10^{13} eV, 25:12071
HARADA, K., Effects of magnetic dipole core polarization in ^{206}Pb and ^{207}Pb, 25:12600
HARASAWA, Susumu, Thermoluminescence of purified LiF powder, 25:11951
HARATYM, Z., Excitation of isomeric activities in ^{71}Ge, ^{79}Br, and ^{79}Br using 14.8-MeV neutrons, 25:12430 (INR-P-1091)
HARBST, H., Functional studies with short-lived reactor isotopes, 25:10943
HARDEN, B. N., Satellite equipment for the measurement of high energy electrons and protons, 25:11813
HARDERS, H., Conference on microcirculation, Goteborg, 6/68, 25:11192
HARDIE, R. W., DPB: dynamic programming code for optimizing short-term operation of a power utility, 25:12919 (WHAN-IR-47)
HARDY, D. M., Deuteron elastic scattering and the (d,p) reaction with polarized ^3He target, 25:12370
HARGROVE, Robert J., Secondary deuterium isotope effects in vinyl cations, 25:10548
HARIHAR, P., Double gamma emission from ^{40}Ca and ^{90}Zr, 25:12495
HARKREADER, W. F., Low temperature transformations in plutonium, 25:11443
HARLAND, H. B., Critical carrier concentration for superconductivity in mixed metal--semiconductor systems, 25:11844
HARMER, D. L., Composition of delta pavonis, 25:11564
HARMS, A. A., Consistent criticality estimates in pulsed neutron experiments, 25:12860
Phase-space reduction in neutron diffusion calculations, 25:12853
HARMS, E., Separable potential calculations on the $^1/_2^+$ neutron--deuteron system, 25:12359
HARMS, Edward, Three-nucleon equations with separable two-body potentials, 25:12687
HAROLDSEN, R. O., Instrument probe for measuring temperature and pressure in the upper plenum of the EBR-II reactor vessel. EBR-II Project, 25:12781 (ANL-EBR-25)
HARPER, E. A., Uranium--plutonium--carbon phase diagram. I, 25:11523
HARRIS, Frederick Allan, Proton polarization in $\Sigma^+ + p\pi^0$, 25:12084
HARRIS, L. A., Characterization and behavior of alkalized alumina during sulfur dioxide sorption--regeneration process, 25:12901 (ORNL-TM-3210)
HARRISON, E., Sodium flow monitoring, 25:12792
HARRISON, E. R., Spirals made simple, 25:11645
HARRISON, J. D. L., Factors affecting the hardness of uranium mononitride at elevated temperatures, 25:11498
HARTMANN, G., Timing of Ge(Li)-detector pulses, 25:10830
HARTMANN, O., Structure, energy, and periodic potential of kinks in screw dislocations for bcc lattices, 25:12027
HARWIT, M., Determining Planck constant of cosmic photons, 25:11665
HASHIMOTO, Tetsuo, Determination of uranium contents in some rocks based on fission track method, 25:10474
HASHITANI, Hiroshi, Spectrophotometric determination of traces of nitrogen in zirconium and zircaloy using thymol, 25:10442
HASS, M., Radiation widths of bound nuclear levels, 25:12447
HATADA, Moyoyoshi, ESR spectra of irradiated beryllium acetylacetonate single crystal, 25:10623 (JAERI-5026, pp 157-60)
HATTORI, Takeshi, Effect of radiation in reactively sputtered Al_2O_3--Si structures, 25:10905
HATTULA, J., Directional correlations of some γ-ray cascades in ^{200}Hg, 25:12527 (NP-18613)
Simultaneous recording of true and random coincidences using a two-parameter analyzer system, 25:10894 (NP-18614)
HATTULA, T., Disintegration of the two isomers of ^{84}Br (31.8 min and 6.0 min), 25:12444
HAUBOLD, U., Clearance studies with ^{131}I-labeled hippuran, ^{203}Hg-salyrgan, ^{51}Cr-EDTA, and ^{51}Cr-inulin, 25:11156
HAUG, Eberhard, Polarization and anisotropy of solar x radiation during flares, 25:11623
HAUSEN, A., Optical anisotropy of β-rhombohedral B, 25:12029
HAUSMANN, Till, Proton decay of analog resonances in ^{93}Nb, 25:12564
HAVINGA, E. E., Critical carrier concentration for superconductivity in mixed metal--semiconductor systems, 25:11844
HAWES, Ralph W., Equipment forecasting simulation models, 25:10757 (RFP-1527)
HAY, S., Effect of β phase-retaining or delta phase stabilizing elements on Pu during alpha--beta thermal cycling, 25:11393
HAYASHI, Kanae, Studies on radiation-induced free-ionic polymerization by electrical conductivity measurements. II, 25:10610 (JAERI-5026, pp 169-71)
HAYASHI, Koichiro, Radiation-induced postpolymerization of trioxane in the solid state. II, 25:10611
Studies on radiation-induced free-ionic polymerization by electrical conductivity measurements. II, 25:10610 (JAERI-5026, pp 169-71)
HAYASHI, Seiju, Determination of uranium contents in some rocks based on fission track method, 25:10474
HAYASHI, T., Magnetic moments of three excited states in ^{149}Pm, 25:12609
HAYDEN, H. C., Analysis of the N^+--Ar and O^+--Kr collisions, 25:11711
HAYON, E., Absorption spectra and kinetics of the intermediate produced from the decay of azide radicals, 25:10643
HAYS, W. W., Seismic response characteristics at NRDS from underground nuclear detonations, 25:10730 (NVO-1163-TM-22)
HAZELTON, W. S., Evaluation by linear elastic fracture mechanics of radiation damage to pressure vessel steels, 25:11470
HAZONY, Y., Electronic structure and anomalous thermal expansion in FeF_2 and VO_2, 25:12015
HAZZAA, I. B., Determination of groundwater flow and quantity of groundwater in Shigaya aquifer in Kuwait using radioisotopes, 25:10700
HEACOCK, R. R., Relation of Pc1 micropulsation source region to plasmasphere, 25:11788
HECHT, K. T., New quasiparticle factorization of the j-shell, 25:12666
HECK, D., Investigations of excited states of ^{96}Mo nucleus from reaction $^{95}Mo(n,\gamma)^{96}Mo$, 25:12598
HECK, Dieter, Computer program for discovery of excited nuclear states according to Ritz combination principle, 25:12519 (KFK-1247)
HEDE, B. B. J., Effect of phonons on the e^+--e^- annihilation rate in metals, 25:11699
HEDGER, H. J., Uranium--plutonium--carbon phase diagram. I, 25:11523
HEDGRAN, Arne, Swedish policy with regard to the limitation of radioactive discharges from nuclear power stations, 25:12757 (SSI-70-27)
HEGEDUS, J. Andras, Determination of traces of foreign matter in molybdenum anuits compounds, 25:10459
HEHL, Wilma Sonia Caiaffa, Fuel development. Program for calculation of a lattice of natural uranium and heavy water and for the calculation of the production of plutonium, 25:12797 (IEA-186)
HEHRLEIN, F. W., Biochemical changes in aortic valve transplants following sterilization, 25:11341
HEIDMANN, J., 21-cm neutral hydrogen line observations of compact galaxies, 25:11638
HEIER, K. S., Concentration of Cs in high grade metamorphic rocks, 25:10508
HEILES, C., Absence of average polarization at 111.5 MHz in pulsar NP 0532, 25:11589
HEIM, Fritz, Inhibition of estrogen-induced radioprotection of placental nucleic acids and proteins by antiestrogen Clomiphene, 25:11104
HEIN, W. W., Decay of ^{95}Ru, 25:12545
HEINZE, H. G., Clearance studies with ^{131}I-labeled hippuran, ^{203}Hg-salyrgan, ^{51}Cr-EDTA, and ^{51}Cr-inulin, 25:11156
Studies on 1-triiodo-thyronine suppression in its dependency on thyroidal function, iodine storage, thyroid size, and age of patients, 25:10944
HEISENBERG, J., Elastic electron scattering from ^{13}C, 25:12376 (AD-710383)
HELLEDAY, E., Study of the precise determination of macroamounts of plutonium in solution by three electrometric oxidation--reduction titration methods, 25:10445
HELLER, Wolfram, Superconductivity and metallurgical problems with Ti--Nb alloys, 25:11416

XUM

HELM, William T., Prog. rpt. on freshwater vertebrate and invertebrate ecology of Amchitka Island, annual, 8/30/67--6/30/68, 25:12871 (BMI-171-104)

HELPPI, M., Directional correlations of some γ-ray cascades in ^{200}Hg, 25:12527 (NP-18613)
Simultaneous recording of true and random coincidences using a two-parameter analyzer system, 25:10894 (NP-18614)

HEMMATI, A., Dependency of protein resorption on acidity and retention time of the stomach, 25:11170

HENDRICKSON, M. M., FFTF containment system alarm and trip criteria, 25:12812 (BNWL-1479)

HENGST, W., Simultaneous blood flow measurements with ^{133}Xe in flexors and extensors of the lower leg under positive and negative load, 25:10913

HENLEY, E. M., High-energy photonuclear reactions and vector-meson dominance, 25:12151

HENNAUT, J., Catalytic decomposition of carbon monoxide on pure iron, mild steels, and alloyed steels, 25:11374 (DP-Report-530)

HENNIG, K., Results of lung scintigraphy in silicosis, 25:11134

HENNION, F., Filling of a magnetic well by injection of neutral atoms at various angles and energies, 25:11859 (EUR-CEA-FC-563)

HENRY, Richard C., Excess background radiation of soft x rays at the galactic pole and plane, 25:11653

HENTZ, Robert R., γ radiolysis of liquids at high pressures. IX, 25:10628

HEPP, K., Renormalized Hamiltonian dynamics and representations of the canonical (anti-) commutation relations, 25:12256

HERAK, R., Stress induced α--U_3O_8--β--U_3O_8 transformation, 25:11528

HERMAN, Jan A., Radiolysis of gaseous isobutene by ^{60}Co γ rays. III, 25:10640

HERMAN, K., Hydrogen--oxygen systems in electrical discharge. IV, 25:10631

HERRMANN, W., Strain hardening and strain rate in one-dimensional wave propagation calculations, 25:12909 (SC-RR-70-471)

HERSHKOWITZ, N., Moessbauer effect studies following Coulomb excitation, 25:10863

HERSKIND, B., Hole-vibration coupling in ^{115}In, 25:12543

HERVE, Alain, Electron spin resonance study of defects produced by irradiation in an ionic solid: beryllium oxide, 25:11950 (CEA-R-3937)

HERZOG, G. F., Protons and alpha particles emitted from ^{79}Br compound nuclei with differing angular-momentum distributions, 25:12461

HESS, S., Thermomagnetic gas torque for collinear static and alternating magnetic fields, 25:11754

HEUSLER, Konrad E., Kinetics of corrosion of Nb in aqueous solutions, 25:11354

HEWITT, G. F., Holdup, heat transfer, and nucleation for steam--water flow in a 0.5 cm bore tube, 25:10766 (AERE-R-3984)

HICKEY, Francis Roger, Small-angle scattering of relativistic particles, 25:12089

HICKS, R. S., Photoneutron cross section of strontium, 25:12456

HIGGINBOTHAM, N., Note on the central star of NGC 3132, 25:11570

HIGHTOWER, Joe W., Catalytic sites for deuterium exchange with benzene over alumina, 25:10530

HILL, C. R., Radiation from ball lightning, 25:11926

HILL, H. H., Kondo effect in Ti, Zr, and Hf alloys containing Pu, 25:12004
Metallic valencies of early transactinium metals, 25:11995

HILL, H. Hunter, Early actinides: the periodic system's f electron transition metal series, 25:11381

HILLENDAHL, R. W., Observational confirmation of a mechanism for the production of extended stellar atmospheres, 25:11571

HILLIARD, R. K., Natural transport effects on fission product behavior in the containment systems experiment, 25:12803 (BNWL-1457)

HILLIS, William D., Genetic effects of radiations in human populations, 25:11025

HILLMANN, H., Multicore superconductors for laboratory-scale magnets and for big magnets, 25:11831

HILSCHER, H., Analogy between radiative pion absorption and muon capture in ^{12}C, 25:12395
Charge exchange of 70 MeV π^- on C, Al, Cu, and Pb, 25:12446
Excitation of the isospin triplet ^{12}B, $^{12}C^*$(15.11 MeV), ^{12}N by pion charge exchange, 25:12397

HILTNER, W. A., Spectroscopic observations of Scorpius X-1, 25:11600

HINAI, Masakatsu, Effects of Ta additions on the properties of Nimalloy, 25:12008

HINOUL, M., Double-wall ultra-high vacuum system with electron gun and evaporation rate monitor, 25:10806

HINRICHS, Roger Albert, Single nucleon transfer reactions, 25:12571

HINTON, J. H., Measurement of time-of-flight using 300 Mc/s scalers, 25:10891 (AERE-R-5422)

HIROTA, Eizi, Microwave spectrum, structure, quadrupole ccupling constant, and force constants of NSCl, 25:10532

HIROTA, Kozo, Radiolysis of cholestanol, 25:10624 (JAERI-5026, pp 160-4)

HIRTH, J. P., Disclination structures in Bloch wall lattices in $BaFe_{12}O_{19}$ and $SmCo_5$, 25:12011

HIWANO, Kunio, Radiation curing of mixture of diallylphthalate prepolymer and vinyl monomer. V, 25:10608 (JAERI-5026, pp 121-9)

HJELLMING, R. M., Further radio observations of novae, 25:11599

HNATOWICH, D. J., Decay of ^{104}Cd, 25:12475

HO, P. S., Observation of void formation induced by electromigration in metallic films. report no. 1447, 25:12899 (NYO-4185-1)

HO, Paul S., Application of pseudopotentials to calculation of vacancy formation energy and volume for alkali metals. report no. 1486, 25:12900 (NYO-4185-2)

HOCHEID, B., Chemical diffusion in epsilon phase of Pu--Cu system, 25:11387
Effect of β phase-retaining or delta phase stabilizing elements on Pu during alpha--beta thermal cycling, 25:11393

HODGES III, Fred J., Normal-pressure hydrocephalus. Role of cisternography in diagnosis, 25:11181

HODGINS, J. W., Gamma-initiated iodination of methane in the gas phase, 25:10620

HODKIN, D. J., Compatibility studies between arc cast ($U_{0.85}Pu_{0.15}$)--C and type 316L stainless steel, 25:11475 (AERE-R-5173)

HOEFER, R., Colloid clearance: effect of particle size and extrahepatic deposition, 25:10918
Conference on radionuclides in circulation research and circulation diagnosis, Vienna, 9/67, 25:11118
Late effects of radiophosphorus therapy of polycythemia vera, 25:11303

HOEGBERG, G., Energy loss of well-channeled H, He, and Li ions in Au, 25:11976

HOEGLUND, A., 190-keV transition in ^{141}La, 25:12540

HOEHLER, G., Discripancies between πN charge exchange forward scattering data and the dispersion relation prediction, 25:12209

HOEKSTRA, E. K., Prog. rpt. on fast reactor program, 1--3/70, 25:12768 (EURFNR-855)

HOER, G., Clearance studies with ^{131}I-labeled hippuran, ^{203}Hg-salyrgan, ^{51}Cr-EDTA, and ^{51}Cr-inulin, 25:11156

HOERZ, Gerhard, Gas-metal reactions in systems of high-melting metals with nitrogen or oxygen, 25:11415

HOFFMANN, Alain, COREGRAF 2: code for computing graphite lattices and their evolution for IBM 360 and CDC 6600, 25:12774 (CEA-N-1344(1))

HOFFMANN, B., Determination of testosterone in peripheral blood of swine and bovines with a double isotope derivative dilution method, 25:10923

HOFFMANN, G., Conference on radionuclides in circulation research and circulation diagnosis, Vienna, 9/67, 25:11118
Evaluation of results of treatment of thyroid carcinoma, 25:11233

HOGLUND, B. M., Pressure distribution for axisymmetric two-dimensional flow in a plenum during coolant expulsion, 25:12808

HOLLADAY, G., Distribution and redistribution of airborne particulates from the Schooner cratering event, 25:10716 (UCRL-72534)

HOLLAND, Eva M., Mutants of E. coli with altered surface properties and sensitive to uv light, 25:11029

HOLLAND, I. B., Mutants of E. coli with altered surface properties and sensitive to uv light, 25:11029

HOLLAND, P. T., Radiolysis of ethane. II, 25:10632

HOLLNAGEL, R., Reactivity measurement in reactor cores on MTR fuel elements with a one-sided heavy water reflector, 25:12818 (FMRB-34/70)

HOLMBERG, S., Interaction between a fully ionized plasma and a neutral gas blanket, 25:11878

HOLSTI, Lars R., Split-course techniques, 25:11223 (BNL-50203, pp 292-307)

HOMAN, F. J., Experiment description and hazards evaluation for the Series I ORNL oxide fuels irradiation in EBR-II, 25:11533 (ORNL-TM-2635(Suppl.))

HOMEYER, H., Reaction ^{15}N(tau,α)^{14}N, 25:12424

HONES, E. W. Jr., Energy spectra and angular distributions of particles in the plasma sheet, 25:11809

HONMA, Kenzo, Irradiation tests of domestic Zircaloy-2 cladding materials in JPDR, 25:12862 (JAERI-Memo-4192)

HOOGLAND, W., Evidence for B(1220) production in an analysis of reaction K$^-$d + p/sub s/Λπ$^+$π$^-$π^0 at 3 GeV/c, 25:12118

HOOKE, William H., Quasi-stagnation levels in the ion motion induced by internal atmospheric gravity waves at ionospheric heights, 25:11800

HOOT, C. G., Gamma-ray production cross sections for the ^{16}O(n,xγ) reaction from 6.35- to 16.52-MeV neutron energy, 25:12406

HOPFIELD, J. J., Infrared optics of high-T/sub c/ superconductors, 25:11824

HOPPE, G., Studies on vasoactive drugs with the ^{133}Xe muscle clearance method, 25:10914

HOREDT, Gp., Gravitational instability of polytropic gas spheres under external pressure, 25:11560

HORI, Satsuko, Comments on the electromagnetic form factors and mass differences, 25:12154
Three-channel model for P_{33} πN scattering, 25:12221

HORIKOSHI, Genichi, Feedback control of the PIG discharge

of the QP machine, 25:11921 (IPPJ-T-2)
HORKAY-BORSOS, Klara, Determination of traces of foreign matter in molybdenum anuits compounds, 25:10459
HORNSBY, James B., Prog. rpt. on powder metallurgy compaction, 9--11/70, 25:12913 (SRO-475-9)
HOROSHKO, R. N., Electromagnetic transitions in ^{51}V, 25:12492
HORSTER, F. A., Successes and failures of fractionated radioiodine therapy among 700 hyperthyroid patients, 25:11230
HORSZOWSKI, S. M., Annealing of electrical properties of electron-irradiated diamond, 25:11966
HOSHINO, Kiyoshi, Species differences of the effects of x-irradiation upon the rat and mouse embryo, 25:11277
HOSODA, Masataka, Comments on the electromagnetic form factors and mass differences, 25:12154
HOSSFELD, F., Pseudorandom and Markov sequences optimizing correlation time-of-flight spectrometry, 25:10850 (JUL-684-FF)
HOSTE, J., Average cross sections of ^{28}Si(n,p)^{28}Al and ^{29}Si(n,p)^{29}Al reactions, 25:12460
HOUGH, A., Creep of UO_2 and $(U,Pu)O_2$, 25:11497
Length changes in actinide metals due to self-irradiation damage at 4^{0}K, 25:11468
HOUSTON, M. D., Thermal creep of polycrystalline UO_2--PuO_2, 25:11496
HOWARD, Alma, Role of oxygen in repair process, 25:11304 (BNL-50203, pp 70-81)
HOWARD, E. B., Immunosuppressive effect of chronic ^{90}Sr administration to miniature swine, 25:10984
HOWARD-FLANDERS, Paul, Repair and reconstruction of chromosomal DNA, 25:11007 (BNL-50203, pp 1-13)
HOWES, A. E., Reoxygenation during fractionated irradiation, 25:11220 (BNL-50203, pp 234-41)
HRADIL, J., Absorption rate of Sr from gastrointestinal tract, 25:10951
Kinetic model of stem-cells population in the postirradiation bone marrow injury. II, 25:11290
Kinetics of radiotellurium in rat, 25:10949
HRYNKIEWICZ, A. Z., Decay of ground state of ^{82}Rb, 25:12507
HSIEH, S. T., Binding energies of p-shell hypernuclei, 25:12393
HUANG, J. S. T., Redistribution of boron in the diffused layer during thermal oxidation, 25:11476
HUBER, O., Computer method for analysis of γ spectra application to fission-fragment mixtures, 25:12535
HUBER, P., Level density parameters for Ge, Ho, and Ta, 25:12536
HUBERT, M., Scientific and industrial applications of nuclear explosives, 25:10743
HUDIS, J., Argon-43 and ^{44}Ar, 25:12499
HUDOKLIN, A., Activation cross sections and integrated cross sections for radiative capture of 14 MeV neutrons, 25:12474
Gamma-ray spectra from radiative capture of 14 MeV neutrons in ^{28}Si and ^{40}Ca, 25:12472
HUDSON, R. F., Bibliography on whole-body irradiation effect related to canine treadmill performance decrement, 25:11251 (AD-705976)
HUEFNER, J., Pion scattering by nuclei in region of (3,3) resonance, 25:12420
HUENIG, R., Simultaneous determination of glomerular filtration rate and renal blood flow with ^{60}Co-cyanocobalamine and ^{131}I-orthohippuric acid, 25:11157
HUFFAKER, J. N., Beta decay and nuclear structure in the mass-14 system, 25:12421
HUGENTOBLER, E., Spontaneous fission of ^{238}U and ^{241}Am, 25:12538
HUGHES, J. A., Levels in ^{47}Ca and ^{41}Ca, 25:12491
HUI, S. W., Doppler-shifted acoustic cyclotron resonance in tungsten, 25:12022
HULTGREN, Ralph, Role of calorimetry in the thermodynamics of metals and alloys, 25:12916 (UCRL-19115)
HUMPHREYS, Roberta M., New Ap stars in NGC 3114, 25:11578
HUNDESHAGEN, H., Determination of central circulation parameters and peripheral blood flow by simultaneous application of ^{133}Xe and ^{131}I-labeled RISA, 25:11123
Determination of coronary blood flow with radioactive indicators as measured by external counting, 25:10911
Determination of lung circulation with the dynapix rapid scanner in pulmonary restrictions, 25:11131
HUNZINGER, W., Nuclear accident dosimetry system at Eurochemic, 25:11082
HURD, C. M., Carcinogen induced immunodepression in mice, 25:10990
HURST, G. S., A sequential neutron and gamma ray monitor, 25:10824
HUSAIN, D., Equivalent local potentials from nonlocal separable ones, 25:12658
HUSSON, J. P., Main decay characteristics of mercury isotopes and their daughter products (182 less than or equal to A less than or equal to 192), 25:12512 (CERN-70-29)
HUTCHISON, Clyde A. Jr., Prog. rpt. on actinide and lanthanide ions and organic molecules in triplet states by magnetic resonance methods, 12/70, 25:10570 (COO-294-10)
HUTTON, R. S., Electron paramagnetic resonance of CD_2 and CHD. Isotope effects, motion, and geometry of methylene, 25:10555
HYDE, Earl K., Production and decay of protactinium isotopes, 25:12592
HYLLERAAS, Egil A., Mathematical and theoretical physics. Volume II, 25:12049
Mathematical and theoretical physics. Volume I, 25:12048
HYLTEN, Gunnar, Investigation of ^{12}C(γ,n)^{11}C reaction for E/sub γ/ up to 1 GeV, 25:12413

I

IBATULLIN, M. S., Cesium-137 in lichen-reindeer man in the extreme north of the USSR, 1962--68, 25:11037 (NP-18381)
IBRAGIMOV, A. P., Gamma radiation effects on pyrimidine oligonucleotides in low-polymer fraction of DNA, 25:11307
ICHIKAWA, F., Co-precipitation of carrier-free ^{31}Si with hydroxides, 25:10675
ICHIKAWA, S., Chromosome number in radiation-induced mutants of Chrysanthemum morifolium, 25:11031
ICHIMORI, T., Gamma-ray discrimination in proton-recoil spectrometer, 25:10857
IGO, G., Proton total reaction cross sections of ^{40}Ca and ^{12}C, 25:12497
Reaction ^{182}W(t,d)^{183}W at 20 MeV triton energy, 25:12611
IIDA, Hiroyoshi, Exposure from ^{147}Pm-activated self-luminous paints, 25:11065
ILBERY, P. L. T., Medical experience of the atomic bombings, 25:11238
ILIFFE, C. E., Assessing the economics of nuclear power stations in an electricity generating system, 25:12724 (TRG-Report-2090)
IL'KHAMDZHANOV, N., Properties of the excited states of ^{147}Sm and ^{149}Pm, 25:12557
IMACHI, Masahiro, Dip-bump structure of cross section and urbaryon rearrangement. II, 25:12219
Exotic resonances, urbaryon rearrangement and hadron structure, 25:12183
IMAI, Isao, Thin airfoil theory in magnetoaerodynamics, 25:11772
INCH, W. R., Multi-component radiation survival curve model, 25:11293
INGVAR, D. H., Variations in regional cerebral blood volume during mental activity, 25:11151
INOGAMOV, Sh. V., Analysis of $\pi^-p \to n\pi^+\pi^-m\pi^0$ (m = 1,2,3) and $\pi^-p \to n2\pi^+2\pi^-m\pi^0$ (m = 1,2) reactions, 25:12204 (JINR-P1-5431)
INOUE, Kazuhiko, Slowing down of neutrons to very low temperature by cold solid hydrogenous moderators, 25:12351
INOUE, Masasi, Superconducting wired-wall cavity for V-band ENDOR experiment, 25:11850
INOUE, S., Inhibition of intestinal absorption of radioactive Sr. IX, 25:10939
INOUE, Yoriteru, Dynamic concentration process of radioactive substances to aquatic organisms, 25:10998
IOSEL'SON, G. L., Feasibility of using the super-high-frequency radiation of a plasma for an accurate measurement of its temperature, 25:11877
IOVNOVICH, M. L., Calculation of the phase volume of the electron--ion bunches in the collective accelerator and the problems of separation, 25:12302 (JINR-P9-5405)
IRVINE, J. M., Shell-model data from realistic N--N interaction, 25:12686
ISABELLE, Didier B., Solid track detectors and their applications to biology, 25:10823
ISAENKO, V. I., Neodymium glass laser with high radiation intensity for producing a high-temperature plasma, 25:11906
ISAKOV, V. V., Investigation of a particle beam with energy up to 70 GeV with a spark spectrometer, 25:10868 (IFVE-SEF/OP-70-13)
ISHIGAKI, Isao, Radiation-induced postpolymerization of trioxane in the solid state. II, 25:10611
ISHII, Kameo, Quasi-gamma bands in ^{152}Gd and possible presence of quasi-K quantum number, 25:12518 (INSJ-123)
ISHII, M., Temperature dependence of dechanneling coefficient in protons in silicon crystals, 25:11969
ISHII, T. Koryu, Electromagnetic radiation from heterogeneous plasma, 25:11890
ISHIZAKI, Y., Numerical differential cross sections of reaction ^{58}Ni(p,t)^{56}Ni with 51.9 MeV protons, 25:12431 (INSJ-124)
ISHIZONE, T., Measurement of the phase constant along a conducting wire in a magnetoplasma, 25:11935
ISKHAKOV, I. F., Polarization of photons during scattering in gravitational field of spherical symmetry, 25:12159
ISO, C., Dual model for diffractive two-pion electroproduction, 25:12137 (DESY-70/56)
ISPIRIAN, K. A., High energy particle identification by x-ray transition radiation (XTR) detectors, 25:10877
ISSINSKII, I. B., Acceleration and extraction of deuterons from the JINR proton synchrotron, 25:12303 (JINR-P9-5442)
ITAGAKI, Gentaro, Effect of x-rays on male germ cells in the mouse, 25:11276
ITIKAWA, Yukikazu, Elementary processes involving electrons in the ionosphere, 25:11810
Rotational excitation of molecules by slow electrons,

XUM

25:11730
ITO, Akihiko, Radiation-induced postpolymerization of trioxane in the solid state. II, 25:10611
ITO, Noboru, Irradiation tests of domestic Zircaloy-2 cladding materials in JPDR, 25:12862 (JAERI-Memo-4192)
ITOH, Junichi, Fluorescent x-ray analysis of tin and zirconium in aluminum alloys, 25:10441
IVANENKO, D. D., Quark stars, 25:12188
IVANNIK, B. P., Radiosensitivity of DNA in vivo and in vitro, 25:10966
IVANOV, A. A., Consumption of complement in irradiated animals, 25:10985
IVANOV, M. P., Neutron detector in search for superheavy elements in nature, 25:10814 (JINR-P13-5391)
IVANOV, V. I., Measurement of scattering angle of particles by Vavilov--Cherenkov radiation, 25:10869 (JINR-E13-5459)
IVANOV, V. N., Protective effects of biogenic amines in the radiation intestinal syndrome, 25:11102
IVANOV, Yu. V., Vulnerability of endothelium of large vessels in radiosensitive and radioresistant animals, 25:11269
IVANOVSKII, M. M., Physico-chemical analysis of handling liquid metal coolants, 25:11342
IVANOVSKII, N. N., Continuously-active indicator for the diffusion of hydrogen in sodium, 25:11400
IWAI, Shigehisa, Dynamic concentration process of radioactive substances to aquatic organisms, 25:10998
IWAI, Tadashi, Radiation-induced postpolymerization of trioxane in the solid state. II, 25:10611
IWAKI, Atsuko, Reaction $\pi^+p \to \pi^0N^{2+}$ at high energy and correction to rho-exchange contribution, 25:12223
IWAO, Syurei, Theory of neutral weak current, 25:12170
IWATA, Shiro, Determination of uranium contents in some rocks based on fission track method, 25:10474
IWAUCHI, Shigeki, Effect of radiation in reactively sputtered Al_2O_3--Si structures, 25:10905
IYENGAR, S. B. D., Calculation of K/sub eff/ for a bare Pu sphere by collision probability method, 25:12849

J

JACKSON, D. D., Low energy secondary electron distribution studies of some light actinides, 25:11999
JACKSON, J. W., Economical beam transport for utilization of post conversion AGS, 25:12296 (BNL-15464)
JACKSON, Jane Chapman, Regge-phenomenological studies of SU(3), exchange degeneracy, and conspiracy, 25:12217
JACOBI, S., Can failure--steam loop, 25:12820 (KFK-1255)
JACOBS, Ralph Raymond, Fine structure measurement of singly ionized He, n = 4, 25:11687
JACOBS, Verne, Low-energy photo-ionization of the 1^1S and 2^1S state of He, 25:11717
JACOBSEN, J. A., Fast breeder reactor static physics methods development and analysis project. Volume 1. FARED: one-dimensional fast reactor physics design and analysis code, 25:12772 (BAW-3867-9(Vol.1)(Rev.1))
JACQUIN, Fernand, Environmental mobility of ^{106}Ru during irrigation processes, 25:10692
JACQUOT, B., Production of intense beams of fast neutral particles using plasma accelerators of the pleiade type, 25:11920 (EUR-CEA-FC-567)
JACQUOT, C., Production of intense beams of fast neutral particles using plasma accelerators of the pleiade type, 25:11920 (EUR-CEA-FC-567)
JAFFE, A., Model estimates and results, 25:12255
JAFFE, A. A., Scattering of protons from ^{128}Te and ^{130}Te, 25:12602
JAFFE, Arthur, Energy--momentum spectrum and vacuum expectation values in quantum field theory, 25:12269
JAGADEESAN, V., Fate of ^{60}Co 1-nitroso 2-naphthol chelate in albino rats after intravenous administration, 25:10958
JAGATBESAN, D., Induced mutations in sugar cane, 25:11030
JAIN, P. L., Mechanism of particle production in nucleon--nucleon interactions at very high energies, 25:12230
JAMES, A. Everette Jr., Normal-pressure hydrocephalus. Role of cisternography in diagnosis, 25:11181
JAMOND, C., Correction of matrix effect in ultraviolet spectrographic analysis, 25:10453
JANKUS, V. Z., LIFE-I: a FORTRAN-IV computer code for the prediction of fast-reactor fuel-element behavior, 25:12794 (ANL-7736)
JANNKE, C. C., Immunosuppressive effect of chronic ^{90}Sr administration to miniature swine, 25:10984
JANOUCH, F., Internal bremsstrahlung and mechanism of direct nuclear reactions, 25:12694
JANOVSKA, Eva, Nature of reparable and non-reparable lethal damage in E. coli, 25:11320
JARVIS, R. G., Theory for least squares description of radial distortions in irradiated fuel sheaths, 25:11368 (AECL-3688)
JASKE, R. T., Effect of Hanford Plant operations on the temperature of the Columbia River 1964 to present, 25:10691 (BNWL-1345)
JAUHO, Pekka, Energy-dependent neutron transport theory in adjacent half-spaces, 25:12857
JAWOROWSKI, Andrzej, Activation energy and frequency factor of 100°K annealing stage of simple defects in n-type Ge, 25:11954
JAWOROWSKI, Z., Incorporation of tritium in hair, 25:10954
JEANJEAN, J., Upper limit on phi in two-π branching ratio, 25:12074
JEANMAIRE, L., Study of two cases of contamination by ^{241}Am, 25:10931 (CEA-CONF-1557)
JEE, Webster S. S., Risk to bone and liver from ^{239}Pu, 25:11301
JEFFERTS, Keith B., Observation of CO emission at 2.6 millimeters from IRC + 10216, 25:11568
JENKINS, R. A., Selective extirpation of oral ciliature of Blepharisma by laser microbeam, 25:11322
JENSEN, J., Odd parity states in ^{238}Pu, 25:12594
JEPPESEN, F., Regional cerebral blood flow, 25:11143
JESDINSKY, H. J., Diagnostic significance of ventricular resorption of ^{131}I-labeled hippuran, 25:11152
JETT, J. H., Rotational states of ^{158}Dy, ^{164}Er, ^{168}Yb, and ^{176}Hf, 25:12544
JEW, Nathan Nay Shew, K⁻--neutron elastic scattering from K⁻d + K⁻d and K⁻d + K⁻pn at 1 GeV/c, 25:12108
JHA, S., Hyperfine-field studies with ^{99}Mo, 25:12568
JNANANANDA, Swami, Gamma spectrum from the thermal neutron capture in cerium, 25:12551
JOELSSON, Ingemar, Applicators for optimum pelvic dose distribution in uterine cervix, 25:11227
JOHANNSEN, K., Stationary heat transfer in infinitely long fuel elements with locally varying heat sources and boundary conditions, 25:12799 (TUBIK-17)
JOHANSEN, Dorothy, N_2 bands of $^{10}BF_3$ and $^{11}BF_3$ at high resolution, 25:10533
JOHANSSON, I., Spectrochemical determination of tracers of impurity elements in Pu by Cu spark method, 25:10444
JOHANSSON, John M., Radiation damage to the surfactant system of the rabbit lung, 25:11267
JOHLIGE, H. W., Electron density at the Be nucleus, 25:12398
JOHN, Joseph, Gamma-ray production cross sections for the $^{16}O(n,x\gamma)$ reaction from 6.35- to 16.52-MeV neutron energy, 25:12406
JOHNS, J. W. C., Spectrum of neutral argon hydride, 25:10535
JOHNSEN, S. W., Energy measurements of 20 to 60 MeV neutron beam of Davis 76-inch isochronous cyclotron, 25:10861
JOHNSON, C. H., Differential scattering of neutrons at narrow levels in ^{17}O, 25:12404
JOHNSON, David John, Reactions $^6Li + ^{12}C$ at bombarding energies from 9.0 to 14.0 MeV, 25:12418
JOHNSON, J., Pi^0 photoproduction from H with linearly polarized photons, 25:12072
JOHNSON, K. A., Melting behavior of (U,Pu) monocarbides, 25:11507
JOHNSON, W. Reed, Gamma-ray attenuation at energies of approximately 6 and 8 MeV, 25:11947
JOHNSON, W. T. K., Magnetic multipole electroexcitation, 25:12657
JOHNSON, Wallace, Elevated levels of ^{137}Cs in common mushrooms (Agaricaceae) with possible relationship to high levels of ^{137}Cs in whitetail deer, 1968--1969, 25:11003
JOHNSON, William Robert, High-temperature creep of Ni--W solid solutions, 25:11408
JOHNSTON, A. R., Response of detectors with cylindrical collimation, 25:10841
JOHNSTON, P. D., Measurement of LTE plasma temperatures below 10,000 K, 25:11876
JOHNY, K. V., Whole-body counter for studies of total body K, 25:10910
JOINER, W. C. H., Voltages induced in superconductors by superimposed ac and dc magnetic fields, 25:11835
JOMBIK, J., Sensitivity of radioisotopes x-ray fluorescence using Ross filters, 25:10479
JONARD, Robert, Host-bacteria relationship in x-irradiated artichokes, 25:11306
JONES, A. H., Photochemical exchange reaction of Michler's ketone, 25:10556
JONES, Arthur, Effect of 14-MeV electrons on blood vessels of the mouse earlobe, 25:11254 (BNL-50203, pp 174-80)
JONES, Frank C., Examination of the leakage-lifetime approximation in cosmic-ray diffusion, 25:11743
JONES, G. D., Angular correlation measurements on excited states of ^{42}Ca, 25:12465
JONES, H. D., Two-quasiparticle states in ^{158}Tb, 25:12578
JONES, K. W., Lifetimes of first four excited states of ^{32}S, 25:12486
JONES, R. E., RUNKUT: computer routine for integrating systems of first order ordinary differential equations, 25:12906 (SC-M-70-868)
JONES, William Philip, Nuclear structure of ^{140}Ce, ^{141}Pr, and ^{142}Nd determined by (d,^{3}He) and (^{3}He,d) reactions, 25:12558
JONKE, Albert A., Annular packed-bed filter, 25:10761
JOOS, Peter, Compilation of photoproduction data above 1.2 GeV, 25:12066 (DESY-HERA-70-1)
JOUBERT, J. C., Systems B_2O_3--MO--MS boracites M--S (M = Mg, Mn, Fe, Cd) and sodalites M--S (M = Co, Zn), 25:11526
JOURET, C., Habit and texture of lunar and meteoritic materials, 25:11671
JOYEUX, Jean, Levitation in ultra-vacuum, 25:10805
JOYNT, Margaret S. K., Effect of a uremic environment on phosphate excretion by a small population of intact and severely diseased nephrons, 25:10963
JUETTE, B. A. H. G., Determination of trace amounts of I.

II, 25:10481
JULEAN, I., Uranyl pyrophosphate complexes. II, 25:10519
JULIAN, Alain, Various vertical sampling devices for aerosols, 25:10754 (NP-18633)
JUN, Choll K., Thermal expansion of polycrystalline graphite, 25:11511
JUNGERMAN, J. A., Medium-energy neutron facility, 25:12331

K

KAFKA, P., Research and development work for Obrigheim Nuclear Power Station, 25:12704 (BMBW-FBK-70-11)
KAGIYA, Tsutomu, Participation of an excited monomer in propagation reaction of the γ-ray induced polymerization of ethylene, 25:10612
KAGIYAMA, Shigenori, DTIE; JA, 25:12152
KAIBA, Masayuki, Regularity of coupling constants of N* + N + π decays, 25:12220
KAIPOV, B., Luminescence of CaF_2—TRF_3 in the gamma-ray field of ^{60}Co, 25:11955
KAISER, G., Determination of regional blood flow with ^{133}Xe in the brain of Parkinson and tumor patients, 25:11147
KAISER, R., Biological effects of the heavy ions in cosmic radiation, 25:11280
Differentiation between maternal, placental, and embryonal hormone production, 25:10982
KAJI, Kanako, Grafting acrylonitrile onto polyvinyl chloride powder and spinning fiber, 25:10595 (JAERI-5026, pp 35-41)
Radiation-induced graft polymerization of acrylonitrile onto poly(vinyl chloride) powder, 25:10596 (JAERI-5026, pp 42-5)
KAKIHANA, Hidetake, Hydrolysis of Cu(II) ion in heavy water, 25:10566
KAKITA, Yachiyo, Determination of Mo in Fe and steel by flame photometry, 25:10439
KALASHNIKOV, O. K., Application of spectral density method to systems with pair interaction, 25:12061
KALINKIN, B. N., Average field of excited nuclei, 25:12632 (JINR-P4-5084)
KALISKI, S., Classical approach to the equations of quantum mechanics in an electromagnetic field, 25:12062
WKB method in classical approach to quantum mechanics, 25:12063
KALKOFEN, Wolfgang, Solar Lyman continuum and the structure of the solar chromosphere, 25:11614
KALKSTEIN, Marvin, International arrangements and control for the peaceful applications of nuclear explosives, 25:10751
KALTENBACH, M., Simultaneous blood flow measurements with ^{133}Xe in flexors and extensors of the lower leg under positive and negative load, 25:10913
KALVIUS, G. M., Magnetic behavior of Np metal and dilute Np alloys from Moessbauer effect studies, 25:12001
KALVIUS, G. Michael, Determination of electronic properties of actinides with Moessbauer effect, 25:12000
KALYANARAMAN, R., Thermochemical studies of some U and Th compounds, 25:10581
KAMATH, P. R., Environmental radiation surveillance laboratory, 25:10763
KAMEL, Ihab, Effect of swelling on radiation-induced grafting of styrene to polyethylene, 25:10613
KAMEYAMA, Yoshiro, Species differences of the effects of x-irradiation upon the rat and mouse embryo, 25:11277
KAMIL, J., Magnetic control of a conducting jet, 25:11775
KAMIMURA, Masayasu, Four-body correlations in light nuclei, 25:12660
KAMINSKAYA, A. N., Experiments on α-particle acceleration by collective method, 25:12305 (JINR-P9-5558)
KAMINSKII, A. K., Experiments on α-particle acceleration by collective method, 25:12305 (JINR-P9-5558)
KAMIYAMA, Hideo, Stability of polyvinyl acetate emulsions produced by radiation-induced polymerization. I, 25:10593 (JAERI-5026, pp 15-25)
Stability of polyvinyl acetate emulsions produced by radiation-induced polymerization. II, 25:10594 (JAERI-5026, pp 26-34)
KAMPMANN, H., Determination of glomerular clearance with radioisotope labeled substances according to the slope method, 25:11154
Experimental scintigraphy of thrombi in animals, 25:11214
Scintigraphic and angiographic studies of the liver of dogs with experimentally produced obstructive jaundice, 25:11213
KANANEN, H., Construction of a scintillation counter telescope for the registration of the meson component of cosmic rays, 25:10871
KANKI, Takeshi, Three-channel model for P_{33} πN scattering, 25:12221
KANO, E., Actinomycin D and radiation fractionation studies in asynchronous and synchronized Chinese hamster cells, 25:11097
KANTELE, J., Directional correlations of some γ-ray cascades in ^{200}Hg, 25:12527 (NP-18613)
Reinvestigation of the decay of ^{200}Tl, 25:12528 (NP-18647)
Semiconductor detector telescope electron spectrometer, 25:10852 (NP-18617)
Table of cross sections of some reactions induced by 14 to 15 MeV neutrons, 25:12353 (NP-18616)
KANTER, H., Response of highly damped Josephson junctions to external, low-frequency noise currents, 25:11822
KANTOR, J., Three-photon ionization of a He atom in excited 2S state, 25:11734
KANWALL, R. P., Boundary-value problems in magnetohydrodynamics, 25:11770
KAPITZA, S. P., Photo-nuclear activation analysis of O in pure materials, 25:10501
KAPLAN, Joan, Repair of UV-irradiated DNA, 25:10959 (BNL-50203, pp 27-40)
KAPLAN, S. A., Interstellar medium, 25:11641
KAPPEY, F., Lung scintigraphy with ^{131}I-labeled MAA in late sequelae following blunt chest concussions, 25:11135
KARAM, RJ A., Analysis of heterogeneity and sodium-void effects in a 2700-liter uranium carbide fast core, ZPR-6 Assembly 5, 25:12825
KARCZ, W., Polarization of protons from $^{12}C(d,p)^{13}C$ reaction at E/sub d/ = 12.4 MeV, 25:12377 (INP-711)
KARG, H., Determination of testosterone in peripheral blood of swine and bovines with a double isotope derivative dilution method, 25:10923
KARIMOV, S. N., Thermo-oxidation degradation of poly(vinyl alcohol) irradiated by γ rays, 25:10591
KAROWSKI, M., Superpropagators, 25:12243
KARTASHOV, P. A., Nonspecific allergic reactions in sheep in chronic radiation sickness, 25:10989
KARUNARATHNE, V. B., Reflexion of a plane wave at a plasma half-space, 25:11939
KASCHL, G. Th., Proton pick-up from ^{19}F, ^{20}Ne, and ^{22}Ne, 25:12385
KASEMO, B., Mean square thermal displacement for surface atoms in nickel (001) surface, 25:12017
KASHY, E., Energy of the second excited state of ^{12}C and the rate of the triple-alpha reaction, 25:11565
KASS, Stanley, Influence of prior corrosion history upon the hydrogen pickup by Zircaloy during subsequent exposure in hot water, 25:11349 (WAPD-TM-906)
KASUNOV, Yu. N., Investigation of possible anapole and electric dipole moment of proton with help of annihilation reaction p anti p reversible e^+e^-, 25:12224
KATHREN, R. L., Intercomparison of portable radiation monitoring instrument evaluations, 25:10809 (BNWL-SA-3565)
KATO, Susumu, Superconducting wired-wall cavity for V-band ENDOR experiment, 25:11850
KATO, Syohei, Elastic scattering of alpha particles by ^{16}O, 25:12419
KATTENBORN, H., j-dependence in l = 2 (^3He,d) reactions on ^{24}Mg, ^{28}Si, and ^{30}Si, 25:12479
KATZ, David H., Radioresistance of cooperative function of carrier-specific lymphocytes in antihapten antibody responses, 25:10987
KATZ, R., DYNA: computer program for determining motions of head of PCRV with complete circumferential crack, 25:10753 (GAMD-7567)
KAUFMAN, A. S., Analysis of the velocity field in plasmas, 25:11875
KAUFMAN, Aaron, Near-surface and near-bottom radon results for the 1969 North Pacific Geosecs Station, 25:10727
Radium-226 measurements from the 1969 North Pacific Geosecs Station, 25:10726
KAUFMANN, P., Night-time anomalies in vlf propagation by galactic x-ray source at Centaurus, 25:11812
KAUFMANN, Pierre, Changes in coronal condensations emission after solar bursts at microwaves, 25:11620
KAUTSKY, H., Measuring instruments for the continuous control of radioactivity in the subsurface water of the oceans, 25:10817
KAVATS, G. E., Predicting radiation effect in seeds of cereal grasses, 25:11314
KAW, P. K., Plasma instabilities in ionospheric heating by radio waves, 25:11806
KAWABE, Mitsuo, Penetration of electrons into anthracene crystals, 25:11673
KAWAGUCHI, Setsuo, Horizontal air showers of energies above 10^{13} eV, 25:12071
KAWAKAMI, Ichiro, Perturbation approach to nonlinear Vlasov equation. II, 25:11933
KAWASAKI, Shoji, Effect of glutathione on the protection against radiation, 25:11098
KAWASAKI, Sunao, Use of comformal mapping to improve uniformity of electric field, 25:12045 (IPPJ-T-4)
KAYE, Stephen V., Dose-estimation studies related to proposed construction of Atlantic--Pacific Interoceanic Canal with nuclear explosives: Phase III, 25:11055 (ORNL-4579)
KAZANSKII, G. S., Acceleration and extraction of deuterons from the JINR proton synchrotron, 25:12303 (JINR-P9-5442)
KAZMAIER, H. E., Prog. rpt. on revegetation of disturbed areas of Amchitka Island, annual, 7/68, 25:12872 (EMI-171-105)
KEEN, B. E., Van der Pol plasma instability, 25:11944
KEIL, G., Design principles of fluorescence radiation converters, 25:10834
KEIRIM-MARKUS, I. B., Emergency personal n-γ radiation dosimeters, 25:10861
KELLEHER, Daniel F., Radiation gauge system for tubular plastic film, 25:10890
KELLER, Donald L., Prog. rpt. on development of fuels and

XUM

technology for advanced reactors,7--9/70, 25:12795 (BMI-1893)
KELLERER, H., Strain-induced phase transformations in Ti-6Al-4V, 25:11453
KELLERSHOHN, C., Application of /sup 99m/Tc for scintigraphic studies of pulmonary circulation, 25:11128
Neutron activation determination of selenium in biological media, 25:10495
Visualization by image intensifier of radioactive indicator flow through the cardiac chambers and the large vessels, 25:11120
KELLEY, Richard D., Isotope effects in the hydrogen-atom addition to olefins at low temperatures, 25:10538
KELLMAN, Sanford A., Scanner observations of the lambda 4430 diffuse interstellar feature, 25:11651
KELLOGG, L. S., EBR-II dosimetry test reaction rate measurements (reactor runs 31E and 31F), 25:12773 (BNWL-1403)
KELLY, W. H., Neutron-deficient Gd isotopes. II, 25:12582
KEMNITZ, H.-P., Results of lung scintigraphy in silicosis, 25:11134
KEMPE, H., Scintigraphic findings in liver diseases identified by laparoscopy and histology, 25:11180
KENDYSH, I. N., Postradiation hyperglycemia, 25:10969
KENEALY, P. F., Nuclear-resonance fluorescence in ^{130}Xe, 25:12560
KENMOKU, Masakatsu, Proper-time formulation in dual resonance model and the subsidiary conditions, 25:12185
KENT, J. J., Threshold effect in ^{93}Nb(d,p)^{94m}Nb, 25:12588
KENT, James J., Proton decay of analog resonances in ^{93}Nb, 25:12564
KENT, R. A., Thermodynamic properties of Pu--C system, 25:11506
KERIMOV, B. K., Investigation of possible anapole and electric dipole moment of proton with help of annihilation reaction p anti p reversible e$^+$e$^-$, 25:12224
KERMAN, A. K., Self-consistent calculations of shell effects, 25:12672
KERN, W., Radioisotope studies on hyperemia producing treatment, 25:10916
KERNEL, G., Angular distribution measurements in inverse photonuclear reactions, 25:10865
KERRISK, J. F., Thermal expansion of extruded graphite--ZrC carbide composites, 25:11512
KHAITOV, R. M., Suppresion of endocolonization in sublethally irradiated mice, 25:10986
KHALILOV, V. R., Effect of induced radiation of electrons moving in planar electromagnetic wave on orientation of their spins, 25:12161
KHAN, H. A., Annealing of fission tracks in tektites: corrected ages of bediasites, 25:10696
KHAN, I. Ali, Solubility and corrosion behavior of iron, steel, molybdenum, niobium, tantalum, vanadium, tungsten, and chromium in molten lead at high temperatures, 25:11376 (JUL-661-RW)
KHAO, Yu., Change in the cellular populations of the bone marrow of mice after single and repeated irradiation, 25:11279
KHARCHENKO, L. A., Cesium-137 in lichen-reindeer man in the extreme north of the USSR, 1962--68, 25:11037 (NP-18381)
KHARITONOV, Yu. N., Barkhausen effect in ferroelectrics during continuous x irradiation, 25:11978
KHARIZANOV, Yu., Plasma cluster in dc arcs with applied inhomogeneous magnetic fields, 25:11905
KHERA, A. K., Rapid determination of Al, Mn, and Na in soils by neutron activation analysis, 25:10909
KHOMYAKOV, K. P., Radioprotective action of polymer salt of cystamine and sulphopropyl ester of dextrane, 25:11108
KHOPKAR, S. M., Liquid--liquid extraction of Gold(III) with diluted tributyl phosphate, 25:10686
KHORVAT, P., Time-coordinate compensator for the time spectrometers with long scintillators, 25:10813 (JINR-P13-5378)
KHRENOV, A. N., Time-coordinate compensator for the time spectrometers with long scintillators, 25:10813 (JINR-P13-5378)
KHRISTOV, V., Pulsed determination of constants of neutron diffusion into heterogeneous water lattices, 25:12861
KHRYLIN, B. A., Estimate of AN interaction in p state, 25:12226
KIELKIEWICZ, M., Bounded positive solutions of nuclear reactor kinetics equations, 25:12845
Periodic positive solutions of nuclear reactor kinetics equations, 25:12846
Volterra functional series for reactors with linear feedback, 25:12843 (INR-1206)
KIHARA-MORISHITA, H., Infra-red reflectance spectra of anodic oxide films formed on pure Ta, 25:11518
KIKUCHI, Tadashi, Determination of oxygen in ferro-boron by the vacuum fusion analysis, 25:10467
KILMER, Nelson G., Temperature effects on the phosphorescence of benzene and toluene, 25:10550
KIM, K. S., Kondo effect in La/sub 1-x/Ce/sub x/ alloys under pressure, 25:11990
KIMEL, S., Far-infrared spectra of ethane, ethylene, and acetylene, 25:10544
KIMURA, Ki-ichi, Optical radiation from gases excited by high-energy electrons. III, 25:10586 (JAERI-5026, pp 155-7)
Optical radiation from gases excited by high-energy electrons. II, 25:10585 (JAERI-5026, pp 153-5)
KIMURA, Toyoaki, Scavengeable electron yield in radiolysis of hydrocarbons, 25:10652
KING, G. W., Ethynylbenzene: the vibrational spectra of some deuterated isomers, 25:10534
KING, L. J., Transuranium processing plant semiannual report of production, status, and plans for period ending June 30, 1970, 25:10654 (ORNL-4588)
KINGSTON, A. E., Use of classical mechanics in the treatment of collisions between massive systems, 25:11733
KINKAID, Donald Eugene, Inelastic scattering of nucleons from ^{7}Li, 25:12384
KIRITANI, Reiko, TC in acidic media, 25:10546
KIRKEGAARD, Peter, FORTRAN IV version of sum-of-exponential least-squares code EXPOSUM, 25:12837 (RISO-M-1279)
KIRKPATRICK, A. E., Gamma densitometry in the study of ventilation and the pulmonary circulation, 25:11116
KISS, A., Three-photon ionization of a He atom in excited 2S state, 25:11734
KISSINGER, H. E., Characterization and annealing behavior of voids in neutron-irradiated nickel, 25:11469
KITAHARA, Akiharu, Thermoluminescence of purified LiF powder, 25:11951
KITAJIMA, Masahiko, Stability of polyvinyl acetate emulsions produced by radiation-induced polymerization. II, 25:10594 (JAERI-5026, pp 26-34)
KITCHIN, C. R., Determining sizes of envelopes surrounding Be stars, 25:11557
KITCHING, J. E., Reactions ^{152}Sm(p,t)^{150}Sm and ^{154}Sm(p,t)^{152}Sm, 25:12612
KIYOKU, Masao, Ecology of insect sterilized by gamma radiation. IV, 25:11338
KIYONO, Kunihiro, Whole body skin eruption combined with radiotherapy, 25:11296
KJELBERG, A., Decay of ^{109}Cd, 25:12475
KLANK, Benno Ernst, Electron-transport solenoid--Si(Li) detector spectrometer, 25:10855
KLARSFELD, S., Stark-broadening functions for nonhydrogenic ions, 25:11892
KLAS, J., Optimum exactness of simple isotope dilution, 25:10471
KLEIN, A., Application of the Hartree--Fock variational method to center-of-mass motion, 25:12653
Theoretical foundation of variable moment of inertia models, 25:12638 (NYO-2171-334)
KLEIN, E., Successes and failures of fractionated radioiodine therapy among 700 hyperthyroid patients, 25:11230
KLEIN, Gerhart P., High resolution print-out of the electronic conductivity distribution of anodic tantalum oxide, 25:12014
KLEIN, H., Wind-tunnel measurements of reactor components to determine flow loads and flow distribution, 25:12706
KLEIN, J. W., Timing of Ge(Li)-detector pulses, 25:10830
KLEIN, Ralph, Isotope effects in the hydrogen-atom addition to olefins at low temperatures, 25:10538
KLEINFELD, A. M., Reorientation effect in the cadmium isotopes, 25:12548
Reorientation effect measurements in ^{106,110}Cd, 25:12619
KLEIN-SZANTO, A. J. P., Microspectrophotometric study of oxidative enzymes in irradiated epidermis, 25:11241
KLEMM, C., Accumulation and excretion of ^{224}Ra (Th X) during treatment of ankylosing spondylitis, 25:11231
KLEMM, J., Brain blood flow measurements (cerebral clearance) with ^{133}Xe, 25:11144
Is ^{133}Xe clearance a routine technique for studying muscular blood flow, 25:11138
Studies on l-triiodo-thyronine suppression in its dependency on thyroidal function, iodine storage, thyroid size, and age of patients, 25:10944
KLEMOVA, L., Estimation of radioactivity of biological samples, 25:11044
KLIEWER, K. L., Electron energy loss due to surface modes in a thin ionic crystal film, 25:11677
KLIMENKO, Yu. I., Forced radiation of neutral Fermi-particles moving in planar wave, 25:12160
KLIMENT, V., Determination of Co and Se by on-stream activation analysis, 25:10500
KLIMKOVA, O. A., Low-temperature lithium drift in silicon, 25:11973
KLIMOVITSKII, V. Ya., Effects of space flight on the central nervous system, 25:11298
KLUYVER, J. C., Evidence for B(1220) production in an analysis of reaction K$^-$d + p/sub s/Ar$^+\pi^-\pi^-\nu^0$ at 3 GeV/c, 25:12118
KLYUSHNIKOV, O. I., Generator for studying superconductivity by a pulse method, 25:10899
KMETKO, E. A., Metallic valencies of early transactinium metals, 25:11995
Single-parameter free-electron exchange approximation in free atoms, 25:11736
KNACKE, R. F., Infrared studies of galactic nebulae. II. The compact nebulae IC 4997, VV 8, and FG sagittae, 25:11569
KNAELMANN, M., Effect of concentration supplied on the iodide sorption by various soils, 25:10694

KNAFJL, J., Use of activated barium sulfate in oral contamination with radiostrontium. I, 25:11049
KNAJFL, J., Assessment of radiotellurium as a fission product, 25:10948
Decrease in radiostrontium accumulation due to activated barium sulphate during repeated and continuous peroral contamination of rats, 25:10940
Use of activated barium sulfate in oral contamination with radiostrontium. III, 25:11047
Use of activated barium sulfate in oral contamination with radiostrontium. II, 25:11048
KNEUBUEHL, F. K., Group theory of paramagnetic resonance, 25:12910 (SC-T-71-3002)
KNIZHNIKOV, V. A., Dietary intake of ^{90}Sr by population of the USSR, 1959--1967 as a result of stratospheric fallout, 25:10934 (NP-18380)
KNOEPFLE, K. T., Reaction $^{90}Zr(^{3}He,d)^{91}Nb$ at 18 MeV, 25:12613
KNOP, Robert Edward, Vector--axial vector current ratio in decay $\Sigma^- \rightarrow n e^- \nu$, 25:12076
KNOTH, Helmut, Investigations of some one-neutron-transfer reactions with ^{18}O and ^{19}F beams, 25:12381 (NP-18541)
KNOX, W. J., Energy measurements of 20 to 60 MeV neutron beam of Davis 76-inch isochronous cyclotron, 25:10861
KNUTH, K. R., Alpha-particle scattering by ^{36}Ar, 25:12455
KNYAZEV, V. A., Emergency personal n-γ radiation dosimeters, 25:10881
KNYSTAUTAS, E. J., Analysis of the N^+--Ar and O^+--Kr collisions, 25:11711
KNYSTAUTAS, Emile John, Coincidence study of nitrogen ion--argon atom collisions at kilovolt energies, 25:11704
KOBA, I. I., Research on 100-MeV electron storage ring of Technical Physics Institute of Ukrainian Academy of Sciences, 25:12307 (KHFTI-69-27)
KOBAYASHI, Akizo, Multiple production processes and rearrangement of sakatons, 25:12186
KOBAYASHI, S., Plastic-strain controlled failure criteria and design parameters. Technical progress report, 25:11373 (COO-2048-1)
KOCH, H., Muon capture probability in isotopes of bromine, 25:12502
KOCH, J., High-stability apparatuses to investigate the angular distribution of charged particles of energies 10^{13}--10^{15} eV in the Galaxy, 25:11742 (KFKI-70-21-HEP)
KOCH, R. D., Differential diagnosis of brain alterations caused by tumor and vascular processes with radioactive isotope blood flow measurements, 25:11149
KOCH, T. H., Photochemical exchange reaction of Michler's ketone, 25:10556
KOCHKIN, V. I., Investigation of ^{8}Li recoil nuclei in $^{9}Be(p,2p)^{8}Li$ reaction at proton energies of 180 and 660 MeV, 25:12378 (JINR-P1-4872)
KODAMA, Takashi, Radiation curing of mixture of diallylphthalate prepolymer and vinyl monomer. III, 25:10606 (JAERI-5026, pp 101-7)
KOELLING, D. D., Electronic band structure of the actinide metals, 25:11992
KOHLER, D., Cross sections for $^{7}Be(p,\gamma)^{8}B$, 25:12400
KOJIMA, Masaharu, Tumor-specific localizing agent for radioisotope image. IV, 25:10921
KOKAME, J., Numerical differential cross sections of reaction $^{58}Ni(p,t)^{56}Ni$ with 51.9 MeV protons, 25:12431 (INSJ-124)
KOKES, R. J., Intermediates in allene--acetylene isomerization over zinc oxide, 25:10558
KOKKONIEMI, J., Construction of a scintillation counter telescope for the registration of the meson component of cosmic rays, 25:10871
KOLAR, D., Magnetic susceptibility of boron nitride, 25:12010
KOLB, K., Radiation protection when handling capsuled radioisotopes in nondestructive testing, 25:11089
KOLESNIKOV, V. V., Preventive diet in internal irradiation with ^{137}Cs and ^{90}Sr, 25:10956
KOLLAR, J., Estimation of radioactivity of biological samples, 25:11044
KOLLIE, T. G., Electrical and thermal properties of NaCl structured metallic actinide compounds, 25:11494
KOLODZIEJ, Bruno J., Neutron activation analysis of manganese and sodium in bacterial cells, 25:10511
KOLOKOL'TSOV, N. A., Cascade rate functions for separating multicomponent isotopic mixtures, 25:10782
KOLOMEITSEVA, I. A., Activity of elements of the optical cortex in animals irradiated in embryogenesis, 25:11283
KOLOMENSKII, A. A., Collective effects in accelerators, 25:12298 (CERN-Trans-70-7)
KOLOT, Z. M., Influence of radial slots in iris disk of waveguide on dispersion properties and quality factor of system of axially-symmetric and nonaxially-symmetric waves, 25:12306 (KFK-tr-334)
KOLOTILOVA, V. G., Use of plastic scintillators in x-ray dosimetry, 25:11072
KOLOUSEK, J., Changes in the number of bone marrow cells, 25:11288
KOMAC, M., Magnetic susceptibility of boron nitride, 25:12010
KOMAKI, K., Temperature dependence of dechanneling coefficient in protons in silicon crystals, 25:11969
KOMENDER, A., Free radicals evoked by radiosterilization in preserved bone grafts, 25:11329
KOMIYA, Hisako, Chromosome abnormalities observed in children receiving roentgenoscope, 25:11113
KONLYAKOVA, N. S., Barkhausen effect in ferroelectrics during continuous x irradiation, 25:11978
KONOCHKOV, M. M., Dose characteristics of protons with energy 200 MeV, 25:11054 (JINR-P16-5383)
KONPPA, T., Reinvestigation of the decay of ^{200}Tl, 25:12528 (NP-18647)
KONDO, M., Resolving time measurements of Geiger counters, 25:10835
KONETSCHNY, W., Nucleon form factors in the Veneziano model, 25:12144
KONGSHAUG, M., Phenyl and hydroxyphenyl radicals. Pulse radiolysis study of their spectra and reactivity, 25:10631
KONNOV, B. A., Dosimetry in radium therapy, 25:11069
KONO, Akira, Tumor-specific localizing agent for radioisotope image. IV, 25:10921
KONO, Yoshimi, Radiation curing of mixture of diallylphthalate prepolymer and vinyl monomer. III, 25:10606 (JAERI-5026, pp 101-7)
KONONENKO, S. G., Research on 100-MeV electron storage ring of Technical Physics Institute of Ukrainian Academy of Sciences, 25:12307 (KHFTI-69-27)
KONOPEL'CHENKO, B. G., Discrete transformations in six-dimensional model of Minkowski space, 25:12252
KONSTANTINIDES, K., Determination of hepatic blood flow in hyperthyroidism with the ^{198}Au blood extraction method, 25:11141
KOOB, Derry D., Prog. rpt. on freshwater ecology of Amchitka Island, annual, 7/68, 25:12870 (BMI-171-103)
KOOPMANN, E. W., Beta--gamma circular polarization correlation in decay of ^{48}V, 25:12471
KOPALEISHVILI, T. I., Effect of rescattering and the absorption mechanism of stopped π^- mesons by Li nuclei, 25:12415
KOPYLOVA, D. K., Analysis of $\pi^- p \rightarrow n\pi^+\pi^- m\pi^0$ (m = 1,2,3) and $\pi^- p \rightarrow n2\pi^+2\pi^- m\pi^0$ (m = 1,2) reactions, 25:12204 (JINR-P1-5431)
KORFF, Serge A., Geiger counters: theory, operation, and manufacture, 25:10807 (AD-708922)
KORNIENKO, L. S., Search for quarks in ferromagnetics using an electrometer with the beams suspension method, 25:12064
KORODENKO, G. D., Thermo-oxidation degradation of poly(vinyl alcohol) irradiated by γ rays, 25:10591
KOROL, B. A., Effects of γ radiation on histones from rat nuclei, 25:10971
KOROLEVSKII, A. P., Effects of space flight on the central nervous system, 25:11298
KORTH, G. E., Surveillance of test reactor beryllium and hafnium, 25:11460 (IN-1437, pp 5-12)
KOSE, V., Maximal output power of point-contact Josephson junctions, 25:11838
Pull-in phenomena of Josephson oscillators, 25:11839
KOSHIBA, Masatoshi, Systematic investigation of ultra high energy interactions. II, 25:12093
KOSHIJIMA, Tokusaburo, Exposure from ^{147}Pm-activated self-luminous paints, 25:11065
KOSTAMIS, P., Determination of hepatic blood flow in hyperthyroidism with the ^{198}Au blood extraction method, 25:11141
KOSTRITSA, A. A., Effect of nuclear motion on neutron pulse, 25:12350
KOS'YANOV, A. N., Nonspecific allergic reactions in sheep in chronic radiation sickness, 25:10989
KOTA, J., High-stability apparatuses to investigate the angular distribution of charged particles of energies 10^{13}--10^{15} eV in the Galaxy, 25:11742 (KFKI-70-21-HEP)
KOTALIK, J., Recovery from radiation damage in mammalian cells, 25:11092 (BNL-50203, pp 41-53)
KOULOUNDJIAN, Jacques, Development of source of polarized deuterons for a synchrocyclotron, 25:12309 (LYCEN-6909)
KOVACS, J. S., Monte Carlo method for multi-particle production processes, 25:12134
KOVETZ, A., Thermodynamics of white dwarf matter, 25:11549
KOWALSKI, L., Protons and alpha particles emitted from ^{75}Br compound nuclei with differing angular-momentum distributions, 25:12461
KOYAMA, Karl, Laser-pulse method of determining thermal diffusivity and thermal conductivity of graphite between 300° and 3300°K, 25:11487 (GA-9168)
KOYAMA, Shin-Ichiro, Gross theory of β decay and application to Fermi matrix element, 25:12690
KOZLOV, B. F., Emergency personal n-γ radiation dosimeters, 25:10881
KOZLOV, F. A., Continuously-active indicator for the diffusion of hydrogen in sodium, 25:11400
KOZLOV, G. I., Method for infrared diagnostics of plasma, 25:11868 (SC-T-70-4054)
KOZLOVA, A. A., Effects of irradiated nutrient medium on chromosome aberrations in mammalian cells in vitro, 25:10970
KOZLOWSKI, T., Excitation of isomeric activities in ^{71}Ge, ^{79}Br, and ^{79}Br using 14.8-MeV neutrons, 25:12430 (INR-P-1091)
KRAFTMAKHER, Ya. A., Equilibrium vacancies in lanthanum, 25:11423
KRAINER, H., CODAC: program to process TIMOC library from ENDF/B file, 25:12339 (EUR-4521)
KRALIOS, A., Determination of hepatic blood flow in

hyperthyroidism with the ^{198}Au blood extraction method, 25:11141
KRAMSKOI, G. D., Influence of radial slots in iris disk of waveguide on dispersion properties and quality factor of system of axially-symmetric and nonaxially-symmetric waves, 25:12306 (KFK-tr-334)
KRANE, K. S., E2/M1 multipole mixing ratios in spherical nuclei ^{124}Te, ^{126}Te, and ^{126}Xe, 25:12515 (COO-1746-51)
KRAUSS, O., Functional studies with short-lived reactor isotopes, 25:10943
KREBS, W.-D., Analogy between radiative pion absorption and muon capture in ^{12}C, 25:12395
Charge exchange of 70 MeV π^- on C, Al, Cu, and Pb, 25:12446
Excitation of the isospin triplet ^{12}B, ^{12}C*(15.11 MeV), ^{12}N by pion charge exchange, 25:12397
KREJS, F. R., Application of the Hartree--Fock variational method to center-of-mass motion, 25:12653
KRESS, Kenneth Albert, Electronic structure of Mo and Ru, 25:11982
KREUTZ, E. W., Changes of surface conductivity in Ge during x-irradiation, 25:11963
KREUZER, H. J., Hartree--Fock approximation for binding energy of ^{6}He, 25:12373
KRIKORIAN, N. H., Anisotropic thermal expansion of refractory carbides by high-temperature neutron diffraction, 25:11509
KRISHNAMOORTHY, P. N., Personnel monitoring for radiation accidents, 25:10885
KRISHNAMURTHY, G. T., False-positive pulmonary photoscans obtained with a dual-probe detector system, 25:11207
KRISHNA SWAMY, K. S., Atmospheres of metal-deficient stars, 25:11546
Thermal emission from grains in H-II regions, 25:11583
KRISS, Joseph P., Radioisotopic angiocardiography: findings in mitral stenosis and mitral insufficiency, 25:11187
KROENERT, E., Quantitative evaluation of ^{131}I-hippuran renal clearance based on a model, 25:11160
Results of renograms evaluated by computer analysis based on a non-compartmental model, 25:11161
KRONGAUZ, A. N., Use of plastic scintillators in x-ray dosimetry, 25:11072
KRTIL, J., Determination of burn-up of nuclear fuel on basis of stable isotopes of Nd. I, 25:10461
Determination of burn-up of nuclear fuel on the basis of stable isotopes of Nd. II, 25:10469
KRUEGER, F. W., Layout of radiation shields against gamma-radiation from spent nuclear fuel, 25:11948
KRUEGER, Woodrow B., Neutron activation analysis of manganese and sodium in bacterial cells, 25:10511
KRUGER, O. L., Thermal creep of polycrystalline UO_2--PuO_2, 25:11496
KRUGLOV, V. T., Nonspecific allergic reactions in sheep in chronic radiation sickness, 25:10989
Strontium-90 upteke by agricultural plants and animals, 25:11050
KRUPNOV, A. F., Millimeter and submillimeter radiospectroscopy, 25:10897
KRUUV, J., Multi-component radiation survival curve model, 25:11293
KU, Teh-lung, Radium-226 measurements from the 1969 North Pacific Geosecs Station, 25:10726
KUAN, H. M., Gamma decay of first two T = $^3/_2$ states of ^{15}N, 25:12416
KUBA, J., Comparison of cerebral blood flow measurements with intravenously administered ^{131}I-labeled hippuran between arteriosclerotic and normal patients, 25:11150
KUBODERA, Kuniharu, Hartree--Fock model of ^{6}Li nucleus, 25:12410
KUCHAK, G. M., Electrical conductivity of liquid indium-bismuth alloys, 25:11398
KUCHAR, Karel, Ground state functional of the linearized gravitational field, 25:12276
KUCHAR, L., Distribution of iron and aluminum during zone melting of uranium, 25:11406
KUCK, V. J., Electron paramagnetic resonance of CD_2 and CHD. Isotope effects, motion, and geometry of methylene, 25:10555
KUDRYASHOV, V. V., Mean energy of electrons ejected from atoms at ionization by electron impact, 25:11727
KUDRYASHOV, Yu. I., Nonspecific allergic reactions in sheep in chronic radiation sickness, 25:10989
KUECHLE, M., Proposal for a standard spectrum to check techniques of fast neutron spectrum measurements, 25:12816 (EACRP-L-74)
KUEHBOECK, J., Late effects of radiophosphorus therapy of polycythemia vera, 25:11303
KUKACKA, R., Investigation of ionizing radiation exposure from cathetrization of the heart, 25:11059
KUKUSHKIN, A. V., Phase fluctuations of the signal of a travelling wave tube generator with superconducting resonator, 25:11853
KULCINSKI, G. L., Characterization and annealing behavior of voids in neutron-irradiated nickel, 25:11469
KULIKOWSKA, T., BIGG code in GIER-ALGOL 4 for the Gier computer, 25:12842 (INR-1193)
KULLANDER, S., Operation of cylindrical wire spark-chambers in low-pressure helium, 25:10872
KUMAR, Satinder, Calculation of charge and current pulses in planar and coaxial Ge-(Li) detectors, 25:10821
KUMER, J. B., Helium I 584-A dayglow radiation between 400 and 1000 km, 25:11789
KUNA, P., Heart rate, mean arterial pressure, and respiratory frequency after zirconium citrate administration in irradiated and non-irradiated rabbits, 25:11289
KUNG, H. W., Nuclear-structure calculations for ^{59}Cu, 25:12451
KUNI, H., Results and importance of quantitative blood flow measurements through parabiotic tissue connections, 25:10915
KUNICKI-GOLDFINGER, Wladyslaw, Mechanism of conjugation and recombination in bacteria. IX, 25:10946
KUNIMASA, Tasaku, Two-body weak-electromagnetic hyperon decays, 25:12169
KUNKEL, R., Simultaneous determination of total potassium and exchangeable sodium in man, 25:10920
Thyroid diagnosis with a whole-body counter in children, 25:11172
KUNKEL, William E., Existence of an upper limit in the activity of solar neighborhood flare stars, 25:11575
KUO, I., Gamma-radioinduced destruction of DNA, nucleosides, and nucleotides, 25:10962
KUPEC, V., Storing of pea seed after γ irradiation, 25:11024
KUPRIYANOV, I. N., Preventive diet in internal irradiation with ^{137}Cs and ^{90}Sr, 25:10956
KURDGELAIDZE, D. F., Quark stars, 25:12188
KURI, Zen-ichiro, Scavengeable electron yield in radiolysis of hydrocarbons, 25:10652
KURIHARA, Masayoshi, Some electrical properties of the uranium--plutonium mixed oxides, 25:11991
KURODA, P. K., Fission products in atmosphere. I, 25:10714 (ORO-2529-28, App. 8)
Fission products in atmosphere. II, 25:10715 (ORO-2529-28, App. 9)
Jet stream and radioactive fallout, 25:10708 (ORO-2529-28, App. 2)
Prog. rpt. on atmospheric radiochemistry, annual, 12/70, 25:10706 (ORO-2529-28)
Temporal distributions of radioactivity and ^{89}Sr/^{90}Sr ratios during rainstorms, 25:10707 (ORO-2529-28, App. 1)
Variation of radiocerium isotope ratio in rain, 25:10709 (ORO-2529-28, App. 3)
KURODA, Tsutomu, Feedback control of the PIG discharge of the QP machine, 25:11921 (IPPJ-T-2)
KURT, V. G., Flux of low-energy protons near the Moon on December 13, 1966, 25:11669
KURTZ, Robert G., Vapor--ion methods of film deposition, 25:12904 (RFP-1568)
KUSHNER, Sidney, Repair of UV-irradiated DNA, 25:10959 (BNL-50203, pp 27-40)
KUSWA, Glenn Wesley, Charged-particle distribution functio measurement in toroidal octupole, 25:11872
KUTZIN, H., Scintigraphic studies in pulmonary tuberculosis, 25:11132
KUUSI, Juhani, Use of radioisotopes for quality and process control analysis in industry, 25:10443
KUZIN, A. M., Effects of γ radiation on histones from rat nuclei, 25:10971
Mutagenesis of T4B phage in γ-irradiated E. coli, 25:11016
KUZMIN, G. G., Astronomy and geodesy in Estonian SSR (1940--1966), 25:11538
KUZ'MIN, V. A., CP noninvariance and baryon asymmetry of Universe, 25:12239
KUZNETSOV, E. A., Dosimetry in radium therapy, 25:11069
KUZNETSOV, E. K., Continuously-active indicator for the diffusion of hydrogen in sodium, 25:11400
KUZNETSOVA, M. A., Effects of space flight on the central nervous system, 25:11298
KWOK, M. A., Isotope separation with the cw hydrogen fluoride laser, 25:10690
KYUNO, Eishin, Thermal properties of deuterated Cu(II) sulfate pentahydrate, 25:10565

L

LABS, Dietrich, Transformation of the absolute solar radiation data into the international practical temperature scale of 1968, 25:11609
LACOMBE, P., Behavior of α U under light stresses during recrystallization process or during the allotropic α/β transformation, 25:11451
LAGRANGE, J. M., Coulomb excitation of ^{123}Te and ^{125}Te, 25:12603
LAHRTZ, Hg., Studies with ^{85}Sr of diseases belonging to the rheumatic complex, 25:11175
LAI, C. S., K/sub 13/ form factors, F/sub K//F/sub π/ and symmetry-breaking parameters of vacuum states, 25:12198
LAIRD, A. R., Electromagnetic drift of the midlatitude F2 layer during a storm, 25:11805
LAIRD, C. E., Beta decay and nuclear structure in the mass-14 system, 25:12421
LAKIN, W. L., Determination of inelastic neutron form factor by scattering of 12-GeV muons on H, C, and Cu, 25:12096
LALERE, J., In-pile loop BANJO, 25:12813 (CEA-CONF-1673)
LALLEMENT, Robert, Mechanical properties of plutonium-based

ceramics at high temperature, 25:11485 (CEA-CONF-1670)
LALOU, C., Use of low-level α spectrometry in the determination of elements occurring in traces in natural mineral substances, 25:10477
LAM, D. J., Crystal-field effect and magnetic properties of NaCl-type actinide compounds, 25:11994
LAMAZE, G. P., Angular correlation study of low-lying levels of ^{29}P, 25:12480
LAMBERIEUX, J., Dosimetry in nuclear accidents, 25:11079
LAMBERT, G., Use of low-level α spectrometry in the determination of elements occurring in traces in natural mineral substances, 25:10477
LAND, C. C., Constitution of plutonium-rich plutonium--osmium alloys, 25:11438
Plutonium--zirconium phase diagram, 25:11439
LANDAU, R. W., Temperature-anisotropy instability for em waves propagating across static magnetic field, 25:11916
LANDBERG, Torsten, Radiosensitivity of mediastinal lymphomas treated with split-course radiotherapy, 25:11226
LANDER, G. H., Interpretation of measurements of magnetic scattering from actinide ions, 25:12002
LANDER, J. J., Chemisorption of I on W(100), 25:11405
LANDIS, D. A., Identification of nuclear fragments, 25:10860
LANDMAN, H. A. A., Proton induced resonance reactions on ^{39}K, 25:12437
LANDOLT, Arlo U., Magnitude sequences for the variable stars UZ Bootis and W Piscium, 25:11579
LANDSHOFF, P. V., Scaling laws in high-energy neutrino reactions, 25:12166
LANDSPERSKY, Hanus, Changes in residual carbon content in UO_2 pellets during decarbonization and sintering, 25:11482
LANE, S., Ion-mobility spectrometer for radiochemical applications, 25:10903
LANGE, D., Sequential use of Anger camera in double-tracer studies, 25:10928
Technical advances of pancreatic scintigraphy with fast scanner (Dynapix), 25:11212
LANGE, Juergen, Estimation of unknown excitation functions for (α,xn)-(α,pxn)-, (d,xn)-, (d,pxn)-, and (p,xn)-reactions, 25:12529 (ORNL-tr-3020)
LANGEVIN-JOLIOT, H., Experimental studies of reactions $^3H(p,p)^3H$, $^3He(p,p)^3He$, and $^3H(p,n)^3He$ at 156 MeV, 25:12365
LANGHOFF, H., Lifetime measurements in ^{131}Xe and ^{129}Xe, 25:12583
LANGSFORD, A., Total neutron cross section of oriented ^{165}Ho, 25:12565
LANGSJOEN, P. H., Significance of red cell aggregation in the vascular complications of angiography, 25:11195
LANGUILLE, Alain, Chemical diffusion and heterodiffusion at infinite dilution of Pu in body centered cubic β Ti, 25:11429 (CEA-CONF-1687)
Effect of a β → α transformation and of oxygen on plutonium distribution in dilute Zr--Pu and Ti--Pu alloys, 25:11431 (CEA-CONF-1691)
LANSIART, A., Visualization by image intensifier of radioactive indicator flow through the cardiac chambers and the large vessels, 25:11120
LANTOS-JARRY, M. F., Coronal magnetic field patterns inferred from radio observations, 25:11605
LANZEROTTI, L. J., Proton drift echoes in the magnetosphere, 25:11801
LAPOINTE, M. H., Achieving uniform spatial response from large area liquid scintillation detectors, 25:10875
LAPSHIN, N. A., Interrelationship of interoceptive unconditioned reflexes after irradiation, 25:11282
LAROSE, James H., Radioiodinated toluidine blue: an unsatisfactory scanning agent, 25:11188
LAROZE, L., Separable potential calculations on the $^1/_2^+$ neutron--deuteron system, 25:12359
LAROZE, Luciano B., Calculations on neutron--deuteron scattering, 25:12227
LARRIMORE, J. A., Considerations on pulsed reactor optimization, 25:12827
LARSEN, O. A., Evaluation of arterial insufficiency of the legs, 25:11139
LARSON, H. V., Intercomparison of portable radiation monitoring instrument evaluations, 25:10809 (BNWL-SA-3565)
LARSON, Steven M., Long-term effects of local irradiation of the marrow on erythron and red cell function, 25:11112
LASKAR, Paul A., Synthesis and biological activity of deuteriobenzyl-d,-penicillin, 25:10560
LASSEN, N. A., Evaluation of arterial insufficiency of the legs, 25:11139
LASSEUR, Claude, Mechanical and electrical properties of aerosols: application to health physics, 25:11036 (CEA-Bib-185)
LAST, G. A., Evaluation of PuO_2 homogeneity in PuO_2--UO_2 fast reactor fuel by scanning electron microprobe, 25:11489 (WHAN-FR-20)
LATAILLADE, F., Chemical diffusion in epsilon phase of Pu--Cu system, 25:11387
LATZKO, D. G., Impact of nuclear engineering on developments in structural mechanics, 25:10758
LAU, K. K., Low-frequency vibrations of molecular solids. X, 25:10529
LAUDISE, R. A., Growth of single crystals of Ta_2C, 25:11484
LAUQUE, R., 21-cm neutral hydrogen line observations of compact galaxies, 25:11638
LAURENCE, J. C., Superconducting magnet research, 25:11851
LAURIE, Victor W., Microwave spectra of the first-excited torsional states and barrier to internal rotation of dimethylamine, 25:10551
LAUSTRIAT, G., Absolute radioluminescence efficiency of liquid benzene and alkylbenzene scintillators, 25:10822
LAUTRUP, B., Sixth-order corrections to the anomalous magnetic moment of the electron, 25:12145
LAVAL, M., Stationary gas detectors for mapping and dynamic studies of organs using x ray or low-energy γ-ray emitters, 25:10810 (CEA-CONF-1668)
LAVERNE, M. E., Performance characteristics of cylindrical heat pipes for nuclear electric space and undersea power plants, 25:10755 (ORNL-TM-2803)
LAVERRIERE, R., Angular distributions and correlations in three-body phase space, 25:12135
Relativistic calculations of angular correlations of particles issued from an interaction-free resonance decay, 25:12176
LAVRENT'EV, L. N., Radiation damages and repair of intestinal tissues, 25:11271
LAWLEY, N., Angular correlation measurements on excited states of ^{42}Ca, 25:12465
LAWRENCE, J. R., Whole-body counter for studies of total body K, 25:10910
LAWRENCE, R. J., Strain hardening and strain rate in one-dimensional wave propagation calculations, 25:12909 (SC-RR-70-471)
LAZARSKA, B., Polarization of protons from $^{12}C(d,p)^{13}C$ reaction at E/sub d/ = 12.4 MeV, 25:12377 (INP-711)
LAZARUS, D., Particle separation in a system of conventional iris-loaded deflectors interspersed with alternate gradient magnets, 25:12295 (BNL-15438)
LEARY, J. A., Differential thermal analysis observations of U--Pu dicarbides, 25:11522
Enthalpies of solution of C, Tm, Ti, Mn, Zr, and Re in liquid Pu, 25:11386
Melting behavior of (U,Pu) monocarbides, 25:11507
Thermal expansion and phase equilibria of the carbon-saturated plutonium carbides, 25:11513
Thermodynamic properties of Pu--C system, 25:11506
LEB, G., Differential scintigraphic representation of the pancreas by means of a computer, 25:11176
Lymph drainage following neck surgery, 25:11178
Studies on techniques for lung scintigraphy, 25:11129
LEBEAU, C., Transition-field enhancement and shape effects due to magnetic inclusions in a superconductor, 25:11840
LEBEDEV, A. N., Collective effects in accelerators, 25:12298 (CERN-Trans-70-7)
LEBEDEVA, N. S., Scattering of neutrons with an energy of 4 MeV at angles close to 180°, 25:12509 (ANL-Trans-855)
LE BOURDONNEC, Yvon, Tests on an automatic air purifying respirator, 25:10752 (CEA-N-1360)
LECLEACH, X., Spark chamber spectrometer for heavy cosmic ions, 25:10873
LEDBETTER, Hassell Marion Jr., Crystal structure and martensitic transformation in near-equiatomic AuCd, 25:11448
LEDERICH, R. J., Interpretation of ellipsometric observations of absorbed oxygen in niobium, 25:11355
LEDOUX-CORBUSIER, M., Effects of Kallikreine on the irradiated skin of swine (large white), 25:11110
LEE, J. A., Length changes in actinide metals due to self-irradiation damage at 4°K, 25:11468
Review of low temperature specific heats of the actinides, 25:11384
Self-irradiation damage induced resistivity changes in actinide metals at low temperatures, 25:11960
Thermal conductivity in the actinide elements, 25:11382
LEE, K., Electromagnetic delay line readout for proportional wire chambers, 25:10846
LEE, K. B., Transmission of ^{133}Xe through activated charcoal adsorber beds, 25:10582
LEE, K. N., Magnetic ordering in PrB_6, 25:11988
LEE, Kyu Yul, Reaction π⁻p → π⁺π⁻π⁻π⁰p at 6 GeV/c, 25:12101
LEE, P., Note on the central star of NGC 3132, 25:11570
LEE, P. W., Studies of the defect structure of nonstoichiometric cerium dioxide, 25:12033
LEE, Patrick A., Effect of noise on I--V characteristics of Josephson junctions, 25:11837
LEE, R. A., Investigation of heat transfer augmentation through use of internally finned and roughened tubes, 25:12891 (NP-18608)
LEE, Roswell, Relativistic beam propagation in magnetized plasma, 25:11886 (NYO-4077-1, Paper 4)
LEE, S. H., Prog. rpt. on air cleaning, semiannual, 3--8/70, 25:10797 (NYO-841-23)
LEE, Sabrina Lin, Decay schemes of ^{131}Ba and ^{192}Ir nucleus, 25:12532 (TID-25592)
LEE, T. Y., Binding energies of p-shell hypernuclei, 25:12393
LEE, Ta-jyh, Photochemistry of some α-ketopropiophenones. Evidence for an unusual cyclic transiton state for hydrogen abstraction, 25:10554

XUM

LEE, Yuan Tseh, Prog. rpt. on dynamics of chemical reactions, annual, 4--12/70, 25:12886 (COO-2092-1)
LEENDERS, L., Experimental and theoretical physics work on Pu enriched LWR's lattices, 25:12796 (EURAEC-2145)
LEFORT, M., Mechanism of single-nucleon and multi-nucleon transfer reactions in grazing collisions of heavy ions on silver, 25:12606
LEFVERT, T., Multiple scattering and collision probability method for neutron transport problems, 25:12347
LEGG, J. C., Spin dependence in inelastic scattering, 25:12454
LEGGETT, R. D., Fission gas bubble precipitation and growth in PuO_2--UO_2 under irradiation, 25:11536
LEGRAND, Jean, Decay scheme of ^{59}Fe and ^{192}Ir, 25:12464
LEHERISSEY, E. S., Excitation of 2s state of atomic H by electron impact, 25:11714
LEHNERT, B., Interaction between a fully ionized plasma and a neutral gas blanket, 25:11878
LEIGH, W. J., Fixed-t dispersion relations for pion photoproduction in the second resonance region, 25:12146
LEINE, L., Research and development work leading up to the ASEA-ATOM BWR, 25:12712
LEISTNER, G. H., Detection and removal of radioactive contaminants in reactor-irradiated NaCl, KCl/K_2CO_3, and NH_4Br, 25:11046
  Method for simultaneous activity measurements of ^{24}Na, ^{42}K, and ^{82}Br in liquid samples, 25:11066
LELAND, W. T., Deuteron scattering from polarized ^{3}He, 25:12358
  Reaction ^{3}He(d,p)^{4}He proton asymmetry, 25:12357
LEMAIRE, G., Yield of hydrogen peroxide in aerated acidified water exposed to tritium β rays, 25:10636
LEMAIRE, H., Free radicals produced by gamma irradiation in bicyclo[2,2,1]heptane, 25:10637
LEMANSKA, Miriam, Solution of one-dimensional, multi-zone, multi-group diffusion equation using Lie series method, 25:12855
LEON, A., Determination of splenic blood flow with ^{51}Cr labeled and heat treated erythrocytes, 25:11142
LEONOVA, L. L., Uranium, Th, and rare-earth elements in thermal waters of the Kamchatka Peninsula, 25:10697
LEPPAEMAEKI, H., Table of cross sections of some reactions induced by 14 to 15 MeV neutrons, 25:12353 (NP-18616)
LEPRETRE, A., Photoneutron cross sections of ^{208}Pb and ^{197}Au, 25:12610
LEQUAIS, J., Visualization by image intensifier of radioactive indicator flow through the cardiac chambers and the large vessels, 25:11120
LERNER, Gerald M., Off-shell effects in knockout reactions, 25:12670
LE ROULLEY, J. C., Use of low-level α spectrometry in the determination of elements occurring in traces in natural mineral substances, 25:10477
LERUSTE, Ph., General theorems on factorization, 25:12292
LESLIE, J. D., Electron tunneling investigation of quench-condensed superconductors, 25:11842
LESSER, P. M. S., Electromagnetic transitions in ^{51}V, 25:12492
LE THANH, Phung, Geometric correction factors relating to the recoil of protons in nuclear emulsions, 25:10867 (CEA-R-4081)
LETOURNEAU, B. W., Critical heat flux and pressure drop tests with parallel upflow of high pressure water in bundles of twenty 1/2-in. rods, 25:12787
LETTAU, H., Reaction ^{15}N(tau,α)^{14}N, 25:12424
LEUCA, I., Separation of Zr from Hf by fractional crystallization, 25:10676
LEUTHAEUSER, Klaus-Dieter, Particular solutions of the monoenergetic transport equation with anisotropic scattering, 25:12055
LEVASSEUR, A., Systems B_2O_3--MO--MS boracites M--S (M = Mg, Mn, Fe, Cd) and sodalites M--S (M = Co, Zn), 25:11526
LEVENTHAL, J. S., Tritium fallout in Pacific United States, 25:10720
LEVIN, A. A., Estimation of potential radionuclide ingestion by native populations of Eastern Panama and Northwestern Colombia. Bioenvironmental and Radiological-Safety Feasibility Studies, Atlantic-Pacific Interoceanic Canal, 25:10995 (BNI-171-45)
LEVIN, E. S., Relation among cross sections of production of 2+, 1+, 0+, and 1-, 0- nonets mesons in meson--baryon interactions in nonrelativistic model of quarks, 25:12203
LEVINGER, J. S., Separable potential calculations on the $^1/_2^+$ neutron--deuteron system, 25:12359
LEVITZ, Norman M., Annular packed-bed filter, 25:10761
LEWAK, G. J., Semi-Lagrangian formulation of Vlasov equation, 25:11897
LEWIS, C. W., X-ray emission induced alpha particles, 25:12488
LEWIS, J. E., Heavy holes and superconductivity in GeTe and SnTe, 25:11847
LEYKO, Wanda, Effect of x-ray upon stored blood, 25:10981
LEZHNEVA, O. M., Surface antigens in methylcholanthrene-induced tumors, 25:10993
LIBBY, H. L., Transformation device using post-detector signal pattern rotators for multiparameter eddy current tester, 25:12878 (BNWL-1469)
LIBBY, R. A., Spectrotitration of ethane-1-hydroxy-1,1-diphosphonic acid (EHDP) with thorium diaminocyclohexanetetra-acetate, 25:10462
LIBBY, W. F., Tritium fallout in Pacific United States, 25:10720
LIBOFF, Richard L., Application of the collective approach to the thermodynamics of an electron gas, 25:11896
LICHNEROWICZ, A., Shock waves in relativistic magnetohydrodynamics, 25:11763
LIEB, Klaus-Peter, Proton decay of analog resonances in ^{93}Nb, 25:12564
LIGEON, Emile, Application of ^{18}O(p,α)^{15}N reaction to study of self-diffusion of oxygen in uranium dioxide, 25:11486 (CEA-R-4095)
LIGGETT, S. L., Spectrotitration of ethane-1-hydroxy-1,1-diphosphonic acid (EHDP) with thorium diaminocyclohexanetetra-acetate, 25:10462
LIKHTAREV, I. A., Irradiation of population in USSR due to global Cs, 25:11073
LILJA, I. A., Limits of validity of Siegert's theorem in nuclear photoabsorption, 25:12649
  Notes on quantum mechanical sum rules, 25:12046 (NP-18619)
LIN, T. K., Alpha-particle model of ^{12}C, 25:12663
LIN, H. E., K/sub 13/ form factors, F/sub K//F/sub π/ and symmetry-breaking parameters of vacuum states, 25:12198
LIN, W. C., K/sub 13/ form factors, F/sub K//F/sub π/ and symmetry-breaking parameters of vacuum states, 25:12198
LIND, D. A., Rotational states of ^{156}Dy, ^{166}Er, ^{168}Yb, and ^{176}Hf, 25:12544
LINDBLAD, Bengt, Mechanism of enzymic formation of homogentisate from p-hydroxyphenylpyruvate, 25:10553
LINDBLAD, P. O., Mean rotational velocities of 56 galaxies, 25:11635
LINDELL, Bo, Swedish policy with regard to the limitation of radioactive discharges from nuclear power stations, 25:12757 (SSI-70-27)
LINDNER, Albrecht, Nuclear reactions with polarized particles of arbitrary spin, 25:12652
LINDOP, Patricia J., Effect of 14-MeV electrons on blood vessels of the mouse earlobe, 25:11254 (BNL-50203, pp 174-80)
LINDSKOUG, Bengt, Radiation damage to the surfactant system of the rabbit lung, 25:11267
LINDSTEDT, Goeran, Mechanism of enzymic formation of homogentisate from p-hydroxyphenylpyruvate, 25:10553
LINDSTEDT, Sven, Mechanism of enzymic formation of homogentisate from p-hydroxyphenylpyruvate, 25:10553
LINDSTROM, Richard Mark, Radionuclides in meteorites and in the lunar surface, 25:11539
LING, Samuel Chen-ying, Exc[illegible]ed states between 18 and 22 MeV in ^{10}B, 25:12389
LINGEMAN, E. W. A., Re-examination of ^{66}Ga decay, 25:12477
LINKE, R., Results and importance of quantitative blood flow measurements through parabiotic tissue connections, 25:10915
LIPCHINA, L. P., Changes in lethal effect of irradiation of cells cultivated outside of organism due to chemical compounds, 25:11106
LITOWSKA, Maria, Effect of gamma radiation on ion exchange resins. II, 25:10646
LITTLE, K., Some effects of sterilizing doses of radiation on biological tissues, 25:11331
LITTLE, W. W. Jr., DPB: dynamic programming code for optimizing short-term operation of a power utility, 25:12919 (WHAN-IR-47)
LITVER, B. Ya., Cesium-137 in lichen-reindeer man in the extreme north of the USSR, 1962--68, 25:11037 (NP-18361)
LIU, T. C., Effective neutron temperatures in reactor core measured by fission track detectors, 25:10836
LIU, Yosen, Handling of fission products in calculation of burnup with regard to new nuclear data applied to graphite reactors, 25:12776 (JUL-678-RG)
LIU, Yu-chien, Continuous moment sum rules, 25:12207
LIVOLSI, A. Z., Fast breeder reactor static physics methods development and analysis project. Volume 1. FAREX: one-dimensional fast reactor physics design and analysis code, 25:12772 (BAW-3867-9(Vol.1)(Rev.1))
LIVSHITS, N. N., Effects of space flight on the central nervous system, 25:11298
LLOYD, R. D., Zirconium-95 in Utah vegetation produced during the 1966 growing season, 25:10999
LOBANOV, Yu. V., Synthesis of element 105, 25:12620
LOEFGREN, Kaj-Erik, Neutron radiation produced by roentgen beam of a betatron, 25:12320
LOEHBERG, Reinhold, Superconductivity and metallurgical problems with Ti--Nb alloys, 25:11416
LOEHKEN, R., Beta spectrum of ^{206}Tl, 25:12615
  Investigation of β spectrum of ^{14}C with a proportional counter with inner anticoincidence screens, 25:12380 (KFK-1222)
LOEPFE, E., Rapid isotopic separation method for the selective determination of short lived radioisotopes, 25:10490 (LIB/Trans-334)
LOEPPERT, H. G., Determination of ^{32}P-labelled adenine nucleotides by chromatography with isotope dilution, 25:10470
LOH, Eddie Lai, Moessbauer-effect studies of Dy metal and $DyCo_2$, 25:12035
LOHEZ, P., Automatic mass spectrometer for the isotopic analysis of hydrogen in natural water samples,

25:10463
LOHSE, U., Thermoluminescent dosimetry with polycrystalline LiF, 25:10879
LONG, W. F., Monte Carlo method for multi-particle production processes, 25:12134
LONGAIR, M. S., Luminosity--volume test for quasi-stellar objects, 25:11664
LONGSON, B., Solubility of carbon in sodium, 25:10579
LOOK, D. C., Nuclear magnetic resonance investigation of the metal-to-semiconductor transition in crystalline CdO, 25:12038
LOPUSHINSKI, Ya., Physical symmetries in field theory framework, 25:12253
LORBER, Steven A., /sup 69m/Zn-chloride. A new scanning agent: a study of its dosimetry and biological fate, 25:11204
LORDELLO, Antonio Roberto, Spectrographic determination of hafnium in zirconium oxide, 25:10431 (IEA-208)
LOREE, T. R., Positron annihilation in Pu--Al delta phase alloys, 25:11998
LORENZ, A., IAEA programs in nuclear data, 25:12343
LORENZ, B., Diagnosis of brain tumors with ^{131}I-labeled albumen particles and with ^{75}Se, 25:11145
LORENZ, W. J., Computer evaluation of scintigraphic studies obtained with a scintillation camera, 25:11122
Functional studies with short-lived reactor isotopes, 25:10943
Quantitative radiocardiographic studies with a scintillation camera, 25:11119
Scintigraphy of renal function evaluated by digital and analog computers, 25:11165
Studies on liver function with computer-scintigraphy, 25:10919
LORENZEN, K., Polarization of protons from the reaction ^{2}H(d,p)^{3}H at deuteron energies between 1.35 to 2.00 MeV, 25:12361
LORENZI, R., Operation of cylindrical wire spark-chambers in low-pressure helium, 25:10872
LORIN, A., X-ray spectrometry using Si (Li) diodes, 25:10812 (CEA-N-1401)
LOSKUTOV, Yu. M., Photon radiation by electrons upon reflection from a magnetic field, 25:11679
LOTTIN, Andre, Measurement and analysis of capture to fission cross section ratio α for ^{239}Pu between 20 keV and 500 keV, 25:12511 (CEA-N-1368)
LOUISE, R., Turbulence in H II regions, 25:11582
LOURENS, J. A. J., Annealing of electrical properties of electron-irradiated diamond, 25:11966
LOVE, W. G., Exchange effects with a realistic interaction for inelastic scattering, 25:12676
LOVELACE, R. V., Precession of a strong E-layer, 25:11924 (NYO-4077-1, Paper 1)
LOWENSTEIN, Derek Irving, $K^0 \rightarrow \pi^+\pi^-$ time dependence, 25:12078
LOZHKIN, O. V., Investigation of ^{8}Li recoil nuclei in ^{9}Be(p,2p)^{8}Li reaction at proton energies of 180 and 660 MeV, 25:12378 (JINR-P1-4872)
LU, K. K., Optimization of time analyzer parameters in multi-cycle experiments with exponential decay, 25:10900
LUBACH, B., Central region of Delft 12 MeV isochronous cyclotron, 25:12330
LUBKIN, Elihu, Simple picture for Dirac's charge-pole quantization law, 25:12150
LUBKOWITZ, J. A., Geiger counters for detection of non-radioactive effluents from gas chromatograph, 25:10888
LUC, H., MHD equilibrium and stability of toroidal plasmas with a quasi-triangular cross section in Tokamak type magnetic configurations, 25:11911 (EUR-CEA-FC-569)
LUCAS, Christopher, Irregularities in proton density deduced from cyclotron damping of proton whistlers, 25:11787
LUCAS, J., Determination of 18 major elements and traces in rocks, 25:10450
LUCAS, J. J., Parity violation in the transition of ^{181}Ta at 482 keV, 25:12621
LUDFORD, G. S. S., Magnetodynamics of fluids without inertia, 25:11767
LUFT, A., Dislocation structure and work-hardening behaviour of Mo single crystals, 25:11422
LUKASHEVITCH, V. V., Lifetime of 2007-keV level for ^{46}Ti nucleus, 25:12508
LUKE, M. O., Hydrogen--deuterium exchange of medium ring cycloalkenes during deuterogenation with tris(triphenylphosphine)chlororhodium(I), 25:10539
LUKENS, H. R. Jr., Neutron activation for measuring bone calcium content, 25:10907 (N-70-31814)
LUKIC, Yovan, Titanium (n,p) cross-section measurements, 25:12504
LUK'YANOVA, L. D., Effects of space flight on the central nervous system, 25:11298
LUNDIN, C. D., Effect of iron on the hot cracking of uranium weld metal. Part I, 25:11427
LUNKE, C., Kinematically complete experiment on reaction n + d → n + n + p, 25:12367
LURIO, Allen, Isotope shift in the (2^1S_0--2^1P_1) line of atomic He, 25:11696
Lifetime of the 2^1P_1 and 3^1P_1 states of atomic He, 25:11695
LUTSENKO, V. N., Flux of low-energy protons near the Moon on December 13, 1966, 25:11669
LUZIO, J., Frozen irradiated peripheral nerve and calvarial homografts in clinical surgery, 25:11334
LYARSKII, P. P., MPC of ^{232}Th and natural Th in drinking water, 25:11051
LYNCH, David W., Optical properties of antiferromagnetic chromium and dilute Cr--Mn and Cr--Re alloys, 25:11987
LYNDS, R., Spectroscopic observations of Scorpius X-1, 25:11600
LYON, L. L., Thermal expansion of extruded graphite--ZrC carbide composites, 25:11512
LYON, W. S., Prog. rpt. on analytical chemistry, annual, 9/30/70, 25:10423 (ORNL-4636)
LYTH, D. H., Fixed-t dispersion relations for pion photoproduction in the second resonance region, 25:12146
LYUBIMOV, G. A., One-dimensional approximation for MHD channel flow, 25:11766
LYUBIMOV, V. B., Analysis of $\pi^-p \rightarrow n\pi^+\pi^-\pi^0$ (n = 1,2,3) and $\pi^-p \rightarrow n2\pi^+2\pi^-\pi^0$ (n = 1,2) reactions, 25:12204 (JINR-P1-5431)

M

MA, Chin-wah, Moment of inertia of the high spin rotational states of deformed nuclei, 25:12654
MAC CONNELL, Darrell J., New Ap stars in NGC 3114, 25:11578
MACDONALD, R. J., Ejection of atomic particles from ion-bombarded solids, 25:11676
MACEFIELD, B. E. F., Numerical evaluation of radiative corrections of order α to allowed nuclear β-decay, 25:12696
MACGREGOR, M. H., Extension of Kemmer-symmetric coupling to meson decays, 25:12199
Meson and kaon structure, 25:12200
MACH, R., Internal bremsstrahlung and mechanism of direct nuclear reactions, 25:12694
MACHABELI, I. Z., Effect of rescattering and the absorption mechanism of stopped π^- mesons by Li nuclei, 25:12415
MACHI, Sueo, Effect of swelling on radiation-induced grafting of styrene to polyethylene, 25:10613
MACHIDA, Takako, Computation of dose distribution and its evaluation by digital computer for the intracavitary irradiation of uterine cervix cancer, 25:11058
MACHLIS, Leonard, Annual review of plant physiology. XIX, 25:10976
MACIAS, A., Ab initio calculations of harmonic force constants. IV, 25:11686
MACIEL, R., Three-band source spectra from color film, 25:10893 (EGG-1183-484)
MACKENZIE, J. K., Neutron activation for measuring bone calcium content, 25:10907 (N-70-31814)
MACKLIN, R. L., Nonresonant neutron capture in ^{207}Pb, 25:12539
MACLENNAN, C. G., Proton drift echoes in the magnetosphere, 25:11801
MACPHERSON, M. R., Magnetic susceptibility of cerium metal under pressure, 25:12018
MACVICAR, M. L. A., Case for a second energy gap in superconducting niobium, 25:11830
MADER, David Lyle, Fine structure measurement in ionized helium, 25:11688
MADEY, Richard, Transmission of ^{133}Xe through activated charcoal adsorber beds, 25:10582
MADIGAN, Denise M., Deuterium isotope effect on competing hydrogen and carbomethoxy migration in benzotropilidene photochemistry, 25:10557
MADISON, D. H., Excitation of 2s state of atomic H by electron impact, 25:11714
MADJID, A. H., Spectral emissivity of Ta in the red and in green and change in emissivity resulting from change in surface structure induced by heat treatment, 25:11395
MADRAZO, A., Radiation nephritis. II. Chronic changes after high doses of radiation, 25:11286
MADSEN, David William, Study of some even isotopes of neodymium by electron scattering, 25:12622
MADUEV, V. L., Flux of low-energy protons near the Moon on December 13, 1966, 25:11669
MAEDA, Masunobu, Hydrolysis of Cu(II) ion in heavy water, 25:10566
MAEDA, Tatsuo, Tumor-specific localizing agent for radioisotope image. IV, 25:10921
MAGER, T. R., Evaluation by linear elastic fracture mechanics of radiation damage to pressure vessel steels, 25:11470
Heavy section steel technology program. Technical report No. 10. Fracture toughness characterization study of A533, grade B, class 1 steel, 25:11380 (WCAP-7578)
MAGI, Attilio, Some measurements on radioactivity in Sweden caused by nuclear test explosions, 25:11004
MAGLIONE, Anthony A., /sup 69m/Zn-chloride. A new scanning agent: a study of its dosimetry and biological fate, 25:11204
MAGNON, Anne, Solution of problems with the Dicke theory, 25:12273
MAGYARI, E., Approach to quantum-mechanical four-body bound-state problem. I, 25:12050
MAHAFFEY, William Raymond, Study of radiation produced by high-energy electrons in a disk-loaded waveguide, 25:12317

MAHLER, Inga, Repair of UV-irradiated DNA, 25:10959 (BNL-50203, pp 27-40)
MAIELLA, G., Crossing-symmetric expansion of πν scattering amplitude, 25:12197
MAIER-BORST, W., Angiocardiography with a scintillation camera, 25:11121
Animal experiments on the suitability of ^{68}Ga compounds for diagnosis in nuclear medicine, 25:11169
Experimental bone scintigraphy in animals, 25:11216
Functional studies with short-lived reactor isotopes, 25:10943
MAIN, I. G., Rotational structure in ^{29}Si, 25:12449
MAINKA, E., Emission spectroscopic determination of traces in nuclear fuel materials, 25:10432 (KFK-1261)
MAIRLE, G., Proton pick-up from ^{19}F, ^{20}Ne, and ^{22}Ne, 25:12385
MAISON, D., Properties of conserved local currents and symmetry transformations, 25:12264
MAISON, J. M., Giant resonance by photon scattering in medium spherical nuclei, 25:12463
MAITA, J. P., Magnetic ordering in PrB_6, 25:11988
MAJEROTTO, W., Nucleon form factors in the Veneziano model, 25:12144
MAJKRZAK, Charles P., Submerged energy converter, 25:10788
MAK, H. B., Beta decay of ^{20}O, 25:12453
MAKARENKO, I. N., Thermal properties of tantalum at high temperatures, 25:11425
MAKEEVA, L. G., MPC of ^{232}Th and natural Th in drinking water, 25:11051
MAKHMAVETSKII, A. S., Comparative heat exchange characteristics of glasses with a radio-protective coating and without one, 25:10770
MAKI, Kazumi, Bound states in a superconductor containing a magnetic impurity, 25:11841
MALAMOS, B., Determination of hepatic blood flow in hyperthyroidism with the ^{198}Au blood extraction method, 25:11141
MALAN, J. G., Investigation of levels in ^{51}Cr, ^{55}Fe, and ^{59}Ni, 25:12476
MALEVICH, M. A., Dosimetry in radium therapy, 25:11069
MALIK, F. B., Application of unified model with Coriolis coupling to ^{22}Ne, ^{29}Al, and ^{30}P, 25:12482
MALINA, Mylan M., Mutagenic effects of near uv and visible radiant energy on E. coli, 25:11032
MALINOVSKII, O. V., Recovery of yeast cells after irradiation, 25:11316
MALKIN, P. M., Protective effects of calcium alginate against chronic ^{90}Sr ingestion, 25:11103
MALOCH, J., Plasma acceleration by means of external magnetic field, 25:11882
MALOVICHKO, I. I., Treatment of acute radiation sickness with bone marrow transplants, 25:11100
MANCHESTER, R. N., Observations of the Crab pulsar at 41(and 1664 MHz, 25:11598
MANDELKERN, L., Fusion of irradiated linear polyethylene crystallized by high speed stirring, 25:10618
MANDELSTAM, Stanley, Feynman-like diagrams in dual-resonance models, 25:12189
MANES, Livio, Infrared properties and specific heat of PuO_2, 25:11996
MANGOLD, E., Level density parameters for Ge, Ho, and Ta, 25:12536
MANN, F., Anisotropy ^{2}H(d,p)^{3}H at low energies, 25:12368
MANNING, P. G., Origin of the iron bands in supernovae spectra, 25:11562
MANNING, Robert Jerome, Resonance production in reaction ν^4d → ppνν from 1.1 to 2.3 GeV/c. I: II, 25:12107
MANOUKIAN, E. B., Equivalence between two field-theoretical models involving pure fermion fields, 25:12241
MANSON, Steven Trent, Theoretical considerations for auto-ionizing states with microsecond lifetimes, 25:11692
MANTLIK, F., Thermokinetics of the fuel element cassette of the fast reactor, 25:12801
MAPLE, M. B., Dependence of s--f exchange on atomic number in rare earth dialuminides, 25:11836
Kondo effect in La/sub 1-x/Ce/sub x/ alloys under pressure, 25:11990
Magnetic susceptibility of cerium metal under pressure, 25:12018
MARACCI, G., Measure of the factor of fast fission epsilon in a D_2O uranium lattice, 25:12817 (EUR-4326)
MARCIAL, Victor A., Relations between dose-time, fractionation, and rest period in radiation therapy, 25:11222 (BNL-50203, pp 280-5)
MARCINKOWSKI, Jan, Use of isotopes in casting practice, 25:10780
MARCINKOWSKI, M. J., Interfaces associated with ordered alloys, 25:12903 (ORO-3935-4)
MARCUS, J. A., Low-temperature phase transitions in alpha uranium, 25:11449
MARCUS, Luc, Germanium detectors and their use for charged particles, experimental study of (d,d'), (d,p), and (d,t) reactions on ^{12}C, 25:10851 (NP-18570)
MARDON, P. G., Compatibility studies between arc cast ($U_{0.85}Pu_{0.15}$)--C and type 316L stainless steel, 25:11475 (AERE-R-5173)
Uranium--plutonium--carbon phase diagram. II, 25:11524
MAREI, A. N., Measurement of ^{90}Sr content in organism of adult persons, 25:10935 (NP-18388)
MARGEN, P., Reactor pressure vessels made of concrete, 25:12788
MARIC, Z., Investigation of ^{8}Li recoil nuclei in ^{9}Be(p,2p)^{8}Li reaction at proton energies of 180 and 660 MeV, 25:12378 (JINR-P1-4872)
MARINO, D., Designing method of switching circuits cascade for analog parameter discrimination, 25:10901
MARINOV, A., Scattering of protons from ^{128}Te and ^{130}Te, 25:12602
MARINOV, V., Determination of low-level ^{90}Sr and ^{137}Cs activation in milk, 25:10480
Possibilities of detecting low-level β-activities by scintillation detectors, 25:10819
MARION, J. B., Nuclear reaction calibration energies by velocity measurements, 25:12402
MARKOWITZ, Eleanor Himoe, Gamma ray-induced mutations in Drosophila melanogaster oocytes: the phenomenon of dose rate, 25:11022
MARLE, C., Grad method extension to solving the relativistic Boltzmann equation, 25:11901
MARMIER, Pierre, Physics of nuclei and particles. II, 25:12662
MAROUN, David, Triton wave function in Feshbach--Rubinow approximation, 25:12364
MARPLES, J. A. C., Creep of UO_2 and $(U,Pu)O_{2-x}$, 25:11497
Length changes in actinide metals due to self-irradiation damage at 4°K, 25:11468
MARRERO, T. R., Diffusion of atoms and molecules, 25:11731
MARSH, Jeffrey Brian, Anomalous transmission and reflection of cyclotron waves, 25:11931
MARSHAK, H., Total neutron cross section of oriented ^{165}Ho, 25:12565
MARSHALEK, Eugene R., Nuclear rotation and boson expansions. I, 25:12671
MARSHALL, J. E., Analysis of heterogeneity and sodium-void effects in a 2700-liter uranium carbide fast core, ZPR-6 Assembly 5, 25:12825
MARTIN, A., Sodium chloride as spectral buffer in emission spectrography, 25:10454
MARTIN, D. J., Review of low temperature specific heats of the actinides, 25:11384
MARTIN, K. J., Production of lithium oxide by electron irradiation of lithium fluoride, 25:11964
MARTIN, W. E., Estimation of potential radionuclide ingestion by native populations of Eastern Panama and Northwestern Colombia. Bioenvironmental and Radiological-Safety Feasibility Studies, Atlantic-Pacific Interoceanic Canal, 25:10995 (BMI-171-45)
MARTIN, W. M., FORTRAN code for analysis of counting data from animal tissues, 25:10937 (UCRL-50957)
MARTINEZ, J. M., Spectral emissivity of Ta in the red and in green and change in emissivity resulting from change in surface structure induced by heat treatment, 25:11395
MARTINSEN, P. O., Electron-nucleus quadrupole interaction and its influence on β-decay, 25:12685
MARTRES, M., Origin of interplanetary sectors from radio observations, 25:11606
MARX, R., EPR spectra of some bicyclic radicals, 25:10638
MASCHKE, E. K., Straight stellarators with strong helical currents, 25:11918 (EUR-CEA-FC-543)
MASINO, A. P., Anion-exchange separation of neptunium from uranium and thorium in basic solution, 25:10655 (ANL-7751)
MASON, A. L., Two-particle unitarity in iterated Regge-cut model, 25:12289
MASON, D. S., Strain hardening and strain rate in one-dimensional wave propagation calculations, 25:12909 (SC-RR-70-471)
MASON, E. A., Diffusion of atoms and molecules, 25:11731
MASON, G. W., Extraction of U(VI) and selected M(III) cations by bis neo-octyl phosphoric acid in two different hydrocarbon diluents, 25:10679
MASON, Rita, Maternal x irradiation and the frequency of mongolism, 25:11300
MASON, W. J., X-ray and nuclear radiation facilities, personnel safety features, 25:11078 (Y-1754)
MASON, W. M., Angular distribution measurements in inverse photonuclear reactions, 25:10865
MASTEL, B., Characterization and annealing behavior of voids in neutron-irradiated nickel, 25:11469
MASUDA, Kohzoh, Penetration of electrons into anthracene crystals, 25:11673
MASUDA, M., Semiautomatic scanning system for nuclear emulsions, 25:10839
MASUMOTO, Hakaru, Effects of Ta additions on the properties of Nimalloy, 25:12008
MATCHERET, Georges, Study of neptunium hexafluoride formation and its adsorption on metallic fluorides, 25:10568 (CEA-R-4051)
MATIN, Philip, Radioisotopic angiocardiography: findings in mitral stenosis and mitral insufficiency, 25:11187
MATSCHAT, Elke, Sliding friction and wear of pure metals under vacuum of 5 x 10^{-8} torr, 25:11413
MATSUDA, Koji, Optical radiation from gases excited by high-energy electrons. II, 25:10585 (JAERI-5026, pp 153-5)
Optical radiation from gases excited by high-energy electrons. III, 25:10586 (JAERI-5026, pp 155-7)
MATSUDA, Shunji, Deposition and translocation of the radioactive fallout, 25:10718
MATSUMOTO, Saburo, Fluorescent x-ray analysis of tin and zirconium in aluminum alloys, 25:10441
MATSUOKA, Takeo, Multiple production processes and

rearrangement of sakatons, 25:12186
MATSUURA, Kiyokata, Feedback control of the PIG discharge of the QP machine, 25:11921 (IPPJ-T-2)
MATTER, Ulrich, Transfer of a neutron between ^{9}Be, ^{13}C, and ^{17}O, 25:12382 (NP-18546)
MATTHIES, S., Supplements to the theory of swelling, 25:12847
MATVEENKO, I. I., Conduction band of IVa and Va subgroup transition metal monocarbides. I, 25:12024
MATYUKHIN, V. V., Continuously-active indicator for the diffusion of hydrogen in sodium, 25:11400
MATZKU, S., Experimental bone scintigraphy in animals, 25:11216
MAURETTE, M., Habit and texture of lunar and meteoritic materials, 25:11671
MAVRYCHEV, Yu. S., Phase of the charge in electrodynamics, 25:12240
MAXEY, Willard A., Prog. rpt. on investigation of initiation and extent of ductile pipe rupture, Phase II, 7--9/70, 25:11369 (BMI-1892)
MAXFIELD, B. W., Direct electromagnetic generation of ultrasound in conducting liquids, 25:12892 (NYO-2150-65)
MAY, J., Safety of heavy water system in Braunschweig research reactor, 25:12822 (NP-18499)
MAY, Joan T., Metallurgical application of solvent extraction. II, 25:10656 (BM-IC-8502)
MAYALL, N. U., Mean rotational velocities of 56 galaxies, 25:11635
MAYANSKII, D. N., Isoenzymatic spectrum of lactic dehydrogenase in xenogenic radiation chimeras, 25:10992
MAYER, S. W., Isotope separation with the cw hydrogen fluoride laser, 25:10690
MAYER-BOERICKE, C., j-dependence in l = 2 (^{3}He,d) reactions on ^{24}Mg, ^{28}Si, and ^{30}Si, 25:12479
Reaction $^{90}Zr(^{3}He,d)^{91}Nb$ at 18 MeV, 25:12613
MAYHUGH, Michael Ray, Color centers and thermoluminescence in LiF, 25:11958
MAYS, Charles W., Risk to bone and liver from ^{239}Pu, 25:11301
MAZARSKII, V. L., Precision apparatus with liquid hydrogen target, 25:12300 (JINR-P8-5212)
MAZESS, R. B., Determining body compositions by radiation absorption spectrometry, 25:11114
MAZIERE, B., Neutron activation determination of selenium in biological media, 25:10495
MAZUR, Claude, Relative thermal neutron flux distribution in core of RV-1 reactor, 25:12826
MAZZA, A. L., A-particle binding in nuclear matter, 25:12668
MCCARTHY, J. S., Elastic electron scattering from ^{13}C, 25:12376 (AD-710383)
MCCRACKEN, K. G., Solar cosmic-ray phenomena, 25:11625
MCCREDIE, J. A., Multi-component radiation survival curve model, 25:11293
MCCUSKER, C. B. A., High transverse momenta observed in air shower cores, 25:11750
MCDERMOTT, M. J., Crystal structure of anhydrous UO_2F_2, 25:10577
MCDIARMID, I. B., Structure observed in solar-particle latitude profiles, 25:11797
MCDOUGAL, J. R., Electron beam welding study on U--Nb--Zr alloy, 25:11377 (MLM-1778)
MCGEE, Thomas D., Prog. rpt. on center of excellence in ceramic and composite materials, 9/68--8/69, 25:11472 (AD-708705)
Prog. rpt. on properties of ceramic materials, 3--5/70, 25:11473 (AD-708712)
MCGINNIS, John T., Quantification of fungus: small arthropod food chains in the soil, 25:10929
MCGOWAN, F. K., Quadrupole moment of first 2+ states of Sn, 25:12587
Reaction list for charged-particle-induced nuclear reactions Z = 1 to Z = 98 (H to Cf), May 1969--June 1970, 25:12366
MCGUIRE, Eugene J., Inelastic scattering of electrons and protons by elements He to Na, 25:11715
MCHARRIS, Wm. C., Neutron-deficient Gd isotopes. II, 25:12582
MCINTYRE, L. C. Jr., Mean lives and angular correlations in ^{35}S, 25:12489
MCLAFFERTY, George H., Gas-core nuclear rocket engine technology status, 25:12834
MCLAREN, J. R., Radiation dose rates from plutonium oxide--beryllium oxide mixtures, 25:11052 (AERE-R-5069)
MCLATCHIE, William, Reactions $^{152}Sm(p,t)^{150}Sm$ and $^{154}Sm(p,t)^{152}Sm$, 25:12612
MCMILLAN, Malcolm, Triton wave function in Feshbach--Rubinow approximation, 25:12364
MCNALLY, J. R. Jr., Use of optical spectra to measure large electric fields in a hot-ion plasma, 25:11874
MCSHERRY, D. H., Deuteron elastic scattering and the (d,p) reaction with polarized ^{3}He target, 25:12370
MCTIGHE, E. P., Development of the UK nuclear power industry, 25:12713
MEABURN, J., Observations of high velocities in H II regions, 25:11587
MEADEN, G. T., Occurrence of different α-phases of U at low temperatures by thermopower and resistivity experiments, 25:12006
MEANLEY, E. S., Backward pion production from π⁻p interactions, 25:12111
MEAUX, R., Substances that react with thiobarbituric acid in irradiated flour, 25:10978
MECCA, Stephen J., Energy and angular distributions of photoneutrons from ^{6}Li and ^{7}Li, 25:12387
MECHLER, P., Application of nuclear explosions to geophysics, 25:10748
MEEKINS, John F., Excess background radiation of soft x rays at the galactic pole and plane, 25:11653
MEHL, J., Nuclear accident dosimetry research and experience, 25:10818
MEHTA, M., Spin isomers of the shape isomer /sup 237m/Pu, 25:12530 (RLO-1388-130)
MEIER, M. M., DWBA analysis of the cross section and polarization data for the $^{14}N(d,n)^{15}O$ reaction at 3.5 MeV, 25:12405
MEIER, R. R., Conjugate excitation of O I 1304-A airglow, 25:11799
MEIRA, Luiz Gylvan Jr., Measurements of upper atmospheric NO, 25:11795
MEISEL, A., System V_2O_5--K_2SO_4, 25:11527
MEISEL, M. N., Thermogenesis of irradiated yeast cells in the process of recovering their reproductive capacity, 25:11324
MEIZEROV, E. S., Effects of space flight on the central nervous system, 25:11298
MELDOLESI, U., First attempts of clinical application of a method for the quantitative interpretation of renogram with radiohippuran, 25:11208
MELEDIN, G. V., Production of muon pairs in interactions of hadrons of high energy, 25:12229
MELLI, G., Scintigraphy of liver, spleen, and pancreas, 25:11200
MELSKI, J., Cobalt-60 teletherapy dosimetry, 25:11061
MELVILLE, P. H., Examination of fluxon behaviour by analogy with a floating magnetic model, 25:11833
MELZNER, F., Electron density measurements in the ionosphere with an improved rf impedance probe, 25:11781
MEN, A. V., Connection between absolute radioluminosity of extragalactic sources and redshift, 25:11581 (CSIRO-Trans-10247)
MENDEL, C. W. Jr., Nonlinear damping of Tonks--Dattner resonances, 25:11942
MENDELSOHN, Mortimer L., Biology of dose-limiting tissues, 25:11253 (BNL-50203, pp 154-73)
MENDELSSOHN, K., Review of low temperature specific heats of the actinides, 25:11384
Self-irradiation damage induced resistivity changes in actinide metals at low temperatures, 25:11960
MENDES, Rui V., Representations of local I-spin charge densities. I, 25:12181
MENDES, Rui Vilela de L., Representations of local currents and related algebras, 25:12127
MENDILLO, Michael, Model relating the radial changes of the plasmapause at dusk to geomagnetic activity, 25:11776 (AD-708495)
MENERET, Jean, Exothermal reaction triggering device, 25:10760
MENON, S., Reactor pressure vessels made of concrete, 25:12788
MERINGDAL, J., Accumulation and excretion of ^{224}Ra (Th X) during treatment of ankylosing spondylitis, 25:11231
MERKEL, G., Al(α,α')Al* compound-nucleus reactions, 25:12422
MERKUR'EV, S. P., Relation between the third virial coefficient and the scattering matrix, 25:12287
MERRILL, Robert P., Scattering of rare gases (He, Ne, Ar, Kr, and Xe) from Pt (111) surfaces, 25:11683
MERTENS, B., j-dependence in l = 2 (^{3}He,d) reactions on ^{24}Mg, ^{28}Si, and ^{30}Si, 25:12479
MERZ, M. D., Deformation of plutonium allotropes, 25:11389
METHASIRI, T., High-energy photofission cross sections of uranium and thorium, 25:12573
METTEL, Denyse, Production of strange particles in π⁺d interactions at 5.1 GeV/c, 25:12100 (NP-18629)
METZGER, F. R., Lifetimes of ^{193}Ir levels, 25:12590
Radiative widths of levels in ^{58}Ni and ^{60}Ni, 25:12478
MEYERER, W. P., Plastic-strain controlled failure criteria and design parameters. Technical progress report, 25:11373 (COO-2048-1)
MICHAELIS, E. G., Target efficiency and multiple traversals in the CERN 600 MeV synchro-cyclotron, 25:12324
MICHAELIS, W., Thermal neutron capture in ^{151}Eu, 25:12547
MICHALIK, J., Quantitative evaluation of irradiated bone grafts resorption rate by the electron spin resonance technique, 25:11340
MICHEL, F. C., Pulsar ejection in supernova events, 25:11588
MICHEL, K., Accumulation and excretion of ^{224}Ra (Th X) during treatment of ankylosing spondylitis, 25:11231
MICHELSEN, Odd B., Separation of Y, Ho, and Er with di-(2-ethylhexyl) phosphoric acid in chloride and nitrate systems, 25:10685
MICLUTIA, M., Dosimetric control in brachycurietherapy, 25:11000
MIDDLETON, R., Level structure of ^{17}O and the $^{13}C(^{6}Li,d)$ and $^{13}C(^{7}Li,t)$ reactions, 25:12425
MIKHAILOV, A. I., Acceleration and extraction of deuterons from the JINR proton synchrotron, 25:12303 (JINR-P9-5442)

MIKHAILOV, I. N., Coupling of collective modes in deformed nuclei, 25:12702
MIKHAILOV, V. G., Influence of radionuclides on enzymes of rat blood and tissues, 25:10968
MIKHAILOVA, A. A., Delay of mitosis in culture of mammalian cells under α and γ rays, 25:11272
MILES, W., Realistic QTDA calculations in odd-mass N = 82 isotones, 25:12616
MILHAUD, G., Metabolism of galactose ^{14}C in blood cells, 25:10485
MILLER, Carl F., Interaction of fallout with fires, 25:10702 (AD-708558)
Properties of radioactive fallout: surface detonation Coulomb C, 25:10734 (AD-708567)
Properties of radioactive fallout: balloon-mounted Shot Priscilla, 25:10733 (AD-708566)
MILLER, J. M., Protons and alpha particles emitted from ^{78}Br compound nuclei with differing angular-momentum distributions, 25:12461
MILLER, M. W., Radiosensitivity of diploid and tetraploid plant species, 25:11020
MILLER, Michael David, Model dependence of the binding energy of nuclear matter, 25:12642
MILLER, Wilmer G., Effect of conformation on isotopic exchange in synthetic polypeptides, 25:10567
MILNER, W. T., Quadrupole moment of first 2+ states of Sn, 25:12587
Reaction list for charged-particle-induced nuclear reactions Z = 1 to Z = 98 (H to Cf), May 1969--June 1970, 25:12366
MIMA, Genjiro, Reheating process of Fe--Cr and Fe--Cr--V alloys, 25:11403
MINER, William N., Conference on plutonium and other actinides, Santa Fe, N. Mex., 10/70, 25:11372 (CONF-701001-(Pt.1))
Conference on plutonium and other actinides, Santa Fe, N. Mex., 10/70, 25:11433 (CONF-701001-(Pt.2))
MINIER, C., Cobalt electron irradiated at 20°K, 25:11949 (AI-Trans-267)
Energy release and electrical resistivity recovery in Ni following electron irradiation, 25:11977
MINKIEWICZ, V. J., Pyrolytic graphite as a high efficiency filter for 13 to 15 MeV neutrons, 25:12352
MINKOWSKI, P., Regge parametrization for low-energy πN scattering, 25:12211
MINOR, M. M., Direct interaction effects in the fission of ^{238}U with 63.5-MeV ^{4}He ions, 25:12526 (MNC-3783-7)
MIQUEL, J., Effects of α particles on longevity of Drosophila melanogaster, 25:11248
MIRIC, I., Accident dosimetry in Yugoslavia, 25:11083
MIRIC, P., Accident dosimetry in Yugoslavia, 25:11083
MIRNA, A., Routine method for determination of low ^{137}Cs activities in biological samples, 25:10482
MIRO, L., Biological effects of the heavy ions in cosmic radiation, 25:11280
MIRONOV, V. I., Experiments on α-particle acceleration by collective method, 25:12305 (JINR-P9-5558)
MISS, H. D., Successes and failures of fractionated radioiodine therapy among 700 hyperthyroid patients, 25:11230
MITCHELL, A., Al(α,α')Al* compound-nucleus reactions, 25:12422
MITYUSHOVA, N. M., Recovery of yeast cells after irradiation, 25:11316
MITZNEGG, Peter, Inhibition of estrogen-induced radioprotection of placental nucleic acids and proteins by antiestrogen Clomiphene, 25:11104
MIURA, Kyoko, Protective effect of ethanol and KI on radiolysis of indole-3-acetic acid, 25:10647
MIYAKE, Shogo, Phenomenological analysis of the infinite resonance model for the nucleon electromagnetic form factor, 25:12153
MIZUGAKI, Hiroshi, Studies on nutritional management in operation. I, 25:11268
MIZUHO, M., Angle information with a gridded ionization chamber and its applications, 25:10837
MIZUNO, Katsuhiro, Parametric excitation of Bernstein waves in plasmas, 25:11934
MIZZAN, E., Multi-cycle irradiation of hollow UO_2 pellets in collapsible Zircaloy-2 sheathing, 25:11530 (AECL-3732)
MKRTCHYAN, M. M., Radiation of a particle in a strong magnetic field at low energy levels, 25:12059
MOAL, J. Y., Quantometer for determination of trace elements in natural materials, 25:10451
MOAZED, Cyrus, Test of the shell model for ^{204}Pb, 25:12574
MOCHESHNIKOV, N. I., Research on 100-MeV electron storage ring of Technical Physics Institute of Ukrainian Academy of Sciences, 25:12307 (KHFTI-69-27)
MOELLER, D. W., Prog. rpt. on air cleaning, semiannual, 3--8/70, 25:10797 (NYO-841-23)
MOGRO-CAMPERO, Antonio, Abundances of C, N, and O nuclei trapped in geomagnetic field, 25:11744
MOISEENKO, V. A., Fast valve of high pressure for bubble chamber, 25:10870 (JINR-P13-5420)
MOISEEV, A. A., Cesium-137 in lichen-reindeer man in the extreme north of the USSR, 1962--68, 25:11037 (NP-18381)
Irradiation of population in USSR due to global Cs, 25:11073
MOKANU, O. V., Accumulation of ^{239}Pu and ^{210}Po by Ascophyllum nodosum and marine phytoplankton, 25:10941
MOLDAUER, P. A., R-matrix shell-model calculations, 25:12423
MOLL, H., Absorption of ^{45}Ca from intestinal tract of rat, 25:10512
MOMENT, Roger L., Annealing and deformation twinning in delta-stabilized plutonium--gallium alloys, 25:11436
MONNAND, E., Isomers of ^{130}I and ^{130}Xe, 25:12572
MONNET, G., Turbulence in H II regions, 25:11582
MONNIER, D., Rapid isotopic separation method for the selective determination of short lived radioisotopes, 25:10490 (LIB/Trans-334)
MONNIN, Michel, Solid track detectors and their applications to biology, 25:10823
MONTANO, P. A., Computerized Moessbauer spectrometer, 25:10866
MONTES, C., Relaxation of a temperature anisotropy in a collisionless plasma, 25:11893
MONTGOMERY, C. G., Dynamic studies of the optical absorption associated with trapped electrons, 25:11967
MONTGOMERY, H., Virtual-bound-state formation in Pd--U alloys, 25:11989
MONTOYA, Orelio, Outdoor aging of adhesive sealants, 25:12908 (SC-RR-70-163)
MONTZ, R., Objective detection of cerebral blood flow disturbances with /sup 99m/Tc, 25:11146
MOOK, D., Spectroscopic observations of Scorpius X-1, 25:11600
MOOKERJEE, Sivatosh, Formation of supernumerary surface layers in radiated amoebae, 25:11249
MOON, Kuk Jin, Highly excited states of ^{12}C and ^{14}O from ^{3}He capture studies, 25:12388
MOONEY, J. R., Higher-order finite-difference solutions of Schroedinger equation for He atom, 25:11697
MOORE, A. D. L., Fabrication and mechanical properties of dispersion hardened Pu--1 wt. percent Ga alloy, 25:11359
MOORE, D. T., Strontium-89 and ^{90}Sr in rain at Fayetteville (36°N, 94°W), Arkansas, 25:10710 (ORO-2529-28, App. 4)
Temporal distributions of radioactivity and $^{89}Sr/^{90}Sr$ ratios during rainstorms, 25:10707 (ORO-2529-28, App. 1)
Variation of radiocerium isotope ratio in rain, 25:10709 (ORO-2529-28, App. 3)
MOORE, J. P., Electrical and thermal properties of NaCl structured metallic actinide compounds, 25:11494
MOORE, W. E., Temperature dependence of neutron inelastic scattering from water, 25:12342 (RPI-328-210)
MORAN, James H., Method and apparatus for simultaneous porosity and chlorinity logging, 25:10889
MORANDI, G., Elimination of thermal shield from Trino Vercellese pressurized water reactor, 25:12715
Experimental irradiation of metallic U fuel elements in the Halden HBWR reactor, 25:11457 (CISE-R-278)
MORAVEC, A., Determination of burn-up of nuclear fuel on basis of stable isotopes of Nd. I, 25:10461
Determination of burn-up of nuclear fuel on the basis of stable isotopes of Nd. II, 25:10469
MORDUKHOVICH, V. V., Nonprotein thiols in tissues after administration of cystamine, 25:11101
MOREH, R., Energy levels of ^{139}La, 25:12585
MOREL, Jean, Decay scheme of ^{59}Fe and ^{192}Ir, 25:12464
MORGAN, D., Nonevasive contributions to forward rho-production and vector dominance, 25:12212
MORGAN, G. L., Neutron--He interaction. II, 25:12360
MORGANDO, E., Interrelationship between cerebral circulation time, pulmonary circulation, and blood pressure, 25:11148
MORGENSTERN, H., Reaction $^{15}N(\tau,\alpha)^{14}N$, 25:12424
MORIARTY, K. J., Instrument probe for measuring temperature and pressure in the upper plenum of the EBR-II reactor vessel. EBR-II Project, 25:12781 (ANL-EBR-25)
MORIMOTO, Ichiro, Rotational hysteresis of alloys of $SmCo_5$--$SmCu_5$ system, 25:11984
MORINO, Yonezo, Microwave spectrum, structure, quadrupole coupling constant, and force constants of NSCl, 25:10532
MORIUCHI, Yasuyuki, Recent tendency of radiation unit, 25:11064
MORLEY, J., Allergic inflammation. I, 25:11193
MOROZ, N. S., Measurement of scattering angle of particles by Vavilov--Cherenkov radiation, 25:10869 (JINR-E13-5459)
MOROZ, V. I., Acceleration and extraction of deuterons from the JINR proton synchrotron, 25:12303 (JINR-P9-5442)
MOROZOV, V. M., Scattering of neutrons with an energy of 4 MeV at angles close to 180°, 25:12509 (ANL-Trans-855)
MOROZUMI, Minoru, Detection of failed fuel at JRR-4, 25:12819 (JAERI-Memo-4196)
MORRIN, P. A. F., Effect of a uremic environment on phosphate excretion by a small population of intact and severely diseased nephrons, 25:10963
MORRISON, J., Chemisorption of I on W(100), 25:11405
MORRISS, R. H., Microstructural effects in critical fields of niobium films, 25:11832
MORSE, R. L., Studies of turbulent heating of H plasma, 25:11862
MORTIMER, M. J., Length changes in actinide metals due to self-irradiation damage at 4°K, 25:11468
Self-irradiation damage induced resistivity changes in actinide metals at low temperatures, 25:11960
MORVAN, Pierre, Visualization of spectra in nuclear

physics, 25:10892 (CEA-N-1363)
MOSER, P., Cobalt electron irradiated at 20°K, 25:11949 (AI-Trans-267)
MOSIER, Stephen Russell, Poynting flux along the geomagnetic field, 25:11780
MOSKALEV, Yu. I., Morphological changes in rats after injection of ^{241}Am, 25:10942
MOSLEY, W. C., Studies of mixed actinide oxides, 25:11521
MOSS, C. E., Angular correlation study of low-lying levels of ^{29}P, 25:12480
MOSZYNSKI, M., Odd parity states in ^{238}Pu, 25:12594
MOTTERSHEAD, Charles Thomas, Analysis of pion--helium scattering for the pion charge form factor, 25:12225
MOTTINGER, J. P., Effects of x rays on the bronze and shrunken loci in maize, 25:11023
MOUSSA, A., Disintegration of the two isomers of ^{80}Br (31.8 min and 6.0 min), 25:12444
Isomers of ^{130}I and ^{130}Xe, 25:12572
Rapid chemical separations: general aspects, 25:10668 (LYCEN-7034, pp 1-8)
MOUTON, R. F., Microbiological evolution under gamma radiation, 25:11019
MOYER, R. A., Excitation of states in ^{207}Pb, 25:12569
MRTEK, Robert G., Synthesis and biological activity of deuteriobenzyl-d_7-penicillin, 25:10560
MUELLER, Guenter, Thermal diffusion column, 25:10783
MUELLER, H. G., Emission spectroscopic determination of traces in nuclear fuel materials, 25:10432 (KFK-1261)
MUELLER, O., Resonator for x-band electron spin resonance spectroscopy for simultaneous measurement and electron radiation of the sample, 25:10626 (KFK-1285)
MUELLER, R. A., Seismic response characteristics at NRDS from underground nuclear detonations, 25:10730 (NVO-1163-TM-22)
MUELLER, W., Studies with ^{85}Sr of diseases belonging to the rheumatic complex, 25:11175
MUELLER-DUYSING, W., Quantitative analysis of the radiorenogram based on ^{131}I-orthohippuric acid clearance, 25:11159
MUENNICH, F., Decay of ^{104}Cd, 25:12475
MUENZEL, Helmut, Estimation of unknown excitation functions for (α,xn)-(α,pxn)-, (d,xn)-, (d,pxn)-, and (p,xn)-reactions, 25:12529 (ORNL-tr-3020)
MUGNOZZA, G. T. S., Radio induced mutation of hard wheat, 25:11033
Radio-induced mutation of hard wheat, 25:11034
MUHLESTEIN, L. D., Investigation of in-band resonant modes in Cr--W alloys by inelastic neutron scattering, 25:12019
MUIRHEAD, E. G., Photoneutron cross sections of ^{28}Si and ^{24}Mg, 25:12469
MUKHIN, S. V., Time-coordinate compensator for the time spectrometers with long scintillators, 25:10813 (JINR-P13-5378)
MUKUNDA, N., Photons and tachyons with continuous spin, 25:12236
MULLAN, Dermott Joseph, Structure of hydromagnetic shocks in regions of very low ionization, 25:11639
MULLANEY, Henry, Influence of the neutral winds in the formation and distribution of the ionospheric evening anomaly, 25:11777 (AD-708496)
MULLER, J., Systems B_2O_3--MO--MS boracites M--S (M = Mg, Mn, Fe, Cd) and sodalites M--S (M = Co, Zn), 25:11526
MULLER, J. C., Radiolytic behavior of ferrous and ferric ions in very dilute solutions, 25:10635
MUMINOV, A. I., Properties of the excited states of ^{147}Sm and ^{149}Pm, 25:12557
MUNDINGER, F., Determination of regional blood flow with ^{133}Xe in the brain of Parkinson and tumor patients, 25:11147
Diagnostic significance of ventricular resorption of ^{131}I-labeled hippuran, 25:11152
MUNDSCHENK, H., Hemodynamic function studies, 25:11184
MUNKBY, L., Superconductivity for ternary fcc Bi--Pb--Tl alloys, 25:11846
MURAKAMI, Ujihiro, Species differences of the effects of x-irradiation upon the rat and mouse embryo, 25:11277
MURAKAMI, Yuetsu, Effects of Ta additions on the properties of Nimalloy, 25:12008
MURPHY, J. H., Stable numerical integration of conservation equations for hydraulic networks, 25:12793
MURRAY, Sylvia A., Growth of mung bean seedlings after x irradiation and shock treatment, 25:11317
MUSHIAKE, Y., Measurement of the phase constant along a conducting wire in a magnetoplasma, 25:11935
MUTA, Taizo, Electromagnetic mass difference of hadrons and the parton model, 25:12155
MYLES, K. M., Thermodynamic properties of solid palladium-rich Pd--Cd, Pd--In, Pd--Sn, and Pd--Sb alloys, 25:11396
MYNATT, F. R., Lateral spread of high-energy (less than or equal to 400 MeV) neutron beams, 25:12332

N

NAD, A., Pulsed reactor potentialities for neutron activation analysis, 25:10489 (KFKI-70-25-NAC)
NADJAKOV, E., Coupling of collective modes in deformed nuclei, 25:12702
NADZHAFKULIEV, N. A., Arsenate method for iodometric determination of scandium in the presence of iron, 25:10465
NADZHAFOV, I. M., Scattering of γ-quantum in field of nucleus with creation of e^-e^+ pair and several photons, 25:12158
NAGAI, Siro, ESR spectra of irradiated beryllium acetylacetonate single crystal, 25:10623 (JAERI-5026, pp 157-60)
ESR study of γ-irradiated pyridine--silica gel system, 25:10622 (JAERI-5026, pp 6-10)
NAGAMIYA, S., Stroboscopic determination of magnetic moment of 8^+ isomeric state of ^{208}Po, 25:12614
NAGANO, Motohiko, Horizontal air showers of energies above 10^{19} eV, 25:12071
NAGAO, Koichiro, Tumor-specific localizing agent for radioisotope image. IV, 25:10921
NAGASAKI, Masayuki, Level structure of hadrons, 25:12182
NAGATA, Sinobu, Reaction matrix theory for cluster states in light nuclei. I, 25:12411
NAGATA, Tsuneo, Two-branch excitation spectrum of liquid ^{4}He, 25:11818
NAGEL, E., Investigations of air currents in the lower Aare river valley with reference to monitoring of atomic installations, 25:10703 (EIR-165)
NAGPAL, T. S., Selenium-75 as a calibration standard for Ge(Li) detectors, 25:10842
NAGY, S., Observation of proton tracks by a plastic detector, 25:10831
NAGY, Stephen W., Charge-exchange scattering of He^+ by He, Ne, and Kr, 25:11716
NAGY, Stephen William, Charge exchange measurements for He^+ on He, Ne, and Kr, 25:11795
NAIDU, M. G. C., Leaching patterns of monazite and zircon, 25:10723
NAJITA, Kazutoshi, White-light events as photospheric flares, 25:11619
NAKADA, Taishi, Effect of glutathione on the protection against radiation, 25:11098
NAKAI, Yohta, Optical radiation from gases excited by high-energy electrons. III, 25:10586 (JAERI-5026, pp 155-7)
Optical radiation from gases excited by high-energy electrons. II, 25:10585 (JAERI-5026, pp 153-5)
NAKAJIMA, T., Resolving time measurements of Geiger counters, 25:10835
NAKAMURA, H., Numerical differential cross sections of reaction ^{58}Ni(p,t)^{56}Ni with 51.9 MeV protons, 25:12431 (INSJ-124)
NAKAMURA, Shoichiro, Coarse mesh acceleration of iterative sollution of neutron diffusion equation, 25:12838
NAKAYAMA, H., Temperature dependence of dechanneling coefficient in protons in silicon crystals, 25:11969
NALBANTOGLU, M., Determination of traces in minerals by spark source mass spectrography, 25:10456
NAMBA, Susumu, Penetration of electrons into anthracene crystals, 25:11673
NAMIKI, Michiko, Determination of Mo in Fe and steel by flame photometry, 25:10439
NARBONI, Ph., Experimental studies of reactions ^{3}H(p,p)^{3}H, ^{3}He(p,p)^{3}He, and ^{3}H(p,n)^{3}He at 156 MeV, 25:12365
NAREBSKA, Anna, Effect of gamma radiation on ion exchange resins. II, 25:10646
NARITA, Kenji, Composition ranges with similar constricted hysteresis loops in Mn--Al--B alloys, 25:11983
NARZULLAEV, B. N., Thermo-oxidation degradation of poly(vinyl alcohol) irradiated by γ rays, 25:10591
NASKALI, Richard John, Effects of acute gamma radiation on chrysanthemum inflorescence morphogenesis, 25:11311
NASONOV, V. S., Phase fluctuations of the signal of a travelling wave tube generator with superconducting resonator, 25:11853
NASSIFF, S. J., Cross section and yield relations for the isomeric pair /sup 90m/Y/^{90}Y obtained by the (d,p) reaction, 25:12428 (CNEA-278)
Cross sections for nuclear reactions produced by deuterons on tantalum, 25:12513 (CNEA-269)
Excitation functions ^{159}Tb(d,p)^{160}Tb and ^{159}Tb(d,4n)^{157}Dy, 25:12595
NASYROV, Yu. S., Mutagenic action of laser radiation on seeds of Arabidopsis thaliana (L) heynh, 25:11027
NATELSON, M., Variational derivation of discrete ordinate-like approximations, 25:12858
NATION, John A., Coupling of a high-current relativistic electron beam to a slow wave structure, 25:11932
NATOWITZ, J. B., X-ray emission induced alpha particles, 25:12488
NATROSHVILI, G. R., Gamma-radiolysis of aqueous solutions of Na_2S, 25:10649
NAUDET, Roger, EL 600: study of core neutronic properties, 25:12775 (CEA-N-1395)
NAUM, Robert G., Thermal expansion of polycrystalline graphite, 25:11511
NAUMANN, R. A., Hole-vibration coupling in ^{115}In, 25:12543
NAVALKAR, M. P., Calculation of K/sub eff/ for a bare Pu sphere by collision probability method, 25:12849
NAYAR, Ram, Avidity of folic acid for carcinogenic metal ions, Al(III), Cr(III), Be(II), Pb(II), and U(VI), 25:10520
NAYFIELD, Chester L., Elevated levels of ^{137}Cs in common mushrooms (Agaricaceae) with possible relationship to high levels of ^{137}Cs in whitetail deer, 1968--1969, 25:11003

NAYLOR, R. S., Uranium--Th--Pb and Rb--Sr systematics in 2700 x 10^6-year old plutons from southern Wind River Range, Wyoming, 25:10701
NECKEL, Heinz, Transformation of the absolute solar radiation data into the international practical temperature scale of 1968, 25:11609
NE'EMAN, Yuval, Representations of local I-spin charge densities. I, 25:12181
NEGITA, Hisao, Fractionation of tritium in crystallization of inorganic hydrates, 25:10688
NEGRINE, S. M., Crossing-symmetric unitarization of the Veneziano amplitude, 25:12196
NEIDIGH, R. V., Use of optical spectra to measure large electric fields in a hot-ion plasma, 25:11874
NEIGE, R., Uranium determination in thin layers of rocks by dielectric detectors, 25:10476
Uranium isotopic determination in rocks by neutron activation, 25:10494
NEIMOTIN, E. I., Effect of nuclear motion on neutron pulse, 25:12350
NEIRINCKX, R. D., Purification of cyclotron-produced ^{123}I by liquid--liquid extraction, 25:10674
Purification of cyclotron-produced ^{203}Pb from Tl, 25:10678
NELLIS, W. J., Magnetism in Pd-actinide alloys, 25:12003
Virtual-bound-state formation in Pd--U alloys, 25:11989
NELP, Wil B., Long-term effects of local irradiation of the marrow on erythron and red cell function, 25:11112
NELSON, C. A., Training manual for fabrication of printed-circuit boards, 25:12864 (ANL-7725)
NELSON, Gary J., Computer processing of gas chromatographic data: quantitative analysis of fatty acid methyl esters using an off-line magnetic tape system, 25:12917 (UCRL-72393)
NELSON, I. C., Build-up of americium-241 in lung containing plutonium-241, 25:11053 (BNWL-B-12)
NELSON, P., High pressure physics, 25:10749
NELSON, Paul Jr., Relationships between various definitions of prompt-neutron lifetime, 25:12856
NELSON, R. D., Beta grain size and $\beta \rightarrow \alpha$ transformation in unalloyed Pu, 25:11444
Deformation of plutonium allotropes, 25:11389
NEMETH, J., Energies of nuclei with different neutron and proton number in Thomas Fermi approximation, 25:12635 (NP-18545)
NEMOV, V. V., Effect of toroidal state on vacuum magnetic configuration of vintotron, 25:11922 (KHFTI-70-25)
NERUDA, O., Absorption of radiostrontium in irradiated organism, 25:10947
Absorption rate of Sr from gastrointestinal tract, 25:10951
Use of activated barium sulfate in oral contamination with radiostrontium. III, 25:11047
NESTOROV, G., Variations of hard solar x rays deduced from radio-wave absorption, 25:11817
NETZBAND, D., DWBA model applied to the $^{24}Mg(d,p)^{25}Mg$ reaction at E/sub d/ = 13.5 MeV, 25:12457
NEUBACHER, H., Electron spin resonance of free radicals in irradiated carbohydrates, 25:10645
NEUHOLD, John M., Prog. rpt. on freshwater vertebrate and invertebrate ecology of Amchitka Island, annual, 8/30/67--6/30/68, 25:12871 (BMI-171-104)
NEUHOLD, R. J., Multiple weighting functions in fast reactor space-energy synthesis, 25:12854
NEVSTRUEVA, M. A., Cesium-137 in lichen-reindeer man in the extreme north of the USSR, 1962--68, 25:11037 (NP-18381)
NEWCOMBE, C. L., Growth of mung bean seedlings after x irradiation and shock treatment, 25:11317
NEWKIRK, Gordon Jr., Magnetic fields and the structure of the solar corona. II, 25:11604
NG, Yook C., Radionuclide body burdens and hazards from ingestion of foodstuffs contaminated by fallout, 25:11038 (UCRL-72716(Rev.1))
NGO, C., Test of DWBA-type model for analysis of heavy-ion transfer reactions, 25:12683
NGUYEN HUU VAN, Use of low-level α spectrometry in the determination of elements occurring in traces in natural mineral substances, 25:10477
NGUYEN-VAN-THANH, Effect of solvent on frequencies of CD and CH stretching band in some haloforms, 25:10540
NI, Tiee-Bor, Prog. rpt. on powder metallurgy compaction, 9--11/70, 25:12913 (SRO-475-9)
NICOLAS-JARLETON, Jacques, Effect of α UO_3 in production of UO_2 and UF_4 from β UO_3--0.05 H_2O, 25:10569 (CEA-R-4074)
NIECKARZ, W. J. Jr., Nuclear structure effects in (p,2 nucleon) reactions on isotopes of Cd, 25:12570
NIEDERLE, J., Matrix elements of finite U(n) transformations, 25:12235
NIEGAWA, Akira, Inelastic π--N and N--N collisions in parton model, 25:12222
NIELSEN, H. L., Odd parity states in ^{238}Pu, 25:12594
NIELSON, C. W., Studies of turbulent heating of H plasma, 25:11862
NIGAM, B. P., Kaon and nucleon form factors using vector dominance, 25:12141
NIGHTINGALE, R. E., Prog. rpt. on reactor fuels and materials development, 4--6/68, 25:11474 (BNWL-842)
NIKITINA, N. S., Radiative polarization of free relativistic electrons in a magnetic field, 25:12060
NIKOLAEV, B. I., Cascade rate functions for separating multicomponent isotopic mixtures, 25:10782
NILSEN, Per Agnar, Visualization of the placenta with a gamma camera and /sup 113m/In, 25:11228
NILSSON, L. B., Construction and installation work at Oskarshamn, 25:12716
NILSSON, Sven Goesta, Low-energy spectrum of ^{29}Si, 25:12503
NINOMIYA, Kansuke, Multiple production processes and rearrangement of sakatons, 25:12186
NIR, D., Properties of ^{95} ^{98}Rh from ^{95} ^{98} Ru(p,n) reaction, 25:12617
NISBET, John S., Diurnal variation of neutral temperature profile at Arecibo, 25:11793
NISHIMURA, Sanae, Effect of glutathione on the protection against radiation, 25:11098
NISHIYAMA, Ronald H., Treatment of thyroid cancer. Death rates after surgery and after surgery followed by sodium iodide ^{131}I, 25:11234
NISSEN, P. E., Metal-to-H ratio for stars in the Hyades and Coma open clusters, 25:11551
NITTA, Isamu, ESR spectra of irradiated beryllium acetylacetonate single crystal, 25:10623 (JAERI-5026, pp 157-60)
ESR study of γ-irradiated pyridine--silica gel system, 25:10622 (JAERI-5026, pp 6-10)
Irradiation effects of oxytocin, 25:10625 (JAERI-5026, pp 164-7)
Radiation effects on gramicidin. II, 25:10587 (JAERI-5026, pp 167-8)
NIX, William D., Prog. rpt. on structure dependence of high temperature deformation of metals, 3/69--3/70, 25:11434 (SU-326-P-17-X-1)
NIYAZOVA, O. R., Low-temperature lithium drift in silicon, 25:11973
NIZHNIKOV, A. I., Cesium-137 in lichen-reindeer man in the extreme north of the USSR, 1962--68, 25:11037 (NP-18381)
NOBLE, J. V., Progenitor sum-rules in nuclear physics, 25:12637 (NYO-2171-328)
Shapes of angular distributions of (^3He,t) and (p,n) transitions to 0^+ antianalog states, 25:12648
NOEL, Janet F., In vitro radioprotection by dimethyl sulphoxide, glycerol, and anoxia, 25:10983
NOERDLINGER, P. D., Can the cosmological constant stabilise galaxy clusters, 25:11642
NOF, A., Energy levels of ^{139}La, 25:12585
NOFAL, Mohammed M., Treatment of thyroid cancer. Death rates after surgery and after surgery followed by sodium iodide ^{131}I, 25:11234
NOGAMI, Y., Coulomb effect on proton--proton scattering parameters, 25:12680
NOGUCHI, M., Angle information with a gridded ionization chamber and its applications, 25:10837
NOGUEIRA, Eduardo Diaz, Bases of a program of investigation for the development of the reprocessing of fuels irradiated in fast reactors, 25:10672
NOMI, Mitsuhiko, Solidification of radioactive sludges, 25:10799
NOMURA, Suso, Irradiation tests of domestic Zircaloy-2 cladding materials in JPDR, 25:12862 (JAERI-Memo-4192)
NOMURA, T., Stroboscopic determination of magnetic moment of 8^+ isomeric state of ^{208}Po, 25:12614
NONAKA, I., Numerical differential cross sections of reaction $^{58}Ni(p,t)^{56}Ni$ with 51.9 MeV protons, 25:12431 (INSJ-124)
NORDEMANN, Daniel, Measurement of radioactivity of recently fallen carbonated chondrite: Allende, 25:11540
NORDEN, H., Energy loss of well-channeled H, He, and Li ions in Au, 25:11976
NORDENFELT, Erik, Method for studying phagocytosis with ^{51}Cr labeled yeast cells, 25:10908
NORTHRUP, C. J. M. Jr., Helium diffusion in $^{238}PuO_2$, 25:11501
NORWOOD III, Thomas Ellis, Energy bands of vanadium oxide, 25:12044
NOVAK, D., Perfusion scintigram of lungs during various stages of pulmonary sarcoidosis (Morbus boeck), 25:11133
NOVIKOV, V. G., Experiments on α-particle acceleration by collective method, 25:12305 (JINR-P9-5558)
NOVOTNY, P., Thermokinetics of the fuel element cassette of the fast reactor, 25:12801
NOYCE, J. R., Strontium-89 and ^{90}Sr in air at Fayetteville, Arkansas, 25:10711 (ORO-2529-28, App. 5)
Temporal distributions of radioactivity and $^{89}Sr/^{90}Sr$ ratios during rainstorms, 25:10707 (ORO-2529-28, App. 1)
NOYES, Robert W., Solar Lyman continuum and the structure of the solar chromosphere, 25:11614
NOZAKI, Tadao, Systematic investigation of ultra high energy interactions. II, 25:12093
NURI, M., Experimental scintigraphy of thrombi in animals, 25:11214

O

O'BAR, P. R., Early detection of injury after nitrogen mustard (HN2) therapy using radioiron, 25:10952
OBATUROV, G. M., Emergency personal n-γ radiation dosimeters, 25:10881

OBERDISSE, K., Successes and failures of fractionated radioiodine therapy among 700 hyperthyroid patients, 25:11230
OBERHAUSEN, E., Determination of renal clearance by external γ-ray measurements, 25:11155
Simultaneous determination of total potassium and exchangeable sodium in man, 25:10920
Thyroid diagnosis with a whole-body counter in children, 25:11172
OBERLEY, L. W., Moessbauer effect studies following Coulomb excitation, 25:10863
O'BOYLE, D. R., Uranium--plutonium--zirconium ternary alloy system, 25:11442
OBRADOVIC, D., Multigroup neutron transport equation in diffusion and P_1 approximation, 25:12345
O'BRIEN, J. R., Detection of thrombosis with ^{125}I fibrinogen, 25:11191
ODDONE, Piermaria Jorge, Deuteron--deuteron elastic scattering at 2.20 GeV/c, 25:12092
ODIEVRE, M., Evaluation of the irradiation of bone marrow resulting from milk contamination by ^{90}Sr after continuous or uneven deposition on pastures, 25:10932 (CEA-CONF-1558)
OEBU, M., Gamma-ray discrimination in proton-recoil spectrometer, 25:10857
OEFF, K., Determination of thyroidal clearance during an automatically controlled and constant ^{131}I blood level, 25:11173
OEGELMAN, H., Extensive air shower arrays as detectors of prompt gamma rays from supernovae explosions, 25:11553
OEKSUEZ, Iskender, Theory of atomic structure including electron correlation, 25:11737
OEKTEM, F., Are the neutrinos an aspect of Riemannian geometry, 25:12280
OESTBERG, Kjell, Study of nonlinear instabilities, 25:11913 (UUIP-722)
OETTING, Franklin L., Half-life of ^{239}Pu by calorimetry, 25:10779
OGANESIAN, Yu. Ts., Synthesis of element 105, 25:12620
OGANESSIAN, A. G., High energy particle identification by x-ray transition radiation (XTR) detectors, 25:10877
OGARD, Allen E., High-temperature heat content of PuO_2, 25:11491
OGATA, H., Numerical differential cross sections of reaction $^{58}Ni(p,t)^{56}Ni$ with 51.9 MeV protons, 25:12431 (INSJ-124)
OGDEN, J. S., Thermophysical properties of (UPu)N, 25:11492
OGILVIE, K. W., Acceleration of protons by interplanetary shocks, 25:11624
Magnetic and thermal pressures in the solar wind, 25:11607
OGITA, N., Cosmic-ray variations during geomagnetic storms, 25:11745
OGRIS, E., Colloid clearance: effect of particle size and extrahepatic deposition, 25:10918
O'HALLORAN, M. W., Whole-body counter for studies of total body K, 25:10910
OHDAN, Koji, Stability of polyvinyl acetate emulsions produced by radiation-induced polymerization. I, 25:10593 (JAERI-5026, pp 15-25)
OHLENSCHLAEGER, L., First aid measures in radiation accidents, especially on radioactively contaminated wounds, 25:11109
OHMER, Melvin C., Voltages induced in superconductors by superimposed ac and dc magnetic fields, 25:11835
OHNISHI, Shun-ichi, ESR spectra of irradiated beryllium acetylacetonate single crystal, 25:10623 (JAERI-5026, pp 157-60)
ESR study of γ-irradiated pyridine--silica gel system, 25:10622 (JAERI-5026, pp 6-10)
Irradiation effects of oxytocin, 25:10625 (JAERI-5026, pp 164-7)
Radiation effects on gramicidin. II, 25:10587 (JAERI-5026, pp 167-8)
OHNO, S., Simultaneous determination of copper and manganese in plants by neutron-activation analysis, 25:10509
OHNO, Shigeru, Simultaneous determination of As and Sb in soil by neutron activation, 25:10506
OHNUMA, H., Nuclear structure of ^{48}Sc, 25:12452
OHSE, Roland W., Evaporation behavior of substoichiometric $(U,Pu)O_{2-x}$, 25:11504
OHTA, Kohichi, Adiabatic theory of fission, 25:12645
OKA, Takefumi, Benzene formation in radiation-induced and photochemical reactions of acetylene, 25:10650
OKADA, Toshio, Grafting acrylonitrile onto polyvinyl chloride powder and spinning fiber, 25:10595 (JAERI-5026, pp 35-41)
Grafting of acrylic acid onto polyester fiber, 25:10602 (JAERI-5026, pp 73-9)
Radiation induced graft copolymerization to polyester. VII, 25:10600 (JAERI-5026, pp 63-7)
Radiation-induced graft copolymerization to polyester. IV, 25:10597 (JAERI-5026, pp 46-51)
Radiation-induced graft copolymerization to polyester. VIII, 25:10601 (JAERI-5026, pp 68-72)
Radiation-induced graft copolymerization to polyester. VI, 25:10599 (JAERI-5026, pp 56-62)
Radiation-induced graft copolymerization to polyester. V, 25:10598 (JAERI-5026, pp 52-5)
Radiation-induced graft polymerization of acrylonitrile onto poly(vinyl chloride) powder, 25:10596 (JAERI-5026, pp 42-5)
OKAMOTO, Hidemasa, Participation of an excited monomer in propagation reaction of the γ-ray induced polymerization of ethylene, 25:10612
OKAMOTO, Paul Rokuro, Initial stages of ordering in Ni_4Mo, 25:11452
OKAMURA, Seizo, Stability of polyvinyl acetate emulsions produced by radiation-induced polymerization. I, 25:10593 (JAERI-5026, pp 15-25)
Stability of polyvinyl acetate emulsions produced by radiation-induced polymerization. II, 25:10594 (JAERI-5026, pp 26-34)
Studies on radiation-induced free-ionic polymerization by electrical conductivity measurements. II, 25:10610 (JAERI-5026, pp 169-71)
OKI, Misaya, Thermal properties of deuterated Cu(II) sulfate pentahydrate, 25:10565
OKITA, Isao, Effect of glutathione on the protection against radiation, 25:11098
OKUMURA, Yoshitaka, Hadron scattering at extremely high energies in the parton model, 25:12187
OLIPHANT, Sir Mark, Interaction of atomic particles with solid surfaces at intermediate energies. III, 25:11675
OLIVEIRA, Jaime M. Costa, Behavior of neutrons in multiplying medium, 25:12341 (LFEN-NI.-46-a)
OLOVSSON, Ivar, Hydrogen bond studies. XXXXVI. Crystal structures of normal and deuterated sodium hydrogen oxalate monohydrate $NaHC_2O_4.H_2O$ and $NaDC_2O_4.D_2O$, 25:10543
OLSEN, A. R., Experiment description and hazards evaluation for the Series I ORNL oxide fuels irradiation in EBR-II, 25:11533 (ORNL-TM-2635(Suppl.))
OLSEN, C. W., Soil strain near a nuclear detonation, 25:10732
OLSEN, Stephen Lars, The /ΔI Vector/ = $^1/_2$ rule and Λ^0 decay, 25:12080
OLSEN, W. C., Electromagnetic properties of ^{58}Fe, 25:12483
OLSON, Arne P., RABID: an integral transport-theory code for neutron slowing down in slab cells, 25:12336 (ANL-7645)
OLSON, D. L., Electrotransport in liquid Na--K, 25:11404
OLSON, Robert, Argon laser micro-irradiation of mitochondria in rat myocardial cells in tissue culture, 25:11242
OLSON, William M., Evaporation behavior of substoichiometric $(U,Pu)O_{2-x}$, 25:11504
OLUWOLE, Abiodun Francis, Nuclear spins, $^3P_1$ and $^3P_2$ hyperfine structures, and nuclear moments of ^{69}Ge and ^{75}Ge, 25:12487
OMALJEV, Veljko, Uranium ore contrasts, 25:10484
ONDRISH, L., Time-coordinate compensator for the time spectrometers with long scintillators, 25:10813 (JINR-P13-5378)
ONG, Ching Ching, Organic oxalates. IV. Pyrolysis of diallyl, disubstituted-allyl, and related oxalates, 25:10526
OP DEN KAMP, A. M. F., Gamma rays from thermal-neutron capture in natural and ^{28}Si enriched silicon, 25:12403
ORLANDINI, K. A., Anion-exchange separation of neptunium from uranium and thorium in basic solution, 25:10655 (ANL-7751)
ORLANDO DE LA TEJA ANGELES, Carlos, EPR of irradiated seeds of Dahlia coccinea, 25:11305 (NP-18394)
ORMAN, P. R., Time jitter due to noise in timing systems, 25:10808 (AERE-R-5561)
OROGUCHI, Takashige, Dip-bump structure of cross section and urbaryon rearrangement. II, 25:12219
Exotic resonances, urbaryon rearrangement and hadron structure, 25:12183
ORPHAN, V. J., Gamma-ray production cross sections for the $^{16}O(n,x\gamma)$ reaction from 6.35- to 16.52-MeV neutron energy, 25:12406
ORRALL, Frank Q., White-light events as photospheric flares, 25:11619
OSBORN, R. K., Use of acoustic waves in nuclear power reactors to determine average void fractions, 25:12779
OSTERMAN, P., Semiconductor detector spectrometer with magnetic electron lens, 25:10864
OSTERTAG, B., Implications of radiation-induced modifications in the comparative teratology of the nervous system, 25:11287
OSTROUMOVA, L. M., Change in blood in prolonged and brief irradiation of guinea pigs, 25:11278
OSTROWSKI, K., Free radicals evoked by radiosterilization in preserved bone grafts, 25:11329
Quantitative evaluation of irradiated bone grafts resorption rate by the electron spin resonance technique, 25:11340
OTSUKI, Shoichiro, Dip-bump structure of cross section and urbaryon rearrangement. II, 25:12219
Exotic resonances, urbaryon rearrangement and hadron structure, 25:12183
OTT, Edward, Finite beta equilibria of relativistic electron beams in toroidal geometry, 25:11887 (NYO-4077-1, Paper 5)
OTT, K. O., Successive space-energy synthesis for neutron fluxes in fast reactors, 25:12780
OTTERSON, P. J., Singularity structure of causal distributions and restricted equal-time limits,

XUM

25:12133
OTTERSON, Paul James, Some distribution theoretic aspects of current algebra, 25:12294
OTTO, H. J., Differential diagnosis of brain alterations caused by tumor and vascular processes with radioactive isotope blood flow measurements, 25:11149
OTWINOWSKI, S., Analysis of D^0 meson in reaction $\pi^+p \rightarrow p\pi^+\pi^+\pi^-\pi^-\pi^0$ at 8 GeV/c, 25:12191 (INR-P-1207)
OUTI, A., Cosmic-ray variations during geomagnetic storms, 25:11745
OVAKIMOV, V. G., Protective effects of biogenic amines in the radiation intestinal syndrome, 25:11102
OVERCASH, Danny Ray, Fermi surface topology changes in In alloys, 25:12032
OVEREND, John, ν_4 bands of $^{10}BF_3$ and $^{11}BF_3$ at high resolution, 25:10533
OVERSBY, V. M., Isotopic analysis of microgram quantities of lead iodide using an electron-bombardment source mass spectrometer, 25:10466
OWEN, L. W., Exchange effects in the nucleon--nucleus optical potential, 25:12689
OZAKI, Kazuhiko, Two-body weak-electromagnetic hyperon decays, 25:12169
OZAKI, S., Lateral distribution of muon pairs in underground cosmic-ray showers, 25:12082
OZIEWICZ, Z., Muon capture in ^{14}N, 25:12386

P

PABST, H. W., Clearance studies with ^{131}I-labeled hippuran, ^{203}Hg-salyrgan, ^{51}Cr-EDTA, and ^{51}Cr-inulin, 25:11156
Renal clearance of ^{133}Xe, 25:11158
Studies on l-triiodo-thyronine suppression in its dependency on thyroidal function, iodine storage, thyroid size, and age of patients, 25:10944
Studies on peripheral circulation with radioisotopes, 25:10912
PACCARD, D., Colinear and noncolinear magnetic structures in rare earth compounds RNi_3 and R_2Ni_7, 25:11979 (CEA-CONF-1704)
PACE, J. V., Lateral spread of high-energy (less than or equal to 400 MeV) neutron beams, 25:12332
PACKAN, Nicolas Hayes, Voids in neutron irradiated aluminum, 25:11465 (ORNL-TM-3109)
PAES DE BARROS, M. H., Night-time anomalies in vlf propagation by galactic x-ray source at Centaurus, 25:11812
PAGE, D. E., Satellite equipment for the measurement of high energy electrons and protons, 25:11813
PAGEL, B. E. J., Composition of delta pavonis, 25:11564
PAGNIA, H., Changes of surface conductivity in Ge during x-irradiation, 25:11963
PAILLERY, A., Energy release and electrical resistivity recovery in Ni following electron irradiation, 25:11977
PAINTER, Robert B., DNA repair in mammalian cells, 25:11008 (BNL-50203, pp 14-26)
PAIS, A., Hadronic helicity conservation and inelastic lepton--nucleon reactions, 25:12165
PAKKANEN, A., Decay of ^{117}In isomers and search for a low-lying $^9/_2^-$ level in ^{117}Sn, 25:12566
Reinvestigation of the decay of ^{200}Tl, 25:12528 (NP-18647)
PAN, P. J., Decay of 6.5 min ^{76}Br, 25:12445
Quasielastic deuteron breakup by protons, 25:12375
PANLENER, R. J., Studies of the defect structure of nonstoichiometric cerium dioxide, 25:12033
PANTUSO SUDANO, J., Particular MHD solutions, 25:11753 (EUR-CEA-FC-571)
PAPADOPULOS, Celso C., Ezeiza semi-industrial irradiation plant, 25:10795 (CNEA-272)
PAPAGIANNIS, Michael D., Influence of the neutral winds in the formation and distribution of the ionospheric evening anomaly, 25:11777 (AD-708496)
Model relating the radial changes of the plasmapause at dusk to geomagnetic activity, 25:11776 (AD-708495)
PAPE, R. P., Factors affecting the hardness of uranium mononitride at elevated temperatures, 25:11498
PARDUE, W. M., Thermal creep of polycrystalline UO_2--PuO_2, 25:11496
Thermophysical properties of (UPu)N, 25:11492
PARENGH, Maurits, Levitation in ultra-vacuum, 25:10805
PARK, John T., Excitation of He^+ in 20- to 100-keV He^+--He collisions, 25:11713
PARK, Won C., Role of radiation therapy in the management of hemangiomas of the liver, 25:11235
PARKER, B. R., Cross section for pair production in proton--proton collision, 25:12231
PARKER, W. C., Geiger counters for detection of non-radioactive effluents from gas chromatograph, 25:10888
PARKIN, Don Merrill, Stage I/sub D/--I/sub E/ recovery in electron-irradiated Cu, 25:11957
PARKS, G. K., Origin of interplanetary sectors from radio observations, 25:11606
PARMEGGIANI, A., Underwater plasma-arc cutting as a powerful dismantling tool for water reactors, 25:12714
PARROT-MICHE, Francoise, Host-bacteria relationship in x-irradiated artichokes, 25:11306
PARSONS, Karl, Nuclear-resonance fluorescence in ^{130}Xe, 25:12560
PASOTTI, G., Preliminary results regarding development of superconducting ribbons of Nb_3Sn, 25:11820 (LNF-70/18)
PASSOJA, A., Semiconductor detector telescope electron spectrometer, 25:10852 (NP-18617)
PASTERNAK, R. A., Hydrogen--deuterium exchange on Mo, 25:10559
PATHAK, A. P., Anomalous transmission of particles through perfect crystals, 25:11971
PATYRA, Ryszard, Radiological protection in management of ^{60}Co teletherapy equipment, 25:11070
PATZELT, A., Safety of heavy water system in Braunschweig research reactor, 25:12822 (NP-18499)
PATZELT, O., Argon-43 and ^{44}Ar, 25:12499
PAUL, J. M., Behaviour of gas Cherenkov counters for electrons, 25:10874
Behaviour of photomultiplier with large photocathode, 25:10847
PAUL, Madhabandra Prasad, Waveform and source-size studies of Jupiter's decametric radiation, 25:11670
PAUL, William E., Radioresistance of cooperative function of carrier-specific lymphocytes in antihapten antibody responses, 25:10987
PAULSON, O. B., Regional cerebral blood flow, 25:11143
PAUTRAT, M., Coulomb excitation of ^{123}Te and ^{125}Te, 25:12603
PAVLOV, N. I., Acceleration and extraction of deuterons from the JINR proton synchrotron, 25:12303 (JINR-P9-5442)
PAVLOVA, O. S., Effect of induced radiation of electrons moving in planar electromagnetic wave on orientation of their spins, 25:12161
Forced radiation of neutral Fermi-particles moving in planar wave, 25:12160
PAVLOVSKAYA, N. A., MPC of ^{232}Th and natural Th in drinking water, 25:11051
PAYNE, G. L., Properties of the K matrix, 25:12669
PEARCE, R. J., Thermodynamics of some metal/coolant reactions in Mk.III reactors, 25:10518 (RD/B/N-1816)
PEARMAN, K., Growth of epitaxial layers by ion beam sputtering, 25:11962
PEARSON, Howard A., Identification of cases of acquired functional asplenia, 25:11117
PECKER, Jean-Claude, Some considerations from the direct comparison between the observations and the theory of solar disk polarization, 25:11610
PEDERSEN, J., Reaction $^{90}Zr(^3He,d)^{91}Nb$ at 18 MeV, 25:12613
PEEKNA, Andres, Strange-particle final states produced by 7-BeV/c π^- on protons, 25:12110
PELEVINA, I. I., Changes in lethal effect of irradiation of cells cultivated outside of organism due to chemical compounds, 25:11106
PELLEGRINI, Claudio, Physics with and physics of colliding electron beams, 25:12325
PELLO, H., Application of nuclear explosives in the mining industry, 25:10747
PELLS, G. P., Virtual-bound-state formation in Pd--U alloys, 25:11989
PENDLETON, R. C., Zirconium-95 in Utah vegetation produced during the 1966 growing season, 25:10999
PENIKIS, E., Isotopic analysis of microgram quantities of lead iodide using an electron-bombardment source mass spectrometer, 25:10466
PENNDORF, K., Stationary state thermal neutron spectrum generated by a Pu Phoenix mixture in high temperature reactors, 25:12778
PENNINGTON, D. G., Isotope bioassay for thrombopoietin, 25:10991
PENNINGTON, E. M., Service routines for multigroup cross-section code MC², 25:12337 (ANL-7654)
PENSTON, M. V., Cloud--intercloud phase change in the interstellar medium, 25:11650
PENZIAS, Arno A., Observation of CO emission at 2.6 millimeters from IRC + 10216, 25:11568
PEPPARD, D. F., Extraction of U(VI) and selected M(III) cations by bis neo-octyl phosphoric acid in two different hydrocarbon diluents, 25:10679
PERCHARD, J. P., Low-frequency vibration spectra of various isotopic varieties of primary aliphatic ethers. I, 25:10542
Low-frequency vibration spectra of various isotopic types of primary aliphatic ethers. II, 25:10562
PERELʹSHTEIN, E. A., Longitudinal instabilities in annular charged beams. I, 25:12312
Longitudinal instabilities in annular charged beams. II, 25:12311
PEREZ-MENDEZ, V., Electromagnetic delay line readout for proportional wire chambers, 25:10846
PERINI, A., Estimate of dose of radiation absorbed by airport personnel, 25:11062
PERJES, Z., Spinor treatment of stationary space--time, 25:12278
PERKINS, F. W., Measuring current distribution in a Tokamak plasma, 25:11867 (MATT-818)
Plasma instabilities in ionospheric heating by radio waves, 25:11806
PERKINS, Francis W., Auroral phenomena driven by the magnetospheric plasma, 25:11804
PERKINS, H. K., Electronic structure and anomalous thermal expansion in FeF_2 and VO_2, 25:12015
PERRIER, Michel, Mechanical activity in a granitic massif subjected to a nuclear explosion, 25:10728 (CEA-R-4059)

PERROTTET, M., Sixth-order radiative corrections to the anomalous magnetic moment of the electron, 25:12065 (CNRS-CPT-70-P-339)
PERROTTET, Michel, Computation of renormalized radiative corrections, 25:12245 (CNRS-CPT-70-P-318)
PERRY, F. C., Electron-beam induced stress waves in solids, 25:10791
PERVEEN, Suraiya, Renormalization problem of Yang--Mills theory with non-zero mass, 25:12250
PESZYNSKI, Jerzy, Radiological protection in management of ^{60}Co teletherapy equipment, 25:11070
PETERMAN, A., Sixth-order corrections to the anomalous magnetic moment of the electron, 25:12145
PETERSEIM, K., Reactions (^{3}He,t) on ^{18}O, ^{22}Ne, ^{26}Mg, and ^{30}Si, 25:12498
PETERSEN, Teri, Detection of positronium hydride, 25:11700
PETERSON, Douglas Vernon, Kaon nucleon total cross sections at low momentum, 25:12120
PETERSON, J. R., Preparation and some properties of berkelium metal, 25:11358
PETERSON, S. F., On-line computer monitoring of pressurized ion exchange process, 25:10664 (DP-MS-70-38)
PETERSON, V. L., Electromagnetic drift of the midlatitude F2 layer during a storm, 25:11805
PETIT, G. Y., Review of experimental works on closed-shell nuclei and the almost closed shell nuclei from ^{40}Ca to ^{210}Pb, 25:12432 (LYCEN-7034, pp 117-46)
PETROFF, Irene Karmilof, Photoelectric emission from W, Ta, and Mo, 25:12040
PETROS'YANTS, A. M., From scientific research to nuclear industry, 25:12709
PETROV, R. V., Suppresion of endocolonization in sublethally irradiated mice, 25:10986
PETROV, V. A., Emissivity of high-temperature materials, 25:11426
PETROVIC, Danilo, New evidence concerning the molecular basis of the restorative effect of DNA in cultured mammalian cells, 25:11243
PETTIGREW, George L., Use of radioactive materials in gas chromatography, 25:10421 (BRH/DMRE-70-5)
PETUKHOVA, E. V., Dietary intake of ^{90}Sr by population of the USSR, 1959--1967 as a result of stratospheric fallout, 25:10934 (NP-18380)
PETUSHKOV, A. A., MPC of ^{232}Th and natural Th in drinking water, 25:11051
PEYRAUD, Nelly, Equilibrium of an ionized atmosphere submitted to an intense radiation field, 25:11585
PEYRET, R., Multiple-scale method applied to magnetohydrodynamic flow inside ducts, 25:11771
PFANNENSTIEL, P., Evaluation of results of treatment of thyroid carcinoma, 25:11233
PFEIFFER, G., Colloid clearance: effect of particle size and extrahepatic deposition, 25:10918
PFIRSCH, D., Influence of electrical conductivity on the equilibrium of low-pressure plasma in stellarators, 25:11912 (MPI-PA-7/62)
PFISTER, A., Biological effects of the heavy ions in cosmic radiation, 25:11280
PFLUG, K., Europium and lanthanum in sunspot and in the undisturbed photosphere, 25:11613
PHAM MAU QUAN, Waves and discontinuities in relativistic magnetohydrodynamics, 25:11762
PHELPS, Michael E., Level structure of ^{101}Rh from the decay of 8.5 h ^{101}Pd, 25:12596
PHELPS, P. L., Distribution and redistribution of airborne particulates from the Schooner cratering event, 25:10716 (UCRL-72534)
PHILIBERT, J., Atomic absorption determination of K, Rb, and Sr, 25:10458
PHILLIPS, Ralph, Role of radiation therapy in the management of hemangiomas of the liver, 25:11235
PHILPOTT, R. J., Core-plus-particle model and the low-lying levels of ^{53}Cr, 25:12494
PICCHI, P., Discussion of some recent results on cosmic-ray muons, 25:12168
PICHON, G., Cauchy problem for the linearized relativistic Boltzmann equation, 25:11902
Mathematical problems of relativistic Boltzman equation, 25:12284
PICK, M., Origin of interplanetary sectors from radio observations, 25:11606
PICOT, A., High efficiency time-of-flight neutron spectometry for random sources, 25:10856
PIEPENBRING, R., Study of different competing coupling mechanisms in deformed nuclei of odd mass, 25:12525 (LYCEN-7034, pp 94-116)
PIERACH, C. A., Assessment of renal blood flow with radioactive labeled compounds excreted by glomerular filtration, 25:11153
Comparison of renal isotope diagnosis with vasoconstrictor content in the renal vein of hypertensive patients, 25:11163
Contribution of scintigraphy for evaluation of vascular renal diseases, 25:11166
PIERCE, Albert W., Positive reactivity from replacement of heavy water by light water in the coolant channels of a heavy-water-moderated reactor, 25:12830
PIERQUIN, B., Dosimetric control in brachycurietherapy, 25:11000
PIERSON, Arthur, Optimization of image location relative to rotor surface Model 739 framing camera, 25:12889 (EGG-1183-542)
PIGORINI, F., Consideration of the clinical interpretation of scintigrams of the pancreas under normal and pathological conditions, 25:11199
PIKELNER, S. B., Interstellar medium, 25:11641
PIKULSKI, A., Muon capture in ^{14}N, 25:12386
PILLAY, Sivasankar K. K., Survival of ^{50}Cr-labeled erythrocytes as studied by instrumental activation analysis, 25:10503
PINEL, J., Transition-field enhancement and shape effects due to magnetic inclusions in a superconductor, 25:11840
PINTA, M., Matrix effects on determination of traces by atomic absorption, 25:10457
Problems of contamination in determination of traces, 25:10427
PIPES, E. W., X-ray and nuclear radiation facilities, personnel safety features, 25:11078 (Y-1754)
PIROTTE, Ch., Relativistic limit of spin tensor operators associated with a vector particle, 25:12128
PISARENKO, N. F., Flux of low-energy protons near the Moon on December 13, 1966, 25:11669
PITIRIMOVA, M. A., Radiation and chemical mutagenes in barley seeds, 25:11315
PITTEL, S., Effects of magnetic dipole core polarization in ^{206}Pb and ^{207}Pb, 25:12600
Structure of the calcium isotopes, 25:12436
PIXBERG, H. U., Determination of central circulation parameters and peripheral blood flow by simultaneous application of ^{133}Xe and ^{131}I-labeled RISA, 25:11123
PIXLEY, R. E., Anisotropy ^{2}H(d,p)^{3}H at low energies, 25:12368
PIZZELLA, G., Energy spectrums for proton intensities in outer radiation zone, 25:11786
PLACE, Thomas Alan, Effect of a thoria dispersion on the yielding and flow of iron, 25:11401
PLANET, J., Evaluation of the irradiation of bone marrow resulting from milk contamination by ^{90}Sr after continuous or uneven deposition on pastures, 25:10932 (CEA-CONF-1558)
PLANTAMURA, V. L., Designing method of switching circuits cascade for analog parameter discrimination, 25:10901
PLATONOV, A. L., Thermogenesis of irradiated yeast cells in the process of recovering their reproductive capacity, 25:11324
PLAUT, L., Variable stars, 25:11550
PLIS, Yu. A., Method for pulsed polarized ion beam production for high-energy accelerators, 25:12304 (JINR-P9-5446)
PLUMEJEAU, Jean, Isodore facility, 25:10794 (CEA-R-4120)
PLUMMER, Mitty Charles, Effects of radiation on thermoelectric properties of Cu_2S, 25:11952
PNIEWSKI, J., Hypernuclei and hypernuclear spectroscopy, 25:12090 (INR-P-1223)
POCOCK, R. F., Nuclear ship propulsion, 25:12836
PODUSHNIKOVA, K. A., Conditions of plasma heating at electron cyclotron resonance, 25:11861 (NP-18635)
POFFE, N., Coulomb excitation of ^{123}Te and ^{125}Te, 25:12603
POGODIN, V. P., Intercrystalline corrosion and corrosion cracking of stainless steel in aqueous solutions, 25:11353
POLASTRI, F., Design of NH_3--H_2 two-temperature plant for heavy water production, 25:10787
POLISHCHUK, R. F., Classification of the curvature tensor by means of principal confluences, 25:12285
POLITZER, Jay Lester, Three-dimensional field emission in the perturbed scattering model, 25:12178
POLLACK, Edward, Charge-exchange scattering of He^{+} by He, Ne, and Kr, 25:11716
POLLACK, Ralph M., Alkaline hydrolysis of p-nitroacetanilide and p-formylacetanilide, 25:10527
POLOSKIN, B. P., Conditions of plasma heating at electron cyclotron resonance, 25:11861 (NP-18635)
POLOSKOV, S. S., Search for quarks in ferromagnetics using an electrometer with the beams suspension method, 25:12064
PONTECORVO, B., Concerning one experimental possibility in neutrino astronomy, 25:11628
POPA, Rodica, Hemorrhagic syndrome in radiation sickness. II, 25:11105
POPEKO, A. G., Neutron detector in search for superheavy elements in nature, 25:10814 (JINR-P13-5391)
POPELKA, M., A contribution to the mechanism of radiostrontium resorption in rats, 25:10938
POPOV, A. S., Delay of mitosis in culture of mammalian cells under α and γ rays, 25:11272
POPOV, A. V., Lifetime of 2007-keV level for ^{46}Ti nucleus, 25:12508
PORSCHING, T. A., Stable numerical integration of conservation equations for hydraulic networks, 25:12793
PORTER, L. E., Light Λ^{0} hypernuclei and lambda--nucleon potential, 25:12232
PORTER, William Hugh Lancelot, Improvements in nuclear reactor plant, 25:12802
POSKANZER, A. M., Identification of nuclear fragments, 25:10860
POSSA, G., Underwater plasma-arc cutting as a powerful dismantling tool for water reactors, 25:12714
POSTMA, Richard William, P-state wave function of two-electron atom and absorption coefficient of H-, 25:11684

XUM

POTAUX, D., Beam--beam effect, 25:12308 (LAL-RT-5-70)
POTOKAR, M., Activation cross sections and integrated cross sections for radiative capture of 14 MeV neutrons, 25:12474
POTTER, P. E., Uranium--plutonium--carbon phase diagram. II, 25:11524
Uranium--Pu--C--O systems, 25:11525
POTTER, R. A., Synthesis, characterization, and fabrication of UN, 25:11480 (ORNL-4608)
POULARIKAS, A. D., Eigenvalues of bounded plasmas with random properties, 25:11945
POUSSIER, C., Spectrometer permitting the analysis of low-energy gammas in the presence of a strong high-energy gamma background, 25:10859
POVEL, H. P., Muon capture probability in isotopes of bromine, 25:12502
POWELL, A. L. T., Composition of delta pavonis, 25:11564
POWELL, Charles H., Review of international microwave exposure guides, 25:11088
POWERS, H. G., Evaluation of PuO_2 homogeneity in PuO_2--UO_2 fast reactor fuel by scanning electron microprobe, 25:11489 (WHAN-FR-20)
POZAR, F., High speed 12 bit register, 25:10816
PRAEG, R., Quantitative evaluation of ^{131}I-hippuran renal clearance based on a model, 25:11160
Results of renograms evaluated by computer analysis based on a non-compartmental model, 25:11161
PRASAD, E. A. V., Leaching patterns of monazite and zircon, 25:10723
PRASAD, G. N. S., Photoproduction of charged pions from ^{12}C, 25:12407
PRATT, J. N., Thermodynamic properties of solid palladium-rich Pd--Cd, Pd--In, Pd--Sn, and Pd--Sb alloys, 25:11396
PRATT, R. H., Exact screened calculations of atomic-field bremsstrahlung, 25:11681
PREINHAELTER, J., Quasi-linear dynamics of ion cyclotron instability in an anisotropic plasma, 25:11915
PREPARATA, Giuliano, Light-cone analysis of massive μ-pair production, 25:12228
PREVOT, F., Vacuum problems encountered in nuclear fusion research, 25:11919 (EUR-CEA-FC-566)
PREVOT, Francois, Getter for vacuum pumps, 25:10804
PREVOT, H., Objective detection of cerebral blood flow disturbances with /sup 99m/Tc, 25:11146
PRINTZ, Morton P., Studies on the secondary structure of phenylalanyl transfer ribonucleic acid, 25:10564
PRIOR, R. M., Absolute tensor-polarization calibration of a polarized deuteron beam, 25:12356
PRITCHETT, John W., MACYL6 hydrodynamic code, 25:10765 (AD-709142)
PROBST, P., Colloid clearance: effect of particle size and extrahepatic deposition, 25:10918
PROBYN, J. E. B., Intergranular embrittlement of an austenitic steel due to impregnation with helium, 25:11456 (AERE-R-5622)
PROFOS, G., New steam generating system for the French nuclear power station EL-4, 25:12766
PROKHOROV, V. I., Effect of irradiation on mechanical properties of fcc alloys of Fe--Cr--Ni system. I, 25:11466 (SRARI-P-78)
PRORIOL, J., Angular distributions and correlations in three-body phase space, 25:12135
Relativistic calculations of angular correlations of particles issued from an interaction-free resonance decay, 25:12176
PROSNITZ, Leonard, Repair and reconstruction of chromosomal DNA, 25:11007 (BNL-50203, pp 1-13)
PROTASEVICH, I. I., Thermogenesis of irradiated yeast cells in the process of recovering their reproductive capacity, 25:11324
PROVOTOROV, A. V., MPC of ^{232}Th and natural Th in drinking water, 25:11051
PRPIC, B., Animal experiments on the suitability of ^{66}Ga compounds for diagnosis in nuclear medicine, 25:11169
Functional studies with short-lived reactor isotopes, 25:10943
PRUNIER, C., Effect of β phase-retaining or delta phase stabilizing elements on Pu during alpha--beta thermal cycling, 25:11393
Plutonium transformation heats, 25:11445
PRUSSIN, S. G., Levels in ^{87}Rb populated in decay of ^{87}Kr, 25:12485
PRZYSTAWA, J., Magnetic structure of U_3P_4, 25:12028
PSHONA, S., Dose characteristics of protons with energy 200 MeV, 25:11054 (JINR-P16-5383)
PUCHKOV, G. P., Acceleration and extraction of deuterons from the JINR proton synchrotron, 25:12303 (JINR-P9-5442)
PUCKNELL, V. F. E., Shell-model data from realistic N--N interaction, 25:12686
PULLEN, D. J., Level structure of ^{17}O and the ^{13}C(^{6}Li,d) and ^{13}C(^{7}Li,t) reactions, 25:12425
PURCELL, J. E., Addendum to potential-scattering model for electrons on helium and other atoms, 25:11722

Q

QUICK, Martin Vinicombe, Nuclear reactor fuel elements, 25:12800
QUIJANO-RICO, M., Highly sensitive rapid methods for boron and lithium determination in stone meteorites and rocks, 25:10493
QUINN III, James L., Year book of nuclear medicine. IV, 25:11209
QUINT, R., Dosimetric control in brachycurietherapy, 25:11000
QUINTIN, M., Nondestructive quantitative determination of trace amounts of elements in rocks, 25:10449
Sodium chloride as spectral buffer in emission spectrography, 25:10454

R

RABBEN, H. H., Electron density measurements in the ionosphere with an improved rf impedance probe, 25:11781
RABE, P., Optical absorption of Ce, Ce oxide, Pr, Pr oxide, Nd, Nd oxide, and Sm in extreme ultraviolet, 25:11698
RADOMANOV, V. B., Measurement of scattering angle of particles by Vavilov--Cherenkov radiation, 25:10869 (JINR-E13-5459)
RADVAN, Rostislav, Pulmonary ascariasis in an irradiated organism. I, 25:11265
RAEVSKAYA, M. V., Interdiffusion in Nb--Zr system, 25:11424
RAFALSKI, Anthony L., Low-temperature deformation mechanisms in delta stabilized Pu--Ga alloys, 25:11435
RAGNARSSON, Ingemar, Low-energy spectrus of ^{29}Si, 25:12503
RAI, D. K., Importance of the kinetic-energy expression for a bound electron in classical theory, 25:11701
RAINES, G. E., Estimation of potential radionuclide ingestion by native populations of Eastern Panama and Northwestern Colombia. Bioenvironmental and Radiological-Safety Feasibility Studies, Atlantic-Pacific Interoceanic Canal, 25:10995 (BMI-171-45)
RAJ, R., Nuclear-structure calculations for ^{59}Cu, 25:12451
RAJAMAEKI, Markku, Energy-dependent neutron transport theory in adjacent half-spaces, 25:12857
RAJPUT, J. S., Transition temperature and temperature dependence of the energy gap in thin film superconductors, 25:11845
RAKOVIC, M., Determination of arsenic in biological material by neutron activation analysis, 25:10510
RAM, Rishi, Normal vorticity jump condition across a magnetogasdynamic discontinuity, 25:11756
RAMAKRISHNAN, Alladi, Weak interaction Hamiltonian in L-matrix theory, 25:12162 (AD-710572)
RAMAN, K., Singular off-mass-shell equation with vector-meson exchange, 25:12192 (NYO-2262-TA-232)
RAMAN, Subramanian, Decay of 3.2 sec ^{58}Cu and an unusually hindered E2 transition in ^{58}Ni, 25:12481
RAMASWAMI, Devabaktuni, Annular packed-bed filter, 25:10761
RAMDOHR, H., Karlsruhe reprocessing plant: objectives and conception of WAK installation, 25:10756 (ORNL-tr-2416)
RAMM, Dietolf, Pressure studies in solid D_2 and solid H_2, 25:10575
RAMUS, Pierre, Isodore facility, 25:10794 (CEA-R-4120)
RAMZAEV, P. V., Cesium-137 in lichen-reindeer man in the extreme north of the USSR, 1962--68, 25:11037 (NP-18381)
RANDOLPH, W. L. Jr., Magnetic moments of the 7/2$^-$ mirror states in ^{37}Ar and ^{37}K, 25:12429 (COO-7-565)
RANDRUP, J., Electron-nucleus quadrupole interaction and its influence on β-decay, 25:12685
RANGER, K. B., Spherical vortex motions of a conducting fluid, 25:11554
RANKIN, A., Fixed-t dispersion relations for pion photoproduction in the second resonance region, 25:12146
RANKIN, J. M., Absence of average polarization at 111.5 MHz in pulsar NP 0532, 25:11589
RANZETTA, G. V. T., Electron metallography of precipitates in irradiated and unirradiated 20 wt. percent Cr--25 wt. percent Ni--0.7 wt. percent Nb stainless steel, 25:11428 (AWRE-O-29/67)
RAO, A. P., Synergistic effects in ion-exchange. I, 25:10681
RAO, K. Srinivasa, Photoproduction of charged pions from ^{12}C, 25:12407
RAO, T. Swamy, Effect of γ irradiation on brown sarson, 25:11318
RAO, U. R., Solar cosmic-ray phenomena, 25:11625
RAO, V. U. S., Calculation of the influence of the crystalline electric field on the spin-disorder resistivity of rare-earth alloys and comparison with results on $CeAl_2$, 25:12009
RAPIN, M., Plutonium transformation heats, 25:11445
RAPP, Robert A., Prog. rpt. on mixed conduction in solid electrolytes, annual, 12/1/70, 25:12883 (COO-1440-21)
RASHEVSKII, V. P., Experiments on α-particle acceleration by collective method, 25:12305 (JINR-P9-5558)
RASHID, Khalid, Energy--momentum tensor of Dirac field with anomalous magnetic moment, 25:12251
RASMUSSEN, J. O., Levels in ^{87}Rb populated in decay of ^{87}Kr, 25:12485
RATTI, A., On the scintigraphy of parenchymatous organs and in particular of the spleen, 25:11201
RATUSKY, J., Reactions of salts of deuterated

benzenecarboxylic acids, 25:10545
RAUTENBERG, I., Can failure--steam loop, 25:12820 (KFK-1255)
RAWAT, S. S., Coupled wave equations for magnetoplasma with anisotropic pressure, 25:11946
RAWITSCHER, G. H., Nuclear size effects in the polarization of elastically scattered electrons, 25:12664
RAWLINS, J. A., Photoneutron angular distributions from $^{2}H(\gamma,n)H$ reactions, 25:12374
RAYNE, J. A., Doppler-shifted acoustic cyclotron resonance in tungsten, 25:12022
RAYNOR, J. B., Atmospheric oxidation of unalloyed plutonium at low humidities, 25:11346 (AWRE-O-100/66)
RAZAVY, M., Construction of the T-matrix from its symmetric part, 25:12673
READ, J., DYNA: computer program for determining motions of head of PCRV with complete circumferential crack, 25:10753 (GAMD-7567)
REAVIS, J. G., Differential thermal analysis observations of U--Pu dicarbides, 25:11522
Melting behavior of (U,Pu) monocarbides, 25:11507
REBA, Richard C., Radioiodinated toluidine blue: an unsatisfactory scanning agent, 25:11188
REBANE, T., Measurement of the $2^{2}S/sub\ {}^{1}/_{2}$--$2^{2}P/sub\ {}^{3}/_{2}$ energy separation in H, 25:11691
REBEL, H., Beta spectrum of ^{204}Tl, 25:12615
Investigation of β spectrum of ^{14}C with a proportional counter with inner anticoincidence screens, 25:12380 (KFK-1222)
RECHTIEN, J. J., Low temperature transformations in plutonium, 25:11443
REDFIELD, J. A., Stable numerical integration of conservation equations for hydraulic networks, 25:12793
REDISH, Edward F., Off-shell effects in knockout reactions, 25:12670
REED, Jack W., Wind and airblast loads on window panes, 25:10792 (SC-RR-70-441)
REEDY, R. C., Protons and alpha particles emitted from ^{78}Br compound nuclei with differing angular-momentum distributions, 25:12461
REEH, H., Properties of conserved local currents and symmetry transformations, 25:12264
REES, M. J., Absorption and scattering of ultraviolet and x-ray photons by intergalactic gas, 25:11654
REESE, Glen Patrick, Model for electronic stopping power of heavy ions, 25:11680
REEVES, H., Energetics of L-nuclei formation in stellar atmospheres and its relevance to x-ray astronomy, 25:11548
Nucleosynthesis of Li, Be, and B, 25:11542 (NP-18591)
REICH, C. W., Gamma-ray studies of the γ-vibrational band of ^{166}Er, 25:12599
REICHSTEIN, I., Study of N + α system, 25:12363
REIMER, G. M., Geometry factor in fission track counting, 25:10695
REINHOLD, Guenther, Thermal diffusion column, 25:10783
REINHOLD, Hulbert S., Response of tumor blood supply to fractionated irradiation, 25:11257 (BNL-50203, pp 210-14)
REINWEIN, D., Successes and failures of fractionated radioiodine therapy among 700 hyperthyroid patients, 25:11230
REISENAUER, A. E., Mathematical model for approximating transient, three-dimensional groundwater systems, 25:12880 (BNWL-SA-3539)
REIST, P. C., Prog. rpt. on air cleaning, semiannual, 3--8/70, 25:10797 (NYO-841-23)
REMY, Clotilde, Effect of a β + α transformation and of oxygen on plutonium distribution in dilute Zr--Pu and Ti--Pu alloys, 25:11431 (CEA-CONF-1691)
RENNER, B., Empirical test of tensor meson dominance, 25:12216
RENNERT, A., Growth, survival, and content of ascorbic acid in cultures of tobacco after γ irradiation, 25:10965
RENNEX, B. G., Achieving uniform spatial response from large area liquid scintillation detectors, 25:10875
RENO, Donna, Repair and reconstruction of chromosomal DNA, 25:11007 (BNL-50203, pp 1-13)
REPRINTSEV, L. V., Research on 100-MeV electron storage ring of Technical Physics Institute of Ukrainian Academy of Sciences, 25:12307 (KHFTI-69-27)
RESHETNIKOVA, K. A., Motion of the charged election ring in the ripple magnetic field, 25:12301 (JINR-P9-5394)
REUSS, Paul, COREGRAF 2: code for computing graphite lattices and their evolution for IBM 360 and CDC 6600, 25:12774 (CEA-N-1344(1))
REVAI, J., Simple model of low-energy K-N scattering on bound nucleons, 25:12213
REVESZ, L., Specific effect of radiation-sterilized tissues on cellular multiplication, 25:11330
RHOADES, Clifford E. Jr., Hagedorn equation of state in neutron stars, 25:11566
RHODES, Wesley, Particle--hole interactions in ^{90}Zr, 25:12537
RIANDEY, C., Matrix effects on determination of traces by atomic absorption, 25:10457
RICCABONA, G., Studies on the uptake of ^{203}Hg-chlormerodrine by brain tumors, 25:11179
RICCI, Enzo, Activation analysis. Recent advances in using charged particles, gamma photons, and ^{252}Cf sources, 25:10497
RICCI, G., Radiotherapy of cancer of the oesophagus, 25:11236
RICCI, M. V., Preliminary results regarding development of superconducting ribbons of Nb_3Sn, 25:11820 (LNF-70/18)
RICCI, R. A., Re-examination of ^{66}Ge decay, 25:12477
RICH, Peter Hamilton, Utilization of benthic detritus in a marl lake, 25:12884 (COO-1599-31)
RICHARD, J.-P., Separation of relativity effects and effects due to a quadrupole moment of the sun in time-delay measurements, 25:11602
RICHARDS, J. M., Measurement of time-of-flight using 300 Mc/s scalers, 25:10891 (AERE-R-5422)
RICHTER, A., Charge asymmetry effects in reaction $d(\alpha,t)^{3}He$, 25:12355
Reaction $^{10}B(\alpha,^{6}Li)^{8}Be$, 25:12392
RICHTER, B., Coincidence spectrometer for fast neutrons, 25:10862
RICHTER, R., T = 3/2 states of ^{25}Mg and ^{29}Si, 25:12450
RICQ, J. M., Activation analysis of rocks and degradation products, application to two types of sands with various mineralogic grades, 25:10492
RIGNEY, D. A., Electrotransport in liquid Na--K, 25:11404
RIJKE, A. M., Fusion of irradiated linear polyethylene crystallized by high speed stirring, 25:10618
RIKHVITSKII, S. V., Time-coordinate compensator for the time spectrometers with long scintillators, 25:10813 (JINR-P13-5378)
RIMAWI, K., Resonance neutron capture in ^{103}Rh, 25:12561
RIMINI, A., Microscopic description of charge form factor of ^{4}He, 25:12651
RINAUDO, G., Spin--parity analysis of B-meson produced in $\pi^{+}p$ reactions, 25:12119
RING, Harvey Michael, Annihilation of 1.6- to 2.2-GeV/c antiprotons into K_1 mesons, 25:12097
RIOTTE, M., Sleep pattern following γ irradiation in cats, 25:11261
RISBERG, J., Regional cerebral blood flow, 25:11143
Variations in regional cerebral blood volume during mental activity, 25:11151
RISHER, Daniel H., Gamma-ray attenuation at energies of approximately 6 and 8 MeV, 25:11947
RISSON, Frederic, Long-term forecasting of cycles of sunspots, 25:11631
RITTENBERG, V., Dual amplitudes for 6 pions with epsilon-tensor couplings, 25:12131
RITTENHOUSE, C. T., Development of pelletized heat sources for thermal batteries, 25:12905 (SC-CR-70-6137)
ROBBINS, J. L., Effect of hot working on room-temperature strength and ductility of Pu--1 wt percent Ga delta-stabilized alloy, 25:11390
ROBBINS, M. F., Proton drift echoes in the magnetosphere, 25:11801
ROBERSON, W. R., Angular correlation study of low-lying levels of ^{29}P, 25:12480
ROBERTS, A. C., Intergranular embrittlement of an austenitic steel due to impregnation with helium, 25:11456 (AERE-R-5622)
ROBERTS, E. C., Strain-induced phase transformations in Ti-6Al-4V, 25:11453
ROBERTS, Jabus Bridges Jr., Relative rate K/sub e2/+/K/sub μ2/+ and upper limit for the structure dependent radiation in K + eνγ, 25:12077
ROBERTSON, B. C., Electromagnetic properties of ^{55}Fe, 25:12483
ROBERTSON, D. E., Trace element calibrations and profiles at Geosecs Test Station in Northeast Pacific Ocean, 25:10428
ROBINSON, A. C., Influence of thermal neutron irradiation on equilibrium temperature of α + β transformation in Pu, 25:11467
ROBINSON, L. C., Electrodynamic analog of wave diffraction phenomena, 25:12156
ROBINSON, R. L., Quadrupole moment of first 2+ states of Sn, 25:12587
ROBISCOE, R. T., Measurement of the $2^{2}S/sub\ {}^{1}/_{2}$--$2^{2}P/sub\ {}^{3}/_{2}$ energy separation in H, 25:11691
ROBOTHAM, P. P. J., Radiation dose rates from plutonium oxide--beryllium oxide mixtures, 25:11052 (AERE-R-5069)
ROBSON, B. A., Scattering and polarization of nucleons and deuterons, 25:12624 (ANU-P-497)
ROCK, R. L., Controlling employee exposure to alpha radiation in underground uranium mines. Volume I, 25:11085
RODENBERG, R., Spin-zero mesons and broken chiral SU_3 x SU_3, 25:12237
RODGERS, A. W., Masses of pulsating stars, 25:11558
ROECKL, E., Decay of ^{84}Se, ^{91}Kr, ^{97}Y, ^{99}Nb, ^{99}Zr, ^{100} ^{101}Nb, and ^{101}Zr, 25:12462
ROESINGER, S., Sulfoxidation of long-chain hydrocarbons with aid of γ radiation, 25:10614
ROESLER, H., Assessment of functional significance for renal artery stenosis confirmed by angiography. comparison of the radiorenogram with the angiotensininfusion test and with the plasma renin content in both peripheral and renal venus blood, 25:11164
Quantitative analysis of the radiorenogram based on ^{131}I-orthohippuric acid clearance, 25:11159
Quantitative radiorenograms as function tests following kidney transplantation, 25:11162

ROETHEMEYER, H., Reactivity measurement in reactor cores on MTR fuel elements with a one-sided heavy water reflector, 25:12818 (FMRB-34/70)
ROGERS, J. D., Reorientation effect measurements in ^{106} ^{114}Cd, 25:12619
ROGERS, James E., Gamma-ray attenuation at energies of approximately 6 and 8 MeV, 25:11947
ROGGE, M., Reaction ^{90}Zr(^{3}He,d)^{91}Nb at 18 MeV, 25:12613
ROGOVIN, Z. A., Radioprotective action of polymer salt of cystamine and sulphopropyl ester of dextrane, 25:11108
ROGOZKIN, V. D., Change in blood in prolonged and brief irradiation of guinea pigs, 25:11278
Radioprotective action of polymer salt of cystamine and sulphopropyl ester of dextrane, 25:11108
ROHWER, Paul S., Dose-estimation studies related to proposed construction of Atlantic--Pacific Interoceanic Canal with nuclear explosives: Phase III, 25:11055 (ORNL-4579)
ROLLAND, Marie Louise, Apparatus for automatic liquid phase chromatography, 25:10659 (CEA-N-1267)
ROMAHN, A., Determination of renal clearance by external γ-ray measurements, 25:11155
Thyroid diagnosis with a whole-body counter in children, 25:11172
ROMANOV, A. S., Neutron-activation analysis of seawater, 25:10507
ROMANOV, E. P., Generator for studying superconductivity by a pulse method, 25:10899
ROMANOV, V. M., Lifetime of 2007-keV level for ^{46}Ti nucleus, 25:12508
ROMANOVA, A. V., Electrical conductivity of liquid indium-bismuth alloys, 25:11398
ROMER, Henry Fiske, Production of neutral mesons in backward π⁻p scattering, 25:12113
ROMMEL, K., Studies on liver function with computer-scintigraphy, 25:10919
RON, A., Far-infrared spectra of ethane, ethylene, and acetylene, 25:10544
RONAMI, G. N., Interdiffusion in Nb--Zr system, 25:11424
RONCARI, G., First attempts of clinical application of a method for the quantitative interpretation of renogram with radiohippuran, 25:11208
RONCHETTI, C., Treatment of water in a nuclear plant for the testing of fuel elements, 25:12821 (LIB/Trans-335)
RONCHI, C., Lattice defects in fluorite structure of UO_2 and UO/sub 2+x/, 25:11520
ROODBERGEN, S., Lifetimes of 2⁺ and 4⁺ rotational states in heavy doubly even nuclei, 25:12542
Lifetimes of rotational states in ^{229}Th and ^{235}U, 25:12541
ROOS, P. G., Test of the shell model for ^{208}Pb, 25:12574
ROQUES, M., Correction of matrix effect in ultraviolet spectrographic analysis, 25:10453
ROSA, Rui, One-dimensional ion--acoustic modes of bounded plasmas, 25:11937
ROSDOLSKY, Hans, Unitarity constraints for multiple resonances, 25:12643
ROSE, E., Accumulation and excretion of ^{224}Ra (Th X) during treatment of ankylosing spondylitis, 25:11231
ROSE, Vernon E., Review of international microwave exposure guides, 25:11088
ROSEN, G., Solution to the initial-value problem for nonlinear classical field equations, 25:12242
ROSEN, Lon Michael, Quantum field theory without cutoffs for self-interacting bosons, 25:12248
ROSENBAUM, Joe B., Metallurgical application of solvent extraction. II, 25:10656 (BM-IC-8502)
ROSENBERG, Ivan, Distribution of brightness and polarization in Cassiopeia A at 5.0 GHz, 25:11590
ROSENBERG, Ronald L., Unified theory of the interplanetary magnetic field, 25:11608
ROSENBERG, T. J., Correlation study of auroral luminosity and x rays, 25:11808
ROSENBLATT, J., Transition-field enhancement and shape effects due to magnetic inclusions in a superconductor, 25:11840
ROSENDORFF, C., Measurement of hypothalamic blood flow in the conscious rabbit by a radioactive inert gas clearance technique, 25:11194
ROSENFELD, Alita, Studies on the secondary structure of phenylalanyl transfer ribonucleic acid, 25:10564
ROSENTHAL, Carey M., Treating perturbation problems, with application to exchange equations for H_2^+ and H_2, 25:11735
ROSENWALD, J. C., Dosimetric control in brachycurietherapy, 25:11000
ROSNER, Herbert Reginald, Relativistic calculations of atomic X-ray and Auger transition rates, 25:11685
ROSNER, Jonathan L., Consistency between low-energy and high-energy hadron scattering, 25:12175 (COO-1764-81)
ROSS, J. R., Recovery of uranium from natural mine waters by countercurrent ion exchange, 25:10657 (BM-RI-7471)
ROSSEL, J., Kinematically complete experiment on reaction n + d → n + n + p, 25:12367
ROSSI, G., Spectrochemical analysis of Zr and its alloys. I, 25:10430 (EUR-4541)
ROSSI, H. H., Relative biological effectiveness of x-rays and 0.43-MeV monoenergetic neutrons on somatic mutations and loss of reproductive integrity in Tradescantia stamen hairs, 25:11313
ROSSI, I., Effect of solvent on frequencies of CD and CH stretching band in some haloforms, 25:10540
ROTE, D. M., Λ-particle binding in nuclear matter, 25:12668
ROTENBERG, Manuel, Theory and application of Sturmian functions, 25:11732
ROTH, G., Differential scintigraphic representation of the pancreas by means of a computer, 25:11176
ROTHHARDT, L., Modern plasma physics as a branch of nuclear engineering, 25:11752
ROUCHAUD, J. C., Uranium isotopic determination in rocks by neutron activation, 25:10494
ROUGE, Pierre, Transmitting motion through reactor wall, 25:12863
ROUNDS, Donald E., Argon laser micro-irradiation of mitochondria in rat myocardial cells in tissue culture, 25:11242
ROUSH, M. L., Nuclear reaction calibration energies by velocity measurements, 25:12402
ROUSSEAU, J., In-pile loop BANJO, 25:12813 (CEA-CONF-1673)
ROUSSEL, Emile, Isodore facility, 25:10794 (CEA-R-4120)
ROUSSEL, P., Transfer reactions (α,t), (α, ^{3}He) in the fp shell, 25:12434
ROUX, C., Plutonium transformation heats, 25:11445
ROUX, G., Visualization by image intensifier of radioactive indicator flow through the cardiac chambers and the large vessels, 25:11120
ROW, T. H., Evaluation of Burgess Fobes Paint Company protective coatings for nuclear plant application, 25:12804 (ORNL-TM-3104)
ROWAN-ROBINSON, M., Extragalactic radio sources. II, 25:11597
ROWLAND, G. F., Carcinogen induced immunodepression in mice, 25:10990
ROY, D. M., Fast breeder reactor static physics methods development and analysis project. Volume 1. FAREI: one-dimensional fast reactor physics design and analysis code, 25:12772 (BAW-3867-9(Vol.1)(Rev.1))
ROYCE, E. B., Dynamic yield strengths of B_4C, BeO, and Al_2O_3 ceramics, 25:11490
ROYER, D., Study of the ^{208}Pb(d,^{3}He)^{207}Tl and ^{206}Pb(d,^{3}He)^{205}Tl reactions at 80 MeV, 25:12575
ROYNETTE, A., Economics of industrial nuclear explosions, 25:10750
RUBENFELD, Sidney, /sup 69m/Zn-chloride. A new scanning agent: a study of its dosimetry and biological fate, 25:11204
RUBIN, N. B., Calculation of the phase volume of the electron--ion bunches in the collective accelerator and the problems of separation, 25:12302 (JINR-P9-5405)
RUBINSTEIN, H. R., Dual amplitudes for 6 pions with epsilon-tensor couplings, 25:12131
RUBINSTEIN, Mark, Investigation of the metal--insulator transition in V_2O_3 by nuclear magnetic resonance, 25:12039
RUCKER, T. R., X-ray and nuclear radiation facilities, personnel safety features, 25:11078 (Y-1754)
RUD, N., M1 admixtures in transitions from γ-vibrational states in ^{152}Sm, ^{154}Gd, and ^{156}Gd, 25:12576
RUDNICK, F. D., Study of decay mode K/sub L/^{0} → π⁺π⁻π⁰, 25:12087
RUDNICK, S. J., Training manual for fabrication of printed-circuit boards, 25:12864 (ANL-7725)
RUDNITSKAYA, E. I., Morphological changes in rats after injection of ^{241}Am, 25:10942
RUEL, G., Quantometer for determination of trace elements in natural materials, 25:10451
RUFF, F., Application of /sup 99m/Tc for scintigraphic studies of pulmonary circulation, 25:11128
RUFFINI, Remo, Hagedorn equation of state in neutron stars, 25:11566
RUH, Arthur Walter, Polarization of protons inelastically scattered on ^{24}Mg, ^{52}Cr, and ^{58}Ni, 25:12433 (NP-16552)
RUNCIMAN, W. A., Origin of diffuse interstellar band at 4430A, 25:11643
RUPP, W. Dean, Repair and reconstruction of chromosomal DNA, 25:11007 (BNL-50203, pp 1-13)
RURARZ, E., Excitation of isomeric activities in ^{71}Ge, ^{79}Br, and ^{79}Br using 14.8-MeV neutrons, 25:12430 (INR-P-1091)
RUSSELL, G. J., Production of lithium oxide by electron irradiation of lithium fluoride, 25:11964
RUSSELL, J. J., Observation of muon trident production in lead and the statistics of the muon, 25:12083
RUSSO, P. A., Mass determinations of neutron-deficient nuclides ^{88}Zr and ^{140}Nd by (p,2n) threshold measurements, 25:12607
Spin isomers of the shape isomer /sup 237m/Pu, 25:12530 (RLO-1388-130)
RUSTGI, M. L., Nuclear-structure calculations for ^{59}Cu, 25:12451
RUSTICHELLI, F., Measure of the factor of fast fission epsilon in a D_2O uranium lattice, 25:12817 (EUR-4326)
RUSTON, W. R., Catalytic decomposition of carbon monoxide on pure iron, mild steels, and alloyed steels, 25:11374 (DP-Report-530)
RUVARAC, A., Thermodynamics of uranyl ion exchange on Zr of various crystallinities, 25:10680
RYABCHENKO, N. I., Radiosensitivity of DNA in vivo and in vitro, 25:10966
RYABININ, A. I., Neutron-activation analysis of seawater, 25:10507
RYABUKHIN, Yu. S., Neutron and neutron-capture therapy,

25:11232
RYAN, Jack L., Halide complexes of pentavalent U, 25:10576
RYBAKOW, Z., Stability and radiochemical purity of some radiopharmaceuticals. III, 25:10642
RYDING, G., Electron capture and loss by fast Br and I ions traversing light gases, 25:11710
RYNDIN, R. M., Verification of vector dominance, 25:12140
RYTER, C., Energetics of L-nuclei formation in stellar atmospheres and its relevance to x-ray astronomy, 25:11548
RZEWUSKI, Henryk, Activation energy and frequency factor of 100°K annealing stage of simple defects in n-type Ge, 25:11954

S

SABO, E., Pulsed reactor potentialities for neutron activation analysis, 25:10489 (KFKI-70-25-NAC)
SACCHETTI, N., Preliminary results regarding development of superconducting ribbons of Nb_3Sn, 25:11820 (LNF-70/18)
SACERDOTI, G., Preliminary results regarding development of superconducting ribbons of Nb_3Sn, 25:11820 (LNF-70/18)
SACHS, Charles, Prognostic value of radioisotopic renal function studies for selecting patients with renal arterial stenosis for surgery, 25:11186
SACKMAN, J. F., Atmospheric oxidation of unalloyed plutonium at low humidities, 25:11346 (AWRE-O-100/66
SADOWSKI, M., Plasma containment in a spherical multipole magnetic trap, 25:11863
SADOWSKI, Marek, Experimental studies of plasma generated by RPI system, 25:11883
SADYKHOV, F. S., Investigation of possible anapole and electric dipole moment of proton with help of annihilation reaction p anti p reversible e^+e^-, 25:12224
SAEBEL, Manfred, Inhibition of estrogen-induced radioprotection of placental nucleic acids and proteins by antiestrogen Clomiphene, 25:11104
SAEKI, B., Numerical differential cross sections of reaction $^{58}Ni(p,t)^{56}Ni$ with 51.9 MeV protons, 25:12431 (INSJ-124)
SAH, R. C., Observation of muon trident production in lead and the statistics of the muon, 25:12083
SAHORES, J., Matrix effects in x-ray fluorescence, 25:10447
SAITOH, Masashi, Thermoluminescence of purified LiF powder, 25:11951
SAJI, Y., Numerical differential cross sections of reaction $^{58}Ni(p,t)^{56}Ni$ with 51.9 MeV protons, 25:12431 (INSJ-124)
SAKAI, Mitsuo, Quasi-gamma bands in ^{152}Gd and possible presence of quasi-K quantum number, 25:12518 (INSJ-123)
SAKAI, Norisuke, Third-order calculation in a nonpolynomial Lagrangian theory, 25:12266
SAKAI, Sunao, Twisting invariant factorization in dual resonance model. I, 25:12184
SAKHAROV, E. S., Optimum dimensions of the operational volumes of radiation circuit joints, 25:12829
SAKURADA, Ichiro, Grafting acrylonitrile onto polyvinyl chloride powder and spinning fiber, 25:10595 (JAERI-5026, pp 35-41)
Grafting of acrylic acid onto polyester fiber, 25:10602 (JAERI-5026, pp 73-9)
Radiation-induced graft copolymerization to polyester. IV, 25:10597 (JAERI-5026, pp 46-51)
Radiation-induced graft copolymerization to polyester. VI, 25:10599 (JAERI-5026, pp 56-62)
SAKURAI, Ko, Effect of glutathione on the protection against radiation, 25:11098
SAKURAOKA, M., Deep inelastic e-p scattering and a reggeization scheme for photon processes, 25:12148
SALAMON, Andras, Activation analysis by charged particles, 25:10504
SALAMON, E., Recovery of skin reactions in mice after split-dose irradiation, 25:11260 (BNL-50203, pp 286-91)
SALEH, F. A., Recovery of U, Th, and Ce from Egyptian monazite sands. I, 25:10683
SALIOU, C., X-ray spectrometry using Si (Li) diodes, 25:10812 (CEA-N-1401)
SALLER, H., Spinor potentials with logarithmic regularization, 25:12261
SALO, Seppo, SYNTH2: two dimensional multigroup flux synthesis calculation code, 25:12844 (TKK-F-A-121)
SALUNKHE, D. K., Effects of γ radiation on Penicillium expansum. II, 25:10979
SALVATELLI, E. R., Collisional-quenching processes in H(2s), 25:11723
SALWIN, A. E., Direct interaction effects in the fission of ^{238}U with 63.5-MeV ^4He ions, 25:12526 (MNC-3783-7)
SALYERS, A., Photodisintegration of ^9Be, 25:12399
SAMOILOV, A. V., Investigation of a particle beam with energy up to 70 GeV with a spark spectrometer, 25:10868 (IFVE-SEF/OP-70-13)
SAMOSYUK, V. N., Photo-nuclear activation analysis of O in pure materials, 25:10501
SAMSON, A. C. R., Mutants of E. coli with altered surface properties and sensitive to uv light, 25:11029
SAMUEL, Mark Aaron, Finite quantum electrodynamics, 25:12247
SANAK, J., Use of low-level α spectrometry in the determination of elements occurring in traces in natural mineral substances, 25:10477
SANDEMAN, T. F., Radiotherapy of kidney and ureter, 25:11225
SANDENAW, Thomas A., Heat capacity behavior of ^{242}Pu between 10° and 373°K, 25:11385
Low-temperature heat capacity of $PuC_{0.81}$, 25:11493
SANDERS, J. B., Spatial distribution of energy deposited by atomic particles in elastic collisions, 25:11682
SANNAZZARI, G. L., Contribution of scintigraphy for the diagnosis of liver diseases, 25:11198
SANO, Katsunori, Solidification of radioactive sludges, 25:10799
SAPP, R. C., Temperature scale for neodymium zinc nitrate below 1K, 25:11852
SARALKAR, A. A., Electric and magnetic resonances of a particulate magnetoplasma, 25:11929
SARANTITES, D. G., Structure of ^{51}Cr, 25:12435
SARANTITES, Demetrios G., Level structure of ^{101}Rh from the decay of 8.5 h ^{101}Pd, 25:12596
SARANTSEV, V. P., Calculation of the phase volume of the electron--ion bunches in the collective accelerator and the problems of separation, 25:12302 (JINR-P9-5405)
Experiments on α-particle acceleration by collective method, 25:12305 (JINR-P9-5558)
SARCIA, A., Contribution of earth sciences to the peaceful applications of nuclear explosions, 25:10740
SARCIA, J. A., Application of nuclear explosives in the mining industry, 25:10747
SARILL, W. J., Centrifugal force and general relativity, 25:12274
SARKAR, D., Magnetic multipole electroexcitation, 25:12657
SARSUNOVA, M., Moisture determination in certain compounds used for pharmaceutical purposes based upon neutron scattering and moderation, 25:10486
Neutron absorption analysis of pharmaceutic preparaticns containing boron, 25:10487
SASAKI, Tadashi, Composition ranges with similar constricted hysteresis loops in Mn--Al--B alloys, 25:11983
SASAYAMA, Tatuo, Some electrical properties of the uranium--plutonium mixed oxides, 25:11991
SASSARD, J., Sleep pattern following γ irradiation in cats, 25:11261
SASTRY, D. L., Gamma spectrum from the thermal neutron capture in cerium, 25:12551
SATCHLER, G. R., Exchange effects in the nucleon--nucleus optical potential, 25:12689
Exchange effects with a realistic interaction for inelastic scattering, 25:12676
SATO, C., Type of radiation cell-killing on human lymphocytes, 25:11299
SATO, Hirokazu, Bound states in a superconductor containing a magnetic impurity, 25:11841
SATO, T., Co-precipitation of carrier-free ^{31}Si with hydroxides, 25:10675
SATO, Teruyuki, Feedback control of the PIG discharge of the QP machine, 25:11921 (IPPJ-T-2)
SAUER, P., Absorption of ^{45}Ca from intestinal tract of rat, 25:10512
SAUNDERS, P. C., Catalytic sites for deuterium exchange with benzene over alumina, 25:10530
SAUS, A., Contributions to the radiation-induced sulfoxidation of paraffins, 25:10592 (BMBW-FBK-70-25)
SAUTER, E., Influence of statistical field errors on stability of longitudinal phase oscillations of a linear accelerator (flatness-problem), 25:12326
SAVIC, Stanley D., Results of a study of color television set assembly and repair workers x-ray safety, 25:11063
SAVOLAINEN, A. W., Progress summary of nuclear safety research and development projects, 25:12805
SAWADA, Katsuro, Two-branch excitation spectrum of liquid ^4He, 25:11818
SAWADA, Shoji, Multiple production processes and rearrangement of sakatons, 25:12186
SAWYER, H. R., Selective extirpation of oral ciliature of Blepharisma by laser microbeam, 25:11322
SAXE, R. F., Prog. rpt. on acoustic emissions from boiling bubbles, 2--11/70, 25:10769 (ORO-3911-3)
SAXENA, S. C., Thermal conductivity of carbon dioxide in temperature range 100 to 1075°C, 25:10574
SCALISE, E. Jr., Changes in coronal condensations emission after solar bursts at microwaves, 25:11620
SCARF, Frederick L., Microscopic structure of the solar wind, 25:11626
SCARONI, A., Behavior of metallic U--Zircaloy-2 fuel element defects and exposure to aqueous corrosion, 25:11347 (CISE-R-222)
Experimental irradiation of metallic U fuel elements in the Halden HBWR reactor, 25:11457 (CISE-R-278)
SCHACHER, J., Level density parameters for Ge, Ho, and Ta, 25:12536
SCHAEFFER, R., Core polarization corrections to DWBA for (p,p') scattering, 25:12678
SCHAEFFER, Richard, Exchange effects for composite particles, 25:12691
SCHALL, Roy F. Jr., Nuclear structure effects in (p,2 nucleon) reactions on isotopes of Te, 25:12581
SCHARFETTER, F., Studies on the uptake of ^{203}Hg-chlormerodrine by brain tumors, 25:11179

SCHATZMAN, E., Nucleosynthesis of Li, Be, and B, 25:11542 (NP-18591)
SCHATZMANN, E., Syrovatskii process, 25:11633
SCHEER, J., Reaction $^{15}N(tau,\alpha)^{14}N$, 25:12424
SCHEER, K. E., Animal experiments on the suitability of ^{68}Ga compounds for diagnosis in nuclear medicine, 25:11169
Computer evaluation of scintigraphic studies obtained with a scintillation camera, 25:11122
Quantitative radiocardiographic studies with a scintillation camera, 25:11119
Scintigraphy of renal function evaluated by digital and analog computers, 25:11165
SCHEER, M. M., Thermodynamic properties of propane as bubble chamber liquid, 25:10876
SCHEER, Milton D., Isotope effects in the hydrogen-atom addition to olefins at low temperatures, 25:10538
SCHELLMAN, R., Radioisotope studies on hyperemia producing treatment, 25:10916
SCHENCK, P., Angiocardiography with a scintillation camera, 25:11121
Lung scintigraphy with ^{131}I-labeled MAA in late sequelae following blunt chest concussions, 25:11135
Sequential use of Anger camera in double-tracer studies, 25:10928
Technical advances of pancreatic scintigraphy with fast scanner (Dynapix), 25:11212
SCHENTER, R. E., Hard-core potential representation, 25:12659
SCHERRER, P. H., Comparison of the mean photospheric magnetic field and the interplanetary magnetic field, 25:11603
SCHEUER, P. A. G., Luminosity--volume test for quasi-stellar objects, 25:11664
SCHIEBER, D., Magnetic control of a conducting jet, 25:11775
SCHLESINGER, Y., Radiation widths of bound nuclear levels, 25:12447
SCHLESSINGER, L., Properties of the K matrix, 25:12669
SCHLIENGER, M., Dosimetric control in brachycurietherapy, 25:11000
SCHLOTT, K., DWBA model applied to the $^{24}Mg(d,p)^{25}Mg$ reaction at E/sub d/ = 13.5 MeV, 25:12457
SCHLUETER, A., Influence of electrical conductivity on the equilibrium of low-pressure plasma in stellarators, 25:11912 (MPI-PA-7/62)
SCHMAHL, Edward J., Magnetic fields and the structure of the solar corona. II, 25:11604
SCHMIDLIN, P., Computer evaluation of scintigraphic studies obtained with a scintillation camera, 25:11122
SCHMIDT, C. G., Some aspects of abdominal lympho-scintigraphy, 25:11177
SCHMIDT, H., Observation windows of synthetic sapphire (leucosapphire) in high-pressure vessels, 25:11488 (KFK-1211)
SCHMIDT, K., Determination of regional blood flow with ^{133}Xe in the brain of Parkinson and tumor patients, 25:11147
SCHMIDT, K. J., Assessment of renal blood flow with radioactive labeled compounds excreted by glomerular filtration, 25:11153
Comparative determination of hepatic blood flow with colloidal ^{198}Au and colloidal /sup 99m/Tc-S, 25:11140
Comparison of renal isotope diagnosis with vasoconstrictor content in the renal vein of hypertensive patients, 25:11163
Contribution of scintigraphy for evaluation of vascular renal diseases, 25:11166
SCHMIDT, R. A., Needed: nuclear engineering standards, 25:12758
SCHMIDT, W., Optical-model analysis for ^{6}Li elastic scattering by ^{16}O at 20 MeV, 25:12408
SCHMIDT-BLEEK, F., Planning an atomic beam apparatus for investigation of elementary chemical processes of neutral particles, 25:10517 (JUL-674-RC)
SCHMIDT-ROHR, U., Proton pick-up from ^{19}F, ^{20}Ne, and ^{22}Ne, 25:12385
SCHMUNK, R. E., Lattice dynamics of zirconium, 25:12026
SCHNABEL, K., Sequential use of Anger camera in double-tracer studies, 25:10928
Technical advances of pancreatic scintigraphy with fast scanner (Dynapix), 25:11212
SCHNEIDER, C., Objective detection of cerebral blood flow disturbances with /sup 99m/Tc, 25:11146
Perfusion scintigram of lungs during various stages of pulmonary sarcoidosis (Morbus boeck), 25:11133
SCHNEIDER, H., Coincidence spectrometer for fast neutrons, 25:10862
SCHOFER, N. L., Extraction of U(VI) and selected M(III) cations by bis neo-octyl phosphoric acid in two different hydrocarbon diluents, 25:10679
SCHOFILL, John Luther Jr., Kinetics of oxidation of Mo, 25:11409
SCHOLZ, A., Determination of thyroidal clearance during an automatically controlled and constant ^{131}I blood level, 25:11173
SCHOONOVER, D. R., Excitation of He^+ in 20- to 100-keV He^+--He collisions, 25:11713
SCHORN, R. A., Improved solar wavelengths between 7780 and 7925 A, 25:11611
SCHOTSMANS, L., Low-lying 0^+ states in ^{12}C and ^{16}O, 25:12412
Projected Hartree--Fock calculation for light nuclei. V, 25:12396
SCHRADER, David M., Detection of positronium hydride, 25:11700
SCHUBERT, G., Stability of rotating stars. III, 25:115[illegible]
SCHUELLER, W., Karlsruhe reprocessing plant: objectives and conception of WAK installation, 25:10756 (ORNL-tr-2416)
SCHULTZ, W. W., 1/v dielectric track detectors for slow neutrons, 25:10820
SCHULZ, H., DWBA model applied to the $^{24}Mg(d,p)^{25}Mg$ reaction at E/sub d/ = 13.5 MeV, 25:12457
SCHUSSLER, F., Disintegration of the two isomers of ^{84}Br (31.8 min and 6.0 min), 25:12444
SCHUTTE, F., Method of measuring the phase angle of a charged particle beam in a cyclotron, 25:12329
SCHWARTZ, E. G., Prog. rpt. on powder metallurgy compaction, 9--11/70, 25:12913 (SRC-475-9)
SCHWARTZ, Leon Joseph, Interactions of refractory metal silicide coatings with substrates, 25:11519
SCHWARTZ, Y. A., Far-infrared spectra of ethane, ethylene, and acetylene, 25:10544
SCHWEIZER, J., Colinear and noncolinear magnetic structures in rare earth compounds RNi_3 and R_2Ni_7, 25:11979 (CEA-CONF-1704)
SCHWERER, F. C., Low field magnetoresistance of nickel polycrystals, 25:12897 (NYO-3087-23)
SCHWERER III, Frederick Carl, Some ferromagnetic effects in the electrical resistivity of nickel, 25:12895 (NYO-3087-17)
SCHWETJE, W., Modal development of the neutron transport equation for plane geometry, 25:12340 (KFK-1223)
SCHWIMMER, A., Charge distributions and multiperipheralism, 25:12179
SCHWOB, J.-L., Multilayer targets as a diagnostic tool for laser-produced plasmas, 25:11870
SCIESINSKA, E., Accuracy of the neutron method of moisture measurement, 25:10887 (INP-709)
SCOTT, D. K., Intermediate structure and reaction $^{28}Si(p,p')^{28}Si$, 25:12470
SCOTT, F. R., Use of optical spectra to measure large electric fields in a hot-ion plasma, 25:11874
SCOTT, V. D., Electron metallography of precipitates in irradiated and unirradiated 20 wt. percent Cr--25 wt. percent Ni--0.7 wt. percent Nb stainless steel, 25:11428 (AWRE-O-29/67)
SEAGREN, R. D., Indexed bibliography on transportation and handling of radioactive materials--2, 25:10798 (ORNL-NSIC-84)
SEAMAN, G. G., Reorientation effect in the cadmium isotopes, 25:12548
SEDRAKIAN, D. M., Battery effect in neutron stars, 25:11591
SEEHARS, R., Reactions (^3He,t) on ^{16}O, ^{22}Ne, ^{24}Mg, and ^{30}Si, 25:12498
SEEMANN, K. W., Temperature dependence of neutron inelastic scattering from water, 25:12342 (RPI-328-210)
SEERY, William N., Low-temperature deformation mechanisms in delta stabilized Pu--Ga alloys, 25:11435
SEILER, H., Thin-layer chromatography as agent in radiochemistry. V, 25:10496
SEJRSEN, P., Blood flow determined by intra-arterial-injection and external recording of ^{133}Xe, 25:11137
Blood flow determined by local injection of ^{133}Xe in skeletal muscle, 25:11136
SEKA, W., Multilayer targets as a diagnostic tool for laser-produced plasmas, 25:11870
SEKIGUCHI, F., Chromosome number in radiation-induced mutants of Chrysanthemum morifolium, 25:11031
SEKIYA, Tamotsu, Neutron ages and slowing down spectra in light water for a fission source and a D-T source, 25:12348
SELIVERSTOVA, L. A., Thermogenesis of irradiated yeast cells in the process of recovering their reproductive capacity, 25:11324
SELLIN, D. L., Relativistic independent-particle model for atoms based on analytical potentials, 25:11738
Semi-empirical atomic-energy formula, 25:11739
SELTZER, Stephen M., Bremsstrahlung and photoneutrons from thick tungsten and tantalum targets, 25:12496
SEMENYUSHKIN, I. N., Time-coordinate compensator for the time spectrometers with long scintillators, 25:10813 (JINR-P13-5378)
SEN GUPTA, N. D., Time-dependent perturbation theory, 25:12054
SENTYUREV, V. P., Intercrystalline corrosion and corrosion cracking of stainless steel in aqueous solutions, 25:11353
SEO, T., Magnetic moments of three excited states in ^{149}Pm, 25:12609
SEPP, G., Analogy between radiative pion absorption and muon capture in ^{12}C, 25:12395
Charge exchange of 70 MeV π^- on C, Al, Cu, and Pb, 25:12446
Excitation of the isospin triplet ^{12}B, $^{12}C^*$(15.11 MeV), ^{12}N by pion charge exchange, 25:12397
SERBO, V. G., Production of muon pairs in interactions of hadrons of high energy, 25:12229
SEREBRYAKOV, V. A., Neodymium glass laser with high radiation intensity for producing a high-temperature plasma, 25:11906

SERGEEV, A. P., Experiments on α-particle acceleration by collective method, 25:12305 (JINR-P9-5558)
SERGOLLE, H., Coulomb excitation of ^{123}Te and ^{125}Te, 25:12603
SERNETZ, F., Effect of neutron irradiation on critical temperature of superconducting Nb, 25:11848
SESHADRI, S. R., Prog. rpt. on plasma instabilities, annual, 12/15/70, 25:11910 (COO-1695-32)
SESLAVINA, L. S., Suppresion of endocolonization in sublethally irradiated mice, 25:10986
SESSLER, Andrew M., Physics with and physics of colliding electron beams, 25:12325
SESTAK, B., Plasma acceleration by means of external magnetic field, 25:11882
SETLIK, L., Comparison of cerebral blood flow measurements with intravenously administered ^{131}I-labeled hippuran between arteriosclerotic and normal patients, 25:11150
SETOGUCHI, Yoshinori, Composition ranges with similar constricted hysteresis loops in Mn--Al--B alloys, 25:11983
SETTI, G., Absorption and scattering of ultraviolet and x-ray photons by intergalactic gas, 25:11654
SEVERA, J., Water solutions of radionuclides for biological experiments, 25:10925
SEVERNY, A., Comparison of the mean photospheric magnetic field and the interplanetary magnetic field, 25:11603
SEXL, R. U., Gravitational field of a massless particle, 25:12283
SEYLER, R. G., Direct radiative capture of ^{3}He by tritons and t + ^{3}He cluster states in ^{6}Li, 25:12372
DWBA analysis of the cross section and polarization data for the ^{14}N(d,n)^{15}O reaction at 3.5 MeV, 25:12405
Polarization and the statistical model, 25:12699
SFONDOURIS, J., Determination of hepatic blood flow in hyperthyroidism with the ^{198}Au blood extraction method, 25:11141
SHABALOV, V. V., Mutagenic action of laser radiation on seeds of Arabidopsis thaliana (L) heynh, 25:11027
SHAKALOVA, V. V., Preventive diet in internal irradiation with ^{137}Cs and ^{90}Sr, 25:10956
SHAKHTAKHTINSKII, G. B., Arsenate method for iodometric determination of scandium in the presence of iron, 25:10465
SHAKIN, C. M., Threshold photodisintegration of ^{208}Pb, 25:12562
SHAMPAI, A. E., Treatment of acute radiation sickness with bone marrow transplants, 25:11100
SHAPIRO, Sidney, rf-induced effects in superconducting tunnel junctions, 25:11827
SHAPPERT, L. B., Indexed bibliography on transportation and handling of radioactive materials--2, 25:10798 (ORNL-NSIC-84)
SHARHAN, A. M., Determination of groundwater flow and quantity of groundwater in Shigaya aquifer in Kuwait using radioisotopes, 25:10700
SHARMA, V. D., Normal vorticity jump condition across a magnetogasdynamic discontinuity, 25:11756
SHATZ, M., Some exact and approximate solutions of the neutron slowing down equation in resonant absorbing media, 25:12346
SHAVIV, G., Thermodynamics of white dwarf matter, 25:11549
SHAW, R. F., Strontium-90 and infant mortality in Canada, 25:11295
SHAW, W. M., Investigation of in-band resonant modes in Cr--W alloys by inelastic neutron scattering, 25:12019
SHCHERBININ, O. N., Determination of the boundary of high frequency wave absorption between the electron cyclotron and the low-hybrid frequency, 25:11927 (FTI-295)
High frequency plasma heating near the low-hybrid frequency, 25:11860 (FTI-282)
SHCHERBOVA, E. N., Vulnerability of endothelium of large vessels in radiosensitive and radioresistant animals, 25:11269
SHCHIGOLEV, P. V., Electrolytic and chemical polishing of metals, 25:11365
SHELDON, Eric, Physics of nuclei and particles. II, 25:12662
SHELINE, R. K., Two-quasiparticle states in ^{158}Tb, 25:12578
SHELTON, W. N., Excitation of 2s state of atomic H by electron impact, 25:11714
SHEN, B. S. P., Photometric history of BL Lacertae, 25:11555
SHENDEROVICH, A. M., Research on 100-MeV electron storage ring of Technical Physics Institute of Ukrainian Academy of Sciences, 25:12307 (KHFTI-69-27)
SHENOY, G. K., Magnetic behavior of Np metal and dilute Np alloys from Moessbauer effect studies, 25:12001
SHEPPARD, D. M., Electromagnetic properties of ^{58}Fe, 25:12483
SHESTAKOV, G. M., Influence of rho^{0}--ω mixing on spin density matrix of ω meson, 25:12208
SHEVCHENKO, V. V., Effects of ^{90}Sr--^{90}Y on chromosomes of Crepis capillaris, 25:11013
SHIBATA, T., Nuclear accident dosimetry by foil group, 25:10884
Nuclear accident dosimetry in Japan, 25:11081
SHIDA, Shoji, Benzene formation in radiation-induced and photochemical reactions of acetylene, 25:10650
SHIHAB-ELDIN, Adnan, Levels in ^{87}Rb populated in decay of ^{87}Kr, 25:12485
SHIKIN, I. S., Relativistic effects for magnetohydrodynamic waves, 25:11764
SHIMIZU, Masami, Evaluation of the influence of the mode of gas flow on the separation factor of a thermal diffusion column, 25:10786
SHIMOKAWA, Junichi, Some electrical properties of the uranium--plutonium mixed oxides, 25:11991
SHIMOYAMA, Koitsu, Radiation curing of mixture of diallylphthalate prepolymer and vinyl monomer. V, 25:10608 (JAERI-5026, pp 121-9)
SHIN, Y. M., Photoneutron angular distributions from ^{2}H(γ,n)H reactions, 25:12374
SHINER, V. J. Jr., α-deuterium effects on rate of solvolysis of 2-adamantyl sulfonate ester, 25:10523 (COO-1008-15)
Dependence of solvolytic α-deuterium rate effects on nature of the leaving group, 25:10522 (COO-1008-13)
Deuterium effects on binding of NADH to alcohol dehydrogenase isoenzyme EE, 25:10525 (COO-1008-17)
SHINN, W. A., Mass spectrometric investigation of volatilization behavior of ($U_{0.8}Pu_{0.2}$)O/sub 2-x/, 25:11503
SHINTOMI, T., Semiautomatic scanning system for nuclear emulsions, 25:10839
SHIRAISHI, Yoshiyuki, Exposure from ^{147}Pm-activated self-luminous paints, 25:11065
SHIRAKATA, K., Gamma-ray discrimination in proton-recoil spectrometer, 25:10857
SHIRANE, G., Pyrolytic graphite as a high efficiency filter for 13 to 15 MeV neutrons, 25:12352
SHIRK, D. G., Gamma decay of first two T = $^{3}/_{2}$ states of ^{15}N, 25:12416
SHISHKIN, A. A., Effect of toroidal state on vacuum magnetic configuration of vintotron, 25:11922 (KHFTI-70-25)
SHIVPURI, R. K., Mechanism of particle production in nucleon--nucleon interactions at very high energies, 25:12230
SHKLOVSKII, J., Momentum conservation and some problems of metagalactic astronomy, 25:11658
SHLENSKAYA, V. I., Analytical chemistry of mixed ligand complexes, 25:10460
SHMIDTKE, B., Fast valve of high pressure for bubble chamber, 25:10870 (JINR-P13-5420)
SHOHET, J. L., Prog. rpt. on plasma instabilities, annual, 12/15/70, 25:11910 (COO-1695-32)
Prog. rpt. on plasma instabilities, 9/15/70, 25:11909 (COO-1695-31)
SHONO, Yoshiyuki, Lipkin's condition and a microscopic theory of the nuclear rotational motion, 25:12647
Unified derivation of the cranking model and the Peierls--Yoccoz method. II, 25:12646
SHOOK, G. B., Coordinated experiment on radar clutter and auroral particle fluxes, 25:11778 (AD-709105)
SHORT, M. D., Use of the gamma camera for ^{131}I renography: a case study on a nephrectomized patient, 25:11206
SHOSHANI, A., Computerized Moessbauer spectrometer, 25:10866
SHOTTER, A. C., Intermediate structure and reaction ^{28}Si(p,p')^{28}Si, 25:12470
SHUFELDT, Warren Eugene, K^{0} proton s^{+} channel in K^{+} proton interactions at 3.2 GeV/c, 25:12114
SHUHAIBER, Y. K., Determination of groundwater flow and quantity of groundwater in Shigaya aquifer in Kuwait using radioisotopes, 25:10700
SHUKLA, P. G., Strong new x-ray object in Cetus region, 25:11592
SHUMAN, Henry E., Ultrasonic measurements on paraelastic impurities in alkali halides, 25:12893 (NYO-2471-47)
SHYN, T. W., Measurement of the $2^{2}S/sub\ ^{1}/_{2}$/--$2^{2}P/sub\ ^{3}/_{2}$/ energy separation in H, 25:11691
SICHELSCHMIDT, F., Reaction ^{15}N(tau,α)^{14}N, 25:12424
SICK, I., Elastic electron scattering from ^{12}C, 25:12376 (AD-710383)
SIDDHANTA, G., Studies on some N-acyl N-phenylhydroxylamines as metal-complexing ligands. IV, 25:10521
SIEDERS, A. A., Proton induced resonance reactions on ^{39}K, 25:12437
SIEGENTHALER, W., Assessment of functional significance for renal artery stenosis confirmed by angiography. comparison of the radiorenogram with the angiotensininfusion test and with the plasma renin content in both peripheral and renal venus blood, 25:11164
SIEGL, H., Lymph drainage following neck surgery, 25:11178
SIGMUND, Peter, Spatial distribution of energy deposited by atomic particles in elastic collisions, 25:11682
SIGNORINI, C., Gamma-ray transition strengths in ^{34}Cl, 25:12493
SILCOX, J., Flux motion through the superconducting surface sheath, 25:11829
Low field magnetoresistance of nickel polycrystals, 25:12897 (NYO-3087-23)
SILVA, A. J., FORTRAN code for analysis of counting data from animal tissues, 25:10937 (UCRL-50957)
SILVA, R. J., New isotopes ^{241}Cf and ^{240}Cf, 25:12593
SILVERMAN, Dennis, Existence of complex poles and oscillatory average multiplicity in multiperipheral models, 25:12122 (NYO-2262-TA-228)
SILVERMAN, Joseph, Effect of swelling on radiation-induced

grafting of styrene to polyethylene, 25:10613
SILVERMAN, S. M., Night airglow phenomenology, 25:11811
SIMARD, P. A., Boson method and the antisymmetrization problem, 25:12697
SIMIC, M., Absorption spectra and kinetics of the intermediate produced from the decay of azide radicals, 25:10643
SIMMS, P. C., Nuclear matrix elements in the first forbidden beta decay of ^{198}Au, 25:12597
SIMON, L., Determination of fluorine by neutron activation analysis in fluorinated ores and concentrates. II, 25:10498
Fast determination of polymetallic Pb + Zn mineralization by gamma--gamma logging, 25:10722
Fast determination of Zn + Cu mineralization by gamma--gamma logging, 25:10693
SIMONDS, R. R., Investigation of heat transfer augmentation through use of internally finned and roughened tubes, 25:12891 (NP-18608)
SIMONENKOVA, V. A., Damage to nerve ganglia and development of intestinal syndrome in mice after neutron irradiation, 25:11270
SIMONS, P. Y., Luminescence of Bi^{+3}-activated LaOCl under x-ray excitation, 25:10590
SIMPSON, F. B., Total neutron cross section and resonance parameters of ^{147}Pm, 25:12550
SIMPSON, J. A., Abundances of C, N, and O nuclei trapped in geomagnetic field, 25:11744
SINAI, P., Correction of optical aberrations by neutron irradiation, 25:11961
SINCLAIR, Warren K., Dependence of radiosensitivity upon cell age, 25:11093 (BNL-50203, pp 97-116)
SINGER, Sidney, Energy spectra and angular distributions of particles in the plasma sheet, 25:11809
SINGH, B., Effects of γ radiation on Penicillium expansum. II, 25:10979
Gamma transitions in ^{102}Ru, 25:12546
SINGH, R. P., Nuclear-structure calculations for ^{59}Cu, 25:12451
SINITSYN, R. V., Dosimetry in radium therapy, 25:11069
SINN, H., Experimental bone scintigraphy in animals, 25:11216
Experimental scintigraphy of thrombi in animals, 25:11214
SIOHAN, F., Achieving uniform spatial response from large area liquid scintillation detectors, 25:10875
SIRI, L. Nicola, Excitation functions ^{159}Tb(d,p)^{160}Tb and ^{159}Tb(d,4n)^{157}Dy, 25:12595
SIRLIN, A., Perturbation theory about the symmetry limit and K/sub 13/ form factors, 25:12173
SIVARAMAKRISHNAN, V. M., Fate of ^{60}Co 1-nitroso 2-naphthol chelate in albino rats after intravenous administration, 25:10958
SIVOLAP, Yu. M., Ionizing radiation and nitrogen metabolism in corn, 25:11309
SIWICKI, R., Radiation accident dosimetry in Poland, 25:11080
SJOEBERG, O., Calculation of effective mass in nuclear matter, 25:12677
SJOELANDER, A., Electron distribution around positrons in metals, 25:12041
SKAREK, P., Target efficiency and multiple traversals in the CERN 600 MeV synchro-cyclotron, 25:12324
SKATULSKA-SURMACKA, Teresa, Effect of x-ray upon stored blood, 25:10981
SKILLMAN, T. L., Magnetopause crossing of the geostationary satellite ATS 5 at 6.6 R/sub E/, 25:11784
SKLADNIK-SADOWSKA, Elzbieta, Experimental studies of plasma generated by RPI system, 25:11883
SKOBEEV, E. M., Influence of x irradiation on maze habit in rats, 25:11273
SKOOG, R., Energy loss of well-channeled H, He, and Li ions in Au, 25:11976
SKOROV, D. M., Diffusion of nickel in beryllium, 25:11399
SKORYNA, S. C., Inhibition of intestinal absorption of radioactive Sr. IX, 25:10939
SKRIPKO, A. L., Physical methods for rapid analysis of substances, 25:10475
SLADEN, Brenda K., Biology of populations, 25:11005
Ecology of animal communities, 25:11006
SLEDZIEWSKI, Zbiniew, Getter for vacuum pumps, 25:10804
SLOUKA, V., Assessment of radiotellurium as a fission product, 25:10948
Distribution and excretion of radiotellurium in rat, 25:10950
Kinetics of radiotellurium in rat, 25:10949
SMID, A., Decrease in radiostrontium accumulation due to activated barium sulphate during repeated and continuous peroral contamination of rats, 25:10940
Kinetic model of stem-cells population in the postirradiation bone marrow injury. II, 25:11290
Use of activated barium sulfate in oral contamination with radiostrontium. II, 25:11048
SMITH, A., Length changes in actinide metals due to self-irradiation damage at 4°K, 25:11468
SMITH, A. P., Strontium-90 and infant mortality in Canada, 25:11295
SMITH, D. F., Towards a theory for Type III solar radio bursts. I, 25:11621
SMITH, D. M., X-ray and nuclear radiation facilities, personnel safety features, 25:11078 (Y-1754)
SMITH, Donald L., Scattering of rare gases (He, Ne, Ar, Kr, and Xe) from Pt (111) surfaces, 25:11683
SMITH, F. G., Generation of radio waves in pulsars, 25:11595
SMITH, H. A., Nuclear matrix elements in the first forbidden beta decay of ^{198}Au, 25:12597
SMITH, H. G., Phonon spectra in TaC and HfC, 25:11986
SMITH, James Alan, Test of the /ΔI Vector/ = 1/2 rule in lambda decay, 25:12086
SMITH, John R., Numerical coefficient of the first exchange inhomogeneity term, 25:11740
SMITH, L. W., Economical beam transport for utilization of post conversion AGS, 25:12296 (BNL-15464)
SMITH, N., FORGOD: FORTRAN IV program for solving the four group neutron diffusion equations in one dimension, 25:12335 (AECL-3671)
SMITH, S. M., Test of the shell model for ^{208}Pb, 25:12574
SMITH, T. F., Pressure dependence of the superconducting transition temperature for niobium, 25:11849
SMUTZ, Morton, Separation of Y, Ho, and Er with di-(2-ethylhexyl) phosphoric acid in chloride and nitrate systems, 25:10685
SNELLING, Robert N., Environmental survey of uranium mill tailings pile, Monument Valley, Ariz, 25:11045
SNIDER, W. D., Investigation of heat transfer augmentation through use of internally finned and roughened tubes, 25:12891 (NP-18608)
SNIHS, Jan Olof, Some measurements on radioactivity in Sweden caused by nuclear test explosions, 25:11004
SNOKE, J. Arthur, Overlapping resonances, 25:12126
SNOVER, Kurt Albert, Study of high isospin states by isospin-forbidden radiative capture reactions, 25:12441
SNYDER, Keith Alan, Structural and related magnetic properties of high angle evaporated cobalt films, 25:12896 (NYO-3087-21)
SNYDER, Lewis E., Observations of radio emission from interstellar hydrogen cyanide, 25:11594
SO, S. P., Ethynylbenzene: the vibrational spectra of some deuterated isomers, 25:10534
SOBOLEVA, G. B., Delay of mitosis in culture of mammalian cells under α and γ rays, 25:11272
SOBOTTKA, H., Level density parameters for Ge, Ho, and Ta, 25:12536
SOBRA, K., Plasma acceleration by means of external magnetic field, 25:11882
SODA, Toshio, Two-branch excitation spectrum of liquid ^{4}He, 25:11818
SOEDERLUND, R., Spectrochemical determination of tracers of impurity elements in Pu by Cu spark method, 25:10444
SOERGEL, V., Analogy between radiative pion absorption and muon capture in ^{12}C, 25:12395
Charge exchange of 70 MeV π$^-$ on C, Al, Cu, and Pb, 25:12446
Excitation of the isospin triplet ^{12}B, ^{12}C*(15.11 MeV), ^{12}N by pion charge exchange, 25:12397
SOIFER, V. N., Radioactive elements and deuterium in underground waters of the Bukhara--Karshin artesian basin, 25:10698
SOK, V., Determination of fluorine by neutron activation analysis in fluorinated ores and concentrates. II, 25:10498
SOKOLOV, A. A., Quantum mechanics and atomic physics, 25:12052
SOKOLOV, O. V., Detector sensitivity for measuring electron current in a betatron, 25:12321
SOKOLOVSKAYA, E. M., Interdiffusion in Nb--Zr system, 25:11424
SOLANILLA, R., Operational formulation of resonance absorption of neutrons, 25:12338 (CNEA-266)
SOLOMATIN, V. I., Leading of accelerated electrons out of small-Gabarite betatrons by means of magnetic method, 25:12334
SOLOMON, Philip, Observation of CO emission at 2.6 millimeters from IRC + 10216, 25:11568
SOLOV'EV, M. I., Fast valve of high pressure for bubble chamber, 25:10870 (JINR-P13-5420)
SOLOVIEV, V. G., Alpha and gamma decays of the high excited states of complex nuclei, 25:12629 (JINR-E4-5135)
Complication of the nuclear state structure with increasing excitation energy, 25:12630 (JINR-E4-5469)
SOMOGYI, A., High-stability apparatuses to investigate the angular distribution of charged particles of energies 10^{13}--10^{14} eV in the Galaxy, 25:11742 (KFKI-70-21-HEP)
SOMOGYI, Antal, Study of the structure of interplanetary space by means of cosmic radiation, 25:11627
SONA, P. G., Macroscopic model for the anelastic scattering of heavy ions, 25:12661
SONE, Kazuho, Wavelengths of transverse oscillations of fast protons in planar channeling, 25:11953
SONNEN, C., Catalytic decomposition of carbon monoxide on pure iron, mild steels, and alloyed steels, 25:11374 (DP-Report-530)
SONNERUP, Bengt U. Ö., Magnetic-field reconnexion in a highly conducting incompressible fluid, 25:11758
SONNTAG, B., Optical absorption of Ce, Ce oxide, Pr, Pr oxide, Nd, Nd oxide, and Sm in extreme ultraviolet, 25:11698
SORENSON, J. A., Determining body compositions by radiation absorption spectrometry, 25:11114
SOVICHE, G., Some aspects of the use of nuclear explosives in the petroleum industry, 25:10746

SOWBY, F. D., Radiation from ball lightning, 25:11926
SPADONI, M., Preliminary results regarding development of superconducting ribbons of Nb_3Sn, 25:11820 (LNF-70/18)
SPANGLER, John D., Temperature effects on the phosphorescence of benzene and toluene, 25:10550
SPARROW, A. H., Relative biological effectiveness of x-rays and 0.43-MeV monoenergetic neutrons on somatic mutations and loss of reproductive integrity in Tradescantia stamen hairs, 25:11313
SPARROW, D. A., Monopole excitations in ^{16}O, 25:12426
SPARROW, Rhoda C., Relative biological effectiveness of x-rays and 0.43-MeV monoenergetic neutrons on somatic mutations and loss of reproductive integrity in Tradescantia stamen hairs, 25:11313
SPEINDE, J., Electromagnetic delay line readout for proportional wire chambers, 25:10846
SPENCER, D. J., Isotope separation with the cw hydrogen fluoride laser, 25:10690
SPENCER, Derek W., Trace element calibrations and profiles at Geosecs Test Station in Northeast Pacific Ocean, 25:10428
SPENCER, Richard P., Identification of cases of acquired functional asplenia, 25:11117
SPENCKER, A., Investigations of radiation resistance of optoelectronic devices for an electronically scanning star sensor in satellites, 25:10904 (HMI-B-97)
SPICER, B. M., Photoneutron cross section of strontium, 25:12456
Photoneutron cross sections of ^{28}Si and ^{24}Mg, 25:12469
SPIERS, E. W., Response of detectors with cylindrical collimation, 25:10841
SPIGER, R. J., Deuteron elastic scattering and the (d,p) reaction with polarized ^3He target, 25:12370
SPINKA, H., Beta decay of ^{20}O, 25:12453
SPITS, A. M. J., Gamma rays from thermal-neutron capture in natural and ^{28}Si enriched silicon, 25:12403
SPOONER, Stephen, Prog. rpt. on magnetic phenomena at metal surfaces, 2--12/70, 25:11981 (ORO-3674-4)
SPRETNAK, J. W., Plastic-strain controlled failure criteria and design parameters. Technical progress report, 25:11373 (COO-2048-1)
SPRING, Erik, Neutron radiation produced by roentgen beam of a betatron, 25:12320
SPRINGER, George S., Prog. rpt. on theoretical and experimental study of film condensation of liquid metal vapors, annual, 12/70, 25:12885 (COO-2032-6)
SPROTT, J. C., Prog. rpt. on plasma instabilities, annual, 12/15/70, 25:11910 (COO-1695-32)
Prog. rpt. on plasma instabilities, 9/15/70, 25:11909 (COO-1695-31)
SQUIRES, E. J., Dual amplitudes for 6 pions with epsilon-tensor couplings, 25:12131
SREENIVASAN, T. B., Induced mutations in sugar cane, 25:11030
SROUR, J. R., Recombination parameters in low-resistivity gamma-irradiated n-type germanium, 25:11968
STACEY, John, Improvements relating to nuclear reactors, 25:12771
STACEY, R., Influence of thermal neutron irradiation on equilibrium temperature of $\alpha + \beta$ transformation in Pu, 25:11467
STACHEL, John, Einstein tensor and 3-parameter groups of isometries with 2-dimensional orbits, 25:12277
STACHELBERGER, H., Influence of γ-radiation on activities of several glycolytic enzymes in rye seeds, 25:10974
STACHOWICZ, W., Free radicals evoked by radiosterilization in preserved bone grafts, 25:11329
Quantitative evaluation of irradiated bone grafts resorption rate by the electron spin resonance technique, 25:11340
STALLINGS, Charles Henry, Ion scattering by electric fields in an inertially confined plasma, 25:11880
STAMP, A. P., Strength of the tensor interaction in the deuteron optical potential, 25:12684
STANEK, Z., Plasma acceleration by means of external magnetic field, 25:11882
STANG, Peter J., Secondary deuterium isotope effects in vinyl cations, 25:10548
STANKO, Alfred F., Radiation gauge system for tubular plastic film, 25:10890
STANNARD, R. W., Uranium--plutonium--carbon phase diagram. I, 25:11523
STANNETT, V., Spontaneous grafting in the presence of swelling agents, 25:10619
STARIKOV, A. D., Neodymium glass laser with high radiation intensity for producing a high-temperature plasma, 25:11906
STARK, W. A. Jr., Helium release from $^{238}PuO_2$ microspheres, 25:11499
STARK, Werner Joseph, Doppler-broadened gamma rays from $^{23}Na(p,\alpha\gamma)^{20}Ne$ reaction, 25:12443
STARTSEV, G. A., Mutagenic action of laser radiation on seeds of Arabidopsis thaliana (L) heynh, 25:11027
STAUDE, J., Europium and lanthanum in sunspot and in the undisturbed photosphere, 25:11613
Line formation in a magnetic field and the interpretation of magnetographic measurements. III, 25:11612
STAVINSKII, V. S., Measurement of scattering angle of particles by Vavilov--Cherenkov radiation, 25:10869 (JINR-E13-5459)
STEAD, A., Sodium flow monitoring, 25:12792
STEADMAN, S. G., Reorientation effect in the cadmium isotopes, 25:12548
Reorientation effect measurements in $^{104,114}Cd$, 25:12619
STEADMAN, Stephen Geoffrey, Reorientation experiments in the even-mass Cd isotopes, 25:12556
STEARN, S. M., Dynamic stress concentration at a chamfered change of section, 25:10790 (RD/B/N-1795)
STEEL, G. Gordon, Kinetics of cell proliferation in tumors, 25:11219 (BNL-50203, pp 130-53)
STEFFEN, R. M., E2/M1 multipole mixing ratios in spherical nuclei ^{124}Te, ^{126}Te, and ^{126}Xe, 25:12515 (COO-1746-51)
STEIGER, R. H., Uranium--Th--Pb and Rb--Sr systematics in 2700 x 10^6-year old plutons from southern Wind River Range, Wyoming, 25:10701
STEIN, W. A., Infrared studies of galactic nebulae. II. The compact nebulae IC 4997, VV 8, and FG sagittae, 25:11569
STEINHOFF, H., Clearance studies with ^{131}I-labeled hippuran, ^{203}Hg-salyrgan, ^{51}Cr-EDTA, and ^{51}Cr-inulin, 25:11156
Renal clearance of ^{133}Xe, 25:11158
STEINITZ, M. O., Low-temperature phase transitions in alpha uranium, 25:11449
STEINNES, E., Rapid determination of Al, Mn, and Na in soils by neutron activation analysis, 25:10909
STELSON, P. H., Quadrupole moment of first 2+ states of Sn, 25:12587
STENDER, H. St., Determination of lung circulation with the dynapix rapid scanner in pulmonary restrictions, 25:11131
STENERSON, R. O., Lateral distribution of muon pairs in underground cosmic-ray showers, 25:12082
STENFLO, L., Solution of Boltzmann equation for electrons in external electric fields, 25:11898
Solution of equations describing explosive instabilities, 25:11914
STEPANOV, B. M., Alpha-representation of Feynman integrals, 25:12288
STEPANOV, Yu. S., Dietary intake of ^{90}Sr by population of the USSR, 1959--1967 as a result of stratospheric fallout, 25:10934 (NP-18380)
STEPHAN, Joachim G., Prog. rpt. on feasibility test to determine Amchitka Sea otter population through photogrammetric techniques, annual 7/68, 25:12875 (BMI-171-108)
STEPHENSON, G. J. Jr., Off-shell effects in knockout reactions, 25:12670
STEPHENSON, L. M., Possible implications of 3K background radiation, 25:11662
STERN, Marvin J., Temperature dependences of kinetic isotope effects, 25:10549
STEVENS, Alan Jerald, Determination of the axial vector to vector ratio in the beta decay of the lambda hyperon, 25:12081
STEVENS, Charles L., Studies on the secondary structure of phenylalanyl transfer ribonucleic acid, 25:10564
STEVENSON, Alan C., Maternal x irradiation and the frequency of mongolism, 25:11300
STEVENSON, P. C., Ion-mobility spectrometer for radiochemical applications, 25:10903
STEWART, J. W., Form-factor ratio G/sub E/(n)/G/sub E/(p) at low momentum transfers, 25:12070
STEWARTSON, K., Resistance between two circular electrodes in presence of a strong magnetic field, 25:11761
STIEGLER, J. O., Transmutation-produced silicon precipitates in irradiated aluminum, 25:11471
Uranium and thorium diffusion in columnar pyrocarbons as influenced by actinide concentration, 25:11378 (ORNL-TM-2989)
STIGERS, Charles Arthur, Electron capture cross sections into H for proton impact on gas targets, 25:11708
STIM, Thomas B., Interference of Cocal virus with Friend leukemia virus-induced splenomegaly in DBA/2J mice, 25:11321
STOCKER, W., Two-body spin--orbit potentials and semi-infinite nuclear matter, 25:12675
STOECKLIN, G., Planning an atomic beam apparatus for investigation of elementary chemical processes of neutral particles, 25:10517 (JUL-674-RC)
STOKSTAD, R. G., Hole-vibration coupling in ^{115}In, 25:12543
STOLARCZYK, L., Radiation-induced graft terpolymerization of poly(ethylene terephthalate). II, 25:10621
STOLL, A. George, Scattering of rare gases (He, Ne, Ar, Kr, and Xe) from Pt (111) surfaces, 25:11683
STOLZ, W., Neutron personnel dosimetry on tissue-equivalent phantoms by solid-state track detectors, 25:10880
Thermoluminescent dosimetry with polycrystalline LiF, 25:10879
STONE, J. A., Radiolysis of ethane. II, 25:10632
STONE, R. G., Type III solar radio burst storms observed at low frequencies. I, 25:11622
STONE, R. S., Controls Department hybrid computer: hardware and applications, 25:10895 (ORNL-TM-3101)
STORB, U., Antibody production by host cells in x-irradiated recipients of allogeneic spleen cells, 25:10994
STOREY, R. N., Growth of single crystals of Ta_2C, 25:11484
STORHOK, V. W., Irradiation studies of (U,Pu)N, 25:11535
STORZER, D., Geometry factor in fission track counting, 25:10695
STOTHERS, R., Internal structure of upper main-sequence

stars, 25:11559
STOTT, M. J., Electron distribution around positrons in metals, 25:12041
STRANIK, D. A., Evaluation of PuO_2 homogeneity in PuO_2--UO_2 fast reactor fuel by scanning electron microprobe, 25:11489 (WHAN-FR-20)
STRAUSS, R., Discripancies between νN charge exchange forward scattering data and the dispersion relation prediction, 25:12209
STRICKER, A., Numerical differential cross sections of reaction $^{58}Ni(p,t)^{56}Ni$ with 51.9 MeV protons, 25:12431 (INSJ-124)
STRITTMATTER, P. A., Atmosphere of white dwarfs. II, 25:11556
STROHBUSCH, U., Optical-model analysis for ^{6}Li elastic scattering by ^{16}O at 20 MeV, 25:12408
STROM, Peter O., Interaction of fallout with fires, 25:10702 (AD-708558)
STROMBERG, H. D., Shear strength of beryllium, uranium, and tungsten as a function of strain, strain rate, and pressure, 25:11379 (UCRL-72477)
STRUVE, Otto, Stellar spectroscopy: normal stars, 25:11543
STRZALOWSKI, A., Real part of the alpha-nucleus potential obtained by double folding procedure, 25:12627 (INP-720)
STUESSI, H. P., Method of measuring the phase angle of a charged particle beam in a cyclotron, 25:12329
STYCZEN, J., Decay of ground state of ^{82}Rb, 25:12507
SU, C. S., Effective neutron temperatures in reactor core measured by fission track detectors, 25:10836
SUBBOTIN, V. G., Neutron detector in search for superheavy elements in nature, 25:10814 (JINR-P13-5391)
SUBBOTIN, V. I., Continuously-active indicator for the diffusion of hydrogen in sodium, 25:11400
Physico-chemical analysis of handling liquid metal coolants, 25:11342
SUCHER, J., Singularity structure of causal distributions and restricted equal-time limits, 25:12133
SUDAN, R. N., E-layer precession in a plasma, 25:11925 (NYO-4077-1, Paper 2)
Finite beta equilibria of relativistic electron beams in toroidal geometry, 25:11887 (NYO-4077-1, Paper 5)
Nonlinear beam--plasma interactions and stochastic acceleration, 25:11885 (NYO-4077-1, Paper 3)
Precession of a strong E-layer, 25:11924 (NYO-4077-1, Paper 1)
Relativistic beam propagation in magnetized plasma, 25:11886 (NYO-4077-1, Paper 4)
SUEHIRO, T., Numerical differential cross sections of reaction $^{58}Ni(p,t)^{56}Ni$ with 51.9 MeV protons, 25:12431 (INSJ-124)
SUGAHARA, Masanori, Suppression of ac hysteresis energy loss in nonideal type-II superconductor, 25:11823
SUGAYA, Reiji, Parametric excitation of Bernstein waves in plasmas, 25:11934
SUGIMOTO, Shun-ichi, Irradiation effects of oxytocin, 25:10625 (JAERI-5026, pp 164-7)
Radiation effects on gramicidin. II, 25:10587 (JAERI-5026, pp 167-8)
SUGIURA, M., Magnetopause crossing of the geostationary satellite ATS 5 at 6.6 R/sub E/, 25:11784
SUGIYAMA, Y., Numerical differential cross sections of reaction $^{58}Ni(p,t)^{56}Ni$ with 51.9 MeV protons, 25:12431 (INSJ-124)
SULABERIDZE, G. A., Cascade rate functions for separating multicomponent isotopic mixtures, 25:10782
SULLIVAN, Robert E., Reduction of the ray effect in discrete ordinates calculations, 25:12852
SULPICE, G., Cobalt electron irradiated at 20°K, 25:11949 (AI-Trans-267)
SUMERLIN, Neal, Radiochemical studies on ^{137}Cs in rain, 25:10713 (ORO-2529-28, App. 7)
SUNAYASHIKI, Tadashi, Shielding against high energy radiations produced by 30 MeV linear accelerator at Hiroshima University, 25:12314
SUNDARESAN, M., Thermochemical studies of some U and Th compounds, 25:10581
SUNDSFJORD, Johan A., Visualization of the placenta with a gamma camera and /sup 113m/In, 25:11228
SUPIOT, F., Mechanical effects of contained underground nuclear explosions, 25:10741
SUSANNA, A., Estimate of dose of radiation absorbed by airport personnel, 25:11062
SUSLENKO, V. C., Investigation of ^{6}Li recoil nuclei in $^{9}Be(p,2p)^{8}Li$ reaction at proton energies of 180 and 660 MeV, 25:12378 (JINR-P1-4872)
SUTCLIFFE, P. W., Review of low temperature specific heats of the actinides, 25:11384
SUTHERLAND, R. M., Multi-component radiation survival curve model, 25:11293
SUZUKI, M., Simultaneous determination of copper and manganese in plants by neutron-activation analysis, 25:10509
SUZUKI, Shuju, Fluorescent x-ray analysis of tin and zirconium in aluminum alloys, 25:10441
SUZUKI, Y., Radiation nephritis. II. Chronic changes after high doses of radiation, 25:11286
SUZUKI, Yasuyuki, Hartree--Fock model of ^{6}Li nucleus, 25:12410
SVAHN-TAPPER, Gudrun, Dosimetric studies in ^{60}Co therapy, 25:11060
SVETLICHNY, George, Generalized operators, 25:12263
SVITEL, J., Sensitivity of radioisotopes x-ray fluorescence using Ross filters, 25:10479
SVOZIL, O., Comparison of cerebral blood flow measurements with intravenously administered ^{131}I-labeled hippuran between arteriosclerotic and normal patients, 25:11150
SWALLOW, A. J., Pulse radiolysis of aqueous solutions of benzonitrile, 25:10639
SWANSON, Jon R., Review of international microwave exposure guides, 25:11088
SWANSON, M. L., Stage I recovery of deformed metals. I, 25:11420
SWARTZ, Wesley E., Diurnal variation of neutral temperature profile at Arecibo, 25:11793
SWEDJEMARK, Gun Astri, Some measurements on radioactivity in Sweden caused by nuclear test explosions, 25:11004
SWENTON, John S., Deuterium isotope effect on competing hydrogen and carbomethoxy migration in benzotropilidene photochemistry, 25:10557
SWINDLE, D. L., Beryllium-7 in Fayetteville, (36°N, 94°W), Arkansas, 25:10712 (ORO-2529-28, App. 6)
SYCHEV, B. S., Dose characteristics of protons with energy 200 MeV, 25:11054 (JINR-P16-5383)
SYNOGROUND, M. O., Effect of Hanford Plant operations on the temperature of the Columbia River 1964 to present, 25:10691 (BNWL-1345)
SYUNYAEV, R. A., Stationary relativistic gas in cosmic objects and γ background in 1 to 20-MeV region, 25:11748
SZABO, Elek, Activation analysis by charged particles, 25:10504
SZE, N. H., Occurrence of different α-phases of U at low temperatures by thermopower and resistivity experiments, 25:12006
SZEGEDI, S., Observation of proton tracks by a plastic detector, 25:10831
SZEGVARI, M., Angiocardiography with a scintillation camera, 25:11121
SZEKERES, P., Colliding gravitational waves, 25:11655
SZICHMAN, H., Radiation widths of bound nuclear levels, 25:12447
SZOTOR, Maria, Effect of x-ray upon stored blood, 25:10981
SZPIKOWSKI, S., New quasiparticle factorization of the j-shell, 25:12666
SZUSZCZEWICZ, Edward Paul, Behavior of low-density plasmas in presence of Langmuir probes, 25:11873

T

TABAKA, Andrzej, Carbon-14 exchange studies in $^{14}CO_2$--CO--quartz wells, 25:10541
TABAKIN, Frank, Nuclear saturation and the smoothness of nucleon--nucleon potentials, 25:12698
TAKADA, Kenjiro, Four-body correlations in light nuclei, 25:12660
TAKAGAKI, Torao, Optical radiation from gases excited by high-energy electrons. II, 25:10585 (JAERI-5026, pp 153-5)
Optical radiation from gases excited by high-energy electrons. III, 25:10586 (JAERI-5026, pp 155-7)
TAKAGI, Fujio, Phenomenological analysis of the infinite resonance model for the nucleon electromagnetic form factor, 25:12153
TAKAHASHI, Junji, Analysis of hyperon nonleptonic decay amplitudes, 25:12171
TAKAHASHI, Kohji, Gross theory of β decay and application to Fermi matrix element, 25:12690
TAKAHASHI, Yasushi, Electromagnetic interaction of a spin-$^3/_2$ field, 25:12267
TAKAMURA, T., Infra-red reflectance spectra of anodic oxide films formed on pure Ta, 25:11518
TAKANO, Masami, Development of reactor enclosure high voltage power cable penetration, 25:12705 (JAERI-Memo-4197)
TAKASHIMA, Yoichi, Evaluation of the influence of the mode of gas flow on the separation factor of a thermal diffusion column, 25:10786
TAKAYANAGI, Kazuo, Elementary processes involving electrons in the ionosphere, 25:11810
Rotational excitation of molecules by slow electrons, 25:11730
TAKEBE, Hiraku, Effect of a potent carcinogen, 4-nitroquinoline 1-oxide, and its reduced from, 4-hydroxylaminoquinoline 1-oxide, on bacterial and bacteriophage genomes, 25:11026
TAKEDA, Minoru, Elastic scattering of alpha particles by ^{16}O, 25:12419
TAKEDA, T., Infra-red reflectance spectra of anodic oxide films formed on pure Ta, 25:11518
TAKESHITA, Kenji, Shielding against high energy radiations produced by 30 MeV linear accelerator at Hiroshima University, 25:12314
TAKESHITA, Noboru, Preparation of Wood--Polymer Composite by ionizing radiation. IV, 25:10603 (JAERI-5026, pp 80-5)
Preparation of Wood--Polymer composite by ionizing radiation. VI, 25:10605 (JAERI-5026, pp 94-100)
TAKETANI, Mituo, Level structure of hadrons, 25:12182
TAKEUCHI, K., R-matrix shell-model calculations, 25:12423
TAKEUCHI, Tamotsu, Radiation curing of monomer--

polybutadiene mixture. I, 25:10609 (JAERI-5026, pp 130-6)
TAKEZAKI, Jun'ichi, Radiolysis of cholestanol, 25:10624 (JAERI-5026, pp 160-4)
TALBOY, James H., Positive reactivity from replacement of heavy water by light water in the coolant channels of a heavy-water-moderated reactor, 25:12830
TALEKAR, V. L., Coupled wave equations for magnetoplasma with anisotropic pressure, 25:11946
TAM, Christopher K. W., Nonlinear dispersion of cold plasma waves, 25:11940
TAMAGAKI, Ryozo, Superfluid state in neutron star matter. I, 25:11545
TAMANIAN, A. G., High energy particle identification by x-ray transition radiation (XTR) detectors, 25:10877
TAMMANN, G. A., Frequency of supernovae as a function of the integral properties of intermediate and late type spiral galaxies, 25:11637
TAMURA, T., Total neutron cross section of oriented ^{165}Ho, 25:12565
TAN, A. H., Examination of various procedures for localization of the counter in isotope renograms, 25:11167
TAN, Chung-I, Existence of complex poles and oscillatory average multiplicity in multiperipheral models, 25:12122 (NYO-2262-TA-228)
TANAKA, Haruhiko, Fractionation of tritium in crystallization of inorganic hydrates, 25:10688
TANAKA, Shigetoshi, Parametric excitation of Bernstein waves in plasmas, 25:11934
TANAKA, Toshio, Effect of radiation in reactively sputtered Al_2O_3--Si structures, 25:10905
TANAKA, Y., Inhibition of intestinal absorption of radioactive Sr. IX, 25:10939
TANDBERG-HANSSEN, E., Orientation of magnetic fields in quiescent prominences, 25:11617
TANG, I-ming, Surface impedance of a clean two-band superconductor near H/sub c2/, 25:11828
TANG, Y. C., Study of N + α system, 25:12363
TANNENBAUM, M. J., Observation of muon trident production in lead and the statistics of the muon, 25:12083
TANNER, N. W., Angular distribution measurements in inverse photonuclear reactions, 25:10865
TANNOCK, Ian F., Effects of pCl_2 on cell proliferation kinetics, 25:11094 (BNL-50203, pp 215-33)
TAO, S. J., Preliminary study on temperature effect on positron annihilation in $KClO_4$, 25:12896 (NYO-3661-33)
TARANDI, T., Reactor pressure vessels made of concrete, 25:12788
TARASENKO, A. S., Research on 100-MeV electron storage ring of Technical Physics Institute of Ukrainian Academy of Sciences, 25:12307 (KHFTI-69-27)
TARKA, John Edward, Mechanisms of radiation-initiated semiconductor device failures, 25:10906
TARRAGO, X., Method for identification of particles from A = 4 to 20, 25:10829
TARSHIS, M. A., Effects of γ radiation on histones from rat nuclei, 25:10971
TATARKINA, A. L., Interdiffusion in Nb--Zr system, 25:11424
TATISCHEFF, B., 166-MeV elastic and inelastic alpha-particle scattering, 25:12549
TATSUKAWA, Toshiaki, Superconducting wired-wall cavity for V-band ENDOR experiment, 25:11850
TATSUNO, T., Chromosome number in radiation-induced mutants of Chrysanthemum morifolium, 25:11031
TAUB, A. H., Variational principles and relativistic magnetohydrodynamics, 25:11769
TAVSHUNSKII, G. A., Luminescence of CaF_2--TRF_3 in the gamma-ray field of ^{60}Co, 25:11955
TAYLOR, D., Processing of pulse trains using rate multipliers, 25:10840
TAYLOR, Glenn N., Risk to bone and liver from ^{239}Pu, 25:11301
TAYLOR, H. W., Decay of 6.5 min ^{78}Br, 25:12445
Gamma transitions in ^{102}Ru, 25:12546
TAYLOR, Harold E., Auroral phenomena driven by the magnetospheric plasma, 25:11804
TAYLOR, J. C., Influence of thermal neutron irradiation on equilibrium temperature of α + β transformation in Pu, 25:11467
TAYLOR, J. M., Expansion properties of segregated Pu--Ga alloys, 25:11388
TAYLOR, John K., Microchemical Analysis Section. Summary of activities, July 1969--June 1970, 25:10422 (NBS-TN-545)
TAYLOR, M. T., Examination of fluxon behaviour by analogy with a floating magnetic model, 25:11833
TAYLOR, Maynard F., Predicted coolant heat transfer and friction compared with nuclear rocket test results, 25:12833
TELLGREN, Roland, Hydrogen bond studies. XXXXVI. Crystal structures of normal and deuterated sodium hydrogen oxalate monohydrate $NaHC_2O_4.H_2O$ and $NaDC_2O_4.D_2O$, 25:10543
TEMKIN, A., Adiabatic theory of rotational excitation of non-Σ states, 25:11725
TENERZ, E., Research and development work leading up to the ASEA-ATOM BWR, 25:12712
TENNERY, V. J., Characterization and behavior of alkalized alumina during sulfur dioxide sorption--regeneration process, 25:12901 (ORNL-TM-3210)
Synthesis, characterization, and fabrication of UN, 25:11480 (ORNL-4608)
TENSHO, Kiyoshi, Iodine and Br in soil-plant system in relation to Reclamation-Akagare disease of rice, 25:10505
TEPEL, J. W., Investigation of levels in ^{51}Cr, ^{55}Fe, and ^{59}Ni, 25:12476
TER-AKOP'YAN, G. M., Neutron detector in search for superheavy elements in nature, 25:10814 (JINR-P13-5391)
TERASIMA, Toyozo, Role of DNA in cell killing by radiation, 25:10960 (BNL-50203, pp 82-90)
TEREKHOV, B. A., Research on 100-MeV electron storage ring of Technical Physics Institute of Ukrainian Academy of Sciences, 25:12307 (KHFTI-69-27)
TERNOV, I. M., Effect of induced radiation of electrons moving in planar electromagnetic wave on orientation of their spins, 25:12161
Quantum mechanics and atomic physics, 25:12052
TERTIAN, R., Determination by x-ray fluorescence of elements in low concentrations in rocks, 25:10448
TESI, R., Diplontic selection in irradiated Gladiolus corms, 25:11035
TESMER, J. R., Spin isomers of the shape isomer /sup 237m/Pu, 25:12530 (RLO-1388-130)
TESSMER, Carl F., Late effects on vascular tissue, 25:11256 (BNL-50203, pp 186-203)
TESTONI, J. E., Transfer reactions (α,t), (α, ^{3}He) in the fp shell, 25:12434
TEWES, Howard A., Radionuclide body burdens and hazards from ingestion of foodstuffs contaminated by fallout, 25:11038 (UCRL-72716(Rev.1))
TEYSSIER, J. L., Registration and counting of alpha particle tracks in cellulose nitrate, 25:10826
THAKUR, Madhukar L., Separation of the oxidation states of some elements with the use of tri-n-butyl orthophosphate, 25:10687
THAYER, W. L., Effect of hot working on room-temperature strength and ductility of Pu--1 wt percent Ga delta-stabilized alloy, 25:11390
THEIN, W., Safety of heavy water system in Braunschweig research reactor, 25:12822 (NP-18499)
THEIS, J. D., Observation of ablation behavior of fibrous carbon--carbon composites, 25:12920 (Y-1752)
THENK, B. K. G., Formation of two-dimensional organic polymers on a mineral surface, 25:10616
THEUS, R. B., Direct interaction effects in the fission of ^{238}U with 63.5-MeV ^{4}He ions, 25:12526 (MNC-3783-7)
THIO, S. K., Investigation of β spectrum of ^{14}C with a proportional counter with inner anticoincidence screens, 25:12380 (KFK-1222)
THOMAS, G. E., States of ^{106}Pd, ^{156}Gd, ^{158}Gd, ^{166}Ho, and ^{168}Er, 25:12586
THOMAS, G. R., Satellite equipment for the measurement of high energy electrons and protons, 25:11813
THOMAS, L. H., Current induced in a plasma by a penetrating electron beam, 25:11894
THOMAS, R. A., Ion-mobility spectrometer for radiochemical applications, 25:10903
THOMASSON, P., Further radio observations of planetary nebulae, 25:11567
THOMLINSON, R. H., Reoxygenation as a function of tumor size and histopathological type, 25:11258 (BNL-50203, pp 242-54)
THOMPKINS, R. W., Radiation in uranium mines, 25:11043
THOMPSON, I. M. G., Intercomparison of portable radiation monitoring instrument evaluations, 25:10809 (BNWL-SA-3565)
THOMPSON, M. A., Vidicon device for ionization measurements, 25:10878
THOMPSON, William L., Gamma-ray attenuation at energies of approximately 6 and 8 MeV, 25:11947
THOMSON, George Michael, Fast electron--scattered ion coincidence studies of the argon ion--atom collision, 25:11709
THONNARD, N., A sequential neutron and gamma ray monitor, 25:10824
THORLEY, A. W., Solubility of carbon in sodium, 25:10579
THORNE, L. F., Design of an insulator which must survive high g-forces, 25:12867 (BDX-613-213)
THORNTON, D. E. J., Computation of asymmetric power divergences in large nuclear reactors, 25:12777 (TRG-Report-2060(Rev.))
THORPE, D. G., Satellite equipment for the measurement of high energy electrons and protons, 25:11813
THRELFALL, E. J., Mutants of E. coli with altered surface properties and sensitive to uv light, 25:11029
THUEMMEL, H.-W., Base of multiple component system analysis by electron and beta ray interaction. I, 25:11674
TIAINEN, O. J. A., Use of nuclear polarization in neutron scattering and transmission measurements, 25:12533 (TKK-F-A-123)
TILFORD, J. M., Fast breeder reactor static physics methods development and analysis project. Volume 1. FARED: one-dimensional fast reactor physics design and analysis code, 25:12772 (BAW-3867-9(Vol.1)(Rev.1))
TILLEY, D. R., Angular correlation study of low-lying levels of ^{29}P, 25:12480
TILLICH, G., Studies on techniques for lung scintigraphy, 25:11129
TISSOT, Roland, Transmitting motion through reactor wall,

25:12863
TITOV, A. V., Nonprotein thiols in tissues after administration of cystamine, 25:11101
TITUS, F., Measurements of the energy response functions of scintillators for monoenergetic electrons, 25:10832
TKACH, V. I., Current structure of phenomenological Lagrangians, 25:12129
TOBAILEM, Jacques, Measurement of radioactivity of recently fallen carbonated chondrite: Allende, 25:11540
TOBUREN, L. H., Distributions of electrons ejected from N_2 by 0.3- to 1.7-MeV protons, 25:11712
TOELGYESSY, J., Determination of boron in boric glasses by a neutron absorption method, 25:10483
Determination of Co and Se by on-stream activation analysis, 25:10500
Moisture determination in certain compounds used for pharmaceutical purposes based upon neutron scattering and moderation, 25:10486
Neutron absorption analysis of pharmaceutic preparations containing boron, 25:10487
TOELGYESSY, Juraj, Activation analysis by charged particles, 25:10504
TOENNESEN, K. H., Blood flow determined by intra-arterial-injection and external recording of ^{133}Xe, 25:11137
Blood flow determined by local injection of ^{133}Xe in skeletal muscle, 25:11136
TOGAMI, Edwin, ^{68}Ga-labeled macroaggregates for lung studies, 25:11205
TOGANO, Kazumasa, Texture of Zn--Cd alloy ingot solidified from the flowing liquid, 25:11450
TOJO, T., Resolving time measurements of Geiger counters, 25:10835
TOMATI, U., Inactivation of β-Fructofuranosidase and Glucosidase by γ radiation of Beta vulgaris, 25:10964
TOMBLIN, F. F., Atmospheric x-ray fluorescence, 25:11790
TOMISELLI, A., Consideration of the clinical interpretation of scintigrams of the pancreas under normal and pathological conditions, 25:11199
TOMPKINS, Donald Harvey, Backward photoproduction of π^0 mesons at 6 to 18 GeV, 25:12069
TOMPSON, C. W., Investigation of in-band resonant modes in Cr--W alloys by inelastic neutron scattering, 25:12019
TON, H., Lifetimes of 2^+ and 4^+ rotational states in heavy doubly even nuclei, 25:12542
Lifetimes of rotational states in ^{229}Th and ^{235}U, 25:12541
TONG, L. S., Thermal analysis of pressurized water reactors, 25:12791
TONNET, Marie L., Solvolysis of sulphonyl halides. V, 25:10537
Solvolysis of sulphonyl halides. VI, 25:10536
TOPSCHOWSKY, M., Scattering of fast electrons by a gas plasma, 25:11879
TOROSSIAN, Claude, Effects of x and γ radiations on the ant, 25:11245
TORSOLI, A., Scintigraphy with ^{198}Au for chronic hepatitis, 25:11196
TOTH, K. S., New isotopes ^{241}Cf and ^{240}Cf, 25:12593
TOTH, Z., Clinical value of liver function appraisal by means of ^{131}I-rose bengal. II, 25:11111
TOTON, Edward Thomas, Mach's principle in scalar tensor theory of gravity, 25:12270
TOUSSAINT, Claude, Continuous control of low-uranium contents of solutions by measurement of radioactivity, 25:10473 (CEA-R-4032)
TOUZEAU, Review on correlation measurements in plasma, 25:11866 (EUR-CEA-FC-570)
TOYODA, Fumihiko, Dip-bump structure of cross section and urbaryon rearrangement. II, 25:12219
Exotic resonances, urbaryon rearrangement and hadron structure, 25:12183
TOYONISHI, Shigekazu, Preparation of Wood--Polymer-Composite by ionizing radiation. V, 25:10604 (JAERI-5026, pp 86-93)
TOYONISHI, Sigekazu, Radiation curing of mixture of diallylphthalate prepolymer and vinyl monomer. IV, 25:10607 (JAERI-5026, pp 108-20)
TRACY, G. D., Validity of the isotope dilution method of measuring extracellular fluid volume, 25:11185
TRAHANOVSKY, Walter S., Organic oxalates. IV. Pyrolysis of diallyl, disubstituted-allyl, and related oxalates, 25:10526
TRAN TUC VI, EL 600: study of core neutronic properties, 25:12775 (CEA-N-1395)
TREFALL, H., Correlation study of auroral luminosity and x rays, 25:11808
TREFNY, J. U., Flux motion through the superconducting surface sheath, 25:11829
TREMEAU, O., Microbiological evolution under gamma radiation, 25:11019
TREMKO, J., Study of Nova Her 1963, 25:11547
TRENTELMAN, G. F., Energy of the second excited state of ^{12}C and the rate of the triple-alpha reaction, 25:11565
TRESCHAU, Elmar, Adsorption of O and N on Ta films. III, 25:11417
TRET'YAK, S. A., Cascade rate functions for separating multicomponent isotopic mixtures, 25:10762
TRIFONOV, V. L., Fast valve of high pressure for bubble chamber, 25:10870 (JINR-P13-5420)
TRINDADE, H. A., Prog. rpt. on air cleaning, semiannual, 3--8/70, 25:10797 (NYO-841-23)
TRIPATHI, D. N., Importance of the kinetic-energy expression for a bound electron in classical theory, 25:11701
TRIPLETT, Larry L., Photodestruction of chloroplast ultrastructure by red light: location of chlorophyll, 25:11310
TROFIMOVA, O. S., Effects of irradiated nutrient medium on chromosome aberrations in mammalian cells in vitro, 25:10970
TROITSKAYA, M. N., Cesium-137 in lichen-reindeer man in the extreme north of the USSR, 1962--68, 25:11037 (NP-18381)
TROMP, R. L., Total neutron cross section and resonance parameters of ^{147}Pm, 25:12550
TRON, P., Metabolism of galactose ^{14}C in blood cells, 25:10485
TROSHICHEV, O. A., Ring current in the magnetosphere and low-latitude magnetic rays, 25:11779
TROSHIN, N. N., Comparative heat exchange characteristics of glasses with a radio-protective coating and without one, 25:10770
TRUE, William W., Core-plus-particle model and the low-lying levels of ^{53}Cr, 25:12494
TRUKHANOVA, L. N., Thermal properties of tantalum at high temperatures, 25:11425
TRUMP, J. G., Use of ionizing radiation for sterilization and preservation of biological tissues, 25:11337
TRUSHINA, M. N., Radioprotective action of polymer salt of cystamine and sulphopropyl ester of dextrane, 25:11108
TSARAPKIN, L. S., Dose effects curves for Ehrlich's ascites cells irradiated with γ rays, 25:11014
TSCHANZ, J. F., Temperature scale for neodymium zinc nitrate below 1K, 25:11852
TSENG, H. K., Exact screened calculations of atomic-field bremsstrahlung, 25:11681
TSIPENYUK, Yu. M., Photo-nuclear activation analysis of O in pure materials, 25:10501
TSKHAI, V. A., Conduction band of IVa and Va subgroup transition metal monocarbides. I, 25:12024
TSUCHIYA, Ryokichi, Thermal properties of deuterated Cu(II) sulfate pentahydrate, 25:10565
TSUEI, C. C., Superconducting metastable simple cubic alloys, 25:11819 (CALT-822-22)
TSUJI, Tadashi, Preparation of Wood--Polymer-Composite by ionizing radiation. V, 25:10604 (JAERI-5026, pp 86-93)
TSUKADA, Masao, Benzene formation in radiation-induced and photochemical reactions of acetylene, 25:10650
TSUKAHARA, Iwao, Determination of Be oxide inclusion in Cu--Be alloy. IV, 25:10440
TSUKUDA, Ritsuko, Ecology of insect sterilized by gamma radiation. IV, 25:11338
TSVINEV, A. P., Precision apparatus with liquid hydrogen target, 25:12300 (JINR-P8-5212)
TUCKER, A. B., Decay of ^{98}Ru, 25:12545
TUCKER, Lee Newbourne Jr., K^- absorption on neon, 25:1210
TUCKFIELD, R. G., Laser-pulse method of determining thermal diffusivity and thermal conductivity of graphite between 300° and 3300°K, 25:11487 (GA-9168)
TUFVESSON, G., Determination of monoamine oxidase activity in human blood serum, 25:10922
TUMERMAN, L. A., Thermogenesis of irradiated yeast cells in the process of recovering their reproductive capacity, 25:11324
TUNG, Wu-ki, Hyperon beta decay, 25:12163 (COO-264-563)
Hyperon beta-decay, 25:12164 (COO-264-563(Add.))
TUNKELO, E., Use of nuclear polarization in neutron scattering and transmission measurements, 25:12533 (TKK-F-A-123)
TUOMINEN, J., Sun as a magnetic rotator, 25:11629
TURALA, M., Time-coordinate compensator for the time spectrometers with long scintillators, 25:10813 (JINR-P13-5378)
TUREK, P., Proton pick-up from ^{19}F, ^{20}Ne, and ^{22}Ne, 25:12385
TUREKIAN, K. K., Trace element calibrations and profiles at Geosecs Test Station in Northeast Pacific Ocean, 25:10428
TURKIN, A. D., Emergency personal n-γ radiation dosimeters, 25:10881
TURNER, P. W., Effect of iron on the hot cracking of uranium weld metal. Part I, 25:11427
TURRICCHIA, A., Underwater plasma-arc cutting as a powerful dismantling tool for water reactors, 25:12714
TURRO, Nicholas J., Photochemistry of some α-ketopropiophenones. Evidence for an unusual cyclic transiton state for hydrogen abstraction, 25:10554
TYUTYUNNIKOV, S. I., Experiments on α-particle acceleration by collective method, 25:12305 (JINR-P9-5558)

U

UDALTSOVA, N. I., Uranium, Th, and rare-earth elements in thermal waters of the Kamchatka Peninsula, 25:10697
UEBERALL, H., Nuclear size effects in the polarization of elastically scattered electrons, 25:12664
UEHARA, Mitsuru, Rotational hysteresis of alloys of $SmCo_5$--$SmCu_5$ system, 25:11984
UGINCIUS, P., Nuclear size effects in the polarization of elastically scattered electrons, 25:12664

ULITOVSKAYA, I. I., Damage to nerve ganglia and development of intestinal syndrome in mice after neutron irradiation, 25:11270
ULLMAN, J. D., Double beta decay of ^{48}Ca, 25:12448
Double gamma emission from ^{40}Ca and ^{90}Zr, 25:12495
ULLRICH, W., Safety of heavy water system in Braunschweig research reactor, 25:12822 (NP-18499)
UMBARGER, C. J., Gamma decay of first two T = $^3/_2$ states of ^{15}N, 25:12416
UMBARGER, Cecil John Jr., Levels in ^{34}Cl and ^{35}Cl from reactions $^{34}S(p,n)$ and $^{31}P(\alpha,n)$, 25:12442
UMEZAWA, H., Systematic behaviour of the most probable charge in the medium-energy fission, 25:12700
UNDERBRINK, A. G., Relative biological effectiveness of x-rays and 0.43-MeV monoenergetic neutrons on somatic mutations and loss of reproductive integrity in Tradescantia stamen hairs, 25:11313
UNDERHILL, D. W., Prog. rpt. on air cleaning, semiannual, 3--8/70, 25:10797 (NYO-841-23)
UNTERREINER, K. H., Magnetization in Yb--Eu alloys, 25:12013
UNVALA, B. A., Growth of epitaxial layers by ion beam sputtering, 25:11962
URAKAMI, Motoaki, Grafting of acrylic acid onto polyester fiber, 25:10602 (JAERI-5026, pp 73-9)
Radiation induced graft copolymerization to polyester. VII, 25:10600 (JAERI-5026, pp 63-7)
Radiation-induced graft copolymerization to polyester. VIII, 25:10601 (JAERI-5026, pp 68-72)
URAY, L., Resistivity decrease due to grain growth in tungsten, 25:12030
URBANO, J. N., Villars theory of nuclear collective rotation and its relation to variable moment of inertia model of Mariscotti et al, 25:12695
USACEV, Sergej, Calculation of ^{90}Sr content changes in atmospheric fallout and on ground in West Slovakia up to year 2000, 25:10719
USADEL, Klaus D., Electrodynamics of strong-coupling superconducting alloys in high magnetic fields, 25:11843
USHAKOVA, A. P., Irradiation of population in USSR due to global Cs, 25:11073
USHER, P. D., Photometric history of BL Lacertae, 25:11555
USMANOV, P. D., Mutagenic action of laser radiation on seeds of Arabidopsis thaliana (L) heynh, 25:11027
USUDA, Hiroshi, Reactor-use structural materials viewed from their fabrication, 25:11364
UZZAN, G., Evaluation of the irradiation of bone marrow resulting from milk contamination by ^{90}Sr after continuous or uneven deposition on pastures, 25:10932 (CEA-CONF-1558)

V

VAANE, J. P., Autoradiography as help for analysing distribution of α-active material in human body after air contamination, 25:10953
VACCARO, G., Design of NH_3--H_2 two-temperature plant for heavy water production, 25:10787
VACLAVIK, J., Quasi-linear dynamics of ion cyclotron instability in an anisotropic plasma, 25:11915
VAGRADOV, G. M., Average field of excited nuclei, 25:12632 (JINR-P4-5084)
VAIDYANATHAN, S., Separation of Pu from ^{95}Zr/+ ^{95}Nb/ and ^{106}Ru, 25:10677
VAISBERG, V. V., Connection between absolute radioluminosity of extragalactic sources and redshift, 25:11581 (CSIRO-Trans-10247)
VAKHIDOV, Sh. A., Luminescence of CaF_2--TRF_3 in the gamma-ray field of ^{60}Co, 25:11955
VALBERG, Peter A., Spin-exchange effects on density-matrix elements, 25:11721
VALENTIN, J., Experimental determination of couplings in deformed nuclei, 25:12523 (LYCEN-7034, pp 58-83)
VALIEV, B. S., Arsenate method for iodometric determination of scandium in the presence of iron, 25:10465
VALLI, Kalevi, Production and decay of protactinium isotopes, 25:12592
VALVERDE, Nilo, Coulometric titrations for determination of homogeneity region of solid silver sulfide, silver selenide, and silver telluride, 25:12865 (ANL-Trans-873)
VAMPOLA, A. L., Access of solar electrons to closed field lines, 25:11783
VAN AUDENHOVE, Jean, Levitation in ultra-vacuum, 25:10805
VAN CAMPEN, D. H., Impact of nuclear engineering on developments in structural mechanics, 25:10758
VAN CRAEYNEST, Annick, Determination of limiting solubilities using heterodiffusion coefficient measurements, 25:11370 (CEA-CONF-1689)
VAN DEN BERGH, Sidney, Optical observations of the pair of galaxies associated with the radio source 4C 31.04, 25:11652
VANDENBOSCH, R., Mass determinations of neutron-deficient nuclides ^{88}Zr and ^{140}Nd by (p,2n) threshold measurements, 25:12607
Spin isomers of the shape isomer /sup 237m/Pu, 25:12530 (RLO-1388-130)
VAN DEN BROECK, H., Experimental and theoretical physics work on Pu enriched LWR's lattices, 25:12796 (EURAEC-2145)
VAN DER LINDE, A., Post-failure examination of the in-pile section of the pressurized water loop in the HFR at Petten, 25:12823 (RCN-125)
VANDERMEULEN, J., Branching ratios of tracks of π mesons emitted from proton--antiproton annihilation, 25:12195
VAN DE WALLE, R. T., Spin--parity analysis of B-meson produced in π⁺p reactions, 25:12119
VAN DE WEYER, K. H., Comparison of renal isotope diagnosis with vasoconstrictor content in the renal vein of hypertensive patients, 25:11163
VAN DIJK, W., Construction of the T-matrix from its symmetric part, 25:12673
VANECKO, J., Plastic-strain controlled failure criteria and design parameters. Technical progress report, 25:11373 (COO-2048-1)
VAN HEMERT, R. L., New detector for keV neutrons, 25:10845
VANHORENBEECK, J., Coulomb excitation of ^{123}Te and ^{125}Te, 25:12603
VANHORENBEECK, Jean, Nuclear reorientation, 25:12522 (LYCEN-7034, pp 42-57)
VAN HOVEN, Gerard, Kinematics and dynamics of nonlinear mode coupling, 25:11943
VAN KOTE, Francis, Apparatus for automatic liquid phase chromatography, 25:10659 (CEA-N-1267)
VAN KRUGTEN, H., Beta--gamma circular polarization correlation in decay of ^{48}V, 25:12471
VAN LIESHOUT, R., Re-examination of ^{66}Ge decay, 25:12477
VAN MAAREN, M. H., Critical carrier concentration for superconductivity in mixed metal--semiconductor systems, 25:11844
VANNIER, M., Quantometer for determination of trace elements in natural materials, 25:10451
VAN NOOIJEN, B., Beta--gamma circular polarization correlation in decay of ^{48}V, 25:12471
VAN WIERINGEN, J. S., Crystal structure and magnetic properties of Ce--Fe compounds, 25:12025
VANYUKOV, M. P., Neodymium glass laser with high radiation intensity for producing a high-temperature plasma, 25:11906
VANZANDT, T. E., Electromagnetic drift of the midlatitude F2 layer during a storm, 25:11805
VARMA, Vijay M., Treatment of thyroid cancer. Death rates after surgery and after surgery followed by sodium iodide ^{131}I, 25:11234
VARNAGY, M., Observation of proton tracks by a plastic detector, 25:10831
VASARU, Gheorghe, Thermal diffusion column, 25:10783
VASS, D. G., Charge collection process in pin junction radiation detectors, 25:10844
VAUGHN, F. J., Cross sections for $^7Be(p,\gamma)^8B$, 25:12400
VAUGHN, Glen A., Phase relationships in U, Np, and Pu, 25:11437
Thermal conductivity of plutonium at high temperature, 25:11383
VEKSLER, A. M., Mutagenesis of T4B phage in γ-irradiated E. coli, 25:11016
VENCHIKOV, V. A., Neodymium glass laser with high radiation intensity for producing a high-temperature plasma, 25:11906
VENDRAMIN, I., Operatorial expansion of the product of two currents, 25:12130
VENDRIK, A. J. H., Double isotope dilution technique in the study of a peripheral vascular system in vivo, 25:10926
VENKATARAMAN, G. S., Radio-resistant auxotrophic strain of R. leguminosarum, 25:11325
VENTER, R., Analytical method applicable to determination of individual concentrations of components, resulting from gamma induced iodination of methane, 25:10615
VERNICKEL, H., Calculation of the ion-trajectories in front of a field emission tip, 25:12299 (IPP-7/2)
VERNON, F. J. Jr., Response of highly damped Josephson junctions to external, low-frequency noise currents, 25:11822
VERNON, P., Use of the gamma camera for ^{131}I renography: a case study on a nephrectomized patient, 25:11206
VERTOGRADOV, L. S., Reaction π⁻p → e⁺e⁻n at 275 MeV, 25:12099 (JINR-P1-5398)
VESELIC, K., Spectral theory for Klein--Gordon equation, 25:12679
VESELY, V., Thermodynamics of uranyl ion exchange on Zr of various crystallinities, 25:10680
VESTERBERG, Viveka, Corrosion of plutonium in argon with small amounts of moisture, 25:11350
VEYSSIERE, A., Photoneutron cross sections of ^{208}Pb and ^{197}Au, 25:12610
VIALETTE, Y., Atomic absorption determination of K, Rb, and Sr, 25:10458
VIALETTES, Henry, Geometric correction factors relating to the recoil of protons in nuclear emulsions, 25:10867 (CEA-R-4081)
VIANNA, E. M., Night-time anomalies in vlf propagation by galactic x-ray source at Centaurus, 25:11812
VIANO, J. B., Parity violation in the transition of ^{181}Ta at 482 keV, 25:12621
VICHNEY, M., What future for advanced reactors in Europe, 25:12707
VIGASSY, J., COBRA: computer program for coolant boiling in rod arrays, 25:12784 (KFKI-70-20-RPT)
VIGNON, B., Boltzmann equation in general relativity, 25:11765

XUM

VIGOULET, Jacques Espagno, Radioactivity sensing apparatus for measuring the blood flow, 25:10828
VIKHRENKO, N. M., Strontium-90 uptake by agricultural plants and animals, 25:11050
VILCEANU, N., Uranyl pyrophosphate complexes. II, 25:10519
VILENCHICH, R., Analytical method applicable to determination of individual concentrations of components, resulting from gamma induced iodination of methane, 25:10615
Gamma-initiated iodination of methane in the gas phase, 25:10620
VILQUIN, A., Irradiation equipment for studying the influence of radiation on marine organisms, 25:10759
VINCENT, C. M., Charge asymmetry effects in reaction d(α,t)^{3}He, 25:12355
VINOGRADOV, N. I., Conditions of plasma heating at electron cyclotron resonance, 25:11861 (NP-18635)
VINOKHODOV, E. V., Procedure for calculating certain parameters of heat-producing elements of VVER type, 25:12798 (IAE-1942)
VIOLA, V. E. Jr., Direct interaction effects in the fission of ^{238}U with 63.5-MeV ^{4}He ions, 25:12526 (MNC-3783-7)
VIRNIK, A. D., Radioprotective action of polymer salt of cystamine and sulphopropyl ester of dextrane, 25:11108
VITALE, V., Radiotherapy of cancer of the oesophagus, 25:11236
VIZDALOVA, Milena, Nature of reparable and non-reparable lethal damage in E. coli, 25:11320
VLADIMIROV, Yu. S., Polarization of photons during scattering in gravitational field of spherical symmetry, 25:12159
VLASOV, A. D., Proton currents that may be obtained with high equilibrium phases in a linear accelerator without particle losses, 25:12313
VLK, J., Storing of pea seed after γ irradiation, 25:11024
VO-DAI, Thien, Coulomb effect on proton--proton scattering parameters, 25:12680
VOGEL, P. Christian, Temperature dependences of kinetic isotope effects, 25:10549
VOGELBRUCH, K., Planning an atomic beam apparatus for investigation of elementary chemical processes of neutral particles, 25:10517 (JUL-674-RC)
VOKROUHLICKY, L., Heart rate, mean arterial pressure, and respiratory frequency after zirconium citrate administration in irradiated and non-irradiated rabbits, 25:11289
VOLKOV, D. V., Current structure of phenomenological Lagrangians, 25:12129
VOLPE, John J., Monte Carlo calculation of the thermal neutron activation in light-water-moderated uranium cells using ENDF/B cross-section data, 25:12859
VON BRANDENSTEIN, Chr, Autoradiography as help for analysing distribution of α-active material in human body after air contamination, 25:10953
VONDRACEK, V., A contribution to the kinetics of radiostrontium in rats after external irradiation, 25:11263
Absorption of radiostrontium in irradiated organism, 25:10947
VON ESSEN, Carl, Repair and reconstruction of chromosomal DNA, 25:11007 (BNL-50203, pp 1-13)
VON ROENNE, P., Safety of heavy water system in Braunschweig research reactor, 25:12822 (NP-18499)
VOROB'EV, E. D., Neutron detector in search for superheavy elements in nature, 25:10814 (JINR-P13-5391)
VORONTSOV-VEL'YAMINOV, B., Masses of galaxies according to radio and optical observations, 25:11634 (CSIRO-Trans-10206)
VOSKRESENSKII, G. V., Linear electron accelerators with intense beams, 25:12315
VOTINOV, S. N., Effect of irradiation on mechanical properties of fcc alloys of Fe--Cr--Ni system. I, 25:11466 (SRARI-P-78)
VRIGAZOV, A., Determination of low-level ^{90}Sr and ^{137}Cs activation in milk, 25:10480
Possibilities of detecting low-level β-activities by scintillation detectors, 25:10819
VRONICH, John J., Positive reactivity from replacement of heavy water by light water in the coolant channels of a heavy-water-moderated reactor, 25:12830
VUKOVIC, Biserka, New evidence concerning the molecular basis of the restorative effect of DNA in cultured mammalian cells, 25:11243
VYHNANKOVA, M., Comparison of cerebral blood flow measurements with intravenously administered ^{131}I-labeled hippuran between arteriosclerotic and normal patients, 25:11150

W

WACKERLING, Lloyd R., Inferred presence of Balmer emission features in the spectra of early-type stars. I. The Hamburg-Case survey, 25:11576
Inferred presence of Blamer emission features in the spectra of early-type stars. II. MK spectral classification and Balmer-line photometry, 25:11577
WADA, Tohru, Ecology of insect sterilized by gamma radiation. IV, 25:11338
WADE, C. M., Further radio observations of novae, 25:11599
WAGEMANN, H. G., Investigations of radiation resistance of optoelectronic devices for an electronically scanning star sensor in satellites, 25:10904 (HMI-B-97)
WAGNER, G. A., Geometry factor in fission track counting, 25:10695
WAGNER, G. J., Proton pick-up from ^{19}F, ^{20}Ne, and ^{22}Ne, 25:12385
WAGNER, H., Electron microprobe to determine layer thicknesses down to monolayer range, 25:11421
WAGNER, Henry N. Jr., Normal-pressure hydrocephalus. Role of cisternography in diagnosis, 25:11181
WAGNER, R., Level density parameters for Ge, Ho, and Ta, 25:12536
WAGNER, Robert F., Even-parity states of the five-nucleon system, 25:12371
WAIDELICH, W., Changes of surface conductivity in Ge during x-irradiation, 25:11963
WAIN, A. G., Potential of Pu(III)--Pu(IV) couple in nitric acid solution and equilibrium constants for nitrato-complexes of Pu(IV), 25:10514 (AERE-R-5320)
WAKAT, M. A., On-line computer monitoring of pressurized ion exchange process, 25:10664 (DP-MS-70-38)
WAKID, A. M., Effects of gamma radiation on cotton leaf worm, 25:11247
WALDMANN, L., Thermomagnetic gas torque for collinear static and alternating magnetic fields, 25:11754
WALDMEIER, M., Structure of the monochromatic corona in the surroundings of prominences, 25:11618
WALDSCHMIDT, M., Semiconductor detector spectrometer with magnetic electron lens, 25:10864
WALEN, R. J., Work carried out in France during recent years on isotopes with Z greater than or equal to 83, 25:12524 (LYCEN-7034, pp 84-93)
WALKER, D. K., Controlling employee exposure to alpha radiation in underground uranium mines. Volume I, 25:11085
WALKER, G. E., Hole-vibration coupling in ^{115}In, 25:12543
WALKER, G. O., Observations of ionospheric electron content across the equatorial anomaly at sunspot minimum, 25:11816
WALKER, R. C., Inductive liquid metal level detector, 25:10896 (RD/B/N-1720)
WALLACE, Peter L., Investigation of the plutonium--silver system, 25:11441
WALLACE, W. E., Calculation of the influence of the crystalline electric field on the spin-disorder resistivity of rare-earth alloys and comparison with results on CeAl$_2$, 25:12009
WALLACE, W. J., Alpha-particle scattering by ^{36}Ar, 25:12455
WALLIN, W. R., Instrument probe for measuring temperature and pressure in the upper plenum of the EBR-II reactor vessel. EBR-II Project, 25:12781 (ANL-EBR-25)
WALLROTH, Carl-Friedrich, Model investigations on conical fluidized beds, 25:11479 (JUL-669-RW)
WALNE, Patricia L., Photodestruction of chloroplast ultrastructure by red light: location of chlorophyll, 25:11310
WALSH, F. D., Strain-induced phase transformations in Ti-6Al-4V, 25:11453
WALTER, E., Determination of regional blood flow with ^{133}Xe in the brain of Parkinson and tumor patients, 25:11147
WALTER, R., Thermoluminescent dosimetry with polycrystalline LiF, 25:10879
WALTER, R. L., DWBA analysis of the cross section and polarization data for the ^{14}N(d,n)^{15}O reaction at 3.5 MeV, 25:12405
Neutron--He interaction. II, 25:12360
WALTER, Roger Kenneth, Polarization of 16.5- and 22.1-MeV neutrons elastically scattered from liquid T and liquid D, 25:12354
WALTERS, W. B., Decay of ^{117}In isomers and search for a low-lying $^{9}/_{2}^{-}$ level in ^{117}Sn, 25:12566
WALTHER, E., Differential diagnosis of ^{85}Sr accumulating processes with the whole-body scintigram, 25:11174
WALTHER, Georg Karl Heinrich, Mathematical treatment of the stationary thermal conductivity in piecemeal homogeneous media, 25:10768 (JUL-657-MA)
WALUS, W., Decay of ground state of ^{82}Rb, 25:12507
WAMBERSIE, A., Recovery of skin reactions in mice after split-dose irradiation, 25:11260 (BNL-50203, pp 286-91)
WANDLING, C. R., Transformation device using post-detector signal pattern rotators for multiparameter eddy current tester, 25:12878 (BNWL-1469)
WARD, D., Reorientation effect in the cadmium isotopes, 25:12548
WARD, Don C., Effects evaluation of gas wells and associated facilities for Project Rulison, 25:10737 (PNE-R-39, Pt.2)
WARD, J. F., Gamma-radioinduced destruction of DNA, nucleosides, and nucleotides, 25:10962
WARD, Samuel, Methods for fractionation and scintillation counting of radioisotope-labeled polyacrylamide gels, 25:10478
WARTENWEILER, M., Further development of Suizer heavy water columns, 25:10764
WARZEE, M., Catalytic decomposition of carbon monoxide on pure iron, mild steels, and alloyed steels, 25:11374 (DP-Report-530)
WASASTJERNA, Frej, Fast method of computing the contribution from interference scattering of neutrons

to the integral J(theta,α,β), 25:12840
WASCHER, H., Differential scintigraphic representation of the pancreas by means of a computer, 25:11176
Lymph drainage following neck surgery, 25:11178
Studies on techniques for lung scintigraphy, 25:11129
WASHUETTL, J., Influence of γ-radiation on activities of several glycolytic enzymes in rye seeds, 25:10974
WASIELEWSKI, P., Application of unified model with Coriolis coupling to ^{22}Na, ^{24}Al, and ^{30}P, 25:12482
WASSBERG, R., Construction and installation work at Oskarshamn, 25:12716
WASSERBURG, G. J., Uranium--Th--Pb and Rb--Sr systematics in 2700 x 10^6-year old plutons from southern Wind River Range, Wyoming, 25:10701
WASSERMAN, E., Electron paramagnetic resonance of CD_2 and CHD. Isotope effects, motion, and geometry of methylene, 25:10555
WASSON, O. A., Gamma rays from resonant neutron capture in ^{169}Tm, 25:12589
WATANABE, Masaaki, Development of reactor enclosure high voltage power cable penetration, 25:12705 (JAERI-Memo-4197)
WATANABE, T., Whole body skin eruption combined with radiotherapy, 25:11296
WATSON, Charles E., Proton decay of analog resonances in ^{93}Nb, 25:12564
WATSON, James Clyde, ESR study of radicals in some irradiated single crystals, 25:10588
WATSON, M. B., Effect of irradiation on tensile and impact properties of 3½ percent and 9 nickel steel weldments, 25:11454 (AECL-3734)
WATSON, R. L., X-ray emission induced alpha particles, 25:12488
WATT, A., Angular momentum projection from non-axial intrinsic states: a calculation for ^{20}Ne, 25:12458
WATT, B. E., Deuteron scattering from polarized ^{3}He, 25:12358
Reaction ^{3}He(d,p)^{4}He proton asymmetry, 25:12357
WATT, C. S., Rising trajectories and singular potentials, 25:12291
WATTECAMPS, E., Proposal for a standard spectrum to check techniques of fast neutron spectrum measurements, 25:12816 (EACRP-L-74)
WATTERS, J. W., Bibliography on whole-body irradiation effect related to canine treadmill performance decrement, 25:11251 (AD-705976)
WAWER, Andrzej, Carbon-14 exchange studies in $^{14}CO_2$--CO--quartz walls, 25:10541
WAYLAND, J. R., Achieving uniform spatial response from large area liquid scintillation detectors, 25:10875
WDOWCZYK, J., Transverse momentum of secondaries from cosmic-ray interactions in region 2 x 10^5 GeV, 25:11749
WEAVER, Lawrence D. Jr., Excitation processes in helium and hydrogen, 25:11702
WEAVER, S. C., Electrical and thermal properties of NaCl structured metallic actinide compounds, 25:11494
WEBB, D. V., Photoneutron cross sections of ^{28}Si and ^{24}Mg, 25:12469
WEBB, H. D., Group rays of internal gravity waves in a wind-stratified atmosphere, 25:11796
WEBB, John, Improvements relating to nuclear reactors, 25:12771
WEBB, Robert B., Mutagenic effects of near uv and visible radiant energy on E. coli, 25:11032
WEBER, T., Microscopic description of charge form factor of ^{4}He, 25:12651
WEEKS, R. W., LIFE-I: a FORTRAN-IV computer code for the prediction of fast-reactor fuel-element behavior, 25:12794 (ANL-7736)
WEETMAN, B. G., Seismic response characteristics at NRDS from underground nuclear detonations, 25:10730 (NVO-1163-TM-22)
WEICHERT, G., Diagnosis of mitral insufficiency with ^{85}Kr, 25:11124
WEIDMANN, P., Assessment of functional significance for renal artery stenosis confirmed by angiography. comparison of the radiorenogram with the angiotensininfusion test and with the plasma renin content in both peripheral and renal venus blood, 25:11164
Simultaneous determination of glomerular filtration rate and renal blood flow with ^{60}Co-cyanocobalamine and ^{131}I-orthohippuric acid, 25:11157
WEILAND, J., Solution of equations describing explosive instabilities, 25:11914
WEINBERG, Alan Henry, Improvements in power supply systems, 25:10762
WEISE, Klaus, Gamma radiation following capture of neutrons, especially of polarized reactor neutrons by oriented nuclei, 25:12626 (FMRB-33/70)
WEISER, R. S., Antibody production by host cells in x-irradiated recipients of allogeneic spleen cells, 25:10994
WEISMAN, Joel, Thermal analysis of pressurized water reactors, 25:12791
WEISS, Edward R., False-positive pulmonary photoscans obtained with a dual-probe detector system, 25:11207
WEISS, M. S., Threshold photodisintegration of ^{208}Pb, 25:12562
WEISS, R. A., Influence of normal cells on the proliferation of tumour cells in culture, 25:11274
WEISSE, J., Review on correlation measurements in plasma, 25:11866 (EUR-CEA-FC-570)
WEISSMAN, Barry, Photodisintegration of deuterium, 25:12362
WELCH, G., Effects of α particles on longevity of Drosophila melanogaster, 25:11248
WELCH, L. C., Study of the ^{14}N(p,2p)^{13}C reaction at 46 MeV, 25:12391
WELLIVER, L. C., Redistribution of boron in the diffused layer during thermal oxidation, 25:11476
WELLS, R. G., Disclination structures in Bloch wall lattices in $BaFe_{12}O_{19}$ and $SmCo_5$, 25:12011
WELTER, H., Calculation of the ion-trajectories in front of a field emission tip, 25:12299 (IPP-7/2)
WELZ, B., Determination of trace elements in serum and urine with flameless atomization, 25:10464
WENDER, S. A., Moessbauer effect studies following Coulomb excitation, 25:10863
WENDT, W., Reactivity measurement in reactor cores on MTR fuel elements with a one-sided heavy water reflector, 25:12818 (FMRB-34/70)
WENESER, Joseph, Nuclear rotation and boson expansions. I, 25:12671
WERBROUCK, A., Spin--parity analysis of B-meson produced in π^+p reactions, 25:12119
WERHEIT, H., Optical anisotropy of β-rhombohedral B, 25:12029
WERNICK, J. H., Magnetic properties of Nb_3X compounds, 25:12037
WEST, C. W., X-ray and nuclear radiation facilities, personnel safety features, 25:11078 (Y-1754)
WEST, J. B., Lung circulation studies using radioactive gases, 25:11125
WEST, L. A., Nuclear reaction calibration energies by velocity measurements, 25:12402
WESTERVELT, Peter J., Scattering electromagnetic and gravitational waves by a static gravitational field, 25:12138 (NYO-2262-TA-222)
WEYER, G., Lifetime of new 194.9 keV level in ^{77}As, 25:12473
WHEELER, A. D., Effect of hot working on room-temperature strength and ductility of Pu--1 wt percent Ga delta-stabilized alloy, 25:11390
WHEELER, K. R., Minimum-creep-rate behavior of polycrystalline vanadium from 0.35 to 0.87 T/sub m/, 25:11397
WHEELER, Richard Merrill, Studies of first 2^+ states of ^{154}Sm and ^{238}U, 25:12559
WHETSEL, H. B., Progress summary of nuclear safety research and development projects, 25:12805
WHITAKER, Robert H., Radioiodinated toluidine blue: an unsatisfactory scanning agent, 25:11188
WHITE, D. H., Levels in ^{47}Ca and ^{51}Ca, 25:12491
WHITE, J. L., Carbonaceous mesophase formed in the pyrolysis of graphitizable organic materials, 25:11529
WHITEHEAD, J. D., Ionization disturbances caused by gravity waves, 25:11798
WHITFIELD, Cyrus E., Method of making metal alloy powders, 25:11362
WHITING, R., Radiation chemical processing, 1969, 25:10617
WHITLOW, G. A., Effect of humidity on the ductility of uranium, 25:11344 (AWRE-C-46/66)
Stress corrosion of uranium alloys, 25:11345 (AWRE-O-49/66)
WHITMORE, G. F., Recovery from radiation damage in mammalian cells, 25:11092 (BNL-50203, pp 41-53)
WHITMORE, James Jonathan, K^+--proton elastic scattering at 2.53, 2.76, and 3.20 GeV/c, 25:12115
WICKENHAEUSER, A., Incorporation of machine data handling in the monitoring of fissionable material in large research centers, 25:10796 (KFK-866)
WICKRAMASINGHE, D. T., Atmosphere of white dwarfs. II, 25:11556
WIEBICKE, H. J., DWBA model applied to the ^{24}Mg(d,p)^{25}Mg reaction at E/sub d/ = 13.5 MeV, 25:12457
WIEDEKING, E., Determination of trace elements in serum and urine with flameless atomization, 25:10464
WIEHR, E., Polarimetry in solar active regions. III, 25:11616
WIESENHAHN, Willem Jacobus, Spins, parities, and electromagnetic transition probabilities in ^{35}Cl, 25:12440
WIESNER, W., Beta spectrum of ^{204}Tl, 25:12615
WIGHTMAN, A. S., Analyticity in the coupling constant, 25:12257
WILCOX, J. M., Comparison of the mean photospheric magnetic field and the interplanetary magnetic field, 25:11603
WILHELM, H. E., Wave-mechanical formulation of many-fluid plasma theory in electromagnetic fields, 25:11899
Wave-mechanical formulation of plasma dynamics in longitudinal electric fields, 25:11891
WILHELMSSON, H., Solution of equations describing explosive instabilities, 25:11914
WILKINSON, D. H., Evaluation of finite nuclear size effects in allowed β-decay, 25:12667
Numerical evaluation of radiative corrections of order α to allowed nuclear β-decay, 25:12696
WILL, H., In-pile arrangement for strain measurements in nuclear fuel and structural materials, 25:11464 (KFK-1281)
WILLARD, J. E., Reactions of electrons and free radicals in

XUM

glassy ethanol, 25:10630
WILLE, Klaus, Luminescent response of anthracene to channeled α particles, 25:11972
WILLIAMS, Clyde M., Evaluation of /sup 99m/Tc-DTPA acid as a brain scanning agent, 25:11189
WILLIAMS, David C., Calculations of He release from $^{238}PuO_2$ microspheres, 25:11500
WILLIAMS, I. R., Deuteron-induced reactions in copper, 25:12438
WILLIAMS, J. L., Spontaneous grafting in the presence of swelling agents, 25:10619
WILLIAMS, R. K., Electrical and thermal properties of NaCl structured metallic actinide compounds, 25:11494
WILLIAMS, W. L., Measurement of the $2^2S/sub\ 1/2/--2^2P/sub\ 3/2/$ energy separation in H, 25:11691
WILLIAMSON, Francis S. L., Prog. rpt. on the avifauna on Aschitka Island, Alaska, 8/14/67--6/9/68, 25:12869 (BMI-171-102)
WILLIS, Clive, Ionic reactions occurring in the irradiation of carbon dioxide--oxygen mixtures at very high dose rates, 25:10633
WILLOWS, R., Effect of humidity on the ductility of uranium, 25:11344 (AWRE-O-46/66)
WILLSON, Charles Frederick, Nuclear reactors, 25:12770
WILLSON, M. A. G., Cluster of galaxies in Coma Berenices, 25:11644
WILNER, B., Interaction between a fully ionized plasma and a neutral gas blanket, 25:11878
WILSKI, H., Stability of phenoplast molding materials towards high-energy radiation, 25:10634
WILSON, B. G., Strong new x-ray object in Cetus region, 25:11592
WILSON, David L., Methods for fractionation and scintillation counting of radioisotope-labeled polyacrylamide gels, 25:10478
WILSON, Kenneth L., Prog. rpt. on powder metallurgy compaction, 9--11/70, 25:12913 (SRO-475-9)
WILSON, M., LS-term dependence of hyperfine-interaction parameters d^3s configurations, 25:11694
WILSON, Margaret D., Structure observed in solar-particle latitude profiles, 25:11797
WILSON, P. R., Three-component model for the formation of the chromospheric Ca II K line, 25:11615
WILSON, Robert N., Derivation of the Vlasov equation, 25:11900
WILSON, Robert W., Observation of CO emission at 2.6 millimeters from IRC + 10216, 25:11568
WINCHELL, P., Diffusion of ^{24}Na in viscosity standard silicate glass, 25:10578
WINGBRO, T., Superconductivity for ternary fcc Bi--Pb--Tl alloys, 25:11846
WINIGER, P., Computer method for analysis of γ spectra application to fission-fragment mixtures, 25:12535
WINIWARTER, P., Isomeric cross-section ratios for reactions $^{192}Os(n,2n)^{191}Os$ and $^{198}Pt(n,2n)^{197}Pt$ at 14 MeV, 25:12618
WINKLER, C., Scintigraphic studies of blood distribution in the pulmonary system, 25:11127
WINKLER, H., Beta decay of ^{22}O, 25:12453
WINN, M. M., High transverse momenta observed in air shower cores, 25:11750
WINN, W. G., Structure of ^{51}Cr, 25:12435
WINSTON, Martin A., False-positive pulmonary photoscans obtained with a dual-probe detector system, 25:11207
WINTER, H., Incorporation of machine data handling in the monitoring of fissionable material in large research centers, 25:10796 (KFK-866)
WINTER, N. J., Gauge-invariant spinor theories, 25:12262
WINTERBON, K. B., Spatial distribution of energy deposited by atomic particles in elastic collisions, 25:11682
WITHERS, H. R., Repair in cells of normal and malignant tissues, 25:11252 (BNL-50203, pp 54-69)
WITHERSPOON, J. P., Differential and combined effects of beta, gamma, and fast neutron irradiation of soybean seedlings, 25:11312
WITTEN, Thomas Jr., Faddeev equations for spin-dependent forces: calculation of ^9Be binding energy, 25:12692
WITTENBERG, Layton J., Phase relationships in U, Np, and Pu, 25:11437
Thermal conductivity of plutonium at high temperature, 25:11383
WITTERS, J., Double-wall ultra-high vacuum system with electron gun and evaporation rate monitor, 25:10806
WITTKOWER, A. B., Electron capture and loss by fast Br and I ions traversing light gases, 25:11710
WLEZEK, Camil, Studies for the optimum design of thermodynamic cycles of helium-cooled high-temperature nuclear power stations, 25:12809
WLODARCZYK, Miroslawa, Mechanism of conjugation and recombination in bacteria. IX, 25:10946
WOEHLBIER, F. H., Diffusion in solid metals and alloys, 25:11411
WOHLLEBEN, D., Magnetic susceptibility of cerium metal under pressure, 25:12018
WOJCIK, Krystyn, Activation energy and frequency factor of 100°K annealing stage of simple defects in n-type Ge, 25:11954
WOJTKOWSKA, J., Excitation of isomeric activities in ^{71}Ge, ^{78}Br, and ^{79}Br using 14.8-MeV neutrons, 25:12430 (INR-P-1091)
WOLF, F., Quantitative evaluation of ^{131}I-hippuran renal clearance based on a model, 25:11160
Results of renograms evaluated by computer analysis based on a non-compartmental model, 25:11161
WOLF, K. L., Spin isomers of the shape isomer /sup 237m/Pu, 25:12530 (RLO-1388-130)
WOLF, L., Stationary heat transfer in infinitely long fuel elements with locally varying heat sources and boundary conditions, 25:12799 (TUBIK-17)
WOLF, R., Assessment of renal blood flow with radioactive labeled compounds excreted by glomerular filtration, 25:11153
Comparative determination of hepatic blood flow with colloidal ^{198}Au and colloidal /sup 99m/Tc-S, 25:11140
Contribution of scintigraphy for evaluation of vascular renal diseases, 25:11166
Determination of splenic blood flow with ^{51}Cr labeled and heat treated erythrocytes, 25:11142
Hemodynamic function studies, 25:11184
Principals of blood flow measurements through organs by clearance methods, 25:10917
Radiation burden in nuclear medicine investigations in childhood, 25:11190
WOLF, Stuart Alan, Superconductivity in silver, 25:11821
WOLFE, A. M., Can the lumpy distribution of galaxies be reconciled with the smooth x-ray background, 25:11686
WOLFENDALE, A. W., Transverse momentum of secondaries from cosmic-ray interactions in region 2 x 10^5 GeV, 25:11749
WOLGEMUTH, K., Barium analyses from first Geosecs test cruise, 25:10468
WOLLENSAK, J., Injuries to eye after ionizing radiations, 25:11284
WOLLER, P., Results of lung scintigraphy in silicosis, 25:11134
WOLLRAB, James E., Microwave spectra of the first-excited torsional states and barrier to internal rotation of dimethylamine, 25:10551
WOLSKI, W., Pressed boride cathodes, 25:12316
WONG, C. Y., Total neutron cross section of oriented ^{165}Ho, 25:12565
WONG, Patrick Tin-choi, Effects of x irradiation on DNA synthesis in salivary gland cells of Drosophila hydei, 25:11246
WONG, S. S. M., Shell-model study of ^{65}Cu and ^{63}Cu, 25:12459
WOOD, David H., Investigation of the plutonium--silver system, 25:11441
WOOD, Louvan Elbert Jr., Chiral dynamics, SU(3) symmetry breaking and Kl, form factors, 25:12194
WOODHOUSE, Denise Micheline Rostan, Preservation of food by irradiation: preliminary studies on commercial shrimp, 25:11326 (NP-18393)
WOODMAN, Ronald F., Inclination of geomagnetic field, 25:11792
WOODS, A. H., Early detection of injury after nitrogen mustard (HN2) therapy using radioiron, 25:10952
WOODS, R., Helium release from alpha-bombarded ThO_2, 25:11502
WORLTON, D. C., Prog. rpt. on reactor fuels and materials development, 4--6/68, 25:11474 (BNWL-842)
WORTHLEY, B. W., Whole-body counter for studies of total body K, 25:10910
WOTTON, B. L., Effect of irradiation on tensile and impact properties of $3^1/_2$ percent and 9 nickel steel weldments, 25:11454 (AECL-3734)
WRIGHT, E. A., In vitro radioprotection by dimethyl sulphoxide, glycerol, and anoxia, 25:10983
WRIGHT, K. A., Use of ionizing radiation for sterilization and preservation of biological tissues, 25:11337
WRIGHT, Ronald A., Prog. rpt. on effects of underwater overpressures on the sea otter and its principal food species, annual, 7/68, 25:12876 (BMI-171-111)
WU, C. S., Double beta decay of ^{48}Ca, 25:12448
Double gamma emission from ^{40}Ca and ^{90}Zr, 25:12495
WU, Ning, Local fields describing an infinite tower of particles, 25:12246
WYATT, P. W., Superconducting Pb--Pb tunnneling near T/sub c/, 25:11826
WYDER, W. C., UV mirror/grating radioisotope heaters fabrication, 25:10776 (MLM-1779)

X

XANTHAKIS, Jean, Correlations between spot areas, number of proton flares, radio diameter of solar corona, and intensity of cosmic rays, 25:11630

Y

YADAV, A. A., Liquid--liquid extraction of Gold(III) with diluted tributyl phosphate, 25:10686
YAEGUCHI, Osami, Superconducting wired-wall cavity for V-band ENDOR experiment, 25:11850
YAGER, W. A., Electron paramagnetic resonance of CD_2 and CHD. Isotope effects, motion, and geometry of methylene, 25:10555
YAGGEE, F. L., Minimum-creep-rate behavior of polycrystalline vanadium from 0.35 to 0.87 T/sub m/, 25:11397
YAGI, Hisao, Superconducting wired-wall cavity for V-band

ENDOR experiment, 25:11850
YAGISHITA, Takashi, Perturbation approach to nonlinear Vlasov equation. II, 25:11933
YAKINTHOS, J., Colinear and noncolinear magnetic structures in rare earth compounds RNi_3 and R_2Ni_7, 25:11979 (CEA-CONF-1704)
YAMADA, Masami, Gross theory of β decay and application to Fermi matrix element, 25:12690
YAMADA, Naohei, Suppression of ac hysteresis energy loss in nonideal type-II superconductor, 25:11823
YAMAGATA, Noboru, Deposition and translocation of the radioactive fallout, 25:10718
YAMAGUCHI, C., Semiautomatic scanning system for nuclear emulsions, 25:10839
YAMAGUCHI, Hikoyuki, Protective effect of ethanol and KI on radiolysis of indole-3-acetic acid, 25:10647
YAMAGUCHI, Masaharu, Reheating process of Fe--Cr and Fe--Cr--V alloys, 25:11403
YAMAKAWA, K., Chromosome number in radiation-induced mutants of Chrysanthemum morifolium, 25:11031
YAMAMOTO, Nobuto, Effect of a potent carcinogen, 4-nitroquinoline 1-oxide, and its reduced from, 4-hydroxylaminoquinoline 1-oxide, on bacterial and bacteriophage genomes, 25:11026
YAMAMOTO, Yasuo, Reaction matrix theory for cluster states in light nuclei. I, 25:12411
YAMAMURA, Yasunori, Neutron ages and slowing down spectra in light water for a fission source and a D-T source, 25:12348
YAMAZAKI, T., Stroboscopic determination of magnetic moment of 8⁺ isomeric state of ^{208}Po, 25:12614
YAMAZAKI, Takashi, Elastic scattering of alpha particles by ^{16}O, 25:12419
YANNITELL, T. W., Training manual for fabrication of printed-circuit boards, 25:12864 (ANL-7725)
YASNOVA, L. N., Effects of irradiated nutrient medium on chromosome aberrations in mammalian cells in vitro, 25:10970
YATAZAWA, M., Simultaneous determination of copper and manganese in plants by neutron-activation analysis, 25:10509
YATAZAWA, Michihiko, Simultaneous determination of As and Sb in soil by neutron activation, 25:10506
YATES, B., Anisotropic thermal expansion of pyrolytic graphite at low temperatures, 25:11510
YATVIN, Milton B., Effect of route of administration and radiation on ^{3}H-actinomycin D binding by mouse hepatocyte DNA, 25:11285
YEATER, M. L., Temperature dependence of neutron inelastic scattering from water, 25:12342 (RPI-328-210)
YEH, K. C., Group rays of internal gravity waves in a wind-stratified atmosphere, 25:11796
YEH, Ko-ling, Iodine and Br in soil-plant system in relation to Reclamation-Akagare disease of rice, 25:10505
YELON, A., Superconducting Pb--Pb tunnneling near T/sub c/, 25:11826
YEN, Huan-Chun, Superconducting metastable simple cubic alloys, 25:11819 (CALT-822-22)
YNTEMA, J. L., Nuclear structure of ^{48}Sc, 25:12452
Spin dependence in inelastic scattering, 25:12454
YOCK, P. C. M., Theory of highly charged subnuclear particles, 25:12132
YOKOYAMA, Kenji, Radiation curing of mixture of diallylphthalate prepolymer and vinyl monomer. III, 25:10606 (JAERI-5026, pp 101-7)
Radiation curing of mixture of diallylphthalate prepolymer and vinyl monomer. IV, 25:10607 (JAERI-5026, pp 108-20)
Radiation curing of mixture of diallylphthalate prepolymer and vinyl monomer. V, 25:10608 (JAERI-5026, pp 121-9)
YOSHIDA, Hideyo, Spectrophotometric determination of traces of nitrogen in zirconium and zircaloy using thymol, 25:10442
YOSHIDA, S., Cosmic-ray variations during geomagnetic storms, 25:11745
YOSHIKAWA, Susumu, Dynamic concentration process of radioactive substances to aquatic organisms, 25:10998
YOSHIZAWA, Y., Systematic properties of nuclei. II, 25:12640 (OU-LNS-70-2)
YOUNG, A. M., Direct radiative capture of ^{3}He by tritons and t + ^{3}He cluster states in ^{6}Li, 25:12372
YOUNG, A. T., Improved solar wavelengths between 7780 and 7925 A, 25:11611
YOUNG, L., Ellipsometric studies of anodic oxide films formed on tantalum in dilute phosphoric acid, 25:11351
YU, Dahsoong, Reduction of the ray effect in discrete ordinates calculations, 25:12852
YU, Y.-W., Reactions of 400 MeV protons with ^{58}Ni and ^{197}Au, 25:12500
YUE, John T., Derivation of the Vlasov equation, 25:11900
YULDASHEV, B. S., Analysis of $\pi^- p$ + $n\pi^+\pi^-\pi^0$ (n = 1,2,3) and $\pi^- p$ + $n2\pi^+2\pi^-\pi^0$ (n = 1,2) reactions, 25:12204 (JINR-P1-5431)
YULE, T. J., Hardware and software for nuclear spectroscopy on the Varian Data Machines 622/i Computer, 25:10848 (ANL-7704)
YUROV, S. S., Mutagenesis of T4B phage in γ-irradiated E. coli, 25:11016
YUSA, H., Prog. rpt. on air cleaning, semiannual, 3--8/70, 25:10797 (NYO-641-23)
YUSSOUFF, M., Anomalous transmission of particles through perfect crystals, 25:11971

Z

ZADGORSKA, Z., Plasma cluster in dc arcs with applied inhomogeneous magnetic fields, 25:11905
ZAITSEVA, K. K., Formation of endogenous colonies of hematogenic tissue in spleens of γ-irradiated mice, 25:11099
ZAITSEVA, T. G., Formation of endogenous colonies of hematogenic tissue in spleens of γ-irradiated mice, 25:11099
ZAK, M., Changes in the number of bone marrow cells, 25:11288
ZAKHARCHUK, A. V., Thermo-oxidation degradation of poly(vinyl alcohol) irradiated by γ rays, 25:10591
ZAKHARTSOV, V. M., Photon radiation by electrons upon reflection from a magnetic field, 25:11679
ZAKI, M. M., Effects of gamma radiation on cotton leaf worm, 25:11247
ZANGHI, Jean-Pierre, Determination of limiting solubilities using heterodiffusion coefficient measurements, 25:11370 (CEA-CONF-1689)
ZAPOL'SKAYA, N. A., Histamine level in blood and tissues of animals under action of radioisotopes, 25:10967
ZATSEPIN, G., Concerning one experimental possibility in neutrino astronomy, 25:11628
ZAVENYAGIN, Yu. A., Interferometric investigations of plasma in a coaxial high-current accelerator using a helium--neon laser, 25:11871
ZEIDMAN, B., Reaction $^{10}B(\alpha,^{6}Li)^{8}Be$, 25:12392
ZEIN EL ABEDINE, A., Application of radiation techniques to water use efficiency studies, 25:10927
ZEL'CHINSKII, M., Dose characteristics of protons with energy 200 MeV, 25:11054 (JINR-P16-5383)
ZEL'TSER, M. R., MPC of ^{232}Th and natural Th in drinking water, 25:11051
ZERKOWITZ, A., Studies on vasoactive drugs with the ^{133}Xe muscle clearance method, 25:10914
ZERWAS, P., Spin-zero mesons and broken chiral $SU_3 \times SU_3$, 25:12237
ZHEREBCHENKO, P. G., Formation of endogenous colonies of hematogenic tissue in spleens of γ-irradiated mice, 25:11099
ZHESTJANIKOV, Vladimir, Nature of reparable and non-reparable lethal damage in E. coli, 25:11320
ZHITARU, R. P., Radiation hardening of NaCl single crystals, 25:11975
ZHUK, I. N., Connection between absolute radioluminosity of extragalactic sources and redshift, 25:11581 (CSIRO-Trans-10247)
ZHURAKOVSKII, E. A., X-ray spectra and band structure of refractory vanadium compounds, 25:12012
ZIELINSKA-PFABE, M., Gamma vibration of nuclei at equilibrium and saddle point, 25:12628 (INR-P-1201)
ZIELINSKI, Mieczysław, Carbon-14 exchange studies in $^{14}CO_2$--CO--quartz walls, 25:10541
ZIELINSKI, R. E., Helium diffusion in $^{238}PuO_2$, 25:11501
ZILLER, Henry Hubert, Metabolic studies on the continuously irradiated rat, 25:10980
ZIMAKOV, V. P., Method for infrared diagnostics of plasma, 25:11868 (SC-T-70-4054)
ZIMMER, W. H., EBR-II dosimetry test reaction rate measurements (reactor runs 31E and 31F), 25:12773 (BNWL-1403)
ZINOV'EV, L. P., Acceleration and extraction of deuterons from the JINR proton synchrotron, 25:12303 (JINR-P9-5442)
ZIONI, J., Properties of ^{96} ^{98}Rh from ^{96} ^{98} Ru(p,n) reaction, 25:12617
ZIPPER, W., Polarization of protons from $^{12}C(d,p)^{13}C$ reaction at E/sub d/ = 12.4 MeV, 25:12377 (INP-711)
ZIPSER, Edith, Repair and reconstruction of chromosomal DNA, 25:11007 (BNL-50203, pp 1-13)
ZITA, Gerlinde, Comparative studies between heart and lung scintigraphy, 25:11130
ZIVANOVIC, D., Level density of system of interacting nucleons in p-shell, 25:12409
ZLOBIN, V. S., Accumulation of ^{239}Pu and ^{210}Po by Ascophyllum nodosum and marine phytoplankton, 25:10941
ZOCHER, R. W., Thermal expansion of extruded graphite--ZrC carbide composites, 25:11512
ZOTOV, V. S., Diffusion of nickel in beryllium, 25:11399
ZOVKO, N., Model of nucleon electromagnetic form factors, 25:12147
ZUBAREV, V. N., Measurement of scattering angle of particles by Vavilov--Cherenkov radiation, 25:10869 (JINR-E13-5459)
ZUBOV, Yu. G., Scattering of neutrons with an energy of 4 MeV at angles close to 180°, 25:12509 (ANL-Trans-855)
ZUCKER, O. S., CO_2 laser heterodyne plasma diagnostics in an adverse environment, 25:11869
ZUCKERMAN, B., Microwave detection of interstellar formic acid, 25:11593
ZUM WINKEL, K., Angiocardiography with a scintillation camera, 25:11121
Scintigraphy of renal function evaluated by digital and analog computers, 25:11165
ZUPAN, J., Magnetic susceptibility of boron nitride,

XUM

25:12010
ZVARA, I., Gasochromatographic separation of nonvolatile metal chlorides using aluminum chloride as eluent, 25:10666 (JINR-P6-5410)
ZVAROVA, T. S., Gasochromatographic separation of nonvolatile metal chlorides using aluminum chloride as eluent, 25:10666 (JINR-P6-5410)
ZWICKER, Ulrich, Superconductivity and metallurgical problems with Ti--Nb alloys, 25:11416
ZYKOV, A. I., Influence of radial slots in iris disk of waveguide on dispersion properties and quality factor of system of axially-symmetric and nonaxially-symmetric waves, 25:12306 (KFK-tr-334)
ZYLICZ, E., Incorporation of tritium in hair, 25:10954

SUBJECT INDEX

Cross references are included in cumulative subject indexes and in *Subject Headings Used by the USAEC Division of Technical Information* (USAEC report TID-5001).

The reader is also referred to *Guide to Abstracting and Indexing for Nuclear Science Abstracts* (USAEC report TID-4576).

Most headings in the subject index are specific materials, things, and processes. The headings are followed by modifiers that describe the properties of, or processes applied to, the headings.

All index entries cite *NSA* volume and abstract numbers; volume number precedes the colon and the abstract number follows it. The designation (R) following the abstract number indicates a progress report; (P) indicates a patent; and (T) indicates a translation. Abstracts for reports other than progress reports carry no letter designation. Report numbers, where applicable, are included in parentheses after the abstract number of the citation. Published literature (journal article or book) can be identified by the absence of a report number.

Ideas presented in the original literature, rather than key words, have been indexed. The indexers have selected what seemed the most probable and logical place to look for typical information. Since it is not always possible to anticipate where a user would look for information, the cumulative indexes include numerous cross references. Consideration of synonymous or closely related terms will prove valuable.

Information is indexed for the greatest use to the greatest number of users. This requires that a topic be indexed to headings that most specifically describe it and not ordinarily to the headings that describe its ultimate use or to the general class headings that include the specific headings. For example, information on boiler design for the Fermi Fast Breeder Reactor would be indexed under the headings BOILERS and FERMI FAST BREEDER REACTOR but not necessarily under the headings REACTORS, FAST or REACTORS, BREEDER.

General or broad headings are reserved for general summaries, reviews, comprehensive reports, and similar literature.

Subject Heading Styles

Generally, the direct form of subject entry is used rather than inverted headings; e.g., AMINO ACIDS rather than ACIDS, AMINO; HELIUM ISOTOPES He-4 rather than HELIUM—ISOTOPES He-4 or HELIUM—He-4 ISOTOPES. Note, however, that in some cases parenthetic modifying terms or inverted headings such as NEUTRONS, FAST, are used where the alphabetical arrangement of a direct entry would cause information to be scattered. In addition, organic compounds are usually entered in the index in the inverted form to facilitate grouping like or related compounds with the parent compounds; e.g., BENZENE, BROMO- rather than BROMOBENZENE. In general, the nomenclature used is that of the subject indexes to *Chemical Abstracts*.

Alphabetization

Subject headings are alphabetized word by word. Parenthetic qualifiers, numbers, and Greek letters within subject headings are disregarded in alphabetizing unless there are two or more headings that are otherwise identical, in which case the qualifier, numerical progression, or spelled names for the Greek letters determine the order.

Examples:

M-Capture
  see ELECTRON CAPTURE
MAGNESIUM
MAGNESIUM ALLOYS AND SYSTEMS
MANGANESE FLUORIDES
MANGANESE FLUORIDES MnF_2
MESONS
MESONS (π)
MESONS (ρ)
1-PENTANOL
2-PENTANOL

Modifying Phrases

The modifiers appearing under a subject heading are written specifically to show the relation between the item being indexed and the heading. The modifier therefore contains a maximum of useful information. Although the modifier begins with the word judged to be of greatest use to the greatest number of users, there is still need for the searcher to consider all modifiers under the heading(s) of interest.

Modifiers usually form meaningful phrases when combined with the subject heading. Some are intended to be read following the subject heading, e.g., the entry HYDROGEN—sorption by charcoal should be read "hydrogen sorption by charcoal." As a result of placing the important word first, however, many modifiers must be rearranged for smooth reading, e.g., FORMALDEHYDE—yields in radiolysis of ethyl ether, effects of deuterium on, should be read "effects of deuterium on formaldehyde yields in radiolysis of ethyl ether" and URANIUM—crystal structure of, effect of cooling rate on allotropic transformations in, should be read "effect of cooling rate on allotropic transformations in crystal structure of uranium."

Special characters are added to modifiers in the fields of physics and reactor technology; if the modifier does not establish the experimental or theoretical character of a reference, a symbol (E), (T), or (E/T) is placed immediately after the modifying phrase and before the abstract number.

Physical States and Configurations of Materials

The specific physical state, if other than normal, or the geometric configuration of the material is included in the modifying phrase; e.g., information on liquid metals is indexed under the specific metal with "liquid" in the modifier and carbon crucibles is indexed under CARBON with "crucibles" appropriately placed in the modifier. The information on carbon crucibles is also indexed under CRUCIBLES.

Nomenclature of Inorganic Compounds

Inorganic compounds are indexed to subject headings in the direct form. Cations are listed in the order of increasing valence for polycationic salts of varying valence and in alphabetic order for polycationic salts in which all cations have the same valence; e.g., SODIUM ALUMINUM SILICATES and POTASSIUM SODIUM SULFATES. If more than one anionic species is presented in a compound, the anions are arranged alphabetically, e.g., BERYLLIUM FLUORIDE HYDROXIDES.

Nomenclature of Organic Compounds

Organic compounds are indexed by subject headings based on the indexes to *Chemical Abstracts* except in the area of enzymes, in which specific enzymes, named according to the 1964 recommendations of the International Union of Biochemistry, are used. In many cases nonproprietary names for drugs are used as subject headings, and cross references are made from the systematic chemical names. Subject headings for hormones appear in the inverted style at HORMONES.

Nomenclature of Life Sciences

Subject headings for plants are names of phyla with one exception: members of the Phylum Tracheophyta are indexed under class or subclass names. Scientific names (genus and species) are used as the initial, or file, word in the modifying phrase. Scientific names are omitted only when the name is not available in the literature or cannot be found in available references.

Subject headings for animals are the names of phyla with the following exceptions: (1) members of Phylum Arthropoda and Phylum Chordata are indexed under appropriate class name, and (2) common names are used for members of Class Mammalia.

Subject headings are entered for various classes of commodities, and specific products are identified in the file-word position of the modifier. In the following examples, approved subject headings are capitalized and typical modifier file words are listed in lower case.

Example 1	Example 2
CEREALS	MEATS
bread	beef
flour	fish
oats	mutton
rice	pork
rye	poultry
wheat	seafood

Diseases, pathological conditions, and in vitro studies of atypical cells and tissues are indexed under subject headings for the organism affected, under the appropriate anatomical structure of physiological phenomenon affected, and under the appropriate disease heading. Subject headings for diseases (defined as any deviation from the norm) are DISEASES; DISEASES, INFECTIOUS; DISEASES, NEOPLASTIC; DISEASES, PHYSIOLOGICAL; DISEASES, PLANT; and DISEASES, TRAUMATIC.

Diseases of mixed etiology are treated in the following manner: neoplastic diseases that are also classified as infectious or physiological are indexed under DISEASES, NEOPLASTIC; diseases in which a microorganism is the etiologic agent are classified under DISEASES, INFECTIOUS; physiological anomalies that are neither neoplastic nor infectious are indexed under DISEASES, PHYSIOLOGICAL; the acute radiation syndrome, nonspecific radiation injuries, trauma, and wounds or incisions inflicted mechanically are indexed under DISEASES, TRAUMATIC.

Specific diseases or pathological conditions are named in the file-word position of the modifier, in the author's terminology, and are set off from the remainder of the modifier by commas. Neoplasms are designated as benign or malignant in the file-word position when more specific information is not available.

Multicomponent Alloys and Other Systems

Multicomponent alloys and systems, except well-known trade names, are indexed under a subject heading for each component in the form "element systems" for nonmetals or "element alloys and systems" for metals. The modifier begins with element symbols for each component arranged alphabetically. In addition, if significance is placed on the base metal of the alloy, this is indicated by adding "-base" to the element symbol.

Example: A 1.5C, 12Cr, 0.25V, 0.8Mo, bal Fe alloy is indexed as

```
CARBON SYSTEMS
  C--Cr--Fe-base--Mo--V, ...
CHROMIUM ALLOYS AND SYSTEMS
  C--Cr--Fe-base--Mo--V,...
IRON ALLOYS AND SYSTEMS
  C--Cr--Fe-base--Mo--V, ...
MOLYBDENUM ALLOYS AND SYSTEMS
  C--Cr--Fe-base--Mo--V, ...
VANADIUM ALLOYS AND SYSTEMS
  C--Cr--Fe-base--Mo--V, ...
```

Well-known alloys, such as ZIRCALOY-2, are indexed under the trade name; cross references from each component of the alloy to the trade name appear in cumulative indexes.

Multicomponent systems in which nonmetallic elements are present in large percentage and which are commonly referred to as systems or mixtures are indexed in a manner similar to alloys.

Example: A tungsten–silicon preparation is indexed as

```
TUNGSTEN ALLOYS AND SYSTEMS
  Si--W, ...
SILICON SYSTEMS
  Si--W, ...
```

Multicompound systems and mixtures of inorganic compounds are indexed under the subject heading for each component compound; the modifiers begin with an alphabetical listing of compound formulas.

Example: A lead titanate–lead zirconate mixture is indexed as

```
LEAD TITANATES
  PbTiO3--PbZrO3
LEAD ZIRCONATES
  PbTiO3--PbZrO3
```

A mixed system of compounds and elements is indexed by a combined form of the preceding conventions; e.g., a dispersion of copper and alumina would be indexed as

ALUMINUM OXIDES
  Al_2O_3--Cu, ...
COPPER ALLOYS AND SYSTEMS
  Al_2O_3--Cu, ...

Mixtures of organic compounds are indexed under subject headings for each component of the mixture; the modifiers begin with an alphabetical listing of compound names.

Example:

ACETIC ACID
  acetic acid--BF_3, ...
BORON FLUORIDES
  acetic acid--BF_3, ...

Example:

BENZENE, CHLORO-
  bromophenol--chlorobenzene, ...
PHENOL, BROMO-
  bromophenol--chlorobenzene, ...

If modifiers for alloys and systems are included with other modifiers under the same subject heading, they are filed last.

Example:

CARBON SYSTEMS
  deposition on nuclear fuel particles
  molecular structure of
  neutron total cross section for
  sorptive properties for xenon
  Young's modulus for
  Al--C--Cr, superconductivity in
  B--C, phase studies for
  C--U--Zr, fabrication and physical properties of

Nomenclature of High Energy Physics

Information on particle-particle events is indexed under subject headings for the specific particles involved. The modifier file word *interactions* is followed by the specific interaction written in symbolic form. Particle nomenclature and symbols follow that of Rosenfeld, et al. *Data on Particles and Resonant States*, UCRL-8030 (latest revision). For consistency the incident particle is always written first. The mass (in MeV) of a resonance state is included in parentheses after the symbol to avoid ambiguity. Hyperfragments are indicated in modifiers as in the following examples: Λ-He^5, Σ-H^3, $\Lambda\Lambda$-Be^{10}. The superscript on the right indicates the total number of baryons in the composite system.

Examples:

MESONS (π^-)
  interactions $\pi^- + p \rightarrow \Lambda + K^+ + \pi^-$ at 6 GeV/c in hydrogen bubble chamber, $\Lambda K(1700)$ enhancement in, (E)
BARYONS, RESONANCE (N^*)
  production of $\Delta^{++}(1236)$ and $\Delta^0(1236)$ from $K^- + p \rightarrow K^- + p + \pi^+ + \pi^-$ interactions at 2.63 and 2.70 GeV/c, (E)
HYPERFRAGMENTS
  binding energy of $\Lambda\Lambda$-He^6, three-body α--Λ--Λ model for

Subject headings are also provided for specific models and theories.

Examples:

ELEMENTARY PARTICLE MODELS (TRIPLET)
  hadron total cross sections in quark, numerical analysis of
CURRENT ALGEBRA
  PCAC hypothesis for A_1 and rho dominance in $\pi \rightarrow e + \nu + \gamma$ decay
REGGE POLE THEORY
  predictions for polarization in $K^- + p \rightarrow$ anti $K^0 + n$, $\pi^- + p \rightarrow \pi^0 + n$, and $\pi^- + p \rightarrow$ eta + n interactions at high energies
SYMMETRY GROUPS
  SU(2) × SU(4) intermediate-coupling model for nucleon and hyperon isobars

Nomenclature of Reactor Technology

Subject headings for reactors are of three types:

(1) Specific reactors, e.g., ARGONNE RESEARCH REACTOR, SAXTON POWER REACTOR

(2) Reactors having a common physics or engineering characteristic, e.g., REACTORS, FAST; REACTORS, ORGANIC-COOLED; REACTORS, PRESSURIZED-WATER

(3) Reactors having a common purpose, e.g., REACTORS, POWER; REACTORS, RESEARCH

Information on specific reactors, type (1), is indexed under the one specific subject heading. Information on classes or types of reactors, types (2) (characteristics) and (3) (purpose), is indexed under all applicable headings. For example, information on a heavy-water-moderated organic-cooled power reactor is indexed under REACTORS, HEAVY WATER-MODERATED; REACTORS, ORGANIC-COOLED; and REACTORS, POWER.

Subject headings exist for selected reactor components, e.g., REACTOR FUEL ELEMENTS. When applicable, headings for components are indexed even though they may have been included in a modifier under a type (1) or (2) heading. The materials in reactor components are indexed when the information is peculiar to the material.

Modifier file words under reactor headings are of two primary types: one type expresses reactor characteristics, e.g., reactivity; the other, components, e.g., control rod. If no subject heading appears for a reactor component, the heading REACTORS is used, and the component is used as the modifier file word.

A

ACCELERATORS
beam optics for, review of collective effects in, 25:12298(T) (CERN-Trans-70-7)
development in U.S.S.R., review of, 25:12709
ion source for high-energy, design of polarized, 25:12304 (JINR-P9-5446)
shielding for high-energy, neutron transport calculations of earthshine for estimating, 25:12332
ACCIDENTS
conference on methods for radiation dosimetry following, 25:11056 (STI/PUB-241)
dosimetry systems for nuclear, intercomparison experiments on, 25:11074(R) (AECL-3777)
planning for nuclear plant, first-aid, 25:11109
radiation dosimetry for criticality, 25:10818
radiation dosimetry of personnel following criticality, methods for γ and fast neutron, 25:11057
radiation protection programs for, 25:11083
ACETAMIDE, TRIMETHYL-
radiation effects on single crystals of, at 77°K, ESR studies on radicals produced by γ, 25:10588
ACETAMIDINE
hydrochloride, radiation effects on single crystals of, at 77°K, ESR studies on radicals produced by γ, 25:10588
ACETIC ACID
acetic acid--acetone--TBP, solvent properties for separation of oxidation states of sixteen elements by paper chromatography, 25:10687
ACETIC ACID, [(CARBOXYMETHYL)IMINO]BIS[[ETHYLENE[(CARBOXYMETHYL)IMINO]ETHYLENE]NITRILO]TETRA-
use of metastable technetium-99-labeled, for scanning of human brain in comparison to metastable technetium-99-labeled pertechnetate, 25:11189
ACETIC ACID, (1,2-CYCLOHEXYLENEDINITRILO)TETRA-
complexes with thorium, uses for spectrotitrimetric determination of (1-hydroxyethylidene)diphosphonic acid, 25:10462
ACETIC ACID, (ETHYLENEDINITRILO)TETRA-
complexes with rare earths, separation by ion exchange, effects of resin crosslinking on, 25:10665 (INR-P-1209)
solvent properties for trace amounts of elements in standard rocks, 25:10671
ACETIC ACID, VINYL ESTER
radioinduced polymerization in aqueous solutions, 25:10594 (JAERI-5026, pp 26-34)
radioinduced polymerization of, effects of cetyltrimethylammonium chloride on γ, 25:10593 (JAERI-5026, pp 15-25)
ACETIC ACID, VINYL ESTER, POLYMERS
stability of emulsions of, produced by radioinduced polymerization, 25:10594 (JAERI-5026, pp 26-34)
stability of emulsions of, produced by radioinduced polymerization, 25:10593 (JAERI-5026, pp 15-25)
ACETIC ANHYDRIDE ($CH_3CO)_2O$
effects on γ- and uv-radioinduced sulfoxidation of alkanes, 25:10592 (BMBW-FBK-70-25)
ACETONE
yields from radiolysis of aqueous diisopropylamine solutions, effects of 2-mercaptoethanol on, 25:10627(R) (NYO-2499-37)
acetic acid--acetone--TBP, solvent properties for separation of oxidation states of sixteen elements by paper chromatography, 25:10687
acetone--HCl--methanol, distribution coefficients of metal ions in, 25:10681
ACETYLCHOLINE
radioprotective effects of, on mice and rats, γ, 25:11102
ACETYLENE
photolysis of, mechanisms of benzene formation in uv, 25:10650
radiolysis of, mechanisms of benzene formation in γ, 25:10650
yields from radiolysis of ethylene and methane, 25:10644
ACIDS
book: Intercrystalline Corrosion and Corrosion Cracking of Stainless Steel in Aqueous Solutions (In Russian), 25:11353
ACRIDINE, 3,6-BIS(DIMETHYLAMINO)-
effects on repair mechanism of uv-irradiated bacteriophages and Escherichia coli, 25:11320
ACRIFLAVINE
effects on ionizing and uv-radiosensitivity of Escherichia coli and Shigella flexneri, 25:11323
ACRYLAMIDE POLYMERS
analysis of gels of, for carbon-14 and tritium by fractionation and scintillation counting, 25:10478
ACRYLIC ACID
effects on electron-induced polymerization of methyl acrylate--1,2-polybutadiene, 25:10609 (JAERI-5026, pp 130-6)
radioinduced polymerization on drawn polyester fibers, properties of products from γ, 25:10599 (JAERI-5026, pp 56-62)
radioinduced polymerization on poly(ethylene terephthalate), effects of solvent on properties of products from γ and electron, 25:10597 (JAERI-5026, pp 46-51)
radioinduced polymerization on polyester fabrics by impregnation method, properties of products from electron, 25:10601 (JAERI-5026, pp 68-72)
radioinduced polymerization on polyester fibers, effects of temperature on γ, 25:10602 (JAERI-5026, pp 73-9)
radioinduced polymerization on polyester films by impregnation method, electron, 25:10598 (JAERI-5026, pp 52-5)
ACRYLIC ACID, BUTYL ESTER
acrylonitrile--bis(2-hydroxyethyl methacrylate) phosphate--butyl acrylate--poly(diallyl phthalate), radioinduced polymerization of coatings of, on metals, electron, 25:10608 (JAERI-5026, pp 121-9)
ACRYLIC ACID, ETHYL ESTER
radioinduced polymerization on cotton, rayon, and wool using water as swelling agent, 25:10619
ACRYLIC ACID, METHYL ESTER
methyl acrylate--polybutadiene, radioinduced polymerization of, effects of catalysts and crosslinking agents on electron, 25:10609 (JAERI-5026, pp 130-6)
ACRYLONITRILE
radioinduced polymerization on poly(vinyl chloride) powders, effects of dose rate on γ and electron, 25:10596 (JAERI-5026, pp 42-5)
radioinduced polymerization on poly(vinyl chloride) powder, properties of fibers from γ, 25:10595 (JAERI-5026, pp 35-41)
acrylonitrile--bis(2-hydroxyethyl methacrylate) phosphate--butyl acrylate--poly(diallyl phthalate), radioinduced polymerization of coatings of, on metals, electron, 25:10608 (JAERI-5026, pp 121-9)
acrylonitrile--poly(diallyl phthalate), radioinduced polymerization in wood, γ or electron, 25:10607 (JAERI-5026, pp 108-20)
ACTINIDE IONS
magnetic properties of, neutron diffraction study of, 25:12002
ACTINIDES
conference on properties and structure of, Sante Fe, New Mexico, Oct. 5 to 9, 1970, 25:11372 (CONF-701001-(Pt.1))
conference on properties and structure of, Sante Fe, New Mexico, Oct. 5 to 9, 1970, 25:11433 (CONF-701001-(Pt.2))
crystal structure of, relation with 5f electrons, 25:11381
determination by spark-source mass spectroscopy, 25:10438 (ORNL-4636, pp 51-3)
determination of, development of methods for, 25:10425 (ORNL-4636, pp 40-2)
effects on thorium and uranium diffusion in columnar pyrocarbons, 25:11378 (ORNL-TM-2989)
electronic properties of, discussion of Moessbauer spectroscopy for determination of, 25:12000
magnetic properties of, relation with 5f electrons, 25:11381
melting points of, relation with 5f electrons, 25:11381
nuclear properties of, summary of work in France on, 25:12524 (LYCEN-7034, pp 84-93)
superconductivity of, relation with 5f electrons, 25:11381
thermal conductivity at low temperatures, review of data on, 25:11382
valence of, nonrelativistic augmented plane wave calculations of metallic, (T), 25:11995
ACTINIUM ISOTOPES Ac-218
alpha decay of, α spectra and half-life for, (E), 25:12592
ACTINIUM ISOTOPES Ac-219
alpha decay of, α spectra and half-life for, (E), 25:12592
ACTINIUM ISOTOPES Ac-220
alpha decay of, α spectra and half-life for, (E), 25:12592
ACTINIUM ISOTOPES Ac-221
alpha decay of, α spectra and half-life for, (E), 25:12592
ACTIVATION ANALYSIS
development for quality and process control in industry, 25:10443
developments in, 25:10472(R) (BMBW-FBK-70-19)
developments in charged-particle, photon, and neutron, 25:10497
developments in charged-particle, review on, 25:10504
neutron sources for, evaluation of pulsed reactors as, 25:10489 (KFKI-70-25-NAC)
ADENOSINE 5'-DIPHOSPHATE
determination of phosphorus-32-labeled, by ion exchange chromatography, isotope dilution, and scintillation counting, 25:10470
ADENOSINE MONOPHOSPHATES
determination of phosphorus-32-labeled, by ion exchange chromatography, isotope dilution, and scintillation counting, 25:10470
ADENOSINE 5'-TRIPHOSPHATE
determination of phosphorus-32-labeled, by ion exchange chromatography, isotope dilution, and scintillation

counting, 25:10470
ADRENAL GLANDS
radiation effects on cortex of, in rats, protective effects of sex hormones against whole-body x, 25:11268
ADVANCED TEST REACTOR
fuel elements for, effects of operating conditions and radiation on performance of, 25:11463 (IN-1437, pp 70-5)
fuel plates for, thermal expansion of, 25:11375 (IN-1437, pp 24-59)
loops for, development of in-pile gas and water, 25:11474(R) (BNWL-842)
AEROSOLS
properties of radioactive, electrical and mechanical, 25:11036 (CEA-Bib-185)
sampling of atmospheric, development and operation of equipment for vertical, 25:10754 (NP-18633)
AGE
effects on accumulation and transport of potassium-42 in leaves, stems, and roots of corn, 25:10930 (CEA-CONF-1517)
effects on mortality in patients with thyroid carcinomas following therapy with iodine-131, 25:11233
effects on x-radiosensitivity on Chinese hamster cells, 25:11093 (BNL-50203, pp 97-116)
AGE ESTIMATION
fission track method for, of glasses and rocks, effects of geometry factor on accuracy of, (E), 25:10695
method for inorganic compounds based on fossil tracks of spontaneous fission, 25:10825
AGUIRRE POWER REACTOR, UNIT 1
design parameters of, revised and additional data on, 25:12752 (DOCKET-50376-7)
operations aspects of, revised and additional data on, 25:12752 (DOCKET-50376-7)
AIR
cleaning of, research program on equipment and methods for, 25:10797(R) (NYO-841-23)
AIR SAMPLERS
operation and performance of, for vertical sampling of atmospheric aerosols, 25:10754 (NP-18633)
AIRGLOW
oxygen excitation in sunlit conjugate ionosphere, O I 1304-A, (E), 25:11799
properties of night, (T), 25:11811
spectral height profiles from 400 to 1016 km, He I 584-A and H I 1216-A euv dayglow, (E), 25:11789
ALARM SYSTEMS
description for criticality accidents, 25:10818
trip levels for reactor containment system radioactivity, 25:12812 (BNWL-1479)
ALASKA
Amchitka marine ecology and oceanography, 25:12877(R) (BMI-171-114)
avifauna of Amchitka Island, 25:12869(R) (BMI-171-102)
ecology of Amchitka Island, freshwater, 25:12870(R) (BMI-171-103)
ecology of Amchitka Island, freshwater vertebrate and invertebrate, 25:12871(R) (BMI-171-104)
geomorphology and pedology of Amchitka Island, 25:12873(R) (BMI-171-106)
plant ecology of Amchitka Island, 25:12874(R) (BMI-171-107)
revegetation of disturbed areas of Amchitka Island, 25:12872(R) (BMI-171-105)
ALBUMINS
removal of iodine-131-labeled, from blood of guinea pigs and rats, estimation of phagocytic coefficient for, 25:10957
sorption of iodine-131-labeled human serum, in man following oral administration, effects of stomach acidity on, 25:11170
use of iodine-131-labeled macroaggregated, for scanning of human lungs, effectiveness of dual-probe detector system and, 25:11207
ALGINIC ACID
calcium salt of, radioprotective effects of, on animals, chronic strontium-90 β, 25:11103
effects of uronic acid components of, on intestinal sorption of radioactive strontium isotopes in rats, 25:10939
ALKALI METAL HALIDES
impurities in, ultrasonic measurement of paraelastic, 25:12893 (NYO-2471-47)
radioinduced M and F centers in crystals of, laser re-excitation and decay of γ, (E/T), 25:11956
ALKALI METAL HYDROXIDES
book: Intercrystalline Corrosion and Corrosion Cracking of Stainless Steel in Aqueous Solutions (In Russian), 25:11353
ALKALI METALS
electron reactions with, cross sections for ionization in, (T), 25:11701
reactions between ground-state atoms of, effects of nuclear spin on evolution of electron angular momentum during spin exchange in, (T), 25:11724
vacancy formation energy and volume in, pseudopotentials in calculations of, 25:12900 (NYO-4185-2)
ALKALINE PHOSPHATASE
radiation effects on activity of, in blood and tissues of rats following injection of mixed radioisotopes, 25:10968
ALKANES
radioinduced sulfoxidation of, comparison of ozone with γ and uv, 25:10592 (BMBW-FBK-70-25)
radioinduced sulfoxidation of, γ, 25:10614
ALKENES
polymers, book: Radiation Chemical Processing, 25:10617
ALLOYS
book: Transport Phenomena in Liquid Metals and Semiconductors, 25:11410
cracks in hcp, orientation effects on twinning in, 25:11474(R) (BNWL-842)
diffusion in, data tabulations on, 25:11411
ductility at high temperatures, factors controlling notch, 25:11373(R) (COO-2048-1)
emissivity of high-temperature, methods for determining, 25:11426
interfaces in ordered, 25:12903 (ORO-3935-4)
preparation of powdered metal, 25:11362(P)
ALPHA PARTICLES
channeling in anthracene crystals parallel to [001] axis, luminescent response to, 25:11972
detection using cellulose nitrate track detectors, 25:10826
distribution of inhaled, in human respiratory tract following inhalation of contaminated aerosols, 25:10953
dose determination during radium therapy, 25:11072
dose to human lung following accidental inhalation of americium-241 and plutonium-241, equations for estimating, 25:11053 (BNWL-B-12)
dosimetry for radium therapy, requirements for accuracy during, 25:11069
effects of longevity of Drosophila melanogaster, lethal, 25:11248
effects on microstructure of neptunium dioxide, plutonium dioxide, and thorium dioxide at 5.5-MeV, 25:11537
effects on mitosis in cultured sat cells, effects of dose on inhibitory, 25:11272
energy losses in argon gas, (E), 25:11726
hazards to bones and liver of personnel following occupational inhalation of plutonium-239 models for, estimation of tumorigenic, 25:11301
hazards to mining personnel, methods for protection against radon and radon decay product, 25:11085
losses from magnetosphere by charge exchange and pitch-angle diffusion, (T), 25:11803
reactions (α,2n) with uranium-235 at 24 to 27 MeV, decay curves and excitation functions for production of isomeric plutonium-237, (E/T), 25:12530 (RLO-1388-130)
reactions (α,2nγ) with dysprosium-162 at 22 and 28 MeV, cross sections and gamma spectra from, (E/T), 25:12544
reactions (α,2nγ) with lead-206 at 29 MeV, anisotropy of γ-ray angular distributions from, (E), 25:12614
reactions (α,3n) with uranium-236 at 34 MeV, decay curves from, (E/T), 25:12530 (RLO-1388-130)
reactions (α,αn), (α,2p) and (α,xn) with niobium-93 at 15 to 41 MeV, excitation functions for, (E), 25:12568
reactions (α,f) with uranium-238 at 63.5 MeV, in- and out-of-phase angular correlations and fission-fragment energy spectra from, (E), 25:12526 (MNC-3783-7)
reactions (α,He-3) and (α,t) with iron-54 and nickel-58, -60, -62, and -64 at 44 MeV, optical-model analysis of angular distributions and energy spectra from, (E/T), 25:12434
reactions (α,He-3) with gold, lead, platinum, tantalum, and tin at 42 to 90 MeV, angular distributions and energy spectra from, (E/T), 25:12604
reactions (α,Li-6) with boron-10 at 46 MeV, DWBA analysis of, (E/T), 25:12392
reactions (α,n) with carbon-13 at 2.9 to 4.9 MeV, polarization excitation functions and angular distributions from, (E), 25:12390
reactions (α,n) with phosphorus-31, threshold energies and excitation functions for, (E), 25:12442
reactions (α,nγ) with magnesium-26 at 5.8 and 6.3 MeV, gamma angular distributions from, (E), 25:12449
reactions (α,nγ), (α,pγ), and (α,α'γ) with titanium-48 at 12 to 15 MeV, gamma spectra from, (E), 25:12435
reactions (α,pn) with oxygen-16 at 42 MeV, gamma spectra from, (E), 25:12553
reactions (α,t) with deuterium at 82 MeV, DWBA analysis of charge-asymmetry effects in, (T), 25:12355
reactions (α,xn) and (α,pxn) with Z = 20 to 100 nuclei, excitation functions and thick-target yields for, (T), 25:12529(T) (ORNL-tr-3020)
reactions in stars, rate of triple, (E), 25:11565
reactions with atoms at 30 to 80 MeV, cross sections for production of K- and L-shell vacancies in, (E), 25:12488
scattering by aluminum at 20 to 27.5 MeV, angular and energy distributions from inelastic, 25:12422
scattering by argon-36 at 12.8 to 17.8 MeV, optical-model analysis of elastic, (E/T), 25:12455
scattering by cadmium-106 and -114 at 9 MeV, correlation functions and hyperfine attenuation coefficients from inelastic, (E), 25:12619
scattering by carbon-12, deuterium, lead, silicon-28, and tin at 166 MeV, optical potentials from DWBA analysis of angular distributions from elastic and inelastic, (E/T), 25:12549
scattering by cobalt-59 at 27.5 MeV, optical-model

XUM

analysis of angular distributions using elementary nucleon--nucleon interactions from elastic, (T), 25:12627 (INP-720)
scattering by copper-63, copper-65, and zinc-67 at 21 MeV, spin dependence in inelastic, (E), 25:12454
scattering by erbium-166, samarium-154, and ytterbium-176 at 27.5 to 32.5 MeV, α spectra and angular distributions for inelastic, (E), 25:12605
scattering by gold, lead, platinum, tantalum, and tin at 42 to 90 MeV, angular distributions and energy spectra from, (E/T), 25:12604
scattering by natural cadmium at 9 and 10 MeV, gamma spectra from inelastic, (E), 25:12548
scattering by natural cadmium at 9 to 10 MeV, gamma angular distributions from inelastic, (E/T), 25:12556
scattering by oxygen-16 at 20 to 24.5 MeV and 176°, differential cross sections and angular distributions for elastic, (E), 25:12419
scattering by phosphorus-31, excitation functions for elastic, (E), 25:12442
scattering by samarium-148 at 27.5 to 32.5 MeV, angular distributions for elastic, (E), 25:12605
scattering by silicon-29 at 15.4 MeV, angular correlations from inelastic, (E), 25:12449
use for determining cross section, thickness, shape, and internal structure, review of, 25:10977

ALUMINUM
crystal structure of quenched, vacancy formation in, 25:10583(R) (AECL-3776)
deformation of, structural dependence of Newtonian, 25:11434(R) (SU-326-P-17-X-1)
determination as impurity in fuel materials by emission spectroscopy, 25:10432 (KFK-1261)
determination by charged particle activation, reactions and sensitivities for, 25:10488 (CEA-R-4072)
determination in sedimentary rocks by direct-reading spectrometry, 25:10450
determination in serum and urine by flameless atomic absorption spectroscopy, 25:10464
determination in soil by neutron activation, 25:10909
determination in tektite by spark source mass spectrometry, 25:10455
determination of trace amounts of, in molybdenum, review on, 25:10459
determination of trace amounts of, in rocks and sand by thermal neutron activation, ion exchange, and γ spectrometry, 25:10492
determination of trace amounts of, in Zircaloy-2 and zirconium, carrier distillation method for spectrographic, 25:10430 (EUR-4541)
distribution in uranium during zone melting, 25:11406
electron beam-induced stress waves in, laser--Doppler interferometric study of, 25:10791
friction and wear of, sliding against copper and iron rings under vacuum, 25:11413
properties for use in screen-type thermal insulation, 25:10778(R) (ORNL-TM-3214)
proton reactions up to 70 GeV, negative particle distributions from, (E), 25:10868 (IFVE-SEF/OP-70-13)
radiation effects on boron carbide-impregnated neutron absorbers of, in-pile, 25:11461 (IN-1437, pp 13-23)
radiation effects on silicon precipitation in, thermal neutron, 25:11471
radioinduced voids in, at 55°C, electron microscopic studies of fast neutron, 25:11465 (ORNL-TM-3109)
reactions with folic acid, stability constants of complexes from, 25:10520
separation of neptunium from, by ion exchange in tetramethylammonium hydroxide--citrate solutions, effects of complexing agents on, 25:10655 (ANL-7751)
stress concentration at chamfered changes of section in plates of, measurement of acoustic, 25:10790 (RD/B/N-1795)

ALUMINUM ALLOYS AND SYSTEMS
analysis of binary, for tin and zirconium, x-ray fluorescent, 25:10441
properties of fuel cladding of Type 2219, 25:11461 (IN-1437, pp 13-23)
radiation effects on boron carbide-incorporating, in-pile, 25:11462 (IN-1437, pp 59-70)
radiation effects on hardness of, in-pile, 25:11461 (IN-1437, pp 13-23)
Al--Ce, electric conductivity of $CeAl_2$, crystal-field effects on spin-disorder contribution to, (T), 25:12009
Al--Cr--Ni-base, creep at high temperatures, effects of cold rolling and shock loading on, 25:11434(R) (SU-326-P-17-X-1)
Al--La, superconducting transition temperature of $LaAl_2$, effects of rare-earth impurities on, (T), 25:11836
Al--Mn, crystal structure of quenched, vacancy formation in, 25:10583(R) (AECL-3776)
Al--Mn, magnetic hysteresis loops of, effects of boron on, 25:11983
Al--Nb, niobium-93 NMR in Nb_3Al, 25:12037
Al--Ni-base, creep at high temperatures, effects of second phases on, 25:11434(R) (SU-326-P-17-X-1)
Al--Pu-base, electronic properties of delta-phase, positron annihilation study of, 25:11998
Al--Pu-base, radiation effects on length of delta-, self-, 25:11468
Al--Si--U, radiation effects on fuels of, at high burnups, in-pile, 25:11462 (IN-1437, pp 59-70)
Al--Ti-base--V, phase transformations at 1000 to 1400°F, effects of strain on, 25:11453
Al--U, analysis for boron using cobalt-60-tagged boron, 25:11375 (IN-1437, pp 24-59)
Al--U, diffusion of fission products from, mechanisms of, 25:11375 (IN-1437, pp 24-59)
Al--U, phase studies of, 25:11375 (IN-1437, pp 24-59)
Al--U, properties of fine-particle UAl/sub x/, for use in fuel plates, 25:11375 (IN-1437, pp 24-59)
Al--U, radiation effects on boron carbide foil-incorporating fuel elements of, in-pile, 25:11461 (IN-1437, pp 13-23)
Al--U, radiation effects on properties of, in-pile, 25:11462 (IN-1437, pp 59-70)
Al-base--Fe, deformation of dilute, structural dependence of Newtonian, 25:11434(R) (SU-326-P-17-X-1)
Al-base--Ni, radiation effects on silicon precipitation in, thermal neutron, 25:11471

ALUMINUM HYDROXIDES
precipitation of carrier-free silicon-31, 25:10675

ALUMINUM ISOTOPES Al-26
abundance in Allende meteorite, (E), 25:11540
energy levels from magnesium-26 (He-3,t) reactions at 16 and 30 MeV, (E), 25:12498
energy levels of, calculation using collective model with Coriolis coupling, (T), 25:12482

ALUMINUM ISOTOPES Al-27
alpha inelastic scattering at 20 to 27.5 MeV, angular and energy distributions from, 25:12422
meson reactions (π^-,π^0) at 70 MeV, integrated cross sections for, (E), 25:12446
neutron capture by, gamma spectra and Q-value for thermal, (E), 25:12403
photon reactions (γ,p) at 85 MeV, proton angular and energy distribution from, (E), 25:12501
proton reactions (p,γ) at 0.9 to 1.9 MeV, excitation function and resonance energy for, (E), 25:12402

ALUMINUM ISOTOPES Al-28
beta decay of, half-life for, (E), 25:12394

ALUMINUM OXIDES
analysis of, neutron activation, 25:11472(R) (AD-708705)
deuterium exchange between benzene and surface of, effects of ammonia, carbon dioxide, carbon monoxide, nitric oxide, and water on catalytic sites for, 25:10530
diffusion of chromium in, research on, 25:11472(R) (AD-708705)
properties of hydrided fuel plate cladding of, 25:11462 (IN-1437, pp 59-70)
radiation effects on interface characteristics of reactively sputtered junctions with silicon, electron, 25:10905
thermal shock resistance of sintered, effects of magnesium oxides on, 25:11473(R) (AD-708712)
yield strength of, dynamic shock-wave, 25:11490
Al_2O_3--Pt, effects on reduction of aqueous uranyl nitrate solutions by hydrogen at low pressure, catalytic, 25:10572 (IEA-184)

AMERICIUM
effects on amperometric or potentiometric determination of plutonium, 25:10445
purification by pressurized cation exchange chromatography, on-line computer monitoring of, 25:10664 (DP-MS-70-38)
separation from aqueous solutions by solvent extraction using bis(2,2-dimethylhexyl) phosphate, 25:10679
structure of fcc, calculation of electronic band, (T), 25:11992

AMERICIUM ALLOYS AND SYSTEMS
Am--Np-base, magnetic behavior of dilute, Moessbauer effect studies of, 25:12001

AMERICIUM ISOTOPES Am-241
buildup in lungs after inhalation of plutonium-241, 25:11053 (BNWL-B-12)
distribution in organs and tissues of animals following intravenous injection as chloride, 25:10942
fission of, half-lives for spontaneous, (E), 25:12538
inhalation in lungs of man, use of sodium iodide crystal detector for measurement of, 25:10931 (CEA-CONF-1557)
use for transmission scanning to measure lean to fat ratios in human tissues, 25:11114

AMERICIUM ISOTOPES Am-243
alpha decay of, time spectrum of alpha--conversion-electron delay in, (E), 25:12542
neon-22 reactions (Ne-22,4n) at 105 to 150 MeV, cross section for, (E), 25:12620
production at TRU, 25:10654(R) (ORNL-4588)

AMERICIUM OXIDES
americium oxides--curium oxides, phase studies of dioxides, intermediate oxides, and sesquioxides of, 25:11521

AMINES
radiolysis of, ESR studies on, 25:10583(R) (AECL-3776)

AMINO ACIDS
content in fossil corals and deep-sea sediments, measurements of, 25:10725(R) (CU-3139-4)

AMMONIA
deuterium exchange between hydrogen and, optimization for heavy water production, 25:10787
effects on radiolysis of ethane, 25:10632

reactions of anhydrous, with ammonium diuranate, preparation of uranium oxides by reduction, 25:10573 (IEA-207)
reactions with α and β uranium trioxide, kinetics of reduction, 25:10569 (CEA-R-4074)
AMMONIUM BROMIDES
purification of bromine-82-labeled, by ion exchange, 25:11046
AMMONIUM CHLORIDES
effects on plutonium-239 and polonium-210 accumulation in Ascophyllum nodosum and marine plankton, 25:10941
AMMONIUM COMPOUNDS, SUBSTITUTED
cetyltrimethylammonium chloride, effects on γ-induced polymerization of vinyl acetate, 25:10593 (JAERI-5026, pp 15-25)
AMMONIUM URANATES
reduction by anhydrous ammonia, preparation of uranium oxides by, effects of temperature and time on, 25:10573 (IEA-207)
AMPHETAMINE
effects on cerebral blood flow in patients with Parkinsons disease, effectiveness of xenon-133 for determining, 25:11147
β-AMYLASE
radioinduced inactivation of, in sugar beets, cobalt-60 γ, 25:10964
ANALYTICAL CHEMISTRY
book: Physical Methods for Rapid Analysis of Substances, in Russian, 25:10475
computer uses in, 25:10424 (ORNL-4636, pp 34-40)
developments in process and quality control, 25:10426 (ORNL-4636, pp 54-7)
developments in, for biochemistry uses, 25:10435 (ORNL-4636, pp 14-20)
developments in, review on NBS, 25:10422 (NBS-TN-545)
instrumentation research and development for, 25:10424 (ORNL-4636, pp 34-40)
methods using mixed ligand complexes in, 25:10460
research progress on, 25:10423(R) (ORNL-4636)
ANGIOSPERMIDAE
Adenostoma sp., radioisotope transport in roots of, cesium-137, ruthenium-106, and strontium-85, 25:10955
Adenostoma sp., radioisotope uptake by, in comparison to beans and tomatoes, 25:10936 (UCB-34-P-23-15)
Arabidopsis sp., genetic variation in quantitative traits of, effects of EMS on, 25:11009(R) (COO-1512-22)
Arabidopsis thaliana, radioinduced mutations in, for pigmentation, effects of seed exposure on laser, 25:11027
Brassica campestris, radiation effects on self-incompatibility in, γ, 25:11318
Ceanothus sp., radioisotope transport in roots of, cesium-137, ruthenium-106, and strontium-85, 25:10955
Ceanothus sp., radioisotope uptake by, in comparison to beans and tomatoes, 25:10936 (UCB-34-P-23-15)
Chrysanthemum morifolium, radiation effects on flower formation by, following plant exposure, x, 25:11311
Chrysanthemum morifolium, radioinduced mutations in, for somatic chromosome number, γ, 25:11031
Crepis capillaris radioinduced chromosome aberrations in, following incorporation of strontium-90--yttrium-90, β, 25:11013
Crepis capillaris, radioinduced aberrations in chromosomes of seedlings of, in combination with caffeine, 25:11015
Dahlia coccinea, radioinduced free radicals in seeds of, EPR analysis of electron, 25:11305 (NP-18394)
Gladiolus sp., radioinduced mutations in, effects of environment on γ, 25:11035
Glycine max, radiation effects on apical meristem mortality, weight, and height of seedlings of, fission neutrons, cobalt-60 γ rays, and strontium-90 and yttrium-90 β particles, 25:11312
Gossypium hirsutum, radioinduced changes in composition and content of pyrimidine nucleotides in DNA in shoots of, following seed exposure, γ, 25:11307
grasses, radiosensitivity of mature, exposed as seeds, mathematical analysis of initial germination rate for predicting, 25:11314
Helianthus tuberosus, radiation effects on tumor production by Agrobacterium tumefaciens in, x, 25:11306
Hordeum sp., growth of seeds of, in soil, effects of dose, fertilizer concentration, and soil chemistry on effects of chemical mutagens on, 25:11315
Hordeum sp., radiation effects on growth of seeds of, in soil, effects of dose, fertilizer concentration, and soil chemistry on γ, 25:11315
Hordeum vulgare, radiation effects on frequency of chlorophyll mutations in, in comparison to effects of EMS and nitrosomethyl urea, x, 25:11021
Lactuca sp., radiation effects on yield of, yttrium-90 β, 25:10936 (UCB-34-P-23-15)
Lycopersicum esculentum, radioisotope uptake by seedlings of, in culture media, in comparison to forage plants, cesium-137, ruthenium-106, and strontium-85, 25:10936 (UCB-34-P-23-15)
Nicotiana tabacum, radiation effects on ascorbic acid content in callus and tumor tissues of, γ, 25:10965
Nicotiana tabacum, radiation effects on growth of callus and tumor tissues of, cultured in standard and enriched media, comparison of γ, 25:10965
Oryza sp., analysis for bromine and iodine by neutron activation, 25:10505
Petunia sp., radiation effects on diploid and tetraploid seedlings of, correlation between dose, LET, and volumes of chromosomes and cell nuclei for x per chromosome, x, 25:11020
Petunia sp., radioinduced somatic mutations in seeds of, for color, effects of dose and presoaking on γ, 25:11011
Petunia sp., somatic mutations induced for color in seeds of, effects of presoaking on methyl methanesulfonate, 25:11011
Phaseolus aureus, radiation effects on growth of seeds of, combined effects of low pressure shock on x, 25:11317
Phaseolus vulgaris, radioisotope uptake by seedlings of, in culture media, in comparison to forage plants, cesium-137, ruthenium-106, and strontium-85, 25:10936 (UCB-34-P-23-15)
Pisum sativum, radiation effects on frequency of chlorophyll mutations in, effects of seed exposure and storage time on γ, 25:11024
Pisum sativum, radiation effects on growth of, phosphorus-32 and strontium-89, 25:10936 (UCB-34-P-23-15)
Quercus sp., radioisotope transport in roots of, cesium-137, ruthenium-106, and strontium-85, 25:10955
Saccharum officinarum, radioinduced mutations in seeds of, effects of 1 to 5 kR doses on γ and x, 25:11030
sorghum, genetic variation in quantitative traits of, effects of EMS on, 25:11009(R) (COO-1512-22)
Tagetes erecta, radiation effects on diploid and tetraploid seedlings of, correlation between dose, LET, and volumes of chromosomes and cell nuclei for x per chromosome, x, 25:11020
Tradescantia sp., radiation effects on somatic mutations and loss of reproductive integrity in stamen hairs of, RBE for fast neutrons, 25:11313
Triticum durum, radioinduced mutations in, effects of 8.38 x 10^{12}/cm² dose on thermal neutron, 25:11034(P)
Triticum durum, radioinduced mutations in, effects of 1.05 x 10^{13}/cm² dose on thermal neutron, 25:11033(P)
Triticum sp., radiation effects on yield of, yttrium-90 β, 25:10936 (UCB-34-P-23-15)
Vicia faba, radiation effects on inhibitors of peroxidase in, seedlings, γ, 25:10973
Vicia faba, radiation effects on, effects of age of neutron and γ, 25:11095 (BNL-50203, pp 308-17)
Vitis sp., radiosensitivity of, in relation to somatic mutation rate, effects of inhibitory and lethal dose rate on chronic, γ, 25:11017
Zea mays, genetic variation in quantitative traits of, effects of EMS on, 25:11009(R) (COO-1512-22)
Zea mays, potassium-42 uptake by roots of, in relation to bioelectric potential, 25:11308
Zea mays, radiation effects on bioelectric potential of roots of, x, 25:11308
Zea mays, radiation effects on male fertility in, role of cytoplasm in, 25:11010(R) (ORO-2583-8)
Zea mays, radiation effects on metabolism of nitrogen compounds in endosperm and seedlings of, following seed exposure, ionizing, 25:11309
Zea mays, radiation effects on random mating populations of, effects of recurrent mass selection on thermal neutron, 25:11009(R) (COO-1512-22)
Zea mays, radiation effects on yield of, yttrium-90 β, 25:10936 (UCB-34-P-23-15)
Zea mays, radioinduced deletion aberrations in chromosomes of, effects of pollen exposure on x, 25:11023
Zea mays, radioinduced mutations in, for necrotic leaf spot, thermal neutron, 25:11009(R) (COO-1512-22)
Zea mays, radioinduced mutations in, for plant height, thermal neutron and uv, 25:11009(R) (COO-1512-22)
Zea sp., evapotranspiration in, use of neutron moisture meters to determine, 25:10927
Zinnia elegans, radiation effects on diploid and tetraploid seedlings of, correlation between dose, LET, and volumes of chromosomes and cell nuclei for x per chromosome, x, 25:11020
ANGIOTENSINS
effects on blood pressure, measurements of, for determining hypertension in combination with kidney scanning and renin content measurements, 25:11164
ANIMALS
americium-241 distribution in organs and tissues of, following intravenous injection as chloride, 25:10942
radiation effects on, 25:11294(R) (EUR-4542)
radiation effects on thyroid gland of, review of iodine-131 β and γ and x, 25:11291
radiation effects on, protective effects of calcium alginate against chronic strontium-90, β, 25:11103
radiation injuries to, evaluation of cosmic, 25:11280
radioisotope metabolism in, use of computers for analysis of counting data from tissues following, 25:10937 (UCRL-50957)
radioisotope uptake and retention by aquatic, statistical analysis of, 25:10998
ANISOLE, VINYL-
radioinduced polymerization on surface of synthetic calcium aluminate hydrate,, 25:10616

XUM

ANOXIA
radioprotective effects of, on growth tail bone transplants in syngeneic recipient mice, x, 25:10983
ANTHRACENE
electron ranges and energy loss profiles in crystals of, at 25 to 40 keV, 25:11673
luminescent response to [001]-channeled α particles in crystals of, 25:11972
ANTIBODIES
formation in cultured cells and animals, tracer studies of, 25:10924
radiation effects on content of auto-, in liver of rabbits, x, 25:10985
ANTIGENS
formation in cultured cells and animals, tracer studies of, 25:10924
radioinduced degradation of, in transplanted tissues, 25:11331
ANTIMONY
content in Black Sea, 25:10507
determination in seawater by neutron activation, 25:10507
determination in seawater by neutron activation, 25:10428
determination in soils by neutron activation and radiochemical separation, 25:10506
determination of trace amounts of, in biotite and tektite by spark source mass spectrometry, 25:10455
determination of trace amounts of, in molybdenum, review on, 25:10459
determination of trace amounts of, in phosphate deposits by spark source mass spectrometry, 25:10456
determination of trace amounts of, in rocks and sand by thermal neutron activation, ion exchange, and γ spectrometry, 25:10492
separation of cyclotron-produced iodine-123 from, by dissolution in hydrochloric acid--hydrogen peroxide and solvent extraction using carbon tetrachloride, 25:10674
separation of trivalent and pentavalent, paper chromatographic, 25:10687
ANTIMONY ALLOYS AND SYSTEMS
Au--Sb, superconducting properties of liquid-quenched simple cubic, 25:11819 (CALT-822-22)
In--Sb, microwave propagation in magnetoplasma of n-type, electric and magnetic resonances in Voigt configuration of, (E/T), 25:11929
In--Sb, superconducting properties of liquid-quenched simple cubic, 25:11819 (CALT-822-22)
Pd--Sb, superconducting properties of liquid-quenched simple cubic, 25:11819 (CALT-822-22)
Pd-base--Sb, thermodynamic properties of, 25:11396
ANTIMONY ISOTOPES Sb-121
neutron capture by, average circular γ polarization in thermal, (E), 25:12601
ANTIMONY ISOTOPES Sb-122
energy levels from thermal neutron capture, spin for compound, (E), 25:12601
ANTIMONY ISOTOPES Sb-123
neutron capture by, average circular γ polarization in thermal, (E), 25:12601
ANTIMONY ISOTOPES Sb-124
beta decay of, gamma spectra from, (E), 25:12531 (TID-25586)
beta decay of, gamma spectra from, (E), 25:12515 (COO-1746-51)
energy levels from thermal neutron capture, spin for compound, (E), 25:12601
ANTIMONY ISOTOPES Sb-126
beta decay of, β--γ angular correlations in, (E), 25:12555
nuclear spin of ground state from β--γ angular correlations, (E), 25:12555
APATITES
age of, effects of geometry factor on accuracy of fission track, (E), 25:10695
APPENDAGES
scanning of blood circulation in feet, of dogs, using double isotope method with iodine-131 and sodium-24 for study of arterio-venus shunts, 25:10926
scanning of blood circulation in leg, of man, effectiveness of xenon-133 for, 25:11138
scanning of leg, for detection of arterial insufficiencies, comparison of arteriography to xenon-133 walking test for, 25:11139
ARGON
alpha-particle energy losses in, (E), 25:11726
argon-36 and -40 concentration in, by thermal diffusion, effects of gas flow mode on, 25:10786
argon-ion reactions at 10 to 30 keV with, coincidence studies of energy spectra of electrons ejected in, (E), 25:11709
deuteron reactions at 30 to 120 keV with, cross sections for electron capture into 3s state of deuterium in, (E), 25:11708
diffusion in solid, isotope effect calculations for self-, neon, and krypton, 25:12042
electron elastic scattering by, calculation of differential cross sections for, using potential-scattering model, 25:11722
electron scattering at low energies by metastable atoms of, total cross sections for, (E), 25:11706
nitrogen-ion (N^+) reactions at keV energies with, statistical-model calculations of ionization probabilities in, 25:11711
nitrogen-ion reactions at 10 to 150 keV with, coincidence study of, 25:11704
plasma of, diagnostics using cylindrical Langmuir probes, (E), 25:11873
plasma of, electron elastic and inelastic scattering from, (E), 25:11879
proton reactions at 30 to 120 keV with, cross sections for electron capture into n = 3 level of hydrogen in, (E), 25:11708
reactions with deuterium ions, 25:10552
reactions with helium, calculation of ionization and stripping cross sections for, using generalized oscillator strengths, 25:11715
scattering by platinum (111) surfaces at thermal energies, (E), 25:11683
ARGON IONS
effects on silicon (111) surface at 150 eV, (E/T), 25:11970
effects on silicon, growth of epitaxial layers by sputtering, 25:11962
implantation into silicon at 50 to 300 keV, sputtering and strain induced by, 25:11959
reactions with argon at 10 to 30 keV, coincidence studies of energy spectra of electrons ejected in, 25:11709
reactions with platinum, angular and energy distributions of charged particles emitted in, (E), 25:11675
ARGON ISOTOPES Ar-36
alpha elastic scattering at 12.8 to 17.8 MeV, optical-model analysis of, (E/T), 25:12455
concentration in argon by thermal diffusion, effects of gas flow mode on, 25:10786
ARGON ISOTOPES Ar-37
energy levels of, lifetimes and magnetic moments for 7/2-, (E), 25:12429 (COO-7-565)
ARGON ISOTOPES Ar-40
concentration in argon by thermal diffusion, effects of gas flow mode on, 25:10786
effects on emission spectra of argon hydride, 25:10535
scattering by natural cadmium at 101 MeV, gamma angular distributions from inelastic, 25:12556
scattering by natural cadmium at 101 MeV, gamma spectra from inelastic, (E), 25:12548
ARGON ISOTOPES Ar-43
decay of, gamma spectra from, (E), 25:12499
half-life, (E), 25:12499
ARGON ISOTOPES Ar-44
decay of, gamma spectra from, (E), 25:12499
half-life, (E), 25:12499
ARGON SYSTEMS
Ar--N, radiation effects on, spectral studies on 1.5-MeV electron, 25:10586 (JAERI-5026, pp 155-7)
ARGONNE RESEARCH REACTOR
reactivity change in, effects of light water additions to coolant channels on positive, (E), 25:12830
ARIZONA
radiation monitoring of uranium mill tailings pile at Monument Valley, 25:11045
ARSENIC
determination in biological materials by neutron activation and radiochemical separations, 25:10510
determination in environmental samples by x-ray fluorescence method, 25:10491 (ORNL-4636, pp 20-33)
determination in soils by neutron activation and radiochemical separation, 25:10506
determination of trace amounts of, in biotite and tektite by spark source mass spectrometry, 25:10455
determination of trace amounts of, in molybdenum, review on, 25:10459
determination of trace amounts of, in phosphate deposits by spark source mass spectrometry, 25:10456
determination of trace amounts of, in rocks and sand by thermal neutron activation, ion exchange, and γ spectrometry, 25:10492
separation of trivalent and pentavalent, paper chromatographic, 25:10687
ARSENIC ISOTOPES As-75
photon inelastic scattering at 12 to 30 MeV, differential cross sections for, (E), 25:12463
proton reactions at 170 MeV to 2.9 GeV, cross sections for spallation products from, (T), 25:12439
ARSENIC ISOTOPES As-77
energy level at 194.9 keV from germanium-77 decay, lifetime and spin-parity assignment for, (E), 25:12473
ARTERIES
radioinduced dilation of, in earlobes of mice, electron, 25:11254 (BNL-50203, pp 174-80)
radiosterilization of transplants of aorta, effects of, on collagen, γ, 25:11341
scanning in human legs for detection of insufficiencies, effectiveness of xenon-133 walking test in comparison to arteriography for, 25:11139
scanning of human aortic, using metastable technetium-99-labeled pertechnetate and Anger camera, method for, 25:11121
ARTHROPODA
food chain studies in soil, use of zinc-65-labeled fungus mycelium for, 25:10929

ASCORBIC ACID
radiation effects on content of, in Nicotiana tabacum callus and tumor tissues, γ, 25:10965
ASPARAGINE
radiation effects on content of, in cooked meats, γ, 25:11339
ASPHALT
radioactive waste solidification in, equipment and method for, 25:10799
ASTATINE ISOTOPES At-213
alpha decay of, α spectra and half-life for, (E), 25:12592
ASTRON DEVICE
E-layer precession in, (T), 25:11924 (NYO-4077-1, Paper 1)
E-layer precession in, (T), 25:11925 (NYO-4077-1, Paper 2)
electron beam equilibria in, finite-beta, (T), 25:11887 (NYO-4077-1, Paper 5)
plasma and E-layer stability in, research on, 25:11923(R) (NYO-4077-1)
plasma diagnostics in, carbon dioxide laser heterodyne system for, 25:11869
ASTRONAUTS
radiation effects on central nervous system of, effects of acceleration, dose, and vibration on ionizing, 25:11298
ASTRONOMY
developments in Estonian SSR, (T), 25:11538
ATLANTIC OCEAN
tritium content of North American coastal waters of, 1963 to 1967, 25:10720
ATMOSPHERE
density at 135 to 195 km, correlation with geomagnetic activity and semiannual effect, (E), 25:11794
fallout content of Fayetteville, Arkansas, July and Aug. 1969, effects of rainstorms on, (E), 25:10707 (ORO-2529-28, App. 1)
fallout monitoring of, review of early research on, 25:10714 (ORO-2529-28, App. 8)
fission products following nuclear explosions in, gamma spectra from, (E), 25:12535
radiation monitoring of surface, over Central, North, and South America during June 1970, gross beta, 25:10721
radiation monitoring of, in North and South America during 1970, β, 25:11039
radioactivity monitoring of, in Ecuador, β, 25:11068
radiochemistry of, University of Arkansas research program on, 25:10706(R) (ORO-2529-28)
radioisotope content of Zugspitze, Germany, April to Dec. 1970, data tabulation on beryllium-7, fallout, and phosphorus-32, 25:10705(R) (NYO-4061-3)
radioisotope content of, in USA during 1968, plutonium-238 and plutonium-239, 25:11039
radioisotope content of, over Central, North, and South America during April to Dec. 1969, plutonium-238 and plutonium-239, 25:10721
radioisotope distribution in, development and operation of equipment for measuring long-lived, 25:10754 (NP-18633)
rotation rate at 135 to 195 km, (E), 25:11794
stable isotope distribution in, development and operation of equipment for measuring, 25:10754 (NP-18633)
strontium-89 and strontium-90 content of Fayetteville, Arkansas ground-level, Aug. 1969 to Aug. 1970, (E), 25:10711 (ORO-2529-28, App. 5)
strontium-90 content of west Slovakia, calculation to year 2000, 25:10719
strontium-90 content of, in Russia, fallout, 25:10934 (NP-18380)
transport processes in, research program at Zugspitze, Germany for studying, (E/T), 25:10705(R) (NYO-4061-3)
x-ray fluorescence in upper, photoelectric-ionized solar-stimulated, (E/T), 25:11790
ATMOSPHERIC PRECIPITATION
fallout monitoring of, review of early research on, 25:10714 (ORO-2529-28, App. 8)
radiation monitoring of, in North and South America during 1970, β, 25:11039
radioisotope content of, in Sweden, during 1959 to 1969, cesium-137 and strontium-90, 25:11004
strontium-90 content of, at worldwide sites, 1956 to 1970, 25:10715 (ORO-2529-28, App. 9)
tritium content of, in USA during 1968, 25:11039
ATOMIC ABSORPTION SPECTROMETRY
effects of matrix on determination of trace amounts by, 25:10457
ATOMIC BEAMS
production for studies on chemical reactions, equipment for, 25:10517 (JUL-674-RC)
ATOMIC ENERGY
book: From Scientific Research to Nuclear Industry. Development and Problems of Nuclear Science and Technology in USSR, 25:12709
ATOMIC ENERGY COMMISSION (USA)
radiation protection standards for environmental exposure of human populations, 25:11076
ATOMIC ENERGY, LEGAL ASPECTS
legislation for control and regulation of nuclear power plants, evaluation of state, 25:11087 (CONF-700408-3)
regulations for handling encapsulated radioisotopes, 25:11089
ATOMIC MODELS
energy-functional formulation of Thomas--Fermi--Dirac statistical, 25:11739
ATOMIC PHYSICS
bibliography on surface and vacuum physics, 25:11678
book: Advances in Atomic and Molecular Physics. Vol. 6, 25:11728
book: Quantum Mechanics and Atomic Physics, 25:12052
ATOMIC STRUCTURE
calculation of, review of relativistic, 25:11741
theory of, including electron correlation, 25:11737
ATOMS
diffusion in gases, review, (E/T), 25:11731
electron elastic scattering by one- and two-electron, infinite-channel close-coupling treatment of charge polarization in, 25:11718
electron exchange interactions in, scale factor for Slater approximation of, 25:11736
electron reactions at 5 keV to 1 MeV with, exact screened calculations of relativistic bremsstrahlung cross sections for, 25:11681
electron reactions with Z = 2 to 11, calculation of ionization cross sections for, using generalized oscillator strengths, 25:11715
electron reactions with, calculation of mean energy of electrons ejected in, from differential ionization cross sections, 25:11727
electron reactions with, kinetic energy of bound electron in calculation of ionization cross sections for, (T), 25:11701
energy of ground states of, calculation using relativistic independent-particle model based on analytic potentials, 25:11738
energy of, numerical coefficient of first exchange inhomogeneity term in calculation of exchange, 25:11740
energy-level transitions in, calculation of rates of Auger and x-ray, using relativistic Hartree--Fock--Slater method, 25:11685
ion reactions at keV energies with, statistical model for calculation of ionization probabilities in, 25:11711
properties of quark, (T), 25:12188
proton reactions with Z = 2 to 11, calculation of excitation and ionization cross sections and stopping power for, using generalized oscillator strengths, 25:11715
reactions with atoms and ions, review of classical mechanical calculations of, 25:11733
reactions with atoms, effects of nuclear spin on electronic spin exchange in, (T), 25:11720
reactions with atoms, effects of nuclear spin on evolution of electron angular momentum during spin exchange in, (T), 25:11724
reactions with atoms, effects of spin exchange on density-matrix elements for, (T), 25:11721
reactions with gases and solids in keV range, spatial distribution of energy deposited in, (T), 25:11682
wave functions for two-electron, calculation of continuum P-state, 25:11684
AURORAE
particle-flux and radar-echo measurements over Alaska, simultaneous, (E), 25:11778 (AD-709105)
x-ray and 5577 O I quasiperiodic pulsations in pulsating, positive correlation of, (E), 25:11808
AURORAL ZONE
arc fields in, current phenomena in, (T), 25:11804
effect of geomagnetic activity in northern, on ionospheric density at 135 to 195 km, (E), 25:11794
electron density in ionospheric, rf impedance probe measurements of, 25:11781
particle energy spectra in oval, effect of magnetic activity in electron and proton, (E), 25:11809
AUTORADIOGRAPHY
methods for determination of inhaled alpha particle distribution in man, review of, 25:10953
AVES
Corturnix sp., radiation effects on immune reactions in, following transplantation of chicken gonads in, x, 25:10988
Corturnix sp., radiosensitivity of immature, x, 25:10988
Gallus sp., radiation effects on immune reactions in, following transplantation of quail gonads in, x, 25:10988
AVIATION PERSONNEL
radiation hazard to supersonic transport, review of monitoring and warning systems to evaluate solar flare, 25:11086
AVR REACTOR
thermal analysis of, mathematical method for, 25:10768 (JUL-657-HA)
AZIDES
radiolysis of aqueous solutions of, reactions and spectra of intermediates from electron pulse, 25:10643

B

BACTERIOPHAGES
radioinduced, from hcr-, rec-, and wild type strains of Salmonella typhimurium, 25:11026
T2, radiation effects on repair mechanisms in, effects of

acridine orange on uv, 25:11320
T3, radiation effects on repair mechanisms in, effects of acridine orange on uv, 25:11320
T4, mutations induced in, by radiotoxins following inoculation into γ-irradiated Escherichia coli, 25:11016
T4, radiation effects on repair mechanisms in, effects of acridine orange on uv, 25:11320
T7, radiation effects on repair mechanisms in, effects of acridine orange on uv, 25:11320

BARBITURIC ACID, THIO-
reactions with molecular by-products from γ-irradiated flour, effects of radiation dose and storage time on, 25:10978

BARIUM
content in Pacific Ocean, 25:10468
determination in seawater by isotope dilution method, 25:10468
determination in sedimentary rocks by direct-reading spectrometry, 25:10450
determination of trace amounts of, in biotite and tektite by spark source mass spectrometry, 25:10455
determination of trace amounts of, in molybdenum, review on, 25:10459
determination of trace amounts of, in phosphate deposits by spark source mass spectrometry, 25:10456
determination of trace amounts of, in rocks, quantometer for spectroscopic, 25:10451
determination of trace amounts of, in silicate rocks, method for elimination of matrix effect in quantometric, 25:10452
determination of trace amounts of, in standard rocks by borate fusion, dissolution in EDTA, and quantometry, 25:10671
determination of trace amounts of, in standard silicate rocks using sodium chloride buffer, emission spectrographic, 25:10454

BARIUM FERRATES
Bloch wall lattices in $BaFe_{12}O_{19}$, disclination structures in, 25:12011

BARIUM FLUORIDES
sorptive properties for neptunium hexafluoride and uranium hexafluoride, 25:10568 (CEA-R-4051)

BARIUM ISOTOPES Ba-131
electron-capture decay of, gamma spectra from, (E/T), 25:12532 (TID-25592)

BARIUM ISOTOPES Ba-138
energy levels from lanthanum-139 (d,He-3) reactions, shell-model calculations of, (E/T), 25:12552

BARIUM ISOTOPES Ba-140
content of milk in South America in 1967, 25:11068
content of milk in USA during February 1970, 25:11040

BARIUM ISOTOPES Ba-141
beta decay of, gamma spectra and beta--conversion-electron delayed-coincidence curves from, (E), 25:12540

BARIUM SULFATES
effectiveness of activated, for inhibiting sorption of metastable strontium-87 from gastrointestinal tract of man, 25:11047
effectiveness of activated, for inhibiting sorption of strontium-90 from gastrointestinal tract, 25:11049
effectiveness of activated, for prevention of strontium-85 deposition in bones of rats, effects of dose and time of administration on, 25:11048
effects on uptake of strontium-85 by rat bones following oral administration, 25:10940

BARIUM TITANATES
electric conductivity of gadolinium-doped, effects of copper on, 25:11472(R) (AD-708705)

BARYONS
asymmetry in universe, model for, (T), 25:12239
interactions with mesons and baryons in parton model, total cross section for, 25:12187
interactions with mesons in parton model, total cross section for, (T), 25:12187
interactions with mesons, scale and chiral symmetry breaking for, 25:12214

BARYONS, RESONANCE
decay of, Jacobian method for angular correlations of particles produced in interaction-free, (T), 25:12176
production in e + N interactions, review of, (E/T), 25:12068 (SLAC-PUB-842)
production in K⁻ + d interactions at 7.3 GeV/c in deuterium bubble chamber, (E), 25:12103
production in two-body and quasi-two-body final states in π⁺ + d and π⁺ + n interactions at 5.1 GeV/c, (E), 25:12100 (NP-18629)
production of exotic, urbaryon rearrangement for, 25:12183
production of overlapping, in three-body systems, (T), 25:12126

BARYONS, RESONANCE (N*)
decay N* → N + π, regularity of coupling constants of, 25:12220
production in γ + p → π⁺ + n interactions at 0.450 to 3 GeV, cross section structure for, (E), 25:12067 (LAL-1239)
production of Δ in anti ν + N and ν + N interactions, form factors and total and differential cross sections for, (T), 25:12174
production of Δ(1236), quark model for, (T), 25:12218
production of Δ⁺⁺ and rho⁻ in π⁻ + p → π⁺ + 2π⁻ + π⁰ + p interactions at 6 GeV/c in hydrogen bubble chamber, associated, (E), 25:12101
production of Δ⁺⁺, Δ⁰, and Δ⁺(1236) in π⁻ + p → π⁺ + 2π⁻ + π⁰ interactions at 6 GeV/c in hydrogen bubble chamber, (E), 25:12101
production of Δ⁺⁺(1236) and N(1400) in pπ⁺ enhancement in K⁺ + p → K⁺ + p + π⁺ + π⁻ interactions at 12.7 GeV/c in hydrogen bubble chamber, diffractive, (E), 25:12102
production of Δ⁺⁺(1236) and Nπ(1400) enhancement in p + p two- and four-charged-prong interactions at 28.5 GeV/c in hydrogen bubble chamber, (E), 25:12091
production of Δ⁺⁺(1236) and Nπ(1400) enhancement in p + p → p + π⁺ + π⁻ + p interactions at 28.5 GeV/c in hydrogen bubble chamber, (E), 25:12091
production of Δ⁺⁺(1236) in π⁺ + d → 2p + π⁺ + π⁻ interactions at 1.1 to 2.3 GeV/c in deuterium bubble chamber, (E), 25:12107
production of N* in K⁺ + p → K_1^0 + p + π⁺ interactions at 3.2 GeV/c in hydrogen bubble chamber, (E), 25:12114
production of pω⁰ and peta⁰ low-mass enhancements in K⁺ + p → K⁺ + p + π⁺ + π⁻ + π⁰ interactions at 12.7 GeV/c in hydrogen bubble chamber, (E), 25:12102
production of rho and Δ(1236) in π⁺ + d → 2p + π⁺ + π⁻ + π⁰ interactions at 4.19 GeV/c in deuterium bubble chamber, one-pion exchange for simultaneous, (E), 25:12112
properties of aleph, determination from 10^{12}-to-10^{13}-eV cosmic showers in emulsions, (E), 25:12093
theory for N(1470), quark model in, (T), 25:12218

BARYONS, RESONANCE (Y*)
contribution to backward K⁻ + N interactions, duality condition for, (T), 25:12215
decay Λ(1815) → Σ + π and Σ(1765) → Σ + π in hydrogen bubble chamber, branching ratios for, (E), 25:12098 (CEA-R-4068)
decay Σ(1385) → Λ + π⁺, branching ratio for, (E), 25:12104
decay Σ(1385) → Σ⁺(Σ⁻) + π⁻(π⁺), branching ratio for, (E), 25:12104
decay Σ(1475) → p(Λ) + anti K⁰(π⁺), branching ratio for, (E), 25:12104
decay Σ(1475) → Σ⁺(Σ⁻) + π⁻(π⁺), branching ratio for, (E), 25:12104
effects of Λ(1405) on K⁻ + N interactions on bound nucleons at low energies, (T), 25:12213
parity and spin of Λ(1670) in K⁻ + p → Σ⁺(Σ⁻) + π⁻(π⁺) interactions at 440 to 1230 MeV/c in hydrogen bubble chamber, (E), 25:12098 (CEA-R-4068)
parity and spin of Λ(1700) and Λ(1830) in K⁻ + p → Σ⁺(Σ⁻) + π⁻(π⁺) interactions at 440 to 1230 MeV/c in hydrogen bubble chamber, 25:12098 (CEA-R-4068)
parity and spin of Σ(1700), Λ(1746), and Ξ(1930) in quark model, (T), 25:12218
parity of Σ(1660) in K⁻ + p → Σ⁺(Σ⁻) + π⁻(π⁺) interactions at 440 to 1230 MeV/c in hydrogen bubble chamber, (E), 25:12098 (CEA-R-4068)
production in strange-particle final states in π⁻ + p interactions at 7 GeV/c, (E), 25:12110
production of Λ(1250) and Σ(1600) enhancement in K⁻ + p and K⁻ + d interactions at 360 to 720 MeV/c, (E), 25:12120
production of Σ in anti ν + N and ν + N interactions, form factors and total and differential cross sections for, (T), 25:12174
production of Σ(1385) and Σ(1475) in π⁺ + p interactions at 1.7 GeV/c, (E), 25:12104
production of Σ(1660), Λ(1670), Λ(1700), Σ(1770), Λ(1815), and Λ(1830) in K⁻ + p → Σ⁺(Σ⁻) + π⁻(π⁺) interactions at 440 to 1230 MeV/c in hydrogen bubble chamber, (E), 25:12098 (CEA-R-4068)
theory for Σ(1700), Λ(1745) and Ξ(1930), quark model in, (T), 25:12218
widths of Σ(1700), Λ(1746), ad Ξ(1930) in quark model, (T), 25:12218

BASALT
analysis for trace amounts of elements, correction of matrix effect in uv spectrographic, 25:10453

BAUXITE
analysis of standard samples of, for trace amounts of elements by x-ray fluorescence, 25:10449

BEAM SEPARATORS
performance parameters for rf, for particles at 1 to 15 GeV/c, 25:12295 (BNL-15438)

BEHAVIOR
radiation effects on mating, of male moths, effects of exposure during pupal stage on γ, 25:11338
radiation effects on maze habit, of rats, effects of dose, fractionation on whole-body x, 25:11273
radiation effects on patterns of sleep, whole-body γ, 25:11261
radiation effects on treadmill performance, bibliography on whole-body, 25:11251 (AD-705976)

BELGIUM
radiation protection programs in, for radiochemical processing plants, 25:11082

BENTONITES
analysis for moisture content by neutron scattering and moderation, 25:10486

BENZANTHRACENE, DIMETHYL-
effects on immunologic properties of mouse spleen cells,

25:10990
BENZENE
determination in effluent from gas chromatograph, performance of Geiger--Mueller counter with external γ source for, 25:10888
deuterium exchange between aluminum oxide surface and, effects of ammonia, carbon dioxide, carbon monoxide, nitric oxide, and water on catalytic sites for, 25:10530
effects of pretreatment with, on properties of products from γ-induced polymerization of vinylidene chloride in woods, 25:10604 (JAERI-5026, pp 86-93)
phosphorescence in polycrystalline cyclohexane and cyclopentane, effects of deuterium and temperature on, 25:10550
scintillation yields of liquid, 25:10822
spectra of monocrystals of, EPR, 25:10570(R) (COO-294-10)
yields from radiolysis and photolysis of acetylene, mechanisms of production of, 25:10650
BENZENE, ALKYL-
scintillation yields of liquid, 25:10822
BENZENE, tert-BUTYL-
radiolysis at 20 and -196°C, scavengeable electron yields from γ, 25:10652
BENZENE, DIVINYL-
radioinduced polymerization on surface of synthetic calcium aluminate hydrate,, 25:10616
BENZENE, IODO-
radiolysis of aqueous solutions of, optical absorption spectra of phenyl radicals produced by electron pulse, 25:10631
BENZOIC ACID
potassium salt, deuterium exchange reaction in transcarboxylation of mixture of deuterated and nondeuterated, mechanism of, 25:10545
BENZONITRILE
radiolysis of aqueous solutions of, spectral studies on short-lived aromatic anions and free radicals produced by electron pulse, 25:10639
BENZOYL PEROXIDE
effects on electron-induced curing of resin coatings on metals, 25:10608 (JAERI-5026, pp 121-9)
BERKELIUM
crystal structure of, 25:11358
melting point of, 25:11358
preparation by lithium reduction of berkelium fluoride at 1025°C, 25:11358
BERKELIUM FLUORIDES
reduction by lithium at 1025°C to prepare berkelium, 25:11358
BERKELIUM ISOTOPES Bk-249
production at TRU, 25:10654(R) (ORNL-4588)
BERYLLIUM
abundance in F and G stars, (T), 25:11544
complexes with 2,4-pentanedione, radiolysis of single crystals of, ESR spectral studies on γ, 25:10623 (JAERI-5026, pp 157-60)
determination by charged particle activation, reactions and sensitivities for, 25:10488 (CEA-R-4072)
determination by charged particle and photon activation, radiochemical separation methods for, 25:10488 (CEA-R-4072)
determination in aluminum by charged particle activation and radiochemical separation, 25:10488 (CEA-R-4072)
determination in serum and urine by flameless atomic absorption spectroscopy, 25:10464
determination of trace amounts of, in biotite and tektite by spark source mass spectrometry, 25:10455
determination of trace amounts of, in molybdenum, review on, 25:10459
determination of trace amounts of, in rocks, quantometer for spectroscopic, 25:10451
determination of trace amounts of, in Zircaloy-2 and zirconium, carrier distillation method for spectrographic, 25:10430 (EUR-4541)
diffusion of nickel in, 25:11399
nucleosynthesis in stellar atmospheres, (T), 25:11548
nucleosynthesis of, (T), 25:11542 (NP-18591)
radiation effects on surfaces and swelling of encapsulated, fast neutron, 25:11460 (IN-1437, pp 5-12)
reactions with folic acid, stability constants of complexes from, 25:10520
separation from ores by solvent extraction, review on, 25:10656 (BM-IC-8502)
shear strength of, effects of pressure and strain rate on, 25:11394
strength of, effects of pressure, strain, and strain rate on shear, 25:11379 (UCRL-72477)
BERYLLIUM ALLOYS AND SYSTEMS
Be--Cu, analysis for beryllium oxide inclusion using bromine--methanol solution, method for, 25:10440
Be-base--Ni, diffusion of nickel in, 25:11399
BERYLLIUM ISOTOPES Be-7
content in atmosphere at Zugspitze, Germany, April to Dec. 1970, 25:10705(R) (NYO-4061-3)
content in Fayetteville, Arkansas rainwater, Jan. 1969 to Mar. 1970, (E), 25:10712 (ORO-2529-28, App. 6)
electron-capture decay in different chemical combinations, effect of electron density on half-life for, (E), 25:12398
proton reactions (p,γ) at 0.95 to 3.28 MeV, cross-section measurements and zero-energy cross-section factor for, (E), 25:12400
BERYLLIUM ISOTOPES Be-8
nuclear binding energies, wave functions, and total-energy curves for, calculations using reaction-matrix theory, (T), 25:12411
BERYLLIUM ISOTOPES Be-9
binding energy of, calculation using angular-momentum decomposition of Faddeev equations, (T), 25:12692
carbon-12 elastic scattering at 12 to 25 MeV, optical-model analysis of angular distributions from, (E/T), 25:12382 (NP-18546)
carbon-12 reactions (C-12,C-13) at 12 and 15 MeV, DWBA analysis of angular distributions from, (E/T), 25:12382 (NP-18546)
helium-3 reactions (He-3,γ) at 3 to 6 MeV, differential cross sections and angular distributions for, (E), 25:12388
oxygen-16 elastic scattering at 12 to 25 MeV, optical-model analysis of angular distributions from, (E/T), 25:12382 (NP-18546)
oxygen-16 reactions (O-16,O-17) at 11 to 18 MeV, excitation functions and DWBA analysis of angular distributions from, (E/T), 25:12382 (NP-18546)
oxygen-18 elastic scattering at 12 to 31 MeV, angular distributions from, (E/T), 25:12381 (NP-18541)
oxygen-18 reactions (O-18,O-19) and (C-18,O-17) at 12 to 20 MeV, DWBA analysis of angular distributions from, (E/T), 25:12381 (NP-18541)
photoneutron cross section of, calculation using Dirac model, (T), 25:12399
proton reactions (p,2p) at 180 and 660 MeV, lithium-8 energy spectra and angular distributions from, (E/T), 25:12378 (JINR-P1-4872)
BERYLLIUM ISOTOPES Be-10
binding energy of ΛΛ hypernucleus of, (T), 25:12393
energy levels of, projected Hartree--Fock calculation of, (T), 25:12396
BERYLLIUM ISOTOPES Be-11
beta decay of, half-life for, (E), 25:12394
BERYLLIUM OXIDES
determination of inclusion of, in beryllium--copper alloy using bromine--methanol solution, method for, 25:10440
radioinduced defects in single crystals of, ESR study of gamma and neutron, 25:11950 (CEA-R-3937)
yield strength of, dynamic shock-wave, 25:11490
BeO--PuO_2, radiation dose rate from, 25:11052 (AERE-R-5069)
BETA DECAY
detection of doub?_, ?alf-lives and sum-energy spectra from, (E), 25:12448
electron--nucleus quadrupole interaction in, numerical solution of, (T), 25:12685
Fermi matrix elements for superallowed and isospin-forbidden, calculation of squared, (T), 25:12690
nuclear-size effects in allowed, wave-function parameterizations including, (T), 25:12667
radiative corrections of order α to allowed, numerical evaluation of, (T), 25:12696
BETA PARTICLES
dosimetry for promethium-147-labeled luminous paints, 25:11065
effects on aerated acidified water, cerium and hydrogen peroxide yields from, 25:10636
effects on soybean seedlings in comparison to effects of cobalt-60 γ rays, fission neutrons, and strontium-90 and yttrium-90 β particles, 25:11312
monitoring in atmosphere and precipitation in North and South America during 1970, 25:11039
monitoring in surface atmosphere over Central, North, and South America during June 1970, 25:10721
monitoring of fallout, in air and milk in Ecuador, 25:11068
scattering by complex materials, calculation of effective atomic number for back-, 25:11674
scattering by crushed dolomite and oxides, particle size determination by, 25:10784
use for determining cross section, thickness, shape, and internal structure, review of, 25:10977
BETA SOURCES
activity in monazites and zircons, 25:10723
activity measurements of low-level, performance of scintillation detectors for, 25:10819
BETA SPECTROMETERS
design and performance of semiconductor detector internal conversion, for γ--e and x--e coincidence measurements, 25:10855
design and performance of telescope semiconductor, 25:10852 (NP-18617)
design of silicon, with superconducting focusing lens, 25:10864
BETA SPECTROSCOPY
research progress on, 25:10437 (ORNL-4636, pp 45-50)
BETATRONS
beam extraction from PMB-6, (E/T), 25:12334
electron currents in, detector sensitivity for measuring, 25:12321
radiation dosimetry around medical, neutron, 25:12320
BIBLIOGRAPHIES
on charged-particle-induced nuclear reactions, 25:12366

XUM

on handling and shipping of radioactive materials, 25:10798 (ORNL-NSIC-84)
on health status of atomic bomb survivors in Hiroshima and Nagasaki during 1968 to 1969, 25:11237(R) (ABCC-68-69)
on nuclear spectroscopy of rare earths, 25:12523 (LYCEN-7034, pp 58-83)
on plasma physics, 25:11857
on plasma physics and fusion reactors, 25:11858
on plasma physics and fusion reactors, 25:11856
on surface and vacuum physics, 25:11678
on treadmill performance of irradiated dogs, 25:11251 (AD-705976)
BICYCLO[2.2.2]OCT-2-ENE
radiolysis of, ESR spectral studies of radicals from γ, 25:10638
BICYCLOPENTYL
yields from γ radiolysis of liquid cyclopentane, effects of pressure on γ, 25:10628
BIG ROCK POINT POWER REACTOR
cooling system for, stress levels for sensitized stainless steel components of, 25:12725 (DOCKET-50155-58)
fuel element storage racks for, permission request for use of new, 25:12726 (DOCKET-50155-59)
fuel elements for, revised physics calculations for gadolinium oxide (Gd_2O_3)--uranium oxide (UO_2), 25:12726 (DOCKET-50155-59)
BIOCHEMISTRY
analytical chemistry uses in, 25:10435 (ORNL-4636, pp 14-20)
BIOLOGICAL MATERIALS
analyses for mercury by neutron activation, 25:10502
analysis for arsenic by neutron activation and radiochemical separation, 25:10510
analysis for carbon-12/carbon-13 and carbon-12/nitrogen-15 abundances by proton reaction methods, 25:10491 (ORNL-4636, pp 20-33)
analysis for cesium-137 by sorption on ammonium molybdophosphate, precipitation, and beta counting, 25:10482
radioisotope content of, gamma scintillation spectrometry method for cerium-144, iron-59, praseodymium-144, 25:11044
radiosterilization of, effects of temperature on sensitivity of contaminating microorganisms during ionizing, 25:11337
BIOLOGICAL MODELS
description of myelocytic leukemia, in mice, similarity of, to radioinduced myelocytic leukemia in man, 25:11302
development for estimation of potential radioisotope ingestion by man in Colombia and Panama, 25:10995 (BMI-171-45)
development for evaluation of changes in genetic parameters resulting from selection in corn, 25:11009(R) (COO-1512-22)
development for human respiratory system, for studies on properties of radioactive aerosols, 25:11036 (CEA-Bib-185)
development of equations for estimating dose to human lungs following accidental inhalation of plutonium-americium-241 aerosol, 25:11053 (BNWL-B-12)
BIOTITES
analysis for trace amounts of elements by spark source mass spectrometry, 25:10455
analysis of thin layers of, for uranium by fission track method using dielectric detectors, 25:10476
BIPHENYL
radiation testing of, design of facility for gamma, 25:10778(R) (ORNL-TM-3214)
BISMUTH
determination of trace amounts of, in biotite and tektite by spark source mass spectrometry, 25:10455
determination of trace amounts of, in molybdenum, review on, 25:10459
determination of trace amounts of, in rocks, quantometer for spectroscopic, 25:10451
superconducting quench-condensed, electron tunneling in, (E/T), 25:11842
BISMUTH ALLOYS AND SYSTEMS
Bi--In, electric conductivity of liquid, effects of composition and temperature on, 25:11398
Bi--In, voltages induced by ac--dc magnetic fields in superconducting foils of, 25:11835
Bi--Pb, superconducting quench-condensed, electron tunneling in, (E/T), 25:11842
Bi--Pb--Tl, superconducting transition temperature of fcc, 25:11846
BISMUTH ISOTOPES Bi-209
neutron elastic scattering at 4 MeV near 180°, differential cross sections and polarizations from polarized, (E), 25:12509(T) (ANL-Trans-855)
BISMUTH ISOTOPES Bi-214
beta decay of, β--γ angular correlations in, (E), 25:12555
nuclear spin--parity assignment of ground state from β--γ angular correlations, (E), 25:12555
BITUMINOUS MATERIALS
radioactive waste solidification in, for storage, 25:10800(P)
BLACK HOLES
formation in ensemble of collisionless zero-rest-mass particles, (T), 25:11660
formation in supernova events, (T), 25:11588
BLACK SEA
antimony content of, 25:10507
BLOOD
circulation in brain of patients with tumors or vascular diseases, effectiveness of iodine-131 for determining, 25:11149
circulation in human brain, effectiveness of iodine-131-labeled hippuran for measurement of, 25:11150
circulation in human brain, effects of pathological processes on, use of xenon-133 for determining, 25:11144
circulation in human brain, measurement of, using xenon-133 in combination with eight or sixteen detectors, evaluation of, 25:11143
circulation in human heart, use of iodine-131 or metastable technetium-99 and scintillation crystals with collimators for measuring, 25:10911
circulation in human kidneys, method for measuring, using cobalt-57-labeled vitamin B 12 in combination with iodine-131-labeled orthohippuric acid, 25:11157
circulation in human kidneys, use of xenon-133 for determining, 25:11158
circulation in human liver, effects of hyperemia on, use of iodine-131-labeled RISA for studying, 25:10916
circulation in human liver, effects of hyperthyroidism on, use of gold-198 and iodine-131 for determining, 25:11141
circulation in human lungs, effectiveness of radioisotopes for evaluating, 25:11126
circulation in human lungs, use of oxygen-15-labeled carbon dioxide or xenon-133 for scanning of, 25:11125
circulation in human muscles, use of xenon-133 for determining, 25:11123
circulation in human organs, radioisotope clearance method for determining, development of method for improved accuracy, 25:10917
circulation in man, detector system for tracer measurement of, 25:10826(P)
circulation measurements in human lungs using iodine-131, use of, for preoperative tumor diagnosis, 25:11127
circulation of, conference on methods for determining, 25:11192
circulation of, development of method using iodine-131 and xenon-133 for assessing peripheral, 25:10912
circulation of, in human spleen, use of chromium-51-labeled heat treated erythrocytes for determining, 25:11142
circulation of, in parabiotic mice, use of chromium-51-labeled erythrocytes for studying, 25:10915
effects on recovery of irradiated blood vessels, 25:11256 (BNL-50203, pp 186-203)
radiation effects on activity of alkaline phosphatase and cholinesterase in, of rats following injection of mixed radioisotopes, 25:10968
radiation effects on circulation of, in tumor cells, effects of dose fractionation in, 25:11257 (BNL-50203, pp 210-14)
radiation effects on coagulation of, in rats, protective effects of cystamine against x, 25:11105
radiation effects on erythrocytes and reticulocytes in peripheral, of guinea pigs, comparison of chronic cesium-137 and single cobalt-60 γ, 25:11278
radiation effects on histamine in, of rats, mechanism of, 25:10967
radiation effects on leukocytes of human, effects of phytohemagglutinin on, 25:11299
radioinduced hemolysis of stored human, low dose x, 25:10981
renin content of, in hypertensive patients, measurements of, in combination with angiotension infusion test and kidney scanning, 25:11164
scanning of circulation in brains of rabbits, using xenon-133, 25:11194
scanning of circulation in feet of dogs, using double isotope method with iodine-131 and sodium-24 for study of arterio-venus shunts, 25:10926
scanning of circulation of, circulation in brain, in patients with brain diseases or thrombosis, use of iodine-131 for scanning of, 25:11148
scanning of circulation of, for detection of brain lesions, effectiveness of metastable technetium-99 for, 25:11146
scanning of circulation of, in human brain, method for iodine-131-labeled RISA, 25:11151
scanning of circulation of, in human lungs, use of metastable technetium-99-labeled macroaggregates of human serum albumin for, 25:11128
scanning of circulation of, in human muscles during work, xenon-133, 25:10913
scanning of circulation of, in kidneys of hypertensive patients, use of radioisotope-labeled compounds for, 25:11153
scanning of circulation of, in lower extremities of man, effectiveness of xenon-133 for, 25:11138
scanning of circulation of, in muscles, comparison of direct measurements to xenon-133, 25:11137
scanning of circulation of, in patients with Parkinsons disease, 25:11147

scanning of circulation of, through heart chambers, use of metastable technetium-99 with stationary detectors for, 25:11120
scanning of circulation time of human, method using dual radioisotopes and multiscaler for, 25:11184
xenon-133 clearance from, in cat muscle, effects of method of administration on, 25:11136
BLOOD PLASMA
analysis for selenium by neutron activation and radiochemical separation, 25:10495
BLOOD PRESSURE
radiation effects on, in rabbits following administration of zirconium citrate, effects of synchronous calcium gluconate administration on whole-body γ, 25:11289
BLOOD SERUM
analysis for trace elements by flameless atomic absorption spectrometry, 25:10464
iodine radioisotope content of human, following oral administration, methods for determining, iodine-127 and iodine-131, 25:10945
radiosterilization of, effects of temperature and 3 Mrad dose on in vivo γ, 25:11333
BLOOD VESSELS
radioinduced damage of, latent, 25:11256 (BNL-50203, pp 186-203)
radioinduced dilation of, in earlobes of mice, electron, 25:11254 (BNL-50203, pp 174-80)
radioinduced tumors in, of mammals, effects of clonogenicity, dose, reproductive integrity, and time on, 25:11253 (BNL-50203, pp 154-73)
BODY FLUIDS
content of extracellular, in splenectomized dogs following acute hemorrhage, radioisotope dilution method for measurement of, 25:11185
radioisotope content of samples of, following neutron activation, use of ion exchange column for simultaneous determination of bromine-82, potassium-42, and sodium-24, 25:11066
BOILERS
fabrication of gas cooled reactor, 25:12766
testing for thermoelectric converters, 25:10778(R) (ORNL-TM-3214)
testing of gas cooled reactor, 25:12766
BONE MARROW
gold-198 colloid deposition in human, effects of particle size on, 25:10918
isoenzymes of lactic dehydrogenase in, of xenogenic radiation chimeras, 25:10992
lymphocyte migration from shielded, in x-irradiated rats, role of, in recovery processes, 25:11077
nonprotein thiol content of, of mice following injection of cystamine in optimum radioprotective dose, 25:11101
radiation effects on cell populations of, of mice, effects of dose fractionation on x, 25:11279
radiation effects on, of rats in relation to stem cell population kinetics, design of model for compartmental analysis of, 25:11290
radioinduced tumors in, of mammals, effects of clonogenicity, dose, reproductive integrity, and time on, 25:11253 (BNL-50203, pp 154-73)
radioprotective effects of homologous, on blood coagulation in rats, x, 25:11105
radioprotective effects of homologous, on spleen mitochondria of rats, against acute x, 25:11100
radiosterilization of human, for use as transplants, γ, 25:11329
scanning using colloidal radioisotopes, baseline studies of stem cell relations for, 25:11112
BONES
calcium content of, of monkeys, method for neutron activation analysis of, 25:10907 (N-70-31814)
cobalt-60 1-nitroso 2-naphthol chelate distribution in, of rats, 25:10958
fluorine-18 distribution in, method for determining, 25:10943
radiation effects on antigenicity of skull, effects of temperature and 2 Mrad dose on ionizing, 25:11334
radiation effects on growth of transplanted tail, from syngeneic donors in recipient mice, protective effects of anoxia, dimethyl sulfoxide, and glycerol against, x, 25:10983
radiation effects on, in man, review of literature on, 25:11209
radioinduced tumors in, of personnel following occupational inhalation of plutonium-239, models for estimating probability of α and γ, 25:11301
radioisotope content of, in rats, effects of estradiol on calcium-47 and strontium-85, 25:10933 (COO-1339-45)
radiosterilization for use as transplants, effects of temperature and storage on osteogenic inductors during γ, 25:11335
scanning of fractured fibia and tibia, in rats using calcium-47, fluorine-18, lutetium-177, and strontium-85, 25:11216
scintiscanning of human, for diagnosis of rheumatic processes, effectiveness of strontium-85 for, 25:11175
strontium-85 deposition in, of rats, effects of dose and time of administration on effectiveness of activated barium sulfate for prevention of, 25:11048
strontium-85 uptake by, following oral administration to rats, effects of barium sulfate on, 25:10940
strontium-85 uptake by, following oral administration to rats, effects of whole-body exposure to γ on, 25:11263
strontium-90 content of human, sampled in USA during 1969, 25:11042
strontium-90 content of, of muskrats and perch in lake contaminated by reactor effluent, 25:11006
tellurium-127m uptake by rat, following intravenous injection, 25:10950
transplantation of γ-radiosterilized, in rabbits, ESR evaluation of resorption rate following, 25:11340
BORANE
BH_3--H_3SiPH_2, deuterium exchange with hydrogen in, 25:10547
BORIC ACID
analysis of pharmaceutical preparations containing, by neutron absorption, 25:10487
BORON
determination as impurity in fuel materials by emission spectroscopy, 25:10432 (KFK-1261)
determination by charged particle activation, reactions and sensitivities for, 25:10488 (CEA-R-4072)
determination by charged particle and photon activation, radiochemical separation methods for, 25:10488 (CEA-R-4072)
determination in aluminum by charged particle activation and radiochemical separation, 25:10488 (CEA-R-4072)
determination in aluminum--uranium fuels using cobalt-60-tagged boron, 25:11375 (IN-1437, pp 24-59)
determination in borate glasses by neutron absorption, 25:10483
determination in sedimentary rocks by direct-reading spectrometry, 25:10450
determination in silicon by proton activation and radiochemical separation, 25:10488 (CEA-R-4072)
determination of trace amounts of, in basalt and granite, correction of matrix effect in uv spectrographic, 25:10453
determination of trace amounts of, in biotite and tektite by spark source mass spectrometry, 25:10455
determination of trace amounts of, in molybdenum, review on, 25:10459
determination of trace amounts of, in phosphate deposits by spark source mass spectrometry, 25:10456
determination of trace amounts of, in rocks and stony meteorites by fluorimetry, 25:10493
determination of trace amounts of, in rocks, quantometer for spectroscopic, 25:10451
determination of trace amounts of, in Zircaloy-2 and zirconium, carrier distillation method for spectrographic, 25:10430 (EUR-4541)
effects on magnetic hysteresis loop of manganese--aluminum alloys, 25:11983
nucleosynthesis in stellar atmospheres, (T), 25:11548
nucleosynthesis of, (T), 25:11542 (NP-18591)
optical properties of β-rhombohedral, anisotropy in, 25:12029
oxidation of, redistribution of impurities in diffused layers during thermal, 25:11476
separation from ores by solvent extraction, review on, 25:10656 (BM-IC-8502)
BORON CARBIDES
yield strength of, dynamic shock-wave, 25:11490
BORON FLUORIDES
determination as impurity in sodium fluoroborate coolants, 25:10434 (ORNL-4636, pp 7-13)
BORON ISOTOPES B-10
alpha reactions (α,Li-6) at 46 MeV, DWBA analysis of, (E/T), 25:12392
effects on ir spectra of boron trifluoride, 25:10533
energy levels from lithium-7 (He-3,γ) reactions, spin-parity assignments for highly-excited, (E), 25:12389
fluorine-19 elastic scattering at 20 and 24 MeV, angular distributions from, (E/T), 25:12381 (NP-18541)
fluorine-19 reactions (F-19,F-18) at 20 and 24 MeV, DWBA analysis of angular distributions from, (E/T), 25:12381 (NP-18541)
nucleosynthesis of, (T), 25:11542 (NP-18591)
oxygen-18 elastic scattering at 12 to 31 MeV, angular distributions from, (E/T), 25:12381 (NP-18541)
oxygen-18 reactions (O-18,O-17) at 20 and 24 MeV, DWBA analysis of angular distributions from, (E/T), 25:12381 (NP-18541)
BORON ISOTOPES B-11
effects on ir spectra of boron trifluoride, 25:10533
nucleosynthesis of, (T), 25:11542 (NP-18591)
reactions (B-11,p) and (B-11,α) with zinc-64 at 49 and 88 MeV, proton and α angular distributions and energy spectra from bromine-75 compound nucleus in, (E), 25:12461
BORON NITRIDES
magnetic susceptibility of, (E), 25:12010
BORON OXIDES
radiation effects on high-pressure polymorphs of, neutron, 25:11474(R) (BNWL-842)
B_2O_3--CdO--CdS, phase studies of, 25:11526
B_2O_3--CdO--La_2O_3, properties and structure of glasses of, 25:11517
B_2O_3--CoO--CoS, phase studies of, 25:11526
B_2O_3--FeO--FeS, phase studies of, 25:11526
B_2O_3--MgO--MgS, phase studies of, 25:11526
B_2O_3--MnO--MnS, phase studies of, 25:11526
B_2O_3--ZnO--ZnS, phase studies of, 25:11526

XUM

BORON SYSTEMS
B--Fe, analysis of powdered, for oxygen, comparison of isotope dilution and vacuum fusion methods for, 25:10467
B--Mg, mechanical properties of composites of, effects of fiber coating and matrix strengthening on, 25:11407
BOSONS
current algebra representations for N identical spin-0, (T), 25:12125
detection of beams of, stochastic theory for, 25:12053
interactions of massive vector, covariant photon amplitudes as zero-mass limit of helicity amplitude for, (T), 25:12177
interactions of, energy--momentum spectrum and vacuum expectation values for, 25:12269
interactions with gravitons, cross sections for, (T), 25:12138 (NYO-2262-TA-222)
interactions with photons, cross sections for, (T), 25:12138 (NYO-2262-TA-222)
quantum field theory without cutoffs for self-interacting, (T), 25:12248
theory for systems of, spectral density method in statistical mechanics in, (T), 25:12061
BRAIN
blood circulation time in human, effects of arteriosclerosis on, effectiveness of iodine-131-labeled hippuran for measuring, 25:11150
blood flow in human, measurement using xenon-133 in combination with eight or sixteen detectors, evaluation of, 25:11143
radiation effects on glucose and lactate production in, of rats, effects of dose rate on strontium-90 β, 25:11262
radiation effects on neural activity in optical cortex of, in rabbits exposed during embryogenesis, x, 25:11283
radioisotope measurement of blood circulation in, of patients with tumors or vascular diseases, effectiveness of iodine-131 for determining, 25:11149
scanning in children with hydrocephalus for openings for ventriculoatriostomy, effectiveness of intraventricular injected iodine-131-labeled hippuran for, 25:11152
scanning of blood circulation in human, for determining mental activity, method for iodine-131-labeled RISA, 25:11151
scanning of blood vessels in human, for diagnosis of brain diseases, use of xenon-133 for, 25:11144
scanning of human, for detection of cerebral lesions, effectiveness of technetium-99m for, 25:11146
scanning of human, for diagnosis of hydrocephalus, use of iodine-131-labeled serum albumin and cisternography for, 25:11181
scanning of human, for differential diagnosis between brain tumors and other brain lesions using mercury-203-labeled chlormerodrin, 25:11179
scanning of human, use of metastable technetium-99-labeled DTPA in comparison to metastable technetium-99-labeled pertechnetate, 25:11189
BREATH
carbon-14-labeled dioxide content of exhaled, in man, method for determining, 25:11168
BREMSSTRAHLUNG
emission from electron cyclotron resonance-heated plasma, free--free, (T), 25:11910(R) (COO-1695-32)
emission from mirror-confined plasma, (E/T), 25:11909(R) (COO-1695-31)
emission from reflected electrons from half-space magnetic fields, 25:11679
production at 5 keV to 1 MeV, exact screened calculations of relativistic cross sections for, 25:11681
production by electron reactions with tungsten at 10 to 60 MeV, 25:12496
reactions (γ,f) with thorium-232 and uranium-238 at 200 to 900 MeV, cross sections for, (E), 25:12573
reactions (γ,n) with carbon-12 at 100 to 1050 MeV, cross sections for, (E), 25:12413
reactions (γ,n) with lithium-6 and -7 at 20 to 75 MeV, differential and integrated cross sections and energy spectra from, (E), 25:12387
reactions (γ,n) with magnesium-24 and silicon-28 at 16 to 31 MeV, cross sections for (E), 25:12469
reactions (γ,n) with strontium up to 27 MeV, cross sections for, (E), 25:12456
scattering by medium spherical nuclei, differential cross sections for, (E), 25:12463
scattering by nickel-58 and -60 at 4.2 MeV, gamma spectra from resonance, (E), 25:12478
spectra for internal, description of direct reactions by triangle mechanisms, (T), 25:12694
BRITTANY POWER REACTOR (EL-4)
boilers for, fabrication and testing of, 25:12766
BROMATES
separation from bromides, paper chromatographic, 25:10687
BROMIDES
separation from bromates, paper chromatographic, 25:10687
BROMINE
determination in soils and lowland rice by neutron activation, 25:10505
determination of trace amounts of, in biotite and tektite by spark source mass spectrometry, 25:10455
determination of trace amounts of, in phosphate deposits by spark source mass spectrometry, 25:10456
energy-level transitions in, rates of Auger and x-ray, (T), 25:11685
separation from seawater by solvent extraction, review on, 25:10656 (BM-IC-8502)
BROMINE IONS
reactions with helium and hydrogen gases at 6 to 15 MeV, cross sections for electron capture and loss in, (E), 25:11710
BROMINE ISOTOPES
decay of fission-product, γ spectra from, 25:10472(R) (BMBW-FBK-70-19)
BROMINE ISOTOPES Br-78
beta and electron-capture decay of, gamma spectra and EC + β^+ branching ratios from, (E), 25:12445
isomeric transition in, half-life and γ energy for, (E), 25:12430 (INR-P-1091)
BROMINE ISOTOPES Br-79
isomeric transition in, half-life and γ energy for, (E), 25:12430 (INR-P-1091)
meson (μ^-) capture probability in, (E), 25:12502
neutron inelastic scattering at 14.8 MeV, isomeric cross section for, (E), 25:12430 (INR-P-1091)
neutron reactions (n,2n) at 14.8 MeV, isomeric cross section for, (E), 25:12430 (INR-P-1091)
BROMINE ISOTOPES Br-81
meson (μ^-) capture probability in, (E), 25:12502
BROMINE ISOTOPES Br-82
determination in body fluid by ion exchange and scintillation counting, 25:11066
BROMINE ISOTOPES Br-84
beta decay of, form factors, gamma spectra, log-ft values, and Kurie plots from, (E), 25:12444
energy levels of, spin and parity of, (E), 25:12462
nuclear spin, half-life, and Q value for, (E), 25:12444
BROMOURANATES
preparation and properties of UBr_6^-, 25:10576
BROOKHAVEN ALTERNATING-GRADIENT SYNCHROTRON (AGS)
beam transport system for post-conversion, parameter study for economical, 25:12296 (BNL-15464)
BROWNS FERRY POWER REACTOR, UNIT 1
site for, environmental survey during January to June 1970, 25:12735 (DOCKET-50259-21)
BROWNS FERRY POWER REACTOR, UNIT 2
site for, environmental survey during January to June 1970, 25:12735 (DOCKET-50259-21)
BROWNS FERRY POWER REACTOR, UNIT 3
site for, environmental survey during January to June 1970, 25:12735 (DOCKET-50259-21)
BRUNSWICK POWER REACTOR, UNIT 1
containment structures for, safety analysis of, 25:12745 (DOCKET-50324-18)
BRUNSWICK POWER REACTOR, UNIT 2
containment structures for, safety analysis of, 25:12745 (DOCKET-50324-18)
BUBBLES
acoustic properties of boiling, in subcooled water, 25:10769(R) (ORO-3911-3)
decay and growth in boiling water, model for, 25:10769(R) (ORO-3911-3)
BUTADIENE POLYMERS
methyl acrylate--polybutadiene, radioinduced polymerization of, effects of catalysts and crosslinking agents on electron, 25:10609 (JAERI-5026, pp 130-6)
2-BUTANOL
yields from γ radiolysis of dilute aqueous sec-butylamine solutions, 25:10627(R) (NYO-2499-37)
2-BUTANONE
yields from γ radiolysis of dilute aqueous sec-butylamine solutions, 25:10627(R) (NYO-2499-37)
sec-BUTYLAMINE
radiolysis of dilute aqueous solutions of, mechanism and yields from γ, 25:10627(R) (NYO-2499-37)
BUTYRIC ACID, 2-AMINO-4-(METHYLSELENYL)-
use of selenium-75-labeled, for scintigraphy of human pancreas, 25:11212

C

CADMIUM
alpha inelastic scattering at 9 and 10 MeV by natural, gamma spectra from, (E), 25:12548
alpha inelastic scattering at 9 to 10 MeV by natural, gamma angular distributions from, (E/T), 25:12556
argon-40 inelastic scattering at 101 MeV by natural, gamma spectra from, (E), 25:12548
argon-40 inelastic scattering at 101 MeV by natural, gamma angular distributions from, (E/T), 25:12556
creep of single crystals of, gradual loading method for determination of room-temperature transient, 25:11412
determination as impurity in fuel materials by emission spectroscopy, 25:10432 (KFK-1261)
determination by photon activation, reactions and sensitivities for, 25:10488 (CEA-R-4072)
determination in serum and urine by flameless atomic absorption spectroscopy, 25:10464
determination of trace amounts of, in biotite and tektite by spark source mass spectrometry, 25:10455

determination of trace amounts of, in molybdenum, review on, 25:10459
determination of trace amounts of, in rocks, quantometer for spectroscopic, 25:10451
determination of trace amounts of, in Zircaloy-2 and zirconium, carrier distillation method for spectrographic, 25:10430 (EUR-4541)
distribution coefficient in mixtures of acetone, hydrochloric acid, and methanol, 25:10681
energy-level transitions in, rates of Auger and x-ray, (T), 25:11685
oxygen-16 inelastic scattering at 38 and 41 MeV by natural, gamma spectra from, (E), 25:12548
oxygen-16 inelastic scattering at 38 to 40 MeV by natural, gamma angular distributions from, (E/T), 25:12556
photon inelastic scattering at 12 to 30 MeV, differential cross sections for, (E), 25:12463
separation from fission products, 25:10472(R) (BMBW-FBK-70-19)
separation from fission products by automatic ion exchange chromatography, design and performance of equipment for, 25:10659 (CEA-N-1267)
separation from indium, molybdenum, niobium, palladium, and rhodium by gas chromatography using aluminum chloride eluent, 25:10666 (JINR-P6-5410)
sulfur-32 inelastic scattering at 64 MeV by natural, gamma spectra from, (E), 25:12548
sulfur-32 inelastic scattering at 64 MeV by natural, gamma angular distributions from, (E/T), 25:12556
superconducting transition temperature of, isotope effect in, (E/T), 25:11825

CADMIUM ALLOYS AND SYSTEMS
Ag--Cd--In-base--Sn, electric conductivity, Fermi surface topology, and superconducting transition temperature of dilute, 25:12032
Au--Cd, crystal structure and martensitic transformation of near-equiatomic, 25:11448
Cd--Pd-base, thermodynamic properties of, 25:11396
Cd--Zn-base, texture of ingot of, solidified from flowing liquid, 25:11450

CADMIUM HYDROXIDES
precipitation of carrier-free silicon-31, 25:10675

CADMIUM ISOTOPES
yields from thermal fission of uranium-235, 25:10583(R) (AECL-3776)

CADMIUM ISOTOPES Cd-104
electron-capture decay of, gamma and conversion-electron spectra, branching ratios, log-ft values, and Q values from, (E), 25:12475

CADMIUM ISOTOPES Cd-106
alpha inelastic scattering at 9 MeV, correlation functions and hyperfine attenuation coefficients from, (E), 25:12619
energy levels from Coulomb excitation, static electric quadrupole moments for first 2+, (E), 25:12619
energy levels from Coulomb excitation, static electric quadrupole moments of 2+, (E/T), 25:12556
energy-level transitions from Coulomb excitation, probabilities for E2, (E), 25:12619
oxygen-16 inelastic scattering at 35 to 40 MeV, correlation functions and hyperfine attenuation coefficients from, (E), 25:12619
proton reactions (p,pn), (p,2n), and (p,2p) at 400 MeV, analysis for nuclear structure effects in, (E), 25:12570
sulfur-32 inelastic scattering at 55 MeV, correlation functions and hyperfine attenuation coefficients from, (E), 25:12619

CADMIUM ISOTOPES Cd-108
energy levels from Coulomb excitation, static electric quadrupole moments of 2+, (E/T), 25:12556
proton reactions (p,pn), (p,2n), and (p,2p) at 400 MeV, analysis for nuclear structure effects in, (E), 25:12570

CADMIUM ISOTOPES Cd-110
effects on superconducting transition temperature of cadmium, (E/T), 25:11825
energy level from Coulomb excitation, static quadrupole moment for first excited 2+, (E), 25:12548
energy levels from Coulomb excitation, static electric quadrupole moments of 2+, (E/T), 25:12556
proton reactions (p,pn), (p,2n), and (p,2p) at 400 MeV, analysis for nuclear structure effects in, (E), 25:12570

CADMIUM ISOTOPES Cd-112
energy level from Coulomb excitation, static quadrupole moment for first excited 2+, (E), 25:12548
energy levels from Coulomb excitation, static electric quadrupole moments of 2+, (E/T), 25:12556
energy levels from photon resonant scattering from, spin assignments for, (E), 25:12554
energy-level transitions from photon resonant scattering from, branching ratios and multipolarities for, (E), 25:12554
proton reactions (p,pn), (p,2n), and (p,2p) at 400 MeV, analysis for nuclear structure effects in, (E), 25:12570

CADMIUM ISOTOPES Cd-113
energy levels from photon resonant scattering from, spin assignments for, (E), 25:12554
energy-level transitions from photon resonant scattering from, multipolarities for, (E), 25:12554
neutron capture by, average circular γ polarization in thermal, (E), 25:12601
nuclear magnetic resonance in cadmium oxide, spin--lattice relaxation and Knight shift in, 25:12038
proton reactions (p,pn), (p,2n), and (p,2p) at 400 MeV, analysis for nuclear structure effects in, (E), 25:12570

CADMIUM ISOTOPES Cd-114
alpha inelastic scattering at 9 MeV, correlation functions and hyperfine attenuation coefficients from, (E), 25:12619
effects on superconducting transition temperature of cadmium, (E/T), 25:11825
energy level from Coulomb excitation, static quadrupole moment for first excited 2+, (E), 25:12548
energy levels from Coulomb excitation, static electric quadrupole moments of 2+, (E/T), 25:12556
energy levels from Coulomb excitation, static electric quadrupole moments for first 2+, (E), 25:12619
energy levels from thermal neutron capture, spin for compound, (E), 25:12601
energy-level transitions from Coulomb excitation, probabilities for E2, (E), 25:12619
oxygen-16 inelastic scattering at 35 to 40 MeV, correlation functions and hyperfine attenuation coefficients from, (E), 25:12619
proton reactions (p,pn), (p,2n), and (p,2p) at 400 MeV, analysis for nuclear structure effects in, (E), 25:12570
sulfur-32 inelastic scattering at 49 to 55 MeV, correlation functions and hyperfine attenuation coefficients from, (E), 25:12619

CADMIUM ISOTOPES Cd-116
effects on superconducting transition temperature of cadmium, (E/T), 25:11825
energy level from Coulomb excitation, static quadrupole moment for first excited 2+, (E), 25:12548
energy levels from Coulomb excitation, static electric quadrupole moments of 2+, (E/T), 25:12556

CADMIUM OXIDES
electric conduction in, NMR study of impurity, 25:12038
B_2O_3--CdO--CdS, phase studies of, 25:11526
B_2O_3--CdO--La_2O_3, properties and structure of glasses of, 25:11517

CADMIUM SULFIDES
B_2O_3--CdO--CdS, phase studies of, 25:11526

CALCIUM
determination as impurity in fuel materials by emission spectroscopy, 25:10432 (KFK-1261)
determination in ores and ore concentrates, intermittent ac arc method for spectrographic, 25:10429 (BARC-468)
determination in sedimentary rocks by direct-reading spectrometry, 25:10450
determination in tektite by spark source mass spectrometry, 25:10455
determination of trace amounts of, in minerals and rocks by x-ray fluorescence, methods for correction of matrix effect in, 25:10448
determination of trace amounts of, in molybdenum, review on, 25:10459
determination of trace amounts of, in rocks and sand by thermal neutron activation, ion exchange, and γ spectrometry, 25:10492
determination of trace amounts of, in standard rocks by atomic absorption spectrophotometry, 25:10671
metabolism of readily exchangeable, in pregnant and lactating cows, 25:12882 (COO-1339-44)

CALCIUM ALUMINATES
radioinduced polymerization of monomers on hydrated, γ, 25:10616

CALCIUM CARBONATES
analysis for thorium and uranium isotopes by α spectrometry, 25:10477

CALCIUM FLUORIDES
analysis of, neutron activation, 25:11472(R) (AD-708705)
diffusion of calcium-45 in monocrystals of, 25:10583(R) (AECL-3776)
radioinduced luminescence of holmium- and erbium-doped crystals of, γ, 25:11955

CALCIUM GLUCONATE
effects on zirconium citrate-induced variations in blood pressure, heart rate, and respiration in whole-body γ-irradiated rabbits following synchronous administration, 25:11289

CALCIUM HYDROXIDES
precipitation of carrier-free silicon-31, 25:10675

CALCIUM IONS
formation of Ca II K line in chromospheric spectra, (T), 25:11615

CALCIUM ISOTOPES Ca-40
binding energy of, Hartree--Fock calculation using effective interaction, (T), 25:12686
center-of-mass motion of, Hartree--Fock treatment of, (T), 25:12653
deuteron elastic scattering at 28 MeV, asymmetries in cross sections for, (E), 25:12309 (LYCEN-6909)
deuteron reactions (d,p) at 7 and 9 MeV, effect of deuteron D-state on DWBA calculations of differential cross sections, proton polarizations, deuteron analyzing powers, and spectroscopic factors from, (T),

XUM

25:12414
energy levels from proton resonances in potassium-39, strengths and spin--parity assignments for, (E), 25:12437
energy levels of, double gamma emission from first-excited, (E), 25:12495
neutron capture at 14 MeV, calculation of γ spectra using statistical and direct-semidirect models, (T), 25:12472
neutron capture by, gamma spectra from thermal, (E), 25:12491
nuclear charge distribution in, second-order perturbation calculation of, (T), 25:12484
proton elastic scattering at 10 to 60 MeV, local Woods--Saxon potentials equivalent to nonlocal analysis including exchange effects in, (T), 25:12689
proton reactions at 10.3 to 21.6 MeV with, total cross sections for, (E), 25:12497
triton reactions (t,p) at 10.1 MeV, angular distributions and reaction amplitudes from finite-range calculations of, (T), 25:12505

CALCIUM ISOTOPES Ca-41
binding energy of, relative to calcium-40, (T), 25:12436
energy levels from thermal neutron capture by calcium-40, 25:12491
energy levels of, Hartree--Fock calculation using effective interaction, 25:12686

CALCIUM ISOTOPES Ca-42
binding energy of, relative to calcium-40, (T), 25:12436
energy levels from proton inelastic scattering, spin-parity assignments for, (E), 25:12465
energy levels of, spin--parity assignments, spectroscopic factors, and wave functions from shell-model calculations of, (T), 25:12436
energy-level transitions from proton inelastic scattering, γ branching and multipole mixing ratios for, (E), 25:12465
nuclear charge distribution in, second-order perturbation calculation of, (T), 25:12484
proton inelastic scattering at 7 MeV, p-γ angular correlations from, (E), 25:12465

CALCIUM ISOTOPES Ca-43
binding energy of, relative to calcium-40, (T), 25:12436
energy levels of, spin--parity assignments and spectroscopic factors from shell-model calculations of, (T), 25:12436

CALCIUM ISOTOPES Ca-44
binding energy of, relative to calcium-40, (T), 25:12436
energy levels of, spin--parity assignments, spectroscopic factors, and wave functions from shell-model calculations of, (T), 25:12436

CALCIUM ISOTOPES Ca-45
binding energy of, relative to calcium-40, (T), 25:12436
diffusion in calcium fluoride monocrystals, 25:10583(R) (AECL-3776)
energy levels of, spin--parity assignments and spectroscopic factors from shell-model calculations of, (T), 25:12436

CALCIUM ISOTOPES Ca-46
binding energy of, relative to calcium-40, (T), 25:12436
energy levels of, spin--parity assignments and wave functions from shell-model calculations of, (T), 25:12436
neutron capture by, gamma spectra from thermal, (E), 25:12491

CALCIUM ISOTOPES Ca-47
binding energy of, relative to calcium-40, (T), 25:12436
content of bones of rats, effects of estradiol on, 25:10933 (COO-1339-45)
energy levels from thermal neutron capture by calcium-46, 25:12491
energy levels of, spin--parity assignments and spectroscopic factors from shell-model calculations of, (T), 25:12436
sorption by intestines of rats, effects of estradiol on, 25:10933 (COO-1339-45)
use for scanning of fibia and tibia bones in rats, 25:11216

CALCIUM ISOTOPES Ca-48
beta decay of, sum-energy spectra and half-lives for double, (E), 25:12448
binding energy of, relative to calcium-40, (T), 25:12436
energy levels of, spin--parity assignments and wave functions from shell-model calculations of, (T), 25:12436
helium-3 reactions (He-3,t) at 30 MeV, exchange effects on differential cross sections from, (T), 25:12691
proton elastic scattering at 10 to 60 MeV, local Woods--Saxon potentials equivalent to nonlocal analysis including exchange effects in, (T), 25:12689

CALCIUM ISOTOPES Ca-49
binding energy of, relative to calcium-40, (T), 25:12436
energy levels of, spin--parity assignments from shell-model calculations of, (T), 25:12436

CALCIUM ISOTOPES Ca-50
binding energy of, relative to calcium-40, (T), 25:12436
energy levels of, spin--parity assignments and wave functions from shell-model calculations of, (T), 25:12436

CALCIUM PHOSPHATES
effects on radioisotope accumulation in rats, dietary, 25:10956

CALIFORNIUM
purification and encapsulation of, hot cell for, 25:10654(R) (ORNL-4588)
purification by pressurized cation exchange chromatography, on-line computer monitoring of, 25:10664 (DP-MS-70-36)

CALIFORNIUM ISOTOPES Cf-240
alpha decay of, α energy spectra and half-life for, (E), 25:12593

CALIFORNIUM ISOTOPES Cf-241
alpha decay of, α energy spectra and half-life for, (E), 25:12593

CALIFORNIUM ISOTOPES Cf-242
alpha decay of, α energy spectra and half-life for, (E), 25:12593

CALIFORNIUM ISOTOPES Cf-250
production at TRU, 25:10654(R) (ORNL-4588)

CALIFORNIUM ISOTOPES Cf-252
alpha decay of, time spectrum of alpha--conversion-electron delay in, (E), 25:12542
production at TRU, 25:10654(R) (ORNL-4588)
use for therapy, oxygen enhancement ratio for, 25:11095 (BNL-50203, pp 308-17)

CALLICREIN
use for treatment of chronic dermatitis in x-irradiated swine, 25:11110

CALORIMETRY
role in thermodynamics of metals and alloys, 25:12916 (UCRL-19115)

CAMERAS
design of rotating mirror framing, 25:12907 (SC-M-70-886)
optimization of image location relative to rotor surface for Model 739 framing, 25:12889 (EGG-1183-542)

CANADA
uranium reserves in, evaluation of ENEA report on estimates of, 25:10724

CANALS
excavation of sea-level, in Central America, estimation of potential radiation dose to human populations following use of nuclear explosives for, 25:11055 (ORNL-4579)

CAPILLARIES
radioinduced dilation of, in earlobes of mice, electron, 25:11254 (BNL-50203, pp 174-80)

CARBOHYDRATES
radiolysis of, saturation of ESR spectra of free radicals from x, 25:10645

CARBON
ablation of fibrous composites of, 25:12920 (Y-1752)
abundance of geomagnetically trapped nuclei of, (E), 25:11744
abundance variations in uranium dioxide pellets during decarbonization and sintering, 25:11482
content in loop sodium, monitoring data on, 25:11348(R) (GEAP-13539-13)
determination by charged particle and photon activation, radiochemical separation methods for, 25:10488 (CEA-R-4072)
determination by charged particle and photon activation, reactions and sensitivities for, 25:10488 (CEA-R-4072)
determination in aluminum by charged particle activation and radiochemical separation, 25:10488 (CEA-R-4072)
determination in iron and niobium by photon activation and radiochemical separation, 25:10488 (CEA-R-4072)
determination in silicon by photon activation and radiochemical separation, 25:10488 (CEA-R-4072)
determination of trace amounts of, in biotite and tektite by spark source mass spectrometry, 25:10455
determination of trace amounts of, in molybdenum, review on, 25:10459
diffusion of thorium and uranium in columnar pyro-, effects of actinide content on, 25:11378 (ORNL-TM-2989)
enthalpy of solution in liquid plutonium, 25:11386
ion stopping in amorphous, electronic, (T), 25:11680
meson (μ^+) inelastic scattering at 12 GeV, determination of neutron form factor from cross section ratios of carbon and copper to hydrogen from, (E), 25:12096
meson reactions (π^-,π^0) at 70 MeV with natural, integrated cross sections for, (E), 25:12446
neutron elastic scattering at 0 to 2 MeV, angular distributions and total cross sections from, (E), 25:12379 (KAPL-P-3901)
neutron total cross sections at 0 to 2 MeV, review of, (E), 25:12379 (KAPL-P-3901)
plasma of, line shapes of resonance multiplets in, (E), 25:11881
solubility in sodium at 600 to 950°C, 25:10579

CARBON DIOXIDES
determination of carbon-14-labeled, in exhaled air for detection of digestion or metabolism disturbances, method for, 25:11168
effects on carburization of iron and steel by decomposing carbon monoxide, relations with composition, surface structure, and temperature, 25:11374 (DP-Report-530)
radiation effects on production of carbon-14-labeled, in rats, continuous, 25:10980
thermal conductivity at 100 to 1075°C, 25:10574
CO_2--O, radiolysis of, effects of sulfur hexafluoride on

yields of ozone from electron pulse, 25:10633
CARBON ISOTOPES
effects on reaction mechanisms, effects of temperature on kinetic, 25:10549
fractionation in stalagmites and stalactites, 25:10684
CARBON ISOTOPES C-12
alpha elastic and inelastic scattering at 166 MeV, optical potentials from DWBA analysis of angular distributions from, (E/T), 25:12549
alpha-particle model of, binding energy, elastic form factor, and rms radius from, (T), 25:12663
determination relative to carbon-13 or nitrogen-15 in biological samples by proton reaction methods, 25:10491 (ORNL-4636, pp 20-33)
deuteron elastic and inelastic scattering at 80 MeV, angular distributions and energy spectra from, (E), 25:10851 (NP-18570)
deuteron elastic scattering at 28 MeV, asymmetries in cross sections for, (E), 25:12309 (LYCEN-6909)
deuteron reactions (d,p) and (d,t) at 80 MeV, angular distributions and energy spectra from, (E), 25:10851 (NP-18570)
deuteron reactions (d,p) at 12.4 MeV, proton polarization from, (E), 25:12377 (INP-711)
energy levels from (p,γ) reactions, widths, branching ratios, and decay strengths for T = 2, (E), 25:12441
energy levels from alpha inelastic scattering at 166 MeV, deformation parameters for, (E/T), 25:12549
energy levels from beryllium-9 (He-3,γ) reactions, (E), 25:12388
energy levels of, projected Hartree--Fock and SU(3) calculations of, (T), 25:12412
energy of second excited state of, (E), 25:11565
helium-3 reactions (He-3,n) at 0.9 to 1.9 MeV, excitation function and threshold energy for, (E), 25:12402
lithium-6 reactions at 9 to 14 MeV, analysis for reaction mechanisms in, (E), 25:12418
meson (μ^-) capture by, relative yields and capture-rate ratios from, (E), 25:12395
meson (π) scattering near 180 MeV, strong absorption mechanism for, (E/T), 25:12420
meson (π^-) capture by, relative yields and capture-rate ratios from, (E), 25:12395
meson (π^+) inelastic scattering at 73 MeV, gamma spectra and cross sections for, (E), 25:12397
meson (π^-) inelastic scattering at 73 MeV, gamma spectra and cross sections for, (E), 25:12397
meson reactions (π^+,π^0) at 71.5 MeV, cross sections for, (E), 25:12397
meson reactions (π^-,π^0) at 73 MeV, cross sections for, (E), 25:12397
neutron elastic and inelastic scattering at 3.03 to 6.94 MeV, phase-shift analysis of angular distributions from, (E/T), 25:12401
neutron elastic scattering at 0 to 2 MeV, angular distributions and total cross sections from, (E), 25:12379 (KAPL-P-3901)
nuclear charge radius from Hartree--Fock treatment of center-of-mass motion, (T), 25:12653
photon reactions (γ,n) at 100 to 1050 MeV, cross sections for, (E), 25:12413
photon reactions (γ,π^+) and (γ,π^-) with, analysis using transition amplitude from impulse approximation, (T), 25:12407
proton scattering at 10.3 to 21.6 MeV, cross sections for, (E), 25:12497
reactions (C-12,C-13) with beryllium-9 at 12 and 15 MeV, DWBA analysis of angular distributions from, (E/T), 25:12382 (NP-18546)
reactions (C-12,p) and (C-12,α) with copper-63 at 49 to 88 MeV, proton and α angular distributions and energy spectra from bromine-75 compound nucleus in, (E), 25:12461
reactions with silver at 86 MeV, analysis for reaction mechanisms in, (E), 25:12606
scattering by beryllium-9 at 12 to 21 MeV, optical-model analysis of angular distributions from, (E/T), 25:12382 (NP-18546)
CARBON ISOTOPES C-13
alpha reactions (α,n) at 2.9 to 4.9 MeV, polarization excitation functions and angular distributions from, (E), 25:12390
concentration in carbonates along stalagmite and stalactite layers, 25:10684
determination relative to carbon-12 in biological samples by proton reaction methods, 25:10491 (ORNL-4636, pp 20-33)
electron elastic scattering by, cross section and form factors for, (E), 25:12376 (AD-710383)
energy levels from neutron elastic and inelastic scattering by carbon-12, spin--parity assignments for, (E/T), 25:12401
helium-3 reactions (He-3,αγ) and (He-3,γ) with, differential cross sections for, (E), 25:12388
lithium-6 reactions (Li-6,d) at 18 MeV, energy levels of oxygen-17 from, (E), 25:12425
lithium-7 reactions (Li-7,t) at 17 MeV, energy levels of oxygen-17 from, (E), 25:12425
oxygen-16 elastic scattering at 14 to 20 MeV, optical- and smooth-cutoff-model analysis of angular distributions from, (E/T), 25:12382 (NP-18546)
oxygen-16 reactions (O-16,O-17) at 14 to 20 MeV, DWBA analysis of angular distributions from, (E/T), 25:12382 (NP-18546)
oxygen-18 elastic scattering at 12 to 31 MeV, angular distributions from, (E/T), 25:12381 (NP-18541)
oxygen-18 reactions (O-18,O-19) at 15 to 24 MeV, DWBA analysis of angular distributions from, (E/T), 25:12381 (NP-18541)
CARBON ISOTOPES C-14
beta spectrum, (E), 25:12380 (KFK-1222)
determination in galactose in blood cells by scintillation counting, 25:10485
determination in high radiation background, spherical proportional detector with anticoincidence scintillation detector for, 25:10843
determination in polyacrylamide gels by fractionation and scintillation counting, 25:10478
determination of, computer system for proportional detector for low-level, 25:10833
exchange between carbon dioxide and carbon monoxide in quartz vessel at 550 to 970°C, 25:10541
proton reactions (p,γ) at 1.3 to 2.6 MeV, γ spectra and angular distributions for, (E), 25:12416
use as tracer for carbon dioxide production from continuously irradiated rats, 25:10980
use of butylamine-incorporated, for determining monoamine oxidase content of human serum, 25:10922
use of glyceryltrioleate- or oleic acid-incorporated for measuring carbon dioxide in exhaled air for detection of digestion or metabolism disturbances, 25:11168
CARBON ISOTOPES C-15
beta decay of, half-life for, (E), 25:12394
CARBON MONOXIDES
effects on carburization of iron and steels, relations with carbon dioxide, composition, oxygen, surface structure, temperature, and water vapor, 25:11374 (DP-Report-530)
radiation effects on, design of apparatus for spectral studies on 1.5-MeV electron, 25:10585 (JAERI-5026, pp 153-5)
radio emission from, in IRC + 10216, (E), 25:11568
CO-He, radiolysis of mixtures of, carbon deposition by gamma, 25:11474(R) (BNWL-842)
CARBON SYSTEMS
C--O--Pu--U, phase equilibria in, prediction of, 25:11525
C--Pu, thermodynamic properties at 900 to 2200°K, 25:11506
C--Pu--U, phase diagrams of, isothermal, 25:11524
C--UO_2, production from uranyl nitrate--sugar solutions by spray calcination, 25:11474(R) (BNWL-842)
C--UO_2, production of mixtures of, by reactions of sugar with uranyl nitrate in spray calciners, 25:11478 (BNWL-843)
C--UO_2, reactions with nitrogen at 1600°C to produce uranium carbide, efficiency of, 25:11478 (BNWL-843)
CARBON TETRACHLORIDE
effects on γ- and uv-radioinduced sulfoxidation of alkanes, 25:10592 (BMBW-FBK-70-25)
solvent properties from iodine in presence of antimony, 25:10674
CARBONACEOUS ROCKS
analysis of standard, for trace amounts of elements by x-ray fluorescence, 25:10449
CARBONATES
isotope fractionation in, of stalagmites and stalactites, carbon and oxygen, 25:10684
CARDIAC PACEMAKERS
development of implantable radioisotope-fueled, fabrication and testing programs for, 25:10777(R) (NUMEC-4189-3)
CASTING
book: Use of Isotopes in Casting Practice (In Russian), 25:10780
CATALASE
effects on x-radiosensitivity of acatalasemic and normal mice, 25:11264
CATALYSTS
particle size in fertilizer, determination by beta backscattering, 25:10784
CATS
radiation effects on reflex response of peripheral systems in, to simultaneous stimulation of mechanoreceptors in different visceral organs, x, 25:11282
radiation effects on sleep patterns in, whole-body γ, 25:11261
CATTLE
strontium-90 uptake by, during 1965 to 1969, 25:11050
testosterone content of blood of, double isotope dilution combined with crystallization technique for measuring, 25:10923
CAVITIES
formation by contained 100 kt underground nuclear explosions, 25:10741
CAVITY RESONATORS
description of superconducting wired-wall, for V-band ENDOR, 25:11850
CELL MEMBRANES
radioinduced deposition of supernumerary surface, in amoeba, x, 25:11249

CELLS
injection of allogeneic spleen, into x-irradiated mice, effects of, on antibody production, 25:10994
radiation effects on carcinoma, in mice, effects of dose fractionation on, 25:11257 (BNL-50203, pp 210-14)
radiation effects on count of bone marrow, in comparison to effects of injection of methioninesulfoximine, x, 25:11288
radiation effects on erythrocyte stem, as baseline studies for scanning radioisotopes, localized, 25:11112
radiation effects on hamster, effects of hypoxia on recovery from, 25:11224 (BNL-50203, pp 318-38)
radiation effects on interrelations of cytoplasm and nuclei of, review of ionizing, 25:10977
radiation effects on lymphoma, effects of age on neutron and γ, 25:11095 (BNL-50203, pp 308-17)
radiation effects on mitotic index in stem, effects of acute exposure and dose fractionation on 500 R x, 25:11279
radiation effects on oxygen supply in carcinoma and sarcoma, in mice and rats, x, 25:11258 (BNL-50203, pp 242-54)
radiation effects on plaque-forming, in mice following injection of spleen cells from mice treated with DMBA, 25:10990
radiation effects on population kinetics of stem, in bone marrow of rats, design of model for compartmental analysis of, 25:11290
radiation effects on sarcoma, in rats in vitro, effects of dose fractionation on fast neutron and x, 25:11240 (BNL-50203, pp 339-52)
radiation effects on survival of rat myocardial, effects of argon laser microbeam exposure of mitochondria on, 25:11242
radiation effects on survival of, review of repair mechanisms for, 25:11252 (BNL-50203, pp 54-69)
radioinduced aberrations in chromosomes in, of Crepis capillaris seedlings in combination with caffeine, 25:11015

CELLS, CULTURED
chromosome aberrations induced in, following growth in x irradiated culture media, 25:10970
radiation effects on growth of Chinese hamster, effects of crowding on x, 25:11239 (BNL-50203, pp 117-29)
radiation effects on mitosis in sot, γ, α, 25:11272
radiation effects on polyoma, Rous, and sarcoma 180 tumor production in fibroblastic, effects of cell population density on x, 25:11274
radiation effects on survival of Chinese hamster, x, 25:11097
radiation effects on survival of Chinese hamster, model for studying γ, 25:11293
radiation effects on, from mice, effects of time between exposure and administration on protective effects of gallic acid propyl ester against γ, 25:11106
radioinduced chromosome aberrations in Ehrlich's ascites, effects of temperature on γ, 25:11014
radioinduced single-strand breaks of DNA of P388 F, effects of dose rate on electron, 25:11028
radiosensitivity of C3H tumor, in mice, effects of oxygen on, 25:11094 (BNL-50203, pp 215-33)
radiosensitivity of Chinese hamster, effects of age on x, 25:11093 (BNL-50203, pp 97-116)
radiosterilization of mammalian, for use as transplants, 25:11330
survival of Chinese hamster, effects of fractionated administration of dactinomycin on, 25:11097

CELLS, HeLa
radiation effects on extraction of DNA from, following lysis, effects of dose and temperature on uv, 25:10975

CELLS, L
radiation effects on DNA synthesis in cultured, molecular basis for effects of exogenous DNA on restoration following x, 25:11243
radiation effects on survival of, effects of DNA on x, 25:10960 (BNL-50203, pp 82-90)
radioinduced lesions in, effects of methotrexate and temperature on, 25:11092 (BNL-50203, pp 41-53)

CEREALS
flour, radiation processing of, effects of, on reactions of molecular by-products with thiobarbituric acid, γ, 25:10978
rye, radiation effects on glycolytic enzyme activity in dormant and sprouting seeds of, γ, 25:10974

CERIUM
determination of trace amounts of, in biotite and tektite by spark source mass spectrometry, 25:10455
determination of trace amounts of, in phosphate deposits by spark source mass spectrometry, 25:10456
determination of trace amounts of, in rocks and sand by thermal neutron activation, ion exchange, and γ spectrometry, 25:10492
magnetic susceptibility of alpha-, effects of pressure and superconducting transition on, 25:12018
separation from aqueous solutions by solvent extraction using bis(2,2-dimethylhexyl) phosphate, 25:10679
separation from Egyptian Monazite sand, process for, 25:10683
spectra of, ultraviolet absorption, 25:11698
spin compensation of alpha-, 25:12016
yields from β radiolysis of aerated acidified water, 25:10636

CERIUM ALLOYS AND SYSTEMS
Al--Ce, electric conductivity of $CeAl_2$, crystal-field effects on spin-disorder contribution to, (T), 25:12009
Ce--Fe, phase diagram, crystal structure, and magnetic properties of, 25:12025
Ce--La-base, Kondo effect in fcc and dhcp, effects of pressure on, 25:11990
Ce--Th, magnetic susceptibility of, temperature dependence of, 25:12016

CERIUM ISOTOPES Ce-140
deuteron reactions (d,He-3) with, energy spectra and angular distributions from, (E/T), 25:12552
energy levels from lanthanum-139 (He-3,d) reactions, shell-model calculations of, (E/T), 25:12552
energy levels from praseodymium-141 (d,He-3) reactions, (E), 25:12558
helium-3 reactions (He-3,d) with, angular distributions for, (E), 25:12558
neutron capture by, gamma spectra from thermal, (E), 25:12551

CERIUM ISOTOPES Ce-141
content in Fayetteville, Arkansas rainwater, Nov. 1968 to Oct. 1969, effects of 1968 Chinese nuclear explosion on, 25:10709 (ORO-2529-28, App. 3)
energy-level transitions from thermal neutron capture by cerium-140, relative intensities of, (E), 25:12551

CERIUM ISOTOPES Ce-144
content in Fayetteville, Arkansas rainwater, July and Aug. 1969, 25:10707 (ORO-2529-28, App. 1)
content in Fayetteville, Arkansas rainwater, Nov. 1968 to Oct. 1969, effects of 1968 Chinese nuclear explosion on, 25:10709 (ORO-2529-28, App. 3)
content of biological materials, gamma scintillation spectrometry method for, 25:11044
content of biological materials, use of γ spectrometry for differentiating iron-59 and praseodymium-144 from, 25:11044

CERIUM OXIDES
spectra of, ultraviolet absorption, 25:11698
structure of nonstoichiometric Ce/sub 1+y/O_2, electric conductivity study of defect, (E/T), 25:12033

CESIUM
determination in metamorphic rocks by neutron activation and γ spectrometry, 25:10508
determination in seawater by neutron activation, 25:10428
determination of trace amounts of, in biotite and tektite by spark source mass spectrometry, 25:10455
determination of trace amounts of, in molybdenum, review on, 25:10459
determination of trace amounts of, in rocks and sand by thermal neutron activation, ion exchange, and γ spectrometry, 25:10492
energy-level transitions in, rates of Auger and x-ray, (T), 25:11685
neutron reactions at 14.8 MeV with, 25:10472(R) (BMBW-FBK-70-19)

CESIUM CHLORIDES
separation of cesium-134 from, using saponite-type montmorillonite, 25:10793 (BARC-506)

CESIUM ISOTOPES Cs-131
energy levels from barium-131 electron-capture decay, spin--parity assignments for, (E/T), 25:12532 (TID-25592)
energy-level transitions from barium-131 electron-capture decay, energies, intensities, internal conversion coefficients, and multipolarities for, (E/T), 25:12532 (TID-25592)

CESIUM ISOTOPES Cs-133
neutron capture by, average circular γ polarization in thermal, (E), 25:12601

CESIUM ISOTOPES Cs-134
energy levels from thermal neutron capture, spin for compound, (E), 25:12601
separation from cesium chloride by treatment with saponite-type montmorillonite, 25:10793 (BARC-506)

CESIUM ISOTOPES Cs-137
accumulation in body of animals, effects of diet on, 25:10956
accumulation in man and mammals of northern Soviet Union, determination of decontamination time, 25:11037 (NP-18381)
content in cow's milk in Bulgaria, 25:10480
content in Fayetteville, Arkansas rainwater, July and Aug. 1969, 25:10707 (ORO-2529-28, App. 1)
content in Fayetteville, Arkansas rainwater, May 1965 to April 1970, effects of Chinese nuclear explosions on, 25:10713 (ORO-2529-28, App. 7)
content of atmospheric precipitation, milk, and reindeer meat in Sweden during 1959 to 1969, 25:11004
content of caribou and reindeer meat in Alaska during 1969, 25:11001
content of human diet in USA during 1969, 25:11040
content of milk in South America in 1967, 25:11068
content of milk in USA during February 1970, 25:11040
content of milk sampled throughout Central, North, and South America during July 1969 to July 1970, 25:11002
content of surface waters sampled in New York State during January to July 1969, 25:11041

content ratio to strontium-90 in worldwide atmospheric and surface soil samples, 25:10718
determination in biological materials by sorption on ammonium molybdophosphate, precipitation, and beta counting, 25:10482
determination in milk by scintillation counting, 25:10480
determination in phosphate glass and spray solidified waste melt samples, direct count method for, 25:10658(R) (BNWL-1533)
energy levels from quasi-particle Tamm--Dancoff approximation, spin--parity assignments, single-particle energies, eigenvectors, electromagnetic moments, and spectroscopic factors for, (T), 25:12616
energy-level transitions from quasi-particle Tamm--Dancoff approximation, rates for M1 and E2, (T), 25:12616
monitoring in Ottawa River in vicinity of Chalk River, 25:11074(R) (AECL-3777)
transport in roots of Adenostoma, Ceanothus, and Quercus, 25:10955
transport through mushroom-deer meat-man food chains, 25:11003
uptake by bean and tomato seedlings in culture media in comparison to forage plants, 25:10936 (UCB-34-P-23-15)
CHALK RIVER AREA (ONTARIO)
radiation monitoring of environs of, 25:11074(R) (AECL-3777)
CHARCOAL
diffusion of xenon-133 through adsorber beds of activated, dispersion model to characterize time-dependent, 25:10582
CHARGED-PARTICLE BEAMS
interactions with magnetized plasma, return current from relativistic, (T), 25:11886 (NYO-4077-1, Paper 4)
interactions with semi-infinite plasma, double Laplace transformations for, 25:11889
potential calculation for, with bi-gaussian charge distribution in transverse plane, 25:12308 (LAL-RT-5-70)
transport magnets for, field harmonic analysis of short, current-dominated, 25:12323
CHARGED PARTICLES
dosimetry of, effects of displacement of target on accuracy in calculations of, 25:11069
interactions with transverse rotating electromagnetic field, electrodynamic analog of wave diffraction phenomena in, (T), 25:12156
motion in magnetic fields, generation of first and second order transformation elements for, 25:12327
precipitation in aurorae, flux measurements of, (E), 25:11778 (AD-709105)
production from Coulomb and transverse-radiation-field interactions, asymptotic states in time development of phase factor and wave function of coherent field for, (T), 25:12249
radiations from, in strong magnetic fields, 25:12059
reactions with Z = 1 to 98 nuclei, nuclear data tables list for, 25:12366
reflection by uniform electric fields, conformal-mapping studies for, 25:12045 (IPPJ-T-4)
theory for dyons, relativistic quantum mechanical, 25:12047 (NYO-3829-65)
trajectories in magnetic fringe fields, (T), 25:12322
CHEMICAL REACTIONS
dynamics of atomic and molecular, 25:12886(R) (COO-2092-1)
mechanisms of electron-transfer, research progress on, 25:10515(R) (COO-1780-14)
CHILE
radioactivity in air and milk in, measurement of fallout, 25:11068
CHIMERAS
spectra of isoenzymes of lactic dehydrogenase in radiation, of mice injected with rat myeloid cells, 25:10992
CHLORATES
separation from chlorides, paper chromatographic, 25:10687
CHLORIDES
radioprotective effects of, on DNA, nucleotides, and nuclectides against γ, 25:10962
separation from chlorates, paper chromatographic, 25:10687
CHLORINE
determination by photon activation, reactions and sensitivities for, 25:10488 (CEA-R-4072)
determination in α-lin-poly-p-xylylene by thermal neutron activation and γ spectrometry, molecular weight from, 25:10512
determination in soils and rocks, neutron radiometric gage for borehole, 25:10889(P)
determination of trace amounts of, in biotite and tektite by spark source mass spectrometry, 25:10455
determination of trace amounts of, in molybdenum, review on, 25:10459
determination of trace amounts of, in rocks and stony meteorites by neutron activation and radiochemical separation, 25:10493
reactions of trivalent, with tetravalent uranium, 25:10515(R) (COO-1780-14)
CHLORINE IONS
spectra in lanthanum chloride monocrystals, ENDOR, 25:10570(R) (COO-294-10)
CHLORINE ISOTOPES Cl-33
energy levels from proton resonances in sulfur-32, spin--parity assignments and resonance parameters for, (E/T), 25:12506
CHLORINE ISOTOPES Cl-34
beta decay of, spectra and end-point energy from, (E), 25:12442
energy levels from sulfur-32 (helium-3,p) reactions, lifetimes, spins, and parities of, (E), 25:12493
CHLORINE ISOTOPES Cl-35
energy levels from alpha resonances in phosphorus-31 and proton resonances in sulfur-34, isospin--spin assignments for, (E), 25:12442
energy levels from sulfur-34 (d,n) and (p,γ) reactions at 1 to 5 MeV, lifetimes and spin-parity assignments for, (E), 25:12440
energy-level transitions from sulfur-34 (d,n) and (p,γ) reactions at 1 to 5 MeV, multipolarities, mixing ratios, and branching ratios for, (E), 25:12440
CHLORINE ISOTOPES Cl-36
abundance in Apollo 11 samples, (E), 25:11539
CHLORINE ISOTOPES Cl-37
effects on microwave spectra, structure, quadrupole coupling constant, and force constants of nitrogen sulfide chloride, 25:10532
CHLORMERODRIN
radiolysis of mercury-203-labeled, yields from γ, 25:10641
thermal decomposition of, yields from, 25:10641
CHLOROFORM
carbon--hydrogen stretching band in, effects of deuterium and solvents on, 25:10540
effects on γ- and uv-radioinduced sulfoxidation of alkanes, 25:10592 (BMBW-FBK-70-25)
radiolysis of vaporous, Arrhenius parameters for hydrogen-atom abstraction reaction of dichloromethyl radicals in x, 25:10629
CHLOROPHYTA
Oedogonium cardiacum, radiation effects on survival of, effects of hypoxia or aerobic conditions on recovery from, 25:11304 (BNL-50203, pp 70-81)
CHLOROPLASTS
radiosensitivity in leaves, effects of red light on γ, 25:11310
CHLOROURANATES
preparation and properties of UCl_6^-, 25:10576
CHOLESTANOL
radiolysis at room temperature, yields of products from γ, 25:10624 (JAERI-5026, pp 160-4)
CHOLINESTERASE
radiation effects on activity of, in blood and tissues of rats following injection of mixed radioisotopes, 25:10968
CHROMATOGRAPHY
equipment for automatic ion exchange, design and performance of, 25:10659 (CEA-N-1267)
CHROMIUM
antiferromagnetic energy gap in, from optical absorption measurements at 4.2°K, 25:11987
corrosion by liquid lead at high temperatures, 25:11376 (JUL-661-RW)
determination as impurity in fuel materials by emission spectroscopy, 25:10432 (KFK-1261)
determination in sedimentary rocks by direct-reading spectrometry, 25:10450
determination in serum and urine by flameless atomic absorption spectroscopy, 25:10464
determination of trace amounts of, in basalt and granite, correction of matrix effect in uv spectrographic, 25:10453
determination of trace amounts of, in biotite and tektite by spark source mass spectrometry, 25:10455
determination of trace amounts of, in molybdenum, review on, 25:10459
determination of trace amounts of, in rocks, quantometer for spectroscopic, 25:10451
determination of trace amounts of, in silicate rocks, method for elimination of matrix effect in quantometric, 25:10452
determination of trace amounts of, in standard silicate rocks using sodium chloride buffer, emission spectrographic, 25:10454
determination of trace amounts of, in zirconium, carrier distillation method for spectrographic, 25:10430 (EUR-4541)
diffusion in aluminum oxide, research on, 25:11472(R) (AD-708705)
photon inelastic scattering at 12 to 30 MeV, differential cross sections for, (E), 25:12463
reactions with folic acid, stability constants of complexes from, 25:10520
separation of trivalent and hexavalent, paper chromatographic, 25:10687
solubility in lead at 350 to 1100°C, 25:11376 (JUL-661-RW)
CHROMIUM ALLOYS AND SYSTEMS
Al--Cr--Ni-base, creep at high temperatures, effects of cold rolling and shock loading on, 25:11434(R) (SU-326-P-17-X-1)

XUM

Cr--Cu--Zr-base, phase transformations in, effects of continuous cooling on, 25:11432 (CEA-N-1310)
Cr--Fe--Ni, radiation effects on mechanical properties of, in water, fast neutron, 25:11466 (SRARI-P-78)
Cr--Fe-base, properties of aged, effects of reheating on electric and mechanical, 25:11403
Cr--Fe-base--V, properties of aged, effects of reheating on electric and mechanical, 25:11403
Cr--Ni-base, production of controlled grain-size, method for, 25:11434(R) (SU-326-P-17-X-1)
Cr--Ni-base, strength and initial work hardening rate of, effects of microstructure on, 25:11402
Cr--Ni-base--ThO_2, strength and initial work hardening rate of, effects of microstructure on, 25:11402
Cr-base--Mn, antiferromagnetic energy gap from optical absorption measurements at 4.2°K, 25:11987
Cr-base--Re, antiferromagnetic energy gap from optical absorption measurements at 4.2°K, 25:11987
Cr-base--W, neutron inelastic scattering study of in-band resonant modes in, 25:12019
Cr-base--W, phonon properties of, inelastic neutron scattering study of in-band resonant modes, 25:11985

CHROMIUM ISOTOPES Cr-50
determination in labeled erythrocytes by neutron activation and γ spectroscopy, 25:10503

CHROMIUM ISOTOPES Cr-51
effectiveness of EDTA-incorporated, for determining renal blood flow in hypertensive patients, comparison studies on, 25:11153
effectiveness of EDTA-incorporated, or inulin-incorporated, for determining renal clearance, evaluation of, 25:11156
effectiveness of inulin-incorporated, for determining renal blood flow in hypertensive patients, comparison studies on, 25:11153
energy levels from titanium-48 (α,nγ) and vanadium-51 (p,nγ) reactions, spin--parity assignments for, (E), 25:12435
energy levels from vanadium-51 (p,n) and (p,nγ) reactions, spin--parity assignments for, (E/T), 25:12476
energy-level transitions from titanium-48 (α,nγ) and vanadium-51 (p,nγ) reactions, branching ratios for, (E), 25:12435
energy-level transitions from vanadium-51 (p,n) and (p,nγ) reactions, intensities and branching ratios for, (E/T), 25:12476
incorporation in yeast cells, 25:10908
use for kidney scanning in hypertensive patients in comparison to /super 99m/Tc scintigraphy and vasoconstrictor content in the renal vein, 25:11163
use for labeling erythrocytes for scanning of human spleen, 25:11200
use for labeling erythrocytes for use in spleen scanning, 25:11201
use of EDTA-incorporated, for determination of glomerular clearance in comparison to inulin, slope method for, 25:11154
use of EDTA-incorporated, for determining renal clearance in combination with whole-body counting, development of method for, 25:11155
use of erythrocyte-incorporated, for studying blood exchange between parabiotic mice, 25:10915
use of heat treated erythrocytes-incorporated, for determining splenic blood flow in man, 25:11142

CHROMIUM ISOTOPES Cr-52
oxygen-16 reactions with, 25:10583(R) (AECL-3776)
proton elastic and inelastic scattering at 5.38 to 5.95 MeV, cross-section and polarization angular distributions and excitation functions from, (E), 25:12433 (NP-18552)

CHROMIUM ISOTOPES Cr-53
energy levels of, core-plus-particle model for low-lying, 25:12494

CHROMOSOMES
aberrations induced in cultured mammalian cells following growth in x-irradiated culture media, 25:10970
radioinduced aberrations of, in corneal epithelium of mice, neutron, x, 25:11018
radioinduced aberrations of, in Crepis capillaris seedlings following incorporation of strontium-90--yttrium-90, β, 25:11013
radioinduced aberrations of, in Crepis capillaris seedlings in combination with caffeine, 25:11015
radioinduced aberrations of, in peripheral lymphocytes of children following diagnostic exposure, x, 25:11113
radioinduced aberrations, in Ehrlich's ascites carcinoma cells, effects of temperature on γ, 25:11014
radioinduced breaks in, review of effects of postexposure time on, 25:10977
radioinduced deletion aberrations in, of maize, effects of pollen exposure on x, 25:11023
radioinduced deletions on proximal heterochromatin of third, in Drosophila melanogaster, x, 25:11012
radioinduced mutations in, of Chrysanthemum morifolium, γ, 25:11031
volume in diploid and tetraploid seedlings of marigolds, petunias, and zinnias, effects of, on x-radiosensitivity of plants, 25:11020

CHROMOSPHERE
spectra of, three-component model for formation of Ca II K line in, (T), 25:11615
structure of, model of upper, (E/T), 25:11614

CIRCUITS
fabrication of printed circuit boards, 25:12864 (ANL-7725)
radioinduced failure of integrated, 25:10906
vibrations of R(t)CL, 25:12911(T) (SC-T-71-3003)

CIRCULATORY SYSTEM
conference on clinical aspects of, 25:11192
conference on scanning of, 25:11118
radiation effects on reflex response of, in cats to simultaneous stimulation of mechanoreceptors in different visceral organs, x, 25:11282

CITRIC ACID
analysis for moisture content by neutron scattering and moderation, 25:10486

CLOMIPHENE
effects on γ-irradiated pregnant rats, 25:11104

CNIDARIA
age of fossil, helium/uranium method for estimation of, 25:10725(R) (CU-3139-4)
amino acid content of fossil, (E), 25:10725(R) (CU-3139-4)

COATINGS
deposition of thin, design of ultrahigh vacuum system for, 25:10805(P)
effects of radioprotective, on heat absorption by glass, 25:10770

COBALT
determination in presence of selenium by on-stream neutron activation and γ spectrometry, design of equipment for, 25:10500
determination in seawater by neutron activation, 25:10428
determination in sedimentary rocks by direct-reading spectrometry, 25:10450
determination in serum and urine by flameless atomic absorption spectroscopy, 25:10464
determination of trace amounts of, in biotite and tektite by spark source mass spectrometry, 25:10455
determination of trace amounts of, in molybdenum, review on, 25:10459
determination of trace amounts of, in rocks and sand by thermal neutron activation, ion exchange, and γ spectrometry, 25:10492
determination of trace amounts of, in rocks, quantometer for spectroscopic, 25:10451
determination of trace amounts of, in silicate rocks, method for elimination of matrix effect in quantometric, 25:10452
determination of trace amounts of, in standard silicate rocks using sodium chloride buffer, emission spectrographic, 25:10454
determination of trace amounts of, in Zircaloy-2 and zirconium, carrier distillation method for spectrographic, 25:10430 (EUR-4541)
distribution coefficient in mixtures of acetone, hydrochloric acid, and methanol, 25:10681
friction and wear of, sliding against copper and iron rings under vacuum, 25:11413
magnetic torque measurements on films of, on copper single-crystal substrate, 25:11981(R) (ORO-3674-4)
properties of films of, magnetic and structural, 25:12896 (NYO-3087-21)
radiation effects on point-defect creation and annihilation in, at 20°K, 1.4-, 2.2-, and 3.0-MeV electron, (E), 25:11949(T) (AI-Trans-267)
separation from copper and zinc by gas chromatography using aluminum chloride eluent, 25:10666 (JINR-P6-5410)
separation of neptunium from, by ion exchange in tetramethylammonium hydroxide--citrate solutions, effects of complexing agents on, 25:10655 (ANL-7751)

COBALT ALLOYS AND SYSTEMS
Co--Sm, sintering of Co_5Sm to high density with high coercive force, 25:11361
Co--Cu--Sm, magnetic rotational hysteresis loss of $SmCo_4Cu$ and $SmCo_{3.5}Cu_{1.5}$, critical field and temperature dependence of, 25:11984
Co--Dy, hyperfine interactions in $DyCo_2$, dysprosium-161 Moessbauer study of, 25:12035
Co--Sm, Bloch wall lattices in $SmCo_5$, disclination structures in, 25:12011
Co--WC, fracture of, electron microscope study of effects of carbide crystal size on, 25:11514
Co--WC, mechanical properties of sintered, continuum mechanics analysis of, 25:11515

COBALT FLUORIDES
reactions in, emf measurements of solid-state displacement, 25:11473(R) (AD-708712)

COBALT ISOTOPES Co-55
energy levels from iron-54 (α,t) reactions at 44 MeV, spectroscopic factors and spin--parity assignments for, (E/T), 25:12434

COBALT ISOTOPES Co-57
effectiveness of vitamin B 12-incorporated, for determining glomerular filtration rate in combination with iodine-131-labeled orthohippuric acid for blood flow measurements, 25:11157
effectiveness of vitamin B 12-incorporated, for determining renal blood flow in hypertensive patients, comparison studies on, 25:11153

use for kidney scanning in hypertensive patients in comparison to /super 99m/Tc scintigraphy and vasoconstrictor content in the renal vein, 25:11163
use of vitamin B 12-incorporated, for determination of glomerular clearance in comparison to inulin, slope method for, 25:11154
COBALT ISOTOPES Co-58
neutron capture cross sections for, thermal, 25:10583(R) (AECL-3776)
COBALT ISOTOPES Co-59
alpha elastic scattering at 27.5 MeV, optical-model analysis of angular distributions using elementary nucleon--nucleon interactions from, (T), 25:12627 (INP-720)
oxygen-16 reactions (O-16,α) and (O-16,p) at 49 to 88 MeV, proton and α angular distributions and energy spectra from bromine-75 compound nucleus in, (E), 25:12461
proton reactions (p,n) and (p,nγ) at 2.4 to 3.3 MeV, gamma spectra and comparison of Hauser--Feshbach theory with neutron and gamma yields from, (E/T), 25:12476
proton reactions at 170 to 370 MeV, cross sections for spallation products from, (T), 25:12439
COBALT ISOTOPES Co-60
abundance in Allende meteorite, (E), 25:11540
metabolism in rats, chelate of 1-nitroso 2-naphthol with, 25:10958
uptake by edible plants in vicinity of Chalk River, 25:11074(R) (AECL-3777)
COBALT OXIDES
preparation of monocrystalline, method for, 25:11472(R) (AD-708705)
B_2O_3--CoO--CoS, phase studies of, 25:11526
COBALT SULFATES
crystallization of hydrates of, from tritiated solutions, fractionations of tritium in, 25:10688
COBALT SULFIDES
B_2O_3--CoO--CoS, phase studies of, 25:11526
COINCIDENCE MEASUREMENTS
method for simultaneous true and random, 25:10894 (NP-18614)
COLLAGEN
radiation effects on, following use of sterilization of aorta transplants, γ, 25:11341
COLLIMATORS
design for irradiation facility sources, 25:10781(P)
COLOMBIA
radioactivity in air and milk in, measurement of fallout, 25:11068
radioisotope ingestion by human population of, for feasibility studies of proposed Atlantic-Pacific interoceanic canal, estimation of potential, 25:10995 (BMI-171-45)
COLUMBIA RIVER
limpet snail growth in, effects of heated effluents on, 25:10996 (BNWL-1537)
temperature of waters of, effects of Hanford reactor effluents on, 1964 to 1970, (E), 25:10691 (BNWL-1345)
COMMUNICATION SYSTEMS
effects of relativity and solar quadrupole moment on time-delay measurements, (T), 25:11602
COMPUTER PROGRAMS
ACOFIS, for quantum field theory renormalized radiative corrections, in LISP for IBM 360-67, 25:12245 (CNRS-CPT-70-P-318)
BIGG 2, for kinetics of bare slab reactors, FORTRAN 63 for CDC 3600, 25:12842 (INR-1193)
COBRA, for coolant boiling in rod arrays of reactors, FORTRAN 4 for IBM 360, 25:12784 (KFKI-70-20-RPT)
CODAC, for processing TIMOC library from ENDF/B file, 25:12339 (EUR-4521)
COREGRAF 2, for kinetics of natural uranium fueled gas cooled graphite moderated reactor, FORTRAN 4 for CDC 6600 or IBM 360, 25:12774 (CEA-N-1344(1))
development for processing data for fissionable materials control in large research centers, FORTRAN, 25:10796 (KFK-866)
DPB, for optimization of short-term operation of electric power utility, for UNIVAC 1108, 25:12919 (WHAN-IR-47)
DYNA, for calculating crack growth and gas flow conditions for prestressed concrete pressure vessel with complete circumferential crack, FORTRAN IV, 25:10753 (GAMD-7567)
ELMOS, for solving the ellipsoidal modified oscillator problem of nuclear single-particle model, 25:12623 (AECL-3730)
EXPOSUM, for least-squares fitting of parameters in sum-of-exponential to given data samples, FORTRAN IV, 25:12837 (RISO-M-1279)
FARED, for liquid metal cooled fast breeder reactor kinetics, FORTRAN for CDC 6600, 25:12772 (BAW-3867-9(Vol.1)(Rev.1))
FOCAL, for control of neutron diffraction experiments, 25:11981(R) (ORO-3674-4)
for analysis of counting data from animal tissues, Fortran for CDC 6600, 25:10937 (UCRL-50957)
for analysis of highly resolved gamma spectra from unknown mixtures of radionuclides, for UNIVAC III, 25:12535
for CDC-211 display package, 25:12918 (WAPD-TM-987)
for constructing Feynman diagrams for calculating electron and meson (μ) anomalous magnetic moments, in LISP for UNIVAC 1108, 25:12136 (CNRS-CPT-70-P-336)
for fuel burnup in heavy water moderated pressure tube type reactors, FORTRAN 2 for IBM 1620, 25:12797 (IEA-186)
for pulse-height analysis for nuclear spectroscopy, in FORTRAN for Varian 622/i, 25:10848 (ANL-7704)
for visualization of nuclear spectra, for CII-90-10, 25:10892 (CEA-N-1363)
FORGOD, for solving the four-group neutron diffusion equations in one dimension, in FORTRAN IV for CDC 6600, 25:12335 (AECL-3671)
FRENEY, for quantum field theory renormalized radiative corrections, in FORTRAN for UNIVAC 1108, 25:12245 (CNRS-CPT-70-P-318)
LIFE 1, for performance of fast reactor cylinder shaped fuel elements, FORTRAN 4 for IBM 360, 25:12794 (ANL-7736)
MACYL6, for calculating incompressible fluid flow at high Reynolds numbers, 25:10765 (AD-709142)
MAGIC, listing and plotting service routine for multigroup cross-section code MC², in FORTRAN, 25:12337 (ANL-7654)
MERMC2, tape-handling service routine for multigroup cross-section code MC², in FORTRAN, 25:12337 (ANL-7654)
RABID, for calculating neutron slowing-down in slab cells by integral transport theory, in FORTRAN IV for IBM 360/75, 25:12336 (ANL-7645)
RITZ, for discovery of excited nuclear states according to Ritz combination principle, in FORTRAN IV for IBM 360 or 7074, 25:12519 (KFK-1247)
SYNTH 2, for neutron flux distribution in reactors, FORTRAN 4G for IBM 360, 25:12844 (TKK-F-A-121)
COMPUTERS
description of hybrid, for reactor control studies, 25:10895 (ORNL-TM-3101)
development at Chicago Univ, 25:12887(R) (COO-2094-2)
development for on-line monitoring of pressurized ion exchange chromatography process for purification of actinides, 25:10664 (DP-MS-70-38)
interface for analog-to-digital converter to Varian 622/i, for nuclear spectroscopy, 25:10848 (ANL-7704)
MUX, simple approach to on-line computing, 25:12890 (LA-4524)
performance for analysis of analog and digital data from radioisotope kidney scans, 25:11165
performance for analysis of renograms, 25:11161
CONCRETES
gamma-ray attenuation at 6 and 8 MeV in, 25:11947
shielding effectiveness of, against point-source γ radiation from fission products, 25:11948
CONNECTICUT YANKEE POWER REACTOR
cooling system components for, revised technical specifications for inspection of, 25:12728 (DOCKET-50213-92)
design parameters of, revised and additional data on, 25:12729 (DOCKET-50213-93)
operations aspects of, revised and additional data on, 25:12729 (DOCKET-50213-93)
owners of, financial statements of, 25:12729 (DOCKET-50213-93)
pressure vessel for, thermal stress analysis for cooldown transient in, 25:12727 (DOCKET-50213-89)
CONNECTIVE TISSUE
radioinduced tumors in, of mammals, effects of clonogenicity, dose, reproductive integrity, and time on, 25:11253 (BNL-50203, pp 154-73)
CONTAINMENT SYSTEMS EXPERIMENT
fission product removal from, effects of natural transport processes on, (E/T), 25:12803 (BNWL-1457)
CONVERSION ELECTRONS
spectra measurements of, solenoid transport system and silicon spectrometer for, 25:10855
CONVEYERS
design of link-type, for transfering radioactive material from shipping container to hot cell, 25:10803(P)
load weight on belts of, radiometric equipment for measurement of, 25:10785(P)
COPPER
alpha reactions at 30 to 80 MeV, cross sections for production of K x rays by, (E), 25:12488
analysis for oxygen by photon activation and radiochemical separation, 25:10501
content with zinc in Czech mineral deposits, gamma--gamma well logging method for determining, 25:10693
creep of, effects of microstructure on, 25:11434(R) (SU-326-P-17-X-1)
determination as impurity in fuel materials by emission spectroscopy, 25:10432 (KFK-1261)
determination by photon activation, reactions and sensitivities for, 25:10488 (CEA-R-4072)
determination in environmental samples by neutron activation, 25:10491 (ORNL-4636, pp 20-33)
determination in seawater by atomic absorption spectrophotometry, 25:10428
determination in sedimentary rocks by direct-reading spectrometry, 25:10450
determination in serum and urine by flameless atomic absorption spectroscopy, 25:10464
determination of trace amounts of, in biotite and tekti... by spark source mass spectrometry, 25:10455

determination of trace amounts of, in granite, correction of matrix effect in uv spectrographic, 25:10453
determination of trace amounts of, in molybdenum, review on, 25:10459
determination of trace amounts of, in phosphate deposits by spark source mass spectrometry, 25:10456
determination of trace amounts of, in rocks and sand by thermal neutron activation, ion exchange, and γ spectrometry, 25:10492
determination of trace amounts of, in rocks, quantometer for spectroscopic, 25:10451
determination of trace amounts of, in silicate rocks, method for elimination of matrix effect in quantometric, 25:10452
determination of trace amounts of, in standard bauxite, carbonate, and silicate rocks by x-ray fluorescence, 25:10449
determination of trace amounts of, in standard silicate rocks using sodium chloride buffer, emission spectrographic, 25:10454
determination of trace amounts of, in Zircaloy-2 and zirconium, carrier distillation method for spectrographic, 25:10430 (EUR-4541)
determination simultaneously with manganese in plants by neutron activation and radiochemical separation, 25:10509
deuteron reactions (d,x) at 5 to 40 MeV with natural, excitation functions for production of copper-61, -62, -64, and -66 and zinc-62, -63, and -65, (E), 25:12438
distribution coefficient in mixtures of acetone, hydrochloric acid, and methanol, 25:10681
effects on electric conductivity of gadolinium-doped barium titanates, 25:11472(R) (AD-708705)
effects on mechanical properties of niobium--titanium alloys, 25:11416
friction and wear of, sliding against copper and iron rings under vacuum, 25:11413
friction and wear on rings of, from sliding metal pieces under vacuum, 25:11413
hydrolysis equilibria in heavy water of divalent, measurement of deuterium ion concentration for determination of, 25:10566
mesons (μ⁺) inelastic scattering at 12 GeV, determination of neutron form factor from cross section ratios of carbon and copper to hydrogen from, (E), 25:12096
meson reactions (π⁻,π⁰) at 70 MeV with natural, integrated cross sections for, (E), 25:12446
radioinduced defects in, I/sub D/--I/sub E/ stage of annealing of electron, 25:11957
separation from cobalt and zinc by gas chromatography using aluminum chloride eluent, 25:10666 (JINR-P6-5410)
separation from ores by solvent extraction, review on, 25:10656 (BM-IC-8502)
separation of neptunium from, by ion exchange in tetramethylammonium hydroxide--citrate solutions, effects of complexing agents on, 25:10655 (ANL-7751)

COPPER ALLOYS AND SYSTEMS
Be--Cu, analysis for beryllium oxide inclusion using bromine--methanol solution, method for, 25:10440
Co--Cu--Sm, magnetic rotational hysteresis loss of $SmCo_5$,Cu and $SmCo_{7-8}Cu_{1-3}$, critical field and temperature dependence of, 25:11984
Cr--Cu--Zr-base, phase transformations in, effects of continuous cooling on, 25:11432 (CEA-N-1310)
Cu--Mo--Zr-base, phase transformations in, effects of continuous cooling on, 25:11432 (CEA-N-1310)
Cu--Ni--Zr-base, phase transformations in, effects of continuous cooling on, 25:11432 (CEA-N-1310)
Cu--Pu, diffusion in epsilon phase on welded couples of plutonium and, chemical, 25:11387
Cu--Zr-base, phase transformations in β phase of, effects of continuous cooling on, 25:11432 (CEA-N-1310)
Cu-base--Si, creep of, effects of microstructure on, 25:11434(R) (SU-326-P-17-X-1)
Cu-base--Zn, creep of, effects of microstructure on, 25:11434(R) (SU-326-P-17-X-1)
Cu-base--Zn, plastic stability of, effects of zinc-induced defect structure on, 25:11373(R) (COO-2048-1)

COPPER CHLORIDES
radiation effects on thermoelectric properties of molten, gamma, 25:11952

COPPER HYDROXIDES
precipitation of carrier-free silicon-31, 25:10675

COPPER IODIDES
radiation effects on thermoelectric properties of molten, gamma, 25:11952

COPPER ISOTOPES Cu-58
beta decay of, beta intensities, log-ft values, and gamma spectra from, (E/T), 25:12481

COPPER ISOTOPES Cu-59
energy levels from nickel-58 (α,t) reactions at 44 MeV, spectroscopic factors and spin--parity assignments for, (E/T), 25:12434
energy levels of, shell-model calculation using Kuo-Brown matrix elements, (T), 25:12451

COPPER ISOTOPES Cu-61
production from natural copper (d,x) reactions at 5 to 40 MeV, excitation functions for, 25:12438

COPPER ISOTOPES Cu-62
production from natural copper (d,x) reactions at 5 to 40 MeV, excitation functions for, 25:12438

COPPER ISOTOPES Cu-63
alpha inelastic scattering at 21 MeV, spin dependence in, (E), 25:12454
carbon-12 reactions (C-12,p) and (C-12,α) at 49 and 88 MeV, proton and α angular distributions and energy spectra from bromine-75 compound nucleus in, (E), 25:12461
deuteron inelastic scattering at 14 MeV, spin dependence in, (E), 25:12454
energy levels of, shell-model calculation of low-lying, 25:12459
helium-3 inelastic scattering at 21 MeV, spin dependence in, (E), 25:12454
neutron reactions (n,γ), 2DB code for calculation of spectral-averaged cross sections for, 25:11474(R) (BNWL-842)

COPPER ISOTOPES Cu-64
effectiveness for scanning of human liver, 25:11198
production from natural copper (d,x) reactions at 5 to 40 MeV, excitation functions for, 25:12438

COPPER ISOTOPES Cu-65
alpha inelastic scattering at 21 MeV, spin dependence in, (E), 25:12454
deuteron inelastic scattering at 14 MeV, spin dependence in, (E), 25:12454
energy levels from nickel-64 (α,t) reactions at 44 MeV, spectroscopic factors and spin--parity assignments for, (E/T), 25:12434
energy levels of, shell-model calculation of low-lying, 25:12459
helium-3 inelastic scattering at 21 MeV, spin dependence in, (E), 25:12454

COPPER ISOTOPES Cu-66
production from natural copper (d,x) reactions at 5 to 40 MeV, excitation functions for, 25:12438

COPPER SULFATES
crystallization of hydrates of, from tritiated solutions, fractionations of tritium in, 25:10688
thermal properties of deuterated pentahydrates of, 25:10565

COPPER SULFIDES
radiation effects on thermoelectric properties of p-type Cu_2S, gamma and neutron, 25:11952

CORROSION
book: Intercrystalline Corrosion and Corrosion Cracking of Stainless Steel in Aqueous Solutions (In Russian), 25:11353
book: Transport Phenomena in Liquid Metals and Semiconductors, 25:11410

CORROSION LOOPS
operation of sodium, for stainless steel testing, 25:11348(R) (GEAP-13539-13)

COSMIC GAMMA SOURCES
luminosity of extended, at center of Milky Way, (T), 25:11636

COSMIC PARTICLES
angular distribution of high-energy primary, detector systems for, (E), 25:11742 (KFKI-70-21-HEP)
diffusion of, leakage-lifetime approximation in, (T), 25:11743
interactions of heavy-mass, production of above-10^{13} eV horizontal air showers from, (E), 25:12071
interactions of meson (μ), production of above-10^{13}-eV horizontal air showers from anomalous, (E), 25:12071
interactions of nucleons with nucleons at very high energies, fireball mechanism for particle production in, 25:12230
interactions with nuclei at 2 x 10^5 GeV, mean transverse momentum of pions from, (E), 25:11749
production in nucleon interactions with nucleons at very high energies, fireball mechanism for, 25:12230
properties of very high-energy meson (μ), review of anomalous, (E), 25:12168
synchrotron emission from high-energy electrons, (T), 25:11747
trapping in geomagnetic field of nuclei of carbon, oxygen, and nitrogen, (E), 25:11744

COSMIC RADIATION
background microwave, explanation of anomalies in, (T), 25:11662
effects on biological materials, quantitation of heavy ion, 25:11280
intensity variations during geomagnetic storms, spherical harmonic analysis of worldwide, (E/T), 25:11745
intensity variations of primary, study of interplanetary space structure from, (E), 25:11627
modulation of galactic, numerical technique for solving solar, (T), 25:11746

COSMIC RADIO SOURCES
detection of, in cluster of galaxies in Coma Berenices, (E), 25:11644
electrons in extragalactic, interaction of relativistic, with cosmic microwave background, (T), 25:11597
formic acid in Sgr B2, detection of emission line of, 25:11593
hydrogen cyanide in, detection of radio emission from, 25:11594
spectral redshifts of galaxies associated with 4C 31.04, (E), 25:11652

COSMIC-RAY SPECTROMETERS
development of magnetostrictive wire spark chamber, for heavy ions, 25:10873
COSMIC RAY TELESCOPES
design of scintillation, for detection of mesons, 25:10871
COSMIC SHOWERS
axes of extensive, detector systems for, (E), 25:11742 (KFKI-70-21-HEP)
meson (μ) pair lateral distribution in underground, (E), 25:12082
moments in cores of extensive air, high transverse, (E/T), 25:11750
particle composition of 10^{12}-to-10^{13}-eV nucleon-interaction-produced, emulsion study of, (E), 25:12093
production of above-10^{13}-eV horizontal air, heavy-mass particle and μ anomalous interactions for, (E), 25:12071
properties of horizontal air, above 10^{13} eV, (E), 25:12071
COSMIC X-RAY SOURCES
Cet-XR2, discovery of, (E), 25:11592
Cet-XR2, intensity of, (E), 25:11592
Cet-XR2, model for, 25:11592
distribution of, (T), 25:11656
effects on nighttime anomalies in vlf radio propagation in the ionosphere, (E), 25:11812
Sco X-1, optical spectroscopic and photometric observations of, (E), 25:11600
COSMOLOGY
constant of, stabilization of galaxy clusters by, (T), 25:11642
radio-source distribution in Lemaitre models, (T), 25:11664
vacuum-like states in Friedman, (T), 25:11659
world models with antipoles for deriving upper bound for density parameter, (T), 25:11667
COULOMETERS
development of cyclic and differential, 25:10424 (ORNL-4636, pp 34-40)
CREEP
model for dislocation climb in diffusional, 25:11434(R) (SU-326-P-17-X-1)
recovery-work hardening model for, 25:11434(R) (SU-326-P-17-X-1)
CRITICAL ASSEMBLIES
conference on radiation protection programs for, 25:11056 (STI/PUB-241)
critical mass of uranium carbide (UC) fueled core in ZPR-6, (E/T), 25:12825
list of worldwide, IAEA, 25:12824 (STI/PUB-248)
neutron multiplication factor for bare plutonium sphere, collision probability method calculation of, (T), 25:12849
neutron spectra measurements in fast, proposed standard assembly for, 25:12816 (EACRP-L-74)
radiation protection at, 25:11080
radiation protection programs for, 25:11084
radiation protection programs for, 25:11081
reactivity of uranium carbide (UC) fueled core in ZPR-6, heterogeneity effects on, (E/T), 25:12825
sodium void effects in uranium carbide (UC) fueled core in ZPR-6, (E/T), 25:12825
thermal column of Harmonie, neutron flux in, (T), 25:12782 (CEA-CONF-1683)
CRITICALITY STUDIES
standards for outside-reactor, description of ANSI N16.1-1969 safety, 25:10802
CROPS
zirconium-95 content of, in Utah during May and June 1966, relation of, to May 9, Chinese atmospheric nuclear explosion, 25:10999
CROSS SECTIONS
excitation functions for (a,xn), (a,pxn), (d,xn), (d,pxn), and (p,xn) reactions with Z = 20 to 100 nuclei, (T), 25:12529(T) (ORNL-tr-3020)
CRUSTACEA
radioisotope content of copepods and crabs in Pacific Ocean, lead-210 and polonium-210, 25:10997(R) (RLO-2225-T-14-1)
CRYSTALS
particle channeling through perfect, Debye-model study of low-temperature, 25:11971
thermal expansion of rutile-type, anisotropic, (T), 25:12015
CULTURE MEDIA
effects on growth of γ irradiated Nicotiana tabacum callus and tumor tissues, comparison of standard and enriched, 25:10965
effects on T_4 phage mutation rate following inoculation into γ-irradiated Escherichia coli, 25:11016
radiation effects on, effects of, on incidence of chromosome aberrations in cultured mammalian cells, x, 25:10970
CUMENE
radiolysis at 20 and -196°C, scavengeable electron yields from γ, 25:10652
CURIUM
determination of, absolute method for, 25:10433 (ORNL-4636, pp 1-7)
purification by pressurized cation exchange chromatography, on-line computer monitoring of, 25:10664 (DP-MS-70-38)
separation from aqueous solutions by solvent extraction using bis(2,2-dimethylhexyl) phosphate, 25:10679
CURIUM ISOTOPES Cm-242
alpha decay of, time spectrum of alpha--conversion-electron delay in, (E), 25:12542
CURIUM ISOTOPES Cm-244
alpha decay of, time spectrum of alpha--conversion-electron delay in, (E), 25:12542
production at TRU, 25:10654(R) (ORNL-4588)
CURIUM ISOTOPES Cm-248
energy levels from californium-252 alpha decay, lifetimes, quadrupole moments, and deformation parameters for, (E), 25:12542
energy-level transitions from californium-252 alpha decay, probabilities for E2, (E), 25:12542
CURIUM OXIDES
americium oxides--curium oxides, phase studies of dioxides, intermediate oxides, and sesquioxides of, 25:11521
curium oxides--plutonium oxides, phase studies of dioxides, intermediate oxides, and sesquioxides of, 25:11521
CURRENT ALGEBRA
commutators in, equal-time limits of matrix elements of, 25:12133
commutators in, Schwinger terms in perturbation theory from equal-time limits of, 25:12294
currents for symmetry transformations in Wightman relativistic quantum field theory, conserved local, 25:12264
currents in field algebra and, representations of local, 25:12127
field theory in, classical Schwinger terms in, 25:12244
hadron spectra from representations of local isospin charge densities in, 25:12181
representations of local nonrelativistic, for N identical particles with spin-0 and $-1/2$, 25:12125
U(3) x U(3) currents, operator expansion of product of two, 25:12130
CUTTING TOOLS
design of milling machine for underwater dismantling of reactor thermal neutron shield, 25:12715
design of plasma arc, for underwater repair of reactor thermal neutron shield, 25:12714
CYCLOHEXANE, METHYL-
radiolysis at 20 and -196°C, scavengeable electron yields from γ, 25:10652
CYCLOPENTANE
radiolysis of liquid, in deuterated ammonia, deuterated ethanol, and nitrous oxide solutions, effects of pressure on yields from γ, 25:10628
CYCLOPENTENE
yields from γ radiolysis of liquid cyclopentane, effects of pressure on γ, 25:10628
CYCLOPHOSPHAMIDE
effects on eosinophil count and phospholipase B content of rats, 25:10961(R) (ORO-3329-6)
CYCLOTRONS
beam phase measurement in, monitoring system for, 25:12329
beam trajectory in central region of Delft 12-MeV isochronous, calculations for, 25:12330
experimental facility for UCD 76-inch isochronous, for neutron production at 20 to 60 MeV, 25:12331
experimental facility for UCD 76-inch isochronous, time-of-flight system for neutron source, 25:10861
CYLINDERS
neutron diffusion in, computer program for solving one-dimensional, (T), 25:12335 (AECL-3671)
CYSTAMINE
effects on content of nonprotein thiols in tissues of mice following injection in optimum radioprotective doses, 25:11101
radioprotective effects of sulfopropyl esters of dextran complexed with, on organisms, γ, 25:11108
radioprotective effects of, on blood coagulation in rats, x, 25:11105
CYSTEAMINE
radioprotective effects of, on activity of lactic dehydrogenase and respiration in embryo organs, x, 25:11096(R) (EUR-4491)
radioprotective effects of, on fish, combined effects of time of injection and temperature on x, 25:11292
CYTOPLASM
role in infectivity of irradiated, of fungi on corn, 25:11010(R) (ORO-2583-8)
volume in thoracic aorta endothelial cells, effects of, on radiosensitivity of rabbits and guinea pigs, 25:11269
CZECHOSLOVAKIA
strontium-90 content of atmosphere and surface soils of, calculations to year 2000, 25:10719

D

DACTINOMYCIN
effects on survival of Chinese hamster cells, effects of dose fractionation on, 25:11097
radiation effects on binding of tritium-labeled, by DNA

of hepatocytes of mice, effects of administration route on x, 25:11285
use for post-surgical treatment of human urinary tract neoplasms during radiotherapy using x, 25:11225
DATA DISPLAY SYSTEMS
development of computer-based, for nuclear spectra, 25:10892 (CEA-N-1363)
DATA PROCESSING SYSTEMS
description of computerized, for simulation modeling of future equipment requirements, 25:10757 (RFP-1527)
development for fissionable materials control in large research centers, 25:10796 (KFK-866)
development of computer-based, for nuclear spectra, 25:10892 (CEA-N-1363)
DATA RECORDING SYSTEMS
circuit of 12-bit register, for scintillation hodoscope, 25:10816
DATA TABULATIONS
hadron production cross sections in γ + d, γ + n, and γ + p interactions above 1.2 GeV, 25:12066 (DESY-HERA-70-1)
DELAY LINES
design of electromagnetic, for readout system for position-sensitive proportional detectors, 25:10846
development of monostable integrated circuit modules, 25:10898
DENSIMETERS
development of radiographic, for fuel elements, 25:11375 (IN-1437, pp 24-59)
DEUTERIUM
alpha elastic and inelastic scattering at 166 MeV, optical potentials from DWBA analysis of angular distributions from, (E/T), 25:12549
alpha reactions (α,t) at 82 MeV, DWBA analysis of charge-asymmetry effects in, (T), 25:12365
content in ground waters of Bukhara--Karshin artesian basin, relations with radium content, 25:10698
determination relative to hydrogen in water, mass spectrometric, 25:10463
deuteron reactions (d,p) at 1.35 to 2.00 MeV, proton spectra and polarizations from, (E), 25:12361
deuteron reactions (d,p) at 90 to 120 keV, angular distributions for, (E), 25:12368
diffusion in Types 304L stainless steel, effects of cold work on, 25:11474(R) (BNWL-842)
effects of alpha, on solvolysis rate as function of leaving group, 25:10522 (COO-1008-13)
effects on biological activity of penicillin D, 25:10560
effects on carbon--hydrogen stretching band in trichloromethane, 25:10540
effects on chemical binding of reduced NAD to alcohol dehydrogenase isoenzyme, 25:10525 (COO-1008-17)
effects on crystal structure of sodium acid oxalate monohydrate, 25:10543
effects on cyclization of cinnamyl radical to indene, 25:10526
effects on electron-impact-induced fragmentation of ethanol in mass spectrometer, 25:10528
effects on emission spectra of argon hydride, 25:10535
effects on EPR spectra of methylene, 25:10555
effects on equilibrium geometries of methyl halides, 25:10561
effects on far ir and Raman spectra of solid 1,1-dichloroethane, 1,1,1-trichloroethane, and 1,1,1-trifluoroethane, 25:10529
effects on γ radiation effects on pyridine--silica gel systems, ESR studies on, 25:10622 (JAERI-5026, pp 6-10)
effects on hydrogen-atom addition reactions with alkenes at low temperatures, 25:10538
effects on hydrolysis equilibria of divalent copper ions, 25:10566
effects on hydrolysis of methanesulfonyl chloride, 25:10537
effects on hydrolysis of methanesulfonyl chloride, 25:10536
effects on hydroxide ion-catalyzed hydrolysis of 4'-nitroacetanilide at 25°C, mechanism of, 25:10527
effects on ir and Raman spectra of ethynylbenzene, 25:10534
effects on ir spectra of acetylene and propyne adsorbed on zinc oxide, 25:10558
effects on ir spectra of acetylene, ethane, and ethylene, 25:10544
effects on ir spectra of carbon-13-labeled ethane and ethylene, studies on frequency shifts in, 25:10563
effects on ir spectra of dimethyl ether, 25:10542
effects on ir spectra of ethyl ethers and ethyl methyl ethers, 25:10562
effects on microwave spectra of first-excited torsional states of dimethylamine, 25:10551
effects on phosphorescence of benzene and toluene in polycrystalline solvents at 2 to 160°K, 25:10550
effects on photochemistry of some α-ketopropiophenones, 25:10554
effects on photolysis of benzonorcaradiene and benzotropilidene, 25:10557
effects on radiolysis of norbornane derivatives, 25:10637
effects on rate of solvolysis of 2,2,2-trifluoroethanesulfonate, 25:10523 (COO-1008-15)
effects on reaction mechanisms, effects of temperature on kinetic, 25:10549
effects on solvolysis of 1-adamantyl carbinyl derivatives, 25:10524(R) (COO-1008-16)
effects on solvolysis of β-styryl trifluoromethanesulfonate, 25:10548
effects on solvolysis of propargyl derivatives in aqueous organic systems, mechanism of, 25:10524(R) (COO-1008-16)
effects on thermal properties of copper sulfate pentahydrates, 25:10565
exchange between aluminum oxide catalyst surface and benzene, effects of ammonia, carbon dioxide, carbon monoxide, nitric oxide, and water on catalytic sites for, 25:10530
exchange between hydrogen and water-d, effects of catalysts on, 25:10583(R) (AECL-3776)
exchange in reactions of cyclododecene, cycloheptene, and cyclooctene with tris(triphenylphosphine)chlororhodium(I), 25:10539
exchange reaction in transcarboxylation of mixture of deuterated and nondeuterated potassium benzenecarboxylates, 25:10545
exchange with hydrogen in ammonia, optimization for heavy water production, 25:10787
exchange with hydrogen in borane--methylphosphine and borane--silylphosphine mixtures, 25:10547
exchange with hydrogen in synthetic polypeptides, 25:10567
exchange with hydrogen on molybdenum surface, low-pressure nonsteady-state, 25:10559
neutron elastic scattering at 0.5 to 49.4 MeV, mixing parameters and phase shifts for, (T), 25:12359
neutron elastic scattering at 16.5 and 22.1 MeV by liquid, polarization in, (E), 25:12354
neutron reactions (n,p) at 14.5 MeV, pole-diagram analysis of cross section for, (E/T), 25:12369
neutron reactions (n,p2n) at 14.1 MeV, cross sections, neutron spectra, and n--p scattering lengths from, (E/T), 25:12367
nucleosynthesis of, effects of energetic proton fluxes on, (T), 25:11544
photoinduced exchange between 4,4'-bis(N,N-dimethylamino)benzophenone and ethanethiol, 25:10556
photon reactions (γ,n) at 10 to 95 MeV, angular distributions of neutrons from, (E), 25:12374
photon reactions (γ,p) at 25 to 55 MeV, absolute differential and total cross sections, and angular distributions for, (E), 25:12362
proton reactions (p,2p) at 100 MeV, proton spectra and angular distributions for, (E), 25:12375
separation from hydrogen using c-w hydrogen fluoride laser, 25:10690
separation from hydrogen, electrochemical, 25:10583(R) (AECL-3776)
thermodynamic properties of solid hydrogen and, under pressure, comparison of, 25:10575
yields from γ radiolysis of liquid cyclopentane in deuterated ammonia and ethanol solutions, effects of pressure on, 25:10628
DEUTERIUM HYDRIDES
yields from γ radiolysis of liquid cyclopentane in deuterated ammonia and ethanol solutions, effects of pressure on, 25:10628
DEUTERIUM IONS
reactions with argon, 25:10552
DEUTERONS
form factors of, e + d → e + d interactions at low momentum transfers for deuteron-to-proton ratio for electric, (E), 25:12070
interactions d + d → d + d at 2.20 GeV/c in bubble chamber, differential cross sections for, (E), 25:12092
interactions e + d → e + d at low momentum transfers, deuteron-to-proton and neutron-to-proton electric form factor ratio and deuteron radius from, (E), 25:12070
interactions γ + d above 1.2 GeV, data compilation on cross sections for hadron production in, (E), 25:12066 (DESY-HERA-70-1)
interactions K⁻ + d → K⁻ + d(p + n) at 810 to 1110 MeV/c, K⁻ + n → K⁻ + n interactions from angular distributions for, (E), 25:12108
interactions K⁻ + d → p + Λ + π⁺ + π⁻ + π⁰ at 3 GeV/c, cross section for B(1220) production in, (E), 25:12118
interactions K⁻ + d at 360 to 720 MeV/c, Λ(1520) and Σ(1600) enhancement production and total cross sections for, (E), 25:12120
interactions K⁺ + d at 360 to 720 MeV/c, total cross sections for, (E), 25:12120
interactions K⁻ + d at 7.3 GeV/c in deuterium bubble chamber, partial and total cross sections, resonance production, and production cross sections for one strangeness-1 neutral hyperon or K⁰ in three-prong, (E), 25:12103
interactions n + d → n + d, amplitudes and scattering length relation with triton binding energy in, (T), 25:12227
interactions π + d at 330 MeV, π production, total and differential cross sections, and momentum and angular distributions for, (T), 25:12105
interactions π⁺ + d → 2p + neutrals at 1.1 to 2.3 GeV/c in deuterium bubble chamber, 2π⁰ mass spectrum in, (E),

25:12107
interactions $\pi^+ + d \rightarrow 2p + \pi^+ + \pi^- + \pi^0$ at 4.19 GeV/c in deuterium bubble chamber, rho, ω^0, A_1, A_2, and phi production and rho Δ(1236) simultaneous production in, (E), 25:12112
interactions $\pi^+ + d \rightarrow 2p + \pi^+ + \pi^-$ at 1.1 to 2.3 GeV/c in deuterium bubble chamber, phase shift analysis on angular distribution moments of π--π scattering and Δ^{++}(1236) production in, (E/T), 25:12107
interactions $\pi^+ + d \rightarrow \pi^+ + \pi^- + \pi^0 + 2p$ at 3.65 GeV/c, H(990) and eta' production in, (E), 25:12121
interactions $\pi^+ + d$ at 5.1 GeV/c, associated production of K anti K and YK, and resonance production from two-body and quasi-two body final states in, (E), 25:12100 (NP-18629)
radius of, interactions $e + d \rightarrow e + d$ at low momentum transfers for determination of, 25:12070
reactions (d,2n) with neptunium-237 at 12.1 MeV, decay curves from, (E/T), 25:12530 (RLO-1388-130)
reactions (d,3nγ) with holmium-165, lutetium-175, terbium-159, and thulium-169 at 18 MeV, cross sections for, (E/T), 25:12544
reactions (d,α) with nitrogen-14 at 30 MeV, internal bremsstrahlung spectra for, (T), 25:12694
reactions (d,γ) with tritium, analysis using shell model and R-matrix formalism, (T), 25:12371
reactions (d,He-3) with cerium-140 and lanthanum-139, energy spectra and angular distributions from, (E/T), 25:12552
reactions (d,He-3) with fluorine-19, neon-20, and neon-22 at 52 MeV, helium-3 spectra and angular distributions for, (E), 25:12385
reactions (d,He-3) with lead-204 and -208 at 80 MeV, energy spectra and DWBA analysis of differential cross sections from, (E), 25:12575
reactions (d,He-3) with praseodymium-141, angular distributions for, (E), 25:12558
reactions (d,He-3) with titanium-49 at 19.5 and 22.4 MeV, angular distributions for, (E), 25:12452
reactions (d,n) with nitrogen-14 at 35 MeV, DWBA analysis of cross section and polarization data in, (T), 25:12405
reactions (d,n) with sulfur-34 at 3.8 to 5.2 MeV, excitation functions and angular distributions from, (E), 25:12440
reactions (d,p) and (d,2n) with tantalum-181 at 27.2 MeV, cross sections for, (E), 25:12513 (CNEA-269)
reactions (d,p) and (d,4n) with terbium-159 at 27.2 MeV, excitation functions for, (E), 25:12595
reactions (d,p) and (d,t) with carbon-12 at 80 MeV, angular distributions and energy spectra from, (E), 25:10851 (NP-18570)
reactions (d,p) with calcium-40 at 7 and 9 MeV, effect of deuteron D-state on DWBA calculations of differential cross sections, proton polarizations, deuteron analyzing powers, and spectroscopic factors from, (T), 25:12414
reactions (d,p) with carbon-12 at 12.4 MeV, proton polarization from, (E), 25:12377 (INP-711)
reactions (d,p) with deuterium at 1.35 to 2.00 MeV, proton spectra and polarizations from, (E), 25:12361
reactions (d,p) with deuterium at 90 to 120 keV, angular distributions for, (E), 25:12368
reactions (d,p) with helium-3 at 6, 8, and 10 MeV using polarized target, proton asymmetries in, (E), 25:12357
reactions (d,p) with lead-206 at 17 MeV, angular distributions for, (E), 25:12569
reactions (d,p) with magnesium-24 at 13.5 MeV, analysis using generalized DWBA model, (T), 25:12457
reactions (d,p) with molybdenum and zirconium isotopes, charge exchange effects and spectroscopic factors in, (E), 25:12571
reactions (d,p) with niobium-93 at 5 to 10 MeV, charge-exchange threshold effects in, (E), 25:12588
reactions (d,p) with nuclei, lectures on polarization in, (T), 25:12624 (ANU-P-497)
reactions (d,p) with polarized helium-3 at 4.8 to 11.9 MeV, proton asymmetries in, (E), 25:12370
reactions (d,p) with yttrium-89 up to 27 MeV, excitation function and isomeric cross-section ratio for, (E), 25:12428 (CNEA-278)
reactions (d,pf) with plutonium-240 and -242 and uranium-234, -236, and -238, fission probabilities and angular correlation coefficients for, (E), 25:12579
reactions (d,pγ) with sulfur-34 at 2 to 3.25 MeV, energy levels of sulfur-35 from, (E), 25:12489
reactions (d,t) with lead-208 at 17 MeV, angular distributions for, (E), 25:12569
reactions (d,t) with terbium-159 at 12 MeV, triton spectra from, (E), 25:12578
reactions (d,x) with natural copper at 5 to 40 MeV, excitation functions for production of copper-61, -62, -64, and -66 and zinc-62, -63, and -65, (E), 25:12438
reactions (d,xn) and (d,pxn) with Z = 20 to 100 nuclei, excitation functions and thick-target yields for, (T), 25:12529(T) (ORNL-tr-3020)
reactions with gases at 30 to 120 keV, cross sections for electron capture into 3s state of deuterium in, (E), 25:11708
scattering by carbon-12 at 80 MeV, angular distributions and energy spectra from elastic and inelastic, (E), 25:10851 (NP-18570)
scattering by carbon-12, calcium-40, and silicon-28 at 28 MeV, asymmetries in cross sections for elastic, (E), 25:12309 (LYCEN-6909)
scattering by copper-63, copper-65, and zinc-67 at 14 MeV, spin dependence in inelastic, (E), 25:12454
scattering by helium-4 at 7.07 MeV and 55°, tensor analyzing power of elastic, (E), 25:12356
scattering by indium-115 at 12 MeV at 125°, energy spectra from inelastic, (E/T), 25:12543
scattering by lead-207 at 17 MeV, angular distributions for inelastic, (E), 25:12569
scattering by nitrogen-14 at 3.5 MeV, optical-model analysis of elastic, (E), 25:12405
scattering by nuclei, lectures on cross sections and polarization from elastic, (T), 25:12624 (ANU-P-497)
scattering by nuclei, strength of tensor interaction in optical potential for, (T), 25:12684
scattering by polarized helium-3 at 4.8 to 11.9 MeV, asymmetries in elastic, (E), 25:12370
scattering by polarized helium-3 at 9.9 and 11.9 MeV, asymmetries in, (E), 25:12358
use for determining cross section, thickness, shape, and internal structure, review of, 25:10977

DEXTRAN
effectiveness of iron-59-labeled, for determining enteral protein loss, 25:11171
effects on aggregation of erythrocytes during angiography in man, 25:11195
radioprotective effects of cystamine complexed with sulfopropyl esters of, on organisms, γ, 25:11108

DIAMONDS
analysis for trace amounts of elements by spark source mass spectrometry, 25:10455
radiation effects on electric properties of semiconducting, annealing of electron, 25:11966

DIET
radioisotope content of human, in USA during 1969, cesium-137, strontium-89, and strontium-90, 25:11040

DIFFERENTIAL EQUATIONS
differential quadrature and long term integration, 25:12914 (TID-25633)
integration of first order ordinary, RUNKUT computer routine for, 25:12906 (SC-M-70-868)

DIFFUSION
data tabulations on alloys, metals, gases, halides, and oxides, 25:11411

DIGESTION
disturbances in human, use of carbon-14-labeled carbon dioxide determination of exhaled air for determining, 25:11168

DIISOPROPYLAMINE
radiolysis of aqueous solutions of, effects of 2-mercaptoethanol on yields from, 25:10627(R) (NYO-2499-37)

DIMETHYLAMINE
spectra of first-excited torsional states of, effects of deuterium and nitrogen-15 on microwave, 25:10551

DIORITES
analysis for trace amounts of elements by spark source mass spectrometry, 25:10455

DISEASES
radiodiagnosis of human liver, effectiveness of radioisotopes for, 25:11198
radiodiagnosis of renal, evaluation of iodine-131-labeled Hippuran renography and clearance procedures in, 25:11210

DISEASES, NEOPLASTIC
carcinoma, radioinduced chromosome aberrations in cells of Ehrlich's ascites, effects of temperature on γ, 25:11014
carcinoma, radiotherapy for human thyroid, combined effects of surgery on iodine-131-labeled sodium iodide, 25:11234
carcinomas, radiodiagnosis of human liver, effectiveness of radioisotopes for, 25:11198
carcinomas, radiodiagnosis of human liver, using gold-198 and iodine-131, 25:11183
carcinomas, radiotherapy in man, 25:11222 (BNL-50203, pp 280-5)
carcinomas, radiotherapy in man, methods for dose fractionation in, 25:11223 (BNL-50203, pp 292-307)
carcinomas, radiotherapy of human bladder, effectiveness of high-energy x radiation for, 25:11229
carcinomas, radiotherapy of human mammary, development of myelocytic leukemia following γ, 25:11302
carcinomas, radiotherapy of human uterine cervix, design of applicator for implant ionizing, 25:11227
carcinomas, radiotherapy of thyroid, in man, effectiveness of iodine-131 for, in relation to mortality, effects of age on, 25:11233
hemangiomas, radiotherapy in man, review of x, 25:11235
leukemia, incidence in man following phosphorus-32 therapy for polycythemia, 25:11303
leukemia, radiodiagnosis of human, using chromium-51 and mercury-197, 25:11201
leukemia, radioinduced myelocytic, in man following therapy of mammary carcinoma, similarity of, to model leukemic diseases in mice, γ, 25:11302
localization in human kidneys, effectiveness of radioisotope scanning for, 25:11115
lymphomas, radiotherapy of human mediastinal,

effectiveness of dose fractionation for ionizing, 25:11226
lymphomas, radiotherapy of human, using γ, 25:11060
lymphosarcomas, radiodiagnosis of human, using chromium-51 and mercury-197, 25:11201
malignant radioinduced, morphological changes preceding appearance of, 25:11271
malignant, radiotherapy in human uterine cervix using implants and computer dose calculations, 25:11058
malignant, radiotherapy of human esophageal, 25:11236
malignant, radiotherapy of human urinry tract, combined effects of dactinomycin on post-surgical x, 25:11225
metastases, radiodiagnosis in bone, using strontium-85 in comparison to x-radiography, 25:11174
metastases, radiodiagnosis of tumor, effectiveness of dcuble isotope method with metastable indium-113 and technetium-99 for, 25:10928
radiodiagnosis of brain, using iodine-131 in combination with three detectors, 25:11148
radiodiagnosis of liver, effectiveness of iodine-131-labeled Rose Bengal for, in comparison to histologic and laparoscopic diagnosis, 25:11180
radiodiagnosis using scintillation cameras, evaluation of, 25:11182
tumors, effects of brain, on cerebral blood flow, use of xenon-133 for determining, 25:11144
tumors, effects of brain, on cerebral blood flow, effectiveness of iodine-131 for determining, 25:11149
tumors, localization of Ehrlich ascites, following transplantation in mice, tracer method using iodine-131 and whole-body autoradiography for, 25:10921
tumors, radiation effects on immunological properties of transplantable, effects of, on antiserum formation following inoculation into syngeneic mice, 25:10993
tumors, radiodiagnosis in pancreas using selenium-75, 25:11199
tumors, radiodiagnosis of brain, effectiveness of mercury-203-labeled chlormerodrin for, method for determining, 25:11179
tumors, radiodiagnosis of human brain, effectiveness of technetium-99 for, evaluation of, 25:11146
tumors, radiodiagnosis of human brain, effectiveness of selenium-75 for, in comparison to iodine-131, 25:11145
tumors, radiodiagnosis of human liver, using gold-198 and iodine-131, 25:11197
tumors, radiodiagnosis of human lung, by scanning with iodine-131-labeled albumin macroaggregates and computers or multichannel analyzers, evaluation of, 25:11131
tumors, radiodiagnosis of pulmonary, in man using iodine-131-labeled albumen macroaggregate, evaluation of, 25:11127
tumors, radioinduced in organs and tissues of mammals, 25:11253 (BNL-50203, pp 154-73)
tumors, radioinduced, in bones and liver of personnel following occupational inhalation of plutonium-239, models for estimating probability of α and γ, 25:11301
tumors, radioinduced, in human tissues, 25:11090
tumors, radioinduced, in zygotes of Drosophila, x, 25:11250
tumors, radiotherapy in dogs, man, mice, and rats, review of, 25:11219 (BNL-50203, pp 130-53)
tumors, radiotherapy in mammals, methods for x, 25:11220 (BNL-50203, pp 234-41)
tumors, radiotherapy of abdominal or retroperitoneal, effects on kidneys, cobalt-60 γ, 25:11275
tumors, radiotherapy of human, review of dose fractionation method for, 25:11221 (BNL-50203, pp 268-79)
tumors, radiotherapy of malignant, in man, development of whole-body skin eruptions following, 25:11296
tumors, radiotherapy of, review of, 25:11259 (BNL-50203, pp 260-7)

DISEASES, PHYSIOLOGICAL

abscesses, radiodiagnosis of human liver, effectiveness of radioisotopes for, 25:11198
angina pectoris, effects on coronary blood circulation, use of external counting of iodine-131 or metastable technetium-99 for determining, 25:10911
arteriosclerosis, effects on cerebral blood circulation time, effectiveness of intravenously injected iodine-131 for measuring, 25:11150
arteriosclerosis, effects on coronary blood circulation, use of external counting of iodine-131 or metastable technetium-99 for determining, 25:10911
arthrosis deformans, radiodiagnosis of, effectiveness of strontium-85 for, 25:11175
asplenia, radiodiagnosis of functional, use of metastable technetium-99, accumulation by spleen for, 25:11117
asplenia, radioinduced, in man following therapy for sarcoma, 25:11117
cataracts, radioinduced lens, in mammalian eyes, comparison of doses for γ and neutron, 25:11284
cataracts, radioinduced, in man, 25:11090
cirrhosis, radiodiagnosis in man using gold-198, effects of blood circulation on, 25:11196
cirrhosis, radiodiagnosis of human, effectiveness of radioisotopes for, 25:11198
cirrhosis, radiodiagnosis of human, using gold-198 and iodine-131, 25:11183
cirrhosis, radiodiagnosis of human, using gold-198, effects of ascites and enlarged spleen on, 25:11203
dermatitis, radioinduced chronic, in swine, callicrein treatment for x, 25:11110
effects of human brain, on cerebral blood flow, use of xenon-133 for determining, 25:11144
effects of vascular, on cerebral blood flow, effectiveness of iodine-131 for determining, 25:11149
effusions, radiodiagnosis of pericardial, by scintiscanning with combinations of iodine-131-labeled RISA and albumin macroagregates, 25:11130
emphysema, radiodiagnosis of honeycomb lung, in man, effectiveness of iodine-131-labeled albumin macroaggregates in comparison to radiography for, 25:11215
hemorrhages, extracellular fluid volume following acute, radioisotope dilution method for measurement of, 25:11185
hepatitis, radiodiagnosis in man using gold-198, effects of blood circulation on, 25:11196
hydrocephalus, radiodiagnosis of normal pressure, in man, use of iodine-131-labeled serum albumin and cisternography for, 25:11181
hydrocephalus, ventriculoatriostomy for human, effectiveness of iodine-131 for testing openings for, 25:11152
hyperglycemia, radioinduced, in rats, role of alarm phase of nonspecific adaptation response in γ, 25:11281
hypertension, effects on renal blood flow, effectiveness of radioisotope-labeled compounds for determining, 25:11153
hypertension, effects on renal blood flow, methods for determining, 25:11164
hypertension, effects on renal blood flow, use of xenon-133 for determining, 25:11158
hypertension, kidney scanning in patients with, using technetium-99m in combination with angiography, evaluation of, 25:11166
hypertension, radiodiagnosis of, in man, evaluation of methods for, 25:11163
hyperthyroidism, effects on hepatic blood flow, use of gold-198 and iodine-131 for determining, 25:11141
hyperthyroidism, radiotherapy using iodine-131 in combination with methylmercaptoimidazol, 25:11230
inflammations, effects on vascular permeability to cells and protein, radioisotope methods for determining, 25:11193
jaundice, radiodiagnosis of, experimental studies in dogs on use of iodine-131-labeled Rose Bengal for, 25:11213
mongolism, incidence in human children x-irradiated in utero, 25:11300
nephritis, radioinduced, in dogs, effects of subsequent uremic condition on phosphate excretion, 25:10963
nephritis, radioinduced, in rats, pathological changes following high dose, 25:11286
Parkinsons disease, blood circulation in brain of patients with, use of xenon-133 for determining effects of amphetamines on, 25:11147
placenta praevia, radiodiagnosis of, use of γ scintillation camera and metastable indium-113 for, 25:11228
polyarthritis, radiodiagnosis of, effectiveness of strontium-85 for, 25:11175
polycythemia vera, radiotherapy of human, latent effects of phosphorus-32 β, 25:11303
radiodiagnosis of arterial, in legs, effectiveness of xenon-133 walking test in comparison to arteriography, 25:11139
radiodiagnosis of brain, effectiveness of mercury-203 for, method for determining, 25:11179
radiodiagnosis of brain, using iodine-131 in combination with three detectors, 25:11148
radiodiagnosis of honeycomb lung, in man, effectiveness of iodine-131-labeled albumin macroaggregates in comparison to radiography for, 25:11215
radiodiagnosis of human heart, using oxygen-15-labeled carbon dioxide or xenon-133, evaluation of method for, 25:11125
radiodiagnosis of human lung, comparison of iodine-131-labeled macroaggregated to RISA for, 25:11129
radiodiagnosis of kidney, effectiveness of double isotope method using iodine-131 and gallium-68 for, 25:10928
radiodiagnosis of kidney, using scanning method in combination with computer analysis, 25:11161
radiodiagnosis of liver, effectiveness of iodine-131-labeled Rose Bengal for, in comparison to histologic and laparoscopic diagnosis, 25:11180
radiodiagnosis of liver, in man, effectiveness of colloidal technetium-99 in comparison to colloidal gold-198, 25:11140
radiodiagnosis of thyroid, in children, effectiveness of iodine-131 and whole-body counting for, 25:11172
renal insufficiency, radiodiagnosis in man using iodine-131 and gamma camera, 25:11206
rheumatoid spondylitis, radiodiagnosis of, effectiveness of strontium-85 for, 25:11175
sarcoidosis, radiodiagnosis of pulmonary, effectiveness of iodine-131-labeled albumen macroaggregate for, 25:11133
sclerosis, radiodiagnosis in pancreas using selenium-75, 25:11199
silicosis, radiodiagnosis lung scintigraphy by patients, comparison of iodine-131-labeled albumin macroaggregate

for, in comparison to radiography, 25:11134
splenomegalie, effects on spleenic blood flow, use of chromium-51-labeled erythrocytes for determining, 25:11142
spondylitis, radiotherapy of ankylosing, using radium-224, excretion measurements and whole-body counting following, 25:11231
stenosis, use of iodine-131-labeled Hippuran for scanning of renal function in patients with renal arterial, 25:11186
thrombi, radiodiagnosis in hind legs of rabbits by metastable indium-113 or iodine-131 scintigraphy, 25:11214
thrombosis, radiodiagnosis in man, method using iodine-125-labeled fibrinogen for, 25:11191
thrombosis, radiodiagnosis of, in major arteries using iodne-131 in combination with three detectors for measuring blood circulation time, 25:11148
tuberculosis, radiodiagnosis in man, comparison of iodine-131-labeled albumin with radiography for, 25:11132

DISEASES, PLANTS
tumors, radiation effects on tissues of, from Nicotiana tabacum cultured in standard and enriched media, comparison of γ, 25:10965
tumors, radiation effects on, in Jerusalem artichokes, x, 25:11306

DISEASES, TRAUMATIC
concussions, lung scintigraphy in patients with chest, effectiveness of iodine-131 in combinaton with radiography and ventilation measurements, 25:11135
fractures, radiation effects on healing of mandibular, in rabbits, x, 25:11266
fractures, radioisotope uptake by rats with bone, 25:11216
radiation injuries, first aid treatment, to nuclear personnel, 25:11109
radiation injuries, induced in human eyes following exposure to high-energy electromagnetic waves, 25:11297
radiation sickness, role of nerve damage in development of intestinal syndrome of, in neutron-irradiated mice, 25:11270

DISPERSION RELATIONS
evaluation of fixed-t, for π^0 and π^+ production in γ + p → $\pi^+(\pi^0)$ + n(p) interactions in second resonance region, 25:12146
predictions for forward π^- + p → π^0 + n interactions, discrepancies between amplitude data and, (E/T), 25:12209
sum rules for model of nucleon electromagnetic form factors, superconvergent, 25:12147
sum rules for π + N, N + N, and γ + N interactions, continuous-moment, 25:12207

DOGS
extracellular fluid content in splenectomized, following acute hemorrhage, radioisotope dilution method for measurement of, 25:11185
radiation effects on sorption of strontium-85 and strontium-89 from gastrointestinal tract of, following injection and ingestion respectively, whole-body γ, 25:10947
radiation effects on treadmill performance behavior in dogs, bibliography on, 25:11251 (AD-705976)
radioinduced nephritis in, effects of subsequent uremic condition on phosphate excretion, 25:10963
radiotherapy of tumors in, review of, 25:11219 (BNL-50203, pp 130-53)
scanning of prostate glands in, use of metastable zinc-69-labeled zinc chloride for, 25:11204

DOLOMITES
particle size in crushed, determination by beta backscattering, 25:10784

DRESDEN POWER REACTOR, UNIT 2
fuel elements for, safety analysis of gadolinium oxide (Gd_2O_3)--uranium oxide (UO_2) replacement, 25:12732 (DOCKET-50237-126)
operations incident of December 21, 1970, possession of unauthorized neutron sources, 25:12719 (DOCKET-50237-128)
operations incident of December 30, 1970, shutdown by instrument air leak, 25:12720 (DOCKET-50237-129)
operations incident of January 5, 1971, failure of A standby gas treatment system discharge damper motor, 25:12718 (DOCKET-50237-127)

DRESDEN POWER REACTOR, UNIT 3
operation of, license for, 25:12734 (DOCKET-50249-53)
technical specifications for, 25:12734 (DOCKET-50249-53)

DRUGS
effects of vasoactive, on muscle activity in man, use of xenon-133 for studying, evaluation of, 25:10914

DUAL-TEMPERATURE PROCESS
optimization of ammonia--deuterium, for heavy water production, 25:10787

DYSPROSIUM
determination of trace amounts of, in biotite and tektite by spark source mass spectrometry, 25:10455

DYSPROSIUM ALLOYS AND SYSTEMS
Co--Dy, hyperfine interactions in $DyCo_2$, dysprosium-161 Moessbauer study of, 25:12035
Dy--Fe, hyperfine interactions in $DyFe_2$, dysprosium-161 Moessbauer study of, 25:12035

DYSPROSIUM ISOTOPES Dy-158
energy levels from terbium-159 (p,2nγ) and (d,3nγ) reactions at 16 to 21 MeV, rotational, (E/T), 25:12544
energy-level transitions from production in (α,3n) and (α,4n) reactions at 42 MeV, intensities and angular distributions from, (E/T), 25:12553
energy-level transitions from terbium-159 (p,2nγ) and (d,3nγ) reactions at 16 to 21 MeV, probabilities for, (E/T), 25:12544
moment of inertia as function of excitation energy, (E/T), 25:12544

DYSPROSIUM ISOTOPES Dy-160
energy-level transitions from production in (α,4n) reactions at 42 MeV, intensities and angular distributions from, (E/T), 25:12553

DYSPROSIUM ISOTOPES Dy-161
Moessbauer hyperfine structure in dysprosium metal and compounds with cobalt and iron, 25:12035
nuclear moments of 75-keV state of, 25:12035

DYSPROSIUM ISOTOPES Dy-162
alpha reactions (α,2nγ) at 22 and 28 MeV, cross sections and gamma spectra from, (E/T), 25:12544

DYSPROSIUM ISOTOPES Dy-164
helium-3 reactions (He-3,3nγ) at 22 MeV, cross sections and gamma spectra from, (E/T), 25:12544

E

EARTH
crust thickness of, calculation using seismic data from underground nuclear explosions, 25:10748

EARTHQUAKES
seismic activity from micro-, in western US, measurement of, 25:10731

ECHINODERMATA
radioisotope content of sea cucumbers and sea urchins in Pacific Ocean, lead-210 and polonium-210, 25:10997(R) (RLO-2225-T-14-1)

ECOSYSTEMS
detritus food chain in Mari Lake, 25:12884 (COO-1599-31)
radioisotope transport in aquatic, statistical analysis of, 25:10998
strontium-90 accumulation by animals in aquatic, 25:11006

ECUADOR
radioactivity in air and milk in, measurement of fallout, 25:11068

EDDY CURRENT TESTING
transformation device for multiparameter, 25:12878 (BNWL-1469)

EGGS
production of viable, by moths, effects of mating with γ-radiosterilized males on, 25:11338
radiation effects on production of, by cotton leaf moths, effects of dose and larval exposure on γ, 25:11247

EINSTEINIUM ISOTOPES Es-253
production at TRU, 25:10654(R) (ORNL-4588)

ELASTOMERS
book: Radiation Chemical Processing, 25:10617
nitroxide free radicals in, 310-MHz NMR study of, 25:12034 (CEA-R-3855)

ELECTRIC ARCS
plasma-cluster production in dc, in inhomogeneous magnetic fields, 25:11905

ELECTRIC DISCHARGE
current and velocity fields between electrodes in mercury, (E/T), 25:11761
plasma wave resonances in, nonlinear damping of Tonks--Dattner, (E/T), 25:11942

ELECTRIC DISCHARGE TUBES
feedback control of PIG, for QP machine, 25:11921 (IPPJ-T-2)

ELECTRIC FIELDS
production of uniform, conformal-mapping analysis of parallel plate, 25:12045 (IPPJ-T-4)

ELECTRIC INSULATORS
design for use under high g-forces, 25:12867 (BDX-613-213)
development of porcelain, for high voltage power cable penetration in reactor containment vessel, 25:12705 (JAERI-Memo-4197)

ELECTRIC PROBES
performance of cylindrical Langmuir, for diagnostics of low-density argon plasma, (E), 25:11873

ELECTRODES
development for molten salts, 25:10434 (ORNL-4636, pp 7-13)

ELECTRODYNAMICS
charge in, phase of, (T), 25:12240

ELECTROJETS
position of ionospheric current, relation with boundary of captured electrons with E greater than or equal to 280 keV in radiation belts, (E/T), 25:11782

ELECTROLYTES
electric conductivity in solid, research on mixed, 25:12883(R) (COO-1440-21)
electric conductivity of solid, 25:11472(R) (AD-708705)
titration of solid, method for coulombic, 25:11472(R) (AD-708705)

XUM

ELECTROMAGNETIC FIELDS
- charged-particle interactions with transverse rotating, electrodynamic analog of wave diffraction phenomena in, (T), 25:12156
- Einstein--Maxwell, invariant transformations for Newman--Penrose constants of motion for coupled, 25:12279
- graviton interactions wth static, photon production from, (T), 25:12272
- photon interactions with static, graviton production from, (T), 25:12272

ELECTROMAGNETIC WAVES
- absorption in plasma between electron cyclotron and lower-hybrid frequency, 25:11927 (FTI-295)
- dosimetry of, effects of displacement of target on accuracy in calculations of, 25:11069
- effects on human eyes, pathological, 25:11297
- electron motion in plane polarized, spin orientation from induced radiation from, (T), 25:12161
- excitation of standing helicon, in cylindrical plasma, (E/T), 25:11908
- fermion motion in planar, induced radiation and spin orientation from neutral, (T), 25:12160
- propagation and reflection of transverse cyclotron, in plasma, (T), 25:11931
- propagation in geomagnetic field, Poynting-flux direction of, (E), 25:11780
- propagation in magnetized plasma with anisotropic pressure, coupled equations for, (T), 25:11946
- propagation of helicon, in uniform nonresistive plasma, (T), 25:11936
- reflection at boundary of plasma half-space, (T), 25:11939
- scattering by static gravitational field, cross sections for, (T), 25:12138 (NYO-2262-TA-222)
- travel time to space vehicles in solar orbits, general-relativistic effects on, (T), 25:11602

ELECTRON BEAMS
- interactions in disk-loaded waveguide at high energy, synchrotron radiation from, 25:12317
- interactions in slow-wave ridged waveguide of high-current relativistic, 25:11932
- interactions with finite-beta plasma, equilibrium of relativistic, (T), 25:11887 (NYO-4077-1, Paper 5)
- interactions with plasma, E-layer precession in, (T), 25:11925 (NYO-4077-1, Paper 2)
- interactions with plasma, induced current from relativistic, (T), 25:11894
- interactions with plasma, stochastic acceleration from nonlinear, (T), 25:11885 (NYO-4077-1, Paper 3)
- monitoring of peak current of linac, digital, 25:12297 (CEA-N-1389)
- polarization from induced radiation from motion in plane polarized electromagnetic wave, (T), 25:12161
- use of high-current relativistic, to generate stress waves in solids, 25:10791

ELECTRON GAS
- electron distribution around positrons in metal, (T), 25:12041
- thermodynamics of, collective theory for, 25:11896

ELECTRON MICROSCOPY
- research progress on, 25:10437 (ORNL-4636, pp 45-50)
- research progress on, 25:10583(R) (AECL-3776)

ELECTRON PAIRS
- production in p + p interactions at 20 to 120 MeV, differential cross section for, (T), 25:12231
- production in photon scattering by nuclear field, polarization in, (T), 25:12158
- production in $\pi^- + p \rightarrow e^+ + e^- + n$ interactions at 275 MeV, energies and angles for, (E), 25:12099 (JINR-P1-5398)

ELECTRON PARAMAGNETIC RESONANCE
- group theory for, 25:12910(T) (SC-T-71-3002)

ELECTRON PROBE MICROANALYSIS
- research progress on, 25:10437 (ORNL-4636, pp 45-50)

ELECTRON-RING ACCELERATORS
- beam instability due to coherent synchrotron radiation, 25:12311
- beam instability due to negative mass effect, longitudinal, 25:12312
- electron--ion bunches in, calculation of phase volume of, 25:12302 (JINR-P9-5405)
- performance for acceleration of alpha particles, 25:12305 (JINR-P9-5558)
- ring motion in ripple magnetic field in, 25:12301 (JINR-P9-5394)

ELECTRON SOURCES
- cathodes for accelerator, properties of lanthanum hexaboride, yttrium hexaboride, and gadolinium hexaboride, 25:12316
- operating characteristics of hollow-anode gas discharge, 25:12319
- use of double gun, with ultrahigh vacuum system for film deposition, 25:10806

ELECTRONIC EQUIPMENT
- design for measuring spectra of boiling bubble acoustic pulses, 25:10769(R) (ORO-3911-3)

ELECTRONS
- detection at 0.25 to 1.25 MeV, energy response functions for scintillation detectors for, 25:10832
- detection of high-energy, development of threshold gas Cherenkov counters for, 25:10874
- effects of fast, on linear polyethylene, NMR spectral studies on compounds produced from, 25:10589
- effects of pulsed, on aqueous benzonitrile solutions, spectral studies on short-lived aromatic anions and free radicals produced by, 25:10639
- effects of pulsed, on aqueous iodobenzene solutions, optical absorption spectra of phenyl radicals produced by, 25:10631
- effects of pulsed, on aqueous solutions of azides, 25:10643
- effects of pulsed, on carbon dioxide--oxygen systems at 10^{24} eV g^{-1} sec^{-1}, 25:10633
- effects of pulsed, on p-bromophenol, optical absorption spectra of phenoxy radicals produced by, 25:10631
- effects on argon--nitrogen, nitrogen--nitrogen oxide, and nitrogen--oxygen systems at 1.5 MeV, 25:10586 (JAERI-5026, pp 155-7)
- effects on carbon monoxide at 1.5 MeV, design of apparatus for spectral studies on, 25:10585 (JAERI-5026, pp 153-5)
- effects on copper at 0.6 to 1.4 MeV, I/sub D/--I/sub E/ stage of annealing of defects induced in, 25:11957
- effects on curing of diallyl phthalate prepolymer--vinyl monomer--wood mixture, 25:10606 (JAERI-5026, pp 101-7)
- effects on curing of resins for coating metals, 25:10608 (JAERI-5026, pp 121-9)
- effects on DNA of P388 F cells, effects of dose rate on degratory, 25:11028
- effects on electric properties of semiconducting diamonds at 1 MeV, annealing of, 25:11966
- effects on free radical in Dahlia seeds, EPR analysis of, 25:11305 (NP-18394)
- effects on gaseous ethane, ethylene, and methane, 25:10644
- effects on impregnation polymerization of acrylic acid on polyester films, 25:10598 (JAERI-5026, pp 52-5)
- effects on lithium fluoride single crystals, lithium oxide precipitation in, 25:11964
- effects on microcirculatory units of blood vessels from earlobes of mice, effects of dose fractionation on, 25:11254 (BNL-50203, pp 174-80)
- effects on n-type germanium at 1 MeV, kinetics of 100°K annealing stage of, 25:11954
- effects on nickel without and with silicon impurities at 2 MeV, 25:11977
- effects on optoelectronic devices at 600 keV and 1.5 MeV, 25:10904 (HMI-B-97)
- effects on phenoplast molding materials, 25:10634
- effects on point-defect creation and annihilation in niobium at 20°K, 1.4-, 2.2-, and 3.0-MeV, (E), 25:11949(T) (AI-Trans-267)
- effects on polymerization of 2-hydroxyethyl methacrylate on polyester fabrics, hydrophilic properties of products from, 25:10600 (JAERI-5026, pp 63-7)
- effects on polymerization of acrylic acid on poly(ethylene terephthalate), effects of solvent on, 25:10597 (JAERI-5026, pp 46-51)
- effects on polymerization of acrylic acid on polyester fabrics by impregnation method, properties of products from, 25:10601 (JAERI-5026, pp 68-72)
- effects on polymerization of acrylonitrile on poly(vinyl chloride) powders, effects of dose rate on, 25:10596 (JAERI-5026, pp 42-5)
- effects on polymerization of acrylonitrile--poly(diallyl phthalate) in wood, 25:10607 (JAERI-5026, pp 108-20)
- effects on polymerization of methyl acrylate--1,2-polybutadiene, effects of catalysts and crosslinking agents on, 25:10609 (JAERI-5026, pp 130-6)
- effects on polymerization of vinylidene chloride in wood, properties of products from, 25:10603 (JAERI-5026, pp 80-5)
- effects on reactively sputtered alumina/silicon junctions at 1 MeV, 25:10905
- effects on water vapor, review on, 25:10651
- emission from radio galaxies, origin of x-ray background in, (T), 25:11657
- energy eigenvalues for, in electric dipole field, variational method for calculation of, 25:12056
- energy losses in lithium fluoride crystal films due to surface vibrational modes, (T), 25:11677
- energy spectra in ionosphere of 40- to 400-keV, (E), 25:11813
- intensity profiles of solar 35 keV, at 2000 to 3000 km, rigidity-dependent latitude, (E), 25:11797
- interaction processes in ionosphere, review of slowdown and recombination, 25:11810
- interaction with cosmic microwave background, (T), 25:11597
- interactions $e + {}^3He \rightarrow {}^3He + \pi^0$, verification of vector dominance in, (T), 25:12140
- interactions e + d → e + d at low momentum transfers, deuteron-to-proton and neutron-to-proton electric form factor ratio and deuteron radius from, (E), 25:12070
- interactions e + N, hadronic s-channel helicity conservation for 2π production in diffractive, (T), 25:12165
- interactions e + N, review of duality and resonance behavior in inelastic, (E/T), 25:12068 (SLAC-PUB-842)
- interactions $e + p \rightarrow e + \pi^+ + \pi^- + p$, cross section for rho' production in dual model for diffractive, (T), 25:12137 (DESY-70/56)
- interactions e + p, Reggeization scheme for photon

processes for deep inelastic, (T), 25:12148
interactions e⁺ + e⁻ + anti p + p, differential and total cross sections and modulus and phase of form factors of proton electric dipole moment from, (T), 25:12224
interactions e⁺ + e⁻ + K + K total cross section for, (T), 25:12141
interactions e⁺ + e⁻ + ν + ν, total cross section for, (T), 25:12141
interactions e⁺ + e⁻ + π⁺ + π⁻, upper limit for phi production in, (E), 25:12074
interactions e⁺ + e⁻ at 0.8 to 1.0 GeV, track analysis and time distribution of elastic, (E), 25:12073
interactions e⁺ + e⁻ at 1.6 to 2 GeV, multiplicities and total cross section for multiple particle production in, (E), 25:12143
interactions γ + e → γ + e, effective field equations for one-electron multi-photon stationary states for Compton, (T), 25:12139
interactions γ + e → γ + e, scale invariance in lambda phi⁴ theory for Compton, (T), 25:12149
magnetic moment of, computer programs for constructing Feynman diagrams for calculating anomalous, (T), 25:12136 (CNRS-CPT-70-P-336)
magnetic moment of, Feynman diagrams with vacuum polarization insertions for sixth-order radiative corrections to anomalous, (T), 25:12065 (CNRS-CPT-70-P-339)
magnetic moment of, sixth-order corrections to anomalous, 25:12145
motion in magnetic fields, radiative polarization of free relativistic, 25:12060
motion in plane polarized electromagnetic wave, spin orientation from induced radiation from, (T), 25:12161
occurrence in magnetospheric quasi-trapping region of, solar, (E/T), 25:11783
polarization from induced radiation from motion in plane polarized electromagnetic wave, (T), 25:12161
production in ionosphere, review of, 25:11810
radiations from, in strong magnetic fields, 25:12059
radioinduced in γ radiolysis of glassy ethanol, mechanism of reactions and trapping of, 25:10630
ranges and energy loss profiles in anthracene crystals at 25 to 40 keV, 25:11673
reactions with atoms at 5 keV to 1 MeV, exact screened calculations of relativistic bremsstrahlung cross sections for, 25:11681
reactions with atoms having Z = 2 to 11, calculation of ionization cross sections for, using generalized oscillator strengths, 25:11715
reactions with atoms, calculation of mean energy of electrons ejected in, from differential ionization cross sections, 25:11727
reactions with atoms, kinetic energy of bound electron in calculation of ionization cross sections for, (T), 25:11701
reactions with diatomic molecules, adiabatic theory of rotational excitation of non-Σ states in, 25:11725
reactions with helium in eV range, absolute cross sections for production of He I 4713-A and He II 4686-A emissions in, (E), 25:11702
reactions with hydrogen atoms at 12.6 to 680.3 eV, distorted-wave calculations of excitation of 2s state and angular distribution of scattered electrons from, 25:11714
reactions with hydrogen molecules at 20 to 400 eV, absolute cross sections for production of Balmer lines in, (E), 25:11702
reactions with ions, review of dissociative recombination in, (E/T), 25:11729
reactions with molecules at low energies, review of rotational excitation in, (T), 25:11730
reactions with potassium polarized atomic beams at 1.6 to 20 eV, depolarization in, (E), 25:11707
reactions with tungsten at 10 to 60 MeV, Monte Carlo calculations of bremsstrahlung and photoneutrons from, 25:12496
reflection by magnetic fields, photon radiation from, (T), 25:11679
reflection from nickel (001) surfaces, surface atom displacement from 1.0- to 600-eV, (E), 25:12017
scattering by argon metastable atoms at low energies, total cross sections for, (E), 25:11706
scattering by argon plasma at 25 keV, angular distributions from, (E), 25:11879
scattering by argon, krypton, and xenon, calculation of differential cross sections for elastic, using potential-scattering model, 25:11722
scattering by atoms having one and two electrons, infinite-channel close-coupling treatment of charge polarization in, 25:11718
scattering by carbon-13, cross section and form factors for elastic, (E), 25:12376 (AD-710383)
scattering by complex materials, calculation of effective atomic number for back-, 25:11674
scattering by helium and hydrogen atoms, effects of charge polarization on differential cross sections for elastic, (T), 25:11718
scattering by hydrogen atoms, review of use of Sturmian functions in calculation of, 25:11732
scattering by lead-208 and vanadium-51 at 1 to 100 MeV, nuclear-size effects on polarization functions for elastic, (T), 25:12664
scattering by light nuclei with M2 electroexcitation, Coulomb-distortion effects in inelastic, (T), 25:12657
scattering by neodymium-142, -146, and -150 at 15 to 60 MeV, angular distributions for, (E), 25:12622
scattering on magnesium and magnesium oxides at 0.25 to 4 keV, secondary electrons from, (E/T), 25:11672
spectra of trapped radiolytic, in glassy ethanol, 25:10648
synchrotron emission from cosmic, (T), 25:11747
yields from radiolysis of hydrocarbons, 25:10652

ELEMENT 104
separation by thermalized recoil atom conversion into volatile chloride, equipment for continuous, 25:10669 (LYCEN-7034, pp 9-22)

ELEMENT 105
fission of A = 261 isotope of, half-life for spontaneous, (E), 25:12620

ELEMENTARY PARTICLE MODELS
anisotropic, for π⁻ + p → n + π⁺(2π⁺) + π⁻(2π⁻) + mπ⁰ interactions at 4 GeV, 25:12204 (JINR-P1-5431)
dual resonance, Feynman-like diagrams in, 25:12189
dual resonance, proper-time formulation in, 25:12185
dual resonance, twisting invariant factorization of n-point amplitudes in, 25:12184
dual, for rho' production in diffractive e + p → e + π⁺ + π⁻ + p interactions, 25:12137 (DESY-70/56)
dual-resonance, characterization of physical states in quantum electrodynamics in, 25:12180
dual-resonance, for backward K⁻ + N interactions, 25:12215
multiperipheral, distribution of charged π from interactions in, 25:12179
multiperipheral, for high-energy total cross sections, complex Regge poles and oscillatory average multiplicity in, 25:12122 (NYO-2262-TA-228)
multiperipheral, review on properties of, 25:12190
parton, hadron electromagnetic mass difference from virtual Compton scattering amplitude in, 25:12155
Reggeized generalized optical, for multiple and diffraction scattering and dips in π⁻ + p → π⁰ + n interactions at high energies, 25:12205
statistical, for π⁻ + p → n + π⁺(2π⁺) + π⁻(2π⁻) + mπ⁰ interactions at 4 GeV, 25:12204 (JINR-P1-5431)
strong-absorption, π + N, anti K + N, and γ + p interactions at high energies for tests of, 25:12206
urbaryon rearrangement, dynamic structure of hadron amplitudes in, 25:12219
urbaryon rearrangement, hadron structure and dynamics in, 25:12183
urbaryon, hadron mass level structure in, 25:12182
vector dominance, for form factor for K → 2π + l + ν decay, (T), 25:12194
vector dominance, form factors and charge radii for K and N in, 25:12141
vector dominance, verification in γ + ³He, π⁺ + ³He, π⁻ + ³He, and e + ³He interactions, 25:12140
vector-meson dominance, for photon reactions with nuclei at high energies, 25:12151
Veneziano, crossing-symmetric unitarization of amplitude for π + π → π + π interactions in, 25:12196
Veneziano, five-body amplitude for diffractive γ + p → π⁺ + π⁻ + p interactions in, 25:12152
Veneziano, for hadron bootstrap, properties of vector currents consistent with, 25:12177
Veneziano, nucleon electromagnetic and axial form factors from π + N → π + N and π + N → N + A_1(rho) interactions in, 25:12144
Veneziano, scaling laws for deep inelastic ν + p interactions in, (T), 25:12166

ELEMENTARY PARTICLE MODELS (BOOTSTRAP)
duality and zero resonance widths for vector currents in hadron, for n-body interactions of spinless mesons, 25:12177
hadrons in, properties of vector currents consistent with Veneziano model for, 25:12177

ELEMENTARY PARTICLE MODELS (TRIPLET)
hadron properties in quark, 25:12218
hadron strong interactions in quark, review of, 25:12175 (COO-1764-81)
interactions of mesons with nucleons in quark, 25:12218
meson classification and form factor ratios in nonrelativistic quark, 25:12203
meson nonet production in π + N interactions in nonrelativistic quark, relations among cross sections for, 25:12203
Pomeranchuk theorem violation relation with isospin dependence of total cross sections at high energies in quark, 25:12218
sakaton rearrangement for multiple production processes, 25:12186

ELEMENTARY PARTICLES
current algebra representations for N identical spin-0 and -1/2, (T), 25:12125
form factors in two dimensions, integral representations for conformal invariant, 25:12142
interactions at high energies, complex Regge poles and oscillatory average multiplicity in multiperipheral models for total cross sections of, (T), 25:12122 (NYO-2262-TA-228)
interactions of heavy-mass, production of above-10^{13} eV horizontal air showers from, (E), 25:12071

XUM

interactions of, dual amplitudes for six-body w production in, (T), 25:12131
interactions of, Monte Carlo method for cross sections for multiparticle production in, 25:12134
interactions of, production of overlapping resonances in three-body systems from, (T), 25:12126
interactions of, relation of classical and quantal predictions for rescattering probabilities in three-body, (T), 25:12194
operators associated with vector, relativistic limit of spin tensor, (T), 25:12128
phase space with constraint functions for, relativistic calculations of angular distributions and correlations in three-body, (T), 25:12135
production of, Monte Carlo method for cross sections for multiple production of, 25:12134
quantum field theory for highly charged subnuclear, 25:12132
strong interactions at high and low energies, review of duality and quark model for, (T), 25:12175 (COO-1764-81)
strong interactions at high energies, quark model numerical selection rule for three-body, (T), 25:12218
strong interactions in multiperipheral model, charged particle distributions from, (T), 25:12179
symmetry for, limiting process m → 0 for Wigner rotations in Poincare group in, (T), 25:12233
symmetry for, matrix elements of finite transformations of U(n), (T), 25:12235
theory for, current structure of phenomenological Lagrangians in, (T), 25:12129
weak interactions of, L-matrix structure of Hamiltonian in, (T), 25:12162 (AD-710572)

ELEMENTARY PARTICLES (TRIPLET)
properties of quark atoms, (T), 25:12188
quark regions inside massive stars, (T), 25:12188
search for quarks in ferromagnetics using electrometers with beam suspension method, (E), 25:12064

ELEMENTS
determination of trace amounts of, in minerals and rocks, conference on, 25:10446
determination of trace amounts of, in rocks and soils by atomic absorption spectrometry, matrix effects on, 25:10457
reactions of beams of atoms of, at 0.1 to 20 eV, 25:10517 (JUL-674-RC)
separation from standard rocks by borate fusion, dissolution in EDTA, and ion exchange, 25:10671
separation of, gaseous and liquid phases of, review on methods for, 25:10669 (LYCEN-7034, pp 9-22)

EMBRYOS
radiation effects on organogenesis in animal and plant, review of ionizing, 25:10977
radiation effects on respiration and lactic dehydrogenase of, protective effects of cysteamine against, x, 25:11096(R) (EUR-4491)
radioinduced teratogenesis in mice, following exposure of mothers, effects of state of pregnancy on x, 25:11287
radiosensitivity of mice and rat, in utero in relation to species differences, x, 25:11277

ENDOCRINE GLANDS
radiation effects on, in man, review of literature on, 25:11209

ENGINEERING
book: Gas Dynamics of Two-Phase Media (In Russian), 25:10772

ENGINEERING TEST REACTOR
fuel element from, analytical examination of failed, 25:11463 (IN-1437, pp 70-5)
fuel elements for, analysis of fabrication breakup defects in plate-type, 25:11461 (IN-1437, pp 13-23)
irradiation facilities in, operation summary on, 25:11474(R) (BNWL-842)

ENVIRONMENT
radiation monitoring of nuclear installation, guide for design, operation, and staffing of facilities for, 25:10763
research programs on, analytical, 25:10433 (ORNL-4636, pp 1-7)

ENZYMES
use for determining uv-radioinduced DNA damage in Micrococcus luteus, 25:10959 (BNL-50203, pp 27-40)

EPITHELIUM
radioinduced aberration of chromosomes in, of mice cornea, neutron, x, 25:11018

EQUIPMENT AND PROCEDURES
requirements for industrial, computerized simulation models for prediction of, 25:10757 (RFP-1527)

ERBIUM
determination of trace amounts of, in biotite and tektite by spark source mass spectrometry, 25:10455
separation from holmium and yttrium in hydrochloric or nitric acid solutions by solvent extraction using DEHPA, 25:10685

ERBIUM ALLOYS AND SYSTEMS
Er--Ni, magnetic structure of intermetallic $ErNi_3$ and Er_2Ni_7, 25:11979 (CEA-CONF-1704)

ERBIUM FLUORIDES
effects on gamma-induced luminescence of calcium fluoride crystals, 25:11955

ERBIUM ISOTOPES Er-162
moment of inertia as function of excitation energy, (E/T), 25:12544

ERBIUM ISOTOPES Er-164
energy levels from holmium-165 (p,2nγ) and (d,3nγ), dysprosium-164 (He-3,3nγ), and dysprosium-162 (α,2nγ) reactions at 16 to 28 MeV, rotational, (E/T), 25:12544
energy levels of, M1 transition probabilities for spin-vibrational, (T), 25:12703
energy-level transitions from holmium-165 (p,2nγ) and (d,3nγ), dysprosium-164 (He-3,3nγ), and dysprosium-162 (α,2nγ) reactions at 16 to 28 MeV, probabilities for, (E/T), 25:12544
energy-level transitions from production in (α,3n) and (α,4n) reactions at 42 MeV, intensities and angular distributions from, (E/T), 25:12553
moment of inertia as function of excitation energy, (E/T), 25:12544
neutron capture by, spectroscopic analysis of, (E), 25:12586

ERBIUM ISOTOPES Er-165
energy levels of, coupling mechanisms between, (T), 25:12525 (LYCEN-7034, pp 94-116)

ERBIUM ISOTOPES Er-166
alpha inelastic scattering at 27.5 to 32.5 MeV, α spectra and angular distributions for, (E), 25:12605
electron--nucleus quadrupole interaction in, numerical solution of, (T), 25:12685
energy levels from alpha inelastic scattering, deformation parameters for, (E), 25:12605
energy levels from holmium-166 and thulium-166 decays, spin-parity assignments and transition probabilities for, (E), 25:12599
neutron capture by, spectroscopic analysis of, (E), 25:12586

ERBIUM ISOTOPES Er-167
neutron capture by, spectroscopic analysis of, (E), 25:12586

ERBIUM ISOTOPES Er-168
energy levels from erbium-167 neutron capture, spin-parity assignments for, (E), 25:12586
neutron capture by, spectroscopic analysis of, (E), 25:12586

ERYTHROCYTES
aggregation of, during angiography, administration of dextran and glucose for reducing complications from, 25:11195
analysis of labeled, for chromium-50 by neutron activation and γ spectroscopy, 25:10503
isoenzymes of lactic dehydrogenase in, of xenogenic radiation chimeras, 25:10992
labeling of human, with chromium-51 and mercury-197 for use in spleen scanning, 25:11201
labeling with radioisotopes for study of inflammatory lesions, 25:11193
radiation effects on, and reticulocytes in peripheral blood of guinea pigs, comparison of chronic cesium-137 and single cobalt-60 γ, 25:11278
use of chromium-51-labeled heat treated, for determining splenic blood flow following injection, 25:11142
use of chromium-51-labeled, for studying blood exchange between parabiotic mice, 25:10915

ESOPHAGUS
radiotherapy of cancer of, recommendations for, 25:11236

ESTERS
polymers, radioinduced polymerization of 2-hydroxyethyl methacrylate on fabrics of, hydrophilic properties of products from γ and electron, 25:10600 (JAERI-5026, pp 63-7)
polymers, radioinduced polymerization of acrylic acid on drawn fibers of, properties of products from γ, 25:10599 (JAERI-5026, pp 56-62)
polymers, radioinduced polymerization of acrylic acid on fibers of, effects of temperature on γ, 25:10602 (JAERI-5026, pp 73-9)
polymers, radioinduced polymerization of acrylic acid on, by impregnation method, electron, 25:10598 (JAERI-5026, pp 52-5)
polymers, radioinduced polymerization of acrylic acid on fabrics of, by impregnation method, properties of products from electron, 25:10601 (JAERI-5026, pp 68-72)

ETHANE
radiolysis of gaseous, low-energy electron, 25:10644
radiolysis of, effects of ammonia or sulfur fluorides on yields from γ, 25:10632

ETHANE, 1,1-DICHLORO-
spectra of solid, far ir, 25:10529

ETHANE, 1,1,1-TRICHLORO-
spectra of solid, effects of deuterium on far ir and Raman, 25:10529

ETHANE, 1,1,1-TRIFLUORO-
spectra of solid, far ir, 25:10529

ETHANOL
effects on γ radiolysis of indole-3-acetic acid, 25:10647
fragmentation in mass spectrometer, effects of deuterium on, 25:10528
radiolysis of glassy, mechanism of electron and free radical reactions and trapping in γ, 25:10630
radiolysis of glassy, spectra and extinction coefficients of trapped electrons and free radicals from γ,

25:10648
ETHANOL, 2-MERCAPTO-
effects on yields from radiolysis of aqueous diisopropylamine solutions, 25:10627(R) (NYO-2499-37)
ETHER, ALKYL VINYL
radioinduced polymerization on surface of synthetic calcium aluminate hydrate,, 25:10616
ETHYL SULFATES
effects on growth of barley seeds in soil, effects of dose, fertilizer concentration, and soil chemistry on, 25:11315
ETHYLENE
polymerization by 2,2'-azobis[2-methylpropionitrile], role of excited monomer in propagation reaction of, 25:10612
radioinduced polymerization of, role of excited monomer in propagation reaction of γ, 25:10612
radiolysis of gaseous, low-energy electron, 25:10644
ETHYLENE, CHLORO-, POLYMERS
radioinduced polymerization of acrylonitrile on powders of, properties of fibers from γ, 25:10595 (JAERI-5026, pp 35-41)
radioinduced polymerization of acrylonitrile on powders of, effects of dose rate on γ and electron, 25:10596 (JAERI-5026, pp 42-5)
ETHYLENE, 1,1-DICHLORO-
radioinduced polymerization in wood, effects of presoaking on properties of products from γ or electron, 25:10603 (JAERI-5026, pp 80-5)
radioinduced polymerization in woods, effects of pretreatment of woods on properties of products from γ, 25:10604 (JAERI-5026, pp 86-93)
radioinduced polymerization in woods, thermal stability of products from γ, 25:10605 (JAERI-5026, pp 94-100)
ETHYLENE POLYMERS
radiation effects on fusion of, crystallized by high-speed stirring at 95, 102, and 105°C, 25:10618
radiation effects on linear, NMR spectral studies on compounds produced from fast electron, 25:10589
radioinduced graft polymerization with styrene, effects of swelling on γ, 25:10613
ETHYLENEIMINE
effects on growth of barley seeds in soil, effects of dose, fertilizer concentration, and soil chemistry on, 25:11315
EUMYCOTA
Agaricaceae sp., cesium-137 concentration by, 25:11003
Helminthosporium maydis, radiation effects on infectivity of, in corn, role of cytoplasma in, 25:11010(R) (ORO-2583-8)
Penicillium expansum, radiation effects on pectinesterase, polygalacturonase, and tissue maceration enzymes of, γ, 25:10979
Phyllosticta sp., radiation effects on infectivity of, in corn, role of cytoplasm in, 25:11010(R) (ORO-2583-8)
radiation effects on survival of, effects of DNA on x, 25:10960 (BNL-50203, pp 82-90)
Saccharomyces cerevisiae, labeling with chromium-51, 25:10900
Saccharomyces vini, radiation effects on heat production and reproduction of, effects of dose on x, 25:11324
Schizosaccharomyces pombe, radioinduced mutations in, effects of dose and temperature on uv, 25:11074(R) (AECL-3777)
Torulopsis sphaerica, radiation effects on heat production and reproduction of, effects of dose on x, 25:11324
use of zinc-65-labeled mycelium of, for arthropod food chain studies in soil, 25:10929
yeasts, radiation effects on survival of, effects of dose fractionation on simultaneous recovery from lethal and sublethal doses in relation to cobalt-60 γ, 25:11316
EUROPE
fuel reprocessing in, economic and legal aspects of, 25:10673
EUROPIUM
abundance in photosphere and sunspots, (E), 25:11613
complexes with EDTA, separation by ion exchange, effects of resin crosslinking on, 25:10665 (INR-P-1209)
determination of trace amounts of, in biotite and tektite by spark source mass spectrometry, 25:10455
determination of trace amounts of, in phosphate deposits by spark source mass spectrometry, 25:10456
determination of trace amounts of, in rocks and sand by thermal neutron activation, ion exchange, and γ spectrometry, 25:10492
energy-level transitions in, rates of Auger and x-ray, (T), 25:11685
separation from aqueous solutions by solvent extraction using bis(2,2-dimethylhexyl) phosphate, 25:10679
EUROPIUM ALLOYS AND SYSTEMS
Eu--Yb-base, magnetic properties, 25:12013
EUROPIUM ISOTOPES Eu-145
energy levels from quasi-particle Tamm--Dancoff approximation, spin--parity assignments, single-particle energies, eigenvectors, electromagnetic moments, and spectroscopic factors for, (T), 25:12616
energy-level transitions from quasi-particle Tamm--Dancoff approximation, rates for M1 and E2, (T), 25:12616
EUROPIUM ISOTOPES Eu-151
neutron capture by, gamma spectra from thermal, (E), 25:12547
EUROPIUM ISOTOPES Eu-152
beta and electron-capture decay of, gamma spectra and e--γ angular correlations from, (E/T), 25:12576
beta decay of, γ singles and coincidence spectra and log ft value for, (E), 25:12518 (INSJ-123)
energy-level transitions from thermal neutron capture by europium-151, intensities of, (E), 25:12547
EUROPIUM ISOTOPES Eu-154
beta decay of, gamma spectra and γ--γ angular correlations from, (E/T), 25:12576
EUROPIUM ISOTOPES Eu-156
beta decay of, gamma spectra and γ--γ angular correlations from, (E/T), 25:12576
EXPERIMENTAL BREEDER REACTOR-II
fuel elements for, fabrication of Type 316 stainless steel clad plutonium nitride (PuN)--uranium nitride (UN) pin type, 25:12795(R) (BMI-1693)
fuel irradiation in, hazards evaluation for higher burnup oxide, 25:11533 (ORNL-TM-2635(Suppl.))
instrumentation for, performance of in-vessel coolant pressure and temperature measuring, 25:12781 (ANL-EBR-25)
neutron flux spectra of, activated foils dosimetry techniques for measurement of fast, 25:12773 (BNWL-1403)
EXPLOSIONS
airblasts from, damage to window panes from, (E/T), 25:10792 (SC-RR-70-441)
EXPLOSIVES
design of nuclear, for industrial and scientific use, criteria for, 25:10739
EXPONENTIAL PILES
neutron buckling and fine structure measurements in HELEN I, (E/T), 25:12828
EYES
radiation dose to lens of human, effects of age and dose fractionation on maximum safe, 25:11284
radioinduced aberrations of chromosomes in corneal epithelium of mice, neutron, x, 25:11018
radioinduced injuries in, of man, following exposure to high-energy electromagnetic waves, 25:11297
radioinduced injuries to tissues of mammalian, effects of dose on acute x, 25:11284
radioinduced lens cataracts in mammalian, comparison of dose for γ and neutron, 25:11284
radiosensitivity of choroid and retinal tissues in, of rats, comparison of, 25:11284

F

FALLOUT
content in atmosphere at Zugspitze, Germany, April to Dec. 1970, 25:10705(R) (NYO-4061-3)
deposition and transport of nuclear explosion-produced, review of early research on, 25:10714 (ORO-2529-28, App. B)
deposition and transport of radioactive, research program on, 25:10706(R) (ORO-2529-28)
deposition of stratospheric, in North American coastal waters and in Crater Lake, Oregon, tritium tracer studies of, 25:10720
deposition of, effects of fires and winds on, 25:10702 (AD-708558)
distribution and redistribution of Project Schooner-produced, measurement of, 25:10716 (UCRL-72534)
distribution from 8th and 9th Chinese nuclear weapons tests, 25:10472(R) (BMBW-FBK-70-19)
monitoring in Japan by measuring iron content of wind-blown surface soil, 25:10718
radiochemical properties of Shot Coulomb C, (E), 25:10734 (AD-708567)
radiochemical properties of Shot Priscilla, (E), 25:10733 (AD-708566)
uptake by human population of Soviet Union, 25:10934 (NP-18380)
uptake by plants and food products following nuclear explosions, predictions for, 25:11038 (UCRL-72716(Rev.1))
FAST FLUX TEST FACILITY
containment system for, atmospheric radioactivity alarm and trip levels for, 25:12812 (BNWL-1479)
materials testing for, in gas and sodium environments, 25:11474(R) (BNWL-842)
FATTY ACIDS
methyl esters, computer analysis of data from chromatographic analysis of, 25:12917 (UCRL-72393)
FECES
americium-241 excretion in human, 25:10931 (CEA-CONF-1557)
cobalt-60 1-nitroso 2-naphthol chelate excretion in, of rats, 25:10958
iron-59 excretion in human, measurement of, for determining enteral protein loss, 25:11171
FERMI POWER REACTOR, UNIT 2
radioactive effluents from, revised and additional data on, 25:12747 (DOCKET-50341-24)
FERMIONS
current algebra representations for N identical spin-$^1/_2$, (T), 25:12125

detection of beams of, stochastic theory for, 25:12053
fields of, equivalence between models for pure, (T), 25:12241
interactions with gravitons, Lagrangian function of tetrad and fermion fields for, (T), 25:12271
motion in planar electromagnetic waves, induced radiation and spin orientation from, (T), 25:12160
theory for systems of, spectral density method in statistical mechanics in, (T), 25:12061

FERMIUM ISOTOPES Fm-257
production at TRU, 25:10654(R) (ORNL-4588)

FERTILITY
radiation effects on human, 25:11090

FERTILIZERS
content of soils, effects of, on growth of chemical mutagen-treated or γ-irradiated barley seeds in soils, combined effects of dose and soil chemistry on, 25:11315
particle size of dolomite and metal oxides in, determination by beta backscattering, 25:10784

FETUSES
radiation effects on human, review of literature on, 25:11209

FIBRINOGEN
radiosterilization of, effects of temperature and 3 Mrad dose on in vivo γ, 25:11333
use of metastable indium-113-labeled, or iodine-131-labeled, for scintigraphy of thrombi in rabbits, 25:11214

FIELD EMISSION MICROSCOPY
ion trajectories in front of tip, calculations, 25:12299 (IPP-7/2)

FIELD THEORY
field equations in, solution to initial-value problem for nonlinear classical, (T), 25:12242
fields in, equivalence between models for pure fermion, 25:12241
models for pure fermion fields in, equivalence between, 25:12241
Schwinger terms in local, 25:12244
superpropagators for arbitrary mass in, mathematical properties of, 25:12243

FILICINIDAE
Osmunda regalis, radioinduced free radicals in, ESR study of ionizing, 25:11319

FILMS
deposition by vapor-ion methods, bibliography, equipment, and summary on, 25:12904 (RFP-1568)
deposition from two sources, ultrahigh vacuum system with double electron gun for, 25:10806
ion scattering by thin, 25:10583(R) (AECL-3776)

FILTERS
design of annular packed-bed, for gases, 25:10761(P)

FIRES
effects with winds on deposition of fallout, 25:10702 (AD-708558)

FISSION
charge distribution in medium-energy, systematic behavior of, (T), 25:12700
nuclear potential energy in, calculation using Strutinski method, (T), 25:12681
theory of, adiabatic, (T), 25:12645

FISSION FRAGMENTS
angular correlations from alpha fission of uranium-238, in- and out-of-plane, (E), 25:12526 (MNC-3783-7)
detection of, uses of dielectric track detectors for, 25:10825
energy spectra from alpha fission of uranium-238, 25:12526 (MNC-3783-7)
mobility in gases, spectrometer for measurement of, 25:10903
tracks in glasses and rocks, effects of geometry factor on counting accuracy for, 25:10695
tracks in meteorites, effects of temperature on annealing of, 25:10696

FISSION PRODUCTS
behavior of aerosols of, following fast reactor accidents, 25:12768(R) (EURFNR-855)
determination in reactors by γ spectrometry, 25:10491 (ORNL-4636, pp 20-33)
diffusion from uranium aluminide fuels, mechanisms of, 25:11375 (IN-1437, pp 24-59)
distribution in graphite moderated thermal reactor, calculation of fuel burnup from, 25:12776 (JUL-678-RG)
gamma spectra at 11 days after thermal neutron fission of uranium-235, (E), 25:12538
removal from reactor containment systems, effects of natural transport processes on post-accident, (E/T), 25:12803 (BNWL-1457)
separation by volatility processes, 25:10472(R) (BMBW-FBK-70-19)
separation from fission products by automatic ion exchange chromatography, design and performance of equipment for, 25:10659 (CEA-N-1267)
sorption of gaseous, efficiency of packed beds for, 25:10797(R) (NYO-841-23)
spectrum for gaseous, calculation of asymptotic bubble, (T), 25:12847

FISSIONABLE MATERIAL
handling of, description of ANSI N16.1-1969 criticality safety standards for outside-reactor, 25:10802

FISSIUM
fissium--U-base, etching of irradiated, materials for, 25:11367

FLANGES
design of high-pressure, for nuclear power plant components, development of deformation and stress analysis methods for, 25:10758

FLOWMETERS
development of a-c operated, for liquid sodium cooled reactors, 25:12792

FLUID FLOW
analysis in reactors, book on, 25:12791
book: Gas Dynamics of Two-Phase Media (In Russian), 25:10772
calculation of free-surface incompressible, at high Reynolds numbers, computer program for, 25:10765 (AD-709142)
heat transfer, holdup, and nucleation in two-phase, calculations for, 25:10766 (AERE-R-3984)
magnetohydrodynamic, around solid and hollow spheres, (T), 25:11760
magnetohydrodynamic, boundary-value problems in, 25:11770
magnetohydrodynamic, correlation functions for velocity and magnetic field in turbulent, 25:11757
magnetohydrodynamic, equations for relativistic and nonrelativistic, 25:11768
magnetohydrodynamic, flow near thin airfoils, 25:11774
magnetohydrodynamic, ionizational and electron thermal nonequilibrium effects in compressible boundary layers of, (T), 25:11755
magnetohydrodynamic, magnetic field re-connection in incompressible, (T), 25:11758
magnetohydrodynamic, multiple-scale solutions for flow inside ducts, 25:11771
magnetohydrodynamic, of ionized jet in tube in magnetic field, (E), 25:11775
magnetohydrodynamic, one-dimensional approximations for channel, 25:11766
magnetohydrodynamic, spherical vortex motions in, (T), 25:11554
magnetohydrodynamic, variational solutions for relativistic, 25:11769
magnetohydrodynamic, wave propagation in relativistic, (T), 25:11764
pressure distribution for axisymmetric two dimensional, during expulsion from cooling system, (T), 25:12808
thermal boundary layer in steady slug-type, with mixed boundary conditions, 25:10771
transients in pressurized water reactor coolant, stable numerical integration of conservation equations for, (T), 25:12793

FLUIDIZED BEDS
efficiency for fission gas sorption, equations for calculating, 25:10797(R) (NYO-841-23)
gases from fuel processing, design of filter for off-, 25:10761(P)
model studies of conical, for fuel particle coating, 25:11479 (JUL-669-RW)
void volume in packed granular, method for calculating, 25:10797(R) (NYO-841-23)

FLUORENONE
photoreduction and quenching of, by dimethylanilines, uv, 25:10627(R) (NYO-2499-37)

FLUORESCEIN, DIIODO-
radiolysis of iodine-131-labeled, yields from, 25:10642
thermal decomposition of iodine-131-labeled, yields from, 25:10642

FLUORINE
determination by charged particle and photon activation, radiochemical separation methods for, 25:10488 (CEA-R-4072)
determination by charged particle and photon activation, reactions and sensitivities for, 25:10488 (CEA-R-4072)
determination in aluminum by charged particle activation and radiochemical separation, 25:10488 (CEA-R-4072)
determination in fluorinated concentrates and ores by activation methods, 25:10498
determination in silicon by photon activation and radiochemical separation, 25:10488 (CEA-R-4072)
determination of trace amounts of, in biotite and tektite by spark source mass spectrometry, 25:10455
determination of trace amounts of, in rocks and stony meteorites by pyrohydrolysis and thorium nitrate titration, 25:10493
reactions with neptunium dioxide and neptunium tetrafluoride, kinetics of, 25:10568 (CEA-R-4051)

FLUORINE ISOTOPES F-18
distribution in bones, method for determining, 25:10943
energy levels from oxygen-18 (He-3,t) reactions at 16 and 30 MeV, (E), 25:12498
use for scanning of fibia and tibia bones in rats, 25:11216

FLUORINE ISOTOPES F-19
deuteron reactions (d,He-3) at 52 MeV, helium-3 spectra and angular distribution for, (E), 25:12385
neutron capture by, gamma spectra and Q-value for thermal, (E), 25:12403
reactions (F-19,F-18) with boron-10 at 20 and 24 MeV, DWBA analysis of angular distributions from, (E/T), 25:12381 (NP-18541)
scattering by boron-10 at 20 and 24 MeV, angular

distributions from elastic, (E/T), 25:12381 (NP-18541)
FLUORITES
analysis of ores containing, for fluorine by activation methods, 25:10498
FLUOROURANATES
preparation and properties of UF_6^-, 25:10576
FOOD
radioisotope contamination of, by fallout, 25:11038 (UCRL-72716(Rev.1))
strontium-90 accumulation in, from fallout in Soviet Union, 25:10934 (NP-18380)
FOOD CHAINS
cesium-137 passage through lichen-reindeer-man, in Soviet Union, 25:11037 (NP-18381)
contamination by radioactive tellurium isotopes, 25:10948
radioisotope transport through plant-caribou and reindeer-man, in Alaska, cesium-137, strontium-89, and stronium-90, 25:11001
tracer study of arthropod, using zinc-65-labeled fungus mycelium, 25:10929
FORBUSH DECREASES
effect on low-energy proton fluxes near Moon, Dec. 16, 1966, (E), 25:11669
FORKED RIVER POWER REACTOR, UNIT 1
design parameters of, requested additional data on, 25:12751 (DOCKET-50363-10)
operations aspects of, requested additional data on, 25:12751 (DOCKET-50363-10)
FORMAMIDE, N,N-DIETHYL-
effects on properties of products from radioinduced polymerization of acrylic acid on poly(ethylene terephthalates), 25:10597 (JAERI-5026, pp 46-51)
FORMIC ACID
effects on properties of products from radioinduced polymerization of acrylic acid on poly(ethylene terephthalates), 25:10597 (JAERI-5026, pp 46-51)
microwave emission from interstellar, detection of, 25:11593
FORT ST. VRAIN POWER REACTOR, UNIT 1
design parameters of, revised and additional data on, 25:12736 (DOCKET-50267-24)
operations aspects of, revised and additional data on, 25:12736 (DOCKET-50267-24)
radioactive effluents from, effects on environment of, 25:12737 (DOCKET-50267-25)
safety aspects of, requested additional information on, 25:12736 (DOCKET-50267-24)
FRANCE
radiation protection programs at critical assemblies in, 25:11079
FRANCIUM ISOTOPES Fr-215
alpha decay of, α spectra and half-life for, (E), 25:12592
FRANCIUM ISOTOPES Fr-216
alpha decay of, α spectra and half-life for, (E), 25:12592
FRANCIUM ISOTOPES Fr-217
alpha decay of, α spectra and half-life for, (E), 25:12592
FREE RADICALS
radioinduced in γ radiolysis of glassy ethanol, mechanism of reactions and trapping of, 25:10630
radioinduced, in ferns, ESR study of, 25:11319
radioinduced, in human bone tissues following processing for sterilization, γ, 25:11329
radioinduced, in seeds of Dahlia, EPR analysis of electron, 25:11305 (NP-18394)
spectra of radiolytic, resonator for simultaneous sample irradiation and measurement of ESR, 25:10626 (KFK-1285)
spectra of radiolytic, saturation of ESR, 25:10645
spectra of, produced in γ-irradiated deuterated and nondeuterated norbornane derivatives, ESR, 25:10637
β-FRUCTOFURANOSIDASE
radioinduced inactivation of, in sugar beets, cobalt-60 γ, 25:10964
FRUITS
dates, infestation with grain beetles, use of γ radiation for control of, 25:11244 (NP-18607)
FUEL CAPSULES
design of high-stability, for thermoelectric converters, 25:10778(R) (ORNL-TM-3214)
FUSED SALTS
electrode development for, 25:10434 (ORNL-4636, pp 7-13)

G

GADOLINIUM
determination of trace amounts of, in biotite and tektite by spark source mass spectrometry, 25:10455
determination of trace amounts of, in phosphate deposits by spark source mass spectrometry, 25:10456
GADOLINIUM BORIDES
properties of electron-emission cathodes of, for accelerator electron sources, 25:12316
GADOLINIUM ISOTOPES Gd-145
decay of isomeric, half-life, branching ratio, and γ and conversion electron spectra from, (E), 25:12582
GADOLINIUM ISOTOPES Gd-152
energy levels from europium-152 decay, properties of low-lying, (E/T), 25:12516 (INSJ-123)
GADOLINIUM ISOTOPES Gd-153
half-life of, 25:10491 (ORNL-4636, pp 20-33)
GADOLINIUM ISOTOPES Gd-154
energy-level transitions following (α,xn) reactions at 42 MeV, branching ratios for, (E), 25:12553
energy-level transitions from europium-154 beta decay, intensities and M1 multipole admixtures for, (E/T), 25:12576
energy-level transitions from production in (α,4n) reactions at 42 MeV, intensities and angular distributions from, (E/T), 25:12553
neutron capture by, spectroscopic analysis of, (E), 25:12586
GADOLINIUM ISOTOPES Gd-155
energy levels of, coupling mechanisms between, (T), 25:12525 (LYCEN-7034, pp 94-116)
neutron capture by, average circular γ polarization in thermal, (E), 25:12601
neutron capture by, spectroscopic analysis of, (E), 25:12586
GADOLINIUM ISOTOPES Gd-156
energy levels from gadolinium-155 neutron capture, spin-parity assignments for, (E), 25:12586
energy levels from thermal neutron capture, spin for compound, (E), 25:12601
energy-level transitions from europium-156 beta decay, M1 multipole admixtures for, (E/T), 25:12576
neutron capture by, spectroscopic analysis of, (E), 25:12586
GADOLINIUM ISOTOPES Gd-157
neutron capture by, average circular γ polarization in thermal, (E), 25:12601
neutron capture by, spectroscopic analysis of, (E), 25:12586
GADOLINIUM ISOTOPES Gd-158
energy levels from gadolinium-157 neutron capture, spin-parity assignments for, (E), 25:12586
energy levels from thermal neutron capture, spin for compound, (E), 25:12601
GADOLINIUM OXIDES
preparation of microspheres of, sol-gel method for, 25:10571 (EUR-4550)
GALACTOSE
analysis for carbon-14 by scintillation counting, 25:10485
GALAXIES
effects of intervening, on radiation from Seyfert galaxies, (T), 25:11584
hydrogen content in M31 and M33, method for measurement of neutral, 25:11646
hydrogen content of M31, neutral, (E), 25:11647
hydrogen content of M33, neutral, (E), 25:11648
masses of, radio and optical observations of, (E), 25:11634(T) (CSIRO-Trans-10206)
plasma ejection from nuclei of, (T), 25:11658
positions of, in direction of quasars with small redshifts, (E), 25:11649
radio observations of cluster of, in Coma Berenices, (E), 25:11644
radio observations of compact, using 21-cm neutral-hydrogen line, (E), 25:11638
rotation of 56, mean velocities of, (E), 25:11635
spectral redshifts of two, associated with 4C 31.04, (E), 25:11652
stability of clusters of, effects of cosmological constant on, (T), 25:11642
structure of, (T), 25:11538
structure of, model for spiral, (T), 25:11645
supernovae in Sb and Sc, frequency of occurrence of, (E), 25:11637
x-ray background in, origin of cosmic, (T), 25:11656
GALLIC ACID, PROPYL ESTER
radioprotective effects of, on cultured cells from mice, effects of time between exposure and administration on γ, 25:11106
GALLIUM
determination in sedimentary rocks by direct-reading spectrometry, 25:10450
determination of trace amounts of, in basalt and granite, correction of matrix effect in uv spectrographic, 25:10453
determination of trace amounts of, in biotite and tektite by spark source mass spectrometry, 25:10455
determination of trace amounts of, in minerals and rocks by x-ray fluorescence, methods for correction of matrix effect in, 25:10448
determination of trace amounts of, in molybdenum, review on, 25:10459
determination of trace amounts of, in rocks and sand by thermal neutron activation, ion exchange, and γ spectrometry, 25:10492
determination of trace amounts of, in rocks, quantometer for spectroscopic, 25:10451
determination of trace amounts of, in standard bauxite, carbonate, and silicate rocks by x-ray fluorescence, 25:10449
determination of trace amounts of, in standard silicate rocks using sodium chloride buffer, emission spectrographic, 25:10454
effects on crack formation in plutonium during α--β

thermal cycling, 25:11393
separation from thallium by gas chromatography using aluminum chloride eluent, 25:10666 (JINR-P6-5410)
superconducting quench-condensed, electron tunneling in, (E/T), 25:11842
GALLIUM ALLOYS AND SYSTEMS
Ga--Pu-base, deformation mechanisms in delta-stabilized fcc, at -196 to 25°C, effects of concentration and strain rate on, 25:11435
Ga--Pu-base, expansion of rolled and segregated, at 25 to 475°C, 25:11388
Ga--Pu-base, fabrication of dispersion-hardened delta-stabilized, 25:11359
Ga--Pu-base, mechanical properties of dispersion-hardened delta-stabilized, at 25 to 400°C, 25:11359
Ga--Pu-base, microstructure and phase composition of heat-treated and as-sputtered, 25:11360
Ga--Pu-base, phase diagram of, proposed, 25:11446
Ga--Pu-base, phase transformations in metastable, 25:11446
Ga--Pu-base, preparation by triode sputtering, 25:11360
Ga--Pu-base, tensile properties of high-purity delta-stabilized, effects of hot working on room-temperature, 25:11390
Ga--Pu-base, tensile properties of rolled, at 25 to 600°C, effects of trace amounts of iron and nickel on, 25:11391
Ga--Pu-base, twinning in delta-stabilized, annealing and deformation, 25:11436
GALLIUM ARSENIDES
recrystallization of amorphous films of, by annealing, 25:12023
GALLIUM ISOTOPES Ga-66
energy levels from germanium-66 beta decay, spin--parity assignments for, (E), 25:12477
energy-level transitions from germanium-66 beta decay, intensities, branching ratios, multipolarities, and conversion coefficients for, (E), 25:12477
GALLIUM ISOTOPES Ga-68
effectiveness of compounds of, for kidney scintigraphy in comparison to iodine-131-labeled hippuran, studies in rats on, 25:11169
effectiveness of EDTA-incorporated, in combination with iodine-131 in double isotope method for diagnosis of kidney diseases, 25:10928
preparation of macroaggregate-incorporated, for lung scanning, 25:11205
use of macroaggregate-incorporated, for scanning of human lungs, 25:11205
GALLIUM ISOTOPES Ga-69
proton reactions at 1.5 GeV, cross sections for spallation products from, (T), 25:12439
GALLIUM ISOTOPES Ga-71
proton reactions at 1.5 GeV, cross sections for spallation products from, (T), 25:12439
GALLIUM PHOSPHIDES
recrystallization of amorphous films of, on gallium-arsenide substrate by annealing, 25:12023
GAMMA CAMERAS
development of multiwire proportional, 25:10810 (CEA-CONF-1668)
performance for scanning iodine-131 in human kidneys for renal insufficiency, 25:11206
GAMMA RADIATION
angular distribution measurements in inverse photonuclear reactions, problems in, 25:10865
attenuation in shielding materials at 6 and 8 MeV, 25:11947
cosmic background, discrete-source interpretation of, (T), 25:11636
cosmic background, origin of, (T), 25:11748
detection of prompt, from supernovae, (T), 25:11553
dose determination during radium therapy, 25:11072
dose to human lung following accidental inhalation of americium-241 and plutonium-241, equations for estimating, 25:11053 (BNWL-B-12)
dose to man in northern Soviet Union, contribution of occupation as reindeer herdsmen on cesium-137, 25:11037 (NP-18381)
dose to population of Soviet Union, assessment of global cesium-137, 25:11073
dosimetry for implant therapy, use of computer calculations for, 25:11058
dosimetry for promethium-147-labeled luminous paints, 25:11065
dosimetry for radium therapy, requirements for accuracy during, 25:11069
dosimetry for therapy using iridium-192 implants, use of computer calculations of isodose curves for, 25:11000
dosimetry for therapy, use of computer calculations for, 25:11061
dosimetry for therapy, use of phantoms for preparation of isodose charts for, 25:11060
dosimetry in accidents, personnel dosimeter for, 25:10881
dosimetry in beryllium oxide mixtures with plutonium oxide, 25:11052 (AERE-R-5069)
dosimetry in nuclear accidents, chemical dosimeter for, 25:10883
dosimetry in tissue-equivalent phantoms following criticality accidents, 25:11057
effects of longevity of Drosophila melanogaster, lethal, 25:11248
effects on acetylene, mechanisms of benzene formation from, 25:10650
effects on activity of glycolytic enzymes in dormant and sprouting rye seeds, 25:10974
effects on alkali metal halides, re-excitation and decay of M and F centers in, (E/T), 25:11956
effects on aorta transplants, damage to collagen following sterilizing, 25:11341
effects on aqueous sodium sulfide solutions, yields from, 25:10649
effects on aqueous solutions of gramicidin, effects of dose rate and concentrations on, 25:10587 (JAERI-5026, pp 167-8)
effects on ascorbic acid content of Nicotiana tabacum callus and tumor tissues, cobalt-60, 25:10965
effects on beryllium oxide single crystals, ESR study of defects induced in, 25:11950 (CEA-R-3937)
effects on bicyclo[2.2.2]oct-2-ene or norbornane, ESR spectral studies of radicals from, 25:10638
effects on biological activity of fibrinogen, 25:11333
effects on blood pressure, heart rate, and respiration in rabbits, effects of calcium gluconate and zirconium citrate on whole-body, 25:11289
effects on bone transplants in rabbits, sterilizing, 25:11340
effects on calcium fluoride crystals doped with holmium or erbium fluoride, luminescence, 25:11955
effects on cell division, γ and uv-radiosensitivity, and nutritional requirements, mutagenic cobalt-60, 25:11019
effects on chloroplasts of leaves, effects of red light on damaging, 25:11310
effects on cholestanol at room temperature, yields of products from, 25:10624 (JAERI-5026, pp 160-4)
effects on chromosomes in Ehrlich's ascites carcinoma cells, effects of temperature on aberrant, 25:11014
effects on chromosomes of Crepis capillaris seedlings in combination with caffeine, aberrant, 25:11015
effects on color, odor, and storage life of shrimp, 25:11326 (NP-18393)
effects on composition and content of pyrimidine nucleotides in DNA in cotton shoots following seed exposure, 25:11307
effects on content of amino acids in cooked meats, 25:11339
effects on corticosterone and glucose content of blood in rats, effects of dianabol and insulin on normalization following whole-body, 25:10972
effects on cotton leaf moths, effects of 2 to 8 krad doses and larval exposure on, 25:11247
effects on cultured cells from mice, effects of time between exposure and administration on protective effects of gallic acid propyl ester against, 25:11106
effects on deuterated and nondeuterated norbornane derivatives, ESR spectral studies of free radicals from, 25:10637
effects on dilute acid solutions of divalent and trivalent iron ions, mechanism for attainment of stationary state produced by, 25:10635
effects on dilute aqueous sec-butylamine solutions, mechanism and yields from, 25:10627(R) (NYC-2499-37)
effects on DNA, nucleosides, and nucleotides, protective effects of chloride ions against, degradatory, 25:10962
effects on endocolonization in spleen of mice, inhibitory effects of dose rate on, 25:10986
effects on enzyme activity in sugar beets, cobalt-60, 25:10964
effects on enzyme synthesis and growth of Penicillium expansum, inhibitory and enhancing, 25:10979
effects on erythrocytes and reticulocytes in peripheral blood of guinea pigs, cobalt-60, cesium-137, 25:11278
effects on ethane in presence of sulfur fluorides or ammonia, 25:10632
effects on flour, effects of, on reactions of molecular by-products with thiobarbituric acid as function of radiation dose and storage time, 25:10978
effects on frequency of chlorophyll mutations in peas, effects of seed exposure and storage time on, 25:11024
effects on gaseous 2-methylpropene, yields of low-boiling-point condensation products from, 25:10640
effects on Gladiolus, effects of environment on mutagenic, 25:11035
effects on glassy ethanol, 25:10648
effects on glassy ethanol, mechanical of electron and free radical reactions and trapping in, 25:10630
effects on graft polymerization of styrene with polyethylene, effects of swelling on, 25:10613
effects on grapes, effects of inhibitory and lethal dose rate on chronic mutagenic, 25:11017
effects on growth of barley seeds in soil, effects of dose, fertilizer concentration, and soil chemistry on, 25:11315
effects on hematopoietic tissue formation in spleen of inbred and noninbred mice, protective effects of cystaphos and mexamine against, 25:11099
effects on histones of rat thymus nuclei, 25:10971
effects on immunological properties of transplantable tumors, effects of, on antiserum formation following inoculation into syngeneic mice, 25:10993

effects on indole-3-acetic acid in presence of ethanol and potassium iodide, 25:10647
effects on inhibitors of peroxidase in broad bean seedlings, inhibitory, 25:10973
effects on iodination of methane in gas phase, 25:10620
effects on iodination of methane, Monte Carlo methods in analysis of, 25:10615
effects on iodine-131-labeled, yields from, 25:10642
effects on kidneys in rabbits, use of iodine-131-labeled hippuran for determining cobalt-60, 25:11275
effects on lens of mammalian eyes, comparison of neutron dose with dose for cataractogenic, 25:11284
effects on liquid and solid hydrocarbons, scavengeable electron yields from, 25:10652
effects on liquid cyclopentane in deuterated ammonia, deuterated ethanol, and nitrous oxide solutions, effects of pressure on yields from, 25:10628
effects on mating behavior of male moths, 20 kR cesium-137, 25:11338
effects on mercury-203-labeled chlormerodrin, yields from, 25:10641
effects on mice, protective effects of acetylcholine, adrenaline, histamine, 5-methoxytryptamine, and serotonin against lethal, 25:11102
effects on mitosis in cultured sot cells, effects of dose on inhibitory, 25:11272
effects on mucous membrane, review of effects of dose fractionation on, 25:11259 (BNL-50203, pp 260-7)
effects on n-type germanium, recombination in, (E/T), 25:11968
effects on Nicotiana tabacum callus and tumor tissues cultured in standard and enriched media, comparison of cobalt-60, 25:10965
effects on nonspecific allergic reactions of sheep, 25:10989
effects on oocytes of Drosophila, effects of 4.8 to 300 R/min dose rate on mutagenic, 25:11022
effects on organisms, protective effects of complexes of cystamine and sulfopropyl esters of dextran against, 25:11108
effects on ovaries of mice, effects of diethylstilbestrol on neoplastic 200 R_0, 25:11107
effects on oxytocin at 25 and -196°C, ESR studies on yields of free radicals from, 25:10625 (JAERI-5026, pp 164-7)
effects on phenoplast molding materials, 25:10634
effects on plant cells in relation to target theory, review of, 25:10977
effects on polymerization of 2-hydroxyethyl methacrylate on polyester fabrics, hydrophilic properties of products from, 25:10600 (JAERI-5026, pp 63-7)
effects on polymerization of acrylic acid on drawn polyester fibers, 25:10599 (JAERI-5026, pp 56-62)
effects on polymerization of acrylic acid on poly(ethylene terephthalate), effects of solvent on, 25:10597 (JAERI-5026, pp 46-51)
effects on polymerization of acrylic acid on polyester fibers, effects of temperature on, 25:10602 (JAERI-5026, pp 73-9)
effects on polymerization of acrylonitrile on poly(vinyl chloride) powders, effects of dose rate on, 25:10596 (JAERI-5026, pp 42-5)
effects on polymerization of acrylonitrile on poly(vinyl chloride) powders, properties of fibers from, 25:10595 (JAERI-5026, pp 35-41)
effects on polymerization of acrylonitrile--poly(diallyl phthalate) in wood, 25:10607 (JAERI-5026, pp 108-20)
effects on polymerization of ethylene, role of excited monomer in propagation reaction in, 25:10612
effects on polymerization of monomers on synthetic calcium aluminate hydrate, 25:10616
effects on polymerization of vinylidene chloride in woods, thermal stability of products from, 25:10605 (JAERI-5026, pp 94-100)
effects on polymerization of vinylidene chloride in woods, effects of pretreatment of woods on properties of products from, 25:10604 (JAERI-5026, pp 86-93)
effects on polymerization of vinylidene chloride in wood, properties of products from, 25:10603 (JAERI-5026, pp 80-5)
effects on pregnant rats, combined effects of cloramiphene on cobalt-60, 25:11104
effects on pregnant rats, protective effects of estrogen against cobalt-60, 25:11104
effects on pure lithium fluoride powder, thermoluminescence, 25:11951
effects on pyridine--silica gel systems, ESR studies on, 25:10622 (JAERI-5026, pp 6-10)
effects on rabbits and guinea pigs, effects of volume of thoracic aorta endothelial cytoplasm on, 25:11269
effects on radiolysis of carbon monoxide--helium mixtures, 25:11474(R) (BNWL-842)
effects on rats, role of alarm phase of nonspecific adaptation response in early glycemic response following, 25:11281
effects on resistance and longevity of ants, effects of 1000 to 150,000 rad doses on, 25:11245
effects on seeds of petunia, effects of dose and presoaking on mutagenic, 25:11011
effects on seeds of sugar cane, effects of 1 to 5 kR doses on γ and x, 25:11030
effects on self-incompatibility of brown sarson, 25:11318
effects on single crystals of acetamidine hydrochloride, amides, and hydrazine compounds, at 77°K, ESR studies on radicals produced by, 25:10588
effects on single crystals of beryllium complex with 2,4-pentanedione, ESR spectral studies on, 25:10623 (JAERI-5026, pp 157-60)
effects on sleep patterns in cats, whole-body, 25:11261
effects on somatic chromosome number of Chrysanthemum morifolium, mutagenic, 25:11031
effects on sorption of strontium-85 and strontium-89 from gastrointestinal tract of dogs following injection and ingestion respectively, whole-body cobalt-60, 25:10947
effects on soybean seedlings in comparison to effects of fission neutrons, cobalt-60 γ rays and strontium-90 and yttrium-90 β particles, 25:11312
effects on subsequent polymerization of solid, in dry and high-vacuum system, kinetics of, 25:10611
effects on sulfoxidation of alkanes, 25:10614
effects on sulfoxidation of alkanes, comparison of ozone and uv radiation with, 25:10592 (BMBW-FBK-70-25)
effects on survival of Chinese hamster cells, model for studying, 25:11293
effects on survival of grain beetles from stored date, effects of dose on, 25:11244 (NP-18607)
effects on survival of lymphoma and Vicia faba cells, effects of age on lethal, 25:11095 (BNL-50203, pp 308-17)
effects on thermal stability of PVA, mechanism of, 25:10591
effects on thermoelectric properties of molten salts and cuprous sulfide, 25:11952
effects on tissues of rabbits, hyperglycemia following destructive, 25:10969
effects on toxin production in Escherichia coli, effects of, on mutagenesis of subsequently inoculated T_6 phage, 25:11016
effects on uptake of strontium-85 by rats, effects of whole-body dose on, 25:11263
effects on yeast cells, effects of dose fractionation on simultaneous recovery from lethal and sublethal cobalt-60, 25:11316
effects on Zerolit FF-IP ion exchange resin, 25:10646
emission from ball lightning, 25:11926
emission from solar nucleosynthesis, 25:11544
hazards to bones and liver of personnel following occupational inhalation of plutonium-239 models for, estimation of tumorigenic, 25:11301
hazards to personnel of teletherapy unit, dosimetry studies for evaluating cobalt-60, 25:11070
monitoring at Van de Graaff accelerator, G--M detector system for, 25:10824
reactions (γ,n) with deuterium at 10 to 95 MeV, angular distributions of neutrons from, (E), 25:12374
reactions (γ,xn) with gold-197 and lead-208 at 6 to 35 MeV, partial cross sections and giant resonance parameters for, (E), 25:12610
scattering by lanthanum-139, γ spectra from elastic and inelastic, (E), 25:12585
scattering by xenon-129 at 318 and 411 keV, cross sections for resonant, (E), 25:12583
scattering by xenon-131 at 364, 637, and 723 keV, cross sections for resonant, (E), 25:12583
spectra of, from fission products in spent nuclear fuel, (T), 25:11948
use as research tool in plant physiology, review of, 25:10977
use for sterilization of bone implants, effects of temperature and storage on, 25:11335
use for sterilization of heart valve homografts, 25:11336
use for sterilization of human bone tissues, effects of 3 Mrad dose on, 25:11329
use for sterilizing mesenchymal tissue for use as transplants, 25:11332
use for therapy of mammary carcinoma, development of myelocytic leukemia following, 25:11302

GAMMA SOURCES
design and operation of, for measuring load weight on conveyor belts, 25:10785(P)
dosimetry of telecobalt, for personnel hazard evaluation, 25:11070
protection of veterinary medical personnel against, recommendations for, 25:11075 (NCRP-36)
use of americium-241 and iodine-125, for transmission scanning of human soft tissues for measurements of lean-fat ratios, 25:11114
use of cesium-137 as, for transmission scanning of human lungs for measurements of blood circulation and ventilation, 25:11116

GAMMA SPECTROMETERS
data analysis of lithium-drifted germanium, method for peak location and calibration for, 25:10858
design and performance of lithium-drifted germanium, for well logging, 25:10849 (CEA-CONF-1694)
performance of lithium-drifted germanium, 25:10851 (NP-18570)
performance of lithium-drifted germanium, for low-energy gamma radiation, 25:10859
spectra analysis for, numerical methods for, 25:10853 (RT/PROT-(70)21)

XUM

GARNETS
formation in atmospheres of cool stars, (E/T), 25:11562
GAS CHROMATOGRAPHY
radioactive material uses in, safety hazards from, 25:10421 (BRH/DMRE-70-5)
GAS FLOW
magnetohydrodynamic, linearized theory for channel and jet, 25:11773
magnetohydrodynamic, normal vorticity jump condition across, (T), 25:11756
magnetohydrodynamic, thermomagnetic torque effect in, (T), 25:11754
magnetohydrodynamic, thin airfoil theory in, 25:11772
GASES
book: Gas Dynamics of Two-Phase Media (In Russian), 25:10772
diffusion in alloys, metals, halides, and oxides, data tabulations on, 25:11411
diffusion of atoms and molecules in, review, (E/T), 25:11731
filtration of fluidized bed exhaust, design of packed-bed filter for, 25:10761(P)
flow from prestressed concrete pressure vessel with complete circumferential crack, DYNA computer program for calculating, 25:10753 (GAMD-7567)
ion mobility in, spectrometer for measurement of, 25:10903
ion reactions in keV range with, spatial distribution of energy deposited in, (T), 25:11682
kinetic theory of relativistic, Boltzmann equation for, 25:11765
kinetic theory of relativistic, general, 25:12058
kinetic theory of relativistic, in strong magnetic fields, 25:11903
kinetic theory of, Cauchy problem for linearized relativistic Boltzmann equation, 25:11902
kinetic theory of, Grad method extension for relativistic Boltzmann equation, 25:11901
photon absorption and scattering by intergalactic, uv and x-ray, (T), 25:11654
GASTROINTESTINAL TRACT
radiation effects on sorption of strontium-85 and strontium-89 from, of dogs following injection and ingestion respectively, whole-body γ, 25:10947
radiation effects on, in man, review of literature on, 25:11209
scanning of human, using colloidal gold-198, 25:11212
strontium-85 sorption from, calculation of rate of, 25:10951
strontium-87m sorption from, of man, effectiveness of activated barium sulfate for inhibiting, 25:11047
strontium-90 sorption from, effectiveness of activated barium sulfate for inhibiting, 25:11049
tellurium-127m sorption from, of rats following ingestion, kinetics of, 25:10949
GENES
radiation effects on bronze and shrunken loci of in maize, effects of pollen exposure on x, 25:11023
GENETIC RECOMBINATION
effects on resistance of Escherichia coli to phosphorus-32 decay, 25:10946
effects on variation in populations of thermal neutron-irradiated corn, 25:11009(R) (COO-1512-22)
GENETIC SELECTION
effects on random mating populations of thermal neutron-irradiated corn, 25:11009(R) (COO-1512-22)
GENETICS
research program at Columbia Univ., 1968-70, 25:12888(R) (CU-1804-34)
GEOMAGNETIC FIELDS
direction of, incoherent scatter measurements at Jicamarca of, (E/T), 25:11792
effects on plasmapause convection at dusk, model of, (T), 25:11776 (AD-708495)
magnetic bays on Earth's surface and at satellite position, relation with magnetospheric ring current, low-latitude, (E/T), 25:11779
nuclei trapping in, carbon, nitrogen, and oxygen, (E), 25:11744
Poynting-flux direction along, source and propagation of magnetospheric, (E), 25:11780
GEONS
formation in ensemble of collisionless zero-rest-mass particles, (T), 25:11660
GERMANIUM
determination of trace amounts of, in biotite and tektite by spark source mass spectrometry, 25:10455
determination of trace amounts of, in molybdenum, review on, 25:10459
determination of trace amounts of, in rocks, quantometer for spectroscopic, 25:10451
effects on mechanical properties of niobium--titanium alloys, 25:11416
neutron inelastic scattering at 14 MeV by natural, neutron spectra and level-density parameters from, (E), 25:12536
radiation effects on electric conductivity of p-type single crystals of, surface effects in 79°K x-, (E), 25:11963
radiation effects on Hall mobility of antimony-doped, kinetics of 100°K annealing stage of 1-MeV electron, 25:11954
radioinduced recombination centers in low-resistivity arsenic- and antimony-doped n-type, γ, (E/T), 25:11968
GERMANIUM ALLOYS AND SYSTEMS
Ge--Si, performance as thermocouple components for thermoelectric converters, 25:11477 (ALO-2510-T-1)
GERMANIUM ISOTOPES Ge-66
beta decay of, gamma spectra, half-lives, log-ft values, Q values, and Kurie plots from, (E), 25:12477
GERMANIUM ISOTOPES Ge-69
hyperfine structure of, 25:12487
nuclear spin and magnetic and quadrupole moments of, determination from hyperfine structure, (E), 25:12487
GERMANIUM ISOTOPES Ge-71
hyperfine structure of, 25:12487
isomeric transition in, half-life and γ energy for, (E), 25:12430 (INR-P-1091)
GERMANIUM ISOTOPES Ge-72
neutron reactions (n,2n) at 14.8 MeV, isomeric cross section for, (E), 25:12430 (INR-P-1091)
GERMANIUM ISOTOPES Ge-75
hyperfine structure of, 25:12487
nuclear spin and magnetic moment of, determination from hyperfine structure, (E), 25:12487
GERMANIUM ISOTOPES Ge-77
beta decay of, γ singles and coincidence spectra from, (E), 25:12473
GERMANIUM TELLURIDES
superconducting transition temperature of, heavy-hole band mechanism of, 25:11847
GLASS
age of, effects of geometry factor on accuracy of fission track, (E), 25:10695
analysis of borate, for boron by neutron absorption, 25:10483
diffusion of sodium-24 in viscosity standard silicate, 25:10578
heat absorption by large-dimension plane, effects of radioprotective coatings on, 25:10770
GLASS TEXTILES
fabrication into holder assemblies, 25:12866 (BDX-613-198)
sorptive properties of Fiberglas E, for water, 25:11472(R) (AD-708705)
sorptive properties of Fiberglas E, for water, 25:11473(R) (AD-708712)
GLOW DISCHARGES
uses in anodizing metals, review on, 25:11343 (AECL-3778)
GLUCOSE
effects on aggregation of erythrocytes during angiography in man, 25:11195
radiation effects on absorption of, in rats, continuous, 25:10980
radiation effects on metabolism of, in rabbits, γ, 25:10969
radiation effects on synthesis of, in ganglia of rats, effects of dose rate on strontium-90 β, 25:11262
GLUCOSE 6-PHOSPHATE DEHYDROGENASE
radiation effects on content of, in epidermis, x, 25:11241
GLUCOSEPHOSPHATE ISOMERASE
radiation effects on activity of, in dormant and sprouting rye seeds, γ, 25:10974
GLUTAMIC ACID
radiation effects on content of, in cooked meats, γ, 25:11339
GLUTATHIONE
radioprotective effects of reduced, on mice, x, 25:11098
GLYCEROL
radioprotective effects of, on growth tail bone transplants in syngeneic recipient mice, x, 25:10983
GLYCINE
sulfates, radiation effects on Barkhausen effect in crystals of tri-, x, 25:11978
GOLD
determination by photon activation, reactions and sensitivities for, 25:10488 (CEA-R-4072)
determination in pyrite by neutron activation and radiochemical separation, 25:10490(T) (LIB/Trans-334)
determination in tektite by spark source mass spectrometry, 25:10455
determination of, photometric, 25:10686
friction and wear of, sliding against copper and iron rings under vacuum, 25:11413
ion channeling in single-crystal foils of, energy loss and straggling of proton, helium, and lithium, 25:11976
separation from diverse ions by solvent extraction using tributyl phosphate in toluene, 25:10686
GOLD ALLOYS AND SYSTEMS
Au--Cd, crystal structure and martensitic transformation of near-equiatomic, 25:11446
Au--Nb, niobium-93 NMR in Nb_3Au, 25:12037
Au--Pd--Te, superconducting properties of liquid-quenched simple cubic, 25:11819 (CALT-822-22)
Au--Sb, superconducting properties of liquid-quenched simple cubic, 25:11819 (CALT-822-22)
GOLD ISOTOPES Au-197
alpha inelastic scattering at 42 to 90 MeV, angular distributions and energy spectra from, (E/T), 25:12604
alpha reactions (α,He-3) at 42 to 90 MeV, angular

distributions and energy spectra from, (E/T), 25:12604
alpha reactions at 30 to 80 MeV, cross sections for production of K and L x rays by, (E), 25:12488
helium-3 inelastic scattering at 50 and 75 MeV, angular distributions and energy spectra from, (E/T), 25:12604
helium-3 reactions (He-3,α) at 50 to 75 MeV, angular distributions and energy spectra from, (E/T), 25:12604
photon reactions (γ,xn) at 6 to 35 MeV, partial cross sections and giant resonance parameters for, (E), 25:12610
proton reactions (p,pn) and (p,p3n) at 400 MeV, angular distribution of recoils from, (E), 25:12500
proton reactions at 2.2 GeV, angular distributions and differential range spectra of terbium-149 recoils from, (E), 25:12580

GOLD ISOTOPES Au-198
beta decay of, matrix elements for first-forbidden, (T), 25:12597
clearance of colloidal, from human liver, effects of particle size on, 25:10918
determination by ion exchange and γ spectroscopy, 25:10490(T) (LIB/Trans-334)
effectiveness for scanning of human liver, 25:11198
effectiveness for scintiscanning of liver and pancreas in combination with selenium-75, computer method for differentiation, 25:11176
effectiveness of colloidal, for scintiscanning of abdominal lymph system, evaluation of interpretation and performance errors for determining, 25:11177
use for determining liver blood flow in patients with hyperthyroidism, 25:11141
use for scanning human liver, 25:11200
use for scanning of human liver, 25:11183
use for scanning of human liver, 25:11201
use for scanning of human liver for diagnosis of cirrhosis, 25:11203
use for scanning of human liver, effects of abscesses, angiomas, hydatid cysts, and tumors on, 25:11197
use for scanning of human liver, effects of blood circulation on, 25:11196
use for studying lymph drainage following neck surgery following subcutaneous injection into mastoid region, 25:11178
use of colloidal, for liver scintigraphy in comparison to colloidal technetium-99, 25:11140
use of colloidal, for scanning of human gastrointestinal tract, effects on pancreas selenium-75 scintigraphy, 25:11212
use of colloidal, for scanning of lateral human liver, effectiveness of, for diagnosis, 25:11211

GOLD ISOTOPES Au-200
beta decay of isomeric, γ singles and coincidence spectra from, (E), 25:12514(R) (COO-1672-21)
energy-level transitions from gold-200 on decay, (E), 25:12514(R) (COO-1672-21)

GRAMICIDIN
radiation effects on aqueous solutions of, effects of dose rates and concentrations on γ, 25:10587 (JAERI-5026, pp 167-8)

GRANITES
analysis for trace amounts of elements, correction of matrix effect in uv spectrographic, 25:10453
motion of Sahara Desert, from underground nuclear explosions, (E), 25:10728 (CEA-R-4059)

GRANODIORITES
age of Wind River, Wyoming, rubidium/strontium method for estimation of, 25:10701
systematics of lead--thorium--uranium and rubidium--strontium distribution in plutonic, at Wind River, Wyoming, 25:10701

GRAPHITE
electron diffraction patterns of polycrystalline, 25:11474(R) (BNWL-842)
fabrication of carbonaceous mesophase-containing, methods for, 25:11529
microstructure of Types AGOT and TSX, effects of microwave-induced oxidation by air or oxygen on, 25:11474(R) (BNWL-842)
morphology of carbonaceous mesophase in, 25:11529
neutron transmission characteristics of filter of pyrolytic fast, 25:12352
radioinduced contraction of, in-pile, 25:11474(R) (BNWL-842)
reactions with helium coolant and gaseous impurities in high-temperature reactors, thermodynamics of, 25:10518 (RD/B/N-1816)
thermal conductivity and diffusivity at 300 to 3300°K, laser-pulse method for determination of, 25:11487 (GA-9168)
thermal emission from grains of, in H II regions, (T), 25:11583
thermal expansion of oriented pyrolytic, Grueneisen parameter study of low-temperature anisotropic, 25:11510
thermal expansion of polycrystalline, to 2400°C, heating--cooling cycle study of, 25:11511
thermal expansion of Types ATJ and ZTA, effects of prestressing on, 25:11474(R) (BNWL-842)

GRAPHITE SYSTEMS
graphite--ZrC, thermal expansion of extruded composites of, to 2500°C, 25:11512

GRAVITATION
Dicke theory of, determinism and space regions with uniform internal space--times and singular fields in, 25:12273
Einstein equations in, plane-wave solution of, (T), 25:12275
Einstein equations in, three-dimensional groups of isometries with two-dimensional orbits for Einstein and Weyl tensors for exact solutions of, 25:12277
field coupling in, event horizons in static scalar-vacuum space times for, (T), 25:12282
Mach principle in scalar--tensor theory of, 25:12270
Riemannian geometry for neutrinos in, 25:12280
stability of polytropic gas spheres under external pressure, (T), 25:11560
theory for photon, 25:12283

GRAVITATIONAL COLLAPSE
event horizons in, (T), 25:11663
formation of geons and black holes in thin-shelled ensemble of (T), 25:11660
light escape during, (T), 25:11663

GRAVITATIONAL FIELDS
Einstein--Maxwell, invariant transformations for Newman--Penrose constants of motion for coupled, 25:12279
electromagnetic wave scattering by static, cross sections for, (T), 25:12138 (NYO-2262-TA-222)
gravitational wave scattering by static, cross sections for, (T), 25:12138 (NYO-2262-TA-222)
ground state functional of linearized, 25:12276
neutrino radiation in, solutions of general relativistic Weyl equation for, (T), 25:12281
photon scattering by spherically symmetric, polarization in, (T), 25:12159
space--times in, spinor treatment of stationary, 25:12278
theory for photon, 25:12283

GRAVITATIONAL RADIATION
collisions of plane waves of, (T), 25:11655
detection of, photon and graviton production respectively from graviton and photon interactions with static electromagnetic field for, (T), 25:12272
Einstein equations for, plane-wave solution of, (T), 25:12275
graviton interactions with fermions, Lagrangian function of tetrad and fermion fields for, (T), 25:12271
graviton interactions with scalar bosons, cross sections for, (T), 25:12138 (NYO-2262-TA-222)
graviton interactions with static electromagnetic fields, photon production from, (T), 25:12272
graviton production from photon interactions with static electromagnetic fields, (T), 25:12272
scattering by static gravitational field, cross sections for, (T), 25:12138 (NYO-2262-TA-222)

GRAVITY WAVES
propagation in ionosphere, vertical ion-motion levels induced by internal atmospheric, (T), 25:11800
propagation in presence of electrostatic field and background wind in ionosphere, ionization irregularities due to internal, (T), 25:11798
propagation in wind-stratified atmosphere, internal, (E/T), 25:11796

GROUND
motion of Nuclear Rocket Development Station, from seismic waves generated by NTS underground nuclear explosions, 25:10730 (NVO-1163-TM-22)

GROUND WATERS
flow and velocity in Shigaya aquifer in Kuwait, iodine-131 tracer measurements of, 25:10700
mineral content of Kamchatka Peninsula thermal, rare earths, thorium, and uranium, (E), 25:10697
model of transient three-dimensional systems of, mathematical, 25:12880 (BNWL-SA-3539)
radioisotope content of Bukhara--Karshin artesian basin, (E), 25:10698
radioisotope content of US, list of reports on 1967 to 1970 measurements of, 25:10699

GROUP THEORY
Lie groups in, diagramatic technique for constructing matrix elements of generators of, 25:12234
Poincare group in, limiting process m → 0 for Wigner rotations in, 25:12233
Poincare group representations for photons and tachyons with continuous spin in, lightlike and spacelike, 25:12236

GROWTH
radiation effects on, of cells, effects of crowding on x, 25:11239 (BNL-50203, pp 117-29)

GUINEA PIGS
iodine-131 removal from blood of, estimation of phagocytic coefficient for, 25:10957
radiation effects on cooperative function of carrier-specific lymphocytes in antihapten responses of, 25:10987
radiation effects on erythrocytes and reticulocytes in peripheral blood of, comparison of chronic cesium-137 and single cobalt-60 γ, 25:11278
radiosensitivity in relation to volume of thoracic aorta endothelial cytoplasm, 25:11269

GUNDREMMINGEN POWER REACTOR
operation during October 1970, 25:12723 (TID-25637)

XUM

H

HI REGIONS
observations of, in compact galaxies, (E), 25:11638
shock structure in, hydromagnetic, (T), 25:11639
HII REGIONS
thermal emission from grains in, (T), 25:11583
turbulence in, (E/T), 25:11582
turbulence in, high-velocity, (E), 25:11587
HADRONS
bootstrap theory for, properties of vector currents consistent with Veneziano model for, 25:12177
helicity conservation in 2π production in e + N and ν + p interactions, (T), 25:12165
interactions at extremely high energies in parton model, total cross section for, (T), 25:12187
interactions with hadrons at high and low energies, review of duality and quark model for, (T), 25:12175 (COO-1764-81)
interactions with hadrons at high energies, quark model numerical selection rule for three-body, (T), 25:12218
mass difference from parton model for forward virtual Compton scattering amplitude, electromagnetic, 25:12155
mass level structure of, urbaryon model for, 25:12182
production in γ + d, γ + n, and γ + p interactions above 1.2 GeV, data compilation on cross sections for, (E), 25:12066 (DESY-HERA-70-1)
spectra of, representations of local isospin charge densities for, (T), 25:12181
structure of, urbaryon model for, 25:12183
HAFNIUM
determination in zirconium oxide, spectrographic, 25:10431 (IEA-208)
determination of trace amounts of, in biotite and tektite by spark source mass spectrometry, 25:10455
determination of trace amounts of, in molybdenum, review on, 25:10459
determination of trace amounts of, in rocks and sand by thermal neutron activation, ion exchange, and γ spectrometry, 25:10492
radiation effects on swelling of shim rods of, fast neutron, 25:11460 (IN-1437, pp 5-12)
separation from ores by solvent extraction, review on, 25:10656 (BM-IC-8502)
separation from zirconium by solvent extraction using tributyl phosphate, 25:10689
separation of zirconium from, by fractional crystallization of potassium hexafluorozirconate, 25:10676
HAFNIUM ALLOYS AND SYSTEMS
Hf-base--Pu, electric conductivity of, 25:12004
HAFNIUM CARBIDES
phonon spectra in, [00ξ] and [110] longitudinal modes in, 25:11986
HAFNIUM ISOTOPES Hf-174
energy level of, half-life of isomeric, (E), 25:12553
energy levels from lutetium-175 (p,2nγ) and (d,3nγ) reactions at 16 to 21 MeV, rotational, (E/T), 25:12544
energy-level transitions from lutetium-175 (p,2nγ) and (d,3nγ) reactions at 16 to 21 MeV, probabilities for, (E/T), 25:12544
energy-level transitions from production in (α,3n) and (α,4n) reactions at 42 MeV, intensities and angular distributions from, (E/T), 25:12553
energy-level transitions in, effect of higher-order deformations on EO, (T), 25:12584
moment of inertia as function of excitation energy, (E/T), 25:12544
HAFNIUM ISOTOPES Hf-176
energy-level transitions from production in (α,4n) reactions at 42 MeV, intensities and angular distributions from, (E/T), 25:12553
HAFNIUM ISOTOPES Hf-178
energy-level transitions in, effect of higher-order deformations on EO, (T), 25:12584
HAFNIUM ISOTOPES Hf-179
decay of metastable, 25:10472(R) (BMBW-FBK-70-19)
HAFNIUM ISOTOPES Hf-181
beta decay of, γ circular polarization of 482-keV γ ray in, (E), 25:12621
HAIR
tritium retention in, of rabbits for use in assessing internal contamination, 25:10954
HALIDES
diffusion in, data tabulations on, 25:11411
HANFORD PRODUCTION REACTORS
thermal effluents from, effects on water temperatures in Columbia River, 1964 to 1970, (E), 25:10691 (BNWL-1345)
HANFORD TEST REACTOR
operating procedures for, revised handbook on, 25:12815 (DUN-7149)
HASTELLOY X
radiation effects on stress rupture of, in-pile, 25:11474(R) (BNWL-842)
HEART
blood volume of human, use of iodine-131-labeled RISA for determining, 25:11123
radiation effects on rate of, in rabbits following administration of zirconium citrate, effects of synchronous calcium gluconate administration on whole-body γ, 25:11289
radiation effects on, in man, review of literature on, 25:11209
radiosterilization of human, in vivo for valve transplants, γ, 25:11336
scanning for diagnosis of mitral valve defects, effectiveness of krypton-85 in combination with pressure measurements for, 25:11124
scanning of human, using iodine-131-labeled RISA in combination with iodine-131-labeled albumin macroaggregate for lung scanning in differential diagnosis of mediastinal processes and pericardial effusion, 25:11130
scanning of human, using metastable technetium-99-labeled pertechnetate and Anger camera, method for, 25:11121
scanning of mitral valve in human, effectiveness of metastable technetium-99 and positioning technique for, 25:11187
scintiscanning of action of, metastable using technetium-99 in combination with Anger camera and computer, evaluation of, 25:11119
HEAT
effects on hepatic blood flow in man following application of compresses to liver area, use of iodine-131-labeled RISA for studying, 25:10916
radiation effects on production of, by yeasts, effects of dose on x, 25:11324
HEAT EXCHANGERS
design parameter for gas cooled reactors, with means to allow for expansion of tubes, 25:12811(P)
design parameters of steam reheater, with U-shaped tube banks in concrete pressure vessel walls, 25:12810(P)
HEAT PIPES
performance characteristics of cylindrical, for space and undersea power plants, 25:10755 (ORNL-TM-2803)
wicks for, development of methods for fabrication of, 25:10778(R) (ORNL-TM-3214)
HEAT SOURCES
development of pelletized, for thermal batteries, 25:12905 (SC-CR-70-6137)
liners for radioisotope, methods for fabrication of, 25:10776 (MLM-1779)
HEAT TRANSFER
analysis in reactors, book on, 25:12791
augmentation using internally finned and roughened tubes, 25:12891 (NP-18608)
calculations of rod type fuel element, comparison of models and methods for, (T), 25:12799 (TUBIK-17)
equations for gas cooled rocket reactors, evaluation of, 25:12833
rates between parallel surfaces, design of barrier for reduction of, 25:10774(P)
rates in steady axially symmetric slug flow, theoretical analysis of, 25:10771
HEAT TRANSFER SYSTEMS
design parameters of 50 MW(e) liquid sodium, for testing boilers of liquid metal cooled power reactors, 25:12708
HEATED EFFLUENTS
effects of Hanford, on temperature of Columbia River waters, 25:10691 (BNWL-1345)
effects on growth of limpet snails in Columbia River, 25:10996 (BNWL-1537)
HELIUM
bromine-ion reactions at 6 to 15 MeV with, cross sections for electron capture and loss in, (E), 25:11710
burning in stars, products of, (E), 25:11565
deuteron reactions at 30 to 120 keV with, cross sections for electron capture into 3s state of deuterium in, (E), 25:11708
diffusion in plutonium-238 dioxide sol-gel microspheres at 25 to 2000°C, anomalous, 25:11501
effects of injected, on density of compacted and sintered nickel powders, 25:11474(R) (BNWL-842)
effects of radioinduced, on intergranular embrittlement of stainless steel, 25:11456 (AERE-R-5622)
electron elastic scattering at 500 eV by, effects of charge polarization on differential cross sections for, (T), 25:11718
electron reactions in eV range with, absolute cross sections for production of He I 4713-A and He II 4686-A emissions in, (E), 25:11702
energy levels of, level-crossing measurement of lifetime of 2^1P_1 and 3^1P_1 states, 25:11695
energy of ground and first-excited states of, calculation using higher-order finite-difference solutions of Schroedinger equation, 25:11697
energy transfer to hydrogen from, efficiency of, 25:11474(R) (BNWL-842)
helium-ion reactions at 1 to 3 keV and at small angles with, charge exchange in, (E), 25:11716
helium-ion reactions at 1 to 3 keV with, charge exchange at small angles in, (E), 25:11705
helium-ion reactions at 20 to 100 keV with, absolute excitation cross sections of He^+ in, (E), 25:11713
iodine-ion reactions at 6 to 15 MeV with, cross sections for electron capture and loss in, (E), 25:11710
photon reactions at 0.20 to 2.40 and 3.15 to 3.30 Ry with 1^1S and 2^1S states of, cross sections for ionization

in, (T), 25:11717
photon reactions with excited 2S atoms of, cross section for ionization in three-, (E), 25:11734
plasma of, electric field measurement from optical spectra in Burnout V, (E), 25:11874
proton reactions at 30 to 120 keV with, cross sections for electron capture into n = 3 level of hydrogen in, (E), 25:11708
reactions between atoms of, calculation of ionization and stripping cross sections for, using generalized oscillator strengths, 25:11715
reactions of coolant, with graphite in high-temperature reactors, thermodynamics of, 25:10518 (RD/B/N-1816)
reactions with argon, calculation of ionization and stripping cross sections for, using generalized oscillator strengths, 25:11715
release from alpha-bombarded polycrystalline thorium dioxide, effects of heat treatments on mechanism of, 25:11502
release from plutonium-238 dioxide microspheres during annealing, calculations of, 25:11499
release from plutonium-238 dioxide microspheres, effects of grain size and thermal history on measurement of, 25:11500
scattering by platinum (111) surfaces at thermal energies, (E), 25:11683
spectra in dc arc, profiles of 4471.5- and 4922-A lines in, as function of electron density, (E), 25:11689
spectral emission of He I 584-A, height profiles from 400 to 1016 km of euv dayglow, (E), 25:11789

HELIUM IONS
abundance in magnetosphere, transport and loss mechanisms of, (E/T), 25:11802
channeling in gold single-crystal foils, energy loss and straggling in, 25:11976
electron recombination coefficient for He_2^+ near 80°K, 25:11690
energy levels of He^-, structure and lifetimes of autoionizing, (T), 25:11692
energy levels of, energy difference between n = 3, (E), 25:11688
energy levels of, energy difference between n = 4, (E), 25:11687
implantation in silicon carbide crystals, cathodoluminescence spectrum in annealing of, 25:11974
losses from magnetosphere by charge exchange and pitch-angle diffusion, (T), 25:11803
reactions with helium at 20 to 100 keV, absolute excitation cross sections of He^+ in, (E), 25:11713
reactions with helium, krypton, and neon at 1 to 3 keV, charge exchange at small angles in, (E), 25:11705
reactions with helium, neon, and krypton at 1 to 3 keV and at small angles, charge exchange in, (E), 25:11716

HELIUM ISOTOPES He-3
deuteron elastic scattering at 4.8 to 11.9 MeV using polarized target, asymmetries in, (E), 25:12370
deuteron reactions (d,p) at 4.8 to 11.9 MeV using polarized target, proton asymmetries in, (E), 25:12370
deuteron reactions (d,p) at 6, 8, and 10 MeV using polarized target, proton asymmetries in, (E), 25:12357
deuteron scattering at 9.9 and 11.9 MeV using polarized target, asymmetries in, (E), 25:12358
proton elastic scattering at 156 MeV, differential cross sections for, (E/T), 25:12365
reactions (He-3,3nγ) with dysprosium-164 at 22 MeV, cross sections and gamma spectra from, (E/T), 25:12544
reactions (He-3,α) with gold, lead, platinum, tantalum, and tin at 50 to 75 MeV, angular distributions and energy spectra from, (E/T), 25:12604
reactions (He-3,α) with nitrogen-15 at 11 MeV, spectroscopic factors for, (E), 25:12424
reactions (He-3,αγ) and (He-3,γ) with carbon-13, differential cross sections for, (E), 25:12388
reactions (He-3,d) with cerium-140 and praseodymium-141, angular distributions for, (E), 25:12558
reactions (He-3,d) with lanthanum-139, energy spectra and angular distributions from, (E/T), 25:12552
reactions (He-3,d) with lithium-6 at 9 and 13 MeV, internal bremsstrahlung spectra for, (T), 25:12694
reactions (He-3,d) with magnesium-24, oxygen-16, silicon-28 and -30, and sulfur-32 at 18 and 20 MeV, DWBA analysis of differential cross sections from, (E/T), 25:12479
reactions (He-3,d) with zirconium-90 at 18 MeV, deuteron spectra and angular distributions for, (E), 25:12613
reactions (He-3,γ) with beryllium-9 at 3 to 6 MeV, differential cross sections and angular distributions for, (E), 25:12388
reactions (He-3,γ) with lithium-7 at 3 to 6 MeV, angular distributions for, (E), 25:12389
reactions (He-3,γ) with tritium at 0 to 20 MeV, direct-capture calculation of excitation functions for, (T), 25:12372
reactions (He-3,n) with carbon-12 at 0.9 to 1.9 MeV, excitation function and threshold energy for, (E), 25:12402
reactions (He-3,t) with calcium-48 at 30 MeV, exchange effects on differential cross sections from, (T), 25:12691
reactions (He-3,t) with magnesium-28, neon-22, oxygen-18, and silicon-30 at 16 and 30 MeV, (E), 25:12498
reactions (He-3,t) with nuclei, shape of angular distributions from, (T), 25:12648
scattering by copper-63, copper-65, and zinc-67 at 21 MeV, spin dependence in inelastic, (E), 25:12454
scattering by gold, lead, platinum, tantalum, and tin at 50 to 75 MeV, angular distributions and energy spectra from inelastic, (E/T), 25:12604
scattering by magnesium-26 at 16 and 30 MeV, elastic and inelastic, (E), 25:12498
spectra of, shift of 2^1S_0--2^1P_1 line of, relative to helium-4, (E), 25:11696

HELIUM ISOTOPES He-4
binding energy of, Hartree--Fock calculation using effective interaction, (T), 25:12686
binding energy of, third-order corrections to the Hartree--Fock approximation for, (T), 25:12373
center-of-mass motion of, Hartree--Fock treatment of, (T), 25:12653
deuteron elastic scattering at 7.07 MeV and 55°, tensor analyzing power of, (E), 25:12356
energy distributions from fission of uranium-236, 25:10583(R) (AECL-3776)
excitation spectra of liquid, sum-rule analysis of two-branch, 25:11818
interactions e + ^{3}He + ^{3}He + π^0, verification of vector dominance in, (T), 25:12140
interactions γ + ^{3}He + ^{3}He + π^0, verification of vector dominance in, (T), 25:12140
interactions π^+ + ^{3}He + ^{3}He + rho$^+$, verification of vector dominance in, (T), 25:12140
interactions π^- + ^{3}He + ^{3}He + rho$^-$, verification of vector dominance in, (T), 25:12140
meson (π^+) elastic scattering by, π charge form factor from differential cross sections for, (T), 25:12225
meson (π^-) elastic scattering by, π charge form factor from differential cross sections for, (T), 25:12225
neutron elastic scattering at 0.2 to 7 MeV, angular distributions for, (E), 25:12360
neutron elastic scattering at 1 to 18 MeV, phase shifts and effective potentials from resonating-group study of, (T), 25:12363
nuclear charge form factor of, microscopic description of, (T), 25:12651
proton elastic scattering at 1 to 40 MeV, phase shifts, cross sections, and polarizations from resonating-group study of, (T), 25:12363
spectra of, shift of 2^1S_0--2^1P_1 line of, relative to helium-3, 25:11696

HELIUM ISOTOPES He-5
energy levels of, Hartree--Fock calculation using effective interaction, 25:12686
energy levels of, shell-model calculation for, (T), 25:12371

HELIUM ISOTOPES He-6
binding energy of ΛΛ hypernucleus of, (T), 25:12393

HELIUM SYSTEMS
CO-He, radiolysis of mixtures of, carbon deposition by gamma, 25:11474(R) (BNWL-842)

HEMATOPOIESIS
radiation effects on, in man, review of literature on, 25:11209
restoration of bone marrow, in whole-body γ-irradiated rats, effects of dianabol and insulin on, 25:10972

HEMATOPOIETIC SYSTEM
radioinduced tumors in, of mammals, effects of clonogenicity, dose, reproductive integrity, and time on, 25:11253 (BNL-50203, pp 154-73)

HEMATOPOIETINS
radioimmunoassay of thrombopoietin in blood plasma of mice using selenium-75-labeled selenomethionine, 25:10991

HEPTANE
determination in effluent from gas chromatograph, performance of Geiger--Mueller counter with external γ source for, 25:10888

HEXANE
determination in effluent from gas chromatograph, performance of Geiger--Mueller counter with external γ source for, 25:10888

HEXOKINASE
radiation effects on activity of, in dormant and sprouting rye seeds, γ, 25:10974

HIGH-ENERGY PHYSICS
High Energy Physics Index. Vol. 8, No. 24, 25:12124
High Energy Physics Index. Vol. 8, No. 25, 25:12123

HIPPURIC ACID
sodium salts, clearance of radioisotope-labeled, from human kidneys, analysis of, 25:11208

HIROSHIMA
atomic bombing of, health status of atomic bomb survivors during July 1968 to July 1969, 25:11237(R) (ABCC-68-69)
radiation injuries to human population exposed to atomic bomb at, review, 25:11238

HISTAMINE
radiation effects on, in blood, intestines, kidneys, and liver of rats, mechanism of, following ingestion of mixed radioisotopes, 25:10967
radioprotective effects of, on mice and rats, γ, 25:11102

HISTIDINE
radiation effects on content of, in cooked meats, γ,

25:11339
radioinduced mutations affecting requirement of Escherichia coli for, cobalt-60 γ, 25:11019
HISTONES
radiation effects on, of rat thymus nuclei, γ, 25:10971
HODOSCOPES
data storage system for scintillation, 12-bit register, 25:10816
efficiency and resolution of Cherenkov, 25:10869 (JINR-E13-5459)
HOLMIUM
complexes with EDTA, separation by ion exchange, effects of resin crosslinking on, 25:10665 (INR-P-1209)
determination of trace amounts of, in biotite and tektite by spark source mass spectrometry, 25:10455
separation from erbium and yttrium in hydrochloric or nitric acid solutions by solvent extraction using DEHPA, 25:10685
HOLMIUM ALLOYS AND SYSTEMS
Ho--Ni, magnetic structure of intermetallic $HoNi_3$, 25:11979 (CEA-CONF-1704)
HOLMIUM FLUORIDES
effects on gamma-induced luminescence of calcium fluoride crystals, 25:11955
HOLMIUM ISOTOPES Ho-165
deuteron reactions (d,3nγ) at 18 MeV, cross sections and gamma spectra from, (E/T), 25:12544
neutron capture by, average circular γ polarization in thermal, (E), 25:12601
neutron capture by, spectroscopic analysis of, (E), 25:12586
neutron inelastic scattering at 14 MeV, neutron spectra and level-density parameters from, (E), 25:12536
neutron total cross section of oriented, at 2 to 135 MeV, (E), 25:12565
proton reactions (p,2nγ) at 16 at 21 MeV, cross sections and gamma spectra from, (E/T), 25:12544
HOLMIUM ISOTOPES Ho-166
beta decay of ground-state and isomeric, γ spectra from, (E), 25:12599
energy levels from holmium-165 neutron capture, spin-parity assignments for, (E), 25:12586
energy levels from thermal neutron capture, spin for compound, (E), 25:12601
HORMONES, ADRENAL
adrenaline, radioprotective effects of, on mice and rats, γ, 25:11102
dexamethasone, effects on eosinophil count and phospholipase B content of rats, relation of, to previous studies on x-irradiated rats, 25:10961(R) (ORO-3329-6)
HORMONES, PANCREATIC
insulin, use for normalization of corticosterone and glucose content of blood in whole-body γ-irradiated rats, 25:10972
HORMONES, PITUITARY
oxytocin, radiolysis at 25 and -196°C, ESR studies on yields of free radicals from γ, 25:10625 (JAERI-5026, pp 164-7)
HORMONES, PLACENTAL
chorionic gonadotropin, radiation effects on production of, in mothers during pregnancy, 25:10982
HORMONES, PLANT
indole-3-acetic acid, radiolysis of aqueous solutions of, effects of ethanol and potassium iodide on γ, 25:10647
HORMONES, SEX
dianabol, use for normalization of corticosterone and glucose content of blood in whole-body γ-irradiated rats, 25:10972
diethylstilbestrol, radioprotective effects of, on γ-radioinduced neoplasms in ovaries of mice, 25:11107
estradiol, effects on calcium-47 and strontium-85 sorption by intestines in rats, 25:10933 (COO-1339-45)
estradiol, effects on calcium-47 and strontium-85 content of bones of rats, 25:10933 (COO-1339-45)
estrogens, radiation effects on production of, in mothers during pregnancy, 25:10982
prednisolone, effects on adrenal cortex of rats, protective effects of nandrolone phenpropionate against atrophic, 25:11268
prednisolone, radioprotective effects of, on adrenal cortex of rats, whole-body x, 25:11268
radioprotective effects of, on pregnant rats, cobalt-60 γ, 25:11104
testosterone, content of peripheral blood of bovines and swine, double isotope dilution combined with crystallization technique for measuring, 25:10923
HORMONES, THYROID
triiodothyronine, effects on iodine-131 uptake by human thyroid, 25:10944
HOT CELLS
design and operation of Isodore, at Saclay for metallurgical examination of irradiated fuels, 25:10794 (CEA-R-4120)
HUMIDITY
corrosive effects on uranium, model for stress, 25:11344 (AWRE-O-46/66)
effects on ductility of uranium, 25:11344 (AWRE-O-46/66)
effects on oxidation rates of plutonium, 25:11346 (AWRE-O-100/66)
HUTCHINSON ISLAND POWER REACTOR, UNIT 1
design parameters of, requested additional information on, 25:12746 (DOCKET-50335-17)
operations aspects of, requested additional information on, 25:12746 (DOCKET-50335-17)
HYDRAZINE
dihydrobromide, radiation effects on single crystals of, at 77°K, ESR studies on Br_2^- radicals produced by γ, 25:10588
dihydrochloride, radiation effects on single crystals of, at 77°K, ESR studies on Cl_2^- radicals produced by γ, 25:10588
dihydrofluoride, radiation effects on single crystals of, at 77°K, ESR studies on radicals and hydrogen atoms produced by γ, 25:10588
HYDRAZINE, METHYL-
effects on ionizing and uv-radiosensitivity of Escherichia coli and Shigella flexneri, 25:11323
HYDROCARBONS
book: Radiation Chemical Processing, 25:10617
HYDROCHLORIC ACID
acetone--HCl--methanol, distribution coefficients of metal ions in, 25:10681
HYDROCYANIC ACID
radio emission from interstellar, detection of, 25:11594
HYDROFLUORIC ACID
properties of c-w laser of, for use in separation of deuterium and hydrogen, 25:10690
reactions of anhydrous, with thorium dioxide, preparation of thorium tetrafluoride by, 25:10516 (IEA-185)
reactions with uranium dioxide, rate of, 25:10569 (CEA-R-4074)
HYDROGEN
abundance of neutral, in M31 and M33, method for measurement of neutral, 25:11646
abundance of neutral, in M31, (E), 25:11647
abundance of neutral, in M33, (E), 25:11648
bromine-ion reactions at 6 to 15 MeV with molecular, cross sections for electron capture and loss in, (E), 25:11710
burning in upper main-sequence stars, (T), 25:11559
determination of trace amounts of, in biotite and tektite by spark source mass spectrometry, 25:10455
determination of trace amounts of, in molybdenum, review on, 25:10459
determination relative to deuterium in water, mass spectrometric, 25:10463
deuteron reactions at 30 to 120 keV with molecular, cross sections for electron capture into 3s state of deuterium in, (E>, 25:11708
diffusion in sodium, design and operation of continuously active indicator for determination of, 25:11400
diffusion in zirconium alloys, effects on corrosion, 25:11343 (AECL-3778)
electron elastic scattering by atomic, effects of charge polarization on differential cross sections for, (T), 25:11718
electron reactions at 13.6 to 680.3 eV with atomic, distorted-wave calculations of excitation of 2s state and angular distribution of scattered electrons from, 25:11714
electron reactions at 20 to 400 eV with molecular, absolute cross sections for production of Balmer lines in, (E), 25:11702
electron scattering by atomic, review of use of Sturmian functions in calculation of, 25:11732
energy eigenvalues for perturbed atom of, variational method for calculation of, 25:12056
energy levels of, atomic-beam radio-frequency measurement of separation between $2^2S_{1/2}$ and $2^2P_{3/2}$, 25:11691
energy transfer from helium to, efficiency of, 25:11474(R) (BNWL-842)
exchange functions for molecular, transform method for solution of, 25:11735
exchange with deuterium on molybdenum surface, low-pressure nonsteady-state, 25:10559
force constant of molecular, comparison of calculations by 5 methods, 25:11686
interaction of interstellar, with solar system, (E/T), 25:11640
iodine-ion reactions at 6 to 15 MeV with molecular, cross sections for electron capture and loss in, (E), 25:11710
meson (μ^+) inelastic scattering at 12 GeV, determination of neutron form factor from cross section ratios of carbon and copper to hydrogen from, (E), 25:12096
plasma of, correlation measurement techniques for, 25:11866 (EUR-CEA-FC-570)
plasma of, heating by hf fields near lower-hybrid frequency, (E), 25:11860 (FTI-282)
plasma of, ion and electron distribution function measurement in toroidal octupoles, (E), 25:11872
plasma of, numerical simulation of turbulent heating of, (T), 25:11862
positron reactions with atomic, generalized-variational-bounds formalism for distortion effects on rearrangement in, 25:11719
positron scattering by atomic, review of use of Sturmian functions in calculation of, 25:11732
proton reactions at 30 to 120 keV with molecular, cross sections for electron capture into n = 3 level of hydrogen in, (E), 25:11708
proton reactions with atomic, review of use of Sturmian

functions in calculation of charge exchange in, 25:11732
reactions with aqueous uranyl nitrate solutions at low pressure, catalytic effects of aluminum oxide--platinum on reduction, 25:10572 (IEA-184)
reactions with dichloromethyl radicals during x radiolysis of chloroform vapor, Arrhenius parameters for abstraction, 25:10629
reactions with neon at 5 keV of metastable 2s atoms of, mechanism of 2s destruction in, (T), 25:11723
scattering of atoms of, by atomic and molecular gases, analytic cross sections for inelastic, (E/T), 25:11703
separation from deuterium using c-w hydrogen fluoride laser, 25:10690
separation from deuterium, electrochemical, 25:10583(R) (AECL-3776)
separation from tritium in crystallization of inorganic hydrates from tritrated solution, 25:10688
sorption by Zircaloy-2 in hot pressurized water, relations with prior corrosion history, 25:11349 (WAPD-TM-906)
spectral emission of H I 1216-A, height profiles from 400 to 1016 km of euv dayglow, (E), 25:11789
target of liquid, for total cross section measurements at high energy, 25:12300 (JINR-P8-5212)
thermodynamic properties of solid deuterium and, under pressure, comparison of, 25:10575
yields from γ radiolysis of aqueous sodium sulfide sclutions, 25:10649
yields from γ radiolysis of liquid cyclopentane in deuterated ammonia, deuterated ethanol, and nitrous acid solutions, effects of pressure on, 25:10628

HYDROGEN IONS
reactions with platinum, angular and energy distributions of charged particles emitted in, (E), 25:11675

HYDROGEN IONS (H^-)
photon absorption by, calculation of coefficients for, 25:11684

HYDROGEN IONS (H_2^+)
exchange functions for, transform method for solution of, 25:11735

HYDROGEN PEROXIDES
yields from β radiolysis of aerated acidified water, 25:10636

HYDROLOGY
data display system for, 25:12879 (BNWL-1525)

HYDROMAGNETIC WAVES
structure of shock, in interstellar regions of very low ionization, (T), 25:11639

HYDROXAMIC ACID
complexes with iron, electronic structure of, effects of pressure on, 25:12881 (COO-1198-777)

HYDROXYLAMINE, N-PHENYL-
complexes of substituted, with uranium, formation constants of, 25:10521

HYPERFRAGMENTS
binding energy of ΛΛ-He^6 and ΛΛ-Be^{10}, (T), 25:12393
hyperon (Λ) binding energy in A-O^{17}, estimate of Λ + N interactions in p state from, (T), 25:12226
hyperon (Λ)--nucleon force in, review of, 25:12232
properties of light, 25:12232
research on, review of, (E), 25:12090 (INR-P-1223)

HYPERONS
binding energy of, Kemmer-symmetric coupling for particle decays for, (T), 25:12199
decay of polarized, beta, (T), 25:12163 (COO-264-563)
decay of, analysis of amplitudes for nonleptonic, 25:12171
decay of, form factors from q^2 spectrum of rate and asymmetry functions for beta, (T), 25:12164 (COO-264-563(Add.))
decay of, Kemmer-symmetric coupling for binding energy and lifetime from, (T), 25:12199
lifetimes of, Kemmer-symmetric coupling for particle decays for, (T), 25:12199
production of single strangeness-1 neutral, in K^- + d interactions at 7.3 GeV/c in deuterium bubble chamber, cross sections for, (E), 25:12103
production of Y and K in π^+ + d and π^+ + n interactions at 5.1 GeV/c, associated, (E), 25:12100 (NP-18629)

HYPERONS (Λ)
binding energy in A-O^{17}, estimate of Λ + N interactions in p state from, (T), 25:12226
binding energy in nuclear matter, calculation using AN tensor force, (T), 25:12668
decay Λ → n + γ, asymmetry parameter and branching ratio for, (T), 25:12169
decay Λ → n + π^0, relative phases and magnitude of amplitude for, 25:12171
decay Λ + n(p) → $\pi^0(\pi^-)$, test of $\Delta I = 1/2$ rule in spark chamber and scintillation counter study of asymmetry parameter ratio for, (E), 25:12086
decay Λ + n(p) → $\pi^0(\pi^-)$, test of $\Delta I = 1/2$ rule from spark chamber study of ratio of parity-violating parameters of, (E), 25:12080
decay Λ → p + e + ν, axial-vector-to-vector ratio from counter ad spark chamber study of up-down asymmetries in, (E), 25:12081
decay Λ → p + π^-, relative phases and magnitude of amplitude for, 25:12171
interactions Λ + N in p-state of A-O^{17}, (T), 25:12226
interactions Λ + N, AN tensor force for scattering, 25:12668
interactions Λ + N, review of, 25:12232
polarization in π^+ + n → A^0 + K^+ interactions at 5.1 GeV/c, (E), 25:12100 (NP-18629)
production in π^+ + p interactions at 1.7 GeV/c, cross sections for, (E), 25:12104

HYPERONS (Σ^-)
decay Σ^- → n + e + ν in bubble chamber, vector to axial vector current ratio for, (E), 25:12076
lifetime in K^- + p → Σ^- + π^+ interactions at 440 to 1230 MeV/c in hydrogen bubble chamber, (E), 25:12098 (CEA-R-4068)
production in K^- + p → Σ^- + π^+ interactions at 440 to 1230 MeV/c in hydrogen bubble chamber, (E), 25:12098 (CEA-R-4068)

HYPERONS (Σ^0)
decay Σ^0 → n + γ, asymmetry parameter and branching ratio for, (T), 25:12169

HYPERONS (Σ^+)
decay in hydrogen bubble chamber, branching ratios for nonleptonic, (E), 25:12098 (CEA-R-4068)
decay Σ^+ → n + π^+, relative phases and magnitude of amplitude for, 25:12171
decay Σ^+ → p + γ, asymmetry parameter and branching ratio for, (T), 25:12169
decay Σ^+ → p + π^0, relative phases and magnitude of amplitude for, 25:12171
decay Σ^+ → p + π^0, spark chamber study of proton polarization for parameters of, (E), 25:12084
lifetime in K^- + p → Σ^+ + π^- interactions at 440 to 1230 MeV/c in hydrogen bubble chamber, (E), 25:12098 (CEA-R-4068)
production in K^- + p → Σ^+ + π^- interactions at 440 to 1230 MeV/c in hydrogen bubble chamber, (E), 25:12098 (CEA-R-4068)
production in π^+ + p interactions at 1.7 GeV/c, cross sections for, (E), 25:12104

HYPERONS (Ξ^-)
decay Ξ^- → Σ^- + γ, asymmetry parameter and branching ratio for, (T), 25:12169

HYPERONS (Ξ^0)
decay Ξ^0 → Λ + γ, asymmetry parameter and branching ratio for, (T), 25:12169

HYPERONS (anti Ξ^0)
decay Ξ^0 → I^0 + γ, asymmetry parameter and branching ratio for, (T), 25:12169

HYPOXIA
effects on irradiated hamster cells, 25:11224 (BNL-50203, pp 318-38)
effects on radiosensitivity of survival in Oedogonium cardiacum, 25:11304 (BNL-50203, pp 70-81)

I

ICE
neutron slowing-down in cold, effective temperature from, (E/T), 25:12351
thermal emission from dirty, in H II regions, (T), 25:11583

IMMUNE REACTIONS
incidence in sheep with β and γ-radioinduced radiation sickness, nonspecific allergic, 25:10989
radiation effects on, in chickens and quail following intra-species transplantation of gonad tissues, x, 25:10988
radiation effects on, in peripheral nerve and skull bone homografts following transplantation in mammals, effects of temperature and 2 Mrad dose on ionizing, 25:11334
radiation effects on, in transplanted tissues, 25:11331
radiation effects on, of guinea pig lymphocytes in antihapten responses, 25:10987
radiation effects on, of mice to sheep red cells, effects of injections of spleen cells from mice treated with DMBA on, 25:10990
radiation effects on, of mice, effects of injections of allogeneic spleen cells and sheep red blood cells on x, 25:10994
radioinduce inhibition of, in miniature swine, strontium-90 β, 25:10984

IMMUNITY
radioisotope tracer studies of, in cultured cells and animals, 25:10924

IN-PILE LOOPS
coolant for CART, chemical and physical properties of water, (E), 25:12821(T) (LIB/Trans-335)
design of sodium cooled Banjo, for OSIRIS reactor, 25:12813 (CEA-CONF-1673)
design parameters of superheated steam, for fuel element failure testing, 25:12820 (KFK-1255)
failure of HFR pressurized water, testing of stainless steel components following, 25:12823 (RCN-125)

1,2,3-INDANTRIONE
effects on ionizing and uv-radiosensitivity of Escherichia coli and Shigella flexneri, 25:11323

INDIUM
determination of trace amounts of, in biotite and tektite by spark source mass spectrometry, 25:10455
determination of trace amounts of, in molybdenum, review on, 25:10459

electric conductivity of, effects of elastic stress on, 25:12032
neutron elastic scattering at 4 MeV, near 180° differential cross sections and polarizations from polarized, (E), 25:12509(T) (ANL-Trans-855)
photon inelastic scattering at 12 to 30 MeV, differential cross sections for, (E), 25:12463
separation from cadmium, molybdenum, niobium, palladium, and rhodium by gas chromatography using aluminum chloride eluent, 25:10666 (JINR-P6-5410)
separation from terbium and zinc by gas chromatography using aluminum chloride eluent, 25:10666 (JINR-P6-5410)
superconducting transition temperature of, effects of elastic stress on, 25:12032

INDIUM ALLOYS AND SYSTEMS
Ag--Cd--In-base--Sn, electric conductivity, Fermi surface topology, and superconducting transition temperature of dilute, 25:12032
Bi--In, electric conductivity of liquid, effects of composition and temperature on, 25:11398
Bi--In, voltages induced by ac--dc magnetic fields in superconducting foils of, 25:11835
In--Pb-base, Kapitza resistance of normal and superconducting, 25:11834
In--Pb-base, superconducting surface sheath response to ac field with triangular waveform, (E/T), 25:11829
In--Pd-base, thermodynamic properties of, 25:11396
In--Sb, microwave propagation in magnetoplasma of n-type, electric and magnetic resonances in Voigt configuration of, (E/T), 25:11929
In--Sb, superconducting properties of liquid-quenched simple cubic, 25:11819 (CALT-822-22)

INDIUM ISOTOPES In-113
decay of isomeric, upper limit for K-electron capture branch in, (E), 25:12591
use of fibrinogen-incorporated, for scintigraphy of induced thrombi in rabbits in combination with scintillation camera and computer, 25:11214
use of metastable, for determining blood circulation time from portal vein to right ventricle in dogs with induced obstructive jaundice, 25:11213
use of metastable, for diagnosis of placenta previa and localization of human placenta by scanning, 25:11228
use of metastable, for diagnosis of tumor metastases in combination with technetium-99m in double isotope method, 25:10928

INDIUM ISOTOPES In-115
deuteron inelastic scattering at 12 MeV at 125°, energy spectra from, (E/T), 25:12543
energy levels from Coulomb excitation and deuteron inelastic scattering, spin--parity assignments for collective, (E/T), 25:12543
energy-level transitions from Coulomb excitation, branching ratios, multipole transition probabilities, and transition strengths for, (E/T), 25:12543
neutron capture by, average circular γ polarization in thermal, (E), 25:12601
oxygen-16 inelastic scattering at 45 MeV, gamma spectra from, (E/T), 25:12543

INDIUM ISOTOPES In-116
energy levels from thermal neutron capture, spin for compound, (E), 25:12601

INDIUM ISOTOPES In-117
beta decay of ground-state and isomeric, gamma spectra and log-ft values from, (E), 25:12566

INDIUM TELLURIDES
radiation effects on high-pressure polymorphs of, fast neutron, 25:11474(R) (BNWL-842)

INDOLE, 3-(2-AMINOETHYL)-5-METHOXY-
radioprotective effects of, on hematopoietic tissue formation in spleen of inbred and noninbred γ-irradiated mice as compared to cystaphos, 25:11099
radioprotective effects of, on mice and rats, γ, 25:11102

INFORMATION CENTERS
description of IAEA Nuclear Data Section, 25:12343
operation of LMFBR fuel cladding, for data analysis, 25:11474(R) (BNWL-842)
operations of Nuclear Safety Information Center, 25:12759

INSECTA
Dahlbominus sp., radioinduced mutations in, for eye color, 25:11074(R) (AECL-3777)
Dolichoderus quadripunctatus, radiation effects on resistance and longevity of, effects of 1000 to 150,000 rad doses on γ and x, 25:11245
Drosophila hydei, radiation effects on synthesis of DNA in salivary glands of larvae of, x, 25:11246
Drosophila melanogaster, radiation effects on survival of, α and γ, 25:11248
Drosophila melanogaster, radiation effects on, effects of, on deletions of the proximal heterochromatin of chromosome three, x, 25:11012
Drosophila melanogaster, radioinduced sex-linked lethal mutations in oocytes of, effects of dose rate on γ, 25:11022
Drosphila melanogaster, radioinduced tumors in, following exposure of zygotes, x, 25:11250
Dryzaephilus surinamensis, radiation effects on survival of female and male, from stored dates, effects of dose on γ, 25:11244 (NP-18607)
Spodoptera exigua, radiation effects on egg production and longevity of, effects of dose and larval exposure on γ, 25:11247
Spodoptera littoralis, radiosterilization of male, effects of, on mating behavior, γ, 25:11338

INSTRUMENTS
radiation effects on optoelectronic, electron and x, 25:10904 (HMI-B-97)

INTERSTELLAR MATERIAL
equilibrium in clouds of, (T), 25:11650
photon absorption by, (E/T), 25:11665
spectra of, origin of 4430-A absorption line in, (E/T), 25:11643

INTESTINES
radiation effects on histamine in, of rats, mechanism of, 25:10967
radiation effects on, of rats following ingestion of mixed radioisotopes, mechanism of damage and repair following chronic, 25:11271
radioactive strontium isotope sorption through, of rats, effects of alginic acid components on, 25:10939
radioinduced damage of mucosal epithelium of, in rats, effects of dose on x, 25:11255 (BNL-50203, pp 181-5)
radioinduced tumors in, of mammals, effects of clonogenicity, dose, reproductive integrity, and time on, 25:11253 (BNL-50203, pp 154-73)
radioisotope sorption by, of rats, effects of estradiol on calcium-47 and strontium-85, 25:10933 (COO-1339-45)
thiol content in, of mice following injection of cystamine in optimum radioprotective dose, nonprotein, 25:11101

INULIN
clearance of radioisotope-labeled, from glomeruli, in comparison to chromium-51-labeled EDTA and cobalt-57-labeled vitamin B 12, methods for studying, 25:11154

INVARIANCE PRINCIPLES
CP noninvariance in model for baryon asymmetry in universe, (T), 25:12239
CP violating parameter phase in $K_1^0 \rightarrow \pi^+ + \pi^-$ decay, spark chamber study of, (E), 25:12078
CP violation in $K_1^0 \rightarrow 2\pi$ and $K_2^0 \rightarrow 2\pi$ decay interference from spark chamber study of proper time dependence of $K^0 \rightarrow \pi^+(\pi^0) + \pi^-(\pi^0)$ decays, 25:12079
CPT invariance in positron and electron g-factor, precision measurement of, (E), 25:12075
parity-violating parameter upper limits from asymmetries in p + N interactions at 210 MeV, (E), 25:12094
scale invariance in meson interactions with baryons, breaking of, 25:12214
time reversal invariance test in total and differential cross sections for n + p + d + γ interactions, (E), 25:12238

IODATES
separation from iodides, paper chromatographic, 25:10687

IODIDES
separation from iodates, paper chromatographic, 25:10687

IODINE
determination in pharmaceuticals using Ross filters for energy selection, x-ray fluorescence, 25:10479
determination in soils and lowland rice by neutron activation, 25:10505
determination of trace amounts of, as iodide by titration using mercury-203, radiochemical, 25:10481
determination of trace amounts of, in biotite and tektite by spark source mass spectrometry, 25:10455
distribution between gas--water systems, effects of pH and temperature on, 25:10513 (AERE-R-4887)
radioinduced reactions with methane, γ, 25:10620
radioinduced reactions with methane, Monte Carlo methods in analysis of γ, 25:10615
reactions with water, 25:10513 (AERE-R-4887)
sorption by soils, effects of initial iodine concentration on, (E), 25:10694
sorption on tungsten (100) surface, LEED study of chemical, 25:11405

IODINE IONS
reactions with helium and hydrogen gases at 6 to 15 MeV, cross sections for electron capture and loss in, (E), 25:11710

IODINE ISOTOPES
decay of fission-product, γ spectra from, 25:10472(R) (BMBW-FBK-70-19)
toxicity of radioactive, to man following ingestion of radiotellurium contaminated food chain components, 25:10948
use of radioactive, for diagnosis of thyroid cancer in man, methods for, 25:11217

IODINE ISOTOPES I-123
separation of cyclotron-produced, from antimony matrix by dissolution in hydrochloric acid--hydrogen peroxide and solvent extraction using carbon tetrachloride, 25:10674

IODINE ISOTOPES I-125
effectiveness for scanning of human liver, 25:11198
effectiveness of protein-incorporated, for measurement of vascular permeability in inflammatory lesions, 25:11193
use for detection of thrombosis in man, scanning method for, 25:11191
use for scanning human liver, 25:11200
use for thyroid scanning in children of man,

considerations of radiation burden during, in comparison to iodine-131 and technetium-99m, 25:11190
use for transmission scanning to measure lean to fat ratios in human tissues, 25:11114
use of isotope dilution measurement of extracellular fluid volume in dogs, 25:11185
use of toluidine blue-incorporated, for scanning of pancreas and parathyroid glands, 25:11188
IODINE ISOTOPES I-126
beta and electron-capture decay of, gamma spectra from, (E), 25:12515 (COO-1746-51)
beta and electron-capture decay of, gamma spectra from, (E), 25:12531 (TID-25586)
IODINE ISOTOPES I-127
content of human blood serum in comparison to iodine-131 following oral administration, methods for measuring, 25:10945
neutron capture by, average circular γ polarization in thermal, (E), 25:12601
IODINE ISOTOPES I-128
energy levels from thermal neutron capture, spin for compound, (E), 25:12601
neutron capture cross section, (E), 25:11539
IODINE ISOTOPES I-129
energy levels from proton scattering, isobaric analog, (E), 25:12602
production in meteorites, cosmic-ray, (E), 25:11539
IODINE ISOTOPES I-131
content of human blood serum following oral administration, in comparison to iodine-127, methods for measuring, 25:10945
content of milk in South America in 1967, 25:11068
content of milk in USA during February 1970, 25:11040
content of milk sampled throughout Central, North, and South America during July 1969 to July 1970, 25:11002
content of thyroid glands from cattle slaughtered in USA from 1962 through 1969, 25:11042
effectiveness for diagnosis of brain tumors in comparison to selenium-75, 25:11145
effectiveness for diagnosis of kidney diseases, review of, 25:11210
effectiveness for diagnosis of thyroid diseases in children in combination with whole-body counting, 25:11172
effectiveness for scanning of human liver, 25:11198
effectiveness for therapy of thyroid carcinomas in man, effects on mortality, 25:11233
effectiveness in combination with methylmercaptoimidazol for therapy of hyperthyroidism, 25:11230
effectiveness of albumen macroaggregate-incorporated, for lung scintigraphy in patients with blunt chest concussions in combination with radiography and ventilation measurements, 25:11135
effectiveness of albumen macroaggregate-incorporated, for evaluating blood circulation in patients with lung tumors in combination with blockage method, 25:11127
effectiveness of albumen macroaggregate-incorporated, for lung scintigraphy in silicosis patients in comparison to x-radiography, evaluation of, 25:11134
effectiveness of albumin macroaggregate-incorporated, for diagnosis of pulmonary sarcoidosis, 25:11133
effectiveness of albumin macroaggregate-incorporated, for diagnosis of honeycomb lung and emphysema in comparison to radiography, 25:11215
effectiveness of albumin macroaggregate-incorporated, for diagnosis of lung diseases in comparison to RISA, 25:11129
effectiveness of albumin-incorporated, for diagnosis of tuberculosis in comparison to radiography, 25:11132
effectiveness of hippuran-incorporated, for determining renal clearance in comparison to chromium-51-labeled EDTA, chromium-51-labeled inulin, and mercury-203-labeled salyrgan, evaluation of, 25:11156
effectiveness of hippuran-incorporated, for determining renal blood flow in comparison to chromium-51-labeled EDTA, chromium-51-labeled inulin, cobalt-57-labeled vitamin B 12, and iodine-125-labeled iothalamate, 25:11153
effectiveness of hippuran-incorporated, for determining radiation damage to kidneys following therapy of abdominal or retroperitoneal tumors, 25:11275
effectiveness of hippuran-incorporated, for function tests following kidney tranplantations, 25:11162
effectiveness of hippuran-incorporated, for kidney scintigraphy in comparison to gallium-68-labeled EDTA, 25:11169
effectiveness of hippuran-incorporated, for measuring cerebral blood circulation time, evaluation of, 25:11150
effectiveness of hippuran-incorporated, for studying renal function in combination with Anger camera, method for evaluating, using computer or oscilloscope, 25:11165
effectiveness of hippuran-incorporated, or RISA-incorporated, for measuring cerebral blood flow in patients with tumors or vascular diseases, evaluation of, 25:11149
effectiveness of hippuric acid-incorporated, in combination with gallium-68-labeled EDTA in double isotope method for diagnosis of kidney diseases, 25:10928
effectiveness of orthohippuric acid-incorporated, for determining renal blood flow in combination with cobalt-57 for glomerular filtration measurements, 25:11157
effectiveness of Rose Bengal-incorporated, for liver scintigraphy for detection of liver diseases in comparison to histologic and laparoscopic methods, 25:11180
effects on thyroid gland of animals and man, review of β and γ, 25:11291
energy levels from proton scattering, isobaric analog, (E), 25:12602
half-life of, 25:10491 (ORNL-4636, pp 20-33)
metabolism in human thyroid gland, use of clearance method at constant blood level for determining, 25:11173
production of, review on developments and patents for, 25:10653 (BLG-442)
removal of albumin-incorporated, from blood of guinea pigs and rats, estimation of phagocytic coefficient for, 25:10957
sensitivity of Rose Bengal-incorporated, for liver function appraisal in comparison to other biochemical tests, 25:11111
sodium iodide-incorporated, for thyroid carcinoma therapy in man, effects of surgery on, 25:11234
sorption of hippuran-incorporated, in hydrocephalic children following intraventricular injection for assessment of surgical shunts, 25:11152
uptake by human thyroid, effects of triiodothyronine on, 25:10944
use as tracer for measuring effects of initial iodine concentration on iodine sorption by soils, (E), 25:10694
use as tracer for measuring ground water flow in Shigaya aquifier in Kuwait, 25:10700
use for determination of heart minute volume in patients with hyperthyroidism, 25:11141
use for evaluating peripheral blood circulation, development of clearance method for, in combination with xenon-133, 25:10912
use for heart scanning in differential diagnosis of mediastinal processes and pericardial effusion in combination with iodine-131-labeled albumen macroaggregate for lung scintigraphy, 25:11130
use for kidney scanning in hypertensive patients in comparison to /super 99m/Tc scintigraphy and vasoconstrictor content in the renal vein, 25:11163
use for scanning of cerebral blood flow in man for determining mental activity, method for, 25:11151
use for scanning of human kidneys for renal insufficiency in combination with gamma camera, 25:11206
use for scanning of human liver, 25:11183
use for scanning of human liver, effects of abscesses, angiomas, hydatid cysts, and tumors on, 25:11197
use for studies on resorption of human albumin and stomach retention time following oral administration, 25:11170
use for thyroid scanning in children of man, considerations of radiation burdens during, in comparison to iodine-125 and technetium-99m, 25:11190
use of albumen-incorporated, for determining coronary blood circulation in patients with arteriosclerosis or angina pectoris in combination with scintillation crystals and collimators, development of techniques for, 25:10911
use of albumin macroaggregate-incorporated, for lung scintigraphy using computers or multichannel analyzers, evaluation of, 25:11131
use of albumin-incorporated, for scanning of arterio-venous shunts in feet of dogs, double isotope method for, 25:10926
use of fibrinogen-incorporated, for scintigraphy of induced thrombi in rabbits in combination with scintillation camera and computer, 25:11214
use of hippuran-incorporated, for determining renal clearanc in combination with mathematical model, 25:11160
use of hippuran-incorporated, for kidney scanning, importance of detector localization for renogram evaluation following, 25:11167
use of Hippuran-incorporated, for scanning of human renal function, 25:11186
use of orthohippuric acid-incorporated, for determining renal clearance, method for, 25:11159
use of orthoiodohippuric acid-incorporated, for kidney scanning in combination with angiotension infusion test and determination of renin content of venous blood, 25:11164
use of RISA-incorporated for scanning of human lungs, effectiveness of dual-probe detector system and, 25:11207
use of RISA-incorporated, for diagnosis of brain diseases or thrombosis in combination with three detectors for measuring blood circulation time, 25:11148
use of RISA-incorporated, for measuring minute cardiac volume, 25:11123
use of RISA-incorporated, for studying minute volume of hepatic blood flow following hyperemia treatment, 25:10916
use of Rose Bengal-incorporated, for liver scintigraphy in dogs, development of computer program for

XUM

improvement of, 25:10919
use of Rose Bengal-incorporated, for study of liver function in dogs with experimentally induced obstructive jaundice, 25:11213
use of serum albumin--incorporated, in combination with cisternography for diagnosis of normal pressure hydrocephalus in man, 25:11181
volatility from sodium peroxide systems, (E), 25:10797(R) (NYO-841-23)
IODINE ISOTOPES I-132
decay of metastable, 25:10472(R) (BMBW-FBK-70-19)
IODINE ISOTOPES I-133
yields from neutron fission of thorium-232, 25:10472(R) (BMBW-FBK-70-19)
IODINE ISOTOPES I-134
yields from neutron fission of thorium-232, 25:10472(R) (BMBW-FBK-70-19)
IODINE ISOTOPES I-135
yields from neutron fission of thorium-232, 25:10472(R) (BMBW-FBK-70-19)
IODINE ISOTOPES I-136
beta decay of, beta and gamma spectra, β--γ delay, and log-ft values for, (E), 25:12572
IODOURANATES
preparation and properties of UI_4^-, 25:10576
ION-ACOUSTIC WAVES
propagation in bounded plasmas, one-dimensional, (T), 25:11937
ION EXCHANGE MATERIALS
radiolysis of Zerolit FF-IP, γ, 25:10646
ION EXCHANGE PROCESSES
methods for rapid, kinetics of effects of complexing on, 25:10668 (LYCEN-7034, pp 1-8)
ION SOURCES
design of Penning-type polarized, 25:12328
design of polarized, for high-energy accelerators, 25:12304 (JINR-P9-5446)
development of polarized deuteron, 25:12309 (LYCEN-6909)
IONOSPHERE
coupling to magnetosphere, dimensional analysis of equations describing, 25:11804
critical frequency in summer hemispheric, effect of neutral winds on evening anomalous, (E/T), 25:11777 (AD-708496)
D region, ionization in daytime, effect of ionospheric nitric oxide NO density at 70 to 110 km on, (E), 25:11795
electrojets in, relation of boundary of captured electrons with E greater than or equal to 280 keV in radiation belts with current, (E/T), 25:11782
electron density in auroral, rf impedance probe measurements of, 25:11781
electron density variations across equatorial anomaly at sunspot minimum, (E), 25:11816
electron density variations at high latitudes, effects on satellite radio scintillations, (E), 25:11601
electron processes in, review of, 25:11810
electron recombination with ions in, review, 25:11729
F region, field-aligned irregularities in, (E), 25:11815
F region, radio-wave accessibility to plasma resonance in, (E), 25:11814
F2 layer, electromagnetic drift of mid-latitude, during magnetic storm, (E/T), 25:11805
gravity wave propagation in, effect of background wind on ray-tracing-typed, (E/T), 25:11796
gravity wave propagation in, vertical ion-motion levels induced by internal atmospheric, (T), 25:11800
heating during Boulder experiment, effect on absorption of probing waves of ordinary and extraordinary polarization, (E/T), 25:11807
magnetic field direction in, incoherent scatter measurements at Jicamarca of, (E/T), 25:11792
nitric oxide density profiles at 70 to 110 km in, effect on daytime D-region ionization, (E), 25:11795
oxygen excitation in sunlit conjugate, O I 1304-A airglow, (E), 25:11799
plasma instabilities in, relevance to heating and radio wave attenuation, (E/T), 25:11806
radiation effects on, solar cosmic, (T), 25:11625
radio propagation in, effects of galactic x-ray source on nighttime anomalies in vlf, (E), 25:11812
radio-wave absorption in, effects of hard solar x rays on, (E), 25:11817
scintillation boundary irregularities at 350 km in, during magnetically quiet and disturbed conditions, (E/T), 25:11791
spread-F irregularities in, aspect sensitivity of, (E), 25:11815
temperature profiles in, relation of incoherent scatter and satellite 1400-hour density measurements, diurnal variation of neutral, (E/T), 25:11793
wave propagation in presence of electrostatic field and background wind in, ionization irregularities due to internal gravity-, (T), 25:11798
IONS
electron reactions with, review of dissociative recombination in, (E/T), 25:11729
mobility in gases, spectrometer for measurement of, 25:10903
reactions with atoms and ions, review of classical mechanical calculations of, 25:11733
reactions with atoms at keV energies, statistical model for calculation of ionization probabilities in, 25:11711
reactions with gases and solids in keV range, spatial distribution of energy deposited in, (T), 25:11682
reactions with solids, review of atom, electron, and ion ejection in, 25:11676
scattering by thin films, 25:10583(R) (AECL-3776)
stopping of heavy, model for electronic, 25:11680
trajectories in front of field emission microscope tip, calculations, 25:12299 (IPP-7/2)
IRIDIUM
determination of trace amounts of, in biotite by spark source mass spectrometry, 25:10455
IRIDIUM ALLOYS AND SYSTEMS
Ir--Nb, niobium-93 NMR in Nb_3Ir, 25:12037
IRIDIUM ISOTOPES Ir-184
beta and electron-capture decay of, γ spectra from, (E), 25:12514(R) (COO-1672-21)
IRIDIUM ISOTOPES Ir-187
electron-capture decay of, γ singles and coincidence spectra from, (E), 25:12514(R) (COC-1672-21)
IRIDIUM ISOTOPES Ir-192
beta and electron-capture decay of, gamma spectra from, (E/T), 25:12532 (TID-25592)
decay scheme, (E), 25:12464
neutron capture by, cascade-theory calculations of gamma spectra from, (T), 25:12626 (FMRB-33/70)
use as γ source for implant therapy, 25:11000
IRIDIUM ISOTOPES Ir-193
energy levels of, lifetimes for, (E), 25:12590
IRON
alpha reactions at 30 to 80 MeV, cross sections for production of K x rays by, (E), 25:12488
analysis for carbon, nitrogen, and oxygen by helium-3 and photon activation and radiochemical separation, 25:10488 (CEA-R-4072)
analysis for molybdenum by solvent extraction and flame photometry, 25:10439
carburization by decomposing carbon monoxide, effects of carbon dioxide, composition, oxygen, surface structure, temperature, and water vapor on, 25:11374 (DP-Report-530)
complexes with hydroxamic acid, electronic structure of, effects of pressure on, 25:12881 (COO-1198-777)
content in wind-blown surface soils, determination for monitoring radioactive fallout, 25:10718
corrosion by liquid lead at high temperatures, 25:11376 (JUL-661-RW)
determination as impurity in fuel materials by emission spectroscopy, 25:10432 (KFK-1261)
determination in ores and ore concentrates, intermittent ac arc method for spectrographic, 25:10429 (BARC-468)
determination in seawater by atomic absorption spectrophotometry or neutron activation, 25:10428
determination in sedimentary rocks by direct-reading spectrometry, 25:10450
determination in serum and urine by flameless atomic absorption spectroscopy, 25:10464
determination in tektite by spark source mass spectrometry, 25:10455
determination of trace amounts of, in molybdenum, review on, 25:10459
determination of trace amounts of, in rocks and sand by thermal neutron activation, ion exchange, and γ spectrometry, 25:10492
determination of trace amounts of, in zirconium, carrier distillation method for spectrographic, 25:10430 (EUR-4541)
dislocation kinks, structure and energy of screw, 25:12027
distribution coefficient in mixtures of acetone, hydrochloric acid, and methanol, 25:10681
distribution in uranium during zone melting, 25:11406
effects on hot cracking of uranium weld metal, 25:11427
effects on tensile properties of rolled gallium--plutonium alloys at 25 to 600°C, 25:11391
friction and wear of, sliding against copper and iron rings under vacuum, 25:11413
friction and wear on rings of, from sliding metal pieces under vacuum, 25:11413
gamma-ray attenuation at 6 and 8 MeV in, 25:11947
mechanical properties at 77 to 373°K, 25:11401
properties for use in thermoelectric converter heat block shield, 25:10778(R) (ORNL-TM-3214)
radioinduced defect clusters in, calculations of in-pile, 25:11474(R) (BNWL-842)
separation of divalent and trivalent, paper chromatographic, 25:10687
separation of neptunium from, by ion exchange in tetramethylammonium hydroxide--citrate solutions, effects of complexing agents on, 25:10655 (ANL-7751)
solubility in lead at 350 to 1100°C, 25:11376 (JUL-661-RW)
IRON ALLOYS AND SYSTEMS
Al-base--Fe, deformation of dilute, structural dependence of Newtonian, 25:11434(R) (SU-326-P-17-X-1)
B--Fe, analysis of powdered, for oxygen, comparison of isotope dilution and vacuum fusion methods for, 25:10467
Ce--Fe, phase diagram, crystal structure, and magnetic properties of, 25:12025

Cr--Fe--Ni, radiation effects on mechanical properties of, in water, fast neutron, 25:11466 (SRARI-P-78)
Cr--Fe-base, properties of aged, effects of reheating on electric and mechanical, 25:11403
Cr--Fe-base--V, properties of aged, effects of reheating on electric and mechanical, 25:11403
Dy--Fe, hyperfine interactions in $DyFe_2$, dysprosium-161 Mcessbauer study of, 25:12035
Fe--ThO_2, mechanical properties at 77 to 373°K, 25:11401
Fe--ThO_2, preparation of fine dispersion of, development of method for, 25:11401
Fe-base--Si, creep at high temperature and low stress, rate controlling factors in, 25:11434(R) (SU-326-P-17-X-1)
Fe-base--Si, strain behavior of solid-solution, 25:11434(R) (SU-326-P-17-X-1)
IRON CARBONATES
neutron inelastic scattering study of magnons and phonons in siderite, 25:11981(R) (ORO-3674-4)
IRON FLUORIDES
reactions in, emf measurements of solid-state displacement, 25:11473(R) (AD-708712)
IRON FLUORIDES FeF_2
thermal expansion of, electronic structure from anomalous, (T), 25:12015
IRON HYDROXIDES
precipitation of carrier-free silicon-31, 25:10675
IRON IONS
radiolysis of divalent and trivalent, in dilute acid solutions, mechanism for attainment of stationary state in γ, 25:10635
IRON ISOTOPES Fe-54
alpha reactions (α,He-3) and (α,t) at 44 MeV, optical-model analysis of angular distributions and energy spectra from, (E/T), 25:12434
neutron capture by, gamma spectra and Q-value for thermal, (E), 25:12403
neutron reactions (n,p), 2DB code for calculation of spectral-averaged cross sections for, 25:11474(R) (BNWL-842)
proton inelastic scattering by, microscopic first-order core polarization corrections to DWBA for, (T), 25:12678
IRON ISOTOPES Fe-55
abundance in Apollo 11 samples, (E), 25:11539
content of blood of Rongelap Atoll residents, 25:10997(R) (RLO-2225-T-14-1)
energy levels from iron-54 (α,He-3) reactions at 44 MeV, spectroscopic factors and spin--parity assignments for, (E/T), 25:12434
energy levels from manganese-55 (p,nγ) and (p,n) reactions, spin--parity assignments for, (E/T), 25:12476
energy levels from manganese-55 (p,nγ) reactions, lifetimes and spin assignments for, (E), 25:12483
energy-level transitions from manganese-55 (p,n) and (p,nγ) reactions, branching ratios for (E/T), 25:12476
energy-level transitions from manganese-55 (p,nγ) reactions, γ-branching and multipole mixing ratios for, 25:12483
IRON ISOTOPES Fe-56
neutron capture by, gamma spectra and Q-value for thermal, (E), 25:12403
proton reactions at 130 MeV to 2.9 GeV, cross sections for spallation products from, (T), 25:12439
IRON ISOTOPES Fe-59
content of biological materials, gamma scintillation spectrometry method for, 25:11044
decay scheme, (E), 25:12464
effectiveness of dextran-incorporated, for determining enteral protein loss, 25:11171
use as tracer in function studies of x-irradiated erythron and reticulo-endothelial cells, 25:11112
use of plasma clearance rate of, for dosimetry of nitrogen mustard therapy, 25:10952
IRON MINERALS
formation in supernovae, (E/T), 25:11562
spectra of, in supernovae, (E/T), 25:11562
IRON OXIDES
effects on electron-induced curing of resin coatings on metals, 25:10608 (JAERI-5026, pp 121-9)
B_2O_3--FeO--FeS, phase studies of, 25:11526
IRON SULFIDES
B_2O_3--FeO--FeS, phase studies of, 25:11526
IRON, TRIS(1,10-PHENANTHROLINE)-
reactions with oxidizing agents, mechanisms of, 25:10515(R) (COO-1780-14)
IRRADIATION FACILITIES
description of Ezeiza semi-industrial, 25:10795 (CNEA-272)
development of 2000 Ci cesium-137, for studying irradiation effects on marine organisms, 25:10759
sources for, design of collimation system for, 25:10781(P)
ISOBUTYRAMIDE
radiation effects on single crystals of, at 77°K, ESR studies on radicals produced by γ, 25:10588
ISOTOPE DILUTION ANALYSIS
radioactivity measurements in, optimum distribution of total time for x, 25:10471
ISOTOPE EFFECTS
effects of temperature on kinetic, 25:10549
ISOTOPE EXCHANGE
kinetics in synthetic polypeptides, effects of conformation on, 25:10567
uses in radiochemical separations, 25:10490(T) (LIB/Trans-334)
ISOTOPE SEPARATION METHODS
book: Thermal Diffusion Column. Theory and Practice with Particular Emphasis on Isotope Separation, 25:10783
cascade rate functions for multicomponent isotopic mixtures, 25:10782
description of liquid--gas exchange, 25:10789(P)
ISOTOPES
determination by mass spectroscopy, 25:10438 (ORNL-4636, pp 51-3)

J

JAPAN
radiation protection programs at critical assemblies in, 25:11081
JAPANESE POWER DEMONSTRATION REACTOR II
containment structure penetration for, development of high voltage power cable porcelain, 25:12705 (JAERI-Memo-4197)
JOINTS
fabrication of rolled, for reactor cooling system fuel channels, 25:11366(P)
JOSEPH M. FARLEY POWER REACTOR, UNIT 1
design parameters of, revised and additional data on, 25:12748 (DOCKET-50348-15)
operations aspects of, revised and additional data on, 25:12748 (DOCKET-50348-15)
JOSEPH M. FARLEY POWER REACTOR, UNIT 2
design parameters of, revised and additional data on, 25:12748 (DOCKET-50348-15)
operations aspects of, revised and additional data on, 25:12748 (DOCKET-50348-15)
JUPITER (PLANET)
radio emission at decametric wavelengths from, waveform and source-size studies of, (E), 25:11670

K

KIDNEYS
americium-241 accumulation in, of animals following intravenous injection as chloride, 25:10942
blood circulation in, use of xenon-133 for determining, 25:11158
chromium-51 clearance from human, use of labeled EDTA and whole-body counting for determining, 25:11155
cobalt-60 1-nitroso 2-naphthol chelate distribution in, of rats, 25:10958
iodine-131 clearance from, use of mathematical model for determining, 25:11160
iodine-131-labeled orthohippuric acid clearance, method for determining, 25:11159
nonprotein thiol content in, of mice following injection of cystamine in optimum radioprotective dose, 25:11101
radiation damage to, in therapy of abdominal tumors, use of renograms obtained with iodine-131-labeled hippuran for evaluating cobalt-60 γ, 25:11275
radiation effects on histamine in, of rats, mechanism of, 25:10967
radiation effects on, of rats, effects of high doses on, 25:11286
radiation hazards to, in human children following scanning with mercury-203 or selenium-75, 25:11190
radioactive hippuran clearance from human, use of computers for quantitative interpretation of renograms of, 25:11208
radiodiagnosis of diseases of, using iodine-131 renography, 25:11210
radioisotope clearance from glomeruli of human, comparison of methods for chromium-51, and cobalt-57, and radioisotope-labeled inulin, 25:11154
radioisotope clearance from human, methods for determining in comparison to standard diagnostic procedures, 25:11156
radioisotope clearance studies in human, for measuring glomerular filtration rate, cobalt-57 and iodine-131, 25:11157
radioisotope scanning of, importance of detector localization for renogram evaluation following iodine-131, 25:11167
scanning in patients with hypertension, in combination with angiography, evaluation of, 25:11166
scanning of blood circulation in, of hypertensive patients, effectiveness of radioisotope-labeled compounds for determining, 25:11153
scanning of function of, using iodine-131-labeled hippuran, computer or oscilloscope methods for evaluating, 25:11165
scanning of human, computer evaluation following, 25:11161
scanning of human, for renal function, use of iodine-131-labeled Hippuran for, 25:11186
scintiscanning of, effectiveness of gallium-68-labeled EDTA in comparison with iodine-131-labeled hippuran for, 25:11169

XUM

tellurium-127m uptake by rat, following intravenous injection, 25:10950
transplantation in man, use of iodine-131 scanning for evaluation of function of, 25:11162
KRYPTON
diffusion in solid argon, isotope effect calculations for, 25:12042
electron elastic scattering by, calculation of differential cross sections for, using potential-scattering model, 25:11722
helium-ion reactions at 1 to 3 keV and at small angles with, charge exchange in, (E), 25:11716
helium-ion reactions at 1 to 3 keV with, charge exchange at small angles in, (E), 25:11705
oxygen-ion (O^+) reactions at keV energies with, statistical-model calculations of ionization probabilities in, 25:11711
scattering by platinum (111) surfaces at thermal energies, (E), 25:11683
KRYPTON IONS
implantation in silicon carbide crystals, cathodoluminescence spectrum in annealing of, 25:11974
implantation into silicon at 50 to 300 keV, sputtering and strain induced by, 25:11959
KRYPTON ISOTOPES Kr-82
energy levels from rubidium-82 decay, spin-parity assignments for, (E), 25:12507
KRYPTON ISOTOPES Kr-84
energy levels from bromine-84 beta decay, spin--parity assignments for, (E), 25:12444
KRYPTON ISOTOPES Kr-85
effectiveness in combination with pressure measurements for diagnosis of mitral valve defects in human hearts, evaluation of, 25:11124
KRYPTON ISOTOPES Kr-87
beta decay of, γ singles and coincidence spectra and log ft value for, (E), 25:12485
KRYPTON ISOTOPES Kr-91
beta decay of, beta and gamma spectra, half-life, log ft, and Q-value for, (E), 25:12462
KUWAIT
ground water flow in Shigaya aquifier in, iodine-131 tracer measurements of, 25:10700

L

LABORATORIES
design, operation, and staffing of environmental radiation surveillance, near nuclear installations, guide for, 25:10763
LACTATE DEHYDROGENASE
radiation effects on activity of, in embryos, protective effects of cysteamine against, x, 25:11096(R) (EUR-4491)
radiation effects on content of, in epidermis, x, 25:11241
spectra of isoenzymes of, in organs of xenogenic radiation chimeras, 25:10992
LACTATES
radiation effects on synthesis of, in ganglia of rats, effects of dose rate on strontium-90 β, 25:11262
LACTOSE
analysis for moisture content by neutron scattering and moderation, 25:10486
LANTHANUM
abundance in photosphere and sunspots, (E), 25:11613
complexes with EDTA, separation by ion exchange, effects of resin crosslinking on, 25:10665 (INR-P-1209)
determination of trace amounts of, in biotite and tektite by spark source mass spectrometry, 25:10455
determination of trace amounts of, in phosphate deposits by spark source mass spectrometry, 25:10456
energy levels of, LS-term dependence of hyperfine interaction parameters in d^2s configurations, 25:11694
vacancy formation in, high-temperature thermal-capacity study of, 25:11423
LANTHANUM ALLOYS AND SYSTEMS
Al--La, superconducting transition temperature of $LaAl_2$, effects of rare-earth impurities on, (T), 25:11836
Ce--La-base, Kondo effect in fcc and dhcp, effects of pressure on, 25:11990
LANTHANUM BORIDES
properties of electron-emission cathodes of, for accelerator electron sources, 25:12316
LANTHANUM HYDROXIDES
precipitation of carrier-free silicon-31, 25:10675
LANTHANUM IONS
spectra in lanthanum chloride monocrystals, ENDOR, 25:10570(R) (COO-294-10)
LANTHANUM ISOTOPES La-139
deuteron reactions (d,He-3) with, energy spectra and angular distributions from, (E/T), 25:12552
energy levels from cerium-140 (d,He-3) reactions, shell-model calculations of, (E/T), 25:12552
energy levels from photon scattering, radiation widths for, (E), 25:12447
energy levels from photon scattering, spin-parity assignments for, (E), 25:12585
energy levels from quasi-particle Tamm--Dancoff approximation, spin--parity assignments, single-particle energies, eigenvectors, electromagnetic moments, and spectroscopic factors for, (T), 25:12616
energy levels of, hyperfine interaction constants and electron g factors for low-lying atomic, (E), 25:11693
energy-level transitions from quasi-particle Tamm--Dancoff approximation, rates for M1 and E2, (T), 25:12616
helium-3 reactions (He-3,d) with, energy spectra and angular distributions from, (E/T), 25:12552
nuclear electric quadrupole moment of, 25:11693
photon elastic and inelastic scattering by, γ spectra from, (E), 25:12585
LANTHANUM ISOTOPES La-141
energy levels from barium-141 beta decay, lifetimes of, (E), 25:12546
energy-level transitions from barium-141 beta decay, intensities, multipolarities, internal conversion coefficients, and hindrance factors for, (E), 25:12540
LANTHANUM OXIDES
B_2O_3--CdO--La_2O_3, properties and structure of glasses of, 25:11517
LANTHANUM OXYCHLORIDES
radiation effects on trivalent bismuth-activated, effects of composition on luminescence produced by x, 25:10590
LARVAE
radiation effects on, of cotton leaf moth, effects of, on pupation and adult emergence, γ, 25:11247
LASER RADIATION
effects on M and F centers in gamma-irradiated alkali metal halides, (E/T), 25:11956
effects on mitochondria of rat myocardial cells, effects of argon microbeam exposure on, 25:11242
effects on oral ciliature of Blepharisma japonicum, in comparison to uv radiation, 25:11322
effects on pigmentation in Arabidopsis, effects of seed exposure on mutagenic, 25:11027
interactions with plasma, stimulated and nonlinear effects from, (T), 25:11884 (CEA-N-1399)
reactions with solid targets, plasma diagnostics from multi-layer, (E/T), 25:11870
scattering on plasma in tokamak configurations, current distributions from, 25:11867 (MATT-818)
scattering on plasma, diagnostic use of Thomson, (T), 25:11865 (CEA-R-4058)
LASERS
development of neodymium, for plasma production, 25:11906
performance of carbon dioxide, for plasma diagnostics in adverse environments, 25:11869
use for light scattering method for study of ribosomal RNA solutions, 25:11074(R) (AECL-3777)
use for plasma diagnostics in coaxial accelerators, 25:11871
use for plasma production, review of, 25:11907
LAWRENCIUM ISOTOPES Lr-256
fission of, half-life for spontaneous, (E), 25:12620
LAWRENCIUM ISOTOPES Lr-257
fission of, half-life for spontaneous, (E), 25:12620
LEAD
alpha elastic and inelastic scattering at 166 MeV, optical potentials from DWBA analysis of angular distributions from, (E/T), 25:12549
alpha inelastic scattering at 42 to 90 MeV, angular distributions and energy spectra from, (E/T), 25:12604
alpha reactions (α,He-3) at 42 to 90 MeV, angular distributions and energy spectra from, (E/T), 25:12604
analysis of microgram quantities of, mass-spectrometric isotopic, 25:10466
content of benthic fish and invertebrates, pelagic fish, and zooplankton of Pacific Ocean, 25:10997(R) (RLO-2225-T-14-1)
corrosive effects of liquid, on iron, refractory metals, and steel at high tempeeratures, 25:11376 (JUL-661-RW)
determination as impurity in fuel materials by emission spectroscopy, 25:10432 (KFK-1261)
determination by beta excitation, 25:10475
determination by photon activation, reactions and sensitivities for, 25:10488 (CEA-R-4072)
determination in sedimentary rocks by direct-reading spectrometry, 25:10681
determination in serum and urine by flameless atomic absorption spectroscopy, 25:10464
determination of trace amounts of, in basalt and granite, correction of matrix effect in uv spectrographic, 25:10453
determination of trace amounts of, in biotite and tektite by spark source mass spectrometry, 25:10455
determination of trace amounts of, in molybdenum, review on, 25:10459
determination of trace amounts of, in phosphate deposits by spark source mass spectrometry, 25:10456
determination of trace amounts of, in rocks, quantometer for spectroscopic, 25:10451
determination of trace amounts of, in standard bauxite, carbonate, and silicate rocks by x-ray fluorescence, 25:10449
determination of trace amounts of, in standard silicate rocks using sodium chloride buffer, emission spectrographic, 25:10454
determination of trace amounts of, in zirconium, carrier distillation method for spectrographic, 25:10430 (EUR-4541)

gamma-ray attenuation at 6 and 8 MeV in, 25:11947
helium-3 inelastic scattering at 50 and 75 MeV, angular distributions and energy spectra from, (E/T), 25:12604
helium-3 reactions (He-3,α) at 50 to 75 MeV, angular distributions and energy spectra from, (E/T), 25:12604
Kapitza resistance of normal and superconducting, 25:11834
mesCn (μ^-) reactions at 10.5 GeV, effective cross sections for μ trident production from, (E), 25:12083
mesCn (μ^+) reactions at 10.5 GeV, effective cross sections for μ trident production from, (E), 25:12083
meson reactions (π^-,π^0) at 70 MeV with natural, integrated cross sections for, (E), 25:12446
mineralization of zinc and, in Horni Benesov ore deposit, gamma--gamma logging method for determination of, 25:10722
neutron elastic scattering at 4 MeV, near 180° differential cross sections and polarizations from polarized, (E), 25:12509(T) (ANL-Trans-855)
reactions with folic acid, stability constants of complexes from, 25:10520
separation of neptunium from, by ion exchange in tetramethylammonium hydroxide--citrate solutions, effects of complexing agents on, 25:10655 (ANL-7751)
solvent properties for iron, refractory metals, and steel at high temperatures, 25:11376 (JUL-661-RW)
superconducting quench-condensed, electron tunneling in, (E/T), 25:11842
superconducting transition temperature and recovery of deformed, 25:10583(R) (AECL-3776)
superconducting tunneling in films of, near transition temperature, (E/T), 25:11826

LEAD ALLOYS AND SYSTEMS
Bi--Pb, superconducting quench-condensed, electron tunneling in, (E/T), 25:11842
Bi--Pb--Tl, superconducting transition temperature of fcc, 25:11846
In--Pb-base, Kapitza resistance of normal and superconducting, 25:11834
In--Pb-base, superconducting surface sheath response to ac field with triangular waveform, (E/T), 25:11829
Pb--Tl, voltages induced by ac--dc magnetic fields in superconducting foils of, 25:11835

LEAD ISOTOPES
determination of abundance ratios of, in microgram quantities of lead iodide, mass-spectrometric, 25:10466

LEAD ISOTOPES Pb-203
separation of cyclotron-produced, from thallium matrix by iron hydroxide precipitation and solvent extraction, 25:10678

LEAD ISOTOPES Pb-204
deuteron reactions (d,He-3) at 80 MeV, energy spectra and DWBA analysis of differential cross sections from, (E), 25:12575

LEAD ISOTOPES Pb-206
alpha reactions (α,2nγ) at 29 MeV, anisotropy of γ-ray angular distributions from, (E), 25:12614
deuteron reactions (d,p) at 17 MeV, angular distributions for, (E), 25:12569
energy levels from lead-208 (p,t) reactions, excitation strengths, form factors, and spin--parity assignments for, (E/T), 25:12574
energy levels of, effect of magnetic dipole core polarization on, (T), 25:12600
proton inelastic scattering by, microscopic first-order core polarization corrections to DWBA for, (T), 25:12678

LEAD ISOTOPES Pb-207
deuteron inelastic scattering at 17 MeV, angular distributions for, (E), 25:12569
energy levels from (d,p) and (d,t) reactions and deuteron inelastic scattering, (E), 25:12569
energy levels of, effect of magnetic dipole core polarization on, (T), 25:12600
neutron capture at 41 keV, gamma spectra from intermediate, (E), 25:12539
neutron capture by, gamma spectra and Q-value for thermal, (E), 25:12403
neutron capture by, resonance effects in thermal, (T), 25:12562

LEAD ISOTOPES Pb-208
deuteron reactions (d,He-3) at 80 MeV, DWBA analysis of differential cross sections from, (E), 25:12575
deuteron reactions (d,t) at 17 MeV, angular distributions for, (E), 25:12569
electron elastic scattering at 1 to 100 MeV, nuclear-size effects on polarization functions for, (T), 25:12664
energy levels from thallium-208 beta decay, particle--hole structure of low-lying, (E/T), 25:12555
photon reactions (γ,xn) at 6 to 35 MeV, partial cross sections and giant resonance parameters for, (E), 25:12610
photoneutron reactions at threshold energy, resonance effects in, (T), 25:12562
proton elastic scattering at 10 to 60 MeV, local Woods--Saxon potentials equivalent to nonlocal analysis including exchange effects in, (T), 25:12689
proton reactions (p,t) at 40.7 MeV, energy spectra and DWBA analysis of differential cross sections from, (E/T), 25:12574

LEAD ISOTOPES Pb-210
abundance in Apollo 11 samples, (E), 25:11539
content of benthic fish and invertebrates, pelagic fish, and zooplankton of Pacific Ocean, 25:10997(R) (RLO-2225-T-14-1)
determination in snow in Antarctica, α spectrometric, 25:10477

LEAD OXIDES
radiation effects on high-pressure polymorphs of, fast neutron, 25:11474(R) (BNWL-842)

LEAVES
potassium-42 accumulation in, of corn, effects of age, potassium deficiency, and temperature on, 25:10930 (CEA-CONF-1517)
potassium-42 transport in, of corn, effects of age, potassium deficiency, and temperature on, 25:10930 (CEA-CONF-1517)

LEPTONS
magnetic moment of, quantum electrodynamics with nonpolynomial interactions for cut-off for anomalous, (T), 25:12157

LEUKOCYTES
count of eosinophilic, in rats, effects of cyclophosphamide and dexamethasone on, relation of, to previous studies on x-irradiated rats, 25:10961(R) (ORO-3329-6)
phagocytosis mechanisms of, in vitro tracer study using chromium-51-labeled yeast cells, 25:10908
radiation effects on, of human blood, effects of phytohemagglutinin on ionizing, 25:11299

LEVEL INDICATORS
development of inductive, for liquid metals, 25:10896 (RD/B/N-1720)

LIFE SPANS
radiation effects on, of Drosophila melanogaster, α and γ, 25:11248

LIGHT
effects on γ radiosensitivity of chloroplasts, red, 25:11310
effects on phage resistance in Escherichia coli, mutagenic, 25:11032
theory of polarized, lectures on, (T), 25:12624 (ANU-P-497)

LIGHTNING
radiation from ball, gamma, 25:11926

LINEAR ACCELERATORS
beam current in electron, digital system for monitoring peak, 25:12297 (CEA-N-1389)
beam current in proton, maximum, 25:12313
book: Linear Electron Accelerators with Intense Beams (Physical Principles of the Theory), 25:12315
particle dynamics in ALICE heavy-ion, 25:12310 (NP-18612)
phase oscillations in, effect of statistical field errors on stability of longitudinal, 25:12326
shielding for 30-MeV, 25:12314
waveguides for, effects of radial slots in iris disks on electromagnetic wave propagation in, 25:12306(T) (KFK-tr-334)

LINEAR ENERGY TRANSFER
effects on x-radiosensitivity of seed plants, 25:11020

LIQUID FLOW
magnetohydrodynamic, inertia effects on channel, (T), 25:11767

LIQUID METAL FAST BREEDER REACTOR
coolant boiling in, research on detection of, 25:10769(R) (ORO-3911-3)
fuel for, program and methods for analysis of, 25:10425 (ORNL-4636, pp 40-2)
fuels for, development of plutonium nitride (PuN)--uranium nitride (UN) and plutonium oxide (PuO_2)--uranium oxide (UO_2), 25:12795(R) (BMI-1893)
kinetics of, FARED computer program for, 25:12772 (BAW-3867-9(Vol.1)(Rev.1))

LITHIUM
abundance in F and G stars, (T), 25:11544
determination in serum and urine by flameless atomic absorption spectroscopy, 25:10464
determination of trace amounts of, in biotite and tektite by spark source mass spectrometry, 25:10455
determination of trace amounts of, in rocks and stony meteorites by neutron activation and radiochemical separation, 25:10493
determination of trace amounts of, in standard rocks by borate fusion, dissolution in EDTA, ion exchange, and atomic absorption spectrophotometry, 25:10671
energy levels of, structure and lifetimes of auto-ionizing, (T), 25:11692
nucleosynthesis in stellar atmospheres, (T), 25:11548
nucleosynthesis of, (T), 25:11542 (NP-18591)
reactions with berkelium fluoride at 1025°C to prepare berkelium, reduction, 25:11358

LITHIUM FLUORIDES
electron energy losses due to surface vibrational modes in films of, (T), 25:11677
radiation damage in single crystals of, lithium oxide precipitation in electron, 25:11964
radioinduced color centers and thermoluminescence in pure and dosimetry-grade, 25:11958
radioinduced thermoluminescence of pure powdered, comparison of glow curves of thermal-neutron and gamma, 25:11951

XUM

LITHIUM IONS
channeling in gold single-crystal foils, energy loss and straggling in, 25:11976
LITHIUM ISOTOPES Li-6
energy levels from tritium (He-3,γ) reactions, evidence for (t + He-3)-cluster, (T), 25:12372
helium-3 reactions (He-3,d) at 9 and 13 MeV, internal bremsstrahlung spectra for, (T), 25:12694
meson (π⁻) reactions (π⁻,2N) with, effect of rescattering and outgoing nucleon interactions in, (T), 25:12415
neutron capture by, gamma spectra and Q-value for thermal, (E), 25:12403
nuclear charge form factor of, phenomenological wave function for calculation of, (T), 25:12383
nuclear radius, binding energy, charge form factors, and wave functions for, calculations using projected Hartree--Fock model, (T), 25:12410
nucleosynthesis of, (T), 25:11542 (NP-18591)
photon reactions (γ,n) and (γ,p) up to 20 MeV, analysis using single-particle model, (T), 25:12417
photon reactions (γ,n) at 20 to 75 MeV, differential and integrated cross sections and energy spectra from, (E), 25:12387
reactions (Li-6,d) with carbon-13 at 18 MeV, energy levels of oxygen-17 from, 25:12425
reactions with carbon-12 at 9 to 14 MeV, analysis for reaction mechanisms in, (E), 25:12418
scattering by oxygen-16 at 20 MeV, optical-model analysis of elastic, (T), 25:12408
triton reactions (t,d) at 9 to 27 MeV, internal bremsstrahlung spectra for, (T), 25:12694
LITHIUM ISOTOPES Li-7
helium-3 reactions (He-3,γ) at 3 to 6 MeV, angular distributions for, (E), 25:12389
meson (π⁻) reactions (π⁻,2N) with, effect of rescattering and outgoing nucleon interactions in, (T), 25:12415
nucleon inelastic scattering by, numerical analysis of differential cross sections for, (T), 25:12384
nucleosynthesis of, (T), 25:11542 (NP-18591)
photon reactions (γ,n) at 20 to 75 MeV, differential and integrated cross sections and energy spectra from, (E), 25:12387
proton reactions (p,n) at 0.9 to 1.9 MeV, excitation function and threshold energy for, (E), 25:12402
reactions (Li-7,t) with carbon-13 at 17 MeV, energy levels of oxygen-17 from, (E), 25:12425
LITHIUM NIOBIUM OXIDES
surface wave production in crystals of, 25:11472(R) (AD-708705)
LIVER
americium-241 accumulation in, of animals following intravenous injection as chloride, 25:10942
blood flow in human, effects of hyperemia on, 25:10916
cobalt-60 1-nitroso 2-naphthol chelate distribution in, of rats, 25:10958
function studies in man, sensitivity of iodine-131-labeled rose bengal in comparison to other biochemical tests for, 25:11111
gold-198 colloid clearance from human, effects of particle size on, 25:10918
isoenzymes of lactic dehydrogenase in, of xenogenic radiation chimeras, 25:10992
radiation effects on content of autoantibodies in, of rabbits, x, 25:10985
radiation effects on histamine in, of rats, mechanism of, 25:10967
radiodiagnosis of diseases of human, using gold-198, effects of blood circulation on, 25:11196
radioinduced tumors in, of personnel following occupational inhalation of plutonium-239, models for estimating probability of α and γ, 25:11301
radioisotope scanning of human, for diagnosis of diseases, 25:11198
radiotherapy of hemangiomas in, of man, review of x, 25:11235
regeneration of human, following hepatectomy, effectiveness of scintigraphy for evaluating, 25:11202
scanning for diagnosis of diseases of human, using gold-198 and iodine-131, 25:11183
scanning of blood flow in, in patients with hyperthyroidism, 25:11141
scanning of human, for diagnosis of cirrhosis using gold-198, effects of ascites and enlarged spleen on, 25:11203
scanning of human, for diagnosis of diseases using gold-198, iodine-125, and silver-111, 25:11200
scanning of human, using gold-198, 25:11201
scanning of human, using gold-198 and iodine-131, effects of abscesses, angiomas, hydatid cysts, and tumors on, 25:11197
scanning of lateral human, use of colloidal gold-198, 25:11211
scintigraphy of function of, in dogs with experimentally induced obstructive jaundice, use of iodine-131-labeled Rose Bengal for, 25:11213
scintiscanning of human, for detection of liver diseases, effectiveness of iodine-131-labeled Rose Bengal in comparison to histology and laparoscopy, 25:11180
scintiscanning of human, using gold-198 and selenium-75 for, computer method for differentiation, 25:11176
scintiscanning of human, using gold-198 colloid or technetium-99 colloid, 25:11140
scintiscanning of, in dogs using iodine-131-labeled Rose Bengal, development of computer program for improving, 25:10919
tellurium-127m uptake by rat, following intravenous injection, 25:10950
LUNAR MATERIALS
analysis by γ spectrometry, 25:10491 (ORNL-4636, pp 20-33)
analysis for chlorine-36, iron-55, and lead-210, radiochemical, (E), 25:11539
properties of fine-grained soil samples, habit and texture, (E), 25:11671
LUNGS
americium-241 inhalation in, of man, use of sodium iodide crystal detector for measurement of, 25:10931 (CEA-CONF-1657)
blood circulation in human, effectiveness of radioisotopes for evaluating, 25:11126
blood circulation in human, use of oxygen-15-labeled carbon dioxide or xenon-133 for measuring, 25:11125
radiation dose to human, following accidental inhalation of plutonium-americium-241 aerosol, equations for estimating α and γ, 25:11053 (BNWL-B-12)
radiation injuries to surface of, in rabbits, 25:11267
scanning for measurements of blood circulation and ventilation in human γ transmission methods for, 25:11116
scanning of human, comparison of iodine-131-labeled albumin with radiography for, 25:11132
scanning of human, for differential diagnosis of mediastinal processes and pericardial effusions, 25:11130
scanning of human, to determine blood circulation, use of metastable technetium-99-labeled macroaggregates of human serum albumin for, 25:11128
scanning of human, use of gallium-68-labeled macroaggregates for, 25:11205
scanning of human, use of iodine-131-labeled RISA and dual-probe detector system for, 25:11207
scintiscanning of human, for diagnosis of sarcoidosis, effectiveness of iodine-131-labeled albumen macroaggregate for, 25:11133
scintiscanning of human, in patients with chest concussions, effectiveness of iodine-131-labeled albumen macroaggregate in combination with radiography, 25:11135
scintiscanning of human, using iodine-131-labeled albumen macroaggregates and computers or multichannel analyzers, evaluation of, 25:11131
scintiscanning with iodine-131 in silicosis patients, comparison of iodine-131 to radiography for, 25:11134
LUTETIUM
determination of trace amounts of, in biotite and tektite by spark source mass spectrometry, 25:10455
LUTETIUM ISOTOPES Lu-175
deuteron reactions (d,3nγ) at 18 MeV, cross sections for, (E/T), 25:12544
energy-level transitions in, parity-nonconserving effects in 343- and 396-keV, (T), 25:12517 (INP-714)
proton reactions (p,2nγ) at 16 and 21 MeV, cross sections for, (E/T), 25:12544
LUTETIUM ISOTOPES Lu-177
use for scanning of fibia and tibia bones in rats, 25:11216
LUTETIUM ISOTOPES Lu-178
decay of, 25:10472(R) (BMBW-FBK-70-19)
LUTETIUM ISOTOPES Lu-180
decay of, 25:10472(R) (BMBW-FBK-70-19)
LYMPH
drainage of, following neck surgery, effectiveness of gold-198 colloids for studying, 25:11178
LYMPH SYSTEM
scintiscanning of human abdominal, evaluation of interpretation and performance errors following colloidal gold-198, 25:11177
LYMPHOCYTES
radiation effects on cooperative function of carrier-specific, in antihapten responses of guinea pigs, 25:10987
radioinduced chromosome aberrations in human peripheral, following, diagnostic exposure, x, 25:11113
role of shielded bone marrow, in recovery of x-irradiated rats, 25:11077

M

MAGNESIUM
determination as impurity in fuel materials by emission spectroscopy, 25:10432 (KFK-1261)
determination by charged particle activation, reactions and sensitivities for, 25:10488 (CEA-R-4072)
determination in sedimentary rocks by direct-reading spectrometry, 25:10450
determination in serum and urine by flameless atomic absorption spectroscopy, 25:10464
determination in tektite by spark source mass spectrometry, 25:10455
determination of trace amounts of, in molybdenum, review on, 25:10459
determination of trace amounts of, in phosphate deposits

by spark source mass spectrometry, 25:10456
determination of trace amounts of, in standard rocks by atomic absorption spectrophotometry, 25:10671
electron inelastic scattering at 0.25 to 4 keV, secondary electrons from, (E/T), 25:11672
friction and wear of, sliding against copper and iron rings under vacuum, 25:11413
MAGNESIUM ALLOYS AND SYSTEMS
B--Mg, mechanical properties of composites of, effects of fiber coating and matrix strengthening on, 25:11407
MAGNESIUM FLUORIDES
sorptive properties for neptunium hexafluoride and uranium hexafluoride, 25:10568 (CEA-R-4051)
MAGNESIUM ISOTOPES Mg-24
deuteron reactions (d,p) at 13.5 MeV, analysis using generalized DWBA model, (T), 25:12457
energy levels from (p,γ) reactions, widths, branching ratios, and decay strengths for T = 2, (E), 25:12441
energy levels from proton resonances in sodium-23, spin--parity assignments and mixing parameters for, (E), 25:12443
helium-3 reactions (He-3,d) at 18 and 20 MeV, energy spectra and DWBA analysis of differential cross sections from, (E/T), 25:12479
photoneutron cross section at 16 to 31 MeV, (E), 25:12469
proton elastic and inelastic scattering at 5.38 to 5.95 MeV, excitation functions and polarization angular distributions from, (E), 25:12433 (NP-18552)
MAGNESIUM ISOTOPES Mg-25
energy levels from magnesium-26 (He-3,α) reactions, spectroscopic factors, l transfers, and spin--parity assignments for T = $^3/_2$, (E/T), 25:12450
MAGNESIUM ISOTOPES Mg-26
alpha reactions (α,nγ) at 5.8 and 6.3 MeV, gamma angular distributions from, (E), 25:12449
helium-3 reactions (He-3,α) at 15.4 MeV, energy spectra and DWBA analysis of differential cross sections from, (E/T), 25:12450
helium-3 reactions (He-3,t) at 16 and 30 MeV, (E), 25:12498
helium-3 scattering at 16 and 30 MeV, (E), 25:12498
MAGNESIUM OXIDES
analysis of, neutron activation, 25:11472(R) (AD-708705)
creep and recovery of, research program on, 25:11472(R) (AD-708705)
effects of sintered, on thermal shock resistance of aluminum oxide, 25:11473(R) (AD-708712)
electron inelastic scattering at 0.25 to 4 keV, secondary electrons from, (E/T), 25:11672
B_2O_3--MgO--MgS, phase studies of, 25:11526
MAGNESIUM SULFIDES
B_2O_3--MgO--MgS, phase studies of, 25:11526
MAGNETIC FIELDS
charged-particle motion in, generation of first and second order transformation elements for, 25:12327
charged-particle trajectories in fringe, (T), 25:12322
disturbances at ATS 1 and surface, variations during Jan.--June 1967, (E/T), 25:11785
electron motion in, radiative polarization of free relativistic, 25:12060
electron reflection from half-space, photon radiation from, (T), 25:11679
intensity variations during magnetic storm, Sept. 27-30, 1969, due to magnetopause recession and magnetosheath exposition, (E/T), 25:11784
lifetime of large-scale solar, (T), 25:11629
orientation in quiescent prominences, (E), 25:11617
polarity of interplanetary, effect of photospheric fields on, (E), 25:11603
polarity pattern of interplanetary, unified theory of, (E/T), 25:11608
production by implosion of thin metal tubes, measurements during, 25:11917 (CEA-R-4024)
proton acceleration in, effect of interplanetary shock wave on 1- to 10-MeV, (E/T), 25:11624
pulsations in, relation of plasmasphere to structured Pc1 source lines, micro-, (E/T), 25:11788
sector structure of interplanetary, origin of, (E), 25:11606
MAGNETIC MIRROR MACHINES
plasma heating by microwaves, off-resonant, (E/T), 25:11909(R) (COO-1695-31)
plasma spectra in Burnout V, electric field determination from, (E), 25:11874
MAGNETIC MONOPOLES
quantization law for, Dirac charge-pole, (T), 25:12150
MAGNETIC STORMS
effect on 350 km-ionospheric scintillation boundary irregularities, (E/T), 25:11791
effect on electromagnetic drift of mid-latitude F2 layer, (E/T), 25:11805
effect on ionospheric density and rotation at 135 to 195 km, (E), 25:11794
effect on magnetic field intensity during Sept. 27-30, 1969, (E/T), 25:11784
effect on worldwide cosmic-ray intensity variations, (E/T), 25:11745
effects on surface and ATS 1 magnetic fields, Jan.--June 1967, (E/T), 25:11785
MAGNETOHYDRODYNAMIC GENERATORS
flow in channels of, one-dimensional analysis of, 25:11766
gas nonuniformities in, electric parameters in, (T), 25:11751
use with fusion and fusion reactors for power generation, review of, 25:11752
MAGNETOHYDRODYNAMICS
airfoil theory in, thin, 25:11772
boundary-value problems in, 25:11770
conference on classical and relativistic, Lille, France, 6/69, 25:11759
equations for system inside neutral sheet, 25:11753 (EUR-CEA-FC-571)
kinetic theory of relativistic plasma in strong magnetic fields, 25:11903
kinetic theory of relativistic, Boltzmann equation for, 25:11765
kinetic theory of, Cauchy problem for linearized relativistic Boltzmann equation, 25:11902
kinetic theory of, Grad method extension for relativistic Boltzmann equation, 25:11901
shock wave theory in, relativistic, 25:11763
variational solutions for relativistic, 25:11769
wave propagation in relativistic, (T), 25:11764
waves and discontinuities in relativistic, 25:11762
MAGNETOPAUSE
magnetic storm effects on, at ATS 1 location, Jan.--June 1967, (E/T), 25:11785
structural observations of, during magnetic storm Sept. 27-30, 1969, at 6.6 R/sub E/, (E/T), 25:11784
MAGNETOSHEATH
magnetic storm effects on, at ATS 1 location, Jan.--June 1967, (E/T), 25:11785
structural observations of, during magnetic storm Sept. 27-30, 1969, at 6.6 R/sub E/, (E/T), 25:11784
MAGNETOSPHERE
coupling to ionosphere, dimensional analysis of equations describing, 25:11804
electrons in quasi-trapping region of, observations of solar, (E/T), 25:11783
helium abundance in, transport and loss mechanisms of ionic, (E/T), 25:11802
helium-ions losses from, by charge exchange and pitch-angle diffusion, (T), 25:11803
Poynting-flux direction in, subprotonospheric whistlers, periodic emission, elf and vlf hiss, chorus, and saucer, (E), 25:11780
proton flux in, drift periodic echoes in solar, (E), 25:11801
proton losses from, by charge exchange and pitch-angle diffusion, (T), 25:11803
proton whistler propagation in, irregularities in proton density determination from cyclotron damping of, (E/T), 25:11787
ring current in, relation with low-latitude magnetic bays on Earth's surface and at satellite position, (E/T), 25:11779
scintillation boundary irregularities at 350 km, effect of magnetic index on, (E/T), 25:11791
MAGNETOTAIL
current variations during magnetic storms, Jan.--June 1967, (E/T), 25:11785
plasma sheet in, electron and proton energy spectra and angular distribution correlation with auroral oval measurements, (E), 25:11809
MAGNETS
analysis of short, current-dominated, beam transport, harmonic, 25:12323
design study for beam transport system for post-conversion Brookhaven AGS, 25:12296 (BNL-15464)
research on superconducting, at Lewis Research Center, 25:11851
superconductors in, multicore, 25:11831
MALEIC ANHYDRIDE
effects on electron-induced polymerization of methyl acrylate--1,2-polybutadiene, 25:10609 (JAERI-5026, pp 130-6)
MALIBU POWER REACTOR
auxiliary systems for, preliminary safety analysis of, 25:12730 (DOCKET-50214-2)
containment systems for, preliminary safety analysis of, 25:12730 (DOCKET-50214-2)
control systems for, preliminary safety analysis of, 25:12730 (DOCKET-50214-2)
design parameters of, requested additional information on, 25:12730 (DOCKET-50214-2)
instrumentation for, preliminary safety analysis of, 25:12730 (DOCKET-50214-2)
operation aspects of, requested additional information on, 25:12730 (DOCKET-50214-2)
operation of, administrative controls for, 25:12730 (DOCKET-50214-2)
personnel for, training of, 25:12730 (DOCKET-50214-2)
shielding for, preliminary safety analysis of, 25:12730 (DOCKET-50214-2)
site for, preliminary safety analysis of, 25:12730 (DOCKET-50214-2)
steam and power conversion systems for, preliminary safety analysis of, 25:12730 (DOCKET-50214-2)
MAMMALIA
cesium-137 accumulation in, in northern Soviet Union, determination of decontamination time, 25:11037 (NP-

XUM

18381)
radioinduced injuries to eyes of, effects of dose on acute x, 25:11284
radioinduced lens cataracts in eyes of, comparison of dose for γ and neutron, 25:11284
MAN
americium-241 inhalation in lungs of, use of sodium iodide crystal detector for measurement of, 25:10931 (CEA-CONF-1557)
cesium-137 accumulation in, in northern Soviet Union, determination of decontamination time, 25:11037 (NP-18381)
health status of atomic bomb survivors in Hiroshima and Nagasaki during July 1968 to July 1969, 25:11237(R) (ABCC-68-69)
iodine radioisotope toxicity to, following ingestion of food chain components contaminated by tellurium radioisotopes, 25:10948
iron-55 content of blood of, in Rongelap Atoll, 25:10997(R) (RLO-2225-T-14-1)
iron-59 clearance from blood plasma of, for dosimetry of nitrogen mustard therapy, 25:10952
kidney function tests in, computer analysis of, 25:11208
mongolism in, effects of in utero x radiodiagnosis of mothers on incidence of, 25:11300
potassium content of, use of potassium-40 activity measurements with whole-body counter for determining, 25:10920
potassium content of, use of whole-body scintillation counter for measuring total-body, 25:10910
radiation dose to lungs of, following accidental inhalation of plutonium-americium-241 aerosol, equations for estimating α and γ, 25:11053 (BNWL-B-12)
radiation dose to ocular lens of, effects of age and dose fractionation on maximum safe, 25:11284
radiation dose to organs of, estimation using tissue equivalent phantom, 25:11067
radiation dose to, in Colombia and Panama following ingestion of radioisotopes and external exposure from use of nuclear explosives for proposed construction of interoceanic canal, estimation of, 25:11055 (ORNL-4579)
radiation effects on infant mortality in, strontium-90 β, 25:11295
radiation effects on thyroid gland of, review of iodine-131 β and γ, 25:11291
radiation injuries of, residing in Hiroshima during atomic bombing, review, 25:11238
radiation injuries to, following medical use of, review of, 25:11209
radiaton effects on hormone production in female, during pregnancy, 25:10982
radioactivity in respiratory tract of, following inhalation of aerosols contaminated by alpha particles, 25:10953
radioinduced chromosome aberrations in peripheral lymphocytes of, following diagnostic exposure, x, 25:11113
radioinduced damage in, radium-224, 25:11294(R) (EUR-4542)
radioinduced hemolysis of stored blood from, low dose x, 25:10981
radioinduced injuries to eyes of, following exposure to high-energy electromagnetic waves, 25:11297
radioinduced leukemia in, following therapy of polycythemia, phosphorus-32 β, 25:11303
radioinduced mutations in populations of, 25:11005
radioinduced mutations in populations of, in relation to natural selection, 25:11025
radioinduced whole-body skin eruptions in, following therapy of malignant tumors, 25:11296
radiosensitivity of organs and tissues of, 25:11090
radiotherapy of ankylosing spondylitis in, using radium-224, excretion measurements and whole-body counting following, 25:11231
radiotherapy of carcinomas in, 25:11222 (BNL-50203, pp 280-5)
radiotherapy of carcinomas of bladder in, effectiveness of high-energy x radiation for, 25:11229
radiotherapy of carcinomas of lung in, methods for dose fractionation in, 25:11223 (BNL-50203, pp 292-307)
radiotherapy of carcinomas of uterine cervix of, design of applicator for implant ionizing, 25:11227
radiotherapy of esophageal cancer in, recommendations for, 25:11236
radiotherapy of hemangiomas in liver of, review of x, 25:11235
radiotherapy of malignant lymphomas of, dosimetry of γ for, 25:11060
radiotherapy of mediastinal lymphomas in, effectiveness of dose fractionation for ionizing, 25:11226
radiotherapy of neoplasms of urinary tract in, combined effects of dactinomycin on post-surgical x, 25:11225
radiotherapy of thyroid carcinomas in, effectiveness of iodine-131 for, in relation to mortality, 25:11233
radiotherapy of tumors in, review of, 25:11219 (BNL-50203, pp 130-53)
sodium content of, use of sodium-22 activity measurements with whole-body counter for determining, 25:10920
strontium-87m sorption from gastrointestinal tract of, effectiveness of activated barium sulfate for inhibiting, 25:11047
strontium-90 accumulation in, following ingestion of contaminated milk, 25:10932 (CEA-CONF-1558)
strontium-90 content in teeth of, methods for measurement of, 25:10935 (NP-18388)
MANGANESE
content in deep-sea sediments, measurements of, 25:10725(R) (CU-3139-4)
content of soil, neutron activation analysis of, 25:10909
determination as impurity in fuel materials by emission spectroscopy, 25:10432 (KFK-1261)
determination in Bacillus megaterium by neutron activation, 25:10511
determination in environmental samples by neutron activation, 25:10491 (ORNL-4636, pp 20-33)
determination in ores and ore concentrates, intermittent ac arc method for spectrographic, 25:10429 (BARC-468)
determination in sedimentary rocks by direct-reading spectrometry, 25:10450
determination in serum and urine by flameless atomic absorption spectroscopy, 25:10464
determination of trace amounts of, in biotite and tektite by spark source mass spectrometry, 25:10455
determination of trace amounts of, in minerals and rocks by x-ray fluorescence, methods for correction of matrix effect in, 25:10448
determination of trace amounts of, in molybdenum, review on, 25:10459
determination of trace amounts of, in phosphate deposits by spark source mass spectrometry, 25:10456
determination of trace amounts of, in rocks and sand by thermal neutron activation, ion exchange, and γ spectrometry, 25:10492
determination of trace amounts of, in rocks, quantometer for spectroscopic, 25:10451
determination of trace amounts of, in standard silicate rocks using sodium chloride buffer, emission spectrographic, 25:10454
determination of trace amounts of, in Zircaloy-2 and zirconium, carrier distillation method for spectrographic, 25:10430 (EUR-4541)
determination simultaneously with copper in plants by neutron activation and radiochemical separation, 25:10509
enthalpy of solution in liquid plutonium, 25:11386
separation of divalent, trivalent, and heptavalent, paper chromatographic, 25:10687
separation of neptunium from, by ion exchange in tetramethylammonium hydroxide--citrate solutions, effects of complexing agents on, 25:10655 (ANL-7751)
MANGANESE ALLOYS AND SYSTEMS
Al--Mn, crystal structure of quenched, vacancy formation in, 25:10583(R) (AECL-3776)
Al--Mn, magnetic hysteresis loops of, effects of boron on, 25:11983
Cr-base--Mn, antiferromagnetic energy gap from optical absorption measurements at 4.2°K, 25:11987
Mn--Ni-base--Ta, properties of, electric and magnetic, 25:12008
MANGANESE CHLORIDES
magnetic spin structure of $MnCl_2.4H_2O$, neutron diffraction study of, 25:11981(R) (ORO-3674-4)
MANGANESE FLUORIDES
reactions in, emf measurements of solid-state displacement, 25:11473(R) (AD-708712)
MANGANESE ISOTOPES Mn-54
abundance in Allende meteorite, (E), 25:11540
MANGANESE ISOTOPES Mn-55
proton reactions (p,n) at 2.4 to 3.3 MeV, comparison of neutron cross sections with Hauser--Feshbach theory, (E/T), 25:12476
proton reactions (p,nγ) at 3.6 to 5.5 MeV, γ spectra and angular distributions for, (E), 25:12483
proton reactions at 170 MeV, cross sections for spallation products from, (T), 25:12439
MANGANESE OXIDES
B_2O_3--MnO--MnS, phase studies of, 25:11526
MANGANESE SULFIDES
B_2O_3--MnO--MnS, phase studies of, 25:11526
MANY BODY PROBLEM
equilibrium solutions of secular variations in restricted three-body problem and their solution, (T), 25:12057
theory for four-body bound-state problem, quantum-mechanical, 25:12050
MASS SPECTROGRAPHY
computer programs for, 25:10436 (ORNL-4636, pp 43-5)
research progress on, 25:10436 (ORNL-4636, pp 43-5)
MASS SPECTROMETERS
developments in on-line, 25:10670 (LYCEN-7034, pp 23-33)
MATERIALS TESTING
electron beam method for generating stress waves in solids, 25:10791
MATERIALS TESTING, NONDESTRUCTIVE
methods for reactor fuels and materials, development of, 25:11474(R) (BNWL-842)
MATHEMATICAL PHYSICS
book: Mathematical and Theoretical Physics, Vol. I, 25:12048
book: Mathematical and Theoretical Physics, Vol. II, 25:12049

MATRICES (MATHEMATICS)
shell structure in anticommuting, manifestation in weak-interaction Hamiltonian of, (T), 25:12162 (AD-710572)
MATTER
separation from antimatter in Universe, (T), 25:11661
thermodynamics of white-dwarf, (T), 25:11549
MATTER, ANTI-
separation from matter in Universe, (T), 25:11661
MEATS
caribou, radioisotope content of, in Alaska during 1969, 25:11001
deer, cesium-137 content of in USA, relation of mushroom consumption to, 25:11003
radiation processing of cooked, effects of, on amino acid composition, γ, 25:11339
reindeer, radioisotope content of, in Alaska during 1969, 25:11001
reindeer, radioisotope content of, in Sweden during 1959 to 1969, 25:11004
seafood, radiation processing of shrimp, effects of, on odor, color, and storage life, γ, 25:11326 (NP-18393)
MECHANICS
spectral density method in statistical, for systems with pair interaction, 25:12061
MEDICAL PERSONNEL
radiation dose to, during radiography for catheterization of the heart, x, 25:11059
radiation protection of veterinary, recommendations for, 25:11075 (NCRP-36)
MEDICAL SUPPLIES
conference on radiosterilization of, effectiveness of γ, 25:11327 (STI/PUB-247)
radiosterilization of, effects of environmental condition on sensitivity of contaminating microorganisms during, 25:11328
MEDICINE
book: Radiation Medicine, 25:11091
book: Year Book of Nuclear Medicine, 25:11209
conference on radioisotopes in nuclear, for diagnosis and research, 25:11118
research on nuclear, revew of literature on, 25:11209
review of Atomic Bomb Casualty Commission research programs on, during July 1968 to July 1969, 25:11237(R) (ABCC-68-69)
MEMBRANES
strontium-85 transport through intestinal epithelial, in rats, reaction mechanisms for, 25:10938
MERCAPTO GROUP
content of nonprotein, in tissues of mice following injection of cystamine in optimum radioprotective doses, 25:11101
MERCURY
determination by beta excitation, 25:10475
determination by neutron activation following chromatographic separation, 25:10496
determination in biological materials by neutron activation, 25:10502
determination in environmental samples by neutron activation, 25:10491 (ORNL-4636, pp 20-33)
determination of trace amounts of, in biotite and tektite by spark source mass spectrometry, 25:10455
determination of trace amounts of, in molybdenum, review on, 25:10459
determination of trace amounts of, in phosphate deposits by spark source mass spectrometry, 25:10456
electric discharges in, current and velocity fields between electrodes, (E/T), 25:11761
energy-level transitions in, rates of Auger and x-ray, (T), 25:11685
magnetization curves of superconducting, containing magnetic inclusions, (E), 25:11840
separation of monovalent and divalent, paper chromatographic, 25:10687
solvent properties for use in radiochemical separations, 25:10490(T) (LIB/Trans-334)
use as working fluid in radioisotope-fueled turboelectric generators, 25:10788(P)
MERCURY ALLOYS AND SYSTEMS
solvent properties for use in radiochemical separations, 25:10490(T) (LIB/Trans-334)
MERCURY IODIDES
electroabsorption and electrophotoluminescence in, 25:12915 (UCLA-34-P-122-X-1)
MERCURY ISOTOPES Hg-197
use for labeling erythrocytes for scanning of human spleen, 25:11200
use for labeling erythrocytes for use in spleen scanning, 25:11201
MERCURY ISOTOPES Hg-199
neutron capture by, average circular γ polarization in thermal, (E), 25:12601
MERCURY ISOTOPES Hg-200
energy levels from thallium-200 decay, spin and parity of, (E), 25:12528 (NP-18647)
energy levels from thallium-200 decay, spin-parity assignments from gamma directional correlations, (E), 25:12527 (NP-18613)
energy levels from thermal neutron capture, spin for compound, (E), 25:12601
energy-level transitions from gold-200 on decay, (E), 25:12514(R) (COO-1672-21)
MERCURY ISOTOPES Hg-203
determination by isotope exchange and γ spectroscopy, 25:10490(T) (LIB/Trans-334)
effectiveness of chlormerodrin-incorporated, for differential diagnosis of brain diseases, method for determining, 25:11179
effectiveness of salyrgan-incorporated, for determining renal clearance, evaluation of, 25:11156
hazards to human children following renal scanning, 25:11190
MESONS
classification of, nonrelativistic quark model for, (T), 25:12203
current algebra representations for N identical spin-0, (T), 25:12125
decay of tensor, test of meson pole dominance from, (T), 25:12216
decay of, extension of Kemmer-symmetric coupling for internal charge configuration, masses, and lifetimes from, (T), 25:12199
detection of cosmic, scintillation detector telescope for, 25:10871
exchange of vector, in meson interactions with mesons at low energies, (T), 25:12192 (NYO-2262-TA-232)
field equations for spinless charged, cellular space--time for solution of, (T), 25:12260
form factors of, nonrelativistic quark model and rho dominance for ratios of, (T), 25:12203
interactions of massive vector, covariant photon amplitudes as zero-mass limit of helicity amplitude for, (T), 25:12177
interactions of spinless, vector currents consistent with hadron bootstrap with duality and zero resonance widths for n-body, (T), 25:12177
interactions with baryons in parton model, total cross section for, 25:12187
interactions with baryons in parton model, total cross section for, (T), 25:12187
interactions with baryons, scale and chiral symmetry breaking for, 25:12214
interactions with mesons at low energies, singular off-mass-shell equation with vector meson exchange for P- and S-wave amplitudes and resonances in, (T), 25:12192 (NYO-2262-TA-232)
interactions with nucleons, formalism with SU(3) symmetry, exchange degeneracy, ad Regge poles for forward, (T), 25:12217
interactions with nucleons, quark model for backward, (T), 25:12218
interactions with nucleons, quark model for total cross section relations for forward elastic, (T), 25:12218
lifetimes of, extension of Kemmer-symmetric coupling for particle decays for, (T), 25:12199
mass level structure of, urbaryon model for, 25:12182
mass of, extension of Kemmer-symmetric coupling for particle decays for, (T), 25:12199
production of nonet, in π + N interactions, relations among cross sections for, (T), 25:12203
MESONS (eta)
production in $\pi^- + p \rightarrow \pi^+ + 2\pi^- + \pi^0 + p$ interactions at 6 GeV/c in hydrogen bubble chamber, (E), 25:12101
production of eta^0 in $\gamma + p \rightarrow \pi^+ + n$ interactions at 0.450 to 3 GeV, resonance structure of cross sections for, (E), 25:12067 (LAL-1239)
production of eta^0 in $K^+ + p \rightarrow K^+ + p + \pi^+ + \pi^- + \pi^0$ interactions at 12.7 GeV/c in hydrogen bubble chamber, (E), 25:12102
production of eta^0 in $\pi^- + p \rightarrow n + 2\gamma$ interactions at 2 to 6 GeV/c, spark chamber study of cross sections for, (E), 25:12113
MESONS (f)
production of f^0 in $\pi^- + p \rightarrow n + \pi^+ + \pi^-$ interactions at 2 to 6 GeV/c, spark chamber study of differential cross sections for, (E), 25:12113
MESONS (K)
decay $K \rightarrow 2\pi + l + \nu$, vector dominance model for form factor for, (T), 25:12194
decay $K \rightarrow e + \nu + \gamma$, counter and spark chamber study of upper limit for branching ratio for, (E), 25:12077
decay $K \rightarrow l + \pi + \nu$, Veneziano-type form factor for, 25:12172
decay $K \rightarrow \pi + l + \nu$ in broken chiral SU(3) x SU(3) group, 25:12237
decay $K \rightarrow \pi + l + \nu$, form factor for, 25:12198
decay $K \rightarrow \pi + l + \nu$, general tests of $\Delta I = 1/2$ and $\Delta S = \Delta Q$ rules in, (T), 25:12167
decay $K \rightarrow \pi + l + \nu$, perturbation theory about SU(3) x SU(3) symmetry limit for form factors of, (T), 25:12173
decay of, chiral Lagrangian with SU(3) symmetry breaking for correlations with spin-1 resonance decay rates for parameters of three- and four-body, (T), 25:12194
form factor ratio F/sub K//F/sub π/ dependence on symmetry-breaking parameter of vacuum states, 25:12198
form factors and mean charge radius from vector dominance model, 25:12141
interactions anti K + N → π + Σ(Λ) at high energies, tests of Regge-pole and strong-absorption models for, (T), 25:12206
interactions K + N at high energies, SU(3) symmetry and exchange degeneracy in Regge pole--cut model for, (T), 25:12217

interactions K + p at high energies, sakaton rearrangement model for, 25:12186
interactions K + π in broken chiral SU(3) x SU(3), S-wave scattering length for, 25:12237
production of anti K and K in π⁺ + d and π⁺ + n interactions at 5.1 GeV/c, associated, (E), 25:12100 (NP-18629)
production of Y and K in π⁺ + d and π⁺ + n interactions at 5.1 GeV/c, associated, (E), 25:12100 (NP-18629)

MESONS (K⁻)
absorption by neon in bubble chamber, general systematics of, (E), 25:12106
decay K⁻ + π⁻ + π⁰ + γ, search for direct processes and upper limit for asymmetries in partial rates for, (E), 25:12085
interactions K⁻ + d + K⁻ + d(p + n) at 810 to 1110 MeV/c, K⁻ + n + K⁻ + n interactions from angular distributions for, (E), 25:12108
interactions K⁻ + d + p + Λ + π⁺ + π⁻ + π⁰ at 3 GeV/c, cross section for B(1220) production in, (E), 25:12118
interactions K⁻ + d at 360 to 720 MeV/c, Λ(1520) and Σ(1600) enhancement production and total cross sections for, (E), 25:12120
interactions K⁻ + d at 7.3 GeV/c in deuterium bubble chamber, partial and total cross sections, resonance production, and production cross sections for one strangeness-1 neutral hyperon or K⁰ in three-prong, (E), 25:12103
interactions K⁻ + n + K⁻ + n at high energies, constancy of total cross sections for, (T), 25:12210
interactions K⁻ + n + K⁻ + n from angular distributions for K⁻ + d + K⁻ + d(p + n) interactions at 810 to 1110 MeV/c, (E), 25:12108
interactions K⁻ + N on bound nucleons at low energies, effect of Λ(1405) on, (T), 25:12213
interactions K⁻ + N, duality condition for resonance contribution to backward, (T), 25:12215
interactions K⁻ + p + anti K⁰ + n at high energies, constancy of total cross sections for, (T), 25:12210
interactions K⁻ + p + K⁻ + p at high energies, constancy of total cross sections for, (T), 25:12210
interactions K⁻ + p + Σ⁺(Σ⁻) + π⁻(π⁺) at 440 to 1230 MeV/c in hydrogen bubble chamber, Λ and Σ resonance production, Σ⁺ decay branching ratio, and Σ⁺ and Σ⁻ lifetimes in, (E), 25:12098 (CEA-R-4068)
interactions K⁻ + p at 360 to 720 MeV/c, Λ(1520) and Σ(1600) enhancement production and total cross sections for, (E), 25:12120
interactions K⁻ + p, urbaryon rearrangement diagrams for amplitudes of, 25:12183

MESONS (K⁰)
decay K⁰ + π⁺(π⁰) + π⁻(π⁰), CP violation in K_1^0 + 2π and K_2^0 + 2π decay interference from spark chamber study of proper time dependence of, (E), 25:12079
decay K_1^0 + π⁺ + π⁻, spark chamber study of K_1^0 lifetime and CP violating parameter phase from, (E), 25:12078
decay K_2^0 + 2π and K_1^0 + 2π, spark chamber study of proper time dependence of K⁰ + π⁺(π⁰) + π⁻(π⁰) decay for CP volation in interference in, (E), 25:12079
decay K_2^0 + e + μ + ν, form factors for, (E), 25:12088
decay K_2^0 + π⁺ + π⁻ + π⁰, wire chamber magnetic spectrometer study of π spectra in, (E), 25:12087
lifetime of K_1^0 from K_1^0 + π⁺ + π⁻ decay, spark chamber study of, (E), 25:12078
mass difference (K⁺ - K⁰), contribution of Born term to electromagnetic, 25:12154
production in anti p + p interactions at 1.6 to 2.2 GeV/c in hydrogen bubble chamber, (E), 25:12097
production of single, in K⁻ + d interactions at 7.3 GeV/c in deuterium bubble chamber, cross sections for, (E), 25:12103

MESONS (anti K⁰)
production of anti K⁰ in π⁺ + p interactions at 1.7 GeV/c, cross sections for, (E), 25:12104

MESONS (K⁺)
decay K⁺ + e⁺(μ⁺) + ν, counter and spark chamber study of relative rate of, (E), 25:12077
decay K⁺ + π⁰ + e⁺ + ν, theory of neutral weak current for, 25:12170
decay K⁺ + π⁺ + e⁻ + e⁺, theory of neutral weak current for, 25:12170
decay K⁺ + π⁺ + ν + anti ν, theory of neutral weak current for, 25:12170
decay K⁺ + π⁺ + π⁰ + γ, search for direct processes and upper limit for asymmetries in partial rates for, (E), 25:12085
interactions K⁺ + d at 360 to 720 MeV/c, total cross sections for, (E), 25:12120
interactions K⁺ + p + K_1^0 + p + π⁺ at 3.2 GeV/c in hydrogen bubble chamber, K⁺ and N* production and momentum transfer distributions in, (E), 25:12114
interactions K⁺ + p + K⁺ + p + K⁺ + K⁻ at 12.7 GeV/c in hydrogen bubble chamber, production of low-mass K⁺phi⁰ enhancement and phi⁰ in, (E), 25:12102
interactions K⁺ + p + K⁺ + p + π⁺ + π⁻ + π⁰ at 12.7 GeV/c in hydrogen bubble chamber, production of low-mass K⁺ω⁰, K⁺eta⁰, pω⁰, and peta⁰ enhancements and ω⁰ and eta⁰ in, (E), 25:12102
interactions K⁺ + p + K⁺ + p + π⁺ + π⁻ at 12.7 GeV/c in hydrogen bubble chamber, resonance diffractive production in, (E), 25:12102
interactions K⁺ + p + K⁺ + p at 2.53 to 3.20 GeV/c in hydrogen bubble chamber, differential and total cross sections for, (E), 25:12115
interactions K⁺ + p at 2.80 GeV/c, phase shift analysis of, (T), 25:12115
interactions K⁺ + p at 360 to 720 MeV/c, total cross sections for, (E), 25:12120
mass difference (K⁺ - K⁰), contribution of Born term to electromagnetic, 25:12154
production in π⁺ + p interactions at 1.7 GeV/c, cross sections for, (E), 25:12104

MESONS (kappa)
mass in broken chiral SU(3) x SU(3), 25:12237

MESONS (μ)
interactions of cosmic, production of above-10^{13}-eV horizontal air showers from anomalous, (E), 25:12071
magnetic moment of, computer programs for constructing Feynman diagrams for calculating anomalous, (T), 25:12136 (CNRS-CPT-70-P-336)
magnetic moment of, sixth-order corrections to anomalous, 25:12145
properties of very high-energy cosmic, review of anomalous, (E), 25:12168
scattering by nuclei at 2.5 to 14.8 GeV/c at small angles in emulsions, multiple scattering techniques and particle energy determination from angular distributions in, (E), 25:12089

MESONS (μ⁻)
capture by bromine-79 and bromine-81, probability for, 25:12502
capture by carbon-12, relative yields and capture-rate ratios from, (E), 25:12395
capture by nitrogen-14, capture rate and gamma--neutrino angular correlations for, (T), 25:12386
distribution of μ⁻ --μ⁺ pairs in cosmic showers underground lateral, (E), 25:12082
production in μ⁻ and μ⁺ reactions with lead at 10.5 GeV, effective cross sections for trident, (E), 25:12083
production of massive μ⁻ --μ⁺ pairs in p + p interactions, light-cone analysis of, (T), 25:12228
production of μ⁺ - μ⁻ pairs in p + p interactions at high energies, cross sections for, (T), 25:12229
reactions with lead at 10.5 GeV, effective cross sections for μ trident production from, (E), 25:12083

MESONS (μ⁺)
distribution of μ⁻ --μ⁺ pairs in cosmic showers underground lateral, (E), 25:12082
production in μ⁻ and μ⁺ reactions with lead at 10.5 GeV, effective cross sections for trident, (E), 25:12083
production of massive μ⁻ --μ⁺ pairs in p + p interactions, light-cone analysis of, (T), 25:12228
production of μ⁺ - μ⁻ pairs in p + p interactions at high energies, cross sections for, (T), 25:12229
reactions with lead at 10.5 GeV, effective cross sections for μ trident production from, (E), 25:12083
scattering by carbon, copper, and hydrogen at 12 GeV, determination of neutron form factor from cross section ratios of carbon and copper to hydrogen for inelastic, (E), 25:12096

MESONS (ω)
mixing rho⁰--ω effects on spin density matrix of ω in π + N + ω + N(Δ) interactions, (T), 25:12208
production in anti p + p interactions at 1.6 to 2.2 GeV/c in hydrogen bubble chamber, (E), 25:12097
production of ω⁰ in K⁺ + p + K⁺ + p + π⁺ + π⁻ + π⁰ interactions at 12.7 GeV/c in hydrogen bubble chamber, (E), 25:12102
production of ω⁰ in π⁺ + d + 2p + π⁺ + π⁻ + π⁰ interactions at 4.19 GeV/c in deuterium bubble chamber, cross sections for, (E), 25:12112
spin density matrix in π + N + ω + N(Δ) interactions, rho⁰--ω mixing effects on, (T), 25:12208

MESONS (phi)
decay phi + π⁺ + π⁻ in e⁺ + e⁻ + π⁺ + π⁻ interactions, upper limit for branching ratio for, (E), 25:12074
production in e⁺ + e⁻ + π⁺ + π⁻ interactions, upper limit for, (E), 25:12074
production of phi⁰ in K⁺ + p + K⁺ + p + K⁺ + K⁻ interactions at 12.7 GeV/c in hydrogen bubble chamber, (E), 25:12102

MESONS (π)
exchange in π⁺ + d + 2p + π⁺ + π⁻ + π⁰ interactions at 4.19 GeV/c in deuterium bubble chamber, simultaneous production of rho and Δ(1236) from, (E), 25:12112
form factor ratio F/sub K//F/sub π/ dependence on symmetry-breaking parameter of vacuum states, 25:12198
interactions γ + π + γ + π, parametrization of amplitude for Compton, (T), 25:12177
interactions K + π in broken chiral SU(3) x SU(3), S-wave scattering length for, 25:12237
interactions π + d at 330 MeV, π production, total and differential cross sections, and momentum and angular distributions for, (T), 25:12105
interactions π + N + K + Σ(Λ) at high energies, tests of Regge-pole and strong-absorption models for, (T), 25:12206
interactions π + N + N + A_1(rho), nucleon electromagnetic and axial form factors from pole dominance and Veneziano model for, (T), 25:12144
interactions π + N + ω + N(Δ), rho⁰--ω mixing effects on spin density matrix of ω in, (T), 25:12208
interactions π + N + π + N, nucleon electromagnetic and

axial form factors from pole dominance and Veneziano model for, (T), 25:12144
interactions π + N at high energies in parton model, cross sections for inelastic, 25:12222
interactions π + N at high energies, SU(3) symmetry and exchange degeneracy in Regge pole-cut model for, (T), 25:12217
interactions π + N at low and intermediate energies, three-channel model for p-wave, 25:12221
interactions π + N at low energies, duality from Regge parametrization for P_{11} and S_{11} partial waves in, (T), 25:12211
interactions π + N in urbaryon rearrangement model, dip-bump structure of cross sections for, 25:12219
interactions π + N, continuous-moment sum rules for, (T), 25:12207
interactions π + N, relations among cross sections of ncnet mesons produced in, (T), 25:12203
interactions π + N, test of tensor meson dominance from f-exchange contribution to, (T), 25:12216
interactions π + p at high energies sakaton rearrangement model for, 25:12186
interactions π + π → π + π, crossing-symmetric unitarization of Veneziano amplitude for, (T), 25:12196
interactions π + π in π⁺ + d → 2p + π⁺ + π⁻ interactions at 1.1 to 2.3 GeV/c in deuterium bubble chamber, phase shift analysis on angular distribution moments of, (E/T), 25:12107
interactions π + π, continuous-moment sum rules for, (T), 25:12207
interactions π + π, crossing-symmetric expansion of amplitude for, 25:12197
interactions π + rho → N + anti N, multichannel N/D equations for bound-state mass of π in, (T), 25:12202
mass of bound-state, in π + rho → anti N + N and anti N + N → π + rho interactions, multichannel N/D equations for, (T), 25:12202
momentum from primary nucleon-nucleus interactions at 2 x 10^{6} GeV, mean transverse, (E), 25:11749
production in e + N diffractive interactions, conservation of hadronic s-channel helicity in, (T), 25:12165
production in γ + N → π + N interactions, continuous-moment sum rules for, (T), 25:12207
production in particle interactions, dual amplitudes for six-body, (T), 25:12131
production in π + d interactions at 330 MeV, (T), 25:12105
production in π + p and p + p interactions in multiperipheral model, charge distributions of, (T), 25:12179
scattering by carbon-12 near 180 MeV, strong absorption mechanism for, (E/T), 25:12420

MESONS (π⁻)
capture by carbon-12, relative yields and capture-rate ratios from, (E), 25:12395
form factor from π⁻ elastic scattering differential cross sections for helium-4, (T), 25:12225
interactions π⁻ + ^{4}He → ^{4}He + rho⁻, verification of vector dominance in, (T), 25:12140
interactions π⁻ + p → e⁺ + e⁻ + n at 275 MeV, emission energies and angles for e⁺ and e⁻ and differential cross sections for, (E), 25:12099 (JINR-P1-5398)
interactions π⁻ + p → Λ + K⁰ at 944 to 1170 MeV/c in hydrogen bubble chamber, differential and total cross sections, polarizations, and partial-wave analysis for, (E/T), 25:12109
interactions π⁻ + p → n + 2γ at 2 to 6 GeV/c, spark chamber study of cross sections for eta⁰ and π⁰ production in, (E), 25:12113
interactions π⁻ + p → n + π⁺ + π⁻ at 2 to 6 GeV/c, spark chamber study of differential cross sections for rho⁰ and f⁰ production in, (E), 25:12113
interactions π⁻ + p → n + π⁺(2π⁺) + π⁻(2π⁻) + mπ⁰ at 4 GeV, statistical and anisotropic models for, (T), 25:12204 (JINR-P1-5431)
interactions π⁻ + p → π⁰ + n at high energies, Reggeized generalized optical model for multiple and diffraction scattering and dips in, (T), 25:12205
interactions π⁻ + p → π⁰ + n, discrepancies between forward amplitude data and dispersion relation prediction for, (E/T), 25:12209
interactions π⁻ + p → π⁺ + 2π⁻ + π⁰ + p at 6 GeV/c in hydrogen bubble chamber, resonance production and cross sections for, (E), 25:12101
interactions π⁻ + p → rho⁰ + n in vector-dominance model, ncnevasive contribution to forward rho production in, (T), 25:12212
interactions π⁻ + p at 2.15 to 6.0 GeV/c, spark chamber study of cross sections for backward π⁻ and π⁺ production in, (E), 25:12111
interactions π⁻ + p at 5 GeV/c in urbaryon rearrangement model, dip-bump structure of cross sections for, (T), 25:12219
interactions π⁻ + p at 7 GeV/c, resonance production in strange-particle final states in, (E), 25:12110
interactions π⁻ + p at high energies, Regge pole fits to charge exchange, differential cross sections, and polarization in, (E/T), 25:12217
interactions π⁻ + p → n + eta⁰ at 5.9 GeV/c, cross sections for backward, (E), 25:12117
interactions π⁻ + p → n + π⁰ at 5.9 to 13.8 GeV/c, cross sections for backward, (E), 25:12117
production in anti p + p interactions, branching ratios for multiple, (T), 25:12195
production in e + p → e + π⁺ + π⁻ + p diffractive interactions, dual model for, (T), 25:12137 (DESY-70/56)
production in π⁻ + p interactions at 2.15 to 6.0 GeV/c, spark chamber study of cross sections for backward, (E), 25:12111
reactions (π⁻,2N) with lithium-6 and -7, effect of rescattering and outgoing nucleon interactions in, (T), 25:12415
reactions (π⁻,π⁰) with aluminum-27 and natural carbon, copper, and lead at 70 MeV, integrated cross sections for, (E), 25:12446
reactions (π⁻,π⁰) with carbon-12 at 73 MeV, cross sections for, (E), 25:12397
scattering by carbon-12 at 73 MeV, gamma spectra and cross sections for inelastic, (E), 25:12397
scattering by helium-4, π charge form factor from differential cross sections for, (T), 25:12225

MESONS (π⁰)
interactions π⁰ + π⁰ → π⁰(π⁺) + π⁰(π⁻), inequalities for s- and p-wave amplitudes of, (T), 25:12193 (SU-1206-234)
mass difference (π⁺ - π⁰), contribution of Born term to electromagnetic, 25:12154
production in anti p + p interactions, branching ratios for multiple, (T), 25:12195
production in γ + p → π⁰ + p interactions at 6 GeV, spectrometer and Cherenkov counter study of asymmetry in, (E), 25:12072
production in γ + p → π⁰ + p interactions at 6 to 18 GeV, differential cross sections for backward, (E), 25:12069
production in γ + p → π⁰ + p interactions in second resonance region, fixed-t dispersion relations for, (T), 25:12146
production in π⁻ + p → n + 2γ interactions at 2 to 6 GeV/c, spark chamber study of cross sections for, (E), 25:12113

MESONS (π⁺)
form factor from π⁺ elastic scattering differential cross sections for helium-4, (T), 25:12225
interactions π⁺ + ^{4}He → ^{4}He + rho⁺, verification of vector dominance in, (T), 25:12140
interactions π⁺ + d → 2p + neutrals at 1.1 to 2.3 GeV/c in deuterium bubble chamber, 2π⁰ mass spectrum in, (E), 25:12107
interactions π⁺ + d → 2p + π⁺ + π⁻ → π⁰ at 4.19 GeV/c in deuterium bubble chamber, rho, ω⁰, A_1, A_2, and phi production and rho Δ(1236) simultaneous production in, (E), 25:12112
interactions π⁺ + d → 2p + π⁺ + π⁻ at 1.1 to 2.3 GeV/c in deuterium bubble chamber, phase shift analysis on angular distribution moments of π⁻-π scattering and Δ⁺⁺(1236) production in, (E/T), 25:12107
interactions π⁺ + d → π⁺ + π⁻ + π⁰ + 2p at 3.65 GeV/c, H(990) and eta' production in, (E), 25:12121
interactions π⁺ + d at 5.1 GeV/c, associated production of K anti K and YK, and resonance production from two-body and quasi-two body final states in, (E), 25:12100 (NP-18629)
interactions π⁺ + n → Λ⁰ + K⁺ at 5.1 GeV/c, Λ polarization in, (E), 25:12100 (NP-18629)
interactions π⁺ + n at 5.1 GeV/c, associated production of K anti K and YK, resonance production from two-body and quasi-two-body final states, and cross sections for two-, three-, four-, and five-body final states in, (E), 25:12100 (NP-18629)
interactions π⁺ + p → 2π⁺ + π⁻ + π⁰ + p at 3 to 5 GeV/c, determination of spin and parity of B meson from, (E), 25:12119
interactions π⁺ + p → A_2⁺ + p at 7 GeV/c in bubble chamber, A_2 mass spectra in, (E), 25:12116
interactions π⁺ + p → p + 3π⁺ + 2π⁻ + π⁰ at 8 GeV/c, D⁰ production in, (T), 25:12191 (INR-P-1207)
interactions π⁺ + p → π⁰ + N*⁺⁺ at high energies, differential cross sections and spin-density matrix elements for, (T), 25:12223
interactions π⁺ + p at 1.7 GeV/c, cross sections for strange-particle final states in, (E), 25:12104
interactions π⁺ + p at 5 GeV/c in urbaryon rearrangement model, dip-bump structure of cross sections for, (T), 25:12219
mass differnce (π⁺ - π⁰), contribution of Born term to electromagnetic, 25:12154
production in anti p + p interactions, branching ratios for multiple, (T), 25:12195
production in e + p → e + π⁺ + π⁻ + p diffractive interactions, dual model for, (T), 25:12137 (DESY-70/56)
production in γ + p → π⁺ + n interactions at 0.450 to 3 GeV, resonance structure of cross sections for, (E), 25:12067 (LAL-1239)
production in γ + p → π⁺ + n interactions in second resonance region, fixed-t dispersion relations for, (T), 25:12146
production in ν + p → p + π⁺ + μ⁻ interactions, hadronic s-channel helicity conservation in, (T), 25:12165

XUM

production in π^- + p interactions at 2.15 to 6.0 GeV/c, spark chamber study of cross sections for backward, (E), 25:12111
reactions (π^+,π^0) with carbon-12 at 71.5 MeV, cross sections for, (E), 25:12397
scattering by carbon-12 at 73 MeV, gamma spectra and cross sections for inelastic, (E), 25:12397
scattering by helium-4, π charge form factor from differential cross sections for, (T), 25:12225

MESONS (rho)
interactions π + rho + N + anti N, multichannel N/D equations for bound-state mass of π in, (T), 25:12202
mixing rho^0--ω effects on spin density matrix of ω in π + N + ω + N(Δ) interactions, (T), 25:12208
production in anti p + p interactions at 1.6 to 2.2 GeV/c in hydrogen bubble chamber, (E), 25:12097
production in π + N + N + rho interactions, nucleon electromagnetic and axial form factors from pole dominance and Veneziano model for, (T), 25:12144
production in π^+ + d + 2p + π^+ + π^- + π^0 interactions at 4.19 GeV/c in deuterium bubble chamber, (E), 25:12112
production in π^- + p + rho^0 + n interactions in vector-dominance model, nonevasive contribution to forward, (T), 25:12212
production of Δ^{++} and rho$^-$ in π^- + p + π^+ + 2π^- + π^0 + p interactions at 6 GeV/c in hydrogen bubble chamber, associated, (E), 25:12101
production of rho and Δ(1236) in π^+ + d + 2p + π^+ + π^- + π^0 interactions at 4.19 GeV/c in deuterium bubble chamber, one-pion exchange for simultaneous, (E), 25:12112
production of rho^0 and rho$^+$ in π^- + p + π^+ + 2π^- + π^0 + p interactions at 6 GeV/c in hydrogen bubble chamber, (E), 25:12101
production of rho^0 in K^+ + p + K^+ + p + π^+ + π^- interactions at 12.7 GeV/c in hydrogen bubble chamber, (E), 25:12102
production of rho^0 in π^- + p + n + π^+ + π^- interactions at 2 to 6 GeV/c, spark chamber study of differential cross sections for, (E), 25:12113

MESONS (X^0)
mass in broken chiral SU(3) x SU(3), 25:12237

MESONS, RESONANCE
decay (2370) + 2K_1^0 + π^+ + π^- + π^0 in hydrogen bubble chamber, (E), 25:12097
decay D^0 + eta + π^+ + π^-, deltar intermediate state in, (T), 25:12191 (INR-P-1207)
decay g' + rho + 2π in hydrogen bubble chamber, (E), 25:12101
decay g' + rho-(A_2) + rho^0(π) in hydrogen bubble chamber, (E), 25:12101
decay in anti p + p interactions, branching ratios for multipion production from, (T), 25:12195
decay of spin-1, chiral Lagrangian with SU(3) symmetry breaking for parameters of three- and four-body K decays from correlations with rates of, (T), 25:12194
decay of, extension of Kemmer-symmetric coupling for internal charge configuration, masses, and lifetimes from, (T), 25:12199
decay of, Jacobian method for angular correlations of particles produced in interaction-free, (T), 25:12176
existence of S^0(730), review of discovery of, (E), 25:12201
lifetimes of, extension of Kemmer-symmetric coupling for particle decays for, (T), 25:12199
mass and width of (1927) and (1950) enhancements in anti p + p interactions at 100 to 750 MeV/c in hydrogen bubble chamber, (E), 25:12095
mass and width of (2370) in anti p + p interactions at 1.6 to 2.2 GeV/c in hydrogen bubble chamber, (E), 25:12097
mass and width of Q(1270) in K^+ + p + K^+ + p + π^+ + π^- interactions at 12.7 GeV/c in hydrogen bubble chamber, (E), 25:12102
mass of, extension of Kemmer-symmetric coupling for particle decays for, (T), 25:12199
mass spectra of K*, tables for, (T), 25:12200
mass spectra of, tables for, (T), 25:12200
parity and spin of B in π^+ + p + 2π^+ + π^- + π^0 interactions at 3 to 5 GeV/c, (E), 25:12119
parity and spin of Q(1270) in K^+ + p + K^+ + p + π^+ + π^- interactions at 12.7 GeV/c in hydrogen bubble chamber, (E), 25:12102
production in anti p + p interactions, branching ratios for multipion production from, (T), 25:12195
production in e + N interactions, review of, (E/T), 25:12068 (SLAC-PUB-842)
production in γ + p + π^+ + n interactions at 0.450 to 3 GeV, cross section structure for, (E), 25:12067 (LAL-1239)
production in K^- + d interactions at 7.3 GeV/c in deuterium bubble chamber, (E), 25:12103
production in meson interactions with mesons at low energies, singular off-mass-shell equation with vector meson exchange for, (T), 25:12192 (NYO-2262-TA-232)
production in strange-particle final states in π^- + p interactions at 7 GeV/c, (E), 25:12110
production in two-body and quasi-two-body final states in π^+ + d and π^+ + n interactions at 5.1 GeV/c, (E), 25:12100 (NP-18629)
production of (1927) and (1950) enhancements in anti p + p interactions at 100 to 750 MeV/c in hydrogen bubble chamber, (E), 25:12095
production of A_1 in π + N + N + A_1 interactions, nucleon electromagnetic and axial form factors from pole dominance and Veneziano model for, (T), 25:12144
production of A_1, A_2, and phi(1650) in π^+ + d + 2p + π^+ + π^- + π^0 interactions at 4.19 GeV/c in deuterium bubble chamber, (E), 25:12112
production of A_2, g'(1700), B, ω(783), and rho-(765) in π^- + p + π^+ + 2π^- + π^0 + p interactions at 6 GeV/c in hydrogen bubble chamber, (E), 25:12101
production of B(1220) in K^- + d + p + A + π^+ + π^- + π^0 interactions at 3 GeV/c, cross section for, (E), 25:12118
production of D^0 in π^+ + p + p + 3π^+ + 2π^- + π^0 interactions at 8 GeV/c, (T), 25:12191 (INR-P-1207)
production of eta (1070) with N and π in strange-particle final states in π^- + p interactions at 7 GeV/c, (E), 25:12110
production of H(990) and eta' in π^+ + d + π^+ + π^- + π^0 + 2p interactions at 3.65 GeV/c, (E), 25:12121
production of K* in K^+ + p + K_1^0 + p + π^+ interactions at 3.2 GeV/c in hydrogen bubble chamber, (E), 25:12114
production of K*(890) and Q in Kπ enhancement in K^+ + p + K^+ + p + π^+ + π^- interactions at 12.7 GeV/c in hydrogen bubble chamber diffractive, (E), 25:12102
production of K*(892) and (2370) in anti p + p interactions at 1.6 to 2.2 GeV/c in hydrogen bubble chamber, (E), 25:12097
production of K*ω^0 and K*eta^0 low-mass enhancements in K^+ + p + K^+ + p + π^+ + π^- + π^0 interactions at 12.7 GeV/c in hydrogen bubble chamber, (E), 25:12102
production of K*phi^0 low-mass enhancement in K^+ + p + K^+ + p + K^+ + K^- interactions at 12.7 GeV/c in hydrogen bubble chamber, (E), 25:12102
production of nonet, in π + N interactions, relations among cross sections for, (T), 25:12203
production of overlapping, in three-body systems, (T), 25:12126
production of rho' in diffractive e + p + e + π^+ + π^- + p interactions, dual model for cross sections for, (T), 25:12137 (DESY-70/56)
structure of A_2, quark model for double peaked, (T), 25:12218
widths of K*, tables for, (T), 25:12200
widths of, tables for, (T), 25:12200

METABOLISM
disturbances in human, use of carbon-14-labeled carbon dioxide determination of exhaled air for determining, 25:11168

METALLIC FILMS
electromigration in, induction of voids by, 25:12899 (NYO-4185-1)

METALLURGICAL EQUIPMENT
performance of laser-pulse, for determining thermal conductivity and diffusivity of graphite from 300 to 3300°K, 25:11487 (GA-9168)

METALS
abundance in atmospheres of giant stars, (T), 25:11546
abundance in delta Pavonis, (E), 25:11564
abundance in photosphere, (E/T), 25:11610
abundance in stars of Hyades and Coma open clusters, (E), 25:11551
anodization of, methods for plasma, 25:11343 (AECL-3778)
book: Electrolytic and Chemical Polishing of Metals, 25:11365
book: Physico-chemical Analysis of Handling Liquid Metal Coolants (In Russian), 25:11342
book: Transport Phenomena in Liquid Metals and Semiconductors, 25:11410
casting of, radioactive tracer methods in USSR for evaluating industrial, 25:10780
condensation of vapors of, (E/T), 25:12885(R) (COO-2032-6)
defects in deformed, review of Stage I recovery of, 25:11420
diffusion in, data tabulations on, 25:11411
dislocations in bcc, model of kinks in screw, 25:12027
ductility at high temperatures, factors controlling notch, 25:11373(R) (COO-2048-1)
electron distribution around positrons in, (T), 25:12041
emissivity of high-temperature, methods for determining, 25:11426
level measurements of liquid, inductive gage for, 25:10896 (RD/B/N-1720)
polishing of, practical and theoretical data on chemical and electrolytic, 25:11365
positron annihilation rate in, effects of phonon interactions on, (T), 25:11699
radioinduced coating of, by polymerization of resins, 25:10608 (JAERI-5026, pp 121-9)
stress wave propagation calculations for, strain hardening and strain rate in one dimensional, 25:12909 (SC-RR-70-471)
thermal properties of liquid and solid, 25:11425

METAMORPHIC ROCKS
analysis for cesium by neutron activation and γ spectrometry, 25:10508

METEORITES
age of, effects of annealing on accuracy of fission track, (E), 25:10696
analysis of stony, for trace amounts of boron by

fluorimetry, 25:10493
analysis of stony, for trace amounts of chlorine and lithium by neutron activation and radiochemical separation, 25:10493
analysis of stony, for trace amounts of fluorine by pyrohydrolysis and thorium nitrate titration, 25:10493
gamma spectrometry of Allende, (E), 25:11540
iodine-129 production in, (E), 25:11539
properties of crushed, habit and texture, (E), 25:11671
x-ray emission from transition metals in, gas proportional counting of, (E), 25:11539
METHACRYLIC ACID, 1,3-BUTYLENE GLYCOL ESTER
radioinduced polymerization on surface of synthetic calcium aluminate hydrate,, 25:10616
METHACRYLIC ACID, ETHYLENE GLYCOL ESTER
radioinduced polymerization on surface of synthetic calcium aluminate hydrate,, 25:10616
METHACRYLIC ACID, 2-HYDROXYETHYL ESTER
radioinduced polymerization on polyester fabrics, hydrophilic properties of products from γ and electron, 25:10600 (JAERI-5026, pp 63-7)
radioinduced polymerization on surface of synthetic calcium aluminate hydrate,, 25:10616
acrylonitrile--bis(2-hydroxyethyl methacrylate) phosphate--butyl acrylate--poly(diallyl phthalate), radioinduced polymerization of coatings of, on metals, electron, 25:10608 (JAERI-5026, pp 121-9)
METHACRYLIC ACID, 3-HYDROXYPROPYL ESTER
radioinduced polymerization on surface of synthetic calcium aluminate hydrate,, 25:10616
METHACRYLIC ACID, METHYL ESTER
radioinduced polymerization on surface of synthetic calcium aluminate hydrate,, 25:10616
METHANE
neutron slowing-down in cold, effective temperature from, (E/T), 25:12351
radioinduced iodination in gas phase, γ, 25:10620
radioinduced iodination of, Monte Carlo methods in analysis of γ, 25:10615
radiolysis of gaseous, low-energy electron, 25:10644
METHANE, CHLORODIFLUORO-
heat transfer to, kinetics of film boiling, nucleate boiling, and under supercritical conditions, 25:10767 (BMBW-FBK-70-24)
METHANE, DICHLORO-
effects on γ- and uv-radioinduced sulfoxidation of alkanes, 25:10592 (BMBW-FBK-70-25)
METHANE, DICHLORODIFLUORO-
heat transfer to, kinetics of film boiling, nucleate boiling, and under supercritical conditions, 25:10767 (BMBW-FBK-70-24)
METHANE, TRIBROMO-
carbon--hydrogen stretching band in, effects of solvents on, 25:10540
METHANESULFONIC ACID, ETHYL ESTER
effects on frequency of chlorophyll mutations in barley in comparison to effects of nitrosomethyl urea and x radiation, 25:11021
effects on genetic variation in Arabidopsis, corn, and sorghum, 25:11009(R) (CCC-1512-22)
effects on growth of barley seeds in soil, effects of dose, fertilizer concentration, and soil chemistry on, 25:11315
effects on seeds of petunia, effects of presoaking on mutagenic, 25:11011
METHANOL
effects of pretreatment with, on properties of products from γ-induced polymerization of vinylidene chloride in woods, 25:10604 (JAERI-5026, pp 86-93)
effects on γ-radioinduced graft polymerization of styrene with polyethylene, 25:10613
acetone--HCl--methanol, distribution coefficients of metal ions in, 25:10681
METHIMAZOLE
effectiveness for treatment of hyperthyroidism in combination with iodine-131 therapy, 25:11230
METHIONINE
effects on radioisotope accumulation in rats, dietary, 25:10956
radioinduced mutations affecting requirement of Escherichia coli for, cobalt-60 γ, 25:11019
METHIONINESULFOXIMINE
effects on bone marrow cell count of x-irradiated mice, 25:11288
METHOTREXATE
effects on survival of L cells, 25:11092 (BNL-50203, pp 41-53)
METHYL SULFOXIDE
effects on properties of products from radioinduced polymerization of acrylic acid on poly(ethylene terephthalates), 25:10597 (JAERI-5026, pp 46-51)
MIAMISBURG AREA (OHIO)
radiation monitoring of environs of, during 1969, 25:11042
MICE
antiserum formation in, following inoculation with γ-irradiated syngeneic tumors, 25:10993
blood exchange in parabiotic, use of chromium-51-labeled erythrocytes for studying, 25:10915
growth of x-irradiated tail bones from syngeneic donors in recipient, 25:10983
nonprotein thiol content of tissues of, following injection of cystamine in optimum radioprotective doses, 25:11101
radiation effects on antibody production in, effects of injections of allogeneic spleen cells and sheep red blood cells on x, 25:10994
radiation effects on bone marrow cell count of, in comparison to effects of injection of methioninesulfoximine, x, 25:11288
radiation effects on immune reactions of, to sheep red cells, effects of injections of spleen cells from mice treated with DMBA on, 25:10990
radiation effects on inbred and noninbred, protective effects of cystaphos and mexamine on hematopoietic tissue formation in spleen against γ, 25:11099
radiation effects on isoenzymatic spectra of lactic dehydrogenase in recipient, after transplantation with rat myeloid cells, 25:10992
radiation effects on nerve ganglia of intestines of, in relation to development of intestinal syndrome, neutron, 25:11270
radiation effects on proliferating cells in, in relation to repair, x, 25:11279
radiation effects on spermatogenesis in, x, 25:11276
radiation effects on survival of, protective effects of acetylcholine, adrenaline, histamine, 5-methoxytryptamine, and serotonin against γ, 25:11102
radiation effects on survival of, protective effects of reduced glutathione against x, 25:11098
radiation effects on virus-induced leukemia in, uv, 25:11321
radiation effects on, combined effects of Ascaris suum invasion of lungs on x, 25:11265
radiation effects on, effects of, on binding of tritium-labeled dactinomycin by hepatocyte DNA of, effects of administration route on x, 25:11285
radioinduced aberrations of chromosomes in corneal epithelium of, RBE for neutron, 25:11018
radioinduced dilation of venules in, blood vessels, electron, 25:11254 (BNL-50203, pp 174-80)
radioinduced inhibition of endocolonization in spleen of, effects of dose rate on cobalt-60 γ, 25:10986
radioinduced neoplasms in ovaries of, protective effects of diethylstilbestrol on γ, 25:11107
radioinduced teratogenesis embryos and infants of, following exposure of mothers, effects of state of pregnancy on x, 25:11287
radiosensitivity of acatalasemic, and normal, x, 25:11264
radiosensitivity of embryos of, in comparison to species differences of rat embryo sensitivity, 25:11277
radiosensitivity of embryos of, in utero in comparison to embryo of rats, role of species differences in x, 25:11277
radiosensitivity of skin of, effects of acute dose and dose fractionation on recovery from, 25:11260 (BNL-50203, pp 286-91)
radiotherapy of tumors in, review of, 25:11219 (BNL-50203, pp 130-53)
thrombopoietin radioimmunoassay in blood plasma of, using selenium-75-labeled selenomethionine, 25:10991
MICROORGANISMS
radiosterilization in biological materials, used as transplants, effects of dry ice temperatures on ionizing, 25:11337
MICROWAVE EQUIPMENT
electron beam coupling in slow-wave ridged waveguide, 25:11932
MICROWAVE SPECTROMETERS
development of, review on, 25:10897
MICROWAVES
cosmic background, explanation of anomalies in, (T), 25:11662
cosmic background, interaction with relativistic electrons in extragalactic radio sources, (T), 25:11597
cosmic background, spectra at low frequencies, (E/T), 25:11666
effects on superconducting tunnel junctions, (E/T), 25:11827
interactions with plasma, heating kinetics from off-resonance, (E/T), 25:11909(R) (CCO-1695-31)
protection of personnel against, review of international standards for, 25:11088
MIDWEST FUEL RECOVERY PLANT
safety analysis for application for operation license, 25:10663 (DOCKET-50268-6)
MILK
analysis for cesium-137 and strontium-90 by scintillation counting, 25:10480
cesium-137 content in cow's, in Bulgaria, 25:10480
radioisotope content of, in Sweden, during 1959 to 1969, cesium-137 and strontium-90, 25:11004
radioisotope content of, sampled throughout Central, North, and South America during July 1969 to July 1970, cesium-137, iodine-131, and strontium-90, 25:11002
radioisotope content of, sampled throughout the USA during February 1970, barium-140, cesium-137, iodine-131, strontium-89, and strontium-90, 25:11040
strontium-90 content in cow's, in Bulgaria, 25:10480
strontium-90 content of, 25:10932 (CEA-CONF-1558)

XUM

MILKY WAY
book: The Interstellar Medium, 25:11641
cosmic-ray diffusion in, 25:11641
dust distribution in, (T), 25:11641
effects on cosmic-microwave background spectrum, (E/T), 25:11666
gamma emission from extended source at center of, (T), 25:11636
gas distribution in, (T), 25:11641
interstellar feature at lambda 4430 in, variation with galactic longitude, 25:11651
Lyman-α brightness in, origin of, (E/T), 25:11640
star distribution in field 3 of Palomar--Groningen survey, variable-, (E), 25:11550
star formation in, (T), 25:11641
supernovae in, frequency of occurrence of, (E), 25:11637
x-ray background at pole and plane of, excess, (E), 25:11653
MILLSTONE POINT POWER REACTOR, UNIT 1
operations incident of December 29, 1970, failure of main steam bypass valves during startup test at 75 percent rated output, 25:12721 (DOCKET-50245-51)
MINERAL DEPOSITS
copper plus zinc content of Czech, gamma--gamma well logging method for determining, 25:10693
MINERALS
analysis for trace amounts of elements by x-ray fluorescence, methods for correction of matrix effect in, 25:10448
analysis for trace amounts of elements, conference on, 25:10446
analysis for trace amounts of potassium, rubidium, and strontium by atomic absorption spectrophotometry, 25:10458
processing of, review on solvent extraction methods for, 25:10656 (BM-IC-8502)
MINES
damage to Project Rulison area, evaluation of structural, 25:10736 (PNE-R-39, Pt.1)
radon concentration in uranium, control and measurement of, 25:11043
MINING
methods using nuclear explosions, review of, 25:10747
MINNESOTA
jurisdiction over nuclear power plants, legality of, 25:11087 (CONF-700408-3)
MITOCHONDRIA
radiation effects on activity of, in rats, continuous, 25:10980
radiation effects on oxidative phosphorylation and respiration in spleen, of rats, protective effects of homologous bone marrow injections against acute x, 25:11100
radiation effects on, of rat myocardial cells, effects of argon laser microbeam exposure on, 25:11242
MITOSIS
radiation effects on, in bone marrow of mice, comparison of effects of acute exposure and dose fractionation on x, 25:11279
radioinduced inhibition of, review of ionizing, 25:10977
radioinduced, following transplantation of sterilized cells, 25:11330
MOESSBAUER SPECTROMETERS
design for Coulomb-excited sources, with closed cycle helium refrigerator, 25:10863
design of computer-based double-ended, for simultaneous calibration, 25:10866
MOISTURE GAGES
accuracy of neutron radiometric, 25:10887 (INP-709)
MOLDS
radiation effects on phenoplast materials for, 25:10634
MOLECULES
diffusion in gases, review, (E/T), 25:11731
electron reactions at low energies with, review of rotational excitation in, (T), 25:11730
electron reactions with diatomic, adiabatic theory of rotational excitation of non-Σ states in, 25:11725
force constants for, comparison of 5 calculation methods for, 25:11686
MOLLUSCA
age of fossil, uranium series method for estimation of, 25:10725(R) (CU-3139-4)
Fisherola nuttalli, growth in Columbia River, effects of heated effluents on, 25:10996 (BNWL-1537)
MOLTEN SALT REACTOR EXPERIMENT
effluent off-gases from, determination of tritium in, 25:10434 (ORNL-4636, pp 7-13)
fuel for, determination of trivalent uranium in, 25:10434 (ORNL-4636, pp 7-13)
fuel for, program and methods for analysis of, 25:10425 (ORNL-4636, pp 40-2)
MOLYBDENUM
analysis for trace amounts of impurities, review on, 25:10459
corrosion by liquid lead at high temperatures, 25:11376 (JUL-661-RW)
determination as fuel burnup monitor, 25:10583(R) (AECL-3776)
determination as impurity in fuel materials by emission spectroscopy, 25:10432 (KFK-1261)
determination by photon activation, reactions and sensitivities for, 25:10488 (CEA-R-4072)
determination in iron and steel by solvent extraction and flame photometry, 25:10439
determination of trace amounts of, in basalt and granite, correction of matrix effect in uv spectrographic, 25:10453
determination of trace amounts of, in biotite and tektite by spark source mass spectrometry, 25:10455
determination of trace amounts of, in minerals and rocks by x-ray fluorescence, methods for correction of matrix effect in, 25:10448
determination of trace amounts of, in phosphate deposits by spark source mass spectrometry, 25:10456
determination of trace amounts of, in rocks and sand by thermal neutron activation, ion exchange, and γ spectrometry, 25:10492
determination of trace amounts of, in rocks, quantometer for spectroscopic, 25:10451
determination of trace amounts of, in Zircaloy-2 and zirconium, carrier distillation method for spectrographic, 25:10430 (EUR-4541)
dislocation kinks, structure and energy of screw, 25:12027
dislocation structure of deformed single crystals of, correlation with work hardening, (E), 25:11422
effects on corrosion resistance of Types 303 and 316 stainless steel in acid media, 25:11352
electron band structure of, photoemission and optical study of, 25:11982
friction and wear of, sliding against copper and iron rings under vacuum, 25:11413
interactions with tantalum silicide coating, 25:11519
oxidation at 1100 to 1500°K, reacting rotating disk method for studying kinetics of, 25:11409
oxidation at 200 to 600°C, ellipsometry method for studying, 25:11355
photoelectric emission by, calculation of direct transition contribution to, 25:12040
reactions with nitrogen and oxygen, review of kinetics, mechanisms, and thermodynamics of degassing and engassing, 25:11415
separation from cadmium, indium, niobium, palladium, and rhodium by gas chromatography using aluminum chloride eluent, 25:10666 (JINR-P6-5410)
separation from fission products by automatic ion exchange chromatography, design and performance of equipment for, 25:10659 (CEA-N-1267)
separation from ores by solvent extraction, review on, 25:10656 (BM-IC-8502)
solubility in lead at 350 to 1100°C, 25:11376 (JUL-661-RW)
sorptive properties for hydrogen and deuterium, exchange in, 25:10559
thickness of surface layers of, electron-microprobe measurements of, 25:11421
MOLYBDENUM ALLOYS AND SYSTEMS
Cu--Mo--Zr-base, phase transformations in, effects of continuous cooling on, 25:11432 (CEA-N-1310)
Mo--Ni, ordering in Ni_4Mo, short-range, 25:11452
Mo--U-base, corrosion by moisture, stress, 25:11345 (AWRE-O-49/66)
MOLYBDENUM CARBIDES
MoC--UC, thermal expansion of $UMoC_2$, high-temperature anisotropic, 25:11509
MOLYBDENUM ISOTOPES
deuteron reactions (d,p) with, charge exchange effects and spectroscopic factors in, (E), 25:12571
proton reactions (p,d) with, charge exchange effects and spectroscopic factors in, (E), 25:12571
MOLYBDENUM ISOTOPES Mo-95
energy level at 204 keV from technetium-95m decay, lifetime and g-factor for, (E), 25:12568
energy levels from technetium-95m decay, (E), 25:12568
neutron capture by, average circular γ polarization in thermal, (E), 25:12601
neutron capture by, γ singles and coincidence spectra and angular correlations for thermal, (E), 25:12598
MOLYBDENUM ISOTOPES Mo-96
energy levels from molybdenum-95 thermal neutron capture, spin-parity assignments and γ-mixing ratios for, (E), 25:12598
energy levels from thermal neutron capture, spin for compound, (E), 25:12601
MOLYBDENUM ISOTOPES Mo-99
effectiveness for scanning of human liver, 25:11198
energy levels of, spin and parity of, (E), 25:12462
MOLYBDENUM ISOTOPES Mo-100
energy levels of, spin and parity of, (E), 25:12462
MOLYBDENUM ISOTOPES Mo-101
energy levels of, spin and parity of, (E), 25:12462
MOLYBDENUM SILICIDES
diffusion of silicon in Mo_3Si, activation energy for, 25:11519
MONAZITES
separation of cerium, thorium, and uranium from, process for, 25:10663
uranium leaching from, using acetic, hydrochloric, nitric, and sulfuric acids, 25:10723
MONKEYS
calcium content of bones of, method for neutron activation analysis of, 25:10907 (N-70-31814)

MONOAMINE OXIDASE
content of human serum, method using carbon-14-labeled butylamine as substrate for measuring, 25:10922
MONTMORILLONITES
preparation of magnesium-rich saponite-type, method for, 25:10793 (BARC-506)
properties for use in separation of cesium-134 from cesium chloride, 25:10793 (BARC-506)
MUCOSA
radioinduced damage of intestinal, in rats, effects of dose on x, 25:11255 (BNL-50203, pp 181-5)
MUSCLES
blood circulation in human gastrocnemius and quadriceps, use of xenon-133 for measuring, 25:11123
cobalt-60 1-nitroso 2-naphthol chelate distribution in, of rats, 25:10958
scanning of blood circulation in human, during work, method for xenon-133, 25:10913
scanning of blood circulation in, comparison of direct measurements to xenon-133, 25:11137
scanning of human, using xenon-133 for studies on effects of vasoactive drugs, 25:10914
xenon-133 clearance from cat, effects of method of administration on, 25:11136
MUSCOVITES
age of, effects of geometry factor on accuracy of fission track, (E), 25:10695
analysis of thin layers of, for uranium by fission track method using dielectric detectors, 25:10476
MUSKRATS
strontium-90 content of, in lake contaminated by reactor effluent, 25:11006
MUTATIONS
induced in T_4 phage by radiotoxins following inoculation into γ-irradiated Escherichia coli, 25:11016
induced, in seeds of petunia for color, effects of presoaking on methanesulfonic acid, ethyl ester, 25:11011
radiation effects on frequency of chlorophyll, in barley in comparison to effects of EMS and nitrosomethyl urea, x, 25:11021
radioinduced sex-linked lethal, in oocytes of Drosophila, effects of dose rate on γ, 25:11022
radioinduced somatic, in grapes, effects of inhibitory and lethal dose rate on chronic, γ, 25:11017
radioinduced somatic, in stamen hairs of Tradescantia, RBE for monoenergetic fast neutron, 25:11313
radioinduced, in Arabidopsis for pigmentation, effects of seed exposure on laser, 25:11027
radioinduced, in Chrysanthemum morifolium, for somatic chromosome number, γ, 25:11031
radioinduced, in corn for necrotic leaf spot, thermal neutron, 25:11009(R) (COO-1512-22)
radioinduced, in Escherichia coli for altered surface properties and radiosensitivity, uv, 25:11029
radioinduced, in Escherichia coli, affecting cell division, γ and uv-radiosensitivity, and nutritional requirements, cobalt-60 γ, 25:11019
radioinduced, in Escherichia coli, for phage T5 resistance, comparison of light with uv, 25:11032
radioinduced, in Gladiolus, effects of environment on γ, 25:11035
radioinduced, in human populations, in relation to natural selection, 25:11025
radioinduced, in peas for chlorophyll content, effects of seed exposure and storage time on frequency of γ, 25:11024
radioinduced, in plants, review of cell lineage studies on, 25:10977
radioinduced, in seeds of petunia for color, effects of dose and presoaking on γ, 25:11011
radioinduced, in seeds of sugar cane, effects of 1 to 5 kR doses on γ and x, 25:11030
radioinduced, in wheat, effects of 1.05×10^{13}/cm² dose on thermal neutron, 25:11033(P)
radioinduced, in wheat, effects of 8.38×10^{12}/cm² dose on thermal neutron, 25:11034(P)
radiosensitivity in Salmonella, repair of Salmonella typhimurium, uv, 25:11026

N

NAGASAKI
atomic bombing of, health status of atomic bomb survivors during July 1968 to July 1969, 25:11237(R) (ABCC-68-69)
NANDROLONE PHENPROPIONATE
effects on adrenal cortex of prednisolone-treated rats, 25:11268
2-NAPHTHOL, 1-NITROSO-
metabolism of chelate of, with cobalt-60 in rats following intravenous administration, 25:10958
NATIONAL REACTOR TESTING STATION
radiation monitoring of environs of, during 1968, 25:11042
NATURAL GAS
analysis of, from wells stimulated by underground nuclear explosions, equipment for, 25:10434 (ORNL-4636, pp 7-13)
NBS RESEARCH REACTOR
operations incident of January 9, 1971, displacement of inlet filter strainer, 25:12814 (DOCKET-50184-24)
NEBULAE
gas densities in comet-shaped, (E), 25:11541(T) (CSIRO-Trans-10286)
infrared sources associated with, (E), 25:11563
masses of comet-shaped, (E), 25:11541(T) (CSIRO-Trans-10286)
physics of, 25:11538
NEMATODA
Ascaris suum, effects on lungs of x-irradiated mice, 25:11265
NEODYMIUM
determination of trace amounts of, in biotite and tektite by spark source mass spectrometry, 25:10455
determination of trace amounts of, in phosphate deposits by spark source mass spectrometry, 25:10456
spectra of, ultraviolet absorption, 25:11698
NEODYMIUM IONS
spectra of photoexcited states of, in lanthanum chloride monocrystals, EPR, 25:10570(R) (COO-294-10)
NEODYMIUM ISOTOPES
determination of stable, by isotope dilution and mass spectrometry, method for measuring burnup from, 25:10469
NEODYMIUM ISOTOPES Nd-140
mass excess of, determination from (p,2n) threshold measurements, (E), 25:12607
NEODYMIUM ISOTOPES Nd-142
energy levels from electron inelastic scattering, transition probabilities for low-lying, (E), 25:12622
energy levels from praseodymium-141 (He-3,d) reactions, (E), 25:12558
nuclear charge distribution of, determination from electron scattering, (E), 25:12622
NEODYMIUM ISOTOPES Nd-146
energy levels from electron inelastic scattering, transition probabilities for low-lying, (E), 25:12622
nuclear charge distribution of, determination from electron scattering, (E), 25:12622
NEODYMIUM ISOTOPES Nd-147
beta decay of, γ-γ directional correlations in, (E), 25:12567
NEODYMIUM ISOTOPES Nd-149
beta decay of, perturbed γ-γ angular correlations from, (E), 25:12609
NEODYMIUM ISOTOPES Nd-150
electron scattering at 15 to 60 MeV, angular distributions for, 25:12622
energy levels from electron inelastic scattering, transition probabilities for low-lying, (E), 25:12622
nuclear charge distribution of, determination from electron scattering, (E), 25:12622
NEODYMIUM ISOTOPES Nd-151
decay of, 25:10472(R) (BMBW-FBK-70-19)
NEODYMIUM OXIDES
spectra of, ultraviolet absorption, 25:11698
NEON
deuteron reactions at 30 to 120 keV with, cross sections for electron capture into 3s state of deuterium in, (E), 25:11708
diffusion in solid argon, isotope effect calculations for, 25:12042
helium-ion reactions at 1 to 3 keV and at small angles with, charge exchange in, (E), 25:11716
helium-ion reactions at 1 to 3 keV with, charge exchange at small angles in, (E), 25:11705
hydrogen-metastable-atom reactions at 5 keV with, mechanism of quenching in, (T), 25:11723
meson (K⁻) absorption in bubble chamber, general systematics of, (E), 25:12106
proton reactions at 30 to 120 keV with, cross sections for electron capture into n = 3 level of hydrogen in, (E), 25:11708
scattering by platinum (111) surfaces at thermal energies, (E), 25:11683
NEON ISOTOPES Ne-20
deuteron reactions (d,He-3) at 52 MeV, helium-3 spectra and angular distribution for, (E), 25:12385
energy levels from (p,γ) reactions, widths, branching ratios, and decay strengths for T = 2, (E), 25:12441
energy levels from oxygen-16 alpha elastic scattering, spins and parities of, (E), 25:12419
energy levels of, analysis of M1 transitions using Tabakin and Serber--Yukawa potentials, (T), 25:12468
energy levels of, projected Hartree--Fock calculation using non-axial intrinsic wave functions, (T), 25:12458
NEON ISOTOPES Ne-22
deuteron reactions (d,He-3) at 52 MeV, helium-3 spectra and angular distribution for, (E), 25:12385
helium-3 reactions (He-3,t) at 16 and 30 MeV, (E), 25:12498
reactions (Ne-22,4n) with americium-243 at 105 to 150 MeV, cross section for, (E), 25:12620
reactions (Ne-22,5n) with uranium-235 at 105 to 150 MeV, cross section for, (E), 25:12620
NEPTUNIUM
compounds of, crystal-field effect and magnetic properties of NaCl-type, 25:11994
energy-level transitions in, rates of Auger and x-ray, (T), 25:11685

magnetic behavior of, Moessbauer effect studies of, 25:12001
phase transformations in, heats and temperatures of, 25:11437
radiation effects on electric conductivity of α-, at low temperatures, self-, 25:11960
separation from plutonium, thorium, and uranium by ion exchange in tetramethylammonium hydroxide--citrate solutions, effects of complexing agents on, 25:10655 (ANL-7751)
thermodynamic properties at low temperatures, review of, 25:11384
NEPTUNIUM ALLOYS AND SYSTEMS
Am--Np-base, magnetic behavior of dilute, Moessbauer effect studies of, 25:12001
Np--Pd-base, magnetic properties of solid solutions of, at 2 to 300°K, 25:12003
Np-base--Pd, magnetic behavior of dilute, Moessbauer effect studies of, 25:12001
NEPTUNIUM CARBIDES
magnetic susceptibility, 25:11980 (CEA-R-4113)
NEPTUNIUM FLUORIDES
reactions with fluorine, kinetics of, 25:10568 (CEA-R-4051)
sorption by barium, magnesium, and sodium fluorides, mechanism of, 25:10568 (CEA-R-4051)
NEPTUNIUM ISOTOPES Np-237
deuteron reactions (d,2n) at 12.1 MeV, decay curves from, (E/T), 25:12530 (RLO-1388-130)
NEPTUNIUM ISOTOPES Np-238
beta decay of, β, γ, and conversion electron spectra from, (E), 25:12594
NEPTUNIUM ISOTOPES Np-239
energy level at 74 keV, lifetime from americium-243 alpha decay, (E), 25:12542
NEPTUNIUM NITRIDES
electric conductivity, 25:11980 (CEA-R-4113)
NEPTUNIUM OXIDES
preparation of monocrystalline neptunium-237 dioxide, high-temperature solution growth method for, 25:11483
radiation effects on microstructure of, 5.5-MeV alpha particle, 25:11537
reactions with fluorine, kinetics of, 25:10568 (CEA-R-4051)
NERVES
radiation effects on antigenicity of peripheral, effects of temperature and 2 Mrad dose on ionizing, 25:11334
radiation effects on, of intestines of mice in relation to development of intestinal syndrome, neutron, 25:11270
radiosensitivity of optic, in rats in comparison to sensitivity of choroid and retinal tissues, 25:11284
NERVOUS SYSTEM
radiation effects on human central, during space flight, effects of acceleration, dose, and vibration on ionizing, 25:11298
radiation effects on, in man, review of literature on, 25:11209
radioinduced injuries of, in embryos and infants of mice, following exposure of mothers, effects of state of pregnancy on teratogenic x, 25:11287
NEUTRINOS
detection of solar, in liquid ionization detectors, (T), 25:11628
interactions ν + N, form factors and differential and total cross sections for Δ and Σ resonance production in, (T), 25:12174
radiation in gravitational fields, solutions of general relativistic Weyl equation for, (T), 25:12281
theory for, discrete transformations in six-dimensional Minkowski space in, 25:12252
theory for, Riemannian geometry in, (T), 25:12280
time variations for sea of, electrodynamic radiative corrections for, (T), 25:11668
NEUTRINOS (ANTI ν)
interactions anti ν + N, form factors and differential and total cross sections for Δ and Σ resonance production in, (T), 25:12174
NEUTRINOS (ν/sub μ/)
interactions ν + p → μ⁻ + hadrons at high energies, scaling laws in Veneziano model for, (T), 25:12166
interactions ν + p → p + π⁺ + μ⁻, hadronic s-channel helicity conservation in, (T), 25:12165
NEUTRINOS (anti ν/sub μ/)
interactions anti ν + p → μ⁺ + hadrons at high energies, scaling laws in Veneziano model for, (T), 25:12166
NEUTRON CAPTURE THERAPY
evaluation of current state and prospects of, 25:11232
NEUTRON CROSS SECTIONS
calculations for off-axis core positions in fast reactors, 25:11474(R) (BNWL-842)
computer service programs for preparing input for diffusion- and transport-theory calculations of, (T), 25:12337 (ANL-7654)
data processing using ENDF/B file, computer program for generating TIMOC library in, 25:12339 (EUR-4521)
information system for, description of IAEA, 25:12343
tables of, for 14- to 15-MeV neutrons, 25:12353 (NP-18616)
vibration effects on, calculation of fuel element, (T), 25:12850
NEUTRON-DIFFRACTION ANALYSIS
control of experiments, FOCAL interpreter for, 25:11981(R) (ORO-3674-4)
NEUTRON SOURCES
description of UCD 76-inch isochronous cyclotron lithium-7-target, for medium-energy neutrons, 25:12331
evaluation of pulsed reactor, for use in activation analysis, 25:10489 (KFKI-70-25-NAC)
fabrication at TRU, 25:10654(R) (ORNL-4588)
spectra measurements of accelerator--target, time-of-flight system for, 25:10861
NEUTRON SPECTROMETERS
data acquisition system for proton-recoil proportional, 25:10848 (ANL-7704)
design and performance of scintillation time-of-flight, 25:10856
design of rotating-disc thermal, 25:10854(P)
design of stilbene and lithium-6-glass scintillation coincidence, 25:10862
development of Bonner multisphere, 25:10811 (CEA-CONF-1685)
performance of time-of-flight, for accelerator--target neutron source, 25:10861
pulse-shape discriminators for gamma discrimination in proton-recoil proportional, 25:10857
NEUTRON SPECTROSCOPY
theory of correlation time-of-flight, 25:10850 (JUL-684-FF)
NEUTRON STARS
battery effect in, (T), 25:11591
equilibrium configurations of, Hagedorn equation of state for, (T), 25:11566
magnetic-field generation in, (T), 25:11591
models for, (T), 25:11596
superfluidity in, (T), 25:11545
NEUTRONS
absorption of, operational formulation of resonance, (T), 25:12338 (CNEA-266)
angular distributions from gamma reactions (γ,n) with deuterium at 10 to 95 MeV, 25:12374
attenuation in resonant absorbing media, exact and approximate calculations of, (T), 25:12346
attenuation in slabs, computer program for calculating resonance absorption, cross sections, and foil reaction rates, (T), 25:12336 (ANL-7645)
attenuation in water, ages and slowing-down spectra from fission and D--T sources, (T), 25:12348
capture by A = 102 to 195 nuclei, spectroscopic analysis of, (E), 25:12586
capture by plutonium-239, uranium-233, and uranium-235, interference effects in average cross sections for, (T), 25:12608
capture by rhodium-103, γ spectra from resonance, (E), 25:12561
capture by thulium-169, low-energy γ spectra and resonance spin assignments for resonance, (E), 25:12589
collision histories of, determination of statistical errors in Monte Carlo calculations of, 25:12839
detection and measurement of slow, boron-impregnated 1/v dielectric detectors for, 25:10820
diffusion calculations for reactors, method for phase space reduction in, 25:12853
diffusion equations for, coarse mesh acceleration of iterative solution of, 25:12838
diffusion in cylinders, plates, and spheres, computer program for solving one-dimensional, (T), 25:12335 (AECL-3671)
diffusion in heterogeneous water moderated lattices, pulsed method for determination of, (E/T), 25:12861
distribution in adjacent half infinite media, energy dependent transport theory for, (T), 25:12857
dosimetry around medical betatron using uranium-loaded dielectric track detectors, 25:12320
dosimetry in accidents, personnel dosimeter for, 25:10881
dosimetry in nuclear accidents, activation foil detectors for, 25:10884
dosimetry in nuclear accidents, chemical dosimeter for, 25:10883
dosimetry of, development of Bonner multisphere detectors for, 25:10811 (CEA-CONF-1685)
dosimetry of, development of dielectric track detectors for personnel, 25:10880
dosimetry of, developments in threshold detectors for personnel, 25:10882
effects on beryllium oxide single crystals, ESR study of defects induced in, 25:11950 (CEA-R-3937)
effects on brittleness of steel by helium-producing reactions with boron, 25:11456 (AERE-R-5622)
effects on chromosomes in corneal epithelium of mice, aberrant, 25:11018
effects on high-pressure polymorphs of boron oxide, 25:11474(R) (BNWL-842)
effects on lens of mammalian eyes, comparison of γ dose with dose for cataractogenic, 25:11284
effects on nerve ganglia of intestines of mice in relation to development of intestinal syndrome, 25:11270
effects on optical aberrations in lenses, 25:11961
effects on survival of lymphoma and Vicia faba cells, effects of age on lethal, 25:11095 (BNL-50203, pp 308-

17)
effects on thermoelectric properties of cuprous sulfide, 25:11952
flux distribution in fast reactors, successive space--energy synthesis for, (T), 25:12780
flux distribution in reactors, reduction of ray effect in discrete ordinates calculations of, 25:12852
flux distribution in reactors, SYNTH 2 computer programs for calculation of, 25:12844 (TKK-F-A-121)
flux distribution in reactors, variational derivation of discrete ordinate-like approximations for, (T), 25:12858
flux in infinite homogeneous systems, effects of cavities on distribution of, (T), 25:12851
flux measurements of, development of Bonner multisphere detectors for, 25:10811 (CEA-CONF-1685)
form factor from cross section ratios for μ^+ inelastic scattering on carbon, copper, and hydrogen at 12 GeV, (E), 25:12096
form factor of, e + d → e + d interactions at low momentum transfers for neutron-to-proton ratio for electric, (E), 25:12070
interactions γ + n above 1.2 GeV, data compilation on cross sections for hadron production in, (E), 25:12066 (DESY-HERA-70-1)
interactions K^- + n → K^- + n at high energies, constancy of total cross sections for, (T), 25:12210
interactions K^- + n → K^- + n from angular distributions for K^- + d → K^- + d(p + n) interactions at 810 to 1110 MeV/c, (E), 25:12108
interactions n + d → n + d, amplitudes and scattering length relation with triton binding energy in, (T), 25:12227
interactions n + p → d + γ, test of time reversal invariance in total and differential cross sections for, (E), 25:12238
interactions n + p from deuterium (n,p2n) reactions at 14.1 MeV, singlet scattering lengths for, (E/T), 25:12367
interactions π^+ + n → A^0 + K^+ at 5.1 GeV/c, Λ polarization in, (E), 25:12100 (NP-18629)
interactions π^+ + n at 5.1 GeV/c, associated production of K anti K and YK, resonance production from two-body and quasi-two-body final states, and cross sections for two-, three-, four-, and five-body final states in, (E), 25:12100 (NP-18629)
kinetic behavior in a multiplying medium, (T), 25:12341 (LFEN-NI.-46-a)
mass difference (n - p), contribution of Born term to electromagnetic, 25:12154
monitoring at Van de Graaff accelerator, proportional detector system for, 25:10824
multiplication factors for bare plutonium spheres, collision probability method calculation of, (T), 25:12849
photoproduction by bremsstrahlung from electron reactions with tungsten, 25:12496
reactions (n,2n) with osmium-192 and platinum-198 at 14.7 MeV, total cross sections and isomeric yield ratios for, (E), 25:12618
reactions (n,f) with plutonium-239, uranium-233, and uranium-235, interference effects in average cross sections for, (T), 25:12608
reactions (n,γ) with copper-63, 2DB code for calculation of spectral-averaged cross sections for, 25:11474(R) (BNWL-842)
reactions (n,p) with iron-54, 2DB code for calculation of spectral-averaged cross sections for, 25:11474(R) (BNWL-842)
reactions with promethium-147 at 0.01 to 1000 eV, total cross sections and resonance parameters for, (E), 25:12550
resonance integral for, calculation of interference scattering contribution to, 25:12840
scattering by natural carbon at 0 to 2 MeV, angular distributions and total cross sections from elastic, (E), 25:12379 (KAPL-P-3901)
scattering by nuclei, lectures on cross sections and polarization from elastic, (T), 25:12624 (ANU-P-497)
scattering by oxygen-16, R-matrix shell-model calculations of cross sections for (T), 25:12423
scattering by plutonium-239, uranium-233, and uranium-235, interference effects in average cross section for resonance, (T), 25:12608
scattering by polarized nuclei, measurement of scattering lengths from elastic, (T), 25:12533 (TKK-F-A-123)
scattering by uranium-238 at 0.075 to 15 MeV, optical potentials for elastic, (T), 25:12510(T) (BNL-tr-366)
scattering by water at 0.04 to 0.632 MeV and 27 to 270°C, double differential cross section for inelastic, (E), 25:12342 (RPI-328-210)
spectra measurements of, fission foil--dielectric track detector for in-core, 25:10836
transport equation solution by discrete ordinates method, reduction of ray effect in, 25:12852
transport equation solutions with anisotropic scattering, monoenergetic, 25:12055
transport in heterogeneous media with sources, calculations using collision-probability method for, (T), 25:12347
transport in media, diffusion and P_1 approximations for multigroup, (T), 25:12345
transport of, solution of Boltzmann equation in plane geometry, (T), 25:12340 (KFK-1223)

NEUTRONS, COLD
production by slowing-down in cold, solid hydrogenous moderators, temperatures and spectra from, (E/T), 25:12351

NEUTRONS, EPITHERMAL
capture by heavy nuclei, cross-section ratios and gamma spectra from cascade theory, (T), 25:12626 (FMRB-33/70)

NEUTRONS, FAST
attenuation by water at 14.7 MeV, removal cross section for, (E), 25:12349
capture by calcium-40 and silicon-28 at 14 MeV, calculation of γ spectra using direct-semidirect and statistical models, (T), 25:12472
capture by nuclei A = 24 to 138 at 14 MeV, integrated cross sections for, (E), 25:12474
capture-to-fission ratio for plutonium-239 at 20 to 500 keV, (E), 25:12511 (CEA-N-1368)
derivation of kerma of, in relation to specific activity produced in threshold detector, 25:11074(R) (AECL-3777)
detection down to 1 keV, coincidence scintillation detector system with uranium-235 fission foil for, 25:10845
dosimetry in beryllium oxide mixtures with plutonium oxide, 25:11052 (AERE-R-5069)
dosimetry in tissue-equivalent phantoms following criticality accidents, 25:11057
effects on fatigue life of Types 304 and 316 stainless steel, 25:11459 (IN-1437, pp 1-4)
effects on high-pressure polymorphs of indium telluride, 25:11474(R) (BNWL-842)
effects on high-pressure polymorphs of lead oxide, 25:11474(R) (BNWL-842)
effects on high-pressure polymorphs of phosphorus, 25:11474(R) (BNWL-842)
effects on high-pressure polymorphs of silicon oxide, 25:11474(R) (BNWL-842)
effects on high-pressure polymorphs of zirconium, 25:11474(R) (BNWL-842)
effects on mechanical properties of chromium--iron--nickel alloys and nickel in water, 25:11466 (SRARI-P-78)
effects on mechanical properties of Type A203 and A353 steel weldments, 25:11454 (AECL-3734)
effects on microstructure and properties of Type 304, 316, and 348 stainless steel, 25:11474(R) (BNWL-842)
effects on sarcoma cells in rats in vitro, effects of dose fractionation on, 25:11240 (BNL-50203, pp 339-52)
effects on somatic mutations and loss of reproductive integrity in Tradescantia stamen hairs, RBE for, 25:11313
effects on sound velocity in steel, 25:11474(R) (BNWL-842)
effects on surfaces and swelling of beryllium, 25:11460 (IN-1437, pp 5-12)
effects on swelling of hafnium shim rods, 25:11460 (IN-1437, pp 5-12)
effects on tensile properties of Type 347 stainless steel, 25:12823 (RCN-125)
effects on void formation in aluminum at 55°C, electron microscopic studies of, 25:11465 (ORNL-TM-3109)
effects on voids in high-purity nickel, relations with annealing, 25:11469
reactions (n,2n) with bromine-79 and germanium-72 at 14.8 MeV, isomeric cross sections for, (E), 25:12430 (INR-P-1091)
reactions (n,p) with deuterium at 14.5 MeV, pole-diagram analysis of cross section for, (E/T), 25:12369
reactions (n,p) with titanium-46 and -48 at 4.91 to 7.04 MeV, cross sections for, (E), 25:12504
reactions (n,p2n) with deuterium at 14.1 MeV, cross sections, neutron spectra, and n--p scattering lengths from, (E/T), 25:12367
reactions with cesium at 14.8 MeV, 25:10472(R) (BMBW-FBK-70-19)
reactions with many nuclei at 14 to 15 MeV, tables of cross sections for, 25:12353 (NP-18616)
reactions with nuclei at 14 MeV, mass dependence of total cross sections for, (T), 25:12344
reactions with oriented holmium-165 at 2 to 135 MeV, total cross section for, (E), 25:12565
reactions with oxygen-16 at 6.4 to 16.5 MeV, γ production cross sections for, (E), 25:12406
scattering by bismuth-209, indium, lead, and tin at 4 MeV near 180° by polarized, differential cross sections and polarizations from elastic, (E), 25:12509(T) (ANL-Trans-855)
scattering by bromine-79 at 14.8 MeV, isomeric cross section for inelastic, (E), 25:12430 (INR-P-1091)
scattering by carbon-12 at 3.03 to 6.94 MeV, differential cross sections for inelastic, (E/T), 25:12401
scattering by carbon-12 at 3.03 to 6.94 MeV, phase-shift analysis of differential cross sections for elastic, (E/T), 25:12401
scattering by deuterium at 0.5 to 49.4 MeV, mixing parameters and phase shifts for elastic, (E), 25:12359
scattering by helium-4 at 0.2 to 7 MeV, angular distributions for elastic, (E), 25:12360

XUM

scattering by helium-4 at 1 to 18 MeV, phase shifts and effective potentials from resonating-group study of elastic, (T), 25:12363
scattering by liquid deuterium and tritium at 16.5 and 22.1 MeV, polarization in, (E), 25:12354
scattering by natural germanium, holmium-165, and tantalum-181 at 14 MeV, neutron spectra and level-density parameters from inelastic, (E), 25:12536
scattering by oxygen-16 at narrow levels in oxygen-17, differential cross sections for, (E), 25:12404
scattering by uranium at 4 MeV near 180° of polarized, differential cross sections from elastic, (E), 25:12509(T) (ANL-Trans-855)
spectra measurements in fast assemblies, proposed standard assembly for, 25:12816 (EACRP-L-74)
spectra measurements of, liquid metal cooled fast reactors, activated foils dosimetry techniques for, 25:12773 (BNWL-1403)
transmission in filters of pyrolytic graphite, characteristics of, 25:12352
transport in silicon dioxide, flux distribution and dose equivalent calculations for, 25:12332

NEUTRONS, FISSION
dose measurements of, using damage track detectors, 25:11074(R) (AECL-3777)
effects on soybean seedlings in comparison to effects of cobalt-60 γ rays and strontium-90 and yttrium-90 β particles, 25:11312
effects on tensile properties of Nimonic PE 16, relations with dose and temperature, 25:11455 (AERE-R-4982)
reactions (n,p) with silicon-28 and -29, average cross sections for, (E), 25:12460
spectra of, SAND-II calculations using activated foil data, 25:11474(R) (BNWL-842)

NEUTRONS, INTERMEDIATE
capture by lead-20 at 41 keV, gamma spectra from, (E), 25:12539
capture-to-fission ratio for plutonium-239 at 20 to 500 keV, (E), 25:12511 (CEA-N-1368)

NEUTRONS, PROMPT
lifetime of, comparison of definitions for, (T), 25:12856

NEUTRONS, THERMAL
activation disadvantage factors in water moderated natural uranium fueled lattices, Monte Carlo calculation of, (E/T), 25:12859
attenuation in moving media, deformation spectra from, (T), 25:12350
capture by calcium-40 and calcium-46, gamma spectra from, (E), 25:12491
capture by cerium-140, gamma spectra from, (E), 25:12551
capture by europium-151, gamma spectra from, (E), 25:12547
capture by lead-207, resonance effects in, (T), 25:12562
capture by molybdenum-95, γ singles and coincidence spectra and angular correlations for, (E), 25:12598
effects on α--β transformation temperature in plutonium, 25:11467
effects on corn, mutagenic for plant height, 25:11009(R) (COO-1512-22)
effects on genetic variation in populations of corn, effects of recombination and selection on, 25:11009(R) (COO-1512-22)
effects on microstructure and tensile properties of Nimonic PE 16, 25:11531 (AERE-R-4913)
effects on pure lithium fluoride powder, thermoluminescence, 25:11951
effects on random mating populations of corn, effects of recurrent mass selection on, 25:11009(R) (COO-1512-22)
effects on silicon precipitation in aluminum and aluminum--nickel alloy, 25:11471
effects on tensile properties of Nimonic PE 16, relations with dose and temperature, 25:11455 (AERE-R-4982)
effects on wheat, effects of 1.05 x 10^{13}/cm² dose on mutagenic, 25:11033(P)
effects on wheat, effects of 8.38 x 10^{12}/cm² dose on mutagenic, 25:11034(P)
flux distribution in swimming pool type research reactors, (E), 25:12826
reactions (n,f) with uranium-235, gamma spectra at 11 days from fission fragments from, (E), 25:12535
reactions with uranium-235, SAND-II calculations of cross sections and spectra of fission, 25:11474(R) (BNWL-842)
scattering by polarized niobium-93, scattering lengths from elastic, (T), 25:12533 (TKK-F-A-123)
spectra in plutonium fueled high temperature gas cooled reactor, calculation of stationary state, 25:12778

NEVADA TEST SITE
soil strain at, effects of Hutch Event underground nuclear explosion on dynamic, 25:10732

NEW YORK
radiation monitoring of environs of Knolls Atomic Power Laboratory, Schenectady, during 1968, 25:11001
radioisotope content of surface waters in, during 1969, cesium-137, strontium-90, and tritium, 25:11041

NICKEL
alpha reactions at 30 to 80 MeV, cross sections for production of K x rays by, (E), 25:12488
coercivity of single crystals of, effects of dislocations on, 25:12894 (NYO-3087-16)
compaction and sintering of powdered, effects of injected helium on, 25:11474(R) (BNWL-842)
determination as impurity in fuel materials by emission spectroscopy, 25:10432 (KFK-1261)
determination by photon activation, reactions and sensitivities for, 25:10488 (CEA-R-4072)
determination in seawater by atomic absorption spectrophotometry, 25:10428
determination in sedimentary rocks by direct-reading spectrometry, 25:10450
determination in serum and urine by flameless atomic absorption spectroscopy, 25:10464
determination of trace amounts of, in basalt and granite, correction of matrix effect in uv spectrographic, 25:10453
determination of trace amounts of, in biotite and tektite by spark source mass spectrometry, 25:10455
determination of trace amounts of, in molybdenum, review on, 25:10459
determination of trace amounts of, in rocks and sand by thermal neutron activation, ion exchange, and γ spectrometry, 25:10492
determination of trace amounts of, in rocks, quantometer for spectroscopic, 25:10451
determination of trace amounts of, in silicate rocks, method for elimination of matrix effect in quantometric, 25:10452
determination of trace amounts of, in standard bauxite, carbonate, and silicate rocks by x-ray fluorescence, 25:10449
determination of trace amounts of, in standard silicate rocks using sodium chloride buffer, emission spectrographic, 25:10454
determination of trace amounts of, in zirconium, carrier distillation method for spectrographic, 25:10430 (EUR-4541)
diffusion in beryllium and beryllium--nickel alloys, 25:11399
diffusion in uranium at 975 to 1075°C, 25:11370 (CEA-CONF-1689)
distribution coefficient in mixtures of acetone, hydrochloric acid, and methanol, 25:10681
effects on tensile properties of rolled gallium--plutonium alloys at 25 to 600°C, 25:11391
electric resistivity of, ferromagnetic effects in, 25:12895 (NYO-3087-17)
friction and wear of, sliding against copper and iron rings under vacuum, 25:11413
magnetoresistance of polycrystals of, low-field, 25:12897 (NYO-3087-23)
properties for use in thermoelectric converter heat block shield, 25:10778(R) (ORNL-TM-3214)
radiation damage in, stored-energy release and resistivity recovery from 20°K electron, 25:11977
radiation effects on mechanical properties of, in water, fast neutron, 25:11466 (SRARI-P-78)
radiation effects on voids in high-purity, relations of annealing with fast neutron, 25:11469
separation of neptunium from, by ion exchange in tetramethylammonium hydroxide--citrate solutions, effects of complexing agents on, 25:10655 (ANL-7751)
solvent properties for uranium at 975 to 1075°C, 25:11370 (CEA-CONF-1689)
strength and initial work hardening rate of, effects of microstructure on, 25:11402
surface atom thermal displacement from electron specular reflectivity, (001), (E), 25:12017

NICKEL ALLOYS AND SYSTEMS
Al--Cr--Ni-base, creep at high temperatures, effects of cold rolling and shock loading on, 25:11434(R) (SU-326-P-17-X-1)
Al--Ni-base, creep at high temperatures, effects of second phases on, 25:11434(R) (SU-326-P-17-X-1)
Al-base--Ni, radiation effects on silicon precipitation in, thermal neutron, 25:11471
Be-base--Ni, diffusion of nickel in, 25:11399
Cr--Fe--Ni, radiation effects on mechanical properties of, in water, fast neutron, 25:11466 (SRARI-P-78)
Cr--Ni-base, production of controlled grain-size, method for, 25:11434(R) (SU-326-P-17-X-1)
Cr--Ni-base, strength and initial work hardening rate of, effects of microstructure on, 25:11402
Cr--Ni-base--ThO_2, strength and initial work hardening rate of, effects of microstructure on, 25:11402
Cu--Ni--Zr-base, phase transformations in, effects of continuous cooling on, 25:11432 (CEA-N-1310)
Er--Ni, magnetic structure of intermetallic $ErNi_3$ and Er_2Ni_7, 25:11979 (CEA-CONF-1704)
Ho--Ni, magnetic structure of intermetallic $HoNi_3$, 25:11979 (CEA-CONF-1704)
Mn--Ni-base--Ta, properties of, electric and magnetic, 25:12008
Mo--Ni, ordering in Ni_4Mo, short-range, 25:11452
Ni--W, creep of solid-solution, parameters for high-temperature, 25:11434(R) (SU-326-P-17-X-1)
Ni-base--Si, radiation damage in, stored-energy release and resistivity recovery from 20°K electron, 25:11977
Ni-base--ThO_2, strength and initial work hardening rate of, effects of microstructure on, 25:11402
Ni-base--W, creep of solid solutions of, high-temperature, 25:11408

NICKEL FLUORIDES
reactions in, emf measurements of solid-state displacement, 25:11473(R) (AD-708712)
NICKEL HYDROXIDES
precipitation of carrier-free silicon-31, 25:10675
NICKEL ISOTOPES Ni-58
alpha reactions (α,He-3) and (α,t) at 44 MeV, optical-model analysis of angular distributions and energy spectra from, (E/T), 25:12434
energy level at 2942.5 keV from copper-58 beta decay, lifetime of, (E/T), 25:12481
energy levels from nuclear resonance fluorescence, radiative widths for, (E), 25:12478
energy-level transitions from copper-58 beta decay, branching ratios and rates for, (E/T), 25:12481
energy-level transitions from nuclear resonance fluorescence, probabilities for M1, (E), 25:12478
photon resonance scattering at 4.2 MeV, gamma spectra from, (E), 25:12478
proton elastic and inelastic scattering at 5.38 to 5.95 MeV, polarization angular distributions from, (E), 25:12433 (NP-16552)
proton reactions (p,pn) and (p,p2n) at 400 MeV, angular distribution of recoils from, (E), 25:12500
proton reactions (p,t) at 51.9 MeV, differential cross sections for, (E), 25:12431 (INSJ-124)
NICKEL ISOTOPES Ni-59
energy levels from cobalt-59 (p,n) and (p,nγ) reactions, spin--parity assignments for, (E/T), 25:12476
energy levels from nickel-58 (α,He-3) reactions at 44 MeV, spectroscopic factors and spin--parity assignments for, (E/T), 25:12434
energy levels of, calculation using modified Tamm--Dancoff approximation, (T), 25:12451
energy levels of, shell-model calculation using Kuo-Brown matrix elements, (T), 25:12451
energy-level transitions from cobalt-59 (p,n) and (p,nγ) reactions, branching ratios for, (E/T), 25:12476
NICKEL ISOTOPES Ni-60
alpha reactions (α,He-3) and (α,t) at 44 MeV, energy spectra from, (E/T), 25:12434
energy levels from nuclear resonance fluorescence, radiative widths for, (E), 25:12478
energy-level transitions from nuclear resonance fluorescence, probabilities for M1, (E), 25:12478
photon resonance scattering at 4.2 MeV, gamma spectra from, (E), 25:12478
proton elastic scattering at 10 to 60 MeV, local Woods--Saxon potentials equivalent to nonlocal analysis including exchange effects in, (T), 25:12689
NICKEL ISOTOPES Ni-61
energy levels of, calculation using modified Tamm--Dancoff approximation, (T), 25:12451
NICKEL ISOTOPES Ni-62
alpha reactions (α,He-3) and (α,t) at 44 MeV, energy spectra from, (E/T), 25:12434
energy levels from photon resonant scattering from, spin assignments for, (E), 25:12554
energy-level transitions from photon resonant scattering from, branching ratios and multipolarities for, (E), 25:12554
NICKEL ISOTOPES Ni-63
energy levels of, calculation using modified Tamm--Dancoff approximation, (T), 25:12451
NICKEL ISOTOPES Ni-64
alpha reactions (α,He-3) and (α,t) at 44 MeV, optical-model analysis of angular distributions and energy spectra from, (E/T), 25:12434
NICKEL ISOTOPES Ni-65
energy levels from nickel-64 (α,He-3) reactions at 44 MeV, spectroscopic factors and spin--parity assignments for, (E/T), 25:12434
energy levels of, calculation using modified Tamm--Dancoff approximation, (T), 25:12451
NICKEL OXIDES
preparation of monocrystalline, method for, 25:11472(R) (AD-708705)
sorptive properties of aqueous suspensions of, for tellurium, 25:10583(R) (AECL-3776)
NICKEL SULFATES
crystallization of hydrates of, from tritiated solutions, fractionations of tritium in, 25:10688
NIMONIC PE 16
radiation effects on microstructure and tensile properties of, thermal neutron, 25:11531 (AERE-R-4913)
radiation effects on tensile properties of, relations of dose and temperature with fission and thermal neutron, 25:11455 (AERE-R-4982)
NIOBIUM
analysis for carbon, nitrogen, and oxygen by helium-3 and photon activation and radiochemical separation, 25:10488 (CEA-R-4072)
corrosion by liquid lead at high temperatures, 25:11376 (JUL-661-RW)
corrosion of oxide-covered, in aqueous solutions to 250°C, electrochemical measurement of, 25:11354
determination of trace amounts of, in biotite and tektite by spark source mass spectrometry, 25:10455
determination of trace amounts of, in molybdenum, review on, 25:10459
diffusion in zirconium at 800 to 1600°C, x-ray spectral study of, 25:11424
dislocation kinks, structure and energy of screw, 25:12027
energy-level transitions in, rates of Auger and x-ray, (T), 25:11685
interactions with tantalum silicide coating, 25:11519
oxidation at 200 to 600°C, ellipsometry method for studying, 25:11355
reactions with nitrogen and oxygen, review of kinetics, mechanisms, and thermodynamics of degassing and engassing, 25:11415
separation from cadmium, indium, molybdenum, palladium, and rhodium by gas chromatography using aluminum chloride eluent, 25:10666 (JINR-P6-5410)
separation from ores by solvent extraction, review on, 25:10656 (BM-IC-8502)
solubility in lead at 350 to 1100°C, 25:11376 (JUL-661-RW)
superconducting critical field in oriented films of, microstructural effects on anisotropy of, (E), 25:11832
superconducting energy gaps for s and d bands in single crystals of, tunneling study, (E/T), 25:11830
superconducting transition temperature of, effect of neutron irradiation at 4.6°K, 25:11848
superconducting transition temperature of, pressure dependence of, (E), 25:11849
surface impedance of, in mixed S/N state, (T), 25:11828
NIOBIUM ALLOYS AND SYSTEMS
Al--Nb, niobium-93 NMR in Nb_3Al, 25:12037
Au--Nb, niobium-93 NMR in Nb_3Au, 25:12037
Ir--Nb, niobium-93 NMR in Nb_3Ir, 25:12037
Nb--Sn, development of superconducting ribbons of intermetallic Nb_3Sn, 25:11820 (LNF-70/18)
Nb--Sn, niobium-93 NMR in Nb_3Sn, 25:12037
Nb--Ti, mechanical properties of, effects of copper and germanium on, 25:11416
Nb--Ti, superconducting critical current density of, effects of annealing, composition, and swaging on, 25:11416
Nb--Ti, superconducting wire of, use in wired-wall cavity for V-band ENDOR, 25:11850
Nb--U-base--Zr, corrosion by moisture, stress, 25:11345 (AWRE-O-49/66)
Nb--U-base--Zr, welding behavior of, electron beam, 25:11377 (MLM-1778)
Nb--Zr, superconducting ac hysteresis losses in wires of, suppression by longitudinal magnetic field, 25:11823
Nb--Zr-base, radiation effects on creep at 300°C, in-pile, 25:11474(R) (BNWL-842)
NIOBIUM ISOTOPES Nb-91
energy levels from zirconium-90 (He-3,d) reactions, spectroscopic factors and spin-parity assignments for, (E), 25:12613
NIOBIUM ISOTOPES Nb-92
energy levels of, particle-hole interactions in, (T), 25:11888
NIOBIUM ISOTOPES Nb-93
alpha reactions (α,αn), (α,2p), and (α,xn) at 15 to 41 MeV, excitation functions for, (E), 25:12568
alpha reactions at 30 to 80 MeV, cross sections for production of K x rays by, (E), 25:12488
deuteron reactions (d,p) at 5 to 10 MeV, charge-exchange threshold effects in, (E), 25:12588
neutron elastic scattering from polarized, scattering lengths for thermal, (T), 25:12533 (TKK-F-A-123)
nuclear magnetic resonance in Nb_3X compounds with X = Al, Sn, Au, Ir, 25:12037
proton reactions at 500 and 720 MeV, cross sections for spallation products from, (T), 25:12439
NIOBIUM ISOTOPES Nb-94
beta decay of, β--γ angular correlations in, (E/T), 25:12555
NIOBIUM ISOTOPES Nb-95
separation of plutonium from, by ion exchange on zirconium phosphate silicate columns, 25:10677
NIOBIUM ISOTOPES Nb-99
beta decay of, beta and gamma spectra, half-life, log ft, and Q-value for, (E), 25:12462
decay of, 25:10472(R) (BMBW-FBK-70-19)
energy levels of, spin and parity of, (E), 25:12462
NIOBIUM ISOTOPES Nb-100
beta decay of, beta and gamma spectra, half-life, log ft, and Q-value for, (E), 25:12462
NIOBIUM ISOTOPES Nb-101
beta decay of, beta and gamma spectra, half-life, log ft, and Q-value for, (E), 25:12462
energy levels of, spin and parity of, (E), 25:12462
NIOBIUM SILICIDES
diffusion of silicon in Nb_5Si_3, activation energy for, 25:11519
NITRIDES
analysis of layers of, on silicon for oxygen by deuteron (d,p) reactions, 25:10583(R) (AECL-3776)
NITROGEN
abundance of geomagnetically trapped nuclei of, (E), 25:11744
determination by charged particle and photon activation, radiochemical separation methods for, 25:10488 (CEA-R-4072)
determination by charged particle and photon activation, reactions and sensitivities for, 25:10488 (CEA-R-4072)

determination in aluminum by charged particle activation and radiochemical separation, 25:10488 (CEA-R-4072)
determination in iron and niobium by photon activation and radiochemical separation, 25:10488 (CEA-R-4072)
determination of trace amounts of, in molybdenum, review on, 25:10459
determination of trace amounts of, in Zircaloy, Zircaloy-2, and zirconium using thymol, spectrophotometric, 25:10442
deuteron reactions at 30 to 120 keV with molecular, cross sections for electron capture into 3s state of deuterium in, (E>, 25:11708
ion stopping in gaseous, electronic, (T), 25:11680
ionization in upper atmosphere, x-ray emission properties of atomic, (E/T), 25:11790
plasma of, line shapes of resonance multiplets in, (E), 25:11881
proton reactions at 0.3 to 1.7 MeV with molecular, angular and energy distributions of electrons ejected from, (E), 25:11712
proton reactions at 30 to 120 keV with molecular, cross sections for electron capture into n = 3 level of hydrogen in, (E), 25:11708
radiation effects on metabolism of, in corn seedlings following seed exposure, ionizing, 25:11309
reactions with carbon--uranium dioxide mixtures to produce uranium nitride, 25:11478 (BNWL-843)
reactions with molybdenum, niobium, tantalum, tungsten, and vanadium, review of kinetics, mechanisms, and thermodynamics of degassing and engassing, 25:11415
sorption by tantalum films at 150 to 500°K, chemical and physical, 25:11419
sorption by tantalum films at 273 to 370°K, 25:11417
yields from γ radiolysis of liquid cyclopentane in nitrous acid solutions, effects of pressure on, 25:10628

NITROGEN IONS
reactions with argon at 10 to 150 keV, coincidence study of, 25:11704
reactions with platinum, angular and energy distributions of charged particles emitted in, (E), 25:11675

NITROGEN IONS (N+)
reactions with argon at keV energies, statistical-model calculations of ionization probabilities in, 25:11711

NITROGEN ISOTOPES
effects on reaction mechanisms, effects of temperature on kinetic, 25:10549

NITROGEN ISOTOPES N-14
deuteron elastic scattering at 3.5 MeV, optical-model analysis of, (T), 25:12405
deuteron reactions (d,α) at 30 MeV, internal bremsstrahlung spectra for, (T), 25:12694
deuteron reactions (d,n) at 3.5 MeV, DWBA analysis of cross section and polarization data in, (T), 25:12405
mesen (μ^-) capture by, capture rate and gamma--neutrino angular correlations for, (T), 25:12386
neutron capture by, gamma spectra and Q-value for thermal, (E), 25:12403
proton reactions (p,2p) at 46 MeV, energy spectra and distorted-wave t-matrix approximation analysis of differential cross sections from, (E/T), 25:12391
reactions with natural silver and silver-109 at 78 and 113 MeV, analysis for reaction mechanisms in, (E), 25:12606
scattering by tellurium-123 and -125 at 44 and 48 MeV, gamma spectra from, (E), 25:12603

NITROGEN ISOTOPES N-15
determination relative to carbon-12 in biological samples by proton reaction methods, 25:10491 (ORNL-4636, pp 20-33)
effects on microwave spectra of first-excited torsional states of dimethylamine, 25:10551
effects on microwave spectra, structure, quadrupole coupling constant, and force constants of nitrogen sulfide chloride, 25:10532
energy levels from carbon-14 (p,γ) reactions, partial widths and spin assignments for first two T = 3/2, (E), 25:12416
energy-level transitions from carbon-14 (p,γ) reactions, branching and multipole mixing ratios for T = 3/2, (E), 25:12416
helium-3 reactions (He-3,α) at 11 MeV, spectroscopic factors for, (E), 25:12424

NITROGEN ISOTOPES N-16
beta decay of, half-life for, (E), 25:12394

NITROGEN MUSTARDS
use for therapy of carcinomas, dosimetry of, using iron-59, 25:10952

NITROGEN OXIDES
free radicals in elastomers, piperidine, and pyrrolidine, NMR study of, 25:12034 (CEA-R-3855)

NITROGEN OXIDES NO
density profiles at 70 to 110 km, effect on daytime D-region ionization, (E), 25:11795
N--NO, radiation effects on, spectral studies on 1.5-MeV electron, 25:10586 (JAERI-5026, pp 155-7)

NITROGEN SYSTEMS
Ar--N, radiation effects on, spectral studies on 1.5-MeV electron, 25:10586 (JAERI-5026, pp 155-7)
N--NO, radiation effects on, spectral studies on 1.5-MeV electron, 25:10586 (JAERI-5026, pp 155-7)
N--O, radiation effects on, spectral studies on 1.5-MeV electron, 25:10586 (JAERI-5026, pp 155-7)

NORBORNANE
radiolysis of deuterated and nondeuterated derivatives of, ESR spectral studies of free radicals from γ, 25:10637
radiolysis of, ESR spectral studies of radicals from γ, 25:10638

NORTH AMERICA
radioactivity of atmosphere and precipitation of, during 1970, gross β, 25:11939

NOVAE
radio observations of Serpentis 1970 and Delphini 1967, (E), 25:11599
velocities in shell of Her 1963, radial, (E), 25:11547

NUCLEAR AUXILIARY POWER SYSTEMS
design of radioisotope-fueled, using submerged heat source to produce mercury vapor, 25:10788(P)
heat pipes for space and undersea, performance of cylindrical, 25:10755 (ORNL-TM-2803)

NUCLEAR BATTERIES
development of radioisotope-fueled, for implantable cardiac pacemakers, fabrication and testing program for, 25:10777(R) (NUMEC-4189-3)

NUCLEAR ELECTRIC MOMENTS
measurements using nuclear reorientation effect, 25:12522 (LYCEN-7034, pp 42-57)

NUCLEAR EMULSIONS
cosmic nucleon reactions with nuclei, at 10^{12} to 10^{13} eV in, particle composition of showers from, (E), 25:12093
meson (μ) scattering at 2.5 to 14.8 GeV/c at small angles in, multiple scattering techniques and particle energy determination from angular distributions in, (E), 25:12089
multiple scattering techniques using, μ scattering by nuclei at 2.5 to 14.8 GeV/c at small angles for study of, (E), 25:12089
particle tracks in, semiautomatic scanning system for analysis of, 25:10839
proton recoil spectra in, geometric correction factors for, 25:10867 (CEA-R-4081)

NUCLEAR ENGINEERING
standards for development of nuclear power plants in U.S, 25:12758

NUCLEAR EXPLOSIONS
book: International Arrangements and Control for the Peaceful Applications of Nuclear Explosives, 25:10751
conference on industrial and scientific uses of, Grenoble, France, May 20 to 22, 1970, 25:10744
conference on industrial and scientific uses of, Grenoble, France, May 20 to 22, 1970, 25:10738
effects on physical properties of porous and solid bodies, 25:10749
fallout from Shot Coulomb C, radiochemical analysis of, 25:10734 (AD-708567)
uses in industry and science, design criteria for explosive charges for, 25:10739
uses in industry, economics of, 25:10750

NUCLEAR EXPLOSIONS, ATMOSPHERIC
acoustic wave propagation from, geophysical uses of data on, 25:10748
airblasts from, damage to window panes from, (E/T), 25:10792 (SC-RR-70-441)
effects of Chinese, on cesium-137 and strontium-90 content of Fayetteville, Arkansas rainwater, May 1965 to April 1970, 25:10713 (ORO-2529-28, App. 7)
effects of Chinese, on strontium-89/-90 ratio in Fayetteville, Arkansas rainwater, 1964 to 1969, relations with jet stream location, 25:10708 (ORO-2529-28, App. 2)
effects of Dec. 1968 Chinese, on fallout content of Fayetteville, Arkansas rainwater, (E), 25:10709 (ORO-2529-28, App. 3)
effects of Dec. 1968 Chinese, on fallout content of Fayetteville, Arkansas rainwater, (E), 25:10707 (ORO-2529-28, App. 1)
effects of Oct. 1969 Chinese, on strontium-89/-90 ratio in Fayetteville, Arkansas rainwater, 25:10710 (ORO-2529-28, App. 4)
fallout from Chinese May 9, 1966, effects on zirconium-95 content of crops in Utah during May and June, 25:10999
fallout from eighth and ninth Chinese, 25:10472(R) (BMBW-FBK-70-19)
fallout from Shot Priscilla, radiochemical analysis of, 25:10733 (AD-708566)

NUCLEAR EXPLOSIONS, HIGH-ALTITUDE
photography of, film analysis and interpretation in, 25:10693 (EGG-1183-484)

NUCLEAR EXPLOSIONS, UNDERGROUND
effects of contained 100 kt, on surrounding medium, mechanical, 25:10741
effects of Hutch Event, on dynamic strain in nearby soils, (E), 25:10732
effects of, review of methods for predicting, 25:10745
effects on seismic activity in western US, (E), 25:10731
Nuclear Rocket Development Station area seismic response to NTS, characteristics of, (E), 25:10730 (NVO-1163-TM-22)
radioisotope distribution and production by, methods for prediction of, 25:10742
safety of contained and cratering, review of chemical,

radiological, and seismic, 25:10743
seismic effects of Sahara Desert, on surrounding granite, 25:10728 (CEA-R-4059)
seismic waves from Sahara Desert, effects of explosion conditions and surrounding medium on amplitude of, (E/T), 25:10729 (CEA-R-4105)
use for construction of interoceanic canal, feasibility studies on, 25:10995 (BMI-171-45)
use for construction of proposed interoceanic canal, dose estimation studies related to, 25:11055 (ORNL-4579)
uses in geophysical research, 25:10748
uses in industry and science, review of, 25:10745
uses in mining, review of, 25:10747
uses in petroleum industry, economic and technical aspects of, 25:10746
uses of, contribution of earth sciences to peaceful, 25:10740

NUCLEAR MAGNETIC MOMENTS
measurements using NMR destruction of nuclear orientation, 25:12521 (LYCEN-7034, pp 34-41)

NUCLEAR MAGNETIC RESONANCE
spectrometer with superconducting solenoid, 310-MHz, 25:12034 (CEA-R-3855)

NUCLEAR MATTER
binding energy of impurity particles in, approximate expression in closed form for, (T), 25:12650
binding energy of, calculations for various potentials, (T), 25:12698
binding energy of, model dependence of, (T), 25:12642
hyperon (A) binding energy in, calculation using AN tensor force, (T), 25:12668
nucleon effective mass in, (T), 25:12677
surface energy of semi-infinite, calculation using two-bcdy spin-orbit potentials, (T), 25:12675

NUCLEAR MODELS
alpha-particle, binding energy, elastic form factor, and rms radius from, (T), 25:12663
cluster, evidence for (t + He-3) clusters in lithium-6, (T), 25:12372
collective, classification of energy levels and interactions in, (T), 25:12631 (JINR-P4-5008)
collective, macroscopic self-consistency relation for deformed nuclei, (T), 25:12655
collective, matrix elements of quadrupole moment operator and E2 transitions in, (T), 25:12633 (JINR-P4-5346)
collective, transition operators for coupling in, (T), 25:12702
optical, exchange effects in nucleon--nucleus, (T), 25:12689
shell, application to nuclear reactions involving two-particle continuum states, (T), 25:12625 (COO-1764-85)
shell, level-density formula for, (T), 25:12688
shell, matrix elements of effective interaction for, (T), 25:12686
single-particle, computer program for calculations using ellipsoidal modified oscillator potential of, 25:12623 (AECL-3730)

NUCLEAR ORIENTATION
temperature scale for, using γ anisotropy of ^{60}Co in neodymium zinc nitrate, 25:11852
theory of polarization of nuclei with ultrasound, 25:12007

NUCLEAR PARTICLES
book: Physics of Nuclei and Particles. Volume II, 25:12662

NUCLEAR PHYSICS
book: Physics of Nuclei and Particles. Volume II, 25:12662
research at Atomic Energy of Canada Limited, Oct. 1 to Dec. 31, 1969, 25:12427(R) (AECL-3666)
research at Central Bureau for Nuclear Measurements during 1969, 25:12516(R) (EUR-4525)
research at Triangle Universities Nuclear Laboratory Oct. 1, 1968 to Sept. 1, 1969, 25:12534(R) (TUNL-2)

NUCLEAR POWER PLANTS
components for, development of deformation and stress analysis methods for design of, 25:10758
development in U. K., program for, 25:12713
development in U.S., nuclear engineering standards for, 25:12758
development in U.S.S.R., review of, 25:12709
economics within a utility system, discounted cash flow method for calculation of, 25:12724 (TRG-Report-2090)
environmental effects of U. S., programs for reduction of, 25:12761
licensing and regulation of, evaluation of state legislation for, 25:11087 (CONF-700408-3)
radioactive effluents from, standards in Sweden of limits for, 25:12757 (SSI-70-27)
regulatory actions on U. S., review of, 25:12762
siting of, long-term ecological effects of radiation releases from, 25:12763
siting of, review of studies for offshore, 25:12765

NUCLEAR REACTIONS
analysis of heavy-ion transfer, using DWBA and Glauber approximation, (T), 25:12683
cross sections for, S-matrix representation for polarized particles of arbitrary spin, (T), 25:12652
K matrix for, properties of, (T), 25:12669
nucleon transfer in heavy-ion induced, macroscopic model for analysis of, (T), 25:12661
off-shell effects in knockout, calculation using impulse approximation and Faddeev equations, (T), 25:12670
polarization phenomena in, statistical analysis of, (T), 25:12699
polarizations for, S-matrix representation for polarized particles of arbitrary spin, (T), 25:12652
resonances in, unitarity constraints for multiple, (T), 25:12643
theory for, research at University of Maryland, 25:12639(R) (ORO-3765-28)

NUCLEAR REACTIONS (DIRECT)
angular distributions of (He-3,t) and (p,n), shapes of, (T), 25:12648
exchange effects for composite particles in, (T), 25:12691
internal bremsstrahlung spectra for, description by triangle mechanisms, (T), 25:12694
shell-model approach to, two-particle continuum states in, (T), 25:12625 (COO-1764-85)
Sopkovich approximation for, test of validity of, (T), 25:12641 (RLO-1388-595)

NUCLEAR STRUCTURE
calculations for deformed even-even nuclei spin-vibrational states, (T), 25:12703
calculations for high-spin rotational states of deformed nuclei using extended cranking model, (T), 25:12654
calculations for light nuclei using four-body correlations, effect of ground-state correlations in, (T), 25:12660
calculations for rare earth region using hexadecapole deformation and rotation-particle coupling, (T), 25:12674
calculations using variational and Hartree methods, hard-core potential representation by delta derivative interaction in, (T), 25:12659
description for ground-state bands in even-even nuclei, 25:12640 (OU-LNS-70-2)
description of rotational, using Beliaev--Zelevinsky method, (T), 25:12671
descriptions for spherical nuclei, survey on shell-model, 25:12634 (LYCEN-7034, pp 147-72)
Faddeev equations for general case of three particles with spin, angular-momentum decomposition for, (T), 25:12692
Hartree--Fock calculations in 2s-1d shell, particle-hole admixtures to, (T), 25:12682
of complex nuclei, information from alpha and gamma transitions, 25:12629 (JINR-E4-5135)
quasi-particle factorization of j shells of nuclei, development of, (T), 25:12666
research at University of Maryland, theoretical, 25:12639(R) (ORO-3765-28)
research on closed-shell and near-closed-shell nuclei, review of, 25:12432 (LYCEN-7034, pp 117-46)

NUCLEAR THEORY
alpha--nucleon potential obtained from double-folding procedure, real part of, 25:12627 (INP-720)
angular-momentum decomposition of the three-body problem in, 25:12644
Coulomb effect on p-p low-energy scattering parameters, 25:12680
derivation of the variable moment of inertia model in, 25:12638 (NYO-2171-334)
electromagnetic transitions and moments, pairing factors, and signs of mixing ratios for, 25:12665
equivalent local potentials in, derivation from nonlocal separable potentials, 25:12658
five-nucleon systems in, 2p-1h shell-model calculation for, 25:12371
gamma vibration of deformed nuclei at equilibrium and the saddle point, 25:12628 (INR-P-1201)
nucleon--nucleon potentials, dependence of saturation on smoothness of, 25:12698
quasi-particle method in, boson method and antisymmetrization in, 25:12697
rotational motion, microscopic theory of, 25:12647
saturation of nuclear forces, implications for nuclear models of, 25:12636 (NP-18580)
spectral theory for the Klein--Gordon equation with an external electrostatic potential, 25:12679
sum rules in nuclear physics, derivation of progenitor, 25:12637(R) (NYO-2171-328)
T-matrix in, construction from symmetric part, 25:12673
three-body problem in, solution using Hilbert--Schmidt kernels in two variables, 25:12693
three-nucleon equations in, derivation using separable two-body potentials, 25:12687

NUCLEAR WEAPONS
control of, problems in establishing international arrangements for, 25:10751

NUCLEI
alpha reactions (α,xn) and (α,pxn) with Z = 20 to 100, excitation functions and thick-target yields for, (T), 25:12529(T) (ORNL-tr-3020)
binding energy of, Thomas--Fermi approximation for, (T), 25:12635 (NP-18545)
charged-particle reactions with Z = 1 to 98, nuclear data tables reaction list for, 25:12366
deuteron elastic scattering, lectures on cross sections and polarization from, (T), 25:12624 (ANU-P-497)
deuteron reactions (d,p) with, lectures on polarization in, (T), 25:12624 (ANU-P-497)

deuteron reactions (d,xn) and (d,pxn) with Z = 20 to 100, excitation functions and thick-target irradiation yields for, (T), 25:12529(T) (ORNL-tr-3020)
deuteron scattering by, strength of tensor interaction in optical potential for, (T), 25:12684
electron inelastic scattering by light, Coulomb-distortion effects in M2 electroexcitation by, (T), 25:12657
energy levels from gamma resonance scattering, level widths for, (E), 25:12490
energy levels of A = 182 to 192, lifetimes and spin--parity assignments for, (E), 25:12512 (CERN-70-29)
energy levels of deformed odd-A, magnetic dipole transition probabilities for ground-state rotational-band, (T), 25:12656
energy levels of deformed, coupling mechanisms between, (T), 25:12525 (LYCEN-7034, pp 94-116)
energy levels of deformed, extended cranking-model calculation of moment of inertia for rotational, (T), 25:12654
energy levels of interacting nucleons in p-shell, effects of pairing correlations on, (T), 25:12409
energy levels of light, effect of ground-state correlations in calculations using four-body correlations, (T), 25:12660
energy levels of, boson method and antisymmetrization of, (T), 25:12697
energy levels of, computer program using Ritz combination principle for discovery of excited, (T), 25:12519 (KFK-1247)
energy levels of, determination of excitation energies for rotational, (T), 25:12695
energy levels of, increasing complication with excitation energy of, (T), 25:12630 (JINR-E4-5469)
energy levels of, structure information from alpha and gamma transitions, (T), 25:12629 (JINR-E4-5135)
energy levels of, unified derivation of cranking-model and Peierls--Yoccoz expressions for energy of rotational, (T), 25:12646
energy-level transitions in A = 182 to 192, relative intensities, internal conversion coefficients, and multipolarities of, (E), 25:12512 (CERN-70-29)
excitation energy of, dependence of average nuclear field on, (T), 25:12632 (JINR-P4-5084)
gamma vibration of deformed, at equilibrium and the saddle point, (T), 25:12628 (INR-P-1201)
heavy ion anelastic scattering by Z = 8 to 26, macroscopic model for, (T), 25:12661
meson (μ) scattering at 2.5 to 14.8 GeV/c at small angles in emulsions, multiple scattering techniques and particle energy determination from angular distributions in, (E), 25:12089
neutron capture at 14 MeV by A = 24 to 138, integrated cross sections for fast, (E), 25:12474
neutron capture by heavy, cross-section ratios and gamma spectra from cascade theory, (T), 25:12626 (FMRB-33/70)
neutron elastic scattering from polarized, measurement of scattering lengths from, (T), 25:12533 (TKK-F-A-123)
neutron elastic scattering, lectures on cross sections and polarization from, (T), 25:12624 (ANU-P-497)
neutron reactions at 14 MeV, mass dependence of total cross sections for, (T), 25:12344
nuclear properties of Z greater than or equal to 83, summary of work in France on, 25:12524 (LYCEN-7034, pp 84-93)
nucleon inelastic scattering by, formalism for, (T), 25:12701
photon absorption by, limits of validity of Siegert's theorem in, (T), 25:12649
photon reactions at high energies, vector-meson dominance model for, 25:12151
photon scattering in field of, polarization of electron pairs and photons from, (T), 25:12158
polarization of, possibility of, using ultrasound, (T), 25:12007
production from proton spallation of medium-weight nuclei at 60 MeV to 2.9 GeV, cross sections for, (T), 25:12439
proton elastic scattering, lectures on cross sections and polarization from, (T), 25:12624 (ANU-P-497)
proton inelastic scattering by, exchange effects with realistic interaction for, (T), 25:12676
proton reactions (p,2p) with, off-shell effects in, (T), 25:12670
proton reactions (p,d) with, lectures on polarization in, (T), 25:12624 (ANU-P-497)
proton reactions (p,xn) with Z = 20 to 100, excitation functions and thick-target yields for, (T), 25:12529(T) (ORNL-tr-3020)
reorientation effect for, review on theory for, 25:12522 (LYCEN-7034, pp 42-57)
symmetry for, matrix elements of finite transformations of U(n), (T), 25:12235

NUCLEI (CELLS)
volume in seed plants, effects of, on x-radiosensitivity, 25:11020

NUCLEIC ACID, DEOXYRIBO-
radiation effects on binding of tritium-labeled dactinomycin by, of hepatocytes of mice, effects of administration route on x, 25:11285
radiation effects on synthesis of, in cultured mammalian cells, molecular basis for effects of exogenous DNA on restoration following x, 25:11243
radiation effects on synthesis of, in salivary glands of Drosophila larvae, x, 25:11246
radiation effects on, extraction of, from HeLa cells, effects of dose on uv, 25:10975
radioinduced chain breaks in, for studies on molecular weight dependence of genetic transcription, 25:10977
radioinduced changes in composition and content of pyrimidine nucleotides in, of cotton shoots following seed exposure, γ, 25:11307
radioinduced damage in, of Micrococcus luteus, use of nucleases for determining uv, 25:10959 (BNL-50203, pp 27-40)
radioinduced damage of, in Escherichia coli, study of repair mechanisms in uv, 25:11008 (BNL-50203, pp 14-26)
radioinduced damage of, protective effects of chloride ions against γ, 25:10962
radioinduced single strand breaks in, of Escherichia coli, effects of temperature on x, 25:11007 (BNL-50203, pp 1-13)
radioinduced single-strand breaks in, of P388 F cells, effects of dose rate on electron, 25:11028
radiosensitivity in vivo and in vitro, comparison of, 25:10966
radiosensitivity of sedimentation rate of, in Bacillus subtilis, effects of dose on x, 25:10960 (BNL-50203, pp 82-90)
repair replication of, in uv-irradiated Escherichia coli, 25:11008 (BNL-50203, pp 14-26)
synthesis in Escherichia coli, effects of, on sensitivity to phosphorus-32 decay products, 25:10946

NUCLEIC ACID, RIBO-
comparison of molecules of, in animal cells by oligonucleotide analysis, 25:11074(R) (AECL-3777)

NUCLEOGENESIS
effects of energetic proton fluxes on, (T), 25:11544
energetics of light-nuclei formation in stellar atmospheres, (T), 25:11548
proton-bombardment reactions for, of light elements, (T), 25:11542 (NP-18591)
rate of triple-alpha reactions, (E), 25:11565

NUCLEONS
coupling constants of, test of tensor meson dominance from, (T), 25:12216
form factor of, phenomenological analysis of infinite resonance model for electromagnetic, 25:12153
form factors and mean charge radius from vector dominance model, 25:12141
form factors from pole dominance and Veneziano model for $\pi + N \to \pi + N$ and $\pi + N \to N + A_1(\mathrm{rho})$ interactions, electromagnetic and axial, (T), 25:12144
form factors of, superconvergent dispersion sum rules for model for electromagnetic, (T), 25:12147
interactions anti $K + N \to \pi + \Sigma(A)$ at high energies, tests of Regge-pole and strong-absorption models for, (T), 25:12206
interactions anti $N + N \to \pi + \mathrm{rho}$, multichannel N/D equations for bound-state mass of π in, (T), 25:12202
interactions anti N + N at high energies, SU(3) symmetry and exchange degeneracy in Regge pole--cut model for, (T), 25:12217
interactions anti ν + N, form factors and differential and total cross sections for Δ and Σ resonance production in, (T), 25:12174
interactions e + N review of duality and resonance behavior in inelastic, (E/T), 25:12068 (SLAC-PUB-842)
interactions e + N, hadronic s-channel helicity conservation for 2π production in diffractive, (T), 25:12165
interactions $\gamma + N \to \pi + N$, continuous-moment sum rules for, (T), 25:12207
interactions in p-shell nuclei, effects of pairing correlations on, (T), 25:12409
interactions K + N at high energies, SU(3) symmetry and exchange degeneracy in Regge pole--cut model for, (T), 25:12217
interactions K^- + N on bound nucleons at low energies, effect of $\Lambda(1405)$ on, (T), 25:12213
interactions K^- + N, duality condition for resonance contribution to backward, (T), 25:12215
interactions Λ + N in p-state of $A\text{-}O^{17}$, (T), 25:12226
interactions Λ + N, ΛN tensor force for scattering, 25:12668
interactions Λ + N, review of, 25:12232
interactions N + N at high energies in parton model, cross sections for inelastic, 25:12222
interactions N + N at high energies, SU(3) symmetry and exchange degeneracy in Regge pole--cut model for, (T), 25:12217
interactions N + N at very high energies in cosmic-ray jets, fireball mechanism for particle production in, 25:12230
interactions N + N, continuous-moment sum rules for, (T), 25:12207
interactions ν + N, form factors and differential and total cross sections for Δ and Σ resonance production in, (T), 25:12174
interactions p + N at 210 MeV, upper limits for two parity-violating parameters from asymmetries in, (E),

25:12094
interactions π + N → K + Σ(Λ) at high energies, tests of Regge-pole and strong-absorption models for, (T), 25:12206
interactions π + N → N + A_1(rho), nucleon electromagnetic and axial form factors from pole dominance and Veneziano model for, (T), 25:12144
interactions π + N → ω + N(Δ), rho^0--ω mixing effects on spin density matrix of ω in, (T), 25:12208
interactions π + N → π + N, nucleon electromagnetic and axial form factors from pole dominance and Veneziano model for, (T), 25:12144
interactions π + N at high energies in parton model, cross sections for inelastic, 25:12222
interactions π + N at high energies, SU(3) symmetry and exchange degeneracy in Regge pole-cut model for, (T), 25:12217
interactions π + N at low and intermediate energies, three-channel model for p-wave, 25:12221
interactions π + N at low energies, duality from Regge parametrization for P_{11} and S_{11} partial waves in, (T), 25:12211
interactions π + N in urbaryon rearrangement model, dip-bump structure of cross sections for, 25:12219
interactions π + N, continuous-moment sum rules for, (T), 25:12207
interactions π + N, relations among cross sections of nonet mesons produced in, (T), 25:12203
interactions π + N, test of tensor meson dominance from f-exchange contribution to, (T), 25:12216
interactions with mesons, formalism with SU(3) symmetry, exchange degeneracy, and Regge poles for forward, (T), 25:12217
interactions with mesons, quark model for backward, (T), 25:12218
interactions with mesons, quark model for total cross section relations for forward elastic, (T), 25:12218
scattering by lithium-7, numerical analysis of differential cross sections for inelastic, (T), 25:12384
scattering by nuclei, formalism for inelastic, (T), 25:12701

NUCLEONS (anti N)
interactions anti N + N → π + rho, multichannel N/D equations for bound-state mass of π in, (T), 25:12202
interactions anti N + N at high energies, SU(3) symmetry and exchange degeneracy in Regge pole--cut model for, (T), 25:12217

NUCLEOSIDES
radioinduced damage of, protective effects of chloride ions against γ, 25:10962

NUCLEOTIDES
radioinduced changes in composition and content of, in DNA of cotton shoots following seed exposure, γ, 25:11307
radioinduced damage of, protective effects of chloride ions against γ, 25:10962

O

OBRIGHEIM POWER REACTOR (GERMANY)
development programs for, review of, 25:12704 (BMBW-FBK-70-11)

OCTANE
determination in effluent from gas chromatograph, performance of Geiger--Mueller counter with external γ source for, 25:10888
effects on γ-radioinduced graft polymerization of styrene with polyethylene, 25:10613

OHIO
radiation monitoring of environs of Goodyear Atomic Corporation, Piketon, during 1969, 25:11001

OOCYTES
radioinduced sex-linked lethal mutations in, of Drosophila, effects of dose rate on γ, 25:11022

OPTICAL SYSTEMS
radioinduced correction of aberrations in lenses, neutron, 25:11961

ORES
analysis for calcium, iron, manganese, and tungsten, intermittent ac arc method for spectrographic, 25:10429 (BARC-468)
analysis of fluorinated, for fluorine by activation methods, 25:10498

ORGANIC COMPOUNDS
pyrolysis of graphitizable, to form carbonaceous mesophase, mechanisms of, 25:11529

ORGANIC COMPOUNDS, HALO-
book: Radiation Chemical Processing, 25:10617

ORGANIC COMPOUNDS, METALLO-
book: Radiation Chemical Processing, 25:10617

ORGANIC COMPOUNDS, NITRO-
book: Radiation Chemical Processing, 25:10617

ORGANIC COMPOUNDS, SULFO-
book: Radiation Chemical Processing, 25:10617

ORGANISMS
radiation effects on marine, development of 2000 Ci cesium-137 irradiator for studies of, 25:10759

ORGANS
blood flow in human, radioisotope clearance method for determining, method for improved accuracy, 25:10917
radioinduced tumors in, of mammals, effects of clonogenicity, dose, reproductive integrity, and time on, 25:11253 (BNL-50203, pp 154-73)

ORGEL REACTOR
uranium-238 fast fission factor measurement in natural uranium fueled lattice of, 25:12817 (EUR-4326)

OSCILLATORS
phase fluctuations of traveling-wave tube, with superconducting resonator, 25:11853
superconducting Josephson junction, pull-in phenomena in, (T), 25:11839

OSKARSHAMN POWER REACTOR
commercial background of, 25:12760
construction of, summary of, 25:12716
control rod drives for, development programs for, 25:12712
cooling system for, development programs for, 25:12712
core physics for, development programs for, 25:12712
design parameters of, 25:12711
design parameters of, 25:12710
illustration of, colored cut-away, 25:12711
site for, description of, 25:12760

OSMIUM
determination of trace amounts of, in biotite and tektite by spark source mass spectrometry, 25:10455
friction and wear of, sliding against copper and iron rings under vacuum, 25:11413

OSMIUM ALLOYS AND SYSTEMS
Os--Pu-base, phase diagram of, 25:11438

OSMIUM ISOTOPES Os-187
energy-level scheme from iridium-187 decay, (E), 25:12514(R) (COO-1672-21)

OSMIUM ISOTOPES Os-192
energy levels from iridium-192 electron-capture decay, spin--parity assignments for, (E/T), 25:12532 (TID-25592)
energy-level transitions from iridium-192 electron-capture decay, energies, intensities, multipolarities, and K and internal conversion coefficients from, (E/T), 25:12532 (TID-25592)
neutron reactions (n,2n) at 14.7 MeV, total cross sections and isomeric yield ratios for, (E), 25:12618

OSTEICHTHYES
Oryzias latipes, radiation effects of survival of, effects of time of injection and temperature on protective effects of cysteamine against x, 25:11292
Perca sp., strontium-90 content of, in lake contaminated by reactor effluent, 25:11006
radioinduced malformations in embryos of, effects of sperm exposure on, 25:11074(R) (AECL-3777)
radioisotope content of benthic and pelagic, from Pacific Ocean, lead-210, polonium-210, 25:10997(R) (RLO-2225-T-14-1)

OTTAWA RIVER
radiation monitoring of liquid effluents in, 25:11074(R) (AECL-3777)

OTTERS
mortality at Amchitka Island, Alaska, 25:12868(R) (BMI-171-101)
population of, feasibility of photogrammetric determination of, 25:12875(R) (BMI-171-108)
underwater overpressure effects on, and its principal food species, 25:12876(R) (BMI-171-111)

OVARIES
radioinduced hyperplasia in, of mice, protective effects of diethylstilbestrol against γ, 25:11107

OXIDES
diffusion in, data tabulations on, 25:11411

OXYBROMOURANATES
preparation and properties of $UOBr_5^{2-}$, 25:10576

OXYCHLOROURANATES
preparation and properties of $UOCl_5^{2-}$,, 25:10576

OXYFLUOROURANATES
preparation and properties of UOF_5^{-}, 25:10576

OXYGEN
abundance of geomagnetically trapped nuclei of, (E), 25:11744
determination by charged particle and photon activation, radiochemical separation methods for, 25:10488 (CEA-R-4072)
determination by charged particle and photon activation, reactions and sensitivities for, 25:10488 (CEA-R-4072)
determination in aluminum by charged particle activation and radiochemical separation, 25:10488 (CEA-R-4072)
determination in boron--iron powders, comparison of isotope dilution and vacuum fusion methods for, 25:10467
determination in copper, steel, and tin by photon activation and radiochemical separation, 25:10501
determination in iron and niobium by helium-3 activation and radiochemical separation, 25:10488 (CEA-R-4072)
determination in nitride layers on silicon surfaces by deuteron (d,p) reactions, 25:10583(R) (AECL-3776)
determination in silicon, comparison of charged particle activation and spectrometric methods for, 25:10488 (CEA-R-4072)
determination in sodium, meter calibration for in-line, 25:11348(R) (GEAP-13539-13)
determination of trace amounts of, in molybdenum, review on, 25:10459

deuteron reactions at 30 to 120 keV with molecular, cross sections for electron capture into 3s state of deuterium in, (E>, 25:11708
diffusion in monocrystalline titanium dioxide, proton resonance method for measurement of coefficient of, 25:11516
diffusion in uranium dioxide, tracer study of self-, 25:11486 (CEA-R-4095)
effects on carburization of iron and steel by decomposing carbon monoxide, relations with composition, surface structure, and temperature, 25:11374 (DP-Report-530)
effects on plutonium distribution in dilute plutonium--titanium and plutonium--zirconium alloys, 25:11431 (CEA-CONF-1691)
effects on radiosensitivity of C3H tumor cells in mice, 25:11094 (BNL-50203, pp 215-33)
effects on radiosensitivity of survival in Oedogonium cardiacum, 25:11304 (BNL-50203, pp 70-81)
effects on radiosensitivity of tumors in mammals, 25:11220 (BNL-50203, pp 234-41)
effects on x-radiosensitivity on Chinese hamster cells, 25:11093 (BNL-50203, pp 97-116)
excitation in sunlit conjugate ionosphere, O I 1304-A airglow, (E), 25:11799
ionization in upper atmosphere, x-ray emission properties of atomic, (E/T), 25:11790
proton reactions at 30 to 120 keV with molecular, cross sections for electron capture into n = 3 level of hydrogen in, (E), 25:11708
pulsations of 5577 O I, positive correlation to x-ray pulsations in pulsating aurorae, quasiperiodic, (E), 25:11808
radiation effects on supply of, in tumor cells, 25:11258 (BNL-50203, pp 242-54)
radiation effects on utilization of, in rats, continuous, 25:10980
radioinduced reactions with alkanes and sulfur dioxide, 25:10614
reactions with molybdenum and niobium at 200 to 600°C, ellipsometry method for studying oxidation, 25:11355
reactions with molybdenum at 1100 to 1500°K, reacting rotating disk method for studying kinetics of oxidation, 25:11409
reactions with molybdenum, niobium, tantalum, tungsten, and vanadium, review of kinetics, mechanisms, and thermodynamics of degassing and engassing, 25:11415
reactions with uranium dioxide, rate of, 25:10569 (CEA-R-4074)
sorption by tantalum films at 77 to 295°K, 25:11418

OXYGEN IONS (O+)
reactions with krypton at keV energies, statistical-model calculations of ionization probabilities in, 25:11711

OXYGEN ISOTOPES
effects on reaction mechanisms, effects of temperature on kinetic, 25:10549
fractionation in stalagmites and stalactites, 25:10684

OXYGEN ISOTOPES O-14
beta decay of, correction factors for Gamow--Teller allowed transitions in, 25:12421

OXYGEN ISOTOPES O-15
effectiveness of carbon dioxide-incorporated, for studying pulmonary circulation for detection of heart disease, 25:11125
proton reactions (p,α) at 16 MeV, internal bremsstrahlung spectra for, (T), 25:12694

OXYGEN ISOTOPES O-16
alpha elastic scattering at 20 to 24.5 MeV and 176°, differential cross sections and angular distributions for, (E), 25:12419
alpha reactions (α,pn) at 42 MeV, gamma spectra from, (E), 25:12553
binding energy of, Hartree--Fock calculation using effective interaction, (T), 25:12686
content ratio to oxygen-18 in deep-sea sediments, (E), 25:10725(R) (CU-3139-4)
energy levels from carbon-13 (He-3,γ) reactions, (E), 25:12388
energy levels of, monopole matrix elements and electron scattering form factors of excited, (T), 25:12426
energy levels of, projected Hartree--Fock and SU(3) calculations of, (T), 25:12412
helium-3 reactions (He-3,d) at 18 and 20 MeV, DWBA analysis of differential cross sections from, (E/T), 25:12479
lithium-6 elastic scattering at 20 MeV, optical-model analysis of, (T), 25:12408
neutron inelastic scattering at narrow levels in oxygen-17, differential cross sections for, (E), 25:12404
neutron reactions at 6.4 to 16.5 MeV, γ production cross sections for, (E), 25:12406
neutron scattering by, R-matrix shell-model calculations of cross sections for, (T), 25:12423
nuclear charge radius from Hartree--Fock treatment of center-of-mass motion, (T), 25:12653
proton elastic scattering at 10 to 60 MeV, local Woods--Saxon potentials equivalent to nonlocal analysis including exchange effects in, (T), 25:12689
proton reactions (p,d) at 25.52, 30, and 31.82 MeV, effect of deuteron D-state on DWBA calculations of differential cross sections, deuteron polarizations, proton analyzing powers, and spectroscopic factors from, (T), 25:12414
reactions (O-16,O-17) with beryllium-9 and carbon-13 at 11 to 20 MeV, excitation functions and DWBA analysis of angular distributions from, (E/T), 25:12382 (NP-18546)
reactions (O-16,p) and (O-16,α) with cobalt-59 at 49 to 88 MeV, proton and α angular distributions and energy spectra from bromine-75 compound nucleus in, (E), 25:12461
reactions with chromium-52, 25:10583(R) (AECL-3776)
scattering by beryllium-9 and carbon-13 at 14 to 25 MeV, optical-model analysis of angular distributions from, (E/T), 25:12382 (NP-18546)
scattering by cadmium-106 and -114 at 35 to 40 MeV, correlation functions and hyperfine attenuation coefficients from inelastic, (E), 25:12619
scattering by indium-115 at 45 MeV, gamma spectra from inelastic, (E/T), 25:12543
scattering by natural cadmium at 38 and 41 MeV, gamma spectra from inelastic, (E), 25:12548
scattering by natural cadmium at 38 to 40 MeV, gamma angular distributions from inelastic, (E/T), 25:12556

OXYGEN ISOTOPES O-17
energy levels from alpha resonances in carbon-13, spin--parity assignments for, (E), 25:12390
energy levels from carbon-13 (Li-7,t) and carbon-13 (Li-6,d) reactions at 17 and 18 MeV, (E), 25:12425
energy levels from oxygen-16 neutron scattering, spin and parity of, (E), 25:12404
energy levels of, Hartree--Fock calculation using effective interaction, 25:12686

OXYGEN ISOTOPES O-18
concentration in carbonates along stalagmite and stalactite layers, 25:10684
content ratio to oxygen-16 in deep-sea sediments, (E), 25:10725(R) (CU-3139-4)
effects on ir spectra of products from electrically dissociated heavy water or water, 25:10531
exchange between oxygen or water and homogentisate from p-hydroxyphenylpyruvate, 25:10553
helium-3 reactions (He-3,t) at 16 and 30 MeV, (E), 25:12498
proton inelastic scattering by, microscopic first-order core polarization corrections to DWBA for, (T), 25:12678
reactions (O-18,O-17) with beryllium-9 and boron-10 at 16 to 24 MeV, DWBA analysis of angular distributions from, (E/T), 25:12381 (NP-18541)
reactions (O-18,O-19) with beryllium-9 and carbon-13 at 12 to 24 MeV, DWBA analysis of angular distributions from, (E/T), 25:12381 (NP-18541)
scattering by beryllium 9, boron-10, and carbon-13 at 12 to 31 MeV, angular distributions from elastic, (E/T), 25:12381 (NP-18541)

OXYGEN ISOTOPES O-19
beta decay of, half-life for, (E), 25:12394

OXYGEN ISOTOPES O-20
beta decay of, analysis using Tabakin and Serber--Yukawa potentials, (T), 25:12468
beta decay of, half-life for, (E), 25:12453

OXYGEN SYSTEMS
C--O--Pu--U, phase equilibria in, prediction of, 25:11525
CO_2--O, radiolysis of, effects of sulfur hexafluoride on yields of ozone from electron pulse, 25:10633
N--O, radiation effects on, spectral studies on 1.5-MeV electron, 25:10586 (JAERI-5026, pp 155-7)
O--Pu--U, diffusion in, effects of temperature gradient on mechanism of, 25:11505

OZHENNITE (ZIRCONIUM ALLOY)
corrosion by organic reactor coolants, review on, 25:11343 (AECL-3778)

OZONE
effects on sulfoxidation of alkanes, comparison of γ and uv radiation with, 25:10592 (BMBW-FBK-70-25)
yields from radiolysis of carbon dioxide--oxygen mixtures, 25:10633

P

PACIFIC OCEAN
barium content in, 25:10468
element content in, 25:10428
radium-226 content of seawater at Geosecs Station in north, relations with depth, 25:10726
radon content of surface and bottom of water column at Geosecs Station in north, 25:10727
tritium content of North American coastal waters of, 1963 to 1967, 25:10720

PAINTS
evaluation of Burgess Fobes, for reactor containment building protective coatings, 25:12804 (ORNL-TM-3104)
properties for reactor containment building protective coatings, effects of accident conditions on, (E), 25:12804 (ORNL-TM-3104)
radiation dose from promethium-147 activation of luminous, β and γ, 25:11065

PALLADIUM
alpha reactions at 30 to 80 MeV, cross sections for production of K x rays by, (E), 25:12488
determination of trace amounts of, in biotite and tektite by spark source mass spectrometry, 25:10455

friction and wear of, sliding against copper and iron rings under vacuum, 25:11413
separation from cadmium, indium, molybdenum, niobium, and rhodium by gas chromatography using aluminum chloride eluent, 25:10666 (JINR-P6-5410)
separation from fission products by automatic ion exchange chromatography, design and performance of equipment for, 25:10659 (CEA-N-1267)
PALLADIUM ALLOYS AND SYSTEMS
Au--Pd--Te, superconducting properties of liquid-quenched simple cubic, 25:11819 (CALT-822-22)
Cd--Pd-base, thermodynamic properties of, 25:11396
In--Pd-base, thermodynamic properties of, 25:11396
Np--Pd-base, magnetic properties of solid solutions of, at 2 to 300°K, 25:12003
Np-base--Pd, magnetic behavior of dilute, Moessbauer effect studies of, 25:12001
Pd--Sb, superconducting properties of liquid-quenched simple cubic, 25:11819 (CALT-822-22)
Pd-base--Pu, magnetic properties of solid solutions of, at 2 to 300°K, 25:12003
Pd-base--Sb, thermodynamic properties of, 25:11396
Pd-base--Sn, thermodynamic properties of, 25:11396
Pd-base--Th, thermal capacity at low temperatures, (E/T), 25:11989
Pd-base--U, magnetic behavior from susceptibility, resistivity, and thermal capacity at low temperatures, (E/T), 25:11989
Pd-base--U, magnetic properties of solid solutions of, at 2 to 300°K, 25:12003
PALLADIUM ISOTOPES Pd-101
beta and electron-capture decay of, γ singles and coincidence spectra and internal conversion electron spectra from, (E), 25:12596
PALLADIUM ISOTOPES Pd-102
neutron capture by, spectroscopic analysis of, (E), 25:12586
PALLADIUM ISOTOPES Pd-104
neutron capture by, spectroscopic analysis of, (E), 25:12586
PALLADIUM ISOTOPES Pd-105
neutron capture by, spectroscopic analysis of, (E), 25:12586
PALLADIUM ISOTOPES Pd-106
energy levels from palladium-105 neutron capture, spin-parity assignments for, (E), 25:12586
PANAMA
radioisotope ingestion by human population of, for feasibility studies of proposed Atlantic-Pacific interoceanic canal, estimation of potential, 25:10995 (BMI-171-45)
PANCREAS
scanning for diagnosis of diseases of human, using selenium-75-labeled methionine, 25:11199
scanning of human, using selenium-75, 25:11197
scanning of human, using selenium-75-labeled methionine, 25:11200
scanning of, use of iodine-125-labeled toluidine blue for, 25:11188
scintigraphy of human, effectiveness of selenium-75-labeled selenomethionine for, effects of simultaneous scanning of gastrointestinal tract with colloidal gold-198 on, 25:11212
scintiscanning of human, using gold-198 and selenium-75 for, computer method for differentiation, 25:11176
PAPER
oxidation of waste, analysis of products from wet, 25:10433 (ORNL-4636, pp 1-7)
PARAMAGNETIC SALTS
temperature scale below 1°K for zinc neodymium nitrate single crystals, gamma-ray anisotropic, 25:11852
PARATHYROID GLANDS
scanning of, use of iodine-125-labeled toluidine blue for, 25:11188
PARTICLE TRACKS
analysis of bubble chamber, vidicon device for ionization measurements for, 25:10878
etching in boron-impregnated dielectric detectors irradiated with slow neutrons, 25:10820
formation and development in dielectric track detectors, 25:10827
scanning of nuclear emulsion, semiautomatic system for, 25:10839
PARTICLES
channeling through perfect crystals, Debye-model study of low-temperature, 25:11971
PECTINESTERASE
radiation effects on synthesis of, in Penicillium expansum, γ, 25:10979
PENICILLIN
biological activity of, effects of deuterium on, 25:10560
PENTANE
determination in effluent from gas chromatograph, performance of Geiger--Mueller counter with external γ source for, 25:10888
PENTANE, 3-METHYL-
radiolysis at 20 and -196°C, scavengeable electron yields from γ, 25:10652
2,4-PENTANEDIONE
complexes with beryllium, radiolysis of single crystals of, ESR spectral studies on γ, 25:10623 (JAERI-5026, pp 157-60)
2-PENTANONE, 4-METHYL-
solvent properties for molybdenum complex with benzoin oxime, 25:10439
1-PENTENE
yields from γ radiolysis of liquid cyclopentane, effects of pressure on γ, 25:10628
PERCH LAKE (ONTARIO)
radioecology of, 25:11074(R) (AECL-3777)
PEROXIDASE
radiation effects on inhibitors of, in broad bean seedlings, γ, 25:10973
PERSONNEL
protection of, automatic air purifying respirator for, 25:10752 (CEA-N-1360)
radiation dose to airport, from intransit radioactive materials, 25:11062
radiation dose to color television assembly and repair, x, 25:11063
radiation dosimetry in, following criticality accidents, use of tissue-equivalent phantoms for γ and fast neutron, 25:11057
radiation hazards to uranium mining, methods for protection against radon and radon decay product α, 25:11085
radiation hazards to, of teletherapy unit, dosimetry studies for evaluating cobalt-60 γ, 25:11070
radiation injuries to nuclear, first aid treatment for, 25:11109
radiation protection of, at storage facilities for radiation sources, standards for, 25:11078 (Y-1754)
radiation protection of, following accidents, programs for, 25:11079
radiation protection of, review of international standards for microwave, 25:11088
radioinduced tumors in bones and liver of, following occupational inhalation of plutonium-239, models for estimating probability of α and γ, 25:11301
requirements for environmental radiation surveillance laboratory, 25:10763
PERTURBATION THEORY
causal distributions in, singularity structure of, 25:12133
Schwinger terms in, equal-time limits of current commutators for derivation of, 25:12294
transform for use in, properties and applications of, 25:11735
wave equation solutions using perturbation expansions, 25:12054
PESTICIDES
determination in tissues by electron-capture gas chromatography, 25:10433 (ORNL-4636, pp 1-7)
PETROLEUM
production stimulation using underground nuclear explosives, economic and technical aspects of, 25:10746
storage in nuclear explosion-produced cavities, economic and technical aspects of, 25:10746
PHAEOPHYTA
Ascophyllum nodosum, radioisotope accumulation by, influence of cellular respiration inhibitors on, polonium-210 and plutonium-239, 25:10941
PHAGOCYTOSIS
mechanisms in leukocytes and yeast cells in vitro, chromium-51 tracer studies of, 25:10908
PHANTOMS
radiation dosimetry in tissue-equivalent, following criticality accident, γ and fast neutron, 25:11057
use of tissue equivalent, to estimate radioactive contamination and dose absorbed at site of human organs, 25:11067
PHARMACEUTICALS
analysis for iodine using Ross filters for energy selection, x-ray fluorescence, 25:10479
analysis of boron-containing, by neutron absorption, 25:10487
PHENIX FAST REACTOR
heat exchangers for, neutron streaming toward, (T), 25:12782 (CEA-CONF-1683)
PHENOL, p-BROMO-
radiolysis of aqueous solutions of, optical absorption spectra of phenoxy radicals produced by electron pulse, 25:10631
PHENOXY RADICALS
yields from electron pulse radiolysis of aqueous p-bromophenol solutions, optical absorption spectra of, 25:10631
PHENYL RADICALS
yields from electron pulse radiolysis of aqueous iodobenzene solutions, optical absorption spectra of, 25:10631
PHOSPHATE DEPOSITS
analysis for trace amounts of elements by spark source mass spectrometry, 25:10456
PHOSPHATES
excretion by nephrons of irradiated kidneys in dogs, effects of uremic condition on, 25:10963
separation of, paper chromatographic, 25:10687
uptake by Ehrlich ascites tumors in mice, tracer study using iodine-131 and whole-body autoradiography for,

XUM

25:10921
PHOSPHINE, SILYL-
BH_3--H_3SiPH_2, deuterium exchange with hydrogen in, 25:10547
PHOSPHOFRUCTOKINASE
radiation effects on activity of, in dormant and sprouting rye seeds, γ, 25:10974
PHOSPHOGLUCOMUTASE
radiation effects on activity of, in dormant and sprouting rye seeds, γ, 25:10974
PHOSPHOLIPASE B
content of rat intestine, effects of cyclophosphamide and dexamethasone on, relation of, to previous studies on x-irradiated rats, 25:10961(R) (ORO-3329-6)
PHOSPHONIC ACID, (1-HYDROXYETHYLIDENE)DI-
determination by spectrometric titration using thorium (1,2-cyclohexylenedinitrilo)tetraacetate, 25:10462
PHOSPHORIC ACID
reactions with tantalum surfaces, anodizing, 25:11351
PHOSPHORIC ACID, BIS(2,2-DIMETHYLHEXYL) ESTER
solvent properties for rare earths and uranium, 25:10679
PHOSPHORIC ACID, BIS(2-ETHYLHEXYL) ESTER
solvent properties for erbium, holmium, or yttrium in hydrochloric or nitric acid solutions, 25:10685
PHOSPHORIC ACID, TRIBUTYL ESTER
solvent properties for gold, 25:10686
acetic acid--acetone--TBP, solvent properties for separation of oxidation states of sixteen elements by paper chromatography, 25:10687
PHOSPHOROTHIOIC ACID, S-(2-AMINOETHYL) ESTER
radioprotective effects of, on hematopoietic tissue formation in spleen of inbred and noninbred γ-irradiated mice as compared to mexamine, 25:11099
PHOSPHORUS
determination of trace amounts of, in biotite and tektite by spark source mass spectrometry, 25:10455
determination of trace amounts of, in molybdenum, review on, 25:10459
development and uses of, 25:10491 (ORNL-4636, pp 20-33)
radiation effects on high-pressure polymorphs of, fast neutron, 25:11474(R) (BNWL-842)
separation from ores by solvent extraction, review on, 25:10656 (BM-IC-8502)
PHOSPHORUS ISOTOPES P-29
energy levels from sulfur-32 (p,αγ) reactions, spin--parity assignments for, (E), 25:12480
energy-level transitions from sulfur-32 (p,αγ) reactions, gamma branching and mixing ratios and strengths for, (E), 25:12480
PHOSPHORUS ISOTOPES P-30
energy levels from silicon-30 (He-3,t) reactions at 16 and 30 MeV, (E), 25:12498
energy levels of, calculation using collective model with Coriolis coupling, (T), 25:12482
PHOSPHORUS ISOTOPES P-31
alpha elastic scattering by, excitation functions for, (E), 25:12442
alpha reactions (α,n) with, threshold energies and excitation functions for, (E), 25:12442
PHOSPHORUS ISOTOPES P-32
content in atmosphere at Zugspitze, Germany, April to Dec. 1970, 25:10705(R) (NYO-4061-3)
decay products of, in Escherichia coli, effects of DNA synthesis in relation to genetic recombination in, 25:10946
determination in liquid scintillation counter by Cherenkov counting, 25:10491 (ORNL-4636, pp 20-33)
effects on growth of dwarf peas, 25:10936 (UCB-34-P-23-15)
effects on polycythemia vera in man, effects on survival and leukemia incidence of therapeutic, 25:11303
PHOTOELECTRIC CELLS
radiation effects on, electron and x, 25:10904 (HMI-B-97)
PHOTOGRAPHIC FILM
analysis and interpretation of color, for recording high-altitude nuclear explosions, 25:10893 (EGG-1183-484)
PHOTOMULTIPLIER TUBES
performance of large photocathode, 25:10847
radiation effects on, electron and x, 25:10904 (HMI-B-97)
PHOTONS
absorption by nuclei, limits of validity of Siegert's theorem in, (T), 25:12649
emission from reflected electrons from half-space magnetic fields, (T), 25:11679
gravitational field of, (T), 25:12283
interactions γ + ^{4}He → ^{4}He + π^0, verification of vector dominance in, (T), 25:12140
interactions γ + d above 1.2 GeV, data compilation on cross sections for hadron production in, (E), 25:12066 (DESY-HERA-70-1)
interactions γ + e → γ + e, effective field equations for one-electron multi-photon stationary states for Compton, (T), 25:12139
interactions γ + e → γ + e, scale invariance in lambda phi^4 theory for Compton, (T), 25:12149
interactions γ + N → π + N, continuous-moment sum rules for, (T), 25:12207
interactions γ + n above 1.2 GeV, data compilation on cross sections for hadron production in, (E), 25:12066 (DESY-HERA-70-1)
interactions γ + p → γ + p, continuous-moment sum rules for Compton, (T), 25:12207
interactions γ + p → K + Σ(Λ) at high energies, tests of Regge-pole and strong-absorption models for, (T), 25:12206
interactions γ + p → π^0 + p at 6 GeV, spectrometer and Cherenkov counter study of asymmetry in, (E), 25:12072
interactions γ + p → π^0 + p at 6 to 18 GeV, differential cross sections for backward, (E), 25:12069
interactions γ + p → π^+ + n at 0.450 to 3 GeV, resonance structure of cross sections for, (E), 25:12067 (LAL-1239)
interactions γ + p → π^+ + π^- + p, five-body Veneziano amplitude for diffractive, 25:12152
interactions γ + p → $\pi^+(\pi^0)$ + n(p) in second resonance region, fixed-t dispersion relations for, (T), 25:12146
interactions γ + p above 1.2 GeV, data compilation on cross sections for hadron production in, (E), 25:12066 (DESY-HERA-70-1)
interactions γ + π → γ + π, parametrization of amplitude for Compton, (T), 25:12177
interactions in e + p deep inelastic interactions, Reggeization scheme for, (T), 25:12148
interactions of, covariant amplitude as zero-mass limit of helicity amplitude for massive vector boson for, (T), 25:12177
interactions of, S-matrix for, 25:12177
interactions with scalar bosons, cross sections for, (T), 25:12138 (NYO-2262-TA-222)
interactions with static electromagnetic fields, graviton production from, (T), 25:12272
Planck constant of cosmic, method for determining, (E/T), 25:11665
production from graviton interactions with static electromagnetic fields, (T), 25:12272
reactions (γ,n) and (γ,p) with lithium-6 up to 20 MeV, analysis using single-particle model, (T), 25:12417
reactions (γ,n) with lead-208 at threshold energy, resonance effects in, (T), 25:12562
reactions (γ,n)2α with beryllium-9, cross-section calculations using Dirac model, (T), 25:12399
reactions (γ,p) at 25 to 55 MeV, absolute differential and total cross sections, and angular distributions for, (E), 25:12362
reactions (γ,p) with aluminum-27 at 85 MeV, proton angular and energy distribution from, (E), 25:12501
reactions (γ,π^+) and (γ,π^-) with carbon-12, analysis using transition amplitude from impulse approximation, (T), 25:12407
reactions with helium 1^1S and 2^1S states at 0.20 to 2.40 and 3.15 to 3.30 Ry, cross sections for ionization in, (T), 25:11717
reactions with helium excited 2S atoms, cross sections for three-photon ionization in, (E), 25:11734
reactions with nuclei at high energies, vector-meson dominance model for, 25:12151
scattering by nuclear field, polarization of electron pairs and photons from, (T), 25:12158
scattering by spherically symmetric gravitational field, polarization in, (T), 25:12159
theory for continuous-spin, lightlike and spacelike representations of Poincare group in, 25:12236
PHOTOREACTIVATION
effects on repair from uv-radioinduced damage in Bacillus subtilis, 25:10960 (BNL-50203, pp 82-90)
radiation effects on, of Escherichia coli, uv, 25:11008 (BNL-50203, pp 14-26)
PHOTOSPHERE
flares in, generation of white-light, (E/T), 25:11619
magnetic field of, comparison with interplanetary field, (E), 25:11603
metal abundance in, (E/T), 25:11610
spectral line profiles in, europium- and lanthanum-ion, (E), 25:11613
spectral polarization of, (E/T), 25:11610
PHTHALIC ACID
potassium salt, deuterium exchange reaction in transcarboxylation of mixture of deuterated and nondeuterated, mechanism of, 25:10545
PHTHALIC ACID, DIALLYL ESTER
poly(diallyl phthalate)--vinyl compound, polymerization for coating woods, electron, 25:10606 (JAERI-5026, pp 101-7)
acrylonitrile--bis(2-hydroxyethyl methacrylate) phosphate--butyl acrylate--poly(diallyl phthalate), radioinduced polymerization of coatings of, on metals, electron, 25:10608 (JAERI-5026, pp 121-9)
acrylonitrile--poly(diallyl phthalate), radioinduced polymerization in wood, γ or electron, 25:10607 (JAERI-5026, pp 108-20)
PHYTOHEMAGGLUTININ
effects on leukocytes in irradiated human blood, 25:11299
PIEZOELECTRIC CRYSTALS
surface waves on, analysis of, 25:11473(R) (AD-708712)
PILGRIM POWER REACTOR
piping systems for, recommendations for codes for power, 25:12741 (DOCKET-50293-33)
PIPERIDINE
nitroxide free radicals in, 310-MHz NMR study of,

25:12034 (CEA-R-3855)
PIPES
crack initiation and growth in reactor cooling systems, effects of low cycle fatigue on, (E), 25:12783(R) (GEAP-10207-22)
failure in reactor cooling systems, probability analysis of, 25:12783(R) (GEAP-10207-22)
fracture behavior of flawed elbows and tees of, review of, 25:11369(R) (BMI-1892)
PLACENTA
scanning of human, use of γ scintillation camera and metastable indium-113 for, 25:11228
PLANETARY NEBULAE
carbon monoxide radio emission at 2.6 mm from IRC + 10216, (E), 25:11568
infrared observations of IC 4997, VV 8, and FG Sge, (E), 25:11569
radio observations of, (E), 25:11567
shell formation in FG Sge, (E), 25:11574
velocity of central star of NGC 3132, radial, (E), 25:11570
PLANETS
orbits of, equilibrium solutions of secular variations in restricted three-body problem for, (T), 25:12057
PLANKTON
radioisotope accumulation by marine phyto-, influence of cellular respiration inhibitors on, polonium-210 and plutonium-239, 25:10941
radioisotope content of, in Pacific Ocean, lead-210 and polonium-210, 25:10997(R) (RLO-2225-T-14-1)
PLANTS
analysis for copper and manganese simultaneously by neutron activation and radiochemical separation, 25:10509
radiation effects on, review of ionizing, 25:10976
radioinduced mutations in, review of ionizing, 25:10977
radioisotope retention in, fallout, 25:11038 (UCRL-72716(Rev.1))
radioisotope uptake and retention by aquatic, statistical analysis of, 25:10998
strontium-90 uptake by, during 1965 to 1969, 25:11050
PLANTS (INDUSTRIAL)
equipment for, computerized simulation models for prediction of requirements for, 25:10757 (RFP-1527)
PLASMA
bibliography on, 25:11857
bibliography on plasma physics and fusion reactors, 25:11858
bibliography on plasma physics and fusion reactors, 25:11856
boundary-value problems in, double Laplace transformations for, 25:11889
charged-particle beam interactions with magnetized, return current from relativistic, (T), 25:11886 (NYO-4077-1, Paper 4)
charged-particle beam interactions with semi-infinite, double Laplace transformations for, 25:11889
collisions in cold, inverse Compton, (T), 25:12537
confinement in spherical multipole magnetic traps, (E), 25:11863
confinement of injected, in minimum-B magnetic traps, 25:11859 (EUR-CEA-FC-563)
diagnostics behind shock fronts, infrared, 25:11868(T) (SC-T-70-4054)
diagnostics in Astron device, carbon dioxide laser heterodyne system for, 25:11869
diagnostics in tokamak-type devices, current distributions from laser scattering, 25:11867 (MATT-818)
diagnostics in toroidal octupoles, distribution functions, (E), 25:11872
diagnostics of hot-ion, optical spectra for measuring electric fields, (E), 25:11874
diagnostics of laser-produced, using multi-layer targets, (E/T), 25:11870
diagnostics of low-density argon, using cylindrical Langmuir probes, (E), 25:11873
diagnostics of, correlation measurements for, 25:11866 (EUR-CEA-FC-570)
diagnostics of, LTE temperatures below 10,000°K, 25:11876
diagnostics using Doppler broadening of spectral emission lines, review, 25:11875
diagnostics using laser scattering, computational method for Thomson, (T), 25:11865 (CEA-R-4058)
diagnostics using shf radiations from, electron temperature, 25:11877
ejection of bodies of, from galactic nuclei and quasars, (T), 25:11658
electron beam interactions with finite-beta, equilibrium of relativistic, (T), 25:11887 (NYO-4077-1, Paper 5)
electron beam interactions with, E-layer precession in, (T), 25:11925 (NYO-4077-1, Paper 2)
electron beam interactions with, induced current from relativistic, (T), 25:11894
electron beam interactions with, stochastic acceleration from nonlinear, (T), 25:11885 (NYO-4077-1, Paper 3)
electron distribution function measurement in toroidal octupoles, (E), 25:11872
electron elastic and inelastic scattering by argon, angular distribution from, (E), 25:11879
equilibrium and stability in Tokamak-type devices, magnetohydrodynamic, 25:11911 (EUR-CEA-FC-569)
equilibrium in stellarators, effects of electric conductivity on, 25:11912 (MPI-PA-7/62)
heating at electron cyclotron resonance, conditions for, 25:11861 (NP-18635)
heating by hf fields near lower-hybrid frequency, (E), 25:11860 (FTI-282)
heating by microwaves, off-resonance, (E/T), 25:11909(R) (COO-1695-31)
heating by microwaves, off-resonance, (E/T), 25:11910(R) (COO-1695-32)
heating by rf fields, efficiency of, (T), 25:11864
heating of toroidal, numerical simulation of turbulent, (T), 25:11862
injection and confinement in minimum-B magnetic traps, neutral atom, 25:11859 (EUR-CEA-FC-563)
injection and confinement in spherical multipole magnetic traps, (E), 25:11863
interactions with neutral gas blanket, in poloidal magnetic fields, (E/T), 25:11878
ion distribution function measurement in toroidal octupoles, (E), 25:11872
ion scattering by electric fields in inertially confined, (E), 25:11880
kinetic theory for electrons in external electric fields, Boltzmann equation for, 25:11898
kinetic theory in electromagnetic fields, wave-mechanical, 25:11899
kinetic theory of relativistic, Boltzmann equation for, 25:11765
kinetic theory of relativistic, general, 25:12058
kinetic theory of relativistic, in strong magnetic fields, 25:11903
kinetic theory of spatially inhomogeneous, with time-independent average properties, 25:11895
kinetic theory of, Cauchy problem for linearized relativistic Boltzmann equation, 25:11902
kinetic theory of, derivation of Vlasov equation for, 25:11900
kinetic theory of, Grad method extension for relativistic Boltzmann equation, 25:11901
kinetic theory of, semi-Lagrangian formulation of Vlasov equation, 25:11897
kinetics in longitudinal electric fields, wave mechanical formalism for, 25:11891
laser beam interactions with, stimulated and nonlinear effects from, (T), 25:11884 (CEA-N-1399)
oscillations in inhomogeneous, Landau damping of resonance, (T), 25:11941
production by standing helicon waves, (E/T), 25:11908
production of clusters of, in dc arcs in inhomogeneous magnetic fields, 25:11905
production of, development of neodymium glass laser for, 25:11906
production using lasers, review of, 25:11907
properties of cylindrical, Maxwell equation for potential, 25:11904
radiations from cold, gyrosynchrotron, (T), 25:12537
radiations from electron cyclotron resonance-heated, free--free bremsstrahlung, (T), 25:11910(R) (COO-1695-32)
radiations from heterogeneous, electromagnetic, (T), 25:11890
radiations from mirror-confined, bremsstrahlung, (E/T), 25:11909(R) (COO-1695-31)
radiations from, electron temperature determination from shf, 25:11877
relaxation of temperature anisotropy in collisionless, (T), 25:11893
research at Fontenay-Aux-Roses, 1969, 25:11854(R) (EUR-CEA-FC-542(Pt.1))
research at Grenoble, April 1969--February 1970, 25:11855(R) (EUR-CEA-FC-542(Pt.2))
shock wave propagation in collisionless, two-fluid model for, 25:11930
simulation of turbulent heating of hydrogen, numerical, (T), 25:11862
spectra of carbon II and nitrogen II, resonance multiplets in, (T), 25:11881
spectra of nonhydrogenic ions in, Stark broadening functions for, 25:11892
stability and equilibrium in Tokamak-type devices, magnetohydrodynamic, 25:11911 (EUR-CEA-FC-569)
stability of anisotropic, quasi-linear dynamics of ion cyclotron, (T), 25:11915
stability of, electromagnetic wave effects on temperature anisotropy, (T), 25:11916
stability of, numerical solutions for explosive, 25:11914
stability of, theory for nonlinear explosive, 25:11913 (UUIP-722)
thermodynamics of electron gas, collective theory for, 25:11896
wave absorption between electron cyclotron and lower-hybrid frequency, boundary of hf, 25:11927 (FTI-295)
wave absorption in heterogeneous layer of, ion hybrid, (T), 25:11928 (IAE-1949)
wave coupling in Van der Pol, growth rate, nonlinear saturation coefficients, and mode--mode, (E), 25:11944
wave coupling in, nonlinear mode, (T), 25:11943
wave damping in inhomogeneous, Landau, (T), 25:11941

XUM

wave excitation in, Bernstein, (E/T), 25:11934
wave propagation along conducting wire in magnetized, electromagnetic, (E), 25:11935
wave propagation and absorption in heterogeneous layer of, ion hybrid, (T), 25:11928 (IAE-1949)
wave propagation and reflection in, transverse cyclotron, (T), 25:11931
wave propagation in bounded, one-dimensional ion--acoustic, (T), 25:11937
wave propagation in cold, nonlinear dispersion of, 25:11940
wave propagation in low-pressure, ion-rarefaction, (T), 25:11938
wave propagation in magnetized bounded, eigenvalues for slow, (T), 25:11945
wave propagation in magnetized with anisotropic pressure, ccupled equations for, (T), 25:11946
wave propagation in magnetized, temperature-anisotropy instability from, (T), 25:11916
wave propagation in uniform nonresistive, dispersion relations for helicon, (T), 25:11936
wave propagation in warm, nonlinear theory for, 25:11930
wave propagation in, nonlinear Vlasov equation for finite-amplitude, (T), 25:11933
wave reflection at boundary of half-space of, electromagnetic, (T), 25:11939
wave resonances in discharge, nonlinear damping of Tonks--Dattner, (E/T), 25:11942

PLASMA ACCELERATORS
jet diagnostics in coaxial, using gas lasers and interferometers, 25:11871
jet diagnostics in rod-plasma-injector, using magnetic probes and photomultipliers, 25:11883
performance of Pleiade-type, for neutral particle production, 25:11920 (EUR-CEA-FC-567)
performance of rail-type, with external magnetic fields, 25:11882

PLASMA JETS
diagnostics using gas lasers and interferometers, in ccaxial accelerators, 25:11871
ion scattering by electric fields in inertially confined, (E), 25:11880
motion in tube in magnetic field, (E), 25:11775

PLASMA, SOLID-STATE
wave propagation in, electric and magnetic resonances in Voigt configuration of micro-, (E/T), 25:11929

PLASMAPAUSE
convection at dusk, geomagnetic activity-related model of, (T), 25:11776 (AD-708495)
pulsation source lines in or near, relation with structured Pcl micro-, (E/T), 25:11788

PLASTICS
thickness measurement of tubular, beta backscatter gage for, 25:10890(P)

PLATES
neutron attenuation in, computer program for calculating resonance absorption, cross sections, and foil reaction rates, (T), 25:12336 (ANL-7645)
neutron diffusion in, computer program for solving one-dimensional, (T), 25:12335 (AECL-3671)

PLATINUM
alpha inelastic scattering at 42 to 90 MeV, angular distributions and energy spectra from, (E/T), 25:12604
alpha reactions (α,He-3) at 42 to 90 MeV, angular distributions and energy spectra from, (E/T), 25:12604
determination of trace amounts of, in biotite and tektite by spark source mass spectrometry, 25:10455
friction and wear of, sliding against copper and iron rings under vacuum, 25:11413
helium-3 inelastic scattering at 50 and 75 MeV, angular distributions and energy spectra from, (E/T), 25:12604
helium-3 reactions (He-3,α) at 50 to 75 MeV, angular distributions and energy spectra from, (E/T), 25:12604
ion reactions with, angular and energy distributions of charged particles emitted in, (E), 25:11675
rare-gas-atom scattering at thermal energies by (111) surfaces of, (E), 25:11683

PLATINUM ALLOYS AND SYSTEMS
Al_2O_3--Pt, effects on reduction of aqueous uranyl nitrate sclutions by hydrogen at low pressure, catalytic, 25:10572 (IEA-184)

PLATINUM CARBIDES
PtC--U_2C, thermal expansion of U_2PtC_2, high-temperature anisotropic, 25:11509

PLATINUM ISOTOPES Pt-192
energy levels from iridium-192 beta decay, spin--parity assignments for, (E/T), 25:12532 (TID-25592)
energy-level transitions from iridium-192 beta decay, energies, intensities, multipolarities, and K conversion coefficients from, (E/T), 25:12532 (TID-25592)

PLATINUM ISOTOPES Pt-195
neutron capture by, spectroscopic analysis of, (E), 25:12586

PLATINUM ISOTOPES Pt-197
energy level at 346 keV, lifetime of isomeric, (E), 25:12618

PLATINUM ISOTOPES Pt-198
neutron reactions (n,2n) at 14.7 MeV, total cross sections and isomeric yield ratios for, (E), 25:12618

PLATINUM ISOTOPES Pt-199
determination by ion exchange and γ spectroscopy, 25:10490(T) (LIB/Trans-334)

PLATINUM METALS
determination using mixed ligand complexes, 25:10460

PLATYHELMINTHES
Echinococcus sp., infection of human liver with cysts of, effects of, on gold-198 and iodine-131 scanning, 25:11197

PLOWSHARE PROJECT
fallout from Project Schooner, distribution and redistribution of, (E), 25:10716 (UCRL-72534)
ground motion from Project Rulison in, effects on nearby gas wells, (E), 25:10737 (PNE-R-39, Pt.2)
ground motion from Project Rulison in, evaluation of structural damage to nearby mines and wells from, 25:10735 (PNE-R-39)
ground motion from Project Rulison in, evaluation of structural damage to mines from, 25:10736 (PNE-R-39, Pt.1)

PLUMES
rise of stack-released, review of methods for predicting, 25:10717

PLUTONIUM
analysis for impurities by copper spark method, spectrochemical, 25:10444
compounds of, crystal-field effect and magnetic properties of NaCl-type, 25:11994
compounds of, review of NMR in NaCl-type, 25:12036
conference on properties and structure of, Sante Fe, New Mexico, Oct. 5 to 9, 1970, 25:11433 (CONF-701001-(Pt.2))
conference on properties and structure of, Sante Fe, New Mexico, Oct. 5 to 9, 1970, 25:11372 (CONF-701001-(Pt.1))
corrosion by water vapor in argon at 50 to 270°C, kinetics of, 25:11350
crack formation during α--β thermal cycling, effects of gallium, titanium, and uranium on, 25:11393
deformation behavior of alpha, beta, and gamma, effects of temperature on, 25:11389
determination in solutions by amperometric or potentiometric titration, effects of americium on, 25:10445
diffusion in epsilon phase on welded couples of copper--plutonium alloy and, chemical, 25:11387
diffusion under hydrostatic pressure, activation voluse study of self-, 25:11371 (CEA-CONF-1690)
distribution in dilute plutonium--titanium and plutonium--zirconium alloys, effects of β and α phase transformation and oxygen content on, 25:11431 (CEA-CONF-1691)
electric potential of trivalent/tetravalent couple of, in nitric acid solutions, 25:10514 (AERE-R-5320)
enthalpy of solution of carbon, manganese, rhenium, thulium, titanium, and zirconium in liquid, 25:11386
grain size of β-, 25:11444
hardness of alpha, at 75 to 375°K, effects of grain size on, 25:11389
oxidation at low humidity, rates of, 25:11346 (AWRE-C-100/66)
phase studies of α--β transformation in monocrystalline, at low temperatures, 25:11443
phase transformation in, comparison of enthalpic analysis and high pressures for determination of heats of α--β, 25:11445
phase transformation in, effects of gamma-phase heat treatments on kinetics of β--α, 25:11444
phase transformations in, review of data on, 25:11437
positron annihilation radiation in, at 4.2 to 623°K, angular correlation of, 25:11997
production by calciothermic reactions, initiation triggering device for, 25:10760(P)
properties of monocrystalline α-, effects of crystallographic orientation on electric and magnetic, 25:12005
radiation effects on α--β transformation temperature in, thermal neutron, 25:11467
radiation effects on electric conductivity of α- and β-, at low temperatures, self-, 25:11960
radiation effects on length of α-, self-, 25:11468
recycle in thermal reactor fuels, Belgian program on physics aspects of, (E/T), 25:12796 (EURAEC-2145)
separation from niobium-95, ruthenium-106, and zirconium-95 by ion exchange on zirconium phosphate silicate columns, 25:10677
separation of neptunium from, by ion exchange in tetramethylammonium hydroxide--citrate solutions, effects of complexing agents on, 25:10655 (ANL-7751)
thermal conductivity at 400 to 800°C, 25:11383
thermal conductivity of high-purity, at 4 to 90°K, 25:11382
thermodynamic properties at low temperatures, review of, 25:11384
thermodynamic properties of bcc and fcc phases of, prediction of effects of elements on, 25:11392
value in nuclear power plants, effects on utility system costs of, (T), 25:12724 (TRG-Report-2090)

PLUTONIUM ALLOYS AND SYSTEMS
Ag--Pu, phase diagram of, 25:11441
Al--Pu-base, electronic properties of delta-phase, positron annihilation study of, 25:11998
Al--Pu-base, radiation effects on length of delta-, self-

, 25:11468
C--O--Pu--U, phase equilibria in, prediction of, 25:11525
C--Pu, thermodynamic properties at 900 to 2200°K, 25:11506
C--Pu--U, phase diagrams of, isothermal, 25:11524
Cu--Pu, diffusion in epsilon phase on welded couples of plutonium and, chemical, 25:11387
Ga--Pu-base, deformation mechanisms in delta-stabilized fcc, at -196 to 25°C, effects of concentration and strain rate on, 25:11435
Ga--Pu-base, expansion of rolled and segregated, at 25 to 475°C, 25:11388
Ga--Pu-base, fabrication of dispersion-hardened delta-stabilized, 25:11359
Ga--Pu-base, mechanical properties of dispersion-hardened delta-stabilized, at 25 to 400°C, 25:11359
Ga--Pu-base, microstructure and phase composition of heat-treated and as-sputtered, 25:11360
Ga--Pu-base, phase diagram of, proposed, 25:11446
Ga--Pu-base, phase transformations in metastable, 25:11446
Ga--Pu-base, preparation by triode sputtering, 25:11360
Ga--Pu-base, tensile properties of high-purity delta-stabilized, effects of hot working on room-temperature, 25:11390
Ga--Pu-base, tensile properties of rolled, at 25 to 600°C, effects of trace amounts of iron and nickel on, 25:11391
Ga--Pu-base, twinning in delta-stabilized, annealing and deformation, 25:11436
O--Pu--U, diffusion in, effects of temperature gradient on mechanism of, 25:11505
Os--Pu-base, phase diagram of, 25:11438
Pd-base--Pu, magnetic properties of solid solutions of, at 2 to 300°K, 25:12003
Pu--Sc, phase diagram of, 25:11440
Pu--Sc, properties of, electric, mechanical, and physical, 25:11440
Pu--Th-base, radiation effects on length of plutonium-238-enriched dilute α-, self-, 25:11468
Pu--Ti, phase studies of, 25:11429 (CEA-CONF-1687)
Pu--Ti-base, plutonium distribution in dilute, effects of β and α phase transformation and oxygen content on, 25:11431 (CEA-CONF-1691)
Pu--U--Zr, phase diagrams at 500 to 700°C, isothermal, 25:11442
Pu--U-base, radiation effects on length of plutonium-238-enriched dilute α-, self-, 25:11468
Pu--Zr, phase diagram of arc cast and heat treated, 25:11439
Pu--Zr-base, plutonium distribution in dilute, effects of β and α phase transformation and oxygen content on, 25:11431 (CEA-CONF-1691)
Pu--Zr-base, transformation processes in dilute, segregation during martensitic, 25:11430 (CEA-CONF-1688)
Pu-base--Ta, phase transformations in sputtered, unusual, 25:11447

PLUTONIUM CARBIDES
entropy of $PuC_{0.81}$ at 298°K, 25:11493
properties of nonstoichiometric, electric and thermal, 25:11494
thermal capacity of $PuC_{0.81}$, at 10 to 375°K, 25:11493
thermal expansion of carbon-saturated Pu_2C_3 and PuC_2 to 2500°C, 25:11513
PuC_2--UC_2, phase diagram of, differential thermal analysis of pseudobinary, 25:11522
PuC_2--UC_2, phase studies of isopleth and melting behavior for, 25:11523
PuC--UC, compatibility of hyperstoichiometric fuels of, with Type 316L stainless steel at 900°C, 25:11475 (AERE-R-5173)
PuC--UC, creep at high temperatures, effects of pressure on, 25:11485 (CEA-CONF-1670)
PuC--UC, properties of, electric and thermal, 25:11494
PuC--UC-base, melting behavior of, 25:11507

PLUTONIUM CARBONITRIDES
PuCN--UCN, creep at high temperatures, effects of pressure on, 25:11485 (CEA-CONF-1670)

PLUTONIUM ISOTOPES Pu-237
energy levels from uranium-235 (α,2n) and neptunium-237 (d,2n) reactions, half-lives, isomer ratios, and production ratios for isomeric, (E/T), 25:12530 (RLO-1388-130)

PLUTONIUM ISOTOPES Pu-238
alpha decay of, time spectrum of alpha--conversion-electron delay in, (E), 25:12542
content of atmosphere in USA during 1968, 25:11039
content of atmosphere over Central, North, and South America during April to Dec. 1969, 25:10721
energy levels from curium-242 alpha decay, lifetimes, quadrupole moments, and deformation parameters for, (E), 25:12542
energy levels from neptunium-238 decay, lifetimes and spin-parity assignments for, (E), 25:12594
energy-level transitions from curium-242 alpha decay, probabilities for E2, (E), 25:12542

PLUTONIUM ISOTOPES Pu-239
accumulation by Ascophyllum nodosum and marine phytoplankton influence of cellular respiration inhibitors on, 25:10941
alpha decay of, time spectrum of alpha--conversion-electron delay in, (E), 25:12541
content of atmosphere in USA during 1968, 25:11039
content of atmosphere over Central, North, and South America during April to Dec. 1969, 25:10721
half-life of, isothermal calorimetric measurement of, 25:10779
inhalation by personnel, hazards to bones and liver following occupational, 25:11301
neutron capture by, interference effects in average cross section for, (T), 25:12608
neutron capture-to-fission ratio at 20 to 500 keV, (E), 25:12511 (CEA-N-1368)
neutron fission of, interference effects in average cross section for, (T), 25:12608
neutron resonance scattering by, interference effects in average cross section for, (T), 25:12608
power output of, isothermal calorimetric measurement of, 25:10779
triton reactions (t,pf) with, fission probability and angular correlation coefficients for, (E), 25:12579

PLUTONIUM ISOTOPES Pu-240
alpha decay of, time spectrum of alpha--conversion-electron delay in, (E), 25:12542
deuteron reactions (d,pf) with, fission probability and angular correlation coefficients for, (E), 25:12579
energy levels from curium-244 alpha decay, lifetimes, quadrupole moments, and deformation parameters for, (E), 25:12542
energy-level transitions from curium-244 alpha decay, probabilities for E2, (E), 25:12542
triton reactions (t,df) with, fission probability and angular correlation coefficients for, (E), 25:12579

PLUTONIUM ISOTOPES Pu-241
inhalation of, americium-241 buildup in lungs after, 25:11053 (BNWL-B-12)

PLUTONIUM ISOTOPES Pu-242
deuteron reactions (d,pf) with, fission probability and angular correlation coefficients for, (E), 25:12579
production at TRU, 25:10654(R) (ORNL-4588)
thermal capacity at 10 to 373°K, 25:11385
triton reactions (t,df) with, fission probability and angular correlation coefficients for, (E), 25:12579

PLUTONIUM NITRIDES
PuN--UN, compatibility with Type 304 stainless steel at 650 to 1000°C, 25:11474(R) (BNWL-842)
PuN--UN, creep at high temperatures, effects of pressure on, 25:11485 (CEA-CONF-1670)
PuN--UN, fabrication of Type 316 stainless steel clad fuel pins of, 25:12795(R) (BMI-1893)
PuN--UN, irradiation testing in liquid sodium cooled fast reactor environment, 25:12795(R) (BMI-1893)
PuN--UN, melting points of, effects of pressure on, 25:11474(R) (BNWL-842)
PuN--UN, properties of, physical, thermal, and thermodynamic, 25:11492
PuN--UN, radiation effects on performance of stainless steel-clad, in-pile, 25:11535
PuN--UN-base, thermal conductivity of carbothermically-produced, at 0 to 1600°C, 25:11474(R) (BNWL-842)

PLUTONIUM OXIDES
curium oxides--plutonium oxides, phase studies of dioxides, intermediate oxides, and sesquioxides of, 25:11521

PLUTONIUM OXIDES PuO_2
diffusion of helium in plutonium-238-enriched sol-gel microspheres of, at 25 to 2000°C, anomalous, 25:11501
enthalpy at 1500 to 2715°K, 25:11491
helium release from plutonium-238-enriched microspheres of, during annealing, calculations of, 25:11499
helium release from plutonium-238-enriched microspheres of, effects of grain size and thermal history on measurement of, 25:11500
radiation effects on microstructure of, 5.5-MeV alpha particle, 25:11537
radiation effects on microstructure of, at high burnups, 25:11474(R) (BNWL-842)
thermal capacity of stoichiometric, vibrational, 25:11996
vibrational frequencies of stoichiometric, ir spectroscopic measurements of, 25:11996
BeO--PuO_2, radiation dose rate from, fast-neutron, γ, and x, 25:11052 (AERE-R-5069)
PuO_2--UO_2, compatibility with Type 304 stainless steel at 650 to 1000°C, 25:11474(R) (BNWL-842)
PuO_2--UO_2, creep at high temperatures, effects of pressure on, 25:11485 (CEA-CONF-1670)
PuO_2--UO_2, creep of polycrystalline, effects of composition, density, grain size, stress, and temperature on compressive, 25:11497
PuO_2--UO_2, creep of, effects of concentration, density, stoichiometry, stress, and temperature on compressive, 25:11495
PuO_2--UO_2, creep testing of, 25:12795(R) (BMI-1893)
PuO_2--UO_2, electric properties of hypostoichiometric, at 25 to 800°C, 25:11991
PuO_2--UO_2, evaporation behavior of hypostoichiometric, at 1800 to 2350°K, 25:11504
PuO_2--UO_2, homogeneity of, mathematical model for describing, 25:11489 (WHAN-FR-20)
PuO_2--UO_2, irradiation testing in liquid sodium cooled

fast reactor environment, 25:12795(R) (BMI-1893)
PuO_2--UO_2, microstructure of fuels of, etching methods for electron microscopic studies, 25:11474(R) (BNWL-842)
PuO_2--UO_2, plutonium dioxide homogeneity in fuel pellets of, scanning electron microprobe analysis of, 25:11489 (WHAN-FR-20)
PuO_2--UO_2, production of monocrystalline, development of methods for, 25:11474(R) (BNWL-842)
PuO_2--UO_2, radiation effects on void distribution in, in-pile, 25:11536
PuO_2--UO_2, volatilization behavior of nonstoichiometric, at 1905 to 2411°K, mass spectrometric study of, 25:11503
PuO_2--UO_2-base, creep of polycrystalline, at 1100 to 1330°C, effects of density, grain size, and stress on compressive, 25:11496

POINT BEACH POWER REACTOR, UNIT 2
design parameters of, revised and additional data on, 25:12744 (DOCKET-50301-26)
operations aspects of, revised and additional data on, 25:12744 (DOCKET-50301-26)
safety injection system piping for, additional data on, 25:12744 (DOCKET-50301-26)

POLAND
radiation protection programs for critical assemblies in, 25:11080

POLAROGRAPHS
development of, 25:10424 (ORNL-4636, pp 34-40)

POLISHING
book: Electrolytic and Chemical Polishing of Metals, 25:11365

POLONIUM ALLOYS AND SYSTEMS
Hf-base--Pu, electric conductivity of, 25:12004
Pu--Ti--Zr-base, electric conductivity of, 25:12004
Pu--Ti-base, electric conductivity of, 25:12004
Pu--Zr-base, electric conductivity of, 25:12004

POLONIUM ISOTOPES Po-208
energy level of, g-factor of 8+ isomeric, (E), 25:12614

POLONIUM ISOTOPES Po-210
accumulation by Ascophyllum nodosum and marine phytoplankton influence of cellular respiration inhibitors on, 25:10941
determination in snow in Antarctica, α spectrometric, 25:10477

POLONIUM ISOTOPES Po-211
content of benthic fish and invertebrates, pelagic fish, and zooplankton of Pacific Ocean, 25:10997(R) (RLO-2225-T-14-1)

POLONIUM ISOTOPES Po-214
energy-level transitions from bismuth-214 beta decay, multipole mixing ratios and γ--γ angular correlations in, (E), 25:12555

POLYGALACTURONASE
radiation effects on synthesis of, in Penicillium expansum, γ, 25:10979

POLYMERS
book: Radiation Chemical Processing, 25:10617
radiation effects on phenoplast molding materials, 25:10634

POPULATIONS
book: Biology of Populations, 25:11005
radiation dose to, of Soviet Union, global cesium-137, 25:11073
radioinduced mutations in human, relation of, to natural selection, 25:11025
radioisotope ingestion by human, in Colombia and Panama for feasibility studies of proposed Atlantic-Pacific interoceanic canal, estimation of potential, 25:10995 (BMI-171-45)
strontium-90 content of rural and urban human, of Soviet Union, 25:10934 (NP-18380)

POROSIMETERS
design of neutron radiometric, for well logging, 25:10889(P)

POSITRONIUM COMPOUNDS
detection of positronium hydride, using Lyman-α radiation from annihilation-product hydrogen atoms, 25:11700

POSITRONS
annihilation in electron gas in metals, (T), 25:12041
annihilation in metals, effects of phonon interactions on rate of, (T), 25:11699
annihilation radiation in plutonium at 4.2 to 623°K, angular correlation of, 25:11997
g-factor of free, CPT invariance in precision measurement of, (E), 25:12075
interactions $e^+ + e^-$ → anti p + p, differential and total cross sections and modulus and phase of form factors of proton electric dipole moment from, (T), 25:12224
interactions $e^+ + e^-$ → K + K total cross section for, (T), 25:12141
interactions $e^+ + e^-$ → π + π, total cross section for, (T), 25:12141
interactions $e^+ + e^-$ → $\pi^+ + \pi^-$, upper limit for phi production in, (E), 25:12074
interactions $e^+ + e^-$ at 0.8 to 1.0 GeV, track analysis and time distribution of elastic, (E), 25:12073
interactions $e^+ + e^-$ at 1.6 to 2 GeV, multiplicities and total cross section for multiple particle production in, (E), 25:12143
reactions with hydrogen atoms, generalized-variational-bounds formalism for distortion effects on rearrangement in, 25:11719
scattering by hydrogen atoms, review of use of Sturmian functions in calculation of, 25:11732

POTASSIUM
content of man, method for determining, 25:10920
content of man, use of whole-body scintillation counter for measuring total-body, 25:10910
determination by photon activation, reactions and sensitivities for, 25:10488 (CEA-R-4072)
determination in serum and urine by flameless atomic absorption spectroscopy, 25:10464
determination in tektite by spark source mass spectrometry, 25:10455
determination of trace amounts of, in minerals and rocks by atomic absorption spectrophotometry, 25:10458
determination of trace amounts of, in molybdenum, review on, 25:10459
determination of trace amounts of, in rocks and sand by thermal neutron activation, ion exchange, and γ spectrometry, 25:10492
determination of trace amounts of, in standard rocks by flame photometry, 25:10671
effects on accumulation and transport of potassium-42 in leaves, stems, and roots of corn, 25:10930 (CEA-CONF-1517)
electron reactions at 1.6 to 20 eV with polarized beams of, depolarization in, (E), 25:11707

POTASSIUM ALLOYS AND SYSTEMS
K--Na, electromigration in liquid, theoretical consideration of, 25:11404

POTASSIUM BROMIDES
defect-induced infrared absorption in lithium ion-doped, isotope effects on, 25:12043
radioinduced M and F centers in crystals of, laser re-excitation and decay of γ, (E/T), 25:11956

POTASSIUM CARBONATES
purification of potassium-42-labeled, by ion exchange, 25:11046

POTASSIUM CHLORATES
positron annihilation in, effects of temperature on, 25:12898 (NYO-3661-33)

POTASSIUM CHLORIDES
defect-induced infrared absorption in lithium ion-doped, isotope effects on, 25:12043
purification of potassium-42-labeled, by ion exchange, 25:11046
radioinduced M and F centers in crystals of, laser re-excitation and decay of γ, (E/T), 25:11956

POTASSIUM IODIDES
defect-induced infrared absorption in chloride- and bromide-doped, isotope effects on, 25:12043
effects on γ radiolysis of indole-3-acetic acid, 25:10647
radioinduced F centers in crystals of, temperature dependence of proton, 25:11965
radioinduced M and F centers in crystals of, laser re-excitation and decay of γ, (E/T), 25:11956

POTASSIUM ISOTOPES K-37
energy levels of, lifetimes and magnetic moments for 7/2-, (E), 25:12429 (COO-7-565)

POTASSIUM ISOTOPES K-39
proton elastic scattering at 1.03 to 3.23 MeV, excitation functions for, (E), 25:12437
proton reactions (p,α) at 1.75 to 3.23 MeV, excitation functions and angular distributions from, (E), 25:12437
proton reactions (p,γ) at 1.03 to 1.75 MeV, excitation functions for, (E), 25:12437

POTASSIUM ISOTOPES K-40
abundance in Allende meteorite, (E), 25:11540
activity measurement of, using whole-body counter for determining total potassium content of man, 25:10920
nucleosynthesis of, effects of energetic proton fluxes on, (T), 25:11544

POTASSIUM ISOTOPES K-42
accumulation in leaves, stems, and roots of corn, effects of age, potassium deficiency, and temperature on, 25:10930 (CEA-CONF-1517)
determination in body fluid by ion exchange and scintillation counting, 25:11066
transport in leaves, stems, and roots of corn, effects of age, potassium deficiency, and temperature on, 25:10930 (CEA-CONF-1517)
uptake in Zea mays roots in relation to bioelectric potential, 25:11308

POTASSIUM SODIUM TARTRATES
radiation effects on Barkhausen effect in crystals of, x-, 25:11978

POTASSIUM SULFATES
K_2SO_4--V_2O_5, phase diagram of, 25:11527

POWDER METALLURGY
compaction research at South Carolina Univ, 25:12913(R) (SRO-475-9)

POWER CYCLES
calculation of optimum high temperature gas cooled power reactor, 25:12809
testing of organic Rankine, design of loop for, 25:10778(R) (ORNL-TM-3214)

POWER SUPPLIES
design and operation of emergency, for reactors, 25:10762(P)

PRASEODYMIUM
complexes with EDTA, separation by ion exchange, effects of resin crosslinking on, 25:10665 (INR-P-1209)
determination of trace amounts of, in biotite and tektite by spark source mass spectrometry, 25:10455
determination of trace amounts of, in phosphate deposits by spark source mass spectrometry, 25:10456
spectra of, ultraviolet absorption, 25:11698
PRASEODYMIUM BORIDES
antiferromagnetic ordering in PrB_6, thermal-capacity and resistivity study of transition order of, (E/T), 25:11988
PRASEODYMIUM ISOTOPES Pr-141
deuteron reactions (d,He-3) with, angular distributions for, (E), 25:12558
energy levels from cerium-140 (He-3,d) reactions, (E), 25:12558
energy levels from quasi-particle Tamm--Dancoff approximation, spin--parity assignments, single-particle energies, eigenvectors, electromagnetic moments, and spectroscopic factors for, (T), 25:12616
energy-level transitions from quasi-particle Tamm--Dancoff approximation, rates for M1 and E2, (T), 25:12616
helium-3 reactions (He-3,d) with, angular distributions for, (E), 25:12558
neutron capture by, average circular γ polarization in thermal, (E), 25:12601
proton reactions (p,2n) at 10 to 15 MeV, cross section and threshold energy for, (E), 25:12607
PRASEODYMIUM ISOTOPES Pr-142
energy levels from thermal neutron capture, spin for compound, (E), 25:12601
PRASEODYMIUM ISOTOPES Pr-144
content of biological materials, gamma scintillation spectrometry method for, 25:11044
PRASEODYMIUM OXIDES
spectra of, ultraviolet absorption, 25:11698
PREAMPLIFIERS
development for lithium-drifted silicon detectors for x-ray spectroscopy, 25:10812 (CEA-N-1401)
PRESSURE GAGES
design of solid galvanic, for oxygen, 25:11472(R) (AD-708705)
performance of liquid metal cooled reactor in-vessel, 25:12781 (ANL-EBR-25)
PRESSURE VESSELS
conference on technology of, Delft, Netherlands, Sept. 29 to Oct. 2, 1969, 25:11357
deformation of prestressed concrete, with complete circumferential crack, DYNA computer program for calculating time-dependent longitudinal, 25:10753 (GAMD-7567)
design, fabrication, and testing of, discussions and lectures on, 25:11357
development of prestressed concrete, for water cooled reactors, 25:12788
fabrication of steel, testing program for, 25:11364
gas flow from prestressed concrete, with complete circumferential crack, DYNA computer program for calculating, 25:10753 (GAMD-7567)
penetrations in reactor, description of hermetically sealed drive shaft assembly for, 25:12863(P)
radiation effects on brittle fracture of steel reactor, method for evaluation of, 25:11470
welds in reactor, equipment for automatic ultrasonic inspection of, 25:12790
windows for, properties of sapphire, 25:11488 (KFK-1211)
PROMETHIUM
complexes with EDTA, separation by ion exchange, effects of resin crosslinking on, 25:10665 (INR-P-1209)
separation from aqueous solutions by solvent extraction using bis(2,2-dimethylhexyl) phosphate, 25:10679
PROMETHIUM ISOTOPES Pm-143
energy levels from quasi-particle Tamm--Dancoff approximation, spin--parity assignments, single-particle energies, eigenvectors, electromagnetic moments, and spectroscopic factors for, (T), 25:12616
energy-level transitions from quasi-particle Tamm--Dancoff approximation, rates for M1 and E2, (T), 25:12616
PROMETHIUM ISOTOPES Pm-147
energy levels from neodymium-147 decay, spin assignments for, (E), 25:12567
energy-level transitions from neodmium-147 decay, multipolarities for, (E), 25:12567
neutron total cross sections and resonance parameters at 0.01 to 1000 eV, (E), 25:12550
PROMETHIUM ISOTOPES Pm-149
energy levels at 114, 189, and 270 keV, nuclear magnetic moments and spins of, (E), 25:12609
energy levels of, magnetic moments of, (E), 25:12557
energy-level transitions from neodymium-149 decay, multipolarities for, (E), 25:12609
energy-level transitions in, angular correlations and probabilities of, (E), 25:12557
PROMETHIUM ISOTOPES Pm-153
decay of, 25:10472(R) (BMBW-FBK-70-19)
PROPANE
thermodynamic properties of, for use as bubble chamber liquid, 25:10876
1,3-PROPANEDIOL, 2-ETHYL-2-(HYDROXYMETHYL)-
trimethacrylate, effects on electron-induced polymerization of methyl acrylate--1,2-polybutadiene, 25:10609 (JAERI-5026, pp 130-6)
2-PROPANOL
yields from radiolysis of aqueous diisopropylamine solutions, effects of 2-mercaptoethanol on, 25:10627(R) (NYO-2499-37)
PROPENE, 2-METHYL-
radiolysis of gaseous, yields of low-boiling-point condensation products from γ, 25:10640
PROPIONITRILE, 2,2'-AZOBIS[2-METHYL-
effects on polymerization of ethylene, role of excited monomer in propagation reaction of, 25:10612
PROSTATE GLAND
scanning of canine, use of metastable zinc-69-labeled zinc chloride for, 25:11204
PROTACTINIUM
radiation effects on electric conductivity of α-, at low temperatures, self-, 25:11960
PROTACTINIUM ISOTOPES Pa-222
alpha decay of, α spectra and half-life for, (E), 25:12592
PROTACTINIUM ISOTOPES Pa-223
alpha decay of, α spectra and half-life for, (E), 25:12592
PROTACTINIUM ISOTOPES Pa-224
alpha decay of, α spectra and half-life for, (E), 25:12592
PROTACTINIUM ISOTOPES Pa-225
alpha decay of, α spectra and half-life for, (E), 25:12592
PROTACTINIUM ISOTOPES Pa-237
decay of, 25:10472(R) (BMBW-FBK-70-19)
PROTACTINIUM ISOTOPES Pa-238
decay of, 25:10472(R) (BMBW-FBK-70-19)
PROTEINS
loss from human intestine, use of iron-59-labeled dextran for determining, 25:11171
radiation effects on cross-linking of, to proteins in HeLa cells, uv, 25:10975
radioisotope content of concentrates of, from pelagic fish, 25:10997(R) (RLO-2225-T-14-1)
PROTON SOURCES
design of polarized, for high-energy accelerators, 25:12304 (JINR-P9-5446)
PROTONS
abundance in magnetosphere, transport and loss mechanisms of, (E/T), 25:11802
acceleration of 1- to 10-MeV, effect of interplanetary shock wave on, (E/T), 25:11624
channeling in gold single-crystal foils, energy loss and straggling in, 25:11976
channeling in silicon (110) planar channel at 0.2 and 1 MeV, calculated wavelength distributions for transverse oscillations in, 25:11953
dechanneling coefficient in silicon crystals of 1.5-MeV, temperature dependence of, (E/T), 25:11969
density irregularities of, deduced from cyclotron damping of proton whistlers, (E/T), 25:11787
detection of, performance of cellulose acetate track detectors for, 25:10831
dose characteristics at 200 MeV, (E/T), 25:11054 (JINR-P16-5383)
effects of fluxes of energetic, on nucleosynthesis at stellar surfaces and on solar system, (T), 25:11544
effects on potassium iodide crystals at 3.5 MeV, F centers induced in, 25:11965
electric dipole moment of, anti p + p → $e^+ + e^-$ and $e^+ + e^-$ → anti p + p interactions for modulus and phase of form factors of, (T), 25:12224
energy spectra in ionosphere of 1- to 30-MeV, (E), 25:11813
energy spectra mirroring near magnetic-equator outer radiation zone, directional differential of 200 eV less than or equal to E less than or equal to 1 MeV, (E), 25:11786
flux in magnetosphere, drift periodic echoes in solar, (E), 25:11801
flux of low-energy, near Moon, Dec. 16, 1966, flare- and Forbush decrease-associated, (E), 25:11669
form factor of, e + d → e + d interactions at low momentum transfers for neutron-to-proton ratio for electric, (E), 25:12070
form factor of, phenomenological analysis of infinite resonance model for electromagnetic, 25:12153
form factors of, e + d → e + d interactions at low momentum transfers for deuteron-to-proton ratio for electric, (E), 25:12070
intensity profiles of solar 1 MeV, 33 MeV, and 114 MeV, at 2000 to 3000 km, rigidity-dependent latitude, (E), 25:11797
interactions anti ν + p → μ^+ + hadrons at high energies, scaling laws in Veneziano model for, (T), 25:12166
interactions anti p + p → $e^+ + e^-$, differential and total cross sections and modulus and phase of form factors of proton electric dipole moment from, (T), 25:12224
interactions anti p + p at 1.6 to 2.2 GeV/c in hydrogen bubble chamber, K^0, $K^*(892)$, ω, rho, and odd-C meson resonance (2370) production and angular distributions for, (E), 25:12097
interactions anti p + p at 100 to 750 MeV/c in hydrogen

bubble chamber, differential elastic and annihilation cross sections and (1927) and (1950) boson resonance production in, (E), 25:12095
interactions anti p + p at high energies, sakaton rearrangement model for, 25:12186
interactions anti p + p, resonance production and branching ratios for multipion production in, (T), 25:12195
interactions e + p + e + π^+ + π^- + p, cross section for rho' production in dual model for diffractive, (T), 25:12137 (DESY-70/56)
interactions e + p, Reggeization scheme for photon processes for deep inelastic, (T), 25:12148
interactions γ + p + γ + p, continuous-moment sum rules for Compton, (T), 25:12207
interactions γ + p + K + $\Sigma(\Lambda)$ at high energies, tests of Regge-pole and strong-absorption models for, (T), 25:12206
interactions γ + p + π^0 + p at 6 GeV, spectrometer and Cherenkov counter study of asymmetry in, (E), 25:12072
interactions γ + p + π^0 + p at 6 to 18 GeV, differential cross sections for backward, (E), 25:12069
interactions γ + p + π^+ + n at 0.450 to 3 GeV, resonance structure of cross sections for, (E), 25:12067 (LAL-1239)
interactions γ + p + π^+ + π^- + p, five-body Veneziano amplitude for diffractive, 25:12152
interactions γ + p + $\pi^+(\pi^0)$ + n(p) in second resonance region, fixed-t dispersion relations for, (T), 25:12146
interactions γ + p above 1.2 GeV, data compilation on cross sections for hadron production in, (E), 25:12066 (DESY-HERA-70-1)
interactions K + p at high energies, sakaton rearrangement model for, 25:12186
interactions K^- + p + anti K^0 + n at high energies, constancy of total cross sections for, (T), 25:12210
interactions K^+ + p + $K_1{}^0$ + p + π^+ at 3.2 GeV/c in hydrogen bubble chamber, K^* and N^* production and momentum transfer distributions in, (E), 25:12114
interactions K^+ + p + K^+ + p + K^+ + K^- at 12.7 GeV/c in hydrogen bubble chamber, production of low-mass K^+phi^0 enhancement and phi^0 in, (E), 25:12102
interactions K^+ + p + K^+ + p + π^+ + π^- + π^0 at 12.7 GeV/c in hydrogen bubble chamber, production of low-mass $K^+\omega^0$, K^+eta^0, pω^0, and peta^0 enhancements and ω^0 and eta^0 in, (E), 25:12102
interactions K^+ + p + K^+ + p + π^+ + π^- at 12.7 GeV/c in hydrogen bubble chamber, resonance diffractive production in, (E), 25:12102
interactions K^+ + p + K^+ + p at 2.53 to 3.20 GeV/c in hydrogen bubble chamber, differential and total cross sections for, (E), 25:12115
interactions K^- + p + K^- + p at high energies, constancy of total cross sections for, (T), 25:12210
interactions K^- + p + $\Sigma^*(\Sigma^-)$ + $\pi^-(\pi^+)$ at 440 to 1230 MeV/c in hydrogen bubble chamber, Λ and Σ resonance production, Σ^+ decay branching ratio, and Σ^+ and Σ^- lifetimes in, (E), 25:12098 (CEA-R-4068)
interactions K^+ + p at 2.50 GeV/c, phase shift analysis of, (T), 25:12115
interactions K^- + p at 360 to 720 MeV/c, $\Lambda(1520)$ and $\Sigma(1600)$ enhancement production and total cross sections for, (E), 25:12120
interactions K^+ + p at 360 to 720 MeV/c, total cross sections for, (E), 25:12120
interactions K^- + p, urbaryon rearrangement diagrams for amplitudes of, 25:12183
interactions n + p + d + γ, test of time reversal invariance in total and differential cross sections for, (E), 25:12238
interactions n + p from deuterium (n,p2n) reactions at 14.1 MeV, singlet scattering lengths for, (E/T), 25:12367
interactions ν + p + μ^- + hadrons at high energies, scaling laws in Veneziano model for, (T), 25:12166
interactions ν + p + p + π^+ + μ^-, hadronic s-channel helicity conservation in, (T), 25:12165
interactions p + N at 210 MeV, upper limits for two parity-violating parameters from asymmetries in, (E), 25:12094
interactions p + p + p + p + π^+ + π^- at 28.5 GeV/c in hydrogen bubble chamber, Δ^{++}(1236) and Nπ(1400) enhancement production in, (E), 25:12091
interactions p + p at 20 to 120 MeV, differential cross section for electron-pair production in, (T), 25:12231
interactions p + p at 210 MeV, upper limits for two parity-violating parameters from asymmetry in, (E), 25:12094
interactions p + p at 28.5 GeV/c in hydrogen bubble chamber, Δ^{++}(1236) and Nπ(1400) enhancement production in two- and four-charged-prong, (E), 25:12091
interactions p + p at high energies, cross sections for μ pair production in two different types of, (T), 25:12229
interactions p + p at high energies, sakaton rearrangement model for, 25:12186
interactions p + p at low energies, Coulomb effect on parameters for, (T), 25:12680
interactions p + p, light-cone analysis of massive μ pair production in, (T), 25:12228
interactions π + p at high energies sakaton rearrangement model for, 25:12186
interactions π^+ + p + $2\pi^+$ + π^- + π^0 + p at 3 to 5 GeV/c, determination of spin and parity of B meson from, (E), 25:12119
interactions π^+ + p + $A_2{}^+$ + p at 7 GeV/c in bubble chamber, A_2 mass spectra in, (E), 25:12116
interactions π^- + p + e^+ + e^- + n at 275 MeV, emission energies and angles for e^+ and e^- and differential cross sections for, (E), 25:12099 (JINR-P1-5398)
interactions π^- + p + A + K^0 at 944 to 1170 MeV/c in hydrogen bubble chamber, differential and total cross sections, polarizations, and partial-wave analysis for, (E/T), 25:12109
interactions π^- + p + n + 2γ at 2 to 6 GeV/c, spark chamber study of cross sections for eta^0 and π^0 production in, (E), 25:12113
interactions π^- + p + n + π^+ + π^- at 2 to 6 GeV/c, spark chamber study of differential cross sections for rho^0 and f^0 production in, (E), 25:12113
interactions π^- + p + n + $\pi^+(2\pi^+)$ + $\pi^-(2\pi^-)$ + $n\pi^0$ at 4 GeV, statistical and anisotropic models for, (T), 25:12204 (JINR-P1-5431)
interactions π^+ + p + p + $3\pi^+$ + $2\pi^-$ + π^0 at 8 GeV/c, D^0 production in, (T), 25:12191 (INR-P-1207)
interactions π^- + p + π^0 + n at high energies, Reggeized generalized optical model for multiple and diffraction scattering and dips in, (T), 25:12205
interactions π^- + p + π^0 + n, discrepancies between forward amplitude data and dispersion relation prediction for, (E/T), 25:12209
interactions π^+ + p + π^0 + N^{*++} at high energies, differential cross sections and spin-density matrix elements for, (T), 25:12223
interactions π^- + p + π^+ + $2\pi^-$ + π^0 + p at 6 GeV/c in hydrogen bubble chamber, resonance production and cross sections for, (E), 25:12101
interactions π^- + p + rho^0 + n in vector-dominance model, nonevasive contribution to forward rho production in, (T), 25:12212
interactions π^+ + p at 1.7 GeV/c, cross sections for strange-particle final states in, (E), 25:12104
interactions π^- + p at 2.15 to 6.0 GeV/c, spark chamber study of cross sections for backward π^- and π^+ production in, (E), 25:12111
interactions π^+ + p at 5 GeV/c in urbaryon rearrangement model, dip-bump structure of cross sections for, (T), 25:12219
interactions π^- + p at 5 GeV/c in urbaryon rearrangement model, dip-bump structure of cross sections for, (T), 25:12219
interactions π^- + p at 7 GeV/c, resonance production in strange-particle final states in, (E), 25:12110
interactions π^- + p at high energies, Regge pole fits to charge exchange, differential cross sections, and polarization in, (E/T), 25:12217
interactions π^- + p + n + eta^0 at 5.9 GeV/c, cross sections for backward, (E), 25:12117
interactions π^- + p + n + π^0 at 5.9 to 13.8 GeV/c, cross sections for backward, (E), 25:12117
losses from magnetosphere by charge exchange and pitch-angle diffusion, (T), 25:11803
mass difference (n - p), contribution of Born term to electromagnetic, 25:12154
reactions (p,2n) with praseodymium-141 and yttrium-89 at 10 to 15 MeV, threshold energies and cross sections for, (E), 25:12607
reactions (p,2nγ) with holmium-165, lutetium-175, terbium-159, and thulium-169 at 16 and 21 MeV, cross sections for, (E/T), 25:12544
reactions (p,2p) with beryllium-9 at 180 and 660 MeV, lithium-8 energy spectra and angular distributions from, (E/T), 25:12378 (JINR-P1-4872)
reactions (p,2p) with deuterium at 100 MeV, proton spectra and angular distributions from, (E), 25:12375
reactions (p,2p) with nitrogen-14 at 46 MeV, energy spectra and distorted-wave t-matrix approximation analysis of differential cross sections from, (E/T), 25:12391
reactions (p,2p) with nuclei, off-shell effects in, (T), 25:12670
reactions (p,α) with oxygen-15 at 16 MeV, internal bremsstrahlung spectra for, (T), 25:12694
reactions (p,α) with potassium-39 at 1.75 to 3.23 MeV, excitation functions and angular distributions from, (E), 25:12437
reactions (p,$\alpha\gamma$) with sodium-23 at 1.1 to 1.5 MeV, α--γ angular correlations in, (E), 25:12443
reactions (p,$\alpha\gamma$) with sulfur-32 at 11.72 to 13.02 MeV, excitation functions, alpha and gamma spectra, and α--γ angular correlations from, (E), 25:12480
reactions (p,d) with molybdenum and zirconium isotopes, charge exchange effects and spectroscopic factors in, (E), 25:12571
reactions (p,d) with nuclei, lectures on polarization in, (T), 25:12624 (ANU-P-497)
reactions (p,d) with oxygen-16 at 25.52, 30, and 31.82 MeV, effect of deuteron D-state on DWBA calculations of differential cross sections, deuteron polarizations, proton analyzing powers, and spectroscopic factors from, (T), 25:12414
reactions (p,γ) with aluminum-27 at 0.9 to 1.9 MeV,

excitation function and resonance energy for, (E), 25:12402
reactions (p,γ) with beryllium-7 at 0.95 to 3.28 MeV, cross-section measurements and zero-energy cross-section factor for, (E), 25:12400
reactions (p,γ) with carbon-14 at 1.3 to 2.6 MeV, γ spectra and angular distributions for, (E), 25:12416
reactions (p,γ) with potassium-39 at 1.03 to 1.75 MeV, excitation functions for, (E), 25:12437
reactions (p,γ) with sulfur-34 at 1.0 to 1.5 MeV, angular distributions from, (E), 25:12440
reactions (p,n) and (p,nγ) with cobalt-59 at 2.4 to 3.3 MeV, gamma spectra and comparison of Hauser--Feshbach theory with neutron and gamma yields from, (E/T), 25:12476
reactions (p,n) and (p,nγ) with vanadium-51 at 2.4 to 3.3 MeV, comparison of Hauser--Feshbach theory with neutron cross sections and gamma angular distributions and anisotropies from, (E/T), 25:12476
reactions (p,n) with lithium-7 at 0.9 to 1.9 MeV, excitation function and threshold energy for, (E), 25:12402
reactions (p,n) with manganese-55 at 2.4 to 3.3 MeV, comparison of neutron cross sections with Hauser--Feshbach theory, (E/T), 25:12476
reactions (p,n) with sulfur-34, threshold energies and excitation functions for, (E), 25:12442
reactions (p,n) with tritium at 156 MeV, spectra and differential cross sections for, (E/T), 25:12365
reactions (p,nγ) and (p,p'γ) with vanadium-51 at 2.3 to 6 MeV, gamma spectra from, (E), 25:12435
reactions (p,nγ) with manganese-55 at 3.6 to 5.5 MeV, γ spectra and angular distributions for, (E), 25:12483
reactions (p,nγ) with rhenium-185 at 12 MeV, γ spectra from, (E), 25:12514(R) (CCO-1672-21)
reactions (p,pn) and (p,p2n) with nickel-58 at 400 MeV, angular distribution of recoils from, (E), 25:12500
reactions (p,pn) and (p,p3n) with gold-197 at 400 MeV, angular distribution of recoils from, (E), 25:12500
reactions (p,pn), (p,2n), and (p,2p) with cadmium-106, -108, -110, -112, -113, and -114 at 400 MeV, analysis for nuclear structure effects in, (E), 25:12570
reactions (p,pn), (p,2n), and (p,2p) with tellurium-122, -123, -124, -125, -126, -128, and -130 at 300 MeV, analysis for nuclear structure effects in, (E), 25:12581
reactions (p,t) with lead-208 at 40.7 MeV, energy spectra and DWBA analysis of differential cross sections from, (E/T), 25:12574
reactions (p,t) with nickel-58 at 51.9 MeV, differential cross sections for, (E), 25:12431 (INSJ-124)
reactions (p,t) with samarium-152 and -154 at 20.6 MeV, angular distributions for, (E), 25:12612
reactions (p,xn) with Z = 20 to 100 nuclei, excitation functions and thick-target yields for, (T), 25:12529(T) (ORNL-tr-3020)
reactions with aluminum up to 70 GeV, negative particle distributions from, (E), 25:10868 (IFVE-SEF/OP-70-13)
reactions with atoms having Z = 2 to 11, calculation of excitation and ionization cross sections and stopping power for, using generalized oscillator strengths, 25:11715
reactions with calcium-40 at 10.3 to 21.6 MeV, total cross sections for, (E), 25:12497
reactions with gases at 30 to 120 keV, cross sections for electron capture into n = 3 level of hydrogen in, (E), 25:11708
reactions with gold-197 at 2.2 GeV, angular distributions and differential range spectra of terbium-149 recoils from, (E), 25:12580
reactions with hydrogen atoms, review of use of Sturmian functions in calculation of charge exchange in, 25:11732
reactions with medium-weight nuclei at 60 MeV to 2.9 GeV, cross sections for spallation products from, (T), 25:12439
reactions with nitrogen molecules at 0.3 to 1.7 MeV, angular and energy distributions of electrons ejected from, (E), 25:11712
reactions with uranium at 5.5 GeV, Z = 5 to 10 mass spectrum from, (E), 25:10860
scattering by atomic and molecular gases, analytic cross sections for inelastic, (E/T), 25:11703
scattering by calcium-42 at 7 MeV, p-γ angular correlations from inelastic, (E), 25:12465
scattering by carbon-12 at 10.3 to 21.6 MeV, cross sections for, (E), 25:12497
scattering by chromium-52 and magnesium-24 at 5.38 to 5.95 MeV, excitation functions, polarization, and angular distributions from elastic and inelastic, (E), 25:12433 (NP-18552)
scattering by helium-3 and tritium at 156 MeV, differential cross sections for elastic, (E/T), 25:12365
scattering by helium-4 at 1 to 40 MeV, phase shifts, cross sections, and polarizations from resonating-group study of elastic, (T), 25:12363
scattering by nickel-58 at 5.38 to 5.95 MeV, polarization from elastic and inelastic, (E), 25:12433 (NP-18552)
scattering by nuclei at 10 to 60 MeV, local Woods--Saxon potentials equivalent to nonlocal analysis including exchange effects in elastic, (T), 25:12689
scattering by nuclei, exchange effects with realistic interaction for inelastic, (T), 25:12676
scattering by nuclei, lectures on cross sections and polarization from elastic, (T), 25:12624 (ANU-P-497)
scattering by nuclei, microscopic first-order core polarization corrections to DWBA for inelastic, (T), 25:12678
scattering by potassium-39 at 1.03 to 3.23 MeV, excitation functions for elastic, (E), 25:12437
scattering by silicon-28 at 12 to 15 MeV, statistical analysis of intermediate structure in inelastic, (E/T), 25:12470
scattering by silicon-29 at 6.5 and 8.7 MeV, gamma spectra and angular correlations from inelastic, (E), 25:12449
scattering by sulfur-32 at 3.200 to 3.385 MeV, phase-shift analysis of excitation functions and energy spectra from elastic, (E/T), 25:12506
scattering by tellurium-128 and -130 at 7.48 to 12.65 MeV, angular distributions and proton and gamma energy spectra from elastic and inelastic, (E), 25:12602
scattering by zirconium-94 at 6 to 8.5 MeV, angular distributions and excitation functions for elastic and inelastic, (E), 25:12564
use for determining cross section, thickness, shape, and internal structure, review of, 25:10977

PROTONS (anti p)
interactions anti p + p → e⁺ + e⁻, differential and total cross sections and modulus and phase of form factors of proton electric dipole moment from, (T), 25:12224
interactions anti p + p at 1.6 to 2.2 GeV/c in hydrogen bubble chamber, K⁰, K⁰(892), ω, rho, and odd-C meson resonance (2370) production and angular distributions for, (E), 25:12097
interactions anti p + p at 100 to 750 MeV/c in hydrogen bubble chamber, differential elastic and annihilation cross sections and (1927) and (1950) boson resonance production in, (E), 25:12095
interactions anti p + p at high energies, sakaton rearrangement model for, 25:12186
interactions anti p + p, resonance production and branching ratios for multipion production in, (T), 25:12195

PROTOTYPE FAST REACTOR
flowmeters for, development of a-c operated, 25:12792

PROTOZOA
Acanthamoeba sp., radiation effects on formation of supernumerary surface layers in, x, 25:11249
Blepharisma japonicum, radiation effects on oral ciliature of, comparison of uv with laser, 25:11322

PUBLIC HEALTH
radiation protection standards affecting, in USA,AEC, ICRP, an NCRP, 25:11076

PULSARS
dynamics of, free, (T), 25:11596
ejection in supernova events, (T), 25:11588
NP 0532, absence of average polarization at 111.5 MHz in, (E), 25:11589
NP 0532, absorption by interstellar gases of photons from, (E/T), 25:11665
NP 0532, magnetic field in, (T), 25:11591
NP 0532, spectral indices of pulses at 410 and 1664 MHz, (E), 25:11598
PSR 1237 + 25, peculiar pulse burst in, (E), 25:11586
pulse variations in, general features of short-term, (E), 25:11586
radio emission mechanisms for, (T), 25:11595

PULSE ANALYZERS
time analyzer for multicycle experiments with exponential decay for multichannel, optimization of parameters for, 25:10900

PULSE CONVERTERS
interface for Varian 622/i computer to analog-to-digital, for nuclear spectroscopy, 25:10848 (ANL-7704)
noise in time-to-pulse height, due to accidental coincidences, 25:10902

PULSE DISCRIMINATORS
circuits for, analysis of cascade switching, 25:10901
development for radiation detectors, review on, 25:10815 (JUL-660-ZE)
performance for gamma discrimination in proton-recoil proportional detector for neutron spectroscopy, 25:10857
time jitter due to circuit noise, 25:10808 (AERE-R-5561)

PULSE GENERATORS (ELECTRONICS)
development of high-current, for studying electric properties of superconductors, 25:10899
efficiency limit of resonance charging of pulse-forming network in, for accelerator power supply, 25:12333

PUREX PROCESS
waste from, treatment of, by pot solidification, 25:10658(R) (BNWL-1533)

PYRIDINE
radiolysis on silica gel, ESR studies on effects of deuterium on γ, 25:10622 (JAERI-5026, pp 6-10)

PYRIDINE, 4-VINYL-
radioinduced polymerization on surface of synthetic calcium aluminate hydrate,, 25:10616

PYRITES
analysis for gold by neutron activation and radiochemical separation, 25:10490(T) (LIB/Trans-334)

PYROPHOSPHATES
separation from meta- and orthophosphates, paper chromatographic, 25:10687
PYRROLIDINE
nitroxide free radicals in, 310-MHz NMR study of, 25:12034 (CEA-R-3855)

Q

Q DEVICES
electric discharge tube for QP, feedback control of PIG, 25:11921 (IPPJ-T-2)
QUANTUM ELECTRODYNAMICS
asymptotic states in, 25:12249
causal distributions in, singularity structure of, 25:12133
charge renormalization in, finite, 25:12247
current commutators in scalar and spinor, singularity structure of causal distributions for, 25:12133
field equations for one-electron multi-photon stationary states for Compton $\gamma + e + \gamma + e$ interactions in, effective, 25:12139
hyperquantization formalism for interacting spin-3/2 field in, 25:12267
lepton anomalous magnetic moment in, cut-off from field with nonpolynomial interaction for, 25:12157
quantization of zero-mass fields in, Poincare covariant, 25:12259
Schwinger terms in second-order, singularity structure of causal distributions for, 25:12133
QUANTUM FIELD THEORY
anharmonic oscillator in, analyticity and singularities in coupling constants for, 25:12257
boson self-interactions in, energy--momentum spectrum and vacuum expectation values for, 25:12269
commutation relations on renormalized space cut-off Hamiltonian in, representations of canonical, 25:12256
conference on, 25:12254
Dirac field with anomalous magnetic moment in, energy-momentum tensor of, 25:12251
Feynman amplitude in nonpolynomial Lagrangian, third-order, 25:12266
field emission in perturbed scattering model in, three-dimensional, 25:12178
formulation of $(phi^4)2$ with interaction, review of, 25:12255
formulation of local infinite-component, Van Hove model of Regge poles in, 25:12246
formulation of spinor, potentials with logarithmic regularization in, 25:12261
formulation without cutoffs for self-interacting bosons, 25:12248
gauge invariance in spinor theories with nonlinear quadratic self-interaction, 25:12262
interactions $\gamma + e + \gamma + e$ in lambda phi^4, scale invariance in Compton, 25:12149
Lee model with arbitrary cutoff in, generalized operators for Ntheta sector of, 25:12263
mesons in, cellular space--time for equations of spinless charged, 25:12260
model of divergenceless nonlocal, 25:12268
operators in, generalized, 25:12263
particles in, highly charged subnuclear, 25:12132
radiative corrections for lambda phi^3, computer programs for calculating renormalized, 25:12245 (CNRS-CPT-70-P-318)
renormalization of Yang--Mills field with nonzero mass in, spectral representation for, 25:12250
renormalizations and dressing transformations in, 25:12258
space--time in, cellular, 25:12260
spinor theory formulation of, potentials with logarithmic regularization in, 25:12261
symmetries in, physical, 25:12253
symmetry transformations generated by conserved local currents in Wightman relativistic, 25:12264
QUANTUM MECHANICS
angular-momentum decomposition of the three-body problem in, 25:12644
book: Mathematical and Theoretical Physics, Vol. I, 25:12048
book: Mathematical and Theoretical Physics, Vol. II, 25:12049
book: Quantum Mechanics and Atomic Physics, 25:12052
formalism considering electromagnetic fields, 25:12062
integral equations for wave vectors of system with discrete set of states, 25:12051
solutions for dyons, relativistic, 25:12047 (NYO-3829-65)
spectral theory for the Klein--Gordon equation with an external electrostatic potential, 25:12679
statistical, generalized operators in, 25:12263
sum rules in, and application, 25:12046 (NP-18619)
wave equation solutions using perturbation expansions, 25:12054
WKB method in classical approach to, 25:12063
QUASARS
galaxies associated with, of small redshift, (E), 25:11649
gravitational lens mechanism for explaining, (T), 25:11584
luminosity-volume test for, (T), 25:11664
models for, featuring antimatter cores, (T), 25:11585
plasma ejection from, (T), 25:11658
radioluminosity as function of redshift for, absolute, (E), 25:11581(T) (CSIRO-Trans-10247)
scintillation of 3C 48, interplanetary, (E), 25:11580(T) (CSIRO-Trans-10204)
spectral redshifts of photons from, (E/T), 25:11665
stability of ionized atmospheres of, (T), 25:11585
ultraviolet background in, origin of, (T), 25:11654
8-QUINOLINOL
complexes with uranium, thermodynamic properties of, 25:10581

R

RABBITS
blood circulation in conscious, methods for xenon-133 scanning of cerebral, 25:11194
bone transplantation in, ESR evaluation of resorption rate following γ-radiosterilized, 25:11340
radiation effects on blood pressure, heart rate, and respiration in, following administration of zirconium citrate, effects of synchronous calcium gluconate administration on whole-body γ, 25:11289
radiation effects on content of autoantibodies in liver of, x, 25:10985
radiation effects on lung surface of, 25:11267
radiation effects on neural activity in optical cortex of, exposed during embryogenesis, x, 25:11283
radioinduced destruction in tissues of, hyperglycemia following γ, 25:10969
radioinduced inhibition of healing of mandibular fractures in, x, 25:11266
radiosensitivity in relation to volume of thoracic aorta endothelial cytoplasm, 25:11269
scanning of x-irradiated bone marrow of, in function studies of erythron and reticulo-endothelial cells, use of iron-59 and metastable technetium-99 colloids for, 25:11112
tritium retention in hair of, 25:10954
RADIATION
book: Intercrystalline Corrosion and Corrosion Cracking of Stainless Steel in Aqueous Solutions (In Russian), 25:11353
book: Radiation Chemical Processing, 25:10617
dose calculation at site of human organs using tissue equivalent phantom, absorbed, 25:11067
dose fractionation for therapy of human mediastinal lymphomas, ionizing, 25:11226
dose to airport personnel from intransit radioactive materials, 25:11062
dose to biological materials, equivalence nomograms for fractionation in, 25:11071
dose to human populations in Colombia and Panama following ingestion and external exposure from use of nuclear explosives for proposed construction of interoceanic canal, estimation of, 25:11055 (ORNL-4579)
dose to lens of human eyes, effects of age and dose fractionation on maximum safe, 25:11284
dosimetry of, classification of ICRU international units for, 25:11064
effects of, morphological changes preceding appearance of neoplastic, 25:11271
effects on activity of alkaline phosphatase and cholinesterase in blood and tissues of rats following injection of mixed radioisotopes, 25:10968
effects on animals and man, genetic, 25:11294(R) (EUR-4542)
effects on antigenicity of peripheral nerve and skull bone homografts for use in mammals, ionizing, 25:11334
effects on antigens in transplanted tissues, effects of 1.5 to 5 Mrad dose on ionizing, 25:11331
effects on aqueous diisopropylamine solutions, effects of 2-mercaptoethanol on yields from, 25:10627(R) (NYO-2499-37)
effects on blood circulation in carcinoma cells of mice, effects of dose fractionation on, 25:11257 (BNL-50203, pp 210-14)
effects on blood vessels, latent damaging, 25:11256 (BNL-50203, pp 186-203)
effects on bone marrow of rats in relation to stem cell population kinetics, design of model for compartmental analysis of, 25:11290
effects on canine treadmill performance decrement, review of whole-body, 25:11251 (AD-705976)
effects on carbon-14-labeled carbon dioxide production, glucose absorption, oxygen utilization and mitochondrial function in rats, continuous, 25:10980
effects on carcinomas in man, relation of dose fractionation and time for, 25:11222 (BNL-50203, pp 280-5)
effects on cellular proliferation following transplantation of sterilized mammalian cells, enhancing and inhibitory, 25:11330
effects on choroid, optic nerve, and retinal tissues in rats, comparison of, in relation to sensitivity, 25:11284
effects on cooperative function of carrier-specific

lymphocytes in antihapten responses of guinea pigs, 25:10987
effects on DNA in vitro and in vivo, comparison of, 25:10966
effects on Escherichia coli and Shigella flexneri, sensitizing effects of acriflavine, indanetrione, and methyl hydrazine on ionizing, 25:11323
effects on free-ionic polymerization of bulk styrene, electric conductivity measurements on, 25:10610 (JAERI-5026, pp 169-71)
effects on germination rate of cereal seeds, mathematical analysis of, for predicting sensitivity of mature plant, 25:11314
effects on growth of C3H tumor cells of mice, effects of oxygen on, 25:11094 (BNL-50203, pp 215-33)
effects on hepatic blood flow, use of iodine-131-labeled RISA for determining microwave, 25:10916
effects on histamine in blood, intestines, kidneys, and liver of rats following ingestion of mixed radioisotopes, mechanism of, 25:10967
effects on hormone production by mother, placenta, and embryo or fetus following exposure during pregnancy, 25:10982
effects on human central nervous system during space flight, effects of acceleration, dose, and vibration on ionizing, 25:11298
effects on human organs and tissues, assessment of, 25:11090
effects on human populations, in relation to natural selection, mutagenic, 25:11025
effects on immune reactions of mice to sheep red cells, effects of injections of spleen cells from mice treated with DMBA on, 25:10990
effects on incidence of whole-body skin eruptions in man following therapy of malignant tumors, 25:11296
effects on infectivity of fungi in sterile corn, role of cytoplasm in, 25:11010(R) (ORO-2583-8)
effects on intestines of rats following ingestion of mixed radioisotopes, mechanism of damage and repair following chronic, 25:11271
effects on kidneys of rats, effects of 4800 to 9600 on histological, 25:11286
effects on leukocytes of human blood, effects of phytohemagglutinin on, 25:11299
effects on lithium fluoride, color centers and thermoluminescence produced in, 25:11958
effects on metabolism of nitrogen compounds in corn endosperm and seedlings following seed exposure, ionizing, 25:11309
effects on nephron function in kidneys of dogs, in dogs, effects of uremic state on phosphate excretion following pathological, 25:10963
effects on organs and tissues, effects of clonogenicity, dose, reproductive integrity, and time on tumorigenic, 25:11253 (BNL-50203, pp 154-73)
effects on oxygen supply in tumor cells, 25:11224 (BNL-50203, pp 318-38)
effects on plants, review of ionizing, 25:10976
effects on polymerization of ethyl acrylate on textiles, 25:10619
effects on polymerization of ethylene terephthalate in aqueous solutions of acryl- or methylacrylamide and unsaturated dicarboxylic acids, 25:10621
effects on polymerization of vinyl acetate in aqueous solutions, stability of emulsions from, 25:10594 (JAERI-5026, pp 26-34)
effects on recipient mice, transplantation of rat myeloid cells following, 25:10992
effects on skin of mice, effects of acute dose and dose fractionation on, 25:11260 (BNL-50203, pp 286-91)
effects on spores of Osmunda regalis, ESR study of, 25:11319
effects on surfactant system in lungs of rabbits, pathological, 25:11267
effects on survival of cells, effects of dose and dose fractionation on, 25:11252 (BNL-50203, pp 54-69)
effects on survival of L cells, effects of lesions on, effects of methotrexate and temperature on, lethal, 25:11092 (BNL-50203, pp 41-53)
effects on survival of Osdogonium cardiacum, effects of hypoxic and aerobic conditions on recovery from, 25:11304 (BNL-50203, pp 70-81)
effects on survival of Rhizobium leguminosarum, effects of dose fractionation on, 25:11325
effects on thyroid in children of man during scanning, comparison of iodine-125, iodine-131, and metastable technetium-99 for, 25:11190
effects on water vapor, review on, 25:10651
use for sterilization of biological materials for use as transplants, effects of temperature on sensitivity of contaminating microorganisms during, 25:11337
use for sterilization of medical supplies, effects of environmental condition on sensitivity of contaminating microorganisms during, 25:11328
use for therapy of cancer of lung in man, methods for dose fractionation in, 25:11223 (BNL-50203, pp 292-307)
use for therapy of carcinomas in esophagus, head, neck, breast, cervix, and bladder in man, 25:11222 (BNL-50203, pp 280-5)
use for therapy of tumor cells, review of effects of dose fractionation on, 25:11259 (BNL-50203, pp 260-7)
use for therapy of tumors in dogs, man, mice, and rats, review of, 25:11219 (BNL-50203, pp 130-53)
use for therapy of tumors in man, review of use of dose fractionation for, 25:11221 (BNL-50203, pp 268-79)

RADIATION CHEMISTRY
research progress on, Osaka Laboratory, Japan, March, 1970, 25:10584(R) (JAERI-5026)

RADIATION DETECTORS
arrangement for radioactivity alarm systems, in reactor containment systems, 25:12812 (BNWL-1479)
description for on-board monitoring of radiation in seawater, 25:10817
design for electron and proton measurements in the ionosphere, 25:11813
development for high-energy particles based on x-ray transition radiation, 25:10877
performance for activity measurements in kidneys following injection of iodine-131, effects of positioning on, 25:11167
sensitivity for measuring electron currents in betatron, 25:12321

RADIATION DETECTORS, ACTIVATION
development for nuclear accident dosimetry, 25:10884
development of Bonner multisphere, for neutron dosimetry and spectroscopy, 25:10811 (CEA-CONF-1685)
development of rhodium-103, for personnel dosimetry, 25:10882
performance for thermal neutron flux distribution measurements in swimming pool type research reactor, 25:12826
performance of foil type, for measurement of fast neutron spectra, 25:12773 (BNWL-1403)

RADIATION DETECTORS, BUBBLE CHAMBER
liquid for, thermodynamic properties of propane, 25:10876
particle tracks in, vidicon device for ionization measurements of, 25:10878
valve for, design and performance of high-pressure fast, 25:10870 (JINR-P13-5420)

RADIATION DETECTORS, CHERENKOV
development of threshold gas, for high-energy electrons, 25:10874
efficiency and resolution of hodoscope, 25:10869 (JINR-E13-5459)

RADIATION DETECTORS, DIELECTRIC TRACK
development for personnel neutron dosimetry, 25:10880
particle track registration and analysis in cellulose nitrate, alpha particle, 25:10826
particle tracks in fission foil--, spark replica method for analysis of, 25:10882
performance of cellulose acetate, for proton detection, 25:10831
performance of fission foil--glass track detector for in-core neutron spectra measurements, 25:10836
preparation and track etching in boron-impregnated 1/v, for slow neutrons, 25:10820
track formation and development in, 25:10827
uses for autoradiography, dosimetry, and microanalysis, 25:10823
uses of, review on, 25:10825

RADIATION DETECTORS, FISSION FOIL
development for neutron detection down to 1 keV using uranium-235 and coincidence scintillation detectors, 25:10845
development of dielectric track--, for personnel dosimetry, 25:10882
performance of fission foil--glass track detector for in-core neutron spectra measurements, 25:10836

RADIATION DETECTORS, GEIGER-MUELLER
calibration of ratemeter using energy-compensated, intercomparison, 25:10809 (BNWL-SA-3565)
design and operation of, review on, 25:10807 (AD-708922)
design of shielded, for monitoring gamma radiation at Van de Graaff accelerator, 25:10824
performance with external γ source for detection of effluents from gas chromatograph, 25:10888
resolving time measurements using time analyzer, 25:10835

RADIATION DETECTORS, IONIZATION CHAMBER
calibration of Cutie Pie, intercomparison, 25:10809 (BNWL-SA-3565)
design and performance of gridded, for angle information, 25:10837
design of high-transmission parallel plate, for measuring ion mobility in gases, 25:10903
performance of liquid, in registration of solar neutrinos, (T), 25:11628

RADIATION DETECTORS, PROPORTIONAL
calibration of cylindrical polyethylene-moderated boron trifluoride, intercomparison, 25:10809 (BNWL-SA-3565)
calibration of spherical polyethylene-moderated helium-3, intercomparison, 25:10809 (BNWL-SA-3565)
data acquisition and analysis system for low-level beta, computer-based, 25:10833
design and performance of flowthrough, for uranium determination in solutions, 25:10473 (CEA-R-4032)
design for tracer measurements of blood flow in man, 25:10828(P)
design of Bragg--Gray, for monitoring neutrons at Van de Graaff accelerator, 25:10824
development of Bonner multisphere boron trifluoride, for

XUM

neutron dosimetry and spectroscopy, 25:10811 (CEA-CONF-1685)
development of helium-3, for detection of fission neutrons from superheavy elements, 25:10814 (JINR-P13-5391)
development of position-sensitive multiwire, for thyroid scanning, 25:10810 (CEA-CONF-1668)
operation and performance of spherical, with anticoincidence detector for carbon-14 determination in high radiation background, 25:10843
pulse-shape discriminators for gamma discrimination in proton-recoil, for neutron spectroscopy, 25:10857
readout system for position-sensitive, electromagnetic delay line, 25:10846
resolution of, statistics of electron avalanches for calculation of ultimate, 25:10838

RADIATION DETECTORS, SCINTILLATION
circuit for long, light transit-time compensator, 25:10813 (JINR-P13-5378)
design of stilbene and lithium-6-glass coincidence, for fast neutron spectroscopy, 25:10862
design of telescope for detection of cosmic mesons, 25:10871
development for neutron detection down to 1 keV using uranium-235 fission foil, 25:10845
development of Bonner multisphere lithium iodide, for neutron dosimetry and spectroscopy, 25:10811 (CEA-CONF-1685)
development of large-area liquid, with uniform spatial response, 25:10875
efficiency of thallium-activated sodium iodide, for gamma spectroscopy, measurement of, 25:10865
light collection systems for, review on, 25:10834
performance for low-level beta detection, 25:10819
performance of stationary, for scanning flow of metastable technetium-99-labeled embolus through heart chambers, 25:11120
response function of thallium-activated sodium iodide, for gamma spectroscopy, 25:10865
response functions for monoenergetic neutrons at 0.25 to 1.25 MeV, 25:10832
response of collimated thallium-activated sodium iodide, to non-axial point gamma sources, 25:10841
scintillation yields of liquid benzene and alkylbenzene, 25:10822

RADIATION DETECTORS, SEMICONDUCTOR
charge collection process in p--i--n junction, 25:10844
design and performance of telescope, for beta spectroscopy, 25:10852 (NP-18617)
development for gamma dosimetry, 25:11074(R) (AECL-3777)
operation of telescope, for identification of A = 4 to 20 particles, 25:10829

RADIATION DETECTORS, SEMICONDUCTOR (GERMANIUM)
calibration of lithium-drifted, selenium-75 gamma source for, 25:10842
efficiency as function of trapping factor for, (E), 25:10851 (NP-18570)
operation and performance for gamma and charged-particle spectroscopy, 25:10851 (NP-18570)
performance of lithium-drifted, for low-energy gamma spectroscopy, 25:10859
pulse trigger with rise time correction for lithium-drifted, zero cross, 25:10830
pulses from lithium-drifted, calculation of charge and current, 25:10821
response to 80-MeV deuterons, 25:10851 (NP-18570)

RADIATION DETECTORS, SEMICONDUCTOR (SILICON)
design with superconducting focusing lens for electron spectroscopy, 25:10864
development of combined time-of-flight and telescope system of phosphorus-diffused, for identification of nuclear fragments, 25:10860
development of lithium-drifted, for x-ray spectroscopy, 25:10812 (CEA-N-1401)
efficiency curves for electrons and γ rays in, absolute, (E), 25:12477

RADIATION DETECTORS, SPARK CHAMBER
development of magnetic, for use in search for quarks, 25:10868 (IFVE-SEF/OP-70-13)
development of magnetostrictive wire, for heavy cosmic ion spectroscopy, 25:10873
operation of cylindrical wire, in low pressure helium, 25:10872

RADIATION DOSE
derivation of numerical values for, 25:11090
maximum permissible ICRP recommendations for, 25:11090
maximum permissible, to personnel from microwaves, review of international, 25:11088

RADIATION DOSIMETERS
conference on development for use following criticality accidents, 25:11056 (STI/PUB-241)
design of multiple detector, for personnel accident dosimetry, 25:10885
development of dielectric track, 25:10825
development of emergency personnel neutron--gamma, review on, 25:10881
standardization and multi-laboratory intercomparisons of nuclear accident, 25:10886

RADIATION DOSIMETERS, CHEMICAL
development for accident dosimetry, 25:10883

RADIATION DOSIMETERS, THERMOLUMINESCENT
development of personnel system and portable instruments for, 25:11074(R) (AECL-3777)
luminescence mechanism of lithium fluoride, role of color centers in, 25:11958
performance of polycrystalline lithium fluoride, 25:10879
preparation of polycrystalline lithium fluoride, 25:10879
standardization of β, construction of 4-π exposure chamber for, 25:10936 (UCB-34-P-23-15)

RADIATION DOSIMETRY
book: Radiation Medicine, 25:11091
conference on methods for use following criticality accidents, 25:11056 (STI/PUB-241)
methods at radiochemical processing plants in Belgium, 25:11082
methods for accidents at critical assemblies in United Kingdom, 25:11084
methods for accidents at critical assemblies in Yugoslavia, 25:11083
methods for critical assemblies in Poland, 25:11080
methods for critical assembly areas and personnel in Japan, 25:11081
methods for critical assembly areas and personnel in France, 25:11079

RADIATION FILTERS
transmission characteristics of pyrolytic graphite, for fast neutrons, 25:12352

RADIATION MONITORING
buildings and facilities for environmental, guide for design, operation, and staffing of, 25:10763

RADIATION PROTECTION
book: Radiation Medicine, 25:11091
programs at critical assemblies in France, 25:11079
programs at critical assemblies in Japan, 25:11081
programs at critical assemblies, in United Kingdom, 25:11084
programs at radiochemical processing plants in Belgium, 25:11082
programs for critical assemblies, in Yugoslavia, 25:11083
programs for reactor personnel in Poland, 25:11080
recommendations for surveys of, in veterinary medicine installations, 25:11075 (NCRP-36)
standards for design of storage facilities for radiation sources, 25:11078 (Y-1754)
standards for environmental exposure of human populations in USA, AEC, ICRP, and NCRP, 25:11076
standards in Sweden for nuclear power plant effluents, 25:12757 (SSI-70-27)

RADIATION RATE METERS
circuit for, binary rate multiplier, 25:10840
deadtime losses in, binary rate multiplier circuit for automatic correction of, 25:10840

RADIATION SOURCES
collimation system for, design of, 25:10781(P)
storage facilities for, safety standards for, 25:11078 (Y-1754)
use of sealed, recommendations for protection of veterinary medical personnel against, 25:11075 (NCRP-36)

RADIATION STANDARDS AND UNITS
classification of international, of ICRU, 25:11064

RADIATION TARGET CANS
design for in-pile creep measurements on fuels and materials, 25:11464 (KFK-1281)

RADIATION TARGET CHAMBERS
design for Moessbauer effect studies following Coulomb excitation, 25:10863
design for Van de Graaff accelerator for charged particle irradiation of materials, 25:12318

RADIATION TARGETS
design of precision liquid hydrogen, for high-energy total cross section measurements, 25:12300 (JINR-P8-5212)
efficiency of internal cyclotron and synchrocyclotron, calculation of, 25:12324
irradiation in reactor cores, optimum volume of sample positions for, (E/T), 25:12829

RADIO GALAXIES
electron leakage from, origin of x-ray background in, (T), 25:11657
radioluminosity as function of redshift for, absolute, (E), 25:11581(T) (CSIRO-Trans-10247)

RADIO WAVES
absorption in ionosphere, effects of hard solar x rays on, (E), 25:11817
attenuation in ionosphere, relevance to ionospheric plasma instabilities, (E/T), 25:11806
emission from Jupiter of decametric, waveform and source-size studies of, (E), 25:11670
ionospheric heating by, effect on absorption of probing waves of ordinary and extraordinary polarization, (E/T), 25:11807
scintillation of satellite, effects of high-latitude ionospheric irregularities on, (E), 25:11601

RADIOACTIVE CONTAMINATION
distribution in human organs, estimation of, using tissue equivalent phantom, 25:11067
distribution in human respiratory tract following inhalation of contaminated aerosols, autoradiographic method for determining, 25:10953

hazards from Project Schooner, effects of atmospheric fallout transport on, (E), 25:10716 (UCRL-72534)
RADIOACTIVE MATERIALS
analysis of, problems in, 25:10491 (ORNL-4636, pp 20-33)
bibliography on handling and shipping of, 25:10798 (ORNL-NSIC-84)
transport from shipping container to hot cell, design of improved link-type conveyer for, 25:10803(P)
RADIOACTIVE WASTE
corrosive effects of boiling solutions of, on stainless steel 304L and 310 and titanium, 25:10658(R) (BNWL-1533)
effects of reactor, on animals in aquatic ecosystem, 25:11006
processing and release at West Valley Processing Plant, 25:10661 (DOCKET-50201-59)
processing of low-level liquid, at West Valley Processing Plant, 25:10660 (DOCKET-50201-58)
processing with saponite-type montmorillonite for separation of cesium-134, 25:10793 (BARC-506)
release from nuclear power plants, long-term ecological effects from, 25:12763
solidification of aqueous solutions and suspensions of, 25:10682(P)
solidification of liquid, in asphalt, equipment and method for, 25:10799
transfer to shipping and storage containers, equipment and method for, 25:10800(P)
treatment of Purex, by pot solidification, 25:10658(R) (BNWL-1533)
RADIOACTIVITY
measurements of, ICRU recommendations for international units for, 25:11064
RADIOAPPLICATORS
design of afterloading, for treatment of human carcinomas of uterine cervix, 25:11227
RADIOBIOLOGY
book: Radiation Medicine, 25:11091
review of Atomic Bomb Casualty Commission research programs on, during July 1968 to July 1969, 25:11237(R) (ABCC-68-69)
RADIOCHEMICAL PROCESSING PLANTS
design and flowsheets for Karlsruhe WAK, for fuel elements, 25:10756(T) (ORNL-tr-2416)
design of Spanish M-1, 25:10667(T) (LIB/Trans-310)
radiation protection programs at, in Belgium, 25:11082
RADIOFREQUENCY SPECTROMETERS
design for simultaneous electron irradiation and ESR measurement, 25:10626 (KFK-1285)
development of, review on, 25:10897
RADIOGRAPHY, BIOMEDICAL
complications in angiographic, in man, administration of dextran and glucose for reducing, 25:11195
effectiveness for diagnosis of bone metastases in comparison to strontium-85 scintigraphy, 25:11174
effectiveness for diagnosis of honeycomb lung and pulmonary emphysema in comparison to scintigraphy with iodine-131-labeled albumin macroaggregates, 25:11215
effectiveness for lung examination in patients with blunt chest concussions in combination with scintigraphy and ventilation measurements, 25:11135
radiation dose to medical personnel during heart catheterization, x, 25:11059
RADIOGRAPHY, INDUSTRIAL
equipment for γ, principles and defects of, 25:11089
RADIOIMMUNOASSAY
methods for studies of allergy and immunology, 25:10924
methods of thrombopoietin, in blood plasma using selenium-75-labeled selenomethionine, 25:10991
RADIOISOTOPE SCANNING
effectiveness for localization of kidney neoplasms, review of, 25:11115
methods for diagnosis of human thyroid cancer using iodine, 25:11217
methods for increased reliability and speed using analog-digital converter, computer, and magnetic tape, 25:11122
methods for measurement of blood circulation time in man, using dual tracers and multiscaler for, 25:11184
methods for positioning maneuver during, of mitral valve in human heart, 25:11187
methods for use of zinc-69-labeled zinc chloride for scanning of prostate glands, to determine dosimetry, and to study biological fate of zinc, 25:11204
performance of colloidal gold-198 for lymph system, evaluation of interpretation errors for determining, 25:11177
RADIOISOTOPES
conference on uses in diagnosis and medical research, 25:11118
content in ground waters of Bukhara--Karshin artesian basin, (E), 25:10698
determination of short-lived, 25:10472(R) (BMBW-FBK-70-19)
distribution and production by underground nuclear explosions, methods for prediction of, 25:10742
distribution in atmosphere, development and operation of equipment for measuring vertical, 25:10754 (NP-18633)
effectiveness for evaluating pulmonary blood circulation in man following injection, 25:11126
effectiveness for evaluating regeneration of human liver by scintigraphy, 25:11202
effects on animals and man, genetic, 25:11294(R) (EUR-4542)
handling of encapsulated, regulations for, 25:11089
incorporation in erythrocytes for study of inflammations in combination with iodine-125 incorporation of proteins, 25:11193
ingestion by man in Colombia and Panama for feasibility studies of proposed Atlantic-Pacific interoceanic canal, estimation of, 25:10995 (BMI-171-45)
metabolism in animals, use of computers for analysis of counting data from tissues following, 25:10937 (UCRL-50957)
production of short-lived, in research reactors for diagnostic use, 25:10943
separation by on-line mass spectroscopy, 25:10670 (LYCEN-7034, pp 23-33)
transport in aquatic ecosystems, statistical analysis of, 25:10998
uptake from fallout by food products, 25:11038 (UCRL-72716(Rev.1))
use for determining blood flow through human organs, development of mathematical formulas for improved accuracy, 25:10917
use for determining testosterone content of blood of bovines and swine by double isotope dilution combined with crystallization, 25:10923
use for kidney scanning, in patients with kidney diseases in combination with computer analysis, 25:11161
use for scanning of blood circulation, methods for, conference on, 25:11192
use in aqueous solutions as tracers, factors affecting behavior and properties during, 25:10925
uses as tracers in USSR metallurgical industry, review of, 25:10780
RADIOPROTECTIVE COMPOUNDS
effects on x-radiosensitivity on Chinese hamster cells, 25:11093 (BNL-50203, pp 97-116)
RADIOSENSITIVITY
estimation for human organs and tissues, 25:11090
RADIOSENSITIZERS
effects on x-radiosensitivity on Chinese hamster cells, 25:11093 (BNL-50203, pp 97-116)
RADIOSTERILIZATION
conference on methods for biological tissues, bacteria, and medical supplies, γ, 25:11327 (STI/PUB-247)
RADIOTHERAPY
book: Radiation Medicine, 25:11091
conference on time relation to radiation dose in, 25:11218 (BNL-50203)
radiation dose calculations for implant, use of computers for, 25:11058
RADIUM
content in ground waters of Bukhara--Karshin artesian basin, relations with deuterium content, 25:10698
RADIUM ISOTOPES Ra-224
effects on man, damaging, 25:11294(R) (EUR-4542)
energy levels from thorium-228 alpha decay, lifetimes, quadrupole moments, and deformation parameters for, (E), 25:12542
energy-level transitions from thorium-228 alpha decay, probabilities for E2, (E), 25:12542
use for therapy of ankylosing spondylitis in man, excretion measurements and whole-body counting following, 25:11231
RADIUM ISOTOPES Ra-226
content in seawater and Pleistocene sediments, (E), 25:10725(R) (CU-3139-4)
content in seawater at Geosecs Station, north Pacific Ocean, relations with depth, 25:10726
effects on oxygen production in algae, 25:11074(R) (AECL-3777)
RADIUM ISOTOPES Ra-228
content in seawater and Pleistocene sediments, (E), 25:10725(R) (CU-3139-4)
RADON
content in surface and bottom of water column at Geosecs Station, north Pacific Ocean, 25:10727
decay products of, content of uranium mines, measurement and control of, 25:11043
diffusion in troposphere, numerical model for, 25:10704 (NP-18609)
RADON ISOTOPES Rn-220
diffusion in troposphere, numerical model for, 25:10704 (NP-18609)
RAINWATER
beryllium-7 content of Fayetteville, Arkansas, Jan. 1969 to Mar. 1970, 25:10712 (ORO-2529-28, App. 6)
radioisotope content of Fayetteville, Arkansas, effects of Dec. 1968 Chinese nuclear explosion on cerium-141, cerium-144, and strontium-90, (E), 25:10709 (ORO-2529-28, App. 3)
radioisotope content of Fayetteville, Arkansas, July and Aug. 1969, cerium-144, cesium-137, strontium-89, and strontium-90, 25:10707 (ORO-2529-28, App. 1)
radioisotope content of Fayetteville, Arkansas, May 1965 to April 1970, effects of Chinese nuclear explosions on cesium-137 and strontium-90, 25:10713 (ORO-2529-28, App. 7)
strontium-89 and strontium-90 content of Fayetteville, Arkansas, Sept. 1969 to Aug. 1970, (E), 25:10710 (ORO-2529-28, App. 4)

XUM

strontium-89/-90 ratio in Fayetteville, Arkansas, 1964 to 1969, effects of jet stream location and Chinese nuclear tests on, 25:10708 (ORO-2529-28, App. 2)
RARE EARTH ALLOYS AND SYSTEMS
electric conductivity of paramagnetic, crystal-field effects on spin-disorder contribution to, (T), 25:12009
phase studies on ternary, 25:10580
RARE EARTH ISOTOPES
nuclear spectroscopy of, survey on, 25:12523 (LYCEN-7034, pp 58-83)
RARE EARTHS
book: Chemistry of Rare Earths and Various Other Elements, in Russian, 25:10580
content in thermal waters of Kamchatka Peninsula, (E), 25:10697
determination by activation methods, review on, 25:10499
determination by spark-source mass spectroscopy, 25:10438 (ORNL-4636, pp 51-3)
determination using mixed ligand complexes, 25:10460
effects as impurity on superconducting transition temperature of lanthanum dialuminide, s--f exchange coupling, (T), 25:11836
energy levels of, calculation using hexadecapole deformation and rotation-particle coupling, (T), 25:12674
separation from ores by solvent extraction, review on, 25:10656 (BM-IC-8502)
RARE GASES
electron reactions with, cross sections for ionization in, (T), 25:11701
RATS
cobalt-60 1-nitroso 2-naphthol chelate metabolism in, following intravenous administration, 25:10958
iodine-131 removal from blood of, estimation of phagocytic coefficient for, 25:10957
radiation effects on activity of alkaline phosphatase and cholinesterase in blood and tissues of, following injection of mixed radioisotopes, 25:10968
radiation effects on adrenal cortex of, protective effects of sex hormones against whole-body x, 25:11268
radiation effects on blood coagulation in, protective effects of cystamine and homologous bone marrow against x, 25:11105
radiation effects on bone marrow of, in relation to stem cell population kinetics, design of model for compartmental analysis of, 25:11290
radiation effects on carbon-14-labeled carbon dioxide production, glucose absorption, oxygen utilization and mitochondrial function in, continuous, 25:10980
radiation effects on corticosterone and glucose content of blood in, effects of dianabol and insulin on normalization following whole-body γ, 25:10972
radiation effects on glucose and lactate production in ganglia of, effects of dose rate on strontium-90 β, 25:11262
radiation effects on histamine in blood, intestines, kidneys, and liver of, mechanism of, following ingestion of mixed radioisotopes, 25:10967
radiation effects on histones in thymus nuclei of, γ, 25:10971
radiation effects on intestines of, following ingestion of mixed radioisotopes, mechanism of damage and repair following chronic, 25:11271
radiation effects on maze habits of, effects of dose, fractionation on whole-body x, 25:11273
radiation effects on oxidative phosphorylation and respiration in spleen mitochondria of, protective effects of homologous bone marrow injections against acute x, 25:11100
radiation effects on pregnant, combined effects of cloramiphene on cobalt-60 γ, 25:11104
radiation effects on pregnant, protective effects of estrogen against cobalt-60 γ, 25:11104
radiation effects on survival of, protective effects of acetylcholine, adrenaline, histamine, 5-methoxytryptamine, and serotonin against γ, 25:11102
radiation effects on uptake of strontium-85 by bones in, whole-body γ, 25:11263
radiation effects on, role of alarm phase of nonspecific adaptation response in early glycemic response following γ, 25:11281
radioinduced damage of mucosal epithelium of intestines of, effects of dose on x, 25:11255 (BNL-50203, pp 181-5)
radioinduced injuries to bone-marrow shielded, role of lymphocytes from shielded marrow on recovery from x, 25:11077
radioinduced injuries to kidneys of, high dose, 25:11286
radioisotope accumulation in, effects of diet on cesium-137 and strontium-90, 25:10956
radioisotope metabolism of bones of, effects of estradiol on calcium-47 and strontium-85, 25:10933 (COO-1339-45)
radiosensitivity of choroid, optic nerve, and retinal tissues in, comparison of, 25:11284
radiosensitivity of embryos of, in comparison to species differences of mice embryo sensitivity, 25:11277
radiosensitivity of embryos of, in utero in comparison to embryos of mice, role of species differences in x, 25:11277
radiotherapy of tumors in, review of, 25:11219 (BNL-50203, pp 130-53)
strontium isotope sorption through intestines of, effects of alginic acid components on, 25:10939
strontium-85 deposition in bones of, effects of dose and time of administration on effectiveness of activated barium sulfate for prevention of, 25:11048
strontium-85 transport through intestinal epithelial membranes in, reaction mechanisms for, 25:10938
strontium-85 uptake by bones of, following oral administration, effects of barium sulfate on, 25:10940
tellurium-127m distribution and excretion in, following ingestion, kinetics of, 25:10949
tellurium-127m distribution and excretion in, following intravenous injection, 25:10950
tellurium-127m sorption from gastrointestinal tract of, following ingestion, kinetics of, 25:10949
REACTION MECHANISMS
isotope effects on, effects of temperature on, 25:10549
REACTOR CONTAINMENT STRUCTURES
coatings for, effects of accident conditions on protective, (E), 25:12804 (ORNL-TM-3104)
penetrations in, development of high voltage power cable porcelain, 25:12705 (JAERI-Memo-4197)
REACTOR CONTAINMENT SYSTEMS
design parameters of pressure suppressing and steam condensing, for pressurized water reactors, 25:12802(P)
REACTOR CONTROL ELEMENTS
drives for boiling reactor, development of electro-hydraulic, 25:12712
REACTOR CONTROL SYSTEMS
design of, hybrid computer for, 25:10895 (ORNL-TM-3101)
REACTOR COOLANTS
boiling of, research on detection of, 25:10769(R) (ORO-3911-3)
book: Physico-chemical Analysis of Handling Liquid Metal Coolants (In Russian), 25:11342
book: Transport Phenomena in Liquid Metals and Semiconductors, 25:11410
REACTOR FUEL ELEMENTS
cladding for, least squares description of radial distortion in irradiated, 25:11368 (AECL-3688)
cladding for, radiation effects on Zircaloy-2, 25:12862 (JAERI-Memo-4192)
cladding materials for fast, radiation damage and corrosion behavior in, 25:12768(R) (EURFNR-855)
coolant flow in hexagonal rod bundle type, (T), 25:12801
creep testing of uranium oxide (UO_2) and plutonium oxide (PuO_2)--uranium oxide (UO_2), 25:12795(R) (BMI-1893)
critical heat flux with parallel upflow of water in bundles of, (E), 25:12787
debris from, description for in-pile receptacle for, 25:12769(P)
design parameters of perforated tapered annular tube particle type, for gas cooled reactors, 25:12800(P)
development of pressurized water cooled Zircaloy clad uranium oxide (UO_2) pin type, 25:12704 (BMBW-FBK-70-11)
dimensional variations in uranium oxide (UO_2) WWER-type, method for calculation of at-power, 25:12798 (IAE-1942)
fabrication of plate-type, by diffusion bonding, 25:11375 (IN-1437, pp 24-59)
fabrication of plate-type, reject reclamation by electron beam welding methods, 25:11375 (IN-1437, pp 24-59)
fabrication of Type 316 stainless steel clad plutonium nitride (PuN)--uranium nitride (UN) pin type, 25:12795(R) (BMI-1893)
failure detection system for water cooled MTR type, performance of, 25:12819 (JAERI-Memo-4196)
fission products in uranium oxide (UO_2) WWER-type, method for calculation of at-power gaseous, 25:12798 (IAE-1942)
heat transfer in hexagonal rod bundle type, (T), 25:12801
heat transfer in rod type, comparison of models for, (T), 25:12799 (TUBIK-17)
heat transfer in uranium oxide (UO_2) WWER-type, method for calculation of at-power, 25:12798 (IAE-1942)
melting of natural uranium gas cooled, causes for, 25:12764
performance of cylinder shaped fast reactor, LIFE 1 computer program for, 25:12794 (ANL-7736)
performance of fast, program for analysis of, 25:12768(R) (EURFNR-855)
power levels in uranium oxide (UO_2) WWER-type, method for calculation of at-power, 25:12798 (IAE-1942)
pressure drop with parallel upflow of water in bundles of, (E), 25:12787
radiation effects on clad uranium, in-pile, 25:11457 (CISE-R-278)
radiation effects on performance of Zircaloy-clad hollow uranium dioxide pellet, in-pile, 25:11530 (AECL-3732)
reprocessing of, design and flowsheet for Karlsruhe WAK plant for, 25:10756(T) (ORNL-tr-2416)
shipping of spent, design of shielded container for, 25:10801(P)
vibrations of, effects on multigroup neutron lattice parameters of, (T), 25:12850
REACTOR FUELS
analysis for impurities by emission spectroscopy, 25:10432 (KFK-1261)

analysis of LMFBR and MSRE, methods for, 25:10425 (ORNL-4636, pp 40-2)
analysis of MSRE, for trivalent uranium, 25:10434 (ORNL-4636, pp 7-13)
burnup determination in, method for calculating, from mass spectrometry of neodymium stable isotopes, 25:10461
burnup determination of, by isotope dilution and mass spectrometry of neodymium stable isotopes, 25:10469
burnup monitoring by molybdenum analysis, 25:10583(R) (AECL-3776)
burnup of ceramic, in EBR-II, hazards evaluation at 10.5 percent FIMA, 25:11533 (ORNL-TM-2635(Suppl.))
burnup of heavy water moderated pressure tube type, digital computer program for, 25:12797 (IEA-186)
coating of particulate, optimization of fluidized beds for, 25:11479 (JUL-669-RW)
creep of, design of in-pile capsule for measuring, 25:11464 (KFK-1281)
inspection of irradiated, design and operation of Isodore facilities at Saclay for metallurgical, 25:10794 (CEA-R-4120)
reprocessing in Europe, economic and legal aspects of, 25:10673
reprocessing of breeder, by chloride volatility methods, 25:10434 (ORNL-4636, pp 7-13)
reprocessing of fast breeder, evaluation of problems in, 25:10672
reprocessing of, Spanish M-1 plant for, 25:10667(T) (LIB/Trans-310)

REACTOR MODERATORS
configuration of pulsed reactor, development of calculations for optimum, 25:12827
keying systems for graphite block, description of, 25:12770(P)

REACTOR SAFETY
incidents reported during August to September 1970, 25:12807
regulation of, administrative activities in, 25:12806
research and development projects on, review of, 25:12805

REACTORS
book: Gas Dynamics of Two-Phase Media (In Russian), 25:10772
burnable poisons for, sol-gel method for preparation of gadolinium oxide microspheres for use as, 25:10571 (EUR-4550)
coolant boiling in rod arrays of, COBRA computer program for, 25:12784 (KFKI-70-20-RPT)
coolant expulsion from, pressure distribution for axisymmetric two dimensional flow during, (T), 25:12808
cooling channels in, power excursion transient heat transfer performance of, 25:10773
cooling system for, method for fabrication of coolant-fuel channels for, 25:11366(P)
criticality analyses of pulsed, method for ensuring consistent, (T), 25:12860
fission gases in, calculation of asymptotic bubble spectrum for, (T), 25:12847
kinetics of bare slab, BIGG 2 computer program for, 25:12842 (INR-1193)
kinetics of, bounded positive solutions of equations for, (T), 25:12845
kinetics of, Lie series method for solution of one dimensional multi-zone multi-group diffusion equation for, (T), 25:12855
kinetics of, periodic positive solutions of equations for, (T), 25:12846
kinetics of, problems of persisting mode time constant in Monte Carlo calculations of, (T), 25:12848
materials for, design of in-pile capsule for measuring creep of, 25:11464 (KFK-1281)
materials for, development of, 25:11458(R) (IN-1437)
neutron diffusion calculations for, method for phase space reduction in, 25:12853
neutron distribution in adjacent half infinite media, energy dependent transport theory for, (T), 25:12857
neutron flux distribution in infinite homogeneous, effects of cavities on, (T), 25:12851
neutron flux distribution in, reduction of ray effect in discrete ordinates calculations of, 25:12852
neutron flux distribution in, SYNTH 2 computer program for calculation of, 25:12844 (TKK-F-A-121)
neutron flux distribution in, variational derivation of discrete ordinate-like approximations for, (T), 25:12858
neutron lattice parameters for, effects of fuel element vibrations on multigroup, (T), 25:12850
neutron lifetime in, comparison of definitions for prompt, (T), 25:12856
physics analysis of one dimensional, multigroup method for, 25:12841 (IAE-1938)
physics analysis of, EXPOSUM code for, 25:12837 (RISO-M-1279)
pressure vessel penetrations for, description of hermetically sealed drive shaft assembly for, 25:12863(P)
pressure vessels for, automatic ultrasonic inspection of welds in, 25:12790
reactivity feedback in, Volterra functional series for linear, 25:12843 (INR-1206)
shielding of, evaluation of computer codes for analysis of, 25:12782 (CEA-CONF-1683)

REACTORS, AIRCRAFT
description of fuselage mounted, with wing mounted propulsion units and auxiliary gas turbine systems, 25:12831(P)
design parameters of fuselage mounted, with wing mounted propulsion units, 25:12832(P)

REACTORS, BOILING
cooling systems for, effects of corrosion on low cycle fatigue life of piping in, (E), 25:12783(R) (GEAP-10207-22)
cooling water radiolysis in, 25:10491 (ORNL-4636, pp 20-33)

REACTORS, BREEDER
development in Germany of 300 MW(e) prototype steam cooled fast, review of, 25:12767 (BMBW-FBK-70-20)
fuel reprocessing for, evaluation of problems in, 25:10672

REACTORS, CANDU-TYPE
coolants for, review of developments in liquid metal, 25:11343 (AECL-3778)
fuel burnup in, digital computer program for calculation of, 25:12797 (IEA-186)
physics measurements for conceptual 600 MW(e) EL 600, 25:12775 (CEA-N-1395)

REACTORS, FAST
accidents in, behavior of fission product aerosols following, 25:12766(R) (EURFNR-855)
core for, heat transfer and hydraulics in, 25:12768(R) (EURFNR-855)
core positions in, neutron cross section calculations for off-axis, 25:11474(R) (BNWL-842)
development at Reactor Centrum Nederland during January to March 1970, 25:12768(R) (EURFNR-855)
development in Germany of 300 MW(e) prototype steam cooled breeder, review of, 25:12767 (BMBW-FBK-70-20)
fuel elements for, heat transfer and coolant flow in rod bundle, (T), 25:12801
fuel elements for, LIFE 1 computer program for performance of cylinder shaped, 25:12794 (ANL-7736)
fuel performance in, program for analysis of, 25:12768(R) (EURFNR-855)
fuel reprocessing for, evaluation of problems in, 25:10672
kinetics analysis of, use of multiple weighting functions in space--energy synthesis method for, 25:12854
neutron flux distribution in, successive space--energy synthesis for, (T), 25:12780
physics of, program for analysis of, 25:12766(R) (EURFNR-855)

REACTORS, GAS-COOLED
cooling system for high temperature power, advantages and disadvantages of helium, 25:12789
cooling systems in high-temperature, thermodynamics of graphite--helium reactions in, 25:10518 (RD/B/N-1816)
core for, keying system for graphite block structure in, 25:12770(P)
development in Europe of high temperature power, 25:12707
fuel element debris receptacles for, with means for securing in place by coolant flow, 25:12769(P)
fuel elements for, description of perforated tapered annular tube particle type, 25:12800(P)
heat exchangers for, with means to allow for expansion of tubes, 25:12811(P)
kinetics of natural uranium fueled graphite moderated, COREGRAF 2 computer program for, 25:12774 (CEA-N-1344(1))
neutron spectra in plutonium fueled high temperature, calculation of stationary state thermal, 25:12778
power cycles for high temperature power, calculation of optimum, 25:12809

REACTORS, GAS-FUELED
development of light bulb and coaxial flow rocket, 25:12834

REACTORS, GERMANY
development of 300 MW(e) prototype steam cooled fast breeder, review of, 25:12767 (BMBW-FBK-70-20)

REACTORS, GRAPHITE-MODERATED
fuel burnup in thermal, manipulation of fission product data for calculation of, 25:12776 (JUL-678-RG)
kinetics of natural uranium fueled gas cooled, COREGRAF 2 computer program for, 25:12774 (CEA-N-1344(1))

REACTORS, HEAVY WATER-MODERATED
moderator for, development of columns for production of heavy water, 25:10764
reactivity change in, effects of light water additions to coolant channels on positive, (E), 25:12830

REACTORS, LIQUID METAL-COOLED
book: Physico-chemical Analysis of Handling Liquid Metal Coolants (In Russian), 25:11342
vessel closure plug for sodium cooled, liquid filled main and secondary seals for, 25:12771(P)

REACTORS, MARITIME
development of, review of, 25:12836

REACTORS, POWER
coolant boiling in pressurized water, acoustic wave technique for monitoring, (T), 25:12779
cooling system for high temperature gas cooled, advantages and disadvantages of helium, 25:12789

XUM

development in Europe of high temperature gas cooled, 25:12707
development in Germany of 300 MW(e) prototype steam cooled fast breeder, review of, 25:12767 (BMBW-FBK-70-20)
fuel elements for CIRENE, water coolant properties in loop for testing prototype, (E), 25:12821(T) (LIB/Trans-335)
physics measurements for conceptual 600 MW(e) CANDU type EL 600, 25:12775 (CEA-N-1395)
power cycles for high temperature gas cooled, calculation of optimum, 25:12809
power divergences in large, calculations of asymmetric, (T), 25:12777 (TRG-Report-2060(Rev.))
power transients in, effects on stability of clad oxide fuel rods, 25:11534 (WAPD-TM-979)
steam reheater units for, with U-shaped tube banks in concrete pressure vessel walls, 25:12810(P)
use with magnetohydrodynamic generators, review of, 25:11752
REACTORS, PRESSURIZED-WATER
book: Thermal Analysis of Pressurized Water Reactors, 25:12791
containment buildings and equipment for, evaluation of protective coatings for, (E), 25:12804 (ORNL-TM-3104)
containment system for, description of pressure suppressing and steam condensing, 25:12802(P)
containment systems for, natural transport effects on fission product removal from, (E/T), 25:12803 (BNWL-1457)
coolant boiling in power, acoustic wave technique for monitoring, (T), 25:12779
coolant loss accidents in, sprays for reducing fission product concentrations in, 25:10491 (ORNL-4636, pp 20-33)
cooling system for, stable numerical integration of conservation equations for flow transients in, (T), 25:12793
core design for, thermal and hydraulic analysis of, 25:12791
fuel elements for WWER-type, calculation of heat transfer, power, dimensional variations, and fission product pressure in, 25:12798 (IAE-1942)
fuel elements for, critical heat flux and pressure drop with parallel upflow in bundles of, (E), 25:12787
REACTORS, RESEARCH
design of Juelich, calculations for optimizing thermal, 25:10768 (JUL-657-MA)
experimental facilities for FR-2, design parameters of superheated steam in-pile loop for fuel element failure testing, 25:12820 (KFK-1255)
fuel element failure detection system for JRR-4, performance of, 25:12819 (JAERI-Memo-4196)
in-pile loop in ESSOR, chemical and physical properties of water coolant in CART, (E), 25:12821(T) (LIB/Trans-335)
in-pile loop in HFR, post-failure properties of stainless steel, (E), 25:12823 (RCN-125)
list of worldwide, IAEA, 25:12824 (STI/PUB-248)
moderator for pulsed, calculation of optimum thickness for, 25:12827
neutron flux distribution in RV-1, measurement of thermal, (E), 25:12826
neutron spectra measurements in THOR, fission foil--dielectric track detectors for, 25:10836
performance of Mainz TRIGA, 25:10472(R) (BMBW-FBK-70-19)
reactivity of coupled core FMRB, (E/T), 25:12818 (FMRB-34/70)
safety of FMRB, effects of coupled core installation on, 25:12822 (NP-18499)
target irradiation in, optimum volume of sample positions for, (E/T), 25:12829
REACTORS, ROCKET
development of light bulb and coaxial flow gaseous core, review of, 25:12834
heat transfer calculations for, revised equations for, (E/T), 25:12833
REACTORS, SUPERHEATING
development in Germany of 300 MW(e) prototype fast breeder, review of, 25:12767 (BMBW-FBK-70-20)
REACTORS, TEST
list of worldwide, IAEA, 25:12824 (STI/PUB-248)
REACTORS, THERMAL
fuel burnup in graphite moderated, manipulation of fission product data for calculation of, 25:12776 (JUL-678-RG)
fuel recycle in, physics aspects of plutonium, (E/T), 25:12796 (EURAEC-2145)
REACTORS, WATER-COOLED
components for, review on corrosion of out-of-core, 25:11343 (AECL-3778)
cooling systems for, design, fabrication, and use of gate, globe and check valves in, 25:12785 (ORNL-TM-3221)
cooling systems for, failure mechanisms in piping of, (E/T), 25:12783(R) (GEAP-10207-22)
cooling systems for, guide for specification of gate, globe, and check valves for, 25:12786 (ORNL-TM-3273)
core components for, review on corrosion of, 25:11343 (AECL-3778)
pressure vessels for, development of prestressed concrete, 25:12788
safety of, review of research and development projects on, 25:12805
REACTORS, WATER-MODERATED
neutron activation in natural uranium fueled lattices, Monte Carlo calculation of thermal, (E/T), 25:12859
neutron diffusion in heterogeneous lattices in, pulsed method for determination of, (E/T), 25:12861
REDUCED NADP DEHYDROGENASE
radiation effects on content of, in epidermis, x, 25:11241
REGGE POLE THEORY
cut model in, two-particle unitarity in, 25:12289
dual amplitudes for six-body ϖ production in, 25:12131
dual model for rho' production in diffractive e + p → e + ϖ⁻ + ϖ⁺ + p interactions in, 25:12137 (DESY-70/56)
duality in e + N inelastic interactions, review of, 25:12068 (SLAC-PUB-842)
duality in hadron bootstrap for vector currents in n-body interactions of spinless mesons, 25:12177
duality in Regge parametrization of partial waves in ϖ + N interactions at low energies in, 25:12211
duality in strong interactions at high and low energies, review of, 25:12175 (COO-1764-81)
interactions e + p in, scheme for photon processes for deep inelastic, 25:12148
model in local infinite-component quantum field theory, Van Hove, 25:12246
model with SU(3) symmetry and exchange degeneracy for hadron interactions with nucleons in, pole--cut, 25:12217
models in, ϖ + N, anti K + N, and γ + p interactions at high energies for tests of, 25:12206
pole fits to charge exchange, differential cross sections, and polarization in ϖ⁻ + p interactions at high energies in, (E/T), 25:12217
poles for oscillatory average multiplicity in multiperipheral models for high-energy total cross sections, complex, 25:12122 (NYO-2262-TA-228)
poles in formalism for forward meson interactions with nucleons in, 25:12217
Pomeranchuk theorem violation relation with isospin dependence of total cross sections at high energies in quark model, 25:12218
trajectories for singular potentials in, rising, 25:12291
RELATIVE BIOLOGICAL EFFECTIVENESS
values for 0.43-MeV monoenergetic neutrons in relation to effects on somatic mutations and loss of reproductive integrity in Trandescantia stamen hairs, 25:11313
values for neutrons in relation to chromosomes in corneal epithelium of mice, 25:11018
RELATIVITY THEORY
Boltzmann equation in general and special, 25:12284
centrifugal force paradox in general, 25:12274
curvature tensor classification in general, principal congruences for, 25:12285
Einstein--Maxwell fields in general, invariant transformations for Newman--Penrose constants of motion for coupled, 25:12279
event horizons in static scalar-vacuum space--times in, 25:12282
gravitational waves in, colliding, (T), 25:11655
Minkowski space in, neutrinos in discrete transformations in six-dimensional model of, 25:12252
Riemannian geometry for neutrinos in general, 25:12280
space--times in general, spinor treatment of stationary, 25:12278
space--times in, event horizons in static scalar-vacuum, 25:12282
spectral theory for the Klein--Gordon equation with an external electrostatic potential, 25:12679
theory for special, empirical foundations of, 25:12265
REMOTE-CONTROL EQUIPMENT
design for triggering calciothermic reactions in plutonium and uranium production, 25:10760(P)
RENIN
content of venous blood in hypertensive patients, method for measuring, 25:11164
REPRODUCTIVE SYSTEM
radiation effects on, of moths, γ, 25:11338
RESINS
effects of crosslinking of Amberlite and Dowex, on ion exchange separation of rare earth complexes with EDTA, 25:10665 (INR-P-1209)
RESPIRATION
radiation effects on rate of, in rabbits following administration of zirconium citrate, effects of synchronous calcium gluconate administration on whole-body γ, 25:11289
radiation effects on, in organs of embryos, protective effects of cysteamine against, x, 25:11096(R) (EUR-4491)
RESPIRATORS
development of model, for studies on properties of radioactive aerosols, 25:11036 (CEA-Blb-185)
testing of automatic air purifying, 25:10752 (CEA-N-1360)
RESPIRATORY SYSTEM
radiation effects on reflex response of, in cats to simultaneous stimulation of mechanoreceptors in different visceral organs, x, 25:11282

radiation effects on, in man, review of literature on, 25:11209
RHENIUM
determination of trace amounts of, in biotite and tektite by spark source mass spectrometry, 25:10455
determination of trace amounts of, in molybdenum, review on, 25:10459
enthalpy of solution in liquid plutonium, 25:11386
friction and wear of, sliding against iron ring under vacuum, 25:11413
interactions with tantalum silicide coating, 25:11519
separation from ores by solvent extraction, review on, 25:10656 (BM-IC-8502)
RHENIUM ALLOYS AND SYSTEMS
Cr-base--Re, antiferromagnetic energy gap from optical absorption measurements at 4.2°K, 25:11987
RHENIUM ISOTOPES Re-185
proton reactions (p,nγ) at 12 MeV, γ spectra from, (E), 25:12514(R) (COO-1672-21)
RHODIUM
determination of trace amounts of, in biotite and tektite by spark source mass spectrometry, 25:10455
friction and wear of, sliding against iron ring under vacuum, 25:11413
separation from cadmium, indium, molybdenum, niobium, and palladium by gas chromatography using aluminum chloride eluent, 25:10666 (JINR-P6-5410)
RHODIUM ISOTOPES Rh-96
beta decay of, gamma spectra, half-lives, and log-ft values from, (E), 25:12617
nuclear mass excess from ruthenium-96 (p,n) reactions, (E), 25:12617
nuclear spin--parity assignment for, (E), 25:12617
RHODIUM ISOTOPES Rh-98
beta decay of, gamma spectra, half-lives, and log-ft values from, (E), 25:12617
nuclear mass excess from ruthenium-98 (p,n) reactions, (E), 25:12617
nuclear spin--parity assignment for, (E), 25:12617
RHODIUM ISOTOPES Rh-101
energy levels from palladium-101 decay, spin-parity assignments for, (E), 25:12596
energy-level transitions from palladium-101 decay, conversion coefficients and multipolarities for, (E), 25:12596
RHODIUM ISOTOPES Rh-102
beta and electron-capture decay of, directional correlations in, (E), 25:12546
RHODIUM ISOTOPES Rh-103
alpha reactions at 30 to 80 MeV, cross sections for production of K x rays by, (E), 25:12488
neutron capture by, γ spectra from resonance, (E), 25:12561
RHODIUM ISOTOPES Rh-104
energy levels from rhodium-103 resonance neutron capture, spin assignments for, (E), 25:12561
RHODIUM SELENIDES
$RhSe_2$--$RuSe_2$, superconductivity in, critical carrier concentration for, 25:11844
RING CURRENT
correlation to low-latitude magnetic bays on Earth's surface and at satellite position, (E/T), 25:11779
effects on magnetic field at ATS 1 during magnetic storms, Jan.--June 1967, /E/T), 25:11785
proton energy spectra in, at L = 5.35 and 5.71 at low magnetic latitudes, July 1, 1966, (E), 25:11786
ROBERT E. GINNA POWER REACTOR, UNIT 1
personnel for, request for respiratory protection procedures for, 25:12733 (DOCKET-50244-54)
ROCKET REACTORS (NERVA)
performance of XE-Prime, test program for, (E), 25:12835
ROCKS
analysis for rubidium and strontium by x-ray fluorescence, correction of matrix effects in, 25:10447
analysis for trace amounts of boron by fluorimetry, 25:10493
analysis for trace amounts of chlorine and lithium by neutron activation and radiochemical separation, 25:10493
analysis for trace amounts of elements by atomic absorption spectrometry, matrix effects on, 25:10457
analysis for trace amounts of elements by thermal neutron activation, ion exchange, and γ spectrometry, 25:10492
analysis for trace amounts of elements by x-ray fluorescence, methods for correction of matrix effect in, 25:10448
analysis for trace amounts of elements, conference on, 25:10446
analysis for trace amounts of elements, quantometer for spectroscopic, 25:10451
analysis for trace amounts of fluorine by pyrohydrolysis and thorium nitrate titration, 25:10493
analysis for trace amounts of potassium, rubidium, and strontium by atomic absorption spectrophotometry, 25:10458
analysis for trace amounts of uranium-235 and uranium-238 by neutron activation and radiochemical separation, 25:10494
analysis for trace elements, problems of contamination during, 25:10427
analysis for uranium, lithium-drifted germanium gamma spectrometer for borehole, 25:10849 (CEA-CONF-1694)
analysis of standard, for trace amounts of elements by borate fusion, dissolution in EDTA, and ion exchange, methods for, 25:10671
analysis of standard, for uranium by fission track method, 25:10474
deformation of surrounding, by contained 100 kt underground nuclear explosions, 25:10741
radioactivity of, measurements on, 25:10583(R) (AECL-3776)
separation of trace amounts of elements from standard, by borate fusion, dissolution in EDTA, and ion exchange, 25:10671
ROOTS
potassium-42 accumulation in, of corn, effects of age, potassium deficiency, and temperature on, 25:10930 (CEA-CONF-1517)
potassium-42 transport in, of corn, effects of age, potassium deficiency, and temperature on, 25:10930 (CEA-CONF-1517)
radiation effects on growth of Zea mays, in relation to bioelectric potential, x, 25:11308
radioisotope transport in, of Adenostoma, Ceanothus, and Quercus, cesium-137, ruthenium-106, and strontium-85, 25:10955
ROSE BENGAL
use of iodine-131-labeled, for liver function appraisal in comparison to other biochemical tests, 25:11111
RUBIDIUM
determination in rocks by x-ray fluorescence, correction of matrix effects in, 25:10447
determination in serum and urine by flameless atomic absorption spectroscopy, 25:10464
determination of trace amounts of, in biotite and tektite by spark source mass spectrometry, 25:10455
determination of trace amounts of, in minerals and rocks by atomic absorption spectrophotometry, 25:10458
determination of trace amounts of, in molybdenum, review on, 25:10459
determination of trace amounts of, in rocks and sand by thermal neutron activation, ion exchange, and γ spectrometry, 25:10492
determination of trace amounts of, in standard bauxite, carbonate, and silicate rocks by x-ray fluorescence, 25:10449
determination of trace amounts of, in standard rocks by borate fusion, dissolution in EDTA, ion exchange, and atomic absorption spectrophotometry, 25:10671
RUBIDIUM ISOTOPES Rb-82
beta decay of isomeric, γ singles and coincidence spectra from, (E), 25:12507
RUBIDIUM ISOTOPES Rb-83
electron-capture decay of, ratios for, (E), 25:12467
RUBIDIUM ISOTOPES Rb-84
beta and electron-capture decay of, K/β⁺ ratio in non-unique first-forbidden, (E), 25:12466
electron-capture decay of, ratios for, (E), 25:12467
RUBIDIUM ISOTOPES Rb-87
content ratio to strontium-86 in Wind River, Wyoming igneous plutons, 25:10701
energy levels from krypton-87 decay, spin--parity assignments for, (E), 25:12485
RUBIDIUM ISOTOPES Rb-91
energy levels of, spin and parity of, (E), 25:12462
RUBIES
analysis for trace amounts of elements by spark source mass spectrometry, 25:10455
RUTHENIUM
determination of trace amounts of, in biotite and tektite by spark source mass spectrometry, 25:10455
electron band structure of, photoemission and optical study of, 25:11982
separation from fission products by automatic ion exchange chromatography, design and performance of equipment for, 25:10659 (CEA-N-1267)
RUTHENIUM ISOTOPES Ru-95
beta and electron-capture decay of, gamma spectra, log-ft values, and branching ratios for, (E), 25:12545
RUTHENIUM ISOTOPES Ru-96
proton reactions (p,nγ) at 5.7 to 7.6 MeV, threshold energy for, (E), 25:12617
RUTHENIUM ISOTOPES Ru-98
proton reactions (p,nγ) at 5.7 to 7.6 MeV, threshold energy for, (E), 25:12617
RUTHENIUM ISOTOPES Ru-102
energy levels from rhodium-102 beta and electron-capture decay, spin--parity assignments for, (E), 25:12546
energy-level transitions from rhodium-102 beta and electron-capture decay, multipolarities, transition probabilities, and multipole-mixing ratios for, (E), 25:12546
RUTHENIUM ISOTOPES Ru-106
determination in phosphate glass and spray solidified waste melt samples, direct count method for, 25:10658(R) (BNWL-1533)
separation of plutonium from, by ion exchange on zirconium phosphate silicate columns, 25:10677
transport in irrigated soils, 25:10692
transport in roots of Adenostoma, Ceanothus, and Quercus, 25:10955
uptake by bean and tomato seedlings in culture media in

XUM

comparison to forage plants, 25:10936 (UCB-34-P-23-15)
RUTHENIUM SELENIDES
$RhSe_2$--$RuSe_2$, superconductivity in, critical carrier concentration for, 25:11844
RUTILES
creep and recovery of, research program on, 25:11472(R) (AD-708705)
creep recovery in stoichiometric, mechanisms of, 25:11473(R) (AD-708712)

S

S-MATRIX
formalism for, asymptotic states in quantum electrodynamics for, 25:12249
formulation for photon and vector current processes, 25:12177
Heisenberg representation for, 25:12290
virial coefficient relation with two- and three-particle-system, third, 25:12287
SACLAY REACTORS (OSIRIS)
in-pile loop for, design of sodium cooled Banjo, 25:12813 (CEA-CONF-1673)
SAINT LAURENT-DES-EAUX REACTOR (EDF-4)
fuel meltdown incident in, causes and cleanup operations for, 25:12764
SALICYLIC ACID, SULFO-
analysis for moisture content by neutron scattering and moderation, 25:10486
SALTS
book: Intercrystalline Corrosion and Corrosion Cracking of Stainless Steel in Aqueous Solutions (In Russian), 25:11353
SAMARIUM
complexes with EDTA, separation by ion exchange, effects of resin crosslinking on, 25:10665 (INR-P-1209)
determination of trace amounts of, in biotite and tektite by spark source mass spectrometry, 25:10455
determination of trace amounts of, in phosphate deposits by spark source mass spectrometry, 25:10456
spectra of, ultraviolet absorption, 25:11698
SAMARIUM ALLOYS AND SYSTEMS
Co--Sm, sintering of Co_5Sm to high density with high ccercive force, 25:11361
Co--Cu--Sm, magnetic rotational hysteresis loss of $SmCo_5Cu$ and $SmCo_{3.5-x}Cu_{1+x}$, critical field and temperature dependence of, 25:11984
Co--Sm, Bloch wall lattices in $SmCo_5$, disclination structures in, 25:12011
SAMARIUM ISOTOPES Sm-147
energy levels of, magnetic moments of, (E), 25:12557
energy-level transitions in, angular correlations and probabilities of, (E), 25:12557
SAMARIUM ISOTOPES Sm-148
alpha elastic scattering at 27.5 to 32.5 MeV, angular distributions for, (E), 25:12605
SAMARIUM ISOTOPES Sm-150
energy levels from samarium-152 (p,t) reactions, spin-parity assignments for, (E), 25:12612
neutron capture by cascade-theory calculations of gamma spectra from, (T), 25:12626 (FMRB-33/70)
SAMARIUM ISOTOPES Sm-152
energy levels from samarium-154 (p,t) reactions, spin-parity assignments for, (E), 25:12612
energy-level transitions from europium-152 beta and electron-capture decay, intensities and M1 multipole admixtures for, (E/T), 25:12576
energy-level transitions in, effect of higher-order deformations on ED, (T), 25:12584
proton reactions (p,t) at 20.6 MeV, angular distributions for, (E), 25:12612
SAMARIUM ISOTOPES Sm-154
alpha inelastic scattering at 27.5 to 32.5 MeV, α spectra and angular distributions for, (E), 25:12605
energy level of, Moessbauer study of first 2^+, (E), 25:12559
energy levels from alpha inelastic scattering, deformation parameters for, (E), 25:12605
nuclear electric quadrupole and magnetic dipole moments of, Moessbauer measurement of, (E), 25:12559
proton reactions (p,t) at 20.6 MeV, angular distributions for, (E), 25:12612
SAN ONOFRE POWER REACTOR, UNIT 2
quality assurance program for, additional information on, 25:12750 (DOCKET-50361-13)
SAN ONOFRE POWER REACTOR, UNIT 3
quality assurance program for, additional information on, 25:12750 (DOCKET-50361-13)
SANDS
analysis for trace amounts of elements by thermal neutron activation, ion exchange, and γ spectrometry, 25:10492
SAPPHIRES
analysis for trace amounts of elements by spark source mass spectrometry, 25:10455
properties of synthetic, for windows in high-pressure vessels, 25:11488 (KFK-1211)
SCANDIUM
book: Chemistry of Rare Earths and Various Other Elements, in Russian, 25:10580
determination in presence of iron, arsenate method for iodometric, 25:10465
determination in seawater by neutron activation, 25:10428
determination of trace amounts of, in biotite and tektite by spark source mass spectrometry, 25:10455
determination of trace amounts of, in phosphate deposits by spark source mass spectrometry, 25:10456
determination of trace amounts of, in rocks and sand by thermal neutron activation, ion exchange, and γ spectrometry, 25:10492
determination of trace amounts of, in rocks, quantometer for spectroscopic, 25:10451
energy levels of, LS-term dependence of hyperfine interaction parameters in d^2s configurations, 25:11694
energy-level transitions in, rates of Auger and x-ray, (T), 25:11685
SCANDIUM ALLOYS AND SYSTEMS
Pu--Sc, phase diagram of, 25:11440
Pu--Sc, properties of, electric, mechanical, and physical, 25:11440
SCANDIUM ISOTOPES Sc-48
energy levels from titanium-49 (d,He-3) reactions, spectroscopic factors for, (E), 25:12452
SCATTERING
amplitudes in dual resonance model, twisting invariant factorization of n-point, 25:12184
amplitudes of, general theorems on factorization near poles of, 25:12292
amplitudes of, role of Schwinger terms in derivation of sum rules and asymptotic limits of, 25:12294
Feynman integrals in, α representation of, 25:12288
Feynman integrals in, physical-region mass-shell properties of renormalized, 25:12293
Feynman path integral formulation of nonrelativistic quantum mechanics for, 25:12286
field emission in perturbed model in, three-dimensional, 25:12178
potential, rising Regge trajectories from singular, 25:12291
T-matrix for two-body, construction from symmetric part, (T), 25:12673
theory of, review of relativistic effects in, 25:11741
theory of, review of use of Sturmian functions in, 25:11732
SCHIZOMYCOTA
Agrobacterium tumefaciens, radiation effects on tumorgenic on qualities of, following inoculation into Jerusalem artichoke tissues, x, 25:11306
Bacillus megaterium, analysis for manganese and sodium by neutron activation, 25:10511
Bacillus subtilis, radioinduced damage in DNA of, effects of photoreactivation on repair of uv, 25:10960 (BNL-50203, pp 82-90)
Escherichia coli, radiation biochemistry of, 25:11074(R) (AECL-3777)
Escherichia coli, radiation effects on cytokinesis, γ and uv-radiosensitivity, and nutritional requirements of, cobalt-60 γ, 25:11019
Escherichia coli, radiation effects on repair mechanisms in, effects of acridine orange on uv, 25:11320
Escherichia coli, radioinduced damage in DNA of, study of repair mechanisms in uv, 25:11008 (BNL-50203, pp 14-26)
Escherichia coli, radioinduced mutations in, for bacteriophage susceptibility, DNA breakdown, and mitosis, 25:11029
Escherichia coli, radioinduced mutations in, for phage T5 resistance, comparison of light and uv, 25:11032
Escherichia coli, radioinduced single strand breaks in, effects of temperature on x, 25:11007 (BNL-50203, pp 1-13)
Escherichia coli, radioinduced toxins in, effects of, on mutagenesis of subsequently inoculated T_4 phage, γ, 25:11016
Escherichia coli, radiosensitivity of, effects of acriflavine, indanetrione, and methyl hydrazine on ionizing and uv, 25:11323
Escherichia coli, resistance to phosphorus-32 decay, effects of DNA synthesis and genetic recombination on, 25:10946
Micrococcus luteus, radioinduced damage of DNA of, use of nucleases for determining, uv, 25:10959 (BNL-50203, pp 27-40)
radiation injuries to, evaluation of cosmic, 25:11280
radiosensitivity on medical supplies during processing for sterilization, 25:11328
Rhizobium leguminosarum, radiosensitivity of, effects of dose fractionation on ionizing, 25:11325
Salmonella sp., radiation effects on survival of, effects of DNA on x, 25:10960 (BNL-50203, pp 82-90)
Salmonella typhimurium, radiosensitivity of 4-nitroquinoline 1-oxide mutants of, uv, 25:11026
Shigella flexneri, radiosensitivity of, effects of acriflavine, indanetrione, and methyl hydrazine on ionizing and uv, 25:11323
SCINTILLATION CAMERAS
effectiveness for function studies and diagnosis of neoplasms, 25:11182
SEALING MATERIALS
aging of outdoor adhesive, 25:12908 (SC-RR-70-163)
SEALS AND GLANDS
design parameters of liquid filled, for sodium cooled

reactor vessel closure plugs, 25:12771(P)
design parameters of reactor pressure vessel penetration hermetic, for drive shaft assembly, 25:12863(P)
SEAWATER
analysis for antimony by neutron activation, 25:10507
analysis for barium by isotope dilution method, 25:10468
analysis for trace elements by atomic absorption, fission track, or neutron activation method, 25:10428
analysis for uranium isotopes by α spectrometry, 25:10477
radiation monitoring of, on-board instruments for, 25:10817
radioisotope content of, measurements of radium-226, radium-228, and thorium-228, 25:10725(R) (CU-3139-4)
SEDIMENTARY DEPOSITS
analysis for major and trace elements by direct-reading spectrometry, 25:10450
SEED
growth of barley, in soils, effects of dose, fertilizer concentration, and soil chemistry on effects of chemical mutagens on, 25:11315
mutation induction in petunia, for color using methanesulfonic acid, ethyl ester, 25:11011
radiation effects on germination rate of cereal, mathematical analysis of, for predicting sensitivity of mature plants, 25:11314
radiation effects on growth of barley, in soil, effects of dose, fertilizer concentration, and soil chemistry on γ, 25:11315
radiation effects on growth of, of mung beans, combined effects of low pressure shock on x, 25:11317
radiation effects on, of corn, latent ionizing, 25:11309
radiation effects on, of cotton, latent γ, 25:11307
radioinduced free radicals in, of Dahlia, EPR analysis of electron, 25:11305 (NP-18394)
radioinduced mutations in, of petunia for color, γ, 25:11011
radioinduced mutations in, of sugar cane, effects of 1 to 5 kR doses on γ and x, 25:11030
SEISMIC WAVES
amplitude of underground nuclear explosion-generated, in Sahara Desert, effects of explosion conditions and surrounding medium on, (E/T), 25:10729 (CEA-R-4105)
characteristics of NTS nuclear explosion-generated, recorded at Nuclear Rocket Development Station, 25:10730 (NVO-1163-TM-22)
generation of micro-, by earthquakes, sonic booms, and underground nuclear explosions, (E), 25:10731
measurement of microearthquake-generated, in western US, 25:10731
propagation from underground nuclear explosions, geophysical uses of data on, 25:10748
SELENIUM
book: Chemistry of Rare Earths and Various Other Elements, in Russian, 25:10580
determination by on-stream neutron activation and γ spectrometry, design of equipment for, 25:10500
determination in blood plasma by neutron activation and radiochemical separation, 25:10495
determination of trace amounts of, in biotite and tektite by spark source mass spectrometry, 25:10455
determination of trace amounts of, in molybdenum, review on, 25:10459
photon inelastic scattering at 12 to 30 MeV, differential cross sections for, (E), 25:12463
SELENIUM ISOTOPES Se-75
effectiveness for diagnosis of brain tumors in comparison to iodne-131, 25:11145
effectiveness of methionine-incorporated, for scintigraphy of liver and pancreas, computer method for differentiation, 25:11176
effectiveness of selenomethionine-incorporated, and fast scanner for scintigraphy of human pancreas, effects of gastrointestinal tract scanning using colloidal gold-198 on, 25:11212
gamma spectrum of, for calibration of lithium-drifted germanium detectors, 25:10842
hazards to human children following renal scanning, 25:11190
labeling of selenomethionine with, for radioimmunoassay of thrombopoietin in plasma of mice, 25:10991
use of methionine-incorporated, for diagnosis of diseases of pancreas by scanning, 25:11199
use of methionine-incorporated, for scanning human pancreas, 25:11200
use of methionine-incorporated, for scanning of human pancreas, 25:11197
SELENIUM ISOTOPES Se-78
energy levels from bromine-78 beta and electron-capture decay, spin--parity assignments for, (E), 25:12445
energy-level trnsitions from bromine-78 beta and electron-capture decay, intensities of, (E), 25:12445
SELENIUM ISOTOPES Se-80
energy levels from photon scattering, radiation widths for, (E), 25:12447
SELENIUM ISOTOPES Se-84
beta decay of, beta and gamma spectra, half-life, log ft, and Q-value for, (E), 25:12462
SEMICONDUCTORS
book: Transport Phenomena in Liquid Metals and Semiconductors, 25:11410
radiation effects on monocrystal, 25:10583(R) (AECL-3776)
radiation effects on, device failures due to, 25:10906
SENA POWER REACTOR
maintenance during October 1970, 25:12722 (TID-25636)
operation during October 1970, 25:12722 (TID-25636)
SEROTONIN
radioprotective effects of, on mice and rats, γ, 25:11102
SERUMS
formation of anti-, in mice following inoculation with γ-irradiated syngeneic tumors, 25:10993
SEYFERT GALAXIES
radiation emission from, operation of gravitational lens mechanism on, (T), 25:11584
SF MATERIALS ACCOUNTING
method for large research centers, computer program for processing data for, 25:10796 (KFK-866)
SHEEP
radiation sickness in, nonspecific allergic reactions following β and γ, 25:10989
SHIELDED CONTAINERS
design for shipping spent fuel elements, 25:10801(P)
SHIELDING
analysis of reactor, evaluation of computer codes for, 25:12782 (CEA-CONF-1683)
cutting of reactor, design of milling machine for underwater, 25:12715
cutting of reactor, design of plasma arc for underwater, 25:12714
design of, for gamma radiation from spent nuclear fuel, 25:11948
recommendations for veterinary medicine, 25:11075 (NCRP-36)
SHIPS
book: Nuclear Ship Propulsion, 25:12836
SHOCK TUBES
plasma diagnostics in, using infrared radiation, 25:11868(T) (SC-T-70-4054)
SHOCK WAVES
effect of interplanetary, on 1- to 10-MeV proton acceleration, (E/T), 25:11624
effects of supersonic flight-generated, on seismic activity in western US, (E), 25:10731
effects of supersonic flight-generated, on window pane damage, (E/T), 25:10792 (SC-RR-70-441)
production in solids by electron beams, 25:10791
propagation in warm plasma, nonlinear theory for collisionless, 25:11930
structure of hydromagnetic, in interstellar regions of very low ionization, (T), 25:11639
theory of magnetohydrodynamic, relativistic, 25:11763
velocity within and at surface of solid materials, effects of high pressure on, (E), 25:10749
SILICATE ROCKS
analysis for trace amounts of elements, method for elimination of matrix effect in quantometric, 25:10452
analysis of standard, for trace amounts of elements using sodium chloride buffer, emission spectrographic, 25:10454
analysis of standard, for trace amounts of elements by x-ray fluorescence, 25:10449
SILICATES
spectra of iron-containing, interstellar absorption, (E/T), 25:11643
SILICON
analysis for boron, carbon, fluorine, and oxygen by charged particle, photon, and proton activation methods, 25:10488 (CEA-R-4072)
analysis of nitride layers on, for oxygen by deuteron (d,p) reactions, 25:10583(R) (AECL-3776)
determination as impurity in fuel materials by emission spectroscopy, 25:10432 (KFK-1261)
determination in sedimentary rocks by direct-reading spectrometry, 25:10450
determination in tektite by spark source mass spectrometry, 25:10455
determination of trace amounts of, in molybdenum, review on, 25:10459
determination of trace amounts of, in Zircaloy-2 and zirconium, carrier distillation method for spectrographic, 25:10430 (EUR-4541)
determination of trace amounts of, in zirconium, carrier distillation method for spectrographic, 25:10430 (EUR-4541)
diffusion in molybdenum silicide, niobium silicide, tantalum silicide, and titanium silicide, activation energies for, 25:11519
growth of epitaxial layers of, by ion-beam sputtering, 25:11962
ion implantation in amorphous films of, sputtering and strain induced by rare-gas, 25:11959
precipitation in aluminum and aluminum--nickel alloy, effects of thermal neutron irradiation on, 25:11471
proton channeling at 0.2 and 1 MeV in (110) planar channel of, calculated wavelength distributions for transverse oscillations in, 25:11953
proton dechanneling coefficient of crystals of, temperature dependence of 1.5-MeV, (E/T), 25:11969
radiation effects on lithium drift at low temperatures in p-type, x-, 25:11973
radiation effects on plasmon loss in electron energy loss

spectra in (111) surface of, argon-ion, (E/T), 25:11970
SILICON CARBIDES
ion implantation in, cathodoluminescence spectrum in annealing of helium- and krypton-, 25:11974
SILICON ISOTOPES Si-28
alpha elastic and inelastic scattering at 166 MeV, optical potentials from DWBA analysis of angular distributions from, (E/T), 25:12549
deuteron elastic scattering at 28 MeV, asymmetries in cross sections for, (E), 25:12309 (LYCEN-6909)
energy levels from (p,γ) and (α,γ) reactions, widths, branching ratios, and decay strengths for T = 2, (E), 25:12441
energy levels from alpha inelastic scattering at 166 MeV, deformation parameters for, (E/T), 25:12549
helium-3 reactions (He-3,d) at 18 and 20 MeV, DWBA analysis of differential cross sections from, (E/T), 25:12479
neutron capture at 14 MeV, calculation of γ spectra using statistical and direct-semidirect models, (T), 25:12472
neutron capture by, gamma spectra and Q-value for thermal, (E), 25:12403
neutron reactions (n,p) in a fission spectrum, average cross section for, (E), 25:12460
nuclear potential energy surface for, (T), 25:12503
photoneutron cross section at 16 to 31 MeV, (E), 25:12469
proton inelastic scattering at 12 to 15 MeV, statistical analysis of intermediate structure in, (E/T), 25:12470
SILICON ISOTOPES Si-29
alpha inelastic scattering at 15.4 MeV, angular correlations from, (E), 25:12449
energy levels from alpha and proton inelastic scattering and magnesium-26 (α,nγ) reactions, spin--parity assignments for, (E), 25:12449
energy levels from silicon-30 (He-3,α) reactions, spectroscopic factors, l transfers, and spin--parity assignments for T = 3/2, (E/T), 25:12450
energy levels from thermal neutron capture, (E), 25:12403
energy levels of, potential energy and spin--parity assignments for, (T), 25:12503
energy-level transitions from alpha and proton inelastic scattering and magnesium-26 (α,nγ) reactions, multipole mixing and gamma branching ratios for, (E), 25:12449
neutron capture by, gamma spectra and Q-value for thermal, (E), 25:12403
neutron reactions (n,p) in a fission spectrum, average cross section for, (E), 25:12460
proton inelastic scattering at 6.5 and 8.7 MeV, gamma spectra and angular correlations from, (E), 25:12449
SILICON ISOTOPES Si-30
energy levels from thermal neutron capture, (E), 25:12403
helium-3 reactions (He-3,α) at 15.4 MeV, energy spectra and DWBA analysis of differential cross sections from, (E/T), 25:12450
helium-3 reactions (He-3,d) at 18 and 20 MeV, DWBA analysis of differential cross sections from, (E/T), 25:12479
helium-3 reactions (He-3,t) at 16 and 30 MeV, (E), 25:12498
neutron capture by, gamma spectra and Q-value for thermal, (E), 25:12403
SILICON ISOTOPES Si-31
energy levels from thermal neutron capture, (E), 25:12403
precipitation of carrier-free, by metal hydroxides, 25:10675
SILICON JUNCTIONS
radiation effects on interface characteristics of reactively sputtered alumina/, electron, 25:10905
SILICON OXIDES
neutron transport in, flux distribution and dose equivalent calculations for, 25:12332
radiation effects on high-pressure polymorphs of, fast neutron, 25:11474(R) (BNWL-842)
radioinduced electron traps in rare earth-doped, absorption--thermoluminescence study of x-, 25:11967
SILICON SYSTEMS
Al--Si--U, radiation effects on fuels of, at high burnups, in-pile, 25:11462 (IN-1437, pp 59-70)
Cu-base--Si, creep of, effects of microstructure on, 25:11434(R) (SU-326-P-17-X-1)
Fe-base--Si, creep at high temperature and low stress, rate controlling factors in, 25:11434(R) (SU-326-P-17-X-1)
Fe-base--Si, strain behavior of solid-solution, 25:11434(R) (SU-326-P-17-X-1)
Ge--Si, performance as thermocouple components for thermoelectric converters, 25:11477 (ALO-2510-T-1)
Ni-base--Si, radiation damage in, stored-energy release and resistivity recovery from 20°K electron, 25:11977
SILTS
amino acid content of deep-sea, (E), 25:10725(R) (CU-3139-4)
analysis for trace elements, problems of contamination during, 25:10427
manganese content of deep-sea, measurements of, 25:10725(R) (CU-3139-4)
radioisotope content of deep-sea, measurements of radium-226, radium-228, and thorium-228, 25:10725(R) (CU-3139-4)
SILVER
alpha reactions at 30 to 80 MeV, cross sections for production of K x rays by, (E), 25:12488
carbon-12 reactions at 86 MeV, analysis for reaction mechanisms in, (E), 25:12606
determination by photon activation, reactions and sensitivities for, 25:10488 (CEA-R-4072)
determination in serum and urine by flameless atomic absorption spectroscopy, 25:10464
determination of trace amounts of, in biotite and tektite by spark source mass spectrometry, 25:10455
determination of trace amounts of, in molybdenum, review on, 25:10459
determination of trace amounts of, in rocks, quantometer for spectroscopic, 25:10451
friction and wear of, sliding against copper and iron rings under vacuum, 25:11413
nitrogen-14 reactions at 78 and 113 MeV, analysis for reaction mechanisms in, (E), 25:12606
superconductivity in, (E/T), 25:11821
SILVER ALLOYS AND SYSTEMS
Ag--Au, activity coefficient and vacancy flow effects on tracer diffusion in, 25:12902 (ORO-2036-20)
Ag--Cd--In-base--Sn, electric conductivity, Fermi surface topology, and superconducting transition temperature of dilute, 25:12032
Ag--Pu, phase diagram of, 25:11441
SILVER BROMIDES
radiation effects on thermoelectric properties of molten, gamma, 25:11952
SILVER CHLORIDES
radiation effects on thermoelectric properties of molten, gamma, 25:11952
SILVER ISOTOPES Ag-104
energy levels from cadmium-104 electron-capture decay, spin--parity assignments for, (E), 25:12475
energy-level transitions from cadmium-104 electron-capture decay, energies, intensities, and conversion coefficients for, (E), 25:12475
SILVER ISOTOPES Ag-109
nitrogen-14 reactions at 78 and 113 MeV, analysis for reaction mechanisms in, (E), 25:12606
SILVER ISOTOPES Ag-110
determination of metastable, by ion exchange and γ spectroscopy, 25:10490(T) (LIB/Trans-334)
SILVER ISOTOPES Ag-111
use for scanning human liver, 25:11200
SILVER SELENIDES
homogeneity region of solid, coulometric titration for determination of, 25:12865(T) (ANL-Trans-873)
SILVER SULFIDES
homogeneity region of solid, coulometric titration for determination of, 25:12865(T) (ANL-Trans-873)
SILVER TELLURIDES
homogeneity region of solid, coulometric titration for determination of, 25:12865(T) (ANL-Trans-873)
SINGLE CRYSTALS
ion reactions with, review of atom, electron, and ion ejection following, 25:11676
SKIN
cobalt-60 1-nitroso 2-naphthol chelate distribution in, of rats, 25:10958
radiation effects on content of oxidative enzymes in epidermal, x, 25:11241
radiation effects on incidence of eruptions in, of man following therapy of malignant tumors, 25:11296
radiation effects on, of mice, effects of acute dose and dose fractionation on recovery from, 25:11260 (BNL-50203, pp 286-91)
radioinduced chronic dermatitis in, of swine, callicrein treatment for x, 25:11110
radioinduced tumors in, of mammals, effects of clonogenicity, dose, reproductive integrity, and time on, 25:11253 (BNL-50203, pp 154-73)
SNOW
accumulation in Antarctica, measurement of, using lead-210/polonium-210, 25:10477
SODIUM
alkaline impurities in loop, monitoring data on content of, 25:11348(R) (GEAP-13539-13)
analysis for oxygen, meter calibration for in-line, 25:11348(R) (GEAP-13539-13)
content of man, method for determining, 25:10920
content of soil, neutron activation analysis of, 25:10909
corrosive effects on stainless steel at 1300°C, effects of oxygen content on, 25:11348(R) (GEAP-13539-13)
corrosive effects on Type 316 stainless steel at 1122 to 1235°F, relations with heat flux, 25:11348(R) (GEAP-13539-13)
determination as impurity in fuel materials by emission spectroscopy, 25:10432 (KFK-1261)
determination by charged particle and photon activation, reactions and sensitivities for, 25:10488 (CEA-R-4072)
determination in Bacillus megaterium by neutron activation, 25:10511
determination in serum and urine by flameless atomic absorption spectroscopy, 25:10464

determination in tektite by spark source mass spectrometry, 25:10455
determination of trace amounts of, in molybdenum, review on, 25:10459
determination of trace amounts of, in rocks and sand by thermal neutron activation, ion exchange, and γ spectrometry, 25:10492
determination of trace amounts of, in standard rocks by flame photometry, 25:10671
diffusion of hydrogen in, design and operation of continuously active indicator for determinaton of, 25:11400
effects on stress rupture of stainless steel at 1150 to 1300°F, 25:11348(R) (GEAP-13539-13)
optical properties of aerosols of, (E), 25:10797(R) (NYO-841-23)
solvent properties of liquid, for carbon at 600 to 950°C, 25:10579
thermal conductivity of layers of elemental, deposited on heat exchanger surfaces, (E), 25:10797(R) (NYO-841-23)

SODIUM ALLOYS AND SYSTEMS
K--Na, electromigration in liquid, theoretical consideration of, 25:11404

SODIUM CHLORIDES
analysis of, neutron activation, 25:11472(R) (AD-708705)
purification of sodium-24-labeled, by ion exchange, 25:11046
radiation hardening of single crystals of, correlation with defects in x-, 25:11975
radioinduced M and F centers in crystals of, laser re-excitation and decay of γ, (E/T), 25:11956

SODIUM CITRATES
analysis for moisture content by neutron scattering and moderation, 25:10486

SODIUM CYANIDES
effects on plutonium-239 and polonium-210 accumulation in Ascophyllum nodosum and marine plankton, 25:10941

SODIUM FLUORIDES
radioinduced M and F centers in crystals of, laser re-excitation and decay of γ, (E/T), 25:11956
sorptive properties for neptunium hexafluoride and uranium hexafluoride, 25:10568 (CEA-R-4051)

SODIUM FLUOROBORATES
analysis for boron trifluoride impurities, 25:10434 (ORNL-4636, pp 7-13)

SODIUM IODIDES
use of iodine-131-labeled, for therapy for human thyroid carcinomas, effects of surgery preceding, 25:11234

SODIUM ISOTOPES Na-22
abundance in Allende meteorite, (E), 25:11540
activity of, whole-body counter for determining total sodium content of man, 25:10920
energy levels from sodium-22 (He-3,t) reactions at 16 and 30 MeV, (E), 25:12498
energy levels of, calculation using collective model with Coriolis coupling, (T), 25:12482

SODIUM ISOTOPES Na-23
proton reactions (p,αγ) at 1.1 to 1.5 MeV, α--γ angular correlations in, (E), 25:12443

SODIUM ISOTOPES Na-24
determination in body fluid by ion exchange and scintillation counting, 25:11066
diffusion in viscosity standard silicate glass, 25:10578
effectiveness of chlorine-incorporated, for scanning of arterio-venus shunts in feet of dogs, double isotope method for, 25:10926
use of isotope dilution measurement of extracellular fluid volume in dogs, 25:11185

SODIUM PEROXIDES
iodine-131 volatilization from, (E), 25:10797(R) (NYO-841-23)

SODIUM SULFIDES
radiolysis of aqueous solutions of, yields from γ, 25:10649

SODIUM TETRABORATES
analysis of pharmaceutical preparations containing, by neutron absorption, 25:10487

SOILS
analysis for aluminum, manganese, and sodium by neutron activation, 25:10909
analysis for antimony and arsenic by neutron activation and radiochemical separation, 25:10506
analysis for bromine and iodine by neutron activation, 25:10505
analysis for trace amounts of elements by atomic absorption spectrometry, matrix effects on, 25:10457
analysis for trace elements, problems of contamination during, 25:10427
contamination by fallout from Shot Coulomb C, (E), 25:10734 (AD-708567)
contamination by fallout from Shot Priscilla, (E), 25:10733 (AD-708566)
deformation of surrounding, by contained 100 kt underground nuclear explosions, 25:10741
effects on growth of chemical mutagen-treated or γ-irradiated barley seeds, combined effects of dose and fertilizer concentration on, 25:11315
iron content of wind-blown surface, determination for monitoring radioactive fallout, 25:10718
properties of nuclear explosion-containing, effects on explosion safety and yield of chemical, mechanical, and physical, 25:10740
ruthenium-106 transport in irrigated, 25:10692
sorptive properties for iodine, effects of initial iodine concentration on, (E), 25:10694
strain in Nevada Test Site, near Hutch Event, measurements of dynamic, 25:10732
strontium-90 content of west Slovakia surface, calculation to year 2000, 25:10719

SOLAR ACTIVE REGIONS
magnetic fields in, strengths of, (E), 25:11616
polarimetry in, (E), 25:11616
radio bursts from, effects of coronal field patterns on, (E), 25:11605

SOLAR CORONA
active centers and condensations in, radio observations of, (E), 25:11606
magnetic fields in, radio study of, (E), 25:11605
radio diameter of, relation to sunspot areas, (E/T), 25:11630
radio emission from condensations of, effect of radio bursts on circular polarization of total, (T), 25:11620
structure of monochromatic, in vicinity of prominences, (E), 25:11618
structure of, during Nov. 12, 1966 eclipse, (E), 25:11604
x-ray emission from, simplified thermal continuum function for, (T), 25:11632

SOLAR FLARES
charged-particle production along neutral line in magnetic field, Syrovatskii mechanism in, (T), 25:11633
effect on low-energy proton fuxes near Moon, Dec. 16, 1966, (E), 25:11669
origin of white-light, (E/T), 25:11619
particle acceleration mechanisms for, (T), 25:11625
radiation hazard from, to supersonic transport personnel, review of, 25:11086
relation to sunspot areas, (E/T), 25:11630
x-ray emission during, polarization and anisotropy of, (E), 25:11623

SOLAR PARTICLES
propagation processes for, review of, (T), 25:11625

SOLAR PROMINENCES
effects on structure of monochromatic corona, (E), 25:11618
magnetic-field orientation in quiescent, (E), 25:11617

SOLAR RADIO BURSTS
effects on coronal condensations emission, (T), 25:11620
emission from active regions, (E), 25:11605
excitation mechanism for Type III, (T), 25:11621
morphology of Type-III, low-frequency storm, (E), 25:11622

SOLAR SYSTEM
element nucleosynthesis in, effects of energetic proton fluxes on, (T), 25:11544
hydrogen interaction with interstellar, (E/T>, 25:11640

SOLAR WIND
cosmic-ray modulation by, numerical technique for solving galactic, (T), 25:11746
cosmic-ray modulation by, primary, (E), 25:11627
effects on polarity pattern of interplanetary field, (E/T), 25:11608
pressures in, magnetic and thermal, (E), 25:11607
propagation processes for, review of, (T), 25:11625
structure of, microscopic, (T), 25:11626

SOLID STATE PHYSICS
research at Atomic Energy of Canada Limited, Oct. 1 to Dec. 31, 1969, 25:12427(R) (AECL-3666)

SOLIDS
compressibility of porous, high-pressure physics research on, 25:10749
conference on thermal expansion of, Santa Fe, N. Mex., June 10 to 12, 1970, 25:11508
ion reactions in keV range with, spatial distribution of energy deposited in, (T), 25:11682
ion reactions with, review of atom, electron, and ion ejection following, 25:11676
physical properties of, high-pressure physics research on, 25:10749
radioinduced displacement spikes in, computer simulation of annealing modes for in-pile, 25:11474(R) (BNWL-842)
thermal expansion of, 1970 conference on, 25:11508

SOLVENT EXTRACTION PROCESSES
methods for rapid, kinetics of effects of acidity and salts on, 25:10668 (LYCEN-7034, pp 1-8)

SOUND
emission by boiling bubbles in subcooled water, 25:10769(R) (ORO-3911-3)

SOUTH AMERICA
radioactivity of atmosphere and precipitation of, during 1970, gross β, 25:11039

SOUTHWEST EXPERIMENTAL FAST OXIDE REACTOR
operations history for August to October 1969, 25:12717 (DOCKET-50231-66)
operations history for May to July 1969, 25:12731 (DOCKET-50231-65)

SOVIET UNION
cesium-137 accumulation by reindeer herdsmen in, 25:11037 (NP-18381)
ground waters of Bukhara--Karshin artesian basin in, radioisotope content of, (E), 25:10698

XUM

ground waters of Kamchatka Peninsula, rare earths, thorium, and uranium contents of thermal, (E), 25:10697
radiation dose to population of, fallout cesium-137, 25:11073
strontium-90 uptake by population of, role of food chain in stratospheric fallout, 25:10934 (NP-18380)
SPACE
book: The Interstellar Medium, 25:11641
structure of interplanetary, (E), 25:11627
SPACE FLIGHT
effects on human central nervous system, effects of acceleration, dose, and vibration on, 25:11298
SPACE VEHICLES
heat sources for Apollo, fabrication of liners for, 25:10776 (MLM-1779)
SPECTRA
analysis of nuclear, computer design and programing for visualization in, 25:10892 (CEA-N-1363)
SPECTROSCOPY
book: Stellar Spectroscopy: Normal Stars, (T), 25:11543
developments in low-energy and nuclear, conference on, 25:12520 (LYCEN-7034)
peak location and calibration in, method for, 25:10858
theory of correlation time-of-flight, 25:10850 (JUL-684-FF)
SPERM
radiation effects on, of moths, γ, 25:11338
SPERMATOCYTES
radiosensitivity of, in mice, x, 25:11276
SPERMATOGENESIS
radiation effects on, in mice, x, 25:11276
SPERMATOGONIA
radiosensitivity of, in mice in relation to mechanisms for depletion and recovery, x, 25:11276
SPHENE
age of, effects of geometry factor on accuracy of fission track, (E), 25:10695
SPHERES
neutron diffusion in, computer program for solving one-dimensional, (T), 25:12335 (AECL-3671)
SPLEEN
blood circulation in human, use of chromium-51-labeled heat treated erythrocytes for determining, 25:11142
enlargement of human, effects of, on selenium-75 scanning of pancreas, 25:11199
isoenzymes of lactic dehydrogenase in, of xenogenic radiation chimeras, 25:10992
nonprotein thiol content of, of mice following injection of cysteine in optimum radioprotective dose, 25:11101
radiation effects on human, Thorotrast, 25:11117
radiation effects on, of inbred and noninbred mice, protective effects of cystaphos and mexamine on hematopoietic tissue formation, against γ, 25:11099
radiodiagnosis of diseases of human, using gold-198, effects of blood circulation on, 25:11196
radioinduced inhibition of endocolonization in, of mice, effects of dose rate on cobalt-60 γ, 25:10986
scanning for diagnosis of diseases of human, using chromium-51 and mercury-197, 25:11201
scanning for diagnosis of functional asplenia, use of metastable technetium-99 for, 25:11117
scanning of human, use of erythrocytes labeled with chromium-51 and mercury-197 for, 25:11200
SPORES
radioinduced free radicals in, of Osmunda regalis, ESR study of ionizing, 25:11319
SPUTTERING
particle-ejection patterns and yields from, review, 25:11676
STABLE ISOTOPES
distribution in atmosphere, development and operation of equipment for measuring vertical, 25:10754 (NP-18633)
STACK DISPOSAL
gases from reactor, effects of lower Aare River Valley air currents on diffusion of, (E), 25:10703 (EIR-185)
plumes from, review of methods for predicting rise of, 25:10717
STADE POWER REACTOR
core components for, wind tunnel testing of coolant flow stresses on, 25:12706
STAINLESS STEEL
analysis for molybdenum by solvent extraction and flame photometry, 25:10439
book: Intercrystalline Corrosion and Corrosion Cracking of Stainless Steel in Aqueous Solutions (In Russian), 25:11353
compatibility of Type 304, with plutonium dioxide--uranium dioxide fuels at 650 to 1000°C, 25:11474(R) (BNWL-842)
compatibility of Type 304, with plutonium nitride--uranium nitride fuels at 650 to 1000°C, 25:11474(R) (BNWL-842)
compatibility of Type 316, with plutonium carbide--uranium carbide fuels at 900°C, 25:11475 (AERE-R-5173)
corrosion by sodium at 1300°C, effects of oxygen content on, 25:11348(R) (GEAP-13539-13)
corrosion of Type 316, by sodium, effects of heat flux at 1122 to 1235°F on, 25:11348(R) (GEAP-13539-13)
corrosion of Types 304L and 310, by boiling waste solutions, 25:10658(R) (BNWL-1533)
corrosion of Types 304L and 310, by glass melts containing boron oxide, silicon dioxide, and sodium oxide, 25:10658(R) (BNWL-1533)
corrosion resistance of resulfurized Types 303, 316, 416, and 430, effects of uranium on, 25:11352
corrosion resistance of Types 303 and 316, effects of molybdenum and uranium in acid media on, 25:11352
diffusion of deuterium in Type 304L, effects of cold work on, 25:11474(R) (BNWL-842)
fabrication of cladding of type 316, for plutonium nitride (PuN)--uranium nitride (UN) fuel pins, 25:12795(R) (BMI-1893)
radiation effects on fatigue life of Types 304 and 316, fast neutron, 25:11459 (IN-1437, pp 1-4)
radiation effects on mechanical properties of Type 347, fast neutron, 25:12823 (RCN-125)
radiation effects on microstructure and properties of Types 304, 316, and 348, fast neutron, 25:11474(R) (BNWL-842)
radioinduced embrittlement of niobium-stabilized, by helium, neutron, 25:11456 (AERE-R-5622)
reactions of Type 304, with sodium at 1150 to 1300°F, effects on stress rupture properties, 25:11348(R) (GEAP-13539-13)
structure of precipitates in niobium-stabilized Type 20-25, metallographic, 25:11428 (AWRE-O-29/67)
tensile properties at 25 and 1000°C, effects of stress aging on, 25:11474(R) (BNWL-842)
STANDARDS
description of ANSI N16.1-1969, for criticality safety in handling fissionable materials outside reactors, 25:10802
STAR CLUSTERS
detection of two Ap, in NGC 3114, (E), 25:11578
stars in Hyades and Coma, metal-to-hydrogen ratio for, (E), 25:11551
STARS
ages of B-type, within 10° of the galactic center, (E), 25:11561
atmospheres of metal-deficient giant, (T), 25:11546
atmospheres of white-dwarf, effects of convection in, (T), 25:11556
atmospheres of, mechanism for production of extended, (E), 25:11571
book: Stellar Spectroscopy: Normal Stars, (T), 25:11543
classification of Feige blue, photometric, (E), 25:11573
detection of two Ap, in NGC 3114, (E), 25:11578
distances of B-type, within 10° of the galactic center, (E), 25:11561
distribution of variable, in field 3 of Palomar--Groningen survey, (E), 25:11550
element nucleosynthesis at surfaces of, effects of energetic proton fluxes on, (T), 25:11544
element nucleosynthesis of beryllium, boron, and lithium in, (T), 25:11548
energy radiated from 21 dMe, under flaring and quiescent conditions, (E), 25:11575
envelopes surrounding Be, method for determining sizes of gaseous, (E/T), 25:11557
formation in HI regions, (T), 25:11639
formation in interstellar clouds, (T), 25:11650
formation of, gravitational instability in, (T), 25:11641
garnet formation in atmospheres of cool, (E/T), 25:11562
gravitational instability of polytropic gas spheres under external pressure, (T), 25:11560
hydrogen depletion in upper main-sequence, (T), 25:11559
magnitude sequences for UZ Bootis and W Piscium, (E), 25:11579
masses of classical Cepheids and RR Lyrae, (T), 25:11558
matter and antimatter in, separation of, (T), 25:11661
metal abundance in delta Pavonis, (E), 25:11564
metal abundances for, in Hyades and Coma open clusters, (E), 25:11551
model for idealized magnetic, generalization of Prendergast, (T), 25:11554
motions of B-type, within 10° of the galactic center, spatial, (E), 25:11561
photoelectric observations of HD 119850, e Boo, and α Tau, (E), 25:11572
photometric history of BL Lac, (E), 25:11555
physics of, 25:11538
quark regions inside massive, (T), 25:12188
spectra of early-type, Balmer emission features in, (E), 25:11577
spectra of early-type, Balmer emission features in, (E), 25:11576
spectra of, scanner observations of lambda 4430 diffuse interstellar feature in, (E), 25:11651
spectra of, variable H and K emission components in, (E), 25:11572
stability of rotating magnetic, nonaxisymmetric modes and diffusivity, 25:11552
structure of upper main-sequence, internal, (T), 25:11559
thermodynamics of white-dwarf matter, (T), 25:11549
velocity of, associated with planetary nebula NGC 3132, radial, (E), 25:11570
x-ray emission from T Tauri, (T), 25:11548
STATISTICS
quantum, generalized operators in, 25:12263
spectral density method in statistical mechanics for

XUM

systems with pair interaction, 25:12061
STEAM
corrosive effects on Zircaloy-2 at 980 to 1340°C, 25:11463 (IN-1437, pp 70-5)
H_2O--steam, corrosive effects on defected Zircaloy-clad uranium fuel elements, 25:11347 (CISE-R-222)
H_2O--steam, flow in tubes, heat transfer, holdup, and nucleation calculations for, 25:10766 (AERE-R-3984)
STEAM POWER PLANTS
environmental effects of U. S., programs for reduction of, 25:12761
STEEL
analysis for molybdenum by solvent extraction and flame photometry, 25:10439
analysis for oxygen by photon activation and radiochemical separation, 25:10501
carburization by decomposing carbon monoxide, effects of carbon dioxide, composition, oxygen, surface structure, temperature, and water vapor on, 25:11374 (DP-Report-530)
corrosion by liquid lead at high temperatures, 25:11376 (JUL-661-RW)
crack initiation and growth in A106B carbon and Type 304 stainless, effects of low cycle fatigue on, 25:12783(R) (GEAP-10207-22)
ductility of Type 4340, relations of strength transition in toughness on notch, 25:11373(R) (COO-2048-1)
fabrication of pressure vessels of, testing program for, 25:11364
fracture toughness of heavy-section notch specimens of Type A533B, effects of fatigue precracking on, 25:11380 (WCAP-7578)
fracture toughness of Type A533B, effects of temperature on, 25:11474(R) (BNWL-842)
properties for use in pressure vessels, lectures on, 25:11357
radiation effects on brittle fracture of pressure vessel, method for evaluation of, 25:11470
radiation effects on mechanical properties of weldments of Types A203 and A353, fast neutron, 25:11454 (AECL-3734)
radiation effects on sound velocity in, fast neutron, 25:11474(R) (BNWL-842)
shear properties of Type 4340, effects of high-temperature strain on, 25:11373(R) (COO-2048-1)
solubility in lead at 350 to 1100°C, 25:11376 (JUL-661-RW)
stress concentration at chamfered changes of section in plates of, measurement of acoustic, 25:10790 (RD/B/N-1795)
toughness of low-carbon rimmed, effects of plastic instability on temperature transition in, 25:11373(R) (COO-2048-1)
STELLAR FLARES
occurrence in 21 dMe stars in solar neighborhood, (E), 25:11575
x-ray emission during, in T-Tauri stars, (T), 25:11548
STELLARATORS
magnet coil windings for Torsatron, properties of, 25:11918 (EUR-CEA-FC-543)
plasma equilibrium in, effects of electric conductivity on, 25:11912 (MPI-PA-7/62)
STEMS
potassium-42 accumulation in, of corn, effects of age, potassium deficiency, and temperature on, 25:10930 (CEA-CONF-1517)
potassium-42 transport in, of corn, effects of age, potassium deficiency, and temperature on, 25:10930 (CEA-CONF-1517)
STOMACH
iodine-131-labeled human serum albumin retention in, effects of acidity on, 25:11170
STORAGE RINGS
beam optics in, 25:12325
development and research at Kharkov 100-MeV, 25:12307 (KHFTI-69-27)
research using, 25:12325
STRANGE PARTICLES
production in final states of π^- + p interactions at 7 GeV/c, (E), 25:12110
STRATOSPHERE
strontium-90 residence time in, comparison of estimates by various investigators, 25:10715 (ORO-2529-28, App. 9)
STRESS
measurement of dynamic, at chamfered changes of section using acoustic waves, 25:10790 (RD/B/N-1795)
STRONTIUM
determination in rocks by x-ray fluorescence, correction of matrix effects in, 25:10447
determination in seawater by atomic absorption spectrometry or neutron activation, 25:10428
determination in sedimentary rocks by direct-reading spectrometry, 25:10450
determination in serum and urine by flameless atomic absorption spectroscopy, 25:10464
determination of trace amounts of, in biotite and tektite by spark source mass spectrometry, 25:10455
determination of trace amounts of, in minerals and rocks by atomic absorption spectrophotometry, 25:10458
determination of trace amounts of, in minerals and rocks by x-ray fluorescence, methods for correction of matrix effect in, 25:10448
determination of trace amounts of, in molybdenum, review on, 25:10459
determination of trace amounts of, in rocks, quantometer for spectroscopic, 25:10451
determination of trace amounts of, in silicate rocks, method for elimination of matrix effect in quantometric, 25:10452
determination of trace amounts of, in standard bauxite, carbonate, and silicate rocks by x-ray fluorescence, 25:10449
determination of trace amounts of, in standard rocks by borate fusion, dissolution in EDTA, ion exchange, and atomic absorption spectrophotometry, 25:10671
determination of trace amounts of, in standard silicate rocks using sodium chloride buffer, emission spectrographic, 25:10454
photoneutron cross section up to 27 MeV, (E), 25:12456
STRONTIUM ISOTOPES
sorption of radioactive, through intestines of rats, effects of alginic acid components on, 25:10939
STRONTIUM ISOTOPES Sr-85
content of bones of rats, effects of estradiol on, 25:10933 (COO-1339-45)
deposition in bones of rats, effects of dose and time of administration on effectiveness of activated barium sulfate for prevention of, 25:11048
effectiveness for diagnosis of bone metastases in man in comparison to x-radiography, 25:11174
effectiveness for diagnosis of rheumatoid spondylitis, and polyarthritis, 25:11175
half-life of metastable, 25:10491 (ORNL-4636, pp 20-33)
radiation effects on sorption of, from gastrointestinal tract of dogs following injection, whole-body γ, 25:10947
radiation effects on uptake of, by rat bones following intravenous or oral administration, whole-body γ, 25:11263
sorption by intestines of rats, effects of estradiol on, 25:10933 (COO-1339-45)
sorption from gastrointestinal tract, calculation of rate of, 25:10951
transport in roots of Adenostoma, Ceanothus, and Quercus, 25:10955
transport through rat intestinal epithelial membranes, mechanisms for, 25:10938
uptake by bean and tomato seedlings in culture media in comparison to forage plants, 25:10936 (UCB-34-P-23-15)
uptake by bones in rats following oral administration, effects of barium sulfate on, 25:10940
use for scanning of fibia and tibia bones in rats, 25:11216
STRONTIUM ISOTOPES Sr-86
content ratio to rubidium-87 in Wind River, Wyoming igneous plutons, 25:10701
energy levels from photon scattering, radiation widths for, (E), 25:12447
STRONTIUM ISOTOPES Sr-87
half-life of metastable, 25:10491 (ORNL-4636, pp 20-33)
sorption of metastable, from gastrointestinal tract of man, effectiveness of activated barium sulfate for inhibiting, 25:11047
STRONTIUM ISOTOPES Sr-88
photoneutron cross section up to 27 MeV, (E), 25:12456
STRONTIUM ISOTOPES Sr-89
content in Fayetteville, Arkansas ground-level atmosphere, Aug. 1969 to Aug. 1970, (E), 25:10711 (ORO-2529-28, App. 5)
content in Fayetteville, Arkansas rainwater, July and Aug. 1969, 25:10707 (ORO-2529-28, App. 1)
content in Fayetteville, Arkansas rainwater, Sept. 1969 to Aug. 1970, (E), 25:10710 (ORO-2529-28, App. 4)
content of caribou and reindeer meat in Alaska during 1969, 25:11001
content of human diet in USA during 1969, 25:11040
content of milk in South America in 1967, 25:11068
content of milk in USA during February 1970, 25:11040
content ratio to strontium-90 in Fayetteville, Arkansas rainwater, 1964 to 1969, effects of jet stream and Chinese nuclear tests on, 25:10708 (ORO-2529-28, App. 2)
effects on growth of dwarf peas, 25:10936 (UCB-34-P-23-15)
radiation effects on sorption of, from gastrointestinal tract of dogs following ingestion, whole-body γ, 25:10947
STRONTIUM ISOTOPES Sr-90
accumulation by animals in aquatic ecosystem, 25:11006
accumulation in body of animals, effects of diet on, 25:10956
accumulation in food products from fallout in Soviet Union during 1959 to 1967, 25:10934 (NP-18380)
accumulation in milk, 25:10932 (CEA-CONF-1558)
content in atmosphere and soils of west Slovakia to year 2000, calculation of, 25:10719
content in atmospheric precipitation at worldwide sites, 1956 to 1970, 25:10715 (ORO-2529-28, App. 9)
content in cow's milk in Bulgaria, 25:10480
content in Fayetteville, Arkansas ground-level atmosphere, Aug. 1969 to Aug. 1970, (E), 25:10711 (ORO-2529-28, App. 5)

XUM

content in Fayetteville, Arkansas rainwater, July and Aug. 1969, 25:10707 (ORO-2529-28, App. 1)
content in Fayetteville, Arkansas rainwater, May 1965 to April 1970, effects of Chinese nuclear explosions on, 25:10713 (ORO-2529-28, App. 7)
content in Fayetteville, Arkansas rainwater, Nov. 1968 to Oct. 1969, effects of 1968 Chinese nuclear explosion on, 25:10709 (ORO-2529-28, App. 3)
content in Fayetteville, Arkansas rainwater, Sept. 1969 to Aug. 1970, (E), 25:10710 (ORO-2529-28, App. 4)
content of atmospheric precipitation, milk, and reindeer meat in Sweden during 1959 to 1969, 25:11004
content of caribou and reindeer meat in Alaska during 1969, 25:11001
content of human bones sampled in USA during 1969, 25:11042
content of human diet in USA during 1969, 25:11040
content of milk in South America in 1967, 25:11068
content of milk in USA during February 1970, 25:11040
content of milk sampled throughout Central, North, and South America during July 1969 to July 1970, 25:11002
content of surface waters sampled in New York State during January to July 1969, 25:11041
content of teeth of man, methods for measurement of, 25:10935 (NP-18388)
content ratio to cesium-137 in worldwide atmospheric and surface soil samples, 25:10718
content ratio to strontium-89 in Fayetteville, Arkansas rainwater, 1964 to 1969, effects of jet stream and Chinese nuclear explosions on, 25:10708 (ORO-2529-28, App. 2)
determination in milk by scintillation counting, 25:10480
effects on animals, protective effects of calcium alginate against chronic, 25:11103
effects on antibody response in miniature swine following chronic ingestion, inhibitory, 25:10984
effects on bone marrow of man following ingestion of contaminated milk, 25:10932 (CEA-CONF-1558)
effects on chromosomes of Crepis capillaris seedlings following incorporation, aberrant, 25:11013
effects on glucose and lactate production in ganglia of rats, effects of dose rate on damaging β, 25:11262
effects on infant mortality in man, β, 25:11295
effects on nonspecific allergic reactions of sheep, β, 25:10989
monitoring in Ottawa River in vicinity of Chalk River, 25:11074(R) (AECL-3777)
residence time in stratosphere, comparison of estimates by various investigators, 25:10715 (ORO-2529-28, App. 9)
separation from solidified waste, leach rates for, 25:10658(R) (BNWL-1533)
sorption from gastrointestinal tract, effectiveness of activated barium sulfate for inhibiting, 25:11049
uptake by cattle and forage plants during 1965 to 1969, 25:11050
Sr-90--Y-90, performance of beta sources of, for determining particle size of solid aggregates, 25:10784

STRONTIUM ISOTOPES Sr-97
half-life, (E), 25:12462

STYRENE
radioinduced free-ionic polymerization of bulk, electric conductivity measurements on, 25:10610 (JAERI-5026, pp 169-71)
radioinduced graft polymerization with polyethylene, effects of swelling on γ, 25:10613
radioinduced polymerization on surface of synthetic calcium aluminate hydrate,, 25:10616

SUBMARINE REACTORS
development of, review of, 25:12836

SUBMARINES
accidents in nuclear powered, discussion of USS Thresher, 25:12836
operations in Arctic Ocean of nuclear powered, 25:12836

SUCCINATE DEHYDROGENASE
radiation effects on content of, in epidermis, x, 25:11241

SUCROSE
boiling of aqueous, bubble behavior in, 25:10769(R) (ORO-3911-3)

SUGARS
reactions with uranyl nitrate to produce carbon--uranium dioxide mixtures, 25:11478 (BNWL-843)
reactions with uranyl nitrates to produce carbon--uranium dioxide mixtures, 25:11474(R) (BNWL-842)

SULFATES
determination of trace amounts of, in molybdenum, review on, 25:10459

SULFITES
yields from γ radiolysis of aqueous sodium sulfide solutions, 25:10649

SULFUR
determination of trace amounts of, in biotite and tektite by spark source mass spectrometry, 25:10455
determination of trace amounts of, in molybdenum, review on, 25:10459

SULFUR DIOXIDES
radioinduced reactions with alkanes and oxygen, γ, 25:10614
sorption-regeneration cycles on sodium aluminate, 25:12901 (ORNL-TM-3210)

SULFUR FLUORIDES
effects on radiolysis of ethane, 25:10632
effects on yields of ozone from radiolysis of carbon dioxide--oxygen mixtures, 25:10633

SULFUR ISOTOPES S-32
energy levels from (p,γ) reactions, widths, branching ratios, and decay strengths for T = 2, (E), 25:12441
energy levels from alpha inelastic scattering, lifetimes of, (E), 25:12486
helium-3 reactions (He-3,d) at 18 and 20 MeV, DWBA analysis of differential cross sections from, (E/T), 25:12479
proton elastic scattering at 3.200 to 3.385 MeV, phase-shift analysis of excitation functions and energy spectra from, (E/T), 25:12506
proton reactions (p,αγ) at 11.72 to 13.02 MeV, excitation functions, alpha and gamma spectra, and α--γ angular correlations from, (E), 25:12480
scattering by cadmium-106 and -114 at 49 to 55 MeV, correlation functions and hyperfine attenuation coefficients from inelastic, (E), 25:12619
scattering by natural cadmium at 64 MeV, gamma angular distributions from inelastic, (E/T), 25:12556
scattering by natural cadmium at 64 MeV, gamma spectra from inelastic, (E), 25:12548

SULFUR ISOTOPES S-34
deuteron reactions (d,n) at 3.8 to 5.2 MeV, excitation functions and angular distributions from, (E), 25:12440
deuteron reactions (d,pγ) at 2 to 3.25 MeV, energy levels of sulfur-35 from, (E), 25:12489
effects on microwave spectra, structure, quadrupole coupling constant, and force constants of nitrogen sulfide chloride, 25:10532
proton reactions (p,γ) at 1.0 to 1.5 MeV, angular distributions from, (E), 25:12440
proton reactions (p,n) with, threshold energies and excitation functions for, (E), 25:12442

SULFUR ISOTOPES S-35
energy levels from deuteron reactions (d,pγ) with sulfur-34 at 2 to 3.25 MeV, 25:12489
use of peroxide-incorporated, for isotope dilution measurement of extracellular fluid volume in dogs, 25:11185

SULFUR OXIDES
radioprotective effects of, on growth tail bone transplants in syngeneic recipient mice, x, 25:10983

SUN
charged-particle production along neutral line in magnetic field, Syrovatskii mechanism in, (T), 25:11633
energy production in, effects of time variations on, (T), 25:11668
magnetic regions of, lifetime of large-scale, (T), 25:11629
quadrupole moment of, effects on electromagnetic signal time delay, (T), 25:11602
spectra of, basic radiation data for, (T), 25:11609
spectra of, improved wavelengths in range 7780 to 7925 A, (E), 25:11611
spectra of, Lyman continuum in, (E/T), 25:11614

SUNSPOTS
area of, relation to proton flares and coronal radio diameter, (E/T), 25:11630
cycle of, forecasting of parameters of twenty-first, (T), 25:11631
magnetic fields of, integrated, (T), 25:11629
magnetic fields of, spectral-line formation in, (T), 25:11612
particle acceleration mechanisms for, (T), 25:11625
spectral line profiles in, europium- and lanthanum-ion, (E), 25:11613

SUPERCONDUCTIVITY
critical carrier concentration for, in mixed metal--semiconductor systems, 25:11844

SUPERCONDUCTORS
bound state in, containing magnetic impurity, (T), 25:11841
current--voltage characteristics of Josephson junctions, effect of noise on, (T), 25:11837
electric properties of, high-current pulse generator for studying, 25:10899
electrodynamics of strong-coupling alloys in high magnetic fields, (T), 25:11843
electron tunneling in quench-condensed, (E/T), 25:11842
energy gap in thin-film, solution of Gorkov equations for temperature dependence of, 25:11845
flux motion through surface sheaths of, (E/T), 25:11829
fluxon behavior in type-II, floating magnet model study of, 25:11833
infrared optics of high-T/sub c/, 25:11824
Josephson junctions as oscillators, pull-in phenomena of (T), 25:11839
Josephson junctions, dc characteristics from low-frequency noise currents in, (T), 25:11822
power output of point-contact Josephson junctions, maximal, (T), 25:11838
properties of silver as, (E/T), 25:11821
surface impedance of pure type-II, two-band expression for mixed state, 25:11826

transition temperature of thin-film, solution of Gorkov equations for, 25:11845
tunnel junctions, standing-wave model of rf-induced effects in, (E/T), 25:11827
use of multicore, in magnets, 25:11831
voltages induced by superimposed ac and dc magnetic fields in foils, dc and harmonic, 25:11835
SUPERFLUIDITY
in neutron-star matter, (T), 25:11545
SUPERNOVA REMNANTS
Cas A, distribution of brightness and polarization at 5 GHz, (E), 25:11590
SUPERNOVAE
gamma emission from, use of EAS array for determining prompt, (T), 25:11553
occurrence in Milky Way, (E), 25:11637
occurrence in Sb and Sc galaxies, frequency of, (E), 25:11637
photon emission from, absorption by interstellar gases, (E/T), 25:11665
pulsar ejection in, (T), 25:11588
spectra of, origin of iron bands in, (E/T), 25:11562
SURFACE WATERS
radioisotope content of US, list of reports on 1967 to 1970 measurements of, 25:10699
radioisotope content of, in New York State during January to July 1969, cesium-137, strontium-90, and tritium, 25:11041
tritium content of Crater Lake, Oregon, 1953 to 1969, 25:10720
SURFACES
bibliography on surface and vacuum physics, 25:11678
SURRY POWER REACTOR, UNIT 1
design parameters of, revised and additional data on, 25:12740 (DOCKET-50280-33)
effluents from, effects on environment of radioactive and thermal, 25:12739 (DOCKET-50280-32)
operations aspects of, revised and additional data on, 25:12740 (DOCKET-50280-33)
SURRY POWER REACTOR, UNIT 2
design parameters of, revised and additional data on, 25:12740 (DOCKET-50280-33)
effluents from, effects on environment of radioactive and thermal, 25:12739 (DOCKET-50280-32)
operations aspects of, revised and additional data on, 25:12740 (DOCKET-50280-33)
SWEDEN
fallout monitoring in, during 1959 to 1969, 25:11004
SWINE
radioinduced chronic dermatitis in, callicrein treatment for x, 25:11110
radioinduced inhibition of antibody response in miniature, strontium-90 β, 25:10984
testosterone content of blood of, double isotope dilution combined with crystallization technique for measuring, 25:10923
SWITCHES
circuits for pulse discriminators, analysis of, 25:10901
SWITZERLAND
meteorological conditions in lower Aare River Valley, effects on diffusion of gaseous effluents from reactors, 25:10703 (EIR-185)
SYMMETRY GROUPS
breaking of chiral, in meson interactions with baryons, 25:12214
fields in physical, quantum, 25:12253
Sp (5,5), description of dynamics of nuclear collective model using, (T), 25:12631 (JINR-P4-5008)
SU(2) x SU(2) gauge invariance in Heisenberg nonlinear spinor theory, 25:12262
SU(3) x SU(3), form factors for K + π + l + ν decay in perturbation theory about limit of, 25:12173
SU(3) x SU(3), properties of spin-0 mesons in broken chiral, 25:12237
SU(n) x SU(n) gauge invariance in spinor theories, 25:12262
transformations in Wightman relativistic quantum field theory, conserved local currents for, 25:12264
U(n), matrix elements of finite transformations of, 25:12235
SYMMETRY GROUPS SU(3)
breaking in chiral Lagrangian for parameters of K three- and four-body decays from correlations with spin-1 resonance decay rates, 25:12194
energy levels of carbon-12 and oxygen-16, calculation of, (T), 25:12412
formalism for forward meson interactions with nucleons in, 25:12217
Regge pole--cut model for hadron interactions with nucleons in, 25:12217
SYNCHROCYCLOTRONS
target efficiency and multiple traversals in CERN 600-MeV, internal, 25:12324
SYNCHROTRON RADIATION
emission from high-energy cosmic electrons, (T), 25:11747
production by high-energy electrons in disk-loaded waveguide, 25:12317
SYNCHROTRONS
operation and performance of JINR proton, for acceleration of deuterons to 11 GeV/c, 25:12303 (JINR-P9-5442)

T

TACHYONS
theory for continuous-spin, lightlike and spacelike representations of Poincare group in, 25:12236
TANTALUM
corrosion by liquid lead at high temperatures, 25:11376 (JUL-661-RW)
determination of trace amounts of, in biotite and tektite by spark source mass spectrometry, 25:10455
determination of trace amounts of, in molybdenum, review on, 25:10459
determination of trace amounts of, in rocks and sand by thermal neutron activation, ion exchange, and γ spectrometry, 25:10492
determination of trace amounts of, in Zircaloy-2, fluorination and arc excitation method for spectrographic, 25:10430 (EUR-4541)
emissivity of, effects of heat treatment on red and green spectral, 25:11395
friction and wear of, sliding against copper and iron rings under vacuum, 25:11413
interactions with tantalum silicide coating, 25:11519
photoelectric emission by, calculation of direct transition contribution to, 25:12040
reactions with dilute phosphoric acid, anodic oxide film formation in, 25:11351
reactions with nitrogen and oxygen, review of kinetics, mechanisms, and thermodynamics of degassing and engassing, 25:11415
separation from ores by solvent extraction, review on, 25:10656 (BM-IC-8502)
solubility in lead at 350 to 1100°C, 25:11376 (JUL-661-RW)
sorptive properties of films of, for nitrogen at 150 to 500°K, chemical and physical, 25:11419
sorptive properties of films of, for nitrogen at 273 to 370°K, 25:11417
sorptive properties of films of, for oxygen at 77 to 295°K, 25:11418
thermal properties at high temperatures, 25:11425
TANTALUM ALLOYS AND SYSTEMS
Mn--Ni-base--Ta, properties of, electric and magnetic, 25:12008
Pu-base--Ta, phase transformations in sputtered, unusual, 25:11447
Ta-base--W, fabrication of fuel capsule liners of, methods for, 25:10776 (MLM-1779)
TANTALUM CARBIDES
phonon spectra in, [001] and [110] longitudinal modes in, 25:11986
preparation of monocrystalline Ta_2C, hollow cathode dc plasma discharge zone melting method for, 25:11484
TANTALUM HYDRIDES
electric properties of Ta_2H at 4 to 408°K, effects of order--disorder transformation on, (E), 25:12021
TANTALUM ISOTOPES Ta-181
alpha inelastic scattering at 42 to 90 MeV, angular distributions and energy spectra from, (E/T), 25:12604
alpha reactions (α,He-3) at 42 to 90 MeV, angular distributions and energy spectra from, (E/T), 25:12604
alpha reactions at 30 to 80 MeV, cross sections for production of K and L x rays by, (E), 25:12488
deuteron reactions (d,p) and (d,2n) at 27.2 MeV, cross sections for, (E), 25:12513 (CNEA-269)
energy-level transitions in, parity-nonconserving effects in 482-keV, (T), 25:12517 (INP-714)
helium-3 inelastic scattering at 50 and 75 MeV, angular distributions and energy spectra from, (E/T), 25:12604
helium-3 reactions (He-3,α) at 50 to 75 MeV, angular distributions and energy spectra from, (E/T), 25:12604
neutron capture by, average circular γ polarization in thermal, (E), 25:12601
neutron inelastic scattering at 14 MeV, neutron spectra and level-density parameters from, (E), 25:12536
TANTALUM ISOTOPES Ta-182
energy levels from thermal neutron capture, spin for compound, (E), 25:12601
TANTALUM OXIDES
electric conductivity distribution in films of anodic, high-resolution redox printout study of, (E), 25:12014
spectra of anodic films of, effects of anodization voltage and thickness on infrared reflectance, 25:11518
TANTALUM SILICIDES
diffusion of silicon in Ta_5Si_3, activation energy for, 25:11519
interactions of coatings of, with molybdenum, niobium, rhenium, tantalum, titanium, tungsten, and zirconium, 25:11519
TECHNETIUM
nucleosynthesis of, effects of energetic proton fluxes on, (T), 25:11544
TECHNETIUM ISOTOPES Tc-95
beta and electron-capture decay of isomeric, γ spectra and γ-γ angular correlations for, (E), 25:12568
energy levels from ruthenium-95 beta and electron-capture decay, spin--parity assignments for, (E), 25:12545
energy-level transitions from ruthenium-95 beta and

XUM

electron-capture decay, (E), 25:12545
TECHNETIUM ISOTOPES Tc-99
effectiveness of metastable, for brain scanning for detection of cerebral lesions, 25:11146
effectiveness of metastable, for scanning of human liver, 25:11198
effectiveness of metastable, for scintiscanning of kidneys in hypertensive patients in combination with angiography, 25:11166
effectiveness of pertechnetate-incorporated metastable, and metastable indium-113 for diagnosis of tumor metastases in combination with Anger camera, 25:10928
effectiveness of pertechnetate-incorporated metastable for determining activity in aorta and heart in combination with Anger camera, effects of patient positioning on, 25:11121
use of colloidal for liver scintigraphy in comparison to colloidal gold-198, 25:11140
use of macroaggregate-incorporated metastable, for scanning of pulmonary circulation, 25:11128
use of metastable for scanning of thyroid in human children, considerations of radiation burden during, in comparison to iodine-125 and iodine-131, 25:11190
use of metastable sulfur colloids of, as tracer for function studies of x-irradiated erythron and reticulo-endothelial cells, 25:11112
use of metastable, for coronary blood circulation in patients with arteriosclerosis or angina pectoris in combination with scintillation crystals and collimators, development of techniques for, 25:10911
use of metastable, for kidney scintigraphy in hypertensive patients, evaluation of, in comparison with radioisotope renograms and vasoconstrictor content of the renal vein, 25:11163
use of metastable, for scanning of mitral valve in human heart, effectiveness of positioning technique for, 25:11187
use of metastable, for scintiscanning of human heart action in combination with Anger camera and computer, 25:11119
use of metastable, with stationary detectors for scanning of blood flow through heart cavities, 25:11120
use of pertechnetate-incorporated metastable, for scanning of human brain in comparison to DTPA-incorporated metastable, 25:11189
use of sulfur colloid-incorporated metastable, for diagnosis of functional asplenia in man, 25:11117
TEETH
strontium-90 content in, of man, methods for measurement of, 25:10935 (NP-18388)
TEKTITES
analysis for trace amounts of elements by spark source mass spectrometry, 25:10455
TELEVISION EQUIPMENT
radiation hazards to personnel during assembly and repair of color, survey of, 25:11063
TELLURIUM
book: Chemistry of Rare Earths and Various Other Elements, in Russian, 25:10560
determination of trace amounts of, in biotite and tektite by spark source mass spectrometry, 25:10455
separation from fission products by automatic ion exchange chromatography, design and performance of equipment for, 25:10659 (CEA-N-1267)
sorption on nickel oxide suspensions in water, 25:10583(R) (AECL-3776)
TELLURIUM ISOTOPES
toxicity of radioactive, to man in relation to generation of radioiodine in food chain, 25:10948
TELLURIUM ISOTOPES Te-122
proton reactions (p,pn), (p,2n), and (p,2p) at 300 MeV, analysis for nuclear structure effects in, (E), 25:12581
TELLURIUM ISOTOPES Te-123
energy levels and transitions from nitrogen-14 inelastic scattering, excitation and transition probabilities for, (E), 25:12603
nitrogen-14 inelastic scattering at 44 and 48 MeV, gamma spectra from, (E), 25:12603
proton reactions (p,pn), (p,2n), and (p,2p) at 300 MeV, analysis for nuclear structure effects in, (E), 25:12581
TELLURIUM ISOTOPES Te-124
energy levels from antimony-124 beta decay, spin--parity assignments for, (E), 25:12531 (TID-25586)
energy-level transitions from antimony-124 beta decay, energies, branching ratios, and relative intensities of, (E), 25:12531 (TID-25586)
energy-level transitions from antimony-124 beta decay, γ--γ angular correlations and E2/M1 mixing ratios for, (E), 25:12515 (COO-1746-51)
proton reactions (p,pn), (p,2n), and (p,2p) at 300 MeV, analysis for nuclear structure effects in, (E), 25:12581
TELLURIUM ISOTOPES Te-125
energy levels and transitions from nitrogen-14 inelastic scattering, excitation and transition probabilities for, (E), 25:12603
nitrogen-14 inelastic scattering at 44 and 48 MeV, gamma spectra from, (E), 25:12603
proton reactions (p,pn), (p,2n), and (p,2p) at 300 MeV, analysis for nuclear structure effects in, (E), 25:12581
TELLURIUM ISOTOPES Te-126
energy levels from iodine-126 beta and electron-capture decay, (E), 25:12515 (COO-1746-51)
energy-level transitions from iodine-126 beta and electron-capture decay, γ--γ angular correlations and E2/M1 mixing ratios for, (E), 25:12515 (COO-1746-51)
proton reactions (p,pn), (p,2n), and (p,2p) at 300 MeV, analysis for nuclear structure effects in, (E), 25:12581
TELLURIUM ISOTOPES Te-127
distribution and excretion of metastable, in rats following intravenous injection, 25:10950
distribution and excretion of metastable, in rats following ingestion, kinetics of, 25:10949
sorption of metastable, from gastrointestinal tract of rats following ingestion, kinetics of, 25:10949
toxicity to organisms, role of daughter nuclides in decay pathway in, 25:10950
TELLURIUM ISOTOPES Te-128
energy levels from proton inelastic scattering, spin and parity of, (E), 25:12602
proton elastic and inelastic scattering at 7.48 to 12.65 MeV, proton angular distributions and proton and gamma energy spectra from, (E), 25:12602
proton reactions (p,pn), (p,2n), and (p,2p) at 300 MeV, analysis for nuclear structure effects in, (E), 25:12581
TELLURIUM ISOTOPES Te-130
energy levels from photon scattering, radiation widths for, (E), 25:12447
energy levels from proton inelastic scattering, spin and parity of, (E), 25:12602
neutron reactions (n,2nβ) in meteorites, (E), 25:11539
proton elastic and inelastic scattering at 7.48 to 12.65 MeV, proton angular distributions and proton and gamma energy spectra from, (E), 25:12602
proton reactions (p,pn), (p,2n), and (p,2p) at 300 MeV, analysis for nuclear structure effects in, (E), 25:12581
TELLURIUM SYSTEMS
Au--Pd--Te, superconducting properties of liquid-quenched simple cubic, 25:11819 (CALT-822-22)
TEMPERATURE
scale below 1°K for zinc neodymium nitrate single crystals, using gamma-ray anisotropy, 25:11852
TERBIUM
complexes with EDTA, separation by ion exchange, effects of resin crosslinking on, 25:10665 (INR-P-1209)
determination of trace amounts of, in biotite and tektite by spark source mass spectrometry, 25:10455
separation from indium by gas chromatography using aluminum chloride eluent, 25:10666 (JINR-P6-5410)
TERBIUM ISOTOPES Tb-158
energy levels from terbium-159 (d,t) reactions, properties of two-quasiparticle, (E/T), 25:12578
TERBIUM ISOTOPES Tb-159
deuteron reactions (d,3nγ) at 18 MeV, cross sections for, (E/T), 25:12544
deuteron reactions (d,p) and (d,4n) at 27.2 MeV, excitation functions for, (E), 25:12595
deuteron reactions (d,t) at 12 MeV, triton spectra from, (E), 25:12578
neutron capture by, average circular γ polarization in thermal, (E), 25:12601
proton reactions (p,2nγ) at 16 and 21 MeV, cross sections for, (E/T), 25:12544
TERBIUM ISOTOPES Tb-160
energy levels from thermal neutron capture, spin for compound, (E), 25:12601
TEREPHTHALIC ACID
potassium salt, deuterium exchange reaction in transcarboxylation of mixture of deuterated and nondeuterated, mechanism of, 25:10545
TEREPHTHALIC ACID, POLYETHYLENE ESTERS
radioinduced graft polymerization in aqueous solutions of acryl- or methylacrylamide and unsaturated dicarboxylic acids, hydrolysis of products of, 25:10621
radioinduced polymerization of acrylic acid on, effects of solvents on properties of products from γ and electron, 25:10597 (JAERI-5026, pp 46-51)
TERPHENYL
corrosive effects on Ozhennite and Zircaloy, review on, 25:11343 (AECL-3778)
TEXTILES
book: Radiation Chemical Processing, 25:10617
radioinduced polymerization of ethyl acrylate on cotton, using water as swelling agent, 25:10619
radioinduced polymerization of ethyl acrylate on rayon, using water as swelling agent, 25:10619
THALLIUM
determination of trace amounts of, in biotite and tektite by spark source mass spectrometry, 25:10455
determination of trace amounts of, in molybdenum, review on, 25:10459
separation from gallium by gas chromatography using aluminum chloride eluent, 25:10666 (JINR-P6-5410)
separation of cyclotron-produced lead-203 from, by iron hydroxide precipitation and solvent extraction, 25:10678
separation of monovalent and trivalent, paper

chromatographic, 25:10687
superconducting transition temperature of fcc, 25:11846
THALLIUM ALLOYS AND SYSTEMS
Bi--Pb--Tl, superconducting transition temperature of fcc, 25:11846
Pb--Tl, voltages induced by ac--dc magnetic fields in superconducting foils of, 25:11835
THALLIUM IODIDES
phase diagram, 25:12912 (SRIA-106-76)
THALLIUM ISOTOPES Tl-200
beta decay of, decay scheme, gamma spectra, and log ft value from, (E), 25:12528 (NP-18647)
THALLIUM ISOTOPES Tl-203
energy levels from lead-204 (d,He-3) reactions, l transfers, spin--parity assignments, and spectroscopic factors for, (E), 25:12575
THALLIUM ISOTOPES Tl-206
beta decay of, spectrum shape and half-life from, (E), 25:12615
THALLIUM ISOTOPES Tl-207
energy levels from lead-208 (d,He-3) reactions, spectroscopic factors for, (E), 25:12575
THALLIUM ISOTOPES Tl-208
beta decay of, β--γ angular correlations in, (E/T), 25:12555
THERMAL DIFFUSION
book: Thermal Diffusion Column. Theory and Practice with Particular Emphasis on Isotope Separation, 25:10783
column operation for isotope separation, effects of gas flow mode on efficiency of, 25:10786
THERMAL EXPANSION
conference on solids, at Santa Fe, N. Mex., June 10 to 12, 1970, 25:11508
THERMAL INSULATION
design for limiting conductive, convective, and radiative heat transfer, 25:10774(P)
development for radioisotope-fueled thermoelectric converters, 25:10778(R) (ORNL-TM-3214)
THERMAL RADIATION SHIELDING
materials for thermoelectric converters, evaluation of, 25:10778(R) (ORNL-TM-3214)
THERMOCOUPLES
performance of liquid metal cooled reactor in-vessel, 25:12781 (ANL-EBR-25)
THERMODYNAMICS
book: Gas Dynamics of Two-Phase Media (In Russian), 25:10772
THERMOELECTRIC CONVERTERS
design, performance, and testing of germanium-silicon air-vac, 25:11477 (ALO-2510-T-1)
THERMOELECTRIC MATERIALS
development for foil-insulated air-vac converter modules, 25:11477 (ALO-2510-T-1)
THERMONUCLEAR REACTORS
bibliography on plasma physics and fusion reactors, 25:11858
bibliography on plasma physics and fusion reactors, 25:11856
electron distribution function measurement in toroidal octupoles, (E), 25:11872
ion distribution function measurement in toroidal octupoles, (E), 25:11872
magnet coil windings for Torsatron, properties of, 25:11918 (EUR-CEA-FC-543)
magnetic configuration of toroidal vintotron, (T), 25:11922 (KHFTI-70-25)
plasma current distribution in tokamak-type, measurement using laser scattering, 25:11867 (MATT-818)
plasma equilibrium and stability in Tokamak-type, magnetohydrodynamic, 25:11911 (EUR-CEA-FC-569)
plasma injection and confinement in minimum-B, neutral atom, 25:11859 (EUR-CEA-FC-563)
plasma injection and confinement in spherical multipole magnetic traps, (E), 25:11863
use with magnetohydrodynamic generators, review of, 25:11752
vacuum systems for power plants, properties of, 25:11919 (EUR-CEA-FC-566)
THERMOSPHERE
gravity wave propagation in, effect of background wind on ray-tracing-typed, (E/T), 25:11796
spectral height profiles from 400 to 1016 km in, He I 584-A and H I 1216-A euv dayglow, (E), 25:11789
THICKNESS GAGES
design of beta backscatter, for tubular plastic film, 25:10890(P)
design of radiometric, for measuring load variations on conveyer belts, 25:10785(P)
use of electron microprobe, to measure thin molybdenum layers on tungsten, 25:11421
THIOSULFATES
yields from γ radiolysis of aqueous sodium sulfide solutions, 25:10649
THORIUM
book: Chemistry of Rare Earths and Various Other Elements, in Russian, 25:10580
complexes with (1,2-cyclohexylenedinitrilo)tetraacetic acid, uses for spectrotitrimetric determination of (1-hydroxyethylidene)diphosphonic acid, 25:10462
content in thermal waters of Kamchatka Peninsula, (E), 25:10697
content of drinking water, calculations of maximum permissible, 25:11051
determination of trace amounts of, in biotite and tektite by spark source mass spectrometry, 25:10455
determination of trace amounts of, in molybdenum, review on, 25:10459
determination of trace amounts of, in phosphate deposits by spark source mass spectrometry, 25:10456
determination of trace amounts of, in rocks and sand by thermal neutron activation, ion exchange, and γ spectrometry, 25:10492
diffusion in columnar pyrocarbons, effects of actinide content on, 25:11378 (ORNL-TM-2989)
effects on solvent extraction of gold by TBP, 25:10686
separation from Egyptian Monazite sand, process for, 25:10683
separation from ores by solvent extraction, review on, 25:10656 (BM-IC-8502)
separation of neptunium from, by ion exchange in tetramethylammonium hydroxide--citrate solutions, effects of complexing agents on, 25:10655 (ANL-7751)
structure of fcc, calculation of electronic band, (T), 25:11992
thermodynamic properties at low temperatures, review of, 25:11384
thermodynamic properties of bcc and fcc phases of, prediction of effects of elements on, 25:11392
THORIUM ACETATES
thermodynamic properties of, 25:10581
THORIUM ALLOYS AND SYSTEMS
Ce--Th, magnetic susceptibility of, temperature dependence of, 25:12016
Pd-base--Th, thermal capacity at low temperatures, (E/T), 25:11989
Pu--Th-base, radiation effects on length of plutonium-238-enriched dilute α-, self-, 25:11468
Th--U--Zr, radiation effects on tube-type fuel elements of, in-pile, 25:11474(R) (BNWL-842)
THORIUM FLUORIDES ThF_4
preparation by reactions of anhydrous hydrofluoric acid with thorium dioxide, 25:10516 (IEA-185)
THORIUM ISOTOPES
determination in stalagmites by α spectrometry, 25:10477
THORIUM ISOTOPES Th-228
alpha decay of, time spectrum of alpha--conversion-electron delay in, (E), 25:12542
content in seawater and Pleistocene sediments, (E), 25:10725(R) (CU-3139-4)
energy levels from uranium-232 alpha decay, lifetimes, quadrupole moments, and deformation parameters for, (E), 25:12542
energy levels of, asymmetric collective model description of negative-parity, (T), 25:12563
energy-level transitions from uranium-232 alpha decay, probabilities for E2, (E), 25:12542
THORIUM ISOTOPES Th-229
energy levels from uranium-233 alpha decay, lifetimes, quadrupole moments, deformation parameters, and gyromagnetic ratios for rotational, (E), 25:12541
energy-level transitions from uranium-233 alpha decay, probabilities for E2 and M1, (E), 25:12541
THORIUM ISOTOPES Th-232
content of, in drinking water, calculations of maximum permissible, 25:11051
neutron fission of, yields of iodine isotopes from, 25:10472(R) (BMBW-FBK-70-19)
photofission at 200 to 900 MeV, cross sections for, (E), 25:12573
THORIUM ISOTOPES Th-235
half-life of, 25:10472(R) (BMBW-FBK-70-19)
THORIUM NITRIDES
magnetic susceptibility, 25:11980 (CEA-R-4113)
properties of, electric and thermal, 25:11494
thermal capacity at low temperatures, 25:11980 (CEA-R-4113)
ThN--UN, magnetic susceptibility, 25:11980 (CEA-R-4113)
ThN--UN, properties of, electric and thermal, 25:11494
THORIUM OXALATES
thermodynamic properties of, 25:10581
THORIUM OXIDES ThO_2
effects on human spleen, pathogenic, 25:11117
electron spectra from (approximately 111) surface of, inelastic secondary, 25:11999
helium release from alpha-bombarded polycrystalline, effects of heat treatments on mechanism of, 25:11502
radiation effects on microstructure of, 5.5-MeV alpha particle, 25:11537
radiation effects on pure and doped, 25:10583(R) (AECL-3776)
reactions with anhydrous hydrofluoric acid, preparation of thorium tetrafluoride by, 25:10516 (IEA-185)
Cr--Ni-base--ThO_2, strength and initial work hardening rate of, effects of microstructure on, 25:11402
Fe--ThO_2, mechanical properties at 77 to 373°K, 25:11401
Fe--ThO_2, preparation of fine dispersion of, development of method for, 25:11401
Ni-base--ThO_2, strength and initial work hardening rate of, effects of microstructure on, 25:11402
ThO_2--UO_2, stability of Zircaloy-clad fuel rods of, in up-power reactor transients, 25:11534 (WAPD-TM-979)
THULIUM
complexes with EDTA, separation by ion exchange, effects

of resin crosslinking on, 25:10665 (INR-P-1209)
determination of trace amounts of, in biotite and tektite by spark source mass spectrometry, 25:10455
enthalpy of solution in liquid plutonium, 25:11386
separation from aqueous solutions by solvent extraction using bis(2,2-dimethylhexyl) phosphate, 25:10679
THULIUM ISOTOPES Tm-166
beta and electron-capture decay of, γ spectra from, 25:12599
THULIUM ISOTOPES Tm-169
alpha reactions at 30 to 80 MeV, cross sections for production of K and L x rays by, (E), 25:12488
deuteron reactions (d,3nγ) at 18 MeV, cross sections for, (E/T), 25:12544
neutron capture by, low-energy γ spectra and resonance spin assignments for resonance, (E), 25:12589
proton reactions (p,2nγ) at 16 and 21 MeV, cross sections for, (E/T), 25:12544
THULIUM ISOTOPES Tm-170
beta decay of, effect of electron--nucleus quadrupole interaction in, (T), 25:12685
THYMUS GLAND
radiation effects on histones in nuclei of rat, γ, 25:10971
THYROID GLAND
iodine-131 content of, from cattle slaughtered in USA from 1962 through 1969, 25:11042
iodine-131 metabolism in human, use of clearance method at constant blood levels for determining, 25:11173
iodine-131 uptake by human, effects of triiodothyronine on, 25:10944
radiation effects on, of animals and man, review of iodine-131 β and γ and x, 25:11291
radiobiology of animal and human, review of, 25:11291
radiotherapy for carcinomas in human, effects of surgery preceding iodine-131-labeled sodium iodide, 25:11234
scanning in children, comparison of iodine-125, iodine-131, and metastable technetium-99 for radiation burden during, 25:11190
scanning of human, for diagnosis of cancer, method for iodine, 25:11217
scanning of, development of multiwire proportional detector for, 25:10810 (CEA-CONF-1668)
tellurium-127m uptake by rat, following intravenous injection, 25:10950
THYROID INHIBITORS
effects of, iodine-131-clearance studies for determining, 25:11173
TIMING CIRCUITS
design of stop clock digitizing system for time-of-flight measurements, 25:10891 (AERE-R-5422)
time jitter due to noise in, 25:10808 (AERE-R-5561)
TIN
alpha elastic and inelastic scattering at 166 MeV, optical potentials from DWBA analysis of angular distributions from, (E/T), 25:12549
alpha inelastic scattering at 42 to 90 MeV, angular distributions and energy spectra from, (E/T), 25:12604
alpha reactions (α,He-3) at 42 to 90 MeV, angular distributions and energy spectra from, (E/T), 25:12604
alpha reactions at 30 to 80 MeV, cross sections for production of K and L x rays by, (E), 25:12488
analysis for oxygen by photon activation and radiochemical separation, 25:10501
determination as impurity in fuel materials by emission spectroscopy, 25:10432 (KFK-1261)
determination by photon activation, reactions and sensitivities for, 25:10488 (CEA-R-4072)
determination in binary aluminum alloys, x-ray fluorescent, 25:10441
determination of trace amounts of, in basalt and granite, correction of matrix effect in uv spectrographic, 25:10453
determination of trace amounts of, in biotite and tektite by spark source mass spectrometry, 25:10455
determination of trace amounts of, in molybdenum, review on, 25:10459
determination of trace amounts of, in rocks, quantometer for spectroscopic, 25:10451
determination of trace amounts of, in zirconium, carrier distillation method for spectrographic, 25:10430 (EUR-4541)
helium-3 inelastic scattering at 50 and 75 MeV, angular distributions and energy spectra from, (E/T), 25:12604
helium-3 reactions (He-3,α) at 50 to 75 MeV, angular distributions and energy spectra from, (E/T), 25:12604
neutron elastic scattering at 4 MeV, near 180° differential cross sections and polarizations from polarized, (E), 25:12509(T) (ANL-Trans-855)
photon inelastic scattering at 12 to 30 MeV, differential cross sections for, (E), 25:12463
superconducting tunnel junctions with oxide, rf-induced effects in, (E/T), 25:11827
TIN ALLOYS AND SYSTEMS
Ag--Cd--In-base--Sn, electric conductivity, Fermi surface topology, and superconducting transition temperature of dilute, 25:12032
Nb--Sn, development of superconducting ribbons of intermetallic Nb_3Sn, 25:11820 (LNF-70/18)
Nb--Sn, niobium-93 NMR in Nb_3Sn, 25:12037
Pd-base--Sn, thermodynamic properties of, 25:11396
TIN ISOTOPES
energy levels from alpha inelastic scattering at 166 MeV, deformation parameters for, (E/T), 25:12549
TIN ISOTOPES Sn-112
energy level from oxygen-16 Coulomb excitation, quadrupole moment of first 2+, (E), 25:12587
TIN ISOTOPES Sn-116
energy level from oxygen-16 Coulomb excitation, quadrupole moment of first 2+, (E), 25:12587
TIN ISOTOPES Sn-117
energy levels from indium-1117 beta decay, lifetimes and spin--parity assignments for, (E), 25:12566
TIN ISOTOPES Sn-118
energy level from oxygen-16 Coulomb excitation, quadrupole moment of first 2+, (E), 25:12587
TIN ISOTOPES Sn-120
energy level from oxygen-16 Coulomb excitation, quadrupole moment of first 2+, (E), 25:12587
energy levels from photon scattering, radiation widths for, (E), 25:12447
proton elastic scattering at 10-60 MeV, differential cross sections and local Woods--Saxon potentials equivalent to nonlocal analysis including exchange effects in, (T), 25:12689
TIN ISOTOPES Sn-122
energy level from oxygen-16 Coulomb excitation, quadrupole moment of first 2+, (E), 25:12587
TIN ISOTOPES Sn-124
energy level from oxygen-16 Coulomb excitation, quadrupole moment of first 2+, (E), 25:12587
TIN OXIDES
properties of electrodes of, 25:10433 (ORNL-4636, pp 1-7)
TIN TELLURIDES
superconducting transition temperature of, heavy-hole band mechanism of, 25:11847
TISSUES
analysis for pesticides by electron-capture gas chromatography, 25:10433 (ORNL-4636, pp 1-7)
conference on radiosterilization of, for use in transplantation, 25:11327 (STI/PUB-247)
radiation effects on activity of alkaline phosphatase and cholinesterase in, of rats following injection of mixed radioisotopes, 25:10968
radiation effects on antigens in transplanted, effects of 1.5 to 5 Mrad dose on ionizing, 25:11331
radioinduced destruction in, of rabbits hyperglycemia following γ, 25:10969
radiosensitivity of human, 25:11090
radiosterilization of human, for use in transplantation, effects of environmental condition on sensitivity of contaminating microorganisms during, 25:11328
radiosterilization of mesenchymal, for use as transplants, γ, 25:11332
radiosterilization of nerve and skull bone, for use as transplants, effects of temperature and 2 Mrad dose on ionizing, 25:11334
radiosterilization of, effects of temperature on sensitivity of contaminating microorganisms during ionizing, 25:11337
scanning of human soft, for measuring lean to fat ratios, γ transmission, 25:11114
TITANIUM
corrosion by boiling waste solutions, 25:10658(R) (BNWL-1533)
determination by photon activation, reactions and sensitivities for, 25:10488 (CEA-R-4072)
determination in sedimentary rocks by direct-reading spectrometry, 25:10450
determination of trace amounts of, in biotite and tektite by spark source mass spectrometry, 25:10455
determination of trace amounts of, in molybdenum, review on, 25:10459
determination of trace amounts of, in Zircaloy-2, carrier distillation method for spectrographic, 25:10430 (EUR-4541)
effects on crack formation in plutonium during α--β thermal cycling, 25:11393
enthalpy of solution in liquid plutonium, 25:11386
friction and wear of, sliding against copper and iron rings under vacuum, 25:11413
interactions with tantalum silicide coating, 25:11519
photon inelastic scattering at 12 to 30 MeV, differential cross sections for, (E), 25:12463
TITANIUM ALLOYS AND SYSTEMS
Al--Ti-base--V, phase transformations at 1000 to 1400°F, effects of strain on, 25:11453
Nb--Ti, mechanical properties of, effects of copper and germanium on, 25:11416
Nb--Ti, superconducting critical current density of, effects of annealing, composition, and swaging on, 25:11416
Nb--Ti, superconducting wire of, use in wired-wall cavity for V-band ENDOR, 25:11650
Pu--Ti, phase studies of, 25:11429 (CEA-CONF-1687)
Pu--Ti--Zr-base, electric conductivity of, 25:12004
Pu--Ti-base, electric conductivity of, 25:12004
Pu--Ti-base, plutonium distribution in dilute, effects of β and α phase transformation and oxygen content on, 25:11431 (CEA-CONF-1691)
TITANIUM BORIDES
electron band structure, 25:12012

TITANIUM CARBIDES
electron band structure, 25:12012
fracture of, electron microscope study of effects of carbide crystal size on, 25:11514
TITANIUM ISOTOPES Ti-46
energy level at 2007 keV, lifetime of, (E), 25:12508
neutron reactions (n,p) at 4.91 to 7.04 MeV, cross sections for, (E), 25:12504
TITANIUM ISOTOPES Ti-48
alpha reactions (α,nγ), (α,pγ), and (α,α'γ) at 12 to 15 MeV, gamma spectra from, (E), 25:12435
neutron reactions (n,p) at 4.91 to 7.04 MeV, cross sections for, (E), 25:12504
TITANIUM ISOTOPES Ti-49
deuteron reactions (d,He-3) at 19.5 to 22.4 MeV, angular distributions for, (E), 25:12452
TITANIUM NITRIDES
electron band structure, 25:12012
TITANIUM OXIDES
diffusion in single crystals of, 25:10515(R) (COO-1780-14)
diffusion of oxygen in monocrystalline, proton resonance method for measurement of coefficient of, 25:11516
performance of TiO, as vacuum pump getter, 25:10804(P)
TITANIUM SILICIDES
diffusion of silicon in Ti_5Si_3, activation energy for, 25:11519
TITRATION EQUIPMENT
development of controlled-current coulometric, 25:10433 (CRNL-4636, pp 1-7)
TOBACCO (the commodity)
combustion of, analysis of smoke from, 25:10433 (ORNL-4636, pp 1-7)
TOKAMAK DEVICES
plasma current distribution measurement in, using laser scattering, 25:11867 (MATT-818)
plasma equilibrium and stability in, magnetohydrodynamic, 25:11911 (EUR-CEA-FC-569)
TOLUENE
phosphorescence in polycrystalline methylcyclohexane, effects of deuterium and temperature on, 25:10550
TOLUIDINE BLUE
use of iodine-125-labeled, for scanning of pancreas and parathyroid glands, 25:11188
TRACE ELEMENTS
determination in rocks, silts, soils, and water, problems of contamination during, 25:10427
TRACER TECHNIQUES
method for study of oxygen self-diffusion in uranium dioxide using proton-induced alpha particles, 25:11486 (CEA-R-4095)
methods for assaying testosterone in peripheral blood, 25:10923
methods using carbon-14-labeled butylamine for monoamine oxidase assays in human serum, 25:10922
methods using radioisotopes in aqueous solutions, factors affecting tracer behavior and properties during, 25:10925
use of iodine-131, for measuring effects of initial iodine concentration on iodine sorption by soils, (E), 25:10694
TRANSACTINIDE ELEMENTS
neutrons from, helium-3 proportional detector for detection of, 25:10814 (JINR-P13-5391)
search for, 25:10472(R) (BMBW-FBK-70-19)
stability of superheavy, self-consistent shell-model calculation for island of, (T), 25:12672
TRANSITION METAL CARBIDES
electron band structure of Group IVa and Va mono-, theory, 25:12024
TRANSITION METALS
determination using mixed ligand complexes, 25:10460
x-ray emission from meteoritic, gas proportional counting of, (E), 25:11539
TRANSITION RADIATION
detection of x-ray, for identification of high-energy particles, development of detector for, 25:10877
TRANSPORT THEORY
solution by discrete ordinates calculations, reduction of ray effect in, 25:12852
solutions of monoenergetic equation with anisotropic scattering, particular, 25:12055
TRANSURANIUM ELEMENTS
neutrons from helium-3 proportional detector for detection of, 25:10814 (JINR-P13-5391)
separation of, electrostatic and hydrodynamic properties for, by physical methods, 25:10669 (LYCEN-7034, pp 9-22)
TRANSURANIUM PROCESSING PLANT
production plans at, review on, 25:10654(R) (ORNL-4588)
TRINO POWER REACTOR
shielding for, design of milling machine for removal of thermal neutron, 25:12715
shielding for, underwater plasma-arc cutting for repair of thermal neutron, 25:12714
TRIOXANES
radioinduced subsequent polymerization of solid, in dry and high-vacuum system, kinetics of γ, 25:10611
TRITIUM
content in coastal waters of eastern US, 1963 to 1967, 25:10720
content in coastal waters of western North America, 1963 to 1969, 25:10720
content in Crater Lake, Oregon, 1953 to 1969, 25:10720
content of atmospheric precipitation in USA during 1968, 25:11039
content of surface waters sampled in New York State during January to July 1969, 25:11041
determination in effluent off-gases from MSRE, 25:10434 (ORNL-4636, pp 7-13)
determination in polyacrylamide gels by fractionation and scintillation counting, 25:10478
determination of, computer system for proportional detector for low-level, 25:10833
deuteron reactions (d,γ) with, analysis using shell model and R-matrix formalism, (T), 25:12371
distribution and production by underground nuclear explosions, methods for prediction of, 25:10742
effects on hydrogen-atom addition reactions with alkenes at low temperatures, 25:10538
effects on reaction mechanisms, effects of temperature on kinetic, 25:10549
energy distributions from fission of uranium-236, 25:10583(R) (AECL-3776)
exchange with hydrogen in organic compounds using tritiated phosphoric acid--boron trifluoride complex, mechanism of, 25:10546
exchange with hydrogen in synthetic polypeptides, 25:10567
exchange with hydrogen to investigate secondary structure of Escherichia coli phenylalanyl transfer RNA, 25:10564
helium-3 reactions (He-3,γ) at 0 to 20 MeV, direct-capture calculation of excitation functions for, (T), 25:12372
monitoring instrument development for, 25:11074(R) (AECL-3777)
neutron elastic scattering at 16.5 and 22.1 MeV by liquid, polarization in, (E), 25:12354
nuclear wave function for, formulation using Feshbach--Rubinow method, 25:12364
proton differential elastic scattering cross sections at 156 MeV, (E/T), 25:12365
proton reactions (p,n) at 156 MeV, spectra and differential cross sections for, (E/T), 25:12365
retention in hair of rabbits for use in assessing internal contamination, 25:10954
separation from hydrogen in crystallization of inorganic hydrates from tritiated solution, 25:10688
TRITIUM SYSTEMS
T--Zr, preparation of gas-free radiation targets of, method for, 25:10775 (KFKI-70-26-HP)
TRITONS
binding energy of, relation with scattering length for n + d + n + d interactions, (T), 25:12227
nuclear wave function for, formulation using Feshbach--Rubinow method, 25:12364
reactions (t,d) with lithium-6 at 9 to 27 MeV, internal bremsstrahlung spectra for, (T), 25:12694
reactions (t,d) with tungsten-182 at 20 MeV, angular distributions for, (E), 25:12611
reactions (t,df) with plutonium-240, plutonium-242, and uranium-236, fission probabilities and angular correlation coefficients for, (E), 25:12579
reactions (t,p) with calcium-40 at 10.1 MeV, angular distributions and reaction amplitudes from finite-range calculations of, (T), 25:12505
reactions (t,pf) with plutonium-239, uranium-233, and uranium-235, fission probabilities and angular correlation coefficients for, (E), 25:12579
scattering by tungsten-182 at 20 MeV, angular distribution for elastic, (E), 25:12611
TROPOSPHERE
diffusion of natural radioisotopes in, numerical model for, 25:10704 (NP-18609)
TRYPTOPHAN
radioinduced mutations affecting requirement of Escherichia coli for, cobalt-60 γ, 25:11019
TUBES
heat transfer from internally-heated, to Freon 12 and 22 at nucleate boiling, film boiling, and under supercritical conditions, 25:10767 (BMBW-FBK-70-24)
joining to hubs in reactor cooling system fuel channels by rolling, 25:11366(P)
TUNGSTEN
corrosion by liquid lead at high temperatures, 25:11376 (JUL-661-RW)
determination in ores and ore concentrates, intermittent ac arc method for spectrographic, 25:10429 (BARC-468)
determination of trace amounts of, in biotite and tektite by spark source mass spectrometry, 25:10455
determination of trace amounts of, in molybdenum, review on, 25:10459
determination of trace amounts of, in rocks and sand by thermal neutron activation, ion exchange, and γ spectrometry, 25:10492
electric conductivity of drawn wires of, grain growth in stage VI annealing of, 25:12030
electron reactions at 10 to 60 MeV, Monte Carlo calculations of bremsstrahlung and photoneutrons from, 25:12496
Fermi surface area derivatives of monocrystals of, Doppler-shifted acoustic cyclotron resonance

measurements of, 25:12022
friction and wear of, sliding against copper and iron rings under vacuum, 25:11413
photoelectric emission by, calculation of direct transition contribution to, 25:12040
reactions with nitrogen and oxygen, review of kinetics, mechanisms, and thermodynamics of degassing and engassing, 25:11415
reactions with tantalum silicide coating, 25:11519
separation from ores by solvent extraction, review on, 25:10656 (BM-IC-8502)
solubility in lead at 350 to 1100°C, 25:11376 (JUL-661-Rw)
sorptive properties of (100) surface of, for iodine, LEED study of chemical, 25:11405
strength of, effects of pressure, strain, and strain rate on shear, 25:11379 (UCRL-72477)

TUNGSTEN ALLOYS AND SYSTEMS
Cr-base--W, neutron inelastic scattering study of in-band resonant modes in, 25:12019
Cr-base--W, phonon properties of, inelastic neutron scattering study of in-band resonant modes, 25:11985
Ni--W, creep of solid-solution, parameters for high-temperature, 25:11434(R) (SU-326-P-17-X-1)
Ni-base--W, creep of solid solutions of, high-temperature, 25:11408
Ta-base--W, fabrication of fuel capsule liners of, methods for, 25:10776 (MLM-1779)

TUNGSTEN CARBIDES
Co--WC, fracture of, electron microscope study of effects of carbide crystal size on, 25:11514
Co--WC, mechanical properties of sintered, continuum mechanics analysis of, 25:11515

TUNGSTEN ISOTOPES W-180
energy-level transitions from production in (α,3n) and (α,4n) reactions at 42 MeV, intensities and angular distributions from, (E/T), 25:12553

TUNGSTEN ISOTOPES W-181
distribution and redistribution of Project Schooner-produced, measurement of, 25:10716 (UCRL-72534)

TUNGSTEN ISOTOPES W-182
energy levels from tantalum-182 beta decay, lifetimes of, (E), 25:12577
energy-level transitions from tantalum-182 beta decay, delay-time spectra and enhancement and retardation factors for, (E), 25:12577
triton elastic scattering at 20 MeV, angular distribution for, (E), 25:12611
triton reactions (t,d) at 20 MeV, angular distributions for, (E), 25:12611

TUNGSTEN ISOTOPES W-183
energy levels from tungsten-182 (t,d) reactions, spectroscopic factors for, (E), 25:12611

U

ULTRASONIC TESTING
equipment for automatic, of pressure vessel welds, 25:12790

ULTRASOUND
generation in conducting liquids, direct electromagnetic, 25:12892 (NYO-2150-65)
use in polarization of nuclei, possibility of, (T), 25:12007

ULTRAVIOLET RADIATION
absorption and scattering by intergalactic gas, (T), 25:11654
cosmic background, origin of, (T), 25:11654
effects on 4-nitroquinoline 1-oxide mutants of Salmonella typhimurium, 25:11026
effects on acetylene, mechanisms of benzene formation from, 25:10650
effects on chain growth of radicals produced by γ-radioinduced polymerization of ethylene, 25:10612
effects on corn, mutagenic for plant height, 25:11009(R) (COO-1512-22)
effects on DNA in Bacillus subtilis, effects of photoreactivation on repair from, damaging, 25:10960 (BNL-50203, pp 82-90)
effects on DNA of Escherichia coli, damaging, 25:11008 (BNL-50203, pp 14-26)
effects on DNA of Micrococcus luteus, use of nucleases for determining, damaging, 25:10959 (BNL-50203, pp 27-40)
effects on Escherichia coli and Shigella flexneri, sensitizing effects of acriflavine and indanetrione on, 25:11323
effects on extraction of DNA from HeLa cells following lysis, effects of dose on, 25:10975
effects on induction of prophage from hcr-, rec-, and wild type strains of Salmonella typhimurium, 25:11026
effects on infectivity of Friend leukemia virus in mice, 25:11321
effects on phage resistance in Escherichia coli, mutagenic, 25:11032
effects on quenching and reduction of fluorenone by dimethylanilines, 25:10627(R) (NYO-2499-37)
effects on repair mechanisms in bacteriophages and Escherichia coli, effects of acridine orange on, 25:11320
effects on sulfoxidation of alkanes, comparison of γ radiation and ozone with, 25:10592 (BMBW-FBK-70-25)
effects on surface properties of Escherichia coli, mutagenic, 25:11029
effects on water vapor, review on, 25:10651
effects on yeast, effects of dose and temperature on mutagenic, 25:11074(R) (AECL-3777)
emission of He I 584-A and H I 1216-A euv dayglow, at 400 to 1016 km, (E), 25:11789

UNITED KINGDOM
radiation protection programs in, for critical assemblies, 25:11084

UNITED STATES
cesium-137 content of deer meat in, in relation of mushroom consumption, 25:11003
radioisotope content of atmosphere during 1968, plutonium-238 and plutonium-239, 25:11039
radioisotope content of human diet in, during 1969, cesium-137, strontium-89, and strontium-90, 25:11040
radioisotope content of milk in, during February 1970, barium-140, cesium-137, iodine-131, strontium-89, and strontium-90, 25:11040
tritium content of atmospheric precipitation in, during 1968, 25:11039

UNIVERSE
density parameters, upper bound for, (T), 25:11667
matter and antimatter in, separation of, (T), 25:11661
model of, baryon asymmetry and CP noninvariance in, (T), 25:12239
time variations in sea of neutrinos, electrodynamic radiative corrections for, (T), 25:11668

URANIUM
aluminum distribution in, during zone melting, 25:11406
complexes with 8-quinolinol, thermodynamic properties of, 25:10581
complexes with N-acetyl, N-chloroacetyl, N-benzoyl, and N-o, -m, and -p-nitrobenzoyl N--phenylhydroxylamines, formation constants of, 25:10521
compounds of, crystal-field effect and magnetic properties of NaCl-type, 25:11994
compounds of, review of NMR in NaCl-type, 25:12036
content in thermal waters of Kamchatka Peninsula, (E), 25:10697
corrosion by humidity, model for stress, 25:11344 (AWRE-O-46/66)
corrosion of defected Zircaloy-clad fuel elements of, by steam--water mixtures, 25:11347 (CISE-R-222)
cracking of weld metal of, effects of iron on hot, 25:11427
crystallization of electrolytically pure, effects of stresses during allotropic α--β transformation on, 25:11451
determination in freeze-dried sea salt by measurement of neutron-induced fission tracks, 25:10428
determination in rocks, lithium-drifted germanium gamma spectrometer for in situ, 25:10849 (CEA-CONF-1694)
determination in seawater by neutron activation, 25:10428
determination in solutions by proportional counting, 25:10473 (CEA-R-4032)
determination in standard rocks by fission track method, 25:10474
determination in thin layers of biotites and muscovites by fission track method using dielectric detectors, 25:10476
determination in uranium ores at pit, radiometric, 25:10484
determination of trace amounts of, in biotite and tektite by spark source mass spectrometry, 25:10455
determination of trace amounts of, in molybdenum, review on, 25:10459
determination of trace amounts of, in phosphate deposits by spark source mass spectrometry, 25:10456
determination of trace amounts of, in rocks and sand by thermal neutron activation, ion exchange, and γ spectrometry, 25:10492
determination of trivalent, in MSRE fuel samples, 25:10434 (ORNL-4636, pp 7-13)
diffusion in columnar pyrocarbons, effects of actinide content on, 25:11378 (ORNL-TM-2989)
diffusion in nickel at 975 to 1075°C, 25:11370 (CEA-CONF-1689)
ductility of, effects of humidity on, 25:11344 (AWRE-O-46/66)
effects on corrosion resistance of resulfurized Types 303, 316, 416, and 430 stainless steel, 25:11352
effects on corrosion resistance of Types 303 and 316 stainless steel in acid media, 25:11352
effects on crack formation in plutonium during α--β thermal cycling, 25:11393
effects on solvent extraction of gold by TBP, 25:10686
ion exchange properties on zirconium phosphate, 25:10680
iron distribution in, during zone melting, 25:11406
leaching from monazites and zircons using acetic, hydrochloric, nitric, and sulfuric acids, 25:10723
neutron elastic scattering at 4 MeV near 180°, differential cross sections for, (E), 25:12509(T) (ANL-Trans-855)
occurrence of different α--phases of polycrystalline, at low temperatures, effects of electric conductivity and thermopower on, 25:12006
phase transformations in, review of data on, 25:11437

phase transition at low temperatures in alpha-, 25:11449
production by calciothermic reactions, initiation triggering device for, 25:10760(P)
proton reactions at 5.5 GeV, Z = 5 to 10 mass spectrum from, (E), 25:10860
radiation effects on clad fuel elements of, in-pile, 25:11457 (CISE-R-278)
radiation effects on electric conductivity of α-, at low temperatures, self-, 25:11960
radiation effects on swelling of, in-pile, 25:11474(R) (BNWL-842)
radiation effects on volume changes in hollow-core fuels of, in-pile, 25:11474(R) (BNWL-842)
reactions of tetravalent, with trivalent chlorine, 25:10515(R) (COO-1780-14)
reactions with folic acid, stability constants of complexes from, 25:10520
reactions with oxidizing agents, mechanisms of, 25:10515(R) (COO-1780-14)
separation from aqueous solutions by solvent extraction using bis(2,2-dimethylhexyl) phosphate, 25:10679
separation from Egyptian Monazite sand, process for, 25:10683
separation from mine water by countercurrent ion exchange, 25:10657 (BM-RI-7471)
separation from ores by solvent extraction, review on, 25:10656 (BM-IC-8502)
separation of neptunium from, by ion exchange in tetramethylammonium hydroxide--citrate solutions, effects of complexing agents on, 25:10655 (ANL-7751)
solubility in nickel at 975 to 1075°C, 25:11370 (CEA-CONF-1689)
strength of, effects of pressure, strain, and strain rate on shear, 25:11379 (UCRL-72477)
structure of bcc, calculation of electronic band, (T), 25:11992
thermal conductivity of high-purity, at 4 to 90°K, 25:11382
thermodynamic properties at low temperatures, review of, 25:11384

URANIUM ALLOYS AND SYSTEMS
radiation effects on swelling of, in-pile, 25:11474(R) (BNWL-842)
Al--Si--U, radiation effects on fuels of, at high burnups, in-pile, 25:11462 (IN-1437, pp 59-70)
Al--U, analysis for boron using cobalt-60-tagged boron, 25:11375 (IN-1437, pp 24-59)
Al--U, diffusion of fission products from, mechanisms of, 25:11375 (IN-1437, pp 24-59)
Al--U, phase studies of, 25:11375 (IN-1437, pp 24-59)
Al--U, properties of fine-particle UAl/sub x/, for use in fuel plates, 25:11375 (IN-1437, pp 24-59)
Al--U, radiation effects on boron carbide foil-incorporating fuel elements of, in-pile, 25:11461 (IN-1437, pp 13-23)
Al--U, radiation effects on properties of, in-pile, 25:11462 (IN-1437, pp 59-70)
C--O--Pu--U, phase equilibria in, prediction of, 25:11525
C--Pu--U, phase diagrams of, isothermal, 25:11524
fissium--U-base, etching of irradiated, materials for, 25:11367
Mo--U-base, corrosion by moisture, stress, 25:11345 (AWRE-O-49/66)
Nb--U-base--Zr, corrosion by moisture, stress, 25:11345 (AWRE-O-49/66)
Nb--U-base--Zr, welding behavior of, electron beam, 25:11377 (MLM-1778)
O--Pu--U, diffusion in, effects of temperature gradient on mechanism of, 25:11505
Pd-base--U, magnetic behavior from susceptibility, resistivity, and thermal capacity at low temperatures, (E/T), 25:11989
Pd-base--U, magnetic properties of solid solutions of, at 2 to 300°K, 25:12003
Pu--U--Zr, phase diagrams at 500 to 700°C, isothermal, 25:11442
Pu--U-base, radiation effects on length of plutonium-238-enriched dilute α-, self-, 25:11468
Th--U--Zr, radiation effects on tube-type fuel elements of, in-pile, 25:11474(R) (BNWL-842)

URANIUM ARSENIDES
structure of paramagnetic, relations of physical properties with calculated electronic band, (T), 25:11993

URANIUM CARBIDES
creep at high temperatures, effects of pressure on, 25:11485 (CEA-CONF-1670)
electric conductivity of U_2C_3, 25:11980 (CEA-R-4113)
magnetic susceptibility of U_2C_3, 25:11980 (CEA-R-4113)
properties of, electric and thermal, 25:11494
radiation effects testing at high temperatures of loose packed particles of, 25:12795(R) (BMI-1893)
structure of paramagnetic, relations of physical properties with calculated electronic band, (T), 25:11993
MoC--UC, thermal expansion of $UMoC_2$, high-temperature anisotropic, 25:11509
PtC--U_2C, thermal expansion of U_2PtC_2, high-temperature anisotropic, 25:11509
PuC_2--UC_2, phase diagram of, differential thermal analysis of pseudobinary, 25:11522
PuC_2--UC_2, phase studies of isopleth and melting behavior for, 25:11523
PuC--UC, compatibility of hyperstoichiometric fuels of, with Type 316L stainless steel at 900°C, 25:11475 (AERE-R-5173)
PuC--UC, creep at high temperatures, effects of pressure on, 25:11485 (CEA-CONF-1670)
PuC--UC, properties of, electric and thermal, 25:11494
PuC--UC-base, melting behavior of, 25:11507

URANIUM CARBONITRIDES
creep at high temperatures, effects of pressure on, 25:11485 (CEA-CONF-1670)
electric conductivity, 25:11980 (CEA-R-4113)
magnetic susceptibility, 25:11980 (CEA-R-4113)
thermal capacity at low temperatures, 25:11980 (CEA-R-4113)
PuCN--UCN, creep at high temperatures, effects of pressure on, 25:11485 (CEA-CONF-1670)

URANIUM FLUORIDES UF_4
production from β uranium trioxide--water, effects of α uranium trioxide on, 25:10569 (CEA-R-4074)

URANIUM FLUORIDES UF_6
sorption by barium, magnesium, and sodium fluorides, mechanism of, 25:10568 (CEA-R-4051)

URANIUM IONS
spectra of photoexcited states of, in lanthanum chloride monocrystals, EPR, 25:10570(R) (COO-294-10)

URANIUM ISOTOPES
decay systematics in Wind River, Wyoming plutons, 25:10701
determination in stalagmites by α spectrometry, 25:10477

URANIUM ISOTOPES U-232
alpha decay of, time spectrum of alpha--conversion-electron delay in, (E), 25:12542
determination in seawater by α spectrometry, 25:10477
energy levels of, asymmetric collective model description of negative-parity, (T), 25:12563

URANIUM ISOTOPES U-233
alpha decay of, time spectrum of alpha--conversion-electron delay in, (E), 25:12541
neutron capture by, interference effects in average cross section for, (T), 25:12608
neutron fission of, interference effects in average cross section for, (T), 25:12608
neutron resonance scattering by, interference effects in average cross section for, (T), 25:12608
triton reactions (t,pf) with, fission probability and angular correlation coefficients for, (E), 25:12579

URANIUM ISOTOPES U-234
determination in seawater by α spectrometry, 25:10477
determination of abundance of, relative to uranium-238 in river water by α spectrometry, 25:10477
deuteron reactions (d,pf) with, fission probability and angular correlation coefficients for, (E), 25:12579
energy levels from plutonium-238 alpha decay, lifetimes, quadrupole moments, and deformation parameters for, (E), 25:12542
energy levels of, asymmetric collective model description of negative-parity, (T), 25:12563
energy-level transitions from plutonium-238 alpha decay, probabilities for E2, (E), 25:12542
half-life of, 25:10583(R) (AECL-3776)

URANIUM ISOTOPES U-235
alpha reactions (α,2n) at 24 to 27 MeV, decay curves and excitation functions for production of isomeric plutonium-237, (E/T), 25:12530 (RLO-1388-130)
determination in seawater by α spectrometry, 25:10477
determination of trace amounts of, in rocks by neutron activation and radiochemical separation, 25:10494
energy levels from plutonium-239 alpha decay, lifetimes, quadrupole moments, and gyromagnetic ratios for rotational, (E), 25:12541
energy-level transitions from plutonium-239 alpha decay, gamma spectra and E2/M1 mixing ratios from, (E), 25:12541
fission by thermal neutrons, SAND-II calculations of cross sections and spectra of, 25:11474(R) (BNWL-842)
neon-22 reaction (Ne-22,5n) at 105 to 150 MeV, cross section for, (E), 25:12620
neutron capture by, interference effects in average cross section for, (T), 25:12608
neutron fission of, charge distribution from thermal, 25:10472(R) (BMBW-FBK-70-19)
neutron fission of, gamma spectra at 11 days from fragments from thermal, (E), 25:12535
neutron fission of, interference effects in average cross section for, (T), 25:12608
neutron fission of, yields from thermal, 25:10472(R) (BMBW-FBK-70-19)
neutron fission of, yields of cadmium isotopes from thermal, 25:10583(R) (AECL-3776)
neutron resonance scattering by, interference effects in average cross section for, (T), 25:12608
triton reactions (t,pf) with, fission probability and angular correlation coefficients for, (E), 25:12579

URANIUM ISOTOPES U-236
alpha reactions (α,3n) at 34 MeV, decay curves from, (E), 25:12530 (RLO-1388-130)
deuteron reactions (d,pf) with, fission probability and angular correlation coefficients for, (E), 25:12579
energy levels from plutonium-240 alpha decay, lifetimes,

quadrupole moments, and deformation parameters for, (E), 25:12542
energy-level transitions from plutonium-240 alpha decay, probabilities for E2, (E), 25:12542
fission of, energy distribution of helium-4 and tritium from, 25:10563(R) (AECL-3776)
triton reactions (t,df) with, fission probability and angular correlation coefficients for, (E), 25:12579
URANIUM ISOTOPES U-238
alpha fission at 63.5 MeV, in- and out-of-plane angular correlations and fission-fragment energy spectra from, (E), 25:12526 (MNC-3783-7)
determination in seawater by α spectrometry, 25:10477
determination of abundance of, relative to uranium-234 in river water by α spectrometry, 25:10477
determination of trace amounts of, in rocks by neutron activation and radiochemical separation, 25:10494
deuteron reactions (d,pf) with, fission probability and angular correlation coefficients for, (E), 25:12579
energy level of, Moessbauer study of first 2⁺, (E), 25:12559
fission of, half-lives for spontaneous, (E), 25:12538
neutron elastic scattering at 0.075 to 15 MeV, optical potentials for, (T), 25:12510(T) (BNL-tr-366)
neutron fission factor in heavy water moderated natural uranium lattice, measurement of fast, 25:12817 (EUR-4326)
photofission at 200 to 900 MeV, cross sections for, (E), 25:12573
URANIUM ISOTOPES U-239
energy levels of, number of nonrotational and fragmentation of single-particle, (T), 25:12630 (JINR-E4-5469)
URANIUM NITRIDES
creep at high temperatures, effects of pressure on, 25:11485 (CEA-CONF-1670)
fabrication of cylinders of, isostatic and uniaxial pressing methods for, 25:11480 (ORNL-4608)
hardness at 20 to 1400°C, effects of impurities on, 25:11498
magnetic susceptibility, 25:11980 (CEA-R-4113)
microstructure of, 25:11480 (ORNL-4608)
preparation of powdered, hydride--dehydride--nitride method for, 25:11480 (ORNL-4608)
production by reactions of nitrogen with carbon--uranium dioxide, 25:11478 (BNWL-843)
properties of, electric and thermal, 25:11494
structure of paramagnetic, relations of physical properties with calculated electronic band, (T), 25:11993
thermal capacity at low temperatures, 25:11980 (CEA-R-4113)
PuN--UN, compatibility with Type 304 stainless steel at 650 to 1000°C, 25:11474(R) (BNWL-842)
PuN--UN, creep at high temperatures, effects of pressure on, 25:11485 (CEA-CONF-1670)
PuN--UN, fabrication of Type 316 stainless steel clad fuel pins of, 25:12795(R) (BMI-1893)
PuN--UN, irradiation testing in liquid sodium cooled fast reactor environment, 25:12795(R) (BMI-1893)
PuN--UN, melting points of, effects of pressure on, 25:11474(R) (BNWL-842)
PuN--UN, properties of, physical, thermal, and thermodynamic, 25:11492
PuN--UN, radiation effects on performance of stainless steel-clad, in-pile, 25:11535
PuN--UN-base, thermal conductivity of carbothermically-produced, at 0 to 1600°C, 25:11474(R) (BNWL-842)
ThN--UN, magnetic susceptibility, 25:11980 (CEA-R-4113)
ThN--UN, properties of, electric and thermal, 25:11494
UN--YN-base, thermal capacity at low temperatures, 25:11980 (CEA-R-4113)
URANIUM ORES
analysis for uranium at pit, radiometric, 25:10484
mining of, methods for protection against radon and radon-daughter radiation hazards during, 25:11085
radiation hazards to environment from mill tailings of, survey of, 25:11045
URANIUM OXALATES
thermodynamic properties of, 25:10581
URANIUM OXIDES
preparation by anhydrous ammonia reduction of ammonium diuranate, effects of temperature and time on, 25:10573 (IEA-207)
URANIUM OXIDES UO_2
creep of polycrystalline, effects of composition, density, grain size, stress, and temperature on compressive, 25:11497
creep testing of, 25:12795(R) (BMI-1893)
decarbonization at 500 to 1400°C, changes in residual carbon content during, 25:11482
diffusion of oxygen in, tracer study of self-, 25:11486 (CEA-R-4095)
elastic constants at 25°C, 25:11474(R) (BNWL-842)
fission gas diffusion and bubble growth in, 25:12795(R) (BMI-1893)
microstructure of hyperstoichiometric and stoichiometric, 25:11520
preparation of controlled-porosity compacts of, methods for, 25:11481(P)
preparation of thin films of irradiated fuels of, for electron microscopy, 25:11532 (AERE-R-5677)
production from β uranium trioxide--water, effects of α uranium trioxide on, 25:10569 (CEA-R-4074)
production of monocrystalline, by electron beam floating method in rhenium capsules, 25:11474(R) (BNWL-842)
radiation effects on performance of Zircaloy-clad hollow pellet fuel elements of, in-pile, 25:11530 (AECL-3732)
reactions with hydrofluoric acid and oxygen, rate of, 25:10569 (CEA-R-4074)
reactivity and reduction of, effects of structure of uranium trioxide on, 25:10569 (CEA-R-4074)
sintering at 800 to 1400°C, changes in residual carbon content during, 25:11482
C--UO_2, production from uranyl nitrate--sugar solutions by spray calcination, 25:11474(R) (BNWL-842)
C--UO_2, production of mixtures of, by reactions of sugar with uranyl nitrate in spray calciners, 25:11478 (BNWL-843)
C--UO_2, reactions with nitrogen at 1600°C to produce uranium carbide, efficiency of, 25:11478 (BNWL-843)
PuO_2--UO_2, compatibility with Type 304 stainless steel at 650 to 1000°C, 25:11474(R) (BNWL-842)
PuO_2--UO_2, creep at high temperatures, effects of pressure on, 25:11485 (CEA-CONF-1670)
PuO_2--UO_2, creep of polycrystalline, effects of composition, density, grain size, stress, and temperature on compressive, 25:11497
PuO_2--UO_2, creep of, effects of concentration, density, stoichiometry, stress, and temperature on compressive, 25:11495
PuO_2--UO_2, creep testing of, 25:12795(R) (BMI-1893)
PuO_2--UO_2, electric properties of hypostoichiometric, at 25 to 800°C, 25:11991
PuO_2--UO_2, evaporation behavior of hypostoichiometric, at 1800 to 2350°K, 25:11504
PuO_2--UO_2, homogeneity of, mathematical model for describing, 25:11489 (WHAN-FR-20)
PuO_2--UO_2, irradiation testing in liquid sodium cooled fast reactor environment, 25:12795(R) (BMI-1893)
PuO_2--UO_2, microstructure of fuels of, etching methods for electron microscopic studies, 25:11474(R) (BNWL-842)
PuO_2--UO_2, plutonium dioxide homogeneity in fuel pellets of, scanning electron microprobe analysis of, 25:11489 (WHAN-FR-20)
PuO_2--UO_2, production of monocrystalline, development of methods for, 25:11474(R) (BNWL-842)
PuO_2--UO_2, radiation effects on void distribution in, in-pile, 25:11536
PuO_2--UO_2, volatilization behavior of nonstoichiometric, at 1905 to 2411°K, mass spectrometric study of, 25:11503
PuO_2--UO_2-base, creep of polycrystalline, at 1100 to 1330°C, effects of density, grain size, and stress on compressive, 25:11496
ThO_2--UO_2, stability of Zircaloy-clad fuel rods of, in up-power reactor transients, 25:11534 (WAPD-TM-979)
URANIUM OXIDES UO_3
effects of structure of, on chemical reactivity and reduction of uranium dioxide, 25:10569 (CEA-R-4074)
physical properties and reactivity of α, 25:10569 (CEA-R-4074)
reduction of α and β, by ammonia, kinetics of, 25:10569 (CEA-R-4074)
H_2O--UO_3, physical properties and reactivity of, 25:10569 (CEA-R-4074)
URANIUM OXIDES U_3O_8
analysis for impurities by emission spectroscopy, 25:10432 (KFK-1261)
phase transformations in, effects of pressure and shear on alpha--beta, 25:11528
URANIUM PHOSPHIDES
magnetic structure of U_3P_4, analysis of neutron-diffraction data on, 25:12028
structure of paramagnetic, relations of physical properties with calculated electronic band, (T), 25:11993
URANIUM RESERVES
estimates of Canadian, evaluation of ENEA report on, 25:10724
URANIUM SELENIDES
structure of paramagnetic, relations of physical properties with calculated electronic band, (T), 25:11993
URANIUM SULFIDES
structure of paramagnetic, relations of physical properties with calculated electronic band, (T), 25:11993
URANYL ACETATES
thermodynamic properties of, 25:10581
URANYL FLUORIDES
crystal structure of anhydrous, 25:10577
URANYL IONS
distribution coefficient in mixtures of acetone, hydrochloric acid, and methanol, 25:10681
exchange equilibrium with hydrogen forms of zirconium phosphate, thermodynamics of, 25:10680
URANYL NITRATES
reactions with sugar to produce carbon--uranium dioxide mixtures, 25:11478 (BNWL-843)
reactions with sugar to produce carbon--uranium dioxide mixtures, 25:11474(R) (BNWL-842)

reduction of aqueous solutions of, by hydrogen at low pressure, catalytic effects of aluminum oxide--platinum on, 25:10572 (IEA-184)
URANYL PYROPHOSPHATES
preparation of anionic complexes of, 25:10519
UREA, 1-METHYL-1-NITROSO-
effects on frequency of chlorophyll mutations in barley in comparison to effects of EMS and x radiation, 25:11021
URIDINE
uptake by Ehrlich ascites tumors in mice, tracer study using iodine-131 and whole-body autoradiography for, 25:10921
URINARY TRACT
radiotherapy of neoplasms of, in man, combined effects of dactinomycin on post-surgical x, 25:11225
URINE
analysis for trace elements by flameless atomic absorption spectrometry, 25:10464
cobalt-60 1-nitroso 2-naphthol chelate excretion in, of rats, 25:10958
UTAH
zirconium-95 content of crops in, during May and June 1966, relation of, to fallout from May 9 Chinese atmospheric nuclear explosion, 25:10999

V

VACUUM PUMPS
performance of getter-ion, using titanium monoxide, 25:10804(P)
VACUUM SYSTEMS
bibliography on surface and vacuum physics, 25:11678
description of ultrahigh, with double electron gun for film deposition from two sources, 25:10806
design of ultrahigh, for use in vapor deposition coating of shaped substrates, 25:10805(P)
properties for use with thermonuclear power plants, 25:11919 (EUR-CEA-FC-566)
VALINE
radiation effects on content of, in cooked meats, γ, 25:11339
VALVES
design and performance of high-pressure fast, for bubble chambers, 25:10870 (JINR-P13-5420)
performance in water cooled reactor systems of gate, globe, and check, engineering guides for reliable, 25:12785 (ORNL-TM-3221)
specifications for water cooled reactor systems gate, globe, and check, guide for, 25:12786 (ORNL-TM-3273)
VAN ALLEN RADIATION BELTS
electron boundary in outer, relation with ionospheric current electrojets position, (E/T), 25:11782
proton energy spectra mirroring near magnetic-equator, directional differential of 200 ev less than or equal to E less than or equal to 1 MeV, (E), 25:11786
VAN DE GRAAFF ACCELERATORS
experimental facility for localized irradiation of materials with charged particles, 25:12318
radiation monitoring at, detector system for neutron and gamma, 25:10824
VANADIUM
corrosion by liquid lead at high temperatures, 25:11376 (JUL-661-RW)
creep rate of polycrystalline, at 477 to 1600°C, effects of stress on minimum, 25:11397
determination as impurity in fuel materials by emission spectroscopy, 25:10432 (KFK-1261)
determination in sedimentary rocks by direct-reading spectrometry, 25:10450
determination of trace amounts of, in basalt and granite, correction of matrix effect in uv spectrographic, 25:10453
determination of trace amounts of, in biotite and tektite by spark source mass spectrometry, 25:10455
determination of trace amounts of, in molybdenum, review on, 25:10459
determination of trace amounts of, in phosphate deposits by spark source mass spectrometry, 25:10456
determination of trace amounts of, in rocks, quantometer for spectroscopic, 25:10451
determination of trace amounts of, in silicate rocks, method for elimination of matrix effect in quantometric, 25:10452
determination of trace amounts of, in standard silicate rocks using sodium chloride buffer, emission spectrographic, 25:10454
determination of trace amounts of, in Zircaloy-2 and zirconium, carrier distillation method for spectrographic, 25:10430 (EUR-4541)
friction and wear of, sliding against copper and iron rings under vacuum, 25:11413
preparation of monocrystalline, electron beam float zone refining method for, 25:11356 (CONF-700546-1)
reactions with nitrogen and oxygen, review of kinetics, mechanisms, and thermodynamics of degassing and engassing, 25:11415
reactions with oxidizing agents, mechanisms of, 25:10515(R) (COO-1780-14)
separation from ores by solvent extraction, review on, 25:10656 (BM-IC-8502)
solubility in lead at 350 to 1100°C, 25:11376 (JUL-661-RW)
VANADIUM ALLOYS AND SYSTEMS
preparation of hardened creep-resistant, composition and methods for, 25:11363(P)
Al--Ti-base--V, phase transformations at 1000 to 1400°F, effects of strain on, 25:11453
Cr--Fe-base--V, properties of aged, effects of reheating on electric and mechanical, 25:11403
VANADIUM BORIDES
x-ray emission spectra, 25:12012
VANADIUM CARBIDES
electron band structure, 25:12012
x-ray emission spectra, 25:12012
VANADIUM ISOTOPES V-48
beta decay of, β-γ circular polarization correlation in, (E), 25:12471
VANADIUM ISOTOPES V-50
nucleosynthesis of, effects of energetic proton fluxes on, (T), 25:11544
VANADIUM ISOTOPES V-51
electron elastic scattering at 1 to 100 MeV, nuclear-size effects on polarization functions for, (T), 25:12664
energy levels from titanium-48 (α,pγ) and vanadium-51 (p,p'γ) reactions, spin--parity assignments for, (E), 25:12435
energy-level transitions from titanium-48 (α,pγ) and vanadium-51 (p,p'γ) reactions, intensities of, (E), 25:12435
energy-level transitions in, measurements and shell-model calculations of, 25:12492
nuclear magnetic resonance in doped vanadium (III) oxide, 25:12039
photon inelastic scattering at 12 to 30 MeV, differential cross sections for, (E), 25:12463
proton reactions (p,n) and (p,nγ) at 2.4 to 3.3 MeV, comparison of Hauser--Feshbach theory with neutron cross sections and gamma angular distributions and anisotropies from, (E/T), 25:12476
proton reactions (p,nγ) and (p,p'γ) at 2.3 to 6 MeV, excitation functions and gamma spectra from, (E), 25:12435
proton reactions at 60 to 240 MeV, cross sections for spallation products from, (T), 25:12439
VANADIUM NITRIDES
x-ray emission spectra, 25:12012
VANADIUM OXIDES
electron band structure calculations, 25:12044
phase transition in doped V_2O_3, NMR study of metal--insulator, 25:12039
thermal expansion of, electronic structure from anomalous, (T), 25:12015
x-ray emission spectra, 25:12012
K_2SO_4--V_2O_5, phase diagram of, 25:11527
VEGETABLES
beets, radiation processing of sugar, effects of, on enzyme activity, γ, 25:10964
soybeans, effects on radioisotope accumulation in rats, diet of proteins from, 25:10956
VEINS (BLOOD)
blood circulation in, comparison of photoelectric drop recorder to ^{133}Xe for measuring, 25:11136
vasoconstrictor content of renal, determination of, for diagnosis of hypertension in combination with radioisotope scintigraphy, 25:11163
VERMONT YANKEE POWER REACTOR
instrumentation for, preliminary safety analysis of, 25:12738 (DOCKET-50271-35)
piping systems for, preliminary safety analysis of, 25:12738 (DOCKET-50271-35)
standby gas treatment system for, control and instrumentation of, 25:12738 (DOCKET-50271-35)
VESSELS
closure plug for sodium cooled reactor, liquid filled main and secondary seals for, 25:12771(P)
VINYL ALCOHOL POLYMERS
radiation effects on thermal stability of, mechanism of γ, 25:10591
VINYL COMPOUNDS
poly(diallyl phthalate)--vinyl compound, polymerization for coating woods, electron, 25:10606 (JAERI-5026, pp 101-7)
VIRUSES
Friend, radiation effects on infectivity of, in mice, uv, 25:11321
polyomas, radiation effects on replication of, in cultured embryo cells from chickens and mice, effects of cell population density on x, 25:11274
Rous, radiation effects on replication of, in cultured embryo cells from chickens and mice, effects of cell population density on x, 25:11274
sarcoma 180, radiation effects on replication of, in cultured embryo cells from chickens and mice, effects of cell population density on x, 25:11274
VITAMIN B GROUP
folic acid, avidity for carcinogenic aluminum, beryllium, chromium, lead, and uranium ions, 25:10520

XUM

W

WATER
analysis for deuterium/hydrogen ratio, mass spectrometric, 25:10463
analysis for trace elements, problems of contamination during, 25:10427
analysis for uranium isotopes by α spectrometry, 25:10477
book: Intercrystalline Corrosion and Corrosion Cracking of Stainless Steel in Aqueous Solutions (In Russian), 25:11353
bubble acoustic emission in subcooled, parameters for boiling, 25:10769(R) (ORO-3911-3)
corrosive effects of hot pressurized, on Zircaloy-2, relations of prior corrosion history with, 25:11349 (WAPD-TM-906)
corrosive effects on zirconium alloys, relations with in-pile radiation, 25:11474(R) (BNWL-842)
decomposition by electric discharges, effects of oxygen-18 on ir spectra of products from, 25:10531
determination in compounds used for pharmaceutical purposes by neutron scattering and moderation, 25:10486
determination of, meters for, 25:10475
effects of hot pressurized, on hydrogen sorption by Zircaloy-2, relations of prior corrosion history with, 25:11349 (WAPD-TM-906)
effects of pretreatment with, on properties of products from γ-induced polymerization of vinylidene chloride in woods, 25:10604 (JAERI-5026, pp 86-93)
effects on polymerization of ethyl acrylate on textiles, 25:10619
effects on properties of products from γ- or electron-induced polymerization of vinylidene chloride in wood, 25:10603 (JAERI-5026, pp 80-5)
effects on properties of products from radioinduced polymerization of acrylic acid on poly(ethylene terephthalates), 25:10597 (JAERI-5026, pp 46-51)
iodine distribution between gases and, 25:10513 (AERE-R-4887)
neutron attenuation at 14.7 MeV, (E), 25:12349
neutron attenuation in, ages and slowing-down spectra from fission and D--T sources, (T), 25:12348
neutron inelastic scattering at 0.04 to 0.632 MeV and 27 to 270°C, double differential cross section for, (E), 25:12342 (RPI-328-210)
neutron removal cross section at 14.7 MeV, (E), 25:12349
radiolysis in loss-of-coolant accidents in PWR or BWR, 25:10491 (ORNL-4636, pp 20-33)
radiolysis of aerated acidified, cerium and hydrogen peroxide yields from β, 25:10636
reactions with water, 25:10513 (AERE-R-4887)
separation of uranium from, by countercurrent ion exchange, 25:10657 (BM-RI-7471)
sorption by Fiberglas E, research on, 25:11472(R) (AD-708705)
sorption by Fiberglas E, research on, 25:11473(R) (AD-708712)
use for irrigation in United Arab Republic, radiation techniques for efficient, 25:10927
D_2O--H_2O, radiolysis of, 25:10583(R) (AECL-3776)
H_2O--steam, corrosive effects on defected Zircaloy-clad uranium fuel elements, 25:11347 (CISE-R-222)
H_2O--steam, flow in tubes, heat transfer, holdup, and nucleation calculations for, 25:10766 (AERE-R-3984)
H_2O--UO_2, physical properties and reactivity of, 25:10569 (CEA-R-4074)
WATER-d_2
decomposition by electric discharges, effects of oxygen-18 on ir spectra of products from, 25:10531
production for heavy water-moderated reactors, development of columns for, 25:10764
production of, optimization of dual-temperature ammonia--deuterium plant for, 25:10787
D_2O--H_2O, radiolysis of, 25:10583(R) (AECL-3776)
WATER SUPPLIES
analysis and sampling of, list of reports on 1967 to 1970 programs for, 25:10699
thorium-232 content of, calculation of maximum permissible, 25:11051
WATER VAPOR
corrosive effects on plutonium in argon at 50 to 270°C, 25:11350
corrosive effects on uranium alloys, stress, 25:11345 (AWRE-O-49/66)
decomposition by electron impact in mass spectrometer, review on, 25:10651
effects on carburization of iron and steel by decomposing carbon monoxide, relations with composition, surface structure, and temperature, 25:11374 (DP-Report-530)
photolysis of, review on, 25:10651
radiolysis of, 25:10583(R) (AECL-3776)
radiolysis of, review on, 25:10651
WATERFORD POWER REACTOR, UNIT 3
auxiliary systems for, preliminary safety analysis of, 25:12755 (DOCKET-50382-4)
buildings and structures for, preliminary safety analysis of, 25:12754 (DOCKET-50382-3)
containment system for, preliminary safety analysis of, 25:12754 (DOCKET-50382-3)
control systems for, preliminary safety analysis of, 25:12755 (DOCKET-50382-4)
cooling system for, preliminary safety analysis of, 25:12754 (DOCKET-50382-3)
electrical systems for, preliminary safety analysis of, 25:12755 (DOCKET-50382-4)
engineered safeguards for, preliminary safety analysis of, 25:12754 (DOCKET-50382-3)
instrumentation for, preliminary safety analysis of, 25:12755 (DOCKET-50382-4)
operations aspects of, preliminary safety analysis of, 25:12755 (DOCKET-50382-4)
radiation protection system for, preliminary safety analysis of, 25:12755 (DOCKET-50382-4)
radioactive waste disposal system for, preliminary safety analysis of, 25:12755 (DOCKET-50382-4)
safety analysis of, 25:12756 (DOCKET-50382-5)
site for, preliminary safety analysis of, 25:12753 (DOCKET-50382-2)
steam and power conversion systems for, preliminary safety analysis of, 25:12755 (DOCKET-50382-4)
technical specifications for, proposed complete, 25:12756 (DOCKET-50382-5)
WATERFORD POWER REACTOR, UNIT 4
auxiliary systems for, preliminary safety analysis of, 25:12755 (DOCKET-50382-4)
buildings and structures for, preliminary safety analysis of, 25:12754 (DOCKET-50382-3)
containment system for, preliminary safety analysis of, 25:12754 (DOCKET-50382-3)
control systems for, preliminary safety analysis of, 25:12755 (DOCKET-50382-4)
cooling system for, preliminary safety analysis of, 25:12754 (DOCKET-50382-3)
electrical systems for, preliminary safety analysis of, 25:12755 (DOCKET-50382-4)
engineered safeguards for, preliminary safety analysis of, 25:12754 (DOCKET-50382-3)
instrumentation for, preliminary safety analysis of, 25:12755 (DOCKET-50382-4)
operations aspects of, preliminary safety analysis of, 25:12755 (DOCKET-50382-4)
radiation protection system for, preliminary safety analysis of, 25:12755 (DOCKET-50382-4)
radioactive waste disposal system for, preliminary safety analysis of, 25:12755 (DOCKET-50382-4)
safety analysis of, 25:12756 (DOCKET-50382-5)
site for, preliminary safety analysis of, 25:12753 (DOCKET-50382-2)
steam and power conversion systems for, preliminary safety analysis of, 25:12755 (DOCKET-50382-4)
technical specifications for, proposed complete, 25:12756 (DOCKET-50382-5)
WEISWEILER POWER REACTOR
boilers for, design parameters of liquid sodium heat transfer system for testing, 25:12708
WELDS
inspection of pressure vessel, automatic equipment for ultrasonic, 25:12750
WELL LOGGING
equipment for radiometric analysis, lithium-drifted germanium gamma spectrometer, 25:10849 (CEA-CONF-1694)
equipment for simultaneous porosity measurement and chlorine determination, neutron radiometric, 25:10889(P)
method for determining copper plus zinc mineralization in Czech mineral deposits, gamma--gamma, 25:10693
WELLS
damage to Project Rulison area gas, postshot evaluation of, 25:10737 (PNE-R-39, Pt.2)
WEST VALLEY PROCESSING PLANT
radioactive waste processing and release at, 25:10661 (DOCKET-50201-59)
radioactive waste treatment plant at, safety analysis of low-level liquid, 25:10660 (DOCKET-50201-58)
safety analysis of cell and crane room extension and sump collection tank for, 25:10662 (DOCKET-50201-71)
WHISTLERS
cyclotron damping of proton, proton density irregularities determination from, (E/T), 25:11787
propagation in geomagnetic field, Poynting-flux direction of magnetospheric, (E), 25:11780
WHOLE-BODY COUNTERS
performance for measuring total body potassium content of man, 25:10910
WILLIAM H. ZIMMER POWER REACTOR, UNIT 1
design parameters of, revised and additional data on, 25:12749 (DOCKET-50358-10)
operations aspects of, revised and additional data on, 25:12749 (DOCKET-50358-10)
WIND
effect of neutral, on evening anomalous critical frequency in summer hemispheric ionosphere, (E/T), 25:11777 (AD-708496)
effects of jet stream, on strontium-89/-90 ratio in Fayetteville, Arkansas rainwater, 1964 to 1969, 25:10708 (ORO-2529-28, App. 2)
effects of lower Aare River Valley, on atmospheric diffusion of gaseous effluents from reactors, (E), 25:10703 (EIR-185)

effects on window pane damage, (E/T), 25:10792 (SC-RR-70-441)
effects with fires on deposition of fallout, 25:10702 (AD-708558)
WIND RIVER DISTRICT (WYO.)
classification and metamorphism of plutons in Wyoming, 25:10701
WIND TUNNELS
use for measuring coolant flow stresses on reactor core components, 25:12706
WINDOWS
damage from explosion airblasts, sonic booms, and winds, (E/T), 25:10792 (SC-RR-70-441)
testing of sapphire, for pressure vessels, 25:11488 (KFK-1211)
WOOD
radioinduced polymerization of acrylonitrile--poly(diallyl phthalate), γ or electron, 25:10607 (JAERI-5026, pp 108-20)
radioinduced polymerization of diallyl phthalate and vinyl monomers for coating of, electron, 25:10606 (JAERI-5026, pp 101-7)
radioinduced polymerization of vinylidene chloride in lauan, effects of presoaking on properties of products from γ or electron, 25:10603 (JAERI-5026, pp 80-5)
radioinduced polymerization of vinylidene chloride in, thermal stability of products from γ, 25:10605 (JAERI-5026, pp 94-100)
radioinduced polymerization of vinylidene chloride in, effects of pretreatment of woods on properties of products from γ, 25:10604 (JAERI-5026, pp 86-93)
WOOL
radioinduced polymerization of ethyl acrylate on, using water as swelling agent, 25:10619

X

X RADIATION
absorption and scattering by intergalactic gas, (T), 25:11654
cosmic background, at the galactic pole and plane, (E), 25:11653
cosmic background, interaction with relativistic electrons in extragalactic radio sources, (T), 25:11597
cosmic background, origin of, (T), 25:11748
cosmic background, origin of, (T), 25:11657
cosmic background, origin of, (T), 25:11656
cosmic background, origin of, (T), 25:11654
dose to color television assembly and repair personnel, low-energy, 25:11063
dose to medical personnel during radiography for heart catheterization, 25:11059
dosimetry for color television assembly and repair personnel, 25:11063
dosimetry in beryllium oxide mixtures with plutonium oxide, 25:11052 (AERE-R-5069)
dosimetry using tissue-equivalent scintillators, 25:11072
effectiveness for post-surgical therapy of human urinary tract neoplasms, 25:11225
effectiveness for therapy of carcinomas of human bladder, high-energy, 25:11229
effects on acatalasemic and normal mice, 25:11264
effects on adrenal cortex of rats, protective effects of sex hormones against atrophic whole-body, 25:11268
effects on antibody production in mice, effects of injections of allogeneic spleen cells and sheep red blood cells on, 25:10994
effects on Barkhausen effect in ferroelectric crystals, 25:11978
effects on binding of tritium-labeled dactinomycin by DNA of hepatocytes of mice, effects of administration route on, 25:11285
effects on bioelectrical potential of Zea mays roots in relation to cell growth, 25:11308
effects on blood coagulation in rats, protective effects of cystamine and homologous bone marrow against, 25:11105
effects on body weight of rat populations, effects of gonad exposure on, 25:11074(R) (AECL-3777)
effects on bone marrow cell count in mice in comparison to effects of injection of methioninesulfoximine, 25:11288
effects on bone marrow cell populations of mice, effects of dose fractionation on, 25:11279
effects on bone-marrow shielded rats, role of lymphocytes from shielded marrow in recovery from pathological, 25:11077
effects on carbohydrates, ESR spectra of free radicals from, 25:10645
effects on Chinese hamster cells, effects of age on, 25:11093 (BNL-50203, pp 97-116)
effects on chloroform vapor, Arrhenius parameters for hydrogen-atom abstraction reaction of dichloromethyl radicals in, 25:10629
effects on chlorophyll in barley in comparison to effects of EMS and nitrosomethyl urea, frequency of mutagenic, 25:11021
effects on chromosome in peripheral lymphocytes of children following diagnostic exposure, aberrant, 25:11113
effects on chromosomes in corneal epithelium of mice, aberrant, 25:11018
effects on chromosomes of maize, effects of pollen exposure on aberrant, 25:11023
effects on content of autoantibodies in liver of rabbits, 25:10985
effects on culture media, effects of, on chromosomes of cultured mammalian cells, 25:10970
effects on diploid and tetraploid seedlings of marigolds, petunias, and zinnias, correlation between dose, LET, and volume of cell nuclei and chromosomes for, 25:11020
effects on DNA of Escherichia coli, effects of temperature on degratory, 25:11007 (BNL-50203, pp 1-13)
effects on DNA synthesis in relation to survival of cultured mammalian cells, molecular basis for effects of exogenous DNA on restoration following inhibitory, 25:11243
effects on electric conductivity of p-type germanium, (E), 25:11963
effects on embryos of mice and rats in utero, effects of species differences on lethal and teratogenic, 25:11277
effects on embryos of mice and rats in utero, effects of species differences on lethal and teratogenic, 25:11277
effects on erythron and reticulo-endothelial cells, radioisotope colloid scanning for, 25:11112
effects on flower formation by chrysanthemum plants, effects of dose on, 25:11311
effects on formation of supernumerary surface layers in amoeba, effects of dose on, 25:11249
effects on fusion of linear polyethylene crystallized by high-speed stirring, 25:10618
effects on growth of Chinese hamster cells, effects of crowding on, 25:11239 (BNL-50203, pp 117-29)
effects on growth of seeds of mung beans, inhibitory, 25:11317
effects on growth of tail bone transplants from syngeneic donor mice, protective effects of anoxia, dimethyl sulfoxide, and glycerol against, 25:10983
effects on healing of mandibular fractures in rabbits, inhibitory, 25:11266
effects on heat production and reproduction of yeasts, 70 to 150 kR, 25:11324
effects on immune reactions in chickens and quail following intra-species transplantation of gonad tissues, 25:10988
effects on lanthanum oxychlorides activated with trivalent bismuth, effects of composition on luminescence produced by, 25:10590
effects on lithium drift in silicon at low temperatures, 25:11973
effects on man following in utero exposure of mothers, pathological, 25:11300
effects on maze habits of rats, effects of dose fractionation on whole-body, 25:11273
effects on mice, combined effects of Ascaris suum invasion of lungs on, 25:11265
effects on mice, protective effects of reduced glutathione against lethal, 25:11098
effects on mucosal epithelium of intestine of rats, effects of dose on, fibrousous, degenerating, and damaging, 25:11255 (BNL-50203, pp 181-5)
effects on nervous system in embryos and infants of mice, effects of stage of pregnancy on teratogenic, 25:11287
effects on neural activity in optical cortex of rabbits exposed during embryogenesis, 25:11283
effects on optoelectronic devices at 100 keV, 25:10904 (HMI-B-97)
effects on oxidative enzymes in epidermis, microspectrophotometric study of, 25:11241
effects on oxidative phosphorylation and respiration in spleen mitochondria of rats, protective effects of homologous bone marrow injections against acute, 25:11100
effects on oxygen supply in tumor cells, 25:11258 (BNL-50203, pp 242-54)
effects on plant cells in relation to target theory, review of, 25:10977
effects on proximal heterochromatin of chromosome three in Drosophila melanogaster, 25:11012
effects on random mating population of corn, effects of mass selection and seed exposure on, 25:11009(R) (COO-1512-22)
effects on rare earth-doped silica, electron traps induced in, (E), 25:11967
effects on reflex response of peripheral systems to simultaneous stimulation of mechanoreceptors in different visceral organs of cats, 25:11282
effects on resistance and longevity of ants, effects of 1000 to 150,000 rad doses on, 25:11245
effects on respiration in organs of embryos, protective effects of cysteamine against, 25:11096(R) (EUR-4491)
effects on sarcoma cells in rats in vitro, effects of dose fractionation on, 25:11240 (BNL-50203, pp 339-52)
effects on sedimentation rate of DNA in Bacillus subtilis, effects of dose on, 25:10960 (BNL-50203, pp 82-90)

XUM

effects on sodium chloride crystals, hardening, 25:11975
effects on spermatogenesis in mice, mechanisms for depletion and recovery from, 25:11276
effects on stored human blood, low dose hemolytic, 25:10981
effects on survival of bacteria, mammalian cells, and yeast, effects of DNA on, 25:10960 (BNL-50203, pp 82-90)
effects on survival of Chinese hamster cells, effects of dactinomycin on lethal, 25:11097
effects on survival of fish, effects of time of injection and temperature on protective effects of cysteamine against, 25:11292
effects on swine, use of callicrein for treatment of chronic dermatitis following, 25:11110
effects on synthesis of DNA in salivary glands of Drosophila larvae, 25:11246
effects on thyroid gland of animals, review of, 25:11291
effects on tissues of mammalian eyes, effects of dose on acute pathological, 25:11284
effects on tumor production by Agrobacterium tumefaciens in Jerusalem artichokes, inhibitory, 25:11306
effects on tumor proliferation in fibroblastic cells, effects of density of cell population on, 25:11274
effects on zygotes of Drosophila, tumorgenic, 25:11250
emission during solar flares, anisotropy and polarization of, (E), 25:11623
emission from coronal plasmas, simplified thermal continuum function for, (T), 25:11632
emission from T-Tauri stars, (T), 25:11548
emission from transition metals in meteorites, gas proportional counting of, (E), 25:11539
fluorescence in upper atmosphere, photoelectric-ionized solar-stimulated, (E/T), 25:11790
intensity of cosmic, the galactic plane, (T), 25:11747
intensity variations of solar hard, deduced from ionospheric radio absorption, (E), 25:11817
pulsations during pulsating aurorae, positive correlation to auroral 5577 O I intensity, quasiperiodic, (E), 25:11808
use as research tool in plant physiology, review of, 25:10977
use for therapy of hemangiomas of liver of man, 25:11235
use for therapy of tumors in mammals, effects of dose fractionation and oxygen on, 25:11220 (BNL-50203, pp 234-41)

X-RAY-DIFFRACTION ANALYSIS
research progress on, 25:10437 (ORNL-4636, pp 45-50)

X-RAY EQUIPMENT
protection of veterinary medical personnel against, recommendations for, 25:11075 (NCRP-36)

X-RAY FLUORESCENCE ANALYSIS
correction of matrix effects in, 25:10447
sensitivity of, using Ross filters for energy selection, 25:10479

X-RAY SPECTROMETERS
development of lithium-drifted silicon, 25:10812 (CEA-N-1401)

X-RAY SPECTROSCOPY
development of radioisotope, for quality and process control in industry, 25:10443

XENON
electron elastic scattering by, calculation of differential cross sections for, using potential-scattering model, 25:11722
plasma of, infrared diagnostics behind shock fronts, 25:11868(T) (SC-T-70-4054)
scattering by platinum (111) surfaces at thermal energies, (E), 25:11683

XENON IONS
implantation into silicon at 50 to 300 keV, sputtering and strain induced by, 25:11959

XENON ISOTOPES Xe-126
energy levels from iodine-126 beta decay, (E), 25:12515 (COO-1746-51)
energy-level transitions from iodine-126 beta decay, γ--γ angular correlations and E2/M1 mixing ratios for, (E), 25:12515 (COO-1746-51)

XENON ISOTOPES Xe-128
energy level of, transition probability of first-excited, (E), 25:12560

XENON ISOTOPES Xe-129
energy levels from nuclear resonance fluorescence, lifetimes for, (E), 25:12583
energy-level transitions from nuclear resonance fluorescence, multipolarities and probabilities for E2 and M1, (E), 25:12583
photon resonant scattering at 318 and 411 keV, cross sections for, (E), 25:12583

XENON ISOTOPES Xe-130
energy level at 536 keV, lifetime and transition probability for, (E), 25:12560

XENON ISOTOPES Xe-131
energy levels from nuclear resonance fluorescence, lifetimes for, (E), 25:12583
energy-level transitions from nuclear resonance fluorescence, multipolarities and probabilities for E2 and M1, (E), 25:12583
photon resonant scattering at 364, 637, and 723 keV, cross sections for, (E), 25:12583

XENON ISOTOPES Xe-132
energy level of, transition probability of first-excited, (E), 25:12560

XENON ISOTOPES Xe-133
clearance from cat muscle in comparison to directy measured venous blood circulation, 25:11136
diffusion through activated charcoal adsorber beds, dispersion model to characterize time-dependent, 25:10582
effectiveness for determining arterial insufficiency in human legs in comparison to arteriography, 25:11139
effectiveness for measuring blood flow in muscle tissue following intraarterial injection, method for, 25:11137
effectiveness for scanning cerebral blood flow for diagnosis of brain diseases in man, 25:11144
effectiveness for scanning of blood flow in lower extremities of man, evaluation of, 25:11138
effectiveness for scanning of pulmonary circulation in man, 25:11125
effectiveness for studying effects of vasoactive drugs on muscles in man, evaluation of, 25:10914
use for determining blood flow in human muscles for assessment of circulatory system, 25:11123
use for determining drug effectiveness for cerebral blood flow in patients with Parkinsons disease, 25:11147
use for determining renal blood flow in hypertensive patients, 25:11158
use for evaluating peripheral blood flow, development of clearance method for, in combination with iodine-131, 25:10912
use for measurement of blood flow in muscles during work, development of method for, 25:10913
use for measuring cerebral blood flow in man following intraarterial injection, evaluation of method with eight detectors in comparison to sixteen detectors, 25:11143
use for scanning cerebral blood flow in conscious rabbits, methods for, 25:11194

XENON ISOTOPES Xe-136
energy level from iodine-136 beta decay, lifetime of isomeric, (E), 25:12572
energy levels from iodine-136 beta decay, spin--parity assignments for, (E), 25:12572
energy-level transitions from iodine-136 beta decay, intensities of, (E), 25:12572

p-XYLENE
polymers, analysis for chlorine by thermal neutron activation and γ spectrometry, molecular weight of α-lin-poly-p-xylylene from, 25:10512

Y

YTTERBIUM
determination of trace amounts of, in biotite and tektite by spark source mass spectrometry, 25:10455
determination of trace amounts of, in rocks, quantometer for spectroscopic, 25:10451
energy-level transitions in, rates of Auger and x-ray, (T), 25:11685

YTTERBIUM ALLOYS AND SYSTEMS
Eu--Yb-base, magnetic properties, 25:12913

YTTERBIUM ISOTOPES Yb-168
energy levels from thulium-169 (p,2nγ) and (d,3nγ) reactions at 16 to 21 MeV, rotational, (E/T), 25:12544
energy-level transitions from production in (α,3n) and (α,4n) reactions at 42 MeV, intensities and angular distributions from, (E/T), 25:12553
energy-level transitions from thulium-169 (p,2nγ) and (d,3nγ) reactions at 16 to 21 MeV, probabilities for, (E/T), 25:12544
energy-level transitions in, effect of higher-order deformations on EO, (T), 25:12584
moment of inertia as function of excitation energy, (E/T), 25:12544

YTTERBIUM ISOTOPES Yb-170
energy levels of, M1 transition probabilities for spin-vibrational, (T), 25:12703

YTTERBIUM ISOTOPES Yb-176
alpha inelastic scattering at 27.5 to 32.5 MeV, α spectra and angular distributions for, (E), 25:12605
energy levels from alpha inelastic scattering, deformation parameters for, (E), 25:12605

YTTRIUM
book: Chemistry of Rare Earths and Various Other Elements, in Russian, 25:10580
complexes with EDTA, separation by ion exchange, effects of resin crosslinking on, 25:10665 (INR-P-1209)
determination of trace amounts of, in biotite and tektite by spark source mass spectrometry, 25:10455
determination of trace amounts of, in phosphate deposits by spark source mass spectrometry, 25:10456
determination of trace amounts of, in rocks, quantometer for spectroscopic, 25:10451
determination of trace amounts of, in standard bauxite, carbonate, and silicate rocks by x-ray fluorescence, 25:10449
friction and wear of, sliding against iron ring under vacuum, 25:11413
separation from aqueous solutions by solvent extraction using bis(2,2-dimethylhexyl) phosphate, 25:10679
separation from erbium and holmium in hydrochloric or

nitric acid solutions by solvent extraction using DEHPA, 25:10685
YTTRIUM BORIDES
properties of electron-emission cathodes of, for accelerator electron sources, 25:12316
YTTRIUM FLUORIDES
reactions in, emf measurements of solid-state displacement, 25:11473(R) (AD-708712)
YTTRIUM ISOTOPES Y-88
half-life of, 25:10491 (ORNL-4636, pp 20-33)
YTTRIUM ISOTOPES Y-89
deuteron reactions (d,p) up to 27 MeV, excitation function and isomeric cross-section ratio for, (E), 25:12428 (CNEA-278)
photon inelastic scattering at 12 to 30 MeV, differential cross sections for, (E), 25:12463
proton reactions (p,2n) at 10 to 15 MeV, cross section and threshold energy for, (E), 25:12607
proton reactions at 240 MeV, cross sections for spallation products from, (T), 25:12439
YTTRIUM ISOTOPES Y-90
effects on chromosomes of Crepis capillaris seedlings following incorporation, aberrant, 25:11013
effects on yield of corn, lettuce, and wheat crops, 25:10936 (UCB-34-P-23-15)
use in 4-π exposure chamber for standardization of thermoluminescent dosimeters, 25:10936 (UCB-34-P-23-15)
Sr-90--Y-90, performance of beta sources of, for determining particle size of solid aggregates, 25:10784
YTTRIUM ISOTOPES Y-97
beta decay of, beta and gamma spectra, half-life, log ft, and Q-value for, (E), 25:12462
YTTRIUM ISOTOPES Y-99
half-life, (E), 25:12462
YTTRIUM NITRIDES
thermal capacity at low temperatures, 25:11980 (CEA-R-4113)
UN--YN-base, thermal capacity at low temperatures, 25:11980 (CEA-R-4113)
YTTRIUM OXIDES
properties of electron-beam-evaporated thin films of, dielectric and electric, 25:12031
YUGOSLAVIA
radiation protection programs in, for critical assemblies, 25:11083

Z

ZINC
content with copper in Czech mineral deposits, gamma--gamma well logging method for determining, 25:10693
determination as impurity in fuel materials by emission spectroscopy, 25:10432 (KFK-1261)
determination in seawater by atomic absorption spectrophotometry or neutron activation, 25:10428
determination in sedimentary rocks by direct-reading spectrometry, 25:10450
determination in serum and urine by flameless atomic absorption spectroscopy, 25:10464
determination of trace amounts of, in biotite and tektite by spark source mass spectrometry, 25:10455
determination of trace amounts of, in molybdenum, review on, 25:10459
determination of trace amounts of, in phosphate deposits by spark source mass spectrometry, 25:10456
determination of trace amounts of, in rocks and sand by thermal neutron activation, ion exchange, and γ spectrometry, 25:10492
determination of trace amounts of, in rocks, quantometer for spectroscopic, 25:10451
determination of trace amounts of, in standard bauxite, carbonate, and silicate rocks by x-ray fluorescence, 25:10449
determination of trace amounts of, in standard rocks by borate fusion, dissolution in EDTA, ion exchange, and atomic absorption spectrophotometry, 25:10671
distribution coefficient in mixtures of acetone, hydrochloric acid, and methanol, 25:10681
energy-level transitions in, rates of Auger and x-ray, (T), 25:11685
friction and wear of, sliding against copper and iron rings under vacuum, 25:11413
mineralization of lead and, in Horni Benesov ore deposit, gamma--gamma logging method for determination of, 25:10722
separation from cobalt, copper, and indium by gas chromatography using aluminum chloride eluent, 25:10666 (JINR-P6-5410)
separation of neptunium from, by ion exchange in tetramethylammonium hydroxide--citrate solutions, effects of complexing agents on, 25:10655 (ANL-7751)
use of zinc-69-labeled zinc chloride to study biological fate of, 25:11204
ZINC ALLOYS AND SYSTEMS
Cd--Zn-base, texture of ingot of, solidified from flowing liquid, 25:11450
Cu-base--Zn, creep of, effects of microstructure on, 25:11434(R) (SU-326-P-17-X-1)
Cu-base--Zn, plastic stability of, effects of zinc-induced defect structure on, 25:11373(R) (COO-2048-1)
ZINC CHLORIDES
use of metastable zinc-69-labeled, to determine dosimetry, for scanning prostate glands, and to study biological fate of zinc in dogs, 25:11204
ZINC ISOTOPES Zn-62
production from natural copper (d,x) reactions at 5 to 40 MeV, excitation functions for, 25:12438
ZINC ISOTOPES Zn-63
production from natural copper (d,x) reactions at 5 to 40 MeV, excitation functions for, 25:12438
ZINC ISOTOPES Zn-64
boron-11 reactions (B-11,p) and (B-11,α) at 49 and 88 MeV, protbn and α angular distributions and energy spectra from bromine-75 compound nucleus in, (E), 25:12461
ZINC ISOTOPES Zn-65
incorporation in fungus mycelium for arthropod food chain studies in soil, 25:10929
production from natural copper (d,x) reactions at 5 to 40 MeV, excitation functions for, 25:12438
ZINC ISOTOPES Zn-66
energy levels from photon scattering, radiation widths for, (E), 25:12447
ZINC ISOTOPES Zn-67
alpha inelastic scattering at 21 MeV, spin dependence in, (E), 25:12454
deuteron inelastic scattering at 14 MeV, spin dependence in, (E), 25:12454
helium-3 inelastic scattering at 21 MeV, spin dependence in, (E), 25:12454
ZINC ISOTOPES Zn-69
use of zinc chloride-incorporated metastable, for scanning prostate gland, to determine dosimetry, and to study biological fate of zinc in dogs, 25:11204
ZINC NEODYMIUM NITRATES
temperature scale below 1°K for $Nd_2Zn_3(NO_3)_{12}.24H_2O$ single crystals, gamma-ray anisotropic, 25:11852
ZINC OXIDES
B_2O_3--ZnO--ZnS, phase studies of, 25:11526
ZINC SULFIDES
B_2O_3--ZnO--ZnS, phase studies of, 25:11526
ZION POWER REACTOR, UNIT 1
containment structure for, information on liner bulge in, 25:12743 (DOCKET-50295-23)
containment structures for, correction of voids at concrete--buttress plate joint of, 25:12742 (DOCKET-50295-22)
ZION POWER REACTOR, UNIT 2
containment structure for, information on liner bulge in, 25:12743 (DOCKET-50295-23)
containment structures for, correction of voids at concrete--buttress plate joint of, 25:12742 (DOCKET-50295-22)
ZIRCALOY
analysis for trace amounts of nitrogen using thymol, spectrophotometric, 25:10442
corrosion of water reactor in-core components of, review on, 25:11343 (AECL-3778)
cracking of, 25:10583(R) (AECL-3776)
ZIRCALOY-2
analysis for impurities, carrier distillation method for spectrographic, 25:10430 (EUR-4541)
analysis for trace amounts of nitrogen using thymol, spectrophotometric, 25:10442
corrosion by hot pressurized water, effects of prior corrosion history on, 25:11349 (WAPD-TM-906)
corrosion by steam at 980 to 1340°C, 25:11463 (IN-1437, pp 70-5)
fracture toughness of, effects of deformation-induced twinning on, 25:11474(R) (BNWL-842)
radiation effects on corrosion and mechanical properties of, in-pile, 25:12862 (JAERI-Memo-4192)
radiation effects on creep at 300°C, in-pile, 25:11474(R) (BNWL-842)
sorptive properties for hydrogen in hot pressurized water, effects of prior corrosion history on, 25:11349 (WAPD-TM-906)
ZIRCALOY-3
corrosion by organic reactor coolants, review on, 25:11343 (AECL-3778)
ZIRCALOY-4
corrosion by organic reactor coolants, review on, 25:11343 (AECL-3778)
stability of oxide fuel cladding of, in up-power reactor transients, 25:11534 (WAPD-TM-979)
ZIRCONIUM
alpha reactions at 30 to 80 MeV, cross sections for production of K x rays by, (E), 25:12488
analysis for impurities, carrier distillation method for spectrographic, 25:10430 (EUR-4541)
analysis for trace amounts of nitrogen using thymol, spectrophotometric, 25:10442
creep behavior at 50 to 840°C, uniaxial tensile, 25:11414
determination by photon activation, reactions and sensitivities for, 25:10488 (CEA-R-4072)
determination in binary aluminum alloys, x-ray fluorescent, 25:10441
determination of trace amounts of, in biotite and tektite by spark source mass spectrometry, 25:10455

determination of trace amounts of, in rocks and sand by thermal neutron activation, ion exchange, and γ spectrometry, 25:10492
determination of trace amounts of, in standard bauxite, carbonate, and silicate rocks by x-ray fluorescence, 25:10449
diffusion in niobium at 800 to 1600°C, x-ray spectral study of, 25:11424
enthalpy of solution in liquid plutonium, 25:11386
friction and wear of, sliding against copper and iron rings under vacuum, 25:11413
oxidation by plasma anodization, 25:10583(R) (AECL-3776)
oxidation of, x-ray analysis of films formed in, 25:10583(R) (AECL-3776)
phonon dispersion relations in [0001] and [01 anti 10] symmetry directions, coherent inelastic neutron scattering study of, 25:12026
radiation effects on high-pressure polymorphs of, fast neutron, 25:11474(R) (BNWL-842)
reactions with tantalum silicide coating, 25:11519
separation from hafnium by fractional crystallization of potassium hexafluorozirconate, 25:10676
separation from hafnium by solvent extraction using tributyl phosphate, 25:10689
separation from ores by solvent extraction, review on, 25:10656 (BM-IC-8502)

ZIRCONIUM ALLOYS AND SYSTEMS
corrosion of, effects of hydrogen diffusion on, 25:11343 (AECL-3778)
oxidation by molten salts, 25:10583(R) (AECL-3776)
oxidation by plasma anodization, 25:10583(R) (AECL-3776)
radiation effects on corrosion by water, in-pile, 25:11474(R) (BNWL-842)
radiation effects on hardness of, 25:10583(R) (AECL-3776)
Cr--Cu--Zr-base, phase transformations in, effects of continuous cooling on, 25:11432 (CEA-N-1310)
Cu--Mo--Zr-base, phase transformations in, effects of continuous cooling on, 25:11432 (CEA-N-1310)
Cu--Ni--Zr-base, phase transformations in, effects of continuous cooling on, 25:11432 (CEA-N-1310)
Cu--Zr-base, phase transformations in β phase of, effects of continuous cooling on, 25:11432 (CEA-N-1310)
Nb--U-base--Zr, corrosion by moisture, stress, 25:11345 (AWRE-O-49/66)
Nb--U-base--Zr, welding behavior of, electron beam, 25:11377 (MLM-1778)
Nb--Zr, superconducting ac hysteresis losses in wires of, suppression by longitudinal magnetic field, 25:11823
Nb--Zr-base, radiation effects on creep at 300°C, in-pile, 25:11474(R) (BNWL-842)
Pu--Ti--Zr-base, electric conductivity of, 25:12004
Pu--U--Zr, phase diagrams at 500 to 700°C, isothermal, 25:11442
Pu--Zr, phase diagram of arc cast and heat treated, 25:11439
Pu--Zr-base, electric conductivity of, 25:12004
Pu--Zr-base, plutonium distribution in dilute, effects of β and α phase transformation and oxygen content on, 25:11431 (CEA-CONF-1691)
Pu--Zr-base, transformation processes in dilute, segregation during martensitic, 25:11430 (CEA-CONF-1688)
T--Zr, preparation of gas-free radiation targets of, method for, 25:10775 (KFKI-70-26-HP)
Th--U--Zr, radiation effects on tube-type fuel elements of, in-pile, 25:11474(R) (BNWL-842)

ZIRCONIUM CARBIDES
electron band structure of ZrC, theory, 25:12024
properties of, relation of band structure to electric, magnetic, and thermoelectric, 25:12024
graphite--ZrC, thermal expansion of extruded composites of, to 2500°C, 25:11512

ZIRCONIUM CITRATES
effects on blood pressure, heart rate, and respiration in whole-body γ-irradiated rabbits, effects of synchronous calcium gluconate administration on, 25:11289

ZIRCONIUM DEUTERIDES
electric properties at 1 to 410°K, 25:12020

ZIRCONIUM HYDRIDES
electric properties at 1 to 410°K, 25:12020
preparation of, methods for, 25:11375 (IN-1437, pp 24-59)

ZIRCONIUM ISOTOPES
deuteron reactions (d,p) with, charge exchange effects and spectroscopic factors in, (E), 25:12571
proton reactions (p,d) with, charge exchange effects and spectroscopic factors in, (E), 25:12571

ZIRCONIUM ISOTOPES Zr-88
mass excess of, determination from (p,2n) threshold measurements, (E), 25:12607

ZIRCONIUM ISOTOPES Zr-90
energy levels of, double gamma emission from first-excited, (E), 25:12495
energy levels of, particle-hole interactions in, (T), 25:11888
helium-3 reactions (He-3,d) at 18 MeV, deuteron spectra and angular distributions for, (E), 25:12613
proton elastic scattering at 10 to 60 MeV, local Woods--Saxon potentials equivalent to nonlocal analysis including exchange effects in, (T), 25:12689
proton inelastic scattering by, microscopic first-order core polarization corrections to DWBA for, (T), 25:12678

ZIRCONIUM ISOTOPES Zr-94
proton elastic and inelastic scattering at 6 to 8.5 MeV, angular distributions and excitation functions for, (E), 25:12564

ZIRCONIUM ISOTOPES Zr-95
content of crops in Utah during May and June 1966, relation of, to fallout from May 9 Chinese atmospheric nuclear explosion, 25:10999
energy levels of, spin-parity assignments for isobaric analog, (E), 25:12564
separation of plutonium from, by ion exchange on zirconium phosphate silicate columns, 25:10677

ZIRCONIUM ISOTOPES Zr-97
energy levels of, spin and parity of, (E), 25:12462

ZIRCONIUM ISOTOPES Zr-99
beta decay of, beta and gamma spectra, half-life, log ft, and Q-value for, (E), 25:12462

ZIRCONIUM ISOTOPES Zr-100
half-life, (E), 25:12462

ZIRCONIUM ISOTOPES Zr-101
beta decay of, beta and gamma spectra, half-life, log ft, and Q-value for, (E), 25:12462

ZIRCONIUM OXIDES
analysis for hafnium, spectrographic, 25:10431 (IEA-208)

ZIRCONIUM PHOSPHATE SILICATES
sorptive properties for plutonium in presence of niobium-95, ruthenium-106, and zirconium-95, 25:10677

ZIRCONS
age of, effects of geometry factor on accuracy of fission track, (E), 25:10655
uranium leaching from, using acetic, hydrochloric, nitric, and sulfuric acids, 25:10723

ZYGOTES
radioinduced tumors in, of Drosophila, x, 25:11250

REPORT NUMBER INDEX

Reports, conference papers and proceedings, numbered translations, and patents are included in this index. Each item is listed by report number; this is followed by the abstract number and a brief notation regarding public availability. The index entries show which reports are on file in the institutions listed on the back of the front cover (Dep.), which reports have been published in open-literature journals (journal citation), and which reports can be purchased (source and price). Whenever a report is identified by more than one number, the availability is given under the primary number, and a cross reference is given under the secondary report number.

The report number codes apply to USAEC reports unless designated otherwise. Non-USAEC reports are identified by parenthetical notes after the report codes; e.g., (non-AEC), (British), (Canadian), (French). The note (Misc.) identifies the codes used for both USAEC and non-USAEC reports. Patents are listed under the heading "PATENTS"; the country of origin is included in parentheses.

A comprehensive list of both USAEC and non-USAEC report codes is contained in the latest revision of TID-85, *Report Number Series Used by the Division of Technical Information in Cataloging Reports.* This information is also included in the Cumulative Report Number Index (issued annually).

Availability of USAEC Reports

All USAEC Reports abstracted in *Nuclear Science Abstracts* are available through one or more of the following sources:

(1) University and public libraries in the United States. A list of these organizations appears on the inside front cover of each issue of *NSA*.

(2) NCR Microcard Editions in Microcard and micronegative form. Orders and inquiries should be sent to: Order Processing Department, 365 South Oak Street, West Salem, Wisconsin 54669.

(3) National Technical Information Service, U. S. Department of Commerce, Springfield, Virginia 22151.

(4) Superintendent of Documents, U. S. Government Printing Office, Washington, D. C. 20402.

(5) National Cash Register Co., P. O. Box 3111, Oak Ridge, Tenn. 37830, in micronegative form. Purchase details available on request.

Availability of Non-USAEC Reports

U. S. Reports. Reports of U. S. Government agencies are available to the public from the National Technical Information Service (NTIS). If specific availability is not shown, inquiries may be directed to NTIS.

Non-U. S. Reports. Reports of atomic energy organizations of other countries are available from NTIS for U. S. sale only. Specific availability in the country of origin is shown, when known, at the report number entry. Otherwise, inquiries should be made to the organizations listed below:

AUSTRALIA

Australian Atomic Energy Commission Research Establishment. Available upon request from the Library, Australian Atomic Research Establishment, Private Mail Bag, Sutherland, New South Wales, Australia.

BELGIUM

Centre d'Étude de l'Energie Nucléaire. Available upon request to individuals and organizations from the Centre d'Etude de l'Energie Nucléaire (C.E.N.), Studiecentrum voor Kernenergie (S.C.K.), Technical Information Dept., MOL-DONK (Belgium).

CERN

CERN European Organization for Nuclear Research. Available without charge from CERN European Organization for Nuclear Research, Geneva 23, Switzerland. Copies are deposited in libraries throughout the world.

FRANCE

Commissariat à l'Energie Atomique. Inquiries for reports numbered 1-2199 should be addressed to Service Central de Documentation du C.E.A., Centre d'Etudes Nucléaires de Saclay, Boîte postale n° 2, 91. GIF-sur-YVETTE, FRANCE. Reports numbered 2200 and above are available from La Documentation Française, 31 quai Voltaire, 75, PARIS (7e), FRANCE.

Service Central de Protection contre les Rayonnements Ionisants. Copies are available from Ministère de la Santé Publique, Service Central de Protection contre les Rayonnements Ionisants, B.P. n° 78 Le Vesinet (France) Telex 25667.

GERMANY

Deutsches Elektronen-Synchrotron DESY. Copies are available from Deutsches Elektronen-Synchrotron DESY, Dokumentation, 2000 Hamburg 52, Notkestieg 1, Germany.

Gesellschaft für Kernforschung mbH (KFK). Copies are available from Gesellschaft für Kernforschung mbH, 75 Karlsruhe, Postfach 947, Germany. Copies are also deposited in many national nuclear centers in the world.

Kernforschungsanlage. Copies may be ordered from Zentralbibliothek der Kernforschungsanlage Jülich, Jülich, Bundesrepublik Deutschland.

Hahn-Meitner-Institute für Kernforschung. Available without charge from Hahn-Meitner-Institute für Kernforschung Ber-

XUM

lin, Bibliothek, Glienicker Strasse 100, 1 Berlin 39, Germany. Copies are deposited in many national nuclear centers in the world.

Johann-Wolfgang-Goethe Universität, Frankfurt Am Main, Institut für Kernphysik, (IKF). Copies are available from Gmelin Institut, 40–42 Varrentrappstrasse, Frankfurt (Main), West Germany.

ISRAEL

Israel Atomic Energy Commission. Available without charge from Israel Atomic Energy Commission, Soreq Nuclear Research Centre, Yavne, Israel.

ITALY

Centro Informazioni Studi Esperienze (CISE). For sale at CISE Press Office, Casella Postale 3986, Milano, Italy. Copies are deposited in the libraries of various nuclear centers in Italy and abroad.

Comitato Nazionale per l'Energia Nucleare. Copies are available from Comitato Nazionale per l'Energia Nucleare, Divisione Affari Internazionali e Studi Economici, Ufficio Pubblicazioni, Via Belisario, 15, Roma, Italy.

JAPAN

Japan Atomic Energy Research Institute (JAERI). Available from the Staff Supply Cooperative of Japan Atomic Energy Research Institute (JAERI), Tokai-mura, Naka-gun, Ibaraki-ken, Japan. Copies are deposited in depositories in Tokyo, Nagoya, and Osaka.

Nagoya University. Copies are available from Research Information Center, Institute of Plasma Physics, Nagoya University, Nagoya, Japan.

University of Tokyo. Available free of charge from Institute for Nuclear Study, University of Tokyo, Tanashi-Machi, Kitatama-gun, Tokyo, Japan.

NETHERLANDS

Reactor Centrum Nederland. For sale by Reactor Centrum Nederland, 112 Scheveningseweg, 's-Gravenhage, The Netherlands. Copies are deposited in university libraries in Holland and in many national nuclear centers in the world.

NEW ZEALAND

Institute of Nuclear Sciences. Copies are available from Librarian, N. Z. Institute of Nuclear Sciences, D.S.I.R., Private Bag, Lower Hutt, New Zealand. Copies are deposited in other countries.

PAKISTAN

Atomic Energy Center. Copies are available from Atomic Energy Center, P. O. Box 658, Lahore, (West Pakistan).

POLAND

Reports of the Polish nuclear institutes are published by the Nuclear Energy Information Center of the Government Commissioner for Use of Nuclear Energy. Copies are available free of charge from Nuclear Energy Information Center, Palace of Culture and Science, Warsaw, Poland.

SPAIN

Junta de Energia Nuclear. "JEN" reports are available without charge from Servicio de Documentation, Junta de Energia Nuclear, Ciudad Universitaria, Madrid (3), España.

SWITZERLAND

Eidgenössisches Institut für Reaktorforschung. "EIR" reports are available from Eidgenössisches Institut für Reaktorforschung, c/o Bibliothek, 5303 Würenlingen/Switzerland.

TURKEY

Turkish Atomic Energy Commission. Copies are available free of charge from T.A.E.C., Çekmece Nuclear Research Center, P. O. Box 1, Airport, Istanbul, Turkey.

Conferences

Published conference proceedings as well as individual unpublished papers from conferences are included in this index. A CONF number is assigned to the conference if published proceedings are received and also if only a single paper is received. The base number used is year-month-sequence. Thus, the number CONF-650101 indicates that the conference was held in 1965, in January, and that this was the first January 1965 conference so received. This number would be assigned to complete published proceedings. If individual papers are received, the base number is extended to include a paper number, e.g., CONF-650101-1. As additional papers are received, they will be assigned consecutive numbers in the series, CONF-650101-1, CONF-650101-2, etc. This numbering system ensures that all papers received from a conference will be associated with that conference in this index.

If published proceedings are received after the receipt of individual papers, the complete proceedings will be abstracted and the abstract number will appear in this index with the base CONF number.

Abbreviations Used in Availability Column

AECL Reports of the Atomic Energy of Canada Limited are for sale by the Scientific Document Distribution Office, Atomic Energy of Canada Limited, Chalk River, Ontario, Canada.

CFSTI See NTIS

DENM Reports of the Atomic Energy Commission Research Establishment, Risö, are available on exchange from the Library, Danish Atomic Energy Commission, Risö, Roskilde, Denmark. Also for sale at the price shown from Jul. Gjellerup, Booksellers, 87 Sölvgade, Kobenhavn K., Denmark.

Reports of Danatom are available on loan from Research Establishment, Risö, Roskilde, Denmark. Copies are available from Danatom, Aurehojvej 2, Hellerup, Denmark.

Dep. AEC reports so designated are maintained in the organizations listed on the inside front cover of *NSA*. Prior to July 1, 1965, reports were deposited either in printed copy form or in microform. After that time, all reports have been in the form of micronegatives.

Reports from other countries so designated are available in the United States at the organizations listed on the inside front cover of *NSA*.

DTIE — Available from the U. S. Atomic Energy Commission, Division of Technical Information Extension, P. O. Box 62, Oak Ridge, Tennessee 37830. (Conference papers are available on loan only.)

EM — Blueprints of AEC engineering drawings are available from NTIS, U. S. Department of Commerce, Springfield, Virginia 22151. Current prices of the CAPE-packages may be obtained from this address. TID-4100, available from the Division of Technical Information Extension, P. O. Box 62, Oak Ridge, Tennessee 37830, contains information on all the CAPE-packages for sale.

EUR — For sale by Centrale de vente des publications des Communautés européennes 37, rue Glesener-Luxembourg.

GPO — For sale by the Superintendent of Documents, Government Printing Office, Washington, D. C. 20402.

IAEA — Available from the International Atomic Energy Agency, Vienna, Austria, and from its sales agencies in various countries throughout the world. A list of these agencies is found in each STI/DOC and STI/PUB publication.

NORW — Reports from Forsvarets Forskningsinstitutt are available from Norwegian Defense Research Establishment, Library, P. O. Box 25, Kjeller, Norway.
"KR" reports are available on an exchange basis from the Library, Institutt for Atomenergi, Box 40, Kjeller, Norway.
Reports of the Norwegian Reactor School are available from the Library, Institutt for Atomenergi, P. O. Box 40, Kjeller, Norway.

NRC — For sale by the National Research Council of Canada, Ottawa, Ontario, Canada.

NTIS — For sale by the National Technical Information Service (NTIS), U. S. Department of Commerce, Springfield, Virginia 22151 at the following prices for eye legible copy:

1–300 pages	$3.00
301–600 pages	$6.00
601–900 pages	$9.00

Documents over 900 pages have special prices which may be obtained from NTIS. Microfiche copy of each separately bound document can be purchased for $0.95.
Reports issued by organizations outside the United States will be sold by NTIS *only to purchasers within the United States.*
Purchasers outside the United States may acquire such reports from the sources described elsewhere in these columns.

OECD — Available from O. E. C. D., Publications 2, rue, André-Pascal, 75 Paris 16e, France, and from its sales agencies in various countries throughout the world. A list of these agencies is found in each OECD publication.

SWED — "AE" reports are for sale from Aktiebolaget Atomenergi, Library Section, Box 43041, Stockholm 43, Sweden. Microcopy of these reports is available from the International Documentation Center, Tumba, Sweden.
Reports of the VDDIT-series may be obtained from Aktiebolaget Atomenergi, Information Office, Scientific and Technical Information, Box 43041, Stockholm 43, Sweden.
Other series are not generally available to the public. Organizations in the Atomic Energy field may obtain copies from Aktiebolaget Atomenergi.

UK — United Kingdom Atomic Energy Authority reports generally may be purchased from Her Majesty's Stationery Office, P. O. Box 569, London S.E.1. Copies of many UKAEA reports (particularly earlier ones) may be purchased in microcopy form from Micro Methods Ltd., East Ardsley, Wakefield, Yorkshire, England. Copies of UKAEA reports are deposited with the National Lending Library for Science and Technology and 10 public libraries in England; with the USAEC and (through USAEC) with NTIS; and in most national nuclear centers throughout the world. In the USA, UKAEA reports are available on a subscription basis, by subject category, from UNIPUB, Inc., P. O. Box 433, New York, N. Y. 10016, USA.

UN — Mail orders should be directed to the Sales Section, Room 1059, United Nations Headquarters, New York, New York 10017.

ZAED — Available from Zentralstelle für Atomkernenergie Dokumentation, 6000 Frankfurt/Main 90, P. O. Box 901069, Westendstr. 21, West Germany

Report No.	Abstract No.	Availability
ABCC-		
68-69	25-11237	Dep. NTIS, 440p.
AD-	(Misc.)	
705976	25-11251	NTIS, 14p.
708495	25-11776	NTIS, 18p.
708496	25-11777	NTIS, 19p.
708558	25-10702	NTIS, 71p.
708566	25-10733	NTIS, 20p.
708567	25-10734	NTIS, 21p.
708705	25-11472	NTIS, 129p.
708712	25-11473	NTIS, 67p.
708922	25-10807	NTIS, 160p.
709105	25-11778	NTIS, 15p.
709142	25-10765	NTIS, 64p.
710383	25-12376	NTIS, 32p.
710572	25-12162	NTIS, 6p.
AECL-	(Canadian)	
3666	25-12427	Dep. CFSTI (U. S. Sales Only). AECL $2.00, 100p.
3671	25-12335	Dep. NTIS (U. S. Sales Only). AECL $1.50, 56p.
3688	25-11368	Dep. NTIS (U. S. Sales Only). AECL $0.50, 19p.
3730	25-12623	Dep. NTIS (U. S. Sales Only). AECL $1.50, 44p.
3732	25-11530	Dep. NTIS (U. S. Sales Only). AECL $1.50, 49p.
3734	25-11454	Dep. NTIS (U. S. Sales Only). AECL $1.00, 33p.
3776	25-10583	Dep. NTIS (U. S. Sales Only). AECL $2.00, 108p.
3777	25-11074	Dep. NTIS (U. S. Sales Only). AECL $1.50, 56p.
3778	25-11343	Dep. NTIS (U. S. Sales Only). AECL $0.50, 24p.
AERE-R-	(British)	
3984	25-10766	Dep. NTIS (U. S. Sales Only), 38p.
4887	25-10513	Dep. NTIS (U. S. Sales Only), 16p.
4913	25-11531	Dep. NTIS (U. S. Sales Only), 36p.
4982	25-11455	Dep. NTIS (U. S. Sales Only), 20p.
5069	25-11052	Dep. NTIS (U. S. Sales Only), 18p.
5173	25-11475	Dep. NTIS (U. S. Sales Only), 26p.
5320	25-10514	Dep. NTIS (U. S. Sales Only), 9p.
5422	25-10891	Dep. NTIS (U. S. Sales Only), 13p.
5561	25-10808	Dep. NTIS (U. S. Sales Only), 4p.
5622	25-11456	Dep. NTIS (U. S. Sales Only), 9p.
5677	25-11532	Dep. NTIS (U. S. Sales Only), 13p.
AFCRL-	(Non-AEC)	
70-257	25-11776	See AD-708495
70-2063	25-11777	See AD-708496
AI-Trans-	(Misc.)	
267	25-11949	Dep. NTIS
ALO-		
2510-T-1	25-11477	Dep. NTIS, 60p.
ANL-		
7645	25-12336	Dep. NTIS, 116p.
7654	25-12337	Dep. NTIS, 74p.
7704	25-10848	Dep. NTIS, 37p.
7725	25-12864	Dep. NTIS, 28p.
7736	25-12794	Dep. NTIS, 63p.
7751	25-10655	Dep. NTIS, 12p.
ANL-EBR-		
25	25-12781	Dep. NTIS, 30p.
ANL-Trans-		
855	25-12509	Dep. NTIS
873	25-12865	Dep. NTIS
ANU-P-	(Australian)	
497	25-12624	Dep. NTIS (U. S. Sales Only), 122p.
AWRE-O-	(British)	
29/67	25-11428	Dep. NTIS (U. S. Sales Only), 17p.
46/66	25-11344	Dep. NTIS (U. S. Sales Only), 11p.
49/66	25-11345	Dep. NTIS (U. S. Sales Only), 18p.
100/66	25-11346	Dep. NTIS (U. S. Sales Only), 15p.
B-	(Misc.)	
2	25-11244	See NP-18607
BARC-	(Non-AEC)	
468	25-10429	Dep. NTIS (U. S. Sales Only), 10p.
506	25-10793	Dep. NTIS (U. S. Sales Only), 22p.
BAW-	(Misc.)	
3867-9(Vol. 1)(Rev.1)	25-12772	Dep. NTIS, 197p.
BDX-		
613-198	25-12866	Dep. NTIS, 17p.
613-213	25-12867	Dep. NTIS, 39p.
BLG-	(Belgian)	
440	25-12796	See EURAEC-2145
442	25-10653	Dep. NTIS (U. S. Sales Only), 25p.
BM-IC-	(Misc.)	
8502	25-10656	
BM-RI-	(Misc.)	
7471	25-10657	
BMBW-FBK-	(West German)	
70-11	25-12704	Dep. NTIS (U. S. Sales Only), 138p.
70-19	25-10472	Dep. NTIS (U. S. Sales Only), 141p.
70-20	25-12767	Dep. NTIS (U. S. Sales Only), 433p.
70-24	25-10767	Dep. NTIS (U. S. Sales Only), 142p.
70-25	25-10592	Dep. NTIS (U. S. Sales Only), 59p.
BMI-	(Misc.)	
171-45	25-10995	Dep. NTIS, 73p.
171-101	25-12868	Dep. NTIS, 5p.
171-102	25-12869	Dep. NTIS, 53p.
171-103	25-12870	Dep. NTIS, 70p.
171-104	25-12871	Dep. NTIS, 60p.
171-105	25-12872	Dep. NTIS, 34p.
171-106	25-12873	Dep. NTIS, 82p.
171-107	25-12874	Dep. NTIS, 21p.
171-108	25-12875	Dep. NTIS, 30p.
171-111	25-12876	Dep. NTIS, 30p.
171-114	25-12877	Dep. NTIS, 79p.
1892	25-11369	Dep. NTIS, 8p.
1893	25-12795	Dep. NTIS, 112p.
BN-	(Misc.)	
7006-3	25-12796	See EURAEC-2145
BNL-		
15438	25-12295	Dep. NTIS, 26p.
15464	25-12296	Dep. NTIS, 70p.
50203	25-11218	Dep. CFSTI, 372p.
BNL-tr-		
366	25-12510	Dep. CFSTI
BNWL-		
842	25-11474	Dep. NTIS, 150p.
843	25-11478	Dep. NTIS, 35p.
1345	25-10691	Dep. NTIS, 288p.
1403	25-12773	Dep. NTIS, 65p.
1457	25-12803	Dep. NTIS, 184p.
1469	25-12878	Dep. NTIS, 19p.
1479	25-12812	Dep. NTIS, 31p.
1525	25-12879	Dep. NTIS, 90p.
1533	25-10658	Dep. NTIS, 32p.
1537	25-10996	Dep. NTIS, 11p.
BNWL-B-		
12	25-11053	Dep. NTIS, 11p.
BNWL-SA-		
3539	25-12880	Dep. NTIS, 14p.
3565	25-10809	Dep. NTIS, 50p.
BRH/DMRE-	(Non-AEC)	
70-5	25-10421	NTIS, 11p.
CALT-		
822-22	25-11819	Dep. NTIS, 4p.
CEA-Bib-	(French)	
185	25-11036	Dep. NTIS (U. S. Sales Only), 63p.
CEA-CONF-	(French)	
1517	25-10930	Dep. CFSTI (U. S. Sales Only), 12p.
1557	25-10931	Dep. CFSTI (U. S. Sales Only), 13p.
1558	25-10932	Dep. CFSTI (U. S. Sales Only), 15p.
1668	25-10810	Dep. NTIS (U. S. Sales Only), 13p.
1670	25-11485	Dep. NTIS (U. S. Sales Only), 17p.
1673	25-12813	Dep. NTIS (U. S. Sales Only), 22p.
1683	25-12782	Dep. NTIS (U. S. Sales Only), 23p.
1685	25-10811	Dep. NTIS (U. S. Sales Only), 21p.
1687	25-11429	Dep. NTIS (U. S. Sales Only), 14p.
1688	25-11430	Dep. NTIS (U. S. Sales Only), 21p.
1689	25-11370	Dep. NTIS (U. S. Sales Only), 15p.
1690	25-11371	Dep. NTIS (U. S. Sales Only), 14p.
1691	25-11431	Dep. NTIS (U. S. Sales Only), 16p.
1694	25-10849	Dep. NTIS (U. S. Sales Only), 26p.
1704	25-11979	Dep. NTIS (U. S. Sales Only), 6p.
CEA-N-	(French)	
1267	25-10659	Dep. NTIS (U. S. Sales Only), 18p.
1310	25-11432	Dep. NTIS (U. S. Sales Only), 23p.
1344(1)	25-12774	Dep. NTIS (U. S. Sales Only), 103p.
1360	25-10752	Dep. NTIS (U. S. Sales Only), 19p.
1363	25-10892	Dep. NTIS (U. S. Sales Only), 57p.
1368	25-12511	Dep. NTIS (U. S. Sales Only), 12p.
1389	25-12297	Dep. NTIS (U. S. Sales Only), 40p.
1395	25-12775	Dep. NTIS (U. S. Sales Only), 57p.
1399	25-11884	Dep. NTIS (U. S. Sales Only), 17p.
1401	25-10812	Dep. NTIS (U. S. Sales Only), 18p.
CEA-R-	(French)	

Report No.	Abstract No.	Availability
3855	25-12034	Dep. NTIS (U. S. Sales Only), 104p.
3937	25-11950	Dep. NTIS (U. S. Sales Only), 160p.
4024	25-11917	Dep. NTIS (U. S. Sales Only), 208p.
4032	25-10473	Dep. NTIS (U. S. Sales Only), 23p.
4051	25-10568	Dep. NTIS (U. S. Sales Only), 80p.
4058	25-11865	Dep. NTIS (U. S. Sales Only), 22p.
4059	25-10728	Dep. NTIS (U. S. Sales Only), 30p.
4068	25-12098	Dep. NTIS (U. S. Sales Only), 133p.
4072	25-10488	Dep. NTIS (U. S. Sales Only), 222p.
4074	25-10569	Dep. NTIS (U. S. Sales Only), 89p.
4081	25-10867	Dep. NTIS (U. S. Sales Only), 29p.
4095	25-11486	Dep. NTIS (U. S. Sales Only), 26p.
4105	25-10729	Dep. NTIS (U. S. Sales Only), 41p.
4113	25-11980	Dep. NTIS (U. S. Sales Only), 153p.
4120	25-10794	Dep. NTIS (U. S. Sales Only), 186p.
CERN-	(European Organization for Nuclear Research)	
70-29	25-12512	Dep. NTIS (U. S. Sales Only), 53p.
CERN-Trans-	(European Organization for Nuclear Research)	
70-7	25-12298	Dep. NTIS (U. S. Sales Only)
CISE-N-	(Italian)	
137	25-12821	For translation see LIB/Trans-335
CISE-R-	(Italian)	
222	25-11347	Dep. NTIS (U. S. Sales Only), 157p.
278	25-11457	Dep. NTIS (U. S. Sales Only), 88p.
CNEA-	(Argentinean)	
266	25-12338	Dep. CFSTI (U. S. Sales Only), 24p.
269	25-12513	Dep. CFSTI (U. S. Sales Only), 11p.
272	25-10795	Dep. NTIS (U. S. Sales Only), 25p.
278	25-12428	Dep. NTIS (U. S. Sales Only), 12p.
CNRS-CPT-	(French)	
70-P-318	25-12245	Dep. NTIS (U. S. Sales Only), 87p.
70-P-336	25-12136	Dep. NTIS (U. S. Sales Only), 131p.
70-P-339	25-12065	Dep. NTIS (U. S. Sales Only), 8p.
CONF-670341-	(Conference on Gas-Metal Reactions in Environments Containing CO_2, London, England, March 1967)	
2	25-11374	See DP-Report-530
CONF-670996-	(5th Conference of the Society of Nuclear Medicine, Vienna, Austria, Sept. 21-23, 1967)	
	25-11118	Nucl.-Med.; 32: Suppl. 7, 1-560(1968)
CONF-680670-	(5th European Conference on Microcirculation, Goteborg, Sweden, June 24-29, 1968)	
	25-11192	Basel; S. Karger AG (1969). 617p. $45.60
CONF-681029-	(National Particle Accelerator Conference, Moscow, U.S.S.R., Oct. 9-16, 1968)	
4	25-12298	See CERN-Trans-70-7
CONF-681205-	(National Conference on Measurement of Elements Occurring in Traces in Rocks, Nancy, France, Dec. 4, 1968)	
	25-10446	Paris; Centre National de la Recherche Scientifique (1970). 466p
CONF-690223-	(Panel on Nuclear Accident Dosimetry Systems, Vienna, Austria, Feb. 17-21, 1969)	
	25-11056	See STI/PUB-241
CONF-690225-	(11th EACRP Meeting, London, England, Feb. 10-14, 1969)	
1	25-12816	See EACRP-L-74
CONF-690447-	(6th Conference of the Temperature Measurements Society, Hawthorne, Calif., Apr. 21-22, 1969)	
1	25-11487	See GA-9168
CONF-690558-	(Conference on Systems With an Infinite Number of Degrees of Freedom, Gif-sur-Yvette, France, May 7-9, 1969)	
	25-12254	Paris; Centre National de la Recherche Scientifique (1970). 200p
CONF-690646-	(Panel on Radiation Sterilization of Biological Tissues For Transplantation, Budapest, Vienna, June 16-20, 1969)	
	25-11327	See STI/PUB-247
CONF-690648-	(Symposium on Classical and Relativistic Magnetohydrodynamics, Lille, France, June 16-20, 1969)	
	25-11759	Paris; Centre National de la Recherche Scientifique (1970). 312p

Report No.	Abstract No.	Availability
CONF-690906-	(1st International Conference on Pressure Vessel Technology, Delft, Netherlands, Sept. 29-Oct. 2, 1969)	
(Pt.3)	25-11357	New York; American Society of Mechanical Engineers (1970). 263p. $20.00
CONF-690915-	(Conference on Time and Dose Relationships in Biology as Applied to Radiotherapy, Carmel, Calif., Sept. 14-19, 1969)	
	25-11218	See BNL-50203
CONF-690968-	(16th Field-Emission Symposium, Pittsburgh, Pa., Sept. 8-14, 1969)	
1	25-12299	See IPP-7/2
CONF-691033-	(8th Eastern Theoretical Physics Conference, Syracuse, N.Y., Oct. 10-11, 1969)	
2	25-12175	See COO-1764-81
CONF-691130-	(5th Japanese Calorimetry Conference, Osaka, Japan, Nov. 20-21, 1969)	
1	25-12916	See UCRL-19115
CONF-700219-	(Conference on Low Energy Spectrometry and Nuclear Spectrometry, Lyon, France, Feb. 18-20, 1970)	
	25-12520	See LYCEN-7034
CONF-700327-	(6th International Colloquium on Plant Analysis and Fertilizer Problems, Tel Aviv, Israel, Mar. 13-17, 1970)	
1	25-10930	See CEA-CONF-1517
CONF-700408-	(2nd Conference on Radiation and Man's Environment, Buck Hill Falls, Pa., Apr. 20-22, 1970)	
3	25-11087	
CONF-700505-	(2nd Congress of the International Radiation Protection Association, Brighton, England, May 3-8, 1970)	
13	25-10931	See CEA-CONF-1557
14	25-10932	See CEA-CONF-1558
CONF-700536-	(12th Meeting on Exploration Techniques Using Radioactive Isotopes, Strasbourg, France, May 22-24, 1970)	
2	25-10810	See CEA-CONF-1668
CONF-700546-	(4th International Conference on Electron and Ion Beam Science and Technology, Los Angeles, Calif., May 10-15, 1970)	
1	25-11356	Dep. NTIS, 33p.
CONF-700547-	(3rd Meeting on the Scientific and Industrial Applications of Nuclear Explosives, Grenoble, France, May 20-22, 1970)	
	25-10738	Bull. Inform. Sci. Tech. (Paris); No. 149, 3-75 (Jun 1970)
	25-10744	Bull. Inform. Sci. Tech. (Paris); No. 150, 3-71 (Jul-Aug 1970)
CONF-700548-	(Symposium on Plasma Diagnostics, Sukhumi, U.S.S.R., May 2-12, 1970)	
1	25-11866	See EUR-CEA-FC-570
CONF-700633-	(Symposium on Thermal Expansion of Solids, Santa Fe, N. Mex., June 10-12, 1970)	
	25-11508	J. Appl. Phys.; 41: 5043-5154(Dec 1970)
CONF-700708-	(6th Interamerican Seminar on Cosmic Rays, La Paz, Bolivia, July 19-24, 1970)	
4	25-11742	See KFKI-70-21-HEP
CONF-700711-	(Meeting of the European-American Committee on Reactor Physics, Richland, Wash., July 7-9, 1970)	
1	25-12782	See CEA-CONF-1683
CONF-700809-	(7th International Congress on Electron Microscopy, Grenoble, France, Aug. 30-Sept. 5, 1970)	
5	25-12903	See ORO-3935-4
CONF-700909-	(Symposium on Survival of Food Crops and Livestock in the Event of Nuclear War, Upton, N. Y., Sept. 15-18, 1970	
3	25-11038	See UCRL-72716(Rev.1)
CONF-700911-	(160th National Meeting of the American Chemical Society, Chicago, Ill., Sept. 14-18, 1970)	
1	25-10664	See DP-MS-70-38
CONF-700928-	(6th Symposium on Fusion Technology, Aachen, Germany, Sept. 22-26, 1970)	
6	25-11919	See EUR-CEA-FC-566
CONF-700933-	(Conference on Hyperfine Interactions Detected by Nuclear Radiation, Rehovot and	

XUM

Report No.	Abstract No.	Availability
		Jerusalem, Israel, Sept. 6-11, 1970)
2	25-12429	See CDO-7-565
CONF-700937-		(Symposium on Hadron Spectroscopy, Balatonfured, Hungary, Sept. 6-11, 1970)
1	25-12068	See SLAC-PUB-842
CONF-700938-		(Fall Meeting of the American Oil Chemists Society, Chicago, Ill., Sept. 27-Oct. 1, 1970)
1	25-12917	See UCRL-72393
CONF-700939-		(International Summer School on Radiation Protection, Dubrovnik, Yugoslavia, Sept. 21-30, 1970)
1	25-10811	See CEA-CONF-1685
CONF-700940-		(International Conference on Magnetism, Grenoble, France, Sept. 14-19, 1970)
3	25-11979	See CEA-CONF-1704
CONF-700941-		(Meeting on Metallurgy, Paris, France, Sept. 28-Oct. 2, 1970)
1	25-11430	See CEA-CONF-1688
2	25-11371	See CEA-CONF-1690
3	25-11429	See CEA-CONF-1687
4	25-11431	See CEA-CONF-1691
5	25-11370	See CEA-CONF-1689
CONF-701001-		(4th International Conference on Plutonium and Other Actinides, Santa Fe, N. Mex., Oct. 5-9, 1970)
(Pt.1)	25-11372	
(Pt.2)	25-11433	
CONF-701002-		(EANDC Symposium on Neutron Standards and Flux Normalization, Argonne, Ill., Oct. 21-23, 1970)
2	25-12379	See KAPL-P-3901
CONF-701019-		(CREST Meeting on Reactivity Effects in Large Power Reactors, Ispra, Italy, Oct. 28-30, 1970)
3	25-12777	See TRG-Report-2060(Rev.)
CONF-701028-		(Meeting of the French Society of High Temperatures, Clermont-Ferrand, France, Oct. 26-27, 1970)
1	25-11485	See CEA-CONF-1670
CONF-701029-		(Euratom Working Group on Irradiation Devices, Karlsruhe, Germany, Oct. 8-9, 1970)
1	25-12813	See CEA-CONF-1673
CONF-701030-		(Meeting on the Use of Radioelements and Nuclear Methods in Geophysics for the Prospection and Exploitation of the Minerals, Nancy, France, Oct. 8-9, 1970)
1	25-10849	See CEA-CONF-1694
CONF-701031-		(Symposium on Economic Integration of Nuclear Power Stations in Electric Power Systems, Vienna, Austria, Oct. 5-9, 1970)
1	25-12724	See TRG-Report-2090
CONF-701106-		(5th Annual Midyear Topical Symposium on Health Physics Aspects of Nuclear Facility Siting, Idaho Falls, Idaho, Nov. 3-6, 1970)
5	25-10716	See UCRL-72534
CONF-701110-		(ASME Winter Annual Meeting, New York, N.Y., Nov. 30-Dec. 3, 1970)
1	25-11379	See UCRL-72477
CONF-701112-		(Symposium on New Developments in Physical and Biological Radiation Detectors, Vienna, Austria, Nov. 23-27, 1970)
2	25-10809	See BNWL-SA-3565
CONF-701201-		(American Geophysical Union National Fall Meeting, San Francisco, Calif., Dec. 7-10, 1970)
1	25-12880	See BNWL-SA-3539
CDO-		
7-565	25-12429	Dep. NTIS, 7p.
264-563	25-12163	Dep. NTIS, 34p.
264-563 (Add.)	25-12164	Dep. NTIS, 7p.
294-10	25-10570	Dep. NTIS, 14p.
1008-13	25-10522	Dep. NTIS, 7p.
1008-15	25-10523	Dep. NTIS, 9p.
1008-16	25-10524	Dep. NTIS, 5p.
1008-17	25-10525	Dep. NTIS, 15p.
1198-777	25-12881	Dep. NTIS, 23p.
1339-44	25-12882	Dep. NTIS, 20p.
1339-45	25-10933	Dep. NTIS, 5p.
1440-21	25-12883	Dep. NTIS, 20p.
1512-22	25-11009	Dep. NTIS, 61p.
1599-31	25-12884	Dep. NTIS, 78p.
1672-21	25-12514	Dep. NTIS, 20p.
1695-31	25-11909	Dep. NTIS, 53p.
1695-32	25-11910	Dep. NTIS, 133p.
1746-51	25-12515	Dep. NTIS, 25p.
1764-81	25-12175	Dep. NTIS, 78p.
1764-85	25-12625	Dep. NTIS, 60p.
1780-14	25-10515	Dep. NTIS, 20p.
2032-6	25-12885	Dep. NTIS, 13p.
2048-1	25-11373	Dep. NTIS, 88p.
2092-1	25-12886	Dep. NTIS, 8p.
2094-2	25-12887	Dep. NTIS, 169p.
CSIRO-Trans-		(Australian)
10204	25-11580	Dep. NTIS (U. S. Sales Only)
10206	25-11634	Dep. NTIS (U. S. Sales Only)
10247	25-11581	Dep. NTIS (U. S. Sales Only)
10286	25-11541	Dep. NTIS (U. S. Sales Only)
CU-		(Misc.)
1804-34	25-12888	Dep. NTIS, 9p.
3139-4	25-10725	Dep. NTIS, 8p.
DESY-		(German)
70/56	25-12137	Dep. NTIS (U. S. Sales Only), 10p.
DESY-HERA-		(West German)
70-1	25-12066	Dep. NTIS (U. S. Sales Only), 142p.
DOCKET-50155-		(Big Rock Point Reactor) (Misc.)
58	25-12725	Dep. NTIS, 19p.
59	25-12726	Dep. NTIS, 4p.
DOCKET-50184-		(National Bureau of Standards Reactor) (Non-AEC)
24	25-12814	Dep. NTIS, 2p.
DOCKET-50201-		(West Valley Reprocessing Plant--Formerly Spent Fuel Processing Plant) (Misc.)
58	25-10660	Dep. NTIS, 45p.
59	25-10661	Dep. NTIS, 1p.
71	25-10662	Dep. NTIS, 10p.
DOCKET-50213-		(Connecticut Yankee Atomic Power Plant) (Misc.)
89	25-12727	Dep. NTIS, 30p.
92	25-12728	Dep. NTIS, 10p.
93	25-12729	Dep. NTIS, 34p.
DOCKET-50214-		(Malibu Nuclear Plant) (Non-AEC)
2	25-12730	Dep. NTIS, 454p.
DOCKET-50231-		(Southwest Experimental Fast Oxide Reactor) (Non-AEC)
65	25-12731	Dep. NTIS, 11p.
66	25-12717	Dep. NTIS, 15p.
DOCKET-50237-		(Dresden Nuclear Power Station, See also DOCKET-50249) (Non-AEC)
126	25-12732	Dep. NTIS, 25p.
127	25-12718	Dep. NTIS, 1p.
128	25-12719	Dep. NTIS, 2p.
129	25-12720	Dep. NTIS, 2p.
DOCKET-50244-		(Robert Emmett Ginna Nuclear Power Plant, Formerly Brookwood Nuclear Station) (Non-AEC)
54	25-12733	Dep. NTIS, 4p.
DOCKET-50245-		(Millstone Point Nuclear Power Station) (Non-AEC)
51	25-12721	Dep. NTIS, 1p.
DOCKET-50249-		(Dresden Nuclear Power Station; See also DOCKET-50237) (Non-AEC)
53	25-12734	Dep. NTIS, 186p.
DOCKET-50259-		(Browns Ferry Nuclear Power Station. See also DOCKET-50260 and DOCKET-50296) (Non-AEC)
21	25-12735	Dep. NTIS, 32p.
DOCKET-50260-		(Browns Ferry Nuclear Power Station. See also DOCKET-50259 and DOCKET-50296) (Non-AEC)
21	25-12735	See DOCKET-50259-21
DOCKET-50267-		(Fort St. Vrain Nuclear Generating Station) (Non-AEC)
24	25-12736	Dep. NTIS, 356p.
25	25-12737	Dep. NTIS, 124p.
DOCKET-50268-		(Midwest Fuel Recovery Plant) (Non-AEC)
6	25-10663	Dep. NTIS, 519p.
DOCKET-50271-		(Vermont Yankee Nuclear Power Station) (Non-AEC)
35	25-12738	Dep. NTIS, 211p.
DOCKET-50280-		(Surry Power Station, See also DOCKET-50281) (Non-AEC)
32	25-12739	Dep. NTIS, 169p.

Report No.	Abstract No.	Availability
33	25-12740	Dep. NTIS, 360p.
DOCKET-50281-	(Surry Power Station, See also DOCKET-50280) (Non-AEC)	
32	25-12739	See DOCKET-50280-32
33	25-12740	See DOCKET-50280-33
DOCKET-50293-	(Pilgrim Nuclear Power Station) (Non-AEC)	
33	25-12741	Dep. NTIS, 4p.
DOCKET-50295-	(Zion Station Nuclear Power Plant. See also DOCKET-50304) (Non-AEC)	
22	25-12742	Dep. NTIS, 30p.
23	25-12743	Dep. NTIS, 25p.
DOCKET-50296-	(Browns Ferry Nuclear Power Station. See also DOCKET-50259 and DOCKET-50260) (Non-AEC)	
20	25-12735	See DOCKET-50259-21
DOCKET-50301-	(Point Beach Nuclear Plant) (Non-AEC)	
26	25-12744	Dep. NTIS, 61p.
DOCKET-50304-	(Zion Station Nuclear Power Plant. See also DOCKET-50295) (Non-AEC)	
22	25-12742	See DOCKET-50295-22
23	25-12743	See DOCKET-50295-23
DOCKET-50324-	(Brunswick Steam Electric Plant, Units 1 and 2, See also DOCKET-50325) (Non-AEC)	
18	25-12745	Dep. NTIS, 130p.
DOCKET-50325-	(Brunswick Steam Electric Plant, Units 1 and 2, See also DOCKET-50324) (Non-AEC)	
18	25-12745	See DOCKET-50324-18
DOCKET-50335-	(Hutchinson Island Plant) (Non-AEC)	
17	25-12746	Dep. NTIS, 11p.
DOCKET-50341-	(Enrico Fermi Atomic Power Plant) (Non-AEC)	
24	25-12747	Dep. NTIS, 54p.
DOCKET-50348-	(Joseph M. Farley Nuclear Plant, Units 1 and 2, Formerly Seala Nuclear Plant, See also DOCKET-50364) (Non-AEC)	
15	25-12748	Dep. NTIS, 349p.
DOCKET-50358-	(Wm. H. Zimmer Nuclear Power Station, Units 1 and 2) (See also DOCKET-50359) (Non-AEC)	
10	25-12749	Dep. NTIS, 958p.
DOCKET-50361-	(San Onofre Nuclear Generating Station) (Units 2 and 3) (See also Docket-50362) (Docket-50206) (Unit 1) (Non-AEC)	
13	25-12750	Dep. NTIS, 139p.
DOCKET-50362-	(San Onofre Nuclear Generating Station) (Units 2 and 3) (See also Docket-50361) (Docket-50206) (Unit 1) (Non-AEC)	
12	25-12750	See DOCKET-50361-13
DOCKET-50363-	(Forked River Nuclear Station) (Unit 1) (Non-AEC)	
10	25-12751	Dep. NTIS, 69p.
DOCKET-50364-	(Joseph M. Farley Nuclear Plant, Units 1 and 2, See also DOCKET-50348) (Non-AEC)	
9	25-12748	See DOCKET-50348-15
DOCKET-50376-	(Aguirre Nuclear Plant) (Non-AEC)	
7	25-12752	Dep. NTIS, 328p.
DOCKET-50382-	(Louisiana Power and Light Plant) (Non-AEC) (See also DOCKET-50383)	
2	25-12753	Dep. NTIS, 500p.
3	25-12754	Dep. NTIS, 314p.
4	25-12755	Dep. NTIS, 228p.
5	25-12756	Dep. NTIS, 286p.
DOCKET-50383-	(Louisiana Power and Light Plant) (Non-AEC) (See also DOCKET-50382)	
2	25-12753	See DOCKET-50382-2
3	25-12754	See DOCKET-50382-3
4	25-12755	See DOCKET-50382-4
5	25-12756	See DOCKET-50382-5
DP-MS-		
70-38	25-10664	Dep. NTIS, 20p.
DP-Report-	(British)	
530	25-11374	Dep. NTIS, 36p.
DUN-		
7149	25-12815	Dep. NTIS, 36p.
EACRP-L-	(European-American Committee on Reactor Physics)	
74	25-12816	Dep. NTIS (U. S. Sales Only), 14p.
EFI-		
70-65	25-12163	See COO-264-563
EGG-		
1183-484	25-10893	Dep. NTIS, 29p.
1183-542	25-12889	Dep. NTIS, 11p.
EIR-	(Swiss)	
185	25-10703	Dep. NTIS (U. S. Sales Only), 60p.
ERI-	(Misc.)	
551	25-11472	See AD-708705
76500	25-11473	See AD-708712
EUR-	(European Atomic Energy Community)	
4034	25-12796	See EURAEC-2145
4326	25-12817	Dep. NTIS (U. S. Sales Only), 52p.
4491	25-11096	Dep. CFSTI (U. S. Sales Only). EUR FF 2.80µ 10p.
4521	25-12339	Dep. NTIS (U. S. Sales Only). EUR FF 7.75, 52p.
4525	25-12516	Dep. NTIS (U. S. Sales Only). EUR FF 11.-, 72p.
4541	25-10430	Dep. NTIS (U. S. Sales Only). EUR FF 5,60, 36p.
4542	25-11294	Dep. NTIS (U. S. Sales Only). EUR DM 3,70, 28p.
4550	25-10571	Dep. NTIS (U. S. Sales Only). EUR FF 6.65, 44p.
EUR-CEA-FC-	(European Atomic Energy Community)	
542(Pt.1)	25-11854	Dep. NTIS (U. S. Sales Only), 121p.
542(Pt.2)	25-11855	Dep. NTIS (U. S. Sales Only), 118p.
543	25-11918	Dep. NTIS (U. S. Sales Only), 38p.
563	25-11859	Dep. NTIS (U. S. Sales Only), 54p.
566	25-11919	Dep. NTIS (U. S. Sales Only), 29p.
567	25-11920	Dep. NTIS (U. S. Sales Only), 33p.
569	25-11911	Dep. NTIS (U. S. Sales Only), 34p.
570	25-11866	Dep. NTIS (U. S. Sales Only), 25p.
571	25-11753	Dep. NTIS (U. S. Sales Only), 10p.
EURAEC-		
2145	25-12796	Dep. NTIS, 220p.
EURFNR-	(European Atomic Energy Community)	
855	25-12768	Dep. NTIS (U. S. Sales Only), 73p.
FMRB-	(German)	
33/70	25-12626	Dep. NTIS (U. S. Sales Only), 120p.
34/70	25-12818	Dep. NTIS (U. S. Sales Only), 54p.
FTI-	(Non-AEC)	
282	25-11860	Dep. NTIS (U. S. Sales Only), 14p.
295	25-11927	Dep. NTIS (U. S. Sales Only), 11p.
GA-	(Misc.)	
9168	25-11487	Dep. NTIS, 9p.
GAMD-	(Misc.)	
7567	25-10753	Dep. NTIS, 61p.
GEAP-	(Misc.)	
10207-22	25-12763	Dep. NTIS, 46p.
13539-13	25-11348	Dep. NTIS, 45p.
HEPL-	(Misc.)	
628	25-12376	See AD-710383
HMI-B-	(German)	
97	25-10904	Dep. NTIS (U. S. Sales Only), 170p.
IAE-	(Russian)	
1938	25-12841	Dep. NTIS (U. S. Sales Only), 40p.
1942	25-12798	Dep. NTIS (U. S. Sales Only), 48p.
1949	25-11928	Dep. NTIS (U. S. Sales Only), 44p.
1962	25-12509	For translation see ANL-Trans-855
IEA-	(Brazilian)	
184	25-10572	Dep. NTIS (U. S. Sales Only), 41p.
185	25-10516	Dep. NTIS (U. S. Sales Only), 26p.
186	25-12797	Dep. NTIS (U. S. Sales Only), 40p.
207	25-10573	Dep. NTIS (U. S. Sales Only), 16p.
208	25-10431	Dep. NTIS (U. S. Sales Only), 16p.
IFVE-SEF/OP-	(Russian)	
70-13	25-10868	Dep. NTIS (U. S. Sales Only), 22p.
IN-		
1437	25-11458	Dep. NTIS, 75p.
INP-	(Polish)	
709	25-10887	Dep. NTIS (U. S. Sales Only), 43p.
711	25-12377	Dep. NTIS (U. S. Sales Only), 27p.
714	25-12517	Dep. NTIS (U. S. Sales Only), 10p.
720	25-12627	Dep. NTIS (U. S. Sales Only), 10p.
INR-	(Non-AEC)	
1193	25-12842	Dep. NTIS (U. S. Sales Only), 65p.
1206	25-12843	Dep. NTIS (U. S. Sales Only), 9p.
INR-P-	(Polish)	
1091	25-12430	Dep. NTIS (U. S. Sales Only), 26p.

XUM

Report No.	Abstract No.	Availability
1201	25-12628	Dep. NTIS (U. S. Sales Only), 25p.
1207	25-12191	Dep. NTIS (U. S. Sales Only), 6p.
1209	25-10665	Dep. NTIS (U. S. Sales Only), 37p.
1223	25-12090	Dep. NTIS (U. S. Sales Only), 25p.
INSJ-	(Japanese)	
123	25-12518	Dep. NTIS (U. S. Sales Only), 16p.
124	25-12431	Dep. NTIS (U. S. Sales Only), 17p.
IPP-	(Non-AEC)	
6/88	25-12299	See IPP-7/2
7/2	25-12299	Dep. NTIS (U. S. Sales Only), 26p.
IPPJ-T-	(Japanese)	
2	25-11921	Dep. NTIS (U. S. Sales Only), 34p.
4	25-12045	Dep. NTIS (U. S. Sales Only), 13p.
IRA-TR-	(Non-AEC)	
1-70	25-10765	See AD-709142
ITP-	(Non-AEC)	
274	25-12635	See NP-18545
JAERI-	(Japanese)	
5026	25-10584	Dep. NTIS (U. S. Sales Only), 171p.
JAERI-Memo-	(Japanese)	
4192	25-12862	Dep. NTIS (U. S. Sales Only), 20p.
4196	25-12819	Dep. NTIS (U. S. Sales Only), 31p.
4197	25-12705	Dep. NTIS (U. S. Sales Only), 44p.
JINR-	(Russian)	
E4-5135	25-12629	Dep. NTIS (U. S. Sales Only), 28p.
E4-5469	25-12630	Dep. NTIS (U. S. Sales Only), 30p.
E13-5459	25-10869	Dep. NTIS (U. S. Sales Only), 10p.
P1-4872	25-12378	Dep. NTIS (U. S. Sales Only), 25p.
P1-5398	25-12099	Dep. NTIS (U. S. Sales Only), 24p.
P1-5431	25-12204	Dep. NTIS (U. S. Sales Only), 19p.
P4-5008	25-12631	Dep. NTIS (U. S. Sales Only), 20p.
P4-5084	25-12632	Dep. NTIS (U. S. Sales Only), 30p.
P4-5346	25-12633	Dep. NTIS (U. S. Sales Only), 18p.
P6-5410	25-10666	Dep. NTIS (U. S. Sales Only), 12p.
P8-5212	25-12300	Dep. NTIS (U. S. Sales Only), 17p.
P9-5394	25-12301	Dep. NTIS (U. S. Sales Only), 17p.
P9-5405	25-12302	Dep. NTIS (U. S. Sales Only), 8p.
P9-5442	25-12303	Dep. NTIS (U. S. Sales Only), 8p.
P9-5446	25-12304	Dep. NTIS (U. S. Sales Only), 9p.
P9-5558	25-12305	Dep. NTIS (U. S. Sales Only), 13p.
P13-5378	25-10813	Dep. NTIS (U. S. Sales Only), 10p.
P13-5391	25-10814	Dep. NTIS (U. S. Sales Only), 18p.
P13-5420	25-10870	Dep. NTIS (U. S. Sales Only), 12p.
P16-5383	25-11054	Dep. NTIS (U. S. Sales Only), 16p.
JUL-	(German)	
657-MA	25-10768	Dep. NTIS (U. S. Sales Only), 64p.
660-ZE	25-10815	Dep. NTIS (U. S. Sales Only), 23p.
661-RW	25-11376	Dep. NTIS (U. S. Sales Only), 62p.
669-RW	25-11479	Dep. NTIS (U. S. Sales Only), 173p.
674-RC	25-10517	Dep. NTIS (U. S. Sales Only), 51p.
678-RG	25-12776	Dep. NTIS (U. S. Sales Only), 248p.
684-FF	25-10850	Dep. NTIS (U. S. Sales Only), 149p.
KAPL-P-		
3901	25-12379	Dep. NTIS, 17p.
KFK-	(German)	
767	25-12529	For translation see ORNL-tr-3020
866	25-10796	Dep. NTIS (U. S. Sales Only), 19p.
1211	25-11488	Dep. NTIS (U. S. Sales Only), 86p.
1222	25-12380	Dep. NTIS (U. S. Sales Only), 33p.
1223	25-12340	Dep. NTIS (U. S. Sales Only), 118p.
1247	25-12519	Dep. NTIS (U. S. Sales Only), 35p.
1255	25-12820	Dep. NTIS (U. S. Sales Only), 92p.
1261	25-10432	Dep. NTIS (U. S. Sales Only), 34p.
1281	25-11464	Dep. NTIS (U. S. Sales Only), 33p.
1285	25-10626	Dep. NTIS (U. S. Sales Only), 42p.
KFK-tr-	(German)	
334	25-12306	Dep. CFSTI (U. S. Sales Only)
KFKI-	(Hungarian)	
70-20-RPT	25-12784	Dep. NTIS (U. S. Sales Only), 14p.
70-21-HEP	25-11742	Dep. NTIS (U. S. Sales Only), 8p.
70-25-NAC	25-10489	Dep. NTIS (U. S. Sales Only), 30p.
70-26-HP	25-10775	Dep. NTIS (U. S. Sales Only), 6p.
KHFTI-	(Russian)	
69-24	25-12306	For translation see KFK-tr-334
69-27	25-12307	Dep. CFSTI (U. S. Sales Only), 9p.
70-25	25-11922	Dep. NTIS (U. S. Sales Only), 19p.
LA-		
4524	25-12890	Dep. NTIS, 16p.
LAL-	(French)	
1239	25-12067	Dep. NTIS (U. S. Sales Only), 113p.
LAL-RT-	(French)	
5-70	25-12308	Dep. NTIS (U. S. Sales Only), 12p.
LFEN-NI.-	(Portuguese)	
46-a	25-12341	Dep. NTIS (U. S. Sales Only), 22p.

Report No.	Abstract No.	Availability
LIB/Trans-	(Australian)	
310	25-10667	Dep. NTIS (U. S. Sales Only)
334	25-10490	Dep. NTIS (U. S. Sales Only)
335	25-12821	Dep. NTIS (U. S. Sales Only)
LMSC-N-	(Non-AEC)	
6-P-70-1	25-11778	See AD-709105
LNF-	(Italian)	
70/18	25-11820	Dep. NTIS (U. S. Sales Only), 12p.
LYCEN-	(French)	
6909	25-12309	Dep. NTIS (U. S. Sales Only), 91p.
7034	25-12520	
MATT-		
818	25-11867	Dep. NTIS, 17p.
MLM-		
1778	25-11377	Dep. NTIS, 17p.
1779	25-10776	Dep. NTIS, 10p.
MNC-		
3783-7	25-12526	Dep. NTIS, 29p.
MPI-PA-	(Misc.)	
7/62	25-11912	Dep. NTIS (U. S. Sales Only), 14p.
N-	(Misc.)	
70-31814	25-10907	NTIS, 84p.
NASA-CR-	(Misc.)	
1606	25-10907	See N-70-31814
72764	25-11480	See ORNL-4608
NBS-TN-	(Misc.)	
545	25-10422	GPO $1.25
NCRP-	(Non-AEC)	
36	25-11075	NCRP $1.50
NP-	(AEC File No. for Non-AEC Reports)	
18380	25-10934	Dep. CFSTI (U. S. Sales Only), 11p.
18381	25-11037	Dep. CFSTI (U. S. Sales Only), 16p.
18388	25-10935	Dep. CFSTI (U. S. Sales Only), 19p.
18393	25-11326	Dep. CFSTI (U. S. Sales Only), 111p.
18394	25-11305	Dep. CFSTI (U. S. Sales Only), 111p.
18499	25-12822	Dep. NTIS (U. S. Sales Only), 24p.
18541	25-12381	Dep. NTIS (U. S. Sales Only), 43p.
18545	25-12635	Dep. NTIS (U. S. Sales Only), 10p.
18546	25-12382	Dep. NTIS (U. S. Sales Only), 42p.
18552	25-12433	Dep. NTIS (U. S. Sales Only), 56p.
18570	25-10851	Dep. NTIS (U. S. Sales Only), 87p.
18580	25-12636	Dep. NTIS (U. S. Sales Only), 27p.
18591	25-11542	Dep. NTIS (U. S. Sales Only), 73p.
18607	25-11244	Dep. NTIS (U. S. Sales Only), 5p.
18608	25-12891	
18609	25-10704	Dep. NTIS (U. S. Sales Only), 152p.
18612	25-12310	Dep. NTIS (U. S. Sales Only), 107p.
18613	25-12527	Dep. NTIS (U. S. Sales Only), 13p.
18614	25-10894	Dep. NTIS (U. S. Sales Only), 9p.
18616	25-12353	Dep. NTIS (U. S. Sales Only), 50p.
18617	25-10852	Dep. NTIS (U. S. Sales Only), 16p.
18619	25-12046	Dep. NTIS (U. S. Sales Only), 15p.
18629	25-12100	Dep. NTIS (U. S. Sales Only), 172p.
18633	25-10754	Dep. NTIS (U. S. Sales Only), 86p.
18635	25-11861	Dep. NTIS (U. S. Sales Only), 15p.
18647	25-12528	Dep. NTIS (U. S. Sales Only), 18p.
NUMEC-		
4189-3	25-10777	Dep. NTIS, 73p.
NVO-		
1163-TM-22	25-10730	Dep. NTIS, 99p.
NYO-		
841-23	25-10797	Dep. NTIS, 83p.
2150-65	25-12892	Dep. NTIS, 8p.
2171-328	25-12637	Dep. NTIS, 28p.
2171-334	25-12638	Dep. NTIS, 10p.
2262-TA-222	25-12138	Dep. NTIS, 18p.
2262-TA-228	25-12122	Dep. NTIS, 11p.
2262-TA-232	25-12192	Dep. NTIS, 46p.
2471-47	25-12893	Dep. NTIS, 86p.
2499-37	25-10627	Dep. NTIS, 21p.
3087-16	25-12894	Dep. NTIS, 174p.
3087-17	25-12895	Dep. NTIS, 208p.
3087-21	25-12896	Dep. NTIS, 73p.
3087-23	25-12897	Dep. NTIS, 25p.
3399-234	25-12193	See SU-1206-234
3661-33	25-12898	Dep. NTIS, 6p.
3829-65	25-12047	Dep. NTIS, 9p.
4061-3	25-10705	Dep. NTIS, 18p.
4077-1	25-11923	Dep. NTIS, 180p.
4185-1	25-12899	Dep. NTIS, 14p.
4185-2	25-12900	Dep. NTIS, 31p.

XUM

Report No.	Abstract No.	Availability
ORNL-		
4579	25-11055	Dep. NTIS, 145p.
4588	25-10654	Dep. NTIS, 35p.
4608	25-11480	Dep. NTIS, 67p.
4636	25-10423	Dep. NTIS, 82p.
ORNL-NSIC-		
84	25-10798	Dep. NTIS, 123p.
ORNL-TM-		
2635(Suppl.)	25-11533	Dep. NTIS, 16p.
2803	25-10755	Dep. NTIS, 75p.
2989	25-11378	Dep. NTIS, 45p.
3101	25-10895	Dep. NTIS, 23p.
3104	25-12804	Dep. NTIS, 23p.
3109	25-11465	Dep. NTIS, 155p.
3210	25-12901	Dep. NTIS, 45p.
3214	25-10778	Dep. NTIS, 24p.
3221	25-12785	Dep. NTIS, 327p.
3273	25-12786	Dep. NTIS, 129p.
ORNL-tr-		
2416	25-10756	Dep. NTIS
3020	25-12629	Dep. NTIS
ORO-		
2036-20	25-12902	Dep. NTIS, 76p.
2529-28	25-10706	Dep. NTIS, 169p.
2583-8	25-11010	Dep. NTIS, 15p.
3329-6	25-10961	Dep. NTIS, 17p.
3674-4	25-11981	Dep. NTIS, 94p.
3765-28	25-12639	Dep. NTIS, 35p.
3911-3	25-10769	Dep. NTIS, 32p.
3935-4	25-12903	Dep. NTIS, 46p.
OU-LNS-	(Japanese)	
70-2	25-12640	Dep. NTIS (U. S. Sales Only), 82p.
P-	(Misc.)	
4407	25-12162	See AD-710572
PATENTS	(British)	
1,213,557	25-12800	
1,214,136	25-12771	
1,214,459	25-12802	
1,214,880	25-10762	
1,214,892	25-12832	
1,214,993	25-12811	
1,214,998	25-12769	
1,215,081	25-10774	
1,215,138	25-12770	
1,215,176	25-12810	
1,215,265	25-10800	
1,215,343	25-11481	
1,215,499	25-12831	
1,215,960	25-12863	
1,217,443	25-10805	
1,218,514	25-11366	
1,218,605	25-11363	
PATENTS	(Canadian)	
853,249	25-10682	
PATENTS	(French)	
1,586,182	25-10854	
1,586,456	25-10801	
1,586,696	25-10803	
1,587,747	25-10804	
1,589,053	25-10789	
1,589,063	25-10760	
1,589,876	25-10781	
2,000,473	25-11033	
2,000,475	25-11034	
PATENTS	(U. S.)	
3,528,407	25-10828	
3,529,160	25-10889	
3,529,163	25-10890	
3,535,103	25-11362	
3,541,332	25-10785	
3,541,342	25-10788	
3,541,762	25-10761	
PWE-R-		
39	25-10735	Dep. NTIS, 58p.
PR-B-	(Canadian)	
87	25-11074	See AECL-3777
PR-CMa-	(Canadian)	
14	25-10583	See AECL-3776
PR-P-	(Canadian)	
84	25-12427	See AECL-3666
RCN-	(Dutch)	
125	25-12823	Dep. NTIS (U. S. Sales Only), 67p.
130	25-12768	See EURFNR-855

Report No.	Abstract No.	Availability
RD/B/N-	(British)	
1720	25-10896	Dep. NTIS (U. S. Sales Only), 27p.
1795	25-10790	Dep. NTIS (U. S. Sales Only), 16p.
1816	25-10518	Dep. NTIS (U. S. Sales Only), 17p.
RFP-		
1527	25-10757	Dep. NTIS, 17p.
1568	25-12904	Dep. NTIS, 12p.
RISO-M-	(Danish)	
1279	25-12837	Dep. NTIS (U. S. Sales Only), 57p.
RLO-		
1388-130	25-12530	Dep. NTIS, 28p.
1388-595	25-12641	Dep. NTIS, 30p.
2225-T-14-1	25-10997	Dep. NTIS, 46p.
RPI-	(Misc.)	
328-210	25-12342	Dep. NTIS, 34p.
RT/PROT-	(Italian)	
(70)21	25-10853	Dep. NTIS (U. S. Sales Only), 47p.
SAM-TR-	(Non-AEC)	
70-22	25-11251	See AD-705976
SC-CR-		
70-6137	25-12905	Dep. NTIS, 95p.
SC-M-		
70-868	25-12906	Dep. NTIS, 4p.
70-886	25-12907	Dep. NTIS, 8p.
SC-RR-		
70-163	25-12908	Dep. NTIS, 25p.
70-441	25-10792	Dep. NTIS, 21p.
70-471	25-12909	Dep. NTIS, 119p.
SC-T-		
70-4054	25-11868	Dep. NTIS
71-3002	25-12910	Dep. NTIS
71-3003	25-12911	Dep. NTIS
SLAC-PUB-		
842	25-12068	Dep. NTIS, 30p.
SRARI-P-	(Russian)	
78	25-11466	Dep. NTIS (U. S. Sales Only), 40p.
SRIA-		
106-76	25-12912	Dep. NTIS, 17p.
SRO-	(Misc.)	
475-9	25-12913	Dep. NTIS, 26p.
SSI-	(Swedish)	
70-27	25-12757	Dep. NTIS (U. S. Sales Only), 25p.
STI/PUB-	(International Atomic Energy Agency)	
241	25-11056	IAEA $5.00
247	25-11327	IAEA $4.00
248	25-12824	IAEA $7.00
SU-	(Misc.)	
326-P-17-X-1	25-11434	Dep. NTIS, 44p.
1206-234	25-12193	Dep. NTIS, 25p.
TID-		
25586	25-12531	Dep. NTIS, 122p.
25592	25-12532	Dep. NTIS, 158p.
25633	25-12914	Dep. NTIS, 6p.
25635	25-12791	Hinsdale, Ill.; American Nuclear Society (1970). 313p. $24.00
25636	25-12722	Dep. NTIS, 18p.
25637	25-12723	Dep. NTIS, 41p.
TKK-F-A-	(Finnish)	
121	25-12844	Dep. NTIS (U. S. Sales Only), 44p.
123	25-12533	Dep. NTIS (U. S. Sales Only), 13p.
TRG-Report-	(British)	
2060(Rev.)	25-12777	Dep. NTIS (U. S. Sales Only), 25p.
2090	25-12724	Dep. NTIS (U. S. Sales Only), 29p.
TUBIK-	(German)	
17	25-12799	Dep. NTIS (U. S. Sales Only), 8p.
TUNL-		
2	25-12534	Dep. NTIS, 72p.
UCB-		
34-P-23-15	25-10936	Dep. CFSTI, 45p.
UCLA-		
34-P-122-X-1	25-12915	Dep. NTIS, 150p.
UCRL-		
19115	25-12916	Dep. NTIS, 16p.
50957	25-10937	Dep. NTIS, 28p.
72393	25-12917	Dep. NTIS, 43p.

XUM

Report No.	Abstract No.	Availability
72477	25-11379	Dep. NTIS, 23p.
72534	25-10716	Dep. NTIS, 21p.
72716(Rev. 1)	25-11038	Dep. NTIS, 79p.
UR-49-1125	25-11020	Radiat. Bot.; 10: 273-9 (Jun 1970)
URS-	(Non-AEC)	
708-4	25-10702	See AD-708558
757-4	25-10733	See AD-708566
757-5	25-10734	See AD-708567
UUIP-	(Swedish)	
722	25-11913	Dep. NTIS (U. S. Sales Only), 33p.
WAPD-TM-	(Misc.)	
906	25-11349	Dep. NTIS, 34p.

Report No.	Abstract No.	Availability
979	25-11534	Dep. NTIS, 11p.
987	25-12918	Dep. NTIS, 34p.
WCAP-	(Misc.)	
7578	25-11380	Dep. NTIS, 39p.
WHAN-FR-		
20	25-11489	Dep. NTIS, 43p.
WHAN-IR-		
47	25-12919	Dep. NTIS, 51p.
Y-		
1752	25-12920	Dep. NTIS, 165p.
1754	25-11078	Dep. NTIS, 71p.

☆U. S. GOVERNMENT PRINTING OFFICE: 1971—436-212/20

UNITED STATES ATOMIC ENERGY COMMISSION

NUCLEAR SCIENCE ABSTRACTS

Volume 25
Numbers 1-6

Abstracts 1-12920

January-March
1971

Division of Technical Information

STAFF OF NUCLEAR SCIENCE ABSTRACTS

John W. Norris
Managing Editor

Donald D. Davis
Assistant Managing Editor

David E. Bost
Production Manager

Sidney F. Lanier
Subject Heading Specialist

J. Paul Meredith
Descriptive Cataloging Specialist

Frederick E. Marsh, Jr.
Computer Index Coordinator

Clara L. Fox
Corporate Author Specialist

Helen W. White
Report Number Specialist

Section Editors

Everett J. Hoffman
Chemistry

Robert C. Kelly
Engineering; Earth Sciences; Metals, Ceramics, and Other Materials

Lee M. Thompson
General Physics

Charles E. Stuber
High Energy Physics; Instrumentation

Helen G. Donald
Life Sciences

Lawrence T. Whitehead
Nuclear Physics

James M. Jacobs
Reactor Technology

Evaluators

Thomas S. Chapman
Rose V. Jermain
John H. Mitchell
Mary H. Newman
Polly C. Summers

Abstractors

F. S. Armstrong*
Ellis R. Bedford
Mary M. Brown
Jane G. Buchanan
D. Lamar Cason
Gloria M. Caton
David C. Cunningham
James R. Dulaney
Helga B. Gerstner
Mary C. Grissom
Phyllis C. Hansen
Carolyn D. Houston
Elaine E. Huber
Rose V. Jermain
W. Hugh Kinser, Jr.
Lisbeth C. Lieberman
Betty L. McDowell
Patricia B. McEwen
Fay M. Martin
William D. Matheny
Dora H. Moneyhun
Jean F. Peckham
Henry D. Raleigh
Mona H. Raridon
Julia S. Redford
Jessie W. Rushing
Robert W. Rutkowski
Francis L. Sachs
Lila B. Smith
Anne G. Ward
Helen L. Ward
Milton O. Whitson
Juanita Wilson

*Atomic Energy of Canada, Ltd.

Charles R. Bruce
Publishing Coordinator

Communication concerning the editorial policy and content of *Nuclear Science Abstracts* should be addressed to the Managing Editor, *Nuclear Science Abstracts*, USAEC Division of Technical Information Extension, P. O. Box 62, Oak Ridge, Tennessee 37830.

Use of funds for printing this publication approved by the Director of the Bureau of the Budget, June 26, 1969.

UNITED STATES
ATOMIC ENERGY COMMISSION
P. O. BOX 62
OAK RIDGE, TENNESSEE 37830

OFFICIAL BUSINESS

POSTAGE AND FEES PAID
U. S. ATOMIC ENERGY COMMISSION

GOVERN

PL

POSTAGE AND FEES PAID
U. S. GOVERNMENT PRINTING OFFICE

UNIVERSITY MICROFILMS 1
ATTN MRS. MARLENE HURST
MANAGER, PUBLISHER RELATIONS
ANN ARBOR MICHIGAN 48106

AEC Critical Review Series

ATMOSPHERIC TRANSPORT PROCESSES, Part 2: Chemical Tracers

Elmar R. Reiter, Colorado State University

January 1971

The use of trace constituents of the atmosphere in estimating the effects of the general circulation has opened into a wide field of research. This book focuses on the large-scale aspects of the atmospheric circulation and on the effect of this circulation on tracer distributions. Future research in this fertile field should produce more cooperation between the chemists, atmospheric dynamicists, and synopticians and thus provide better returns from the intricate and complex experiments necessary in exploring the many aspects of our global atmosphere and of the atmospheres of other planets. (388 pages, 7 x 9¾ inches, Library of Congress Catalog Card Number: 76-603262)

Contents

- Introduction and Theoretical Considerations
  - The Spreading of Tracers
  - The Structure of the Upper Atmosphere
  - General Comments on the Photochemistry of the Upper Atmosphere
- Water Vapor as a Tracer
  - Tropospheric Distributions
  - Water Vapor in the Stratosphere
  - Water Vapor in the Mesosphere
- Carbon Dioxide
  - The Secular Trend of CO_2 Concentrations
  - Diurnal Variations
  - Seasonal Variations and Interhemispheric Exchange
- Ozone
  - The Chemistry and Photochemistry of Ozone
  - The Vertical Distribution of Ozone
  - Surface [O_3] and Its Variations
  - Solar Relations of Ozone Variations
  - Ozone and the Biennial Oscillation
  - Theoretical Models of Ozone Transport
- Oxygen as a Tracer
  - Molecular and Atomic Oxygen
  - The Oxygen Green Line, 5577 Å
  - The Oxygen Red Line, 6300 Å
  - The Hydroxyl Radical
- Other Chemical Tracers
  - Carbon Monoxide
  - Methane
  - Sulfur
  - Nitrogen Compounds
  - The Halogens
  - Sodium and Other Alkali Metals
  - Dust
- Conclusions and Outlook

This book is available for $6.00 as TID-25314 from National Technical Information Service, U. S. Department of Commerce, Springfield, Virginia 22151

XUM

XUM